# EANM'13


Annual Congress
of the
European Association of Nuclear Medicine

October 19 - 23, 2013

Lyon, France

Abstracts

European Journal of Nuclear Medicine and Molecular Imaging

Volume 40, Supplement 2

DOI 10.1007/s00259-013-2535-3

**This supplement was not sponsored by outside commercial interests. It was funded entirely by the association's own resources.**

Springer

Eur J Nucl Med Mol Imaging (2013) 40 (Suppl 2):S1–S477
DOI 10.1007/s00259-013-2535-3

# Welcome to the EANM Congress 2013 in Lyon!

On behalf of the European Association of Nuclear Medicine, it is my great honour and pleasure to welcome you in Lyon for the 26th Annual Congress of the European Association of Nuclear Medicine, following the successful 25th anniversary in Milan last year. After "Paris 2000", this is the second time that France has had the privilege of hosting our annual congress.

The EANM Congress is now a key international scientific event attracting specialists from all over the world. Its exciting and diverse scientific programme offers the full spectrum of our specialty, ranging from continuing education to cutting-edge lectures on the newest research.

As each year, the scientific programme is the result of the joint efforts and productive collaboration of the scientific committee, all the committees and the working groups, whose suggestions – regarding topics and lecturers – were of major importance. The programme highlights the fields in which nuclear medicine is most essential for patient management but also features the most appealing issues for future developments. It will take us from molecular biology and new achievements in physics and dosimetry to the recent results of radiopharmaceutical research and the implementation of hybrid imaging. The best experts and speakers have been invited to teach us about the latest developments in our discipline in both diagnostic and therapeutic areas. Much room has been allowed for collaboration with other medical specialties through the high number of joint symposia with other scientific societies.

As in 2012, we have paid special attention to the education of our young colleagues. The Young EANM Daily Forum will provide young specialists with an opportunity to meet with their peers and more experienced colleagues, and to learn more about research and career development. For medical students a special event has been organised: the "Offspring Day", very successful last year, will be repeated and will consist in a one-day guided visit to the congress, with attendance at the Marie Curie Lecture, a visit to the exhibition and a final meeting with peers and teachers.

Four plenary sessions will focus on the present status and future of nuclear medicine, with contributions from high-level lecturers along with 7 joint symposia with related medical societies, 7 free symposia and 13 continuing medical education sessions. Several daily interactive sessions successfully launched at previous congresses will be continued, including the "Pitfalls & Artefacts & Physiology" sessions. A high-standard technologist programme will include courses, continuing technologist education sessions, and oral and poster sessions.

This year the programme of the EANM Congress has again stimulated high scientific interest. The Scientific Committee received a total of 1867 abstracts, of which 1671 were accepted; over 570 oral presentations and more than 1000 posters will finally be presented during the congress.

The EANM Congress is also an opportunity to stress the strategic importance of our Association. It has a major role in promoting nuclear medicine and its broad applications in modern medical practice, as well as in spreading knowledge of functional and molecular imaging modalities throughout Europe and worldwide.

One last innovation must be emphasised: the EANM "goes green": no more abstract book – we have replaced it by a digital on-line version; which means that the congress bags will be lighter too!

Finally, a great debt of gratitude is owed to the Local Organising Committee for taking care of the social programme, which will dovetail perfectly with the busy scientific programme.

On behalf of the EANM Executive Committee, the Scientific Committee, the Technologist Programme Committee, the Local Organising Committee and all the excellent professionals working in the EANM Headquarters in Vienna and the French Association of Nuclear Medicine, it is my great pleasure to welcome you to the 26th EANM Congress and to wish you a very pleasant stay in Lyon.

Dominique Le Guludec, MD, PhD
EANM Congress President 2013

# Saturday, October 19, 2013

**TIME SCHEDULE**

| Time/ Halls | Amphithéâtre | Saint-Clair 2 | Saint-Clair 1 | Rhône 3A/3B | Salon Pasteur | Rhône 2 | Gratte-Ciel 1/2/3 | Grand Salon Prestige Gratte-Ciel | Tête D'Or 1/2 | | Poster Exhibition Bellecour Area |
|---|---|---|---|---|---|---|---|---|---|---|---|
| Cap. | 3140 | 80 | 80 | 220 | 280 | 100 | 250 | 280 | 180 | | |
| 08:00 - 18:00 | | EANM Advisory Council Meeting (11:00 - 13:00) | ESNM Meeting (14:00 - 16:00) | EANM Delegates Assembly (14:00 - 16:00) | EANM Committee Meetings (16:00 - 18:00) | UEMS / EBNM Delegates Assembly (16:40 - 18:00) | Pre-Symposium 1: Quantitative Imaging and Dosimetry: Steps Towards Personalised Nuclear Medicine Treatments (09:30 - 16:30) | Pre-Symposium 2: Molecular Cardiovascular Imaging: From New Tracers to Hybrid Technology (08:45 - 17:45) | Pre-Symposium 3: MRI-PET: Current Status and Future Perspectives (09:00 - 12:45)<br>* * * * * * * *<br>Pre-Symposium 4: New Imaging Targets for Dementia (13:30 - 16:15) | | Poster Setup: Technologist Posters Poster Walks Poster Group 1 (08:00 - 18:00) |
| 19:00 - 20:00 | OPENING CEREMONY (19:00 - 20:00) & WELCOME RECEPTION (20:00 - 22:30) | | | | | | | | | | |

# Sunday, October 20, 2013

**TIME SCHEDULE**

| Time/ Halls | Amphithéâtre | Auditorium Lumière | Forum 3 | Bellecour 1/2/3 | Auditorium Pasteur | Grand Salon Prestige Gratte-Ciel | Salon Pasteur | Gratte-Ciel 1/2/3 | Rhône 3A/3B | Tête D'Or 1/2 | Poster Exhibition Bellecour Area |
|---|---|---|---|---|---|---|---|---|---|---|---|
| Cap. | 3140 | 880 | 700 | 390 | 290 | 280 | 280 | 250 | 220 | 180 | |
| 08:00 - 09:30 | 101 CME 1: Oncology & Drug Development PET and SPECT in Oncology Drug Development | 102 Symposium 1: FDG-PET in Early Alzheimer: Why do they look so Heterogeneous? | 103 Technologists 08:00 - 08:12 Opening Ceremony 08:15 - 09:45 CTE 1: Radionuclide Therapy in Oncology | | | | 107 Pitfalls & Artefacts & Physiology (Interactive): Oncology | | | | Poster Walks: PW01 - PW05 (08:30 - 09:30) |
| 10:00 - 11:15 | 201 Plenary Session 1 incl. Marie Curie Lecture: Functional and Molecular Imaging in Heart Disease | | 203 In Hall Amphithéâtre: Plenary Session 1 incl. Marie Curie Lecture: Functional and Molecular Imaging in Heart Disease | | | | | | | | |
| 11:30 - 13:00 | 301 CME 2: Radionuclide Therapy & Dosimetry PRRT: New Approaches | 302 Symposium 2: Assessment of Patients Suspected of CAD | 303 Technologists CTE 2: Multiprofessional Round Table on Entry Level and Advanced Practice (Interactive) | 304 Featured - Conventional & Specialised Nuclear Medicine: Renal Function | 305 Oncology Basic Science: Preclinical Tumour Targeting | 306 Physics & Instrumentation & Data Analysis: Image Reconstruction | 307 Oncology Clinical Science: Melanoma, Sarcoma, CUP & Other | 308 Molecular & Multimodality Imaging: Metabolism in Preclinical Models | 309 Radiopharmaceuticals & Radiochemistry & Dosimetry: PET Radiopharmaceuticals | | |
| 13:00 - 14:30 | | GE Healthcare Symposium | | EARL: Visions for the Future of European Nuclear Medicine | Bayer HealthCare Symposium | | | Clinical Audit Beyond Europe | | Young EANM Daily Forum: Back to the Future | |
| 14:30 - 16:00 | 401 CME 3: Physics Motion Correction | 402 Symposium 3: From Cell to Scanner 2013: Hypoxia | Technologists 403a 14:30 - 15:30 Mini Course 1: Reconstructions: TrueX + TOF, PSF, OSEM * * * * * * * * * 403b 15:45 - 16:45 Mini Course 2: EANM-TC/SNMMI-TS Joint Session: Technologists Perspective in Radionuclide Therapy * * * * * * * * * 403c 17:00 - 18:00 Mini Course 3: Dose Reduction | 404 Featured - Cardiovascular: Plaque Imaging | 405 Radionuclide Therapy & Dosimetry: Preclinical Models | 406 Molecular & Multimodality Imaging: Hybrid Imaging - Image Processing & Quantitation | 407 Conventional & Specialised Nuclear Medicine: Bone Infection & IBD | 408 Radionuclide Therapy & Dosimetry: Thyroid Cancer | 409 Radiopharmaceuticals & Radiochemistry & Dosimetry: Radiopharmaceuticals - SPECT | 410 Oncology Clinical Science: Upper GI Tract Tumours | Posters Group 1: P01-1 - P74-1 (16:00 - 16:30) |
| 16:30 - 18:00 | 501 CME 4: Radiopharmacy & Drug Development State of the Art of Radiopharmaceuticals | 502 Symposium 4: EANM/EORTC Joint Session: Imaging Biomarkers for Early Response Assessment in Clinical Oncology Trials | | 504 Featured - Physics & Instrumentation & Data Analysis: Image Reconstruction, TOF | 505 Conventional & Specialised Nuclear Medicine: Bone 1 (Oncology) | 506 Cardiovascular: Myocardial Perfusion SPECT II | 507 Conventional & Specialised Nuclear Medicine: FVO - Sjögren - Sarcoidosis | 508 Radionuclide Therapy & Dosimetry: Peptide Receptor Radionuclide Therapy | 509 Oncology Clinical Science: Brain Tumours | 510 Neurosciences: Data Analysis & Management | |

# Monday, October 21, 2013

**TIME SCHEDULE**

| Time/ Halls | Amphithéâtre | Auditorium Lumière | Forum 3 | Bellecour 1/2/3 | Auditorium Pasteur | Grand Salon Prestige Gratte-Ciel | Salon Pasteur | Gratte-Ciel 1/2/3 | Rhône 3A/3B | Tête D'Or 1/2 | Poster Exhibition Bellecour Area |
|---|---|---|---|---|---|---|---|---|---|---|---|
| Cap. | 3140 | 880 | 700 | 390 | 290 | 280 | 280 | 250 | 220 | 180 | |
| 08:00 - 09:30 | CME<br>601<br>CME 5:<br>Cardiovascular<br>Myocardial Viability | 602<br>Symposium 5:<br>EANM/EAU Joint Session:<br>Diagnostics and Therapy of Bone Metastases in Patients with Advanced Prostate Cancer | 603<br>Technologists<br>Oral Presentations 1 | | | | 607<br>Pitfalls & Artefacts & Physiology (Interactive):<br>Paediatric Hybrid Imaging | | | | Poster Walks:<br>PW06 - PW10<br>(08:30 - 09:30) |
| 10:00 - 11:15 | 701<br>Plenary Session 2:<br>Use of PET in Assessment of Therapy | | 703<br>In Hall Amphithéâtre:<br>Plenary Session 2:<br>Use of PET in Assessment of Therapy | 704<br>Featured - Cardiovascular:<br>Advances in MPI SPECT | | | | | | | |
| 11:30 - 13:00 | CME<br>801<br>CME 6:<br>Bone & Joint<br>The Limping Patient - Multimodality Imaging | 802<br>Symposium 6:<br>SNMMI Session:<br>NM Brain Imaging Update | 803<br>Technologists<br>Oral Presentations 2 | 804<br>Featured - Oncology Basic Science:<br>New Tracer Development | 805<br>Featured - Molecular & Multimodality Imaging:<br>Optical Imaging | 806<br>Cardiovascular:<br>Cardiac PET | 807<br>Physics & Instrumentation & Data Analysis:<br>Modelling / Simulation | 808<br>Radionuclide Therapy & Dosimetry:<br>Dosimetry & Radiobiology | 809<br>Oncology Clinical Science:<br>Prostate Cancer | 810<br>Conventional & Specialised Nuclear Medicine:<br>Paediatrics - Kidney / Lung / Liver | |
| 13:00 - 14:30 | | Sirtex Medical Europe Symposium | Technologist Interest Meeting:<br>EANM Technologist Committee 20th Anniversary Celebration | Eli Lilly and Company Symposium:<br>Update on Amyloid Imaging with PET | Genzyme Symposium | EANM/OECD NEA/AIPES Joint Symposium:<br>Mo-99/Tc-99m Supply in 2013 and Beyond | | | | Young EANM Daily Forum:<br>Tools for Nuclear Medicine | Poster Dismantling:<br>Posters Group 1<br>(13:00 - 14:30) |
| 14:30 - 16:00 | CME<br>901<br>CME 7:<br>Paediatrics<br>Thyroid Diseases in Children | 902<br>Symposium 7:<br>EANM/ESMO Joint Session:<br>Bringing Molecular Imaging into Clinical Practice in Medical Oncology | 903<br>Technologists<br>CTE 3:<br>Challenge and Perspective in Health Care: Nuclear Medicine Role | 904<br>Featured - Conventional & Specialised Nuclear Medicine:<br>Cardiovascular Infections | 905<br>Oncology Clinical Science:<br>Gynaecological Tumours | 906<br>Cardiovascular:<br>Innervation | 907<br>Conventional & Specialised Nuclear Medicine:<br>Parathyroid | 908<br>Radionuclide Therapy & Dosimetry:<br>Dosimetry for Molecular Radiotherapy | 909<br>Physics & Instrumentation & Data Analysis:<br>CZT - Gamma Probes | 910<br>Molecular & Multimodality Imaging:<br>Novel Tools for Preclinical Imaging | Poster Setup:<br>Posters Group 2<br>(14:30 - 18:00) |
| 16:30 - 18:00 | CME<br>1001<br>CME 8:<br>Inflammation & Infection<br>The Diabetic Patient | 1002<br>Symposium 8:<br>EANM/ESTRO Joint Session:<br>PET/MR and Radiation Oncology | 1003<br>Technologists<br>CTE 4:<br>PET/MR in Neurology | 1004<br>Featured - Neurosciences:<br>Amyloid Quantification | 1005<br>Oncology Clinical Science:<br>Lower GI Tract Tumours | 1006<br>Molecular & Multimodality Imaging:<br>Assessment of Receptor Expression - Preclinical Studies | 1007<br>Physics & Instrumentation & Data Analysis:<br>QA & Phantoms | 1008<br>Radionuclide Therapy & Dosimetry:<br>Treatment of Bone & Joint Diseases | 1009<br>Radiopharmaceuticals & Radiochemistry & Dosimetry:<br>Radiometals | 1010<br>Conventional & Specialised Nuclear Medicine:<br>Uronephrology | |

# Tuesday, October 22, 2013

**TIME SCHEDULE**

| Time/ Halls | Amphithéâtre | Auditorium Lumière | Forum 3 | Bellecour 1/2/3 | Auditorium Pasteur | Grand Salon Prestige Gratte-Ciel | Salon Pasteur | Gratte-Ciel 1/2/3 | Rhône 3A/3B | Tête D'Or 1/2 | Poster Exhibition Bellecour Area |
|---|---|---|---|---|---|---|---|---|---|---|---|
| Cap. | 3140 | 880 | 700 | 390 | 290 | 280 | 280 | 250 | 220 | 180 | |
| 08:00 - 09:30 | 1101 CME 9: Neuroimaging (Interactive) Brain PET Imaging | 1102 Symposium 9: EANM/BIR Joint Session: Current Evidence and Future Directions of SPECT/CT Imaging | In Poster Exhibition Area: Technologists Poster Sessions TP01, TP02, TP03 | | | | 1107 Pitfalls & Artefacts & Physiology (Interactive): Advances in Cardiac SPECT & SPECT/CT | | | | Technologist Posters: TP01, TP02, TP03 (08:00 - 09:30) Poster Walks: PW11 - PW15 (08:30 - 09:30) |
| 10:00 - 11:15 | 1201 Plenary Session 3: New Insights in Molecular Neuroimaging | | 1203 In Hall Amphithéâtre: Plenary Session 3: New Insights in Molecular Neuroimaging | 1204 Featured - Oncology Clinical Science: Lymphoma | | | | | | | |
| 11:30 - 13:00 | 1301 CME 10: ESNM Faculty (Interactive) PET/CT in Cancers of Unknown Origin or Paraneoplastic Syndromes | 1302 Symposium 10: The Nuclear Medicine Diagnosis of Bone and Cardiovascular Infections | 1303 Technologists Oral Presentations 3 | 1304 Featured - Radiopharmaceuticals & Radiochemistry & Dosimetry: New PET Radiopharmaceuticals | 1305 Featured - Radionuclide Therapy & Dosimetry: PRRT of Neuroendocrine Tumours | 1306 Oncology Clinical Science: Sentinel Node | 1307 Oncology Clinical Science: Paediatrics | 1308 Molecular & Multimodality Imaging: Precinical - Methods & Instrumentation | 1309 Neurosciences: Miscellaneous | 1310 Physics & Instrumentation & Data Analysis: SUV Quantification | |
| 13:00 - 14:30 | | | Technologist Lunch Meeting: Preparing for a Congress: How to Present your Scientific Work | | Endocyte Symposium | | | | EANM MEMBERS' ASSEMBLY | Young EANM Daily Forum: From Bench to Bedside | |
| 14:30 - 16:00 | 1401 CME 11: ESNM Faculty (Interactive) Pitfalls in Nuclear Medicine | 1402 Symposium 11: Combination Therapies | 1403 Technologists CTE 5: EANM-TC/ESTRO-Radiation Therapist Committee Joint Session: Evolution of RT Planning | 1404 Featured - Cardiovascular: Arrhythmias & CRT | 1405 Featured - Oncology Clinical Science: Breast Cancer | 1406 Oncology Clinical Science: Sentinel Lymph Node & Radioguided Surgery | 1407 Neurosciences: Psychiatry | | 1409 Radiopharmaceuticals & Radiochemistry & Dosimetry: Antibodies & Peptides | 1410 Physics & Instrumentation & Data Analysis: Radiation Protection Patient | Posters Group 2: P01-2 - P74-2 (16:00 - 16:30) |
| 16:30 - 18:00 | | 1502 Symposium 12: Multimodality Tracers | | 1504 Featured - Oncology Clinical Science: Lung Tumours | 1505 Cardiovascular: Myocardial Perfusion SPECT I | 1506 Molecular & Multimodality Imaging: Hybrid Imaging - Methods & Tracer Development | 1507 Neurosciences: Movement Disorders | 1508 Radionuclide Therapy & Dosimetry: Treatmeat of Benign Thyroid Diseases | 1509 Radionuclide Therapy & Dosimetry: Radioembolisation of Primary & Metastatic Liver Cancer | 1510 Physics & Instrumentation & Data Analysis: Radiation Protection Occupational / Image Quantification & VOI Delineation | |

# Wednesday, October 23, 2013

TIME SCHEDULE

| Time/ Halls | Amphithéâtre | Auditorium Lumière | Forum 3 | Bellecour 1/2/3 | Auditorium Pasteur | Grand Salon Prestige Gratte-Ciel | Salon Pasteur | Gratte-Ciel 1/2/3 | Rhône 3A/3B | Tête D'Or 1/2 | Poster Exhibition Bellecour Area |
|---|---|---|---|---|---|---|---|---|---|---|---|
| Cap. | 3140 | 880 | 700 | 390 | 290 | 280 | 280 | 250 | 220 | 180 | |
| 08:00 - 09:30 | 1601 CME 12: Oncology Cross-sectional Imaging in Nuclear Medicine | 1602 Symposium 13: EANM/MDS Joint Session: Biomarkers for Dementia with Lewy-bodies | 1603 Technologists 09:30 - 10:45 CTE 6: Focus on Children | 1604 Featured - Physics & Instrumentation & Data Analysis: PET/MR | | 1606 Oncology Clinical Sciences: Thyroid Cancer | 1607 Conventional & Specialised Nuclear Medicine: Bone 2 (Benign) | 1608 Radionuclide Therapy & Dosimetry: Miscelaneous Therapy | 1609 Radiopharmaceuticals & Radiochemistry & Dosimetry: Drug Development | 1710 Physics & Instrumentation & Data Analysis: Standardisation | |
| 10:00 - 11:30 | 1701 CME 13: Translational Molecular Imaging: Joint EANM/ESMI Session: Optical and Nuclear Imaging | 1702 Symposium 14: EANM/ELI Joint Session: PET in Lymphoma: The New Proposals for Staging and Response Assessment with Illustrations and Research Perspectives in Follicular Lymphoma | | 1704 Featured - Radionuclide Therapy & Dosimetry: Liver Directed Treatments | 1705 Oncology Clinical Sciences: Head & Neck Tumours | 1706 Oncology Clinical Sciences: Neuroendocrine Tumours | 1707 Neurosciences: Dementia | | 1709 Radiopharmaceuticals & Radiochemistry & Dosimetry: Miscellaneous | | |
| 11:45 - 13:15 | 1801 11:45 - 12:00: Awards Ceremony 12:00 - 13:00: Highlights Lecture 13:00 - 13:15: Closing Ceremony | | 1803 In Hall Amphithéâtre: 11:45 - 12:00: Awards Ceremony 12:00 - 13:00: Highlights Lecture 13:00 - 13:15: Closing Ceremony | | | | | | | | |

Pre-Congress Meetings/Sessions
Special Features
Industry/Lunch Symposia
Plenary
Symposia
UEMS/EBNM/CANMD Session
Poster Sessions
Parallel Sessions
Featured Scientific Sessions
Presidential Awards/Highlights
Technologist Sessions

# Continuing Medical Education at the Annual Congress of the European Association of Nuclear Medicine, October 19 – 23, 2013, Lyon/France

The 'CME Sessions during EANM'13 Annual Congress of the European Association of Nuclear Medicine' have been accredited by the European Accreditation Council for Continuing Medical Education (EACCME) and are designated for a maximum of 2 European CME credits per session, with a maximum of 3 credits for half a day and a maximum of 6 credits for a whole day. Through an agreement between the European Union of Medical Specialists and the American Medical Association, physicians may convert EACCME credits to an equivalent number of AMA PRA Category 1 Credits™.

## Educational Objectives for CME Topics

**CME Session I – ONCOLOGY & DRUG DEVELOPMENT**
**October 20, 2013, 08:00–09:30**
**PET and SPECT in Oncology Drug Development**

Chairs: F. Giammarile (Lyon), A.D. Windhorst (Amsterdam)

Speakers: J.Y. Blay (Lyon): The Basis of Drug Development in Oncology: General Point of View; from Pre-clinical to Clinical Aspects
M. Bergström (Basel): Translational PET and SPECT Imaging in Oncology Drug Development: A Pharmaceutical Industry Point of View
W.J.G. Oyen (Nijmegen): Current Application of PET and SPECT Imaging in Drug Development in Oncology: The Nuclear Physician Point of View

**Educational Objectives:**

1. To have an overview of drug development in oncology
2. To learn the necessary basic requirements of imaging evaluation in the field of drug development in oncology
3. To show the possibilities and limits of PET and SPECT imaging in pre-clinical and clinical drug development in oncology

**Summary:**
This continuing education session is directed primarily towards nuclear medicine physicians, who are interested in drug development in oncology.

Despite remarkable progress in our understanding of cancer biology, the identification and characterization of novel therapeutic targets and new drugs need a precise analysis of the oncogenic process and of the therapeutic response. In this setting, PET and SPECT offer the potential to give robust, reliable and well characterised answers to scientific questions in cancer research. In particular, PET and SPECT may show a reduction in tumour cell proliferation and an induction of necrotic or apoptotic cell death. New developments in targeted therapies in oncology drug development require assessment of targeted drug kinetics in a non-invasive manner. Both PET and SPECT can offer these, either by using the radiolabeled drug as radiopharmaceutical or by a surrogate imaging biomarker, like [18F]FDG or [18F]FLT.

The CME will thus give an overview of drug development in oncology for the nuclear medicine physician with a focus on pre-clinical and clinical aspects related to PET and SPECT imaging.

**Key Words:**
Drug Development, Oncology, PET, SPECT

**CME Session II – RADIONUCLIDE THERAPY & DOSIMETRY**
**October 20, 2013, 11:30–13:00**
**PRRT: New Approaches**

Chairs: L. Bodei (Milan), G. Flux (Sutton Surrey)
Speakers: I. M. Modlin (New Haven): The Genomics of Neuroendocrine Tumours: From Gnosis to Sunesis
G. Flux (London): Dosimetry and Radiobiology for PRRT: Clinically Relevant or is it just a Physicist's Hobby?
L. Bodei (Milan): PRRT: from the EANM-IAEA-SNM Guidance Document towards Standardisation of Individualised Treatments

**Educational Objectives:**

1. To learn the necessary basic knowledge on the genomics underlying the development and progression of neuroendocrine tumours, as well as their response to therapies
2. To show the possibilities and limits of a dosimetric approach to PRRT and the potential for radiobiology
3. To have an overview of the current status of clinical protocols of PRRT in neuroendocrine tumours and the possibility of personalised treatments

**Summary:**
This continuing education session is directed primarily towards nuclear medicine physicians who are interested in performing PRRT in a comprehensive and modern environment and, hence, to deliver the treatment in a safe and effective manner.

Peptide Receptor Radionuclide Therapy (PRRT) consists of the systemic administration of a synthetic somatostatin analog, radiolabeled with a suitable beta-emitting radionuclide. The compound is able to irradiate tumours and their metastases via internalisation through somatostatin receptors over-expressed on the cell membrane. As a result, the radiopharmaceutical is concentrated in the tumour cell, where sensitive molecules, such as DNA, can be targeted.

In more than 15 years of academic phase I/II trials, despite the lack of homogeneity among studies, PRRT has proved to be efficient and consistent in efficacy and has, ultimately, demonstrated an impact on survival. Side effects of PRRT typically affect the kidneys and the bone marrow. These, however, are mild, provided adequate protective measures are undertaken.

Despite the large body of evidence regarding efficacy and clinical safety of the fixed dose approach, PRRT still has grey zones of inefficient treatments due to the administration of inadequate absorbed doses to the target or excessive absorbed doses to normal organs.

The first lecture of this CME will give an overview on the genomics that sustain the development and progression of neuroendocrine tumours (NET), defining the interactome of neuroendocrine cells and its relevance to the development of (drone) therapy, providing a platform to understand the development of Master regulator genes and their role in identifying druggable addiction points, defining the mutational spectrum of NET tumourigenesis to understand the induction of NET neoplasia, establishing the basis of blood transcript analysis in diagnosis of NET disease and the role of molecular transcripts as a surrogate marker for the efficacy of PRRT.

The second lecture will examine dosimetric and radiobiologic approaches to PRRT with either 90Y or 177Lu radiopeptides as a basis for personalisation of treatment. The advantages and disadvantages of this over a population based approach will be considered and radiobiological aspects of ‘cocktail’ administrations of more than one radiopharmaceutical will be explored. The practicalities of a dosimetric approach to treatment in terms of resource requirements will also be taken into account.

The third lecture will give an overview on the current clinical protocols of PRRT, which are reflected in the common document that has been written by experts reunited under the auspices of IAEA, EANM and SNMMI. The lecture will give an overview on the current advantages and limitations of PRRT, will define the parameters of standardisation that can be regarded as milestones today, and will explore the possibility of going towards personalised treatments, capitalising the input deriving from the biologic and dosimetric approaches.

**Key Words:**
PRRT, 90Y-Octreotide, 177Lu-Octreotate, Genomic Approach, Radiobiology, Dosimetry

**CME Session III – PHYSICS**
**October 20, 2013, 14:30–16:00**
**Motion Correction**

Chairs: K. Thielemans (London), C. Hindorf (Lund)
Speakers: K. Thielemans (London): Principles of Motion Correction and Gating
P. Knaapen (Amsterdam): Clinical Use of Cardiac Gating within PET and SPECT
D. Thorwarth (Tuebingen): 4D PET/CT for Radiotherapy Treatment Planning

**Educational Objectives:**

1. Understand the principle of gated acquisition.
2. Have knowledge about devices and methods to detect cardiac/respiratory motion.
3. Understand the impact of motion on image quality and quantification and recognise image artefacts caused by respiratory motion within attenuation corrected PET images.
4. Understand the clinical use of cardiac gated SPECT/PET – when do we need it, what does it provide and what can we measure with it (functional imaging).
5. Have knowledge about methods to compensate for motion during dynamic imaging.
6. Understand the use of dynamic PET imaging– when do we need it, what does it provide and what can we measure with it (functional imaging).

**Summary:**
This continuing education session is directed towards medical physicists and physicians who would like to have a deeper understanding on how motion correction is performed and how it is used in a clinical setting.

Devices and methods for motion correction (cardiac gating, respiratory gating and dynamic imaging) will be reviewed and the impact on image quality as well as the impact on quantification will be analysed. The clinical use of cardiac gated SPECT and PET imaging will be reviewed. Dynamic PET imaging (functional imaging) will also be reviewed.

**Key Words:**
Motion Correction, Cardiac Gating, Respiratory Gating, Dynamic Imaging, PET, SPECT

**CME Session IV – RADIOPHARMACY & DRUG DEVELOPMENT**
**October 20, 2013, 16:30–18:00**
**State of the Art of Radiopharmaceuticals**

Chairs: M. Behe (Villigen), A. Gee (London)
Speakers: R. Schibli (Zurich): New SPECT Tracers
P. Elsinga (Groningen): New Radiopharmaceuticals for PET
G. Meyer (Hannover): New Radiopharmaceuticals for Therapy

**Educational Objectives:**

1. To learn about new imaging radiopharmaceuticals for PET and SPECT
2. To learn about new developments in radiopharmaceuticals for therapy
3. To learn about the scope and limitations of new radiopharmaceuticals

**Summary:**
New radiopharmaceuticals are being developed on a continuous basis in all major disease areas. It is important that Nuclear Medicine physicians and researchers are frequently updated about new radiopharmaceuticals that might become part of their practice in a few years' time. These new radiopharmaceuticals will address new applications, opening new possibilities for Molecular Imaging research and clinical research supported by PET and SPECT. In addition quit some effort is being addressed to new radiopharmaceuticals for therapy, predominantly in cancer.

The three contributions will address the above topics in a comprehensive manner.

**Key Words:**
New PET Tracer, New SPECT Tracer, New Therapy Tracer

**CME Session V – CARDIOVASCULAR**
**October 21, 2013, 08:00–09:30**
**Myocardial Viability**

Chairs: H.J. Verberne (Amsterdam), T.H. Schindler (Baltimore)
Speakers: H.J. Verberne (Amsterdam): Critical Appraisal of Viability Assessment
C. Übleis (Munich): SPECT and PET/CT Assessment
M. Lombardi (Pisa): Cardiac Magnetic Resonance Assessment
T.H. Schindler (Baltimore): Multimodality Interpretation and Comparison

**Educational Objectives:**

1. To show a critical appraisal of myocardial viability assessment
2. To have an overview of viability assessment with different imaging modalities
3. To outline the value of multimodality clinical interpretation

**Summary:**
This continuing education session is directed primarily towards nuclear physicians active in clinical cardiology studies, cardiologists, radiologists and trainees who are interested to know more on how to perform a clinical evaluation of myocardial viability with different imaging modalities. The prognosis for patients with chronic coronary artery disease and severe left ventricular dysfunction is poor, despite advances in different therapies. The assessment of myocardial viability has become an important aspect of the diagnosis, prognosis and management of patients with ischemic cardiomyopathy. Imaging techniques utilize several methods to assess myocardial viability: left ventricular function, morphology, perfusion, and metabolism. Each technique (nuclear imaging techniques and magnetic resonance imaging) has the ability to assess one or more of these parameters. The primary goal of viability assessment in such patients is to guide therapeutic decisions by determining which patients would most likely benefit from revascularisation. Multimodality clinical interpretation is useful to reach to this important goal.

The CME will give an overview of the imaging modalities can be used to assess myocardial viability, and reviews the relative strengths and limitations of each technique.

**Key Words:**
Myocardial Viability, Imaging Modalities, Multimodalities Interpretation

**CME Session VI – BONE & JOINT**
**October 21, 2013, 11:30–13:00**
**The Limping Patient – Multimodality Imaging**

Chairs: F. Paycha (Paris), T. Van den Wyngaert (Edegem)
Speakers: H. K. Mohan (London): The Unexplained Hip Pain
K. Strobel (Luzern): SPECT/CT in Knee Joints – What is Left for Nuclear Medicine Tests at the Era of MRI?
F. Paycha (Paris): Foot Pain Unexplained by X-Rays
W. van der Bruggen (Nijmegen): The Referred Pain – When the Causative Lesion Lies Far from the Aching Joint

**Educational Objectives:**

1. To gain an overview of the main conditions involving the lower limb joints responsible for limping
2. To understand the technical requirements of SPECT/CT protocols adapted to rheumatological or orthopaedic indications
3. To recognise the most important semiological SPECT/CT patterns and their causes
4. To illustrate how to avoid common diagnostic pitfalls (e.g. referred pain) and review recent insights

**Summary:**
This continuing medical education session is directed towards a broad audience of nuclear medicine practitioners and will be of special interest for skeletal imaging-oriented colleagues.

A vast spectrum of lower limb bone and joint disorders (hip, knee, ankle, foot) present with a common clinical presentation (limping) and too often generates a cascade of less than efficient imaging studies, 99mTc-bisphosphonates bone scintigraphy included.

Emphasis will be placed on optimising the diagnostic effectiveness of bone scintigraphy, such as correct clinical indication, optimal scintigraphy procedure and updated image pattern-oriented reporting.

Beyond frustrating, and often misleading, dichotomous diagnosis of fatigue fractures and CRPS type I (formerly reflex sympathetic dystrophy), frequent lower limb conditions never suggested on a planar bone scan report but evidenced or suspected on SPECT/CT bone scan will be sketched out.

Clinical and imaging pitfalls, such as referred pain (e.g. originating from spine lesion), incipient chronic rheumatic diseases (e.g. spondyloarthropathies) and malignant conditions, will be reviewed. Clinical and paraclinical red flags for such instances will be recalled.

Lyon EANM bone and joint CME is an updated and focused seminar in keeping with the 2010 EANM Vienna

congress session which was dedicated to musculo-skeletal pain:

(http://www.eanm.org/education_esnm/cme_cte/cme_2010/cme_session10.php?navId=83)

**Key Words:**
Bone and Joint Disorders, Lower Limb, Bone Scintigraphy, SPECT/CT, Imaging Patterns, Pitfalls

**CME Session VII – PAEDIATRICS**
**October 21, 2013, 14:30–16:00**
**Thyroid Diseases in Children**

Chairs: C. Vaylet (Paris), D. de Palma (Varese)
Speakers: B. Helal (Orsay): Hypothyroidism and Hyperthyroidism in Children: Role of Nuclear Medicine
R. Howman-Giles (Sydney): Paediatric Thyroid Cancer
F. A. Verburg (Aachen): Dosimetry and Short/Long-Term Consequences of Radioiodine Treatment in Children and Teenagers

**Educational Objectives:**

1. To set actual state-of-the-art knowledge about use of radionuclide imaging in functional abnormalities of the Thyroid in paediatric age
2. To define criteria for modern diagnostic and follow-up of children and adolescents affected by Differentiated thyroid carcinoma (DTC) in the era of hybrid imaging
3. To analyse the potential side effects and future harm for children and adolescents due to radioiodine treatment

**Summary:**
This session is aimed towards all physicians caring for children affected by congenital or acquired Thyroid diseases. Firstly, functional impairment will be discussed, with special focus on usefulness and the method of radionuclide imaging in congenital hypothyroidism. Thereafter, the session will discuss the management and treatment of thyroid carcinoma in children and adolescents, analysing the impact of the technical evolution represented by hybrid imaging and the use of positron emitters, finishing with a review of our knowledge about the lifelong effects of radionuclide therapy on these patients with a long life expectancy and the methods available to minimise them.

**Key Words:**
Children, Teenager, Differentiated Thyroid Carcinoma, Hyperthyroidism, Radionuclide

**CME Session VIII – INFLAMMATION & INFECTION**
**October 21, 2013, 16:30–18:00**
**The Diabetic Patient**

Chairs: J. Buscombe (Cambridge), A. Signore (Rome)
Speakers: O. Israel (Haifa): Nuclear Medicine Procedures and Clinical Indications in Diabetic Patients with Infection (With Special Emphasis on FDG Imaging)
J. Buscombe (Cambridge): Diabetic Nephropathy and Imaging of Kidney Infections and Graft Rejection
R. Slart (Groningen): Imaging Cardio-Vascular Diseases in Diabetic Patients

**Educational Objectives:**

1. To identify clinical unmet needs in patients with diabetes
2. To define nuclear medicine procedures that can be used to diagnose and monitor infectious and inflammatory processes in patients with diabetes
3. To address specific clinical entities such as diabetic nephropathy and atherosclerosis and define the role of nuclear medicine in monitoring disease progress or response to therapeutic procedures

**Summary:**
This continuing education session is directed primarily towards nuclear medicine practitioners and clinicians involved in the care of patients with diabetes. Infectious and inflammatory processes occur with a high incidence in diabetic patients and pose significant clinical challenges both for diagnosis and management. Diabetic nephropathy, atherosclerotic cardiovascular disease, impaired myocardial sympathetic innervation and orthopaedic infection, such as osteomyelitis in the "diabetic foot" are severe complications occurring as consequences of prolonged or poorly controlled diabetes. These, as well as additional clinical entities, can be tracked by the use of nuclear medicine techniques. In addition to the use of single photon emitting tracers, imaging with positron emitting radioisotopes has gained wide applications in infection supplemented by the successful implementation of hybrid SPECT/CT and PET/CT. Caution in the use of FDG in patients with diabetes has been previously advocated and was considered to limit its clinical value in this subgroup of patients.

This CME will present an overview of clinical questions in patients with diabetes and diagnostic keys that can be provided by a variety of nuclear medicine procedures.

**Key Words:**
Diabetes, Infection, Kidney, Atherosclerosis, PET/CT, SPECT

**CME Session IX – NEUROIMAGING (INTERACTIVE)**
**October 22, 2013, 08:00–09:30**
**Brain PET Imaging**

Chairs: J. Darcourt (Nice), P. Payoux (Toulouse)
Speakers: F. Nobili (Genoa): FDG-PET in the Context of the other Biomarkers in Prodromal AD
P. Payoux (Toulouse): How to Read Amyloid Images?
S. Hesse (Leipzig): PET-MRI Brain Imaging
J. Darcourt (Nice): DOPA PET Neuroimaging

**Educational Objectives:**

1. Review the criteria for reading brain PET images using 18F-FDG; 18F-DOPA, radiolabelled amino acid analogues and amyloid plaques tracers (18F-FET?)
2. Identify the possible difficulties and pitfalls
3. Understand the relevance of multidimensional information: clinical, biological, neuropsychological and neuroradiological

**Summary:**
Imaging of the brain is becoming the second most common indication of PET imaging. This CME session is directed primarily to nuclear physician who want to improve their knowledge about this topic. The session will address brain imaging with 18F-FDG; 18F-DOPA, radiolabelled amino acid analogues (11C-Methionine and 18F compounds as 18F-FET and 18F-DOPA) and amyloid plaques markers. It will consist in interactive clinical cases presentation. Voting systems will allow the attendees to express their opinion and to test their skills.

Common and less common forms of neurodegenerative diseases will be presented. Imaging and clinical overlaps will be shown in order to illustrate how reading relies on the knowledge of multidimensional information. This part will include dementias and Parkinson disease using 18F-FDG and 18F-DOPA. Amyloid plaques imaging will also be addressed focusing on image acquisition, reading criteria and on the use of the corresponding information in patients' management.

For brain tumour imaging, cases will illustrate how radiolabelled amino acid analogues can add important information for patient management. Mutlimodal imaging including MRI will be described as well as the advantages and limitations of 18F-FDG in that field.

**Key Words:**
PET, Brain Imaging, Dementia, Parkinson, Brain Tumours

**CME Session X – ESNM FACULTY (INTERACTIVE)**
**October 22, 2013, 11:30–13:00**
**PET/CT in Cancers of Unknown Origin or Paraneoplastic Syndromes**

Chairs: C. Hoefnagel (Amsterdam), J.N. Talbot (Paris)
Speakers: S. Balogova (Bratislava): Cancer of Unknown Origin (CUP)
F. Montravers (Paris): Neuroendocrine Cancer of Unknown Origin (CUPNET)
J.N. Talbot (Paris): Paraneoplastic Syndromes

**Educational Objectives:**

Interactive presentation of real cases of patients, to illustrate the impact of PET/CT:

1. In case of metastatic cervical lymph node with no primary cancer detected on physical examination and anatomical imaging
2. In case of other revealing non-endocrine metastases in the whole body (lymph node, liver, lung, bone, cerebral…)
3. Is there an added value of PET/CT when the primary tumour cannot be clearly delineated?
4. In case of metastases of an unknown neuroendocrine tumour (CUPNET), how to choose the optimal PET tracer?
5. Specific aspects of exploration of CUPNETs, interaction with biology
6. What is the best trade-off between a sensitive and a specific reading in this setting?
7. In case paraneoplastic syndrome with neurologic symptoms, are the clinical data effective to indicate PET/CT? Interaction with biology
8. Experience available in case of non-neurologic paraneoplastic syndrome

The audience will be equipped with voting systems. The aims are:

1. To favour a better prescription of PET/CT among the diagnostic tools in those settings. The performance of PET/CT depends on the localisation and the histologic type of the revealing metastasis
2. To discuss the specific aspect of PET/CT tracer choice and image acquisition in cancer of unknown origin
3. To improve interpretation of PET/CT imaging by the attendees (avoiding pitfalls)
5. To document the impact on patient management of a skilled interpretation of PET/CT integrating the imaging patterns, the biological results and the clinical context

**Summary:**
The presentations will cover the current and potential role of nuclear medicine in case of cancer of unknown origin or paraneoplastic syndrome. With the help of newer histologic and biologic technologies, the indications and the imaging protocol of PET/CT may be optimised. With a great number of small anatomical structures and the presence of physiologic lymphoid tissue, head and neck which are the most frequent location of revealing lymph node metastases request the most skilled FDG PET/CT interpretation. The session will also address the particularities and main results of the PET detection of the primary lesion in neuroendocrine metastasis of an unknown origin, and in which paraneoplastic syndromes PET/CT is the most effective. Voting systems will allow the attendees to express their opinions and to evaluate their experience and skills in this field.

**Key Words:**
Interactive Session, Cancer of Unknown Origin, Paraneoplastic Syndrome, PET/CT, FDG, FDOPA, Somatostatin Analogues for PET

**CME Session XI – ESNM FACULTY (INTERACTIVE)**
**October 20, 2013, 14:30–16:00**
**Pitfalls in Nuclear Medicine**

Chairs: L. Mansi (Napoli), A. Britten (London)
Speakers: S. Agostini (Trento) and D. Donner (Trento): How to Avoid Pitfalls "Before the Scan"
A. Britten (London): Technical Pitfalls and Solutions
J. Buscombe (Cambridge): Unusual Clinical Pitfalls

**Educational Objectives:**

1. Define pitfalls and understand the concept of error in nuclear medicine; how to define and apply standard operating procedures (SOP); knowledge of Total Quality Management (TQM) as a "new" attitude in daily work; how to apply a PDCA (plan, do, check, act) cycle
2. Review common and important sources of technical problems in Nuclear Medicine, including examples from Gamma camera, SPECT/CT, PET/CT and intraoperative probe work. Learn good practice to follow in order to avoid such problems
3. Understand how technical aspects or imaging, pathology and the drugs taken by a patient may alter the appearances of nuclear medicine and PET images

**Summary:**
This interactive CME session is directed primarily towards nuclear physicians, radiopharmacists, radiochemists, physicists and technologists. Starting from the definitions of pitfall and error in medicine, all the major radiochemical and radiopharmaceutical issues that have to be checked before the radiocompound's administration to the patient will be discussed. The choice of examination and precise procedures for the subject are discussed, including any medical issues, such as contraindications and interferences. Problems connected with Radiology Information Systems, Systems of picture archiving and medical billing software will be also analysed. Solutions will be identified through a TQM (total quality management) approach and the application of quality controls, regarding both the radiopharmaceutical's preparation and its release. At the end of this first part, the application of a PDCA cycle system in the routine work to improve the "before the scan" SOP (Standard Operating Procedure) will be shown. In the second lecture, common and important sources of technical problems in Nuclear Medicine, including examples from Gamma camera, SPECT/CT, PET/CT and intraoperative probe work will be discussed. This will include issues in the data acquisition, image processing and study analysis. There will be a debate of good practice to follow in order to avoid such problems. In the 3rd and final lecture, unusual images will be presented, obtained after ensuring a correct radiopharmaceutical and the physics is right and therefore depending on the patient themselves. The causes may be technical, due to pathology changing the way a radiopharmaceutical is handled or interaction with drugs. A good knowledge of these pitfalls is needed for accurate interpretation. The CME's panel aims to give to nuclear physicians elements of knowledge able to avoid and/or interpret pitfalls that may arise during all the steps preceding the clinical diagnosis. Non-medical professionals may be interested both for a better knowledge of their specific arguments and for an improvement of the interactive dialogue between all the parties involved in the final common goal: a correct diagnosis.

**Key Words:**
Pitfalls, Quality Control, SOP (Standard Operating Procedure), TQM (Total Quality Management), Technical Artefacts, Drug Interaction

**CME Session XII – ONCOLOGY**
**October 23, 2013, 08:00–09:30**
**Cross-sectional Imaging in Nuclear Medicine**

Chairs: F. Giammarile (Lyon), P.J. Valette (Lyon)
Speakers: SPECT-CT: The Example of Musculoskeletal Pathologies
G. Tognini (La Spezia): CT and MR in Musculoskeletal Pathologies: What the Nuclear Physician Should Know
G. Mariani (Pisa): SPECT-CT in Benign Bone Diseases
PET-CT: The Example of l Abdominal Cancers
P.J. Valette (Lyon): CT and MR in Abdominal Cancers: What the Nuclear Physician Should Know
C. Tychyj-Pinel (Lyon): PET-CT in Abdominal Cancers

**Educational Objectives:**

1. To have an overview of Cross-sectional Imaging, in particular in the fields of musculoskeletal pathologies and abdominal cancers
2. To learn the necessary basic requirements of anatomical imaging for clinical nuclear medicine studies interpretation
3. To show the possibilities and limits of Cross-sectional Imaging

**Summary:**
This continuing education session is directed primarily towards nuclear medicine physicians, who are interested to perform Cross-sectional Imaging.

Cross-sectional Imaging has a central role in the management of patients with malignant diseases and it is used at all point in the patient pathway. In particular, in abdominal cancers, the monitoring of the response to treatment and the presurgical evaluation of suspected masses represent key issues in order to reach a perfect tailored treatment. On the other hand, many traditional imaging modalities may contribute to the diagnosis, treatment planning, or post-treatment evaluation of patients with musculoskeletal pathologies, but cross-sectional imaging has assumed an increasing important role.

The CME will thus give an overview of Cross-sectional Imaging for the Nuclear Physician with a focus on aspects related to bone pathologies and abdominal cancers.

**Key Words:**
Cross-sectional Imaging, Bone Diseases, Abdominal Cancers

**CME Session XIII – TRANSLATIONAL MOLECULAR IMAGING: Joint EANM/ESMI Session**
**October 23, 2013, 10:00–11:30**
**Optical and Nuclear Imaging**

Chairs: B. Tavitian (Orsay), T. Lahoutte (Brussels)
Speakers: R. Pleijhuis (Groningen): Nuclear and Fluorescent Tracers for Intraoperative Application
F. Ducongé (Orsay): PET and Optical Tomography in Small Animals
S. Maitrejean (Paris): Cerenkov Luminescence Imaging

**Educational Objectives:**

1. To have an overview of optical and isotope-based methods
2. To learn the options for preclinical development of these methods
3. To show the possibilities for clinical application

**Summary:**
This continuing education session is directed primarily towards radiochemists, radiopharmacists and nuclear medicine physicians, who are interested to perform preclinical studies and finally clinical application with molecules for optical and nuclear imaging. This CME will give an overview of established and new methods for optical imaging in comparison to or complementing isotope based methods. Furthermore the demands, the problems and possible solutions for the preclinical development and the possible clinical application e.g. intraoperative visualisation of lesions for both methods will be discussed. The third talk is intended to show the opportunity to visualise accumulation of beta-emitting tracers in the setting of endoradiotherapy with optical methods.

**Key Words:**
Radiopharmacy, Optical Imaging, Preclinical Development, Intraoperative Detection

## ORAL SESSIONS

101 — Sunday, Oct. 20, 08:00 — 09:30, Amphithéâtre

### CME 1 - Oncology & Drug Development: PET and SPECT in Oncology Drug Development

**OP001**
**The Basis of Drug Development in Oncology: General Point of View; from Pre-clinical to Clinical Aspects**
J.Y. Blay, FRANCE

**OP002**
**Translational PET and SPECT Imaging in Oncology Drug Development: A Pharmaceutical Industry Point of View**
M. Bergström, SWEDEN

**OP003**
**Current Application of PET and SPECT Imaging in Drug Development in Oncology: The Nuclear Physician Point of View**
W.J.G. Oyen, NETHERLANDS

102 — Sunday, Oct. 20, 08:00 — 09:30, Auditorium Lumière

### Symposium 1 - FDG-PET in Early Alzheimer: Why do they look so Heterogeneous?

**OP004**
**Presenile and Senile Presentation**
K. Herholz, UNITED KINGDOM

**OP005**
**The Impact of ApoE Genotype**
G. Chételat, FRANCE

**OP006**
**The Impact of Education and Cognitive Reserve**
S. Morbelli, ITALY

103 — Sunday, Oct. 20, 08:15 — 09:45, Forum 3

### CTE 1: Radionuclide Therapy in Oncology

**OP007**
**Radionuclide Therapy in Neuroendocrine Tumours**
L. Bodei, ITALY

**OP008**
**Radionuclide Therapy in Thyroid Carcinoma**
D. Piciu, ROMANIA

**OP009**
**Radioimmunotherapy in Lymphoma**
F. Kraeber-Bodéré, FRANCE

107 — Sunday, Oct. 20, 08:00 — 09:30, Salon Pasteur

### Pitfalls & Artefacts & Physiology (Interactive): Oncology

**OP010**
**Pitfalls in PET**
T. Mognetti, FRANCE

**OP011**
**Pitfalls in SPECT**
A.L. Giraudet, FRANCE

**OP012**
**Pitfalls in Paediatric Oncology**
F. Giammarile, FRANCE

201/203 — Sunday, Oct. 20, 10:00 — 11:15, Amphithéâtre

### Plenary 1 (incl. Marie Curie Lecture): Functional and Molecular Imaging in Heart Disease

**OP013**
**Myocardial Perfusion and Blood Flow in Clinical Decision Making**
M. Di Carli, USA

**OP014**
**Marie Curie Lecture: Imaging of Coronary Artery Disease: Stenosis versus Perfusion**
J.J. Bax, NETHERLANDS

**OP015**
**Molecular Imaging from Bench to Bedside**
M. Schwaiger, GERMANY

301 — Sunday, Oct. 20, 11:30 — 13:00, Amphithéâtre

### CME 2 - Radionuclide Therapy & Dosimetry: PRRT: New Approaches

**OP016**
**The Genomics of Neuroendocrine Tumours: From Gnosis to Sunesis.**
I.M. Modlin, USA

**OP017**
**Dosimetry and Radiobiology for PRRT: Clinically Relevant or is it just a Physicist's Hobby?**
G. Flux, UNITED KINGDOM

**OP018**
**PRRT: from the EANM - IAEA - SNM Guidance Document towards Standardisation of Individualised Treatments.**
L. Bodei, ITALY

302 — Sunday, Oct. 20, 11:30 — 13:00, Auditorium Lumière

### Symposium 2: Assessment of Patients Suspected of CAD

**OP019**
**Anatomical Assessment First**
J.F. Deux, FRANCE

**OP020**
**Physiological Assessment First**
P.G. Camici, ITALY

303 — Sunday, Oct. 20, 11:30 — 13:00, Forum 3

### CTE 2: Multiprofessional Round Table on Entry Level and Advanced Practice (Interactive)

## OP021

### Multiprofessional Round Table on Entry Level and Advanced Practice

**K. Waterstram-Rich, USA**

304 - Sunday, Oct. 20, 11:30 - 13:00, Bellecour 1/2/3

## Featured - Conventional & Specialised Nuclear Medicine: Renal Function

## OP022

### Renal Function and NM

**A. Prigent, FRANCE**

## OP023

### Assessment of Dynamic Contrast-enhanced MR Urography in Comparison to Dynamic Renal Scintigraphy to Assess Relative Renal Function in 295 Hydronephrotic Patients

**E. Durand**[1], M. CLAUDON[2], P. CHAUMET-RIFFAUD[3], F. GUILLEMIN[2], N. GRENIER[4], E. MICARD[5], C. PASQUIER[5], M. SOUDANT[6], J. FELBLINGER[5], A. PRIGENT[3]; [1]Université de Strasbourg, Strasbourg, FRANCE, [2]Université de Lorraine, Nancy, FRANCE, [3]Université Paris-Sud, LE KREMLIN-BICETRE, FRANCE, [4]Université de Bordeaux, Bordeaux, FRANCE, [5]IADI - Université de Lorraine, Nancy, FRANCE, [6]Service d' Épidémiologie et Évaluation Cliniques, Nancy, FRANCE.

**Aim** Dynamic renal scintigraphy (DRS) is the gold standard to assess relative renal function. Dynamic contrast-enhanced magnetic resonance urography (MRU) provides functional information with fair spatial resolution, without ionising radiation. Like DRS, MRU can use either the area under the curve (AUC) technique or the Patlak technique to assess renal function. However, MRU with Patlak technique had never been tested on a large scale against DRS. The Aim of the present study was therefore to assess both AUC-MRU and Patlak-MRU against DRS on a population of patients presenting with hydronephrosis. Patients and Methods Fourteen centres included 369 patients (both adults and children) presenting with hydronephrosis and referred for functional and morphological evaluation. Dynamic renal scintigraphy was carried out with 99mTc-MAG3 or 99mTc-DTPA and analysed with Patlak analysis. MRU was also performed with a low dose (0.05 µmol/kg) of macrocyclic gadolinium chelate and analysed with both AUC and Patlak Methods, using a parenchymal ROI on a slice; the result was then normalised for the whole kidney parenchymal volume determined on a 3D MRI acquisition. The analysis was first performed by a panel of 12 senior physicians then by 3 experts. DRS was analysed by Patlak-Rutland analysis using a left ventricular ROI with lung ROI subtraction for input function. When bolus poor quality precluded Patlak analysis, the area technique was used, as recommended by the international consensus. Another panel of 12 physicians plus 3 experts analysed the DRS data. **Results** After secondary exclusion for technical protocol violation (74 patients) or failure to analyse data (48 patients), 247 patients were finally analysed. Intraobserver reproducibility was excellent. Interobserver reproducibility was good (ICC≥0.75) but for MRU-AUC. On the average, MRU provided valued that were equivalent to DRS. However, a notable scattering was found (SD for the difference with DRS was 12% for Patlak-MRU and 17% for AUC-MRUfor the expert review). Furthermore, function of highly dilated kidneys, was underestimated by MRU by ca. 4% on the average. **Conclusion** Additionally to morphological information, MRU provides an unbiased estimation of the relative renal function compared to DRS except for highly dilated kidneys. Precision is limited by a standard deviation of about 12%. Patlak-MRU should be preferred over AUC-MRU.

## OP024

### Standardization of the diuresis renography report by the implementation of International Atomic Energy Agency Software Package for the Analysis of Scintigraphic Renal Dynamic Studies

**S. BEATOVIC**[1,2], E. Jaksic[1,2], J. Marinkovic[3,2], R. Rebic[1], M. Blagic[1], V. Obradovic[1,2]; [1]Center for Nuclear Medicine Clinical Center of Serbia, Belgrade, SERBIA, [2]Belgrade University School of Medicine, Belgrade, SERBIA, [3]Institute for Medical Statistics, Belgrade, SERBIA.

**Introduction**: Under the auspices of The International Atomic Energy Agency (IAEA) a "Software Package for the Analysis of Scintigraphic Renal Dynamic Studies" was recently developed and distributed among developing countries. It is expected that implementation of the Software will reduce the heterogeneity in acquisition and processing among centers and improve standardization of renography reports. The Software enables comprehensive analysis of renal dynamic studies with calculation of curve parameters, excretory parameters and transit times through kidney. The Aim of our study was to implement the IAEA Software Package in the analysis of 99mTc-MAG3 diuretic renography. We tend to define the normal ranges for time to maximum counts (Tmax), time to half-peak counts (T1/2), normalized residual activity (NORA 20/2), postvoid normalized residual activity (NORA PM/2), ), twenty-minute/maximum count ratio (20min/max), postvoid/maximum count ratio (PM/max), output efficiency (ROE 20), post-furosemide output efficiency (ROE F+20 whole-kidney mean transit time (MTT) and mean parenchymal transit time (MPTT). Patients and Methods: 46 healthy potential kidney donors aged 20 to 73 years (mean: 43.2 years) were included in the study. Dynamic scintigraphy was done 40 minutes after bolus injection of 50 MBq Tc-99m MAG3. 240 images of 10 seconds were recorded. Furosemide was injected in 20 minute. Post void static image was performed in 50 minute. **Results**: For all parameters, mean values, lower and upper bound of 95% confidence interval were calculated: Values of Tmax (min) were: Left kidney: 3.5; 2.5; 5.2; Right kidney: 3.6; 2.6; 5.0. Values of T1/2 (min): Left kidney: 6.6; 4.4; 10.2; Right kidney: 7.2; 4.9; 10.7. Values of NORA 20/2: Left kidney: 0.31; 0.22; 0.46; Right kidney: 0.31; 0.26; 0.43. Values of NORA PM/2: Left kidney: 0.01; 0.01; 0.03; Right kidney: 0.02; 0.01; 0.04. Values of 20min/max: Left kidney: 0.22; 0.16; 0.31; Right kidney: 0.24; 0.19; 0.31. Values of PM/max: Left kidney: 0.01; 0.01; 0.02; Right kidney: 0.01; 0.01; 0.03. Values of ROE 20 (%): Left kidney: 93; 89; 96; Right kidney: 92; 90; 93. Values of ROE F+20 (%): Left kidney: 98; 97; 98; Right kidney: 97; 96; 98. Values of MTT: Left kidney: 2.4; 1.5; 3.5; Right kidney: 2.5; 2.0; 2.8. Values of MPTT: Left kidney: 1.7; 1.2; 2.5; Right kidney: 1.8; 1.4; 2.1. **Conclusion**: The implementation of IAEA Software Package enables the normal limits of quantitative MAG3 parameters to be established. That would improve the standardization of renography and facilitates the comparison of reports between physicians and departments.

## OP025

### 99mTc-MAG3 dynamic renal scintigraphy (DRS): a tool for short a long-term monitoring for ischemic damage after laparoscopic partial nefrectomy

T. Angusti, F. Porpiglia, R. Bertolo, C. Fiori, I. Morra, E. Pilati, **V. Podio**; Ospedale San Luigi Gonzaga, Orbassano, ITALY.

**Introduction**: laparoscopic partial nephrectomy (LPN) is a minimally invasive approach for renal cell neoplasm. The success of LPN depends on a bloodless operative field: ischemia obtained by transient renal hilar clamping ("warm ischemia") causes a direct hypoxic injury to the kidney. Every minute of ischemia has deleterious effects on the outcome of renal function. Few studies have evaluated the long-term effects of warm ischemia time (WIT) on kidney function in patients after LPN. Moreover, most of the studies evaluated function using serum creatinine (SCr) and/or estimated glomerular filtration rate (eGFR), disregarding the masking effect of the normal controlateral kidney. **Aim**: to evaluate long-term effect of WIT on renal function, using split renal function (SRF) and ERPF, as estimated by DRS. Materials and Method: between 2004 and 2007, we prospectively examined kidney function of 54 patients (tumor size ≤ 4.0 cm, GFR ≥ 60 ml/min, SRF 45%÷55%) before LPN; follow-up: 48 months. DRS was performed preoperatively, at 3, 12, 24, 36 and 48 months after surgery (POMs). We computed "baseline weighted differential" (bWD) representing (in per cent) the loss of SRF or ERPF from baseline: 1) SRF bWD = (nPOM SRF-baseline SRF)/baseline SRF, 2) ERPF bWD = (nPOM ERPF-baseline ERPF)/baseline ERPF where n = 3, 12, 24, 36 and 48, respectively Results: at 3 months, both SRF bWD and ERPF bWD of kidney after LPN decreased significantly in comparison with their baseline values: (48.05±4.33 vs 44.76±2.40, p=0.0030 and 182.70±34.01 vs 153.54±42.34, p=0.0001, respectively). This decrease remained stable at subsequent DRS. On the other hand, serum creatinine and eGFR did not change significantly during follow-up (p=0.83 and p=0.92, respectively). To predict renal damage, the regression model showed statistical significance at month 3 for WIT and age, whereas at 48 months, statistical significance was reached only by WIT. **Conclusion**: this is one of the largest long-term study using DRS to evaluate the renal function after LPN. Our results confirmed that SCr and eGFR measures have low sensitivity for evaluating kidney damage in patients with normal or moderately reduced kidney function. In contrast, both SRF and ERPF estimated by DRS identified loss of renal function at 3-months POM. This loss remained stable over time, as confirmed by follow-up measurements of both SRF bWD and ERPF bWD. These findings may suggest that future studies of early kidney damage should focus on the results of DRS and should accurately record SRF and ERPF data.

## OP026

### Detection of pleuroperitoneal communication as a complication of peritoneal dialysis: peritoneal scintigraphy or peritoneal CEUS?

**L. BERTHET**[1], C. POROT[2], P. MANZONI[3], C. CAODURO[1], C. UNGUREANU[1], B. HARACHE[1], O. ANGOUE[2], M. YANNARAKI[4], H. BOULAHDOUR[1]; [1]Nuclear Medicine Department, University Hospital of Besancon, F-25000, FRANCE, [2]Radiopharmacy Unit, University Hospital of Besancon, F-25000, FRANCE, [3]Radiology Department, University Hospital of Besancon, F-25000, FRANCE, [4]Nephrology Department, University Hospital of Besancon, F-25000, FRANCE.

**Background**: Hydrothorax that arises from a pleuroperitoneal communication is a known complication of continuous ambulatory peritoneal dialysis (CAPD). Confirmation or not of this breach by further techniques is essential to provide the

most appropriate treatment to the patient. Indeed, the switch to hemodialysis is compulsory in case of diaphragmatic breach. Among several techniques, peritoneal scintigraphy seems to be the most informative. Nevertheless, only case reports were reported literature. **Material and Methods**: Seven patients in CAPD with suspected pleuroperitoneal communication were studied retrospectively. We compared the diagnostic value of peritoneal scintigraphy and of peritoneal contrast-enhanced ultrasound (CEUS, 5 patients), a promising technique not studied yet in this indication. Glucose, albumin, protein and CRP concentration were also measured in pleural fluid and plasma of the patients. **Results**: Pleural effusion was unilateral, lateralized to the right (6/7). Three patients had a final diagnosis of pleuroperitoneal communication made by the referring nephrologists. For the other 4 patients, 3 diagnosis of vascular overload and one diagnosis of pneumonia were made. The 3 patients with pleuroperitoneal communication were switched to hemodialysis and had no recurrence of hydrothorax. These 3 patients had a pleural effusion lateralized to the right. There was no significant difference in the pleural/plasma ratio of glucose, protein and CRP between patients with and those without a pleuroperitoneal communication. However, there was a significant difference between the two groups regarding the pleural/plasma ratio of albumin ($p = 0.03$) with a lower ratio for patients with a pleuroperitoneal communication. Peritoneal scintigraphy sensitivity, specificity, positive predictive value, negative predictive value and diagnostic accuracy were 100%. The interobserver agreement was excellent, evaluated at 100%. Peritoneal CEUS sensitivity was 50%, specificity 67%, positive predictive value 50%, negative predictive value 67% and diagnostic accuracy 43 %. **Conclusion**: this study in a little group of patients demonstrated a high sensitivity and specificity of peritoneal scintigraphy comparing to CEUS which nevertheless presents some limits in this indication. An acquisition protocol and a decision algorithm are proposed with peritoneal CEUS used at first intention because of no irradiation and peritoneal scintigraphy in second intention in front of any suspected pleuroperitoneal communication in a patient with CAPD.

## OP027

### Extracellular fluid volume (ECV) is a proper variable for Cr-51-EDTA-glomerular filtration rate (Cr-51-GFR) indexation across the entire GFR range: a study through the stages of chronic kidney disease (CKD)

G. Arsos[1], **C. Sachpekidis**[2], D. Katsampoukas[1], E. Manou[3], G. Miserlis[4], A. Vainas[5], I. Tsechelidis[6], D. Tsakiris[3], N. Karatzas[1]; [1]3rd Department of Nuclear Medicine, Aristotle University of Thessaloniki Medical School, Papageorgiou Hospital, Thessaloniki, GREECE, [2]Clinical Cooperation Unit Nuclear Medicine, German Cancer Research Center, Heidelberg, GERMANY, [3]Department of Nephrology, Papageorgiou Hospital, Thessaloniki, GREECE, [4]Transplantation Clinic, Aristotle University of Thessaloniki Medical School, Hippokration Hospital, Thessaloniki, GREECE, [5]Department of Nephrology, 424 Military Hospital, Thessaloniki, GREECE, [6]1st Department of Nuclear Medicine, Aristotle University of Thessaloniki Medical School, Hippokration Hospital, Thessaloniki, GREECE.

**Introduction**: GFR is traditionally, although unreasonably, indexed by body surface area (BSA). ECV is an attractive, physiologically meaningful variable suitable for GFR indexation, and its main determinants have been studied in detail in healthy population. However, both the disease process and the treatment could alter ECV in CKD patients. We Aim to explore ECV changes in a representative CKD population across a wide GFR range. **Subjects and Methods**: Three hundred patients (58.0±16.1 years, 33.0% females) with CKD of various aetiologies, most of them regularly being on different combinations of antidiabetics, a- and b-blockers, calcium channel blockers, ACE-I, ARB, and diuretics, were referred for routine GFR measurement. No patients with excessive, diffuse oedema or ascites were included. After bolus i.v. injection of 3.7 MBq Cr-51-EDTA and 10 plasma samples between 5 min-4 hours p.i., GFR and ECV were calculated by biexponential kinetic analysis based on a two-compartment model. GFR was indexed by BSA (ml/min/1.73 m2) and CKD staging was made according to KDIGO-2012 as G1, G2, G3 and G4-5 (≥90, 60-89, 30-59 and ≤29 ml/min/1.73 m2 respectively). Age, BSA, body mass index (BMI), ECV and ECV/10kg body weight (ECV/BW) differences between the KDIGO-2012 groups were studied by ANOVA and Bonferroni post hoc analysis where needed. Because both GFR and ECV are derived from the same kinetic parameters, the correlation between GFR and ECV/BW was examined by linear regression analysis. Significance was accepted for $p<0.05$. Results: 36, 65, 143 and 54 patients were allocated to G1, G2, G3 and G4 groups with GFR values of 109.0±17.0, 72.3±9.3, 44.3±8.5 and 21.3±5.7, respectively. KDIGO-2012 groups did not differ for BSA, BMI, ECV and ECV/BW. Patients in groups G1 and G2 were younger than in groups G3 and G4-5. ECV (l) and ECV/BW (l/10kg BW) were (mean±SD, CV% in parentheses): 16.4±4.1 (25.0), 2.05±0.43 (21.0); 15.6±4.5 (28.8), 1.95±0.39 (20.0); 15.3±3.7 (24.2), 1.98±0.33 (16.7) and 16.5±4.0 (24.2), 2.11±0.41 (20.8) for G1, G2, G3 and G4-5 groups respectively. No correlation was evident between GFR and ECV/BW ($r=0.037$, $p=0.527$). **Conclusions**: Despite the potentially volume-modifying effects of disease process and treatment, ECV and ECV/BW show remarkable stability across the stages of CKD in patients routinely referred for GFR measurement with Cr-51EDTA. This finding substantiates the suitability of ECV as an GFR indexing variable in GFR measurement with exogenous tracer plasma clearance studies both in health and CKD.

## OP028

### Evaluation of Hepatic Uptake Rate Relationship with the Time Difference of Radiopharmaceutical Preparation and Application at Dynamic Renal Scintigraphy with Tc-99m Mag-3

**S. ISGOREN**, E. ALKAN CIFTCI, G. DAGLIOZ GORUR, M. GUR, C. HAKSAL, H. DEMIR; Kocaeli University School of Medicine, KOCAELI, TURKEY.

**PURPOSE:** The duration of time between the preparation of Tc-99m Mag-3 and application to the patient may vary in relation to the number of patients scheduled. During renal scintigraphy, variable rates of hepatic radiopharmaceutical (RF) uptake are frequently observed. We Aimed to evaluate the relation of the hepatic uptake of Tc-99m Mag-3, with the time difference between RF preparation and patient application. **METHOD:** We analyzed 376 patients with normal or near normal renal scintigraphy findings in between February 2012 and December 2012.On the fifth minute images of dynamic images, rectangler ROI of a median size were drawn to the area of liver and to the background, and then mean counts of these regions were recorded. Hepatic uptake rates were calculated by dividing the counts from liver to that of background. The times that the RF were prepared and that were applied to the patients were recorded and the durations in between them were calculated in terms of minutes. The patients were grouped as group 1 to 5 according to the time elapsed in between preparation and application like 0-60 min, 61-120 min, 121-180 min, 181-240 min, 241-360 min, respectively. Optimum imaging time was accepted as 60 minute after preparation of RF (group 1) so hepatic uptake rates of all other groups was compared with that of group 1 statistically. Besides that, to assess the effectiveness of binding of the RF, we performed quality control (QC) test at each hour up to 5 hours at 5 different days. **RESULTS:** For group 1 to 5, number of patients were 96, 108, 92, 54, 26 and hepatic uptake rates were 1.69, 1.64, 1.69, 1.70, and 1.67, respectively. No statistically significant difference was found in between the hepatic uptake rate of group 1 and other groups. A total of 25 QC analyses which were performed at each hour up to 5 hours and at 5 different days, showed high binding efficiency values of %94 to 96 and there was no statically significant difference between hours and days. **CONCLUSION:** We found that there is no significant effect of the duration of time between the preparation and application to the patient of Tc-99m Mag-3 on hepatic uptake ratio. These results show us the reliable stability of Tc-99m Mag-3 and let us use of the RF up to 5 hours without a deterioration of image quality.

305 - Sunday, Oct. 20, 11:30 - 13:00, Auditorium Pasteur

## Oncology Basic Science: Preclinical Tumour Targeting

## OP029

### Increase of HER2 expression in prostate cancer cell lines as reaction on external irradiation

**J. Malmberg**, M. Rosestedt, A. Orlova; Uppsala University, Uppsala, SWEDEN.

**Aim:** Treatment of aggressive prostate cancer remains to be a great challenge in current oncology. High-dose external beam radiotherapy is among standard-care therapeutic for localised prostate cancer. Ultimately, the objective of local therapy is to control disease with minimal collateral damage, thereby optimizing both cancer and toxicity outcomes. However, biochemical recurrence occurs in 20–40% of patients within 10 years and one third of them will eventually progress to clinical disease, often more aggressive with progression to androgen independent stage. It can be hypothesised that survival mechanism of prostate cancer cells after external beam radiotherapy includes activation mechanism of resistance to apoptosis and increased proliferation. Receptor tyrosine kinase expression, and particularly receptors of HER family, is associated with such behaviour of cancer cells. We have studied expression of HER2 expression in prostate cancer cells lines in vitro in response to external irradiation. **Method:** Prostate cancer cell lines with different origin and HER2 expression were used in this study: LNCaP, local LN metastasis, $30{\cdot}10^3$ receptors/cell[1], PC-3, bone metastasis, $25{\cdot}10^3$, and DU145, brain metastasis, $50{\cdot}10^3$. Cells were irradiated using $^{137}$Cs γ-ray photon radiation source. HER2 receptor expression was quantified using anti-HER affibody molecule $^{99m}$Tc-$Z_{HER2:2395}$ 24, 48 h and 7d post irradiation and compared with non-irradiated cells. **Result:** The HER2 expression in prostate cancer cell lines as a reaction on external irradiation differs in cell line origin, but not in their initial HER2 expression. HER2 expression in LNCaP cells, local LN metastasis, did not change after irradiation. On the opposite, PC-3 and DU145 (both distant metastasis and more aggressive prostate cancer forms) demonstrated a rapid increase of HER2 receptor expression at 24 and 48 h after irradiation (2- and 3-fold, respectively). At 7 d after irradiation HER2 expression level in these cell lines decreased to the level in un-treated cells. **Conclusion:** The study demonstrated that more aggressive prostate cancer may react on high-dose irradiation with increasing of HER2 expression (apoptosis suppressing factor). Additional anti-TKR therapy might be an option for prostate cancer patients undergoing radical prostatectomy with high-dose external beam radiotherapy. 1. Malmberg et al. Exp Ther Med 2011;2:523-528.

## OP030

### DNA double strand breaks as predictor of efficacy of the alpha-particle emitter Ac-225 and the electron emitter Lu-177 for somatostatin receptor targeted radiotherapy

F. Graf[1], J. Fahrer[1], S. Maus[1], A. Morgenstern[2], F. Buchertseifer[2], S. Venkatachalam[1], C. Fottner[1], M. Weber[1], J. Huelsenbeck[1], M. Schreckenberger[1], B. Kaina[1], **M. Miederer**[1]; [1]Universitätsmedizin Mainz, MAINZ, GERMANY, [2]European Commission, Karlsruhe, GERMANY.

**Aim** In this study, we investigated biologic effects of alpha-particle emitter Actinium-225 in comparison to beta-particle emitter Lutetium-177 labeled somatostatin analogue DOTATOC in vitro and in vivo. Methods Radiolabelling of DOTATOC was performed at pH=5.0 with a sodium acetate buffer for Lu-177 and at pH=9.0 with Tris buffer for Ac-225, respectively. In order to determine the relative biological effectiveness (RBE) between the two isotopes somatostatin expressing AR42J cells were incubated with Ac-225-DOTATOC and Lu-177-DOTATOC (0.005 - 250 kBq/ml and 0.005 - 30 MBq/ml) up to 48 h and viability was analyzed using the MTT colorimetric assay. DNA double strand breaks were quantified by microscopy after immunofluorescence staining of γH2AX. Furthermore, cell cycle was analyzed by flow cytometry. In vivo, uptake of both radiolabeled somatostatin-analogues into subcutaneous AR42J tumors in nude mice was measured and number of cells displaying γH2AX-foci was assessed by confocal immunofluorescence microscopy. Therapeutic efficacy was assayed by monitoring tumor growth after treatment with activities translated from in vitro cytotoxicity (n=3-4). Results Ac-225-DOTATOC was synthesized with specific activities between 0.2-0.4 MBq/µg and radiochemical purity of > 90%. ED50 values were 30 kBq/ml after 24 h and 14 kBq/ml after 48 h. Lu-177-DOTATOC displayed radiochemical purity of >95% and ED50 values of 10 MBq/ml after 48 h. Number of DNA double strand breaks increased with increasing concentration of Ac 225 DOTATOC and Lu-177-DOTATOC similarly, if a factor of approximately 700 of Lu-177 activities over Ac-225 activities was applied. Already 24 h after incubation with 2.5, 5, and 10 kBq/ml Ac 225 DOTATOC cell cycle studies showed an increment of the percentage of tumor cells in G2/M phase up to 60%. After 72 h an apoptotic subG1 peak was also detectable. Tumor uptake for both radio peptides at 48 h was identical with 7.5 %ID/g, though overall number of cells with γH2AX-foci was higher for tumors treated with 48 kBq Actinium-225-DOTATOC than tumors treated with 30 MBq Lutetium-177-DOTATOC (35% vs. 21%). Tumors with a mean volume of 0.34 ml reached exponential tumor growth (tumor size of 1.5 ml) after 25 days (44 kBq Ac-225-DOTATOC), after 21 days (34 MBq Lu-177-DOTATOC) and after 5 days (control). **Conclusions** On basis of a factor of 700 between Lu-177 and Ac-225 activities and taking into account the different physical properties, a RBE of approximately 10 can be calculated. This predicts downstream killing effects as determined in vitro and in vivo.

## OP031

### Evaluation of a 99mTc-labelled porphyrin (2CPP) complex as a tumour image agent

P. M. Santos[1], M. Laranjo[2], A. M. Abrantes[2], J. E. Casalta-Lopes[3], A. C. Serra[4], **J. G. Tralhão**[5], J. M. Maia[6], A. M. Rocha-Gonsalves[4], M. F. Botelho[2]; [1]Biophysics Unit, IBILI, Faculty of Medicine, University of Coimbra, Coimbra; Faculty of Health Sciences, University of Beira Interior, Covilhã, PORTUGAL, [2]Biophysics Unit, IBILI, CIMAGO, Faculty of Medicine, University of Coimbra, Coimbra, PORTUGAL, [3]Biophysics Unit, IBILI, Faculty of Medicine, University of Coimbra, Coimbra, PORTUGAL, [4]Quimiotecnon, Chemistry Department, Faculty of Sciences and Technology, University of Coimbra, Coimbra, PORTUGAL, [5]Biophysics Unit, IBILI, CIMAGO, Faculty of Medicine, University of Coimbra; Surgical Department, Surgery A, HUC, Coimbra, PORTUGAL, [6]Faculty of Sciences, University of Beira Interior, Covilhã, PORTUGAL.

**Introduction**: In the last years many advances were achieved in the development of novel imaging agents specific for tumour detection. Porphyrins are good agents for photodynamic treatment of various types of cancer. Moreover, porphyrins are excellent metal chelators, they can form highly stable metallo-complexes with radioisotopes. Therefore, radiolabelled porphyrins could potentially be used as tumour imaging agents. In this context, the Aim of this work was to continue the studies with the 99mTc-labelled porphyrin ((meso-bis[3,4-bis(carboxymethyleneoxy)phenyl]porphyrin) (2CPP)) complex, in order to evaluate its biodistribuition and pharmacokinetics in vivo as well as its potential use as tumour imaging agent. **Material and Methods**: After synthesis of 2CPP, the optimization of the radiolabelling procedure led to the incubation of 0.4mg 2CPP, pH=7 plus 15µg of stannous chloride dihydrate with 162.8±2.6 MBq 99mTc at room temperature for 20 minutes for an optimal labelling reaction. Biological properties of 99mTc-2CPP were evaluated in vitro and in vivo. Uptake of 99mTc-2CPP by colorectal adenocarcinoma (WiDr) and non-small cell lung cancer (H1299) cell was studied using suitable equipment, the LigandTracer® (Ridgeview Instruments AB). For this, to 2x106 cells plated in a petri dish were added 25 µCi/mL of 99mTc-2CPP. In vivo, biodistribution studies were carried out in balb/c nu-nu mice with xenografts of the same cell lines. After administration of the 99mTc-2CPP, the animals were killed at different time intervals and samples were collected from organs and fluids. The percent of the injected activity per gram of organ was calculated. **Results:** Labelling procedure lead to an efficiency of 92.52±0.48. The complex remained stable for more than 4h. Uptake studies showed that uptake increases over time for both cells lines. WiDr and H1299 cells showed a maximum uptake of 2.44±0.60 and 2.63±0.99, respectively. Biodistribution studies showed that the complex was largely eliminated through the renal and hepatobiliary systems. The tumour/muscle ratio increases over time for both tumour types, at 360 min post injection the tumour/muscle ratio in WiDr-bearing mice and H1299-bearing mice was 3.33±1.22 and 3.55±1.29, respectively. **Conclusion**: The labelling of 2CPP with 99mTc was stable, as was proved by biodistribution, and was also reproducible. This complex has a quickly clearance, being eliminated by renal and hepatobiliary system. Both in vitro and in vivo studies showed a higher uptake by H1299 cell line than WiDr cell line.

## OP032

### Imaging HNSCC Xenografts Before and After Irradiation with USPECT $^{111}$In-cetuximab-F(ab')$_2$ and PET $^{18}$F-FDG

**L. K. van Dijk**, J. Bussink, G. M. Franssen, O. C. Boerman; Radboud University Nijmegen Medical Centre, Nijmegen, NETHERLANDS.

**Aim:** A select group of patients with head and neck squamous cell carcinomas (HNSCC) show an improved response when treated with radiotherapy and concurrent epidermal growth factor (EGFR)-inhibitor cetuximab. It would be beneficial to non-invasively image the EGFR to determine receptor availability and potentially predict cetuximab treatment response. The Aim of this study was to visualize the change in systemically accessible EGFR with $^{111}$In-cetuximab-F(ab')$_2$ before and after treatment with radiotherapy, while simultaneously evaluating tumor metabolism with $^{18}$F-FDG PET. **Material and Methods:** $^{111}$In-cetuximab-F(ab')$_2$ optimal protein dose and imaging time point was determined in athymic mice with s.c. FaDu xenografts. Subsequently, mice with patient-derived HNSCC xenografts, SCCNij202 and 167, were imaged with microSPECT/CT using $^{111}$In-cetuximab-F(ab')$_2$ followed by PET/CT imaging with $^{18}$F-FDG. Scans were made 7 days prior to radiotherapy (10 Gy) and 1, 7 and 14 days post treatment. Validation of $^{111}$In-cetuximab-F(ab')$_2$ as an EGFR-specific tracer was evaluated in biodistribution studies as well as by autoradiography and immunohistcohemical staining of the EGFR. **Results:** The highest uptake of $^{111}$In-cetuximab-F(ab')$_2$ in FaDu tumors was obtained at doses of 5 µg/mouse (13.5 ± 5.2 %ID/g). Due to the rapid blood clearance, tumor-to-blood ratios were highest for $^{111}$In-cetuximab-F(ab')$_2$ at 24 h p.i (31.4 ± 3.8). EGFR fractions (fEGFR) of the two tumor xenografts as determined immunohistochemically were significantly different: 0.8 ± 0.1 (SCCNij202), 0.2 ± 0.1 (SCCNij167). Intratumoral distribution of $^{111}$In-cetuximab-F(ab')$_2$ as determined by autoradiography correlated well with the immunohistochemical distribution of EGFR ($r$ = 0.64 ± 0.06, p<0.0001). Growth of irradiated SCCNij202 tumors was significantly inhibited as compared to controls (p<0.05). No significant difference in tumor volume was detected between the control and experimental group for SCCNij167 (p=0.06). MicroSPECT images showed a significant increase in uptake of $^{111}$In-cetuximab-F(ab')$_2$ in SCCNij202 after irradiation (tumor-to-liver ratio 1.9 ± 0.2 *versus* 3.8 ± 0.7, 7 d pre- and 14 d post-treatment respectively, p<0.05), but not in SCCNij167 (p=0.36). A decrease in uptake of $^{18}$F-FDG was observed in both xenografts after radiation therapy. **Conclusion:** EGFR expression can be visualized with $^{111}$In-cetuximab-F(ab')$_2$ and SPECT imaging with $^{111}$In-cetuximab-F(ab')$_2$ has the potential to monitor the effects of radiation therapy. In addition, $^{111}$In-cetuximab-F(ab')$_2$ could potentially be used to predict treatment response to EGFR-inhibitors such as cetuximab.

## OP033

### Cetuximab treatment reduces the accumulation of $^{111}$In-bevacizumab in breast cancer xenografts

**S. Heskamp**[1], H. W. M. van Laarhoven[2], J. D. M. Molkenboer-Kuenen[1], W. J. G. Oyen[1], W. T. A. van der Graaf[1], O. C. Boerman[1]; [1]Radboud University Nijmegen Medical Centre, Nijmegen, NETHERLANDS, [2]Amsterdam Medical Center, Amsterdam, NETHERLANDS.

**Introduction:** Bevacizumab (anti-VEGF) and cetuximab (anti-EGFR) are approved for the treatment of cancer. However, in advanced colorectal cancer, the combination of bevacizumab and cetuximab did not improve survival. The reason for the lack of activity remains unclear. Previously, we have shown that bevacizumab reduced the vascular density of tumor xenografts and consequently limited the delivery of cetuximab to tumors. Thus bevacizumab could limit the therapeutic efficacy of cetuximab. Alternatively, cetuximab could alter VEGF expression, limiting tumor targeting by bevacizumab. The Aim of this study was to determine the effect of cetuximab on targeting of bevacizumab to the tumor. **Material and Methods:** Mice with s.c. SUM149 or WiDr (EGFR and VEGF positive) tumors were treated twice a week intraperitoneally with 1 or 40 mg/kg cetuximab. Before start of treatment (day 0) and after 7 and 21 days, the uptake of

radiolabeled bevacizumab in the tumor was measured by immunoSPECT/CT. Three days prior to scanning, mice received 15 MBq of $^{111}$In-Bevacizumab. After scanning, tumors were dissected to determine the activity concentration ex vivo. **Results:** Cetuximab treatment significantly delayed growth of SUM149 xenografts, while growth of WiDr tumors was not affected. SPECT/CT imaging revealed that cetuximab caused reduced tumor targeting of radiolabeled bevacizumab to SUM149 xenografts. The tumor uptake of $^{111}$In-bevacizumab at day 7 and 21 decreased with 24% and 37%. Tumor-blood ratios before treatment and at day 7 and 21 of treatment were 2.4 ± 0.3, 1.6 ± 0.2, and 1.4 ± 0.2, respectively (p=0.004). In the WiDr model, tumor-blood ratios did not change significantly during treatment (ratios day 0, 7 and 21: 1.3 ± 0.2, 1.2 ± 0.1, and 1.1 ± 0.1, respectively). **Conclusion:** Cetuximab can reduce the targeting of radiolabeled bevacizumab to cetuximab sensitive tumors. This reduced targeting may partly explain why the combination of bevacizumab and cetuximab does not result in improved therapeutic efficacy.

## OP034

### In Vivo Tumor Targeting and Drug Delivery with Mesoporous Silica Nanoparticles

**F. Chen**, H. Hong, H. F. Valdovinos, T. E. Barnhart, W. Cai; University of Wisconsin-Madison, Madison, WI, UNITED STATES.

**Aim:** In vivo targeting of mesoporous silica nanoparticles ($mSiO_2$) to either tumor cells or tumor vasculature has been a major challenge since their initial use as novel drug delivery nanoplatforms. We sought to overcome this challenge by functionalizing uniform $mSiO_2$ with a tumor targeting antibody and a radioisotope for in vivo tumor targeting and drug delivery, which can be non-invasively monitored by positron emission tomography (PET) imaging. **Materials and Methods:** A soft-template method was used to synthesize uniform $mSiO_2$, which were functionalized with thiol groups and conjugated to TRC105 (an anti-CD105 antibody) and 1,4,7-triazacyclononane-N,N'N''-triacetic acid (NOTA) through polyethylene glycol (PEG) linkers. Transmission electron microscopy (TEM), dynamic light scattering (DLS), and zeta-potential measurements were performed to confirm successful synthesis of NOTA-$mSiO_2$-PEG-TRC105. In vitro CD105 imaging was carried out with FITC-conjugated nanoparticles in HUVECs (CD105 positive) and MCF-7 (CD105 negative) human breast cancer cells. After labeling with $^{64}$Cu, PET imaging, biodistribution, and blocking studies were performed in 4T1 murine breast tumor-bearing mice to evaluate the tumor targeting capability of $^{64}$Cu-NOTA-$mSiO_2$-PEG-TRC105, where $^{64}$Cu-NOTA-$mSiO_2$-PEG was used as the control. Histology studies were performed to confirm CD105 specificity of the nanoconjugate. **Results:** Uniform $mSiO_2$ (~ 80 nm) nanoparticles were synthesized and little changes in particle size or morphology were observed during surface functionalization, as demonstrated by serial TEM studies. Changes in zeta-potential and DLS measurements confirmed the success of each reaction step (e.g. thiolation, PEGylation, NOTA/TRC105 conjugation). Incubation with FITC-$mSiO_2$-PEG-TRC105 resulted in greatly enhanced fluorescence signal on HUVECs compared to FITC-$mSiO_2$-PEG. $^{64}$Cu-labeling was achieved with high yield and specific activity. Serial PET imaging revealed that 4T1 tumor uptake of $^{64}$Cu-NOTA-$mSiO_2$-PEG-TRC105 peaked at 5 h post-injection (5.9±0.4 %ID/g; n=3), significantly higher than that of $^{64}$Cu-NOTA-$mSiO_2$-PEG (2.9±0.9 %ID/g), indicating CD105 specific tumor targeting of $^{64}$Cu-NOTA-$mSiO_2$-PEG-TRC105 which was confirmed by blocking and histology studies. We further demonstrated successful targeted delivery of doxorubicin (DOX) in 4T1 tumor-bearing mice after intravenous injection of DOX-loaded $mSiO_2$-PEG-TRC105, which holds potential for image-guided drug delivery and targeted cancer therapy. **Conclusion:** This is the first report of in vivo tumor (vasculature) targeting with $mSiO_2$, one of the most promising drug delivery nanoplatforms. Successful surface modification, 64Cu-labeling, and in vitro/in vivo CD105 targeting was demonstrated, which opened up new perspectives on the use of biocompatible $mSiO_2$ for cancer targeted imaging and therapy. Since CD105 expression correlates with poor survival in >10 solid tumor types, this strategy can be generally applicable to all solid tumors.

## OP035

### Biopolymeric nanoprobes for improved efficacy of PRRT

**G. Arora**[1], J. Shukla[2], S. Ghosh[3], S. Ballal[1], G. Bandopadhyaya[1]; [1]All India Institute Of Medical Sciences, Delhi, INDIA, [2]Post Graduate Institute of Medical Education and Research, Punjab, INDIA, [3]Indian Institute of Technology, Delhi, INDIA.

**Aim** - The potential of peptide receptor radionuclide therapy (PRRT) with 177Lu-DOTATATE therapy for Neuroendocrine tumors (NETs) is limited by the associated renal radiation dose. Application of nanoparticles in drug delivery has yielded promising results in chemotherapy both in terms of enhanced efficacy while simultaneously reducing the associated side effects. Based on these facts, we have developed biopolymeric nanoparticles containing 177Lu-DOTATATE for NETs therapy. **Methods** - Nanoparticles (NPs) of PLGA, alginate and alginate/chitosan were prepared followed by 177Lu-DOTATATE encapsulation and PEG-coating. They were compared in-vitro with respect to various parameters such as ease of formulation, particle size, stability at physiological pH (7.4), drug-loading efficiency and release kinetics over 21 days. The most suitable NPs were evaluated in vivo in tumor-induced wistar albino rats (C6 glioma cell) by imaging followed by blood and organ counting upto 24 h. Uptake ratio of tumor (T) to kidney (K), liver (L) and bone (B) were calculated and compared to that of control group injected with 177Lu-DOTATATE. **Results** - All NPs were spherical in shape as seen on electron microscope with size range between 200-300 nm. PLGA NPs, however, had smoother surface. Optimum size (303.8 ± 67.2 nm), better stability, drug-loading capacity (65.385 ± 5.67%) and minimum release till 6 h (27.89 ± 4.60%) favored the use of PLGA NPs over alginate and alginate/chitosan NPs. T:K, T:L and T:B values were 8.58, 5.68 and 8.00 in the group injected with 177Lu-DOTATATE-NPs at 24 h post-injection compared to 2.17 ($p<0.001$), 6.82 ($p=0.2$) and 8.71 ($p=0.3$) for the control group, respectively. Further, the uptake in tumor with 177Lu-DOTATATE-NPs (43%) was significantly higher than the control group (33%; $p<0.05$). **Conclusion** - A 4-fold increase in tumor-to-kidney ratio and higher tumor uptake of 177Lu-DOTATATE indicates the high potential of these nanoprobes in enhancing the efficacy of PRRT by reducing the associated renal radiation dose. NPs can play a significant role for delivery of radiopharmaceuticals, particularly in patients who otherwise remain undertreated owing to increased side effects at high doses. Radiolabeled nanoparticles have yet not found a widespread clinical application in nuclear medicine therapy. This study will therefore serve as a foundation for further trials in human subjects, so that NPs can be applied in routine PRRT and also encourage nano-biotechnology-based research in nuclear medicine and molecular imaging.

306 - Sunday, Oct. 20, 11:30 - 13:00, Grand Salon Prestige Gratte-Ciel

## Physics & Instrumentation & Data Analysis: Image Reconstruction

## OP036

### Filtering of 3D PET images using compressed sensing

**D. Richter**[1], T. C. Basse-Lüsebrink[2], T. Kampf[2], A. Fischer[3], P. M. Jakob[2], S. Samnick[1]; [1]Department of Nuclear Medicine, University of Würzburg, Würzburg, GERMANY, [2]Department of Experimental Physics 5, University of Würzburg, Würzburg, GERMANY, [3]Institute of Radiology, University of Würzburg, Würzburg, GERMANY.

**Aim**: It has been shown, that in positron emission tomography (PET) noise and reconstruction artefacts in analytically reconstructed 2D images can be reduced using compressed sensing (CS) [1]. With the development of modern computers, the trend is heading for 3D image reconstruction Methods. Data of oblique sinograms can accurately be used in the reconstruction process reducing statistical noise and yielding an improved signal-to-noise ratio (SNR) compared to 2D reconstructions. The 3D reprojection (3DRP) algorithm is a widely used analytic method to reconstruct 3D PET data [2]. Especially for low count statistics, however, iterative Methods can outperform 3DRP e.g. in view of contrast. Unfortunately, iterative Methods can need long computation times [3]. Furthermore, a large amount of memory can be required if the system matrix is pre-computed and stored. We investigate if a CS-based post processing filtering method can be extended to 3D. Thus, to improve the contrast, this technique was applied to 3DRP reconstructed images. **Materials and Methods**: Raw data are reconstructed using 3DRP. Subsequently, the image is transformed to Fourier-space where the completely sampled dataset is reduced by multiplication with an incoherently undersampled sampling pattern. Afterwards, undersampled data are reconstructed using CS. The procedure is repeated several times using different sampling patterns and the average of the reconstructed images is calculated. The method is tested both on data generated by GATE and on data acquired on an Inveon small-animal PET scanner (Siemens Medical Solutions) [4]. The results are compared to a 3D ordered subset expectation maximization (3D-OSEM) reconstruction [5]. For quantification purposes, the SNR is calculated. **Results and conclusion**: The proposed filtering method using CS can be extended to 3D. It is possible to considerably improve the contrast of 3DRP reconstructed images especially if raw data contained only few counts. This is displayed in clearly improved SNR. For several undersampling factors and noise levels, the SNR can be more than doubled. However, with increasing undersampling, images are notably smoothed and blurred. With regard to contrast, the filtered images are comparable to and, especially in case of low count data, can even outperform those reconstructed using 3D-OSEM. References: [1] Richter D et al., 2013 (unpublished data) [2] Kinahan PE, Rogers JG, IEEE Trans. Nucl. Sci. 1989, 36:964-8 [3] Reader AJ, et al., Phys. Med. Biol. 1998, 43:823-34 [4] Jan S et al., Phys Med Biol 2004, 49:4543-61. [5] Hudson HM, Larkin RS, IEEE Trans. Med. Imaging 1994, 13:601-9

## OP037

### Joint integration of temporal regularization and respiratory motion corrections inside the reconstruction algorithm in dynamic PET imaging for applications in oncological studies

**T. Merlin**[1], P. Fernandez[1], D. Visvikis[2], F. Lamare[1]; [1]Hôpital de Bordeaux, INCIA, CNRS UMR 5287, Bordeaux, FRANCE, [2]UMR 1101 INSERM, LaTIM, Brest, FRANCE.

**Purpose**: Respiratory motion reduces both the qualitative and quantitative accuracy of PET images in oncology. This impact is more significant for quantitative applications based on kinetic modeling, where dynamic acquisitions are associated with limited statistics due to the necessity of enhanced spatiotemporal resolution. While previous works have concentrated either on the correction of respiratory motion or on the improvement of dynamic PET images, the Aim of this study is to address these drawbacks by combining within a unique reconstruction algorithm, a respiratory motion correction for dynamic PET imaging based on a temporal basis functions' regularization. In oncology applications such as lung cancer, developed method represents the first step towards quantitative analysis based on kinetic modelling. **Materials and Methods**: The acquired dynamic list-mode is sorted according to the amplitude of the recorded respiratory cycle and independent reconstructions of each PET gated frame is performed. Elastic transformation parameters for the motion correction are estimated from the registration of the reconstructed PET gated images. The derived displacement matrices are subsequently used in a modified version of the OPL-EM reconstruction algorithm integrating a temporal regularization between the 3D dynamic PET frames based on temporal basis functions. These functions are simultaneously estimated at each iteration along with their relative coefficients for each image voxel. Quantitative evaluation was performed using dynamic Monte-Carlo simulations of the NCAT phantom including respiratory motion, as well as dynamic FDG PET/CT acquisitions of lung cancer patients acquired on a GE DRX system. The proposed method was compared with the performance of a standard multi-frame OPL-EM reconstruction algorithm. **Results:** The proposed method achieved significant improvements in terms of bias reduction and contrast enhancement while accounting for respiratory motion artifacts. Results on simulated data show contrast and error positioning improvements as high as 80% and 95% respectively for a realistic lung lesion, in comparison to a standard reconstruction. **Conclusion**: Incorporation of the elastic model based respiratory motion correction along with a temporal regularization in the reconstruction process of the PET dynamic series led to activity estimation improvement and motion artefacts reduction. Future work will include the integration of a linear FDG kinetic model in order to directly reconstruct parametric images.

## OP038

### Clinical evaluation of penalized likelihood reconstruction in whole-body PET studies

H. Ma[1], E. Asma[2], S. Ahn[2], S. Ross[3], R. Manjeshwar[2], D. Wilson[4], R. P. Tonseth[4], A. Tran[4], A. Celler[1], **F. Benard**[1,4]; [1]University of British Columbia, Vancouver, BC, CANADA, [2]GE Global Research, Niskayuna, NY, UNITED STATES, [3]GE Healthcare, Milwaukee, WI, UNITED STATES, [4]BC Cancer Agency, Vancouver, BC, CANADA.

**Aim**: Iterative reconstruction algorithms such as ordered subsets expectation maximization (OSEM) are widely used for oncologic PET image reconstruction. However, OSEM creates "mottling" in uniform organs due to clustering of voxels, which becomes more prominent as the number of subsets/iterations increase. Penalized likelihood algorithms such as block sequential regularized expectation maximization (BSREM) have been proposed to reduce voxel clustering and improve image quality. The purpose of this study was to evaluate the performance of BSREM in comparison to OSEM on routine clinical data. **Methods**: Sinograms from 30 consecutive cases of suspected lung cancer were reconstructed by OSEM (with point spread function or PSF modeling), time-of-flight OSEM (TOF-OSEM, also with PSF), and BSREM. Algorithms used consistent parameters across patients (2 iterations/32 subsets, 6.4 mm Gaussian filter for OSEM and TOF-OSEM; gamma 2, beta 525, run at full convergence for BSREM). For each scan, 3D regions-of-interest (ROI) were drawn around the smallest and largest visible lesions, adjacent background, liver, mediastinal blood pool activity and white adipose tissue. Signal-to-noise (SNR) was defined as the SUV peak divided by the standard deviation in the adjacent background ROI. Contrast was calculated as the SUV peak divided by the average activity in adjacent background ROI. Each reconstructed data set was assigned a randomized identifier and blindly assessed by 3 physicians for evaluation of overall image quality, noise and lesion conspicuity. Quantitative and qualitative data sets were analyzed using non-parametric one-way ANOVA with correction for multiple comparisons. **Results:** The SNR of FDG avid lesions were significantly higher with BSREM compared to OSEM and TOF-OSEM (adjusted p<0.01). Contrast was significantly higher with BSREM compared to OSEM (adjusted p<0.0001), but lower than TOF-OSEM (p<0.0001). BSREM showed less variability in uniform organs than OSEM and TOF-OSEM (p<0.001) while maintaining similar SUV values. Lesion SUV peak and SUV max were similar between BSREM and TOF-OSEM (p=ns); all were significantly higher than OSEM (p<0.0001). Lesion conspicuity was ranked significantly better with BSREM and TOF-OSEM compared to OSEM by 2 of 3 readers, and not significantly different by the third reader. Lesion conspicuity was similar between BSREM and TOF-OSEM. **Conclusion**: Our results show that non-TOF penalized likelihood reconstruction Methods improve lesion contrast and signal-to-noise compared to OSEM, while maintaining SUV values that are comparable to TOF-OSEM reconstructions. Ongoing work includes evaluating the algorithms in a larger group of patients (n=90).

## OP039

### Evaluation of the iterative reconstruction algorithms with resolution recovery for reducting patient dose in MPI: transmural defect contrast and left-ventricular wall thickness

O. Zoccarato[1], C. Scabbio[2], E. De Ponti[3], M. Brambilla[4], R. Matheoud[4], S. Morzenti[3], S. Garancini[5], M. Menzaghi[5], **M. Lecchi**[2]; [1]Unit of Nuclear Medicine, IRCCS S. Maugeri Foundation, Veruno, ITALY, [2]Department of Health Sciences, University of Milan; Department of Diagnostic Imaging, San Paolo Hospital, Milan, ITALY, [3]Medical Physics, San Gerardo Hospital, Monza, ITALY, [4]Unit of Medical Physics, University Hospital 'Maggiore della Carità', Novara, ITALY, [5]Unit of Nuclear Medicine, Ospedale di Circolo, Varese, ITALY.

**Introduction.** Recent clinical studies have highlighted the ability of the new iterative reconstruction algorithms with resolution recovery (IR-RR) to halve the patient dose in SPECT MPI, while retaining the same diagnostic accuracy as the standard procedure. **Aim**. The CILDA (Cardiac Imaging Low Dose Algorithms) project Aims to establish the lower limit of radioactivity that can be administered to patients in SPECT MPI, independently of the equipment/IR-RR used while preserving diagnostic accuracy. **Materials and Methods.** In four different nuclear-medicine centers, an anthropomorphic phantom was used to simulate clinical STRESS scans with [$^{99m}$Tc]tetrofosmin. In each center, two sets (with and without a transmural defect, TD) of five separate scans were acquired with total counts of 6(standard *in vivo* counting statistics), 4(75% of standard counts), 3(50%), 1.5(25%) and 0.8 Mcounts(12.5%). For each nuclear medicine center and each scan, three sets of SPECT images were reconstructed with: 1)FBP, 2)OSEM and 3)the new IR-RR available in the different centers: *Evolution for cardiac* (GE), *Astonish* (Philips), *Flash 3D* (Siemens) and *Wide beam reconstruction, WBR* (UltraSPECT). In the case 3), the IR-RR dataset included no correction(NC), correction for attenuation (AC), for scatter (SC) or for both(ACSC). To date, all image sets have been centrally analyzed in order to evaluate: **a)**TD contrast in LV wall; **b)**LV wall thickness (FWHM of the medial sections). The difference (Diff) of IR-RR analysis results from FBP and OSEM ones was finally evaluated (t test). **Results. a)**For all counting-statistics and all IR-RR algorithms, Diff in TD contrast was significant (p<0.01) from both FBP (9.7%±6.9%; 15.2%±5.8%; 8.3%±6.8% and 14.5%±6.8% for NC, SC, AC, ACSC, respectively) and OSEM (7.9%±3.9%; 13.5%±4.0%; 6.6%±4.9% and 12.7%±4.1% for NC, SC, AC, ACSC, respectively). **b)**LV wall thickness was significant (p<0.01) smaller for IR-RR compared to FBP and OSEM until 50% of the standard counts (Diff at 50% from FBP: 4.0±3.4mm, 5.4±2.3mm, 3.6±3.1mm, 4.6±3.1 for NC, SC, AC, ACSC, respectively). The FWHM of the LV wall for all WBR image sets increased with decreasing counting statistics, being found to be comparable to or worse than FBP and OSEM at 25% of the standard dose. **Discussion and conclusion**. The IR-RR algorithms provide significant better results up to 50% of standard counting statistics when LV wall thickness was considered. The attenuation and scatter corrections should be included in the reconstruction process: AC alone must be applied carefully, while SC shows better results for both the LV wall thickness and for the TD contrast.

## OP040

### Reduction of Staircasing Artifacts in Tomographic Reconstruction with Total Variation Regularization

S. Li[1], **A. Krol**[2], Z. Wu[1], J. Zhang[3], L. Vogelsang[4], L. Shen[3], Y. Xu[3], E. Lipson[3], D. Feiglin[2]; [1]Sun Yat-sen University, Guangzhou, CHINA, [2]SUNY Upstate Medical University, Syracuse, NY, UNITED STATES, [3]Syracuse University, Syracuse, NY, UNITED STATES, [4]VirtualScopics, Rochester, NY, UNITED STATES.

**Aim:** To reduce staircasing artifacts in tomographic reconstruction with total variation regularization. **Materials and Methods:** We have generalized our previously developed preconditioned alternating projection algorithm (PAPA) for maximum a posteriori (MAP) ECT reconstruction, by introducing the modified total variation (TV) regularization and have accordingly developed a "generalized PAPA" (GPAPA) algorithm. The second order TV regularization term $R(f)= lam_1Phi(B_1f)+ lam_2Psi(B_2f)$ was directly added to the objective function, where $B_1$ and $B_2$ are first and second order difference matrices, respectively; $f$ is the expected image vector, and $lam_1$ and $lam_2$ are hyperparameters. Because of separability of the proximity operator on $R(f)$, i.e. $prox_R=[prox_{lam1Phi}(B_1f), prox_{lam2Psi}(B_2f)]$ , our previously derived PAPA algorithm can be applied to solve the modified MAP ECT problem. This leads to the following iterative scheme: Step 1: $S^{(k)}=diag(f^{(k)}/A1)$; Step 2: $h^{(k)}=P_R^d(f^{(k)}- cS^{(k)}grad_fH(f^{(k)},b^{(k)}))$; Step 3: $b^{(k=1)}=[b_1^{(k+1)}, b_2^{(k+1)}]^T=Q_{h(k)}{}^{-1}([b_1^{(k+1)}, b_2^{(k+1)}]^T)$; and Step 4: $f^{(k+1)}= P_R^d(f^{(k)}- cS^{(k)}grad_fH(f^{(k)},b^{(k+1)}))$, where A is system matrix, $H(f,b)$ =

*<Af,1>-<ln(Af+r), g>+mu<Bf,b>, mu* is constant, *r* are random counts, *g* are observed data, and $Q_{h(k)}$ $([\ b_1^{(k)},\ b_2^{(k)}]^T=[(I\text{-}prox_{lam1/muPhi})(\ b_1^{(k)}+ B_1f),(I\text{-}prox_{lam2/muPsi})(\ b_2^{(k)}+ B_2f)]$. Using Monte Carlo Methods, we simulated a fan-beam (f =43 cm) SPECT projection set (120 views, 128x64 matrix, 3.56 mm pixel size, 35,000 counts per view) from a cylinder (20.8 cm diameter) containing objects with linear and quadratic (concave and convex) activity gradients. These projection data were reconstructed using the new GPAPA algorithm. The derived GPAPA algorithm requires estimation of three hyperparameters, while the original PAPA requires only two. The hyperparameters were obtained by performing sets of trial reconstructions (50 iterations each) and plotting spatial resolution and coefficient of variation (a surrogate measure of noise) versus hyperparameter value. The best hyperparameter values were obtained using these plots. We also reconstructed the same data using our previously developed PAPA algorithm with only first order TV. The 100 noise realizations were reconstructed (200 iterations each) for both algorithms. We performed quantitative analyses (line profiles, noise power spectra, uniformity, bias, contrast-to-noise ratio and recovery coefficient) and qualitative analyses of image quality. **Results:** In the images obtained using GPAPA the staircasing artifacts are partially suppressed, as compared to PAPA, without significant loss of spatial resolution. **Conclusions**: The total variation regularization can be augmented to contain second order derivatives resulting in improved imaging performance with the suppressed staircasing artifacts.

## OP041

### Low-Noise Reconstruction of the Monte Carlo Simulated SPECT Data Using a Preconditioned Alternating Projection Algorithm

**A. Krol**[1], S. Li[2], J. Zhang[3], L. Vogelsang[4], L. Shen[3], Y. Xu[3], E. Lipson[3], D. Feiglin[1]; [1]SUNY Upstate Medical University, SYRACUSE, NY, UNITED STATES, [2]Sun Yat-sen University, Guangzhou, CHINA, [3]Syracuse University, SYRACUSE, NY, UNITED STATES, [4]VirtualScopics, Rochester, NY, UNITED STATES.

**Aim**: To apply the preconditioned alternating projection algorithm (PAPA) to realistic SPECT data, ascertain its low-dose performance, and compare the performance with that of conventional maximum-likelihood expectation maximization (MLEM) with Gaussian post-filter. **Materials and Methods**: We previously developed the preconditioned alternating projection algorithm for solving the maximum a posteriori (MAP) emission computed tomography reconstruction problem using total variation (TV) regularization. We applied the PAPA algorithm to reconstruction of realistic, Monte Carlo simulated, fan-beam (f = 43 cm) SPECT data (120 views, 128×128 matrix, 3.6 mm pixel size). We simulated a cylinder with 20.8 cm diameter, containing two sets, in transverse planes, of seven hot spheres (relative activity-to-background ratio 2:1; diameters 0.66−3.08 cm) and one plane with seven cold spheres (zero activity). A reference cylinder had uniform background activity only. The mean total number of counts per view was 35,000. We created 100 noise realizations for each phantom (200 datasets total). The PAPA algorithm requires estimation of two hyperparameters, obtained by performing sets of trial reconstructions (50 iterations each) and plotting spatial resolution and coefficient of variation (a surrogate measure of noise) versus hyperparameter value. The best hyperparameter values were obtained using these plots. We performed 200 reconstructions (200 iterations each) of all noise realizations of both phantoms with selected hyperparameter values. We also performed 200 reconstructions (100 iterations each) of the same data using conventional MLEM with Gaussian post-filter and with spatial resolution set to match the spatial resolution of PAPA. The reconstructed images so obtained were used to estimate the following for each sphere: contrast-to-noise ratio, bias, and recovery coefficient. In addition, the noise (coefficient of variation for a uniform region), noise power spectrum (NPS), image uniformity, and global bias were estimated. We also performed channelized Hotelling observer (CHO) studies of simulated lesion detectability, and obtained corresponding receiver operating characteristic (ROC) curves. **Results**: We observe that PAPA produced images with significantly better image quality, compared to MLEM/Gauss, because of much better control of the noise. While the spatial resolution, bias, and recovery coefficient are comparable for both algorithms, the NPS is significantly lower for PAPA with correspondingly higher contrast-to-noise ratio for PAPA, compared to MLEM/Gauss. Further, the area under the ROC curve (AUC) is significantly higher for PAPA. **Conclusions**: Our new PAPA algorithm significantly outperforms the conventional MLEM/Gauss in terms of noise performance and thus might allow very low-dose SPECT scans.

## OP042

### Quantitation of Lu-177 SPECT: OSEM and Bayesian Reconstruction with State-of-the-Art Compensation Methods

**E. Hippeläinen**[1,2], A. Sohlberg[3]; [1]HUS Medical Imaging Center, Helsinki, FINLAND, [2]University of Helsinki, Department of Physics, Helsinki, FINLAND, [3]Joint Authority for Päijät-Häme Social and Health Care, Department of Clinical Physiology and Nuclear Medicine, Lahti, FINLAND.

**Introduction** Patient specific internal dosimetry is essential for safe treatment of neuroendocrine tumors with Lutetium-labeled peptides. The key part of internal dosimetry is the quantitative accuracy of the single photon emission computed tomography images (SPECT), which serve as a starting point for the dose calculations. SPECT images are degraded by photon attenuation, scatter and collimator blurring, which have to be accurately compensated. In addition to compensations, also the reconstruction algorithm itself has a big impact on the reconstructed image. Conventionally ordered subsets expectation maximum (OSEM) algorithm has been used for dosimetry, but Bayesian reconstruction Methods might offer advantages compared with OSEM. Bayesian Methods can produce smoother, less noisy images than OSEM, which might be beneficial especially for dose volume histogram-based quantitation. The **Aim** of this study is to compare OSEM and Median Root Prior (MRP), which served as our Bayesian reconstruction method, in terms of quantitative accuracy using different combinations of the compensations Methods. **Material and Methods** The reconstructions were performed with OSEM and MRP reconstruction algorithms. CT-based attenuation compensation, Monte Carlo- based scatter modeling and Gaussian-based collimator compensation were applied in different combinations to the images. A cylindrical calibration and RDS Alderson thorax phantoms were imaged using Siemens Symbia T SPECT/CT camera. The calibration phantom was uniformly filled with $^{177}$Lu and calibration coefficients for quantification were defined from images. The thorax phantom was filled with 9 active spherical tumor models with different sizes, which were filled with the same concentration of $^{177}$Lu solution. The thorax phantom also had low background activity in thorax and in other lung. Images were analyzed using VOIs delineated from CT images. Relative quantification error was calculated for all active spheres and histograms of the voxel values were generated. **Results** The quantitative accuracy of both the algorithms was very similar. The lowest quantification error, which ranged from 5% to 88% for OSEM and from 6% to 89% for MRP depending on the sphere size, was achieved when all the corrections were applied. The quantitative accuracy was heavily dependent on the compensations and got better as more compensation Methods were applied during reconstruction. MRP images were more homogenous than OSEM images. Also the voxel value histograms were less dispersed with MRP indicating more accurate distribution of voxel values inside the VOIs. **Conclusion** Quantitative accuracy of the OSEM and MRP reconstruction algorithms were very similar. MRP produced images whose voxel value dispersion was smaller in homogenous areas.

## OP043

### Performances of the iterative reconstruction algorithm in a last-generation SPECT/CT hybrid system

**A. Ferretti**[1], M. Gava[1], A. M. Maffione[1], S. Chondrogiannis[1], M. C. Marzola[1], G. Grassetto[1], L. Rampin[1], E. Bolla[2], L. Gallo[2], D. Rubello[1]; [1]Santa Maria della Misericordia Hospital, ULSS 18, Rovigo, ITALY, [2]Castelfranco Veneto Hospital, ULSS 8 Asolo, Castelfranco Veneto (TV), ITALY.

**Aim:** To evaluate the accuracy of volumetric tomographic reconstruction of a last-generation SPECT/CT system, in particular for quantitative applications. **Materials and Methods:** We utilized a cylindrical phantom filled with a solution of Tc-99m (activity 57 MBq in a volume of 6.5 l), equipped with 6 hot spheres (internal diameters from 31.3 to 9.8 mm) filled with a concentration of 70 kBq/ml, i.e. intrinsic contrast of 8:1 to the background, in order to simulate the clinical settings. The attenuation correction (AC) was performed through the 16-slices CT installed in the hybrid system. The reconstruction iterative OSEM algorithm was evaluated using different settings. The AC and scatter corrections (SC) were evaluated in terms of axial flatness and noise (coefficient of variation CV) of the images, both evaluated in the uniform part of the phantom. The partial volume effect (PVE) was evaluated calculating the recovery coefficient of the 6 small spheres. The tomographic acquisition included 120 views, covering 360°, with a duration of 45 sec per view. Moreover the tomographic spatial resolution with scatter was computed, using a similar cylindrical phantom, equipped with 3 capillary tubes (activity of 40 MBq of Tc-99m). **Results:** Both uniformity and noise improved by decreasing the number of iterations and increasing the critical frequency of the post-reconstruction filter. No-AC images had very poor uniformity in comparison to AC images (underestimation of the central counts was 71% in no-AC images vs. 2.1% in AC images). The PVE recovery coefficients increased significantly with the diameter of the spheres (22% for the 9.8 mm sphere vs. 100% for the 31.3 mm sphere) and slightly with the critical frequency (22% with f = 0.48 vs. 26% with f = 0.80, for the smallest sphere) or the number of iterations (22% with 2 iterations vs. 24% with 3 iterations, for the smallest sphere). Only the smallest sphere detectability appeared critical. The spatial resolution improved when the critical frequency of the filter increased, while it appeared unchanged when the number of iterations was increased. **Conclusion:** The SPECT/CT reconstruction settings appeared decisive to obtain accurate emissive images. In particular the reconstruction parameters affected inversely the spatial resolution and the noise, so the best compromise between these two important image characteristics should be investigated.

307 - Sunday, Oct. 20, 11:30 - 13:00, Salon Pasteur

## Oncology Clinical Science: Melanoma, Sarcoma, CUP & Other

### OP044

#### F-18 FDG-PET/CT in the follow-up of patients (pts) with stage II-III malignant melanoma (MM) : the experience of the National Cancer Institute of Milano

**B. Padovano**, A. Alessi, A. Maurichi, G. Serafini, C. Bampo, M. Santinami, F. Crippa; Fondazione IRCCS Istituto Nazionale dei Tumori, Milano, ITALY.

**Aim**: In our Institute [18F]FDG-PET/CT (PET) is routinely used for the follow-up of pts with MM with high risk of relapse for the first 5 yrs after the initial diagnosis. Aim of our study was to retrospectively evaluate the results of PET in monitoring the disease and to investigate the incremental added value of extending standard total body scan (from upper thigh to skull base) to lower extremities in every patient, independently from the location of the primary lesion. **Material and Methods**: We retrospectively analyzed 338 consecutive pts with advanced histological proved MM (from stage IIA to IIIC) who underwent whole body PET extended to lower limbs every 6 months from the initial diagnosis. Scans were performed using PET/CT systems, 60 minutes after the injection of FDG (activity range 250-450 MBq) in pts in fasting status (≥6 hrs) and blood glucose levels <140 mg/dl. Images were evaluated looking for abnormal FDG findings consistent with MM localizations. Results were compared with data coming from the clinical/instrumental follow-up and, when available, with post-surgery pathological analysis. **Results**: PET demonstrated MM metastases in 57/338 pts (17%). In 47/57 pts (82%), the metastases were amenable for surgical treatment, and precisely we found cutaneous/subcutaneous metastases in 27/57 pts (47%) and lymph nodes metastases in 20/57 pts (35%); in the remaining 10 pts (18%), PET showed multiple localizations on skin, liver, lymph nodes, lung and bone. In the subgroup of pts with cutaneous/subcutaneous metastases, 19 cases (70%) have lesions located only in the lower limbs with primary placed on torso in 3 cases (16%) and in the lower limbs in 16 cases (84%). Six of 57 patients had false-positive findings (3 skin inflammatory lesions, 2 inflammatory lymp-node, 1 Warthin tumor) and no false negative was found (sensitivity: 100%; specificity: 98%). **Conclusion**: Our results confirm the clinical utility of PET for the surveillance of pts with advanced stage MM and emphasize that in the majority of relapsed pts (82%), PET could detect the disease when still amenable to surgery, with a potential favorable impact in the patient's quality of life and survival. In our experience, all pts should be studied with PET/CT scans extended to their lower limbs. In fact, even if lower limbs metastases were more common in pts with primary placed in this area (70%), about 16% of pts with torso or arms primary MM showed unexpected metastases in lower limbs.

### OP045

#### Impact of 18F-FDG PET/CT for staging, restaging and assessment of response to treatment in bone and soft tissue sarcomas

**L. Locantore**[1], M. Tredici[1], D. Volterrani[1], I. Paglianiti[1], F. Betti[1], L. Coccoli[2], G. Mariani[1]; [1]Regional Center of Nuclear Medicine, University of Pisa, Pisa, ITALY, [2]UO Oncoematologia Pediatrica, AOUP, Pisa, ITALY.

**Background/Aim**: Sarcomas are a histologically heterogeneous group of uncommon malignant tumors with high propensity for hematogenous metastases that constitute a relevant diagnostic and therapeutic challenge. While standard imaging consists especially of MRI and CT, the role of [18F]FDG-PET/CT is still under evaluation. The purpose of this study was to assess the diagnostic usefulness and the added value of [18F]FDG-PET/CT in patients with bone and soft tissue sarcomas. **Patients and Methods**: Data from 48 consecutive patients with sarcomas (21 women, 27 men; mean age 36 yr) were retrospectively evaluated. Ten patients had soft tissue sarcoma, 38 had osseous sarcoma. All patients underwent at least an [18F]FDG-PET/CT scan for initial staging (n=8), restaging (n=28), assessment of response to therapy (n=43), or follow-up (n=25), for a total of 104 scans. [18F]FDG (3.7 MBq/kg) was injected i.v. in fasting conditions. Images were acquired 60 minutes after tracer administration with a Discovery ST/8 scanner (GE Healthcare, Milwaukee, USA). A low-dose CT was performed for attenuation correction and image co-registration. PET/CT interpretation was based on abnormal uptake and SUVmax. Whenever possible, the PET/CT results were compared with those obtained with MRI (n=20) and/or CT (n=24). **Results**: In 30/44 cases [18F]FDG-PET/CT confirmed the MRI and/or CT findings. [18F]FDG-PET/CT correctly changed therapeutic strategy in 31% patients, by disclosing previously unknown distant metastases in 6 patients, by discriminating loco-regional scar from sarcomatous tissue in 3 patients, and by providing early assessment of response to therapy in 5 patients. [18F]FDG-PET/CT was falsely negative in 5/35 patients (3 lung and 2 pelvic lesions) and falsely positive in 2/61 (1 mediastinal and 1 inguinal lymphoadenopathy). In 8 cases PET/CT was inconclusive (uncertain findings). **Conclusion**: Because of good agreement with conventional imaging tecniques in the evaluation of locoregional disease, [18F]FDG-PET/CT resulted to be an accurate diagnostic tool in patients with sarcomas. PET/CT also provided relevant additional information on the presence of distant metastases or for identifying the relative extension of scar and of locoregional disease, thus changing clinical management in a high proportion of patients. Moreover, the PET/CT scan was useful for assessing response to treatment, by identifying clinically relevant responses and thus providing predictive information as to the patient outcome.

### OP046

#### Dynamic FDG PET-CT in patients with unresectable aggressive fibromatosis following imatinib therapy

**C. Sachpekidis**[1], B. Kasper[2], L. G. Strauss[1], P. Hohenberger[3], A. Dimitrakopoulou-Strauss[1]; [1]Clinical Cooperation Unit Nuclear Medicine, German Cancer Research Center, Heidelberg, GERMANY, [2]Interdisciplinary Tumor Center Mannheim, Sarcoma Unit, Mannheim University Medical Center, University of Heidelberg, Mannheim, GERMANY, [3]Division of Surgical Oncology and Thoracic Surgery, Mannheim University Medical Center, Mannheim, GERMANY.

**Aim**: Imatinib is a competitive tyrosine-kinase inhibitor applied in various malignancies. Dynamic PET-CT (dPET-CT) studies with 18F-FDG were performed in patients (pts) with unresectable aggressive fibromatosis (desmoid tumors) who received therapy with imatinib. Aim of the study was to evaluate FDG metabolism with regard to the preliminary therapy outcome. **Materials and Methods**: The ongoing evaluation includes 23 pts (mean age 50 years) with primary disease (n=8), recurrent disease (n=14) or residual tissue (n=1). All pts were examined prior and after therapy with imatinib. The mean interval period between baseline and 1st follow-up dPET-CT scan was 116 days (4 months). In 16 pts (70%) also a third dPET-CT exam was performed. The mean interval between baseline and 2nd follow-up study was 274 days (9 months). The evaluation of dPET-CT studies was based in addition to the conventional SUV evaluation, on a 2-tissue compartment model and a non-compartmental approach. Clinical evaluation according to the Response Evaluation Criteria in Solid Tumors (RECIST) was performed and served for reference. **Results**: Prior therapy mean SUV was 3.6, maximum SUV was 6.1, k1 was 0.4 1/min and k3 was 0.08 1/min. The 1st follow-up study after imatinib therapy displayed the following values: mean SUV was 2.7 (25% reduction), maximum SUV was 4.6 (25% reduction), k1 was 0.34 1/min and k3 was 0.09. Respectively, the 2nd follow-up study revealed: mean SUV was 2.4 (33% reduction), maximum SUV was 3.8 (38% reduction), k1 was 0.37 and k3 was 0.08. **Conclusions**: Generally, desmoid tumors' SUVs range in low levels compared with other malignancies. The perfusion-dependent kinetic parameter k1 is high while the phosphorylation-dependent parameter k3 is low (in comparison with reference areas). The patients responded to imatinib treatment with reduction of mean and maximum SUV as well as with reduction of the value of k1. k3 remained almost stable. These results are consistent with the clinical data, which revealed in 15 pts non-progressive disease (stable disease, partial response) and only in 8 progressive disease.

### OP047

#### Utility of 18F-FDG PET with a semi-quantitative index in the detection of sarcomatous transformation in patients with neurofibromatosis type 1

**T. MOGNETTI**[1], P. COMBEMALE[1], B. BENSAID[1], L. VALEYRIE-ALLANORE[2], S. PINSON[1], B. GUILLOT[3], D. MARIANO-GOULART[3], P. WOLKENSTEIN[2], J. BLAY[1], F. GIAMMARILE[4]; [1]Centre Léon Bérard, LYON, FRANCE, [2]Hopital Henri Mondor, CRETEIL, FRANCE, [3]Hopital Universitaire Saint-Eloi, MONTPELLIER, FRANCE, [4]Centre Hospitalier Lyon Sud, LYON, FRANCE.

**Background**: Malignant peripheral nerve sheath tumors (MPNSTs) are one of the most serious complications of neurofibromatosis type 1 (NF1), with an estimated lifetime risk of 8 to 13%. Late diagnosis is associated with poor prognosis, and deeper lesions can be difficult to diagnose. $^{18}$F-FDG positron emission computed tomography (PET) improves the detection of malignancies. However, criteria of malignancy, notably $SUV_{max}$ threshold, are not standardized. Therefore, the Aim of the present study was to evaluate a semi-quantitative index for the reproducible detection of malignant transformation with FDG PET. **Methods:** This multicenter study was carried out between 2000 and 2012. All patients with NF1 and suspected MPNST underwent PET. Instead of the absolute standardized tumor uptake value ($SUV_{max}$), we used the uptake ratio between the tumor and the normal liver (T/L ratio). A preliminary study suggested a T/L ratio of 1.5 as the cut-off for malignancy. Thus, based on a semi-quantitative analysis of PET images, patients were compared using this cut-off value. **Results**: A total of 113 patients with 145 tumors were included. PET assessment revealed 65 suspected lesions with T/L > 1.5, and among these, 40 were MPNSTs. A total of 80 tumors were classified as non-suspicious, and 79 were finally benign according to histology results or long-term monitoring. The 1.5 T/L cut-off had a negative predictive value (NPV) of 98% and a positive predictive value of 61%. The positive likelihood ratio (LR) was 4,059 and the negative LR was 0,0,32 with 97% sensitivity and 75% specificity. **Conclusions:** This

study, which is among the largest published, confirms the utility of PET for detecting NF1-associated MPNSTs. A semi-quantitative index, the T/L ratio with a cut-off of 1.5, allowed sensitive and specific differentiation of malignant from benign tumors and enabled appropriate surgical treatment, better than $SUV_{max}$. When T/L was < 1.5, MPNSTs were ruled out with 99% NPV, thus avoiding unnecessary surgery. When T/L was > 1.5, there was a strong suspicion of malignancy. However, there was a risk of false positives, and thus medico-surgical assessment was necessary before making therapeutic decisions. No significant correlation was found between $SUV_{max}$ and malignancy. This semi-quantitative analytical method is as simple as $SUV_{max}$, but more sensitive, more reproducible and non user-dependent.

## OP048

### Role of 68Ga-DOTA-NOC PET/CT in detection of unknown primary neuroendocrine tumors (CUP-NET)

**C. Jora**, P. Pankaj, R. Verma, E. Belho, A. Jain, N. Sharma, P. Gupta, H. Mahajan; Department of Nuclear Medicine, Sir Gangaram Hospital, Delhi, INDIA.

**Purpose:** This study Aimed to determine the role of $^{68}$Ga-DOTA-NOC PET/CT in the detection of undiagnosed primary sites of neuroendocrine tumors (NETs) and to understand the tumor biology of the primarily undiagnosed tumors. **Methods:** Overall 31 patients (21 men and 10 women, age: 50±9 years) with documented NET metastases and unknown primary were enrolled. PET/CT was performed after injection of approximately 100 MBq (46-260 MBq) of $^{68}$Ga-DOTA-NOC.Any area with intensity greater than background was considered to be indicative of tumour tissue and the maximum standardised uptake values (SUVmax) were calculated. CECT was done in all the patients prior to PET/CT study and the results were compared. **Results** In 24 of 31 patients (77%), $^{68}$Ga-DOTA-NOC PET/CT localised the site of the primary: stomach (2), duodenum (4), jejunum (5), ileum (1), pancreas {Neck (1), Uncinate process(1) and Tail (2)}, rectum (3), lungs (2), kidney (1) and gall bladder (2). CT alone (on retrospective analyses) confirmed the findings in only 2 of 31 patients (6%). The mean SUVmax of the identified primary tumors was 20 ±9.8. Size of primary tumor was less than 1 cm in 3 of 31 detected cases. Focal $^{68}$Ga-DOTA-NOC uptake at the site of primary without underlying CT abnormality was seen in 3 cases. Rare sites of primary NET in horseshoe kidney and gall bladder were identified. Besides the usual metastases to lymph nodes, liver and bone, atypical metastases to lung, pancreas, adrenal gland, orbit, brain and bone marrow were detected in some cases. Osteolytic bone metastases were detected in one case. Metastases to distant cervical, supraclavicular and internal mammary lymph nodes were noted in few cases. Portal vein thrombus and splenic vein thrombus were additional findings in three cases. **Conclusion:** Our study shows that $^{68}$Ga -DOTA-NOC PET/ CT detects both usual and unusual sites of primary tumor and metastases. Tumor size is an unreliable predictor of metastatic potential, as metastases is seen in primary tumors less than 1 cm in diameter. Early detection of rare atypical sites of primary NET like kidney and gall bladder helps in individualising treatment approach. Our data clearly indicate that $^{68}$Ga -DOTA-NOC PET/ CT is a promising imaging modality for evaluation of patients with CUP-NET. Keywords: Unknown primary . Neuroendocrine tumour . 68Ga-DOTA-NOC PET/CT.

## OP049

### 18F-FDG-PET/CT, 99mTc-MIBI and MRI in the Prediction of Outcome of Patients with Multiple Myeloma

**R. Fonti**[1], L. Pace[2], C. Cerchione[3], L. Catalano[3], S. De Luca[3], F. Pane[3], M. Salvatore[3], S. Del Vecchio[3]; [1]Institute of Biostructures and Bioimages, National Research Council, Naples, ITALY, [2]University of Salerno, Salerno, ITALY, [3]University "Federico II", Naples, ITALY.

In the last years, newer imaging techniques are assuming a continuously growing role in the management of multiple myeloma (MM) including prediction of patient outcome. **Aim.** Compare the relative contribution of 18F-FDG-PET/CT, 99mTc-MIBI and MRI in the prediction of progression-free (PFS) and overall survival (OS) in MM patients. **Methods.** In a previous study 33 newly diagnosed MM patients had been prospectively studied by whole-body 18F-FDG-PET/CT, whole-body 99mTc-MIBI and spine and pelvis MRI within 10 days. The number of eventual focal lesions and/or the presence or absence of diffuse bone marrow involvement assessed by each imaging methodology were recorded. Twenty-seven patients (7 females, 20 males; mean age 62±11 y) were then subjected to a mean follow-up period of 60 months while 6 patients were lost. Univariate and Multivariate Analysis were performed including imaging findings and clinical prognostic parameters widely used in MM to test their capability in predicting PFS and OS. **Results.** 18F-FDG-PET/CT, 99mTc-MIBI and MRI were positive in 26, 24 and 22 patients, respectively, showing diffuse bone marrow involvement in 4, 6 and 7 patients and a total of 185, 56 and 39 focal lesions, respectively. At follow-up, 18 patients were in complete or partial remission, while 9 patients developed progressive disease, 7 of which died of myeloma. Univariate analysis showed that 18F-FDG-PET/CT focal uptake ($\chi^2$=8.773 p=0.0031), 99mTc-MIBI focal uptake ($\chi^2$=4.633 p=0.0314), 99mTc-MIBI diffuse uptake ($\chi^2$=7.368 p=0.0066), MRI diffuse distribution ($\chi^2$=6.567 p=0.0104), haemoglobin ($\chi^2$=8.007 p=0.0047), β2-microglobulin ($\chi^2$=4.468 p=0.0345), stage ($\chi^2$=7.044 p=0.0080) and ISS ($\chi^2$=4.885 p=0.0271) were all predictive of PFS. When these variables were entered in the multiple regression model, only 18F-FDG-PET/CT focal uptake and 99mTc-MIBI focal and diffuse uptake were retained in the model ($\chi^2$=17.205 p=0.0006). Moreover, univariate analysis showed that 18F-FDG-PET/CT focal uptake ($\chi^2$=8.654 p=0.0033), 99mTc-MIBI focal uptake ($\chi^2$=7.596 p=0.0058), 99mTc-MIBI diffuse uptake ($\chi^2$=5,109 p=0.0238), MRI diffuse distribution ($\chi^2$=4.583 p=0.0323) and β2-microglobulin ($\chi^2$=3.772 p=0.0521) were predictive of OS. When these variables were entered in the multiple regression model, only 18F-FDG-PET/CT focal uptake and 99mTc-MIBI focal uptake were retained in the model ($\chi^2$=13.892 p=0.0010). **Conclusion.** 18F-FDG-PET/CT and 99mTc-MIBI may be used in the prediction of PFS and OS in myeloma patients, while the role of spine and pelvis MRI is more controversial probably due to its limited field of view.

## OP050

### $^{18}$F-Fluoromisonidazole PET/CT Is A Valuable Tool for Predicting Primary Endocrine Therapy Resistance in Breast Cancer

**J. Cheng**; Fudan University Cancer Center Nuclear Medicine Department, Shanghai, CHINA.

Endocrine therapy is an important method to treat hormone receptor positive breast cancer. However, approximately 30%-40% of hormone receptor positive breast cancers have got primary resistance to endocrine therapy. Our current study was to analyzed whether $^{18}$F-FMISO PET/CT could predict the primary resistance of hormonal therapy in ER positive breast cancer. **Methods:** 28 post-menopausal women with ER-alpha positive, stages II-III breast cancer, and endocrine treatment-naive were enrolled prospectively in this study and preformed $^{18}$F-FDG and $^{18}$F-FMISO PET/CT scan before and after treatment. The clinical outcomes of primary endocrine therapy with letrozol were evaluated after at least 3-month treatment by WHO criteria. Immunohistochemistry (IHC) test of tumor markers of proliferation (ki67) and hypoxia(HIF-1-alpha) were also undertaken for a subset of tumors received biopsy or surgery. Pearson and Spearman correlation coefficient test and Wilcoxon test were used to determine the correlations between the parameters of $^{18}$F-FDG /$^{18}$F-FMISO uptake and clinical or IHC outcomes with a 0.01 threshold for statistical significance. **Results:** All 28 primary lesions of primary breast cancer underwent $^{18}$F-FMISO PET/CT scans prior to the treatment. There was a significantly correlation between $^{18}$F-FMISO uptake (TBR4h) and clinical outcomes after treatment (P=0.002, Spearman's test). The cut off value of TBR4h=1.2 was an optimal predictable value to define hypoxia in breast cancer. Breast cancers with higher TBR4h (≥1.20) were less likely to achieve a reduction in Ki67 score after 3 months of primary endocrine therapy compared with those whose TBR4h was lower (< 1.20) (P=0.5 versus P=0.002, Wilcoxon test,). A good correlation was observed between pre-treatment HIF-1-alpha expression (overall score) and clinical outcomes (P=0.012, Spearman's test), as well as the reduction of Ki67 score(P=0.002, Spearman's test). In addition to this, it was found that the HIF-1-alpha expression level in the post-treatment samples was significantly increased compared with that at baseline, regardless of the scoring Methods applied (overall score or intensity score, P=0.001 or P=0.001, respectively; Wilcoxon test,) And such changes were also consistent regardless of the response types: PRs, SDs or PDs . As for ER-alpha, its expression level was slightly decreased after endocrine therapy, but this difference did not attain the statistical significance level (P=0.239). **Conclusion:** The primary endocrine resistance of ER-positive breast cancer could be predicted by $^{18}$F-FMISO PET/CT.

## OP051

***Shifted to poster P360b***

308 - Sunday, Oct. 20, 11:30 - 13:00, Gratte-Ciel 1/2/3

## Molecular & Multimodality Imaging: Metabolism in Preclinical Models

## OP052

### Effects of starvation and chemotherapy on glucose uptake in colon murine cancer line cells. An in vitro 18F-FDG study.

**C. Marini**[1], M. MASSOLLO[2,3], L. Raffaghello[4], G. Bianchi[4], R. Martella[4], C. Massara[2], A. Democrito[2], S. Capitanio[2,3], S. Morbelli[2], G. Sambuceti[2,3]; [1]CNR Institute of Bioimages and Molecular Physiology, Milan, Section of Genoa, ITALY, [2]IRCCS San Martino IST, Nuclear Medicine Unit, Genoa, ITALY, [3]University of Genoa, Genoa, ITALY, [4]Laboratory of Oncology, G. Gaslini Institute, Genoa, Genoa, ITALY.

**Aim**. Effectiveness of anticancer chemotherapy is limited by its toxicity and by the ability of cancer cells to become resistant. Thus, it is essential to develop treatment modalities able to increase chemotherapy efficacy and tolerability. Growing evidence indicates that starvation/caloric restriction might afford this task by two major pathways: it selectively protects normal cells and tissues from chemotherapy

toxicity, simultaneously sensitizing tumor to drug action. We Aimed to directly verify in vitro effects of starvation and chemotherapy on glucose uptake in colon (CT26) murine cancer line cells. **Materials and Methods**. CT-26 cells were cultured under normal (1 g/L glucose, 10% FBS) and starved (Short term starvation: STS) (0.5 g/L glucose, 1% FBS) conditions for 24 hours before and 24 hours during treatment with Oxaliplatin (OXP). The following evaluations were performed: 1) glucose uptake was estimated by measuring labeling yield after incubation with 18F-fluoro-deoxyglucose (FDG) at a fixed concentration of 1 microCi/mL for 60 minutes at 37°C; 2) cell apoptosis was tested by Annexin V FITC staining; 3) Western blot and flow cytometry were applied to study expression of proteins involved in glucose metabolism such as glucose transporters (GLUT) and hexokinases (HK) and, finally, 4) the same Methods were used to evaluate the following components of PI3K/AKT/mTOR nutrient-sensing pathway: phosphorylated AKT (p-AKT), p-S6Kinase as well as phosphatase and tensin homolog (PTEN). **Results and Conclusion.** FDG uptake was similarly inhibited by STS (from 35±5% in control cells to 23±3% in STS cells, p<0.05) and chemotherapy (from 35±5% to 26±4% in treated cells, p<0.05). The effect of the two treatment protocols was additive, as their combination decreased tracer uptake to 14±2% (p=0.01 versus all other conditions). This profound metabolic impairment was paralleled by a reduced availability of GLUT-1 and HK-1 followed by a concomitant decrease in p-AKT and p-S6Kinase facing an increased expression of PTEN. Similarly, the metabolic derangement caused by STS plus chemotherapy significantly increased the prevalence of apoptosis with respect to chemotherapy alone (81±9% vs 30±3%, respectively, p<0.0001). In conclusion, monitoring cancer cell metabolism with FDG in addition to molecular analysis permits to identify the additive effect of STS and chemotherapy and thus might represent an important tool in the development of innovative approaches to improve chemotherapy effectiveness.

## OP053

### Assessment of Lung Inflammation After Inhalation of ZnO Nanoparticles Using PET-[$^{18}$F]FDG

C. Pérez-Campaña[1], V. Gómez-Vallejo[1], M. Puigivila[1], A. Martin[1], T. Calvo-Fernández[1], S. E. Moya[1], S. Thor Larsen[2], J. D. Gispert[3], **J. Llop**[1]; [1]CIC biomaGUNE, San Sebastian, SPAIN, [2]National Research Centre for the Working Environment, Copenhagen, DENMARK, [3]Fundacio Pasqual Maragall, Barcelona, SPAIN.

**Aim** The unique properties of nanoparticles (NPs) have promoted a rapid increase in the use of nanoparticulate materials in industrial processes which, in turn, has raised many concerns about potential risks for the health and the environment. During environmental or occupational exposure, the lung is usually the targeted organ and NPs inhalation might lead to lung inflammation. To date, no Methods for the *in vivo* assessment of lung inflammation after exposure to NPs have been reported. In the current work, a method for the *in vivo* and noninvasive assessment of inflammatory response in rat lungs after exposure to ZnO NPs is presented. **Materials and Methods** Healthy, female Sprague-Dawley rats (n=15) were submitted to ZnO NPs inhalation in a specially designed chamber. A control group (n=15) was also exposed following the same procedure but no NPs were introduced into the chamber. Six animals per group were submitted to [$^{18}$F]FDG-PET studies at days 1, 7 and 28 after exposition. The [$^{18}$F]FDG influx constant (*Ki*) for the lungs was calculated using Patlak analysis and an image derived blood input function. Nine animals per group were sacrificed at 1, 7 and 28 days after exposure (n=3 per group and time point), the lungs were harvested and submitted to immunohistochemical analysis. **Results** Significantly higher mean whole-lung *Ki* values were obtained for animals exposed to NPs at days 1 and 7 after exposure (0.0045 ± 0.0016 and 0.0047 ± 0.0015, respectively) compared to controls (0.0024 ± 0.0010 and 0.0019 ± 0.0011 at 1 and 7 days, respectively). The $K_i$ value for exposed animals dropped to 0.0023 ± 0.0010 at day 28. This value was not significantly different from the values obtained at 1, 7 and 28 days for the control group. Immunofluorescence staining on lung tissue slices from animals exposed to ZnO NPs showed an increase of CD11b reactivity at days 1 and 7, followed by a decrease of CD11b positive cells at 28 days. **Conclusions** The [$^{18}$F]FDG influx rate constant ($K_i$) for lungs of rats exposed to ZnO NPs inhalation could be determined by Positron Emission Tomography using Patlak analysis and a corrected image derived input function. Higher *Ki* values were obtained for exposed animals with respect to control at days 1 and 7 after exposition. These results were in good concordance with immunohistochemical assays performed on harvested tissue samples.

## OP055

### New application of FDG microPET imaging for research investigation in a non-model organism: Octopus vulgaris

**M. MASSOLLO**[1,2], L. Zullo[3], M. Riondato[1,2], F. Benfenati[3,4], G. Bottoni[1,2], C. Marini[5], A. Democrito[1], S. Morbelli[1], F. Fiz[1,2], A. Zanini[1], F. Bongioanni[1,2], G. Sambuceti[1,2]; [1]IRCCS San Martino IST, Nuclear Medicine Unit, Genoa, ITALY, [2]University of Genoa, Genoa, ITALY, [3]Department of Neuroscience and Brain Technologies, Istituto Italiano di Tecnologia, Genoa, ITALY, [4]Department of Experimental Medicine, University of Genoa, Genoa, ITALY, [5]CNR Institute of Bioimages and Molecular Physiology, Milan, Section of Genoa, ITALY.

**Aim**: Here we present the first application of FDG microPET technique for the metabolic evaluation of a non-model organism, the marine invertebrate Octopus vulgaris. Octopuses are cephalopods endowed with unique properties amongst invertebrates. They have a large nervous system and amazing motor capabilities. They have been used in various research areas from neuroscience to behavior and motion kinetics for their high motor and learning capability and their ready adaptability to captivity. The octopus thus represents an emerging interesting non-model animal. Our Aim is to verify the feasibility of microPET imaging of glucose metabolism in the octopus and the possible changes in metabolic rate in response to environmental stimuli. **Material and Methods**: Four animals were brought to our lab in oxygenated artificial sea water (ASW) water. Anesthesia was obtained adding a solution of MgCl2 to the final concentration of 3.7% in ASW. Afterwards, each octopus was injected with 18-25MBq of isosmotic 18F-FDG by accessing the brachial heart or the vena cava. After an uptake time of 50 minutes, the animal was sacrificed, placed on a bed of a microPET scanner (Albira, Carestream, US inc) and submitted to a 15 minutes static three beds acquisition, in order to visualize the entire body. Thereafter, the animal was dissected for the collection of all the internal organs of interest, brain and muscle portions. All collected organs were counted in a gamma-counter (Cobra II- Packard Bell). **Results and Conclusion**: The entire animal was clearly visible documenting a full body distribution with a high mantle radioactivity facing a relatively low tracer uptake in the arms. In particular, the following organs were clearly identified: brain (SUV max 2,05), optic lobes (SUV max 3,17), and arms (SUV max 1,15) and a good correlation was found between the "in vivo" and "ex vivo" counting. Given the remarkable ability of the Octopus vulgaris to regenerate its arms, this technique can be also applied for the study of regenerative processes. As a proof of concept, we performed a pilot study on one animal with a single regenerating arm. Interestingly, FDG uptake was increased in the regenerating arm (mean SUV 3,24 vs 1,15 in the intact arms). This study represents a first step toward the use of nuclear medicine imaging techniques in new emergent research areas, such as neurophysiology of non-model invertebrates and neurobiology of regeneration.

## OP056

### Metabolic PET/CT investigations on shellfish: biomarker feasibility of important environmental sentinel organisms

D. Máthé[1], B. Szczupak[2], I. Horváth[3], M. González[2], V. Gómez-Vallejo[2], **K. Szigeti**[3], E. San Sebastián[2], J. Llop Roig[2]; [1]CROmed Ltd, Budapest, HUNGARY, [2]CICbiomaGUNE, San Sebastián, SPAIN, [3]Semmelweis University, Budapest, HUNGARY.

**Introduction**. One of the most important "sentinel" animal groups of marine pollution is that of mussel shellfish. Being very effective filter feeders, these animals are the main target of accumulation among others, of heavy metals, highly dangerous biotoxins from algae e.g. saxitoxin, and metallic nanoparticles (NPs). **Aims**. Glucose metabolism being a universal mechanism of energy gain our expectation was that FDG will be a marker of live tissues with high metabolism of the healthy animal. Our other presumption was that the pallial organ being responsible for shell production and metabolism will be effectively depicted with 18F-fluorine PET. **Materials and Methods**. For these PET/CT imaging studies that are, to our knowledge the first ever reported in the literature, we used commercially available species, Veneropsis philippinarum and Mytilus edulis. Animals (six of both species) gently opened to be able to inject radiopharmaceuticals in volumes circa 0.5 mL/4 to 8 MBq using 22G needles and left at room temperature for 110 minutes. Injections were directed at the main body fluid channel for FDG and into the pallial tissue for 18F-fluorine. PET/CT static data acquisitions were performed on GE Vista eXplore and Mediso nanoScan PET systems combined with CT (40 kV, 140 uA and 55 kV, 145 uA respectively) for 30 minutes. **Results.** Using FDG-PET in M. edulis, we could observe highest uptake (28.8% of total injected activity) in the heart of animals, while pedal gland, pedal muscles and hepatopancreas also contributed to FDG uptake in V. philippinarum. Interestingly and in accordance with known biophysics and physiology, internal abductor muscle did not show visually judged FDG uptake. 18F-fluorine uptake was observed throughout the body of the animals, with high uptake (16.4% of total injected activity) in pedal muscle, in the region of the internal abductor muscle and also co-localized with inner shell layer of cca. 2 mm. CT volumes were able to depict gross internal anatomy of the animals. **Conclusions**. Our group is the first in reporting imaging of live shellfish using PET/CT. The uptake in the heart and non-uptake of 18F-FDG in the "clam" muscle indicates that specific metabolic patterns will be further imaged in shellfish. The results of this study are reinforcing to warrant exploration of the "in vivo biomarker" area for biomarker species. Acknowledgement. This study was in part supported by EC-FP7 Transnational Access Facilities grant QNANO.

## OP057

### Assessment of Treatments Against Staphylococcus Aureus Biofilms Using in Vivo 18F-FDG-PET in an Animal Model

**M. Collantes**[1], V. Garrido[2], M. Barberán[3], J. Arbizu[4], B. Amorena[2], S. Abadía[1], M. Ecay[1], M. J. Grilló[2], I. Peñuelas[5]; [1]MicroPET Research Unit, Center for Applied Medical Research, Pamplona, SPAIN, [2]Animal Health, Agrobiotechnology Institute (CSIC-UPNA), Pamplona, SPAIN, [3]Animal Pathology, Faculty of Veterinary, University of Zaragoza, Pamplona, SPAIN, [4]Department of Nuclear Medicine, University Clinic of Navarra, Pamplona, SPAIN, [5]Radiopharmacy Unit, Department of Nuclear Medicine, University Clinic of Navarra, Pamplona, SPAIN.

Biofilms are aggregates of microorganisms that may be formed on different surfaces as medical implants. Their appearance is associated to almost undetectable and persistent infections that hardly respond to antibiotic treatments. Consequently, the development of new antibiotic therapies and of adequate techniques to confirm their effectiveness is of utmost importance. **Aim**: to evaluate the feasibility of 18F-FDG-PET imaging for in vivo monitoring of bacterial biofilm infections and quantifying the response to antibiotic treatments in an animal model. **Methodology:** sealed catheters of VialonTM biomaterial were pre-colonized with Staphylococcus aureus ATCC15981 and subcutaneously implanted in CD1 mice (n=14). Half of these animals (n=7) received oral rifampicin (0.5 mg/day) for 7 days. The infection was monitored in vivo by 18F-FDG-PET imaging at days 1, 7 and 14 after catheter implantation. For this, an 18F-FDG dose (18,3±1,6 MBq) was injected in the tail vein, and after 60 minutes under continuous isoflurane anesthesia, a static PET image was performed. 18F-FDG uptake was quantified by means of SUV, drawing volumes of interest over the catheters and lymph nodes. In parallel, an additional group of untreated mice (n=9) was used to determine both the number of colony forming units (CFU) per catheter and the histopathological changes (i.e. presence of inflammatory cells and bacteria) in the surrounding area of the catheter. **Results**: 18F-FDG-PET produced a quantifiable signal already at 1 day post-implant. The signal was found associated with the appearance of bacteria and polymorphonuclear cells in the area of the catheter. Moreover, a high 18F-FDG-PET uptake in lymph nodes was observed in the non-treated group at days 7 and 14. At day 7, the rifampicin-treated group showed a statistically significant reduction in both SUV values ($p=0.006$) and number of viable CFU ($p<0.001$) in catheters, and lymph node images became negative. At day 14 (one week after treatment was stopped), the SUV values of catheter and lymph nodes increased in the treated group, reaching levels similar to those of the control group, compatible with the growth of surviving bacteria. **Conclusions:** 18F-FDG-PET could be an innovative and useful technique to detect in vivo biofilm infections, in follow-up studies and evaluation of the efficacy of antibiotic therapies in living mice.

## OP058

### Multimodal Imaging of Tumor Perfusion, Permability, Metabolism and Hypoxia after Antiangiogenic Treatment with Fc-Endostatin

**P. Hofner**[1,2], T. Rackwitz[1,2], C. Melzig[1,2], M. Moustafa[1,2], K. Leotta[3], F. Giesel[3], T. Bäuerle[1], W. Mier[3], J. Debus[1,2], K. Javaherian[1], U. Haberkorn[3], A. Abdollahi[1,2]; [1]Molecular & Translational Radiation Oncology, Heidelberg Ion Therapy Center (HIT), Heidelberg Institute of Radiation Oncology (HIRO), University of Heidelberg Medical School and National Center for Tumor Diseases (NCT), German Cancer Research Center(DKFZ), Heidelberg, GERMANY, [2]German Cancer Consortium (DKTK), Heidelberg, GERMANY, [3]Department of Nuclear Medicine, University of Heidelberg Medical School and National Center for Tumor Diseases (NCT), German Cancer Research Center (DKFZ), Heidelberg, GERMANY.

**Aim:** Endostatin is a 20 kDa proteolytic fragment of collagen XVIII and a broad spectrum endogenous angiogenesis inhibitor. Generation of fusion protein consisting of murine Endostatin and the Fc-fragment of murine immunoglobuline (mFc-Endostatin) has substantially prolonged its halflife allowing long term investigation of endostatin effects in-vivo. The Aim of our study was to decipher the effects of Fc-endostatin treatment on the tumor perfusion, metabolism and hypoxia in a syngenic murine lung cancer model. **Materials and Methods:** Lewis lung carcinoma (LLC) cells were implanted subcutaneously in the hindlimb of C57 BL/6 mice. The mFc-Endostatin treatment (100 µg/mouse/every 6$^{th}$ day) was initiated two days after tumor cell implantation. Sized match (200-250 mm$^3$) tumors, endostatin vs. sham treated control (n: 9 per group), were selected for multimodal non-invasive imaging based analysis of tumor pathophysiology. In particular, glucose metabolism and tumor hypoxia were detected by fluorodeoxyglucose (18FDG) and [18F]-MISO PET/CT scans, respectively. Dynamic contrast enhanced (DCE) MRI was applied to evaluate tumor perfusion (permability and vascularity). Diffusion weighted imaging (DWI) was used to detect intratumoral cellularity (DWI). Tumor tissue was further excised for immune-histopathology assessing tumor microvascular index (CD31), proliferation (Ki67) and apoptosis (TUNEL). **Results:** Fc-Endostatin treatment led to significant inhibition (>74%) of tumor growth after day 18 ($p<0.001$) post tumor implantation. This inhibition was accompanied by increased apoptosis (TUNEL), reduced microvascular density (CD31) and tumor proliferation index (Ki67) as determined by immunohistochemistry. DCE-MRI revealed reduced perfusion after endostatin administration. In particular, the Kep was markedly reduced after Fc-Endostatin treatment indicating decreased vascular permeability and contrast agent extravasation. Different Methods for calculation of ROI vs. SUV-max and normalization of hypoxia (FMISO) vs. metabolism (FDG) PET are employed to correlate both parameters with MRI which, together with histopathology data, will be presented at the meeting. **Conclusion:** Fc-Endostatin elicits potent long term tumor growth inhibitory effect in this syngenic C57/Bl6 lung cancer model via inhibition of tumor angiogenesis. Multimodal non-invasive imaging provides excellent surrogate markers for detecting the therapeutic efficacy of novel antiangiogenic compounds such as Fc-Endostatin.

309 - Sunday, Oct. 20, 11:30 - 13:00, Rhône 3A/3B

## Radiopharmaceuticals & Radiochemistry & Dosimetry: PET Radiopharmaceuticals

## OP059

### Development of a Pro-drug Tracer for Functional Imaging of Multiple Drug Resistance

**K. Sander**[1], E. Galante[1], E. Yiannaki[2], N. Patel[3], F. Bauer[4], M. Robson[5], S. P. Johnson[5], A. Badar[3], D. Dickens[6], O. Langer[7], M. Koepp[8], E. Årstad[1]; [1]University College London, Institute of Nuclear Medicine and Department of Chemistry, London, UNITED KINGDOM, [2]University College London, Department of Chemistry, London, UNITED KINGDOM, [3]University College London, Centre for Advanced Biomedical Imaging, London, UNITED KINGDOM, [4]University of Vienna, Department of Medicinal Chemistry, Vienna, AUSTRIA, [5]University College London, Cancer Institute, London, UNITED KINGDOM, [6]University of Liverpool, Institute of Translational Medicine, Department of Molecular and Clinical Pharmacology, The Wolfson Centre for Personalised Medicine, Liverpool, UNITED KINGDOM, [7]Austrian Institute of Technology, Molecular Medicine, Health and Environment Department, Seibersdorf, AUSTRIA, [8]University College London, Institute of Neurology, Department of Clinical and Experimental Epilepsy, London, UNITED KINGDOM.

**Objectives**: Multiple drug resistance is a major clinical challenge for the treatment of many neurological diseases. It has been shown that increased activity of drug efflux transporters at the blood-brain barrier, particularly P-glycoprotein (P-gp), is a major contributor to drug resistance [1]. Non-invasive imaging of P-gp activity in the brain can therefore help to clarify the underlying mechanisms of drug resistance, and facilitate diagnosis, patient stratification and treatment monitoring, thereby improving the efficacy of therapeutic drug treatment. This study Aims at the development of a pro-drug tracer for the functional imaging of P-gp activity with positron emission tomography (PET). **Methods**: Novel P-gp substrates as well as their corresponding pro-drugs were designed in order to make use of the 'metabolite extrusion method' (MEM). This strategy involves the passive diffusion of a pro-drug tracer into the brain, its subsequent trapping by metabolic conversion and the transporter-mediated extrusion of the active metabolite, which is a selective substrate for the respective transporter. Exploiting MEM potentially allows for quantitative imaging of a membrane transporter since it is expected that the clearance of radioactivity from the brain correlates with the efflux pump's activity. Labelling of P-gp pro-drug tracers with fluoride-18 was achieved using triarylsulfonium salts as precursors for aromatic fluorination. Selected compounds were investigated in vivo in order to characterize tissue distribution, metabolic conversion, and P-gp interaction. **Results**: A library of fluorinated compounds was tested in vitro to evaluate their P-gp activity and identify suitable labelling positions. A new labelling strategy was developed in order to access pro-drug tracers bearing fluorine-18 attached to the aromatic backbone to avoid defluorination in vivo. In preclinical studies in mice, selected pro-drug tracer candidates showed excellent initial brain uptake and a favourable clearance. Brain metabolism of a designated lead tracer was exceptionally clean as only the pro-drug tracer and the desired tracer metabolite were detected with radio-HPLC. Blocking studies with the P-gp inhibitor tariquidar demonstrated that extrusion of the metabolite tracer from the brain is mediated by P-gp. **Conclusions**: We have developed a fluorine-18-labelled pro-drug tracer for non-invasive imaging of P-gp activity with PET. The preclinical studies have produced highly encouraging data which suggest that the lead tracer can be used to monitor efflux pump function in vivo. Reference: [1] Löscher W and O Langer (2011), Curr Top Med Chem, 10 (17), 1785-1791.

## OP060

### Preclinical Evaluation of Al$^{18}$F- and $^{68}$Ga-labeled GRPR-antagonist for PET Imaging of Gastrin-Releasing Peptide Receptor Expression in Prostate Cancer

**K. L. S. Chatalic**[1], G. M. Franssen[2], W. J. McBride[3], L. M. van der Graaf[1], R. M. Sharkey[3], P. Laverman[2], D. M. Goldenberg[3], B. Hajjaj[4], J. A. Fehrentz[4], J. Martinez[4], O. C. Boerman[2], M. de Jong[1]; [1]Departments of Nuclear Medicine and Radiology, Erasmus MC, Rotterdam, NETHERLANDS, [2]Radboud University Nijmegen Medical Centre, Nijmegen, NETHERLANDS, [3]Immunomedics, Morris Plains, NJ, UNITED STATES, [4]Institut des Biomolécules Max Mousseron, UMR 5247, CNRS-UM1-UM2, Montpellier, FRANCE.

**Objectives:** Gastrin-Releasing Peptide Receptor (GRPR) is overexpressed in prostate cancer and is being used as a target for high sensitivity molecular imaging based on Positron Emission Tomography (PET). Recently, it was shown that GRPR-targeting using antagonists offers good tumor retention of radioactivity and fast washout from receptor-positive normal organs without inducing any side effects. In this study we compared the tumor targeting properties of 3 novel radiolabeled GRPR-antagonists: $^{68}$Ga-JMV4168, $^{68}$Ga-JMV5132 and Al$^{18}$F-JMV5132. **Materials and Methods:** The JMV594-based peptide conjugates (JMV4168= DOTA-ßAla-ßAla-JMV594, JMV5132= NODA-MPAA-ßAla-ßAla-JMV594) were synthesized on solid support and purified by RP-HPLC. Their affinity for the human GRPR was evaluated on PC-3 xenograft sections in a competitive binding assay, using [$^{125}$I-Tyr$^4$]BBN as radioligand. Labeling with $^{68}$Ga was achieved by heating the peptide with $^{68}$Ga eluate for 10 min at 95 $^0$C, followed by RP-HPLC purification. Labeling with Al$^{18}$F was achieved by heating a buffered solution containing the peptide, $AlCl_3$, and $^{18}F^-$ for 15 min at 105 $^0$C with no need for purification. Imaging was performed using an Inveon PET/CT 1 or 2 h after injection of labeled peptide (200 µL, 5 MBq, 200 pmol peptide) in mice bearing s.c. human PC-3 xenografts. After imaging, the biodistribution of the radiolabeled peptides was determined. **Results:** $IC_{50}$ values (in nM ± SD) for GRPR of JMV5132 (NODA-MPAA, 6.3 ± 4.0) and JMV4168 (DOTA, 13.7 ± 9.0) were not significantly different. Biodistribution studies revealed a comparable tumor uptake of the tracers, while GRPR-positive pancreas uptake was not. For example, at 1 h post injection tumor uptake (in %ID/g ± SD) was 4.46 ± 0.33, 4.73 ± 0.68 and 4.96 ± 1.20, while pancreas uptake was 6.14 ± 0.68, 11.42 ± 0.84, 4.21 ± 1.34 for $^{68}$Ga-JMV4168, $^{68}$Ga-JMV5132 and Al$^{18}$F-JMV5132, respectively. Interestingly, the biodistribution of Al$^{18}$F-JMV5132 after 2 h p.i. showed tracer washout from the pancreas (1.08 ± 0.25 %ID/g) with preserved tumor uptake (4.04 ± 0.13 %ID/g). PET images clearly visualized s.c. tumors with all radiolabeled peptides. Higher resolution was observed with Al$^{18}$F-JMV5132 as a tracer. **Conclusions:** High sensitivity and receptor-specific imaging of prostate cancer with PET/CT can be achieved using $^{68}$Ga- and $^{18}$F-labeled GRPR-antagonists. $^{18}$F has good characteristics for GRPR-based PET imaging: the half-life (109.7 min) matches the pharmacokinetics of the peptide, and the low positron energy of 635 keV results in a short penetration range in tissue and good imaging resolution. Therefore Al$^{18}$F-JMV5132 is an interesting tracer for further studies.

## OP061

### Shifted to poster P566b

## OP062

### One step n.c.a. $^{18}$F-Labeling of unprotected aromatic and heteroaromatic carboxylic acids

**B. Hooshyar Yousefi**[1], M. Bollinger[2], H. Kessler[2], H. Wester[1]; [1]Pharmaceutical Radiochemistry, Technische Universtät München, Garching, GERMANY, [2]Institute for Advanced Study and Center of Integrated Protein Science,Technische Universtät München, Garching, GERMANY.

Due to its optimal half-life and its low positron emission energy, n.c.a $^{18}$F-fluoride is widely used for the labeling of PET-biomarkers by nucleophilic aliphatic and aromatic substitution. Very early in the history of $^{18}$F-labeling on the no-carrier-added level it has been accepted that precursors consisting of carboxylates do not lend themselves for a direct fluorination and thus need to be protected. Consequently, two-step reactions, comprising of $^{18}$F-fluorination and subsequent deprotection, are necessary. In this study we report on the results of a re-evaluation of the direct $^{18}$F-fluorination of carboxylic acids, i.e. aromatic and heteroaromatic carboxylates. A method is presented allowing for the n.c.a. radiofluorination of aromatic carboxylates that can improve the separation of the desired tracer by minimizing side reactions during deprotection and thus might also facilitate the automated production of such compounds under GMP conditions. For the direct labeling of a series of carboxylates and precursors with unprotected aromatic and heteroaromatic carboxylates the compounds were converted to corresponding salts, i.e. cryptates, quaternary ammonium salts or combinations thereof. Subsequently, the precursor salts were directly used for n.c.a. nucleophilic substitution under otherwise typically employed reaction conditions. N.C.A. $^{18}$F-fluorination of different precursor salts, such as a GCP-II (PSMA) ligand, salts of tirofiban analogs, 2-amino-3-(4,5-dimethoxy-2-nitrophenyl)propanoate , (2S)-2-amino-3-(6-chloropyridin-3-yl)propanoate, benzoate and pyridine carboxylates with various leaving groups, such as nitro, chloro or bromo groups, was carried out at 100-150 °C for 10-60 min by $[K^+\subset 2.2.2]^{18}F^-$ in the presence of $[K^+\subset 2.2.2]CO_3$ or $[K^+\subset 2.2.2]CO_3$ and $[K^+\subset 2.2.2]C_2O_4$ in $CH_3CN$, *t*BuOH/$CH_3CN$ and DMSO yielded the desired $^{18}$F-labeled product with radiochemical yields up to 30%. Interestingly, very low yields obtained by $^{18}$F-fluorination of fully protected $\alpha_{IIb}\beta_3$ integrin antagonist and were significantly improved by using the nonprotected precursor salts according to the presented method. In conclusion, we successfully labeled several aromatic and heteroaromatic nitro and halo consisting of carboxylates. Among the examples are novel $^{18}$F-labeled PSMA and $\alpha_{IIb}\beta_3$ binding radiotracers for the visualization of prostate cancer and activated platelets involved in thromboembolic disorders, respectively. Upon further improvement of the overall labeling yields, the one-step direct fluorination of aromatic carboxylates might become an interesting alternative to the commonly used two step procedures, i.e. for automated tracer production.

## OP063

### PET of Tumor Angiogenesis with $^{61/64}$Cu-Labeled Fab and F(ab')$_2$ Antibody Fragments

**H. Hong**, Y. Zhang, H. Orbay, T. E. Barnhart, W. Cai; University of Wisconsin-Madison, Madison, WI, UNITED STATES.

**Aim**: To characterize the in vitro and in vivo properties of the Fab and F(ab')$_2$ fragments of TRC105, a monoclonal antibody that binds with high affinity to human and murine CD105, and investigate their potential for positron emission tomography (PET) imaging of tumor angiogenesis after $^{61/64}$Cu-labeling. **Materials and Methods**: TRC105-Fab was generated by enzymatic papain digestion, while TRC105-F(ab')$_2$ was generated by pepsin digestion. The integrity and CD105 binding affinity of TRC105-Fab and TRC105-F(ab')$_2$ was evaluated before NOTA (i.e. 1,4,7-triazacyclononane-1,4,7-triacetic acid) conjugation and $^{61/64}$Cu-labeling. Serial PET imaging and biodistribution studies were carried out to quantify tumor targeting efficacy and distribution of $^{61/64}$Cu-NOTA-TRC105-Fab and $^{61/64}$Cu-NOTA-TRC105-F(ab')$_2$ in 4T1 murine breast tumor-bearing mice. Blocking and histology studies were performed to confirm CD105 specificity of both tracers in vivo. **Results**: Both TRC105-Fab and TRC105-F(ab')$_2$ were produced with high purity by enzymatic digestion of TRC105, confirmed by SDS-PAGE, HPLC analysis, and mass spectroscopy. CD105 binding affinity and specificity of both fragments were maintained based on flow cytometry analysis. $^{64}$Cu-labeling of NOTA-TRC105-Fab and NOTA-TRC105-F(ab')$_2$ were both achieved with good yield and specific activity. PET imaging revealed rapid uptake of $^{64}$Cu-NOTA-TRC105-F(ab')$_2$ (5.8±0.8, 7.6±0.6, 5.6±0.4, and 3.8±0.7 %ID/g at 0.5, 3, 16, and 48 h post-injection respectively; n = 4), as well as $^{64}$Cu-NOTA-TRC105-Fab (3.6±0.4, 4.2±0.5, 4.9±0.3, and 4.6±0.8 %ID/g at 0.5, 2, 5, and 24 h post-injection respectively; n = 4), in the 4T1 murine breast cancer model. Since tumor uptake peaked quickly, both $^{61}$Cu-NOTA-TRC105-Fab and $^{61}$Cu-NOTA-TRC105-F(ab')$_2$ were also able to provide good tumor contrast at a few hours post-injection. CD105 specificity of both tracers was confirmed with blocking and histology studies. Overall, similar tumor contrast was observed for the two tracers, although the absolute tumor uptake was higher for $^{61/64}$Cu-NOTA-TRC105-F(ab')$_2$ due to bivalency, higher molecular weight, and longer circulation half-life. **Conclusion**: Both $^{61/64}$Cu-NOTA-TRC105-Fab and $^{61/64}$Cu-NOTA-TRC105-F(ab')$_2$ had rapid, prominent, and CD105-specific uptake in the 4T1 tumor. The use of Fab and F(ab')$_2$ fragments allowed much faster tumor uptake (peaking at a few hours after injection) than radiolabeled intact antibody (often peaking after 24 h), which may be translated for same day immunoPET imaging in the clinic. Besides a shorter $t_{1/2}$ of 3.3 h that is more suitable for labeling of antibody fragments, $^{61}$Cu also has much higher $\beta^+$ branching ratio than $^{64}$Cu (62% vs 17%). Therefore, it can offer stronger signal intensity and require lower tracer dose for PET than $^{64}$Cu, which will facilitate clinical translation.

## OP064

### Dual-label approach: optical dye conjugates of the PET tracer $^{68}$Ga-PSMA-HBED-CC

**M. Eder**[1], M. Schäfer[1], U. Bauder-Wüst[1], M. Benesova[1], A. Afshar-Oromieh[2], U. Haberkorn[2], M. Eisenhut[1], K. Kopka[1]; [1]German Cancer Research Center, Heidelberg, GERMANY, [2]Department of Nuclear Medicine, University Hospital Heidelberg, Heidelberg, GERMANY.

**Aim** First clinical experiences with the $^{68}$Ga-labelled prostate-specific membrane antigen (PSMA) targeting inhibitor Glu-urea-Lys-HBED-CC (PSMA-HBED-CC) demonstrated high and specific tracer uptake in local relapses and metastases of prostate cancer as well as low background activity [1]. Fluorescence dye conjugates of PSMA-HBED-CC might allow further characterization of urea-based small molecule inhibitors of PSMA in respect to their intracellular distribution. In addition, the results of this initial study might serve as a proof of principle and as a platform for the development of novel bimodal contrast agents targeting PSMA in order to further improve the clinical management of prostate cancer. **Materials & Methods** The formation of the binding motif Glu-urea-Lys was carried out by an isocyanate reaction of protected Glu with resin immobilized lysine. The resulting product was reacted with the bi-activated TFP-ester of HBED-CC and *2,2*

(ethylenedioxy)bis(ethylamine) to form the precursor for dye conjugation. For this initial study, the optical dye- labelled tracer PSMA-HBED-CC-fluorescein was synthesized using the respective isothiocyanate (FITC). The binding properties were analyzed in a competitive cell binding assay followed by internalization experiments. The intracellular distribution of the tracer was investigated by confocal fluorescence microscopy using PSMA expressing LNCaP cells. **Results** The $^{68}$Ga-labelling of PSMA-HBED-CC-fluorescein resulted in a high radiochemical yield of >99% after 2 minutes at room temperature with specific activities of 500-1000 GBq/µmol. Comparative cell binding experiments revealed a high affinity to PSMA expressing cell lines ($IC_{50}$= 6.3 ± 1.4 nM) which is in line with the excellent values obtained with the parental molecule PSMA-HBED-CC (12.0 ± 2.8 nM). The dual-labelled molecule was effectively internalized into the PSMA expressing cell line LNCaP which is considered crucial in respect to its *in vivo* tumor targeting properties. First confocal fluorescence microscopy images of the intracellular distribution were obtained at different time points. **Conclusion** As the cell binding properties were not affected by the conjugation of the fluorescent dye, PSMA-HBED-CC-fluorescein might represent a tool to follow the intracellular distribution of $^{68}$Ga-labelled PSMA-HBED-CC. Moreover, conjugated with a near-infrared fluorescent dye the dual-labelled PSMA-HBED-CC might serve as a multimodal imaging agent offering staging by PET imaging on the one hand and intraoperative fluorescence signals on the other hand which might help to distinguish between prostate cancer and healthy tissue during surgery. Reference [1] Afshar-Oromieh et al. (2013) *Eur J Nucl Med Mol Imaging*; 40: 486-95

## OP065

### Radiochemical Evaluation of Phosphinic, Carboxylic and Mixed Chelators for Gallium-68

**G. Máté**[1], J. Šimeček[2], J. Notni[2], L. Galuska[1], H. J. Wester[2], I. Kertész[1]; [1]Department of Nuclear Medicine, University of Debrecen, Debrecen, HUNGARY, [2]Department of Pharmaceutical Radiochemistry, Technische Universität München, Munich, GERMANY.

**Aims***:* Due to its attractive physical and radiochemical properties, generator-produced PET radionuclide Gallium-68 has recently gained importance in nuclear medicine. As part of our research is to develop new $^{68}$Ga-PET radiopharmaceuticals, we intended to select the most promising chelator for further preparation of conjugates with new biologically active targeting molecules. Previously it was shown that chelators based on 1,4,7-triazacyclononane (TACN), particularly those comprising three (methylene)phosphinic acid side arms, possess markedly improved $^{68}$Ga-labelling properties. Therefore, we prepared two mixed phosphinic/carboxylic chelators: Ac-TACN-$PH_2$ and NOP-2A, and compared them with the carboxylic-type chelator NOTA and the phosphinic-type chelator NOPO. **Methods:** NOPO and NOTA were synthesised according to published procedures. Ac-TACN-$PH_2$ [1,4,7-Triazacyclononane-1,4-di-(methylenephosphinic acid)-7-acetic acid] and NOP-2A ([1,4,7-Triazacyclononane-1-(methylene(2-carboxyethyl)phosphinic acid)-4,7-di(acetic acid)] were synthesised in multistep Moedritzer-Irani reactions. A $^{68}$Ge/$^{68}$Ga-generator (iThemba Labs, South Africa) was eluted with 1 M HCl manually. The eluate fraction with the highest activity (≈ 50 MBq in 1.25 ml) was further used for labelling. These studies were performed at room temperature (r.t.) and 95 °C with HEPES buffering. pH was adjusted by the addition of HCl (pH 0-2) or NaOH solution (pH 4-8). All used chemicals and solvents were of ultrapure grade. Radionuclide incorporation was determined by radio-TLC. **Results:** Concentration dependency (5 min, pH 3) at 95°C showed labelling efficiency in order NOTA≈NOP-2A<<Ac-TACN-$PH_2$≈NOPO. At r.t. NOP-2A was generally more efficient chelator for $^{68}Ga^{3+}$ compared to NOTA. Nevertheless, after reaching 90 % activity incorporation at 10 µM concentration, the labelling did not improve upon ascending ligand concentration. At the same concentration, NOTA was labelled only to 50 %, quantitative labelling (>95%) was reached at 100 µM concentration. R.t. labelling yields of NOPO and Ac-TACN-$PH_2$ were almost identical. To reach the same yield with NOTA and NOP-2A, both ligands had to be used at 10 times higher concentration. Labelling efficiency along pH 0-8 (at constant ligand concentration) strongly correlated with TACN substitution pattern. NOPO with 3 phosphinic acids could be quantitatively labelled already at pH 1. At 95 °C and pH 1-3, the labelling efficiency increased in order NOTA<<NOP-2A≈Ac-TACN-$PH_2$<<NOPO. Labelling between pH 3 and 4 was comparable, at pH 5-7 activity incorporation decreased in order NOP-2A>>Ac-TACN-$PH_2$>NOPO≈NOTA. **Conclusion:** TACN-based chelators bearing 2 or 3 phosphinic acids showed much better labelling characteristics for $^{68}$Ga compared to those with 3 carboxylates or only 1 phosphinate. Among the investigated chelate systems, NOPO seems to be a decent choice for further development of new $^{68}$Ga-radiopharmaceuticals.

## OP066a

### Promising Prospects for PET Imaging with Scandium-44: Cyclotron Production and Preclinical Evaluation in Tumor-Bearing Mice

**C. Müller**[1], M. Bunka[2,3], J. Reber[1], K. Zhernosekov[2], A. Türler[2,3], R. Schibli[1,4]; [1]Center for Radiopharmaceutical Sciences ETH-PSI-USZ, Paul Scherrer institute, Villigen-PSI, SWITZERLAND, [2]Laboratory of Radiochemistry and Environmental Chemistry, Paul Scherrer Institute, Villigen-PSI, SWITZERLAND, [3]Laboratory of Radiochemistry and Environmental Chemistry, University of Bern, Berne, SWITZERLAND, [4]Department of Chemistry and Applied Biosciences, ETH Zurich, Zurich, SWITZERLAND.

**Aim:** Herein, we propose the use of $^{44}$Sc ($t_{1/2}$ = 3.97 h, $E\beta^+_{av}$ = 632 keV) as a valuable alternative to $^{68}$Ga ($t_{1/2}$ = 68 min, $E\beta^+_{av}$ = 830 keV) for imaging of cancer prior to $^{177}$Lu-based radionuclide therapy. The Aim of the study was the preclinical evaluation of a folate conjugate labeled with cyclotron-produced $^{44}$Sc and to compare these data with those of the $^{177}$Lu-labeled match. **Material and Methods:** $^{44}$Sc was produced via the $^{44}$Ca(p,n)$^{44}$Sc-nuclear reaction at a cyclotron (~ 17 MeV, 50 µA, 30 min) using highly enriched $^{44}$Ca-targets (10 mg $^{44}CaCO_3$, 97.00%). Separation from the target material was carried out by a semi-automated process using extraction chromatography and cation exchange chromatographies. Radiolabeling of a DOTA-folate conjugate (cm09) with $^{44}$Sc was performed at 95°C within 10 min. $^{44}$Sc-cm09 was investigated in vitro using FR-positive KB tumor cells and in vivo by PET/CT imaging of tumor-bearing mice. **Results:** Under the given irradiation conditions and amount of $^{44}$Ca, cyclotron-produced $^{44}$Sc was obtained in a maximum yield of 350 MBq at high radionuclide purity (> 99%). Semi-automated isolation of $^{44}$Sc from $^{44}$Ca-targets allowed formulation of up to 300 MBq $^{44}$Sc in a volume of 200-400 µL within 10 min. Radiolabeling of cm09 was achieved with a radiochemical yield of > 96% at a specific activity of 5.2 MBq/nmol. In vitro, $^{44}$Sc-cm09 showed specific binding to KB tumor cells. PET/CT imaging studies of mice injected with $^{44}$Sc-cm09 allowed excellent visualization of tumor xenografts. Moreover, $^{44}$Sc-cm09 and $^{177}$Lu-cm09 showed an equivalent in vivo distribution profile and the same pharmacokinetics. **Conclusion:** In this study we demonstrated the feasibility of using cyclotron-produced $^{44}$Sc for the preparation of a folate radioconjugate. A proof-of-concept study revealed favorable features of $^{44}$Sc as for PET imaging. The excellent analogy of $^{44}$Sc-cm09 and $^{177}$Lu-cm09 holds promise for future application of $^{44}$Sc-radiopharmaceuticals in cancer patients prior to the application of $^{177}$Lu-based radionuclide therapy.

LS — Sunday, Oct. 20, 13:00 — 14:30, Bellecour 1/2/3

## EARL: Proving the Quality of Nuclear Medicine

## OP066b

### Introduction: EANM and EARL - A Strong Commitment to Quality

**J.F. Verzijlbergen, NETHERLANDS**

## OP066c

### The Success Story of EARL - History, Projects and Aims

**K. Tatsch, GERMANY**

## OP066d

### How to Reach Quality Standards for Successful EU Grant Applications

**M. Gotthardt, NETHERLANDS**

## OP066e

### Part 1: EARL's Dedication to Quality - The EARL FDG-PET/CT Accreditation Programme & Guideline Developments: Results of more than 65 Successfully Accredited Sites and Future Perspectives

**R. Boellaard, NETHERLANDS**

## OP066f

### Part 2: EARL FDG-PET/CT Accreditation in Practice - Easily Implemented and Performed

**R. Boellaard, NETHERLANDS**

LS — Sunday, Oct. 20, 13:00 — 14:30, Gratte-Ciel 1/2/3

## Clinical Audit - Europe and Beyond

### OP067
**Updated Policy of UEMS/EBNM Accreditation Committee**

**S. Mirzaei, AUSTRIA**

### OP068
**Clinical Audit in Algier**

**S.E. Bouyoucef, ALGERIA**

### OP069
**Clinical Audit in Switzerland**

**J.O. Prior, SWITZERLAND**

### OP070
**General Talk on Clinical Audit**

**A. Garcia-Burillo, SPAIN**

### OP071a
**Clinical Report Audit**

**A.J.W. Hilson, UNITED KINGDOM**

### OP071b
**Update of Quanum Manual**

**T. Pascual, IAEA**

YE1 — Sunday, Oct. 20, 13:00 — 14:30, Tête D'Or 1/2

## Young EANM Daily Forum 1: Back to the Future

### OP072
**Welcome and Introduction**

**I.Zerizer, UNITED KINGDOM, F. Jamar, SPAIN**

### OP073
**Historical Perspective: From the Discovery of Radioactivity to the Production of Images**

**H.J. Biersack, GERMANY**

### OP074
**Hybrid Technologies in Molecular Imaging**

**F.M. Mottaghy, GERMANY**

### OP075
**Radioactivity for Treatment?**

**L. Bodei, ITALY**

### OP076
**Discussion**

**All Participants**

401 — Sunday, Oct. 20, 14:30 — 16:00, Amphithéâtre

## CME 3 - Physics: Motion Correction

### OP077
**Principles of Motion Correction and Gating**

**K. Thielemans, UNITED KINGDOM**

### OP078
**Clinical Use of Cardiac Gating within PET and SPECT**

**P. Knaapen, NETHERLANDS**

### OP079
**4D PET/CT for Radiotherapy Treatment Planning**

**D. Thorwarth, GERMANY**

402 — Sunday, Oct. 20, 14:30 — 16:00, Auditorium Lumière

## Symposium 3 - From Cell to Scanner 2013: Hypoxia

### OP080
**HIF Pathways**

**T. Acker, GERMANY**

### OP081
**Importance of Hypoxia in Radiotherapy: Past - Current - Future**

**A. Abdollahi, GERMANY**

### OP082
**Hypoxia PET Imaging, What Tracer To Use?**

**P. Lambin, NETHERLANDS**

403a — Sunday, Oct. 20, 14:30 — 15:30, Forum 3

## Mini Course 1 - Reconstructions: TrueX + TOF, PSF, OSEM

### OP083
**Reconstruction Techniques used in Nuclear Medicine and PET/CT Imaging**

**S. Rep, SLOVENIA**

### OP084
**Overview of State of the Art PET Image Reconstruction Technologies**

**R. Boellaard, NETHERLANDS**

403b — Sunday, Oct. 20, 15:45 — 16:45, Forum 3

## Mini Course 2 - EANM-TC/SNMMI-TS Joint Session: Technologists Perspective in Radionuclide Therapy

### OP085
**Dosimetry in Radionuclide Therapy**

**G. Flux, UNITED KINGDOM**

### OP086
**Radiopharmaceuticals in Radionuclide Therapy**

**E. Mantel, USA**

403c — Sunday, Oct. 20, 17:00 — 18:00, Forum 3

## Mini Course 3: Dose Reduction

### OP087
**The Importance of Understanding Dosing**

**K. Bacher,BELGIUM**

### OP088
**Dose Optimisation: A European Perspective**

**M. Lassmann, GERMANY**

404 - Sunday, Oct. 20, 14:30 - 16:00, Bellecour 1/2/3

## Featured - Cardiovascular: Plaque Imaging

### OP089

#### The Many Ways to Address Atherothrombosis

**F. Rouzet, FRANCE**

### OP090

#### Comparison 18F-FDG PET/CT with Immunohistochemical Analysis of CD68 in the Assessment of Carotid Atherosclerotic Vulnerable Plaques

**A. Niccoli Asabella**[1], A. Di Palo[1], D. Rubini[1], A. Notaristefano[1], C. Mandurino[2], A. Marzullo[3], M. M. Ciccone[2], G. Rubini[1]; [1]Nuclear Medicine Unit, D.I.M., University of Bari "Aldo Moro", Bari, Italy, ITALY, [2]Cardiovascular Diseases Section, Department of Emergency and Organ Transplantation (DETO), University of Bari, Bari, Italy, Bari, Italy, ITALY, [3]Department of Anatomic Pathology, University of Bari, Bari, Italy, Bari, Italy, ITALY.

**Background**: Carotid atherosclerotic vulnerable plaque represents an important cause of morbidity and mortality worldwide due to cerebral-vascular ischemic events. Inflammation is traditionally associated with plaque vulnerability, whereas calcification with plaque stability. **Aim**: To investigate the role of 18F-FDG PET/CT in the assessment of carotid vulnerable plaques, we compared 18F-FDG PET/CT findings with data obtained from the histological analysis of carotid plaques of patients underwent carotid endarterectomy. **Methods**: we studied thirty-two consecutive patients (20 men and 12 women, mean age ± SD 74±8 years) who performed 18F-FDG PET/CT and underwent carotid endarterectomy within one week. Maximum and mean standardized uptake value (SUV) and Target Background Ratio (TBR) were used to quantify 18F-FDG uptake while surgical samples were analyzed to identify inflamed carotid plaques, with evaluation of macrophages infiltration by mean of immunohistochemistry. CD68 staining was analyzed and categorized in a blinded manner. Immunochemical setting was evaluated using a four level arbitrary score as follows: (-) absence of immune-positivity; (+) presence of sporadic positive cellular elements, mostly isolated; (++) presence of positive sporadic cellular elements arranged in small heaps; (+++) presence of positive cellular elements scattered in the plaque and organized into big piles. The immunohistochemical analysis distinguished two groups: group A, patients with inflamed carotid plaques and group B, patients with non inflamed ones; the histological data were compared with PET/CT findings. **Results**: 12/32 (37%) patients resulted in group A and 20/32 (63%) in group B. Group A patients showed a large inflammatory component [(+++) in 8 (67%) cases and (++) in the other 4 (33%) cases] composed by CD68 positive cells (macrophages). Group B patients showed absence of immune-positivity [(-) in 17 (85%) cases] or presence of sporadic positive CD68 cellular elements mostly isolated [(+) in 3 (15%) cases]. No statistical significant differences were found between the two groups as regard SUVmax [2.38±0.92 in group A vs. 1.79±0.37 in group B, p=ns] and SUVmean [1.99±0.68 group A vs. 1.64±0.34 group B, p=ns], while we found statistical significant differences among TBRmax [1.42±0.32 group A vs. 1.16±0.19 group B, p=0.02] and TBRmean [1.34±0.26 group A vs. 1.03±0.20 group B, p<0.001] and carotid inflammation. **Conclusion**: TBRmax and TBRmean proved to be a more reliable parameter then SUV in identifying inflamed plaques. Although limited by the small population, our partial results suggested the important role of 18F-FDG PET/CT in the identification of vulnerable carotid atherosclerotic plaques at high rupture risk.

### OP091

#### Suppression of myocardial FDG-uptake for vulnerable coronary plaque imaging: Is fatty acid loading or the use of calcium channel blockers really needed?

**F. Demeure**[1], F. Hanin[1], A. Bol[2], P. Sprimont[1], B. Gerber[1], A. Pasquet[1], J. Vanoverschelde[1], D. Vancraeynest[1]; [1]Institut de Recherche Clinique et Expérimentale, IREC, Université Catholique de Louvain. Cliniques Universitaires Saint-Luc, Bruxelles, BELGIUM, [2]Institut de Recherche Clinique et Expérimentale, IREC, Université Catholique de Louvain, Bruxelles, BELGIUM.

**Background**: $^{18}$F-FDG-PET/CT is a promising approach for imaging atherosclerotic plaque inflammation. However, to image coronary plaque inflammation, this application requires the suppression of background signal from adjacent myocardium. To this Aim, overnight fasting, fatty acids loading and calcium channel blocker (CCB) treatment have been proposed. **Aim**: To compare the efficacy of different interventions in suppressing myocardial FDG-background in a randomized prospective trial. **Methods**: 36 healthy volunteers (mean age 25.5±5.1 years) were randomized to 4 different types of intervention after 12 hours overnight fasting preceded by a high fat-low carbohydrate (HFLC) meal. Group 1 did not receive any additional preparation and served as reference. Group 2 and group 3 consumed 1 hour before FDG-injection respectively, a high fat solution containing 43.8 g of lipids (Ketocal®), or 50 mL of olive oil, to evaluate the additive value of fatty acid loading on myocardial FDG-uptake suppression. Group 4 received 120 mg of Verapamil PO. In all groups, PET/CT of the heart (Philips Gemini-TF) was performed 60 minutes after injection of 370 MBq of $^{18}$F-FDG. Images were acquired for 5 minutes per bed position and the myocardial uptake suppression was assessed either by using a qualitative visual scale (QVS) and by measuring the maximum standardized uptake value ($SUV_{max}$) at the level of the papillary muscle. **Results** QVS of myocardial background suppression was similar in all groups of volunteers (0.8±1.1, 1.3±1.4, 1.4±1.2, 0.9±0.9, for groups 1-4 repectively, p=0.28 NS by $\chi^2$ test). Good myocardial background suppression (i.e. QVS 0 or 1) was observed in respectively 8/9, 5/9, 4/9 and 8/9 subjects of group 1,2,3 and 4 (p=0.08). Myocardial $SUV_{max}$ tended to be lower in group 1 (2.3±0.8) than in the 3 other groups ( 4.6±3.0, 5.5±5.1, 3.0±2.7 respectively), however differences were not statistically significant (p=0.18 by ANOVA). Myocardial $SUV_{max}$ of volunteers from the reference group (2.3±0.8) was lower than that of 100 consecutive patients who underwent FDG PET for oncological diagnosis after overnight fasting only (6.8±4.8, p=0.045). **Conclusion:** A HFLC meal followed by a fast of 12 hours before FDG injection allows to obtain a good myocardial FDG-uptake suppression in 90% of subjects. Fatty acid loading or Verapamil 1 hour before FDG injection did not confer any additional benefit.

### OP092

#### Pathophysiology of calcium deposition as a marker of the ongoing aortic plaque: an 18F-Fluoride PET study

**F. Fiz**[1], A. Piccardo[2], L. Picori[1], M. Massollo[1], E. Pestarino[2], C. Marini[3], M. Cabria[2], A. Democrito[1], G. Sambuceti[1], S. Morbelli[1]; [1]Nuclear Medicine Unit, Department of Health, IRCCS SAn Martino-IST, University of Genoa, Genoa, ITALY, [2]Nuclear Medicine Unit, Ente Ospedaliero Ospedali Galliera, Genoa, ITALY, [3]CNR Institute of Bioimages and Molecular Physiology, Milan, Section of Genova, Genoa, ITALY.

**Background and Aims**: Several studies have highlighted the role of vascular $^{18}$F-NaF uptake as a marker of ongoing calcium deposition. However, visible $^{18}$F-NaF accumulation often showed inconsistent co-localization with arterial plaque. It has been hypothesized that "active" calcification processes, which can be imaged with $^{18}$F-NaF PET, prevail in the early stages of plaque formation; conversely, in later stages of plaque development, "passive" and gradient-driven phenomena of calcium deposition predominate. In order to test this hypothesis, we evaluated $^{18}$F-NaF uptake in three stages of plaque evolution, using Hounsfield density as a marker of calcification progression. We also tested whether attenuation weighted image reconstruction affected $^{18}$F-NaF uptake values in the different plaque stages considered. **Methods:** 64 oncologic patients (14 males, mean age 65.3±8.2 range 26-81) underwent 18F-NaF PET/CT for either breast or prostate cancer. All visible calcific plaques within the wall of infrarenal aorta were identified; a volume of interest (VOI), created using a growing region algorithm on the CT images, was drawn on each plaque to assess mean SUV and mean Hounsfield value (HU). Plaques were then stratified according to an ordered distribution in tertiles, in light plaques (LP) having a mean HU <185, medium plaques, with HU values ranging from 185 to 480 and heavy plaques, having mean HU >480. SUV was normalized for blood $^{18}$F-NaF activity, assessed on a VOI drawn within the inferior vena cava, to obtain plaque target-to background ratio (TBR). In all patients, TBR was calculated in a sample non-calcified aortic segment, serving as control. In 35 patients TBR was also calculated on non-attenuation-corrected (NAC) images. **Results**: Average TBR values were largely different in the three sets of plaques, being highest in LP (2.09±1.09) and significantly lower in MP (1.35±0.57, p<0.001). HP presented an even lower TBR, which was 1.01±0.55 (p<0.01 with respect to MP, p<0.001 compared with LP). Control segment TBR was similar to the one of HP and MP (1.26±0.45, p=ns), while it was significantly lower than LP's (p<0.01). Considering TBR values originated from NAC reconstruction didn't modify these figures. **Conclusion:** The present pathophysiological study is in keeping with the concept that $^{18}$F-NaF is a feasible option in imaging molecular calcium deposition in the early stages of plaque formation, when active uptake mechanism are the main determinants of calcium presence. From a technical point of view, our data suggest that NAC reconstruction doesn't significantly affect output when evaluating plaques of any thickness.

### OP093

#### Characterization of the Mineral Deposition and the Inflammatory Metabolism of the Carotid Atheroma by 18F-FLUORIDE and 18F-FDG PET/CT in the Subacute Fase of Stroke

**R. Quirce**, I. Martínez-Rodríguez, I. Banzo, J. F. Jiménez-Bonilla, S. Ibánez-Bravo, N. Martínez-Amador, C. Lavado, Z. Bravo-Ferrer, M. Rebollo Alvarez-Amandí, M. Revilla, E. Palacio, J. M. Carril; Hospital Univ. M. Valdecilla. Universidad de Cantabria., Santander, SPAIN.

**Aim**: To evaluate the mineral deposition by 18F-Fluoride and inflammatory metabolism by 18F-FDG in the carotid atheroma in patients starting statine

therapy. **Material and Methods**: This prospective study included 11 patients with carotid atheroma detected by angioCT and neurological symptoms. Statine treatment was started within ten days before PET/CT examinations. There were 23 plaques, 12 in relation with the symptomatology. In all patients 18F-Fluoride PET/CT and 18F-FDG PET/CT were done 180 minutes after injection of the radiotracer within no more than 7 days between both explorations. A semiquantitative analysis by Target to Background Ratios -TBR- was done, being the target the carotid plaque and the background the cava lumen. **Results**: The mean TBR values for the 18F-Fluoride and the 18F-FDG uptake in the 12 symptomatic plaques were 2.53 ± 1.01 and 1.84 ± 0.45 and for the 11 asymptomatic 2.19 ± 0.71 and 1.77 ± 0.5 respectively. **Conclusions**: The different behaviour of 18F-Fluoride may indicate an association of the mineral deposition and symptomatology. The results are encouraging to continue this work including a larger number of patients.

## OP094

### Circulating free fatty acid levels predict the myocardial FDG-uptake suppression. Implications for vulnerable plaque imaging.

**F. Demeure**[1], F. Hanin[1], A. Bol[2], P. Sprimont[1], M. Vincent[3], B. Gerber[1], A. Pasquet[1], J. Vanoverschelde[1], D. Vancraeynest[1]; [1]Institut de Recherche Clinique et Expérimentale, IREC, Université Catholique de Louvain. Cliniques Universitaires Saint-Luc, Bruxelles, BELGIUM, [2]Institut de Recherche Clinique et Expérimentale, IREC, Université Catholique de Louvain, Bruxelles, BELGIUM, [3]Faculté de Pharmacie et des Sciences Biomédicales, FASB, Université Catholique de Louvain. Cliniques Universitaires Saint-Luc, Bruxelles, BELGIUM.

**Background**: $^{18}$F-FDG PET/CT is a promising method for imaging coronary atherosclerotic plaque inflammation. However, the avid myocardial glucose uptake may preclude the correct visualization of coronary arteries. The Randle cycle (fatty acid - glucose cycle competition) establishes that fatty acid loading suppresses glucose metabolism by the myocardium. **Aim**: We hypothesized that circulating free fatty acid (FFA) levels might predict the magnitude of myocardial FDG-uptake suppression. **Methods:** 36 healthy volunteers underwent cardiac PET/CT (Philips Gemini-TF) after overnight fasting preceded by a high fat-low carbohydrate meal. A 5 minutes per bed position image of the heart was obtained 60 minutes after injection of 370 MBq of $^{18}$F-FDG. Myocardial uptake suppression was assessed by using a qualitative visual scale (QVS) while maximum standardized uptake value ($SUV_{max}$) of the left ventricle was measured at the level of the papillary muscles. Both parameters were correlated to insulin, glucose and FFA levels measured immediately before, and respectively 1 and 2 hours post injection. **Results:** Mean glycemia was 81.5±4.1 mg/dL, mean insulin level was 6.0±4.1 UI/L, mean FFA was 0.72±0.30 mmol/L before FDG injection. The mean glycemia and insulin level decreased and the mean FFA increased over time. By QVS, background suppression was optimal in 24 subjects (mean $SUV_{max}$ 2.11±0.41) and suboptimal in 12 (mean $SUV_{max}$ 7.37±4.20), the mean myocardial $SUV_{max}$ being significantly lower in the first group ($p<0.001$). We note a good correlation between the FFA level and the reciprocal of $SUV_{max}$ ($R = 0.59$). Furthermore, the amount of FFA was higher in volunteers with a good suppression compared with volunteers with a poor suppression (0.81±0.31 vs. 0.53±0.14 mmol/L; $p=0.005$). The ROC curve analysis identified 0.65 mmol/L as the cut-off value with the best positive predictive value (88%). However no correlation existed between glycemia or insulin level and the reciprocal of $SUV_{max}$ ($R = -0.25$ and 0,02 respectively). There was no difference in glycemia or insulin level between volunteers with a good or poor suppression. **Conclusion:** Myocardial FDG-uptake suppression is inversely correlated with FFA level and is significantly better in volunteers with high FFA level. The measurement of FFA at the time of $^{18}$F-FDG injection represents an interesting way for predicting the quality of myocardial FDG-uptake suppression.

## OP095

### Detection of apoptotic cells in atherosclerotic plaques of rabbits with the PET radiotracer 18F-ML-10

**F. Hyafil**[1], A. Tran Dinh[2], R. Ben Azzouna[1], L. Louedec[3], A. Petiet[4], M. Milliner[1], S. Leygnac[1], S. Burg[1], O. Meilhac[3], M. Ben-Ami[5], A. Reshef[5], D. Le Guludec[1]; [1]Department of Nuclear Medicine, Bichat Hospital, AP-HP, Paris, FRANCE, [2]Inserm 698, Bichat Hospital, AP-HP, Paris, FRANCE, [3]Inserm 698, Bichat Hospital, Paris, FRANCE, [4]IFR 02, UFR de Médecine, Université Paris Diderot, Paris, FRANCE, [5]Aposense Ltd, Petach-Tikva, ISRAEL.

**Aim**. High-risk atherosclerotic plaques contain higher densities of apoptotic cells as compared to stable plaques. 18F-ML-10 (Aposense) is a PET radiotracer that accumulates in cells presenting apoptosis-specific alterations, collectively designated as the apoptotic membrane imprint. The Aim of this study was to test whether the presence of apoptotic cells in atherosclerotic plaques induced experimentally in rabbits could be detected with 18F-ML-10 and PET. **Materials and Methods**. Atherosclerotic plaques were induced in the aorta of 5 New-Zealand White rabbits by a repeated balloon injury (4 weeks apart) and 4 months of hyperlipemic diet. Five non-injured rabbits fed a chow diet were used as controls. Rabbits were imaged in vivo 150 minutes after intravenous injection of 15 Mbq/kg of 18F-ML-10 using a clinical PET-CT system. At the end of the PET, the abdominal aorta was located with computed tomographic angiography during a bolus injection of iodinated contrast agent. Maximal SUVs adjusted for weight were measured in 2D regions of interest placed on the abdominal aorta and averaged over 10 axial slices. Aortas were then imaged ex vivo with a micro-PET system. Activities were measured in aortic segments using a gamma counter. In addition, activities were located in atherosclerotic and control aortic segments by autoradiography and compared to the presence of apoptotic cells (TUNEL-positive) on histological sections **Results**. Activities measured in vivo were higher in the aorta of atherosclerotic as compared to control rabbits (maximal SUV = 0,15 ± 0,07 vs. 0,06 ± 0,05; $p < 0,05$). Activities measured ex vivo were higher in the atherosclerotic aortas as compared to control aortas (23,9 ± 11,2 vs. 1,1 ± 2,4 counts/pixel; $p < 0,05$). Activities measured with a gamma-counter in atherosclerotic plaques were higher as compared to control aortic segments (3,78 ± 2,01 vs. 0,08 ± 0,01 counts/g wet weight; $p < 0,05$). In addition, activities detected in atherosclerotic plaques by autoradiography were associated to the presence of apoptotic cells on corresponding histological sections. **Conclusions**. In this preliminary study, accumulation of 18F-ML-10 was significantly higher in atherosclerotic plaques as compared to normal aortic wall of rabbits, and associated to the presence of apoptotic cells on histology. 18F-ML-10 could represent an interesting radiotracer for the identification of high-risk atherosclerotic plaques in patients with PET.

405 - Sunday, Oct. 20, 14:30 - 16:00, Auditorium Pasteur

## Radionuclide Therapy & Dosimetry: Preclinical Models

## OP096

### $^{188}$Re-$Z_{HER2:V2}$, a promising targeting agent against HER2-expressing tumors: in vitro and in vivo assessment.

**M. Altai**[1], H. Wållberg[2], H. Honarvar[1], J. Strand[1], A. Orlova[3], J. Löfblom[4], Z. Varasteh[3], M. Sandström[5], S. Ståhl[4], V. Tolmachev[1]; [1]Oncology, Radiology And Biomedical Radiation Sciences, Uppsala, SWEDEN, [2]Karolinska Institutet, Solna, SWEDEN, [3]Preclinical PET Platform, Uppsala, SWEDEN, [4]Royal Institute of Technology, Stockholm, SWEDEN, [5]Akademiska Sjukhuset, Uppsala, SWEDEN.

**Aim**. Rhenium-188 (T1/2 =17 h) is a promising radionuclide for therapy applications. This generator-produced high energy beta-emitter is suitable for eradication of bulky non-operable tumors. Low abundance 155 KeV photons permit SPECT imaging of biodistribution of Rhenium-188 labeled targeting agents during therapy for personalized dosimetry. Affibody molecules are small (7 kDa) non-immunoglobulin scaffold proteins with good tumor targeting properties and favorable kinetics. Optimization of the targeting properties of Technetium-99m and Rhenium-188 labeled anti-HER2 affibody molecules demonstrated that the variant with C-terminal glycyl-glycyl-glycyl-cysteine (-GGGC) chelating sequence (designated ZHER2:V2) has the best biodistribution profile in vivo and the lowest renal uptake of radioactivity. The Aim of this study is to evaluate 188Re-ZHER2:V2 as a potential candidate for affibody-based radionuclide targeted therapy against HER2-expressing tumors. **Methods**. ZHER2:V2 was labeled with Rhenium-188 using gluconate-containing kit at pH 4.2. Binding specificity to HER2-expressing cells in vitro was evaluated. Targeting of HER2-overexpressing SKOV-3 ovarian carcinoma xenografts in NMRI nu/nu female mice was studied for a preliminary dosimetry assessment. **Results**. The labeling method provided labeling yields over 95%. The release of free 188Re was negligible after incubation in serum. Binding of 188Re-ZHER2:V2 to living SKOV-3 cells was HER2-mediated (KD = 13 pM). The biodistribution study showed a rapid blood clearance (1.2±0.1 %IA/g at 1h p.i.). Bone uptake was 1.2±0.1 %IA/g at 1h p.i. and remained below 0.15 %IA/g after 4 h p.i. The tumor uptake was 11±3, 10±1, 4±2 and 1.6±0.5 %IA/g at 1, 4, 24 and 48 h p.i., respectively. Pre-saturation of HER2 in xenografts by a pre-injection of a large excess of non-labeled affibody molecules reduced tumor uptake to 2±0.1 %IA/g at 4h p.i., suggesting receptor specificity of the targeting. Already at 4 h pi, the tumor uptake exceeded uptake in kidneys (1.9±0.2 %IA/g). Overall, an area under curve (AUC) for tumor exceeded AUC for kidney by 4-fold, and AUC for bone by 70-fold. γ-camera imaging, performed at 1 and 4 h showed that tumor xenografts was the only sites with prominent accumulation of radioactivity. Kidney visualization was possible 1 h after injection, but only the HER2-expressing tumor xenografts were visible at 4 h p.i. **Conclusion**. Current results suggest that the use of 188Re-ZHER2:V2 can deliver high dose to tumors sparing kidneys and bone marrow. Biodistribution profile suggests that therapy fractionation is possible, providing re-oxygenation of quiescent malignant cells in tumors.

## OP097

### DNA repair inhibitor, Dbait, enhances internal radiotherapy efficacy in melanoma preclinical models

**C. VIALLARD**[1], B. DIRAT[1], F. MISHELLANY[2], I. RANCHON-COLE[3], N. JACQUEMOT[3], B. PEREIRA[4], S. BESSE[1], P. LABARRE[1], E. MIOT-NOIRAULT[1], J. CHEZAL[1], Y. SUN[5], M. DUTREIX[6], F. DEGOUL[1]; [1]UMR990, INSERM, Université d'Auvergne, Clermont-Ferrand, FRANCE, [2]Centre Jean Perrin, Clermont-Ferrand, FRANCE, [3]UMR1107, INSERM, Université d'Auvergne, Clermont-Ferrand, FRANCE, [4]DRCI,CHU Clermont-Ferrand, Clermont-Ferrand, FRANCE, [5]DNA Therapeutics, Evry, FRANCE, [6]CNRS-UMR3347, INSERMU1021, Institut Curie, Orsay, FRANCE.

**Aim:** Despite significant improvement in metastatic melanoma therapeutics, research is still needed for patients not eligible for targeted chemotherapy or without successful treatment. Our laboratory develops melanin-targeting ligands (e.g. ICF01012) for both melanoma PET/SPECT imaging and targeted radionuclide therapy (TRT). [131I]ICF01012 TRT led to a significant growth inhibition of B16Bl6 syngenic tumors and human xenografts (Bonnet-Duquennoy M et al., Int J Cancer, 2009; Bonnet M et al.,PCMR, 2010). Mechanistic studies on B16Bl6 model demonstrated that TRT treatment induced characteristic cellular responses to radiations (Degoul F et al., Int J Cancer, 2013). To increase TRT efficacy, we used the DNA repair inhibitor, DBait, that has been shown to potentiate external radiotherapy effects (Quanz M et al., Clin Cancer Res, 2009).**Material and Methods**: Preclinical models of murin (B16Bl6) and human melanomas (SKMel3) were treated by intravenous injection of 131I]ICF01012 (18.5 MBq and 75 MBq, respectively) and/or with intra and subcutaneous injections of Dbait (10 mg). Tumoral growth and survival were followed. Anatomopathological and molecular studies were performed on in vivo samples and in cell cultures. Statistical analyses were done by ANOVA and log Rank tests and considered significant when $p<0.05$. **Results and conclusion**: In the syngenic B16Bl6 model and in SKMel3 xenografts, we observed a significant decrease of tumoral growth accompanied by an increased of median survival in [131I]ICF01012+Dbait group vs control and single treatment groups. Furthermore, despite of a large systemic distribution of Dbait after subcutaneous injection, DBait association with TRT did not induce any general toxicity nor increase of secondary side effects in pigmented tissues (e.g.. skin, eyes). γH2AX immunofluorescence labelling suggested an increase of DNA double strand breaks in melanomas treated by [131I]ICF01012+Dbait compared to other groups. This preclinical study allows to show that melanoma radioresistance could be overcome by association of internal radiotherapy and DNA repair inhibitors. Combination of [131I]ICF01012 with Dbait could be then considered as a potential treatment for patients with pigmented metastatic melanoma.

## OP098

### A new route toward enhancing the uptake of [$^{111}$In/$^{177}$Lu-DOTA,Leu$^{15}$]MG11 in CCK2R-positive xenografts in mice

A. Kaloudi[1], B. A. Nock[1], E. Lymperis[1], P. J. Marsouvanidis[1,2], E. P. Krenning[2], M. de Jong[2,3], **T. Maina-Nock**[1]; [1]Molecular Radiopharmacy, INRASTES, NCSR Demokritos, Athens, GREECE, [2]Department of Nuclear Medicine, Erasmus MC, Rotterdam, NETHERLANDS, [3]Department of Radiology, Erasmus MC, Radiology, NETHERLANDS.

**Aim**: Previous studies have shown that [$^{111}$In-DOTA]MG11 ([(DOTA)DGlu$^{10}$]gastrin(10-17)), and other *des*-Glu$^{6-10}$ gastrin analogs attractive for their low renal accumulation, poorly localize in CCK2R-expressing tumors *in vivo* due to very rapid enzymatic degradation. We have recently proposed the co-injection of the neutral endopeptidase (NEP) inhibitor phosphoramidon (PA) to increase the stability and tumor uptake of [$^{111}$In-DOTA]MG11. In the present study, we investigated the effect of PA co-injection on the biological profile of [$^{111}$In/$^{177}$Lu]SG5, a [DOTA]MG11 analog with Leu$^{15}$ replacing the oxidation-susceptible Met$^{15}$. Conclusions on the efficacy of this novel approach in improving tumor diagnosis and therapy are drawn. **Materials and Methods**: SG5 was labeled with $^{111}$In or $^{177}$Lu, as previously described. Radioligand internalization was tested by 1 h incubation at 37°C in human epidermoid carcinoma A431 cells transfected to stably express the human CCK2R. Blood samples collected 5 min postinjection (pi) of [$^{111}$In/$^{177}$Lu]SG5 in healthy Swiss albino mice without or with PA co-injection were analyzed by RP-HPLC. Biodistribution was conducted in SCID mice bearing a double A431 tumor model expressing (Tu+) or not (Tu-) the CCK2R. Radioligand was injected (100 µL, 2 µCi, 10 pmol total peptide) with vehicle (100 µL) or with PA (100 µL, 0.5 µmol PA) and animals were sacrificed at 4 h and 24 h pi; for [$^{177}$Lu]SG5 the 48 h and 72 h time points were also studied. **Results**: Both radioligands efficiently internalized in A431-CCK2R-positive cells via a CCK2R-mediated process. While 27% of [$^{111}$In]SG5 and 34% of [$^{177}$Lu]SG5 were detected intact in mouse blood at 5 min pi, by PA-treatment percentages impressively rose to 85% and >90%, respectively. A likewise profound PA impact on tumor uptake was observed in the CCKR-expressing tumors at all time intervals. Thus, by PA co-injection tumor values astonishingly increased from 3.7%ID/g to 12.8%ID/g for [$^{111}$In]SG5 and from 3.9%ID/g to 11.9%ID/g for [$^{177}$Lu]SG5 at 4 h pi and the PA effect remained evident up to 72 h pi. In contrast, renal values as well as uptake in the (Tu-) xenografts remained low and unaffected by PA. **Conclusions**: This study has shown the efficacy of PA treatment in improving the stability of circulating [$^{111}$In/$^{177}$Lu]SG5 in mice. Moreover, radioligand uptake in CCK2R-expressing tumors impressively increased whereas renal values remained low. Enhancement of tumor uptake was evident as long as 72 h pi highlighting the significance of this new approach for tumor therapy.

## OP099

### Radioimmunotherapy of small cell lung cancer xenograft mice with a $^{90}$Y anti-ROBO1 monoclonal antibody : Pathological study of effects on tumor and normal organs

**K. Fujiwara**[1], K. Koyama[1], K. Suga[2], T. Kitada[1], M. Takahashi[1], T. Momose[1]; [1]The University of Tokyo, Tokyo, JAPAN, [2]Sankyo Labo Service Corporation. INC., Tokyo, JAPAN.

**Introduction:** ROBO1 is a membrane protein that is concerned about axon guidance. It is reported that ROBO1 contributes to tumor metastasis and angiogenesis. ROBO1 is specifically expressed at high levels in small cell lung cancer (SCLC). In this study, we performed radioimmunotherapy (RIT) to SCLC models, and analyzed pathological alteration of tumor and organs. **Methods:** For the biodistribution study, $^{111}$In-DOTA anti-ROBO1 IgG (about 370kBq, $^{111}$In anti-ROBO1) was injected into NCI-H69 xenograft mice via tail vein. To evaluate antitumor effect, RIT study was performed. $^{90}$Y-DOTA anti-ROBO1 IgG (about 7.4 MBq, $^{90}$Y anti-ROBO1) was injected. The experiments measured tumor volume, mouse weights and blood cell counts periodically. The tumors and organs (liver, kidney, intestine, spleen, femoral and sternum) of mice were obtained, and histopathologic analysis were carried out. **Results:** As a result of biodistribution study, the specific accumulation in the tumor of $^{111}$In anti-ROBO1 was observed. Liver, kidney, spleen and lung showed comparatively high accumulation of $^{111}$In anti-ROBO1. In the RIT study, $^{90}$Y anti-ROBO1 significantly reduced tumor volume compared with original volume and increased median survival time to 58 days ($p<0.01$, versus saline, 28 days), while $^{90}$Y anti-ROBO1 induced transient pancytopenia. Histopathologic analysis of tumors and organs further validated the therapeutic efficacy and the systemic toxicity of $^{90}$Y anti-ROBO1. In day 7 when tumor volume reduced to 60% compared with original volume, irreversible nuclear denaturation and fibrosis were observed. The percentage of TUNEL-positive cells increased to 11.4% ± 5.1 in the day 7 ($p<0.01$, versus control, 4.14% ± 1.4), which showed increase of DNA fragmentation and apoptosis in the tumor tissues. Normal organs excluding spleen and sternum showed no significant injury. In day7 post injection, spleen showed transient reduction of hematopoietic cells. Hematopoietic cells in sternum reduced to about 20% compared with control. They were recovered in day28. On the other hand, femoral did not show reduction of hematopoietic cells. In the biodistribution study, we found previously that the difference of accumulation of $^{111}$In anti-ROBO1 to between sternum and femoral has no significant. Therefore, these findings suggest that the myelosuppression of RIT is caused also by radiation exposure from $^{90}$Y in blood pool of tumor, heart and liver. **Conclusion***:* Histopathologic analysis showed significant antitumor effect to SCLC by $^{90}$Y anti-ROBO1. The pathological changes of normal organs were limited to hematopoietic system. It is suggested that $^{90}$Y anti-ROBO1 might become one of the effective treatment for SCLC.

## OP100

### Combination of 177Lu-labeled anti-L1CAM mAb chCE7 and paclitaxel improved survival and enhanced tumor uptake of the radioimmunoconjugate in nude mice bearing human ovarian cancer

**D. Lindenblatt**[1], E. Fischer[1], S. Cohrs[1], R. Schibli[1,2], J. Grünberg[1]; [1]Paul Scherrer Institut, Villigen-PSI, SWITZERLAND, [2]ETH Zurich, Zurich, SWITZERLAND.

**Aim:** Recently we could show that radioimmunotherapy with $^{177}$Lu-labeled anti-L1CAM monoclonal antibody chCE7 is a valuable option for treatment of ovarian cancer [Fischer et al. Int J Cancer 2012, 130:2715]. Based on these results we investigated if the efficacy of radioimmunotherapy can be improved by combination with paclitaxel (PTX). Furthermore *in vitro* data of induced G2/M phase cell cycle arrest and cell growth upon different combination treatment conditions were collated. **Material and** Methods**:** Cell viability for different treatment conditions was measured *in vitro* by MTT assays and cell cycle arrest by flow cytometry. *In vivo* therapy was performed in nude mice (n=8) with subcutaneous IGROV1 ovarian cancer xenografts. Mice were injected with a single dose of 6 MBq $^{177}$Lu-chCE7 alone or in combination with 600 µg PTX administered 24 h post radioimmunotherapy. Control groups received an accordant treatment scheme containing an unspecific $^{177}$Lu-labeled antibody in combination with PTX. Tumor growth delay was measured and mice reaching a defined end point were euthanized. Biodistribution (n=4) and SPECT images were acquired post treatments with injections of 2 MBq $^{177}$Lu-chCE7 alone or in combination with 600 µg PTX 24 h post radioimmunoconjugate administration. **Results***: In vitro* combination revealed a decreased cell viability of ovarian carcinoma cells compared to monotherapy treatments. Quantification of cell cycle arrest of PTX pretreated cells resulted in 65 % of cells being arrested in the radiosensitive G2/M-phase peaking at 24 h post PTX treatment with half maximal inhibitory concentration ($IC_{50}$). *In vivo* combination therapy of $^{177}$Lu-chCE7 and PTX reduced tumor burden with a significant decrease in tumor size of 80% (+/- 8,2%) compared to monotherapies (16 days post

treatment; P<0.05). Median survival of control groups varied between 21 and 34 days whereas 6 out of 8 mice are still alive after 54 days in the combination treatment group. Biodistribution studies revealed a significant higher tumor uptake of $^{177}$Lu-chCE7 72 h post injection by 12% (P<0.05) in mice treated in combination with PTX. In addition SPECT scans and microautoradiography studies confirmed a higher uptake at the tumor site. **Conclusion:** Combination of $^{177}$Lu-chCE7 and paclitaxel is a promising treatment modality resulting in a prolonged survival of tumor-bearing nude mice compared to monotherapies. Whether enhanced tumor uptake is a consequence of increased blood vessel permeability caused by PTX treatment is subject of current investigations.

## OP101

### GRP-R expression in Breast Cancer as target for Nuclear Imaging and Therapy; correlation with ER

**S. U. Dalm**[1], A. M. Sieuwerts[2], M. Melis[1], J. W. M. Martens[2], M. de Jong[3]; [1]Department of Nuclear Medicine, Erasmus MC, Rotterdam, NETHERLANDS, [2]Department of Medical Oncology, Erasmus MC, Rotterdam, NETHERLANDS, [3]Department of Nuclear Medicine and Radiology, Erasmus MC, Rotterdam, NETHERLANDS.

**Introduction**: Breast cancer (BC) is a complex and heterogeneous disease: several molecular characteristics reflect subtypes, partly overlapping with therapeutic targets. Examples include the expression of the oestrogen receptor (ER), expressed in ~approximately 75 % of all breast cancer cases. Currently mammography, MRI, $^{99m}$Tc-Sestamibi scintigraphy, and $^{18}$F-FDG PET are commonly used for diagnostic imaging to accurately localize BC. Since it has been reported that the gastrin releasing peptide receptor (GRP-R) is expressed in BC, targeting this receptor with radiolabeled GRP analogues might offer opportunities for SPECT/CT or PET/CT imaging as well as radionuclide therapy in BC. In this study GRP-R expression was determined in human BC specimens and BC cell lines and correlated with ER status. **Methods**: GRP-R mRNA levels of 90 human breast cancer specimens, with known ER status (48 ER-positive and 42 ER-negative) were determined using qRT-PCR in a Taqman Gene expression assay. Furthermore a panel of 21 BC cell lines characterized for ER expression (13 ER-positive, 8 ER-negative) was analysed for GRP-R expression at the protein level. Internalisation studies were performed with $10^{-9}$ M $^{111}$In-AMBA (an receptor-agonist GRP analogue) for 1 hour and 15 minutes at 37ºC. Thirteen of these BC cell lines were also analyzed for GRP-R expression at mRNA level using qRT-PCR. **Results**: Clinical BC specimens with high GRP-R mRNA level were all ER-positive, resulting in a significant positive correlation *(p=0.03)*. Fifty-two percent of the analyzed BC cell lines showed the ability to internalize $^{111}$In-AMBA, although high variation between cell lines was observed. GRP-R mRNA levels of the BC cell lines significantly correlated with the internalisation rate *(p=0.0003)*, indicating that the amount of internalized $^{111}$In-AMBA is partly determined by the level of receptor expression. However, no correlation was found between ER status and GRP-R expression in the BC cell lines. **Conclusion/Discussion**: GRP-R is expressed on human clinical BC specimens, with high correlation with the ER positive subtype. Characterization of a panel of 21 BC cell lines demonstrated that 52 % of the BC cell lines express the GRP-R, though without strict correlation with ER. This observed discrepancy might be explained by a lack of power of the study on the BC cell lines. A radiolabeled GRP peptide analogue demonstrated specific GRP-R mediated and quantitative uptake in BC cell lines, proving that the GRP-R is a promising target for nuclear imaging and therapy of BC using radiolabeled GRP analogues.

## OP102

### Investigation of $^{177}$Lu-Folate Based Radionuclide Tumor Therapy in Combination with Pemetrexed

**C. Müller**[1], J. Reber[1], S. Haller[1], C. P. Leamon[2], R. Schibli[1,3]; [1]Center for Radiopharmaceutical Sciences ETH-PSI-USZ, Paul Scherrer Institute, Villigen-PSI, SWITZERLAND, [2]Endocyte Inc., West Lafayette, IN, UNITED STATES, [3]Department of Chemistry and Applied Biosciences, ETH Zurich, Zurich, SWITZERLAND.

**Aim:** The antifolate pemetrexed (PMX) was shown to improve the tissue distribution profile of radiofolates by reducing undesired renal accumulation without affecting uptake in the tumor. We hypothesized that PMX would have a dual role in combination with therapeutic radiofolates as it may protect kidneys from radionephrotoxicity and contribute to the anticancer effect as a chemotherapeutic and/or radiosensitizing agent. Therefore, the Aim of the study was to investigate the combined application of $^{177}$Lu-folate and PMX in vitro an in vivo. **Material and Methods:** The DOTA-folate conjguate (EC0800, Endocyte Inc.) was labeled with $^{177}$Lu at high specific activity. In vitro the effects of $^{177}$Lu-EC0800 alone and in combination with PMX was tested with FR-positive KB tumor cells using MTT and clonogenic assays. In vivo, undesired effects of $^{177}$Lu-EC0800 (20 MBq/mouse) with/without co-application of PMX were investigated in non-tumor bearing mice over six months. Kidney function was monitored by determination of renal accumulation of $^{99m}$Tc-DMSA using SPECT. Therapy studies in KB tumor-bearing mice were performed with $^{177}$Lu-EC0800 (20 MBq) combined with subtherapeutic (0.4 mg) and therapeutic amounts (1.6 mg) of PMX. **Results:** Determination of the combination index revealed a synergistic inhibitory effect of $^{177}$Lu-EC0800 and PMX on the viability of both FR-positive cancer cell lines in vitro (CI < 0.8). In vivo application of 20 MBq $^{177}$Lu-EC0800 impaired kidney function 6 months as demonstrated by a significantly reduced renal uptake of $^{99m}$Tc-DMSA and elevated plasma levels of blood urea nitrogen. Pre-injection of subtherapeutic amounts of PMX (0.4 mg) protected kidneys effectively as demonstrated by parameters which were in the same range as those of untreated control animals. Therapy studies revealed a 3-fold more pronounced anticancer effect and 25% increased survival if $^{177}$Lu-EC0800 was combined with therapeutic amounts of PMX compared to the combination with subtherapeutic amounts of PMX. **Conclusion:** In this study it was for the first time possible to demonstrate the favorable effect of PMX to protect kidneys from radiotoxic side effects of $^{177}$Lu-folate therapy. Moreover, we demonstrated that PMX enhances the therapeutic effect of FR-targeted radionuclide therapy. These findings proved the anticipated dual role of PMX.

## OP103

### Synergistic anti-cancer response to chemotherapy and $^{177}$Lu-labelled APOMAB® radioimmunotherapy in a preclinical model of lung cancer.

**A. H. Staudacher**[1], M. P. Brown[1,2,3]; [1]Experimental Therapeutics Laboratory, Hanson Institute, Adelaide, AUSTRALIA, [2]Cancer Clinical Trials Unit, Royal Adelaide Hospital, Adelaide, AUSTRALIA, [3]School of Medicine, University of Adelaide, Adelaide, AUSTRALIA.

**Aim**: We have identified a murine monoclonal antibody (APOMAB®) which targets the La antigen. La is a ribonucleoprotein which is over-expressed in malignancy and is only accessible to antibody binding when tumour cells die, making APOMAB® a dead tumour cell-specific marker. We hypothesise that APOMAB® radio-labelled with the β-particle emitting radionuclide Lutetium-177 ($^{177}$Lu) will be an effective anti-tumour treatment *in vivo*, particular after chemotherapy, as the targeting of radio-labelled APOMAB® specifically to dead tumour cells within the tumour tissue will result in the surrounding viable tumour cells being irradiated with a therapeutic dose of β-radiation. **Material and Methods**: The binding of APOMAB® to viable and dead murine Lewis Lung cells (LL2) was examined *in vitro* by flow cytometry. Subsequently, C57Bl/6 mice bearing syngeneic LL2 tumours were treated with chemotherapy (gemcitabine/cisplatin) and the tumour uptake of biotinylated APOMAB® was determined. We then administered escalating activities of $^{177}$Lu-labelled APOMAB® or a $^{177}$Lu-labelled isotype control antibody either alone or 24 hours after chemotherapy and monitored tumour growth and survival. We also analysed the bio-distribution of $^{177}$Lu-labelled APOMAB® in LL2 tumour-bearing mice which had or had not been treated with chemotherapy to determine whether the uptake of APOMAB® after chemotherapy treatment was tumour-specific. **Results**:*In vitro* analysis revealed that APOMAB® did not bind viable LL2 cells, but bound with high avidity to cisplatin-treated, dead LL2 cells. Chemotherapy increased tumour cell death *in vivo*, and was associated with increased tumour uptake of APOMAB® compared to LL2 tumour-bearing mice that did not receive chemotherapy. Administration of escalating doses of $^{177}$Lu-labelled APOMAB® alone to tumour-bearing mice was well tolerated but showed only modest anti-tumour activity which was comparable to the response seen after chemotherapy. However, combination of chemotherapy and $^{177}$Lu-labelled APOMAB® had a synergistic response, resulting in a significant decrease in tumour growth and increased survival of tumour-bearing mice. Bio-distribution analysis revealed that radio-labelled APOMAB® targeted tumour tissue, and chemotherapy specifically increased tumour uptake of radio-labelled APOMAB®. Importantly, chemotherapy was not associated with increased normal tissue uptake of radio-labelled APOMAB®. **Conclusions***:* We have demonstrated both *in vitro* and *in vivo* that APOMAB® is a dead tumour-cell specific antibody, and that $^{177}$Lu-labelled APOMAB® is a safe and effective anti-cancer treatment when combined with chemotherapy. Given the safety and efficacy of a single cycle of β-radioimmunotherapy, multiple cycles of treatment, the substitution of an alpha-emitting radionuclide, or both, may provide further benefit and increase the anti-tumour response.

406 - Sunday, Oct. 20, 14:30 - 16:00, Grand Salon Prestige Gratte-Ciel

## Molecular & Multimodality Imaging: Hybrid Imaging - Image Processing & Quantitation

## OP104

### Development of PET in Western Europe

**A. N. Stevens**; Medical Options, London, UNITED KINGDOM.

**Aims** To track the development of PET in Europe. The provision of PET and PET/CT in Europe is extremely heterogeneous with a large variation in scans per head of population between countries; while within countries workload varies widely between different providers. The high level of variation between facilities, the number of new installations and the rapid growth in workload at existing sites precluded a sampling approach and required identification of all European PET providers. **Materials and Methods** Facilities with PET, PET/CT and or cyclotron(s) were identified from a number of sources including records of the IAEA,

manufacturers of diagnostic equipment and sites providing nuclear medicine services. Sites were invited to describe their operation including their equipment profile, the number and types of patient studies performed and their use of radiotracers. We were able to identify over 95% of the PET, PET/CT and cyclotrons operating in Western Europe. 67.5% of these sites provided workload numbers for 2012. To project total workload we employed a segmentation scheme for each country or region which identified ten types of facility allowing us to estimate more accurately patient numbers at sites who did not contribute workload data. **Results** In 2012 there were 577 providers of PET and/or PET/CT in Western Europe of which 18 were mobile. PET/CT accounted for 92% of the installed systems. PET cameras were located in countries where reimbursement or replacement was regulated and in research departments. PET/MR accounted for 0.02% of systems. FDG accounted for 95% of the studies. Of the FDG studies the majority 92% were oncology. Fluorinated molecules made up the majority (49%) of other compounds and are used at ~33% of sites. F-Choline accounted for 62% of these fluorinated studies. NaF studies accounted for less than 10%. Carbon 19% and Gallium 17% were the other significant nuclei in use. Scan numbers rose by 19.6% from the 921,000 scans estimated for 2010 but is slowing as the technique matures. There are wide variations across Europe both in terms of scans performed and patient throughput. In some cases this is due to reimbursement and in others working practices and patient catchment. **Conclusions** Across Europe there is an opportunity to double the use of FDG if the proportion of patients in regions with low adoption meets that of high adopters. The growing use of compounds other than FDG bodes well for the Introduction of new molecular entities over the coming years.

## OP105

### Variation in Thoracic Lesions SUVmax as a Function of Respiratory Phase Based on the Optical Flow Motion Estimation: A Simulation Study Using 4D XCAT Phantom

P. Geramifar[1], **M. Shamsaei Zafarghandi**[1], M. R. Ay[2,3,4]; [1]Faculty of Nuclear Medicine Engineering and Physics, Amir Kabir University of Technology, Tehran, IRAN, ISLAMIC REPUBLIC OF, [2]Medical Imaging Group, Research Center for Molecular and Cellular Imaging, Tehran University of Medical Sciences, Tehran, IRAN, ISLAMIC REPUBLIC OF, [3]3Department of Medical Physics and Biomedical Engineering, Tehran University of Medical Sciences, Tehran, IRAN, ISLAMIC REPUBLIC OF, [4]Research Center for Nuclear Medicine, Tehran University of Medical Sciences, Tehran, IRAN, ISLAMIC REPUBLIC OF.

**Aim**: This study introduces an optical flow based method for estimating the respiratory induced voxel motions as a function of CT respiratory phase. We investigated the impact of respiratory motion on thoracic tumor quantification in terms of SUVmax and determined the SUVmax variations for different respiratory motion traces and various lesion sizes in different locations of the lung. **Methods**: Respiratory motion traces were simulated based on the common patient breathing cycle and three diaphragm motion amplitudes of 15 mm, 25 mm and 35 mm as used to drive the 4D XCAT phantom. Spherical Lesions with diameters of 15 mm, 21 mm and 27 mm were simulated in different locations of the lung. The optical flow method, a deformable image registration, was used to estimate the respiratory induced voxel motions and calculate the motion field as a function of respiratory phase for 10 phases of CT breathing cycle. The generated PET sinograms based on analytic simulation were subsequently corrected for attenuation using the CT images generated by averaging of the respiratory cycle to prevent the effect of misalignment between CT and PET images. Attenuation correction and reconstruction of PET images were performed using the STIR package. The lesions SUVmax were then measured and analyzed for each respiratory phase. **Results:** The lesion motion vectors and the SUVmax percentage change were consistently larger in the Superior Inferior direction. The maximum SUVmax change was 27% for the 15 mm lower lung lesion in its extreme phase of inhalation. The SUVmax variations for end inhalation were nearly significant for all simulated lesions except for the upper and the middle lung lesions were the variations were lower than 5%. Meanwhile, the SUVmax variations are smaller during the exhalation phases and the least variations were belonging to the upper lung lesions in the middle phase of exhalation. **Conclusion**: Our results show that optical flow method could precisely calculate the maximum displacements of the tumor motion in respiration. The results also show that increased variation in SUVmax has a significant degree of association with the amplitude of the motion field and the percentage change was higher with lower lobe lesions.

## OP106

### The Effects of Single Photon Contamination in FDG PET

**A. Hughes**; Royal Preston Hospital, Preston, UNITED KINGDOM.

**Aim** Many cancer patients, especially those enrolled on clinical trials, are often subjected to a range of imaging procedures which require multiple hospital visits. Being able to perform several examinations in one visit has advantages for both the patient & the hospital. The Aim of this study was to investigate whether the presence of single photon tracers in the patient from a prior nuclear medicine study can affect FDG PET studies. **Method** Three phantom arrangements were used in the study. (a) NEMA PET phantom (NU2) without inserts and filled with a uniform solution of F18. Localised Tc99m soources (20ml in a 50ml syringe) were then attached to the outer surface of the phantom. The measurements were repeated with I131 replacing Tc99m in the syringe (b) NEMA PET phantom filled with uniform solutions of both F18 & Tc99m. (c) NEMA IEC body phantom with all spheres filled with F18 (contrast 4:1). Increasing amounts of Tc99m were then added to the body of the phantom. All data were acquired on a GE Discovery STE PET/CT scanner in 3D mode. For each dataset the maximum and mean SUV were calculated along with image uniformity and image contrast. **Results** (a) Increasing levels of single photon tracer in the PET FOV decreased both the maximum & mean SUV, but had no effect on image uniformity. The activity needed for a 2% reduction in SUV was 250MBq Tc99m and 160MBq I131 respectively. (b) Uniform distributions of Tc99m within the phantom decreased the calculated SUV to a similar extent as localised sources on the periphery, but had no effect on uniformity. (c) For activities up to 100MBq Tc99m in the PET FOV there was a ~1% reduction in the maximum & mean SUV for each sphere, but no change in measured image contrast**. Conclusion** The presence of single photon tracers in the detector FOV can introduce dead time effects in FDG PET. For typical nuclear medicine procedures where the activity of Tc99m in the FOV is likely to be ≤100MBq the SUV is decreased by ≤1% with no change in image uniformity or contrast. Furthermore, these effects were independent of the source distribution. Therefore, it is feasible to perform both SPECT & PET studies on the same day with no loss of diagnostic information. However, FDG PET immediately following iodine therapy may need to be avoided as I131 doses ≥400MBq will decrease the SUV by ≥5%.

## OP107

### Impact of CT Dose Reduction Strategy on CT Diagnostic Value in Oncologic PET/CT

**A. Ross**[1], E. Tonkopi[1], A. MacDonald[2]; [1]Dalhousie University, Halifax, NS, CANADA, [2]Capital District Health Authority, Halifax, NS, CANADA.

**Aim**: Our hypothesis was significant dose reduction could be obtained from the CT component of PET/CT studies with no significant impact on the diagnostic information provided by this component of the exam. **Methods**: All data were acquired on a GE Discovery STE 16 PET/CT scanner. The CT protocol used at installation was that recommended by the vendor for attenuation correction and anatomic localization. Modification of scanning parameters was performed in three steps with decrease in x-ray tube rotation time from 0.8 s to 0.5 s; x-ray beam collimation changed from 16x0.625 to 16x1.25 and pitch from 1.75:1 to 1.35:1; and the noise index increased from 25 to 27.1. Resultant dose reduction was estimated from the dose length product (DLP) values from the scanner-generated dose reports and conversion factor. Twenty six patients who had studies before and after optimization were included in the image quality analysis. All patients maintained the same weight between examinations and were scanned in the same position. Studies were anonymized and reviewed by an experienced PET/CT interpreter blinded to the acquisition parameters. Images of the region of primary pathologic concern were graded for diagnostic quality of the CT component and their usefulness for anatomic localization. A 4-point system of diagnostic acceptability as follows was used: score of 1 - nondiagnostic ; 2 - suboptimal ; 3 - acceptable; and 4 - excellent. Mean values and standard deviations were determined in each category, and a two-tail paired t-test with a probability level of 0.05 used to evaluate the difference between two patient samples in each graded category. Results: Comparison of the WB CT dose used for attenuation correction and anatomic localization of the PET data demonstrated a 32% reduction of mean CT radiation dose for the patients studied: CTDIvol decreased from 6.4±2.4 mGy to 4.3±1.6 mGy, and effective dose was reduced from 8.0±3.3 mSv to 5.5±2.1 mSv. Analyses of the diagnostic acceptability of the CT images for the region of primary pathology pre and post dose optimization demonstrated no statistically significant difference between exams. Anatomic localization gave a P= 0.820 and structural detail in the area of pathology was P=.653**. Conclusion**: A dose reduction strategy for the CT compnent of a PET/CT resulted in an overall reduction of 32% and had no statistically significant effect on the diagnostic information of the CT in the region of primary pathologic concern.

## OP108

### Image quality characterization of time-of-flight information and point-spread-function recovery in PET imaging

**S. Gnesin**[1], J. Delacoste[1], P. Martinez[1], C. Praz[1], M. Pappon[2], J. O. Prior[2], S. Baechler[1], F. R. Verdun[1]; [1]Institute of Radiation Physics, Lausanne University Hospital, Lausanne, SWITZERLAND, [2]Department of Nuclear Medicine, Lausanne University Hospital, Lausanne, SWITZERLAND.

**Aim**: Latest generation commercial PET devices incorporate the time-of-flight (TOF) information and the point spread function (PSF) recovery to improve the image quality and the quantitative accuracy of PET images. The purpose of this study was to investigate the true impact of TOF-based reconstruction algorithms and PSF

correction used in the clinical setting**. Materials and Methods**: We characterised the performances of TOF and PSF information in terms of recovery coefficients (RCs), image noise estimated by the coefficient of variation (COV), and contrast. A GE Discovery 690 PET/CT (GE Healthcare) was used to image 18F-FDG-filled standard NEMA IEC body phantoms (activity concentration 2:1, 4:1 and 10:1) using clinical reconstruction parameters used in oncology. A custom chest phantom was used to better characterise the impact of TOF information and PSF recovery in cold regions of clinical interest. We also explored whether PSF recovery lead to any quantitative bias. Furthermore, we varied reconstruction parameters (number of iterations, image smoothing, and integration time) to identify optimal reconstruction parameters for oncologic PET imaging. Results: TOF increased cold lesions contrast by 20% as compared to non-TOF reconstructions and improved the quantitative accuracy in cold regions (lung inserts). No appreciable benefit of TOF was found in terms of COV and RCs. PSF recovery (as compared to non-PSF corrected images) significantly improved hot lesion contrast and RCs, in particular for small-sized lesions (~30% RC improvement for lesions <10 mL) and contributed to reduce image noise (20% COV reduction in average as compared to non PSF-recovered reconstructions). The reduced spatial correlation of noise (inherent to TOF) and improved spatial resolution (inherent to PSF) contributed synergistically and dramatically to reduce partial volume effects. Quantitative bias, potentially affecting SUV quantification, was observed at the edge of large (>10mL) hot lesions. However PSF recovery induced artefacts (ringing/edge) can be controlled by adopting appropriate image smoothing. **Conclusions**: Our results suggest the synergistic use of TOF information and PSF recovery that demonstrate the best overall quantitative performances provided appropriate image smoothing and iterations are used. Under these conditions, image quality can significantly be improved and patient dose potentially reduced thanks to favorable noise behavior and reduced PVE effects.

## OP109

### Optical Flow Based Method for Generation of Virtual Average CT: A Simulation Study Using 4D XCAT Phantom

**P. Geramifar**[1], M. Shamsaei Zafarghandi[1], M. R. Ay[2,3,4]; [1]Faculty of Physics, Amir Kabir University of Technology, Tehran, IRAN, ISLAMIC REPUBLIC OF, [2]Medical Imaging Group, Research Center for Molecular and Cellular Imaging, Tehran University of Medical Sciences, Tehran, IRAN, ISLAMIC REPUBLIC OF, [3]Department of Medical Physics and Biomedical Engineering, Tehran University of Medical Sciences, Tehran, IRAN, ISLAMIC REPUBLIC OF, [4]Research Center for Nuclear Medicine, Tehran University of Medical Sciences, Tehran, IRAN, ISLAMIC REPUBLIC OF.

**Aim**: Averaging the CT data over many respiratory cycles, derived from cine average CT (CACT), reduces the respiratory-induced artifacts and misalignments in the attenuation corrected PET image during CT-based attenuation correction. However, the radiation dose to patients is higher with CACT. This study introduces an optical flow based method that uses two low dose CT images in order to virtually generate average CT (VACT) for PET image attenuation correction. **Methods**: Using the digital 4D XCAT phantom, we simulated different respiration motions and produced 10 phases of CT breathing cycle and respiration averaged CT (ACT) as a surrogate for the true values. Each time, two of the generated breathing phases, one in the inhalation phase and another one in the exhalation phase, were used as the two original phases. The optical flow method, a deformable image registration, was used to estimate the respiratory induced voxel motions and calculate a voxel-to-voxel motion matrix between aforementioned original CT sets. The VACT is then generated form the motion matrix and the original CT phases. Using four different pairs of inhale/exhale CT phase and their corresponding calculated velocity field, four VACT image entitled VACT1 to VACT4 were generated. For analytic simulation, the PET sinograms with attenuation modeling were then corrected for attenuation with generated maps from ACT and VACT images. Attenuation correction and reconstruction of PET images were performed using STIR (Software for Tomographic Image Reconstruction). The stationary (no respiratory motion) PET/CT image was also reconstructed as the "stationary truth" value for the quantification done by visual assessment, mutual information (MI), and standardized uptake value (SUV). **Results**: The PET reconstructed images with attenuation correction using ACT showed least difference as compared to the stationary truth, followed by VACT1, VACT3, VACT4 and VACT2, each generated by different original phases. The MI and SUV differences between VACT1 and ACT were 2% and 6.5% respectively. With a slight misplacement of the exhalation phase, VACT3 and VACT4 were still comparable to VACT1 with MI and SUV differences of 4% and 9% respectively. The maximum SUV difference between the use of different pairs of VACT and ACT was 23%, and it was less than 14% between the use of ACT and the stationary truth. **Conclusion**: This feasibility study shows VACT could be a suitable approximation on CACT with lower patient dose for CACT of PET data, where reduces misalignments artifact and improves the quantification accuracy in PET/CT.

## OP110

### The perfusion and metabolic characteristics of various tumors as assesed by dynamic FDG PET

**M. Tuncel**, O. Kupik, B. Erbas; Hacettepe University, Ankara, TURKEY.

**Aim**: Blood flow of tumors can be quantified using 15-H2O PET. However, it is not readily available in many centers and not practical for routine studies. It has been suggested that first-pass uptake of 18F-FDG might provide an estimate of perfusion of tumor and well correlated with 15H2O. Therefore, we Aimed to investigate the pattern of early 18-FDG uptake in various tumors by the means of dynamic 18-FDG PET/CT study. **Materials and Methods**: Dynamic 18 FDG PET/CT study was performed in 27 patients (49±11yrs) with various tumors ranging from 20 mm to 100 mm. According to type of tumor, patients were divided into 3 subgroups; breast ca (n=12), lung ca (n=7) and others (n=8). Serial images were obtained following i.v. injection of 18FDG for 30 minutes. Time activity curves were generated using ROIs drawn on tumor, contralateral normal tissue and aortic arch. Slope of the curves and SUVmax values for 2., 5., 10., 30.minutes were calculated. Using 2nd minute data, perfusion volume (PV) and perfusion index (PI=SUVmeanxvolume) values were calculated. SUV max and SUV mean values were obtained using standard PET/CT images and corrected for body wight (bw), lean body mass(lean) and body surface area(bsa). In addition, metabolic volume (MV) and glycolytic index (GI=SUVmeanxvolume) were measured using standard PET/CT data. **Results**: SUVmax values were increased gradually from 2.min to 30 min.(SUV2:2.77±1.4, SUV5:3.28±1.6, SUV10:3.9±2.1, SUV30:5.7±3.7, respectively). Slope of the tumor curve had a significant correlation with SUV5 (r=0,74), SUV10 (r=0,87), and SUV30 (r=0,95) values. Perfusion volume (11±16) and metabolic volume (33±44) differed significantly (p=0.01), as well as perfusion index (21±45) and glycolytic index (221±343) (p=0.004). There was significant difference between subgroups. Breast tumor groups had lower values for SUV2, SUV5, SUV10, SUV30 than other tumors, but not for PV and PI. SUVmean lean and SUV mean bsa was also different between subgroups, being lower in breast tumors (2.6±1,2 vs 4,9±1,3 and 0,9±0,4 vs 1,6±0,4). **Conclusion**: Tumor hemodynamics can be evaluated using dynamic 18-FDG PET/CT study. It can be easily performed in addition to standard PET/CT imaging.

407 - Sunday, Oct. 20, 14:30 - 16:00, Salon Pasteur

## Conventional & Specialised Nuclear Medicine: Bone Infection & IBD

## OP111

### Diagnostic value of FDG PET/CT in diabetic patients with suspicion of foot osteomyelitis.

**M. A. DUFOUR**, P. VIAU, R. MERIC, E. BERNARD, M. RAZZOUK; CHU de Nice - Hopital l'Archet, Nice, FRANCE.

**Aim**: The gold standard of diabetic foot osteomyelitis (OM) is bone biopsy. However, it is not performed in clinical routine (painful procedure, risk of haemorrhage, bone sample contamination). The Aim of this study is to evaluate the FDG PET/CT performances in the detection of diabetic foot osteomyelitis. **Materials and Methods**: The retrospective study included 10 patients with diabetis mellitus type 2 (range: 48-84 yo) with suspected foot osteomyelitis. The locations of suspected osteomyelitis were the forefoot (3 ptts), the midfoot (2 ptts) and hindfoot (4patts). They underwent FDG PET/CT on the same machine (GE discovery ST). None of the patients were withdrawn from the study because of high blood glucose levels. One patient was excluded because he had undergone a bone biopsy and 6 weeks antibiotics before PET. The most important criterion for interpretation was the precise anatomic localisation of FDG uptake on the fused PET/ CT images in order to distinguish between soft tissue infection and osteomyelitis. The final diagnosis was based on clinical follow-up and other imaging modality. Most patients had deep soft tissue biopsy but no bone biopsy. **Results** : FDG PET/CT localised correctly 6 foci to bone stuctures in 6 ptts, consisting with the diagnosis of osteomyelitis and 3 ptts with FDG uptake limited to soft tissue infection, excluding bone involvement. The mean SUVmax was 6.7 (range 3.9-13.6) in OM and 3.7 (range 2.6-6.7) in soft tissue infection. The two patients who had the lowest SUVmax in OM and soft tissue infection had the highest blood glucose levels . Patients with soft tissue infection had no evidence of an infectious process on clinical follow-up after 3 weeks of antibiotics. 4 of 5 patients were cured from OM after 6 weeks of antibiotics and imaging follow-up and only 1 patient had a recurrence of foot infection. One patient with suspected OM is still on antibiotics. In our short series of patient, the FDG PET/CT accuracy in differentiation of OM from soft tissue infection was 100%. **Conclusion** : Our results are concordant with some recent studies. FDG PET/CT can be considered as a useful, simple and non invasive imaging modality for detection of diabetic foot infection. It can help to accurately differentiate between osteomyelitis and soft-tissue infection.

## OP112

### Dual time point imaging with F-18 FDG-PET/CT in Spondylodiscitis

**B. Yilmaz Gunes**[1], C. Onsel[1], S. Sager[1], M. Halac[1], K. Sonmezoglu[1], F. Tabak[2], R. Ozaras[2], B. Mete[2], B. Kanmaz[1]; [1]1. Istanbul University, Cerrahpasa Medical Faculty, Department of Nuclear Medicine, Istanbul, TURKEY, [2]2. Istanbul University, Cerrahpasa Medical Faculty, Department of Infectious Diseases and Clinical Microbiology, Istanbul, TURKEY.

**Purpose***:* Spondylodiscitis (SPD) is an infectious processes of the vertebral bodies and intervertebral discs. FDG PET/CT is a promising imaging method that may outreach the diagnostic challenges in SPD. However, the uptake of FDG is shown to be not only in malignant tissues but also in infectious lesions. Dual time point imaging is said to be useful in differentiating malignant from infective lesions by showing declining of the activity in delayed images. The Aim of our prospective study was to investigate the value of dual time point imaging with FDG-PET/CT in the diagnosis of SPD. **Materials and Methods***:* Nineteen patients (nine female, ten male, mean age 55,5 ±18,8 ) with suspected SPD referred to our unit for FDG-PET/CT scan between December 2009 and January 2012. PET/CT studies were performed with a 6-slice multidetector CT integrated high-resolution PET system. After fasting state, 11-21 mCi FDG was injected intravenously. First images were obtained approximately after ninety minutes (early) and second imaging was performed approximately after seventy-five minutes (delayed). The SUV max values were obtained in early (SUVmax1) and delayed images (SUVmax2). **Results:** All patients had the final diagnosis of SPD. In diagnosed SPD patient population, the mean early SUVmax1 of FDG was 11,1 (SD ± 5,1) and the mean delayed SUVmax2 of FDG was 10,9 (SD ± 5,2). In only 3 patients, SUVmax levels decreased over time. No statistical difference was found between early and delayed SUVmax results of 19 patients (p>0,05). **Conclusion***:* Our preliminary data suggest that dual time imaging might be insignificant in discriminating malignant from infectious lesions.

## OP113

### FDG PET/CT Imaging in Diabetic Foot Infections

**D. Franceschi**, R. Matthews, V. Brunetti, A. M. Franceschi, E. Safaie, C. J. Carcamo, N. K. Relan; Stony Brook University Hospital, Health Sciences Center, STONY BROOK, NY, UNITED STATES.

**Introduction**: Osteomyelitis is a common complication of diabetic foot Infections. Accurate diagnosis of osteomyelitis in the setting of complicated diabetic foot is a diagnostic challenge. We evaluated the use of FDG PET/CT to determine bone involvement in diabetic patients with chronic foot infection. **Material and Methods**: Thirty nine diabetic patients with chronic foot infection (24 men and 15 women; age range, 21-84y) were studied using dedicated, high resolution FDG PET/CT imaging of the feet. In 17 patients surgery was performed and the final diagnosis was determined based on surgical and histopathologic findings. **Results**: PET/CT findings indicated bone involvement in 27 patients, and excluded osteomyelitis in 12 patients. Abnormal focal FDG uptake was found in the bones in all 13 patients with surgical or histopathologic diagnosis of osteomyelitis. PET/CT correctly excluded osteomyelitis in 3 patients with no histopathologic evidence of osteomyelitis. In 1 patient with focal FDG uptake in the bone there was no definite findings of bone infection on histopathology. Sensitivity of FDG PET/CT was 100% and specificity 75% with overall accuracy of 94%. **Conclusion**: In our experience FDG PET/CT proved to be highly accurate in the diagnosis of osteomyelitis in diabetic patients with chronic foot infections.

## OP114

### Usefulness of 99m-Tc-HMPAO Leukocyte Scintigraphy in Paediatric Patients with Inflamatory Bowel Disease

**A. MARTINEZ LORCA**, M. DE GREGORIO VERDEJO, M. MARIN FERRER, Y. RAMIREZ ESCALANTE, M. CORONADO POGGIO, C. ESCABIAS DEL POZO, L. MARTÍN CURTO; HOSPITAL UNIVERSITARIO LA PAZ, MADRID, SPAIN.

**Aim** The Aim of this study is to asses $^{99m}$Tc-HMPAO leukocyte scintigraphy findings as a useful test for the diagnosis or control activity in paediatric patients with suspicious of inflammatory bowel disease (IBD). **Material and Methods** $^{99m}$Tc-HMPAO leukocyte scintigraphy studies were evaluated retrospectively between February 2008 and January 2013 in 49 children (p), 30 boys and 19 girls from 2 to 17 years (mean age: 12.61±3.99). Scintigraphy was performed as part of the initial diagnostic work-up of IBD (47/49p) or re-evaluation of their disease (2/49p).Radiobelled leukocyte scintigraphy with $^{99m}$Tc-HMPAO was undertaken using conventional protocols in our Radiopharmacy Unit and the dose being scaled in proportion to body weight. Anterior abdomen and pelvis images and caudal images were acquired at 30 minutes and 3 hours after injection of the labelled blood sample by using a single-headed gamma camera. The leukocyte scintigraphy was reported as positive, negative or undefined using this qualitative score due to isotope uptake. The anatomical area of inflammation was noted involving 6 segments (stomach/duodenum; small intestine; right colon; transverse colon; descending colon and sigmoid colon/rectum). The final diagnosis of IBD were considered by histopathology features (42p; 85,71%) or clinical follow-up for at least 24 months (7p, 14,28%). **Results** In relation with the isotope uptake localization (20 studies positive uptake): 4 small intestine and right colon, 9 right colon, 2 colon frame, 1 right and transverse colon, 1 right and descending colon, 3 sigmoid colon/rectum. As a diagnostic test in children with suspected IBD leukocyte scintigraphy has found 15/49p true positive (10/15p Crohn´s Disease, 3/15p Ulcerative Colitis, 2/15 IBD non-defined); 26/49p true negative (7/26p clinical follow-up without outbreak, 6/26p no histological findings, 9/26p unspecific inflammation, 2/26p follicular lymphoid hyperplasia, 1/26p intestinal atrophy, 1/26p bacterial translocation); 4/49p false positive for IBD (2/4p no histological findings, 2/4p acute and chronic inflammation) and 3/49p false negative (2/3p Crohn´s Disease, 1/3p Ulcerative Colitis). 1/49p was undefined (positive leukocyte scintigraphy and biopsy studied from other localization). Leukocyte scintigraphy was found to have a sensitivity, specificity, positive predictive value and negative predictive value of 83,33%, 86,67%, 78,95% and 89,66%, respectively. **Conclusion** Our results suggest that $^{99m}$Tc-HMPAO leukocyte scintigraphy is a valuable and complementary technique for detection and localization of IBD, although the number of paediatric patients is reduced.

## OP115

### Contribution of the SPECT and SPECT/CT with radiolabeled leucocytes in the evaluation of the inflammatory bowel disease

**O. Puig**, J. Martin-Comin, A. Benítez Segura, A. Sabaté-Llobera, P. Notta, T. Lobatón, L. Camacho Berné, R. Puchal, J. Guardiola Capo; Hospital Universitari de Bellvitge, Hospitalet de Llobregat, SPAIN.

**Objective** To evaluate the contribution of the SPECT and SPECT-CT over the planar scintigraphy with radiolabelled leucocytes in assessing the degree of activity and the extent in the inflammatory bowel disease (IBD). **Material and Methods** 44 studies were performed in 28 patients (64% male) with IBD (89% ulcerative colitis, 11% Crohn's disease) at different stages. Autologous leukocytes were labeled with 99mTc-HMPAO according to the method proposed by the ISORBE. Planar images were acquired in anterior and caudal projections at 30 and 180 minutes p.i. and an abdominal SPECT / CT at 180 minutes. Two groups of physicians determined the number of affected segments, its intensity and a scintigraphic activity index (SAI) in both planar imaging and SPECT or SPECT-CT if needed. When both groups had different results, studies were evaluated by a third doctor. **Results** We obtained a Kappa index of 0.91 in the assessment of the SAI using the planar images and a 0.84 when using the SPECT. In 11 studies the SAI was the same in the planar and SPECT images. In the 33 remaining studies differences were found in the assessment of activity and, on 22 of them also of the extension, both being higher in the SPECT. In 3 studies the SPECT obtained a positive result when the planar study was negative, in 4 the SPECT dismissed intestinal involvement when the result of the planar image was interpreted as positive. The SPECT-CT was found to be useful in the assessment of 24 studies (55%). **Conclusion** The diagnosis using both planar and SPECT studies obtained a very good agreement between the two groups of observers in the evaluation of the SAI being slightly higher when using the planar study. The SPECT showed a higher number of affected segments and more activity the same affected segments over planar scintigraphy. The CT was considered useful in assessing the localisation of the affection in 55% of the studies but was not considered essential for diagnosis.

## OP116

### Assessment of Crohn's disease activity by FDG PET-CT and Tc-99m HmPAO labeled white blood cell SPECT-CT in a prospective study

**L. Galuska**[1], S. A. Kiss[1], N. Fedinecz[2], K. Palatka[3], S. Lovas[4], I. Garai[2], J. Varga[1]; [1]Department of Nuclear Medicine, University of Debrecen MHSC DEBRECEN, HUNGARY, [2]ScanoMed Ltd, DEBRECEN, HUNGARY, [3]Department of Internal Medicine, Gastroenterology, University of Debrecen MHSC, HUNGARY, [4]Department of Internal Medicine, Gastroenterology2, University of Debrecen MHSC, HUNGARY.

**Objectives.** Crohn's disease (CD) may start and persist at different parts of the gastrointestinal tract. The endoscopic evaluation is the gold standard to assess inflammatory lesions, but it is limited in the small bowels and in characterizing the inflammatory activity (IA) in the whole abdominal cavity that is crucial for staging, prognosis, treatment and follow up. A good sensitivity and specificity of $^{18}$F-FDG PET-CT (PET) was shown in pilot studies in detecting lesions of CD. White blood cell $^{99m}$Tc-HmPAO labeling (WBC) is also known as an effective method for identifying inflammatory sites. Our Aim was to assess the value of PET for determining the location and inflammatory activity of CD, and compare them with the WBC SPECT-CT results. **Patients.**Eleven non-treated patients with active CD (18-39, mean 25 years old; 6 M, 5 FM) were entered into the prospective study, with a Clinical Disease Activity Index (CDAI) above 300, and ileocolonoscopic results typical of CD. **Methods**. Ileocolonoscopy, FDG PET (TOF PET-CT, Philips) and WBC-SPECT-CT (Anyscan, Mediso) were performed within 2 weeks, before and 10-11 months after the initiation of biological immunosuppressive therapy. (Only 4 patients had a second SPECT study.) The FDG SUV score (bowel SUV/liver SUV from 0 to 3) of the

PET and activity uptake score of SPECT-CT (bowel CPS/ background CPS from 0 to 2 ) were calculated for the terminal ileum, 3 colon and a sigma bowel region. The summarized scores of these 5 segments gave the global PET and SPECT scores, which were compared to the Simple Endoscopic Score **(**SES-CD) and CDAI before and after treatment. **Results.**CDAI, SES-CD ($p<0.001$) and PET score values ($p<0.01$) decreased significantly as a result of the therapy (paired t-test), to 33% (SD 22%), 32% (SD 22%) and 52% (SD 37%) of the initial values, respectively. Neither the initial scores, nor the absolute or relative changes of the different parameters correlated with each other significantly; the initial values of SES-CD and the SPECT score were closest to significant correlation (Kendall's tau-b, $p=0.07$). Initially SPECT showed significantly less abnormal segments than either PET ($p<0.05$) or SES-CD $p<0.01$). **Conclusions.** PET is a promising tool for the management of CD patients, who may benefit from staging before and after systemic therapies. However, further studies are needed to compare the diagnostic efficiency of different modalities.

## OP117

### Role of 18F-FDG PET/CT in diagnosis of possible septic endoprosthetic arthroplasty loosening.

**J. M. Nogueiras Alonso**, O. Rivas Domínguez, C. Castillo Berrio, D. Ruiz Hernández, A. Serena Puig, L. Campos Villarino, F. Loira Bamio, R. Guitian Iglesias; Hospital do Meixoeiro, Vigo, SPAIN.

**Objective**: Our intention is to determine the value of 18F-FDG PET/CT in the differentiation between septic/aseptic endoprosthetic loosening in arthroplasty from different locations. **Methods**: Retrospective analysis of a prospective cohort. Nineteen patients with clinically suspected endoprosthetic loosening, which has been acquired a located 18FFDG-PET/TC performed in our center from 2011 to 2012.Correlated with the analytical data of ESR, WBC, CRP and the joint synovial fluid analysis before, during surgery and clinical follow-up longer than 6 months. **Results**: A total of 19 patients (4♂/15♀), with a mean age of 68.5 ± 15.6 years (27-86y). Arthroplasty located in: hip (8), knee (9), shoulder (1) and femur (1). A total of 10 patients had normal findings on 18F-FDG PET/CT, coincident with absence of infection in synovial fluid or biopsy; however the analytical results of inflammatory activity (ESR, WBC and CRP) were elevated in the majority of cases. We did not get any false negative. Nine patients with 18F-FDG PET/CT positive for inflammation showed SUVmax average value of 4,5g/ml. Of these, 8 cases had a good correlation with the analytical altered synovial fluid data and clinical signs of infection after 8 months of follow up. In one patient the result was considered as a false positive by normal synovial fluid analysis, however surgery synovial biopsies showed infection. **Conclusions**: The 18F-FDG-PET/TC is useful and highly accurate in the diagnosis of infection in endoprosthetic loosening, showing good agreement with bacteriological and histological data.

## OP118

### 18F-FDG PET-CT accuracy in osteomyelitis and prosthetic joint infections decision making and therapy monitoring

**M. CATALANO**[1], T. Ascione[2], S. Piccolo[2], M. Bifulco[2], F. Porcaro[2], C. Landolfi[2], P. Pagliano[3], G. Borrelli[3], P. Muto[3]; [1]AORN A. Cardarelli, Naples, ITALY, [2]Ospedale dei Colli, Naples, ITALY, [3]Ospedale dei Colli, Naples, ITALY.

**Introduction** Prosthetic joint infections and osteomyelitis require antibiotic and surgical therapy. The choice between different therapeutic approaches and their optimal timing are still debated. Clinical data often are doubtful and also normal C-reactive protein (CRP) value may be observed in infected pts. 18F-FDG PET-CT could play a role in decision making about antibiotic start or break and surgical management, particularly regarding antibiotic withdrawal and new surgical procedures feasibility in patients with uncertain infection diagnosis. **Aim** To evaluate 18F-FDG PET-CT accuracy in osteoarticular and prosthetic joint infections diagnosis and therapy monitoring and in prosthesis two-stage reimplant optimal timing. **Method** Patients (pts) with prosthetic joint infection (PJI) undergoing two-stage exchange or with chronic osteomyelitis were included. Infection diagnosis was based on commonly accepted criteria. Laboratory data (CRP, Erythrocyte sedimentation rate and white blood cells), microbiological data (cultures attempted form sinovial liquid, intraoperative tissue samples or swabs from sinus tract) and PET-CT scan were evaluated before antibiotic therapy beginning and 3-6 months post-therapy in patients affected with osteomielitis or prosthetic joint infection. **Results** Fifty-six (56) pts (71% males, median 60 years, range 27-78) were enrolled, 26 pts with prosthetic infection (12 hip and 14 knee prosthesis) and 30 pts with chronic osteomyelitis. At baseline, median CRP value above the normal was reported in 45 patients (median value 22 mg/dl, range 10-78) and within the normal range in 11 cases and PET-CT scan median SUV value in region of interest (osteomyelitis foci or bone-implant interface) was 7 (range 5-12) in all pts. At post-therapy follow-up 44 pts were clinically healed. In this group, in 42 pts a correlation was observed between SUV reduction and therapy efficacy, established on symptoms disappearance. Discordant results were obtained in 2 pts, where a successful therapy was instead coupled with positive PET-CT finding. In the remaining 12 cases, showing therapeutic failure, based on clinical and microbiological data, SUV was high even in presence of normal CPR value in 8 pts. **Conclusions** Because of low diagnostic accuracy of CRP value in prosthetic joint infection and osteomielitis diagnosis and follow-up , PET-CT can represent a complementary diagnostic tool, especially in presence of co-morbidity. Infact we report negative PET-CT findings (SUV <3), at post-therapy follow-up, in 75% disease free pts and positive PET-CT findings in pts with infection persistence, despite antibiotic or surgical therapy.

408 - Sunday, Oct. 20, 14:30 - 16:00, Gratte-Ciel 1/2/3

## Radionuclide Therapy & Dosimetry: Thyroid Cancer

## OP119

### Experimental peptide receptor radionuclide therapy in radioiodine negative somatostatin receptor positive thyroid cancer

**B. Nilica**, A. Kroiss, D. Putzer, C. Uprimny, B. Warwitz, D. Kendler, D. Waitz, I. Virgolini; Universitätsklinik für Nuklearmedizin, Innsbruck, AUSTRIA.

**Purpose**: This retrospective analysis evaluated the time to progression (TTP), progression free survival (PFS) and overall survival (OS) in patients with radioiodine negative thyroid cancer who had undergone peptide receptor radionuclide therapy (PRRT) with $^{177}$Lu-DOTA-TATE, $^{177}$Lu-DOTA-LAN, $^{90}$Y-DOTA-TOC or $^{90}$Y-DOTA-LAN after tumor progression. **Methods**: Data derived from twenty patients with either differentiated (n=15), anaplastic (n=1) or medullary (n=4) somatostatin receptor positive thyroid cancer who had received treatment with PRRT after tumor progression. TTP, PFS and OS were defined according to the clinical trial endpoints suggested by the FDA (Food and Drug Administration). Progressive disease was defined by sonography, FDG-PET, Ga-DOTA-TOC-PET, or CT (RECIST Criteria). **Results**: In 17 patients the median overall survival time after the first PRRT was 17.3 (range: 0.1 - 109.7) months. Three patients still alive are actually showing stable disease. The median of PFS in 20 Patients (6 with more than one PRRT-cycle or PRRT-substance) has been 10.9 (range: 0.1 - 44.0) months. The median TTP was 15.6 (range 4.4 to 29.2) months. **Conclusion**: PRRT appears to be useful in patients with somatostatin receptor positive but radioiodine negative thyroid cancer as a complementary palliative cytotoxic therapy.

## OP120

### Salivary gland dosimetry using 124I-PET/CT imaging and MIRD method.

**C. Pettinato**[1], M. Celli[2], S. Cima[3], F. Monari[3], S. Civollani[1], C. Nanni[2], V. Allegri[2], P. Zagni[2], R. Mazzarotto[3], E. Spezi[4], S. Fanti[2]; [1]AOU S.Orsola Malpighi, Medical Physics Unit, Bologna, ITALY, [2]AOU S.Orsola Malpighi, Nuclear Medicine Unit, Bologna, ITALY, [3]AOU S.Orsola Malpighi, Radiotherapy Unit, Bologna, ITALY, [4]Velindre Cancer Centre, Department of Medical Physics, Cardiff, UNITED KINGDOM.

**Aim**: Salivary gland toxicity is often of concern on radioiodine therapy of thyroid cancer. The major problem is that toxicity could occur even if the absorbed doses are below the expected limits (26 Gy for EBRT). In the past this was associated to the fact that the poor accuracy of standard dosimetric Methods, based on planar I131 images, assuming that calculated absorbed doses were underestimated. The Aim of this work was the evaluation of the feasibility of using serial 124I-PET/CT scans for the measurement of absorbed doses to salivary glands. **Material and Methods**: Twenty-five patients affected by metastatic thyroid cancer (MTC) were enrolled in a study approved by the ethical Committee of our Institution, with the Aim to evaluate the usefulness of 124I PET/CT sequential scans to predict absorbed doses to metastatic thyroid cancer patients undergoing 131I therapy. Fifteen patients had salivary glands included in the PET FOV and were used for absorbed dose measurements to submandibular salivary glands and parotids. For each of the four PET/CT scans the mean activity concentration in the glands were obtained, corrected for partial volume effect and scaled to 131I decay time. Absorbed doses were calculated using the sphere model of the MIRD formalism, with volumes segmented on CT images. **Results**: The 131I administered activity was 3700 MBq for patients presenting negative PET/CT finding and 7400-11100 MBq for patients with iodine avid metastases. Mean dose per administered 131I activity was respectively 0.67 ± 0.35 mGy/MBq and 0.56 ± 0.37 mGy/MBq for parotids and submandibular glands. The corresponding mean absorbed doses were 4.11 ± 2.55 Gy (range: 0.19 - 11 Gy) and 3.38 ± 2.62Gy (range: 0.26 - 10.3 Gy). Two patients complained for mild salivary complications and none of the patient had severe impairment. Discussion and **Conclusion**: 124I-PET/CT imaging can usefully be used for salivary gland dosimetry following the MIRD formalism. Although the values found in this work are slightly lower than similar data published in literature, they are quite below the toxicity thresholds. Considering the mean doses per unit of 131I administered activity, the toxicity limit would not be exceeded even following high dose protocols. However the clinical toxicity occurs and probably the reason

should be related with a possible higher radiosensitivity of the glands and the influence of cumulative dose due to multiple treatments.

## OP121

### Comparison between spect and planar techniques for internal dosimetry of patients submited to a thyroid ablative therapy

**S. M. Carvalho**[1], R. Biancardi[2], S. Gabbay[2], N. D. Corrêa[2], S. Rozenblum[2], C. D. Ramos[3], S. Q. Brunetto[3], S. M. V. Oliveira[1]; [1]Instituto de Radioproteção de Dosimetria, Rio de Janeiro, BRAZIL, [2]Hospital Federal dos Servidores do Estado, Rio de Janeiro, BRAZIL, [3]Universidade Estadual de Campinas, São Paulo, BRAZIL.

The absolute image quantification is the most usually method for the individualized organ dosimetry. The Aim of this study was two. First, to compare the results of image quantification based on emission computed tomography (SPECT) with the results of the conventional planar imaging quantification. Second, to compare the dose obtained by external radiation monitoring with that obtained by the whole-body quantification. The study was performed with 7 patients (48,9+11,4) years old and thyroid ablation (4,9+1,4 GBq), submited a thyroid ablative therapy. The images were performed in a dual-head gamma camera detection system. The whole-body scans were quantified by planar images conjugate-view method, single source model, attenuation correction, triple-energy windows for scatter correction and considering organs homogeneous uptake. SPECT was performed directly after the whole-body scans over the upper abdomen, with 64 projections and 40s exposure time per projection. Reconstruction was performed with OSEM algorithm (4 subsets and 2 iterations) followed by Butterworth filtering with a cut-off of 0.28 and power 14. Regions of interest were drawn with contour lines. The external radiation monitoring was performed with a Geiger-Muller detector (GM). Two different sensibility calibrations for the SPECT were performed, first with the cylinder water phantom (Jaszczak Phantom) with a centrally placed cylinder I-131 source (5ml, 37MBq), and another with the source placed in the periphery at the phantom. The sensibilities calculated with the source placed at the central and periphery at the phantom were 2.2 (ctg/µCi.Voxel) and 4.18 (ctg/µCi.Voxel), respectively. The average activity on whole-body for the 7 patients monitored with external radiation monitoring (GM) was 62.4+17,1% greater than quantification with planar imaging. The quantification of the stomach for 3 patients with planar images was 114.9+51,5% greater in comparison to SPECT. As expected, the uptake is 17.93+6,8% when using the peripheral calibration value for SPECT aquisition. For intestine, patient with great uptake in the peripheral port of the strap, the planar imaging overcomes in 253.2+143,1% the values obtained with SPECT for central calibration and in 85.9+59,7% for peripheral calibration. Otherwise, for the patient with homogeneous uptake the relatives deviations were 33.48% and 33.05% respectively. The results demonstrated that the images quantification are more accurate than external radiation monitoring for the whole-body activity estimative. Also suggest the need to use the correct calibration factor. peripheral or central, depending on the location of the organ of interest.

## OP122

### rh-TSH (Thyrogen) Aided Radioiodine Therapy in Children and Adolescents with Differentiated Thyroid Cancer.

**D. Handkiewicz-Junak**, J. Roskosz, T. Gawlik, O. Tomasz, J. Barbara; Centre of Oncology - MSC Memorial Institue, Gliwice, POLAND.

**Background.** Although recombinant human TSH (rhTSH) is widely used to aid radioiodine treatment of differentiated thyroid cancer (DTC), almost in all clinical studies it was used in adults and there are very few data concerning paediatric group of patients. The Aim of our retrospective study was to evaluate the effectiveness and safety of rhTSH-aided radioiodine treatment in DTC patients 18 yr old or younger. **Material and Methods:** Twenty five children/adolescents (median age 15, range 7-18) with the diagnosis of DTC were treated using the approved adult regimen (one 0.9 mg im. injection daily on two consecutive days) and therapeutic activity of $^{131}$I (median 3.7 GBq, range 2.2-3.8 GBq). Thyroglobulin concentration was evaluated on the 1$^{st}$ and 6$^{th}$ day of stimulation, and whole body scan (WBC) on the 6$^{th}$ day. Subsequently the patients were followed-up every 6 months, including single diagnostic $^{131}$I WBS. The median follow up after the treatment was 28 months. **Results:** In 16 children radioiodine treatment was given as an adjuvant treatment after total/near total thyreoidectomy. In another 9 children distant metastases (mainly to lungs) were recognized. Peak TSH concentration post-rhTSH exceeded 25 mU/liter in all children. In all children the peak stimulated thymoglobulin was achieved on day 6 of stimulation (median 4 ng/ml, range 0.17-1080.0 ng/ml). In children treated with radioiodine as an adjunct to total thyreoidectomy, in all but two cases complete remission was achieved. Two patients needed subsequent radioiodine retreatment. All are now free of disease. Among patients with distant metastases in 3 (33%) complete remission and in 6 (67%) partial remission (decrease in thyroglobulin concentration and decrease in radioiodine uptake on WBS) was achieved. In none but one patients there were side effects after rhTSH application. In one patient on the second day after the first rhTSH dose rush was observed, that resolved after anti-histaminic treatment. There were no signs of hyperthyreosis and in all patients fT3 was within normal range. There were no late side effects. **Conclusions**. rhTSH-aided radioiodine treatment in children/adolescents with DTC is safe and effective treatment. It allows to avoid hypothyroidism during L-thyroxin withdrawal, without any significant side effects. The so far observed results of the therapy suggest that the treatment is effective both as an adjuvant and radical treatment but longer follow up is necessary.

## OP123

### Does remnant from differentiated thyroid microcarcinoma patients really not be treated with Iodine-131 ablation?

**F. D'Antuono**[1], R. Gallicchio[1], A. Venetucci[1], A. Nardelli[2], S. Giacomobono[1], T. Pellegrino[2], A. Tempone[1], A. Di Leo[1], D. Gattozzi[3], G. Storto[1]; [1]IRCCS CROB, Rionero in Vulture, ITALY, [2]IBB CNR, Napoli, ITALY, [3]University of Texas Southwestern, Dallas, TX, UNITED STATES.

**Aim**: Remnant ablation by radioiodine is generally not recommended in patients presenting uni- or multifocal cancer <1 cm, without other higher risk features. We retrospectively studied low-risk patients (pts) with differentiated thyroid cancer (DTC) less than 1 cm recruited for radioiodine therapy (RAI). **Methods**: 91 pts (79 women, age 49.4 ± 10 yrs) with DTC were recruited for RAI. Pts underwent pre-therapy ultrasonography (US), those with suspected/ambiguous lymph-nodes were excluded and proposed for cytology. Treated pts underwent post-therapeutic whole body scan (WBSt) completed by neck/chest SPECT-CT, when necessary (e.g. evidence of uptake outside of thyroid bed). A target lesion on SPECT-CT was defined as an identifiable lymph-nodal site presenting a matched significant iodine uptake. Patients were followed up for 13 ± 2 months thereafter. **Results**: All pts/cancers were pT1. Mean histological diameter was 0.66 ± 0.25 cm. Six patients were excluded because of clear nodal involvement at US. Thirty (35%) out of 85 pts had suspicious WBSt as per lymph-nodal involvement which was confirmed at the following SPECT-CT acquisition in most part of pts (25/30; 83 %). Overall detected target lesions was 34, ten (29%) had interim positive fine needle cytology. **Conclusions**: a significant part of low risk DTC patients, for whom RAI is not recommended, presents an incidental evidence of lymph-nodal involvement at WBSt confirmed by SPECT-CT, when performed. Such setting would have not been treated by I-131. Indications for RAI in DTC low risk patients could be revised at least considering a different dimensional cut-off for the primary lesion.

## OP124

### Treatment of patients with Hürthle cell thyroid carcinoma using [Lu-177-DOTA0,Tyr3]octreotate

**B. L. R. Kam**, J. J. M. Teunissen, R. P. Peeters, W. W. de Herder, E. P. Krenning, D. J. Kwekkeboom; Erasmus MC Rotterdam, Rotterdam, NETHERLANDS.

**Aim**: Hürthle cell thyroid carcinoma (HCTC) is a variant of follicular thyroid carcinoma. Although radioiodine (I-131) is given for ablation of the thyroid remnant to enable serum thyroglobulin levels for follow-up, it is rarely used for the treatment of residual or metastatic disease, related to the Hürthle cell tumour's poor capacity of taking up radioiodine. Since thyroid tumour cells express somatostatin receptors, peptide receptor radionuclide therapy using radiopharmaceuticals such as [Lu-177-DOTA0,Tyr3]octreotate (Lu-177-octreotate) has been proposed as a potential treatment option. **Materials and Methods**: fifteen patients with pathology proven HCTC treated with Lu-177-octreotate between January 2000 and April 2012 were studied. CT or MRI scans were analysed using SWOG criteria for response outcome. Thyroglobulin levels were analysed and a decrease of more than 50% was considered as a significant biochemical response. All patients had received radioiodine to ablate the thyroid remnant. Six patients received an additional treatment dose of I-131 (total cumulative dose range: 0.7 to 14.8 GBq I-131). **Results**: Acute side effects such as nausea, vomiting, pain, and hair loss were present during 22%, 2%, 8% and 27% of all administrations respectively. WHO grade 3 bone marrow toxicity for both platelets and leukocytes was present in 2% of all treatment cycles. No long-term side effects such as myelodysplasia or kidney failure were found during a median follow-up of 25 months (range 2-119 months). Twelve patients received the intended cumulative dose (22.2-29.6 GBq) of Lu-177-octreotate whereas 3 did not, due to persisting thrombocytopenia, concomitant cardiac atrial fibrillation, or to the diagnosis of rectal adenocarcinoma as a second primary tumour. In 11 out of the 12 remaining patients sufficient follow-up data were available for evaluation. Four (36%) patients had a partial response (PR) at 3 months after the last treatment. Stable disease (SD) was found in 7 (64%) patients of whom all had progressive disease within one year prior to treatment with Lu-177-octreotate, demonstrated with either anatomical imaging (6) or an increase of more than 50% in thyroglobulin levels (1). During follow-up, a decrease of more than 50% in thyroglobulin was found in 4 patients of whom 3 also had a PR on CT or MRI. **Conclusion**: Lu-177-octreotate therapy may be effective in patients with HCTC who have non-iodine avid lesions at diagnosis considering the 36% of patients with PR. SD was accomplished in 64%, of whom all patients had proven progressive disease prior to treatment.

## OP125

### Previsional Red Marrow Dosimetry in Differentiated Thyroid Cancer with I131 and I124: is a Reliable Value?

**G. ROSSI**[1], M. Camarda[1], P. D'Avenia[1], E. Di Nicola[1], L. Montani[1], C. Bartolozzi[1], A. Dente[1], N. Gasparrini[1], E. Brianzoni[2], S. Fattori[1]; [1]Medical Physic, Macerata Hospital AREA VASTA 3 ASUR Marche, Macerata, ITALY, [2]Nuclear Medicine, Macerata Hospital AREA VASTA 3 ASUR Marche, Macerata, ITALY.

**Aim** For patients affected by with differentiated thyroid cancer (DTC) we always consider a dosimetric limit of 2 Gy/treatment for the red marrow protection. Aim of this work was to evaluate confidence between previsional and post therapy red marrow dosimetry in order to guarantee patients safety. **Material and Methods** We studied 7 patients (pts) affected by DTC at multiple treatment phase, enrolled for subsequent radioiodine therapy. For 5/7 pts we administered a trace activity of $I^{131}$ (74 MBq) and for 2/7 we administered a trace activity of $I^{124}$ (74 MBq). Then we collected 6 blood samples the week before therapy and 6 blood samples during therapy after administration of $I^{131}$ (range 5550-9213 MBq). We analyzed 10 whole body counts before and during therapy, considering the ant-post geometric mean. We calculated the residence times for blood and remainder of the body. By the use of OLINDA/EXM we had the values of dose/administered activity (mSv/MBq), allow for proportionality between blood and red marrow. **Results** We found that for 6/7 the red marrow behaviour is different from pre and post administration of radioiodine therapy. The cumulated activity were always higher during therapy till the $50^{th}$ hours and then are superimposable with the previsional ones. In one patient we found that previsional value are higher than post therapy evaluation, both for red marrow and for whole body. The variability range of the residence times between pre-and post-therapy dosimetry was 38%-84%. Regarding to whole body analysis, we found that the residence times are superimposable for 4/7 patients. For 1/4 we found a oscillating behaviour of the cumulated activity but resulting in an overlapping of the residence times pre and post therapy. For 2/7, we found a higher value during therapy, probably due to the presence of diffuse bone metastases. For 1/7 we found a lower value during therapy. No patients received a dose to the red marrow higher than the accepted limit of 2 Gy. **Conclusion** The different behaviour of red marrow residence times point out the need to validate the absorbed dose during therapy. Our work will carry on with the analysis of the follow up of the patients, with particular focus on their red marrow safety. Moreover, it is important to consider localization and uptake values of bone metastases in order to try to hypothesize the behaviour during therapy and any eventual variation in the prediction.

## OP126

### The quantitative comparison of low dose and standard dose radioiodine therapy effectiveness in patients with low risk differentiated thyroid cancer

**U. Abdulrezzak**[1], A. Tutus[1], M. Kula[1], Y. Kurt[1], E. Kocaagaoglu[1], Y. Sarıkaya[1], I. Isık[2], [1]Erciyes University, Nuclear Medicine Department, Kayseri, TURKEY, [2]Dumlupınar University, Nuclear Medicine Department, Kutahya, TURKEY.

**Background:** Currently, the lower dose radioiodine administration instead of standard 3700 MBq for low-risk differentiated thyroid cancer (DTC) is discussed. In this study, we compared the results of postoperative I-131 remnant ablation using a quantitative data in the low activity (1110 MBq; 30 mCi) and standard dose (3700 MBq; 100 mCi). **Patients and Methods**: The study included two groups of patients with low risk differentiated thyroid cancer: group 1 included 43 patients who were treated with 30 mCi I-131 and group 2 included 32 patients treated with 100 mCi (control group) for postoperative thyroid remnant ablation. In both groups, following a near total or total thyroidectomy, postoperative thyroid remnants of all patients were assessed with thyroid uptake test (TUT). Whole body scans (WBS) of all patients were performed in 7-10th days after the administering I-131 treatment for the ablation of residual thyroid. We obtained counts from ROI (region of interest) analysis of several regions (thyroid bed, liver, thigh and whole body). Thyroid/liver ratios were calculated by comparing counts that in the thyroid region to that in the liver. Sixth month whole body scans after the treatment was performed to 52 patients (24 patients of group 1 and 28 patients of group 2) for evaluating success of ablation treatment. **Results**: A significant difference in pretreatment TUT and thyroid remnant counts in post treatment scans wasn't found between both groups (p>0.05). However, in post treatment scans, liver, thigh, whole body count were significantly higher and thyroid/liver ratio was significantly lower in group 2 compared with group 1 (p<0.001). Although the percentage of ablation based on 6th month scans was higher in group 2 compared with group 1 (25 of 28 patients, %89.3 versus 17 of 24 patients, %70.8), statistical difference was not significant (p>0.05).**Conclusion**: In low risk DTC patients, low dose radioactive iodine can ablate thyroid remnant as effectively as a higher dose with other non-target organs and whole body less exposure to radiation.

409 - Sunday, Oct. 20, 14:30 - 16:00, Rhône 3A/3B

## Radiopharmaceuticals & Radiochemistry & Dosimetry: Radiopharmaceuticals - SPECT

## OP127

### [$^{111}$In-DOTA]MG11 revisited: Successful visualization of CCK2R-expressing cancer following a new concept

**M. de Jong**[1,2], T. Maina-Nock[3], A. Kaloudi[3], E. P. Krenning[1], B. A. Nock[3]; [1]Department of Nuclear Medicine, Erasmus MC, Rotterdam, NETHERLANDS, [2]Department of Radiology, Erasmus MC, Rotterdam, NETHERLANDS, [3]Molecular Radiopharmacy, INRASTES, NCSR Demokritos, Athens, GREECE.

**Aim**: Truncated gastrin radioligands lacking the $(Glu)^{6\text{-}10}$-sequence of the human heptadecapeptide gastrin, such as [DOTA]MG11 ([(DOTA)$DGlu^{10}$]gastrin(10-17)), are less prone to accumulate in the kidneys than their $(Glu)_5$-chain containing counterparts. However, they can poorly visualize CCK2R-expressing cancer in animal models and in man, mainly as a result of very fast *in vivo* degradation. We now propose the co-injection of the neutral endopeptidase (NEP) inhibitor phosphoramidon (PA) together with [$^{111}$In-DOTA]MG11 in mice to enhance radioligand stability and tumor uptake without compromising the favorably low renal radioactivity uptake. **Materials and Methods**: [$^{111}$In-DOTA]MG11 was injected in healthy mice without or with PA. Blood samples were collected 5 min post injection (pi) and analyzed by RP-HPLC. Likewise, [$^{111}$In-DOTA]MG11 was injected without or with PA in SCID mice bearing AR4-2J xenografts and biodistribution was conducted at 4 h pi. Furthermore, dynamic and static images were acquired by small-animal NanoSPECT/CT after injection of [$^{111}$In-DOTA]MG11 without or with PA. **Results**: After entry in the mouse blood stream [$^{111}$In-DOTA]MG11 was rapidly degraded with only <5% detected intact at 5 min pi. However, by co-injection of PA the percentage of intact peptide enormously rose above 75% for the same time interval. This astonishing effect on metabolic *in vivo* stability translated into a dramatic increase of tumor uptake in SCID mice. Thus, the initial value of 1.22±0.06%ID/g found in the AR4-2J xenografts at 4 h pi raised to 16.18±3.0%ID/g in the animal group treated with PA. Of particular interest is the fact that kidney values remained unchanged (≈2%ID/g, $P$>0.05). These observations were reproduced in the SPECT/CT images of mice after co-administration of PA. **Conclusions**: Co-injection of the NEP inhibitor PA stabilized the rapidly biodegradable [$^{111}$In-DOTA]MG11 in mice leading to efficient radioligand delivery at the target and vast increase of tumor uptake. The effectiveness of this exciting new approach, currently studied for other radioligand/inhibitor combinations in mice, holds great promise for eventual application in the clinic.

## OP128

### Diagnostic efficacy of a single vial kit preparation of 99mTc-DTPA-bis-methionine (MDM) for the detection of primary lesions in breast cancer and gliomas : A clinical evaluation

**B. Singh**[1], S. Sharma[1], H. Verma[1], K. Chutani[2], A. Mishra[2], P. Kumar[1], B. R. Mittal[1], G. Singh[1]; [1]PGIMER, CHANDIGARH, INDIA, [2]INMAS, Delhi, INDIA.

**Aim**: To evaluate the diagnostic efficacy of a single vial kit preparation of 99mTc-MDM as a breast cancer and brain tumor scintigraphic agent. **Methods**: 30 female patients with proven breast cancer and 6 patients (4M: 2F) having brain tumor (4 - had post-surgery residual tumor; 1each with primary glioblastoma and recurrent disease) were prospectively enrolled in the study.Briefly, 555-740 MBq of 99mTc-MDM was injected intravenously in all the patients. Breast cancer patients were subjected to scintimammography at 1h, 2h & 4h and glioma patients to brain SPECT at 1.5 h following 99mTc-MDM administration. All the scans were visually inspected and also subjected to semi-quantitative analysis (drawing ROI over the lesion) to calculate lesion to background ratios (LBR) at different time intervals. **Results**: An excellent radio-labeling efficiency (97 ± 1.5%) was obtained for all the kit preparations of MDM used in the study. Scan findings were positive in 27 breast cancer patients (29 breast lesions) Semi-quantitative analysis of positive breast lesions revealed mean LBR of 3.64 ± 1.26, 3.01 ± 0.98 and 2.42 ± 0.77 at 1h, 2h & 4h respectively. The sensitivity and specificity of methionine scanning was calculated to be 93% and 100% respectively as compared with the histopathological findings. 99mTc-MDM scans findings were positive in 4/6 glioma patients . Two negative cases were patients (1-each) with residual tumor and recurrent glioma. **Summary**: Evaluation of LBR can be used to differentiate between the benign and malignant lesions and combined with 99mTc-MDP bone scanning offers a near complete diagnostic work-up of breast cancer patients both for primary lesions and skeletal metastases. 99mTc-MDM showed increased and focal tracer uptake in brain tumors. However, large numbers of patients are required to prove its diagnostic efficacy in glioma cases.

## OP129

### Improvement of Beta Cell Imaging by Multi-chelation of Exendin-3

**L. Joosten**, M. Brom, H. Peeters, C. Frielink, O. Boerman, M. Gotthardt; Radboud University Nijmegen Medical Centre, Nijmegen, NETHERLANDS.

**Aim** Exendin-3 is a stable glucagon-like peptide-1 (GLP-1) analogue with high affinity for the GLP-1 receptor (GLP-1R), specifically expressed on pancreatic beta cells. The beta cell mass (BCM) can be measured *in vivo* with In-111-labelled DTPA-exendin-3. For SPECT high specific activities are required to avoid receptor saturation. We examined two exendin-3 derivatives that contain multiple DTPA-moieties in order to enhance the specific activity of the tracer. **Materials and Methods** Exendin-3 was modified by C-terminally adding five Lysine residues. DTPA was conjugated to the ε-amino group of these C-terminal Lysine residues. Two DTPA moieties were conjugated at position 40 and 41 for 6Lys(DTPA(40+41))-exendin-3 and 6Lys(DTPA(40-45))-exendin-3 had a DTPA moiety attached to each of the six Lysine residues. Both peptides were labelled with In-111 and the affinity for the GLP-1R was determined in competitive binding assays using INS-1 cells expressing the GLP-1R. Biodistribution studies were performed with equimolar doses of the In-111 labelled analogues in BALB/c nude mice with subcutaneous INS-1 tumours to examine *in vivo* GLP-1R targeting properties. SPECT was performed in Brown Norway (BN) rats to assess visualisation of pancreatic beta cells. **Results and conclusion** Labelling of 6Lys(DTPA(40+41))-exendin-3, 6Lys(DTPA(40-45))-exendin-3 and Lys(DTPA(40)-exendin-3 (reference peptide with one DTPA) with In-111 resulted in a maximum specific activity of 4.2 GBq/nmol, 3.9-6.5 GBq/nmol and 0.65 GBq/nmol. $IC_{50}$ values were 36.8, 75.1 and 9.9 nM for 6Lys(DTPA(40+41))-exendin-3, 6Lys(DTPA(40-45))-exendin-3 and Lys(DTPA(40)-exendin-3, respectively. In mice with s.c. INS-1 tumours 6Lys(DTPA(40+41))-exendin-3, 6Lys(DTPA(40-45))-exendin-3 and Lys(DTPA(40)-exendin-3 showed high uptake in the tumour (22.9 ± 7.3, 19.9 ± 9.2 and 33.8 ± 7.6 %ID/g, respectively), which could be blocked by excess of unlabelled exendin (1.8 ± 0.4, 1.2 ± 0.2 and 1.6 ±0.5 %ID/g). Accumulation in the pancreas was similar for all peptides (10.8 ± 2.9, 9.8 ± 2.7 and 12.0 ± 4.0 %ID/g, respectively). Blocking with excess of unlabelled peptide showed receptor-mediated uptake in the pancreas. All tracers showed high kidney uptake (199.0 ± 18.0, 184.7 ± 5.3 and 196.4 ± 20.5 %ID/g), which could not be blocked by unlabelled peptide. Uptake in receptor-expressing organs (lung, stomach and duodenum) and non-target organs was similar for all exendin-3 derivatives. Imaging studies in BN rats clearly showed higher absolute accumulation of activity of 6Lys(DTPA(40-45))-exendin-3 in the pancreas compared to Lys(DTPA(40))-exendin-3, due to higher specific activities. In conclusion, the addition of 6 Lysines and multiple DTPA molecules to exendin-3 improved the specific activity and the tracers had similar *in vivo* pharmacokinetic characteristics.

## OP130

### Optimized delivery of an anti-amyloid VHH-2H heavy chain antibody fragment to the mouse brain

**M. M. Welling**[1], M. Rotman[1], M. E. de Backer[2], J. Rip[2], P. J. Gaillard[2], L. van der Weerd[1]; [1]Leiden University Medical Center, Leiden, NETHERLANDS, [2]ToBBB, Leiden, NETHERLANDS.

This study investigated the enhanced delivery of heavy chain antibody fragment VHH pa2H (VHH-2H) to accumulate on vascular and parenchymal amyloid-β deposits in APP/PS1 murine brains as a model for clinical pathologies in Alzheimer's disease. VHH-2H was conjugated with a DTPA chelator to facilitate radiolabeling with $^{111}$In, directly and after encapsulation in two different liposome preparations, LIPO-6 and LIPO-7 each with specific pharmacokinetic properties. Immuno reactivity of VHH-2H after conjugation with DTPA and radiolabeling was assessed with immuno-histochemical staining and autoradiography on human brain sections of Alzheimer patients. Blood clearance and biodistribution including brain uptake were studied using SPECT imaging and tissue counts after bolus injection of radiolabeled VHH-2H either non-encapsulated or in liposomal preparations in APP/PS1 mice or wildtype littermates (WT). Radiochemical analysis showed robust and stable labeling of $^{111}$In-DTPA-VHH-2H with high yield (>95%), either non-encapsulated or in liposomes. After conjugation to DTPA, VHH-2H specifically detects amyloidal plaques in human brain sections. In both APP/PS1 and WT mice, non-liposomal $^{111}$In-DTPA-VHH-2H showed rapid renal 1-phase clearance (T½ ca. 20 min) with 90% of the injected dose removed from the mice by urinary excretion at 24 hr post injection. Liposomal clearance of VHH-2H LIPO-6 and LIPO-7 showed two-phase decay with T½=13 and 17 min respectively in the first phase and very slow clearance in the second phase for LIPO-6 (T½ >500 min, 27%) and LIPO-7 (T½ >600 min, 42%). From SPECT imaging and calculating standard uptake values (SUV) in mice injected with LIPO-6 or LIPO-7 radioactivity patterns were significantly higher in blood, heart, muscle, lungs, spleen, liver, and kidneys compared to mice injected with non-encapsulated $^{111}$In-DTPA-VHH-2H. Most remarkable, compared to non-encapsulated $^{111}$In-DTPA-VHH-2H, 24 hours post-injection liposomal $^{111}$In-DTPA-VHH-2H resulted in a significant higher (19-31x for LIPO-6 and 51-121x for LIPO-7) cerebral uptake in both WT and APP/PS1 mice. Despite the brain uptake of $^{111}$In-DTPA-VHH-2H is too low for in vivo imaging of amyloidal plaques, this study provides evidence that VHH-2H delivery in brains can be significantly enhanced by liposomal encapsulation, making them promising tools for further development as diagnostic tracers or therapeutic agents for the immunological treatment of Aβ plaques. Acknowledgements.Research was supported by the Center for Translational Molecular Medicine (LeARN) and the Center for Medical Systems Biology (CMSB2).

## OP131

### ABCB1 gene, but not gender may influence Tc-99m-2-methoxyisobutylisonitril (Tc-99m-MIBI) imaging findings

**S. Dizdarevic**[1,2], M. Aplin[1], M. J. Newport[1,2], N. Ryan[1], S. G. Holt[1,3], S. Goubet[1], L. Goldberg[1], K. A. Miles[4,5], A. M. Peters[1,2]; [1]Brighton and Sussex University Hospital NHS Trust, BRIGHTON, UNITED KINGDOM, [2]Brighton and Sussex Medical School, Brighton, UNITED KINGDOM, [3]Royal Melbourne Hospital, Melbourne, AUSTRALIA, [4]University College London, London, UNITED KINGDOM, [5]Molecular Imaging Centre, Princess Alexandra Hospital, Brisbene, AUSTRALIA.

**Aim:** Inter-individual expression of P-glycoprotein (P-gp) is known to be associated with C3435T polymorphism in exon 26 of *ABCB1* (formerly known as *MDR1 gene)*. A possible role for P-gp in gender-dependent differences in drug availability, however, remains unresolved. It has been reported, for example, that hepatic P-gp expression in men is 2.4-fold higher than in women. In contrast, others have demonstrated that P-gp is not differentially expressed between genders. Tc-99m-MIBI elimination involves ATP-binding cassette (ABC) transporter proteins, including P-gp, so studying Tc-99m-MIBI kinetics allows inference of P-gp status. The Aim of this study, therefore, was to investigate organ elimination rates of Tc-99m-MIBI in relation to gender and genetic variation in *ABCB1*. **Methods:** Thirty healthy prospective kidney transplant donors (17 female, 13 male) were imaged for 30 min following injection of 400 MBq Tc-99m-MIBI. Posterior static 5-minute images of the abdomen, including myocardium, were acquired at 30 and 120 min. The 30 min/peak ratio and the exponential 2 point (30 and 120 min) rate constant (*k*) were calculated. Nineteen donors were genotyped for the C3435T (exon 26), G2677T (exon 21), C1236T (exon 12) and G1199A (exon 11) *MDR1* polymorphisms using a PCR-based technique. Homozygous negative (TT), heterozygous (TC) and homozygous positive (CC) genotypes were correlated with renal and hepatic 30 min/peak ratios and *k* values using ANOVA. Two-tailed *t*-testing was used to assess differences in renal and hepatic Tc-99m-MIBI elimination rates between males and females. **Results:** There was a negative trend between the hepatic 30 min/peak ratio and C3435T genotype (CC: 0.8374 ± 0.0502; TC: 0.6806 ± 0.1300; TT: 0.6919 ± 0.1506; p = 0.083). Splenic, myocardial and renal 30 min/peak ratios did not correlate with any genotype. Renal *k* ($min^{-1}$) showed a negative trend with C3435T genotype (CC: 0.0021 ± 0.0020; TC: 0.0037 ± 0.0013; TT: 0.0040 ± 0.0012; p = 0.087), but with no other genotypes. Hepatic, splenic and myocardial *k* values did not correlate with any genotype. No significant gender differences in renal and hepatic 30 min/peak ratios and *k* values between females and males were found.**Conclusion:** Tc-99m-MIBI handling is not gender-dependant, implying that P-gp expression is not differentially expressed between genders. Although limited, our preliminary data, however, suggests that C3435T polymorphism of *ABCB1* gene may influence Tc-99m-MIBI kinetics. In the era of personalised medicine, further prospective trials are required to investigate the impact of genotype variation on Tc-99m-MIBI imaging findings in routine clinical practice and research.

## OP132

### $^{99m}$Tc-DPD Binding to Synthetic Amyloid Fibrils

F. E. Buroni, L. Lodola, F. Lavatelli, V. Valentini, **C. Aprile**; Fond. Policlinico San Matteo Hospital, IRCCS, Pavia, ITALY.

**Background** Amyloidotic cardiomyopathy is the worst prognostic factor and early detection is mandatory for appropriate clinical management. Bone seekers, such as $^{99m}$Technetium-labeled pyrophosphate ($^{99m}$Tc-PPi), $^{99m}$Tc-methylenediphosphonate ($^{99m}$Tc-MDP), and $^{99m}$Tc-3,3,-diphosphono-1,2-propanodicarboxylic acid ($^{99m}$Tc-DPD) have been reported as potential radiopharmaceuticals able to image cardiac amyloid deposits, being DPD the most sensitive tracer especially for ATTR deposits. **Aim** To investigate: 1. the in vitro binding affinity of DPD for synthetic insulin amyloid fibrils , 2. the role of Ca++ ions on binding. 3. the relative affinity of DPD in comparison to HMDP and PPi **Methods** Synthetic h-insulin fibrils were prepared according to the standard method. Commercially available kits of $^{99m}$Tc-HMDP, $^{99m}$Tc-PPI and $^{99m}$Tc-DPD was reconstituted according to the manufacturers' instructions. To assess affinity constant of $^{99m}$Tc-DPD, increasing amounts from 0 up to 400 nmol in 1.4 mmol/L of $Ca^{++}$ were added to 1 mg of fibrils. After 2 h at RT incubation, bound/free fraction was assessed for each sample and data were fitted to Scatchard analysis. In a separate run, equimolar amount of the three radiopharmaceuticals (140 nmol) were added to 1 mg of fibrils at various concentrations of $Ca^{++}$ (0, 0.7, 1.4, 2.8, 4.2 mmol/L). After 2h at RT incubation, bound activity for each radiopharmaceutical was assessed. **Results** Synthetic fibrils demonstrated the characteristic apple-green birefringence with polarized light after Congo red staining. Labelling yield of the radiopharmaceuticals was >98% in any preparation. Scatchard analysis of the binding affinity for $^{99m}$Tc-DPD revealed a Kd of 167.1 nmol. The radioactivity bounds to fibrils increases with $Ca^{++}$ ions concentration from 0 to 2.8 mmol/L, thereafter it remains stable. The comparison between the three radiopharmaceuticals shows that $^{99m}$Tc-DPD has the highest

binding in comparison to the other compounds: $^{99m}$Tc-HMDP 72% and $^{99m}$Tc-PPI 44% of DPD respectively. **Conclusions** $^{99m}$Tc-DPD shows a high affinity for amyloid fibrils, and its binding is significantly higher in comparison to the other two compounds tested, thus confirming the results obtained in humans. Calcium ions content of the media seems to play an important role in binding process up two times the physiological ion concentration, thereafter a further increase does not influence the binding. The synthetic fibrils we employed, however, does not answer the question if the affinity is the same for any kind of naturally occurring fibrils (ATTR and AL). In addition other test could be mandatory to assess binding specificity to amorphous proteinaceous material, for instance.

## OP133

### Radiosynthesis of 99mTc-HYNIC-NH-BG: A new Tc-99m radiotracer to visualise specific cells in vivo via SNAP-tag

**R. O. Awais**[1], B. Mills[2], J. C. A. Luckett[2], P. Duncanson[3], V. Griffiths[3], P. Williams[2], P. Hill[4], A. C. Perkins[1]; [1]Radiological & Imaging Sciences, University of Nottingham, Nottingham, UNITED KINGDOM, [2]Centre for Biomolecular Sciences, University of Nottingham, Nottingham, UNITED KINGDOM, [3]School of Biological and Chemical Sciences, Queen Mary University of London, London, UNITED KINGDOM, [4]School of Biosciences, University of Nottingham, Nottingham, UNITED KINGDOM.

**Introduction** SNAP-tag is a protein based on human O6-alkylguanine-DNA alkyltransferase (hAGT) and can bind specifically and covalently to substrates bearing a benzylguanine functional group. The SNAP-tag has successfully been expressed in yeasts, mammalian cells and bacteria. For imaging applications, SNAP-tag substrates linked to fluorophores have been used for optical imaging. Such agents can provide spatial and kinetic data in real time and also reduce the number of animals required. We have previously shown that the SNAP-tag can be used to label Gram positive bacteria where it can be expressed in S. aureus and specifically anchored to the cell wall via sortase A. Preliminary data show that the surface-localized SNAP tag can be targeted by fluorescent probes in vitro and here we present the design of a new radioligand. 6-Hydrazinonicotinic (HYNIC)(i) is a widely employed bifunctional chelating agent for Tc-99m. In this study we prepared 99mTc-HYNIC-NH-BG which allows a novel use for SNAP-tag technology in nuclear imaging. **Methods** HYNIC-NH-BG (3) was synthesised by coupling the tert-Boc protected HYNIC-NHS (1) with BG-NH2 (2) in DMF. The product was purified by chromatography on silica-gel eluting with DCM/Methanol mixtures and the ligand (180 mg 80%) fully characterised by 1H-NMR, 13C-NMR, IR, and LC-MS. The procedure used for labelling Tc-99m with HYNIC was similar to that described by King et al(ii) with Tricine as the co-ligand. Approximately 200 MBq of Na99mTcO4 was mixed with SnCl2, serving as a reducing agent, added to the HYNIC-NH-BG with thorough mixing and the mixture incubated at 37oC for 30 min. The corresponding rhenium reference standard was synthesised in the same manner but with NaReO4. **Results & Conclusion** The radiochemical yield of the radiotracer exceeded 99% (n=5) as determined by iTLC and RP-HPLC. In vitro studies have demonstrated that the novel radiotracer 99mTc-HYNIC-NH-BG is able to specifically bind to surface displayed SNAP-tag. This radiotracer may facilitate investigation of experimental staphylococcal infections and screening of potential antimicrobials. References (i)- Babich et al., J. Nucl. Med., 1993, 34, 1964. (ii)-King et al., Dalton Trans., 2007, 4998-5007

## OP134

### Synthesis, biological evaluation and radiopharmaceutical efficacy of Catecholamine vehicle for studying dopaminergic system

**P. Singh**[1,2], A. K. TIWARI[1], R. PRATAP[2], K. CHUTTANI[1], A. K. MISHRA[1]; [1]INMAS, DELHI, INDIA, [2]DEPARTMENT OF CHEMISTRY ,UNIVERSITY OF DELHI, Delhi, INDIA.

**Introduction**: Dopamine, epinephrine, and nor-epinephrine are the most abundant catecholamine neurotransmitter found in mammals, which are biosynthesized by enzymatic pathway starting from phenylalanine to tyrosine and the respective catecholamine. Alteration in this biosynthesis has been associated with various neuropsychiatric disorders such as schizophrenia, depression, Parkinson's disease and Alzheimer's disease. To monitor these alterations, EDTA or DTPA based various radiopharmaceuticals are synthesized for the diagnosis on labeling with radio-metals like, 68Ga, 99mTc, 111In, 153Sm, 188Re. Out of these, 99mTc is of great approach in this field due to its short half life of 6.02 hrs and low absorbed radiation dose to patient. In the present study, EDTA-bis(tyramide) was synthesized and studied for imaging of dopaminergic system and to fulfill the imaging purpose, 99mTc-EDTA-bis(tyramide) and 68Ga- EDTA-bis(tyramide) was studied for in-vivo applications. **Materials and Methods**: The compounds was characterized by different spectroscopic techniques (NMR and mass spectroscopy) and later radiolabeled with 99mTc and 68Ga. In vivo biodistribution and blood kinetics studies were performed for radiolabeled EDTA-bis(tyramide) and SPECT image was taken for 99mTc-EDTA-bis(tyramide) using gamma camera. MAO-B Inhibition assay was studied spectrophotometrically and AChE binding affinity using Ellman method. **Result:**-The novel compound was labeled with 99m Tc and 68Ga at optimum pH and temperature, which results to forms stable complex with high radiochemical purity 98% and 87% respectively. Blood kinetic and biodistribution showed a quick wash out from the circulation via renal route and 3.96% brain uptake respectively. IC50 value was calculated for MAO-B inhibition, and it was found 18.60 µM, shows effective inhibition. Additionally to go more into the neuronal pathway AChE binding affinity was investigated using Ellman method, which shows 90% binding for the 10 mM concentration. Furthermore, an excellent quality SPECT image confirms that this compound is potential candidate for dopaminergic imaging. **Conclusion**: Scintigraphy image in rabbit showed brain uptake of the ligand which suggested brain imaging application to see more into the neuronal pathway. Enzyme inhibition assay confirmed the activity of the ligand as a MAO-B inhibitor, which shows that ligand can go more insight the dopaminergic system and affect the dopamine synthesis.

410 - Sunday, Oct. 20, 14:30 - 16:00, Tête D'Or 1/2

## Oncology Clinical Science: Upper GI Tract Tumours

## OP135

### A prospective trial for the evaluation of esophageal cancer patients: fluorodeoxyglucose (FDG) positron emission tomography (PET)/computed tomography (CT) vs. contrast enhancement (c.e.)CT vs. FDG PET/c.e.CT

**L. Evangelista**[1], F. Pomerri[2], E. Scagliori[2], R. Alfieri[3], C. Castoro[3], R. Alberto[4], S. Galuppo[1], V. Chiarion Sileni[5], A. R. Cervino[1]; [1]Radiotherapy and Nuclear Medicine Unit, Istituto Oncologico Veneto I.R.C.C.S., Padova, ITALY, [2]Radiology Oncology Unit, Istituto Oncologico Veneto I.R.C.C.S, Padova, ITALY, [3]Surgery Oncology Unit, Istituto Oncologico Veneto I.R.C.C.S., Padova, ITALY, [4]Department of Surgery and Organ Transplant, Clinica Chirurgica III, University of Padova School of Medicine, Padova, ITALY, [5]Oncology 2 Unit, Istituto Oncologico Veneto I.R.C.C.S, Padova, Italy, Padova, ITALY.

**Introduction**. The present study was conceived on a population of esophageal cancer patients (ECP) who have been undergoing FDG PET/CT and c.e.CT in a single session, both at initial staging and after more than 4 weeks from the end of neoadjuvant treatment. The prospective trial was approved by our institutional Ethical Committee. Herein, we reported the preliminary data about the comparison of diagnostic performance among PET/CT, c.e.CT and PET/c.e.CT. **Materials and Methods**. The multidisciplinary team of our Institute started the recruitment from January 2012. To date, 60 ECP (46 male, 14 female, 62±12years) were recruited, with adenocarcinoma or squamous cell carcinoma who underwent basal PET/CT plus c.e.CT in a single session. The glycemic recorded value was not higher than 170mg/dL and insulin-dependent diabetic patients were excluded from recruitment, according to RECIST guideline. After 60min from the injection of 3MBq/Kg of FDG, a whole body PET/CT scan was acquired. At the end of standard acquisition, a neck-thorax-abdomen c.e.CT was performed; in particular three c.e. phases for the liver evaluation were made. Three specialized physicians (two radiologists and two nuclear medicine specialists) read the images, separately. The diagnostic performances of PET/CT, PET/c.e.CT and c.e.CT were evaluated by using the standard method and then compared with clinical staging (by patient-based analysis). **Results**. 60 patients performed both PET/CT and c.e.CT while 57 of them had all three scans. The imaging co-registration (PET and c.e.CT) was good in 88% of patients, discrete in 7% and scarce in only 5%. The agreement among the three scans was present in 35% of subjects. In the remnant 65% of patients, c.e.CT demonstrated more lymph node metastases than both PET/CT and PET/c.e.CT (15% and 11%, respectively), similarly PET/c.e.CT showed more loco-regional/distant lymph nodes and distant metastases than PET/CT (increase in positive rate=30%). The clinical staging was recovered in 28 (41%) patients. The positive predictive value of PET/c.e.CT was higher than PET/CT and c.e.CT for the identification of loco-regional/distant lymph nodes and distant metastases (81% vs. 78% and 70%, respectively). **Conclusions**. In ECP, at initial staging FDG PET/c.e.CT represents an accurate and feasible method for recognizing a major number of pathological findings in comparison with PET/CT and c.e.CT.

## OP136

### The Role of FDG PET/CT Findings in Predicting Survival in Patients with Esophageal Cancer

**B. Vatankulu**[1], Y. Sanli[1], E. Kaytan Saglam[2], S. Kuyumcu[1], E. Yilmaz[1], G. Ozkan[1], S. Purisa[3], I. Adalet[1]; [1]Istanbul University Istanbul Medical Faculty Department of Nuclear Medicine, Istanbul, TURKEY, [2]Istanbul University Istanbul Medical Faculty Department of Radiation Oncology, Istanbul, TURKEY, [3]Istanbul University Istanbul Medical Faculty Department of Biostatistics, Istanbul, TURKEY.

**Background-Aim:** It is known that FDG PET/CT imaging has an important role for staging in patients with esophageal cancer. There are contradictory results for

PET/CT findings in predicting survival for esophageal cancer. We Aimed to investigate the value of PET/CT findings in predicting survival in patients with pretreatment esophageal cancer. **Methods:** We retrospectively analyzed patients with esophageal cancer between May 2009 and December 2011 who had FDG PET/CT for staging. All patients were followed up to March 2013. Histopathology, localization, clinical staging, presence of distant metastasis, SUV max value of primary tumor and metastatic lymph node were evaluated. The association of these findings and overall survival were analyzed using univarient and multivarient Cox regression. **Results:** A total of 107 patients (48 female, mean age ;56.6±12.3) were included in the study. All patients were followed up between 2 and 49 months (median month :20.2 ± 2.1). Eighty-eight (82.2%) patients had squamous cell carcinoma, 19 (17.8%) had adenocarcinoma. The localization of tumor was seen as 45.8 % in lower thoracic esophagus. The majority of patients were in advanced disease group ( stage 1-2: 27.1%, stage 3: 42.1%, stage 4: 30.8% ). The mean SUVmax value of primary tumor and metastatic lymph node were 19.3 ± 8.8 and 10.4 ± 9.1, respectively. The lymph node metastasis were seen in 65% of all patients, and of 43% of these patients lymph node metastasis were seen in thoracic region. The liver was the most common sites of distant metastasis (10.3%). Metastatic lymph node SUVmax value had an effect in predicting survival whereas primary tumor SUVmax value had no effect. (p: 0.014 and p: 0.262, respectively). Furthermore, lymph node metastasis had also been associated with survival (p: 0.04). Multivarient Cox Regression analysis showed that clinical stage of the disease was the only independent factor predicting survival. Stage 3 had a 4.2 fold risk for predicting survival as compared stage 2, whereas stage 4 had 2.8 (p:0.001). **Conclusion:** Among patients with esophageal cancer, the value of primary tumor SUVmax had no effect in predicting survival. Clinical stage assessed with FDG PET/CT imaging, was found to predict survival in esophageal carcinoma. Additionally, we found that lymph node SUVmax value was showed as a new parameter in predicting survival in the present study

## OP137

### SUVmax of 18 F- FDG PET CT predicts survival in oesophageal cancer

N. Alam, F. Bayam, R. Hanlon, E. Kneale, **H. Wieshmann**; Aintree University Hospitals, Liverpool, UNITED KINGDOM.

18 F- fluorodeoxyglucose (FDG) Positron-Emission Tomography Computed Tomography (PET CT) is increasingly used in staging, restaging, surveillance of recurrence, and monitoring treatment response in oesophageal cancer. The prognostic and predictive value of initial maximum standardised uptake value (SUVmax) has been described for non-small cell lung cancer, lymphoma, and colorectal cancer, but only in a limited manner for patients with oesophageal cancer. **Aim** Assess the correlation between SUVmax of less versus higher than 5 at the primary cancer site and overall survival in patients with oesophageal cancer. **Methods** All biopsy-proven oesophageal cancer patients who underwent PET CT as part of their initial cancer staging and discussed at the regional upper Gastrointestinal Cancer Multidisciplinary Team at Aintree University Hospital between April 2008 and March 2011 were reviewed. Information regarding overall survival was obtained for each patient. Data collected from the hospital records included the SUVmax of the primary cancer, patient follow-up data, and death records. Overall survival was defined as the time period from diagnosis to death or last follow-up, whichever occurred first. Patients who were alive at the time of the last follow-up were treated as censored. The Kaplan-Meier method was used to estimate the probability of overall survival. **Results** 195 patients with biopsy-proven oesophageal cancer underwent PET CT between April 2008 and March 2011. The SUVmax of the primary cancer in 38 patients was less than 5 and higher than 5 in 157 patients. The follow up intervals were at 6, 12, 18 and 24 months. In the group of patients with SUVmax of less than 5 the survival was 90%, 75%, 65%, 65% and in the group with SUVmax of higher than 5 the survival was 95%, 60%, 40%, 34%. The Kaplan Meier analysis demonstrated an improved overall survival among the patients with SUVmax less than 5 compared to the group with SUVmax higher than 5. **Conclusion**: Our data suggests that SUVmax <5 of the primary cancer is associated with a better overall survival in patients with oesophageal cancer.

## OP138

### FDG-PET/CT to adapt radiotherapy target volume and dose during chemo-radiotherapy (CRT) in esophageal cancer patients

**L. NKHALI**[1,2,3], S. THUREAU[1,2,3], A. EDET-SANSON[4,2,3], K. DOYEUX[1,2,3], A. BENYOUCEF[1,2,3], I. GARDIN[4,2,3], P. MICHEL[5,2,3], P. VERA[4,2,3], B. DUBRAY[1,2,3]; [1]Department of Radiation Oncology and Medical Physics - QuantIF-LITIS (EA4108), Henri Becquerel Cancer Center, Rouen, FRANCE, [2]Rouen University Hospital, Rouen, FRANCE, [3]University of Rouen, Rouen, FRANCE, [4]Department of Nuclear Medicine – QuantIF-LITIS (EA4108), Henri Becquerel Cancer Center, Rouen, FRANCE, [5]Department of Hepatogastroenterology, Rouen, FRANCE.

**Aim** of the study: the standard treatment of esophageal cancer is a concomitant combination of cis-platinum-based chemotherapy (CT) and radiotherapy (RT) to a total dose of 50.4Gy. Higher RT doses are likely to improve the poor results of concomitant CRT. We investigated whether RT target volumes reduction, as assessed on FDG-PET/CT before and during CRT, would allow RT dose escalation to 66Gy without compromising normal tissue tolerance. **Methods and Materials**: a prospective study (RTEP3, NCT 00934505) included 57 patients with stage IIB, III or IVA (TNM 2002) esophageal squamous cell carcinomas. FDG-PET/CT was performed before (PET1) and at 21 days (PET2) of CRT. The present analysis is restricted to 13 patients in whom FDG-PET/CTs were acquired in radiotherapy position. The Gross Target Volume (GTVPET) was delineated by a nuclear physician and a radiation oncologist on PET1 and PET2. Adequate margins were added to account for microscopic disease around GTVPET (Clinical Target Volume CTV) and set-up uncertainties around CTV (Planning Target Volumes PTV). RT plans were calculated to deliver either 50 or 66Gy to PTV1 or PTV2, according to ICRU 83 report. The Organs At Risk (OAR) were the spinal cord, the lungs, and the heart. Results: a 45% decrease in SUVmax was observed between PET1 and PET2 (p = 0.001). Due to acute esophagitis, GTVPET-2 could not be delineated in 3 patients. In the 10 remaining patients, GTVPET decreased by 61% (p=0.01) during CRT. The PTV66Gy-1 and PTV66Gy-2 were 149±18cm3 and 102±8cm3, respectively, i.e. a 31% reduction (p=0.05). Adequate PTV coverage was achieved for all the treatment plans. The doses to the OAR's were similar when a conventional 50 Gy dose was to be delivered to PTV1 or PTV2. The doses to the spinal cord and the lungs were significantly lower when planning 66 Gy to PTV2, as compared to 66 Gy to PTV1. **Conclusion**: the reduction in metabolic tumor volume during CRT allows the escalation of RT total dose with a better protection of the spinal cord and the lungs. This approach deserves clinical validation in a prospective trial.

## OP139

### The role of FDG PET/CT in staging gastric cancer: comparison with laparoscopic staging

**I. Zerizer**[1], A. Parsai[2], E. Manca[1], Y. Du[1], B. Sharma[1], B. Mohammadi[1]; [1]Royal Marsden Hospital, London, UNITED KINGDOM, [2]Bart's and the Royal London, London, UNITED KINGDOM.

**Introduction** FDG PET/CT is increasingly used for staging operable gastric carcinoma with a superior performance to conventional imaging (CT) in detecting metastatic disease. Laparoscopic staging is also currently recommended in gastric and type 2/3 oesophageal cancer to detect occult disease. The Aim of this study is to compare PET/CT with laparoscopy in staging gastric and type 2/3 oesophageal cancer. **Material and Methods** 41 patients with gastric (n= 21) and type 2/3 oesophageal cancer (n= 20) considered for radical surgery underwent PET/CT and laparoscopic staging from January 2012 to January 2013. PET/CT data were reviewed independent of laparoscopy results by an experienced nuclear medicine physician. The site of the primary tumour, locoregional lymph node involvement, presence of peritoneal nodules and metastases were recorded. Laparoscopic results were extracted from the operation notes recorded on the electronic patient record. Histopathological correlation was made whenever samples were taken during laparoscopy. **Results** PET/CT correctly excluded metastases in 35/41 patients. The calculated sensitivity of PET/CT for excluding peritoneal metastases was 85%, specificity 85%. Laparoscopic staging identified 6 patients (n = 4 gastric cancer, n = 2 oesophageal cancer) with peritoneal disease not shown on PET/CT (14%). In this cohort, the primary tumours were all signet ring or mucinous with only low grade FDG uptake (SUVmax range 3.4 -4) except for one oesophageal lesion where the SUVmax was 12.6. The latter also had a mucinous peritoneal metastasis in the hemidiaphragm. 12/41 patients in our cohort had a primary tumour with SUVmax ≤ 4. The sensitivity of PET/CT for excluding peritoneal metastases in these patients was 66%, specificity 85%. However, using SUVmax cut-off > 4 in the primary tumour, the sensitivity of PET/CT for excluding peritoneal metastases increased to 96%, specificity 97%. Receiver operating characteristic analysis has shown a primary tumour threshold SUV max >4 had a sensitivity of 96% for excluding metastases (Area under the curve 0.965, p<0.005). **Conclusion** PET/CT is useful in selecting patients that would benefit from laparoscopic staging. Based on our findings, laparoscopy should be performed in signet ring/mucinous tumours and a primary lesion with SUVmax < 4. Our results indicate that laparoscopy could be omitted in tumours with SUVmax > 4 but larger studies are required to validate our findings.

## OP140

### The Role of F-18 FDG PET/CT in the Evaluation of Gastric Cancer Recurrence

**H. Cayvarli**[1], R. Bekis[2], T. Akman[3], D. Altun[4]; [1]GATA Haydarpasa Training Hospital, Department of Nuclear Medicine, Istanbul, TURKEY, [2]9 Eylul University, Faculty of Medicine, Department of Nuclear Medicine, Izmir, TURKEY, [3]9 Eylul University, Faculty of Medicine, Department of Medical Oncology, Izmir, TURKEY, [4]9 Eylul University, Faculty of Medicine, Department of Public Health, Izmir, TURKEY.

**Purpose** F-18-fluorodeoxyglucose positron emission tomography/computed tomography (F-18 FDG PET/CT) has been widely used for staging, re-staging and for

monitoring therapy-induced changes and response to therapy in patients with various types of cancer, but its utilization for gastric cancer has been limited. This study Aimed to assess the diagnostic performence of F-18 FDG PET/CT for detecting recurrence in gastric cancer patients with radiologic or clinical suspension of recurrence. **Materials and Methods** We performed a retrospective review of 130 consecutive patients who underwent PET/CT scans for post treatment surveillance of gastric cancer between January 2008 and March 2012. The number and site of positive FDG uptakes were analyzed and were correlated with the final diagnosis by calculating the diagnostic values. We evaluated the diagnostic accuracy of PET/CT for detecting the recurrence in the patients with histopathologic types of signet ring cell carcinoma (SRC) and mucinous adenocarcinoma. Cut-off SUVmax values in differentiating benign lesions from recurrence in different organs and the changes in the clinical management of patients according to the results of PET/CT were also evaluated. **Results** Of all 130 patients, 91 patients were confirmed to have true recurrence. The sensitivity, specificity, positive predictive value, negative predictive value and the dignostic accuracy of PET/CT for diagnosing true recurrence on a per-person basis were 91.2 %, 61.5 %, 84.6 %, 75.0 % and 82.3 % respectively. In the subgroup with SRC and mucinous adenocarinoma differentiation of the primary tumor, there was no statistically significant difference in terms of diagnostic accuracy of PET/CT on a per-person basis. PET/CT had also detected second primary cancer in two patients and the PET/CT results changed the patients' management in 20 (15 %) cases. **Conclusion** FDG PET/CT was highly effective in discriminating true recurrence in patients with gastric cancer and had important impacts on clinical decisions in a considerable portion of patients.

## OP141

### Diagnostic accuracy of 11C-choline PET (CHO-PET) in patients affected by hepatocellular carcinoma (HCC): comparison with CT/MRI

**E. Lopci**[1], J. Guerra Sabongi[2], G. Torzilli[1], A. Palmisano[1], F. Alongi[1], M. Scorsetti[1], A. Chiti[1]; [1]Humanitas Clinical and Research Center, Rozzano (Mi), ITALY, [2]Hospital de Cancer de Barretos, Barretos, BRAZIL.

**Aim**: In our study, we Aimed assessing the role of 11C-choline PET (CHO-PET) in patients affected by hepatocellular carcinoma (HCC) and comparing its diagnostic performance to conventional imaging with CT/MRI. **Materials and Methods**: We prospectively enrolled 28 consecutive patients (M:F=25:3; mean age 70years) affected by HCC: 11 patients at initial presentation and 17 patients at restaging after HCC relapse. In all cases, we performed a whole-body CHO-PET and compared findings with dedicated CT (n=25) and/or MRI scanning (n=12), for a total of 30 paired scans. The reference standard for imaging validation was either histology (10 patients) or a multidisciplinary work-up. Diagnostic performance was then determined for both imaging modalities on a scan-based and on a lesion-based analysis. **Results** : Out of the 30 paired scans, CHO-PET resulted positive in 25 cases. On a scan-based analysis, the sensitivity for PET was 83.3%, whereas for CT/MRI it was 100% (p=0.0613). Overall we detected 128 lesions, of which 62 in the liver and 66 in extra-hepatic sites. On a lesion-based analysis, the two imaging modalities demonstrated an overall sensitivity of 78.1% for PET and 66.4% for CT/MRI (p=0.0511). When considering only liver lesions, CHO-PET and CT/MRI showed a sensitivity of 62.9% and 87.1% respectively (p=0.0037). On counterpart, for extra-hepatic lesions PET showed a sensitivity of 92.4% versus a sensitivity for CT/MRI of 40.7% (p<0.0001). According to CHO-PET result, in 7 patients (25%) a change in treatment planning was determined. **Conclusions** : Our findings demonstrate that CHO-PET has a potential role in investigating patients with HCC. The principal advantage compared to CT/MRI appears its ability to detect extra-hepatic lesions, which can lead to treatment modification in a good proportion of patients.

## OP142

### First clinical experience with [$^{68}$Ga]TRAP(RGD)$_3$ for PET imaging of $A_v B_3$ expression in cancer patients

**J. Notni**[1], R. Braren[2], A. Beer[2], K. Steiger[3], A. Schlitter[3], I. Esposito[2], J. Siveke[2], M. Erkan[2], M. Schwaiger[2], H. Wester[1]; [1]Pharmaceutical Radiochemistry, Garching, GERMANY, [2]Technische Universität München, München, GERMANY, [3]Helmholtz-Zentrum München, Neuherberg, GERMANY.

**Introduction**: Radiopharmaceuticals based on cyclic RGD pentapeptides were previously used for in vivo imaging of $A_vB_3$-integrin status. We recently introduced [$^{68}$Ga]TRAP(RGD)$_3$, a cyclo(RGDfK) trimer with very high $A_vB_3$ affinity ($IC_{50}$=0.19 nanomolar), and report on first clinical PET studies using this tracer. The novel probe is based on the TRAP- (triazacyclononane-phosphinate) chelator which allows for efficient $^{68}$Ga-labelling and, optionally, high specific activity. **Materials & Methods**: Production of [$^{68}$Ga]TRAP(RGD)$_3$ was done on an automated module (GRP, Scintomics), using non-purified eluate of a $^{68}$Ge/$^{68}$Ga-generator with $SnO_2$-matrix (iThembaLABS). Clinical PET/MR or PET/CT studies were done either on a Biograph mMR or a mCT system (Siemens). PET studies were performed for nine patients ~30 min after injection of 120-150 MBq of [$^{68}$Ga]TRAP(RGD)$_3$, four of them with metastatic pancreatic adenocarcinoma (PDAC), four with hepatocellular carcinoma (HCC) and one with cholangiocellular carcinoma (CCC). Expression of $B_3$-integrin (clone SAP) in five resected tumors (formalin-fixed, paraffin-embedded tissue) was investigated semiquantitatively by immunohistochemistry. **Results**: [$^{68}$Ga]TRAP(RGD)$_3$ was produced with 97.4% RCY. Injected doses ranged from 121-149 MBq (100±23 GBq/µmol, 4.4±1.3 µg). [$^{68}$Ga]TRAP(RGD)$_3$ exhibited favourable biodistribution, showing only renal excretion and negligible uptake in background (i.e., muscle) tissue. Moderate tracer uptake was observed in salivary glands, thyroid, intestines, liver, spleen, and partially in pancreas, well corresponding to preclinical results which showed specific uptake in these tissues. [$^{68}$Ga]TRAP(RGD)$_3$ mostly showed intense uptake in both the primary PDAC tumors and in PDAC metastases. For one PDAC patient, a liver metastasis could be detected which was neither visible in CT nor in MRI including diffusion weighted imaging performed for staging. Heterogeneous but also partly intense uptake was seen in HCC and CCC; however, liver uptake was generally higher in these patients, resulting in somewhat lower tumor-to-liver ratios. SUV (mean/max) were 3.98/5.72 in tumors, 2.66/3.47 in liver, and 0.50/0.83 in muscle. Tumor/liver ratios ranged from 1.09-2.23 (mean 1.61), tumor/muscle ratios from 4.74-11.64 (mean 9.41). Preliminary immunohistochemistry showed $B_3$-integrin positivity in intra- and peritumoral vessels and in a part of the tumor cells with a patchy membranous and/or intracytoplasmatic pattern. **Conclusions**: [$^{68}$Ga]TRAP(RGD)$_3$, the first TRAP-based radiopharmaceutical being tested in a clinical setting, shows high $A_vB_3$-affinity (190 pM) and highly integrin-specific target binding without unspecific uptake, which is fully in line with preclinical data and was confirmed by immunohistochemistry. The resulting high target-to-background contrast and an excellent pharmacokinetic profile (only renal / no hepatobiliary excretion) render [$^{68}$Ga]TRAP(RGD)$_3$ a powerful substitute for [$^{18}$F]Galacto-RGD, thus warranting use in further patient studies.

501 — Sunday, Oct. 20, 16:30 — 18:00, Amphithéâtre

## CME 4 - Radiopharmacy & Drug Development: State of the Art of Radiopharmaceuticals

### OP143
**New SPECT Tracers**

**R. Schibli, SWITZERLAND**

### OP144
**New Radiopharmaceuticals for PET**

**P.H. Elsinga, NETHERLANDS**

### OP145
**New Radiopharmaceuticals for Therapy**

**G.J. Meyer, GERMANY**

502 — Sunday, Oct. 20, 16:30 — 18:00, Auditorium Lumière

## Symposium 4 - EANM/EORTC Joint Session: Imaging Biomarkers for Early Response Assessment in Clinical Oncology Trials

### OP146
**DW-MR: Ready for Prime Time?**

**N.M. deSouza, UNITED KINGDOM**

### OP147
**PET Imaging Biomarkers: Is FDG Unbeatable?**

**K. Herrmann, GERMANY**

### OP148
**Integrated PET/MR - The Future or just a Fancy Machine?**

**A.J. Beer, GERMANY**

504 - Sunday, Oct. 20, 16:30 - 18:00, Bellecour 1/2/3

## Featured - Physics & Instrumentation & Data Analysis: Image Reconstruction, TOF

### OP149

#### State of the Art PET Reconstruction using Time of Flight Information

**S. Vandenberghe, NETHERLANDS**

### OP150

#### Impact of PSF and ToF on the EANM procedure guideline for tumour PET imaging.

**E. H. de Groot**, J. R. de Jong, R. A. J. O. Dierckx, A. T. M. Willemsen; University Medical Center Groningen, University of Groningen, Groningen, NETHERLANDS.

**Aim** One of the Aims of the "FDG PET and PET/CT: EANM procedure guidelines for tumour PET imaging: version 1.0" (EJNMMI (2010) 37:181-200) is to harmonize SUV values in multicenter trials by specifying a bandwidth for the recovery coefficients (RC's) of the spheres inside the NEMA NU2-2001 Image Quality (NEMA-IQ) Phantom. Since this publication, time of flight (ToF) and position dependent point spread function (PSF) correction have been widely adopted. These additions improve both the RC's and the uniformity as expressed by the coefficient of variation (COV). The Aim of this study was to investigate whether these additions are compatible with the current guideline, what the minimum combinations of scan time and activity concentration are and what the potential improvement in RC values with ToF and PSF are. **Materials and Methods** A NEMA-IQ phantom was prepared conform the guideline, and was after a delay scanned on a Siemens TrueV mCT-64, mimicking a 75 kg patient injected with 3 MBq/kg FDG scanned one hour after injection. Emission scans during 1, 2 or 3 minutes per bedposition were performed, and repeated after 1, 2, 3 and 4 hours simulating lower dose scans. Scans were reconstructed using OSEM3D, PSF and PSF+ToF, using various matrix sizes and Gaussian filters. Using a 50% isocontour, the RC's and the maximum pixel value for each sphere were calculated and compared to the guideline values. The COV was determined in the background of the phantom. The maximum allowed COV was set at 15%. **Results** PSF and ToF resulted in higher RC's showing an improvement of image quality. Smaller matrices and larger filters reduced the COV. Larger Gaussian filters also lowered the RC's. For PSF+ToF, only a reconstruction using a 256x256 matrix and an 8 mm filter was within the current boundaries. PSF gave comparable results, while less filtering was needed for OSEM3D. Depending on the reconstruction, reduced counts scans were still within RC and COV boundaries. **Conclusion** PSF and PSF+ToF reconstructions have superior resolution compared to OSEM3D, explaining the higher RC's for all spheres. To obtain RC's within the current boundaries, resolution has to be sacrificed by employing large Gaussian filters which degrade image quality. Once PSF+ToF is more generally adopted, it should be considered to update the guidelines. PSF and PSF+ToF also improve signal to noise ratio explaining the improved COV. This shows the potential for further reductions in dose or scan time of about 30%.

### OP151

#### Improving TOF-PET by Studying Scintillation Photon Propagation and the Cherenkov Effect

**S. E. Brunner**[1], L. Gruber[1], J. Marton[1], K. Suzuki[1], T. Beyer[2], A. Hirtl[3]; [1]Stefan Meyer Institute for Subatomic Physics - Austrian Academy of Sciences, Vienna, AUSTRIA, [2]Center for Medical Physics and Biomedical Engineering, Medical University of Vienna, Vienna, AUSTRIA, [3]Department of Radiology and Nuclear Medicine, Medical University of Vienna, Vienna, AUSTRIA.

**Aim** Cherenkov radiation is emitted when charged particles traverse non-conductive matter, e. g. a scintillator, faster than the speed of light. In PET, Cherenkov photons are emitted instantaneously when electrons, ionized by an incident 511 keV photon, propagate within the scintillator crystal. Previous studies indicated a resulting improvement in timing resolution in PET coincidence measurements using the Cherenkov effect, e. g., [1]. Our goal is the quantitative assessment of this improvement in timing resolution when considering Cherenkov photons during the coincidence measurements. **Materials and Methods** This study is based on Monte Carlo simulations using Geant4 (4.9.4_p3). 511 keV photons produced by a point source impinging on a scintillator (LSO) crystal were simulated for single crystal setups and for basic coincidence setups (two opposing crystals). The propagation of the created optical photons (scintillation and Cherenkov) was analysed using single photon tracking. Parameters such as number of optical photons, energy, propagation path length, the location and process of photon creation and the location and time of detection were recorded. Due to the precise knowledge of the time stamps of individual photons, variations of the photon arrival rates at the detector can be determined and, therefore, the rise time of the scintillation signals can be calculated. The data were analysed by comparing the achievable timing resolution from coincidence measurements only and by adding the Cherenkov effect. **Results** Coincidence timing resolution for the basic coincidence setup with varying crystal lengths ranged from 32 ps (1 mm) to 144 ps (30 mm) FWHM for scintillation light based coincidence detection. With the additional detection of Cherenkov photons, the coincidence timing resolution was improved significantly (at least 20 ps). The signal rise time increased linearly with the depth of interaction (DOI) of the annihilation photon in the crystal. This increase was lower with the added detection of Cherenkov photons. Additionally, the normalized photon yield decreased exponentially with the DOI. **Conclusion** The added detection of Cherenkov photons improves the timing resolution of scintillator-based PET detectors. Rise time and photon yield measurements allow the determination of the DOI and, thus, the deduction of the real time of photon interaction inside the scintillator. These findings may help improve timing resolution and reduce parallax errors in PET imaging. Motivated by these first results, further investigations (simulations and measurements) of more complex setups will be performed and presented. References [1] P. Lecoq et al., IEEE Transactions on Nuclear Science 57, 2411 (2010).

### OP152

#### Impact of Point Spread Function and Time-of-Flight Reconstruction on the Sensitivity of SUVmax and SUVpeak to Decreasing Image Counts

I. S. Armstrong[1,2], **H. A. Williams**[1], M. D. Kelly[3], J. C. Matthews[2]; [1]Nuclear Medicine, Central Manchester University Hospitals, Manchester, UNITED KINGDOM, [2]MAHSC, University of Manchester, Manchester, UNITED KINGDOM, [3]Molecular Imaging, Siemens Healthcare, Manchester, UNITED KINGDOM.

**Aims**: New reconstruction algorithms should be introduced to clinical practice in a manner that enables reporters to apply experience with previous algorithms. Hence, reconstruction parameters for new algorithms are often adjusted so that image metrics such image noise and SUV recovery are matched to previous algorithms. This work assesses the impact of reconstruction algorithms incorporating point spread function (PSF) and time-of-flight (TOF) on the sensitivity of SUVmax and SUVpeak to image counts when matching image noise or SUV recovery. **Materials and Methods**: 10 replicate images of a NEMA image quality phantom with hot spheres at 8:1 contrast were reconstructed with OSEM, PSF, TOF and PSF+TOF algorithms on a Siemens Biograph mCT. Acquired net true counts were 60, 30, 15, 10 and 5 million. Gaussian filter FWHMs were chosen to either match background image noise (PSF: 3.8mm, TOF: 4.4mm, PSF+TOF: 2.9mm) or SUVmax recovery (PSF: 6.6mm, TOF: 4.8mm, PSF+TOF: 6.5mm) to OSEM with a 5.0mm filter. SUVmax and SUVpeak were measured in all spheres at each count level and expressed as the ratio of SUVmax and SUVpeak for the 60M count image. Two-tailed T-tests were performed to assess the significance ($p<0.05$) of SUV change with decreasing counts and also the effect of the four algorithms on SUV with decreasing counts. **Results and conclusions**: For SUVmax, values (measured relative to 60M SUVmax) increased as counts decreased and sphere size increased. At matched noise, there were no significant differences in values when comparing reconstructions. At matched recovery, significant reductions in were achieved with PSF and PSF+TOF in the 17 to 37mm spheres in 5 to 30M count images. As counts decreased, the values for SUVpeak were smaller in magnitude than for SUVmax. No significant changes with counts were observed in the 10, 17, 22, and 37mm spheres, for either matched noise or matched SUV recovery. The table shows a subset of SUV ratios illustrating these trends (5M/60M count images; 37mm sphere). **Conclusions**: SUVpeak is less sensitive to image counts and reconstruction algorithm than SUVmax. Sensitivity of SUVmax to image counts can be reduced by matching SUVmax recovery instead of noise to OSEM and using PSF-based reconstructions.

### OP153

#### Impact of Time-of-Flight and Point-Spread Function FDG PET/CT on the Optimization of Time Acquisition.

**M. J. Garcia-Velloso**, E. Prieto, J. M. Marti-Climent, M. J. Ribelles, C. J. Caicedo, L. Sancho, M. Rodriguez-Fraile, J. A. Richter; CLINICA UNIVERSIDAD DE NAVARRA, Pamplona, SPAIN.

**Objective** : We investigated the effect of Time-of-Flight (TOF) algorithm and point spread function (PSF) based reconstruction on tumor detection and quantification in short time FDG PET/CT acquisitions. **Methods** : whole-body FDG PET/CT examinations were performed on a Siemens Biograph mCT in 30 patients, 19 men, mean age 62 y.o. (25-82), mean BMI 24,6 (18-34). Emission data were acquired 60 min after i.v. injection of 5 MBq/kg of FDG. A 3 min list-mode acquisition was resampled to simulate 180 s, 120 s, 90 s, 60 s, 30 s and 15 s acquisitions. PET images were reconstructed using AW-OSEM with TOF and PSF (3 iter, 21 subsets, Gaussian filter 2 mm). Individual lesions were detected on the sets of images and semiquantitative analysis using volumes of interest was performed. The relative change in SUVmax, SUVpeak, and SUVmean with shorter scan times was reported. Furthermore, SUV values were measured for a 2 cm spherical region in the liver

and SNR was determined. Statistical analysis was performed to evaluate differences across different time acquisitions. **Results** : Visual analysis showed an increase in noise and a decrease in image quality as the acquisition time decreased. SNR progressively decreased as scan time decreased (SNR: 9.4 - 7.7 - 6.8 - 5.7 - 3.9 - 2.8 respectively) with significant differences in SUVmean in liver tissue among the different times per bed position (p<0,01). One hundred and twelve lesions were detected in 180 s, 120s, 90 s; 109 lesions were detected in 60 s; 99 lesions were detected in 30 s and only 77 lesions were detected in 15 s. Decreasing the time per bed position to 120 s, 90 s, and 60s produced a <10% variation in SUVmax and SUVmean values (p<0,05). Scan times of 30 s and 15 s produced a significant increase in both SUVmax (12.3% and 29.5% respectively) and SUVmean (11.8 %, and 28.2% respectively). The increase in SUVpeak values was <5% in every time acquisition. **Conclusions** : In whole-body FDG-PET/CT with TOF algorithm and PSF-based PET reconstruction the time per bed position affects SUVmax measurements. PET acquisition time can be reduced to 60 s/bed position with similar tumor detection, improving patient comfort and efficiency, and with a <5% variation in quantification with SUVpeak values.

## OP154

### Time of Flight and Resolution Recovery for PET in Clinical Praxis

**J. Trnka**, J. Kubinyi, V. Ptacnik; General University Hospital, Prague, CZECH REPUBLIC.

**Introduction:** Time Of Flight (TOF) and Resolution Recovery (RR) belong to the most advanced image processing techniques for improvement of PET images. However they are still quite new, and there is no general consistency how to use them properly. Many believe that they can be used to shorten acquisition time or to reduce applied activity. Therefore they are often purchased as an investment to reduce costs or other resources. But is this true? Is it even somehow possible to compensate for the lack of acquired counts ? **Methods:** After the installation of TOF (VPFX) and RR (SharpIR) options to our GE Discovery 690 PET/CT scanner, both these new techniques were substantially examined regarding qualitative and quantitative image quality for both the phantom studies and patient data. They were tested both separately and working together, as well as with different filter widths and various numbers of iterations and subsets. The results were assessed both visually and quantitatively, especially regarding partial volume effect (PVE) influencing SUV's of small lesions. **Results and Discussion:** TOF noticeably improves spatial resolution and moderately improves contrast, whereas RR noticeably improves constrast and moderately improves spatial resolution. The best results are achieved when both options are applied together. For optimal image quality it is necessary to set proper reconstruction parameters. The combination of 3 iterations, 32 subsets and 4-5 mm filter seems to be close to an optimum. With these settings (VPFX-S, 32/3, 4.5mm), the visual quality of both slice view and MIP rendering is apparently better regarding the original reconstruction (VPHD, 24/2, 6.4mm), as well as the PVE is measurably better suppressed. This makes some small lesions (formerly false negative) more easily detectable. However, by reduction of acquired counts, the (visual) image quality rapidly descends due to noise increase. Conversely, the contribution of new algorithms to image quality is much more considerable when acquired counts are increased (prolonged time per bed). TOF and RR can improve the acquired data, but they can not compensate for the missing counts. **Conclusion:** TOF and RR provide relevant improvement of PET image quality regarding the spatial resolution, contrast and suppression of PVE, which represents the most important clinical impact. However, they need enough counts to work properly. Attempts to reduce dosage or acquisition time are totally contraproductive.

505 - Sunday, Oct. 20, 16:30 - 18:00, Auditorium Pasteur

# Conventional & Specialised Nuclear Medicine: Bone 1 (Oncology)

## OP155

### Interobserver variation in the evaluation of bone scans in newly diagnosed prostate cancer

**H. D. Zacho**[1,2], J. Manresa[3], J. C. Mortensen[4], H. Bertelsen[1,5], L. J. Petersen[1,3]; [1]Dept. of Nuclear Medicine, Aalborg University Hospital, DENMARK, [2]Dept. of Clinical Physiology, Viborg Hospital, DENMARK, [3]Institute of Health Science and Technology, Aalborg University, DENMARK, [4]Dept. of Nuclear medicine, Herning Hospital, DENMARK, [5]Dept. of Nuclear Medicine, Randers Hospital, DENMARK.

**Aim**: The objective of this study was to assess variability among trained observers in the interpretation of bone scans in an unselected population of patients with newly diagnosed prostate cancer. **Materials and Methods:** A total of 671 consecutive patients were referred to three sites from March 2008 to October 2009 for bone scintigraphy as a part of the staging workup for newly diagnosed prostate cancer. Standard whole body bone scans were independently reviewed by three experienced nuclear medicine physicians in a separate session. The three observers were blinded to clinical and laboratory data. Each scan was classified according to two grading systems, A) a four category scale (1: normal scan and/or benign changes, 2: equivocal, 3: most likely malignant findings, and 4; multiple bone metastases), and B) a dichotomous scale (bone metastasis present or absent). **Results:** Uniform classification of bone scans on the 4-point scale was observed in 440/671 (66%) patients. A difference of one category scale was observed in 225/671 (34 %) and only in 6 (0.9%) patients was the scale difference > 1. The linear weighted Cohens kappa ranges between the three observers is 0.71, 0.72 and 0.72, and the Intraclass Correlation Coefficient 0.835, 0.835 and 0.839. The agreement among individual observers and the median category scale was very similar (76% - 78%). There was uniform agreement in 45% of patients with category 2 and 3 scans (representing 38% of all patients) with more than one scale of difference in 6/247 (2.4%) of these patients.Uniform agreement between the three reviewers was observed in 641/671 (96%) patients based on evaluation on a dichotomous scale. **Conclusion:** There is a low variation among trained observers for evaluation of bone scans in patients with newly diagnosed prostate cancer. The variation was very low using a dichotomous grading scale. Variation in classification of patients with equivocal and suspected malignant findings may have significant impact on subsequent imaging workup and therapeutic decisions.

## OP157

### Discordant Findings Between Choline-PET/CT and Bone Scintigraphy in Detecting Bone Metastases of Prostate Cancer: Bicentric Experience and Meta-analysis of the Literature.

**G. Treglia**[1], L. Evangelista[2], C. Vigneri[3], L. Ceriani[1], G. Paone[1], G. Giovacchini[4], G. Saladini[2], L. Giovanella[1]; [1]Nuclear Medicine and PET/CT Center, Oncology Institute of Southern Switzerland, Bellinzona, SWITZERLAND, [2]Radiotherapy and Nuclear Medicine Unit, Venetian Oncology Institute, Padua, ITALY, [3]Nuclear Medicine Unit, University of Messina, Messina, ITALY, [4]Department of Radio-Oncology and Nuclear Medicine, Stadtspital Triemli, Zürich, SWITZERLAND.

**Aim**: Radiolabelled choline-PET/CT and bone scintigraphy are both used for detecting bone metastases of prostate cancer. To date, there is an open debate between the experts whether choline-PET/CT could substitute bone scintigraphy to this regard. The Aim of our study was to evaluate the pooled prevalence of discordant findings between these Methods in this setting presenting the results of a bicentric experience associated to a meta-analysis of the literature, in order to establish whether one of these Methods could be really omitted. **Methods**: Choline-PET/CT and bone scintigraphy both performed in patients with prostate cancer for staging or restaging at the Oncology Institute of Southern Switzerland and Venetian Oncology Institute were retrospectively reviewed. Scintigraphic findings were considered positive or negative based on histology or clinical/imaging follow-up. The prevalence of discordant findings on a per patient-based analysis was calculated. Furthermore a systematic review of the literature was carried out including articles in which both Methods were performed in prostate cancer patients without selection bias. Data about discordant findings were retrieved by these articles. Finally, the overall pooled prevalence of discordant findings (including 95% confidence intervals) was calculated using the statistical software StatsDirect. **Results**: One hundred fifty-two patients (mean age: 70.1±6.9) who performed both Methods were included in our centers. Concordant findings were found in 126 cases (82.9%), discordant in 26 (17.1%). In 11 cases (7.2%) choline-PET/CT was positive and bone scintigraphy was negative/inconclusive for metastases, whereas in 15 cases (9.9%) bone scintigraphy was positive and choline-PET/CT was negative. Pooling these data with those obtained from 14 articles in the literature including other 782 patients, the overall prevalence of discordant findings was 8.2% (95%CI: 5-12%). Choline-PET/CT was positive and bone scintigraphy negative/inconclusive in 5.8% (95%CI: 3.4-8.7%) of cases, whereas bone scintigraphy was positive and choline-PET/CT negative in 2.4% (95%CI: 0.8-4.9%), without a statistically significant difference about the prevalence of these two groups. **Conclusions**: Discordance rate between choline-PET/CT and bone scintigraphy in prostate cancer patients is not negligible. There is not a statistically significant difference between the prevalence of patients with choline-PET/CT positive and bone scintigraphy negative/inconclusive and those with bone scintigraphy positive and choline-PET/CT negative. Therefore, to date, a clear superiority of one method on the other in detecting bone metastases of prostate cancer is not evident. Large prospective studies are needed to assess the factors which could guide the choice of the best scintigraphic method in this setting.

## OP158

### Bone metastasis: comparison between 18F-fluoride PET/CT and 99mTc-MDP bone scintigraphy

**L. Antunovic**[1], G. Ciocia[2], A. Chiti[1]; [1]Humanitas Clinical and Research Center, Milan, ITALY, [2]Humanitas Gavazzeni, Bergamo, ITALY.

**Purpose**: Sodium 18F-fluoride (FLU) is a bone seeking radiopharmaceutical for PET/CT imaging, demonstrated to have some advantages over bone scintigraphy

with 99mTc-MDP. High quality PET/CT images give answers to clinical questions on presence/absence of skeletal metastasis, thus improving patient management and therapy decisions; faster tracer uptake and shorter imaging time improve patient comfort. We present our experience on the clinical impact of FLU PET/CT compared with MDP bone scintigraphy. **Methods**: 17 patients (11 breast cancer, 1 sarcoma, 3 prostate cancer, 2 occult primary tumor) were submitted to MDP followed by FLU. Of these, 5 patients underwent MDP for staging, 9 for restaging, 1 for systemic therapy response evaluatio and 2 were in follow-up. In 3 cases there was previous clinical and radiological evidence of bone metastatic disease: one patient had multiple bone metastases from breast cancer and was already in therapy with bisphosphonates; one prostatic cancer patient had a single bone metastasis on previous evaluations; in one patient there was evidence of bone lesions from unknown neoplasia. All images were reviewed and interpreted by 2 board certified nuclear medicine physicians with experience in oncologic imaging**. Results**: MDP gave pathological results in 13 of 17 patients, but in 9/13 cases further imaging was recommended; in 4/17 cases, although there was no clear metastatic disease, further investigation was suggested. On FLU PET/CT evaluation, 6/17 patients were disease free and 10/17 patients showed bone metastasis; in one case FLU PET images were suggesting a benign bone lesion, but further imaging was required. PET/CT showed a higher number of bone metastases than MDP due to better spatial resolution and three-dimensional imaging. The evaluation of CT images allowed better definition of the lesions nature: in two cases areas of suspicious uptake in bone scintigraphy were related to unrecognized traumatic fractures, as seen by PET/CT. In the patient undergoing bone scintigraphy for evaluation of therapy response, PET/CT provided a clearer interpretation of new areas of tracer uptake previously visualized by bone scintigraphy. **Conclusions**: Further studies are needed to assess the impact on patient management, but our initial experience indicates that FLU PET/CT is a valuable tool in the evaluation of bone metastatic disease and offers distinctive advantages over MDP, particularly for accuracy and sensitivity of lesion detection.

## OP159

### Bone scan index as a biomarker of systemic metastatic bone involvement in prostate cancer can be easily obtained using an expert system

A. Namazian[1], **G. Berding**[1], F. Wilke[2], A. Böker[3], L. Geworski[2], M. A. Kuczyk[3], F. Bengel[1], I. Peters[3]; [1]Department of Nuclear Medicine, Hannover Medical School, Hannover, GERMANY, [2]Department of Medical Physics and Radiation Protection, Hannover Medical School, Hannover, GERMANY, [3]Clinic for Urology, Hannover Medical School, Hannover, GERMANY.

**Aim**: Bone scintigraphy is sensitive for the detection of metastases but its summary into one parameter of systemic bone involvement is a challenge. The bone scan index (BSI) has been suggested for this purpose, but it is complex to determine it. The present study evaluates the helpfulness of an expert system in this context. **Methods**: In 44 patients (69±6yrs.) scanned for bone metastases of prostate cancer (median Gleason score: 8, range 5-10) the EXINI bone software (EXINI, Lund, Sweden) has been employed to facilitate the determination of BSI. The software is based on artificial neural networks that have been trained using a large database of bone scans interpreted by fully-fledged experts. BSI as a measure of the extent of skeletal involvement and the number of metastases (NUM) were determined twice in 193 scans: (i) fully automated as provided by the software (available within seconds after data loading) and (ii) including individual selection and adaptation of lesions by a nuclear medicine physician (necessitating a few minutes). Furthermore, correlation of (i) physician modified parameters (BSI, NUM) to Gleason score and (ii) therapy related change in these parameters to change in tumor-marker PSA (prostate-specific antigen, baseline range 7-1046ng/ml) after 11 months of chemotherapy (Docetaxel) were evaluated. **Results**: In a small number of cases (4%) the automated scan analysis was cheated and included the bladder as a "bone metastasis". In all other cases a high correspondence between the automated and physician-modified result of analysis was observed for both parameters (BSI: r2=0.99, p<0.0001, NUM: r2=0,98, p<0.0001). There was no significant difference between automated and modified analysis for BSI (2.92 vs. 2.96, p greater than 0.05) but a small, significant difference in NUM (29 vs. 31, p<0.0001). In patients with a Gleason score ≥8, a tendency of more hotspots with increasing score was seen (r2=0.27, p=0.0197). With respect to chemotherapy monitoring the correlation to change in PSA was significant for change in BSI (r2=0.81, p<0.0001) and at the borderline of significance for NUM (r2=0.32, p=0.0569). **Conclusion**: In the vast majority of cases the expert system suggests lesions for BSI calculations, which require only minor modifications, and the few cases of program failure (due to bladder-activity) are easy to notice. Considering the minimal time requirement the program is most suitable for a clinical context. Moreover, preliminary analysis shows correlation of BSI with other biological parameters indicating BSI to be a valuable marker of systemic bone involvement.

## OP160

### Relationship of Bone Scan Index and Bone Alkaline Phosphatase in Prostate Cancer Patients with Bone Metastases

**H. WAKABAYASHI**[1], K. NAKAJIMA[1], A. MIZOKAMI[2], M. NAMIKI[2], A. INAKI[1], J. TAKI[1], S. KINUYA[1]; [1]Dept of Nuclear MEdicine, Kanazawa University Hospital, KANAZAWA, JAPAN, [2]Dept of Urology, Kanazawa University Hospital, KANAZAWA, JAPAN.

**Purpose** A computer-aided diagnosis system for bone scan using semiquantitative index [Bone Scan Index (BSI)] has been used to measure the tumor burden of bone metastases. However, BSI has the possibility to overestimate the extent and activity of bone metastases during treatment for reflecting healing process of the bone lesions compared with clinical bone metabolic markers. Therefore, we examined relationships of BSI, serum bone alkaline phosphatase (BAP), and serum prostate specific antigen (PSA) between before and after bone scan**. Methods** A total of 109 scans of 37 prostate cancer patients with bone metastases (number of median scans/person 2, range 1 to 8; median age 72 years, range 47 to 86) were included. BSI was automatically calculated by BONENAVI® software version 1 (FUJIFILM RI Pharma, Co. Ltd., Tokyo, Japan; Exini Bone, Exini Diagnostics, Sweden). Serum BAP and PSA were examined 3 times (1 month before, around same time with, and 1 month after each bone scan). Since serum BAP and PSA covered a large range of scales, we also used the logarithms. The Pearson product-moment correlation coefficient measures the strength of the linear relationship. For multiple comparison, subjects were divided into 3 groups according to BSI; Group A: 0 to <4, Group B: 4 to <8, and Group C: over 8. If the ANOVA F-test shows a significant difference between the groups, Dunnett's test was used for multiple comparisons. **Results** All bone scans showed high uptake with bone metastases. BSI was correlated significantly with the serum BAP [r=0.69 (1 month before), 0.66 (around the same time with), and 0.60 (1 month after bone scan)], logBAP (r=0.73, 0.71, and 0.64, respectively), and logPSA (r=0.44, 0.41, and 0.36, respectively). BSI was correlated with the serum PSA [r=0.17 (before 1 month)]. The statistical F value by ANOVA were 52 (1 month before), 47 (around same time with), and 20 (1 month after bone scan) in the serum BAP, 37, 42, and 25 in logBAP, and 15, 13, and 8 in logPSA, respectively. Comparison by Dunnett's test showed significantly higher values in Group B and C for the serum BAP, log BAP, and logPSA compared with Group A. **Conclusion** The BSI showed close relationships with BAP compared with PSA in prostate cancer patients with bone metastases and was effective to monitor the clinical course during treatment.

## OP161

### FDG-PET/CT versus bone scintigraphy for detection of bone metastases in breast cancer

**D. Grigolato**, M. Cucca, M. Zuffante, A. Arini, L. Bonfante, L. E. Etta, M. Ferdeghini; Azienda Ospedaliera Universitaria Integrata UOC Medicina Nucleare, Verona, ITALY.

FDG-PET/CT is a sensitive tool for tumor staging in different malignant diseases and bone scintigraphy is the standard procedure to evaluate bone metastases in breast cancer. **Purpose**: To assess the diagnostic accuracy of whole-body FDG-PET/CT and bone scintigraphy for the detection of bone metastases in breast cancer patients and to describe their distribution in the skeleton. **Material and Methods**: We retrospectively evaluated one hundred forty women (range 33-89 years) with histologically proven breast cancer who underwent bone scintigraphy and FDG-PET/CT from April 2010 to December 2012. Both examinations were performed during the initial staging in 9 patients, during the restaging in 127 patients with a history of advanced breast cancer and in 6 patients for doubtful findings at conventional imaging. Concordant readings between bone scintigraphy and FDG-PET/CT were considered true. In case of discordant readings, the results were verified with additional MR imaging , follow-up studies or biopsies. **Results**: Forty-six patients harbored bone lesions both on bone scintigraphy and FDG-PET/CT while 88 patients were free of bone metastases. There were four false results in bone scan: one woman had benign lesion at MRI (1 FP) and three patients were positive for metastases at biopsy and FU (3 FN). In the same patients PET/CT correctly identified the results. Two lesions remained unclear at FU. The distribution of bone metastases in the total of metastatic patients (50) was central (involving the proximal third of humerus and femur) in all patients and included the skull in eleven. There were no lesions in the peripheral extremities. There was significant discrepancy on a lesion-basis evaluation in 6 women in favour of PET/CT. The sensitivity of bone scintigraphy was 92% (47/50) compared to 98% (49/50) for FDG-PET/CT. The specificity of bone scintigraphy and FDG-PET/CT was 98% and 99% respectively. FDG-PET/CT depicted visceral lesions (in lymph nodes, lung, liver, breast, thorax and others) in 27/50 patients (54%) with bone metastases and surprisingly in 49/89 patients (55%) who had negative bone scans. **Conclusion**: FDG-PET/CT is more sensitive and specific for the detection of bone metastases compared with bone scintigraphy. None of the patients in this study had peripheral metastases excepted for the skull which can be included in the standard whole body PET/CT proving a sufficient staging and restaging in breast cancer metastases, as additional imaging of the periphery. Moreover FDG PET/CT had the advantage of allowing chest and abdomen examination in a single session.

## OP162

### Skeletal Muscle Metastases detection by 18F-FDG PET-CT imaging

**R. Jaller**, A. Domènech, V. Camacho, A. Flotats, A. Fernández, L. Geraldo, J. Deportos, I. Carrió; Hospital De la Santa Creu i Sant Pau, Barcelona, SPAIN.

**Aim**: To assess the role of 18F-FDG PET-CT to detect muscle metastases (MM) in oncologic patients. **Methods**: 18F-FDG PET-CT studies from 3213 patients referred for oncologic imaging at our hospital between June 2010 and December 2012, were retrospectively reviewed. Patients with hypermetabolic muscle lesions suggestive of metastases were included in the study. The incidence of MM in our setting as well as the source and the diagnostic implications of MM were studied. Results: Suspicious lesions for MM were identified in 32 patients. The presence of MM was confirmed in 18 patients: 7 by biopsy, 1 by MRI, 6 by a follow-up PET-CT and 4 by TC. Malignancy was ruled out in 2 patients: one by biopsy and another by MRI. In the 12 remaining patients the MM was not confirmed due to the poor clinical condition of the patients. The overall incidence of MM was close to 1% (30/3213). The primary sources of MM were lung cancer (6 patients [20%]), lymphomas (6 patients [20%]) and head and neck malignancy tumors (6 patients [20%], followed by esophagogastric tumors (3 patients [10%]) , breast neoplasm (2 patients [6.7%]), sarcomas (2 patients [6.7 %]), bladder and genitourinary malignancies (1 patient [3.3%]), colon cancer (1 patient [3.3%]), histiocytoma (1 patient [3.3%]), apocrine glands tumor (1patient [3.3%]) and adenocarcinoma of unknown origin (1 patient [3.3%]). The most affected muscle group was the upper extremity (9 patients [30%]). Twenty-nine patients (97%) had widespread disease in the PET-CT. Therefore, neither the staging nor the treatment of the patients were altered by the presence of MM. **Conclusions**: Our results demonstrate that PET-CT is a useful technique for detecting unsuspected MM. Tumors found to metastasize more frequently to the muscular system were lung cancer, lymphomas, and head and neck tumors. Patients with MM are in advanced stages of their disease and therefore, they are generally not upstaged.

506 - Sunday, Oct. 20, 16:30 - 18:00, Grand Salon Prestige Gratte-Ciel

## Cardiovascular: Myocardial Perfusion SPECT II

## OP163

### Stress-only Myocardial Perfusion Imaging: Which should be followed by a rest study? Intra- and interobserver agreement for physicians on different training levels

**J. A. Ejlersen**[1], J. Mortensen[1], G. L. Nielsen[1], O. May[2], J. K. Lauridsen[3], A. Johansen[3]; [1]Department of Nuclear Medicine, Regional Hospital West Jutland, HERNING, DENMARK, [2]Cardiovascular Research Unit, Regional Hospital West Jutland, HERNING, DENMARK, [3]Department of Nuclear Medicine, Odense University Hospital, Odense, DENMARK.

**Aim** Several studies have convincingly shown that a normal stress myocardial perfusion study implies a good prognosis. Focus on radiation safety and efficient patient flow has led to increased attention on stress-only protocols for myocardial perfusion imaging. This study focused on the observer agreement whether the stress perfusion is considered completely normal or a rest study is needed to achieve a final diagnosis. **Materials and Methods** In a prospective study, patients with stable angina and no known ischemic heart disease referred for coronary angiography underwent a two-day Sestamibi (10 MBq/kg) exercise/rest myocardial perfusion protocol with attenuation correction (AC). The stress images were blinded and evaluated twice by two experienced nuclear physicians (E1 and E2) and two novice nuclear physicians (N1 and N2) from two institutions (I1 and I2). Both institutions routinely use the stress-only approach, but only I1 routinely use AC. The time frame between the two evaluations was at least two weeks. Two weeks after the second evaluation, E1 and E2 met in person and performed a consensus reading. Agreement was expressed as exact agreement (percent) and by Kappa statistics. Comparisons between observers were made by the McNemar test. A Kappa-value >0.80 was considered as "excellent", 0.61-0.80 as "good", 0.41-0.60 as "moderate" and 0.40 or less as "poor". **Results** All 109 patients (80 males, mean aged 61.2[SD 9.0]) years were stressed sufficiently. The consensus-readers required a rest-study for 47 (43%) patients. Rest studies were requested by physicians as follows: E1: 37%, E2: 42%, N1: 43% and N2: 51%; p(E)=0.13, p(N)=0.03, p(I1)=0.02; p(I2)=0.02). The intraobserver kappa-values were: E1:0.97 [95% confidence interval 0.91-1.00]; E2:0.77[0.65-0.90]; N1:0.91[0.82-0.99] and N2:0.96[0.91-1.00]. The interobserver kappa-values for the first reading made by observers at the same level or institution were: E:0.69[0.56-0.83], N:0.68[0.56-0.82], I1:0.83[0.72-0.95] and I2:0.67[0.63-0.81]. The interobserver kappa-values between the consensus reading and the observers' first reading were E1:0.81[0.70-0.92], E2:0.81[0.70-0.92], N1:0.80[0.68-91] and N2:0.74[0.62-0.86]. **Conclusion** Overall, the inter- and intraobserver agreement whether a stress study should be followed by a rest study or not was good or excellent, respectively. Physicians familiar with AC tended to have the highest degree of agreement. The novice physicians and physicians not familiar with AC required more rest-studies. Comparing the individual observers with the consensus reading showed excellent agreement except for the novice physician unfamiliar with AC, for whom the agreement was good. Hence, it seems acceptable to let physicians on different training levels judge if a rest-study is needed.

## OP164

### Incremental Prognostic Value of Gated SPECT Myocardial Perfusion Scans With Dipyridamole Stress in Patients With Left Bundle Branch Block

**N. Fatima**[1,2], M. Zaman[3,4], M. Ishaq[2], R. Omar[5]; [1]Department of Nuclear Medicine, Dr Ziauddin Medical University, Karachi, PAKISTAN, [2]Karachi Institute of Heart Diseases (KIHD), Karachi, PAKISTAN, [3]Department of Radiology, The Aga Khan University Hospital (AKUH), Karachi, PAKISTAN, [4]Karachi Institute of Heart Disease (KIHD), Karachi, PAKISTAN, [5]Karachi Institute of Heart Diseases (KIHD), Karachi, PAKISTAN.

**Objective:** Gated single photon emission computerized tomography (GSPECT) myocardial perfusion imaging (MPI) has well validated incremental prognostic value. The Aim of this study was to find out the prognostic value of abnormal dipyriodamole GSPECT MPI in patients with left bundle branch block (LBBB). **Material and Methods:** This was a prospective study conducted at Nuclear Cardiology Department of Karachi Institute of Heart Diseases (KIHD), Karachi from August 2010 till February 2011. Total 345 patients (135 with LBBB comprised Group A and 210 without LBBB comprised Group B) with adequate dipyridamole GSPECT MPI were included. These patients were followed-up for 18-24 months (mean 20 ±3 months) for fatal or non-fatal infarctions (MI). **Results:** GSPECT scans were positive for abnormal in 47/135 (35%) in Group A and in 90/210 (43%) in Group B patients (non-significant p values). However, fixed perfusion defects were significantly higher in Group A (27%) than Group B (15%) while reversible defects were significantly higher in Group B (28%) than Group A (08%). Similarly incidence of transient ischemic dilatation (TID) was significantly higher in Group B (16%) than Group A (02%). Mean sum stress score (SSS) was higher in Group A (6 ±5) while mean sum difference score (SDS) was higher in Group B (4 ±2). Left ventricular ejection fraction (LVEF) was significantly lower in Group A (42 ±16) than Group B (58 ±8) with significantly higher end diastolic and end systolic volumes (EDV, ESV) in Group A. At 18-24 months follow up, 09 (4.3%) non-fatal events were reported in Group B while in Group A it was 04 (2.9%, non-significant p values). Total 8 (5.90%) fatal MIs were reported, all in Group A and none in Group B (significant p values). Kaplan Meier survival plot for non-fatal MI shows a similar event free survival in both groups with a Log Rank value 0.217 (non-significant p value) [Figure 2]. Kaplan Meier survival plot for fatal MI show significantly low event free survival for patients with LBBB (Group A) with a Log Rank value 10.552 (significant p value). **Conclusions**: We conclude that dipyridamole GSPECT MPI provides important prognostic information in patients with LBBB. LBBB group had lower LVEF which was a strong predictor of cardiac deaths while perfusion parameters were predictors of non-fatal MIs in patients with or without LBBB.

## OP165

### Adenosine Myocardial Perfusion Imaging: Increased workload reduces disturbing bowel activity, decreases the side effects and facilitates patient flow

**J. A. Ejlersen**[1], L. C. Gormsen[2], L. E. Nielsen[2], M. S. Hansen[1], J. Madsen[2], J. Mortensen[1], K. Bouchelouche[2]; [1]Department of Nuclear Medicine, Regional Hospital West Jutland, HERNING, DENMARK, [2]Department of Nuclear Medicine & PET Centre, Aarhus University Hospital, Skejby, Aarhus, DENMARK.

**Aim** Physiological exercise is preferred over vasodilator stress for several reasons. Besides gaining clinical information from the exercise test, imaging can be performed shortly after the tracer injection, no oral fat intake is needed and the image quality is almost always excellent. This makes the examination time short and logistics easy, which is favourable to both patient and staff. Patients undergoing vasodilator stress are not suited for a regular physiological test, but most are capable of exercising to a certain extent. To gain benefits from exercise and to minimize the side effects from adenosine, it is routine to perform light treadmill exercise (approximately 25 Watt) during the adenosine infusion in suitable patients (Ado-25 protocol). We studied if the frequency of visually acceptable images obtained within 1 hour after the Sestamibi injection was increased if the adenosine infusion was preceded by 5 minutes increasing bicycle exercise (25 Watt/minute) up to maximum 125 Watt (Ado-Ex protocol). **Materials and Methods** From November 2011 to February 2013, we prospectively and consecutively included all patients scheduled for Ado-25 adenosine stress at the two departments. At department A (West) all suitable participants performed the Ado-Ex protocol, at department B (Skejby) they performed the standard Ado-25 protocol. Groups were compared by un-paired t-test (continuous variables) and chi squared test or Fishers Exact test as appropriate (categorical variables). **Results** 411

patients (A: 157, B: 254) aged 64.5(10.7) years (mean(SD)) (A: 65.1(10.8), B: 63.2(10.4), p=0.11) were included. 59.9% were male (A: 63.7., B: 52.8, p=0.03). Fewer severe adenosine side effects (severe discomfort, chest pain or dyspnoea, 2°/3° degree AV-block, vomiting) were observed in the Ado-Ex group (A: 6.4%, B: 16.9%, p=0.001). Imaging was performed 5-200 minutes after Sestamibi injection (p.i.) and 376 of the included patients (91.5%) had an acceptable image quality on the first scan, p=0.34. One-hundred-eight patients were scanned 5-30 minutes p.i. (A: 96, B: 12, no difference in age or gender) and 89 of these (82.4%) had an acceptable image quality (A: 81(84.4%), B: 8(66.7%), p=0.10). One-hundred-thirty-two patients were scanned 30-60 p.i. (A: 46, B: 86, no difference in age or gender) and 122 (92.4%) had an acceptable image quality (A: 46(100%), B: 76(88.4%), p=0.01). **Conclusion** Five minutes stepwise increasing workload prior to adenosine infusion seems to reduce the incidence of severe adenosine side effects and improve early image quality. Our results indicate that the optimal scan time is 30-60 minutes after the Sestamibi injection.

## OP166

### Transient Ischemic Dilation in Diabetic Patients: Prognostic Value and Impact on Clinical Outcome after Coronary Revascularization

**R. Assante**[1], M. Petretta[1], W. Acampa[2], S. Daniele[2], M. P. Petretta[1], E. Zampella[1], M. Plaitano[1], A. Cuocolo[1]; [1]University of Naples - Federico II, Napoli, ITALY, [2]National Council of Research, Napoli, ITALY.

**Aim**: Transient ischemic dilation (TID) on myocardial perfusion single-photon emission computed tomography (MPS) provides incremental diagnostic information to standard myocardial perfusion analysis for the identification of severe coronary artery disease (CAD) in diabetic patients. However, investigations on the prognostic value of TID in large cohorts of diabetic patients are still lacking. We prospectively evaluated the incremental prognostic value of TID in patients with type-2 diabetes during long-term follow-up and estimated cardiac death and nonfatal myocardial infarction using traditional approaches of prognostication to more recent Methods. We also assessed the relationship between clinical outcome and coronary revascularization procedures according to gated MPS findings. **Material and Methods**: A total of 672 consecutive diabetic patients with available rest and stress gated MPS data were enrolled. Multivariable Cox proportional hazards models were employed to estimate cardiac death and nonfatal myocardial infarction. Risk reclassification was calculated and the effect of coronary revascularization on event-free survival was evaluated. **Results**: At multivariable analysis, post-stress LV ejection fraction (EF) (hazard ratio, HR, 2.3, 95% confidence interval, CI, 1.4-3.9, P<0.005), MPS ischemia (HR 1.9, 95% CI 1.1-3.5, P<0.01), and TID (HR 2.7, 95% CI 1.6-4.6, P<0.0001) were independent predictors of events. The addition of TID improved the power of a model including clinical cardiac risk, LVEF, and ischemia (P<0.0001). The addition of TID resulted in reclassification of 169 patients (25% of the sample). The reclassification was correct in 123 and incorrect in 46 patients with a net reclassification improvement of 0.14 (95% CI 0.02-0.26, P<0.05). Overall, 120 patients were reclassified to a lower risk category (estimated probability of event 1.2%/year), 503 were unchanged (estimated probability of event 2.3%/year), and 49 were reclassified to a higher risk category (estimated probability of event 4.1%/year) (P<0.05). Revascularization had a significant effect on event-free survival (HR 0.28, 95% CI 0.09-0.88, P<0.05), which was more evident in patients with impaired LV function, severe MPS ischemia, and TID. **Conclusions**: TID provides independent and incremental prognostic information for the prediction of cardiac death and nonfatal myocardial infarction in diabetic patients. The addition of TID to a prediction model based on clinical data, LV ejection fraction, and MPS ischemia, results in correct reclassification of approximately one fifth of the study population. The beneficial effect of revascularization was more evident in patients with severe ischemia and was related to the severity of LV systolic dysfunction and TID.

## OP167

### Very High Coronary Calcium Score Confers High Diagnostic Added Value for Detecting Coronary Artery Disease in Patients with Normal Myocardial Perfusion Imaging

**S. Fukuzawa**, J. Sugioka, A. Ikeda, S. Okino, J. Maekawa, S. Ichikawa, N. Kuroiwa, s. Okamoto, M. Inagaki; Funabashi Municipal Medical Center, FUNABASHI, JAPAN.

**Background** Measure coronary artery calcium (CAC) serve as a quantitative reflection of the severity of coronary artery atherosclerosis, and greater calcium burdens correlate with more advanced disease. By comparison, gated myocardial perfusion scintigraphy (MPS) is a well-established noninvasive imaging modality that is a core element in evaluation of patients with stable chest pain syndromes. Stress MPS is the most commonly used stress imaging technique for patients with suspected or known coronary disease. **Objectives** The Aim of study was to evaluate the clinical impact of a very high coronary artery calcium score (CAC ≥ 1000) in patients with no known coronary artery disease (CAD) and normal MPS. Furthermore, we evaluated whether triple vessel disease would support the notion of balanced ischemia as an underlying mechanism of false negative MPS in patients with very high CAC. **Methods** Twenty-five patients with suspected CAD and normal stress/rest MPS and CAC ≥ 1000 prospectively underwent invasive coronary angiography as the standard of reference. When coronary lesions with ≥ 50% luminal diameter narrowing on invasive coronary angiography were shown, intracoronary pressure measurements to determine fractional flow reserve (FFR) are increasingly performed during coronary angiography. FFR was performed using a pressure wire with hyperemia from intravenous adenosine. Abnormal FFR ≤ 0.80 were considered to represent significant stenosis. **Results** The median total CAC was 1344 (range 1002-3118). In 19 (76%) of twenty-five patients, invasive analysis with FFR on coronary angiography revealed one-vessel disease (1-VD) (n=8), 2-VD (n=6), 3-VD (n=9) or left main disease (n=2). **Conclusions** In patients with gated single photon emission computed tomography MPS, a CAC ≥ 1000 confers a high diagnostic added value for detecting CAD. This is not solely based on unmasking balanced ischemia due to epicardial 3-VD or left main disease on MPS, as it occurred predominantly in patients with 1-VD and 2-VD. The relative prognostic value of each modality needs to be determined by a follow-up of this cohort.

## OP168

### Impact of CT-based Attenuation Correction on the Diagnostic Performance of Myocardial Perfusion Imaging

**C. A. Savvopoulos**, P. Barla, V. Lakiotis, E. Rapti, T. Spyridonidis, P. J. Vassilakos, D. Alexopoulos, D. J. Apostolopoulos; University Hospital of Patras, Patras, GREECE.

**Aim**: The purpose of this study was to assess the impact of CT-based attenuation correction on SPECT myocardial perfusion imaging (MPI) in the evaluation of coronary artery disease (CAD). **Materials and Methods**: We retrospectively analyzed 120 patients (90 males and 30 females) who underwent coronary angiography (CANG) <2 months after routine stress/rest Tl-201 SPECT MPI with CT-based attenuation correction. Of them, 24% had a history of AMI and 35% had previously been subjected to revascularization. Acquisition was performed by means of a "Hawkeye" hybrid system (GE healthcare). Data was analyzed quantitatively in order to avoid observer interference. 20-segment polar maps of non-corrected (NAC) and attenuation corrected (AC) studies were used to obtain overall summed-stress (SSS), summed-rest and summed-difference (SDS) score values as well as corresponding scores for LAD and combined RCA/LCx domains. Using CANG findings as reference, ROC curves were created to determine SSS and SDS diagnostic cut-offs for AC and NAC in LAD and RCA/LCx domains separately for males and females. Studies were considered abnormal if either their SSS or SDS lay above the respective cut-off value. Sensitivity, specificity and accuracy of each MPI technique were then calculated. The areas under the ROC curves (AUC) were also compared. **Results**: In our cohort, CAD prevalence for ≥50% coronary artery stenosis was 62% in males and 33% in females. In males, NAC sensitivity, specificity and accuracy was 67%, 72%, 70% in the LAD and 90%, 54%, 73% the RCA/LCx domain. Corresponding AC figures were 77%, 68%, 71% and 65%, 83%, 73%. The McNemar's test verified statistical significance for higher NAC sensitivity (p=0.003) and higher AC specificity (p=0.003) in the RCA/LCx territory, but yielded non-significant results regarding accuracy (p=0.8). No notable NAC/AC disparity was substantiated in the female subgroup. Results were similar when the CANG ≥70% stenosis criterion was selected. AUC comparison produced no difference between NAC and AC in either males or females, LAD or RCA/LCx, ≥50% or ≥70% stenosis definition, by either SSS or SDS approach. **Conclusion**: Our findings suggest that AC improves Tl-201 MPI SPECT specificity in the RCA/LCx domain in males at the cost of reduced sensitivity in the same area. These results challenge the necessity of CT-based AC in routine clinical practice.

## OP169

### CT-Based Attenuation Correction in Myocardial Perfusion Scintigraphy - Risk Stratification and Prognostic Significance

**C. A. Savvopoulos**, N. Papandrianos, S. Alexiou, E. Rapti, T. Spyridonidis, P. J. Vassilakos, D. Alexopoulos, D. J. Apostolopoulos; General Hospital of Patras, Patras, GREECE.

**Aim** To investigate the impact of CT-based attenuation correction on the prognostic efficacy of myocardial perfusion imaging (MPI). **Materials and Methods** Seven-hundred and twenty consecutive patients from our daily routine underwent stress/rest Tl-201 SPECT MPI with CT-based attenuation correction. A "Hawkeye" hybrid system (GE Healthcare) was used. Non-corrected (NAC) and attenuation-corrected (AC) studies were interpreted blindly. Summed-stress scores (SSS) were calculated for NAC and AC from corresponding 20-segment polar maps. Left ventricular dilation (LVD) and transient ischemic dilation were also recorded. Follow-up was conducted by telephone interview and/or review of hospital records. Study endpoints were all-cause mortality and the composites of death/non-fatal AMI and death/AMI/late revascularization. SSS cut-offs were determined independently for AC and NAC results according to event rate distribution across SSS values. Subsequently, Kaplan-Meier curves were drawn and compared. Univariate Cox proportional hazards analysis was employed to examine

the prognostic significance of clinical and scintigraphic variables. Statistically significant parameters were then entered into the multivariate Cox model. **Results** Our final cohort involved 637 patients after excluding 25 technically unacceptable studies, 32 early revascularizations (<2 months) and 26 lost during follow-up. Thirty-two percent had previously documented coronary artery disease. Of the remaining, 26% had low, 38% intermediate and 36% high 10-year risk of cardiac events according to the "HEART" scoring system. During follow-up (Mean±SD=42.3±12.8 months) 24 patients expired (7 cardiac deaths), 13 experienced non-fatal AMI, while 28 were subjected to late revascularization. Selected SSS cut-offs categorized perfusion results into three groups: 0-4; 5-13; >13 (NAC) and 0-2; 3-9; >9 (AC). In the Kaplan-Meier analysis, NAC demonstrated statistical significance between SSS 5-13 and >13 for all-cause mortality and between all SSS groups for both composite endpoints. AC was only able to discriminate between 0-2 and >9 for death/AMI and between 0-2 and 3-9 for death/AMI/late revascularization. In the univariate analysis, abnormal NAC (SSS>4), male sex, age>65 y.o. and LVD predicted all-cause mortality whereas abnormal AC (SSS>2) was not significant. Regarding composite endpoints, abnormal AC was a significant predictor but its hazards ratio nearly halved that of abnormal NAC (2.14 vs. 4.15 for death/AMI and 2.10 vs. 3.28 for death/AMI/revascularization). In the multivariate model, only NAC SSS results proved to be independent from other scintigraphic and clinical covariates. **Conclusion** In our study cohort AC failed to perform effective risk stratification, apparently due to underestimation of perfusion defects. On the contrary, NAC MPI managed to preserve its established prognostic value.

## OP170

### SPECT wall thickening prognostic value

**L. Dercle**, O. Lairez, T. Cognet, S. Méjean, D. Bastié, M. Galinier, D. Carrié, I. Berry; CHU Toulouse, Toulouse, FRANCE.

**Introduction** New echocardiographic technics have shown that myocardial deformation is a strong predictor of outcome, superior to ejection fraction (EF). The **Aim** of this study was to assess the correlation between global wall thickening (GWT) obtained by gated single photon emission computed tomography (SPECT) and echocardiographic measures (EF and global longitudinal strain (GLS) and strain rate (GLSR)) and to compare their prognostic value for all-cause mortality. Subjects and Methods 74 patients referred for dipyridamole myocardial perfusion SPECT were prospectively included and underwent a transthoracic echocardiography at the peak of stress to measure left ventricular EF, GLS and GLSR. **Results** Mean EF, GWT, GLS and GLSR were 54.1±13.7%, 36.4±14.8%, - 16.4±4.6% and - 1.3±0.4%, respectively. The strongest correlation with GWT was for EF (R = 0.63, P < 0.001), followed by GLSR (R = -0.57, P < 0.001) and GLS (R = -0.53, P < 0.001). There were 10 deaths over a period of 14.6±5.7 months. By multivariate Cox analysis, only diastolic blood pressure (HR 0.86; P = 0.005), EF (HR 1.01, P = 0.031), GLS (1.593, P = 0.001) and GWT (HR 0.898, P = 0.034) remained independent predictors of all-cause mortality. The presence of myocardial ischemia was not statistically significant. The areas under the ROC curve of GLS (0.905) with a best cutoff point of -11.9%; GWT (0.816) with a best cutoff point of 24% and EF (0.743) with a best cutoff point of 38% were not statistically different. Mean survival evaluated by Kaplan-Meier analysis was longer in patients with GWT ≥ 24% (21.9±0.6 months) than those with GWT < 24% (13.6±2.7 months; P < 0.001). **Conclusion/Discussion** GWT assessed by gated SPECT is a highly sensitive tool to detect early myocardial systolic dysfunction and brings additive prognostic information, over myocardial ischemia.

507 - Sunday, Oct. 20, 16:30 - 18:00, Salon Pasteur

# Conventional & Specialised Nuclear Medicine: FVO - Sjögren - Sarcoidosis

## OP171

### Comparison between Gallium-68 citrate PET-CT and Gallium-67 citrate scintigraphy for infection imaging

**T. Segard**[1], L. Morandeau[1], A. Evans[1], M. Dunne[2], O. Robinson[2], R. Murray[1], E. Geelhoed[3], R. Francis[3]; [1]Sir Charles Gairdner Hospital, Nedlands, AUSTRALIA, [2]Royal Perth Hospital, Perth, AUSTRALIA, [3]University of Western Australia, Crawley, AUSTRALIA.

**Aim:** Preliminary studies have been published demonstrating the potential utility of Ga-68 citrate PET-CT for infection imaging. In addition to improved image quality with Ga-68 citrate PET-CT, there are several other potential benefits over the current 'gold standard' nuclear imaging technique Ga-67 citrate scintigraphy: reduced radiation dose to patients, significantly shorter time between injection and imaging and reduced time required for image acquisition. The Aim of this study is to prospectively evaluate Ga-68 citrate PET-CT, in a multicentre public hospital setting and to compare it to Ga-67 scintigraphy, to ascertain whether Ga-68 citrate PET-CT is of equivalent diagnostic efficacy to Ga-67 citrate scintigraphy for bone and joint infection or pyrexia of unknown origin (PUO), and assess image quality and reporter confidence for the interpretation of Ga-68 citrate PET-CT compared to Ga-67 citrate scintigraphy. **Materials and Methods**: Ga68 citrate was synthesized using an ITG silica based 68Ge/68Ga generator coupled to the iQS Ga-68 Fluidic Labeling Module. Patients with PUO, bone and joint infection or vascular infection were eligible for enrolment. In addition to a Ga-67 citrate planar wholebody and SPECT-CT study, patients were injected with 98MBq of Ga-68 citrate for PUO and imaged from vertex to below knees or 140 MBq for limited view bone and joint or vascular infection. Imaging was performed with time-of -flight PET-CT at one hour post administration of Ga-68 citrate. The radiation dose to patients from the Ga-68 citrate PET-CT was less than 5mSv. No patient preparation was required for either the Ga-68 citrate or Ga-67 citrate scans. Patients were followed up for 3 months post-imaging to record subsequent treatments and results: antibiotic therapy, surgery, biopsy results when performed, radiological and clinical responses to therapy. **Results**: Eight patients have been recruited: six for bone and joint infection, one for PUO and one for vascular infection. There have been no adverse events related to Ga-68 citrate injection in the first eight patients. Image quality has been good, despite low administered doses of Ga-68 citrate. There is prominent blood pool activity at one hour on the Ga-68 citrate PET images, which, in the initial patient group, limits interpretation of vascular infection. Identification of bone or joint infection however appears promising. **Conclusion**: Initial experience confirms that Ga-68 citrate PET-CT is safe and feasible, with promising images obtained at 1 hour post injection. Expanded recruitment of this multicentre clinical trial will therefore be undertaken.

## OP172

### 68Ga-DOTANOC PET/CT in sarcoidosis: scope beyond Neuroendocrine tumours

**A. Malhotra**, S. Singla, R. Kumar, S. Sharma, S. K. Sharma; All India Institutes of Medical Sciences, New Delhi, INDIA.

**Aim:** The present study Aims to compare the diagnostic performance of 68Ga-DOTANOC PET/CT with conventional investigations in treated and untreated sarcoidosis. **Materials and Methods**: Fifteen patients (M/F=10/5), known cases of sarcoidosis were referred for 68Ga-DOTANOC PET-CT study. The patients were injected 3 mCi (111MBq) and scans extending from skull base to mid-thigh region were acquired one hour post-injection. Region of Interests (ROIs) were drawn on nodal lesions, lung fields and mediastinum to calculate SUVmax and lesion to mediastinum ratio. The findings of PET/CT were compared with HRCT chest, clinical findings, pulmonary function test (PFT), and serum Angiotensin-converting enzyme (ACE) levels. Written informed consent was obtained from all patients and the study was approved by the institutional ethics committee**. Results**: The mean age of the patients was 41±10 years. Four patients had stage 1 disease, eight patients had stage 2, two patients had stage 3 and one case with stage 4 disease. There was past history of treatment with steroids in 10 cases, no treatment in three and two cases were on steroids at time of study. The findings of PET and HRCT were 80% concordant in detection of active nodal disease and 60% for active pulmonary lesions (p=0.250; p=0.688). Addional lymph nodal lesions than HRCT were detected in 3 (20%) cases in axillary, internal mammary and inguinal regions. The average serum ACE levels were 50±17 (20 - 80), serum Vitamin D levels were 30±16 (4 - 56), SUVmax nodal lesions was 4.2±3.5 and lung was 1.6±1.2. There was no significant correlation between node/mediastinum ratio, lung/mediastinum ratio and lesion SUVmax with serum ACE levels (p=0.109; p=0.654; p=0.078). However, the lung SUVmax was 2.3±1.1 in patients with exacerbation of pulmonary symptoms which was significantly higher compared to 0.8±0.5 in patients with normal PFT (p=0.018). There was an increased tracer uptake in lesions of both the patients on steroid treatment requiring addition of immnosuppresants. Also, discontinuation of treatment was attempted successfully in two cases with inactive lesions on PET. **Conclusion**: 68Ga-DOTANOC PET can identify active lesions of sarcoidosis and increased uptake in lungs is associated with deranged PFTs. Additional lesions can be detected in 20% cases compared to HRCT and change in management in 27% cases was observed with PET/CT.

## OP173

### Is In-111 WCC SPECT/CT of value in patients with pyrexia of unknown origin (PUO)?

**F. Dambha**, E. Nowosinska, J. Buscombe; Cambridge University, Cambridge, UNITED KINGDOM.

**Objectives:** Assessment of In-111 leukocyte SPECT/CT in patients with PUO. **Methods**: 18 Patients underwent a whole-body In-111 leukocyte scintigraphy and SPECT/CT of chest, abdomen/pelvis or long bones/prosthetic joints at 24 hours. The final diagnosis was based on microbiology, histopathology or imaging follow- up. **Results**: Within 12 month period, 18 patients were identified (11 female), mean age 63 (range 16-93). 12 patients had imaging appearances consistent with soft tissue infection: liver (2), bowel (1), vascular (3), muscular (2), subcutaneous tissue (1),multifocal (1) in the right tibia (1), and 2 had prosthetic joint infection (PKJI). Of these, 7/12 were confirmed as infection. Multifocal WCC uptake (1) and vascular

uptake (1) were thought to represent inflammatory changes whereas increased white cell concentration in the right tibia was related to post surgical changes. Of 6/18 patients with negative In-111WCC studies 4 had negative radiological follow up. In a further 2 In-111 WCC (-) ve patients radiological imaging demonstrated pneumonia and pyelonephritis. Overall sensitivity was 78%, specificity of 44%, PPV 58 % and NPV 67%. The In-111 SPECT/CT leukocyte study changed the management in 44% patients. **Conclusion**: In-111 leukocyte SPECT/CT is useful in identifying and localising both soft tissue and bone infection.

## OP174

### Diagnostic Contribution of F-18 FDG-PET/CT on the Management of FUO

**H. Tokmak**[1], Ö. Ergönül[2], O. Demirkol[1], M. Çetiner[2], B. Ferhanoglu[2]; [1]American Hospital, Istanbul, TURKEY, [2]Koc University Medical Faculty, Istanbul, TURKEY.

**Objectives:** With the wide range of possible underlying causes, fever of unknown origin (FUO) is the one of the most compelling diagnostic issues for clinicians. The present study Aimed to evaluate the clinical contribution of F-18 FDG-PET/CT on the identification of the underlying cause of FUO as well as providing a guiding role in the further management of these group patients. **Material and Methods:** This retrospective analysis was performed on the twenty five (12 men, 13 women; age rage 17-88) of fifty consecutive patients (27 men, 23 women; age range 17-91), who diagnosed as FUO based on the revised definition criteria of FUO, for the diagnostic contribution of F-18 FDG-PET/CT. Final diagnosis was based on biochemistry, histopathology, microbiologic results, or clinical and imaging follow-up. PET-CT images were obtained with the Gemini Philips TF F-18 FDG-PET/CT camera after a 60-minute "standard uptake" period following an injection of mean 330 MBq (range 290-370 MBq) IV 18-fluoro-2-deoxyglucose ($^{18}$F-FDG). **Results:** F-18 FDG-PET/CT results were reevaluated with the final diagnoses. In the present study; findings were focal infectious process in five patients, sepsis and focal infection in one patient, systemic infection in two, inflammatory non-infectious disease in ten, and malignancy in three patients. In four patients, fever normalized spontaneously without a subsequently identified pathology during the clinical follow-up period of twelve months. In one patient, vasculitis had been detected by F-18 FDG-PET/CT findings. F-18 FDG-PET/CT precisely detected the cause of fever in 56 % of the patients (fourteen TP pts) and contributed to the final diagnosis or elimination of a focal pathologic process of the febrile state in 72 % of patients (eighteen TP+TN patients). The accuracy of the F-18 FDG-PET/CT test was calculated as 90%, the sensitivity was calculated as 93%, whereas the specificity was 80%. **Conclusions:** F-18 FDG-PET/CT should be considered as one of diagnostic imaging procedures in the initial diagnostic workup of the patients with FUO, if further studies indicate similar diagnostic contribution rate as the present study.

## OP175

### FDG PET/CT in the management of patients with fever of unknown origin

**M. Sollini**[1], A. Froio[1], A. Fraternali[1], M. L. Di Paolo[1], A. Filice[1], M. Roncali[1], M. Casali[1], G. Pazzola[2], F. Muratore[2], P. A. Erba[3], A. Versari[1]; [1]Nuclear Medicine Dept -S. Maria Nuova Hospital-IRCCS, REGGIO EMILIA, ITALY, [2]Rheumatology Dept -S. Maria Nuova Hospital-IRCCS, REGGIO EMILIA, ITALY, [3]Nuclear Medicine Center-Dept of Translational Research and Advanced Technologies in Medicine, Pisa, ITALY.

**Aim:** to evaluate the clinical value of Fluoro-18-fluoro-2-deoxy-D-glucose positron emission tomography/computed tomography ([$^{18}$F]FDG-PET/CT) in patients with FUO. **Materials and Methods:** we retrospectively evaluated [$^{18}$F]FDG-PET/CT diagnostic performances in 167 patients (man=85; women=82; mean age 58 years; median age 60 years; range 17-92 years) with fever of unknown origin (FUO) referred to Nuclear Medicine Unit of the Arcispedale Santa Maria Nuova - IRCCS, Reggio Emilia from 2007 to 2013. In all patients FUO was classified as classic, neutropenic, nosocomial and HIV-associated according to the clinical features. Final diagnosis was obtained with microbiology or histology except in case of endocarditis and uveitis/allergies where diagnosis was confirmed by echocardiography and by clinical or instrumental examination, respectively. [$^{18}$F]FDG-PET/CT results were compared to final diagnosis. **Results:** FUO was classified as classic in 161/167 cases, neutropenic in 3/167 patients, nosocomial in 2/167 cases and HIV-associated in 1/167 case. Final diagnosis was obtained in 106/167 cases (63%) while in the remained 61/167 patients the cause of FUO remained indetermined. Final diagnosis was obtained with microbiology in 30/106 cases, histology in 63/106 cases, echocardiography in 5/106 cases and clinical or laboratory examination in 4/106 patients each. Final diagnosis resulted in infection in 36/106 cases (sepsis=14, pneumonitis=5, spondilodiscitis=4, endocarditis=4, urinary infection=3, cutaneous infection=2, pericarditis=1, pace-maker infection=1, vascular prosthesis infection=1, peritonitis=1), neoplasms in 14/106 cases, rheumatoid arthritis in 10/106 cases, vasculitis in 8/106 cases, uveitis in 2/106 cases, and miscellaneous (inflammatory-non infectious disease=16, autoimmune disease=8, other benign conditions=12) in 36/106 cases. [$^{18}$F]FDG-PET/CT resulted positive in 111/167 (66%) cases. [$^{18}$F]FDG-PET/CT resulted true positive, true negative, false positive and false negative in 61/106, 7/106, 23/106 and 15/106 cases, respectively. False positive PET/CT results were due to [$^{18}$F]FDG accumulation in bowel (n=9), muscles and soft tissues (n=6), peri-prosthetic soft tissues (n=4), myocardium (n=2), ovary (n=1). False negative PET/CT results were diagnosed as rheumatoid arthritis (n=4), E. Coli (n=2), Chlamydia pneumoniae (n=1) and Mycoplasma pneumoniae (n=1) infections, urinary tract infections (n=1), endocarditis (n=1), cutaneous basocellular carcinoma (n=1), acute cholangitis (n=1), uveitis (n=1), acute thyroiditis (n=1), chronic lymphadenitis (n=1), visceral leishmaniasis (n=1). [$^{18}$F]FDG-PET/CT showed sensitivity and accuracy of 80% and 64%, respectively in identify the cause of FUO. Positive and negative predictive values resulted 73% and 32%, respectively. **Conclusions:** FDG PET/CT has an important role in the study of FUO, allowing to evaluate all its main causes ( inflammatory and infectious diseases; neoplasms)

## OP176

### 18F-FDG PET could be an objective tool for assessing disease activity in Sjögren's syndrome

C. Cohen[1], A. Mekinian[1], Y. Uzunhan[2], V. Eder[3], R. Dhote[4], H. Nunes[2], D. Valeyre[2], P. Brillet[5], O. Fain[1], **M. Soussan**[3]; [1]Jean Verdier Hospital, Department of Internal Medicine, Bondy, FRANCE, [2]Avicenne Hospital, APHP, Department of Pneumology, Bobigny, FRANCE, [3]Avicenne Hospital, APHP, Department of Nuclear Medicine, Bobigny, FRANCE, [4]Avicenne Hospital, APHP, Department of Internal Medicine, Bobigny, FRANCE, [5]Avicenne Hospital, APHP, Department of Radiology, Bobigny, FRANCE.

**Purpose** To determine the value of 18F-Fludeoxyglucose (FDG) Positron Emission Tomography/CT (PET/CT) to assess disease activity in patients with Sjogren's syndrome (SS). **Methods** Thirty-two patients with SS who underwent PET/CT were retrospectively analyzed (median age 57 years, male/female ratio 7/25). PET/CT activity score was measured using a 6-point scale including the 6 following items, each taking a value of 1 in case the argument listed below is true and 0 otherwise: CT lymph-nodes (small diameter > 1cm), HRCT evidence of interstitial lung disease, parotid glands SUVmax > 3, submandibular glands SUVmax > 3, lymph node uptake higher than background, interstitial lung disease FDG uptake (>liver uptake). Combined PET/CT score was correlated to ESSDAI (EULAR Sjögren's syndrome disease activity index) score and other parameters of SS activity. **Results** Pathological FDG uptake was observed in 75% of patients (24/32), located as follows: lymph nodes (n=19 (60%), median SUVmax =4.2 [2.5-10.6]); salivary glands (n=17, 53%), symmetrical in all patients with a median SUVmax = 2.7 [2.5-4.8]; lung (n=9, 28%), median SUVmax=3 [2.3-12], and thyroid (n=2). Median PET/CT and ESSDAI scores were 2 [0; 6] and 10 [1; 19], respectively. PET/CT activity score correlated with ESSDAI (r=0.49; p=0.005). Patients with an ESSDAI score higher than the median had a higher PET activity score than patients with an ESSDAI score lower than the median (3 vs 1, respectively, p= 0.004). PET was also correlated with gammoglobulin levels (r=0.43, p=0.02), but not with the presence of cryoglobulinemia, activated complement or beta2microglobulin levels. The presence of FDG salivary glands' uptake was not correlated with the presence of glandular swelling, xerostomia or high Chisholm score. The FDG uptake in patients with lymphoma (n=4) was higher than in patients without lymphoma (SUvmax 5.4 vs 3.2, respectively, p=0.05). In remained cases, the presence of hypermetabolic lymph nodes was considered related to immunological hyperstimulation observed is SS patients, with the absence of lymphoma during a median of 2.4 years follow-up. **Conclusions** We described a new PET/CT activity score which correlates to ESSDAI and could help to assess disease activity in SS patients. PET can also help in the diagnosis of lymphoma, even if lymph node FDG uptake can be frequently observed in SS patients in the absence of underlying lymphoma.

## OP177

### Diagnostic Value of Cardiac Dynamic FDG-PET/CT for Cardiac Sarcoidosis

**A. LEBASNIER**[1], C. LASNON[1], D. LEGALLOIS[1], S. COSTO[1], B. BIENVENU[1], G. ZALCMAN[1], D. PEYRONNET[1], E. BERGOT[1], D. AGOSTINI[1,2], A. MANRIQUE[1,2]; [1]University Hospital of Caen, Caen, FRANCE, [2]Normandie Université, EA4650, Caen, FRANCE.

**Aim** The heterogeneity of cardiac FDG uptake has been reported in patients with cardiac sarcoidosis (CS). We Aimed to evaluate the diagnostic value of dynamic cardiac 18FDG-PET/CT in patients with suspected CS. **Material and Methods** Data obtained from 14 patients with proven sarcoidosis and suspected cardiac involvement who underwent cardiac 18F-FDG PET/CT as part of clinical routine were reviewed. A 60-min list-mode cardiac 18FDG-PET/CT (injected dose: 278±29 MBq) was acquired (Biograph, Siemens®) after a 24h high-fat and low-carbohydrate diet. Blood glucose level before 18F-FDG injection was 98±17 mg/dL. Dynamic PET images (6x5s, 6x10s, 3x20s, 5x30s, 5x60s, 10x300s frames) were reconstructed using OSEM (4 iterations, 8 subsets) with a gaussian postfilter (FWHM= 5 mm). A normalized coefficient of variation (NCOV) of the metabolic rate of glucose, reflecting the heterogeneity of myocardial glucose metabolism, was determined by using a validated software (Carimas® 2.4, Turku PET Centre) and a 17-segment model. The metabolic rate of glucose was calculated using the Gjedde-Patlak plot method, without plasma sampling. NCOV was calculated as the ratio: (standard deviation of the metabolic rate of glucose among all 17 segments [mmol.min-1.g-

1]) / (global metabolic rate of glucose [mmol.min-1.g-1]). Patients were classified according to their NCOV values, using a cut-off value determined from receiver operating characteristic (ROC) curve. CS was diagnosed using the Japanese Ministry of Health and Welfare (JMHW) criteria as a gold standard. **Results** Among the 14 patients, 3 were excluded because of non-compliance to diet. In the 11 remaining patients (mean age = 52±21, males: 10), 4 (36%) were considered to have CS according to the JMHW criteria. NCOV values were significantly higher for CS patients as compared to CS free patients (1.14 ± 1.26 and 0.28 ± 0.17 respectively, p= 0.024). NCOV cutoff value was 0.53 (AUC= 0.92, p= 0.033). Seven patients out of 8 showing a NCOV <0.53 were free of CS. The 3 remaining patients with NCOV≥0.53 were considered as CS according to the JMHW criteria. There was one case with false negative result, yielding a sensitivity and specificity of 87.5% and 100% for the diagnosis of CS using cardiac dynamic 18FDG-PET/CT. **Conclusion** Quantitative analysis of the metabolic rate of glucose from cardiac dynamic 18FDG-PET/CT may be an appropriate tool to diagnose cardiac involvement in patients with systemic sarcoidosis.

## OP178

### Inflammatory activity assessment by F18-FDG-PET/CT in patients with sarcoidosis

**C. GAMEZ CENZANO**[1], J. MAÑA REY[2], P. CARESIA ARÓZTEGUI[1], F. MARTINEZ TORRENS[2], M. CORTES ROMERA[1], I. PUIG POVEDANO[1], L. RODRIGUEZ BEL[1], E. ANDIA NAVARRO[1], S. ROSSI SEOANE[1], R. LLATJOS SANUY[2], J. ROBLES BARBA[1], M. DE ALBERT DE DELAS-VIGO[2], F. FERNANDEZ ALARZA[2]; [1]IDI - HOSPITAL UNIVERSITARI DE BELLVITGE, L'HOSPITALET DE LLOBREGAT. BARCELONA, SPAIN, [2]HOSPITAL UNIVERSITARI DE BELLVITGE, L'HOSPITALET DE LLOBREGAT. BARCELONA, SPAIN.

**Aim** To assess the presence of inflammatory activity using FDG-PET/CT in patients with sarcoidosis. **Materials and Methods** A prospective study was undertaken of 75 whole-body F18-FDG-PET/CT scans performed in 63 patients with biopsy-proven sarcoidosis. Patients characteristics included: 34w/29m, 29-76y, diabetes:6, chronic sarcoidosis: 35 (5 to 30 y), neurosarcoidosis:1. Prolonged fasting was required. Unfractionated heparine (50 IU/Kg) was administered 15 min before of FDG in 2 patients. In 21 scans patients received corticosteroids. Positive findings were classified as thoracic and/or extrathoracic, measuring SUVmax in all active lesions. Thoracic findings in the CT were classified as typical or atypical. The left myocardial FDG uptake was quantified on a scale of 0-4, with grade 0 being no apparent activity, grades 1-2-3 physiological pattern with diffuse activity (3>liver) and grade 4 abnormal. **Results** Indications included (75 scans): 1) assessment of presence of inflammatory activity in systemic sarcoidosis and detection of occult activity sites (n=28); 2) assessment of presence of pulmonary activity in chronic fibrotic pulmonary sarcoidosis (n=17), 3) characterization of mediastinal lymph nodes (n=13), 4) monitorization of response to corticosteroids (n=9), 5) detection of occult primary malignancy (n=3); 6) staging in cancer patients with previously known sarcoidosis (n=2), 7) cardiac sarcoidosis (n=2) and 8) characterization of lung nodules (n=1). PET/CT showed pulmonary activity in 13/17 patients with chronic fibrotic pulmonary sarcoidosis. All second PET scans after corticosteroid therapy showed a significant reduction in pulmonary uptake. Positive findings were seen in 60/75 scans (80%): 22 thoracic, 4 extrathoracic and 34 both. The most common positive sites were mediastinal lymph nodes, lung and abdominal lymph nodes with ranges of SUVmax of 2,2 to 44. Sixteen scans showed occult sites in abdominal lymph nodes, muscle, skin and spleen. An incidental prostate cancer was detected in 1 patient. Left ventricular FDG uptake was present in 65 scans: physiological pattern in 61 (grade 3 in 29) and grade 4 in 4 (3 with normal MRI and/or a negative second PET with heparine). In 33/75 (44%) PET scan changed the management of the patient, guiding biopsy/other tests (17) or corticosteroids (16). **Conclusion** FDG-PET/CT appeared to be a sensitive method to detect inflammatory activity in sarcoidosis. It seems to be useful in the assessment of residual activity in fibrotic pulmonary sarcoidosis and may help to therapeutic decisions. In addition, it is a valuable tool to detect occult activity sites identifying extrathoracic involvement (>60% patients) and may be used to guide biopsies.

508 - Sunday, Oct. 20, 16:30 - 18:00, Gratte-Ciel 1/2/3

## Radionuclide Therapy & Dosimetry: Peptide Receptor Radionuclide Therapy

## OP179

### Critical issues in drafting Investigational Medicinal Product Dossier (IMPD) of radiolabeled peptides for radiometabolic therapy in metastatic neuroendocrine tumors

**M. Di Franco**[1], T. Scotognella[1], T. Angusti[2], D. Ielo[1], V. Podio[2]; [1]Ospedale San Luigi Gonzaga - Pharmacy, Orbassano (TO), ITALY, [2]Ospedale San Luigi Gonzaga - Nuclear Medicine, Orbassano (TO), ITALY.

**Aim** Applications to conduct clinical trials are required to be submitted to the competent authority for approval prior to beginning a clinical trial separately in each member state in which the trial is proposed to take place. Radiometabolic therapy of neuroendocrine tumors often requires in situ labelling procedure to obtain final radiopharmaceutical and IMPD is the most critical document to be submitted to authorities. We intended to focus the most critical points to be solved in drafting IMPD of radiolabeled peptides for radiometabolic therapy of neuroendocrine tumors, Aiming to guarantee efficacy and safety to patients. **Materials and Methods** IMPD structure stated by national and European law was analysed and two main sections were identified: the first contains information concerning biological, chemical and pharmaceutical quality of active substance and the second concerning the same aspects referred to Investigational Medicinal Product (final formulation of radiopharmaceutical to be administered) under test. Preclinical and clinical studies on active substance are required to be listed in the final section of IMPD to support the clinical study. **Results** Critical issues in drafting IMPD concerned both main sections. 1) Precise information about chemical and physical properties are required and exact aminoacidic sequence of chosen peptide (DOTA-TOC, DOTA-TATE, DOTA-NOC or others) is critical to define affinity to receptors and consequent pharmacology and pharmacokinetics. 2) Quality assurance in terms of chemical and microbiological stability must be evaluated and separately reported for non-radioactive precursors and for final radiopharmaceutical; analytical Methods must be described in details also in terms of validation. In particular, solid phase extraction (SPE) and/or thin layer chromatography (TLC) must be validated to test radiochemical purity of radiolabeled peptides. It is also necessary to choose method of detection, depending on radionuclide emission: phosphor imager for quantitative filmless autoradiography, radiochromatography and beta counter are the most common, each of them with advantages and limits. 3) Main radiometabolic treatment limit is renal toxicity , due to high renal uptake, related to chemical structure of the chosen peptide. As consequence, both administered activity of radiopharmaceutical and the most appropriate mixture of protective aminoacids must be carefully evaluated and declared in IMPD. **Conclusion** A critical analysis of IMPD shows the most critical aspects in starting a clinical trial in nuclear medicine when a radiolabeled peptide for radiometabolic therapy of neuroendocrine tumors is involved. Appropriately addressing those quality attributes that may impair patient's safety, a high quality investigational medicinal product is guaranteed.

## OP180

### Mild erythrocytopenia is the Most Frequent Long-term Sequel after Peptide Receptor Radionuclide Therapy: Results of Long-term Follow-up in more than 500 Patients from a Single Centre

**J. Schmidl**[1], Y. Menghui[2], H. R. Kulkarni[1], R. P. Baum[1]; [1]THERANOSTICS Center for Molecular Radiotherapy and Molecular Imaging, Bad Berka, GERMANY, [2]Tang-du Hosptial, Xi'an, CHINA.

**Aim:** Peptide receptor radionuclide therapy (PRRT) is highly effective in well differentiated neuroendocrine neoplasms (NENs) and lends a benefit in overall survival of several years. Renal toxicity is a well-known adverse effect of PRRNT. Hematological toxicity as possible long-term sequel has been hardly examined. Therefore we investigated the effect of PRRT on the hematological status (erythrocytes, leukocytes, thrombocytes) of patients who received individualized therapy at our centre. **Materials and Methods**: Out of over 500 patients, fifty-nine chemotherapy naïve patients with well-differentiated NENs who were treated with at least 3 cycles of PRRT with 177Lu- and/or 90Y- labeled DOTATATE / DOTATOC and long-term follow-up were selected for this analysis. Blood counts were documented before the first cycle and repeated at monthly intervals between further cycles and during restaging examinations after PRRT for many years. Comparisons were done between the hematological status before the first cycle and the one 3 years after the last cycle of PRRT. **Results**: All three cell lines were significantly decreased 3 years after the last radionuclide therapy (erythrocytes, leukocytes: p=0,000; thrombocytes: p=0,002; confidence interval 95%). But only erythrocytes showed a significant decrement, i.e., below the reference level of our in-house laboratory (mean value ± standard deviation: 4.07 ± 0.69 / l; reference level: 4.1-5.4 / l). **Conclusions**: Mild erythrocytopenia is the most frequent long-term sequel after PRRT. Although it has to be considered that repeated cycles probably cause impoverishment in bone marrow reserve (or red cell precursors), PRRT achieves both significant improvement in clinical symptoms and excellent palliation. Thus it remains a safe procedure if performed at specialized centres with interdisciplinary and long-term care.

## OP181

### The role of 177LuDotatate peptide receptor radionuclide treatment in patients with metastatic well differentiated gastroenteropancreatic neuroendocrine neoplasms (GEP-NETs)

**S. Severi**[1], M. Sansovini[1], A. Ianniello[1], A. Ambrosetti[1], M. Monti[1], E. Scarpi[1], V. Di Iorio[1], V. D'Errico[1], T. Ibrahim[1], G. Paganelli[2]; [1]IRCCS IRST, Meldola, ITALY, [2]IEO, Milano, ITALY.

**Purpose**: We evaluated the activity and safety profile of 177LuDotatate peptide receptor radionuclide therapy (LU-PRRT) in patients with advanced well differentiated gastroenteropancreatic neuroendocrine neoplasms (GEP-NETs). **Patients and Methods**: 87 consecutive patients with tumor progression at baseline were treated with a cumulative activity of 18.5 - 27.8 GBq in five cycles, according to the patient's kidney function and/or bone marrow reserve, both known to be dose-limiting factors in LU-PRRT. **Results**: All 87 patients with metastatic pancreatic (52), ileal (27), appendicular (1), stomach (3) or sigma-rectum (4) NETs had well differentiated tumors with positive Octreoscan® scintigraphy or 68Ga PET-CT at enrollment. Forty-eight patients received a mean full dosage (FD) of 25.6 GBq (range 21-28) and 39 a mean reduced dosage (RD) of 18.2 GBq (range 11-20.3). Overall response in the 87 patients was CR in 5 (5.7%) cases, PR in 14 (16.1%), and SD in 52 (59.8%) and PD in 16 (18.4), with a disease control rate (DCR) of 81.6%. Median progression-free survival (PFS) was 31 months (95 CI 20-nr) and median overall survival (OS) has not been reached yet. In the FD (48 patients) group we observed 3 (6%) CR, 9 (19%) PR and 28 (58%) SD (DCR 83%), while 8 (17%) patients showed PD. In the RD group (39 patients) 2 (5%) had CR, 5 (13%) har PR and 24 (61%) had SD (DCR 79%), while 8 (21%) showed PD. Statistical analysis of the results obtained comparing FD and RD patients was not statistically significant for DCR (p=0.461), median PFS (p=0.123) and median OS (p=0.079). None of the patients, including those previously treated with chemotherapy or those with hypertension or diabetes, all known to be risk factors for toxicity, showed significant side-effects after LU-PRRT. **Conclusion:** Our results confirm that LU-PRRT was a suitable therapeutic option in patients with advanced GEP-NETs, with a DCR of 81.6% and a PFS of 31 months. It was well tolerated and proved safe in all patients. Both activities of 27.8 GBq and 18.5 GBq administered in five cycles were effective and should be selected on the basis of kidney function and bone marrow reserve.

## OP182

### Uncertainties in measurement of $^{90}$Y and $^{177}$Lu activities in an ionisation chamber

**J. R. Ballinger**, R. Fernandez, S. J. Allen; Guy's & St Thomas' Hospital, London, UNITED KINGDOM.

Accurate measurement of administered activity is essential in radionuclide therapy. However, this can be difficult to perform using a standard ionisation chamber, particularly with beta emitting radionuclides where measurements are greatly affected by the type of container (e.g. glass vial vs plastic syringe) in which the activity is contained, as well as the shape and volume of the sample. **Methods:** All measurements were taken with one of two ionisation chambers of the same model (Capintec CRC-15R). Shipments were received from two different suppliers of $^{90}$Y (Polatom; Eckert&Ziegler-E&Z) and two suppliers of $^{177}$Lu (ITG Munich; Advanced Accelerator Applications-AAA). The quantities of $^{90}$Y varied from 2.5-7.4 GBq and of $^{177}$Lu from 3.3-8.4 GBq. The calibration factors used to make measurements in the glass vials supplied were 62x10 for $^{90}$Y and 450x10 for $^{177}$Lu. A reference sample of $^{177}$Lu was sent to the UK National Physical Laboratory, Teddington, for absolute calibration. **Results:** Compared to the manufacturer's calibration, the activities received were 88±23% for Polatom $^{90}$Y (n=7), 103±5% for E&Z $^{90}$Y (n=56), 94±2% for ITG $^{177}$Lu (n=93) and 112±5% for AAA $^{177}$Lu (n=14). The large variation in measurements on Polatom $^{90}$Y was due to one shipment at 36%; without that value the mean was 96±4% (n=6). With AAA $^{177}$Lu there was a step change during the process with the initial shipments reading significantly higher than the later ones: 115±1% (n=10) vs 105±4% (n=4). With $^{90}$Y a different calibration factor was required for doses drawn into syringes (49x10), whereas with $^{177}$Lu the same value could be used; this is presumably due to the contribution of the gamma emissions of $^{177}$Lu. Cross calibration with the national metrology institute showed that our measurements were within ~1% of the accepted value for $^{177}$Lu. **Conclusions:** Accurate measurement of beta emitters used in radionuclide therapy requires careful attention to geometry and dialogue with suppliers over the calibration factors which they have used and any changes which might have occurred.

## OP184

### Dual-isotope receptor based 68Ga-DOTANOC and metabolic 18F-FDG PET/CT helps in treatment planning of patients with advanced NETs. A single institute experience.

**A. Malhotra**, R. Kumar, P. Sharma, N. Naswa, C. S. Bal; All India Institutes of Medical Sciences, New Delhi, INDIA.

**Aim**: Multitude of treatment options are available for patients with metastatic NETs. The choice of one particular regime depends on the tumor histology with emphasis on degree of tumor cell differentiation. Octreotide based regimes are offered to patients with well differentiated NETs while the more aggressive chemotherapy for patients with anaplastic NETs.This is an oversimplification of the management protocol and doesn't take into account the entire burden of tumor cell differentiation. With two fold objectives, one whether it is possible to establish a total whole body tumor cell differentiation map and 2nd to analyze whether it is feasible to select an appropriate treatment plan for patients with advanced NETs. It was based on the results of dual functional imaging with the metabolic tracer 18F-FDG and receptor (somatostatin) based agent 68Ga-DOTANOC. **Methods:** Biopsy confirmed lesions with evidence of metastasis on either CT/MRI (n=75), patients underwent dual imaging two weeks apart. 57 patients had advanced gastro-enteropancreatic (GEP-NETs) while 18 patients had metastatic pulmonary NETs.Based on the dual imaging patients were grouped into four categories.Group A- 68Ga-PET (+), 18F-FDG (-) , Group B - 68Ga-PET (-), 18F-FDG (+), Group C- Both (+) with 68Ga-PET predominant and Group D - Both (+) with 18F-FDG predominant.Group-A patients were treated with Octreotide based regimes (either cold or radiolabeled) while group-B patients were treated with chemotherapy. Group-C and D were treated with octreotide and chemotherapy respectively depending on predominant tumor cell differentiation profile. **Results**: After dual imaging, groups-A, B, C, and D had 38, 10, 19 and 8 patients respectively. 33/38 patients in group-A, showed a stable pattern after a median follow-up of 30 months, while 3/5 patients who progressed died.Group-B had worst prognosis with all 10 patients who showed initial response to chemotherapy had eventual disease progression, 7/10 patients died. Stable disease was noted in 12/19 patients in group-C and 5/8 patients in group-D with progression in the rest.After appropriate triaging an overall progression rate of 31% was observed. This rate was lower compared to the 39% progression rate when facilities for triaging patients based on PET/CT were not available. However a statistically significant association could not be reached. **Conclusion:** Based on these initial results it seems feasible to use dual PET/CT imaging Methods using 18F-FDG and 68Ga-DOTANOC to choose the best mode of treatment in this patient group.Obtaining a whole body tumor cell differentiation map also seems possible using this approach.

## OP185

### Optimization of gamma-camera extrinsic spatial resolution for improved organ delineation during internal dosimetry with 177-Lu peptide receptor radionuclide therapy - a phantom study

**J. A. M. Santos**; Instituto Português De Oncologia Do Porto Francisco Gentil E.P.E., Porto, PORTUGAL.

**Aim** Data for patient dosimetry in peptide receptor radionuclide therapy with 177-Lu-DOTA-X is generally obtained by planar or tomographic emission imaging (e.g. SPECT). Since internal dosimetry may involve appreciable inaccuracies, accurate organ delineation, based on the highest Extrinsic Spatial Resolution (ESR) available, is mandatory. Since 177-Lu presents the highest photopeak energy of 208 keV, a medium energy collimator, such as a Medium Energy Low Penetration (MELP), is usually indicated, with two energy windows at 113 keV and 208 keV, and with lower ESR associated to higher energy collimators. The Aim of the present work is to suggest strategies to obtain higher ESR images using other acquisition parameters. **Material and Methods** This study used a Siemens e-Cam with Low Energy High Resolution (LEHR) and Medium Energy Low Penetration (MELP) collimators. ESR with and without scatter was measured by calculating the Full Width at Half Maximum (FWHM) of a 100 mm length linear radioactive source image obtained using a capillary tube. The profiles orthogonal to the linear source (Linear Spread Function; LSF) were fitted using one to three Gaussian curves depending on the experimental data and accounting for the trans-septal scatter component. The Modulation Transfer Function was calculated by Fourier transforming the fitting function. **Results and Conclusions** A 177-Lu linear source image was acquired at 10 cm from the collimator with both photopeak windows at 20% using the MELP collimator. A FWHM = 11.6 mm was calculated. Another image was acquired in the same conditions using the LEHR collimator. The new profile presented different features than that obtained with the MELP collimator. Although one could notice a degradation of the image due to lateral scatter, the central profile peak presented a FWHM = 7.2 mm, lower than that obtained with the MELP (FWHM = 7.7 mm for 99m-Tc with LEHR). The FWHM of the central peak profile for 177-Lu with MELP is thus lower than this value suggesting that it could be possible to attain higher ESR with LEHR if the scatter component could be attenuated without prejudice of the narrower peak. That was achieved by acquiring the image using only the lower energy window (20%), reaching a FWHM = 7.5 mm with almost no scatter. The drawback is a lower count rate (~50%), which can be compensated by longer acquisition times. Similar improvements were found in SPECT. This approach can thus constitute a higher accuracy alternative for internal dosimetry organ delineation.

509 - Sunday, Oct. 20, 16:30 - 18:00, Rhône 3A/3B

## Oncology Clinical Science: Brain Tumours

### OP187

### Differentiating glioma recurrence from treatment induced necrosis. Comparison of Diffusion Tensor, Dynamic Susceptibility Contrast MRI and 99mTc-Tetrofosmin Brain SPECT.

**G. A. ALEXIOU**, A. Zikou, S. Tsiouris, A. Goussia, P. Kosta, A. Papadopoulos, S. Voulgaris, P. Tsekeris, A. P. Kyritsis, A. D. Fotopoulos, M. I. Argyropoulou; University Hospital of Ioannina, Ioannina, GREECE.

**Introduction:** Malignant gliomas are the most common type of primary brain tumor and carry a dismal prognosis. Treatment induced necrosis is a relative frequent finding in patients treated for high-grade gliomas. Differentiation by imaging modalities between glioma recurrence and treatment induced necrosis is not always possible. We set out to compare diffusion tensor, dynamic susceptibility contrast MRI and $^{99m}$Tc-Tetrofosmin brain SPECT for the differentiation of glioma recurrence from treatment induced necrosis. **Methods:** We prospectively studied thirty patients who were treated for high-grade glioma and had a suspicion of recurrent tumor on follow-up MRI. All patients received surgical resection of the tumor, followed by postoperative standard radiotherapy with chemotherapy. No residual tumor had been found in the imaging follow-up immediately after initial treatment. All patients underwent brain MRI and within a week underwent $^{99m}$Tc-Tetrofosmin brain SPECT. **Results:** Both $^{99m}$Tc-Tetrofosmin brain SPECT and dynamic susceptibility contrast MRI could discriminate the two clinical entities with 100% sensitivity and 100% specificity. An ADC ratio cut-off value of 1.27 could differentiate recurrence from treatment induced necrosis with 65% sensitivity and 100% specificity and a FA ratio cut-off value of 0.47 could differentiate recurrence from treatment induced necrosis with a 57% sensitivity and 100% specificity. A significant correlation between $^{99m}$Tc-Tetrofosmin uptake ratio and rCBV was found ($P$=0.002). A significant negative correlation was also found between $^{99m}$Tc-Tetrofosmin uptake ratio and ADC ratio ($P$=0.031). **Conclusions:** Dynamic susceptibility contrast MRI and brain SPECT with $^{99m}$Tc-Tetrofosmin had the same accuracy and may be used to detect recurrent tumor. DTI also showed promise for the detection of recurrent tumor, but was inferior to both dynamic susceptibility contrast MRI and brain SPECT.

### OP188

### Correlation of biological data and metabolic information on 11C-methionine PET in primary brain tumours.

**E. Lopci**, L. Bello, F. Raneri, M. Riva, M. Rodari, A. Chiti; Humanitas Clinical and Research Center, Rozzano (Mi), ITALY.

**Aim**: in our study we Aimed assessing the correlation of metabolic information on 11C-methionine PET and biological data in patients affected by primary brain tumour and eligible for surgical resection. **Materials and Methods**: we analysed data deriving from 54 consecutive patients (M:F=34:20; mean age 45, range 19-77 years) affected by pathologically proven gliomas and referred to our institution for primary tumour resection. Before surgery, patients underwent 11C-methionine PET performed according to standard procedure. In all cases semi-quantitative analyses were obtained by taking into consideration SUVmax, SUVratio, and whole tumour metabolic activity (WTMA), expressed as a product of metabolic tumour volume and lesion SUVmean. Functional data on PET were then correlated with biological information obtained by histology (WHO grade/MIB1) and gene profiling, including isocitrate dehydrogenase 1 gene (IDH1) mutation, 1p/19q co-deletion and $O^6$-methylguanine-DNA methyltransferase (MGMT) promoter methylation. **Results**: according to WHO classification, in our series we analysed 23 low-grade gliomas (LGG: grade II), and 31 high-grade gliomas (HGG: 16 grade III and 15 grade IV). Based on semi-quantitative analyses, we determined a statistically significant correlation between SUVmax, SUVratio and WTMA versus tumour grading (p<0.001). In our series we could also define some optimal cut-off points able to differentiate between LGG and HGG: respectively SUVmax >2.8, SUVratio >2.08 and WTMA >6.63. Among the biological data, we determined a statistically significant correlation with tumour uptake only for IDH1 mutation, which was expressed in patients with lower SUVmax (mean 5.63 versus 2.32; p=0.003) and SUVratio (mean 2.99 versus 1.86; p=0.002). The correlation was not confirmed for WTMA (p=0.8). In addition, no significant difference was found in tumour grade/MIB1 and IDH1 mutation, 1p/19q co-deletion or MGMT methylation. **Conclusions**: as expected, semi-quantitative information obtained by 11C-methionine PET significantly correlated with histological grading in primary brain tumours. Among other biological data, only IDH1 mutation resulted correlated to tumour uptake, with a prevailing expression in gliomas with lower SUVmax and SUVratio, suggesting a better prognosis in these cases.

### OP189

### Comparison of visual and semi-quantitative analysis of F-DOPA-PET/CT for recurrence detection in glioblastoma patients

**K. Herrmann**[1], J. Czernin[2], T. Cloughesy[2], C. Bluemel[1], A. Lai[2], K. Pomykala[2], M. Benz[2], A. Buck[1], M. Phelps[2], W. Chen[2]; [1]University Hospital, Wuerzburg, GERMANY, [2]University of California, Los Angeles, CA, UNITED STATES.

**Aim:** Aminoacid transport imaging with 18F-DOPA PET imaging is increasingly used for detection of glioblastoma (GBM) recurrence. However, a standardized image interpretation for 18F-DOPA brain PET studies has not yet been established. This study compares visual and semi-quantitative analysis parameters for detection of tumor recurrence and correlates them with progression free survival (PFS). **Materials**: A total of 111 patients (74 m /37 f) with suspected tumor recurrence who underwent 18F-DOPA PET imaging were included. PET scans were analyzed visually (5-point scale) and semi-quantitatively (lesion to striatum- and lesion to normal brain tissue-ratios using both SUVmean and SUVmax-). Accuracies for recurrence detection were calculated using histopathology and clinical follow-up for validation. ROC- and Kaplan-Meier-Survival-analysis were performed to derive imaging based prediction of progression free and overall survival. Results: Accuracies for detection of GBM recurrence were similar for visual (82%) and semi-quantitative (range 79%-82%) analysis. Both visual and semi-quantitative indices were significant predictors of PFS, with mean lesion-to normal brain tissue ratios providing the best discriminator (median survival: 39.4 vs. 9.3 mo; p<0.001). Visual analysis resulted in a p-value of 0.00012 (median survival: 25.4 vs. 8.2 mo; p<0.001). None of the investigated parameters was predictive for overall survival **Conclusion**: Both visual and semi-quantitative indices detected glioblastoma recurrence with a high accuracy and were predictive for PFS. Lesion to normal tissue ratios were the best discriminators of PFS. However, none of the investigated parameters predicted overall survival Moreover, these retrospectively established analysis parameters need to be confirmed prospectively.

### OP190

### Evaluation of the use of SUV for glioma grading using static and dynamic 18F-FDopa PET/CT

**C. NIOCHE**[1], M. SORET[1], E. GONTIER[1], G. BONARDEL[1], I. BUVAT[2]; [1]HIA du Val-de-Grace, Paris, FRANCE, [2]IMNC, UMR 8165 CNRS, Orsay, FRANCE.

**Aim**: The Aim of this study was to compare the accuracy of brain tumor grading based on SUV measured on static or dynamic 18F-FDopa PET. **Materials and Methods:** 54 patients with a brain tumor were included. Each patient underwent a 40 minute dynamic brain PET 3 minutes after injection of 120 to 200 MBq of 18F-FDopa. A static PET volume corresponding to the last 5 minutes of the dynamic acquisition was reconstructed. In addition, 40 frames of 1 minute were reconstructed for dynamic analysis. For each tumor, a large VOI encompassing the tumor was manually drawn on the 5-minute static volume and the maximum SUV value ($SUV_{max}$) in that VOI was calculated from the static volume. An $SUV_{peak}$ value was also calculated in a 1 cm3 spherical region located in the large VOI so as to get the maximum $SUV_{peak}$. For dynamic imaging, the $SUV_{max\text{-}t}$ was calculated as the maximum SUV in the large VOI over all 1-min time frames. ROC curve analysis was used to characterize the performance of the 3 SUV indices in distinguishing between HG and LG tumors. **Results**: 28 tumors were classified as high grade (HG) and 26 as low grade (LG) by histopathologic analysis. The average $SUV_{peak}$ was significantly different (t-test, p<0.001) between HG ($SUV_{peak\text{-}HG}$=2.5±0.9) and LG tumors ($SUV_{peak\text{-}LG}$=1.7±0.6), and the same was true for $SUV_{max}$ ($SUV_{max\text{-}HG}$ = 3.1±0.9 vs $SUV_{max\text{-}LG}$ = 2.2±0.8, p<0.005). $SUV_{max\text{-}t}$ was also significantly different (t-test, p<0.005) between HG ($SUV_{max\text{-}t\text{-}HG}$=6.5±1.8) and LG tumors ($SUV_{max\text{-}t\text{-}LG}$=4.9±0.9). With $SUV_{peak}$, HG tumors could be distinguished from LG tumors with a specificity of 61% and a sensitivity of 84% for an $SUV_{peak}$ threshold of 1.9. With $SUV_{max}$, a specificity of 50% and a sensitivity of 88% were obtained for a threshold set to 2.1. With $SUV_{max\text{-}t}$, a specificity of 46% and a sensitivity of 100% for identifying HG tumors were obtained with a threshold set to 3.9. The comparison of the areas under the ROC curves corresponding to the 3 SUV indices did not show any statistically significant difference ($AUC_{peak}$= 0.78, $AUC_{max}$= 0.74, $AUC_{max\text{-}t}$=0.75). **Conclusion**: SUV measurements from static or dynamic 18F-FDopa PET can discriminate between LG and HG gliomas. No significant difference was found between the 3 SUV indices. Good discrimination was obtained by calculating $SUV_{peak}$ of a 5-minute static scan performed 38 minutes after injection. Full kinetic analysis is under way to determine whether classification performance can further be improved.

## OP191

### 18F-FDOPA PET-CT for predicting survival in patients with recurrent glioma: A prospective study

**S. Karunanithi**, P. Sharma, A. Kumar, D. Gupta, R. Kumar, A. Malhotra, C. Bal; All India Institute of Medical Sciences, New Delhi, INDIA.

**Objective**: To evaluate the role of 18F-FDOPA PET-CT for predicting survival in a group of patients with suspected recurrent glioma. **Methods**: A total of 33 previously treated histopathologically proven glioma patients (mean age-39.1 years, median-38 years, range: 11-62); with clinical and conventional imaging findings suspicious of recurrence were included in this study. All patients underwent FDOPA PET-CT study. Ratios of tumor uptake to normal tissue uptake were generated by dividing the tumor SUVmax by the SUVmax of the contralateral normal hemispheric brain tissue (T/N), the normal striatum (T/S), the normal white matter (T/W) and the normal cerebellum (T/C). Patients were followed up clinically and by repeated imaging. Data was censored, if the patient died of disease or at the end of the study. Survival analysis was done in the distributions of each variable and by multivariate analysis. **Results:** Mean lesions size obtained from contrast enhanced area in MRI was 3.4cm (± 0.24 cm) and median size was 3.3 cm (range 1.1 cm-6.2 cm). FDOPA PET-CT findings were positive for recurrence in 25 patients and negative in 8 patients. All patients were followed up. Median follow up period was 20.23 months (range: 1.0 - 42.87). Total nineteen patients died within median follow up period. Median survival in this study was 39.22 months. Five patients underwent reoperation and histopathology revealed recurrence in all five. ROC analysis was done to derive a cut-off value for continuous variables like age and 18F-FDOPA quantitative parameters (SUVmax, T/S, T/W, T/N and T/C). In univariate analysis significant association of survival was noted with age, size of the recurrent tumor, histological grade of the primary tumor, mode of treatment after recurrence, clinical symptoms at the time of recurrence and visual FDOPA results (p 0.0071). Significant correlation with survival was noted for all the ROC analysis derived cut-off values of FDOPA quantitative parameters namely SUVmax (p 0.0011), T/S (p 0.0059), T/W (p 0.0004), T/N (p 0.0006) and T/C (p 0.003). But on multivariate analysis only size of the recurrent tumor (p 0.002) and T/N ratio of FDOPA PET (p 0.005) were found to be significantly associated with survival. T/S ratio of FDOPA PET was found to be borderline significant predictor of survival (p 0.076). **Conclusion**: Intensity of FDOPA uptake (FDOPA uptake in tumors higher than that of grey matter) on PET-CT is a strong predictor of survival in patients with imaging findings of recurrent glioma.

## OP192

### 18F-DOPA PET impact on decision making of a multidisciplinary neuro-oncology tumour board

**J. Darcourt**[1,2], J. Barriere[1], V. Bourg[3], D. Fontaine[3], S. Chanalet[3], L. Mondot[3], P. Bondiau[1], F. Vandenbos[3], R. Guignard[1], N. Sapin[1], E. Saada[1]; [1]Centre Antoine Lacassagne, NICE, FRANCE, [2]University of Nice Sophia Antipolis, Nice, FRANCE, [3]CHU, Nice, FRANCE.

L-AAT amino-acid transporter is overexpressed in brain tumours. Among 18F labelled amino-acids, F-DOPA has demonstrated high diagnosis performances. We investigated prospectively the practical clinical impact of F-DOPA PET on the intended management of patients suspected of brain tumour recurrence during the multidisciplinary neuro-oncology board meetings (MNOBM). **Materials and Methods** 31 patients, 17 males and 14 females mean age 55 y (16 glioblastomas, 9 oligodendrogliomas II and III, 1 astrocytoma III and 5 metastases) underwent 52 18F-DOPA PET studies during their follow-up after initial treatment for diagnosis of recurrence versus pseudo-progression or radiation necrosis. Patients received 100 mg of carbidopa 1 hour prior to the injection of 2 MBq/kg of 18F-DOPA. A 10 minutes static acquisition was performed 20 min post injection using a PET-CT camera (mCT-Siemens; OSEM 5 iterations and 24 subsets). MRI images were obtained within 3 weeks and coregistered to PET data. Images were analysed visually comparing tumour uptake with striatal activity. Images were considered positive when tumour activity was > to 75% of striatal uptake. During the MNOBM, clinical and MRI data (including perfusion and spectrometry) were discussed first and a decision proposed for patient management. Then F-DOPA PET images were shown and the decision considered again. The impact was measured by the number of changes in patients' management between the two decisions. When unchanged, the level of confidence was taken into account. **Results** Considering the 52 PET studies, 35 were considered positive and 17 negative. MNOBM decision was changed in 20 cases (38.5%) and unchanged in 32 (61.5%). Within the changed decisions only 3 (6%) were for down staging. Within the unchanged decisions, TEP results increased the confidence in the decision in 8 cases (15.5%). In 15 cases confirmation of the diagnosis was available by surgery (5) or after 6 months follow-up (10): only 1 false positive results related to radiation necrosis was found. **Conclusion** Multimodality MRI is used to monitor patients' brain tumours. However, after initial treatment, the assessment of recurrence is complicated by pseudoprogression and radiation necrosis. These results show that 18F-DOPA PET imaging had a direct impact on the intended management of such patients in more than one third of the cases.

## OP193

### Shortened scan duration of static [18F]-FET PET does not relevantly affect diagnostic quality

**S. B. Andersen**, M. L. Lassen, I. Law; Department of Clinical Physiology, Nuclear Medicine and PET, Rigshospitalet, Copenhagen, DENMARK.

**Aim** Reduction of either PET scan duration or injected radioactive dose may diminish patient discomfort or radiation burden and optimize use of scanners. The Aim of this retrospective study was to investigate the effects of static O-(2-[18F]Fluoroethyl)-L-tyrosine ([18F]-FET) PET scan time duration on the diagnostic quality in glioma patients and thereby exploit the increased sensitivity in modern PET/CT scanners. **Materials and Methods** Fifty patients with metabolically active gliomas (45 high grade) were injected with 200 MBq [18F]-FET i.v. and scanned on a Siemens mCT PET/CT system with static reconstructions at 20-40 min and 25-35 min p.i. On co-registered PET and T1w MRI images average background activity (B), tumor mean (Tmean) and tumor max activity (Tmax), tumor volume (Vol) at values > 1.6 B were sampled. Analyses were performed for Tmax/B, Tmean/B and Vol at 20-40 and 25-35 min including paired t-tests, linear correlation and Bland-Altman method comparison. The magnitude of the noise in the two scans was characterized by the coefficient of variation (COV) from a 2 cm in diameter spherical ROI in pons**. Results** Tmax/B, Tmean/B and Vol were 3.50±1.16, 2.06±0.26 and 45.34mL±37.29mL at 20-40 min and 3.52±1.15, 2.06±0.26 and 45.00mL±37.16mL at 25-35 min, respectively. For scan duration 25-35 min Tmax/B was significantly increased by 0.02 ($p < 0.05$). Tmean/B and Vol were not significantly different. Correlation for Tmax/B, Tmean/B and Vol was r2 = 0.996, 0.996 and 0.998 respectively with no systematic deviation from y = x. Bias, SD and 95 % confidence interval in Bland-Altman % difference plots were 0.9 %, 2.2 % and [-3.4 %;5.2 %] for Tmax/B, -0.1 %, 0.8 % and [-1.6 %; 1.4 %] for Tmean/B and -1.0 %, 5.4 % and [-11.6 %;9.5 %] for Vol. In absolute values these results were 0.02, 0.07 and [-0.12;0.17] for Tmax/B, 0.00, 0.02 and [-0.03;0.03] for Tmean/B and -0.34 ml, 1.72 mL and [-3.72 mL ;3.04 mL] for Vol. The noise level (COV) increased significantly from 20-40 min to 25-35 min from 8.4 % to 9.9 % (Wilcoxon test, $p > 0.0001$). **Conclusion** Reduction in scan time did not affect scan quality of [18F]-FET PET in a clinically relevant manner. Therefore, it seems possible to utilize the increased sensitivity of modern PET/CT scanners to implement a scan time reduction or reduce injected dose in the future clinical use of [18F]-FET.

## OP194

### 13N-ammonia PET/CT can predict progression free survival in patients with suspected recurrent glioma

**B. C. Khangembam**, P. Sharma, C. S. Bal, R. Kumar, G. P. Bandohpadhyaya, A. Malhotra; All India Institute of Medical Sciences, New Delhi, INDIA.

**Aim** The Aim was to evaluate the efficacy of $^{13}$N-ammonia PET/CT ($NH_3$) in predicting progression free survival (PFS) in patients with suspected recurrent glioma. **Materials and Methods** Fifty-two patients of histopathologically proven glioma (38 low-grade, 14 high-grade) who had been previously treated (surgery/radiotherapy/both with or without chemotherapy), and presented with suspicion of recurrence on clinical evaluation and/or MRI were prospectively enrolled and evaluated with $NH_3$. Data was censored, if the patient had clinical progression or at the end of the follow up. ROC analysis was done for continuous variables to find out the optimal cut off values associated with progression. Univariate and multivariate Cox regression with forward stepwise method was applied to find out the variable(s) with the strongest prediction potential for progression. **Results** On univariate analysis, patients with age ≤45 years were associated with shorter PFS. Variables associated with better PFS included involvement of only one lobe, negative $NH_3$, T/W ≤1.51, T/G ≤0.62, T/P ≤0.56, absence of debilitating symptoms, recent corticosteroid therapy, and size of contrast enhancement on MRI ≤2.4 cm (Table). However on multivariate analysis, only negative $NH_3$ findings emerged as the only independent predictor for PFS (HR, 0.08; 95% CI, 0.01-0.39; P value, 0.002). **Conclusion** $^{13}$N-ammonia PET/CT is an independent predictor of progression free survival in patients with suspected recurrent glioma.

510 - Sunday, Oct. 20, 16:30 - 18:00, Tête D'Or 1/2

## Neurosciences: Data Analysis & Management

## OP195

### Quantification and accuracy of clinical [11C]-PiB PET/MRI: The effect of MR-based attenuation correction

**I. Law**[1], F. L. Andersen[1], T. Beyer[2], A. E. Hansen[1], S. Hasselbalch[3], C. Ladefoged[1], S. H. Keller[1], S. Holm[1], L. Højgaard[1]; [1]Rigshospitalet, The Department of Clinical Physiology, Nuclear Medicine and PET, Copenhagen, DENMARK, [2]Center for Medical Physics and Biomedical Engineering, Vienna, AUSTRIA, [3]Rigshospitalet, Memory Disorders Research Group, Copenhagen, DENMARK.

**Aims:** The Dixon-Water-Fat segmentation (DWFS) method (1) is a standard attenuation correction (AC) method in PET/MRI and has demonstrated a systematic and spatially variable quantitative bias in [18F]-FDG-PET/MRI studies of the brain (2) compared to PET/CT. The Aim of this study was to measure the regional and absolute bias of DWFS -AC in combined PET/MR images of the brain using [11C]-PiB for cerebral amyloid binding and evaluate the impact on the clinical reading of these images. **Methods**: Twenty-one healthy volunteers, 1 MCI patient and 3 patients with clinical Alzheimers disease (14 M, 10 F, age: 51-78 y, median: 66 y) underwent a simultaneous PET/MRI (Siemens mMR) acquisition 40 min pi of (201-838) MBq [11C]-PiB. A single 30 min frame was reconstructed (OSEM-3D, 21it4sub, 5 mm Gauss) with the only difference being the AC calculation. AC was performed using either DWFS or a head CT scan acquired independently on the same day and co-registered to DWFS using rigid body transformation. AC-PET images were fused with T1w-MRI and activity concentration (Bq/mL) was sampled from symmetrically delineated cortical ROI's in lateral frontal, lateral and medial parietal, lateral temporal, lateral occipital cortical areas, deep white matter, and the caudate nuclei. Ratios of region-to-cerebellar grey matter (SUVr) were calculated. Amyloid uptake was considered abnormal at cortical SUVr ≥1.5 or increased amyloid uptake in two or more grey matter regions on visual evaluation. Bland-Altman analysis was used to compare AC Methods. **Results**: The overall activity concentration in the average of all ROI's was biased by -23 % (95% CI: -14%; -37%) in DWFS-AC compared to CT-AC. The SUVr were spatially variable from the center of the brain to the periphery. SUVr using DWFS-AC compared to CT-AC was biased by 0.12 (95% CI: -0.03;0.26) in the caudate nuclei and 0.04 (95% CI: -0.05; 0.12) in lateral cortical ROI's. Although the visual categorization of both, amyloid-positive (n=5) and -negative (n=20) scans was unaffected by DWFS-AC, 2 healthy subjects were quantitatively reclassified as amyloid positive. **Conclusion**: The visual and quantitative consequences of MR-AC using DWFS in the brain with [11C]-PiB resemble those described for [18F]-FDG (2). Following DWFS-AC [11C]-PiB images exhibit a noticeable radially variable bias. The quantitative diagnostic criteria using this biomarker with DWFS-AC may need to be modified. References (1) Martinez-Moller A et al. J Nucl Med. 2009;50:520-526. (2) Andersen, F. L. et al. Eur J Nucl Med Mol Imaging (2012) 39 (Suppl 2): S174, OP116

## OP196

### Potential value of quantitative estimate of cortical to cerebellar SUVr in aiding visual interpretation of florbetapir PET scans

M. J. Pontecorvo, **A. K. Arora**, M. Devine, M. Lu, A. Siderowf, MD, C. Devadanam, A. D. Joshi, C. Breault, S. L. Heun, D. M. Skovronsky, M. A. Mintun; Avid Radiopharmaceuticals, Philadelphia, PA, UNITED STATES.

**Aim**: To evaluate inter reader reliability of nuclear medicine physicians interpreting florbetapir PET scans with and without access to cortical to cerebellum SUVr quantitation **Materials and Methods**: Six radiologist/nuclear medicine physicians agreed to participate. Each reader was asked to use standard visual interpretation techniques for florbetapir (http://www.amyvidtraining.com) to interpret 50 florbetapir PET images randomly selected from a previous clinical trial that enrolled patients seeking diagnosis for cognitive decline. The readers were subsequently given instructions in the use of quantitative software as a potential adjunct for interpreting florbetapir images. Readers then reviewed all 50 images again while using MIMneuro 5.6.3 to provide a quantitative estimate (SUVr) of florbetapir amyloid binding. For each case, the reader reassessed their previous interpretation in light of the quantitation results and provided a final interpretation. Cohen's kappa statistic, κ, was used to assess pairwise agreement between readers. Fleiss's kappa statistic was used to estimate overall reader agreement prior to and after access to quantitative processing. Accuracy was also calculated as the percent of cases in agreement with an expert (AKA) visual interpretation. **Results**: With standard visual interpretation approach, reader-to-reader paired κ values ranged from 0.64 to 0.88 with an overall Fleiss κ of 0.76 (95% CI 0.69-0.83). After obtaining quantitative processing information, interreader agreement improved significantly ($p < 0.05$), with paired κ values ranging from 0.80 to 0.96 and an overall Fleiss κ = 0.88 (95% CI 0.81-0.95). 22 of the 50 cases were rated amyloid positive by the expert reader. The accuracy of reader interpretation (agreement with the expert reader) ranged from 80-94% with a mean of 89 ± 5.2%. After obtaining SUVrs, the range of accuracy scores narrowed to 92-96% with a mean of 94 ± 1.5% (p=0.052 vs prequantitation). The only two readers that did not increase accuracy with quantitation were those with the highest pre-quantitation accuracy (94%). **Conclusions**: Interreader reliability increased significantly after obtaining quantitative estimates of florbetapir PET amyloid binding (SUVr). There was a trend toward increased accuracy (compared to expert read) although the study may have been limited by a ceiling effect for some readers who already agreed with the expert reader in 94% of the cases prior quantitative information. The results suggest that quantitative information may improve performance of individual physician readers.

## OP197

### Improving amyloid PET brain imaging

**K. Knesaurek**, J. Machac, Z. Zhang, A. Rafique; The Mount Sinai Medical Center, New York, NY, UNITED STATES.

**Objectives:** The Aim of our study was to improve amyloid PET brain imaging by applying partial volume corrections (PVC). **Methods:** In a continuing study, 22 patients were imaged on a GE STE 16 slice PET/CT system with 370 kBq of florbetapir F-18. The data were reconstructed using vendor's reconstruction software. When available, the corresponding MRI data were taken from the PACS system and both PET and MRI data, of the same subjects, were transferred to a common platform. Two PVC corrections, which utilize MRI segmentation into grey matter (GM), white matter (WM) and cerebrospinal fluid (CSF) regions, were use and compared. First method was a geometric transfer matrix (GTM) method and second, a simplified Muller-Gartner (MG) or Meltzer's method (sMG), which uses only brain spill out. **Results:** For an amyloid-negative and cognitively normal subject, MRI segmented WM corresponded well with the florbetapir F-18 uptake. In this case, WM values were 7.2-9.6 kBq/cc and GM values 2.3-6.2 kBq/cc in the original images, 6.8-9.2 kBq/cc in WM and 3.9-6.3 in GM for sMG images and for GMT PVC in WM the value was 8.7 kBq/cc and in GM 5.4-6.4 kBq/cc. For the same subject, SUVr values for original, sMG and GTM were 0.98±0.45, 1.12±0. 75 and 1.12±1.26, respectively. For a typical amyloid-positive patient with AD, the WM and GM values were inseparable and in the range of 2.5-5.3 kBq/cc in original images, 3.1-5.9 kBq/cc for sMG images and for GMT PVC the same value for both WM & GM was 4.2 kBq/cc. In this case, the SUVr values were 1.19±0.46, 1.17±0.60 and 1.20±0.95, for original, sMG and GTM, respectively. **Conclusions:** Applied partial volume corrections did not significantly change or improve original images. GTM method seems to outperform sMG method because it provided smoother and more uniform images. The activity concentration and SUVr values in original and corrected images were close and not significantly different.

## OP198

### 123I-FP-CIT brain SPECT study: Analysis of Clinical Impact and Utility of Different Semi-Quantification of Striatal Uptake

**J. Lepej**[1,2], L. Skicka[3], R. Sudzina[3], T. Puskas[2], E. Kahancová[3], B. Marinová[1]; [1]Institut of Nuclear and Molecular Medicine, Kosice, SLOVAKIA, [2]Faculty of Medicine UPJS, Kosice, SLOVAKIA, [3]Dpt. Neurology University Hospital L. Pasteura, Kosice, SLOVAKIA.

**Aim**: Many different semi-quantitative analyses were suggesting to proving DaT-SPECT to be a sensitive neuroimaging method for the assessment of dopaminergic system degeneration in patients with suspected Parkinson´s disease. We tried to find a semi-quantitative method and presentation of results for more clear differentiation between patients with Essential Tremor (ET), Parkinson´s disease (PD) and other forms of Parkinsonism. **Material and Methods**: DaT-SPECT was performed in patients mainly with no clear symptoms of ET or PD. In a retrospective study, from the referring physicians, we acquired data of the 69 patients (age ± SD), 40 female (59.5 ± 8.5 years) and 29 male (56.0 ± 14.6 years). The final clinical diagnosis, obtained in average 23.0 ± 15.8 months after the initial SPECT scanning served as a golden standard. A brain SPECT (128 projections per 30", matrix 128x128) was acquired 4h post injection of mean 181.6 ± 9.2 MBq 123I-Ioflupane. Acquired data were reconstructed in a standard manner of protocol Milano. The composite image was used to draw separate pairs of symmetrical ROIs of nucleus caudate (NC), putamen (PU), whole striatum (ST) and occipital region (OR) used for calculation of specific uptake indexes (SUI). From obtained data were suggested the diagram method which uses different x-y plots (for example: SUI mean ST - mean PU vs. lower value of PU). It was clearly differentiating all patients to 2 subgroups with ET and PD. **Results:** The sensitivity, specificity, positive and negative predictive values was calculated for each from 3 evaluation Methods: 1) Visual evaluation method (0.97, 0.75, 0.78, and 0.96); 2) SUI of putamen (1.00,

0.67, 0.73, and 1.00) and 3) Diagram method (1.00, 0.89, 0.89, and 1.00). False positive result in diagram method was Willson´s disease (1), Dementia Lewy Bodies (1) and Subcortical Arteriosclerotic Encephalopathy (2). **Conclusion**s: The best results of semi-quantitative evaluation 123I-FP-CIT brain SPECT were obtained by diagram method, mainly in specificity and positive predictive value. This method in case of large cohort offer better differentiation between ET and PD patients which is lower dependent on comparison the normal values and diminish the subjectivity in decision-making. It shows high importance to individualize these quantitative Methods for each nuclear medicine department.

## OP199

### Evaluation of pituitary adenoma and craniopharyngioma by Methionine positron emission tomography

**J. Abe**, N. Tsuyuguchi, Y. Terakawa, K. Ishibashi, T. Nagata, K. Ohata; Osaka City University Graduate School of Medicine, Osaka, JAPAN.

**Aim**. Methionine (MET) positron emission tomography (PET) is known to be useful for evaluation of extent and malignancy of several types of brain tumours; however, only a few reports are available regarding the role of MET PET in the evaluation of suprasellar brain tumours. Accordingly, this study was conducted to assess the role of MET PET in pituitary adenomas and craniopharyngiomas. **Materials and Methods**. A total of 64 patients, 32 men and 32 women with the mean age of 48.8 years, were included in this study. Among them, 50 were pituitary adenomas and 14 were craniopharyngiomas. MET uptake on PET was calculated and the correlation between MET uptake and histopathological results was assessed. Of the 50 pituitary adenomas, 16 cases were hormone producing pituitary adenomas which were under medical treatment. In these medically treated pituitary adenomas, the relationship between MET uptake and serum hormone levels were also examined. **Results.** The mean of the lesion to normal (L/N) ratio, generated by dividing the mean standardized uptake value (SUV) of the lesion by the mean SUV of the contralateral normal frontal lobe gray matter, was 1.6 in normal pituitary glands, 2.1 in non-functioning adenomas, and 3.1 in functioning adenomas. The mean L/N ratio in pituitary adenomas was significantly higher than that in normal pituitary glands. Among pituitary adenomas, the mean L/N ratio in functioning adenomas was significantly higher than that in non-functioning adenomas. MET uptake was correlated weakly with the serum level of prolactin and growth hormone. MET uptake in craniopharyngiomas was generally low in both newly diagnosed and recurrent cases. There was no significant correlation between MET uptake and tumour proliferation in craniopharyngiomas. **Conclusion**. In pituitary adenomas, MET PET may be used to detect and localize a microadenoma as even small lesions often show higher MET uptake than normal pituitary glands. MET PET may also be used to evaluate the effect of medical treatment in functioning pituitary adenomas. The role of MET PET in the assessment of craniopharyngiomas may be limited as most of craniopharyngiomas show low MET uptake.

## OP200

### Computation of cerebral blood volume from single PET scan with sequential administration of $^{15}O_2$ and $H_2{}^{15}O$

**N. Kudomi**[1], Y. Maeda[2], Y. Yamamoto[3], Y. Nishiyama[3], H. Iida[4]; [1]Faculty Of Medicine, Kagawa University, KAGAWA, JAPAN, [2]Clinical Radiology, Kagawa University, KAGAWA, JAPAN, [3]Radiology, Kagawa University, KAGAWA, JAPAN, [4]Investigative Radiology, National Cerebral and Cardiovascular Center, Osaka, JAPAN.

**Objectives:** PET with $^{15}O$-labeled tracers is capable of providing unique and essential information in patients with cerebro-vascular disorders, and has been promoted as a clinical diagnostic tool. A novel DBFM method, allowing an extremely shortened examination period <10 min scan time, has been developed to quantitatively assess functional images of cerebral blood flow (CBF), oxygen extraction fraction (OEF) and metabolic rate of oxygen ($CMRO_2$), from a dynamic single PET scan in conjunction with sequential administration of $^{15}O_2$ and $H_2{}^{15}O$ [1]. The DBFM, however, misses information of cerebral blood volume (CBV) due to elimination of $C^{15}O$ scan. This study was intended to develop a further improved technique for providing CBV, from the single scan data. **Methods:** The technique was based on a basis-function method, provides the CBF, OEF, $CMRO_2$ and CBV images. The sensitivity on CBV is high to appearance time of cerebral blood (ATB), namely, error in input function. We estimated the ATB by accounting for differences in the computed CBF values in a pixel-basis manner using two analyses: DARG [2] and DBFM. Then, those functional images were computed again after correcting for the ATB. Validity was tested by comparing CBV values from region of interest (ROI) on frontal, temporal, occipital and cerebellum regions, between the present ($V_{B,Dual}$) and CO scan Methods ($V_{B,CO}$), on normal ($n$=7) and patient subjects with cerebro-vascular disorder ($n$=8). **Results:** The estimated ATBs were 0.6±2.9, -1.4±3.2, -0.1±2.0 and 3.4±1.4 s for frontal, temporal, occipital and cerebellum, respectively, in normal and 1.1±2.5, 0.9±1.5, 0.3±1.8 and 3.2±0.9 s for those regions, respectively, in patient subjects. The obtained CBV values in normal subject were 0.038±0.014 and 0.039±0.023 (N.S.) for $V_{B,CO}$ and $V_{B,Dual}$, respectively and those in patient were 0.030±0.012 and 0.028±0.014 (N.S.) for $V_{B,CO}$ and $V_{B,Dual}$, respectively. Regional contrast, namely, ROI values between $V_{B,CO}$ and $V_{B,Dual}$ showed tight correlation, i.e., r=0.72 for normal and r=0.68 for patient, but without ATB correction, r=0.53 for normal and r=0.23 for normal and patient, respectively. The obtained $V_B$ images were similar, particularly CBV elevated regions due to ischemia were identical between the Methods, though those by DBFM were suffered from noise more. **Conclusion:** The present method is of use to assess CBV as well CBF, OEF and $CMRO_2$ rapidly in clinical settings. [1] Kudomi et al JCBFM (2013) 33; 440-448 [2] Kudomi et al JCBFM (2005) 25; 1209-1224

## OP201

### Initial evaluation of [$^{18}$F]F13714, a novel 5-HT$_{1A}$ receptor agonist in non-human primates

A. TAVARES[1], G. BECKER[2], O. BARRET[3], T. MORLEY[3], D. ALAGILLE[3], B. VACHER[4], A. NEWMAN-TANCREDI[5], G. TAMAGNAN[3], **L. ZIMMER**[2]; [1]Molecular NeuroImaging, New Haven, New Haven, CT, UNITED STATES, [2]Hospices Civils de Lyon & Univ. Lyon 1, Lyon, FRANCE, [3]Molecular NeuroImaging, New Haven, CT, UNITED STATES, [4]Laboratoires Pierre Fabre, Castres, FRANCE, [5]Neurolixis, San Diego, CA, UNITED STATES.

**Aim.** Brain serotonin 1A receptors (5-HT$_{1A}$) exist in high- and low-affinity states. It is known that agonists bind preferentially to the high-affinity state of the receptors and therefore could provide a measure of the functional 5-HT$_{1A}$ receptors. Since all available fluorinated PET 5-HT$_{1A}$ radiopharmaceuticals are antagonists, it is of great interest to develop a fluorine-18 labelled agonist. [$^{18}$F]F13714 is a novel ligand with high affinity (0.05 nM) for 5-HT$_{1A}$ receptors (J Nucl Med 2012; 53:969-976). Its nitro-precursor was synthesized and radiolabelled via a fluoronucleophilic substitution. Radiopharmacological evaluations included *in vitro* and *ex vivo* autoradiographies in rat brain and PETscans on rats and cats. With the Aim to prepare the transfer of this radiotracer in humans, we now report the first studies of [$^{18}$F]F13714 in non-human primates. **Materials and Methods.** Four baseline PET studies, two blockade and one displacement studies with WAY-100635 (a 5-HT$_{1A}$ antagonist) were performed in two anaesthetized rhesus. Blood quantifications were done for each PET acquisition. **Results and conclusion.** The brain distribution of [$^{18}$F]F13714 was consistent with 5-HT$_{1A}$ receptor distribution and confirmed data previously obtained in rodent and cat. No displacement was observed with WAY-100635 (1 mg/kg iv) but a blockade was observed when WAY100635 (1 mg/kg iv) was administered before the radiotracer. The blood profiles were reproducible between baselines acquisitions. The kinetic modelling using the two-tissue compartment model and $k_4$=0 yielded the best results (i.e. lowest AIC and highest MSC). Test-retest of Ki was < 10%. In conclusion, if [$^{18}$F]F13714 binds *in vivo* the high-affinity states of the 5-HT$_{1A}$ receptors, the modelling data and the competition studies suggest that it binds to the target in a quasi irreversible manner (ie very low $k_4$), probably because of its particular high affinity.

601 — Monday, Oct. 21, 08:00 — 09:30, Amphithéâtre

## CME 5 - Cardiovascular: Myocardial Viability

## OP202

### Critical Appraisal of Viability Assessment

**H.J. Verberne, NETHERLANDS**

## OP203

### SPECT and PET/CT Assessment

**C. Übleis, GERMANY**

## OP204

### Cardiac Magnetic Resonance Assessment

**M. Lombardi, ITALY**

## OP205

### Multimodality Interpretation and Comparison

**T.H. Schindler, USA**

602 — Monday, Oct. 21, 08:00 — 09:30, Auditorium Lumière

## Symposium 5 - EANM/EAU Joint Session: Diagnostics and Therapy of Bone Metastases in Patients with Advanced Prostate Cancer

### OP206
**Diphosphonate Imaging of Bone Metastases**

**I. Fogelman, UNITED KINGDOM**

### OP207
**Choline & Fluoride PET-CT Imaging of Bone Metastases**

**W. Langsteger, AUSTRIA**

### OP208
**Treatment of Bone Metastases: State of the Art**

**B. Djavan, USA**

### OP209
**Alpharadin: New Horizons for Systemic Therapy**

**J. Tennvall, SWEDEN**

603 - Monday, Oct. 21, 8:00 - 9:30, Forum 3

## Technologist Oral Presentations 1

### OP210
**Energy window optimization in 99mTc-technetium MDP bone scan in obese patients**

**M. Smolen**[1], P. Cegla[1], J. Kazimierska[2], W. Cholewinski[2]; [1]Department of Nuclear Medicine, Greater Poland Cancer Center, Poznan, POLAND, [2]Chair and Department of Electroradiology, Medical University in Poznan, Poland, Poznan, POLAND.

The WB bone scans has a particular role in assessment of metabolic function of bone and therefore in oncology. The standard energy window used for technetium studies consist on the peak set on 140keV with 10% window on both sides. In obese patients the Compton scattering decreases the quality of the images and requires special treatment as higher injected activity and longer scan time. The Aim of the study was to evaluate the diagnostic quality of the bone scan image acquired in modified energy window settings. **Material and Methods***:* The study population consist of 105pts (40M,65F) with histologically confirmed prostate, breast or lung cancer. Bone scans were performed 2.5 hour post injection of 800MBq of 99mTc-MDP using BrightView XCT gammacamera (Philips,USA). Whole body bone scans (continous mode, speed 15cm/min, 1024x256 matrix size, body contouring) were performed simultanously in 3 different energy window (WB1:140keV±10%, WB2:147keV±10% and WB3:140keV±5%). Depending on BMI patients were divided into two groups: A-BMI>30 (14M,10F, 63±8y) and B-BMI<30 (26M,55F, 62±13y). Images were analysed using Xeleris workstation (GE,USA). Image parameters were assessed using semiquantitative ROI method assessing counts ratio between normal bone and background (L4 vertebrae was taken as reference) and between metastatic lesion and normal bone. ROI counts ratios were compared in three different acquisition protocols. For statistic analysis T-test was used. **Results***:* As expected decreased number of total counts were found in WB2 and WB3 as compared to reference WB1 (1,4±0,3 Mcts for WB1, 1,1±0,3 Mcts for WB2 (18% decrease; p<0.05) and 1,0±0,2 Mcts for WB3 (29% decrease; p<0.05). L4/backgroung ratio increases with energy window change in patients with BMI>30 [(3,4±0,8 for WB1, 3,8±1,0 for WB2 (12% increase) and 3,9±1,1 for WB3 (15% increase)] and in patients with BMI<30 [(3,8±1,0 for WB1, 4,3±1,3 for WB2 (13%increase) and 4,5±1,4 for WB3 (18%increase)]. Differences in and between patients groups were significant (p<0.05). Significant changes in metastasis/L4 ratio were also found between two analysed groups - for group with BMI>30: 2,29±1,48 for WB1 2,42±1,63 for WB2 (5%increase) and 2,45±1,66 for WB3 (7%increase) and on group with BMI<30 - 1,73±0,66 for WB1 1,82±0,74 for WB2 (5%increase) and 1,80±0,73 for WB3 (4%increase). There were no significant differences between meta/L4 ratios in WB2 and WB3 in analysed patient groups (p>0.05). **Conclusion***:*Changing energy window setting in studies with obese patients may improve diagnostic image quality by increse target/nontarged ratio and the 147±10% window seems to be option with resonable low decrease in total counts.

### OP211
**Does enhanced CT influence the biological GTV measurement on FDG-PET images?**

**P. Vera**[1], R. Modzelewski[1], S. Hapdey[1], P. Gouel[1], H. Tilly[1], F. Jardin[1], S. Ruan[2], I. Gardin[1]; [1]Centre Henri Becquerel, Rouen, FRANCE, [2]Rouen University - School of Medicine, Rouen, FRANCE.

**Objectives:** To test the influence of media injection in PET/CT on the functional or gross tumor volume measurement. **Patients and Methods**: Thirty-three patients (56 ± 19 years) with non-Hodgkin lymphoma (n=22) or Hodgkin disease (n=11) were prospectively studied at staging. PET/CTs were performed 60 min after injection of FDG. Iopamiron 300® (Iopamidol, 1.5 cc/kg) was injected immediately after, followed 50 seconds later by a second craniocaudal CT (CT+). PET images were successively reconstructed using the unenhanced CT (PET-) and the CT+ (PET+) for attenuation correction using iterative reconstruction (4 iterations, 8 subsets, 5 mm post-filtering). The SUVmax, SUVmean, SUVpeak and functional tumoural volume were measured in tumoural lymphadenopathies or malignant tissues (n = 56 VOIs) using 5 3D-thresholding Methods on PET- and PET+ images: absolute SUV value of 2.5; 40% of SUVmax, and 3 adaptative thresholding Methods (Vauclin, Black and Nestle/Schaefer Methods**). Results**: The SUVmean and the volume measurement were significantly different (p<0.001) for the five segmentation Methods for PET- (p<0.001) and PET+ (p<0.001). The SUVmax, SUVmean and SUVpeak increased significantly in PET+ compared to PET- (2 to 5%). The SUVpeak was not significantly different for the five segmentation Methods. The functional volume measurements were significantly different between PET- and PET+ only for the 2.5 segmentation method (+3%; p=0.001), but not for the 40%, Vauclin, Black and Nestle/Schaefer Methods. **Conclusion**: The functional volume could be measured in PET/CT when CT was performed with enhanced media. Caution should be taken when using the volume delineation method. Volume delineation Methods using absolute threshold may artefactually increase the functional volume when enhanced CT is used for attenuation correction. The delineation volume using the relative or adaptative method should be preferred when contrast media is used for PET/CT

### OP212
**Leveraging the Complimentary Power of Concurrent Multimodality PET-CT and Multiparametric MRI via Retrospective Coregistration of Separately Acquired Datasets**

**S. Raja**[1], H. GhunAim[2], S. Rumyantsev[2], A. AlRashed[2], K. Das[2]; [1]Baylor College of Medicine, Houston, TX, UNITED STATES, [2]KFMC, Riyadh, SAUDI ARABIA.

**Introduction:** Concurrent dual and multimodality oncologic imaging such as PET-CT and PET-MR is being increasingly used utilized in oncologic imaging, and more importantly for radiotherapy treatment planning. With the recent Introduction of PET-CT in our institution, we have observed that multimodality co-registration and fusion of PET-CT datasets with multiparametric MRI scans is complimentary. Retrospectively fused datasets have significantly increased the specificity and accuracy of interpretation of the two modalities, and helped in precise localization of PET-CT abnormalities. We present a portfolio of cases that demonstrate the power of retrospective co-registration and fusion of multimodality noninvasive medical imaging with PET-CT and MRI, in oncologic patients. **Methods and Materials:** We retrospectively reviewed all PET-CT studies performed in KFMC from Aug 2012 to present. We identified 21 pts wherein retrospective fusion of PET-CT with MRI led to significant changes in the initial interpretation of either preregistered PET-CT or MRI and/or changed clinical management prospectively. All PET-CT and multiparametric MRI scans were obtained on a GE STE 960 PET-CT scanner and a GE 1.5 tesla HDX MRI scanner (GE - Wakusha, Milwaukee, USA) respectively. The PET-CT and MRI datasets were co-registered, fused and reviewed on GE AW4.6 workstation for final interpretation. **Results**: The histopathology of the 21 cases were as follows: colon/rectal Ca (5),cervical/uterine Ca (5), sarcoma (4), lymphoma/hodgkins (3), recurrent GBM (1), Sq cell Ca (1), intracranial tuberous sclerosis (1), neuroendocrine tumor (1) respectively. In 5/21 pts (23%) co-registration PET with MRI improved localization of abnormality on PET and also enhanced accuracy of PET-CT interpretation. While in 8/21 pts (38%) indeterminate or suspicious lesions on MRI, were clarified as definitely positive/negative for viable tumor by PET, information from PET-CT also improved the specificity and accuracy of findings on MRI. In 2/21 pts. (9%), the initial falsely negative observations on PET-CT, were in retrospect amended as positive for viable tumor following review of fused PET- MR images. In 5/21 pts (24%) whole body PET detected additional lesions outside the FOV of MRI, and in 2/2 pts with suspected hepatic metastasis MR detected additional lesions as compared to PET. **Conclusion:** Retrospective co-registration and fusion of concordantly acquired (but acquired separately, on different scanners and days) multimodality PET-CT and multiparametric MRI imaging is complimentary; significant incremental improvements in the localization of abnormalities, and diagnostic accuracy can be attained, with associated change in subsequent clinical management.

## OP213

### Simultaneous PET/MR in breast cancer-first results

**C. Meisinger**, I. Dregely, S. Schachoff, M. Schwaiger; Klinikum rechts der Isar, München, GERMANY.

**Aim**: MR is a very sensitive diagnostic method in breast cancer imaging. It is well established for mammography and therapy monitoring in high-risk patients. Novel, integrated PET /MR systems combine the advantages of both modalities and thus yield excellent soft tissue contrast and functional information about tumor biology. However, technological challenges in the application of this fairly new method, such as patient position and PET photon attenuation of the breast coil, have to be considered. This work shows our first results using a newly developed 16 channel breast coil (RAPID Biomedical, Rimpar, Germany) specifically developed for simultaneous PET/MR. **Material and Methods**: To obtain accurate PET quantification we characterised and corrected photon attenuation of the new breast coil. Therefore we measured two phantoms (1-liter-water bottles with 75MBq of F-18-FDG each) with and without the coil. Next we obtained a CT map of the coil, which was then fused with the standard patient attenuation correction (AC) map. The patient AC-map was obtained after segmentation of a Dixon-MR sequence. PET was reconstructed using this combined AC map. We measured 4 patients with breast cancer. Approximately 100 min. after injecting F-18-FDG (according to patient's weight) we positioned the patient in the coil, prone with arms over the head. It is important to ensure the patient is fairly comfortable to minimize motion artefacts. **Results**: We found that the presence of the MR coil caused 15% PET photon count loss, which however can be accurately corrected using the described CT template AC map of the coil. Using the MR breast coil, MR image quality in the simultaneous PET/MR exam was comparable to our routine MR-only exams. After implementation of the combined AC map, which accounts for both patient and coil attenuation, the previously observed underestimation of SUV values could be corrected for and accurate PET quantification and image quality was restored. A major focus has to be set on patient positioning, taking into consideration that the examination will take about twice as long as conventional breast scanning. **Conclusion**: Using a dedicated PET/MR breast coil with proper implementation of attenuation correction, state-of-the-art image quality of both, PET and MR, can be achieved. Altogether, simultaneous breast PET/MR is an elegant method of obtaining substantial morphological and functional information for diagnosis and therapy monitoring.

## OP214

### Establishing a radiography program in Denmark with specialization in nuclear medicine included in the curriculum

**S. Holm**[1], L. K. Jeppesen[2]; [1]University College Lillebaelt, Odense, DENMARK, [2]University College Metropol, Copenhagen, DENMARK.

**Aim**: A decree from the Ministry of Education stated that the Radiography education in Denmark should establish and include specialization in nuclear medicine in the curriculum. **Materials and Methods**. The program was developed in collaboration between Metropol University College of Copenhagen, University College Lillebaelt of Odense, Escola Superior de Tecnologia da Saúde de Lisboa, Portugal, and collaboration of staff from the University Hospital of Odense and Rigshospitalet Copenhagen. The course counted a total number of 3 radiography students, and 1 Lecturer. Theoretical teaching is offered by both University Colleges, and students traveled between the destinations. Parts of the course were taught in English from Escola Superior de Tecnologia da Saúde de Lisboa in Portugal, as distance learning using telepresence. Clinical teaching was planned in conjunction with a Clinical Physiological Departments of Nuclear Medicine, approved by either of the schools in Denmark. The radiography program is a 3½ year bachelor degree, and the last 1½ year, students follow their chosen specialization. Two dedicated nuclear medicine modules, each lasting 10 weeks have been established; module 10 focusing on conventional nuclear medicine, and module 11 focusing on PET/CT. Each module equally divided into theoretical teaching counting 7,5 ECTS and clinical teaching counting 7,5 ECTS Assessment involves a two-part examination. The theoretical part, students choose at random one of number of selected nuclear medicine examinations presented in case histories including images/results. Students explain the pathologies and theoretical perspectives in connection to the case. The clinical part of the examination involves an assessment where the student first performs an examination, followed by a session where the care provided and actions taken are discussed. Each module has been orally evaluated by focus group interview including all students and separate interviews with the clinical supervisors additionally a written evaluation of the two modules assembled, has been performed by all students. **Results** : Students have been very satisfied with both their theoretical and clinical learning outcomes. They have been well prepared for performing in clinical practice. Clinical supervisors have been very satisfied with the student's level of meeting the clinical learning outcomes and are ready to welcome the first formally trained Nuclear medicine technologists in Denmark **Conclusion** : The radiography program in Denmark, has succeeded in establishing specialization in nuclear medicine and students have satisfyingly met the learning outcomes established by the Ministry of Education for modules 10 and 11.

## OP215

### Influence of 18F FDG-PET/CT on radiotherapy planning in patients with cervical cancer

**P. Cegla**[1], W. Cholewinski[2], A. Roszak[2], M. Smolen[1], J. Kazmierska[2], B. Urbanski[2]; [1]Department of Nuclear Medicine, Greater Poland Cancer Center, Poznan, POLAND, [2]Chair and Department of Electroradiology, Medical University in Poznan, Poznan, POLAND.

**Objectives**: Cervical cancer is one of the most common cancers to affect woman's reproductive organs. The effectiveness of radiation therapy depends to a large extent on the exact determination of the area of irradiation. FDG-PET/CT has been shown to be a very useful tool in the diagnosis and staging of various cancerous diseases. As a functional imaging it may aid the radiotherapy planning not only by providing three-dimensional conformational images of primary tumour but also by accurate staging and narrowing proper therapeutic options. The Aim of the study was to evaluate the added value of FDG-PET/CT in radiotherapy planning in cervical cancer with the focus on metabolic properties of primary tumour. **Material and Methods:** Between Jan 2012 and Apr 2013, 103 patients (mean age 55±10y) with histologically confirmed cervical cancer underwent PET/CT examinations performed for radiation therapy planning. In 80 pts no treatment was introduced prior to PET scan, in 23pts surgical hysterectomy was performed. PET scans were acquired on Gemini TF PET/CT scanner (Philips) 60min after IV injection of 2-[(18)F]-fluoro-2-deoxy-D-glucose (FDG-FCON, Germany) with the mean activity of 364±75 MBq, with the area being examined extending from the calvaria, to half way down the thigh. The reconstructed PET images were evaluated on a dedicated Philips EBW workstation with time-of-flight reconstruction algorithms. Tumour volumes were calculated using semiautomatic segmentation method; for metabolic activity maximum SUV was used. **Results:** In 36 cases FDG-PET scan didn't show active proliferative process outside the cervix, suggesting of metastases. In 33 cases metastases were found in iliac lymph nodes and in 34 patients scans showed metastases above the aortic bifurcation including lymph nodes, abdominal organs, lung and bone. There was no significant difference in tumour volume (p=0.62) and tumour metabolic activity (p=0.87) between patient group with localized disease (519±561cc; SUVmax 11.7±5.7) and patient group with metastases (439±807cc; SUVmax 12.0±5.7). **Conclusion:** 18F-FDG-PET/CT has a significant influence in assessing the severity of the disease, especially in the evaluation of lymph nodes outside the pelvis and in the selection of the appropriate method of radiotherapy. PET-CT is a powerful tool in the treatment planning of cervical cancer with the regard to the optimal choice of therapeutic procedure.

## OP216

### Qualitative and semi-quantitative comparison of early and late $^{68}$Ga-DOTANOC PET/CT images.

**C. Del Mastro**, A. Papa, F. Trapasso, S. Tetti, I. Baldazzi, F. Cicone, A. Lenza, F. Scopinaro; Department of Nuclear Medicine, Sant'Andrea Hospital, Rome, ITALY.

**Aim.** It's generally recommended to acquire $^{68}$Ga-DOTANOC PET/CT images 50-60 minutes after tracer injection. Based on the expected kinetic of peptides and $^{68}$Ga physical half-life, we postulated that earlier imaging may be possible, without degrading the quality and readability of the scans. The Aim of this study was to evaluate differences between early and late $^{68}$Ga -DOTANOC PET/CT acquisitions, in order to standardise our acquisition protocol and to maximize performances. **Materials and Methods.** Ten patients were enrolled in this prospective study. For each patient, two PET scans were performed in sequence on a Philips Gemini camera, 20 ± 5 minutes (early images) and 50 ± 10 minutes (late images) post injection. Patient position was not modified between scans, in order to use only one low-dose CT (120 kV, 60mA) and to obtain two comparable images. A dynamic scan (5 frames of 3 minutes each) was also obtained in 3 patients to evaluate uptake kinetic in known lesions and in normal tissues. Whole body scans were acquired from mid femora to vertex (3 minutes/bed position, 50% bed overlap). Early and late images were evaluated both qualitatively and semi-quantitatively by five well experienced nuclear medicine physicians from our department, blinded to the acquisition time settings. Semi-quantitative parameters were expressed in terms of SUVmax calculated on normal organ tissues (i.e. liver, spleen, adrenal and pituitary glands), tumor lesions and background (lung and mediastinum). Early vs late organ tissue/background and tumor/background ratios were also compared. **Results**. Four out of five nuclear physicians considered the early images qualitatively better than the late ones. Median early and late SUVmax of normal organ tissue (i.e. liver) were 4.1±0.73 and 3.87±1.03, respectively. Median early and late SUVmax of 3 latero-cervical lesions from medullary thyroid cancer (MTC), were 3.4± 0.5 and 2.5±0.6, respectively. Median early and late SUVmax of 3 lesions from pancreatic neuroendocrine tumors (pNETs) were 25±6 and 20±3, respectively. SUVmax background values were 1.35±0.37 and 0.9±0.2 in early and late images, respectevely. Early and late tumor/background ratios in MTC lesions were 2.5 and 2.7, respectively. Early and late tumor/background ratios in pNETs lesions were 18.5 and 22.2, respectively. SUVmax diffences between early and late images were not significant. **Conclusions.** Our results suggest that early and late acquisitions of $^{68}$Ga-DOTANOC PET/CT images can be considered equivalent.

## OP217

### Evaluation of protein-losing gastroenteropathy in pediatrics with 99mTc-Human Serum Albumin - technical and methodological developments

**B. M. Martins**[1], D. Dantas[1], A. Canudo[1], V. Santos[1], S. Chaves[1], B. Freitas[1], C. Oliveira[2], D. C. Costa[2], I. Santos[3], C. Fernandes[3]; [1]Medical Consult, SA / Fundação Champalimaud, Lisboa, PORTUGAL, [2]Fundação Champalimaud, Lisboa, PORTUGAL, [3]Centro Tecnológico e Nuclear, Instituto Superior Técnico, Lisboa, PORTUGAL.

**Introduction** Protein-losing gastroenteropathy (PLGE) is characterized by an excessive loss of proteins into the bowel lumen due to abnormal mucosal permeability. The clinical presentation is variable, depending on the underlying cause. 99mTc labeled Human Serum Albumin (HSA) has been used to confirm and localize PLGE. First results date back to 1986. Nevertheless, HSA supply is limited, since it is produced from human plasma, involving potential immunological and infectious risks. Therefore, it has been impossible to acquire pre-prepared cold kits of HSA to label with 99mTc. **Materials & Methods** HSA used to treat the underlying pathology was screened for infectious diseases and utilized in this work. The kit formulation was 25 mg of HSA and 0.25 mg of SnCl2.2H2O in 4mL of nitrogen-purged sterilized water (pH 2.5). Labeling was accomplished by addition of 2ml (1174 MBq) of Na99mTcO4 and incubation for 30 minutes at room temperature. Radiochemical purity (RCP) was assessed by ITLC-SG using methanol 85% as eluent (99mTc-HSA remains at Rf=0 and 99mTcO4- migrate to Rf=1) and by size exclusion chromatography (SEC) with Biogel P6 (100-200 µm) in which eventual colloidal species are retained in the top of the column. The radiolabeled solution was tested for endotoxins with a Limulus Amebocyte Lysate Kit (Lonza Pyrogent®) using negative and positive controls incubated for one hour at 37ºC. 99mTc-HSA was then intravenous administrated (111-185MBq) to 3 pediatric patients and a dynamic study of 30 frames, 1 min/frame, was performed. Sequential abdominal static images were acquired at 1h, 2h, 4h and 24h post-injection. **Results** 99mTc-HSA was obtained with high radiochemical purity (~ 100% by ITLC) and pH 4-5. By SEC, the recovered activity was 87%, higher than the required by European Pharmacopeia. The negative result found by the endotoxin test assured a safe administration of the preparation. All children tolerated well the procedure. No one showed specific adverse effects or major complaints, either immediately or at later than 2 months questionnaire to parents and referring physician. Areas of enteric protein loss were demonstrated in one patient. **Conclusion** Preparation of 99mTc-HSA is simple and adequate for "in vivo" administration: convenient pH, high RCP level as well as extended in vitro stability can be readily achieved. Detection, localization and follow-up of cases with occult or intermittent PLGE benefit from 99mTc-HSA reliable serial imaging for up to 24h, with impact on therapeutic strategies.

## OP218

### Nuclear Medicine Education and Training in Europe

**A. C. P. F. Matos**, R. C. Massa, T. F. Vaz, F. Lucena; Nuclear Medicine - Escola Superior de Tecnologia da Saúde de Lisboa, Instituto Politécnico de Lisboa, Lisbon, PORTUGAL.

Nuclear Medicine Technologist is a highly specialized health professional, with competences to undertake the whole range of Nuclear Medicine procedures (diagnosis by imaging, non-imaging and therapy) working in a multidisciplinary team at Nuclear Medicine departments. The education and training of Nuclear Medicine Technologist is not homogeneous among European countries, which leads to different scope of practices and, therefore, different technical skills are assigned. The goal of this research was to characterize the education, training and the scope of practice of Nuclear Medicine Technologists in Europe. This study was based on two different approaches, performing an online survey (multiple choice and open answers) and by literature research. The online survey was developed in two modules. The first was intended to identify the education and the scope of practice of Nuclear Medicine Technologists and the second module was intended to characterize the training of these professionals. The main organization of the survey was based on the following scope of practice: Radiopharmacy, Conventional Nuclear Medicine, Positron Emission Tomography, Radionuclide Therapy, Nuclear Hematology, Cyclotron, Radiation Safety and Protection, Dual-Energy X-ray Absorptiometry and Research. After pre-testing the survey we sent it by e-mail to 48 European countries, namely for Directors of Nuclear Medicine departments and Coordinators of Nuclear Medicine Technologists. Regarding the literature research, it was Aimed to characterize the education, training and scope of practice of Nuclear Medicine Technologists and support the historical evolution of this profession. It was based on scientific research platforms (PubMed and b-on); websites of representative international and national associations and societies in the field of Nuclear Medicine and websites of European higher education institutions. The keywords used in the research were: Nuclear Medicine, Nuclear Medicine Technologist, Biomedical Laboratory Technologist, Radiographer, Education, Training, Career, Scope of practice, Professional Development, Nuclear Medicine Departments and Europe. There was no exclusion criteria based on publishing date since it is Aimed to characterize also the professional evolution of Nuclear Medicine Technologists. The results of the survey will be analyzed and discussed with the results from the literature review. The results are expected to reflect the reality of Nuclear Medicine departments and the Practice of Nuclear Medicine Technologists. It is hoped that the discussion of the results might contribute to the reflection about the role and professional identity of the Nuclear Medicine Technologists in Europe.

607 — Monday, Oct. 21, 08:00 — 09:30, Salon Pasteur

## Pitfalls & Artefacts & Physiology (Interactive): Paediatric Hybrid Imaging

## OP219

### Patient Preparation and Image Acquisition

**R. Kluge, GERMANY**

## OP220

### Interpretation of PET/CT

**L. Kurch, GERMANY**

## OP221

### Interpretation of PET/MRI

**T. Pfluger, GERMANY**

701/703 — Monday, Oct. 21, 10:00 — 11:15, Amphithéâtre

## Plenary 2: Use of PET in Assessment of Therapy

## OP222

### FDG Standardisation

**F.M. Mottaghy, GERMANY**

## OP223

### What Tracer beyond FDG

**C. Nanni, ITALY**

## OP224

### Usefulness of Tailored Treatment in Various Cancer Patients

**B. You, FRANCE**

## OP225

### PET and Radionuclide Therapy

**F. Kraeber-Bodéré, FRANCE**

704 - Monday, Oct. 21, 10:00 - 11:15, Bellecour 1/2/3

## Featured - Cardiovascular: Advances in MPI SPECT

## OP0226

### Advances in MPI SPECT

**S. Ben-Haim, ISRAEL**

## OP227

### Impact of CZT cameras in the daily practice of Nuclear Cardiology: results from a French survey

**A. Manrique**[1,2], F. Rouzet[3], W. Djaballah[4], The French Working Group of Nuclear Cardiology; [1]Normandie Université - EA 4650, Caen, FRANCE, [2]CHU de Caen, Caen, FRANCE, [3]CHU Bichat, Paris, FRANCE, [4]CHU de Nancy, Nancy, FRANCE.

**Objectives**: Previous studies documented the impact of Cadmium-Zinc-Telluride (CZT) cameras in reducing injected radiopharmaceutical doses and radiation dosimetry in selected patients. However, the impact in a routine setting of Nuclear Cardiology remains poorly documented. **Materials and Methods**: A first national survey was conducted in France during 3 days in February 2013 to enhance the

knowledge of current practice in myocardial perfusion imaging (MPI). Centres were screened in December 2011, and all participating centres were asked to provide data obtained from all consecutive myocardial perfusion SPECT performed during a 3-day period (from 4th to 6th February). **Results**: 49 centres replied to the screening phase and 24 finally participated to the survey. Data were obtained from 644 consecutive MPI procedures. Among the 49 centres that participated to the screening phase, 30 utilize a dedicated gamma camera for MPI, including 13 CZT-based cameras. In most centres (93%), quality controls are supervised by a medical physicist. All patients received specific instructions (including refrain from caffeine-containing beverages) prior to the examination (written: 40%, oral: 7%, both: 53%). The indication for MPI were: diagnostic of CAD (378, 59%), post-PCI (159, 25%), post-CABG (46, 7%), medical therapy evaluation (129, 20%), or pre-operative evaluation (35, 5%), and viability (18, 3%). Stress tests were performed using exercise alone (52%) or combined with dipyridamole (28%), dipyridamole alone (15%), or dobutamine (1%) infusion. MPI were performed using sestamibi (43%), tetrofosmin (30%) or thallium (27%). A CZT camera was used in 54% of the SPECT procedures. Radiation dosimetry was strongly related to the type of injected radiopharmaceutical (p< 0.0001) and to the type of camera (conventional vs. CZT, p< 0.0001). Radiation dosimetry was particularly reduced in cases of stress only procedures, leading to doses of 2.69±1.83 mSv, 1.46±0.64 mSv and 16.45±5.06 mSv for sestamibi, tetrofosmin and thallium respectively when using stress only procedures with CZT camera. **Conclusion:** Using CZT based camera significantly reduced radiation dosimetry in the routine practice of myocardial perfusion imaging, particularly when associated to the injection of 99mTc labeled radiopharmaceuticals.

## OP228

### How does cardiac morphing affect cardiac volume, perfusion defects and image quality in CZT MPS?

**J. Oddstig**[1], F. Hedeer[2], C. Hindorf[1], C. Kullberg[2], M. Carlsson[2], J. Jögi[2], H. Engblom[2]; [1]Radiation Physics, Skånes University Hospital, Lund, SWEDEN, [2]Department of Clinical Physiology and Nucalear Medicine, Skånes University Hospital, Lund, SWEDEN.

**Background** During myocardial perfusion SPECT (MPS) the myocardial wall is moving during the cardiac cycle. The clinical evaluation of regional myocardial perfusion is traditionally performed on so called summed images acquired over the entire cardiac cycle. The myocardial motion thereby blurs the summed images which presumably lead to a decrease in image resolution potentially affecting the diagnostic accuracy of regional ischemia and/or infarction. Commercial software is now available to compensate for myocardial motion. Motion-frozen correction is performed by morphing the gated images to the end-diastolic (ED) phase of the cardiac cycle. The Aim of this study was to investigate how this cardiac morphing affects the appearance of regional perfusion compared to traditional summed, non-morphed images using the recently introduced cadmium zinc telluride (CZT) gamma camera. **Material and Methods** In total, 100 patients were included in the study. All underwent a 1-day $^{99m}$Tc-tetrofosmin stress-rest protocol (4 MBq/kg at stress) and were examined with a CZT gamma camera. The images were reconstructed using the reconstruction parameters recommended by the manufacturer. Correction for myocardial motion was performed using the Cardiac morphing software supplied by GE (Cardiac Morphing). From the two set of images, summed and morphed, the following diagnostic parameters were derived using QPS (version 4.0, Cedars Sinai Medical Centre, Los Angeles, CA): Summed stress score (SSS), summed rest score (SRS), summed difference score (SDS). **Results** There was a statistically significant increase (p< 0.001) in all parameters when comparing the morphed images to the summed images (10.7 vs 7.7 for SSS, 6.1 vs 4.9 for SRS and 5.3 vs 3.8 for SDS, respectively). **Conclusions** The use of morphed images in CZT MPS result in more pronounced ischemia. This may improve the diagnostic sensitivity in regional ischemia.

## OP229

### Impact of image processing in the detection of ischemia using CZT-SPECT/CT

D. Koopman[1], **J. van Dalen**[2], C. Slump[1], D. Vink[2], D. Lots[2], P. Jager[2]; [1]University of Twente, Enschede, NETHERLANDS, [2]Isala, Zwolle, NETHERLANDS.

**Objective:** The new multipinhole cardiac SPECT/CT cameras with cadmium zinc-telluride (CZT) detectors are highly sensitive, produce high image quality but rely on dedicated reconstruction algorithms. The influence of image processing steps may be different as compared to standard SPECT protocols. We determined the intra- and inter-operator variability of these processing steps on the final result of myocardial perfusion imaging studies. **Methods:** The population consisted of 20 consecutive patients (7 women and 13 men, BMI 22-40, age 34-79) who underwent a one-day protocol stress- and rest CZT-SPECT/CT (GE Discovery NM/CT 570c) using Tc99m-tetrofosmin. Data were processed twice by three experienced operators. Processing steps include determining of myocardial axes and boundaries, masking of the myocardium and manual SPECT/CT co-registration for attenuation correction. We used a 17-segment cardiac model and calculated the difference between stress and rest of % segmental uptake values (after normalization of peak activity to 100%) for non-corrected (NC) and attenuation-corrected (AC) image sets. AC includes one extra processing step, i.e. SPECT/CT co-registration. Operator variation was considered significant for the diagnosis of ischemia when greater than 5%. **Results:** As a measure of inter-operator variation, the mean operator variation was 2.4% (Q1-Q3: 1.8-2.7%) for the NC images and 3.8% (Q1-Q3: 3.0-4.5%) for the AC images (p<0.01). In 6% (NC) and 23% (AC) of the cases, inter-operator variation was greater than 5%. The mean intra-operator variation was 2.2% (Q1-Q3: 1.5-2.2%) for the NC images and 3.5% (Q1-Q3: 2.6-3.9%) for the AC images. In 5% (NC) and 13% (AC) of the cases, intra-operator variation was greater than 5%. **Conclusion:** Intra- and inter-operator variation in image processing of SPECT-CT CZT gammacamera data is significant and may influence the final diagnosis of ischemia. Especially the use of attenuation correction significantly increases this variation, in particular because of SPECT/CT misregistrations. Clearer guidelines for image processing are necessary in order to improve the reproducibility of the results and to obtain a more reliable diagnosis of ischemia.

## OP230

### Global and regional LV function assessment using two different semiconductor cadmium zinc telluride (CZT) cameras: a dynamic cardiac phantom study compared to conventional gamma camera with cardiofocal collimators.

**A. Bailliez**[1,2], T. Blaire[1,2], D. Legallois[3], C. Desmonts[3], D. Agostini[3], A. Manrique[3,2]; [1]Nuclear Medicine, IRIS, Polyclinique du Bois, Lille, FRANCE, [2]Normandie Université - EA 4650, Caen, FRANCE, [3]Nuclear Medicine, CHU de Caen, Caen, FRANCE.

**Objectives**: Available cadmium-zinc-telluride (CZT) cameras (DNM 530c, GE Healthcare and D-SPECT, Spectrum Dynamics) are not equivalent in terms of sensitivity and spatial resolution. This phantom study compared DNM 530c and D-SPECT to a conventional Anger camera with cardiofocal collimators (Symbia IQ, Siemens) for LV function assessment. **Methods:** The Amsterdam gated (AGATE) dynamic cardiac phantom (Vanderwilt techniques, Boxtel, NETHERLANDS) was used. Eighteen acquisitions were processed on each CZT cameras and Anger camera (IQSPECT). Stop conditions varied from 0.25 Kcts, 0.5 Kcts, 0.75 Kcts, 1 Mcts, 1.25 Mcts and 1.5 Mcts within a myocardial VOI. Left ventricular ejection fraction (EF) was set to 33%, 45% or 60%. Hypokinetic segments were in the antero-septal wall. EDV, ESV, EF, regional wall thickening and motion (17-segment model) were assessed using QGS. **Results:** Myocardial volumes were higher with the DNM 530c compared to D-SPECT and IQ SPECT, respectively EDV (mL): 88±40 vs. 76±32 vs.65±37 (P<0.001), ESV (mL): 40±3 vs. 32±6 vs. 24±2 (P<0.001), resulting in a non significant decreased LVEF: EF (%): 52±23 vs. 53±23 vs. 59±21 (p= NS). Bland Altman plots and Lin's concordance correlation coefficient (CCC) showed a poorer concordance between DNM 530c and IQSPECT (CCC=0.55 for EDV and CCC=0.78 for EF) than between D-SPECT and IQSPECT (CCC=0.79 for EDV and CCC=0.89 for EF). In contrast, the concordance was better between the two CZT cameras (CCC=0.81 for EDV, CCC=0.96 for EF). For ESV, CCC was <0.1 within all cameras. No significant difference was found in total wall thickening (%) and motion (mm) values. Using Kruskal Wallis test, the only parameter that significantly impacted on myocardial wall thickening assessment was EF (chi-squared = 709, P<0.0001). Segmental analysis showed that thickening (segments 1, 2, 3, 7, 8) and motion assessment (segments 1,3) were different between cameras in hypokinetic segments (P<0.05). **Conclusion:** In this phantom study, new CZT cameras, with higher resolution and sensitivity yielded different results compared to Anger camera with cardiofocal collimators for global LV function assessment. Segmental thickening and motion were also different, especially in hypokinetic segments.

## OP231

### Possible use of IQ-SPECT protocol in myocardial perfusion imaging in the evaluation of Patients with suspected or known coronary artery disease: preliminary results.

**F. Caobelli**, C. Pizzocaro, V. Massetti, A. Mostarda, A. Soffientini, M. Andreoli, U. P. Guerra; Fondazione Poliambulanza, Brescia, ITALY.

**Aim:**Quantification of myocardial perfusion scintigraphy is often performed to assist physicians in detecting coronary artery disease (CAD).Modern software and hardware packages provide improvements able to shorten scan time and/or to reduce administered activity,maintaining comparable image quality in radionuclide myocardial perfusion imaging (MPI).Recently,multifocal collimators with dedicated reconstruction software,named IQ-SPECT,are available,able to considerably shorten scan time.The Aim of our study was to compare this new protocol to the already validated standard ones. **Methods**:43 patients with suspected or diagnosed CAD underwent a two-days protocol MPI at rest and after a standard stress test using 99mTc-tetrofosmin.Images were acquired on a 2-head gamma camera and reconstructed with attenuation correction.All the images were scored using a 17 segment model by 3 experienced physicians,blind to clinical data and acquisition and processing modality. **Results**:Overall 17 segments, mean SSS was respectively

5.37 ± 7.01 for IQ-SPECT and 5.65 ± 7.46 for standard acquisition(p=0.65);mean SRS was respectively 3.42 ± 4.61 for IQ-SPECT and 4.23 ± 6.92 for standard acquisition(p=0.13);mean SDS was respectively 2.40 ± 4.94 for IQ-SPECT and 1.74 ± 4.52 for standard acquisition (p=0.23). In the segments of the LAD distribution,mean SSS was respectively 3.23 ± 4.06 for IQ-SPECT and 3.46 ± 4.67 for standard acquisition (p=0.60);mean SRS was respectively 2.46 ± 3,05,61 for IQ-SPECT and 3.03 ± 4.90 for standard acquisition (p=0.24);mean SDS was respectively 1.16 ± 2.32 for IQ-SPECT and 0.74 ± 2.19 for standard acquisition (p=0.27). In the segments of the LCX distribution,mean SSS was respectively 2.13 ± 4.32 for IQ-SPECT and 2.18 ± 3.78 for standard acquisition (p=0.87);mean SRS was respectively 0.95 ± 2.49 for IQ-SPECT and 1.20 ± 2.80 for standard acquisition (p=0.17);mean SDS was respectively 1.23 ± 3.28 for IQ-SPECT and 1 ± 2.70 for standard acquisition (p=0.34). In the segments of the RCA distribution,mean SSS was respectively 3.76 ± 4.93 for IQ-SPECT and 3.93 ± 5.18 for standard acquisition (p=0.68);mean SRS was respectively 2.30 ± 3.22 for IQ-SPECT and 2.58 ± 3.79 for standard acquisition (p=0.28);mean SDS was respectively 1.76 ± 3.56 for IQ-SPECT and 1.41 ± 3.58 for standard acquisition (p=0.29). There were no significant differences on paired t-test and Wilcoxon test in perfusion scores among the full-time images reconstructed with standard protocol or IQ-SPECT,overall on a 17-segments evaluation and when considering different territories of distribution. **Conclusion**:MPI with IQ-SPECT protocol can be acquired at about a quarter scan time without disagreement compared to full time scan acquisition performed with standard protocols.

## OP232
### How smart is SMARTZOOM? A direct comparison between IQ-SPECT and traditional clinical myocardial perfusion SPECT

**U. Talleruphuus**, M. L. Davidsdottir, M. N. Lonsdale; Bispebjerg Hospital, Copenhagen NV, DENMARK.

**Aim** The Aim of this study was to compare left ventricular end diastolic (EDV) and systolic (ESV) volumes and ejection fraction (EF) obtained with IQ-SPECT (IQ) versus conventional parallel-hole LEHR imaging (LI). The Siemens IQ-SPECT system consists of SMARTZOOM collimators (magnifying collimators with a complex design), gantry movement control and special reconstruction software. Thus the system manages to focus on the cardiac region, yielding the opportunity to reduce acquisition time from approximately 20 min to less than 10 minutes**. Materials and Methods** Eleven consecutive patients with suspected angina referred for MPI were included. All patients performed a stress study and two days later a rest study each with both collimators. The stress study was performed in accordance with international guidelines either as bicycle or pharmacological stress using adenosine. The injected activity for both stress and rest study was approximately 750 MBq 99mTc labeled tetrofosmin (Myoview). For patients larger than 100 kg the injected dose was increased to 1000MBq. Gated image acquisition (8 frames) was performed 1h p.i. on a combined Symbia T16 SPECT/CT using IQ and LI. The order of IQ/LI acquisition was alternated for consecutive patients. Acquisition- and reconstruction-parameters were as recommended by the vendor. Left ventricular volumes and EF were estimated using automatic quantification (QGS. Cedars Sinai). Image quality and left ventricular wall delineation was visually assessed by an experienced nuclear medicine specialist without subsequent change. Differences in ESV, EDV and EF between the two collimators were computed, and evaluated using a paired t-test and Bland-Altmann plots. **Results and Conclusions** Eighteen stress and rest studies, each study consisting of both IQ and LI acquisition, were suitable for comparison. All investigated parameters showed highly significant and clinically relevant differences between IQ and LI. For LI the mean (+-SD) values of EF, ESV and EDV were 60.8 ±3.0; 44.2 ± 6.6; 101.6 ±10.1 respectively. For IQ the corresponding values were 66.9 ± 4.2; 32.2 ±6.2 and 79.2 ±9.3. The discrepancy in EF values increased with increasing average value of EF. To conclude, IQ studies exhibit systematic deviations from LI studies concerning EDV, ESV and EF (as estimated by QGS). Care must be taken when moving from one method to the other. This study emphasizes the ever-persistent importance of verifying new equipment before use in clinical practice.

801 — Monday, Oct. 21, 11:30 — 13:00, Amphithéâtre

## CME 6 - Bone & Joint: The Limping Patient - Multimodality Imaging

## OP233
### The Unexplained Hip Pain

**H.K. Mohan, UNITED KINGDOM**

## OP234
### SPECT/CT in Knee Joints - What is Left for Nuclear Medicine Tests at the Era of MRI?

**K. Strobel, SWITZERLAND**

## OP235
### Foot Pain Unexplained by X-rays

**F. Paycha, FRANCE**

## OP236
### The Referred Pain - When the Causative Lesion Lies Far from the Aching Joint

**W. van der Bruggen, NETHERLANDS**

802 — Monday, Oct. 21, 11:30 — 13:00, Auditorium Lumière

## Symposium 6 - SNMMI Session: NM Brain Imaging Update

## OP237
### Dementia Imaging with Amyloid Agents

**P. Herscovitch, USA**

## OP238
### Non-Dementia Related NM Brain Imaging

**G.L. Dillehay, USA**

## OP239
### New Agents for NM Brain Imaging

**K.A. Frey, USA**

803 - Monday, Oct. 21, 11:30 - 13:00, Forum 3

## Technologist Oral Presentations 2

## OP240
### Use of a mobile lead shield to effectively reduce radiation exposure in the PET suite

**J. Trinckauf**, S. Kaltsuni, E. Loga, V. Weichselbaumer, M. Hofbauer, S. Epp, G. Warnock, A. Buck; University Hospital Zürich, ZÜRICH, SWITZERLAND.

**Aim:** Investigate the use of a mobile lead shield to reduce the radiation exposure received by PET technologists while positioning and supervising patients in the PET suite. **Materials and Methods:** The use of a fully automatic injection system reduces the radiation exposure received by PET technologists during tracer injection. However, radiation exposure due to the positioning and supervising of the patient in the PET camera remains an issue. This exposure can be reduced by putting a mobile lead shield between patient and technologist. Such a shield was built by the in-house workshop. The dimensions of the shield are 117x74x85cm, it has wheels for ease of movement and contains a 25mm thickness lead shield, equivalent to approximately 4 times the Half Value Layer (HVL). The total weight is around 250kg and it protects the lower part of the body from the chest down. We measured the reduction in radiation exposure by wearing 2 dosimeters, one above and one below the height of the lead shield. Measurements were performed by 3 technologists while handling 71 patients. The dosimeters were worn during injection, while leading the patients to the PET suite, positioning them on the camera and assisting them off the camera at the end of scanning. Patients were injected with 18F- FDG (4MBq/kg bodyweight) using an automatic injector (Medrad INTEGO) and positioned on the camera after an uptake time of 60 minutes. **Results:** The radiation dose measured with each dosimeter (above and below the lead shield, respectively) was 29 vs 13, 36 vs 20 and 44 vs 26 microSv/h for the 3 technologists, representing reductions of 55, 44 and 40 percent. **Conclusion:** This study demonstrates that the use of a mobile lead shield in the PET suite effectively reduces the radiation exposure received by the technologists by a factor of nearly two. The method is easy to implement and there were no acceptance problems.

## OP241
### Impact of Weight Loss and Weight Gain in Cancer Patients During the Waiting Time for Quantitative 18F-FDG PET Imaging

**T. Mylvaganan**, M. J. Romano-Fraai, B. G. Hoving, W. V. Vogel; NETHERLANDS Cancer Institute – Antoni van Leeuwenhoek Hospital (NKI-AVL), Amsterdam, NETHERLANDS.

**Aim:** Weight loss and weight gain is a common problem for oncology patients. PET/CT imaging has the ability to visualize and quantify tumor metabolism. Tracer uptake is quantified using the standardized uptake value (SUV), but this depends strongly on body weight. The body weight may be measured at the time of referral or at the time of actual imaging, but it may change significantly in this interval especially in patients who are on treatment. In this study we explored the influence of changes in patient body weight on quantification of $^{18}$F-FDG images. **Methods:** We included 234 patients who underwent $^{18}$F-FDG PET/CT in NKI-AVL in January 2013 in a retrospective analysis. Patient details and scan parameters were retrieved from our clinical database (radiology information system, RIS). Available data included the registered height and body weight of the patient at the time of referral for PET/CT (measured by the referring doctor), and the actual height and body weight at the day of imaging (measured by PET technicians). The body mass index (BMI) was calculated from these values. We evaluated the difference in the registered and actual patient body weight, and its influence on the PET quantification with the $SUV_{max}$ measured in a volume of interest (VOI) in the tumor. **Results:** In 75 of the 234 patients (32%) there was a difference between actual and registered body weight. 60% of these weight differences occurred in male patients. In 19 cases (25%) the weight difference was 5 kilograms or more. In those 19 cases we calculated the $SUV_{bw,max}$ in the same tumor lesions with the actual and registered body weight. The average difference in $SUV_{bw,max}$ related to weight differences in these patients was 11%, range 5-17%. **Conclusion:** We conclude that significant weight differences were commonly encountered between the time of referral and actual imaging. This may be related to real changes in patient weight or to inaccurate measurements by referring doctors. These differences may lead to significant under- or overestimation of $SUV_{bw,max}$. Therefore, SUV quantifications should always be performed using the actual patient weight at the time of imaging. This is especially important for patients who are in quantitative response monitoring studies.

## OP242

### $^{18}$F-FDG PET-CT respiratory gating for evaluation of lung lesions: a scan protocol

**F. Van Der Pluijm**, D. A. Kuijper, C. H. Grievink; Erasmus Mc, Rotterdam, NETHERLANDS.

**Introduction:** The evaluation of lesions in the lower lung regions with a PET-CT scan using $^{18}$F-FDG is difficult because of respiratory motion artefacts. These artefacts can be minimized by using a respiratory gating system. **Aim:** The Aim of this study was to make a respiratory gated $^{18}$F-FDG PET-CT scanprotocol. **Materials and Methods:** For this study the Anzai Respiratory Gating System and the Anzai Respiratory Phantom were used in combination with the Siemens software. The gating system registers the breathing profile which will be postspectively linked to the scandata. A syringe with 6,24 MBq was attached to the side of the phantom. At t=0 a scan of 10 minutes was made, directly followed by a scan of 5 minutes. This was repeated every 30 minutes, until t=120. All scans were acquired with the Siemens Biograph mCT. All scans were attenuation corrected and reconstructed UltraHD with 3 iterations, 21 subsets, image size 200, zoom 1.0, Gaussian filter, FWHM 3 mm. For every scan a static reconstruction and three gated reconstructions were made. The gated reconstructions consisted of 4, 8 and 16 gates. For every reconstruction the coronal plain was viewed in the Hermes viewer. The gates with the least respiratory motion were selected and summed and VOI's were drawn. Subsequently gated reconstructions were compared to the static reconstructions and to each other. **Results:** There is a significant difference between the static and gated reconstructions. The static reconstructions show an obvious respiratory motion artefact. The gated reconstructions however, show minimal respiratory motion artefacts, due to the selected and summed gates. The difference in volume between the static and the summed 16 gates reconstruction from t=0 to t=120 is 19 to 24 %. There is no significant difference between the VOI's drawn on the 5 and 10 minute scans. **Conclusion and discussion:** The summed gated reconstructions show better results than the static reconstruction. Comparing the summed 4 and 8 gates reconstructions, they can be considered to be alike. The summed 16 gates reconstruction is recommended because it shows a more precise result, but reconstructing costs more time and it takes more PACS data storage. The difference between the 5 and 10 minute scans is minimal. Considering attenuation and respiratory signal loss in patient studies, it's preferable to scan 10 minutes. Loss of image quality between t=60 and t=90 is minimal. The respiratory gated scan can be acquired subsequently to the whole body scan.

## OP243

### The effects of weight and injected dose on the Signal-to-Noise Ratio of the liver in adult FDG-PET/CT scans

**D. Duarte**[1], M. Janssen[2], D. Vriens[2], W. van den Broek[2]; [1]Escola Superior de Tecnologia da Saúde de Coimbra, Portugal/Radboud University Nijmegen Medical Centre Nijmegen,Netherlands, Coimbra, PORTUGAL, [2]Radboud University Nijmegen Medical Centre, Nijmegen, NETHERLANDS.

**Context & Aim:** The quality of the image of $^{18}$F-FDG PET/CT scans in overweight patients is commonly degraded, despite increasing the injected radiopharmacon dose. This study retrospectively evaluates the relation between signal-noise-ratio (SNR), bodyweight and $^{18}$FDG-dose injected in PET/CT-scans performed in 65 adult patients. Assuming that the liver has homogenous FDG-uptake, the SNR of this organ was chosen as measure of image quality. A new dosing scheme, based on Poison statistics and the measured relation between SNR and bodyweight, is proposed. **Material and Methods:** All adult non-diabetic patients scanned between 12/11/2012 and 28/01/2013, without known or suspected liver disease were eligible. All patients included in this study underwent the department's standard acquisition protocol on a Siemens' Biograph mCT, had proven normoglycemia, no major artefacts and were fasted at least 6 hours at time of the scan. They were injected with 1.6MBq/kg FDG 60 +/- 5 min prior to scanning. Five liver Regions of Interest were drawn on consecutive PET-slices to obtain the liver's mean uptake value and its standard deviation, the ratio of which was defined as the SNR. Loglinear regression analysis was used to describe the relation between bodyweight and SNR. **Results:** The FDG-PET/CT scans of 65 patients were analysed. The patient's bodyweight ranged from 35 to 120 kg. Despite the use of the current linear FDG-dosing scheme, there was a negative relation between SNR and bodyweight, supporting our hypothesis that increasing the FDG-dose linearly with respect to the bodyweight does not fully solve the negative impact of bodyweight on image quality. Using Poisson statistics, we proposed a new dosing scheme in the form $D=c_1 \times BW \times c_2^{BW}$ (D: FDG-dose in MBq, BW: bodyweight in kg, $c_1/c_2$ constants). As reference image quality, the SNR of a patient of 86 kg (the median in our population) was used. With this reference level, the total amount of FDG activity, needed for our population, would be the same as with the current dosing scheme. **Conclusion:** There is a negative exponential relation between image quality (measured by the liver's SNR) and the patient's bodyweight, despite linear dose-increase in FDG-PET/CT scans. A new dosing scheme was proposed, which is expected to be economically neutral with similar population effective doses. A prospective study using this proposed dosing scheme will be undertaken to validate, whether it leads to image quality independent of patient's bodyweight.

## OP244

### PET with low dose CTAC: how low can we go without affecting PET quantification?

**T. F. Vaz**[1], D. C. Costa[2], R. Parafita[3]; [1]Nuclear Medicine - Escola Superior de Tecnologia da Saúde de Lisboa, Instituto Politécnico de Lisboa, Lisbon, PORTUGAL, [2]Nuclear Medicine - Radiopharmacology, Champalimaud Centre for the Unknown, Champalimaud Foundation, Lisbon, PORTUGAL, [3]Nuclear Medicine - Radiopharmacology, Champalimaud Centre for the Unknown, Champalimaud Foundation / Medical Consult, Lisbon, PORTUGAL.

**Aim** To determine the minimum acquisition parameters values for kVp and mAs, for low dose Computed Tomography (CT), that do not compromise the attenuation correction (AC) of Positron Emission Tomography (PET) data during semi-quantitative assessment. **Materials and Methods** PET acquisition (Philips Gemini TF PET/CT 16) of Jaszczak® phantom (filled with 15.16 kBq/ml [18F]FDG), in 3D mode, 10minutes/bed, 5mm slice thickness, FOV=576mm and matrix=144x144 pixels. CT acquisition with different protocols, varying voltage (90, 120, 140 kVp) and exposure (20, 25, 30, 35, 40, 45, 50, 55, 60, 100, 230, 265, 305 mAs), keeping all remaining acquisition parameters of the standard protocol of low dose CT constant (viz. thickness=5mm; increment=-5mm; collimation=16x1.5mm, pitch=0.813; rotation=0.5s, FOV=600mm; matrix=512x512 pixels). CT data were resampled to the resolution of PET images and the Hounsfield Units (HU) were converted to linear attenuation coefficient values at 511 keV, for AC purposes. We measured the HU in the CT images, drawing regions of interest (ROI) in the flood area and in the larger acrylic sphere, obtaining the average HU and their standard deviation (SD). Additionally, we performed semi-quantitative analyses of PET data (mean and SD for standardized uptake value (SUV) and radioactive concentration) corrected for AC from different CT scans, using the same ROI locations as for CT. To evaluate image quality (i.e. noise) of PET and CT, we used measures of coefficient of variation (CV). Analysis of variance (one-way ANOVA) and multiple mean comparisons with the Games-Howell test were used for the HU, SUV, radioactive concentration and CV. In all analyzes, p value < 0.05 was considered to indicate statistical significance. Results SUV did not show statistically significant differences. However there were significant differences in the CT numbers obtained from the CT different characteristics (mainly kVp) used for AC. Radioactive concentration values were significantly affected by the CTAC with 90 kVp. These AC didn't affect the CV of the [18F]FDG radioactive concentration, but affected the average radioactive concentration and, therefore degradation of contrast resolution in PET images is to be expected, apparently with no significant clinical impact. Finally, there were no statistically significant differences when different mAs were used in the CTAC. **Conclusion** Low dose CT (i.e. low values of kVp and mAs) enables efficient AC of PET images for quantification purposes, with phantom acquisitions.

## OP245

### PET/CT imaging of head-neck patients: Comparison of a one-step protocol and a two-step protocol

**C. S. Knudsen**, A. Ljunggren, T. Beyer, F. Andersen, T. L. Klausen, K. Cappelen, A. K. Berthelsen, S. Holm, A. Loft; Rigshospitalet, Copenhagen, DENMARK.

**Aim**: The 2009 EANM Guidelines for FDG PET and PET/CT tumour imaging[1], a two-step protocol is recommended for head-neck patients (torso: arms-up and head-neck: arms-down). This procedure is time consuming, increases radiation exposure to staff, and challenges the benefit of contrast-enhanced CT. Our Aim was to assess the feasibility and quality of a one-step protocol for contrast-enhanced high-quality PET/CT imaging of head-neck patients. **Materials and Methods**: This study included 15 head-neck patients referred for 18F-FDG PET/CT imaging (Siemens Biograph mCT, 4MBq/kg 1h pi). Patients were subject to either (A, n=5) standard EANM protocol or (B, n=10) proposed 1-step protocol: (A) supine, head-neck: arms-down, torso: arms-up, repositioning, 2min/bed (B) supine, head-neck-torso: arms-up, 2min/bed in torso region and 5min/bed in head-neck. In both protocols IV contrast were administered once and optimized for head-neck. PET images were attenuation corrected using the diagnostic CT (CT-AC). ROIs were placed in tongue, neck muscle, lung and liver of the CT and copied to the PET images using Mirada XD3 (Mirada Imaging, Oxford, UK). The coefficient-of-variance (CV= SD/mean* 100%) was used to assess image quality. Total PET scan time including repositioning was measured for all exams. Visual PET image quality was evaluated by an experienced nuclear medicine physician on a scale from 1-5 (poor to excellent). Comparisons were performed using unpaired t-statistics. **Results:** CV in the reference regions for protocols (A) and (B) were: Tongue: 15.2 and 11.1 ($p=0.4$ n.s.), Neck muscle: 16.1 and 11.2, ($p<0.01$), Lung: 23.5 and 20.6, ($p=0.3$ n.s.), and Liver: 15.0 and 16.3 ($p=0.4$ n.s.) Mean scan time for protocols (A) and (B) were 23:41 min and 20:46 min, respectively. Visual grading of AC-PET quality showed no significant difference in the mean scores between (A) and (B): head-neck: 4.4 and 4.5, and thorax: 4.6 and 4.8. **Conclusion**: A one-step imaging protocol with adjusted emission time and single CT contrast injection is feasible and results in image quality comparable to that from a two-step protocol as recommended in the EANM guidelines. Furthermore, the one-step protocol reduced overall scan time and staff exposure due to the reduced requirements on repositioning patients.

## OP246

### Triple-phase 18F-choline PET/CT imaging in the diagnosis of primary hyperparathyroidism

**S. Rep**[1], M. Hocevar[2], B. Vidovic[1], S. Sustar[1], L. Lezaic[1]; [1]University Medical Centre Ljubljana, Ljubljana, SLOVENIA, [2]Institute of Oncology, Ljubljana, SLOVENIA.

**Introduction**: Scintigraphy of parathyroid adenomas based on the accumulation and distribution of radiopharmaceutical, usually 99mTc-MIBI. Most centers used for the diagnosis of parathyroid adenomas dual-phase, subtraction scintigraphy, SPECT and SPECT/CT. The disadvantage of these Methods is a poor image resolution and sensitivity of the systems. Some PET tracers may be clinically useful to image parathyroid adenomas with advantage of superior image resolution. AIM: To define the diagnostic value of PET/CT 18F-choline compares with 99mTc-MIBI and with kinetic analysis of 18F-cholin determines the optimal timing to performed scintigraphy. **Methods**: We covered 20 patients (18 women and 2 men, mean age 52 years) with suspected primary hyperparathyroidism. In all patients, we performed PET/CT in three phases, immediately, one and two hours after administration of 100MBq 18F-choline. SPECT/CT and subtraction scintigraphy (99mTc-MIBI - 99mTcO4) were performed after administration of 600MBq 99mTc-MIBI and 150MBq 99mTcO4. All scans were diagnostically evaluated as positive, equivocal and negative. In all PET/CT scans, SUV value were calculated in parathyroid adenomas and thyroid gland. Based on these results, we sought to determine the optimal time for scanning. **Results**: In 20 patients, 28 adenomas were found and confirmed histologically. PET/CT with 18F-choline, correctly localized in the first phase23/28, in the second phase 24/28 and in the third phase 22/28, together 25/28 adenomas. SUV value in the parathyroid adenomas was in the first phase between 2.1 and 10.2, in the second phase between 1.9 and 12.1 and in the third phase between 1.9 and 10.2. In the thyroid SUV value was in the first phase between 1.6 and 4.1, in the second phase between 1.5 and 3.2 and in the third phase 1.3 and 3.4. SPECT/CT correctly localized 19/28 adenomas and subtraction scintigraphy 16/28 adenomas. **Conclusion**: Advantages of 18F-choline PET/CT according the SPECT/CT and subtraction scintigraphy have better sensitivity, reduced time imaging and lower radiation burden. The optimal are performed 18F-choline PET/CT immediately and one hour after administration.

## OP247

### Very early pelvic acquisition of 18 F-Choline PET/CT in patients with prostate cancer avoids radioactive urine interference.

A. Massaro[1], **M. C. Marzola**[1], S. Chondrogiannis[1], L. Rampin[1], A. Ferretti[2], A. M. Maffione[1], G. Grassetto[1], D. Rubello[1]; [1]Nuclear Medicine PET/CT Centre, Santa Maria della Misericordia Hospital, Rovigo, ITALY, [2]Medical Physics and Biostatistics Unit, Santa Maria della Misericordia Hospital, Rovigo, ITALY.

**Purpose:** To evaluate the usefulness and feasibility of a "very early" pelvic acquisition of 18F-Choline PET/CT in order to have a "clean" vision of the prostatic region avoiding radioactive urine interference. **Materials and Methods**: 55 consecutive patients (mean age 72 years, mean PSA 7.9 ng/ml) with prostate cancer who performed 18F-Choline PET/CT (November 2012-February 2013) were prospectively evaluated. 50 patients undergone 18FC-PET/CT for restaging (40 after surgery/radiotherapy and biochemical relapse and 10 after treatment with hormonal therapy only) and 5 patients for staging. New protocol consisted on a very early scan of the pelvic region (1 bed position of 4 min) followed by a whole body scan 1 hour p.i. Patients were asked to drink 500 ml of water before PET/CT and were positioned on the tomograph without voiding the bladder. 18F-Choline was injected (3 MBq/kg) after the CT scan for attenuation correction. PET acquisition started right after the injection. A comparison between very early and 1 hour images of the pelvic region was performed by visual/semiquantitative analysis evaluating 1) activity in the urinary tract (bladder, ureters, urethra) and whether it interferes with the reading of the scan 2) pathologic findings (prostate region, lymphnodes, bone). **Results**: The overall detection rate of 18F-Choline was 56% (31/55 pts). 14/31 (45%) of PET positive patients showed local pathologic uptake: in 8 cases confined to the prostatic bed only, in 3 cases to the locoregional lymphnodes only and in 3 cases to both sites. 10/31 (32%) showed distant localizations only: in 6 cases confined to the bone and in 4 cases to distant lymph nodes. The remaining 7 patients (23%) showed both local and distant localizations. In all patients the very early images showed absence of radioactive urine in ureters, bladder or urethra which allowed a "clean" evaluation of the prostatic region. Moreover uptake in the prostatic region, confirmed also in the late images, was better visualized in the early phase in 45% (5/11) of the patients. Other pelvic pathologic findings (bone and lymphnodes) were visualized both in the early and late images. **Conclusion:** The overall detection rate of 18F-Choline PET/CT was 56 %. In all patients the "very early" pelvic acquisition offered a very "clean" evaluation of the prostatic region without any interference of physiologic activity in the urinary tract. All pathologic deposits in the pelvic region (prostate, lymphnodes, bone) were visualized both in the early and late images.

## OP248

### Comparison of PET/CT acquisition protocols in lung carcinoma: effective radiation dose and image quality

**H. Eckhart**, A. v. Langen, E. Vleeming, S. Lazarenko, G. Gommans, R. Knol, F. v. d. Zant; Medisch Centrum Alkmaar, Alkmaar, NETHERLANDS.

**Aim:** To compare the effective dose and image quality of two frequently used PET/CT protocols in patients with suspected lung carcinoma. **Methods:** Seventy patients were included after informed consent. Patients unable to position the arms above the head were excluded. Patients were randomly assigned to group 1 or 2. Group1: PET/CT scan was performed with a radiocontrast enhanced diagnostic CT (110mAs/130kV) without breath hold command. Group 2: PET/CT was performed with low-dose CT (25mAs/130kV) without breath hold command, followed by a diagnostic radiocontrast enhanced CT scan of the thorax and upper abdomen (110mAs/130kV) with breath hold command. For patients with body weight <60kg, tube voltage was reduced to 110kV. Acquisitions were performed using a Siemens Biograph 16-slice PET/CT, using Care Dose4D™. Effective doses of the CT-scan were calculated using the ImPACT dosimetry tool. The parameters age, sex, length, weight and BMI were recorded. The CT image quality of the basal lung segments, the upper abdomen, and extra-thoracic areas was scored as moderate, reasonable or good. Continuous data were tested for normal distribution with a Kolmogorov-Smirnov test and expressed as mean±standard deviation (SD). Differences between group 1 and 2 were tested using Fisher's exact, Mann-Whitney U or two-sided unpaired t-tests, where appropriate. $P \leq 0.05$ was considered significant. **Results:** There were no significant differences in age (67±10y vs 66±11y), weight (76±17kg vs 75±17kg), length (173±8cm vs 175±9cm) and BMI (25±5 vs 24±5) or gender (17 M:18 F vs 23 M:12 F) between both groups. The number of patients that were scanned using tube voltage of 110kV (6 patients in group 1 vs 3 in group 2, $p=0.48$) did not differ significantly. The mean effective radiation dose was significantly higher in group 1 than in group 2: 14±4.5mSv compared to 12±3.6mSv, $p=0.048$. CT image quality of the basal lungs was significantly better in group 2 (35 good) compared to group 1 (13 moderate, 22 reasonable), $p<0.0001$. CT image quality in the other areas was significantly higher in group 1 (35 good) compared to group 2 (10 moderate, 25 reasonable), $p<0.0001$. **Conclusions:** The PET/CT protocol with low-dose CT followed by diagnostic CT thorax/upper abdomen results in a lower effective radiation dose and better CT image quality of the basal lungs as compared to the protocol with diagnostic PET/CT. However, the latter protocol provides better CT-image quality in areas outside the thorax and upper abdomen.

804 - Monday, Oct. 21, 11:30 - 13:00, Bellecour 1/2/3

## Featured - Oncology Basic Science: New Tracer Development

### OP249

#### New Radiopharmaceuticals for Molecular Imaging of Tumours

**O.C. Boerman, NETHERLANDS**

### OP250

#### Immuno-SPECT Imaging of IGF-1R Expression with Radiolabeled R1507 and F(ab')2-R1507 in Bone Sarcoma Models: Predicting R1507 Therapy Response and Improving IGF-1R targeting

**E. D. G. Fleuren**, Y. Versleijen-Jonkers, S. Heskamp, M. Roeffen, J. Molkenboer-Kuenen, H. van Laarhoven, W. Oyen, W. van der Graaf, O. Boerman; Radboud University Nijmegen Medical Centre, Nijmegen, NETHERLANDS.

**Aim:** To image Insulin-like Growth Factor-1 Receptor (IGF-1R) expression in bone sarcomas with the radiolabeled anti-IGF-1R antibody R1507 and F(ab')$_2$-R1507 fragments with a special focus on predicting R1507 therapy response and improving IGF-1R targeting. **Materials and Methods:** BALB/c nude mice were subcutaneously implanted with IGF-1R-expressing human bone sarcoma xenografts (OS-1, EW-5 and EW-8) which showed high, modest or no response, respectively, to R1507. An IGF-1R-negative tumour (OS-33), unresponsive to IGF-1R inhibitors, was examined as well. Mice were injected with In-111-labeled R1507 ($^{111}$In-R1507) or $^{111}$In-F(ab')$_2$-R1507. The localization of $^{111}$In-R1507 and $^{111}$In-F(ab')$_2$-R1507 in the mice was determined in biodistribution and immuno-SPECT/CT imaging studies. **Results:** Biodistribution studies showed specific accumulation of $^{111}$In-R1507 in OS-1 and EW-5 xenografts (27.5±6.5%ID/g and 14.0±2.8%ID/g, 3 days p.i., respectively). Most importantly, $^{111}$In-R1507 uptake in IGF-1R-positive, but unresponsive, EW-8 xenografts (6.5±1.5%ID/g, 3 days p.i.) was comparable to that of IGF-1R-negative OS-33 tumours (5.5±0.6%ID/g, 3 days p.i.). Uptake in normal tissues was low. Corresponding immuno-SPECT images correlated with the response to anti-IGF-1R treatment by showing homogeneous (OS-1), heterogeneous (EW-5) or non-specific (EW-8 and OS-33) uptake of $^{111}$In-R1507 in the tumours. Because EW-5 and EW-8 xenografts demonstrated modest or no $^{111}$In-R1507 uptake despite apparent IGF-1R expression, we selected these models to further investigate IGF-1R-targeting properties of $^{111}$In-F(ab')$_2$-R1507. Biodistribution studies showed specific accumulation of $^{111}$In-F(ab')$_2$-R1507 in EW-5 xenografts from 2 h p.i. onwards (3.6±0.2 %ID/g, t=24 h p.i.) and $^{111}$In-F(ab')$_2$-R1507 immuno-SPECT showed almost homogeneous intratumoural distribution at 24 h p.i. Tumour-to-blood ratios of $^{111}$In-F(ab')$_2$-R1507 were significantly higher than those of $^{111}$In-R1507 at t=24 h p.i. (2.4±0.4 vs. 0.5±0.1, respectively; p<0.05). More importantly, $^{111}$In-F(ab')$_2$-R1507 also specifically accumulated in EW-8 tumours (3.7±0.7 %ID/g, t=24 h p.i). In both EW-5 and EW-8 tumours, there was a good spatial correlation between IGF-1R expression and intratumoural $^{111}$In-F(ab')$_2$-R1507 uptake as measured by autoradiography. **Conclusion:** $^{111}$In-R1507 tumour uptake as determined by immuno-SPECT correlates to anti-IGF-1R therapy (R1507) response in bone sarcoma models. Because $^{111}$In-F(ab')$_2$-R1507 fragments have superior tumour penetrating and IGF-1R-targeting properties as compared to $^{111}$In-R1507, this suggests that anti-IGF-1R therapies in bone sarcomas and other tumours may be improved by using smaller therapeutic compounds. Further *in vivo* studies addressing this topic are warranted.

### OP251

#### [$^{68}$Ga]CPCR4.2-PET for Imaging of CXCR4-Chemokine Receptors opens a new and exciting field of clinical research

**H. Wester**[1], U. Keller[2], A. B. Beer[2], M. Schottelius[1], F. Hoffmann[1], H. Kessler[1], M. Schwaiger[2]; [1]Technische Universität München, Garching, GERMANY, [2]Technische Universität München, Munich, GERMANY.

It is well reported that the CXCL12/CXCR4 signaling pathway is of vital importance to various pathophysiological phenomena, including cancer growth, metastasis, hematopoiesis, angiogenesis, atherosclerosis, and human immunodeficiency virus infection. CXCR4 and its endogenous ligand CXCL12 (SDF-1) are one of the major receptor/ligand systems consistently overexpressed in the majority of solid tumors and hematological malignancies such as B-cell lymphomas. Recently, we reported on a newly developed cyclic pentapeptide, [$^{68}$Ga]CPCR4.2, a PET imaging agent that binds with high affinity and selectivity to CXCR4. Here we report on the preclinical evaluation of this probe and first clinical PET results. [$^{68}$Ga]CPCR4.2 emerged from the screening of a wide variety of c(D-Tyr$^1$-Arg$^2$-Arg$^3$-2-Nal$^4$-Gly$^5$) (FC131) derivatives. Competition binding studies on Jurkat cells with [$^{125}$I]FC131 demonstrated high affinity binding of [$^{68}$Ga]CPCR4.2 to CXCR4 ($IC_{50}$ of 5.0±07 nM). Binding studies with iodinated [$^{nat}$Ga]CPCR4.2 on transiently transfected CHO-K1 cells revealed high specific binding to hCXCR4 and no binding to mCXCR4, rCXCR4 or hCXCR7. Based on very promising in vivo data in mice bearing OH1 hSCLC and HT19 colon cancer xenografts, first human CPCR4.2-PET scans were performed at 1h p.i. of 100-150 MBq [$^{68}$Ga]CPCR4.2. [$^{68}$Ga]CPCR4.2 showed only little to moderate uptake in normal organs and background tissue ($SUV_{mean}$ /$SUV_{max}$ blood pool 1.87/3.38, muscle 0.77/1.38, lung 0.75/1.20, liver 1.46/2.99, spleen 5.69/7.53, bone marrow 4.00/5.05, kidney 5.06/11.89, bladder 36.4/71.0). CPCR4.2-PET/MR revealed excellent image quality in a patient with chronic lymphocytic leukemia and suspected transformation into aggressive B-cell lymphoma. All nodal lesions were detected with even higher tracer uptake compared to [$^{18}$F]FDG-PET/CT ($SUV_{mean}$ /$SUV_{max}$ [$^{18}$F]FDG: 3.66/5.94; [$^{68}$Ga]CPCR4.2: 5.05/6.64). In a patient with histologically proven non-small cell adenocarcinoma of the lung and CD30+ aggressive T-cell lymphoma CPCR4.2-PET/CT showed high tracer uptake in the lymphoma lesions (SUVmean /SUVmax [$^{18}$F]FDG: 29.82/50.91; [$^{68}$Ga]CPCR4.2: 9.91/16.95) but lower uptake in the lung cancer lesions ($SUV_{mean}$ /$SUV_{max}$ [$^{18}$F]FDG: 26.36/38.57; [$^{68}$Ga]CPCR4.2: 2.70/3.86). Assessment of peripheral blood stem cell (PBSC) mobilization using pre- and post-imaging standard CD34+ flow cytometry did not show any change in the frequency of PBSC. To the best of our knowledge we could demonstrate for the very first time successful PET imaging of CXCR4 expression in humans. [$^{68}$Ga]CPCR4.2 exhibits high affinity and selectivity for CXCR4, excellent pharmacokinetics, low unspecific uptake and high target/non-target ratios. Based on the wide spectrum of diseases that has been linked with CXCR4 expression, CPCR4.2-PET opens a new and exciting field of clinical research.

### OP252

#### $^{111}$In-DOTA-E-[c(RGDfK)]$_2$ for specific in vivo imaging of angiogenesis

**S. Terry**[1], K. Abiraj[2], L. van Dijk[1], C. Frielink[1], J. Bussink[1], W. Oyen[1], O. Boerman[1]; [1]Radboud University Nijmegen Medical Centre, Nijmegen, NETHERLANDS, [2]Hoffmann-LaRoche AG, pRED, PharmaResearch & Early Development, Basel, SWITZERLAND.

**Aim:** An early event during angiogenesis, a key process during tumor growth and development, is the overexpression of integrin $\alpha_v\beta_3$ on activated endothelial cells. Anti-angiogenic therapy is being applied and investigated for the treatment of an increasing number of types of cancer. Being able to non-invasively image angiogenesis could help stratify patients and monitor therapy response as well as determine the optimal window for a combination of chemo- and radio-therapy. Previously, most preclinical imaging studies utilized tumor models where integrin $\alpha_v\beta_3$ is expressed on both the tumor cell surface and the vasculature. Here, it was determined whether $^{111}$In-DOTA-E[c(RGDfK)]$_2$ allows specific visualization of $\alpha_v\beta_3$ integrin expression on the vasculature of the tumor only. **Materials and Methods:** $^{111}$In-DOTA-E-[c(RGDfK)]$_2$ was used for its high specific affinity for integrin $\alpha_v\beta_3$ as well as high tumor uptake *in vivo* and was prepared to a radiochemical purity above 95%. Biodistribution and SPECT/CT imaging studies as well as immunohistochemistry and autoradiography were used to validate $^{111}$In-DOTA-$RGD_2$ as a specific tracer for angiogenesis. This was accomplished in nude mice with patient-derived squamous cell head and neck carcinoma (HNSCC; SCCNIJ3 and SCCNIJ202) and FaDu tumor xenografts in which integrin $\alpha_v\beta_3$ is solely expressed on angiogenic vessels. Integrin $\alpha_v\beta_3$ binding specificity was studied by co-injection of an excess of unlabeled DOTA-E-[c(RGDfK)]$_2$, macroautoradiography and immunohistochemistry. **Results:** The HNSCC tumor models all showed only vascular integrin $\alpha_v\beta_3$ expression; none was present on the cell surface of tumor cells. The optimal dose of $^{111}$In-DOTA-$RGD_2$ at 1 hour post injection in the head and neck tumor xenografts was determined to be ≤ 1 µg per mouse. Tumor uptake at one hour post injection was 2.25 ± 0.02%, 1.94 ± 0.54% and 1.21 ± 0.04% ID/g for $^{111}$In-DOTA-E-[c(RGDfK)]$_2$ (1 µg) and 0.74 ± 0.41%, 0.60% and 0.49 ± 0.10% ID/g for $^{111}$In-DOTA-E-[c(RGDfK)]$_2$ plus cold excess (50 µg) for FaDu, SCCNIJ3 and SCCNIJ202, respectively. SPECT/CT imaging showed clear uptake of the tracer around the tumor edges, corresponding with well-vascularized areas of the tumor. Correlation analysis allowed us to further determine areas within the tumor where $^{111}$In-DOTA-$RGD_2$ was located, as determined by autoradiography, coincided with vascular integrin $\alpha_v\beta_3$ expression, as measured after immunohistochemical staining. **Conclusion:** $^{111}$In-DOTA-$RGD_2$ shows potential as a tracer to monitor angiogenesis, which could lead to the use of this tracer to ultimately aid the stratification of patients and monitor treatment response of anti-angiogenic therapy.

### OP253

#### Preclinical in vivo imaging of pheochromocytoma using the MIBG-analog PET tracer [18F]LMI1195

**F. C. Gaertner**[1], T. Wiedemann[2], B. H. Yousefi[1,3], M. Lee[2], I. Repokis[2], T. Higuchi[4], S. G. Nekolla[1], M. Yu[5], S. Robinson[5], M. Schwaiger[1], N. S. Pellegata[2]; [1]Klinikum rechts der Isar der Technischen Universitaet Muenchen, Munich, GERMANY, [2]Helmholtz Zentrum Muenchen, Deutsches Forschungszentrum fuer Gesundheit und Umwelt, Neuherberg, GERMANY, [3]Technische Universitaet Muenchen, Pharmaceutical Radiochemsitry, Faculties of Chemistry and Medicine, Munich, GERMANY, [4]Universitaetsklinikum Wuerzburg, Comprehensive Heart Failure Center, Wuerzburg, GERMANY, [5]Discovery Research, Lantheus Medical Imaging, Billerica, MA, UNITED STATES.

**Aim**: [18F]LMI1195 [1-(3-bromo-4-(3-[18F]fluoro-propoxy)benzyl)guanidine] is a novel MIBG-analog PET tracer. In this study we evaluated the feasibility of [18F]LMI1195 for in vivo imaging of tumors overexpressing the norepinephrine transporter using the preclinical MENX rat model of neuroendocrine tumors. Due to a germline mutation in the cell cycle regulatory gene Cdkn1b (encoding p27Kip1), MENX-affected rats develop endogenous bilateral pheochromocytomas with 100% penetrance. **Materials and Methods**: Dynamic small animal PET imaging was performed to evaluate the uptake kinetics of [18F]LMI1195 in Wistar control rats (n=6). Biodistribution studies and small animal PET imaging were performed to evaluate the tracer distribution of [18F]LMI1195 in pheochromocytoma-bearing MENX rats (n=10) in comparison to healthy wild-type control rats (n=4). Tracer uptake of [18F]LMI1195 and [123I]MIBG were compared using co-injection biodistribution studies (n=6). Tumor volume (assessed by histology) and norepinephrine transporter expression (assessed by real-time RT-PCR) were correlated with tracer uptake of [18F]LMI1195. In vivo blocking experiments were conducted after i.v. injection of the norepinephrine transporter inhibitor desipramine (n=2). Autoradiography of the adrenal glands was performed to visualize the intra-organ distribution of [18F]LMI1195. **Results**: Dynamic PET showed rapid accumulation of [18F]LMI1195 in the adrenal glands after i.v. injection. 45 minutes after tracer injection, PET imaging showed significantly higher tracer accumulation in the pheochromocytoma-bearing adrenal glands of MENX rats compared to the normal adrenal glands of control animals (mean SUVmax 10.3 vs 6.1, $p < 0.01$). Desipramine significantly inhibited tracer uptake in the adrenal glands of MENX rats (mean SUVmax 4.6, $p < 0.01$). Biodistribution studies 60 minutes p.i. confirmed the PET imaging results. Mean adrenal uptake values were 0.16 %ID in MENX rats, 0.09 %ID in control rats ($p < 0.01$) and 0.08 %ID in MENX rats after previous blocking of the norepinephrine transporter with desipramine ($p < 0.01$). Adrenal uptake of [18F]LMI1195 correlated highly with [123I]MIBG uptake. Moderate correlations were observed between [18F]LMI1195 uptake, histologic tumor volume and NET expression. [18F]LMI1195 showed an overall favorable tracer distribution for tumor imaging, however increased uptake in bone tissue was observed at late time points. **Conclusion**: [18F]LMI1195 shows high and specific accumulation in pheochromocytomas in the preclinical in vivo MENX tumor model. Its overall favorable biodistribution properties make it a promising PET tracer for imaging of tumor entities overexpressing the norepinephrine transporter. Further studies are warranted to evaluate its clinical value in oncologic indications.

## OP254

### FEMAET: a Cationic Amino Acid PET Probe Targeting the Concentrative Amino Acid Transporter $ATB^{0,+}$

**S. D. Krämer**, A. Müller, A. Chiotellis, L. Mu, C. Keller, S. M. Ametamey, R. Schibli; Center for Radiopharmaceutical Sciences ETH-PSI-USZ, Zürich, SWITZERLAND.

**Aim** $ATB^{0,+}$ (SLC6A14) is an unidirectional concentrative influx transporter for neutral and cationic amino acids. It accepts a broad variety of natural and non-natural amino acids as substrates. The transporter is upregulated in several cancers and is currently investigated as drug target in oncology. The goal was to provide a PET probe for the imaging of $ATB^{0,+}$ overexpressing tumors and the in vivo evaluation of $ATB^{0,+}$ inhibitors. **Methods** The cationic tyrosine analog O-2((2-[$^{18}$F]fluoroethyl)methyl-amino)ethyltyrosine (FEMAET) was synthesized by nucleophilic substitution with non-carrier added [18F]KF-K2.2.2. Cell uptake and efflux were characterized in vitro with prostate cancer PC-3 and small cell lung cancer NCI-H69 cells. Radioactivity accumulation in PC-3, NCI-H69 and breast cancer MDA-MB-231 xenografts in NMRI nu/nu mice was studied by PET after intravenous injection of 6-14 MBq FEMAET. For blocking studies, 100 mg/kg alpha-methyl-DL-tryptophan was injected intraperitoneally 15 min before FEMAET injection. $ATB^{0,+}$ expression in cultured cells and xenografts was quantified by real time PCR. **Results** FEMAET radiochemical yield was 9 %, radiochemical purity > 95% and specific activity > 28 GBq/µmol. FEMAET accumulated in PC-3 and NCI-H69 cells in vitro at 37°C but hardly at 4°C. Uptake in PC-3 cells at 37°C was inhibited to > 90 % by 10 mM BCH and to 66 % by 1 mM alpha-methyl-DL-tryptophan, both are inhibitors of LAT1/2 and $ATB^{0,+}$. The basic amino acids L-arginine, L-lysine and L-histidine, all 10 mM, reduced FEMAET uptake in PC-3 cells by 39±9, 61±8 and 75±12 %, respectively (n≥3). While addition of 1 mM LAT1/2 substrate L-leucine depleted PC-3 cells within 5 min from radiolabeled LAT1/2 substrates, neither 1 mM L-leucine nor 10 mM L-lysine had this effect on FEMAET, indicative of an unidirectional uptake transport. In vivo, FEMAET reached a tumor-tissue ratio of 2.5 at 140 min after injection in a PC-3 xenograft-bearing mouse. alpha-Methyl-DL-tryptophan reduced the tumor-tissue ratio in NCI-H69 xenograft-bearing mice significantly ($P<0.05$) from 2.1±0.4 to 1.7±0.2 at 60-90 min after FEMAET injection (n≥5 xenografts). MDA-MB-231 xenografts did not accumulate FEMAET. Real-time PCR confirmed high expression of $ATB^{0,+}$ in PC-3 and NCI-H69 but negligible expression in MDA-MB-231 cells and xenografts. No radiometabolites were detected in mouse blood plasma 60 min after FEMAET injection. **Conclusion** The $^{18}$F-labeled cationic tyrosine analog FEMAET is most probably a selective substrate of $ATB^{0,+}$. It offers the possibility to image $ATB^{0,+}$-positive tumors and to investigate the inhibitory potential of $ATB^{0,+}$ inhibitor candidates in vivo by non-invasive imaging.

## OP255

### Tumor Vasculature Targeting and PET Imaging in Living Mice with Reduced Graphene Oxide

**S. Shi**, K. Yang, H. Hong, T. E. Barnhart, Z. Liu, W. Cai; University of Wisconsin-Madison, Madison, WI, UNITED STATES.

**Aim**: Graphene-based materials exhibit unique properties for biomedical applications including cancer therapy (e.g. drug/gene delivery, photothermal ablation, etc.). Among the different subtypes of graphene-based nanomaterials, reduced graphene oxide (RGO) is an excellent photothermal agent that enables highly efficient in vivo tumor ablation. In addition, RGO can be used to integrate imaging and therapeutic components for cancer theranostics. Our goal was to employ RGO for in vivo tumor targeting, and quantitatively evaluate the pharmacokinetics and tumor targeting efficacy with positron emission tomography (PET), using $^{64}$Cu as the radiolabel. **Materials and Methods**: RGO sheets, with amino group-terminated PEG chains on the surface, were conjugated to NOTA (1,4,7-triazacyclononane-1,4,7-triacetic acid, for $^{64}$Cu labeling) and TRC105 (an antibody that binds to human and murine CD105, a receptor overexpressed on tumor vasculature). FACS analyses, size measurements, and serum stability studies were performed to characterize the RGO conjugates before in vivo investigation (PET, biodistribution, and blocking studies) in 4T1 murine breast tumor-bearing mice. Imaging results were validated by histological assessment. **Results**: The RGO conjugate, $^{64}$Cu-NOTA-RGO-TRC105, had a size range of 20-80 nm. It exhibited CD105 specificity and superb stability in vitro and in vivo. Nearly 90% of $^{64}$Cu remained on the RGO conjugates after incubation in complete mouse serum at 37 ºC for 48 h, which ensured that the signal observed with PET imaging (based on $^{64}$Cu detection) truly reflects distribution of the RGO conjugates. Serial PET imaging and biodistribution studies revealed that 4T1 tumor uptake of $^{64}$Cu-NOTA-RGO-TRC105 was clearly visible at 0.5 h post-injection (p.i.) and remained stable over time (5.0±0.6, 5.6±0.2, 5.7±0.2, 4.5±0.4, and 4.0±0.5 %ID/g at 0.5, 3, 6, 24, and 48 h p.i.; n = 4), which gave excellent tumor contrast and was several fold higher than the non-targeted RGO conjugate. Various in vivo (e.g. blocking with TRC105), in vitro (e.g. flow cytometry), and ex vivo (e.g. histology) studies further confirmed the specificity of $^{64}$Cu-NOTA-RGO-TRC105 for targeting CD105 on the tumor vasculature. Little extravasation was observed, confirming that tumor vasculature targeting is an ideal approach for RGO. **Conclusion:** This is the first report of in vivo tumor targeting and imaging with RGO. This proof-of-principle study opened up new perspectives for future research and cancer theranostics using graphene-based materials, which are desirable nanoplatforms for biomedical applications because of the versatile chemistry and low toxicity.

805 - Monday, Oct. 21, 11:30 - 13:00, Auditorium Pasteur

## Featured - Molecular & Multimodality Imaging: Optical Imaging

## OP256

### Optical Imaging in Image Guided Surgery

**C.W.G.M. Löwik, NETHERLANDS**

LS — Sunday, Oct. 20, 13:00 — 14:30, Bellecour 1/2/3

## EARL: Proving the Quality of Nuclear Medicine

## OP257

### Improving (real-time) surgical visualization of lymphatic drainage using fluorescein

**T. Buckle**[1], N. S. van den Berg[1], P. T. K. Chin[1], H. G. van der Poel[2], F. W. B. van Leeuwen[1]; [1]LUMC, Leiden, NETHERLANDS, [2]NKI-AvL, Amsterdam, NETHERLANDS.

**Aim:** Conventional sentinel node procedures are performed using a combination of preoperative injection of radiocolloid and an intraoperative injection of vital blue dye. The radiocolloid enables preoperative identification of the SN while the dye allows intraoperative detection of the lymphatic drainage. However, in area's such as the prostate and the kidney blue dyes have shown to be of limited value. Fluorescent dyes such as Indocyanine Green (ICG) and Fluorescein have also been

used. Where ICG has an emission in the near-infrared range, fluorescein has a much higher quantum yield, meaning light efficiency. Moreover, fluorescein can be seen with the naked eye; use of a near-infrared fluorescence camera is not required. In this study the value of fluorescein in intraoperative lymphatic drainage was evaluated. **Material and Methods**: Non-tumor bearing male mice were anesthetized with a hypnorm/dormicum/water solution (1:1:2; 5ul/g) prior to injection of 10-20uL of fluorescein solution (1mg/mL into the left lobe of the prostate (n=6) or directly in the cortex of the kidney (n=3). To increase lymphatic drainage the injection site was massaged for up to 1 minute post injection. Intraoperatively dynamic fluorescence imaging was performed using a self-made fluorescence camera exciting fluorescein (ex = 488 nm; em = 520 nm) in order to visualize draining lymph vessels and the SN. **Results**: In all mice drainage from the injection site into a lymphatic vessel could be visualized directly after injection. Injection of fluorescein into the prostate allowed real-time intraoperative visualization of the lymphatic vessels and the inguinal SNs. Dependent on the location of dye injection (e.g. in the prostate or seminal vessels) bi-lateral inguinal drainage and SN visualization was seen. When unilateral drainage was seen, re-injection in the contralateral lobe resulted in drainage to the contralateral SN. Visualization of the SN after injection into the kidney proved to be more complicated, but feasible.In one of the animals a lymphatic vessel and SN located below the hilus were found. In the other animals drainage into a vessel was found, but the location of the possible SN was not explored. **Conclusion**: Dynamic fluorescence imaging enabled real-time visualization of the draining lymphatic vessels into the SNs. Implementation of this technique into the current clinical setting might increase guidance to and the detection of SNs during SN biopsy procedures in challenging malignancies such as the kidney and prostate.

## OP258

### Fluorescence feature of hybrid tracer is more effective than blue dye in confirmation of sentinel node detection in 199 patients

**G. H. KleinJan**[1,2], N. S. Van den Berg[1,2], O. R. Brouwer[1], H. Mathéron[2], H. Simon[2], O. E. Nieweg[2], K. M. Martin[2], B. Van der Hiel[2], R. A. Valdés Olmos[1,2], F. W. B. Van Leeuwen[1]; [1]Leiden University Medical Centre, Leiden, NETHERLANDS, [2]NETHERLANDS Cancer Institute, Amsterdam, NETHERLANDS.

**Aim** A combination of radiocolloid and blue dye is conventionally used for sentinel node (SN) biopsy in the operating room. The radiocolloid allows for preoperative lymphoscintigraphy and intraoperative probe-guided tracing of the radioactive signal, while the intraoperative injection of blue dye is used for visual detection of the lymph vessel that leads to the sentinel node. Recently, the hybrid tracer ICG (indocyanine green)-99mTc-nanocolloid that is both radioactive and fluorescent was introduced for SN biopsy. One single injection with this hybrid tracer enables both lymphoscintigraphy and intraoperative radio- and fluorescence-guided SN detection. This study evaluated the performance of this hybrid tracer for SN biopsy. **Materials and Methods** One hundred ninety-nine patients with different types of cancer were included in the study: melanoma of head and neck (n=23), of an extremity (n=19) or trunk (n=35) as well as carcinoma of the penis (n=108) or vulva (n=14). Following hybrid tracer injection lymphoscintigraphy and SPECT/CT images were obtained to determine the number and location of the SN(s). Prior to operation vital blue dye was injected around the tumor site. Intraoperatively, the SN(s) were pursued with a gamma probe and a portable gamma camera. Subsequently, the SN(s) were evaluated for the presence of fluorescence and blue dye. **Results** At least one sentinel node was found in each patient with a mean of 2,98 (range:1-10) The nodes were significantly more often fluorescent than blue for all indications. In head and neck melanoma, 93% was fluorescent and 33% had stained blue ($p<0.001$). In both melanoma of the trunk (96% vs. 71%, $p<0.001$) and extremities (100% vs. 76% $p=0.025$) the findings were similar. In patients with vulvar cancer the percentages were 93 and 55 ($p<0.001$) and for penile cancer 93 and 56 ($p<0.001$). **Conclusion** In all indications studied, the SNs were significantly more often fluorescent than blue ($p<0.001$). The addition of fluorescence detection to the SN procedure appears to be highly effective. These findings suggest that the hybrid tracer ICG-99mTc-nanocolloid has the potency to become an alternative of the conventional approach of radiocolloid and blue dye.

## OP259

### An opto-nuclear probe for combined radio- and fluorescence guided sentinel node biopsy

**N. S. van den Berg**[1], G. H. KleinJan[1], D. D. D. Rietbergen[1], H. Simon[2], J. Chambron[2], R. Valdés Olmos[3], F. W. B. van Leeuwen[1]; [1]Leiden University Medical Center, Leiden, NETHERLANDS, [2]Eurorad, Strasbourg, AUSTRIA, [3]Netherlands Cancer Institute - Antoni van Leeuwenhoek Ziekenhuis, Amsterdam, NETHERLANDS.

**Introduction** The clinical implementation of hybrid tracers, such as ICG-99mTc-nanocolloid stimulates the generation of more sophisticated imaging modalities. The opto-nuclear probe prototype (Eurorad, Strasbourg, Austria) used in this study is a modified gamma probe allowing acoustic tracing of the gamma signal produced by 99mTc. Additionally, switching the system to the 'opto' settings allows the acoustic tracing of the near-infrared fluorescence signal produced by ICG. In this study the potential of this first prototypical opto-nuclear probe was evaluated. **Materials and Methods** Nineteen patients scheduled for sentinel node biopsy were included. Following hybrid tracer injection conventional lymphoscintigraphy and SPECT/CT images were performed to determine the number and location of the sentinel node(s). Intraoperatively, sentinel nodes were removed using a combination of conventional gamma tracing (Neoprobe, Johnson&Johnson Medical, Hamburg, Germany) and near-infrared fluorescence imaging (PhotoDynamic Eye, Hamamatsu Photonics, Hamamatsu, Japan). In three patients, intraoperatively, sentinel nodes were pursued using the opto-nuclear probe; here firstly the gamma signal was traced after which the fluorescence signal was traced. Following sentinel node excision ex vivo all excised nodes were measured with the opto-nuclear probe. Measured 5-second count rates were noted. Obtained results were compared to the results obtained with the conventional tools. **Results** In the three patients in which the opto-nuclear probe was used in vivo (3 sentinel nodes were pursued) only in 1 patient the sentinel node could be successfully detected in vivo via acoustic tracing of the fluorescence signal. Ex vivo, a total of 62 lymph nodes was studied. Among them were 56 sentinel nodes, which were both radioactive and fluorescent and 6 non-sentinel nodes that were neither radioactive nor fluorescent. With the opto-nuclear probe, radioactivity was confirmed in 100% of the nodes that were also found to be radioactive with the conventional gamma probe. In 68% of the nodes fluorescently identified with the PhotoDynamic Eye, the fluorescence signal could be acoustically traced using the opto-nuclear probe. **Discussion** The potential of hybrid imaging systems into the clinical situation is great. The opto-nuclear probe allows detection of both labels, radioactive and fluorescence, of ICG-99mTc-nanocolloid. Though further optimization of the settings for acoustic tracing of the fluorescence signal still is required.

## OP260

### Best of both worlds: dual modality imaging of clear cell renal cell carcinoma xenografts using dual label anti-Carbonic Anhydrase IX antibody In-111-DTPA-G250-IRDye800CW

**C. H. J. Muselaers**, D. L. Bos, M. Rijpkema, E. Oosterwijk, P. F. A. Mulders, W. J. G. Oyen, O. C. Boerman; Radboud University Medical Centre, Nijmegen, NETHERLANDS.

**Aim**: Optical imaging using antibodies labeled with near-infrared (NIR) dyes is a very sensitive imaging modality which can be used during surgery. However, because of the low tissue penetration depth of the emitted light, the addition of a radioactive signal to the probe remains indispensible. For this reason, we constructed a dual label anti-Carbonic Anhydrase IX (CAIX) antibody In-111-DTPA-G250-IRDye800CW and investigated the feasibility of dual modality imaging in a intraperitoneal clear cell renal cell carcinoma model. **Materials & Methods**: Forty athymic female BALB/c mice were injected intraperitoneally with 3 x 10^6 SK-RC-52 cells. The mice were divided in two groups; one group received 10 µg DTPA-G250-IRDye800CW labeled with 15 MBq of In-111 prior to imaging, the other received dual labeled aspecific antibody NUH82. To evaluate when tumors could be detected, 4 mice per group were imaged with both the USPECT SPECT/CT and the IVIS Lumina optical imager 48 hours post injection every week. **Results**: Already one week after inoculation, SPECT/CT and optical images showed clear delineation of the CAIX-expressing ccRCC xenografts, with very good concordance between the SPECT/CT and optical images. This high and preferential accumulation of the dual label construct in the CAIX-expressing tumors was confirmed with biodistribution data confirmed these results**. Conclusion**: This is the first imaging study with the dual label antibody In-111-DTPA-G250-IRDye800CW. Very good concordance between the SPECT/CT and optical images was observed. These results strongly suggest that intra-operative detection of CAIX-expressing tumor depositions such as primary renal tumors, positive surgical margins and/or tumor-infiltrated lymph nodes might be feasible.

## OP261

### SPECT/fluorescence dual-modality imaging of carcinoembryonic antigen-expressing tumors: a pretargeting study

**M. Rijpkema**[1], R. Sharkey[2], D. Bos[1], W. McBride[2], W. Oyen[1], D. Goldenberg[2,3], O. Boerman[1]; [1]Nuclear Medicine, Radboud University Nijmegen Medical Centre, Nijmegen, NETHERLANDS, [2]Immunomedics, Inc., Morris Plains, NJ, UNITED STATES, [3]Garden State Cancer Center, Morris Plains, NJ, UNITED STATES.

**Aim** Intraoperative tumor detection with specific radiotracers is a useful tool for accurate localization and resection during surgery. These techniques could benefit from the addition of an optical tracer, since this may allow more accurate intraoperative delineation of the tumor and resection margins. Both tracers in such a dual-modality approach need to show a high specificity and tumor-to-background ratio. We investigated the potential of a pretargeting system using the anti-

CEACAM5 x anti-HSG (histamine-succinyl-glycine) bispecific antibody TF2, and a new hapten-peptide (RDC-018) derived from IMP288, bearing both DOTA for radiolabeling and a fluorescent moiety (IRdye800CW). In this study, we assessed the radiolabeling, in vivo biodistribution and tumor localization properties of RDC-018 in a pretargeting setting compared to IMP288. **Materials and Methods** Three groups of BALB/c nude mice bearing s.c. CEA-expressing LS174T human colonic tumors (left flank) and CEA-negative SK-RC-52 human renal cell tumors (right flank) were injected with saline or with TF2 (0.6 or 6 nmole), and then after 16 h, a 0.05x molar equivalent of either $^{111}$In-labeled IMP288 or $^{111}$In-labeled RDC-018 was administered. Mice were euthanized 2 and 24 hours p.i. (5 mice/group) and optical images were acquired using an IVIS Lumina system and organs of interest were dissected and counted in a gamma counter. **Results and Conclusion** The biodistribution of the dual-label hapten peptide showed specific CEA-expressing tumor targeting (LS174T: 22.0 and 10.0 % injected dose per gram (ID/g), SK-RC-52: 6.0 and 0.9 %ID/g at 2 h and 24 h p.i., respectively) and clearance via the kidneys (22.2 and 12.3 %ID/g at 2 h and 24 h p.i., respectively), similar to IMP288. The optical images confirmed this pattern of high tumor-to-background ratio and renal clearance of RDC-018. Tumor accumulation of RDC-018 was only observed in the mice who received the bispecific antibody (not in the saline control group). In conclusion, the high tumor targeting and excellent tumor-to-background ratio of RDC-018 illustrate the feasibility of this pretargeted dual-modality (SPECT/fluorescence) imaging approach, and show the potential for dual-modality guided intraoperative delineation of tumors and resection margins.

## OP262

### Dual modality imaging of PSMA-expressing prostate cancer with a new radiolabeled anti-PSMA monoclonal antibody conjugated with IRDye800CW

**S. Lütje**[1], M. Rijpkema[1], G. M. Franssen[1], W. Helfrich[2], G. Fracasso[3], W. J. Oyen[1], M. Colombatti[3], O. C. Boerman[1]; [1]Department of Nuclear Medicine, Radboud University Medical Centre Nijmegen, Nijmegen, NETHERLANDS, [2]Department of Surgery, University Medical Centre Groningen, Groningen, NETHERLANDS, [3]Department of Pathology and Diagnostics, University of Verona, Verona, ITALY.

**Aim:** Both radionuclide and near-infrared fluorescence imaging have a high sensitivity to detect tumor lesions *in vivo*. The combination of these modalities using dual labeled antibodies may allow both preoperative tumor identification and intraoperative delineation of tumor lesions using real-time image-guided surgery. Here, we evaluated the prostate cancer targeting characteristics of the new monoclonal antibody D2B, directed against an extracellular domain of prostate-specific membrane antigen (PSMA). D2B was labeled both with $^{111}$In and with the near-infrared fluorescent dye IRDye800CW. **Material and Methods:** D2B was conjugated with NHS-IRDye800CW and ITC-DTPA and subsequently radiolabeled with $^{111}$In. The immunoreactive fractions of $^{111}$In-labeled DTPA-D2B-IRDye800CW and single label $^{111}$In-DTPA-D2B were determined using freshly trypsinized PSMA$^+$ B16-PSMA cells. For biodistribution studies, 2 µg $^{111}$In-DTPA-D2B-IRDye800CW (0.37 MBq/mouse) was injected intravenously into BALB/c nude mice with subcutaneous PSMA$^+$ B16-PSMA tumors (right flank) and PSMA$^-$ B16-wildtype tumors (left flank) as a negative control. The biodistribution was determined at 24, 48 and 72 hours after injection. **Results and Conclusion:** The immunoreactive fractions of $^{111}$In-DTPA-D2B-IRDye800CW and $^{111}$In-DTPA-D2B on B16-PSMA cells were 71.9% and 82.4%, respectively. $^{111}$In-DTPA-D2B-IRDye800CW specifically accumulated in the s.c. PSMA$^+$ B16-PSMA tumors with an uptake ranging from 55.7 %ID/g at 24 h p.i. to 69.8 %ID/g at 72 h p.i., while tumor uptake in PSMA$^-$ B16-wildtype xenografts was much lower at all time points (6.27 %ID/g at 24 h p.i. to 4.23 %ID/g at 72 h p.i.). Highest uptake of $^{111}$In-DTPA-D2B-IRDye800CW was observed at 72 h after injection. In conclusion, in this first proof-of-principle study, we showed that dual-label $^{111}$In-DTPA-D2B-IRDye800CW can be used for specific and sensitive detection of prostate cancer lesions *in vivo*. While the $^{111}$In label allows preoperative delineation of tumor lesions, fluorescent imaging adds the possibility for real-time image guided surgery. These preclinical findings encourage future clinical studies with $^{111}$In-DTPA-D2B- IRDye800CW for pre- and intraoperative guidance for resection of prostate cancer lesions.

806 - Monday, Oct. 21, 11:30 - 13:00, Grand Salon Prestige Gratte-Ciel

## Cardiovascular: Cardiac PET

## OP263

### Interobserver reproducibility of myocardial perfusion quantification with $^{13}$N-ammonia and $^{82}$Rb PET studied with Carimas

**S. V. Nesterov**[1], E. Deshayes[2], L. Settimo[3], C. Han[1], D. V. Ryzhkova[4], I. S. Kostina[4], M. Mäki[1], J. O. Prior[2], R. Sciagrà[3], J. Knuuti[1]; [1]Turku PET Centre, Turku, FINLAND, [2]University of Lausanne, Lausanne, SWITZERLAND, [3]University of Florence, Florence, ITALY, [4]Almazov Federal Heart, Blood and Endocrinology Centre, St. Petersburg, RUSSIAN FEDERATION.

**Aim:** To study the interobserver reproducibility of myocardial perfusion (MP) quantification with the two most frequently used PET tracers_$^{13}$N-ammonia and $^{82}$Rb. **Methods**: The analysis was done on two sets of MP studies used in two multicenter projects (C-AMMO: 48 stress studies of HCM patients; RUBY-10: 48 rest and 48 stress studies of suspected or known CAD patients). Studies were analyzed with Carimas software (Turku, Finland) by 4 observers in Turku, Florence, Lausanne and St. Petersburg. One-tissue compartment models (1TCMs) were used for MP quantification (DeGrado et al., 1996, for $^{13}$N-ammonia; Lortie et al., 2007, for $^{82}$Rb). The reproducibility was assessed on global and regional (LAD, LCx, and RCA) levels. The reproducibility was evaluated using two metrics: pairwise differences between the MP values and corresponding intraclass correlation coefficients (ICC). Both the metrics were obtained from a custom-built linear mixed model for the repeated measures. **Results:** $^{13}$N-ammonia: the smallest difference between a pair of observers for global MP was 0.08±0.04 mL/min/g (4.7% of global MP average), the largest 0.28±0.04 (17.5% of the average); ICCs were 0.97 and 0.85, respectively. LAD: from 0.03±0.03 (2.3% of LAD MP average) to 0.23±0.03 (16.0%), ICCs - 0.96 and 0.91; LCx: from 0.07±0.06 (3.5%) to 0.38±0.06 (19.4%), ICCs - 0.96 and 0.80; RCA: from 0.02±0.08 (1.3%) to 0.34±0.08 (19.0%), ICCs - 0.74 and 0.63. For $^{82}$Rb we only provide the largest differences_the smallest were negligible (0.1% of the average global rest MP and 0.3% of the average global stress MP). $^{82}$Rb rest: at a global level 0.01±0.02 (1.0%) mL/min/g, ICC=0.95; LAD: 0.02±0.02 (1.6%), ICC=0.95; LCx: 0.01±0.01 (1.3%), ICC=0.95; RCA: 0.05±0.02 (4.2%), ICC=0.94. $^{82}$Rb stress: at a global level 0.11±0.05 (4.5%) mL/min/g, ICC=0.95; LAD: 0.20±0.05 (8.2%), ICC=0.97; LCx: 0.05±0.04 (2.0%), ICC=0.98; RCA: 0.07±0.07 (2.3%), ICC=0.98. **Conclusions**: We demonstrated good interobserver reproducibility for $^{13}$N-ammonia and excellent - for $^{82}$Rb myocardial perfusion quantification with PET using Carimas software. In our experimental setting, the results suggest that interobserver reproducibility is better for MP quantification with $^{82}$Rb than with $^{13}$N-ammonia PET.

## OP264

### Project AQUA: towards standardization of software tools for myocardial perfusion quantification with $^{15}$O-water PET

**S. V. Nesterov**[1], H. J. Harms[2], R. Sciagrà[3], V. Berti[3], C. Han[1], R. Klein[4], R. deKemp[4], K. L. Gwet[5], K. Yoshinaga[6], C. Katoh[6], P. Knaapen[2], J. Knuuti[1]; [1]Turku PET Centre, Turku, FINLAND, [2]VU University Medical Centre, Amsterdam, NETHERLANDS, [3]University of Florence, Florence, ITALY, [4]University of Ottawa Heart Institute, Ottawa, ON, CANADA, [5]Advanced Analytics, LLC, Gaithersburg, MD, UNITED STATES, [6]Hokkaido University Graduate School of Medicine, Sapporo, JAPAN.

**Aim**. $^{15}$O-labelled water PET myocardial blood flow (MBF) quantification can have additional diagnostic value in patients with coronary artery disease (CAD). However, the application of MBF quantification in clinical setting has been limited, and it would require standardized measurement tools. As the first step of the standardization, we evaluate agreement between the five software (SW) tools--Carimas, CardiacVUer, FlowQuant, PMOD, and HOQUTO--for myocardial blood flow (MBF) and myocardial flow reserve (MFR) obtained from $^{15}$O-water PET/CT data. **Methods**. Rest and pharmacological stress $^{15}$O-labelled water PET/CT scans of 100 patients_two cohorts of 50 coming from PET Centers in Amsterdam and Turku_with suspected coronary artery disease (CAD) were to be analyzed in five collaborating centers. An expert in each center used one of the five SW tools to analyze global and regional (LAD, LCx and RCA) MBF and MFR. The agreement was evaluated using two metrics: pairwise differences between the MBF or MFR values and corresponding intraclass correlation coefficients (ICC). **Results.** By the time of submission to EANM 2013 two centers--using Carimas and PMOD--provided accomplished results for 40 patients from the Amsterdam cohort. At the studied levels only one difference between PMOD and Carimas was statistically significant ($P<0.05$)-stress MBF in LCx: 0.27±0.48 mL/min/g. This difference, however, is only 8.3% of average stress MBF in LCx and was therefore considered clinically non-significant; ICC was 0.89. The other differences follow. Global: rest - 0.03±0.13 mL/min/g, ICC=0.93; stress - 0.10±0.39 mL/min/g, ICC=0.92; MFR - 0.01±0.47, ICC=0.88. LAD: rest - 0.00±0.17 mL/min/g, ICC=0.90; stress - 0.04±0.47 mL/min/g, ICC=0.91; MFR - 0.06±0.55, ICC=0.82. LCx: rest - 0.09±0.11 mL/min/g, ICC=0.95; MFR - 0.02±0.51, ICC=0.87; RCA: rest - 0.06±0.30 mL/min/g, ICC=0.69; stress - 0.15±0.66 mL/min/g, ICC=0.80; MFR - 0.02±0.85, ICC=0.81. The results of all 100 patients obtained from the participating SW tools will be available by autumn 2013. **Conclusions**. At this moment in the AQUA project we can state that when used for MP quantification with $^{15}$O-water PET, PMOD and Carimas provide nearly identical results in measuring myocardial blood flow and myocardial flow reserve on global and regional levels.

## OP265

### Is one single CT enough for attenuation correction of both rest and stress studies for Rb-82 cardiac PET myocardial blood flow quantitation ?

**E. DESHAYES**[1], M. SILVA MONTEIRO[2], R. KLEIN[3], R. DEKEMP[3], J. O. PRIOR[2]; [1]Montpellier Cancer Institute, Montpellier, FRANCE, [2]Lausanne University Hospital, Lausanne, SWITZERLAND, [3]University of Ottawa Heart Institute Cardiac PET Center, Ottawa, ON, CANADA.

**Aim**: Quantitation of myocardial blood flow (MBF) requires PET images to be attenuation-corrected with a co-registered CT scan (AC-CT). Our current Rb-82

cardiac PET acquisition protocol includes two CT scans: One for rest (R) and one for adenosine-induced pharmacological stress (S). The Aim of this study was to determine whether the use of only one single AC-CT for the two PET series (rest and stress) was enough and if yes, when to perform it. **Materials:** Thirty patients with suspected or known CAD underwent a cardiac PET/CT (Discovery FX690, GE Healthcare) with a low-dose AC-CT1 (120kV, 10mA) performed just before Rb-82 administration at rest (10MBq/kg) and PET acquisition started simultaneously in list mode for 8minutes. Then, an adenosine-induced pharmacological stress acquisition was acquired in list mode for 8 minutes before performing a second, low-dose, AC-CT2. MBF was quantified at rest (R) and stress (S), as well as the myocardial flow reserve (MFR) with FlowQuant® (FQ, Ottawa Heart Institute, Canada). Co-registration of PET and CT was performed manually by the same person using the vendor ACQC program. Concordance between MBF for the different series was assessed by comparing: (1) series reconstructed with the first AC-CT1 to those reconstructed using both AC-CTs; and (2) series reconstructed with the second AC-CT2 to those reconstructed with both AC-CTs. Pearson's correlation r [95%CI], Bland-Altman 95% limits of agreement (LoA), Lin's concordance correlation ρc [95%CI] and the bias coefficient (Cb= ρc/r) were computed (R software). **Results:** Intra-operator FQ reproducibility is excellent at rest, stress and for MFR (r respectively 0.99, 0.99, 0.98; ρc respectively 0.99, 0.99, 0.98), which allows its use as a comparison tool for the study (AC-CT1 vs. AC-CT2). Concordance between MBF at rest using AC-CT1 or AC-CT2 (RCT1 vs. RCT2) was good (r=0.89 [0.78-0.95]; ρc = 0.84 [0.74-0.91]). Similarly, the concordance between MBF at stress using AC-CT1 or AC-CT2 (SCT1 vs. SCT2) was slightly but not significantly lower (r=0.78 [0.59-0.89]; ρc = 0.76 [0.57-0.87]). Similar results were obtained for MFR, using CT1 or CT2 without statistical difference (r=0.82 [0.66-0.91], 0.86 [0.72-0.93], respectively; ρc = 0.80 [0.63-0.89], 0.86 [0.72-0.93], respectively). Bias coefficient was always Cb>0.95, indicating that no systematic error was performed. **Conclusion**: It seems acceptable to use only one CT (AC-CT1 or AC-CT2) for attenuation correction of both rest and stress series of Rb-82 cardiac PET to perform quantitative measurement of myocardial blood flow.

## OP266

### A cross-comparison study of 10 software tools for quantification of $^{82}$Rb myocardial perfusion PET

**S. V. Nesterov**[1], R. Sciagrà[2], A. M. Alessio[3], J. M. Declerck[4], E. Ficaro[5], P. J. Slomka[6], K. Yoshinaga[7], S. Nekolla[8], J. Case[9], R. A. deKemp[10], J. O. Prior[11]; [1]Turku PET Centre, Turku, FINLAND, [2]University of Florence, Florence, ITALY, [3]University of Washington, Seattle, WA, UNITED STATES, [4]Siemens Molecular Imaging, Oxford, UNITED KINGDOM, [5]University of Michigan Health Systems, Ann Arbor, MI, UNITED STATES, [6]Cedars-Sinai Medical Center, Los Angeles, CA, UNITED STATES, [7]Hokkaido University Graduate School of Medicine, Sapporo, JAPAN, [8]Technical University, Munich, GERMANY, [9]Cardiovascular Imaging Technologies, Kansas City, MO, UNITED STATES, [10]University of Ottawa Heart Institute, Ottawa, ON, CANADA, [11]University of Lausanne, Lausanne, SWITZERLAND.

**Aim**. To cross-compare myocardial blood flow (MBF) estimates derived from $^{82}$Rb PET data for 8 mathematical models implemented in ten software (SW) tools: Carimas, Corridor4DM, FlowQuant, HOQUTO, ImagenQ, MunichHeart, PMOD, QPET, syngo.MBF, and UW-QPP. **Methods**. Rest and stress $^{82}$Rb PET/CT scans (10MBq/kg and 3D data acquisition) of 48 patients with suspected or known coronary artery disease (CAD) were analyzed in 10 centers. Each center used one of the 10 SW tools to analyze global and regional (LAD, LCx and RCA) MBF. Values were considered to agree well if they simultaneously had an intraclass correlation coefficient (ICC)>0.75 and a difference <20% of median values of all models for the studied parameter. **Results.** The flow estimates from all the seven SW tools implementing one-tissue compartment model (1TCM) as in Lortie et al. (2007) were in agreement with one another on global and regional levels. Results of the model by El Fakhri et al. (2009) as implemented in Corridor4DM were also in excellent agreement with the Lortie's 1TCM, so were the results of the axially-distributed blood flow model (Alessio et al. 2011) implemented in UW-QPP, yet, with occasional differences of more than 20% of median values from the Lortie's 1TCM. The MBF estimates using other kinetic models, though producing similar results were less correlated with Lortie's 1TCM (ICC<0.75): 2TCM (PMOD, Herrero et al. 1992), and net retention models (ImagenQ, Yoshida et al., 1996, MunichHeart, Lautamäki et al., 2008). Results of 1TCM (Murthy et al. 2011) in Corridor4DM and 1TCM (Katoh et al. 2012) in HOQUTO could not be directly compared to results from other models on global and regional levels. **Conclusions**. Software packages using the same kinetic model, specifically the 1TCM as described in Lortie et. al. (2007), provide nearly equivalent results in measuring global and regional MBF (rest and stress), suggesting that they may be clinically interchanged for the benefit of multicenter trials in future.

## OP267

### Clinical application of F-18-Fluorodeoxyglucose PET/CT with long-term low-carbohydrate diet preparation for the diagnosis of patients with cardiac sarcoidosis

**Y. Kobayashi**, K. Ishihara, Y. Fukushima, H. Sato, K. Akiyama, S. Kumita; Nippon Medical School, Tokyo, JAPAN.

**Introduction**: Long-term carbohydrate-restriction preparation for F-18-fluorodeoxyglucose (FDG)-positron emission tomography (PET) has been reported to suppress physiological myocardial uptake sufficiently enough that assessing myocardial inflammation activity is possible. The Aim of this study was to evaluate the inflammation activity caused by cardiac sarcoidosis through utilizing this preparation. **Materials and Methods**: Thirty eight patients (15 males and 23 females with the mean age of 57.9±14.3 years) diagnosed or suspected to have cardiac sarcoidosis were included in this study. All patients underwent FDG-PET/CT with long-term carbohydrate restriction preparation. As part of the 24-hour carbohydrate-restriction preparation, the patients took prescribed meals at lunch and dinner the day before FDG-PET examinations, either of which included less than 3g glucose. Foodstuffs and fluid containing glucose between the meals were prohibited. Visual assessment of myocardial uptake was carried out on PET images taken 120 minutes after the FDG administration. Focal myocardial uptake which did not correspond to coronary artery territory was considered to be active inflammation. Moreover, septal accumulation presenting with wall thinning or ventricular aneurysm was considered to be positive identification of active inflammation. However, complete suppression of myocardial uptake, uptake with indistinct boundaries, diffuse myocardial uptake, or uptake corresponding to coronary artery territory was considered to be negative. Subendocardial slight uptake with wall thickening was also designated as a negative finding**. Results**: Only 2 patients were excluded due to poor blood sugar control and disregard of dietary instructions, which resulted in a 96% accomplishment of this preprocessing management. Forty three examinations of the remaining 36 patients were analyzed through FDG-PET images. Twenty four patients showed positive patterns such as focal myocardial uptake. Of these patients, only 1 could be designated a classical positive finding, the widely known 'focal on diffuse.' In cases wherein the patient was identified as cardiac sarcoidosis negative by FDG-PET, complete myocardial physiological uptake suppression was observed in 13 participants. In addition, diffuse or subendocardial uptakes were detected in 6 participants. Eventually, 19 patients were diagnosed as negative in FDG-PET examinations. The sensitivity and specificity were 68% and 75%, respectively. The basal antero-septal abnormal uptake was noted in 17 (71%) of the 21 true positive patients. **Conclusions**: It was found that the cause behind the low diagnostic accuracy of FDG-PET is due to the fact that FDG-PET detects only 'present active' inflammatory lesions. Long-term carbohydrate-restriction preparation promises to detect the active inflammatory lesions by suppressing myocardial physiological uptake.

## OP268

### Complete Somatostatin Induced Insulin Suppression Combined with Heparin Loading does not Significantly Suppress Myocardial 18F-FDG Uptake in Patients with Suspected Cardiac Sarcoidosis

**L. C. Gormsen**, N. L. Christensen, K. M. E. Bendstrup, L. P. Tolbod, S. S. Nielsen; Aarhus University Hospital, Aarhus C, DENMARK.

**Aim:** Cardiac 18F-FDG PET after 12 hours fasting has shown promising results in demonstrating active cardiac sarcoidosis . However, physiological myocardial 18F-FDG uptake (MGU) may in some patients significantly obscure 18F-FDG uptake in inflammatory sarcoid lesions. We therefore Aimed to completely suppress insulin mediated MGU in patients with suspected cardiac sarcoisosis. We did this by blocking endogenous insulin secretion with a continous somatostatin infusion combined with heparin to increase circulating free fatty acids (FFAs). **Materials and Methods**: 6 patients with suspected cardiac sarcoidosis (male:female ratio 4:2, age (mean, SD); 54 +/- 14 years (range 40-76)) were studied in a randomized cross-over design separated by 7 days: 1) After 12 hours fasting with a 2 h infusion of saline (SALINE), and 2) after 12 hours fasting with infusions of somatostatin (300 µg/hour) and heparin (70 mIE/kg/min)(SOMA). Infusions were started at t=0 and at t=60 minutes, a bolus 18F-FDG (5 MBq/kg) was injected. At t=120 minutes all infusions were discontinued and a whole body 18F-FDG scan was performed (GE Discovery 690). Glucose, insulin and FFA levels were measured during the 2 hour infusion period. The cardiac region was subsequently identified, reoriented and segmented using Carimas software and regional and global SUV-values of the left ventricle were recorded. **Results**: Baseline (t=0) insulin , glucose and FFAs were comparable between study days. During the SALINE study day, insulin (~40 pmol/liter), glucose (5.2 mmol/liter) and FFAs (0.45 mmol/liter) did not change. By contrast and design, the somatostatin/heparin infusion (SOMA) resulted in rapid (<60 min) complete suppression of insulin to below detection threshold (< 2 pmol/liter), whereas FFA levels increased to peak values of 1.13 +/- 0.23 mmol/liter and glucose decreased to 4.1 +/- 1.0 mmol/liter. In general, 12 h fasting (SALINE) did not completely abolish physiological 18F-FDG uptake in the cardiac region. Contrary to our expectations though, the SOMA infusions only decreased cardiac 18F-FDG uptake modestly and insignificantly [SUVglobal (ml/g): 4.0 +/- 3.3 (SALINE) vs. 2.4 +/- 1.2 (SOMA), p=0.15]. This pattern was the same when SUV values for cardiac vascular territories were compared. One patient had the particular focal 18F-FDG uptake pattern consistent with cardiac sarcoidosis; this was evident regardless of study day. **Conclusion:** Complete insulin suppression combined with a 3-fold increase in circulating FFAs does not result in clinically meaningful suppression of physiological MGU. Insulin-independent MGU therefore must account for a significant proportion of total MGU.

## OP269

### Comparison of exercise FDG direct ischemia imaging with stress-MPS in detecting ischemia in patients with coronary artery disease.

**A. Sasikumar**, R. Kumar Manoj, A. Bhattacharya, B. Mittal; Post Graduate Institute of Medical Education and Research (PGIMER), Chandigarh, INDIA.

**Objective**: To compare stress 99mTc- tetrofosmin myocardial perfusion scintigraphy (MPS) with exercise 18F-FDG PET in detection of ischemia in patients with suspected coronary artery disease (CAD). **Methods**: 45 patients with clinical suspicion of CAD without history of myocardial infarction (MI), were prospectively and they underwent stress-MPS and exercise FDG imaging on two separate days; with coronary angiography done within 30 days of imaging. Suppression of physiological FDG uptake in myocardium was achieved by high fat, high protein, low carbohydrate diet. 5mCi of 18F-FDG was injected intravenously at peak stress and gated cardiac PET study was acquired. These patients were followed up clinically thereafter for any adverse cardiac outcome. **Results**: 37 males and eight females with mean age 51yrs (27-71 yrs) was studied. 18 patients had a normal and 27 patients had abnormal coronary angiography (at least one coronary artery with stenosis > 50%) findings. 17 patients had single vessel disease (SVD), five patients had double vessel disease (DVD) and five patients had triple vessel disease (TVD). Both stress-MPS and exercise FDG were compared with angiography as the gold standard for detecting ischemia on the basis of vascular territory, number of vessels involved, patient basis considering separate cut off of >50% and >70% as critical stenosis for ischemia. In SVD patients exercise FDG is far superior imaging modality compared to stress-MPS (McNemar P value-0.0005) with equally good performance parameters as stress-MPS in multi vessel disease (McNemar p value DVD- 0.683 & TVD-1.0). Exercise FDG performed statistically better than stress-MPS in LAD and LCX territory with comparably good performance in RCA territory. In patients with >70% stenosis both modalities perform equally good (Mcnemar p value: 0.61). In patients with stenosis of >50% exercise FDG has significantly high sensitivity of 96% vs 56% sensitivity of stress-MPS and reasonable high accuracy of 76% compared to 62% of stress-MPS (Mcnemar p value: 0.0004). Mean follow up period was ~18 months (range 12-25months). One patient with concurrent findings in stress-MPS and exercise FDG died of MI and four others developed an acute coronary event requiring hospitalization. One of ten patients with ischemia on exercise FDG and normal stress-MPS developed an acute coronary event requiring hospitalization. **Conclusion**: Exercise FDG performs significantly better than stress-MPS in detecting ischemia in patients with stenosis >50%, with equally good performance in patients with stenosis >70%, thus making it a better imaging modality for detecting ischemia in patients with stenosis between 50-70%.

## OP270

### Sepsis effect on heart oxidative metabolism: 11C Acetate TEP approach

**J. Aboab**[1], B. Kuhnast[2], G. Pottier[3], A. Mansart[4], C. Adam[1], J. Cayla[5], A. Pouilly[6], P. Merlet[7], D. Annane[1], R. Boisgard[3]; [1]Service de Réanimation - Hôpital Raymond Poincaré, APHP, Garches, FRANCE, [2]CEA, DSV, I2BM;SHFJ,, Orsay, FRANCE, [3]CEA, DSV, I2BM;SHFJ, INSERM U1203, Orsay, FRANCE, [4]Laboratoire d'Étude de la Réponse Neuroendocrine - E4342, Université de Versailles-Saint –Quentin-en-Yveline, FRANCE, [5]CEA, DSV, I2BM;SHFJ, Orsay, FRANCE, [6]Pulssion Medical Systems, Feldkirchen, GERMANY, [7]Service de Médecine Nucléaire, Hopital Saint Louis APHP, Paris, FRANCE.

**Introduction**: Sepsis shock associated with cardiovascular failure is one of the most important reasons of death in Intensive Care Units. The mechanisms of this complication of sepsis remain unclear. Pro-inflammatory mediators that are abundantly released in blood and tissues may induce oxidative metabolism alterations as already demonstrated in striated muscles. **Purpose:** This experiment **Aims** to investigate heart oxidative metabolism in an endotoxin pig model characterised by an early and heavy cardiovascular impairment. **Methods**:. Five anesthetized and mechanically ventilated pigs (mean weight = 25 kg) were challenged with intravenous LPS to achieve a status of profound hypodynamic shock. No vasopressor were used. Animals were exclusively fluid resuscitated as needed following standard hemodynamic parameters. Heart rate (HR) and mean arterial blood pressure (ABP) were continuously monitored throughout the study period (Picco- Pulssion Feldkirchen Deutschland). Animals were imaged before and after endotoxin shock using [11C] acetate as tracer for the combined assessment of mean blood flow (MBF, in ml/min/g) and oxidative metabolism (VO2. Imaging was performed with a dedicated PET device (Ecat HR+ Siemens). Definition of regions of interests (ROIs) and kinetic modeling were performed using PMOD software (Pmod 3.4). LV blood ROI was defined to monitor input function. **. Results**: HR and ABP changed respectively from 97±8 beat per min (bpm) bpm and 97±8 mmHg to 131±31 bpm and 90±15 mmHg between the early phase of sepsis (T0) and T-60min. This variation corresponds to a relative change of +22% in HR and -10% for ABP. Quantification of PET images performed before and after the endotoxin shock does not reveal significant changes in values of MBF and VO2. The mean MBF value was 1.66±0.9 ml/min/g and 1.86±1 ml/min/g and the mean VO2 was 0.27±0.07 l/min/g and 0.32±0.18 l/min/g during the first PET and the second PET experiments, respectively. **Discussion** These preliminary results suggest that despite the early and major increased metabolic demand caused by sepsis, as illustrated by the increase in HR and the drop of ABP, no significant changes in myocardial flow or oxidative metabolism were found to occur concomitantly. The deregulation of these adaptive phenomena may participate in the onset of myocardial involvement in sepsis.

807 - Monday, Oct. 21, 11:30 - 13:00, Salon Pasteur

## Physics & Instrumentation & Data Analysis: Modelling / Simulation

## OP271

### Monte Carlo simulations in PET: what should be the spatial sampling of the input activity map?

**P. Huet**[1], S. Burg[2,1], S. Stute[3], D. Le Guludec[2], I. Buvat[1]; [1]IMNC-UMR 8165 CNRS, Orsay, FRANCE, [2]Service de Médecine Nucléaire, Bichat Hospital, AP-HP, Paris, FRANCE, [3]SHFJ - CEA, Orsay, FRANCE.

**Aim**: PET simulations require a numerical description of the radiotracer spatial concentration. Sampling with a Cartesian grid is the most frequently used method to represent this spatial distribution. This sampling introduces potential errors in the source location that might be a concern when simulating very small structures. Yet, using high voxel density maps may be unnecessarily memory expensive because of the limited detector crystal size. We evaluated the impact of the input activity map sampling on the tissue fraction effect introduced in the reconstructed images. **Materials and Methods**: Using the GATE simulation tool v6.1, PET acquisitions of two line sources parallel to the scanner axis (6 cm long, 2.2MBq of 18F) were simulated, considering a model of the Gemini GXL system (cystal size: 4x4x22 mm). A first line was off-centered by 10 cm in the transaxial direction while the second was located 0 mm to 6 mm (step of 0.2 mm) from the first line towards the center of the FOV. Images were reconstructed with an OP-OSEM algorithm (10 iterations, 10 subsets) including corrections for random and multiple coincidences. The point spread function of the imaging system was modeled in the image space during reconstruction, using a 4.0 mm FWHM Gaussian. Voxel size was 1 mm in the 3 directions and no post-filtering was applied. Slices were summed and a profile along the line perpendicular to the two sources was plotted. **Results**: A single maximum in the profile was observed only when the distance between the two lines was less than 5 mm, suggesting that the system could not distinguish objects that were that close. For line distances smaller than 5 mm, the FWHM of the single-peak profile was constantly equal to 4.7 mm +/- 3.6% when the line distance varied between 0 and 1.2 mm. This suggests that the reconstructed images are the same whatever the sampling of the activity map up to 1.2 mm. **Conclusions**: We introduced a method to determine which sampling should be used to describe the activity map in PET Monte Carlo simulations without introducing artificial tissue fraction effect in the reconstructed images. For the PET scanner and reconstruction protocol that we considered, we found that defining the activity map using voxels up to 1.2 mm did not introduce any sampling-related tissue fraction effect in the reconstructed data.

## OP272

### Is Monte Carlo Scatter Correction (MCSC) including full collimator and detector response modelling superior to object only MCSC for I-123 SPECT?

**C. M. Brown**[1,2], A. O. Sohlberg[3], J. Prosser[1], M. Dempsey[1], G. Gillen[1]; [1]NHS Greater Glasgow & Clyde, GLASGOW, UNITED KINGDOM, [2]University of Glasgow, Glasgow, UNITED KINGDOM, [3]HERMES Medical Solutions, Stockholm, SWEDEN.

**Introduction**: Current MCSC algorithms based on Gaussian collimator and detector response offer a good approximation for single low energy photopeak isotopes such as Tc99m. Isotopes with higher energy photons such as I123 require more complex collimator detector and response models due to collimator septal penetration and scatter with low energy collimators. However, full MCSC with modelling of collimator and detector response during simulation is computationally very demanding. A recently developed implementation of fast MC-simulator with full detector modelling was evaluated against the current commercially available MCSC which only modelled scatter in the patient. **Method:** Multiple SPECT-CT acquisitions were made of I123 point sources in air and in scatter material, and of the PET NEMA IEC Body phantom filled with I123 containing a sphere to background concentration ratio of ~4:1. All data were acquired using a Siemens Symbia T2 and acquisitions were OSEM reconstructed from 2-160 iterations with Resolution Recovery (RR), Attenuation Correction (AC) and MCSC, with and without collimator detector response modelling. The FWHM and FWTM of the point sources in air and scatter material were measured using a Gaussian fit of the Line

Spread Function (LSF). Contrast recovery for the six spheres in the NEMA phantom were also assessed. Noise in background regions of the reconstructed volumes were assessed using the Coefficient of Variation (COV) and the lung insert residual error was calculated to evaluate the effectiveness of attenuation and scatter correction. **Results**: The FWHM and FWTM of the point sources in air and in scatter material showed no statistically significant difference between all MCSC reconstructions with and without collimator detector response modelling. The addition of collimator response modelling to the MCSC algorithm improved I123 contrast recovery (measured from 0-1) significantly ($p<0.05$): the contrast recovery of the 37mm, 28mm, 22mm and 17mm spheres was improved by as much as 0.33±0.09, 0.26±0.05, 0.28±0.05 and 0.16±0.04 respectively. There was no statistically significant difference in measured COV between both Methods of MCSC. Similarly, measured lung insert residual error showed no significant difference between both Methods. **Conclusions**: The addition of full collimator detector response modelling to the MCSC algorithm has demonstrated a significant improvement in I123 contrast recovery. Although the novel algorithm does not significantly affect resolution or noise properties, the improvement in contrast recovery increases image quality to an extent that may be of clinical significance.

## OP273

### Deadtime count-loss compensation method for quantitative SPECT/CT imaging

W. Siman[1,2], M. Silosky[1], **S. C. Kappadath**[1,2]; [1]University of Texas MD Anderson Cancer Center, Houston, TX, UNITED STATES, [2]UT Graduate School of Biomedical Sciences, Houston, TX, UNITED STATES.

**Objective:** Modern SPECT/CT systems can correct for scatter and photon attenuation that improves SPECT accuracy. Count loss due to deadtime contributes to bias and uncertainty in quantitative SPECT, especially post-therapy where count losses can be >10%. The Aim of this study is to evaluate the accuracy of a frame-based pixel-wise deadtime count loss compensation model to improve SPECT quantification. **Materials and Methods**: A Jaszczak phantom initially containing ~4 GBq 99mTc-pertechnatate was imaged using Siemens Symbia SPECT/CT system with LEHR collimation, 22-cm circular orbit, 4.8-mm pixels, 128x128 matrix, 128 views over 360 degrees. SPECT acquisitions were repeated 12 times over 5 half-lives with time-per-view adjusted as the source decayed to yield 250 kcounts/view. Different projection count rates were extracted as a function of time from multiple ROIs drawn on corresponding views over 12 SPECT acquisitions. The degree of correlation between the measured count rates, Mi, amongst different ROIs was evaluated by calculating the Pearson correlation coefficient ($r$). The deadtime for each projection view, $\tau i$, was estimated via non-linear least-squares fit of measured data over time following Silosky (Medical Physics, 2013). The input frame count rate, Ni, can be calculated for a known $\tau i$ as $Ni=(1-\sqrt{(1-4.Mi.\tau i)})/2\tau i$ based on paralyzable detector model. Deadtime correction factors were computed for each frame as Ci=Ni/Mi. Pixel data in each frame were multiplied by Ci to compensate for deadtime count losses. SPECT images were reconstructed using filtered back-projection from the acquired and deadtime corrected projections. For both projections and SPECT images, the deadtime corrected counts were compared against counts extrapolated from the last acquisition (with low count rate) assuming physical decay only. **Results**: Measured count rates in ROIs with different input count rates were found to be proportional to each other ($r>0.998$ in all cases); demonstrating similar fractional count loss for all input count rates and justifying a single frame-based correction factor to correct the measured pixel count in planar and SPECT images. The system deadtime was estimated via least-squares fit to be 1.25 +/- 0.05 µs. The frame-based pixel-wise correction method was found to compensate for deadtime count losses of over 16% in planar images to less than 0.3%, and losses of over 15% in SPECT to less than 2%. **Conclusions**: The frame-based pixel-wise count loss correction method proposed can compensate for deadtime count loss to with greater than 98% accuracy for quantitative planar and SPECT imaging. Evaluations are underway for clinical imaging.

## OP274

### Estimating Cardiac Kinetic Parameters Using Dynamic Time-of-Flight PET

**S. J. McQuaid**[1], M. F. Kijewski[2,3], S. C. Moore[2,3], M. Park[2,3], A. Sitek[4,3], E. Gualtieri[5], A. Perkins[6], M. Daube-Witherspoon[5], J. S. Karp[5]; [1]Royal Surrey County Hospital, Guildford, UNITED KINGDOM, [2]Brigham and Women's Hospital, Boston, MA, UNITED STATES, [3]Harvard Medical School, Boston, MA, UNITED STATES, [4]Massachusetts General Hospital, Boston, MA, UNITED STATES, [5]University of Pennsylvania, Philadelphia, PA, UNITED STATES, [6]Philips Healthcare, Philadelphia, PA, UNITED STATES.

**Aim.** The advantages of time-of-flight (TOF) PET for estimating parameters of static activity distributions have previously been demonstrated and it is also expected that TOF would be beneficial in the estimation of kinetic parameters in dynamic acquisitions. The Aim of this study was to quantify these benefits for myocardial perfusion imaging with N-13 ammonia. **Methods.** High-count PET data were acquired on the $LaBr_3$ PET system at the University of Pennsylvania, with timing resolution of 375ps, using the Anthropomorphic Torso Phantom (Data Spectrum). Data were acquired from three of the fillable organs (myocardium, liver and torso) separately, with the remaining organs filled with non-radioactive water. The list-mode datasets were binned into sinograms of 40 TOF bins, each of width 125ps. A low-noise dynamic sinogram dataset of a N-13 ammonia study was synthesized by scaling each organ dataset according to the assumed time-activity curves (TAC), sampled at 34 time points, and summing. TACs for the three organs had the same functional form, with kinetic parameters describing the fractional blood volume (fv), and the rate constants for the exchange of activity between compartments (k1, k2 and k3). fv(liver) was assumed to be zero, so that there were 11 unknown parameters. The input function was assumed to be known. The Cramer-Rao lower bound (CRB) was calculated for each of the kinetic parameters, to measure the theoretically best precision that could be obtained by an unbiased estimator. The calculation was performed both for TOF data and for non-TOF data, obtained by summing sinograms over TOF bins. **Results.** Incorporation of TOF information led to improved CRB on parameter estimates for all 11 parameters. For the myocardium, the ratios of the square roots of the CRB with and without TOF were 0.53, 0.63, 0.65 and 0.66 (for fv, k1, k2 and k3, respectively). The corresponding values for the torso were 0.91, 0.86, 0.86 and 0.75 and for the 3 liver kinetic parameters were 0.59, 0.64 and 0.68. These results imply that TOF information would lead to much better performance in estimating myocardial kinetic parameters and, consequently, better tissue characterization and improved discrimination between normal and diseased myocardial tissue. **Conclusions.** The use of TOF in N-13 ammonia imaging has the potential to substantially improve the precision with which cardiac kinetic parameters can be estimated, compared with non-TOF PET data. Further work will assess the impact of TOF in estimating kinetic parameters when a myocardial defect is present.

## OP275

### How accurate is the scintigraphic estimation of split renal function?

L. Tímár[1], **J. Varga**[2]; [1]JAON Ltd., Nyíregyháza, HUNGARY, [2]University of Debrecen, Debrecen, HUNGARY.

**Aim:** Scintigraphy provides the only routine way for estimating the split kidney function, an information crucial when deciding about the surgical removal of a kidney. Usually we calculate the ratio of kidney functions from the geometric mean of count rates measured from posterior and anterior views, since for point sources in a homogeneous medium it is theoretically independent of the source position. In our present work we investigated the extent of inaccuracy obtained by the geometric mean method, when varying the kidney size and position (depth) as well as background activity level in a phantom experiment. **Materials and Methods**: We inserted a simple kidney phantom in a rectangular water tank (thickness: 35 cm). We varied the volume of the "kidney" (0.5, 50, 100, 150, 200, 250 mL), activity concentration in the scattering medium (0, 33 or 65% of the concentration inside the "kidney"), and the position (in one centimeter steps from 4 to 31 cm). We acquired images simultaneously by two detector heads positioned on opposite sides of the tank, and analyzed the changes in the geometric mean of the two count rates. Then we processed clinical studies in the way found optimal in the phantom study, and compared the obtained ratios with those estimated by the routinely used Methods. **Results**: We obtained almost identical geometric mean values, independent of the position, volume, and also of the background concentration when applying a suitable background correction method. For the low-background patient studies with DMSA (n=30), the routine processing method gave similar results to the "optimized" one (all differences <5%; <3% in 90% of cases). When utilizing dual detector acquisition data for the clinical studies with higher background (40 DTPA studies), the deviations from the target values were small in most cases (<5% difference in 70% of cases). However, estimations based on only posterior images resulted in quite high errors (up to 19%; >5% difference in 72% of all cases) because of the unknown differences between kidney depths. **Conclusion**: Based on the phantom study, the size and position of the kidney do not significantly influence the geometric mean obtained from anterior and posterior views; however, the method for background correction is critical. DTPA studies with traditional posterior acquisition are not suitable for the accurate estimation of split renal function. Quite good estimation can be obtained when utilizing dual-detector acquisition and a suitable background correction based on background ROIs surrounding both kidneys.

## OP276

### Interpolation-free 3D data rebinning in prolate spheroidal coordinates for robust estimation of morphofunctional parameters in nuclear cardiology

**M. Tripodi**, D. Panetta, P. Salvadori; CNR Institute of Clinical Physiology, Pisa, ITALY.

**Aim:** Estimation of morphological parameters of the heart from nuclear cardiology images such as gated SPECT or PET is usually performed by model-based fitting of radial 1D activity profiles through the left ventricle (LV) wall after image reorientation in short-axis. In this study, we evaluate a new data rebinning scheme based on 3D prolate spheroidal coordinates. The proposed method does not require image reorientation and hence it is less prone to suffer from image degradation due to voxel interpolation; furthermore, the method is robust with respect to noise because it employs all the voxels in the reconstructed images instead of just line profiles. **Materials and Methods**: The frame of reference of the LV with respect to the scanner is first defined by selecting three points in the reconstructed image: the center of the LV base (P1), the apex (P2) and the center of the RV cavity (P3). Once the above three points are defined, 3D prolate spheroidal coordinates are computed for each voxel; afterwards, activity profiles are obtained by partitioning the half-space containing the heart in several solid sectors, each covering a small interval of the azimuthal and radial coordinates. Angular intervals were kept small enough to avoid inhomogeneity within each sector, but ensuring a sufficient number of points within it. The curvilinear activity profile of each sector was then fitted to the common 1D model to find optimal values of LV cavity radius (R) and wall thickness (d). Anisotropy and shift-variance of the PSF are also included in the model. The proposed method was tested on computational phantoms with various levels of additive gaussian noise and realistic anisotropic PSF and voxel size. Initial tests were also performed on gated PET images of healthy patients. **Results and Conclusion**: Good agreement was observed between measurements on the noisy phantom and the ground truth. Both the LV cavity volume and the myocardial thickness for each sector were within 10% of the true value. In some sector, the fit failed to converge probably because of a bad choice of initialization parameters. In such cases, bilinear interpolation was used to recover the values of R and d. The proposed method is alternative to standard cardiac analysis based on image reorientation and linear profiles, avoiding interpolation and providing robustness due to the full data utilization. Furthermore, the prolate spheroidal coordinates are optimal because they minimize the angle of incidence to the endocardial surface.

## OP277

### Inaccuracy in parameter estimation with background subtraction method in dual injection PET based on simulation study

X. Huang[1,2], H. Merisaari[1], V. Oikonen[1], M. Teräs[1], T. Tolvanen[1], A. Saraste[1], J. Knuuti[1], **C. Han**[1]; [1]Turku PET Centre, Turku University Central Hospital, Turku, FINLAND, [2]Dept. of Mathematics, Beijing Jiaotong University, Beijing, CHINA.

**Aim**: In dual injection PET protocol with long half-life isotopes, such as novel myocardial 18F-labeled perfusion tracers, the second injection usually starts with a high background radioactivity. Currently, in modeling of the second injection, the background activity is simply subtracted (Nekoll et al. 2009). This study is designated to investigate the accuracy of background subtraction method on parameter estimation with simulated data. **Materials and Methods**: The input function was generated by a multi-exponential function with three decay components, i.e. Ca(t)= (1-exp(-t/d0))*(A1*exp(-t/d1)+ A2*exp(-t/d2)+ A3*exp(-t/d3)). Irreversible two-tissue compartment model (T2CMK3) with three parameters (K1, k2 and k3) was employed, and the four-order Runge-Kutta method was used to solve the ordinary differential equation system. The second injection started at 45 minutes after the first injection. The radioactivity just before the second injection was considered as the background activity. The background activity was subtracted from tissue-time activity curves before performing parameter estimation with T2CMK3. Simulation was performed in MATLAB, modeling was performed using Carimas2 (PET modeling package developed in Turku PET Centre, Finland. http://www.turkupetcentre.fi/carimas). **Results:** Our simulation study showed that the background subtraction method contributes to a significant error in parametric estimation in the dual injection protocol. When the second injection started at 45 minutes after the first injection with ground truth values of K1 as 0.25, 0.50, 1.06, 1.55 and 2.04 ml/ml/min (k2=0.07/min, k3=0.009/min), respectively, the estimated K1 values were 0.236(-8.1%) , 0.511(1.3%) 1.23(16%), 2.05(30.3%) and 3.02(47.2%) ml/ml/min, respectively. The estimated parameter error increased when K1 becomes greater. The study also showed that the non-zero initial condition is responsible for the parameter estimation error in background subtraction method. **Conclusions**: Our simulation study shows, the background subtraction method in dual injection protocol introduces a significant error for parameter estimation. New algorithms need to be investigated for better accuracy in modeling the second injection in dual injection PET method. Reference: Nekolla et al. Evaluation of the novel myocardial perfusion position-emission tomography tracer 18F-BMS-747158-02. Circulation. 2009;119:2333-2342

## OP278

### 18F-6-Fluoro-6-Dexoxy-D-Glucose Modeling for Evaluating Insulin Resistance

**K. Su**[1,2], V. Chandramouli[2], F. Ismail-Beigi[3], R. F. Muzic, Jr.[1,2,4]; [1]Case Center for Imaging Research, Case Western Reserve University, Cleveland, OH, UNITED STATES, [2]Department of Radiology, University Hospitals Case Medical Center, Case Western Reserve University, Cleveland, OH, UNITED STATES, [3]Department of Medicine, University Hospitals and Cleveland VA Medical Center, Case Western Reserve University, Cleveland, OH, UNITED STATES, [4]University Department of Biomedical Engineering, Case Western Reserve University, Cleveland, OH, UNITED STATES.

**Aim:** The purpose of this study is to evaluate the possibility of identifying mechanisms of insulin resistance in vivo using PET imaging. **Materials and Methods**: Seventeen Spring-Dawlay rats were separated into three, different groups: five normal controls under basal conditions (Ctrl); five controls under insulin stimulation (Ctrl+I); and seven insulin-resistant rats under glucose stimulation wherein dexamethasone, i.e. 100 µg/kg SC for two days before PET, was used to induce insulin resistance (DEX+I). To facilitate blood sampling and infusion of glucose and insulin during PET-scanning, arterial and venous catheters were surgically placed. Allowing at least seven days for recovery before scanning, rats were fasted overnight prior to scanning for which rats were anesthetized with isoflurane and, for the insulin groups, administered insulin (5 mU/kg/min). The glucose infusion rate (GIR) was adjusted to maintain euglycemia (7.22 mM). Dynamic PET scanning was performed using 18F-fluoro-6-dexoxy-D-glucose (6FDG), a PET tracer for glucose transport, while arterial blood samples were collected and used as the input function of a Michaelis-Menten-based kinetic model that was fit to the data in order to assess the insulin response. For this purpose, we extended our model to account for the time-varying blood glucose concentration as the untreated control rats (Ctrl) exhibited a slowly increasing blood glucose concentration. Maximal transport capacities of the glucose transporter and hexokinase (VG and VH), the cellular influx and efflux of glucose (CI and CE), and the glucose phosphorylation rate (PR) were estimated with the model and were compared among those groups. **Results:** The average GIRs during scans were 69.8±9.0 and 47.1±19.9 µmol/kg/min for Ctrl+I and DEX+I. The VG values for Ctrl, Ctrl+I, and DEX+I, respectively, were 0.09±0.02, 0.31±0.08, 0.20±0.03 mmol/mL/min; VH were 0.12±0.02, 0.26±0.07, 0.18±0.07 mmol/mL/min; CI were 0.06±0.01, 0.17±0.04, 0.11±0.01 mmol/mL/min; CE were 0.00±0.00, 0.03±0.03, 0.02±0.02 mmol/mL/min; and the PR were 0.06±0.01, 0.14±0.02, 0.09±0.02 mmol/mL/min. Significant differences were found for VG, CI, and PR in any pair of the three groups. The p-values comparing Ctrl+I and DEX+I for GIR, VG, CI, and PR were 0.03, 0.02, 0.04, and 0.00, respectively. These results suggest that the parameters, VG and PR, are better able than GIR to distinguish the difference between control and DEX-treated rats. Furthermore, the model parameters provide insight into the nature of insulin resistance. **Conclusion:** The parameters estimated with the extended 6FDG model showed a better discriminatory power than those of the standard approach used to monitor a DEX-induced, insulin-resistant model.

808 - Monday, Oct. 21, 11:30 - 13:00, Gratte-Ciel 1/2/3

## Radionuclide Therapy & Dosimetry: Dosimetry & Radiobiology

## OP279

### A model for inverse dose-rate effects / low dose-rate hypersensitivity in response to targeted radionuclide therapy

**I. Murray**[1], S. J. Mather[2]; [1]Royal Marsden NHS Foundation Trust, Sutton, UNITED KINGDOM, [2]Queen Mary, University of London, London, UNITED KINGDOM.

The **Aim** of this work was to test the hypothesis that the Linear-Quadratic (LQ) model of cell survival, developed for external beam radiotherapy (EBRT), could be extended to targeted radionuclide therapy (TRT) in order to predict dose-response relationships in a cell line exhibiting low dose hypersensitivity (LDH). **Methods**: Aliquots of the PC-3 cancer cell line were treated with either EBRT or an in-vitro model of TRT (Irradiation of cell culture with Y-90 EDTA over 24, 48, 72 or 96 hours). Dosimetry for the TRT was calculated using radiation transport simulations with the Monte Carlo PENELOPE code. Clonogenic as well as functional biological assays were used to assess cell response. An extension of the LQ model was developed which incorporated a dose-rate threshold for activation of repair mechanisms**. Results:** Accurate dosimetry for in-vitro exposures of cell cultures to radioactivity was established. LQ parameters of cell survival were established for

the PC-3 cell line in response to EBRT. The standard LQ model did not predict survival in PC-3 cells exposed to Y-90 irradiation over periods of up to 96 hours. In fact cells were more sensitive to the same dose when irradiation was carried out over 96 hours than 24 hours. I.e. at a lower dose-rate. Deviations from the LQ predictions were most pronounced below a threshold dose-rate of 0.5Gy/hr. These results led to an extension of the LQ model based upon a dose-rate dependent sigmoid model of single strand DNA repair. This extension to the model resulted in predicted cell survival curves that closely matched the experimental data. **Conclusion**: The LQ model of cell survival to radiation has been shown to be largely predictive of response to low dose-rate irradiation. However, in cells displaying LDH, further adaptation of the model was required.

## OP280

### Biological effects of positron emitters in thyroid cell cultures

**C. Breunig**[1], L. Flämig[1], M. Bache[1], A. Odparlik[1], J. Meller[2], D. Vordermark[1], M. Bähre[1], B. Meller[1]; [1]Martin-Luther-University Halle, Halle/Saale, GERMANY, [2]Georg-August-University Göttingen, Göttingen, GERMANY.

**Aim:** Today, the use of $^{124}I^-$ ($ß^+$, half life 4.2 d) is an increasing field in positron emission tomography (PET). In principle, positrons deposit their energy in the surrounding material like electrons. Therefore, we investigated the biological effects of positron emitters in comparison to electrons in vitro. **Materials and Methods:** Two different thyroid cell lines (Fischer Rat Thyroid Cell Line No. 5 (FRTL5) and human papillary thyroid cancer cell line BCPAP) were investigated in vitro. While FRTL5 has been described to express a high level of sodium iodine transporter (NIS), the NIS expression of BCPAP is known to be low. Parallel cultures were incubated with either 50 -400 kBq/ml $^{124}I^-$ (IBA) or 50 -400 kBq/ml $^{131}I^-$ (GE Healthcare). Cell count and radioiodine uptake were determined 24 h to 144 h after isotope application. Additionally, 4',6-diamidino-2-phenylindole (DAPI) staining of ethanol fixed cells was performed and induced apoptosis was determined by morphological analysis of the cell nucleus (condensation, fragmentation) by fluorescence microscopy. **Results:** BCPAP showed no significant uptake (<0.1 % per one million cells). The proliferation of BCPAP cells was not significantly influenced by radioiodine incubation. The uptake of NIS-expressing FRTL5 cells ranged between 0.6 % and 4 % per one million cells, independently of the isotope. In FRTL5 cells the incubation with $^{131}I^-$ induced a significant dose-dependent inhibition of proliferation ($p<0.05$). The positron emitter $^{124}I^-$ induced analogue effects on proliferation compared to the electron emitter $^{131}I^-$ (30-40 % inhibition, 144 h incubation with 400 kBq/ml). In parallel, in FRTL5 cell lines an isotope-independent increase of morphological changes in the cell nuclei (up to 5 fold) could be determined. In contrast, no significant changes could be verified in BCPAP cell nuclei. **Conclusions:** As expected from the physical point of view, the biological effects of positrons in vitro are very similar to those of electrons. On the one hand our results indicate a potential of new possible therapeutic applications of positron emitters. However, on the other hand these results should be considered when positron emitters with long half life are applied for PET investigations.

## OP281

### Investigation of early DNA damage after radioiodine therapy in patients with thyroid cancer using the gamma-H2AX focus assay

**U. Eberlein**[1], M. Lassmann[1], C. Nowak[2], C. Bluemel[1], V. Meineke[2], A. K. Buck[1], H. Scherthan[2]; [1]Department of Nuclear Medicine, University of Würzburg, Würzburg, GERMANY, [2]Bundeswehr Institute of Radiobiology, Munich, GERMANY.

**Objectives**: The Aim of the study is to investigate the DNA damage formation in blood lymphocytes and the correlation to the absorbed dose to the blood in patients with differentiated thyroid carcinoma (DTC) after their first radionuclide therapy with I-131 as measured by the induction, persistence and decay behaviour of γ-H2AX and 53BP1 DNA damage-induced foci. Radiation-induced DNA double strand breaks (DSBs) cause in their vicinity the formation of microscopically visible foci of the phospho-histone H2AX (γ-H2AX) and the 53BP1 protein that binds to and signals damaged chromatin at the DSB site. Nuclear foci containing both markers thus represent radiation-induced DSBs. **Methods**: We investigated 19 patients with DTC during the first treatment with 3.5±0.3 GBq I-131. Between 7 and 10 sequential peripheral blood samples (at least four within the first 5 hours) were taken before and between 0.5h and 144h post administration. The physical dosimetry procedures were performed according to the EANM DTC SOP. White blood cells were recovered by density centrifugation in CPT tubes (BD Biosciences) and subjected to two-colour immunofluorescence staining. The average frequencies of the radiation-induced γ-H2AX foci/nucleus that colocalized with 53BP1 foci were derived from immunostained mononuclear peripheral blood lymphocyte samples. The number of foci was counted manually using a red/green double band pass filter (Chroma) in a Zeiss microscope by an experienced observer. **Results:** The mean I-131 absorbed dose to the blood was 0.04±0.01Gy at t=2h, 0.07±0.02Gy at t=4h, and 0.21±0.05Gy at t=24h, respectively. The mean value of the total absorbed dose to the blood was 0.36±0.08Gy. The highest number of radiation-induced foci per nucleus (RIF) and per absorbed dose (median: 8.8 RIF/Gy, range 3.1-10.9 RIF/Gy) was observed in the first three hours post administration. Four hours after radioiodine administration the number of RIF reached a maximum in most patients (median: 0.51 RIF at t=4h, range 0.36-0.74 RIF). This corresponded to a mean absorbed dose of 0.07±0.02Gy. Later time points were characterized by a considerable decrease of RIF, agreeing with a diminished dose rate. An elevated number of excess RIF were still detectable 144h after therapy. **Conclusions**: A combinatorial measurement of RIF and the absorbed dose to the blood at early time points after systemic administration of I-131 may be used to obtain data on the individual dose-response relationships after nuclide incorporation in-vivo.

## OP282

### Redefining the relative biological effectiveness (RBE) in the context of the EQDX formalism

**R. F. Hobbs**[1], R. Howell[2], H. Song[1], S. Baechler[3], G. Sgouros[1]; [1]Johns Hopkins University, Baltimore, MD, UNITED STATES, [2]Rutgers New Jersey Medical School, Newark, NJ, UNITED STATES, [3]University Institute of Radiation Physics, University of Lausanne, Lausanne, SWITZERLAND.

**Objective:** The relative biological effectiveness (RBE) of high-LET radiation (alpha-particles, e.g.) is defined as the ratio of the absorbed dose of a reference radiation (usually external beam) to a test radiation absorbed dose for a same biological endpoint, often a surviving fraction of cells. However, as it is currently defined, the RBE is dependent on the dosimetric end point as well as the dose values and is therefore limited in its utility, as a range of experimental values are often reported and it is unclear which value should be used in which context. We propose adoption of a quantity, called the RBE2, which relates the high-LET absorbed dose to 2-Gy fraction megavoltage external beam equivalents. **Method:** Recently, the ICRU has promulgated the use of the equieffective dose EQDX for bioeffect modeling of radiation responses. EQDX is defined as the total absorbed dose delivered by the external beam reference treatment plan of fraction size X that leads to the same biological effect as a test treatment plan. It was proposed that 2-Gy fractions of megavoltage x-rays should be the reference. Therefore, within this context relating the high-LET absorbed dose, not to a single fraction of external beam or β-emitter radiation, but to 2-Gy fraction external beam equivalent is a logical step, and more readily understood. We propose to call this new ratio RBE2, in keeping with the EQDX naming convention. Furthermore, for high-LET radiations typically used in nuclear medicine, α-particles and Auger electrons, the RBE2 value is dose-independent. The theoretical framework for the proposed new formalism is presented as is the application to two tumor cell lines. **Results:** The radiobiological parameters are obtained by fitting the curves to dose-response data from α-particle ($^{213}$Bi) and β-particle ($^{137}$Cs) radiation to two cell lines: a murine breast cancer cell line, NT2.5 and a human breast cancer cell line, MDA-MB-231. From these, the l RBE values are derived: 2.4 - 9.0 for the murine NT2.5 cell line and 2.4 - 6.0 for the human MDA-MB-231 cell line. The invariant RBE2 values were 5.9 and 4.5. **Conclusion:** RBE2 defined as a ratio between the electron-mediated (photon or electron) 2-Gy fraction equivalent EQD2 and the high-LET response provides a more logical formalism for data reporting and dose conversions. Moreover, it provides a much needed foundation for the ongoing development of an α-particle dosimetry paradigm as well as for rational (i.e. safe and effective) dosimetrically-based combination therapies.

## OP283

### Development of a Hybrid Multiscale Phantom for Monte Carlo Based Internal Dosimetry

**S. Marcatili**, D. Villoing, M. Bardiès; UMR 1037 INSERM/UPS, Centre de Recherche en Cancérologie de Toulouse, Toulouse, FRANCE.

**Aim** In recent years several phantoms were developed for radiopharmaceutical dosimetry in clinical and preclinical settings. "Voxel-based" models (Zubal, Max/Fax, ICRP110) were developed to reach a level of realism that could not be achieved by mathematical models. In turn, "hybrid" models (XCAT, MOBY/ROBY, Mash/Fash) allow a further degree of versatility by offering the possibility to finely tune each model according to various parameters. However, even "hybrid" models require the generation of a voxel version for MC modeling of radiation transport. Since absorbed dose simulation time is strictly related to geometry spatial sampling, a compromise should be made between phantom realism and simulation speed. This trade-off leads on one side in an overestimation of the size of small radiosensitive structures such as the skin or hollow organs' walls, and on the other hand to unnecessarily detailed voxellization of large, homogeneous structures. The Aim of this work is to develop a hybrid multi-resolution phantom model for Geant4 and Gate, to better characterize energy deposition in small structures while preserving reasonable computation times. **Materials and Methods** We developed a pipeline for the conversion of preexisting phantoms into a multi-scale Geant4 model. Meshes of each organ are created from raw binary images of a phantom and then voxellized to the smallest spatial sampling required by the user. The user can then decide to resample the internal part of each organ, while leaving a layer of

smallest voxels at the edge of the organ. In this way, the realistic shape of the organ is maintained while reducing the voxel number in the inner part. For hollow organs, the wall is always modeled using the smallest voxel sampling. This approach allows choosing different voxel resolutions for each organ according to a specific application. **Results** Preliminary results show that it is possible to reduce MC simulation time whilst maintaining a high resolution in the absorbed dose distribution in the selected volumes (bladder, kidneys). We will present absorbed doses obtained in more critical organs in comparison to those obtained in a non-modified version of the ICRP110 model used in a parallel project (Dositest), and compare respective simulation times. **Conclusions** The proposed multi-resolution approach offers the possibility to accurately model internal structures of some organs (i.e. kidney medulla and cortex, bone marrow) while performing whole body absorbed dose calculations, in an effort to better take into account the functional consequences of irradiation induced by radiopharmaceuticals.

## OP284

### Absorbed dose to the urinary bladder wall for different radiopharmaceuticals using dynamic S-values.

**M. Andersson**[1], L. Johansson[2], D. Minarik[1], S. Mattsson[1], S. Leide-Svegborn[1]; [1]Medical Radiation Physics, Department of Clinical Sciences Malmö, Lund University, Malmö, SWEDEN, [2]Department of Radiation Sciences,Umeå University, Umeå, SWEDEN.

**Aim and background**: The urinary bladder wall is a radiosensitive organ that can receive a high absorbed dose from radiopharmaceuticals used in diagnostic nuclear medicine. Current dynamic models estimate the photon and electron absorbed dose at the inner surface of the bladder wall. The Aim of this work has been to create a more realistic estimation of the mean absorbed dose to the urinary bladder wall from different radiopharmaceuticals. This calculation also uses dynamic specific absorption fractions (SAF) that changes with bladder volume and are gender specific. **Materials and Methods**: The volume of the urinary bladder content was calculated using a spherical approximation with a urinary inflow of 1.0 ml/min and 0.5 ml/min during day and night time, respectively. The activity in the bladder content was described using a bi-exponential extraction from the body. The absorbed dose to the bladder wall was estimated using linear interpolation of SAF values from different bladder volumes, ranging from 10 ml to 800 ml. Administration of the activity was assumed to start at 09:00 with an initial voiding after 40 minutes and a voiding interval of 3.5 hours during the day. A six hour night gap, starting at midnight, with a voiding right before and after the night period, was used. Calculations were made, with the same assumptions, for an earlier dynamic bladder model and with a static SAF value from the ICRP/ICRU adult reference computational phantoms for a bladder containing 200 ml. Values for the absorbed dose per unit administered activity for 19 commonly used radiopharmaceuticals were calculated, e.g. 18F-FDG, 99mTc-pertechnetate, 99mTc-MAG3 and 123I-NaI. Results and conclusion: The results of the estimates of the absorbed doses to the inner bladder wall were a factor of ten higher than the estimates mean absorbed doses. The mean absorbed doses to the bladder wall were slightly higher for females than males, due to a smaller female bladder wall. Calculations with a constant SAF value for 200 ml bladder content resulted in an average of 50% lower absorbed dose for all radiopharmaceuticals when compared to calculations using dynamic SAF values, indicating that the 200 ml approximation is not optimal for static calculations. The new dynamic model that calculates the mean absorbed dose to the bladder wall instead of the dose to its inner surface will give a more realistic dose estimate. The use of Monte Carlo simulated electron SAF values also improves the accuracy of the estimates.

## OP285

### Validation of Monte Carlo code GATE on the ICRP/ICRU female reference computational phantom for internal dosimetry aspects.

**D. VILLOING**, T. MAUXION, S. MARCATILI, M. POIROT, M. BARDIES; INSERM / UPS, Toulouse, FRANCE.

**Aim** The Monte Carlo code GATE[1] is widely used for scintigraphic image modelling, both for preclinical and clinical PET/SPECT studies. However, it is now possible (since version 6.0) to use Gate for absorbed dose calculations, both for External Beam (or Hadron) Radiotherapy and Nuclear Medicine. Molecular radiotherapy dosimetry implies combining quantitative imaging and absorbed dose calculations. Therefore the possibility to use the same code to model both aspects of radiopharmaceutical dosimetry is an asset. This study Aims at validating GATE for clinical internal dosimetry applications by comparing S values (Gy.Bq-1.s-1) obtained with Gate and the radiation transport code MCNPX[2], assumed as a reference in dosimetry. **Materiel and Methods** The ICRP/ICRU female reference computational phantom[3] derived from the "ICRP reference female"[4] was used to compare S values between Gate (V6.2) and MCNPX (v2.7a). Amongst the 141 anatomical regions segmented in the model, 23 source and target organs relevant to Nuclear Medicine were selected. For each of the 53 constituting materials, the elemental composition and density were detailed in media definition for both codes. Monoenergetic photons and electrons (100&500 keV, 1&2 MeV) and 4 radionuclides (18F, 177Lu, 131I, 90Y) were studied. Radionuclide emission yields were taken from the MIRD: Radionuclide Data and Decay Schemes book[5]. MCNPX was used to score the energy deposition in target organs, whereas an absorbed dose distribution "dose actor" was selected in Gate to define a scoring grid overlaid on the voxel geometry. **Results** Less than 3% relative differences were observed between GATE and MCNPX for self-absorbed doses (i.e. source=target), with less than 0.2% of associated uncertainties. Up to 5% relative differences were obtained for close source-target configurations, with acceptable uncertainties. Finally for distant source-target configurations, even though higher relative differences were observed, the absolute differences resulting from very small S values can be considered as non-significant. **Conclusion** S values obtained with GATE and MCNPX showed a very good agreement for monoenergetic photon and electron emissions and for a range of relevant radionuclides, in a reference clinical dosimetric model. This study confirms results obtained at the preclinical scale[6] and highlights the relevance of Gate for radiopharmaceutical dosimetry. [1] Jan et al. Phys Med Biol 2011. [2] Pelowitz et al. 2008. Los Alamos National Laboratory. [3] Publication 110. Annals of the ICRP 2009. [4] Publication 89. Annals of the ICRP 2002. [5] Eckerman & Endo. 2nd ed. SNM 2008. [6] Mauxion et al. Med Phys 2013, in press

## OP286

### Influence of lung/soft-tissue interfaces in Targeted Radionuclide Therapy (TRT) dosimetry: Implication for the Voxel-S-Values (VSV) fast convolution

A. Srour[1], I. Gardin[2,3], F. Maurel[4], S. Burg[5,6], D. Le Guludec[5,1,6], R. Lebtahi[1,7], **A. Dieudonné**[1,7]; [1]APHP - Service de Médecine Nucléaire - Hôpital Beaujon, Clichy, FRANCE, [2]Service de Médecine Nucléaire - Centre Henri Becquerel, Rouen, FRANCE, [3]LITIS (EA 4108), Rouen, FRANCE, [4]Service de Médecine Nucléaire - Hôpital de Nice, Nice, FRANCE, [5]APHP - Service de Médecine Nucléaire - Hôpital Bichat, Paris, FRANCE, [6]INSERM U698, Paris, FRANCE, [7]INSERM U773, Clichy, FRANCE.

Introduction The Aim of our work was to study the influence of lung/soft-tissue (L/ST) interfaces on dosimetry in Targeted Radionuclide Therapy (TRT) by fast convolution of Voxel-S-Values (VSV). **Materials and Methods** Two simple anthropomorphic phantoms have been simulated with the Monte Carlo software tool MCNPX in order to calculate the dose deposition of 131I, 177Lu and 90Y. Phantom 1 was a lung composed of lung tissue (LT, 0.26 g.cm-3) surrounded by soft tissue (ST, 1.04 g.cm-3). Phantom 2 was Phantom 1 plus a tumour of variable diameter (1,2 and 4 cm). For each phantom, two simulations have been computed, the first one takes into account L/ST interfaces (heterogeneous simulation - HT) and the other one doesn't (homogeneous simulation - HM), as it's computed when using VSV fast convolution. Dose distributions have been compared in terms of dose ratio between HM and HT (RHM/HT=DHM/DHT) at the organ (ORHM/HT) and voxel levels (VRHM/HT). Results In phantom 1, ORHM/HT for 90Y, 131I and 177Lu were respectively 0.989, 0.992 and 0.998 and mean values for VRHM/HT were 0.987, 0.996 and 0.999. Profiles on VRHM/HT show very few perturbations inside the lung (RHM/HT≈1.00) and at interfaces (0.99 ≤ RHM/HT ≤ 1.01). In phantom 2, ORHM/HT for the three tumour sizes was 1.00 for 177Lu, 1.01 ≤ ORHM/HT ≤ 1.02 for 131I and 1.03 ≤ ORHM/HT ≤ 1.24 for 90Y. The highest values are found for the 1 cm tumour. At the voxel level, for every tumour size, mean VRHM/HT were respectively 1.49 ± 0.30, 1.05 ± 0.03 et 1.05 ± 0.10 for 177Lu, 1.04 ± 0.03, 1.01 ± 0.01 and 1.03 ± 0.17 for 90Y and 1.00 for 131I with standard deviations below 0.0044. **Conclusion Results** in our phantoms showed that L/ST interfaces have a minor impact on dosimetry of lungs and tumour bigger than 2 cm. Validation with clinical data containing intra-organ density heterogeneities will definitely validate the VSV dosimetry in lungs.

809 - Monday, Oct. 21, 11:30 - 13:00, Rhône 3A/3B

## Oncology Clinical Science: Prostate Cancer

## OP287

### Is the detection rate of 18F-Choline PET/CT influenced by androgen deprivation therapy in restaging patients with prostate cancer?

**S. Chondrogiannis**[1], M. C. Marzola[1], A. Ferretti[2], A. M. Maffione[1], L. Rampin[1], G. Grassetto[1], D. Rubello[1]; [1]Nuclear Medicine - PET/CT Centre, Santa Maria della Misericordia Hospital, Rovigo, ITALY, [2]Medical Physics and Biostatistics Unit, Santa Maria della Misericordia Hospital, Rovigo, ITALY.

**Purpose**: To evaluate whether the detection rate of 18F-Choline is influenced by androgen deprivation therapy (ADT), at the time of the examination, in patients with prostate cancer already treated with radical intent and who present biochemical relapse. **Materials and Methods**: We have retrospectively evaluated 18F-Choline PET/CT scans (November 2009 - December 2012) of 187 patients

(mean age 70 years, range 49-86) with prostate cancer previously treated with radical intent through surgery (104 patients), radiotherapy (37 patients) or both (46 patients) and who presented biochemical relapse (mean PSA 2.1 ng/ml, range 0.5-5 ng/ml). At the time of the examination 72 patients were under hormonal therapy. The relationship between 18F-Choline PET/CT findings and possible clinical predictors was investigated using univariate and multivariate binary logistic regressions, including PSA trigger and androgen deprivation therapy as predictors. The odds ratios (ORs) together with their 95% confidence intervals were computed. The statistical correlation between categorical variables (PET findings and ADT or not at the time of the examination) was stated according to Pearson's chi-squared test applied to the contingency table. Statistical significance was always taken at $p<0.05$. **Results**: The overall detection rate of 18F-Choline was 56.7% (106/187 pts). 39/106 (37%) of PET positive patients showed local pathologic uptake: in 27 cases confined to the prostatic bed and in 12 cases to the locoregional lymphnodes. 47/106 (44%) showed distant localizations only: in 23 cases confined to the bone, in 14 cases to lymphnodes and in 10 cases to both bone and lymphnodes. The remaining 20 patients (19%) showed both local and distant localizations. In the univariate and multivariate logistic regression analysis trigger PSA was significantly correlated with the detection rate of 18F-Choline PET/CT ($p < 0.001$), while ADT at the time of the examination was not statistically correlated to the detection rate of 18F-Choline PET/CT ($p=0.062$ and 0.089 respectively). In patients under ADT the detection rate was 65.3%, while in patients not under ADT the detection rate was 51.3%; the lack of correlation between detection rate and ADT was also confirmed by the Pearson's chi-squared test ($p >0.061$). **Conclusion**: The overall detection rate of 18F-Choline PET/CT was 56 % and was significantly correlated to trigger PSA. Androgen deprivation therapy at the time of the examination does not influence the 18F-Choline PET/CT detection rate and it should not be interrupted.

## OP288

### Impact of 18F-Flurocholine PET/CT in therapeutic strategy of biochemical recurrent prostate cancer

**M. Colombié**[1], C. Bailly[1], D. Rusu[1], M. Lacombe[1], L. Ferrer[2,3], T. Rousseau[4], F. Kraeber-Bodéré[1,3], C. Rousseau[1,3]; [1]Nuclear Medicine, ICO Cancer Center, Saint Herblain, FRANCE, [2]Physics Unit, ICO Cancer Center, Saint Herblain, FRANCE, [3]CRCNA U892, Nantes, FRANCE, [4]Urologic Clinic Nantes-Atlantis, Saint Herblain, FRANCE.

**Aim**: Biochemical recurrent prostate cancer (PC), rising PSA after initial treatment, is an important challenge because imaging modalities as CT, MRI or bone scan often failed to localize local or metastatic disease especially for low level of PSA. Location is important to provide a personalized curative or palliative treatment depending on the extent of disease. The Aim of this study is to evaluate the impact of 18F-Fluorocholine (FCH) PET/CT in therapeutic strategy of biochemical recurrence in PC. **Materials and Methods**: We retrospectively studied 123 consecutive patients (pts) (age 50-81, median 67) who underwent FCH PET/CT. One hundred and three patients (83.74 %) were referred due to biochemical recurrence of PC, after a negative or equivocal conventional imaging. PSA values were collected, PSA doubling time (months) and velocity (ng/ml/yr) calculated. FCH PET/CT list mode acquisition (8 minutes) was performed on pelvic area right after injection and followed by a whole body PET acquisition. All hotspots, excepted physiological uptake, were classified as positive. Positive studies were classified in 3 groups, according to disease's location: prostatic bed, loco-regional disease (ie: pelvic lymph nodes ± prostate area), or distant metastases**. Results:** Biochemical recurrence patients were initially classified as intermediate or high risk of recurrence (79% Gleason ≥ 7, and mean PSA 34.09 ± 92.33). Most common initial treatments were radical prostatectomy (23 pts), radiotherapy (37 pts) and both modalities (30 pts). Biochemical recurrence time after initial diagnosis and mean rising PSA were respectively 4.14 yr ± 3.32 and 10.41 ng/ml ± 41.99. Metastatic patients had significant shorter PSA doubling time (median 3.99 months) than patients with local recurrence (median 7.07 months) ($p = 0.02$). Eighty (77.67%) FCH PET/CT, analyzed as positive, tended to have higher PSA (mean PSA = 12.03 ng/ml), as compared to negative FCH PET/CT examination (mean PSA = 4.93 ng/ml). Among positive FCH PET/CT examinations, 21, 39 and 20 were respectively prostatic recurrence (26.25%), pelvic lymph node ± prostatic recurrence (48.75%), and bone and/or lung metastases (25%). FCH PET/CT changed treatment plan in 52 pts (50.49%). For positive FCH PET/CT, treatments changed in 60 % of cases (48 pts): from curative to palliative treatment (4 pts), from palliative strategy to another one (19 pts), and more importantly from palliative to curative treatment (25 pts). **Conclusion**: In aggressive biochemical recurrent prostate cancer, 18F-Fluorocholine PET/CT results have a major impact on the therapeutic strategy, allowing tailoring treatment.

## OP289

### Evaluation of Unexpected Tracer Uptakes in Prostate Cancer Patients in Whole-body 18F-Fluorocholine PET studies

**A. Baskin**[1], O. Rager[2], G. Amzalag[2], F. Buchegger[2], R. Miralbell[2], O. Ratib[2], T. Zilli[2], V. Garibotto[2]; [1]Ankara Training and Research Hospital, Ankara, TURKEY, [2]Geneva University Hospital, Geneva, SWITZERLAND.

**Aim**: Our Aim was to assess the occurrence and the clinical value of unexpected tracer uptakes in whole body 18F-Fluorocholine (FCH) PET in prostate cancer (PC) patients. We defined unexpected uptakes as visible tracer uptake in regions other than prostate, regional lymph nodes and bones. **Methods**: We retrospectively included all 267 PC patients who were referred for FCH study (either PET/CT or PET/MRI) for staging or restaging. 44 patients were evaluated by PET/MRI. We recorded all unexpected uptakes described in the final report. The final diagnoses for these incidental findings were sought from the hospital archives. **Results**: Out of 267 patients, 131 patients had unexpected uptakes in 183 regions. Among these, 8 were localized in the brain, 28 in the neck, 126 in thorax (axillary and mediastinal lymph nodes and pulmonary uptake), and 21 in the abdomen. Among the 8 brain lesions, 4 of them were further investigated: 3 of them corresponded to a meningioma and 1 of them was a pituitary adenoma. In the neck, 9 uptakes out of 28 were investigated, detecting 4 malignant pathologies (1 thyroid papillary ca, 1 Whartin tumor with cervical lymph node involvement, 1 Hodgkin lymphoma) and 5 benign pathologies (2 benign thyroid nodules, 1 parathyroid adenoma, 1 cervical lymph node with normalization at follow-up, 1 subclinic hyperthyroidism correlated with laboratory findings). In the thorax 14 out of 126 uptakes were further evaluated: 6 were malignant pulmonary lesions (5 primary pulmonary lesions, 1 PC metastasis), 7 were benign pulmonary lesions and 1 was Hodgkin lymphoma. The most common finding in the thorax was mediastinal lymph nodes uptake (in 93 patients): however, among these, only patients with concomitant pulmonary nodules (3 patients of whom 2 of them had primary lung tumors and 1 of them had PC metastases) were malignant In the abdomen among 21 uptakes 4 were investigated: 2 were malignant (2 pancreatic tumors) and 2 were benign pathologies (1 liver hemangioma, 1 adrenal gland adenoma). **Conclusion**: In our group 5.5 % of unexpected FCH uptakes corresponded to a second primary cancer other than PC (10/183). These were localized in the lung, pancreas, parotid, thyroid and in lymph nodes (lymphoma). We conclude that incidental findings of FCH uptake in these organs as well as multiple nodal uptakes should be carefully assessed, even if presumably unrelated with PC, in order to exclude malignant lesions.

## OP290

### Evaluation of choline PET/CT in therapy response monitoring of standardized docetaxel first-line chemotherapy in patients with advanced castration refractory prostate cancer

**S. M. Schwarzenböck**[1,2], M. Thalgott[3], M. Souvatzoglou[1], U. Treiber[3], M. Eiber[4], M. Retz[3], R. Nawroth[3], E. J. Rummeny[4], J. E. Gschwend[3], M. Schwaiger[1], B. J. Krause[1,2]; [1]Department of Nuclear Medicine, Technical University of Munich, TUM, Munich, GERMANY, [2]Department of Nuclear Medicine, University Medical Centre of Rostock, Rostock, GERMANY, [3]Department of Urology, Technical University of Munich, TUM, Munich, GERMANY, [4]Department of Radiology, Technical University of Munich, TUM, Munich, GERMANY.

**Aim** Evaluation of C-11 choline PET/CT for re-staging and therapy response monitoring of docetaxel as first-line chemotherapy in patients with advanced castration refractory prostate cancer. **Methods** 32 patients (mean age 70 years, range 53-83 years) with advanced castration refractory prostate cancer were referred for C-11 choline PET/CT for primary staging before initiation of the first cycle of docetaxel chemotherapy (baseline scan), after 1 (day 1-7) and after 10 cycles of docetaxel chemotherapy (or - in case of discontinuation - after their last chemotherapy cycle) for re-staging and therapy response assessment. 27/32 patients received 2 follow up PET/CTs (after 1 and 10 cycles of chemotherapy), 5/32 were lost to follow up due to death and therefore received 1 follow up PET/CT after the first cycle of docetaxel only). SUVmax, SUVmean, HU max, HU mean and volume of bone, lung and nodal metastatic lesions as well as of local recurrence site were measured semi-automatically in PET/CT at these three timepoints (before chemotherapy, after 1 and after 10 cycles of chemotherapy) (in the mean 7 lesions per patient, range 2-11). PSA values were followed up. Statistics were performed using SPSS. **Results**: SUVmax as well as SUVmean showed a statistically significant decrease in comparison to the baseline scan as early as one week after the initiation of the first cycle of docetaxel ($p$-value < 0.001, respectively). Decrease of choline uptake between the first and the 10th cycle of docetaxel was less pronounced but also significant ($p$-value < 0.001, respectively). Decrease of choline uptake during docetaxel therapy was accompanied by a significant decrease in PSA levels. No statistically significant change was shown for HU max and mean as well as volumetric measurements**. Conclusion**: Choline PET/CT depicts early decreases in choline uptake in metastatic lesions following initiation of standardized first-line docetaxel chemotherapy in patients suffering from advanced castration refractory prostate cancer.

## OP291

### [11C] Choline PET/CT Predicts Prostate Cancer-Specific Survival in Patients with Biochemical Failure During Androgen Deprivation Therapy

**G. Giovacchini**[1], M. Picchio[1], R. Garcia-Parra[2], A. Briganti[3], F. Abdollah[3], L. Gianolli[1], C. Schindler[4], F. Montorsi[3], C. Messa[5], F. Fazio[1]; [1]Department of Nuclear Medicine, San Raffaele Scientific Institute, Milan, ITALY, [2]Department of Health Sciences, Tecnomed Foundation, University of Milano-Bicocca, Milan, ITALY, [3]Department of Urology, San Raffaele Scientific Institute, Milan, ITALY, [4]Swiss Tropical and Public Health Institute, Basel, SWITZERLAND, [5]Department of Nuclear Medicine, San Gerardo Hospital, Monza, ITALY.

**Aim**. Several studies have shown that [11C]choline PET/CT may be useful for restaging prostate cancer (PCa) patients with biochemical failure after radical prostatectomy. However, validation of [11C]choline PET/CT findings scarcely relied on histological findings and prognostic implications of [11C]choline PET/CT are currently unknown. Aim of the study was to assess whether [11C]choline PET/CT predicts survival in PCa patients. **Materials and Methods**. This retrospective study included 195 PCa patients treated with radical prostatectomy that underwent [11C]choline PET/CT from December 1st, 2004 to July 31st, 2007 owing to biochemical failure (prostate specific antigen, PSA > 0.2 mg/ml) during androgen deprivation therapy. PCa-specific survival was computed as the interval from radical prostatectomy to PCa-specific death. **Results.** Median interval after radical prostatectomy was 8.9 years (95% CI, 1.7-18.9 years). Median follow-up after [11C]choline PET/CT was 4.5 years (95% CI, 0.4-8.5 years). [11C]choline PET/CT was positive in 57% of patients. Median PCa-specific survival was 16.4 years (95% CI, 14.0-18.8 years) in patients with negative [11C]choline PET/CT and 11.2 years (95% CI, 9.8-12.6 years) in patients with positive [11C]choline PET/CT (log Rank: Chi-Square=19.3, P<0001). At multivariate analysis, statistical significance was obtained for [11C]choline PET/CT (hazard ratio=2.53, 95% CI, 1.41-4.53, P=0.002), PSA (hazard ratio= 1.03, 95% CI, 1.00-1.05, P=0.037), and Gleason score (Gleason score > 7: hazard ratio=2.49, 95% CI, 1.25-4.95, P=0.009). Patients with pathological [11C]choline uptake in the prostatic bed and/or in retroperitoneal lymph nodes had longer PCa-specific survival (median = 12.1 years, 95% CI: 10.5-13.7 years) in comparison to patients with pathological tracer uptake in the skeleton (median = 9.9 years, 95% CI: 6.8-13.1 years) (log-rank: Chi-Square: 6.5, P=0.010). Two internally validated nomograms predicted 10-year and 15-year PCa-specific survival probability with an accuracy of 76% and 74%, respectively. In an ancillary analysis we also showed that [11C]choline PET/CT predicts PCa-specific survival after PET/CT with very similar statistical power. **Conclusion**. [11C]choline PET/CT predicts PCa-specific survival in PCa patients treated with radical prostatectomy that develop biochemical failure during androgen deprivation therapy. If independent or multicenter confirmation of these findings is obtained, [11C]choline PET/CT might be more widely used in the follow-up of PCa patients for tailoring salvage therapy.

## OP292

### 11C-Choline-PET/CT can detect the site of recurrence in the majority of prostate cancer patients showing biochemical relapse after EBRT

**F. Ceci**[1], P. Castellucci[1], T. Graziani[1], C. Fuccio[2], R. Schiavina[3], J. J. Morigi[1], S. Sanfilippo[1], R. Mazzarotto[4], F. Lodi[1], S. Fanti[1]; [1]Nuclear Medicine, Policlinico S.Orsola-Malpighi, Bologna, ITALY, [2]Nuclear Medicine, Fondazione Salvatore Maugeri, Pavia, ITALY, [3]Urology, Policlinico S.Orsola-Malpighi, Bologna, ITALY, [4]Radiotherapy, Policlinico S.Orsola-Malpighi, Bologna, ITALY.

**Aim:** To investigate the detection rate of 11C-Choline-PET/CT in prostate cancer (PC) patients treated exclusively with external-beam radiotherapy (EBRT) as primary treatment, which showed biochemical relapse (BR). **Materials and Methods**: 182 patients treated with EBRT as primary treatment for PC who showed rising PSA levels were retrospectively enrolled. All patients were previously treated with EBRT in the prostatic fossa, and /or iliac LNs with doses ranging from 74Gy to 81Gy. Mean PSA at the time of 11C-Choline-PET/CT was 6,92ng/ml (median=4.5ng/mL; range=0,4-60ng/mL), mean PSA doubling time (PSAdt)=6,59 months (median=4,71mo; range=0,4-48mo) and mean PSA velocity (PSAVel)=11,13ng/mL//y (median=5,25ng/mL//y; range=0,3-87ng/mL//y). At the time of the scan 55 patients were receiving androgen-deprivation-therapy (ADT) with a continuous ADT scheme (CADT), 27 patients were in therapy suspension with intermittent ADT scheme (IADT) and 68 were not treated with ADT. Positive findings were validated by: a) TRUS-guided biopsy in cases of local recurrence, b) surgical lymphoadenectomy, c) other imaging procedures including repeated 11C-Choline-PET/CT. **Results**: 11C-Choline-PET/CT was positive in 150/182 patients (82,4%): 65 patients were positive in prostate only; 24 showed positive LNs only; 23 bone lesions only; 17 were positive in prostate and LNs; 7 were positive in prostate and bones; 10 were positive in local, LN and bone and 4 patients were positive in LNs and bone. In patients with positive findings mean PSA=7,67ng/ml (median=4,05ng/mL; range=0,4-60ng/mL), mean PSAdt=5,97 months (median=4,25mo; range=0,4-48mo) and mean PSAVel=12,7ng/mL//y (median=6,9ng/mL//y; range=0,4-87ng/mL//y). According to PSA cut-off value for BR proposed by EAU guidelines (BR=PSA>2ng/ml) in PC patients treated with EBRT as primary treatment, we divided our population in two subgroups. In patients with PSA>2ng/ml 11C-Choline-PET/CT was positive in 123/139 patients (88,5%) showing extra-prostatic findings in 75/123 patients. **Conclusion:** 11C-Choline PET/CT can detect the site of relapse in the majority (82,4%) of patients showing BR after EBRT as primary treatment. In particular 11C-Choline-PET/CT has been able to detect extra-prostatic findings in the majority of patients showing rising PSA>2ng/ml.

## OP293

### Accuracy of [11C]CHOLINE PET/CT in patients with prostate cancer recurrence localized to a single lymph node at imaging: Results from a pathological-validated series

**M. Kirienko**[1], N. Passoni[2], N. Suardi[2], F. Abdollah[2], G. Giovacchini[3,4], M. Freschi[5], F. Montorsi[2], A. Briganti[2], C. Messa[6,7,8], M. Picchio[4,6]; [1]University Milano-Bicocca, Milan, ITALY, [2]Urology Department, San Raffaele Scientific Institute, Milan, ITALY, [3]Department of Radiooncology and Nuclear Medicine, Stadtspital Triemli, Zurich, SWITZERLAND, [4]Nuclear Medicine, Scientific Institute San Raffaele, Milan, ITALY, [5]Department of Pathology, Vita-Salute University, San Raffaele Scientific Institute, Milan, ITALY, [6]Institute for Bioimaging and Molecular Physiology, National Research Council (IBFM-CNR), Milan, ITALY, [7]Tecnomed Foundation, University of Milano-Bicocca, Milan, ITALY, [8]Nuclear Medicine, San Gerardo Hospital, Monza, ITALY.

**Aim** to assess [11C]choline Positron emission tomography (PET)/Computed tomography (CT) validity in detecting a single positive lymphnode (LN) compared to pathological examination in men affected by prostate cancer with biochemical recurrence (BCR) after radical prostatectomy (RP), in regards to an increasing interest in lesion-targeted salvage therapies. **Materials and Methods** We perspectively enrolled 46 patients with BCR after RP and a single positive nodal uptake at [11C]choline PET/CT. All the patients underwent pelvic and/or retroperitoneal salvage lymphnode dissection (sLND), according to the results of [11C]choline PET/CT. [11C]choline PET/CT positive predictive value (PPV) in identifying the exact positive LN was assessed in the overall population and according to androgen deprivation therapy (ADT), PSA value and site of PET/CT positivity. **Results** Overall, 32/46 (69.5%) patients were true positive, defined as a single spot of uptake pathologically verified as a metastatic lesion after salvage LND. However, of these only 16/32 (50%) patients had that single lymphatic landing site identified at [11C]choline PET/CT as the only region of recurrence at pathology. Of these, only 11/16 (69%) had a single positive LN at pathological examination corresponding to that detected at imaging. Of the other 5/16 (31%) patients, 3 had 2 positive LNs, 1 had 4 metastasis and 1 had 5 metastatic lymph nodes but all in the same landing station. The overall [11C]choline PET/CT PPV was 35% and 24% when exact concordance was defined according to lymphatic landing site and single positive LN, respectively. The PPV ranged from 33 to 44% and from 18 to 29%, according to lymphatic landing site and single positive LN, in men with and without ADT respectively. PPV was of 24% for both PSA <1 ng/mL or ≥ 1 ng/mL. **Conclusions** [11C]choline PET/CT PPV in correctly identifying patients with a single positive lymph node compared to sLND is limited (24%). Therefore, extensive salvage treatment approaches are needed in order to maximize the chance of cure.

810 - Monday, Oct. 21, 11:30 - 13:00, Tête D'Or 1/2

## Conventional & Specialised Nuclear Medicine: Paediatrics - Kidney / Lung / Liver

## OP294

### Exploring a method to overcome the problem of assessing differential renal function in pediatric patients, when unilaterally large, hypoactive kidneys are present.

**R. Ferreira**, G. Costa, A. Moreira, J. Pedroso de Lima; Centro Hospitalar e Universitário de Coimbra, Coimbra, PORTUGAL.

**Aim**: The Aim of this study was to explore a way to overcome the usual problem posed by the presence of large pathologic kidneys. A method to calculate the differential renal function based on the calculation of function per unit of renal area is proposed**. Materials and Methods**: 37 pediatric patients (15 female and 22 male, age <18 years, mean 4.30 ± 4.53) referred for renal scintigraphy with 99mTc-MAG3, between January 2012 and February 2013, who showed unilaterally large and hypoactive kidneys, were evaluated. Pathologic kidneys (PK) (n= 37) had a mean area of 42.32 ± 22.59 cm2 and normal kidneys (NK) (n= 37) had a mean area of 31.61 ± 17.12 cm2. Differential renal function obtained using a standard ROI procedure was recorded (group A). Subsequently, the uptake in these kidneys was corrected for the area of the contralateral normal kidney using the formula: differential function of the PK (%) / area of the PK (cm2) X area of the NK (cm2) (group B). In all cases, the area of the PK was ≥ 7.25% greater than the NK. Groups A and B were compared by statistical analysis using Pearson Chi-Square test. **Results**: For pathologic kidneys (PK) the values of differential renal function calculated by the standard ROI procedure (group A) had mean 50.30% ± 6.08, range 32-62%; the values corrected for the area (group B) had mean 37.94% ± 6.51, range

21-50%. When the two groups were statistically compared, a very significant difference was obtained (p<0.001). **Conclusions**: In large, pathologic kidneys our results show an overestimation of the renal function calculated by the standard method, when compared to the method which uses an area correction factor. We believe that the proposed method, based on function per unit of kidney area, may reflect a more accurate information on the renal function of pathologic large kidneys, allowing a better management and follow-up, especially in children where is greatest the expectation of benefits from an early intervention. Nevertheless, this methodology needs to be tested in a large clinical setting.

## OP295

### The usefulness of normalized residual activity, output efficiency and post void indices in the interpretation of Tc-99m MAG3 scans in children with renal pelvic dilatation

**S. BEATOVIC**[1,2], E. Jaksic[1,2], A. Ljubic[3,2], Z. Mikovic[4,2], Z. Krstic[5,2], V. Obradovic[1,2]; [1]Center for Nuclear Medicine Clinical Center of Serbia, Belgrade, SERBIA, [2]Belgrade University School of Medicine, Belgrade, SERBIA, [3]Department of Obstetrics and Gyneacology Clinical Center of Serbia, Belgrade, SERBIA, [4]Clinic for Gyneacology and Obstetrics Narodni Front, Belgrade, SERBIA, [5]University Children's Hospital, Belgrade, SERBIA.

**Introduction**: In protocols for follow-up of antenatal hydronephrosis (HN), diuretic renography plays important role. It is method of choice for investigation of upper urinary tract to evaluate renal function and drainage. The Aim of our study is to analyze quantitative parameters of renal output during F+2 diuretic renography in children. We tend to define a normal range for normalized residual activity (NORA 20/2), output efficiency (OE), postvoid normalized residual activity (NORA PM/2) and postvoid to maximum count ratio (PM/Max) and to assess their diagnostic accuracy in children with HN. Patients and Methods: 57 children aged one month to 12 years (median 17 months) were investigated. 109 kidneys were analyzed. Dynamic scintigraphy was done 22 minutes after Tc-99m MAG3 injection. Furosemide was injected at the end of second minute (F+2). Postvoid static image was performed in 60 minute. Renograms were analyzed and according to Tmax, T½ and assessment of dynamic and postvoid images were classified into three groups: Group A: 47 normal curves; Group B: 14 obstructive curves; group C: 34 hypotonic non obstructive curves. There were also 14 equivocal findings. For quantitative analysis, "The International Atomic Energy Agency Software Package for the Analysis of Scintigraphic Renal Dynamic Studies" was used. **Results**: For all parameters, mean value, lower and upper bound of 95% confidence interval were calculated. Values of Tmax (min) were: Group A: 3.3; 2.2; 4.7; Group B: 16.0; 5.5; 21.8; Group C: 5.0; 3.2; 11.3. Results of NORA 20/2 were: Group A: 0.3; 0.1; 0.5; Group B: 1.9; 1.3; 2.6; Group C: 0.5; 0.2; 0.7. Results of ROE 20 (%) were: Group A: 95; 91; 98; Group B: 61; 42; 73; Group C: 89; 83; 94. Values of NORA PM/2 were: Group A: 0.01; 0.01; 0.03; Group B: 0.26; 0.10; 0.44; Group C: 0.02; 0.01; 0.07. Values of PM/Max were: Group A: 0.01; 0.01; 0.02; Group B: 0.13; 0.05; 0.43; Group C: 0.02; 0.01; 0.03. Statistical difference was significant between Group B and C for all parameters (p<0.01). Among kidneys with equivocal finding, 10 were found to be non obstructive and 4 obstructive. Significant linear correlation between NORA 20/2 and ROE 20 was found (r=-0.97). **Conclusion**: The range of normal values for these four parameters in F+2 diuretic renography are: NORA 20/2: 0.1-0.5, ROE 20: 91%-98% NORA PM/2: 0.01-0.03 and PM/Max: 0.01-0.02. Cut off values that exclude obstruction are: ≤ 1.0, ≥ 80%, < 0.1 and ≤ 0.04, respectively.

## OP296

### How accurate is the classification of renal drainage patterns assessed by scintigraphy in pediatric patients with hydronephrosis? Comparison with clinical findings during follow-up.

**R. Ferreira**, G. Costa, A. Moreira, J. Pedroso de Lima; Centro Hospitalar e Universitário de Coimbra, Coimbra, PORTUGAL.

**Aim**: Renal scintigraphy is an important method to assess renal drainage. In adults, it is usually easier to classify the pattern of drainage as obstructive or non-obstructive. In pediatric patients, namely in children, due to renal immaturity and a wide range of "normal variants", this is more difficult, especially when dilated collecting systems are present. The Aim of this study was to evaluate whether the renal drainage patterns, scintigrafically assessed, are consistent with clinical follow-up in pediatric patients with hydronephrosis. **Materials and Methods**: 108 pediatric patients (70 male and 38 female) with hydronephrosis , age 0-18 years, mean 5.31 ± 5.12 years, referred between January 2012 and February 2013 for renal scintigraphy with 99mTc-MAG3 were included in this study. Whenever stasis was observed after the standard 20 minute basal study, a diuretic stimulation with furosemide was conducted (protocol F+20). In all cases, the pattern of renal drainage was evaluated and classified into three categories: good drainage (T1/2 of elimination < 20 min in the basal study or after furosemide administration); poor drainage (T1/2 of elimination > 20 min after furosemide administration and no significant change in the late post micturition image), and inconclusive (T1/2 of elimination > 20 min after furosemide administration but with some improvement after the post-micturition image). A clinical follow-up during 2-12 months, which included ultrasound, was undertaken, and a qualitative comparison has been established. **Results:** 94 patients (87%) were classified has having good drainage, 7 (6.5%) with poor drainage and 7 (6.5%) with an inconclusive pattern. During the follow-up, 11 children needed corrective surgery for hydronephrosis. In nine of them, the renal drainage pattern has been classified as either "poor drainage" or "inconclusive". Nevertheless, in two of those cases (1.8% of the total) the scintigraphic pattern of drainage has been classified as "good drainage", in opposition of what was verified in follow-up. This had an important clinical impact (corrective surgery). **Conclusions**: In this study scintigraphic drainage patterns and clinical follow-up compared favourably in 98.1% of the cases. However, a discrepancy was observed in 2 cases (1.9%) and had an important clinical impact. Scintigraphy is helpful in this setting but a particular caution must be taken in a case by case basis.

## OP297

### MAG3- scintigraphy in the follow-up of children with upper tract dilatation or obstruction: how long the Follow-up ?

**M. Castellani**[1], M. Testoni[1], G. Selvaggio[2], E. Seregni[1], M. Maccauro[1], G. Aliberti[1], C. Vellani[1], A. Lorenzoni[1], G. Riccipetitoni[2]; [1]Istituto Nazionale di Tumori, Milan, ITALY, [2]2Ospedale dei Bambini Buzzi- A.O. Istituti Clinici di Perfezionamento, Surgical Division, Milano, Italy, Milan, ITALY.

**Introduction** In infants with an ultrasound diagnosis of hydronephrosis a conventional cystography or cystoscintigraphy is performed to exclude the presence of a Vesicoureteral.reflux (VUR). Anyway, hydronephrosis could coexist with a VUR In addition to the other examinations a 99mTc-MAG3-scintigraphy can be performed to differentiate a dilating reflux from an obstructive condition only. In most cases of hydronephrosis with no significant loss of percentage of renal relative uptake (RRU), no treatment is necessary but a surveillance with MAG3 can be clinically useful. AIMS We performed a retrospective analysis of MAG3(± diuretic study) in patients who underwent two or more scans for two or more years, with the primary end point to assess the changes in scan findings during Follow-up and with the secondary end point to define the lasting of the MAG3surveillance. **Results** From July 1994 to December 2012 224 patients performed two or more MAG3 scans (±voiding study) in an interval time ranging from 12 months to 13 years. A diuretic study was added to MAG3 only in the case of a persistence of more than 75% of activity in the renal pelvis after 20/30 minutes from starting time, with the patient standing and following bladder voiding. 175 patients underwent 2 scans, 30 patients 3 scans, 13 patients 4 scans, 6 patients 5 scans, with the median interval time period of two years between each study. At basal study, 163 patients presented with a monolateral hydronephrosis (HYD), 61 showed a bilateral HYD. In more than one third of patients mono or bilateral upper tract obstruction were associated with other malformative conditions. The ranges of RRU found were: 40%-53% in 130 patients (58%); 30-40% in 47 pts (21%), 20-30% in 36 pts (16%); ≤20% in 11 pts (5%). Most patients with RRU values lower than 40% underwent surgical correction. Unrespectively to surgery, in follow-up scans RRU values remained stable in about 95% with a significant decline only in 2-3 % of cases. Except for the above mentioned patients, we observed a progressive improvement of excretory function, with an eventual normalization in about 2/3 of patients. When the follow-up was longer than 4 years we did not observed any further significant change of the findings. **Conclusions** In our experience a four-year time frame follow-up is enough to determine prognosis in patients with dilatation or obstruction when no decline of RRU or excretory function are observed after the second study.

## OP298

### Unilateral Multicystic Dysplastic Kidney (MCDK): Assessment of Initial and Long-term Renal Function with Dynamic Renography (RG).

N. Keller[1], P. Ramseyer[2], B. Meyrat[2], H. Chehade[3], P. Frey[2], **A. Boubaker**[1]; [1]Nuclear Medicine, Centre Hospitalier Universitaire Vaudois, Lausanne, SWITZERLAND, [2]Pediatric surgery, Centre Hospitalier Universitaire Vaudois, Lausanne, SWITZERLAND, [3]Pediatric Nephrology, Centre Hospitalier Universitaire Vaudois, Lausanne, SWITZERLAND.

**Aim**: To assess whether function of the contralateral kidney measured by scintigraphy at initial assessment, during and after the maturation phase in children with unilateral MCKD could predict long-term outcome. **Materials and Methods**: Children with unilateral MCKD and normal contralateral kidney (NK) referred for $^{123}$I-hippuran RG between 1985 and 2009 were reviewed. Inclusion criteria were: at least 3 RG and a minimum of 2 years follow-up. A 20-min 2-phase dynamic acquisition was started immediately after injection of 0.5 MBq/kg of $^{123}$I-hippuran. Absolute single kidney function was measured by an accumulation index (AI) defined as the percent of injected activity (%ID) extracted 30-90 sec after heart-peak activity. Normal AI of a single kidney unit is 11±2 %ID in children aged more

than 2 years. **Results**: 75 children (45 boys and 30 girls) were identified. 2 groups were defined based on age at first examination: group 1 (55 children) had RG performed before 3 months of age (6 d-3 mo; 1.2±0.3 mo), and group 2 (20 children) after 3 months (4 mo-8.5 y; 2.9±2.7 y). Age at last follow-up renography ranged from 2.2 to 21.7 y in group 1 (mean 9.6±5.3 y), and from 5.2 to 20.8 y in group 2 (14.5±4.9 y; p<0.001). Observation period ranged from 2.1 to 21.6 y in group 1 (9.5±5.3 y), and from 4.6 to 18.7 y in group 2 (11.6±4.0 y). Interval between first and last RG was similar in both groups. In group 1, AI at first RG was superior to upper normal limit in 28 (5.4 -23.6; 12.0±3.2), within normal limits in 23 (7.2-11.2) and inferior to normal in 4 (5.7-6.9). At last examination AI was above normal limit in all children (13.4-29.4; 19.8±3.2), being totally compensatory in 34 (62%). In group 2, all children had a supranormal AI (13.3-22.0; 17.4±3.6) at first examination, being totally compensatory in 12 of them (60%). At last follow-up AI was totally compensatory in 13 of 20 (range: 13.8-24.1; 19.0±2.4).**Conclusion** Children with simple MCDK have an excellent prognosis and early compensation is common. A first RG should be performed before the age of 3 months to assess early renal function compensation. Close follow-up with I-123-OIH renography is not mandatory and should be performed only in case of complication (infection, urolithiasis, trauma, nephrotoxic drug) or in children with no or incomplete compensation at first assessment.

## OP299

### Correlation of the Findings of Quantitative 99mTc MAA Lung Scintigraphy and Cardiac Catheterization in pediatric patients with Pulmonary Vein Stenosis

**L. A. Drubach**[1], E. L. Palmer[2], C. Stamoulis[1], K. J. Jenkins[1], A. C. Marshall[1], X. Cao[1], E. Y. Lee[1]; [1]Boston Children's Hospital, Boston, MA, UNITED STATES, [2]Massachusetts General Hospital, Boston, MA, UNITED STATES.

**Aim** To evaluate the correlation of the findings on quantitative 99m TC MAA lung scintigraphy and cardiac catheterization in the initial evaluation of pediatric patients with pulmonary vein stenosis. **Materials and Methods** The lung scans and cardiac catheterization of 36 consecutive pediatric patients (age range 1 to 120 months) were retrospectively reviewed. The findings on catheterization were assessed for presence or absence of obstruction in the right upper (RU), right lower (RL), left upper (LU) and left lower (LL) pulmonary vein. The lung scans were assessed by the presence or absence of obstruction in the RU, RL, LU and LL lung zones and a percent distribution of blood flow in each zone was calculated. Correlation of the findings from lung scans and cardiac catheterization were assessed using both simple contingency tables and logistic regression models. The models also included age at scan and time interval between lung scan and catheterization, to assess the potential effects of these variables on the correlation between lung scan and catheterization outcomes. **Results** All 36 patients had pulmonary vein stenosis involving at least one pulmonary vein. The locations of pulmonary vein stenosis were: 1) 27 (75%) of 36 patients at cardiac catheterization and 22 (61%) of 36 patients on lung scan for the RU pulmonary vein; 2) 18 (50%) of 36 patients at cardiac catheterization and 13 (36%) of 36 patients on lung scan for the RL pulmonary vein; 3) 22 (61%) of 36 patients at cardiac catheterization and 22 (61%) of 36 patients on lung scan for the LU pulmonary vein; and 4) 27 (75%) of 36 patients at cardiac catheterization and 14 (39%) of 36 patients on lung scan for the LL pulmonary vein. Statistically significant correlations between findings from lung scan and cardiac catheterization was found, for each of the four zones, when both outcomes were dichotomized (obstructed lobe versus unobstructed lobes). There were statistically significant correlations between percentage reduction of perfusion scan tracer on lung scan and catheterization findings of obstruction for both lower lobes (p=0.001 for right lower lobe, and p=0.017 for left lower lobe), but there was no statistically significant correlation between the two variables for upper lobes. No statistically significant effects of age at lung scan or time between procedures were found. **Conclusions** Quantitative 99mTc MAA perfusion lung scintigraphy is a reliable method to noninvasively diagnose primary pulmonary vein stenosis in pediatric patients.

## OP300

### Correlation between liver function tests and intrapulmonary shunts studied with lung perfusion scintigraphy in paediatric patients with liver disease

**T. Saraiva**[1], R. Silva[1], A. Moreira[1,2], I. Gonçalves[1], J. Pedroso de Lima[1,2], G. Costa[1]; [1]Centro Hospitalar e Universitário de Coimbra, Coimbra, PORTUGAL, [2]Instituto de Ciências Nucleares Aplicadas à Saúde - ICNAS, Coimbra, PORTUGAL.

**Aim**: Hepatopulmonary Syndrome (HPS) is more common in advanced liver disease and in severe portal hypertension, but it may occur in both well compensated and decom¬pensated liver disease, and in situations in which portal hypertension is present in the absence of cirrhosis. The Aim of our study was to determine if there is a correlation between liver function tests and intrapulmonary shunts using lung perfusion scintigraphy in paediatric patients with chronic liver disease and/or portal hypertension. **Material and Methods**: A total of 47 children (22 female and 25 male, age range 1-19 years, mean of 9.9 ± 5.4) were submitted to lung perfusion scintigraphy from February 2010 to March 2013, for a total of 63 studies. After i.v. administration of an adjusted number of MAA particles labelled with 99mTc, with activity calculated according to the EANM pediatric dosage card, anterior and posterior images of the lungs and lateral images of the brain were obtained and brain activity calculated. Biochemical liver function parameters were obtained within an average interval of 7.9 days from lung scintigraphy acquisition and included ALT, AST, GGT, ALP, LDH and Albumin. Each one of these parameters was correlated with the degree of intrapulmonary shunting using a non parametric Mann-Whitney U test. **Results**: Liver disease was due to extrahepatic biliary atresia (n=19), autoimmune hepatitis (n=6), alpha 1-antitrypsin deficiency (n=4), progressive familial intrahepatic cholestasis (n=3), Wilson's disease (n=2) and other pathologies (n=13). HPS was diagnosed (brain activity>6%) in 30.2% (19 studies / 10 children). Statistical analysis showed a strong correlation between GGT and ALP (P<0.01) and the degree of intrapulmonary shunting, and a week correlation with LDH (P<0.05). No correlation was found concerning ALT, AST and Albumin. Discussion: The high incidence of HPS is explained by the fact that in our study has been included the follow-up of children with known positive findings on previous lung scintigraphies. Nonetheless, biochemical liver function parameters, namely GGT, ALP and in a lesser extent LDH values, showed a direct correlation with the degree of intrapulmonary shunting. The diagnosis of HPS requires a high degree of clinical suspicion which can increase in the presence of elevated values of these parameters.

## OP301

### Measuring effective renal plasma flow with I-123-hippurate in liver transplanted children - evidence for its impairment and validation of a simplified procedure for its determination provided by Sapirstein's method

**G. Berding**[1], F. Wilke[2], U. Baumann[3], L. Geworski[2], F. Bengel[1], D. Haffner[3]; [1]Department of Nuclear Medicine, Hannover Medical School, Hannover, GERMANY, [2]Department of Medical Physics and Radiation Protection, Hannover Medical School, Hannover, GERMANY, [3]Clinic for Paediatric Nephrology, Hepatology and Metabolic Disorders, Hannover Medical School, Hannover, GERMANY.

**Aim**: Immuosuppression after organ transplantation might cause impaired kidney function. The Aim of the present study was to demonstrate reduced effective renal plasma flow (ERPF) in liver transplanted children (even when plasma creatinine is normal) using I-123-hippurate and Sapirstein's procedure as a gold standard. Furthermore, prerequisites (e.g. adequate blood sampling times) for the use of a simpler method for ERPF determination according Oberhausen should be validated in children. **Methods**: 48 children (age 5-18 years, mean 12) were studied 1 to 16 years (mean 6) after liver transplantation. Commencing with a bolus injection of 40kBq I-123-hippurate per kg body weight activity at the right shoulder was registered continuously with a probe for 1h. Additionally ten blood samples were collected up to 4h at increasing time intervals. Radiotracer clearance was calculated according to: (i) Sapirstein based on all blood samples (ERPF-SAP) and (ii) Oberhausen at the basis of probe measurements and blood samples at 10, 15 or 25min post injection (ERPF-OH-10, -15, -25, assuming equal activity concentration in arteries and veins at the respective time). Plasma creatinine was 69±35µmol/l in the mean and pathologically increased in 42% of the children. An age according normal mean of 518 ml/min/1.73qm (standard deviation 81) was used for judgement with respect to normal or impaired ERPF. Significance of differences between Sapirstein and Oberhausen method, 95% confidence intervals (c.i.) and r-squared (rsq) coefficients were calculated. **Results**: ERPF-SAP was 404±162 ml/min/1.73qm and impaired more than 1 standard deviation in 60% and more than 2 standard deviations in 46% of the children. Mean differences of ERPF determined with Oberhausen's algorithm compared to ERPF-SAP were: (i) for ERPF-OH10: +9 ml/min/1.73qm (p=0.542), c.i.: +39/-21 ml/min/1.73qm rsq 0.56; (ii) for ERPF-OH15: -28 ml/min/1.73qm (p=0.074), c.i.: +3/-58 ml/min/1.73qm rsq 0.50 and (iii) for ERPF-OH25: -95 ml/min/1.73qm (p<0.0001), c.i.: -61/-128 ml/min/1.73qm, rsq 0.37. **Conclusions**: I-123-hippurate clearance reveals impaired kidney function in up to 18% of liver transplanted children with normal plasma creatinine. With respect to substitution of the demanding Sapirstein procedure by the simpler Oberhausen method the use of early blood samples at 10 min post injection (in contrast to 20 min in adults) provides accurate results with less than 10% over- or underestimation of ERPF in 95% of the cases. Using late samples results in significant underestimation of ERPF with the Oberhausen method. Our results indicate a faster equalization of venous and arterial tracer concentration in children compared to adults.

LS — Monday, Oct. 21, 13:00 — 14:30, Grand Salon Prestige Gratte-Ciel

## EANM/OECD NEA/AIPES Joint Symposium: Mo-99/Tc-99m Supply in 2013 and Beyond

### OP302
**Current and Future Mo-99/Tc-99m Needs**

**J. Kubinyi, CZECH REPUBLIC**

### OP303
**Potential Consequences from Ceased Production of Medical Radioisotope Production at the NRU Reactor**

**B. Ponsard, BELGIUM**

### OP304
**Necessary Changes in the Mo-99/Tc-99m Supply Chain to Improve the Availability of Medical Radioisotopes and Implications for the Nuclear Medicine Community**

**R. Cameron, FRANCE**

YE2 — Monday, Oct. 21, 13:00 — 14:30, Tête D'Or 1/2

## Young EANM Daily Forum 2: Tools for Nuclear Medicine

### OP305
**Welcome and Introduction**

**F. Cicone, ITALY, F. Giammarile, FRANCE**

### OP306
**Radionuclide Production**

**J. Barbet, FRANCE**

### OP307
**Preparation and Synthesis of Radiopharmaceuticals**

**P. Peitl, SLOVENIA**

### OP308
**Technological Development in SPECT**

**T. Kuwert, GERMANY**

901 — Monday, Oct. 21, 14:30 — 16:00, Amphithéâtre

## CME 7 - Paediatrics: Thyroid Diseases in Children

### OP309
**Hypothyroidism and Hyperthyroidism in Children: Role of Nuclear Medicine**

**B.O. Helal, FRANCE**

### OP310
**Paediatric Thyroid Cancer**

**R. Howman.Giles, AUSTRALIA**

### OP311
**Dosimetry and Short/Long-Term Consequences of Radioiodine Treatment in Children and Teenagers**

**F.A. Verburg, GERMANY**

902 — Monday, Oct. 21, 14:30 — 16:00, Auditorium Lumière

## Symposium 7 - EANM/ESMO Joint Session: Bringing Molecular Imaging into Clinical Practice in Medical Oncology

### OP312
**Unmet Needs in Clinical Oncology: The Role of Molecular Imaging**

**J. Gligorov, FRANCE**

### OP313
**Evidence-based Molecular Imaging in Oncology: Current Status**

**W.A. Weber, GERMANY**

### OP314
**Assessing the Clinical Utility of New Diagnostic Technology: The Epidemiologic Perspective**

**K.G. Moons, NETHERLANDS**

### OP315
**Round Table Discussion: Bringing Molecular Imaging to Clinical Practice: The Road Ahead**

903 — Monday, Oct. 21, 14:30 — 16:00, Forum 3

## CTE 3 - Challenge and Perspective in Health Care: Nuclear Medicine Role

### OP316
**Impact of GMP Introduction in Nuclear Medicine Daily Practice**

**J. Ballinger, UNITED KINGDOM**

### OP317
**Global Availability of Molybdenum 99, Is There a Crisis?**

**S. Holbrook, USA**

### OP318
**Drug Registration: Opportunities and Difficulties**

**J. Koziorowski, DENMARK**

904 - Monday, Oct. 21, 14:30 - 16:00, Bellecour 1/2/3

## Featured - Conventional & Specialised Nuclear Medicine: Cardiovascular Infections

### OP319
**Nuclear Medicine and Cardiovascular Infections: What the Clinician needs**

**N. Petrosillo, ITALY**

### OP320
**FDG PET/CT in large vessel vasculitis: correlation between SUV and disease activity**

M. Casali[1], G. Pazzola[2], F. Muratore[2], M. Sollini[1], L. Boiardi[2], M. L. Di Paolo[1], A. Froio[1], N. Pipitone[2], C. Salvarani[2], **A. Versari**[1]; [1]Nuclear Medicine Dept - S. Maria Nuova Hospital-IRCCS, Reggio Emilia, ITALY, [2]Rheumatology Dept - S. Maria Nuova Hospital-IRCCS, Reggio Emilia, ITALY.

**Aim**: 18F-Fluorodeoxyglucose (FDG) positron emission tomography/computerized tomography (PET/CT) is useful in diagnosis of large vessel vasculitis (LVV) but its role in distinguishing between active and inactive disease is still debated. Objective of this study is to evaluate the utility of vascular standardized uptake value (SUV) assessment in differentiating between patients with clinical active and inactive LVV. **Methods**: All patients with LVV seen in our center undergo clinical, laboratory (ESR, CRP) and imaging assessment with FDG PET/CT scans. We retrospectively compared 14 consecutive evaluations of 12 patients with active disease according to clinical indices ITAS (Indian Takayasu activity score) and Kerr/National Institute of Health (Kerr/NIH) with 15 evaluations of 10 patients with inactive disease. ITAS, Kerr/NIH scores, ESR, CRP, values were obtained within 20 days of PET/CT scans. PET/CT scans were reviewed by two expert nuclear medicine physicians blinded to clinical information. Vascular uptake was assessed using visual 4-point semiquantitative scale (0:no uptake, 1-2-3: <, =, > to liver uptake, respectively) ,

vascular $SUV_{max}$ and vascular $SUV_{max}$/liver $SUV_{max}$ ratio (SUV ratio) in 12 vessel segments. The highest $SUV_{max}$ among the different vessel segments was used for the analysis. **Results**: Patients with active disease according to ITAS and Kerr/NIH indices compared to patients with inactive disease had higher vascular $SUV_{max}$ (mean ± SD 4.31 ± 1.63 vs 2.89 ± 0.99 p= 0.008) and higher SUV ratio (1.71 ± 0,74 vs 1.1 ± 0.54 p=0.016).Patients with visual grade >2 (high vascular uptake) compared to patients with visual grade <1 (low vascular uptake) had higher vascular max SUV (mean ± SD 4.62 ± 1.50 vs 2.6 ± 0.52 p< 0.0001) and SUV ratio (1.78 ± 0.78 vs 1.05 ± 0.41 p=0.004).Correlations between $SUV_{max}$ and ESR or CRP (r = 0.551 p = 0.002 vs. ESR; r = 0.565 p = 0.001 vs. CRP) and between SUV ratio and ESR or CRP (r = 0.522, p = 0.004 vs. ESR; r = 0.586 p = 0.001 vs. CRP) were significant.**Conclusions**: Our results show higher values of $SUV_{max}$ and SUV ratio in active than in inactive LVV patients. Both $SUV_{max}$ and SUV ratio correlates significantly with ESR and CRP. The assessment of $SUV_{max}$ and SUV ratio is a promising tool in differentiating between active and inactive disease during follow-up of patients with LVV.

## OP321

### Role of PET/CT in diagnosis of infected vascular prosthetic graft.

**J. M. Nogueiras Alonso**, D. Ruiz Hernández, C. Castillo Berrio, O. Rivas Domínguez, L. Campos Villarino, A. Serena Puig, F. Loira Bamio, A. M. López López, J. Outomuro Perez, R. Guitian Iglesias; Hospital do Meixoeiro, Vigo, SPAIN.

**Objective**: What is the diagnostic role of 18F-FDG PET/CT in infection suspected of vascular prosthetic graft? **Method**: We prospectively evaluated a cohort of 16 patients with clinical suspicion of vascular prosthetic infection by 18F-FDG-PET/CT scan performed in our center from 2011 to 2012. While we compared our findings with Angiography studies (angioCT,angioMR) and Tc99m-HMPAO labeled leukocyte scintigraphy. Finding surgical/histopathological and clinical follow-up at 6 months was the gold standard. **Results**:16 patients (13 men and 3 women), with a total of 22 studies PET/CT, mean age 60±10.6 years (32y to 77y), with location of the vascular prosthesis: thoracic aortic root(1), aorta descending thoracic(2), thoraco-abdominal(2), aorto-bifemoral(7), aorto-iliac(1), femoral-popliteal(1). The correlation of abnormal uptake on PET/CT with histopathology and clinical follow suggestive of infection was obtained in 10 patients, of whom 9 correlated with angioCT and 7 with angioMR findings, the leukocyte scintigraphy was positive only in 5 patients. SUVmax average: 6.4±1.8g/ml (range 4.0-9.0). All cases with abnormal uptake of FDG studies were concordant with CT angiography and/or angioMR positive for infection. In 6 patients with PET/CT negative, angiography studies confirmed the absence of infection in three cases and in the remaining 3 patients by one year clinical follow. In 4 patients with positive baseline PET was repeated PET/CT after antibiotic treatment for 4-6 months, with no abnormal uptake in 2 cases and persistence in the other 2 (it is striking pathological finding in leukocyte scintigraphy in two patients with negative basal scan). **Conclusions**: PET/CT-FDG is a useful tool in the diagnosis and follow up of vascular prosthesis infection, showing very good correlation with angiography studies, and better sensitivity than Tc99m-HMPAO-leukocytes scintigraphy.

## OP322

### Diagnostic Performance of PET/CT in Patients with Newly Diagnosed, Biopsy-Proven Giant-Cell Arteritis. A Prospective, Case-Control Study.

**M. Depetris**[1], S. Prieto Gonzalez[2], A. Perissinotti[1], M. Mayoral[1], I. Tavera-Bahillo[2], J. Hernandez Rodriguez[2], F. Lomeña[3,1], M. C. Cid[3,2]; [1]Nuclear Medicine Department. Hospital Clinic, Barcelona, SPAIN, [2]Systemic Autoinmune Diseases Department. Hospital Clinic, Barcelona, SPAIN, [3]Institut d'Investigacions Biomèdiques Agustí Pi i Sunyer, Barcelona, SPAIN.

**Aim**: To assess the diagnostic utility of 18-F-fluordesoxyglucose (FDG)-PET/CT for giant cell arteritis (GCA) using a receiver operating characteristic (ROC) analysis of FDG uptake at different vascular beds, in a cohort of newly diagnosed biopsy proven patients. **Materials and Methods**: From November 2006 to March 2011, PET/CT with FDG was performed in all patients with newly diagnosed, biopsy-proven GCA who met at least 3 diagnostic criteria for American College of Rheumatology classification (ACR). PET/CT results were compared with a control group consisting of patients, who underwent PET/CT for staging of solid tumor, with no metastases or lesions in contact with main vascular structures. Patients and controls were matched by gender, age and cardiovascular risk factors. The Standardized uptake value (SUV) was calculated at four aortic segments (ascending thoracic aorta, aortic arch, descending thoracic aorta and abdominal aorta), as well as at the supraaortic (subclavian, carotid and axillary arteries) and the iliofemoral vessels. ROC curves were used to calculate sensitivity and specificity in each vascular territory. **Results**: 30 patients and 20 controls were included. The SUV in each territory was significantly higher in GCA patients than in controls. The SUV at supraaortic vessels showed the best area under the curve (AUC) (0.826). According to this, a FDG uptake cut-off of 1.70 achieved a sensitivity and specificity of 81 and 79%, respectively, for GCA diagnosis (p<0.001). FDG uptake at the aorta showed a more limited utility (AUC = 0.740), with a sensitivity and specificity of 80 and 48%, respectively, using a cut-off of 2. 48 (p=0.001). **Conclusion**: PET- FDG shows a remarkable sensitivity and specificity for the diagnosis of GCA, using an objective and reproducible FDG uptake cut-off. Supraaortic branches may be the most suitable vascular field for this purpose.

## OP323

### 18F-FDG-PET/CT Distant Septic Foci Detection in Patients with Infective Endocarditis

**A. Marí Hualde**, M. Kestler, A. Rotger Regí, J. Orcajo Rincón, F. Jimenez Requena, P. Muñoz, E. Bouza, J. Alonso Farto, Nuclear Medicine Department, Microbiology Department; Gregorio Marañon Universitary Hospital, Madrid, SPAIN.

**Introduction**: Peripheral septic foci detection in infective endocarditis (IE) can change the management and prognosis of this serious entity. They are life-threatening complications and asymptomatic in a high percentage of cases. The objective of this study is to assess the clinical utility of PET / CT in identifying these foci and compare its usefulness versus CT. **Material and Methods**: 18F-FDG-PET/CT results were retrospectively reviewed in 36 patients incuded between January 2012 and March 2013 in the context of an ongoing prospective study (PET-END). 18F-FDG-PET/CT was performed after the diagnosis of IE (34 days of average). Other diagnostic imaging technics (CT/US/MRI), clinical follow-up (6 months) and microbiological samples were taken as gold standard. The results were considered significant if they had an impact on the total duration of the treatment or unexpected surgery was necessary. **Results**: The following values for sensitivity, specificity, positive predictive value and negative predictive value for PET/CT were obtained: 96.29%, 88.24%, 92.86%, 93.75% and respectively for CT: 55.56%, 100%, 100%, 58.62%. 26 distant foci were detected in 18 of the 36 patients. 23.07% corresponded to septic pulmonary embolism (SUVmax mean: 3.75), of which 66.67% were not suspected and were of special relevance in these cases. 19.23% belonged to spondylodiscitis (SUVmax mean: 5.39), 80% of these were previously suspected. 15.38% of the foci were identified as intra / endovascular material infection (SUVmax mean; 7.39). The remaining lesions belonged to DAI-associated infection, splenic and cerebral septic emboli, pleural empyema, recto-anal abscess, intraatrial aspergiloma and coronary sinus infection. 15 out of 44 lesions were found (34.09%) that were previously unsuspected belonging to 11 out of the 36 patients (30.56%). There were 73.34% of lesions (11/15) that were identified by PET and were not seen on CT. None of the patients with negative outcome in PET/CT received additional treatment and only one relapsed. A positive PET/CT result for infection led to intensification of treatment in all cases (increasing antibiotic treatment duration or surgery). 7 unrelated lesions were found: 4 belonged to benign pathology and 3 to unknown neoplasms. **Conclusions**: In IE, a negative 18F-FDG-PET/CT outcome almost completely excluded the presence of distant septic foci. PET/CT performs better than CT alone in detecting hidden septic foci in up to one third of the patients and promoting treatment intensification.

## OP324

### The role of 18F-FDG PET/CT in patients with feverish symptoms: can FUO criteria be overlooked?

**J. J. Morigi**[1], V. Ambrosini[1], M. Zompatori[2], C. Nanni[1], F. Ceci[1], R. Bonfiglioli[1], S. Cambioli[1], S. Nicolini[1], E. Tabacchi[1], P. Castellucci[1], S. Fanti[1]; [2]Nuclear Medicine Unit, S.Orsola-Malpighi Hospital, Bologna, ITALY, Radiology Unit, S.Orsola-Malpighi University Hospital, Bologna, Bologna, ITALY.

**Aim:** Fever is a complex body reaction that can be triggered by several physiological or pathological events. Fever of unknown origin (FUO) criteria are well known (body Temperature >38.3 °C for at least 3 weeks, 3 days hospitalisation/3 visits for out-patients, negative blood cultures) but often challenging for the correct diagnostic management of the patient (pt), as no standardized procedure has been determined yet. The Aim of this study is to establish the sensitivity and specificity of $^{18}$F-FDG PET/CT (PET/CT) in a variegated group of patients (pts) with feverish symptoms (FS) and to correlate such data to inflammatory markers (C-reactive protein or CRP) gathered on a short time lapse. **Materials & Methods:** Clinical, microbiological and imaging data from all the pts who underwent PET/CT with an indication of FS in our center between July 2008 and January 2013 were recorded. PET/CT scan was performed following standard procedure (images acquired 60 minutes after the injection of 370 MBq of $^{18}$F-FDG in pts with 6 hours fasting). When available, a blood test from the same day of the PET/CT scan was gathered and the CRP value was assessed. Clinical and histological follow up data were collected for each pt. **Results:** This study included 120 pts (mean age 59,6 yrs [10-90]), organized into groups based on FUO criteria: complete criteria (GROUP 1 or G1=47 pts; mean SUVmax of positive lesions=11.6) vs incomplete criteria (GROUP 2 or G2=73 pts; mean SUVmax of positive lesions=7.8). A cause underlying FS was clinically/histologically available in 77% of pts in G1 and in 64% of pts in G2. PET/CT sensitivity in G1 was 83% while specificity was 91%. Sensitivity in G2 was 87% while specificity was 65%. Accuracy rates were 85% and 80% respectively. 34 pts had lab tests available from the same day of the PET/CT scan: CRP mean values were 7.3 for G1 and 6.8 for G2. **Conclusions:** Results show that all pts with FS can be successfully investigated through PET/CT. However, matching FUO criteria will improve the specificity rate of the exam, thus drastically reducing the number of false positive reporting (9 FP pts in G2 vs 1 FP pt in G1). In our experience, meeting

FUO criteria did not correlate with CRP mean value, though higher CRP values were generally related to a positive PET/CT scan in both groups (4,0 vs 8,6 in G1, 2,6 vs 8,1 in G2).

## OP325

### $^{18}$FDG PET CT imaging for infected cardiac implantable electronic devices

**J. James**, D. Tout, F. Ahmed, P. Arumugam, A. Zaidi, M. Prescott; Central Manchester University Hospitals, Manchester, UNITED KINGDOM.

**Aims**: Cardiac implantable electronic devices (CIEDs) are increasingly used in the management of patients with arrhythmias and cardiac failure. Infection, particularly in relation to intravascular leads, can be challenging to diagnose and subsequent CIED extraction is associated with significant morbidity, mortality and extended hospital stay. The extent of infection also influences the timing of CIED replacement. Studies have indicated good sensitivity and specificity for diagnosis and localisation of CIED infection from $^{18}$FDG uptake in attenuation corrected (AC) PET images, despite concern that streaking artefacts from the metal CIED on the CT may affect AC PET quantitation. A semi-quantitative ratio (SQR) between maximal CIED uptake and mean lung parenchyma uptake on non-AC PET images has also been reported. This study assesses the affect of CIED CT artefacts on AC PET quantitation, and reports preliminary results of correlation between location and extent of $^{18}$FDG uptake and SQR with microbiological findings from extracted CIEDs. **Materials and Methods**: A CIED was attached to an anthropomorphic torso phantom and associated leads wrapped around the cardiac insert. The phantom was filled with $^{18}$FDG at typical patient activity concentrations and imaged using the routine PET CT infection protocol. AC and non-AC PET data were reconstructed. At the time of writing, 10 patients have been imaged for CIED infection. Patients received 350 MBq $^{18}$FDG and were imaged at 90 and 180 minutes post injection. AC and non-AC images were reconstructed to assess $^{18}$FDG uptake and SQR. The presence and extent of infection was determined by microbiological results from the CIED and leads following device removal. **Results**: Phantom AC PET images showed a reduction in $^{18}$FDG uptake in areas surrounding the CIED compared to background, but no change in uptake in relation to the leads. Patient AC PET images showed a range of $^{18}$FDG uptake surrounding both the CIED and leads, with SQR on the non-AC images ranging from <2 to >7. Microbiological findings were in good agreement to those reported from the PET images. **Conclusion:** Phantom data showed that increased activity surrounding the CIED or leads is a true reflection of $^{18}$FDG uptake, although the magnitude of uptake surrounding the CIED may be underestimated in this region. Early patient results indicate good correlation between PET and microbiological findings with respect to the extent of infection. The PET findings therefore impact on the timing of device replacement.

905 - Monday, Oct. 21, 14:30 - 16:00, Auditorium Pasteur

## Oncology Clinical Science: Gynaecological Tumours

## OP326

### Prospective evaluation of FDG PET-CT in predicting progression free survival in patients with recurrent carcinoma cervix: results from a single centre study

**V. Dhull**, P. Sharma, K. K. Agarwal, B. C. Khangembam, S. Arora, C. Bal, A. Malhotra, R. Kumar; AIIMS, New Delhi, INDIA.

**Aim:** To assess the role of Fluorodeoxyglucose Positron Emission Tomography-Computed Tomography (FDG PET-CT) in response assessment of patients with recurrent carcinoma cervix and evaluating the predictive value of metabolic response for progression free survival (PFS) and overall survival (OS). **Methods:** 40 patients with histopathologically or clinically evident recurrent cervical carcinoma underwent a baseline and a post-therapy FDG PET-CT for treatment response evaluation. PET-CT images were analysed by two experienced nuclear medicine physicians. Response was categorised using EORTC criteria into complete metabolic response (CMR), partial metabolic response (PMR), stable metabolic disease (SMD) and progressive metabolic disease (PMD). Clinical/imaging follow-up (minimum 6 months) and/or histopathology were taken as reference standard. Patients were categorized into two groups, those with PMD and those without PMD (i.e. CMR, PMR and SMD). PFS and OS based on PET-CT response were measured from the date of post-therapy PET-CT to the first documentation of progression of disease and death respectively. **Results**: On the basis of metabolic response on post-therapy PET-CT, 7 patients had CMR, 13 patients had PMR, 8 patients had SMD and 12 patients had PMD. PFS for patients with cervical carcinoma ranged from 0.5 to 26.5 months (mean 6.7 ± 6.1 months). Median PFS for patients with PMD was 3.1 months while median PFS for those without PMD was not reached. Patients who did not show PMD on post-therapy PET-CT had a significantly better PFS than patients who showed PMD (p<0.0001, HR: 0.14). There was no statistically significant difference in OS between the two groups (p= 0.187; HR: 0.39). **Conclusion:** FDG PET-CT is an effective tool for response evaluation in recurrent carcinoma cervix. FDG PET-CT can prognosticate recurrent cervical cancer. Patients with metabolically progressive disease on post-therapy FDG PET-CT had a significantly shorter progression free survival.

## OP327

### Role of 18F-FDG PET/CT in detection of recurrence in patients with carcinoma cervix

**S. Jeph**[1], S. A. Shamim[1], P. Sharma[2], A. Kumar[2], R. Tumma[1], N. Jain[1], B. Aggarwal[1]; [1]DCA Imaging and Research Centre, New Delhi, INDIA, [2]All India Institute of Medical Sciences, New Delhi, INDIA.

**Aim** To evaluate the role of 18F-FDG PET/CT in early detection of recurrence in follow up patients of carcinoma cervix. **Method** Patients with history of histopathological proven carcinoma cervix underwent chemotherapy, radiotherapy and/or surgery and were on follow up. Fifty-two patients underwent 18F - FDG PET/CT for detection of recurrence. The median age was 51.5 (average= 53.4) years. PET/CT studies were evaluated and analyzed by two experienced nuclear medicine physicians independently. The physicians were blinded for the patient history. PET/CT results were validated with histopathologic correlation/conventional radiologic imaging and clinical follow up. **Results** Out of 52 patients, 34 patients were reported as positive for recurrence, 17 of these were having active local recurrence and 31 patients had regional lymphnode metastases, 14 patients had distant metastases (out of them 6 patients had distant lymphnode metastases, 6 had lung metastases, four had bone metastases and two had liver metastases). Remaining 18 patients were reported as negative for recurrence. The lung was the most common site for distant metastases. Patient were then further evaluated based on histopathological correlation, conventional radiologic imaging and follow up and five were found to be false positive and one patient was identified as false negative. The sensitivity, specificity, positive and negative predictive value were derived to be 96.7%, 77.3%, 85.3% and 94.4 %, respectively. Accuracy was calculated to be 88.5%. **Conclusions** 18F FDG PET/CT is a very useful non-invasive modality for the early detection of recurrence and metastatic workup in patients with carcinoma cervix with a very high sensitivity and negative predictive value. It is also useful in targeting biopsy sites in suspected cases of recurrence.

## OP328

### Correlation between SUVmax of $^{18}$F-FDG PET-CT scan and depth of invasion in early stage endometrial cancer.

**J. Cordero Garcia**, A. Palomar Muñoz, A. García Vicente, G. Giménez Londoño, O. Gómez López, A. Soriano Castrejón; Hospital General de Ciudad Real, Ciudad Real, SPAIN.

**Aim** To compare the relationship between de depth of invasion in histologically proven stage I endometrial cancer and the SUVmax value obtained on PET-CT study with $^{18}$F-FDG. **Material and Methods** Retrospective study, carried out as a part of a FISCAM grant (PI 2009/31), initially including 47 patients with histologically proven endometrial cancer, in clinical stage I of the FIGO 2009 classification. A standard PET-CT study with $^{18}$F-FDG was performed. A total hysterectomy and double anexectomy was performed in all patients, as well as pelvic lymphadenectomy. Those patients with definitive histological stage I after surgery were selected, being classified into stage IA and IB according to the FIGO 2009 criteria, The SUVmax of the endometrial lesion of each patient was obtained, and the statistical significance of the difference between both groups was calculated (U Mann Whitney test). **Results** Thirty six out of 47 patient fit the criteria, being the rest excluded due to final stage higher than I (7 patients) or absence of residual tumour after the diagnostic biopsy in the surgical specimen (4 patients). The final stage of the patient included was IA in 16 patients (2 clear cell tumours, 1 sarcoma and 13 adenocarcinoma) and IB in 20 patients (18 adenocarcinoma, 2 sarcoma). The mean SUVmax of the IA group was 6,8 (range between 3 and 13,3; median 7,3), being that of the group IB 12,1 (range 6,4 and 22,2; median 11,35). The difference between both means compared using the U Mann Whitney test was statistically significant (p=0,02). **Conclusion** There is a significant relation between the depth of tumoral invasion and the SUVmax obtained in the presurgical PET-CT 18F-FDG study in early stage endometrial cancer (stage I), being lower in histologically proven stage IA tumours.

## OP329

### The preoperative SUVmax (maximum standardized uptake value) measured by 18F-FDG PET/CT as an independent prognostic factor of overall survival in high risk endometrial cancer patients.

**B. Malkowski**[1], M. Walentowicz-Sadlecka[2], P. Walentowicz-Sadlecka[2], P. Walentowicz-Sadlecka[2], P. Sadlecki[2], A. Marszalek[3], T. Pietrzak[4], M. Grabiec[2]; [1]Oncology Centre, Bydgoszcz, POLAND, [2]Department of Obstetrics and Gynecology, The Ludwik Rydygier Collegium Medicum in Bydgoszcz, Bydgoszcz, POLAND, [3]Department of Clinical Pathology, The Ludwik Rydygier Collegium Medicum in Bydgoszcz, Bydgoszcz, POLAND, [4]Department of Nuclear Medicine Oncology Centre, Bydgoszcz, POLAND.

The Aim of this study was to determine if the preoperative maximum standardized uptake valve (SUVmax) measured by 18F-FDG PET/CT in the primary tumor has

prognostic value in the group of patients with endometrial cancer. **Methods:** A total of 101 consecutive endometrial cancer patients, mean age 62 years, range 40 - 82 (FIGO I - IV stage) who underwent 18-FDG-PET/CT one to two weeks prior radical surgery, were enrolled to the study. The maximum SUV was measured and compared with the various clinicopathologic findings obtained after surgery. The relationship between SUVmax and overall survival was analyzed**. Results**: The mean preoperative SUV max was 14.34; range (3.90 - 33.80) and was significantly lower for FIGO I than for higher stages (p=0.0012), for grade 1 than for grade 2 and 3 (p=0.018), myometrial invasion (p=0.0016) and for high risk group (p=0.0005). The analysis of survival ROC curve revealed SUV max cut-off value of 17.7 to predict high risk of recurrence. Endometrial cancer patients with SUV max higher than 17.7 characterized by lower overall survival. **Conclusion**: The preoperative SUVmax measured by 18F-FDG PET/CT is considered very informative index reflecting tumor aggressiveness which may predict poor prognosis. High value of SUVmax would be useful for making noninvasive differentiation between patient's groups and assigning the appropriate therapeutic strategy for patients with endometrial cancer.

## OP330

### Re-staging FDG PET/CT changes management of patients considered for pelvic sidewall resection in relapsed gynaecological tumours

**I. Zerizer**, E. Brockbank, C. Caro, D. Barton, A. Sohaib; Royal Marsden Hospital, London, UNITED KINGDOM.

**Introduction** Pelvic sidewall resection surgery (PSWR) is a novel highly specialised technique for the treatment of relapsed single site pelvic disease in gynaecological tumours. Patient selection, usually performed using conventional MRI and CT, requires accurate delineation of tumour extent, its proximity to adjacent neurovasculature, exclusion of additional pelvic sites of disease and distant metastases. The Aim of this study is to evaluate the role of PET/CT in re-staging patients considered for PSWR. **Materials and Methods** 29 female patients underwent PET/CT and MRI/CT for re-staging pelvic sidewall recurrence prior to surgery. 22 patients had cervical cancer, 3 ovarian, 1 vulval, 1 germ cell tumour and 1 vaginal cancer. The PET/CT data were reviewed independent of the MRI/CT studies and reports on a HERMES workstation by a dual accredited nuclear medicine and radiology practitioner. The site of the recurrence, additional pelvic sites of disease and distant metastases were recorded. The MRI/CT images were then reviewed by the same practitioner 10 days after reading the PET/CT studies in a different order from the first read to avoid interpretation bias. Again the site of recurrence, pelvic disease and distant metastases were recorded. These results were then compared noting additional sites of disease and their impact on clinical management provided on the electronic patient record. **Results** PET/CT and pelvic MRI were concordant in identifying the pelvic sidewall recurrence. Although MRI remains the gold standard imaging modality for delineating local extent of the recurrence, PET/CT identified additional sites of disease in 10/29 patients. 5 patients had additional pelvic lymph nodes (1 inguinal, 1 presacral, 4 external iliac), 4 patients had additional pelvic sites of disease (3 peritoneal, 1 vesical) and 1 pulmonary metastases. FDG PET/CT has resulted in a change in management in 34% of patients compared to using conventional imaging alone (CT/MRI). 3/10 patients in this cohort underwent subsequent PSWR with modification of the surgical plan to take into account the PET/CT findings. 7 patients were referred for chemotherapy or palliative care. **Conclusion** Re-staging FDG PET/CT is highly recommended in patients who are considered for PSWR, resulting in a 34% change in management plan.

## OP331

### Role of 18F-FDG PET/CT in prognostication of advanced ovarian carcinoma patients in complete remission after primary treatment - a prospective study

**R. Soundararajan**, S. Singla, S. Karunanithi, P. S. Chakraborty, R. Kumar, L. Kumar, S. Kumar, G. P. Bandopadhyaya, A. Malhotra; All India Institute of Medical Sciences, New Delhi, INDIA.

**Aim**: To evaluate the role of $^{18}$F-FDG PET/CT in prognostication of advanced ovarian carcinoma patients who were in complete remission after primary treatment. **Materials and Methods**: In this prospective study, 38 patients (median age - 47 yrs, range 24-75) were recruited from July 2010-November 2011.Patients in complete remission(CR) [negative physical examination + normal CA-125 &CT scan] were selected for $^{18}$F-FDG PET/CT (positron emission tomography-computed tomography) after 6 to 8 weeks of primary treatment. Patients with normal PET/CT were kept on follow up. Patients with abnormal tracer uptake on PET/CT scan were considered to have residual disease and offered three cycles of salvage chemotherapy and kept on follow up (Range- 1.4-20.1 months, Median duration of follow up - nine months). Progression Free Survival(PFS), Disease Free survival(DFS) and Overall Survival(OS) of patients with residual disease detected on PET/CT after primary treatment was compared with patients having normal PET/CT scan. **Results**: Among total 38 patients, $^{18}$F-FDG PET/CT detected residual disease in 10 patients; and remaining 28 patients had normal scan. Histopathology (HPE)/follow up imaging/clinical examination/CA-125 levels were used as reference standard. There were nine true positives, 20 true negatives, eight false negatives and one false positive in the study. The sensitivity, specificity, positive and negative predictive values of $^{18}$F-FDG PET/CT in detection of residual disease were 53%, 95%, 90% and 71% respectively. The median PFS, DFS and OS was 5.7, 6.4 and 27.6 months respectively in whom $^{18}$F-FDG PET/CT detected residual disease after primary treatment and treated with salvage chemotherapy and 6.4, 7.6 and 20.7 months respectively in patients with normal post treatment PET-CT. No statistically significant difference was found in PFS [p value = 0.62, Hazards ratio = 0.84, 95% CI = 0.42-1.68), DFS (p value = 0.73, Hazards ratio = 0.8, 95% CI = 0.43-1.79) OS (p value = 0.13, Hazards ratio = 0.59, 95% CI = 0.31-1.15) between patients with residual disease detected on $^{18}$F-FDG PET/CT and patients with negative PET scan after primary treatment. **Conclusion**: $^{18}$F-FDG PET/CT is a useful imaging modality in detecting residual disease in patients of advanced epithelial ovarian carcinoma who are in complete clinical , radiological and biochemical remission after primary treatment and it has a subsequent bearing on patients management. But the impact of $^{18}$F-FDG PET/CT in prognosis of such group of patients is not significant.

## OP332

### Role of $^{18}$F-FDG PET/CT in detection of suspected recurrent ovarian cancer: correlation with serum CA-125 and CT imaging

M. Rensi, F. Giacomuzzi, M. Povolato, L. Bastianutti, **O. Geatti**; University Hospital S.M.M., Udine, ITALY.

**Objective:** This study Aimed to evaluate the efficiency of $^{18}$F-FDG PET/CT in detection of suspected epithelial ovarian cancer recurrence and to compare the accuracy of the technique with those of CA-125 assay and CT scan. **Methods:** Data from 124 women, mean age 62,3 years (range 44-78 years), who underwent CA 125 assay, CT scan and PET/CT for suspected recurrence of epithelial ovarian cancer were reviewed retrospectively, having as gold standard, histological data or clinical and imaging follow-up. **Results:** At the time of PET/CT scan, pts had an average CA 125 of 182.2 U/mL (range 3-2600, SD 472,2), being the marker above the pathological reference level of 35 in only 84 of them. Recurrent disease was confirmed by final diagnosis in 101 pts (81%). PET/CT scans were consistent for recurrence in 102 pts (82%), of them 97 were true positive and 5 false positive. Of the 22 pts with a negative PET/CT scan, 18 were true negative and 4 false negative. Sensitivity, specificity, accuracy, positive predictive value (PPV) and negative predictive value (NPV), of FDG-PET were 96%, 78%, 93%, 95%, and 85% respectively and were significantly better than those of CT (88%, 71%, 85%, 93% and 58%) or CA125 levels (79%, 83%, 80%, 95%, 48%). **Conclusions:** FDG PET/CT had excellent sensitivity in detection of recurrent ovarian cancer and yielded better than CT imaging and serum CA 125 assay. Moreover PET/CT showed the highest negative predictive value (85%) when compared with other modalities (58% and 48% respectively) and was able to detect recurrent disease even in case of normal CA 125 levels and negative CT scan.

## OP333

### Clinical value of 18F-FDG PET/CT in the follow up and recurrence detection of patients with cancer of the ovary

**S. Jeph**[1], A. Chauhan[2], S. A. Shamim[1], B. Aggarwal[1], P. Sharma[3]; [1]DCA Imaging and Research Centre, New Delhi, INDIA, [2]MD Anderson Cancer Center, Houston, TX, UNITED STATES, [3]All India Institute of Medical Sciences, New Delhi, INDIA.

**Aim** To evaluate the role of 18F-FDG PET/CT in detection of recurrence in patients of carcinoma ovary. **Method** Histopathologically proven patients of carcinoma ovary underwent chemotherapy and/or surgery and were on follow up. Thirty-seven patients with clinically suspected recurrence underwent 18F - FDG PET/CT for detection of recurrence. The median age was 53 (average= 52.16) years. PET/CT studies were evaluated and analyzed by two experienced nuclear medicine physicians independently. The physicians were blinded for the patient history. Histopathologic correlation/conventional radiologic imaging and clinical follow up were considered as gold standards. **Results** Out of thirty-seven patients, 23 patients were reported as positive for recurrence. Only six patients had local recurrence. While 22 patients had locoregional metastatic disease. Six patients presented with distant metastases with three having lung metastases two with liver metastases and one had bone metastasis. Remaining 14 patients were reported as negative for recurrence. Lung was the most common site for distant metastases. Patients were further evaluated based on histopathological correlation, conventional radiologic imaging and follow up. Two patients were reported as false positive and one patient was reported as false negative. The sensitivity, specificity, positive and negative predictive value were derived to be 95.5%, 86.7%, 91.3% and 92.8 %, respectively. Accuracy was calculated to be 91.9%. **Conclusions** 18F FDG PET/CT is a very good non-invasive modality for the detection of recurrence and metastatic workup in patients with carcinoma ovary

with high accuracy. It shows good positive correlation with CA-125 levels. It is also useful for guiding biopsy.

906 - Monday, Oct. 21, 14:30 - 16:00, Grand Salon Prestige Gratte-Ciel

## Cardiovascular: Innervation

### OP334

### Evaluation of the sympathetic innervation in diabetic/nondiabetic patients with dilated cardiomyopathy in class I indication for implantable cardioverter defibrillator

**M. COZAR SANTIAGO**[1], P. GONZALEZ GARCIA[2], J. AGUILAR BARRIOS[1], R. SANZ LLORENS[1], F. RIDOCCI SORIANO[2]; [1]UNIVERSITY GENERAL HOSPITAL. ERESA-NUCLEAR MEDICINE DEPARTMENT, Valencia, SPAIN, [2]UNIVERSITY GENERAL HOSPITAL. CARDIOLOGY DEPARTMENT, Valencia, SPAIN.

**Objective**: evaluate the usefulness of MIBG scintigraphy in patients with and without diabetes, to assess the state of the sympathetic innervation. **Material and Methods**: We studied 64 patients (44male ,20 female; mean age 64±10.06 years), with severe heart failure (LVFE 23,78±9%) and dilated cardiomyopathy in class I indication for implantable cardioverter defibrillator (ICD) and properly treated. All of them underwent a metaiodobenzilguanidina (MIBG) scintigraphy. Planar early images in the anterior view were obtained 20 minutes and 4 hours after injection (370 MBq). We use the analysis of the region of interest (ROI) drawn on the heart and upper mediastinum, in the early and late planar anterior images. We calculate the early (e) and late (l) heart to mediastinum (H/M) ratios and the washout according to the protocol (Eur J Nucl Med Mol Imaging (2010) 37:1802-1812). **Results**: Patients were classified into two groups according to the presence (36) or absence (28) of diabetes. No differences in age or other cardiovascular risk factors were found. All of them had similar treatment. MIBG scintigraphy shows significantly lower values of H/Ml (1.27±1.17) in diabetic patients compared to non-diabetic (1.38±0.22) (p< 0.041) with a washout rate without significant differences (41,64±21.83 y 38,31±22.43 respectively) . **Conclusion**: Our results indicate a worse state of myocardial sympathetic innervation in diabetic patients compared to non-diabetics (lower H/Ml ratio) and MIBG scintigraphy can evaluated effectively these patients. Further studies are needed to conclude that these patients may have worse prognosis with increased of frequency of cardiac events.

### OP335

### Reliability and Agreement of Planar and Single-Photon Emission Computed Tomography 123I-Metaiodobenzylguanidine Cardiac Imaging in Patients with Heart Failure

**T. Pellegrino**[1], M. Petretta[2], S. De Luca[2], A. Boemio[2], R. Carotenuto[2], M. P. Petretta[2], S. Paolillo[2], P. Perrone Filardi[2], A. Cuocolo[2]; [1]National Council of Research, Napoli, ITALY, [2]University of Naples - Federico II, Napoli, ITALY.

**Aim**: This study assessed the reliability and agreement of planar and single-photon emission computed tomography (SPECT) 123I-metaiodobenzylguanidine (MIBG) cardiac sympathetic imaging in patients with heart failure (HF). **Material and Methods**: Seventy-four patients (62 men, age 67±10 years) with HF and left ventricular systolic dysfunction (ejection fraction 31±7%) underwent planar and SPECT 123I-MIBG (111 MBq) cardiac imaging. A 10-minute planar image was acquired from an anterior thoracic view 15 minutes ("early" image) and 3 hours and 50 minutes ("late" image) after tracer administration. Four hours after tracer administration, a SPECT study was performed using a dual-head camera system. From planar images early and late heart-to-mediastinum (H/M) ratios were computed. From SPECT images, 123I-MIBG defect score was calculated using the 17-segment model by the summation of segmental tracer uptake scores (summed score) and separately for each of the individual vascular territories. The intraclass coefficient of correlation (ICC) and Lin's concordance correlation coefficient were used to evaluate the reliability, and the Bland-Altman analysis the agreement of early and late H/M ratios on planar images and defect score on SPECT images. **Results**: The difference between measurements obtained twice by the same examiner and by two different examiners was negligible for both early and late H/M ratios. ICC and Lin's coefficient values were excellent (>0.90) for all measurements. At Bland-Altman analysis, the intraobserver limits of agreement were -0.111 to 0.141 for early and -0.116 to 0.145 for late H/M ratio, and the interobserver limits of agreement were -0.108 to 0.179 for early and -0.118 to 0.195 for late H/M ratio. No correlation between difference and mean was found for both early and late H/M ratios. For SPECT defect score, the difference between measurements obtained twice by the same examiner and by two different examiners was not significant with ICC and Lin's coefficient values >0.90. At Bland-Altman analysis, the intraobserver and interobserver limits of agreement were -2.72 to 3.12 and -7.10 to 5.29, respectively, and no correlation between difference and mean was found. Finally, for each of the individual vascular territory the reliability and agreement was excellent for both intraobserver and interobserver analysis (ICC and Lin's coefficient values >0.90 for all measurements). **Conclusions**: The present study showed a high reliability and agreement of planar H/M ratios and SPECT defect score with 123I-MIBG cardiac imaging in patients with HF.

### OP336

### Combined Cardiac magnetic resonance and I-123 MIBG imaging improves risk stratification in patients evaluated for cardiac defibrillator implantation

**M. COZAR SANTIAGO**[1], P. GARCIA GONZALEZ[2], J. ESTORNELL ERILL[3], F. RIDOCCI SORIANO[2]; [1]GENERAL UNIVERSITARY HOSPITAL, NUCLEAR MEDICINE DEPARTMENT-ERESA, SPAIN, [2]GENERAL UNIVERSITARY HOSPITAL, CARDIOLOGY DEPARTMENT, SPAIN, [3]GENERAL UNIVERSITARY HOSPITAL, RADIOLOGY DEPARTMENT-ERESA, SPAIN.

**Purpose:** Risk stratification in patients with heart failure and left ventricular systolic disfunction (LVSD) remains challenging. We assessed the usefulness of the presence of myocardial scarring by cardiac magnetic resonance Imaging (MRI) in conjunction with 123-iodine metaiodobenzylguanidine (I-123 MIBG) Imaging to predict cardiac events in patients evaluated for implantable cardioverter defibrillator (ICD) implantation**. Methods**: Forty one patients (80% males, mean age 63.7±10.1 years) with heart failure and optimal medical treatment referred for ICD implantation were prospectively enrolled and underwent cardiac MRI assessment of LVEF and scar, as well as Cardiac I-123 MIBG Imaging with calculation of early and late heart-to-mediastinum (H/M) ratios, washout rate, and summed defect score from single-photon emission computed tomography (SPECT) to assess cardiac innervation. During follow-up, cardiac events were documented. **Results**: During a mean follow-up of 546 days, 13 patients (31%) experienced a cardiac event (1 sudden death, 6 appropriate ICD therapy, 5 heart failure hospitalizations, 1 myocardial infarction). Late gadolinium enhancement (LGE) was detected in 35/41 (85%) patients. Median value for late H/M was 1.38. Patients with late H/M below median showed significantly more cardiac events (84% vs 15%, p= 0.013) than patients with late H/M above median. In addition, when combined LGE and late H/M ratio < 1.38 were highly predictive of events (p=0.035). As shown in table no patient without LGE by MRI and late H/M ratio above median (1.38) suffered a cardiac event. **Conclusion:** Our preliminary results suggest that combining the presence of myocardial scarring detected by cardiac MRI with late H/M ratio by cardiac I-123 MIBG identified a subgroup of primary prevention ICD candidates with a very low risk for adverse cardiac events and might become a clinical risk stratification tool.

### OP337

### Standardization of I-123 meta-iodo benzyl guanidine heart-to-mediastinum ratio in 33 hospitals and 101 camera-collimator combinations in Japan

**K. Nakajima**[1], K. Okuda[2], Y. Kirihara[3], T. Hosoya[3], S. Matsuo[1], S. Kinuya[1]; [1]Kanazawa University Hospital, Kanazawa, JAPAN, [2]Kanazawa Medical University, Kanazawa, JAPAN, [3]FUJIFILM RI Pharma, Tokyo, JAPAN.

**Aim.** I-123 meta-iodo benzyl guanidine (MIBG) has been used in patients with chronic heart failure and neurological diseases. Using heart-to-mediastinum (H/M) ratio, however, normal values and thresholds between normal and abnormal conditions differ significantly. The purpose of this study was to create cross-calibration method among hospitals and to examine the possibility to unify the H/M ratios using calibration phantom method. **Materials and Methods**. I-123 MIBG calibration phantoms were created for planar MIBG imaging. The calibration phantoms, each of which provided a single fixed H/M ratio, were made to calculate 4 different H/M ratios. The theoretical H/M ratios were calculated mathematically. The phantom experiments were performed in 101 camera-collimator combinations in 41 Japanese hospitals, which included 30 camera types, 9 major collimator groups and 8 camera vendors. The software for automatically calculating the phantom H/M ratio was also created to obtain reproducible results of H/M ratios. Conversion formula was determined for two possible camera-collimator combinations based on a specific linear regression equation. In addition conversion formula to the theoretical H/M ratio were determined for each camera-collimator set. **Results**. A total of 53 low-energy (LE) type and 48 medium-energy (ME) type collimators were included in the experiments. In all settings, linear conversion coefficients between two systems were successfully determined. The effects of septal penetration and scatter were not identical among vendor-camera-collimator settings, and H/M ratios could not be interchangeably used among hospitals and even in the same hospital after camera renewal. For example, a phantom type with true H/M ratio =1.55 was calculated as mean and SD of 1.46±0.08 (range 1.30-1.73) and another type with true H/M ratio =2.60 was calculated as 2.21 ±0.25 (range 1.81-2.80). The average coefficients to convert from the individual camera-collimator condition to the theoretical H/M ratio were 0.56 for LEHR (LE high resolution), 0.63 for LEGP (LE general purpose), 0.73 for ELEGP (extended LEGP), 0.83-0.86 for LMEGP (low-medium energy GP), ME and MEGP, and 0.94 for MELP

(ME low-penetration) types. By using the theoretical H/M ratio as a reference value, we developed a method to calculate any conversion coefficients between two arbitrary systems. **Conclusion.** I-123 MIBG H/M ratios differ significantly among 101 conditions, which depended on the vendor-camera-collimator combinations, and cannot be interchangeably used without correction. The conversion method using calibration phantoms might be practically used for multi-center comparisons and standardization.

## OP338

### Impact of collimator choice on $^{123}$I-MIBG calculated late heart-to-mediastinum ratio: Is there a need to account for liver and lung activity?

**D. O. Verschure**[1,2], T. C. de Wit[1], V. Bongers[3], P. J. Hagen[3], C. Sonneck-Koenne[4], K. Huber[4], B. L. F. van Eck - Smit[1], P. Knoll[4], G. A. Somsen[2,5], S. Mirzaei[4], H. J. Verberne[1]; [1]Academic Medical Center, Amsterdam, NETHERLANDS, [2]Onze Lieve Vrouwe Gasthuis, Amsterdam, NETHERLANDS, [3]Diakonessenhuis, Utrecht, NETHERLANDS, [4]Wilhelminenspital, Vienna, AUSTRIA, [5]Cardiology Centers of NETHERLANDS, Amsterdam, NETHERLANDS.

**Aim:** The $^{123}$I-metaiodobenzylguanidine ($^{123}$I-MIBG) semi-quantitatively assessed late heart-to-mediastinum (H/M) ratio is a well-established semi-quantitative prognostic parameter in patients with chronic heart failure (CHF). However, $^{123}$I presents imaging problems owing to high photon emission. In addition the knowledge on the clinical impact of collimator choice on the calculation of the H/M ratio is relatively limited. In this prospective multicenter study we compared the difference in late (H/M) between low energy high resolution (LEHR) and medium energy (ME) collimators in subjects with CHF. **Materials and Methods:** 53 subjects with CHF (age 63±8.3 years, 87% male, LVEF 29±7.8) referred for $^{123}$I-MIBG were enrolled. At 4 hours (late H/M) after the administration of 185 MBq $^{123}$I-MIBG anterior planar thoracic images were acquired with both LEHR and ME collimators. Late H/M was calculated based on the mean count densities from the manually drawn regions of interest (ROI) over the left ventricle and a predefined fixed ROI placed in the upper mediastinum. Additional ROIs were drawn over liver and lungs. To estimate scatter from liver and lung activity in the myocardial and mediastinal ROIs, liver/lung to myocardium and liver/lung to mediastinal ratios were calculated. **Results:** The LEHR collimator derived parameters were lower compared to the ME collimator (late H/M 1.41±0.18 vs. 1.80±0.41, p<0.001). However Bland-Altman analysis showed that with increasing late H/M the difference between the 2 collimator types increased ($R^2$ 0.73, p=0.001). Multivariate regression analysis showed that almost 90% of the variation in the difference between ME and LEHR late H/M could be explained by scatter from the liver in both the mediastinal and myocardial ROIs ($R^2$: 0.90, p=0.001). The liver-to-heart ratio and the liver-to-mediastinum on both ME (standardized coefficient of -1.69 and 1.16, respectively) and LEHR (standardized coefficient of 1.24 and -0.90, respectively) were independent predictors for the difference in the late H/M between ME and LEHR (p<0.001 for all). **Conclusion:** Comparing ME and LEHR collimator showed a linear increase in difference in favour of the ME derived late H/M. These differences could be explained by scatter from both liver and lung in the mediastinum and myocardium in favour of the ME collimator. These results strengthen the recommendation that for a straightforward implementation of semi-quantitative $^{123}$I-MIBG studies the use of ME collimators is essential.

## OP339

### Clinical evaluation of simultaneous 123I-MIBG / 201Tl imaging with cardiac CZT camera

**F. Rouzet**[1], R. Chequer[1], M. Milliner[1], F. Hyafil[1], S. Burg[1], S. Askienazy[2], D. Le Guludec[1]; [1]Bichat Hospital, Paris, FRANCE, [2]Cyclopharma, Clermont Ferrand, FRANCE.

**Objectives:** Currently, imaging of cardiac innervation using sequential dual isotope (123I-MIBG and 201Thallium) SPECT is hampered by poor quality of images (low count statistics with 123I-MIBG and downscatter in 201Tl energy window) and duration of the procedure. Dedicated cardiac CZT cameras offer, additionally to greater sensitivity, better energy resolution and hence are likely to overcome main limitations of conventional gamma cameras (CC). The Aim of this study was to compare 123I-MIBG / 201Tl imaging acquired simultaneously with CZT vs. sequentially with CC in a clinical setting. **Methods**: 32 patients (age: 55±14 years, males: 22, informed consent obtained) referred for cardiac sympathetic innervation assessment in the setting of familial amyloid neuropathy (n=20) or heart failure (n=12) underwent the same day, following injection of 209±32 MBq of 123I-MIBG: planar (20 min and 4 h) and SPECT (3h30 post-injection, 123I energy window) acquisitions on a CC (Infinia, GEMS). 201Tl (111 MBq) was then injected and SPECT (201Tl energy window) was acquired with the same camera 20 min later. Immediately after completion of conventional imaging, patients were asked to move to the CZT camera (DSPECT, Spectrum Dynamics) for a 12 min acquisition (list mode) specifically for the study. Post-processing performed on a dedicated workstation included dual isotope scatter correction with multiple energy windows model. The following parameters were recorded: MIBG heart/mediastinum ratio (H/M) at 20 min and 4 h, washout rate (WOR) (CC only) and summed score (SS, 17 segments model, each segment quoted from 0 [normal uptake] to 4 [no uptake]) for both isotopes on both cameras**. Results**: MIBG SS was (mean ± SD) 28±14 with CZT and 28±19 with CC (p=0.6). Tl SS was 10±9 with CZT and 8±10 with CC (p=0.3). There was a good correlation between simultaneous CZT and sequential CC acquisitions for MIBG and Tl defect extent and severity (notwithstanding an error proportional to SS value), as well as parameters derived from planar imaging (see table). Conclusions: simultaneous 123I-MIBG / 201Tl SPECT with CZT camera yields results similar to those obtained sequentially with CC, and may thus represent a relevant alternative since acquisition duration is much shorter and potentially allows for dose reduction.

## OP340

### Sympathetic innervation in patients with idiopathic heart failure disease before and after cardiac resynchronization therapy evaluated by 11C-HED PET/CT.

**S. Capitanio**[1], C. Nanni[2], L. Picori[1], C. Martignani[3], R. Bonfiglioli[2], G. Boriani[3], F. Lodi[2], M. Massollo[1], C. Marini[4], S. Fanti[2], G. Sambuceti[1]; [1]Nuclear Medicine Unit, Department of Health Sciences, University of Genoa and IRCCS AOU San Martino-IST, Genoa, ITALY, [2]Nuclear Medicine Unit, Hematology-Oncology and Laboratory Medicine Department, Azienda Ospedaliero-Universitaria di Bologna Policlinico Sant' Orsola-Malpighi, University of Bologna, Bologna, ITALY, [3]Istitute of Cardiology , Azienda Ospedaliero-Universitaria di Bologna Policlinico Sant' Orsola-Malpighi, University of Bologna, Bologna, ITALY, [4]CNR Institute of Bioimages and Molecular Physiology, Milan, Section of Genoa, Genoa, ITALY.

**Aim** Cardiac resynchronization therapy (CRT) is an accepted treatment modality in patients with end- stage heart failure despite optimal pharmacologic therapy. In this setting, PET represents the only technique that permits the absolute quantification of global and regional homogeneity in cardiac sympathetic innervation. We Aimed to evaluate the variation of cardiac adrenergic activity in a population of patients affected by idiopathic heart failure (IHF) disease (NYHA III-IV) after CRT using 11C-hydroxyephedrine (HED) PET/CT. **Materials and Methods** We evaluated ten IHF patients (mean age=68; range=55-81; average left ventricular ejection fraction 26±4%) implanted with a resynchronization device. All patients underwent three HED PET/CT studies as following: PET1 one week after device implantation but before its switching on; PET2, one week after PET1 under stimulated rhythm; PET3, at 6 months under active CRT. Images were acquired 10 minutes after i.v. injection of HED (370-555 MBq). A dedicated software (PMOD 3.4 version) was used to estimate global and regional cardiac uptake of HED that was represented in polar maps using the 17 segments model proposed by the American Heart Association Guidelines. **Results** HED uptake was heterogeneously distributed throughout the left ventricle with a variation coefficient of 18±5%. CRT progressively reduced this variable that did not change after one week (19±5%, ns vs baseline) while markedly decreased at six months (12±5%, p<0.01 vs baseline). Overall, standardized uptake value (SUV) of HED did not significantly change in the myocardium throughout the study (from 3.20±1.06 at baseline to 3.43±1.51 at late follow up, respectively, ns). However, this observation reflected a different behaviour according to the baseline status of cardiac innervation. To test this hypothesis, the 170 segments were divided into 85 regions with "relatively preserved innervation" and 85 with "impaired innervation", according to the median value of relative tracer uptake expressed as % of maximal myocardial uptake (76%). This analysis showed that HED uptake did not change in segments with relatively preserved sympathetic neuronal function, as their SUV was 3.79±0.86 at baseline and 3.69±1.45 at late follow up (ns). On the contrary, in segments with more evident sympathetic neuronal damage, SUV increased from 2.61±0.92 at PET1 up to 3.05±1.67 at six months, (p<0.01). **Conclusion** PET/CT imaging of HED uptake and distribution indicates that CRT improves the homogeneity of cardiac neuronal function throughout the left ventricular myocardium. This effect is mostly caused by a selective improvement of tracer uptake in regions with more severe neuronal damage.

907 - Monday, Oct. 21, 14:30 - 16:00, Salon Pasteur

## Conventional & Specialised Nuclear Medicine: Parathyroid

## OP341

### Superiority of Digital Subtraction over Visual Interpretation of Co-Imaged 99mTc-MIBI and 123I-NaI Planar Parathyroid Scintigraphic Images

**M. Pelletier-Galarneau**, O. O. Sogbein, S. Dinning, L. S. Zuckier; University of Ottawa, Ottawa, ON, CANADA.

**Objective:** $^{99m}TcO_4^-$ or $^{123}$I-NaI thyroid imaging is often used to supplement $^{99m}$Tc-sestamibi parathyroid scintigraphy. While both EANM and SNMMI guidelines recommend the use of digital subtraction over visual interpretation alone, very few studies have formally compared these Methods. The purpose of this study is to rigorously assess the added value of digital subtraction to visual interpretation. **Materials:** Three experienced nuclear medicine residents retrospectively reviewed 90 parathyroid studies in patients with primary hyperparathyroidism, consisting of simultaneously acquired early $^{99m}$Tc-MIBI and $^{123}$I-NaI planar images. (Delayed MIBI images were not included in this analysis). Studies were interpreted with and without digital subtraction of $^{123}$I-NaI from $^{99m}$Tc-MIBI on a commercially-available workstation (Hermes Medical Solutions, Sweden) and compared to histopathologic findings, which served as ground truth. Sensitivity, specificity, and area under ROC curve (AUC) were compared for the two modalities using an ROI-based approach. **Results:** 90 patients had a total of 91 histopathologically confirmed parathyroid adenomas (2 in 1 patient). Inter-observer agreement was significantly improved ($p<0.01$) with digital subtraction versus visual interpretation. All 3 readers had significantly greater sensitivity ($p<0.05$) with digital subtraction (74%, 73% and 82%) vs. visual interpretation alone (49%, 64% and 59%) while specificity was not significantly diminished (93%, 96% and 95% vs 94%, 94% and 97%, $p>0.13$). ROC AUC was significantly greater with digital subtraction in 2 of 3 readers. In one reader, ROC AUC increased from 0.7561 to 0.8533 ($p=0.0001$). In a second reader, ROC AUC increased from 0.7974 to 0.8846 ($p=0.0006$). In a third reader, ROC AUC increased from 0.8340 to 0.8617 ($p=0.26$). **Conclusion**: Using an optimized dual-isotope co-imaging technique, digital subtraction significantly improves inter-observer agreement and increases sensitivity by 9-23%, without diminishing specificity. Digital subtraction should be performed on simultaneously acquired dual-isotope parathyroid images.

## OP342

### Pre-Operative Localization with $^{11}$C-Methionine PET/CT and $^{99m}$Tc-sestamibi in patients with confirmed parathyroid adenoma.

**N. Martinez-Amador**, I. Martínez-Rodríguez, M. De Arcocha-Torres, I. Banzo, R. Quirce, J. Jiménez-Bonilla, F. Ortega-Nava, S. Ibáñez-Bravo, Z. Bravo-Ferrer, C. Lavado-Pérez, J. M. Carril; "Marqués de Valdecilla" University Hospital. University of Cantabria, Santander, SPAIN.

**Aim:** To evaluate the usefulness of $^{11}$C-methionine PET/CT (MET) in the pre-operative localization of parathyroid adenomas and to compare the results with those obtained with the technique of choice, the double-phase $^{99m}$Tc-sestamibi scintigraphy (MIBI). Also, we evaluated the optimal timing for MET imaging. **Methods:** This prospective study included 15 patients (mean age: 65.5±9.7 years) with primary hyperparathyroidism (PH) underwent surgery. MIBI (planar and SPECT) was obtained 10′ and 2-3 hours after injection of 740 MBq (20 mCi) of $^{99m}$Tc-sestamibi. MET was obtained 10′ and 40′ after injection of 740 MBq (20 mCi) of $^{11}$C-methionine. MIBI and MET images were visually evaluated and compared. A score for 10′ and 40′ MET images from 0 (no abnormal uptake) to 3 (intense uptake) was assigned. **Results**: MIBI and MET were positive and concordant in 12/15 patients (80%). In 11 of these 12 patients the adenoma was correctly localized, in 2 of them the adenoma was ectopic and the anatomic information provided by the CT component of the PET/CT was essential to address surgery. In 1 patient MIBI and MET incorrectly localized the adenoma. In 3/15 patients (20%) MIBI was positive (adenoma correctly localized in 2 of them) and MET negative. According to the timing of MET imaging, the 10′ and 40′ acquisition showed the same score in 11 patients, it was higher at 10′ acquisition in 3 and in 1 the adenoma was only detected at 40′. **Conclusion**: Double-phase MIBI-SPECT is still the technique of choice for the localization of parathyroid adenomas in patients with PH and MET-PET/CT may have a complementary role in selected patients. Although the early MET acquisition allowed a more confident report, the delayed acquisition was also helpful and should be included in the protocol.

## OP343

### Usefulness of 18F-fluorocholine PET/CT for preoperative localization of parathyroid adenomas

**L. Lezaic**[1], S. Rep[1], T. Kocjan[1], M. Jensterle Sever[1], M. Hočevar[2], J. Fettich[1]; [1]Klinicni Center Ljubljana, Ljubljana, SLOVENIA, [2]Onkološki Inštitut, Ljubljana, SLOVENIA.

**Background:** Accurate localization of parathyroid adenomas allows use of minimally invasive surgical techniques. Some PET tracers may be clinically useful to image parathyroid adenomas with advantage of superior image resolution and mechanism of uptake not affected by P-glycoprotein expression. Aim: to assess usefulness of 18F-fluorocholine PET/CT for preoperative localization of parathyroid adenomas. **Materials, Methods:** in 17 patients with clinical primary hyperparathyroidism (elevated Ca2+ and iPTH) 99mTc-sestaMIBI SPECT/CT (600 MBq) and 18F-fluorocholine (100MBq) PET/CT were performed. Intraoperative localization and histology were used as gold standard for comparison of diagnostic performance of both imaging techniques. **Results**: 20 lesions were found intraoperatively and confirmed histologically. 18F-fluorocholine correctly localized 16/20 lesions (80%) and the affected side in 18/20 adenomas (90%). 99mTc-sestaMIBI SPECT only localized lesions in 10/20 cases (50%) and the affected side in 11/20 cases (55%). Moreover, 18F-fluorocholine PET/CT correctly localized 2/2 adenomas occurring in one patient and 7/8 hyperplastic glands in two patients with hyperplasia. **Conclusion:** 18F-fluorocholine PET/CT appears to be clearly superior to 99mTc-sestaMIBI SPECT for localization of parathyroid adenomas, especially in cases of multiple localizations. Our results are currently limited by small sample size and need to be expanded.

## OP344

### Title: An analysis of the ability of three parathyroid scintigraphy protocols of increasing complexity to successfully guide minimally invasive surgical approach with histopathological correlation.

**J. C. Fowler**[1,2], D. Ravichandran[1], N. Bassett[1]; [1]Luton and Dunstable NHS Foundation Trust, Luton, UNITED KINGDOM, [2]Royal Brompton and Harefield NHS Foundation Trust, Harefield Hospital, UNITED KINGDOM.

**Background:** Correct parathyroid adenoma localisation facilitates successful minimally invasive surgical approach. There are many different scintigraphic protocols available for successful parathyroid adenoma localisation. In our centre 3 different scintigraphic strategies of increasing complexity have been utilised for preoperative parathyroid adenoma localisation: Protocol 1: Early and late Tc99m-sestamibi planar imaging with late Tc99m-sestamibi SPECT scanning Protocol 2: Early and late Tc99m-sestamibi planar imaging with late Tc99m-sestamibi SPECT scanning supplemented with planar thyroid imaging with Tc99m-pertechnetate Protocol 3: Early and late Tc99m-sestamibi and Tc99m-pertechnetate imaging, all performed as SPECT acquisitions, resulting in three volumetric datasets to allow cross sectional analysis of all datasets and surface rendered image comparison The increasingly complexity of these protocols and time taken to process and report images require additional camera and staff resources. An analysis of the success of more complex protocols to successfully localise adenomas would be helpful to justify these additional resources. **Aim:** To assess whether increasing complexity of different scintigraphic protocols can be justified in terms of success of parathyroid adenoma localisation. **Material and Methods**: A retrospective analysis of the ability of the three strategies to correctly localise the side of adenomas was carried out. 106 parathyroid scintigraphic studies were performed using the three described protocols and reported by a single radionuclide radiologist. 73 had surgery performed by a single endocrine surgeon. 65 of these had a proven histopathological diagnosis of parathyroid adenoma with side of lesion confirmed from operative findings. Operative/histopathological findings were compared with scintigraphic results for the three scanning techniques to assess the ability of the three protocols to correctly localise the side of lesions. **Results**: Correct side localisation of adenomas was achieved in 76% of patients examined with Protocol 1 (n=33), 83% with Protocol 2 (n=24) and 100% with protocol 3 (n=8). **Conclusion**: There appears to be good correlation of parathyroid adenoma localisation success with scintigraphic protocol complexity. The most recent strategy of triple phase SPECT appears to be highly successful although numbers of patients who have had this technique and completed surgery is relatively small at this stage

## OP345

### The oxyphilic cell amount in parathyroid adenomas is an important determinator of scintigraphy outcome.

**J. Schildt**, A. Ahonen, P. Pulkkinen, L. Halme, E. Ryhänen, C. Schalin-Jäntti; Helsinki University Central Hostpital, Helsinki, FINLAND.

**Aim** The exact mechanism of visualization of parathyroid adenomas is not clear. The detection of parathyroid adenomas by 99mTc-sestamibi scanning is influenced by several factors, including the predominant cell type, different wash-out of sestamibi in parathyroid adenomas and in thyroid tissue, expression of P-glycoprotein, tumour size, serum levels of calcium and parathyroid hormone. Some imaging centers still prefer a single tracer scanning with sestamibi over a double tracer subtraction scanning (sestamibi/I-123), although it seems that the latter has a significantly better accuracy to detect parathyroid adenomas. The Aim of this study was to assess the various factors influencing the visualization and wash-out of sestamibi in parathyroid adenomas. **Materials and Methods** 46 patients (33 women, 13 men) with surgically removed parathyroid adenomas and prior laboratory tests were included. The cell types and the weight of the removed adenomas were obtained. In 36 patients, the adenoma was visualised before the operation with parathyroid scintigraphy using double tracer scanning and in 10 patients not. In the patients with a positive scintigraphy the kinetics of the wash-out of sestamibi was visually analysed by two experienced nuclear medicine physicians. The visualization of adenomas and the wash-out kinetics were compared with pre-operative laboratory tests, histology and weight of the adenomas. **Results** Of the 36 patients with a positive scintigraphy, 24 had a slow and 12 a rapid or stable wash-out of sestamibi. Adenomas with a slow wash-out had significantly more oxyphilic cells than those with a rapid or stable wash-out

(p=0,027). The kinetics groups did not differ significantly concerning the weight of the adenoma or the laboratory tests. There were no significant differences between visualized or non-visualized adenomas in the weight or in serum calsium or PTH level. The amount of the oxyphilic cells in the visualized adenomas were not significantly higher than in those not visualized. **Conclusions** The amount of oxyphilic cells in a parathyroid adenoma is an important factor influencing the visualization and wash-out kinetics of the parathyroid adenomas. Some adenomas had a low oxyphilic cell count and probably therefore a rapid or stable wash-out of sestamibi and could be visualized with double isotope scanning but not with a single tracer scintigraphy. This seems to be one important reason why double tracer subtraction scanning is better than single tracer scanning in the imaging of parathyroid adenomas.

## OP346

### Imaging of renal hyperparathyroidism using SPECT/CT with low-dose localizing CT

A. G. G. Doruyter, T. Hartley, J. W. Ameyo, M. R. Davids, **J. M. Warwick**; Stellenbosch University, Cape Town, SOUTH AFRICA.

**Background:** Hybrid imaging using SPECT with low dose x-ray CT (SPECT/LDCT) is of benefit in preoperative scintigraphy of primary hyperparathyroidism. The role of SPECT/LDCT in preoperative assessment of renal hyperparathyroidism has not yet been examined. The Aim of the study was to determine whether SPECT/LDCT conferred any benefit over SPECT alone in terms of detection and/or localization of hyperfunctioning parathyroid tissue in this patient group. **Methods**: A retrospective study of patients with renal hyperparathyroidism and positive planar and SPECT scintigraphy was undertaken. Patient records were examined for renal disease and management data. All patients underwent planar scintigraphy using $^{99m}$Tc-pertechnetate immediately followed by $^{99m}$Tc-sestamibi as well as SPECT/LDCT 60 min after sestamibi injection and a delayed static image to assess for differential washout at 2-3 hours. Planar subtraction images were generated. Planar + SPECT images were reported on followed by planar + SPECT/LDCT images. Confidence for the presence of hyperfunctioning parathyroid tissue as well as confidence of location was scored on a Likert-type scale. Interpretation of planar + SPECT was compared with interpretation of planar + SPECT/LDCT using least squares means analysis. McNemar tests were used to determine the impact of LDCT on equivocal lesions and number of ectopic lesions detected**. Results**: Twenty patients with renal hyperparathyroidism who had lesions positive on planar and SPECT component of SPECT/LDCT imaging were included. Thirty-five lesions were detected on planar + SPECT and this was unchanged after assessment of the LDCT data. Confidence for the presence of parathyroid pathology changed in 5 patients (5 lesions) with mean confidence of parathyroid pathology increasing (p=0.16). The number of equivocal lesions decreased from 18 (14 patients) to 14 (10 patients) (p=0.13). Localization changed in 4 lesions (3 patients), and confidence in localization changed in 9 lesions (7 patients) (p=0.002). The number of lesions classified as ectopic increased from 5 to 8 (p=0.25). **Conclusion**: Addition of LDCT changed localization in 4/35 lesions (11%) (3/20 patients) and identified possible second pathology in 1/35 lesions (1/20 patients). Although clinical impact of LDCT was not measured, the addition of LDCT had potential clinical impact in 1/7 lesions (14%) or 1/5 patients (20%). The addition of LDCT confers no benefit over planar + SPECT imaging alone in renal hyperparathyroidism in terms of sensitivity. The likely improvement in localization of disease supports the use of LDCT in renal hyperparathyroidism when surgery is considered.

## OP347

### 99mTc-sestamibi/123I subtraction SPECT-CT for parathyroid scintigraphy: 180° or 360°of SPECT acquisition?

**V. Tunninen**[1], P. Varjo[1], A. Holm[1], T. Kauppinen[2]; [1]Satakunta Central Hospital, Pori, FINLAND, [2]Helsinki University Central Hospital, Helsinki, FINLAND.

**Aim**. 99mTc-sestamibi/123I subtraction SPECT/CT is a valuable tool for localization of parathyroid ade-noma. Currently SPECT acquisition is performed with 360° and acquisition takes approximately half an hour. The Aim of this study is to evaluate if the total length of the study may be shortened by half using 180° acquisition with 90° detector configuration (L-mode) with similar acquisition parameters. **Materials and Methods**. 99mTc-sestamibi/123I subtraction SPECT/CT was performed for 21 patients with primary hyperparathyroidism. Due to the possibility of the rapid washout of 99mTc-sestamibi, the evaluation of the two acquisition Methods (360° vs. 180°) was performed by reconstructing half of the 360° data to mimic a 180° acquisition. Attenuation corrected SPECT/CT images were reconstructed on the Siemens Syngo workstation using the FLASH 3D-algorithm with 360° of rotation (8 iterations, 8 subsets, Gaussian 9.00 filter) and with 180° of rotation (the anterior half, 8 iterations, 4 subsets, Gaussian 9.00 filter). Two anonymized image sets (360° and 180°) with 123I, 99mTc-sestamibi, and subtraction SPECT/CT images were generated. Image sets were reviewed and each quadrant in relation to the thyroid gland was classified on a 3-point scale. Scores of 0-1 were considered negative and scores of 2 were considered positive. Findings were classified with histologic analysis as the reference standard. The false-positive image rate was defined as the ratio of false-positives to the sum of true-positives plus false-positives. **Results**. There were 22 adenomas in 21 patients. Twenty-one patients had solitary adenomas, one patient had double adenoma. 20 abnormal parathyroid glands were found in both image sets. The sensitiv-ities and specificities of both reconstructions (90,9% and 91,9%, respectively) were similar. There was no visual difference in reconstructed slices. **Conclusion**. This study indicates that the total length of the 99mTc-sestamibi/123I subtraction SPECT-CT may be shortened by half without compromising quality using 180° acquisition with detectors in L-mode.

## OP348

### 99mTc-sestamibi/123I subtraction SPECT/CT for parathyroid scintigraphy: additional planar pinhole image decreases false-positive findings

**V. Tunninen**[1], P. Varjo[1], A. Holm[1], T. Kauppinen[2]; [1]Satakunta Central Hospital, Pori, FINLAND, [2]Helsinki University Central Hospital, Helsinki, FINLAND.

**Aim**. 99mTc-sestamibi/123I subtraction SPECT/CT is a valuable tool for localization of parathyroid adenomas. However, false-positive findings are common due to uneven iodine uptake in thyroid. The iodine uptake in thyroid may be evaluated more reliably from anterior pinhole images, as the resolution of the pinhole collimator is superior compared to the reconstructed SPECT resolution (with parallel hole collimator). The Aim of this study was to evaluate whether the review of additional planar pinhole image decreases the number of false-positives in 99mTc-sestamibi/123I subtraction SPECT/CT. **Materials and Methods**. Dual-isotope parathyroid scintigraphy with 99mTc (550MBq) and 123I (20MBq) was performed for 21 patients with primary hyperparathyroidism. Two simultaneous 99mTc /123I acquisitions were performed (anterior planar pinhole image and SPECT/CT). Two anonymized image sets were generated. The first set ("SPECT/CT") consisted of 99mTc-sestamibi, 123I, and subtraction SPECT/CT images. The second set ("SPECT/CT+Pinhole") consisted of 99mTc-sestamibi, 123I, and subtraction SPECT/CT images and anterior planar pinhole images (99mTc-sestamibi,123I, and subtraction images). Image sets were reviewed and each quadrant in relation to the thyroid gland was classified on a 3-point scale. Scores of 0-1 were considered negative and scores of 2 were considered positive. Findings were classified with histologic analysis as the reference standard. The false-positive image rate was defined as the ratio of false-positives to the sum of true-positives plus false-positives. A McNemar test was performed to compare the sensitivities and specificities between the image sets. **Results**. There were 22 adenomas in 21 patients. Twenty-one patients had solitary adenomas, one patient had double adenoma. Four of the patients had thyroid nodules which did not take up iodine, thus creating erroneous residual activity in subtraction images. Twenty adenomas were correctly localized by SPECT/CT, but five false-positive findings were generated. Twenty-one adenomas were correctly localized by SPECT/CT+Pinhole, and only one false-positive finding was generated. Both sensitivity and specificity were higher with SPECT/CT+Pinhole than with SPECT/CT (95,5% vs. 90,9% and 98,4% vs. 91,9%, respectively. p = 0,08). False-positive rate was 20% with SPECT/CT, and decreased to 4,6% with SPECT/CT+Pinhole. **Conclusion**. This study indicates that the use of additional pinhole image with 99mTc-sestamibi/123I subtraction SPECT/CT increases both sensitivity and specificity of parathyroid scintigraphy. Although the difference was not statistically significant due to the small number of patients, we find that the decrease of the false-positive rate is of high importance. The use of additional planar pinhole image with 99mTc-sestamibi/123I subtraction SPECT/CT is thus recommended.

908 - Monday, Oct. 21, 14:30 - 16:00, Gratte-Ciel 1/2/3

# Radionuclide Therapy & Dosimetry: Dosimetry for Molecular Radiotherapy

## OP349

### Evaluation of Radiobiological Effects in Three Distinct Biological Models

**J. Lemos**[1,2], P. Costa[1,2], L. Cunha[1,2,3], A. P. Carvalho[4], V. Vasconcelos[4], P. Genésio[5], F. Ponte[5], P. S. Costa[5], P. Crespo[6], L. F. Metello[1,3,2]; [1]ESTSP.IPP, V N Gaia, PORTUGAL, [2]CADCTR, Porto, PORTUGAL, [3]IsoPor SA – Isotopes for Diagnostic & Therapeutics, SA, Porto, PORTUGAL, [4]Biology Dept, Sciences Faculty, CIIMAR, Univ. of Porto, Porto, PORTUGAL, [5]Radiotherapy Dept, Julio Teixeira SA, Porto, PORTUGAL, [6]LIP, Univ. of Coimbra, Coimbra, PORTUGAL.

The present work Aims to share the process of development of advanced biological models to study radiobiological effects. Recognizing several known limitations and difficulties of the current monolayer cellular models, as well as the increasing difficulties to use advanced biological models, our group has been developing advanced biological alternative models, namely three-dimensional cell cultures and

a less explored animal model (the Zebrafish - Danio rerio - which allows the access to inter-generational data, while characterized by a great genetic homology towards the humans). These three models (monolayer cellular model, three-dimensional cell cultures and zebrafish) were externally irradiated with 100mGy, 500mGy or 1Gy. The consequences of that irradiation were studied using cellular and molecular tests. Our previous experimental studies with 100mGy external gamma irradiation of HepG2 monolayer cells showed a slight increase in the proliferation rate 24h, 48h and 72h post irradiation. These results also pointed into the presence of certain Bystander effects 72h post irradiation, constituting the starting point for the need of a more accurate analysis realized with this work. At this stage, we continue focused on the acute biological effects. Obtained results, namely MTT and clonogenic assays for evaluating cellular metabolic activity and proliferation in the in vitro models, as well as proteomics for the evaluation of in vivo effects will be presented, discussed and explained. Several hypotheses will be presented and defended based on the facts previously demonstrated. This work Aims to share the actual state and the results already available from this medium-term project, building the proof of the added value on applying these advanced models, while demonstrating the strongest and weakest points from all of them (so allowing the comparison between them and to base the subsequent choice for research groups starting on the field) for the study of biological effects of low doses of ionizing radiation, believing that there is a clear lack of data related with the biological effects of low doses of ionizing radiation. It is our goal to study the radiobiological effects of those levels of radiation - the medical imaging levels, that characterizes the Nuclear Medicine and Radiology typical environments.

## OP350

### Individual dosimetry planning using the conjugate view mode with reduced scan time for improved patient compliance

**G. Dobrozemsky**[1], S. Witoszynskyj[1], T. Beyer[2], M. Hoffmann[1]; [1]Department of Radiology and Nuclear Medicine, Clinical Department of Nuclear Medicine, Medical University Vienna, Vienna, AUSTRIA, [2]Centre for Biomedical Technology and Medical Physics, Medical University Vienna, Vienna, AUSTRIA.

**Aim** Subject-specific dosimetry planning (DP) for radionuclide therapy (RNT) is mandatory. The conjugate view method (CVM) is a well-established method for DP whereby dynamic data is derived from a series of whole-body, planar scintigraphies to determine pharmacokinetics of target tissue and organs at risk. However, many patients experience pain during these scans and cannot remain still for extended imaging times. Therefore, our goal is to reduce the scan duration by shortening the scan length during CVM without compromising data integrity. **Materials and Methods** This is a retrospective study based on 10 patients subject to RNT with [Lu-177]-DOTATATE. All patients underwent routine DP following the injection of 3,7 GBq [Lu-177]-DOTATATE. Six whole body scans were performed from 30 min to 140 hours p.i. with a speed of 10 cm/min. Our assumption is that the activity in distal legs can be extrapolated from the activity in the upper thighs covered in the upper 70% of the scan (head, torso and upper thighs only). We therefore compare the measured total body counts for each of the scans (anterior and posterior view) to the counts calculated from the upper 70% of the scan (simulating a partial body scan of head, torso and upper thighs only), while extrapolating for the lower 30%. This was performed by multiplying the counts in the upper thighs for all scans following the initial scan by the ratio of counts for total legs to upper thighs derived from the first scan. **Results** Preliminary evaluation of 10 patients indicated the extrapolation method to reproduce the counts in the "disregarded" extremities with a mean error of 12% (max. 16%). The resulting difference in whole-body counts was less then 2%. This small impact is based on the fact that the counts in the legs only contribute 5% to 16% to the total body counts for this tracer. **Conclusion** Our data indicate that the total scan length in the CVM can be reduced by covering the torso only, thereby reducing the total scan duration by about 30%, or 5 min, respectively. The resulting difference in DP was less then 2% for the determination of total body counts in later scans.

## OP351

### Liver Internal Selective Radiation Therapy with 90Y microspheres: comparison between different pre-treatment activity calculation Methods

**M. Bernardini**[1], C. Smadja[1], M. Faraggi[2], P. Weinmann[1], S. Orio[1], N. Ghazzar[1]; [1]European Georges Pompidou Hospital, Paris, FRANCE, [2]Princesse Grace Hospital, Monaco, MONACO.

**Aim**: Our purpose was to compare different Methods of calculating $^{90}$Y microspheres activity for liver treatment by Internal Selective Radiation Therapy (SIRT). Such comparison is not yet available and is needed in clinics to optimize patient specific dosimetry. We also investigated lungs breakthrough (LB) calculation and its impact on the maximum injectable activity. **Materials and Methods:** 31 consecutive evaluations based on $^{99m}$Tc macro-aggregates (MAA), followed by 25 treatments with $^{90}$Y microspheres SIR-spheres® (SIRTEX) were performed. Tumor and healthy liver volumes were determined by the interventional radiologist on anatomical images acquired with a standard contrast enhanced CT (ceCT) protocol. To determine the Tumor to Normal liver uptake ratio (T/N), regions of interest (ROIs) were drawn on $^{99m}$Tc MAA SPECT/CT images acquired with a hybrid gamma camera Infinia-Hawkeye (GE). The ROIs were drawn by both a nuclear physicist and a physician via a triple fusion between SPECT/CT data, ceCT and either PET or MRI. For each treatment, four different Methods of calculating $^{90}$Y activity were applied retrospectively: three based on Body Surface Area (BSA-1, BSA-2 and BSA Kennedy) and one based on MIRD formalism (Partition Model). Relationships between calculated activities, LB, T/N ratio and tumor involvement were investigated. In the same way, lobar and total liver treatments were analysed separately. **Results:** When attenuation correction was not considered, overestimation of LB was on average 65%, but in any case the estimated lungs' doses were below 30 Gy. Moreover, LB was not significantly related to the T/N ratio, neither to tumor involvement nor Radiochemichal Purity. Differences in calculated $^{90}$Y activities were extremely large, being greater for lobar treatments (from -85% to 417%) than whole liver treatments (from -49% to 58%). Besides, two values of T/N ratio were identified as thresholds: one for BSA-based Methods (average dose to healthy liver is higher than 30 Gy for T/N≤3) and one for partition model (average dose to tumor is higher than 120 Gy for T/N≥4). **Conclusion:** The maximum injectable activity is not limited by lungs' irradiation. As the partition model accounts for differences in uptake between normal and tumour liver, thus optimizing the risk-benefit ratio, this method should be preferred over BSA-based Methods. Nevertheless, partition model assumes an adequate match between MAA and $^{90}$Y microspheres that should be investigated with further studies. Calculating doses with partition model partially introduces a bias that would be removed using a gold standard method such as Monte Carlo simulations.

## OP352

### Absorbed Dose in Molecular Radiotherapy: a Comparison Study of Monte Carlo, Dose Voxel Kernels and Phantom Based Dosimetry

**S. Marcatili**[1], T. Mauxion[1], D. Villoing[1], B. J. McParland[2], M. Bardiès[1]; [1]UMR 1037 INSERM/UPS, Centre de Recherche en Cancérologie de Toulouse, Toulouse, FRANCE, [2]Imaging Technology Group, GE Healthcare Medical Diagnostics, Amersham, UNITED KINGDOM.

**Aim** The Aim of this study was to perform a critical comparison of three dosimetric approaches in Molecular Radiotherapy: phantom based dosimetry, Dose Voxel Kernels (DVKs) and full Monte Carlo (MC) dosimetry. The objective was to establish the impact of the absorbed dose calculation algorithm on the final result. **Materials and Methods** We calculated the absorbed dose to various organs in six healthy volunteers injected with a novel 18F-labelled PET radiotracer from GE Healthcare. Each patient underwent from 8 to 10 whole body 3D PET/CT scans. The first 8 scans were acquired dynamically in order to limit co-registration issues. Eleven organs were segmented on the first PET/CT scan by a physician. We analysed this dataset using the OLINDA/EXM software taking into account actual patient's organ masses; the commercial software Stratos by Philips implementing a DVK approach; and performing full MC dosimetry on the basis of a custom application developed with Gate. The calculations performed with these three techniques were based on the cumulated activities calculated at the voxel level by Stratos. **Results** All the absorbed doses calculated with Gate were higher than those calculated with OLINDA. The average ratios between the Gate absorbed dose and OLINDA's was 1.38±0.34 σ (from 0.93 to 2.23) considering all patients. The discrepancy was particularly high for the thyroid, with an average Gate/OLINDA ratio of 1.97±0.83 σ for the 6 patients. The lower absorbed doses in OLINDA may be explained considering the inter-organ distances in the MIRD phantom. These are in general overestimated, leading to lower absorbed doses in target organs. The differences between Stratos and Gate resulted to be the highest. The average ratios between Gate and Stratos absorbed doses were 2.51±1.21 σ (from 1.09 to 6.06). The highest differences were found for lungs (average ratio 4.76±2.13 σ), as expected, since Stratos considers unit density material. The high discrepancies observed also depend on the relative small size of the DVK matrix implemented in Stratos, that underestimates the photon contribution to the absorbed dose. **Conclusions** Though OLINDA and Stratos can produce reliable absorbed doses for beta emitting radionuclides, they may be too approximate for photon dosimetry. For target organs, whose dose mainly depends on photon irradiation, the stylized geometry of the MIRD phantom is not able to reproduce realistic photon ballistics. At the same time, the reduced size of the Stratos DVK matrix prevents the propagation of photons from the source organs to the targets.

## OP353

### Absorbed dose distributions from 99mTc-MAA-SPECT and 90Y-PET in selective intravascular radionuclide therapy (SIRT): a phantom and patient study

**T. Eugene**[1], T. Carlier[1], A. Faivre-Chauvet[1], F. Kraeber-Bodere[1], R. Lebtahi[2], I. Gardin[3], A. Dieudonné[2]; [1]Nuclear Medicine Department, Nantes University Hospital, Nantes, FRANCE, [2]Nuclear Medicine Department,

Beaujon Hospital, Paris, FRANCE, [3]Nuclear Medicine Department, Cancer Center, Rouen, FRANCE.

**Objectives**: Pre-treatment 99mTc-MAA-SPECT is the standard tool for managing patients in hepatic SIRT and 90Y-PET proved to be a reliable post-treatment dosimetry index. This study Aims at comparing absorbed dose (AD) distributions obtained from these 2 modalities, in both experimental and clinical situation. **Methods:** The study involved 8 procedures (lobar injection) on 6 patients treated with SIRT using resin micro-spheres for HCC. For the experimental part, we used the IEC torso-shaped phantom with six spheres (0.5 to 26.5 mL) filled with free 90Y: 5.6 MBq/mL and 99mTc: 1.4 MBq/mL. All the images were acquired on a mCT PET/CT (Siemens) and a Symbia SPECT/CT (Siemens) and reconstructed with OP-OSEM-PSF-TOF for PET and OSEM including, attenuation and scatter corrections for SPECT. AD maps were subsequently computed with the software VoxelDose (Dieudonné et al). The PET-based dosimetry was performed using direct absolute quantification and the SPECT-based dosimetry from the 90Y prescribed activity. The average absorbed dose (AAD) and dose volume histograms (DVH) were calculated in the treated lobe, and D20 and D50 (median) subsequently derived. PET and SPECT differences were calculated using the SPECT as reference . **Results:** In the phantom study, for spheres between 1.5 and 26.5 mL, the AAD differed from -1 to 6% and the DVH curves looked similar in shape. The D20 and median differed from -6 to 13 % except for the median of the 10.5 mL sphere being 20 %. In patients, the AAD differed by 20 % [-24 to 52 %], D20 by 23 % [-0.7 to 61 %] and D50 by 43 % [-12.4 to 168 %]. The prescribed activity was 990 MBq in average [450 - 1900 MBq], while the average activity measured on PET dataset was slightly superior: 1167 MBq [433 - 2776 MBq]. When correcting the activity differences between prescription and PET measurements, the differences were reduced to 6 % for AAD, 11 % for D20 and 24 % for D50, underlying the impact of 90Y activity measurement. **Conclusions:** Our work suggests that PET and SPECT data lead to similar results for experimental object larger than 1.5 ml (difference < 10 %). However, in our small sample of clinical data AD distributions appear to be significantly different, partly due to errors in the Y90 activity measurement, and potentially because of different distributions of tracers.

## OP354

### The NUKDOS Software for Dosimetry in Molecular Radiotherapy

**P. Kletting**[1], S. Schimmel[1], H. Hänscheid[2], M. Fernandez[2], J. Bröer[3], D. Noßke[3], M. Laßmann[2], G. Glatting[4]; [1]Klinik für Nuklearmedizin, Universität Ulm, Ulm, GERMANY, [2]Klinik für Nuklearmedizin, Universität Würzburg, Würzburg, GERMANY, [3]Bundesamt für Strahlenschutz, Fachbereich Strahlenschutz und Gesundheit, Oberschleißheim, GERMANY, [4]Medical Radiation Physics/Radiation Protection, Medical Faculty Mannheim, Heidelberg University, Mannheim, GERMANY.

**Aim**: The NUKDOS software is developed to improve and standardize therapy planning in molecular radiotherapy (MRT). **Methods**: NUKDOS is developed in Matlab, based on the MIRD formalism, modularly structured and currently allows dosimetry for Y-90, Lu-177, I-131. First, the user enters the basic patient data and specifies the injected activities. Second, 3D or 2D images can be loaded. Based on the voxel-size and the used nuclide the corresponding voxel S-values (>1 mm) are calculated. Serum, probe or urine data can be entered and processed. To get the activity distribution of the organs for all serial measurements, the user is led to the image processing tool. This tool includes all functionality for defining the regions or volumes of interest (ROIs/VOIs). ROIs/VOIs can also be created in a corresponding CT image and subsequently transferred to the SPECT/PET images. Time activity curves (TACs) derived from 2D scans are scaled using the averaged organ activity of a 3D image. To determine the time-integrated activity coefficients $\tilde{a}$, the areas under the time activity curves are calculated. For this purpose, a set of fit functions can be chosen. The selection of the most suitable function is based on the Akaike Information Criterion and statistical measures. The most suitable TACs are integrated analytically and including the standard errors. Absorbed dose coefficients are calculated by convolution using the voxel based $\tilde{a}$ and S value matrices. Depending on the absorbed dose (or biologically effective dose) for the limiting organ the activity to administer along with the pertaining organ doses is calculated using the absorbed dose coefficients. **Results**: Proper implementation of the mathematical Methods of each module of the software was tested by comparing the results to currently available software. The applicability of the software was investigated using phantom measurement and examples from MRT. User interaction is minimized; plausibility checks are available. The results are reproducible; the error propagation calculation of the absorbed doses adds additional benefit. **Conclusion**: The software represents a summary/unification of currently used Methods from image data processing to the absorbed dose and biological effective dose calculation for specific treatment scenarios. Features like the assignment of errors for all results, an objective method for model selection and inference are provided. NUKDOS promises to increase accuracy, reproducibility and documentation as a prerequisite for determining a dose-effect relationship in MRT dosimetry.

## OP355

### Generation of scintigraphic images in a virtual dosimetry trial based on Monte Carlo modelling

**D. VILLOING**[1], M. GARCIA[1], I. BERRY[2], F. BOTTA[3], S. BRILLOUET[1], O. CASELLES[4], E. CASSOL[2], F. COURBON[1], M. CREMONESI[5], M. FERRARI[3], L. FERRER[6], M. POIROT[1], D. VALLOT[4], M. BARDIES[1]; [1]INSERM / UPS, UMR 1037, CRCT, Toulouse, FRANCE, [2]CHU Rangueil, Département de Médecine Nucléaire, Toulouse, FRANCE, [3]European Institute of Oncology, Milano, ITALY, [4]Institut Claudius Régaud, Toulouse, FRANCE, [5]European Institute of Oncology, Toulouse, FRANCE, [6]ICO René Gauducheau, Saint-Herblain, FRANCE.

**Aim** The purpose of dosimetry calculations in therapeutic nuclear medicine is to maximize tumour absorbed dose while minimizing normal tissue toxicities. However a wide heterogeneity of dosimetric approaches is observed: there is no standardized dosimetric protocol to date. The DosiTest project (www.dositest.com) intends to identify critical steps in the dosimetry chain by implementing clinical dosimetry in different Nuclear Medicine departments, on scintigraphic images generated by Monte Carlo simulation from a same virtual patient. This study Aims at presenting the different steps contributing to image generation, following the imaging protocol of a given participating centre, Milano's European Institute of Oncology (IEO). **Materiel and Methods** The chosen clinical application is that of 111In-pentetreotide (OctreoscanTM). Pharmacokinetic data from the literature are used to derive a compartmental model. The kinetic rates between 6 compartments (liver, spleen, kidneys, blood, urine, remainder body) were obtained from WinSaam[3]: the activity in each compartment is known at any time point. The TestDose[1] software (computing architecture of DosiTest) implements the NURBS-based phantom NCAT-WB[2] to generate anatomical data for the virtual patient. IEO gamma-camera was modelled with GATE[4] v6.2. Scintigraphic images were simulated for each compartment and the resulting projections were weighted by the respective pharmacokinetics for each compartment. The final step consisted in aggregating each compartment to generate the resulting image**. Results** Following IEO's imaging protocol, planar and tomographic image simulations were generated at various time points. Computation times (on a 480 virtual cores computing cluster) for "step and shoot" whole body simulations (5 steps/time point) and acceptable statistics were: 10 days for extra-vascular fluid, 28h for blood, 12h for liver, 7h for kidneys, and 1-2h for bladder, spleen and 1-2 cm3 tumours. With 15 projections per head (on a virtual 4-headed gamma-camera), tomographic simulations were 3 times longer. GateLab[5] was used to reduce computation times by a factor 2. **Conclusion** The generation of realistic scintigraphic images was successful with an acceptable computation time. We are now able to send a complete dosimetry dataset to our first participating centre (IEO). The next step will be to compare their dosimetric results with a GATE-based reference dosimetry derived directly from the pharmacokinetics. The results of that comparison will be presented. [1] Garcia et al. Proc. SPIE, Medical Imaging. 2013 [2] Segars et al. IEEE Trans Nucl Sci. 1999. [3] Stefanovski et al. Metabolism. 2003 [4] Jan et al. Phys Med Biol. 2011 [5] Camarasu-Pop et al. Future Generation Computer Systems. 2013

## OP356

### IDAC2.0 a new generation of internal dosimetric calculations for diagnostic examinations in nuclear medicine using the adult ICRP/ICRU reference computational voxel phantoms

**M. Andersson**[1], L. Johansson[2], D. Minarik[1], S. Mattsson[1], S. Leide-Svegborn[1]; [1]Medical Radiation Physics, Department of Clinical Sciences Malmö, Lund University, Malmö, SWEDEN, [2]Department of Radiation Sciences, Umeå University, Umeå, SWEDEN.

**Aim and background**: The International Commission on Radiological Protection (ICRP) Task Group 36 (TG 36) has the commission to propose biokinetic data and estimates of absorbed doses to organs and tissues and the effective dose to patients from various radiopharmaceuticals. To this date the program IDAC1.0 has been used to perform the dose calculations and OLINDA-EXM as an independent validation of the calculations. Both these calculations are based on photon specific absorption fractions (SAF) simulated from the mathematical phantoms created by Cristy and Eckerman in 1987 while the kinetic energy of electrons is mainly assumed to be absorbed locally. To improve the accuracy of the calculations, ICRP has now adopted a more realistic voxel phantom to incorporate in Monte Carlo (MC) simulations of new electron and photon SAF-values. The internal dosimetry computer program, IDAC, has been substantially upgraded (IDAC2.0) and incorporates these new SAF-values for calculations of the absorbed doses and the effective dose. **Material & Methods**: With IDAC2.0 it is possible to calculate the dose from 1252 different radionuclides. The program uses the latest biokinetic models and assumptions of the ICRP TG 36, which also includes the incorporation of the Human Alimentary Tract Model (ICRP 100) and the latest tissue weighting factors (ICRP 103). The S-values are generated through mono-energetic photon and electron SAF-values from the new voxel phantom and decay data of ICRP publication 107. The input data of the source regions included in the model for the absorbed doses and effective dose calculations in IDAC2.0 can be given in a

descriptive biokinetic model or by constructing a compartment model with defined transfer coefficients or just as the total number of disintegrations per unit administered activity. Absorbed doses and the effective dose are calculated and presented here for 120 different radiopharmaceuticals based on earlier published biokinetic data (ICRP 53, ICRP 80 and ICRP 106). **Results & Conclusions**: The effective doses are in general lower (in 60 % of the cases) with the voxel phantom and the latest tissue weighting factors compared to data for the previous phantom and old tissue weighting factors. Absorbed doses and the effective dose calculated with IDAC2.0 are consistent with the prior published results using the same voxel phantom. Calculations with IDAC2.0 will give a more realistic estimation of the radiation-induced risk from nuclear medicine examinations.

909 - Monday, Oct. 21, 14:30 - 16:00, Rhône 3A/3B

## Physics & Instrumentation & Data Analysis: CZT - Gamma Probes

## OP357

### Dual isotope global and regional left ventricular function using semi-conductor cadmium zinc telluride (CZT) camera: a dynamic cardiac phantom study

**T. Blaire**[1,2], A. Bailliez[1,2], D. Legallois[3], C. Desmonts[3], D. Agostini[3], A. Manrique[3,2]; [1]Nuclear Medicine, Polyclinique du Bois, Lille, FRANCE, [2]Normandie Université - EA4650, Caen, FRANCE, [3]Nuclear Medicine, CHU de Caen, Caen, FRANCE.

**Objectives:** New Cadmium-zinc-telluride (CZT) cameras have dramatically increased sensitivity and energy resolution. Combining the use of 123I-metaiodobenzylguanidine with technetium-99m myocardial perfusion agents could allow simultaneous assessment of myocardial perfusion, LV function and sympathetic innervation in patients with dilated cardiomyopathy. This phantom study compared the evaluation of global and regional left ventricular function in dual isotope conditions using a CZT camera (DNM 530c, GE Healthcare). **Materials and Methods:** The Amsterdam gated (AGATE) dynamic cardiac phantom (Vanderwilt techniques, Boxtel, NETHERLANDS) was successively filled with a solution of 123I alone, 99mTc alone, and a mixture of 123I and 99mTc. A total of 36 datasets were acquired using both energy windows (99mTc or 123I) in all cases, with the following parameters: 10-minute acquisition, contraction rate of successively 70 and 85 bpm, and ejection fraction (EF) set to 33%, 45% and 60%. EDV, ESV, EF, regional wall thickening and motion (17-segment model) were assessed using QGS. **Results:** Myocardial volumes using single (123I, 99mTc) and dual isotope (reconstructed using both 123I and 99mTc energy windows) acquisitions were respectively for EDV (mL): 89±47 vs. 89±50 vs.91±47 vs. 90±47, ESV (mL): 41±2 vs. 41±3 vs. 42±3 vs. 42±2, EF (%): 52±23 vs. 51±23 vs. 51±24 vs. 51±22 (p= NS), regional thickening (%): 48±64 vs. 46±59 vs. 46±63 vs. 45±57, regional motion (mm): 6.6±5.3 vs. 6.8±5.5 vs. 6.7±5.8 vs. 6.6±5.4. Using MANOVA and Kruskal Wallis test, no significant difference was found between successive and simultaneous dual isotope acquisitions in wall thickening (%), regional motion (mm), EF and EDV values (All p values = NS). Only ESV was significantly underestimated with 123I acquisitions in the 99mTc energy window, leading to overestimate EF (p<0,001). Bland Altman plots and Lin's concordance correlation coefficient (CCC) showed an excellent concordance between regional wall thickening and motion (CCC>0.91). **Conclusion:** In this phantom study, the DNM 530c CZT camera, with higher energy resolution and sensitivity yielded no significant difference between single (successive) isotope and simultaneous dual isotope acquisition.

## OP358

### Comparison of Gated Blood-Pool Ejection Fraction Techniques using a CZT SPECT system and a reference free ranking approach.

**Y. R. PETEGNIEF**[1], R. SABBAH[1], M. LEFORT[2], S. PERLONGO[1], C. CAODURO[1], F. FROUIN[2], H. BOULAHDOUR[1]; [1]CHRU Jean Minjoz, Besançon, FRANCE, [2]LIF UMR S678 UPMC, Paris, FRANCE.

We proposed to compare the accuracy of four previously described Methods for the measurements of left and right ventricular ejection fractions (LVEF and RVEF) using a cadmium-zinc-telluride (CZT) camera for gated blood pool (GBP) SPECT studies and a scintillation camera for equilibrium radionuclide ventriculography (ERNV). The reference-free statistical regression method, "extended Regression without Truth" (eRWT), relies on a parameterized Beta distribution of the EF and a linear relationship between calculated EF and the true values. eWRT was applied to rank Methods according to their accuracy derived by a figure of merit (Fm). Sixty seven patients (75% male) with known or suspected heart disease underwent a 5 minutes GBP SPECT study (list-mode, 16 gated bins) using a stationary pin-hole CZT system. GBP analysis were performed with 3 different segmentation Methods i) a semi-automated iterative threshold segmentation technique coupled to a count-based (M1) or a volume-based (M2) EF calculation, ii) a watershed immersion algorithm (M3), and an automated ventricular surface calculation (M4). Thirty six patients with known cardiac pathologies underwent also a LAO ERNV using a gamma camera and a semi-automated technique (M5) was used for EF assessment. In 2 GPB studies, automated Methods failed because of large dyskinetic abnormalities. The ranking of the 4 SPECT techniques gave the most accurate estimates -i.e. lower Fm- for M2 estimates of both the LVEF (Fm for M2=0.0042 vs. 0.0061-0.0068 for others) and the RVEF (0.003 for M2 vs. 0.006-0.018 for others). When ERNV was included in eWRT, the most accurate techniques were M3 and M2 (Fm = 0.0039 and 0.0046 respectively) for LVEF and still M2 (Fm:0.005) for RVEF. Planar estimates were less accurate. Fast and accurate GBP studies were obtained with a CZT system and analyzed with available segmentation software. The eWRT ranking approach clearly exhibited the superiority of a semi automated approach (M2) for the two databases designed with different sizes and clinical background.

## OP359

### Optimized dose regimen for myocardial perfusion imaging using CZT-SPECT

**J. D. van Dijk**[1,2], P. L. Jager[1], M. Mouden[3], C. H. Slump[2], J. A. van Dalen[1]; [1]Isala klinieken, Department of Nuclear Medicine, Zwolle, NETHERLANDS, [2]University of Twente, MIRA Institute for Biomedical Technology and Technical Medicine, Enschede, NETHERLANDS, [3]Isala Klinieken, Department of Cardiology, Zwolle, NETHERLANDS.

**Aim** Guidelines for SPECT myocardial perfusion imaging (MPI) traditionally recommend a fixed amount of administered Tc-99m dose for all patients which has also been implemented for Cadmium Zinc Telluride (CZT) SPECT based-protocols. However, clinical practice shows degraded image quality in more obese patients, and currently there is a strong general towards lower radiation exposure. Therefore the objective was to optimize the administered dose and scan time for CZT SPECT, to provide constant image quality, less depending on the patient's physical characteristics. **Materials and Methods**: 126 patients underwent CZT-based SPECT MPI (Discovery NM 570c, GE Healthcare) using 370 MBq and 500 MBq Tc-99m tetrafosmin for patients > 100 kg. Adenosine stress imaging was performed 60 min post injection using 5 min acquisitions. For each patient the number of photon counts was measured within a 20% energy window centered at 140 keV and normalized to the administered amount of radioactivity ($C_{norm}$). Subsequently, various parameters (body mass, BMI, mass per length, lean body mass, fat mass, waist size) were correlated with $C_{norm}$, to find the best predictive parameter. Each patient specific parameter (P) was fitted to $C_{norm}$ using the power-law function: $C_{norm} = a \cdot P^{-b}$, with a and b as fit parameters. Consequently, the recommended dose to administer was determined, described by $A_{admin} = C \cdot P^{b} / (a \cdot Tscan)$, with C being the preferred number of counts for adequate images and $T_{scan}$ the scan time in min. **Results**: $C_{norm}$ decreased with increasing values of all patients' specific parameters ($p<0.001$), implying an image degradation for more obese patients. Body mass proved to be the best predictive parameter, with an absolute mean fitting error of 15% and $R^2$ of 0.62. The best fitting results were obtained when fit parameter b was equal to 1, i.e. an inversely linear relation between body mass and $C_{norm}$ was found. Consequently, the recommended dose is linearly related to body mass. In order to obtain a constant preferred number of counts (based on the current mean number of 1.2 Mcounts) we derived the following dose calculation formula: $A_{admin}(MBq) = 23.8 \cdot \text{body mass (Kg)} / \text{Tscan (min)}$. **Conclusion**: A fixed amount of Tc-99m dose is suboptimal for CZT-based SPECT MPI. It is preferable to administer a dose that depends linearly on patient's body mass to provide more constant image quality which is less depending on patient's physical characteristics.

## OP360

### Role of Contrast Enhanced CT (CECT) PET/CECT in Staging Of Carcinoma Gall Bladder Over Non Enhanced Low Dose CT (NECT) PET/NECT

**A. Tiwary, Jr.**[1], A. G. Vyas, Sr[2]; [1]Army Hospital R&R, New Delhi, INDIA, [2]NMC Imaging at VIMHANS Hospital, New Delhi, INDIA.

**Aim:** To evaluate the additional role of Contrast Enhanced CT (CECT) F-18FDG PET/CECT in Staging of Carcinoma Gall Bladder over Non Enhanced Low Dose CT (NECT) PET/NECT **Methods**: Total 88 F-18FDG PET/CT scans were performed in patients with carcinoma of gall bladder, for attenuation correction whole body NECT was performed followed by a diagnostic CECT with intravenous contrast agent. Criteria for evaluation were signs of vital tumor tissue (extent of lesions, contrast enhancement & maximum standardized uptake value -SUVmax) specially in N and M staging. Combined analysis of PET/NECT and PET/CECT were evaluated separately by two different PET experts. Findings were verified histologically (where ever possible), tumor markers and/or clinical follow up (12 months). **Results**: Total 237 lesions were analyzed and 161 proved to be metastatic. The sensitivity, specificity, positive predictive value, negative predictive value & accuracy of PET/NECT were 88%, 78.9%, 85.7%, 86.3% and 83% respectively and for PET/CECT were 95%, 93%, 94%, 96.7% and 95% respectively. Compared to

PET/NECT the PET/CECT obtained additional 23 lesions -perihepatic/ peritoneal deposits (n=5), hepatic metastases (n=7) and small abdominal lymph nodes (n= 9), serosal deposit (n=1) and brain lesion (n=1). On.PET/NECT had 13 false negative findings (retroperitoneal lymph nodes (n = 5), liver lesions (n= 3), meditational lymphnodes (n= 3), lung metastasis (n= 1) & peritoneal deposit (n=1) .On PET/CECT had 3 false negative findings bone (n= 2) & liver (n= 1). **Conclusion:** Overall PET/CECT changed staging of 8 patients. Our results indicate that PET/CECT instead of PET/NECT may be a better tool for staging of carcinoma gall bladder, prior to selection of most appropriate treatment. The ability to fully evaluate the patient in a single combined imaging modality rather than multiple conventional imaging studies is advantageous if the performance is equal to or better as it adds to better patient care.

## OP361

### Evaluation of 177Lu-SPECT Quantification Using the 112 and 208 keV Photopeaks for Tumor Dosimetry

**A. Dieudonné**[1,2], M. Ben Reguiga[1,3], S. Burg[4,5], I. Buvat[6], D. Le Guludec[1,4,5], R. Lebtahi[1,3]; [1]APHP - Service de Médecine Nucléaire - Hôpital Beaujon, Clichy, FRANCE, [2]INSERM U773, CLichy, FRANCE, [3]INSERM U773, Clichy, FRANCE, [4]APHP - Service de Médecine Nucléaire - Hôpital Bichat, Paris, FRANCE, [5]INSERM U698, Paris, FRANCE, [6]IMNC, UMR 8165 CNRS, Orsay, FRANCE.

**Introduction** 177Lu-peptide receptor radionuclide therapy (177Lu-PRRT) is based on the 177Lu beta emission (500 keV, 100 %). The associated photon emissions enable SPECT imaging for tumor dosimetry. The purpose of this study was to evaluate the use of the 112 (6.5 %) and 208 keV (10 %) photo-peaks for tumor dosimetry. **Materials and Methods** The experiment was set up to meet clinical constraints (i.e. activity concentrations and acquisition parameters), with a cylindrical Jaszczak phantom (Data Spectrum Corporation) including 6 fillable spheres (0.5 to 16 mL, 1.18 MBq/mL activity concentration) and 0.127 MBq/mL in the background. The phantom was scanned with a Symbia T2 (Siemens Healthcare) SPECT/CT device (3/8" NaI crystal) with the 112 keV±10 % and 208 keV±7.5 % photopeak windows, and 3 10%-wide energy windows to record scatter centered on 92, 137 and 189 keV. Three acquisitions of 60 projections each in a non-circular orbit were performed with 10, 50 and 100 kcounts per projection in the 208 keV window. The data were reconstructed using Flash3D (Siemens Healthcare), including attenuation and scatter corrections. The number of iterations was chosen so as to get the same signal-to-noise ratio (SNR) in the homogeneous part of the phantom. Activity measurements were performed within regions of interest (ROI) defined on the CT and using partial volume effect compensation (PVC) based on the inversion of the geometric transfer matrix (GTM), assuming an isotropic point spread function (PSF) with full width at half maximum (FWHM) estimated from independent line source experiments. **Results** For PVE compensation, the PSF FWHM was 12 mm in the reconstructed 10k dataset and 7 mm in the 50k and 100k datasets. For the 10k dataset, the activity recovery was 91, 86, 71, 66, 84 and 77 % in the 16, 10, 4, 2, 1 and 0,5 mL spheres respectively. For the 50k dataset, these activity recovery values were 96, 91, 80, 62, 53 and 44 % respectively. For the 100k dataset, they were 98, 98, 86, 64, 56 and 46 % respectively. **Conclusion** 177Lu-SPECT (112 & 208 keV) quantification with clinical tools and additional PVC allows for accurate activity recovery in spheres above 4 mL in volume for both high and low statistical levels. Feasibility of accurate PVC in realistic patient activity distributions remains to be studied.

## OP362

### Preliminary evaluation of a novel high-resolution hybrid gamma/optical camera for intraoperative imaging

**S. Bugby**[1], J. Lees[1], D. Bassford[1], E. Blackshaw[2], A. Perkins[2]; [1]University of Leicester, Leicester, UNITED KINGDOM, [2]Queen's Medical Centre, Nottingham, UNITED KINGDOM.

**Introduction** We have developed a novel handheld hybrid gamma/optical small field of view (SFOV) camera that provides an optical image overlaid with a scintigraphic image. The compact size and fused image display makes it ideal for use in the operating theatre where the optical information can aid surgeons in localising the site of uptake, such as in sentinel node detection. This study investigates the performance characteristics of the system and compares images from the hybrid and a standard large field of view (LFOV) gamma camera. **Materials and Methods** The hybrid camera consists of a 0.5mm thick CsI(Tl) columnar scintillator coupled to an electron multiplying CCD. A 0.5mm diameter pinhole collimator gives a 40mm x 40mm nominal field of view for an 8mm x 8mm detector area. An optical camera is aligned to provide the same field of view as the gamma camera. Optical and gamma images are taken simultaneously and fused to produce an augmented reality image display, providing information from the gamma camera within an optical context. Performance characteristics including sensitivity, spatial resolution, and count rate response, were investigated based on NEMA protocols adapted for use with high resolution SFOV systems. Images were obtained in laboratory simulations and from patients attending the nuclear medicine clinic with further scenarios investigated through Monte Carlo simulations. **Results** The characteristics of the hybrid camera compared favourably with SFOV cameras currently in use. Spatial resolution of less than 1mm was recorded with a system sensitivity of up to 165cps/MBq. Experimental simulations demonstrated the ability to differentiate between adjacent hot sources (ratio of activities less than 1:20) in close proximity, as would be required for differentiation of sentinel nodes from the injection site. Initial clinical studies showed that the site of uptake could be visualised in the patient. **Conclusion** The performance characteristics and small hybrid camera have been described and initial images demonstrate that it is ideally suited for intraoperative imaging. The anatomical context provided by the optical camera aids the physical localisation of radiopharmaceutical uptake. These studies encourage us to carry out further evaluation in the surgical theatre setting.

## OP363

### Hand-held imaging γ-camera for intraoperative use: performances and comparison with a large-FOV γ-camera

**A. Ferretti**, S. Chondrogiannis, M. C. Marzola, L. Rampin, G. Grassetto, A. M. Maffione, D. Rubello; Santa Maria della Misericordia Hospital, Rovigo, ITALY.

**Aim**: In recent years hand-held imaging γ-camera have been increasingly used for intraoperative imaging to perform scintigraphic imaging during surgery. Aim of the present work was to evaluate the physical characteristics of a new high-sensitivity hand-held mini γ-camera through specific phantom measurements. **Materials and Methods**: In order to characterize the hand-held imaging γ-camera Guardian2, we measured its sensitivity and depth transmission curve, the spatial uniformity, extrinsic spatial resolution in depth and the count-rate linearity. We compared the extrinsic spatial resolution of the hand-held γ-camera with a large field-of-view (FOV) γ-camera routinely used for pre-operative lymphoscintigraphy. For this comparison, we also measured the resolution in depth (from 0 to 5 cm of plexiglass). Finally we estimated the whole image quality through the contrast-to-noise ratio of 4 hot spheres (internal diameters ranging from 4.9 to 9.8 mm), evaluated both at contact to the collimator and with a 5cm-thick plexiglass slab interposed. **Results**: The sensitivity of the hand-held γ-camera was 204 counts/sec/MBq, allowing to obtain scintigraphic images of good quality (i.e. sentinel lymph nodes) in few seconds. It showed optimal counts linearity ($R^2$ = 0.999). The uniformity resulted better or similar to previously described portable γ-cameras: integral uniformity of 8.8% and differential uniformity of 4.0% in the central FOV. The system spatial resolution resulted equal to 2.5 mm FWHM at contact to the collimator. In comparison with the large-FOV γ-camera, the hand-held γ-camera showed better spatial resolution at small depth (-40% at contact and -20% with 1 cm of plexiglass interposed between the capillary source and the collimator); this discrepancy decreased until a depth of 4 cm of plexiglass (about 4.8 cm water-equivalent), when the spatial resolution of the two γ-cameras became similar. The system was able to detect and distinguish all the four small spheres used for the whole quality test in both configurations. A limitation of the hand-held γ-camera is the lack of energy calibration tools, to adjust on-site the center of the energy window of acquisition. **Conclusions**: The γ-imaging probe we evaluated demonstrated good sensitivity, count-rate linearity and overall image quality, together with a better spatial resolution in comparison with usual lymphoscintigraphy imaging, allowing confidently use for specific clinical applications in radio-guided surgery.

## OP364

### Development and characterization of a compact gamma-ray spectrometry system for quality control of PET radiopharmaceuticals

S. Vichi[1,2], **A. Infantino**[1,2], G. Cicoria[2], D. Pancaldi[2], M. Marengo[2], F. Lodi[3], D. Mostacci[1]; [1]Nuclear Engineering Laboratory of Montecuccolino, Industrial Engineering Department, University of Bologna, Bologna, ITALY, [2]Medical Physics Department, "S. Orsola-Malpighi" Hospital, Bologna, ITALY, [3]Nuclear Medicine Unit, "S. Orsola-Malpighi" Hospital, Bologna, ITALY.

**Introduction**: In this work we characterized and validated a very compact, USB powered, CdZnTe (CZT) detector for gamma-ray spectrometry applications in Radiopharmacy. This type of detector operates at room temperature, i.e., without need for expensive and cumbersome cooling equipment. The detector was calibrated in energy and efficiency for different geometries and all the acquisition chain was developed for application to quality control of positron emission tomography (PET) radiopharmaceuticals. **Materials and Methods**: a GR1 model (by KromekTM , Sedgefield, UK) a 1 cm3 CdZnTe crystal with all the electronics enclosed in a 25x25x63mm containment, was utilized. The detector was placed in a 5 cm thick lead shielding; a plastic sample holder was used to secure a reproducible acquisition geometry. Acquisitions were recorded using the software driver KSpect 1.1.6. Energy and efficiency calibrations were performed using certified standard sources in three different geometries: point source, 1 cm3 tube and 5 cm3 vial, all at 6 cm distance. Samples of [18F]FDG and [68Ga]-DOTANOC were measured to

assess radionuclidic purity and results were compared with those of an HPGe detector ( relative efficiency 15% , resolution 1.8 keV @ 1332 keV). **Results and Conclusions**: The energy resolution obtained for the Kromek GR1 was 1.5% (10.3 keV) at 662 keV and to 1.1% (14.5 keV) at 1332 keV, while the efficiency response at the same energies was 7E-3 % and of 2E-3 %, respectively, in 1 cm3 tube geometry. The energy resolution obtained is fully adequate for QC of PET radiopharmaceuticals, even though, at energies lower than 100 keV, peak resolution is suboptimal. Analysis of [18F]FDG and [68Ga]-DOTANOC samples proved to be comparable to those obtained using a HPGe detector (max activity deviation 2%). The order of magnitude of the minimum detectable activity (MDA) at 511 keV was of 2 Bq for annihilation photons of 18F and 68Ga. For impurities like 57Co, 60Co, 52Mn and 54Mn the MDA varies from 40 Bq to 120 Bq, whereas for 51Cr it is about 3500 Bq. In conclusion, the performance of small sized CZT detectors seems promising; its reduced dimensions and the energy resolution intermediate between those of NaI(Tl) and HPGe detectors, make this type of devices an extremely attractive tool for QC applications in Radiopharmacy.

910 - Monday, Oct. 21, 14:30 - 16:00, Tête D'Or 1/2

## Molecular & Multimodality Imaging: Novel Tools for Preclinical Imaging

### OP365

### Preliminary evaluation of [18F]DPA-714 in inflammatory processes related to Inflammatory Bowel Diseases (IBD)

**N. Bernards**[1], G. Pottier[1], F. Dollé[2], R. Boisgard[1]; [1]CEA/DSV/I2BM/SHFJ/U1023, Orsay, FRANCE, [2]CEA/DSV/I2BM/SHFJ, Orsay, FRANCE.

Abstract: **Aim**: Inflammatory bowel disease (IBD) is defined as a chronic relapsing idiopathic inflammation of the gastrointestinal tract. The two main clinical forms of this disease family are Crohn's Disease (CD) and Ulcerative Colitis (UC). IBD affects an estimated 3.6 million individuals in Europe and North America. To date it is thought that IBD is the result of continual activation of the mucosal immune system. In order to better understand this disease family an in-house developed animal model was implemented and characterized with [18F]FDG (used to illustrate the increased glucose consumption associated with inflammatory processes) and also with TSPO 18 kDa radioligand [18F]DPA-714, an established radiotracer for the study of inflammation within the central nervous system. **Materials and Methods**: Colonic inflammation was induced in male Wistar rats weighing between 200-250 g by rectal administration of trinitrobenzenesulfonic acid (TNBS) at 4cm from the anal orifice. Control animals were administered, 0.9% aq. sodium chloride analogously. A Siemens Inveon PET/CT tomograph, dedicated to small animals, was used to acquire [18F]FDG images on day 7 post TNBS administration and [18F]DPA-714 images the following day. Rats were then sacrificed by an i.v. injection of pentobarbital, and then the lower intestine was extracted and analyzed by immunohistochemistry to determine macrophage infiltration and the presence of TSPO. **Results**: PET image analysis clearly shows an important accumulation of both radiotracers within the intestinal walls of treated animals in comparison to control animals. Mean levels of [18F]FDG uptake in treated and control animals were 1.20 ± 0.56 %ID/cc and 0.43 ± 0.18 %ID/cc, respectively. Comparable results were found when using [18F]DPA-714, with mean level of uptake in treated and control animals of 1.21 ± 0.62 %ID/cc and 0.46 ± 0.23 %ID/cc, respectively. Immunohistochemistry analysis revealed a higher presence of macrophages in TNBS treated animals. Expression of TSPO was largely increased in the treated animals, when compared to the controls animals, and mainly localized in macrophages cells. **Conclusion:** Preliminary results seem to indicate that [18F]DPA-714 is an adapted tracer for the study of inflammation of IBD in our animal model. Beyond this, data demonstrating that [18F]DPA-714 could be used to characterize and quantify the level of inflammation during the disease evolution, within the TNBS treated animals, will also be presented.

### OP366

### Surface displayed SNAP-tag as a novel tool for study of Gram-positive bacterial infections.

**B. Mills**[1], V. Steele[1], J. C. A. Luckett[1], R. O. Awais[2], P. Duncanson[3], V. Griffiths[3], A. Cockayne[1], M. Xu[4], I. Correa[4], A. C. Perkins[2], P. Williams[1], P. Hill[5]; [1]School of Molecular Medical Sciences, University of Nottingham, Nottingham, UNITED KINGDOM, [2]Radiological and Imaging Sciences, University of Nottingham, Nottingham, UNITED KINGDOM, [3]School of Biological and Chemical Sciences, Queen Mary University of London, London, UNITED KINGDOM, [4]New England Biolabs, Inc, Ipswich, ME, UNITED STATES, [5]School of Biosciences, University of Nottingham, Nottingham, UNITED KINGDOM.

**Introduction**: The design of specific probes for *in vivo* molecular imaging of microbial infections remains one of the greatest challenges to overcome before useful, functional data can be obtained. An increasingly attractive approach for probe design is to express a ligand-binding protein within a cell, which may then covalently bind specific synthetic ligands with attached imaging moieties. One such labelling system is the commercially available SNAP-tag. SNAP-tag specifically and covalently binds O2-benzylguanine (BG) compounds, which may have fluorophores or other functional elements attached at the 4' position of their benzyl ring. We have designed a BG ligand labelled with $^{99m}$Tc, suitable for SPECT imaging. We propose to utilise this technology for the imaging of *Staphylococcal* infection *in vivo* with the view to investigate bacterial pathogenicity and to visualise the effect potential antimicrobials may have on bacterial load. **Methods**: The SNAP-tag gene was codon optimised for expression in the Gram positive bacterium *Staphylococcus aureus* and fused with an N-terminal *spa* secretion leader sequence and a C-terminal *spa* cell-wall anchoring domain. The N-terminal fusion directs the expressed SNAP-tag towards the cell exterior where the C-terminal domain is recognised by the cell-wall sorting enzyme sortase A, covalently anchoring SNAP-tag in such a way that the ligand binding domain decorates the cell surface. A novel $^{99m}$Tc-HYNIC–NH-BG ligand for SPECT imaging was prepared by coupling BG to HYNIC and radiolabelling with $Na^{99m}TcO_4$ in the presence of tricine as co-ligand. Radiochemical yields >99% were obtained. nanoSPECT-CT imaging will be used to assess the functional data produced by using SNAP-tag expressing *S. aureus* cells in *in vivo* infection models. **Results:** We have demonstrated that SNAP-tag was expressed and exported to the cell wall where it was covalently anchored. Deletion of the sortase A enzyme prevented attachment of the SNAP-tag to the cell wall, as determined by Western blot. Once situated within the cell wall, SNAP-tag was functional and able to specifically bind cell-impermeable fluorescent BG ligands and our synthesised precursor HYNIC-$NH_2$-BG ligand, as determined by confocal microscopy and fluorometry assay. Pilot *in* vivo studies for fluorescence optical imaging and nanoSPECT-CT imaging with the novel $^{99m}$Tc-HYNIC-NH-BG ligand are currently under development to visualise *S. aureus* infections in mouse models. **Conclusions**: This approach should allow a higher sensitivity to be achieved when investigating bacterial infections in real time compared to current molecular imaging techniques, thus allowing bacterial virulence and the potential effects of new antimicrobials to be assessed.

### OP367

### Dual imaging of lipopolysaccharides (LPS) by SPECT-CT and Confocal Microscopy.

**M. Moreau**[1], V. Duheron[1,2], B. Collin[1], W. Sali[2], C. Bernhard[1], C. Goze[1], T. Gautier[2], J. Pais de Barros[2], V. Deckert[2], F. Brunotte[3], L. Lagrost[2,4], F. Denat[1]; [1]ICMUB - UMR CNRS 6302, Dijon, FRANCE, [2]INSERM - UMR866, Dijon, FRANCE, [3]Centre Georges-François Leclerc, Dijon, FRANCE, [4]Centre Hospitalier Universitaire, Dijon, FRANCE.

**Introduction**: Lipopolysaccharides (LPS) or endotoxins are found inserted in the outer membrane of Gram-negative bacterias. Their appearance in blood stream triggers a massive secretion of pro-inflammatory cytokines in mammals. A controlled response allows the neutralization and elimination of LPS, whereas an excessive inflammatory response leads to severe circulatory and respiratory defects. It is the endotoxemic shock or septic shock that can leads to death. Many approaches are used to study LPS, including labeling with radiochemicals (3H, 125I, 99mTc or 51Cr) or with fluorophores (FITC, Alexa488, Bodipy). Bimodality is attracting more and more interest in the field of molecular imaging since the combination of two different techniques may provide complementary information, thus improving the accuracy of diagnosis. Combining nuclear modalities (PET or SPECT) with optical imaging is of particular interest, and the similar sensitivities of the two techniques allows to fuse the signaling moieties into a unique molecule, called monomolecular multimodality imaging agent (MOMIA), ensuring a same biodistribution of the two probes. **Method**: A recently described bimodal probe, namely DOTA-Bodipy-NCS, has been covalently attached to LPS. The integrity of the LPS after labeling procedure was checked by SDS-PAGE electrophoresis and β-hydroxymyristate titration (BHM). Pro-inflammatory activity of LPS was assessed by quantification of cytokines released by differentiated THP-1 cells. This bioconjugate was then radiometallated for SPECT-CT biodistribution imaging. **Results:** DOTA-Bodipy-LPS was metallated with 111In to yield a high specific activity (600 MBq.mg-1), with a radiochemical purity >98 % after purification. Biodistribution of the radiolabeled compound was then evaluated in vivo in WT mice by SPECT-CT imaging. Radiolabeled LPS is rapidly eliminated from the bloodstream and accumulates in spleen and liver. Liver slices were then analyzed by confocal microscopy, and specific fluorescent signals in the cytoplasm of hepatocytes were detected, confirming the accumulation of 111In-DOTA-Bodipy-LPS in the liver. **Conclusion**: These results demonstrate the efficiency of the conjugation process of our bimodal probe. It made it possible to perform both non-invasive SPECT and ex vivo fluorescence imaging of LPS biodistribution, underlining its liver uptake for further detoxification. The 111In-DOTA-Bodipy-LPS probe arises here as a relevant tool to identify key components of LPS detoxification in vivo paving the way to therapeutic issues in the field of sepsis. Acknowlegement: Support was provided by the CNRS, the University of Burgundy, the Conseil Régional de Bourgogne.

## OP368

### Detecting Genitourinary Cancer Ex Vivo: Correlation with Histopathologic Findings

S. K. Tripathi, K. Zhang, R. C. Birbe, P. Cotzia, P. A. McCue, C. Solomides, L. G. Gomella, E. J. Trabulsi, **M. Thakur**; Thomas Jefferson University, Philadelphia, PA, UNITED STATES.

**Objectives:** Bladder urothelial cancer (BC) is the 5th most commonly diagnosed malignancy in the USA and one of the most common worldwide. The recurrence rate of BC is >50% mandating long-term surveillance. CT, MR and F-18-FDG imaging demonstrate serious limitations and have low sensitivity in detection of recurrent papillary tumors. C-11-Choline, which has demonstrated high sensitivity for BC suffers from short t½ of C-11. Our long term goal is to target VPAC1 genomic biomarkers, expressed in high density on BC cells, with VPAC1 specific (Kd=3.1x10$^{-9}$M) Cu-64-TP3805 and TP4303 for imaging BC**. Method:** TP3805 was synthesized, characterized, and labeled with Cu-64 for digital autoradiography (DA) or with a near infrared fluorophore (TP4303) for optical imaging (OI). Formalin-fixed paraffin embedded sections from a tissue microarray of 100 patients (75M, mean age 70.2±11 yrs. (45-89), and 25F, mean age 71.4±9.3 yrs. (54-89) with high grade BC (stage pT1-T4b) and 5 normal subjects (3M, 2F)), were obtained from institutional tissue library and incubated at ambient temperatures for 15 min, either with Cu-64-TP3805 (10±2 μCi) or TP4303 (1 nm). After thorough PBS washes, tissues were air dried, DA was performed using Kodak Image Station 4000R (Bruker) and OI was carried out using FX-Pro OI system (Bruker). ROI analysis was performed and malignant lesions to background image intensity ratios were calculated for tissue slice of each subject. Data were correlated with histologic findings**. Results:** All histologically malignant and healthy tissue specimens demonstrated Cu-64-TP3805 and TP4303 uptake, with 100% corroboration. The Cu-64-TP3805 mean signal to noise ratio (SNR) was 4.9 (SD 1.3, range 1.9-10.7) and 2.1 (SD 0.4, range 1.4-2.7) for malignant and benign tissue, respectively (p=0.01). The TP4303 mean SNR was 4.7 (SD 1.6, range 2.4-8.5) and 1.4 (SD 0.9, range 0.3-2) for malignant and benign tissue, respectively (p=0.02). All malignant specimens with low SNR had denuded, inflammatory or necrotic cells present on histopathology, and accounted for a low SNR, as inflammatory and necrotic cells barely express VPAC1 oncogenic biomarker. Aggressive BC samples had higher uptake than lower grade BC samples on both DA and OI. (Previous data in our laboratory in humans have shown absence of urinary excretion of Cu-64-TP3805**). Conclusion:** Cu-64-TP3805 demonstrates strong binding to BC tissue which together with its absence in urinary excretion, renders Cu-64-TP3805 worthy of future investigations to image BC in humans. Support: NIH, RO1 CA157372-01 (MLT)

## OP369

### Predicting response to vintafolide therapy using the folate receptor-specific imaging agent, $^{99m}$Tc-etarfolatide

**C. P. Leamon**, J. A. Reddy, P. J. Klein, I. R. Vlahov, M. Vetzel, A. Bloomfield, R. Dorton, M. Nelson; Endocyte Inc., West Lafayette, IN, UNITED STATES.

**Background:** The folate receptor (FR) is overexpressed in many of cancers and represents a potentially relevant target for biomarker and drug development. Vintafolide is a potent folate-targeted vinca alkaloid conjugate currently being evaluated in clinical programs, including a global phase 3 trial for treatment of platinum-resistant ovarian cancer in combination with pegylated doxorubicin, and a randomized phase 2 study for advanced NSCLC. $^{99m}$Tc-etarfolatide is a small-molecular-weight folate-targeted imaging agent that can be used for non-invasive, real-time assessment of functionally active and anatomically accessible FRs. As seen in preclinical models as well as in the clinic, response to vintafolide is dependent on FR expression. Therefore, the ability to screen patients for FR-positive disease in real time is of high value. The Aim of these studies was to determine if $^{99m}$Tc-etarfolatide has the potential to predict response to vintafolide therapy. **Methods:** $^{99m}$Tc-etarfolatide was investigated *in vitro* and *in vivo* using cell lines and mouse xenograft models to evaluate its pharmacologic properties. Relative FR binding affinity of $^{99m}$Tc-etarfolatide was determined using tumor cells in the presence and absence of increasing competitor concentrations of folic acid or vintafolide. The ability of $^{99m}$Tc-etarfolatide to target tumors *in vivo* was examined using BALB/c mice with subcutaneously inoculated tumor cells that could yield 0.1-0.5 g tumors in 20 days. **Results:** $^{99m}$Tc-etarfolatide and vintafolide bind to the FR with high affinity (Kd ~3 nM) in a saturable manner that is dependent on FR expression, but independent of cell type. This was validated by demonstrating the specificity of $^{99m}$Tc-etarfolatide in preclinical models, specifically showing that i) binding of $^{99m}$Tc-etarfolatide to cells and its accumulation within solid tumors correlated with FR expression, and ii) excess folic acid competitively blocked $^{99m}$Tc-etarfolatide's cell/tissue binding. Vintafolide was also found to block $^{99m}$Tc-etarfolatide binding to FR-positive tumors in mice. In cells where $^{99m}$Tc-etarfolatide demonstrated uptake, vintafolide was found to have a correlative cytotoxic effect. Further, cytotoxic effect of vintafolide could be blocked by excess un-labeled etarfolatide. Taken together, these data strongly suggest that vintafolide and $^{99m}$Tc-etarfolatide are distributed similarly *in vivo* and that $^{99m}$Tc-etarfolatide can identify tumors that may respond to vintafolide therapy. **Conclusions:** These findings indicate that the FR mediates tissue binding of $^{99m}$Tc-etarfolatide, and that this radiodiagnostic agent may identify tumors and predict response to folate-targeted drugs, such as vintafolide. This novel approach to predictive medicine may allow for the identification of patients who are likely to benefit from FR-targeted therapy.

## OP370

### HaloTag as a Reporter Gene for Positron Emission Tomography

**H. Hong**, H. A. Benink, H. T. Uyeda, T. E. Barnhart, F. Fan, W. Cai; University of Wisconsin-Madison, Madison, WI, UNITED STATES.

**Aim**: As a versatile tool, the HaloTag technology has attracted much attention for a broad array of biomedical applications such as in vitro optical imaging, in vivo cell labeling/imaging, protein purification/trafficking, study of protein-protein and protein-DNA interactions, high-throughput assays, etc. The HaloTag technology involves two key components: the HaloTag protein and HaloTag ligands (HTLs). The goal of this study is to employ the HaloTag technology as a reporter gene for positron emission tomography (PET), which involves two components: the HaloTag protein (a modified hydrolase which covalently binds to synthetic ligands) and HaloTag ligands (HTLs). **Materials and Methods**: 4T1 murine breast cancer cells were stably transfected to express HaloTag protein on the surface (termed as 4T1-HaloTag-ECS, ECS denotes extracellular surface). Two new HTLs were synthesized and termed NOTA-HTL2G-S and NOTA-HTL2G-L (2G indicates second generation, S stands for short, L stands for long, NOTA denotes 1,4,7-triazacyclononane-N,N'N''-triacetic acid). Microscopy studies were performed to determine the cellular distribution of HaloTag, as well as to evaluate the HaloTag binding efficiency of NOTA-HTL2G-S/L in vitro. $^{64}$Cu-NOTA-HTL2G-S/L was studied by PET imaging in mice bearing both 4T1-HaloTag-ECS and 4T1 tumors. Autoradiography and histology studies were carried out to confirm the HaloTag specificity of $^{64}$Cu-NOTA-HTL2G-L in vivo. **Results:** Microscopy confirmed surface expression of HaloTag in 4T1-HaloTag-ECS cells, which specifically bind NOTA-HTL2G-S/L. The radiochemical yield was ~25% for $^{64}$Cu-NOTA-HTL2G-S and >80% for $^{64}$Cu-NOTA-HTL2G-L, with purity of >95%. Uptake of $^{64}$Cu-NOTA-HTL2G-L in 4T1-HaloTag-ECS tumors (4.3 ± 0.5, 4.1± 0.2, 4.0 ± 0.2, 2.3 ± 0.1, and 2.2 ± 0.1 %ID/g at 0.5, 3, 6, 18, and 24 h post-injection; n = 4) was significantly higher than that in the 4T1 tumors (3.0 ± 0.3, 3.0± 0.1, 3.0 ± 0.2, 2.0 ± 0.4, and 2.4 ± 0.3 %ID/g at 0.5, 3, 6, 18, and 24 h post-injection respectively; n = 4) at early time points. Other organs with significant tracer uptake included kidneys and liver, which indicated renal/hepatobiliary clearance. In comparison, $^{64}$Cu-NOTA-HTL2G-S did not demonstrate significant uptake in either 4T1-HaloTag-ECS or 4T1 tumors. Blocking studies and autoradiography of tumor lysates confirmed that $^{64}$Cu-NOTA-HTL2G-L binds specifically to HaloTag protein in the 4T1-HaloTag-ECS tumors, corroborated by histology. **Conclusion**: HaloTag protein-specific targeting and PET imaging in vivo was achieved with $^{64}$Cu-NOTA-HTL2G-L, which serves as a proof-of-principle for future non-invasive and sensitive tracking of HaloTag-transfected cells with PET, as well as many other studies of gene/protein/cell function in vivo.

## OP371

### Study on In-vivo Tumor Imaging by Telomerase Targeted Radiolabeled RNA Probe

**R. Wang**, L. Kang, P. Yan, C. Zhang, M. Liu, Y. Cui; Department of Nuclear Medicine,Peking University First Hospital, Beijing, CHINA.

**Objective:** This study is to explore the value of telomerase targeted radiolabeled small interference RNA in tumor imaging in vivo. **Methods:** hTERT-targeted and human gene non-targeted siRNAs were chemically synthesized. Through the conjugation with the chelator N-hydroxysuccinimidyl derivative of S-acetylmercaptoacetyltriglycine (NHS-$MAG_3$), siRNAs were radiolabeled with $^{99m}$Tc. HE and immunohistochemical staining were used to identify the pathological characteristics. 7.4 MBq of $^{99m}$Tc-siRNAs were injected in hepatocarcinoma bearing mice via the tail vein. At 0.5, 1, 3 and 6 h post injection, mice were laid on a face-up detector and imaged by SPECT. Ratio of radioactive counts in tumor to that in the contralateral equivalent region was calculated by drawing regions of interest (ROI) at each time point. Statistical comparisons of variables were performed by *t*-test. **Results:** The labeling efficiency reached 73.4 ± 3.0 %. After purification, the radiochemical purity was no less than 92 % and the specific activity was up to 25.9 Gbq/μmol. HE staining showed pathological mitotic figure in nucleus of tumor cells. hTERT immunohistochemical staining demonstrated deep brown dyed spots were found in the cell nucleus. hTERT-targeted $^{99m}$Tc-siRNA administrated xenografts could show tumor images clearly after the administration, especially at 6h. In contrast, $^{99m}$Tc-control-siRNA showed no tumor image. Ratios of uptake in tumor to that in contralateral region of hTERT-targeted siRNA increased from 2.68 ± 0.21 to 5.86 ± 0.30 in 6 hours, while those of control siRNA decreased from 1.55 ± 0.16 to 1.28 ± 0.12 ($P < 0.01$). **Conclusion**: $^{99m}$Tc radiolabeled telomerase-targeted siRNA probe allows for noninvasive visualization of tumor telomerase in vivo.[Keywords] Human telomerase reverse transcriptase (hTERT), Small interference RNA (siRNA), Tumor, Imaging

## OP372

### Experimental study on 99mTc-RRL as a novel molerule probefor tumor angiogenesis imaging

**R. Wang**, Q. Zhao, P. Yan, C. Zhang, X. Lu, L. Li, L. Yin; Department of Nuclear Medicine, Peking University First Hospital, Beijing, CHINA.

**Objective:** Tumor angiogenesis plays an important role in the growth and metastasis of malignant tumor, which supplies metabolites to helping tumor cells surviving and metastasis. Radionuclide imaging as a noninvasive technique have played critical roles in cancer clinical diagnosis and treatment. Arginine-arginine-leucine (RRL) peptide is considered as a tumor endothelial cell specific binding sequence. The overall Aim of this study was to evaluate whether the $^{99m}$Tc-radiolabeled RRL can be used for imaging of malignant tumors, and be a new targeted tumor angiogenesis molecular probe in vivo and nonivasively. **Methods:** The RRL (arginine-arginine-leucine) peptide targeting tumor angiogenesis was redesigned, synthesized and radiolabeled with $^{99m}$Tc by one step method. Then the radiolabeling efficiency and radiochemical purity was characterized in vitro. $^{99m}$Tc-RRL was injected intravenously in HepG2 xenograft-bearing BALB/c nude mice. Biodistribution and in vivo imaging was performed periodically. All data were analyzed by statistical software. **Results:** The labeling efficiencies of 99mTc-RRL reached 76.9% ± 4.5% ($n$ = 6) within 30-60 min at room temperature, and the radiochemical purity exceeded 96% after purification. $^{99m}$Tc-RRL showed complete stability at room temperature, especially in fresh 37℃ human serum. In nude mice bearing HepG2 xenografts, tumor radioactivity uptake of $^{99m}$Tc-RRL after injection was significantly higher than that of unlabeled RRL after injection ($P < 0.05$). The tumor-to-skeletal muscle ratio exceeded 8.0, and the tumor-to-blood ratio reached 2.0. In SPECT imaging of nude mice bearing HepG2, U87, B16 xenografts, the tumors were clearly imaged at 2-6 h noninvasively after the administration of $^{99m}$Tc-RRL, whereas the xenografts were not clearly imaged at any time after injection of unlabeled RRL first. **Conclusion:** $^{99m}$Tc-RRL can be used as a potential candidate for visualization of tumor angiogenesis in malignant carcinomas. Key Words: $^{99m}$Tc; peptide; tumor angiogenesis; molecular imaging; biodistribuiton

1001 — Monday, Oct. 21, 16:30 — 18:00, Amphithéâtre

## CME 8 - Inflammation & Infection: The Diabetic Patient

## OP373

### Nuclear Medicine Procedures and Clinical Indications in Diabetic Patients with Infection (With Special Emphasis on FDG Imaging)

**O. Israel, ISRAEL**

## OP374

### Diabetic Nephropathy and Imaging of Kidney Infections and Graft Rejection

**J.R. Buscombe, UNITED KINGDOM**

## OP375

### Imaging Cardiovascular Diseases in Diabetic Patients

**R.H.J.A. Slart, NETHERLANDS**

1002 — Monday, Oct. 21, 16:30 — 18:00, Auditorium Lumière

## Symposium 8 - EANM/ESTRO Joint Session: PET/MR and Radiation Oncology

## OP376

### PET/MR: The Future is Now

**A.J. Beer, GERMANY**

## OP377

### Technical Implementation of PET/MR for Radiotherapy Treatment Planning

**D. Thorwarth, GERMANY**

## OP378

### Clinical Applications of PET/MR in Radiation Oncology

**D. Zips, GERMANY**

1003 — Monday, Oct. 21, 16:30 — 18:00, Forum 3

## CTE 4: PET/MR in Neurology

## OP379

### The Challenge of Attenuation Correction in PET/MR Studies of the Brain

**Y. Berker, GERMANY**

## OP380

### Simultaneous PET/MRI - Clinical Applications and Current Development of Neuroimaging with PET/MRI

**P. Werner, GERMANY**

## OP381

### Integrated Brain PET/MR in Clinical Routine and Research

**S. Schachoff, GERMANY**

1004 - Monday, Oct. 21, 16:30 - 18:00, Bellecour 1/2/3

## Featured - Neurosciences: Amyloid Quantification

## OP382

### Remembering the Complexities of PET Amyloid Imaging

**J. Price, USA**

## OP383

### Correction of partial volume effects in an Alzheimer's disease mouse model using [18F]florbetaben PET

**M. Brendel**[1], A. Delker[1], G. Boning[1], E. Mille[1], F. Gildehaus[1], K. Baumann[2], C. Haass[1], J. Herms[1], P. Bartenstein[1], A. Rominger[1]; [1]University of Munich, Munich, GERMANY, [2]Hoffmann-La Roche, Basel, SWITZERLAND.

**Aim:** We previously investigated the progression of β-amyloid deposition in brain of mice over-expressing amyloid-precursor protein (APP-Swe), a model of Alzheimer's disease (AD), in a longitudinal PET study with the novel β-amyloid tracer [18F]florbetaben. Signal loss due to partial volume effects (PVE) is a well-known problem especially in microPET studies and envisioned by discrepancies between PET quantitation and autoradiography findings. Therefore we Aimed to investigate the magnitude of PVE as well as to validate a correction algorithm (PVC) for the mouse brain. **Methods**: A phantom study using cannula filled with cross-calibrated activity was performed to assess the full-width-at-half-maximum (FWHM) of the Siemens Inveon DPET. Subsequently a volume-of-interest (VOI)-based PVC algorithm using the appropriate FWHM was applied on in vivo microPET data. Therefore 90 min dynamic emission recordings were acquired following administration of [18F]florbetaben. A total of 32 PET scans in groups of APP-Swe (N=8) and age-matched wild-type (WT) mice (N=8) at 13 and 16 months of age were performed. After spatial normalization, VOI-based cortex-to-cerebellum ratios (SUVR) were calculated. Ex vivo autoradiography was accomplished in a subset of animals immediately after PET scans and analyzed using corresponding regions. Uncorrected and PVE-corrected results were contrasted and statistical power analyses (α=0.05) were performed for longitudinal comparisons in APP-Swe mice. These PET data were compared with autoradiographic results through calculation of root-mean-square-errors (RMSE). **Results**: The phantom study revealed a FWHM of 1.72 mm. Uncorrected cortical SUVR increased over time in APP-Swe mice compared to baseline estimates (+5.4%; $p<0.005$) while PVE-corrected SUV increased by +12.2% ($p<0.005$). Wild-type animals showed significant changes neither in uncorrected nor in PVE-corrected data. Statistical analyses revealed a higher power in PVE-corrected APP-Swe longitudinal comparison. RMSE for uncorrected cortical SUVR in PET were 24.6% in contrast to autoradiographic data and declined to 3.9% for PVE-corrected values. **Conclusion**: The application of PVC to the currently largest dataset of the novel β-amyloid tracer [18F]florbetaben in an AD mouse model increased differences between groups and reduced discrepancies to autoradiography results. As statistical power shifted towards higher levels in the longitudinal analysis, PVE-correction improves the APP-Swe model in detecting early amyloidogenesis more sensitively, finally requiring less animals in disease-modifying treatment studies.

## OP384

### Evaluation of software tools for automated identification of neuroanatomical structures in β-amyloid PET imaging to diagnose Alzheimer's disease

**T. Tuszynski**, M. Rullmann, J. Luthardt, A. Seese, D. Butzke, S. Tiepolt, S. Hesse, H. Barthel, O. Sabri; University of Leipzig, Department of Nuclear Medicine, Leipzig, GERMANY.

For regional quantification of nuclear brain imaging data, defining volumes of interest (VOIs) by hand is still the gold standard approach. As this procedure is time-consuming and definer-dependent, a variety of software tools for automated identification of neuroanatomical structures emerged over the past few years. As the quality and performance of those tools are not systematically investigated so far for β-amyloid PET data, we compared in this project three software tools for automated VOI definition (PMOD, Hermes Brass, Freesurfer) against the conventional method. We systematically analysed florbetaben brain PET (summed 90-110 min p.i. images) and MRI (T1 3D MPRAGE) data of 10 patients with probable Alzheimer's disease (AD) and 10 age-matched healthy volunteers (HVs) collected in a Phase 0 trial [Eur J Nucl Med Mol Imaging 2011]. Florbetaben is a 18F-labeled β-amyloid PET tracer which underwent successful phase 0 to 3 clinical development and which was recently submitted for clinical approval in the USA and Europe. To analyse the florbetaben PET data in this project, VOIs were defined on the data manually as well as through the automated workflows of PMOD, Hermes Brass and Freesurfer. Florbetaben standardized uptake value ratios (SUVRs) with cerebellar cortex as reference region were obtained for each VOI. SUVR comparisons between ADs and the HVs were carried out using student's t-tests and calculating the effect sizes (Cohen's d). SUVRs of the automatically generated VOIs were correlated with the SUVRs of conventionally derived VOIs (Pearson's tests). The composite neocortex SUVRs obtained by manually defined VOIs were significantly higher for ADs vs. HVs (p=0.022, d=1.17). For the automated approaches of PMOD, Hermes Brass and Freesurfer even better group discrimination was achieved (p=0.007, d=1.42; p=0.005, d=1.47; p=0.008, d=1.46). SUVRs of the automatically generated VOIs correlated significantly with those of the hand-drawn VOIs in distinct brain regions, but strong regional differences in this correlations were observed (r=-0.224 to r=0.946, p=0.375 to p<0.001). Regions of best and weakest correlation were different depending on the software approach. Best overall correlation was observed in the frontal cortex VOI for all tested software tools (r=0.555 to r=0.942, p=0.011 to p<0.001). In conclusion, automated VOI definition by the software tools tested has a great potential to substitute the current standard procedure to manually define VOIs in β-amyloid PET data analysis. In a next step, we will test these promising tools in larger cohorts and for other PET tracers. Research support: Piramal Imaging, Berlin (Germany)

## OP385

### Automated analysis of 18F-florbetaben PET scans

**V. Dicken**[1], F. Weiler[1], B. S. Geisler[1], J. Strehlow[1], J. Hirsch[1], F. Semah[2], P. Payoux[3], A. Drzezga[4], L. M. Dinkelborg[5], M. Pessel[6], H. K. Hahn[1]; [1]Fraunhofer MEVIS, Bremen, GERMANY, [2]Nuclear Medicine, University of Lille, Lille, FRANCE, [3]Nuclear Medicine, University of Toulouse, Toulouse, FRANCE, [4]Nuclear Medicine, University of Cologne, Cologne, GERMANY, [5]Piramal Imaging GmbH, Berlin, GERMANY, [6]Bayer Healthcare, Berlin, GERMANY.

**Aim**: Development and evaluation of a software tool for automated z-score analysis of florbetaben (FBB) PET scans to facilitate image interpretation. **Materials and Methods**: Based on 58 FBB-PET scans and high-resolution MRI from neurologically normal and amyloid-negative subjects from a clinical phase-II trial a normal FBB-template was compiled using MRI based MNI-atlas registration and a cerebellum histogram peak-position normalization strategy. A software prototype was developed for analysis of FBB-PET images using a dedicated registration method aligning PET images directly to MNI geometry without reliance on individual MRI-data. Following registration quality control and optional corrections, the regions with significant deviation from normal uptake are identified by means of high z-scores (standard-deviations away from the mean) and displayed in 2D-overlay and 3D surface maximum-intensity projections. Statistical parameters on the SUVR and z-score distribution were obtained within 15 grey matter regions defined per hemisphere as well as white matter and cerebellum regions. The prototype software was analyzed by the three nuclear medicine physicians among the authors and refined upon their suggestions. Subsequently, 4 non-expert readers (1 MD, 3 non-MD) analysed FBB-PET images (90-110min p.i.) from 150 subjects (AD-patients and normal controls) and mean sensitivity and specificity values were calculated. Further a fully automated binary classification was developed based on regional quantitative values with greatest difference between positive and normal FBB scans and white matter SUVR to compensate for variability in the white-matter/cerebellum uptake-ratio. **Results:** With clinical diagnosis as reference a sensitivity of 77.8% and specificity of 91.3% was obtained for the majority rating of the 3 non-MD readers with limited or no experience in reading amyloid PET scans using this software prototype. This is in good accordance with the published data of this data set (Barthel et al. Lancet Neurol. 2011) where an external expert panel rated the images in qualitative visual reads. The results of a majority read of the 3 non-MD readers using the software prototype showed 93.3% agreement (kappa=0.87) with the external expert panel, similar levels of agreement were obtained with the automated classifier. **Conclusion:** This new software is user-friendly and can be used to assist and facilitate the interpretation of FBB-PET scans. Using z-score analysis less experienced readers can rate amyloid load in florbetaben PET with similar sensitivity and specificity in good agreement with expert readers without software support. Results of the automated classification are comparable to human readers but need further confirmation on data not available during development.

## OP386

### Comparison of two brain VOI templates to quantify β-amyloid radioligand binding

**M. J. Santiago-Ribeiro**, C. Hommet, M. Bailly, J. Vercouillie, E. Beaufils, K. Mondon, D. Guilloteau, V. Camus; CHRU, INSERM 930, Université François Rabelais, Tours, FRANCE.

**Objectives**: PET of β-amyloid (Aβ) in vivo has had an important impact in research progress in Alzheimer's (AD) disease during the past decade. Several studies have demonstrated that Aβ PET could differentiate patients with AD from normal controls. Visual qualitative assessment of Aβ PET is able to differentiate between negative and positive Aβ loading images. However, software tools for quantitative evaluation of Aβ binding relative to the uptake by cerebellum are mandatory to potentially provide additional diagnostic information when used as an adjunct to the visual analysis. In this study we compared two templates of Volumes of Interest (VOI) to obtain SUVr ratios after 18F-Florbetapir (18F-AV45) injection. Material and **Methods**: Sixteen subjects, 71.0±8.6 y (8 heath controls, HC; 5 AD, 5 MCI) were submitted to a cerebral 10 min PET study, 50 min after the injection of 18F-AV45 (266±50 MBq) using a Gemini Dual PET tomograph (Philips). All the images were co registered using the same template VOI were defined for frontal, posterior cingulate, precuneus, parietal, temporal and occipital cortex as also for whole cerebellum (used as reference region to obtain SUVr values) for 18F-AV45 images using two softwares: Syngo.via with the VOI template developed by Siemens and Pmod 3.4 (Pmod Technologies) using MNI VOI. **Results:** For the 3 groups of subjects and for the 6 VOI, all the SUVr were higher using MNI VOI. SUVr mean±SD whole brain obtained using Pmod were: 1.25±0.04, 1.41±0.17, 1.21±0.30 for HC, MA and MCI respectively. Using Syngo, also for whole brain, SUVr were: 0.97±0.03, 1.15±0.29, 1.02±0.38, for the same groups. The highest SUVr were founded for the MA group independently of the VOI method used. The highest values obtained using Pmod were possibly du to the fact that VOI included gray and white matter while Syngo VOI only take in account gray matter. None of the Methods takes into account partial volume. **Conclusions**: The results obtained confirm that a quantitative analysis provides accuracy in the diagnosis of the AD. However, these results also show that a standardized VOI template for the calculation of SUVr is mandatory. This work has been supported in part by grants from French National Agency for Research called Investissements d'Avenir ANR-11-LABX-0018-01 and FEDER (Radex programme).

## OP387

### Whole brain gray matter and white matter contrast analysis of 18F-florbetapir (AV-45) for diagnosis Alzheimer's disease

**H. Sato**[1], K. Ishihara[2], M. Suda[2], A. Tateno[1], Y. Okubo[1], S. Kumita[1]; [1]Nippon Medical School Main Hospital, Tokyo, JAPAN, [2]Clinical Imaging Center for Healthcare Nippon Medical School, Tokyo, JAPAN.

**Aim**: Recently amyloid positron emission tomography (PET) is spread and widely used for Alzheimer's disease (AD) research. There are some techniques of evaluation for amyloid PET images, most popular method is estimating standard uptake value ratio (SUVR); SUV of cerebral gray matter (GM) is divided by that of cerebellum. Essentially diagnosis of AD on amyloid PET is detecting amyloid burden of brain gray matter, however amyloid burden is observed on brain white matter (WM) normally. Purpose of this study is more directly calculating an amyloid accumulation contrast between whole brain GM and WM with using 18F-florbetapir (AV-45). **Materials:** This study recruited 33 subjects (15 AD patients and 18 healthy controls (HC)). MRI images T1WI and T2WI were scanned before PET scanning, and then 5 AD patients and 4 healthy controls were excluded because of their over aging cerebral vascular diseases. AD patients were 1 male and 9 females, and healthy controls were 8 males and 6 females. For all subjects, MMSE test was undergone before registration on this study and written consent were provided. *Methods*: All subjects received intravenous injection of 370MBq of AV-45 while lying on scanning bed. After 50min. from injection whole brain scanning is performed for 10min. All amyloid PET images were coregistered based on individual T1WI. Personal templates of GM and WM for VOI analysis were made from T1WI. About coregistered amyloid PET images, standard uptake values (SUV) of whole brain GM and WM were obtained using original template, and GM SUV average / WM SUV average contrast ratio (SUVCR) were calculated individually. **Results:** Significantly difference SVCR was found among AD and HC. SUVCR of AD (0.79 ± 0.057) is higher than that of HC (0.67 ± 0.032) (P < 0.001). Diagnosis AD based on SUVCR method showed a sensitivity of 100% and specificity of 92% with a cut-off value of 0.704 (area under the curve 0.992). **Conclusion:** This preliminary study indicated usefulness of SUVCR method for diagnosis AD on amyloid PET.

## OP388

### Quantification of florbetapir F18 PET: Comparison of two Methods

**C. Hutton**[1], J. Declerck[1], M. A. Mintun[2], M. J. Pontecorvo[2], A. Joshi[2]; [1]Siemens Molecular Imaging, Oxford, UNITED KINGDOM, [2]Avid Radiopharmaceuticals, Philadelphia, PA, UNITED STATES.

**Aim:** Two Methods for quantitative analysis of florbetapir F18 PET were compared in a diverse clinical population from the Alzheimer's Disease Neuroimaging Initiative (ADNI). Cortex-to-cerebellum standard uptake ratios (SUVr) were calculated using syngo.PET Amyloid Plaque (sPAP) developed by Siemens [Peyrat et al., SNM, 2012] and the method developed by Avid [Joshi et al., JNM, 2012]. **Materials and Methods:** Florbetapir data from 604 subjects were downloaded from ADNI. Using sPAP, PET data were automatically affine-registered to a synthetic florbetapir PET template in MNI atlas space (Evans et al., 1993). Registration results were visually assessed and sPAP Manual Fusion Tools were used to apply manual affine transformations to cases requiring adjustments. SUVr values were calculated from mean uptake in six cortical regions (medial orbital frontal, parietal, temporal, precuneus, posterior cingulate and anterior cingulate) with reference to whole cerebellum Fleisher et al. (2011). The Avid method used SPM2 (Friston et al., 2007) for non-linear registration of PET data to MNI space with reference to florbetapir PET template. Mean cortex-to-cerebellum SUVr values were calculated for six similar cortical regions (as per sPAP). **Results:** All 604 subjects were successfully registered to MNI space using both Methods. Using sPAP, 14/604 cases (2.3%) required manual registration adjustments. Using the Avid method, 15/604 cases (2.5%) required additional preprocessing for successful registration. Mean cortical SUVrs from the two Methods were correlated (r=0.99) over the range from 0.77 to 2.25 SUVr units. The linear regression of sPAP SUVr values on Avid SUVr was y=0.04264+0.9782*x with a mean (SD) difference Avid-sPAP of -0.02 (0.04). The regression equation was used to convert the Avid proposed SUVr threshold for florbetapir positivity (SUVr>1.10, Joshi et al., 2012) to a corresponding threshold for sPAP (SUVr>1.12). There was agreement between Avid and sPAP SUVr in categorization for 96.3% of the scans with 45% in the positive range and 51.3% in the negative range. In 1.2% only the Avid method classified as positive and in 2.5% only the sPAP classified as positive. **Conclusion:** Cortex-to-cerebellum SUVr values calculated from florbetapir PET data using sPAP provides similar results as Avid method. Linear conversion of the Avid proposed SUVr (>1.10) threshold to sPAP threshold (>1.12) for florbetapir positivity resulted in similar categorization in 96.3% of subjects despite methodological differences in registration approach.

1005 - Monday, Oct. 21, 16:30 - 18:00, Auditorium Pasteur

## Oncology Clinical Science: Lower GI Tract Tumours

## OP389

### Role of FDG PET-CECT in suspected recurrence of non CEA secreting colorectal malignancies - A prospective study

**S. Dash**[1], A. Gupta[2]; [1]SARAL ADVANCED DIAGNOSTICS, Delhi, INDIA, [2]ACTION CANCER HOSPITAL, New Delhi, INDIA.

**Aim**: To determine the diagnostic efficiency of FDG PET-CECT in non CEA secreting colorectal malignancy recurrence. **Material and Methods:** A prospective study of 28 treated patients of colorectal malignancy with normal serum CEA was carried out using whole body FDG PET with contrast enhanced diagnostic CT scan and dual time point imaging of suspicious lesion(s). Suspicious lesions detected on FDG PET-CECT were subjected to pathological evaluation to confirm or refute recurrence. The lesions which were not amenable to FNA cytology or biopsy were followed up. **Result:** FDG PET-CECT detected 37 suspicious lesions in 21 patients (histology types were poorly differentiated adenocarcinoma - 5, mucinous adenocarcinoma - 12, adenocarcinoma with neuroendocrine differentiation - 3, squamous cell carcinoma - 1) out of which 33 lesions were subjected to cyto / histpathological evaluation. 26 lesions were consistent with disease recurrence. 4 lesions which could not be biopsied were followed up for 3-6 months with serial USG or CECT scan. Subsequently one lesion was biopsied and was consistent with disease recurrence. Rest of the 3 lesions remain unchanged on follow up and were concluded to be probably benign. 7 patients in whom PET-CECT did not reveal any obvious abnormality (histology types were poorly differentiated adenocarcinoma - 1, mucinous adenocarcinoma - 4, adenocarcinoma with neuroendocrine differentiation - 2) were also followed up for 6 months and 2 patients (mucinous adenocarcinoma - 2) developed recurrent disease. Out of 27 true positive (for recurrence) lesions (in 18 patients), 11 lesions showed abnormal FDG uptake. 16 non FDG avid lesions were considered suspicious due to abnormal CT morphology and / or abnormal contrast enhancement pattern. 7 of the 10 false positive lesions had granulomatous inflammation. Rest of the false positive lesions were either fibrous scar tissue or non specific inflammatory pathologies. Overall FDG PET-CECT showed 93.10 % sensitivity and 72.97 % positive predictive value in detecting recurrent lesion of non CEA secreting colorectal malignancies. Accuracy of the modality was 71.43 % in the evaluation of such patients. **Conclusion:** FDG PET scan is being traditionally known of having no additional advantage in the evaluation of non CEA secreting colorectal malignancies. However dual time point PET imaging along with diagnostic quality CT scan (with intravenous and oral contrast administration) improves the performance of the modality and hold promise to be one stop approach for surveillance in this clinical scenario. Key Words: FDG PET, CECT, non CEA secreting colorectal Malignancy, Recurrence

## OP390

### Comparison of 18F FDG PET/CT and CECT scan in assessing chemotherapy response in Metastatic Colorectal Cancer.

**R. Kumar**, J. R. Mohan, M. L. Abrar, B. Anish, B. R. Mittal; Postgraduate Institute of Medical Education & Research, PGIMER, CHANDIGARH, INDIA.

**Aim**: To compare the performance of 18F-FDG PET/CT and Contrast enhanced CT (CECT) scan in assessing response to chemotherapy in Metastatic Colorectal Cancer. **Materials and Methods**: The population for this retrospective study comprised of 34 patients (26 males, 8 females, mean age of 58yrs), who were treated for metastatic colorectal cancer. All the patients underwent CECT and 18F-FDG PET/CT before and after 4 courses of chemotherapy. PET and CT data were interpreted separately by experienced reviewers and were used to assess metabolic and morphological tumour response after chemotherapy. Response Evaluation Criteria In Solid Tumors (RECIST 1.1) and Positron Emission tomography Response Criteria In Solid Tumors (PERCIST) criteria were used to evaluate CT and PET respectively. **Results**: Of the 34 patients, discrepancies between the findings of CT and PET/CT were evident in 24 patients. 19 patients with morphologically stable disease (SD) on CT were evaluated as 3 CMR, 15 partial metabolic responses (PMR) and 1 progressive metabolic disease (PMD). 8 morphological partial responses (PR) were evaluated as 2 CMR, 3 PMR, 1 stable metabolic disease (SMD) and 2 PMD. 4 morphologically complete responses (CR) were correlated with complete metabolic response (CMR). 3 morphologically progressive diseases (PD) were correlated with progressive metabolic disease (PMD). Concordance between PET and CT findings were noted in a total of 7 patients belonging to morphologically CR (4 patients) and morphologically PD (3 patients). PET revealed progressive disease in 6 patients compared to only 3 patients on CECT. On clinical follow up of the 6 patients who showed PMD at end of chemotherapy 3 had expired, 2 were lost to follow up and 1 patient was switched over to alternate chemotherapy regimen. **Conclusion**: Assessment of chemotherapy response in metastatic colorectal cancer is fundamental in order to change an ineffective but possibly toxic chemotherapy protocol. Our result has revealed that 18 F FDG PET/CT fares better than CT scan in assessing the complete response and progressive disease to chemotherapy. The findings suggest a potential role for PET/CT in altering therapeutic management in such patients.

## OP391

### PET-CT in patients with metastatic colorectal cancer undergoing treatment with an experimental bevacizumab schedule in combination with standard chemotherapy: evaluation of early changes

**L. Aloj**, A. Avallone, C. Caraco', L. Silvestro, F. Izzo, P. Delrio, G. Nasti, A. Budillon, S. Lastoria; INT Fondazione Pascale, Napoli, ITALY.

**Aim**: We have recently shown that FDG-PET/CT is capable of predicting pathologic response as early as 11 days from the beginning of treatment, in patients with locally advanced rectal cancers undergoing neo-adjuvant radiochemotherapy in combination with the anti-angiogentic drug bevacizumab administered with a novel schedule in which the monoclonal antibody is given 4 days prior to chemotherapy. This schedule has shown to significantly improve pathologic response compared to chemotherapy alone or chemotherapy with bevacizumab using a standard administration schedule. A prospective study is underway to evaluate whether this approach is valid also in patients with metastatic colorectal cancer. **Methods** Between May 2012 and February 2013, 34 patients with inoperable metastatic colorectal cancer have been enrolled in this study at our center. Patients undergo standard 5-FU/oxaliplatin regimens (12 biweekly cycles) and are sequentially assigned to receive bevacizumab (5mg/kg) either on the same day as chemotherapy (standard) or 4 days prior (experimental). FDG-PET/CT is performed at baseline and 11 days from the beginning of therapy to assess response. **Results**. Highest SUV max values at baseline were recorded for lesions in liver (22 pts), lung (4 pts), colon (7 pts) and lymph nodes (2 pts). PET response was highly variable with reduction in SUVmax of the target lesion ranging from -39 to 82 % with the standard schedule and 0 to 51% using the experimental schedule. In 16 patients, 9 treated under the standard regimen and 7 under the experimental schedule, early reduction in target lesion SUVmax was 30% or more. **Conclusion**. The reduction of FDG uptake 11 days from the beginning of treatment is very dramatic in some lesions. Further follow-up will determine whether this parameter can aid in predicting response and long term outcome with this novel bevacizumab schedule.

## OP392

### Role of $^{18}$F FDG PET/CT as pathologic response predictor of locally advanced rectal cancer treated by neoadjuvant chemoradiation therapy: from PERCIST to PReDiST?

**A. Maffione**, A. Ferretti, G. Grassetto, E. Bellan, C. Capirci, S. Chondrogiannis, M. Marzola, L. Rampin, C. Bondesan, D. Rubello; S.M. della Misericordia Hospital, Rovigo, ITALY.

**Aim**: the purpose of this study was to correlate qualitative visual response and some different PET quantification factors with Mandard's Tumour Regression Grade (TRG) classification of pathologic response to neoadjuvant chemo-radiotherapy (CRT) in patients affected by locally advanced rectal cancer (LARC). **Materials and Methods:** sixty-nine consecutive LARC patients were retrospectively included. FDG-PET/CT scans were performed at staging time and after the CRT end (mean time 6.7 weeks). We calculated tumour SUVmax and its related arithmetic and percentage decrease (Response Index - RI). Qualitative and semiquantitative analysis was performed by visual response assessment (VRA), PERCIST criteria 1.0 and a new classification (PReDiST: PET Residual Disease in Solid Tumour) based on a new definition of residual disease (FDG uptake > 1.5 × $SUV_{mean\_liver}$ + 2 × standard deviations). We split the TRG system into responders (TRG1-2) and non-responders (TRG3-5). **Results:** SUVmax-post and RI, parameters were significantly correlated with pathological treatment response ($p<0.01$) with a ROC curve cut-off of 5.1 and 61.8%, respectively. SUVmax-post had the bigger ROC-curve (0.846) with sensitivity 86% and specificity 80%. VRA and PReDiST classification were also statistical predictive of TRG response (VRA with the best accuracy: sensitivity 86% and specificity 55%). On the contrary, PERCIST was not statistically correlated to TRG. **Conclusions**: FDG PET/CT scan is actually accurate to stratify preoperatively LARC patients, independently of the chosen tool to interpret the images. Among many PET parameters, the most commonly used in clinical practice (SUVmax-post and VRA) have shown the best accuracy to predict TRG. PReDiST seems to be a novel promising semiquantitative predictive criterion for response assessment.

## OP393

### The Influence of Radiation Enteritis on Predicting pathological Response of Locally Advanced Rectal Cancer after Neoadjuvant Radiochemotherapy by PET/CT

**J. Xu**, Y. Zhang, Z. Zhang, W. Sun, Z. Yao; Shanghai Cancer Center, Shanghai, CHINA.

**Background and purpose**: Neoadjuvant radiochemotherapy (neoRCT) is proved to lower the risk of local recurrence and downstage the primary tumor of locally advanced rectal cancer (LARC). In recent years, $^{18}$F-FDG PET/CT has been applied to monitor the response and distinguish pCR of LARC after neoRCT, but radiation enteritis may result in misestimating the tumor response. The objective of our prospective study was to investigate the value of PET/CT for evaluating the response to neoRCT in LARC and the influence of radiation enteritis on predicting the response. **Methods:** 52 patients were diagnosed with LARC, treated with capecitabine-based chemoradiation and resection 7~8 weeks later. $^{18}$F-FDG PET/CT was performed before and after RCT (PET1&2) in all patients and additional one before surgery (PET3) in 32 of whom. PET indices including $SUV_{max}$, $SUV_{mean}$ and volume were calculated by delineation of VOI. Responders (TRG2~4) and non-responders (TRG1) were determined in histopathology. The correlation between pathological response and the percentage decrease in PET indices was analyzed in consideration of radiation enteritis. **Result:** The pathological response rate was 80.7% (42/52 for TRG2~4). The rate of morphological change between PET1 and PET2 was 71.2%, which correlated with the percentage of Δvolume ($p=0.005$). No significant differences in all the relevant PET parameters concluding the percentages of Δvolume, $\Delta SUV_{max}$ and $\Delta SUV_{mean}$ were observed between responders and non-responders ($p=0.973$, 0.075 and 0.142). We found over half of patients suffered radiation enteritis within one month after RCT, but most of them recovered before surgery. So, firstly, according to the high uptake in the gut around the rectal lesions in PET2, all the patients were divided into two groups. In 31 patients with radiation enteritis, absolute SUVmax in PET2 was a predictor of pathological response, which was significantly higher ($p=0.033$) in non-responders (18.59±17.52) than in responders (12.11±3.50). While, of 21 patients without radiation enteritis, only the percentage of $\Delta SUV_{mean}$ between PET1 and PET2 was significantly different ($p=0.029$) between nonresponders (mean 36.31%) and responders (mean 53.94%). Secondly, we analyzed the parameters in PET3 and observed no correlation between the percentages of Δvolume, $\Delta SUV_{max}$, $\Delta SUV_{mean}$ and pathological response ($p=0.657$, 0.791, 0.701). **Conclusion:** PET/CT after neoRCT plays an important role in accessing the pathological response in LARC. $SUV_{max}$ in PET2 and the percentage of $\Delta SUV_{mean}$ between PET1&2 could be predictors in patients with and without radiation enteritis. PET/CT before surgery was not necessary for evaluating the response.

## OP394

### Prospective analysis of 18F-FDG PET/CT' predictive value in patients with low rectal cancer treated with neoadjuvant chemoradiotheraphy and conservative surgery.

**C. Altini**[1], A. Niccoli-Asabella[1], R. De Luca[2], V. C. Loseto[1], A. Notaristefano[1], M. Fanelli[1], S. Montemurro[2], G. Rubini[1]; [1]Nuclear Medicine Unit, D.I.M., University of Bari "Aldo Moro", Bari, Italy, ITALY, [2]Department of Surgical Oncology, Istituto Tumori G. Paolo II, IRCCS Bari, Italy., Bari, Italy, ITALY.

**Aim**. This study prospectively assessed the value of 18F-FDG PET/CT for predicting the response of low rectal cancer (LRC) to neoadjuvant chemoradiation (nCRT). **Matherials and Methods**. 56 consecutive patients with LRC were enrolled (38 M, 18 F; mean age 62.25) and performed 18F-FDG PET/CT scans twice (baseline and 5-6 weeks after the end of nCRT). The nCRT consists of concurrent 5-fluorouracil-based chemotherapy and pelvic radiation (25 fractions of 180cGy/d). All patients performed 8 weeks later surgery with preservation of the sphinther. Post-nCRT 18F-FDG PET/CT sensitivity, specificity, PPV and NPV were evaluated. SUVs max and mean values on the baseline scan (SUVmax1, SUVmean1) and post-nCRT scan (SUVmax2, SUVmean2) were employed to assess tumor response to therapy also by calculating response index (RI=[(SUV1−SUV2)/SUV1]x100). Assessment of nCRT' tumor response was performed according the Mandard's Tumor Regression Grade (TRG) and the T parameter of the TNM staging on the surgical specimen. TRG I-II was considered responders while TRG III-V no-responders. T0 was considered as completely responder, T1-3 was considered as partially/no-responder. The diagnostic capability of 18F-FDG PET/CT was calculated by ROC analysis and expressed as area under curve (AUC). **Results:** Post-nCRT 18F-FDG PET/CT sensitivity, specificity, PPV and NPV were respectively 88.6%, 66.7%, 90.7%, 61.5%. TRG responders were 33/56 (58.9%). Mean values of SUVmax2, SUVmean2, RImax and RImean in TRG responders were respectively 5.22, 2.33, 65.72% and 70.18%; in TRG no-responders were 7.73, 3.57, 52.52%, 54.39%. According TRG, statistical differences between responders and no-responders were significant in the analysis of SUVmax2 (t=-3.140, p=0.003), SUVmean2 (t=-3.220, p=0.002), RImax (t=2.278, p=0.027) and RImean (t=2.698, p= 0.009). T parameter responders were 12/56 (21.5%). Mean values of SUVmax2, SUVmean2, RImax and RImean in T parameter responders were respectively 4.17, 1.92, 70.32%, 73.73%; in T parameter partially/no-responders were 7.38, 3.38, 54.57%, and 57.37%. According the T parameter, statistical differences between responders and partially/no-responders were significant in the analysis of SUVmax2 (t=-4.353, p=0), SUVmean2 (t=-3.976, p=0), RImax (t=2.26, p=0.027) and RImean (t=2.595, p= 0.016). AUCs of the analysis in relation to TRG were: SUVmax2=0.737, SUVmean2=0.736, RImax=0.672, RImean=0.695. AUCs of the analysis in relation to T parameter were: SUVmax2=0.798, SUVmean2=0.782, RImax=0.742, RImean=0.741. **Conclusion:** Dual time 18F-FDG PET/CT is a reliable technique for evaluating response to nCRT in LRC, in patients scheduled for a conservative surgical treatment. Furthermore, the combination of the visual and semiquantitative analysis of the PET data increases the diagnostic validity of the examination.

## OP395

### Radiotherapy planning in anal cancer: role of Biological Target Volume (BTV)

**O. Bagni**[1], L. Filippi[1], A. Fontana[2], G. Arcangeli[2], R. Salvatori[1], F. Scopinaro[3], O. Schillaci[4]; [1]Section of Nuclear Medicine, Santa Maria Goretti Hospital, Latina, ITALY, [2]Section of Radiotherapy, Santa Maria Goretti Hospital, Latina, ITALY, [3]Section of Nuclear Medicine, Sant'Andrea Hospital, Roma, ITALY, [4]Section of Nuclear Medicine, Tor Vergata Hospital, Roma, ITALY.

**Purpose:** In anal cancer (AC) the standard for treatment is combined radiochemotherapy. A dose of 30 Gy was delivered to the pelvis with a Boost of 30 Gy only on tumor site using CT images as a guide with 2 cm margin. Therefore, a total dose of 60 Gy in association 5fluoro-uracile chemotherapy continuous infusion was administered to every patient. FDG PET/CT was demonstrated of value for the radiation therapy planning by the definition of the Biological Target Volume (BTV). In the present study, we assessed the clinical impact when BTV is used for the treatment planning in AC instead of the more conventional CT guide. **Materials and Methods**: ten patients (7 females, 3 male) affected by AC were included in the study. All performed non-PET staging by clinical examination, CT and/or RM. In every patient whole body PET/CT scan (GE Discovery ST) was performed. In the same session the isocenter points of radiation plan was defined. PET images were qualitatively evaluated and then were processed with a dedicated software (PET-VCAR, GE). BTV was calculated on the primitive site and the node localizations by using a threshold of segmentation set on the 42% of the SUV max. Follow up was made by clinical and instrumental examination for the following 24 months. **Results:**. According to clinical and CT examination, four patients were at Stage II, three were at Stage IIIA, and 3 were at Stage IIIB. PET/CT detected focal and intense tracer uptake corresponding to anal lesion in every subject. In all cases, node involvement was detected. According to PET/CT tumor staging was stage II in 2 case, IIIA in 3 cases, IIIB in 5 cases. The BTV was contoured also taking into account node localizations. PET/CT at 3 months after treatment showed complete metabolic response in every patient. At 24/36 months' follow up, patients were still free from disease according to all parameters. On the basis of FDG PET/CT, the margin around the gross volume target (GTV) was reduced of the 45% (from 2 cm to 1.2 cm). In our series, toxicity was limited to erythema and dry epidermiolisis (G1-G2) and transitory rectal tenesmus which went to spontaneous resolution

within 30 days. **Conclusions**: FDG PET can be useful for radiation planning of AC, with poor toxicity in terms of side effects both acute and delayed.

## OP396

### Assessment of response to Imatinib mesylate by F-18 FDG PET/CT in Gastro intestinal stromal Tumors (GIST) by PERCIST criteria

**A. G. Vyas, Sr.**[1], A. Tiwary, Jr[2]; [1]NMC Imaging at VIMHANS Hospital, New Delhi, INDIA, [2]Army Hospital R&R, New Delhi, INDIA.

**Aim**: The role of F-18 FDG PET/CT in response assessment by PERCIST criteria of adjuvant treatment with imatinib mesylate (selective tyrosine kinase inhibitor) for metastatic and recurrent Gastro intestinal stromal Tumors (GIST) after localised resection of primary tumor. **Material & Methods**: Prospective analysis of 62 patients (39 males, 23 females) of GIST (with metastatic and recurrent after localised resection of primary tumor ) was done , which was confirmed surgically /histopathologically. Patient age ranged between 28-76 years with mean age of 52 years. Patients underwent F-18 FDG PET/CT scans before imatinib mesylate treatment (400mg /day or more) and response was assessed as per PERCIST criteria, after 6 months of treatment. Data was interpreted using qualitative (compared to liver & mediastinal blood pool) & semi-quantitative (Standardized Uptake Value- SUV max) Methods. Resolution of metabolic activity was used as a marker of response to therapy**. Results** were further confirmed by clinical follow up, biopsy (were ever possible) or conventional imaging findings. Results: 22 ( 35.4%) lesions originated from stomach, 20 ( 32.2%) from small intestine, 09 ( 14.5%) from large intestine, 06 ( 9.6%) from rectum and0 5 ( 8.0 %) from peritoneum respectively. GIST were almost equally prevelant in stomach & small intestine, unlike in other studies where stomach is the most common site. Mean SUV in the GIST lesions was 6.3 with a range of 4.4 to 12.7 .Out of 62 patients for response assessment there was complete metabolic response (CMR) in 15 (24.1%), partial metabolic response (PMR) in 30 (48.3 %), stable metabolic disease in 12 (19.3 %) & progressive disease (PD) in 05 (8.0 %) cases respectively. Retroperitoneal lymph nodes was the most common site of metastasis (48%) followed by liver (21%) and peritoneal deposits (08%) respectively. 08/15 patients who attained CMR had abdominal / retroperitoneal lymph nodal metastases. Disease progression was observed in liver in 03/05 patients, peritoneal / omental deposits in 01/05 & pulmonary metastasis in 01/05 patients respectively. Responders showed decrease in SUV max of the lesions earlier than decrease in size. **Conclusion**: F-18 FDG PET/CT scan is a valuable tool in response assessment of GIST and PERCIST criteria may be helpful to assess the degree of response accurately. Further large prospective studies may be needed to establish the criteria.

1006 - Monday, Oct. 21, 16:30 - 18:00, Grand Salon Prestige Gratte-Ciel

# Molecular & Multimodality Imaging: Assessment of Receptor Expression - Preclinical Studies

## OP397

### Molecular imaging of somatostatin receptor 2 in brain tumors with Ga-68-DOTA-TOC-PET

**M. Rodrigues**[1], D. Waitz[1], A. Kroiss[1], D. Putzer[1], B. Nilica[1], H. Kostron[2], I. Virgolini[1]; [1]1. Department of Nuclear Medicine, Innsbruck Medical University, Innsbruck, AUSTRIA, [2]2. Department of Neurosurgery, Innsbruck Medical University, Innsbruck, AUSTRIA.

It has been assessed in vitro that meningioma and glioma cells are able to express somatostatin receptor subtype 2 (SSTR 2). Therefore, therapy with radiolabeled peptides is an encouraging new approach in the treatment of these tumors. The present experience is however limited and a clinical protocol is missing. The Aim of this study was to evaluate the correlation between the expression of SSTR 2 (investigated with Ga-68-DOTA-TOC-PET) in brain tumors and the age and gender of patients, the tumor type and size, and the survival. **Materials and Methods**: 50 consecutive patients (25 female, 25 male; age 21-81 years, mean age 50.02 years) with brain tumors (meningioma 25, glioblastoma 16, glioma 4, anaplastic astrocytoma 3, meduloblastoma 2 patients) were prospectively investigated with Ga-68-DOTA-TOC-PET (150 MBq, intravenously applied). Expression of SSTR 2 was classified in 4 grades [0, no uptake; 1, faint uptake; 2, moderate uptake; 3, high uptake (equal or higher than pituitary uptake)]. The tumor size was based on recent (time interval < 48 hours) MRI and/or CT data. **Results:** Grade 0 or 1 were found in 2 patients with meningiomas and 15 patients with other tumor types, whereas grade 2 or 3 were found in 23 patients with meningioma but only in 10 patients with other tumor types. The tumor size ranged 0.5-8.1 cm (meningiomas 0.7-6.0 cm, other tumors 0.5-8.1 cm, mean 2.86 cm). No correlation was found between the expression of SSTR 2 and the gender, age of the patient, tumor size or survival. However, the survival time (from date of Ga-68-DOTA-TOC-PET study to death or latest follow-up) in meningioma patients was found to be longer than that of patients with other tumor types (6-91 months and 2-72 months, respectively). **Conclusion**: Because of the complexity of brain tumors, assessment of the receptor expression status with Ga-68-DOTA-TOC-PET/CT has to be conducted on an individual basis in order to evaluate the eligibility of each patient to this new therapeutic approach.

## OP398

### Lessons from 11C-DTBZ imaging in a xenograft mouse model of rat insulinoma: is PET imaging of pancreatic β cell mass feasible?

**I. Peñuelas**[1,2], M. Collantes[2], M. Barajas[3], S. Rodríguez[3], G. Quincoces[1], M. Ecay[2], S. Abadía[1], F. Prósper[3], J. Á. Richter[4]; [1]Radiopharmacy Unit, Clínica Universidad de Navara, Pamplona, SPAIN, [2]MicroPET Research Unit, CIMA-CUN, Pamplona, SPAIN, [3]Cell Therapy Unit, Clinica Universidad de Navara, Pamplona, SPAIN, [4]Nuclear Medicine Department, Clínica Universidad de Navara, Pamplona, SPAIN.

Diabetes mellitus is associated with functional loss of β cell mas (BCM), and most therapeutic efforts in this field have focused on preserving this kind of cells and their function. For such purpose, the availability of imaging biomarkers to precisely quantify BCM would be of great interest. Among these, tetrabenazine-based VMAT2 cognate ligands for PET imaging have received main interest in the last years, albeit substantial controversy about their usefulness has recently been raised[1]. **Objectives:** The feasibility of BCM imaging with PET and $^{11}$C-(+)-α-dihidrotetrabenazine ($^{11}$C-DTBZ) in the pancreas is controversial. To overcome some of the limitations of pancreas PET imaging, we have herein used a xenograft model of rat insulinoma implanted in nude mice to study the relationship among in-vivo $^{11}$C-DTBZ-MicroPET imaging, ex-vivo $^{11}$C-DTBZ-autoradiography and different metabolic, immunohistochemical and molecular biomarkers. **Methodology:** $10^5$ RIN cells were subcutaneously implanted in nude mice (n=8). Tumour size and glycaemia levels were determined daily. Rat C-peptide was measured by ELISA to demonstrate rat insulin production. $^{11}$C-DTBZ PET was performed at 3 and 4 weeks and compared with $^{18}$FDG and $^{18}$FDOPA studies in the same mice. Ex-vivo autoradiography with $^{11}$C-DTBZ was carried out in frozen sections of explanted tumours. VMAT2 expression was measured by Western-blot in tumour homogenates and cultured RIN cells. Immunohistochemistry against VMAT2 and insulin was done in consecutive parafine tumour slices and RIN cells. **Results:** After 15-20 days, >120 $mm^3$ tumours were visible in all cases. Functional rat insulin production in mice was demonstrated by substantial decrease in glycaemia (<50 mg/dL by week 4) while rat C-peptide production was 7.28±2.65 ng/mL, not substantially different to peptide-C production in normal rats. MicroPET imaging with $^{11}$C-DTBZ or $^{18}$FDG was negative at both time points (4 and 5 weeks), and only bigger tumours could in some cases be seen with $^{18}$FDOPA. In explanted tumours, VMAT2 expression was detected by Western-blot, albeit as well as VMAT2 and insulin immunohistochemistry, it was much lower than in cultured RIN cells. $^{11}$C-DTBZ autoradiography was negative in explanted tumors. **Conclusions:** Although insulinomas are fully functional as demonstrated by rat insulin production and express VMAT2, it does not seem feasible to use $^{11}$C-DTBZ for in vivo measuring of BCM. This might either be due to inherent technical limitations of PET, decrease in VMAT2 expression in the tumours due to unknown reasons or other biological limiting facts. [1]Mol.Imaging Biol.(2013);15:1-2: β-cell mass imaging with DTBZ PET: Is it possible?

## OP399

### Biological evaluation of the new glutamate-urea-based PSMA ligand Df-DUPA-Pep

**G. Winter**[1], B. Baur[1], E. Andreolli[2,1], T. Kull[1], B. Witulla[1], C. Solbach[1], H. Machulla[1]; [1]University Hospital, Nuclear Medicine Clinic, Ulm, GERMANY, [2]University of Milano-Bicocca, Milan, ITALY.

**Aim**: For diagnosis of prostate carcinoma the glutamate carboxypeptidase II or PSMA (prostate-specific membrane antigen) is a very appropriate target for labeled urea-based peptides, as it is highly overexpressed in these tumor cells. Previously presented [Ga-68]-DOTA-DUPA-Pep already showed promising characteristics like very good binding affinities and excellent tumor specificity. Based on the same pharmacophoric group for Df-DUPA-Pep the ligand is coupled with desferal(Df), which can be labeled by various radionuclides at room temperature. **Methods**:Df-DUPA-Pep was labeled with Zr-89 as well as Ga-68 for characterization in vitro and in vivo. Binding affinity was determined using the PSMA-positive cell lines LNCaPand LNCaP C4-2. Peptide concentration ranged from 2 to 400 nM, while 2-PMPA was used as competitive inhibitor in excess. The stability of the peptide in serum, whole blood and buffer was determined via HPLC after 1, 2 and 24 hours. Biological distribution was detected by PET/CT measurements and calculated by tumor-to-tissue ratio in %ID/g by means of γ counter analysis of SCID mouse xenografts. Negative controls included cells and tumors of the PC-3 cell line. **Results:** The peptide was labeled with Zr-89 and Ga-68 for biological evaluation. No radionuclide-dependent difference in binding affinity or biological distribution was

observed. An average KD value of 42 ± 5nM was determined for the PSMA-positive cell lines. A cellular uptake of 8.6 ± 0.4 %IDin PSMA-positive cell lines was calculated from the γ-counter measurements. The inhibitor 2-PMPA completely abolished peptide binding, demonstrating the peptide-specificity for PSMA. Concerning stability the peptide showed no alteration under all conditions tested up to 24 hours. PET/CT images depicted a specific accumulation in PSMA-positive tumor xenografts. Further uptake was detected in kidney and bladder. For biological distribution values up to 13.7 %ID/g were detectable in PSMA-positive tumors and an average tumor-to-tissue ratio of 27 ± 10 was calculated. PSMA-negative xenografts showed a tumor-to-tissue ratio of 1.15 ± 0.28. **Conclusions**: The new ligand Df-DUPA-Pep shows all characteristics of a promising candidate for prostate cancer diagnosis and therapy. Similar to DOTA-DUPA-Pep the affinity is within the expected order of magnitude and the peptide is highly specific for PSMA. Desferal can be labeled by various radionuclides, for example Zr-89, allowing a longer follow-up in biological evaluations and an extended clearance improving signal-to-noise ratio.

## OP400

### Pilot Prospective Evaluation of Early Response to Bevacizumab Treatment Using the Novel PET/CT Radiopharmaceutical 18F FPPRGD2

**A. Iagaru**, C. Mosci, G. Davidzon, M. Kumar, B. Shen, F. Chin, S. S. Gambhir; Stanford University School of Medicine, Stanford, CA, UNITED STATES.

**Objectives**: Angiogenesis is essential for tumor growth and the expression of activated αvβ3 integrins plays a key role in this process. 18F FPPRGD2 (US FDA IND #113269) is a PET radiopharmaceutical based on a dimeric RGD peptide sequence that targets the αvβ3 integrins. We now present data on early evaluation of response to bevacizumab treatment in patients with glioblastoma multiforme (GBM) and non-small cell lung cancer (NSCLC). **Methods**: We recruited 5 participants (2 women, 3 men), 45-76 year-old (average: 59 ± 12.5). All patients had biopsy-proven malignancy (2 NSCLC, 3 GBM) and were treated with bevacizumab. One dynamic 18F FPPRGD2 PET and two static 18F FPPRGD2 PET/CT scans were obtained up to 3 hours post-injection. SUVmax values in the detected lesions, as well as in normal background areas were measured. Vital signs and EKGs were obtained at regular intervals. Blood samples were collected before injecting 18F FPPRGD2, at 24 hours and 1 week post-injection. All participants were scanned before and at 1-week after starting bevacizumab treatment**. Results**: 18F FPPRGD2 was well tolerated, with no significant changes in vital signs, EKGs, or laboratory values. The 18F FPPRGD2 uptake at 1 week after starting bevacizumab decreased by 29.5% in one NSCLC patient and by 16.8% in the other. The patient with 29.5% decrease in 18F FPPRGD2 uptake had stable disease at 4 months follow-up, but died after another 5 months. The patient with 16.8% decrease in 18F FPPRGD2 uptake had stable disease at 10 months follow-up. For the three GBM patients, the 18F FPPRGD2 uptake at 1 week after starting bevacizumab decreased by 28.8%, 64.3% and 59.1%, respectively. The patient with 28.8% decrease in 18F FPPRGD2 uptake had recurrent disease after another 2 months and died soon after. However, the patient with 64.3% decrease in 18F FPPRGD2 uptake had no recurrent GBM on follow-up brain MRI up to 11 months. The patient with 59.1% decrease in 18F FPPRGD2 uptake has not been seen in follow-up yet. Background SUVmax values were 0 - 1.02 (average 0.53 ± 0.12) for cerebellum, 0.63 - 1.67 (average 1.29 ± 0.29) for aortic arch, and 2.29 - 4.11 (average 3.09 ± 0.7) for liver. **Conclusions**: 18F FPPRGD2 is a safe PET radiopharmaceutical that may allow for evaluation of early response to bevacizumab treatment in patients with GBM and NSCLC.

## OP401

### In vivo characterization of CD44v6-targeting Fab fragments for molecular imaging of squamous cell carcinoma: a dual isotope study

**D. Spiegelberg**; Radiology, Oncology and Radiation Sciences; Uppsala University, Uppsala, SWEDEN.

**Aim** The strategy of selective tumour targeting based on cell surface molecules makes new personalized diagnosis and treatment available, and promises to lower redundant adverse effects. We have developed a fully humanized Fab fragment (AbD15179) for radioimmunotargeting that binds to CD44v6, an alternative splice variant of the adhesion receptor CD44. CD44v6 is overexpressed in squamous cell carcinomas (SCC), especially in the head and neck region. The Aim of this study was to assess the *in vivo* targeting properties of $^{111}$In and $^{125}$I -labelled Abd15197. By simultaneously injecting the two differently labelled tracers into mice carrying double SCC tumours with different CD44v6 expression, biodistribution, tumor uptake, contrast, as well as specificity and sensitivity of the tracers could be evaluated while eliminating inter-subject variability. **Materials and Methods** AbD15179 fragment was radiolabeled with $^{125}$I using Chloramine-T ($^{125}$I-Fab), or $^{111}$In using the chelate CHX-A"-DTPA ($^{111}$In-Fab). For specificity studies at 24h p.i, $^{125}$I-Fab and $^{111}$In-Fab were injected simultaneously into nu/nu mice bearing tumours with high (3x10$^6$ antigens/cell) and low (no detectable antigens) CD44v6 expression. For biodistribution studies, nu/nu mice bearing tumours with high and intermediate (7x10$^5$ receptors/cell) CD44v6 expression was used. Animals were sacrificed at 6, 24, 48 and 72h p.i. and radioactivity in different organs was measured. **Results** Both $^{111}$In-Fab and $^{125}$I-Fab demonstrated favourable biodistributions with a tumour specific uptake. The $^{111}$In labelled fragment demonstrated higher tumour uptake, slower tumour retention, and a more favourable biodistribution in organs of the head and neck region compared to $^{125}$I-Fab, whereas uptake of $^{125}$I labelled fragment in liver, kidneys and spleen was lower than the $^{111}$In-Fab uptake. Tumour to blood ratios increased with time, exceeding 15 for $^{111}$In-Fab in high CD44v6-expressing tumours at 72h p.i. Furthermore, $^{111}$In-Fab demonstrated better ability to discriminate between tumours with intermediate and high CD44v6-expression. **Conclusion** Radiolabeled AbD15179 is an excellent tracer for both intermediate and high CD44v6-expressing tumours. In this study, $^{111}$In-Fab demonstrated superior targeting properties. However, radiohalogens may also be suitable for this fragment, and targeting properties may be additionally improved by further optimizing the radiolabeling method. We believe that radiolabeled AbD15179 is a good candidate for developing individualized diagnosis and therapy in head and neck SCC.

## OP402

### HAHAHA-, HIHIHI-. HKHKHK. HHHHHH- and HEHEHE-tags: Influence of position and composition of histidine-containing tags on biodistribution of [99mTc(CO)3]+- labeled affibody molecules.

**V. Tolmachev**[1], C. Hofström[2], M. Altai[1], H. Honarvar[1], J. Strand[1], J. Malmberg[1], S. J. Hosseinimehr[1,3], A. Orlova[1], T. Gräslund[2]; [1]Uppsala Univesity, Uppsala, SWEDEN, [2]KTH Royal Institute of Technology, Stockholm, SWEDEN, [3]Mazandaran University of Medical Sciences, Sari, Iran, ISLAMIC REPUBLIC OF.

**Aim** Affibody molecules are a promising class of small (7 kDa) high-affinity probes for in vivo molecular imaging. Extending a recombinantly produced affibody molecule with a histidine-containing tag allows for convenient purification by immobilized metal-ion affinity chromatography (IMAC) and labeling with $[^{99m}Tc(CO)_3]^+$. Earlier, we have shown that the use of hexahistidine tag increases radioactivity uptake in the liver, while placement of a glutamate-containing HEHEHE-tag at N-terminus provides a $^{99m}$Tc – labeled conjugate with a low hepatic uptake. The Aim of this study was to investigate further the impact of charge, lipophilicity and position of histidine-containing tags on biodistribution of $^{99m}$Tc – labeled $Z_{HER2:342}$ affibody molecule. **Materials and Methods**. Ten variants of a HER2 binding affibody molecule were produced. Besides hexahistidine, tags containing glutamate (HEHEHE), isoleucine (HIHIHI), alanine (HAHAHA) and lysine (HKHKHK) were placed on N- or C-termini of affibody molecule. Affibody molecules were labeled with $^{99m}$Tc and characterized in vitro. Biodistribution of $^{99m}$Tc – labeled conjugates was investigated in NMRI mice at 4 and 24 h pi. **Results**. An IMAC purification and efficient labeling with $[^{99m}Tc(CO)_3]^+$ was possible for all ten variants. Affinity of all variants was in a narrow range of 26-88 pM. Stability under challenge with 5000-fold excess of histidine was higher for variants with N-terminal placement of tags. The influence of the tags on biodistribution was the most pronounced in the case of N-terminal modification. For N-terminally placed histidine-tags containing glutamate (E), alanine (A), histidine (H) and isoleucine (I), liver uptake and hepatobiliary excretion correlated with the lipophilicity of the side-chain. The liver uptake was the highest for the most lipophilic I (32±4 %ID/g at 4 h pi) and in decreasing order I>H>A>E (to1.5±0.1 %ID/g at 4 h pi). However, the hepatic uptake of $[^{99m}Tc(CO)_3]^+$-HKHKHK-$Z_{HER2:342}$ with a hydrophilic tag was also high (23±4 %ID/g at 4 h pi). The influence of tags at C-terminus was similar but the variation range was smaller (3.9 to 13 %ID/g). However, the blood radioactivity was higher in this case, and the level of blood radioactivity correlated with instability under histidine challenge. **Conclusion**, Composition of histidine-containing tags can be used for modification of biodistribution of $[^{99m}Tc(CO)_3]$-labeled affibody molecules. N-terminal HEHEHE-tag provided the lowest uptake in normal organs and tissues. The use of positively charged HKHKHK-tag is undesirable due to high hepatic uptake.

## OP403

### Feasibility of radionuclide imaging of HER3-expressing tumours using technetium-99m labeled affibody molecules

**A. Orlova**[1], M. Malm[2], H. Lindberg[2], Z. Varasteh[1], R. K. Selvaraju[1], N. Kronqvist[2], S. Ståhl[2], J. Löfblom[2], V. Tolmachev[3]; [1]Uppsala University, Preclinical PET Platform, Uppsala, SWEDEN, [2]Royal Institute of Technology, Stockholm, SWEDEN, [3]Uppsala University, Biomedical Radiation Sciences, Uppsala, SWEDEN.

**Aim.** Human epidermal growth factor type 3 (HER3) is a transmembrane receptor tyrosine kinase belonging to HER (ErbB) receptor family. Clinical data suggest that membranous expression of HER3 is associated with trastuzumab resistance in breast cancer and transition to androgen independence in prostate cancer. Thus,

imaging of HER3 expression in malignant tumours may provide important diagnostic information influencing patient's management. The Aim of the study was to investigate feasibility of HER3 imaging using radiolabelled affibody molecules, small (7 kDa) scaffold-based affinity proteins. **Materials and Methods.** High-affinity HER3-binding affibody molecules $Z_{HER3:5}$ and $Z_{HER3:6}$ were obtained by affinity maturation and produced with $(HE)_3$- and $H_6$-tags. Their affinity ($K_D$) was measured by SPR. $Z_{HER3:5}$ and $Z_{HER3:6}$ were labelled with $^{99m}Tc(CO)_3$ using histidine-containing tags as a chelators. In vitro binding specificity and cellular processing of labelled affibody molecules was evaluated using a panel of cancer cell-lines. To determine cross-reactivity with murine ErbB3, biodistribution was measured in NMRI mice after injection of three protein doses (0.1, 1 and 10 μg per mouse). Biodistribution in BALB/C nu/nu mice bearing LNCaP, MCF7, BT474 and LS174T xenografts was studed. **Results.** Affinity ($K_D$) of $Z_{HER3:5}$ and $Z_{HER3:6}$ binding to extracellular domain of HER3 were in low picomolar range (50 and 21 pM, respectively). The labelling yield was in range of 45-75% depending on molecule, and the purity of all conjugates was over 98% after purification using disposable size-exclusion column. Conjugates demonstrated specific binding to several carcinoma cell lines: BT474 and MCF7 (breast), DU145 and LNCaP (prostate), NCI-N87 (gastric), LS174T (colon), and A549 (lung). Cellular processing was characterised by rapid internalisation with up to 40% cell associated radioactivity being internalised already at 2 h of incubation, and 70% at 24 h. In normal mice, uptake of $^{99m}Tc(CO)_3$-$Z_{HER3:5}$-$H_6$ was saturable in liver, stomach, salivary gland, and intestines, which indicate cross-reactivity of conjugates with murine ErbB3 and makes mice a valid model for targeting studies. Uptake in liver, lungs, and intestine tissue decreased when $(HE)_3$-tag was used for labelling in comparison with $H_6$-tag. In tumour-bearing mice the tumour uptake was receptor mediated (saturable). Tumor-to-organ ratios for all tested xenografts were 4-5 for blood, 10-15 for muscle, and 5-4 (for LNCaP and LS174T) and 35-50 (for BT474 and MCF7) for bone. BT474 xenografts were visualized after injection of $^{99m}Tc(CO)_3$-$(HE)_3$-$Z_{HER3:5}$ by microSPECT/CT. **Conclusion.** The results of this study suggest feasibility of HER3-imaging in malignant tumours using affibody molecules.

## OP404

### Priliminary evaluation of 18F-FP-FSH1 for FSHR PET imaging

**M. Yang**, Y. Xu, D. Pan, L. Wang, S. Luo; Jiangsu Institute of Nuclear Medicine, Wuxi,Jiangsu, CHINA.

**Aim***:* Follicle-stimulating hormone receptor (FSHR) is an interesting new target, which was overexpressed in various solid tumors while negative in normal tissues. FSHβ(81-95) peptide (QCHCGKCDSDSTDCT, FSH1) has been proven as the antagonist of FSHR. Based on this peptide, we want to develop a new $^{18}$F-labeled FSHR probe, $^{18}$F-FP-FSH1 and evaluate its feasibility for PET imaging. **Materials and Methods***:* FSH1 peptide was labeled with $^{18}$F using 4-nitrophenyl 2-$^{18}$F-fluoropropionate ($^{18}$F-NFP) as a prosthetic group. The stability of $^{18}$F-FP-FSH1 was also determined in PBS and human serum. With none or excess FSH1, microPET imaging was done in PC-3 human prostate cancer xenograft model. **Results***:* Starting with $^{18}F^-$, the total reaction time for $^{18}$F-FP-FSH1 was about 120 min. The decay-corrected radiochemical yield for $^{18}$F-FP-FSH1 was 27±5% (calculated from $^{18}$F-NFP, n=5) and the radio purity was greater than 95%. The tracer was stable in PBS and human serum. HPLC analysis showed that more than 95% of the labelled peptide was still intact after 2h at room temperature. The tumors were clearly visible with good tumor-to-background contrast. Quantitative microPET studies demonstrated that the tumor uptakes of $^{18}$F-FP-FSHβ (81-95) were 3.71±0.42%ID/g, 3.25±0.24%ID/g and 2.69±0.36%ID/g at 30, 60 and 120 min postinjection respectively. The tumor to muscle uptake ratios were 4.14±0.60, 5.19±0.51 and 6.75±0.81 at the corresponding time. In addition, the tracer showed relatively high kidney accumulation at the early time points (7.96±1.40%ID/g at 30min p.i.) then dropped significantly afterward, indicating rapid renal clearance. In the presence of excess FSH1, the tumor uptake was completely blocked (0.54±0.06%ID/g at 1 h p.i.). **Conclusion***:* $^{18}$F-FP-FSH1 was prepared firstly with favorable characteristic in vivo. With this new probe, FSHR positive tumor such as prostate cancer can be clearly visualized by PET. Further study should be undertaken to test its diagnostic value. Research Support: NSFC (81171399 and 81101077), NSNDCP (2012ZX09505-001-001), Jiangsu Province SFC (BE2012622, BK2011166, BL2012031, RC2011095, H201028, BM2012066)

1007 - Monday, Oct. 21, 16:30 - 18:00, Salon Pasteur

## Physics & Instrumentation & Data Analysis: QA & Phantoms

## OP405

### Interpolated Average CT for Reducing Cardiac PET/CT Artifacts

**G. S. Mok**, C. Y. Ho, T. Sun; University of Macau, Macau, MACAO.

**Aim**: Previously we evaluated the interpolated averaged CT (IACT) method for improved attenuation correction (AC) in noise-free cardiac PET/CT simulations. This study Aims to demonstrate its effectiveness in realistic noisy simulations and clinical data. **Materials and Methods**: We first simulated realistic noisy 18F-FDG distribution based on the clinical count level using the digital 4D Extended Cardiac Torso phantom (XCAT) with respiratory motion amplitudes of 2 cm, 3 cm and 4 cm. The average activity and attenuation maps represented static PET and cine average CT (CACT) respectively, while the end-inspiration and end-expiration phases of the attenuation maps represented 2 helical CTs (HCT-1 and HCT-8). We used B-spline registration method combined with an empirical sinusoidal function to generate interpolated phases between 2 extreme phases. IACT was obtained by averaging the original and interpolated phases. The noisy sinograms with attenuation modeling were generated and reconstructed with CACT, HCTs and IACT by STIR (Software for Tomographic Image Reconstruction). Later we recruited 4 patients who had their scheduled whole body PET/CT scans under local ethics approval. They were scanned 1 hr post 315~428 MBq 18F-FDG injection. The PET sinograms were reconstructed with AC using: (i) standard HCT (120 kV, smart mA (30-150 mA), 0.984:1 pitch); (ii) IACT from 2 end-inspiration and end-expiration breath-hold HCTs (120 kV, 10 mA, 0.984:1 pitch) aided by an active breathing controller; (iii) CACT (120 kV, 10 mA, 5.9 s duration). Bull's eye plots were generated from the short-axis images and the corresponding circumferential profiles were analyzed. Effective dose of different CT protocols were also estimated. **Results**: The bull's eye plots of PET-IACT were more similar to PET-CACT from visual inspection in both simulations and clinical data. Artifacts were observed in various locations including anterior, anterolateral, apical lateral, anteroseptal and inferior segments in PET-HCT. The circumferential profiles from different apex-to-base distances consistently showed that PET-IACT closely approached to PET-CACT while PET-HCT showed substantial variations. The mean effective doses were 0.38 mSv, 2.26 mSv and 2.01 mSv for IACT, HCT and CACT respectively. The IACT reduced ~83% effective dose as compared to HCT. **Conclusion:** The IACT based AC reduced respiratory artifacts in cardiac PET. It is a promising low dose alternate of CACT to improve cardiac PET/CT imaging.

## OP406

### How to gain comparable low-dose protocols for different hybrid and stand-alone CT-scanners based on image-noise measurement-results - using a Tissue-Characterization-Phantom and an Alderson-Phantom

**S. Kerschbaumer**, C. Gstettner, A. Triebl, B. Schröttner, R. Aigner; Division of Radiology, Graz, AUSTRIA.

Comparability of image quality is a basic requirement for standardized clinical and scientific results. Aim of this study was to find a method and criteria to adjust the protocol parameters at various different CT-scanners. The method has been developed on SPECT/CT, PET/CT and stand-alone CT-scanners across different types, generations and manufacturers from 2 up to 320 detector lines. There are a growing number of technologies available to gain improved image impression with less radiation dose. For comparable image quality the appropriate settings of protocol-parameters have to compensate the influence of scanner hardware boundaries and reconstruction software characteristics. Provided, that the geometric parameters of the images (pixel size, slice thickness, pitch, filter kernel) are comparable, image-noise is the main criteria for accessing results from different scanners. A Tissue-Characterization-Phantom (Model 461A, GAMMEX-rmi, Middleton, WI, USA) and an Alderson-Phantom (Radiology Support Devices Inc. , Carson, CA, USA) were investigated. The tube current-time was modified in steps from 7mAs up to 600mAs (depending on the scanner) for both phantoms on each scanner. The dose modulation was "off" for the tissue characterization phantom and "on" for the Alderson-Phantom. The analysis was done on a HERMES Workstation (Hermes Medical Solutions AB., Stockholm, Sweden). The measured deviation of Houndsfield-Units within a spherical VOI (between 6 and 20mm diameter) was taken as a parameter for the image noise. The examination were performed on a SYMBIA-T2, SYMBIA-T16, BIOGRAPH-mCT-S(40)-4R, SOMATOM DEFINITION-AS+128 (Siemens Healthcare, Erlangen, Germany), DISCOVERY ST-16 (GE Healthcare, Chalfont St Giles, UK), AQUILION ONE (Toshiba Medical Systems, Nasu, Japan). For the Tissue-Characterization-Phantom up to a factor of 4 in the tube current-time settings (mAs) is required to gain the same noise value for the different observed scanners. Comparing the measured noise value on the Alderson-Phantom including dose modulation shows that image noise increases in the abdomen with lower current-time. This was up to a factor of 2 comparing the noise at 30mAs and 100mAs for each scanner. For the VOI within the brain, this effect was less pronounced. For lounge and bone regions, the noise value kept constant for the whole measurement range. The study has shown that phantom measurement can be used to compare the resulting image quality between CT protocols on scanners of different technological solutions and generations. The results impressively show that for comparable scanner protocols image quality and subsequent radiation-exposure must be perfectly adjusted with respect to the associated scanner hardware and software.

## OP407

### Accuracy of the Iterative Adaptive Dual Thresholding Method in SPECT and PET Phantom Experiments

**J. Grimes**[1], P. L. Esquinas[1], S. Zhang[2], M. Blaickner[3], T. Layer[3], B. Knäusl[4], D. Georg[4], A. Celler[5]; [1]Department of Physics and Astronomy, University Of British Columbia, Vancouver, BC, CANADA, [2]British Columbia Cancer Agency, Vancouver, BC, CANADA, [3]Austrian Institute of Technology, Health & Environment Department – Biomedical Systems, Vienna, AUSTRIA, [4]Department of Radiotherapy and Christian Doppler Laboratory for Medical Radiation Research for Radiation Oncology, Medical University of Vienna, Vienna, AUSTRIA, [5]Department of Radiology, University Of British Columbia, Vancouver, BC, CANADA.

**Aim**: The iterative adaptive dual thresholding (IADT) method applies two thresholds - one for segmenting target volume and one for recovering total activity in an object. These thresholds are semi-automatically obtained from experimentally generated calibration curves for each situation based on the signal-to-background ratio (SBR) and reconstruction algorithm. Our objectives were to test performance of IADT when applied to SPECT and PET cameras different than those used for calibration and to investigate bias and variance of volume and activity estimates from repeated acquisitions. **Materials and Methods**: SPECT and PET experiments were performed using Tc-99m and F-18 filled spheres (0.27-115ml) inside phantoms containing background activity. Five SPECT/CT acquisitions of the same phantom with a SBR of 10 were performed on a GE Infinia/Hawkeye and a sixth scan was acquired on a Siemens Symbia T camera. All scans were reconstructed using in-house software. Sphere volumes and activities were estimated using IADT with calibration curves previously generated using a different phantom configuration scanned on Infinia/Hawkeye. PET/CT studies were performed on a GE Discovery-690 and a Siemens Biograph-64-TruePoint system. Scans acquired at SBRs ranging from 2-10 were reconstructed using manufacturer's software and IADT calibration curves were generated for each camera. Calibration curves from the GE scan were used to estimate sphere volumes and activities from the experiment performed on the Siemens camera, and vice versa. Percent differences between true and measured volumes and activities were assessed. **Results**: SPECT image segmentation using the Infinia-based calibration for spheres greater than 4ml produced percent differences for the volume (activity) estimates averaging 0.3±12.4% (1.0±4.2%) for GE and 3.5±9.8% (-0.9±7.5%) for Siemens images. Repeated volume/activity measurements had low variance with relative standard deviations of 2.3% or less. IADT did not perform well for spheres less than 4ml in the SPECT study, where percent differences rose above 100%. In segmentation of PET images using Siemens calibration curves applied to the GE data, IADT performed best for SBRs of 4 and higher, and for spheres 2.57ml and larger. In this range, the average volume (activity) percent difference was 6.6±5.3% (7.2±5.6%). When the GE calibration curves were applied to the Siemens data, these percent differences were -10.4±8.5% (-10.9±6.8%). **Conclusion**: We have shown that IADT segmentation performs well for SPECT and PET studies, except for situations with low SBR and small objects. Most importantly, calibration curves from different cameras can be used as long as the data is reconstructed using comparable Methods.

## OP408

### Creation and Assessment of a 3D-Printed Subresolution Sandwich Phantom for the Simulation of HMPAO SPECT Images

**R. Holmes**[1], K. Jordan[2], I. Negus[1], G. Thorne[1], M. Saunders[1]; [1]University Hospitals Bristol, Bristol, UNITED KINGDOM, [2]University of Bristol, Bristol, UNITED KINGDOM.

**Background**: Data simulation is an essential step in SPECT and PET, especially in the validation of quantitative analysis techniques intended for clinical application. Software simulation allows the generation of known realistic ground truth but does not include the actual scanning process. Phantoms using the subresolution sandwich method (SSM) allow the simulation of realistic uptake patterns and provide a physical object to be scanned, thereby including the scanner in the simulation process. We have previously studied the usefulness of SSM phantoms to simulate 18F-FDG and 99Tcm-HMPAO in oncology and neurology. These studies used either cylindrical or elliptical perspex phantoms. Although they have produced highly realistic and flexible uptake patterns without the use of glass walls these phantoms cannot realistically simulate the attenuation and scatter properties of the head. Consequently we have investigated the feasibility of using a 3D printer to create subresolution phantoms using tissue equivalent plastic. **Materials and Methods:** BrainWeb MRI segmentation maps were used to create a 3D head volume suitable for 3D printing. Individual 4mm slices from the volume were printed using a commercial RepRap Mendel 3D printer using standard plastic feedstock to create a 3DP-SSM phantom. A brain pattern template with a 2:1 ratio of printed intensity for grey and white matter segments was derived from the same BrainWeb MRI segmentation maps and printed with a HP Deskjet 930 printer using black ink mixed with 99Tcm pertechnetate. Lesions were simulated in the template by reducing the printed intensity at various locations at various levels of severity. The printout slices were then placed within the 3DP-SSM phantom and scanned with a dual-headed gamma camera. **Results**: Unlike previous versions of the phantom, the increased realism of the 3DP-SSM version meant that standard clinical software could be used to reconstruct phantom data. All lesions were clearly visible in the reconstructed slices. **Conclusions**: This work has verified the feasibility of creating subresolution sandwich phantoms using 3D printing. Increased realism, in terms of improved simulation of the scatter and attenuation properties of the head, has been demonstrated which significantly improves the usefulness of this type of phantom.

## OP409

### Quality assurance of gamma-camera measurement of 99mTc-MAG3 renal clearance

**M. Samal**[1,2], V. Ptacnik[1,2], D. Skibova[1,2], H. Jiskrova[1,2], J. Kubinyi[1,2]; [1]Charles University Prague, 1st Faculty of Medicine, Prague, CZECH REPUBLIC, [2]General University Hospital, Prague, CZECH REPUBLIC.

Gamma-camera measurement of renal clearance is mostly based on empirical equations derived from regression of renal uptake on plasma clearance obtained with multiple blood samples. It is considered precise but not accurate. The Aim is to demonstrate 2 model-based Methods that can be used per se or as quality control of renal clearance calculated by regression. **Method** 'A' derives renal clearance Z from the slope of Patlak-Rutland plot k which is fraction of plasma volume in the heart ROI, k = Z/Vh, cleared per unit time. Plasma volume Vh is estimated as Vh = P(0)/c(0) = P(0)Vp/D where c(0) is plasma concentration at time t = 0, P(0) is the point of the heart ROI curve P(t) extrapolated to t = 0 by mono-exponential fit through uptake interval, D is injected activity and Vp is total plasma volume estimated from body surface area as Vp = 1645 BSA. Method 'B' derives renal clearance from Stewart-Hamilton principle R(t) = Z∫c(t)dt where R(t) is the renogram value at time t within the period of renal uptake and c(t) is plasma concentration curve estimated as P(t)/Vh. Renal clearance estimated by 'A' and 'B' was compared with each other, with the results of 2 regression Methods (Taylor et al 1995 and Gates modified for MAG3) and 2 in vitro Methods using one blood sample (Russell et al 1989, Bubeck et al 1992) in 107 patients with a wide range of renal function. The results demonstrate that although 'A' and 'B' are similar, they differ in handling renal and background counts and in dependence on background subtraction (none, tissue, vascular, both) they produce different results. Background subtraction affects 'A' much less than 'B'. Both Methods perform comparably well after subtraction of both tissue and vascular background from the kidney ROI. Using Taylor's kidney-depth estimation, agreement of 'A' and 'B' was best with Taylor's method (correlation coefficient r = 0.981 and 0.982, mean absolute difference 6 and -19 ml/min). Modified Gates was best predicted by 'B' without vascular background subtraction (0.983, 9 ml/min). Correlation of 'A' and 'B' with in-vitro Methods was lower (Russell 0.917, Bubeck 0.918). In conclusion, model-based Methods applied to individual patients provide quality control tool for checking the results of regression Methods. They can be also used independently of the regression Methods to provide additional information on renal function. The study was partly supported by the Czech Science Foundation grant GACR 303/07/0950.

## OP410

### Performance Evaluation of a Small Field of View Portable Gamma Camera for Localization of Sentinel Lymph Nodes

**N. Gorjizadeh**[1,2], N. Zeraatkar[1], A. Kaviani[3], S. Farzaneh far[4], M. Farahani[1,5], A. Akbarzadeh[1], S. Sajedi[1,5], B. Teimourian[1,5], M. Ay[1,2,6]; [1]Medical Imaging Group,Research Center for Molecular and Cellular Imaging,Tehran University of Medical Sciences, Tehran, IRAN, ISLAMIC REPUBLIC OF, [2]Department of Medical Physics and Biomedical Engineering,Tehran University of Medical Sciences, Tehran, IRAN, ISLAMIC REPUBLIC OF, [3]Department of Surgery,Tehran University of Medical Sciences, Tehran, IRAN, ISLAMIC REPUBLIC OF, [4]Department of Nuclear Medicine,Valiasr Hospital,Tehran University of Medical Sciences, Tehran, IRAN, ISLAMIC REPUBLIC OF, [5]Parto Negar Persia Co,, Tehran, IRAN, ISLAMIC REPUBLIC OF, [6]Research Center for Nuclear Medicine,Tehran University of Medical Sciences, Tehran, IRAN, ISLAMIC REPUBLIC OF.

**Aim**: This study Aimed to evaluate and characterize the performance of a newly developed pixelated portable gamma camera system that we called it SURGEOSIGHT. Radio-guided surgery using a gamma probe has been widely introduced in sentinel lymph node biopsies.However, gamma probe cannot provide any visual information of the region of interest. The use of a portable gamma camera in combination with a surgery gamma probe incorporates intraoperative real time imaging with improved sentinel node identification in different cancers. A compact, portable mini gamma camera with excellent intrinsic and extrinsic performance has been developed in our group for identification and localization of sentinel lymph nodes during the surgery of various cancers. **Materials and Methods**: The portable gamma camera consists of CsI(Na) scintillation crystal, coupled with a Hamamatsu H8500 position sensitive photomultiplier tube (PSPMT).

The detector elements have a size of 1.2 ×1.2×5 mm. This camera is equipped with 27 mm thick parallel-hole collimator with 1.6 mm hole size and 0.2 mm septa and dedicated electronics for data acquisition,processing, and transmission. The useful field of view of the camera is 42×42 $mm^2$. Performance measurements and the data analysis were done according to the procedures of the NEMA standard for human gamma cameras, NU 1-2001, due to the fact there is no dedicated standard for this kind of imaging system. **Results**: The system spatial resolution varied linearly with distance from the collimator; the FWHM was measured to be 2.25 mm at collimator surface and 4.9 mm at 3cm distance. Also, the system sensitivity was about 225 cpm/µci at distance 5cm from the collimator. The measured side shielding sensitivity was 98.2%. **Conclusion**: In this study, we have evaluated the performance of developed small field Gamma Camera in our group. This camera has an acceptable planar sensitivity, spatial resolution and energy resolution that are comparable to other commercially available gamma cameras with the same applications. The SURGEOSIGHT imaging performance, however, can still be improvedby optimizing collimator design, crystal dimension.

## OP411

### Image quality for advanced iterative reconstruction schemes with SPECT/CT

Y. Petegnief[1], J. Vrigneaud[2], C. Barrau[3], M. Guilhem[4], J. Coulot[5], **S. Hapdey**[6]; [1]CHU Besancon, Besancon, FRANCE, [2]Centre Georges-Francois Leclerc, Dijon, FRANCE, [3]CHU Nimes, Nimes, FRANCE, [4]CHR Orleans, Orleans, FRANCE, [5]Institut Gustave Roussy, Villejuif, FRANCE, [6]Centre Henri Becquerel, Rouen, FRANCE.

**Background:** Advanced iterative reconstruction Methods are now widely used for SPECT-CT. The Aim of this study was to evaluate the gain in image quality for clinical settings currently used for brain and body SPECT studies. Material and **Methods**: Data from the IEC image quality head and body phantoms were obtained with different SPECT/CT systems. Spheres (inner diameters varying from 10 to 37 mm) were filled with Tc-99m for spheres to background contrasts of 4:1 and 6:1 and the 'body' filled with 150 MBq. Camera settings were those used routinely for brain and body SPECT studies except pixel size that was adjusted as close as 3 mm. SPECT data were reconstructed with clinical parameters for OSEM (number of iterations and subsets, post-filter) using CT-based attenuation correction, scatter compensation based on multiple windowing estimates and nonuniform collimator response compensation for recovering isotropic resolution. Image quality was assessed following NEMA NU2-2007 definitions for hot spheres percent contrasts and background variability for the 37 mm sphere for 24 background ROIS (8 ROIs on three slices). **Results**: Visual analysis exhibited that all spheres were detected in brain studies whereas in body studies, in one case the smaller sphere was not visible for the 4:1 contrast. Spatial distorsions due to incomplete collimator response correction were present in all body transaxial images. Image noise was substantially decreased with resolution recovery correction. Despite different reconstruction parameters depending on manufacturers recommendations, hot sphere contrasts were quite similar from one system to the other and exhibited strong variations with sphere size (from 10% for 10 mm to 66% for 37 mm). Contrast recovery was mainly affected by post filtering. **Conclusion:** We proposed an image quality test for evaluation of image quality and contrast recovery in SPECT-CT. Advanced iterative reconstructions including collimator modelling demonstrated important spatial distorsions for body like studies and limitations of contrast recovery.

## OP412

### Interlaboratory comparison of SPECT image quality

**G. Köchle**[1], A. Hirtl[2], F. König[3], B. Ibl[4], B. Kroupa[5], M. Schaffarich[6], C. Sonneck-Koenne[7], A. Kurtaran[1], S. Mirzaei[7], H. Bergmann[6], M. Figl[6], P. Knoll[7]; [1]Dept. of Nuclear Medicine, Rudolfstiftung, Vienna, AUSTRIA, [2]Dept. of Radiology and Nuclear Medicine, Medical University of Vienna, Vienna, AUSTRIA, [3]Dept. of Nuclear Medicine, Donauspital, Vienna, AUSTRIA, [4]Staff Unit for Medical Physics, Medical Directorate, Rudolfstiftung, Vienna, AUSTRIA, [5]Institute of Hospital Physics, Hospital Hietzing, Vienna, AUSTRIA, [6]Center for Biomedical Engineering, Medical University of Vienna, Vienna, AUSTRIA, [7]Dept. of Nuclear Medicine, Wilhelminenspital, Vienna, AUSTRIA.

**Background/Aim**: Using the Jaszczak phantom for quality assurance of SPECT-capable gamma cameras is common practice in clinical routine. Nevertheless, up to now, image quality has been rated by visual inspection and comparison of the obtained phantom images with previous data. With our recently developed software it is now possible to quantify Jaszczak phantom data in terms of contrast and homogeneity. In addition, the software is capable of detecting potential ring artefacts by using the Hough transform. This makes the observation of SPECT-image quality much easier and more accurate. Prior to an Austria-wide interlaboratory comparison, we collected Jaszczak-phantom data from seven SPECT cameras in Vienna and tested our method for its practicability. **Material and Methods:** The participating departments were instructed to use standardized parameters for the data acquisition (106 counts on first view, 3° angular steps, attenuation correction) while for image reconstruction department-specific parameters were applied. For quantification of homogeneity and contrast, ImageJ plugins were developed and optimized for semi-automated ROI recognition. Furthermore, by performing a Hough transform and searching for circular objects in the homogeneity sector of the phantom, ring artefacts can be identified by our software. **Results**: For our sample of participating gamma cameras (n=7), homogeneity varied from 6.2% to 15.4%, the Total Contrast Quality Index (TCQI) for the four largest cold spheres was between 97.16 and 195.36 and for the rod sector (sector 1-6) between 6.17 and 60.56. No ring artefacts were found in our sample. **Conclusion:** This preliminary study showed that SPECT image quality control using the Jaszczak phantom, combined with our software, provides an easy way to obtain quantitative data. Expressing image quality in numbers is an important step to provide objective quality standards and to compare interlaboratory results.

1008 - Monday, Oct. 21, 16:30 - 18:00, Gratte-Ciel 1/2/3

## Radionuclide Therapy & Dosimetry: Treatment of Bone & Joint Diseases

## OP413

### Absorbed dose distributions in patients with bone metastases from hormone refractory prostate cancer treated with Re-186 HEDP

**A. M. Denis Bacelar**[1], A. Divoli[2], S. Chittenden[2], Y. Du[2], D. P. Dearnaley[1], J. M. O'Sullivan[3], G. D. Flux[2]; [1]Institute of Cancer Research, Sutton, UNITED KINGDOM, [2]Royal Marsden Hospital, Sutton, UNITED KINGDOM, [3]Queen's University Belfast / Belfast City Hospital, Belfast, UNITED KINGDOM.

**Aim:** Intravenous administration of Re-186 hydroxyethylidene-diphosphonate (HEDP) is used for metastatic bone pain palliation in hormone refractory prostate cancer patients. Dosimetry for bone seeking radionuclides is challenging due to the complex structure with osteoblastic, osteolytic and mixed lesions. The Aim of this study was to perform image-based patient-specific 3D convolution dosimetry to obtain a distribution of the absorbed doses to each lesion and estimate inter- and intra-patient variations. **Materials and Methods**: Twenty-eight patients received a fixed 5 GBq activity of Re-186 HEDP followed by peripheral blood stem cell rescue at 14 days in a phase II trial. A FORTE dual-headed gamma camera was used to acquire sequential Single-Photon-Emission Computed Tomography (SPECT) data of the thorax and pelvis area at 1, 4, 24 48 and 72 hours following administration. The projection data were reconstructed using filtered-back projection and were corrected for attenuation and scatter. Voxelised cumulated activity distributions were obtained with two different Methods. First, the scans were co-registered and the time-activity curves were obtained on a voxel-by-voxel basis. Second, the clearance curve was obtained from the mean number of counts in each individual lesion and used to scale the uptake distribution taken at 24 hours. The calibration factors required for image quantification were obtained from a phantom experiment. An in-house developed EGSnrc Monte Carlo code was used for the calculation of dose voxel kernels for soft-tissue and cortical/trabecular bone used to perform convolution dosimetry. Cumulative dose-volume histograms were produced and mean absorbed doses calculated for each spinal and pelvic lesion. **Results:** Preliminary results show that the lesion mean absorbed doses ranged from 25 to 55 Gy when the medium was soft tissue and decreased by 40% if bone was considered. The use of the cumulated activity distribution obtained from the scan acquired at 24 hours following administration reduced the number of artefacts introduced by the registration and voxelised cumulated activity calculations. **Conclusion**: Patient-specific convolution dosimetry calculations show that the absorbed dose to each lesion changes significantly depending on the medium density considered. This suggests that specific lesion and surrounding tissue compositions should be considered to overcome the limitations of convolution dosimetry, which could explain the range of absorbed doses observed. Future work will include the correlation of absorbed dose with patient outcome.

## OP414

### Palliative Treatment of Bone Metastases with Sm-153 EDTMP at Pain Onset

**F. D'Antuono**[1], A. Nardelli[2], R. Gallicchio[1], S. Giacomobono[1], A. Venetucci[1], T. Pellegrino[2], F. Leggiadro[1], N. D'Errico[1], D. Gattozzi[3], P. Mainenti[2], G. Storto[1]; [1]IRCCS CROB, Rionero In Vulture, ITALY, [2]IBB CNR, Napoli, ITALY, [3]University of Texas Southwestern, Dallas, TX, UNITED STATES.

**Aim:** we evaluated the pain response and the daily discomfort in patients suffering from a borderline degree of bone pain due to breast or prostate cancer bone metastases, who had undergone early palliative radionuclide treatment. The results were compared with those from patients who had received standard analgesic therapy. **Methods**: 22 patients (10 women; 66.4 ± 3 yrs) with metastatic bone cancer underwent Samarium-153 EDTMP administration (group A) and 18 patients (8 women; 67.7 ± 4 yrs) continued to receive standard analgesics (group B; control

group). The patients kept a daily pain diary assessing both their discomfort and the pain of specific sites by means of a visual analog scale (VAS), rating from 0 (no discomfort-no pain) to 10 (worst discomfort-pain). These diaries were reviewed weekly for 2 months and three physicians rated the pain response on a scale from −2 (considerable deterioration) to +2 (considerable improvement). **Results**: Baseline characteristics were similar in both groups. The reduction of total discomfort and of bone pain in the group A was significantly greater as compared to group B ($p < 0.0001$). A significant improvement of clinical conditions was observed in the group A, where the physician rate changed from −1 to 1, as compared to groups B in which the rate changed from −1 to 0. **Conclusion**: Sm-153 EDTMP therapy can be considered for patients with bone pain from breast and prostate cancer in advance, before the establishment of a severe pain syndrome.

## OP415

### Lutetium-177-ethylenediamine tetramethylene phosphonate (EDTMP) for bone pain palliation in metastatic prostate and breast cancer: A single institutional experience

**K. K. AGARWAL**, C. BAL, S. SINGLA, A. MALHOTRA; ALL INDIA INSTITUTE OF MEDICAL SCIENCES, NEW DELHI, INDIA.

**Aim**: The Aim of this study was to assess the viability of 177Lu-EDTMP as an effective bone palliation radiopharmaceutical and characterise the toxicity profile. **Materials & Methods**: 32 patients of prostate carcinoma (61 ± 15 yrs) and 12 patients of breast carcinoma (60 ± 13 yrs) with painful bone metastases were recruited into the study. The patients were randomised in two groups who were administered dose of 1295 and 2590 MBq of 177Lu-EDTMP intravenously. Patients were observed for toxicity and decrease in pain score using Visual Analogue Scale (VAS) upto 16 weeks. **Results**: There was a significant decrease in VAS score from the time of administration upto 16 weeks ($p <0.001$). The median time taken for response to therapy was found to be 9 days. The VAS decreased by 23% at 1st week, 57% at 4th week and 40% at 16th week compared to baseline score ($p <0.05$). However, no significant decrease was observed in VAS score from 4 to 8 weeks ($p <0.128$). Decrease of ≥50% in VAS score was observed in 26 (59%) patients and more than ≥70% in five (11%) patients. There was no statistically significant difference in the decrease in VAS from 2nd to 16th week in both the groups ($p <0.05$). The median duration of response was 90 days. The degree of effective pain palliation (maximum decrease in VAS) was not influenced by bone lesion score (BLS), baseline VAS and type of cancer and group on univariate analysis ($p=0.216$; $p=0.981$; $p=0.320$; $p=0.201$). The median duration of response in prostate carcinoma was 74 days compared to 88 days in breast carcinoma ($p=0.291$). The duration of response was unaffected by the dose of radiopharmaceutical ($p=0.845$) and BLS ($p=0.095$) but was associated with baseline VAS ($p=0.038$) and degree of response ($p=0.034$). No serious acute adverse events were observed post-treatment. Non-serious haematoxicity were observed in 15 patients and gr-3 /gr-4 haematoxicity occurred in eight patients. The median time to nadir was at third weeks and the median time to recovery at six weeks. **Conclusion:** 177Lu-EDTMP was found to be a safe and effective radioisotope for bone pain palliation in patients with metastatic prostate and breast carcinoma. The maximum pain relief was observed at 4th week which persisted upto 16th week.

## OP416

### Assessment of Patients with Diffuse Pigmented Villonodular Synovitis of Knee Before and After Radiosynovectomy

G. Koca, H. Ozsoy, H. I. Atilgan, **A. Baskin**, D. Koray, O. Fakioglu, M. Korkmaz; Ankara Training and Research Hospital, Ankara, TURKEY.

**Aim**: The Aim of this study was to evaluate subjective and objective findings of patients with diffuse pigmented villonodular synovitis (DPVNS) of knee before and after treatment with Yttrium-90 (Y-90) radiosynoviectomy. **Materials and Methods**: Between years 2005 and 2013, 23 patients, 15 female and 8 male, who had adjuvant radiosynoviectomy after arthroscopic surgery were included to our study. Five mCi of Y-90 radiocolloid was administered under local anesthesia at least 6 weeks after arthroscopic surgery. The patients were reevaluated 6 months after radiosynovektomy. All the patients were assigned a Lysholm knee score prior to surgery, prior to radiosynovectomy and 6 months after radiosynoviectomy. Lysholm score was calculated according to patients' pain, swelling, instability, locking, limping, support, climbing the stairs, squatting and the highest evaluation score was 100. In addition Modified Marshall scoring system was calculated according to objective and subjective findings of the patients prior to surgery and six months after radiosynovectomy. The highest evaluation score was 30 in modified Marshall scoring system where 19 points were provided by objective findings and 11 points were provided by subjective findings. Scores higher than 26 were defined as very good, between 21-25 was good, between 16-20 was medium, and values less than 16 points are considered to be poor. The obtained points using scoring systems were evaluated statistically. **Results**: The mean age was 31.7 ± 13.2 years. The average time period between the operation and radiosynoviectomy was 12.8 ± 8.14 weeks. The calculated Lysholm scores prior to surgery, prior to radiosynovectomy and 6 months after radiosynoviectomy were 38.8 ± 4.1, 60.0 ± 4.4 and 82.9 ± 6.5, respectively ($p <0.001$). Modified Marshall scores prior to surgery, and 6 months after radiosynoviectomy, was 12.4 ± 2.7 and 25.5 ± 3.1 respectively ($p <0.001$). CONCLUSION: We conclude that Y-90 therapy in patients with DPVNS of knee is efficient in treatment of objective and subjective symptoms. In addition both scoring systems are reliable predictors of effectiveness of the Y-90 therapy.

## OP417

### SPECT/CT: Can It Be Helpful In The Evaluation Of The Distribution Of The Radionuclide in the Joint Following Radiosynovectomy

**F. Özülker**, A. Küçüköz Uzun, T. Özülker; Okmeydanı Training and Education Hospital, Department of Nuclear Medicine, İstanbul, TURKEY.

Planar control scintigraphies have been utilized for the detection of any possible extra articular leakage after radiosynovectomy in patients with haemophilic arthropathy. In this study we Aimed to assess whether utilization of SPECT-CT for the same purpose can provide additional information. Patients who fullfilled the following prerequisites were included for radiosynovectomy application: (1) more than four hemorrhagic episodes in six months (2) at least a Stage II haemophilic arthropathy according to the classification of Arnold and Hilgartner (3) persistent synovitis. Six male patients (5 hemophilia A, 1 hemophilia B) who suffered from haemophilic arthropathy with a mean age of 10.5 (range between 8-15) were included in this study. We administered 148-185 MBq Yttrium 90 silicate (Y-90) to 5 knee joints, 74 MBq Rhenium 186 (Re-186) to 1 elbow joint and 74 MBq Re-186 to two ankle joints of these patients. The median number of bleedings into the target joints was 10.1 ± 1.4 in the six months prior to the procedure. All patients were admitted to the hospital and treated with factor replacement so as to raise the factor level of the patient to 80% the following morning and 50% for three days thereafter. The effusion in the joint was evacuated before the injection of the radiocolloid. Intraarticular injections in ankle and elbow joints were done under fluoroscopic guidance. The joint was moved rapidly a few times to distribute the radiocolloid, after which a plaster of paris cast was applied for 72 hours. One hour after the RS, planar images of the treated joints and the regional lymph nodes were obtained with gamma camera and SPECT-BT acquisitions were obtained from treated joints to confirm the appropriate distribution of the radionuclide in the joint. Distribution of the radionuclide in joint spaces was normal and we haven't encountered any extraarticular leakage. In one patient there was loculation af activity in suprapatellar recess detected with SPECT-CT which was not deliniated in planar image. We concluded that SPECT-CT might be superior to planar imaging in the detection of any possible extraarticular leakage and intraarticular loculation of radionuclide when the poor anatomic deliniation of the images obtained with radionuclides used for radiosynovectomy is concerned.

## OP418

### Hematologic Safety Profile of Radium-223 Dichloride (Ra-223) From the Phase 3 ALSYMPCA Trial in Castration-Resistant Prostate Cancer (CRPC) Patients With Bone Metastases

**A. Widmark**[1], S. I. Helle[2], N. James[3], A. Larsson[1], K. Staudacher[4], I. Haugen[4], J. Garcia-Vargas[5], S. Nilsson[6]; [1]Umeå University, Umeå, SWEDEN, [2]Haukeland University Hospital, Bergen, NORWAY, [3]Cancer Research UK Clinical Trials Unit, School of Cancer Sciences, Birmingham, UNITED KINGDOM, [4]Algeta ASA, Oslo, NORWAY, [5]Bayer HealthCare, Montville, NJ, UNITED STATES, [6]Karolinska University Hospital, Stockholm, SWEDEN.

**Aim:** Ra-223 is a targeted alpha-emitter that selectively binds to bone metastases and emits high-energy, short-range (<100 µm) alpha-particles. In the phase 3, double-blind, randomized, multinational ALSYMPCA trial, Ra-223 significantly improved overall survival (OS) in CRPC patients with bone metastases by a median increase of 3.6 months versus placebo (median OS: 14.9 vs 11.3 mo; HR = 0.695; 95% CI, 0.581-0.832; $P = 0.00007$) and was associated with a highly favorable safety profile. Updated hematologic safety data are presented. **Methods:** Eligible patients had progressive, symptomatic CRPC with ≥2 bone metastases on scintigraphy and no known visceral metastases; were receiving best standard of care (BSoC); and had received docetaxel, or were unfit for or declined docetaxel. Patients were randomized 2:1 to 6 injections of Ra-223 (50 kBq/kg IV) q4wk or matching placebo and stratified by prior docetaxel use, baseline alkaline phosphatase level, and current bisphosphonate use. The primary endpoint was OS. An updated analysis, based on 528 deaths, was performed on data from all randomized patients. Hematology values at baseline, week 24, and follow-up visit 2 (40 weeks after first study drug administration), were compared for clinically meaningful differences between treatment groups. **Results:** Updated analyses included 901 patients (safety population: Ra-223, n = 600; placebo, n = 301). Overall grade 3/4 hematologic adverse events (AEs) were similar between Ra-223 and placebo groups (19% vs 16%), with neutropenia in 2% and 1%, thrombocytopenia in 6% and 2%, and anemia in 13% and 13% of Ra-223 and placebo groups, respectively. Grade 3 febrile neutropenia was reported in 1 patient (0.2%) receiving Ra-223 and 1 patient

(0.3%) receiving placebo. Median neutrophil values decreased from baseline at week 24 in the Ra-223 group, but recovered in follow-up (Ra-223: $4.5\times10^9$/L; $3.3\times10^9$/L; $3.9\times10^9$/L vs placebo: $4.6\times10^9$/L; $4.5\times10^9$/L; $4.3\times10^9$/L). A similar decline in median platelet values was observed in the Ra-223 group, but recovered during follow-up (Ra-223: $244\times10^9$/L; $202\times10^9$/L; $216\times10^9$/L vs placebo: $240\times10^9$/L; $232\times10^9$/L; $218\times10^9$/L). Median hemoglobin values decreased over time in both groups (Ra-223: 12.2 g/dL; 11.4 g/dL; 10.8 g/dL vs placebo: 12.1 g/dL; 11.6 g/dL; 11.2 g/dL). **Conclusions:** Overall, the incidence of hematologic AEs was relatively low with Ra-223 treatment. Laboratory assessment of hematology parameters was consistent with the hematologic AE findings. Ra-223 is an effective therapy with a highly favorable safety profile in CRPC patients with bone metastases.

## OP419

### Updated Analysis of Radium-223 Dichloride (Ra-223) Impact on Survival, Safety, and Skeletal-Related Events in Castration-Resistant Prostate Cancer (CRPC) Patients With Bone Metastases From the Phase 3 ALSYMPCA Trial

**S. Wedel**[1], T. W. Kranert[2], A. Chodacki[3], K. Staudacher[4], J. Garcia-Vargas[5], C. Parker[6]; [1]Ortenau Klinikum Offenburg Gengenbach, Klinik für Urologie und Kinderurologie, Offenburg, GERMANY, [2]Universitätsklinikum Frankfurt, Klinik für Nuklearmedizin, Frankfurt/M, GERMANY, [3]Hospital Kochova, Chomutov, CZECH REPUBLIC, [4]Algeta ASA, Oslo, NORWAY, [5]Bayer HealthCare, Montville, NJ, UNITED STATES, [6]Royal Marsden NHS Foundation Trust and Institute of Cancer Research, Sutton, UNITED KINGDOM.

**Aim:** Ra-223, a first-in-class alpha-emitting pharmaceutical, targets bone metastases with high-energy, short-range (<100 µm) alpha-particles. ALSYMPCA, a phase 3 double-blind, randomized, multinational study, compared Ra-223 plus best standard of care (BSoC) versus placebo plus BSoC in CRPC patients with bone metastases. Updated survival, safety, and skeletal-related event (SRE) data are presented. **Methods:** Eligible patients had progressive, symptomatic CRPC with ≥2 bone metastases on scintigraphy and no known visceral metastases; were receiving BSoC; and had received docetaxel, or were unfit for or declined docetaxel. Patients were randomized 2:1 to 6 injections of Ra-223 (50 kBq/kg IV) q4wk or matching placebo and stratified by prior docetaxel use, baseline alkaline phosphatase level, and current bisphosphonate use. The primary endpoint was overall survival (OS); secondary endpoints included SREs and safety. Updated analysis, based on 528 deaths, was performed on data from all randomized patients. Pathologic bone fractures, reported as an SRE component, were required to be clinically relevant, not asymptomatic fractures. **Results:** 921 patients were randomized (Ra-223, n = 614; placebo, n = 307); 40% had >20 metastases. Compared to placebo, Ra-223 significantly improved OS (median OS: 14.9 vs 11.3 mo; HR = 0.695; 95% CI, 0.581-0.832; *P* = 0.00007) and delayed time to first SRE (median time to first SRE: 15.6 vs 9.8 mo; HR = 0.658; 95% CI, 0.522-0.830; *P* = 0.00037). In addition, Ra-223 reduced risk for all 4 SRE components versus placebo (external beam radiotherapy [EBRT]: HR = 0.67; 95% CI, 0.53-0.85; *P* = 0.001; spinal cord compression [SCC]: HR = 0.52; 95% CI, 0.29-0.93; *P* = 0.025; pathologic bone fracture: HR = 0.62; 95% CI, 0.35-1.09; *P* = 0.095; and surgical intervention: HR = 0.72; 95% CI, 0.28-1.82; *P* = 0.479). Ra-223 was associated with a low incidence of myelosuppression (eg, grade 3/4 neutropenia in 2% and 1%, and grade 3/4 thrombocytopenia in 6% and 2% with Ra-223 and placebo groups, respectively) and fewer adverse events versus placebo. **Conclusions:** Ra-223 significantly prolonged OS, significantly delayed time to first SRE, and reduced risk for all 4 SRE components when compared to placebo in CRPC patients with bone metastases. Ra-223 patients had an approximately 50% reduction in risk for SCC. Ra-223 is an effective therapy with a highly favorable safety profile in CRPC patients with bone metastases.

1009 - Monday, Oct. 21, 16:30 - 18:00, Rhône 3A/3B

## Radiopharmaceuticals & Radiochemistry & Dosimetry: Radiometals

## OP420

### A tripodal tris(hyroxypyrdinone) ligand for immunoconjugate PET imaging with zirconium-89

**M. T. Ma**[1], L. K. Meszaros[1], B. M. Paterson[2], D. J. Berry[1], M. S. Cooper[1], Y. Ma[3], J. R. Ballinger[1], R. C. Hider[3], P. J. Blower[1]; [1]Division of Imaging Sciences and Biomedical Engineering, King's College London, London, UNITED KINGDOM, [2]University of Melbourne, Melbourne, AUSTRALIA, [3]Institute of Pharmaceutical Science, King's College London, London, UNITED KINGDOM.

**Aim:** Due to its long half-life (78.4h) and decay properties (23% β$^+$, 897keV), $^{89}$Zr is an appealing radionuclide for immunoPET imaging with antibodies. Desferrioxamine-B (DFO) is the most widely used bifunctional chelator to coordinate $^{89}Zr^{4+}$ because the radiolabelling of the resulting immunoconjugates is rapid under mild conditions. $^{89}$Zr-DFO complexes are stable *in vitro* but recent data demonstrated the release and subsequent bone uptake of the radiometal *in vivo*. We Aim to evaluate a tripodal tris(hydroxypyridinone) ligand CP256 (Berry DJ, *et al.* (2011) ChemComm, 47, 7068-70) developed in our laboratory, as a $^{89}Zr^{4+}$ chelator and compare it with DFO. **Methods:** To compare the ability of CP256 to complex $Zr^{4+}$ with that of DFO, decreasing concentrations of each chelator were labelled with $[^{89}Zr(oxalate)_4]$. Competition experiments were also undertaken. The radiolabelled products and radiochemical yields were evaluated by ITLC and reverse phase HPLC-MS coupled to a scintillation detector. To assess the stability of DFO/CP256-immunoconjugates radiolabeled with $^{89}$Zr, maleimide derivatives of the chelators were conjugated to the monoclonal antibody trastuzumab *via* reduced cysteine side chains. Serum stability studies and *in vivo* biodistribution and microPET/CT studies with normal C57Bl/6j mice were undertaken on the $^{89}$Zr-radiolabelled immunoconjugates. **Results:** CP256 coordinates $Zr^{4+}$ (natural abundance) and comparison of HPLC-MS/scintillator chromatograms confirms that addition of $[^{89}Zr(oxalate)_4]$ to CP256 results in formation of $[^{89}Zr(CP256)]^+$. DFO and CP256 can be radiolabelled with $[^{89}Zr(oxalate)_4]$ at ambient temperature in quantitative yield at pH 6-7 at millimolar concentrations. Competition experiments demonstrate that $^{89}Zr^{4+}$ does not substantially dissociate (<10%) from $[^{89}Zr(CP256)]^+$ in the presence of a ten-fold greater concentration of DFO relative to CP256. However, $^{89}Zr^{4+}$ dissociates from $[^{89}Zr(DFO)]^{2+}$ in the presence of one equivalent of CP256 (relative to DFO), resulting largely in $[^{89}Zr(CP256)]^+$. The immunoconjugates, CP256-trastuzumab and DFO-trastuzumab, can be labelled with $^{89}$Zr in >98% yield at specific activities of 55MBq mg$^{-1}$ and 91MBq mg$^{-1}$ respectively. Both $^{89}$Zr-labelled immunoconjugates are stable in serum with respect to dissociation of the radiometal. MicroPET/CT and biodistribution studies indicate that after one day, $^{89}Zr^{4+}$ dissociates from CP256-trastuzumab with significant amounts of activity associated with bones and joints (25.88±0.58% ID g$^{-1}$ after one week). In contrast, <8% ID g$^{-1}$ of $^{89}$Zr activity is associated with bone for animals administered $^{89}$Zr-DFO-trastuzumab over the course of one week. **Conclusion:** The tris(hydroxypyridinone) ligand, CP256 coordinates $^{89}Zr^{4+}$ rapidly under mild conditions, but the $^{89}$Zr-labelled immunoconjugate, $^{89}$Zr-CP256-trastuzumab, was observed to release significant amounts of $^{89}Zr^{4+}$ *in vivo*, demonstrating inferior stability when compared with $^{89}$Zr-DFO-trastuzumab.

## OP421

### Using Low Energy Medical Cyclotrons to Produce 99mTc - Technetium

**L. F. Metello**[1,2], W. Gelbart[3], L. Cunha[1], S. Carmo[4], C. Artner[5], F. Alves[4]; [1]Nuclear Medicine Department, High Institute for Allied Health Technologies, Polytechnic Institute of Porto (ESTSP.IPP), VILA NOVA GAIA, PORTUGAL, [2]IsoPor, SA, Porto, PORTUGAL, [3]Advanced Systems Design (ASD), Garden Bay, BC, CANADA, [4]Institute for Health Applied Nuclear Sciences (ICNAS), University of Coimbra, Coimbra, PORTUGAL, [5]IASON (ARGOS Zyklotron Betriebs-GesmbH), Linz, AUSTRIA.

This paper refers to work in progress, addressing the global trouble in delivering 99mTc to Nuclear Medicine Departments, Aiming to develop an efficient, safe and economical way to directly produce Technetium 99metastable (99mTc) using low-energy - so-called "medical" - cyclotrons. The present delivery strategy has intrinsic limitations because it is not only based on old nuclear reactors, but also limits the weekly agenda workflow. Our approach is distinct, and is based on the broad distribution network of the low energy cyclotrons and the accessibility of Molybdenum 100 (100Mo) as the target material, so the system here presented, is not based on the use of Nuclear Reactors and highly enriched (or even low enriched) Uranium 235 (235U), but entirely complying with the current international trends and directives, concerning the need to reduce the use of this potential highly critical target material. The direct production technique is based on the nuclear reaction 100Mo(p,2n)99mTc whose production yields have already been widely documented. The 99mTc is produced in a routine, reliable and efficient manner that, remaining always flexible, entirely blends with established protocols. An additional advantage is that there are no more agenda constraints (daily workflow could be the maintained). A solid target station, that can be installed in most of the existing low energy cyclotrons has been developed; it will tolerate up to 400 µA of beam by allowing it to strike the solid target material at an oblique angle, under controlled circumstances, while allowing the remote and automatic loading and discharge of the targets. Concerning the solid target itself, several Methods of target material deposition and substrates are being studied and compared. The rationale was to create a cost effective means of depositing and intermediate the target material thickness (75 - 300µm) with a minimum of loss on a substrate that is able to easily transport the heat inherently associated with high beam currents. Finally, the separation techniques are yet under development, using a combination of both physical and column chemistry. The ultimate goal is to extract and deliver 99mTc in the identical form now in use in radiopharmacies worldwide. In addition, the solid target material needs - due to its price and relevance - to be recovered and should be recycled, adding an extra degree of complexity. This simpler, cleaner and more efficient way of producing 99mTc will bring a new solution to the present 99mTc shortage problem.

## OP422

### Cyclotron Produced $^{99}$Mo as a Source of $^{99m}$Tc via Generator-Like Automated Extraction Procedure

**S. V. Selivanova**[1], J. Sader[2], E. J. van Lier[2], A. Zyuzin[2], J. E. van Lier[1,3], R. Lecomte[1,3], B. Guérin[1,3]; [1]Centre Hospitalier Universitaire de Sherbrooke, Sherbrooke, QC, CANADA, [2]Advanced Cyclotron Systems Inc., Vancouver, BC, CANADA, [3]Université de Sherbrooke, Sherbrooke, QC, CANADA.

**Aim:** Technetium-99m ($^{99m}$Tc) is the most widely used radioisotope in nuclear imaging. Current route of $^{99m}$Tc manufacturing requires irradiation of highly-enriched weapon-grade uranium-235 ($^{235}$U) in nuclear reactors. One of the most promising alternatives is cyclotron production method via $^{100}$Mo(p,2n)$^{99m}$Tc nuclear reaction. Besides $^{99m}$Tc itself, a considerable amount of $^{99}$Mo is co-produced at medium irradiation energies (>20 MeV). Normally, processed target solute containing $^{100}$Mo/$^{99}$Mo in ammonium carbonate buffer would be collected for further $^{100}$Mo recycling. The goal of this work was to investigate if cyclotron-produced $^{99}$Mo can serve as a source of $^{99m}$Tc and to develop a suitable procedure and automated apparatus for repetitive $^{99m}$Tc extraction. **Methods:** Enriched (>99%) $^{100}$Mo targets were irradiated in a TR24 cyclotron at 24 MeV beam energy and 15 µA target current. Irradiated targets were dissolved and $^{99m}$Tc was isolated from the crude mixture as sodium $^{99m}$Tc-pertechnetate by passing the solution through a set of biphasic and ion exchange resins. Reserved target solute was kept for 24 h after processing to allow for $^{99m}$Tc growth. After this time, $^{99m}$Tc was extracted again following the same protocol. The extraction procedure was repeated after every 24 h, as it is common for $^{99}$Mo generators. Radiochemical identity and purity of the extracted $^{99m}$Tc-pertechnetate from $^{99}$Mo target solute were determined by TLC. Gamma-ray spectrometry was used to verify radionuclidic purity of the product. **Results:** $^{99m}$Tc was repetitively extracted from $^{99}$Mo/$^{100}$Mo solution in a generator-like manner using an automated system. Recovery of $^{99m}$Tc from the target solute followed the rules for $^{99}$Mo/$^{99m}$Tc transient equilibrium. Radiochemical purity of the isolated $^{99m}$Tc was above 98%. Presence of $^{99}$Mo was not detected. The extraction can be done starting next day after $^{99}$Mo production, unlike for reactor produced $^{99}$Mo, which requires a week to be shipped and assembled into a generator. Since the same automated procedure was used for $^{99m}$Tc elution day after day, total $^{99m}$Tc-pertechnetate solution volume remained the same, while radioactivity was decreasing with daily elutions. Optimisation of resins amounts and elution solvent volume is required to achieve higher radioactivity concentration of final product. **Conclusions:** We demonstrated that $^{99}$Mo, co-produced with $^{99m}$Tc in a cyclotron during bombardment of $^{100}$Mo targets, can be used for the subsequent repetitive $^{99m}$Tc extraction in an automated device, resembling generator principle.

## OP423

### The Somatostatin Receptor Antagonist Ga-68-NODAGA-BASS (sst2-ANT) has Significantly Better in vivo Performance, as PET Imaging Probe, than Ga-68-DOTA-BASS (sst2-ANT)

**M. Fani**[1], M. L. Tamma[1], G. P. Nicolas[1], E. Gourni[2], J. C. Reubi[3], H. R. Maecke[2]; [1]University of Basel Hospital, Basel, SWITZERLAND, [2]University Hospital of Freiburg, Freiburg, GERMANY, [3]University of Bern, Bern, SWITZERLAND.

**Aim:** Imaging and treatment of somatostatin receptor (sst)-expressing tumours with radiolabelled somatostatin agonists are routinely applied nowadays in many hospitals, especially in Europe. Recent preclinical studies showed superiority of the antagonists compared to agonists, in terms of tumour uptake and pharmacokinetics. SPECT imaging data of the first radiolabelled somatostatin antagonist, namely $^{111}$In-DOTA-BASS, in patients showed that imaging with antagonists is clinically feasible. The Aim of our work was to develop and evaluate this antagonist as a $^{68}$Ga-PET imaging probe. **Materials and Methods:** The somatostatin antagonist DOTA-BASS and the new conjugate NODAGA-BASS were labelled with $^{68}$Ga. Labelling with $^{67}$Ga was performed for long time-points investigations. The affinity of the conjugates after complexation with natural Ga was determined by receptor autoradiography. Two cell lines expressing the somatostatin receptor subtype 2, one transfected (HEK-sst2) and one natural (AR42J), were used for the evaluation of the probes *in vitro* and *in vivo*. **Results:** The affinity and the pharmacokinetics of the new probes depend on the chelator. $^{nat}$Ga-NODAGA-BASS has 2.5-fold higher affinity than $^{nat}$Ga-DOTA-BASS ($IC_{50}$ = 16.7±0.6 and 40.0±5.0, respectively) and more than 2-fold higher tumor uptake in HEK-sst2 xenografts (33.9±4.9 and 14.2±4.9 %IA/g, respectively, 1 h p.i.). Blood clearance and also clearance from non-tumour organs was faster for $^{68}$Ga-NODAGA-BASS while tumor washout was slower compared to $^{68}$Ga-DOTA-BASS (74% and 37% remained in the tumour at 4 h p.i., respectively). The tumor-to-background contrast was significantly higher and increasing over time for $^{68}$Ga-NODAGA-BASS while decreasing for $^{68}$Ga-DOTA-BASS. The differences *in vivo* was even more profound in the AR42J xenografts, where the tumour uptake of $^{68}$Ga-NODAGA-BASS was 17.0±3.1 %IA/g while of $^{68}$Ga-DOTA-BASS only 1.2±0.4 %IA/g, at 1 h p.i. The uptake and washout from the non-tumour organs was very similar in both xenograft models. Specificity of the probes was demonstrated by successful blocking of HEK-sst2 and AR42J tumour uptake with excess of cold peptide. Small-animal PET images demonstrated high contrast images of HEK-sst2 and AR42J tumours for $^{68}$Ga-NODAGA-BASS and quantitatively confirmed the ex-vivo biodistribution data. Additionally, PET imaging of the same animal with both probes highlighted the significant differences found in the biodistribution studies. **Conclusion:** $^{68}$Ga-NODAGA-BASS has significantly better *in vivo* performance, as PET imaging probe, than $^{68}$Ga-DOTA-BASS. The results are in agreement with our previous findings showing that in the family of radiolabelled somatostatin antagonists the chelate makes the difference.

## OP424

### Synthesis and Zr-89 labeling of Df-DUPA-Pep: A new peptide ligand for molecular imaging of prostate carcinoma.

**B. Baur**[1], E. Al-Momani[1], E. Andreolli[2], G. Winter[1], H. Machulla[1], C. Solbach[1]; [1]Clinic of nuclear medicine, Ulm, GERMANY, [2]University of Milano-Bicocca, Milan, ITALY.

**Aim**: Using molecular imaging for diagnosis and therapy of prostate carcinoma the prostate-specific membrane antigen (PSMA) is a valid target due to its high expression in prostate carcinoma. Therefore, various peptides for diagnostic and therapeutic approaches were developed. Previous investigations with the Ga-68 labeled DOTA conjugated PSMA ligand DUPA-Pep (2-[3-(1,3-dicarboxypropyl) ureido]pentanedioic acid (DUPA) linked via 8-aminooctanoic acid to two phenylalanine residues) showed a high PSMA affinity with a KD of 21 nM. In-vivo experiments with [Ga-68]GaDOTA-DUPA-Pep showed promising results. The Aim of this study was the synthesis of desferal conjugated DUPA-Pep and the radiolabeling with Zr-89. The advantages of the use of Zr-89 for labeling of Desferal linked peptides are the mild labeling conditions (room temperature) and its t½ of 3.3 d allowing long term investigations. . **Materials and Methods**: Desferal-DUPA-Pep was synthesized in a one step reaction with custom made DUPA-Pep-trifluoroacetate and p-isothiocyanatobenzyl-desferal. Characterization of the synthesized desferal conjugated peptide was achieved using HPLC, 1H-NMR and LC/MS. Radiosynthesis was developed regarding reaction-time and amount of precursor. Labeling was performed by adding 50-200 µl of Zr-89 activity in neutralized aqueous solution to a solution of 5-100 µg peptide in 500 µl 0.25 M HEPES buffer of pH 7.4. The reactions were carried out at room temperature and monitored after 5, 10, 30 and 60 min. Radiochemical yield (RCY) and radiochemical purity were determined by radio-TLC and radio-HPLC. PSMA-affinity was determined in cell experiments using LNCaP cells. **Results:** The structure of the peptide was verified by 1H-NMR and LC/MS. A purity of 99% was determined by HPLC (254 nm). The best result was obtained after reaction time of 60 min and using 100 µg of peptide with a RCY of 96 % ± 0.7 %. In cell experiments the radiolabeled peptide showed high affinity towards PSMA with a KD value of 42 ± 5 nM. **Conclusion**: An efficient method for the preparation of the new PSMA-ligand [Zr-89]Zr-Df-DUPA-Pep was developed. Under the shown conditions a nearly quantitative labeling yield was observed. Moreover, the ability to label desferal conjugated biomolecules under mild conditions (room temperature) avoids heat-based side reactions or decomposition.

## OP425

### Feasibility study of direct cyclotron production of 227-Th.

J. Kozempel[1], **M. Vlk**[1], P. Mičolová[1], O. Lebeda[2], M. Moša[3], A. Morgenstern[4]; [1]Czech Technical University in Prague, Prague 1, CZECH REPUBLIC, [2]UJF AV ČR, Řež, CZECH REPUBLIC, [3]General University Hospital in Prague, Prague 2, CZECH REPUBLIC, [4]ITU, Karlsruhe, GERMANY.

Aim Alpha emitting radiometals are promising tools for cancer treatment. One of them is $^{223}$Ra (half-life of 11.4 days) together with its mother nuclide, $^{227}$Th (half-life of 18.7 days).These nuclides can be obtained from $^{227}$Ac/$^{227}$Th/$^{223}$Ra generator produced via $^{226}$Ra(n,γ)$^{227}$Ra/$^{227}$Ac reaction using nuclear reactor. This fact puts, however, high requirements on radiation stability of such a generator. Aim of this study was to develop alternative method for direct cyclotron production of $^{227}$Th via $^{226}$Ra(α,3n) reaction. **Methods** Cross-sections of the $^{226}$Ra(α,3n) reaction were adopted from TENDL-2012 library based on TALYS nuclear model code. Using these data, thick target yields of this reaction were calculated. Experimental verification of the predicted values was performed on a U-120M isochronous cyclotron of the Nuclear Physics Institute of the Academy of Science of the Czech Republic by irradiating single thin $^{226}$Ra targets. The targets were then analysed using alpha and gamma spectrometry. **Results** According to TENDL-2012, the maximum of the excitation function of the $^{226}$Ra(α,3n)$^{227}$Th reaction is around 33 MeV, while of the $^{226}$Ra(α,2n)$^{228}$Th reaction is around 26 MeV. Irradiation of $^{226}$Ra target with 30 µA alpha particle beam degraded from 40 to 30 MeV for 10 hours should result in ca 74 MBq (2 mCi) of $^{227}$Th that contains 0.09 MBq (2.5 µCi) of $^{228}$Th radionuclidic impurity (<0.2% at EOB). High purity $^{227}$Th could be obtained by proper selection of the beam energy window. **Conclusion** Relevant quantities of $^{227}$Th of high radionuclidic purity may be produced using medium energy alpha particle beam on $^{226}$Ra targets. We have shown that production of $^{227}$Th is feasible and sufficient

activities of of $^{227}Th/^{223}Ra$ for therapy purposes can be produced on medium energy cyclotrons.

## OP426

### Heteroligand Yttrium-90 dialkyldithiocarbamate complexes with 1,10-Phenanthroline for the potential application in therapy of hepatocellular carcinoma

**N. Lepareur**[1], A. Lopez[1,2], N. Noiret[2], E. Garin[1]; [1]Centre Eugene Marquis, Rennes, FRANCE, [2]ENSCR, Rennes, FRANCE.

**Aim** Hepatocellular carcinoma (HCC) ranks third in terms of cancer mortality worldwide, with an increasing incidence in western countries. Due to often late detection and underlying hepatopathy, it is a pathology for which curative treatment is only accessible to a minority of patients. Radiolabelled Lipiodol has shown promising results for internal radiotherapy of inoperable hepatocellular carcinomas. Literature has shown that yttrium-90 is a radionuclide of choice for HCC treatment. We thus propose a new labelling of Lipiodol with yttrium-90 as a potential treatment modality for HCC. **Materials and Methods** A series of long-chain alkyl dithiocarbamate (dtc) yttrium complexes, which could easily be extracted in Lipiodol due to their high lipophilicity, have been synthesised, both at millimolar (non-radioactive) and radiotracer levels. Coordination sphere is completed with 1,10-phenanthroline, giving a complex of general formula $[Y(dtc)_3Phen]$, as determined by analytical Methods. Various conditions have been investigated (pH, temperature, reaction time···). Lipiodol labelling yield and *in vitro* stability have been determined by counting of organic and aqueous phases, over a period of 8 days. **Results** Five heteroligand complexes with alkyl chain ranging from ethyl to hexadecyl were prepared and fully characterised. At tracer level, three radiocomplexes were prepared and used to successfully label Lipiodol. Preparation is quick and efficient, at room temperature. Too long an alkyl chain seems to have a deleterious influence on the labelling yield, as well as on the stability, presumably for steric reasons. **Conclusion** A new simple and reliable method for the $^{90}Y$-labelling of Lipiodol has been demonstrated. *In vivo* biodistribution and stability are now to be investigated.

1010 - Monday, Oct. 21, 16:30 - 18:00, Tête D'Or 1/2

## Conventional & Specialised Nuclear Medicine: Uronephrology

## OP427

### Quantitative analysis of angiotensin converting enzyme inhibition renography: a step forward toward standardization and harmonization of reports

**S. BEATOVIC**[1,2], E. Jaksic[1,2], M. Dragas[3,2], J. Marinkovic[4,2], R. Rebic[1], V. Obradovic[1,2]; [1]Center for Nuclear Medicine Clinical Center of Serbia, Belgrade, SERBIA, [2]Belgrade University School of Medicine, Belgrade, SERBIA, [3]Clinic for Vascular and Endovascular Surgery Clinical Center of Serbia, Belgrade, SERBIA, [4]Institute for Medical Statistics, Belgrade, SERBIA.

**Introduction**: Captopril renography (CR) is established for screening of renovascular hypertension. Prolongation of time to maximum activity and increasing of 20 min/ peak ratio are the main criteria to define a positive test result. The analysis of cortical renograms is useful in distinguishing parenchymal from pelvic retention. Our study Aimed at assessing the significance of several parameters of kidney transit in the analysis of CR: Tmax, 20min/ Tmax ratio, whole kidney mean transit time (MTT) and mean parenchymal transit time (MPTT). **Patients and Methods**: 57 patients aged 20 to 78 years were evaluated. All patients were first investigated with a captopril-stimulated renogram. A baseline study was added only in patients showing abnormal finding on ACEI study. Dynamic scintigraphy was done 20 minutes after bolus injection of 74 MBq Tc-99m MAG3. 120 images of 10 seconds were recorded. For data processing, "The International Atomic Energy Agency Software Package for the Analysis of Scintigraphic Renal Dynamic Studies" was used. **Results:** Analysis of sequential images and time-activity curves revealed 11 patients (19%) with significant unilateral parenchymal retention after captopril (Group A). Group B consisted of 28 patients with normal finding on ACEI renography. In 18 patients both CR and basal study were abnormal (Group C). For all parameters, mean value, lower and upper bound of 95% confidence interval were calculated. Group A: CR: Tmax(min): 12.0; 7.2; 16.2; 20min/ Tmax ratio: 0.70; 0.35; 0.94; MTT: 6.5; 5.0; 8.2; MPTT: 4.0; 2.4; 6.9. Baseline finding: Tmax: 4.9; 3.0; 6.2; 20min/ Tmax ratio: 0.39; 0.26; 0.56; MTT: 3.3; 2.0; 5.1; MPTT: 2.1; 1.5; 2.9. Increasing of Tmax after ACEI was between 2.4 and 10.5 min (33-73%). 20min/ Tmax ratio increased between 0.12 and 0.54, and MPTT between 18% and 76%. Group B: Tmax: 3.6; 2.3; 5.0; 20min/ Tmax ratio: 0.23; 0.13; 0.40; MTT: 2.2; 1.4; 3.2; MPTT: 1.6; 1.1; 2.4. Group C: CR: Tmax: 9.1; 3.5; 19.8; 20min/ Tmax ratio: 0.64; 0.24; 0.98 MTT: 4.4; 2.1; 8.4; MPTT: 2.7; 1.6; 5.3. Baseline finding: Tmax: 9.4; 3.2; 21.5; 20min/ Tmax ratio: 0.70; 0.32; 0.98; MTT: 5.1; 2.1; 10.5; MPTT: 3.0; 1.7; 6.5. In this group 7 patients showed decreasing of MTT after ACEI between 14% and 55%. **Conclusion:** Quantitative analysis of CR facilitates the comparison between studies. The evaluation of cortical transit can increase the specificity of the test. Decreasing of MTT after ACEI could help to select hypertensive patients who can benefit from ACE inhibitors.

## OP428

### DMSA split function as a predictor of outcome in pediatric patient with unilateral vesicoureteric reflux

**H. R. S. Farghaly**[1,2], H. Nasr[3,2], N. Al Shobely[4]; [1]Nuclear Medicine Unit-Assiut University, Assiut, EGYPT, [2]Nuclear Medicine Div. Prince Sultan Military Medical City, Riyadh, SAUDI ARABIA, [3]Cairo University, Cairo, EGYPT, [4]Radiology dept. Prince Sultan Military Medical City, Riyadh, SAUDI ARABIA.

**Objective:** To emphasize the value of DMSA split function in predict the outcome of unilateral vesicouereteric reflux (VUR) in pediatric patients. **Patient and Methods:** Retrospectively we reviewed 136 pediatric ( 0 - 14 years) patients (79 boys and 57 girls) with unilateral VUR diagnosed by VCUG study with normal contralateral kidney who underwent DMSA scan in period from Jan 2006 to Feb 2013. VCUG exam was performed and reported by consultant pediatric radiologist and DMSA scan was reviewed by consultant nuclear medicine. Other imaging modality (ultrasound, Renogram) or follow up DMSA scan was recorded and tabulated. Split renal function (SRF) in both baseline and follow-up DMSA in each kidney in each patient was recorded and compared with VUR grades. Statistical analysis was performed using chi square statistics to get the statistical significance (P value). **Result:** There were 36 patients with low grade (I &II) VUR, 31 of them (86%) have normal RSF (≥40%) and 5 (14%) have abnormal SRF (< 40%). 100 patients are high grade (III, IV &V), 19 of them have RSF ≥40% and 81 have RSF < 40%. 48 patients have follow-up DMSA scan, 32 of them have baseline SRF of < 20% only 2 (6%) out of these 32 showed interval increased in RSF (>30%) upon treatment the other 30 (94%) patients showed no improvement or even deterioration of SRF despite treatment. 16 patients out of 48 with follow-up DMSA have baseline SRF between 20-40%, 13 (81%) of them showed no improvement or even deterioration of SRF despite treatment and only 3 (19) out of these 16 patients showed interval increased in RSF (>30%) upon treatment. Statistical analysis of 20% cutoff value of SRF in predicting outcome result in Chi square= 4.83 and P value=0.028 (< 0.05).**Conclusion**: RSF with cutoff of 20% is a good predictor of outcome in pediatric patients with unilateral VUR and patients with baseline SRF of < 20% have poor outcome despite treatment.

## OP429

### Predictors of surgical outcome in antenatally diagnosed hydronephrosis: A prospective study

**M. L. Abrar**, A. Bhattacharya, K. L. N. Rao, K. S. Sodhi, B. R. Mittal; Postgraduate Institute of Medical Education & Research, PGIMER, CHANDIGARH, INDIA.

**Objectives**: To define parameters that predict surgical outcome in infants with antenatally detected hydronephrosis (ANH). Methods: 38 patients with a diagnosis of ANH were enrolled in this prospective study and had a postnatal ultrasonography (USG) and Technetium99m-EC (Ethylene Dicysteine) dynamic renal scintigraphy (DRS). Quantitative parameters like APD (Antero-posterior diameter of renal pelvis) on USG and clearance T1/2 value and differential renal function (DRF) on DRS were measured. Visual analysis of drainage pattern on done on DRS was as following: Grade 1: Unobstructed drainage: Adequate tracer clearance during dynamic study (20 minutes) Grade 2: Slow unobstructed drainage: Tracer retention noted during dynamic study tracer clearance seen at 3 hours Grade 3: Equivocal drainage: Slow drainage with delayed images showing tracer retention Grade 4: Obstructed drainage: Significant retention of tracer in the kidney in the delayed image. Univariate analysis was done using Chi square test with YATES correction and Fischer's exact test where applicable to evaluate which parameter predicted surgical outcome Results: Two patients had single kidney and the other kidney remained non-visualized. A total of 74 renal units were hence analysed. The APD of the hydronephrotic kidneys ranged from 4 to 100mm (mean APD of 15.9 ± 19.2mm); 14 renal units had APD>15mm; 8 renal units had a DRF of 20 minutes that was suggestive of pelvi-ureteric junction obstruction (PUJO). 72% renal units showed unobstructed drainage. 27% of renal units showed Grade 4 drainage pattern suggestive of PUJO; APD>15 mm (p value 0.002), clearance T1/2 >20 minutes (p <0.001) and Grade 4 pattern of drainage (p <0.001) predicted surgical outcome. DRF 15mm, clearance T1/2 >20 minutes and Grade 4 pattern of drainage are significant predictors of pyeloplasty. DRF of <40% does not predict surgical outcome. Tc99m EC DRS plays a complementary role with USG in evaluation of ANH and is particularly important in identifying infants who are at high risk of PUJO.

## OP430

### Brief report: Short term prognostic utility of Tc-99m DMSA renal imaging in sepsis induced acute renal failure; Provisional data

**A. Amin**, H. Nasr, H. Gamal; NEMROCK, Faculty of Medicine; Cairo University, Cairo, Egypt, Cairo, EGYPT.

**Background**: Sound prognostic data in sepsis induced acute renal failure (SARF) are lacking especially on the short term outcome [STO] in the intensive care unit [ICU]. We addressed the use of Tc-99m DMSA [2, 3-dimercaptosuccinicacid] renal cortical imaging as a prognostic tool in SARF. **Methods:** Forty patients with acute renal failure due to sepsis [age range 15-74 years; median 44.5] were subjected for full history taking; complete physical examination, routine ICU monitoring, routine laboratory investigations, APACHE II [Acute Physiology and Chronic Health Evaluation] and SOFA [Sequential Organ Failure Assessment] together with Tc-99m DMSA cortical renal scintigraphy. Patients' death in the ICU or discharge was considered as the end point of the study representing the so-called short term outcome [STO]. **Results:** 25% mortality rate [10/40] was found along the admission period in the ICU. All non-survivors were abnormal with DMSA imaging [NPV & PPV 100% & 66.7% respectively]. Abnormal DMSA cases showed significant positive associations with serum creatinine at admission [r=0.5; P 0.02]; admission duration [r=0.4; P 0.002]; APACHE II score [r=0.5; P 0.004] and STO [r=0.4; P 0.03]. Statistically significant difference was elicited between subjects with normal and abnormal DMSA regarding the same parameters. **Conclusion**: This preliminary data could raise Tc-99m DMSA renal imaging as a prognostic tool in SARF that could allow influential interference to prohibit dramatic outcomes as mortality.

## OP431

### F+0 Diuresis Renography in children : experience of nuclear medicine department in Ibn Rochd Hospital in Casablanca

**S. TALEB**, M. AIT IDIR, G. CHERKAOUI, A. GUENSI, M. KEBBOU; Nuclear Medicine Department in Ibn Rochd, Casablanca, MOROCCO.

Dynamic renography is a non-invasive functional procedure which presents a big interest for exploration of urinary tracts drainage, while estimating relative renal function. There are several protocols. Simultaneous administration of diuretic and radiotracer or F+0 protocol, allows increasing number of patients able to complete dynamic acquisition without interference, and to overcome injection difficulties in children. Aim of this study was to evaluate usefulness of this protocol and to appreciate different patterns in our experience. Fifty one patients (32 M and 18 F), aged 17 days to 16 years (mean: 8.55 yrs), were studied in nuclear medicine department of Ibn Rochd UH, in Casablanca, between January 2010 and December 2012. The investigation was indicated to assess: uretero-hydronephrosis (22 cases), obstruction and renal function in patients with pelvi-ureteric junction syndrome (17 cases), mega-ureter (7cases), renal lithiasis (2case), vesicoureteral reflux (1case), urethra posterior valve (1case) and post-surgical evaluation of a previously obstructed system (1 cases). Diuretic and radiotracer were administered intravenously at the same time, 99mTc-MAG3 in 24 cases (47%) and 99mTc-DTPA in 27 cases (52%). Qualitative and quantitative parameters were included for interpretation (dynamic display, relative renal function, time to maximum activity, clearance half time and residual renal activity). Interpretation criteria were those currently recommended by European associations of Nuclear medicine. Data of dynamic renal scintigraphy were used to classify our patients into three groups. Group I: absence of urinary tracts drainage impairment in 18 cases (36%). Group II: with urinary tracts drainage impairment and functional consequences, in 34 cases (68%), unilateral alteration for 54% and bilateral alteration for 14% of cases. Group III : unclear findings in 7 cases (14%) (no kidney uptake making it impossible to assess quality of drainage). F+0 diuresis renography study of children, is a valid method for investigation of urinary tract drainage. In addition, F+0 protocol has a shorter imaging time and is less invasive compared with the F+20 study.

## OP432

### Superiority, after motion correction of renal studies, of pinhole SPECT on parallel hole SPECT

**G. Demonceau**[1], M. Hesse[2], S. Walrand[2]; [1]St Elisabeth Hospital, Zottegem, BELGIUM, [2]UCLouvain, Brussels, BELGIUM.

Pinhole SPECT studies (PHS) were previously demonstrated to be of general better quality than parallel hole SPECT for Tc-DMSA studies. Motion badly affects the reconstructed image quality and is frequent in long lasting imaging, especially with children. Motion correction is particularly challenging in renal pinhole SPECT, due the pinhole magnification that is strongly spatially dependent, unlike what happens in parallel hole collimation. We wonder if, after motion correction, the advantage of pinhole SPECT would still remain. Six hours after a weight-dependant injection of $^{99m}$Tc-DMSA, four 5min-dynamic views and two 25min-SPECT were performed in 25 patients (pts) aged between 1 month and 47 years (mean: 5.4 y) and suspected for acute pyelonephritis. A motion correction was applied on each data: on planar imaging, an irregular ROI was manually applied on each frame; the frames were adjusted according to the ROI center of mass, then summed together. On both SPECT imaging, the acquired projections were shifted to match as well as possible the re-projections of a first reconstruction of the set of good incidences only. Reconstruction of both SPECT was made with an OSEM algorithm with, in the case of PHS, geometric correction and adaptive filters. Both SPECT studies were visually compared side-by-side on the same screen. Criteria were the blurring of the contours, the cortex/cavity contrast and the depth and volume of the cortical defects. In case of doubt, the planar imaging was used as gold standard. Compared to parallel hole SPECT, pinhole SPECT had a better quality of imaging in 13 pts, the same in 6pts and a lower quality in 6 pts. A significant relation was observed with the registered counts for PHS: a large number of counts (i.e. above 150.000) is associated with a greater chance to be superior to parallel hole SPECT, and a similar quality is expected in a zone between 110.000 and 150.000 registered counts. The amount of registered counts is depending on the injected dose, the body attenuation and the kidney-pinhole distance. The superiority of PHS was thus clearer for patients with age between 2 and 18 years. In conclusion, the difficulty to correct for motion in PHS doesn't preclude the superiority of this method on parallel hole SPECT for children. In adults, both techniques seem equal, probably due to the higher kidney-pinhole distance and attenuation.

1101 — Tuesday, Oct. 22, 08:00 — 09:30, Amphithéâtre

## CME 9 - Neuroimaging (Interactive): Brain PET Imaging

### OP433
**FDG-PET in the Context of the other Biomarkers in Prodromal AD**

**F.M. Nobili, ITALY**

### OP434
**How to Read Amyloid Images?**

**P. Payoux, FRANCE**

### OP435
**DOPA PET Neuroimaging**

**J. Darcourt, FRANCE**

### OP436
**PET-MRI Brain Imaging**

**S. Hesse, GERMANY**

1102 — Tuesday, Oct. 22, 08:00 — 09:30, Auditorium Lumière

## Symposium 9 - EANM/BIR Joint Session: Current Evidence and Future Directions of SPECT/CT Imaging

### OP437
**Added Value of SPECT/CT in Endocrinology**

**S. Navalkissoor, UNITED KINGDOM**

### OP438
**SPECT/CT in Benign and Malignant Bone Disease: Moving beyond Planar & SPECT**

**G. Gnanasegaran, UNITED KINGDOM**

### OP439
**Added Value of SPECT/CT in Miscellaneous Scenarios**

**J.R. Buscombe, UNITED KINGDOM**

1107 — Tuesday, Oct. 22, 08:00 — 09:30, Salon Pasteur

## Pitfalls & Artefacts & Physiology (Interactive): Advances in Cardiac SPECT & SPECT/CT

### OP440
**Clinical Use of IQ-SPECT**

**E. Gremillet, FRANCE**

### OP441
**Clinical Use of CZT-SPECT**

**A. Gimelli, ITALY**

## OP442
### Clinical Use of SPECT/CT & Flow Quantification

**C. Anagnostopoulos, GREECE**

1201/1203 — Tuesday, Oct. 22, 10:00 — 11:15, Amphithéâtre

## Plenary 3: New Insights in Molecular Neuroimaging

## OP443
### Is FDG still the Gold Standard for Early and Differential Diagnosis of AD? Comparison to Amyloid and other Biomarkers

**K. Herholz, UNITED KINGDOM**

## OP444
### Cerebral Pattern Recognition in Neurodegenerative Brain Diseases using FDG Uptake and Principal Component Analysis

**K.L. Leenders, NETHERLANDS**

## OP445
### Role of Molecular Imaging in the Treatment and Follow-up of Brain Tumours

**C. la Fougère, GERMANY**

1204 - Tuesday, Oct. 22, 10:00 - 11:15, Bellecour 1/2/3

## Featured - Oncology Clinical Science: Lymphoma

## OP446
### Lymphoma Management: Towards Personalised Therapy

**E. Itti, FRANCE**

## OP447
### Lymphoma newly diagnosis: initial results with 18F-FDG PET/CT and whole body MRI-DWIBS

**A. Niccoli Asabella**[1], C. Ferrari[1], M. Ficco[2], N. Maggialetti[3], F. Iuele[1], C. Altini[1], C. Minoia[4], A. Guarini[4], C. M. Florio[2], G. Rubini[1]; [1]1Nuclear Medicine Unit, D.I.M., University of Bari "Aldo Moro", Bari, Italy, ITALY, [2]2Department of Radiology, Istituto Tumori G. Paolo II, IRCCS Bari, Italy., Bari, Italy, ITALY, [3]3Ricerche Radiologiche srl, Molfetta (BA), Italy", Bari, Italy, ITALY, [4]4Department of Hematology, Istituto Tumori G. Paolo II, IRCCS Bari, Italy., Bari, Italy, ITALY.

**Aim**: 18F-FDG PET/CT is the reference standard in HL and high-grade NHL staging, but its role in the other histotypes remains to be demonstrated. Diffusion-weighted whole body imaging with body signal suppression (DWIBS), is an emerging functional imaging modality, which can be complementary to 18F-FDG PET/CT. The Aim of this study was to evaluate the role of whole-body MRI/DWIBS compared with 18F-FDG PET/CT in the initial staging of lymphomas. **Methods & Materials**: 25 patients (14 men, 11 women; mean age 40,6 years) with newly diagnosed lymphoma (11/25 HL, 14/25 NHL) prospectively performed staging 18F-FDG PET/CT and whole-body MRI (coronal T1-weighted, coronal STIR, axial DWIBS sequences) within 2 weeks interval. Lymphnodes larger than 10 mm, in the coronal plane on T1-weighted and STIR images, were considered positive. Lymphnodes positive on PET/CT images were included even if lower than 10 mm. The comparison between the different sites involved (nodal and extranodal) was performed by K of Cohen. The overall agreement in lymphoma staging, according to Ann Arbor criteria, was evaluated. **Results**: 18F-FDG PET/CT showed 75 nodal and 10 extranodal sites involved, while WB-MRI/DWIBS showed 80 nodal and 12 extranodal sites. The two techniques were discordant in 10/25 patients (40%), 5 HL and 5 NHL (2 DLBCL, 1 FL, 1 SLL/CLL, 1 sMZL), for a total of 21 lymphnodal stations. Of these, 18FDG-PET/CT was positive and WB-MRI/DWIBS was negative in 8/21 lymphnodal stations, while in 13/21 lymphnodal stations 18F-FDG-PET/CT was negative and WB-MRI/DWIBS positive. The Cohen's K performed for each lymphonodal basins involved, was: 0.754 (95%CI,0.494-1.014) for cervical, 0.918 (95%CI,0.761-1.075) for axilla, 0.838 (95%CI,0.622-1.053) for mediastinum, 0.679 (95%CI,0.392-0.967) for abdominals and 0.851 (95%CI,0.654-1.048) for inguinal basins. In according to Ann Arbor criteria, the two Methods were concordant for staging in 22/25 cases (88%) and the agreement was moderate-good. 2/25 patients (8%; 1 DLBCL, 1 SLL/CLL) showed a different stage with the 2 techniques, with an over staging by WB-MRI/DWIBS. 1/25 patient (4%) was under staged by WB-MRI/DWIBS. **Conclusion**: agreement between 18F-FDG PET/CT and WB-MRI/DWIBS is moderate-good. In a minority of patients, WB-MRI/DWIBS over staged or under staged the disease. 18F-FDG PET/CT remains the gold standard for lymphoma staging, but WB-MRI/DWIBS can be useful in histotypes not FDG-avid. The information provided by the 2 Methods can be complementary, because they are based on different biophysical underpinnings.

## OP448
### Role assessment of FDG-PET on involved node radiotherapy (INRT) implementation in Hodgkin lymphoma patients.

V. Edeline1, A. Aupérin2, V. Ribrag3, M. Elleuch-Ghrab4, Ch. Fermé3, G. Bonniaud5, C. Ruelle6, J.-L. Albérini1, A. Celebic2, T. Girinsky7; 1Department of Imaging, Institut Curie, R. Huguenin Hospital, Saint-Cloud, France, 2Biostatistics and Epidemiology unit, Institut Gustave Roussy, Villejuif, France 3Department of Medicine, Institut Gustave Roussy, Villejuif, France, 4Department of Imaging, Institut Gustave Roussy, Villejuif, France, 5Department of Medical Physics, Institut Gustave Roussy, Villejuif, France, 6Department of Information Technology, Institut Gustave Roussy, Villejuif, France 7Department of Radiation Oncology, Institut Gustave Roussy, Villejuif, France.

**Purpose**: To assess the role of FDG-PET in the implementation of INRT in patients treated for a stage I-II supra-diaphragmatic Hodgkin lymphoma. **Methods**: Patients with early-stage Hodgkin lymphoma enrolled in the EORTC-LYSA-FIL H10 trial and participating in a real-time prospective quality assurance program were prospectively included in this study. Data was electronically obtained from 18 French cancer centres. Patients underwent a pre-chemotherapy PET/CT and a post-chemotherapy CT simulation performed 3-4 weeks after the end of chemotherapy. Co-registration of PET/CT and CT simulation were performed according to previously published procedures. First, gross tumor volume (GTV) and clinical target volumes (CTV) were delineated on CT only by the radiation oncologist. After planning PET coregistration, an analysis of the delineated volumes was jointly performed by the radiation oncologist and the nuclear medicine physician. Lymph nodes undetected on CT, but FDG-avid were recorded. GTV and CTV were modified according to FDG-PET results. **Results**: From March 2007 to February 2010, 135 patients were included. PET/CT identified at least one additional FDG-avid lymph node in 95/135 patients (70.4%; CI 95%: 61.9-77.9) and one additional lymph node area in 55/135 (40.7%; CI 95%: 32.4-49.5). Mean increase in GTV and CTV were 8.8% and 7.1%, respectively. The systematic addition of PET to CT led to a CTV increase in 60% of the patients and in most cases, radiation volumes remained smaller than those of classical involved field radiotherapy (IFRT). **Conclusions**: Pre-chemotherapy FDG-PET imaging leads to a significantly better INRT delineation without necessarily increasing radiation volumes.

## OP449
### Characterizing Bone Marrow Involvement in Hodgkin's Lymphoma by FDG-PET/CT

**M. Weiler-Sagie**, O. Kagna, E. Dann, A. Ben-Barak, O. Israel; Rambam Health Care Campus, Haifa, ISRAEL.

**Aim:** FDG-PET/CT has been shown to be superior to bone marrow (BM) biopsy in detecting bone marrow involvement in the staging of Hodgkin's lymphoma (HL). The present study Aims to define the prevalence and distribution of BM involvement in Hodgkin's lymphoma as determined by FDG-PET/CT in a single large referral center. **Materials and Methods**: Reports of FDG-PET/CT studies performed for staging of HL between January 2001 and January 2013 were reviewed. Patients who had an additional malignancy and patients who did not perform post-treatment follow up studies were excluded. Reports indicating the presence of pathological foci in the skeleton that resolved in the post-treatment scan were defined as positive for BM involvement. Number of foci and location were recorded. Change in stage of disease following diagnosis of BM involvement by FDG-PET/CT was recorded. **Results:** Four hundred and fifty one patients with HL met the inclusion criteria. The study group included 226 males and 225 females with an age range of 3-86 (median 30). Sixity three patients (14%) had evidence of BM involvement by FDG-PET/CT. Twelve patients had a single focus, 12 had 2 foci and 39 had 3 or more foci of pathological FDG uptake in the skeleton. Vertebrae were involved in 44 patients, pelvis in 41, long bones in 28, ribs in 17, sternum in 16, scapula in 10, skull in 9 and clavicle in 3 patients. The BM was the only extra-nodal site in 44/63 patients (70%). BM involvement, defined by FDG-PET/CT, upstaged 34/63 patients (54%) from stage 3 to 4 and 10/63 patients (16%) from stage 2 to stage 4. **Conclusion**: FDG-PET/CT demonstrated a prevalence of 14% of BM involvement in patients with newly diagnosed HL. Diagnosis of BM involvement in HL by FDG-PET/CT was higher as compared to reports using BM biopsy and led to upstaging of 70% of patients. Multifocal pattern of BM involvement was found in 62% and single foci were found in 19% of positive studies. The most common sites of BM involvement were the spine and pelvis.

## OP450

### Limited 18F-FDG PET-CT for monitoring early chemotherapy response in lymphoma for reducing total radiation exposure

**L. I. Sonoda**, B. Sanghera, T. Wagner, P. Hoskin, W. Wong; Paul Strickland Scanner Centre, Mount Vernon Hospital, London, UNITED KINGDOM.

**Introduction:** There is ever-increasing evidence of 18F-FDG-PET-CT being useful in monitoring early response to chemotherapy in curable lymphoma. With a concern of radiation burden this study Aimed to assess if the early follow-up PET-CT acquisition area could be minimised and limited to the original sites of disease in order to reduce radiation dose and acquisition time without missing any significant findings. **Materials and Methods**: Retrospective analysis of 1000 consecutive lymphoma patients (553 male, mean 42.4years-old, 421 Hodgkin's Lymphoma (HL), 579 Non-HL) was performed to record sites of disease on pre-chemotherapy PET-CT and the first early follow-up post-chemotherapy PET-CT. The body is divided into four conventional parts (head-and-neck, thorax, abdomen and pelvis) for recording sites of disease. The potential reduction in radiation dose and time-saving achieved by limiting to the sites of known disease identified on pre-chemotherapy PET-CT was calculated. **Results:** No FDG-uptake was seen in 744/1000 first post-chemotherapy PET-CT, indicating complete metabolic response. FDG-uptake at known disease sites was seen in 256/1000 cases indicating residual disease. 902/1000 of the patients had disease confined to only one or two body parts out of four. Incidental synchronous non-lymphomatous malignancy (such as colonic or lung carcinoma) was identified in 48/1000 cases in pre-chemotherapy PET-CT. Post-chemotherapy PET-CT did not reveal any further unexpected sites of lymphoma or incidental interval malignancy. Limiting PET-CT to the sites of known disease would have reduced a mean radiation dose by 3.6 mSv (24.3 %), with a mean time-saving of 16 minutes (66.6%), without missing any significant findings. **Conclusion**: In order to assess early response to chemotherapy in curable lymphoma with 18F-FDG-PET-CT it may be sufficient to limit scan to the sites of known disease without missing any significant or unexpected findings. This will lead to reduce the total radiation dose in patients' journey with multiple radiation exposure, and hence reduce the incidence of secondary cancers caused by medical radiation. This is particularly important in young patients with curable lymphoma.

## OP451

### %ΔSUVmax is a Better Predictor of Outcome than Deauville 5-PS after One Cycle of Therapy in Diffuse Large B-Cell Lymphoma (DLBCL)

**Y. Rydzinski**[1], M. Hutchings[2], A. Knight-Greenfield[1], K. Mylam[2], J. Stern[1], J. Doucette[1], M. Coleman[3], L. Kostakaglu[1]; [1]Icahn School of Medicine at Mount Sinai, New York, NY, UNITED STATES, [2]Rigshospitalet, Copenhagen, DENMARK, [3]Weill Cornell Medical Center, New York, NY, UNITED STATES.

**Objectives :** To determine the best predictor of response and progression free survival (PFS) among various Methods and variables of tumor metabolic parameters at baseline and at interim PET/CT after one cycle compared to conventional prognostic measures in DLBCL. **Methods :** Retrospective evaluation of prospectively acquired data in 51 DLBCL patients, all stages (16 stage I-II, 35 stage III-IV). Eligibility: PET/CT prior to and after 1 cycle (PET1), with standard therapy (R-CHOP), imaging at 60min+15min. Baseline clinical parameters included stage and international prognostic index (IPI), and PET parameters included metabolic tumor volume (MTV), total lesion glycolysis (TLG), SUVmax, and SULpeak, by PERCIST criteria (1), determined using adaptive threshold method (PETVCAR2, GE Healthcare). Data were also evaluated at PET1 using Deauville 5-PS (2), %ΔMTV, %Δ SUVmax, %ΔTLG, and PERCIST. Variables were correlated with PFS and response evaluated by revised international working group criteria (rIWG) (3). **Results :** Median follow-up: 26.1 months. Results for PFS and response are displayed in supplemental Tables 1 and 2, respectively. At baseline, the only variable predictive of PFS or response was IPI > 2 (p=0.03 for both). At interim analysis, %ΔSUVmax and %ΔTLG both bordered on significance for prediction of PFS (p=0.05 for both). Deauville 5-PS, %ΔMTV and PERCIST were not predictive of PFS. The best predictor of response at interim was %ΔSUVmax, followed by Deauville 5-PS and PERCIST (p=0.01, 0.02, and 0.04, respectively). %ΔMTV and %ΔTLG were not predictive of response. **Conclusions :** Interim %ΔSUVmax predicts PFS and response better than Deauville 5-PS in DLBCL. At baseline, IPI best predicts PFS, while at interim, %ΔSUVmax best predicts response. Risk-stratification of DLBCL using tumor metabolic volumetry and PERCIST criteria probably requires a larger sample size and further assessment of various volumetric methodologies. References : (1) Wahl RL, Jacene H, Kasamon Y et-al. From RECIST to PERCIST: Evolving Considerations for PET response criteria in solid tumors. J. Nucl. Med. 2009;50 Suppl 1 : 122S-50S. (2) Meignan M, Gallamini A, Meignan M et-al. Report on the First International Workshop on Interim-PET-Scan in Lymphoma. Leuk. Lymphoma. 2009;50 (8): 1257-60. (3) Cheson BD, Pfistner B, Juweid ME et-al. Revised response criteria for malignant lymphoma. J. Clin. Oncol. 2007;25 (5): 579-86. Supplemental Table 1. Predictors of PFS in DLBCL

## OP452

### Relative reduction of residual tumor improves outcome prediction of PET after effective chemotherapy for patients with advanced stage Hodgkin Lymphoma

**C. Kobe**[1], M. Dietlein[1], G. Kuhnert[1], D. Kahraman[1], H. Haverkamp[2], M. Fuchs[2], H. Eich[1], P. Borchmann[1], A. Engert[1], A. Drzezga[1]; [1]University Hospital of Cologne, Cologne, GERMANY, [2]German Hodgkin Study Group, University Hospital of Cologne, Cologne, GERMANY.

**Background:** Positron emission tomography (PET) after chemotherapy is established to guide consolidating radiotherapy in advanced stage Hodgkin Lymphoma (HL). This analysis Aims to assess if prediction may be improved using additional criteria derived by computed tomography (CT). **Patients and Methods**: The analysis set consisted of 739 patients from the HD15 trial qualified for the PET question. A central panel reviewed PET and CT scans and performed image measurements and interpretation. Prognosis was evaluated using progression free survival (PFS); groups were compared with the log rank test. Potential prognostic factors were investigated using ROC analysis and logistic regression**. Results**: 548 of 739 patients (74%) were PET negative with a 4-year PFS after panel of 91.5%. 191 PET positive patients (26%) had a 4-year PFS of 86.1% (p=0.022). When investigating further potential predictive factors, ROC analysis showed that relative reduction of the largest residual tumor diameter was significantly associated with outcome (AUC 0.65, 95% CI 0.57 to 0.73). Comparing the 54 PET-positive patients with a reduction of at most 40% to the 135 PET-positive patients with a larger reduction revealed an odds ratio for recurrence within a year of 5.6 (95% CI 2.1 to 15.2). In contrast to PET, CT alone was unable to separate patients by risk of recurrence (p=0.9). **Conclusion:** PET after chemotherapy is able to divide patients into risk groups. In this situation a low percentage change of tumor shrinkage identifies PET positive patients with a higher risk for progression or relapse who may need additional treatment.

1301 — Tuesday, Oct. 22, 11:30 — 13:00, Amphithéâtre

## CME 10 - ESNM Faculty (Interactive): PET/CT in Cancers of Unknown Origin or Paraneoplastic Syndromes

## OP453

### Cancer of Unknown Origin (CUP)

**S. Balogova, SLOVAKIA**

## OP454

### Neuroendocrine Cancer of Unknown Origin (CUPNET)

**F. Montravers, FRANCE**

## OP455

### Paraneoplastic Syndromes

**J.N. Talbot, FRANCE**

1302 — Tuesday, Oct. 22, 11:30 — 13:00, Auditorium Lumière

## Symposium 10: The Nuclear Medicine Diagnosis of Bone and Cardiovascular Infections

## OP456

### The Clinical Role of Nuclear Medicine in Osteomyelitis and Common Diagnostic Flow Charts

**A.Signore, ITALY**

## OP457

### The Clinical Role of Nuclear Medicine in Vascular Graft Infections and Common Diagnostic Flow Charts

**F. Jamar, BELGIUM**

## OP458

### The Clinical Role of Nuclear Medicine in Endocarditis and Common Diagnostic Flow Charts

**E. Lazzeri, ITALY**

1303 - Tuesday, Oct. 22, 11:30 - 13:00, Forum 3

## Technologist Oral Presentations 3

### OP459

#### BSGI imaging optimalisation using Dillon 6800 Camera; two versus four imaging directions

**R. van der Boor**, M. van de Meulengraaf, M. van Rutte, O. Suna; St Antonius Hospital, Nieuwegein, NETHERLANDS.

**Motivation:** Breast cancer is one of the most common forms of cancer. If results of mammography are not conclusive or mammography is not possible, Breast Specific Gamma Imaging (BSGI) is a sensitive and specific alternative or supplemental method in the detection of malignant breast lesions. **Problem statement:** In patients BSGI is performed after intravenous administration of 740MBq Tc-99m Sestamibi, using the Dilon 6800 single head gamma camera. Per breast, lateral and caudal images are obtained in a preset time of eight minutes. Concerns have risen that lesions can be missed when located farther from the detector. Such a situation may arise in larger breasts. In our study, we investigated the influence of detector-lesion distance and acquisition time, on the sensitivity of the imaging method. This in order to determine which patients should be imaged using three of four image directions and in which cases two image directions will be sufficient. **Approach:** A phantom study was conducted with a contrast-detail phantom with a maximum contrast ratio of 2.5. Images were made using four and eight minutes acquisition time, corrected for decay, at a distance of 0, 25, 50 and 75mm from the detector. Lesions with a diameter of 4, 5, 7.5 and 10mm were investigated. **Results:** Analysis of the phantom study shows that visibility of lesions decreases when the distance to the detector increases. For example with an acquisition time of eight minutes, the 10mm lesion is not seen at 75mm from the detector and a lesion with a diameter of 5mm is not seen at 50mm from the detector. Lesions smaller than 5mm are not visible at any distance. While the above mentioned 5mm lesion was visible at 25mm using eight minutes acquisition time, while after four minutes acquisition time it was not visualized anymore. **Conclusions:** This phantom study suggests that, depending on the size of the breast, additional medial and/or caudal images may be necessary to increase the sensitivity of the single head BSGI exam. As expected acquisition time is of great influence. **Discussion:** The phantom study was executed using a homogeneous background and without an anatomically correct phantom. The study should be repeated in real life BSGI patients.

### OP460

#### How low can you go: Dose-reduction in Low-Dose CT-scans for attenuation correction in myocardial perfusion imaging

**N. de Wit**, B. J. Vermolen, P. J. G. Peeters, A. M. Scholtens, J. C. M. Buijs, H. W. A. M. de Jong; UMC Utrecht, Utrecht, NETHERLANDS.

**Aim** Dose reduction is a continuing topic of interest in radiology and nuclear medicine. Since the Introduction of SPECT/CT, Low-Dose CT is easily and often performed as an adjunct to nuclear imaging techniques due to the added diagnostic value of anatomical correlation and attenuation correction. However this added CT leads to an increase in radiation dose, which should be kept to a minimum according to the ALARA-principle. The Aim of this study was to determine the feasibility of dose-reduction in Low-Dose CT scans, while not affecting the attenuation correction of the myocardial perfusion scintigraphy. **Materials & Methods** In this study two SPECT/CT systems were used: Siemens Symbia T16 and T2 (16- and 2- slice CT system, Siemens Healthcare). An anthropomorphic thorax-phantom with a static myocardial insert. The insert with a volume of ~120 ml was filled with 10 MBq 99mTc-pertechnetate solution. SPECT data was acquired according to our clinical myocardial perfusion acquisition protocol. A series of CT-scans with different parameters (80-130 kV, 12-44 mAs) and all with adaptive dose modulation were performed. CT-dosages were compared to the clinical Low-Dose CT (130 kV, 29 mAs, CTDI of 2.48 mGy) On every CT-scan a 3D map, giving linear attenuations coefficients (μ-map), was made which were sequentially used to reconstruct volumes using an iterative reconstruction algorithm. Quantitative analysis was performed on the μ-maps to determine the value of the average attenuation coefficient in several regions (compartments with water, tightly packed styrofaom beads in water and teflon, mimicking tissue, lungs and bone respectively) and compare these to known values for 140 keV photons. After reconstruction and processing using 4DM SPECT (Invia Medical Imaging Solutions), the resulting Bull's-eyes were scored automatically using the 17 segment model. Both the Bull's-eye and the volume images where reviewed by a nuclear physician. **Results** CT-dose ranged (CTDI) from 2.48 mGy (130 kV,29 mAs) to 0.56 mGy (80 kV, 12 mAs) Except for teflon, there were no differences in attenuation coefficients between the various μ-maps in corresponding regions and only minor differences with the known μ-values. There were no statistical differences in automated Bull's-eye scoring or visual interpretation by the nuclear physician between the different datasets. **Discussion** Dose reduction in Low-Dose CT with a factor 4.4 on the tested systems is feasible without affecting attenuation correction. This study was conducted using a phantom, patient data is needed to validate the results for patient care, especially in obese patients.

### OP461

#### Importance of Technologist Involved in a Multimodal Preclinical Imaging Department

**J. DILLENSEGER**, A. SAYEH, C. GOETZ, A. CONSTANTINESCO, P. CHOQUET; Hôpitaux Universitaires de Strasbourg - Preclinical Imaging Lab UF6237, Strasbourg, FRANCE.

**Aim**: Combined multimodal acquisitions have already demonstrated their added value, both in clinical and preclinical fields. It is stated that coupling scintigraphic modalities with CT and/or MRI is a benefit for data interpretation. A short time multimodal protocol was developed in our imaging laboratory, to facilitate coregistration between images acquired on a 1.5T preclinical MRI and microSPECT-CT data, when the animal is moved between systems. Our experience shows that skilled and trained technologists could give an advantage to optimize protocols implementation. This presentation will describe the different steps of such procedure, the technologist's roles, and emphasize why its competence could be a benefit in a preclinical imaging department, and an opportunity for himself. **Material and Methods**: MRI system (OPTImouse, RS2D, Bischwiller, France) uses a 1.5T cryogen-free superconducting magnet. It takes up a floor area of 1.20m x 2m while the 5G line is at 80cm away from the center of the magnet in the worst case. For mice whole body imaging, a RF coil (RapidBiomedical, Würzburg, Germany) of 40mm in diameter is used, which remains inside the magnet. The microSPECT-CT (eXplore speCZT Vision 120, GE, Waukesha, USA) is installed 2 to 3m away from the MRI, thanks to the short extension of the magnet fringe field. Imaging cells (Minerve, Esternay, France) share common support on each imaging instrument, allowing for quick and efficient docking. Mice are kept anesthetised and warmed in the imaging cells during acquisitions. Multimodality imaging is achieved sequentially by moving the chamber from one system to the other, which takes approximately 20s. Amide (http://amide.sourceforge.net/) is used for coregistration of acquired data. **Results**: The total multimodal procedure (animal handling, CT, SPECT and MRI acquisitions, and multimodal coregistration) could be done in less than 2 hours with one skilled technologist. **Conclusion**: Our experience shows that the integration of a technologist in a preclinical imaging department can be an added value to all researchers as well as to scientific projects. Technologist collaboration with a research team improves and facilitates procedures organization and consequently increases the throughput. In France, in preclinical imaging labs, few places are currently made available for Medical Imaging Technologists. We believe that preclinical imaging competences could be one of the key issues for technologist success.

### OP462

#### Can Sestamibi kits be prepared with more than the recommended Tc-99m activity? A validation study

**C. Kammies**, S. Rubow; Tygerberg Hospital, Tygerberg, SOUTH AFRICA.

**Background:** Radiopharmaceutical kit manufacturers provide instructions for radiolabelling of kits, including details of activity and volume of pertechnetate to be added to their specific product, and shelf-life after radiolabelling. If a user wants to deviate from the manufacturer's instructions, any changes in the Methods should be validated to ensure that the product will still be safe and effective. According to the manufacturer's instructions, our MIBI kits should be prepared with a maximum of 2280 MBq Tc-99m pertechnetate in 1 to 3 ml, and be used within 6 hours. Due to the number of myocardial perfusion studies requested, we would like to add considerably more Tc-99m to the kit. **Aim:** To verify the quality of MIBI kits if labelled with higher than the recommended Tc-99m activity. **Methods:** Details of 109 MIBI kits were reviewed in a retrospective study. For each kit, the labelling efficiency (LE) was determined shortly after preparation. The number of doses withdrawn from each vial was noted. Anonymised planar images of 20 patients whose doses were withdrawn more than 4 hours after labelling of kits with more than 11 GBq were reviewed. In a small number of kits, chromatography was repeated more than six hours post labelling and after withdrawal of multiple doses. **Results:** The LE of kits was always more than 90%, and there was no correlation between activity added and LE ($r = 0.012$). There was no significant difference between kits labelled with more than 11 GBq (mean 95.9%) and those labelled with less activity (mean 95.7%) ($p > 0.07$). LE remained above 90% after 6 hours and repeated withdrawals and there was no correlation between LE after more than 6 hours and the number of doses withdrawn from the vial ($r = 0.19$). No abnormal biodistribution was seen on images of patients whose doses were obtained from high activity kits. **Discussion:** Up to 15 GBq Tc-99m can be added to the MIBI kits used at our institution without significant effect on LE. Even with such high activity added to the kits, the LE remained above 90% for more than 6 hours post labelling and image quality was not affected. In view of these results it is justified to exceed the recommended activity for the product tested.

## OP463

### The use of stress CT attenuation correction map for the resting study in myocardial perfusion scintigraphy - feasibility and potential reduction of radiation exposure

**G. Barth**[1], E. Hillinger[1], J. Holzmannhofer[1], C. Pirich[1], I. Ortner[2]; [1]Universitätsklinik für Nuklearmedizin und Endokrinologie, Salzburg, AUSTRIA, [2]Fachhochschule Puch/Salzburg, Puch, AUSTRIA.

**Aim:** Hybrid imaging systems (SPECT/CT) allow the use of attenuation correction (AC) in myocardial perfusion SPECT. Further reduction in radiation exposure and scanning time might be achieved by the use of the same CT attenuation correction map for both stress and resting studies. **Material and Methods:** 50 patients referred for the evaluation of coronary artery disease underwent myocardial perfusion scintigraphy (mean age 70 years; BMI 28.2±5.2) using adenosine or regadenosone stress/rest gated Tc-99m tetrofosmin SPECT on a SPECT/CT dual-head gamma camera with IQ SPECT equipment (Siemens, Germany). Images were processed using iterative reconstruction and AC was applied using the following CT acquisition parameters: 130 kV, 13 mAs, slice thickness 5mm, collimation 6x3mm. Analysis was performed with 4DM processing software. Scores were assessed in 17 segment model and related to angiographic and clinical data. All processing was done independently by two technologists with different levels of professional experience to evaluate the impact of inter-observer variability. Images were interpreted separately by a board-certified specialist in nuclear cardiology. **Results:** The use of stress CT map for AC of resting studies did no influence diagnostic quality and accuracy in any case when careful alignment was applied by the technologists. The agreement in clinical interpretation was 100 %. Quantitative polar map analysis demonstrated that the summed difference score was equal or different by not more than 2 score points in 78 % of the patients. The approach was feasible for technologists with short or long professional experience requiring 5 minutes more workload on average per patient. Using 4 MBq /kg body weight radiation exposure due to scintigraphy alone was 0.0073 mSv/MBq that is 0.0292 mSv/kg bw. The effective dose was approximately 2 mSv in a patient with 70 kg bw. Radiation exposure due to CT is reduced by 50 % (CTDI: 1.36, DLP: 25-30, mAs: 150-160) and study time by 2 minutes per patient. **Conclusion:** The use of stress CT maps for AC of resting studies is feasible and does not impair diagnostic accuracy in visual analysis. This is also true for polar map analysis in the majority of cases. The use of stress CT maps for AC of resting studies reduces patient scanning time and radiation exposure at the price of increased workload for technologists. Radiation exposure can be markedly reduced by the use of state-of-art GC systems.

## OP464

### Position sensitive domestic normal database for myocardial perfusion scintigraphy

**A. Oszlánszki**[1], N. Nagy[2], B. Pongrácz[1], K. Kukucs[1], A. Kiss[1]; [1]ScanoMed Ltd., Debrecen, HUNGARY, [2]University of Medical Diagnostics, Debrecen, HUNGARY.

**Background**: Dedicated cardiac sofwares are used to evaluate myocardial perfusion studies in clinical routine. These softwares generally include normal database regardless patient's position. However recently dedicated cardiac cameras have launched into the market applied bed position differs from laying one. Based on our daily routine practice we experienced that the examination can differ according to the patient position. Our Aim was to create a new database based on ECG gated myocardial perfusion acquired sitting position. Method: 40 patients (17 women and 23 men) were enrolled our prospective study. Gated myocardial perfusion SPECT protocols were used in different cardiac cameras using different patient position (Cardio C, with lying position, Cardio Desk, with sitting position, Mediso, Hungary). Every patient was examined on both of scanners. The order has been randomly chosen for the two position to exclude bias caused by radioactive decay. After the acquisition (stress or rest protocol) the data were processed with Interview XP, and Emory Cardiac Tool Box to create polar map. For the creation of a new database we used Emory Normal Database Generator (ENDG). While the different patient position results different image quality, different patient database need to be created for different cameras applying altered patient position. For technologist there are the possibilities to create a normal database. We propose to present the importance of this method in the clinical practice.

## OP465

### Evaluation of myocardial image acquisition, processing condition optimization of processing conditions by short acquisition of myocardial SPECT images using 1231-BMIPP

**T. Takase**[1], C. Noda[1], J. Suyama[2], H. Satou[3], Y. Nakazawa[3]; [1]Showa University Hospital Department of Radiology, Tokyo, JAPAN, [2]Showa University School of Medicine Department of Radiology, Tokyo, JAPAN, [3]Showa University Graduate School of Nursing and Rehabilitation Science, Tokyo, JAPAN.

**Background**: In myocardial scintigraphy, long acquisition time can be a burden to patients and prone to motion artifact. We had a firsthand experience with IQ•SPECT scanner system in which acquisition, collimator and image reconstruction are different from conventional Methods. In IQ•SPECT, cardiac-dedicated multifocal collimator called SMARTZOOM collimator is used. IQ•SPECT allows reduction of acquisition time or injected dose. Here, we compared acquisition, post-processing conditions associated with different collimators in 123I-BMIPP myocardial fatty acid metabolism imaging with regard to the duration of acquisition and the image quality. **Materials and Methods**: Low Energy High Resolution (LEHR) and SMARTZOOM collimators were used with Symbia S scanner system (Siemens). Data were processed on Symbia.net. The DSSCP Cardiac Phantom was loaded with 123I-BMIPP. Injected activity was calculated from the product label under the assumption that approximately 5% and 10 % of injected dose were taken up in myocardium and in the liver, respectively. Clinical cardiac images were obtained from patients who underwent 123I-BMIPP myocardial SPECT examination. Myocardial phantom acquisition was conducted using the conventional protocol (64x64 matrix, 30sec/view, 24steps, FBP) using LEHR collimator. Short axis cardiac images were also obtained with IQ•SPECT. LEHR and IQ•SPECT images were compared and the IQ•SPECT acquisition and processing conditions that can give rise to equivalent image quality to the conventional scans were assessed. Moreover, the processing conditions were determined through contrast, uniformity and QPS data. **Results**: In the phantom study, the necessary acquisition conditions through IQ•SPECT to acquire counts comparable to LEHR were 128x128 matrix, 9 sec/view and 34 steps. In clinical evaluation, the necessary acquisition time for IQ•SPECT to acquire counts comparable to LEHR was 13sec/view. Total acquisition time was 720 sec in LEHR and 442 sec in IQ•SPECT. IQ•SPECT data processed through OSEM (subset 3, iteration10) resulted in images comparable to those through LEHR. **Conclusion**: These results indicated that in myocardial SPECT using 123I-BMIPP, IQ•SPECT can be used to acquire comparable images to conventional LEHR with reduced acquisition time.

## OP466

### MIBG-I123 myocardial innervation: we do need standardization of acquisition parameters and processing analysis

**A. Ghilardi**, G. Medolago, C. Bianchi, L. Pozzi, M. Caloiero, A. Bruno; AO Papa Giovanni XXIII, Bergamo, ITALY.

Clinical application of MIBG-$I^{123}$ myocardial innervation is not yet well defined also because of lack of standardization of acquisition parameters and processing analysis. **Aim** of the study is to illustrate homogeneous and reproducible procedures to overcome any inter-intra operator variability, especially for semi-quantitative calculation **Methods**: We studied 90 pts [74 M; 16 F] with LV dysfunction [EF 32.5± 9.5%], NYHA II-III. All pts underwent 15min early wholebody scan + 2 static images[10min/each] at 15min 4hrs later in Anterior view [MTX 128x128pxls, Zoom 1.46] using LEHR collimator and 15min, 4hrs SPECT using Siemens Smartzoom Cardiac Focusing collimator. For static images we focused our attention to center correctly myocardial and thyroid images to better identify similar mediastinum area in early/late study. Total counts of wholebody scan was used as input function. From static images we calculated Heart/Mediastinum, wash-out rate, Heart/Whole Body at 15min, 4hrs; on 4hrs static image we drew 3 ROIs on remote, bordeline and infarcted myocardium. To obtain semi_quantitative data DICOM images were analyzed by 3 different operators using a specific off-line software we developed [**C**ardiac**S**ympatic**I**nnervation**B**ergamo] allowing to draw ROIs of the same size in the same position in different patients and in the same patient in repeated study.SPECT was performed using Smartzoom Cardiac Focusing Siemens collimator [high sensitivity] able to detect low MIBG myocardial uptake. All pts underwent also stress-test G-SPECT to assess extent of perfusion defect and LV ventricular dysfunction. **Results:** As expected values of H/M, washout rate and Heart/Whole Body Ratio showed less variability, more reproducibility when CSIB was used. The quality of early and 4hrs SPECT images was very good to be compared with perfusion study. Regarding SPECT MIBG uptake score, a good correlation was found with Perfusion score even if a normal data base is needed. **Conclusions:** In our experience to validate MIBG-$I^{123}$ myocardial innervation as specific and adjunctive prognostic tool in LV dysfunction, we need standardization of acquisition but mainly of processing analysis to overcome any discrepancy, which is relevant in repeated studies[follow_up]. SPECT MIBG is very useful when compared to Perfusion Imaging but still shows some drawbacks: instrumentation [low count rate] and quantification[normal data base]

## OP467

### Clinical usefulness of quantitative $^{201}$Tl myocardial uptake index at stress with normal $^{201}$Tl SPECT-MPI

**S. Haneta**[1], S. Tomiguchi[2], M. Tanaka[3]; [1]Department of Radiology, Kagoshima Medical Center, Kagoshima, JAPAN, [2]Faculty of Life Sciences, Kumamoto University, Kumamoto, JAPAN, [3]Graduate School of Health Sciences, Kumamoto University, Kumamoto, JAPAN.

**Aim:** We developed a Quantitative $^{201}$Tl myocardial uptake index at stress (stress uptake index: SUI) for the evaluation of myocardial perfusion reserve. The Aim of study was to evaluate the clinical usefulness of SUI in patients with ischemic heart disease. **Subjects and Methods:** A total of 25 patients without any perfusion

abnormality on stress $^{201}$Tl single photon emission computed tomography-myocardial perfusion imaging(SPECT-MPI) with adenosine were enrolled in this study. The normal values of SUI were defined in 10 patients without coronary arterial disease (CAD). The clinical usefulness of SUI was assessed in 14 patients (5 with CAD and 9 without CAD). A SUI was calculated by dividing the myocardial radioactivity converted from automatically estimated whole left ventricular counts using cross-calibration factor by total injected dose. The SUI under 1 SD of mean value was defined as abnormal. **Results:** The mean value of normal SUI was 14.4±2.4% at stress. Normal value of SUI was observed in all of 9 patients without CAD. On the other hands, abnormal value of SUI was observed in 4 of 5 patients with CAD. Moderate to severe multi-vessel diseases were found in 4 patients. Only a patient with mild stenosis of right coronary artery showed normal SUI. **Conclusion:** SUI adding to visual assessment is useful for the diagnosis of multi-vessel CAD.

1304 - Tuesday, Oct. 22, 11:30 - 13:00, Bellecour 1/2/3

## Featured - Radiopharmaceuticals & Radiochemistry & Dosimetry: New PET Radiopharmaceuticals

## OP468

### Trends of New PET Radiopharmaceuticals

**D. Guilloteau, FRANCE**

## OP469

### Synthesis and preclinical evaluation of serotonin 5-HT$_6$ receptor radioligands for PET imaging

G. BECKER[1], J. COLOMB[2], T. BILLARD[2], **L. ZIMMER**[1]; [1]Hospices Civils de Lyon & Univ. Lyon 1, Lyon, FRANCE, [2]CNRS & Univ. Lyon 1, Lyon, FRANCE.

**Aims.** According to their brain localization, the serotonin 5-HT$_6$ receptors are potent therapeutic targets for psychiatric and neurological diseases, i.e., schizophrenia and Alzheimer's disease. However, the understanding of the serotonin 5-HT$_6$ pharmacology is currently partial and its exploration is limited to animal models, particularly because of the current lack of fluorinated PET 5-HT$_6$ radiopharmaceuticals. In this context, we developed several 5-HT$_6$ fluorinated radioligands and, through a translational approach, evaluated their suitability for PET imaging. **Material and Methods.** Various quinoline and pyridine-based ligands have been synthesized, inspired by the known 5-HT$_6$ receptor pharmacophore. These non-radioactive fluorinated ligands and their radiolabelling's precursors were obtained from *bis*-functionalized heteroaromatic core followed by coupling reactions in three steps. Only ligands with the higher *in vitro* affinities toward 5-HT$_6$ receptors and the lower affinities toward 5-HT$_{2A}$ receptors (a close pharmacophore) were radiolabeled via $^{18}$F-nucleophilic aromatic substitution. These potential radiotracers were evaluated by *in vitro* autoradiography in rat brain. The most interesting radioligands of these were later evaluated by microPET scans on anaesthetized rats, PET scans on anaesthetized cat. Finally, the selected 5-HT6 radioligand was used in postmortem PET autoradiography in brain tissue (control subjects and Alzheimer disease patients). **Results and conclusion.** Eight molecules were initially synthesised. Three molecules with low *in vitro* affinity for 5-HT$_6$ receptors were discarded (Ki >10 nM). The chemical and radiochemical purities of the five remaining fluorine radiotracers were > 99%, with a radiochemical yield of 5-45% (EOB) and specific activities in the range of 40-104 GBq/µmole (EOS). Three radiolabelled molecules presented a high *in vitro* binding in the striatum area rich in 5-HT$_6$ receptors and a dose-dependent displacement after SB258585 addition (a 5-HT$_6$ receptor antagonist). The microPET studies in anesthetized rats showed that one among these three molecules (2FNQ1P) had a good brain penetration and a striatal fixation. PETscans in cats gave additional information about 2FNQ1P pharmacokinetic, showing a good brain penetration and a binding to striatal 5-HT$_6$ receptors. The further evaluations in post-mortem human tissues were in accordance with the known distribution of 5-HT$_6$ receptors in the brain. In conclusion, our study allowed us to select a radiotracer-candidate with suitable characteristics for PET imaging of 5-HT$_6$ receptors, justifying further evaluations and quantitative approach using kinetic models.

## OP470

### Synthesis, radiolabeling and pre-clinical evaluation of [$^{18}$F]MA3 as a candidate PET-tracer for in vivo mapping of the type 2 cannabinoid receptor

**D. van Veghel**; KU Leuven, Leuven, BELGIUM.

**Aim.** The type 2 cannabinoid receptor (CB2), a member of the endocannabinoid system, is known for its important role in neuroinflammation. Many neuropathogenic disorders are characterized by a neuroinflammatory component and CB2-overexpressing microglia have been detected in β-amyloid plaques of Alzheimer's disease patients, active plaques of patients with multiple sclerosis and striatal lesions of Huntington's disease patients. Therefore, CB2 became an attractive therapeutic and molecular imaging target. Here, we report the synthesis, radiolabeling and preliminary biological evaluation of a fluorine-18 labeled analogue of the highly potent CB2 agonist *N*-(3-(3-(2-chloro-4-fluorophenyl)-(1,2,4,-oxadiazol-5-yl)propyl)-6-(trifluoromethoxy)quinolin-3-amine (GTP binding EC$_{50}$ = 0.015 nM).[1] **Materials & Methods.** The precursor (MA1) and non-radioactive reference (MA3) were synthesized in 8 steps according to previously described Methods.[1,2] The binding profile of MA3 for hCB2 was investigated by means of cAMP assays and competition binding assays using [$^3$H]CP55940 as radioligand. [$^{18}$F]MA3 was synthesized via a nucleophilic substitution reaction on the phenol moiety of precursor MA1 using [$^{18}$F]fluoroethyl bromide ([$^{18}$F]FEtBr). The kinetics and tissue distribution of [$^{18}$F]MA3 were studied in mice at 2, 10, 30 and 60 min after injection of the tracer. **Results.** Fluorine-18 alkylation yields ranged from 24% to 68% with corresponding isolated amounts of 617 MBq to 706 MBq. MA3 behaved as an agonist with an EC$_{50}$ of 0.13 nM for hCB2 and an efficacy of 102% in the cAMP assays. Its binding affinity (K$_i$) for hCB2 was 0.8 nM and 3.5-fold higher than that of the lead compound (K$_i$ hCB2 = 2.8 nM). [$^{18}$F]MA3 was efficiently cleared from blood (% ID 2 min/60 min ratio = 5.2) and all studied organs, except the liver (SUV = 2.1 at 60 min p.i.). The high brain uptake of [$^{18}$F]MA3 (1.2 % ID at 2 min p.i.) was followed by a rapid wash-out from brain (% ID 2 min/60 min ratio = 9.2). Elimination of the tracer occurred predominantly via the hepatobiliary pathway with excretion of the radioactivity into the intestines (64.4 % ID at 60 min p.i.). **Conclusion.** MA1 was synthesized and successfully labeled with [$^{18}$F]FEtBr to obtain [$^{18}$F]MA3. MA3 displayed a high *in vitro* binding affinity for hCB2 and the $^{18}$F-labeled analogue showed favorable biodistribution characteristics in mice. Work is in progress to further evaluate the potential of [$^{18}$F]MA3 for in vivo mapping of CB2. References. [1] Cheng Y et al. J. Med. Chem. 2008, 51, 5019-34; [2] DiMauro EF et al. Bioorg. Med. Chem. Lett. 2008, 18, 4267-74.

## OP471

### N-[11C]methyl - AMD3465 a new tracer for PET imaging of CXCR4 receptors

**S. V. Hartimath**, R. Dierckx, E. d. Vries; University of Groningen, Groningen, NETHERLANDS.

**Aim I**n the last few decades, chemokines and their receptors have been studied as new drug targets in wide variety of diseases, such as neurodegenerative diseases, allergy, autoimmune diseases, AIDS and cancer. CXCR4 and its ligand, stromal cell derived factor (SDF-1/CXCL-12), play an important role in tumour progression and metastasis. It has been demonstrated in preclinical studies that position emission tomography (PET) with radiolabelled a small molecule allows noninvasive monitoring of CXCR4 expression. In this work, we labelled the selective CXCR4 receptor antagonist AMD3645 with carbon-11 and evaluated its imaging properties using small animal PET. **Materials and Methods** Synthesis of N-[$^{11}$C]methyl-AMD3465 was performed by reaction of [$^{11}$C]methyl triflate with AMD3465 in acetone, in the presence of NaOH as base. For *in vitro* characterization, partition coefficient, serum and microsomal stability were analyzed. In addition, binding affinity, cellular uptake and internalization of tracer were measured in C-6 cells. Furthermore, biodistribution, blocking and invivo PET imaging experiments were performed in C6 glioma-bearing rats. **Results** N-[$^{11}$C]methyl -AMD3465 was prepared with a high radiochemical yield (60±2 %) and purity (>99 %). The specific activity of the tracer was 30±5 MBq/nmol. *In vitro* characterization showed that the tracer is hydrophilic (logD -0.860±0.054) and stable in both serum and liver microsomes (>98% intact, at 2h). *In vitro* binding and cellular uptake of tracer was found to be receptor-mediated. Blocking with the selective CXCR4 antagonists AMD3465, N-methyl-AMD3465 and AMD3100 gave IC50 values of 0.68µM, 1.13µM and 2.95µM, respectively. The internalization of tracer was rapid and reached a plateau around 40% after 15 min. Biodistribution at 60 min after injection of N-[$^{11}$C-]methyl-AMD3465 showed specific tracer uptake in the tumor (SUV: 0.48±0.05), bone marrow (0.98±0.07) and spleen (1.01±0.06).. Furthermore, blocking experiments with AMD3100 (50 mg/kg, s.c.) significantly reduced tracer uptake in tumor (65 %), bone marrow (80%), spleen(62%), and lymph nodes (76%). Despite moderate expression of CXCR4 in the tumor (as compared to transgenic CXCR4 overexpressing tumors), N-[$^{11}$C]methyl-AMD3465 PET images clearly visualized the tumor. The tracer showed fast uptake in the tumor, followed by slow wash-out. **Conclusion** In conclusion, we labelled AMD3465 with carbon-11 with high yield and purity. The tracer is stable *in vitro* and *in-vivo*. The tracer showed specific CXCR4 receptor-mediated uptake in cell experiments and in tumor-bearing rats. Moreover, N-[$^{11}$C]methyl -AMD3465 showed favorable kinetics in PET imaging experiments. These results justify further evaluation of N-[$^{11}$C]methyl-AMD3465 as a potential tracer for non-invasive CXCR4 receptor imaging.

## OP472

### Development and Preclinical Evaluation of a Novel F-18 Labeled SCH442416 Analog for Imaging Adenosine A2A Receptors

**S. Khanapur**[1], S. Paul[1], A. Anup Shah[2], G. Luurtsema[1], R. Zijlma[1], R. A.J.O.Dierckx[1], P. Garg[2], A. Van waarde[1], P. Elsinga[1]; [1]University Medical Center, Groningen, Groningen, NETHERLANDS, [2]Department of Pharmacoinformatics, National Institute of Pharmaceutical Education and Research, Mohali, INDIA.

**Introduction and Aim**: Adenosine A2A receptors (A2AR) highly concentrated in the striatum, are an attractive therapeutic target for Parkinson's disease (PD). Radiolabeled A2AR antagonists can be important research and diagnostic tools for PD. Several [11C]-labeled A2AR antagonists have been evaluated for A2AR imaging, including [11C]SCH442416. However, the short half life of 11C (20.4 min) limits their use. The purpose of this project was to develop a F-18 labeled SCH442416 derivative with a longer physical half-life (109.8 min), allowing tracer distribution to remote imaging centers without cyclotron facilities and longer scanning times. For this purpose, we prepared the 18F-labeled fluoropropyl derivative of SCH442416 ([18F]FPSCH) and evaluated kinetics and biodistribution in healthy rats. The fluoropropyl analogue was selected based on favorable in-silico modeling and in vitro autoradiography data. **Methods**: For preparation of [18F]FPSCH, a two-pot radiosynthesis method was adopted. 1. intermediate (3-[18F]-fluoropropyltosylate) synthesis , 2. O-fluoroalkylation of SCH phenolic precursor with 3-[18F]-fluoropropyltosylate. The time-dependent regional brain uptake of 18F in living Wistar rats was studied with a microPET camera, after i.v. injection of [18F]FPSCH. Animals were either untreated or pretreated with the selective adenosine antagonist, KW-6002 (1 mg/kg). Metabolism of [18F]FPSCH was studied both in vitro, using rat hepatic microsomes and LC-MS, and in rat plasma in vivo, using radio-TLC. **Results**: Total Synthesis time including UPLC quality control was 138-145 min. Radiochemical yield was 6-10% (EOB), radiochemical purity > 99%, and specific radioactivity 136 ± 13 GBq/µmol. In microPET scans, A2AR-mediated tracer accumulation was observed. Striatum-to-cerebellum ratios of radioactivity reached maximum of 2.8 ± 0.2 at 15 min; the striatum was clearly visualized. This ratio was reduced (1.1± 0.2) after pretreatment with KW-6002. The value at baseline is higher than was previously observed for the [18F]fluoroethyl derivative of SCH442416 (2.2). UPLC-MS analysis of chemical species produced in vitro by rat liver microsomes indicated an increase in m/z by 16, which is probably the result of hydroxylation. Radio-TLC indicated presence of a hydrophilic metabolite in rodent plasma which is not expected to cross the blood-brain-barrier. Metabolism in rats showed more than 20% plasma activity was due to parent compound at 60 min. Tracer uptake in the skeleton was rather high, suggesting defluorination. **Conclusion**: [18F]FPSCH can be prepared using a two-step procedure. The specificity of its in vivo binding, the good signal to noise ratios and the low amounts of radioactive metabolites suggested that this tracer has potential for mapping cerebral A2AR with PET.

## OP473

### Development of Novel F-18 Labeled Deuterated Analogues of Fluorodeprenyl and Fluororasagiline by PET to Study MAO-B Activity

**S. Nag**[1], L. Lehmann[2], G. Kettschau[2], T. Heinrich[2], A. Thiele[2], M. Toth[1], C. Halldin[1]; [1]Karolinska Institutet, Stockholm, SWEDEN, [2]Bayer HealthCare AG, Global Drug Discovery, Berlin, GERMANY.

**Introduction:** Monoamine oxidases (MAO) are important enzymes regulating the levels of monoaminergic neurotransmitters and of bioactive monoamines by catalyzing their deamination. MAO-B inhibitor such as L-deprenyl has been labeled with $^{11}$C and used in PET studies to image the distribution of available MAO B in the human brain. In high MAO-B regions the tracer is trapped at a rate which exceeds the rate at which it is delivered by the plasma. Deuterium-substituted L-deprenyl ([$^{11}$C]L-deprenyl-D2) has been introduced to reduce the rate of radiotracer trapping in the human brain. We recently reported novel fluorine-18 labeled fluoro analogue of L-deprenyl and fluoro analogue of rasagiline to image MAO-B in monkey brain[2-4]. In this project we developed a fast and efficient synthetic method for labeling two novel deuterium substituted compounds (**6**, [$^{18}$F]fluorodeprenyl-D2 and **8**, [$^{18}$F]fluororasagiline-D2) with fluorine-18. **Experimental:** Precursors and reference standards were synthesized in multi-step syntheses. Radiolabeling was accomplished by a one-step nucleophilic substitution reaction. *In vitro* MAO inhibition was determined for both deuterated fluorodeprenyl and fluororasagiline. Uptake and binding were examined in a cynomolgus monkey brain by PET. Radiometabolites were measured in monkey plasma using gradient HPLC. **Results and discussion:** Radiolabeling of both compounds were accomplished successfully with an incorporation radiochemical yield from fluorine-18 ion >60%. The radiochemical purity was higher than 99% and the specific radioactivity was >200 GBq/µmol at the time of administration for both comounds **6** and **8**. The *in vitro* inhibition of deuterated fluorodeprenyl gave an $IC_{50}$ of 227 ± 36,8 nM for its MAO-B whereas deuterated fluororasagiline inhibited MAO-B activity with an $IC_{50}$ of 173,0±13,6. *In vivo* for both radioligands there were high uptake in the monkey brain (>300 SUV (%) at 4 min) with higher amounts in the striatum and thalamus compared to the cortex and cerebellum. Metabolite studies demonstrated 45% unchanged radioligand at 120 min post injection. **Conclusion**: Radiolabeling of a novel fluorine-18 analogue of deuterium substituted L-deprenyl (**6**) and rasagiline (**8**) were performed. Both compounds bind specifically to MAO-B rich region in monkey brain are both potential candidates for human PET studies. **References:** (1) Fowler, J. S.; et. al. *Science* **1987**, *235*, 481. (2) Nag, S.; et.al. *J Med Chem* **2011**, *54*, 7023. (3) Nag, S.; et.al. *Synapse* **2012**, *66*, 323. (4) Nag, S.; et.al. *Bioorg Med Chem* **2012**, *20*, 3065.

## OP474

### [18F]afatinib as imaging biomarker of EGFR tyrosine kinase in NSCLC.

**P. Slobbe**[1], A. D. Windhorst[1], M. Stigter-van Walsum[1], H. Niessen[2], G. A. M. S. van Dongen[1], A. J. Poot[1]; [1]VU University Medical Center, Amsterdam, NETHERLANDS, [2]Boehringer Ingelheim Pharma GmbH & Co. KG, Biberach, GERMANY.

**Aim:** The increased understanding of the tumors molecular biology has led to innovative targeted therapies. An important class of targeted therapies in cancer treatment are the Tyrosine Kinase Inhibitors (TKIs). Unfortunately, TKI therapies have limited clinical efficacy. Especially for EGFR targeting molecules only 10-30% of the patients respond to the treatment, which has been shown to be related to mutations in the receptors catalytic site.[1,2] We envision that PET imaging with TKIs (TKI-PET) is uniquely qualified to study and understand the behaviour of these therapeutics *in vivo*.[3] This studies Aim was to label irreversible EGFR inhibitor afatinib with fluorine-18, perform an initial preclinical analysis in tumor bearing mice and gain an increased understanding of the behaviour of this therapeutic. Ultimately, the Aim is to distinguish between responding and non-responding tumors. **Material and Methods:** The synthesis of [$^{18}$F]afatinib was explored using an innovative three step radiosynthesis. Key step is an unprecedented BOP mediated condensation of 3-chloro-4-[$^{18}$F]fluoro-aniline with a cyclic amide precursor. [$^{18}$F]afatinib as TKI-PET tracer was evaluated in mice bearing a panel of three clinically relevant EGFR expressing human NSCLC (Non-Small Cell Lung Cancer) xenografts. The three selected cell lines are: A549 with wild-type EGFR, H1975 with the sensitizing mutation L858R and the acquired resistance related mutation T790M and HCC827 cell line with the sensitizing exon 19 deletion. All tumor types were successfully xenografted in nude mice and [$^{18}$F]afatinib was preclinically evaluated in a PET study and in an *ex vivo* biodistribution. Furthermore a metabolite analysis was performed. **Results:** [$^{18}$F]afatinib was successfully synthesized in an overall decay corrected yield of 17±2.3% with a radiochemical purity of >97% and a specific activity of >200 GBq/µmole at end of synthesis. [$^{18}$F]afatinib is stable in vivo with 80% of parent tracer still present in the blood 60 minutes post injection**.** PET imaging and *ex-vivo* biodistributions showed a rapid tumor uptake and good retention of [$^{18}$F]afatinib, where background tissues were rapidly cleared. Furthermore, the afatinib sensitive cell lines showed an increased signal-to-background ratio compared to the insensitive cell line A549. **Conclusion:** The new TKI-PET tracer [$^{18}$F]afatinib has been synthesized successfully. The tracer shows good metabolic stability and good tumor retention. Further optimization of [$^{18}$F]afatinib PET imaging conditions is ongoing. [1] P. Slobbe et al., *Drug Discov. Today*, 2012, *17*, 1175; [2] A.J. Poot et al., *Clin. Pharmacol. Ther.*, *93*, 239; [3] I. Bache et al., Clin. Cancer Res., *19*, 183

1305 - Tuesday, Oct. 22, 11:30 - 13:00, Auditorium Pasteur

## Featured - Radionuclide Therapy & Dosimetry: PRRT of Neuroendocrine Tumours

## OP475

### PRRT in the Therapeutic Algorithm of Neuroendocrine Tumours

**K. Öberg, SWEDEN**

## OP476

### Peptide receptor radionuclide therapy proves to be safe and immediately efficient in elderly patients with symptomatic neuroendocrine tumours.

**H. Duan**, P. Dolliner, G. Dobrozemsky, M. Raderer, M. Hoffmann; Medizinische Universität Wien, AKH Wien, Vienna, AUSTRIA.

**Background:** Peptide receptor radionuclide therapy (PRRT) with radiolabelled somatostatin analogues is a promising treatment modality in patients with neuroendocrine tumours. It is known not only to reduce tumour burden but also leads to symptomatic relief. Although used for several years, little is known about the safety and efficacy of PRRT in the elderly patient. **Methods:** 13 patients (8 females and 5 males) aged over 80 years (83 ± 5 yrs) with a progressing and symptomatic neuroendocrine tumour (7 of the small intestine, 3 of the pancreas, 1 of the stomach, 1 of the appendix) and 1 oxyphillic thyroid carcinoma underwent PRRT with Lu-177 labelled somatostatin analogues. The therapy was given along with nephroprotective (Arginin 25mg and Lysin 25mg) and antiemetic agents

(Odansetron 8mg). Dosimetry was performed during the first cycle in all patients. Patients were scheduled to receive 4 cycles. **Results:** Prior to the first cycle, 11 patients out of 13 had severe symptoms related to their disease, e.g. flush symptoms, diarrhoea, and dyspnoea. In 6 out of the 11 symptomatic patients an improvement in the frequency of their flush symptoms and diarrhoea started after just one cycle. At the end of the last cycle all symptomatic patients showed relief of tumour associated symptoms. In the conducted blood collections a slight decrease in the leucocytes count was seen after every cycle, which improved over time. Kidney parameters were within the normal range during therapy and follow up. **Conclusion:** We conclude that Lu-177 PRRT is an efficient and safe, non-invasive therapy for elderly patients suffering from the symptoms of their neuroendocrine tumours.

## OP477

### Comparison of tumour and whole body absorbed doses of 177-Lu-DOTA-TATE and Lu-177 DOTA-NOC treatment in the same patient group

N. Yeyin[1], L. Kabasakal[1], **R. Akyel**[1], M. Ocak[2], T. Toklu[3], N. Selçuk[3], M. Demir[1], B. Kanmaz[1]; [1]University of Istanbul, Cerrahpasa Medical Faculty, Istanbul, TURKEY, [2]University of Istanbul, Faculty of Pharmacy, Department of Pharmaceutical technology, Istanbul, TURKEY, [3]Yeditepe University, Medical Faculty, Department of Nuclear Medicine, Istanbul, TURKEY.

Peptide Receptor Radionuclide Therapy (PRRT) with Lu-177 labelled peptides in patients with neuroendocrine tumours (NETs) aroused great interest. An estimation of actual radiation doses to tumours is very important for therapy planning. There are several radiolabelled peptides, which can be used for PRRT with different biological behaviour. **Aim**: The Aim of the study was to compare the tumour and normal organ absorbed doses in patients who have received Lu-177-DOTA-TATE and Lu-177 DOTA-NOC. **Materials and Methods**: Study was composed of 20 patients (M/F: 10/10, mean age: 51.5±14.9) with histologically proven inoperable NETs. All patients received Lu-177-DOTA-NOC treatment 6 to 12 weeks after last Lu-177-DOTA-TATE treatment. Dosimetric calculations were performed using MIRD scheme and lesion doses were calculated using post therapy whole body images obtained at 4, 20, 44, and 68 hours after injection. Tumour volumes were determined from CT images. Thirteen blood samples beginning from time zero to 4 days after injection were obtained for bone marrow and whole body dosimetry. **Results**: There were 53 lesions in Lu-177-DOTA-TATE post therapy whole body images and 49 lesions in Lu-177 DOTA-NOC post therapy images. Lesions were selected according to lesion delineation and superimposed lesions were excluded. Mean lesion absorbed dose is calculated to be 47.4±53.4 and 42.9±52.8 Gy per 370 MBq for Lu-177-DOTA-TATE and DOTA-NOC respectively ($p>0.5$). There were significantly higher absorbed doses for kidney and bone marrow after Lu-177-DOTA-NOC treatment as compared to Lu-177-DOTA-TATE treatment, which were 6.9±2.7 vs 3.9±1.7 ($p<0.05$) and 0.12±0.0 vs 0.10±0.0 ($p<0.05$) Gy, respectively. There was not any difference in plasma elimination times between two tracers. On the other hand the whole body absorbed dose was significantly higher after Lu-177-DOTA-NOC treatment, which was 0.24±0.07 vs 0.20±0.06 Gy ($p<0.05$), respectively. **Conclusion**: The radiation absorbed doses to kidney, bone marrow and whole body after Lu-177-DOTA-NOC treatment are significantly higher then those of Lu-177-DOTA-TATE so it should be performed carefully and with patient dosimetric calculations.

## OP478

### Does Molecular Response Assessment after Peptide Receptor Radionuclide Therapy using Ga-68 Somatostatin Receptor PET/CT Offer an Additional Benefit?

**H. R. Kulkarni**, R. P. Baum; THERANOSTICS Center for Molecular Radiotherapy and Molecular Imaging, Bad Berka, GERMANY.

**Aim**: The Aim of this study was to examine the value of molecular response evaluation to peptide receptor radionuclide therapy (PRRNT) using Ga-68 somatostatin receptor PET/CT (SSTR PET/CT) in patients with neuroendocrine neoplasms (NENs). **Materials and Methods**: One hundred and fifty three patients with metastasized inoperable well-differentiated NENs (G1 and G2) and evidence of morphological or clinical progression (progressive disease, PD) within the last 1 year underwent SSTR PET/CT using Ga-68 DOTATOC or DOTATATE before and 10 - 14 weeks after each cycle of PRRNT. The 4 cycles of PRRNT were administered with an interval of 11 to 16 weeks between successive cycles, administering a cumulative radioactivity of 19.6 - 41.8 GBq of Lu-177 and/or Y-90. The maximum standardized uptake values (SUVmax) were determined for each patient on pre- and post- therapy SSTR PET/CT. Molecular response was evaluated according to the EORTC criteria, i.e., with percentage change in SUVmax of the target lesion. Morphological response was determined calculating percentage change in the longest diameter of target lesions on CT. Patients were followed up prospectively for PFS and OS as the end-points after SSTR PET/CT post-4th PRRNT cycle. **Results:** According to molecular response criteria, partial remission (PR) was observed in 54 patients, stable disease (SD) in 78, and PD in 21 patients after the 4th cycle of PRRNT. Response based on morphological criteria was as follows: PR in 27, SD in 98 and PD in 28 patients. The median PFS was 25 months and OS 59 months. There was a statistically significant difference in probability of OS after 4th cycle of PRRNT based on the molecular response status ($p=0.013$), but not with morphological response status as determined by CT ($p=0.71$). The probability of PFS also differed significantly based on the molecular response status, i.e., between patients who had PR and those with SD ($p=0.024$) **Conclusion**: Evaluation of molecular response to PRRNT using SSTR PET/CT offers additional information over morphologic response assessment alone since molecular response precedes morphology, and may predict OS and PFS after PRRNT in patients with NENs.

## OP479

### Somatostatin Receptor Expression in the Human Spleen - Answer to an Enigma by Ex vivo and In vitro Autoradiography after $^{177}$Lu-DOTA-octreotate Administration

**M. Melis**[1], D. Kaemmerer[2], J. de Swart[1], H. R. Kulkarni[3], A. Lupp[4], J. Saenger[5], H. C. Groen[1], M. W. Konijnenberg[1], L. M. van der Graaf[1], M. de Jong[6], R. P. Baum[3]; [1]Dept, of Nuclear Medicine, Erasmus MC, Rotterdam, NETHERLANDS, [2]Dept. of General and Visceral Surgery, Zentralklinik, Bad Berka, Bad Berka, GERMANY, [3]THERANOSTICS Center for Molecular Radiotherapy and Molecular Imaging, ENETS Center of Excellence, Zentralklinik Bad Berka, Bad Berka, GERMANY, [4]Dept.of Pharmacology and Toxicology, Jena University Hospital, Jena, GERMANY, [5]Laboratory of Pathology and Cytology, Zentralklinik Bad Berka, Bad Berka, GERMANY, [6]Dept, of Nuclear Medicine and Radiology, Erasmus MC, Rotterdam, NETHERLANDS.

**Aim**: Radiolabelled somatostatin analogues are being used for diagnostic and therapeutic (PRRT) purposes in patients with somatostatin receptor (SSTR) expressing tumours. During PRRT a significant spleen uptake may lead to radiation doses of > 20 Gy. Yet, the threshold dose for spleen radiation induced toxicity is currently unknown. Based on previous $^{68}$Ga-DOTATOC PET/CT studies, demonstrating higher uptake in spleen than in splenosis, white pulp (WP) localization of radioactivity was suggested. This hypothesis was investigated in the current pilot study using the longer lived $^{177}$Lu-DOTA-octreotate. **Methods**: A patient diagnosed with neuroendocrine neoplasm of the pancreatic tail ($SUV_{max}$ on $^{68}$Ga-DOTATOC PET/CT 100.4) with liver metastasis (SUV 47.3, normal liver SUV 12.5) and uptake in the spleen (SUV 41.0) received 1 GBq $^{177}$Lu-DOTA-octreotate. 2h after administration whole-body planar scintigraphy and SPECT/CT of the upper abdomen was performed, followed by laparoscopic resection of the pancreatic tumour and splenectomy the next day. After spleen transport from Bad Berka to Rotterdam *ex vivo* micro-SPECT of the removed spleen was acquired for 73min using 2.5mm diameter pinholes. Spleen fragments (~10 x 10 x 5mm) were either snap-frozen in liquid nitrogen or fixed in 10% formalin and paraffin embedded. *Ex vivo* autoradiography of 10µm cryosections was performed and serial sections were used for $^{111}$In-DOTA-octreotate *in vitro* autoradiography after decay of $^{177}$Lu. FFPE sections were used for HE- and immunostaining for SSTR2A and cell subsets CD4 (Th-cell), CD8 (Ts-cell), CD20 (B-cell) and CD68 (macrophage). **Results**: $^{177}$Lu-DOTA-octreotate scintigraphy and SPECT/CT demonstrated high uptake in the pancreatic tumor, hepatic metastasis and homogenously in the normal spleen. High resolution micro-SPECT imaging of the isolated spleen also revealed a relatively homogeneous uptake (calculated rest activity 60 MBq $^{177}$Lu). The vast majority of retained radioactivity was located in the red pulp (RP) as visualized in *ex vivo* autoradiograms, though some radioactivity was found in WP. *In vitro* autoradiography, however, demonstrated strongest $^{111}$In-DOTA-octreotate binding in WP, and less in RP. Immunostaining showed SSTR2A expression in lymphoid follicles in the WP, also stained for CD20, and in cells lining the marginal zone, but most SSTR2A staining was observed in foci scattered throughout RP. Also CD4- and CD68-staining abundantly was found in RP. **Conclusion**: The highest retention of radioactivity in spleen shortly after administration of $^{177}$Lu-DOTA-octreotate appeared to be located in the RP, for which CD68 positive cells (macrophages) seem to be responsible. *In vitro* autoradiography demonstrated preferential binding of $^{111}$In-DOTA-octreotate to SSTR positive B-cells in WP.

## OP480

### Quantification of the Pancreatic Beta Cell Mass with $^{111}$In-exendin in Patients with Type 1 Diabetes and Healthy Controls

**W. van der Weg**[1], M. Brom[1], M. J. R. Janssen[1], M. Béhe[2], W. J. G. Oyen[1], C. J. J. Tack[1], O. C. Boerman[1], M. Gotthardt[1]; [1]Radboud University Nijmegen Medical Centre, Nijmegen, NETHERLANDS, [2]Center for Radiopharmaceutical Sciences, Paul Scherrer institute, Villingen-PSI, SWITZERLAND.

**Aim**: To date, many questions remain concerning the role of beta cell mass (BCM) in the pathophysiology and course of type 1 and type 2 diabetes (T1D and T2D). Various tests exist to quantify beta cell (BC) function (insulin secretion), but do not necessarily provide information on BCM, while BCM seems the most important predictor of future BC failure. A method that reliably can quantify BCM would be a tremendous asset to better elucidate the pathophysiology of T1D and T2D, and to

determine effects of therapeutic interventions. We developed a non-invasive imaging technology based on targeting of $^{111}$In-labelled Exendin to the glucagon-like peptide-1 (GLP-1) receptor, which is specifically expressed on beta cells. Here, we report the first results of an ongoing clinical trial using single photon emission computed tomography (SPECT) with $^{111}$In-Exendin for BCM quantification in patients with T1D and in healthy controls. **Materials and Methods**: Patients with long standing T1D (no measurable C-peptide after glucagon stimulation, BMI below 27, age 21-60 yr) and healthy controls (normal glucose tolerance, matched for age, gender and BMI) are eligible for the study. 24 hours after i.v. injection of 150 MBq $^{111}$In-Exendin-4, SPECT/CT was acquired for quantification of pancreatic BC targeting. A volume of interest (VOI) of the pancreas was delineated on SPECT/CT images and counts within this VOI were corrected for administered activity and time after injection. **Results**: So far, 5 T1D patients and 5 matched healthy volunteers were studied. The pancreatic uptake of $^{111}$In-Exendin varied widely among these subjects. In healthy volunteers, it ranged from $0.9x10^5$ to $3.8x10^5$ counts/MBq (mean $2.3x10^5$ counts/MBq). The uptake was decreased in T1D patients, but interestingly not completely absent in all, ranging from $0.5x10^5$ to $1.5x10^5$ counts/MBq (mean $1.0x10^5$ counts/MBq). Our main observations: a) up to 8-fold lower pancreatic uptake in T1D patients than in healthy volunteers, b) pancreatic uptake varied by a factor of 3-4 amongst individuals within one group, and c) in some T1D patients, the radiotracer uptake suggests a substantial residual BCM. **Conclusion**: Our results suggest that quantification of BCM with $^{111}$In-Exendin SPECT is feasible. Our *in vivo* imaging data are in line with autopsy data from the literature, suggesting that T1D patients may have a relevant remaining BCM, and that large inter-individual differences in BCM exist. $^{111}$In-Exendin SPECT seems a valuable tool for non-invasive determination of BCM. Support: NIH 1R01 AG 030328-01 and EC (FP7/2007-2013), BetAimage, grant n° 222980

## OP481

### Biological effective doses in 300 patients undergoing therapy with $^{177}$Lu-octreotate

**M. Sandstrom**[1,2], U. Garske-Roman[2], D. Granberg[3], B. Eriksson[3], A. Sundin[2], H. Lundqvist[2], M. Lubberink[1,2]; [1]Medical Physics, Uppsala, SWEDEN, [2]Nuclear medicine & PET, Uppsala University, Uppsala, SWEDEN, [3]Endocrine Oncology, Uppsala University, Uppsala, SWEDEN.

**Aim:** Fractionated therapy with $^{177}$Lu-octreotate has been reported to be an effective treatment option for patients with generalized neuroendocrine tumors. The main Aim of this study was to calculate the biological effective dose (BED) to the kidneys using an individualized dosimetry protocol, and to assess differences in the number of possible treatment cycles based on BED compared to those based on absorbed dose. **Methods***:* A total of 148 female and 152 male patients with neuroendocrine tumors with high somatostatin receptor expression (grade 3 or 4) were included. After infusion of 7.4 GBq of $^{177}$Lu-octreotate SPECT/CT images over the abdomen were acquired at 24, 96 and 168 h after infusion. Absorbed dose to kidneys was calculated based on pharmacokinetic data obtained from SPECT/CT. From this the effective half-life of $^{177}$Lu-octreotate in the kidneys was estimatesd, and BED was calculated using the equation described by Barone *et al.*[1]. **Results and discussion***:* For a single treatment cycle of 7.4 GBq, median (1:st-3:rd quartiles) BED was 5.0 Gy (3.9-6.1) in the right kidney and 4.7 Gy (3.7-5.8) in the left kidney. For the same treatment cycle, BED was 9.0% (7.1-11.3) and 8.7% (7.0-10.9) higher than absorbed dose in right and left kidneys, respectively. In patients with high absorbed doses, BED could be more than 20% higher than absorbed dose. Assuming an absorbed dose limit of 23 Gy and a BED limit of 45 Gy to the kidneys, the possible number of treatment cycles was 5.4 (4.5-6.8) based on absorbed dose while using BED increased the number of possible cycles to 9.8 (8.1-12.5). **Conclusions***:* Although biological effective dose to the kidneys is higher than absorbed dose, use of BED to estimate the number of possible treatment cycles in $^{177}$Lu-octreotate therapy may allow for more treatment cycles than the use of absorbed dose. [1] Barone R *et al*. Patient-specific dosimetry in predicting renal toxicity with (90)Y-DOTATOC: relevance of kidney volume and dose rate in finding a dose-effect relationship. J Nucl Med. 2005;46 Suppl 1:99S-106S

1306 - Tuesday, Oct. 22, 11:30 - 13:00, Grand Salon Prestige Gratte-Ciel

## Oncology Clinical Science: Sentinel Node

## OP482

### The feasibility of axillary reverse mapping with lymphoscintigraphy and selective axillary dissection to prevent breast-cancer related lymphedema.

**M. Maccauro**[1], M. Gennaro[2], A. Lorenzoni[1], G. Aliberti[1], C. Sigari[3], C. Vellani[1], L. Bedodi[3], M. Castellani[1], E. Seregni[1], A. Caraceni[3], R. Agresti[2], E. Bombardieri[1]; [1]Foundation IRCCS Istituto Nazionale dei Tumori, Nuclear Medicine, Milan, ITALY, [2]Foundation IRCCS Istituto Nazionale dei Tumori, Breast Unit Surgery, Milan, ITALY, [3]Foundation IRCCS Istituto Nazionale dei Tumori, Rehabilitation and Palliative Care, Milan, ITALY.

**Aim** The lymphendema is a chronic, progressive and invaliding disease. Axillary reverse mapping (ARM) is a technique to distinguish the lymphatic pathway of the arm from that of the breast. In patient with indication for axillary lymph node dissection (ALND) the use of ARM may preserve upper extremity drainage preventing breast-cancer-related lymphedema (BCRL). The Aim of this study was to assess the feasibility of selective axillary dissection (SAD) after ARM and to evaluate the rate of related lymphedema. **Materials and Methods** Between June 2009 and February 2012 seventy-three patients stage with II-III breast cancer and positive sentinel lymph node (SLNB) were enrolled in the study. Sixty patients underwent to selective axillary dissection (SAD) after ARM. Lymphoscintigraphy was performed 4-6 hours prior SAD to identify the draining lymph node by mean three subcutaneous injection of $^{99m}$Tc-nanocolloid (15 MBq, 0.3 ml) into the dorsum of hand. SAD was performed up to Berg's level III with the gamma probe to identify and preserve the arm's lymphatic hot spot. Thirteen patients were treated with ALND due to a positive SLNB being found during the same surgery.Breast-cancer-related lymphedema was evaluated by physiatric assessment (increase > 2 cm of the arm circumference) and lymphoscintigraphy of the upper extremities at 1, 6 and 12 months after SAD. **Results** SAD was performed in 45/60 (75%) patients who underwent ARM. The draining lymph nodes were located medially to where the thoracodorsal merged with the axillary vein in 40/60 pts or laterally to the thoracodorsal vein in 5/60 pts. In 15/60 (25%) patients hot nodes were removed during surgery because located below the second intercostobrachial nerve, where metastatic spread from breast carcinoma is most likely to occur. The incidence of secondary lymphedema was compared in patient underwent to SAD (45/73 pts, group A) and ALND (28/73 pts, group B). The mean number of lymph nodes removed was 17 in group A and 20 in group B. BCRL presented in 4/45 pts (9%) of group A and in 8/28 pts (29%) of group B (29%) (p=0.048). At a mean follow-up of 16 months (range 6-36) none of the patients had nodal relapses. **Conclusion** Selective axillary dissection using axillary reverse mapping is a feasible and safe procedure to reduce BCRL.

## OP483

### Detecting near-the-injection-site sentinel nodes in the neck: a phantom study comparing a portable pinhole gamma-camera with a gamma-probe, conventional gamma-camera and SPECT/CT.

**D. Hellingman**, L. J. de Wit - van der Veen, R. A. Valdés Olmos; Department of Nuclear Medicine, NETHERLANDS Cancer Institute - Antoni van Leeuwenhoek hospital, Amsterdam, NETHERLANDS.

**Aim**: Traditionally, sentinel nodes (SNs) are preoperatively depicted by means of planar lymphoscintigraphy and intraoperatively acoustically localized with a gamma-probe. In head/neck cancer, especially in the preauricular or submandibular region, near-the-injection-site (NIS)-SNs may be missed on planar images. SPECT/CT visualizes more SNs than conventional images but has sometimes difficulties to detect these NIS-SNs too. In our hospital, a high-resolution portable gamma-camera is used prior to and after SN excision to confirm removal of all SNs. In some clinical situations with non-visualization on SPECT/CT this portable gamma-camera is able to depict NIS-SNs. The Aim of the present study was to compare the performance of this portable gamma-camera with a gamma-probe, conventional planar images and SPECT/CT in a phantom set-up simulating NIS-SNs **Materials and Methods**: Five plastic eppendorf tubes filled with 0.1ml Technetium-99m-nanocolloid were used to simulate four radiotracer deposit sites (range 14.5-23.6 MBq), as traditionally injected in melanomas, and one NIS-SN (range 0.3-0.6 MBq). The five tubes were placed in a self-made adjustable plastic holder, in order to regulate the distance between the SN and injection deposits with a 1mm accuracy. A portable gamma-camera (Sentinella 102, Oncovision) was used with pinhole collimators of 2.5 and 4.0mm. Image acquisition time was 1min with the camera positioned at fixed positions of 1.5 to 15.5cm distance. A conventional gamma-probe (Neoprobe3, Johnson&Johnson) positioned at a 1cm distance was used to detect the NIS-SN in the phantom set-up. Planar images were acquired with a dual-head SPECT/CT (SymbiaT; Siemens) and evaluated by an experienced nuclear physician. SPECT (128x128 matrix, 40 frames, 30 s/frame, zoom 1.00) was performed using a low-energy-all-purpose collimator. For CT (130 kV, 40 mAs, B30s kernel), 2-mm slices were obtained. **Results**: The simulated NIS-SN was detected with the 4mm-pinhole at 6mm and 12mm distance from the injection site with the portable gamma-camera positioned at 1.5 and 5.5cm respectively. Using the 2.5mm-pinhole collimator the NIS-SN was detected at 3mm and 12mm from the injection site with the camera at 1.5 and 7.5cm respectively. The conventional gamma-probe, planar lymphoscintigraphy and SPECT/CT detected the NIS-SN at distances from the injection site of 22, 14 and 12mm respectively. **Conclusion**: In a simulation phantom-model, the high-resolution portable gamma-camera, positioned close to the skin, is able to detect SNs at distances of at least 3mm from the injection site. The incorporation of this device to localize head/neck SNs may contribute to reduce the number of false-negative procedures and potential recurrences.

## OP484

### Sentinel node mapping in anal canal cancer: systematic review and meta-analysis of the literature.

S. Tehranian[1], G. Treglia[2], D. Krag[3], V. Dabbagh Kakhki[4], S. Zakavi[4], **N. Ayati**[4], R. Sadeghi[4], M. Keshtgar[5]; [1]Mashhad University of Medical Science, Mashhad, IRAN, ISLAMIC REPUBLIC OF, [2]Department of Nuclear Medicine and PET/CT Centre, Oncology Institute of Southern Switzerland, Bellinzona, SWITZERLAND, [3]Department of Surgery, College of Medicine, University of Vermont, Burlington, VT, UNITED STATES, [4]Nuclear Medicine Research Center, Mashhad University of Medical Science, Mashhad, IRAN, ISLAMIC REPUBLIC OF, [5]Consultant Surgical Oncologist, Royal Free Hospital and University College London, London, UNITED KINGDOM.

**Background and Aims:** The pathological condition of inguinal lymph nodes is an independent prognostic factor in predicting tumor recurrence and overall survival in anal canal cancer. Sentinel node mapping is a non-invasive method for detection of inguinal lymph node involvement in anal cancer. In the current study, we conducted a comprehensive search of literature in this regard and then interpreted the final results in a systematic review and meta-analysis format. **Methods:** Medline, SCOPUS, and ISI web of knowledge were searched with the following search terms: ((anal OR anus) AND sentinel). Outcomes of interest were inguinal detection rate and inguinal recurrence in the patients received inguinal sparing radiotherapy due to pathologically negative inguinal sentinel nodes (false negative cases). **Results:** Overall 16 studies (323 patients) included in the meta-analysis. Pooled inguinal detection rate was 86.2% [73.4-93.4%] (for studies used both blue dye and radiotracer was 90.1%[78.7-95.8] and for studies used radiotracer alone was 72.4% [46.3-88.9]). Pooled sensitivity was 90% [79-97%].**Conclusions:**Sentinel node biopsy is a promising method for inguinal lymph node staging in anal cancer. Combined blue dye and radiotracer technique can maximize the inguinal detection rate. Location of the tumor is highly associated with detection of inguinal sentinel nodes. Despite fairly high pooled sensitivity, no definite conclusion can be made regarding false negative rate of this technique due to low sample size and sub-optimal quality of the included studies. Large multicenter studies with long and consistent follow up are needed to definitely validate this technique in the future.

## OP485

### Is pre-operative identification of sentinel lymph node (SLN) by lymphoscintigraphy (LS) reproducible ? experience in 110 patients with melanoma of head/neck and trunk

M. Rensi, F. Giacomuzzi, L. Bastianutti, **O. Geatti**; S.M.M., Udine, ITALY.

**Aim**: as trunk and especially head/neck have complex lymphatic drainage systems, we always precede (within 3 weeks), the LS to be performed the day of surgery, by a strictly similar procedure (which could be done by a different staff from the same team), so surgical approach can be correctly planned before to improve operation management. A high reproducibility is obviously crucial, so we decided to analyze our data as concerning basin site location and exact SLNs detection. **Methods**: 110 melanoma pts who had 2 separate LS studies as previously mentioned, were included: 79 pts (72%) had primary tumors on the trunk (mean Breslow thickness 1,8 mm; ulceration: 25%; mean mitosis/mm$^2$: 3.8; Clark's level II 17%, III 37%, IV 44%, V 2%) and 31 pts (28%) had primary tumor on the head/neck (mean Breslow thickness 2,2 mm; ulceration: 32%; mean mitosis/mm$^2$: 2.9; Clark's level II 5%, III 50%, IV 40%, V 5%). The first LS was carried out in 8 to 34 days (m 20d) after excision biopsy of the primary melanoma, while the second LS was obtained 6 to 21 days later (m 16d). All pts had planar acquisition and 46 (42%) an additional SPECT-CT. Those cases with a failure or a mismatch in SLN localization were defined as non reproducible. **Results**: lymphatic drainage was shown in all studies but one and at least one SLN was identified. More than 1 lymphatic basin was visualized in 36 pts (33%) in the first series of LS and in 39 pts (35%) in the second series. In 96/110 pts (87%), the findings of the two series of LS matched exactly, while in 14 patients (13%) did not: 6 of them had melanomas of the trunk and 8 of the head/neck; metastases were found in SLN in 2/14 of them. The unreproducibility of SLN localization was 8% (6/79) for primary trunk lesions and 26% (8/31) for head/neck ones. **Conclusion**: reproducibility in SLN detection was pretty good (92%) in pts with melanoma of trunk but only acceptable (74%) as could be expected, for head/neck primaries. This must be kept in mind as it may be crucial in case of metastatic involvement.

## OP486

### Radio-Guided Sentinel Lymph Node Identification by Lymphoscintigraphy Fused with an Anatomical Vector Profile: Clinical Applications

**A. Niccoli Asabella**, F. Antonica, A. Nicoletti, D. Rubini, M. A. Renna, G. Rubini; Nuclear Medicine Unit, D.I.M., University of Bari "Aldo Moro", Bari, Italy, ITALY.

**Aim**: To develop a method to fuse lymphoscintigraphic images with an adaptable anatomical vector profile and to evaluate its role in the clinical practice. **Methods**: We used Adobe Illustrator CS6 to create different body vector profiles, in which every anatomical structure is divorced from the rest of the picture. In Adobe Photoshop we imported lymphoscintigraphic image and the corresponding body vector profile. Once the vector profile fits well to scintigraphic image the 2 different layers were fused. We processed 197 lymphoscintigraphies performed in patients with cutaneous melanomas, breast cancer or delayed lymph drainage. To validate the profile positioning on the planar lymphoscintigraphic (PLS) we compared the scintigraphic alignment to an external radionuclide marker image. Validation was done by placing a small external radionuclide source on the relevant anatomical structures in a new static scan. Images were evaluated by 5 nuclear medicine specialists and 5 surgeons. Two panels of different cases were shown: the first containing PLS images, the second containing vector fused images. The confidence image interpretation was evaluated on a 4-point scale. **Results**: Our models can be adapted to every patient attitude or position and contain different levels of anatomical details ranging from external body profiles to the internal anatomical structures like bones, muscles, vessels, and lymph-nodes. Average fusion processing times for all 3 operators involved in this procedure progressively decreased by 62% after the first 20 procedures, from a mean of 225 seconds to a mean of 85 seconds. Operators reported no particular difficulties during the fusion process. The image fusion validation showed a shift between the profile and Marker Image in a small number of procedures (15%) with a displacement of less than 13 mm (range 4-13 mm). The mean confidence score evaluated by the 5 nuclear medicine specialists was 1.9 for PLS and 3.0 for vector fused images (36.6% increase). The mean confidence score evaluated by the 5 surgeons was 0.7 for PLS and 2.4 for vector fused images (70,8% increase). The observers evaluated vector fused images always better than the PLS. **Conclusions**: We have created a new, practical, inexpensive digital technique for fusing lymphoscintigraphic images with built-in anatomical reference profiles. It's easily reproducible, does not alter the original scintigraphic image and increase the confidence in image interpretation. Our method allows a more meaningful interpretation of lymphoscintigraphies, an easier recognition of the anatomical site and better lymph-node dissection planning.

## OP487

### Comparison of SPECT/CT and Planar Sentinel Node Lymphoscintigraphy in Breast Cancer Patients

**A. Jimenez-Heffernan**[1], C. Ramos[1], E. Sanchez de Mora[1], J. Lopez-Martin[1], C. Salgado[1], D. Ladrero[1], H. Sado[2], T. Pascual[3]; [1]Hospital Juan Ramon Jimenez, Huelva, SPAIN, [2]Instituto do Câncer do Estado de São Paulo - ICESP, Sao Paulo, BRAZIL, [3]Division of Human Health. International Atomic Energy Agency, Vienna, AUSTRIA.

**Aim** To assess the impact of SPECT/CT as an adjunct to conventional planar lymphoscintigraphy for the detection of sentinel lymph nodes (SLN) in areas of unpredictable drainage patterns in patients with breast cancer. We present the patients included from December 2010 to March 2013 at a single site participating in the IAEA Coordinated Research Project CRP E1.30.37. **Materials and Methods** We studied 213 patients (3 men), mean age: 55.9 years (r: 28-86) with breast cancer (stages T1a: 5, T1b: 39, T1c: 87, T2: 78 and T3: 4 patients respectively). Mean tumor size was 1.7 cm (r: 0.4-6.5). The left breast and the upper outer quadrant were the most frequent tumor locations (125 and 124 patients respectively). Carcinomas were invasive ductal: 179, "in situ": 20, invasive lobular: 9; mucinous: 4, medular: 1 and carcinosarcoma: 1. 99mTc-Nanocoll (74-111MBq in 0.2-0.8 ml) injection was tumoral: 88, areolar: 38 or both: 87; guided by sonography in 33 nonpalpable tumors. Planar and SPECT/CT imaging was performed during the first 2 hours following injection in 72 patients and between 2-3 hours in the rest. The study was approved by the local ethical committee and all patients gave informed written consent. Planar images were 300s, 256x256 matrix, anterior, oblique and lateral; SPECT/CT comprised 90, 20s projections, 128x128 matrix, all imaging with high resolution collimation. Estimated effective doses were approximately 2,5 mSv for the sum of emission and transmission imaging. **Results** More sentinel nodes were identified on SPECT/CT (492, mean:2.3) versus planar imaging (466, mean:2.1). The number of SNL increased from planar to SPECT/CT in 27 patients (7 changing from 0 to 1-2 axillary SLN) with a change in drainage territory in 14 patients. There was a change in territory in 21 additional patients. The most frequent change was from axillary to interpectoral (14) followed by clavicular to infraclavicular (4) and axillary to intramammary (3) nodes respectively. In four patients no nodes were identified on either imaging modality. No significant differences were observed in the following parameters between patients with or without an increase in SLN number or a change in territory: age, weight, BMI, tumor size, injection (number and site), and tumor pathology. **Conclusion** Adding SPECT/CT to planar imaging identifies more SLN and provides better anatomic localization, with special relevance in the cases with negative planar images and nodes depicted on SPECT/CT. The approach increases camera time in 35 minutes and is suitable in most patients.

## OP488

### Usefulness of Radioguided Occult Lesion Localization and Sentinel Node Occult Lesion Localization guided by breast magnetic resonance imaging for nonpalpable breast carcinoma. Preliminary results

**S. Fuertes Cabero**, V. Martínez de Vega, S. Linares González, G. Hernández Cortés, R. Sainz de la Cuesta, A. Maldonado Suárez; Universitary Quiron Madrid Hospital, Pozuelo de Alarcón (Madrid), SPAIN.

**Aim:** Breast Magnetic Resonance Imaging (MRI) is more sensitive for detecting breast cancer than mammography and ultrasound. There are breast cancers that are only detected by MRI. The Aim of this study is to evaluate usefulness of Radioguided Occult Lesion Localization (ROLL) and Sentinel Node and Occult Lesion Localization (SNOLL) guided by breast MRI for nonpalpable breast carcinoma. **Material and Methods**: This is a retrospective study performed from April 2012 to April 2013. 12 newly diagnosed breast carcinoma patients were enrolled in this study. All patients Histological diagnosis was made by MRI-guided vacuum assisted biopsy. A total of 21 lesions were marked with ROLL technique: 6 patients showed 1 lesion, 3 patients showed 2 lesions and 3 patients showed 3 lesions. The day before surgery an intralesional dose of 99mTc-nanocolloid (activity of 4 mCi and 0.2 ml volume) was injected guided with MRI using a titanium needle. The site of injection and lymphatic drainage were confirmed by scintigraphy image. Intraoperative lesion and sentinel lymph node were localized and excised during surgery using a gamma probe. In some cases were necessary to administer blue day. **Results**: In 9 patients got a complete surgical excision of primary breast tumour with free margins (minimum 3 mm of distance). In 3 patients, microscopic examination stumble across invasive lobular carcinoma (two cases) and new focus < 1mm ( 1 case). In these cases, underwent a re-excision of the margins ( distance<1mm). Lymphoscintigraphy showed drainage in 9 patients. In 2 patients the SLN was positive and 10 patients the SLN was negative. **Conclusions**: Our results demonstrate that ROLL/SNOLL guided by MRI is useful technique for complete excision nonpalpable breast lesions and to localize the sentinel lymph node.

## OP489

### Sentinel node mapping in thyroid cancer patients: experience on 30 patients

**R. Sadeghi**[1], M. Mehrabibahar[2], M. Assadi[2], S. Zakavi[1], M. Yarani[2]; [1]Nuclear Medicine Research Center, Mashhad University of Medical Sciences, Mashhad, IRAN, ISLAMIC REPUBLIC OF, [2]Surgical Oncology Research Center, Mashhad University of Medical Sciences, Mashhad, IRAN, ISLAMIC REPUBLIC OF.

**Purpose:** In the current study, we evaluated the accuracy of sentinel node mapping in thyroid cancer patients using both radiotracer and blue dye. **Material and Methods:** 30 patients with diagnosis of papillary thyroid carcinoma (PTC) were included in the study. 2-3 hours before surgery, 0.5 mCi 99m-Tc-Antimony Sulfide Colloid was injected intratumoraly. 30 minutes post-injection lymphoscintigraphy images of the neck was perfored. Immediately before surgery 1cc patent blue V was also injected in the same fashion. Sentinel lymph nodes were detected intraoperatively using gamma probe and blue dye. Near total thyroidectomy was performed for all patients with dissection of central neck lymph nodes as well as sampling of the lateral neck lymph nodes. **Results:** At least one sentinel node could be identified during surgery in 19 patients (63.3%). Median number of sentinel nodes per patient was 1. Sentinel nodes in 16 patients were pathologically involved. No false negative case was noted. Upstaging occurred in 6 patients (20%). **Conclusion:** Sentinel node mapping is feasible in PTC. This method can upstage and change the treatment plan of the patients.

1307 - Tuesday, Oct. 22, 11:30 - 13:00, Salon Pasteur

## Oncology Clinical Science: Paediatrics

## OP490

### Sedation procedures in Pediatric Nuclear Medicine Imaging: an all-around patients approach to reduce them

**A. Grossi**, C. Bia, C. Chiaramonte, G. Baldari, A. Belletti, L. Ruffini; Nuclear Medicine Department, University Hospital Parma, Parma, ITALY.

Pediatric nuclear medicine procedures are noninvasive and painless, but they involve several aspects to consider: - are founded on the molecular activity pinpointed by injected radiotracers - can takes a long time scan - require absolute stillness - use massive and peculiar equipment These reasons often involve the need of a sedation approach to patients, but targeted paths and Methods can avoid it. AIM To develop an all-around approach to nuclear medicine pediatric imaging which connects every patient's need, from babies to young children and teenagers, and reduces sedation procedures. MATERIAL AND METHODS Our all-around approach consists of: - a multidisciplinary group (nuclear medicine physician, pediatrician, oncohaematologist physicist, technologist, nurse) who cares each patient according to scientific and evidence-based guidelines (i.e. appropriateness criteria, dosimetry) - a collaboration agreement with a pediatric no profit association (Giocamico Onlus®) who meets patient/parents 'not health' needs (talking, playing, emotional comprehension) - a dedicated examination session for patients that need sedation with a pediatric anesthesiologist - a risk communication strategy before examination (brochures, phone calls, access to see exam room) - a dedicated and colored children waiting room with toys, colored pencils, etc. RESULTS From Jan 2009 to Sep 2012, 190 pediatric patients performed a nuclear medicine examination, 39 had a PET/CT scan and 136 had a traditional nuclear medicine procedure to evaluate organ systems (kidneys and bladder, bones, liver and gallbladder, gastrointestinal tract, heart, lungs, brain, thyroid m-IBG). No patients had not performed the booked procedure, 9 patients had postponed it due to the worsening of their clinical condition. A sedation procedure was practiced on 2 PET/CT patients, due to their very young age (12 and 9 mo). On traditional nuclear medicine we performed a sedation procedure on 12% of patients, almost all on m-IBG scan (19 patients). CONCLUSION While sedation is a necessary procedure for much paediatric imaging (i.e very young patients, long procedure, not compliant patients) our experience shows that a multidisciplinary (nuclear medicine physician, pediatrician, oncohaematologist physicist, technologist, nurse), social (parents involving, supporting associations) and well structured (procedures) approach can cut it down. On one hand patients and relatives are more confident and compliant and, on the other hand, the healthcare system saves a time/cost-consuming and without no risks procedure.

## OP491

### Visualization of brown adipose tissue recruitment in human adults by means of dynamic and static [$^{18}$F]FDG PET/CT-imaging

A. van der Lans[1], W. van Marken Lichtenbelt[1], J. Hoeks[1], G. Vijgen[2], M. Visser[2], M. Vosselmans[1], J. Hansen[1], J. Jorgensen[1], J. Wu[3], F. Mottaghy[4], P. Schrauwen[1], **B. Brans**[2]; [1]University Maastricht, Maastricht, NETHERLANDS, [2]Maastricht University Medical Center, Maastricht, NETHERLANDS, [3]Dana-Farber Cancer Institute and Harvard Medical School, Boston, MA, UNITED STATES, [4]University Hospital RWTH Aachen, Aachen, GERMANY.

**Aim.** Upon mild cold exposure people can increase their energy expenditure (EE) without shivering, which is defined as non-shivering thermogenesis (NST). In rodents, brown adipose tissue (BAT) is the major contributor to NST. When chronically exposed to cold shivering gradually disappears, while EE remains elevated and BAT recruitment takes place. Nowadays, it is well recognized that active BAT depots are present in human adults, and recruitment of BAT might have favorable effects on body weight regulation. This study uses static and dynamic $^{18}$F-fluoro-deoxyglucose ([$^{18}$F]FDG) PET/CT-imaging to study BAT activity in human adults, before and after a cold acclimation period. **Materials and Methods.** 17 healthy, young and lean humans participated, of which 9 females and 8 males. Cold acclimation was achieved by exposure to an ambient temperature of 15-16 °C for 6 hours a day during 10 consecutive days. Before and after this period, a PET/CT dynamic scan of the supraclavicular region (74 MBq of [$^{18}$F]FDG) assessed BAT activation, while cooling subjects with a water-perfused suit. Energy expenditure was measured simultaneously (indirect calorimetry). From the dynamic PET/CT scans, glucose uptake rates were calculated according to a two-compartment model for FDG and Patlak curve fitting. Afterwards, a static scan of 6-7 bed positions assessed BAT presence and distribution. **Results.** The cold acclimation period increased glucose uptake rate in BAT from 11.1±8.7 to 17.0±12.4 µmol/min ($p<0.05$), and increased detectable BAT volume from 665±451 to 913±458 cc ($p<0.01$). In parallel, cold acclimation increased NST from 10.8±7.5 before to 17.8±11.1 % after ($p<0.01$). A significant correlation between maximal BAT activity (SUVmax) and NST (%) was found, both before ($R^2$ 0.55; $p<0.01$) and after ($R^2$ 0.32; $p<0.05$) the cold acclimation period. **Conclusion.** Both dynamic and static imaging by [$^{18}$F]FDG PET/CT were able to show human BAT recruitment after cold acclimation.

## OP492

### Spinal cord visualization in children on 18FDG PET/CT study

O. Kupik, M. Tuncel, **B. Erbas**; Hacettepe University, Ankara, TURKEY.

**Aim :** 18-FDG uptake of spinal cord may be seen in some patients without any spinal pathology. This retrospective study was performed to investigate the pattern of spinal cord visualization on 18-FDG PET/CT study in children and its relation with clinical parameters. **Material and Methods :** Eighty 18-FDG PET/CT studies of 50 children (13±4 yrs) were reviewed. Additional 33 studies of 20 adults were included for comparison. Subjects had no known spinal pathology or history of radiation therapy. Images were evaluated visually and semi-quantitatively. Spinal cord was visible on 18FDG at the level of middle servical and lower thorasic region. Therefore, ROIs were drawn on axial images on the spinal cord at the level of C5, T5, T12, L5 vertebrae. In addition ROIs were placed on the liver as a referance value. SUVmax and SUVmean values were measured for each ROIs and ratios to liver were calculated. Glucose level and imaging season were recorded for each

patients. **Results :** Pediatric age group has significantly higher ratios compared to adults (C5/L: 1.06±0.02 vs 0.88±0.04; T5/L: 0.8±0.6 vs 0.02±0.03; L12/L:1.03±0.02 vs 0.71±0.03; L5/L:0.6±0.02 vs 0.46±0.02). In pediatric group, C5/L SUVmax and T12/L SUVmax ratios were significantly higher compared to T5/L SUVmax and L5/L SUVmax ratios. C5/L, T5/L, T12/L ratios were higher than 1 in % 62, % 19 and % 56 % of subjects, respectively. Ratios were not related with glucose level or post injection time, however C5/L, T5/L and T12/L ratios showed significant negative correlation with age (p<0.01, r=-0.29, p<0.07, r=-0,3, p<0.0001, r=-0.44, respectively). Although there was no significant difference between girls and boys, when compared according to the imaging season, girls had higher values for C5/L and T12/L ratios than boys in winter compared to summer time. 23 children had two studies and 10 had more than two studies. Ratios were different between studies indicating transient spinal visualization. **Conclusions :** 18-FDG uptake of spine is not uncommon finding in children, especially in middle servical and lower thoracic level. Amount of uptake seems to be more pronounced with decreasing age, female sex and winter time. It should be taken into consideration as a physiological finding.

## OP493

### The Role of FDG PET/CT in Evaluation of Residual Disease in Pediatric Patients Diagnosed with Tumors Originated from Neural Crest

**A. Oral**[1], E. Tekin[1], Z. Burak[1], B. Demirağ[2], H. Öniz[3], S. Aksoylar[4], A. Çelik[5]; [1]Ege University, Faculty of Medicine; Department of Nuclear Medicine, Izmir, TURKEY, [2]Dr. Behcet Uz Children's Hospital, Department of Pediatrics, Division of Pediatric Oncology, Izmir, TURKEY, [3]Izmir Tepecik Training and Research Hospital, Department of Pediatrics, Division of Pediatric Oncology, Izmir, TURKEY, [4]Ege University, Faculty of Medicine; Department of Pediatrics, Division of Pediatric Oncology, Izmir, TURKEY, [5]Ege University, Faculty of Medicine; Department of Pediatric Surgery, Izmir, TURKEY.

**Aim**: 123I/131I-MIBG scintigraphy is used for determining primary focus, staging and follow-up of pediatric patients with neural crest originated tumors. In some cases MIBG scintigraphy shows residual tumor tissues which can not be confirmed by any radiological technique. The clinical approach for those patients is controversial; the children are usually followed by multiple MIBG scans until the scintigraphy becomes negative. We investigated the contribution of 18F-FDG PET/CT in differential diagnosis of 123I-MIBG positive residual disease which was not confirmed by other imaging modalities in pediatric cases with neural crest tumors. **Methods**: Between January 2009 and December 2012, a total of 121 123I-MIBG scintigraphies in 40 children were examined retrospectively. In 5 cases with positive and persistent 123I-MIBG findings indicating residual disease concomitant FDG-PET/CT results were evaluated. **Results**: Patients' age-range varied between 2 and 11 years (mean age 5.3 ± 2.5 years). Three of them had ganglioneuroblastoma, 37 were diagnosed as neuroblastoma. 57 of 121 123I-MIBG scintigraphies were pathologic. During follow-up, there was residual disease or relapse in 5 patients whose recent FDG- PET/CT is available. In 3 of them there was no FDG uptake in 6 MIBG positive lesions. In one child focal 123I-MIBG uptake was prominent consistent with minimal residual disease, while there was only mild FDG uptake (SUVmax;1.9) in PET/CT. This case is clinically stable and minimal 123I-MIBG uptake is still positive in follow-up scintigraphies. In last case hypermetabolic foci in brain parenchyma and medulla spinalis consistent with neuroblastoma involvement was observed in PET/CT. The lesions were 123I-MIBG positive as well. The child had aggressive clinical course with significant neurological symptoms and lost during treatment course. **Conclusion**: 123I-MIBG scintigraphy is highly sensitive and specific in evaluation of tumors with neural crest origin. However, the clinical importance of residual and consistent uptakes seen on 123I-MIBG scintigraphy is still unknown. Our limited series shows that the tumor may be more differentiated if the residual tissue has low FDG uptake. Such cases can be considered as low risk clinically. We believe that FGD-PET/CT positivity may contribute to indicate more aggressive types in high risk patients and may help to get the prognostic information in addition to MIBG scintigraphy.

## OP494

### The use of F18 FDG PET-CT in children and young adults with Ewing Sarcoma diagnosed in Norway 2005-2012. A national, population based study

**B. Johnsen**[1], K. Boye[2], K. Rosendahl[3], C. Trovik[1], M. Biermann[3], S. Aukland[3]; [1]Haukeland University Hospital, Bergen, NORWAY, [2]Oslo University Hospital/ Oslo University, Oslo, NORWAY, [3]Haukeland University Hospital & University of Bergen, Bergen, NORWAY.

**Objective:** Ewing sarcoma is a malignant bone tumour that typically affects children and young adults. X ray, Ultrasound, CT, MRI and skeletal scintigraphy constitute the "conventional" imaging. Methods reflecting the biology of the tumour like PET-CT are now emerging. This national, population based study summarizes the use of PET-CT in diagnostics and follow- up of patients with Ewing sarcoma. We investigate whether the use of PET-CT is influenced by tumour biology (expressed by Picci grade of operation specimen), disease stage at diagnosis, patient age, time since histological diagnosis or regional site. **Material and Methods:** All patients diagnosed with Ewing Sarcoma in Norway in the period 2005-2012 (age below 30 years at diagnosis) were identified from the Sarcoma databases in Oslo and Bergen. Medical records, pathology results and total imaging records were gathered from the four regional tumour centres in Norway: University Hospital in Northern Norway, St. Olav's Hospital, Oslo University Hospital and Haukeland University Hospital. The study population consists of 57 patients (27 females) (Oslo database no 37, Bergen database no 22). Mean age 17 years (range 4-28 y). Mean time since histological diagnosis 41 moths (range 2- 94 months). At diagnosis 28 patients had localized disease, 6 patients had tumour extending to nearby organs and 23 patients had metastases. Among the 36 operated patients twenty had Picci grade 1, six Picci grade 2 and ten Picci grade 3. **Results:** Of the 57 patients 22 (39%) had no PET-CT, 21 (37%) had one, 6 (10%) had two, and 8 (14%) had three or more PET-CT studies. There was a significant group difference in the use of PET-CT between the two regional sites; mean no of PET-CT pr. patient in the Oslo database was 0.9 vs. 1.8 pr. patient in the Bergen database (p = 0.035). There was a clear association between *disease stage at diagnosis* and the number of PET-CT studies performed (p = 0.018). The number of PET-CT studies was not associated to *Picci grade of operation specimen* (p= 0.646), *patient age* (p= 0.807) or *time since histological diagnosis* (p= 0.602). **Conclusion** In this study of patients with Ewing Sarcoma in Norway in the period 2005- 2012, we found a significant group difference in the use of PET-CT between the two regional sites. The extent of PET-CT imaging is related to the disease stage at diagnosis but unrelated to patient age, tumour biology or time since histological diagnosis.

## OP495

### The use of $^{18}$F-FDG PET SUV thresholds for target volume delineation in external beam treatment of pediatric Hodgkin's lymphoma

**R. F. Hobbs**, A. Walker, A. Chirindel, M. Huynh-Le, J. Moore, M. Wharam, S. Cho, S. Terezakis, R. Wahl; Johns Hopkins University, Baltimore, MD, UNITED STATES.

**Purpose:** Accurate target volume delineation in Hodgkin lymphoma (HL) is becoming more important as external beam radiotherapy (XRT) moves toward more conformal techniques and smaller treatment fields. FDG-PET imaging is used in staging and management of HL and shows potential as a planning tool for XRT. One approach to reduce tumor volume definition variability is to apply segmentation Methods such as $SUV_{max}$ percentage thresholding. We apply various $SUV_{max}$ thresholds in treatment planning and examine their effects in involved field (IFRT) and involved nodal radiation therapy (INRT) in regards to target volumes and dose to normal structures. **Materials/Methods:** 15 pediatric and young adult patients with HL treated with IFRT at our institution were included in this retrospective analysis. PET/CT datasets were reviewed and clinical target volumes (CTVs) generated using the standard qualitative visual method (QVM, so called $CTV_{QVM}$). The following $SUV_{max}$ thresholds were applied to the pre-chemotherapy PET: 15, 20, 25, 30, 35, and 40%. CTVs for IFRT and INRT plans ($CTV_{PET}$) were manually generated based on $SUV_{max}$ threshold volumes, and INRT treatment plans were designed using 15% and 40% $SUV_{max}$ threshold volumes. **Results:** Among pre-chemotherapy PET/CTs, the mean $SUV_{max}$ was 13.8 +/- 6.9. When applying the seven $SUV_{max}$ thresholds in the design of target volumes for IFRT, only 1 out of 15 patients had a change in treatment volume. On average there was an eight-fold increase in PET volume between 40% and 15% $SUV_{max}$ (range 2-18). The mean INRT CTV was 353 ml with 15% $SUV_{max}$, 299 ml with 25% $SUV_{max}$, and 184 ml with 40% $SUV_{max}$. When comparing INRT plans that were generated using 15% $SUV_{max}$ and 40% $SUV_{max}$ volumes, the absolute mean difference in dose was 47.8 cGy to heart, 15.3 cGy to breast tissue, and 28.4 cGy to lung. The optimal threshold, defined as the $CTV_{QVM}$ and $CTV_{PET}$ ratio closest to 1, ranged from 15-30% $SUV_{max}$. **Conclusions:** In IFRT planning, $SUV_{max}$ thresholding had very little effect on final target volumes. In INRT planning there was a significant amount of variability both within and between patients when $SUV_{max}$ thresholds were used in generating CTVs, which resulted in differences in dose to normal structures. The "best fit" $SUV_{max}$ threshold was 15 or 20% in the majority of patients; however, accurate target volume delineation with FDG-PET in HL is challenging and may require more precise and reproducible segmentation Methods as conformal therapy with involved site radiation therapy becomes standard.

## OP496

### Utility of 124I-MIBG PET/CT in the follow-up of patients with advanced neuroblastoma: first report of the AIMN PET-Pediatric Study InterGroup

U. Ficola[1], **N. Quartuccio**[2], R. Paratore[1], G. Treglia[3], A. Piccardo[4], A. Cistaro[5,6]; [1]Department of Nuclear Medicine, La Maddalena Hospital, Palermo, ITALY, [2]Nuclear Medicine Unit, Department of Biomedical Sciences and of the Morphological and Functional Images, University of Messina, Messina, ITALY, [3]Department of Nuclear Medicine and PET/CT Centre, Oncology Institute of Southern Switzerland, Bellinzona,

SWITZERLAND, [4]Nuclear Medicine Unit, Galliera Hospital, Genoa, ITALY, [5]Positron Emission Tomography Centre IRMET S.p.A., Euromedic Inc., Turin, ITALY, [6]Co-ordinator of National PET Pediatric Group, Turin, ITALY.

**Aim**: 124I-MIBG is a novel and promising PET radiotracer. At present there is lack of data about its value in the follow-up of patients with neuroblastoma due to its limited use. We present the first report of our study group on the usefulness of 124I-MIBG PET/CT in the follow-up of a small group of pediatric patients. **Materials and Methods:** 4 children with advanced (stage III-IV) neuroblastoma have been scanned with post-therapeutic 131I-MIBG-whole-body scan, 123I-MIBG SPECT and 124I-MIBG-PET/CT within an interval time of 3 months. **Results:** Patient n.1 (female; age: 136,9 months) presenting with left abdominal neuroblastoma underwent post-therapeutic 131I-MIBG scan with detection of a doubtful uptake in the postero-basal region of the right lung, which was better visualized by 123I-MIBG SPECT and 124I-MIBG PET/CT. In patient n.2 (male; age: 256,5 months), affected by focal relapse of neuroblastoma, post-therapeutic 131I-MIBG study depicted a focal uptake in three vertebrae (D10, L1, L2) and in the left 10th rib. Three months later, 124I-MIBG-PET/CT documented disappearance of the lesions. Patient n.3 (male; age: 73,4 months) diagnosed with abdominal neuroblastoma presented multiple lesions on 131I-MIBG scan (skull, left clavicle, right humerus, right femur, pelvis and left tibia). 124I-MIBG PET/CT resulted to be helpful in the follow-up, demonstrating improvement in most of the sites but worsening of the skull lesions. Clinical/imaging follow-up confirmed 124I-MIBG-PET/CT findings. In patient n.4 (female; age: 63.6 months) 123I-MIBG SPECT documented pathological uptake in the posterior mediastinum. 124I-MIBG PET/CT was performed and correctly confirmed the findings. **Conclusion**: Thanks to its high spatial distribution in tumors at high resolution and sensitivity, 124I-MIBG-PET/CT may be used used in the follow-up of patients with advanced neuroblastoma as a complementary imaging method or to clarify doubtful lesions. Multicenter investigations are warranted to validate these preliminary data.

## OP497

### Impact of Reconstruction Incorporating Point Spread Function and Time-of-Flight (PSF+TOF) on Dynamic 18FDOPA PETCT of the pancreas in children with Congenital Hyperinsulinism (CHI)

**H. A. Williams**[1], D. Tout[1], N. Wright[2], J. James[1]; [1]Nuclear Medicine, Central Manchester University Hospitals, Manchester, UNITED KINGDOM, [2]Paediatric Radiology, Central Manchester University Hospitals, Manchester, UNITED KINGDOM.

**Aims**: $^{18}$FDOPA PETCT can distinguish between focal and diffuse CHI, and guide curative surgery for focal CHI. Published work typically uses OSEM reconstruction and visual interpretation. Developments in reconstruction offer potential improvements in image quality, and quantitative analysis may assist disease classification. This work characterises the variation of $^{18}$FDOPA uptake with time post-injection and assesses the impact of OSEM+PSF+TOF reconstruction on uptake measures. **Materials and Methods**: 27 children presenting clinically with CHI were referred for quantitative $^{18}$FDOPA PETCT, with median (range) age 1.9 (0.1-11.2) years and weight 11.8 (3.5-43.5) kg. Intravenous $^{18}$FDOPA (mean 4 MBq/kg) was followed by CT for attenuation correction, dynamic PET and bi-phase contrast CT. Uptake patterns were classified visually as focal or diffuse. SUVmax and SUVmean were determined for volumes of interest (VOIs) over the focus and remainder of the pancreas (focal pattern, 5/27) or over the head, body and tail (diffuse pattern, 22/27) on dynamic frames representing 5-15, 15-30, 30-45, 45-60 and 65-90 minutes post-injection, reconstructed using OSEM and OSEM+PSF+TOF. SUVmax and SUVmean for each VOI, and focal VOI : remainder VOI, were plotted against time post-injection for both reconstructions. The impact of OSEM+PSF+TOF was quantified as the average change (%) in SUVmax and SUVmean with OSEM+PSF+TOF relative to OSEM, across all time-points, for specified VOIs. **Results**: SUVmax and SUVmean showed similar relationships with time post-injection, for both reconstructions. For diffuse patterns, SUVmax and SUVmean typically decreased with time post-injection, linearly ($r^2$> 0.8) in 149/264 plots. Average change was + 22% for SUVmax and +11% for SUVmean across all VOIs. For focal patterns, SUVmax and SUVmean tended to decrease slightly with time post-injection for 4/5 focal VOIs and all remainder VOIs, linearly ($r^2$> 0.8) in 14/40 plots. For one focal VOI (latterly confirmed as insulinoma) SUVmax and SUVmean increased until 60 minutes post-injection. For focal VOIs, average change was +69% for SUVmax and +26% for SUVmean; for remainder VOIs, average change was +20% for SUVmax and +14% for SUVmean. For focal VOI:remainder VOI, average change was +44% for SUVmax and +11% for SUVmean. **Conclusion:** For both uptake patterns, $^{18}$FDOPA uptake tends to decline with time post-injection, the exception being a single focal pattern subsequently proven to represent insulinoma, where uptake increased. OSEM+PSF+TOF does not alter the general relationship between uptake and time post-injection, but does enhance uptake relative to OSEM, particularly for focal VOIs. OSEM+PSF+TOF may therefore be useful in improving disease visualisation and classification.

1308 - Tuesday, Oct. 22, 11:30 - 13:00, Gratte-Ciel 1/2/3

## Molecular & Multimodality Imaging: Preclinical - Methods & Instrumentation

## OP498

### PIXSIC, a wireless radiosensitive intracerebral probe to monitor PET radiotracers in anaesthetized and awake rat

L. BALASSE[1], J. MAERK[2], S. FIEUX[1], F. PAIN[3], P. GISQUET[3], C. MOREL[2], **L. ZIMMER**[4], P. LANIECE[3]; [1]CERMEP, Lyon, FRANCE, [2]CNRS & Université Marseille, Marseille, FRANCE, [3]CNRS & Univ. Paris Sud, Orsay, FRANCE, [4]Hospices Civils de Lyon & Univ. Lyon 1, Lyon, FRANCE.

**Aim.** In neuroscience, PET functional imaging and behavioural assays in rodents are complementary approaches, despite the fact that they are rarely associated simultaneously because general anaesthesia inherent to PET precludes behavioural studies. To address this methodological limit, we have developed a radiosensitive pixelated intracerebral probe, PIXSIC, that provides access to the combination of simultaneous observations of molecular and behavioural parameters on rodents. **Material and Methods**. PIXSIC proposes a novel strategy for *in vivo* recording of the local time-activity curves of PET radiopharmaceuticals. It relies on a sub-millimetre pixelated probe of Si (17 mm long hosting 10 pixels with dimension 200 µm x 500 µm) implanted into the brain region of interest by stereotaxic surgery. Positrons are detected by reverse-biased, high-resistivity silicon diodes. The system Aims at time-resolved high sensitivity measurements in a volume of a few mm$^3$. The pixelated detection scheme adds "imaging" features as it allows recording of the time-activity curves in different brain regions along the probe position. PIXSIC has a compact and autonomous design based on a radiofrequency data exchange link that allows for full freedom in the animals motion and behavioural activity while limiting stress during acquisition. **Results and Conclusion**. The first biological validations were performed on anaesthetized rats implanted with two probes, one in the region of interest (hippocampus or striatum, according to the radiotracer) and the other one in a control region (cerebellum). We used [$^{11}$C]-raclopride for dopamine $D_2$ receptors and [$^{18}$F]-MPPF for serotonin $5HT_{1A}$ receptors. According to our previous studies with the Beta-Microprobe (*J Nucl Med 2002, 43(2):227-33; Eur J Nucl Med 2002 29(9) 1237-47*), the radioactive signals measured with the PIXSIC pixels are reproducible and well-correlated with the distributions of the targeted receptors. The simultaneous measurement of implanted rats in a small animal PET camera confirmed the similarity between PIXSIC and microPET time-activity curves. Moreover, the binding curves highlighted the possibility for PIXSIC to distinguish different tracer kinetics within the structure of interest (cortex/striatum or cortex/hippocampus) in accordance to the stereotaxic location of the pixels. In addition, PIXSIC allowed us to perform the first kinetic measurements of [$^{11}$C]-raclopride and [$^{18}$F]-MPPF on awake and freely moving rats. In conclusion, PIXSIC constitutes an unprecedented instrumental methodology for connecting PET molecular imaging and behavioral measurements with freely-moving rodents.

## OP499

### Radiation safety issues in small animals preclinical imaging: a careful approach to evaluate staff exposures

**S. Prevot**[1], J. Vrigneaud[1], O. Raguin[2], L. Houot[1], M. Moreau[1], C. Dejucq[2], L. Morgand[2], M. Février[1], C. Mary[1], A. Courteau[1], A. Oudot[1], B. Collin[1], F. Brunotte[1], P. Fumoleau[1]; [1]Centre Georges-François-Leclerc, Dijon, FRANCE, [2]Oncodesign, Dijon, FRANCE.

**Introduction:** The growing use of preclinical imaging raises the question of whether staff exposures are maintained well below the regulation limits when handling radioactive sources and animals without a shield. Considering the low activity injected to a mouse in few seconds (s) and the small number of injections performed on a daily basis, the risk of external exposure may be very low compared to standard clinical procedures. Is that hypothesis true? The Aim of this study was to investigate the level of protection when holding a monoclonal antibody labeled with 111Indium. A series of measurements was performed during four steps considered critical: dispensing doses from an unshielded test tube, injecting & positioning mice on the scanning bed, dissecting animals at the end of the process. **Material & Methods:** Time was kept for all tasks. Injections were performed with a 5mm-tungsten syringe shield, behind a bench screen (15 mm lead, 20 mm lead glass, Medisystem) that was also used for dissections. Whole-body (WB) doses Hp(10) were monitored with 2 electronic dosimeters (DMC2000 XB, Mirion) one placed in front of the screen, the other behind. Exposure rates were measured with a pen ratemeter (fieldSPEC, Aries) at distances of 0 and 10 cm. TLD rings (LANDAUER Europe) were used to investigate finger doses Hp(0.07) during dissections. A prospective series of 15 mice was studied. Mean activity was 8.2 ± 1.2 MBq per animal. **Results:** Average time was 30 s when preparing the syringe, 60 to 90 s per injection, 20-35 s when positioning simultaneously 3 animals in the scanning bed and 15 minutes per dissection. Hp(10) without shield was 17 µSv for injections, 19 µSv for dissections. WB doses were kept below 1 µSv behind the screen. Exposure rates at short distance are high: 10 µSv.MBq-1.h-1 to fingers

on contact with the test tube, 300 µSv.h-1 at 10 cm when dispensing the syringe, 200 µSv.h-1 at 10 cm when injecting a mouse, 300 to 1000 µSv.h-1 on contact with the multi-mouse bed of the imaging system. Finger dose Hp(0.07) measured during dissections was 840 µSv. **Discussion**: Measurements confirm the risk of exposure should not be underestimated. Clinical shielding devices are not always appropriate to procedures involving small animals. Therefore specific protective techniques must be developed so that unshielded sources are not held directly. Adherence to standardized handling procedures and close monitoring of finger doses are recommended so that exposures can be maintained ALARA.

## OP500

### Application of the optically stimulated luminescence (OSL) technique for mouse dosimetry in micro-CT imaging

**J. M. Vrigneaud**[1], A. Courteau[1], J. Ranoull[2], L. Morgand[3], O. Raguin[3], A. Oudot[1], B. Collin[1], F. Brunotte[1]; [1]Centre Georges-François Leclerc, Dijon, FRANCE, [2]Landauer Europe, Fontenay-aux-roses, FRANCE, [3]Oncodesign, Dijon, FRANCE.

**Aim:** Micro-CT is considered to be a powerful tool to investigate various models of disease on anesthetized animals. However, the radiation dose is known to be much higher than in clinical CT. The Aim of this work was to assess the dose delivered by the CT component of the nanoSpect/CT plus™ camera (Bioscan Inc.) during a typical whole-body mouse study. To this end, OSL dosimeters (OSLDs) were used in association with the InLight™ MicroStar™ reader (Landauer Inc.). **Materials and Methods:** OSLDs were first checked for reproducibility and linearity in the range of doses delivered by the micro-CT. A pencil ionization chamber properly calibrated at radiation quality encountered in micro-CT imaging was used to derive an energy correction factor for OSLDs. Doses to tissue were then investigated in phantoms and cadavers. A 30 mm diameter phantom was specifically designed to insert OSLDs and assess radiation dose over a typical whole-body mouse imaging study. Eighteen healthy female BALB/c mice weighing 27.1 ± 0.8 g (1 SD) were euthanized for small animal measurements. OLSDs were placed externally or implanted internally in 9 different locations by an experienced animal technician. Five commonly used micro-CT protocols were investigated and each experiment was repeated three times. **Results:** OSLDs exhibited a reproducibility of 2.4 % and good linearity was found in the dose range of the micro-CT, i.e. between 60 and 450 mGy. The energy scaling factor was calculated to be between 1.80 and 1.86, depending on protocol used. In phantoms, mean doses to tissue over a whole-body CT examination were ranging from 189.5 ± 3.6 mGy to 234.9 ± 4.5 mGy. In mice, mean doses to tissue in the mouse trunk (thorax, abdomen, pelvis and flanks) were between 215.1 ± 13.1 mGy and 251.2 ± 10.9 mGy. Skin doses (3 OSLDs) were much higher with average doses between 350.6 ± 24.6 mGy and 436.4 ± 44.0 mGy. Use of the multi-mouse bed of the system gave a significantly 20 to 40 % lower dose per animal ($p < 0.05$). **Conclusion:** Absorbed doses were found to be relatively high with the micro-CT component of the NanoSpect/CT plus™ camera. Given the low soft-tissue contrast capabilities of the system, users should pay attention to adjustable CT parameters so as to get the smallest radiation doses for a given purpose. This is even more critical in micro-SPECT/CT studies where CT is only used to produce a localisation frame.

## OP501

### Non-parametric bootstrap method for small animal Y-90 PET image enhancement

**T. Nam**, S. Woo, G. Min, J. Kim, J. Kang, K. Kim, S. Lim; Korea Institute of Radiological and Medical Sciences, Seoul, KOREA, REPUBLIC OF.

**Aim:** Yttrium-90 (Y-90) has been studied being received much interest by many researchers after Y-90 showed potential as a new treatment for unrespectable stage of hepatocellular carcinoma (HCC) since most existing treatments for HCC is palliative. Y-90 Imaging has been performed commonly with gamma camera. However, Y-90 PET imaging is required due to the fact that sensitivity and resolution are not sufficient. The Aim of this study was evaluating statistical characteristics and improving count rate to enhance Y-90 PET image quality using non-parametric bootstrap method for diagnosis and treatment. **Materials and Methods:** List mode data for 20 min using was acquired from small animal PET scanner (Inveon™, Siemens) after injection of 74 MBq Y-90 to mouse. List mode data format consists of 48 bit space composed of 8 bit for header and 40 bit for payload. The first bit of header is always zero and the next three bits are gray code to prevent fault of binary code and it was used to evaluate sequence of packet. Realigned sinogram was generated using resampled data of original list mode data using non-parametric bootstrap method producing new data set whose elements was extracted randomly from the original data set with buffer size of 50 million. The number of elements of resampled data set was 10 times, 100 times and 1000 times of original data set in this study. The realigned sinogram was reconstructed using ordered subsets expectation maximization (OSEM) 2D algorithm with 4 iterations. **Results:** PET image quality was evaluated by uniformity and signal to noise ratio (SNR). Estimated uniformity and SNR was 2.25, 1.99 (11.6% improved), 1.90 (15.6% improved), 1.92 (14.7% improved) and 0.73, 0.98 (34.2% improved), 0.98 (34.2% improved), 0.97 (32.9% improved) for original and bootstrapped data of 10 times, 100 times and 1000 times, respectively. **Conclusions**: The results showed that Y-90 PET image can be improved using non-parametric bootstrap method. 100 times bootstrapped data showed better result than 10 and 1000 times bootstrapped data in both of uniformity and SNR. The non-parametric bootstrap method will be useful tool for enhancing Y-90 PET image and it will be expected to reduce time for acquisition and to elevate performance for diagnosis and treatment.

## OP502

### High Resolution microSPECT imaging of Bi-213

**J. de Swart**[1], M. Segbers[1], A. Morgenstern[2], F. van der Have[3,4], H. Chan[1], S. C. Berndsen[1], F. Bruchertseifer[2], M. de Jong[1], F. J. Beekman[3,4], M. W. Konijnenberg[1]; [1]Erasmus MC, Rotterdam, NETHERLANDS, [2]European Commission, Joint Research Centre, Institute for Transuranium Elements, Karlsruhe, GERMANY, [3]Delft University of Technology, Delft, NETHERLANDS, [4]MILabs, Utrecht, NETHERLANDS.

**Aim** VECTor is an option to U-SPECT preclinical SPECT systems (MIlabs, NETHERLANDS) to perform high resolution imaging of high energy photons, including 511 keV photons ("pinhole PET"). Here we investigate the feasibility to use VECTor for quantitative high spatial resolution $^{213}$Bi imaging in small animals. **Methods** The VECTor high resolution mouse collimator uses 162 clustered pinholes of 0.7 mm. Acquisition is performed in list mode. An energy window of 16% around 440.5 keV was applied with 20 keV scatter windows on each side. Data was reconstructed with pixel-based OSEM [Branderhorst, Phys. Med. Biol 2010]. The calibration factor for $^{213}$Bi to perform absolute quantitative imaging was determined by scanning a 3 mL syringe containing 20.4 MBq $^{213}$Bi. To test spatial resolution a Jaszczak phantom with fillable rods (0.7 to 1.5 mm) containing 119 MBq $^{213}$Bi was scanned for 45 minutes. Dynamic scans, one with 15 frames of 30 minutes and one with 45 frames of 5 minutes, were made of a syringe containing respectively 7.8 MBq and 13.2 MBq. The syringe was placed inside a saline filled attenuator. The measured activity by the VECTor in each frame was then compared to the known amount of activity. As an in-vivo pilot experiment, 7 MBq $^{213}$Bi-DTPA was administered i.v. to a mouse. The mouse was scanned for 45 minutes using frames of 5 minutes. **Results** In the resolution phantom images rods with a diameter of 0.8 mm could be resolved. On the the 30 minute dynamic series the syringe was still visible when it contained an activity of 0.1 MBq. Radioactivity measurements by the VECtor had an accuracy within 11% for activities > 0.1 MBq. For lower activities there was an increasing overestimation. On the second dynamic series the syringe was visible at the lowest activity as well (0.5 MBq). The accuracy was within 10% for activities > 1.0 MBq. Below this activity there was increasing overestimation. On the in vivo mouse SPECT using $^{213}$Bi-DTPA kidneys and the bladder were clearly visible. Using VOIs, time activity curves were obtained. **Conclusion** VECTor enables sub-mm resolution $^{213}$Bi microSPECT in mouse sized objects. Absolute quantification was possible, but could be improved for low amounts of activities and/or short scan times. In vivo imaging of $^{213}$Bi compounds was feasible and may have applications in preclinical research on $^{213}$Bi therapy and dosimetry.

## OP503

### Feasibility of novel ICG-radiocolloid sentinel node detection technique in head and neck region using animal model

**S. Kosuda**, K. Araki, D. Mizokami, M. Tomifuji, T. Yamashita, A. Shiotani; National Defense Medical College, Tokorozawa, JAPAN.

Sentinel node biopsy (SNB) allows head and neck surgeons to avoid unnecessary neck dissection. Popular SNB method using radioisotope (RI) has some drawbacks, such as the strict legal regulations for RI use in Japan. Recently, SNB technique using real time indocyanine green (ICG) fluorescence image becomes prevalent in breast cancer. Some report demonstrated improved detection sensitivity with this method. However the major problem of ICG method is its quick migration through the lymphatic system, which results in a limited diagnostic time window and detection of downstream subsequent nodes. To overcome this problem, we modified ICG detection method by making ICG-colloid and demonstrated the feasibility study of this technique in mouse model. [Methods] ICG-colloid or ICG-99mTc-colloid was formed by mixing ICG and phytate colloids which is commercially available as a kit for 99mTc-radiocolloid. Twenty microliter of ICG or ICG-colloid or ICG-99mTc-colloid was injected into tongue of nude mouse and the fluorescence images were observed with time until 48Hrs after injection. The fluorescence intensity in detected SN was analyzed. [Results] In ICG injected animals, SNs were detected soon after injection, and second echelon lymph nodes were detected after 30-60min. In ICG-colloid injected animals, SNs were also detected after 30-60 min and no second echelon lymph node was detected. Peak fluorescence intensity was 6-12Hr in both animals. No SN was detected after 24Hr in ICG animals, whereas SNs were still detectable in ICG-colloid or ICG-99mTc-colloid animals. [Conclusions] SNB using ICG-colloid or ICG-99mTc-colloid technique

may have advantages of prolonged diagnostic time window and prevention of downstream subsequent nodes detection.

## OP504

### Positron range corrected MLEM and cascade-gamma removal for I-124 in small animal PET imaging

**S. Sauerzapf**[1], F. Braun[1], W. Weber[2], U. Pietrzyk[3], M. Mix[1]; [1]University Hospital Freiburg, Freiburg, GERMANY, [2]Memorial Sloan-Kettering Cancer Center, New York, NY, UNITED STATES, [3]Research Center Juelich, Juelich, GERMANY.

**Aim:** Small Animal PET Imaging with the non-pure positron emitter I-124 implies two well-known major difficulties: Due to its high energy and its resultant long positron range, resolution is degraded. Furthermore absolute quantification is complicated due to the emission of cascade-gammas in conjunction with the positron decay. Aim of this work was the implementation of corrections for both effects to be applied to simulated and measured PET data. **Materials and Methods:** To quantify the impact of cascade-gamma coincidences on energy, sinogram- and image-based level, an animal PET scanner (MicroPET Focus 120) was modeled with GATE Monte-Carlo software. A reconstruction pipeline for measured and simulated data was established. To enable quantification with I-124, a sinogram-based scatter estimation involving an edge-finding tail-fitting procedure combined with a uniform background subtraction for cascade-gammas and randoms correction is proposed. To restore the resolution loss, a modified Maximum Likelihood Expectation Maximization algorithm with positron range correction (PR-MLEM) was implemented which involves the convolution of the estimated activity before projection. The convolution kernel was determined from over 700 measurement positions across the FOV for I-124 and F-18 and verified by GATE simulations. The implemented correction procedure was tested on simulated as well on measured data for several phantoms (Image Quality, hollow spheres, resolution, a self-made attenuation phantom and versions of the MOBY mouse voxel phantom) and on 20 mouse scans. **Results:** The additional uniform background contribution due to cascade-gamma and randoms depends on object geometry and is between 30% and 42% of all coincidences. Quantification accuracy over all phantoms increased to 7±5% compared to 17±2% without corrections. The mean change in quantification over all mouse scans was 37±20%. The optimal kernel, describing the difference between I-124 and F-18 across the whole FOV, has a Full Width at Half Maximum (FWHM) of 1.8±0.1mm. Applying the PR-MLEM on phantoms, increased the mean recovered resolution by 17% up to an FWHM of 2.5±0.4mm. For a single line source, an artifact-free increase in resolution of 46% is possible. For the small animal studies, the mean maximum contrast and Contrast-to-Noise-Ratio could be increased by 77±39% and 30±13%. The large standard deviation is due to heterogeneities within the study group itself. **Conclusion:** With the aid of GATE, it was possible to implement a complete correction technique for non-pure high energy positron emitters. The method was verified by several phantom simulations and measurements and could be successfully transferred to real animal PET data.

1309 - Tuesday, Oct. 22, 11:30 - 13:00, Rhône 3A/3B

## Neurosciences: Miscellaneous

## OP505

### High discriminant value of 18FDG-PET in Amyotrophic Lateral Sclerosis

**M. Pagani**[1], A. Chiò[2], J. Öberg[3], A. Calvo[2], C. Moglia[2], F. Nobili[4], P. Fania[5], S. Morbelli[6], M. Valentini[7], A. Cistaro[5]; [1]ISTC-CNR, Rome, ITALY, [2]ALS Center, Department of Neuroscience University of Turin, Turin, ITALY, [3]Department of Nuclear Medicine, Karolinska Hospital, Stockholm, SWEDEN, [4]Clinical Neurophysiology Unit, Dept of Neurosciences, Ophthalmology and Genetics University of Genoa, Genoa, ITALY, [5]Positron Emission Tomography Center IRMET S.p.A., Turin, ITALY, [6]Department of Internal Medicine, Nuclear Medicine Unit, University of Genoa, Genoa, ITALY, [7]Department of Neuroradiology, CTO Hospital, Turin, ITALY.

**Background.** Amyotrophic lateral sclerosis (ALS) is a selective corticospinal tract degeneration. The Aim was to assess the discriminant value of 18FDG-PET at rest in the largest series of ALS patients investigated so far by PET. **Methods**. 195 ALS patients (77 women and 118 men, mean age 63±12) and 40 control subjects (11 women and 29 men, mean age 62±14) underwent brain [18F]FDG PET. Twenty-six cortical and sub-cortical brain regions were segmented by the Pick Atlas tool in SPM2 and relative metabolic uptakes individually normalized by whole brain values. Factorial (FA) and Discriminant (DA) analysis were performed using the 52 bilateral regions as well as age and sex. The strict statistical constraint of post-hoc cross-validation was applied. **Results**. FA identified 8 factors in CTRL and 10 factors in ALS explaining 90% and 87% of total variance, respectively. As compared to CTRL, ALS showed factors with stronger laterality, networking separately left and right temporal lobes and left somatosensory and superior parietal cortex. In ALS FA gathered also selectively insulas and central structures (nc.caudati and thalami). DA performed on all 235 subjects showed following cross-validation an accuracy of 88% (sensitivity 89% and specificity 83%) when all 52 regions were taken into account and of 80% (equal sensitivity and specificity) when analyzing the discriminant value of the 10 factors. **Conclusions**. In ALS different cortical and subcortical networks were found as compared to normal controls. When 52 functional regions were submitted to discriminant analysis the overall accuracy was 88% with a very high sensitivity of 89%. This results show for the first time the usefulness of 18FDG-PET in differentiating ALS patients from normal controls and paves the way to a larger implementation of such methodology in ALS diagnosis.

## OP506

### Cortical 18F FDG-PET changes during olfactory stimulation in normal subjects

**A. Chiaravalloti**[1], M. Pagani[2], M. Alessandrini[3], A. micarelli[1], B. Di Pietro[1], D. Di Biagio[1], A. Lacanfora[1], B. Napolitano[3], R. Danieli[1], O. Schillaci[1]; [1]Department of Biomedicine and Prevention, University Tor Vergata, Rome, ITALY, [2]Institute of Cognitive Sciences and Technologies, CNR, Rome, ITALY, [3]Department of Medical Science and Translational Medicine, University Tor Vergata, Rome, ITALY.

**Aim**: The Aim of our study was to assess the cortical metabolic changes related to a pure olfactory stimulation using 18F FDG-PET/CT in normal subjects**. Materials and Methods**: Fifty-eight normosmic individuals without otorhinolaryngologic or neurological diseases were enrolled in the study. The global sample of individuals was then divided in two groups of thirty-five (nineteen women and sixteen men; mean age 49.5 ± 12 years; control group, CG) and twenty-three (thirteen women and ten men; mean age 48.5 ± 10 years; experimental group, EG) subjects. All of them were assessed as normosmic when evaluated with the multiple-forced choice Sniffin' Sticks Screeinng (SSS) test . The subjects of the experimental group, underwent a simple olfactory stimulation by using a common aerosol facial mask containing in its ampoule a solution of 1.5 ml of lavender 100% and 5 ml of saline sodium chloride (NaCl) 0.9% conveyed by an oxygen flow rate of 3.5 liters per minute; the stimulation consisted of one continuous 6 minute block without any sniffing generated instructions. At the end of the third minute each subject was injected with 185-210 MBq of 18F-FDG and after continued the olfactory stimulation until the end of the sixth minute. Control subjects breathed normal room air before and after 18F-FDG injection. Differences in brain 18F-FDG uptake were analyzed using statistical parametric mapping (SPM2, Wellcome Department of Cognitive Neurology, London, UK) implemented in Matlab 6.5 (Mathworks, Natick, Massachusset, USA). **Results**: A significantly higher glucose metabolism was found in EG as compared to CG in the following regions of the right hemisphere: superior (BA 9) and middle (BA 46) frontal gyrus, sub-lobar insula (BA 13), inferior parietal lobule (BA 40), superior temporal gyrus (BA 22) and supramarginal gyrus (BA 40) (Figure 1 and Table I). No statistically significant differences were found when data of EG subjects were subtracted to those of CG subjects. **Conclusions**: the results of our study suggest that neural responses associated to a pure olfactory stimulation via FDG-PET highlights several metabolic changes in cortical sites related to on-line olfactory i) working memory (BA 9 and 46, prefrontal and BA 40, parietal), ii) short term recognition (BA 13, insula) and iii) discrimination (BA 22, STG). The present results also confirmed the right hemisphere dominance in a task likely engaging recognition processes.

## OP507

### Cerebral Glucose Metabolism in Sarcoidosis Patients With and Without Cognitive Failure.

**S. Jentjens**[1], C. Urbach[1], M. Drent[2,3], R. Wierts[1], P. Wijnen[1], E. Hoitsma[4], R. Ponds[1], M. van Kroonenburgh[1]; [1]Maastricht University Medical Center, Maastricht, NETHERLANDS, [2]Maastricht University, FHML, Maastricht, NETHERLANDS, [3]Hospital Gelderse vallei, Ede, NETHERLANDS, [4]Dept of Neurology, Diaconessenhuis, Leiden, NETHERLANDS.

**Introduction** Sarcoidosis is a disease characterized by granulomas in multiple organs including the central nervous system. Neurosarcoidosis accounts for 5-16% of systemic sarcoidosis cases. Cognitive failure can be a serious problem in patients suffering from sarcoidosis. Although PET with $^{18}$F-FDG can depict granulomas in several organs, only a few cases of proven neurosarcoidosis have been studied with PET. Not much is known about brain involvement detected by PET in patients with proven sarcoidosis or in patients complaining of cognitive failure. **Methods** The clinical records of 166 known sarcoidosis patients visiting the outpatient clinic between June 2005 and October 2011, who underwent a $^{18}$F-FDG PET scan (Philips Gemini TOF), performed according to the EANM guidelines, were reviewed. The brain was cropped from the whole body PET-images using Pmod software (version 3.0 PMOD Ltd, Zurich, Switzerland). Cognitive failure was measured by the CFQ-scores. Statistical software (SPM-8, Welcome Trust, London UK) was used on the cropped brain data for group comparisons and to study co-variability. Normalisation to MNI-space, smoothing with 8 mm FWHM and a 2-sample T-test was used to find differences between the groups with high (>43) and low CFQ scores and between patients who had a PET positive and negative scan, corrected for age and sex. A threshold with a p-value of 0.001 was used for a cluster

containing 100 voxels. **Results** Our population yielded 50 patients with a PET scan that could be analysed and who completed the CFQ questionnaire. Nineteen patients had a high CFQ score, 31 scored normal. On visual analysis all PET images were without obvious abnormalities. In patients with high CFQ score we found higher metabolism in the right thalamus. We did not find a significant difference in cerebral glucose metabolism between patients with normal and abnormal PET scans. **Conclusion** This is an attempt to systematically study changes in brain glucose metabolism as measured by PET in patients with proven sarcoidosis. Our data indicate that even in patients with several organs involved as detected by PET imaging, changes in brain glucose metabolism could not be detected either statistically or visual reading. Of great interest however are the increased metabolism observed in the thalamus in patients with cognitive failure, compared to patients without cognitive complaints. Although the data are derived from retrospective analysis and more reliable cognitive tests are known, it warrants further investigation in order to study the consistency and the meaning of our findings.

## OP508

### Structural MRI and FDG-PET modifications induced by one year multdidomain intervention in elderly.

**D. Adel**[1,2,3], K. Boulanouar[1,2], N. Chauveau[1,2], J. Delrieu[3,4], T. Voisin[3,2,4], B. Vellas[3,4,2], P. Payoux[1,3,2]; [1]INSERM U825, Toulouse, FRANCE, [2]Paul Sabatier Toulouse University, Toulouse, FRANCE, [3]Toulouse University Hospital, Toulouse, FRANCE, [4]INSERM U1027, Toulouse, FRANCE.

Multidomain intervention (physical and cognitive training, nutritional advices), is supposed to reduce the risk of cognitive decline in prefrail older people. FDG-PET and MRI have been proposed as biomarkers of neurodegeneration. The Aim of this study is to assess the effect of Multidomain Alzheimer preventive program on brain metabolism and gray matter change after one year practice. **Methods**: All subjects were enrolled in MAPT neuroimaging study, an ancillary study of MAPT (3-year, randomized controlled trial), who don't meet the criteria of dementia or AD, on the basis of at least one of following criteria: subjective memory complaints spontaneously expressed, limitation in one instrumental activity of daily living, and slow walking speed (speed≤0.8m/s). We enrolled 68 subjects (77±4 yo) in Toulouse University Hospital. They were randomized in two groups, the active multidomain group and the control group. Among them 15 controls and 15 multidomain intervention underwent a FDG-PET and MRI scans at baseline and 12 months. We used SPM8 software to assess the differential maps of PET-FDG uptake and cortical thickness between the two times. Cortical thickness was computed according to the methodology developed in our research unit (Querbes et al.Brain 2009). The maps of differences were thresholded at p<0.005 (uncorrected) and spatial extent k>300. **Results:** They were no difference at baseline in FDG or MRI assessment. Multidomain group demonstrated an increase of FDG uptake at 12 months compared to baseline in right hippocampus, parahipppocampus, left fusiform and left cerebellum. No voxel survived in the inverse contrast. In this group, after 12 months, the cortical thickness showed an increase at left in insula, cerebellum, fusiform, inferior temporal, precuneus and post-central gyrus, and a decrease at right in insula, inferior frontal, mid-temporal, inferior temporal, fusiform and left caudate, In control group, FDG uptake decreased in anterior cingulum, frontal medial, right mid-frontal, superior and orbitofrontal, right temporal, right insula. FDG uptake increased in left temporal. The cortical thickness decreased in right temporal, left inferior frontal and left orbitofrontal. No increase was seen. These results show an effect on both, FDG uptake and cortical thickness. The metabolism structural changes in multidomain group are not seen in control group. These changes are partly co-localized, they both increase in left fusiform and cerebellum. FDG-PET seems to be a more sensitive biomarkers in the follow up of cognitive improvement induced by multidomain intervention than structural MRI.

## OP509

### Effects of ECT against depression on [11C]raclopride binding

**M. Tiger**, C. Halldin, L. Farde, J. Lundberg; Karolinska Institutet, Stockholm, SWEDEN.

Depression is a significant contributor to the global burden of disease. Electroconvulsive therapy (ECT) is a highly effective antidepressant treatment where the mechanism of action still remains largely unknown. ECT can alleviate symptoms of parkinson's disease, implying a potential dopaminergic effect of the treatment. [$^{11}$C]raclopride binds selectively to dopamine (D) 2/3 receptors. Aim: to examine [$^{11}$C]raclopride binding with positron emission tomography (PET) before and after ECT for major depressive episodes, data that previously not have been reported in the litterature. **Materials and Methods**: 8 patients hospitalized for a major depressive episode were included. Patients with medication with known effect on the dopamine system were excluded. [$^{11}$C]raclopride PET was performed before ECT and when the patients were in remission or within one week after termination of treatment. The PET system used was ECAT HRRT (High Resolution Research Tomograph). The patients were assessed with MADRS (Montgomery-Åsberg Depression Rating Scale), the Consortium for research on electroconvulsive therapy scale (CORE) and clinical global impression (CGI) by a psychiatrist at time of PET. **Results**: All patients responded to treatment with at least 50 % reduction of depressive symptoms. A preliminary analysis of PET data suggest that half of the patients had a pronounced increase of [$^{11}$C]raclopride binding potential ($BP_{ND}$), 98 %, in the ventral striatum after ECT, while the remaining patients had virtually no difference in $BP_{ND}$ with treatment . Similar results were observed also for other examined regions of interest in the brain. **Conclusions**: Alteration of D2/3 binding is not required for the antidepressant effect of ECT. The increased [$^{11}$C]raclopride seen with half of the patients is probably due to upregulation of D2/3 receptors, since decreased dopamine levels with ECT is unlikely, given its effect against parkinsonian symptoms. The response rate for ECT effect on D2/3 binding is similar to what has been observed in clinical trials of ECT for parkinson's disease.

## OP510

### Microglia activation after acute stroke demonstrated using 18F-DPA-714 PET. Correlation with MRI.

**M. J. Santiago-Ribeiro**[1], J. Vercouillie[1], J. P. Cottier[1], S. Debiais[2], I. Bonnaud[2], N. Arlicot[1], B. Erra[1], S. Maia[1], M. Kassiou[3], D. Guilloteau[1]; [1]CHRU, INSERM 930, Université François Rabelais, TOURS, FRANCE, [2]CHRU, TOURS, FRANCE, [3]School of Chemistry, University Sydney, BMRI, Medical Radiation Sciences, Sydney,, AUSTRALIA.

**Objectives:** Stroke induces inflammatory reaction with glial cells activation and leukocyte infiltration, with an increase in the cerebral expression density of the translocator protein 18 kDa (TSPO) that could be visualised by PET. In this study we evaluate the expression of TSPO after a recent stroke using 18F-DPA-714. Material and **Methods:** Eight patients (4 women, 4 men; age range: 55 to 82 years) with a unilateral recent infarct have been submitted to two imaging studies 8 to 15 days after an acute insult. MRI with gadolinium injection and a 90 dynamic PET acquisition followed an iv injection of a mean dose of 3.4 MBq/kg of 18F-DPA-714 were performed. A visual analysis between MRI and PET images were done by two physicians. Pmod® 3.4 software is also used to achieve co registration between MRI and PET images and to define manually regions of interest (ROI) on the region corresponding to the tissue infarct, and on the contralateral region as also on the cerebellum. Time activity curves (TAC) were obtained from each ROI. **Results:** Visual analysis shows an increase uptake of 18F-DPA-714 corresponding to the infarct tissue observed on MRI images. However, radiotracer increase uptake area is larger than the region corresponding to the blood brain barrier (BBB) rupture observed on MRI. This could be to an increasing neuronal loss associated to the inflammatory reaction on penumbra area. For all the subjects, higher binding values are observed for the region infarcted decreasing slowly from 10 minutes pi to the end of the PET acquisition. The uptake of the 18F-DPA-714 by the infarct region remains higher than that observed for the other two regions until the end of the acquisition Conclusions: Our results show: 1) the uptake of the 18F-DPA-714 is due to the BBB breaking and to activation of microglia in the penumbra area; 2) the kinetics of the 18F-DPA-714 is different in the injured and normal tissue. These results allow the use of the 18F-DPA-714 in the analysis of the intensity of neuroinflammation reaction associated to the penumbra area as well as in the evaluation of the possible use of anti-inflammatory drugs in the future. This work has been supported in part by grants from: French National Agency for Research called Investissements d'Avenir ANR-11-LABX-0018-01. FEDER (Radex programme) FP7-HEALTH-2011 (INMiND-Imaging of Neuroinflammation in Neurodegenerative Diseases and the Fondation Thérèse Planiol.

## OP511

### Imaging of cyclooxygenase-1 in activated microglia by PET with S-enantiomer of $^{11}$C-ketoprofen-methyl ester

M. Shukuri[1,2], A. Mawatari[1], M. Ohno[1], H. Doi[1], M. Suzuki[1], Y. Watanabe[1], **H. Onoe**[1]; [1]RIKEN Center for Life Science Technologies, Hyogo, Kobe, JAPAN, [2]National Center of Neurology and Psychiatry, Kodaira, JAPAN.

**Aim:** Neuroinflammation is known to be involved in various neurological and neurodegenerative diseases. Recently, we reported that $^{11}$C-labeled ketoprofen-methyl ester (KTP-Me), a derivative of cyclooxygenase-1 (COX-1) selective inhibitor, could be a useful PET probe for monitoring activated microglia during the process of neuroinflammation (J Nucl Med. 52:1094-101, 2011). For further improvement of specificity, we have successfully obtained S-enantiomer of $^{11}$C-KTP-Me ($^{11}$C-(S)KTP-Me), which is considered to be more pharmacologically active than R-, by chiral HPLC separation. In this study, we have evaluated $^{11}$C-(S)KTP-Me as a PET probe for neuroinflammation in rat model and have applied it to Alzheimer's disease model mice (APP-Tg). **Methods:** The specificity of $^{11}$C-(S)KTP-Me for COXs was examined in PET studies with rats which had hemi-intrastriatal injection of lipopolysaccharide (LPS), and compared with $^{11}$C-(R)KTP-Me. To determine the details of changes in COXs expression and microglial activation during progressive accumulation of amyloid β-peptides (Aβ) in APP-Tg mice (8-24 months old, ♀), we performed *ex vivo* autoradiography with $^{11}$C-(S)KTP-Me, and immunohistochemical study. **Results:** The accumulation level of $^{11}$C-(S)KTP-Me in LPS-induced inflammatory region of rat was almost 2-fold higher than that of $^{11}$C-(R)KTP-Me,

which was well correlated with the potency of each enantiomer of ketoprofen for inhibition of COX-1 obtained from *in vitro* assay. Though PET image of $^{11}$C-(R)KTP-Me also showed some amounts of accumulation in the inflammatory region, simultaneous injection of unlabeled (R)KTP-Me with $^{11}$C-(R)KTP-Me did not show any reduction in both inflammatory and normal region of rat brain. These data indicate that $^{11}$C-(S)KTP-Me could detect neuroinflammation more specifically than R-enantiomer and also racemic mixture of $^{11}$C-KTP-Me. In APP-Tg mice, the apparent increase in accumulation of $^{11}$C-(S)KTP-Me was seen from 15 months old, at which histopathological appearance of abundant Aβ plaque and activated microglia were also observed. Especially, $^{11}$C-(S)KTP-Me was highly accumulated in the frontal cortex and hippocampus, where COX-1 expressing activated microglia tightly surrounded and enclosed Aβ plaque. **Conclusion**: $^{11}$C-(S)KTP-Me is a potent and highly specific PET probe for neuroinflammation. The studies using APP-Tg mice indicated that $^{11}$C-(S)KTP-Me could recognize COX-1 expressing activated microglia surrounding Aβ plaque, which suggests that the imaging of activated microglia by PET with $^{11}$C-(S)KTP-Me could be a valuable tool for monitoring pathological process of AD. 362 words/ limited in 400 words

1310 - Tuesday, Oct. 22, 11:30 - 13:00, Tête D'Or 1/2

## Physics & Instrumentation & Data Analysis: SUV Quantification

## OP512

### Factors Affecting Liver SUV in $^{18}$F-FDG PET

**A. Melessen**[1], N. Rizvi[1], O. S. Hoekstra[1], C. Kobe[2], J. J. B. van Lanschot[3], J. Zijlstra[1], L. M. Velasquez[4], C. J. J. Mulder[1], P. M. van de Ven[1], R. Boellaard[1]; [1]VU University Medical Center, Amsterdam, NETHERLANDS, [2]University Hospital of Cologne, Cologne, GERMANY, [3]Erasmus Medical Center, Rotterdam, NETHERLANDS, [4]Bristol-Myers Squibb, Princeton, NJ, UNITED STATES.

**Objectives:** Liver SUV can be used as a quality control (QC) measure as suggested in PET Response Criteria in Solid Tumors (PERCIST 1.0). The Aim of this study was to evaluate potential factors that may affect liver SUV. **Methods :** Using 214 $^{18}$F-FDG PET scans of 106 patients we investigated the potential impact of (a) different types of disease [steatosis, steatohepatitis, non-small cell lung cancer (NSCLC), esophageal cancer, diffuse large B-cell lymphoma (DLBCL), advanced gastrointestinal malignancy and non-Hodgkin lymphoma (NHL)], (b) treatment [baseline and during or after treatment], (c) SUV normalizations [BW, BSA, LBM], (d) VOI sizes and locations [19 mL in right superior and inferior and left lobe, 77 mL in right lobe, and entire liver VOI], (e) gender, (f) age and (g) uptake interval (60 vs. 90 min ) on liver SUV; finally, we measured repeatability of liver SUV in a subset (n=9). **Results:** The $SUV_{LBM}$ in the 77 mL VOI in the right superior lobe had the highest correlation with the total liver VOI (0.93) and this correlation differed significantly with correlations of other VOIs with the total liver VOI. Minor (<5%), yet significant (p=.04), differences were seen when a VOI was placed in the left lobe compared with VOIs placed in the right lobe. Multivariate analysis suggested that women have a significantly lower liver SUV than men when normalized for LBM: 20% lower (p=.00) and weight: 14% lower (p=.04) but not for BSA: 8% lower (p=.28). Moreover, liver SUV was not affected by tracer uptake time. Average $SUV_{LBM}$ at baseline for different populations from different centers ranged from 1.21±0.23 (NSCLC stage IV, n=26) to 1.62±0.21 (Steatohepatitis, steatosis). Mean test-retest variability of liver $SUV_{LBM}$ (1 week apart, n=9) was 12%. In 10 patients with DLBCL who received R-CHOP+G-CSF (granulocyte colony-stimulating factor) we found significant increase of liver $SUV_{LBM}$ (1.41±0.23 at baseline; 1.59±0.22 during therapy, p=.01) **Conclusions:** Liver SUV can be obtained with low test-retest variability, but liver $SUV_{LBM}$ and $SUV_{BW}$ may be gender specific. VOI size seems positively related with accuracy of the measurement. Moreover, Liver SUV data are different between various patient groups and research centers and can change during or after treatment. Use of liver SUVs as reference or QC measure should therefore be validated thoroughly.

## OP513

### Comparison of liver SUV using unenhanced CT versus contrast enhanced CT for attenuation correction in 18F-FDG PET/CT

**E. G. W. ter Voert**[1], H. W. M. van Laarhoven[1,2], P. J. M. Kok[1], W. J. G. Oyen[1], E. P. Visser[1], L. F. de Geus-Oei[1]; [1]Radboud University Nijmegen Medical Centre, Nijmegen, NETHERLANDS, [2]Academic Medical Center, University of Amsterdam, Amsterdam, NETHERLANDS.

**Aim** To quantify differences in standardized uptake value (SUV) in liver tissue between PET images corrected for attenuation with unenhanced low-dose CT data and PET images corrected with contrast enhanced high-dose CT based data. The liver is the organ of interest since PERCIST 1.0 requires calculation of background SUV in the liver. **Methods** Ten patients, scheduled for FDG-PET and contrast enhanced abdominal CT were included. All patients fasted for 6hr prior to injection of FDG. Sixty minutes post-injection, a standard whole-body low-dose CT (care dose at 50mAs, 130kV) and a whole-body PET was performed on an integrated PET/CT scanner. Afterwards IV CT contrast media (100ml Optiray 300) was administered and an abdominal high-dose CT (care dose at 110mAs, 130kV) was performed. During CT scanning an end expiration breath-holding protocol was used for optimal comparability with free breathing PET scans. Per patient two PET datasets were created: one corrected for attenuation using the unenhanced and one using the contrast enhanced CT. In both datasets, three spherical regions of interest (ROI), with median diameter of 25 mm were drawn in healthy liver segments V/VI, II/III, VII/VIII to also assess within-liver variation. For each patient the average SUVmean and SUVmax were calculated per ROI location and per dataset and the differences between datasets were compared using the Wilcoxon signed rank test. Additionally, the differences in SUVmean and SUVmax values per location were compared using the Wilcoxon signed rank test. **Results** The average SUVmean and SUVmax of all lesions were 2.43±0.47 and 2.91±0.45 g/cm$^3$ (mean±std), respectively, in the PET dataset corrected for attenuation using the unenhanced CT and 2.53±0.48 and 3.17±0.47 g/cm$^3$ in the PET dataset corrected for attenuation using the contrast enhanced CT. The measured SUVmean and SUVmax were significantly elevated (3.7%, p<0.01 and 8.3%, p<0.01, respectively) in liver tissue corrected for attenuation with contrast enhanced high-dose CT compared to unenhanced low-dose CT. Another interesting finding is that liver segments II/III appear to have more elevated SUVmean and SUVmax values compared to other liver regions. **Conclusions** SUVmean and SUVmax values were significantly higher in liver tissue when using PET images corrected for attenuation using contrast enhanced high dose CT compared to unenhanced low dose CT. Although the differences may not be relevant in daily clinical practice, unenhanced and contrast enhanced CT should not be used randomly for attenuation correction if exact quantitative results are required.

## OP514

### Prospective evaluation in NHL patients of a strategy to minimise reconstruction dependent variation in SUV

**E. Quak**, N. Hovhannisyan, C. Fruchart, J. Vilque, D. Musafiri, N. Aide; Francois Baclesse Cancer Centre, Caen, FRANCE.

**Aim** To prospectively evaluate a strategy to harmonise SUVs when using point-spread function (PSF) reconstruction for both visual and quantitative analysis in non-Hodgkin lymphoma (NHL) patients, with special emphasis on the tumour-to-liver ratio used in the Deauville criteria for interim FDG-PET/CT risk adapted treatment planning. **Materials and Methods** All FDG-PET acquisitions were performed on a Siemens Biograph PET/CT system equipped with PSF. First, the NEMA NU-2 phantom was used to determine the optimal filter to apply to PSF-reconstructed images in order to obtain recovery coefficients (RCs) fulfilling the EANM guidelines for tumour PET imaging (here-after referred to as $PSF_{EANM}$). The phantom study was performed as described in the EANM guidelines. Second, we reconstructed the PET data of 23 NHL patients with PSF High Definition reconstruction for optimal visual interpretation (3 iterations, 21 subsets, no filtering, here-after referred to as $PSF_{HD}$), $PSF_{EANM}$, and with a conventional OSEM algorithm known to meet EANM guidelines (4 iterations, 8 subsets, 5 mm Gaussian filter). SUVs for $PSF_{HD}$ and $PSF_{EANM}$ reconstruction were compared to SUVs for OSEM reconstruction. As the tumour-to-liver ratio is the discriminator between a positive and negative FDG-PET/CT in the Deauville criteria, the ratios of the tumour SUVmax to the liver SUVmax were compared for the different reconstructions. **Results** The phantom studies showed that with a 7 mm Gaussian filter RCs fulfilled the EANM criteria. In 23 consecutive NHL patients (15 DLBCL, 5 follicular and 3 other subtypes) 388 lesions were studied. Bland-Altman analysis showed that the mean ratios for tumour SUVmax were 1.54 (95% CI: 0.95-2.14) for $PSF_{HD}$ /OSEM and 1.04 (95% CI: 0.93-1.14) for $PSF_{EANM}$ /OSEM. The mean tumour-to-liver ratios for $PSF_{HD}$, $PSF_{EANM}$ and OSEM were 3.45 ± 3.57, 2.82 ± 2.93 and 2.71 ± 2.88 respectively. Regarding the tumour-to-liver ratio, Bland-Altman analysis showed that the mean ratio for $PSF_{HD}$/OSEM was 1.31 (95% CI: 0.79-1.82) and 1.06 (95% CI: 0.93 - 1.18) for $PSF_{EANM}$/OSEM. **Conclusion** Our data show that $PSF_{HD}$ significantly increases SUVmax and tumour-to-liver ratios, and that it is possible to get rid of this reconstruction dependent variation by using the proposed strategy. This strategy can be useful in the setting of multicentre trials, or in the case of patients undergoing pre- and post treatment scans on different PET-systems, for example in centres running two or more PET systems or after a system update.

## OP515

### Effect of the GE SharpIR PET reconstruction on contrast convergence and measured SUV values in the NEMA image quality phantom and patients

**K. E. Kenny**, D. R. McGowan; Oxford University Hospitals NHS Trust, Oxford, UNITED KINGDOM.

**Aim** A study has been undertaken to investigate the benefit of using the GE Resolution Recovery (SharpIR) algorithm and its effect on PET image quality for

both a phantom and patients. **Materials and Methods** A NEMA Image Quality phantom was scanned on a GE Discovery 690 PET/CT scanner. The scan data was processed using a time of flight (TOF) iterative reconstruction with and without SharpIR, with one to four iterations, 24 and 32 subsets and 4mm and 6.4mm Gaussian filters. Image quality was assessed in terms of contrast recovery curves. Following this, the optimum clinical processing parameters were determined, and used on a variety of patients to investigate the improvement in imaging small lesions. **Results** A significant increase in contrast recovery was observed for small spheres (of the order of 10mm). As expected for the large spheres there was no significant increase in contrast recovery. For the SharpIR reconstructions an additional iteration was needed to achieve contrast convergence. In our phantom studies using a TOF SharpIR reconstruction had an increase in contrast of up to 40% (17% absolute increase) compared to the standard TOF reconstruction. For patient studies reconstructed using TOF SharpIR a significant increase in maximum standardised uptake value (SUVmax) of up to 78% was found for small legions. For larger legions the increase in SUVmax was less significant. **Conclusion** We conclude that the SharpIR algorithm gives a significant benefit in terms of contrast recovery for small lesions. This requires an additional iteration in the reconstruction parameters. For clinical studies this leads to an increase in SUVmax values, particularly for small legions. Due to this care must be taken when comparing SUVmax values for longitudinal studies. The recommended reconstruction parameters for clinical practice will be presented.

## OP516

### Effect of Hepatosteatosis on Different SUV Measurement Techniques in $^{18}$F-FDG PET-CT Imaging.

**M. Bozkurt**, B. Temelli; Hacettepe University Medical School, Ankara, TURKEY.

**Objectives:** Liver is generally used as a reference organ for semiquantitative evaluation of $^{18}$F-FDG uptake in oncologic PET/CT studies. However, as being an organ which suffers from steatosis frequently, glucose metabolism in liver is expected to be decreased in the state of hepatosteatosis which may result with misleading measurements. The Aim of this study is to assess the effect of hepatosteatosis on different SUV measurement techniques in $^{18}$F-FDG PET/CT imaging and to find out the most suitable SUV measurement technique for the patients with hepatosteatosis. **Materials and Methods**: A total of 444 patients who are recruited to PET/CT imaging were retrospectively evaluated. Hepatosteatosis was diagnosed by calculation of the difference of attenuation between liver and spleen in HU (DHU) on non-enhanced CT images from PET/CT and defined as prominent hepatosteatosis, mild fatty infiltration and normal liver density if DHU≤-10, -9<DHU<10 and DHU≥10 respectively. On the basis of non-enhanced CT component of PET/CT imaging, 37 patients were found to have prominent hepatosteatosis, 279 patients displayed mild fatty infiltration while the rest 131 had normal liver density. SUVmean measurements from PET images were both normalized to body weight as $SUV_{bw}$ and to lean body mass as $SUV_{lbm}$ and both values were measured in liver, spleen and mediastinum for comparative analysis. Density measurements in HU units from CT component of PET/CT imaging were also done in liver, spleen and mediastinum for comparative analysis. **Results**: $SUV_{bw}$ measurements in all 3 sites showed no significant difference between 3 groups, while liver $SUV_{lbm}$ measurements in hepatosteatosis group were lower than the other 2 groups showing that the decrease in glucose metabolism in the state of hepatosteatosis can only be measured with $SUV_{lbm}$ technique (p=0,05). Among the groups, only hepatosteatosis group showed significant positive correlation between liver $SUV_{lbm}$ and HU measurements. For the whole group of patients $SUV_{bw}$ measurements displayed significant correlation with body weight, BMI, VLDL, LDL, total cholesterol and trigliseride levels which proves that $SUV_{bw}$ measurement technique is actually affected by all these parameters, while there was no such significant correlation for $SUV_{lbm}$. **Conclusion:** In case of hepatosteatosis, $SUV_{bw}$ measurement technique cannot reflect the changes in liver glucose metabolism and therefore, $SUV_{lbm}$ as being a more reliable method should be the technique of choice in oncologic $^{18}$F-FDG PET/CT imaging when liver is used as a reference organ.

## OP517

### Shape indices derived from baseline 18F-FDG PET images can predict response to concomitant radio-chemotherapy in esophageal cancer

F. Tixier[1], M. Hatt[1], C. Valla[2], **D. Visvikis**[1], C. Cheze Le Rest[2]; [1]INSERM UMR 1101 LaTIM, Brest, FRANCE, [2]Department of Nuclear Medicine, CHU Milétrie, Poitiers, FRANCE.

**Aim**: It has been recently demonstrated that it is possible to extract from 18F-FDG PET images several quantitative parameters that can be useful to improve patient's management. Among these parameters are the maximum or mean standardized uptake value (SUVmax, SUVmean), the metabolic tumor volume (MTV), the total lesion glycolysis (TLG) and the quantification of tracer uptake heterogeneity. Another kind of parameters which can be investigated on these images is the shape quantification (SC). However, the predictive value of parameters belonging to this category has not been thoroughly assessed yet. Consequently the Aim of this study was the investigation of the predictive value of 7 parameters derived from SC of PET images functional tumor activity distributions within the context of esophageal cancer treated by concomitant radio-chemotherapy. **Methods**: Baseline 18F-FDG PET scans of 50 patients with locally advanced esophageal cancer were retrospectively analyzed. Primary tumors were delineated with the fuzzy locally adaptive bayesian algorithm and 7 features describing the shape of the delineated volumes were extracted from these segmented volumes. Response to therapy (complete (CR), partial (PR) and non-response (NR)) was evaluated according to RECIST criteria 1 month after the end of treatment. The correlation between SC parameters was assessed using Pearson coefficients and their corresponding predictive value regarding the identification of non responders or complete responders, was evaluated with receiver operating characteristic (ROC) curves analysis. **Results**: 3D surface and MTV were highly correlated (r=0.97). All other SC parameters were moderately correlated (r<0.75). Maximum diameter within the MTV, as well as the smoothness of its surface allowed the identification of NR (vs. PR+CR) or CR (vs. PR+NR) with areas under the ROC curves of 0.78 and 0.80 respectively, whereas SUVmax or SUVmean standard indices led to significantly lower AUCs of 0.55 to 0.6 (p<0.02). **Conclusion**: In this study we have identified that the SC performed on baseline 18F-FDG PET image can provide useful information for the prediction of the response to the concomitant radio-chemotherapy. Future studies will investigate their potential combination with other parameters previously demonstrated as predictive of response, such as intra-tumor heterogeneity quantification.

## OP518

### Texture indices for tumor characterization in FDG PET: robustness and relationship with SUV and metabolic volumes

**F. Orlhac**[1], M. Soussan[1,2,3], J. A. Maisonobe[1], C. A. Garcia[4], B. Vanderlinden[4], I. Buvat[1]; [1]IMNC, UMR 8165 CNRS, Paris 11 University, Orsay, FRANCE, [2]Paris 13 University, Sorbonne Paris Cité, Bobigny, FRANCE, [3]AP-HP, Avicenne University Hospital, Departement of Nuclear Medicine, Bobigny, FRANCE, [4]Department of Nuclear Medicine, Institut Jules Bordet, Université Libre de Bruxelles, Brussels, BELGIUM.

**Aim**: Texture indices (TI) are of growing interest for tumor characterization in FDG PET. Yet, based on results published in the literature, it is unclear which TI should be measured. We investigated 31 TI on a variety of tumors to determine how they relate one to another and to Standardized Uptake Values (SUV), metabolic volume (MV) and total lesion glycolysis (TLG). We also studied their sensitivity to the tumor segmentation method. The consistency of our conclusions as a function of the tumor type was investigated. **Materials and Methods**: We analyzed 31 TI together with 3 SUV indices, MV and TLG in tumors observed in three cancer types at baseline: metastatic colorectal (72 lesions), non-small cell lung (24 lesions) and breast (54 lesions) cancers. For each tumor group, the linear correlation between each pair of indices was analyzed. All indices were calculated for two tumor segmentation Methods: using a threshold of a 40% of SUVmax, or using a threshold depending on SUVmax and surrounding activity. The relative difference between the 2 values V1 and V2 was deduced as RD=2*(V1-V2)/(V1+V2)*100 and the standard deviation of RD (sdRD) for all tumors of one type was used as an index of robustness. **Results:** Grouping together indices that were highly correlated (Pearson r > 0.85), 9 groups were identified. MV was highly correlated with 5 TI (Gray-Level Non-Uniformity for Run, Run Length Non-Uniformity, Long-Zone High Gray-level Emphasis, Gray-Level Non-Uniformity for Zone, Zone Length Non-Uniformity) while the correlation between SUVmax and TI was always less than 0.56. Comparing the sensitivity of TI to the segmentation method, no TI had an sdRD less than that of SUVpeak or SUVmax. 5/31 TI had an sdRD less than that of SUVmean, 12 had an sdRD greater than that of SUVmean but lower than that of MV, while 14 had an sdRD greater than that of MV. All results were highly consistent across the 3 tumor types, demonstrating the validity of our findings for a broad range of tumors. **Conclusions:** No more than 8 TI need to be considered in addition to SUV for tumor characterization, as other TI are strongly correlated with them. Indices from 3 groups are not robust with respect to the tumor segmentation method, including Busyness. Therefore, only 5 TI, such as Homogeneity, Entropy or Zone Length Non-Uniformity (highly correlated with MV) should be further investigated in addition to SUV for tumor characterization in FDG PET.

## OP519

### Can image quality variation in optimized FDG-WB PET scanning be reduced using multiple patient dependent parameters?

**E. H. de Groot**[1], J. A. van Dalen[2], N. R. L. Wagenaar[3], A. T. M. Willemsen[1]; [1]University Medical Center Groningen, University of Groningen, Groningen, NETHERLANDS, [2]Isala Klinieken, Zwolle, NETHERLANDS, [3]Ziekenhuisgroep Twente, Hengelo, NETHERLANDS.

**Aim** Earlier research (Eur J Nucl Med Mol Imaging 39(Suppl.2):S185,2012) showed that a linear relation between FDG dosage and patient weight in FDG-WB PET examinations results in a decreasing image quality (IQ) with increasing patient weight. We showed that a quadratic dose-weight relation results in an IQ that is independent of weight. However, the remaining variation in IQ may still be correlated with other patient characteristics, e.g. BMI or length. In this study, these correlations were investigated in an attempt to further harmonize IQ between patients. **Materials and Methods** In our first study, 102 whole-body FDG-PET scans using a linear dose-weight relation were included; the second study included 42 scans using a quadratic dose-weight relation. In all cases, the signal to noise ratio (SNR) in the liver was a measure for the IQ of the scan. In the first study, IQ was normalized for injected activity and scan time per bed position and then fitted to a power law. In the second study, IQ was indeed independent of patient weight and the mean IQ was subtracted. For both studies, the residue was fitted to different patient dependent parameters: length, mass per length, lean and fat mass (both James' and Hume's definitions) and BMI for both groups. Using linear regression, dependence of the IQ variation on the different patient dependent parameters was explored. In addition, the correlation between patient weight and the other patient dependent parameters was determined. **Results** For both groups, none of the tested patient dependent parameters showed significant correlation with the IQ variation. The correlation between weight and other patient dependent parameters was high (0.72-0.94), except for length, where the correlation was 0.43. **Conclusion** Using an optimized quadratic relation between FDG dose and weight, IQ cannot be further harmonized between patients by using other patient dependent parameters. Even the use of body length, which has the lowest correlation with weight, in dose calculations will not further harmonize IQ between patients. This is surprising since IQ in PET is not only determined by the Poisson statistics of the measured counts but also depends on for example attenuation and scatter which are related to patient size. Apparently, the effect of other patient dependent parameters on IQ is only moderate, or it is not distinct because of uncertainties in the data.

YE3 — Tuesday, Oct. 22, 13:00 — 14:30, Tête D'Or 1/2

## Young EANM Daily Forum 3: From Bench to Bedside

### OP520
**Welcome and Introduction**

**P. Pilkington, SPAIN, M. de Jong, NETHERLANDS**

### OP521
**Methods of Preclinical Research**

**O.C. Boerman, NETHERLANDS**

### OP522
**Methods of Clinical Research**

**I.M. Modlin, USA**

### OP523
**Public Funding of NM Research in Europe**

**M. Gotthardt, NETHERLANDS**

### OP524
**Industry Funding for Equipment and Drug Development**

**R. Zimmermann, FRANCE**

### OP525
**Discussion**

**All Participants**

1401 — Tuesday, Oct. 22, 14:30 — 16:00, Amphithéâtre

## CME 11 - ESNM Faculty (Interactive): Pitfalls in Nuclear Medicine

### OP526
**How to Avoid Pitfalls "Before the Scan"**

**D. Donner, ITALY, S. Agostini, ITALY**

### OP527
**Technical Pitfalls and Solutions**

**A.J. Britten, UNITED KINGDOM**

### OP528
**Unusual Clinical Pitfalls**

**J.R. Buscombe, UNITED KINGDOM**

1402 — Tuesday, Oct. 22, 14:30 — 16:00, Auditorium Lumière

## Symposium 11: Combination Therapies

### OP529
**Combination Therapies in PRRT of Neuroendocrine Tumours**

**D.J. Kwekkeboom, NETHERLANDS**

### OP530
**Combination Therapies in the Treatment of Thyroid Cancer**

**M. Hoffmann, AUSTRIA**

### OP531
**Combination Therapies in the Treatment of Haematologic Malignancies**

**D. Bunjes, GERMANY**

1403 — Tuesday, Oct. 22, 14:30 — 16:00, Forum 3

## CTE 5 - EANM-TC/ESTRO-Radiation Therapist Committee Joint Session: Evolution of RT Planning

### OP532
**The Role of PET/CT for Radiotherapy Treatment Planning in Head & Neck Carcinoma**

**F. Moura, PORTUGAL**

### OP533
**From 2D to 4D Radiotherapy - When Bony Landmarks are Replaced by Biological Tumour Information for Adaptive Treatment**

**E.G.C. Troost, NETHERLANDS**

### OP534
**Inter-Observer Variation in Delineation of Tumours**

**A.K. Berthelsen, DENMARK**

1404 - Tuesday, Oct. 22, 14:30 - 16:00, Bellecour 1/2/3

## Featured - Cardiovascular: Arrhythmias & CRT

### OP535
**Is There a Place for Cardiac Radionuclide Imaging in Electrophysiology?**

**P. Milliez, FRANCE**

### OP536
**Assessment of left ventricular function and mechanical dyssynchrony using equilibrium radionuclide angiography to evaluate the significance of percentage ventricular pacing in patients with permanent right ventricular pacemakers.**

**H. Singh**, C. Patel, P. Sharma, G. Sharma, N. Naik, A. Malhotra; All India Institute of Medical Sciences, New Delhi, INDIA.

**Aim**: Permanent right ventricular pacing can adversely affect left ventricular mechanical dyssynchrony (LVMD) and function, both of which can be objectively quantified using equilibrium radionuclide angiography (ERNA). The Aim of the study was to assess LVEF and LVMD using ERNA in patients with permanent pacemakers over 1 year follow up, and to assess significance of percentage ventricular pacing (%VP) in such patients. **Material and Methods**: 51 patients who underwent permanent pacemaker implantation and had normal LV function were

prospectively included, irrespective of pacing site. All patients underwent ERNA within 2 week post pacemaker implantation, at 6 months and 12 month follow-up. All studies were performed under forced ventricular pacing a rate of 100/minute. Standard deviation of LV mean phase angle (SD LVmPA) expressed in degrees, which was derived by Fourier first harmonic analysis of phase images was used to quantify left intra-ventricular synchrony and LVEF were used to measure outcome. As %VP can affect long term LV function in these patients, its significance was assessed by dividing the patients into 2 groups: those with %VP≥90 (n=27) and %VP<90 (n=24). **Results**: Mean LVEF was 55.1±6.37% (range 45-65) in group with %VP≥90 & 56.2±4.82% (range 48-64) in group with %VP<90 (p <0.519). The mean %VP was 98.4±1.69% (range 92-99) in group with %VP≥90 & 16.4±21.79% (range 1-75) in group with %VP<90 (p <0.0001). In group with %VP≥90, LVEF decreased from 55.1±6.37% at baseline to 51.5±8.49% at 12 months follow up (p 0.006) whereas in group with %VP<90, LVEF changed from 56.2±4.82% at baseline to 55.7±5.08% at 12 months follow up (p 0.523). At 12 month follow up, difference in LVEF between 2 groups became statistically significant (p 0.037). However, no significant change in SD LVmPA was noted in both groups [%VP≥90, from 13.6±5.72° at baseline to 13.9±5.49° at 12 months (p 0.764); and %VP<90 (from 10.8±3.98° at baseline to 11.7±5.10° at 12 months (p 0.204)]. **Conclusion**: ERNA can objectively quantify LVMD and function both, and can be routinely employed as a tool in follow up assessment of patients with permanent RV pacemakers. Percentage ventricular pacing is a predictor of functional outcomes after permanent RV pacing.

## OP537

### Global and regional left ventricular synchrony parameters on phase analysis in normal gated myocardial perfusion scintigraphy using quantitative gated SPECT software

**P. Kundu**, G. K. Arun Reddy, A. Sood, M. Parmar, A. Bhattacharya, B. R. Mittal; Postgraduate Institute of Medical ,Education & Research, Chandigarh, INDIA.

**Aim** The Aim of study was to assess global and regional parameters of left ventricular (LV) synchrony on phase analysis on $99^{m}$Tc tetrofosmin gated myocardial perfusion scintigraphy (MPS) using quantitative gated SPECT (QGS) software in patients having moderate to high pretest probability of CAD and normal MPS. **Materials and Methods** In this retrospective study, 55 patients (male 21, female 34; mean age 57.6, range 27-80 years) underwent one day $99^{m}$Tc tetrofosmin stress/ rest gated SPECT MPS. Inclusion criteria was non-diagnosed CAD, normal MPS study, QRS<120ms, LV ejection fraction >50%. Patients with non-ischemic cardiomyopathies with normal MPS were excluded from the study. Phase analysis was done using QGS software. Fourier transformed time dependent signals of varying myocardial thickness over a cardiac cycle were obtained and then first harmonic phase angles were used to obtain various parameters automatically. Global parameters of LV synchrony comprised histogram SD (S), bandwidth (B), and entropy (E) and regional (wall based) parameters included mean (μ, average over mean), SD (σ), mode(M, location of the peak of the distribution of values) bandwidth(b) and entropy(e). Values are expressed as mean±SD in degrees. Entropy is expressed in percentages. Shape index (SI) defined as ratio of maximum dimension of LV in short axis planes to mid ventricular long axis plane was also calculated which is postulated as marker of heart failure. **Results** Left ventricular global synchrony parameters obtained for all the patients were mean (137.2±14.1), SD (7.1±4.4), M (138.7±14.1), B (29.5±15.7), E (48.3%±8.8%). For female and male patients LV global parameters were mean (133.7±17.8), SD (7.3±3.6), M (133.8±16.8), B(30±15.8), E(52.3%±9.4%) and mean (139.4±11.0), SD (7.1±4.8), M (141.7±11.4), B(29.1±16.3), E(45.8%±7.5%) respectively. Regional (wall based) synchrony parameters for all patients were: apex μ(135.9±13.9), σ(2.9±1.5), M(138.8±14.1), b(13.9±6.1), e(15.5%±8.3%) ; lateral wall μ(137.7±14.4), σ(5.5±2.3), M(140.1±14.3), b(24.3±14.4), e(28.0%±9.3%) ; inferior wall μ(138.7±14.8), σ(6.9±5.1), M(140.0±14.5), b(28.5±19.7), e(29.2%±11.6%) ; septal wall μ(138.0±15.8), σ(5.4±5.1), M(139.9±14.7), b(22.5±16.2), e(24.6%±12.5%) ; anterior wall μ(135.1±13.9), σ(5.5±2.6), M(136.6±13.2), b(23.9±11.5), e(27.5%±9.2%). Apical wall regional parameters phase SD, histogram bandwidth and entropy showed significant difference as compared to other walls of LV myocardium (p<0.001). Gender specific phase analysis comparison suggested significant difference in LV phase entropy (p=0.006, 95% CI- 1.92 to 11.16) with no significant difference in other parameters. SI for end diastole was 0.74±0.11 and for end systole was 0.42±0.12. **Conclusion** Normal database of detailed phase analysis using QGS with gated MPS provides a platform to assess global and regional LV dyssynchrony.

## OP538

### Evaluation of LV Mechanical Dyssyncrony by Gated-MPI SPECT Phase Analysis at Stress and at Rest in Patients with No Reversible Perfusion Defects and in Patients with Fully Reversible Perfusion Defects

**V. M. Alves**, P. Oliveira, T. Vieira, A. Oliveira, E. Martins, T. Faria, M. B. Perez, J. G. Pereira; Centro Hospitalar de São João, Porto, PORTUGAL.

**Objectives**: To characterize left ventricular (LV) mechanical dyssynchrony at stress and at rest in patients with no reversible perfusion defects and in patients with fully reversible perfusion defects. **Materials and Methods**: From all patients (pts) that performed gated SPECT myocardial perfusion imaging (MPI) with $^{99m}$Tc-tetrofosmin at stress with adenosine, and at rest, at our department around 2010, we retrospectively selected 31 with myocardial infarction history and no reversible perfusion defects (summed difference score <4), 30 pts with fully reversible perfusion defects (ischemia) and a control group of 20 pts that had normal MPI and no history of heart or coronary disease. Pts with left bundle branch block, fascicular blocks, ventricular pacing and atrial fibrillation were excluded. Parameters of LV mechanical dyssynchrony evaluated were phase standard deviation (SD) and histogram bandwidth (Bw). They were compared within each group (between stress and rest) and between groups, both at stress and at rest. **Results**: Mean pts ages were 59.9 years (±11.1 years) in the infarction group, 65.1 years (±10.2 years) in the ischemia group and 59.9 years (±9.4 years) in the control group. Only in the ischemia group, the parameters of mechanical dyssynchrony derived from stress were significantly higher than those derived from rest [stress SD 19.5º vs. rest SD 12.6° (p<0.001); stress Bw 63.4º vs. rest Bw 40.8º (p<0.001)]. In the infarction and control groups, there were no statistically significant differences between values in stress and rest (infarction group: stress SD 28,1º vs. rest SD 30,1º; stress Bw 88.3º vs. rest Bw 94.6º. Control group: stress SD 11.4º vs. rest SD 11.1º; stress Bw 37.4º vs. rest Bw 35.2º). The comparison between groups showed that SD and Bw were significantly higher in the infarction group, both during stress and at rest, as compared to the ischemia group (stress: p=0.01 and p=0.02 respectively; rest: p<0.001 for both) and the control group (p<0.001, all situations). Among the ischemia group and the control group, the SD and Bw were significantly higher in the former only in stress (p=0.001 for both). **Conclusion:** The presence of myocardial infarction without significant residual ischemia is associated with an overall increase of mechanical dyssynchrony. However, in such pts the stress testing does not induce additional dyssynchrony. In contrast, this study strengthens the evidence that stress-induced mechanical dyssynchrony is associated to ischemia, even when the adenosine protocol for stress testing is used.

## OP539

### The effect of preceding beat duration on left ventricular ejection fraction during atrial fibrillation.

**A. Small**[1], W. Martin[2], A. Rankin[3]; [1]NHS Lothian, Edinburgh, UNITED KINGDOM, [2]NHS Greater Glasgow and Clyde, Glasgow, UNITED KINGDOM, [3]University of Glasgow, Glasgow, UNITED KINGDOM.

**Aim:** The substantial beat-to-beat variation in R-R interval seen in atrial fibrillation (AF) results in images which are heavily subject to artefact and often unreportable; these problems are compounded when images are used quantitatively e.g. in left ventricular ejection fraction (LVEF) measurement. The Frank-Starling mechanism states that LVEF is dependent on end-diastolic volume (EDV). EDV is dependent on the duration of diastole which is reflected in the R-R interval. This suggests that single beat LVEF should be dependent on the preceding beat length. Our principal Aim was to investigate the extent of this dependence in AF. A secondary objective was to assess parameters to maximise the reproducibility of LVEF using radionuclide ventriculography (RNVG). **Methods:** RNVG was used to measure LVEF in images created from list-mode acquisition using beats selected on the duration of both the preceding and indexed beat. 15 minute acquisitions were each formatted into 36 images using each combination of six indexed and six preceding beat selection windows defined by (a-d) the quartile durations, (e) 300 ms centred on the modal beat, and (f) all the beats. To minimise possible geometric variations LVEF was calculated using a single region of interest technique with the same regions applied to each image. Comparison was also made between LVEFs assessed in only the first or second half of the acquisition for each pair of beat selection criteria. The study investigated 378 patients in AF and a comparative group of 385 patients in sinus rhythm (SR). **Results**: In AF, LVEF was found to be greater when preceded by a longer beat ($p < 1x10^{-7}$). A weaker negative correlation with the indexed beat was also found. In SR no significant associations were seen. Different beat selection criteria were found to give a mean variation in LVEF of 14.4 ± 13.2 EF points in AF and of 8.2 ± 10.2 EF points in SR. The smallest differences (1.45 ± 3.16 in AF and 1.74 ± 3.50 in SR) between the halves of the acquisition were found when all beats were accepted, while the greatest (up to 6.09 ±13.21 in AF, 5.05 ± 9.54 in SR) were found with the longest preceding beats and tightly windowed index beats. **Conclusion:** LVEF measured in patients with AF depends more on the duration of the preceding beat than that of the indexed beat. LVEF is most reproducibly measured in AF when all beats are included without windowing.

## OP540

### Myocardial Perfusion SPECT for cardiac resynchronization therapy(CRT)

**M. Kostkiewicz**[1], W. Szot[2], P. Podolec[3]; [1]Jagiellonian University, Hospital John Paul II, Dept of Nuclear Medicine, KRAKOW, POLAND, [2]Hospital John Paul II, Dept of Nuclear Medicine, KRAKOW, POLAND, [3]Jagiellonian

University, Hospital John Paul II, Dept of Cardiovasc. Diseases, Krakow, POLAND.

Cardiac resynchronization therapy (CRT) has been accepted as a treatment for heart failure patients refractory to conventional therapy. QRS prolongation in such patients is associated with delayed electrical activation of the left ventricle, leading to uncoordinated ventricular motion, decreased stroke volume, and mitral regurgitation. Comparison of TVI for two basal segments can assess dyssynchrony. A delay of ≥60ms between the septal and lateral wall or ≥65ms between the anteroseptum and posterior wall predicts increased ejection fraction after CRT implantation. It has also been found that LV dyssynchrony measured by SPECT phase analysis correlates with TVI data but the former obtains more reproducible results. Aim of the study was to assess the relationship between mechanical dyssynchrony described by TVI and phase analysis by SPECT. We studied 29 NYHA class III-IV heart failure patients with ejection fraction ≤ 35% referred for CRT. LV dyssynchrony was evaluated with TVI by recording all basal and mid segments from the apical 4-, 2- and 3-chamber views and deriving the standard deviation between all segments. TVI assessment of delayed contraction was based on the time from onset of the QRS complex to the peak of the S2 component of the velocity trace. Myocardial perfusion, viability, ejection fraction and optimal cutoff values for the prediction of response to CRT were assessed by SPECT. TVI and SPECT substantially agreed on the diagnosis of dyssynchrony. TVI identified LV dyssynchrony in 22 patients. In patients with TVI SD ≥ 33 ms, histogram bandwidth (PHD) and phase SD (PSD) measured by SPECT were significantly higher than in patients with TVI SD <33 ms: 186°±52° versus 74°±24° (p<0.0001) and 55.3°±13.6° versus 25.1°±7.6° (p<0.0001), respectively. SPECT identified severe LV dyssynchrony in 21 patients with a mean PHD of 225.2° ± 36.7° and a mean PSD of 68.7° ± 11.3°. Also, scar visualization in SPECT helped to determine optimal pacing sites and prospective targeting LV lead placement. TVI is a useful method, but it is angle-dependent, providing data only on timing in the longitudinal plane, potentially resulting in an incomplete assessment of dyssynchrony. Histogram bandwidth and phase SD measured by SPECT showed a strong correlation with the values assessed with TVI; hence these appear to be optimal variables for assessment of LV dyssynchrony. The results of this study confirm the feasibility of evaluation of LV dyssynchrony with SPECT and its applicability in the clinical setting.

## OP541

### gSPECT Phase Analysis in CRT Patients

**G. Cantinho**[1], H. Pena[1], A. Veiga[2], A. Magalhães[2], F. Godinho[1]; [1]Atomedical & IMN-FML, Lisboa, PORTUGAL, [2]S. Cardiologia - H. Santa Maria, Lisboa, PORTUGAL.

**Introduction** Cardiac resynchronization therapy (CRT) reduces morbidity and mortality in patients (pts) with heart failure and dyssynchrony, responders (R). However, 20-30% are non-responders (NR). Methods based on phase analysis from myocardial perfusion (gSPECT) have proved to be promising. To access this technique's performance, we used it before and after CRT to evaluate patients' selection by conventional criteria (LVEF≤35%; EDV≥130ml and QRS≥120ms. **Material & Methods** We selected 21 pts who met conventional criteria for CRT, 68±9 years, 90% male; 14 pts (70%) with ischemic heart disease and the remaining with non ischemic dilated cadiomyopathy. 13 pts where in NYHA class II and 8 in class III All pts underwent 30 mCi 99mTc-Tetrofosmin gSPECT (rest and pharmacological stress) before and after CRT. Time between CRT implantation and gSPECT analysis: 21±9 months. We analyzed the onset of LV mechanical contraction by phase histogram based on Garcia's method, with the determination of peak phase (PP), standard deviation (SD), histogram bandwidth (HB), skewness (HS) and kurtosis (KH). We calculated the mean percentage difference and standard deviation of the phase histogram parameters before and after CRT and correlated them with LV function parameters on gSPECT (LVEF, EDV and ESV) as well as with QRS duration (ECG)in R and NR pts. We also compared the R and NR before CRT. Favorable response was defined as an end-diastolic LV volume reduction ≥15% or LVEF increase >15%. **Results** 10 pts were considered R, with LVEF pre and post CRT: 25±8 vs 33±2%; VTD=222±88 vs 165±67 and VTS= 170±81 vs 123±79ml (p<0,05 for all). A significant decrease was also present in QRS duration: 177±4 vs 145±13 ms (p<0,05). PP, SD and HB from phase histogram showed a significant decrease of LV dyssynchrony parameters that follows LV functional improvement. SD showed the most significant decrease. 60±18 vs 43±26º (p=0,002). In NR patients, no changes were found in LV functional and phase histogram parameters pre and post CRT (p>0,05). The analysis of pre CRT parameters (R and NR) didn't reveal statistically significant differences for LV functional and phase histogram parameters. **Conclusions** The evolution of dyssynchrony assessed by gSPECT in CRT patients reflects the response to therapy (R vs NR). SD may be the best marker of ventricular remodelling. In this small population, we haven't found in phase histogram parameters a real discriminative tool to help select patients for CRT. Further correlation studies with conventional parameters are needed to improve this method validation.

1405 - Tuesday, Oct. 22, 14:30 - 16:00, Auditorium Pasteur

## Featured - Oncology Clinical Science: Breast Cancer

## OP542

### Delineating Clinical Perspectives for FDG Molecular Imaging in Breast Cancer

**R. Valdes Olmos, NETHERLANDS**

## OP543

### FDG-PET/CT textural features in triple negative breast tumors

**M. Soussan**[1], F. Orlhac[2], M. Boubaya[3], L. Zelek[4], M. Ziol[5], V. Eder[1], I. Buvat[2]; [1]Avicenne Hospital, APHP, Department of Nuclear Medicine, Bobigny, FRANCE, [2]IMNC - UMR 8165 CNRS - Paris 7 and Paris 11 Universities, Orsay, FRANCE, [3]Avicenne Hospital, APHP, Clinical Research Unit, Bobigny, FRANCE, [4]Avicenne Hospital, APHP, Department of Oncology, Bobigny, FRANCE, [5]Jean Verdier Hospital, Department of Pathology, Bondy, FRANCE.

**Purpose** Triple negative (TN) breast tumors are associated with aggressive histological features and poor prognosis in breast cancers. We studied whether intratumoral heterogeneity as measured using textural indices in FDG PET/CT images could identify TN breast tumors. **Methods** Fifty-four patients with locally advanced biopsy-proven breast cancer who had an initial PET were retrospectively included. Four textural features extracted from 3D matrices were selected according to their robustness: High-Gray-level Run Emphasis (HGRE), Short-Run Emphasis (SRE), Entropy, and Homogeneity. HGRE and SRE are extracted from a gray-level run length matrix describing the alignment of voxels with the same intensity and are related to textural heterogeneity at a regional level. Homogeneity and entropy are extracted from a co-occurrence matrix describing pairwise arrangement of voxels in a 3D matrix and are related to textural heterogeneity at a local level. Maximum SUV, metabolic volume and total lesion glycolysis were also measured. A logistic regression was used to identify parameter values associated with triple negative tumors. The parameters predictive performance was assessed based on reclassification measures. **Results** Homogeneity, entropy, HGRE, and SRE were not correlated with SUV max (Pearson correlation r=-0.05, 0.15, 0.29, and -0.07). In univariate analyses, only SUVmax, Homogeneity and HGRE were able to identify TN tumors. TN tumors exhibited higher SUVmax (p=0.004), lower homogeneity (p=0.05) and higher HGRE (p=0.005) than non-TN tumors. After adjustment for SUVmax, HGRE remained associated with TN tumors (Odd Ratio [95%CI]: 5.27 [1.12-1.38], p=0.03), unlike Homogeneity. Combining SUVmax with HGRE improved the probability of correct classification in 77% of the TN tumors and in 71% of the non-TN tumors. **Conclusion** TN tumors exhibit more heterogeneous textural pattern on FDG PET compared to non-TN tumors, suggesting that intratumoral heterogeneity is correlated with breast tumor aggressiveness. Combining SUV with PET textural analysis at regional level may improve identification of TN breast tumors.

## OP544

### Evaluation of primary tumour and regional lymph node metastases with FDG PET/CT in breast cancer patients: prone versus supine position.

**S. Teixeira**, B. B. Koolen, W. V. Vogel, M. P. Stokkel, M. P. Stokkel, M. Vrancken-Peeters, E. J. T. Rutgers, H. van Tinteren, R. A. Valdés Olmos; Dutch Cancer Institute, Amsterdam, NETHERLANDS.

**Aim:** Standard 18F–FDG PET/CT acquired in supine position has been shown valuable for staging in breast cancer. In analogy with MRI, currently performed in prone position, an additional PET/CT study of the thorax in prone position was incorporated in our hospital for breast cancer patients scheduled to receive neoadjuvant chemotherapy (NAC). The objective of the present study was to evaluate the differences in visualization and uptake quantification of FDG–avid primary tumours and lymph node metastases between PET/CT scans acquired in prone and in supine position. **Materials and Methods**: We included 198 patients (mean age 51, range 26–81) with stage II/III breast cancer from August 2010 to April 2012. An intravenous 18F–FDG dose (180–240 MBq) was administered. After a minimum of 60 minutes an optimized PET/CT of the thorax was performed in prone position using a mock-up MR coil stripped from all metal parts, with PET acquisition 3.00 min per bed position and high–resolution reconstruction in 2x2x2 mm voxels. Subsequently, a standard PET/CT was performed in supine position from skull base to thighs, with 1.30 min per bed position and standard reconstruction in 4x4x4 mm voxels. The prone and supine PET scans were compared by measuring the SUVmax of FDG–avid PTs, and of regional LNs in the axillary and non-axillary regions. Detection of PT multifocality and the occurrence of an anatomical mismatch between PET and CT were compared visually for both scans. **Results.** Prone PET/CT images resulted in significantly higher SUVmax values both in primary tumours (average 7,5 versus 6,4, P=0.015) and in non–axillary lymph nodes (average 7,6 versus 6,0; P<0.001). The measured volume of the FDG uptake was larger in prone images (average 9,1 versus 6,24; P<0.001) with a more

round form of shape. In four patients multifocality was visualized only in prone position (P=0.134). A visually relevant anatomical mismatch between PET and CT was less often identified on prone than on supine images, especially at the location of non-axillary lymph nodes (N=4 versus N=9). **Conclusion**: Optimized thoracic PET/CT in prone position leads to higher quantitative SUVmax values, a sharper tumour delineation and more adequate loco–regional assessment in breast cancer patients. These results may also contribute to an appropriate correlation of FDG–PET/CT with MRI in the monitoring of therapy response in patients receiving NAC.

## OP545

### Diagnostic accuracy of a full-ring dedicated PET scanner for breast imaging

**Y. Nakamoto**, S. Kanao, K. K. Miyake, K. Nakatani, K. Togashi; Kyoto University Hospital, Kyoto, JAPAN.

**Objectives:** The purpose of this study was to investigate the diagnostic performance of a dedicated breast positron emission tomography (dbPET) scanner with full-ring detectors in patients with known or suspected breast cancer. **Methods**: The study was comprised of 175 female patients (26-89 yr, mean 55 yr) with known or suspected breast cancer who underwent whole body FDG-PET scanning, followed by breast scanning in prone position for 5 min per each side using our dbPET scanner between Sep 2009 and Sep 2012. A total of 207 lesions (198 malignant, 7 benign, and 2 unclassified) were visually evaluated. Based on final diagnosis obtained by biopsy and/or surgery, diagnostic performance of the scanner was assessed. **Results**: The maximal diameter of lesions ranged from 2 to 116 mm with the average of 23 mm. Of 198 malignant lesions, 161 lesions were depicted, 14 lesions were not detected, and the remaining 23 lesions were out of scanning range, while 182 lesions were identified by a conventional PET/CT scanner. The lower-inner (4/19) and lower-outer (8/32) lesions tended to be missed due to outside the field of view, as compared with the upper-outer lesions (5/86) and lesions close to nipple (0/20). The sensitivity of the dbPET scanner was 83% in patient-basis, and 81% in lesion-basis, respectively. After excluding lesions which located outside the field of view, they were 95% and 92%, respectively. For lesions of ductal carcinoma in situ, size of which was ranging from 2 to 48 mm, the lesion-based sensitivity was 71%, excluding three lesions outside the field of view. The breast-based specificity was 97%. For two unclassified lesions, the flat epithelial atypia was depicted, while the adenomatous ductal hyperplasia was not depicted in this population. **Conclusion**: The dbPET scanner with full-ring had comparable diagnostic performance for detecting breast cancer, although some lesions especially in lower portion of the breast can be missed due to out of scanning range in dbPET.

## OP546

### Early and delayed prediction of axillary lymph node neoadjuvant response by18F-FDG PET /CT in patients with locally advanced breast cancer.

**A. Garcia Vicente**[1], A. Soriano Castrejón[1], A. León Martín[2], F. Relea Calatayud[3], M. Cruz Mora[4], I. Chacón López-Muñiz[4], M. Muñoz Sanchez[5], V. Muñoz Madero[6], R. Espinosa Aunión[7], A. Gonzalez Ageitos[8]; [1]Nuclear Medicine Department. University General Hospital, Ciudad Real, SPAIN, [2]Investigation Unit. University General Hospital, Ciudad Real, SPAIN, [3]Histopathology Department. University General Hospital, Ciudad Real, SPAIN, [4]Oncology Department. Complejo Hospitalario., Toledo, SPAIN, [5]Oncology Department. Virgen de la Luz Hospital, Cuenca, SPAIN, [6]Surgery Department. Provincial Hospital, Toledo, SPAIN, [7]Oncology Department. La Mancha Centro Hospital. Alcázar., Ciudad Real, SPAIN, [8]Oncology Department. Ntra Sra del Prado Hospital. Talavera., Toledo, SPAIN.

**Aim:** To determine the utility of 18F-FDG (FDG) PET/CT performed in an early and delayed phase during the neoadjuvant chemotherapy treatment in the prediction of lymph node histopathologic response in patients with locally advanced breast cancer (LABC). **Methods**: Prospective multicenter study (FISCAM grant 2009/40). Analysis of FDG PET/CT studies performed in 76 patients with LABC, mean age: 51.5 y, at baseline (PET-1, 76 studies), after the second course of chemotherapy (PET-2, 58 studies) and after the last course (PET-3, 44 studies). Inclusion criteria: lymph node involvement detected by PET-1, non-sentinel node biopsy previous or after the baseline PET/CT and the establishment of histopathological confirmation of lymph node status after chemotherapy. For diagnostic purposes a qualitative evaluation was used. Attending to visual analysis, lymph node FDG uptake decreasing to background was considered metabolic complete response (mCR). The predictive value of a negative lymph node status (mCR) in the PET-2 for pathological complete response (pCR) was assessed in 58 patients (group 1 with early evaluation) and in the PET-3 in 44 patients (group 2 with delayed evaluation). Lymph nodes were histopathological classified into pCR or not pCR (type A/D or B/C of Miller and Payne grading system respectively). The relation between mCR and pCR was established (X2 Pearson). **Results:** The sensitivity and specificity of FDG PET-1 in the detection of lymph node involvement was 86.7% and 81.2% respectively. Group 1: 36 out of 58 cases with lymph node involvement previous to chemotherapy, reached mCR in PET-2. By histological analysis 33 cases showed a pCR after chemotherapy. No statistical relation was observed between mCR and pCR (p=0.182). 22/33 cases with pCR had mCR. On the contrary, 14/25 cases with non pCR have mCR (FN). Group 2: 34 out of 44 cases reached mCR in PET-3 whereas 21 cases had pCR. 3 cases with persistent metabolism after chemotherapy showed pCR. The Se, Sp, PPV and NPV for PET-2 and PET-3 in the establishment of axillary final status after chemotherapy was 44%, 67%,50% and 61% and 35%,88%, 70% and 62% respectively. **Conclusions**: FDG PET/CT seems to have limitations, both in the early or delayed evaluation of lymph node status after neoadjuvant chemotherapy. The NPV is not accurate enough for the establishment of final lymph node response in order to avoid their histopathological confirmation.

## OP547

### HER2-overexpressing breast cancer: Interim PET after two cycles of chemotherapy predicts the outcome of neoadjuvant treatment

**D. Groheux**[1], S. Giacchetti[1], M. Hatt[2], M. Marty[1], L. Vercellino[1], C. Cuvier[1], F. Coussy[1], M. Espié[1], E. Hindié[3]; [1]Hopital Saint Louis, Paris, FRANCE, [2]INSERM, UMR 1101 LaTIM, Brest, FRANCE, [3]Haut-Lévêque Hospital, CHU Bordeaux, Bordeaux, FRANCE.

**Aim**: Pathological complete response (pCR) to neoadjuvant treatment correlates with improved survival of patients with HER2-positive breast cancer. We prospectively investigated the ability of interim PET to predict pathology outcomes early. **Materials and Methods**: During 61 months, consecutive patients with locally-advanced or large HER2-positive breast cancer patients without distant metastases were included. All patients received neoadjuvant treatment with 4 cycles of epirubicin+cyclophosphamide, followed by 4 cycles of docetaxel+trastuzumab. 18F-FDG-PET/CT was performed at baseline and after two cycles of chemotherapy (PET2). The correlation between pathologic response and SUV parameters (SUVmax at baseline, at two cycles, and ΔSUVmax) was examined. **Results**: Thirty consecutive patients were included. At baseline, 22 patients had PET-positive axilla and in nine of them FDG uptake was higher than in the primary tumor. At surgery, 14 patients (47%) showed residual tumor (non-pCR) while 16 had pCR. There was a strong correlation between the highest residual FDG uptake at PET2 and pathological response. Any site of residual FDG uptake with a SUVmax >3 whether in breast or axilla was predictive of non-pCR. The risk of non-pCR was 92.3% in patients with any site of residual uptake >3 on interim PET vs. 11.8% in patients with uptake ≤3 (p = 0.0001). **Conclusions**: The level of FDG uptake after two cycles of chemotherapy predicts residual disease at completion of neoadjuvant treatment with chemotherapy+trastuzumab. Because many innovative therapeutic strategies are now available (e.g., addition of a second HER2-directed therapy or an anti-angiogenic), early prediction of poor response is critical.

## OP548

### Response evaluation during primary systemic therapy of breast cancer

**T. Tőkés**[1,2], L. Torgyík[2], A. Tóth[2], J. Kulka[3], Z. Lengyel[4], H. Galgóczy[5], T. Györke[6,5], M. Dank[2]; [1]Semmelweis University School of Ph.D. Studies, Budapest, HUNGARY, [2]Semmelweis University 1st Department of Internal Medicine, Oncological Division, Budapest, HUNGARY, [3]Semmelweis University 2nd Department of Pathology, Budapest, HUNGARY, [4]Pozitron Diagnosztika Ltd., Budapest, HUNGARY, [5]Scanomed Ltd., Budapest, HUNGARY, [6]Semmelweis University Department of Nuclear Medicine, Budapest, HUNGARY.

**Aim:** Our Aim was to analyze the relationship between the metabolical and radio-morphological response of tumors and changes in the expression of the Ki-67 proliferation marker in a group of breast cancer patients treated with primary systemic therapy (PST). **Materials and Methods**: We report 42 patients in whom staging FDG-PET-CT scans were carried out before and after the PST (just before surgery). Maximal SUVs (Standardized Uptake Values) and morphological changes in the primary tumor (PT) and the axillary lymph node (AL) region were evaluated. SUVs were compared with Ki-67 labeling index (LI) (measured semiquantitatively in the core-biopsies and surgical specimens by immunohistochemistry). Furthermore, we analyzed the relationship between the changes of the Ki-67 LI (using our 4 grade scoring system) and the well-known response evaluation systems (Chevallier, Sataloff, WHO, RECIST, EORTC, PERCIST). **Results:** The decrease of SUVmax was significant in the PTs (12 vs. 1,6, p<0,001) and in the ALs (10,15 vs. 1,58, p<0,001). A significant reduction in the size of the PTs (29 vs. 8,5 mm, p<0,001) as well in the ALs was also observed (21 vs. 11 mm, p=0,027). Decrease of Ki-67 LI was significant (48,9 vs. 13,3%, p<0,001). Significant correlation was found between Ki-67 LI and SUV before the PST (r=+0,31, p=0,04), and ΔKi-67 and ΔSUV, both regarding the absolute values (r=0,427; p=0,005) and percentage changes (r =+0,51, p=0,0007). Moreover, we found significant correlation between the Chevallier and Sataloff grades and the RECIST (r=+0,502, p=0,0007; r=+0,404, p=0,009) and WHO score (r=+0,537, p=0,0002; r=0,462, p=0,0025); the PERCIST (r=+0,36; p=0,019; r=+0,349, p=0,025) and EORTC score (r=+0,361; p=0,019; r=+0,344, p=0,027); and the Ki-67 score (r=+504; p=0,0007; r=+0,463, p=0,002), as well. Between PERCIST and RECIST scale values a stronger correlation (r=+0,448, p=0,003) was observed compared

with that between PERCIST and Ki-67 score (r=+0,332 p=0,031), although the Ki-67 score correlated slightly better with the EORTC score results (r=+0,353, p=0,021). **Conclusions:** The metabolical remission measured by FDG-PET-CT correlated well with the pathological response and the overall proliferation of the tumors, even better than it did with the radio-morphological remission. This could be particularly important in the axillary lymph node region, wherein, the morphological measurement has limited efficiency. Because of these findings, the FDG-PET-CT results may play an essential role in the indication of PST, and can be successfully used in assessing the early therapeutic response of tumors. However - for the most accurate and effective response evaluation criteria - further investigations are needed.

1406 - Tuesday, Oct. 22, 14:30 - 16:00, Grand Salon Prestige Gratte-Ciel

## Oncology Clinical Science: Sentinel Lymph Node & Radioguided Surgery

### OP549

#### Evaluation of lymphedema following axillary lymph node dissection for breast cancer by combined lymphoscintigraphic studies of superficial and deep system

**G. Villa**, F. Boccardo, F. Bongioanni, A. Buschiazzo, E. Monteverde, G. Sambuceti; IRCCS Az. Ospedaliera Universitaria San Martino - IST, Genoa, ITALY.

***Aim*:** Arm lymphedema is a frequent complication of breast cancer therapy and axillary lymph node dissection, with an estimated frequency of 5%-30%. This incidence is based primarily on studies that use volume and circumference criteria in the first years after surgery. In the extremities, the lymphatic system consists of a superficial system that collects lymph from the skin and subcutaneous tissue, and a deeper system that drains subfascial structures such as muscle, bone, and deep blood vessels. The superficial and deep systems drain at markedly different rates. In the normal arm, subfascial transport is slower than the superficial system and transports less lymph. **Material and Methods**: A retrospective study of 62 patients with breast cancer-related lymphedema was performed. The ages of the patients ranged from 38 to 81 years old with a mean of 57 years. They underwent both subcutaneous and intradermal injections in order to differentiate various mechanisms of edema. Superficial system was studied injecting 15 MBq of 99mTc-Nanocoll in 0.1 mL. 4 injections were performed in the web space between the first and second and the second and third digits of the hands. Both arms receive injection to use one side as a control for patients with unilateral lymphedema. Deep system was demonstrate using a single 37 MBq dose in aponeurotic sites of the palms. Time for transport to regional lymph nodes, appearance of lymph vessels and nodes and distribution pattern were scored. These scores were compiled into a modified Kleinhans transport index (TI) in order to quantitate visual findings in lymphoscintigraphy. This method designes a numeric index of transport kinetics by combining visual assessment of five criteria: temporal and spatial distribution of the radionuclide, appearance time of lymph nodes, and graded visualization of lymph nodes and vessels. For assessment, scores were used ranging from 0 to 9. Thus, the resulting TI ranged from 0 (normal) to 45 (pathological). **Results and conclusions:** TI of both systems in healthy extremities was less than 10. TI was found to be increased in 93% of the affected arms. Average TI for superficial and deep systems were respectively 22.6 and 22.3. Lymphoscintigraphic semiquantitative evaluation has proved to be very sensitive and able to measure the arm lymph flow in axillary lymphadenectomy related lymphedema; investigation of the subfascial transport does not seem to provide additional informations respect the assessment of superficial circulation.

### OP550

#### 99m Tc-Nanocolloid and Indocyanine Green: a Synergistic Alliance for a Better Result in Breast SLN Detection

A. Peloso, A. Ferrari, A. Della Valle, V. Gallo, A. D'Addiego, F. De Marco, A. Mimmo, A. Presazzi, G. Cavenaghi, I. Di Salvo, M. Maestri, A. Sgarella, **C. Aprile**; Fond. Policlinico San Matteo Hospital, IRCCS, Pavia, ITALY.

**Introduction** - Sentinel lymph node biopsy (SLNB) currently represents the standard of care in early-phase axilla staging of breast cancer patients. To identify sentinel node, different techniques can be used. The most common method is based upon the use of radioactive colloid (99mTc-NanoColloid, NC) as a direct guidance on the operation field. Recently, a new and innovative method for axillary node mapping has been implemented in breast surgery. Such technique is based on the use of a fluorescent dye (indocyanine green -ICG-) and a specific camera able to detect it. AIM - The intent of the current study is to test the potential synergism between the traditional radioactive method (NC) and the fluorescent method with ICG, in order to increase sensibility and specificity in SLNB. **Material and Methods** - We enrolled a total of 70 female patients (mean-age 63 years, range 40-84 years).with T1-T2 primary early breast cancer. According to protocol, all patients underwent a linfoscintigraphy NC-based the day before (or the same day of) the surgical procedure, while an intradermal and periareolar injection with 2 ml of ICG was performed 30 min before the intervention. A gentle pumping pressure was applied to the injection site in order to favor the lymphatic flow. Operating room's lights were turned off during the analysis of the ICG fluorescence. Nodes were thus removed after control and confirmation with the gamma probe which was used by the surgeon only following the 15 min after the skin incision. **Results** - In all patients undergoing NC and ICG procedures, SLNB was successful. Trancutaneous fluorescent lymphography was visible in all 70 procedures. In 69/70 (98,57 %), removed node were gamma-emitting and positive to gamma probe. Only in one case (1/70; 1,42%), nodes were NC negative , but positive to ICG-detection. In 68/70 (97,14 %), removed node were ICG fluorescent (in two patients nodes were ICG-negative and, consequently, node incision was performed after 99TC-detection). **Conclusion** - The use of fluorescence-dye introduces, into surgical operatiing room, the lymphography method in order to detect sentinel lymphnodes. The ICG-based approach permits a real-time navigation following breast subcutaneous lymphatic flow and allows SLN identification. The combined use of ICG system and radioisotope seems to improve sensitivity and specificity of SLN detection leading, at the same time, to a safer patients' treatment.

### OP551

#### SPECT/CT mixed-reality combined with freehand SPECT augmented-reality for intraoperative navigation in sentinel node biopsy during laparoscopic procedures

**N. S. Van den Berg**[1,2], G. H. KleinJan[1,2], O. R. Brouwer[1], T. Wendler[3,1], R. A. Valdés Olmos[1,2], H. Van der Poel[2], F. W. B. Van Leeuwen[1]; [1]Leiden University Medical Centre, Leiden, NETHERLANDS, [2]NETHERLANDS Cancer Institute, Amsterdam, NETHERLANDS, [3]Surgic Eye, Munich, NETHERLANDS.

**Aim** For prostate cancer, the more intricate anatomy asks for improved orientation during laparoscopic sentinel node biopsy. This study provides a proof of concept on how a protocol of mixed-reality intraoperative navigation based on the preoperatively acquired SPECT/CT images may facilitate radio- and fluorescence-guided surgery. Also a proof of concept is given regarding the generation of intraoperative SPECT visual data, thereafter allowing for real-time augmented-reality based navigation with a freehand-SPECT device. **Materials and Methods** Prostate cancer patients received a (transrectal) intraprostatic injection with the hybrid tracer indocyanine green (ICG)-99mTc-nanocolloid. Conventional lymphoscintigraphy and SPECT/CT imaging were performed to determine the number and location of the sentinel node(s). As proof of principle for SNs outside the extended pelvic dissection area were located. Prior to SPECT/CT imaging a reference tracker (ReT) was placed on the patient and marked with indelible ink. An identical sterile ReT was placed on the exact same location on the patient prior to the start of the robot assisted laparoscopic prostatectomy. This allowed registration of the SPECT/CT image onto the patient. By placing a second ReT on the laparoscopic gamma probe, the probe could be navigated in 3D SPECT/CT-based mixed-reality to the sentinel node. In the freehand-SPECT situation, after placing a ReT on the patient, an area of interest was "scanned" with the laparoscopic gamma probe for the presence of radioactivity. This was done in three different directions. After reconstruction, this provided the surgeon with real time SPECT data to visualize the location of the sentinel node. Thereafter the laparoscopic gamma probe could be used to navigate to the sentinel node. During surgery the fluorescence of the SN was used to confirm the location of the SN. **Results** Both 3D SPECT/CT-based mixed-reality and freehand SPECT-based augmented-reality navigation allowed the identification of 4 sentinel nodes in 4 patients. The optical guidance of the fluorescence could be used for confirmation of the SN. The current challenge is to place the ReT onto the body on a location that the ReT can be visualized by the system during the robot assisted procedure. Intraoperative positioning of the instrumentation is a factor can block the tracking of the ReTs. In 3D SPECT/CT we noticed a learning curve in the accuracy of the placement of ReT. **Conclusion** 3D SPECT(/CT)-based navigation in the operating seems feasible. Both presented techniques have the potential to help further improve the sentinel node biopsy for prostate cancer.

### OP552

#### Radioguided Seed Localization for breast cancer excision: an ex-vivo specimen-based study to establish accuracy of a freehandSPECT device in predicting resection margins

**B. Pouw**[1], L. J. de Wit- van der Veen[1], J. A. Van der Hage[2], J. Wesseling[3], M. T. F. D. Vrancken Peeters[2], M. P. Stokkel[1], R. A. Valdés Olmos[1]; [1]Department of Nuclear Medicine, NETHERLANDS Cancer Institute, Amsterdam, NETHERLANDS, [2]Department of Surgical Oncology, NETHERLANDS Cancer Institute, Amsterdam, NETHERLANDS, [3]Department of Pathology, NETHERLANDS Cancer Institute, Amsterdam, NETHERLANDS.

**Aim**. Positive margins after breast-conserving surgery are associated with a 2 to 3 times increase in the chance of recurrence when compared to negative margins; therefore, reexcision of the positive margins or other additional treatment options are required. Various techniques like wire-localization and radioguided occult lesion localisation have been used in the past to guide tumour excision. Radioguided seed localisation (RSL) is a relatively new technique and uses an Iodine-125 (125I)-seed as a marker for the tumour location. The 125I-seed is implanted into the tumour and enables intra-operative localisation with a conventional gamma-probe. However, specimen margins in relation to the 125I-seed are estimated only based on gamma-countings. A novel technique, freehand-SPECT (DeclipseSPECT; SurgicEye GmbH, Germany), is able to generate images of the 125I-seed within minutes and is capable of measuring the distance from the resection plane to the 125I-seed. The Aim of the present feasibility study was to establish the accuracy of this device in predicting resection margins in ex-vivo breast cancer specimens of patients operated using RSL-guidance. **Materials and Methods**. In this feasibility study 10 patients (mean age: 52.7 years, range: 36-71) with non-palpable breast cancer and scheduled for wide local excision with RSL were included. Six patients had received neo-adjuvant chemotherapy. After surgery, the specimens containing the breast tumour and the 125I-seed were scanned using freehand-SPECT and 3D-images were generated. Measurements from 5 directions were performed and compared with distances measured on an ex-vivo CT-scan of the specimen obtained in the exact same orientation. Finally, the measurements were related to the pathology report. **Results**. For the freehand-SPECT an average error in predicting margins compared to CT of 2.9 mm (SD: 2.7 mm, range: 0-13 mm) was found on the basis of 60 measurements (5 measurements per 125I-seed). Only one patient had positive margins, this specimen contained a focal irradical resection (< 4 mm2) of ductal carcinoma in-situ grade III, the narrowest margin to the tumour was at the ventral side (2 mm) based on the pathology report. The smallest distance to the 125I-seed measured from ventral side was 4 mm for the freehand-SPECT and 5 mm for the CT-scan. **Conclusion**. In patients scheduled for breast-conserving surgery an accurate ex-vivo measurement of the tumour resection margins using 125I-seed and freehand-SPECT is feasible. Incorporation of the freehand-SPECT device to RSL protocols may enable a real-time estimation of resection margins, which may be useful for surgeons in adjusting local tumour excisions.

## OP553

### Value of sentinel lymphnode biopsy in papillary thyroid cancer - initial results of a prospective trial

**E. Etchebehere**, R. Cabrera, C. Chone, D. Zantut-Wittmann, A. Santos, R. Ferrari, P. Pereira, P. Matos, D. Miranda, G. Pinto; UNICAMP, SÃO PAULO, BRAZIL.

**Aim**: Evaluate the performance of sentinel lymph node (SLN) biopsy in detecting occult metastases in papillary thyroid cancer (PTC) and the correlation of occult LN metastases to histology of the primary tumor and patient characteristics. **Materials and Methods:** Twenty-three patients (21 females, mean age 48.4 years) with PTC diagnosed by fine-needle aspiration biopsy and without evidence of loco-regional LN metastases by clinical exam and ultrasound were prospectively enrolled. Patients with prior neck surgery or radiotherapy, cervical lymphadenopathy and pregnancy were excluded. All patients were submitted to SLN lymphoscintigraphy prior to total thyroidectomy. An ultrasound guided peritumoral injection of 7.4 MBq of phytate-$^{99m}$Tc was performed as either a single injection or two injections (in multifocal diseases). SPECT/CT images of the cervical region were acquired 15 minutes after radiotracer injection and 2 hours prior to surgery. Intra-operatively, a hand-held gamma probe was used to locate the SLN. SLNs were removed along with non-SLNs located in the same neck compartment level. Histopathology of PTC was divided into: aggressive type (solid, tall and oxyphilic cells) and non-aggressive type (papillary, follicular and classic variants). All SLNs and non SLNs were submitted to histopathology analysis. **Results**: SLNs were located in levels VI in 82,6% of patients, level II in 34.7%, level III in 26%, level IV in 30.4%, and one in level VII (4.3%). One single metastatic SLN in level V occurred in one patient (4.3%) with a 3.5 cm multifocal PTC, aggressive variant, extra-thyroid extension, positive surgical margins and vascular invasion with a metastatic. Metastases in the SLN were noted in 7 patients (30.4%) and SLN was false-negative in 3 patients. Histology of SLN and non-SLNs was: aggressive (4/23), positive surgical margins (3/23) and extra-thyroid extension (3/23) and vascular invasion (4/23). SLNs contra-lateral to the primary tumor were also noted in 4/23 patients (levels II, III and IV) and none were metastatic. There were significant associations between LN metastases and tumor vascular invasion (p = 0.045; Fisher´s exact test), extra-thyroid extension (p = 0.052; Fisher´s exact test) and tumor size (p value = 0.07; T Test). No associations were noted among LN metastases and patient age, sex, stimulated thyroglobulin levels, positive surgical margins, aggressive histology and multifocal lesions. **Conclusion**: SLN biopsy can detect occult metastases in PTC. The risk of a metastatic SLN is increased in larger tumors, with extra-thyroid extension and vascular invasion. This may help guide future patient surveillance and radioiodine therapy doses.

## OP554

### First clinical experiences with a hybrid portable camera for simultaneous scintigraphic and optical imaging of head and neck sentinel nodes.

**D. Hellingman**[1], J. Catret[2], L. J. de Wit-van der Veen[1], W. M. Klop[3], R. A. Valdés Olmos[1]; [1]Department of Nuclear Medicine, NETHERLANDS Cancer Institute - Antoni van Leeuwenhoek hospital, Amsterdam, NETHERLANDS, [2]Oncovision GEM-Imaging S.A., Valencia, SPAIN, [3]Department of Head and Neck Surgery & Oncology, NETHERLANDS Cancer Institute - Antoni van Leeuwenhoek hospital, Amsterdam, NETHERLANDS.

**Aim:** Traditionally, sentinel nodes (SNs) are localized with a gamma ray detection probe. However, in areas such as the head and neck often SNs in the vicinity of the injection site can be missed. To optimize the procedure we incorporated a hybrid radioactive/fluorescent tracer in our hospital. A high-resolution portable gamma-camera is used prior to and after SN excision to confirm removal of all SNs. Unfortunately, this current intra-operative approach is hampered by difficulties in the interpretation of the portable gamma-camera images due to a lack of anatomical information. The Aim of the present study was to establish the feasibility of a novel portable hybrid-camera for simultaneous scintigraphic/optical imaging of the head and neck in a coordinated one-screen display for SN detection. **Materials and Methods:** Validation was performed using a multimodality hybrid prototype based on a currently available portable gamma-camera (Sentinella 102, Oncovision, Valencia, Spain). This prototype combines an optical stereo-camera module and a pinhole gamma-camera in a configuration that offers real-time superimposition of an optical image onto a scintigraphic image. Spatial accuracy of the image registration was evaluated by obtaining images of a head phantom with iodine-seeds ($^{125}$I-seeds) at different distances (range 2-20cm). Secondly, spatial accuracy was tested in five head/neck melanoma patients, evaluated by means of preoperatively marked skin marks by a experienced nuclear physician with a cobalt-57-source pen, undergoing a standard clinical SN procedure (including SPECT/CT using a conventional gamma-camera). **Results:** In the phantom model the best image registrations were achieved at distances ≥8cm corresponding to a field of view (FOV) of ≥10.4cm$^2$. Superimposition failed for distances ≤4cm and a FOV of ≤5.2cm$^2$. In the five patients, a total of 13 SNs (mean 2.6 a person, range 1-4) were depicted using SPECT/CT. All $^{125}$I-seeds in the head phantom and all SNs were depicted pre- and intra-operatively with the hybrid-camera with an accuracy between 0-2cm (mean 1cm, for distances ≥8cm). In the border of the FOV is more spatial distortion (0-3cm). **Conclusion:** Simultaneous optical/scintigraphic imaging is feasible in a clinical setting with an 2cm accuracy in the FOV centre, but FOV border distortion needs to be corrected. This hybrid prototype enables easier interpretation of the images in a pre-operative and intra-operative setting. The hybrid prototype opens the possibility to incorporate in a later stage a fluorescent-camera into the optical module to enable work with hybrid tracers, which have been introduced for simultaneous scintigraphic/fluorescence imaging in head/neck SN procedures.

## OP555

### Hybrid sentinel node biopsy in vulvar cancer

**N. S. van den Berg**[1], G. H. KleinJan[1], W. van Driel[2], M. Stokkel[2], H. Trum[2], F. W. B. van Leeuwen[1], R. A. Valdés Olmos[2]; [1]Leiden University Medical Center, Leiden, NETHERLANDS, [2]NETHERLANDS Cancer Institute - Antoni van Leeuwenhoek Hospital, Amsterdam, NETHERLANDS.

**Introduction** Sentinel node biopsy has proven to be a minimally invasive technique to accurately determine the regional lymph node status. Conventionally, a radiocolloid is injected surrounding the lesion after which lymphoscintigraphy is performed to determine the number of sentinel nodes. Intraoperatively, sentinel nodes are pursued with a gamma ray detection probe and blue dye detection. The Aim of this study was to evaluate the added value of intraoperative fluorescence imaging to the radioguided procedure for sentinel node localization in patients with vulvar carcinoma. For this, the hybrid tracer ICG-99mTc-nanocolloid was used, which is both radioactive and fluorescent. **Materials and Methods** Fourteen patients with vulvar carcinoma (FIGO stage 1) scheduled for a sentinel node biopsy procedure were peritumorally injected with ICG-99mTc-nanocolloid 5-18 hours before the start of the operation. Following injection, lymphoscintigraphy (dynamic and static (15 min and 2 hours) and SPECT/CT images were obtained to determine the number and location of the sentinel node(s). Prior to the start of the operation, blue dye was injected intradermally around the lesion. Sentinel nodes were harvested using a combination of radio- and fluorescence guidance, and optical blue dye detection. SN removal was confirmed using a portable gamma camera. **Results** Early and late lymphoscintigraphy revealed 24 and 34 sentinel nodes, respectively. Following SPECT/CT a total of 37 sentinel nodes were identified dispersed over 24 groins. Non-visualization occurred in 2 groins. Intraoperatively, all but 3 sentinel nodes could be localized and excised. Intraoperatively, 95% was radioactive and 91% fluorescent. In contrast, only 59% had stained blue at the time of excision. Fluorescence identification of the sentinel node was mainly beneficial when these had not taken up blue dye. In 2 patients, sentinel nodes could be

identified with fluorescence imaging before they were detected with blue dye. Pathological examination revealed 6 tumor-positive sentinel nodes in 4 patients. **Discussion** Sentinel node biopsy using the hybrid tracer ICG-99mTc-nanocolloid proved feasible. ICG-99mTc-nanocolloid enabled the combination of unaltered preoperative sentinel node identification using lymphoscintigraphy and SPECT/CT with an improved bimodal (radioactive and fluorescent) signal for intraoperative sentinel node detection.

## OP556

### Contribution of SPECT/CT in the sentinel node detection in early cervical cancer

**C. M. Hernández Heredia**, P. Paredes Barranco, S. Vidal-Sicart, F. Pons, P. Fusté, S. Martinez-Roman, J. Pahisa; Hospital Clinic, Barcelona, SPAIN.

**Objective**: To evaluate the utility of SPECT/CT in the detection of sentinel lymph node (SLN), in patients with early cervical cancer. **Material and Methods** We included 39 patients with cervical cancer (38 stage IB1 and 1 stage IIa), with mean age of 42 years (22-74 years), who underwent sentinel node biopsy (39 / 39) and eventually primary surgery of the tumour. The day before surgery a peritumoral / periorificial injection of 111 MBq of 99mTc-albumin nanocolloid was performed. Planar images were acquired (30 minutes and 2 hours p.i.) and SPECT/CT at 2 hours post injection. All images were evaluated and agreed by three observers, in order to determine the number and location of the SLN. During surgery, SLN were removed by means of a gamma-probe and a portable gamma camera. The study was completed with histological analysis with haematoxylin/eosin and immunohistochemistry. RESULTS Drainage was observed in all patients (39/39) both on planar and SPECT/CT images. Bilateral drainage was observed in 69% of the patients (27/39). SPECT/CT detected more SLNs compared to the planar (109/162) in 69% of patients (27/39). Laterality of drainage was modified in 15% of the patients (6): 3 cases with unilateral drainage presented bilateral SLNs on SPECT/CT and in 3 patients misinterpretations were identified. In 5% of patients, SPECT/CT detected paraaortic SLNs that were not visualized on planar images. During surgery 132 SLNs were removed, and 13% of patients (5/39) had metastatic infiltration. **Conclusions** The SPECT/CT is a useful technique in the detection of SLN in patients with early cervical cancer, allowing greater accuracy in the anatomical location and SLN number identification.

1407 - Tuesday, Oct. 22, 14:30 - 16:00, Salon Pasteur

## Neurosciences: Psychiatry

## OP557

### Changes in Cerebral CB1 Receptor Availability in Chronic Cannabis Users by the PET radioligand [18F]MK-9470

**J. Ceccarini**[1], R. Kuepper[2], D. Kemels[1], J. van Os[2,3], C. Henquet[2,4], K. Van Laere[1,5]; [1]Division of Nuclear Medicine, University Hospitals and KU Leuven, Leuven, BELGIUM, [2]Department of Psychiatry and Psychology, Maastricht University Medical Centre, Maastricht, NETHERLANDS, [3]Department of Psychosis Studies, Institute of Psychiatry, King's Health Partners, King's College London, London, UNITED KINGDOM, [4]PsyQ Heerlen, Mondriaan, South Limburg, NETHERLANDS, [5]LIND, Leuven Institute for Neurobiology and Disease, KU Leuven, Leuven, BELGIUM.

**Aim**: Δ9-tetrahydrocannabinol (Δ9-THC), the main psychoactive component of cannabis, exerts its central effects through activation of the cerebral type 1 cannabinoid receptor (CB1R). Chronic exposure to cannabis has been linked to decreased CB1R availability and this is thought to be a component underlying drug tolerance and dependence. The Aim of the current study was to investigate in vivo CB1R availability in chronic cannabis users using a selective high-affinity CB1R radioligand [18F]MK-9470 in comparison to healthy subjects. **Materials and Methods**: Ten chronic cannabis users (8 men, 2 women, age 26.0 ± 4.1 years) and ten healthy control subjects (7 men, 3 women, age 23.0 ± 2.9 years) were investigated using positron emission tomography (PET) with [18F]MK-9470. Cannabis users were scanned within the first week (4.0 ± 1.7 days) following the last cannabis consumption. For the cannabis consumption, 60% of the cannabis users were heavy users (several times a day). CB1R PET scans were started 120 min after [18F]MK-9470 injection (146.8 ± 6.7 MBq) with 60 min scanning session. Parametric modified Standardized Uptake Value (mSUV) images, reflecting CB1R availability, were calculated. Changes in CB1R availability were analyzed by predefined volume-of-interest (VOI) analysis and voxel-based statistical parametric mapping (pheight = 0.005; kext = 50). **Results**: Compared to controls, cannabis users had a global decrease in CB1R availability (-11.7%). Regional VOI-based analysis demonstrated that the CB1R decrease was significant in the temporal lobe (-12.7%, p = 0.04), anterior (-12.6%, p = 0.04) and posterior cingulate cortex (-13.5%; p = 0.04), and nucleus accumbens (-11.2%, p = 0.04). Voxel-based analysis confirmed this decrease and regional pattern in CB1R availability in cannabis users. There were no associations between CB1R availability and the level of cannabis consumption. However, low cannabis consumption did not produce similar CB1R downregulation: the subject with a lowest cannabis use showed the smallest global CB1R decrease (-5.8%) compared to the cannabis users with a moderate/heavy use (-15.8%). **Conclusion**: In conclusion, this study shows that chronic cannabis use downregulates in vivo CB1R availability in mainly neocortical regions. Considering that subjects who occasionally smoke cannabis do not develop tolerance to the level that heavy chronic daily smokers do, and that occasional cannabis users likely differ in term of CB1R downregulation, these preliminary results may indicate that CB1R downregulation may contribute to the development of tolerance to cannabis.

## OP558

### Transcranial magnetic stimulation in fibromyalgia: a randomized trial evaluating quality of life and its brain metabolic substrate

**E. Guedj**, A. Dousset, L. Boyer, P. Roussel, S. Cammilleri, O. Mundler, A. Donnet; CHU Timone, Marseille, FRANCE.

**Objective.** This double-blind randomized placebo-controlled study investigates the impact of rTMS on QoL of patients with fibromyalgia, and its possible brain anatomo-functional substrate. **Methods**. Thirty-eight patients were randomly assigned to receive high-frequency rTMS (n=19) or sham stimulation (n=19), applied to left primary motor cortex. An induction phase of 10 sessions over 2 weeks was followed by a maintenance phase of 4 sessions until week 10. Primary clinical outcomes were QoL changes at the end of week 11, measured by FIQ and SF-36. Secondary clinical outcomes were pain, mood, and anxiety. Resting-state 18FDG-PET metabolism was assessed at baseline, week 2, and week 11. Whole-brain voxel-based analysis was performed to study between-group metabolic changes over time. **Results.** At week 11, patients of the active rTMS group had significantly greater QoL improvement in FIQ (p=0.034) and in mental component of SF36 (p=0.016), than in the sham stimulation group. No significant impact was found for other clinical outcomes. In comparison to sham stimulation group, patients of the active rTMS group presented a significant increase in right medial temporal metabolism between baseline and week 11 (p<0.001), which was correlated with FIQ and mental component of SF36 concomitant changes (r =-0.38, p=0.040; r=0.51, p=0.009). QoL improvement involved mainly affective, emotional, and social dimensions. **Conclusion**. Our study shows that rTMS improves QoL of patients with fibromyalgia. This improvement is associated with a concomitant increase in right limbic metabolism, arguing for a neural substrate to the impact of rTMS on affective, emotional, and social dimensions involved in QoL.

## OP559

### Deep Brain Stimulation Induces Endogenous Striatal Dopamine Release in Obsessive-compulsive Disorder

**M. Figee**, G. van Wingen, J. Booij, D. Denys; Academic Medical Center, University of Amsterdam, Amsterdam, NETHERLANDS.

**Background***:* Obsessive-compulsive disorder (OCD) is a chronic psychiatric disorder related to dysfunctional dopaminergic neurotransmission. Molecular imaging studies consistently showed decreased dopamine $D_{2/3}$ receptor binding in OCD, most prominently in the ventral striatum. Deep Brain Stimulation (DBS) targeted at the ventral striatum (nucleus accumbens, NAc) has recently become an effective treatment for therapy-refractory OCD, but its effects on dopaminergic transmission are unknown. We investigated dopaminergic changes related to NAc DBS treatment of OCD. **Methods:** We measured the effects of DBS in 15 patients and 18 healthy controls on the dopamine $D_{2/3}$ receptor binding potential ($D_{2/3}$R BP) in the striatum and in the stimulation area with [$^{123}$I]iodobenzamide single photon emission computed tomography ([$^{123}$I]IBZM SPECT). All patients were investigated on three separate occasions: during chronic stimulation (1 year stable DBS treatment), DBS OFF (after 8 days of DBS inactivation) and during acute stimulation (1 hour after DBS activation). Healthy controls were investigated once. For administration of the radiotracer, we used a sustained equilibrium/constant infusion technique, with acquisition of the images 2 hours after the bolus injection when a stable state of sustained binding equilibrium can be expected. SPECT scans were acquired on a 12-detector single slice brain-dedicated scanner (Neurofocus 810). For quantification of $D_{2/3}$R BP we defined standard regions of interest in the striatum (putamen and caudate) and around the electrodes we defined regions of interests using individual co-registered MRI scans. We correlated DBS-induced dopaminergic changes with clinical changes. **Results:** Acute and chronic DBS decreased striatal $D_2$R BP compared to the non-stimulated condition. Repeated measures ANOVA showed a significant time by hemisphere interaction ($P$ = 0.012). Contrasts showed a general increase of $D_2$R BP in the putamen from chronic stimulation to DBS OFF over both hemispheres ($P$ = 0.04), which rapidly reversed after acute stimulation in the left putamen ($P$ = 0.02). $D_{2/3}$R BP decreases in the stimulated area were significantly correlated with changes in clinical symptoms (45% symptom decrease). Irrespective of DBS condition, OCD patients had significantly lower striatal $D_{2/3}$R BP and than healthy controls **Conclusion:** DBS targeted at the NAc for OCD induces a reduction in striatal $D_{2/3}$R binding. These $D_{2/3}$R BP decreases most likely reflect dopamine release because they occurred

already during the first hour of stimulation. DBS induced dopamine release at the NAc electrode was associated with improved clinical symptoms. Our findings suggest that DBS may compensate for a defective dopaminergic system in OCD.

## OP560

### Evidence for an involvement and therapeutic relevance of the serotonergic system in Tourette syndrome with co-morbidities

**G. Berding**[1], F. Wilke[2], S. Bokemeyer[3], C. Haense[1], L. Geworski[2], F. Bengel[1], K. Müller-Vahl[3]; [1]Department of Nuclear Medicine, Hannover Medical School, Hannover, GERMANY, [2]Department of Medical Physics and Radiation Protection, Hannover Medical School, Hannover, GERMANY, [3]Clinic of Psychiatry, Socialpsychiatry and Psychotherapy, Hannover Medical School, Hannover, GERMANY.

**Aim**: In Tourette syndrome (TS) a pathophysiologic relevance of the serotonergic system has been suggested, but reports on changes of serotonin transporter (SERT) binding in TS are inconsistent. The present study employs radiotracer imaging to improve understanding of: (i) the role of SERT for TS in consideration of co-morbidities like obsessive compulsive behaviour (OCB) and (ii) the therapeutic potential of SERT inhibitors (SRI) in TS. **Methods**: Ten patients with TS (according to DSM-IV criteria) and without OCB (age 40±14 years), eight with TS and OCB (33±10) and ten healthy control subjects (40±16) were enrolled. TS patients with OCB were treated with the SRI escitalopram (maximum dose 30mg per day) for 12 to 16 weeks. Patient symptoms were assessed at baseline and after treatment using the Yale Global Tic Severity Scale (YGTSS), Yale Brown Obsessive Compulsive Scale (YBOCS) and Becks Depression Inventory (BDI). SERT binding was measured with the radioligand I-123-ADAM (185MBq) and SPECT (Siemens ECAM). Tracer uptake at equilibrium (280-320min p.i.) was analysed using PMOD2.8 and SPM2 software. First an ADAM template complying with the MNI stereotaxic space was generated based on MRT and SPECT data from healthy controls including fiducial markers. All SPECT studies were spatially normalised using this template. Employing the WFU PickAtlas mean count densities in volumes of interest with specific binding (hypothalamus, midbrain, pons, caudate, putamen, thalamus, mesial temporal cortex) and the cerebellum as a reference region were extracted. Specific to non-specific binding ratios as well as percentage decrease in specific over non-specific binding (SERT occupancy) were calculated. **Results**: SERT binding ratios showed for none of the regions a significant difference between TS without OCB and healthy controls, but ratios were significantly elevated in the hypothalamus of TS patients with OCB (2.38±0.14 vs. 2.13±0.26, p=0.023). Comparison of clinical scores at baseline vs. during treatment revealed no significant difference for YGTSS (23 vs. 23) and YBOCS (21 vs. 18, p=0.225) but a significant reduction in BDI (8 vs. 13, p=0.042). SERT binding ratios decreased due to SRI intake significantly for all regions (p<0.05, at least 19%) with the highest occupancy in midbrain (57%, p<0.001) and hypothalamus (50%, p=0.001). **Conclusions**: We found no evidence for changed SERT binding in TS without OCB and no tic reduction in this patient group as a result of SRI intake. Nevertheless, TS patients with OCB showed altered SERT binding in the hypothalamus and a significant reduction of co-morbid depression with SRI.

## OP561

### Synaptic Neurotransmission in Schizophrenic Patients

**S. Nikolaus**, H. Hautzel, H. W. Müller; University Hospital Düsseldorf, Düsseldorf, GERMANY.

**Aim**: Various factors are discussed in the pathophysiology of schizophrenia including dysfunctions of the (DA)ergic, serotonin(5-HT)ergic, GABAergic and glutamatergic system. In the present investigation, we assessed the contribution of the individual synaptic constituents by subjecting all available in vivo imaging studies on schizophrenic patients to a retrospective analysis. **Materials & Methods**: In a total of 2238 schizophrenic patients (mean age: 33.7±8.6 years, mean disease duration: 7.1±6.5 years, mean PANSS score: 67.6±17.5) and 2902 controls (mean age: 33.3±8.8 years) investigations were performed on DA synthesis, DA release, VMAT2, DAT and SERT binding as well as D1, D2, 5-HT1A, 5-HT2A, GABA(A), mACh, nACh, NMDA, H1 and CB1 receptor binding in various cortical and subcortical brain regions with either PET or SPECT. For each study, the percentual difference of transporter or receptor binding in patients relative to the respective controls was computed. Studies were pooled over all patients and median values and interquartile ranges of percentual differences relative to controls were determined for the individual brain regions. Differences between patients and controls were assessed with the Mann-Whitney-U-test for unrelated samples. **Results:** When all patients were pooled, analysis revealed a significant increase of striatal DA synthesis (+12%) and striatal DA release (+94%) relative to healthy individuals. Findings, moreover, showed significant decreases of striatal DAT (-2%) as well as striatal (-14%), thalamic (-8%), frontal (-18%) and temporal D2 receptor binding (-29%). Furthermore, midbrain 5-HT1A (-6%), temporal 5-HT1A (-5%) as well as frontal 5-HT2A (-27%) and temporal 5-HT2A receptors (-25%) were significantly diminished (0.037<p<0.0001). Numerous synaptic constituents were assessed merely once. Thereby, amygdalar and mesencephalic DA synthesis, and striatal 5-HT2A as well as pontine CB1 receptor binding were significantly elevated, while insular D1, amygdalar and insular D2, striatal, thalamic, neocortical, cingulate and cerebellar NMDA as well as frontal and cingulate H1 receptors were significantly diminished relative to controls (p<0.05). **Conclusion:** The elevation of striatal DA synthesis and release leading to increased concentrations of available DA may be surmised to induce a compensatory down-regulation of excitatory D1 and inhibitory D2 receptors in striatum and thalamocortical projection areas. As both the 5-HT1A and 5-HT2A receptor subtype are known to stimulate DA release, the observed decrease of 5-HT receptors in both midbrain and neocortex of schizophrenic patients may reflect a further compensatory mechanism Aiming to reduce DA efflux in mesencephalic and neocortical projection areas. In addition, there is in vivo evidence of altered histamine, acetylcholine and glutamate function.

## OP562

### Relationship between brain glucose metabolism and depression symptoms in patients with refractory temporal lobe epilepsy measured by positron emission tomography

**S. Divošević**[1], H. Hećimović[2], A. Balenović[1], I. Mihaljević[3], D. Bedek[4], T. Sajko[5]; [1]Medikol Outpatient Clinic, PET/CT Centre, Zagreb, CROATIA, [2]University Hospital Centre "Sestre milosrdnice", Department of Neurology, Zagreb, CROATIA, [3]Clinical Hospital Centre Osijek, Department of Nuclear Medicine, Osijek, CROATIA, [4]University Hospital Centre "Sestre milosrdnice", Department of Radiology, Zagreb, CROATIA, [5]University Hospital Centre "Sestre milosrdnice", Department of Neurosurgery, Zagreb, CROATIA.

**Aim:** The Aim of this study was to establish the relationship between regional brain glucose metabolism with the degree of depressive symptoms in examinees with refractory temporal lobe epilepsy, and thereby establishing the importance of positron emission tomography (PET) in these patients. **Materials and Methods:** 73 examinees signed compliance for this study and filled in the BDI questionnaire immediately before $^{18}$F FDG PET brain imaging. They were divided into two groups, with BDI<15, without clinically significant depressive symptoms, and those with BDI≥15, with pronounced symptoms. We have analyzed qualitatively and quantitatively brain glucose metabolism, as well as interconnection between regional brain glucose metabolism and clinical parameters: overall BDI, localization of epileptogenic zone and brain MRI. **Results:** A total of 30.1% of examinees had depressive symptoms. Through a qualitative analysis of PET we have established the highest frequency of reduced glucose metabolism in temporal region. No difference was found in the overall BDI between examinees with normal and pathological PET. Patients with right-sided temporal glucose hypometabolism and right-sided hippocampal sclerosis on average had lower overall BDI score. An exceptionally high level of correspondence between PET findings and EEG and MRI findings was perceived, with pathological PET in 90,1% of examinees with normal brain MRI findings. Through a quantitative analysis of PET we did not found any differences neither in glucose hypometabolism intensity, nor in the number of hypometabolic brain regions, including frontal regions. We detected lateralising asymmetry in frontal and temporal regions, parietal and primary visual cortex. Examinees with depression have statistically significant lower values of brain glucose metabolism in the anterior and posterior medial temporal region, with right-left asymmetry and correlations between frontal and temporal regions, while examinees without depression show no correlation between those regions. Correlations between frontal and temporal regions are different depending on EEG localization of temporal focus, MRI findings and depressive symptoms. **Conclusion:** By using $^{18}$F FDG PET, we have established a clear correlation between individuals, mostly frontal and temporal regions, depending on diverse structural brain changes and localization of epileptogenic zone, as well as correlation with existence of depressive symptoms. Since there are still some neurobiological uncertainity regarding ethiology of depression commorbidity in persons with epilepsy, and considering the fact that such depression significantly reduces the quality of life for those persons, the results obtained in this study may contribute to early recognition, and consequently to timely choice of optimal treatment of persons with epilepsy.

## OP563

### In-vivo norepinephrine transporter availability in obesity

**S. Hesse**[1,2], G. A. Becker[1], J. Luthardt[1], M. Rullmann[2], F. Zientek[2], P. M. Meyer[1], G. Reissig[2], M. Patt[1], K. Arelin[3], D. Lobsien[4], M. Blüher[5,2], M. Faßhauer[5,2], M. Stumvoll[5,2], Y. S. Ding[6], O. Sabri[1,2]; [1]Dept. of Nuclear Medicine, University of Leipzig, Leipzig, GERMANY, [2]IFB AdiposityDiseases, Leipzig University Medical Centre, Leipzig, GERMANY, [3]Max-Planck-Institute for Human Cognitive and Brain Sciences, Leipzig, GERMANY, [4]Dept. of Neuroradiology, University of Leipzig, Leipzig, GERMANY, [5]Dept. of Internal Medicine, University of Leipzig, Leipzig, GERMANY, [6]Dept. of Radiology and Psychiatry, New York University School of Medicine, New York, NY, UNITED STATES.

**Aim** Central noradrenergic pathways are involved in feeding control, stress and reward system activation, physiological processes altered by obesity. In particular, the norepinephrine transporters (NET), which terminate noradrenergic synaptic transmission, seems to play a key role since they are regulated by insulin, a hormone critical for the regulation of metabolism, and target of feeding-suppressive drugs (e.g. NET inhibitors). Due to the lack of suitable NET radiotracers, in-vivo NET availability has not yet been investigated in obesity. Hence, the Aim of our study was to explore NET availability in heavily obese subjects (BMI>35 kg/m²) compared with healthy normal-weight controls as measured with PET using a NET-selective tracer [$^{11}$C]MRB. Materials and Methods Seven obese subjects (BMI 41±3 kg/m², age 37±8 years, 2 females) and 10 controls (BMI 24±2 kg/m², age 33±8 years, 4 females) underwent dynamic PET (ECAT EXACT HR+) acquisition after IV application of 355±16 and 361±7 MBq [$^{11}$C]MRB, respectively. Standardized uptake value ratios (SUVR) were computed from the time-activity-curves to estimate NET availability in 29 brain regions based on individual PET-MR coregistration and using the occipital cortex as a reference region. To test for biological plausibility, the SUVR were additionally plotted against BIS-11 (Barrett Impulsivity scale), a marker for impulsive behaviour. Results There was no difference of SUVR between obese subjects and age- and gender-matched lean, healthy controls (e.g. in the dorsolateral prefrontal cortex p=0.84 to 0.98; the insula p=0.82 to 0.88; the amygdala p=0.40 to 0.88; the nucleus accumbens p=0.19 to 0.49; the locus coeruleus p=0.78; and the hypothalamus p=0.33 to 0.69). SUVR and BIS-11 total score, however, correlated in some of the investigated brain regions such as the right hippocampus (r=-0.640; p=0.006), the right caudate (r=-0.655, p=0.004), and the hypothalamus (r=-0.492, p=0.045). **Conclusion** These preliminary data do not indicate an overall alteration of central NET availability in obesity. The correlation between the BIS-11 and NET availability, however, point to an involvement of the NET system in impulsive behaviour also in obese subjects; and this can be measured with [$^{11}$C]MRB. Currently, extended neuropsychological testing, pharmacological stress tests, peripheral hormones (leptin, ghrelin, insulin) and joint PET MR data are being included in our analyses to further sub-characterize the phenotype of obesity.

## OP564

### Impulsivity and in-vivo serotonin-transporter availability in obesity

**D. Korth**[1], A. Bresch[2], J. Luthardt[2], M. Rullmann[1], F. Zientek[1], G. Becker[2], M. Patt[2], K. Arelin[3], A. Hilbert[1], C. Schinke[4], M. Blueher[1,5], M. Fasshauer[1,5], M. Stumvoll[1,5], O. Sabri[2], S. Hesse[1,2]; [1]IFB AdiposityDiseases, Leipzig University Medical Center, Leipzig, GERMANY, [2]Department of Nuclear Medicine, University of Leipzig, Leipzig, GERMANY, [3]Max-Planck- Institute for Human Cognitive and Brain Sciences, Leipzig, GERMANY, [4]Department for Neurology, University of Leipzig, Leipzig, GERMANY, [5]Department for Internal Medicine, University of Leipzig, Leipzig, GERMANY.

**Aim** Impulsivity, a predisposition toward uncontrolled behaviour, strongly predicts the risk for externalizing psychiatric conditions; it is prominent in eating disorders and a potential factor for developing obesity. Although central serotonergic mechanisms in the aetiology of impulsive behaviour are discussed, no literature data are available on the linkage between the serotonergic system and impulsivity in obesity. Hence, we Aimed to explore for the first time the association between in-vivo SERT availability in a group of heavily obese subjects (BMI > 35 kg/m$^2$) and lean, healthy controls. **Materials and Methods** Nine obese subjects (body mass index, BMI, 40±6 kg/m$^2$, age 42±12 years, 3 females) and 13 healthy controls (BMI 22±2 kg/m$^2$, age 35±7 years, 4 females) underwent dynamic 3D PET acquisition (ECAT EXACT HR+) after the IV injection of (mean) 485 MBq [$^{11}$C]DASB. From the PET data, parametric image data of the binding potential (BP) were calculated by using MRTM2 (Ichise et al., 2003) and evaluated by regional VOI analysis with two standardized brain atlases (automated anatomical labeling/Hammers) based on an individual MR coregistration. The impulsivity was measured by means of the Barratt Impulsivity Scale, version 11 (BIS-11) including the subscales: attentional (rapid shifts of attention and impatience with complexity), motor (impetuous action), and nonplanning (lack of future orientation) impulsivity. **Results** VOI analysis revealed a significant negative correlation between the BIS-11 total score and BP in distinct brain regions including the limbic system (e.g. BIS-11 total score vs. right amygdala r = -0.45, pn= 0.03; right hippocampus r = -0.60 p = 0.003; left hippocampus r = -0.61, p = 0.002) as well as the frontal and anterior cingulate cortex r = -0.50, p=0.01). On a subscale level, BIS-11 attentional, BIS-11 motor and BIS-11 nonplanning significantly correlated with the BP in the hippocampus or parahippocampal region (e.g. BIS-11 attentional r = -0.56, p = 0.006; BIS-11 motor r = -0.47, p = 0.027; BIS-11 non-planning r = -0.43, p = 0.048). However, BIS-11 total score and the respective subscales did neither differ between obese and non-obese healthy controls nor there was a correlation between BIS-11 and BMI. **Conclusion** These preliminary findings underscore that impulsivity is related to the serotonergic neurotransmission in fronto-limbic areas. Whether such variation also contributes to response inhibition in particular in obese subjects with binge eating and hence to the vulnerability to develop obesity in distinct phenotypes, is currently under investigation.

1409 - Tuesday, Oct. 22, 14:30 - 16:00, Rhône 3A/3B

## Radiopharmaceuticals & Radiochemistry & Dosimetry: Antibodies & Peptides

## OP565

### Novel radioiodinated CXCR4-Ligands with high affinity for human and murine CXCR4 receptors

**M. Schottelius**, F. Hoffmann, U. Keller, S. Hintze, M. Schwaiger, H. Kessler, H. J. Wester; TU Munich, Munich, GERMANY.

Due to its role in a multitude of physiological and pathophysiological processes, such as tumor growth and metastasis, neoangio-/vasculogenesis, tissue remodeling, atherosclerosis, the chemokine receptor CXCR4 attracts considerable interest as a target for radiolabeled CXCR4-imaging probes. Recently, [$^{68}$Ga]CPCR4.2 has been successfully applied for high-contrast PET-imaging of CXCR4 positive tumors in patients. This tracer, however, shows high specificity for human CXCR4 (*h*CXCR4). To enable preclinical studies on CXCR4 function in murine models (*m*CXCR4), species-independent radioiodinated CXCR4-ligands were developed and compared. Phe$^5$-AcTZ14011 (Ac-RRNal-*cyclo*$_{S,S}$(CFCitRkPYRCitC)R-NH$_2$), CPCR4-HG (*cyclo*(ya(HexGua)RNalG)) and the FC131 (cyclo(yRRNalG)) were radioiodinated via the Iodogen-method. For the determination of IC$_{50}$ values, Jurkat (*h*CXCR4$^+$) and EuMyc-1080 (*m*CXCR4$^+$) cells were used with [$^{125}$I]FC131 and [$^{125}$I]CPCR4-HG as radioligands, respectively. Ligand internalization and externalization kinetics were investigated using transiently transfected (*h*CXCR4/*m*CXCR4) CHO-K1 cells. Both in Jurkat and EuMyc1080 cells, CPCR4-HG showed subnanomolar CXCR4-binding affinity: the IC$_{50}$ of CPCR4-HG for *h*CXCR4 was 0.04±0.02 nM (Phe$^5$-AcTZ14011: 5.9±3.0) and 0.76±0.11 nM (Phe$^5$-AcTZ14011: 34.0±6.3 nM) for *m*CXCR4. This more than 40-fold improvement in *m*CXCR4-binding affinity for CPCR4-HG compared to Phe$^5$-AcTZ14011 was confirmed in an inverse competition binding experiment (higher IC$_{50}$ = stronger binding) in EuMyc1080 cells for the respective radioiodinated peptides using Phe$^5$-AcTZ14011 as competitor: here, the IC$_{50}$ of [$^{125}$I]CPCR4-HG was 283 nM vs 7.1 nM for [$^{125}$I]Phe$^5$-AcTZ14011. Interestingly, despite strong differences in *h*CXCR4-binding affinity, both [$^{125}$I]CPCR4-HG and [$^{125}$I]Phe$^5$-AcTZ14011 showed the same internalization efficiency into *h*CXCR4$^+$ CHO-K1 cells (app. 20% of applied dose internalized after 30min at 37°C). In contrast, internalization of [$^{125}$I]CPCR4-HG into *m*CXCR4$^+$ CHO-K1 cells was almost threefold increased compared to [$^{125}$I]Phe$^5$-AcTZ14011 (21 vs 8% of added dose), leading to enhanced cellular retention of [$^{125}$I]CPCR4-HG over 60min due to more efficient ligand recycling (68 vs 46% ([$^{125}$I]Phe$^5$-AcTZ14011) of initial cellular activity). However, when recycling was inhibited (100µM AMD3100) ligand retention was independent of the radioligand and CXCR4-subtype used (10-13% of initial activity). In first in vivo biodistribution studies (60min p.i., Balb/c mice), [$^{125}$I]CPCR4-HG showed moderate (2-4%iD/g) accumulation in lung, spleen, adrenals (*m*CXCR4$^+$) and in kidney (5±0.6%iD/g), but high uptake in liver and intestines (25±6 and 21±4%iD/g). Uptake of [$^{125}$I]Phe$^5$-AcTZ14011 was 2-5fold higher in all organs, indicating a high extent of non-specific binding. Given its excellent binding affinity to both *h*CXCR4 and *m*CXCR4 and its efficient internalization into *h/m*CXCR4$^+$ cells, [$^{125}$I]CPCR4-HG shows distinct advantages over [$^{125}$I]Phe$^5$-AcTZ14011 and represents the first non-species-selective high affinity CXCR4-ligand suitable for investigation of CXCR4-function in vitro and in vivo in a variety of murine models.

## OP566

### Selection of an optimal cysteine-containing peptide-based chelator for labeling of Affibody molecules with $^{188}$Re.

**M. Altai**[1], H. Honarvar[1], H. Wållberg[2], J. Strand[1], Z. Varasteh[3], A. Orlova[3], F. Dunås[4], M. Sandström[5], M. Rosestedt[3], J. Löfblom[6], V. Tolmachev[1], S. Ståhl[7]; [1]Oncology, Radiology and Biomedical Radiation Sciences, Uppsala, SWEDEN, [2]Korliniska institutet, Stockholm, SWEDEN, [3]Preclinical PET Platform, Uppsala, SWEDEN, [4]Affibody AB, Solna, SWEDEN, [5]Akademiska sjukhuset, Uppsala, SWEDEN, [6]Royal Institute of Technology, Stockholm, SWEDEN, [7]Royal Institute of Technology, Uppsala, SWEDEN.

**Introduction:** Affibody molecules are novel class of small (7 kDa) scaffold proteins with good tumor targeting properties and favorable in vivo kinetics. Affibody molecules are readily filtered through the glomerulus and efficiently reabsorbed by the kidney tubular cells. This property hampered development of efficient affibody based radionuclide therapeutic agents. We have found earlier that biodistribution properties(especially renal and hepatic uptake) of recombinant $^{99m}$Tc-labeled Affibody molecules can be optimized by modifying the amino acid composition and position of mercaptoacetyl/cysteine containing peptide based chelators. Rhenium is a chemical analogue of Technetium and translating of the previous findings may result in $^{186/188}$Re labeled Affibody molecule for therapeutic applications is possible.**Methods:** A series of $Z_{HER2:2395}$ derivatives containing, -GGGC ($Z_{HER2:V2}$), -GGSC and -GSGC ($Z_{HER2:V3}$ and $Z_{HER2:V6}$), -GGEC and -GEGC ($Z_{HER2:V4}$ and $Z_{HER2:V7}$), or -

GGKC and -GKGC ($Z_{HER2:V5}$ and $Z_{HER2:V8}$) moieties on C-terminus were labeled with $^{188}$Re and evaluated in vitro and in vivo. $Z_{HER2:2395}$, the parental variant bearing a C-terminal -KVDC sequence was sued as a comparator.**Results:** All 8 variants were efficiently labeled with Rhenium-188 and preserved capacity to bind the receptor. They displayed picomolar affinities to HER2. The biodistribution of all $^{188}$Re-labeled Affibody molecules was in general comparable, with the main difference found in uptake and retention of radioactivity in excretory organs. All variants were highly stable with the low levels of stomach and salivary gland uptake indicating no in vivo reoxidation of Rhenium-188. The lysine containing variants $Z_{HER2:2395}$ (-KVDC), $Z_{HER2:V5}$ (-GGKC) and $Z_{HER2:V8}$ (-GKGC) showed 2-10 fold higher liver uptake in comparison with the remaining 5 variants at 4 h p.i. The renal retention of radioactivity of $Z_{HER2:2395}$ (172±32%IA/g), $Z_{HER2:V5}$(152±24%IA/g) and $Z_{HER2:V8}$ (136±23%IA/g) was also high. Interestingly, changing the position of a single amino acid in the chelator in $Z_{HER2:V6}$ vs. $Z_{HER2:V3}$ and $Z_{HER2:V7}$ vs. $Z_{HER2:V4}$ resulted in an appreciable difference in radioactivity retained both in liver and kidneys. The best variant, $^{188}$Re-$Z_{HER2:V2}$, with the C-terminal chelating sequence -GGGC, provided the lowest radioactivity retention in all organs including the kidneys (3.1±0.5%IA/g 4 h p.i.). Comparative γ-camera imaging of $Z_{HER2:2395}$, $Z_{HER2:V2}$ and $Z_{HER2:V4}$ performed at 4 h p.i. confirmed the biodistribution results. **Conclusion:** These results suggest that $^{188}$Re-$Z_{HER2:V2}$ is a promising candidate for further development as a scaffold-based therapeutic radiolabeled conjugate against HER2 expressing tumors.

## OP567

### Imaging of PDGFRbeta expression in vivo using Affibody molecule 111In-DOTA-Z09591.

**V. Tolmachev**[1], Z. Varasteh[1], H. Honarvar[1], S. J. Hosseinimehr[1,2], O. Eriksson[1], P. Jonasson[3], F. Y. Frejd[1,3], L. Abrahmsen[4], A. Orlova[1]; [1]Uppsala Univesity, Uppsala, SWEDEN, [2]Mazandaran University of Medical Sciences, Sari, IRAN, ISLAMIC REPUBLIC OF, [3]Affibody AB, Stockholm, SWEDEN, [4]Algeta ASA, Oslo, NORWAY.

A receptor tyrosine kinase, platelet derived growth factor receptor beta (PDGFRbeta) is often overexpressed in cancers, atherosclerosis, and in a variety of fibrotic diseases. In vivo visualization of PDGFRbeta-expression using radionuclide molecular imaging might help to stratify patients for a PDGFRbeta-targeting treatment for these diseases. Affibody molecules are small (7 kDa) scaffold proteins that can be selected to bind with high affinity to different proteinaceous targets. Affibody molecules with subnanomolar affinity to PDGFRbeta have been selected earlier. The goal of this study was to evaluate the feasibility of in vivo radionuclide imaging of PDGFRbeta-expression using a specific Affibody molecule. **Methods**. The PDGFRbeta-binding Z09591 Affibody molecule was site-specifically conjugated at C-terminus with a maleimido derivative of DOTA and labeled with 111In. Targeting of PDGFRbeta-expressing U-87 MG glioblastoma cell line using 111In-DOTA-Z09591 was evaluated in vitro and in vivo. In vivo receptor saturation experiment was performed to demonstrate that targeting xenografts in mice was PDGFRβ-specific. Imaging of U-87 MG-bearing mice was performed microSPECT/CT to confirm capacity of 111In-DOTA-Z09591 to visualize PDGFRbeta-expressing tumors. **Results**. DOTA-Z09591 was stably labeled with 111In with a yield of 99.3±0.6% (specific radioactivity up to 14 GBq/μmol). The dissociation constant for 111In-DOTA-Z09591 binding to U-87 MG cells was determined to be 84 pM. The cell line expressed 32000 binding sited per cell in vitro. In mice bearing U-87 MG xenografts, 111In-DOTA-Z09591 showed specific (saturable) tumor uptake. An optimal injection dose was 0.13 nmol per mouse. At this dose, the tumor uptake of 111In-DOTA-Z09591 was 5.7±0.6, 5.9±1.7, and 4.0±0.8 %ID/g at 1, 2 and 4 h after injection, respectively. The tumor-to-blood ratio was 11 ±1, 17±3 and 21±6 at these time points. In vivo receptor saturation experiments demonstrated that targeting of U-87 MG xenografts in mice was PDGFRbeta-specific. U-87 MG xenografts were clearly visualized using microSPECT/CT at 3 h after injection. **Conclusions**. This study demonstrated the feasibility of in vivo visualization of PDGFRbeta-expressing xenografts using an Affibody molecule. Further development of radiolabeled Affibody molecules might provide a useful clinical imaging tracer for PDGFRβ-expression visualization during various pathological conditions.

## OP568

### Personalized imaging of cancer via evaluation of functional biomarker expression

**T. Buckle**, J. Kuil, S. Poort, N. S. van den Berg, A. Bunschoten, F. W. B. van Leeuwen; LUMC, Leiden, NETHERLANDS.

**Aim** The inability to accurately distinguish aggressive cancerous lesions from early stage tumor or normal tissue is limiting for the therapeutic follow up of cancer patients. Evaluation of biomarker expression levels in biopsy tissue prior to targeted diagnostic imaging could increase the feasibility of a targeted imaging approach. Here functional factors such as the localization and level of (membrane) expression play a crucial role in the feasibility of in vivo biomarker targeting. We developed a fresh tissue-based assay for characterization and quantification of functional biomarkers in breast and prostate cancer. Hereby, inclusion of multiple biomarkers is instrumental in addressing the heterogeneity in and between lesions. **Material and Methods** Fresh tumor cell suspensions derived from prostate (PC3, DU145 and C4-2B4) and breast (MIN-O and 4T1) tumors served as a model for biopsy tissue. Cell suspensions were incubated with different targeting peptides (e.g. CXCR4 and PSMA) labeled with both a fluorescent dye and a DTPA chelate. Functional biomarker expression was evaluated using flow cytometry. By using fluorescent labels with different excitation and emission spectra biomarkers were evaluated simultaneously. For in vivo detection of tumor lesions, tumor bearing mice were imaged using SPECT/CT. By specifically scoring membranous staining patterns, screening-results could be validated with ex vivo (fluorescence) immunohistochemistry ((F)IHC). **Results** Flow cytometric analysis of functional biomarker expression revealed different functional biomarker expression patterns in individual lesions. Prostate specific PSMA was only seen in C4-2B4 (ratio = 4 compared to unstained cells) while CXCR4 expression was highest in the PC3. Evaluation of functional CXCR4 expression enabled discrimination between CXCR4 positive MIN-O tumors from 4T1 control lesions. The predictive value of biomarker screening was validated in vivo; tumors that were deemed positive for either PSMA or CXCR4, could be visualized with the biomarker specific imaging agent. Uptake of the targeting imaging agent in the tumor was comparable to the difference in expression found with flow cytometry. Both were consistent with an increase of membranous staining for CXCR4 as seen with IHC. **Conclusion** The membranous fraction of the biomarkers, measured with flow cytometry, proved predictive for in vivo targeting (SPECT and fluorescence imaging) using the same (multimodal) imaging agent. The screening approach can thus enables individualized selection of a diagnostic molecular imaging approach.

## OP569

### Influence of macrocyclic chelators on biodistribution and targeting properties of 68Ga-labeled synthetic Affibody molecules. Comparison with 111In-labeled counterparts.

**J. Strand**, H. Honarvar, A. Perols, A. Orlova, R. Kumar, A. Eriksson Karlström, V. Tolmachev; Uppsala University, Uppsala, SWEDEN.

**Aim** Detection of cancer-associated molecular alterations by molecular imaging can help to select an optimal therapy and personalize cancer treatments. Affibody molecules are 7 kDa small scaffold proteins with good tumor targeting properties and rapid kinetics. Labeling of Affibody molecules with positron emitting radionuclide 68Ga may further increase diagnostics accuracy because of the higher sensitivity and quantification accuracy provided by PET. In this study, HER2-targeting synthetic Affibody molecule, ZHER2:S1 was used as a model to obtain information on how chemical nature of radionuclide and chelators can influence the biodistribution profile. The Aim of the study was to compare the biodistribution profile between Affibody molecules labeled with 111In and 68Ga using DOTA, NOTA and NODAGA at N-terminus of ZHER2S:1 and to select the conjugate with the highest tumor-to-organ ratio. **Methods**: DOTA, NOTA and NODAGA were conjugated to N-terminus of synthetic ZHER2:S1 via amide bond. The conjugates were labeled with 68Ga. In vitro binding and internalization assays were performed using HER-expressing SKOV-3 cells. The tumor targeting properties of 111In- and 68Ga-labelled conjugates were compared in mice bearing SKOV-3 xenografts. **Results** All three conjugates were successfully labeled with 68Ga. The purity of conjugates was over 97% after purification using NAP-5 column. The conjugates demonstrated preserved binding specificity to HER2 expressing cells in vitro. Cells studies showed that all 68Ga labeled conjugates were slowly internalized by SKOV3 cells. In mice bearing SKOV3 xenografts, pre-saturation of the receptors in vivo demonstrated specific binding to HER2 receptors. The tumor uptake for 68Ga-DOTA-ZHER2:S1 (17.9±0.7 %IA/g) was significantly higher than for both 68Ga-NODAGA-ZHER2:S1 (16.13±0.67 %IA/g) and 68Ga-NOTA-ZHER2:S1 (13±3%IA/g) at 2h after injection. Further, 68Ga-NODAGA-ZHER2:S1 had the highest tumor-to-blood ratio (60±10) in comparison with both 68Ga-DOTA-ZHER2:S1 (28±4) and 68Ga-NOTA-ZHER2:S1 (42±11). The tumor-to-liver ratio was also higher for 68Ga-NODAGA-ZHER2:S1 (7±2) than the DOTA and NOTA conjugates (5.5±0.6 vs.3.3±0.6) offering the advantage of better visualization of liver metastases. The influence of chelator on the biodistribution and targeting properties was less pronounced for 68Ga than for 111In. MicroPET/CT imaging confirmed that 68Ga-NODAGA-ZHER2:S1 can visualize HER2-expressing xenografts with high contrast. **Conclusion** In conclusion, macrocyclic chelators conjugated at N-terminus have substantial influence on biodistribution of HER2 targeting Affibody molecule labeled with 68Ga.This can be used to enhance imaging contrast of PET imaging using Affibody molecules and improve sensitivity of molecular imaging. The study has demonstrated appreciably difference of chelator influence for 68Ga and 111In.

## OP570

### Different Mechanisms of Kidney Retention of Radiolabeled Minigastrin Analogues and their Potential Metabolites

**P. Kolenc Peitl**[1], M. Kroselj[1], D. Gerrits[2], L. Joosten[2], R. Mansi[3], H. R. Maecke[3], O. C. Boerman[2], P. Laverman[2]; [1]University Medical Centre Ljubljana, LJUBLJANA, SLOVENIA, [2]Radboud University Nijmegen Medical Centre, Nijmegen, NETHERLANDS, [3]University of Freiburg, Freiburg, GERMANY.

**Aim** High kidney retention of minigastrin (MG) analogues hampers their suitability for peptide receptor radionuclide therapy (PRRT) of medullary thyroid carcinoma and other CCK2/gastrin receptor-expressing tumors. Until recently it was assumed that solely the charge of the ligand determines its retention in the kidneys. We demonstrated that also spacer amino acid chirality and corresponding secondary structure determines the kidney retention of MG analogues [1]. In the present study we Aimed to further investigate the influence of secondary structure and charge on kidney retention of stereochemical pairs of MG analogues to get more insight into mechanisms involved in kidney retention of radiopeptides which could help to improve kidney protection in PRRT in the future. **Materials and Methods** MG analogues, DOTA-(L-Glu)6-Ala-Tyr-Gly-Trp-Met-Asp-Phe-NH2 and its D-Glu spacer congener and 6 potential metabolites of each parental peptide, were synthesized on solid phase. The secondary structure of selected pairs of the L- and D- series was determined by circular dichroism (CD) spectroscopy. Biodistribution and SPECT studies of the 111In-labeled peptides were carried out in female BALB/c mice. **Results** CD spectroscopy revealed differences in secondary structure for both MG analogues and for selected pairs of metabolites. Biodistribution and SPECT studies showed large differences in kidney retention between L- and D- analogues and also within each series. Kidney retention of the parental (L-Glu)6-spacer-MG analogue was 116.9 ± 15.2 %ID/g tissue vs. only 6.6 ± 1.0 %ID/g for its D-Glu spacer congener, 1 h p.i.. Deleting Phe at C-terminus - which causes loss of CCK2R binding affinity - lowered kidney retention by 30% in case of L-Glu series and by almost 50% in case of its D-Glu congener. Deleting Asp, at C-terminus, further lowered kidney retention by additional 50% in both series. By repeating the process to the short metabolites DOTA-(L-Glu)6-Ala-COOH the kidney retention drops to 3.5 ± 1,1 %ID/g tissue vs. 1.8 ± 0.6 %ID/g for its D-Glu pair, namely DOTA-(D-Glu)6-Ala-COOH. **Conclusion** There is strong evidence that the intact radiopeptides are retained in the kidneys. Next to well-known megalin-related reabsorption of small radiopetides we observed CCK2-specific receptor uptake in the kidneys. Differences in the kidney retention of stereoisomeric pairs indicate involvement of yet another retention mechanism. Literature 1. Kolenc-Peitl P, Tamma ML, Kroselj M, Behe M, Reubi JC, Maecke HR, et al. Stereochemistry of amino acid spacers determines the pharmacokinetics of 111In-DOTA-minigastrin analogues for targeting of the gastrin receptor. Eur J Nucl Med Mol Imaging. 2012;39:S418.

## OP571

### First Bimodal Fluorinated and Iodinated Prosthetic Group TFIB. Application to the Radiolabelling of Bioactive Compounds

**A. Vidal**, E. Billaud, L. Rbah-Vidal, A. Vincenot, S. Besse, E. Miot-Noirault, J. Chezal, P. Auzeloux; UMR990 INSERM Université d'Auvergne, Clermont-Ferrand, FRANCE.

**Aim:** We developed the first bimodal fluorinated and iodinated prosthetic group tetrafluorophenyl fluoro-iodobenzoate (TFIB) as a suitable acylating agent for labelling of a large variety of compounds (e.g. small organic ligands, peptides, proteins, nanoparticles,…). In this approach, this new compound allowed applications in diagnosis (PET imaging/$^{18}$F) and therapy (Targeted Radionuclide Therapy/$^{131}$I). Herein we present the fully automated three steps two-pots radiosynthesis of [$^{18}$F]TFIB as well as the optimized protocol for radiosynthesis of [$^{125}$I]TFIB. Some examples of bioactive compounds radiolabelling are also given. **Methods:** *Chemistry:* TFIB, ICF15096 (quaternary ammonium for $^{18}$F-radiolabelling) and ICF15098 (perfluorostannane for $^{125}$I and $^{131}$I-radiolabelling) were synthesized in 2 to 4 steps and their structures were confirmed by NMR, IR and MS. *$^{18}$F-Radiolabelling:* Fully automated radiosynthesis of [$^{18}$F]TFIB has been developed on a SynChrom®R&D bi-reactor synthesizer (Raytest). First step was the formation of methyl [$^{18}$F]fluoro-iodobenzoate from methyl (*N,N,N*-trimethylammoniumtriflate)-iodobenzoate precursor. Subsequent alkaline saponification yielded the [$^{18}$F]benzoic acid intermediate purified by C18+ SPE cartridge. This acid was further converted into [$^{18}$F]TFIB by treatment with tetrafluorophenol and DCC with a final purification by semi-preparative RP-HPLC. A final formulation on C18+ SPE cartridge allowed to obtain [$^{18}$F]TFIB ready to react with bioactive compounds. *$^{125}$I-Radiolabelling:* [$^{125}$I]TFIB was produced at high specific activity in one step starting from ICF15098 ([$^{125}$I]NaI, AcOH, iodogen, rt), purified by fluoroflash® F-SPE cartridge and formulated on a C18 SPE cartridge. *Radiolabelling examples: N,N*-diethylethylenediamine has been radiolabelled in one step with [$^{18}$F]TFIB and [$^{125}$I]TFIB and purified by C18 SPE before *in vivo* evaluation. Radiolabelling of peptides NDP-MSH and PRGD2 are currently in progress. **Results:** TFIB, ICF15096 and ICF15098 were synthesized in very few steps, with 54%, 49% and 15% overall yields, respectively. [$^{18}$F]TFIB was produced within 75 min, a decay-corrected yield (RCY) of 27% and a radiochemical purity (RCP)>99%. [$^{125}$I]TFIB was obtained in 60 min with 54% overall RCY and a RCP>99%. *N,N*-diethylethylenediamine was successfully radiolabelled in less than 15 minutes with [$^{18}$F]TFIB and [$^{125}$I]TFIB to afford [$^{18}$F]*N*-[2-(diethylamino)ethyl]-fluoro-iodobenzamide and [$^{125}$I]*N*-[2-(diethylamino)ethyl]-fluoro-iodobenzamide in 80% (decay-corrected) and 92% RCY, respectively. **Conclusion:** [$^{18}$F]TFIB and [$^{125}$I]TFIB were synthesized with excellent RCY and RCP. $^{125}$I-radiosynthesis was optimized and the purification by F-SPE avoided the use of HPLC. $^{18}$F-radiosynthesis was fully automated and provided [$^{18}$F]TFIB in a short time with reproducible yields. We demonstrated that TFIB can be a good bimodal prosthetic group which could be used with a large variety of small organic ligands, peptides, proteins, as well as nanoparticles.

## OP572

### Development and pre-clinical evaluation of a new glucose-dependent insulinotropic polypeptide (GIP) based radioligand for PET imaging of a broad spectrum of neuroendocrine tumors

**E. Gourni**[1], B. Waser[2], R. Tönnesmann[1], V. Gigoux[3], P. Clerc[3], D. Fourmy[3], J. Reubi[2], H. Maecke[1]; [1]University Hospital, Department of Nuclear Medicine, Freiburg, GERMANY, [2]University of Berne, Berne, SWITZERLAND, [3]Institut de la Santé et de la Recherche Médicale, Toulouse, FRANCE.

**Aim:** The overexpression of the glucose-dependent insulinotropic polypeptide (GIP) receptor on many neuroendocrine tumors (NET) is of great importance because it allows the *in vivo* peptide based receptor targeting of the NETs which don't express somatostatin or glucagon-like peptide-1 (GLP-1) receptors. The Aim of this study was to develop and evaluate a new class of radioligands with the potential to be used for the *in vivo* targeting of GIP-receptor positive tumors. **Materials and Methods:** GIP(1-42) was modifed C-terminally and the truncated peptide [Nle$^{14}$, Lys$^{30}$(Ahx-DOTA)]GIP(1-30)NH$_2$ (EG4) was conjugated with Ahx-DOTA via the Lys$^{30}$ side chain. The GIP receptor affinity ($IC_{50}$ value) of EG4 was determined using $^{125}$I-GIP as radioligand and GIP(1-30) as control peptide. EG4 was labeled with $^{111}$In and $^{68}$Ga. *In vitro* evaluation included determination of lipophilicity, Kd and Bmax. Furthermore, internalization - dissociation studies were performed using the glucagonoma cell line INR1G9 transfected with the human-GIP receptor (INR1G9-hGIPR). The *in vivo* evaluation was consisted of biodistribution and PET animal studies in INR1G9-hGIPR tumor bearing mice. **Results:** The GIP receptor affinity of EG4 in human tumors was found to be 1.49 ± 0.72 nmol/L. The labeling yield for $^{111}$In-EG4 was greater than 95% at a specific activity of 7 - 8 GBq/μmol. EG4 was labeled with $^{68}$Ga with a labeling yield greater than 98% and a specific activity ranging between 30 and 40 GBq/μmol. Saturation binding studies revealed a Kd value of 10.12 ± 2.05 nmol/L and Bmax equal to 1.36 ± 0.08 nmol/L. Specific internalization was found in the cell culture with a maximum of 18.3 ± 1.1 % at 6 h. Dissociation studies revealed fast dissociation with approx 60 % dissociated within 10 min. No further dissociation was observed up to 4 h. $^{111}$In-EG4 and $^{68}$Ga-EG4 were shown to target specifically INR1G9-hGIPR xenografts with the tumor uptake 10.36 ± 2.16 and 16.99 ± 4.35 %IA/g, 1h p.i., respectively. Kidneys showed the highest uptake which could be reduced by approximately 40 % by Gelofusine. PET imaging studies were also performed and the images very well represented the data acquired from the biodistribution studies. **Conclusion:** The evaluation of EG4 as a proof-of-principle radioligand indicated feasible imaging of GIPr-positive tumors. The acqiured results prompt us to further continue on the development of this family of radioligands which allow to image a broad spectrum of NETs.

1410 - Tuesday, Oct. 22, 14:30 - 16:00, Tête D'Or 1/2

## Physics & Instrumentation & Data Analysis: Radiation Protection Patient

## OP573

### Information of Stakeholders about the Risk of Nuclear Medicine Patients

**E. De Geest**[1], P. Covens[2], F. Jamar[3]; [1]AV Controlatom, Vilvoorde, BELGIUM, [2]VUB, Brussels, BELGIUM, [3]UCL, Brussels, BELGIUM.

**Introduction** Although nuclear medicine is an established part of the diagnosis and treatment of patients, the perception about the related risk is not always realistic. Neither the minimizing of the risk related to ionizing radiation nor the absolute demonization of radiation, are attitudes that are helping patients. Therefore the Health Counsel of Belgium has taken the initiative to develop information in an objective way and in a day to day language for stakeholders who are professionally involved. **Method** The brochure gives in the Introduction a general overview of the classical radiological risk and emphasizes on the justification of the practice. This part has to be seen as background information for people who like to know more. In the second part, the stakeholders are divided in groups around the patient. The nuclear medicine department in the first shell around the patient, in the second shell you find the referring physician, the treating physician, the ward personnel, the personnel of radiology and the external workers (maintenance, housekeeping,⋯) For every group a leaflet in an adapted vocabulary was made. The leaflets have all the same structure, they exist on their own, they contain practical examples and they try to keep the balance between enough and correct information without the ballast that nobody reads. The first part 'sets the scene' about who is the target group, then nuclear medicine is explained and what are the

ways the target group can be exposed. In the third part the radioprotective measures are described with examples and at the end some extra information is given e.g. reanimation by ward personnel. The referring physicians receive a FAQ leaflet with daily practices and simple demands such as: can I go to the hairdresser, what if I'm pregnant, is there an alternative examination... **Result** The leaflets will be distributed to the management of the hospitals and the stakeholders' professional associations. The nuclear medicine departments are encouraged to use the leaflets as pro-active information to their stakeholders and in case of difficulties with groups that have been disinformed about the risks and/or are not willing to help nuclear medicine patients. An evaluation of the efficiency of the information will be made in a second stage.

## OP574

### Radiation Risks from Nuclear Cardiology Procedures as a Function of Patient Age & Gender

**A. Hughes**; Royal Preston Hospital, Preston, UNITED KINGDOM.

**Aim** Radiation risks from medical exposures are often calculated from the effective dose for the procedure. Effective dose was introduced by ICRP as a tool for evaluating & comparing radiation protection practices and was never intended to be used for estimating radiation risks to individuals from medical exposures. In this study, the radiation risks for patients undergoing nuclear cardiology procedures have been calculated as a function of age & gender of patients. **Method** Three radiopharmaceuticals commonly used in nuclear cardiology were analysed; Tc99m-MIBI, Tc99m-tetrofosmin and Tl201. The simulated activities for a one-day protocol were 250/750MBq stress/rest respectively and 500/500MBq for two-day protocols. The activities assumed for Tl201 were 80MBq (rest-redistribution) and 120MBq (re-injection studies). Organ doses for each radiopharmaceutical were taken from ICRP 80 and used to compute the effective dose/MBq using the methodology outlined in ICRP 103. Cancer risk for each study was then computed by multiplying the effective dose by the ICRP nominal risk coefficient of 5.5% per Sv. Cancer risks as a function of age & gender of adult patients were then calculated from the organ doses & the risk models described in ICRP 103 and the values compared with those predicted by the effective dose. Heritable risks were also computed using the gonad doses and a risk coefficient of 0.5% per Sv. **Results** For all three tracers the cancer risk decreased with age over the range 20-70yr. For tetrofosmin, the risk for males <60yr was greater than that for females. For MIBI the risk was higher to male patients <40yr, while for Tl201 the risk was greater for females at all ages. The cancer risk derived from the effective dose overestimated the risk for all patients >35yr using Tc99m tracers and patients at any age using Tl201. From these data the estimated cancer risk/unit effective dose for a median age of 45yr was 4.4% (M) & 3.7% (F) per Sv for tetrofosmin, 4.1% per Sv (M & F) for MIBI and 2.0% (M) & 2.7% (F) per Sv for Tl201. Heritable risks were greater for females for all three tracers. The heritable risks calculated for Tl201 re-injection studies were 10-15 times higher than those for Tc99m tracers. **Conclusion** Cancer risks for nuclear cardiology studies vary with age and gender and cannot be accurately predicted from the effective dose & the ICRP nominal risk coefficient.

## OP575

### Dose reduction of CT-based attenuation correction in myocardial perfusion CZT-SPECT using iterative CT reconstruction

**J. van Dalen**, J. van Osch, M. Mouden, J. Timmer, J. Ottervanger, S. Reiffers, S. Knollema, P. Jager; Isala, Zwolle, NETHERLANDS.

**Objective**: CT-based attenuation correction (CT-AC) is commonly applied to improve diagnostic accuracy in myocardial perfusion SPECT imaging. Reliable attenuation maps can be obtained corresponding to exposure levels down to 0.4 mSv effective dose, using traditional filtered back projection (FBP) for CT image reconstruction. The Aim of this study was to further reduce radiation dose of CT-AC using iterative CT reconstruction, without degrading image quality of myocardial perfusion SPECT with cadmium-zinc-telluride (CZT) technology. **Methods**: CZT-SPECT/CT imaging was performed of a cardiac phantom filled with Tc-99m to simulate myocardial uptake. Multiple CTs were acquired using different currents and levels of adaptive statistical iterative reconstruction (ASIR). SPECT images were then reconstructed using these different CTs for AC, to derive reliable AC with a minimal dose (CT-$AC_{ASIR}$). Next, both default CT-AC using FBP and CT-$AC_{ASIR}$ were applied to 10 patients who underwent a stress SPECT examination. For each patient two SPECT image sets were obtained and compared using the 17-segment cardiac model. **Results**: The phantom study resulted in CT-$AC_{ASIR}$ using half the radiation exposure of the default CT-AC with 70% ASIR. The patient study showed similar CZT-SPECT image quality using either the default or ASIR-based AC, with minimal variation in segmental myocardial uptake (≤ 4 percent points in 95% of cases). **Conclusion**: A dose reduction of 50% for CT-AC is feasible using iterative CT reconstruction, without impairing myocardial perfusion CZT-SPECT image quality. The corresponding effective dose can be reduced to values below 0.2 mSv.

## OP576

### Patient dose and image quality of a cone-beam CT system for SPECT/CT: comparison with 16 slice CT

C. Vandevoorde[1], D. Vandendriessche[1], Y. D'Asseler[2], B. Lambert[2], I. Goethals[2], **K. Bacher**[1]; [1]Ghent University, Gent, BELGIUM, [2]Ghent University Hospital, Gent, BELGIUM.

**Aim**: Recently, a combination of a low-dose cone-beam CT (CBCT) and a SPECT camera became available. As detailed data on image quality and patient radiation dose linked with this CBCT system is missing, a phantom study was set up to compare the effective dose and corresponding image quality of the CBCT system with a diagnostic 16-slice CT scanner. **Materials and Methods**: An anthropomorphic Rando phantom was filled with 150 calibrated LiF thermoluminescent dosemeters (TLD's) at representative locations for radiosensitive organs as included in the ICRP 103 publication. CT scans of the neck, abdomen and pelvis of the phantom were acquired using clinical protocols of the Brightview XCT CBCT and the Brilliance 16-slice CT systems respectively (both systems: Philips). Scan regions and volumes for the acquisitions at both systems were taken identical. TLD values were converted into organ and effective doses according using the ICRP 103 weighting factors. The image quality was evaluated by acquiring scans of a Catphan 504 phantom (Phantom Laboratories) at a wide range of dose levels. Noise, resolution and low-contrast performance were evaluated. **Results**: For the CBCT system, the measured effective doses were 0.5, 3.2 and 2.5 mSv for the neck, abdomen and pelvis CTs. For the 16-slice CT the corresponding values were 2.0, 11.7 and 8.9 mSv. At the current clinical dose settings, the 16-slice CT system significantly outperformed the CBCT with respect to noise and low-contrast performance. Resolution performance was only better with the CBCT system, using the high-resolution mode. Reducing the CT doses of the 16-slice CT to the dose level of the CBCT system, resulted in similar image quality of both systems. **Conclusion**: The CBCT is operated at significantly lower radiation doses compared to a conventional 16-slice CT system. However, if the image quality level of the CBCT system is considered to be sufficient, the dose levels of the 16-slice CT system could be reduced to approximately the same level as for the CBCT.

## OP577

### Estimation of CT Radiation Doses in SPECT/CT and PET/CT Examinations

**T. Sera**[1], T. Porubszky[2], M. Papos[1], Z. Besenyi[3], A. Bartha[2], R. Elek[2], S. Pellet[2], L. Pavics[1]; [1]University of Szeged, Szeged, HUNGARY, [2]"Frédéric Joliot-Curie" National Research Institute for Radiobiology and Radiohygiene, Budapest, HUNGARY, [3]Euromedic Diagnostics, Szeged, HUNGARY.

The performance characteristics of the SPECT/CT and PET/CT hybrid devices have proved to be superior to those of the standalone SPECT or PET, therefore the use of hybrid devices has become more and more widespread in nuclear medicine. However, the new techniques lead to higher patient doses; in addition to the doses from the radiopharmaceuticals the CT component has to be included too. The Aim of our study was to estimate the CT doses by phantom studies for bone and myocardial SPECT/CT and 18-FDG whole body PET/CT examinations and compare them with overall (nuclear medicine investigation and CT) doses. **Materials and Methods**: The calculation of the CT effective doses was based on the CT Dose Index (CTDIvol) values which were determined on 4 sets of SPECT/CT and 4 sets of PET/CT equipment (manufactured by GE, Siemens, Philips and Mediso), the total number of hybrid devices in our country in 2011. The measurements were performed with cylindrical PMMA body (diameter 32 cm) 15 cm long phantom, with a 10 cm long calibrated pencil ionization chamber (IEC 1999). The CTDIvol values were used for the calculation of Dose Length Product (DLP) values using an average scan length (for cardiac studies 15 cm, for thorax 40 cm and for pelvis 10 cm, respectively). The CT effective doses were then determined from DLP and region specific conversion factors (mSv/mGy-1cm-1) based on the publication: Radiation Protection No 154/2008, EC. For the calculation of the effective doses from radiopharmaceuticals conversion factors (mSv/MBq) were taken from Publication ICRP80. Collective effective doses were calculated for the investigations performed in 2011. **Results**: The collective effective dose (manSv) from SPECT/CT examinations due to the radiopharmaceuticals (labeled with 99m-Tc) for 1186 bone examinations was 5 and for 1100 myocardial examinations 5.92 respectively. The corresponding CT doses were 0.535 and 0.455, respectively. The collective effective dose for 12674 whole body PET/CT examinations from 18-FDG radiopharmaceutical was 91, and from CT 16.9 manSv. **Conclusion**: The CT doses of SPECT/CT examinations for the two most common (bone and myocardial) investigations give a contribution of 10 - 7% of the overall doses, in the case of PET/CT examinations the impact of the CT is even higher, 15.6%, therefore the contribution of the CT component to the overall doses should be taken into consideration.

## OP578

### Optimization of radiation protection by automation: a dosimetric study in PET

**F. Rinaldi**[1], D. Bruel[1], N. Machefert[1], C. Cottet[2], C. Boursot[3], C. Naveau-Ploux[4]; [1]Radiopharmacy, Le Mans Hospital, Le Mans, FRANCE, [2]Radiation

Protection Unit, Le Mans Hospital, Le Mans, FRANCE, [3]Nuclear Medicine, Le Mans Hospital, Le Mans, FRANCE, [4]Pharmacy, Le Mans Hospital, Le Mans, FRANCE.

18 Fluorodeoxyglucose (18FDG) is used in positron emission tomography (PET) at Le Mans hospital since 2005. Radiopharmacy unit is equipped with "Unidose" (Trasis), a fluorinated radiopharmaceuticals dispenser since 2011. A dosimetric study was performed to analyse the influence of the automation of 18FDG preparations on radiation protection of the staff unit. Whole body dosimetry was estimated from operational dosimetries. Balance sheet before and after installation of Trasis was done : before automation, from January 1st, 2010 to February 28th, 2011, on 226 doses and after automation, from March 1st, 2011 to April 30th, 2012, on 264 doses. Extremities dosimetry was given thanks to handling durations and dose rates in contact with the 18FDG. Handling durations were estimated according to the course of the 18FDG (reception, syringe preparation and waste) and according to the course of patient (preparation, injection, installation, examination). The whole body dosimetry was measured to a total of 3725 µSv for the first period and of 2982 µSv for the second period, which represents a 20% reduction of received radiations. The effective dose of whole body for one technician decreased from 16 µSv per day in 2010 to 9 µSv per day in 2012 (43% reduction) which corroborates Trasis data indicating a maximum exposure of 9.317 µSv per day. For extremities dosimetry, received radiations decreased by 38% between the first period (5312 µSv) and the second period (3296 µSv). While the Trasis study estimates the equivalent doses at extremities with 190 µSv for 10 PET scans of 370 MBq, our study evaluated the received amount at 90 µSv by technician for 7 PET scans of 200 MBq, "Time of flight" technology allowing to reduce doses administrated to the patient for a definition of image equivalent to a classical TEP. The annual extrapolation of this amount (3.6 mSv per technician) is consistent with the operational dosimetry of extremities done during the second period. Amounts received after automation are concordant with values announced by the manufacturer. Using Trasis automat allows an exposure to radiations lower than 1 µSv per patient for whole body dosimetry and lower than 20 µSv at the extremities per patient. These values extrapolated over one year represent less than 2% of the maximum exposure authorized to the thorax and the extremities. The radiation protection of medical staff has been optimized by conditioning multidoses of 18FDG.

## OP579

### Study on PET internal dosimetry estimates using different region-of-interest delineation Methods. Analysis of intra- and inter- operator variability

**N. López-Vilanova**[1,2], M. Duch[1], J. Pavía[2,3,4], A. Catafau[4,5], D. Ros[2,4,6], S. Bullich[7]; [1]Institut de Tècniques Energètiques (INTE), Universitat Politècnica de Catalunya (UPC), Barcelona, SPAIN, [2]Centro de Investigación Biomédica en Red en Bioingeniería, Biomateriales y Nanomedicina (CIBER-BBN), Barcelona, SPAIN, [3]Nuclear Medicine Dept., Hospital Clínic i Provincial de Barcelona, Barcelona, SPAIN, [4]Institut d'Investigacions Biomèdiques August Pi i Sunyer (IDIBAPS), Barcelona, SPAIN, [5]Barcelona Imaging Group (BIG), Barcelona, SPAIN, [6]Unitat de Biofísica i Bioenginyeria, Universitat de Barcelona, Barcelona, SPAIN, [7]Molecular Imaging Centre (CRC-CIM), Barcelona Biomedical Research Park, Barcelona, SPAIN.

**Aim***:* Human dosimetry studies play a central role in positron emission tomography (PET) radioligand development. Internal dosimetry estimates are necessary to minimize the associated risks to patients that have been administered a radiopharmaceutical. In order to estimate internal dosimetry, it is necessary to measure the time course of the radioligand in each organ. This is achieved by drawing regions of interest (ROIs) on PET images and quantifying the radiotracer uptake. The present study seeks to evaluate the impact of ROI delineation Methods and intra- and inter-operator variability in the calculation of internal dosimetry estimates. **Methods:** $^{11}$C-GSK931145 PET studies of a Zubal phantom were simulated by using Monte Carlo techniques (SimSET). $^{11}$C-GSK931145 biodistribution simulated high activity in the liver in the case of early scans, and intestinal elimination. The time course of the radioligand was estimated using three ROI delineation Methods varying in complexity and execution time. ROIs were drawn on a) antero-posterior compressed PET images (AP), b) subsamples of the organs (S), and c) a 3D-volume covering the whole-organ (W). Residence times for each organ were calculated from the time course of the radioligand. The OLINDA/EXM software package was used to obtain dosimetry estimates. Inter- and intra-operator variability ROI drawing was evaluated by using human data (n=8 scans). **Results:** Measured time activity curves (TACs) showed a close agreement with the simulated TACs when S and W ROI delineation Methods were used. The percentage difference in effective dose (ED) estimates between S and W Methods was 2%. The ED using AP were 25% and 22% higher than those obtained by using S and W, respectively. S and W Methods showed the lower intra and inter-operator variability in the ED estimates (intra-operator variability: 7.8% (AP), 1.7% (S), 5.5% (W); inter-operator variability: 15.1% (AP), 4.9% (S) and 5.3% (W)). **Conclusions***:* ED estimations are sensitive to the delineation method applied. AP method overestimated doses due to a combination of delineating and overlapping between ROIs. Among the three Methods compared to delineate ROIs, the S method showed the best balance between quantitative accuracy and inter- and intra-operator variability.

## OP580

### Changes in Noise Index: An Effective Manner to Reduce Radiation Exposure in Patients Undergone PET/CT scans

**P. C. Santana**[1], A. P. Mourão[2], P. A. Morais[1], T. A. Silva[3], M. Mamede[1]; [1]Universidade Federal Minas Gerais, BELO HORIZONTE - MG, BRAZIL, [2]Centro Federal Ensino Tecnológico, BELO HORIZONTE - MG, BRAZIL, [3]Centro de Desenvolvimento Tecnologia Nuclear, BELO HORIZONTE - MG, BRAZIL.

**Aim:** The Aim of this study was to determine the best relationship between image quality and dose reduction in computed tomography (CT) by changing the Noise Index (NI) in the . automated tube current modulation (ATCM) technique using a phantom. **Material and Methods:** To assess the radiation level from CT , TLD100 detectors embedded in a male anthropomorphic Alderson® Random phantom were imaged underwent the clinical PET/CT protocol. The CT scanning parameters were: 120kVp; auto mA range, 10-120; time, 0.7 second; pitch 0,984 and reconstruction slice thickness 3.75mm. Three NI (18.5, 22 and 25) values were applied during the acquisition protocol. This investigation was undertaken on PET/CT model GE Discovery 690. In addition, the effective dose from positron emitter (F-18) was estimated using the ICRP106 model. The activity applied was 0.1 mCi/kg in a 70 kg subject for the determination of the effective dose for PET. **Results:** The effective doses from CT were 10.7 mSv, 7.5 mSv and 6.5 mSv using NI 18.5, 22 and 25, respectively. Meanwhile, the effective dose from positron emitter was 5.3 mSv. These measurements resulted in a maximum effective dose reduction of 26%. **Conclusions:** The ATCM is a technique used to reduce overall patient dose by rapidly altering the mA as the gantry rotates around the patient. The mA modulation is determined from the attenuation and shape of scout scan projections of the patient. In order to have good image quality with lower effective dose during PET/CT study, it is important to understand all technical parameters that interfere with imaging acquisition. Thus, the present study showed a preliminary data in a phantom where changes in NI at CT acquisition resulted in significant dose reduction.

1502 — Tuesday, Oct. 22, 16:30 — 18:00, Auditorium Lumière

## Symposium 12: Multimodality Tracers

## OP581

### Exploiting Multimodality for Sentinel Lymph Node Imaging using Bimodal PET-MRI Nanoparticles

**R.T.M. de Rosales, UNITED KINGDOM**

## OP582

### PET-Optical

**G.A.M.S. van Dongen, NETHERLANDS**

## OP583

### Bimodal Imaging Probes

**E. Boros, USA**

1504 - Tuesday, Oct. 22, 16:30 - 18:00, Bellecour 1/2/3

## Featured - Oncology Clinical Science: Lung Tumours

## OP584

### 18 FDG-PET in Lung Tumors - An Old Success Story with New Perspectives

**U. Nestle, GERMANY**

## OP585

### Role of [18F]-FDG-PET-CT in Prediction of Kras and EGFR Molecular Profile in Advanced Non-Small-Cell Lung Cancer Patients

**C. Caicedo**, M. García-Velloso, M. Lozano, C. Vigil Diaz, J. López-Picazo, A. Gúrpide, J. Zulueta, J. Richter Echevarria, M. Rodríguez-Fraile, J. Pérez Gracia; Clínica Universidad de Navarra, Pamplona, SPAIN.

**Aim**: Tumor molecular profile predicts activity of epidermal growth-factor receptor (*EGFR*) inhibitors in non-small cell lung cancer (NSCLC). Besides, KRAS mutation has been described as a factor which induce a lack of activity to that treatment.

However, tissue availability and tumor heterogeneity limit its assessment. We evaluated whether [18F]-fluorodeoxyglucose positron-emission tomography ([18F]-FDG-PET) might help to predict *KRAS* and *EFGR* molecular profile in patients with NSCLC. **Methods**: One hundred and two stage III or IV NSCLC untreated patients who were tested for KRAS and EGFR mutations, and underwent an [18F]-FDG-PET-CT were included in this study. Standardized uptake values (peak SUV [SUVpeak], maximum SUV [SUVmax], and isocontour at 50% of the maximum pixel value [SUVmean]), were calculated in the single hottest tumor lesion using a volume of interest. Their association with *EGFR* and *KRAS* mutation status were assessed. Reciver operator characteristic (ROC) curves and Area Under the Curve (AUC) for each SUV were calculated. A descriptive multivariable model was designed, including age, gender, American Joint Committee on Cancer stage and the SUV with the best AUC value, obtaning a predicted probability of KRAS mutation for each patient. The discriminating ability of this model for predicting the mutation was evaluated through the AUC of the predicted probabilities. Sensitivity and specificity of the model were also evaluated. **Results:** Twenty-eight patients (27%) had *KRAS* mutations (*KRAS+*), 22 (22%) had *EGFR* mutations (*EGFR+*), and 52 (51%) had a wild-type *KRAS* and *EGFR* profile (WT). The *KRAS+* patients presented significantly higher SUVpeak (11.6 vs. 6.8 vs. 8.8, p<0.001), SUVmax (13.8 vs. 8.6 vs. 9.9, p<0.001) and SUVmean (9.5 vs. 5.7 vs. 6.6, p<0.001), compared to *EGFR+* and WT patients. The Bonferroni test for post-hoc multiple comparisons was applied, showing differences depending on the presence or absence of *KRAS* mutation for any of SUV measures. ROC curve analysis yielded an AUC of 0.738 for SUVpeak, 0.725 for SUVmax and 0.740 for SUVmean (p<0.001 for all of them). AUC of the descriptive multivariable model was 0.773, with a sensitivity of 78.6% (CI: 60.5% - 89.8%) and specificity of 62.2% (CI: 50.8% - 72.4%). **Conclusion**:The [18F]-FDG uptake, measured with SUV peak, max and mean, was significantly higher in patients with *KRAS* mutation. In our series, there were no significant differences on SUVs between EGFR+ tumors and wild-type tumors. The descriptive model including SUV, might help to predict KRAS mutation in advanced NSCLC.

## OP586

### FDG-PET during radio-chemotherapy is predictive of outcome at 1 year in non small cell lung cancer patients: a prospective multicentric study (RTEP2)

**P. Vera**[1], S. Mezzani-Saillard[2], A. Edet-Sanson[2], J. F. Ménard[2], R. Modzelewski[2], S. Thureau[2], M. E. Meyer[3], S. Bardet[4], C. Houzard[5], P. Olivier[6], C. Rousseau[7], I. Brenot-Rossi[8], B. Dubray[1], RTEP2 study group; [1]Centre Henri Becquerel, Rouen, FRANCE, [2]Centre Henri Becquerel, ROUEN, FRANCE, [3]CHU Amiens, Amiens, FRANCE, [4]Centre Francois Baclesse, Caen, FRANCE, [5]CHU Lyon, Lyon, FRANCE, [6]CHU Nancy, Nancy, FRANCE, [7]Institut Cancerologie de l'Ouest, Nantes, FRANCE, [8]Centre Paoli Calmette, Marseille, FRANCE.

**Objectives**. Prospective multicentric study to assess the prognostic value of FDG PET/CT during curative-intent (chemo-)radiotherapy in patients with non small cell lung cancer (NSCLC). **Patients and Methods**. Patients with histological proof of invasive localized NSCLC, evaluable tumour (RECIST1.1), and candidate for curative-intent chemo-radiotherapy (CRT) or radiotherapy (RT) were pre-included after written informed consent. Definitive inclusion was conditional to significant FDG uptake before RT (PET1). All included patients had a FDG PET/CT during radiotherapy (PET2, mean dose 43 Gy) and were evaluated by FDG PET/CT at 3 months and 1 year after RT. The main endpoint was overall survival or tumour progression at 1 year. Results. Seventy-seven patients were pre-included, 57 definitively included. Fifty-two patients were evaluable, after 2 consent withdrawals, 2 general condition degradations and 1 early death. Among the evaluable patients, 77% received initial chemotherapy and 73% concomitant chemoradiotherapy. At 1 year, 40 (77%) patients were dead or had tumour progression. No statistically significant association was found between stage (IIIB vs. others), histology (SCC vs. others), induction or concomitant CT, and death/tumour progression at 1 year. The Maximum Standard Uptake Value (SUVmax) at PET2 was the single variable predictive of death or tumour progression at 1 year (odd ratio: 1.97, 95% CI: 1.25 - 3.09, p=0.003) in multivariate analysis. The area under the Receiver Operating Curve (ROC) was 0.85 (95% CI 0.73-0.94, p<10-4). A SUVmax value of 5.3 at PET2 yielded a sensitivity of 70% and a specificity of 92% for predicting tumour progression or death at 1 year**. Conclusion**. This prospective multicentric study demonstrates the prognostic value on disease-free survival of SUVmax assessed during the 5th week of curative intent (chemo-) radiotherapy in NSCLC patients (ClinicalTrials.gov NCT01261598; RTEP2 study).

## OP587

### High FDG uptake areas on pre-radiotherapy PET/CT identifies preferential sites of local recurrence in non small cell lung cancer (NSCLC) patients

**J. Calais**[1,2], S. Thureau[1,3,2], B. Dubray[3,2], R. Modzelewski[1,3,2], I. Gardin[1,3,2], P. Vera[1,2]; [1]Department of Nuclear Medicine, Centre Henri Becquerel, Rouen, FRANCE, [2]QuantIF (Litis EA4108), Centre Henri Becquerel, Rouen, FRANCE, [3]Radiotherapy and Oncology, Centre Henri Becquerel, Rouen, FRANCE.

**Purpose:** Conventionally-dosed radiotherapy (RT) in non-operable stage II-III NSCLC is associated to high rates of local recurrence. The tolerance of the surrounding organs (lung, spinal chord) limits the total RT dose that can be safely administered. The areas with FDG uptake (hotspot) on pre-RT FDG-PET/CT have been reported to identify intra-tumour sites with high risk of relapse after RT [Aerts, Lung Cancer, 2012]. The present study Aimed at confirming earlier reports, opening the way to localized dose increase on selected tumour volumes. **Patients and Methods**: Thirty-three patients with inoperable stage II-III NSCLC, treated with chemo radiation (CTRT) or with RT alone, underwent FDG-PET/CT scans at initial staging, before and during radiotherapy (42 Gy), and during systematic follow-up (3 month and 1 year). All FDG-PET/CT acquisitions were co-registered on the initial scan. The hotspot volumes in the initial tumour (using 90 % and 70% of SUVmax as thresholds) and in the subsequent local recurrence (90 % and 40% SUVmax thresholds), were delineated, pasted on the initial scan and compared. **Results:** Eight patients remained in complete metabolic response at last follow-up (mean follow-up : 23 months, range: 6-55). Twenty-five patients had an intra thoracic local recurrence documented on FDG-PET/CT. In 17 (68%) patients, the hotspot volumes in the initial tumour and in the local recurrence were superimposable. The remaining 8 patients (32%) had recurrences in distant sites, mostly controlateral lymph nodes. **Conclusion**: We confirm that high FDG uptake areas in the initial tumour volume are preferential sites of subsequent local failure after CTRT or RT. We are presently investigating the possibility of selective RT dose-increase targeted to high FDG uptake areas on pre-RT FDG-PET/CT in NSCLC patients.

## OP588

### Effects of respiratory gated positron emission tomography on quantification of lesion volume and FDG uptake in clinical practice

**W. Grootjans**, L. F. de Geus-Oei, A. P. W. Meeuwis, M. Gotthardt, W. J. G. Oyen, E. P. Visser; Radboud University Nijmegen Medical Centre, Nijmegen, NETHERLANDS.

**Aim:** To determine the effects of amplitude-based optimal respiratory gating (ORG) in PET imaging on quantification of lesion volume and FDG uptake in patients with lung tumours. **Materials and Methods**: Whole body FDG-PET imaging was performed in 60 patients with lung tumours using a Siemens Biograph 40 mCT PET/CT scanner. Gated and non-gated bed positions were acquired during free breathing for 6 and 2 minutes, respectively. The respiratory signal was obtained using an Anzai AZ-733 V pressure sensor integrated in an elastic belt placed around the patient's thorax. ORG, as implemented in the Syngo 2011A software of the mCT scanner ("HD·Chest"), was performed on the list-mode data of bed positions covering the thorax and upper abdomen. Images were reconstructed with duty cycles of 20%, 35%, and 50%. Differences in lesion volume between gated and non-gated images, as determined by a 40% $SUV_{max}$ isocontour, and mean FDG uptake of the corresponding volumes ($SUV_{mean}$) were calculated. Furthermore, lesions were grouped according to their anatomical location within the lungs (central, upper-, middle and lower lobes). Statistical analysis was performed using the Wilcoxon signed-rank test for paired variables. Statistical significance was defined for p<0.05 and a Bonferroni correction was performed on statistically significant p-values to correct for multiple testing. **Results:** For lesions in the middle and lower lobes, ORG-images demonstrated a significant increase in $SUV_{mean}$ and concomitant decrease in volume, compared to non-gated images. This increase in $SUV_{mean}$ for duty cycles of 50%, 35%, and 20%, was 16.3±21.1% (p<0.0001), 19.2±25.2% (p<0.0001), and 21.9±25.5% (p<0.0001) respectively. An associated volume decrease of 15.4±27.2% (p=0.02), 16.4±24.4% (p=0.004), and 20.4±23.5% (p=0.0006) was observed. The $SUV_{mean}$ increase for lesions in the upper lobes was 3.3±10.7% (p=0.1), 5.4±11.7% (p=0.05), and 7.5±15.0% (p=0.01), with a concomitant volume decrease of 1.6±16.7% (p=0.6), 5.3±19.1% (p=0.1), 6.7±22.5% (p=0.05). The centrally located lesions demonstrated a $SUV_{mean}$ increase of 3.5±9.0% (p=0.1), 4.8±11.2% (p=0.06), 5.4±9.9% (p=0.07) and volume decrease of 3.7±18.7% (p=0.8), 5.1±18.3% (p=0.4), 5.7±13.7% (p=0.1). **Conclusion**: The effects of ORG on quantification of lesion volume and FDG uptake are typically dependent on anatomical location and the percentage duty cycle used for image reconstruction. Statistically significant effects have been observed for tumours in the upper, middle and lower lobes. The effects on centrally located tumours are not significant. Our data suggest that ORG could influence clinical PET imaging with respect to response monitoring, radiotherapy planning and small lesion detection. This should be addressed in clinical studies.

## OP589

### Comparative assessment of Different Tumor Delineation Methods and Derived Indices for Early Metabolic Response Monitoring in Locally Advanced Non-Small Cell Lung Cancer

E. A. Usmanij[1], O. C. J. Schuurbiers[2], E. G. C. Troost[3], L. Peters-Bax[4], E. H. F. M. van der Heijden[2], E. Visser[1], J. H. A. M. Kaanders[5], W. J. G. Oyen[1], J.

Bussink[5], **L. de Geus-Oei**[1]; [1]Department of Nuclear Medicine, Radboud University Medical Centre Nijmegen, Nijmegen, NETHERLANDS, [2]Department of Pulmonary Diseases, Radboud University Medical Centre Nijmegen, Nijmegen, NETHERLANDS, [3]Department of Radiation Oncology (MAASTRO), GROW School for Oncology and Developmental Biology, Maastricht University Medical Centre, Maastricht, NETHERLANDS, [4]Department of Radiology, Radboud University Medical Centre Nijmegen, Nijmegen, NETHERLANDS, [5]Department of Radiation Oncology, Radboud University Medical Centre Nijmegen, Nijmegen, NETHERLANDS.

The Aim of this prospective study was to find the most optimal tumor delineation method in combination with the most appropriate derived indices to be used for early metabolic response prediction during chemo-radiotherapy in patients with locally advanced non-small cell lung cancer (NSCLC). **Methods**: In twenty-eight patients with NSCLC, 18F-FDG-PET was performed pre-treatment, at the end of the second week of treatment, two weeks and three months after completion of treatment. Different delineation Methods for metabolic tumor volume segmentation were used: a background-subtracted relative-threshold level (RTL) method, a method based on signal-to-background ratio (SBR), a gradient based watershed and hierarchal clustering method, a method using a 50% threshold level of the maximum signal intensity and a fixed SUV threshold level of 2.5 g/cm3. Different PET indices were calculated: standardized uptake value (SUV), maximum SUV (SUVmax), metabolic tumor volume (MTV) and total lesion glycolysis (TLG). TLG was calculated as a summation of both primary tumor and metastatic lymph nodes. Progression free survival was used as the primary outcome measure. Cox proportional hazards regression analysis and Kaplan-Meier estimations were performed. **Results:** Different metabolic tumor volume segmentation techniques led to substantially different metabolic volume measurements. In-treatment decrease in SUV, SUVmax or MTV, however, was not associated with clinical outcome for any of the delineation techniques, whereas baseline TLG, in-treatment TLG and decrease in TLG (ΔTLG) were predictive for clinical outcome. TLG was calculated using a 50% threshold level delineation method: decrease in TLG ≥ 38% was associated with increased progression free survival (PFS); (1-y PFS 80% vs. 38% and 2-y PFS 33% vs 0%; P = 0.02). Furthermore, three risk groups were identified; favourable prognosis (baseline TLG < 500 and ≥ 38% decrease in ΔTLG), intermediate risk (baseline TLG < 500 or ≥ 38% decrease in ΔTLG) and unfavourable risk (baseline TLG ≥ 500 and < 38% decrease in ΔTLG). Median survival in months in the favourable risk group was 17.1 months (range 4.8 - 34.0 months), in the intermediate risk group 11.8 months (range 3.3 - 31.7) and in the unfavourable risk group 2.3 months (range 2.1 - 4.5); (log rank test; P < 0.02). **Conclusion**: Change in TLG measured early during concomitant treatment using 18F-FDG-PET is predictive of PFS in NSCLC patients; TLG calculation using a 50% threshold delineation technique was found best method for early metabolic response monitoring.

## OP590

### 18F-FLT PET/CT for Detection of Functional Cross-talk between MET and EGFR in Non-small Cell Lung Cancer Resistant to EGFR Inhibitors

F. Iommelli[1], V. De Rosa[1], S. Gargiulo[1], M. Panico[1], M. Monti[2], G. Ortosecco[1], A. Greco[2], M. Gramanzini[1], R. Fonti[1], A. Brunetti[2], **S. Del Vecchio**[2]; [1]Institute of Biostructures and Bioimages, National Research Council, Naples, ITALY, [2]Department of Advanced Biomedical Sciences, University, Naples, ITALY.

Targeting epidermal growth factor receptor (EGFR) with tyrosine kinase inhibitors (TKIs) is one of the most promising treatment strategies in patients with advanced non-small cell lung cancer (NSCLC). Despite the initial response, most tumors may become resistant to EGFR TKIs for different molecular mechanisms including MET amplification. A high copy number of MET is reported indeed to cause EGFR TKI resistance through HER3-dependent activation of EGFR signaling pathway. Here we tested whether 18F-FLT PET/CT is able to detect the functional cross-talk between MET and EGFR signaling pathways in NSCLC and to monitor the effects of treatment with MET inhibitors. **Methods**: NSCLC cell lines H1993 and H820 with a high and low level of MET amplification, respectively, and HCC827 expressing MET but without oncogene amplification were selected and tested for the effects of MET inhibitors on EGFR pathway and proliferation both in vitro and in vivo. The sensitivity of cells to MET inhibitors and EGFR TKIs was preliminarily tested and levels of total and phosphorylated forms of HER3, EGFR, MET, AKT and ERK1/2 as well as cyclin D1 were analyzed in untreated and treated cells. Nude mice bearing NSCLCs with and without MET amplification were injected with 7.4 MBq of 18F-FLT and subjected to PET/CT before and after treatment with MET inhibitor or EGFR TKI (50 mg/Kg p.o. for 3 days). Untreated and treated tumors were then removed and subjected to Ki67 immunostaining. **Results**: H1993 cells showed a high responsiveness to MET inhibitor and were resistant to EGFR TKIs. Conversely, HCC827 cells showed a high sensitivity to EGFR TKIs and were resistant to MET inhibitor. Accordingly, EGFR pathway was blocked by MET inhibitor in H1993 cells whereas it remained unchanged in HCC827 cells. In agreement with in vitro findings, a strong reduction of 18F-FLT uptake was observed in tumors bearing MET amplification in response to treatment with MET inhibitor whereas no post-therapy changes of 18F-FLT uptake was observed in lung tumors lacking MET amplification. Furthermore a persistently high 18F-FLT uptake was observed in tumors bearing MET amplification after treatment with EGFR TKIs. Imaging findings were confirmed by Ki67 immunostaining of tumor sections. **Conclusion**: 18F-FLT PET/CT is able to detect the functional cross-talk between MET and EGFR causing resistance to EGFR TKIs and to monitor the reversal of such resistance by MET inhibitors.

1505 - Tuesday, Oct. 22, 16:30 - 18:00, Auditorium Pasteur

## Cardiovascular: Myocardial Perfusion SPECT I

## OP591

### Comparison of Incremental Prognostic Value of Gated and Non-Gated SPECT Myocardial Perfusion Imaging: Does Gating Matters?

**M. u. Zaman**[1,2], N. Fatima[3,4], M. Ishaq[5], Z. Rasheed[2], D. Baloch[2]; [1]AKUH, Karachi, PAKISTAN, [2]Karachi Institute of Heart Disease (KIHD), Karachi, PAKISTAN, [3]Dr Ziauddin Medical University, Karachi, PAKISTAN, [4]Karachi Institute of Heart Diseases (KIHD), Karachi, PAKISTAN, [5]Karachi Institutev of Heart Disease (KIHD), Karachi, PAKISTAN.

**Objectives:** Gated Single photon emission computerized tomography (SPECT) myocardial perfusion imaging (MPI) has better diagnostic accuracy than non-gated SECT MPI. The objective of this study was to evaluate prognostic strength of gated and non-gated SPECT MPI in same patients' population. **Material and Methods:** This was a prospective study conducted at Nuclear Cardiology Department of Karachi Institute of Heart Diseases (KIHD), Karachi from March 2009 till January 2011. We recruited 452 consecutive patients (mean age of 57 ± 12 years; male: female ratio of 280: 172) who were referred for stress (exercise or dipyridamole) SPECT scan for evaluation of known or suspected CAD. Stress SPECT MPI was acquired in gated and non-gated modes while resting SPECT were acquired only in non-gated mode in all patients. Patients were followed up for a period of 18-24 months regarding major adverse cardiac events (MACE). **Result:** For gated and non-gated MPI, SSS of 0, 1-3 and 4-8 were seen in 150 (33%): 80 (18%), 130 (29%) : 165 (37%) and 90 (20%) : 87(19%) respectively (significant p values). While a non-significant SSS >8 was found in 82 (18%) : 87 (19%) for gated and non-gated MPI. During 18-24 months follow-up, no MACE was observed for SSS 0 in both sets of studies while significantly higher event rate was noted for GMPI than NGMPI group [ 5(3.80%) Vs 1 (0.60%)] for SSS 1-3. For SSS 4-8 and >8, non-significant but higher event rates were seen in both sets of studies [ 7(7.70%) Vs 8 (6.60%) and 8(9.80%) Vs 11 (12.60%) respectively]. Kaplan Meier survival plot for fatal MI in combination with left ventricular function (LVEF) showed significantly lower event free survival for GMPI than NGMPI studies (Log Rank = 4.68, p <0.05). Kaplan Meier survival plot for non-fatal MI in combination with left ventricular function showed lower but non-significant event free survival for GMPI than NGMPI studies (Log Rank = 2.799, p <0.094). **Conclusions:** We conclude that gating adds better incremental prognostic value to SPECT MPI and SSS 0 has high NPV for both GMPI and NGMPI. SSS 1-3 for GMPI has better diagnostic accuracy than NGMPI but for SSS ≥4 the event rates are similar. LVEF estimated by GMPI with higher SSS is a predictor of fatal MI than non-fatal MI.

## OP592

### Could Administered Activity for Myocardial Perfusion Scintigraphy be Reduced in Obese Patients?

**C. Kullberg**[1], M. Hansson[1], F. Hedeer[1], J. Jögi[1], H. Engblom[1], C. Hindorf[2], J. Oddstig[2]; [1]Department of Clinical Physiology and Nuclear Medicine, Skåne University Hospital Lund, SWEDEN, [2]Department of Radiation Physics, Skåne University Hospital Lund, SWEDEN.

**Aim** Obesity is a worldwide problem which also affects diagnostic performance of nuclear medicine examinations. A large body size means that a higher proportion of the photons is attenuated within the patient and this must be compensated for in order to have a sufficient number of counts in the image. Traditionally, this has been performed either by prolonged acquisition time or by the administration of a proportionally higher activity. The Aim of this study was to evluate the number of counts in myocardial perfusion images for obese patients in relation to non-obese patients in order to enable a decresase of the administered activity in patients with high body weight with a preserved number of counts in the image. **Material and Methods** Ninety-two (92) patients with a body weight >100 kg (range 100-156kg) and 75 patients with a body weight <100kg (mean 78kg) were included in the study. Patients with a body weight ≤110kg received 2.5MBq/kg body weight, whilst patients >110kg received a fixed activity (111-120 kg: 430MBq; >120kg: 570MBq) according to clinical routine. The SPECT acquisition was performed with a conventional gamma camera (scan time 12 minutes) or a solid-state gamma camera (scan time 8 minutes). The total number of counts was acquired from the DICOM information. In order to simulate reduced activity, the total number of counts in the images for patients with body weight >110kg was re-calculated to

correspond to the number of counts if an activity of 2.5MBq/kg body weight was administered assuming a linear relationship between administered activity and number of counts. **Result** The number of counts in the images was constant for patients with a body weight less than approximately 110kg (administered activity 2.5MBq/kg). The total number of counts in the images for patients >110kg increased up to 130% when the fixed activity administration schedule was applied. The re-calculation of number of counts to correspond to an administered activity of 2.5MBq/kg resulted in the same level of counts as for the <100 kg group. A patient with a body weight of 120kg would receive 30% lower administered activity (and absorbed dose) with the new administration schedule (2.5MBq/kg, 300MBq) compared to the old (430MBq) for the stress examination. **Conclusion** The results show that the administered activity can be significantly reduced in obese patients by applying a administration schedule based on a linear increase of activity (2.5MBq/kg) without loss of counts due to attenuation.

## OP593

### Preliminary report of randomized clinical trial for assessment of the short term Folate therapy on transient ischemic dilatation in myocardial perfusion scan of diabetic patients

A. Emami Ardekani[1], M. Abousaidi[1], S. Abdollahi[1], A. Esteghamati[2], B. Fallahi[1], M. Abbasi[3], D. Beiki[1], A. Fard-Esfahani[1], **M. Eftekhari**[1], S. Farzanefar[3]; [1]Research Center for Nuclear Medicine, Tehran University of Medical Sciences, Tehran, Iran, ISLAMIC REPUBLIC OF, [2]Endocrinology and Metabolism Research Center (EMRC), Vali-Asr Hospital, School of Medicine, Tehran University of Medical Sciences, Tehran, Iran, Tehran, Iran, ISLAMIC REPUBLIC OF, [3]Nuclear Medicine Department, Vali-asr Hospital, Tehran University of Medical Sciences,, Tehran, Iran, ISLAMIC REPUBLIC OF.

Endovascular dysfunction (ED) is one of the risk factors in coronary artery disease which directly or indirectly causes ischemic heart disease. There are speculations indicating beneficial effects of folate supplementation to improve ED. Transient ischemic dilation (TID) is one of the presentations of endovascular dysfunction and coronary artery disease in myocardial perfusion imaging (MPI). We intended to study the therapeutic effect of folate therapy on ED employing TID in randomized clinical trial. **Method:** 40 diabetic patients were recruited without history or symptoms of coronary artery disease (CAD). They underwent MPI SPECT (20 mCi Tc-99m MIBI) employing two head gamma camera with two days stress (dipyridamole 0.56 mg/kg/4 min) and rest protocol. The patients received 5 mg folate daily (group A) or placebo tablets (group B) for about 1 month when the MPI SPECT was repeated with the same radionuclide and protocol. TID was determined as an output of the QPS semi-quantification. **Results:** Till now 37 diabetic patients (20 females, 17 males) aged 52.7±6.8, were referred to our center and underwent primary and secondary MPI, 19 patients in group A and 18 in group B. TID decreased in group A from 1.00±0.08 to 0.96±0.09 in contrast to the increase of these values for the group B (0.95±0.13 to 1.02±0.16). General linear analysis indicated significant different change in the TID values between the therapy and placebo groups (age and sex adjusted; F=10.4 and p=0.004). **Conclusion:** The endovascular dysfunction of the diabetic patients may be reversed by folate supplementation therapy. This supplementation could be considered of potential value in treatment of these patients. Key words: endothelial dysfunction; folic acid; transient ischemic dilation.

## OP594

### Warranty Period of Normal Stress Myocardial Perfusion Imaging in Diabetic and Non-diabetic Patients: a Propensity Score Analysis

**E. Zampella**[1], W. Acampa[2], M. Petretta[1], S. Daniele[2], R. Assante[1], M. Plaitano[1], V. Cantoni[2], A. Cuocolo[1]; [1]University of Naples - Federico II, Napoli, ITALY, [2]National Council of Research, Napoli, ITALY.

**Aim**: Stress myocardial perfusion single-photon emission computed tomography (MPS) variables are robust estimators of prognosis. In diabetic patients a normal MPS seems to be less reassuring than in non-diabetic subjects. However, potential confounding may affect the results reported in previous studies. We sought to evaluate the relationship between diabetes and the temporal characteristics of cardiac risk in a cohort of diabetic and non-diabetic patients with normal myocardial perfusion using a propensity score analysis approach. **Material and Methods:** The study population consisted of 828 consecutive patients with known or suspected coronary artery disease (CAD) that underwent stress MPS and had normal myocardial perfusion (summed stress score <3). Of these patients, 402 (48%) had a history of type-2 diabetes. To account for differences in baseline characteristics between diabetics and non-diabetics we created a propensity-matched cohort considering the following clinical variables: age, sex, hypertension, hypercholesterolemia, family history of CAD, smoke, and history of CAD. After propensity score matching, baseline clinical characteristics were comparable in 260 diabetic and 260 non-diabetic subjects. Cardiac events were CAD death and nonfatal myocardial infarction (MI) whichever occurred first. All patients were followed for at least one year (mean 58±17 months). **Results**: During follow-up, the cumulative event rate was 6.9% in diabetic and 2.3% in non-diabetic patients (P<0.05). At multivariable Cox analysis, diabetes (hazard ratio 3.7, 95% confidence interval 1.5-9.1, P<0.005) and abnormal (<45%) post-stress left ventricular (LV) ejection fraction (EF) (hazard ratio 3.6, 95% confidence interval 1.5-8.5, P<0.01) resulted independent predictors of events. For parametric (Weibull) analysis, the survival model included diabetes and post-stress LVEF (chi-square 12.8, P<0.001). Patients with diabetes had a higher probability of CAD death or nonfatal MI accelerating over time as compared to those without diabetes. The highest probability of CAD death or nonfatal MI and the major risk acceleration was observed in patients with diabetes and abnormal post-stress LVEF. In these patients, the time to achieve a defined cardiac risk level (>2%) was <12 months. Conversely, in patients without diabetes and with normal post-stress LVEF the time to achieve >2% risk of events was >60 months. **Conclusion:** From our data, it emerged that the warranty period of a normal stress MPS is lower in diabetic patients compared to non-diabetic subjects also after balancing baseline clinical characteristics in a propensity score-matched cohort analysis. In particular, the poorest outcome was observed in diabetic patients with normal myocardial perfusion and reduced post-stress LVEF.

## OP595

### Phase Gated SPECT in LBBB Heart Failure

H. Pena[1], **G. Cantinho**[1], A. Veiga[2], F. Godinho[1]; [1]Atomedical & IMN-FML, Lisboa, PORTUGAL, [2]S. Cardiologia - H. Santa Maria, Lisboa, PORTUGAL.

**Aim** Phase analysis applied to gated SPECT myocardial perfusion studies (GMPS) allows determining the regional onset timing evaluation of mechanical left ventricular contraction. This method (E. Garcia) uses 5 indices in its normal database, four of which are consistently abnormal in LBBB patients without heart failure (HF). In our study, we pretend to evaluate how powerful these indices are to discriminate LBBB patients with and without HF, allowing a more accurate selection of potential candidates for cardiac resynchronization therapy (CRT). **Material & Methods** G1: 21 men (65±10 y/o) (G1m) and 11 women (67±11 y/o) (G1w) with LVEF≤35%, EDV≥130 ml, QRS≥120ms and no CAD. G2: 36 men (65±10 y/o) (G2m) and 66 women (67±11 y/o) (G2w) with LVEF>35%, EDV<130 ml, QRS≥120ms and no CAD. All were submitted to GMPS rest and gated stress with 20 mCi 99mTc-Tetrofosmin, reconstructed iteratively by WBR Xpress3. Germano's QGS and QPS were used to quantify LV function and perfusion. E. Garcia's Phase Analysis was used to evaluate LV desynchrony with determination of peak phase (PP), phase standard deviation (SD), as well as histogram bandwidth (HB), skewness (HS) and kurtosis (HK).. We calculated the mean and its standard deviation and applied unpaired student t test for G1 and G2 subgroups comparison. These parameters were also correlated with QRS duration, LVEF and volumes. We used 1 and 2 SD from the normal mean database values to determine the percentage of patients outside that range. **Results** In the phase histogram, 4 of the 5 indices were consistently abnormal (p<0.01). All the HF patients had SD and HB above normal range and 95% showed low HS (even with 2SD), while the same doesn't happen for G2. LV functional parameters (LVEF, EDV and ESV) were statistically different (p<0.005) We found no statistically significant differences in age, heart rate or QRS duration. There were no significant differences between sexes, except for the functional parameters in dilated LVs (G2). **Conclusions** GMPS phase analysis of in HF seems to be a useful/feasible method to evaluate LV dyssynchrony. HB, phase SD and HS are the most consistently and greater abnormal variables, depicting a greater dyssynchrony (independently of LVEF or QRS duration), as a potential independent discriminative parameter. The lower number of patients with low HK (2SD) is yet to be explained.These 4 GMPS phase analysis parameters may therefore play a potential adjuvant role in the future to select HF patients for CRT.

## OP596

### The relevance of adenosine induced ST-segment depression during myocardial perfusion imaging in different risk category patients for coronary artery disease.

**J. R. Mohan**, M. L. Abrar, S. Arun, S. Ashwani, B. Anish, B. R. Mittal; Postgraduate Institute of Medical Education & Research, PGIMER, Chandigarh, INDIA.

**Aim**: The Aim of this study was to evaluate the relevance of adenosine induced ST-segment depression during myocardial perfusion imaging (MPI) in different risk category patients for coronary artery disease (CAD). **Materials and Methods**: We reviewed retrospectively 145 patients who had undergone adenosine stress MPI. Patients with baseline ECG abnormalities, history of coronary artery bypass graft surgery or myocardial infarction (MI) were not included. Patients were stratified into different risk categories for CAD based on Diamond-Forrester clinical risk score. All patients were administered adenosine at a rate of 140 mcg/kg/min for a total of 6 min and 99m Tc-Tetrofosmin was injected at 3 min into the protocol. The ECG changes were interpreted as positive for ischemia in the presence of ≥1mm horizontal or down-sloping ST-segment depression during adenosine stress testing. The SPECT perfusion analysis was performed by experienced nuclear physician.

**Results**: Of the 145 patients (76 males, 69 females, mean age of 60.6 yrs), 60 had evidence of ischemia on MPI, 24 of them accompanied with ischemic ECG changes. 18 patients had ischemic ECG changes with normal MPI. Of the 28 high risk category patients, 10 had both ischemic ECG changes and perfusion defects on MPI, 2 had only ischemic ECG changes and 6 had only perfusion defects on MPI. The sensitivity and specificity of stress ECG changes in predicting ischemia on perfusion in these patients were 63% and 83% respectively, with a positive predictive value (PPV) of 83% and a negative predictive value (NPV) of 63%. Of the 117 intermediate and low risk category patients, 14 had both ischemic ECG changes and perfusion defects on MPI, 16 had only ischemic ECG changes and 30 had only perfusion defects on MPI. The sensitivity and specificity of stress ECG in predicting ischemia on MPI in these patients were 32% and 78% respectively, with PPV of 47% and a NPV of 65%. There was a significant difference in the PPV of stress ECG changes in predicting ischemia on MPI between high and combined intermediate & low risk groups (p<0.03) **Conclusion**: In patients with high risk of CAD, ischemic ECG changes during adenosine stress are specific for ischemia on MPI, whereas in patients with low-intermediate risk of CAD the ability of stress ECG changes in predicting ischemia on perfusion is not significantly specific. Hence ECG changes during adenosine stress MPI must be interpreted with caution.

## OP597

### Gated SPECT Indicators of the Focal Inflammation of the Myocardium in Patients with Dilated Cardiomyopathy before Heart Transplantation. Comparison with Explanted Hearts Histology

E. Ostroumov[1], **E. Kotina**[2], V. Ploskikh[2], I. Ilyinsky[1], N. Mozheiko[1], R. Voilokova[1], M. Naumova[1], I. Muminov[1], V. Zakharevich[1], R. Saitgareev[1], D. Shumakov[1]; [1]Academician V.I. Shumakov Federal Research Center of Transplantology and Artificial Organs, Moscow, RUSSIAN FEDERATION, [2]Saint-Petersburg State University, Saint-Petersburg, RUSSIAN FEDERATION.

**Aim**. To clarify the differentiation of focal myocardial inflammation from other forms of DCM, we compared the results of gated SPECT performed before transplantation with histological examination of the hearts explanted during transplantation. **Materials and Methods**. 54 explants have been investigated. Histological criteria were based on the inflammatory lymphocytic infiltration associated with myocyte injury in the absence of ischemia (DCMP+Inf). Histological samples were taken and compared with the results of gated SPECT topographically on 3 sides of left ventricular: anterior, posterior and septum. Criteria of gated SPECT were foci of regional topographic coincidence of the segmental akinesia (wall motion), of the pathological asynchrony (phase) and the maximum, and/or normal end diastolic LV myocardial perfusion (bull's eye). Gated SPECT criteria were selected as the specific for inflammation. **Results.** According to the histological characteristics: dilated cardiomyopathy (DCMP) - 13 patients (p-ts); the development of dilated cardiomyopathy in 16 p-ts was associated with inflammation (DCMP + Inf) among them 1 patient (p-t) - granulomatous myocarditis, 1p-t - rheumatoid, other p-ts - eosinophilic myocarditis; ischemic cardiomyopathy (ICMP) - 7 p-ts; left ventricular aneurysm (LVa) - 16 p-ts; others - 2 p-ts, including valve disease (1 p-t), hypertrophic cardiomyopathy (1 p-t). Valve disease patient showed no histological evidence of inflammation, but the PCR in the myocardium had revealed the presence of viral genomes of CMV, EBV, and HSV. By gated SPECT criteria: DCMP - 10 p-ts; DCMP + Inf - 19 p-ts; ICMP - 10 p-ts; LVa - 15 p-ts. The agreement between histology and SPECT results in the diagnosis of inflammation was observed in 16 p-ts. The discrepancy between the histological and SPECT criteria in the diagnosis of inflammation: DCMP + Inf diagnosed by gated SPECT criteria included so others (2 p-ts) and DCMP (1 p-t) by the histological characteristics. **Conclusion**. Phase-assisted topographical image analysis can be useful in the diagnosis of active inflammatory process in the myocardium in patients with chronic heart failure.

## OP598

### Assessment of left ventricular diastolic function by myocardial perfusion scintigraphy: validation of 4D-MSPECT software

**D. C. Mitea**, I. Al Younis, A. J. H. A. Scholte; Leiden University Medical Center, Leiden, NETHERLANDS.

**Aim** To validate 4D-MSPECT software for the assessment of cardiac diastolic function and to determine which parameters can be used to evaluate diastolic function. **Materials and Methods** In 106 selected patients (mean age 62.6± 10.5 years) rest/stress myocardial perfusion scintigraphy (MPS) and echocardiography were performed (mean interval 23.4 days). Peak filling rate (PFR), mean filling rate in the first 1/3 of the diastole (MFR/3) and time to peak filling rate (TPFR) 4D-MSPECT software parameters were calculated in the rest images. Diastolic dysfunction was also assessed by transthoracic echocardiography and graded from 1 to 4. In addition specificity and sensitivity of the 4DM-SPECT parameters for assessing diastolic dysfunction was calculated. **Results** Rest-MPS derived parameters PFR and MFR/3 showed statistically significant difference between the patients with and without diastolic dysfunction as diagnosed by transthoracic echocardiography (mean PFR in patients without diastolic dysfunction 2.75 EDV/sec vs 1.85 EDV/sec for patients with diastolic dysfunction, p<0.01 and mean MFR/3 1.3 ms in patients without diastolic dysfunction vs 0.88 ms in patients with diastolic dysfunction, p<0.5), while TPFR was not able to discriminate between these patient's groups (177 ms in patients without diastolic dysfunction vs 183 ms in patients with diastolic dysfunction). However, PFR and MFR/3 could not differentiate between the different grades of diastolic dysfunction as being diagnosed by echocardiography. In our study PFR showed a sensitivity of 70% and specificity of 86% and MFR/3 60% and 77% respectively for the detection of diastolic dysfunction. **Conclusion** The 4D-MSPECT software derived parameters PFR and MFR/3 can be used with good sensitivity and specificity for the evaluation of the cardiac diastolic function as showed by the comparison with transthoracic echocardiography.

1506 - Tuesday, Oct. 22, 16:30 - 18:00, Grand Salon Prestige Gratte-Ciel

## Molecular & Multimodality Imaging: Hybrid Imaging - Methods & Tracer Development

## OP599

### DCE-MRI parameters to predict delivery and binding of radiolabeled peptides for SPECT imaging of prostate carcinoma

**J. Haeck**, K. Bol, C. de Ridder, H. Groen, L. van der Graaf, J. Veenland, W. van Weerden, M. Bernsen, M. de Jong; Erasmus Medical Centre, Rotterdam, NETHERLANDS.

**Aim** In recent years, the cell-surface gastrin-releasing peptide receptor (GRPR), expressed on multiple prostate cancer sub-types, has become a target for both imaging and therapy studies. The delivery and binding efficacy of radiopeptides binding GRPR rely on multiple properties; cells must have high levels of GRPR expression on the cell surface and the peptide should reach the tumor cells sufficiently. Despite the fact that GRPR distribution appeared homogenous in tumor xenografts as assessed by in vitro autoradiography, SPECT images showed substantial heterogeneity of peptide accumulation with higher levels in the tumor periphery. We hypothesized that delivery of peptide relies on local tumor perfusion characteristics. To study the relationship between tumor perfusion and peptide uptake, sequential SPECT/CT and MRI was used to image mice with PC295 xenografts after injection with a radiolabeled GRPR antagonist. Since tumor size plays a role in both vascularization and peptide uptake, tumors were studied at different sizes. **Materials and Methods** Male NMRI mice weighing approximately 30 grams were implanted subcutaneously with PC295 tumor fragments harbouring tumour cellsthat overexpress GRPR. At different time-points after tumour implantation and growth, the tumors were imaged by SPECT/CT and MRI. Two hours prior to SPECT imaging, animals received 25 MBq 111In-JMV-4168 (25 pmol). Images were acquired using a 4-head multipinhole NanoSPECT/CT camera. Directly after SPECT/CT imaging, MR images were acquired. Imaging was performed on a 7.0 T dedicated animal scanner. During injection of a contrast agent dynamic contrast enhanced-MR images were acquired with a temporal resolution of 4.7 seconds over 8 minutes. **Results** Quantification of the SPECT/CT uptake revealed that there is a high %ID in small tumors, and the %ID decreases as tumor volume increases. SPECT images show that in the large tumors the periphery accumulates more peptide, coincidentally; DCE-MR images revealed that in large tumors higher contrast uptake is found in the tumor periphery than in the center, in line with the SPECT radiopeptide pattern. Preliminary voxel-based correlation data show a clear relationship between SPECT uptake values and the amount of perfusion measured by DCE-MRI **Conclusions** Multi-modality functional imaging makes it possible to assess the relationship between perfusion properties (DCE-MRI parameters) and targeted peptide uptake. Global assessment and direct voxel-based comparison shows that adequate perfusion is necessary for efficient accumulation of peptide in tumors. DCE-MRI parameters are potential biomarkers to predict the distribution and uptake of targeted peptides in tumors.

## OP600

### Imaging performance of Ingenuity TF PET/MR versus Gemini TF PET/CT

**M. Yaqub**, P. Horstman, D. Oprea-Lager, M. Huisman, I. Pieters - van den Bos, O. Hoekstra, A. Lammertsma, R. Boellaard; VU University Medical Centre, Amsterdam, NETHERLANDS.

**Aim**: To compare the quantitative accuracy of PET studies performed on the Ingenuity TF PET/MR with the Gemini TF PET/CT (Philips) using phantoms and preliminary patient data. **Methods**: Several phantom experiments were performed on both PET/MR and PET/CT. Calibration and uniformity were measured using a

cylindrical phantom filled with known 18F-FDG solution. The same phantom was also filled with short lived isotopes (15O and 11C) in order to asses count rate linearity. To further assess image quality and (SUV) contrast recovery, the NEMA-NU2-2007 IQ and a 3D anthropomorphic brain phantom (Data Spectrum) were filled with 18F-FDG solutions. In the IQ phantom sphere to background radioactivity concentration ratio was set to ~10:1. Various acquisition modes (whole body, body dynamic, brain) and reconstruction algorithms (BLOB-OS-TF, 3D-Ramla, LOR-Ramla) were applied. For PET/MR special attention is required in order to generate accurate phantom attenuation correction maps (atMR), such as adding saline to the solutions and/or using predefined or separately acquired templates to compensate for lack of MR signal from the phantom walls. Finally, a pilot clinical PET/CT-PET/MR comparison study using 18F-FDG/ 18F-Choline WB scans (n=5, same patient scanned on PET/CT followed by PET/MR) was performed. **Results:** Calibration accuracy and image uniformities were comparable between PET/MR and PET/CT (within ~5%). However, PET/MR studies with additional MR coils showed image artefacts (up to 15%) due to use of metal objects within the coils which are not fully compensated in the atMR templates. The linearity of the system, as function of activity (1 - 170 MBq in VOF), was more accurate on PET/CT (error = -0.01±1.03%) than on PET/MR (error = -6.3±3.17%). SUV or contrast recoveries in the IQ phantom were comparable on both systems and met the EANM/EARL requirements (for WB mode). Contrast recovery in the brain phantom was slightly (5%) lower on PET/MR compared to PET/CT, possibly due to limitations in the experimental atMR. Initial clinical PET/CT - PET/MR evaluations based on 18F-FDG/ 18F-Choline WB studies (n=5) showed qualitatively comparable PET image quality between both modalities. **Conclusion:** PET/MR and PET/CT showed comparable performance regarding calibration accuracy, image uniformity and contrast recovery. Initial clinical evaluation revealed similar qualitative image quality between both systems, although some artefacts are visible in/near bones and lungs, as expected. Presence of MRI coils may result in (additional) image non-uniformities up to 15%, possibly due to inaccuracies in the attenuation map (MR coil) templates.

## OP601

### PET/MR imaging of head/neck in the presence of dental implants: reducing image artifacts and increasing accuracy through inpainting

**C. N. Ladefoged**[1], T. Beyer[2], S. H. Keller[1], I. Law[1], L. Højgaard[1], A. Kjær[1], F. Lauze[3], F. L. Andersen[1]; [1]Rigshospitalet Copenhagen, Copenhagen, DENMARK, [2]Center for Medical Physics and Biomedical Engineering, Vienna, AUSTRIA, [3]Dept. of Computer Science, University of Copenhagen, Copenhagen, DENMARK.

**Aim**: In combined PET/MR, attenuation correction (AC) is performed indirectly based on the available MR image information. Implant-induced susceptibility artifacts and subsequent signal voids challenge MR-based AC (MR-AC). We evaluate the accuracy of MR-AC in PET/MR in patients with metallic dental implants or braces, and propose a clinically feasible correction method. Materials and **Methods**: This study includes subjects selected retrospectively from our routine PET/MR referral base of patients with neurological disorders. Seven patients with metallic implants and implant-induced signal voids > 100 mL were included. In all patients simultaneous PET/MR imaging (mMR, Siemens Healthcare) of the head was performed at 40 min (n=5) and 80 min (n=2) p.i. of 200 MBq [18F]-FDG. MR-AC was performed using (A) standard Dixon water-fat segmentation (DWFS), and (B) as (A) but with the implant-induced signal voids semi-automatically filled with soft tissue (Soft). Following MR-AC, both PET emission images were reconstructed on 344x344 matrices using AW-OSEM (3iter, 21sub, 4mm Gauss). We report the volume of the inpainted area and the relative difference (Δ%) of PET(/MR)Soft to PET(/MR)DWFS for reference regions in the inpainted region, tongue and cerebellum. Furthermore, PET ratio images are computed for visual inspection. Results: The mean volume of implant-induced signal voids was (232±68) mL (min: 152mL, max: 348mL). The relative difference in mean SUV following inpainting as part of MR-AC (PET(/MR)Soft) was (217±65)% and (340±121)% in the inpainting region and tongue, respectively. Of note, comparatively large relative differences were noted also in the cerebellum: (6±3)% (max: 11%). Visual inspection of the ratio images indicated a marked regional variation of PET uptake depending on the shape and size of the signal void. **Conclusion:** Metallic dental work causes severe MR signal voids and PET/MR artifacts that exceed the actual implant volume. The resulting bias in AC-PET is severe in regions in and near the signal voids. Notably, the bias is present also in areas further away from the implants. In selected cases this bias may markedly affect regions used commonly as reference for kinetic modeling. Artifacts and bias can be corrected to a first degree by inpainting with soft tissue prior to MR-AC.

## OP602

### Studies On The Specific Activity Of $^{18}$F-Labelled $MnFe_2O_4$@$Al(OH)_3$ And $CoFe_2O_4$@$Al(OH)_3$ Nanoparticles For PET/MR Imaging

**S. Belo**[1], X. Cui[2], P. J. Blower[2], J. R. Ballinger[1,2]; [1]Guy's and St. Thomas' NHS Foundation Trust, London, UNITED KINGDOM, [2]King's College London, London, UNITED KINGDOM.

**Aim**: Superparamagnetic nanoparticles coated by aluminium hydroxide are suitable for one-step labelling with [$^{18}$F]Fluoride, and could perform as a bi-modal agent for PET/MRI, provided their specific activity allows detection of PET signal. Our Aim is to estimate the maximum theoretical specific activity attainable by labelling $MnFe_2O_4$@$Al(OH)_3$ and $CoFe_2O_4$@$Al(OH)_3$ nanoparticles with [$^{18}$F]Fluoride. **Methods**: Aqueous suspensions of $MnFe_2O_4$@$Al(OH)_3$ and $CoFe_2O_4$@$Al(OH)_3$ were reacted with aqueous [$^{18}$F]$F^-$ to assess labelling efficiency. The mass of fluoride absorbed per mass unit of nanoparticles was determined by incubating known nanoparticle masses with varying concentrations of [$^{19}$F]Fluoride (0.01,0.1,1.0 and 10 mM) and measuring the fluoride concentration in the supernatants by potentiometric assay. The absorbed masses allowed for estimation of maximum specific activities at end of bombardment; these were decay-corrected for one-hour post EOB to represent more realistic conditions. Labelling efficiencies for the cold labelling were equally assessed. **Results**: Labelling efficiencies of both $MnFe_2O_4$@$Al(OH)_3$ and $CoFe_2O_4$@$Al(OH)_3$ with $^{18}$F were consistently higher than 96%, excluding the need for a purification step. The cold labelling efficiencies were dependent on the [$^{19}$F]Fluoride concentration. These were( for $MnFe_2O_4$@$Al(OH)_3$ and $CoFe_2O_4$@$Al(OH)_3$ respectively) 65% and 80% when the samples were incubated with 0.01mM [$^{19}$F]Fluoride, 90% and 89% at 0.1mM, 94% and 85% at 1mM and 24 and 19% at 10 mM..The lower labelling efficiencies found for samples incubated with 0.01 mM [$^{19}$F]Fluoride are likely to be due to the method used, since radiolabelling yielded much higher efficiency with lower [$^{18}$F]Fluoride concentration. The decrease in labelling efficiency when samples were incubated with 10mM [$^{19}$F]Fluoride indicates saturation of inorganic binding sites at a lower concentration. The maximum Specific Activities (GBq/mg) calculated for $MnFe_2O_4$@$Al(OH)_3$ and $CoFe_2O_4$@$Al(OH)_3$ were $3.4x10^8$ and $4.0x10^8$ respectively if samples were reacted with 0.01mM [18F]F- , $4.7x10^9$ and $4.7x10^9$ with 0.1mM, $4.9x10^{10}$ and $4.4x10^{10}$ with 1mM and $1.2x10^{11}$ and $9.7x10^{10}$ with 10 mM. Below 10mM [$^{19}$F]Fluoride , the increase in specific activity is proportional to the [$^{19}$]Fluoride concentration. A slower increase between 1 and 10mM confirms saturation. **Conclusion**: The radiolabelling of $MnFe_2O_4$@$Al(OH)_3$ and $CoFe_2O_4$@$Al(OH)_3$ nanoparticles with [$^{18}$F]Fluoride is quantitatively achieved by a one-step reaction. The molarity of [$^{18}$F]Fluoride in reaction is not a limiting factor regarding labelling efficiency since the molarities commonly used for labelling with [$^{18}$F]F are considerably below the site saturation level demonstrated. The specific activities attainable by labeling $MnFe_2O_4$@$Al(OH)_3$ and $CoFe_2O_4$@$Al(OH)_3$ nanoparticles with [$^{18}$F]Fluoride make them a suitable contrast agent for bi-modal imaging by PET/MR.

## OP603

### Functionalized Magnetic Nanoparticles for biomedical applications: radiolabelling and preliminary magnetically-driven biodistribution study

**M. De Simone**, D. Panetta, L. Gherardini, C. Cinti, P. Salvadori; CNR Institute of Clinical Physiology, Pisa, ITALY.

Magnetic nanoparticles (MNPs) are becoming extremely diffused in biomedical field due to their unique physical properties and perspective use in theranostics. Although MNPs have been used as contrast media in MRI, obtaining multiprobe performance of these may also be useful to apply multimodality imaging. A particular feature of MNPs is that their disposition in vivo can be targeted in presence of an external magnetic field to achieve higher concentration and confinement in specific regions.We developed a simple strategy for labeling polymer-coated nanosystem based on magnetite ($Fe_3O_4$) nanoparticles and performed preliminary biodistribution studies to assess their use in targeted applications. **Material and Methods**: We used commercially-available aminodextran-coated iron oxide nanoparticles. N-hydoxylamine groups were produced by fuctionalisation of amino groups on the MNPs surface with BOC protected aminoxyacetic acid and conjugated with routinely produced 2-[$^{18}$F]Fluoro-2-deoxy-D-glucose ([$^{18}$F]FDG) by a chemoselective reaction based on the formation of an oxime with the aldehyde of the acyclic sugar. Radiochemically pure FDG-labelled MNPs were recovered by ultrafiltration (Microcon®, Merck) and formulated in saline. The obtained nanoparticles were characterized by TEM and FTIR using non-radioactive FDG. PET/CT is being used in healthy CD-1 mice to assess biological distribution of the radiolabelled construct and study the influence of an external magnet on the nanosystem to drive MNPs biodistribution. In particular, [$^{18}$F]FDG-MNPs were administered after a cylindrical magnet (N52, 1T) was placed on one tigh only. After MNPs administration, the mice were kept immobilized for 30 minutes and then sacrificed by inhalation of an anesthetic overdose. Afterwards, the magnet was removed and animals were scanned by microCT and the micro-PET for *post-mortem* whole-body imaging. Image were reconstructed and Volumes of Interest (VOIs) were drawn on both tighs. **Results**: A procedure for the radiolabelling of MNPs was achieved developing ad-hoc functionalised MNPs and [$^{18}$F]FDG solution. The whole-body PET scan revealed higher radioactivity concentration in the bladder, kidneys and myocardium (@ 30′ from injection). The

ratio of measured activity in the two VoIs (magnet vs control) was M/C = 1.4-3.4 (min-max). The asymmetry of the radioactivity distribution can be ascribed to the presence of the magnetic field. **Conclusion**: A quick procedure for MNPs radiolabelling has been set up by simple oxime-forming reaction and the ability of external magnetic field to localise MNPs in a specific region was demonstrated. Further characterisation of the in vivo biodistribution is in progress as the study of specially designed magnets to achieve shaped MNPs concentration.

## OP604

### Convenient Route towards Gallium-68 Labelled Gadolinium Contrast Agents for Simultaneous in vivo PET/MR Imaging

**J. Notni**[1], P. Hermann[2], I. Dregely[3], M. Schwaiger[3], H. Wester[1]; [1]Pharmaceutical Radiochemistry, Garching, GERMANY, [2]Charles University, Prague, CZECH REPUBLIC, [3]Nuclear Medicine, Technische Universität München, München, GERMANY.

**Introduction**: With the advent of integrated whole-body scanners allowing for simultaneous recording of PET and MRI data, the interest in dual-mode contrast agents (CA) awakened, for two reasons: Targeted bimodal PET/MRI probes would release the full synergy between high sensitivity of PET and high resolution of MRI. Furthermore, application of responsive MRI-CA (whose relaxivity is determined by tissue pH, serum metal ions, enzyme activity etc.) seem to be of special interest. However, such probes require quantification of their in vivo concentration; for PET-labelled smart MRI probes, these data could be taken from simultaneously recorded PET. We Aimed at labelling of gadolinium-CA with $^{68}$Ga because this nuclide is widely available at low cost. **Materials & Methods**: The bifunctional $^{68}$Ga-chelator TRAP (triazacyclononane-triphosphinate) was functionalized with 1,6-hexanediamine (HMDA) linkers and DOTA moieties, resulting in the conjugate TRAP(HMDA-DOTA)$_3$ (1). The MRI-CA GaTRAP(HMDA-GdDOTA)$_3$ (2) was obtained by complexation of $Gd^{3+}$ and, subsequently, $Ga^{3+}$. The precursor for PET labelling, TRAP(HMDA-GdDOTA)$_3$, was obtained by complexation of (1) with $Gd^{3+}$ and subsequent removal of TRAP-bound Gd(III) with aq. DTPA. $^{68}$Ga-labelling was done in a standard automated procedure (HEPES-buffered generator eluate, pH 3, 5 min at 95°C), affording the PET-tracer [$^{68}$Ga]TRAP(HMDA-GdDOTA)$_3$ (3). Simultaneous PET/MRI imaging was done on a Wistar rat, using a formlation of 20 µmol of (2) and 27 MBq of (3) in PBS. Simultaneous PET/MRI was recorded 25 min p.i. on a Siemens Biograph mMR scanner, (3D VIBE (GRE) coronal sequence, TR = 4.9 ms, TE = 2.4 ms). Listmode PET was recorded throughout MRI acquisition. Results: The main difficulty in preparation of $^{68}$Ga-labelled gadolinium-CAs is that common chelators (e.g. DOTA) form stable complexes with both Gd(III) and Ga(III). An exception is TRAP, which is highly selective for Ga(III). In conjugates of TRAP and DOTA, Gd(III) and Ga(III) were found to be selectively complexed by the DOTA and TRAP unit, respectively. A chemically homogenous dual-mode probe, comprising identical CA molecules for MR and PET, thus can be synthesized in a straightforward manner. PET/MRI scans showed suitability for in vivo application, MRI contrast enhancement being superimposable with PET images. **Conclusions:** We have established a universally applicable method for preparation of TRAP-based, $^{68}$Ga-labelled gadolinium-CA. Such agents enable PET/MRI with truly identical pharmacokinetics, making cross-validation of the two modalities obsolete. As TRAP can be equipped easily with additional molecular entities, a vast variety of applications are possible, including targeted PET/MRI and inclusion of further imaging modalities.

## OP605

### Cyclotron activated nanoparticles: application in PET/SPECT imaging

D. Máthé[1], I. Horváth[2], F. Budán[1], S. Hóbor[3], P. Koncz[3], F. Simonelli[4], U. Holzwarth[4], G. Németh[3], **K. Szigeti**[2], N. Gibson[4]; [1]CROmed Ltd, Budapest, HUNGARY, [2]Semmelweis University, Budapest, HUNGARY, [3]Mediso Ltd, Budapest, HUNGARY, [4]JRC, IHCP, Ispra, ITALY.

**Introduction:** Nanoparticles (NP) are widely used in everyday life. Pigments, cosmetic products, some foods, suncream, and many other products may contain NPs, and possible environmental pollution may be associated with wastes and NP release. Investigation of possible toxicological effects from exposure to NPs requires in vivo bio-distribution studies. Three frequently applied NPs: silver (Ag), zinc oxide (ZnO) and titanium dioxide (TiO2) were tested by our research group in activated form for quantification and tomographic detection using PET and SPECT. **Materials and Methods**: Activated NPs were produced in the JRC Cyclotron (Scanditronix MC40). Dry NP powders were placed in sample holders and activated for several hours by proton or deuterium irradiation. The resulting target material was left to decay for 2 weeks to allow irrelevant short-lived isotopes to decay away. Ag-105 (Ag-NP), Zn-65 (ZnO-NP) and V-48 (TiO2-NP) isotopic purity and radioactivity were determined precisely with gamma spectroscopy (Canberra GX2518 HPGe) using Genie 2000 software. The data were used to adjust quantification factors for imaging instruments NanoSPECT/CTPlus (Mediso Ltd.) and nanoScan PET/MRI (Mediso Ltd.). Using SPECT several peaks of the different gamma photon energies characteristic of the specific isotope spectra were applied. We detected 64.0, 280.5, 443.4 and 344.5 keV peaks for Ag-105, and the 560 keV peak for V-48 in addition to detecting the 511 keV annihilation peak of Zn-65 for PET. The HiSPECT (SciVis Gmbh, Germany) reconstruction algorithm was used to calculate volumes from multiplexing overlapping multi-pinhole SPECT while Tera-Tomo (Mediso Ltd) 2-D and 3-D iterative reconstruction algorithms were used to calculate PET volumes**. Results**: The specific activity of all the NP types used was between 1-1.5 MBq/mg. The radiation emission of Zn-65 was detected using PET, Ag-105 and V-48 were detected with both PET and SPECT. All nanoparticle samples have shown adequate signal-to-noise ratio in their spectral properties for SPECT (Ag-105, V-48) and PET (Ag-105, Zn-65 and V-48) imaging in durations between 40 minutes and 120 minutes of signal integration. **Conclusion**: All PET and SPECT imaging data were capable of determining the original radioactivity and distribution of the nanoparticles. Quantitation error was 24,3%. These findings provide the basis for the application of non-conventional long-lived isotope tracking of nanoparticles. The actual practicality and usefulness of the technique at realistic NP doses and at lower doses in various organs after biodistribution still has to be studied. Acknowledgement. This study was in part supported by EC-FP7 Transnational Access Facilities grant QNANO.

1507 - Tuesday, Oct. 22, 16:30 - 18:00, Salon Pasteur

## Neurosciences: Movement Disorders

## OP606

### Reduced Cardiac 123I-Metaiodobenzylguanidine Uptake in Patients with Spinocerebellar Ataxia Type 2: a Comparative Study with Parkinson's Disease

**A. Boemio**[1], T. Pellegrino[2], R. Carotenuto[1], A. De Rosa[1], M. F. De Leva[1], A. Roca[1], A. Filla[1], G. De Michele[1], S. Pappatà[2], M. Petretta[1], A. Cuocolo[1]; [1]University of Naples - Federico II, Napoli, ITALY, [2]National Council of Research, Napoli, ITALY.

**Aim**: Spinocerebellar ataxia type 2 (SCA2) is an autosomal dominant neurodegenerative disorder characterized by cerebellar ataxia, supranuclear ophthalmoplegia, and peripheral neuropathy. Autonomic nervous system dysfunction is often present. We evaluated the cardiac sympathetic function in patients with SCA2 using 123I-metaiodobenzylguanidine (MIBG) in comparison with patients with Parkinson's disease (PD) and control subjects. **Material and Methods**: Nine patients (6 men, age 42±14 years) with SCA2 and 9 patients (6 men, age 55±7 years) with PD were studied. All patients underwent planar 123I-MIBG (111 MBq) cardiac imaging. A 10-minute planar image was acquired from an anterior thoracic view 15 minutes ("early" image) and 3 hours and 50 minutes ("late" image) after tracer administration. Early and late heart-to-mediastinum (H/M) ratios were computed by dividing the mean counts per pixel within the myocardium by the mean counts per pixel within the mediastinum. 123I-MIBG washout rate was also calculated. Nine subjects (5 men, mean age 40±15 years) who underwent 123I-MIBG scintigraphy to rule out a disease of the adrenal medulla, served as control group. **Results**: At one-way ANOVA, significant differences in early ($F=12.3$, $P<0.0001$) and late ($F=16.8$, $P<0.0001$) H/M ratios among control subjects, SCA2 patients, and PD patients were found. In control subjects, early and late mean H/M ratios (2.2±0.12 and 2.1±0.20, respectively) were significantly higher as compared to both SCA2 patients (1.94±0.23 and 1.81±0.20; $P<0.05$) and PD patients (1.66±0.27 and 1.47±0.31; $P<0.001$). Early ($P<0.05$) and late ($P<0.001$) mean H/M ratios were higher in patients with SCA2 compared to those with PD. A significant difference in washout rate values among groups was also found ($F=11.7$; $P<0.0001$). In control subjects, mean washout rate (19.9±9.6%) was significantly lower compared with PD patients (47.9±24.1%; $P<0.005$), but not different compared with SCA2 patients (19.5±9.4.1%; $P=0.99$). Mean washout rate was significantly lower in patients with SCA2 compared to those with PD ($P<0.001$). In patients with SCA2, at multivariable linear regression analysis the ataxia score was independently associated ($\beta=-0.12$, $P<0.05$) with early H/M ratio. **Conclusions:** 123I-MIBG myocardial scintigraphy demonstrated an impairment of cardiac sympathetic function in patients with SCA2, which is less marked than in PD patients. The results suggest that this tool may be useful not only to identify PD patients, but also to detect subtle autonomic alterations in other neurodegenerative disorders such as SCA2 where the autonomic system is involved.

## OP607

### Evaluation of an Automated Age Independent Atlas-based Method for DaTscan™ Diagnosis

**J. Piper**, A. Nelson, S. Pirozzi, M. Horvat; MIM Software Inc., Cleveland, OH, UNITED STATES.

**Purpose:** In a previous study automatically computed DaTscan SPECT uptake ratio cutoffs separated Parkinson's disease (PD) patients from healthy controls (HC) with 90-95% consistency within age-specific patient groups. The Aim of this study was to further explore the accuracy of DaTscan in classifying Parkinson's disease with

age-independent cutoffs derived by combining multiple quantitative end-points. **Methods:** DaTscan SPECT imaging data for 60 PD and 60 HC subjects were acquired from the Parkinson's Progression Markers Initiative database (ages 50-79). Half of the subjects from each group were used for training and the other half for testing. Affine registration was used to align images to a PD and HC template simultaneously. Through this registration pre-defined atlas volumes of interest (VOIs) were transferred from the template back to the patient image for computation of uptake ratios for the following structures: occipital normalized putamen (P), anterior putamen (AP), posterior putamen (PP), caudate (C), and striatum (STR), caudate normalized putamen (P/C), and asymmetry indices for the putamen (ASYM_P) and striatum (ASYM_S). Linear combinations of two or three variables were used as classifiers. The classifiers were characterized by their consistency on the 60 training subjects and accuracy on the 60 testing subjects. **Results:** Combining the AP uptake ratio value with P/C in a 1:11 ratio separated HC from PD with 93% consistency (30/30 HC and 26/30 PD). Combining ASYM_S with AP and P/C in a 4.3:1:30 ratio improved the consistency to 95% (30/30 HC and 27/30 PD). The AP and P/C classifier resulted in 90% accuracy on the test subjects (28/30 HC and 26/30 PD). The ASYM_S, AP, and P/C classifier also resulted in 90% accuracy (30/30 HC and 24/30 PD). **Conclusion:** A completely automated method for DaTscan analysis achieved 93-95% consistency and 90% accuracy in separating PD from HC across all age groups. One likely cause of the incorrect classifications is misregistration, which might be detected and corrected if this tool were to be used clinically. At 90% accuracy, this method would be a helpful aid to visual interpretation of DaTscan SPECT images.

## OP608

### Standardized semi-quantitative evaluation of 123I-FP-CIT SPECT in a multicenter study: striata binding potential assessed by BASGAN (V2)

**A. Skanjeti**[1,2], G. Castellano[3], B. Elia[4], T. Angusti[1], S. Grimaldi[3], M. Balma[3], S. Romana[1], M. Zotta[3], M. Iudicello[5], M. Zibetti[6], P. Ferrero[7], P. Filippi[8], R. Pellerito[4], G. Bisi[3], V. Podio[1]; [1]Nuclear Medicine Unit, San Luigi Gonzaga Hospital, University of Turin, Orbassano, ITALY, [2]Medical Science Department, University A. Avogadro, Novara, ITALY, [3]Nuclear Medicine Unit, San Giovanni Battista Hospital, University of Turin, Turin, ITALY, [4]Nuclear Medicine Unit, Umberto I Hospital, Mauriziano, Turin, ITALY, [5]Neurology 1, San Luigi Gonzaga Hospital, Orbassano, ITALY, [6]Neurology 4, San Giovanni Battista Hospital, University of Turin, Turin, ITALY, [7]Neurology 2, San Giovanni Battista Hospital, University of Turin, Turin, ITALY, [8]Neurology, Maria Vittoria Hospital, Turin, ITALY.

**Introduction.** In nuclear medicine field various acquisition protocols, data analysis and interpretation/presentation of results are observed and comparability of semi-quantified results is still to be assured. The Aims of this multicentre study were: 1) to assess the accuracy of semi-quantitative evaluations of DAT-SPECT in pooled samples and 2) to identify the best threshold as well as sensitivity, specificity and accuracy in a patient population with suspected parkinsonian syndrome. **Materials and Methods**. Two-hundred-twenty patients (age 67±10 y) with movement disorders and suspected for neurodegenerative parkinsonian syndrome (NPS), were included. They underwent DAT-SPECT in three centres (San Luigi Gonzaga, with Philips Axis; San Giovanni Battista, with GE Varicam; Mauriziano, with Siemens E.cam) from January 2006 to July 2010. After at least 2 years interval, initial diagnosis were reviewed for fulfilment of Step 1 of UK Brain Bank criteria for Parkinson Disease and of Findley & Koller criteria for Essential Tremor by experienced neurologists, independently from DAT-SPECT report. All exams were reconstructed on a single device with the same filter and the same attenuation correction. Semi-quantitative data of each patient were obtained after processing by BASGAN and were correlated with diagnosis. In particular, the analysis were performed from the values of the most deteriorated putamen and caudate using ROC analysis and area under the curve (AUC). All data were normalized for age according to BASGAN database. **Results**. In NPS-free patients, both putamen and caudate data were not comparable among the three centres. Then, each patient data were normalised dividing by the mean value of NPS-free patients of the respective centre. Further analysis showed high AUCs (0.88, 0.866, 0.92 and 0.891 for each centre and for pooled data, respectively) demonstrating high accuracy for each centre and for the whole population. The best cut-off were 0.71 and 0.80 for putamen and caudate, respectively. These thresholds yielded similar sensitivities and specificities (78% and 94%, 82% and 81%, 88% and 94%, 82% and 91%) in each centre and in the entire population. **Conclusion.** A unique threshold for all centres with high and similar accuracy is possible if semi-quantitative assessment is performed by BASGAN. However, high accuracy regardless the device used can be obtained with correction of semi quantitative data by results of "normal" subjects.

## OP609

### DaTSCAN™ (Ioflupane I 123 Injection) for Prediction of Clinical Diagnosis of Early Parkinsonian Syndromes: Sensitivity, Specificity, Positive and Negative Predictive Values, and Accuracy

**M. Plotkin**[1], I. D. Grachev[2], R. A. Hauser[3], J. Seibyl[4], K. Marek[4], A. Kupsch[5], N. Bajaj[6]; [1]Leiter des Vivantes Instituts für Nuklearmedizin Mitte/Nord, Berlin, GERMANY, [2]GE Healthcare, Princeton, NJ, UNITED STATES, [3]USF Byrd Parkinson's Disease and Movement Disorders Center, Tempa, FL, UNITED STATES, [4]The Institute for Neurodegenerative Disorders, New Haven, CT, UNITED STATES, [5]Otto-von-Guericke-University, Magdeburg, GERMANY, [6]University of Nottingham, Nottingham, United Kingdom, Nottingham, UNITED KINGDOM.

**Background:** Neurodegenerative Parkinsonian syndromes (PS) is the second most common neurodegenerative disorder. DaTSCAN™ ([$^{123}$I]Ioflupane Injection) is a radiopharmaceutical, approved in Europe and the USA (under the name DaTscan™) for SPECT imaging to visualize the dopamine transporter in the brain. In practice, clinical diagnosis is sufficient and accurate for many patients with advanced and typical manifestations of PS. However, there is a subset of patients with early-stage disease with insufficient or atypical signs and symptoms, who may benefit from DaTSCAN™. **Objective:** To assess the diagnostic efficacy data from clinical trial PDT409 (Kupsch et al, 2012; data not previously published) conducted using DaTSCAN™. **Patients and Methods:** Study PDT409 (n=92 imaging group) was used to assess the diagnostic accuracy of DaTSCAN™ in subjects with early, clinically uncertain PS after 1 year follow-up. The reference standard was final clinical diagnosis 1 year after imaging (with DaTSCAN™ results available), and it was compared to baseline clinical diagnosis (without DaTSCAN™) and to baseline imaging diagnosis. Visual assessment of DaTSCAN™ images was performed by local nuclear medicine physicians, which is consistent with current clinical practice. Acquisition of SPECT data with DaTSCAN™ and their reconstruction were performed using a standardized imaging protocol. **Results:** The sensitivity of clinical diagnoses at baseline using clinical data was 92% when compared to final clinical diagnosis at 1 year, but the specificity was only 52.4%. For the comparison of baseline DaTSCAN™ images to the clinical diagnosis at 1 year, the sensitivity was 93.9%; specificity was 95.4% (p=0.0005 as compared to baseline clinical diagnosis). The PPV, NPV and diagnostic accuracy for baseline clinical diagnosis or baseline imaging diagnosis vs. final clinical diagnosis at 1 year (reference standard) were respectively: 69.7% vs. 95.8% (p<0.0001), 84.6% vs. 93.2%, and 73.9% vs. 94.6%. **Conclusion:** High sensitivity and specificity, PPV, NPV and diagnostic accuracy of DaTSCAN™ in diagnosis of early clinically uncertain PS were demonstrated. Performance of DaTSCAN™ compares favorably in this study to the performance of clinical diagnosis relative to final clinical diagnosis. Improving early diagnostic accuracy may help avoid unhelpful treatments and their potential side effects. Study Supported by: GE Healthcare, Princeton, NJ, USA. References: Kupsch AR, Bajaj N, et al. Impact of DaTscan SPECT imaging on clinical management, diagnosis, confidence of diagnosis, quality of life, health resource use and safety in patients with clinically uncertain parkinsonian syndromes: a prospective 1-year follow-up of an open-label controlled study. J Neurol Neurosurg Psychiatry 2012 Jun; 83(6):620-8.

## OP610

### Different cerebellar regional metabolic patterns in MSA, SCA and CCD

**M. Oh**, J. Kim, J. Oh, S. Chung, C. Lee; Asan Medical Center, Seoul, KOREA, REPUBLIC OF.

**Purpose** Ataxia, the predominant manifestation of different types of cerebellar degenerative disorders such as multiple system atrophy (MSA) and spinocerebellar ataxia (SCA), often makes clinical diagnosis difficult. Based on their different pathophysiology, we evaluated quantitatively whether they show distinct regional cerebellar metabolic pattern compared to crossed cerebellar disachisis (CCD) and normals on FDG PET. **Methods** We retrospectively analyzed FDG PET in patients with 44 cerebellar (median age 57.0 yrs, M:F=24:20) and 53 parkinsonian (61.0 yrs, M:F=37:16) types of MSA (MSA-C and MSA-P), 6 SCA2 (38.5 yrs, M:F=3:3), 5 SCA6 (63.0 yrs, M:F=3:3), and 15 CCD (48.0 yrs, M:F=7:8), compared to 30 normal controls (52.5 yrs, M:F=16:14). PET images were spatially normalized to MNI template and analyzed with 13 predefined cerebellar subregional [bilateral anterior lobes (ANT), superior/mid/inferior posterior lobes (SUPP, MIDP, INFP), dentate nuclei (DN), anterior vermis (ANTV), and superior/inferior posterior vermis (SUPV/INFV)] and 2 parietal volume-of-interests (VOIs) template. Metabolic ratios (cerebellar subregion to parietal cortex) of each VOI, anterior to posterior lobe (AP) ratio and asymmetric ratios were calculated. **Results** Compared to normal controls, MSA-C and SCA2 showed severely decreased metabolic ratios in all cerebellar subregions (ANT: 0.79 vs 0.59 and 0.47, respectively, $p$<0.001). MSA-P showed less degree of decreased metabolic ratios in all subregions (ANT: 0.70, $p$=0.001), but no difference in DN. SCA6 showed decreased metabolic ratios only in ANT, ANTV and SUPV ($p$<0.001). In comparison among disease groups, SCA2 showed more decreased metabolic ratios in DN than MSA-C ( 0.64 vs 0.78, $p$<0.001). SCA2 and SCA6 showed lower AP ratios than normal controls and CCD (0.79 and 0.69 vs 0.87 and 0.96, respectively, $p$<0.001). Compared to normal controls, CCD and MSA-C showed high asymmetric ratios (0.03 vs 0.22 and 0.11, respectively, $p$<0.001), whereas MSA-P, SCA 2 and 6 did not. **Conclusion** In conclusion, regional patterns of cerebella metabolic deficits in cerebellar degenerative disorders differ not only

from each other, but from other diseases causing reduced cerebellar metabolism such as CCD in terms of AP ratio and asymmetry. These results may provide diagnostic clues in case of clinical dilemma.

## OP611

### Diagnosis of movement disorders in clinical routine: the challenging issue of building a 18F-DOPA normal database

**R. Guignard**[1], A. Ochin[1], J. Barriere[1], V. Bourg[2], M. Borg[2], M. Ouvrier[1], J. Darcourt[1]; [1]Centre Antoine Lacassagne, Nice, FRANCE, [2]University hospital, Nice, FRANCE.

**Aim** 18F-DOPA can be used to diagnose presynaptic dopaminergic deficits in early phases of Parkinson's Disease (PD). Adding semi-quantitative analysis to visual reading is an important issue. As DOPA is also an amino acid PET tracer which demonstrates a high uptake in brain tumors (BT), the first endpoint was to assess the feasibility of building a normal database using patients without any movement disorders (MD) studied by 18F-DOPA PET for BT. The second endpoint was to assess several semi-quantitative parameters applicable in clinical routine and to compare them with our reference database. **Materials and Methods** Sixty minutes after oral administration of carbidopa (100 mg), patients received intravenously 2 MBq/kg of 18F-DOPA. Only late PET acquisitions (90 minutes post-injection; 10 minutes duration; OSEM 5 iterations 24 subsets; noTOF; noHR; mCT Siemens) were considered to analyze the nigrostriatal dopaminergic (NSD) function. 18F-DOPA striatal uptake (StUp) was quantified using SUVmean, both on striatal VOI using a semi-automatic isocontour delineation method, and on manually-drawn VOI for caudate, anterior and posterior putamen. Specific activity was assessed using striatal-to-occipital ratio (SOR), as well as caudate- (COR) and putamen-to-occipital ratio (POR). **Results** Ten HC patients studied for BT (18 PET procedures; 55.8±13.6 years) were prospectively included in our reference database (T0). StUp was comparable on both sides (SOR: 3.6±1.2; p=0.3); no difference was observed for gender (p=0.2); StUp was negatively correlated with age (p=0.04). 18F-DOPA uptake was significantly higher in the anterior putamen (PORAnte: 3.7±1.3; p=0.04). Forty-eight older patients (73.3±10.1 years; p<0.001) referred for MD diagnosis were considered as normal (T1) on the basis of visual analysis. StUp in T1 was significantly lower than in T0 (PORAnte: 3.1±0.1; p=0.02). Men (n=31) demonstrated higher StUp than women (p=0.002). Right PORAnte was superior to left PORAnte (p=0.01). In multivariate analysis, taking into consideration age-related effects, it appears that NSD function might be quantitatively assessed in clinical practice using simple semi-quantitative parameters, like the right PORPost (p=0.004). **Conclusion** A non-invasive and accurate detection of NSD alteration at the earliest stages of PD is a challenging issue. Despite some methodological limits of this preliminary study, it shows that 18F-DOPA PET data acquired in the neuro-oncological setting can be used to define reference values. When compared to an older population of visually normal patients studied in the MD setting, some discrepancies are found in particular in the putamen, emphasizing the requirement to collect data across a wide age range.

## OP612

### [18F]PR04.MZ for Quantification of Striatal and Extrastriatal Dopamine Transporters in Patients with Idiopathic Parkinson's Disease

H. Amaral[1], **V. Kramer**[1], R. Pruzzo[2], P. Chana[3], C. Juri[4], M. Piel[5], R. Galaz[2], I. Coudeu[2], F. Rösch[5]; [1]PositronPharma SA, Santiago de Chile, CHILE, [2]Fundacion Arturo Lopez Perez, Santiago de Chile, CHILE, [3]CETRAM, Universidad de Santiago, Santiago de Chile, CHILE, [4]Universidad Catolica, Santiago de Chile, CHILE, [5]Universität Mainz, Mainz, GERMANY.

**Objectives:** The dopamine transporter (DAT) is considered to be a valuable target for preclinical detection of neurodegenerative diseases and its availability correlates with striatal dopamine concentration and clinical severity of Parkinson's disease (PD). To evaluate the diagnostic utility of [18F]PR04.MZ for idiopathic PD we measured presynaptic cell loss by comparison of PD patients with a group of age matched health volunteers. **Methods**: 10 patients (mean age 50 ± 10 a) with idiopathic PD underwent a static PET scan (Siemens mCT) for a duration of 15 min, 75 min after bolus injection of 231 ± 51 MBq (mean ± SD) [18F]PR04.MZ. PET scans were co-registrated to CT images and normalized to a standardized brain template. Binding potentials (BPnd) in different brain regions were calculated as region/cerebellum-1. **Results**: Idiopathic PD was diagnosed after clinical onset (mean disease duration 4 ± 3.4 a) by standardized neurological examination at least one year prior to PET scans. In all patients Binding potentials in all striatal brain regions were significantly reduced. Dopaminergic cell loss was more pronounced in putamen (mean reduction 72 ± 12 %) vs. caudate nucleus (mean reduction 42 ± 20 %) and in posterior putamen (83 ± 6 %) vs. anterior putamen (61 ± 17 %). Furthermore dopaminergic cell loss correlates with disease progression by comparing results of patients with different severities of PD. Also in patients in early clinical stages asymmetric cell loss in putamen and caudate nucleus was observed, corresponding to the clinically affected side. **Conclusions**: [18F]PR04.MZ seems to be a promising tool for precise quantification of striatal DAT and thereby measuring presynaptic cell loss in PD patients. Especially the high binding potential in DAT rich brain regions may provide the possibility of detecting small changes in preclinical phases of PD. Further evaluation of a larger group of patients has to be conducted to confirm these promising results.

## OP613

### Human brain PET imaging of PDE10A in Parkinson's and Huntington's disease

**R. U. Ahmad**[1], S. Bourgeois[1], A. Postnov[1], M. E. Schmidt[2], G. Bormans[1], W. Vandenberghe[1], K. Van Laere[1]; [1]University Hospital Leuven, Leuven, BELGIUM, [2]Janssen R&D, Beerse, BELGIUM.

**Objective:** Phosphodiesterase 10A (PDE10A) is an enzyme that hydrolyzes cAMP and cGMP. PDE10A is strongly expressed in striatal medium spiny neurons and is assumed to be involved in several brain disorders. We have used the novel tracer 18F-JNJ-42259152 and Positron Emission Tomography (PET) to evaluate PDE10A activity in patients with Huntington's (HD) and Parkinson's (PD) disease in vivo. **Methods:** Five patients with PD and 5 patients with HD were compared to 11 healthy controls (CON). Patients were clinically evaluated using the Unified Parkinson's Disease Rating Scale (UPDRS), and Unified Huntington's Disease Rating Scale (UHDRS), respectively. All subjects received a slow bolus of 168.3±11.5 MBq 18F-JNJ-42259152, were scanned dynamically for 90 minutes with full arterial sampling. Dynamic VOI analysis of the striatum and substantia nigra was done on individual volumetric MRI data. Distribution volume VT, obtained with a two tissue compartment model (2TCM) and binding potential (BPND) using a Reference Tissue Model (MRTM) with frontal cortex as a reference region was used with partial volume correction (PVC). **Results:** HD patients showed a strongly reduced VT and BPND in the striatum compared to CON. After PVC BPND values where significantly different between HD en CON for putamen (PT) and caudate nucleus (CNc) ($p = 0.02$ and $p < 0.001$ respectively), but not for ventral striatum (VSt) or substantia nigra (SN). There was no significant difference between PD and CON (PT $p = 0.77$; CNc $p = 0.79$; VSt $p = 0.23$; SN $p = 0.46$). **Conclusion**: In vivo, PDE10A activity is severely reduced in PT and CNc of patients with HD, whereas it is preserved in PD. Modulation of PDE10A activity may be of interest in HD as a potential novel target.

1508 - Tuesday, Oct. 22, 16:30 - 18:00, Gratte-Ciel 1/2/3

## Radionuclide Therapy & Dosimetry: Treatment of Benign Thyroid Diseases

## OP614

### Therapy planning and dose prescription in radioiodine therapy for hyperthyroidism using SPECT/CT

**M. Hosono**[1], K. Hanaoka[2], K. Ishii[1], S. Im[1], K. Sakaguchi[1], Y. Yagyu[1], Y. Matsukubo[1], Y. Ohno[1], H. Ikegami[1]; [1]Kinki University School of Medicine, Osaka-Sayama, JAPAN, [2]Osaka University, Suita, JAPAN.

**Aim:** Functional thyroid weight is one of the most important factors for prescribing radioiodine doses in the iodine-131 therapy for hyperthyroidism. Thyroid weight is usually determined using planar scintigraphic Methods such as Allen's method, which may include deviations especially in cases of atypical thyroid morphology. In this study, we assessed the usefulness of SPECT/CT in the measurement of functional thyroid weight for radioiodine therapy. **Methods**: Patients with Grave's disease who underwent radioiodine therapy along with preceding I-123 planar scintigraphy and SPECT/CT scan were enrolled in this study (n=19). On planar images, thyroid weight was measured using Allen's method and another conventional method of Okubo, a modified Allen's method. Thyroid iodine uptake was estimated using 2-demensional (2D) regions of interest (ROI). On SPECT/CT images, 3D volumetric regions of interest (VOI) were placed over the thyroid on SPECT images by adjusting thresholds with referring to CT images. Cross calibration of I-123 scan was performed with SPECT/CT scanner to measure thyroid iodine uptake. 4 operators performed measurements of thyroid weight and radioiodine uptake for each patient. Weight values and iodine uptake estimated by these three Methods were analyzed and compared by regression analysis. **Results**: In estimation of thyroid weight, a good correlation was observed between the SPECT/CT method and the planar scintigraphic method ($r=0.96$, $p<0.01$ and $r=0.95$, $p<0.01$ for Allen's and Okubo's Methods, respectively). Variations in the estimated thyroid weight among 4 operators were 4.66, 10.32, and 10.52% for SPECT/CT method, Allen's method, and Okubo's method, respectively. On iodine uptake, a good correlation was observed between the SPECT/CT method and the two planar scintigraphic Methods ($r=0.82$, $p<0.01$). Using values on these SPECT/CT Methods, among 19 patients, the prescribed I-131 dose in capsules was changed as compared with the conventional method as follows; increase in 2 and decreased in 2 using weight alone, increase in 3 and decreased in 2 using uptake alone, and increase in 4 and decreased in 5 using both weight and uptake. Among the patients, an ectopic uptake and non-functional mass were confirmed on SPECT/CT fusion image. **Conclusions**: Our method of estimating radioiodine thyroid uptake

using SPECT/CT facilitated more personalized planning by adding morphological information to functional images in 3D.

## OP615

### The influence of single low dose of recombinant human thyrotropin on I-131 treatment of large multinodular goitre.

**M. N. Mojsak**, S. Abdelrazek, F. Rogowski, P. Szumowski, J. Myśliwiec, A. Kociura-Sawicka; Medical University, Bialystok, POLAND.

Recombinant human thyrotropin (rhTSH) is a substance that after single intramuscular injection can increase thyroid radioiodine uptake (RAIU) and improve the results of radioiodine therapy (RIT) in patients with nontoxic multinodular goitre (MNG). These effects are very important especially in cases of large MNG with relatively low RAIU or contraindications to surgery. The Aim of the study. The evaluation of the influence of the single low dose of rhTSH to RAIU and the effects of RIT in patients with benign large nontoxic MNG. **Material and Methods**: 40 patients (14 male, 26 female, age 41-80 yr) with large MNG > 100 grams and with baseline RAIU < 40% (33,37+/-7,96%) were included to the study and divided into two groups. First group received the single intramuscular injection of 0,03 mg rhTSH and the second received placebo. The RAIU were measured again 48 hours after the rhTSH (24 hours after diagnostic dose of I-131). After this, all the patients were administered the therapeutic doses of I-131 recalculated according to new RAIU. The patients follow up was continued for minimum 12 months. **Results**: The mean RAIU after rhTSH increased more than twice, to 75% from 33%. One year after RIT the mean volume goitre reduction were significantly greater in group with rhTSH than in patients with placebo (48±16% vs. 37±18%). Decrease of compression symptoms has taken place earlier and was more important in patients after rhTSH. 12 months after RIT two patients stay in hypothyroid state (from the group with rhTSH), other patients are euthyroid. **Conclusions**: Even the single very low dose of rhTSH increases the values of RAIU in significant way. Efficacy of rhTSH-augumented RIT in patients with large nontoxic MNG is greater than standard RIT. It allows to reduce administered doses of I-131, decreases the need of repeating RIT, makes the radiation adsorbed doses for whole body lower and the RIT shorter.

## OP616

### Factors influencing the success of Radio-iodine dose in the treatment of Graves disease: one year outcome

**T. Kamoun**[1], R. Sfar[1], H. Regaieg[1], A. Toumi[1], H. Zanzouri[1], M. Nouira[1], M. Ben Fredj[1], N. Ayachi[1], K. Chatti[1], M. Guezguez[1], N. Sakly[2], H. Essabbah[1]; [1]Nuclear Medicine department, Sahloul University Hospital, SOUSSE, TUNISIA, [2]Laboratory of Immunology, F. Bourguiba University Hospital, MONASTIR, TUNISIA.

**Aim**: Radioiodine (131I) is increasingly used as the definitive treatment of Graves' disease (GD). Many factors influence the curative effects of the 131I, thus there are some difficulties to define the optimal dose of 131I for the treatment of GD. The purpose of our study is to evaluate the factors influencing the success rate in patients having GD and treated with radioiodine dose modulated by thyroid mass. **Materials and Methods**: This is a prospective study of 86 patients (aged 43 ±11, 58 women and 28 men) treated for Graves disease by radioiodine during the year 2011 in Nuclear Medicine department CHU Sahloul, Sousse. Radioiodine dose are modulated by thyroid mass: 370MBq, 444MBq and 555MBq respectively for mass strictly less than 30gr, between 30gr and 40gr and greater than to 40gr. Some patients received more than 555MBq for other causes to reach hypothyroidism precociously. The thyroid function outcome (hyperthyroidism or euthyroidism/hypothyroidism) was verified 6 months and 1 year after 131I treatment. Patient gender, age, ophthalmopathy, thyroid size, antithyroid drugs used prior to 131I treatment and anti-TSH receptor antibodies (TRAb), anti-thyroid peroxydase antibodies (ATPO) and anti-thyroglobulin antibodies (ATG) plasma concentrations before 131I treatment were studied as potential interference factors for 131I treatment success. **Results:** Thirty patients received 370 MBq, 29 received 444 MBq, 14 received 555MBq and 13 more than 555MBq. Outcome after treatment was determined in a total of 66 patients at 6 months and 63 at one year. Post-therapy follow-up revealed that treatment failed in 29% of the patients at 6 months and in 20% of patients at one year. No correlation was noted between the outcome of treatment and age, sex, ophthalmopathy, antithyroid drugs taking and ATG titer. A significant correlation was noted between the disease outcome at one year and TRAb titer; High TRAb levels are associated with relative resistance to therapy. A significant correlation was noted between the disease outcome and ATPO titer at 6 months; High ATPO levels are associated with precocious hypothyroidism, which can be transient. This finding was justified by the fact that there was no correlation between ATPO titer and disease outcome at one year. A significant correlation was noted between the disease outcome and the size of the thyroid gland; Huge thyroid mass was predictive of therapeutic failure. **Conclusion:** High thyroid mass and TRAb levels are significantly associated with the failure of Radioiodine for treating GD.

## OP617

### Correlation of recurrence of Graves Disease with thyroid gland mass, 24h radioiodine uptake and the administered therapeutic activity.

**L. P. Pires**, C. Moreno, G. Costa, A. Albuquerque, J. Pedroso de Lima; Centro Hospitalar e Universitário de Coimbra, Coimbra, PORTUGAL.

**Aim**: In our department, calculation of radioiodine activity to treat patients with Graves Disease (GD) is based on thyroid mass and on the 24h radioiodine uptake (24h-RIU). The Aim of this study was to evaluate the importance of those parameters and of the administered activity in the outcome of radioiodine therapy in patients with GD, considering the need for an additional 131I treatment. **Material and Methods**: Clinical charts of 251 GD patients (202 females, 49 males, mean age 47±15.3 yr) treated with radioiodine between January 2003 and February 2011 were reviewed. From those, 42 patients relapsed and needed additional 131I therapy (Group A = 34 females, 8 males; mean age 49.5±16.2 yr). The average time between first treatment and recurrence was 15.9±11.9 months. To obtain a case-control group (Group B), 42 patients successfully submitted to a single course of 131I therapy, were randomly selected between 2003 and 2007 (33 females, 9 males; mean age 47.3±15.5yr). Success of 131I therapy was defined as an euthyroid or hypothyroid status at 3 years post-therapy without the need for additional radioiodine treatment, surgery or antithyroid medication. Each group was characterized for thyroid mass, 24h-RIU, and radioiodine therapeutic activity administered. A non parametric Mann-Whitney U test has been used for comparison of those parameters between the two groups. **Results**: Four Group A, the mean (and range) of 24h-RIU, thyroid mass, and therapeutic activity administered were, respectively: 59.1%±10.7 (36-82); 78.2g±35.5 (28-172) and 414.4MBq±170.2 (111-814). For Group B were: 53.6%±10.9 (32-75); 48g±25.7 (20-170); 362.6MBq±114.7(196.1-740). Statistical analysis showed that the need for a second treatment in GD patients was significantly correlated with thyroid mass ($p<0.01$) and to 24h-RIU ($p<0.033$) but not with the administered activity ($p>0.05$). **Conclusions**: In our experience, recurrence of Graves Disease after radioiodine therapy is associated with heavy thyroid glands and high values of 24h-radioiodine uptake and but not with the administered therapeutic activity.

## OP618

### Radioidine therapy - a review

**R. Teixeira**, R. Brito, R. Castro, I. Amorim; CHP, Porto, PORTUGAL.

**Aim:** In this study, we analysed the results of radioiodine therapy for treatment of toxic multinodular goiter, toxic diffuse goiter,and functional autonomy, performed in the Nuclear Medicine Department of Centro Hospitalar do Porto during 2012 **Methods:** Retrospective study analysis of 52 patients (47 women, 5 men; age: 58,25 +/- 15,33 years) records who received RAI treatment for hyperthyroidism the Nuclear Medicine Department of Centro Hospitalar do Porto between 2011 and 2012 were treated and analyzed. 28 patients were diagnosed with toxic diffuse goiter. The other ones, had functional autonomy (16) and Goiter (8). The administered activity ranged between 370 and 740MBq, according to the clinical situation. **Results:** The treatment of hyperthyroidism had a global success rate of 85%, with 44 of 52 patients achieving euthyroidism or hypothyroidism. The frequency of normalized TSH was 35% (18/52) and the rate of post-treatment hypothyroidism reached 50% (26/52). 15% of the patients (8/52) had residual hyperthyroidism after the treatment, and this number was more significant in the group of patients with toxic diffuse goiter disease (5/28 - 18%), as was expected, regarding the data from similar studies. The rate of residual hyperthyroidism in toxic multinodular goiter and functional autonomy patients was 12% (1/8 and 2/16, respectively). There was no significant difference in the response rate to different doses of RAI treatment groups. **Conclusions:** Radioactive iodine treatment is an effective modality for definitive treatment of hyperthyroidism. We had a success rate of 85%, which is acceptable according to the references from larger studies (80-100%)., Response rate was related to etiology ( lower in toxic diffuse goiter) but was not related to gender or RAI dosage etiology.

## OP619

### Can dosimetry help to predict euthyroidism after 131I radioiodine treatment of solitary thyroid nodule?

**A. Skanjeti**[1,2], A. Pia[3], G. M. Delgado[1], D. Bianciotto[1], A. Galati[1], E. Trevisiol[1], V. Podio[1]; [1]Nuclear Medicine Unit, San Luigi Gonzaga Hospital, University of Turin, Orbassano, ITALY, [2]Medical Science Department, University A. Avogadro, Novara, ITALY, [3]Medicine 1, San Luigi Gonzaga Hospital, Orbassano, ITALY.

**Introduction.** Recent SNM guidelines suggest to administer 3-8 MBq for each gram of thyroid tissue in order to reach a non hyperthyroid status, while EANM guidelines suggest to reach a dose of 100-400 Gy depending on type of disease. This second point of view is based on the principle that dosimetry, i.e. the metabolism of radioiodine within the thyroid can determine the outcome of radiation in the gland. However, although reasonable, it has not been shown unequivocally that dosimetry allows better outcome. The Aim of this pilot study

was to evaluate whether dosimetry and parameters that consent a dose evaluation can be useful in order to predict outcome in hyperthyroid patients with solitary nodule and successfully treated with radioiodine. **Material and Methods**. Thirty-one consecutive patients with solitary nodule and successfully treated with 131I radioiodine were included. In 27 patients euthyroidism was durably reached during the follow up, while in 4 hypothyroid state was the final outcome. All of them underwent Radioiodine Uptake Test (RUT) with 5 measurements (6h, 24h, 48h, 72h, and 96h), thyroid scintigraphy to estimate gland mass and radioiodine administration. Bi-compartimental model was used to estimate residence time and dose was estimated according to EANM guidelines based on administered activities of radioiodine. Uptake at 6h, uptake at 24h, mass gland, dose, age, residence time, activity and activity/mass were compared in patients with stable euthyroidism versus patients with hypothyroidism in the follow up. **Results.** Only uptake at 6h was different in these groups of patients (p=0.05 at Welch t-test), the logistic regression seemed to confirm the significant correlation (p=0.08) between uptake at 6h and outcome of the treatment. The other parameters were not significantly correlated with the treatment effect. **Conclusion**. This pilot study, performed in a very small population, did not show any significant correlation between dose and treatment outcome; however, uptake at 6h, a parameter that allows to define radioiodine metabolism, predicted euthyroidism versus hypothyroidism. Consequently, we are engaged to examine in depth the potential correlations of iodine metabolism with radioiodine treatment outcome in hyperthyroid patients.

## OP620

### The influence of radioiodine therapy in 1470 patients with subclinical hyperthyroidism

**S. Abdelrazek**, P. Szumowski, J. Mysliwiec, M. Mojsak, A. Kraszynska, A. Amelian-Filonowicz; Department of Nuclear Medicine, Medical University of Bialystok, Bialystok, POLAND.

The Aim of our study was to assess the influence of radioiodine ($^{131}$I) therapy on the achievement of euthyroidism, prevention of adverse effects on the cardiovascular and prevent evolvement to overt hyperthyroidism. **Material and Methods:** We treated 1470 patients refeerd to our department during the last 7 years, aged 24-76 years; 88% of them were female and 12% male; 490 patients with multinodular goitre (MNG), and 980 patients with autonomous nodule (ATN). Some of the patients were treated with antithyroid drugs for 1 to 3 months before $^{131}$I therapy (140 patients). Malignant changes were excluded in all nodules by fine needle aspiration biopsy. All the patients had serum TSH levels <0.1 mU/l and effective T-half was more than 3 days at the time of treatment. The activity dose was calculated by the use of Marinelli's formula and ranged between 200 and 800 MBq. The absorbed dose (Gy) ranged between 180 and 300, and was proportional to thyroid volume. Follow up control was done every 6 weeks. **Results:** Euthyroidism achieved in 99% of patient with ATN and 94% of MNG; 1% of patients with ATN and 5% of patients with MNG develop hypothyroidism. 1% of patients with MNG were in subclinical hyperthyroidism and received second dose of radioiodine therapy. In all of the patients, the symptoms and signs of subclinical hyperthyroidism disappeared (palpitation, tachycardia, atrial fibrillation, exercise tolerance improved, the blood pressure normalised and the quality of life improved). **Conclusions**: Our result is good and is in the range of the existing literature. The achievement of euthyroidism and the remission of the symptoms and signs of subclinical hyperthyroidism, were due to good diagnosis, well preparation of the patients; accurate measurement of administered activity, effective half-life, and well-organised follow up. We recommend early treatment of subclinical hyperthyroidism, and long period of follow up visits in our department to evaluate the long term effect of radioiodine therapy.

## OP621

### Radioiodine 131 therapy in hyperthyroidism Evaluation of French nuclear medicine practices

**D. BERNARD**[1], C. BOIN[1], J. ROUX[2], M. WOLF[2], B. ALLENET[3], L. FORONI[3], D. FAGRET[2], M. DESRUET[1]; [1]Radiopharmacy, University Hospital, Grenoble, FRANCE, [2]Nuclear Medicine Unit, University Hospital, Grenoble, FRANCE, [3]Pharmacy, University Hospital, Grenoble, FRANCE.

**Aim** Radioiodine 131 (RAI) is currently used routinely in the treatment of hyperthyroidism including Graves' disease (GD), toxic multinodular goitre (TMNG) and toxic solitary nodule (TSN), It has proved to be safe, efficacious and relatively inexpensive therapy. But after more than 60 years, many protocols are coexisting and no consensus exists on the most appropriate way to prescribe RAI dose: fixed dose regime or calculated doses based on gland size or turnover of RAI. This is the first nationwide French survey assessing the current practices about radioiodine treatment in thyrotoxicosis. **Methods** We sent a questionnaire to French nuclear medicine hospital units and cancer treatment centres (n=69) about their practices in 2012. Questions were asked about RAI treatment: objectives, way to prescribe the therapeutic dose and its factors, radioisotope use to explore thyroid function and method of gland size measurement. **Results** We received 40 responses. Euthyroidism was a successful treatment outcome for 33% of French respondents whereas hypothyroidism was the Aim for 26%. Antithyroid drugs were stopped 7 days on average (range 3-21 days) before therapy. 68% of physicians used ultrasound for thyroid volume measurement. Calculated doses were used by 40% of clinicians (Marinelli's formula: 80%). Factors influencing prescription were thyroid uptake (100%) based on radiotracer iodine-131 (33%) or iodine-123 (67%), thyroid volume (93%) and disease (80%). Fixed activities represented 60% of the prescribed doses (72,5% for TMNG and TSN). The administered dose was chosen between 1 to 3 levels of standard doses, according to the patient characteristics. Factors influencing this choice were disease, with respectively a median of 370MBq (range:185-740), 555MBq (185-740), 555MBq (296-925) for GD, TSN and TMNG, thyroid volume (59%) and thyroid uptake (52%) with the radiotracer iodine-123 (30%) or technetium-99m (70%). Even physicians using fixed doses performed pretherapeutic thyroid scan and uptake (98%). RAI therapy was administrated in capsule form (64%), intravenous (20%) or liquid form (16%). **Conclusion** This study shows that practices about prescription of therapeutic dose of iodine-131 are heterogeneous, but the actual trend in France as in Europe, is administration of fixed doses which are cost and time effective. Meta-analysis should be performed to clarify this debate especially about treatment outcome after fixed or calculated doses. Another point is highlighted: liquid form of $^{131}$I is still used despite existence of substitutes (for thyroid uptake e.g. iodine-123; for the treatment e.g. iodine-131 capsule) which prevents high exposition to medical personnel and increased risk of contamination.

1509 - Tuesday, Oct. 22, 16:30 - 18:00, Rhône 3A/3B

## Radionuclide Therapy & Dosimetry: Radioembolisation of Primary & Metastatic Liver Cancer

## OP622

### Feasibility of temporary protective embolization of normal liver tissue using degradable starch microspheres during radioembolization of liver metastases

**H. Ahmadzadehfar**[1], C. Pieper[2], S. Ezziddin[1], K. Wilhelm[2], H. Schild[2], C. Meyer[2]; [1]University Hospital Bonn-Department of Nuclear Medicine, BONN, GERMANY, [2]University Hospital Bonn-Department of Radiology, BONN, GERMANY.

**Purpose:**To describe and evaluate a new approach to protect non-target healthy liver tissue during radioembolization of liver metastases with 90Y microspheres using degradable starch microspheres (DSM) as a short-term embolization. **Methods**: 5 patients underwent protective temporary embolization using DSM (Embocept S) of normal liver tissue that could not be excluded from the area treated with radioembolization through catheter repositioning. Clinical symptoms, laboratory findings, preinterventional imaging, 99mTc-MAA and Bremsstrahlung SPECT/CT as well as baseline and follow-up imaging with 18F-FDG PET/CT and MRI were evaluated regarding technical and clinical success of protective embolization. **Results:** Temporary embolization of arteries supplying normal liver tissue using DSM was technically successful in 5/5 cases. 99mTc-MAA and Bremsstrahlung SPECT/CT as well as follow-up imaging 4 weeks after radioembolization demonstrated satisfactory irradiation of the tumor and successful protection of normal liver tissue. There were only mild hepatotoxic effects (grade 1) on laboratory follow-up exams and no adverse events associated with DSM embolization or radioembolization were recorded. No peri - or postinterventional complications occurred. **Conclusion:** Temporary embolization with DSM before radioembolization is feasible and can effectively protect areas of normal liver tissue from irradiation and permanent embolization if other Methods such as catheter repositioning are not possible due to location of the metastases.

## OP623

### Selective internal radiotherapy for unresectable liver tumours: The Lausanne experience

**S. Adib**[1], S. Baechler[2], S. Gnesin[2], N. Cherbuin[1], Y. Lachenal[3], P. Bize[3], J. O. Prior[1], A. Denys[3], A. Boubaker[1]; [1]Department of Nuclear Medicine, Lausanne University Hospital, Lausanne, SWITZERLAND, [2]Institute of Radiation Physics, Lausanne University Hospital, Lausanne, SWITZERLAND, [3]Department of Radiology, Lausanne University Hospital, Lausanne, SWITZERLAND.

**Aim**: Ongoing prospective study to evaluate the Y-90 microsphere therapy feasibility and clinical efficacy in patients with primary or metastatic unresectable liver tumours. **Materials and Methods:** We reviewed our prospective hepatic arterial therapy registry for patients who had received Selective Internal Radiotherapy (SIRT) for unresectable hepatic malignancies from January 2010 to December 2012. A simulation study with Tc-99m-MAA was performed to measure the degree of shunt to the lungs and evaluate the relative amount of activity deposited in the tumoral and the non-tumoral liver. Out of 54 cases, 11 patients could not be treated due to lung/intestinal shunting or rapidly progressive disease.

The prescribed radio microspheres activity was calculated using a partition model adjusted, in some cases by the body surface area method. Baseline PET/CT and MRI or CT scans were performed in all patients. Response was assessed early using PET/CT-imaging for FDG-avid tumors (n=28/45) and/or MRI-CT at 4-6 weeks (total of 42/45), then at 3 and 6 months. **Results:** A total of 43 patients (27 men/16 women) with a median age of 67 y (range 39-87), received 48 treatments (21 right-lobe, 9 left-lobe, 16 dual-lobe, and 3 radiation segmentectomy). The disease types were hepatocellular carcinoma (n=15), colorectal carcinoma (n=8), cholangiocarcinoma (n=6), neuroendocrine tumor (n=5), breast cancer (n=4), melanoma (n=3), adrenal cortical carcinoma (n=1), and leiomyosarcoma (n=1). The injected activity ranged from 0.4 to 3.5 GBq (mean 1.5 GBq) of Yttrium-90 resin microspheres. Follow-up data was available for 45 treatments. Overall response to therapy was seen in 34 patients (76%) at the first control; three patients had a complete response, 28 patients had partial response and 3 patients had stable disease. Progression-free survival rate at 3 months was 56% (25/45 patients). **Conclusions:** SIRT with Y-90 microspheres is feasible in most patients with unresectable liver tumors, but requires a multidisciplinary team. Our results support the idea that it is a safe procedure achieving good local control of disease in most cases.

## OP624

### Is it possible to perform voxel dosimetry in a simple way in patients treated with Selective Internal Radio Therapy using 90Y microspheres?

**C. Pettinato**[1], A. Fracchetti[2], S. Civollani[1], F. Monari[3], G. Gavaruzzi[4], E. Giampalma[5], B. Angelelli[6], C. Mosconi[5], C. Nanni[4], R. Golfieri[5], R. Mazzarotto[3], S. Fanti[4]; [1]AOU S.Orsola Malpighi, Medical Physics Unit, Bologna, ITALY, [2]ASAA Ospedale di Bolzano, Medical Physics Unit, Bolzano, ITALY, [3]AOU S.Orsola Malpighi, Radiotherapy Unit, Bologna, ITALY, [4]AOU S.Orsola Malpighi, Nuclear Medicine Unit, Bologna, ITALY, [5]AOU S.Orsola Malpighi, Radiology Unit, Bologna, ITALY, [6]AOU S.Orsola Malpighi, Oncology Unit, Bologna, ITALY.

**Aim:** Several Methods have been used to perform dosimetry in SIRT and most of them involve the pre-therapeutic study made using the 99mTc-MAA scan. Although it presents several limitations, it is still the only pre-therapeutic dosimetric approach available. The Aim of this work was the evaluation of the use of an homemade program, based on ImageJ, to calculate Dose Volume Histograms (DVHs) and to compare the average dose with the mean dose calculated assuming a uniform distribution into the treated volume. **Material and Methods**: twenty-eight patients affected by HCC liver cancer have been retrospectively included in this study. Each patient underwent a SPECT scan after the injection of about 100 MBq of 99mTc-MAA into the hepatic artery. Dosimetry was performed assuming that: a) each voxel receive dose for local deposition only; b) total counts of the 99mTc-MAA images represent the total injected activity. MIRD formalism was used to calculate the absorbed dose at voxel level as the product between the cumulated activity and the self-irradiation S factor, calculated dividing the mean energy of beta radiation of Y90 by the mass of the voxel. Dose at voxel level was calculated by scaling the 99mTc-MAA images by a factor which take into account the S value, the injected activity and the total counts into the liver: dose maps were obtained. Scaled images were processed with the dedicated ImageJ plugin by positioning ROIs on treated volume and DVHs were plotted. Mean dose and maximum dose were calculate at voxel level. **Results**: The average absorbed doses calculated using the DVHs and considering only the uniform distribution on the entire treated volume were respectively 130.3 ± 76.4 Gy (range: 29.1 - 338.3 Gy) and 142.1 ± 72.4 Gy (range: 48.97 - 917.2 Gy). Although the average values look quite similar the differences found using these two Methods were often very high, ranging from 0.6% up to 400%. A preliminary comparison with DVH obtained on post-treatment Y90 PET/CT images revealed even higher differences. **Conclusion**: The homemade plugin in ImageJ is a useful tool to create DVH of selected volumes, in an easy and chip way. Our results confirm that dosimetry of SIRT treatments, simple in principle, is complicated by several limitations and, in our opinion, one of the most important is related to the fact that treated volumes represent perfusion territories that can be sensibly different from anatomical segment volumes as evaluated with CT.

## OP625

### Occupational Exposure Following Yttrium-90 Microspheres SIR Therapy

P. FONTAINE[1], G. BOIRIE[2], A. DIEUDONNE[2,3], D. LEGULUDEC[4], R. LEBTAHI[1,3], **M. BEN REGUIGA**[1,3,2]; [1]APHP - Hôpital Beaujon - Service de Médecine Nucléaire, Clichy, FRANCE, [2]APHP - Hôpital Beaujon - Unité de Radioprotection - Radiophysique, Clichy, FRANCE, [3]INSERM U773, Paris, FRANCE, [4]APHP - Hôpital Bichat - Service de Médecine Nucléaire, Clichy, FRANCE.

**Introduction** Selective Internal Radiation Therapy (SIRT) is a promising technique for solid hepatic neoplasms treatment. SIRT consists in implanting radioactive microspheres (RMS)in targeted hepatic lesions via femoral artery. Two RMS - Therapspheres® [glass-microspheres/TSR] and Sir-Spheres® [resin-spheres/SSR]- are marketed in the European market, both radiolabeled with Yttrium-90. The objective of this study is to assess occupational exposure for nuclear medicine, radiology and clinical staff involved in Y90-RMS preparation and implantation. **Materials & Methods** The study was conducted on 20 patients treated for Hepato-Cellular Carcinoma: 10 treated with TSR and 10 with SSR. Dose rate (DR, mSv/h) or absorbed doses (mSv) measurements were made during all steps of TSR and SSR handling: sources receipt and unpacking, preparation, transport to radiology, implantation, and patient care. Measurements were made with portable ionization chamber(Babyline®/Nardeux), spectrometer(FieldSpect®/Aries), digital dosimeter (NED®/Unfors) and operational dosimeter (Mk2/Siemens). Values were expressed as mean±SD. **Results** Patients received of 1.8GBq to 3.1GBq of TSR and 0.55GBq to 2.4GBq of SSR. TSR were delivered ready-to-use with the prescribed activity. For SSR only one activity was commercially available and shipped (3GBq at calibration-time)requiring a preparation step to adjust needed activity. DR measured during RMS was 1723±157µSv/h SSR and 1189±92µSv/h for TSR. When preparing spheres in radiopharmacy, fingers and whole body doses were respectively 8326±2360µSv and 12.3±5,2µSv for Sir-Spheres® vs. 33.5±7.8µSv and 1.1±0.3µSv for TSR. DR in contact with carrying case during RMS transfer to radiology were 299±102µSv/h for SSR and 5.3±1.2µSv/h for TSR. During RMS infusion, radiologist's finger doses were limited to 3.6±1µSv for SSR and 0.7±0.3µSv for TSR. Finally, following RMS implantation in patients, DR were respectively for SSR and TSR 23.8±14.2 and 56.3±69.6 in contact with patient's abdomen right and 0.77±0.31µSv/h.GBq and 0.92±0.60µSv/h.GBq when measured at 1m from sternum. Discussion and **Conclusion** Occupational exposure related to SSR was greater than with TSR, particularly finger doses during preparation phase. In addition, due to the longer duration of SSR administration (60-90min vs. <10min for TSR), exposure of radiologists is higher with resin spheres. Finally, the absence of lead in carrying cases shielding of SSR makes DR higher during SSR transport to radiology. However, once implanted, DR were not significantly different, less than 1µSv/h.GBq at 1m from patient for both products. These results show that prior to SIRT implementation particularly with resin RMS, a special attention should be devoted to procedures optimization and staff training, in order to control and limit workers occupational exposure.

## OP626

### Dose-response evaluation after Yttrium-90 resin microsphere radioembolization of breast cancer liver metastases

**S. Gnesin**[1], A. Boubacker[2], S. Adib[2], N. Cherbuin[2], P. Bize[3], A. Denys[3], J. O. Prior[2], F. R. Verdun[1], S. Baechler[1]; [1]Institute of Radiation Physics, Lausanne University Hospital, Lausanne, SWITZERLAND, [2]Department of Nuclear Medicine, Lausanne University Hospital, Lausanne, SWITZERLAND, [3]Department of Radiology, Lausanne University Hospital, Lausanne, SWITZERLAND.

**Aim**: Yttrium-90 resin microsphere radioembolization is a valuable therapeutic option in metastatic breast cancer patients with progressive disease refractory to chemotherapy. The goal of this study was to evaluate the dose-response relationship of liver metastasis based on a 3D voxelized 90Y PET dosimetry. **Materials and Methods**: We studied the dose-response relationship of twelve hepatic lesions in four selected patients with metastatic breast cancer who underwent 90Y radioembolization (Sirtex SIR-Spheres Pty Ltd.). The administered activity ranged from 1 to 1.3 GBq. Ten days before treatment, patients underwent a baseline 18F-FDG PET/CT. The determination of the 90Y-microsphere activity to administer for treatment was based on the BSA method refined with the partition model derived from a 99mTc-MAA SPECT/CT performed a week prior to radioembolization. Within 24 hours after treatment, 90Y TOF PET/CT imaging was performed. A follow-up 18F-FDG PET/CT was performed 1 month after the treatment to evaluate response to radioembolization. For each patient, 3D voxelized dose-maps were obtained from the post-treatment 90Y TOF PET/CT. A volume of interest (VOI) was drawn for each selected hepatic lesion using the baseline 18F-FDG PET/CT. To obtain dose-volume histogram (DVH) for each lesion, image coregistration and VOI masks were generated using the PMOD 3.4 software and then exported in Matlab for dose calculation. Furthermore, the average absorbed dose in lesions was corrected for PVE effects by multiplication for appropriate (phantom-based) recovery coefficients according to the lesion size. Early metabolic lesion response was assessed in terms of variation in the maximum standard uptake value (ΔSUVmax) between baseline and follow-up 18F-FDG PET/CT. The average absorbed dose for each lesion was associated with the respective metabolic response. **Results**: For the 12 selected lesions, the average volume was 35 cm3 (range 8-147 cm3) and the average absorbed dose was 92 Gy (range 32-137 Gy). We observed a reduced average absorbed dose as the volume of the lesion increased. Metabolic response was observed for all lesions with a measured average ΔSUVmax of -66% (range -28% to -83%). The observed dose-response relationship suggests that better metabolic response was obtained in lesions receiving the higher dose. **Conclusions:** Three-dimensional voxelized dose-map based on 90Y TOF PET/CT imaging is an effective tool for assessing tumor dose-response relationship. Patients with breast cancer liver metastases showed good short-term metabolic responses with average absorbed doses to lesions

ranging between 32 and 137 Gy. A trend showing improved metabolic response in lesions receiving higher doses was observed.

## OP627

### Voxel-based dose heterogeneity and dose-volume effects in 90Y-microsphere therapy dosimetry

J. Mikell[1,2], F. Mourtada[3], **S. C. Kappadath**[1,2]; [1]University of Texas MD Anderson Cancer Center, Houston, TX, UNITED STATES, [2]UT Graduate School of Biomedical Sciences, Houston, TX, UNITED STATES, [3]Christiana Care Health System, Newark, DE, UNITED STATES.

**Objective:** Standard 90Y-microsphere therapy planning (STD) conservatively assumes uniform uptake to total liver (normal-liver and tumor) to minimize radiation induced toxicities but fails to provide tumor doses. The three-compartment model (3CM) that accounts for preferential uptake in tumor has been used to estimate tumor doses (Ho 1996). However, ambiguity in estimation of tumor uptake and differences between planning 99mTc-MAA and post-therapy 90Y-microsphere images lead to significant dose uncertainties (MacLellan SNMMI 2012). We propose a new method for calculating 3-dimensional dose distributions (3Ddose) based on post-therapy quantitative 90Y SPECT/CT to investigate dose heterogeneity and dose-volume effects. **Materials and Methods**: 3Ddoses were generated from DOSXYZnrc Monte Carlo (MC) simulations and ATTILA a grid-based Boltzmann solver (GBBS). We retrospectively computed normal-liver and tumor doses for 5 patients after 90Y-microsphere therapy using MC and GBBS. Cumulative dose-volume histograms (DVH) were calculated for total liver using 3Ddose, 3CM, and STD. For evaluation of heterogeneity, we computed ratios of maximum to minimum dose in normal-liver and tumor; the integral uniformity of the 3Ddose in normal liver (IUNL) and tumor (IUT) was also calculated. We computed percent differences of minimum doses covering 100% of normal-liver (DL100) and tumor (DT100) and median dose to normal-liver (DL50) and tumor (DT50) for 3Ddose and 3CM. **Results:** The average total liver dose calculated by 3Ddose (using both MC and ATTILA) agreed to within 5% of the STD. 3Ddose calculations showed large dose heterogeneity with over 400% variation in both normal-liver and tumor compartments relative to 3CM. The ranges of max/min doses in normal-liver and tumor were 1.8-to-5.0 and 2.3-to-6.4, respectively. IUNL ranged from 29% to 67%. IUT ranged from 40% to 73%. Compared to 3CM, 3Ddose estimates of DL100 were higher (mean 400%, range -50% to 1600%), while those of DT100 were lower (mean -40%, range -67% to +3%). Compared to 3CM, 3Ddose estimates of DL50 were higher (mean 900%, range 38% to 2600%) while those of DT50 were lower (mean -13%, range -56% to +69%). **Conclusion**: Doses quantified from 3Ddose exhibited substantial heterogeneity in normal-liver and tumor. While previous works have shown lower normal-liver and higher tumor doses with the 3CM compared to STD, 3Ddose suggests that 3CM may be under/over estimating normal-liver/tumor doses. Dose heterogeneity and dose-volume effects likely play a key role in understanding tumor response and normal tissue toxicity in 90Y-microsphere therapy. 3Ddose evaluations for N=20 patients are ongoing.

## OP629

### 3D-Personalized Monte Carlo Dosimetry in 90Y-Microspheres Therapies of Primary and Secondary Hepatic Cancers: Absorbed dose and Biological Effective Dose considerations

A. Petitguillaume[1], M. Bernardini[2], C. de Labriolle-Vaylet[3], D. Franck[1], **A. Desbrée**[1]; [1]Institut de Radioprotection et de Sûreté Nucléaire, Fontenay-aux-Roses, FRANCE, [2]Hôpital Européen Georges Pompidou, Paris, FRANCE, [3]Hôpital Trousseau - UPMC Univ Paris 06, Paris, FRANCE.

**Purpose**: A 3D-Personalized Monte Carlo Dosimetry (PMCD) was developed for treatment planning in nuclear medicine. The method was applied to Selective Internal Radiation Therapy (SIRT) using 90Y-microspheres for unresectable hepatic cancers. **Methods**: The PMCD method was evaluated for 20 patients treated for hepatic metastases or hepatocellular carcinoma at the Hôpital Européen Georges Pompidou (France). First, regions of interest were outlined on the patient CT images. Using the OEDIPE software, patient-specific voxel phantoms were created. 99mTc-MAA SPECT data were then used to generate 3D-matrices of cumulated activity. Absorbed doses and Biologically Effective Dose (BED) were calculated at the voxel scale using the MCNPX Monte Carlo transport code. Finally, OEDIPE was used to determine the maximum injectable activity (MIA) for tolerance criteria on organs at risk (OARs), i.e. the lungs and non tumoral liver (NTL). Tolerance criteria based on mean absorbed doses, mean BED, Dose-Volume Histograms (DVHs) or BED-Volume Histograms (BVHs) were considered. Those MIAs were compared to the Partition Model with tolerance criteria on mean absorbed doses, which is a conventional method applied in clinical practice. **Results**: Compared to Partition Model recommendations, performing dosimetry using the PMCD method enables to increase the activity prescription while ensuring OARs' radiation protection. Moreover, tolerance criteria based on DVHs allow to enhance treatment planning efficiency by taking advantage of the parallel characteristic of the liver and the lungs, whose functions are not impaired if the level of irradiation to a fraction of the organ is kept sufficiently low. Finally, multi-cycle treatments based on tolerance criteria on mean BED and BVHs, were considered to go further in the dose optimization, taking into account biological considerations such as cell repair or radiosensitivity. **Conclusion:** Besides its feasibility and applicability in clinical routine, the interest of a personalized Monte Carlo dosimetry for treatment planning in SIRT was confirmed from those patient studies. Finally, the PMCD is a general purpose method that could be used to perform treatment planning and dosimetry for different therapies and isotopes in nuclear medicine.

1510 - Tuesday, Oct. 22, 16:30 - 18:00, Tête D'Or 1/2

## Physics & Instrumentation & Data Analysis: Radiation Protection Occupational / Image Quantification & VOI Delineation

## OP630

### Dosimetric evaluation to medical workers operating in a PET/CT department after the use of dynamic techniques.

**K. Dalianis**, F. Vlachou, K. Gogos, V. Fillippi, A. Nikaki, D. Kechagias, S. Merisoglou, V. Papoutsis, R. Efthymiadou, V. Prassopoulos; DTCA Hygeia Department of PET/CT, Athens, GREECE.

**Purpose** Positron Emission Tomography is considered to be one of the most relevant diagnostic imaging techniques having peculiar characteristic to provide both functional and morphological information for the patient. Due to the high-energy tracers emitting 511 KeV used in PET/CT departments and considering the risks associated to ionizing radiation that have been derived from previous studies, special attention is needed when dealing with radiation protection aspects in a PET/CT modality . Since new radiopharmaceuticals such us [18F]-fluorothymidine and 18F fluoromethylcholine are used, new imaging dynamic techniques are performed and new measurements concerning the doses to medical staff are needed. The Aim of this study was to measure the effective wholebody dose of the personnel in comparison with measurements that have been made in the past. **Material - Method** The estimation of equivalent dose from external dosimetry for all seven members of the staff was monitored with the use of TLDs badges and electronic dosimeters worn at the upper pocket of their overall. The average workload of the department is 6-8 patients per day. In 2012, 983 patients were examined. In our department 18F-FDG, 18F-FCT, 18F-FCH is available in multi dose vials. Data were collected day-to-day concerning the interaction of the staff during PET/CT procedures. **Results:** We compared the first six months of 2012 a period in which no FLT or FCH procedures were performed, with the second semester in which 96 FLT and 66 FCH examinations were performed. The average number of FDG patients was the same for every day, and all patients received 330-390 MBq dose each. Regarding the whole body doses no changes were observed concerning medical physicist. The measurements for the nurses show increased wholebody dose of about 7-12% and that is due to the longer time spent near the patient. Concerning the technologist doses, an increase of about 15-21% was measured because they are near to patient at the time of the injection. **Conclusions** Regulations exist to ensure safety of the medical workers according to ALARA principles. From our results we can observe that although there is an increase of the doses for technologists and nurses the numbers are significantly lower than the recommended annual dose limit by Euratrom 97/43.

## OP631

### Occupational Radiation Exposures of Professionals - Historic Analysis of a Nuclear Medicine Department

**P. Gil**[1], J. Isidoro[1], G. Costa[1], J. Pedroso de Lima[1,2]; [1]Centro Hospitalar Universitário de Coimbra, Coimbra, PORTUGAL, [2]Instituto de Ciências Nucleares Aplicadas à Saúde, Coimbra, PORTUGAL.

**Aim**: The Aim of this work was to analyze the historic records of the 'personal dose equivalent' from all workers. We evaluated the results taking into account the different professional groups, the number of working professionals and the workload. **Materials and Methods**: The personal dose equivalent (deep dose-Hp(10)) data records, over 23 years (1990-2012), were analyzed. Film badge dosimeters were used until 1997, and then replaced by thermoluminescent dosimeters. Professionals were subdivided in 6 groups: medical doctors (MD), NM technicians (NMT), auxiliary personnel (AUX), medical physicist (MP), radio-pharmacist (PHARM), and administrative personnel (ADM). The annual total work load was calculated by adding the number of scintigraphic, therapeutic and PET/CT procedures. The department average dose, dose per professional, and dose per professional normalized to the annual work load (number of exams) were calculated. Several events were identified and their impact evaluated, namely: the beginning of in-patient iodine-131 therapy procedures (1993), hiring a medical physicist (1995) and significant number of PET/CT procedures (2004), PET/CT was installed in 2003. **Results**: The annual average dose (mSv) and standard deviation for each professional group was evaluated (in parenthesis is the group percentage):

MD 1.0±1.4(24.2%); NMT 3.3±1.6(52.5%); MP 0.3±0.3(0.7%); PHARM 1.1±1.6(3.3%); AUX 1.3±0.8(18.5%); and ADM 0.1±0.2(0.8%). The maximum dose reported was 8.30mSv in 1995 and 6.85mSv in 2003. The number of procedures has increased over the years, with the number of PET/CT rising substantially since 2005. In 2012 the work load distribution was: scintigraphy 80.1%, therapeutic 1.7%, and PET/CT 18.2%. The average dose per worker (mSv/worker) for: 1990-1992, 1993-1995, 1996-1998, 2002-2004, 2005-2007, 2010-2012 was 2.0, 2.2, 1.0, 1.5, 1.4 and 1.1 respectively. The average dose per worker normalized to the number of procedures in 1990-1992 was 0.8μSv and in 2010-2012 was 0.1μSv which corresponds to a reduction of 88%. **Conclusion**: In 1993 (Introduction of therapeutics) there was a slight dose increase of 12%. In 1996 there was significantly dose reduction of 55%, probably explained by changes in radiation protection procedures. Although higher exposure risk in PET/CT we had little or no dose change. The highest record dose (8.3mSv) is punctual and well bellow the whole body dose limit (20mSv) for professionals exposed. From 1990 to 2012 globally the number of procedures has increased, but the average dose per worker normalized to the number of procedures has declined in 88%, showing good work practices.

## OP632

### A Method for the Identification of Hand Exposure by Annihilation Photons and Positrons During the Handling of 18F Radiopharmaceuticals

**M. Fulop**[1], J. Hudzietzová[2], J. Sabol[2], O. Bělohlávek[3], I. Makaiová[4], P. Povinec[5], J. Veselý[4], A. Vondrák[6], P. Mihalová[3]; [1]Slovak Medical University, Bratislava, SLOVAKIA, [2]Faculty of Biomedical Engineering of Czech Technical University in Prague, Kladno, CZECH REPUBLIC, [3]PET Centre, Na Homolce Hospital, Prague, CZECH REPUBLIC, [4]Oncology Clinic of St. Elizabeth, Bratislava, Bratislava, SLOVAKIA, [5]Nuclear Medicine Clinic, BIONT, Bratislava, SLOVAKIA, [6]Izotopcentrum, Nitra, SLOVAKIA.

**Introduction**: During the preparation and administration of radiopharmaceuticals to patients at nuclear medicine departments, the exposure received by the hands of nuclear medicine staff from photons and especially positrons due to possible local surface contamination of the workplace as well as of some tools may be rather significant in some cases. Some of the most energetic positrons may easily penetrate the thin walls of syringes and infusion cannulas and thus contribute to the skin dose. At present, there is insufficient data available about the positron exposure of the hands, which would serve as a basis for the optimization of procedures, including the preparation and administration of positron radiopharmaceuticals. This deficiency impedes the improvement of protective shielding of relevant tools against positrons and the availability of more accurate specifications of the distribution of local exposure of the skin of hands. **Methods:** Individual exposure due to photons and positrons has been identified using two types of TLDs with different sensitivities to photons and positrons. The dosimeters MCP-7 of thickness 0,9 mm and MCP-Ns with an active layer of 0.05 mm calibrated in terms of H(0.07) have been used for hand dose mapping in PET centres in the Czech Republic and Slovakia. Altogether 34 measurements of 16 workers in the Czech Republic were performed. The personnel was monitored during 50 preparations and administrations of radiopharmaceuticals where they wore special gloves with 12 twin TLDs. Similar measurements were carried out in the Slovak Republic where 60 measurements were performed on 6 workers serving FDG patients. **Results:** Based on the measurements of the PET personnel's local exposure of the skin of their hands to photons and positrons, about 25% of cases of significant exposures to positrons were identified. The forefinger pads and thumbs appeared to be the most exposed locations corresponding to more than 5mSv.GBq-1. In some cases the assessment showed an increase of local exposure to positrons up to 100%. Some appropriate radiation protection procedures Aimed at the reduction of local exposure have been proposed. **Conclusion:** Although the standard finger dosimeters used for monthly monitoring of the personnel at PET departments demonstrate that exposures are lower that the relevant reference levels, our more detailed measurements have revealed that in some cases the exposure of certain spots on hands may reach levels comparable with or even higher than the dose limits for both skin and fingers.

## OP633

### Cyclotron production of 99mTc: contribution of impurities to effective and absorbed doses

**G. Lucconi**[1], G. Cicoria[2], F. Zagni[2], A. Infantino[3], M. Marengo[2]; [1]Postgraduate School in Medical Physics, University of Bologna, Bologna, ITALY, [2]Medical Physics Department, S.Orsola – Malpighi University Hospital, Bologna, Bologna, ITALY, [3]Nuclear Engineering Laboratory of Montecuccolino, Industrial Engineering Department, University of Bologna,, Bologna, ITALY.

**Aim:** There is growing interest in the production of 99mTc via the 100Mo(p,2n)99mTc reaction; this work investigates the contribution of impurities to the effective and organ absorbed doses for cyclotron produced 99mTc-radiopharmaceuticals. **Material and Methods:** MonteCarlo simulations have been performed considering a 97.46% enriched 100Mo target irradiated by a (16.03→13.3)MeV proton beam. We simulated irradiations of 3h at a current of 50 μA for tests (case A) and 6h at 100 μA granting the production of an amount of 99mTc sufficient for local supply (case B). ICRP72 dose-activity (Sv/Bq) coefficients for 99mTc and the principal impurities (97mTc, 96mTc, 96Tc, 95Tc, 94mTc, 94Tc, 99Mo, 93mMo, 97Nb, 96Nb, 95mNb) have been used; male and female ingestion coefficients were evaluated for the two irradiation cases. According to ICRP60 estimates, the fractional contribution of each radionuclide to the total effective and organ adsorbed doses has been calculated. Male and female bio-distribution and dosimetry of 99mTc-Pertechnetate, 99mTc-Methyldiphosphonate and 99mTc-Sestamibi have been obtained from ICRP80; the contribution of the impurities has been valuated considering the fraction of dose due to the impurity relative to dose from ICRP60 estimates. We considered clinical activities of 130 MBq for 99mTc-Pertechnetate and 740 MBq for 99mTc-Methyldiphosphonate and 99mTc-Sestamibi. **Results:** With no purification, isotopic and non-isotopic impurities contribute to the effective dose for a 22.4% for male and female in case A and for 29.2% and 34.3% in case B. This percentage corresponds to an extra male effective dose of 0.49 mSv (A) and 0.69 mSv (B) for 99mTc-Pertechnetate, 1.22 mSv (A) and 1.74 mSv (B) for 99mTc-Methyldiphosphonate, 1.93 mSv (A) and 2.74 mSv (B) for 99mTc- Sestamibi. An efficient purification of the target allows to remove non-isotopic impurities, reducing the effective dose due to impurities to 0.88% for male and female in case A and 1.25% and 1.58% in case B: 15 μSv (A) and 21 μSv (B) for 99mTc-Pertechnetate, 37 μSv (A) and 53 μSv (B) for 99mTc-Methyldiphosphonate, 59 μSv (A) and 84 μSv (B) for 99mTc-Sestamibi. For all radiopharmaceuticals the lower large intestine resulted the organ receiving the highest relative dose due to impurities: 1.9% for both sexes in case A and 2.8% and 3.4% for male and female in case B. **Conclusion**: The contribution of impurities in absence of purification is unjustified; the removal of non-isotopic impurities strongly reduces the effective and organ doses due to impurities to an acceptable level ( <4%) compared to generator 99mTc.

## OP634

### Evaluation of several automatic PET-segmentation algorithms for radiotherapy treatment planning in H&N using a printed sub-resolution sandwich phantom

**B. Berthon**[1], R. B. Holmes[2], C. Marshall[1], V. S. Jayaprakasam[1], M. Evans[3], E. Spezi[4]; [1]Wales Research and Diagnostic PET Imaging Centre, Cardiff, UNITED KINGDOM, [2]University Hospitals Bristol NHS Foundation Trust, Bristol, UNITED KINGDOM, [3]Velindre Cancer Centre, Cardiff, UNITED KINGDOM, [4]Department of Medical Physics, Velindre Cancer Centre, Cardiff, UNITED KINGDOM.

**Aims**: Accurate tumour localization for Radiotherapy Planning (RT) is particularly challenging for H&N cancer due to low image resolution of PET and complex anatomy of the H&N area. At present, there is still a need for evaluation and cross-comparison of automatic H&N segmentation techniques on clinically realistic data. Sub-resolution printed phantoms allow the gap between unrealistic plastic phantom studies and tests on clinical data, for which the ground truth is unknown, to be bridged. The Aim of this study was to qualitatively and quantitatively assess the performance of several automatic optimized segmentation Methods, using the sub-resolution printed phantom to recreate conditions clinically relevant to the H&N. In addition, this work investigated the feasibility of using such a phantom for evaluating segmentation techniques. **Materials and Methods**: Grey level patterns representing typical 18F-FDG uptake in the normal H&N, were generated from PET images with help from a radiologist. Three irregular lesions were drawn in the tonsils, base of tongue and side of the oropharynx. Their texture was changed to represent necrotic and randomly heterogeneous uptake. Patterns were printed with a HP Deskjet 930 printer using black ink mixed with 18F-FDG. The printed slices were assembled with 2mm spacing in a Perspex sub-resolution sandwich phantom and imaged on a GE 690 Discovery PET-CT scanner. Nine segmentation Methods, developed and optimized in house, were applied to these test images: relative thresholds, gradient-based contouring, region growing, watershed segmentation, K-means, Fuzzy C-means and Gaussian Mixture clustering and active contours. The volumes obtained were compared to the ground truth derived from the printed pattern using several performance metrics, including Dice Index (DSI) and volumetric error (VE). **Results**: Adaptive Thresholding (AT), Region-Growing and Fuzzy C-means (FCM) Methods yielded the highest DSI (0.76) on the whole dataset, and the lowest VE were obtained for AT and Gaussian Mixture Models clustering (GMC), with 8% and 4% of the true volume respectively. Preliminary results also highlighted the superiority of clustering algorithms FCM and GMC in the case of heterogeneous lesions (8% and 10% VE and 0.74 and 0.76 DSI respectively). **Conclusions**: The use of a sub-resolution printed phantom facilitates the evaluation of the performance of automatic segmentation techniques on a range of test images clinically relevant to the H&N. The GMC and FCM clustering Methods demonstrated performance superior to other techniques.

## OP635

### Performance of 18F-FDG PET automated segmentation Methods for non-spherical objects

**B. Berthon**[1], C. Marshall[1], M. Evans[2], A. Edwards[3], E. Spezi[3]; [1]Wales Research and Diagnostic PET Imaging Centre, Cardiff, UNITED KINGDOM, [2]Velindre Cancer Centre, Cardiff, UNITED KINGDOM, [3]Department of Medical Physics, Velindre Cancer Centre, Cardiff, UNITED KINGDOM.

**Aim**: Current radiotherapy treatments (RT) of H&N cancer are limited by the lack of a technique to accurately delineate the tumour volume on PET scans. The low image resolution of PET and complex anatomy of the H&N area make this task particularly challenging. Although the use of automatic segmentation (AS) has been recommended, there is still a need for a solid cross-comparison of such techniques on clinically useful data. This phantom study Aimed to quantitatively assess and compare the performance of several automatic segmentation Methods on different objects geometries relevant to clinical H&N anatomy. **Materials and Methods**: Nine segmentation Methods were developed in the Matlab environment (Mathworks, Natick, USA). These included fixed (FT) and adaptive thresholding (AT), gradient-based contouring (GC), region-growing (RG), watershed (WT), K-means (KM), Fuzzy C-means (FCM) and Gaussian mixture clustering (GCM) and active contours (AC). 17 different non-spherical volumes were manufactured with a vacuum-moulding technique, which allowed the production of sub-millimeter thin plastic walls. Volumes including tubes, ellipses, drop- and pear-shaped objects and tori, were used to investigate the effect of thin shapes, sharp corners and necrotic regions. These volumes were scanned on a GE 690 Discovery PET/CT scanner in a custom plastic phantom at a Tumour-to-Background Ratio of 5. The contours obtained on the test PET images for each method were compared to the ground truth in terms of volumetric error (VE), sensitivity, specificity, Dice similarity index (DSI) and recovered dimensions. **Results:** All automatic Methods except FCM performed significantly better ($p<0.01$) than fixed thresholding. AT performed best, with an average DSI of 0.88 and VE of 20%, followed by RG and KM method (DSI of 0.86 and 0.85, VE of 33% and 24% respectively). FCM performed worst of all automatic method because of a low sensitivity. RG systematically showed the highest errors in recovering the shape length, in particular for thin objects (up to 33% error). **Conclusions:** Results demonstrated the superiority of automatic segmentation Methods compared to fixed thresholding for the delineation of non-spherical volumes. AT, RG and KM clustering are proposed as superior Methods for the delineation of tumour volume in H&N RT Planning.

## OP636

### Automatic background determination for contrast-based threshold segmentation in PET imaging based on histograms

**U. Christ**, T. Fechter, M. Mix, J. Hennig, U. Nestle; University Hospital, Freiburg, GERMANY.

**Aim:** PET based volumes are increasingly used in radiotherapy planning e.g. for gross tumor volume (GTV) delineation. To ease this process, automatic segmentation Methods have been developed. Several widely used Methods apply thresholding based on contrasts. For those types of algorithms it is necessary to determine a background value. A drawback in the implementation of these Methods is the user dependence and the high sensitivity of the background value against highly accumulating structures in the neighborhood. To cope with this problem, we here propose a presumably more robust histogram based background computation (HBGC). **Materials and Methods**: For calculating the mean background value the histogram of the whole image is used. The mean background value is calculated as the average value of the voxels inside fixed boundaries. To avoid the contribution of the empty space around the body the lower boundary is set to 1% of the maximal voxel intensity. The upper boundary is 15% to be certain to have an adequate distance to the tumor to avoid the contribution of the partial volume effect. This HBGC is implemented in MITK Workbench software. Phantom (cylindrical phantom with 4 fillable spheres, contrasts: 16.5:1, 8.25:1, 5.5:1) and patient data (n=10) with both homogeneous and heterogeneous background are used to evaluate HBGC against another semi-automatic background determination, where the background is calculated in a so called nutshell as the average of all voxels inside a user-drawn mask and outside the tumor ROI, within a certain range depended on the estimated spatial resolution of the scanner. For both implementations the same contrast-based threshold algorithm is used to delineate the target volume. For comparison the deviation in volumes and the concordance index is used. **Results**: The deviation from the true volume in the phantom data was in mean 1.33±1.25 % whereas the nutshell implementation has a mean deviation in volume of 1.22±1.45 %. Regarding the background computation for the patient data the values of HBGGC versus nutshell implementation differ in mean 9.21±43.2 % resulting in a difference in the threshold about 0.29±2.9 %. Applied on the data this deviation in the threshold causes a difference in volume of -0.73±1.9 % in mean with a mean concordance index of 0.983. **Conclusion:** With the validation of this background implementation it can be shown, that it is possible to determine the background in a more user-independent way. For lesions in homogeneous background this computation leads to the same results.

## OP637

### Effect of calibration source geometry on shape on absolute activity quantification in SPECT

**N. Anizan**, E. C. Frey; Johns Hopkins University School of Medicine, Baltimore, MD, UNITED STATES.

**Objectives:** An essential element for achieving absolute quantification in SPECT is the calibration factor used to convert reconstructed voxel values to activity concentration. The calibration factor is related to the geometric sensitivity of the collimator, which is difficult to measure accurately for radionuclides emitting high-energy photons due to septal penetration and scatter effects. In this work we used a simulation study to evaluate the effects of source shape and acquisition geometry on the measurement of this calibration factor. **Methods:** We investigated the calibration factor in the context of Ba-133 because of its long half-life, which facilitates phantom experiments, and similarity to I-131. Cylindrical Ba-133 calibration sources with diameters and lengths ranging from 0.5 mm to 10 cm were simulated using the SIMIND code. The axis of the cylinder was positioned parallel or perpendicular to the detector and centered on or between the collimator holes. The source-detector distance (SDD) was varied from 5 cm to 20 cm; pixel sizes of 4.42, 2.21 and 1.11 mm were simulated. The calibration factor was calculated as the ratio between the ROI count rate and source activity. The ROI dimensions were based on the source size and geometric resolution in order to limit the number of non-geometrically collimated photons. The factor was applied to quantify activity in each of four Ba-133 rod sources (total activities of 0.4-1.2 MBq and diameters from 0.8-2.9 cm) in a water-filled cylindrical phantom. Images were reconstructed using OSEM with compensation for attenuation, scatter, and the full collimator-detector response compensation. **Results:** A source size equivalent to a vial used for dosimetry in internal radionuclide therapy (2 cm diameter and 5 cm length) placed parallel to the detector, leads to a relative error in the geometric sensitivity of 25.18% with a SSD of 20 cm and a 1.11 mm pixel size. Activity in the large rod is estimated using this factor with an error of -20.29%. A 1 cm diameter and 2 cm long source, long axis perpendicular to collimator, a 5 cm SSD and 1.11 mm pixels size gave an error of 0.49% in the geometric sensitivity. The relative error in the activity estimate for the large rod was 0.79% using this calibration factor. **Conclusions:** This study shows the importance of the calibration factor measurement method on the accuracy of activity quantification. The results provide data that aid in standardizing calibration factor measurement in order to provide the best accuracy.



1601 —Wednesday, Oct. 23, 08:00 — 09:30, Amphithéâtre

## CME 12 - Oncology: Cross-sectional Imaging in Nuclear Medicine

## OP638

### CT and MR in Musculoskeletal Pathologies: What the Nuclear Physician Should Know

**G. Tognini, ITALY**

## OP639

### SPECT-CT in Benign Bone Diseases

**G. Mariani, ITALY**

## OP640

### CT and MR in Abdominal Cancers: What the Nuclear Physician Should Know

**P.J. Valette, FRANCE**

## OP641

### PET-CT in Abdominal Cancers

**C. Tychyj-Pinel, FRANCE**

1602 —Wednesday, Oct. 23, 08:00 — 09:30, Auditorium Lumière

## Symposium 13 - EANM/MDS Joint Session: Biomarkers for Dementia with Lewy-bodies

## OP642

### Do we need Biomarkers in DLB?

**I.G. McKeith, USA**

## OP643
**Pre-synaptic Dopaminergic Deficit**

**Z. Walker, UNITED KINGDOM**

## OP644
**[I-123] MIBG Cardiac Scintigraphy**

**G. Treglia, SWITZERLAND**

1603 —Wednesday, Oct. 23, 09:30 — 10:45, Forum 3

## CTE 6: Focus on Children

## OP645
**Updates in Paediatric MIBG Scintigraphy**

**M.F. Golvet, FRANCE, M. Adam, FRANCE**

## OP646
**Multimodality Imaging in Paediatric Oncology**

**T. Pfluger, GERMANY**

## OP647
**Radionuclide Measurement of Mucociliary Clearance**

**J. Mortensen, DENMARK**

1604 - Wednesday, Oct. 23, 8:00 - 9:30, Bellecour 1/2/3

## Featured - Physics & Instrumentation & Data Analysis: PET/MR

## OP648
**New Strategies for MR-based Attenuation Correction of PET**

**H.H. Quick, GERMANY**

## OP649
**Value of 18F-DOPA PET/MRI fusion in pediatric patients with supratentorial infiltrative astrocytomas. A pilot study.**

**A. PICCARDO**[1], G. Morana[2], G. Villavecchia[1], N. Mehrdad[3], M. Cabria[1], M. Garre'[2]; [1]AZIENDA OSPEDALIERA GALLIERA, Genova, ITALY, [2]Gaslini Hospital, Genova, ITALY, [3]IRCCS San Martino Hospital-University of Genoa, Genova, ITALY.

**Purpose** To investigate the diagnostic role, clinical contribution, and prognostic value of fused 18F-DOPA PET/MRI images in pediatric patients with supratentorial infiltrative astrocytomas (IAs). **Methods** Pediatric patients with histologically proven supratentorial IAs involving at least two cerebral lobes, both newly diagnosed and with suspected disease progression, were studied with 18F-DOPA PET and MRI. 18F-DOPA-PET data were interpreted qualitatively and semiquantitatively, fusing images with MRI. Correlations between the degree and extent of 18F-DOPA uptake, MRI tumor characteristics, and histopathologic results were investigated. Contribution of 18F-DOPA-PET/MRI fusion was also evaluated concerning the determination of biopsy sampling site, discrimination between disease progression and treatment related changes, and subsequent treatment strategy. Patient's outcome was finally correlated with DOPA uptake. **Results** 13 patients (8 boys and 5 girls) were eligible for the study (5 diffuse astrocytomas, 2 anaplastic astrocytomas, 4 gliomatosis cerebri, and 2 glioblastoma multiforme). Fusion technology allowed for precise anatomical localization of 18F-DOPA activity. The DOPA uptake pattern was heterogeneous in all positive scans (9/13), revealing metabolic heterogeneities within each tumor; increased DOPA uptake was concordant with MRI tumor extent. Significant differences in terms of DOPA uptake were found between low- and high-grade lesions ($p< 0.05$). The diagnostic and therapeutic contribution of 18F-DOPA PET/MRI fusion was relevant in 9 out of 13 patients (69%). Significant differences of progression free survival (PFS) were found between patients with absent to moderately increased DOPA uptake and those with markedly increased uptake ($p< 0.01$). **Conclusion** Our preliminary results support the reliability of 18F-DOPA PET/MRI fusion as a biological marker of IAs. Information gathered by this combined imaging approach can be readily transferred to the everyday practice and may help clinicians to better stratify patients with IAs for diagnostic, therapeutic and prognostic purposes.

## OP650
**The effects of MR-based attenuation correction on the evaluation of gliomas using [18F]-FET PET/MRI**

**I. Law**[1], F. L. Andersen[1], T. Beyer[2], A. E. Hansen[1], M. Lundemann[3], C. Ladefoged[1], S. H. Keller[1], S. Holm[1], L. Højgaard[1]; [1]Rigshospitalet, The Department of Clinical Physiology, Nuclear Medicine and PET, Copenhagen, DENMARK, [2]Center for Medical Physics and Biomedical Engineering, Vienna, AUSTRIA, [3]Rigshospitalet, The Department of Radiation Oncology, Copenhagen, DENMARK.

**Aim**: Single-injection/dual-imaging protocols are standard in PET/MR evaluation today (1), but may be adversely affected by tracer redistribution, mis-registration, and PET-system specific differences. Further, the standard Dixon-Water-Fat segmentation (DWFS) attenuation correction (AC) method in PET/MRI (2) has demonstrated a systematic and spatially variable quantitative bias in [18F]-FDG-PET/MRI studies of the brain compared to PET/CT (3). Our Aim was to evaluate DWFS-AC in glioma patients using [18F]-FET PET/MRI and co-registered cerebral CT images using single-imaging (PET/MRI-DWFS vs. PET/MRI-CTAC) and dual-imaging (PET/CT vs. PET/MRI-CTAC). **Methods**: Fourteen patients with gliomas were imaged in a single-injection/dual-imaging protocol consisting of a single-bed 20 min PET/CT acquisition (Siemens Biograph mCT) 20 min pi of 200 MBq [18F]-FET followed by a single-bed 20 min simultaneous PET/MRI acquisition (Siemens Biograph mMR) (70 +/- 12 min pi). AC of the PET/MRI data was performed using either DWFS or a co-registered (minctracc, McConell Imaging Center, Montreal), low-dose head CT scan. AC-PET images were reconstructed using identical parameters (OSEM-3D 21i4s, 5 mm Gauss). The cortical background SUV activity (SUVb), metabolic tumor volume (vol) at an isocontour threshold of >1.6 SUVb, max tumor SUV to SUVb (Tmax/SUVb) and inter-PET dislocation of Tmax were measured and reported. The DICE similarity coefficient was calculated for vol > 8mL. Wilcoxon matched-pairs signed rank test was used for statistical evaluation ($p < 0.05$) using PET/MRI-CTAC as the reference. **Results**: 13/14 patients had a metabolically active tumor. PET/MRI-DWFS vs. PET/MRI-CTAC: DICE: 0.92 [0.88; 0.95]; largest Tmax dislocation: 2 mm. The clinical interpretation was not affected. PET/CT vs. PET/MRI-CTAC: DICE: 0.79 [0.71; 0.81]*; largest Tmax dislocation: 36 mm. The clinical interpretation was affected in 3/13 patients. Metric PET/MRI-DWFS PET/MRI-CTAC PET/CT SUVb 1.0 [0.9; 1.3]* 1.2 [1.1; 1.6] 1.0 [0.8; 1.3]* Tmax/SUVb 2.9 [2.2; 4.0] 2.8 [1.8; 3.8] 2.8 [2.2; 4.3] Volume (mL) 34 [19; 73]* 31 [17; 73] 29 [15; 68] Median and interquartile range; * $p < 0.05$. Tmax/SUVb: no significant differences. **Conclusion**: The single-injection/dual-imaging protocol approach is suboptimal for evaluating consequences of MR-AC using DWFS in gliomas using [F18]-FET. From this patient sample it can be expected that PET/MRI-DWFS will be sufficiently reliable without supplementary head CT for AC to detect regional tissue activity for two main clinical FET indications: biopsy planning and identification of recurrent tumor. References: 1. Souvatzoglou M et al. J Nucl Med.2012;53(Supp1):256 2. Martinez-Moller A et al. J Nucl Med.2009;50:520-526. 3. Andersen, F. L. et al. Eur J Nucl Med Mol Imaging.2012;39;Suppl2:S174,OP116

## OP651
**Radiotherapy Planning of Glioblastoma using $^{11}$C-Methionine-PET/CT and MRI: Prediction of Recurrence and Survival Analysis.**

**C. Vigil**, E. Prieto, M. Hernández, C. Caicedo, M. Rodríguez-Ruiz, M. García-Granero, G. Quincoces, I. Peñuelas, J. Aristu, J. Arbizu; Clínica Universidad de Navarra, Pamplona, SPAIN.

**Aim:** The Aim of this study was to evaluate the contribution of MET-PET/CT to the standard MRI in radiotherapy planning, to explore the relationship between MET-PET/CT distribution and recurrence location, and its influence in patient survival. **Materials and Methods:** 40 patients (mean age 57.7 years, range: 18 to 73) newly diagnosed of Glioblastoma Multiforme (GBM) and referred to radiotherapy planning 4-6 weeks, after total (n=22) or subtotal (n=18) surgery resection, were prospectively included. Integrated boost intensity-modulated-radiotherapy (IMRT) planning was performed using standard MRI and MET-PET/CT. Total Gross Tumor Volume ($GTV_T$) was defined as the union of standard gadolinium contrast-enhancement volume on $T_1$ MRI ($GTV_{Gd}$) and MET-PET/CT volume ($GTV_{MET}$). Differences between $GTV_{Gd}$ and $GTV_{MET}$ were calculated in order to evaluate their individual contribution to $GTV_T$. Tumor-to-Non Tumor ratio (T/NT) and maximum Standard Uptake Value (SUVmax) were calculated on the MET-PET/CT. Tumor recurrences were delineated on the follow-up MRI, and co-registered with the initial MRI and MET-PET/CT images. Spatial correlation between highest uptake area of $GTV_{MET}$ (isocontour at 50% of SUVmax) and MRI recurrence volume was explored. The association between variables studied, Progression-Free Survival (PFS) and Overall Survival (OS) period was evaluated using Chi Square tests, Kaplan-Meier method and log-rank test. **Results:** $GTV_{MET}$ added to the $GTV_T$ a median tumor volume that was not identified by MRI of 3.95cc (Interquartile range: 1.3 to 10.2). MRI recurrence volume matched the highest uptake area of $GTV_{MET}$ in 30/40 patients (75%). Using Chi-square goodness-of-fit test, recurrence match with the highest uptake was statistically significant in sample distribution ($Chi^2Coef=16.7$; $p=0.02$). Median PFS was 29 weeks (95%CI: 19.3 to 38.7), and OS was 20 months (95%CI: 16.4 to 23.6) after a median follow-up of 28.8 months (95%CI: 23.7 to 34). Patients with a T/NT ratio over 2.5 exhibited a shorter pattern of PFS (<24 weeks) ($p=0.006$; OddsRatio: 6.6; 95%CI: 1.8-24.7), and a shorter OS (<14 months)

(p=0.008; OddsRatio: 6.3; 95%CI: 1.7-23.7). Besides, when $GTV_{MET}$ exceeded 9 cc median PFS was significantly shorter ($GTV_{MET\geq}$ 9 cc: 20.4 weeks vs. $GTV_{MET}$<9 cc: 35 weeks; p=0.02). **Conclusion:** MET-PET before IMRT in resected GBM patients provides additional diagnostic information that modifies the GTV delineation. Tumors with higher T/NT values might have a significant influence in PFS, and possibly in OS. These findings could be applied to redirect IMRT towards areas of high risk in future studies.

## OP652

### Lean Body Mass Correction of Standardized Uptake Values in Simultaneous Whole-Body PET-MRI - proof of principle trial

**B. Sattler**[1], T. H. Jochimsen[2], J. Schulz[3], P. Werner[2], A. Seese[2], H. Barthel[2], O. Sabri[2]; [1]University Hospital Leipzig, Leipzig, GERMANY, [2]University Hospital Leipzig, Dept of. Nuclear Medicine, Leipzig, GERMANY, [3]Max Planck Institute for Human Cognitive and Brain Sciences, Leipzig, GERMANY.

**Aim:** In this study, we explore the possibility to use simultaneous PET-MRI to measure the lean body mass (LBM) in order to obtain standardized uptake values ($SUV_{MR}$) that are less dependent on the patient's adiposity compared to conventional Methods that are based on body weight. Body surface area or predicted lean body mass. We hypothesize that an MRI-based correction of SUV is superior to the clinically widely applied normalization to the total body weight ($SUV_{BW}$) and the correction based on predictive equations for the LBM ($SUV_{LBM}$) due to a more precise estimation of body composition by MR. **Method:** Corresponding whole body PET-MR and PET-CT datasets of 22 patients (age: 31-75 yrs, 10 female) were acquired on the same day using one application of FDG (258-441MBq) after uptake times of 182±52min (PET/MRI) and 120±37min (PET/CT). A straightforward approach to calculate an MRI-based LBM was developed and tested. It is based on the fat and water information obtained by the two-point Dixon MR sequence. The respective datasets were used to calculate a water fraction for each voxel. Integration over the whole body yielded the weight-normalized LBM. The principle and performance of the approach in terms of reducing variations of the mean SUV in brain in FDG studies across subjects is proven by comparing it with results for the respective $SUV_{BW}$ and $SUV_{LBM}$. Furthermore, using the body surface area (BSA) as a predictive method to calculate the SUV was considered. For a quantitative comparison, the relative standard deviation (rSD), i.e. the SD of the SUVs divided by the mean SUV of the patients' brains, was calculated for the different Methods. **Results:** The MRI-measured-LBM method outperformed the other Methods to determine brain FDG SUVs. In particular, the rSD of $SUV_{MR}$ was reduced by 41% compared to thevconventional $SUV_{BW}$ whereas for the predictive $SUV_{LBM}$ and $SUV_{BSA}$ the reduction of the rSD was 28% and 22%. **Conclusion:** We could proof the principle of using MRI-measured LBM to calculate SUVs and reduce their variance across subjects. Employing simultaneous PET-MRI to measure and calculate the LBM provides an $SUV_{MR}$ which is less dependent on the patient's adiposity than those derived by predictive Methods. Therefore, it is more comparable across patients. The technique does not impose an overhead in measurement time and its implementation is straightforward.

## OP653

### Use of 4D PET images for the derivation of respiratory synchronised MR images in PET/MR

H. Fayad[1], H. Schmidt[2], C. Wuerslin[2], **D. Visvikis**[1]; [1]INSERM UMR1101, Brest, FRANCE, [2]University Hospital of Tübingen, Tübingen, GERMANY.

**Aim**: One of the parameters compromising both qualitative and quantitative accuracy of PET /MR images is patient physiological motion. Respiratory motion correction approaches in combined PET/MR are based on the use of sequences allowing the acquisition of respiratory synchronized MR images. These are subsequently used to derive deformable transformations for motion correction in PET. However, such protocols are most of the time incompatible with the use of diagnostic MR acquisitions, while on the other hand the acquisition of 4D MR datasets is not currently common clinical practice. The objective of this work is to propose the use of acquired 4D non-attenuation corrected (NAC) PET images in order to generate 4D MR images based on a single static MR image acquisition and deformation matrices derived from the 4D NAC PET images. This approach removes the need for 4D MR acquisitions, allowing an accurate MR based attenuation correction (AC) for the simultaneously acquired 4D PET images. **Methods**: Five patient datasets acquired on a SIEMENS mMR PET/MR system were used. 4D PET acquired datasets were retrospectively binned into multiple amplitude frames corresponding to simultaneously acquired 4D gradient echo MR images. For PET attenuation correction purposes a single MR Dixon scan was acquired at end expiration. The reconstructed 4D NAC PET images were registered using a deformable registration algorithm to the end expiration NAC PET image. The obtained deformation fields were subsequently applied to the end expiration 3D gradient echo MR volume to obtain respiratory synchronized MR images. A comparison between the original 4D MR images and those derived based on the proposed approach was used to assess the accuracy of the developed methodology. Two metrics were use in this validation stage, considering a global correlation coefficient and expert validation by identifying multiple anatomical landmarks in both the original and generated 4D MR image series. **Results:** A high mean correlation coefficient of 0.90± 0.05 was obtained for the five patient datasets considered. The expert validation results comparing the generated and acquired 4D MR image series demonstrated also a good accuracy with differences of <2.8 mm in the transverse and coronal planes). **Conclusions**: This study demonstrates the potential of using 4D NAC PET images to derive matching 4D MR series from a single respiratory state MR image volume. This may allow for accurate PET AC and respiratory motion correction in PET/MR without the need for patient specific 4D MR acquisitions.

## OP654

### Role of dual-point FDG PET/CT in prone position and fused PET/MR; correlation with biologic prognostic parameters in breast cancer.

**D. Grigolato**[1], M. Cucca[1], M. Zuffante[1], E. Manfrin[2], F. Pellini[3], G. Pollini[3], R. Pozzi Mucelli[4], M. Ferdeghini[1]; [1]Nuclear Medicine Unit, Azienda Ospedaliera Universitaria Integrata Verona, ITALY, [2]Dept of Pathology, Azienda Ospedaliera Universitaria Integra Verona, ITALY, [3]Dept of Surgery, Azienda Ospedaliera Universitaria Integrata Verona, ITALY, [4]Dept of Radiology, Azienda Ospedaliera Universitaria Integrata Verona, ITALY.

**Aim**: to evaluate the utility of dual-time point $^{18}$F-FDG PET/CT in newly diagnosed breast tumours and to correlate the metabolic behaviour with pathologic and immunohistochemical prognostic factors. **Methods:** twenty-one consecutive patients, histologically proved breast cancers (cT1- cT2), consented to undergo FDG PET/CT for initial staging in the second semester of 2012. They performed FDG PET/CT for staging within 10 days from dynamic contrast-enhanced MR of the breast. It was acquired a standard whole body PET/CT scan in supine position followed by a delayed prone acquisition 2 hours post-injection with a dedicate breast device equal to the one utilized in MR. All patients underwent surgery without neoadjuvant chemotherapy. Twelve women had single lesions (group A) and 9 patients had multicentric/multifocal lesions (group B). There were five suspected bilateral lesions. The maximum standard uptake values (SUV) in all lesions at 1and 2 hours acquisition and the percentage of SUV variation were registered respectively as SUV1, SUV2 and ΔSUV. The metabolic results were correlated to biologic prognostic parameters: the expression of estrogen receptors (ER), progesterone receptors (PR), human epidermal growth factor receptor-2 (HER2), proliferation rate (Ki-67), tumor histology and grade, lesion dimension and PET stage. **Results**: In 31/36 lesions there were increased FDG uptake and five lesions showed either no change or a decrease in the SUV max over time. PET/CT detected 11/12 lesions in group A (sensitivity of 92%). In group B with 23 multicentric/multifocal lesions FDG PET/CT depicted 19/23 with a sensitivity of 83%. In 5 contralateral breasts with suspicious findings at MR, PET correctly identified four true negative lesions and missed a lobular invasive cancer of 9 mm. The overall sensitivity of MR alone was 98%, FDG-PET alone was 84%, and fused FDG PET/MR was 89%. ΔSUV, SUV1 and SUV2 correlated with high grade, HER2 positivity, invasive ductal histology, lesion dimension and PET stage. **Δ**SUV had a slight correlation with Ki67. Four lesions had negative **Δ**SUV and were ER+, HER2-, Ki67 < 20. **Conclusion:** Integrated information between PET and MR images increased the sensitivity, specificity and accuracy in diagnostic work-up of breast cancer. FDG uptake and ΔSUV are influenced by biological tumor features. There is a subgroup of invasive breast lesions, Luminal A subtype, characterized by low glycolytic metabolism and a decrease uptake over time, which could be misinterpreted as benign lesions. The knowledge of all these factors is important for a better interpretation of metabolic results.

1606 - Wednesday, Oct. 23, 8:00 - 9:30, Grand Salon Prestige Gratte-Ciel

# Oncology Clinical Science: Thyroid Cancer

## OP655

### Cost-Effectiveness of FDG-PET/CT for Cytologically Indeterminate Thyroid Nodules

**D. Vriens**[1], E. M. M. Adang[2], R. T. Netea-Maier[3], J. W. A. Smit[3], J. H. W. de Wilt[4], W. J. G. Oyen[1], L. de Geus-Oei[1]; [1]Radboud University Medical Centre (RUMC), Dept. of Nuclear Medicine, Nijmegen, NETHERLANDS, [2]Radboud University Medical Centre (RUMC), dept. of Health Evidence, Nijmegen, NETHERLANDS, [3]Radboud University Medical Centre (RUMC), Dept. of Medical Endocrinology, Nijmegen, NETHERLANDS, [4]Radboud University Medical Centre (RUMC), Dept. of Oncological Surgery, Nijmegen, NETHERLANDS.

**Aim:** Screening for malignancy in thyroid nodules (TNs) is performed using ultrasonography guided fine-needle aspiration cytology (FNAC). In approximately 25% of patients FNAC is inconclusive, mostly due to follicular neoplasia or cellular atypia, and diagnostic (hemi)thyroidectomy is proposed to patients. This strategy

results in futile surgery in 75% of these patients as histology reveals a benign TN. Consequently, this leads to unnecessary costs and burden for the patients. Our recent meta-analysis reported a high negative predictive value of 96% for FDG-PET/CT in this category of patients. As over a third of patients do have a negative FDG-PET/CT, we hypothesized that its routine use in FNAC-indeterminate TNs leads to better and more cost-effective patient care. In a decision analytic approach we set out to calculate the efficacy and economical value of FDG-PET/CT in order to support implementation. **Materials and Methods:** We developed an 8-state Markov decision model. Based on literature, reimbursement schedules of diagnosis/treatment combinations and expert panel opinion, we attributed distributions to the transition probabilities, costs and utility scores. Analysis of the model was performed by probabilistic sensitivity analysis for hypothetical adult patients with FNAC-indeterminate TNs over a duration of 5 years. Means and confidence intervals of discounted costs and QALYs were determined. Efficiency of FDG-PET/CT was presented by the incremental cost effectiveness ratio (ICER). One-way sensitivity analysis was performed over a plausible range for FDG-PET/CT costs, sensitivity, and specificity, prevalence of malignancy, the fraction of operated patients that primarily undergo hemithyroidectomy and the yearly fraction of patients that will undergo surgery after a negative FDG-PET/CT. **Results:** Modifying current practice with routine use of FDG-PET/CT resulted in 47.9% fewer surgeries for benign nodules. Compared to surgery in all patients, the fraction of untreated cancers was 1.3%, similar as reported in literature. Over 5 years, mean discounted cost estimates were €10,007 (95%-CI: €9,948-€10,066) for current practice and €8,398 (95%-CI: €8,293-€8,501) with the routine use of FDG-PET/CT. Current practice and FDG-PET/CT produced no significantly difference in QALYs (4.59 and 4.61 QALY, respectively). FDG-PET/CT therefore saved €1,609 per 0.02 QALY gained: i.e. the dominant alternative. One-way sensitivity analysis showed no incremental costs for an FDG-PET/CT-driven strategy for the ranges of the variables tested. **Conclusion:** Markov decision modeling showed the potential cost-effectiveness of FDG-PET/CT in TN patients with inconclusive FNAC. A prospective randomized study is necessary to confirm these observations.

## OP656

### Follow-up of cervical lymph node metastases detected in first radioablation in patients with well differentiated thyroid carcinoma - a bicentric study

**H. Ilhan**[1], M. Mustafa[1], B. Peter[1], T. Kuwert[2], D. Schmidt[2]; [1]Clinic of Nuclear Medicine, Ludwig Maximilian University Munich, München, GERMANY, [2]Clinic of Nuclear Medicine, University of Erlangen-Nürnberg, Erlangen, GERMANY.

**Aim:** So far there are no clearly defined guidelines for the management of radioiodine-positive lymph node metastases (LNMs) identified by SPECT/CT in patients with thyroid carcinoma (DTC) at first radioablation (RA). Surgical reintervention might be indicated after the detection of LNMs. However, iodine-positive LNMs might not survive radioablation. Thus, a reoperation could be an overtreatment in these patients. The Aim of this study was to investigate the outcome of patients with LNMs identified by SPECT/CT after radioablation. **Methods:** At the Clinics of Nuclear Medicine of the Ludwig-Maximilians-University of Munich and the Friedrich-Alexander-University of Erlangen-Nuremberg SPECT/spiral-CT is routinely performed in all patients with DTC at the time of RA. Screening the SPECT/CT databases for DTC patients revealed 81 patients with 97 lymph node metastases identified by SPECT/CT at RA after thyroidectomy. Follow-up data including serum thyreoglobulin (Tg) values and diagnostic I-131 scans was available in 73 patients (papillary 62/ follicular 10/ insular 1; staging: 33 pT1, 12 pT2, 24 pT3, 2 pT4; 25 pN1, 48 pNx or 0). Surgery was carried out in 8 patients with 13 LNMs due to the presence of additional suspicious iodine-negative LNMs. These patients were removed from further analysis. **Results:** 72 LNMs were successfully eliminated by radioiodine as demonstrated by negative radioiodine scans and Tg values at follow-up. 12 LNMs persisted and 8 new LNMs were detected at follow-up. 66/70 LNMs smaller than 0,9 ml were eliminated by radioiodine, whereas this was the case of only 6/14 nodes exceeding this threshold (Chi-Square test: 25,2; $p < 0,01$). **Conclusion:** In this study 85,7 % (CI 75,4 - 92,4 %) of iodine-positive LNMs persisting after thyroidectomy in DTC (94% of LNMs < 0,9 ml) were successfully treated by radioiodine given at RA. Surgical reintervention, however, has to be discussed in patients with additional iodine-negative LNMs or if pathological radioiodine accumulation persists in the follow-up.

## OP657

### Can the position of malignant thyroid nodule be considered as additional risk factor for recurrent and/or metastatic disease in patients affected by low risk differentiated thyroid cancer ?

**A. Campennì**[1], R. M. Ruggeri[2], R. Gentile[1], M. E. Stipo[1], S. Giovinazzo[2], M. Cucinotta[1], S. Baldari[1]; [1]Nuclear Medicine Unit, Department of Biomedical Sciences and of the Morphological and Functional Images, University of Messina, Messina, ITALY, [2]Department of Clinical Medicine, Unit of Endocrinology, University of Messina, Messina, ITALY.

**Aim:** The utility of radioiodine thyroid remnant ablation (TRA) is still debated in patients with low-risk differentiated thyroid cancer (DTC), although not rarely they develop recurrent disease or metastases (often loco-regional) during follow-up. Recently, a risk re-stratification based on 131I-post-dose whole body (pWBS) or at the time of the first clinical control (after initial therapy) has been proposed. We investigated if the position of the malignant thyroid nodule can be considered as additional risk factor for recurrent or metastatic disease in patients with pT1a-pT1b lesions (TNM 7th edition). **Materials and Methods**: We have retrospectively reviewed the records of 133 patients (F= 114, M= 19; F/M ratio 6:1; age 47.4 ± 11.8 years, range 22-75) with DTC [(122/133 with papillary histotypes (PTC), and 11/133 with follicular histotypes (FTC)] admitted to our Nuclear Medicine Unit for the radioiodine therapy (RAIT) after total thyroidectomy. All patients, without known metastasis at the time of the recruitment, underwent: - Neck ultrasonography; - Measure serum of: TSH, Thyroglobulin and anti-Thyroglobulin Antibody; - Radioiodine thyroid uptake obtained 24 hours after 131I (1.8 MBq) administration; - RAIT (555-4588 MBq) in hypothyroidism (TSH ≥ 30 μUI/ml) or after recombinant human TSH (rhTSH) stimulation for TRA; - pWBS obtained 5-7 days after RAIT. **Results**: Metastases were discovered by pWBS in 13/133 (9,7%) patients (F=10, M=3). All metastatic patients had papillary histotype; 9/13 had pT1a lesions. Malignant lesions were localized in: right lobe 5/65 (7.6%; F=4, M=1, mean age 45 years, range 23-65; histological variants: classic (CV)=3, follicular (FV)=2); left lobe 3/52 (5,6%; F=3; mean age 48 years, range 42-55; CV=1, FV=2); isthmus 5/15 (33,3%; F=3, M=2; mean age 43 years, range 22-70; CV=4, FV=1); pyramidal lobe 0/1 (0%). All metastatic patients but one (with lung metastases) had lymph-node metastasis (upper mediastinum=4, left lateral neck=2, right lateral neck=3; anterior central compartment=3). Among metastatic patients, only a woman had associated Hashimoto Thyroiditis. The incidence of metastases was significantly higher in patients with DTC located in the isthmus, respect to other sites (33,3%, 7.6%, 5.6% respectively), ($\chi 2$ 4.8, $p<0.05$). **Conclusion**: The overall frequency of metastases in patients with pT1a-pT1b lesions was relatively low but their prevalence was higher in the patients with isthmic lesion. Our preliminary data suggest that the isthmic location of DTC can be considered an additional risk factor in the patients with pT1a or pT1b lesions regardless of age and sex of the patients and of the histological variant.

## OP658

### Tumor Heterogeneity for Assessment of Response to Tyrosine Kinase Inhibitors in Patients with Thyroid Cancer

**R. A. Bundschuh**[1,2], J. Hartl[1], N. Zsótér[3], L. Papp[3], J. Biko[1], A. K. Buck[1], C. Lapa[1]; [1]Universitätsklinikum Würzburg, Wuerzburg, GERMANY, [2]Klinikum rechts der Isar der Technischen Universität München, Munich, GERMANY, [3]Mediso Medical Imaging Systems Ltd., Budapest, HUNGARY.

**Introduction:** Tyrosine kinase inhibitors (TKIs) are used as treatment option in patients with progressive iodine-negative thyroid cancer. However, response assessment can be demanding. RECIST criteria underestimate the response due to small changes in tumor size also in patients responding to TKIs [1]. Textural parameters for tumor analysis in CT in patients with renal cell cancer were found to be an independent factor associated with time to progression [1]. FDG-PET is directly reflecting the tumor metabolism and may therefore even superior when used for textural analysis of the tumor. Therefore we investigated the correlation between textural parameters assessed in FDG-PET with time to progression in patients with iodine-negative thyroid cancer treated with TKIs. **Methods:** 11 patients with iodine-negative thyroid cancer treated with TKIs were examined with FDG-PET before initiation and 9 month after start of therapy. In clinical follow-up 8 patients developed progress after a mean of 310 days, 3 patients are still stable after 389, 703 and 704 days.In FDG-PET images metastases were analyzed for heterogeneity using entropy, homogeneity and coefficient of variation (COV) with Interview Fusion Software (Mediso), for comparison the mean SUV was measured. For statistical analysis for each patient the mean value of the parameters over all analyzed metastases were used for correlation with time to progress as well as the changes of these mean values between the pretherapeutic examination and the examination 9 month after begin of therapy. **Results:** A strong correlation between the homogeneity and COV measured in the pretherapeutic PET with the time to progression ($r^2$=0.82 and 0.79) was found, whereas a higher COV and a lower homogeneity showed a worse prognosis in accordance to the findings in [1]. Entropy and mean SUV in the pretherapeutic examination did not show any correlation with the time to progression ($r^2$=0.03 and 0.08). Changes between the pretherapeutic PET and the examination 9 month after initiation of therapy did not show good correlation ($r^2$ ranging between 0.27 and 0.10). **Conclusion:** Tumor homogeneity and COV in the pretherapeutic FDG-PET correlate well with time to progress in patients with iodine-negative thyroid cancer treated with TKIs whereas the conventional mean SUV only showed worse correlation. Therefore these textural parameters seem to be promising for therapy response assessment and potential therapy decisions. *Reference:* [1] Goh V, Ganeshan B, Nathan P, et al.. Assessment of Response to Tyrosine Kinase Inhibitors in Metastatic Renal Cell Cancer: CT Texture as Predictive Biomarker. *Radiology,* 261:165-171, 2011.

## OP659

### 18F FDG PET/CT or 131I SPECT/CT Imaging of Rare Metastases in Differentiated Thyroid Cancer; on Behalf of the French Tuthyref (Tumeurs de la Thyroide Refractaires) Network

I. FAUGERON[1], F. BONICHON[2], C. SCHVARTZ[3], C. DEJAX[4], C. BOURNAUD[5], D. BENISVY[6], S. LEBOULLEUX[7], O. SCHNEEGANS[8], **M. TOUBERT**[1]; [1]Saint-Louis Hospital, APHP, PARIS, FRANCE, [2]Institut Bergonie, Bordeaux, FRANCE, [3]Centre Jean Godinot, REIMS, FRANCE, [4]Centre Jean Perrin, Clermont-Ferrand, FRANCE, [5]Hospices Civils de Lyon, GH Est,, Bron, FRANCE, [6]Centre Antoine Lacassagne, Nice, FRANCE, [7]Institut Gustave Roussy, Villejuif, FRANCE, [8]Centre Paul Strauss, Strasbourg, FRANCE.

**Introduction:** Rare metastatic sites of differentiated thyroid cancer (DTC) should be differentiated from 131I False Positive uptake, as it may impact on the clinical decision and prognosis of patients. Refractory thyroid cancers are rare with an estimated global incidence in France of 350 cases per year of whom about 200 cases per year are of DTC origin). Most of them present multiple metastases (M+). 18F FDG PET/CT imaging which has a well-known prognosis impact on their management, also allows describing unexpected rare M+. **Methods:** In France, the management of refractory thyroid cancer patients has benefited from the TUTHYREF network, a unique system where individual cases are collectively discussed twice a month during web conferences among 30 regional expert centres throughout France. Among the TUTHYREF network, we are collecting rare M+ (*defined as sites other than lung and bone localizations*) imaged with either 18F FDG or 131I, and confirmed by histology whenever possible or follow-up procedures. **Results:** We have already collected 13 different rare metastatic sites (liver, brain, choroidal, adrenal, muscular, sub-cutaneous, pleural, endobronchial, mesenteric, peritoneal, gastric, pancreatic M+, and iliac lymph node) from18 patients (very frequent multiple M+). Of note, the whole population, except one patient (with a histological proven renal M+ only visible with 131I imaging), occurred in patients with a refractory thyroid cancer, and mostly with an aggressive histology (at least 5 pts with follicular or poorly differentiated tumors, 3 T3 or T4 papillary DTC pts, 10 pts to be precised). Histology, TNM, age at diagnosis, possible association with lung and/or bone metastases, and delay since primary diagnosis will be collected. Treatments such as surgery, cumulative 131I dose, external beam radiation therapy, local treatment modalities and even targeted therapy will be listed. **Conclusions:** Work is still in progress and updated findings will be presented. The final Aim will be to present an atlas of rare metastatic localizations either with 18F FDG or even 131I imaging, which could allow a more appropriated knowledge of those very rare sites, and management of our patients.

## OP660

### Clinical value of 18F-FDG-PET/CT in the follow-up of patients with recurrent differentiated thyroid carcinoma in relation to the thyroglobulin levels: a retrospective analysis

**T. Traub-Weidinger**, S. Spandri, G. Dobrozemsky, M. Mayerhöfer, R. Marculescu, W. Wadsak, M. Hoffmann, G. Karanikas; Medical University of Vienna, Vienna, AUSTRIA.

During the last decade 18F-FDG PET has been established for detecting local recurrency and/or distant metastases in patients with differentiated thyroid carcinoma (DTC) especially with negative 131I-whole body scintigraphy and increasing tumor marker thyreoglobulin (Tg). A Tg cut-of level of 10 ng/ml is widely used for decision of PET performance. The Aim of this study was to evaluate the sensitivity and specificy of 18F-FDG-PET in combination with computer tomography (CT) as a hybrid device system in radioiodine negative TC patients with elevated Tg levels and to estimate the Tg cut-off level for a positive 18F-FDG-PET/CT**. Methods**: Sixty-six TC patients (papillary TC, n=45, follicular TC, n=19, Hürtle-cell TC, n=2) with elevated Tg levels (≥ 2 ng/ml) under thyroid stimulating hormone (TSH) suppressive thyroid hormone therapy, were investigated by 18F-FDG-PET/CT under exogenous TSH stimulation. An appropriate TSH stimulation was considered, if the TSH level was ≥ 25 mU/l. The results of the hybrid device system were compared to additional imaging modalities as well as to the clinical follow-up. **Results**: Analyzing 125 FDG-PET/CT examinations in 66 TC patients 92 examinations (74%) showed positive and 33 negative results (26%). True positive PET/CT results were detected in 86 of the 92 positive PET/CTs (93%). Of the 33 negative FDG-PET/CTs, 30 (92%) were confirmed to be true-negative. Therefore, an overall sensitivity and specificity of the hybrid FGD-PET/CT device of 97% and 83% was observed. The positive predictive value, negative predictive value (NPV) and accuracy of FDG-PET/CT were 93%, 91%, and 93%, respectively. At a Tg level of only 4.4.ng/ml the accuracy was 79% and the sensitivity 85% for positive FDG-PET/CT results. **Conclusion**: These results suggest that 18F-FDG PET/CT is a valuable technique in TC patients even with only slightly elevated Tg levels.

## OP661

### Metabolic status using FDG PET and oncogene mutations status of Iodine refractory thyroid metastatic cancer.

**A. Giraudet**[1], C. Bournaud-Salinas[2], M. Fondrevelle[3], M. Decaussin-Petrucci[4], Q. Wang[3], P. Bringuier[5], J. Lopez[6], V. Isnardi[1], T. Mognetti[1], F. Giammarile[7], J. Lifante[8], J. Peix[8], F. Borson-Chazot[9], C. De La Fouchardière[3]; [1]Centre LUMEN, Centre Léon Bérard, Lyon, FRANCE, [2]Federation d'Endocrinologie Lyon-Est, Lyon, FRANCE, [3]Centre Léon Bérard, Lyon, FRANCE, [4]CHLS, Dpt. of Anatomic Pathology, Lyon, FRANCE, [5]Hôpital Edouard Herriot, Lyon, FRANCE, [6]Hôpital de la Croix-Rousse, Lyon, FRANCE, [7]Centre LUMEN, Hôpital Lyon Sud, Lyon, FRANCE, [8]Hôpital Lyon Sud, Lyon, FRANCE, [9]Fédération d'Endocrinologie Lyon-Est, Lyon, FRANCE.

**Introduction:** Iodine refractory thyroid metastatic cancer (IRTMC) is a poor prognosis disease. The Aim of this retrospective study was to determine the metabolic status using FDG PET and oncogene mutations (BRAF, NRAS, PI3KCA) status in IRTMC patients treated in our cancer center. **Material and Method:** only patients with at least one FDG PET performed and one oncogene mutation study successfully done (using PCR on primary tumors or metastases) were selected in our IRTMC patients database. Iodine refractory disease is defined as a progressive disease after $^{131}$I treatment despite $^{131}$I uptake and/or persistant disease after a cumulative activity of at least 600 mCi of $^{131}$I (group 1) or no $^{131}$I uptake in at least one metastatic lesion (group 2). **Results:** 53 patients were included (25 males and 28 females; median age at time of cancer diagnosis 58.6 years [29-77]) including 17 patients in group 1 and 36 in group 2. Histology revealed 18 poorly differentiated thyroid carcinoma and the rest well differentiated carcinoma in primary tumors. 46 patients presented with lung metastases, 27 with bone mets, 9 with liver mets, 10 with brain mets. 47 patients (15/17 in groupe 1 and 32/36 in group 2) demonstrated FDG uptake in at least one lesion. At least one oncogene mutation was found in 19 patients (4/17 in group 1 and 15/36 in group 2). **Conclusion:** positive FDG status is more frequently observed in IRTMC than mutations in BRAF, NRAS or PI3KCA. It could therefore be more representative of the poor prognosis of this type of cancer evolution. However, oncogene mutations might be related to the lack of Iodine uptake in metastases that leads to a sooner use of targeted therapy. Prospective studies are warranted.

1607 - Wednesday, Oct. 23, 8:00 - 9:30, Salon Pasteur

## Conventional & Specialised Nuclear Medicine: Bone 2 (Benign)

## OP662

### Blood Pool SPECT/CT Imaging of Benign and Malignant Processes of Bone: Does It Give Additional Information?

T. Ones, **M. Aras**, F. Dede, S. Ozgüven, S. Gungor, R. Maleki, T. Y. Erdil, S. Inanir, H. T. Turoglu; Marmara University School of Medicine Nuclear Medicine Department, Istanbul, TURKEY.

Skeletal scintigraphy is seldom used in the workup of primary bone neoplasms due to it's limited role in the definition of tumor margins and assessment of soft tissue extension. A three-phase bone scan is usually needed to assess blood flow/pool phase and soft tissue activity for cases of infection and trauma. The Aim of the current study was to investigate whether blood pool SPECT/CT imaging gives additional information to standard planar whole-body/spot images and late phase SPECT/CT imaging in benign and malignant processes of bone. 7 patients aged between 12-56 years-old (mean age: 32±14 years) with known or suspected bone lesions were included in this prospective study. Blood Pool SPECT/CT imaging was performed with a dual detector gamma camera in combination with 2-slice multidetector CT scanner (Symbia T®, Siemens Healthcare, Erlangen, Germany). A perfusion study and delayed blood pool studies were performed. Radionuclide angiography was performed with 2-second images obtained for 44 seconds after a i.v. bolus injection of 555 - 740 MBq (15 - 20 mCi) technetium-99m-methylene diphosphonate (Tc-99m-MDP). The perfusion study was followed immediatly by an early blood pool SPECT/CT study. Sixteen projections of 12-15 seconds each, with 64 x 64 matrix, in 360º non-circular rotation were acquired. All images were interpreted visually by two experienced nuclear medicine physicians. Three hours after the radiopharmaceutical administration, standard whole-body anterior and posterior images of each patient were obtained. Spot images of suspected lesions were also taken. Late phase SPECT/CT images were obtained if needed for better visualization of the primary lesions. Blood pool SPECT/CT, whole-body/spot images and late phase SPECT/CT images were compared in terms of lesion visualization and soft tissue extension. We have been evaluated 16 bone lesions in 7 patients. In two patients with diagnosed fibrous dysplasia the lesions showed variable patterns of uptake in the blood pool SPECT/CT images. Additionally the soft-tissue component of the primary malignant lesions and the meta- tarsal lesions could be evaluated more accurately with the blood pool SPECT/CT images. This pilot study is the only one to date that to assess the impact of blood pool SPECT/CT imaging over bone scan in benign and malign process of bone. It seems that blood pool SPECT/CT

imaging of the suspected bone lesions may provide additional information in the evaluation of routine standard bone scintigraphy.

## OP663

### Diagnostic dilemma: The clinical significance of a solitary rib lesion visualized on Sodium Flouride-PET-low dose CT (NaF-PET) in patients with prostate or breast cancer.

**C. Haarmark**, C. Madsen, H. W. Hendel; Department of Clinical Physiology and Nuclear Medicine, Herlev, DENMARK.

**Introduction**: The better sensitivity of NaF-PET compared with bone scintigraphy has yielded some diagnostic dilemmas. One troublesome dilemma is the seemingly increased number of patients with a solitary rib lesion, as there is no well established image modality to determine whether a given rib lesion is malignant or not. Bone metastasis dramatically changes the patient management and prognosis. Therefore we wanted to investigate the significance of a single rib lesion seen on NaF-PET. **Method**: Through retrospective review of our records we included patients who on NaF-PET had a solitary rib lesion without any other suspect foci present. Exclusion criteria were less than 1 year of available follow-up or multiple bone lesions. Lesions were classified as malignant upon follow-up if biopsy proven or imaging confirmed (other modalities). In patients without follow-up imaging, the lesions were also considered malignant if the patient was treated as having bone disseminated disease by the referring clinician. Lesions were classified as benign if proven by biopsy or if follow-up imaging were without suspicious lesions. Without follow-up imaging the lesions were considered benign in prostate group when the PSA level remained stable or dropped. In the breast cancer group, no clinical suspicion of recurrence of disease was considered to confirm the benign nature of the lesion. Patient data and imaging results was retrieved from the hospital's electronic database. **Results**: In all 28 patients were identified (79% male, mean age 67±11 years) as having solitary rib lesion. Mean follow-up was 18±4.6 months. The majority of patients had prostate cancer (79%) with PSA values of mean 39±72 µg/l, mean Gleason score 7.4. Additional imaging procedures (MRI, CT, FDG-PET, NaF-PET) were preformed in 13 patients (46%) with MRI being most prevalent. Three patients had their NaF-PET repeated. In only two patients biopsies were taken (both benign). Upon follow-up two patients proved to have malignant bone involvement (7%) compared with twenty-two patients showing no evidence of bone disseminated disease (79%). In four patients (14%) the status remained undetermined, due to lack of follow-up imaging combined with slowly increasing PSA (most in watchful waiting protocol). **Conclusion**: In the majority of cases (79%), solitary rib lesions seen on NaF-PET in patients with either prostate or breast cancer are benign as determined by follow-up for at least 12 months. Two out of 28 patients proved to have malignant bone involvement. Biopsy was taken in a minority of the patients.

## OP664

### Incremental value of SPECT/CT in identifying pain generators post-lumbar fusion surgery

**R. Mandegaran**[1], S. Ridgeway[2], J. Dooley[2], M. Nathan[1]; [1]Royal Free London NHS Trust, London, UNITED KINGDOM, [2]The Hillingdon Hospitals NHS Foundation Trust, London, UNITED KINGDOM.

**Introduction**: Pain persistence/recurrence remains a cause of great morbidity in a significant proportion of patients post-lumbar fusion surgery. Although CT remains the preferred choice, diagnosis on the basis of clinico-radiological findings using conventional imaging is challenging. Our study demonstrates the incremental value of SPECT/CT in localising and characterising areas of increased uptake to determine the possible underlying pain aetiologies in this patient cohort. **Methods**: SPECT/CT findings were compared to CT and SPECT alone in 20 consecutive patients referred for SPECT/CT for persistence/recurrence of back/leg pain post-lumbar fusion. Four criteria were assessed: (1) Possible screw loosening (2) Non-union within/around interbody cages suggestive of pseudoarthrosis (3) Active facet joint degeneration (4) Active sacroiliac degeneration SPECT versus SPECT/CT were assessed for localisation of abnormal areas of uptake. RESULTS: SPECT/CT versus CT alone: (1) Possible screw loosening: identified in 5 patients on CT, 10 patients on SPECT/CT (12 patients across both modalities). 17 screws identified across both modalities: concordance in 5/17 screws (29%), SPECT/CT in 10/17 screws (59%), CT in 2/17 screws (12%). (2) Non-union into cages (3 patients underwent fusion without interbody devices and not included): identified in 7 patients on CT, 6 patients on SPECT/CT (8 patients across both modalities). Concordance in 5/8 patients (62.5%), SPECT/CT in 1/8 patients (12.5%), CT in 2/8 patients (25%). (3) Facet joint degeneration: identified in 19 patients on CT, 18 patients on SPECT/CT (20 patients across both modalities). 100 possible degenerative facet joints identified across both modalities: concordance in 34/100 joints (34%), active degenerative disease on SPECT/CT without gross changes on CT in 13/100 joints (13%), degenerative changes on CT in 53/100 joints (53%) without associated metabolic activity. (4) Sacroiliac degeneration: identified in 10 patients on CT, 9 patients on SPECT/CT (15 patients across both modalities). Concordance in 4/15 patients (27%), CT in 6/15 patients (40%), SPECT/CT in 5/15 patients (60%). Subjective diagnostic confidence improved with SPECT/CT versus CT in above four categories in 50%, 59%, 90% and 60% of patients respectively. SPECT/CT improved localisation of uptake versus SPECT in 19/20 patients. **Conclusion**: Our findings suggest that diagnostic confidence regarding possible pain generators in the post-fusion spine is significantly improved with SPECT/CT versus CT, particularly regarding non-union, active facet joint disease and active SIJ degeneration. As would be expected, SPECT/CT also significantly improves accurate localisation of abnormal uptake.

## OP665

### A pharmacokinetic modeling approach of 18F-fluoride PET/CT scans to assess bone graft incorporation in posterior lumbar interbody fusion

**R. Wierts**[1], M. Peters[2], P. C. Willems[1], E. M. C. Jutten[1], F. M. Mottaghy[1,3], B. Brans[1]; [1]Maastricht University Medical Centre, Maastricht, NETHERLANDS, [2]Eindhoven University of Technology, Eindhoven, NETHERLANDS, [3]University Hospital RWTH Aachen, Aachen, GERMANY.

**Aim** Posterior Lumbar Interbody Fusion (PLIF) is a surgical procedure to treat patients with symptomatic spondylolisthesis which involves the insertion of interverbal cages filled with autologous bone. The development of pseudarthrosis may limit clinical success. Presently, no non-invasive technique is available to reliably assess bone graft incorporation after PLIF. Using static $^{18}$F-fluoride PET/CT imaging, an increased bone metabolism in patients with persisting symptoms after PLIF surgery has been shown. In this study, a pharmacokinetic modeling approach using dynamic $^{18}$F-fluoride PET/CT scanning to assess bone graft incorporation after PLIF is evaluated. **Materials and Methods** Twenty patients who underwent PLIF were included. Following a low-dose CT scan, a 30 minutes dynamic PET acquisition (Philips, Gemini TF PET/CT) covering the PLIF region was started directly after intravenous injection of $^{18}$F-fluoride (mean: 187 MBq). One hour post-injection a static PET/CT scan was acquired (5 min/bed position). The dynamic data was analyzed using two different pharmacokinetic models: the irreversible two-tissue-compartment model (2TCM) and the Patlak model. For each patient, six regions of interest (ROIs) were defined, including the intervertebral disc space and upper and lower endplates of both the operated segment and a normal reference segment. For each region three parameters reflecting overall bone metabolism were determined: $SUV_{mean,stat}$, $K_{bone,2TCM}$, $K_{bone,Patlak}$. For the 2TCM the rate constants, $K_{1,2TCM}$, $k_{2,2TCM}$ and $k_{3,2TCM}$ were determined as well. Using the 2TCM rate constants the $SUV_{mean,2TCM}$ at one hour after administration, was estimated from the dynamic scan. **Results** As expected, $K_{bone,2TCM}$ and $K_{bone,Patlak}$ were highly correlated (R=0.99). Furthermore, a high correlation (R=0.90) was observed between $SUV_{mean,stat}$ and $SUV_{mean,2TCM}$. $SUV_{mean}$ and $K_{bone,2TCM}$ and $SUV_{mean}$ and $K_{bone,Patlak}$ were correlated to a lesser degree (R=0.84 and R=0.85, respectively) which could explained by the fact that the SUV is not corrected for patient-specific arterial blood clearance of the tracer, whereas this effect is taken into account in the $K_{bone}$ measures. Adjusting for this effect increased the strength of correlation (R=0.90). All investigated parameters except $k_{3,2TCM}$ (p=0.112) showed a significant increase for the PLIF segment compared to the control segment (p<0.05). **Conclusion** Our study shows that the one hour post-injection $SUV_{mean,stat}$ can be reliably calculated from the 30 minutes dynamic PET scan, allowing a substantial shortening of the total PET/CT procedure. Moreover, the 2TCM provides additional information concerning the individual rate constants. The clinical relevance of dynamic $^{18}$F-fluoride PET/CT for bone graft incorporation needs to be evaluated in a prospective study.

## OP666

### Diagnostic Value of quantitative SPECT/CT versus MRI for the assessment of Sacroiliitis in Early Axial Spondyloarthritis.

**L. Sancho**, E. Ornilla, E. Prieto, M. Ribelles, M. García-Velloso, C. Caicedo, M. Hernández, C. Vigil, J. Richter; Clínica Universidad de Navarra, Pamplona, SPAIN.

**Aim**: To assess the diagnostic value of quantitative bone SPECT/CT versus MRI for the detection of sacroiliitis in patients with early active axial spondyloarthritis (SpA) and patients with inflamatory low back pain (IBP). **Materials and Methods:** Twenty-three patients were explored two hours after intravenous injection of 9.3 MBq/Kg 99m-Technetium-hydroxi-di-phosphonate ($^{99m}$Tc-HDP) by means of SPECT/CT. Fourteen of them had active SpA (symptom duration < 10 years) and nine had IBP according to the new ASAS classification criteria for axial spondyloarthritis. Besides, Magnetic Resonance (MRI) of sacroiliac joints was performed in all of them. The SPECT/CT indices were obtained quantifying each joint area (J) with the sacrum promontory (P). Sensitivity (S), specificity (Sp), positive predictive value (PPV) and negative predictive value (NPV) of SPECT/CT were calculated, considering MRI and clinical diagnosis as the gold standard techniques for the diagnosis of sacroiliitis. ROC curve was calculated to define the cutoff value of J/P index to asses the diagnostic performance of quantitative bone SPECT/CT. **Results:** Both imaging techniques (SPECT/CT and MRI) were analyzed. Taking J/P ratio ≥ 1.21 as cut-off value of the ROC curve and the clinical diagnosis as gold standard, the results for SPECT/CT were S: 53.6%, Sp: 83.3%, PPV: 83.3% and NPV: 53.6%. Taking MRI as gold standard, the results were: S:70%, Sp: 69.4%, PPV:

38.9% and NPV: 89.3%. **Conclusion:** Even though these results should be considered preliminary, it is concluded that quantitative bone SPECT/CT is a valuable alternative to MRI for the early diagnosis of sacroiliitis in patients with SpA. Moreover, SPECT/CT has high Sp, crucial for the test validity since we are trying to discriminate between healthy subjects (IBP) and patients (SpA) in early stages of the illness.

## OP667

### Role of 99mTc MDP bone scan with SPECT/CT of the pelvic region and clinical disease activity scoring in diagnosis of sacroiliitis in Spondyloarthropathy

**R. V. PARGHANE**, B. SINGH, B. R. Mittal, A. Bhattacharya, A. Sharma, P. Singh; PGIMER, Chandigarh, INDIA.

**Aim:** To evaluated role of 99mTc MDP bone scan with SPECT/CT of the pelvic region, clinical disease activity scoring in diagnosis of sacroiliitis in spondyloarthopathies patients. **Material and Methods**: We evaluate prospectively 155 diagnosed cases of spondyloarthropathies according to ESSG criteria. There were 83 male and 72 female patients in the age range 18 to 60 years with mean age of 35 years. The average duration of lower backache was 15 months. The smallest duration was 3 months and the largest was 96 months. All patients were subjected 99mTc MDP bone scan with SPECT/CT of the pelvic region, MRI, X ray of the pelvic region, clinical assessment, pain score, functional score (BASDAI, BASFI, BASMI) and acute phase reactants such as ESR, CRP and HLA B27 for detection of sacroiliitis. The sensitivity, specificity, and positive and negative predictive values in diagnosis of sacroiliitis were determined using MRI as the gold standard method. **Results**: Comparing with MRI as the gold standard, sensitivity, specificity, positive predictive value and negative predictive value of 99mTc MDP planar bone scan was 42%, 80%, 85%, and 36% respectively. The sensitivity, specificity, positive predictive value and negative predictive value of 99mTc MDP bone scan with SPECT/CT of the pelvic region and clinical disease activity scoring was 90%, 80%, 92%, and 75% respectively. Pearson chi square value was P <0.001. **Conclusions**: Our results indicate that 99mTc MDP planar bone scan has low sensitivity for detection of sacroiliitis as compared to MRI. With use of SPECT/CT of the pelvic region and clinical disease activity scoring diagnostic accuracy of 99mTc MDP bone scan for detection of sacroiliitis in spondyloarthropathies patients were significantly improved and similar to MRI, so 99m Tc MDP bone scan with SPECT/CT of the pelvic region and clinical disease activity scoring was useful in patients having claustrophobia, pacemakers, and metal implants and where MRI equipment or a skilled staff are not available and on economic grounds. With use of delayed whole body 99mTc MDP bone scan helpful in detection of other joints inflammation and enthesitis in spondyloarthropathies patients.

## OP668

### Radiographic suspicious changes in the sacroiliac joints: the role of bone single photon emission computed tomography (SPECT) scintigraphy

T. Pipikos[1], **J. Koutsikos**[1], S. Bakalis[1], S. Episkopopoulou[1], K. Athanasiou[1], G. Koniaris[1], D. Kassimos[2]; [1]401 General Military Hospital, Nuclear Medicine dept., Athens, GREECE, [2]401 General Military Hospital, Rheumatology dept., Athens, GREECE.

**Introduction**: The early changes of sacroiliitis are an important feature for establishing the early diagnosis of seronegative spondyloarthropathy (SpA). X-ray may be negative or indefinite (New York criteria=1) at the early changes of sacroiliitis. The role of bone scintigraphy (BS) in the evaluation of patients with SpA is not clear, while magnetic resonance imaging (MRI) is considered as the most sensitive and specific procedure for sacroiliitis. The Aim of our study was to evaluate the role of bone single photon emission computed tomography (SPECT) scintigraphy in the detection of sacroiliitis in patients with SpA and suspicious changes of sacroiliitis on X-ray. **Materials & Methods**: X-ray, MRI, and SPECT of the sacroiliac joints of 46 SNSpA patients (41 males, 5 females, mean age 28.2 y.o.) were evaluated retrospectively. The maximum time interval between these studies was 5 days. X-rays of the sacroiliac joints were grading according to the NY criteria and radiographs with suspicious findings were characterized as grade 1. MRI scans were examined for the presence of joint fluid, abnormalities in articular cartilage and subchondral marrow edema. BS was performed 3 hours after IV administration of 18 mCi Tc-99m HDP using a single-head gamma-camera (SPECT data: patient at prone position, 180o rotation, 32 projections of 60 seconds, matrix 64x64, iterative reconstruction method). A qualitative assessment of radiopharmaceutical uptake in the SI joints was derived from SPECT scans. Markers of inflammation (CRP and ECR) were also evaluated. All studies were read without knowledge of patient identification. **Results**: Fourteen patients were classified as grade 1; 8/14 pts had increased CRP and ECR suggesting disease activity. MRI detected features of sacroiliitis in 10/14 patients (71%); 7/10 pts had increased CRP and ECR. SPECT detected active sacroiliitis in 11/14 pts; in all 10 MRI identified pts as well as in one more male with increased CRP and ECR. In a 2-year follow up period, ankylosing spondylitis was established for this patient. **Conclusion**: Bone SPECT seems to be an excellent tool for detecting active sacroiliitis in suspicious changes on conventional radiography. Its application on conventional planar bone scan, an economic and widely available diagnostic technique, appears to be a valuable aid for the clinician and can be used as first choice diagnostic modality to define the activity of the disease.

## OP669

### Role of planar bone scintigraphy and hybrid SPECT/CT in localising the site for corticosteroid injection in patients with plantar fasciitis

**K. KAMALESHWARAN**, A. BHATTACHARYA, B. RAI MITTAL; PGIMER, Chandigarh, INDIA.

**Aim** : The Aim of this study is to localize the site for corticosteroid injection in the treatment of plantar fasciitis using bone scintigraphy and to compare the efficacies of planar and hybrid SPECT/CT imaging for successful localization as measured by pain relief score. **Methods**: A total of 30 heels of 30 patients with clinical diagnosis of plantar fasciitis were randomly assigned to two steroid injection groups: Planar scintigraphy-guided (Group A) and hybrid SPECT/CT guided injection(Group B ).Patients were evaluated for pain intensity before the injections and at the follow-up of 6 weeks with a 100- mm visual analog scale (VAS). **Results**: There was significant improvement in VAS score in both the groups. Before treatment, VAS values in group A were 7.4 ± 1.3 and after treatment were 3.3 ± 2.4 In group B VAS before treatment were 7.4 ± 1.2 and after treatment were 1.6 ±1.5 and so there was a statistically significant difference between the before-injection and follow-up values for VAS (P < 0.05). Between the groups, there was no difference between the VAS values before injection(P=0.98,MWU=-0.021). Between the groups, there was statistically significant difference in the VAS values after injection (P=0.048, MWU=1.97). Three patterns of blood pool abnormality such as focal calcaneal hyperemia, proximal third of plantar fascia involvement and diffuse pattern were noted. **Conclusion**: Bone scintigraphy helped in identifying the inflammatory focus and guide in injection of corticosteroid at a specific site in the treatment of this condition .SPECT/CT guided steroid injection demonstrated a significantly better treatment patient outcome as compared to planar scintigraphy guided injection. We are of opinion that steroid injections should be performed using bone scintigraphy.

1608 - Wednesday, Oct. 23, 8:00 - 9:30, Gratte-Ciel 1/2/3

# Radionuclide Therapy & Dosimetry: Miscellaneous Therapy

## OP670

### A Phase Ib Study of Fractionated $^{90}$Y-Clivatuzumab Tetraxetan in Patients with Metastatic Pancreatic Cancer after ≥ 2 Prior Therapies.

**D. M. Goldenberg**[1], V. J. Picozzi[2], R. K. Ramanathan[3], P. Conkling[4], M. J. Guarino[5], E. P. Mitchell[6], A. J. Ocean[7], W. A. Wegener[1], S. J. Goldsmith[7]; [1]Immunomedics, Morris Plains, NJ, UNITED STATES, [2]Virginia Mason Medical Center, Seattle, WA, UNITED STATES, [3]Virginia G. Piper Cancer Center/TGen, Scottsdale, AZ, UNITED STATES, [4]Virginia Oncology Associates, Norfolk, VA, UNITED STATES, [5]Helen F. Graham Cancer Center, Christiana Care, Newark, DE, UNITED STATES, [6]Kimmel Cancer Center of Thomas Jefferson University, Philadelphia, PA, UNITED STATES, [7]New York Presbyterian Hospital-Weill Cornell Medical College, New York, NY, UNITED STATES.

**Background:** Radioimmunotherapy (RAIT) with $^{90}$Y-clivatuzumab tetraxetan ($^{90}$Y-hPAM4) may be an attractive option for patients with metastatic pancreatic cancer (mPC) to avoid the side effects of further chemotherapy. This multicenter, phase Ib study of fractionated $^{90}$Y-hPAM4 alone or combined with low radiosensitizing doses of gemcitabine was undertaken in patients with mPC treated with > 2 prior gemcitabine- or 5FU-containing regimens. A prior frontline study showed a median overall survival (OS) of 11.8 months for patients given repeated treatment cycles (Ocean et al., *Cancer* 2012;118:5497-506). **Methods:** Patients were alternated to arm A (4-week cycles: once-weekly 200 mg/m$^2$ gemcitabine; 6.5 mCi/m$^2$ $^{90}$Y-hPAM4 once-weekly the last 3 weeks) or B (3-week cycles: 6.5 mCi/m$^2$ $^{90}$Y-hPAM4 once each week), with cycles repeated at 4-week intervals until unacceptable toxicity or patient deterioration. Safety, efficacy and survival were evaluated. To determine if this approach is sufficiently active in this population and if gemcitabine adds to the therapeutic activity requires a sample size of 50 patients (25 per arm). **Results:** A total of 58 patients (33M /25F;median age 65) were enrolled on arm A (N=29) or B (N=29), 1.6 median years from initial diagnosis after a median of 3 (2-6) prior treatments. Accrual has been rapid with 50/58 patients currently having completed cycle 1, including 11 patients now also having received 2 (N=8) or 3 (N=3) cycles. RAIT has been feasible, with dose reductions for cytopenias required infrequently, and only one case of severe consumptive coagulopathy during cycle 2 considered

as possible dose-limiting toxicity. CT scans currently evaluated 4 weeks after cycle 1 show no difference between arms A and B, with predominantly stable disease and no partial responses by RECIST criteria. Of the initial combined A and B patients now with mature data assessable for survival analysis (N=18), the median estimated OS is 3.0 mos. **Conclusions:** Fractionated RAIT appears well-tolerated in these mPC patients after a median of 3 prior therapies, with manageable myelosuppression and current survival estimate of 50% (9/18) at 3.0 mos.

## OP671

### Correlation of administered activity and dosimetric data in patients treated with 131MIBG therapy

**M. Castellani**[1], C. Chiesa[1], R. Luksch[2], G. Aliberti[1], M. Maccauro[1], E. Seregni[1], A. Lorenzoni[1]; [1]Foundation IRCCS National Cancer Institute Of Milan, Nuclear Medicine, Milano, ITALY, [2]Foundation IRCCS National Cancer Institute Of Milan, Pediatric Oncology Unit, Milano, ITALY.

**Aims** The purpose of the study was to optimized 131-MIBG therapy in children and adults patients with neural crest tumors, by correlating the administered pro/kg activity to whole-body dosimetry and hematologic toxicity. **Materials and Methods** From September 2003, to June 2012 twenty-four patients (9 children, 15 adults) (13 neuroblastoma, 9 pheochromocytoma/paraganglioma, 2 medullary thyroid carcinoma) treated with 131I-MIBG were enrolled in the study. In each patient dosimetric estimation was carried out with MIRD method after patient therapy, using imaging acquisition or probe determination (from 1 to 168 hours). Haematological toxicity was evaluated according to WHO grade by weekly blood count for at least 6 weeks or until recovery. Whole Body Dose (WBD) was correlated with administered pro/kg activity and bone marrow toxicity. **Results** A total of forty-five dosimetric studies have been performed, 16/45 in children and 29/45 in adult patients. Administered activity ranged from 7.4 to 16.65 GBq, corresponding in children to 5-21 mCi/kg (median 10 mCi/kg) and in adults to 3-7 mCi/kg. (median 5 mCi/kg). In four patients (3 children, 1 adult) 2 weeks after 131I-MING therapy autologous stem cell transplantations were performed. Grade II-III heamatological toxicity was observed in all children and in 6/15 adult patient. Whole Body Dose ranged from 1 Gy to 3.6 Gy (median 1.7 Gy) in children, meanwhile it ranged between 0.55 and 1.87 Gy (median 0.96 Gy) in adults. In 5/16 children studies WBD was about 2 Gy and one child received a dose of 3.6 Gy (0.4 Gy/GBq), corresponding to an activity of 18 mCi/kg. **Conclusion** Contrary to published data in children the pro/kg activity is not a good predictor of WB dose. In these cases WB dose calculation can affect by the presence of large tumor masses which overestimate the absorbed dose. In any case the administration of activity superior to 15 mCi/kg is known to be associated with bone depression and the necessity of stem cells reinfusion. In adult patients WBD correlated with administered activity (Spearman coefficient 0.84 ). Indeed bone marrow toxicity cannot be predictable even if WBD is inferior to 2Gy, especially in case of further treatments. Probably in adult patients the hematological toxicity depends on the extension of disease and in these cases a caution approach is recommended even if WBD is low.

## OP672

### Individualised $^{131}$I-mIBG Therapy in the Management of Refractory and Relapsed Neuroblastoma

**S. L. George**, S. J. Kirk, D. Lancaster, S. J. Vaidya, H. Mandeville, F. Saran, S. J. Chittenden, A. D. J. Pearson, Y. Du, G. D. Flux; Royal Marsden Hospital, Sutton, Surrey, UNITED KINGDOM.

**Introduction** $^{131}$I labeled mIBG is used as targeted radionuclide therapy for relapsed and refractory neuroblastoma. An individualized form of $^{131}$I-mIBG-therapy using whole body dosimetry has been developed at our institution. We report toxicity and outcome data. **Methods** A retrospective review of children treated at the Royal Marsden Hospital (RMH) from 1994-2012. The overall Aim was initially to deliver a whole body dose (WBD) of 2 Gy based on a tracer study, or in later years a total 4 Gy WBD in two fractions, with cell support, was delivered by a first therapeutic activity of 444 mBq/Kg and a subsequent therapy adjusted according to the measured WBD. Toxicity and outcome data were collated by clinical note review. Institutional review board approval was obtained. **Results** 45 treatments were given to 26 patients (16 male, 10 female). Median age at first mIBG: 72 months (range 17-241), median 2 treatments per patient. Indication: Primary refractory disease (12), relapse (8), other (6). Administered mean mIBG activity 10951mBq (range 3539-32871). Mean mIBG whole body dose 1.8Gy, (range: 1-3.5). Recorded toxicities: grade 3-4 neutropenia in 20/24 treatments, grade 3-4 thrombocytopenia in 20/26 treatments. Acute toxicity occurred following 21/45 treatments, including 9 cases of febrile neutropenia and 1 hypertensive crisis. The only long-term toxicity was prolonged thrombocytopenia in a patient where there was no hematopoietic stem cell rescue. There were no toxic deaths related to mIBG therapy. Response rates as reported on first post-treatment mIBG scan were complete response (4.5%), partial response (52%), stable disease (30%), progression (9%) and mixed response (4.5%). Median time to progression was 3 months (range 6 weeks to 11 months). 6 patients were alive with disease at last follow up (mean 11 months) and 3 are alive and disease-free at last follow up (4 months, 20 months and 10 years). **Conclusions** In children with relapsed and refractory neuroblastoma the disease burden and heterogeneous presentation requires an individualised approach. Personalised $^{131}$I-mIBG therapy based on WBD is a viable treatment option and allows higher activities to be administered than standard population based treatments. It is well tolerated and haematological toxicity is the dose-limiting side effect. Using the individualised protocol developed at RMH, our overall response rate of 57% compares very favourably with the response rates of 27-39% in other series. Prospective European multi-centre clinical trials are in preparation to define the role of $^{131}$I-mIBG therapy in the patient pathway.

## OP673

### Targeted Alpha Therapy of Glioblastoma Multiforme: Initial Clinical Experience with $^{213}$Bi-Substance P

**A. Morgenstern**[1], L. Królicki[2], J. Kunikowska[2], H. Koziara[3], B. Królicki[3], M. Jakuciński[4], R. Mikołajczak[5], D. Pawlak[5], C. Apostolidis[1], F. Bruchertseifer[1]; [1]European Commission, Joint Research Centre, Institute for Transuranium Elements, Karlsruhe, GERMANY, [2]Department of Nuclear Medicine, Medical University of Warsaw, Warsaw, POLAND, [3]Department of Neurosurgery, Institute of Psychiatry and Neurology, WARSAW, POLAND, [4]Department of Imaging Diagnostic, Masovia Hospital, Warsaw, POLAND, [5]National Centre for Nuclear Research, Otwock, POLAND.

**Aim:** Glioblastoma, the most common primary brain tumor in adults, has a very poor prognosis with a median overall survival of 15 months despite of aggressive therapy including surgery, chemotherapy and radiation therapy. New therapy options are urgently needed. Targeted alpha therapy with the short range, high LET alpha emitter $^{213}$Bi offers the potential for selective irradiation of tumors, while minimizing damage to adjacent, functional critical areas of the brain. The peptide carrier substance P is targeting neurokinin type 1 (NK-1) receptors, which are consistently over-expressed on glioblastoma cells. Here we report the first clinical experience with $^{213}$Bi-labeled DOTA-SubstanceP in patients with recurrent glioblastoma. **Materials and Methods:** 17 patients with histologically confirmed recurrence of glioblastoma multiforme after standard therapy (surgery, radio- and chemotherapy) were included. Following intracavitary or intratumoral insertion of 1- 2 catheter systems, patients were treated with 1 to 4 doses of 50 mCi $^{213}$Bi-substanceP in intervals of 2 months. $^{68}$Ga-DOTA-SubstanceP was co-injected to assess biodistribution using PET/CT. Blood sampling was performed up to 2 hours post injection to determine $^{213}$Bi activity in the blood pool. Therapeutic response was monitored with repetitive MRI and FDG-PET. **Results:** Treatment with doses up to 200 mCi $^{213}$Bi-SustanceP was tolerated very well with only mild transient adverse reactions, including a transient increase of focal neurological symptoms (n=2) and episodes of epileptic seizures several days after treatment (n=4). PET/CT imaging of co-injected $^{68}$Ga-DOTA-SubstanceP showed high retention of the radiolabeled peptide at the tumor site. In all cases leakage of $^{213}$Bi activity into the blood pool was below 8% I.D. Out of 16 evaluable patients, 5 patients died due to progressive disease (n=4) or non-treatment related causes (n=1), within the follow up period of 2 - 12 months. 2 patients showed progressive disease, while in 9 patients stabilization of disease (n=4) or reduction of tumor (n=5) was observed. Long term follow up of therapeutic responses is continued and patient recruitment is ongoing. **Conclusions:** Treatment of recurrent GBM with $^{213}$Bi-substanceP is safe with a favorable toxicity profile. Tumor control could be achieved in particular in patients that have received multiple doses of $^{213}$Bi-substanceP (e.g. 4 x 50 mCi). Targeted alpha therapy with $^{213}$Bi-substanceP may evolve as a promising novel option for treatment of recurrent GBM. **Acknowledgements:** The authors are indebted for use of parts of $^{225}$Ac/$^{213}$Bi to the U.S. Department of Energy's, Office of Nuclear Physics, Isotope Development and Production for Research and Applications Program.

## OP674

### PET-based Target Volume Delineation in Radiation Therapy Planning: Are Different Implementations of the Same Automatic Delineation Method Really Equal?

**C. Doll**[1], C. Parcq[2], R. Modzelewski[3], A. S. Dewalle-Vignion[4], U. Christ[1], K. Loquin[3], F. Valenti[5], I. Gardin[3], M. Vermandel[4], L. Massoptier[2], U. Nestle[1]; [1]University Medical Center Freiburg, Freiburg, GERMANY, [2]AQUILAB, Lille, FRANCE, [3]Centre Henri Becquerel, Rouen, FRANCE, [4]University of Law and Health - INSERM Unit U703, Lille, FRANCE, [5]UMANIA, Bergamo, ITALY.

**Aim**: The integration of FDG-PET into radiation treatment planning is now routine in many centers. For PET-based target volume delineation, automatic Methods are in the focus of research with their quantity on the rise. For performance comparisons of different automatic Methods, their implementation in different platforms is often necessary. Although in the majority of cases assuming so, the equality of different implementations of the same algorithm has not been studied in detail yet. Therefore this study compares the performance of implementations on different platforms, including different algorithms and different image data sets. **Materials and Methods**: Three PET-based automatic segmentation Methods are

included in this study: Two adaptative thresholding Methods (Method 1: Schaefer et al, Eur J Nucl Med Mol Imaging 2008; Method 2: Vauclin et al, Phys Med Biol 2009) and the MIP-based method (Method 3: Dewalle-Vignion et al, IEEE Trans Med Imaging 2011), each from a different center. Each of these Methods is implemented in each institution's individual platform and in the new AQUILAB ARTIVIEW segmentation platform being developed in the EUREKA-EUROSTARS project "Segmentation applied to lesions delineated on PET images: Optimization of Methods (SALOME)". This research project features an innovative consensus method evolving from the three different automatic Methods for PET-based target volume delineation. The equality of the different implementations was tested on four image data sets: Method 2 and 3 each on a distinct FDG-PET/CT physical phantom data set acquired at these centers, method 1 on a FDG-PET/CT physical phantom data set and on a clinical lung cancer data set. The gross tumor volumes of each institution's implementation and of the SALOME implementation were compared for each sphere or lesion using the mean volume difference (VD) and/or the mean Concordance Index (CI). **Results**: The implementation in each institution's platform and in the SALOME platform showed good agreement: For method 1 on phantom data a CI of 0.92 and a relative VD of 0.83%, on lung data a CI of 0.89 and a relative VD of 3.0%; for method 2 on phantom data an absolute VD of 1.2ml with mean volume of 17.3ml; for method 3 on phantom data a CI of 0.96 and a relative VD of 3.28%. **Conclusion**: The implementation of PET based automatic segmentation algorithms on different platforms is possible and produces concordant target volumes. The innovative consensus segmentation method of the SALOME project is a promising approach combining the benefits of multiple segmentation algorithms.

## OP675

### Radioimmunotherapy (RAIT) with anti-CD22 90Y-epratuzumab in adults with refractory or relapsed CD22+ ALL: preliminary results of a phase I/II study.

**T. Eugene**[1], C. Bodet-Milin[1,2], P. Chevallier[3], A. Faivre-Chauvet[1,2], A. Rauscher[1,2], N. Robillard[4], J. Barbet[2,5], W. Wegener[6], D. Goldenberg[7,δ], F. Kraeber-Bodere[1,2,8]; [1]Nuclear Medicine Department, Nantes University Hospital, Nantes, FRANCE, [2]Cancer Research Center, Université de Nantes, Inserm UMR 892, Nantes, FRANCE, [3]Hematology Department, Nantes University Hospital, Nantes, FRANCE, [4]Biology/Hematology Department, Nantes University Hospital, Nantes, FRANCE, [5]GIP ARRONAX, St Herblain, FRANCE, [6]Immunomedics, Inc.,, Morris Plains, NJ, UNITED STATES, [7]Garden State Cancer Center, Center for Molecular Medicine and Immunology, Morris Plains, NJ, UNITED STATES, [8]Department of Nuclear Medicine, ICO Gauducheau, St Herblain, FRANCE.

**Objectives:** The outcome is dismal for many adults with acute lymphoblastic leukemia (ALL) and there remains a need for new therapeutic approaches. This study evaluated fractionated radioimmunotherapy (RAIT) using anti-CD22 90Y-epratuzumab in adults with refractory or relapsed CD22 + ALL . **Methods**: Patients initially received cold epratuzumab on days 1, 4, 8, and 11. 90Y-epratuzumab was administered on days 30 and 37, with 111In-epratuzumab on day 30 for serial SPECT-CT imaging and dosimetry. Injections were followed by weekly blood samples and bone marrow aspirates (BMA) 4 weeks later. For dose escalation, dose-limiting toxicity (DLT) was defined (NCI CTC v4.0) as: non-blastic (<5%) pancytopenia grade 4 ≥ 6 weeks or other toxicities ≥ grade 3. Responses were assessed by Cheson 2003 criteria. **Results:** Eight patients have now been treated without infusion reactions, receiving 90Y doses of 92.5 MBq/m2 x 2 (N=5) and 185 MBq/m2 x 2 (N=3). 111In imaging showed bone marrow uptake but after the first 2 patients the cold epratuzumab was discontinued to avoid blocking tumour uptake of the radiolabeled epratuzumab. One month after RAIT, 7/8 patients showed blood and/or bone marrow evidence of disease progression (PD). However, one Philadelphia-positive patient in third relapse achieved a complete phenotypic and molecular response (CR) at the second dose level and is currently still in CR, after receiving a second cycle of RAIT as consolidation, waiting for allogenic transplantation. In PD patients, hematologic decreases were attributed to disease progression while pancytopenia in the CR patient duration resolved within 6 weeks. No other toxicities were observed. **Conclusions:** This radioimmunotherapy approach was well tolerated and appears promising in advanced ALL with one refractory patient having achieved a CR at the current dose level. Dose escalation is continuing and additional dosimetric data will be available at the time of congress.

## OP676

### Association among heterogeneity of intratumoral anti-CD20 antibody distribution, glucose metabolism and therapeutic response in radioimmunotherapy for B-cell lymphoma

**M. Hosono**[1], K. Hanaoka[2], K. Ishii[1], S. Im[1], K. Sakaguchi[1], Y. Yagyu[1], Y. Komeya[1], N. Tsuchiya[1], Y. Tatsumi[1], I. Matsumura[1]; [1]Kinki University School of Medicine, Osaka-Sayama, JAPAN, [2]Osaka University, Suita, JAPAN.

**Aim**: In Zevalin therapy for CD20 positive low-grade lymphoma, heterogeneity of intratumoral anti-CD20 antibody distribution as well as status of lesional glucose metabolism prior to therapy may affect tumor response. The Aim of this study was to evaluate association of heterogeneity of intratumoral In-111 Zevalin (In-Zevalin), accumulation of F-18 FDG (FDG), and therapeutic response in patients receiving Zevalin therapy. **Methods**: Sixteen patients with CD20 positive B-cell non-Hodgkin's lymphoma who underwent Y-90 Zevalin therapy after imaging with In-Zevalin SPECT/CT and FDG PET/CT were enrolled. Patients received In-Zevalin, followed by SPECT/CT scanning at 48 hrs after administration. SUVmax of FDG of lesions was measured on PET/CT while lesion accumulation of In-Zevalin as %ID/g and SUVmax of In-Zevalin (In-Zevalin SUVmax) was measured on SPECT/CT. To evaluate heterogeneity of anti-CD20 antibody distribution, skewness and kurtosis of voxel distribution were calculated by placing there-dimensional volumes of interest (3-D VOIs) on SPECT/CT images. As another intratumoral heterogeneity index, cumulative SUVmax-volume histograms describing percentage of total tumor volume above thresholds of In-Zevalin SUVmax (AUC-CSH) were calculated by placing 3-D VOIs. All lesions (n=42) were classified into responders and non-responders lesion-by-lesion on pre- and post-therapeutic CT images. **Results**: By lesion-based analysis, a positive correlation was observed between FDG SUVmax and accumulation of In-Zevalin. Accumulation of In-Zevalin was 0.0022 ± 0.0009 and 0.0024 ± 0.0008 %ID/g (n.s.), and 2.74 ± 1.43 and 3.29 ± 1.47 SUVmax (n.s.) for responders and non-responders, respectively. In contrast, voxel distribution of In-Zevalin demonstrated skewness of 0.58 ± 0.16 and 0.73 ± 0.24 ($p<0.05$), kurtosis of 2.39 ± 0.32 and 2.78 ± 0.53 ($p<0.02$), and AUC-CSH of 0.37 ± 0.04 and 0.34 ± 0.05 ($p<0.05$) for responders and non-responders. **Conclusions:** Pretherapeutic glucose metabolism was predictive of tumor response; higher glucose metabolism corresponded to poorer tumor response. There was a positive correlation between glucose metabolism and anti-CD20 antibody distribution, and heterogeneity rather than the absolute levels of anti-CD20 antibody correlated well with tumor response.

## OP677

### Preparation & quality control of 177Lu-DOTA-Rituximab for radioimmunotherapy of relapsed and refractory B-cell NHL patients

**P. Thakral**, M. K. Yadav, S. Singla, S. Lata, A. Vashist, A. Sharma, S. K. Gupta, C. S. Bal, A. Malhotra; ALL INDIA INSTITUTE OF MEDICAL SCIENCES, New Delhi, INDIA.

**Background**: The prerequisite of radioimmunotherapy is stable binding of a radionuclide to monoclonal antibodies, which are specific to the tumor-associated antigen. Most B-cell lymphomas express CD20 antigen on the surface of the tumor cells, making it a suitable target for therapeutic radioactive monoclonal antibodies. In the present study, the immunoconjugate of Rituximab and macrocyclic chelator, p-SCN-Bz-DOTA, was prepared and radiolabelled with Lutetium-177 followed by quality control procedures. **Methods:** Rituximab was desalted with sodium bi-carbonate (0.1M, pH 9.0) and incubated with DOTA-SCN (1:50). The effectiveness of the conjugation was evaluated by determining the number of chelators per antibody molecule. This conjugate was radiolabelled with Lutetium-177 and purified using PD10 column. The quality control parameters like pH, clarity, radiochemical purity, in-vitro stability and pyrogenicity were studied. Immunoreactivity of 177Lu-DOTA-Rituximab was assessed using RAMOS cells. The radioimmunoconjugate (RIC) after stringent quality assurance was injected in three patients and the biodistribution profile was analysed. **Results**: An average of 4.02 ± 1.04 p-SCN-Bz-DOTA molecules could be randomly conjugated to a single Rituximab antibody. The radiochemical purity of the labelled antibody was >95 % with preserved affinity for CD20 antigen. The final preparation was stable up to ~120 hrs when tested under different conditions. Bacterial endotoxin level in the sample was less than the permissible levels(<0.2 EU/ml).A favourable biodistribution profile was observed with liver showing the maximum uptake of the RIC. **Conclusion**: A favorable radiochemical purity, stability and biodistribution of the radiolabelled immunoconjugate indicated that 177Lu-DOTA-antiCD20 antibody-Rituximab might be a promising therapeutic agent for the treatment of relapsed and refractory Non Hodgkin's Lymphoma.

1609 - Wednesday, Oct. 23, 8:00 - 9:30, Rhône 3A/3B

## Radiopharmaceuticals & Radiochemistry & Dosimetry: Drug Development

## OP678

### Influence of DOTA chelator position on biodistribution and targeting properties of 68Ga-labeled synthetic anti-HER2 Affibody molecules. Comparison with 111In-labeled counterparts.

**H. Honarvar**[1], J. Strand[2], A. Perols[3], A. Orlova[4], A. Eriksson Karlström[3], V. Tolmachev[1]; [1]Unit of Biomedical Radiation Sciences, Uppsala, SWEDEN, [2]Biomedical Radiation Sciences, Uppsala, SWEDEN, [3]Division of Molecular

Biotechnology (KTH), Stockholm, SWEDEN, [4]Preclinical PET Platform,, Uppsala, SWEDEN.

**Aim**: Affibody molecules are three-helix-scaffold-based affinity proteins (7kD) with high potential as imaging agents. Preclinical and clinical studies have demonstrated that HER2-targeting Affibody molecules enable high contrast imaging within hours after injection. The use of a generator-produced positron emitter 68Ga (T1/2=68 min) might further increase sensitivity of Affibody-mediated imaging. Earlier, we have shown the influence of DOTA chelator positioning on blood clearance rate and tissue uptake of a synthetic variant of anti-HER2 Affibody molecule ZHER2:342 radiolabeled with 111In. The Aim of this study was to compare tumor-targeting properties of 68Ga and 111In-labeled synthetic Affibody molecules having different position of DOTA chelator**. Material and Methods**. ZHER2:S1, a synthetic variant of anti-HER2 ZHER2:342 Affibody molecule, was conjugated with DOTA via amide bond at three different positions: N-terminus ([DOTA]-A1-ZHER2:S1), C-terminus ([DOTA-K58]-ZHER2:S1), and middle of helix 3 ([DOTA-K50]-ZHER2:S1). These Affibody molecules were labeled with 68Ga, and their HER2 binding specificity was evaluated using HER2-expressing SKOV3 cells. Biodistribution of 111In and 68Ga labeled conjugates was compared (at 2 h pi) in NMRI nu/nu mice bearing SKOV3 xenografts. To verify in vivo specificity, control groups of mice were pre-injected with a large excess amount of unlabeled Affibody molecule ZHER2:342 to saturate HER2 in xenografts. **Results:** The specificity tests confirmed that binding of the 68Ga-labeled compounds to SKOV3 cells was HER2-mediated both in vitro and in vivo. The tumor uptake did not differ significantly between 68Ga-labelled conjugates (12.5±1.4, 10.0±1.4, 12.7±1.6 %ID/g, for [DOTA-A1]-ZHER2:S1, [DOTA-K50]-ZHER2:S1, and [DOTA-K58]-ZHER2:S1, respectively). However, position of DOTA had an influence on blood clearance rate and uptake in normal tissues. The variant with the best imaging properties, 68Ga-[DOTA-A1]-ZHER2:S1 had significantly higher tumor-to-blood, tumor-to-liver and tumor-to-bone ratios (38±12, 7.2±2, and 94±42, respectively), than the worse variant [DOTA-K50]-ZHER2:S1 (14±4, 4.0±2, and 25±4, respectively). Surprisingly, tumor uptake of 111In-labeled variants was significantly ($p<0.05$ in the paired t-test) higher (15.7±1.83, 12.8±1.8, 15.4±1.7 %ID/g, for [DOTA-A1]-ZHER2:S1, [DOTA-K50]-ZHER2:S1, and [DOTA-K58]-ZHER2:S1, respectively). Head to head comparison of 111In- and 68Ga-labeled conjugates demonstrated also higher tumor-to-organ and tumor-to-blood ratios for 111In-labeled conjugates. **Conclusion**. 68Ga-[DOTA-A1]-ZHER2:S1 provides the high tumor-to-organ ratios among 68Ga-labeled variants. Not only positioning of the DOTA chelator, but also selection of radionuclide influences biodistribution pattern of radiolabeled Affibody molecules creating pre-conditions for optimization of their imaging properties.

## OP679

### Clinical evaluation of a simple kit formulation for the preparation of $^{99m}$Tc-MIP-1404 for prostate cancer imaging

**S. Vallabhajosula**[1], A. Nikolopoulou[1], L. Solnes[1], P. D. Mozley[1], S. T. Tagawa[1], S. J. Goldsmith[1], J. B. Stubbs[2], T. Armor[3], J. W. Babich[4]; [1]Weill Cornell Medical College, New York, NY, UNITED STATES, [2]Radiation Dosimetry Systems, Inc, Palo Alto, CA, UNITED STATES, [3]Progenics Pharmaceuticals, Inc, Tarrytown, NY, UNITED STATES, [4]3Progenics Pharmaceuticals, Inc, Tarrytown, NY, UNITED STATES.

**Introduction:** $^{99m}$Tc-MIP-1404, a small molecule with specific binding to prostate specific membrane antigen is in phase II clinical trial for imaging prostate cancer (PCa) in patients undergoing radical prostatectomy. For the initial phase I studies, the preparation of $^{99m}$Tc-MIP-1404 involved a labor intensive, multi-step procedure (Preparation-B) taking several hours to complete. In order to facilitate multi-center clinical trials, a "kit formulation" which is rapidly and easily prepared has been developed (J Nucl Med. 2012; 53:S523) (Preparation-A). We report here the results of a phase I study to assess the radiochemical purity (RCP) and image quality of $^{99m}$Tc-MIP-1404 prepared using both Methods. **Methods:** In preparation-B, $^{99m}$Tc pertechnetate (200 mCi) was first added to a carbonyl kit followed by the addition of precursor (MIP-1404). The mixture was incubated for one hour at 100°C and then neutralized by the addition of 0.2 mL of 2N HCl. $^{99m}$Tc-MIP-1404 was then isolated using a Sep-Pak cartridge and ethanol, diluted in physiological saline and sterilized by membrane filtration. In contrast, preparation-A is a simplified procedure using lyophilized precursor and reducing agent. RCP of both formulations was determined using HPLC and a simple solid phase extraction (SPE) cartridge. In a phase I clinical trial, 3 normal control subjects and 3 patients with metastatic PCa received both preparations 1-2 weeks apart. Following intravenous injection of 20 mCi of $^{99m}$Tc-MIP1404, planar whole body images (WBI) were obtained at 15 min, 2, and 4 hours. Based on the region of interest (ROI) analysis, the percent injected dose (%ID) in major organs was estimated. **Results**: The RCP of both $^{99m}$Tc-MIP-1404 preparations was similar (A: 94.2±1.2% vs. B: 93.4±1.4%). For both preparations, the kinetics of distribution and the %ID in major organs were also similar; salivary gland (A: 2.6±0.5% vs. B: 2.6±0.5%), liver (A: 17.2±6.0% vs. B: 16.5±6.0%), kidney (A: 16.4±5.8% vs. B: 13.2±4.7%), and gut (A: 9.8±0.5%vs.B: 9.3± 0.6%). Based on the clinical read of images, there were no apparent differences in the normal organ distribution or image quality. Also, in the 3 patients with PCa, the tumor/background ratios were comparable. **Conclusions**: The results of this study show that a simple kit is feasible and performance is comparable to a more elaborate preparation method that includes a separation step to remove unbound ligand; image quality is unaffected as is lesion detection. A simple kit approach should allow for convenient and widespread preparation of $^{99m}$Tc-MIP1404 for molecular imaging of prostate cancer.

## OP680

### Radiosynthesis and first small animal microPET imaging of [$^{18}$F]UCB-H, a new fluorine-18 labelled tracer targeting synaptic vesicle protein 2A (SV2A)

**J. Aerts**[1], M. Otabashi[1], F. Giacomelli[1], G. Warnock[1], M. Bahri[1], F. Bretin[1], X. Sauvage[1], C. Thielen[2], C. Lemaire[1], E. Salmon[1], A. Plenevaux[1], A. Luxen[1]; [1]Liege University, Liège, BELGIUM, [2]Liege University, Liege, BELGIUM.

**Aim.** We report the radiosynthesis and first rat microPET imaging of a new fluorine-18 tracer targeting the synaptic vesicle protein 2A, SV2A, identified as the binding site of the antiepileptic drug levetiracetam. **Materials and Method.** Two different nucleophilic radiosynthesis pathways were tested to obtain [$^{18}$F]UCB-H, a no-carrier-added tracer in the 2-[$^{18}$F]fluoropyridine family. The Methods were automated on FastLab™ synthesizers. PET studies in rodents were carried out using male SD rats, imaged under isoflurane anaesthesia in a Siemens Concorde Focus 120 microPET scanner. Arterial input function was measured using an arteriovenous shunt method and beta microprobe system. All animal protocols were reviewed and accepted by animal ethical committees. **Results and conclusion.** A radiosynthesis yield of 30% was obtained (uncorrected for decay, 150 minutes of synthesis). Analytical Methods were developed and validated to demonstrate that the quality of the tracer solution was compatible with *in vivo* injection. After intravenous injection, the tracer rapidly entered the brain, followed by rapid washout. PET imaging revealed high uptake of the tracer in the brain and spinal cord, matching the expected SV2A homogeneous distribution. Results indicate that [$^{18}$F]UCB-H is suitable to quantify SV2A proteins *in vivo* and to estimate target occupancy of drugs targeting SV2A. Acknowledgments. The authors thank UCB Pharma SA Belgium for collaboration and the Walloon Region Belgium and the FRNS Belgium for financial support.

## OP681

### Whole body biodistribution of intravenously administered acetylcholinesterase inhibitor in the normal rat : C11-Donepezil PET study.

**T. Watabe**[1], S. Naka[2], Y. Kanai[1], E. Shimosegawa[1], G. Horitsugi[1], H. Ikeda[1], I. Mochida[1], K. Isohashi[1], H. Kato[1], H. Watabe[1], J. Hatazawa[1]; [1]Osaka University Graduate School Of Medicine, SUITA/OSAKA, JAPAN, [2]Osaka University Hospital, Suita/Osaka, JAPAN.

**Objective** Acetylcholinesterase inhibitor (AChEI) has been used for the patients with Alzheimer's disease to protect against the reduction of acetylcholine in the brain. However, biodistribution of AChEI other than the brain has not been clarified yet. The purpose of this study was to evaluate the whole body biodistribution of $^{11}$C-Donepezil (DNP) in the normal rat. **Methods** The biodistribution of $^{11}$C-DNP was investigated by means of PET/CT in 4 normal male Wister rats (8 weeks old, body weight=218±4.8g) under isoflurane anesthesia. A 30-min dynamic scan was started simultaneously with an intravenous bolus injection of $^{11}$C-DNP (44.7±13.8MBq) from tail vein. Metabolite analysis was performed from the blood sample immediately after the PET/CT study. Regions of interests were placed on the major organs of the PET images with reference to the CT images. **Results** Time activity curves of major organs showed following dynamics; wash-out pattern in the lung and the heart, rapid increase and wash-out pattern in the brain, kidney, and spleen (peak SUVmean=2.5±0.3, 6.0±2.0, and 3.9±1.3, respectively), gradual increase to 4 min and slow decrease pattern in the thymus (peak SUVmean=2.3±0.8), gradual increase pattern in the liver, stomach, Herderian gland, and submandibular gland (peak SUVmean=5.4±1.6, 2.0±0.2, 3.5±0.1, 3.3±0.2, respectively), and gradual increase and variable high accumulation in the small intestine, suggesting enterohepatic circulation (peak SUVmean=3.2±0.6). Adrenal grand showed the highest accumulation among the major organs 10 min after the administration and slowly decreased (peak SUVmean=5.7±2.2). Accumulation in the pancreas was stable 5 min after the administration and relatively low compared to the other abdominal organs (peak SUVmean=1.5±0.2). Urine bladder showed gradual increase, reflecting the excretion from the kidney (peak SUVmean=5.9±3.3). Metabolite analysis showed 23.9% of $^{11}$C-DNP in the blood plasma remained unchanged after the PET/CT study. **Conclusions** This study demonstrated the whole body biodistribution of $^{11}$C-DNP by PET in the normal rat. It was suggested that AChEI had potential to be used for the diagnosis and new therapeutic targets of diseases other than Alzheimer's disease.

## OP682

### Biodistribution and Dosimetry of $^{111}$In PSMA Minibody (IAb2-M-DOTA): First Results

**C. Schuchardt**[1], S. Wiessalla[1], H. R. Kulkarni[1], D. Mueller[1], D. Bartlett[2], D. Ho[2], C. P. Behrenbruch[2], A. Wu[2], R. P. Baum[1]; [1]THERANOSTICS Center for Molecular Radiotherapy and Molecular Imaging, BAD BERKA, GERMANY, [2]ImaginAb, Inc., Inglewood, CA, UNITED STATES.

**Aim** IAb2-M-DOTA minibody binds with high affinity to Prostate Specific Membrane Antigen(PSMA) and is potentially an important tool for the detection and treatment of metastatic prostate cancer. The Aim of our pilot study was to determine organ and tumor kinetics of the $^{111}$In labeled PSMA-minibody (fragment), from the parent huJ591 antibody, and to estimate the mean absorbed dose to normal organs and tumor lesions. **Materials and Method** 2 patients (65.5 and 74.1years) suffering from metastatic prostate cancer received 1mg of the minibody, labeled with 731 and 306MBq $^{111}$In, respectively. Based on 5 conjugated planar whole-body scans, the time-dependent activities (whole-body/tumor) were determined, and dosimetric calculations performed according to the MIRD scheme using OLINDA/EXM software. To describe the kinetics, we used the following parameters: mean half-life (hours) and uptake (%IA, fraction of injected activity), which were calculated using the fit of the time-dependent activity curve to a mono- or bi-exponential function. Blood samples were drawn (determine blood-kinetics, estimate the absorbed dose to red marrow). **Results** The whole body uptake showed an exponential decline, half-lives being 50h/47h, respectively in the patients. The liver showed the highest uptake (28%IA and 25%IA at 20h p.i. respectively), the corresponding half-life being 52h in both patients. The kidneys exhibited an increase in uptake until 3h p.i. in one patient and an increase until 20h p.i. in the second patient. After 20h p.i., the renal uptake followed an exponential clearance with half-lives of 56h and 48h, respectively. The maximum kidney uptake was 5%IA in both patients. Given the liver clearance of the fragment, this is most likely due to free radiolabel. Spleen uptake: 2%IA (20h p.i.), effective half-lives 49h and 38h Blood-kinetics (fitted to a tri-exponential function): first half-life: 50min (both patients), second half-life: 10h (both patients), and third half-life: 53h and 24h respectively. Tumor uptake: increased until 20h p.i. followed by a fall (half-life of 45-60h). The following mean absorbed doses (in mGy/MBq, both patients) were calculated: whole body 0.1, liver 0.9, spleen 0.4, metastases 0.2. Kidneys: 0.5/0.7 mGy/MBq, respectively, The resulting dose to the red marrow was 0.1 mGy/MBq. **Conclusions** Despite the high liver accumulation when using only 1mg of the $^{111}$In labelled PSMA-minibody, a significant uptake was demonstrated in the metastatic lesions. Using higher antibody dose, lower hepatic uptake is probable (based on the findings when using the intact J591 parent antibody), making IAb2-M-DOTA minibody a potentially attractive agent for radioimmunotherapy of prostate cancer.

## OP683

### Influence of animal heating on PET imaging quantification and kinetics: results on the biodistribution of 18F-tetrafluoroborate in mice

**C. GOETZ**[1,2], M. Podein[3], F. Braun[3], P. Choquet[1,2], M. Mix[3]; [1]Hopitaux Universitaires de Strasbourg - Preclinical Imaging Lab UF6237, Strasbourg, FRANCE, [2]ICube,CNRS, Strasbourg, FRANCE, [3]University Hospital of Freiburg, Freiburg, GERMANY.

**Aim:** varying environmental conditions under anesthesia are known to modify physiological parameters in rodents including body temperature, heart and breathing rates - leading in unstable homeostatic conditions. These varying environmental conditions could modify uptake of molecular imaging tracers [Fueger & al. J Nucl Med 2006] thus inducing quantification errors. The Aim of this study was to evaluate the impact of heating conditions on PET imaging quantification. **Materials and Methods**: tumor cells transfected with hNIS were implanted subcutaneously in 6 adult female balb-c nude mice (mean weight 18.7 +/- 0.3 g). After 4 days of tumor growth (tumors size 5-7 mm), animals were monitored (heart rate, temperature), maintained under anesthesia using a 1.5% isoflurane / oxygen mix and heated using a dedicated imaging cell (Minerve, France). Mice were administered twice with 3.1 +/- 0.2 MBq of 18F-tetrafluoroborate via tail vein inside the cell. Interval between injections was 4 hours - animals were awaken and fed. Both PET dynamic acquisition were conducted for each animal covering the first 45 minutes after injection (Focus 120 microPET, Concorde Microsystems, US). Heating temperature of the holder was changed between acquisitions leading to either optimal conditions (defined by holder temperature set to 35°) or sub-optimal conditions (defined by holder temperature set to 33°). Time-activity curves were obtained for each animal and for both acquisitions from ROI placed over the liver, thyroid, stomach, implanted tumor and blood compartment (heart ROI). Bi-exponential fitting conducted to calculation of uptake and washout time constants for each ROI (proFit, Quantumsoft, Switzerland). **Results:** optimal animal heating showed stable heart rates during acquisition (515 +/- 35 bpm) as well as stable body temperature (37.1 +/- 0.3°) whereas sub-optimal heating leads to lower heart rates with higher standard deviation (470 +/- 84 bpm) and lower body temperature (36.8 +/- 0.5°). Both uptake and washout time constants were faster ($p < 0.01$) in animals maintained under optimal heating conditions for liver, thyroid, stomach and implanted tumor. **Conclusion**: different heating conditions during anesthesia led to slight but statistically significant differences in heart rate during PET imaging as well as larger standard deviation associated with sub-optimal heating. Despite these slight differences optimal heating showed different distribution with faster uptake and washout kinetics of the radiotracer over all studied compartments in mice.

## OP684

### Using the biodegradable PLGA microsphere to evaluated a new drug delivery system for the brachytherapy of hepatoma in animal model.

**L. Chang**[1], C. Peng[2], P. Chiang[1], H. Wang[1], T. Luo[1]; [1]Institute of Nuclear Energy Research, Taoyuan, TAIWAN, [2]Institute of Biomedical Engineering, National Taiwan University, Taipei, TAIWAN.

**Aims**. The Aim of this study is to establish a new biodegradable drug delivery system for hepatoma embolization brachytherapy. We try to solve the unabsorbed problems appeared at the commercial microspheres products for transarterial embolization (TAE) to hepatoma therapy. **Materials and Methods**. PLGA (poly-lactic-co-glycolic acid) was chosen as the material to make the biodegradable microsphere. The characteristics of DOTA-PLGA-microspheres were identified by FTIR, MALDI-TOF, SEM and size analyzer. We further modified PLGA-microspheres to DOTA-PLGA-microspheres by EDC/NHS/DOTA mixed solution. The modified PLGA-microspheres were labeled with 111In-radioisotope. SD rat implanted N1S1 hepatoma cell line was used as our animal model to evaluate the targeting potential of 111In-PLGA-microspheres via (TAE). **Results**. The results from FTIR and MALDI-TOF Methods demonstrated the existence of NH2 functional group and DOTA conjugation to PLGA-microsphere. The sizes of PLGA-microspheres were ranged between 15±10μm~47±10μm. The radiochemical purity (RCP) of 111In-PLGA-microspheres is more than 95% and kept stable for one week in serum. The Nano-SPECT/CT images and biodistribution data of SD rats obtained at 4, 24 and 48 hr post-injected with 111In-PLGA-microsphere demonstrated that most of radioactivity accumulated in the tumor and liver tissues. The data also showed that less than 0.1% (I.D/g %) of radioactivity could be detected in blood sampling from tail veins at 24 hour post-injected with 111In-PLGA- microsphere via TAE. **Conclusions**. We have established the manufacturing Methods of PLGA-microsphere and 111In-In Cl3 labeling Methods to obtain the high RCP of 111In-PLGA-microspheres. The animal data confirmed that 111In-PLGA-microsphere stably distributed in the tumor site and only little radioactivity was leaked out to the blood. We suppose that our highly- uniformed PLGA-microspheres with isotope labeling have great potential to be applied in the hepatoma therapy.

## OP685

### GRPR antagonist NOTA-P2-RM26 labeled with fluorine-18: radiochemistry, in vitro and in vivo evaluation

**Z. Varasteh**[1], O. Åberg[1], G. Lindberg[1], G. Antoni[1], I. Velikyan[1], M. Sandström[2], M. Larhed[1], V. Tolmachev[3], A. Orlova[1]; [1]Medicinal Chemistry, Uppsala, SWEDEN, [2]Uppsala University Hospital, Uppsala, SWEDEN, [3]Biomedical Radiation Sciences, Uppsala, SWEDEN.

**Aim.** Expression of the Gastrin Releasing Peptide Receptor (GRPR) in prostate cancer suggests that this receptor can be a potential molecular target for visualisation and treatment of these tumors. Previously we have investigated bombesin antagonistic analog (D-Phe-Gln-Trp-Ala-Val-Gly-His-Sta-Leu-NH2, RM26) conjugated to 1,4,7-triazacyclononane-N,N',N''-triacetic acid (NOTA) via a diethylene glycol (PEG2) spacer (NOTA-P2-RM26) and labeled with 68Ga and 111In for visualisation of GRPR1 and have found favorable properties of the conjugate for in vivo imaging of GRPRs. The focus of this study was to develop a high affinity antagonistic 18F-labelled PET GRPR-ligand. **Materials and Methods**. NOTA-P2-RM26 was radiolabeled with 18F using aluminum fluoride chelation2. Labeling stability, in vitro specificity and cellular processing of the [18F]AlF-NOTA-P2-RM26 have been investigated. Inhibition efficiency (IC50) of the [natF]AlF-NOTA-P2-RM26 was compared to that of the natGa-loaded peptide. Pharmacokinetics and in vivo binding specificity of the compound have been studied in mice bearing PC-3 xenografts. The potential of [18F]AlF-NOTA-P2-RM26 for visualization of GRPR-positive tumors was studied using PET camera**. Results**. NOTA-P2-RM26 was stably labelled with 18F resulting in 60-65% decay corrected radiochemical yield within 1 h. Radiochemical purity was >99% after HLB cartrige purification and specific radioactivity was 55 GBq/μmol. The labelled peptide was stable in PBS for at least 3 h at RT and showed high specific binding to PC-3 cells. Both natF- and natGa-NOTA-P2-RM26 have shown low nanomolar inhibition efficiency (IC50=4.3±0.2 nM and 3.1±0.2 nM, respectively). The internalization rate of the radiolabeled peptide was low, only 14% of cell associated radioactivity was internalized after 4 h continuous incubation at 37 °C. Biodistribution was in a good agreement with our previously reported data for 111In- and 68Ga-labeled analogs1 and demonstrated rapid blood clearance, low liver uptake and low kidney retention. Tumor uptake at 3 h pi was 5.5±0.7%IA/g and tumor-to-blood, -muscle and -bone ratios were 87±42, 159±47, 38±16, respectively. Uptake in tumors, pancreas and other GRPR expressing organs, was significantly reduced when excess of non-labeled peptide was co-injected. The low uptake in bone suggests high in vivo stability. PET image with high contrast was obtained 3 h after injection of [18F]AlF-NOTA-P2-RM26.

**Conclusions**: The Al18F-labelled bombesin antagonist was obtained in sufficient yield, purity and specific activity. The inititial biological results suggest Al18F-NOTA-P2-RM26 is a promising candidate for PET imaging of GRPR in vivo. 1. Varasteh et al. Bioconjug Chem, conditionally accepted. 2. McBride et al. J Nuc. Med, 2009,50:991.

1701 —Wednesday, Oct. 23, 10:00 — 11:30, Amphithéâtre

## CME 13 - Translational Molecular Imaging: Joint EANM/ESMI Session: Optical and Nuclear Imaging

### OP686
**Nuclear and Fluorescent Tracers for Intraoperative Application**

**R.G. Pleijhuis, NETHERLANDS**

### OP687
**PET and Optical Tomography in Small Animals**

**F. Ducongé, FRANCE**

### OP688
**Cerenkov Luminescence Imaging**

**S. Maitrejean, FRANCE**

1702 —Wednesday, Oct. 23, 10:00 — 11:30, Auditorium Lumière

## Symposium 14 - EANM/ELI Joint Session: PET in Lymphoma: The New Proposals for Staging and Response Assessment with Illustration and Research

### OP689
**New Proposals for Staging and Response Assessment in Lymphoma**

**S. Barrington, UNITED KINGDOM**

### OP690
**Staging and Response Assessment in Lymphoma: Role of Quantitative PET**

**M. Meignan, FRANCE**

### OP691
**PET in Follicular Lymphoma (Management and Research Perspectives)**

**S. Luminari, ITALY**

1704 - Wednesday, Oct. 23, 10:00 - 11:30, Bellecour 1/2/3

## Featured - Radionuclide Therapy & Dosimetry: Liver Directed Treatments

### OP692
**Intra-arterial Treatments in the Management of Primary and Metastatic Liver Cancer**

**B. Lambert, BELGIUM**

### OP693
**Liver directed treatment with selective internal radiation therapy (SIRT) : 4 year experience in a UK tertiary referral centre**

**M. Kay**, S. Leach, B. Stedman, F. Sundram; University Hospital, Southampton, UNITED KINGDOM.

**Introduction** Liver metastases are a common feature of neoplastic disease and currently surgery is the only curative option, however 75% of patients are unsuitable. Selective internal radiation therapy (SIRT) is an emerging liver directed treatment modality, which Aims to improve survival in unresectable disease. We present our data from our tertiary referral centre in South Central England for patients treated over a 4 year period. SIRT is currently not routinely available or publically funded by the UK National Health Service (NHS). The Cancer Drugs Fund (CDF) in England was established in 2011. CDF is intended to fund patient treatments if these treatments are not accessible after consideration by local funding bodies, the primary care trust (PCT) **Methods** Patients were identified from the departmental database over a 4 year period (January 2009 - December 2012). Information on patient demographics, primary malignancy, administered activity and funding source were obtained retrospectively. All patients had pre-SIRT planning angiography and $^{99m}$Tc-macroaggregated albumin (Tc-MAA) SPECT/CT. SIRT was performed 7-14 days later followed by Bremsstrahlung imaging within 24 hours. **Results** 41 patients had SIRT work-up ( 24 male, 17 female ; age range 40- 77 ), 31 (76%) proceeded to treatment. 6 patients were unsuitable for treatment due to either significant lung shunt or extra-hepatic gut uptake, and 4 not treated for non-technical reasons. The average lung shunt was 7.6% (range 2-25%). On post-therapy Bremsstrahlung imaging, all treated patients demonstrated no extra-hepatic uptake, 1 treated patient refused imaging. Primary malignancies included colorectal (28/41, 68%), ocular melanoma (8/41, 20%), neuroendocrine tumour (2/41, 5%), and 1 each of breast, cholangiocarcinoma and SCC tongue (3/41, 7%). The activity administered ranged from 1.0 - 2.25 GBq. Referrals have exponentially increased over the last 4 years, from 5 in 2009, to 21 in 2012. Funding sources include research trials (2/41, 5%) private funding (10/41, 25%), individual funding requests from PCT (17/41 41%) and the CDF (12/41, 29%). **Discussion** SIRT has exponentially increased over the last 4 years, from 5 in 2009, to 21 in 2012, increasingly funded by the CDF. 90% of our patients were colorectal cancer or ocular melanoma patients. Other patients are increasingly been referred as data from published studies show increased time to progression and progression-free survival. In patients with unresectable liver metastases, nuclear medicine guides treatment planning and dosimetry and assesses post SIRT activity distribution. This optimises the therapeutic strategy and minimises complications.

### OP694
**Treatment of hepatocellular carcinoma (HCC) with intra-arterial Yttrium-90 microspheres for downstaging patients to transplantation**

**K. DE MAN**, L. DEFREYNE, E. DELANGHE, P. SMEETS, X. VERHELST, A. GEERTS, H. VAN VLIERBERGHE, X. ROGIERS, R. TROISI, B. LAMBERT; UZ Gent, Gent, BELGIUM.

**Introduction and Aim**: In our hospital, patients are referred for intra-arterial treatment with Yttrium-90 microspheres if they present with an HCC confined to the liver, but are ineligible for curative treatment options such as liver transplantation, partial hepatectomy or radiofrequent ablation. Additional eligibility criteria for radioembolisation consist of Child-Pugh score <B8, Karnofsky status ≥70% and bilirubin <2 mg/dL. Portal vein thrombosis is not considered a contra-indication. In the presented study we assessed retrospectively how successful we were in downstaging patients to liver transplantation. **Methodology**: We retrospectively analyzed all HCC patients who were treated with Yttrium-90 microspheres in our hospital since 2008 and who presented at an age <70 and with a disease load exceeding the Milan criteria (single tumour ≤5 cm or ≤3 lesions ≤3cm). We recorded whether the patient was downstaged to a tumour load complying with the Milan criteria, and if so, whether transplantation was carried out. **Results**: 40 patients aged <70 years and with a tumour load exceeding the Milan criteria (all treated with TheraSphere, Nordion except 1 with SIR-Spheres, Sirtex) were evaluable. 35 had Barcelona Clinic Liver Cancer (BCLC) B stage disease and 5 had BCLC C. Overall median survival was 12.9 months. 16 out of 40 patients were downstaged to the Milan criteria (40%, all BCLC B), of whom 8 were actually transplanted so far. Two patients are on the waiting list, 1 patient refuses to be listed and 1 patient suffers comorbidity that excludes him from abdominal surgery. Unfortunately 4 patients died before or during work-out for transplantation: 1 unexplained sudden death, 1 lung embolism and 2 due to liver failure. The overall median survival was 30,4 months in the downstaged patients. 24 out 40 patients (60%) did not have a tumour load within the Milan criteria at any point of their follow up and had a significant worse median survival of only 5.5 months (p 0.007 LogRank). 8 patients suffered intrahepatic disease progression and 4 developed metastatic disease. 7/24 were not assessable because of drop-out (2), too short interval since radioembolisation (3) or sudden death within 6 months following treatment (2). **Conclusion:** In our series of BCLC B and C patients aged <70 who underwent radioembolisation, we obtained a successful downstaging to the Milan criteria in 40% of patients, with an actual transplantation rate of 20%. No patients presenting initially with BCLC C disease stage could be successfully downstaged.

### OP695
**Lower biological efficacy of $^{90}$Y-loaded glass microspheres results from microspheres transport in the arterial hepatic tree**

**S. Walrand**[1], M. Hesse[1], C. Chiesa[2], F. Jamar[1], R. Lhommel[1]; [1]Université Catholique de Louvain, Brussels, BELGIUM, [2]National Cancer Institute, IRCCS Foundation, Milan, ITALY.

**Aim:** $^{90}$Y resin and glass microspheres liver radioembolizations delivering liver dose of 40 and of 120 Gy, respectively, display similar hepatic toxicity risk than 40 Gy fractionated EBRT. We investigated why. **Materials and Methods**: The microscopic dose distribution was assessed in the realistic liver model developed by Gulec et al., but using the Russels dose deposition kernel: $D(r) = 0.989\ A\ (1\text{-}r/8) / r^2$ (1). r: radial distance in mm, D: dose in Gy and A : microsphere activity in kBq. A lattice of hexagonal prisms represented the hepatic lobules. The central vein and the six portal tracts were located in the hexagon centre and corners, respectively. Each branch segment of the arterial tree was assumed to split in two smaller branch daughters owing different curvatures which results in a 40-60% microspheres repartition as derived by Kennedy et al. from computer modelling. We performed four 120 Gy to liver simulations. Two uniform: 1 and 6 glass microspheres trapped in all and in only 1 portal tract per lobule, respectively. Two random: glass microspheres trapping assuming an equal probability for all the portal tracts or a variable probability depending on the successions of artery connections leading to the portal tract. **Results**: Eq. 1 fitted well the $^{90}$Y dose kernel obtained from Monte Carlo simulation by Gulec et al. For the two uniform simulations all hepatic structures received at least 110 Gy. The fast decrease of the $^{90}$Y kernel (eq. 1) as the inverse of the square distance r is counterbalanced by the number of contributing microspheres that increases as the square of this distance r. The major part of a dose everywhere in a lobule does not arise from the microsphere tapped in the portal tracts of this lobule, but arises from the farther lobules (75%) as already pointed out by Gulec et al. The Russels law clearly explains this observation. The first random simulation gave for the less irradiated tissue a dose distribution centred around 103 Gy (FWHM = 20 Gy). In the last simulation the dose distribution became significantly asymmetric with a shift of the maximum from 103 Gy to 30 Gy and about 35% of lobules got a dose lower than 40 Gy for the hepatocytes, the central vein and the portal tracts. **Conclusions:** The larger microspheres non-uniform trapping produced by their transport in the arterial tree seems to explain the lower biological efficacy of the glass microspheres.

## OP696

### Comparison of standard versus dosimetrically individualized treatment in intermediated/advanced hepatocellular carcinoma (HCC) radioembolization with glass microspheres

**C. Chiesa**[1], M. Mira[2], M. Maccauro[1], A. Facciorusso[3], C. Spreafico[4], C. Morosi[4], R. Romito[3], C. Sposito[3], S. Bhoori[3], E. Civelli[4], T. Camerini[5], E. Seregni[1], A. Marchiano'[4], E. Bombardieri[1], V. Mazzaferro[3]; [1]Nuclear Medicine, Fondazione IRCCS Istituto Nazionale Tumori, MILAN, ITALY, [2]Post graduate Health Physics School, University of Milan, MILAN, ITALY, [3]Surgery 1, Fondazione IRCCS Istituto Nazionale Tumori, MILAN, ITALY, [4]Radiology B , Fondazione IRCCS Istituto Nazionale Tumori, MILAN, ITALY, [5]Scientific Direction, Fondazione IRCCS Istituto Nazionale Tumori, MILAN, ITALY.

**Aim**: Comparison of standard versus dosimetrically individualized treatment in intermediated/advanced hepatocellular carcinoma (HCC) radioembolization with glass microspheres (Therasphere). **Methods**: 52 highly selected patients (first series) had been treated according to the prescription of an absorbed dose D of 120 Gy averaged on the injected lobe. Tumor and parenchyma (including non irradiated voxels) mean D and Equivalent Uniform Dose (EUD) were retrospectively calculated. 99mTc MAA pre-treatment SPECT voxel dosimetry was performed using the simple local energy deposition method (no convolution). Lesion below 3 grams had not been considered. Only the uptaking region of large lesion had been considered as "lesion" and contoured. The Normal Tissue Complication Probability (NTCP) curve for liver decompensation and the Tumor Control Probability (TCP) curve for >50% density reduction (EASL) had been obtained. A second series of 96 treatments of unselected patients were then planned and performed using these curves. An EUD constraint of 60 Gy for parenchyma was assumed for Child A5, corresponding to a risk of radiation induced liver decompensation less than 20%, with the Aim of delivering a tumor EUD larger than 500 Gy (TCP>50%). Infiltrating lesions with no definable border were included in parenchyma (safety oriented calculation). Median lesion volumes were significantly larger in the second series (median 55 versus 35 cc). **Results:** For the second series, EUD gave only a slight improvement in dose effect correlation, being linearly correlated with D (r = 1.00, 0.92 for lesions and parenchyma respectively). The administered activity was increased with respect to the 120 Gy prescription in 47% of patients (average increase +88%, maximum +370%), reduced in 24% (average -26%, maximum -54%), and in unaltered in 29%. Median parenchyma D and EUD were statistically higher in the first series (D=59 vs 54 Gy, p=0.026; EUD=56 vs 48 Gy, p=0.0062), while median tumor D and EUD in the two series were not statistically different. Child A5-A6 patients showing liver decompensation were 12/43 (28%, first series) versus 13/52 (25%), with non significant difference, in spite of more advanced disease of the second series. Discussion: the mean dose D is a good planning parameter. Moreover, in the framework of local deposition hypothesis, D can be calculated using ROI on rescaled SPECT images, without need of voxel dosimetry. **Conclusion**: mean dose evaluation through ROI evaluation on 99mTc-MAA SPECT without voxel dosimetry is a very simple and effective tool for highly individualized treatment planning in HCC radioembolization with glass microspheres.

## OP697

### Yttrium 90 PET assessment of delivered Sir-spheres concentrations in patients undergoing single liver lobe radioembolization

**L. Aloj**[1], C. Arrichiello[2], L. D'Ambrosio[1], P. Gaballo[1], F. Di Gennaro[1], V. Albino[1], F. Fiore[1], R. D'Angelo[1], F. Izzo[1], S. Lastoria[1]; [1]INT Fondazione Pascale, NAPOLI, ITALY, [2]Current Address: AUSL Valle D'Aosta, SC Fisica Sanitaria, Aosta, ITALY.

**Aim:** The success of Selective Internal Radiotherapy (SIR) with 90Y-spheres in patients with primary or metastatic liver tumors relies at least in part on achieving adequate concentration of spheres in the target tissue. Different Methods with varying degrees of complexity can be utilized to define administered doses. Most Methods cannot accurately take into account the volume of liver that will be irradiated. This may be determined only by performing pre therapy 99mTc-MAA distribution analysis, albeit with some limitations. Many factors may influence the volume of liver into which the microspheres distribute following injection, particularly in single lobe treatment such as catheter position, shunting that may occur through vasculature of the lesions, back-flow due to the embolization effect and so on. The Aim of this study is to determine the degree of variability of 90Y-sphere concentration obtained in the target tissue using administered doses not based on pre-therapy distribution analysis. **Methods:** We evaluated 90Y PET studies performed in 22 patients (15 with hepatocellular carcinoma and 7 with metastatic disease) immediately following single lobe treatment with Sir-spheres. 90Y images were collected by scanning two adjacent 15 minute bed positions over the liver. Administered activities were determined with the body surface area (BSA) method. Volume of interest analysis using a threshold method was utilized to estimate the volume of liver containing radioactive spheres on the PET images. Average activity concentrations were derived by dividing the injected activity by the observed distribution volume. **Results**: Administered activities ranged from 535 to 2450 MBq. The average activity obtained in the irradiated portion of the liver was 1753 KBq/ml however this activity ranged from 624 to 4188 KBq/ml. This translates to average absorbed doses between approximately 30 and 200 Gy. **Conclusions**: Using non-image based Methods to define administered dose yields very high variability in effective concentrations of microspheres in the target volume. Such variability may have negative impact on treatment outcome and toxicity. Pre-treatment estimation of irradiated liver volume should aid in better treatment planning. 90Y-PET imaging provides very useful clinical information and should be employed to estimate effective absorbed doses after treatment regardless of which method is utilized to determine administered doses.

## OP698

### Boosted selective internal radiation therapy (B-SIRT) using 90Y-loaded glass microspheres induces prolonged overall survival for PVT patients.

**E. Garin**, L. Lenoir, J. Edeline, S. Laffont, H. Mesbah, P. Porée, E. Boucher, Y. Rolland; Cancer Instutute Eugène Marquis, F-35042 Rennes, FRANCE.

**Goal**: Evaluation of the response rate and survival of hepatocellular carcinoma PVT patients treated with Therasphere® using the boost concept. **Material and Methods**: Therasphere® was administered in 40 PVT hepatocellular carcinoma patients (main= 11, lobar = 23, segmental= 6). MAA SPECT/CT quantitative analysis was used for the calculation of the tumour dose (TD), the healthy injected liver dose (HLD) and the injected liver dose (LD). Response was evaluated at 3 months using EASL criteriae. OS was evaluated using Kaplan and Meyer tests. **Results**: Mean 90Y-loaded microspheres injected activity was 3.1±1.5 GBq. Mean LD was 143±49Gy. Median TD was 316Gy for responding lesions versus 133Gy for non responding lesion ($p<0.0001$). With a threshold TD of 205Gy, MAA-SPECT/CT was predictive of response with a sensibility of 100%, and an overall accuracy of 90% (0FN, 4FP). Knowing the TD and the HLD, 40% of the patients received an intensification of the treatment (increase of the injected activity with the goal to achieve a TD> 205Gy with a LD > 150 Gy and a HLD<120Gy) with a good response rate (81%) and without increased liver grade III toxicity (6.2% as against 12.5% in the non boosted patients, ns). 6 patients were dowstaged, 5 received a lobar hepatectomy. Median OS was 18.2 months [12-27]. It was 4m [12-27] for patients with a TD<205Gy versus 21.5m [12-28.5] for patients with a TD>205Gy. OS was 12m [3-∞] for patients with main PVT versus 21.5m [12-28.7] for patients segmental or lobar PVT (ns). Finally Os was 23.2m for patients with a TD>205Gy and a good PVT targeting (n= 34). **Conclusion**: Boosted selective internal radiation therapy using 90Y-loaded glass microspheres induces prolonged overall survival for PVT patients without increasing liver toxicity.

1705 - Wednesday, Oct. 23, 10:00 - 11:30, Auditorium Pasteur

**Oncology Clinical Science: Head & Neck Tumours**

## OP699

### Role of pre-therapy FDG PET/CT to predict outcome in head and neck cancer patients undergoing radiation treatment

**M. Kirienko**[1], I. Castiglioni[2], I. Dell'Oca[3], E. Villa[3], F. Gallivanone[2], P. Mapelli[4], L. Gianolli[4], C. Messa[5,6,7], M. Picchio[2,4]; [1]University Milano-Bicocca, Milan, ITALY, [2]Institute for Bioimaging and Molecular Physiology, National Research Council (IBFM-CNR), Milan, ITALY, [3]Radiation Oncology, Scientific Institute San Raffaele, Milano, ITALY, [4]Nuclear Medicine, Scientific Institute San Raffaele, Milan, ITALY, [5]Institute for Bioimaging and Molecular Physiology, National Research Council (IBFM-CNR), Milano, ITALY, [6]Tecnomed Foundation, University of Milano-Bicocca, Milan, ITALY, [7]Nuclear Medicine, San Gerardo Hospital, Monza, ITALY.

**Aim** To evaluate the predictive role of pre-therapy FDG PET/CT on radiotherapy treatment outcome in head and neck cancer patients. **Materials and Methods** We retrospectively included 19 pts (15 men, **4** women, mean age 59.2 yrs, range 23-81 yrs). Tumour sites were 12 (63.1%) oropharynx, 5 (26.3%) rynopharynx and 2 (10.5%) larynx. Twelve (63.1%) pts were in stage IV, 3 (15.8%) in stage III, 3 (15.8%) in stage II and 1 (5.3%) in stage I. All pts underwent FDG PET/CT before treatment with Simultaneous Integrated Boost Intensity-Modulated Radiotherapy guided by Biological Target Volume defined on PET/CT images. The median follow-up was 19.3 months (range 4 - 24). The prognostic role of SUVmean and SUVmean corrected for Partial Volume Effect (PVC-SUVmean) of the primary lesion, was assessed with respect to the lymphnodes PET/CT negativity (G1, n=6) or positivity (G2, n=13), using ROC analysis, considering 2-year disease free survival (DFS), local relapse free survival (LRFS) and distant metastasis free survival (DMFS). **Results** No statistical significance was found by the Log-Rank test (p>0.05) with regard to DFS, LRFS and DMFS for the differentiation of (G1) and (G2) pts. The small number of G1 pts did not allow the correlation analysis between SUVmean and survival endpoints. A SUVmean cut-off value could separate the G2 pts into two groups (G2-A and G2-B), with SUVmean lower and higher than 10.8, characterized by DFS of 100 vs 33.3% (p<0.05), LRFS of 100 vs 44.4% (p>0.05) and DMFS of 100 vs 76.2% (p>0.05), respectively. When PVC was applied, DFS was 75 vs 20% (p<0.05), LRFS was 75 vs 40% (p>0.05) and DMFS was 100 vs 60% (p≈0.05), with PVC-SUVmean lower and higher than 15, respectively.The results of the ROC analysis for G1, G2-A and G2-B patients with respect to LRFS, DMFS and DFS didn't show statistical significance (p>0.05) by the Log-Rank test in the correlations when PVC was not applied. A statistically significant correlation was found for DFS: 83.3%, 75% and 20% for G1, G2-A and G2-B, respectively when PVC was considered. **Conclusions** SUVmean was found to be a surrogate biomarker with prognostic value for lymphnode positive patients with respect to DFS, while PVC-SUVmean was found to be predictive for both DMFS and DFS. When PVC was considered, SUVmean associated with lymphnode PET/CT detection was statistically correlated to DFS in all patients.

## OP700

### Impact of F-18 FDG PET/CT on management in head and neck cancer patients

**H. H. Tam**, N. Patel, R. Sandhu, Z. Win; Department of Nuclear Medicine, Imperial College Healthcare NHS Trust, London, UNITED KINGDOM.

**Aim:** $^{18}$F FDG PET/CT is well established as the technique of choice for staging in head and neck squamous cell carcinoma (HNSCC). While previous studies have reported on its usefulness in guiding management in HNSCC as a group, its impact on the management of individual tumour sites have not been reported. In this study, we present an analysis of PET/CT impact on the management of the subgroups of HNSCC based on tumour location. **Materials and Methods**: Retrospective review of 47 patients between 2009 to 2012. Site of primary tumour, location of lymph nodes and presence of metastases on PET/CT, CT and/or MRI were recorded. PET/CT was then compared with CT and/or MR with regards to nodal staging and any other addition feature which would have influenced the management plan. **Results**: 29 tonsillar (7 females, 22 males) and 18 tongue-base (4 females, 14 males) SCC patients were identified. In tonsillar SCC, PET/CT nodal downstaged 6 patients, nodal upstaged 7 patients, identified the primary site in 2 patients, identified a second primary in 2 patients. In total, PET/CT changed the management plan of 17 patients (59%). In tongue-base SCC, PET/CT nodal downstaged 1 patient and nodal upstaged 8 patients, thus changing the management plan of 9 patients (50%). **Conclusion**: $^{18}$F FDG PET/CT changed the management plan of a substantial proportion of patients with tonsillar SCC and tongue-base SCC. A detailed analysis and results from other HNSCC tumour subgroups will be presented.

## OP701

### Clinical impact of increased oral $^{18}$F- FDG tracer-uptake in follow up of oral squamous cell carcinoma.

**C. Gstettner**, S. Kerschbaumer, R. Aigner; Medical University Graz,Departement of Radiology, Division of Nuclear Medicine, Graz, AUSTRIA.

**Aim:** We want to demonstrate the clinical impact of increased tracer- uptake in the follow- up PET- CT after therapy in patients presenting oral squamous cell carcinoma. **Materials and Methods**: The study covers a sample of 40 patients (30 male, 10 female with an average age of 54 years). Each patient suffered from a histological proven oral squamous cell carcinoma. In 38 patients a curative tumour resection with a neck dissection was done with an additional local radiation in 19/38 patients. Two patients underwent only chemotherapy and local radiation. A routinely follow up $^{18}$ F- FDG PET-CT was performed on a PET-CT scanner (GE, Discovery ST). The diagnostic CT scan was done with iodinated contrast (biphasic bolus of 80 - 110ml of Visipaque™ 320 mg iodine/ ml intravenously was applicated) 20min after the PET-CT. The $^{18}$F FDG uptake was measured and stated as normalised SUV-BW (standard uptake value per body weight and injected activity). Pathological enhanced tracer was observed in comparison to the uptake of neck muscle or the salivary glands. An oral tissue sample had been taken in every patient in case of an increased FDG uptake or clinical suspicious sings. **Results:** In Group A (13/40 patients) an oral focal tracer-uptake with a SUV max 5,3- 8,4 was detected. In Group B (9/40 patients) an oral elongated uptake with a SUV max 3,3-14,6 was measured and in Group C (15/40 patients) an oral inhomogeneous extensive FDG uptake with a SUV max 4,2- 31 was detected. 3/40 patients were diagnosed as local unsuspicious. The histological sample leads to the following results: In Group A in 8/13 patients an inflammation, in 2/13 patients a remaining tonsil tissue, in 2/13 patients a soft tissue and in 1/13 patients an atrophic salivary gland was diagnosed. In Group B in 6/9 patients an inflammation, in 1/9 patient a granulation tissue, in 1/9 patient a hyperplasia and in 1/9 patient a soft tissue was diagnosed. In Group C all of the 15 patients had a histological proven tumour relapse. **Conclusion**: Increased $^{18}$F- FDG oral tracer-uptake in follow up of oral squamous cell carcinoma needs further evaluation. In most cases inflammation leads to focal or elongated results without malignancy. Independently from the SUV max inhomogeneous extensive tracer-uptake is caused by tumour relapse.

## OP702

### Compensatory lingual muscles hyperfunction after hemiglossectomy : A potential cause of false positive PET interpretation in oral cancer patients

**V. Soubeyran**, K. Sandu, K. Khanfir, P. Brachet, S. Monteiro, E. M. Kamel; CHCVs, Sion, SWITZERLAND.

**Aim** : To describe the typical pattern of contralateral compensatory FDG accumulation within lingual muscles in patients underwent partial- or hemi-glossectomy for oral cancer. **Methods** : Eleven patients with tongue cancer (n=8) and mouth floor cancer infiltrating the tongue (n=3) were studied. These cancerous lesions were all squamous cell carcinomas. Surgical intervention of those patients consisted of hemi-glossectomy (n=8) and partial-glossectomy (n=3). Partial-glossectomy was defined as removing less than half the tongue. All patients had uneventful post-operative recovery and usual speech- rehabilitation programs. Follow-up FDG PET/CT without I.V contrast media was requested for all patients and the images were analysed for any potential local disease recurrence. Abnormal FDG accumulation was defined as that exceeded normal background activity with or witout correlative nodular pattern on the native CT. **Results** : Abnormal contralateral FDG accumulation was observed in 9 (82%) out of 11 patients (SUVmax 8.11 ±5.2). Correlative CT referred these metabolically active areas to the extrinsic muscles of the tongue (hyoglossus, n=7, genioglossus, n=1, and both muscles, n=1) that appeared homogenous without suspicious nodular pattern on CT. Clinical and radiological follow-up (mean 8 ± 3.5 month) did not reveal local disease recurrence in any patients and hence the benign entity of these muscular FDG accumulations was confirmed. Interestingly, these findings were observed in 8/8 (100%) patients with hemi-glossectomy, and 1/3 (33%) patient with partial-glossectomy suggesting a propable relation between the resected tongue bulk and the aforementioned compensatory phenomena. **Conclusion** : After incomplete tongue resection, compensatory contalateral extrinsic lingual muscles' FDG accumulation is a frequent finding occured in 100% of patients with hemi-glossectomy and 33% of patients with partial-glossectomy. This abnormal FDG uptake should not be mistaken for local disease recurrence on PET interpretation.

## OP703

### Incremental Value of FDG PET CT Imaging Over Conventional Neck Nodal Staging in Therapeutic Decision Making in Patients with Cervical Nodal Metastases from Unknown Primary

**M. SARMA**, C. BORDE, P. SUBRAMANYAM, P. S. SUNDARAM; AMRITA INSTITUTE OF MEDICAL SCIENCES (AMRITA VISHWA VIDYAPEETHAM), COCHIN, INDIA.

**Aim**: This study was undertaken to evaluate the incremental value of FDG PET CT imaging over conventional neck nodal staging (AJCC 2010 7th edition) in

therapeutic decision making in patients with cervical nodal metastases from unknown primary. FDG PET CT attempted to assess the presence of infraclavicular lymphnodal or distant organ metastasis. **Materials & Methods**: 26 patients, (age 44-70 yr, M:F = 19:7) diagnosed to have metastatic neck lymph nodes with unknown primary tumour site inspite of thorough physical, panendoscopy examination, anatomical imaging underwent AJCC 7th edition staging & 18F FDG PET CT imaging (head to mid thigh, 8 bed positions) between Jan 2011 & Oct 2012. Patients were grouped as Group I (N1/N2a) and Group II (N2b/N2c/N3) as per AJCC nodal staging. Relevant clinical, other anatomical imaging findings, surgical, subsequent histopathological findings as and when available, were used to correlate with FDG PET/CT findings. Fisher Exact Test was performed to analyse any association between pre PET CT AJCC N staging (for Gp I, II) and FDG PET CT findings with reference to unsuspected infraclavicular lymphnodal or distant organ metastases. **Results**: Infraclavicular lymphnodal metastases and distant organ metastases were detected in 4/26 patients. Gp I patients showed no distant metastasis while 4 of 20 Gp II patients showed distant metastases (N2b: N2c: N3 = 1:2:1 patients). Fischer exact Test was performed to analyze any association between AJCC neck nodal staging and presence of distant metastases. P value of 0.542 (>0.05) was found which is not statistically significant suggesting presence or absence of distant metastases is independent of the neck nodal staging in unknown primary with metastatic cervical lymph nodes patients.This implies that an FDG PET CT whole body evaluation is essential for accurate staging & therapeutic decision making. Thus a radical treatment can be planned in patients with no distant metastases even in higher N staged patients. Patients with lower N staging but with PET CT detected distant metastases can be planned for a conservative approach. **Conclusion**: Patients with cervical nodal metastases from unknown primary will need FDG PET CT imaging irrespective of the neck nodal status at presentation.

## OP704

### The role of 18FDG-PET/CT for response assessment after (chemo)radiotherapy for head and neck squamous cell carcinoma

**B. Van Den Heuvel**[1,2], D. Roothans[1,2], N. Helsen[2], T. Van Den Wyngaert[2], D. Van den Weyngaert[1,3], L. Carp[2], S. Stroobants[1,2]; [1]University of Antwerp, Antwerp, BELGIUM, [2]Department of Nuclear Medicine, Antwerp University Hospital, Edegem, BELGIUM, [3]Department of Radiotherapy, ZNA Middelheim, Antwerp, BELGIUM.

**Aim** To evaluate dedicated FDG-PET/CT for the assessment of treatment response in patients with head and neck squamous cell carcinoma (HNSCC). **Materials and Methods** Patients with histologically proven HNSCC treated with radiotherapy with or without concomitant chemotherapy were studied retrospectively. Histopathology or clinical follow-up (≥12 months) provided the reference standard. Sensitivity, specificity, positive (PPV) and negative predictive value (NPV), and accuracy were calculated on a patient level. The impact of the imaging interval post-treatment was analysed using logistic regression. For survival outcomes, Kaplan Meier-analysis was used. Within the subgroup of patients who also underwent conventional imaging including computed tomography (CT) and/or magnetic resonance imaging (MRI), comparison between FDG-PET/CT and conventional imaging was performed using the McNemar test. **Results** 104 patients were included (median age 61y; male n=84). Median follow-up was 28.3 months (range 0.4 - 60.7 months). FDG-PET/CT was performed at a median of 13 weeks post-treatment (range 5.4- 19.0 weeks). Sensitivity, specificity, PPV, NPV, and accuracy for FDG-PET/CT were 89% (95% CI 75% - 97%), 90% (95% CI 80% - 96%), 83% (95% CI 67% - 93%), 94% (95% CI 85% - 98%) and 89% (95% CI 82% - 95%), respectively. FDG-PET/CT was significantly more accurate when performed >11 weeks after treatment (p=0.008), due to a higher specificity (97% vs 44%, p<0.001). The odds of FDG-PET/CT correctly discriminating between complete response and residual disease increased with 33% for every additional week between end of therapy and imaging (OR 1.33; 95% CI 1.07 - 1.66; p=0.01). A complete response on FDG-PET/CT was associated with a significantly longer median overall survival (50.7 vs 10.3 months; p<0.001). 57 patients also underwent conventional imaging. Within this subgroup, the specificity of FDG-PET/CT was significantly higher (86% vs 56%, p=0.007). There was no significant difference in sensitivity (95% vs 90%, p=0.56). **Conclusion** FDG-PET/CT has a high diagnostic value to detect residual disease after (chemo)radiotherapy, with significantly higher accuracy when performed >11 weeks after the end of therapy. Furthermore, FDG-PET/CT can be used to identify patients with poor prognosis. When compared to conventional imaging modalities, FDG-PET/CT has significantly better specificity, with comparable sensitivity.

## OP705

### FDG-PET/CT in the assessment of retro- and parapharyngeal metastases in head and neck squamous cell carcinoma

**S. Siepmann**[1], J. Brömme[1,2], A. Arnold[3], M. Schmücking[2], R. Giger[3], D. Aebersold[2], T. Krause[1], B. Klaeser[1]; [1]Department of Nuclear Medicine, Inselspital, Bern University Hospital, and University of Bern, Bern, SWITZERLAND, [2]Department of Radiation Oncology, Inselspital, Bern University Hospital, and University of Bern, Bern, SWITZERLAND, [3]Department of Oto-Rhino-Laryngology, Head and Neck Surgery, Inselspital, Bern University Hospital, and University of Bern, Bern, SWITZERLAND.

**Background** The detection of retro- and parapharyngeal lymph node metastases (RPLN) of head and neck squamous cell carcinoma (HNSCC) is essential for surgical planning and correct dose prescription in radiotherapy. 18F-fluorodeoxyglucose-Positron emission tomography/ computed tomography (FDG-PET/CT) has been proved as an accurate imaging modality to assess lateral cervical lymph nodes. We investigated the detection rate of RPLN with FDG-PET/CT in patients with HNSCC. **Materials & Methods** Patients undergoing PET/CT for staging or restaging of HNSCC between January 2011 and October 2012 were included. Patients with known secondary malignancies were excluded. All patients underwent a PET/CT of the trunk (90 min p.i., matrix size 200x200, 5 mm Gauss filtering, acquisition time per bed position 2 min) and a dedicated high-resolution PET/CT acquisition of the head & neck area (110 min p.i., matrix size 512x512, 2 mm Gauss filtering, acquisition time per bed position 10 min). PET/CT was coregistered either with an unenhanced or contrast-enhanced CT of the head and neck region. Patients that had MRI examinations within 6 weeks prior or after PET/CT were included in a comparative analysis of PET/CT and MRI. Written reports of PET/CT and MRI examinations were reviewed to assess the rate of RPLN metastases. **Results** 302 patients with PET/CT examinations in the study period met the inclusion criteria. PET/CT was done for primary staging in 234 (77%) and re-staging for recurrent disease in 68 patients (23%). The most common tumour site in primary disease was the oropharynx (44%), most frequent AJCC stages were III and IVa (75%). FDG-PET/CT detected RPLN in 35/302 patients (11.6%) (primary staging 27/234 (11.5%), recurrence 8/68 (11.8%)). The highest rate of RPLN was found in oropharyngeal cancer (17.4%) compared to hypopharyngeal cancer (5%) and other HNSCC (0.8%). A total of 185 patients had MRI and PET/CT examinations and were included in the comparative analysis. MRI detected RPLN in 9/185 (4.9%) vs. PET/CT in 23/185 patients (12.4%). Of 23 RPLN detected with PET/CT, MRI detected 8 (34.8%, p=0.015). One RPLN was exclusively detected in MRI (1/24, 5%). **Conclusion** FDG-PET/CT revealed a considerable rate of RPLN in patients with HNSCC, especially in case of primary tumours of the oropharynx and in recurrent disease. In our study group, PET/CT detected significantly more RPLN than MRI.

## OP706

### Diagnostic Value of FDG-PET/CT in Laryngeal Nerve Palsy

**A. L. Nielsen**[1], A. Thomassen[1], S. Hess[1], H. Petersen[1], A. Johansen[1], M. Rohde[2], A. R. Madsen[2], C. Godballe[2], P. Hoeilund-Carlsen[1]; [1]Department of Nuclear Medicine, Odense University Hospital, Odense C, DENMARK, [2]Department of ENT Head and Neck Surgery, Odense University Hospital, Odense C, DENMARK.

**Aim** Paresis of the recurrent laryngeal nerves may be a symptom of malignancy due to the anatomical course of the nerves in the neck and mediastinum. Therefore, FDG-PET/CT may be useful as an ancillary examination for diagnosing malignancy. The Aim was to investigate the frequency of malignant findings and the diagnostic yield of FDG-PET/CT in patients presenting with recurrent laryngeal nerve palsy. **Materials and Methods** We retrospectively included all patients referred for FDG-PET/CT scans with recurrent laryngeal nerve palsy from the Department of ENT Head and Neck Surgery at our hospital from January 2011 until March 2013. Scan results were compared to clinical workup including biopsy and pathology results. A scan was considered true positive if PET/CT was suggestive of malignancy along the pathway of the recurrent laryngeal nerves, and this finding was confirmed by biopsy and false positive if not confirmed by biopsy and/or follow-up. A true negative scan was one without abnormal FDG-uptake and a follow-up demonstrating non-malignancy, whereas a false negative scan was present if follow-up was consistent with malignancy in a patient in whom PET/CT failed to detect a malignancy suspicious lesion**. Results** The study comprised 48 patients, 23 females and 25 males with a mean age of 66 years (range 37-89). Nine of these had a history of radically treated cancer. Twenty-one (44 %) were diagnosed with cancer during follow-up, most frequently of the lung, breast and oesophagus. The palsy was right-sided in 13 patients, left-sided in 32 and bilateral in 3. Mean follow-up was 6 months (range 1-24). PET/CT was suggestive of malignancy in 27 patients (21 true positive, 6 false positive) and showed no malignancy in 21 (21 true negative, 0 false negative). Thus, the sensitivity, specificity, accuracy, positive and negative predictive values were 100% [85%-100%], 78% [59%-89%], 88% [75-94%], 78% [59%-89%], and 100% [85%-100%], respectively (Wilson score based 95% confidence intervals in brackets). **Conclusion** In this retrospective survey, biopsy proven malignancy (whether newly diagnosed or relapsed) was the cause of recurrent laryngeal nerve palsy in almost half of the patients. FDG-PET/CT was excellent in finding (sensitivity 100%) and ruling out malignancy (negative predictive value 100%).

1706 - Wednesday, Oct. 23, 10:00 - 11:30, Grd. Salon Prestige Gratte-Ciel

**Oncology Clinical Science: Neuroendocrine Tumours**

## OP707

### $^{68}$Ga-DOTATOC PET has a higher sensitivity, on a lesion-by-lesion comparative analysis, than $^{111}$In-pentetreotide SPECT in neuroendocrine tumor patients

**S. Van Binnebeek**[1], B. Vanbilloen[1], K. Baete[1], C. Terwinghe[1], M. Koole[2], F. M. Mottaghy[3,4], P. M. Clement[5], L. Mortelmans[1], K. Bogaerts[6], K. Haustermans[7], E. Van Cutsem[8], C. Verslype[8], A. Verbruggen[9], C. M. Deroose[1]; [1]Nuclear Medicine, University Hospitals Leuven and Department of Imaging & Pathology, KU Leuven, Leuven, BELGIUM, [2]Department of Nuclear Medicine, University Medical Center Groningen, Groningen, NETHERLANDS, [3]Department of nuclear medicine, University Medical Center, Maastricht, Maastricht, NETHERLANDS, [4]Department of Nuclear Medicine, University Hospital Aachen, Aachen, GERMANY, [5]Medical Oncology, University Hospitals Leuven and Laboratory of Experimental Oncology, KU Leuven, Leuven, BELGIUM, [6]Department of Public Health and primary Care (I-BioStat), KU Leuven, Leuven, BELGIUM, [7]Radiation Oncology, University Hospitals Leuven and department of Oncology KU Leuven, Leuven, BELGIUM, [8]Division of Digestive Oncology, University Hospitals Leuven and Department of Oncology, KU Leuven, Leuven, BELGIUM, [9]Laboratory for Radiopharmacy, KU Leuven, Leuven, BELGIUM.

**Aim**: In this prospective study, including patients with neuroendocrine tumors (NET), the detection efficiency of metastatic lesions using $^{111}$In-pentetreotide SPECT or $^{68}$Ga-DOTATOC PET was compared. We specifically looked for incremental lesions, defined as lesions only observed on one modality even after extensive retrospective evaluation of the other modality. **Materials and Methods**: Fifty-five patients with a metastasized NET underwent 185 MBq $^{111}$In-pentetreotide SPECT 24 hours post-injection and 185 MBq whole-body $^{68}$Ga-DOTATOC PET/CT 30 minutes post-injection. As most of the patients had intra-abdominal tumoral lesions, the SPECT-images were acquired from the abdominal region; in 1 patient with a medullar thyroid carcinoma and lung metastasis, a SPECT Thorax was executed. For the SPECT-PET comparison, only the field of view of the SPECT was taken into account on the PET-images (=$PET_{FOVSPECT}$). A lesion-by-lesion analysis was performed for all tumoral foci on both somatostatin receptor imaging Methods whereby total lesions as well as incremental lesions were determined for both modalities. **Results**: $^{111}$In-pentetreotide SPECT and $^{68}$Ga-DOTATOC PET was performed in the same week, except for 5 patients in whom scintigraphy was performed 1 to 5 months after PET/CT and for 2 patients in whom $^{68}$Ga-DOTATOC PET was executed 18 and 22 days after $^{111}$In-pentetreotide SPECT. Significantly more lesions were detected on $PET_{FOVSPECT}$ compared to SPECT, 1139 (range: 1-105; median: 15) versus 675 (range: 0-73, median: 9) respectively ($p = 8.1*10^{-6}$ (paired t-test)). In one patient (2%), one single incremental lesion was detected on SPECT. Further on, in 10 patients (18%), SPECT- and PET-images showed the same number of tumoral lesions. In the remaining 44 out of 55 patients (80%), a total of 465 incremental lesions were noticed on $PET_{FOVSPECT}$. When expressed as fraction of all lesions seen on PET in those 44 patients, the incremental lesions on $PET_{FOVSPECT}$ represented on average 46% (median: 38%; IQR: 28-63%). **Conclusion**: $^{68}$Ga-DOTATOC PET is superior for the detection of NET metastases, compared to $^{111}$In-pentetreotide SPECT, picking up a significantly higher number of tumoral lesions. $PET_{FOVSPECT}$ detected hereby, in 80% of the patients, an average of 11 incremental lesions per patient, which represents 46% of all the lesions detected on $PET_{FOVSPECT}$. One must therefore be aware of the potential higher clinical impact of $^{68}$Ga-DOTATOC PET due to its higher sensitivity for tumor detection.

## OP708

### Should 68Ga-DOTANOC PET/CT be the first imaging investigation in patients with clinical or biochemical suspicion of neuroendocrine tumors?

**S. Jain**, P. Sharma, S. Arora, C. Bal, A. Malhotra, R. Kumar; ALL INDIA INSTITUTE OF MEDICAL SCIENCES, New Delhi, INDIA.

**Aim:** To evaluate whether 68Ga-DOTANOC PET/CT be the first imaging investigation in patients with clinical or biochemical suspicion of neuroendocrine tumors. **Material and Methods**: Data of 164 patients (mean age: 42.5±17.3 years; 54.8% male) who underwent 68Ga-DOTANOC PET/CT for suspected NET was retrospectively analysed. NET was suspected based on clinical signs/symptoms and/or raised biochemical markers. These patients were divided into two groups: Group A-93 patients with conventional imaging suspicious for NET [CT (n=71), MRI (n=12), ultrasonography (n=5), endoscopic ultrasound (n=4), 131I-Metaiodobenzylguanidine scintigraphy (n=3) and 18F-FDG PET/CT (n=3)], and Group B-71 patients where conventional imaging was either negative (n=18) [CT (n=15), MRI (n=2), USG (n=4)] or not available (n=53). PET/CT images were reviewed by two experienced nuclear medicine physicians in consensus. Histopathology (n=55) and clinical/imaging follow up (n=109; median-11 months) was used as reference standard. Based on reference standard 97 of 164 patients had NET. **Results**: 68Ga-DOTANOC PET/CT was positive for NET in 101 and negative in 63 patients. Primary tumor was demonstrated in 90 patients (commonest site-pancreas) and metastasis in 30 (commonest site-liver). The site of suspicious primary lesion on conventional imaging were pancreas (n=20), stomach (n=8), duodenum (n=8), ileum (n=2), colon (n=3), rectum (n=1), lung (n=24), adrenal (n=13) and paraganglioma (n=10). The site of suspicious metastatic lesion on conventional imaging were liver (n=21), lung (n=3), lymph node (n=6) and bone (n=1). 68Ga-DOTANOC PET/CT showed sensitivity of 93%, specificity of 84%, PPV of 94.2%, NPV of 91.3% and accuracy of 93.5% in Group A patients. 68Ga-DOTANOC PET/CT showed sensitivity of 89.6%, specificity of 88.1%, PPV of 83.8%, NPV of 92.5% and accuracy of 88.7% in Group B patients. No significant difference was found in the accuracy of 68Ga-DOTANOC PET/CT between these two groups (P=0.420). In patients where other radiological imaging was available (n=111; suspicious=93; negative=18), 68Ga-DOTANOC PET/CT was superior for detection of NET (P<0.0001). **Conclusion**: 68Ga-DOTANOC PET-CT shows comparable high accuracy in patients with suspected NET, with positive conventional imaging and in patients where conventional imaging is negative or not available. Hence, it should be used as a first imaging investigation in patients with clinical or biochemical suspicion of NET.

## OP709

### Role of 68Ga-DOTATATE in patients with known or suspected Neuroendocrine Tumours.

**E. Panagiotidis**[1], M. Al-Harbi[1], R. Sajjan[1], Z. Saad[1], M. Caplin[2], J. Bomanji[1]; [1]Institute of Nuclear Medicine, UCL, London, UNITED KINGDOM, [2]Royal Free Hospital, London, UNITED KINGDOM.

**Aim:** In patients with newly diagnosed neuroendocrine tumors (NETs), correct mapping of disease is important for prognostic stratification and therapeutic tailoring. Moreover in patients with suspected NETs, early diagnosis and delineation of the disease extent is crucial for accurate treatment. In spite of several radiotracers, imaging of the NETs appears challenging. Hence, the role and the impact of [68Ga-DOTA, Tyr3]-octreotate (68Ga-DOTATATE) PET/CT in the clinical practice were examined in patients with either diagnosed or suspected NETs. **Materials and Methods**: Three hundred twenty patients (pts) (152 male; 168 female; range: 7-86years, median age 56 years) that underwent 381 68Ga-DOTATATE PET/CT exams in our department with known (n=218) or with suspected (n=102) NETs enrolled this study. Main indications for the known NETs were staging, follow up and recurrence, and for the suspected NETs were elevated blood levels of tumour markers, clinical symptoms, and findings in conventional imaging. Comparison was made when available with 18FDG PET/CT (n=62), 123I-MIBG (n=14) and 111In-Octreoscan (n=38) studies. **Results:** 68Ga-DOTATATE PET/CT was positive in 63 of 102 suspicious for NETs pts (61.7%) with the most frequently lesions located in the liver (29/63), in the lymph nodes (15/63) and in the small bowel (8/63). Twenty nine out of 63 pts (46%) had additional radionuclide imaging, 5 of which (17%) had negative additional radionuclide imaging, leading 68Ga-DOTATATE in changing patient management. In the remaining 39 pts with suspected NETs (38.3%), 68Ga-DOTATATE PET/CT was negative with 2 false negative results in high grade NETs, revealed by 18FDG PET/CT. In pts with known NETs most frequently primary site was in pancreas (49/218), lung (35/218), large bowel (31/218) and small bowel (30/218). 68Ga-DOTATATE PET/CT mapped correctly the extent of the disease in 161 of 218 (73.8%) pts with known NET. Six out of 57 pts (10.5%) had false negative 68Ga-DOTATATE PET/CT study with poorly differentiated NETs, as one pt had recurrence revealed by the 123I-MIBG and 5 pts by the 18FDG PET/CT. **Conclusion**: 68Ga-DOTATATE PET/CT has significant role in patients with suspected or known NETs, supporting its daily use in clinical diagnostics. Only in high grade/poorly differentiated NETs 18FDG PET/CT should be considered as a complimentary imaging modality.

## OP710

### 68Ga-DOTANOC PET/CT in patients with Pheochromocytoma

**P. Sharma**, V. S. Dhull, S. Arora, C. Bal, A. Malhotra, R. Kumar; All India Institute of Medical Sciences, New Delhi, INDIA.

**Aim:**The Aim of the present study was to evaluate the diagnostic accuracy of 68Ga-DOTANOC PET/CT in patients with suspicion of pheochromocytoma. **Methods**: Data of 62 patients (Age: 34.3±16.1 years; 14 with MEN 2) with clinical/biochemical suspicion of pheochromocytoma and suspicious adrenal lesion on CT (n=70), who had undergone 68Ga-DOTANOC PET/CT, was retrospectively analyzed. PET/CT images were analyzed visually as well as semi-quantitatively, with measurement of SUVmax, SUVmean, SUVmax/SUVLiver and SUVmean/SUVLiver. Results of PET/CT were compared with 131I-MIBG imaging, which was available in 40 patients (45 lesions). Histopathology and/or imaging/clinical/biochemical follow up (minimum 6 months) was used as reference standard. **Results**: The sensitivity, specificity and accuracy of 68Ga-DOTANOC PET/CT was 90.4%, 85% and 88.7% respectively on patient wise analysis and 92%, 85% and 90% respectively on lesion wise analysis. 68Ga-DOTANOC PET/CT showed 100% accuracy in patients with MEN 2 syndrome and malignant pheochromocytoma. On direct comparison, lesion wise accuracy of 68Ga-DOTANOC PET/CT for pheochromocytoma was significantly higher than 131I-MIBG imaging (91.1% vs. 66.6%; P=0.035). SUVmax was higher for pheochromocytomas than other adrenal lesions (P=0.005), MEN 2 associated vs. sporadic pheochromocytoma (P=0.012), but no difference was seen between

benign vs. malignant pheochromocytoma (P=0.269). **Conclusion**: 68Ga-DOTANOC PET/CT shows high diagnostic accuracy in patients with suspicion of pheochromocytoma and is superior to 131I-MIBG imaging for this purpose. Best results of 68Ga-DOTANOC PET/CT is seen in patients with MEN 2 associated and malignant pheochromocytoma.

## OP711

### 68Ga-DOTANOC PET/CT for staging and restaging of patients with pancreatic neuroendocrine tumors

**S. Arora**, P. Sharma, H. Singh, A. Mukherjee, A. Malhotra, C. Bal, R. Kumar; All India Institute of Medical Sciences, New Delhi, INDIA.

**Aim**: To evaluate the role of 68Ga-DOTANOC PET/CT for staging and restaging of patients with pancreatic neuroendocrine tumors (NETs). **Material and Methods**: Data of 141 patients (Mean age: 46.2±15.2 years; Male/Female-85/56) who underwent 178 68Ga-DOTANOC PET/CT studies for staging or restaging of pancreatic NET, was retrospectively analyzed. The indication for PET/CT were diagnosis and staging (n=30), staging alone (n=58) and restaging (n=90). Two nuclear medicine physicians reviewed the PET/CT studies in consensus, blinded to clinical/biochemical and imaging findings. Histopathology and/or clinical/imaging follow up (minimum-4 months) were used as reference standard. **Results**: Out of the 178 68Ga-DOTANOC PET/CT studies, 137 studies were positive and 41 were negative. 68Ga-DOTANOC PET/CT studies were positive for primary tumour (n=106), lymph node metastasis (n=60), liver metastasis (n=84), bone metastasis (n=14) and metastasis at other sites including breast, myocardium and lung (n=12). In 7 PET/CT studies, second primary lesions were demonstrated (duodenal NET-4, ileal NET-1, hemangioblastoma-1, ectopic pituitary adenoma-1). When PET/CT results were compared to the reference standard, 132 68Ga-DOTANOC PET/CT were found to be true positive, 19 were true negative, 5 were false positive and 22 were false negative. Sensitivity of 68Ga-DOTANOC PET/CT for pancreatic NET was 85.7% [95% CI: 79.1-90.8], specificity was 79.1% [95% CI: 57.8-92.8], PPV was 96.3% [95% CI: 91.6-98.8], NPV was 46.3% [95% CI: 30.6-62.5] and accuracy was 84.8%. Majority of false negative PET/CT (19/22) were in patients with known or suspected insulinomas. In 110 patients, comparable conventional imaging (CECT, MRI, USG) were available. On analysis of these patients, overall accuracy of 68Ga-DOTANOC PET/CT was found to be superior to conventional imaging (p<0.001). Conclusion: 68Ga-DOTANOC PET/CT is useful for staging and restaging patients with pancreatic NET. However, it can have a low sensitivity in patients with insulinoma.

## OP712

### The perplexing pancreas: when is pancreatic 68Ga DOTATATE uptake suspicious?

**P. Mapelli**[1], H. H. Tam[2], L. Portigliotti[1], E. Aboagye[1], A. Al-Nahhas[2], R. Sharma[3]; [1]Department of Surgery and Cancer, Imperial College, London, UNITED KINGDOM, [2]Department of Nuclear Medicine, Hammersmith Hospital, London, UNITED KINGDOM, [3]Department of Experimental Medicine, Imperial College, London, UNITED KINGDOM.

**Aim:** 68Ga DOTATATE positron emission tomography (PET/CT) is largely used for staging, treatment planning and response assessment in pancreatic and non pancreatic neuroendocrine tumours (NETs). Pancreas has been reported as a possible site of physiological 68Ga DOTATATE uptake especially in the head and uncinate process. The Aim of the present study is to compare the pancreatic 68Ga DOTATATE incidental findings with morphological imaging modalities (CT, MRI, US and EUS) to assess the incidence of pathological and physiological uptakes. **Material and Methods** We reviewed 178 68Ga DOTATATE PET/CT reports of patients (80 women and 98 men; mean age: 53 yrs; range: 17-83 yrs) with pancreatic NET (n=41) or non-pancreatic NET (n=137) who underwent 68Ga DOTATATE PET/CT between January 2011 and March 2013. Scans were performed for staging, detection of somatostatin receptors status prior to peptide receptor radionuclide therapy or for therapy response assessment. Any pancreatic areas reported as having intensity greater than background was considered for analysis (head, neck, body, tail, uncinate process); maximum standardized uptake value (SUVmax) was also considered for analysis. Pancreatic 68Ga DOTATATE PET/CT findings were compared with CT, MRI or EUS**. Results** 68Ga DOTATATE uptake was detected in 69 pancreatic sites, 60 of which were confirmed as pathological on morphological imaging modalities (mean SUVmax 31.6, range: 9-27). In 6 sites (5 in the uncinate process and 1 in the tail) pancreatic uptake was interpreted as physiological; the highest SUVmax observed among physiological uptakes was 7.4. In 3 sites tracer uptake was interpreted as suspicious: two were located in the uncinate process; one was located in the head of pancreas and showed a SUVmax higher than physiological uptake (SUVmax 14). In those cases with suspicious uptake (n=3), subsequent CT imaging performed to characterize the pancreatic lesions did not show any pathological findings**. Conclusion** Physiological uptake was predominantly observed in the uncinate process. Despite the small number of suspicious pancreatic uptake on 68Ga DOTATATE PET/CT reported in this series, we believe that morphological imaging modalities should be always required to characterize unequivocal findings. Larger cohort of patients and further studies are necessary to better understand the mechanisms of physiologic versus pathologic uptake in the pancreatic tissue, and whether the assumption of non-pathological uptake is correct.

## OP713

### Role of 68Ga-DOTANOC, 18F-DOPA and 131I-MIBG imaging in the evaluation of multiple endocrine neoplasia.

**A. Kumar**, P. Sharma, A. Mukherjee, S. Karunanithi, R. Kumar, G. Bandhopadhyaya, A. Malhotra, C. Bal; All India Institute Of Medical Sciences, New Delhi, INDIA.

**Aim**: Multiple endocrine neoplasia(MEN) are characterized by occurrence of tumors of endocrine system that may be associated with hyperfunction and malignancy. Nuclear imaging plays a pivotal role in the in the diagnosis and management of these syndromes.This retrospective study was done to evaluate role of 68Ga-DOTANOC PET/CT, 18F-DOPA PET/CT and 131I-MIBG imaging in MEN syndromes. **Materials and Methods** : Fourteen patients with MEN syndrome ( MEN I : 8 & MEN II : 6) were identified who underwent both 68Ga-DOTANOC and 18F-DOPA PET/CT. Patients with MEN II syndrome also underwent 131I - MIBG scintigraphy for evaluation of pheochromocytoma. **Results**: MEN I group consisted of post parathyroidectomy patients with proven pancreatic tumors or were being evaluated for pancreatic tumors. Six out of eight patients were positive for pancreatic tumors on both the studies, however it was 68Ga-DOTANOC which identified more number of lesions as compared to 18F-DOPA (14 vs 8). The MEN II patient group was evaluated for staging/restaging of Medullary thyroid carcinoma ( MTC )or for suspicion of pheochromocytoma. In case of MTC 68Ga - DOTANOC showed higher sensitivity and identified more number of lesions as compared to 18F-DOPA. In evaluation of pheochromocytoma 18F-DOPA seemed to be a superior modality as compared to 68Ga - DOTANOC and 131I-MIBG. 4 out of 6 MEN II patients were confirmed to have pheochromocytoma on histopathology. 18F-DOPA was positive in all of these cases. 68Ga - DOTANOC being equivocal in one of these cases and 131I-MIBG scintigraphy being negative in another. **Conclusion** : 68Ga-DOTANOC PET/CT, 18F-DOPA PET/CT and 131I-MIBG imaging modalities are complimentary to one another and should be used with discretion depending upon the clinical suspicion for accurate detection, staging and surveillance in this diverse patient group. While 68Ga-DOTANOC PET/CT appears to be a modality of choice for staging of pancreatic tumors and MTC , 18F-DOPA should be preferred for evaluation of pheochromocytoma in these patients with MEN.

## OP714

### 18F-FDG-PET/CT and 111In-Octreotide SPECT in Patients with Metastatic Medullary Thyroid Carcinoma

**S. De Luca**[1], R. Fonti[2], C. Mainolfi[1], A. Anzivino[1], L. Camera[1], A. Faggiano[3], A. Colao[3], M. Salvatore[1], S. Del Vecchio[1]; [1]Department of Advanced Biomedical Sciences, University Federico II, Naples, ITALY, [2]Institute of Biostructures and Bioimages, National Research Council, Naples, ITALY, [3]Department of Clinical Medicine and Surgery, University Federico II, Naples, ITALY.

**Aim.** To test the role of combined imaging with 18F-FDG-PET/CT and 111In-Octreotide SPECT in the evaluation of patients with metastatic medullary thyroid carcinoma (MMTC). **Methods.** We evaluated 13 MMTC patients (age 59.7±15.8 y) who had undergone 18F-FDG-PET/CT and 111In-Octreotide SPECT within an interval of 6 weeks. 18F-FDG-PET/CT scans were acquired after fasting for 8 h and 60 min after i.v. injection of 370 MBq of 18F-FDG. All patients underwent diagnostic contrast-enhanced CT alone or as part of 18F-FDG-PET/CT examination. All areas of focal 18F-FDG uptake not corresponding to physiological tracer uptake were considered to be positive and SUVmax was recorded. 111In-Octreotide whole body scan, SPECT of the head and neck and of other districts eventually involved were performed 4 and 24 h after i.v. injection of 200 MBq of 111In-Octreotide using a dual-head large field-of-view gamma camera. Levels of calcitonin at the time of imaging examinations were also recorded. **Results.** Contrast-enhanced CT detected 34 enlarged lymph nodes, 5 hypodense liver lesions, 7 lung nodules, 5 diffuse micro-nodular lung involvements, 13 bone lesions, 2 brain metastases, 3 pancreatic lesions and 3 masses in the thyroid bed. A total of 44 lesions were detected by 18F-FDG-PET/CT showing SUVmax values ranging between 1.5 and 8.3 (mean 4.0±1.74) while 111In-Octreotide SPECT showed a total of 40 areas of tracer uptake. In particular, 18F-FDG uptake was found in 29 lymph nodes (SUVmax 3.41±1.38), 22 of which (75%) corresponded to enlarged lymph nodes at CT whereas 111In-Octreotide uptake was detected in 20 lymph nodes, 13 of which (65%) were positive at CT. In the remaining districts, 18F-FDG uptake was found in only one of the 5 hypodense liver lesions (SUVmax 8.3), 4 out of 7 lung nodules (SUVmax 4.90±2.38), 6 out of 13 bone lesions (SUVmax 5.98±0.81), 3 masses in the thyroid bed (SUVmax 3.4 ±0.17) and 1 pancreatic nodule (SUVmax 3.5) whereas no 18F-FDG uptake was detected in all cases of micro-nodular lung involvement and brain metastases. Furthermore, 111In-Octreotide SPECT showed focal tracer uptake in 1 liver lesion, 5 lung nodules, 8 bone lesions, all confirmed at CT and diffuse uptake in 6 thyroid regions. Finally, calcitonin levels were greater than 1000

pg/ml in 9 out of 13 patients. **Conclusion.** Our findings indicate that in MMTC patients, 18F-FDG-PET/CT provides a useful contribution mainly in the evaluation of lymph node involvement whereas 111In-Octreotide SPECT is more helpful in the detection and receptor characterization of bone lesions.

1707 - Wednesday, Oct. 23, 10:00 - 11:30, Salon Pasteur

## Neurosciences: Dementia

### OP715

### Beta-Amyloid PET Imaging in Alzheimer's Disease in a Close to Clinical Routine Situation - Results of a Multi-Center Phase 2 Trial

**O. Sabri**[1], J. Seibyl[2], K. Ishihara[3], A. Taneto[3], A. Drzezga[4], T. Grimmer[5], M. Senda[6], Y. Yamamoto[7], H. Gertz[1], C. Reininger[8], H. Barthel[1]; [1]University Leipzig, Leipzig, GERMANY, [2]MNI, New Haven, CT, UNITED STATES, [3]Nippon Medical School, Tokyo, JAPAN, [4]University Cologne, Cologne, GERMANY, [5]Technical University Munich, Munich, GERMANY, [6]IBRI, Kobe, JAPAN, [7]Kobe University, Kobe, JAPAN, [8]Bayer Healthcare, Berlin, GERMANY.

**Introduction:** Florbetaben, a $^{18}$F-labeled β-amyloid PET tracer, recently demonstrated efficacy in discriminating Alzheimer's disease (AD) patients from healthy volunteers (HVs) in an exploratory phase 2A trial [Lancet Neurol 2011] and in an in vivo PET vs. post mortem histopathology phase 3 trial. Consequently, this tracer was recently submitted for clinical approval in the USA and in Europe. With florbetaben soon envisaging clinical approval, the question arises as to how the tracer performs in a situation akin to future clinical routine use, i.e. in suspected AD patients at earlier dementia stages, and as employed by non-β-amyloid-PET-expert nuclear physicians who evaluate the PET Images visually. **Methods***:* To address this question, the 90-110 min p.i. florbetaben PET data of 116 patients with probable AD (age≥55yrs, MMSE=18-26, CDR=0.5-2) and of 120 cognitively normal elderly HVs as acquired within the confirmatory phase 2B trial in 22 centers across four continents were visually assessed using a pre-established scoring system by five so far un-experienced blinded readers after running a web-based training program. The consensus panel clinical diagnosis served as a surrogate standard of truth to evaluate the tracer performance**. Results:** For the five blinded readers, sensitivity for discrimination between AD patients and HVs was 78.5% (median value; range: 69.0% (95% CI: 60.6-77.4%) to 81.0% (95% CI: 73.9-88.2%)), and specificity 89.2% (median value; range: 81.7% (95% CI: 74.7-88.6%) to 95% (95% CI: 91.1-98.9%)). Inter-Reader agreement was substantial to almost perfect with a kappa of 0.81 (95% CI: 0.77-0.86) across the five readers. **Conclusions***:* Taken together, the training procedure developed leads to reproducible visual assessments of florbetaben PET data which allow for an accurate discrimination between AD patients and HVs. Thus, the results of this to date largest phase 2 trial of a $^{18}$F-labeled β-amyloid-PET tracer confirm the great potential of florbetaben to supplement the clinical routine toolbox to diagnose AD. *Research support:* Bayer Healthcare/Piramal Imaging, Berlin (Germany)

### OP716

### Interobserver agreement in visual analysis of Florbetapir PET studies

**V. Camacho**, A. Fernández, A. Domènech, M. Lagreca, J. Deportós, M. Estorch, A. Flotats, J. Duch, I. Carrió; Hospital de la Santa Creu i Sant Pau. Nuclear Medicine Department, Barcelona, SPAIN.

Amyloid positron emission tomography (PET) is an important noninvasive method for detecting amyloid burden in Alzheimer's disease (AD) patients, and it has been suggested as a core biomarker for AD. Florbetapir (18F-AV-45) is an 18F-labeled PET imaging tracer thought to bind to fibrillar forms of amyloid. The objective of the study was to evaluate the interobserver agreement in visual analysis of Florbetapir PET in patients with cognitive impairment. **Material and Methods**: Twenty-two patients with clinical diagnosis of cognitive impairment were evaluated with Florbetapir PET-TC (Philips Gemini TF). The images were obtained 50 minutes after injection of 370mBq of tracer. After transmission data was obtained, brain PET dynamic acquisition was acquired (2x5min or 3x5min frames). The reconstruction method was iterative (LOR RAMBLA, 3 iterations and 33 subsets) with a 128x128 image size, 2mm pixel size and 2mm pixel slice thickness. Florbetapir PET images were assessed visually by four independent nuclear medicine physicians using a semiquantitative score ranging from 0 (no cortical amyloid) to 2 (high levels of cortical amyloid) in four cortical brain regions (frontal, temporal, parietal and cingulated posterior regions). The Fleiss' Kappa was used to assess the interobserver agreement. **Results**: The fixed-marginal Kappa was 0.698 in frontal region, 0.623 in temporal region, 0.518 in temporal region and 0.654 in cingulated posterior region. We observed the highest concordance in negative patients and in patients with high level of cortical amyloid, higher interobserver variability was found in the intermediate patients. **Conclusion**: The interobserver agreement in visual analysis of Florbetapir PET images is higher in negative cases and in cases with important amyloid burden. A training period with learning curve may be necessary to evaluate Florbetapir images in clinical practice, particularly to assess patients with mild or intermediate amyloid burden.

### OP717

### Imaging of Amyloid Deposition in Alzheimer's Disease using a novel Radioligand [$^{18}$F]FIBT: Preclinical and First Clinical Results

**B. Hooshyar Yousefi**[1], S. Förster[2], A. Manook[2], B. von Reutern[2], G. Henriksen[2], I. Yakushev[2], T. Grimmer[3], M. Schwaiger[2], A. Drzezga[4], H. Wester[1]; [1]Pharmaceutical Radiochemistry, Technische Universtät München, Garching, GERMANY, [2]Department of Nuclear Medicine, Technische Universtät München, Munich, GERMANY, [3]Department of Psychiatry and Psychotherapy, Technische Universtät München, Munich, GERMANY, [4]Department of Nuclear Medicine, University Hospital of Cologne, Cologne, GERMANY.

As demonstrated in a previous study, [$^{18}$F]FIBT, a novel $^{18}$F-fluorinated imidazo[2,1-b]benzothiazole derivative, shows very high affinity towards Aβ ($K_i$=2.1±0.8nM) in a competition binding assay with [$^3$H]PiB. FIBT also shows high selectivity for Aβ with almost no affinity for neurofibrillary tangles ($K_i$>10μM) and α-synuclein aggregates ($K_i$>10μM). Furthermore, [$^{18}$F]FIBT seems to address at least three binding sites on Aβ fibrils in saturation binding assays ($K_{d1}$ of 0.12±0.02nM, $K_{d2}$ of 5.6±2.04nM and $K_{d3}$ of 26.2±2.80nM). On cortical sections of post-mortem human AD brain [$^{18}$F]FIBT selectively labeled Aβ in gray matter with very low non-specific binding in plaque devoid white matter. In this study we report on the in vivo evaluation of [$^{18}$F]FIBT in APP/PS1-tg mice and present first clinical results. Biodistribution studies with [$^{18}$F]FIBT in balb-C mouse demonstrated that this new agent exhibits an excellent in vivo characteristics, i.e. rapid and high brain uptake, fast clearance from normal mouse brain (brain uptake 5 min p.i. 7.2±0.34 %ID/g and 30 min p.i. 1.27±0.24) and high in vivo stability in mouse brain (10 min p.i. 92±4 and 30 min p.i. 88±6). The single dose intravenous $LD_{50}$ of FIBT in normal mouse was found to be >33.3nmol/kg (>11.4μg/kg). Selective binding and high-contrast imaging of Aβ deposits (VOI ratio $^{cortex}/_{cerebellum}$ for 12m.o. tg mice: 1.38±0.11 vs. 1.60±0.14 for 24m.o. tg mice) was demonstrated in vivo by PET imaging in 12 and 24 month old APP/PS1 tg mice after i.v. administration of 10±3MBq [$^{18}$F]FIBT. These data were cross evaluated by ex vivo autoradiography and immunohistochemistry. The preclinical results, high affinity and selectivity for Aβ, excellent pharmacokinetics in vivo, high in vivo stability and low unspecific uptake in white matter encouraged us to perform a first-in-human [$^{18}$F]FIBT PET study in a patient with the diagnosis of moderate probable AD dementia with evidence of the pathophysiological process (MMSE score 8; age 58). Dynamic [$^{18}$F]FIBT-PET was performed over a period of 90 min after i.v. injection of the tracer (200 MBq). Visually [$^{18}$F]FIBT accumulated in cortical regions expected to be high in Aβ deposition (e.g., bilateral precuneus and frontal and temporal cortices) as well as in subcortical regions such as the bilateral thalamus. Standardized uptake values to cerebellum standardized uptake value ratios (SUVRs) were calculated in different predefined brain regions (e.g., SUVR bilateral precuneus 2.0, SUVR bilateral temporal cortex 1.8). These pilot findings highly recommend further investigations in a larger number of subjects, in comparison with well-established [$^{11}$C]PiB for amyloid imaging.

### OP718

### A post-mortem study to compare the 5-HT$_{1A}$ receptor binding of a PET agonist and a PET antagonist in Alzheimer's disease

G. BECKER[1], N. STREICHENBERGER[1], T. BILLARD[2], B. VACHER[3], A. Newman-Tancredi[4], **L. ZIMMER**[1]; [1]Hospices Civils de Lyon & Univ. Lyon 1, Lyon, FRANCE, [2]CNRS & Univ. Lyon 1, Lyon, FRANCE, [3]Laboratoires Pierre Fabre, Castres, FRANCE, [4]Neurolixis, San Diego, CA, UNITED STATES.

**Aim.** The 5-HT$_{1A}$ serotonin receptors located in hippocampus are known to be linked to memory processes. PET clinical imaging studies with [$^{18}$F]MPPF have documented the decrease of 5-HT$_{1A}$ receptor expression in Alzheimer's disease patients, interpreted as neuronal loss. Interestingly, other [$^{18}$F]MPPF PET studies have reported a specific increase in hippocampal 5-HT$_{1A}$ receptor binding during a pre-dementia stage of Alzheimer's disease (mild cognitive impairment). If this increase in [$^{18}$F]MPPF binding may be explained by compensatory mechanisms, the pharmacological properties of this PET radiotracer limit its biological interpretation. It is known indeed that [$^{18}$F]MPPF, which is an antagonist like a majority of available PET receptor radioligands, binds non-specifically to the high-affinity state of 5-HT$_{1A}$ receptors (functional) and to the low-affinity state of these receptors (decoupled from G proteins and non-functional). On the contrary, an agonist binds selectively to the high-affinity state of the receptor which are functional. The Aim of this study is demonstrate that the binding of a 5-HT$_{1A}$ PET agonist provides complementary information to the binding of a 5-HT$_{1A}$ PET antagonist, to improve understanding of the functional impairment of 5-HT$_{1A}$ receptors during Alzheimer's disease. **Materials and MJethods.** We compared in postmortem human brain sections the specific binding of [$^{18}$F]F15599, a 5-HT$_{1A}$ PET agonist we developed previously, with

the specific binding of [$^{18}$F]MPPF, a 5-HT$_{1A}$ PET antagonist. Thirty-µm coronal sections were cut across hippocampi of 18 patients at different Braak's stages (from 0 to VI). The days of radiotracers synthesis, the brain slides were incubated in a saline buffer containing 37 kBq/mL of [$^{18}$F]MPPF or [$^{18}$F]F15599. Hippocampal subregions were drawn according to a brain atlas and binding quantification was performed with extemporaneous fluorine-18 scales. The specific binding of both radiotracers was determined by addition of 100 nM of serotonin and the agonist binding of [$^{18}$F]F15599 was revealed by addition of 10 µM of Gpp(NH)p. **Results and Conclusion.** The autoradiography distribution of both 5-HT$_{1A}$ PET radiotracers varied across hippocampus regions. The highest binding density was found in the pyramidal layer of CA1, followed by the molecular layer of the dentate gyrus. The incubation with 10 µM of Gpp(NH)p, a non-hydrolysable analogue of GTP, reduced significantly [$^{18}$F]F15599 binding, confirming its specific binding to G-coupled 5-HT$_{1A}$ receptors. [$^{18}$F]F15599 binding compared to [$^{18}$F]MPPF binding revealed specific modifications of the density of functional 5-HT$_{1A}$ correlated to the Braak's stages. These results justify an extension of this concept of functional PET imaging in clinical studies.

## OP719

### External Globus Pallidus and pontine nuclei are involved in RSBD in Dementia with Lewy bodies: a DAT/SERT statistical parametric mapping 123I-FP-CIT SPECT study.

**A. Niccoli Asabella**[1], D. Liuzzi[2], P. Taurisano[2], F. Roselli[2], A. Notaristefano[1], D. Rubini[1], C. Altini[1], E. P. Mossa[1], G. Defazio[2], P. Livrea[2], G. Rubini[1]; [1]Nuclear Medicine Unit, D.I.M., University of Bari "Aldo Moro", Bari, Italy, ITALY, [2]Department of Neuroscience and Sensory Organs, University of Bari, Bari, Italy, Bari, Italy, ITALY.

**Aims**: REM sleep behavior disorder (RSBD) is a prominent feature of synucleinopathies and a major diagnostic item for Dementia with Lewy Bodies (DLB). In Parkinson's disease and in DLB, the presence of RSBD is thought to highlight a distinct subgroup of patients. Although dopaminergic and serotoninergic loss are prominent in DLB, their involvement in RSBD development is unclear. **Methods**: Twenty-one DLB patients (8 with RSBD, 13 without RSBD) underwent brain SPECT with the DAT and SERT specific radiotracer 123I-FP-CIT. Reconstruction was performed by Butterworth filter. Attenuation correction was performed according to Chang method. System spatial resolution at a radius of rotation of 15.9 cm was 11 mm. The raw 123I-FP-CIT SPECT data of each subject were normalized on the SPECT template in MNI space with a 12-parameter affine transformation. A mean image of the previously normalized raw data acquisitions was then computed and used as a template image. V2 was a no specific 123I-FP-CIT SPECT binding area and was calculated with a ROI of the occipital lobe from the WFU PickAtlas. The spatially normalized parametric images were convolved with a Gaussian kernel (6×6×6 mm) for smoothing. One-way ANOVAs were used to evaluate potential differences between groups with a statistical threshold of p<0.05, with further FWE (Family Wise Error) whole brain correction for multiple comparisons. Secondary analysis were performed on Pons and thalamus ROI from WFU PickAtlas, with a statistical threshold of p=0.05 with FWE ROI correction for multiple comparisons. **Results**: DLB patients with RSBD displayed decreased DAT levels in external part of Globus Pallidus (GPe k=81, Z=3.93, p=0.027 FWE corrected; x -20, y -10, z 4); among SERT-rich structures, DLB patients with RSBD displayed reduced uptake in a large cluster located in the pons (k=156, Z=2.59, p=0.005; x 8 y -24 z -40) and in a smaller cluster in the right anterior thalamus (k=10, Z=3.93, p=0.005 FWE corrected; x -19 y -14 z 1). **Conclusions**: Our data support the identification of DLB with RSBD as a possible DLB subgroup with a distinct patter of degeneration of dopaminergic fibers and more severe degeneration of serotoninergic neurons; our findings provide a tentative in vivo marker for the subgroups and provide evidence for the involvement of dopaminergic and serotoninergic inputs in the onset of RSBD. Furthermore, our work underscore the power of voxel-wise radiotracer uptake analysis for DAT-specific tracers like 123I-FP-CIT.

## OP720

### Predictors of dopamine transporter DaTSCAN™ (Ioflupane $^{123}$I) SPECT imaging results in subjects with possible Dementia with Lewy Bodies

**F. Lomeña**[1], G. Oliver[2], C. Barber[3], E. Moreno[4], D. Volterrani[5], J. Daumal[6], D. Flores[7], A. Serena[8], Z. Walker[9], DaTSCAN DLB Study Group; [1]Hospital Clinic i Provincial, Barcelona, SPAIN, [2]John Radcliffe Hospital, Oxford, UNITED KINGDOM, [3]Princess Alexandra Hospital, Essex, UNITED KINGDOM, [4]GE Healthcare, London, UNITED KINGDOM, [5]Ospedale Santa Chiara, Pisa, ITALY, [6]Hospital Universitari Son Espases, Palma de Mallorca, SPAIN, [7]Consorcio Hospitalario Provincial de Castellón, Castellón, SPAIN, [8]Hospital do Meixoeiro, Vigo, SPAIN, [9]University College London, London, UNITED KINGDOM.

**Background:** The diagnosis of dementia with Lewy bodies (DLB) can be clinically challenging. Patients with possible DLB (dementia + one core or one or more suggestive feature) are a particularly difficult group to diagnose. Although the diagnosis becomes clearer over time this can be supported by the evaluation of the dopamine transporter uptake as suggested by the International Consensus Criteria[1] **Objective:** To analyse clinical predictors of dopamine transporter receptor deficit in a cohort of possible DLB patients using DaTSCAN™ (Ioflupane $^{123}$I)SPECT imaging . **Methods:** One hundred and eighty seven patients with possible DLB were randomized to have a DaTSCAN™ or to follow routine clinical care.114 subjects underwent dopamine transporter imaging and were subdivided into normal or abnormal uptake depending on the visual reading of their scans. To identify the most predictive baseline DLB features for normal vs. abnormal DaTSCAN™ images, logistic regression analyses were performed. Diagnosis, DLB features and a comprehensive neuropsychiatric battery were assessed at baseline, 8 and 24-weeks. **Results:** Forty nine patients (43%) had abnormal scans and 65 patients had normal scans (57%). Changes in diagnostic category were more frequent in the DaTSCAN™ group than in the control group (71 vs 16% p<0.0001), and particularly in those subjects with abnormal images (82%, 87% for abnormal and 46%, 58% for normal scans, at weeks 8 and 24 respectively). Patients with abnormal scans had higher UPDRS-III score at baseline (11.3 ± 9.0) than patients with normal scans (7.8 ± 7.7; p=0.0284) and the change of this score was more pronounced after 24-weeks (3.5 ± 5.7 and 0.2 ± 3.8; p=0.004). Stepwise logistic regression analysis showed that only "spontaneous features of Parkinsonism" was a significant predictor of an abnormal DaTSCAN™ image (p=0.0006). There was no difference between the groups with regard to any other clinical features at baseline or at 24-weeks follow-up except the presence of "preserved medial temporal lobe structures on CT/MRI scan" that accounted for 57% in subjects with abnormal scans as compared to 26% with normal scans (p=0.001) The evolution of core and suggestive DLB features followed a tendency to increase during follow up in subjects with abnormal scans. **Conclusion:** Changes in diagnostic category were highly impacted by the DaTSCAN™ results. Although the prevalence of spontaneous features of Parkinsonism was low in this population it seems to be the only predictor for abnormal scans in possible DLB. Reference [1]McKeith IG, Dickson DW, Lowe J, et al. Neurology. 2005;65:1863-72.

## OP721

### Changes in Dementia Diagnostic Category and Diagnostic Confidence following dopamine transporter SPECT imaging with DaTSCAN™ (Ioflupane $^{123}$I) in Subjects with an Uncertain Diagnosis of Dementia with Lewy Bodies (possible DLB)

**B. Paghera**[1], J. Prosser[2], T. Leitha[3], K. Howe[4], E. Moreno[5], F. Dore[6], S. Dizdarevic[7], U. Stabell[8], Z. Walker[9], DaTSCAN DLB Study Group; [1]Nuclear Medicine Dpt. AO Spedale Civile, Brescia, ITALY, [2]Gartnavel Hospital, Glasgow, UNITED KINGDOM, [3]SMZ-Ost/Donauspital, Vienna, AUSTRIA, [4]Royal Victoria Infirmary, Newcastle upon Tyne, UNITED KINGDOM, [5]GE Healthcare, Madrid, SPAIN, [6]Ospedale Cattinara, Trieste, ITALY, [7]Royal Sussex County Hospital, Brighton, UNITED KINGDOM, [8]Praxen fur Diagnostische und Terepeutische Nuklearmedizin, Berlin, GERMANY, [9]UCL, London, UNITED KINGDOM.

**Background:** Dementia with Lewy Bodies (DLB) is often unrecognized with the accuracy of the clinical diagnosis having good specificity but low sensitivity. This is particularly an issue in patients with an uncertain diagnosis and results in many cases of true DLB being missed. The International Consensus Criteria[1] include the presence of low dopamine transporter uptake in basal ganglia as a 'suggestive' feature for the diagnosis of DLB. **Objectives:** To evaluate the impact of DaTSCAN™ (Ioflupane $^{123}$I) imaging on dementia diagnostic category and the diagnostic confidence in patients with possible DLB. **Methods:** One hundred and eighty seven patients with a diagnosis of possible DLB were recruited from 21 centers in 6 European countries. After baseline evaluation, patients were randomized in a 2:1 ratio to have a DaTSCAN™ (n=127) or no-imaging ( n=60). DaTSCAN™ images were visually assessed and categorized as normal, abnormal type 1-3, or other abnormal patterns. The proportion of patients with changes in clinical diagnosis (to probable DLB or non-DLB) and changes in the confidence of diagnosis were compared between the two groups at 8 and 24 weeks. **Results:** DaTSCAN™ imaging showed dopaminergic deficit in 50/116 (43%) subjects. 38 subjects showed abnormal images type 1-3 and 12 subjects other patterns of abnormality. Significantly more patients in the DaTSCAN™ group had a change in diagnostic category after 8 weeks (61% vs 4%; *p*<.0001) and after 24 weeks (71% vs 16%; *p*<.0001) compared to the control group. Clinicians were more likely to change the diagnostic category if the DaTSCAN™ was abnormal (82%) than if the result was normal (46%). Confidence in diagnosis measured by a visual analogue scale (0-100, mean baseline 49) significantly increased in the imaging group during follow-up compared to the control group (+17.5 vs 1 at week 8 and +21 vs 3 at week 24; both p<.0001). Similarly clinician`s confidence of diagnosis was higher when the DaTSCAN™ images showed evidence of dopaminergic deficit. Two adverse events (anxiety, bruising at injection site) were reported as possibly related to DaTSCAN™ **Conclusions:** DaTSCAN™ SPECT imaging has a significant impact on diagnostic category in subjects with an uncertain diagnosis of DLB, proving to be a useful adjunct in the diagnostic work-up of patients with possible DLB. DaTSCAN™ SPECT imaging significantly improved the diagnostic confidence. Changes in diagnostic category

were less frequent in the control group despite a 24-weeks prospective follow-up.
**Reference** [1]McKeith IG, Dickson DW, Lowe J, et al. Neurology. 2005;65:1863-72.

## OP722

### Hypometabolism, gray and white atrophy in Behavioral variant of Fronto-temporal Dementia (bvFTD): a combined 18F-FDG PET and MRI study.

**S. Morbelli**[1], M. Ferrara[2], F. Fiz[1], D. Arnaldi[3], A. Picco[2], I. Bossert[1], A. Buschiazzo[1], J. Accardo[3], G. Sambuceti[1], F. Nobili[2]; [1]Nuclear Medicine Unit, IRCCS AOU San Martino - IST, DISSAL, University of Genoa, Genoa, ITALY, [2]Clinical Neurophysiology, Department of Neurosciences, Ophthalmology and Genetics, University of Genoa, Genoa, ITALY, [3]Clinical Neurophysiology, Department of Neurosciences, Ophthalmology and Genetics, University of Genoa, Genoa, Italy, Genoa, ITALY.

To provide a comprehensive map of functional and structural abnormalities across the whole brain in a group of patients with bvFTD and to relate these abnormalities with behavioral profile. **Methods:** Twenty-five bvFTD patients (12 males; mean age:74.9±6.8; mean MMSE score:27.2±2.4) and 20 normal controls (CTR) (8 males; mean age:68.9±7.9) underwent both 18F-FDG PET/CT (Siemens Biograph 16, 3D acquisition) and T1-weighted 3D MRI. Behavioural profile was assessed by means of the Neuropsychiatric Inventory (NPI). Imaging preprocessing was performed in SPM8. MRI scans were segmented using a modified optimized Voxel Based Morphometry technique. FDG PET, as well as segmented gray (GM) and white (WM) matter maps were compared between patients and CTR. Moreover, patients were divided in two subgroups according to prevalence of positive (bvFTD+) or negative (bvFTD-) symptoms and each subgroup was compared with CTR. Both analyses were performed using two-sample t-test of SPM8 (height threshold: uncorrected $p< 0.001$ at peak level and $p<0.05$ FDR-corrected at cluster level; age as nuisance). **Results**: With respect to controls, the whole bvFTD group showed lower GM density in the left inferior frontal gyrus (BA 47). Reduced WM density was found in the left side of corpus callosum, anterior cingulate and parahippocampal gyrus as well as in the subgyral white matter of left frontal and temporal cortex. Glucose hypometabolism was found in bvFTD group with respect to CTR in a wide cluster involving bilateral inferior, middle and superior frontal cortex (BA 8-9-10 and 45-46-47) as well as in caudate nuclei in both hemispheres. Moreover, bvFTD+ patients (n=11; mean age:74.8±7.2; mean MMSE score:27.2±2.5) showed hypometabolism in bilateral frontal cortex (BA 47, 9-10), caudate nucleus, thalamus and superior temporal gyrus (BA 22) in the left hemisphere. By contrast, bvFTD- (n=14; mean age:75.0±6.5; mean MMSE score:27.3±2.6) showed hypometabolism in small clusters within right middle frontal gyrus (BA 6-8) and left inferior frontal gyrus (BA 47). No significant differences were highlighted in GM and WM density between CTR and each bvFTD subgroup. **Conclusion:** More severe cortical hypometabolism and WM atrophy than GM atrophy demonstrates early functional network damage. This is reflected by extended hypometabolism to temporal lobe and by functional impairment in distant brain regions, such as the caudate n., thalamus (PET) and limbic cortex (WM). Patients with different behavioural presentation have different cortical functional impairment; further correlation analysis with neuropsychological and genetic data is ongoing.

1709 - Wednesday, Oct. 23, 10:00 - 11:30, Rhône 3A/3B

## Radiopharmaceuticals & Radiochemistry & Dosimetry: Miscellaneous

## OP723

### Profound enhancement of PC-3 tumor uptake of the pan-bombesin radiotracer [$^{111}$In]PanSB1 in mice applying a new promising strategy

B. A. Nock[1], M. de Jong[2,3], P. J. Marsouvanidis[1,2], E. P. Krenning[2], **T. Maina-Nock**[1]; [1]Molecular Radiopharmacy, INRASTES, NCSR Demokritos, Athens, GREECE, [2]Department of Nuclear Medicine, Erasmus MC, Rotterdam, NETHERLANDS, [3]Department of Radiology, Erasmus MC, Rotterdam, NETHERLANDS.

**Aim**: The degradation of bombesin (BBN) analogs by neutral endopeptidase (NEP) may be, at least in part, responsible for the sub-optimal performance of many BBN-radioligands in animal models and in man. We decided to investigate this hypothesis and to improve tumor uptake of BBN-related radiopeptides by the novel approach of co-injection of a NEP inhibitor (phosphoramidon, PA). As a first example, we studied the effects of PA co-administration on the *in vivo* profile of [$^{111}$In]PanSB1 ([$^{111}$In-[(DOTA)PEG$_2^0$,DTyr$^6$,βAla$^{11}$,Phe$^{13}$,Nle$^{14}$]BBN(6-14)), a BBN analog with high affinity for all three human BBN receptor subtypes, expressed in e.g. prostate, breast and lung cancer. **Materials and Methods**: [$^{111}$In]PanSB1 was injected in healthy Swiss albino mice without or with PA. Blood samples were collected 5 min post injection (pi) and radiopeptide degradation was monitored by RP-HPLC. Furthermore, [$^{111}$In]PanSB1 was injected (100 µL, 2 µCi, 10 pmol total peptide) with vehicle (100 µL) or with PA (100 µL, 0.5 µmol PA), or with PA plus excess [Tyr$^4$]BBN (0.5 µmol and 40 nmol, respectively; BBN-receptor-block group) in SCID mice bearing human PC-3 xenografts; animals were sacrificed at 4 h pi and biodistribution was conducted. Furthermore, dynamic and static images were acquired by small-animal NanoSPECT/CT after injection of [$^{111}$In]PanSB1 with or without PA. **Results**: [$^{111}$In]PanSB1 degraded in mice very fast with only ≈12% of parent radiopeptide still detectable in blood at 5 min pi. By co-injection of PA this percentage vastly rose above 85%. This profound stabilization effect was accompanied by an impressive increase of [$^{111}$In]PanSB1 uptake in the PC-3 xenografts at 4 h pi. Thus, the initial value of 3.75±0.73%ID/g in the control animal group reached 20.96±2.58%ID/g in the group co-injected with PA. Interestingly, this value dropped to 0.69±0.03%ID/g in the animals co-receiving PA and [Tyr$^4$]BBN implying BBN-receptor-specificity. These results were visualized in the SPECT/CT images after co-administration of PA. **Conclusions**: Co-injection of PA with [$^{111}$In]PanSB1 in mice had a remarkable effect on peptide-stability, promoting delivery at the target and drastically improving tumor uptake. The success of this strategy, currently being studied by us in an increasing number of radiopeptides, reveals a broad role of NEP in the metabolic fate of several (radio)peptides and may have significant implications for their clinical applicability.

## OP724

### [$^{111}$In-DOTA]SS14 can successfully target sst$_{1\text{-}5}$-expressing tumors in vivo with the aid of a new "recipe"

**T. Maina-Nock**[1], A. Tatsi[1], E. P. Krenning[2], M. de Jong[2,3], B. A. Nock[1]; [1]Molecular Radiopharmacy, INRASTES, NCSR Demokritos, Athens, GREECE, [2]Department of Nuclear Medicine, Erasmus MC, Rotterdam, NETHERLANDS, [3]Department of Radiology, Erasmus MC, Rotterdam, NETHERLANDS.

**Aim**: The very rapid *in vivo* degradation of native somatostatin-14 (SS14) renders it unsuitable for somatostatin receptor-targeting radioligand development. On the other hand, stabilized cyclic octapeptide analogs, currently applied with success in the diagnosis and therapy of neuroendocrine tumors, are sst$_2$-prefering having lost their pansomatostatin-like character. In an exciting new approach, we have co-injected [$^{111}$In-DOTA]SS14 together with the neutral endopeptidase (NEP) inhibitor phosphoramidon (PA) to prolong the *in vivo* survival of the radioligand and thereby to enhance delivery and uptake in somatostatin receptor-expressing tumors in mice. **Materials and Methods**: [$^{111}$In-DOTA]SS14 was injected in healthy Swiss albino mice without or with PA co-injection and blood samples collected 5 min post injection (pi) were analyzed by HPLC to detect radiometabolite formation. Moreover, biodistribution experiments were conducted in SCID mice bearing sst$_2$-positive AR4-2J or HEK-sst$_3$ xenografts at 4 h pi. [$^{111}$In-DOTA]SS14 was injected (100 µL, 2 µCi, 10 pmol total peptide) with vehicle (100 µL) or with PA (100 µL, 0.5 µmol PA). **Results**: While [$^{111}$In-DOTA]SS14 hardly survived in the blood of mice (<2.5% intact at 5 min pi), by co-injection of PA >90% of radioligand remained intact. This profound stabilization effect of PA translated into an impressive increase of tumor uptake in both the sst$_2$- and the sst$_3$-expressing xenografts in SCID mice. Thus, these values in the control groups of animals were 0.67±0.10%ID/g (AR4-2J xenografts) and 0.53±0.16%ID/g (HEK-sst$_3$ xenografts) at 4 h pi, but in the respective animal groups co-injected with PA these values rose to 13.87±2.4%ID/g (AR4-2J xenografts) and 8.74±1.10%ID/g (HEK-sst$_3$ xenografts). **Conclusions**: Co-injection of the NEP inhibitor PA stabilized [$^{111}$In-DOTA]SS14 promoting its safe delivery on tumor sites and leading to vast improvement of tumor uptake. This approach may facilitate the advantageous use of pansomatostatin-like radioligands in cases of lesions showing sst$_{1\text{-}5}$ co-expression. Ongoing studies will show the effectiveness of this promising new strategy in other radiopeptide-enzyme inhibitor systems.

## OP725

### Dimerization is not always the best option for upgrading the in vivo profile of peptide radioligands

**T. Maina-Nock**[1], B. A. Nock[1], P. Laverman[2], P. J. Marsouvanidis[1], E. P. Krenning[3], O. Boerman[2], M. de Jong[3,4]; [1]Molecular Radiopharmacy, INRASTES, NCSR Demokritos, Athens, GREECE, [2]Department of Nuclear Medicine, Radboud University MC, Nijmegen, NETHERLANDS, [3]Department of Nuclear Medicine, Erasmus MC, Rotterdam, NETHERLANDS, [4]Department of Radiology, Erasmus MC, Rotterdam, NETHERLANDS.

**Aim**: A mono- (CY313) and dimer (CY314) analog of the bombesin (BBN) antagonist JMV594 (H-D-Phe-Gln-Trp-Ala-Val-Gly-His-Sta-Leu-NH$_2$) both coupled to DOTA have been synthesized via a two-stage "click" approach. [$^{nat/111}$In]CY314 showed higher affinity and metabolic stability during *in vitro* testing. However, [$^{111}$In]CY314 showed high levels of background radioactivity compromising its higher uptake in human PC-3 xenografts in mice. As an alternative strategy to peptide dimerization, we propose co-injection of the neutral endopeptidase (NEP) inhibitor phosphoramidon (PA) to improve the *in vivo* stability of the monomer [$^{111}$In]CY313 and to enhance supply and localization in the tumor. **Materials and Methods**:

[$^{111}$In]CY313 and [$^{111}$In]CY314 were labeled as previously described. Radiopeptides were injected in healthy Swiss albino mice without or with PA. Blood samples were collected 5 min postinjection (pi) and formation of metabolic products was monitored by RP-HPLC. [$^{111}$In]CY313 and [$^{111}$In]CY314 were injected (100 µL, 2 µCi, 10 pmol total peptide) with vehicle (100 µL) or with PA (100 µL, 0.5 µmol PA), or with PA plus excess [Tyr$^4$]BBN (0.5 µmol and 40 nmol, respectively; *in vivo* BBN-receptor-blockade group) in SCID mice bearing human PC-3 xenografts. Animals were sacrificed at 4 h pi and biodistribution was conducted. **Results**: While dimeric [$^{111}$In]CY314 remained practically stable 5 min after entering the mouse blood stream, the monomer [$^{111}$In]CY313 degraded substantially with 52% detected intact in blood at 5 min pi by HPLC analysis. By co-injection of PA this percentage remarkably rose above 85%. This strong stabilization effect resulted in sharp increase of uptake in the PC-3 xenografts at 4 h pi. Thus, the control tumor value of 4.3±1.9%ID/g vastly rose to 24.7±5.3%ID/g by PA treatment, but dropped to 1.5±0.2%ID/g when both PA and [Tyr$^4$]BBN were administered, demonstrating BBN-receptor-specificity. Interestingly, tumor values achieved by [$^{111}$In]CY313 with the aid of PA exceeded those registered for [$^{111}$In]CY314 without or with PA co-injection (≈10%ID/g). In contrast to the dimer, however, the monomer exhibited significantly higher tumor-to-background ratios by PA co-injection. **Conclusions**: Although multimerization has often been successfully pursued to enhance receptor affinity, metabolic stability and tumor uptake of small-size hydrophilic radioligands, in the case of bigger and more lipophilic analogs, such as the [$^{111}$In]CY314 dimer, can lead to unfavorably high background levels. Instead, stabilization of the monomer [$^{111}$In]CY313 by PA turned out to be a more advantageous alternative for improving *in vivo* profile.

## OP726

### Comparison of iodine-125 and gallium-67 labeled GRAS protein nanoparticles for long-lasting biodistribution studies by SPECT-CT

**G. Quincoces**[1], E. Larrañeta[2], C. Vigil[3], M. Dávila[2], M. Ecay[4], S. Abadía[4], A. Vidal[1], M. Agüeros[2], J. M. Irache[2], I. Peñuelas[1]; [1]Radiopharmacy Unit, Department of Nuclear Medicine, University Clinic of Navarra, Pamplona, SPAIN, [2]Department of Pharmaceutics and Pharmaceutical Technology, University of Navarra, Pamplona, SPAIN, [3]Department of Nuclear Medicine, University Clinic of Navarra, Pamplona, SPAIN, [4]Small Animal Imaging Research Unit. CIMA-CUN, Pamplona, SPAIN.

GRAS Nanoparticles (NP) are made from Generally Recognised As Safe proteins that facilitate oral administration of NP encapsulated substances with medical application. Gallium-68 radiolabelling of these NP for PET imaging would not permit delayed imaging of biodistribution due to short 68Ga half-life. Consequently, longer-lived radioisotopes are required for this kind of studies. Objective: We have radiolabeled GRAS-NP with gallium-67 by citrate-NOTA transchelation and, after oral administration, compared their biodistribution with that of iodine-125 labeled NP by in vivo imaging by SPECT-CT for up to one week. **Methodology**: Radioiodination of lyophilized GRAS-NP was made by standard mild oxidative iodination using iodo-beads™ and 125INa. For radiolabelling with gallium-67, the GRAS protein was first tagged with NOTA by reaction with p-SCN-Bn-NOTA, purified by dialysis and used to build NP by spray-drying of NOTA-tagged and untagged protein; NOTA-NP were then purified by ultracentrifugation and lyophilized. NOTA-NP were labeled by citrate-NOTA transquelation with gallium-67 citrate1. Both iodine-125 and gallium-67 radiolabelled NP were purified by centrifugation. 125I-NP were incubated in dialysis cassettes with simulated gastric or intestinal media and deiodination measured by TLC of samples for up to 48 h. In vivo biodistribution studies were done for up to one week by SPECT-CT imaging of Wistar rats after oral administration of free 125INa, 67Ga-citrate or 10 mg of 125I or 67Ga-radiolabelled NP. Animals with 67Ga-citrate and 67Ga-NP were imaged at 2, 24, 48 and 72 h, while those with 125INa and 125I-NP were imaged at 2, 24, 48, 72 and 168 h. Images were exported to PMOD and Volumes of Interest drawn on CT images for quantification. Results: 67Ga-citrate to NOTA-NP transchelation proceeded with moderate yield (~20%) while 125I-iodination occurred with >70% yield. After purification, both radiolabelled NP were >99% pure. 125I-NP were progressively deiodinated both in gastric and intestinal medium after 20h. SPECT-CT images showed that 67Ga-NP were stable in vivo, were not absorbed and were readily eliminated by the gastrointestinal tract in <48h, while for 125I-NP substantial thyroid (and presumably gastric) uptake was seen after 24 h, complicating image analysis and quantification. **Conclusions**: 67Ga-citrate transchelation to NOTA-tagged protein NP is feasible, and can be used for biodistribution imaging by SPECT-CT of orally administered NP at long times. Albeit GRAS-NP labeling with radioiodine is much easier and proceeds with higher yields, 125I-NP are readily deiodinated and can hence not be used for such purposes. 1 Morfin JF & Tóth E. Inorg.Chem. (2011)50:10371-10378.

## OP727

### Radionuclides for nuclear medicine: a nuclear physicists' view

M. Cantone[1], F. Haddad[2], S. Harissopoulos[3], M. Jensen[4], A. Jokinen[5], **U. Köster**[6], O. Lebeda[7], B. Ponsard[8], U. Ratzinger[9], T. Stora[10], F. Tarkanyi[11], P. Van Duppen[12]; [1]Università degli Studi di Milano, Milano, ITALY, [2]ARRONAX, Nantes, FRANCE, [3]IAEA, Vienna, AUSTRIA, [4]Risø DTU, Roskilde, DENMARK, [5]University of Jyväskylä, Jyväskylä, FINLAND, [6]Institut Laue Langevin, Grenoble, FRANCE, [7]NPI - CAS, Řež, CZECH REPUBLIC, [8]SCK-CEN, Mol, BELGIUM, [9]Goethe-Universität, Frankfurt, GERMANY, [10]CERN, Geneva, SWITZERLAND, [11]ATOMKI, Debrecen, HUNGARY, [12]KU Leuven, Leuven, BELGIUM.

NuPECC (the Nuclear Physics European Collaboration Committee, an expert committee of the European Science Foundation) has the mission to strengthen European Collaboration in nuclear science through the promotion of nuclear physics and its trans-disciplinary use and application. NuPECC is currently working on a report on "Nuclear Physics for Medicine" and has set up a working group to review the present status and prospects of radionuclides for nuclear medicine. An interim report will be presented to seek comments and constructive input from EANM members. In particular it is investigated how nuclear physics Methods and nuclear physics facilities are supporting the development and supply of medical radionuclides and how this support could be further strengthened in future. Aspects that will be addressed: •In recent years, the reactor-based supply chain of $^{99}$Mo/$^{99m}$Tc generators was repeatedly challenged by unforeseen outages. This triggered the proposition and development of complementary accelerator-based production Methods of $^{99m}$Tc. Long-term prospects for $^{99m}$Tc supply in Europe will be discussed. •The emergence of new applications as well as rising costs and regulations for radioactive transport of individual doses lead to a renewed interest in radionuclide generators such as $^{68}$Ge/$^{68}$Ga, $^{82}$Sr/$^{82}$Rb or even $^{44}$Ti/$^{44}$Sc. For long time such generator nuclides were mainly produced at non-European accelerators (BNL, LANL, TRIUMF, iThemba Labs) that are mainly devoted to support nuclear physics facilities. The recent addition of ARRONAX, a dedicated production facility in Nantes, France, and the upcoming inauguration of a 70 MeV cyclotron at the nuclear physics facility SPES at Legnaro, Italy will greatly improve Europe's production capabilities of these nuclides. •Ongoing accelerator R&D for new nuclear physics facilities led to improved technologies for linear accelerators which could in future be used for providing intense beams of alpha particles cost-efficiently, thus facilitating access to nuclides such as $^{211}$At, $^{43}$Sc, $^{67}$Cu, etc. •The evaluation of trends in radionuclide demand requires reliable statistical data. The working group is promoting the collection of data on the production and use of medical radionuclides in European countries. Trends and prospects, in particular for non-conventional radionuclides will be discussed. •Nuclear medicine departments interested in using, or performing research with non-conventional radionuclides are sometimes faced with the problem of identifying an adequate supplier since many of these nuclides are not yet commercially available. The working group is preparing a database of regular and potential producers of emerging radionuclides such as $^{64}$Cu, $^{67}$Cu, $^{44}$Sc, $^{89}$Zr, $^{211}$At, etc. in Europe.

## OP728

### Improved bombesin based antagonists for PET imagingdiagnosis of prostate cancer

**E. Gourni**[1], R. Mansi[1], M. Jamous[2], B. Waser[3], Y. Kiefer[1], F. Buchegger[4], J. Reubi[3], H. Maecke[1]; [1]University Hospital, Department of Nuclear Medicine, Freiburg, GERMANY, [2]University Hospital, Basel, SWITZERLAND, [3]University of Berne, Berne, SWITZERLAND, [4]CHUV, Lausanne, SWITZERLAND.

**Aim:** Bombesin receptors are overexpressed on a variety of human cancers such as prostate, breast, ovarian and gastrointestinal stromal tumors providing the opportunity for peptide receptor targeting via radiolabeled bombesin-based peptides. The mitogenic properties in combination with the side effects that have been observed after administration of radiolabeled bombesin agonists prompted us to develop a family of antagonistic radioligands targeting the GRPr. Taking into acount our previous findings which support that the presence of a positevely charged spacer improves the binding affinity of the derived ligand, statine based bombesin analogues were synthesized and evaluated. This study Aims at developing bombesin antagonist-based radioligands for PET of GRPr-positive tumors with the potential to be used in clinical application. **Materials and Methods:** The potent bombesin antagonist Pip-D-Phe-Gln-Trp-Ala-Val-Gly-His-Sta-Leu-$NH_2$ (MJ9) where Pip stands for 4-amino-1-carboxymethyl-piperidine, conjugated to the chelators 1,4,7-triazacyclononane (NODAGA) and 1,4,7 acetic acid 1,4,7-triazacyclononane (NOTA); and radiolabeled with $^{68}$Ga. The GRP receptor affinity of $^{nat}$Ga-NODAGA-MJ9 and $^{nat}$Ga-NOTA-MJ9 was determined using $^{125}$I-Tyr$^4$-BN as radioligand. The labelling efficiency of $^{68}Ga^{3+}$ was compared for NODAGA-MJ9 and NOTA-MJ9 at room temperature and at 95 °C. The $^{68}$Ga-conjugates were further evaluated *in vivo* in PC3 xenografts by biodistribution along with PET animal studies. Specificity of binding was demonstrated by co-injection of 20 nmol of the cold peptide in each case. **Results:** The GRP receptor affinity ($IC_{50}$ values) of $^{nat}$Ga-NODAGA-MJ9 and $^{nat}$Ga-NOTA-MJ9 were found to be in the low nmolar range. NODAGA-MJ9 is able to incorporate $^{68}$Ga nearly quantitatively (>95%) at room temperature and at much lower peptide concentrations ($1.4x10^{-6}$ M) compared to NOTA-MJ9 where the labeling yield was found to be approx. 45% under the same conditions which was increased to 73% after heating for 5 min at 95 °C. Biodistribution studies showed high and persistent tumor uptake with a maximum

of 23.34 ± 2.00 %IA/g for $^{nat}$Ga-NOTA-MJ9 and 16.72 ± 2.03 %IA/g for $^{nat}$Ga-NODAGA-MJ9 at 1 h p.i.. The pancreas uptake was about 65 %IA/g for both radiotracers at 1 h p.i. but faster washout compared to the tumor was observed resulting in an increased tumor to background ratio at later time points. Competition binding studies showed specific uptake in tumor and GRPr-positive tissues. PET images confirmed the results from the biodistribution studies. **Conclusion:** We have developed two bombesin-based antagonist radioligands for the imaging of GRPr-positive tumors. Their promising *in vivo* pharmacokinetic performance may contribute to the improvement of the diagnostic imaging of tumors overexpreesing GRPr.

## OP729

### New chelator-conjugated PSMA ligands for functional imaging and endoradiotherapy of prostate cancer

**M. Weineisen**, M. Schottelius, J. Simecek, H. Wester; Chair of Pharmaceutical Radiochemistry, Garching, GERMANY.

Due to its consistently high expression in metastatic and non-metastatic prostate cancer, PSMA (Prostate-specific membrane antigen) represents an ideal target for both diagnostic imaging and endoradiotherapeutic approaches. Several radiometallated PSMA-inhibitors based on the Glu-urea-Lys (EuK)-scaffold have been evaluated preclinically, but only EuK-Ahx-[68Ga]HBED-CC has been successfully applied in patients[1]. Due to its chelation chemistry, however, this compound is not suitable for radiolabeling with therapeutic radionuclides, which prompted us to the development and comparative evaluation of a series of chelator-coupled EuK-sub-KFF/KYF-analogs, which allow radiolabeling with the alternative diagnostic/therapeutic pairs 68Ga/177Lu or 68Ga/131I. For the synthesis of the previously published reference compound EuK-sub-KFF-DOTA [2] as well as the new compounds EuK-sub-KFF-DOTAGA, EuK-sub-KFF-NOPO and EuK-sub-KYF-NOPO, EuK(tBu)3 was conjugated with NHS-sub-NHS and then reacted with the respective peptide sequences KFF/KYF-DOTA/DOTAGA/NOPO, which had been prepared by solid-phase-synthesis. Determination of PSMA-affinity (IC50) of the respective natGa-DOTA/DOTAGA/NOPO- and natLu-DOTA/DOTAGA-analogs was performed using PSMA-positive LNCaP cells and EuK(4-[125I]Benzoyl) as radioligand. Internalization kinetics of the respective 68Ga- or 177Lu-labeled ligands were investigated by incubating LNCaP and PSMA-negative PC-3 cells (non-specific binding). Generally, radiochemical yields for 68Ga- and 177Lu-labeling of the ligands investigated were almost quantitative. While specific activities of [68Ga]DOTA/DOTAGA-analogs did not exceed 250-300 GBq/µmol, >7000 GBq/µmol were obtained for the [68Ga]NOPO-derivatives. With an IC50 of 39.5±10.2 nM, EuK-sub-KYF-natGa-NOPO showed the highest PSMA-affinity of the compounds investigated, followed by EuK-sub-KFF-natLu-DOTAGA (45.7±3.8 nM), EuK-sub-KFF-natGa-DOTAGA (55.3±20.3 nM), EuK-sub-KFF-natGa-NOPO (56.5±3.5 nM), EuK-sub-KFF-natLu-DOTA (100.0±59.7 nM) and EuK-sub-KFF-natGa-DOTA (131.5±7.4 nM). Internalization kinetics were fast for all ligands, with an ≥2fold increase in internalization efficiency for the [68Ga/177Lu]DOTAGA-derivatives compared to their [68Ga/177Lu]DOTA-counterparts. The highest internalization efficiencies were observed for EuK-Sub-KFF-[68Ga]DOTAGA and EuK-sub-K[125I]YF-natGa-NOPO (10.2% and 14.6% of applied dose internalized after 60 min, respectively). In initial biodistribution studies in normal mice, the EuK-sub-KFF-[68Ga]DOTAGA construct showed significantly lower non-specific tracer accumulation in lungs, liver, spleen and intestine than EuK-Ahx-[68Ga]HBED-CC. Further in vivo studies in tumor-bearing mice for comparative evaluation of the compounds in this study are currently performed. In conclusion, the respective diagnostic/therapeutic pairs EuK-Sub-KFF-[68Ga/177Lu]DOTAGA and EuK-sub-KYF-[68Ga]NOPO/EuK-sub-K[131I]YF-natGa-NOPO show high PSMA-affinity and efficient internalization into PSMA-expressing cells and might open new perspectives as theranostic agents for imaging and endoradiotherapy of prostate cancer. References [1] Afshar-Oromieh AA, et al (2013) Eur. J. Nucl. Med. Mol. Imaging, 40, 486-95. [2] Banergee SB, et al (2010) J. Med. Chem., 53, 5333-5341.

## OP730

### Synthesis and in Vitro and in Vivo Evaluation of Iodine-124-Labeled Folates: Potential PET Radiopharmaceuticals

**I. Aljammaz** B. Al-Otaibi, S. Amer, N. Al-Hokbani, S. Okarvi; F. Al-Rumayan Cyclotron and Radiopharmaceuticals Department, King Faisal Specialist Hospital and Research Centre, Riyadh, SAUDI ARABIA.

Receptor-targeted radiotracers have shown promises in improvement of the specificity and sensitivity of nuclear medicine imaging procedures. Membrane-folic acid receptor is a glycosylphospstidylinositol protein that overexpressed in approximately 100% of serious ovarian adenocarcinomas and various epithelial cancers including cervical, colorectal and renal cancers. Meanwhile, this receptor is highly restricted in most normal tissues which make these receptors as excellent candidates for molecular targeting through the folate receptor system. Folic acid has been conjugated with various chelates via its carboxylate of the glutamic acid fragment. These conjugates have shown considerable success for delivering various radionuclides to folate-receptor-positive KB cell tumor xenografts in athymic mouse models. Among these radionuclides Ga-67/68, In-111, Tc-99m and F-18 appeared to be feasible in targeting folate receptor expressing tumors *in-vivo*. With the increased use of positron emission tomography (PET), there has been a great interest in the development of positron emitting radiopharmaceuticals for earlier detection and characterization of cancer, molecular assessment of treatment effects and more fundamental understanding of the disease process. Thus, as part of our on-going research effort to develop prosthetic precursors for halogenation of bioactive molecules, we here report the synthesis and biological evaluation of [$^{124}$I]fluorobenzene and pyridine carbohydrazide-folates. The synthetic approaches for the preparation of [$^{124}$I]iodobenzene and pyridine carbohydrazide-folates entailed sequence of reactions. The key precursors N-hydroxysuccinimide 3-tri-n-butylstannyl-benzoate and 3-tri-n-butylstannyl-pyridine carboxylate were radioiodinated using classical method involving 0.1% acetic acid/methanol, iodogen and Na$^{124}$I (50 MBq) at room temprature. The N-succinimidyl-*p*-[$^{124}$I]-iodobenzoate ([$^{124}$I]-SIB) and N-succinimidyl-*m*-[$^{124}$I]-iodopyridine carboxylates ([$^{124}$I]-SIP) were purified using Sep-pak silica cartridge. Hydrazide-folate was then reacted with [$^{124}$I]-SIB and [$^{124}$I]-SIP to give [$^{124}$I]-SIB-folate and [$^{124}$I]-SIP-folate conjugates. Radiochemical yields were quantitative and synthesis times were ranging between 30-40 min. Radiochemical purity was also greater than 98% without HPLC purification. These synthetic approaches hold considerable promise as rapid and simple method for the radioiodination of folate in high radiochemical yield and in short time. *In vitro* tests on KB cell line has shown that the significant amount of the radioconjugate associated with cell fractions. Initial *in vivo* characterization in normal Balb/c mice revealed rapid blood clearance of these radioconjugate with excretion predominantly by the hepatobiliary system for the [$^{124}$I]-SIB-folate and renal system for [$^{124}$I]-SIP-folate conjugates. *In vivo* tumor targeting capacity of this radioconjugate in athymic mice with folate-recptor-positive human KB cell tumor xenografts is currently in progress and will be reported.

1710 - Wednesday, Oct. 23, 10:00 - 11:30, Tête D'Or 1/2

# Physics & Instrumentation & Data Analysis: Standardisation

## OP731

### Feasibility of Absolute SPECT Quantitation Across Continents

**A. Celler**[1], J. Gear[2], C. Uribe[1], P. L. Esquinas[1], X. Hou[1], J. Grimes[1], G. Flux[2]; [1]University of British Columbia, Vancouver, BC, CANADA, [2]Dept of Physics & Royal Marsden Hospital & Institute of Cancer Research, Sutton, UNITED KINGDOM.

**Aim** The demand for absolute SPECT quantitation is rapidly increasing. Particularly, dosimetry calculations which are necessary for personalized molecular therapies require a series of quantitative scans following radionuclide administration. These, however, often present logistic difficulties, particularly in smaller local centers, where patients are tertiary referrals and have been discharged. One solution to this would be for the community to develop a network of centres whereby scanning can be performed at satellite centres, but still processed by the lead centre. This will require data transfers and remote processing. To assess feasibility of this approach, quantitative accuracy of images reconstructed from data acquired on different cameras at different sites was evaluated. **Materials and Methods** Phantoms containing 4 to 6 inserts with volumes 4-200ml were filled with $^{99m}$Tc, $^{111}$In and $^{131}$I and scanned on Philips (2 studies, Adac, Brightview) in London (UK) and on GE (4 studies, Infinia/Hawkeye) and Siemens (1 study, Symbia) cameras in Vancouver (Canada). Both SPECT/CT and separate SPECT and CT systems were used. All studies were processed by three operators in Vancouver who were blinded to the true activity distributions scanned in London. The in-house qSPECT reconstruction algorithm (Shcherbinin et al., PMB-2008) with attenuation, scatter and resolution recovery was used. Accuracy of blinded versus non-blinded reconstructions for data from different systems were compared. **Results** The initial results are promising with agreement varying according to isotope and object size. The accuracy of absolute activity recovery ranged from 1-3% for Vancouver and 3-6% for London acquisitions of $^{99m}$Tc phantoms to 8-18% for London studies with other isotopes. Higher accuracy was achieved for SPECT/CT acquisitions demonstrating the importance of attenuation map alignment. Hand-drawn and thresholded regions-of-interest were used. Understandably, larger errors were observed for small objects. In general, the accuracy of the Vancouver studies was about twice better than from blinded London data which requires further investigation. Additional acquisitions using other isotopes (including beta emitters), more complex phantoms with background activity and non-uniform density will be performed and commercial reconstruction algorithms will be tested. As segmentation is crucial for accurate quantitation, our adaptive iterative thresholding method (Grimes et al., NMC-2012) will be applied. **Conclusions**: Our results indicate that remote processing of SPECT data is challenging, but feasible. In most cases the achieved accuracy would be sufficient for clinical applications. This approach could be especially valuable for multicenter clinical trials with distributed data acquisition and advanced data processing by specialized centers.

## OP732

### Assessing the quality of parathyroid scintigraphy across a large hospital network using a patient simulator: Can we improve image and interpretation quality?

**L. M. Fig**[1], D. Bonta[2], K. P. Friedman[3], P. E. Christian[4], S. H. Abreu[5], M. D. Gross[1]; [1]VAMC, Ann Arbor, MI, UNITED STATES, [2]VAMC, Atlanta, GA, UNITED STATES, [3]NYU Langone Medical Center, New York, NY, UNITED STATES, [4]University of Utah, Salt Lake City, UT, UNITED STATES, [5]Consultant, Oklahoma City, OK, UNITED STATES.

**Aim**: Preoperative parathyroid scintigraphy to guide minimally invasive parathyroidectomy has become routine. Given this central role, quality assurance of scintigraphic imaging and clinical interpretation is essential. As part of an annual quality enhancement exercise for US Department of Veterans Affairs (DVA) nuclear medicine laboratories, we evaluated our first utilization of a patient simulator (phantom) designed to mimic a parathyroid adenoma. **Materials and Methods**: A neck phantom designed by the Society of Nuclear Medicine & Molecular Imaging (SNMMI) Quality Assurance Committee (QAC) simulated a solitary parathyroid adenoma. An insert to simulate a normal "thyroid gland" was filled with a low concentration of Tc-99m. A separately injected Tc-99m circuit simulated a 10 mm right lower pole parathyroid adenoma. Washout from the "thyroid" for delayed imaging was mimicked by a second "thyroid" insert of lower activity. The phantom was imaged at 124 DVA laboratories by planar and SPECT techniques (SPECT-CT at 44 sites) using each facility's usual clinical protocol. Data collection included quality control information, imaging and processing parameters, and DICOM images. After review of a simulated "case history" interpreting physicians (N=322) reported lesion location/s, number of visualized glands, and answered questions concerning imaging and management of hyperparathyroidism. We analyzed factors associated with poor performance to identify and remediate problems related to image acquisition, processing and scan interpretation. **Results**:Most commonly, inappropriate acquisition parameters e.g. unsuitable collimator in 5.6% (low energy all purpose instead of high resolution) and/or incorrect matrix in 13% (64x64 matrix without zoom) caused suboptimal image quality. Short acquisition times (< 10 min/view for planar imaging and <15 sec/projection for SPECT in 4%) also resulted in poor quality images. Improper reconstruction parameters caused excessively smoothed or noisy images. Errors specific to SPECT-CT included image misregistration and inappropriately high CT mA. Erroneous lesion detection/localization and/or lack of knowledge of the embryological origins of ectopic lesions resulted in lower interpretative performance scores. **Conclusions**: To our knowledge, these data are the first report on the performance of parathyroid imaging using a clinical simulator across a large number of laboratories in a single hospital system. Identification of factors involved in suboptimal performance allows us to recommend system-wide changes in acquisition/reconstruction parameters. The SNMMI QAC phantom testing program provides a valuable benchmarking tool to standardize acquisition, processing and interpretative methodology and enhance the quality of parathyroid imaging in the DVA. The data highlight the desirability of national standardization and harmonization of imaging and interpretative procedures.

## OP733

### Innovative methodology for dose calibration inter-comparison studies using in-situ prepared 99m-Tc sources

**P. A. Oliveira**, A. L. Bastos, J. A. M. Santos; Instituto Português De Oncologia Do Porto Francisco Gentil E.P.E., Porto, PORTUGAL.

**Aim** The inter-comparison of accuracy performance and traceability achievement of dose calibrators between Nuclear Medicine centers, through measurement with calibrated sources is commonly recommended [1]. It is however only possible using isotopes of relatively long half-lives, allowing the source to be sent from a calibration laboratory. For 99m-Tc, its relatively short half-life makes this inter-comparison methodology virtually impossible. In this work, the implementation of an innovative new approach using this isotope is described. A validation study was performed confirming it as a possible and useful tool to conduct inter-comparison studies between Nuclear Medicine centers. **Materials and Methods** The proposed inter-comparison procedure involve an in-situ preparation of a 99m-Tc source, which will be used to irradiate a radiochromic film (Gafchromic XRQA2 [2]) inside a specially designed irradiator under strict conditions. The cumulated activity, Ã, is calculated based on the initial activity and total irradiation time. This irradiation will originate an increase in the film optical density (OD) dependent on the cumulated activity, OD (Ã). A calibration curve is established for a given irradiator geometry and a calibrated dose calibrator. It is thus possible to send the irradiator plus detailed irradiation instructions to a distant Nuclear Medicine centre to be exposed using a locally prepared source. The dose calibrator activity read-out as well as the accurate irradiation time is recorded and used to calculate the cumulated activity. Back to the controlling centre, the corresponded OD is measured using a dedicated scanner (EPSON Expression 10000XL), and compared with a reference value obtained from a previous measured calibration curve. If the irradiation time is accurately determined (<0.07%) the differences between the measured OD and the calibration curve OD (Ã) can only be attributed to the initial activity (dose calibrator read-out), or to the Gafchromic XRQA2 measurement and associated errors. This allows the comparison of both activity read-outs and the deviation between the calibrated and the tested device. **Results and Conclusion** To estimate the total expected measurement errors, a careful analysis of this methodology was performed: reproducibility determination (<0.1%), scanning conditions optimization, and possible fadeout effects. It can be also used for verification of correct syringe positioning inside the dose calibrator [3]. This methodology shows potential for accurate dose inter-comparison studies for 99m-Tc between Nuclear Medicine centers. References [1] AAPM Report 181 (2012) [2] Giaddui, T. *et al.*, Med. Phys. 39 (2012) 842 [3] Santos *et al.*, Appl. Rad. and Isot. 67 (2009) 1104-1109

## OP734

### Variability Evaluation of Mebrofenin-99mTc Liver Clearance with Hepato-Biliary Schintigraphy

**A. Olivier**, C. Baillet, S. Truant, A. Deshorgue, F. Pruvot, D. Huglo; CHRU Lille, Lille, FRANCE.

**Aim**: In pre-operative and post-operative major hepatectomy, hepatobiliary scintigraphy allows liver function assessment which may provide additional information to the data volume. Liver function evaluation is particularly useful in patients with liver disease or earlier hepatotoxic treatment. The purpose of this study was to investigate some of the parameters able to influence Tc-mebrofenin hepatic clearance calculation and inter-and intra-observers reproducibility to optimize further multicentric studies. **Materials and Methods**: Scintigraphies were performed before surgery (8 patients) or after major hepatectomy (22 patients). Hepatic clearance (% / min.m²) was calculated from the values of hepatic, cardiac, and total activities, 150 and 350 s post-injection, in accordance with the method recommended in the literature. We had studied: 1) Impact of injection-acquisition delay variations (calculation of clearances beginning 110, 130, 150, 170 or 190 s after injection), 2) Clearances calculated either from anterior acquisitions only (FA) or from the geometric mean (GM), 3) Clearances calculated either from the four most used body surface area (BSA) formulas, 4) Reproducibility intra-and inter-observers for three observers (two evaluations for each scintigraphy). **Results**: 1) Clearance differences between different studied intervals were statistically significant. These differences were more important if the studied interval is far from reference interval (150-350s) and even more when the interval studied is too early (110-310s). 2) There was a statistically significant difference between the measurements of clearance on FA or GM images. This difference was on average 0.85% / min.m² or a decrease of approximately 13.3% of the average FA clearance ($p < 0.001$). 3) Clearances comparisons using different BSA formulas put in evidence of statistically significant differences for four of them (Dubois formula versus other Methods and Boyd formula versus Mosteller formula). These differences were small, at most 2% of the mean clearance, 4) Despite differences in size of cardiac and hepatic ROI, intra-observer reproducibility of hepatic clearance was excellent for each observer (observer 1: 0.996 [0.991 to 0.998], observer 2: 0.998 [0.995 to 0.999] and observer 3: 0.982 [0.963 to 0.991]). Inter-observers reproducibility was also excellent (R = 0.982). **Conclusion**: Hepatic clearance of mebrofenin appears to be a highly reproducible method provided to standardize acquisition and clearance calculation. It allows functional assessment of the liver which is complementary to morphological and biological data usually performed before major hepatectomy. Thereby, the definition of a standardized protocol would make possible realization of multicentric studies.

## OP735

### Optimization of brain PET imaging for a multicenter clinical trial: the french CATI experience

**R. TREBOSSEN**[1], S. MARIE[2], A. KAS[2], M. REYNAL[2], J. MARTINI[2], H. BERTIN[2], M. GUYOT[2], M. Habert[3,2]; [1]CEA, Orsay, FRANCE, [2]UMR_S 678, INSERM UPMC, Paris, FRANCE, [3]Hopital Pitie Salpetriere, Paris, FRANCE.

**Objectives** : The CATI is a French initiative Aiming at improving multicentric data acquisition and processing for clinical research in Alzheimer disease. The objective is to optimize acquisition and reconstruction parameters, to reduce variability across centers for the MEMENTO trial. **Methods** : Jaszczak (with 4 hot and 2 cold spheres) and 3D-Hoffman phantoms were acquired in 21 PET centers. The hot sphere radiuses were respectively 3.9, 8.4, 11.4, and 16.2 mm. The phantom background (BG) was filled with 5 kBq/ml radioactive solution and the sphere to BG concentrations equaled 3. The recovery coefficients (RC) obtained with different parameters were compared. The Hoffman phantom was filled with a 30-45 kBq/ml radioactive solution. Left to right (L/R), anterior to posterior (A/P), putamen to grey matter (P/GM) and grey to white matter (GM/WM) ratios were computed. In house softwares were developed for an automated phantom analysis. **Results** : All tomographs were 3D PET-CT, installed between 2003 and 2012, and consisted of 9 GE, 3 Philips and 9 Siemens systems and 10 different scanners. Optimized RC of the 2 smallest spheres ranged respectively from 0.23 to 0.55 (mean±SD 0.33±0.09) and from 0.56 to 0.87 (mean±SD 0.71±0.08). Compared to center routine parameters, SD on RC were reduced by a factor 1.7. Spatial resolution increased for the coarsest

scanners and decreased for the recent ones since reconstruction algorithms with PSF correction were discarded. Optimized average P/GM ratio was 0.80±0.012 (range 0.80-0.88), L/R ratio was 0.95±0.01 (range 0.97-1.01), A/P ratio was 0.97±0.01 (range 0.97-1.05) and GM/WM ratio was 2.87±0.14 (range 2.70-3.37). **Conclusions :** P/GM values suggest that spatial resolution was preserved and homogenous across the centers. GM/WM values exhibited a larger variability, which could partly be due to segmentation issues. A/P and L/R values suggest that uniformity across the scanners fields of view was correct. The residual center effect will be accounted for the subject data analysis, thanks to an adequate modeling.

## OP736

### An international multicentre comparison of true administered F-18 radioactivity in patients undergoing [F-18]FDG-PET exams

**A. Del Sole**[1], M. Lecchi[1], S. Gaito[2], G. Lucignani[1]; [1]Department of Health Sciences, University of Milan; Department of Diagnostic Imaging, San Paolo Hospital, Milan, ITALY, [2]Department of Computer Science, University of Milan, Milan, ITALY.

**Introduction**: In [$^{18}$F]FDG PET imaging the radiation dose received both by patients and by operators depends directly on the radioactivity injected into the patients. The guidelines issued by national and international professional associations (as SNMMI and EANM), allow widely heterogeneous protocols. **Aims**: To analyse variability of injected $^{18}$F radioactivity across international sites in order to provide support for clinical, industry and regulatory initiatives to standardise practice and decrease radiation exposure in [$^{18}$F]FDG-PET imaging. **Material and Methods:** A database of 24,781 [$^{18}$F]FDG injections performed in 15 PET centres was collected. Participating PET sites included large institutional hospitals and outpatient clinics in Australia (n. 3), Europe (n. 4), and the United States of America (US) (n. 8), where an automatic combined dispenser and injector system, the Intego™ (Medrad, Inc., Indianola, PA), was available. This device records the effective activity injected into each patient. Data were provided by MedRad in an anonymous form. Univariate statistics (SPSS v. 20) and t-tests (two-tailed with Welch-Satterthwaite correction for unequal variances) were used to determine differences between sites using weight-based and standard [$^{18}$F]FDG dosing protocols, and between different geographical areas. **Results:** The mean radioactivity administered in US centres (n=8,066 injections) was 500.8 MBq [SD = 87.6, SEM=1.0], as opposed to 266.2 MBq [SD = 72.5, SEM=0.6] in the European and Australian ones (n=16,715 injections). The 0.95 confidence interval for the difference between means was: 232.4-236.8 MBq ($p<0.0001$), allowing a 61.2% difference in patient dose. This result could be due to different [$^{18}$F]FDG dosing protocols: a standard [$^{18}$F]FDG activity protocol was used in 92.5% of the injections performed in the US, versus only 10.4% of those performed in Europe and Australia. In particular, in Europe 98.8% of the [$^{18}$F]FDG injections were based on the patient's body weight, versus 75.5% in Australia. However, the mean radioactivity administered in the US sites (n=605 injections) using a weight-based protocol was 469.2 MBq [SD = 97.0, SEM=3.9], only 6.5% less than that administered using a standard [$^{18}$F]FDG dosing protocol. **Conclusions:** There emerged large differences in injected [$^{18}$F]FDG activity across the PET imaging centres considered in this study: assuming a similar population of patients, PET centres outside the US and/or sites using weight-based [$^{18}$F]FDG dosing administered 60% less $^{18}$F radioactivity than centres located in the US and/or using standardised dosing. This could be due to differences in PET scanner sensitivity, uptake times and/or scan durations.

## OP737

### Multicenter Evaluation of Renography with a New Automated Physical Phantom: Reports

**J. Heikkinen**[1], A. Nykänen[1], J. Aarnio[1], P. Rautio[2]; [1]Mikkeli Central Hospital, Mikkeli, FINLAND, [2]North Karelia Central Hospital, Joensuu, FINLAND.

The Aim of this study was to evaluate the quality of the study reports of renography in Finnish hospitals. Twenty nuclear medicine departments participated in the study which was organised by Labquality Ltd. (Helsinki). Three renography simulations were made with a new dynamic renal phantom (Foundation for Finnish Inventions). It was imaged as well as interpreted as a renal patient according to the clinical routine of each centre. An experienced (30 years) nuclear medicine physician evaluated all reports and images blindly and scored each of them according to what was stated about the structure and the location of the kidneys, the parameters, the curves and the conclusion. Interpretation, description and overall quality were judged, too. Average points for the reports were 17.2 ± 9.1 (from 0.0 to 35.0). The terminology used varied and was sometimes misleading and often inconsistent with recommended national terminology. Language could have been better and clearer. The position of the patient (sitting/supine) was seldom reported, although it affects the interpretation and reference values. Difference between kidney size was clearly under-reported and a scar in one simulation was often not detected. Sometimes interpreters used inconsistent or non-physiological parameters. A few reports used two different relative function parameters, de convoluted and Patlack-plot, which differed too much and were confusing for the reader. There were undetected errors in mean transit time (MTT) calculations although the error should have been clear from the visual interpretation or in relation to other parameters. For example some hospitals reported MTT of 2.0 - 3.0min when the curve was rising all the time and Tmax was > 20min. In this respect renal outflow efficiency (ROE) seemed quite robust, but it was only used by 4 sites, so the sample size is too low for clear judgements. Residual cortical activity (RCA) was sometimes used additionally and sometimes misleadingly with more sophisticated parameters like MTT and ROE for obstruction evaluation. Using Tmax and relative function and ROE or MTT, if it was calculated correctly, lead usually to correct interpretation. The findings were often well described but what the findings meant in the situation of the individual patient, could have been discussed more. Although, the results were mostly satisfactory, there was a quite large variation in the quality. Standardisation and regular external tests for renography reports is needed to ensure correct outcome for the referrals.

## OP738

### Development and implementation of a website for quality assurance of clinical studies

**P. J. Collins**[1], R. Barnett[2]; [1]Royal Adelaide Hospital, Adelaide, AUSTRALIA, [2]Westmead Hospital, Sydney, AUSTRALIA.

**Background and Aim:** It is important that clinical studies are evaluated to ensure both their accuracy and reproducibility. Software audits are used for benchmarking against national standards, internal validation of new software releases and training of operators within a site. They can be conducted either locally or nationally but considerable resources are usually required to administer the process. The Aim of this project was to develop an online software audit tool to streamline the audit procedure. **Method and Results:** The software enables users to (i) participate in an existing audit (ii) test their study results against a training dataset or (iii) setup and administrate their own audit (subject to adjustable privileges). The online site uses open source software including PHP (scripting language) and MySQL (database). The design is modular so that additional data entry and report forms can be added without changing the existing code. Moodle (freeware educational software) is used for password authentication to simplify management of the site. Datasets are downloaded from the website, processed on the users clinical workstation and the results entered online. Gated blood pool and renal datasets are currently available (in Interfile and DICOM format). Audits are identified by dataset and institution. Users are able to participate in any audit, without a password, regardless of the purpose of the audit; however, the person administering the audit has the authority to either include or exclude results where appropriate. The results can be downloaded by the administrator in a format suitable for statistical analysis. Audits can also be utilised as a training tool to evaluate operator proficiency. In this mode, participants are provided with an immediate online report after data entry - a statistical comparison of their data with the audit results. Several mechanisms are available to delegate administration of the site. A user can initiate a new software audit (using current datasets) by registering a request to the site administrator. The user can also be given privileges to administer existing audits. **Conclusion:** An online software audit tool has been developed that allows users to either (i) conduct/participate in small to large audits, or (ii) test their analysis skills against audited results using the training mode.

1801/1803 —Wednesday, Oct. 23, 12:00 — 13:00, Amphithéâtre

## Plenary 4: Highlights Lecture

## OP739

### Highlights Lecture

**F.M. Bengel, GERMANY, S. Fanti, ITALY**

# POSTER WALKS

PW 01 - Sunday, Oct. 20, 8:30 - 9:30, Poster Exhibition Area

## Poster Walk 1 - Oncology: Head & Neck

### PW001

### FLT-PET/CT for Brain Lesions Evaluation: a Semi Quantitative Approach in a Prospective Study

**A. Nikaki**[1], V. Prassopoulos[1], V. Fillippi[1], D. Kechagias[1], F. Vlachou[1], S. Merisoglou[1], E. Razi[2], P. Nomikos[3], R. Efthymiadou[1], P. Georgoulias[4]; [1]DTCA Hygeia Department of PET/CT, Athens, GREECE, [2]DTCA Hygeia 3rd Oncology Department, Athens, GREECE, [3]DTCA Hygeia Neurosurgery Clinic, Department of Spinal Surgery & Scoliosis and Gamma Knife Brain Radiosurgery, Athens, GREECE, [4]University of Thessaly/ University Hospital of Larissa, Larissa, GREECE.

**Purpose**: The purpose of this study is to record and examine the potential role of semi quantitative FLT-PET/CT analysis utilization in addition to visual assessment of brain in differential diagnosis of a brain lesion as primary or metastatic in recurrent or treated brain masses. **Method-Material**: 16 patients with primary or metastatic brain tumor underwent 19 FLT-PET/CT examinations at a Siemens Biograph LSO PET/CT device, 50-60 min after intravenous administration of the radiopharmaceutical. In 10 cases, patients underwent PET for evaluation of possible recurrence, in 9 cases for treatment response evaluation. 9 patients (11 PET cases) suffered from metastatic brain disease, 1 patient (2 PET) from recurrent Non Hodgkin Lymphoma (NHL, initial localization at the base of the tongue, recurrence at brain) and 6 from primary brain tumor (2 Grade II, 2 Grade III, 2 Grade IV). SUVmax and Tumor-to-Background ratio (T/B) was calculated for each lesion (totally 20 lesions). Comparison of SUVmax and T/B values was attempted between primary (grade included) and metastatic lesions. **Results**: 15 PET examinations, 8 for metastatic disease, 6 for primary brain tumor and 1 NHL (total 20 lesions), were characterized as positive and 4 as negative. Accordingly, 11 lesions were metastatic, 7 primary and 2 NHL. For one PET examination for evaluation of treatment response in metastatic breast cancer (4 lesions), FLT uptake was definitely visible in one lesion (SUVmax 2.3, T/B 4), while at the rest, 3 FLT uptake was slightly above background (SUVmax 0.6-0.9, T/B 1.2-1.8). In one case- evaluation of radiotherapy response in metastatic thymoma- (1 lesion) FLT uptake was diffuse and low and the examination was characterized as negative. Average SUVmax and T/B was 2.3±1.1 and 5.1±1.9 for primary; accordingly 2.1±1.2 and 4.1±3.4 for metastatic tumors respectively- while when excluding the 3 equivocal lesions, SUVmax and T/B became 2.6±1 and 5.2±3.5. Average SUVmax and T/B for NHL were 8.9 and 19.5 respectively. Overlap was identified among the different grades of recurrent or treated primary tumors. **Conclusions**: With respect to our small sample and the fact that all patients had been treated sometime in the course of disease, NHL lesions exhibited high SUVmax and T/B values. Average SUVmax between primary and metastatic lesions did not substantially differ. Variability in T/B values were noted in metastatic lesions, perhaps due to differences in primary site and treatment response. Overlap among different grades could, at least partially, attributed to increased aggressiveness of recurrent tumors.

### PW002

### Novel metrics to assess changes to C-11-methionine PET uptake in pituitary adenoma and normal tissue after surgical or chemical intervention

**S. Heard**, D. Gillett, O. Koulouri, N. Vennart, M. Gurnell; Cambridge University Hospitals NHS Foundation Trust, Cambridge, UNITED KINGDOM.

**Aim**: Uptake of C11-methonine in pituitary adenoma is currently quantified using SUVmax, usually normalised to background brain regions. The validity of this approach is compromised by uptake in normal pituitary tissue and by the partial volume effect (PVE) because the tumours are small. We aimed to optimise PET imaging for these small tumours and to develop novel metrics to assess change following intervention. Methods were designed particularly to obtain functional data for co-registration with MRI scans on which it can be difficult to distinguish metabolically active adenoma from necrotic tissue or post-operative scar tissue. **Methods**: We started by optimising image reconstruction parameters using time-of-flight (TOF) and Sharp IR point-spread-function (PSF) algorithms on a GE Discovery 690 PET/CT scanner. Phantom and patient studies were reconstructed with a range of parameters and compared blindly by physicists and clinicians. The optimised images were then analysed using GE's AW and Xeleris processing systems. Regional uptake was quantified with thresholded SUVmean and volume together with histogram analysis of SUV values on a pixel-by-pixel basis. All uptake values were normalised to the cerebellum, which has been found to give a more constant ratio than whole body activity. We then determined uptake in a smoothed region encompassing the entire pituitary, including any suspected adenoma. The region was copied to a co-registered post-intervention image and subtracted from the first to create a difference image which was then co-registered with a post-intervention MRI scan. **Results**: The optimum reconstruction parameters were TOF with PSF using 3 iterations, 24 subsets and a 2 mm Gaussian filter. The various metrics derived from image analysis have shown changes post-intervention that were not obvious from SUVmax values alone. Observed changes included tumour shrinkage, a reduction in the histograms of mean and median uptake values, and displacement of maximum uptake from adenoma to normal tissue. **Conclusions**: We have shown that changes to pituitary adenoma post-intervention can be more definitively and accurately assessed on C-11 methionine PET scans by using a range of metrics that we have developed to improve upon the normalised SUVmax approach. We have automated the methodology for use by clinicians and radiologists when reporting on the efficacy of interventional treatment.

### PW003

### F-18 fluorodeoxyglucose positron emission tomography for squamous carcinoma of the upper and lower gum

**K. Hayasaka**[1,2], T. Komatsu[2], H. Inanami[2], T. Nihashi[3]; [1]Fukujyuuji Hospital, Tokyo, JAPAN, [2]Iwai Medicheck Imaging Center, Tokyo, JAPAN, [3]Graduate School of Nagoya University, Nagoya, JAPAN.

**Purpose** We aimed to determine whether F-18 fluorodeoxyglucose (FDG) positron emission tomography (PET) imaging can diagnose and stage upper and lower gum squamous cell carcinoma. **Materials and Methods** We used FDG-PET to evaluate 75 patients aged 70 (SD, 9.9) y who had been pathologically diagnosed with squamous cell carcinoma of the upper (n = 31) and lower (n = 44) gums. Normal glucose levels were confirmed in all patients, who fasted for at least 5 h before being intravenously injected with 185 - 300 MBq of F18-FDG. Images were acquired one hour later using a GE Discovery ST Elite PET/CT machine. Regional FDG uptake in the affected area is expressed as maximal uptake values (SUV). Data were statistically analyzed using SPSS Version 11.0 software (SPSS Inc. Chicago, IL, USA). **Results** Hypermetabolic lesions with intense focal uptake (SUVmax > 2.5) were considered malignant. Positive FDG uptake was identified in primary lesions among 73 (97.3%) of 75 patients. The SUVmax of primary lesions of the lower and upper gums, respectively, were 10.3 (SD, 6.6) and 12.9 (SD, 7.5), respectively. The SUV max was 6.3 (SD, 2.9) in T1 (N = 24), 11.7 (SD, 6.6) in T2 (N = 24), 16.1 (SD, 6.6) in T3 (N=5) and 15.5 (SD, 7.6) in T4 (N=22). Lymph node metastasis was found in 21 patients and 51 of 54 patients were diagnosed as having N0 by PET/CT. The sensitivity, specificity and accuracy of FDG-PET were 80.0%, 85% and 81.3% for N0, 83.3%, 82.5% and 82.6% for N1, and 70%, 100% and 96% for N2, respectively, but FDG-PET detected distant metastasis in only one patient (100%). The SUVmax at primary lesions in males and females (P = 0.624), or location in the upper or lower gums (P = 0.479) did not significantly differ. On the other hand, differences were statically significant between T1 and T2, T1 and T4, T1 and T2, T2 and T4, T1-2 and T3-4, stages 1-2 and 3-4 (P < 0.05 for all). **Conclusion** Using F-18 FDG PET/CT imaging to evaluate squamous cell carcinoma of the upper and lower gums had good accuracy and predictive value in determining T factor, lymph node status and tumor staging. The SUV max significantly differed among T factors and stages in primary lesions, but not with respect to lymph node metastasis.

### PW004

### Evaluation of Tumor Heterogeneity: Textural Features and SUV Discriminate Different Biological Phenotypes in Squamous Cell Carcinoma of the Head and Neck

**R. A. Bundschuh**[1], R. Heinrich[1], A. Pickard[1], J. Dinges[1], G. Piontek[1], N. Zsótér[2], L. Papp[2], E. Scherer[1], M. Essler[1]; [1]Klinikum rechts der Isar der Technischen Universität München, Munich, GERMANY, [2]Mediso Medical Imaging Systems Ltd., Budapest, HUNGARY.

**Introduction:** Tumor heterogeneity assessed in PET imaging was found to be a prognostic factor for overall survival and time to progression as well as a predictive factor for therapy response assessment in several tumor entities [1]. However no correlation between tumor heterogeneity assessed in PET imaging and tumor biology as assessed by histological parameters was performed up to now. Therefore the aim of this study was to correlate different textural parameters assessed in FDG-PET/CT with various histopathological parameters in patients with squamous cell carcinoma of the head and neck (HNSCC). **Methods:** 21 patients with histologically proven HNSCC were examined with FDG-PET/CT 1 to 4 days before head and neck dissection. For the primary tumor the coefficient of variation (COV), skewness and kurtosis was estimated using Interview Fusion Software (Mediso). In addition the maximum and mean SUV were measured. After resection the primary tumor was worked up histopathological and quantitatively analyzed for the expression of p16, p53, Ki67, EGFR, E-Cadherin (ECAD), CD31, CD44, aldehyde dehydrogenase (ALDH) and GLUT1 was performed. Afterwards correlations

between histological parameters and textural parameters were analyzed. **Results:** We found statistical significant correlation ($p<0.05$) for COV with E-Cad and EGFR expression, for kurtosis with ALDH, CD44 and E-Cad, and for skewness with ALDH, GLUT1 and p53. Mean SUV did correlate with CD31, EGFR, GLUT1, Ki67 and p53 while maximum SUV showed correlations with CD31, CD44 and p53. The other histological parameters did not correlate with the examined imaging parameters. **Discussion:** Our data suggest that textural markers and SUV may reflect different aspects of cancer biology. Interestingly, kurtosis is correlated with the stem cell markers ALDH and CD44, skewness only with ALDH. In contrast, COV is associated with EGFR- and E-Cadherin expression, general markers of tumor aggressiveness. Mean SUV showed a correlation with markers of proliferation and angiogenesis as well as glucose transporter expression. Maximum SUV showed an additional correlation with CD44. Analysis of tumor biology by textural markers may emerge as tools for phenotyping of tumors in the future. Reference: [1] Chicklore S, Goh V, Siddique M, et al.. Quantifying Tumour Heterogeneity in (18)F-FDG PET/CT Imaging by Texture Analysis. Eur J Nucl Med Mol Imaging, 40:133-140, 2013.

## PW005

### Prognostic value of 18F-FDG PET/CT parameters and human papillomavirus in patients with oropharyngeal squamous cell carcinoma

**S. Koyasu**[1], M. Kikuchi[2], Y. Nakamoto[1], K. Nakatani[1], K. Kurihara[1], K. K. Miyake[1], N. Hayakawa[1], M. K. Arimoto[1], S. Shinohara[2], K. Itoh[2], K. Togashi[1]; [1]Kyoto University Graduate School of Medicine, Kyoto, JAPAN, [2]Kobe City Medical Center General Hospital, Kobe, JAPAN.

**Aim:** 18F-FDG PET/CT parameters have been proposed as potential prognostic imaging markers for patient outcome in solid tumours including head and neck cancer. Human papillomavirus (HPV) positivity is associated with favourable survival in oropharyngeal squamous cell carcinoma (OPSCC). The aim of this study was to evaluate whether PET/CT parameters have independent prognostic information in addition to HPV infection status in patients with OPSCC. Material and **Methods**: A prospective data acquisition and retrospective review of pre-treatment FDG-PET/CT scans from August 2005 to July 2012 for 46 consecutive patients (M:F = 37:9) who were histopathologically diagnosed OPSCC and who received definitive therapy (surgery:radiation therapy = 16:30) without any co-existing malignancies or other organ metastases was performed. On FDG-PET/CT images, regions of interest was placed over a primary tumour and lymph node metastases to calculate PET/CT parameters_maximum standardized uptake value (SUVmax), metabolic tumour volume (MTV), and total lesion glycolysis (TLG). Pretreatment tumour biopsy specimens were studied by polymerase chain reaction or immunohistochemistry (p16) to determine HPV infection status. The prognostic value of these parameters was evaluated using univariate and multivariate Cox regression analysis in order to investigate predictors of the disease specific survival (DSS), disease free survival (DFS), and the local control (LC). A two-sided P value of $< 0.05$ was considered significant. **Results:** The median follow-up period was 25 months. Of 46 patients, 28 patients were HPV positive. Between these two groups, there was no significance for any PET parameters. In univariate analysis, MTV and TLG (primary, nodal, and total) as well as HPV status and UICC staging were significant prognostic factor, while SUVmax was not significant factor for DSS, DFS, nor LC. In multivariate analysis adjusted for HPV infection status, MTV (primary, nodal and total) and TLG (primary and total) were independently associated with LC. Among them, the larger primary MTV yielded the higher risk (hazard ratio, HR: 9.2). As for DFS, MTV and TLG (nodal and total, for both) were independently significant factors and the larger nodal TLG yielded the higher HR (3.7). As for DSS, MTV (nodal and total) and TLG (primary, nodal and total) were independently significant factors and the larger total TLG yielded the higher HR (4.9). **Conclusions**: Our data indicate that the pretreatment PET/CT parameters had independent prognostic value adjusted for HPV infection status in patients with OPSCC.

## PW006

### In-vivo metabolic tumour volume correlation with ex-vivo pathological volume in laryngeal SCC

N. Patel[1], **H. H. Tam**[1], A. Sandison[2], Z. Win[1]; [1]Departmetn of Nuclear Medicine, Imperial College Healthcare NHS Trust, London, UNITED KINGDOM, [2]Departmetn of Histopathology, Imperial College Healthcare NHS Trust, London, UNITED KINGDOM.

**Aim**: Accurate estimation of gross tumour volume in head and neck cancer is important for radiotherapy planning, especially with 3D dose calculation and intensity modulated radiotherapy treatment beams. In this pilot study, we evaluate the accuracy of automated volume segmentation of laryngeal tumour in comparison to resected pathological specimen. **Materials and Methods**: Pre-treatment 18F-FDG PET/CT studies of five patients who underwent laryngectomy for laryngeal SCC were reviewed. The gross tumour volume (GTV) was recorded by automated segmentation using SUV threshold (percentage of maximum SUV) methodology. The PET/CT data was reconstructed using both Iterative (OSEM, 4 iterations, 8 subsets) and Point Spread Function (PSF) algorithms (TrueX, 4 iterations,16 subsets). This was compared with the tumour volume derived by cross-sectional area from macroscopic pathology specimens. **Results**: For the PSF and OSEM PET data, a significant difference was observed between both the SUVmax and the threshold for accurate volume delineation using paired t-test statistics ($p=0.002$, $p = 0.017$ respectively). The PSF data showed larger SUVmax and smaller threshold for accurate GTV delineation. No significant difference was found between the gross target volumes for the PSF and OSEM data ($p=0.139$). Inter- and intra-observer variations were very small and always far below the residual variance. The gross target volumes delineated using threshold-based PET Methods were found to overestimate the histology volumes. Despite this, they were closer to histology than those determined using CT alone. Comparing the two reconstruction algorithms showed that the PET volumes using the PSF algorithms were found to be closest matched to the histology volumes due to improved spatial resolution. **Conclusion**: Compared with GTVs on CT, GTVs on FDG PET were smaller and closest match to the histology specimen volumes. Accurate point spread algorithms have improved spatial resolution improving the accuracy of the volume delineation.

## PW007

### 131I SPECT/CT False Positive Imaging in Differentiated Thyroid Cancer; on Behalf of the French Tuthyref (Tumeurs de la Thyroide Refractaires) Network

T. MEAS[1], A. KELLY[2], Y. GODBERT[3], R. CIAPPUCCINI[4], A. BERNARD[5], I. FAUGERON[1], **M. TOUBERT**[1]; [1]Saint-Louis Hospital, APHP, PARIS, FRANCE, [2]Centre Jean Perrin, CLERMONT-FERRAND, FRANCE, [3]Institut Bergonie, BORDEAUX, FRANCE, [4]Centre François Baclesse, CAEN, FRANCE, [5]Centre Eugène Marquis, RENNES, FRANCE.

**Introduction:** Multimodality imaging using 131I SPECT/CT has allowed a better knowledge of atypical foci that may be related either to unusual sites of differentiated thyroid cancer (DTC) metastasis or false positive (FP) 131I uptake. 131I FP uptake should be differentiated from metastases, as it has a major impact on the clinical decision and prognosis of patients. **Methods:** In France, through the TUTHYREF network, a unique system allowing collective discussion twice a month during web conferences among 30 regional expert centres, we have the opportunity to collect unusual 131I SPECT/CT imaging. Our results are confirmed by histology whenever possible, and taking in account the other parameters of the clinical decision, such as the seric thyroglobulin level; in the other cases, results are confronted to follow-up procedures. **Results:** We have already collected 11 atypical FP images (biliary lithiasis, benign peritoneal kystic mesothelioma, benign renal cyst, benign ovarian cyst, benign ovarian teratoma, uterine fibroid, post-lactation mammary gland, pneumonectomy cavity and bronchial secretions) of which histology was sometimes required to eliminate rare metastasis (kidney, ovary and peritoneal lesions). Histology, TNM, age at diagnosis, Thyroglobulin level will be precised. Biological (and sometimes imaging) follow-up procedures will be described to assess our diagnosis. **Conclusions:** Work is still in progress and updated findings will be presented. The final aim will be to allow a better knowledge of very unusual FP I131 images, today accessible with SPECT/CT technique, to gather them in an atlas, and permit a more appropriated management of our patients.

## PW008

### The impact of FDG PET/CT imaging in the initial work-up of patients with high risk differentiated thyroid carcinoma.

**G. U. Vural**, B. B. Demirel, B. E. Akkas, A. K. Fidan, N. Ercakmak; Ankara Oncology Research and Training Hospital Department of Nuclear Medicine, Ankara, TURKEY.

The aim of this study was to evaluate the impact of FDG PET/CT imaging in the initial work-up of patients with high risk differentiated thyroid carcinoma (DTC). **Method**: Thirty-one patients with high risk DTC (21F, 10M, age:46±17 yr, 25 papillary, 6 non-papillary cancer), who were referred to radioiodine ablation therapy to our nuclear medicine clinic, underwent FDG PET/CT as a part of initial work-up. PET/CT was indicated to define disease extent; in 22 patients with serum Thyroglobulin (Tg) levels out of proportion to the identified disease, in 4 patients with unfavorable histopathology (Hurthle cell cancer n:3, tall cell variant n:1), in 4 patients with suspected distant metastasis before thyroidectomy and in 1 patient with rising anti-Tg antibody levels. Patient management was planned based on clinical, laboratory and PET/CT findings. The contribution of PET/CT findings to patient management was evaluated. **Results**: PET/CT detected metastatic cervical and/or mediastinal lymph nodes in 14 patients, lung metastasis in 12 patients, bone metastasis in 2 patients and multiple sites of metastasis in 2 patients. In a patient with tall cell variant, PET/CT was negative. In the light of PET/CT findings, 9 patients were referred to surgery for focused neck dissection or completion compartmental neck dissection and/or metastatectomy. 4 patients received external beam radiotherapy for bone metastasis. 18 patients received I-131 radioiodine therapy with doses of 150-250 mCi. Of these, the findings of PET/CT and post-ablation radioiodine whole body scan were comparable in 13 patients,

PET/CT detected non-radioiodine avid lung and mediastinal metastasis in 4 patients, and 1 patient had radioiodine avid micronodular lung metastasis without FDG uptake. PET/CT provided a change in treatment plans for patients who were referred to surgery or radiotherapy (13/31 patients, 42%). In addition, PET/CT defined extra sites of distant metastasis and changed TNM stage in 4 patients (13%). Totally, in 55% of patients with high risk DTC, PET/BT contributed to patient management in the initial work-up. **Conclusion**: FDG PET/CT, as a part of initial staging algorithm, has an important role on the management of patients with high risk DTC. We consider that, especially in patients with Tg levels out of proportion to the identified disease, PET/CT provides unique opportunity to select patients who may benefit from treatment choices to reduce tumor burden (such as metastatectomy, debulking surgery or external beam radiotherapy) and help to increase therapeutic response to further radioiodine therapies which all result in an improvement of progression-free survival.

## PW009

### $^{131}$I-SPECT/CT in the follow-up of thyroidectomized patients with differentiated thyroid carcinomas (DTC)

**A. Spanu**, F. Chessa, I. Gelo, L. Mele, S. Sanna, S. Nuvoli, G. Madeddu; University of Sassari, Sassari, ITALY.

**Aim**. Conventional planar $^{131}$I-Whole body scan (WBS), which represents routine diagnostic procedure of choice in DTC patients, has some limitations, such as low sensitivity and lack of anatomic land markers which can cause difficulties for foci localizations. We further investigated whether $^{131}$I-SPECT/CT may have an incremental value than WBS contributing to DTC current diagnosis and therapeutic post-operative protocol reassessment. **Method**. We enrolled 612 thyroidectomized DTC patients, 147 classified at high risk (H), 242 of low risk (L) and 223 at very low risk (VL), 14 observed after thyroidectomy before radioiodine therapy and 598 in chronic follow-up; 553/612 patients underwent diagnostic and 59/612 post-therapeutic $^{131}$I-scintigraphy, with total 699 exams. WBS was followed by SPECT/CT in the neck and chest and other suspect regions using dual head gamma cameras (Millennium VG and Infinia Hawkeye; GE Medical System) including low dose x-ray tube. **Results**. In 207/612 patients SPECT/CT identified 459 iodine fixing foci, 348 in the neck and 111 outside the neck. Planar WBS in 154 patients evidenced 328 foci, 260 in the neck and 68 outside the neck, all positive at SPECT/CT. In 65 patients, SPECT/CT evidenced 130 foci occult at WBS which was completely negative in 38/65 cases, with 93/130 foci being malignant. Globally, SPECT/CT ascertained 153 neoplastic lesions in 459 iodine foci, while planar WBS 59, 29 of which classified unclear and only characterized by SPECT/CT. Only SPECT/CT evidenced 7 neck lymph node metastases in 3L and 3VL patients and small size bone metastases in 2H cases with undetectable TG serum levels as well as 8 neck lymph node metastases in 8 patients (1L, 3VL, 4H) and pulmonary small size metastases in 1L and 1H cases with TG levels <2.5 ng/ml. SPECT/CT also characterized 38 physiologic foci unclear at WBS. SPECT/CT obtained an incremental value than planar in 101/207 cases (48.8%) and changed therapeutic management in 66/207 (31.9%). **Conclusion**. $^{131}$I-SPECT/CT improved WBS image interpretation allowing a more accurate iodine fixing foci localization and characterization in our DTC patients showing an incremental value than planar WBS, particularly when the latter is inconclusive and TG levels are undetectable or very low in L and VL cases. Moreover, SPECT/CT correctly modified patients classification defined by WBS permitting more appropriate therapeutic management. Thus, SPECT/CT wider use is suggested and it can contribute to reassess DTC current management protocol.

## PW010

### Comparison of $^{18}$F-FLT PET/CT and $^{18}$F-FDG PET/CT in detection of metastases of differentiated thyroid cancer

**K. Kato**[1], S. Abe[2], T. Odagawa[1], Y. Fujita[1], A. Niwa[1], S. Iwano[1], S. Ito[1], M. Ikeda[1], S. Naganawa[1]; [1]Nagoya University Graduate School of Medicine, NAGOYA, JAPAN, [2]Nagoya University Hospital, Nagoya, JAPAN.

**Purpose:** 3′-deoxy-3′-18F-fluorothymidine ($^{18}$F-FLT) has been recently developed as a PET/CT proliferation tracer. At present, there are no studies investigating its role in differentiated thyroid carcinoma (DTC). The aim of this study was to assess the efficacy of $^{18}$F-FLT PET/CT for the detection of metastases in DTC in comparison with 2-deoxy-2-18F-fluoro-D-glucose ($^{18}$F-FDG) PET/CT. **Methods**: We examined 14 patients (6 women, 8 men; mean age,±14.5 years) with DTC who had undergone total thyroidectomy and were hospitalized to be given $^{131}$I therapy. All patients were examined by $^{18}$F-FLT PET/CT and $^{18}$F-FDG PET/CT before the therapy, and they were examined by $^{131}$I scintigraphy after the therapy. All scans were evaluated by 2 experienced nuclear medicine physicians who were unaware of the clinical data and the results of other imaging studies. The sites of metastases were identified as areas of focally increased uptake, exceeding that of surrounding normal tissue. When the results between the 2 readers differed, they reached a consensus. For semi-quantitative analysis, the maximal standardized uptake value (SUVmax) was calculated in $^{18}$F-FLT PET/CT and $^{18}$F-FDG PET/CT. Radioiodine scintigraphy after the therapy was used to confirm the sites of metastases. **Results**: There were a total of 61 metastases in various regions of all the 14 patients. Forty-one of 61 metastases were detected by $^{18}$F-FLT PET/CT and 43 of 61 metastases were detected by $^{18}$F-FDG PET/CT. The SUVmax values in metastases in various regions were 0.51-14.79 (mean±SD, 2.58±2.58) for $^{18}$F-FLT PET/CT and 2.31-28.21 (7.40±6.38) for $^{18}$F-FDG PET/CT, respectively. The differences between SUVmax for $^{18}$F-FLT PET/CT and that for $^{18}$F-FDG PET/CT were statistically significant in metastases of lungs and lymph nodes, whereas the differences were not significant in metastases of bones, pleura, adrenal gland, liver, and thyroid bed. The sensitivity of $^{18}$F-FDG PET/CT for the detection of bone metastases was higher than that of $^{18}$F-FLT PET/CT, because $^{18}$F-FLT tended to accumulate in normal bones. **Conclusion**: These results suggest that the sensitivities in detecting of metastases of DTC are almost the same in $^{18}$F-FLT PET/CT and $^{18}$F-FDG PET/CT. However, the sensitivity of $^{18}$F-FLT PET/CT for detecting bone metastases of DTC is inferior to $^{18}$F-FDG PET/CT.

PW02 - Sunday, Oct. 20, 8:30 - 9:30, Poster Exhibition Area

# Poster Walk 2 - Radionuclide Therapy & Dosimetry: Internal Dosimetry

## PW011

### Quantitative 177Lu-SPECT/CT imaging and validation of a commercial dosimetry software

**L. D'ambrosio**[1], L. Aloj[1], D. Madesani[2], A. Morisco[1], M. Aurilio[1], A. Prisco[1], F. Di Gennaro[1], S. Lastoria[1]; [1]SC Medicina Nucleare, Fondazione Pascale, Napoli, ITALY, [2]GE Healthcare, Milano, ITALY.

**Aim** 3D dosimetry is an appealing yet complex application of SPECT/CT in patients undergoing radionuclide therapy. In this study we have developed a quantitative imaging protocol and we have validated commercially available dosimetry software (Dosimetry Toolkit Package, GE Heathcare) in patients undergoing 177Lu-DOTATATE therapy. **Materials and Methods** Dosimetry toolkit uses multi SPECT/CT and/or WB planar datasets for quantifying changes in radiopharmaceutical uptake over time to determine residence times. This software includes tools for performing reconstruction of SPECT/CT data, registration of all scans to a common reference, segmentation of the different organs, creating time activity curves, curve fitting and calculation of residence times. All acquisitions were performed using a hybrid dual-head SPECT-CT camera (Discovery 670, GE Heathcare) equipped with medium energy collimator using a triple-energy window. SPECT images were reconstructed using an iterative reconstruction algorithm with attenuation, scatter and collimator depth-dependent three-dimensional resolution recovery correction. Camera sensitivity and dead time were evaluated. Accuracy of activity quantification was performed on a large homogeneous source with addition of attenuating/scattering medium. A NEMA/IEC body phantom was utilized to measure the recovery coefficient that the software does not take into account. The residence times for organs at risk were calculated in five patients. OLINDA-EXM software was used to calculate absorbed doses. **Results** 177Lu-sensitivity factor was 13 counts/MBq*s. Dead time was <3% with 1.11 GBq in the field of view. The measured activity was consistent with the decay-corrected calibrated activity for large volumes (>100 cc). The recovery coefficient varied from 0.71 (26.5 ml) to 0.16 (2.5 ml) in the absence of background activity and from 0.58 to 0.13 with a source to background activity concentration ratio 20:1. The activity concentration measured in the spheres depended on the reconstruction parameter and for the smallest sphere the accuracy increased with increasing numbers of iterations and subsets. The residence time range was 0.33-1.46 hours for lungs, 0.57-3.54 hours for spleen, 0.93-3.58 hours for kidneys and 3.74-8.33 hours for liver. The mean absorbed dose was 0.69 Gy/GBq for liver, 0.76 Gy/GBq for spleen, 0.55 Gy/GBq for kidneys and 0.08 Gy/GBq for lungs. **Conclusion** Quantitative SPECT with Lu-177 has high accuracy both in our phantom and in clinical practice. Dosimetry toolkit simplifies the procedure for quantifying absorbed dose reduces the processing time and improves accuracy of results compared to manual Methods. Software implementation of partial volume correction in the dosimetric workflow is desiderable to obtain more accurate dose estimations.

## PW012

### Cumulated blood activity measurements and modelling in patients with differentiated thyroid carcinoma

**A. Kluczewska-Galka**, J. Roskosz, K. Gorczewski, D. Borys, D. Handkiewicz-Junak, J. Krajewska, B. Jarząb; Comprehensive Cancer Center and M. Skłodowska-Curie Memorial Institute of Oncology, Gliwice, POLAND.

**Introduction:** The purpose of the radioiodine therapy in differentiated thyroid carcinoma (DTC) formulated by the EANM Therapy Committee is to provide advice to nuclear medicine clinicians on how to ablate thyroid remnant or treat inoperable advanced DTC or both employing large 131-iodine activities. The therapy of DTC with radioactive iodine is a standard procedure for the ablation of remnant thyroid tissue following surgery and for the treatment of iodine avid metastases. The level of administered activity in radionuclide therapy is often limited by hematological toxicity resulting from the absorbed dose delivered to the bone marrow. The

purpose of this study is to validate models for calculation of an effective half-life (Teff) of 131I, blood and bone marrow dose in patients with DTC. **Materials and method:** The measurements of 131I concentration in blood samples have been used to estimate the marrow absorbed dose. The administered activity was 100-103 mCi (about 3.7 GBq). In 328 patients, the measurement of the exposure rate was performed at 4, 8, 18, 24, 30, 42, 54, 66 hours after administration of Na131I using well counter ISOMED 1010 for studying the absorbed dose (according to the MIRD schema) and Teff evaluation. To obtain cumulated activity in blood/red marrow two mathematical models of radioisotope elimination were used: mono-exponential and bi-exponential. **Results:** The majority of the activity is excreted by the patients in the first 24 hours after Na131I administration. The effective half-life of 131I ranged from 2 to 37 hours due to the first model. According to the administrated activity, the evaluation of the total absorbed dose by patients to red marrow ranged from 5.5×10-4 to 3.1×10-1 Gy. Bi-exponential model allows estimating an initial income of the 131I concentration, as well as later excretion. More precise model found two subgroups of patients: with fast (~37%) and slow (~63%) kinetics of the 131I in the blood according to the one of the parameters. Slow uptake in the blood cannot be properly estimated by a mono-exponential model. Therefore, it was found that the dose estimated with mono-exponential model was over-estimated. **Conclusions:** Using the two compartment model allows discriminating the patients in two groups with different iodine biokinetics. It is noteworthy that the second model is essential for the patients with the slow kinetics of radioiodine.

## PW013

### A Novel Method for Calculating the Personalized 131I-Iodide Activity for Graves' Disease Patients Based on the Reduction of Thyroid Mass: Results of a Prospective, Randomized Study

**F. Guidoccio**[1], M. Grosso[1], A. Traino[2], F. Orsini[1], G. Puccini[1], E. Tardelli[1], E. Fiasconaro[1], S. Margotti[1], A. Svirydenka[1], R. Boni[1], D. Volterrani[1], G. Mariani[1]; [1]Regional Center of Nuclear Medicine - University of Pisa, Pisa, ITALY, [2]Health Physics Unit, University Hospital of Pisa, Pisa, Italy, Pisa, ITALY.

**Aim:** There is no consensus regarding the most appropriate dosimetric approach to cure Graves' disease with 131I-Iodide. In this study we explored the efficacy of a personalized approach based on the desired therapy-induced volume (mass) reduction in order to define the optimal activity of 131I-Iodide to be administered. **Methods**: A model for calculating the "optimal" final thyroid mass has already been published by our group. Based on sequential measurements of changes in thyroid volume, uptake and kinetics obtained in 40 patients with Graves' disease following 131I-iodide therapy. Based on this model, the optimal thyroid final mass (mfin) can be estimated as follows: mfin=0.24*m0/U0 where m0 and U0 are baseline mass and maximum thyroid uptake, respectively. Starting from the MIRD approach and the Linear Quadratic Model in radiobiology, a final equation was developed to calculate the therapeutic activity based on the desired final mass of the gland. A total of 160 Graves' disease patients treated in our Department were randomly divided into 5 groups based on the level of Absorbed Thyroid Dose (ATD) from 131I-iodide, equal respectively to 100 Gy (Group A, n=29), 200 Gy (Group B, n=25), 300 Gy (Group C, n=27), 400 Gy (Group D, n=29); Group V included 64 patients who received a 131I activity calculated on the basis of the "optimal" desired final thyroid mass. **Results**: At one-year follow-up, 14/29 patients of Group A (48%), 16/25 patients of Group B (64%), 25/27 patients of Group C (93%), 28/29 patients of Group D (97%), and 60/64 patients of Group V (94%) were cured. A significantly higher proportion of patients were cured in Groups C, D and V than in Groups A and B (P<0.01), while there was no statistical difference between cure rate in Groups C and D versus Group V. The average ATD was 300±13 Gy for Group C and 407±23 Gy for Group D, significantly higher than for Group V (277±75 Gy, P<0.01), as also significantly higher was the administered 131I activity (452 ±190 MBq and 524±201 MBq respectively versus 386±173 MBq, P<0.01). Administered activities in Groups A and B were 223±201 MBq and 266±129 MBq, respectively, with average ATDs of 106±12 Gy and 204±9 Gy. **Conclusions**: These results confirm that our novel method based on thyroid-mass reduction allows optimization of 131I-iodide therapy for Graves' disease on an individual basis, achieving a high therapeutic efficacy and avoiding administration of unjustified higher activities of 131I-Iodide.

## PW014

### SPECT/CT Images in the Calculation of Absorbed Dose Ratio Between Radiosynovectomy Procedures with 153Sm-HA and 90Y-HA

M. E. G. Seren, M. L. Oliveira, F. C. Rocha, **S. Q. Brunetto**, C. H. P. V. Cerqueira, A. O. Santos, R. P. M. Oliveira, C. D. Ramos; University of Campinas, Campinas, BRAZIL.

Heterogeneity in the intra-articular distribution of hydroxyapatite (HA) labeled with $^{90}$Y or $^{153}$Sm at radiosynovectomy (RSV) procedures can be detected by use the fusion between transmission (SPECT) and emission (CT) tomographic images. To avoid this heterogeneity, commonly it is preferred to use $^{90}$Y over $^{153}$Sm assuming that the larger penetration range of the emitted beta particles will make the absorbed dose distribution more uniform. In this study, we evaluated the validity of this assumption by determining the affected area of RSV procedures in human joints treated with $^{90}$Y-HA and $^{153}$Sm-HA. Using SPECT/CT images of 3 patients treated with $^{90}$Y-HA (185MBq) or $^{153}$Sm-HA (740MBq), a voxel-by-voxel (voxel size=9.06mm$^3$) analysis was performed to build 3D distribution of $^{90}$Y and $^{153}$Sm activity. With the 3D image of the activity correlated to the mass of each voxel, provided by CT images via Housfield scale, the absorbed dose was calculated using the generic equation of absorbed dose rate and the average range of beta particles emitted from $^{90}$Y and $^{153}$Sm. We have chosen the generic dose equation rather than the MIRD model of voxel dosimetry or the Dose-Point Kernel method because the later models do not allow for a voxel mass dependent dose calculation. In addition, there is little information on $^{153}$Sm data and voxel sizes in these models. Considering the average energy and the therapeutic range of emitted beta particles we concluded that the dose in each voxel is not affected by the activity of neighboring voxels. Difference in the RSV procedures using $^{90}$Y-HA and $^{153}$Sm-HA should be just the dose difference per activity injected. Collisional Stopping Power shows us that the relative dose between these two compounds is 4.12:1. With these results we conclude that beta particles emitted from $^{90}$Y and $^{153}$Sm do not have range enough to reach cold spots found in heterogeneous distributions of radionuclide at RSV. Hence the spatial dose distribution of both $^{90}$Y and $^{153}$Sm are the same with respect to their activity distribution and HA distribution. The use of relative activities of approximately 1:4 of $^{90}$Y-HA or $^{153}$Sm-HA should provide similar therapeutic effects for RSV.

## PW015

### Relationship of tumor absorbed doses of 177Lu-DOTA-TATE treatment and uptake in pre-therapeutic Ga68 DOTA-TATE PET/CT imaging

**E. Demirci**[1], L. Kabasakal[1], N. Yeyin[1], M. Ocak[2], T. Toklu[3], N. Selcuk[4], B. Kanmaz[1]; [1]Istanbul University, Cerrahpasa Faculty of Medicine, Department of Nuclear Medicine, Istanbul, TURKEY, [2]Istanbul University, Pharmacy Faculty, Department of Pharmaceutical Technology, Istanbul, TURKEY, [3]Yeditepe University Medical School, Department of Nuclear Medicine, Istanbul, TURKEY, [4]Yeditepe University Medical School, Department of Nuclear Medicine, Istanbul, Turkey, Istanbul, TURKEY.

**Introduction/Background** Peptide Receptor Radionuclide Therapy (PRRT) with labeled Lu-177 labeled peptide in patients with neuroendocrine tumors (NETs) aroused great interest. An estimation of actual radiation doses to tumors is very important for therapy planning. It is well known that uptake of Ga-68 DOTATATE very well correlated with sst2 expression. The uptake of radiolabelled peptides calculated from SUV max values may predict the radiation-absorbed dosimetry of lesions treated with PRRT. AIM: The aim of the study was to evaluate the relationship between the tumor absorbed doses and pre-therapeutic Ga-68 DOTA-TATE PET/CT uptake calculated from SUV values. **Materials and Methods**: PRRT results of patients (M/F: 8/5, mean age: 55.5±12.5) with histologically proven inoperable NETs were retrospectively analyzed. Dosimetric calculations were performed using MIRD scheme and lesion doses were calculated using post therapy whole body images obtained at 4, 20, 44, and 68 hours after injection. Calculated tumor absorbed doses were compared with SUVmax of 68 Ga-DOTA-TATE PET/CT, which were performed before the therapy. Tumor volumes were determined from CT images. Thirteen blood samples beginning from time zero to 4 days after injection were obtained for bone marrow and whole body dosimetry. **Results**: There were 38 lesions in 13 patients. Lesions were selected according to lesion delineation and superimposed lesions were excluded. Mean lesion volume was 19.58±25 cm3. Median tumor dose for all lesions, bone lesions, lesions on other sites (lung, liver, lymph nodes) were 15.08 Gy, 19.34 Gy, 14.05 Gy per 370 MBq respectively. Median SUVmax values of those were 25.8, 13.7, 23.05, respectively. Correlation between calculated tumor dose and uptake of 68Ga-DOTA-TATE was modarete (R=0.42). Also a moderate correlation was found for radiation absorbed doses of bone metastases. A very low correlation was found for radiation absorbed doses of lung, liver and lymph nodes metastases. **Conclusion**: The uptake of radiolabelled peptides calculated from SUV max values may predict the radiation-absorbed dosimetry of lesions treated with PRRT and it may be used for prognostic evaluation and therapy outcome. KEYWORDS Tumor absorbed doses, PRRT, PET imaging

## PW016

### Calculation of voxel S values for electrons and photons in different human tissues

**E. AMATO**[1], A. Italiano[2], S. Baldari[1]; [1]UNIVERSITA' di MESSINA, Messina, ITALY, [2]Istituto Nazionale di Fisica Nucleare, Messina, ITALY.

**Aim** Voxel dosimetry is the simplest and most widespread approach to internal dosimetry of nonuniform activity distributions in radionuclide therapies and in estimations of radiation hazard due to internal contamination. However, voxel S value (VSV) data are currently available only for soft tissues. Aim of the present

work is to extend our approach to the calculation of VSVs to materials different from the soft tissue. **Materials and Methods** We developed a Monte Carlo simulation in Geant4 of a voxelized region of each material in which the source of monoenergetic electrons or photons is uniformly distributed within the central voxel, and the energy deposition was scored over the surrounding 11x11x11 voxels. VSVs were obtained for the following standard ICRP materials: Adipose tissue, Bone cortical, Brain, Lung, Mucle skeletal and Tissue soft. We also considered the standard ICRU materials: Bone compact and Tissue soft with four elemental components. Our results were compared with literature data, when available. **Results** VSVs were represented as a function of the "normalized radius", defined as the ratio between the distance between source and target voxel centers and the voxel side. We found that VSVs and related analytical fit functions are mainly affected by the tissue density, while the material composition gives only a slight contribution to the difference between VSV data series, which is negligible for the practical purposes. **Conclusions** Our results can be useful to broaden the dosimetric three-dimensional approach based on VSVs to other tissues where diagnostic and therapeutic radionuclides can be taken up and radiation can propagate.

## PW017

### Correlation between radiolysis of $^{111}$In- or $^{177}$Lu-labelled methionine-containing regulatory peptides and absorbed dose (Gy).

**E. de Blois**, M. Konijnenberg, H. S. Chan, R. de Zanger, W. A. P. Breeman; Erasmus MC, Rotterdam, NETHERLANDS.

**Aim:** Radiopeptides in small volumes are prone to radiation damage with initial dose rates ≥10 Gy/h. High specific activities (high activity (MBq) and at low peptide mass (nmoles)) are needed for optimal imaging and therapy in preclinical studies of receptor-mediated processes with peptides, like minigastrin (MG) and bombesin. These small methionine-containing regulatory peptides oxidise rapidly. Radiolysis of radiopeptide means decreased RCP. Radiolysed radiopeptide has lost receptor affinity with subsequent decreased imaging quality and therapeutic effect. Here, we present our method how to measure radiochemical purity (RCP) and quantify radiolysis of these radiolabelled peptides by using reversed phase HPLC $C_{18}$ gradient. Absorbed doses were calculated in the reaction vial during radiolabelling and storage of radiopeptides. We investigated the relation of the absorbed dose (Gy) and RCP of $^{111}$In- or $^{177}$Lu-labelled methionine-containing peptides. **Materials and Methods:** Absorbed dose rates were determined assuming a spherical geometry as obtained in the reaction vials. RCP of these peptides was measured without quenchers and relation between radiation dose and radiolysis established. The presence of quenchers will underestimate the influence radiolysis. DOTA-MG11 and DOTA-Tyr$^4$-bombesin was used as models for methionine-containing regulatory peptides. **Results:** According to our calculations, 110 MBq $^{111}$In and 23 MBq $^{177}$Lu in a final volume of 200 µL have similar dose rates (4.3 mGy/s vs. 4.2 mGy/s), leading to doses at 24h of 255 Gy and 209 Gy, respectively. If under these conditions no radiolysis can be detected, HPLC-separation need optimalisation. We found a linear correlation between RCP and absorbed dose during these 24h. This provides the possibility to predict RCP of radiopeptides, using the absorbed dose as indicator. **Conclusions:** Radiation induced radiolysis of radiopeptides shows a linear relation with absorbed dose. High activities of radiolabelled peptides in small volumes, should always be combined with quenchers to maintain high RCP.

## PW018

### Absorbed Dose Calculation of the Energy Deposition close to Bone, Lung and Soft Tissue Interfaces in Molecular Radiotherapy

**M. Fernandez**, M. Lassmann; (Department of Nuclear Medicine) University of Würzburg, Würzburg, GERMANY.

**Aim**: For voxel-based dosimetry in molecular radiotherapy (MRT) based on tabulated voxel S-Values these values are usually obtained only for soft tissue. In order to study the changes in the dose deposition patterns at interfaces between different materials we have performed Monte Carlo simulations. **Methods:** The deposited energy patterns were obtained using the Monte-Carlo radiation code MCNPX v2.7 for Lu-177 (medium-energy) and Y-90 (high-energy). The following interfaces were studied: soft tissue-bone and soft tissue-lungs. For this purpose a volume of soft tissue homogeneously filled with Lu-177 or Y-90 was simulated at the interface to three different volumes containing no activity: soft tissue, lungs and bone. The emission was considered to be isotropic. The dimensions were chosen to ensure that the energy deposited by all generated particles was scored. The materials were defined as recommended by ICPR46; the decay schemes of Eckerman and Endo were used. With these data the absorbed dose patterns normalized to the maximum absorbed dose in the source region (soft tissue) were calculated. **Results**: The absorbed dose fractions in the boundary with soft tissue, bone and lungs are 50%, 47% and 57%, respectively, for Lu-177 and 50%, 47% and 51% for Y-90. The distances to the interface at which the absorbed fractions are at 0.1% are 1.0, 0.6 and 3.0 mm for Lu-177 and 7.0, 4.0 and 24 mm for Y-90, for soft tissue, bone and lungs respectively. **Conclusions**: In MRT, the changes in the absorbed doses at interfaces between soft tissue and bone/lungs need to be considered for isotopes emitting high energy particles.

## PW019

### Methodological Effects in Kidney Dosimetry in Lu-177 Radionuclide Therapy

**J. Heikkonen**, H.Mäenpää, M.Tenhunen; Helsinki University Central Hospital, Department of Oncology, Helsinki, FINLAND.

The aim of this study was to calculate the absorbed radiation dose in Lu-177 DOTATATE treatments to the kidneys of patients with metastasized neuroendocrine tumours and compare the radiation doses obtained with small volume and kidney volumetric analysis. **Methods**: For 40 patients (23 males, 17 females) in 120 treatments absorbed doses to both kidneys were calculated. One patient had five cycles, 19 patients four cycles, 8 patients three cycles, 3 patients two cycles and 9 patients one cycle. Each patient received amino acid solution 30 minutes before and 8 hours after treatment to reduce the kidney dose. The injected activity was 7.4 GBq (88 treatments) or 3.7 GBq (32 treatments) and therapy cycles were repeated every eighth week. SPECT/CT studies were made 24h, 48h, 72h (or 120h) and 168 h after injection with Siemens Symbia T2. The window was set over the 208 keV photopeak. Attenuated and scatter corrected counts from kidney volumes were registered with volumetric analysis both from right and left kidney and also with small volume (4 cm3) technique. Dosimetric calculations were done with OLINDA/EXM software using mono-exponential time activity curve fitting. Results: The mean radiation dose for kidneys (67-208 cm3) in one cycle was 2.9 Gy (0,48 mGy/MBq) range 0.8-7.7 Gy using kidney volumetric analysis and 4.8 Gy (0.80 mGy/MBq) range 1.3-15.4 Gy using small volume analysis. Twenty patients received four cycles. In this group radiation dose to the kidneys in the first cycle was 2.8 Gy (range 1.0-5.3 Gy) in second 2.5 Gy (range 0.7-3.9 Gy), in third 3.2 Gy (range 1.3-6.4 Gy) and in fourth cycle 3.2 Gy (range 1.5-7.7 Gy). Small volume technique yielded 1.7 times (range 1.0-2.2) higher radiation doses compared with volumetric analysis. The cumulative administered doses in four cycle treatments were 14.0-29.3 GBq. The effective half live for kidneys was 45 h (range 30-110 h). The highest kidney dose was 20,5 Gy and this patient received activity of 21.9 GBq in four cycles. Treatments of one patient was stopped after three cycles because of high kidney doses. Upper limit for kidney dose 23 Gy would have been exceeded. **Conclusions:** Because of considerable large variation between patients in absorbed radiation kidney doses, individual dosimetry is desirable. Especially dosimetry during the first and third cycle are important. There is a need for separate cut off levels for absorbed doses depending on method used for calculation.

## PW020

### Patient-Specific Dosimetry of $^{99m}$Tc-HYNIC-Tyr$^3$-Octreotide in Patients with NeuroEndocrine Tumors

**M. T. Chalkia**, A. P. Stefanoyiannis, A. Prentakis, S. N. Chatziioannou, E. P. Efstathopoulos; University General Hospital of Athens "Attikon", Athens, GREECE.

**Aim:** A high concentration of somatostatin receptors is expressed in NeuroEndocrine Tumors (NETs). The relatively new radiopharmaceutical $^{99m}$Tc-HYNIC-TOC ($^{99m}$Tc-hydrazinonicotinamide-Tyr$^3$-Octreotide) is a somatostatin analogue which binds to somatostatin receptors with high affinity (particularly subtype 2 and, to a lesser extent, subtypes 3 and 5). Consequently, its use in clinical practice for the diagnosis of NETs is gradually gaining acceptance. The aim of this study is to present a 2-dimensional image-based dosimetric protocol for the commercially available $^{99m}$Tc-HYNIC-TOC. Application of this protocol results in the estimation of absorbed dose values for several organs and tumors, shedding light to the eligibility of patients for potential subsequent Peptide Receptor Radionuclide Therapy (PRRT). **Materials & Methods:** Four patients (three females, one male) with metastatic NETs were administered with 725-920 MBq of $^{99m}$Tc-HYNIC-TOC. Anterior and posterior whole-body scans were acquired at 0, 2, 4, 5, 24 and 27 h p.i. using a single-head gamma camera. A SPECT scan was additionally obtained at 4 h p.i. for tumor localization. Quantitative analysis of planar images was based on the conjugate view method. Raw data were corrected for attenuation, self-attenuation, scatter and background activity. Absorbed doses were estimated using the MIRD schema. Volumes of organs and tumors were also obtained from planar images. Preliminary phantom-based validation of activity and volume estimated values was carried out. The % deviation of nominal and estimated activity and volume values was subsequently introduced in the dosimetric protocol, in the form of corresponding correction factors, which further enhance the precision of patients' dosimetric results. **Results:** The ranges of absorbed doses per unit of administered activity estimated for organs and tumors are: § Kidneys: 0.010 - 0.026 mGy/MBq § Spleen: 0.041 - 0.065 mGy/MBq § Liver: 0.005 - 0.021 mGy/MBq § Urinary bladder: 0.007 - 0.042 mGy/MBq § NETs: 0.005 - 0.028 mGy/MBq **Conclusion:** The dosimetric results of this study are in agreement with other published data, demonstrating that even a simple patient-specific 2-dimensional dosimetric protocol, relatively easily adopted in clinical routine, can be proved

efficient. Despite the fact that spleen receives the highest absorbed dose, kidneys are considered to be the dose-limiting organs in case of subsequent PRRT, due to their higher radiosensitivity. Significant interpatient dose and volume variations in organs and tumors necessitate the application of patient-specific dosimetry.

PW03 - Sunday, Oct. 20, 8:30 - 9:30, Poster Exhibition Area

## Poster Walk 3 - Conventional & Specialised Nuclear Medicine: Infection

### PW021

### Hybrid SPECT-WBC/MRI in Detection of Osteomyelitis in Patients with Diabetic Foot

**M. Zorkaltsev**, V. Zavadovskaya, O. Kilina, A. Kurazhov, V. Udodov, M. Zamyshevskaya; Siberian State Medical University, Tomsk, RUSSIAN FEDERATION.

The aim of the study was to evaluate the diagnostic value of SPECT-WBC/MRI in detection of osteomyelitis in patients with diabetic foot. **Material and Methods**. 76 patients were examined (35 males and 41 females, aged 59.4±7.1 years), with diabetes mellitus type I and II, and with suspicion of osteomyelitis. 76 scintigraphies with 99mTc-HMPAO labeled leukocytes (370 MBq; SPECT Philips Brightview) and 30 MRI (Siemens Essenza 1.5T; T1WI, T2WI, PD-FSat) were obtained. 39 results were verified by a morphological study, other cases were observed conservatively. Fusion of SPECT and MRI (T1WI, PD-FSat) was performed in the program RView 9.06 (Colin Studholme). **Results**. When used alone of WBC-SPECT in the case of diagnosis of intraosseous inflammation, 25 TP, 38 TN, 12 FP and 1 FN results were obtained. FP results were caused by difficulty in determining the localization of the pathological accumulation of WBC due to the low resolution of the method and the small size of the object. One FN result was identified in the ischemic form of diabetic foot, because of the reduced blood flow. When using MRI 15 TP, 10 TN, 3 FP and 2 FN results were obtained. Relatively low specificity of MRI was due to the presence of false positive results due to the complexity of the differential diagnosis of bone marrow edema and inflammatory infiltration. In the case of SPECT-WBC/MRI (the diagnostic criterion was the maximum accumulation of radiopharmaceutical in the projection of the bone, determined by MRI), was obtained 17 TP, 11 TN, 1 false positive (FP) and 1 FN results. Identified FP and FN results were due to the complexity of fusion of toes. **Conclusion**. Comparison of the MRI (sensitivity - 88.2%, specificity - 76.9%, accuracy - 83.3%), WBC-scintigraphy (sensitivity - 96.2%, specificity - 76.0%, accuracy - 82.9%) and WBC-SPECT/MRI showed higher diagnostic performance of hybrid research method (sensitivity, specificity, and accuracy were 94.4%, 91.7%, and 93.3%, respectively). There remains a need of a separate assessment of MRI data for a detailed assessment of periarticular structures and bones.

### PW022

### The value of 18FDG-PET for the detection of infected hip prosthesis.Can we find a specific uptake pattern for septic loosening?

**E. Tabacchi**[1], S. Cambioli[1], C. Nanni[1], E. Zamparini[2], J. Morigi[1], P. Viale[2], L. Raumer[2], M. f. Ciliberti[2], G. Pignatti[3], S. Fanti[1]; [1]Nuclear Medicine Department, University Hospital S.Orsola-Malpighi, Bologna, ITALY, [2]Infective Diseases Unit, University Hospital S.Orsola-Malpighi, Bologna, ITALY, [3]Revision Surgery of Hip Prosthesis and Development of New Implants Division, Rizzoli Orthopaedic Istitute, Bologna, ITALY.

**Aim:** The Aim of this study is to evaluate the sensitivity and specificity of fluorine-18 labelled 2-fluoro-2-deoxy-D-glucose positron emission tomography (18FDG PET/CT) in the detection of infected hip prosthesis and to find a possible specific uptake pattern related to septic loosening. **Materials & Methods**: 18 patients (pts) were enrolled: 9 pts with hip prosthesis and clinical suspected infection and high CRP value, 9 patients with hip prosthesis without clinical suspected infection (asyntomatic control group). PET/CT scan was performed following standard procedure (images acquired 60 minutes after the injection of 370 MBq of $^{18}$F-FDG in pts with 6 hours fasting). Coltural exam of samples obtained by surgery or by needle aspiration and/or clinical follow up were used as the gold standard. The 18FDG-PET scans of pts with clinical suspected infection of the prosthesis were compared with the distribution pattern of the tracer in the asymptomatic control group. **Results**: In 9 pts with hip prosthesis without clinical suspected infection a recurrent pattern of slightly increased tracer uptake (mean SUVmax 2,5) around the femoral neck (in proximity to the anterior-lateral portion of the femoral head) and, to a lesser degree, around the trochanter major, were detected. In the remaining 9 pts with a diagnosis of infected prosthesis (confirmed by gold standard), a significant increased uptake (mean SUVmax 7,6) was observed at the head, neck and stem-prosthesis interface (in 4\9 cases in the femoral head and neck area and in a part of the bone-acetabular cup, in 5\9 cases in the femoral head and neck area and in the proximal portion of the steam) and in periprosthetic soft tissue. Based on ROC analysis, a SUVmax cut-off of 5,7 yielded to a sensitivity and specificity of 77% and 89%, respectively and AUC (area under the ROC curve) to 0,97 (97%). **Conclusions**: Positron emission tomography based on 18FDG PET could be a valid option when a septic loosening specific uptake pattern is identified. In this preliminary study, 18FDG PET scans were suggestive of sepsis when increased uptake was observed at the head, neck and stem-prosthesis interface and in periprosthetic soft tissue, while a limited uptake (around the femoral neck and in proximity to the anterior-lateral portion of the femoral head of the prosthesis) was aspecific and considered to be the normal pattern of a hip prosthesis on a PET/CT scan. However no clear explanation for this phenomenon is currently available.

### PW023

### The connection between joint inflammation activity and myocardial perfusion alterations in patients with rheumatoid arthritis.

**D. N. Shulgin**, D. R. Olisaeva, O. A. Fomicheva, V. B. Sergienko, K. P. Ivanov; Russian Cardiology Research and Production Complex, Moscow, RUSSIAN FEDERATION.

With increasing frequency the scientists point out inflammation factor as the key mechanism, resulting in incidence of myocardial diseases. Wherefore it is particularly challenging to study not only myocardial perfusion, but also inflammation activity in joints in cases of rheumatoid arthritis (RA) by means of single-photon emission computed tomography (SPECT), as a possible diagnostic criterion for diagnostics and subsequent approach to patients. Purpose: Study of the patients, suffering from RA, by means of SPECT of the clinical features of myocardial perfusion with the application of 99mTc-MIBI (4,2-methoxyisobutyl isonitrile). Detection of relation between changes of myocardial perfusion and activity of arthritis on the basis of quantitative assessment data by means of bone scintigraphy with 99mTc-pyrophosphate. **Materials and Methods**: 50 patients, aging from 30 to 65 years old with confirmed RA, were included into the study. 23 men and 27 women. Patients took cytostatics, glucocorticosteroids, non-steroidal anti-inflammatory drugs. All patients underwent SPECT-scanning of myocard with subsequent assessment of perfusion and whole-body scintigraphy and quantitative scintigraphy of knee joints. DAS28 scale was used to asses RA activity of the patients. **Results**: In the course of the result analysis there were detected the following correlation dependences between the number of affected joints and activity index r=0,457 (p=0,01); the number of affected joints and DAS-28 r=0,688 (p=0,05); accumulation index and DAS-28 r=0,3 (p=0,05); accumulation index and volume of transient ischemia r=0,342 (p=0,05); area of myocardial injury and accumulation index r=0,503 (p=0,01); depth of myocardial injury and accumulation index r=0,389 (p=0,01). **Conclusion**: Presence of correlation dependence between accumulation index and DAS-28 suggests that quantitative scintigraphy is an important diagnostic criterion in evaluation of RA activity. Correlation between accumulation index and myocardial injury indicates the necessity of preventive evaluation of myocardial perfusion of the patients with RA.

### PW024

### Detection of Abdominal Infections using Radiolabeled Antibiotic

**V. Artiko**[1,2], D. Sobic-Saranovic[2], N. Petrovic[2], M. Petrovic[2], S. Pavlovic[2], V. Obradovic[2]; [1]Clinical Center of Serbia, BELGRADE, SERBIA, [2]Faculty of Medicine, University of Belgrade, Belgrade, SERBIA.

**Introduction**: Among a lot of radionuclide Methods currently used, only radiolabeled antibiotic is claimed to be the one able to distuinguish inflammation from infection. Purpose: The aim of the study is detection of the abdominal infective foci using 99mTc-ciprofloxacin obtained by original method from Laboratory for radioactive isotopes, Vinca. **Patients and Methods**:Total of 65 patients with clinical suspicion on abdominal or gastrointestinal infection were investigated. Labeling og 3,5 mg ciprofloxacin chloride was performed with 555 MBq 99mTc in 3 ml of physiological solution, mixed and incubated for 20 min. Scintigraphy was performed after 4h (whole body, SPECT) and 24h (spot views) after slow i.v. injection. **Results**: There were 34 true positive (TP) findings (5 perianal fistulas, 11 subhepatic, 12 abdominal and 6 liver abscesses), 20 true negative (TN) (5 pneumonias, 4 liver cysts, paravertebral lipoma, 2 Tu pp Wateri, 8 FUO), 8 were false negative (FN) (4 abscesses subphrenic and 4 M.Crohn) while 4 were false positive (3 intestinal obstructions,vascular tumour). The smallest lesion found was 18x18 mm. SPECT increased the number of TP findings from 25 to 34. Infections were caused by: Echerihia coli (20), Proteus mirabilis (6), Pseudomonas aeruginosa (4) and Klebsiella (2), while in 2 patients only surgicaly confirmation existed. In 4 FN patients, infection was caused by anaerobes, while in the remaining 4 E.coli was found. **Conclusion**: Scintigraphy with 99mTc-ciprofloxacin is useful method for detection and assessment of exact localization of deep seated bacterial infections, which is very important for surgical intervention.

### PW025

### Tc99m-HMPAO-labeled leucocyte scan in the diagnosis of OM complicating fractures in the appendicular skeleton

**S. Georga**[1], D. Lo-Presti[1], S. Fares[2], I. Iakovou[1], P. Christodoulou[3], K. Badiavas[1], V. Balaris[1], D. Katsaboukas[1], V. Nikos[1], A. Doumas[1], G. Kapetanos[2], N. Karatzas[1]; [1]3rd Dept of Nuclear Medicine, Aristotle University Medical School, Papageorgiou Hospital, Thessaloniki, GREECE, [2]3rd Clinic of Orthopaedic Surgery, Aristotle University Medical School, Papageorgiou Hospital, Thessaloniki, GREECE, [3]2nd Orthopaedic Dept, 424 General Military Hospital, Thessalonoki, GREECE.

**Introduction-Aim:**Diagnosis of osteomyelitis (OM) complicating fractures is often difficult. Multiphase bone scan (BS) is highly sensitive but not specific for diagnosing infection in injured bone, while CT and MRI are frequently unable to diagnose infection around metallic implants. The aim of the study was to evaluate the efficacy of $^{99m}$Tc-HMPAO-labeled leucocyte scan (LS), alone and combined with $^{99m}$Tc-tin-colloid bone marrow scan (BMS), for diagnosing OM complicating fractures in the appendicular skeleton. **Patients and Methods:** Forty two patients with clinical suspicion of OM in sites of fractures in the appendicular skeleton, with or without surgical intervention, were enrolled in the study. Sites of suspected infection were: femur (n=16), tibia (n=14), ankle joint (n=6), calcaneous (n=4) and humerus (n=2). Seventeen patients had metallic implants, in 17 the endoprostheses had been previously removed, while 8 had non-union fractures. All patients underwent LS followed by BMS in 23 of them. LS images showing markedly increased leucocyte uptake at the site of suspected infection, compared with leucocyte uptake in the adjacent or contralateral bone, was compatible with infection. When LS were interpreted together with BMS, incongruent LS/BMS images indicated infection, while congruent LS/BMS images indicated active bone marrow. Final diagnosis was based on clinical evolution or bone biopsy. **Results:** Among the 42 fracture sites investigated, 13 cases of OM and 29 uninfected fracture sites were finally diagnosed. Sensitivity,specificity, accuracy, positive (PPV) and negative predictive value (NPV) of LS alone for diagnosing OM complicating fractures were 92.3%, 93.1 %, 92.8%, 85.7% and 96.4% respectively.The same parameters for combined LS/BMS were 85.7%, 94.1%, 95.7%, 85.7% and 94.1% respectively. There were 2 false positive LS results due to leucocyte accumulation at sites of active bone marrow or inflammatory reaction associated with healing process. There was one false negative LS result, in a patient with tibial fracture and clinical evidence of extended soft tissue infection, attributable to regional elevated tissue pressure, secondary to inflammatory response, causing reduced leucocyte inflow in the infected site.The addition of BMS improved accuracy of LS from 92.8% to 95.7%reducing false positive results on LS. **Conclusion:** LS is an effective imaging modality for diagnosing OM complicating fractures in the appendicular skeleton. The addition of bone marrow scan is useful, in cases of nondiagnostic positive leucocyte scans, to differentiate infection from active bone marrow. With an accuracy of 95.7%, combined LS/BMS represents the optimal procedure to diagnose OM complicating fractures.

## PW026

### The impact of PET/CT in the management of patients with Wegener's Granulomatosis

**O. OZMEN**[1], E. TATCI[1], A. GOKCEK[2], D. KOKSAL[3], Y. DADALI[2], E. OZAYDIN[4], N. ARSLAN[5]; [1]Atatürk Chest Diseases and Thoracic Surgery Training and Research Hospital, Nuclear Medicine Department, Ankara, TURKEY, [2]Atatürk Chest Diseases and Thoracic Surgery Training and Research Hospital, Radiology Department, Ankara, TURKEY, [3]Atatürk Chest Diseases and Thoracic Surgery Training and Research Hospital, Chest Diseases Clinic, Ankara, TURKEY, [4]Atatürk Chest Diseases and Thoracic Surgery Training and Research Hospital,Pathology Department, Ankara, TURKEY, [5]Gulhane Military Medical Academy and Medical Faculty, Nuclear Medicine Department, Ankara, TURKEY.

**Background:** Wegener's granulomatosis (WG) is a rare disorder characterized by granulomatous necrotizing vasculitis which mainly affects small and medium-sized vessels. While the classical triad of involvement is upper and lower respiratory system and glomerulonephritis, WG may involve any part of the body. The aim of this study is to investigate the role of PET/CT (positron emission tomography/ computed tomography) in the evaluation and follow-up of patients with WG. **Methods:** Thirteen FDG-PET/CT imagings obtained from 12 patients with WG were retrospectively evaluated. The demographic data, clinical and laboratory findings of each patient were recorded from the hospital files. **Results:** Six males and six females with a mean age of 44±11.8 years (range: 28-63) were retrospectively analyzed. Lung (n=12), parafaryngeal space (n=7), nose (n=7), and ear (n=4) were the most common disease sites detected on PET/CT. All of the patients have solitary or multiple pulmonary nodular/ mass lesions on CT sections. SUVmax of these lesions were all increased with a mean SUVmax value 12 ± 4.1 (range: 3.53-19.51). In two PET/CT scans performed after treatment, there were no significant FDG uptakes. Upper respiratory system and additional organ involvements such as great vessels, ear, spleen, duedonum, trachea, and adrenals are more accurately detected by PET/CT. Urine analysis, BUN and creatinine levels are still the best way for diagnosis of renal involvement. **Conclusion:** In patients with WG, PET/CT is valuable in the evaluation of disease extention, hence, to initiate appropriate immunosupressive therapy. PET/CT may also help to determine therapy response and detect appropriate site for biopsy.

## PW027

### PET/CT study with 18F-FDG-labeled leukocytes: the first experience

T. Dautov[1], T. Nurgozhin[2], **A. Saduakassova**[3], Y. Ilin[3], I. Tleulessova[3], M. Jakanova[3]; [1]National Research Cardiac Surgery Center, Astana, KAZAKHSTAN, [2]Nazarbayev University, Astana, KAZAKHSTAN, [3]Republican Diagnostic Center, Astana, KAZAKHSTAN.

The aim of our study is the identification of differential diagnostic criteria of inflammatory and cancer diseases using 18F-FDG-labeled autologous leukocytes. This work started in 2012. Before basing on the method of labeling leukocytes by 18F-FDG, we decided to conduct studies on healthy individuals and verify the effectiveness of labeling leukocytes, holding control of radionuclide purity of the samples and determining the most effective exposure time of 18-FDG-labeled leukocytes substance with the calculation of equivalent dose of radioactivity. **Materials and Methods**: When obtaining informed consent, we examined 20 healthy volunteers (17 women and 3 men). The study population had a mean age of 47-48 years (age range 27-68 years). PET/CT imaging was performed in "Total body mode" on "Gemini GXL-16" unit by Philips. Same patient underwent PET\CT study twice, firstly with 18-FDG and then with 18F-FDG-labeled autologous leukocytes in 3-5 days. The coincidence of injected doses of radiopharmaceutical was strictly accounted during the first and repeated examinations. The availability of results of detailed blood analysis was a mandatory for volunteers for further analysis of the correlation with the quantitative results of accumulation. As important stage of work was marked the examination of smears of blood after centrifugation to assess and quantify the "living leukocytes" in the resulting substance. To perform the research a physicist, chemist-analyst, radiofarmaceut, physician-cytolog and nuclear medicine physicians were involved. **Results:** The results of monitoring radionuclide purity showed a 56% match of the measurements to theoretical calculated data. The exposure time of made substance was 1 hour for the most patients (70%). Evaluation of PET\CT image was built on comparison of accumulation of 18F-FDG and 18F-FDG-labeled autologous leukocytes in the parenchyma of liver and spleen. There was observed the increase of accumulation of 18F-FDG-labeled autologous leukocytes in spleen parenchyma compared to accumulation in liver parenchyma, with the following percentage rate: 11% in 4 patients, 17% in 2 patients, 19% in 6 patients, 22% in 3 patients, 24% in 4 patients and 27% in 1 patient. The correlation between number of leukocytes in blood and SUV index with the accumulation in the spleen parenchyma was quite important, as with an increase of leukocytes in blood the increase of the accumulation of 18F-FDG-labeled autologous leukocytes in spleen was observed. **Conclusion**: The effectiveness of labeling leukocytes by 18F-FDG has a place in PET/CT study, which we will use in the future at the differential diagnosis of malignant and inflammatory diseases.

## PW028

### Differentiating pedal osteomyelitis from Charcot osteoarthropathy: value of labeled leucocyte scan and MRI

**S. Georga**[1], G. Arsos[1], C. Manes[2], D. Skoutas[2], V. Nikos[1], G. Tsiantas[2], I. Iakovou[1], V. Balaris[1], D. Katsaboukas[1], D. Lo-Presti[1], A. Doumas[1], N. Karatzas[1]; [1]3rd Dept of Nuclear Medicine, Aristotle University Medical School, Papageorgiou Hospital, Thessaloniki, GREECE, [2]Diabetes Center, Papageorgiou Hospital, Thessaloniki, GREECE.

**Introduction-Aim**: Clinical and radiographic identification of osteomyelitis (OM) superimposed on Charcot arthropathy (CA) is difficult. The aim of the study was to evaluate the diagnostic accuracy of 99m Tc-HMPAO-labeled leucocyte scan (LS) and MRI for diagnosing OM complicating CA in diabetics.Patients and Methods:Forty four diabetic patients with radiographic evidence of CA (5 bilateral) and clinical suspicion of mid/hind foot OM were included in the study. 26 patients had concomitant plantar ulcers. All patients underwent 99mTc-MDP-three phase bone scan (BS) and LS. In 4 patients 99m Tc-tin-colloid bone marrow scan (BMS) was also performed to interpret multifocal leucocyte uptake. Seventeen patients also underwent MRI. LS images showing uni-/multifocal increased leucocyte uptake at the site of suspected infection, greater than surrounding soft tissue/bone uptake, indicated OM. When LS were interpreted together with BS, spatially congruent BS/LS findings indicated OM. Increased leucocyte uptake without corresponding BMS uptake confirmed the diagnosis of OM. Principal MRI findings compatible with OM were low signal intensity on T1-combined with high signal intensity on T2-weighted images. Final diagnosis was based on clinical and radiological follow-up or bone biopsy. **Results:** Among the 49 Charcot feet investigated, 15 cases of OM, 11 cases of acute CA and 23 uninfected Charcot joints were finally diagnosed. 10/15 patients with OM had concomitant ulcers. Sensitivity, specificity, accuracy, positive (PPV) and negative predictive value (NPV) of MRI for diagnosing OM complicating CA were 100%, 62.5%, 82.3 %, 75% and 100% respectively. There were 3 false positive MRI results due to bone marrow oedema in acute CA. Sensitivity,

specificity, accuracy, PPV and NPV of LS alone for diagnosing OM superimposed on CA were all high: 92.3%, 96.3 %, 95%, 92.3 % and 96.3% respectively, not further improved with the addition of BS. LS showed mild diffuse or no uptake in all uninfected Charcot joints and in 10/11 cases of acute CA. There was only 1 false positive LS result due to active bone marrow in acute CA. The addition of BMS in that case helped to establish the correct diagnosis. **Conclusion**: MRI is highly sensitive but not specific enough for diagnosing OM superimposed on CA. LS although slightly less sensitive than MRI is considerably more specific (96.3% vs 62.5%) for diagnosing OM complicating CA. The addition of BS does not improve LS accuracy. The addition of BMS is helpful in cases of multifocal leucocyte uptake on CA to discriminate OM from acute Charcot process.

## PW029

### The effect of prednisolone on Tc99m-HMPAO pure eosinophil and neutrophil radiolabelling efficiency, and their kinetics in vivo, in real time

**J. Lukawska**[1], L. Livieratos[1], B. Sawyer[1], T. Lee[2], M. O'Doherty[1], P. Blower[1], P. Blower[1], M. Kofi[3], J. R. Ballinger[1], G. Gnanasegeran[3], C. Corrigan[1], G. Mullen[1]; [1]King's College London, London, UNITED KINGDOM, [2]HK Sanatorium and Hospital, Hong Kong, HONG KONG, [3]Guy's Hospital, London, UNITED KINGDOM.

**Aim**: Here we present a study of Tc99m radiolabelling efficiency and kinetics of pure eosinophils and pure neutrophils obtained from healthy human volunteers and asthmatic volunteers pretreated with steroids. **Methods**: 105 mL of venous blood was obtained on two separate occasions from two groups of volunteers: healthy (4), asthmatics (4) pretreated with prednisolone at 0.5mg per kg for 5 day. Granulocytes were separated using gradient Ficoll-Paque PLU 1.084 centrifugation. Superparamagnetic particles coupled to a monoclonal antibody against CD16, a surface marker present in neutrophils, were incubated with the granulocytes (mixed eosinophils and neutrophils). CliniMACS system (Miltenyi biotec, Bergisch-Gladbach, Germany) was used to obtain highly purified (>95% pure) human blood eosinophils (negative selection) or neutrophils (>97%, positive selection). Purified cells were labelled with Tc-99m HMPAO (Ceretec, GE Healthcare) under aseptic cGMP conditions and 75-100 MBq of labelled cells were administered intravenously. **Results**: Lung migration of eosinophils differed significantly from that of neutrophils in both groups of volunteers, with eosinophils showing a significantly faster efflux and shorter transit times ($T_{1/2}$) than neutrophils. There was marginal difference in lung $T_{1/2}$ observed between healthy volunteers ($T_{1/2}$ = 4.1±0.1 min) and asthmatics pre-treated with steroids ($T_{1/2}$ =5.6±1.2 min ) for eosinophils (p = 0.052), and no statistically significant difference for neutrophils (healthy:$T_{1/2}$ =13.7±4.1 min, pre-treated: $T_{1/2}$ =16.0±2.0 min, p = 0.762). There was a marked difference in spleen and liver migration of eosinophils and neutrophils with large percentage difference between liver and spleen uptake in neutrophil migration. Such differences were exaggerated in the steroid treated group compared to healthy volunteers. Tc99m-HMPAO radiolabelling efficiency of pure eosinophils was better in the absence of steroids (mean = 70%) compared to steroid pre-treated group (mean = 47%); for pure neutrophils radiolabelling efficiency improved with steroid treatment (mean = 27% for no steroids group, mean = 55% for steroid treated group). **Conclusions**: Treatment with prednisolone results in altered Tc99m-HMPAO radiolabelling efficiency, kinetics and migration to body organs of pure eosinophils and neutrophils. The effect of the drug should be taken into account when assessing pure eosinophil and neutrophil as well as mixed granulocyte studies.

## PW030

### Combined $^{99m}$Tc-besilesomab and bone marrow imaging in diagnosis of prosthetic joint infection

**A. Tsaroucha**, O. Bourogianni, K. Galanopoulos, M. Alefantinou, M. Stathaki, E. Papadaki, S. Koukouraki, K. Balalis, N. Karkavitsas; University Hospital of Heraklion, Heraklion,Crete, GREECE.

**Aim**: The aim of the study was to assess the diagnostic value of combined $^{99m}$Tc-besilesomab and bone marrow imaging in the diagnosis of prosthetic joint infection. **Materials and Methods**: Twelve patients, with total hip or knee arthroplasty, were prospectively enrolled in the study.They were referred with the suspicion of delayed or late prosthetic infection. All of them underwent $^{99m}$Tc-besilesomab examination .10 min and 20 min planar spot views were obtained 4h and 24h respectively after iv injection of 740 MBq $^{99m}$Tc-besilesomab. If increased periprosthetic activity was shown, additional bone marrow imaging was performed .10 min planar spot views were obtained 1h after iv injection of 340 $^{99m}$Tc-sulfur colloid.The combined study was considered positive for infection when increased activity in the first scan was depicted without corresponding increased activity on the bone marrow scan.Any other pattern was considered negative.The images were visually evaluated independently by two nuclear medicine physicians. Considering the small patient population no statistical analysis was performed.The definite diagnosis of prosthetic joint infection was based on positive cultures of two or more separate tissue or fluid samples obtained surgically from the prosthetic joint. Two of the patients did not undergo surgery and were excluded from the study. **Results:** $^{99m}$Tc-besilesomab scan alone correctly detected 2 out of the 4 cases with prosthetic joint infection (2 true positive),however it was false negative in 2 cases. It correctly ruled out infection in 1 out of the 6 cases without infection(1 true negative), but it was false positive in the rest 5 cases. Further bone marrow imaging was performed in 7 cases,in which increased periprosthetic activity was shown in the first scan. The combined study correctly diagnosed one out of the 2 cases with prosthetic joint infection(1 true positive), but it was false negative in the other one. It was true negative in all 5 cases without infection. No false positive case was observed in the combined study. Both the combined study and $^{99m}$Tc-besilesomab scan alone missed cases of infection. However it is worth noting, that the combined study correctly ruled out infection in all 5 cases of false positive $^{99m}$Tc-besilesomab scan. **Conclusion**:In this small series of patients, combined $^{99m}$Tc-besilesomab and bone marrow imaging seems to be highly specific in the diagnosis of prosthetic joint infection, by ruling out the cases of bone marrow expansion around the prosthesis , which lead to false positive results.

PW04 - Sunday, Oct. 20, 8:30 - 9:30, Poster Exhibition Area

## Poster Walk 4 - Cardiovascular: Cardiovascular

## PW031

### Long-term Prognostic Value of Stress Tetrofosmin-Tc-99m Right Ventricular to Left Ventricular Uptake Ratio Assessment in Dilated Cardiomyopathy

**T. Vieira**[1], R. Godinho[2], I. Rangel[2], V. Alves[1], A. Oliveira[1], T. Faria[1], P. Oliveira[1], A. Sousa[2], E. Martins[2], J. G. Pereira[1]; [1]Nuclear Medicine Department of Hospital de São João, Porto, PORTUGAL, [2]Cardiology Department of Hospital de São João, Porto, PORTUGAL.

**Aim:** Dilated cardiomyopathy (DCM) is a progressive disease of the myocardium that is characterized by ventricular chamber enlargement and contractile dysfunction with normal left ventricular (LV) wall thickness. The prognosis of patients with heart failure depends on several factors, and higher mortality rates are associated with increased age and male sex. Patients with DC may have both myocardial ischemia and pulmonary hypertension. A relative increase in right ventricular to left ventricular uptake of myocardial perfusion agents for SPECT was previously reported as a marker of LV hypoperfusion and of pulmonary hypertension. We aimed to study the prognostic value of right ventricular to left ventricular uptake ratio (RV/LV) in DCM. **Materials and Methods**: The study included 50 DCM patients (38 males) consecutively referenced for stress tetrofosmin-Tc-99m gated myocardial perfusion SPECT between January 2006 and May 2008 because of suspected or known coronary artery disease. The stress imaging was performed 30-60min after tetrofosmin-Tc-99m administration and LV perfusion and function were assessed. For RV/LV calculation an investigator with no knowledge of the patients' follow-up placed 6×6 pixel ROIs in the RV and LV free walls of a mid-ventricular short-axis SPECT slice. RV/LV was calculated as the ratio of myocardial total counts in each ROI. Follow-up was obtained for major adverse cardiac events (MACE) (cardiac death and hospitalization for any cardiac reasons, including worsening of heart failure, non-fatal myocardial infarction, unstable angina and coronary revascularization). Statistical analysis was conducted**. Results:** Mean age was 60.6 years-old (range 38 to 79). Mean summed stress score was 6.56 ± 6.13 and mean post-stress LV ejection fraction was 29.92 ± 12.17%. Mean RV/LV was 0.47 ± 0.15. Fifteen patients had MACE, including 3 cardiac deaths. The area under the receiver operating characteristic (ROC) curve for RV/LV to predict MACE revealed the optimal threshold was 0.45. Cox regression analysis showed that RV/LV was a predictor of MACE (hazard ratio (HR) = 3.437 [95% CI 1.081-10.931; p = 0.036]). In a multivariate analysis adjusted to age and sex RV/LV remained a significant predictor of MACE (HR = 3.418 [95% CI 1.061-11.008; p = 0.039]). **Conclusion:** RV/LV obtained during tetrofosmin-Tc-99m myocardial perfusion SPECT adds value to the prediction of cardiac events independent of age and sex in DCM patients.

## PW032

### Simultaneous evaluation of coronary and peripheral artery disease with 99mTc-MIBI scintigraphy in diabetic and non-diabetic patients. A pilot study

**N. Ristevska**[1], D. Pop Gjorcheva[1], L. Todorovska[2], M. Vavlukis[3], I. Ahmeti[4], S. Stojanoski[1], M. Zdraveska Kocovska[1]; [1]Institute of Pathophisiology and Nuclear Medicine, SKOPJE, MACEDONIA, THE FORMER YUGOSLAV REPUBLIC OF, [2]Institute of Physiology, SKOPJE, MACEDONIA, THE FORMER YUGOSLAV REPUBLIC OF, [3]Clinic of Cardiovascular Disease, SKOPJE, MACEDONIA, THE FORMER YUGOSLAV REPUBLIC OF, [4]Clinic of Endocrinology, Diabetes and Metabolic disorders, SKOPJE, MACEDONIA, THE FORMER YUGOSLAV REPUBLIC OF.

**Aim** of the study: to establish one-day rest-Dypiridamol 99mTc-MIBI protocol for lower limb muscle perfusion scintigraphy (LLMPS), as a complement to myocardial perfusion scintigraphy (MPS) for simultaneous evaluation of coronary and

peripheral artery disease (CAD, PAD), in non-diabetic (NDpts) and diabetic patients (Dpts), as well as to estimate diagnostic value of various parameters of LLMPS in assessment of PAD. **Materials and Methods**: 41 pts, 20/41 NDpts (49%) and 21/41 Dpts (51%) were included in the study. No significant difference was found in gender distribution, BMI and presence of risk factors for PAD and CAD among the groups, except for diabetes. At rest, LLMPS was performed as "dynamic phase of the calves" (0-7 min p.i. and the early arterial phase of left calf (LC) and right calf (RC) was characterized using time of maximum activity (Tmax). Acquisition of whole-body scan (WBS-PA) and MPS at rest followed. At stress, LLMPS (WBS-PA) was performed immediately after Dypiridamol/99mTc-MIBI application, followed by MPS. Index of asymmetry of activity left/right thigh (LT/RT) and left/right calf (LC/RC) and intra-extremity index LT/L-knee, RT/R-knee, LC/L-ankle and RC/R-ankle, at rest and stress were determined. Perfusion reserve (PR) of thighs (LT, RT) and calves (LC, RC) was calculated as "(ROI Stress-ROI Rest)x100%/ROI Rest". Results: Dpts showed prolonged value of Tmax of LC, RC (108±23s, 113±29s. vs. 93±25s, 91±20s in NDpts, p<0.01). 7/20 NDpts (35%) and 13/21 Dpts (62%) showed pathological values of index of asymmetry of activity at rest and stress. PR was significantly lower in Dpts compared with NDpts: LT-28±19% vs. 43±24% in NDpts, p<0.05; RT-27±17% vs. 40±25% in NDpts, p<0.05; LC-22±15% vs. 36±15% in NDpts, p<0.01; RC-25±15% vs. 38±14% in NDpts, p<0.01. Identically, significantly lower perfusion reserve in Dpts was obtained comparing the Δ values of stress-rest ratio of LT/L-knee, RT/R-knee (p<0.05) and LC/L-ankle and RC/R-ankle (p<0.01). PR estimated as percentage of counts over ROI of thighs and calves at rest and stress, as a part of whole body counts, although lower in D pts, did not show significant difference among the groups. **Conclusion:** LLMPS performed simultaneously with Rest-Dypiridamol 99mTc-MIBI MPS seems to be useful procedure in assessing PAD along with CAD. This pilot study suggests a significant role of LLMPS in estimation of tissue perfusion by measuring the PR in lower limb muscles in patients at risk for PAD, especially diabetic pts.

## PW033

### Radionuclide evaluation of cardiac dysfunction in young patients with ventricular arrhythmias

**Y. Lishmanov**, V. Saushkin, K. Zavadovsky; Institute of Cardiology, Tomsk, RUSSIAN FEDERATION.

**Aim:** to estimate the diagnostic possibilities of quantitative blood pool single photon emission computer tomography (QBP-SPECT) in diagnostic of arrhythmogenic heart dysfunction in children and teenagers with ventricular arrhythmias (VA). **Material and Methods**: The study included 64 children and teenagers (mean age 12,9±3,2 years) with VA. Electrophysiological study followed by radiofrequency ablation was performed 24 patients. The comparison group included 18 patients of similar age and sex, with the exclusion of cardiac arrhythmias. All patients underwent gated blood pool SPECT. In addition, we calculated the sensitivity, specificity, diagnostic accuracy, positive and negative predictive value. As a reference method, we used electrophysiological study of the heart. **Results:** In all patients with VA we observed the areas of asynchronous contraction - the sign of myocardium mechanical heterogeneity. The most common site of these areas is the right ventricle. When the source of arrhythmia located in the right ventricular outflow tract - preliminary contraction areas are located in the anterior wall of the right ventricle. And when source of arrhythmia located in the left sinus of Valsalva, the asynchrony appears in the interventricular septum. In children and teenagers with VA versus comparison group, we observed a moderate dilatation and reduced contractile function of the heart. This phenomenon is most expressed in patients with arrhythmia from the left sinus of Valsalva. For the further analysis of diagnostic opportunities of QBP-SPECT the patients were divided into 2 groups according to the quantity of focuses of premature contraction according to QBP-SPECT. The first group included 36 children with single area of premature contraction, the second group - 43 patients with multiple similar areas. RV peak ejection rate, peak filling rate, mean filling rate for first third of cardiac cycle, RV EF was significantly more in the first group of patients. Standard deviation of mean contraction time of LV and RV in the second group was significantly more. **Conclusion**: The presence of areas of asynchronous contraction on the phase-polarity maps can be considered as pathognomonic scintigraphic symptom of VA existence. The most pronounced hemodynamic changes were observed in patients with arrhythmia originating from the left sinus of Valsalva.

## PW034

### Computation of myocardial blood flow and metabolic rate of O2 in right ventricle at rest and during exercise using H215O and 15O2 PET

**N. Kudomi**[1], K. K. Kalliokoski[2], V. J. Oikonen[2], C. Han[2], J. Kemppainen[2], M. Luotolahti[3], H. Sipilä[2], D. J. Duncker[4], J. Knuuti[2], I. Heinonen[2]; [1]Faclty of Medicine, Kagawa University, KAGAWA, JAPAN, [2]Turku PET Centre, Turku, FINLAND, [3]Clinical Physiology and Nuclear Medicine, Turku, FINLAND, [4]Division of Experimental Cardiology,MC, University, Rotterdam, FINLAND.

**Objectives:** Myocardial blood flow (MBF) and metabolic rate of oxygen ($MMRO_2$) can be quantified using $H_2{}^{15}O$ and $^{15}O_2$ PET [1]. This study aimed to develop a computational method for MBF and $MMRO_2$ in the right ventricle (RV) as well as left (LV), applying to resting and physiologically relevant exercise condition. **Methods**: We studied 10 healthy young men (age: 30 ± 5 years, height: 180 ± 7 cm, weight: 72 ± 7 kg) at rest and during exercise, and developed a method for LV and RV input functions for $H_2{}^{15}O$ scan. With the two inputs, we generated MBF, perfusable tissue fraction (PTF) and blood volume ($V_B$) images, and subsequently $MMRO_2$ were computed from the $^{15}O_2$ scan data using the obtained MBF and PTF for partial volume correction [1]. The obtained MBF was compared with that by previously established Methods [2,3], the PTF with extra vascular density ($D_{ev}$) for testing quantitative validity, and the $V_B$ with that from $C^{15}O$ scan for testing validity of LV and RV inputs. The obtained MBF and $MMRO_2$ were compared between resting and exercise conditions. **Results:** The LV MBF was similar between the two Methods. Tight correlations were measured between PTF and $D_{ev}$ for left (r = 0.89) and right (r = 0.78) regions. No significant differences were found in $V_B$ both in LV and RV. The obtained MBF and $MMRO_2$ values were similar between LV and RV in the resting condition: resting MBF was 0.67±0.13 and 0.64±0.26 ml/min/g in the LV and RV, respectively, and resting $MMRO_2$ was 0.14±0.04 and 0.12±0.04 ml/min/g, in the LV and RV, respectively. In response to exercise, MBF and $MMRO_2$ were significantly increased, as MBF in LV was 147±82% (P<0.05) and MBF in RV 53±37% (P<0.05) higher compared to rest, and respective increases in $MMRO_2$ were 174±82% (P<0.05) in LV and 88±50% (P<0.05) in RV. **Conclusions**: These results suggest that the MBF and $MMRO_2$ in the RV can be quantified, indicating that it could provide new avenues for the assessment of right MBF and $MMRO_2$ not only during exercise, but also in pathophysiological states. [1] Iida et al Circulation (1996) 94: 792-807 [2] Iida et al Circulation (1988) 78: 104-115 [3] Watabe et al JNM (2005) 46; 1219-1224

## PW035

### Quantification of myocardial blood flow in cardiac 82Rb-PET: comparison of 4 different softwares

**M. L. Lassen**, F. Andersen, T. E. Christensen, A. A. Ghotbi, A. Kjær, P. Hasbak; Dept. of Clinical Physiology, Nuclear Medicine & PET, Rigshospitalet, University of Copenhagen, Copenhagen, DENMARK.

**Aim.** With an increasing number of studies using 82Rb and multiple software options for myocardial perfusion estimation it is required to have robust and reproducible myocardial blood flow (MBF) estimates. The goal of this study was to evaluate the correlation and reproducibility of MBF estimates in four programs (Syngo MBF (Siemens), PMOD (PMOD technologies), Carimas (Turku PET centre) and Corridor4DM (Invia)). **Methods.** MBF and coronary flow reserve (CFR, (stress MBF)/(rest MBF)) were evaluated in 20 patients (17 men, mean age 53±10.2 (range 37 - 68 years)). Dynamic rest and stress studies were performed for all patients in a Siemens mCT (PET/CT scanner). All scans were evaluated in all four programs using a 1-tissue compartment model. The global blood flow was used for all patients due to different levels of user interaction in the respective programs. Pearson R^2 values and Bland-Altman plots were generated for all combinations for comparison of the programs. **Results.** The data was automatically processed in Syngo MBF and Corridor 4DM, while different levels of user interaction was required in PMOD and Carimas. R^2 values above 0.63 between the programs were found when pooling rest and stress studies, indicating different estimates on MBF when using different programs. Good R^2 values (above 0.88) were found for rest studies when separating the studies. For stress studies R^2 values down to 0.47 between two programs were found, indicating great differences in the estimated MBF. R^2 values for CFR were found to be above 0.52, indicating non-homogenous MBF estimates for the programs. Great variations in the flow estimates were found for the patients. Mean±SD were calculated to be 0.97±0.47 for Syngo MBF, 0.90±0.45 in PMOD, 0.92±0.44 in Corridor4DM using a Lortie approach, 1.52±0.81 in Corridor4DM using a Yoshida approach and 1.37±0.77 in Carimas for rest studies. For stress studies mean flow and standard deviations were calculated to be 2.44±0.79 for Syngo MBF, 2.39±1.4 for PMOD, 2.26±0.79 for Corridor4DM (Lortie approach), 3.86±1.29 for Corridor4DM (Yoshida approach) and 3.11±0.69 for Carimas. R^2 values were calculated to be above 0.93 when repeating the MBF calculations in all programs. **Conclusion.** The MBF estimated using a 1-tissue compartment model cannot be used as a definite measurement, as different tools available give different flow estimates. The high R^2 values for the reproducibility study indicate that one can use the same program for evaluation of the patients, if a normal material for the given program exists.

## PW036

### A Comparison of Iterative Reconstruction and Prone Imaging in Reducing the Inferior Wall Attenuation in Tc- 99m Sestamibi Myocardial Perfusion SPECT

**D. KUSLU**, E. BALKAN, E. OZTURK; Ufuk University Medical Faculty Nuclear Medicine Department, Ankara, TURKEY.

**Aim**: The most common artifact of the inferior wall in myocardial perfusion SPECT (MPS) is diaphragmatic attenuation, that reduces the specificity of the exam. There are limited numbers of studies that suggest gated imaging, prone imaging and iterative reconstruction (IR-OSEM) Methods to reduce this problem. The purpose of this study was to compare the effects of gating, prone imaging and IR-OSEM in reducing inferior wall artifact. **Materilas and Methods**: The images of the 45 patients (42 M, 3 F), who had been examined a combined supine and prone 99m-Tc MIBI MPS imaging were retrospectively evaluated. Both images were reconstructed with IR-OSEM [supine (SIR), prone (PIR)] and compared with FBP [supine (SFBP), prone (PFBP)] reconstructed images. Clinical perfusion assesment was made by using 5-point, wall motion (WM) 6 point, wall thickening (WT) 5 point scale and grouped as normal/abnormal. Segmental myocardial tracer uptake values (percent of maximum) were noted from 4 of the reconstructed images from the 17 segment model of bullseye. Statistical analysis was made using repeated measures variant analysis, McNemar test and correlation analysis. **Results**: The difference of the % tracer activities of the inferior wall segments were significant between SFBP, PFBP, SIR and PIR images (p=0,000). But in the apical segment there was significant difference between SFBP, SIR and PIR (p<0,01), but PFBP and SIR images (p=0,314). Normalcy rates were the highest in PIR images with the rate of 86,7%; followed by PFBP images with 73,3% and SIR images with the rate of 28,9%. The differences between the groups were significant (p=0,00). The number of patients that considered abnormal in SFBP, PFBP, SIR and PIR images were 42, 12, 32, and 6, respectively. Rest images of the 6 patients that still considered abnormal in stress PIR images were re-evaluated and summed difference scores (SDS) were calculated to be '0' that indicates fixed perfusion defect. There were 29 and 11 patients that WM and WT were considered normal, respectively. The correlation was significant between WM and PFBP (p=0,008, r=0,392); PIR images (p=0,000, r=0,528). Although there were 16 patients that WM considered abnormal, only 6 patients' perfusion considered abnormal in PIR. **Conclusion**: Prone stress MPS imaging significantly reduces the infeior wall attenuation, particularly when reconstructed with IR-OSEM. Since PFBP and WM is well correlated, ECG-gating can also be helpful with a lower normalcy rate than PIR.

## PW037

### Reference values for left ventricular systolic synchrony assessed by phase analysis of gated myocardial perfusion SPECT

**T. Laitinen**[1], H. Hämäläinen[1], T. Laitinen[1], A. Hedman[2], M. Hedman[2], A. Kivelä[2]; [1]Department of Clinical Physiology and Nuclear Medicine, Kuopio University Hospital and University of Eastern Finland, Kuopio, FINLAND, [2]Heart Center, Kuopio University Hospital and University of Eastern Finland, Kuopio, FINLAND.

**Aim**: The phase analysis of gated myocardial perfusion SPECT is a useful method for examining left ventricular mechanical dyssynchrony in cardiac patients especially when planning cardiac resynchronization therapy for patients with severe heart failure. There are only few studies in which reference values have been presented for phase analysis measures. Furthemore, reference values may not be generalized across different analysis Methods. The aim of this study was to define reference values for measures reflecting left ventricular synchrony and to investigate physiological correlates for these parameters. **Materials and Methods**: We evaluated data of 384 consecutive patients who were sent to myocardial perfusion SPECT/CT study during the year 2012 in the Department of Clinical Physiology and Nuclear Medicine, Kuopio University Hospital. Exclusion criteria were 1) previously diagnosed cardiac disease, 2) abnormal ECG at rest, 3) signs of advanced coronary artery calcification in CT, and 4) abnormal myocardial perfusion in stress/rest myocardial perfusion SPECT study. Final study population consisted of 50 subjects (40 women and 10 men) aged 42-84 years. Left ventricular dyssynchrony was assessed by phase analysis of gated myocardial perfusion SPECT (QGS 2012, Cedars Sinai) both at rest and related to stress. Age, gender, body mass index and blood pressure were taken into consideration as possible physiological correlates for measures reflecting mechanical synchrony. Due to skewed distribution in phase analysis parameters, statistical analyses were done using nonparametric tests and values are presented as medians [95$^{th}$ percentiles]. **Results:** Phase histogram bandwidth at the rest study was 18 [57] degrees. Standard deviation of phase element distribution at the rest study was 4.3 [15.9] degrees. Entropy at the rest study was 25 [49]. All these measures were comparable between men and women (NS for all). All parameters reflecting left ventricular systolic synchrony tended to be higher at the stress study as compared with the rest study (Bandwidth: P=0.070; Standard deviation: P=0.035, Entropy: P=0.045). We did not find any statistically significant correlations between measures of phase analysis and age, body mass index and diastolic blood pressure. Systolic blood pressure correlated negatively with phase histogram bandwidth (r=-0.290, P=0.041). **Conclusions**: In subjects without signs of cardiac diseases left ventricular systolic function is well synchronized and measures of phase analysis are not dependent on subject's age, gender or body mass index, and influence of blood pressure on mechanical synchrony is likely to be only modest.

## PW038

### "In silico" simulation of SPECT recording with a new-generation cardiac Semi-Conductor Gamma-camera

**L. Imbert**[1,2,3], E. Galbrun[3], S. Poussier[2,4], D. Wolf[3], A. Noel[3], G. Karcher[1,2,4], P. Marie[1,2,5]; [1]CHU Nancy - Department of Nuclear Medicine, Nancy, FRANCE, [2]Nancyclotep Experimental Imaging Platform, Nancy, FRANCE, [3]CRAN - UMR 7039, Université de Lorraine - CNRS, Vandoeuvre-lès-Nancy, FRANCE, [4]INSERM, U947 and Université de Lorraine, Nancy, FRANCE, [5]INSERM, U1116 and Université de Lorraine, Nancy, FRANCE.

**Introduction.** Recently, significant improvements have been proposed for cameras dedicated to myocardial perfusion imaging, including the use of new cadmium-zinc-telluride (CZT) detectors and new collimation systems. Monte-Carlo simulations are widely used to model imaging systems, to develop acquisition process and to assess reconstruction algorithms. Up to now, however, no CZT camera has been analyzed with such simulations systems. This study was aimed at analyzing the CZT "D.SPECT" camera by using the "Geant4 Application for Emission Tomography" (GATE), a Monte-Carlo simulation system, which is currently used for both SPECT and PET medical imaging. The D.SPECT gamma-camera involved 9 mobile blocks of pixelated Cadmium Zinc Telluride (CZT) detectors with wide-angle square-hole tungsten collimators. Each block records a total of 120 projections by means of a 'region-centric' acquisition. **Materials and Methods**. Placements and movements of detector-blocks were tried to be simulated by GATE, as well as the detector response in terms of intrinsic spatial and energy resolutions. This simulation was applied to point and linear sources of $^{99m}$Tc, as well as to a cardiac phantom. Simulation results were compared to what was obtained by real recordings for the following parameters: 1) detection sensitivity assessed on a point source, 2) energy resolution assessed on a point source by the full width at half maximum (FWHM) of the $^{99m}$Tc photopeak, 3) spatial resolution assessed by FWHM on orthogonal images of linear sources and 4) for the cardiac phantom, a contrast-to-noise ratio and a sharpness index of the external myocardial border, a parameter that reflects spatial resolution. The real and simulated recorded data were similarly reconstructed with a dedicated algorithm of iterative reconstruction, which compensates for the collimator-related loss in spatial resolution. **Results**. Results from the simulated data exhibited an excellent agreement with those from real recordings with only differences of: 1) 1% for count sensitivity, 2) 5% for energy resolution, 3) 7% for spatial resolution and 4) 3% for contrast-to-noise ratio and 5) 5% for the sharpness index. **Conclusion**. The modeling of the D.SPECT CZT gamma-camera has been successfully achieved with the GATE code, as evidence by the close analogy between simulated and real recorded data. It is now possible to use this simulation for optimizing the recorded and reconstruction processes, especially for complex protocols such as dual-radionuclide acquisition and kinetics first-pass studies.

## PW039

### Impact of modulation of inflammatory response by LR-12, after myocardial infarction in rats

**F. MASKALI**[1], S. POUSSIER[1], M. DERIVE[1,2], M. LHUILLIER[1], J. LEMARIE[1,2], H. BOUTLEY[1], S. GIBOT[1,2], G. KARCHER[1,3], P. MARIE[1,3]; [1]GIE-NANCYCLOTEP, VANDOEUVRE-LES-NANCY, FRANCE, [2]UNITE INSERM U1116, Vandoeuvre-les-nancy, FRANCE, [3]NUCLEAR MEDICINE DEPARTMENT, Vandoeuvre-les-nancy, FRANCE.

**Purpose**: The receptor "triggering-receptor-expressed-on-myeloid-cells-1" (TREM-1) enhances downstream signalling of molecules implicated in inflammatory responses and might contribute to the deleterious cardiac remodelling observed after myocardial infarction. This seems be downregulated by a TREM-like transcript 1-derived peptide (LR-12). However the effect of this LR-12 peptide on the deleterious cardiac ventricular remodelling has yet to be elucidated. Our aim was to study the impact of treatment by LR-12 after myocardial infarction in rats. **Materials and Methods**: Two hours after induction of a myocardial infarction by coronary ligation and FDG microPET acquisition, 35 adult male rats were randomized to receive LR-12 (n =17; 5mg/kg ; peritoneal administration up to 5 days) or its vehicle alone (saline solution, n = 18). Extent of myocardial infarction and left-ventricular parameters were analysed by using FDG microPET at 2-hours and 6 weeks after ligation. Left ventricular function was also assessed at 6 weeks by conductance catheter in order to quantify systolic myocardial elastance, ventriculo-arterial coupling and diastolic relaxation constant Tau. **Results:** 2-hours after ligation, the extent of infarction at FDG microPET was equivalent between treated and control rats (in % of the left ventricle, 22±11 vs. 23±9, respectively). End-diastolic volume (EDV in mL; 417±92 vs. 431±75, respectively) and ejection fraction (EF in%, 48±8 vs. 48±8, respectively) were also similar in the two groups. At 6 weeks, the increase of end-diastolic volume, which reflects the evolution towards ventricular remodelling was largely attenuated by LR-12 administration (difference between 6-weeks and 2-hours in treated rats: + 198±95µL control-rats: + 273±77µL; p = 0.005). Similarly in the two groups, LV systolic function expressed by slope of the LV end-systolic pressure volume relationship (Ees) and preload recruitable stroke work (PRSW) were significantly enhanced. **Conclusion:** modulation of the inflammatory response by the LR-12 peptide limits deleterious

ventricular remodelling after myocardial infarction in rats. It constitutes a mean therapeutic class in this setting in addition to beta-blockers and ACE inhibitors.

## PW040

### FDG-uptake by PET/CT in an Uncoupling Protein 3 Transgenic Murine Model of Myocardial Infarction

**S. Gargiulo**[1,2], M. P. Petretta[3], M. Gramanzini[1], A. Greco[3], G. Schiattarella[3], G. Esposito[3], A. Brunetti[3], A. Cuocolo[3]; [1]National Council of Research, Napoli, ITALY, [2]CEINGE scarl, Napoli, ITALY, [3]University of Naples - Federico II, Napoli, ITALY.

**Aim**: Uncoupling protein 3 (UCP3) is a member of the mitochondrial anion carrier super-family of proteins uncoupling mitochondrial respiration. UCP3 is required to maintain high rates of glucose aerobic metabolism, while deficiency in UCP3 might result in a metabolic shift that favored anaerobic glycolytic metabolism. We investigated the effects of UCP3 genetic deletion on $^{18}$F-fluorodeoxyglucose (FDG) uptake by a high-resolution positron emission tomography (PET)/computed tomography (CT) dedicated animal system after myocardial infarction (MI). **Material and Methods**: Mice (C57Bl/6J, aged 9-16 weeks) were studied by $^{18}$F-FDG PET/CT (eXplore Vista, GE Healthcare) one to four weeks after induction of MI (15 wild type mice and 5 UCP3 knockout mice) by permanent coronary occlusion or sham procedure (n=20). Mice were warmed with an infrared lamp and injected in tail vein with a bolus of 7.4 MBq/100 µl of $^{18}$F-FDG. In the MI group animals, infarction was obtained trough the ligation of the left coronary artery. Regional ischemia was confirmed by visual inspection under a dissecting microscope by discoloration of the occluded distal myocardium. Sham-operated animals underwent the same procedure without occlusion of the left coronary artery. PET images were processed using a 2D-OSEM iterative algorithm including random, scatter correction, dead time, decay, and attenuation correction using CT data. An automated software (MunichHeart) was used to measure left ventricular surface area and volume. Left ventricular $^{18}$F-FDG myocardial uptake was measured in a representative mid-ventricular axial slice and expressed as standardized uptake value (SUV): radioactivity in the heart by PET (Bq/ml) × (g) body weight/injection dosage of $^{18}$F-FDG (Bq**). Results**: In the entire group of mice with MI, left ventricular total surface area and volume (measures of left ventricular chamber dilatation) were significantly greater (both P<0.05) as compared to mice of the sham group (+20.5% and +17.7%, respectively). At one-way ANOVA, significant differences (P<0.01) in SUV among mice of the sham group, wild type mice with MI, and UCP3 knockout mice with MI were found. In UCP3 knockout mice with MI, SUV (4.48±1.21) was significantly higher as compared to both mice of the sham group (2.02±0.98, P<0.005) and wild type mice with MI (2.57±0.73, P<0.05). **Conclusions:** The results of this study demonstrate that in a mice model of permanent coronary occlusion UCP3 is required to maintain high rates of glucose aerobic metabolism and its deficiency results in a metabolic shift that favored anaerobic glycolytic metabolism and increased $^{18}$F-FDG uptake.

PW05 - Sunday, Oct. 20, 8:30 - 9:30, Poster Exhibition Area

## Poster Walk 5 - Neurosciences: Basic Science

## PW041

### Comparison of (-)-[$^{18}$F]-Flubatine and 2-[$^{18}$F]FA-85380 Binding to Nicotinic alpha4beta2 Acetylcholine Receptors in Human Brains

**G. A. Becker**[1], S. Wilke[1], P. Schönknecht[2], M. Patt[1], J. Luthardt[1], S. Hesse[1], P. M. Meyer[1], H. Barthel[1], D. Sorger[1], A. Seese[1], G. Wagenknecht[3], A. Höpping[4], S. Fischer[5], P. Brust[5], O. Sabri[1]; [1]Department of Nuclear Medicine, University of Leipzig, Leipzig, GERMANY, [2]Department of Psychiatry, University of Leipzig, Leipzig, GERMANY, [3]Multimodal Image Processing, Central Institute ZEA-2 Electronic Systems, Forschungszentrum Jülich GmbH, Jülich, GERMANY, [4]Advanced Biochemical Compounds (ABX), Radeberg, GERMANY, [5]Institute of Radiopharmaceutical Cancer Research, Helmholtz-Zentrum Dresden-Rossendorf, Research Site Leipzig, Leipzig, GERMANY.

**Aim:** Nicotinic α4β2* acetylcholine receptors (nAChR) are an important target for diagnostic neuroimaging because of their involvement in Alzheimer's disease, Parkinson's disease, tobacco and alcohol addiction. 2-[$^{18}$F]FA-85380 (2-FA) has been used extensively for PET imaging of α4β2* receptors but is limited as biomarker by its unfavourable slow kinetic. The newly developed radiotracer (-)-[$^{18}$F]-Flubatine (Flubatine) shows a significantly improved brain uptake, receptor affinity and selectivity (1). Here we estimated the compartmental parameters of both tracers by full kinetic modeling and compared them. **Materials and Methods***:* After intravenous administration of ~370 MBq radiotracer PET brain imaging was performed in 20 healthy controls with Flubatine (age 70.6±4.6, scan duration 90 min) and in 7 healthy controls with 2-FA (age 60.7±9.0, scan duration 420 min) using an ECAT EXACT HR+ system. PET frames were motion corrected with SPM2 and kinetic modeling using a 1-tissue compartment model (1TCM) with arterial input-function was applied to the volume of interest (VOI) based tissue time-activity curves (TACs) generated for 29 brain regions (anatomically defined via MRI co-registration). The model-based receptor parameter used was the total distribution volume $V_T$ (ml/cm$^3$), tracer uptake was measured by $K_1$ (ml/cm$^3$/min) and tracer tissue clearance by $k_2$ (1/min). ***Results****:* For both tracers TACs of all 29 brain regions could be described appropriately with the 1TCM and all kinetic parameters could be reliably estimated from the PET data. Regional $V_T$ increased as expected with regional nAChR density. Parameters of Flubatine in characteristic regions with very low, medium and high receptor density were: Corpus callosum ($K_1$= 0.18±0.04, $k_2$= 0.032±0.004, $V_T$= 5.68±1.01), Frontal cortex ($K_1$= 0.37±0.04, $k_2$= 0.040±0.003, $V_T$= 9.18±0.59), Thalamus ($K_1$= 0.48±0.06, $k_2$= 0.020±0.003, $V_T$= 25.03±3.33). The respective parameters of 2-FA were: Corpus callosum ($K_1$= 0.063±0.009, $k_2$= 0.014±0.003, $V_T$= 4.45±0.65), Frontal cortex ($K_1$= 0.099±0.013, $k_2$= 0.018±0.001, $V_T$= 5.42±0.56), Thalamus ($K_1$= 0.13±0.019, $k_2$= 0.010±0.001, $V_T$= 13.06±2.62). ***Conclusions****:* Flubatine is superior to 2-FA in tracer uptake velocity (characterized by $K_1$), velocity of washout (characterized by $k_2$) and in the amount of measured specific binding (characterized by $V_T$-target - $V_T$-reference). It shows a threefold higher uptake rate constant $K_1$ and a twofold higher washout rate constant $k_2$, providing the rational for much shorter scan durations in case of Flubatine. These results are in good agreement with our former findings in an animal (pig) model (1). *Reference:* 1. P. Brust, ..O. Sabri: In vivo measurement of nicotinic acetylcholine receptors with [$^{18}$F]Norchloro-Fluoro-Homoepibatidine (Flubatine). Synapse 2008;62:205-218.

## PW042

### The effect of estrogen replacement on neural responses of rats to stress in the forced swim test: a [18F]FDG micro PET study

**M. A. Khayum**, J. Doorduin, S. Copray, J. A. den Boer, R. A. J. O. Dierckx, E. F. J. de Vries; University Medical Center Groningen, Groningen, NETHERLANDS.

**Introduction:** Estrogens are known for their role in reproduction in females, but are also associated with changes in cognition, anxiety, and depression. In postmenopausal women, hormone replacement therapy (HRT) with estrogens was found to have an antidepressant effect and to enhance the effect of antidepressants. However, there appears to be a critical window for HRT, which depends on age and stage of menopause. Ovariectomy in rats is often used to reduce the levels of circulating estrogens to mimic a state of menopause. The forced swim test (FST) is a stressful test, often used to assess antidepressant properties of new drugs. In this study, we used the FST to evaluate the antidepressant properties of estrogen replacement in ovariectomized rats and to measure the neuronal response to stress using [$^{18}$F]FDG positron emission tomography (PET). The effect of estrogen replacement was compared to acute treatment with the conventional antidepressants fluoxetine and escitalopram. **Methods:** Female rats were ovariectomized (OVX) and divided in 5 groups (n=8 per group): 1, placebo treatment; 2, estradiol treatment starting at day 7 post-OVX; 3 estradiol treatment from day of OVX. Group 4-5 received 3 injections of 10 mg/kg fluoxetine or escitalopram before the test FST on day 16 post-OVX (-24, -19 and -1 h). Rats were subjected to a baseline [$^{18}$F]FDG scan on day 14 post-OVX and a pretest FST on day 15. On day 16 post-OVX, rats were injected with [$^{18}$F]FDG and immediately subjected to a 30-min test FST. After the FST, the rats were anesthetized and a 30-min PET scan was acquired. **Results:** In 16 days estradiol treated rats (group 3), immobility was significantly reduced (58%, p<0.01), whereas swimming was increased (46%, p<0.05), compared to the placebo treated rats. [$^{18}$F]FDG PET analysis revealed a significant reduction (40%; p<0.001) in [$^{18}$F]FDG uptake in all brain regions between the baseline and stress scan for all groups. No differences in [$^{18}$F]FDG uptake between groups were found at baseline or during stress. When corrected for blood glucose levels, [$^{18}$F]FDG uptake during FST was significantly lower (32%; p<0.01) in all brain regions of 16 day estradiol-treated rats. **Conclusion:** Our results suggest that estrogen replacement for 16 days immediately after ovariectomy has an antidepressant effect in the FST and reduces brain glucose metabolism during stress. In contrast, 1-week delayed treatment with estradiol or acute treatment with conventional antidepressants did not have any effect.

## PW043

### Brain uptake of novel NMDA and GABAergic PET tracers in a Model of Traumatic Brain Injury in Rat

**F. R. Lopez Picon**[1], O. Shatillo[2], A. Snellman[1], P. A. Jones[3], W. Trigg[3], P. Lehtiniemi[1], P. Marjamäki[1], O. Solin[1], A. Pitkänen[2,4], M. Haaparanta-Solin[1]; [1]Turku PET Centre, University of Turku, Turku, FINLAND, [2]Department of Neurobiology, A.I. Virtanen Institute, University of Eastern Finland, Kuopio, FINLAND, [3]Medical Diagnostics, GE Healthcare Ltd., Amersham, UNITED KINGDOM, [4]Kuopio University Hospital, Kuopio, FINLAND.

BACKGROUND: Severe traumatic brain injury (TBI) is associated with a number of co-morbidities, including somatomotor, cognitive, and behavioral impairments. In

addition, TBI can trigger epileptogenesis in up to 50% of patients, and about 10% of symptomatic epilepsy is caused by TBI. The molecular mechanisms determining the post-TBI recovery and epileptogenesis are unknown. Here we tested a hypothesis that functional impairments after TBI are associated with acquired ligand-gated channelopathies which can be detected by novel PET tracers. METHODS: TBI was induced with lateral fluid-percussion in adult Spraque-Dawley rats. Sham-operated controls underwent all surgical procedures without impact. Ex vivo autoradiography was performed using new 18F-labelled PET tracers for NMDA ([18F]GE-179) and GABA ([18F]GE-194) at the acute (5-6 days after TBI) or chronic stage (40-42 days after TBI). RESULTS: At the acute stage, the uptake of NMDA tracer [18F]GE-179 was increased within the primary cortical lesion as well as in the perilesional cortex as compared to the contralateral side ($p<0.05$). At the chronic stage, the increased [18F]GE-179 uptake was more widespread, including also the ipsilateral capsula externa and the thalamus. The magnitude and distribution of the GABA tracer [18F]GE-194 binding was quite different from that of the NMDA tracer. Acutely the binding of [18F]GE-194 was reduced at the primary lesion and the ipsilateral thalamus. At chronic stage, reduced binding of [18F]GE-194 was still present in the lesioned cortex and ipsilateral thalamus and the reduction in binding had expanded to the perilesional cortex. CONCLUSIONS: Our data demonstrate that both PET tracers [18F]GE-179 and [18F]GE-194 successfully bind to active NMDA and GABA receptors, respectively, with a good profile. Second, [18F]GE-179 is a promising tracer to investigate the overactivation of glutamate receptors and pathologies related to them. By applying these tracers we demonstrated that within 7 wk post-TBI, abnormalities in NMDA and GABA binding expand from the cortical lesion and perilesional cortex to the thalamus, which likely relates to the progressive damage in thalamo-cortical pathways. Finally, the increase in NMDA binding and decrease in GABA binding suggest a development of acquired channelopathy in thalamo-cortical circuits or locally in the perilesional cortex and the thalamus. It remains to be demonstrated whether the magnitude of these changes can be used to predict post-TBI recovery and development of hyperexcitability.

## PW044

### Impact of Carisbamate on metabolic markers of epileptogenesis in an experimental rat model of epilepsy

**G. VEXIAU**[1], F. MASKALI[1], B. CHALON[1], M. LHUILLIER[1], L. IMBERT[1], S. POUSSIER[1], E. RAFFO[1,2], G. KARCHER[1,3], P. MARIE[1,3]; [1]GIE-NANCYCLOTEP, VANDOEUVRE-LES-NANCY, FRANCE, [2]UNIVERSITY HOSPITAL OF NANCY, Vandoeuvre-les-nancy, FRANCE, [3]NUCLEAR MEDICINE DEPARTMENT, Vandoeuvre-les-nancy, FRANCE.

**Purpose**: Although the number of antiepileptic drugs (AEDs) is increasing, none displays neuroprotective or antiepileptogenic properties that could prevent the development of drug-resistant epilepsy. Carisbamate is proposed as an alternative treatment in epilepsy. Our aim, was to assess the neuroprotective et/or antiepileptogenic effect of this drug in a well-characterized model of mesial temporal lobe epilepsy induced by lithium-pilocarpin in adult rats. **Material and Methods**: 21 adult male Sprague-Dawley rats were subjected to lithium-pilocarpin and allocated to 2 groups: (i) a control group with this injection of saline solution (0.1 mL/kg; n =10), and (ii) a treated group with injection of Carisbamate (90mg/Kg; n=11). These rats were referred to: (i) serial brain FDG-PET, at 4-hours, 48-hours, 8-days, 1-month and 3-months, (ii) brain MRI with a dedicated T2-weighted sequence at 24-hours and 3-months and (iii) a sacrifice with histological analyses at 3-months. PET images were coregistered on MRI anatomical images in order to facilitate the anatomic determination of the regions of interest (ROI). Mean voxel activity of FDG was determined in each ROI and expressed relative to mean voxel activity of the overall brain volume**. Results**: After lithium-pilocarpine, all untreated rats evolved into chronic epilepsy, whereas only 36% of treated rats became epileptic ($p<0.05$). A decrease in FDG uptake was documented during the initial 48-hours of the untreated rats in hippocampal areas and in residual cortical foci (entorhinal, piriform and sensorimotor) and persisted up to 3-months only in hippocampal areas and sensorimotor cortex. This decrease in FDG uptake was lowered by the Carisbamate treatment, especially in the hippocampal areas at 48-hours and 3-months and in sensorimotor cortex at 3-months. **Conclusion:** Carisbamate improves significantly the FDG-uptake of the damaged brain areas of the lithium-pilocarpin rat model giving evidence of his antiepileptogenic and neuroprotective potential.

## PW045

### Six Weeks of Hypercaloric High-Fat-High-Sugar Snacking decreases Diencephalic Serotonin Transporters, but not Dopamine Transporters, in Lean Men

**K. E. Koopman**, S. E. la Fleur, E. Fliers, M. J. Serlie, J. Booij; AMC, Amsterdam, NETHERLANDS.

Aim and background Brain dopamine and serotonin systems are affected in obese subjects. We recently found a decrease in serotonin transporter (SERT) immunoreactivity in hypothalamic post-mortem tissue of overweight compared to lean subjects which is in line with a previously described negative correlation between cerebral SERT (striatum, (hypo)thalamus and midbrain) and BMI. We furthermore found a decrease in striatal dopamine D2/3 receptor availability in morbidly obese women, also in line with a previously described negative correlation between brain dopamine and BMI. Both dopamine and serotonin are involved in food intake regulation, but whether changes in serotonin and dopamine in obesity are related to eating behaviour or absolute body weight is unclear. We hypothesized that brain serotonin and dopamine systems are altered by both macronutrient content and eating pattern during a hypercaloric diet. Materials and Methods Twenty five lean male subjects (age: 22.1yrs±2.5; BMI: 22.5±1.3 kg/m2) followed a hypercaloric diet with 40% caloric surplus on top of their regular diet for 6 weeks. Subjects were randomised into a high-fat-high-sugar (HFHS) diet or a high-sugar (HS) diet group. Within the HFHS- and the HS-group, subjects consumed the caloric surplus with meals (increase in meal size) or in between meals (increase in meal frequency). We also included a control group (N=5) who did not follow a diet. At baseline and after 6 weeks subjects underwent SPECT imaging using the well-validated radiotracer 123I-FP-CIT to measure SERT and dopamine transporter (DAT) availability in the diencephalon and striatum, respectively, using a brain-dedicated system (Neurofocus). Specific-to-nonspecific binding ratios (SNS-BR) were calculated and used as the outcome measure. Results Weight gain was significantly increased to the same degree in all diet groups, yet BMI remained within normal ranges (19-25 kg/m2) in almost all subjects. SERT SNS-BR in the diencephalon decreased significantly only in the HFHS-group with increased meal frequency. Striatal DAT SNS-BR was not altered by any of the hypercaloric diets. None of the measurements were changed in the control group. Conclusion The reduction in SERT was only found in the HFHS meal frequency group. This finding suggests that specifically snacking high-fat-high-sugar products induces changes in the human brain which may predispose to a disturbed food intake resulting in obesity.

## PW047

### Preliminary exploration of dynamic I-123-FP-CIT imaging in rats using a cadmium zinc telluride (CZT) ring detector SPECT system

F. Wilke[1], C. Schütze[1], **G. Berding**[2], L. Geworski[1], F. Bengel[2], J. P. Bankstahl[2]; [1]Department of Medical Physics and Radiation Protection, Hannover Medical School, Hannover, GERMANY, [2]Department of Nuclear Medicine, Hannover Medical School, Hannover, GERMANY.

**Aim**: Reliably determining the equilibrium binding phase of I-123 labelled ligands in small animals would be a major achievement for the evaluation of new radiopharmaceuticals. However, up to recently this was hampered by the limited sensitivity of conventional small animal SPECT scanners. The appearance of new cadmium zinc telluride (CZT) solid-state ring-detector systems offers fundamentally new options in this context. The present study aims to elaborate basic data with respect to a dynamic CZT-SPECT imaging protocol for the dopamine transporter ligand I-123-FP-CIT in rats. **Methods**: A mean activity of 46 MBq (range 23-80) I-123-FP-CIT was injected into 4 rats. In these animals the following data were acquired: (i) eight static scans starting 16 to 272 min p.i., (ii) one dynamic scan for 216 min and (iii) one bio-distribution study of the brain (removed at 5.5 h p.i.) using a well counter. For Imaging an explore SPECZT/CT 120 (GE-Healthcare/Gamma Medica) equipped with a 5 slit collimator was employed. In static scans slit projections were always registered over 360° but with acquisition times per projection ranging between 4 and 40 sec. Total acquisition times per scan ranged between 5 and 24 min. After iterative reconstruction (OSEM) regions of interest were drawn manually over striatum (ST) and cerebellum (CB) using the PMOD software. Finally, specific over non-specific binding ratios were calculated: (ST-CB)/CB. **Results**: The bio-distribution study revealed a specific over non-specific binding contrast of 3.0. This is in good agreement with earlier reports in the literature. Static scans showed three ranges of binding ratios: (i) ≤1.0, (ii) 1.5-1.6 and (iii) ≥2.0. The lowest range of ratios was associated with the lowest applied activity (23 MBq) and the shortest acquisition times (4-15 sec per projection, 5 min total), while considerably higher activity (≥53 MBq) and acquisition times (20-40 sec per projection, 20-24 min total) produced ratios of the highest range. Consequently such parameters were selected for the dynamic scan. In this scan a mean specific binding ratio of 1.33±0.09 could be demonstrated with minor variations (-10% to +12%) over the entire imaging period. **Conclusions:** If activity or acquisition time is selected too low even sensitive imaging technology could not retrieve adequate contrast of specific over non-specific binding. However, using sufficient activity and acquisition time constant equilibrium binding could be demonstrated up to three hours as it has been reported in the literature for the same radiopharmaceutical based on bio-distribution studies.

## PW048

### Evaluating Effects of Daily Rhythm on Central SERT Activity Using 4-[$^{18}$F]-ADAM PET/CT

**M. Wang**[1,2], C. Chien[2], P. Wang[2,3], T. Kuo[2], J. Kuo[2], C. Yang[2], C. Ho[2], W. Lin[2], W. Huang[4,5]; [1]Institute of Biotechnology, National Taiwan University, Taipei, TAIWAN, [2]Institute of Nuclear Energy Research, Taoyuan, TAIWAN,

[3]School of Veterinary Medicine, National Taiwan Univesity, Taipei, TAIWAN, [4]Departments of Research and Nuclear Medicine, Changhua Christian Hospital, Changhua, TAIWAN, [5]National Defense Medical Center, Taipei, TAIWAN.

***Background***: Serotonin transporter (SERT) is crucial in management of patients with major depression. It also reported to be related to daily rhythm with higher uptake in dark phase than light phase. N, N-dimethyl-2-(2-amino-4-[$^{18}$F] fluorophenylthio)benzylamine (i.e. 4-[$^{18}$F]-ADAM) has been served as a SERT specific PET radioligand. The study was undertaken to observe changes of SERT activity in different brain regions including the Harderian gland after periods of dark and light on status using 4-[$^{18}$F]-ADAM PET. ***Methods***: Twelve Sprague-Dawley rats (aged 6-8 wks, weighted 200-250g) were raised in 48h consecutive light and dark phases (n=6 for each phase). The rats were then scanned 30min with nanoPET/CT 1hr after 1mCi of 4-[$^{18}$F]-ADAM intravenous injection under 5% isoflurane anesthesia. Imaging data were reconstructed and analyzed by InVivo Scope and PMOD software and expressed as specific region-to-cerebellar uptake ratios (SURs). Immunohistochemical stain (IHS) and Western blot assay (WBA) were also applied to verify presence and quantity of SERT in corresponding brain regions. ***Results***: Our preliminary data revealed a trend yet not statistically significant of increased 4-[$^{18}$F]-ADAM uptake in the striatum, thalamus and midbrain in the dark group compared to that of the light group. The averaged SURs in Harderian gland were 5.23±0.45 and 5.14±0.93 in the light and dark groups respectively. Results of IHS and WBA were consistent with imaging findings. However, there was no significant uptake of SERT in Harderian gland using both IHS and WBA. ***Conclusions***: The central SERT changes might be not apparently affected by daily rhythm as evaluated by 4-[$^{18}$F]-ADAM PET. The commonly found high uptake in the Harderian gland is more likely due to nonspecific accumulation which is also not associated with the light/dark rhythm.

## PW049

### Brain nor-β-CIT Binding Is Related to the Short Term Heart Rate and Cardiac Repolarisation Interval Variability on ECG in l Homozygotes by Serotonin Transporter Gene Polymorphism (5-HTTLPR)

**E. Kauppila**[1,2], J. Lipponen[2], M. Tarvainen[2], S. Kaurijoki[2], L. Karhunen[2], K. H. Pietiläinen[3,4], A. Rissanen[3,4], J. Kaprio[5,4], U. Pesonen[6], J. Tiihonen[5,2,7], E. Vanninen[1]; [1]Kuopio University Hospital, Kuopio, FINLAND, [2]Univeristy of Eastern Finland, Kuopio, FINLAND, [3]Helsinki University Hospital, Helsinki, FINLAND, [4]University of Helsinki, Helsinki, FINLAND, [5]National Institute for Health and Welfare, Helsinki, FINLAND, [6]University of Turku, Turku, FINLAND, [7]Karolinska Institutet, Stockholm, SWEDEN.

**Background**: Intrabrain structural correlation or functional connectivity is related to serotonin transporter gene polymorphism (5-HTTLPR) with more integrated pattern in l homozygotes than in s carriers. S carriers have been reported more fragile and at risk for depression. We previously reported heart rate (HR) corrected repolarisation interval (QTc) on ECG was related to brain serotonin transporter binding (SERT) in healthy young l homozygotes, but not in s carriers. Whether this relationship reflects association between autonomic control of the heart and brain SERT needs further clarification. **Aim**: To explore the relationship between brain nor-β-CIT binding and autonomic cardiac function by using spectral analyses of HR and cardiac repolarisation interval variability on ECG. **Methods**: Twenty-eigth young adults (26 ± 1.7 yrs, fifteen women) were studied; fifteen l homozygotes and twelve s carriers according to 5-HTTLPR genotyping, (including seven and five twin pairs, respectively). Brain imaging was performed with iodine-123 labeled 2β-carbomethoxy-3β-(4-iodophenyl) nortropane (nor-β-CIT) SPECT. Continuous ECG recording was obtained from each subject at rest. Computed analyses of the short term fluctuations of HR and ventricular repolarisation interval (from the beginning of R wave to the end of T wave, or RTe), as metrics of autonomic cardiovascular control, were performed. Brain imaging and ECG data were analysed blindly to the other study data. Significant level was set as $P < 0.05$. **Results**: High frequency, or HF(= parasympathetic), and low frequency, or LF, (=mixed parasympathetic and sympathetic) fluctuations of HR and RTe variability were related to striatal and thalamic nor-β-CIT binding in l homozygotes by 5-HTTLPR, but not in s carriers. [In l homozygotes correlations for HF HR and RTe variability and thalamic SERT were -0.64 ($p = 0.01$) and -0.67 ($p = 0.006$), and correlations for LF HR and RTe variability and thalamic SERT were 0.64 ($p = 0.01$) and 0.68 ($p = 0.006$), respectively.] HF/LF variability, or striatal/thalamic nor-β-CIT binding, were not related to body mass index, HR, or blood pressure in l homozygotes. Midbrain nor-β-CIT binding was not related to HF/LF HR or RTe variability**. Conclusions**: In line with studies with interest on functional connectivity in the brain our results showed differentiated coupling patterns of autonomic control of the heart and thalamic/striatal nor-β-CIT binding by 5-HTTLPR genotype.

## PW050

### The Role of Acetyl-L-Carnitine in the Mice Brain Glucose Uptake

**L. Cunha**[1,2], S. Fernandes[2], J. Bravo[2], D. Máthé[3], I. Horváth[3], D. S. Veres[3], K. Szigeti[3], L. F. Metello[1], T. Summavielle[2]; [1]Nuclear Medicine Department, High Institute for Allied Health Technologies, Polytechnic Institute of Porto (ESTSP.IPP), VILA NOVA GAIA, PORTUGAL, [2]Neuroprotection Lab, Institute for Molecular and Cell Biology (IBMC), Porto, PORTUGAL, [3]Nanobiotechnology & In Vivo Imaging Center, Semmelweis University, Budapest, HUNGARY.

Acetyl-L-Carnitine (ALC) has been described as playing a role on metabolic compromising diseases, especially those related to mitochondria. Considering that deficiencies in mitochondrial energy metabolism play a pivotal role in the pathogenesis of the main human neurodegenerative diseases, we aim to clarify the role of ALC in neuronal metabolism. In vivo assays using C57BL/6J mice were performed to assess brain glucose uptake under the action of ALC. Methamphetamine (METH) was used due to its potential to reduce the rate of cerebral glucose uptake. Mice were divided into 4 groups, according to different treatments: group 1 (control), group 2 (ALC, 100 mg/kg), group 3 (METH, 10 mg/kg) and group 4 (ALC+METH). 18F-FDG was injected and images were acquired in a PET/MRI scanner (nanoScan, Mediso, Hungary). Images were co-registered and visualized using Interview FusionTM (Mediso, Hungary) and VivoQuant (inviCRO, USA) dedicated image processing software. We have also used advanced post processing Hybrid Viewer™ software, (HERMES Medical Solutions, Sweden). 18F-FGD brain uptake was calculated using the standardized uptake value. Due to the known role of insulin growth factor (IGF) signaling cascade in brain metabolism, Igf1 and Igf1R transcript levels were also determined in the striatum by real-time polymerase chain reaction (RT-PCR). Results show that the tested dose of METH had no significant impact on glucose uptake, while ALC led to a nearly significant reduction. However, when ALC was administered previously to METH, a significant increase in glucose uptake was evidenced. Prefrontal cortex was one of the most affected regions, displaying increased glucose uptake in the ALC/METH group that was significant when compared to all other conditions ($p<0.001$ to ALC and METH and $p<0.01$ to control). The right striatum was also a highly affected region, displaying a very similar increase in uptake in the ALC/METH group ($p<0.001$ to ALC and METH and $p<0.01$ to control). In the left striatum differences were significant when compared to ALC ($p<0.001$) and METH ($p<0.01$), but not to control. Decreased Igf1 levels were observed in the striatum, induced by METH ($p<0.001$); this was prevented by the previous administration of ALC. ALC by itself increased Igf1 levels ($p<0.05$). Transcript levels of Igf1R were significantly increased in the ALC/METH group ($p<0.01$). The present results show that the administration of ALC in mice preconditioned with a single dose of METH led to a robust increase in glucose uptake, paralleled by increased Igf1R transcript levels.

PW06 - Monday, Oct. 21, 8:30 - 9:30, Poster Exhibition Area

## Poster Walk 6 - Oncology: Lung, Breast, Endometrial Cancers & Lymphoma

## PW051

### The Imaging Characteristics of F-18 FDG PET-CT on Epidermal Growth Factor Receptor Mutations in Non-small cell Lung Cancer

**B. Degirmenci Polack**[1], Y. Baskin[2], N. Karahan[1], G. Calibasi[3], O. Unal[4], I. Oztop[4], R. Bekis[1], A. Akkoclu[5]; [1]Dokuz Eylul University Medical School Nuclear Medicine Department, Izmir, TURKEY, [2]Dokuz Eylul University Institute of Oncology Basic Oncology Department, Izmir, TURKEY, [3]Dokuz Eylul University Institue of Oncology Basic Oncology Department, Izmir, TURKEY, [4]Dokuz Eylul University Medical School Medical Oncology Department, Izmir, TURKEY, [5]Dokuz Eylul University Medical School Chest Disease Department, Izmir, TURKEY.

**Aim**: We aimed to compare F-18 FDG PET-CT imaging charactericitics in non-small cell lung cancer (NSCLC) with and without epidermal growth factor (EGFR) reseptor mutation. **Methods**: A total of 47 NSCLC patients (38 male, 9 female, mean age : 47±10.45 )were included in this retrospective study. All patients underwent EGFR mutation resting and pretreatment F-18 FDG PET-CT scan. The maksimum standardized uptake (SUVmax) of the primary tumor and metastases was calculated for all lesions in all patients. We compared the SUVmax values for primary tumor and metastatic lesions in patients with and without EGFR receptor mutation. **Results**: In our study group, there were 17 adeno, 10 squamous, 2 large cell, 1 mixt-type and 17 non-small cell cancer patients. Seven patients had EGFR-mutant and 40 patients had EGFR wild-type tumors. There was a trend for higher SUVmax in primary tumors among patients with EGFR-mutant (mean SUVmax: 14.20±10.40) versus patients with wild-type EGFR (mean SUVmax:11.53±6.46). In patients with wild-type EGFR, the mean SUVmax was 7.05±3.39, 7.83±4.66, 6.10±4.44, 12.83±4.89 for hilar(17 pts), unilateral mediastinal (23 pts), contralateral mediastinal (13pts) and supraclavicular (3 pts) lymph node metastates (LNM), respectively. In 5 patients with EGFR-mutant , SUVmax was 6.48±3.39 for unilateral mediastinal LNM. There was no hilar, contralateral and supraclavicular LNM which

can be demonstrated by F-18 FDG PET-CT in EGFR-mutant patients. The mean SUVmax was 7.97±6.67, 8.98±4.31 and 5.85±3.39 for lung (6 pts), bone (9 pts) and adrenal (6 pts) metastases in wild- type EGFR patient group. In EGFR-mutant group , one patient had lung, bone and adrenal metastases in which SUVmax was 4.2, 11.20 and 22.20, respectively. **Conclusion**: Higher FDG uptake was found in primary tumors among EGFR-mutant patients than wild-type EGFR patients. In this study group, the incidence of hilar, contralateral mediastinal and supraclavicular LNM were higher in wild-type EGFR group than that in EGFR-mutant group. Bone and adrenal metastases in a patient with EGFR-mutant showed markedly increased FDG uptake. Further analyses with large number of patients are needed to describe a predictive role of FDG uptake on EGFR mutations in NSCLC patients.

## PW052

### An early timeframe allows a better evaluation of local metabolic response to stereotactic radiotherapy (SBRT) in early stage non-small cell lung cancer (NSCLC).

**B. Dib**[1], M. Marcenaro[2], M. Massollo[1], A. Fozza[2], G. Cittadini[3], E. Monteverde[1], C. Marini[4], G. Sambuceti[1], S. Morbelli[1]; [1]Nuclear Medicine Unit, IRCCS AOU San Martino - IST, DISSAL, University of Genoa, Genoa, ITALY, [2]Radiation Oncology Department, IRCCS AOU San Martino - IST, DISSAL, University of Genoa, Genoa, ITALY, [3]Radiology Department, IRCCS AOU San Martino - IST, Genoa, ITALY, [4]Institute of Molecular Bioimaging and Physiology, CNR, Section of Genoa, ITALY, Genoa, ITALY.

**Purpose**: To assess the more suitable timeframe for the evaluation of metabolic response to SBRT in patients with early stage NSCLC. **Methods**: Thirty-seven patients with stage 1 NSCLC were treated with SBRT (dose = 48-60 Gy, 4-8 Fx). All patients underwent 18F-FDG PET scan three times: at baseline before SBRT (PET1), 4-5 (PET2) and 10-12 months (PET3) post-SBRT. PET-based metabolic response was evaluated by means of EORTC criteria. Standardized uptake value (SUVmax) of the residual lesion after SBRT was recorded and visual assessment was performed to assess demarcation of residual lesion with respect to surrounding tissues (ill/diffuse or focal/well-defined). Histopathology when available or clinical-radiological follow up with contrast-enhanced CT of at least 1year served as standard reference. **Results**: The thirty-six NSCLC were T1N0 =86% and T2aN0 =14% respectively. Average SUV max at baseline was 6.5±4.2(range 2.5-12.7). EORTC metabolic Complete or Partial Response (CR and PR) were 44% and 47.2 % for PET2 and 19% and 77.8% for PET3 respectively. Metabolic stable disease was evident in 2 patients both in PET2 and PET3. Average SUVmax was 2.9±2 for PET2 and 3.6±2.2 for PET3. In particular, in 14 patients (38.9%) SUVmax increased from PET2 to PET3 but none of these patients was proven to have residual disease or disease relapse. Only in 5 patients (13.9%) SUVmax significantly decreased from PET2 to PET3 while it remained stable in 17 patients (47.2%). However more than a half of patients with decreased/stable SUVmax between PET2 and PET3 were already classified as CR in PET2. At visual analysis 5/36 lesions still showed focal/well-defined FDG uptake at PET2 and only 3/36 at PET3, while all the remaining lesions showed diffuse/ill defined uptake. In agreement with their diffuse metabolic pattern, all lesions with ill defined FDG uptake were also judged as flogistic at contrast-enhanced CT. **Conclusion:** Metabolic response after SBRT is rapid and well evident as soon as 4 months after SBRT. A later evaluation of metabolic response did not improve accuracy of metabolic EORTC-based evaluation. On the contrary in a significant number of patients SUVmax value might increase from 4 to 12 months after therapy due to late post-actinic inflammatory response. The present data further testify that metabolic profile of lung lesions treated with SBRT is extremely different from what evident after conventional radiotherapy. Accordingly after SBRT an earlier evaluation is more likely to avoid false positive results due to late inflammatory response.

## PW053

### Correlation between (18)F-FDG uptake on PET/CT and time intensity curve on dynamic MRI in patients with breast cancer

**K. TAMURA**[1], K. Suzuki[1], I. Sakata[1], K. Yoshikawa[2], S. Ohashi[2], S. Toubaru[2], N. Shigematsu[3], K. Murakami[3], S. Kosuda[4], K. Hayashi[4], J. Ishida[1]; [1]Tokorozawa PET Diagnostic Imaging Clinic, Tokorozawa, JAPAN, [2]National Institute of Radiological Sciences, Chiba, JAPAN, [3]Keio University Hospital, Department of Radiology, Tokyo, JAPAN, [4]National Defense Medical College, Department of Radiology, Tokorozawa, JAPAN.

**OBJECTIVE:** The objective of this study is to investigate the relationship between accumulation of 2-deoxy-2-[(18)F] fluoro-D: -glucose (FDG) and dynamic contrast enhanced MRI in patients with breast cancer **METHODS:** Consecutive 64 patients who had histologically proven breast cancer and underwent FDG-PET/CT and dynamic contrast enhanced MRI on a same day in Jan. 2012- Feb.2013 were evaluated. FDG uptake in the breast cancer lesion was evaluated by means of SUVmax both 60 and 120min after FDG injection. The MRI data analysis was designed to assess the value of lesion enhancement kinetics using time intensity curve (TIC). We categorized TIC into three types: Type1: steady increase; Type2: plateau; Type3: wash-out. Probavility value (p-value) < 0.05 indicated a statistically difference when we compared the two groups. **RESULTS:** The average patient age was 58.5±13.7years (range 34-86 years). The average maximum tumor size measured by MRI was 27.7±21.0mm (range 9-130 mm). Mean SUVmax 60 min after FDG injection was 5.12±4.60 (range 0.50-20.3), and SUV max 120min after injection (d-SUVmax) was 6.30±6.37 (range 0.50-29.3). TIC was Type1 in 16 (26.6%) patients, Type2 in 6 (9.3%) patients and Type3 in 41 (64.0%) patients. Mean SUVmax was 2.77±2.63 in Type1, 7.60±6.93 in Type2, and 5.73±4.57 in Type3. Mean d-SUV max was 3.03±3.64 in Type1, 9.22±9.22 in Type2, and 7.22±6.42 in Type3. Mean SUVmax of Type1 was significantly lower than that of Type2 and Type3 (p=0.022 and p=0.016, respectively). Also mean d-SUVmax of Type1 was significantly lower than that of Type2 and Type3 (p=0.028 and p=0.015, respectively). No significant difference wad found between Type2 and Type3 both in SUVmax and d-SUVmax (p=0.39 and p=0.50, respectively). **CONCLUSIONS:**In breast cancer, Type1 time intensity curve which is representative of benign breast lesions showed significantly lower FDG uptake than Type2 and 3 that are common in breast cancer. We consider that our study indicates a good correlation between FDG uptake and TIC.

## PW054

### The clinical utility of tumor SUVmax for predicting axillary lymph node metastasis in invasive breast cancer with clinically negative axillary lymph node

Y. Kim[1], **B. Kim**[2]; [1]Department of dentistry, Ewha Womans University, school of medicine, Seoul, KOREA, REPUBLIC OF, [2]Department of nuclear medicine, Ewha Womans University, school of medicine, Seoul, KOREA, REPUBLIC OF.

**Objective**:The aim of this study was to evaluate the clinical value of 18F-fluorodeoxyglucose (FDG) uptake and the clinicopathologic or immunohistochemical findings of the primary tumor to predict axillary lymph node (ALN) metastasis in breast cancer with clinically negative ALN. **Methods** :This study retrospectively enrolled 104 women (49.43 ± 9.9 years) having breast cancer with clinically negative ALN using all types of preoperative imaging modalities including ultrasonography, FDG positron emission tomography (PET), and magnetic resonance imaging. All cases of breast cancer in this study were proven as invasive ductal carcinoma with ≥ 1 cm in size. The final diagnosis of ALN status was confirmed by permanent pathology after operation. **Results:**Among 104 breast cancers with clinically negative ALN, 21 breast cancers (20.2%) were proven to have ALN metastasis. The ROC curve analysis showed that the best cut-off value of SUVmax for identifying ALN metastasis was 9.8 with 33.3 % sensitivity and 92.8 % specificity (AUC = 0.656; $p$ = 0.027). The multivariable analysis revealed that primary tumors with SUVmax > 9.8 ($p$ = 0.011) and D2-40 positivity ($p$ = 0.027) were independently associated with ALN metastasis with odds ratios of 5.516 (CI = 1.475-20.6333) and 3.409 (CI = 1.154-10.072), respectively. **Conclusion**: Our study demonstrates that the incidence of ALN metastasis in even rigorously clinically evaluated breast cancer without suspiciously positive ALN is still not negligible, and while a high SUVmax of the primary tumor may be associated with a higher incidence of ALN metastasis in breast cancer with clinically negative ALN, a low SUVmax does not exclude ALN metastasis. (This research was funded by Basic Science Research Program (2012R1A1A1012913) and Bio & Medical Technology Development Program (2012M3A9B6055379) through the National Research Foundation of Korea (NRF) funded by the Ministry of Education, Science and Technology).

## PW055

### Are Standard uptake value and total lesion glycolisis of 18F-FDG PET/CT useful tools to predict neoadjuvant chemotherapy response in breast cancer?

**R. Jaller**, A. Domènech, M. Estorch, J. Duch, A. Montes, A. Fernández, V. Camacho, I. Carrió; Hospital De la Santa Creu i Sant Pau, Barcelona, SPAIN.

**Objectives:** This study was conducted to evaluate the role of 18F-fluorodeoxyglucose (18F-FDG) PET/ CT in the assessment of neoadjuvant chemotherapy response in breast cancer patients based on Standard uptake value (SUV) and total lesion glycolisis (TLG) values. **Methods**: Forty four women affected with breast cancer (mean age, 55 years, range, 29-86 years) and scanned with whole body 18F-FDG PET/CT prior to neoadjuvant chemotherapy were prospectively studied. Data from the 18F-FDG PET/CT studies were analyzed qualitatively and quantitatively taking the parameters (SUVmax and TLG) . Correlations between the parameters obtained on the 18F-FDG PET/CT studies and pathologic response observed in surgical specimens after the completion of chemotherapy were assessed and compared with the Miller and Payne grading system (MPGS). The association between the parameters analyzed and the MPGS was evaluated with one-way ANOVA test. **Results**: From 44 patients, 38 (77%) had locoregional disease and 6 (23%) had both locoregional disease and distant metastasis. The parameters measured gave the following results: mean SUVmax 8,61 (range 1,56-30,1) and mean TLG 223,36 (range 3-2046,36). Seven patients (16%) showed a MPGS response grade 1, 8 patients (18%) grade 2, 15 patients (34%) grade 3, 6 patients (14%) grade 4 and 8 patients (18%) grade 5. No statistical

differences were seen between SUVmax and TLG values and the MPGS (p > 0.05). Conclusions: The results obtained show no trend that relates values of the parameters measured (SUVmax and TLG) with histological response evaluated with MPGS. Therefore, these parameters are not useful to be considered as prognostic values for predicting the response to neoadjuvant chemotherapy. However, further studies as well as a larger patient cohort are needed to evaluate these findings.

## PW056

### Tumor Response Evaluation to Neoadjuvant Chemotherapy by Functional Imaging Technologies

**M. SIMO**, M. GONZALEZ CAO, B. UBEDA, F. TRESERRAS, C. ARA, J. BROWN, R. FABREGAS, S. BAULIES, A. MARTINEZ, M. CUSIDO; INSTITUTO UNIVERSITARIO QUIRON-DEXEUS, BARCELONA, SPAIN.

**Background**: Current Methods for tumor response evaluation during neoadjuvant chemotherapy (NCx) in breast cancer have shown limited success. Functional imaging technologies as FDG-PET and MRI could have a role. Objectives:Evaluate the accuracy of FDG-PET and MRI for tumor response evaluation to sequential NCx and explored correlation between SUVmax and size decrease with pathologic response. Design/population:Patients were treated with neoadjuvant chemotherapy (AC 4 cycles and taxol for 12 cycles). Tumor evaluation by FDG-PET and MRI was performed both pretreatment and following each treatment sequence. Pathologic response was evaluated by Miller-Payne criteria. EORTC criteria for PET response and RECIST criteria for RMI. 41 patients with histologically breast cancer T1-T4N0-3M0 were evaluated.FDG-PET and MRI were performed in 37patients. **Results**:SUVmax was higher in patients with HR negative tumors and tumors with high ki67. There were significant differences in median pretreatment SUV max value between patients with HR positive tumors versus HR negative (4.44 vs 8.68 p=0.002). There were also significant differences in median preSUVmax between tumors with low and high ki67 index:4.2 (1.5-8.5) versus 7.9(1.5-24)(p 0.049) The absolute value of SUVmax pretreatment was not predictive of pCR. Median SUV max in patients with pCR was 5(2.1-24), versus 5.7(1.5-17) in patients without pCR(p=0.59) There were no significant differences in SUVmax decrease after chemotherapy between patients with or without pathologic complete response. Relative decrease in FDG uptake after 3 months of chemotherapy tends to be greater in patients that had a pCR(75.8% vs 54.8%, p =0.069). There were significant differences in tumor size decrease by MR after chemotherapy between patients with pathologic complete response versus patients without response. Residual disease after chemotherapy: PET-CT had a high rate of false negative results before surgery. PET-CT performed before surgery had high specificity for residual disease(93.8%) but low sensitivity(21.4%), with an unaceptable rate of FN(78.6%) and an accuracy of 60% MR performed before surgery had high sensitivity for residual disease. MR performed before surgery had low specificity for residual disease(50%) but high sensitivity(100%), with a positive predictive value of 66.7% and an accuracy of 79% **Conclusion**: Pretreatment SUVmax was higher in HR negative and high KI67 tumors but was not predictive of pCR. MR was a better test for detecting residual disease after chemotherapy. Patients with a pathologic complete response had a significant decrease in tumor size by MR but did not have significant change in SUVmax comparing with non responding patients.

## PW057

### Feasibility of a dedicated breast PET for response monitoring during neoadjuvant chemotherapy.

**S. Teixeira**, B. B. Koolen, M. P. Stokkel, R. A. Valdés Olmos; Dutch Cancer Institute, Amsterdam, NETHERLANDS.

**Aim:** Both MRI and, more recently, 18F– FDG PET/CT have been shown to be useful for tumour response monitoring during neoadjuvant chemotherapy (NAC). In analogy with the hanging breast device for MRI used for these purposes a prone position PET/CT was introduced recently. However, PET/CT has limitations for small tumours, is often not able to detect uptake heterogeneity in tumours and it is mostly full– time planned with other diagnostic procedures. Against this background, the aim of the present study was to evaluate the feasibility of a dedicated breast PET for hanging breast imaging (MAMMI-PET) for response monitoring during NAC and to compare these results with those of prone position PET/CT. **Materials and Methods:**Patients referred for PET/CT in the context of NAC and who gave informed consent for an additional MAMMI – PET scan were included. The MAMMI – PET is a high – resolution device equipped with 12 LYSO – detectors and able to work with low 18F – FDG dosages. At baseline and during chemotherapy all patients were scanned with a prone position PET/CT, 60 ±10 minutes after injection of 180 – 240 MBq 18F – FDG. The MAMMI – PET was performed approximately 110 min after injection. Sixteen patients (mean age 50y) with completely visualised FDG – avid tumours were evaluable for response monitoring with both scans. The correlation for the differences were tested using the Pearson s exact test ( Δ – SUVmax) and an Interclass Correlation Coefficient (ICC) test (Δ – FTV) Uptake heterogeneity of the tumours visualized with the MAMMI – PET scan, before and after therapy, was compared according to the number of high intensity areas within the tumour.**Results:** A strong correlation was found for Δ – FTV with an ICC of 0,88. The SUVmax showed a correlation of 0,82 (P<0,001). A higher number of high intensity areas (range 1 – 8) was found in tumours with a larger FTV. In most tumours (N=10) FDG – avid areas within the tumours reduced in quantity during chemotherapy. **Conclusions:** Although different scanning timeframes were used, this study shows a correlation between PET/CT and MAMMI/PET regarding assessment of primary tumour parameters for therapy response. The MAMMI – PET may be of utility in primary tumour response monitoring alleviating PET/CT planning. Detection of tumour uptake heterogeneity by the MAMMI – PET needs further to be evaluated in response monitoring protocols.

## PW058

### Clinical value of F18-FDG PET/CT imaging for preoperative evaluation in patiens with endometrial cancer

B. Atmaca Saglık[1], **F. Canbaz Tosun**[1], M. Tosun[2], H. Celik[2], A. Kokcu[2], T. Alper[2]; [1]Ondokuz Mayis University Hospital, Faculty of Medicine,Nuclear Medicine, SAMSUN, TURKEY, [2]Ondokuz Mayis University Hospital, Faculty of Medicine, Gynecology and Obstetrics, SAMSUN, TURKEY.

**Aim**: Our aim was to evaluate the value of dual time F-18 FDG PET-CT imaging in patients with uterine cancer, compared to surgical-pathological findings.Moreover, agreement of MRI was investigated compared with surgery and F-18 FDG/CT findings. **Materials and Methods**: Thirty-four patients with endometrial carcinoma, underwent preoperative dual-phase FDG PET/CT were included in this study. A subgroup of 14 patients had also MRI preoperatively. Imaging results were evaluated using FIGO2009-staging system in both lesion and patient basis. Sensitivity, specificity, positive and negative predictive value(PPV,NPV) and accuracy values of both standard -delayed PET/CT scan and MRI results were calculated in detecting myometrial invasion, lymph node and distant metastasis. **Results:** Both standard and delayed-PET /CT results showed good agreement with the pathology(kappa: 0.68 to 0.79, p <0.001) in all regions. In region-based analysis, the sensitivity, specificity, PPV, NPV and accuracy of standard PET/CT for detecting myometrial invasion were 95%, 64%, 83%, 88% and 84%,respectively.Sensitivity,specificity,PPV, NPV and accuracy of delayed PET/CT for detecting myometrial invasion were 100%, 64%, 83%, 100% and 87% and the values were as %29, %86, %67, %55 and %57,respectively for MRI. Region-based analysis showed that sensitivity, specificity, PPV, NPV and accuracy of sPET/CTand dPET/CT for lymph node metastasis were 80%, 92%, 67%, 96% and 90%,respectively.The agreement was complete in the evaluation of pathologic lymph node detection between MRI and PET/CT(kappa= 1, p<0.001). For the evaluation of distant metastasis, the sensitivity, specificity, PPV, NPV and accuracy of both sPET/CT and dPET/CT were 100%, 97%, 67%, 100% and 97%, respectively. There was complete agreement in only 7/14 patients (50%) between sPET-CT staging and MRI results regarding myometrial invasion. On patient basis, according to FIGO 2009-staging system, there was a strong correlation between surgical staging compared with both standard and delayed PET/CT results (kappa = 0.61, p=0.000, R=0.60, p=0.000). **Conclusion:** F-18 FDG PET/CT examination showed a strong correlation with surgical staging and had a complete agreement with the MRI examination results in our patients with endometrial cancer. In regional basis, F-18 FDG PET/CT showed better results than MRI in the evaluation of myometrial invasion. Our results suggest that F-18 FDG PET/CT imaging is an efficient imaging modality for patient selection before surgical staging due to the high NPV in the evaluation of metastatic lymph nodes. This functional imaging is also effective inpatients with advanced stages of the uterine cancer to complete the staging evaluation .

## PW059

### PET/CT Staging of Cutaneous Lymphoma

**P. J. Peller**, G. B. Johnson, C. H. Hunt; Mayo Clinic, ROCHESTER, MN, MN, UNITED STATES.

**OBJECTIVE**: The purpose of this study is to identify the utility of FDG PET/CT in staging patients presenting with lymphoma involving the skin, to quantify the frequency of extracutaneous disease and measure the degree of FDG avidity in specific disease subtypes. **MATERIALS AND METHODS**: A HIPPA compliant, retrospective review of patients with biopsy proven lymphoma involving the skin who underwent PET/CT examination for initial disease staging from 2000 to 2011 a single institution. The PET/CT scans were review without knowledge of clinical data and sites of disease involvement were documented according to cutaneous, nodal, splenic, hepatic and extranodal locations. The maximum standardized uptake value (SUV) was recorded for each disease site. The PET/CT results were compared to pathology and imaging data in the patient's electronic medical record. Lymphoma subtypes were grouped according to World Health Organization categorization. **RESULTS**. A total of 123 cutaneous lymphoma patients were evaluated with PET/CT from vertex to toes. There were 61 men and 62 women with a mean age of 49.8±17.5 year (range 19-86) and the majority, 92 (74.8%) patients had T-cell lymphomas (29 or 23.6% B-cell). All patients referred had T2 skin disease or greater. The cutaneous disease on PET/CT ranged from subtle, barely visible

plaques to thick bulky tumors with a wide range of SUVmax (1.0-21.2). In 89 (72.4%) patients only skin involvement was present. Nodal disease was present in 34 patients and the mean SUVmax was 4.5 with a range of 1.4-19.8. All patients with mycosis fungoides had positive nodes on PET/CT and biopsy. The highest nodal uptake was seen in patients with large cell transformation. There was splenic involvement in 6, liver in 2 and other extranodal disease in 4 patients, but all also had nodal disease. **CONCLUSION.** Cutaneous lymphoma is a very heterogeneous disease and FDG PET/CT identifies patients with biologically aggressive skin lesions and extracutaneous disease.

## PW060

### The Effect of Lymphoma Chemotherapy on Standard Uptake Value of Liver, in Positron Emission Tomography Imaging

H. P. Jonsson[1], A. Forgács[2], F. Bátyi[3], S. Barna[2], L. Papp[4], J. Varga[5], **I. Garai**[2]; [1]Medical School, University of Debrecen, HUNGARY, [2]ScanoMed Ltd., DEBRECEN, HUNGARY, [3]Nuclear Medicine, Kenézy Hospital, Debrecen, HUNGARY, [4]Mediso Ltd, Budapest, HUNGARY, [5]Nuclear Medicine, University of Debrecen, HUNGARY.

**Background**: Positron emission tomography, combined with computer tomography (F18-FDG PET/CT), has increasing importance in the management of Lymphoma. When evaluating the early response to a chemotherapy treatment, a F18-FDG PET/CT scan is performed and choice of treatment affected by its outcome. By measuring the standard uptake value (SUV) of a tumor, its metabolic activity may be assessed and thereby the efficacy of the treatment. For quantifying changes of the tumor metabolism, the liver activity is commonly used as a reference. Considering the cost and morbidity of chemotherapy and the importance of correct treatment, we aimed to see if chemotherapy has any effect on liver SUV and thereby possibly have an impact on the evaluation of treatment efficacy. Aim of our study was to see if lymphoma chemotherapy has any effect on liver SUV. **Materials and Methods**: 32 lymphoma patients were included this retrospective study. We analyzed 3 consecutive F18-FDG PET/CT scans in all of these patients: Before (P1-Staging), during (P2- Interim) and after chemotherapy (P3-Restaging) studies. All of the PET/CT evaluations were performed in 1 year. We drew three 50 mm diameter sherical volume of interests- VOIs- (InterViewFusion1.8) on the right lobe of the liver and measured the density (HU) and tracer uptake (SUV) in them.We statistically analyzed the changes in the density and uptake values during the follow up studies. **Results**: The localisation of the VOIs did not singificantly influence on the measured values (nor HU neither SUV). There was no significant change in HU. (Paired Friedman test, p=0.058) We found no significant change in SUV mean between P1 and P3 (Paired Friedman Test, p>0.1). However we found significant, increase in SUV mean of the liver between P1 and P2 (Wilcoxon Signed Ranks Test, p=0.045) **Conclusion**:During visual assesment of FDG-PET/CT studies, the liver is widely accepted as a reference region. However, based on our results, we propose that the changes in hepatic uptake values should be taken into account.during visual analysis. Extended number of patients is needed to confirm these preliminary results.

PW07 - Monday, Oct. 21, 8:30 - 9:30, Poster Exhibition Area

## Poster Walk 7 - Radionuclide Therapy & Dosimetry: Treatment of Benign & Malignant Thyroid Diseases

## PW061

### Non-inferiority of 30 versus 100 mCi of 131-I in post-surgical ablation in patients with differentiated thyroid carcinoma

V. Markovic, A. Punda, **D. Eterovic**; University Hospital Split, Split, CROATIA.

**Background:** Meta-analysis reported inconclusive comparison of 30 vs. 100 mCi 131-I ablative activities for post-surgical remnants in patients with differentiated thyroid carcinoma (DTC), apparently due to heterogeneity. We use measures to maximize the likelihood of success of ablation and present our results. **Methods**: In the period 2008-2010, at the University Hospital Split, 221 patients with non-metastatic T1/T2 DTC underwent radioiodine ablation. In order to avoid stunning the diagnostic 5 mCi 131-I imaging was omitted; the patients were also advised on low iodine diet. According to referring physician preferences the activities of I-131 were either 30 mCi (N=108) or 100 mCi (N=113). The unsuccessful ablations were repeated. **Results**: The groups were well balanced. The success of ablation, defined by negative scintigraphy at 6-12 months follow-up, was achieved in 85 (79%) of patients in 30 mCi arm (average total activity 41 mCi), and in 91 (89%) of patients in 100 mCi arm (average total activity 107 mCi). In the subset of 96 (43%) patients the thyroglobulin (Tg) concentration could not be used to monitor the success of ablation, due to presence of antibodies to Tg (N=45) or Tg being negative at baseline (N=51). The success of ablation, assessed by Tg changes in the rest of patients, was 79% in 30 mCi arm and 83% in 100 mCi arm. **Conclusion**: Avoiding of diagnostic scintigrahy and low iodine diet was associated with better success of radioiodine ablation of post-surgical thyroid remnant tissue than reported in meta-analysis. Relatively small greater efficacy of 100 vs. 30 mCi of 131-I does not seem to pay-off for about 2.6 times grater radiation exposure.

## PW062

### Negative predictive value of 124I-PET/CT imaging in patients affected by metastatic thyroid cancer and treated with 131I.

**C. Pettinato**[1], C. Nanni[2], M. Celli[2], V. Allegri[2], F. Monari[3], S. Cima[3], S. Civollani[1], P. Zagni[2], R. Mazzarotto[3], E. Spezi[4], S. Fanti[2]; [1]AOU S.Orsola Malpighi, Medical Physics Unit, Bologna, ITALY, [2]AOU S.Orsola Malpighi, Nuclear Medicine Unit, Bologna, ITALY, [3]AOU S.Orsola Malpighi, Radiotherapy Unit, Bologna, ITALY, [4]Velindre Cancer Centre, Department of Medical Physics, Cardiff, UNITED KINGDOM.

**Aim:** Patients affected by metastatic Differentiated Thyroid Cancer (mDTC) are treated with 131I even in presence of negative diagnostic 131I whole body scan. Actually, very often, these patients present positive post therapy 131I whole body scan, showing iodine avid metastases that were not seen with the diagnostic imaging. The aim of this work was the evaluation of the feasibility to use 124I PET/CT images to predict patients who will not benefit from the iodine therapy, because of the absence of avidity, avoiding useless treatments. Material and **Methods**: Twenty-five patients affected by mDTC were enrolled in the study approved by the ethical Committee of our Institution, with the aim to evaluate the usefulness of 124I PET/CT sequential scans to predict absorbed doses to metastatic thyroid cancer patients undergoing 131I therapy. Patients were divided into 4 groups, based on their histology: groupA, 4 pts with follicular cancer; groupB, 13 pts with papillary cancer; groupC, 2 pts with papillary tall cells cancer; groupD, 6 patients with papillary cancer with follicular variant. Patients showing negative 124I-PET/CT were treated with a reduced dose of 131I (3700 MBq) and post treatment WB scans were acquired 96 hours after the therapeutic administration. **Results**: Twelve patients showed at least one metastatic lesion at 124I PET/CT imaging, and most of the lesions were visible at the 24 hours scan (4 pts groupA, 3 pts groupB, 5 pts groupD). The remaning 13 patients did not show any uptake of all known metastatic lesions at each PET/CT time points (10 pts groupB, 2 pts groupC, 1 pt groupD). Negative PET/CT findings were confirmed by post therapy WB scan. **Discussion and Conclusion**: 124I-PET/CT scan is a useful diagnostic tool to discriminate patients with iodine avid metastases. Actually, when they are present, the superiority of PET/CT resolution and sensitivity, compared to standard 131I planar imaging, allow the characterization of all lesions leading to a more precise dosimetry. Furthermore, the negative predictive value of 124-PET/CT is useful to avoid useless treatments, sparing organ at risk such as salivary glands and red marrow. To conclude we encourage the use of 124I-PET/CT imaging to select patients candidate to 131I therapy that will have chance to benefit by the treatment.

## PW063

### Is It Necessary to Perform Control Diagnostic $^{131}$I Whole Body Scan After Remmant Ablation in Differentiated Thyroid Carcinoma Patients Who Have Stimulated Tg Levels Under 2 ng/ml?

E. Kalender[1], **U. Elboga**[1], Y. Celen[1], H. Demir[1], E. Sahin[2], M. Yilmaz[1]; [1]Gaziantep University, GAZIANTEP, TURKEY, [2]Namik Kemal University, Tekirdag, TURKEY.

**Introduction:** The aim of this retrospective study is to evaluate whether diagnostic I-131 whole body scan (DWBS) performed 6-12 months after thyroid remnant ablation is necessary or not in differentiated thyroid carcinoma (DTC) patients with thyroglobulin (Tg) levels under 2 ng/ml and negative anti-Tg antibodies. **Materials and Methods:** The study included 812 DTC patients undergoing the first control DWBS with Tg levels under 2 ng/ml and negative anti-Tg antibodies in the hypothyroid state, 6 months after postsurgical radioablation of residual thyroid tissue. Second DWBS was performed 18 months after ablative I-131 treatment (AIT) to 572 patients who had negative first control DWBS. These 572 patients had a stimulated Tg level under 2 ng/ml at 18th month control. **Results:** The first control DWBS, 6 months after thyroid ablation, was negative in 789 (97.2%) patients and was positive for minimal residual uptake in the thyroid bed in 23 (2.8%) patients. Nine of the 23 patients with residual thyroid bed uptake, received a second dose of radioiodine therapy for complemantary ablation of residual thyroid. Fourteen patients were not retreated. Second DWBS performed 18 months after AIT, was negative in all patients. **Conclusion:** Our data suggest that in patients with stimulated Tg level under 2 ng/ml, DWBS performed 6 months after AIT, is informative only in minority of patients for residual uptake in the thyroid bed which is usually clinically not relevant. Therefore, we suggest that the DWBS may be avoided in patients with stimulated Tg level under 2 ng/ml.

## PW064

### Influence of radioiodine therapy on ocular changes and their relation to urine cotinine level in patients with Graves' ophthalmopathy

A. Czarnywojtek[1], M. Zgorzalewicz-Stachowiak[2], **R. Czepczynski**[1], B. Budny, MD[1], E. Florek, MD PhD[3], K. Komar-Rychlicka[4], M. Ruchała, MD, PhD[1]; [1]Dept. of Endocrinology, Poznan University of Medical Sciences, Poznań, POLAND, [2]Department of Health Prophylaxis, Poznan University of Medical Sciences, Poznań, POLAND, [3]Department of Toxicology, Poznan University of Medical Sciences, Poznań, POLAND, [4]Dept. of Ophthalmology, Poznan University of Medical Sciences, Poznań, POLAND.

Radioiodine therapy (RIT) is frequently used as the definitive treatment in patients with Graves' hyperthyroidism when remission is not achieved with anti-thyroid drugs (ATDs). In this observational study, we intended to examine whether the use of high doses of radioiodine (RAI) [22 mCi (814 MBq)] with prophylaxis of oral glucocorticoids (oGCS) does not exacerbate Graves ophthalmopathy (GO) in smokers and non-smokers, especially with regard to cotinine concentrations and ocular changes before and after RIT. **Material and Methods**: The studied group consisted of 26 smokers, aged 28-61 years and 25 non-smoker patients, aged 21-54 years, respectively. The patients were qualified to RAI after one-year of ineffective ATDs treatment. Criterion for inclusion in the study were patients with mild GO with hyperthyroidism at diagnosis based on the severity (NOSPECS) and activity (CAS) scale. All the patients were subjected to RIT with oGCS prophylaxis and evaluated prospectively during a one-year follow-up. The ophthalmological examination was performed at various stages of RIT: initial pre-radioiodine administration, at the time of treatment 6, and 12 months after RAI. Urine cotinine measurement was employed to detect nicotine exposure, also in regard to smoking intensity. **Results**: TSHR-Abs concentration was higher in smokers ($P < 0.05$), rising from 22.9±1.2 IU/L before therapy to 29.6±5.3 IU/L at 2 months, 32.6±8.6 IU/L at 6 months, and 28.9±10.6 IU/L at 12 months after RIT. These observed changes were statistically different between groups at baseline ($P < 0.05$) and after one-year follow-up ($P < 0.005$). Mean urine cotinine were considerably higher in smokers comparing to non smokers in each point of. CAS values in the smoking group before RIT increased statistically from 2.8 ± 0.2 points at baseline to 4.3 ± 0.3 after 6 months, and 4.0 ± 0.5 (12 months), while in the non-smoking patients it was 1.4 ± 0.2, 2.8 ± 0.3 and 2.2 ± 0.2, respectively. Urinary cotinine excretion correlated positively with CAS and TSHR-Ab in the smoking group ($r = 0.41$; $P <0.05$) at baseline and during follow-up. In the NOSPECS classification, the symptoms changed from mild to moderate, mostly in smoking patients. **Conclusions:** Ablative RIT dose with prophylactic oral prednisone is a safe treatment in both smokers and non-smokers with mild GO. The post hoc analysis showed that urinary level of cotinine can be very helpful in the assessment of exacerbation of ophthalmological clinical symptoms before and after RIT particularly in smokers.

## PW065

### The prognostic value of BRAF mutation and lymph node metastases in patients with papillary thyroid cancer

**E. Takacsova**; St. Elisabeth Cancer Institute, Bratislava, SLOVAKIA.

**Aim:** To assess the prognostic significance of BRAF mutation and lymph node metastases in patients with papillary thyroid cancer. **Method**: Between January 2010 and March 2012, we retrospectively analysed 172 patients after total thyroidectomy with neck dissection for papillary thyroid cancer. Mutation in the BRAF gene (V600E) was assessed in all of the enrolled patients. According to TNM classification, 56 (33%) patients were in low risk group and 116 (67%) patients in high risk group. Among high risk group, 105 out of 116 (90%) patients were presented with lymph node metastases. Thyroablation with radioactive iodine was performed in all of the patients enrolled in the study. Persistent or recurrent disease was diagnosed in 42 (24%) patients during radioiodine therapy. **Results and conclusion**: BRAF mutation did not appear to be significant unfavourable prognostic factor in our cohort: it was present in 55% of low risk patients, in 48% of high risk patients and in 46% of patients with lymph node metastases. In patients with persistent or recurrent disease, BRAF mutation was found in 48%. But we confirmed that presence of lymph node metastases in time of initial surgery (61% of all patients) appeared to be prognostically significant: neck dissection enabled a more precise classification of patients into the high risk group - up to 95% of patients with persistent or recurrent disease diagnosed during radioiodine therapy belonged to the high risk group in the beginning of therapy. Key words: papillary thyroid cancer, BRAF mutation, neck dissection, lymph node metastases

## PW066

### Stimulated Tg Level Measurements May be Avoided in Differentiated Thyroid Carcinoma Patients Who Have Undetectable Basal Tg Levels

E. Kalender[1], **U. Elboga**[1], Y. Celen[1], H. Demir[1], E. Sahin[2], M. Basibuyuk[1], M. Yilmaz[1]; [1]Gaziantep University, Gaziantep, TURKEY, [2]Namik Kemal University, Tekirdag, TURKEY.

**Objective:** The aim of this retrospective study is to evaluate the diagnostic value of undetectable basal thyroglobulin (Tg) levels measured 6 months after ablative $^{131}$I treatment (AIT) in patients with differentiated thyroid carcinoma (DTC). **Materials and Methods:** The study included 159 patients (140 women, 19 men with , mean age 43.4±15.6) who had undetecable basal Tg levels (<0.2 ng/ml) and negative anti-Tg antibodies, 6 months after AIT. Histologic examination was papillary thyroid carcinoma in 151 patients and follicular thyroid carcinoma in 8 patients. To control the AIT efficacy, diagnostic whole body scan (DWBS) was planned 6 months after AIT. Before DWBS, basal and stimulated Tg levels were measured and compared. Then all patients underwent DWBS. **Results:** All patients (with undetectable basal Tg level) had a stimulated Tg level under 2 ng/ml. Stimulated Tg levels were undetectable (<0.2 ng/ml) in 142 (89.3%) patients and 0.58±0.26 ng/ml (range 0.3-1.3 ng/ml) in 17 (10.7%) patients. The control DWBS, 6 months after thyroid ablation, was negative in 151 (95%) patients and was positive for minimal residual uptake on the thyroid bed in 8 (5%) patients. Stimulated Tg levels of patients with residual thyroid bed uptake on control DWBS, were undetectable (<0.2 ng/ml) in 4 patients and 0.8±0.19 ng/ml (range 0.3-1.3 ng/ml) in 4 patients. **Conclusion:** Our data suggest that stimulated Tg level measurements may be avoided in DTC patients with undetectable basal Tg levels. Thus, unnecessary Tg stimulation with rhTSH or endogen TSH, diagnostic procedures (DWBS) and radiation exposure can be reduced.

## PW067

### Thyroid Cancer in Pediatric Patients treated with Iodine-131: A retrospective analysis

**A. Silva**, S. Vaz, T. C. Ferreira, P. Ratão, A. Daniel, L. Salgado; Department of Nuclear Medicine, Instituto Português de Oncologia de Lisboa Francisco Gentil, E.P.E., Lisboa, PORTUGAL.

**Aim**: To evaluate pediatric patients (pts) with differentiated thyroid cancer (DTC) treated with Iodine-131 (I131) in terms of clinical presentation of disease, histological findings, treatment response and follow-up (f-up). Patients and **Methods**: Retrospective analysis of pts with DTC, with age ≤18 years at diagnosis, treated with I131 (RAI) in our institution between 1997-2012. Fourty-six of the 51 DTC pediatric pts were included in the study. Five pts were excluded due to: insufficient f-up (<1y) - 1 pt; lost to f-up - 4 pts. The administered activity of I131 was based on clinical features, histological findings and patient's weight (20-110 MBq/kg). A whole body scan after therapy (WBI131) was obtained 2-3 days after administration of I131. **Results**: Pediatric pts corresponded to 1,3% of the total of pts treated during the period analysed. Mean age at the time of diagnosis was 13,5 y (range 5-18). Thirty-five pts (76%) were females and 11 pts (24%), males. At presentation, 31 pts (67,4%) had cervical involvement and 1 pt, lung metastases. One pt had familiar history of DTC and 2 pts (4,3%), cervical RT due to previous hematologic malignancy. All pts were submitted to thyroidectomy and cervical lymph node dissection (bilateral in 28,3%). Most pts (93,5%) had papillary cancer; 1 pt, follicular cancer; 1 pt, poorly differentiated cancer and 1 pt, a non specified epithelial-derived differentiated cancer. The primary tumor size ranged from 0,6-7,1 cm (2,75±1,38). Extrathyroidal extension was found in 26 pts (56,5%), multifocal disease in 22 pts (47,8%) and vascular invasion in 23 pts (50%). The WBI131 showed cervical iodine uptake in all the pts; 11 pts (24%) had mediastinal uptake and 10 pts (22%), pulmonary metastases. Twenty-nine pts (63%) had a single RAI. The RAI was repeated due to lung metastases in 10 pts (21,7%), lymph node metastases in 2 pts (4,3%) and increased thyroglobulin (Tg) levels in 5 pts (10,9%). At the last evaluation all the pts were alive. According to clinical, biochemical and imagiologic criteria 35 pts (76%) are considered without evidence of disease. In 11 pts (24%) the only evidence of disease are detectable levels of Tg (0,3-5,3 ng/mL). **Conclusion:** Pediatric pts with DTC usually present with extensive and aggressive disease. However, with appropriate therapy, they have favorable prognosis. The RAI plays an important role in the DTC staging and management in children and, therefore, should be used without hesitation in order to achieve remission and avoid recurrence.

## PW068

### Weight gain after stimulated thyroid-stimulating hormone for $^{131}$I-therapies in patients with thyroid cancer

**H. Seo**[1,2], J. Chung[1], G. Cheon[1], J. Paeng[1], K. Kang[1], D. Lee[1]; [1]Seoul National University Hospital, Seoul, KOREA, REPUBLIC OF, [2]WCU Graduate School of Convergence Science and Technology, Seoul National University College of Medicine, Seoul, KOREA, REPUBLIC OF.

**Purpose:** The extent and association of weight gain after TSH stimulation for $^{131}$I-therapies remains unclear. To evaluate the association factors of irreversible weight gain after $^{131}$I-therapies, we evaluated variable clinical factors. **Methods** : The studied population included 301 adult patients (69 men, 232 women). The enrolled patients were all asian and the average age was 53.4 ± 12.2. To prepare $^{131}$I therapy, 293 patients had experience of stimulated TSH during 4 weeks, 7 patients used both recombinant TSH and stimulated TSH during 4 weeks and 1 patient used recombinant TSH once. Clinical data including irreversible weight change before and after $^{131}$I-therapy, BMI, use of recombinant TSH drug, number of $^{131}$I-therapies, history of chronic diseases, exercise, diet, current thyroid cancer,

laboratory results of thyroid hormone, and subjective discomfort due to irreversible weight gain, were reviewed using questionnaire, interview, and electronic medical records. Subjective discomforts due to weight gain and body mass index (BMI) between pre-treatment and post-treatment of $^{131}$I-therapy were scored. Inter-rater agreement between subjective discomfort score and BMI increase was estimated. Logistic regression analysis was performed to evaluate multiple associating factors for irreversible weight gain. Statistical significance was less than 0.05. **Results** : Stimulated TSH level was 139.7 ± 74 and usual TSH was 1.30 ± 2.8 (normal range:0.4-4.1). TSH level was not associated with weight gain. All the studied patients showed normal range or suppressed level of TSH during follow-up. The associating factors for irreversible weight gain were diabetic mellitus, presence of thyroid cancer and initial BMI in multivariate analysis ($P$<0.05). 13% of studied patients showed irreversible weight gain (>5kg) after stimulated TSH for $^{131}$I-therapies. **Conclusions** : Association factors to the significant weight gain after $^{131}$I-therapies were diabetic mellitus, presence of thyroid cancer and initial BMI. TSH level were not correlated with irreversible weight gain. Therefore, further individual biologic factors should be evaluated to clarify the mechanism of obesity due to stimulated TSH period.

## PW069

### Efficacy of $^{131}$I SPECT/CT in the Initial Nodal Staging in Patients with Differentiated Thyroid Carcinoma at the First Ablative Radioiodine Therapy

**N. Kisiel**, A. Garcia-Burillo, M. Barios, F. Dellepiane, J. Castell-Conesa; Hospital Vall D'Hebron, Barcelona, SPAIN.

**Background:** After the first radioiodine ablative dose, planar Whole-Body Scanning (WBS) offers the possibility for detecting thyroid remnant, loco-regional node involvement and distant metastases. Nevertheless, available anatomic information is scarce and the high activity of thyroid remnants can interfere with the detection of cervical lymphatic nodes. **Objective:** To determine the additional value of the SPECT-CT over planar WBS, performed seven days after ablative treatment with $^{131}$I, in patients who were operated on for Differentiated Thyroid Cancer (DTC). **Methods:** From January 2009 to December 2012, 132 patients with DTC were admitted for radioablation with $^{131}$I after thyroidectomy. All of them underwent WBS seven days after ablation, and 91 had an additional SPECT-CT, 71 women and 20 men, with ages ranged from 15 to 89 yo (mean, age 54 yo). All patients had histological confirmed DTC (73 papillary, 17 follicular -2 cases with double tumour, papillary and follicular-, and 1 insular type). In addition to the thyroidectomy, lymph node dissection was performed in 54 patients (59%): 20 patients were classified as N0 and 29 as N1. The remaining 42 patients were classified as Nx. Planar and tomographic images were independently evaluated by two experienced nuclear medicine physicians. **Results:** 195 cervical focal uptake were observed in the 91 planar WBSs. No additional foci were observed in SPECT-CT. Compared to the nodal staging prior to ablation based on the histopathological diagnosis, we had an upstaging from N0 to N1 in 4 of 20 patients and from Nx to N1 in 2 of 42 patients, changing the stage in 6.6% of the patients. **Conclusions:** Iodine $^{131}$I SPECT-CT imaging adds relevant information to determine the nodal involvement compared to planar WBS. The indeterminate pattern in WBS was completely clarified en SPECT-CT image.

## PW070

### Impact of post-therapy SPECT-CT with 131I in the assesment of patients with differenciated thyroid cancer

**P. García-Talavera**[1], A. Sainz-Esteban[1], J. G. Villanueva[1], C. Gamazo[1], G. Díaz-Soto[2], M. L. González[1], M. Á. Ruiz[1], R. Olmos[1]; [1]Nuclear Medicine. Hospital Clinico Universitario de Valladolid, Valladolid, SPAIN, [2]Endocrinology. Hospital Clinico Universitario de Valladolid, Valladolid, SPAIN.

**Aim** To assess the role of SPECT-CT performed after treatment with 131I, in the localization and characterization of equivocal or doubtful foci detected by whole body scintigraphy (WBS) in differentiated thyroid cancer (DTC) patients. **Material and Methods** 30 patients (mean age=53.75 ±13.73; 17 women) with DTC (25 papillary, 3 follicular, 2 mixed) in stages I (18), II (3), III (4) and IV (8) were included in the study. A WBS and a SPECT-CT were performed to all patients (33 studies) 8 days after the administration of a therapeutic dose of 131I (from 3.4 to 6.7 GBq) and four weeks after withdrawal of hormone replacement therapy (28) or postinjection of recombinant TSH (5). The SPECT-CT was performed for the localization and characterization of one or more foci of uptake previously visualized in the WBS. The findings were correlated with histology, radiology or posterior follow-up. **Results** The WBS detected 77 foci (48 in the neck and 29 in other localizations) and the SPECT-CT 79 (49 in the neck; 30 in other localizations). The SPECT-CT visualized four new foci compared to the WBS and dismissed 2 doubtful foci which were neither confirmed by other imaging test. It improved the localization and characterization of 48 foci, 23 in the neck and 25 in other localizations. Among these, it detected 19 false positive in salivary glands (3), bowel (5), thymus (6), nasal cavity (3), kidney (1) and ovary (1). In 16 out of 19, the stage of the patient could have been increased erroneously had not they been properly characterized. Moreover, SPECT-CT allowed restaging a patient by means of the identification of unsuspected neck adenopathys. **Conclusion** SPECT-CT is a usefull technique to improve the localization and characterization of foci previosly detected by a WBS performed after treatment with 131I of patients with DTC, in the neck region or in other localizations, with implication in the restaging of patients.

PW08 - Monday, Oct. 21, 8:30 - 9:30, Poster Exhibition Area

# Poster Walk 8 - Conventional & Specialised Nuclear Medicine: Paediatric Kidney Diagnostics

## PW071

### The use of SPECT-CT for determining the volume of sclerotic and cystic changes in children with the autosomal dominant polycystic kidney disease.

V. Solodky, A. Pavlov, V. Dlin, D. Fomin, **O. Lugay**; Russian Scientific Center of Roentgenoradiology., Moscow, RUSSIAN FEDERATION.

The use of SPECT-CT for determining the volume of sclerotic and cystic changes in children with the autosomal dominant polycystic kidney disease. **Objective**: determining the volume of sclerotic and cystic changes in children with the autosomal dominant polycystic kidney disease by means of SPECT-CT. **Materials and Methods** of research: 25 children with the ADPKD condition aged 12 to 17 (18 boys and 7 girls) were examined in the course of research. In 16 of the children the disease progress was latent, while in 9 cases it was accompanied by arterial hypertension. None of the children revealed symptoms of renal insufficiency. All of the children underwent an US of kidneys, static nephroscintigraphy and SPECT-CT. SPECT-CT was carried out on the hybrid diagnostic system “Precedence”. Two hours prior to the examination children were intravenously injected 50-120 Technetium-99 m (DMSA), depending on the weight and emotional state of each child, followed by the planar nephroscintigraphy and SPECT . **Results:** We have developed our own protocol of processing reconstructed images. The first stage was the setting of cut-offs for the maximal brightness according to the anatomic boundaries of a kidney (CT -slice) and its size on the planar nephroscintigraphy. Next came the setting of the background so that the accumulation deficiency in the renal pelvis coincided with the one on the planar nephroscintigraphy. Subsequently, with the help of the available software, we summed up the cut-offs (1 to 10, 11 to 20 and so on), defining of the volume of the vitality renal parenchyma (the tissue with an invariable density based on the CT data, accumulating a radionuclide label), scar changes (absence of major changes in the X-ray density and in the accumulation of radioisotope), as well as cysts. The average volume of revealed cysts made up 13700mm$^3$, which corresponded to 47% of the kidney volume. It’s important to notice that on the hybrid tomograms of 7 children there was detected an accumulation of radioisotope in the cyst cavity as well as in the renal pelvis and group of cups. Such accumulation which accounts for 11 to 48% of the label activity above the background is certainly responsible for the substantial miscalculation of the renal tissue vitality. **Conclusion**: the use of SPECT-CT, along with the suggested protocol of processing the data, allows to obtain an easy-to-use examination result, which allows to estimate a dynamic of cyst growth and nephrosclerosis.

## PW072

### Surgical and nonsurgical follow up results of ureteropelvic junction obstruction without diuretic response in pediatric patients

**Z. Koç**, M. Gurgoze, U. Bakal, T. Balci; Firat University Hospital, Elazig, TURKEY.

**Aim:** Diuretic response is one of the most important parameters in the management of ureteropelvic junction obstruction. Usually patients without diuretic response are candidates for surgery. We aimed to retrospectively compare the surgical and nonsurgical follow up results of ureteropelvic junction obstruction without diuretic response. Materials and **Methods**: Forty one pediatric patients (16 F, 25M; mean: 4,2±4,3 years old, range: 0-15) without diuretic response were subject of this study. The diuretic renography results and additional intravenous pyelography, voiding and ultrasonography results performed within one month were compared with control ultrasonography and/or diuretic renography results in 7,9±8 month follow up. **Results**: All of the patients were non responsive to diuretic administration in diuretic renography. Simultaneous intravenous pylographies of 6 of the patients revealed present excretion to the ureter. 17 patients underwent surgical approaches (14 pyeloplasty, one ureterocele resection, one double J stent placement and one nephrolitotomy operation) mean 5,3±5,8 months after scintigraphy. Three patients were out of follow up. Among patients with surgical follow up 13 (87%) had recovery and 2 had stabile disease. 10 out of 23 patients

without surgery had recovery, 7 had stabile disease and 6 had additional pathologies (one ureter dilatation, one kidney failure, infection in two, one worsening of diuretic response, one volume loss). **Conclusion:** In patients without diuretic response in scintigraphy even without conclusive morphological results, surgery is more appropriate management approach. Key Words: diuretic response, intravenous pyelography, pyeloplasty, scintigraphy.

## PW073

### Assessment of differential renal function in unilateral hydronephrosis by unit area formula against classic method in Tc-99m DMSA scintigraphy before and after intervention

F. Kepenek[1], **Z. Koç**[1], I. Orhan[1], T. Balci[1], F. Aydin[2], A. Gungor[2]; [1]Firat University Hospital, Elazig, TURKEY, [2]Akdeniz University Faculty of Medicine, Antalya, TURKEY.

**Aim**: Relative kidney function of an affected kidney sometimes may be estimated exaggerated by Tc-99m DMSA scintigraphy in unilateral hydronephrosis. What is being aimed in this survey is to compare the effectiveness of both Methods; relative kidney functions measured by classical method and by unit area method in unilateral hydronephrosis by Tc99m DMSA scintigraphies before and approximately three-six mounts after surgical intervention. **Materials and Methods**: For this purpose 20 patients (12 M, 8F; mean:42,6 ±18,5 years old) who were operated due to unilateral hydronephrosis were included to the study. Patients were evaluated by physical examination, laboratory tests and ultrasonography later on Tc99m DMSA scintigraphy images were obtained before and after the surgical interventions. Relative kidney functions obtained by unit area method which is obtained by ratio of the counts in region of interest of the kidney and area of the kidney as pixel and by classical method in hydronephrotic kidney in preoperative and postoperative period. The relative renal functions before and after surgery with classical and unit area Methods were compared by Bland Altman analysis. **Results**: In the preoperative period both Methods were in positive correlation however not in agreement which level of the discrepancy might influence surgical decision (mean: 2,3, ±1,96 SD:5,2). In the postoperative period both Methods were both in positive correlation and in agreement with each other (mean: 0,53, ±1,96 SD: 2,3). **Conclusion**: According to these results the classical method is not reliable in unilateral hydronephrosis and unit area method might provide reliable relative kidney function estimation. Keywords: Hydronephrosis, DMSA, Scintigraphy

## PW074

### The Reproducibility of Measurements of Function and Drainage in Pediatric $^{99m}$Tc-ethylenedicysteine Dynamic Renal Scintigraphy

C. LABRIOLLE-VAYLET[1], E. DURAND[2], P. X. FERNANDEZ[3], L. D. NGUYEN[4], F. BONNIN[5], D. DELIU[6], **P. D. CHAUMET-RIFFAUD**[4]; [1]Hôpital Trousseau AP-HP, PARIS 75012, FRANCE, [2]Hôpitaux Universitaires de Strasbourg, STRASBOURG, FRANCE, [3]Hôpital Pellegrin, BORDEAUX, FRANCE, [4]Hôpitaux universitaires Paris-Sud Bicêtre AP-HP, LE KREMLIN BICETRE, FRANCE, [5]Centre Hospitalier René Dubos, PONTOISE, FRANCE, [6]Hôpitaux universitaires Paris-Sud Antoine Béclère AP-HP, CLAMART, FRANCE.

**Aim:** The differential renal function (DRF) of kidneys is calculated using dynamic renal scintigraphy (DRS) with $^{99m}$Tc labelled organic anions radiopharmaceuticals. It plays a central role in the management of various diseases of the kidneys and urinary tract in paediatric medicine and urology. DRS is the gold standard to assess relative renal function. The aim of this study was to evaluate the reproducibility of the analysis of $^{99m}$Tc-ethylènedicystéine (EC) renography by nuclear physicians in 3 centres and a panel of specialists. **Patients and Methods**: It was a prospective non-interventional trial where the radiopharmaceutical product was prescribed in the usual manner in accordance with the terms of the marketing authorisation. No additional diagnostic or monitoring procedures was applied to the patients and approval of the local IRB and CNIL was obtained for the analysis of collected data. Three centres included 109 patients over a period of 9 months. The population was composed of children (less than 12 years old) presenting with hydronephrosis and referred for functional and morphological evaluation. Dynamic renal scintigraphy was carried out with 99mTc-EC according to standard procedures of each centre and analysed. Two nuclear physicians (1 senior and 1 junior) performed the analysis in each centre with local solutions (area under the curve (AUC) technique or Patlak technique). Then 3 experts analysed the data using the same software installed on an electronic platform. Agreement between observers was the primary criterion of the statistical analysis. **Results**: Most of the young patients were in the range 2-4 years with a mean weight about 12 kg. The mean injected activity of $^{99m}$Tc-EC was close to 2.5 MBq/kg. Using Bland-Altman representation, the mean difference between senior's measure and junior's measure was inferior to 0.1%. The 95% confidence interval of this difference was [-3.1% , +3.2%] in both major centres of recruitment. The intra-centre reproducibility of measurements was excellent. **Conclusion**: The results are very similar to those reported in prior studies estimating the reproducibility and accuracy of $^{99m}$Tc-mercaptoacetyltriglycine.

## PW075

### Scintigraphic Role in Unilateral Pelvi-ureteral Junction Obstruction in Pediatrics: Long Term Follow-up

**H. M. Gad**, A.A. Shokeir, M. Dawaba, A.T. Hafez & R.T. Abouelkheir; Urology& Nephrology Center. Mansoura University., Mansoura, EGYPT.

**Aim** Assess the role of scintigraphy in diagnosis and management of unilateral pelvi-ureteral junction obstruction in pediatrics as well as regular long term follow-up. **Materials and Methods** One hundred and thirty children were suspected to have unilateral pelvi-ureteral junction obstruction by ultrasonography. Dynamic 99m Tc-MAG3 diuretic renographic studies were done for all cases. The children were classified into two groups, Group I (n=70) who are symptomatic or those with split function 40% or less, they underwent pyeloplasty & Group II (n=60) who are symptomatic or those with split function greater than 40%, were treated conservatively. Follow-up 99m Tc-MAG3 dynamic studies were performed every 3 months for both groups. Patients who showed renal function deterioration in group II underwent pyeloplasty. **Results** After pyeloplasty, Group I had improvement in the glomerular filtration rate and split function in 60 cases (85.7%), stabilization in 4 cases (5.7%) and deterioration in 6 cases (8.6%). In group I, the comparison between the mean value of the base line GFR (17+ 7.7 ml/min) and its mean value at follow up (28 + 6.3 ml/min) showed an increase in the statistical significance (P ⍰ 0.01). In group II patients, conservative management resulted in improvement in the GFR in 24 (40%), stabilization in 6 (10%) and deterioration in 30 (50%) patients. In group II, no significant difference was found between the mean baseline GFR (29.8 + 9.8 ml/min) and its mean value at follow up ( 31.2 + 5.6 ml/min). **Conclusion** Dynamic renal scintigraphy is the golden method for diagnosing and management of postnatal pelvi-ureteral junction obstruction as well as regular long term follow-up.

## PW076

### Correlation of 99mTc-DMSA scan with radiological and laboratory examinations in childhood acute pyelonephritis: a time-series study

K. Ghasemi[1], S. Montazeri[2], A. Mahmoud Pashazadeh[2], H. Javadi[3], **M. Assadi**[2]; [1]Department of Paediatrics (division of nephrology), Bushehr Medical Center Hospital, Bushehr University of Medical Sciences, BUSHEHR, IRAN, ISLAMIC REPUBLIC OF, [2]The Persian Gulf Nuclear Medicine Research Center, Bushehr University of Medical Sciences (BUMS), BUSHEHR, IRAN, ISLAMIC REPUBLIC OF, [3]Golestan Research Center of Gastroenterology and Hepatology (GRCGH), Golestan University of Medical Sciences (GUOMS),, Gorgan, IRAN, ISLAMIC REPUBLIC OF.

**Background**: Urinary tract infections (UTIs) are one of the most common diseases in children. They may lead to hypertension and renal failure later in life. Renal scintigraphy with technetium-99m dimercaptosuccinic acid (99m Tc-DMSA) is one method used to diagnose acute pyleonephritis (APN) and renal parenchymal scars. The aim of the present study was to determine the ideal time to perform a follow-up DMSA scan to detect renal scars and also to evaluate factors predicting the development of permanent renal damage after APN. **Methods**: Sixty-four children with a first episode of APN underwent a 99mTc-DMSA scan. If there were abnormal findings on this scan, another scan was performed 6 and 12 months later. **Results:** The baseline 99mTc-DMSA scan showed cortical changes in 35 patients (54.6%). One the 6- and 12-month follow-up scans, 25 patients (39.06%) and 21 patients (32.8%), respectively, had cortical lesions. In multiple logistic regressions with the final 99mTc-DMSA scan results as the dependent variable, only the age range of the patients (β = 1.062; 95% CI: 1.014-1.113; p = 0.01) showed an independent and significant association. Gender, therapeutic delay time (TDT), ultrasonography, and voiding cystourethrogram (VCUG) results, as well as laboratory test results including the erythrocyte sedimentation rate (ESR), C-reactive protein (CRP) level, white blood cell (WBC) counts, and type of bacteria in the urine, did not show such an association (p >0.05). **Conclusion**: There is not a significant difference between the results of 6- and 12-month 99mTc-DMSA follow-up scans. A follow-up 99mTc-DMSA scan should be performed 12 months after the acute scan to yield a more accurate diagnosis of permanent renal damage. If present, long-term follow up of patients is necessary.

## PW077

### Split Renal Function and Drainage Pattern in Infants with Antenatal Hydronephrosis

**B. Z. AJDINOVIC**[1], B. BAZIC[1], Z. KRSTIC[2], L. D. JAUKOVIC[1]; [1]INSTITUTE OF NUCLEAR MEDICINE, MILITARY MEDICAL ACADEMY, BELGRADE, SERBIA, [2]UNIVERSITY PEDIATRIC CLINIC, BELGRADE, SERBIA.

**Aim** of this study was to assess the renal function determined by the pattern of drainage and split renal function (SRF) on diuretic renography in infants with antenatal hydronephrosis. **Patients and metods**: Thirty infants with 60 renal units (RU) (25 boys and five girls, median age 6.0 months, range 2-24) who presented with unilateral mild to moderate hydronephrosis on ultrasound in newborn period

underwent DTPA diuretic renalscintigraphy (F+15). Images and Tmax/2 on the background subtracted renographic curves were used as the criteria for classifying the drainage as 1) good or almost good, 2) partial and 3) poor or no drainage. SRF was calculated with integral method. Micturation cystourethrography was done in 22/30 infants ruling out the presence of vesicoureteral reflux in all but two of them. **Results**: Median antero posterior pelvic diameter evaluated on perinatal ultrasound was 15mm (range 5-30). Good or almost good drainage was shown in 36/60, partial drainage in 13/60 and poor or no drainage in 11/60 RU. Split renal function (SRF)>40% was observed in 55/60 RU, with no RU showing SRF less than 23.5%. The postnatal associated clinical diagnosis were pelviureteric junction obstruction, simple hydronephrosis, megaureter, VUR and posterior urethrae valves in 11, 10, 6, 2 and one infant respectively. **Conclusion**: Our results suggest that even in presence of partial, poor or no drainage, the split renal function may not be significantly impaired. Diuretic renography in antenataly detected hydronephrosis should be a useful tool in follow up and making the therapeutic strategy of these infants.

## PW078

### 99mTechnetium-dimercaptosuccinic Acid Renal Scintigraphy in Children with Antenatal Hydronephrosis

**B. Z. AJDINOVIC**[1], D. PUCAR[1], B. BAZIC[1], Z. KRSTIC[2]; [1]MILITARY MEDICAL ACADEMY, BELGRADE, SERBIA, [2]UNIVERSITY PEDIATRIC CLINIC, BELGRADE, SERBIA.

The purpose of this study was to evaluate renal parenchyma damage with 99mTc-dimercaptosuccinic acid (DMSA) scintigraphy in children with antenatal hydronephrosis (ANH) detected by ultrasound. The study presents results of DMSA scintigraphy in 38 children (13 girls, 25 boys), aged from two months to 5 years (median 13,8 months) with ANH (29 unilateral, 10 F, 19 M and 9 bilateral, 3 F, 6 M). Morpholgycal irregularity, clear cortical abnormalities and/or differential separate uptake less than or equal to 40% were considered as pathological findings. The postnatal associated clinical diagnosis were: megaurether in 9 pts, *pyelo-ureteric* junction (PUJ) stenosis in 4 pts, duplication *ureter or duplex system in 5 pts,* posterior urethral valve in 1 pt. Micturating cystourethrogram (MCUG) was performed in 30/38 children and vesicoureteric reflux (VUR) was not found in 16/30, low grade VUR (I-II) in 5 and high grade VUR (III-V) in 11 pts. DMSA findings in children with unilateral hydronephrosis were: decreased or enlarged kidney in 12 pts, irregular shape in 1, connected (fused) kidney in 1 and poorly or non visual kidney in 8 pts. Regular kidney morphology was found in 7 patients. In children with bilateral hydronephrosis we found out regular morphology in 3 pts, four cases with decreased or enlarged kidneys, irregular shape in 1 pt and one case with non visible right kidney. Typical renal parenchymal damage were found in 5/38 pts and all had separate uptake less than 40% (separate uptake were less than 40% in 31,5% pts, 12/38). On the basis of these results we recommend DMSA scintigraphy in the evaluation renal parenchyma damage in children with ANH.

## PW079

### Radionuclide Evaluation of Compensatory Activity and Renal Parenchyma State in Children after Kidney Surgery

N. P. Gerasimova, I. E. Smirnov, V. I. Vidyukov, N. L. Komarova, **L. S. Kogtev**; Scientific Centre of Children's Health, Moscow, RUSSIAN FEDERATION.

**Aim**: To assess the compensatory activity and state of renal parenchyma in children, who has undergone kidney surgery. **Materials and Methods**: Total of 31 children, at the age of 4-17 years have been studied, including 11 children with hydronephrosis, 6 children with ureterohydronephrosis, 10 children with megaloureter, and 10 children with vesicoureteral reflux. Examinations have been implemented within range from 0.5 to 5 years after kidney surgery. Reference group was composed of 10 children without renal pathologies. Static acquisitons of kidneys with DMSA-$^{99m}$Tc as tracer (four projections for each kidney) were conducted using gamma-camera Millenium-MG (GE HEALTHCARE). Injected activity was considered. Quantitative indexes, namely, renal capture, kidney volume, specific activity, relation between activities, and dimensions of afflicted and contralateral kidneys with regard to anthropometric data have been determined. **Results**: In the assessment of functional status and volume of parenchyma, the most responsive indexes were: specific activity and relation between specific activities of healthy and afflicted kidneys in combination with kidney volume. Kidneys as the whole organ are responsible for the decrease of parenchymal volume of the afflicted kidney, increase of kidney volume by means of involvement of reserve nephrons and hypertrophy of the present nephrons. In the course of study, 2 groups of children were defined. In the first group the mean value for the relation of specific activities for afflicted and contralateral kidneys in the course of kidney volume changes was of -0.52 + -0.04, and was considered as unfavorable fact, indicative of insufficiency of nephronal function, that may be the trait of renal parenchyma functional reserve depletion. Children from this group were ranged in the risk group (14 children). In the second group the mean value for the relation of specific activities was of 1.0-0.9 and renal function was assessed as good. In cases of increased or normal kidney volume this data could be explained by the involvement of nephrons, composing renal functional reserve. Patients with the single kidney and megaloureter demonstrated good specific activity of parenchyma. In patients with the single kidney and diagnosed ureterohydronephrosis, in case of increased kidney volume specific activity was low (0.32,-0.46). These patients were also ranged in the risk group. **Conclusion**: Relation of specific activities and volumes between afflicted and contralateral kidneys is the most informative index in the compensatory activity assessment of renal parenchyma, and can be used for the case follow-up of post-surgical patients.

## PW080

### Verification of quantitative assessment of the separate renal function ratio in planar DMSA scan using SPECT 3D method

**D. Chroustová**[1], J. Trnka[2], I. Urbanová[3], J. Langer[4], V. Ptáčník[1], J. Kubinyi[1]; [1]Department of Nuclear Medicine, General Teaching Hospital and 1th Faculty of Medicine Charles University Prague, Czech Republic, PRAGUE 2, CZECH REPUBLIC, [2]Department of Medical Physics, General Teaching Hospital Prague, Czech Republic, PRAGUE 2, CZECH REPUBLIC, [3]Department of Paediatrics, University Hospital Bulovka, Prague, Czech Republic, PRAGUE 8, CZECH REPUBLIC, [4]Clinic of Paediatrics and Adolescent Medicine, General Teaching Hospital and 1th Faculty of Medicine Charles University Prague, Czech Republic, PRAGUE 2, CZECH REPUBLIC.

**Aim:** The primary parameter of static renal scintigraphy using $^{99m}$Tc- DMSA (dimercaptosuccinic acid) is the determination of separate renal function. In our work we proceed from the assumption that the most accurate values of this parameter are obtained from SPECT (Single Photon Emission Tomography) examination. We compared the separate renal function values obtained by routinely provided planar scintigraphy (DMSA scan) using two different gamma cameras with SPECT 3D method. **Patients and Methods**: A total of 146 patients (64 boys and 94 girls aged from 5 to 19 years) with various renal diseases and congenital abnormalities were examined. DMSA scan was performed 2 hours after administration of 99mTc-DMSA in all patients. Separate renal function was determined using 3 Methods: A) planar scintigraphy performed on gamma camera MB 9200 (Mediso), ANT and POST projections with changing the patient´s position between ANT and POST acquisitions, and correction for kidney depth calculated by the geometric mean, B) the same planar procedure without changing the patient's position re-produced on two heads gamma camera Infinia (GE), C) SPECT images taken on the Infinia system, using locally developed SW for proper kidney segmentation and voxel-based analysis. The values of the separate renal function provided by all three Methods were mutually compared via paired t-test. **Results:** Statistically, method C was significantly different from both planar Methods A and B (p-values 1.9E-9 and 1.7E-9 respectively), whereas both planar Methods remained mutually similar (p-value 0.8). However, from the clinical point of view, the observed differences between tomographic and planar Methods represented no impact on the evaluation (mean average difference between tomography and planar imaging was approx. 2 percentage points in both cases). **Conclusion:** Based on these results, routinely evaluation of separate renal function using planar technique with correction of the renal position depth can be considered valid.

PW09 - Monday, Oct. 21, 8:30 - 9:30, Poster Exhibition Area

# Poster Walk 9 - Radiopharmaceuticals & Radiochemistry & Dosimetry: PET Radiopharmaceuticals

## PW081

### Development of $^{18}$F-AlF-NOTA-FSH2, a Novel FSHR targeting probe

**S. Luo**, D. Pan,, Y. Xu, F. Chen, L. Wang, M. Yang; Jiangsu Institute of Nuclear Medicine, Wuxi, CHINA.

**Aim:** Overexpression of the follicle-stimulating hormone receptor (FSHR) in prostate cancer provides a promising target for staging and monitoring tumor. $FSH_{33-53}$ peptide (FSH2) is a FSHR antagonist exhibiting high affinity for the receptor. In this study $^{18}$F-labeled NOTA-MAL-FSH2 was prepared by Al$^{18}$F method and the potential of $^{18}$F-AlF-NOTA-MAL-FSH2 for prostate tumor PET imaging was also evaluated. **Materials and Methods***:* NOTA-MAL-FSH2 was radiolabeled with $^{18}$F via new AlF complex strategy. PET studies were performed with $^{18}$F-AlF -NOTA- MAL-FSH2 in PC-3 tumour bearing mice and $^{18}$F-FDG was used as a reference. The tumor targeting and pharmacokinetic profiles of $^{18}$F-AlF-NOTA- MAL-FSH2 were also analyzed with biodistribution experiments. FSHR binding specificity was evaluated by coinjection with an excess of unlabeled FSH2. **Results:** $^{18}$F-AlF-NOTA-MAL-FSH2 can be produced within 30 min with a decay-corrected yield 48.6±2.1% and a radiochemical purity of more than 98%. The specific activity was at least 20 GBq/μmol. From small-animal PET images, the PC-3 tumors were clearly visible with high contrast after injection of$^{18}$F-AlF-NOTA- MAL-FSH2. It also showed that

the tumor uptakes and tumor to muscle uptake radios of $^{18}$F-AlF-NOTA-MAL-FSH2 were significantly higher than those of $^{18}$F-FDG. At 60min postinjection, the tumor uptakes of $^{18}$F-AlF -NOTA-MAL-FSH2 and $^{18}$F-FDG were 2.68±0.23%ID/g and 1.58±0.15%ID/g, and tumor to muscle uptake radios for two tracers were 13.28±2.97 and 1.78±0.32 respectively.$^{18}$F-Al-NOTA-MAL-FSH2 excreted mainly through the kidneys, as evidenced by the higher renal uptake at early time points and excretion via the bladder. The kidney uptake reached a peak (24.52±3.37%ID/g) at 30 min after injection and then decreased to 18.86±2.34 ID/g at 120 min p.i.. The results of the biodistribution study were in line with with the PET quantification. High PC-3 tumor uptake of the radiotracer was found at 30min after injection (3.09±0.35 %ID/g). At 1h p.i., the normal organs expect kidney uptakes were all below 1%ID/g. At the presence of excess FSH2, the tumor uptake of $^{18}$F-AlF -NOTA- MAL-FSH2 reduced to 0.56±0.09%ID/g at 1h postinjection . **Conclusions***:* NOTA- MAL-FSH2 could be labeled rapidly and efficiently with $^{18}$F using one step method. Favorable preclinical data showing $^{18}$F-AlF-NOTA- MAL-FSH2 may have higher diagnostic accuracy than $^{18}$F-FDG in PET for prostate cancer. *Research Support:* NSFC (81171399 and 81101077), NSNDCP (2012ZX09505-001-001), Jiangsu Province SFC (BE2012622, BK2011166, BL2012031, RC2011095, H201028, BM2012066) Corresponding author: yangmin@jsinm.org

## PW082

### Linker Modifications of DOTA-conjugated Inhibitors of the Prostate-Specific Membrane Antigen (PSMA)

**M. Benesova**[1], M. Schäfer[1], U. Bauder-Wüst[1], W. Mier[2], U. Haberkorn[2], M. Eisenhut[1], K. Kopka[1], M. Eder[1]; [1]German Cancer Research Center, Heidelberg, GERMANY, [2]Department of Nuclear Medicine, University Hospital, Heidelberg, GERMANY.

**Introduction** Since the Prostate-specific membrane antigen (PSMA) is up regulated in nearly all prostate cancers while showing rather low expression levels in normal tissue, PSMA can be considered as an attractive target for the diagnosis and therapy of prostate cancer (1). Due to the similarity of the coordination chemistry of $^{68}$Ga and that of therapeutic radionuclides such as $^{90}$Y and $^{177}$Lu, the combination of DOTA with PSMA targeting inhibitors might open the possibility of using the same vector molecule for imaging and therapeutic purposes. The putative $^{68}$Ga-labelled DOTA-conjugated imaging agents consist of the PSMA binding motif, a variable linker and the DOTA chelator. The linker region is designed in order to increase the distance between the biologically active site and the bulky chelator and at the same time to further elucidate the resulting structure-activity relationships (SAR). **Materials & Methods** The synthesis of DOTA-conjugated PSMA inhibitors were performed by solid-phase chemistry. After formation of the resin immobilized Glu-urea-Lys structure, the subsequent synthesis of the varied linker region was performed according to standard Fmoc protocols. The chelator was finally conjugated by using HBTU activated DOTA-tris(tert-Bu)ester or DOTA-NHS ester. In order to compare the series of novel compounds in respect to their cell binding properties the binding affinity and the specific internalization was studied using the PSMA expressing human prostate cancer cell line LNCaP. **Results** All compounds revealed a high affinity for PSMA on LNCaP cells. Four compounds were found to bind with nanomolar affinity ($K_i$ = 0.07 ± 0.01, 0.49 ± 0.06, 1.33 ± 0.07, 2.06 ± 0.09 nM). Since internalization is considered crucial in respect to the tumor targeting properties, the compounds were ranked according to their specific internalization rates. The two most promising substances showed improved cellular uptake compared to the reference $^{68}$Ga labelled Glu-urea-Lys-Ahx-HBED-CC. The PSMA-targeting and pharmacokinetic properties will be further investigated by means of *in vivo* biodistribution studies as well as microPET imaging. **Conclusion** DOTA-based $^{68}$Ga-PSMA-PET imaging possesses a high potential to become a valuable diagnostic method for recurrent prostate cancer or therapy monitoring. The here intended evaluation of a series of linker variations resulted in DOTA-conjugated PSMA inhibitors with maintained or even improved PSMA binding potential. This approach could lead to favourable pharmacokinetic properties, but especially to an improved management of recurrent prostate cancer with one and the same precursor for diagnostic and therapeutic purposes. References (1) Silver et al., Clin. Cancer Res. 1997, 3, 81-5.

## PW083

### Characterization of Binding of $^{18}$F-Labeled 2-Arylquinoline Derivatives to Tau Deposition in the Brain of Alzheimer's Disease

**S. Furumoto**[1], R. Harada[1], N. Okamura[1], T. Tago[2], H. Arai[3], R. Iwata[2], K. Yanai[1], Y. Kudo[4]; [1]Tohoku University School Of Medicine, SENDAI, JAPAN, [2]Cyclotron and Radioisotope Center, Tohoku University, SENDAI, JAPAN, [3]Institute of Development, Aging and Cancer, Tohoku University, SENDAI, JAPAN, [4]Clinical Research, Innovation and Education Center, Tohoku University Hospital, Sendai, JAPAN.

**Aims**: Abnormal accumulation of tau aggregates in the brain is one of the key pathological features of Alzheimer's disease (AD). To visualize the tau deposition by PET, we developed novel 2-arylquinoline derivatives containing a racemic [$^{18}$F]$FCH_2CH(OH)CH_2$ structure. Among them, [$^{18}$F]THK-5105 and [$^{18}$F]THK-5117 showed excellent brain kinetics in the normal mouse brain and high binding affinities for fibrils of K18d280 (tau constructs). In this study, we performed further evaluation of their binding properties using AD brain tissue samples. **Methods**: Fluorine-18 labeled THK-5105 (racemate, (R)-body, and (S)-body) and THK-5117 (racemate) were prepared from the corresponding tosylate precursors using [$^{18}$F]KF/Krypt222 and used for binding assay and autoradiography (ARG) after HPLC purification. Tissue homogenates of several brain regions were prepared for binding assay. The amount of insoluble tau and amyloid-β (Aβ) in the brain samples were measured by ELISA. Saturation binding assay using tau-rich/Aβ-poor homogenate (hippocampus) was carried out to determine Kd value. Binding property of [$^{3}$H]THK-5117 was compared with that of [$^{3}$H]PiB by binding assay and ARG to evaluate the binding selectivity for tau. **Results**: THK-5105 (racemate, (R)-body, and (S)-body) and THK-5117 (racemate) displayed high binding affinity for the tau-rich/Aβ-poor homogenates with Kd values of 5.76, 3.29, 6.70, and 5.11 nM, respectively. While binding assay gave different Kd values between the (R)- and (S)-bodies, ARG study using serial hippocampal sections showed no difference in radioactivity distribution between the two radiotracers. The amount of [$^{3}$H]THK-5117 bound to the homogenates was significantly correlated with that of insoluble tau (r = 0.63, P = 0.02), but not with that of Aβ (r = -0.20, P = 0.51). By contrast, there was no correlation between the level of [$^{3}$H]PiB binding and insoluble tau (r = -0.17, P = 0.57). ARG study of AD brain section clearly demonstrated that [$^{3}$H]THK-5117 bound to the tau deposition selectively. **Conclusions**: The novel 2-arylquinoline derivatives, THK-5105 and THK-5117, showed high affinity to the pathological insoluble tau in the AD brain and good correlation between the level of binding and insoluble tau, suggesting that they are potentially suitable for imaging of tau pathology in AD.

## PW084

### Assessment of recovery of regional sympathetic reinnervation after myocardial ischemia-reperfusion using a new cardiac sympathetic nerve imaging agent: $^{11}$C-N-methyldopamine

**X. Wang**[1], Y. He[1], W. Fang[2], W. Zhou[1], X. Wang[1], B. Bao[1], G. Zhang[1], C. Wang[1], C. Wang[1], C. Han[3]; [1]Dept. of Nuclear Medicine, Inner Mongolia Medical University, Hohhot, CHINA, [2]Dept. of Nuclear Medicine, Fuwai Hospital, Chinese Academy of Medicine, Beijing, CHINA, [3]Turku PET Centre, Turku University Hospital, Turku, FINLAND.

**Aim:** PET imaging of cardiac sympathetic function is of importance in evaluating heart diseases. To overcome the limitations of current sympathetic radiolabeled tracers, this study was to develop $^{11}$C-N-methyldopamine as a new PET tracer for imaging cardiac sympathetic nervous system. The secondary goal was to investigate the cardiac regional sympathetic recovery of ischemia-reperfusion in animals using this tracer. **Materials and Methods:** $^{11}$C-N-methyldopamine was synthesized by direct N-methylation of dopamine with $^{11}$C-methyl iodide and purifed by semi-preparation reverse HPLC. About 3.7 MBq of $^{11}$C-N-methyldopamine in 0.1mL solution were injected through the tail vein of normal Kunming mice. The tissues and organs including heart, lung, liver, spleen, kidney, stomach, intestine, brain, muscle, bone and blood were collected, weighted wet and counted in a γ-counter. Chinese mini pigs, 20-30 kg, were used in this study: five pigs as control group and ten pigs as ischemia-reperfusion group. Acute myocardial infarction model was made by ligaturing left descending coronary artery (LAD) with stenosis (>90%) for 30 min and then releasing for reperfusion. PET/CT imaging was performed with $^{13}$N-ammonia and one hour later with $^{11}$C-N-methyldopamine. Same animal underwent these studies six times; before the operation and one hour, one day and one, three and six months after operation **Results:** $^{11}$C-N-methyldopamine was synthesized with the overall decay corrected radiochemical yields about 20% and the chemical purity >97%. Biodistribution data in mice showed that myocardium had a high $^{11}$C-N-methyldopamine uptake. At 2, 5, 10, 20, 30 min after the tracer injection the radioactivity uptake was 0.65 ± 0.18, 0.50 ± 0.26, 0.44 ± 0.07, 0.30 ± 0.08 and 0.25 ± 0.03 %ID/g, respectively. In healthy pigs, PET/CT imaging showed that myocardium had a clear $^{11}$C-N-methyldopamine uptake with an even distribution. After acute ischemia and reperfusion, defect scores ($^{11}$C-N-methyldopamine /$^{13}$N-ammonia) were at day 1, and at 1, 3, and 6 months after the ischemia 12.1 ± 1.3/7.3 ± 0.8 ($p > 0.05$), 28.3 ± 2.0/8.4 ± 1.0 ($p < 0.001$), 47.7 ± 2.1/8.4 ± 1.3 ($p < 0.001$), and 7.7 ± 1.6/7.4 ± 1.1 ($p < 0.001$); meanwhile, recovery of uptake of $^{11}$C-N-methyldopamine was significantly later than $^{13}$N-ammonia. **Conclusion:** This study suggested $^{11}$C-N-methyldopamine is a promising new radiotracer for imaging cardiac sympathetic nervous system, and $^{11}$C-N-methyldopamine PET imaging is potentially a sensitive method for assessing myocardial ischemia and the sympathetic reinnervation after myocardial ischemia-reperfusion.

## PW085

### Rapid and One-Step Radiofluorination of Bioactive Peptides: Potential PET Radiopharmaceuticals

**I. Aljammaz**, B. Al-Otaibi, A. Aboussekhra, S. Okarvi; Cyclotron and Radiopharmaceuticals Department, King Faisal Specialist Hospital and Research Centre, Riyadh, SAUDI ARABIA.

Peptide-based agents have attracted enormous attention as biological vehicles to deliver radioactivity to tumor cells for receptor-targeted imaging and radiotherapy. Several radiolabeled peptides are currently under investigation to determine their clinical potential as imaging and therapeutic agents for different cancers. With the increased use of positron emission tomography (PET), there has been a great interest in the development of positron emitting radiopharmaceuticals for earlier detection and characterization of cancer, molecular assessment of treatment effects and more fundamental understanding of the disease process. Due to the favorable nuclear and chemical characteristics of fluorine-18 ($^{18}$F) for PET diagnostic imaging applications, various techniques including aliphatic and aromatic radiofluorinated substrates such as N-succinimidyl-4-[$^{18}$F]-fluorobenzoate ([$^{18}$F]SFB) and N-succinimidyl-4-F-fluoropyridine carboxylate ([$^{18}$F]SFP) have been developed to allow labeling of peptides via free amino group on lysine residue without affecting their receptor-binding properties. These classical Methods which are routinely used for radiolabeling peptides with $^{18}$F are multi-steps and time consuming (>100 min). Thus, as part of our on-going research effort to develop new and effective prosthetic precursors for radiofluorination of bioactive molecules, we here report a rapid and one-step radiofluorination of bombesin (BBN) and mucin (MUC1) peptide analogs as representative peptides examples and their biological evaluation. The synthetic approaches for preparation of [$^{18}$F]-BBN and [$^{18}$F]-MUC1 peptide analogs entailed only a one-step reaction. The key precursors 4-N,N,N-trimethylammonium benzoate-BBN and MUC1 triflates were prepared by reacting *N*-succinimidyl 4-N,N,N-trimethylammonium benzoate with BBN and MUC1 peptide analogs to furnish 4-N,N,N-trimethylammonium benzoate-BBN and MUC1 peptide triflates in almost 70% yield and >97% purity for both precursors. Both precursors were treated using catalyzed nucleophilic no-carrier-added radiofluoride produced by the $^{18}$O(p,n)$^{18}$F nuclear reaction on $^{18}$O-enriched (98%) water and Kryptofix 222 as nucleophilic catalyst in anhydrous ACN at 80°C for 5 min. The radiofluorinated peptides were purified by C-18 Sep-Pak column to give [$^{18}$F]-BBN and [$^{18}$F]-MUC1 peptide analogs in >70% radiochemical yield and >95% radiochemical purity in less than 30 min. This synthetic approach hold considerable promise as a rapid and efficient method amenable for automation for the radiofluorination of peptides with high radiochemical yield and short synthesis time. *In vitro* tests on T47D breast cancer cell line has shown that significant amount of the [$^{18}$F]-MUC1 peptide analog associated with cell fractions. *In vivo* tumor targeting capacity of this radioconjugate in athymic mice with T47D cell tumor xenografts is currently in progress and will be reported.

## PW086

### Characterization of 123I- and 18F-labeled radiopharmaceuticals for imaging dopamine D2-receptors in the high-affinity state

**J. van Wieringen**[1], V. Shalgunov[2], H. M. Janssen[3], P. M. Fransen[3], M. C. Michel[4], J. Booij[1], P. H. Elsinga[2]; [1]Academic Medical Center, University of Amsterdam, Amsterdam, NETHERLANDS, [2]University Medical Center Groningen, University of Groningen, Groningen, NETHERLANDS, [3]SyMO-Chem BV, TU/e, Eindhoven, NETHERLANDS, [4]Johannes Gutenberg University, Mainz, GERMANY.

**AIM** Dopamine D2 receptors play a central role in several neuropsychiatric disorders including schizophrenia, addiction and Parkinsonism. Using agonist tracers for PET/SPECT imaging of D2 receptors is considered advantageous over the use of antagonist tracers because they may selectively label the high-affinity state of the receptor which is the active form. In addition, agonist tracers may be more sensitive to detect endogenous dopamine release. Carbon-11 labeled agonist tracers to visualize dopamine D2/3 receptors have been developed successfully (e.g., [11C]PHNO). The aim of the project is to develop 123I- and 18F-labeled agonist radiopharmaceuticals to visualize and quantify the high-affinity state of the D2 receptor also in centers without an on-site cyclotron. Here we report the in-vitro results of a series of novel compounds representing a family of D2/3-ligands in the development of PET/SPECT tracers and autoradiography evaluation of two of the most promising compounds. **MATERIALS AND METHODS** Based on a 2-aminomethylchroman (AMC) scaffold, a series of 10 potential dopaminergic ligands were synthesized incorporating iodine or fluorine atoms in their structures. Binding experiments were done on membrane homogenates from HEK-293 cells expressing the different dopamine receptors, [3H]spiperone and [3H]SCH23390 were used as radioligands. Agonism was determined by a cAMP accumulation assay, and lipophilicity of the structures was calculated. The two most promising compounds, termed AMC-13 and AMC-15, were labeled with fluorine-18 and evaluated by means of in-vitro autoradiography in Sprague-Dawley rats. **RESULTS** Competition studies showed that several of the compounds have an affinity in the desired low nanomolar range and that they are selective for the D2/3 receptors over the D1 receptor. Agonism of the compounds was shown by the inhibition of forskoline stimulated cAMP synthesis and by biphasic competition curves in the radioligand binding experiments. According to these results, AMC-13 and AMC-15 were selected and labeled with fluorine-18. In the autoradiography study, [18F]AMC-15 showed specific binding to striatal dopamine D2/3-receptors. **CONCLUSION** We synthesized a new series of agonist radiopharmaceuticals that bind selectively and with high affinity to dopamine D2/3 receptors in-vitro. In addition, two of these compounds were labeled successfully with fluorine-18, and one of them showed specific striatal binding in rats using autoradiography. These findings stimulate further in-vivo evaluations.

## PW087

### Alveolar Echinococcosis Metabolic Imaging: from In Vitro Testing to Small Animal Positron Emission Tomography

C. Porot[1], J. Knapp[1], J. Wang[2,3], D. Camporese[4], S. Germain[5], H. Boulahdour[1], Y. Seimbille[5], B. Gottstein[3], D. A. Vuitton[2], **O. Blagosklonov**[1]; [1]University of Franche-Comté and University hospital, Besançon, FRANCE, [2]University of Franche-Comté, Besançon, FRANCE, [3]University of Bern, Bern, SWITZERLAND, [4]Advanced Accelerator Applications SA, Saint Genis Pouilly, FRANCE, [5]University of Geneva and University hospital, Geneva, SWITZERLAND.

FDG-PET including delayed acquisition is a valuable method for initial staging and follow-up of patients with alveolar echinococcosis (AE). Since inflammatory reaction surrounds the parasitic tissue, metabolic activity of inflammatory cells could explain the FDG uptake. However, the cells responsible for FDG uptake have never been identified. The main goal of our study was to test in vitro the most widely used fluorinated tracers in order to provide clinicians with more specific staging tools of AE, based on direct assessment of E. multilocularis viability. We designed a radiolabelling protocol which could be transposed to each type of cells, composing the AE host-parasite interface. Candidate molecules - [18F]-fluorotyrosine (FET), [18F]-fluorothymidine (FLT), [18F]-fluorometylcholine (FMC), and sodium [18F]-fluorine (NaF) - were tested and compared to FDG by in vitro studies on human leukocytes and in vitro-cultivated E. multilocularis vesicles. Each experiment, for each molecule, was performed on 3 independent pools of AE vesicles and of human leukocytes. We determined mean radiolabelling efficiency (%) and mean uptake by volume of cells (MBq/µm3) from 3 tests. Our results showed that FLT was the best candidate tracer for parasite metabolism and confirmed that FDG was mainly consumed by periparasitic immune cells. Leukocytes had the worst radiolabelling efficiency with FLT (6%) and the best one with FDG (59%). On the other hand, in parasitic vesicles, FLT showed the highest radiolabelling efficiency (93%), and the radiolabelling efficiency with FDG was poor (32%). The difference of radiolabelling efficiency with other tracers was not discriminant between the parasitic vesicles and leukocytes (cf. Table). Based on average uptake value by cell volume, leukocytes were 1,000 to 10,000 times more avid for fluorinated tracers than E. multilocularis vesicles. We also performed FDG-PET/CT scans in mice infected intraperitoneally and orally with E. multilocularis metacestodes at late infection stage. We observed moderate FDG uptake by granuloma-rich parasitic lesions. In conclusion, our study confirmed in vitro and in vivo the role of inflammatory periparasitic process in FDG-PET imaging of AE; thus, this technique only indirectly reflects E. multilocularis viability. FLT, a proliferation tracer, might be suitable for direct functional imaging of AE. Further in vivo experiments are needed to confirm this hypothesis, and we are currently developing protocols for FLT-PET scan in AE mice. This preliminary study is a good basis for the development of a specific PET tracer for AE lesions in order to improve their detection and treatment of human echinococcosis.

## PW088

### $^{68}$Ga-Labeled FSHR antagonist for Prostate Cancer Imaging

**Y. Xu**, D. Pan, L. Wang, F. Chen, S. Luo, M. Yang; Jiangsu Institute of Nuclear Medicine, Wuxi, CHINA.

**Aim:** Prostate cancer is the most frequently diagnosed cancer among men. PET is an important functional imaging modality in the field of oncology. Development of specific PET probes is crucial for the successful diagnosis and therapy of tumor. Recent studies showed that the follicle stimulating hormone receptor (FSHR) is an attractive target for prostate cancer because its expression is largely limited at the tumor periphery. In this study, a FSHR antagonist, $FSH_{33-53}$ peptide (YTRDLVYKDPARPKIQKTCTF) was labeled with $^{68}$Ga via maleimide-NOTA (MAL-NOTA) conjugates and the targeting potentials of $^{68}$Ga-NOTA-MAL-$FSH_{33-53}$ in prostate cancer imaging were investigated. **Materials and Methods:** The NOTA conjugated $FSH_{33-53}$ peptide was synthesized and radiolabeled with $^{68}$Ga. In vitro stability and the log $P_{octanol/water}$ value of the radiotracer were determined. The tumor targeting characteristics of the compound were assessed in mice with subcutaneously growing PC-3 xenografts. FSHR binding specificity was studied by coinjection of an excess of unlabeled $FSH_{33-53}$ peptide. Small animal PET images and biodistribution studies were performed. **Results:** The synthesis of NOTA-MAL-$FSH_{33-53}$ is straightforward with 50% yield. This precursor can be labeled with $^{68}$Ga within 20 min with a decay corrected yield ranging from 90 to 95% .The radiochemical purity was more than 98% and the specific activity was greater than 18 GBq/µmol. The radiotracer was stable in phosphate buffered saline and human serum for at least 2 hours at 37°C. The log P value of $^{68}$Ga-NOTA-MAL-$FSH_{33-53}$ was -3.12±0.05. In mice

bearing PC-3 xenografts, the tumor uptakes of $^{68}$Ga-NOTA-MAL-FSH$_{33-53}$ were 2.67±0.47, 2.20±0.27 and 1.57±0.15 %ID/g at 0.5, 1h and 2h p.i. respectively. The corresponding tumor to blood and tumor to muscle ratios were 2.81±0.50 ,12.94±1.35, 15.70±2.16 and 10.26±0.46, 31.4±2.99, 41.25±4.54 respectively. The accumulation of $^{68}$Ga-NOTA-MAL-FSH$_{33-53}$ in the subcutaneous PC-3 tumors could be visualized via small animal PET. Radioactivity was also concentrated in the kidney at early time points, suggesting that this compound was mainly excreted through the renal urinary route. FSHR binding specificity was demonstrated by reduced tumor uptake of $^{68}$Ga-NOTA-MAL-FSH $_{33-53}$ after coinjection an excess of unlabeled FSH $_{33-53}$ peptide in both noninvasive PET imaging and biodistribution studies. **Conclusion:** NOTA-MAL-FSH$_{33-53}$ has been successfully prepared and labeled with $^{68}$Ga. The favorable in vivo performance of $^{68}$Ga-NOTA-MAL-FSH$_{33-53}$ warrant its further investigation for prostate cancer imaging. Research Support: NSFC (81171399 and 81101077), NSNDCP (2012ZX09505-001-001), Jiangsu Province SFC (BE2012622, BK2011166, BL2012031, RC2011095, H201028, BM2012066)

## PW089

### Synthesis and in vitro application of 2'-[18F]fluoroethylrhodamine B for detecting multidrug resistance

**I. Kertész**, L. Kárpáti, G. Máté, J. Péli Szabó, T. Nagy, G. Trencsényi, T. Márián; University of Debrecen, Department of Nuclear Medicine, Debrecen, HUNGARY.

**Introduction** Resistance of malignant tumors to chemotherapeutic agents is a major cause of treatment failure in patients with cancer. Pgp is a 140-180 kDa plasma membrane transporter and one of the best characterized mediators of multidrug resistance. This protein is responsible for altering the membrane permeability to cytotoxic compounds and/or enhances the efflux of these agents out of cancer cells. Detection of the emergence of Pgp mediated multidrug resistance in tumors could be beneficial for patients treated with anticancer drugs. Rhodamine dyes are well-known substrates of PgP, and they are used for in vitro measurements. Recently, the synthesis of 18F-labeled rhodamine B has been reported. This substance seemed to be the most suitable compound, as the ethyl substituents on the amine moieties of rhodamine B protect them from side reactions. This radiolabelled compound-family can give us a possibility for using them in in vivo experiments of the multidrug resistance of tumors. Our objective was to improve the formerly published synthesis of 2'-[18F] fluoroethylrhodamine B ([18F]FEtRB) and to test this compound on three different types of multidrug resistance- and sensitive cancer cell line pairs. **Materials and Methods** We have performed a two-step radiosynthesis. The first step was the preparation of [18F]fluoroethyltosylate ([18F]FETos) from ethyleneglycol-1,2-ditosylate with a standard method (Kryptofix 2.2.2./K[18F], abs. AcCN). After HPLC purification of the intermedier, the synthesis of [18F]FEtRB was performed from rhodamine B lactone using [18F]FETos and ionic liquid [bmim][BF4]. After the final HPLC the radiochemical purity was higher than 98%. For the in vitro studies human cervix carcinoma Pgp negative (KB-3.1) and positive (KB-V-1), human ovarian carcinoma (A2780 and A2780AD), and mouse fibroblast (3T3 nad 3T3MDR1) cell lines were used. The accumulation of the ([18F]FEtRB was measured by gamma counter. **Results** All of the Pgp positive cell lines demonstrate the Pgp-substrate nature of [18F]FEtRB. The accumulations were much higher in the Pgp negative cell lines in contrast to their Pgp positive counterparts. The treatment of the PgP positive cell lines with cyclosporine A resulted in comparable accumulation levels of [18F]FEtRB in both type of cells. The functionalities of the Pgp pumps were assessed using a validated PgP substrate (rhodamine 123) by flow-cytometry. **Discussion** The 18F-labelled rhodamine B can sensitively visualize the operation of the Pgp pump in multidrug resistant tumor cell lines. Further biological studies are needed to demonstrate the applicability of the [18F]FEtRB in in vivo by PET imaging.

## PW090

### Evaluation of $^{124}$I-Labeled 3E8ΔCH$_2$ and 3E8ΔCH$_2$ (dPEG®$_4$)$_{12}$ Antibodies as PET/CT Imaging Agents in Mice

**K. KUMAR**[1], H. Ding[1], M. M. Carlton[1], K. Milium[1], S. Kothandaraman[1], K. Davis[2], P. D. Davis[2], A. Pokora[2], S. P. Povoski[3], E. W. Martin, Jr[3], M. F. Tweedle[1]; [1]Department of Radiology, The Wright Center for Innovation in Biomedical Imaging, The Ohio State University, Columbus, OH, UNITED STATES, [2]Quanta Biodesign, Ltd., Powell, OH, UNITED STATES, [3]Department of Surgery, The Ohio State University, Columbus, OH, UNITED STATES.

**Aim.** The objective of the present study was to develop novel micro PET/CT imaging agents based on $^{124}$I-labeled antibodies, i.e., a mouse monoclonal IgG$_1$ (3E8ΔCH$_2$) and a novel antibody, 3E8ΔCH$_2$(dPEG®$_4$)$_{12}$ (where dPEG®$_4$ is a discrete PolyethyleneGlycol compound that is a single compound, and has a specific chain length and molecular weight). **Materials and Method.** 3E8ΔCH$_2$ with molecular weight 120,000 was custom produced. The novel antibody, 3E8ΔCH$_2$ (dPEG®$_4$)$_{12}$, was prepared by the reaction of m-dPEG®$_4$-NHS ester and 3E8ΔCH$_2$ and purified by a size-exclusion method. The 3E8ΔCH$_2$(dPEG®$_4$)$_{12}$ was characterized by a UV/Vis method for potency and by a Glycine curve method for determination of number of dPEG®$_4$ groups attached to the antibody. Both antibodies were radiolabeled, with $^{124}$I, by using the Iodogen method. The radiolabeled antibodies were purified by a size-exclusion method and radiochemical purities were measured by a Thin Layer Chromatography method. All bio distribution and micro PET/CT imaging studies were conducted by using xenograft mice bearing TAG-72 expressing LS174T human colon carcinoma tumors. **Results and Conclusions.** Blood clearance kinetics of the 3E8ΔCH$_2$(dPEG®$_4$)$_{12}$ antibody showed significantly lengthened blood retention vs. the blood retention of 3E8ΔCH$_2$ (%ID/g as 53.53, 35.56, 12.76, 2.86, 1.12 vs. 17.75, 8.43, 0.52, 0.09, 0.05 at 1, 5, 24, 48, and 72 h, respectively. Bio distribution studies of the 3E8ΔCH$_2$(dPEG®$_4$)$_{12}$ showed increased tumor concentration (by 200%) in excised tissues at 72 h. For example, 6.69 ± 0.82 %ID/g observed for 3E8ΔCH$_2$ (dPEG®$_4$)$_{12}$ vs. 3.28 ± 0.77 %ID/g for 3E8ΔCH$_2$ at 72 h. Increased blood retention and significantly higher tumor uptake of the 3E8ΔCH$_2$(dPEG®$_4$)$_{12}$ was supported by the micro PET/CT studies. From these studies, it was concluded that by making subtle changes in the structure of the antibody by discrete PEGylation, we can create significantly altered biological behavior.

PW10 - Monday, Oct. 21, 8:30 - 9:30, Poster Exhibition Area

## Poster Walk 10 - Molecular & Multimodality Imaging: Preclinical - Tumorative Tracers

## PW091

### 18F[FLT]PET and imaging post-processing for non -invasive assessment of siRNA treatment efficacy in experimental glioblastoma

M. Gramanzini[1,2], **S. Gargiulo**[1,2], A. Greco[1,2], A. Feliciello[3], L. Lignitto[3], A. Brunetti[1,2], M. Salvatore[1]; [1]Institute of Biostructures and Bioimages of National Council of Research, Via T. De Amicis 95 and Department of Advanced Medical Sciences, University of Naples Federico II, Via Pansini 5, 80145, Naples, ITALY, [2]CEINGE scarl, Via G. Salvatore 486, 80145, Naples, ITALY, [3]Department of Molecular Medicine and Advanced Biotechnologies, University of Naples Federico II, Via Pansini 5, 80145, Naples, ITALY.

**Introduction** The development of novel anticancer therapies demands advances in the early assessment of their efficacy in the preclinical phase. $^{18}$F-FLT PET has been successfully used to evaluate brain tumor proliferation and its uptake correlate with Ki67 proliferation markers. Semi-automated and standardized quantification techniques are crucial to achieve a reproducible analysis of preclinical PET data. This study aimed to monitor the effects of praja2-siRNA on tumor metabolic activity and growth in an orthotopic mouse model of glioblastoma by $^{18}$F-FLT PET and dedicated images post-processing technology. **Materials and Methods** U87MG cells transfected with *praja2* or control siRNA were implanted into the brain of seven CD1 nude mice.$^{18}$F-FLT PET (9.5 MBq, static, 30 minutes) was performed after 2 and 4 weeks with eXplore Vista GE PET/CT (<1.8mm FWHM; sensitivity 4.2% ACS; CT: 200 µm, 200 µA, 35 kVp, energy windows 250-700keV). PET datasets were reconstructed by 2D FORE/3D OSEM algorithm and corrected for random coincidences, scatter, physical decay to the time of injection, and attenuation with a CT-based method. Counting rates were converted to Standardized Uptake Values (SUV=Tissue activity (MBq/cc)/[Injected dose (MBq)/body weight (g)] ) by use of a system calibration factor (1035 Bq/mL/cps/voxel) derived from the imaging of a mouse-size water-equivalent phantom containing $^{18}$F. Quantitative analysis were performed using Osirix. To avoid over-segmentation problem, calvarial boundaries were manually drawn and pixel values outside ROIs were set to 0. Maximum SUV (SUVmax) and volume lesions were calculated on the base of an interactive 3D growing region procedure, by adding all spatially connected voxels with SUV>50%. Intraobserver and interobserver post-processing reproducibility was evaluated by the intraclass coefficient correlation (ICC) with ANOVA random effects model. **Results** SUVmax were 0.46±0.10 in control and 0.24±0.10 in treated subjects 2 weeks after cells transplantation (>43%). SUVmax were 1.19 in control and 1.1 in treated mice after 4 weeks (>15%). Tumor volume increased from 0.02±0.002 to 0.14 cc in control group and from 0.0093±0.002 to 0.12 cc in siRNA treated one, resulting 55% and 14% greater in control group 2 and 4 weeks post-injection, respectively. SUV without AC underestimate the true activity by 5% ($P < 0.05$). The intraobserver and interobserver ICC were 0.99 (F value 47) for SUVmax and 0.99 for volume (F value 40)(95% interval confidence; $p<0.0001$). **Conclusions** Our results indicate that $^{18}$F-FLT PET quantification allow to test in vivo siRNAs gene-knockdown capability in preclinical glioblastoma tumor model with excellent intraobserver and interobserver reproducibilities.

## PW092

### Dynamic monitoring of gemcitabine induced apoptosis in pancreatic cancer bearing mice with $^{18}$F-ML-10 microPET/CT

**S. Hu**[1], M. Wang[1], Y. Zheng[1], X. Bao[1], J. Zhang[1], Y. Zhang[1], Z. Zhou[2]; [1]Department of Nuclear Medicine, Fudan University Shanghai Cancer Center; Department of Oncology, Shanghai Medical College, Fudan University, Shanghai, CHINA, [2]Department of Diagnostic Radiology, Fudan University Shanghai Cancer Center; Department of Oncology, Shanghai Medical College, Fudan University, Shanghai, CHINA.

**Aim:** Chemotherapy is known to induce apoptotic cell death in malignant tumors. This study aims to evaluate the performance of microPET/CT with $^{18}$F-labeled 5-fluorpentyl-2-methyl-malonic acid ($^{18}$F-ML-10) for the visualization and quantification of cell death induced by gemcitabine in a human pancreatic cancer cell SW1990 tumor xenograft model. **Materials and Methods:** Established SW1990 tumors in nude mice were treated with a single dose of gemcitabine (120 mg/kg, administrated intraperitoneally). $^{18}$F-ML-10 microPET/CT scans were performed at 6h, 24h, 48h and 72h after initiating treatment and in not treated mice. After imaging, TUNEL staining of tumor sections was performed to determine the apoptotic index (AI) and confirm the accuracy of PET quantification. **Results:** One dose of gemcitabine treatment induced a significant increase in tumor uptakes of $^{18}$F-ML-10 as early as 24h after treatment. The accumulations of $^{18}$F-ML-10 were visualized clearly by microPET/CT in local tumor at 24h, 48h and 72h after chemotherapy. Sustained increase of $^{18}$F-ML-10 uptake was observed until 72h after treatment and the AIs from TUNEL staining were consistent with microPET/CT imaging results. The %ID/g for tumor uptake of $^{18}$F-ML-10 were 0.30±0.03 in untreated tumors, 0.33±0.03, 0.65±0.07, 0.67±0.07 and 0.87±0.08 in tumors 6h, 24h, 48h and 72h after treatment, respectively. The corresponding AIs(%) of tumor were 1.40±0.55, 1.60±0.55, 5.00±1.22, 5.20±1.30 and 7.80±1.30, respectively. The differences of both %ID/g and AI among these groups were significant ($P < 0.001$). The tumor uptake of $^{18}$F-ML-10 was significantly correlated with the AI($r = 0.89$, $P < 0.001$). **Conclusions:** $^{18}$F-ML-10 microPET/CT can visualize chemotherapeutic-agent-induced apoptosis in pancreatic cancer xenograft model as early as 24h after treatment. The optimal time window for the detection of apoptosis with $^{18}$F-ML-10 microPET/CT could be 72h after chemotherapy.

## PW093

### A Disulfide Stabilised Diabody Fragment of mAb J591 for SPECT Imaging of Prostate Specific Membrane Antigen

**F. Kampmeier**, J. Williams, L. K. Meszaros, S. Nawaz, G. E. D. Mullen, P. J. Blower; King's College London, London, UNITED KINGDOM.

**Purpose:** Sensitive and specific detection of nodal status, sites of metastases and low volume recurrent disease could greatly improve management of patients with advanced prostate cancer. Prostate specific membrane antigen (PSMA) is a well-established marker for prostate carcinoma with increased levels of expression in late stage, hormone refractory and metastatic disease. The monoclonal antibody J591 is directed against an extracellular epitope of PSMA and has been shown to efficiently target disseminated disease including metastases in lymph nodes and bone. Its use as an imaging agent however is limited due to its slow pharmacokinetics. In this study a diabody fragment derived from mAb J591 was developed as a SPECT tracer for the detection of PSMA in prostate cancer. Experimental: A diabody in $V_H$-$V_L$ orientation and with a stabilising C-terminal cysteine was expressed in HEK293T cells and purified by IMAC/SEC. Specificity and affinity were determined in cell binding studies. For SPECT imaging, the diabody was site specifically labelled with $[^{99m}Tc(CO)_3]^+$ via the C-terminal His tag and evaluated in a subcutaneous DU145/DU145-PSMA prostate carcinoma xenograft model. **Results:** J591C diabody binds to PSMA expressing cells with low nanomolar affinity (2.3±0.4 nM). SPECT studies allowed imaging of tumour xenografts with high contrast from 4h post injection (p.i.). Ex vivo biodistribution studies showed peak tumour uptake of the tracer of 12.1±1.7%ID/g at 8h p.i. and a tumour to blood ratio of 8.0. The Tc-99m-labelled J591 diabody allows SPECT imaging of PSMA within a short time frame. Feasibility of LN and metastasis imaging should be investigated.

## PW094

### Preclinical Development of a Novel Radiolabeled Peptide for Breast Tumor Imaging

**M. Wang**[1,2], J. Kuo[2], K. Lin[2], M. Weng[2], C. Chien[2], W. Lin[2]; [1]Institute of Biotechnology, National Taiwan University, Taipei, TAIWAN, [2]Institute of Nuclear Energy Research, Taoyuan, TAIWAN.

Nowadays peptide targeted delivery has been rapidly applied for cancer therapy. According to the statistics of American Cancer Society, one fourth of the death in the US was due to cancer. However, there is still tremendous unmet need in the early and accurate cancer detection. L-peptide, a kind of 12-mer peptide sequenced by RLLDTNRPLLPY, were used as anticancer drugs recently because of its high recognition to nasopharyngeal carcinoma, breast cancer and lung cancer. In this study, we established an L-peptide imaging platform for detection of breast or lung cancer. L-peptide and L-peptide-cysteine were produced by automated microwave peptide synthesizer. The latter provided free-thio group reacting with the maleimido-PEG for L-peptide PEG formation. I-123 iodination of L-peptide and L-peptide PEG were performed by Iodogen method, then proceeded for in vitro cellular binding of MB231 and in vivo tumor imaging studies, including kinetics of biodistribution in NOD-SCID mice bearing breast or lung cancer. The chemical purity and radio-labelling efficiency were more than 90%. The cellular uptake indicated its rapidly and significant uptake by cancer cell. In vivo images, there is no radio-activity accumulation in the tumor site by I-123-L-peptide in saline, however, with pegylation assistance, there is significant activity accumulation in tumor site by I-123-L-peptide-PEG in 24hr. The kinetics of biodistribution was established for protocal design of tumor targeting and our results indicate a radioiodinated L-peptide PEG with high labeling efficiency for tumor targeting has been successfully developed.

## PW095

### 99mTc-Au-BSA Fluorescent Nanoclusters as Potential Multimodal Imaging Agents

**M. Stalnionis**[1,2], M. Matulionyte[1,2], R. Rotomskis[1,2]; [1]Institute of Oncology, Vilnius University, Vilnius, LITHUANIA, [2]Faculty of Physics, Vilnius University, Vilnius, LITHUANIA.

**Aim**: Diagnostics in oncological diseases is important throughout the treatment. And various imaging modalities have been employed for that purpose. However, diagnosis is not always so easy to obtain. Optical imaging techniques are limited by low penetration through the tissue. The idea of combining optical imaging with other imaging modalities has brought scientific attention, and it could lead to important advances in cancer imaging and other applications. It is also relevant to develop more sensitive and specific contrast agents than the conventional ones. The aim of this study is to develop a SPECT/Fluorescence agent for the imaging and intraoperative guidance. **Materials and Methods**: Bovine serum albumin (BSA) embedded fluorescent gold nanoparticles (Au-BSA) can be one of promising optical imaging tracer. Au-BSA was synthesized by mixing tetrachlorauric acid (HAuCl4) with BSA and then adding sodium hydroxide (NaOH) as a reducing agent in the final step. Radiolabeling was done by mixing Au-BSA with the stannous chloride (SnCl2) solution and sodium pertechnetate (NaTcO4). Labeling efficiency and stability were performed by means of thin-layer chromatography (TLC) analysis using acetone as solvent. The stability of the fluorescent properties of the 99mTc-Au-BSA complex were investigated spectroscopically. Biodistribution imaging of the fluorescent Au-BSA clusters with technetium-99m in a small animal model was performed using clinical SPECT/CT gamma camera. 99mTc-Au-BSA complex (0.2 ml, 100 MBq) was intravenously administered into the tail vein of Wistar rats. The dynamic planar and SPECT/CT imaging of the 99mTc-Au-BSA complex accumulation and distribution was performed**. Results**: Spectroscopic analysis revealed that the optical properties of the synthesized 99mTc-Au-BSA nanocluster remained unchanged after the labeling. The radiochemical purity was above 99%. Biodistribution studies exhibited uptake of the tracer by heart, lung, liver, and kidney immediately after the injection. Dynamic study revealed gradual decrease of activity in heart and lung, whereas organs with the highest activity at 1h30min post injection were liver, kidney, bowel, and bladder. **Conclusion**: The dual-labeled complex 99mTc-Au-BSA was synthesized. High uptake in the urinary system could represent the excretion of 99mTc-Au-BSA via the kidneys. Moderate uptake of liver and bowel might be caused by the excretion of 99mTc-Au-BSA through the hepatobiliary system. The investigation has shown that 99mTc-Au-BSA could be used as a platform for designing a multimodal SPECT/Fluorescence agent for imaging and intraoperative guidance in cancer diagnostics and treatment. Nevertheless, further investigation is required.

## PW096

### Imaging of PDE10A Knockout Mice with a Novel Radiotracer: [11C]T-773

**M. Tóth**[1], J. Häggkvist[1], V. Stepanov[1], A. Takano[1], R. Nakao[1], N. Amini[1], H. Kimura[2], T. Taniguchi[2], S. Miura[1,3], B. Gulyás[1], C. Halldin[1]; [1]Karolinska Institutet, Department of Clinical Neuroscience, Center for Psychiatric Research, Stockholm, SWEDEN, [2]TAKEDA Pharmaceutical Company, Ltd., Pharmaceutical Research Division, CNS Drug Discovery Unit, Fujisawa, JAPAN, [3]Pharmaceutical Company, Ltd., Pharmaceutical Research Division, Medicinal Chemistry research lab, Fujisawa, JAPAN.

**Aim**: [11C]T-773 is a new PET radioligand targeting phosphodiesterase 10A (PDE10A). PDE10A is highly expressed in the striatum by the medium spiny neurons, and it has been demonstrated to be involved in the regulation of striatal signaling through the reduction of medium spiny neuronal sensitivity towards glutamatergic excitation. PDE10A is associated with different neuropsychiatric disorders such as Parkinson's disease, Huntington's disease and schizophrenia. Studies have indicated that PDE10A inhibition may be a novel therapeutic approach to the treatment of the aforementioned diseases characterized by a reduced activity of the medium spiny neurons. An appropriate PET radioligand for PDE10A would help to facilitate drug development and drug evaluation. **Materials and Methods**: Six Homozygous (HOM), 6 Heterozygous (HET) B6.D1-Pde10a/J (JAX® Mice and Services, The Jackson Laboratory, USA) and 6 Wild-Type (WILD) control C57BL/6J mice were imaged. After the induction of 4% isoflurane, anaesthesia was

maintained on 1.5-2% concentration. The bolus injection of [11C]T-773 was given through tail vein cannulation upon the start of a 63 min PET scan in a nanoScan® PET/MRI and PET/CT scanners (Mediso Ltd, Budapest Hungary). PET scans were co-registered with PMOD's mice brain MRI template (PMOD 3.3 Zurich, Switzerland) to acquire time-activity curves (TAC) for the striatum, cortex and cerebellum. Percentage standard uptake values (%SUV) were calculated on a 15-63 minute time period (equation: %SUV=c(t) x body weight / injected dose(t0) x 100). Binding potential (BPND) values were estimated with simplified reference tissue modeling (SRTM) using the cerebellum as reference. **Results**: The regional %SUV values in the striatum were 48.2±1.0, 63.6±5.3, 85.1±6.3, in the cortex 46.1±1.2, 49.7±2.3, 54.5±5.2, and in the cerebellum 58.5±1.9, 57.7±3.9, 54.1±5.4 (HOM, HET and WILD, respectively). Between each animal group (HOM vs HET, HOM vs WILD, HET vs WILD) the striatal %SUV values were significantly different ($p < 0.001$). The striatal BPND values were 0.0±0.0, 0.14±0.07, 0.56±0.15 (HOM, HET and WILD, respectively). The values were significantly different between HOM and WILD and between HET and WILD ($p < 0.001$). **Conclusions:** [11C]T-773 has reached acceptable level of uptake in the striatum and there was a significantly higher uptake and binding potential in wild-type mice compared to heterozygous and homozygous mice. We can conclude that the novel PDE10A radioligand [11C]T-773 shows increased signal with higher level of PDE10A and good binding in the striatum.

## PW097

### A new bifunctional chelating agent, DOTAGA anhydride, shows high potential for labeling biological vectors

C. Bernhard[1], M. Moreau[1], M. Larrouy[1], D. Lhenry[1], **C. Goze**[1], F. Boschetti[2], Y. Rousselin[1], O. Raguin[3], X. Tizon[3], O. Duchamp[3], B. Collin[1,4], J. Vrigneaud[5], F. Brunotte[5], F. Denat[1]; [1]Université de Bourgogne, Dijon, FRANCE, [2]Chematech, Dijon, FRANCE, [3]Oncodesign, Dijon, FRANCE, [4]Centre Georges François Leclerc, Dijon, AUSTRIA, [5]Centre Georges François Leclerc, Dijon, FRANCE.

**Introduction**: The use of so-called bifunctional chelating agents (BFCA) has proved to be the most reliable and commonly employed method for attaching a metal ion (radiometal or paramagnetic metal) to a biomolecule for molecular imaging application (PET, SPECT, MRI, bimodality SPECT-PET/Optical imaging).1 DOTA (1,4,7,10-tetrakis(carboxymethyl)-1,4,7,10 tetraazacyclododecane) and its derivatives represent a major class of chelating agents for biomedical applications, due to their excellent complexation properties towards many trivalent metal ions, and the high kinetic stability of the metal complexes.2, 3 **Method**: in this work, we report the synthesis and reactivity investigations of a new bifunctional chelator so-called DOTAGA-anhydride, readily obtained thanks to the key reaction step of cyclic anhydride formation. With the aim of demonstrating the potential of this new building block for labeling biomolecules, we used it to prepare dual labeled peptides and DOTAGA-antibodies conjugates. **Results:** DOTAGA-Anhydride was prepared in a one-step reaction starting from the macrocycle DOTAGA. The resulting anhydride is stable enough to be stored but may react readily with amino groups, allowing for instance the attachment of bimodal probe on peptidic moiety (Octreotide). 111In labeled DOTAGA-antibodies conjugates were also prepared, leading to a high specific tumor targeting shown in a model of human breast tumors overexpressing HER2/neu antigen.4 **Conclusion**: this work demonstrates the usefulness of DOTAGA-anhydride for the preparation of metal-based imaging agents, whose stability is essential to obtain high quality imaging and for radioprotection purposes. Research support: Support was provided by the CNRS, the University of Burgundy and the Conseil Régional de Bourgogne through the 3MIM project. References: 1) L. Lattuada, A. Barge, G. Cravotto, G. B. Giovenzana, L. Tei. Chem. Soc. Rev. 2011, 40, 3019. 2) T. J. Wadas, E. H. Wong, G. R. Weisman, C. J. Anderson. Chem. Rev. 2010, 110, 2858. 3) G.J.Stasiuk, N. J. Long, Chem. Commun. 2013, 49, 2732.

## PW098

### New macrocyclic imaging agents for targeting chemokine receptor CXCR4

**S. Poty**[1], P. Désogère[1], K. Nicholson[2], S. Nigam[2], C. Goze[1], F. Boschetti[3], H. Maëcke[4], S. Archibald[2], F. Denat[1]; [1]ICMUB, Dijon, FRANCE, [2]University of Hull, Hull, UNITED KINGDOM, [3]Chematech, Dijon, FRANCE, [4]Universitätsklinikum, Freiburg, GERMANY.

**Introduction** : The chemokine receptor 4 (CXCR4) is overexpressed in diseases such as cancer where it plays a role in, among others, the metastatic spread. For this reason, it is an interesting biomarker for the field of diagnostic oncology, and therefore, it is gaining interest for applications in molecular imaging. CXCR4 inhibitors, both peptide-based and small molecules, such as AMD3100 and AMD3465, have been extensively studied. To image CXCR4 expression in tumor models, macromolecular agents such as 111In- and 18F-labeled peptides and 125I-labeled monoclonal antibodies have been investigated using either SPECT (Single Photon Emission Computed Tomography) or PET (Positron Emission Tomography). Recently, AMD3100 and AMD3465 were directly radiolabeled with 99mTc and 64Cu, but these complexes have a low in vivo stability leading to the decomplexation of the metal. Subject : In this work, we investigate the synthesis of new AMD3100 and AMD3465 analogues. The AMD-like moiety will serve as a carrier for specific delivery of radionucleide (64Cu, 68Ga, 111In) to cancer tissues. Then, we consider the introduction on the AMD-like moiety of a chelator selective of the targeted metal. This route also offers the possibility of attaching a fluorescent tag for optical imaging or a bimodal system for both radio-(PET/SPECT) and fluorescence imaging**. Results** : Here, we present the synthetic pathway toward our new AMD3100 and AMD3465 derivatives for nuclear imaging. Biological studies were performed at the University of Hull to validate our concept on our compounds. Flow cytometry and invasion assays were carried out and preliminary results will be shown. **Conclusion** : New CXCR4 inhibitors were synthesized. We are currently working on the radiometallation of our AMD-derivatives and the first CXCR4 imaging on small animals with these new compounds.

## PW099

### Study on the feasibility of a novel cancer-specific molecular imaging method based on the translational control of the 5′-untranslated region

**F. Kang**, W. Ma, W. Yang, L. Li, J. Wang; Xijing Hospital, Xi'an, CHINA.

**Aim:** Cancer targeting strategies based on the translational control of the 5′-untranslated region (5′-UTR) have been well established for gene therapies targeting cancers overexpressing the eukaryotic translation initiation factor eIF4E. Here, we aimed to extend the 5′-UTR candidate range for this strategy and confirm the feasibility of this cancer targeting strategy for molecular imaging in vitro and in vivo. **Materials and Methods:** The optical imaging reporter gene, firefly luciferase (Fluc), was modified with the complex 5′-UTRs of cyclin D1 and vascular endothelial growth factor (VEGF), which limited efficient translation in cells overexpressing eIF4E. The simple-structured 5′-UTR of β-actin was used as a negative reference of cancer specificity, and the blank Fluc vector was used as a blank control. In vitro transfection of the above Fluc reporter gene vectors was conducted in U87MG cancer cells and GES normal cells. The cancer specificity of the 5′-UTRs of cyclin D1 and VEGF was quantified by dual luciferase analysis and optical imaging. The feasibility of this 5′-UTR-based cancer targeting strategy for cancer-specific molecular imaging was also assessed in a U87MG xenograft mouse model. **Results:** Dual luciferase analysis identified significant differences between U87MG and GES cells in groups transfected with pGL3-UTR containing 5′-UTRs of cyclin D1 ($p < 0.05$) and VEGF ($p < 0.05$). In vitro optical imaging showed 5.22- and 11.44-fold enhanced Fluc intensities in cancer cells transfected with pGL3-UTR containing the 5′-UTR of cyclin D1 or VEGF, respectively, as compared with normal cells. A higher tumor/liver optical signal ratio was detected in U87MG xenograft models transfected with pGL3-UTR containing the 5′-UTR of cyclin D1, as compared with the blank Fluc vector group ($p < 0.05$). **Conclusion:** The 5′-UTRs of cyclin D1 and VEGF were sufficient for this novel 5′-UTR-based cancer targeting strategy, which has potential as a cancer-specific molecular imaging modality in vitro and in vivo.

PW11 - Tuesday, Oct. 22, 8:30 - 9:30, Poster Exhibition Area

## Poster Walk 11 - Oncology: Prostate Cancer & Miscellaneous

## PW100

### Usefulness of 18F-choline PET in prostate cancer patients with an unexplained rising of PSA.

**H. Kolesnikov-Gauthier**, H. Lahousse, A. Oudoux, P. Nickers, R. Renard, E. Lartigau, P. Carpentier; Centre Oscar Lambret, Lilli Cedex, FRANCE.

**Aim**: To determine the clinical value of 18F-fluorocholine (FCH)-PET in the management of patients with rising prostate specific antigene (PSA) level after initial treatment. **Methods:** 83 patients with suspected prostate cancer recurrence were addressed for FCH-PET. Patients were initially treated by radical prostatectomy (n=44), external beam radiotherapy or curietherapy (n=39). All of them had rising of PSA levels (mean : 7.3 ng/ml). Accuracy of PET results was determined by histology, clinical and radiological follow-up and changes of PSA values. **Results:** Mean follow-up was 18 months. TEP was positive for 54 patients and negative for 29 patients. In 2/54 PET-positive patients, PSA level decreased during the follow-up without additional treatment. Therefore PET results were considered false positive. Disease relapse was confirmed in 52/54 patients. It was a loco-regional relapse in 34 patients. The others 18 patients had bone metastasis. In 18/29 PET-negative patients, the follow-up of PSA level confirmed the recurrence. However, radiological imaging remained negative. In 11/29 PET-negative patients, a decrease of PSA level was observed in the follow-up and the recurrence was not confirmed. Due to the FCH-PET results, treatment was given in 34 out of the 52 patients with positive PET results. Salvage radiotherapy was proposed for 11 patients, hormonotherapy for 10, radiotherapy combined with hormonotherapy

for 3 and chemotherapy for 5. Two patients had bone radiotherapy only. For 3 others patients, modification of hormonotherapy was proposed. **Conclusion** FCH-PET had major implication in the management of patients with recurrent prostate cancer. It leads to therapeutic changes in 41% (34/83) of the cases. In particularly, salvage radiotherapy was performed in 11 of 34 patients, leading to differ hormonotherapy.

## PW101

### Interest of Early Pelvic Dynamic Acquisition for 18f-Choline PET/CT in Prostate Cancer Patients

**F. DELFORT**, M. EBERLE, S. GUILLEMARD, P. FAUROUS, P. KOTZKI, E. DESHAYES; Cancerology Institute of Montpellier, Montpellier, FRANCE.

**Aim** Literature shows a lack of uniformity in the imaging procedures of 18F-Choline PET/CT in the management of prostate cancer. In our department we perform dual-phase exams but they appear to be time consuming and logistically complicated. The aim of this study was to evaluate the impact of an early dynamic pelvic acquisition on our interpretation. Methods According to the French Society of nuclear medicine guidelines, dual-phase exam was realized with initial dynamic imaging during the first 10 minutes after injection, centered on the pelvis, completed by a late acquisition at 90 minutes on the whole body, with use of intravenous diuretic. 50 patients were included in this retrospective review. All exams were randomized and anonymised two times, one with only the late data, and the other with all acquisition data (early phase and late phase). They were reviewed separately by a resident and a senior nuclear physician; discordant results were reviewed with a third senior physician. Interpretation - blinded to the clinical features - was focused on the pelvis and used objective criteria on prostatic lodge, iliac nodes and bones. For nodes, high uptake was considered as pathological, absence of uptake as normal and an uptake comparable to the gluteal muscle as equivocal. In prostate lodge, median uptake suspect of urinary focus was equivocal. Uptake kinetic in dynamic acquisition was used to better classify foci: a decrease of uptake over time was considered as normal, an increase as pathological. Inguinal lymph nodes were excluded from the analysis. **Results** 60 foci were found on late data alone: 25 in prostatic lodge, 9 in bones and 26 in iliac nodes. With full data acquisition (late and early phases), 52 foci were found: 21 on prostatic lodge, 9 in bones and 22 in iliac nodes. No foci were missed by late data alone except in one difficult case with local inflammation. In 14 foci among 10/50 patients, performing early dynamic acquisition changed the status of foci. In most cases (11/14), it down-staged the status: 6 times from equivocal to normal, 4 from pathological to normal,1 from pathological to equivocal. In prostatic lodge, 3 median foci retained as equivocal on late data alone were better classified with the help of dynamic early phase. There were no differences in bones metastasis. **Conclusion** Early dynamic pelvic acquisition showed a slight improvement on iliac nodes and prostatic lodge final interpretation, but not for bone metastasis.

## PW102

### Diagnostic impact of F-18 FDG PET/CT after diuretic for the upper urinary tract carcinomas: comparison with standard PET/CT and PET/ contrast-enhanced CT

**M. Nogami**[1], Y. Kataoka[1], S. Kohsaki[2], K. Miyatake[1], N. Akagi[1], Y. Ogawa[1]; [1]Kochi University Hospital, NANKOKU, KOCHI, JAPAN, [2]Hosogi Hospital, Kochi, Kochi, JAPAN.

**PURPOSE**: To determine the diagnostic impact of F-18 FDG PET/CT after administration of diuretic for upper urinary tract carcinomas by comparing with standard PET/CT and PET/contrast-enhanced CT. **MATERIALS AND METHODS**: Nineteen consecutive patients with known bladder cancer (n=7) and positive urinary cytology without bladder lesion (n=12) underwent PET/CT with multiphase contrast-enhanced CT (ceCT). After whole-body standard PET/CT scan after an uptake phase of 50 min, furosemide was administrated 120 minutes after FDG injection. Delayed PET/CT was performed after an uptake phase of 180 min, followed by ceCT. To determine the diagnostic impact of diuretic PET/CT for upper urinary tract lesions, ceCT, standard PET/CT (stdPET/CT), PET/ceCT and delayed PET/CT with diuretic (diuPET/CT) were separately and visually assessed for 14 divided regions in the upper urinary tract by using a 5-point visual scoring system. The ROC analysis followed by the McNemar's test were performed based on the reference standard determined by the histopathological results. The distribution of the scoring of each method was statistically compared by the Wilcoxon signed-rank test. The interobserver variability of each was evaluated by the kappa statistics. **RESULTS:** 13 in 266 regions were diagnosed as upper urinary tract carcinomas by the reference standard. The area under the curves of ceCT (0.997) and PET/ceCT (0.997) were significantly higher than stdPET/CT (0.888) ($p<0.05$) but were not significantly different from diuPET/CT (0.952) ($p>0.05$). The number of equivocal scorings was significantly smaller in diuPET/CT than stdPET/CT ($p<0.001$). The interobserver agreement for diuPET/CT was almost perfect (0.85) and significantly higher than stdPET/CT (0.60). **CONCLUSIONS**: Diuretic F-18 FDG PET/CT is superior in diagnostic performance to standard PET/CT and equivalent to contrast-enhanced Methods for the upper urinary tract carcinomas. The diagnostic confidence and interobserver agreement are raised by the PET/CT with administration of diuretic.

## PW103

### Role of 18F-Choline PET/CT in restaging patients with prostate cancer with trigger PSA < 1 ng/ml.

**M. C. Marzola**[1], S. Chondrogiannis[1], A. Ferretti[2], A. M. Maffione[1], L. Rampin[1], A. Massaro[1], G. Grassetto[1], D. Rubello[1]; [1]Nuclear Medicine - PET/CT Centre, Santa Maria della Misericordia Hospital, Rovigo, ITALY, [2]Medical Physics and Biostatistics Unit, Santa Maria della Misericordia Hospital, Rovigo, ITALY.

**Purpose**: To assess the role of 18F-Choline PETCT in patients with prostate cancer already treated with radical intent and who present biochemical relapse with very low trigger PSA < 1 ng/ml, evaluating: a) the positive detection rate of 18F-Choline PET/CT, b) its possible correlation with trigger PSA c) the possible influence of androgen deprivation therapy (ADT) and d) the metastatic spread distribution. **Materials and Methods**: We have retrospectively evaluated 18F-Choline PET/CT scans (November 2009 - December 2012) of 112 patients (mean age 67 years, range 49-82) with prostate cancer previously treated with radical intent through surgery (80 patients) or surgery and radiotherapy (32 patients) with biochemical relapse with very low PSA values of less than 1 ng/ml (mean PSA 0.39 ng/ml, range 0.1-0.99 ng/ml). At the time of the examination 34 patients were under androgen deprivation therapy. The relationship between 18F-Choline PET/CT findings and possible clinical predictors (age, PSA trigger and ADT) was investigated using univariate and multivariate binary logistic regressions. Histology and/or clinical and imaging follow up were taken as gold standards. Correlation between categorical variables (PET findings and ADT) was stated according to Pearson's chi-squared test applied to the contingency table. Comparisons between PET-positive and PET-negative patients in relation to PSA were performed using the non-parametric Mann-Whitney test. **Results**: The overall detection rate of 18F-Choline was 23.2% (26/112 pts). 9/26 (35%) of PET positive patients showed local pathologic uptake: in 5 cases confined to the prostatic bed and in 4 cases to the locoregional lymphnodes. 15/26 (58%) showed distant localizations only: in 9 cases confined to the bone, in 4 cases to non-pelvic lymphnodes and in 2 cases to both bone and non-pelvic lymphnodes. The remaining 2 patients (7%) showed both local and distant localizations. In the univariate and multivariate logistic regression analysis the detection rate of 18F-Choline PET/CT was correlated to trigger PSA ($p< 0.05$, confirmed by the Mann Whitney test: $p<0.05$) and not influenced by androgen deprivation therapy at the time of the examination ($p>0.05$, confirmed by Pearson's chi-squared test $p>0.05$). **Conclusion**: 18F-Choline PET/CT was able to detect local and/or distant relapse in 23.2% of the patients with very low PSA values (<1 ng/ml) and could guide precociously the further treatment. The detection rate of 18F-Choline PET/CT was significantly correlated to trigger PSA while was not influenced by androgen deprivation therapy at the time of the examination even in very low PSA values.

## PW104

### Role of 18F-Choline PET/CT in suspicion of relapse following definitive radiotherapy for prostate cancer.

**M. C. Marzola**[1], S. Chondrogiannis[1], A. Ferretti[2], A. M. Maffione[1], L. Rampin[1], G. Grassetto[1], D. Rubello[1]; [1]Nuclear Medicine - PET/CT Centre, Santa Maria della Misericordia Hospital, Rovigo, ITALY, [2]Medical Physics and Biostatistics Unit, , Santa Maria della Misericordia Hospital, Rovigo, ITALY.

**Purpose**: a) To evaluate the diagnostic role, by means of positive detection rate (PDR), of 18F-Choline (18F-CH) PET/CT, in patients with prostate cancer treated with radiotherapy with curative intent and suspicion of relapse during follow up, b) to correlate the PDR with trigger PSA, c) to investigate the possible influence of androgen deprivation therapy (ADT) at the time of scan on PDR and d) to assess the metastatic spread distribution. **Materials and Methods**: 18F-CH PET/CT exams from 46 consecutive patients (mean age 71.3 years, range 51-84 years) with prostate cancer (mean Gleason score 6.4, range 5-8) previously treated by definitive radiotherapy and with suspicion of relapse with negative or inconclusive conventional imaging were retrospectively evaluated. Twelve patients were treated with brachytherapy and 34 with external beam radiation therapy. Twenty-three patients were under ADT at the time of the examination. Trigger PSA was measured within 1 month before the exam (mean value 6.5 ng/ml, range: 1.1- 49.4 ng/ml). Patients were subdivided in four groups, according to their PSA level: $1.0 < PSA \leq 2.0$ ng/ml (11 patients), $2.0 < PSA \leq 4.0$ ng/ml (16 patients), $4.0 < PSA \leq 6.0$ ng/ml (9 patients) and PSA > 6.0 ng/ml (10 patients). Correlation between ADT and PDR was investigated as well as between PSA and metastatic spread distribution. **Results:** The overall detection rate of 18F-Choline PET/CT was 80.4% (37/46 patients), increasing with the increase of trigger PSA. PDR of 18F-CH PET/CT is not influenced by ADT ($p = 0.710$) even if PET performed under ADT demonstrated an overall higher PDR (82.6%). The majority of the patients 59% (22/37 patients) showed local relapse only, confined to the prostatic bed; 22% of the PET/CT positive patients (8/37 patients) showed distant relapse only (bone localizations in all of them),

while the remaining 19% (7/37 patients) showed both local and distant spread (lymph node and bone). **Conclusion:** 18F-Choline PET/CT showed a high overall detection rate (80%), increasing with trigger PSA (for both local and distant relapse) not influenced by ADT. 18F-Choline PET/CT could be proposed as a first line imaging procedure in restaging prostate cancer patients primarily treated with radiotherapy.

## PW105

### Comparison of FDG-PET/CT with bone scan and chest CT in the staging of bone sarcomas

**J. Alberini**[1], L. Champion[1], V. Edeline[1], M. Wartski[2], N. Jehanno[2], S. Petras[2], M. Gauthe[1], P. Anract[3]; [1]Institut Curie - Hôpital René Huguenin, SAINT-CLOUD, FRANCE, [2]Institut Curie - Hôpital Claudius Regaud, PARIS, FRANCE, [3]Hôpital Cochin, Paris, FRANCE.

***Purpose:*** FDG-PET/CT is not systematically performed in the staging of bone sarcomas. The purpose of this prospective study was to compare FDG-PET/CT scans with bone scan (BS) and chest CT in the detection of bone and lung metastases from bone sarcomas. ***Methods:*** PET/CT (including lower limbs), BS and chest CT were performed with a mean interval between examinations of less than 2 weeks in 135 patients (mean age: 17.5years ±9.8) with histologically confirmed osteosarcoma (n=94) or Ewing sarcoma (n=41). 10 French centres participated to this multicentric study. ***Results:*** primary tumors had a higher FDG uptake in osteosarcoma ($SUV_{max}$±SD 9.2±4.6) than in Ewing sarcoma ($SUV_{max}$±SD 5.4±3.4). PET/CT was positive in 32 patients for bone (n=12), lung metastases (n=12) or bone and lung (n=5). Concordance in PET and BS positive results was obtained in 13 patients: multiple distant lesions (n=3), isolated distant lesion (n=5), skip metastases (n=2), benign lesion (n=1), lesion contiguous to the primary (n=2). Skip metastases were detected only by PET in 2 patients. Discordance in positive BS and negative PET was found in 13 patients: lesions classified as benign in 11 patients: uptake in contralateral lower limb (n=4), post-traumatic (n=3), arthritis (n=2), enthesopathy (n=1) and chondroma (n=1), and remained undetermined in 2 patients. BS was positive for multiple lung metastases in 2 osteosarcoma patients. Concordance in PET and chest CT positive results was found in 17 patients, but in other 25 patients, chest CT was positive for lung nodules, measuring generally less than 5 mm and not active metabolically. No significant difference was found in the performance of BS or chest CT compared to PET in patients with osteosarcoma or Ewing sarcoma. ***Conclusion:*** Compared with BS, PET allowed detection of skip metastases and avoided false positive results in benign lesions. Compared with chest CT, PET failed in the detection of lung nodules especially with a diameter less than 5 mm.

## PW106

### 18F-fluoride kinetics in patients with multiple myeloma. A dynamic PET-CT study

**C. Sachpekidis**[1], L. G. Strauss[1], H. Goldschmidt[2], H. Dirk[2], C. Cheng[1], L. Pan[1], A. Dimitrakopoulou-Strauss[1]; [1]Clinical Cooperation Unit Nuclear Medicine, German Cancer Research Center, Heidelberg, GERMANY, [2]Department of Medicine V, Multiple Myeloma Section, University of Heidelberg, Heidelberg, GERMANY.

**Aim**: During recent years the role of 18F-fluoride has been revalidated as a highly sensitive and reliable biomarker of bone reconstruction, with potential indications in a wide range of bone diseases. A 3-compartment model best describes the incorporation of 18F-fluoride into the skeleton, with influx rate Ki [Ki = k1xk3/(k2+k3)] being the kinetic parameter most closely representing bone remodeling rate. Aim of the study was to acquire quantification data regarding bone influx rate and bone blood flow in patients (pts) with multiple myeloma (MM). **Materials and Methods**: Dynamic PET-CT (dPET-CT) studies of the lower lumbar spine and pelvis were performed after the administration of 200-250 MBq of 18F-fluoride in 41 pts with MM. Sites of focal increased tracer uptake that showed correlation with FDG PET-CT scans, performed 1 day before, were considered as highly suspicious of metastatic lesions. The kinetic parameters' values of these lesions were compared with the respective values of lower lumbar spine and pelvic skeleton that served as reference. A 3-compartment model and standardized uptake value (SUV) calculation were applied for evaluation of the tracer's kinetic data. **Results:** The number of MM-indicative lesions was 22. The kinetic parameter k1 (1/min) that represents regional blood flow was 0.26 for MM lesions and 0.19 for reference areas. Respectively, the influx rate (ml/min/ml) was 0.11 for MM lesions and 0.07 for reference region. Besides the MM-indicative lesions, 18F-fluoride uptake was enhanced in inflammatory sites, traumatic lesions, old fractures, joint disease and other degenerative bone lesions not related to the MM. **Conclusion**: Increased bone blood flow and influx rate in MM lesions of the lower lumbar spine and pelvis, as demonstrated by 18F-fluoride dPET-CT studies, represent the intense bone reconstruction that takes place in this malignancy. 18F-fluoride dPET-CT studies may have a potential role in MM in combination with 18FDG for monitoring and therapy response. Since nearly all causes of increased new-bone formation cause increased localization of the radiopharmaceutical, single 18F-fluoride dPET-CT studies cannot be recommended due to the false positive results.

## PW107

### Prognostic value of FDG PET/CT in patients with hepatocellular carcinoma treated with liver transplantation

**L. Govaerts**, O. Detry, N. Bletard, G. Verset, P. Honoré, A. De Roover, J. Delwaide, R. Hustinx; CHU Liège, Liège, BELGIUM.

**Objectives** : FDG uptake has been shown to predict the outcome in large series of patients with hepatocarcinoma (HCC) in Asia, but few data are available regarding European populations. Our aim was to evaluate the prognostic value of pretreatment FDG PET-CT in patients treated by liver transplantation. **Methods**: We retrospectively analyzed the data of 27 patients (24 M and 3 W, mean age 58 ± 9 years). The mean follow-up was 26 ± 18 months (min 1 month, max 66 months). All patients had an FDG PET-CT before the transplantation. The FDG PET/CT was performed according to a standard clinical protocol: 4 MBqFDG/kg body weight, uptake 60 min., low-dose non-enhanced CT. We measured the SUVmax and SUVmean of the tumor and the normal liver. The tumor/liver activity ratios (RSUVmax and RSUVmean) were tested as prognostic factors and compared to the following conventional prognostic factors: MILAN, CLIP, OKUDA, TNM stage, alphafoetoprotein level, portal thrombosis, size of the largest nodule, tumor differentiation, microvascular invasion, underlying cirrhosis and liver function. **Results** : The DFS was 87.2% at 1y and 72.1% at 3y. The OS was 85.2% at 1y and 80.7% at 3y. According to an univariate Cox model, RSUVmax, RSUVmean and healthy liver were predictors of DFS and RSUVmax, RSUVmean, size of the largest nodule, CLIP, liver involvement>50%, and healthy liver predicted the OS. According to a multivariate Cox model, only RSUVmax predicted DFS and RSUVmax and liver involvement>50% predicted OS. An ROC analysis of the ratios showed that the 1.15 cut-off for RSUVmax was best for predicting both the DFS (Cox regression:HR 14.4, p=0.02) and OS (HR 5.6, p=0.049). The Kaplan-Meier curves and Logrank tests confirmed those results. Even though the MILAN criteria alone were not predictive, it is worth noting that none of the patients outside the MILAN criteria and with RSUVmax<1.15 relapsed. **Conclusions**: The RSUVmax is a strong prognostic factor for recurrence and death in patients with HCC treated by liver transplantation with a cut-off value of 1,15. further prospective studies should test whether the metabolic index should be systematically included in the preoperative assessment.

## PW108

### Hypothyreosis induced myopathia in patients with DTC undergoing radioiodine treatment

**T. M. Haslerud**, A. Schreiber, A. Sabet, H. Ahmadzadehfar, M. Muckle, F. Khalaf, S. Ezziddin; Nuclear medicine; Uniklinikum Bonn, Bonn, GERMANY.

**Objectives:** Patients undergoing radioiodine therapy because of DTC must have elevated TSH levels to assure a sufficient radioiodine uptake in the target lesions. An elevated TSH level can be achieved through thyroid hormone withdrawal or rTSH injection. Hypothyroidism can lead to a number of metabolic changes such as elevated cholesterol levels and reduced kidney function as well as myopathia with elevation of serum creatine kinase (CK). We have investigated the CK levels in patients with DTC undergoing radioiodine treatment after hormone withdrawal and after rTSH injection. **Methods**: We compared three groups of patients undergoing radioiodine treatment. Group 1 underwent a first ablative therapy in hypothyreosis (n= 72), group 2 underwent a second or third radioiodine treatment in hypothyreosis (n= 100) and the patients in group 3 underwent radioiodine treatment without hormone withdrawal using rTSH (n=35). In all patients TSH levels, thyroid hormone status (T3 and fT4), CK, creatinine levels, GFR and liver enzymes were measured on the day of treatment. The mean CK levels were compared between the groups and correlated with the blood parameters above, age, gender and BMI of the patients. It was also noted if the patients had any record of statin medication. Results: The mean CK values for group one were 336,9 (range 28-3670), for group two 325,6 (range 44-4432) and for group three 118,8 (range 46-656). In total 6 of 35 patients (17,1%) in group three had elevated CK levels, in group one 41 of 72 patients (56,9%) showed elevated CK levels and in group two 69 of 100 (69%) had an elevation in CK levels. In total 8 of the 208 patients in this study were on statin medication regularly. **Conclusions**: More than 50% of the patients with manifest hypothyroidism and DTC undergoing radioiodine treatment have an incidence of elevated CK levels. These patients have a more than twice as high mean CK level compared to patients undergoing radioiodine treatment using only rTSH. Which other parameters influence the CK levels demand further studies.

## PW109

### The impact of persistently high or rising anti-thyroglobulin antibodies on follow-up of patients with differentiated thyroid carcinoma

G. Ucmak Vural, **I. Sahiner**, B. B. Demirel, S. Demirtas, A. K. Fidan, B. E. Akkas, N. Ercakmak; Ankara Oncology Research and Training Hospital Department of Nuclear Medicine, Ankara, TURKEY.

Measurement of serial serum thyroglobulin (Tg) levels is of great value in patients with differentiated thyroid carcinoma (DTC). We aimed to investigate the added value of presence of high serum anti-thyroglobulin antibody (TgAb) levels in the postoperative work-up of patients with DTC. **Materials and Methods**: A total of 582 patients with DTC, who were previously treated with total thyroidectomy and radioiodine therapy were referred to nuclear medicine department for routine follow-up control. Among these, 86 patients with elevated serum TgAb levels (>100 IU/ml) were identified and enrolled in this retrospective study. We evaluated the clinical significance of elevated TgAb levels on clinical follow-up (range: 11-276 months). **Results**: The average TgAb levels were 486 IU/ml (range: 105-2070 IU/ml) in the whole patient group. Of 86 patients, 80 patients had elevated TgAb levels at the time of post-operative, preablation evaluation, and 6 patients with negative initial TgAb had rising TgAb levels on follow-up. In 53 of 80 patients, serum TgAb levels were decreased (<20 IU/ml) and no evidence of disease was detected on follow-up. In 27 of 80 patients, TgAb levels remained persistently high or increased. When evaluated for the etiology of TgAb elevation, we observed that 11 patients had either cervical/mediastinal lymph node metastasis or distant disease at the time of diagnosis, 6 patients had cervical lymph node metastasis on follow-up, 1 patient with previous cervical nodal metastasis on diagnosis progressed with lung metastasis, whereas no histopathological confirmation of disease could be established despite suspicious findings on neck ultrasound in 9 patients. In the assessment of patients with rising TgAb levels on follow-up, 5 patients had local-regional disease at the time of initial diagnosis and had progressive disease on follow-up; however, no site of disease was detected in 1 patient with rising TgAb. The frequency of lymph node metastasis in initial diagnosis was significantly higher in patients with persistently high or increasing TgAb levels compared to patients with decreasing levels in further follow-up (p=0.02). **Conclusions**: Persistently high TgAb levels as well as rising TgAb levels on follow-up period in patients with DTC may predict presence of recurrent or metastatic disease especially in regional lymph nodes. Thus, we consider that, similar to patients with high Tg levels on post-ablative follow-up, patients with elevated TgAb levels should be closely monitored for recurrent or metastatic disease.

PW12 - Tuesday, Oct. 22, 8:30 - 9:30, Poster Exhibition Area

## Poster Walk 12 - Radionuclide Therapy & Dosimetry: Radioisotope Therapy - Preclinical

### PW110

#### Absorbed doses to mice for three [18F]-tracers calculated from experimental kinetic data and Monte Carlo simulations

**F. Bretin**[1], T. Mauxion[2], M. A. Bahri[1], A. Luxen[1], A. Plenevaux[1], M. Bardiès[2], A. Seret[1]; [1]University of Liege, Cyclotron Research Centre, Liege, BELGIUM, [2]Inserm UMR 1037 INSERM/UPS, Centre de Recherche en Cancérologie de Toulouse, Toulouse, FRANCE.

In preclinical microPET imaging small rodents often have to undergo longitudinal studies involving multiple scans combined with microCT imaging to gather anatomical information. The radiation exposure of the animals needs to be addressed since the impact of the radiation might compromise the validity of the results. The aim of the study was to use experimentally obtained kinetic data of three [$^{18}$F]-tracers and S-values derived by Monte Carlo simulations to calculate absorbed doses in mice and estimate radiation exposure in longitudinal studies. The bio-distribution of 6-[$^{18}$F]fluoro-L-DOPA, 2-[$^{18}$F]fluoro-L-Tyrosine and a [$^{18}$F] compound under development ([$^{18}$F]X) was obtained using organ harvesting (OH) at multiple time points, dynamic microPET imaging (DI) and hybrid method (HM), where organs are harvested post scan to improve quantification of the microPET. Monte Carlo simulations were carried out using GATE v6.1 and the MOBY phantom to determine S-values of multiple source and target organs. Time activity curves were derived from experimental data and residence times for multiple source organs were calculated and used for absorbed dose calculations. The total body absorbed dose for all three [$^{18}$F]-tracers and all Methods was almost identical with 14.19 ± 0.11 mGy/MBq. The critical organ for 6-[$^{18}$F]fluoro-L-DOPA were the kidneys with 23.61 ± 6.34 mGy/MBq for OH and the bladder wall for DI and HM with 552.44 ± 316.55 mGy/MBq and 569.73 ± 326.48 mGy/MBq, respectively. The high derived bladder wall absorbed dose is similar to values provided in literature for bladder wall from [$^{18}$F]FDG in mice. For 2-[18F]fluoro-L-Tyrosine the highest dose was absorbed by the liver for all three Methods with 48.23 ± 8.32 mGy/MBq derived by OH (DI: 41.57 ± 7.69 mGy/MBq; HM: 54.75 ± 11.03 mGy/MBq). For [$^{18}$F]X the critical organ was the liver for OH with 65.14 ± 8.47 mGy/MBq and the bladder wall for DI with 57.63 ± 28.36 mGy/MBq. The calculated absorbed doses derived from the three experimental Methods showed good agreement. When assuming multiple injected activities of 10 MBq plus additional radiation from microCT (multiple scan average absorbed dose of approx. 80 mGy for full body soft tissue scan, GE eXplore 120 microCT) an accumulated total body absorbed dose of more than 1 Gy and much higher absorbed doses for single organs can be reached possibly introducing stochastic effects. The lethal absorbed dose for a mouse is considered 6 Gy, however, studies have shown that far lower absorbed doses can alter the physiology and compromise results.

### PW111

#### Preclinical models for an innovative glioblastoma therapeutical strategy by 188Re-SSS encapsulated in nanotools: translational view

**A. Cikankowitz**[1,2,3], C. Belloche[1,2], G. Chassain[3], B. Fellah[3], E. Verger[1,2], F. Davodeau[4], J. Abadie[3], E. Garcion[1,2], D. Couez[5,2], N. Chouin[3], N. Lepareur[6], F. Lacoeuille[1,7,2], P. Menei[8], C. Ibisch[3], F. Hindré[1,2]; [1]INSERM UMR_S 1066, MINT, ANGERS, FRANCE, [2]LUNAM – University of Angers, Angers, FRANCE, [3]AMaROC, ONIRIS, Veterinary school of Nantes, Nantes, FRANCE, [4]INSERM UMR_S 892, teams 7 and 13, CRCNA, Nantes, FRANCE, [5]INSERM UMR_S 892, teams 7 and 13, CRCNA, Angers, FRANCE, [6]CRLCC Eugène Marquis, Rennes, FRANCE, [7]Nuclear medicine department, CHU of Angers, Angers, FRANCE, [8]Neurosurgery department, CHU of Angers, Angers, FRANCE.

**Aim**: Glioblastoma (GBM) is the most frequent cancer of the nervous system and therapies currently used cannot treat definitively this disease. By the way of NucSan (Nuclear for health) program which supports research development about the use of radiopharmaceutics in oncology, the aim of the proposed work is to provide evidences that internal radiotherapy through lipid nanocapsules loaded with Rhenium-188 (LNC188Re-SSS) is an alternative therapeutic strategy for GBM that can be translated to human medicine. Previous works have shown a remarkable efficiency of this tool among syngeneic rats linked with local and peripheral recruitments of the immune system's effectors. In this context, two animal models have been chosen to validate the feasibility of this new innovative therapy design (LNC188Re-SSS stereotactic injection). **Materials & Methods**: The syngeneic six weeks old C57BL/6J female mice were treated 6 or 12 days after stereotactic GL261 cells implantation, by a single injection of increasing activities of LNC188Re-SSS (0,925; 1,85 and 2,7 MBq/5µL). MRI was used to follow tumor progression to determine the mass volume through the selection of regions of interest. The increased median survival time (IMST) was also assessed for treated mice versus control mice (stereotactic injection of saline solution). For long time survival animals (3 times the median survival time), they were rechallenged through the same procedure in the other hemisphere. The brachycephalic dog bearing spontaneous tumor will lead to additional evidences to specifically highlight the potential of this innovative technology for GBM treatment. In order to validate procedures of intracerebral injections, a stereotactic head frame specially designed for dog has been conceived which allow both images acquisition (MRI-SPECT and PET) and the achievement of biopsies. **Results/Perspectives**: As previously observed on rat models, the preliminary data show interesting results on treatment efficiency in GL261 mice model with the long time survival animals assessed by the absence of tumor progression (IMST: 41%). Thanks to the dog head frame accuracy, brain biopsy targeted by pre/post-surgery MRI has been validated. These two preclinical models will give us additional evidences for a translational approach with the help of CGO-2012 (IRAD) and ANR-12-EMMA-003301 Radiohead projects. They aim at collecting data on in vivo feasibility and efficiency of LNC188Re-SSS for GBM treatment, especially in a spontaneous model linked with immune response. Finally, the objective of this work is to set up a phase I/II clinical trial.

### PW112

#### Lutetium-177-G250 radioimmunotherapy in an intraperitoneal clear cell renal cell carcinoma xenograft model

**C. H. J. Muselaers**, D. L. Bos, P. F. A. Mulders, E. Oosterwijk, W. J. G. Oyen, O. C. Boerman; Radboud University Medical Centre, Nijmegen, NETHERLANDS.

**Aim**: Despite the good results achieved with agents targeting the VEGF and mTOR pathways, the treatment of advanced clear cell renal cell carcinoma (ccRCC) still poses a great challenge. A new approach in the treatment of ccRCC is radioimmunotherapy (RIT) using anti-carbonic anhydrase IX (CAIX) antibody G250. To investigate the potential of RIT with Lutetium-177 (Lu-177) labeled G250, we conducted protein dose escalation study and subsequently a RIT study with Lu-177-G250 in an intraperitoneal ccRCC mouse model. **Materials & Methods**: Twenty-five athymice female BALB/c mice were injected intraperitoneally with 3 x 106 SK-RC-52 cells. To determine the optimal G250 protein dose, three weeks after inoculation the mice were injected with either 1, 3, 10, 30 or 100 µg G250 radiolabeled with 15 MBq indium-111 (In-111). SPECT/CT images were made with the microSPECT USPECT II camera 48 hours p.i. After imaging, the mice are euthanized and the biodistribution of In-111-G250 was determined. The optimal protein dose was used in a subsequent therapy experiment in three groups of mice with i.p. SK-RC-52 tumors. One group (n=10) was injected with 13 MBq Lu-177-G250, a control group received nonspecific antibody MOPC21 labeled with 13 MBq Lu-177 (n=10) and the

second control group received 20 MBq In-111-G250 (n=10). Tumor growth was monitored with SPECT/CT imaging before treatment and with 3 week intervals. Primary endpoints were overall survival and toxicity. **Results**: The optimal G250 protein dose to target ccRCC in this model was 10 μg G250, as determined with SPECT/CT imaging and biodistribution. Treatment with 13 MBq Lu-177-G250 was well tolerated. Treatment with Lu-177-G250 resulted in significantly prolonged median survival of 139 days, in comparison with 49 days (Lu-177-MOPC21) and 53 days In-111-G250 (p=0.015). **Conclusion**: This is the first RIT study with radiolabeled G250 protein in mice with i.p. growing ccRCC. Treatment with Lu-177-G250 resulted in significantly improved median survival, indicating that this model is suitable to further investigate the potential of RIT of ccRCC.

## PW113

### Tumor targeting with Y-90 or Lu-177 radiolabeled αvβ3 binding RAFT-RGD in a Nude mouse model

**A. Petitprin**[1], D. Marti Batlle[1], S. Martin[1], M. Ahmadi[1], P. Perret[1], D. Fagret[1,2], A. Gauchez[1,3], C. Ghezzi[1], J. Vuillez[1,2,4]; [1]Radiopharmaceutiques Biocliniques / INSERM U1039 / Université Joseph Fourier, La Tronche, FRANCE, [2]Service de médecine nucléaire / CHU Grenoble, La Tronche, FRANCE, [3]Plateforme radioactivité / Pôle biologie / CHU Grenoble, La Tronche, FRANCE, [4]Société Française de Médecine Nucléaire et Imagerie Moléculaire, Paris, FRANCE.

The αvβ3 integrin is known to play an important role in tumor-induced angiogenesis, tumor proliferation, survival and metastasis. Because of its overexpression on neoendothelial cells and on tumor cells of various origins, αvβ3 integrin is an attractive molecular target for diagnosis and therapy of the rapidly growing and metastatic tumors. A tetrameric RGD-based peptide, regioselectively addressable functionalized template-(cyclo-[RGDfK])4 (RAFT-RGD), specifically targets integrin αvβ3 in vitro and in vivo. RAFT-RGD has been used for tumor imaging and drug targeting. This study is the first to evaluate the therapeutic potential of the β- emitters radiolabeled tetrameric RGD peptide RAFT-RGD in a Nude mouse model of αvβ3-expressing tumors. **Material and Methods** We evaluated and compared RAFT-RGD peptides radiolabeled with two β- emitters: yttrium-90 (90Y) and lutetium-177 (177Lu). All mice received an intravenous pre-injection of gelofusine® 4% for renal protection. A biodistribution study of 90Y-RAFT-RGD and scintigraphic images after 177Lu-RAFT-RGD injection were realized in a U-87 MG subcutaneous αvβ3-expressing xenograft model in Nude mice. For experimental targeted radionuclide therapy study, 90Y-RAFT-RGD or 177Lu-RAFT-RGD and 90Y-RAFT-RAD or 177Lu-RAFT-RAD (non-specific controls) were injected intravenously to mice bearing U-87 MG tumors of different size (small vs. large, approximately 200-800 mm3) or αvβ3-non expressing TS/A-pc tumors. Tumor volume doubling times (TVDT) was used to evaluate the efficacy of each type of treatment. Hematologic and renal toxicities of the different treatments were assessed by comparison of blood cells and creatinine levels of the treated groups with the control groups. **Results** An injection of 37 MBq 90Y-RAFT-RGD in mice bearing αvβ3-positive tumors caused a significant growth delay compared to mice treated with 37 MBq 90Y-RAFT-RAD or untreated mice. The treatment was more efficient in large rather than small tumors: TDVT was multiplied by 2.4 in mice bearing large tumors and by 1.33 in mice bearing small tumors as compared with untreated mice. In comparison, an injection of 30 MBq 90Y-RAFT-RGD had no efficacy for the treatment of αvβ3-negative tumors. An injection of 37 MBq 177Lu-RAFT-RGD in mice bearing small αvβ3-positive tumors caused a significant growth delay compared to mice treated with 37 MBq 177Lu -RAFT-RAD or untreated mice. TDVT was multiplied by 1.44 as compared with untreated mice. We observed a reduced toxicity of the 177Lu-RAFT-RGD treatments as compared with the 90Y-RAFT-RGD treatments (no acute nephrotoxicity revealed and decreased leukopenia and thrombocytopenia for the 177Lu-RAFT-RGD treatments). **Conclusion** 90Y-RAFT-RGD and 177Lu-RAFT-RGD are potent αvβ3-expressing tumor targeting agents for internal targeted radiotherapy.

## PW114

### Evaluation of direct rhenium-188-labeled NGR-VEGI for radiotherapy of murine breast tumor 4T1

W. Ma, **J. Wang**, W. Yang; Department of Nuclear Medicine, Xijing Hospital, Fourth Military Medical University, Xi'an, CHINA.

**Aim** NGR-VEGI (asparagine-glycine-arginine-Vascular Endothelial Growth Inhibitor) is a humanized fusion protein directed targeting the CD13 receptor expressed on neurovascular endothelial cell surface, found on some tumor cell lines too. It is being developed for the treatment of tumor and other diseases with angiogenesis. This study focused on synthesis, quality control, in vitro evaluation and imaging of $^{188}$Re-NGR-VEGI for radiotherapy of murine breast tumor 4T1. **Materials and Methods** $^{188}$Re-NGR-VEGI was synthesized using a direct radiolabeling method using sodium gluconate as weak chelator and SnCl2 as reducing agent. Quality control was done using instant thin-layer chromatography. Female BALB/c mice with 4T1 breast cancer were imaged at different time points after intravenously injection of 7.4MBq $^{188}$Re-NGR-VEGI. The inhibitory effects of $^{188}$Re-NGR-VEGI(18.5MBq), NGR-VEGI(10μg), NGR(10μg ) and saline control(200μl) were evaluated by measurement of tumor growth, hematoxylin and eosin and TdT mediated dUTP nick end labeling (TUNEL) staining. All data were analyzed Software and P value of less than 0.05 was considered statistically significant. **Results** $^{188}$Re-NGR-VEGI was prepared achieving high radiochemical yields of more than 90% under optimal reaction conditions and showed good stability in vitro, remaining intact at 24 h after radiolabeling. $^{188}$Re-NGR-VEGI showed tumor visualized at 4h p.i. and the highest uptake was at 12h p.i. The main excretion organ was kidney. $^{188}$Re-NGR-VEGI group showed significantly longer half life (48d) than other groups ($p<0.05$) and higher tumor growth inhibitory($p<0.05$). **Conclusion** $^{188}$Re-NGR-VEGI can be prepared with high radiochemical yield and purity and would be a promising candidate for tumor radiotherapy.

## PW115

### Preclinical Incorporation Dosimetry of (+)-[18F]flubatine in piglets

**B. Sattler**[1], M. Kranz[2], M. Patt[1], C. K. Donat[2], W. Deuther-Conrad[2], S. Fischer[2], T. Sattler[3], R. Smits[4], A. Hoepping[4], J. Steinbach[5], P. Brust[2], O. Sabri[1]; [1]University Hospital Leipzig, Dept of. Nuclear Medicine, LEIPZIG, GERMANY, [2]Helmholtz Center Dresden-Rossendorf, Research Site Leipzig, LEIPZIG, GERMANY, [3]University of. Leipzig, Large Animal Clinic for Internal Medicine, LEIPZIG, GERMANY, [4]ABX advanced biochemical compounds, Dresden, GERMANY, [5]Helmholtz Center Dresden-Rossendorf, Institute for Radiopharmacy, Dresden-Rossendorf, GERMANY.

***Aim:*** (+)-[18F]flubatine is the mirror image isomerof (-)-[18F]flubatine, hich is successfully used for neuroimaging of alpha4beta2 nAChRs with PET. To assess the radiation risk by this new radiotracer, biodistribution, organ doses (OD) and the effective dose (ED) were investigated in a preclinical trials using piglets. ***Method:*** Whole body dosimetry of (+)-[18F]flubatine was performed in 3 female piglets (age: 43±1.2d, weight: 14±1.0kg). The animals were narcotized using 20 mg/kg Ketamine, 2mg/kg Azaperone; 1.5% Isoflurane in 70% N2O/30% O2 and sequentially PET-imaged up to 5h post i.v. injection of 183.5±9.0MBq on a SIEMENS Biograph16 PET/CT-system on 7 bed positions (BP) per frame, 1.5 to 6 min/BP, CT-attenuation correction (AC) and iterative reconstruction. All relevant organs were defined by volumes of interest. Exponential curves were fitted to the time-activity-data (%ID/g, and %ID/organ). Time- and mass-scales were adapted to the human order of magnitude. The ODs were calculated using the adult male model with OLINDA. The ED was calculated using tissue weighting factors as published in the ICRP103. ***Results:*** The highest OD was received by the urinary bladder (71.7±26.3μSv/MBq), the kidneys (45.1±6.5 μSv/MBq) and the brain (32.3±3.24μSv/MBq). The highest contribution to the ED was by the urinary bladder (2.9±1.1 μSv/MBq), the lungs (1.7±0.02μSv/MBq) and the red marrow (1.4±0.1μSv/MBq). According to this data, the ED to humans is 14.3±0.3 μSv/MBq. ***Conclusion:*** Considering 40% underestimation of the ED to humans by preclinical dosimetry [1] the expected ED to humans after 300MBq i.v. is 7.2 mSv, which is about the ED by (-)-[18F]flubatine (6.8 mSv/300MBq) and well within the range of what other 18F-labeled compounds cause to humans. This risk assessment encourages to transfer (+)-[F-18]flubatine from preclinical to clinical study phases and to further develop as a clinical tool for PET imaging of the brain. References: [1] Sattler B, ⋯, Sabri O. Incorporation dosimetry of F-18-Flubatine - Comparison of animal model data with first-in-man results J. Nucl. Med. 2012; 53(suppl): 1503. The trial is partly co-funded by Strahlenschutzseminar in Thüringen e.V. and by Helmholtz Validation Fonds.

## PW116

### Potential renal toxicity biomarkers indicating radiation injury after 177Lu-octreotate treatment

**J. Dalmo**[1], E. Westberg[2], L. Svedbom[3], M. Törnqvist[2], L. Barregård[3], E. Forssell-Aronsson[1]; [1]Institute of clinical sciences, Sahlgrenska Cancer Center, Gothenburg, SWEDEN, [2]Department of Materials and Environmental Chemistry, Stockholm, SWEDEN, [3]Institute of Medicine, Gothenburg, SWEDEN.

The kidneys are one of the most exposed non-tumor tissues and regarded as one of the main dose-limiting organs in peptide receptor radionuclide therapy (PRRT). [177Lu-DOTA0, Tyr3]-octreotate (177Lu-octreotate) has shown promising results in the treatment of somatostatin receptor overexpressing neuroendocrine tumors, but optimization is still needed. The ability to give each patient as much 177Lu-octreotate as possible without inducing nephrotoxicity is necessary for an efficient treatment. However, due to large inter-individual differences in uptake and retention in the kidneys, there is a need for efficient Methods that early can indicate renal injury. A possible way is to identify biomarkers for high risk of radiation nephrotoxicity. The aim of this study was to investigate the potential of using urinary retinol binding protein (RBP), and blood valinhydantoin (VH) as biomarkers of nephrotoxicity on adult mice after 177Lu-octreotate treatment. BALB/c nude mice (n=6/group) were i.v. injected with 60 MBq or 120 MBq of 177Lu-octreotate. The control group was mock treated with saline. Spot urine samples were collected before injection, and 14, 30, 60 and 90 days after injection. Analysis of RBP4 and creatinine was performed using Mouse RBP4 ELISA kit and

Poster Walks

Creatinine kit from R&D Systems, respectively. Erythrocytes were separated from whole blood samples collected 90 days after injection, and analysed for VH by LC-MS/MS. The ratio between VH and a volumetric standard was calculated. The RBP/creatinine level increased with time in both groups given 177Lu-octreotate, with earlier and higher response for the 120 MBq group. No clear change in VH level between the different groups was observed. The result show that RBP may be a promising new biomarker for radiation induced kidney toxicity. The presently used method based on VH was not sensitive enough to be used as kidney toxicity marker. Further studies on mice are ongoing to validate if RBP4 may be efficient in predicting late nephrotoxicity. In patients, RBP/creatinine levels are followed in urine samples after treatment with 177Lu-octreotate.

## PW117

### Dose-response study of the hematological toxicity induced by vectorized radionuclides in a mouse model

**J. Rousseau-Poivet**[1], N. Sas[1], F. Nguyen[1], J. Abadie[1], N. Chouin[1], J. Barbet[2]; [1]LUNAM Université, Oniris, "AMaROC", Nantes, F-44307, FRANCE, [2]CRCNA, INSERM, Université de Nantes, UMR_S 892, Nantes, FRANCE.

**Aim** In internal radiotherapy, the dose-limiting factor is often the bone marrow (BM) toxicity. In patients, its relationship with the BM absorbed dose seems to be elusive. Most probable reasons are the BM depletion following previous treatments associated to dose assessment complexity. To avoid this and better understand myelotoxicity mechanisms, we investigated hematopoiesis from BM to blood after radionuclide injections in healthy mice associated to individual BM dosimetry. Based on these data, a compartmental model was developed to predict the depletion of each mouse hematopoietic cell in a dose-dependent manner. **Materials and Methods** C57/Bl6 mice were injected with increasing activities of 18FNa, an osteotropic agent. Mean absorbed doses to the BM were calculated using the MIRD formalism with the mineralized bone considered as the principal source of 18FNa. Time-integrated activities within the skeleton were derived from dynamic microPET-CT images. Hematological toxicity was monitored via blood cell counts and myeloid progenitor colony assays over time after injection. The myelotoxicity model consists in compartments for each hematopoietic cell. Its parameters were adjusted to reproduce experimental toxicities. **Results** For an absorbed dose to the BM of 0.8±0.1 Gy, myeloid progenitors showed a 84% depletion 84% at day 7 post-injection (D7) and a recovery at D14 for all precursors and D21 for the less differentiated progenitor. In blood, neutrocytopenia was observed at D3 (80% decrease) and recovered at D7. Thrombocytopenia was also noticed between D7 and D17 with a nadir at D7 (26% of depletion). The compartmental model predicted platelets kinetics in a satisfying manner. The nadir value, time to nadir and time to recovery were estimated with errors of 4.9%, 10.2% and 10% respectively. Whereas higher absorbed doses only increased platelets depletion (62% associated to 1.4 Gy), they extended the recovery time for all studied progenitor and blood cells. As compared to 0.8 Gy, one more week was necessary at 1.4 Gy. A mild anemia (21% erythrocyte depletion) was noticed only at this higher absorbed dose between D3 and D10. Conclusion Absorbed doses to the BM between 0.8 and 1.4 Gy induced hematological toxicity expressed by transient BM aplasia, neutropenia, thrombocytopenia and inconsistent anemia. These depletions and time to recovery were both dose-dependent. Higher absorbed doses will be achieved to better investigate the dose-response relationship and to further develop our compartmental model for platelets. Neutrophils and erythrocytes kinetics are also under investigation to generate satisfying simulations with the model.

## PW118

### Optimization of combination of peptide receptor radionuclide therapy (PRRT) and temozolomide therapy using SPECT/CT and MRI in mice.

**S. M. Bison**[1,2], J. C. Haeck[1,2], S. J. Koelewijn[1], H. C. Groen[1], S. Berndsen[1], M. Melis[1], M. R. Bernsen[1,2], M. de Jong[1,2]; [1]Erasmus MC, Department of Nuclear Medicine, Rotterdam, NETHERLANDS, [2]Erasmuc MC, Department of Radiology, Rotterdam, NETHERLANDS.

**Aim**: Successful treatment of patients with somatostatin receptor overexpressing neuroendocrine tumours (NET) with Lutetium-177-labelled octreotate, (PRRT) or temozolomide (TMZ) as single treatments has been described. Their combination might result in additive response, so we studied tumour characteristics and therapeutic responses after different administration schemes in mice to obtain the optimal strategy to combine PRRT and TMZ. **Materials and Methods**: Initially we performed imaging studies of nu/nu mice, (n=5-8) bearing somatostatin receptor-expressing human H69 small cell lung carcinoma xenografts, after single administration of $^{177}$Lu-octreotate (30MBq/µg) or TMZ therapy (50mg/kg/day (d) 5x/week for 2 weeks). Weekly tumour perfusion was measured by DCE-MRI and tumour $^{111}$In-uptake 24h after administration of 30MBq $^{111}$In-octreotide was quantified using SPECT/CT. Based on the imaging results, seven groups were included in a combination therapy study in H69 tumour-bearing mice (n=8-9): 1: control (saline), 2: TMZ, 3: PRRT, 4: PRRT + TMZ both d1, 5: PRRT d1, TMZ from d15, 6: TMZ from d1, PRRT d15, 7: PRRT d1 and d15. Study endpoint was tumour volume >1800-2000 mm$^3$. **Results:** Single treatment with $^{177}$Lu-octreotate or TMZ therapy resulted in reduction of tumour size, which led to changes in MRI characteristics such as intrinsic T2, T2* and perfusion values. Moreover, TMZ treatment not only showed tumour size reduction 9d after start of treatment and an increase in MRI perfusion parameters but uptake of $^{111}$In-octreotide peaked at d15 followed by a decrease afterwards. In the combination therapy study no complete cure was found in control, single TMZ and single and double PRRT groups, while in the TMZ/PRRT combination groups resp. 44%, 38% and 55% of mice (groups 4, 5 and 6) showed cure without recurrence of tumour growth during follow-up. This was also reflected in an extended median survival time (MST), resp. 101, 107 and 120d. MST for controls only was 35d; single TMZ resulted in a MST of 83d, while PRRT showed a MST of either 56d after single and 74d after double administration. **Conclusions**: All three TMZ and PRRT combination groups showed additional anti-tumour effect compared to the single treatment groups, including fractioned PRRT. MRI tumour perfusion and SPECT/CT uptake studies proved that administration of $^{177}$Lu-octreotate 15d after start of TMZ treatment is the optimal combination as confirmed in the best anti-tumour effects in the model studied. Therefore TMZ administration prior to PRRT might be the best option for clinical practice to increase tumour responses in NET patients as well.

PW13 - Tuesday, Oct. 22, 8:30 - 9:30, Poster Exhibition Area

# Poster Walk 13 - Conventional & Specialised Nuclear Medicine: Pulmonology

## PW119

### How common is cancer suspected CT findings in the lungs when V/P SPECT-CT hybrid imaging is used in patients with stable COPD or healthy smokers?

J. Jögi[1], H. Markstad[2], J. Olsson[3], L. Bjermer[3], **M. Bajc**[1]; [1]Dept. of Clinical Physiology & Nuclear Medicine, Lund University and Skåne University Hospital, Lund, SWEDEN, [2]Dept. of Radiology, Lund University and Skåne University Hospital, Lund, SWEDEN, [3]Dept. of Respiratory Medicine & Allergology, Lund University and Skåne University Hospital, Lund, SWEDEN.

Chronic obstructive lung disease (COPD) is an inflammatory disease that predominantly affects small airways. COPD is a heterogeneous condition and patients with COPD are prone to co-morbid diseases such as heart failure, ischemic heart disease and lung malignancy. Ventilation/Perfusion (V/P) SPECT is used for pulmonary embolism diagnosis but has also shown to be a sensitive method to detect obstructive lung changes. Today it is more and more common to use hybrid SPECT/CT systems that combine anatomical and physiological imaging. The combined low dose CT (LDCT) can show unexpected changes in the lungs that give suspicion of malignancy and need to be followed-up. In this study the aim was to investigate how common it was with tumour suspected changes in the lungs among healthy smokers and patients with stable COPD that was investigated with V/P SPECT/CT hybrid imaging METHOD: 69 subjects, either healthy smokers or with stable COPD (GOLD 0-4) were evaluated with Clinical questioners (CCQ) and were examined with V/P SPECT and low-dose CT (LDCT) in a hybrid system. Spirometry was performed. The physicians that reviewed the V/P SPECT and LDCT images were blinded to other information. V/P SPECT was interpreted in accordance with the guidelines of EANM. Tumour suspected changes in LDCT images were reported and follow-up was performed by referring physicians in accordance with local guidelines. RESULTS: Nodular or other tumour suspected findings in LDCT images were reported in 19 cases (27.5%). Nine patients (13%) needed further follow-up and out of these, 3 patients (4,3%) were found to have lung cancer. One of the patients died due to this malignancy during the follow up period. CONCLUSION: LDCT performed in combination with V/P SPECT In healthy smokers and patients with COPD shows that malignancy suspected changes that need further evaluation is quite common. Follow-up identified unexpected cancer among 3 (4.3%) of the subjects in this study. The effects of introducing hybrid systems in lung imaging needs to be further evaluated.

## PW120

### Impact of V/P tomography on treatment duration of pulmonary embolism

**A. Begic**[1], E. Opankovic[1], V. Cukic[1], M. Rustempasic[1], A. Basic[1], M. Miniati[2], J. Jögi[3], M. Bajc[3]; [1]Clinical Center University of Sarajevo, Sarajevo, BOSNIA AND HERZEGOVINA, [2]Università degli Studi di Firenze, Firenze, ITALY, [3]Lund University and Skåne University Hospital, Lund, SWEDEN.

As stated in the guidelines of the European Association of Nuclear Medicine, Ventilation/perfusion tomography (V/P SPECT) is a method of choice for the diagnosis and follow-up of pulmonary embolism (PE). PE is treated with

anticoagulantia. The optimal duration of anticoagulantia therapy is still a subject of debate. Usually 6 months treatment is recommended. Therapy length is today based on the estimated risk of recurrence, considering thrombophilic risk factors and if the cause of the the PE event is established. As anticoagulation in itself can cause serious adverse events, a better way to individualize therapy is desirable. Under treated, PE can become chronic and contribute to pulmonary hypertension. **The objective** of this study was to investigate if V/P SPECT follow-up could be of benifit to identify patients who would be eligable for shortened anticoagulation therapy (3 months) as well as those who might need indefinite therapy. The long term aim is to better individualize PE therapy. **Material and method**: 54 consecutive patients with acute PE were followed-up clinically and by V/P SPECT at 3 and 6 months. Therapy was terminated after 3 months if V/P SPECT was normal, patients were clinically normalized and were without risk of hypercoagulability. **Results:** PE extension varied from 10% to 70% in acute stage. Complete resolution of PE was found in 63% (45 patients) of the patients after 3 months. PE extent decreased significantly between acute stage and first control after 3 months ($p<0.01$). The treating pulmologist decided to terminate therapy in 30 patients (56%). On second control, 6 months later, PE extent showed no further reduction ($p=0.5$). PE extent at acute stage did not have an impact on the teraphy decision. 24 patients (44%) were treated for 6 months. Nine of them had perfusion defects at 3 months. No recurrency was identified at 6 months in the 30 patients who terminated therapy after 3 months. **Conclusion:** In the presented study it was showed that V/P SPECT can be used as an objective tool for follow-up of patients with PE and that V/P SPECT can be of help for individualized therapy decisions.

## PW121

### Correlation between the extent&number of perfusion abnormalities in V/Q SPECT/CT and Pulmonary Vascular Resistance (PVR) in CTEPH patients

**S. Ozguven**[1], F. Dede[1], B. Yıldızeli[2], S. Tas[3], M. Yanartas[3], S. Gungor[1], T. Ones[1], S. Inanir[1], T. Y. Erdil[1], H. T. Turoglu[1]; [1]Marmara University Department of Nuclear Medicine, Istanbul, TURKEY, [2]Marmara University Department of Thoracic Surgery, Istanbul, TURKEY, [3]Kartal Kosuyolu EAH Department of Cardiovascular Surgery, Istanbul, TURKEY.

**Objective**: Systolic pulmonary arterial pressure (SPAP) can estimated by echocardiography to assess the severity of pulmonary hypertension in chronic thromboembolic pulmonary hypertension (CTEPH). When this value is high; mean pulmonary arterial pressure (MPAP) and pulmonary vascular resistance (PVR) measurements were performed with Swan-Ganz catheter before endarterectomy procedure. On the other hand when differentiating CTEPH from other causes of PH; ventilation/perfusion scintigraphy (V/Q) which is in the diagnostic algorithm is used. In this study, we investigated the relationship between the extent of 'mismatch' perfusion defects detected by V/Q SPECT/CT and pulmonary hypertension pressure parameters. **Methods**: In this retrospective study, we investigated the comparison between the number of abnormally perfused segments in V/Q SPECT / CT studies and SPAP, MPAP and PVR measurements in patients with a diagnosis of CTEPH and undergoing endarterectomy. **Results:** 10 patients (4 women, 6 men) with a mean age of 49.8 ± 10.8 years were included in this retrospective study. The average number of abnormally perfused segment detected in V/Q SPECT/CT was 10.5±6.7. The average PVR value was 1196.4 ± 582 (240 -2176) in these patients and was correlated with the number of affected segments ($r=0.66$, $p<0.039$). However, there was no significant correlation between the mean SPAB (74.5 ± 27.3mmHg, 30 -108 mm / Hg, and $r = 0.46$, $p = 0.18$) and MPAB (49.5 ± 17.2mmHg, 30 -108 mm / Hg, and $r = 0.38$, $P = 0.23$) with perfusion abnormalities. **Conclusion**: Pulmonary hypertension should be evaluated hemodynamically in patients with CTEPH. PVR is the most important parameter for prognosis of the disease and determination of the risk associated with the pulmonary endarterectomy procedure. In this study, increased number of abnormally perfused segments in V/Q SPECT/CT showed significant correlation with increased pulmonary vascular resistance

## PW122

### Outpatient treatment of pulmonary embolism in patients with small or submassive embolic burden

J. Elf[1], N. Isma[2], J. Jögi[3], **M. Bajc**[3]; [1]Dept of Vascular Surgery, Skåne University Hospital and Lund University, Malmö, SWEDEN, [2]Dept of Cardiology, Skåne University Hospital and Lund University, Malmö, SWEDEN, [3]Center for Medical Imaging and Physiology, Skåne University Hospital and Lund University, Lund, SWEDEN.

**Objectives:** To assess safety of outpatient treatment in hemodynamically stable patients with scintigraphically small or submassive pulmonary embolism Design: A prospective outcome study Setting: Single center, tertiary care hospital **Patients and Methods**: Consecutive patients with acute pulmonary embolism diagnosed by V/P SPECT (ventilation /perfusion tomography), were risk stratified by clinical judgement in combination with a quantitative estimation of embolic burden, between January 2007 and December 2011. Patients were treated at home if they were hemodynamically stable, did not require oxygen or parental analgetics, had no contraindications to anticoagulant treatment and had an obstruction of the pulmonary vascular bed less than 40%, quantified by V/P SPECT. Patients who were admitted but had a total stay in the hospital less than 24 hours were also included in the analysis of outpatient treatment. The primary outcomes were venous thromboembolic (VTE) recurrences, major or clinically relevant bleeding and overall mortality during the 3-month follow up. **Results:** Eight hundred and thirty six patients were diagnosed during the study period, of whom 416 (49.8%) were diagnosed as outpatients. In those patients diagnosed as outpatients 260 (62.5%) were treated at home. In total 307 (36.7%) patients were treated at home and during follow up 1 patient (0.3%) had a recurrent thrombotic event and another 8 patients (2.8%) had to be readmitted due to VTE related symptoms. Eleven patients (3.6%) had a major or clinically relevant bleed. The overall mortality was 2 % (n=6) in the outpatient group with no PE-related mortality, compared to 15.5% (n=82) in the inpatient group. **Conclusion**: Outpatient management in patients with pulmonary embolism is safe and should be considered if the clinical risk estimate is low and V/P SPECT excludes massive obstruction of the pulmonary vascular bed.

## PW123

### Ventilation/ perfusion lung scan results in patients with chronic thromboembolic pulmonary hypertension: A Comperative study Between V/Q SPECT/CT and pulmonary thromboendarterectomy surgery

**S. Ozguven**[1], F. Dede[1], B. Yıldızeli[2], S. Tas[3], M. Yanartas[3], S. Gungor[1], M. Aras[1], R. Maleki[1], T. Ones[1], S. Inanir[1], T. Y. Erdil[1], H. T. Turoglu[1]; [1]Marmara University Department of Nuclear Medicine, Istanbul, TURKEY, [2]Marmara University Department of Thoracic Surgery, Istanbul, TURKEY, [3]Kartal Kosuyolu EAH Department of Cardiovascular Surgery, Istanbul, TURKEY.

**Introduction**: Chronic thromboembolic pulmonary hypertension (CTEPH) is a poor prognostic disease occurs approximately 1% of patients after acute pulmonary embolism and can be treated with pulmonary thromboendarterectomy (PTEA) once diagnosed. In this study, we compared "mismatch" perfusion defects seen in ventilation-perfusion (V/Q) SPECT/CT with PTEA surgical specimen findings in patients with CTEPH **Methods**: In this retrospective study we investigated the CTEPH patients who performed V/Q-SPECT/CT imaging and PTEA operation from January to December 2012 period. V/Q SPECT/CT images assessed according to "EANM guidelines for ventilation / perfusion scintigraphy, 2009". "Mismatch" perfusion defects were expressed with lobes (0-5 lobes / patient) and compared with macroscopic findings of the post-extracted material in PTEA operation. **Results:** 13 patients (4 females, 9 males) with a mean age of 50.5 ± 11.2 years (32-67 years) with a diagnosis of CTEPH were included. V/Q SPECT/CT sensitivity on the basis of patient was 84.6% (11/13) and on the basis of the lesion was in 75% (48/64 lobe), respectively. **Conclusion**: Diagnostic performance of V/Q scintigraphy in CTEPH was investigated with planar imaging technique in the majority of studies. Another limitation is that these studies compared V/Q scintigraphy results with angiography ( CT pulmonary angiography or digital substraction angiography) or clinically instead of comparing directly with PTEA operation material. Few in number, but a selected group of our patients, showed the results of V/Q SPECT/CT has a high sensitivity on the basis of the patient. Although V/Q SPECT/CT has a key role in the pre-selection of the patient to PTEA, albeit low, false negativity on the basis of the patient and the lesion was observed. Relative decrease of sensitivity is due to difference between vascular physiopathology of acute pulmonary thromboembolism and CTEPH. Vascular pathology in CTEPH is due to fibrosis of partially recanalised clot, disappearance of tunica intima and infiltration of tunica media, instead of a simple thrombus occlusion . In conclusion, V/Q scintigraphy is a successful method for differential diagnosis of CTEPH in patients with pulmonary hypertension. Albeit low, false-negative cases in V/Q scintigraphy should be taken into consideration.

## PW124

### Can Thoracic Low-dose Multidetector CT Replace Pulmonary Ventilation Scintigraphy in the Follow-up of Patients with Pulmonary Embolism?

**C. Achury**, A. Flotats, A. Domenech, R. Jaller, L. Geraldo, J. Deportos, A. Montes, I. Carrió; Hopital de la Santa Creu i Sant Pau, Barcelona, SPAIN.

**Objectives** : Planar ventilation/perfusion (V/Q) scintigraphy is currently the standard method in the follow-up of patients with pulmonary embolism. With the advent of hybrid SPECT/CT systems it is possible to study both the anatomical lung space and its functionality. We hypothesized that anatomic findings using the low-dose CT component of the hybrid SPECT/CT system may potentially replace the functional findings of the ventilation scan. Therefore, the aim of the study was to assess the agreement between the planar ventilation scan and the low-dose CT scan. **Methods**: Fifty-three consecutive patients underwent planar V/Q and lung perfusion SPECT/CT imaging as follow-up of acute pulmonary embolism. A hybrid double headed SPECT/CT system equipped with a six slice multidetector scanner was used (Philips Precedence). Planar ventilation images and low-dose CT images

were separately interpreted by consensus of two nuclear medicine physicians. Kappa statistics were calculated to determine the agreement between both Methods. **Results**: Only 15 (28.3%) of the patients showed one or more ventilation defects and/or anatomical changes in the CT, with a total of 20 abnormalities registered (2 ventilation defects with no corresponding CT changes; 6 CT changes with no corresponding ventilation defects; and 12 matched ventilation and CT changes). Thirty-eight patients showed no defects on the planar ventilation scan or CT scan. The overall agreement between the planar ventilation scan and the low-dose CT scan was good (kappa =0,657, p<0.0001). **Conclusions:** Low-dose CT scan used for lung perfusion SPECT/CT imaging in the follow-up of patients with acute pulmonary embolism shows good agreement with planar ventilation scan, thus potentially avoiding the need of the ventilation scan, reducing total exploration time and cost, and increasing patient comfort.

## PW125

### Single subsegmental mismatched defect on Ventilation/Perfusion SPECT: single centre review and follow up of a small cohort of patients

S. Rodney, T. Wagner, P. Kyrtatos, **S. Navalkissoor**; Royal Free London NHS Foundation Trust, London, UNITED KINGDOM.

**Introduction**: According to the EANM guidelines for ventilation perfusion (V/Q) SPECT scans in pulmonary embolus (PE), a positive scan is diagnosed when there is at least 2 subsegmental or one segmental wedge-shaped mismatch. There is no current guidance for 1 subsegmental mismatch. Aim: To determine the incidence of single subsegmental wedge-shaped mismatched defects and to determine the rate of treatment/ what influenced treatments in these patients. **Methods:** Retrospective review of V/Q scans performed for a year between April 2012 and March 2013 was performed. In the patients with single subsegmental defects, we looked at which patients went on to have treatment (and what influenced these treatments) and determine if any of the patients not treated went on to develop PE **Results:** 11/402 (2.7%) patients were identified. Of these 11, 4 patients were diagnosed with a PE and three were treated. The reason for treatment was positive computed tomography pulmonary angiogram (CTPA) in 1 patient, repeat V/Q showing resolution of mismatch whilst on Warfarin in 1 patient and high pre-test probability in 1 patient. One further patient was diagnosed as having a small PE but was not warfarinised as repeat V/Q scan showed resolution of mismatch. In the 7 patients who were not treated, the decision not to treat was based on patients having low pre-test likelihood Wells score (3 patients) or a moderate pre-test likelihood Wells score and a negative subsequent CTPA (4 patients). Telephone follow up of all non-treated patients revealed no further clinical development of a PE. **Conclusion:** Although the majority of VQ SPECT scans can be reported in a binary fashion i.e. PE present or not present, single subsegmental wedge shaped mismatches, although infrequent, represent a diagnostic conundrum. As a small PE is possible in all these patients, careful discussion with referring clinicians should be instituted before deciding on treatment and/or follow up.

## PW126

### Lung scintigraphy performed on SPECT/CT hybrid cameras in pulmonary embolism diagnostics

**A. Mazurek**, M. Dziuk, S. Piszczek, Z. Stembrowicz-Nowakowska, A. Gizewska-Krasowska; Military Institute of Medicine, Warsaw, POLAND.

**Aim** The main aim of this study was to evaluate the accuracy of SPECT/CT scintigraphy in the diagnosis of pulmonary embolism (PE). The additional objectives were to compare the existing Methods (planar and SPECT) with SPECT/CT **Materials and Methods** In 84 consecutive patients suspected of PE, perfusion (Q) scintigraphy (planar, SPECT, SPECT/CT ) was performed.PE was diagnosed when: there was at least 1 segmental or 2 subsegmental perfusion defects with the absence of abnormalities in the lungs parenchyma (visualized in CT). PE was excluded when there was: normal perfusion pattern, perfusion defects that were not located according to the lungs vascularity, perfusion defects caused by abnormalities in the lungs parenchyma (visualized in CT). Ventilation scintigraphy (V) was done in 24 patients in which lung perfusion abnormalities were equivocal.Final clinical diagnosis was established by physician responsible for patient care ( based on clinical symptoms, laboratory tests, other imaging studies, the treatment). To establish the performance of SPECT/CT all patients were followed up for 6 months. **Results**. According to the reference test, pulmonary embolism was diagnosed in 31% of patients (n = 26). The sensitivity and specificity of each imaging Methods were as follows: planar (Q) 73% and 43.1%, SPECT (Q) of 88.5% and 46.6%, SPECT/CT (Q) 100% and 82.8%, SPECT/CT (Q / V, n = 24) 96% and 96.6%. The SPECT/CT (Q) method demonstrated a statistically significant higher diagnostic accuracy compared to the planar method (p <0,001) and the SPECT method (p <0,001). There were no statistically significant differences in diagnostic accuracy after adding ventilation to perfusion studies in SPECT/CT method (p = 0,083). The SPECT/CT method versus planar and SPECT Methods revealed more segmental and subsegmental perfusion defects, there were no differences in the amount of visualized lobar perfusion defects. For the SPECT/CT method there was no statistically significant correlation between the need of performing the ventilation studies and the occurrence of chronic obstructive pulmonary disease spearman rho (rs) = 0,03; p=0,769 and heart failure rs= 0,1; p=0,375. **Conclusions** Lung scintigraphy combined with computed tomography performed by hybrid SPECT/CT gamma cameras has a high diagnostic efficacy in the diagnosis of pulmonary embolism. Lung ventilation scintigraphy in addition to perfusion SPECT/CT scintigraphy does not increase the effectiveness of detection of pulmonary embolism. Lung perfusion scintigraphy performed by hybrid SPECT/CT device has a significantly higher accuracy compared to those performed by planar or SPECT technique.

## PW127

### Grading obstructive lung disease using V/P SPECT in COPD patients and long time smokers

**J. Jögi**[1], H. Markstad[2], J. Olsson[3], L. Bjermer[3], M. Bajc[1]; [1]Dept. of Clinical Physiology & Nuclear Medicine, Lund University and Skåne University Hospital, Lund, SWEDEN, [2]Dept. of Radiology, Lund University and Skåne University Hospital, Lund, SWEDEN, [3]Dept. of Respiratory Medicine & Allergology, Lund University and Skåne University Hospital, Lund, SWEDEN.

Chronic obstructive lung disease (COPD) is characterized by not fully reversible airflow limitation. COPD is predominantly a small airways disease. The severity of COPD is defined by the degree of flow limitation measured as forced expiratory volume in 1 s (FEV1). However, COPD is a heterogeneous condition and early changes are likely missed by FEV1. Therefore better diagnostic tools are needed. Ventilation/Perfusion (V/P) SPECT has shown to be a sensitive method to detect obstructive lung changes. AIM: To define criteria to stage obstructive airway disease with V/P SPECT and to compare this to GOLD grade. METHOD: 69 subjects, either healthy smokers or with stable COPD (GOLD 0-4) were examined with V/P SPECT and low-dose CT (LDCT) in a SPECT/CT system. Spirometry was performed. V/P SPECT and LDCT were reviewed independently. The physicians were blinded to other information. V/P SPECT was interpreted in accordance with the guidelines of EANM. Preserved lung function (%) was evaluated semi-quantitatively. In addition, the degree of airway obstruction (ObstrV/P SPECT) was graded according to distribution of Technegas from central to peripheral parts of the lungs as: 0) Normal - even distribution of Technegas with good peripheral penetration and without accumulation in large or small airways. 1) Mild airway obstruction - uneven distribution with some deposition of aerosol in small airways. 2) Moderate airway obstruction - diminished peripheral penetration with maximum accumulation in central half of the lung. 3) Severe airway obstruction - central deposition with severely impaired penetration of Technegas and partial absence of lung ventilation. Data was compared to GOLD. RESULTS: Mean GOLD was 1.8±0.1 (mean±SEM). Mean ObstrV/P SPECT was 2.0±0.1. ObstrV/P SPECT increased with increasing GOLD and was 1.5±0.2 at GOLD 0-1, 2.0±0.1 at GOLD 2 (p=0.004) and 2.8±0.1 for GOLD 3-4 (p<0.001 compared to GOLD 2). Mean ObstrV/P SPECT was elevated (1.5±0.2) among long time smokers at GOLD 0. Total preserved lung function decreased in relation to higher GOLD stage (73±4.0% at GOLD 0-1, 53±3.0% at GOLD 2, p<0.001, and 32±4.0% at GOLD 3-4, p<0.001 vs. GOLD 2). Mean CT emphysema extent was 3.9±2.2% at GOLD 0-1, 11.4±2.7% at GOLD 2 (p=0.01) and 20.0±4.4% at GOLD 3-4 (p=0.04) CONCLUSION: Functional imaging with V/P SPECT enables grading of airway obstruction and reduced lung function, which both are in relation with GOLD stage. V/P SPECT shows that long time smokers already at GOLD 0 have signs of airway obstruction, not shown by spirometry or LDCT.

## PW128

### Comparison of 2D planar and 3D SPECT-CT quantification of lung function in patients with lung cancer

**A. V. Thillainathan**[1], S. Gregg[2], A. Elsner[3], J. Avondo[3], J. Bailey[2], E. Reyes[2], S. R. Underwood[1], K. Wechalekar[2]; [1]Imperial College, LONDON, UNITED KINGDOM, [2]Royal Brompton Hospital, LONDON, UNITED KINGDOM, [3]Hermes Medical Solutions, Stockholm, SWEDEN.

**Introduction & Objective** Conventionally, differential and regional lung function has been measured from the geometrical mean of anterior and posterior planar images of lung perfusion (Q) and ventilation (V), using whole lung and upper, middle and lower zones. However, these do not represent the true anatomical lobes. The purpose of this study was to compare, the conventional planar technique with fused SPECT-CT images using both the functional and anatomical images to define the lobes (Hermes Medical Solutions). The SPECT-CT technique was validated using a phantom with known activity in simulated lobes. **Methods** Ten patients (5 male, mean age 66.6 years) undergoing partial lung resection were studied. Planar and SPECT-CT perfusion (99mTc-MAA) and ventilation (81mKr) images were acquired using a GE Infinia Hawkeye camera. In the planar method, the relative percentage contribution of each zone to total lung activity was measured. In the SPECT-CT method, attenuation corrected V and Q SPECT images were co-registered with diagnostic quality CT images, acquired separately. The fissures were defined on CT images and volumes of interest (VOIs) were created for each lobe. These were used to assess lobar counts in the SPECT V and Q images and

lobar contribution to total lung function was calculated and compared with the planar results. Similar techniques were applied to a three-part single lung phantom with known volumes and activity. **Results** In the phantom study, the difference between true and measured activity by planar imaging was 3.5%. The activity ratios for the 3 phantom compartments were 1.00, 1.96 and 2.02, which compared well with calculated SPECT ratios of 1.00, 1.97 and 2.04. In the patients, there was a good correlation between planar and SPECT techniques for the assessment of differential lung function (r=0.9, P<0.0001). The mean contribution of individual lobes by both V and Q SPECT differed significantly from the corresponding zones on planar imaging (median SPECT-planar difference ranged from 3% [0.5%, 26%] to -18% [-20%, +4%]; P<0.05) but correlation was moderate (r=0.7, P<0.01) for all lobes. This is expected due to differences in lobar definition between techniques. **Conclusion** SPECT-CT can assess simulated lobar lung function in a phantom. In patients, there was good correlation between planar and SPECT-CT techniques for the assessment of differential lung function and moderate correlation for the assessment of lobar function. The SPECT-CT technique may become the method of choice for assessing differential and lobar lung function in pre-operative assessment for lung resection surgery.

PW14 - Tuesday, Oct. 22, 8:30 - 9:30, Poster Exhibition Area

## Poster Walk 14 - Radiopharmaceuticals & Radiochemistry & Dosimetry: Antibodies & Peptides

### PW129

#### Study on interactions of radiolabelled bombesin analogues with selected renal transporters using cellular models

**M. Volková**, J. Mandikova, A. Laznickova, M. Laznicek, F. Trejtnar; Faculty of Pharmacy Charles Univerzity in Prague, Hradec Kralove, CZECH REPUBLIC.

Bombesin is a neuropeptide with high affinity for the gastrin-releasing peptide (GRP) receptor, which is overexpressed by a variety of cancers. High expression of BN/GRP receptors provides an attractive target for BN/GRP receptor scintigraphy and radionuclide therapy. However, renal accumulation of radiopeptides resulting in toxicological injury may limit potential clinical use of the tested compounds. Preclinical studies point out the role of endocytic receptor megalin in the transport but handling of the radiopeptides in the renal tubules is still not fully explained. This study was aimed at evaluation of potential interaction of radiolabelled bombesin analogues with several membrane transporters abundantly expressed in the kidney. Interaction of the radiopeptides with transporters OAT1, OCT2, megalin, MDR1 and BCRP was evaluated in vitro using several cellular models. To evaluate a contribution of active endocytosis by megalin, pig kidney epithelial cell line LLC-PK1, stably expressing this system was affected by RAP as a competitive inhibitor, and by albumin as a proven substrate of megalin. Rottlerin was used as a known inhibitor of fluid phase endocytosis. Incubations under low temperature (4°C) served to reveal general role of active transport process in the cell uptake. Possible inhibitory effect of the radiopeptides on BCRP and MDR1 transport activity was investigated employing stably transduced MDCKII cells. HeLa cells transiently transfected with hOAT1 and MDCKII cells with hOCT2 were used to reveal the contribution of the transporters on peptide uptake. Three bombesins were tested: $^{177}$Lu-DOTA-[Pro$^{1}$,Tyr$^{4}$]bombesin, $^{177}$Lu-DOTA-[Lys$^{3}$]bombesin and $^{177}$Lu-PCTA-[Lys$^{3}$]bombesin. Cellular accumulation in the used cellular models was significantly inhibited under lower incubation temperature, so we confirmed that this process is at least partly active. Incubation with the specific megalin substrate and inhibitor, albumin and RAP, respectively, resulted in a significant inhibition of the accumulation of all radiolabelled bombesins. Therefore, this transporter seems to be responsible for active endocytosis of the peptides. Fluid-phase endocytosis plays a minor role, because rottlerin decreased accumulation of bombesins in a smaller rate compared to aforementioned substances. OATs and OCTs seem to play no significant role in the renal handling of the radiobombesins as well as transporters BCRP and MDR1. The study was supported by Charles University in Prague (Project SVV 267003) and grant GAUK No.376411/FaF/C-LEK.

### PW130

#### Synthesis and Evaluation of $^{68}$Ga-NOTA-cRGDyK-S-S-CPLHSpT for diagnosis of tumor

**M. Yim**, S. Kim, E. Ryu; Korea Basic Science Institute, Ochang Cheongwon-gun, KOREA, REPUBLIC OF.

Polo-like kinase 1 (Plk1) is overexpressed in many different tumors. Plk1 are characterized by the presence of a highly conserved C-terminal polo-box domain (PBD) that regulates the localization of plk1 during mitosis. The phosphopeptide Pro-Leu-His-Ser-p-Thr (PLHSpT) has been reported as a potent and selective inhibitor of the PBD of human plk1 in cancer cells. However, one of the major limitations of using this phosphopeptide as an anticancer agent is membrane impermeability. Therefore, we designed and synthesized cRGDyK-S-S-CPLHSpT (**1**) not only to penetrate cell membrane, but also to evaluate as a radioligand for tumor diagnosis. The peptides were prepared using Fmoc-based solid-phase peptide synthesis on Rink amide resin, which involves sequential condensation of Fmoc-protected amino acids. *N*-succinimidyl-3-(2-pyridyldithio) propionate was conjugated with the lysine side chain of the protected cRGDyK peptide under basic conditions. The peptides were purified with HPLC and identified with MALDI-TOF mass spectroscopy. NOTA-conjugated peptide was synthesized with **1** and SCN-Bz-NOTA in 0.1 M sodium carbonate buffer (pH 9.5). The NOTA-activated peptide was labeled with $^{68}$Ga from a $^{68}$Ge/$^{68}$Ga generator and then gently stirred at room temperature for 10 min. The in vitro cell-binding affinity of $^{68}$Ga-NOTA-**1** was assessed by incubating the cells with $^{68}$Ga-NOTA-**1** for 30, 60, and 120 min. The radioligand was used in a specific binding assay with cRGDyK peptide (100 μg/mL) after the 120 min incubation. For the preparation of **1**, after the assembly of the peptides on the resin, activated cRGDyK with the heterobifunctional cross-linking reagent was covalently conjugated at the N-terminal cysteine via a disulfide bond. The decay-corrected radiochemical yield of $^{68}$Ga-NOTA-**1** was 20-35%. In binding affinity studies, the uptake at 30, 60, and 120 min was 1.51 ± 0.03, 2.10 ± 0.13, and 3.10 ± 0.20 % of uptake in HeLa cancer cells, and 1.49 ± 0.10, 1.35 ± 0.22, and 2.82 ± 0.15 % of uptake in U87MG cancer cells, respectively. The $\alpha_v\beta_3$ integrin receptor specificity was demonstrated by co-incubation with cRGDyK (100 μg/mL), an $\alpha_v\beta_3$ integrin-positive inhibitor, and radiolabeled phosphopeptide in U87MG tumor cells, which significantly reduced radioactivity by 50%. This result means that the radioligand was specifically bound to the $\alpha_v\beta_3$ integrin receptor. In conclusion, we overcame the limitation of a lack of membrane penetration of the PLHSpT peptide by using receptor-targeting peptide conjugation. Our results demonstrated that the new fusion peptide is promising as a radioligand for tumor diagnosis.

### PW131

#### Post-conjugation purification of DOTA-anti-CD20 (Rituximab®) and influence on $^{177}$Lu-labeling yield

**U. Karczmarczyk**, W. Wojdowska, M. Maurin, E. Byszewska-Szpocinska,P. Garnuszek, R. Mikolajczak; National Centre for Nuclear Research, Radioisotope Centre POLATOM, Otwock, POLAND.

Aim Monoclonal antibodies (mAb) are attractive molecules in the field of molecular imaging agent development. In 2011 the IAEA initiated a Coordinated Research Project (CRP) on the "Development and preclinical evaluations of therapeutic radiopharmaceuticals based on $^{177}$Lu and $^{90}$Y labelled monoclonal antibodies and peptides". Our aim in this project is the preparation of DOTA-anti-CD20 conjugate and radiolabelling optimization of $^{177}$Lu-DOTA(SCN)-Rituximab for further in vitro and in vivo studies. Materials and Methods The commercially available solution of the anti-CD20 (Rituximab, Mabthera, Roche) was initially purified by ultrafiltration using Amicon Ultra-2ml filter (Millipore, MWCO 30,000) and coupling buffer (0.2 M sodium carbonate buffer pH 8.0) to remove excipients such as polisorbate 80, sodium citrate and sodium chloride. Then the chelator p-SCN-Bn-DOTA was conjugated to anti-CD20 antibody basing on published procedures, using 20 mg of antibody (molar ratio mAb:chelator as 1:10). The conjugation reaction was carried out for 1.5 hours at 37$^0$C in carbonate buffer 8.0, with gentle mixing. Then the conjugate was purified to remove the excess of chelator using three different Methods: column chromatography (PD-10), ultrafiltration (Amicon Ultra, MWCO 30,000, Millipore) and dialysis (membrane avg. diameter 6 mm). Final concentration of the conjugated anti-CD20 antibody was quantified colorimetrically using Bradford method (BioRad). The number of conjugated DOTA molecules was determined by titration with the Cu(II)-arsenazo(III) complex. The $^{177}$Lu-labelling was performed using dry kit of DOTA-anti-CD20 (1.5 mg of DOTA-antiCD20; 5 mg of mannitol; 9.62 mg of ammonium acetate) and Lu-177 of radioactivity in the range 200-1400 MBq at 40$^0$C for 2 hours. The labelling yield was determined by GF-HPLC. The in vitro binding affinity of the radiolabelled Rituximab to specific receptors was confirmed in RAJI cell line (ATCC). Results and Conclusion From three tested Methods of purification of the immunoconjugate the ultrafiltration system significantly saves purification time and results in the high recovery efficiency (65%) comparing to dialysis (40%) and PD-10 column chromatography (ca. 35%). After radiolabelling with Lu-177 the most stable complexes were obtained using the conjugate, which was purified by ultrafiltration. HPLC analysis at 1h, 4h and 24 h showed the RCP above 95%. No release of free $^{177}$Lu was detected up to 24 hours. $^{177}$Lu-DOTA-anti-CD20 radioimmunoconjugate with high radiolabeling yield and radiochemical purity (> 97%) and specific activity of 0.6-0.7 GBq/mg was obtained. The preliminary in vitro studies confirmed the immunoreactivity of $^{177}$Lu-DOTA-anti-CD20.

### PW132

#### Dual-targeting bombesin-shepherdin radioconjugate for targeting extracellular GRP-receptor and intracellular Hsp90

**C. A. Kluba**[1], S. Vomstein[1], M. Zimmermann[2], I. Valverde[1], A. Bauman[1], T. L. Mindt[1]; [1]University of Basel Hospital, Department of Radiology and Nuclear Medicine, Division of Radiopharmaceutical Chemistry, Basel, SWITZERLAND, [2]University of Basel, Department of Biomedicine, Basel, SWITZERLAND.

**AIM:** Different receptors overexpressed by certain cancer cells have been identified in the past. As a result, a number of radiolabeled peptide analogues, specific for such receptors, have been developed for targeted diagnosis and therapy of cancers in nuclear medicine. However, after specific receptor-mediated uptake of the radiopeptides into cancer cells a rapid washout of the radioactivity can be observed, which is against the initial targeting efforts. To overcome this limitation, we envision the use of dual-targeting radiopeptides. Such tumor-specific, radiolabeled conjugates bear an additional moiety for interaction with an intracellular target. Through interactions of the conjugate with the intracellular target, cellular retention of radioactivity could be enhanced and thus, the efficacy of the radiopharmaceutical could be improved. For intracellular targeting we chose shepherdin, a peptidic inhibitor of the chaperon heat shock protein 90 (Hsp90), which is present in high concentrations in the cytosol. The peptide bombesin (BBS) was used for extracellular targeting of gastrin-releasing peptide receptors (GRPr) that are overexpressed on, e.g., prostate cancer cells. **MATERIALS AND METHODS:** The trifunctional dual-targeting radioconjugate described is built of 1) a modified bombesin binding sequence, [Nle$^{14}$]BBS(7-14), 2) the shepherdin (KHSSGCAFL) sequence, and 3) $^{99m}$Tc-tricarbonyl as a SPECT imaging probe. The required amino acid sequences were synthesized by solid phase peptide synthesis (SPPS) and the three building blocks were assembled by Cu(I)-catalyzed azide-alkyne cycloaddition (CuAAC, click chemistry). For comparison, we synthesized three control compounds; BBS-reference, shepherdin-reference, and BBS-scrambled-shepherdin. All four peptidic conjugates were radiolabeled with $[^{99m}Tc(CO)_3(H_2O)_3]^+$ for physicochemical characterization and biological evaluation. **RESULTS:** Dual-targeting BBS-shepherdin conjugate and the three reference compounds were successfully synthesized and characterized by HPLC and mass spectrometry. Radiolabeled conjugates were obtained in high radiochemical yield and purity (≥95%). All compounds were shown to be stable in PBS and cell culture medium (1% FBS) and exhibited appropriate lipophilicities (LogD: -1 to -0.8). With exception of the shepherdin-reference, all radiolabeled compounds showed receptor-specific uptake into GRPr overexpressing PC-3 cells. Further biological evaluations including control experiments are currently ongoing and the results will be presented. **CONCLUSION:** Application of dual-targeting radioconjugates to retain radioactivity inside cancer cells is an innovative approach and has the potential to improve the efficacy of peptidic radiopharmaceuticals. The described assembly for trifunctional conjugates is modular and thus, can be extended to different dual-targeting radiolabeled conjugates.

## PW133

### In Vitro Targeting of Trastuzumab-resistant Breast Cancer Cells and In Vivo Biodistribution and Acute Toxicity Studies Using a High Specific Radioactivity Auger Electron Radioimmunotherapeutic Agent Composed of Trastuzumab and PAMAM Dendrimer Displaying Multiple DTPA Chelators for $^{111}$In

**C. Chan**, K. Lam, D. Bergstrom, S. Done, Z. Cai, R. M. Reilly; Departments of Pharmaceutical Sciences and Medical Imaging, University of Toronto and Toronto General Research Institute, University Health Network, Toronto, ON, CANADA.

**Aim:** To evaluate the cytotoxicity on trastuzumab-resistant (TrR1) breast cancer (BC) cells *in vitro* of a high specific radioactivity (SA) Auger electron-radioimmunotherapeutic agent composed of trastuzumab conjugated to polyamidoamine (G4) dendrimers that display multiple DTPA chelators for $^{111}$In and modified with nuclear localization sequence (NLS) peptides (NLS-trastuzumab-G4-DTPA). To examine the biodistribution in mice with HER2-expressing tumour xenografts and acute toxicity in non-tumour bearing mice. **Methods:** NLS-trastuzumab-G4-DTPA was labeled with $^{111}$In to high SA (5.9 MBq/μg). Clonogenic assays were performed on TrR1 cells exposed to NLS-trastuzumab-G4-DTPA-$^{111}$In or low SA NLS-trastuzumab-DTPA-$^{111}$In (0.4 MBq/μg) for 20h. DNA damage was assessed by immunofluorescence for phosphorylated histone H2AX (γH2AX). Biodistribution studies were performed at 5, 24, 48 and 72h p.i. in mice bearing s.c. SK-Ov-3 tumour xenografts ($10^6$ HER2/cell). Acute toxicity was assessed by serum alanine aminotransferase (ALT) and creatinine (Cr), complete blood counts (CBC), and histopathological examination of tissues following i.v. injection of 2 or 8 μg of NLS-trastuzumab-G4-DTPA-$^{111}$In, 8 μg of NLS-trastuzumab-G4-DTPA or saline. **Results:** The surviving fraction (SF) of TrR1 cells exposed to NLS-trastuzumab-G4-DTPA-$^{111}$In (0.8±0.3%) was dramatically decreased compared to low SA NLS-trastuzumab-DTPA-$^{111}$In (50.8±6.2%), with a corresponding increase of γH2AX foci. No morphological abnormalities in normal tissues were detected in mice and no differences were found for CBC between mice treated with high or low doses of NLS-trastuzumab-G4-DTPA-$^{111}$In, NLS-trastuzumab-G4-DTPA or saline. ALT and Cr levels in mice treated with 8 μg of NLS-trastuzumab-G4-DTPA-$^{111}$In were 58.2±22.1 U/L and 67.1±24.5 μmol/L, respectively, which was not different (one-way ANOVA, $p$ = 0.866 and $p$ = 0.467, respectively) than mice treated with non-labeled NLS-trastuzumab-G4-DTPA (41.1±21.8 U/L and 49.9±12.6 μmol/L, respectively) or saline (36.9±9.2 U/L and 35.4±5.1 μmol/L, respectively). Tumour localization of NLS-trastuzumab-G4-DTPA-$^{111}$In was 0.9±0.1, 1.1±0.2, 1.0±0.4 and 1.0±0.3% i.d./g at 5, 24, 48 and 72 p.i, respectively. Blood levels were 5-fold lower at 72h compared to 24h p.i. (0.1±0.03 vs 0.5±0.2% i.d./g; P<0.05), yielding tumour/blood ratios that were higher (10.6±4.3 vs 3.5±3.2; P<0.05). **Conclusion:** NLS-trastuzumab-G4-DTPA-$^{111}$In displayed potent cytotoxicity *in vitro* on trastuzumab-resistant BC cells. Although tumour uptake was low, the absence of toxicity *in vivo* combined with the very high SA may permit effective treatment of trastuzumab-resistant tumours.

## PW134

### 1,2,3-Triazole Backbone-Modified Peptidomimetics for Improved Tumor Targeting

**I. E. Valverde**, A. Bauman, C. A. Kluba, S. Vomstein, T. L. Mindt; University of Basel Hospital, Basel, SWITZERLAND.

**Aim:** Regulatory peptides have been shown to be suitable vectors for the specific delivery of radioactivity to tumors and metastasis for diagnostic and therapeutic applications in nuclear oncology. A potential drawback of such vectors is represented by their instability in vivo as the result of rapid degradation by proteases. Thus, new strategies are needed for the stabilization of radiolabelled peptides in order to improve their specific accumulation in the targeted tissue. It has been suggested that 1,4-disubstituted 1,2,3-triazoles, obtained by the Cu(I)-catalyzed azide-alkyne cycloaddition (CuAAC; click chemistry), might represent suitable amide bond isosters, which are resistant to proteases. We herein wish to report the synthesis and biological evaluation of radiolabelled, 1,2,3-triazole containing analogs of the GRP-receptor (GRPr) targeting bombesin binding domain BBN(7-14). **Materials and Methods**: Azide and alkyne analogs of amino acids were used for the synthesis by CuAAC of peptidomimetics in which amide bonds are replaced systematically by 1,2,3-triazoles. Conjugation of the peptide analogs with the chelator DOTA via a PEG linker provided the means for radiolabelling with Lu-177. In vitro GRPr binding affinity (KD) and cell internalization kinetics of the radioconjugates were determined using GRPr-overexpressing PC-3 cells. Metabolic stability of the conjugates was evaluated in blood serum. Biodistribution experiments were performed in PC-3-xenografted nude mice. **Results:** We have synthesized "clickable" chiral azido acids and amino alkynes by straightforward procedures from commercial amino acids. These building blocks were used for the synthesis of a series of DOTA-conjugated BBN(7-14) analogs by combination of standard Fmoc-solid phase peptide synthesis (SPPS) and CuAAC on solid support. Radiolabelling of the novel compounds with Lu-177 provided the corresponding radiolabeled conjugates in excellent radiochemical yields and purity (>95%). A side by side comparison in vitro revealed that all triazole-containing peptides exhibited a significantly increased half-life in blood serum (up to 20-fold). Also, single-digit nanomolar affinity of the sequence [Nle14]BBN(7-14) towards the GRPr could be retained in several cases. The results of the in vivo evaluation of the most promising compounds will be presented. **Conclusion:** To the best of our knowledge, this is the first report of the systematic replacement of amide bonds with 1,2,3-triazoles in linear, high affinity peptides. The methodology developed (termed "triazole scan") can potentially be applied to a variety of peptide vectors and thus, holds great promise for the development of novel, stabilized peptidomimetic-based radiopharmaceuticals.

## PW135

### $^{111}$In-Maxadilan, a new radiotracer for PAC1 receptor targeting

**M. Brom**[1], L. Joosten[1], E. Weihe[2], O. Boerman[1], M. Gotthardt[1]; [1]Radboud University Nijmegen Medical Centre, Nijmegen, NETHERLANDS, [2]Philipps University Marburg, Marburg, GERMANY.

**Aim** The PACAP preferring type 1 (PAC1) receptor is expressed in several tumour types such as insulinomas, ovarian carcinoma, breast cancer and pheochomocytoma. Therefore, the PAC1 receptor could potentially be used for targeting of these tumours. Maxadilan is a 61 amino acid peptide specifically binding to the PAC1 receptor. We developed two DTPA-conjugated Maxadilan derivatives and determined their *in vitro* and *in vivo* tumour cell binding characteristics. **Materials and Methods** Maxadilan was labelled with $^{125}$I via the chloramine T reaction. DTPA was conjugated C- (Maxadilan-DTPA) or N-terminally (DTPA-Maxadilan) and labelled with $^{111}$In. The affinity of the unlabelled and labelled compounds was determined in an $IC_{50}$ experiment using PAC1 expressing INS-1 cells (rat insulinoma cell line) in suspension. The *in vivo* targeting properties were investigated in biodistribution studies and by SPECT 2 h after injection of $^{111}$In-DTPA-Maxadilan and Maxadilan-DTPA-$^{111}$In in BALB/c nude mice with a subcutaneous INS-1 tumour. **Results and Conclusion** $^{125}$I-Maxadilan, $^{111}$In-DTPA-Maxadilan and Maxadilan-DTPA-$^{111}$In could be labelled with a specific activity of 25, 55 and 680 MBq/nmol, respectively. The $IC_{50}$ value of Maxadilan was 3.2 nM. Conjugation of DTPA resulted in a slight decrease in affinity: 18.3 and 13.2 nM for DTPA-Maxadilan and Maxadilan-DTPA, respectively. Interestingly, labelling of Maxadilan with $^{nat}$I resulted in a marked decrease in affinity (188 nM). $^{nat}$In-labelling only had a moderate effect on the affinity of both DTPA-Maxadilan and Maxadilan-DTPA (21 nM for both compounds). Biodistribution studies showed efficient accumulation of $^{111}$In-DTPA-Maxadilan and Maxadilan-DTPA-$^{111}$In in the INS-1 tumour (4.8 ± 0.9 %ID/g and 7.8 ± 1.4 %ID/g, respectively) and the uptake could be

blocked with an excess unlabelled Maxadilan (1.2 ± 0.5 %ID/g and 1.5 ± 0.5 %ID/g). Besides specific accumulation in the tumour, specific uptake was observed in various organs (liver, adrenals, pancreas, stomach and intestines). The tumour uptake of $^{111}$In-DTPA-Maxadilan and Maxadilan-DTPA-$^{111}$In was higher than the uptake in non-target organs. High uptake of $^{111}$In-DTPA-Maxadilan and Maxadilan-DTPA-$^{111}$In was observed in the kidneys (148.2 ± 2.9 %ID/g and 145.6 ± 19.0 %ID/g, respectively) and this uptake could not be blocked with an excess unlabelled Maxadilan (136.3 ± 7.7 %ID/g and 155.6 ± 21.9 %ID/g, respectively). Subcutaneous INS-1 tumours were visualized by SPECT after injection of $^{111}$In-DTPA-Maxadilan and Maxadilan-DTPA-$^{111}$In. Maxadilan-DTPA-$^{111}$In had superior *in vivo* binding characteristics. In conclusion, $^{111}$In-DTPA-Maxadilan and Maxadilan-DTPA-$^{111}$In accumulate efficiently and specifically in INS-1 tumours and could potentially be used for visualization of PAC1 expressing tumours.

## PW136

### Targeting the disialoganglioside GD2 in neuroblastoma using a phage display derived oligopeptide

**J. Müller**, S. Vogt, R. Reichel, K. Fielitz, S. Müller, W. Brandau, A. Schramm; University Duisburg-Essen, Essen, GERMANY.

**Aim:** High expression of GD2 on neuroblastoma cells renders this disialoganglioside an attractive target for novel therapeutic and diagnostic approaches. Anti-GD2 antibodies have already entered the clinical stage, but GD2-based markers could also serve in diagnostics and for imaging purposes. Our aim was to generate peptides specifically binding to GD2, to test their tumor-homing capability in vivo and to show their diagnostic potential using radioactively labeled peptides and tumor-bearing mice in PET studies. **Materials and Methods**: To obtain such peptides we performed a combined in vivo and in vitro phage display screen to identify GD2-specific peptides. Therefore we first selected phages binding to human GD2. In a further screen we used these phages to generate a phage pool binding to the tissue of neuroblastoma tumor xenografts. The resulting phages were tested for their binding specificity and their ability to home to xenografted neuroblastoma tumors in mice. Phage-derived peptides were further characterized using MTT-Assays and radioactively labeled with either In111 or Ga68 to analyze their tumor homing capacity using in vivo imaging. **Results:** Phages specifically binding to GD2 were identified in vitro and their in vivo accumulation in xenografted tumors was confirmed. The displayed peptides derived from the phages were shown to competitively inhibit the phage binding to GD2 in vitro and to tumor tissue in vivo. GD2-binding peptides were shown to reduce cell viability of neuroblastoma cells in vitro when compared to control peptides. Furthermore we found an accumulation of the In111 labeled peptides in tumor tissue. Finally, we used Ga68 labeled GD2-binding peptides for PET/MR imaging and observed an accumulation in the tissue of xenografted neuroblastoma tumors. **Conclusion**: We demonstrate that peptide ligands to the human disialoganglioside GD2 generated via a phage display screen can home to neuroblastoma tumor-tissue. Furthermore the accumulation of the Ga68 labeled peptides in tumor tissue could be shown by PET imaging. Therefore this peptide may be a new useful tool for diagnostic and therapeutic procedures in neuroblastoma and other tumors expressing GD2.

## PW137

### Kit preparation of Lysyl-3-(Trimethylstannyl)Benzamide Immunoconjugates for 211At Labeling of Antibodies

**S. Lindegren**[1], E. Aneheim[1], J. Hallerö[1], H. Jensen[2]; [1]Clinical Sciences, Gothenburg, SWEDEN, [2]Cyclotron and PET Unit, Copenhagen, DENMARK.

**Aim:** The objective of this study was to investigate the shelf life of immunoconjugates for astatination of antibodies. Different immunoconjugates were evaluated regarding shelf life prior to labelling, and were analysed for radiochemical yield, radiochemical purity, structure integrity, immunoreactive fractions following astatination. If a significant shelf-life of these immunoconjugates is feasible it would enable KIT formulation for astatination and distant shipping to facilities that can produce astatine-211. **Materials and Methods**: The monoclonal antibodies MX35 and Trastuzumab (Herceptin) were used in the study. Antibody immunoconjugates of m-MeATE and MX35 or Trastusumab were prepared in advance at different time prior to labeling. The stored conjugates were compared freshly prepared immunoconjugates. The immunoconjugates were labeled with At-211 and evaluated with regard to radiochemical yields, radiochemical purity as determined by methanol precipitation and FPLC, and immunoreactivity by binding to tumor cells. **Results** and conclusion: Yields in the astatination of the different immunoconjugates produced were in the range 70-80% and there were no signs of decline in radiochemical yield on immunoconjugates prepared up to ten days prior to labeling. At further storage the labeling efficacy decreased. Radiochemical purity was in the range 97-99 % for all preparations made in the study as determined by methanol precipitation. There were no significant differences in immunoreactivity between freshly prepared or stored immunoconjugates. The structural integrity of the astatinated antibodies were also investigated by FPLC before labeling on unmodified antibody and immunoconjugates as well as after labeling. The results from the chromatography could not reveal any structural changes after the conjugation of the antibody or after labeling of the immunoconjugates.

## PW138

### Anti-CEA antibody fragments labeled with [$^{18}$F]AlF for PET imaging of CEA-expressing tumors

**G. M. Franssen**[1], P. Laverman[1], K. L. S. Chatalic[2], W. J. G. Oyen[1], R. M. Sharkey[3], D. M. Goldenberg[3], E. Rossi[3], W. J. McBride[3], O. C. Boerman[1]; [1]Radboud University Nijmegen Medical Centre, Nijmegen, NETHERLANDS, [2]Erasmus Medical Centre, Rotterdam, NETHERLANDS, [3]Immunomedics, Morris Plains, NJ, UNITED STATES.

**Aim:** A facile and rapid method for $^{18}$F-radiolabeling of chelated peptides has been developed recently. So far, this method has been applied to labeling peptides that could be heated to 100 ºC. Here, we applied a two-step procedure to prepare $^{18}$F-labeled heat-labile proteins using the [$^{18}$F]AlF method based on a hot maleimide conjugation. The NODA-MPAEM ligand was labeled with [$^{18}$F]AlF and then conjugated to partly reduced humanized anti-CEA antibody fragments (i.e., hMN-14 Fab', a diabody and a Dock-and-Lock engineered dimeric fragment designated as hMN-14 Fab-AD2) at room temperature. The biodistribution of each of these agents was monitored by PET imaging of mice bearing s.c. CEA-expressing LS174T tumors. **Material and Methods:** NODA-MPAEM was radiolabeled with [$^{18}$F]AlF (1.5 -2.0 GBq) in a solution of 70% acetonitrile for 15 min at 105 °C. The [$^{18}$F]AlF-NODA-MPAEM labeling mixture was evaporated to dryness, dissolved in PBS (pH 7.2) and conjugated to hMN14-Fab', hMN14-Fab-AD2 or hMN14-diabody. After incubating for 20 min at room temperature, the radiolabeled conjugates were purified using PD10 gel permeation columns. For biodistribution and PET imaging, 1 nmol (10.2-13.8 MBq/mouse) antibody fragment was injected intravenously into BALB/c nude mice with s.c. CEA$^+$ LS174T xenografts (right flank) and CEA$^-$ SK-RC-52 xenografts (left flank, negative control). Two days before injecting the radiolabeled conjugates, separate groups were injected with an excess of unlabeled MN-14 IgG to determine nonspecific uptake. PET imaging and biodistribution was performed 4 h p.i. **Results**: NODA-MPAEM ligand could be labeled at a specific activity of 29-39 MBq/nmol, resulting in [$^{18}$F]AlF-labeled MN14 antibody fragments with a specific activity of 15-17 MBq/nmol. After PD10 purification (yield 43-56%), all radiolabeled conjugates had a radiochemical purity >95%. All radiolabeled [$^{18}$F]AlF conjugates showed specific uptake in the CEA$^+$ LS174T xenografts with an uptake ranging from 1.85 - 4.73 %ID/g. Uptake in CEA$^-$ SK-RC-52 xenografts, as well as in blocked LS174T tumors, were significantly lower (0.62 %ID/g to 2.30 %ID/g), indicating that the uptake in LS174T tumors was specific. Uptake in organs was low, except for the kidneys. Tumors were clearly visualized on PET images. **Conclusion:** Antibody fragments could be radiofluorinated rapidly (<60 min) and efficiently at a high specific activity using and [$^{18}$F]ALF-labeled maleimide functionalized chelator. MN14 antibody fragments showed specific targeting to CEA-expressing tumors.

PW15 - Tuesday, Oct. 22, 8:30 - 9:30, Poster Exhibition Area

# Poster Walk 15 - Physics & Instrumentation & Data Analysis: Physics & Instrumentation & Radiation Protection

## PW139

### Evaluation of lesion detectability for four different PET/CT scanners using a whole-body anthropomorphic phantom

**A. Martineau**[1], M. Waryn[2], J. Filmont[3], M. Bernardini[4]; [1]Hopital Saint Louis, Paris, FRANCE, [2]Hopital Avicenne, Paris, FRANCE, [3]American Hospital, Paris, FRANCE, [4]Hopital Europeen Georges Pompidou, Paris, FRANCE.

Aim : The purpose of this study was to evaluate the influence of Time-of-Flight (TOF) PET reconstruction and Point Spread Function (PSF) correction on lesion detectability of 18F-FDG images acquired with four different PET/CT scanners. Materials and Methods: We compared images acquired on four PET/CT scanners in three different nuclear medicine departments: one non-TOF PET (Gemini GXL - Philips), one TOF PET (Gemini TF - Philips), and two TOF PET with PSF correction (Discovery 690 - General Electric and mCT - Siemens). In order to simulate a whole-body patient acquisition, three phantoms were employed: a homogenously filled cylinder representing the brain, an anthropomorphic phantom (Radiology Support Devices) with lungs and liver inserts, representing the thorax and a NEMA/IEC image quality phantom with bladder insert, representing the pelvis. Lesions were simulated by seven spheres with volumes ranging from 0.5 ml to 2 ml placed in the axillary and mediastinal regions, in the lungs and the liver of the anthropomorphic phantom. The spheres were filled to obtain lesion-to-background ratio (L/B) ranging from 2.5:1 to 12:1. 18F-FDG PET/CT imaging was performed to acquire emission data with an equal scan length and duration as well as the same 18F-FDG background activity concentration. PET images were reconstructed using manufacturer-supplied iterative reconstruction algorithms and clinical

reconstruction parameters. For each sphere, lesion detectability was quantified by measuring recovery coefficients (RC) in three different ways by the use of 3D volumes of interest (VOI): RC_max was calculated with the maximum voxel value in a 3D-VOI, RC_T40 with the average concentration value in a 3D isocontour at 40% of the maximum value and RC_A50 with the average concentration value in a 3D isocontour at 50% of the maximum value adapted for background correction. Results and conclusion: TOF PET reconstruction and PSF correction improved lesions detectability (RC increased) in comparison with non-TOF PET and TOF PET without PSF correction. In particular, for 0.5 ml sphere and L/B equal to 2.5:1, RC coefficients were increased by up to 67%, 74% and 76% respectively for RC_max, RC_T40 and RC_A50. Differences in lesions detectability and their impact on quantification should be take into account in multi-center PET studies.

## PW140

### Comparison of different reconstruction algorithms for evaluation of bone metastases in 18F-Fluoride PET images using a TOF PET/CT system

**D. D'AMBROSIO**, C. FUCCIO, E. G. SPINAPOLICE, I. CARNE, P. L. CUCCHI, E. BRUGOLA, G. TRIFIRO', D. FANTINATO; Fondazione S. Maugeri, Pavia, ITALY.

**Aim:** Bone metastases detection is important in patient with cancer in order to correctly decide patient treatment. Thus, the uptake of bone lesion have to be estimated accurately. The aim of this study was to investigate the effect of different PET reconstruction algorithms on $^{18}$F-Fluoride uptake in bone metastases. **Materials an Methods:** Seven patients (average BMI=25.4) were injected with 2.8 MBq/kg of $^{18}$F-Fluoride. List mode PET data (3 minutes/bed position) were acquired using GE-MS Discovery VCT 690 PET/CT tomograph. PET data were reconstructed using several iterative reconstruction algorithm (3 and 5 iterations, 16 subsets): 3D-OSEM, 3D-OSEM with time of flight (TOF), 3D-OSEM with point spread function (PSF) and 3D-OSEM incorporating both TOF and PSF information. Images were analyzed by drawing VOIs on the 21 bone metastases and maximum uptake was calculated in each lesion. Maximum uptake percentage difference was estimated with respect to the maximum uptake measured on 3D-OSEM images. Metastases with volume less than 4mm$^3$, were considered as small lesions. **Results:** TOF PET yielded a lesion uptake increase over non TOF PET of 1.6%±0.8% and 11.0%±3.1% for small and homogeneous lesions located in- and off-axis, respectively. PSF inclusion in the reconstruction algorithm provided an maximum uptake increase equal to 9.2%±3.6% and 13.5%±6.6% for in- and off-axis metastases, respectively. The overall effect of TOF and PSF incorporated in 3D-OSEM was a maximum uptake percentage difference equal to 15.3%±5.5% and 16.2%±9.6% for in- and off axis metastases with respect to 3D-OSEM algorithm. Different results were found analyzing PET images of larger bone lesions. The maximum uptake increased up to 2.1%±1.2% and 5.5%±4.7% for in- and off-axis lesions, respectively. Incorporating PSF in the reconstruction process, a maximum uptake percentage difference equal to 3.9%±2.3% and 11.3%±6.2% was measured for in- and off-axis metastases, respectively. Comparing OSEM and OSEM+TOF+PSF, an increase equal to 8.8%±4.7% and 12.1%±6.1% was estimated for in- and off axis metastases, respectively. No significant differences in maximum uptake percentage difference were found comparing images reconstructed by using 3 or 5 iterations. **Conclusions:** Within the limitations of this work due to the limited number of patients and lesions that were considered, the inclusion of PSF and TOF information increased the maximum uptake of bone lesion up to 16% for small lesions and 12% for larger lesions. These results have to be taken into account for quantitative comparisons between $^{18}$F-Fluoride PET images reconstructed using different algorithms, in follow-up studies as in multicenter works.

## PW141

### Simultaneous Algebraic Reconstruction Technique for Time-of-Flight Dual Photons Emission Computed Tomography System

**C. C. Chiang**[1], K. S. Chuang[1], H. H. Lin[1], M. L. Jan[2]; [1]Department of Biomedical Engineering and Environmental Sciences, National Tsing Hua University, Hsin-Chu, TAIWAN, [2]Institute of Nuclear Energy Research, Atomic Energy Council, Taoyuan, TAIWAN.

Aim: In the past decades, extensive researches have been done on time-of-flight positron emitter tomography (TOF-PET), but the use of the time information in dual-photon imaging has not yet been much explored. Our previous studies demonstrated the time-of-flight information can be applied in dual-photon emission tomography. We successfully employed a simple back-projection (SBP) to reconstruct images of time-of-flight dual photons emission computed tomography (TOF-DuPECT). Despite SBP could effectively obtain the distribution of radionuclides, it suffered serious streak artifact. Therefore, the purpose of this study is to use simultaneous algebraic reconstruction technique (SART) to improve image quality and reduce artifact. Method: TOF-DuPECT simulations were achieved by an in-house developed SimGATE Monte Carlo code, which was the integration of SimSET and GATE simulation codes. The geometry of Siemens Biograph 6 PET scanner and a hot-rod phantom had been used in simulation. Se-75 was used for its characteristic of emitting two angularly uncorrelated photons of energies 136keV and 264.7keV in cascades. According to the TOF information of each coincidence event, the surface of hyperboloid could be determined in three-dimensional space representing the possible locations of decay. All images were reconstructed by SART and SBP reconstruction algorithm. In addition, the half-life of isotopes' energy levels was also taken into account in this study. Results: The Monte Carlo simulation study indicates that the TOF-DuPECT technique is feasible and able to provide high sensitivity, on account of the elimination of collimators. The rod-phantom images show that SART method achieved higher image quality than previous SBP method. Conclusion: SART method has been proved to be useful in TOF-DuPECT system. Furthermore, SART algorithm can be used to reduce artifact, improve spatial resolution, and increase image quality. Future works include more phantom studies and develop other iterative reconstruction algorithms (e.g., MLEM, OSEM) for TOF-DuPECT.

## PW142

### SPECT/CT imaging of dopamine transporters in diagnosis of corticobasal degeneration

**G. Pina**[1,2], C. De Charry[3], A. Vighetto[4], C. Scheiber[1]; [1]Médecine Nucléaire, Groupement Hospitalier Est, Hospices Civils de Lyon, Université de Lyon, BRON, FRANCE, [2]Centre de Recherche en Neuroscience, Equipe BioRan, Université Lyon 1, Université de Lyon, France, FRANCE, [3]Hôpital d'Instruction des Armées Desgenettes, Lyon, FRANCE, [4]Service de Neurologie D, Groupement Hospitalier Est, Hospices Civils de Lyon, Université de Lyon, Bron, FRANCE.

Aim: To illustrate the contribution of hybrid imaging for the diagnosis of corticobasal degeneration (CBD), a rare disorder typically presenting as an asymmetrical Parkinsonism. Materials and Methods: Retrospective study of 21 subjects (9 with probable CBD, and 12 with normal scintigrams) referred for 123I-FP-CIT SPECT/CT (DaTSCAN®, GE Healthcare, UK). The method is based on the transformation of anatomical and functional images into an anatomical reference space enabling statistical analysis (Statistical Parametric Mapping : SPM5) and the use of a labeled anatomical atlas for computerized semi-quantitative analysis by volume of interest. Results: Visual and semi-quantitative analysis showed moderate and asymetrical presynaptic involvement in DCB patients, more severe on the side contralateral to the clinical motor symptoms. The binding potential was 1.69 +-0.38 vs 2.62+-0.37 for the affected striatum for DCB patients and control subjects respectively ($p<0.0001$). Statistical analysis conducted on the DCB population confirms asymmetrical striatal impairment (including caudate nucleus impairement) controlateral to the clinical motor signs. These elements were sought on individual comparison of each CBD patients vs control patients: striatal uptake asymmetry and caudate nucleus impairment were found in 7/9 and 8/9 CBD patients respectively. Asymmetrical cortical atrophy contralateral to the clinical motor symptoms on CT was reported on 6/9 DCB patients Conclusion: The combined interpretation of cortical asymmetry, semi-quantitative and voxel-based statistical analysis on 123I-FP-CIT SPECT/CT provided pertinent information for the differential diagnosis of Parkinsonian syndrome by simultaneously showing signs of cortical atrophy and presynaptic impairment of the homolateral nigrostriatal pathway.

## PW143

### Improved PET Functional Segmentation Using 4D Reconstruction of Dynamic Acquisitions: Application to Pig Pancreas Imaging

S. Stute[1], I. Buvat[2], **R. Boisgard**[1]; [1]CEA/SHFJ, Orsay Cedex, FRANCE, [2]CNRS/IMNC, Orsay Cedex, FRANCE.

**Aim.** In dynamic PET studies, the different time frames are usually reconstructed independently using standard 3D reconstruction Methods. This leads to high image noise, especially in the first time frames that must be short enough to capture the rapid kinetic changes of the injected radiotracer. 4D reconstruction Methods have been proposed to better handle noise. In (Reader *et al* IEEE MIC 2007), the time activity curve $TAC_i$ of any voxel $i$ is assumed to be a linear combination of a set of $K$ predefined temporal functions $f_k$. All frames are reconstructed together, taking advantage of the whole acquisition statistics hence reducing image noise. Here, we propose to use the coefficients $w_{ik}$ of the linear combination to identify different functional regions of interest. We apply the method on dynamic PET scans of pigs acquired on the HR+ scanner using [$^{18}$F]FP-DTBZ. For this application (no anatomical information available), segmentation of the pancreas is a challenge due to the vicinity of kidney. **Materials and Methods.** 4D reconstruction was performed with the $K$ temporal basis functions $f_k$ modeled as 12 exponential decaying functions (from a constant to a delta function) convolved by the image-derived input function, enabling a description of the entire range of possible kinetics. For the time being, one pig scan was reconstructed. We compared the volumes of the pancreas manually delineated from the 3D images and from the images of the $w_{ik}$ derived from the 4D reconstruction. We also compared the mean activity inside

Poster Walks

these volumes. **Results.** The manual delineation of pancreas from the $w_{ik}$ images was much easier than from the 3D images. Some $w_{ik}$ images included the whole pancreas without kidney signal and conversely. The pancreas volume was 23% smaller when derived from the $w_{ik}$ images compared to the 3D images. This is because voxels at the pancreas-kidney border were erroneously included in the segmentation from the 3D images, though a lobe of the pancreas was actually absent in the 3D segmentation. The mean activity values in the pancreas differed from -36% to 6% depending on the time frame. **Conclusion.** Initial results suggest that the 4D reconstruction method greatly facilitates the segmentation of different functional regions through the use of the $w_{ik}$ images. Twenty additional pig scans will be included to better assess the significance of the 4D method, both for segmentation and quantification accuracy.

## PW144

### Inter-software variability of SUVmax, SUVmean and functional volume with FDG-PET/CT imaging in primary lung cancer: GEHC vs. ROVER software.

**M. H. Vilstrup**; Odense University Hospital, Odense C, DENMARK.

Aim Standardized uptake values (SUV) are used to characterise tumour metabolism. Different software with different corrections models ad variability, and partial volume correction (PVC) is necessary to compensate for insufficient recovery. We compared values obtained by two semi-automatic analysis systems, one provided by General Electrical Healthcare (GEHC) and another, named ROVER, allowing also PVC. Materials and Methods We performed PET/CT in 173 consecutive, operable lung cancer patients using 4 MBq/kg of FDG, low dose CT, and image acquisition with 2½ min per bed position 60 minutes following tracer injection. SUVmax, SUVmean and functional volume (50% of SUVmax) were measured retrospectively by applying 3D-ROIs using Advanced Workstation/GEHC software (Volume Computer Assisted Reading) and ROVER software (+/- PVC) over the primary lung cancer lesion. Bland-Altman analyses were performed to assess agreement. Results With GEHC software, measurement of 154 lesions was possible, while ROVER allowed measuring 164 lesions. With GEHC, the range of SUVmax values was 0.8 - 36.4 g/ml, average 9.8 g/ml compared to 0.8 - 36.2 g/ml, average 9.9 g/ml with ROVER. ROVER-GEHC SUVmax differences ranged from -1.65 to 2.01 g/ml, mean difference (D) = -0.07 g/ml ± 0.34, lower limit of agreement (LLOA) = -0.74 and upper limit of agreement (ULOA) = 0.59. Similarly, SUVmean values differed from -4.2 to 0.95 g/ml, D = -0.80g/ml ± 0.84, LLOA = -2.45 and ULOA = 0.85. Differences were positive for lower values of SUVmean (< 3 g/ml) shifting to negative for higher values. With ROVER software, comparing partial volume corrected SUVmean (cSUVmean) and non-corrected (SUVmean) the difference ranged from -1.43 to 10.63 g/ml, D = 2.72 g/ml ± 2.2, LLOA = -1.49 and ULOA = 6.94. As expected, the cSUVmean values were all higher than the SUVmean values. Functional volume showed differences ranging from -27.3 to 127.6 cm3, D = 6.77 cm3 ± 15.1, LLOA = -22.77 and ULOA = 36.3. Conclusion The inter-software variability was small for both SUVmax and uncorrected SUVmean values. As expected, the poorest agreement was found between SUVmean and cSUVmean values. There was a good correlation between all measured, but uncorrected, variables, albeit with a rather large difference (-27 to 128 cm3) in functional volume. Thus, the variability in software calculation of SUVmax, SUVmean and functional volume must be taken into account when used in cancer PET/CT imaging to quantify focal metabolic activity. In particular, the big difference between SUVmean and cSUVmean values calls for serious consideration.

## PW145

### How does the inclusion of the entire brain in a whole body FDG PET/CT scan affect the effective dose for the patient

S. Ivanova, **P. Bochev**, A. Klisarova; Mbal St. Marina Varna, Varna, BULGARIA.

Brain is not routinely included in the scanned field during a whole body FDG PET/CT scan, which is usually performed from scull base to mid-thigh. However data exists that in patients with solid extracranial tumors inclusion of the brain in the scanned field could reveal unexpected metastases or other brain abnormalities. The yield of routine brain scanning as a part of a whole body exam is modest, so there should be a meaningful trade-off between effective dose increase and expected benefits. The additional dose is entirely due to increase in CT dose, while the dose from the injected activity is constant. **Aim:** To calculate the additional effective dose from low dose CT scan of whole body PET/CT examination if the entire brain is included in the scanned field. **Materials and Method:** Objects of study were 50 consecutive patients with solid extracranial tumors without particular indications for brain scanning. All patients underwent a routine whole body FDG PET/CT (Phillips Gemini TF, 16slice). Using the capabilities of the acquisition software in its scan field planning part, the CT scan was planned twice per patient with and without brain in the field (standard and extended scan field). All other imaging parameters remain constant. The values of the dose-length product (DLP) from the standard and extended field of view were used for further calculations. The data from the patient is collected without additional exposure of the patients caused from the experiment. The additional effective dose is calculated as a product of DLP difference (extended scan field minus standard scan field) and a conversion factor for multislice head CT. **Result:** The average additional effective dose from a low dose CT as a part of whole body FDG PET/CT when the scanned field is extended to cover the whole brain is 0,14mSv (0,07mSv to 0,18mSv) which is less than 1% of the average FDG PET/ CT whole body dose (CT dose plus FDG dose) **Conclusion:** The increase of the effective dose from a whole body FDG PET/CT when the scanned field is extended to include the whole brain is low (less than 1%). This could justify routine brain scanning in patients with solid extracranial tumors as part of a whole body scans, given the expected metastases detection rate.

## PW146

### Radiation Doses Received During Sm-153 Therapy

**Y. Parlak**, D. Goksoy, N. Incili, F. Gumuser, E. Sayit; Celal Bayar University Department of Nuclear Medicine, Manisa, TURKEY.

Aim: Samarium-153 (153Sm-EDTMP) emits a range of medium-energy therapeutically useful beta particles that have been found beneficial in the palliation of metastatic bone cancer pain. The aim of the study is to determine the dose received by the skin of the fingers of clinical and laboratory staff during injections of Sm-153, as the hands are the critical parts of the body during 153Sm-EDTMP therapy. Material and Methods: In this study, eleven patients were treated with Sm153. Thermoluminescent dosemeters (TLD-100 chips) were used for absorbed dose measurements. TLDs were annealed at 400C for 1 h and at 100C for 2 h. For each treatment, 15 TLDs detectors were placed in 13 different points (10 TLDs to fingers, 1 TLD to thyroid, 1 TLD to chest and 1 TLD to abdomen). Two TLDs were placed at a 5 m distance from the patient, to determine the level of background radiation. A total of 165 TLD chips were used for eleven patients. These were read with a manual TLD reader (Harshaw, TLD 3500, Holland). These values were graphed, and the graphs were used to interpret the exposed TLDs. Background was systematically evaluated and subtracted from measurements before each reading. Each chip was calibrated individually in the same radiation beam. The average values of absorbed doses (skin of all fingers, chest, thyroid and abdomen) measured separately with TLD100. Results: Treating staff was right-handed. Right hand had been exposed to more radiation than left hand (the difference is 77%). The highest finger radiation dose is the right hand thumb (3.74±1.96 mGy). The second and third high radiation doses are right hand index finger (3.10±1.43 mGy) and left hand index finger (2.46±1.00 mGy). The results of TLD under the lead apron for thyroid, chest and abdomen were calculated as 0.60±0.15 mGy, 0.41 ± 0.18 and 0.57 ± 0.09 mGy, respectively. Conclusion: In view of the ICRP (International Commission Radiation Protection) recommended weekly skin dose limit is 10 mGy. According to the results of our study, we recommend that one staff should give therapy at most two patients in one week on the basis of radiation safety.

## PW147

### Advantages and disadvantages of out-patient treatment with radium-223 dichloride

**B. Szermerski**, C. Wanke, A. Solle, L. Geworski; Mezinische Hochschule Hannover, Hannover, GERMANY.

Aim: The administration of radium-223 dichloride in patients suffering from CRPC with bone metastases provides palliative pain reduction and OS improvement. Similar to established therapies in nuclear medicine, legal, regulatory and clinical criteria for radiation protection of medical staff and relatives have to be met regarding treatment in a hospital and out-patient setting. In this work, consequences for performing this therapy concerning the German legal regulatory environment are shown. Methods: The decision, whether the patient can be released immediately after administration or has to be hospitalised, must be based on the estimation of the possible exposure of relatives. Therefore we calculated external expositions of relatives. The dose rate constant of Ra-223 including all daughter nuclides was derived based on decay data available in the NuDat database of the Brookhaven National Lab and following the German standard DIN 6844-3. For estimating the internal exposition, different exposition pathways (inhalation and ingestion) were considered. The results are evaluated with regard to German legal and regulatory requirements. Results: The dose-rate constant derived in this work is 0.0468 (µSv m²) / (MBq h) and implies an exposition of relatives well below the German annual dose limit value of 1 mSv. However, this dose limit would already be exceeded by the internal exposition due to the inhalation of about 100 Bq of Ra-223, which has to be prevented for the whole series of six administrations. Although it is highly unlikely that relatives inhale significant amounts of Ra-223 excreted or exhaled by the patient, it has to be kept in mind that 100 Bq Ra-223 corresponds to less than 0.001 % of the administrated activity. On the other hand, hospitalisation requires a minimum stay of 48 h for every administration according to German guidelines. This is not medical necessary and causes a high burden to the patient. Conclusion: Both in-patient and out-patient Ra-223 therapy is feasible. Exceeding the dose limit values of relatives seems to be rather unlikely, however, measurements of contaminations by the

patient and potential incorporations are still to be performed. Concerning the aim of the therapy and the social impact of hospitalisation, out-patient therapy may be preferred.

## PW148

### Radio-iodine Therapy of a Dialysis Patient

**H. CARPENET**[1], S. VERBEKE[1], N. GOMBERT[2], J. MONTEIL[1], I. QUELVEN[1]; [1]Nuclear Medicine Department, University Hospital Dupuytren, LIMOGES, FRANCE, [2]Biomedical Department, University Hospital Dupuytren, Limoges, FRANCE.

**INTRODUCTION** Every year, more than 100 patients are treated with radio-iodine in Limoges Nuclear Medicine department. According to the indication, Iodine-131 activity, ranged from 1110 to 3700 MBq, is administered, representing a strong challenge for medical and paramedical team radiation protection. Most of the time, patients, hospitalized in protected room for 2 to 3 days, are under videosurveillance with staff limited contact. However, in some cases, patient proximity care is necessary because of an associated pathology. The aim of this work is to present dosimetric study and protocol implemented in particular situation of a dialysis patient. **PATIENT AND METHODS** A young patient (26 years old), who must receive 1110 MBq of Iodine-131, is treated with hemodialysis every 2 days due to a terminal renal failure with anuria. Radiation protection problems mainly concern organization of dialysis sessions (4 hours) during and after hospitalization. Three points have been assessed: staff radiation protection during dialysis, dialysis waste (solid and liquid) and machine management. At each dialysis until Iodine-131 elimination, dosimetric measures have been executed on dialysis staff with an active dosimeter and on patient, waste or device with doserate meter. **RESULTS** Treatment day was chosen depending on dialysis sessions organization: iodine intake was carried out the day after dialysis. The first dialysis post-iodine therapy was performed in the sealed room with a dialysis mobile machine. Sealed screen was used to limit staff exposure (14 μSv during the first dialysis). As for normal renal function patients, this first dialysis eliminated radioactivity major part (dosimetry at 1 m from patient before dialysis: 43 μSv/h - after: 14 μSv/h). Dialysates were eliminated as usual liquid effluents, directly from device output to toilets connected with decay tanks. Disposables were collected with Nuclear Medicine department solid usual waste. After system disinfection, no residual activity was measured on dialyser and its evacuation manifolds. Thus, device could be restored to Hemodialysis department. Subsequent dialysis sessions took place at regular dialysis center. Since accurate data wasn't available on the radiation protection necessary duration, equipment counts were made after each dialysis and contaminated waste were returned to Nuclear Medicine department. Four dialysis allowed to obtain counts inferior to twice the background noise. **CONCLUSION** Patients with specific care can be treated with Iodine-131 provided to establish dosimetric studies and follow-up. Radiation protection process carried in the particular case of a dialysis patient, constitutes a feedback which may be of interest to other hospitals.

# POSTER SESSIONS – GROUP 1

P01-1 - Sunday, Oct. 20, 16:00 - 16:30, Poster Exhibition Area

## Physics & Instrumentation & Data Analysis: Instrumentation

### P001

### The electromagnetic interference of mobile phones on the function of a gamma camera

**M. Assadi**[1], H. Javadi[2], Z. Azizmohammadi[3], A. Mahmoud Pashazadeh[1], T. Moazzeni[4], N. Baharfar[3], B. Shafiei[3], S. Delavari[3], I. Nabipour[1], A. Babaei[3], I. Neshandar Asli[3]; [1]The Persian Gulf Nuclear Medicine Research Center, Bushehr University of Medical Sciences (BUMS), BUSHEHR, IRAN, ISLAMIC REPUBLIC OF, [2]Golestan Research Center of Gastroenterology and Hepatology (GRCGH), Golestan University of Medical Sciences (GUOMS),, Gorgan, IRAN, ISLAMIC REPUBLIC OF, [3]Department of Nuclear Medicine, Taleghani Hospital, Shahid Beheshti University of Medical Sciences, Tehran, IRAN, ISLAMIC REPUBLIC OF, [4]Department of Electrical and Computer Engineering, University of Nevada, Las Vegas, NV, UNITED STATES.

**Purpose**: The aim of the present study is to evaluate whether or not the electromagnetic field generated by mobile phones interferes with the function of a single-photon emission computed tomography (SPECT) gamma camera during data acquisition. **Methods and Materials**: We tested the effects of seven models of mobile phones on one SPECT gamma camera. The mobile phones were tested when making a call, in ringing mode, and in standby mode. The gamma camera function was assessed during data acquisition from a planar source and a point source of technetium-99m with activities of 10 mCi and 3 mCi, respectively. A significant decrease in count number was considered to be electromagnetic interference (EMI). **Results:** The percentage of induced EMI with the gamma camera per mobile phone was in the range of 0-100%. The incidence of EMI was mainly observed in the first seconds of ringing and then mitigated in the following frames. **Conclusion**: Mobile phones are portable sources of electromagnetic radiation, and there is interference potential with the function of SPECT gamma cameras leading to adverse effects on the quality of the acquired images.

### P002

### Implementation and optimization of automatic 18F-FDG PET segmentation Methods

**B. Berthon**[1], C. Marshall[1], M. Evans[2], E. Spezi[3]; [1]Wales Research and Diagnostic PET Imaging Centre, Cardiff, UNITED KINGDOM, [2]Velindre Cancer Centre,, Cardiff, UNITED KINGDOM, [3]Department of Medical Physics, Velindre Cancer Centre, Cardiff, UNITED KINGDOM.

**Aim**: The use of automatic segmentation techniques for the delineation of tumour volumes on Positron Emission Tomography (PET) scans is of increasing interest. Optimization of the delineation algorithms is required in order to overcome the low image resolution and high noise levels encountered in PET. Promising automatic delineation Methods have been suggested recently with various implementations schemes. The aim of this phantom study was to investigate these automatic segmentation Methods and the influence of the algorithm implementation on their performance. In particular, the difference between 3D and slice-by-slice schemes, and the inclusion of Partial Volume Correction (PVC) before gradient-based segmentation were investigated. **Materials and Methods**: Nine different segmentation Methods were developed in the Matlab environment (Mathworks, Natick, USA). These included thresholding (AT), gradient-based contouring (GC), region-growing (RG), watershed (WT), clustering Methods and active contours segmentation (AC). PET scans were acquired on a GE 690 Discovery PET-CT scanner with the NEMA IEC body phantom, for six spherical inserts of 10-38mm diameter with Tumour-to-Background Ratios (TBRs) of 3,5 and 7. Each algorithm was implemented in 2D and 3D versions. Gradient-based algorithms were tested with and without the addition of a Partial Volume Correction (PVC) pre-processing step. The PVC included de-noising with a bilateral Wiener filter, followed by de-blurring with the Landweber algorithm. Performance metrics used to evaluate the delineation included Dice index (DSI) and volumetric error (VE). **Results**: AT, RG, and the clustering Methods performed significantly better ($p<0.01$) when implemented in a 3D mode. The 3D WT method performed better in 83% of cases, with improvements up to 0.15 DSI and 80% VE, although not statistically significant. GC and AC were not improved by 3D implementation. Gradient-based Methods AC, GC and WT method showed higher DSI values (up to 40%, 71% and 227% respectively) after PVC, for objects smaller than 13mm diameter at TBR =3. **Conclusions**: PVC preceding segmentation improves small volume delineation for the gradient-based segmentation Methods GC and WT at low TBRs. Threshold-based, region-growing and clustering Methods should be implemented in 3D.

### P003

### Energy spectrum and point spread function comparison of pin-hole and parallel-hole collimators for $^{90}$Y bremsstrahlung imaging.

**S. Walrand**[1], M. Hesse[1], A. Seret[2], G. Demonceau[3], F. Jamar[1]; [1]Université Catholique de Louvain, Brussels, BELGIUM, [2]Université de Liège, Liège, BELGIUM, [3]Sint-Elisabeth Ziekenhuis, Zottegem, BELGIUM.

**Aim:** recent phantom studies prove pinhole being superior to parallel hole collimator for $^{90}$Y bremsstrahlung SPECT. We compared their energy spectra and PSF. **Materials and Methods:** a camera (1/2"-thick NaI), successively equipped with a medium energy general purpose (MEGP) parallel hole and a 9mm-diameter aperture medium energy pinhole (MEPH) collimator was used. A $^{90}$Y point source surrounded by 1cm-thick perpex wall and a 1cm-diameter $^{99m}$Tc source, both located at 10 cm far away the collimator, were acquired. **Results:** MEGP $^{90}$Y energy spectrum matched published Monte Carlo (MC) simulations. Compared to MEGP, the lead fluorescence x-rays were reduced by 4 in the MEPH $^{90}$Y energy spectrum which displayed an exponential decrease pattern. The MEPH collimator sensitivity was 1.5 times higher than that of the MEGP one, but for a FOV area 6 times smaller. The FWHM (FWTM) in the object space for $^{90}$Y were 1.2 (2.0) and 1.5 (3.1) cm for the MEPH and MEGP collimators, respectively. Farther than 3 cm, the MEGP PSF was typically 6 fold higher than the MEPH one. By subtracting from the $^{90}$Y PSF the $^{99m}$Tc one, the geometric to total x-rays ratios in a [50,150] keV window were 68% and 31% for the MEPH and MEGP collimators, respectively. This last value is in line with published MC simulations. **Conclusions:** for $^{90}$Y, the MEPH collimator displayed a twice better geometric to total x-rays ratio and a sharper PSF with 6 fold lower tail than the MEGP ones explaining the better spatial resolution and quantification accuracy obtained by helical pinhole bremsstrahlung SPECT. Further MEPH collimator MC modelling will assess the different components contribution: tungsten insert, lead housing, camera compartments.

### P004

### SURGEOGUIDE: a Gamma Probe for Localization of Sentinel Lymph Nodes

**M. Ay**[1,2,3], N. Zeraatkar[1], N. Gorjizadeh[3], A. Kaviani[4], S. Farzaneh Far[5], S. Sajedi[1], H. Arabi[1], M. Farahani[6], B. Teimourian[1]; [1]Medical Imaging Group, Research Center for Molecular and Cellular Imaging, Tehran University of Medical Sciences, Tehran, IRAN, ISLAMIC REPUBLIC OF, [2]Research Center for Nuclear Medicine,, Tehran University of Medical Sciences, Tehran, IRAN, ISLAMIC REPUBLIC OF, [3]Department of Medical Physics and Biomedical Engineering, Tehran University of Medical Sciences, Tehran, IRAN, ISLAMIC REPUBLIC OF, [4]Department of Surgery, Tehran University of Medical Sciences, Tehran, IRAN, ISLAMIC REPUBLIC OF, [5]Depatment of Nuclear Medicine, Valiasr Hospital, Tehran University of Medical Sciences, Tehran, IRAN, ISLAMIC REPUBLIC OF, [6]Parto Negar Persia Co, Tehran, IRAN, ISLAMIC REPUBLIC OF.

**Aim**: We aimed to develop a gamma probe for localizing sentinel lymph nodes during surgery. Due to high prevalence of breast cancer in females, there are annually lots of breast surgical operations for removal of malignant tumors. However, failure in discovery and removal of cancerous lymph nodes will lead to metastasis of cancer in the patient. Currently, there are various Methods with different degrees of accuracy to detect sentinel nodes. Amongst all of them, still the most common and most favorite device for surgeons is gamma probe providing an easy-to-use small hand-held tool with the capability of detection and localization of sentinel lymph nodes not only in breast cancer but also for some masculine types of cancers where detection of sentinel nodes is mandatory. We developed such a gamma probe system: SURGEOGUIDE. **Materials and Methods**: A CsI(Tl) scintillator crystal joint to a Silicon Photomultiplier was placed into a Tungsten head to form the detection subsystem. Tungsten provided almost ideal features for both collimation and side and back shielding. The head was covered by a thin layer of stainless steel. The largest diameter of the probe is in head part; 16mm. The probe is connected to a control basement using a cable with removable connectors at both ends. A multi-touch tablet plays the role of control panel and display of the system which is connected to the basement by WiFi protocol. Different features and performance parameters can be obtained by altering the collimator design. However, the following results are related to the current design and were measured according to NEMA Standards for Gamma Probes, NU 3-2004. **Results**: Although the system is capable of working in 60-600keV range, it is optimal for being used with Tc-99m. The system sensitivity was about 1.1cps/kBq at at 3cm distant from the probe. In addition, the extrinsic spatial resolution was measured about 4cm at 3cm distant from the collimator. Also, the angular resolution of the probe was 75° FWHM. Finally, side shielding sensitivity was about 99.3%. **Conclusion**: We developed a gamma probe usable for localizing sentinel lymph nodes by displaying count rate (or counts number) and sound signals. Regarding the physical size and performance parameters of the probe, it is optimal for being used in breast cancer surgery. We are now receiving some clinical test

feedbacks to improve the current version and manufacture other versions of the gamma probes according to the customers' needs.

## P005

### A Commercial Low Cost SPECT System, Suitable for Small Animal Imaging

G. Kagadis[1], M. Georgiou[2,3], E. Fysikopoulos[2], N. Efthimiou[2], K. Mikropoulos[2], P. Papamichalis[2], P. Papadimitroulas[1,3], E. David[2], **G. Loudos**[2]; [1]University of Patras, Patras, GREECE, [2]Technological Educational Institute of Athens, Athens, GREECE, [3]BETsolutions, Athens, GREECE.

Small animal imaging, using nuclear medicine techniques, is a valuable tool in preclinical research. We present a new commercial, low cost system, suitable for small animal SPECT imaging. Design constraints include i) adoption to user needs, ii) high performance, iii) minimization of dimensions, iv) minimization of cost, v) user friendly environment and vi) robustness. The system is inspired by the facts that: i) most in vivo studies can be conducted with simple cameras; ii) the purchase of a high cost system can be justified and exploited only by large centers; iii) most groups can attract resources for a system that would cost 5 to 10 times less than the standard commercial ones and will give them the opportunity to shift from in vitro and ex vivo to in vivo. The prototype has a 10x10cm field of view and is suitable for imaging mice, rats and rabbits. The camera head is based on 4 position sensitive photomultipliers -PSPMTs (H8500), coupled to a CsI(Na) scintillator with 1.5x1.5x6mm$^3$ pixels. The 128x128 PSPMT signals are multiplexed using a resistive readout circuit and result to 2X and 2Y position signals, which are amplified and digitized using programmable ADCs controlled by an FPGA. The digitized signals are transferred to a laptop using Ethernet protocol. The gamma camera head is mounted on a rotating gantry. For gantry rotation a stepper motor has been selected, which is controlled by an AVR microcontroller using serial over USB communication. Image visualization interface was developed using Qt toolkit, while SPECT reconstruction is carried out using the QSPECT opensource software developed by our group. Overall dimensions are less than 1x1x1m$^3$ and weight less than 100kg. The system has been evaluated in both planar and tomographic mode. The spatial resolution is 2.3mm on the surface of the collimator and reaches 3.5mm at 5cm distance from the camera, using a hexagonal hole collimator, with 1.2mm holes, 0.16mm septa and thickness of 28mm. Tomographic tests have shown spatial resolution better than 4mm at 7.5cm, which is the maximum distance required to image larger animals such as rabbits. The system has been tested using capillary phantoms, mice and rodents. Current work includes further miniaturization of the system, to provide a prototype suitable for dedicated mouse imaging, with improved performance, at even lower cost and overall dimensions 50x50x50cm$^3$. The system is distributed by BETsolutions (www.betsolutions.gr).

## P006

### Physical and clinical validation of myocardial perfusion images generated using multi-focus fan beam collimator SPECT/CT

**H. ONISHI**[1], N. Matsutomo[2], S. Kenda[3], Y. Kangai[1], T. Saho[4], H. Amijima[5]; [1]Program in Biological System Sciences, Graduate School of Comprehensive Scientific Research, Prefectural University of Hiroshima, MIHARA, Hiroshima, JAPAN, [2]Department of Radiology, Kurashiki Central Hospital, Kurashiki, Okasyama, JAPAN, [3]3) Department of Radiology, Hiroshima prefectural Hospital, Hirosahima, Hiroshima, JAPAN, [4]Program in Health and Welfare Sciences, Graduate School of Comprehensive Scientific Research, Prefectural University of Hiroshima, Mihara, Hiroshima, JAPAN, [5]School of nursing, Hyogo University of Health Sciences, Kobe, Hiyougo, JAPAN.

**Aims:** We compared the quality between IQ-SPECTTM myocardial perfusion images (MPI) in conventional (180° apart: C-mode) and L-mode (90° apart). We assessed image resolution and image quantitation with use of a physical phantom and performed a clinical study. **Methods**: Images were acquired with standard parallel-hole collimations (LEHR) and the same system with the IQ-SPECT (IQ-mode) modification employing SMARTZOOM. Both C- and L-mode images were acquired over 180°contoured orbits with 30 and 34 views per detector for 12.5 s into 64 ⊆ 64 matrices and 4.8 mm pixels. IQ-SPECT images were acquired over 208° cardio-centric orbits with 17 views per detector for 6.25 s per view to 128 ⊆ 128 matrices and 4.80 mm pixels. Both images were attenuation corrected using CT images. The reconstruction soft-ware was used of Flash3DTM, and with specific Flash3DTM (OSCGM) for IQ-mode. Image resolution and total image quality were evaluated using the myocardial torso phantom. Five healthy volunteers were injected with 370MBq 99m-TC Tetrofosmin and then the quality of MPI SPECT images acquired using C-, L-, and IQ-modes were compared. Segmental values were calculated based on 17-segment models for phantoms and polar maps of the volunteers. **Results**: The myocardial wall thickness of the phantom determined from short-axis images resulted in significant correlations among C-, L-, and IQ-modes (25.1±1.1, 24.7±0.97 and 18.2±1.2 mm, respectively; $p < 0.001$). Image distortion occurred in L-mode system. The maximal difference in %uptake among the three modes was 13% in the quantitative 17-segment model, and the mismatch was more affected by L- and IQ-modes than C-mode. Homogeneity was significantly more affected in basal, mid, and apical regions by C-mode than by IQ-mode (C-mode vs. L-mode: p=0.07, 0.061 and 0.058, C-mode vs. IQ-mode: p<0.05 for all three regions). Percent uptake in the mid anteroseptal, apical septal, and apex regions was significantly more decreased in IQ- than in C-mode ($p < 0.05$) in healthy individuals. Discrepancies in the apical region were against clinical for phantom study with use of IQ-mode. The results were false positive in the apical segment. **Conclusions**: Myocardial perfusion images acquired by IQ-SPECT were comparable to those acquired by conventional and L-mode SPECT, but with significantly improved resolution and quality. Our results suggest that IQ-SPECT is the optimal technology for myocardial perfusion SPECT imaging.

## P007

### Correction of the Collimator Aperture Effect in Fan-beam SPECT System

**K. Ogawa**, R. Kamiya; Hosei University, Faculty of Science and Engineering, Tokyo, JAPAN.

**Aim:** Collimator holes of a fan-beam collimator have a physical dimension, and so the fan-beam collimator used in the SPECT system introduces an aperture effect as well as a parallel-hole collimator. The purpose of the present study is to develop an accurate aperture correction method of the fan-beam collimator. **Materials and Methods:** The fan-beam collimator focused on in this study has a hole whose diameter is the same at both ends (object and detector sides). And the septa of this fan-beam collimator differ in thickness at both ends of the hole. In this situation the aperture angle changes at the center and periphery of the collimator. And so the effect of the collimator aperture depends on the hole position in the detector. To overcome this problem, we modeled the aperture effect with an asymmetric Gaussian function and corrected it in the process of an iterative image reconstruction with the OS-EM method, in which we calculated projection data by multiplying the ideal projection data with an asymmetric Gaussian function. To confirm the validity of our method, we conducted some simulations with three point source phantoms and brain phantom. The distance between the focal point and surface of the collimator was 400 mm. The thickness of the collimator was 40 mm, the hole size 2 mm at both ends of the collimator surface, and the thickness of the septum at the object side 0.3 mm. The hole shape was assumed to be a square. The number of projection data was 90 over 360 degrees, and the number of pixels in the projection data was 256. To reconstruct an image, the OS-EM method (iterations: 5) was used and the number of subsets was 15. The size of an image matrix was 128 x 128 x 128. Moreover, to confirm the validity of our proposed method clinically, we applied it to the projection data measured with a gamma camera system (GCA9300-A) with fan-beam collimators. **Results:** The results showed that the blurrings of corrected images were much reduced by about 1/3 of the uncorrected image, and the validity of the proposed method was confirmed. The results obtained with the brain phantom and clinical data showed that thequality of the reconstructed image was much improved with our method. **Conclusions:**Our proposed aperture correction method was effective in improving the spatial resolution of SPECT images acquired with the fan-beam collimator.

P02-1 - Sunday, Oct. 20, 16:00 - 16:30, Poster Exhibition Area

## Physics & Instrumentation & Data Analysis: Data Analysis & Management

## P008

### An utilization of SUV navigator interface for precise measurement of SUV on F-18 FDG PET/CT.

**A. Okizaki**[1], M. Nakayama[1], T. Uno[2], J. Sato[2], M. Sakaguchi[2], M. Takeda[3], K. Watanabe[3], N. Yamaguchi[3], T. Nakamura[3], S. Ishitoya[1], K. Nakayama[2], N. Nakagami[2]; [1]Department of Radiology, Asahikawa Medical University, Asahikawa, JAPAN, [2]Radiological Technorogy Section, Asahikawa Medical University Hospital, Asahikawa, JAPAN, [3]Nursing Department, Asahikawa Medical University Hospital, Asahikawa, JAPAN.

**Objectives** Standardized uptake value (SUV) is widely used in positron emission tomography (PET) imaging for an semi-quantitative index. A maximum of SUV (maxSUV) is important to evaluate the activity of malignancy. A malignant lesion often extends to all directions, and therefore, it may be difficult to find the location of maxSUV in the lesion. To solve this issue, we devised SUV navigator interface (SUVnavi). This interface designed for fast and easy measurement of maxSUV in malignant lesion. It shows maxSUV in upper and lower several slices at the same time without paging. The purpose of this study was to investigate the utility of SUVnavi for precise measurement of maxSUV on 2-[18F]Fluoro-2-deoxyglucose positron emission tomography /computed tomography (F-18 FDG PET/CT).**Methods** Fifty patients with various malignant tumors were studied. The maxSUVs were measured in 349 lesions. F-18 FDG PET/CT scans were performed,

and the data were independently diagnosed by 2 radiologists with and without SUVnavi. True maxSUVs were obtained by remeasurements on both Methods. An accuracy of the measurements of maxSUV with and without SUVnavi were calculated using true maxSUV. To test the difference of the maxSUV with and without SUVnavi, paired t-test was used.**Results** The maxSUV agreed with true maxSUV in 348 of 349 lesions (99.7%) with SUVnavi, but 250 of 349 lesions (71.6%) without SUVnavi. Six lesions (1.7%) were overestimated and 94 lesions (26.9%) were underestimated without SUVnavi. On the other hand, only 1 lesion (0.3%) was overestimated with SUVnavi. Furthermore, the average of maxSUV without SUVnavi was smaller than with SUVnavi (5.67 +/- 48.7 vs 5.85 +/- 52.5, p < 0.000001).**Conclusions** A maxSUV might sometimes be underestimated with ordinarily method. The SUVnavi may be useful for accurate measurement of maxSUV on F-18 FDG PET/CT.

## P009

### Quantification of myocardial infarction in cardiac FDG PET

R. Klaassen[1], R. H. J. A. Slart[2], E. H. de Groot[2], R. Dierckx[2], **A. T. M. Willemsen**[2]; [1]University of Twente, Enschede, NETHERLANDS, [2]University Medical Center Groningen, Groningen, NETHERLANDS.

**Background** Current commercial software for the assessment of myocardial infarction based on static, dynamic or gated FDG PET, offers limited or no access to internal results, e.g. contour points, and has little flexibility in, or not even the option for, pharmacokinetic modeling or the determination of infarct size and transmurality. **Objective** The final goal of this study is to develop a computer application for myocardial PET analysis as a research tool to integrate several parameters, for example, tracer uptake, quantified perfusion and metabolism as well as wall thickness and motion to ultimately assess and quantify ischemia and infarction. Here we focus only on the core of this program i.e. the contour detection in nine patients with known myocardial infarction to quantify the infarct volume and left ventricle (LV) function, as a proof of principle. **Materials and Methods** Gated FDG PET (Siemens/CTI HR+) and delayed enhancement MRI (Siemens 1.5T Sonata) patient scans were performed. After transformation of the LV to "heart-coordinates" the only remaining optimization variable was the radius. A 3D *Snake* based contour detection algorithm to detect the epi- and endocardial contours was developed. Optimization is based on both image and contour characteristics. The resulting contours were evaluated based on the resulting end-diastolic volumes (EDV), end-systolic volumes (ESV), LV ejection fractions (LVEF) and myocardial volumes and were compared with the commercial package QGS. Infarct size was quantified using different threshold techniques. Myocardial and infarct volumes were compared to MRI data using the commercial package QMass. **Results** The *Snake* method created contours which were visually convincing, giving high correlations with QGS for EDV ($r$=0.98), ESV ($r$=0.99) and LVEF ($r$=0.92). However, image signal to noise ratio (SNR) of gated FDG-PET was low resulting in only fair correlation for total myocardial volume (r=0.72) and infarct size (r=0.63-0.79 depending on threshold). Infarct transmurality could not be derived due to the limited resolution of the PET images. **Conclusion** The current *Snake* contour detection is hampered by the data rather than by the algorithm. For static scans, the effective image resolution is to low due to respiratory and wall motion. For gated scans the SNR is to low because of the short scan duration. Fortunately, current High-Definition and Time-of-Flight PET/CT scanners have improved resolution and SNR. In addition, respiration gating may remove respiratory motion. Finally, the Snake algorithm can be improved further by including additional optimization criteria allowing, for example, 4D contour detection.

## P010

### Exploring the Precision of Textural Features in 18F-FDG-PET Scans of Oesophageal Cancer

**G. Doumou**[1], M. Siddique[1], C. Tsoumpas[1], V. Goh[1,2], G. Cook[1,2]; [1]Division of Imaging Sciences and Biomedical Engineering, Kings College London, London, UNITED KINGDOM, [2]Guy's & St Thomas' Hospitals NHS Foundation Trust, London, UNITED KINGDOM.

**Aim:** $^{18}$F-FDG PET provides clinically relevant information in oncology for diagnosis, staging and to determine early response to therapy. Additional quantification of the heterogeneity of FDG PET tracer uptake within tumours may be a significant predictor of response and prognosis [1]. This study aims to evaluate the precision of these measurements with respect to smoothing, segmentation and quantisation changes. **Materials and Methods:** 66 oesophageal cancer patients underwent a staging $^{18}$F-FDG PET/CT. The PET raw data were processed by using different smoothing levels (2.0, 2.5, 3.0, 3.5 or 4.0mm), percentage $SUV_{max}$ thresholds (45%, 50%, 55% or 60%) and bin widths (8, 16, 32, 64 or 128). Textural analysis was performed using first, second and high-order features (including ROI, SUV, FD, GLCM, GLRL, NGTDM, GLDM, GLSZM matrices). Precision Error was described by the percentage of Coefficient of Variance (CV%) between the different levels for each of the 3 variables. **Results:** Many textural features showed a Precision Error > 50% between different bin widths. However, the following features (fractal dimension, coarseness, correlation, inverse different moment normalized, inverse difference normalized and information correlation measure 1) presented low Precision Errors < 15%. Different Segmentation and Smoothing levels had only small effects on precision errors. GLCM and GLRL matrices were the most robust, showing precision error below 10% in both segmentation and smoothing changes. **Conclusions:** This study showed that applying different smoothing levels or $\%SUV_{max}$ thresholds has little effect on the precision of heterogeneity measurements in $^{18}$F-FDG PET oesophageal data. However, quantisation often has larger effects and a normalization process is being investigated in order to reduce this effect [2]. Further evaluation and standardization of parameters for multicentre studies is needed. References: [1] Chicklore S, Goh V, Siddique M, Roy A, Marsden PK, Cook GJ. *Quantifying tumour heterogeneity in 18F-FDG PET/CT imaging by texture analysis*. Eur J Nucl Med Mol Imaging. 2013 Jan;40(1):133-40 [2] Tixier F, Le Rest CC, Hatt M, Albarghach N, Pradier O, Metges JP, Corcos L, Visvikis D. *Intratumor heterogeneity characterized by textural features on baseline 18F-FDG PET images predicts response to concomitant radiochemotherapy in esophageal cancer*. J Nucl Med. 2011 Mar;52(3):369-78

## P011

### Adaptive threshold algorithm for Metabolic Tumor Volume estimation based on lesion-to-background ratio measured on clinical 18F-FDG PET oncological images

**F. Gallivanone**[1], F. Fazio[2], M. Paganoni[2], L. Gianolli[3], M. Gilardi[1], I. Castiglioni[1]; [1]IBFM-CNR, Segrate, ITALY, [2]University of Milan-Bicocca, Milan, ITALY, [3]San Raffaele Scientific Institute, Milan, ITALY.

**AIM** Adaptive thresholding algorithms (ATA) for the estimation of 18F-FDG PET Metabolic Tumor Volume (MTV) have been proposed based on actual signal-to-background ratio, a parameter not available for real oncological lesions measured by 18F-FDG PET images. Aim of this work was to assess the accuracy of an operator-independent ATA for the estimation of 18F-FDG PET Metabolic Tumor Volume (MTV) based on PET measured lesion-to-background ratio. **MATERIALS AND METHODS** NEMA IQ phantom with spheres of different diameter (10, 13, 17, 23, 29, 37 mm) was filled at different actual sphere-to-background ratio (from 2.65 to 65) and acquired (9 acquisitions) on the Discovery STE PET/CT scanner (General Electric Medical Systems). PET measured Sphere-to-Background ratio (S/Bm) and PET measured sphere-equivalent diameter (dm) were calculated using a fixed threshold at 60% from the maximum uptake value and a background contribution defined as the mean uptake in 4 circular regions of 3 cm surrounding the sphere, according to published studies proving accuracy and operator-independency of the measurement approach [Gallivanone et al., 2011]. For each sphere, once measured dm and S/Bm, the threshold was furtherly optimized (Optimal Threshold, OT) as the percentage threshold from the maximum uptake value allowing to define an "isocontour" volume matching actual sphere volume (minimum percentage difference). OT values were fitted with different models with respect to S/Bm and dm. Three anthropomorphic oncological phantoms, simulating oncological lesions of different diameter (9.8, 12.3, 15.6, 25.8, 31.3 mm) in different body regions (thorax, breast and brain) were used for the validation of the MTV estimation using the adaptive fitted-model threshold method. The accuracy of the method was evaluated by the percentage difference between MTV and the actual sphere volume. **RESULTS**: The best model for fitting OT values was: $OT((S/B)m,dm) = \alpha(1/(S/B)m)+\beta1dm+\beta2(dm)2+ \beta3(dm)3+\beta4(dm)4$. The fit resulted accurate (adjusted R-square = 0.89) and both S/Bm and dm were confirmed as significant independent predictors of OT. Considering the percentage difference between actual sphere volume and MTV obtained by the fitted OT, our method developed for the estimation of MTV achieved an accuracy > than 95% for sphere diameter < 1cm and of 93% for sphere diameter < 1cm. **CONCLUSIONS** This work provides an accurate operator independent method to extract MTV by using an adaptive threshold obtained as a function of parameters always available on clinical PET oncological images (S/Bm and sphere-equivalent dm).

## P012

### Effect of NaI(Tl) Crystal Hydration on Co-57 and Tc-99m Imaging

**F. H. Barrack**, S. J. McQuaid, S. A. Kilfeather, S. L. Manoy, J. W. Scuffham, P. J. Hinton; Royal Surrey County Hospital, Guildford, UNITED KINGDOM.

***Aim.*** Sodium-iodide scintillation crystals can suffer from hydration, which changes the optical properties of the crystal and consequently produces areas of non-uniformity in gamma camera images. Although the only long-term solution is to replace the crystal, new uniformity maps can overcome the problems in the short-term and extend the life of the system. The aim of this study was to characterise the hydration in terms of its effect on the Tc-99m and Co-57 energy spectra and to assess if hydration affects the ability of Co-57 flood images to be used for assessing Tc-99m uniformity. ***Method.*** Flood images of Tc-99m and Co-57 were acquired on a GE Infinia Hawkeye that is suffering from crystal hydration in several regions. To investigate the energy spectra for the hydrated and non-hydrated regions, data were acquired in multiple adjacent energy windows. For Tc-99m, 5 keV windows were used over 105-155 keV and for Co-57, 2.5 keV windows were used, from 84 to

135 keV. Regions of interest were drawn on the acquired images around the four most prominent areas of crystal hydration and a region containing no apparent crystal hydration. The mean counts in the hydrated and non-hydrated regions were plotted as a function of central energy of the window to determine the apparent position of the photopeak, and the FWHM. The effect of the increasing hydration of the crystal was also assessed, by plotting the mean counts in the hydrated areas as a function of time. ***Results.*** For Tc-99m, the apparent photopeak energy was found to be 133 keV and 140 keV for the hydrated and non-hydrated regions respectively, and for the Co-57 flood, these figures were 104 keV and 123.4 keV. The photopeak was therefore shifted by a much greater amount for Co-57. The ratio of the mean counts in the hydrated and non-hydrated ROIs for photopeak images was found to increase over time, with a more rapid change seen for Co-57. ***Conclusions.*** The apparent photopeak position was seen to decrease for both Tc-99m and Co-57 in regions affected by hydration. The increased degradation to Co-57 uniformity indicates that in hydrated crystals, Co-57 daily floods cannot be used as surrogate for Tc-99m uniformity and instead Tc-99m floods need to be performed. It can also be seen that in the presence of hydration, Tc-99m uniformity maps are not appropriate for other radioisotopes, even if their photopeak energy is close to 140 keV.

## P013

### Effect of Statistical Noise on DVR Parametric Images depends on the Kinetic Analysis Method in the PiB-PET Dynamic Scan

K. Adachi[1], M. Senda[2,3], **R. Ueda**[1], Y. Ikari[2,4,3], T. Nishio[2,4,3]; [1]Kobe University, Kobe, JAPAN, [2]Institute of Biomedical Research and Innovation, Kobe, JAPAN, [3]J-ADNI PET QC core, Kobe, JAPAN, [4]MICRON Inc., Kobe, JAPAN.

**Aim**: Dynamic PiB-PET scan provides distribution volume ratio (DVR) of cerebral amyloid deposition, and the DVR parametric images (PIs) could visualize spatial distribution of cerebral amyloid deposition in more details than the ROI analysis. However the quantitative capability of pixelwise DVR estimation is undermined by large pixel-based statistical noise. In this study, we evaluated the effect of statistical noise in pixel-based time activity curves (TACs) on the DVR PI and how it depends on the kinetic analysis method. **Materials and Methods**: Pixel-based TACs were acquired for 70 min on a PiB-positive patient with Alzheimer's disease. In each pixel, the DVR value was estimated by the two-parameter multilinear reference tissue model (MRTM2) and by Logan graphical analysis with reference region (LGAR). First, the pixelwise DVR values were calculated from noise free TACs to generate the DVR PI "original," in which noise free TACs were obtained by the pixelwise fitted TACs of MRTM2. The noise at each pixel was simulated as a Gaussian with the standard deviation related to the pixel count. Three different average noise levels (9%, 34% and 40%) were tested, of which noise level 34% corresponded to that of the measured TACs. The simulated noise was added to the noise free TACs to generate the DVR PI "add noise." Finally, the effects of statistical noise were evaluated by the pixelwise difference (ΔDVR) between DVR PI "original" and DVR PI "add noise." **Results:** For the noise level of measured data (34%), DVR PI generated by MRTM2 looked noisy due to statistical noise. The mean±S.D. of ΔDVR was 0.0825±1.891, indicating that DVR was slightly positively biased. The mean±S.D. of ΔDVR for DVR PI generated by LGAR was -0.4680±1.389, i.e. DVR was negatively biased. As the noise level increased, DVR PI generated by MRTM2 became noisier, and DVR PI generated by LGAR was more negatively biased. On the other hand, for small noise level (9%), DVR PIs were less affected by statistical noise. As a result, DVR PI generated by MRTM2 was slightly positively biased and the noise expanded as the noise level increased, which was more pronounced for high uptake pixels than for low uptake pixels. DVR PI generated by LGAR was negatively biased as the noise level increased. **Conclusions**: According to the simulation, the effect of statistical noise is a serious matter in the DVR parametric images and the effect strongly depends on the kinetic analysis method.

## P014

### Evaluation of Two Automated Methods for PET Region of Interest Analysis

**M. Schain**[1,2], K. Varnäs[1], Z. Cselényi[1,3], C. Halldin[1,2], L. Farde[1,2,3], A. Varrone[1,2]; [1]Karolinska Institutet, Stockholm, SWEDEN, [2]Stockholm Brain Institue, Stockholm, SWEDEN, [3]AstraZeneca Translational Science Center, Stockholm, SWEDEN.

**Background** Manual definition of regions of interest (ROIs) has been considered the reference standard method in PET data evaluation. The procedure is labor-intensive, prone to rater bias and show low reproducibility. These limitations become particularly challenging for large datasets, and when pooling a large number of measurements is required, for example in multicenter studies. Automatic Methods for ROI definition may overcome these limitations and thereby facilitate large scale analysis. **Aim** The aim of the study was to validate the two automated Methods FreeSurfer and the AAL template for definition of ROIs for the analysis of PET data. **Materials and Methods** PET data obtained using the radioligands [$^{11}$C]AZD2184 (amyloid-β radioligand) and [$^{11}$C]AZ10419369 (5-HT$_{1B}$ receptor radioligand) were evaluated. Since both brain atrophy and PET system resolution may impact the performance of the automated Methods, this study included both patients with Alzheimer's disease and healthy subjects, and PET measurements acquired on one high and one lower resolution PET system. Outcome measures obtained using automated Methods were compared to those obtained using manual ROIs, using linear regression analysis, intra class correlation coefficients, and repeated measures ANOVA. **Results** Almost all ROIs provided by the automatic Methods were significantly larger than the manually delineated regions, which in some cases introduced biased estimates of the regional outcome measures due to increased partial volume effects or heterogeneity of radioligand binding. Of the 12 ROIs included in the analysis, systematic and significant differences in outcome measures between manual and automated ROIs was found in a total 3 regions per automated method (AAL: caudate, sensorimotor cortex, and hippocampus; FreeSurfer: caudate, posterior cingulate cortex, and laterotemporal cortex). For [$^{11}$C]AZD2184, differences between the automated and manual Methods were only observed among patients, and for the lower resolution system, significant difference was also observed for the prefrontal cortices. The overall percent difference between automated and manual ROIs was less than 2% percent for controls, and less than 5% for patients for both systems. The ICC scores were generally greater than 0.8, and the regression analysis resulted in slopes close to 1 and intercepts close to 0. **Conclusion** Both AAL and FreeSurfer can be used for quantification of PET data. Since their accuracy in the estimates of outcome measures are similar, the choice of method could be based upon other factors, such as necessity of fast analysis as provided by AAL, or more detailed ROIs and measures of cortical thickness as provided by FreeSurfer.

## P015

### Performances evaluation of Big Bore PET/CT for virtual treatements simulation in radiothérapy

**T. MONFORT**; Léon Bérard, Lyon, FRANCE.

***Introduction*** The Big Bore PET/CT is the model which offers the widest opening of tunnel (a diameter of 85 cm) due to the absence of external septa. The use of bulky restraint systems like those used in radiotherapy is possible. Therefore the Big Bore is presented like the PET/CT dedicated to virtual simulation of radiation treatment. Few studies have been conducted on performances evaluation of the PET/CT Big Bore. Besides, none bears to pay particular attention to the absence of external septa. ***Aim*** The purpose of this study is to compare the Big Bore performances to the standard model TF 16, used as a reference in this work, to assess the impact of the tunnel enlargement on the quantification and the target volumes definition in radiotherapy. Meanwhile, this study offers to carry out new tests, more specific to the characteristics of the PET/CT Big Bore. ***Material & Methods*** The Big Bore is composed of 28336 crystals of 4x4x22 mm$^3$ Cerium doped Lutetium Yttrium Orthosilicate (LYSO) spread over 44 rings of 90 cm diameter. Wide bore opening is 85 cm. The axial () and transverse () fields of view axial are 18 cm and more than 67.6 cm, respectively. It doesn't have any septa and can operate in 3-dimensional (3D) mode. The coincident window width is 3.8 ns. The energy is greater than 440 keV. The electronic system allows using the Time Of Flight (TOF). The CT scanner is the Brillance 16 slice. In comparison, PET/CT Gemini TF 16 has same characteristics except a wide bore opening of 70 cm because of presence of external septa of 7.5 cm. The performances of both PET/CT are evaluated using "classical" experiments found in literature: the NEMA NU 2-2007 Protocol, measurement of intrinsic radioactivity from LYSO and evaluation of temporal and energy resolutions. The original experiment, created for this work, consists on assessment of an external radioactivity source influence, over multiple distances, on the image quality of test phantom. ***Results*** The preliminary results of the first experiment underline that the absence of external septa has an influence on the image quality. Carrying out other experiments would permit to characterize the phenomenon in depth. ***Conclusion*** This study proposes the performances evaluation of the Big Bore. Results of the different experiments are being processed and will be presented.

## P016

### Population averaged image derived arterial input function in 15-O Water PET

**F. Hofheinz**[1], J. Langner[1], B. Beuthien-Baumann[2], I. G. Steffen[3], I. Apostolova[3], R. Buchert[3], J. Steinbach[1], J. Kotzerke[2], J. van den Hoff[1]; [1]Helmholtz-Zentrum Dresden-Rossendorf, Dresden, GERMANY, [2]University Hospital Carl Gustav Carus, Dresden, GERMANY, [3]Charite - Universitätsmedizin Berlin, Berlin, GERMANY.

Arterial input function (IF) determination is traditionally based on arterial blood sampling which is invasive and ill-suited for clinical routine. Alternatively, one can use a population averaged IF determined via blood samples (BSIF) in a separate study. We present a strategy for generation of a population averaged image derived IF (IDIF) in brain investigations. **Methods**: An image subvolume enclosing the carotid arteries is manually defined. Further processing is fully automated: 1: peak phase detection of the IF, 2: threshold based, background aware delineation using peak phase optimized for small structure size (~ 5 mm), 3: time activity curve

generation, 4: model free recovery coefficient (R) determination 5: recovery and spillover correction according to Cm = R x Ct + (1 - R) x B, Cm/Ct: measured/true signal/IF, B: local background. This method was applied to 48 15-O Water brain studies (acquired with an ECAT HR+ PET). The resulting IFs were averaged, leading to a population averaged image derived IF (IDIF). Gray matter perfusion was computed from the Kety-Schmidt model assuming a partition coefficient in gray matter of 0.9 (f1). Perfusion was also computed using a BSIF from a different institution (f2). f1 and f2 were compared. **Results:** f1 and f2 are strongly correlated (Pearson 0.999) and differences are small: (f2-f1)/f2 = (4.6 +/- 0.9)% (mean +/- sd), range 1.8% - 7.4%. **Conclusion**: The presented method allows to generate an IDIF which reproduces the results achieved with BSIF with good accuracy. For the investigated data an individual IF determination is not possible with this method due to the modest reconstructed resolution of the HR+ data and the resulting vessel delineation errors. First evaluations of data measured with a Philips Gemini TF PET scanner indicate that individual IF determination becomes possible with increased spatial resolution of the images.

P03-1 - Sunday, Oct. 20, 16:00 - 16:30, Poster Exhibition Area

## Physics & Instrumentation & Data Analysis: Radiation Exposure & Protection

### P017

### The Evaluation of Urine Activity and Dose Rate from Patients Administired SM-153 Therapy

**Y. Parlak**, D. Goksoy, G. Gumuser, N. Incili, G. Topal, E. Sayit; Celal Bayar University Department of Nuclear Medicine, Manisa, TURKEY.

**Aim**: Samarium-153 ethylenediaminetetramethylene phosphonic acid (153Sm-EDTMP) emits medium-energy beta particles and gamma photon with a physical half-life of 46.3 h. The aim of the study is to determine the excretion of Sm-153 in urine and to calculate dose rate of Sm-153 retention in the body as a function of time. **Materials and Methods**: Ten prostate cancer patients (mean age: 69±5.8years; age range from 59 to 79 years) were treated with 153Sm-EDTMP at dose of 37 MBq/ kg. Urine samples were collected at 2nd, 4th, 6th, 8th and 24th hours from 10 patients after iv injection of Sm-153. After collecting urine samples, the measurements of dose rate were acquired by Geiger-Muller (GM) probe (Ludlum, 14C, USA); and it was expressed as retained Sm-153 body activity versus dose rate. **Results:** Effective half life that is calculated from urine samples measurements were found as 7.11± 2.9h within the first 24h. Urinary excretion at first 8 h were 26.97%±10.66% of administered activity. Median value urinary excretion at 24 h were 33.30% ±14.17% with a range of 18.5%- 64.0%. Whole body dose rates before collecting urine of patients were 60.0±15.7 µSv /h for within 1 h following Sm-153 administration and dose rate per MBq was calculated as 0.018 ± 0.005. Effective half life that was calculated from dose rate measurements with GM probe was 17.61±6.6 hr within the first 24 h. **Conclusion**: According to the regulations of our country, the dose rate for discharge of patients should not exceed 20 µSv/h. In respect to this criteria, the results of our study imply that patients who recieved 153- Sm therapy should be kept a minumum of 8 hours in an isolated room at hospital.

### P018

### Radiation exposure of surgical staff during sentinel node surgery for breast cancer

**M. BAILLY**, A. ZINSIUS, S. MAIA, M. J. SANTIAGO RIBEIRO; CHRU Tours, Hôpital Bretonneau, Tours, FRANCE.

***Aims***: Assess the radiation exposure of surgical staff and determine controlled areas around the patient according the Council Directive 96/29/EURATOM during sentinel node surgery in gynecology at the University Hospital of Tours. ***Materials and Methods***: A prospective study was conducted during 3 months representing 40 sentinel node surgical procedures with different dosimetric measurements. Dosimeters were used to evaluate the whole body and the fingers radiation exposure for all exposed workers (surgeon, nurse and surgical assistant). Another dosimeter was used to estimate the atmospheric radiation level. We also measured the dose rate at 1 m, 30 cm and in contact with the patient in the operating room to determine controlled areas. ***Results***: The activity of $^{99m}$Tc-microalbumin injected was 50,1 ± 2,4 MBq when the surgery was performed the same day and 90,4 ± 3,2 MBq when the surgery was performed the day after. Radiation exposure of the surgical staff is very low. Doses received during one surgical procedure by the surgeon, surgical assistant and nurse are 5 µSv, 3,8 µSv and undetectable for whole body exposure, 17,5 µSv, 15,6 µSv and 16,2 µSv for extremities respectively (highest dose received by the surgeon). Atmosphere dosimeter didn't detect any radiation over this period. On average, 200 procedures are performed each year in our hospital by 7 surgeons. Surgeon's radiation exposure remains below the threshold of 1 mSv annual for whole body and 50 mSv annual for fingers set for public by the International Commission on Radiological Protection n°103. According to the French order N° 137 of June 15th 2006, when the radiopharmaceutical injection is performed the day before surgery, controlled area in the operating room around patient's breast is 14 cm diameter, and 32 cm diameter when the surgery is performed the same day. ***Conclusions***: During sentinel node surgery for breast cancer, the radiation exposure of surgical staff is weak. The surgeon is the most exposed and receives a dose below the limits of the public radiation exposure. This study shows there is no need for special dosimetric monitoring during the sentinel node surgery using $^{99m}$Tc-microalbumin injection; the real danger lying in the risk of contamination by the radiopharmaceutical during injection.

### P019

### An utilization of a shielded syringe for administration of radioactive tracer: investigation about the direction and location of the syringe

**M. Takeda**[1], K. Watanabe[1], N. Yamaguchi[1], T. Nakamura[1], A. Okizaki[2], M. Nakayama[2], T. Uno[3], J. Sato[3]; [1]Nursing Department, Asahikawa Medical University Hospital, Asahikawa Hokkaido, JAPAN, [2]Department of Radiology, Asahikawa Medical University, Asahikawa Hokkaido, JAPAN, [3]Radiological Technology Section, Asahikawa Medical University Hospital, Asahikawa Hokkaido, JAPAN.

**Objectives** Nuclear medicine is one of the useful diagnostic and therapeutic Methods in all over the world. The administration of radioactive tracer is performed by doctors and nurses. Protection from radiation exposure is very important especially for full-time staff. A tungsten shielded syringe was widely used for this issue, however, it designed to protect the radioactivity in the lateral direction. Therefore, the distribution of radioactivity around the syringe may be spread asymmetric. We hypothesized that the reduction of radiation exposure on administration of radioactive tracer could be achieved to pay attention the distribution of radioactivity. The purpose of this study was to investigate the distribution of radioactivity around the syringe. Moreover, the direction and location of the shielded syringe were estimated to minimize the radiation dose to docrors and nurses. **Methods** A shielded syringe filled with Tc-99m (2.5 mCi, 2ml) was placed on X-ray film to obtain the distribution of radioactivity. The film was developed after 1 hour of the exposure, and the distribution was evaluated. Furthermore, actual radiation dose from syringe with shield, which filled with Tc-99m (10 mCi, 2ml) , in a vartical direction and a 45 degree angle to aline the syringe axis, and at a distance of 15 and 30 centimeters, using a pocket dosimeter. The dose from same syringe without shield in a vartical direction and a 45 degree angle at a distance of 30 centimeters were measured to confirm the effect of the shield. **Results** The distribution of radioactivity was spreded out like a comet tail shape, it aline the syringe axis. The radiation dose from shielded syringe in a vartical direction at a distance of 15 and 30 centimeters were 95.85 µSv/h, and 24.85 µSv/h, and a 45 degree angle at those distance were 0.85µSv/h and 0.23µSv/h, respectively. On the other hand, the dose from unshielded syringe in a vartical direction and a 45 degree angle at a distance of 30 centimeters were 56.0µSv/h and 51.0µSv/h, respectively. **Conclusions** The radiation dose with shielded syringe was smaller than unshielded syringe. The dose were smaller in a 45 degree angle and at a larger distance compared with another conditions. When an administration of radioactive tracer, to keep a 45 degree angle and maximum distance with a shielded syringe is important to protect from radiation exposure.

### P020

### Monte Carlo evaluation of dose to fingers from handling radiopharmaceuticals

**P. J. Collins**, Y. Matyagin; Royal Adelaide Hospital, Adelaide, AUSTRALIA.

**Background and Aim:** Dispensing/administering radiopharmaceuticals can result in a high radiation dose to staff fingers. Although syringe shields will significantly reduce this exposure, staff often do not use them as it can lengthen the time needed to find a vein and the risk of extravasation is increased. The aim of this study was to use Monte Carlo simulation to estimate the finger dose from diagnostic and therapeutic radiopharmaceuticals in shielded/unshielded syringes. **Methods:** The dose-rate at a depth of 0.25 mm in a tissue equivalent "finger" positioned over the radioactivity (A) (worse case) or at the rear of a syringe (B) containing a solution of either Tc-99m, F-18, Y-90 or Lu-177 was simulated using DOSRZnrc/EGSnrc. The geometries (radiopharmaceutical volume (syringe size)) evaluated were 0.3 (1) and 1 (1) (Tc-99m), 2 (3) (F-18, Lu-177) and 1.3 (2) (Y-90). The activities (MBq) were 1000 (Tc-99m), 320 (F-18), 200 (Y-90) and 8000 (Lu-177) and the exposure times were 20 seconds (Tc-99m, Y-90) and 60 seconds (F-18, Lu-177). The thicknesses of the tungsten syringe shields were 2.03 mm (Tc-99m) and 2.21 mm (F-18, Lu-177). The perspex shield for Y-90 was 7.21 mm thick. The shields were only simulated for position A. **Results:** The following doses (mGy) to the unshielded (shielded) "fingers" were obtained. Tc-99m: 4.11 (0.0022) and 1.56 (0.00077) in Position A and 0.0183 (-) and 0.150 (-) in Position B for the 0.3 and 1 ml active volumes respectively. F-18: 16.0 (5.73) in Position A and 0.462 (-) in Position

B. Y-90: 105 (0.020) in Position A and 0.546 (-) in Position B. Lu-177: 19.1 (0.385) in Position A and 0.316 (-) in Position B. **Conclusions:** (a) The annual extremities dose limit (500 mGy) may be exceeded after 122 (Tc-99m), 32 (F-18), 27 (Lu-177) or 5 (Y-90) studies with typical exposure times and poor technique (unshielded syringe and fingers over radioactivity). (b) Finger exposure is reduced by 1 - 2 orders of magnitude if the (partially filled) syringe is held at the end (cf. holding over radioactivity). (c) Syringe shields are highly effective and should be used whenever possible.

## P021

### Contribution of Ring Dosimeters in Revealing Increased Radiation Burden of the Staff in a Nuclear Medicine and PET/CT Department

**K. Gogos**, F. Vlachou, A. Nikaki, D. Papoutsani, V. Papoutsis, K. Dalianis, T. Pipikos, R. Efthymiadou, V. Prassopoulos; DTCA Hygeia Department of PET/CT, Athens, GREECE.

**AIM:** To determine whether hand dose, measured by ring dosimeters in a nuclear medicine and PET/CT department, contributes significantly to the overall radiation burden of the personnel and also to compare it with the wholebody radiation dose measured by routine chest dosimeters. **MATERIALS - METHOD:** Four members of the nuclear medicine and PET/CT department authorized for radiopharmaceutical preparation, dose drawing, and intravenous administration of the radiopharmaceuticals were monitored by ring and chest TLD dosimeters for a 1 year period. The staff wore the ring dosimeters on the middle finger of right hand with the TLD detector facing in. **RESULTS:** The total annual hand dose that was recorded by the ring dosimeters was 38mSv (7.6% of annual 500mSv dose limit for the hands (IAEA,ICRP 2007)) and 45mSv (9% of the 500mSv limit) concerning the personnel charged with the nuclear medicine radiopharmaceuticals binding procedure and the drawing of the PET radiopharmaceutical ($^{18}$F FDG) doses. Regarding the personnel responsible for the intravenous administration of the PET radiopharmaceutical, the annual measured hand dose was 33.5mSv (6.7% of the 500mSv limit) and for the personnel responsible for dose drawing and intravenous administration of conventional nuclear medicine radiopharmaceuticals (mainly $^{201}$Tl and $^{99m}$Tc bonds) the measured hand dose was 15.7mSv (3.2% of the 500mSv limit). The corresponding chest doses that were recorded for the same period of time were 1.5mSv, 0.3mSv, 3.16mSv and 1.66mSv (7.5%, 1.5%, 15.8% and 8.3% of the annual 20mSv limit) respectively. In comparison with chest doses, hand dose represented 50%, 85%, 30% and 28%, respectively, of the total radiation burden of the involved personnel. **CONCLUSION:** Hand dose is a component of the radiation burden that escapes routine chest dosimeters' monitoring of the personnel in nuclear medicine and PET/CT departments. The implementation of ring dosimeters in routine personnel dosimetry revealed a mean of 48% contribution of the hand dose to the overall radiation dose of the staff, reaching 85% contribution individually, and showed that it is a crucial means of assessing the actual radiation burden of the personnel authorized for radiopharmaceutical handling tasks.

P04-1 - Sunday, Oct. 20, 16:00 - 16:30, Poster Exhibition Area

## Physics & Instrumentation & Data Analysis: Quality Control & NEMA

## P022

### Use of wall-less radionuclide doped gel phantoms to determine the influence of non-active phantom walls in 18F PET/CT and 123I SPECT/CT activity quantification and outlining of tissue volume

**M. Sydoff**, M. Andersson, S. Mattsson, S. Leide-Svegborn; Department of Clinical Sciences, Malmö, Lund, SWEDEN. Skåne University Hospital Malmö, Malmö, Sweden

**Introduction and aim:** Activity quantification of tomographic images, such as Single photon emission computed tomography (SPECT) images and Positron emission tomography (PET) images is an important tool to convert imaging data into activity concentration values. It is of great importance to have a high level of accuracy in the quantification of activity, since it is the basis for the determination of biokinetics and dosimetry of radiopharmaceuticals used in nuclear medicine. It is also of utmost importance that the volume assessment is highly accurate for the correct delineation of tumor volumes for radiation therapy planning. The most common types of phantoms used in activity quantification in SPECT and PET utilize fillable, hollow spheres placed in a circular or elliptical cylinder which could be filled with a selected activity concentration to imitate tumors in a hot or cold background. However, the occurrence of a cold sphere wall surrounding the hot-spot activity in images of this kind of phantoms could pose a problem since the lesion-to-background contrast is decreased and the delineation of volumes becomes less accurate on account of the cold sphere wall. **Materials and Methods**: We have developed a new type of phantom without cold sphere walls for the quantification of activity and outlining of tissue volume in both SPECT and PET measurements. Gelatin hot-spots of three different sizes were molded and placed in a Jaszczak phantom together with hollow plastic spheres of the same sizes containing the same activity concentration. 18F PET and 123I SPECT measurements were made with zero background activity and with lesion-to-background activity concentrations of 10:1 and 5:1.The background corrected relative volume reproducing threshold, T was calculated for both the gelatin and the plastic spheres. **Results and conclusion**: The results show that the threshold, T drops with increasing background for the plastic spheres. For the gelatin spheres, this background dependence is not present. A decrease of the lesion-to-background contrast is seen for the plastic spheres compared to the gelatin spheres; this effect is more pronounced in the SPECT images than in the PET images.

## P023

### The essay of Iodine-123 revisited

**M. N. Lonsdale**; Bispebjerg Hospital, Copenhagen, DENMARK.

**Aim** Iodine-123 is an isotope with a wide range of applications in nuclear medicine, e.g. for labeling FP-CIT (DaTSCAN). Essaying I-123 in a well counter imposes some challenges as the dominant 159 KeV gamma line used for imaging is not (!) the dominant gamma line in a well counter. Due to a significant amount of secondary X-ray radiation (about 30 KeV), the near-4π geometry of modern well counters and the small degree of self-absorption in samples, summed peaks appear in the spectrum, notably at about 60 KeV and about 190 KeV. The aim of this study was to establish a simple model that qualitatively and quantitatively describes observed spectra of I-123 in order to optimize gamma counting parameters. **Materials and Methods** A probability tree was generated using detailed decay information of I-123. Particles that for physical reasons could not contribute to the features of the spectrum, were disregarded. The model included the probability graph for three types of X-rays and gamma lines together with parameters such as population of the relevant energy levels, branching ratios, detection efficiency and geometry of the crystal and sample position. Experimental verification of the model was performed on a Wallac Wizard 1480 well counter (Perkin-Elmer). The number of counts contributing to each peak in the spectrum was calculated as height multiplied by the FWHM from a fitted Gaussian curve. In an additional experiment, the low-energy X-rays were selectively attenuated and the effect on the resulting spectra investigated. **Results and conclusion** Four distinct peaks were visible on the spectra. The number of counts in each peak was (relative to the 159 KeV peak): 30% (20 KeV), 16% (53 KeV), 100% (159 KeV) and 131% (190 KeV). (Note the non-linearity in energy resolution of the counter.) The model predicted 67%, 17%, 100% and 133%. Despite its simplicity, the model predicts the actually measured counts in the summed peaks very well. Selective attenuation of low-energy X-rays attenuated the 190 KeV peak accordingly. When used with appropriate parameters, the model can be used to predict consequences of altered procedures and may also be easily extendible to other isotopes such as Indium-111.

P05-1 - Sunday, Oct. 20, 16:00 - 16:30, Poster Exhibition Area

## Physics & Instrumentation & Data Analysis: Standardisation

## P024

### The use of Fluoroscopic X-Ray Flat Panel Based CT in SPECT/CT Examinations. Optimizing the Acquisition Parameters

**K. Gogos**, F. Vlachou, E. Tsiakas, A. Nikaki, T. Pipikos, K. Dalianis, D. Papoutsani, V. Prassopoulos; DTCA Hygeia Department of Nuclear Medicine, Athens, GREECE.

**AIM**: To optimize the use of flat panel based CT in SPECT/CT studies and to reveal the most common artifacts that are encountered, in comparison with conventional CT based SPECT/CT systems. **METHOD**: In our department SPECT/CT is used in nuclear cardiology, bone disorders, lung scintigraphy as well as tumor diagnosis. SPECT/CT acquisitions are performed with a PHILIPS XCT BVW dual head SPECT/CT camera that includes x-ray flat panel technology for the CT part. The flat panel as well as the x-ray tube are mounted on the γ-camera gantry and acquire an axial FOV of 15cm(segment) for each revolution. The revolution time varies from 60s(slowest) to 12s(fastest), and it is significantly slower than in any conventional CT. We applied the different exposure and revolution time parameters provided by the manufacturer in various SPECT/CT examinations, in order to optimize image quality taking into consideration the patient's dose. **RESULTS:** In myocardial perfusion, SPECT/CT is used exclusively for attenuation correction so the lowest exposure(5mA) and the slowest revolution time(60s) are used. The additional effective dose imparted to the patient is limited to 0.2mSv. In lung perfusion, the fastest revolution time(12s) with average exposure (10-20mA) and breathhold

requirement are adopted in order to prevent motion artifacts. In bone scans, an average revolution time(24s) with high exposure(80mA) is found to perform better CT images, except for the thorax region, where breathing can be responsible for motion artifacts, especially on the ribs. Finally, for whole-body examinations, fast revolution time(12s) with average exposure settings(20mA) are preferred in order to prevent motion artifacts. It is also important to mention that in the thorax and upper abdomen region, where breathhold is required, the breathhold for each segment should be the same because the non-consecutive manner in which the CT is acquired on the z-axis can cause organ displacement artifacts. **CONCLUSION**: Slower tube revolution time and non-consecutive imaging that a flat panel based CT performs, introduce new aspects in SPECT/CT acquisition that are not met in the SPECT/CT systems that use conventional CT. Optimization of the parameters that are selected for each examination is essential for avoiding artifacts and obtaining clinically useful images

## P025

### Variability in PET quantitation within a multicenter studies in Japan

**K. MATSUMOTO**[1], K. Suzuki[2], H. Fukukita[3], Y. Ikari[4], K. Oda[5], Y. Kimura[6], S. Sakamoto[2], N. Shimada[7], T. Shiraishi[8], T. Nishio[4], H. Nishida[4], T. Terauchi[7], M. Senda[4]; [1]Kyoto College of Medical Science, Kyoto, JAPAN, [2]Dokkyo Medical University Hospital, Tochigi, JAPAN, [3]International University of Health and Welfare, Tochigi, JAPAN, [4]Institute of Biomedical Research and Innovation, Kobe, JAPAN, [5]Tokyo Metropolitan Institute of Gerontology, Tokyo, JAPAN, [6]Kinki University, Wakayama, JAPAN, [7]National Cancer Center, Tokyo, JAPAN, [8]National Institute of Radiological Sciences, Chiba, JAPAN.

**Aim:** Among clinicians who use positron emission tomography (PET), the standardized uptake value (SUV) is a popular semi-quantitative value that can be easily assessed whenever a PET study is performed under physiological and pathological conditions. However, many factors affect SUV, such as patient preparation procedures, scan acquisition, image reconstruction and data analysis settings, and the variability in methodology across centers prohibits exchange of SUV data. The purpose of this study was to evaluate the variability in quantitation of positron emission tomography (PET) data acquired within the phantom test of a multicenter studies. **Materials and method**: A image quality phantom of the NEMA NU-2 2007 Standard filled with F-18 was scanned with sixteen PET/CT and PET scanner in 3D mode. The all six hot spheres, with internal diameters of 10, 13, 17, 22, 28 and 37 mm, were filled with F-18 at an 4:1 concentration with respect to the background area. Data were acquired with a list mode for 30 min, from which PET images of 30 min acquisition duration were reconstruction. The phantom image is reconstructed with all available corrections applied, was optimized using a Japanese guideline for the oncology FDG-PET/CT data acquisition protocol. Twelve ROIs of the same size were drawn throughout the background at a distance of 15 mm from the edge of the phantom, and measured activity in each background ROI was recorded. **Results:** An average SUV of sixteen PET/CT and PET scanner was 1.00±0.07, and the range of SUV mean was 0.87 to 1.14 (95% confidence interval [CI], 0.96-1.04). **Conclusion**: Our preliminary data suggest that the variability of SUV is small if a Japanese guideline is used and quality assurance and quality control procedures are followed.

P06-1 - Sunday, Oct. 20, 16:00 - 16:30, Poster Exhibition Area

## Physics & Instrumentation & Data Analysis: New & Innovative

## P026

### Comparison of different Tc-99m mebrofenin liver clearance calculation Methods using hepatobiliary scintigraphy in Y-90 microsphere therapy planning

**H. Tanyildizi**[1], L. Kabasakal[2], R. O. Tutar[3], S. Yilmaz[2], N. Yeyin[2], A. Aygün[2], M. Ocak[4], Y. Oktem[1], B. Akkus[1], B. Kanmaz[2]; [1]Istanbul University, Faculty of Science, Department of Nuclear Physics, Istanbul, TURKEY, [2]Istanbul University, Faculty of Medicine, Department of Nuclear Medicine, Istanbul, TURKEY, [3]Istanbul University, Faculty of Engineering, Department of Physical Chemistry, Istanbul, TURKEY, [4]Istanbul University, Faculty of Pharmacy, Department of Pharmaceutical Technology, Istanbul, TURKEY.

**Aim:** Ytrium-90 microsphere (Y90) therapy data depicted that local efficacy correlated to tumor absorbed dose and the mean absorbed dose is associated with toxicity. Accurate measurement of liver function before Y-90 therapy is crucial especially in patients with underlying paranchymal disease. Nuclear imaging techniques have the advantage of measuring both lobar and total liver function. Several liver function tests, like biochemical parameters can measure only global liver function and fail to calculate segmental or lobal functions. In this study, we aimed to measure gamma camera mebrofenin (M) clearance (C) and extraction rate and compare results with blood M C. **Material and Method:** Thirty two patients with primary or metastatic liver malignancy, who were planned to give Y-90 microsphere therapy were included in study. After iv injection of Tc-99m M, dynamic hepatobiliary scintigraphy was performed. To determine global and lobar liver functions, region of interest (ROI) around right lobe, left lobe and heart was drawn. Radioactivity counts acquired between 150 and 350 seconds postinjection were used for calculation as described previously. Also in 13 patients blood samples were obtained at 2, 5, 10, 20, 30 minutes after injection and they were also used for calculation. In 9 patients Tc-99m M C were measured using single compartment model. **Results:** Two different C rates, which are called liver C (LClr) and blood pool C (BClr) were calculated. Mean LClr and BClr were found to be 9,17±0,52%/min and 12,64±0,61%/min, respectively. Correlation was found between LClr and BClr (r=0,90), when ROI (region of interest) around larger vessels and geometric mean for liver and blood pool counts were taken into consideration for M C rate (MCR). Mean C of left and right liver lobes were found to be 3,29±0,31%/min and 5,84±0,42%/min, respectively. Mean golden C (GK) was calculated as 393,33± 2,20%/min. Correlation was found between GK and calculated C according to Ekman's formalism (r=0,57). **Conclusions:** Tc-99m labelled M was found to be a useful method to show visual and quantitative information of hepatobiliary scintigraphy. Both total and regional liver uptake functions can be determined by MCR calculations. It seems to be a valuable liver function test especially in Y-90 microsphere therapy planning. Optimal method to calculate LClr and BClr were found to be the technique using both geometric data and larger blood pool ROI. We found that calculated C according to the Ekman's formalism is correlated with the GK.

## P027

### FLT PET-CT Functional Texture Analysis Has Potential To Distinguish Breast Cancer Patients

**B. Sanghera**[1], L. Sonoda[1], D. Woolf[2], A. Makris[2], W. Wong[1]; [1]Paul Strickland Scanner Centre, Mount Vernon Hospital, Northwood, UNITED KINGDOM, [2]Mount Vernon Hospital, Northwood, UNITED KINGDOM.

**Objectives:** Establish if FLT PET-CT scanned breast cancer displays functional fractal or lacunarity textural properties pre and during therapy. Ascertain if potential fractal and lacunarity signatures enable normal contralateral breast tissue to be distinguished from breast cancer tissue. Investigate value of potential fractal and lacunarity relationships pre and during therapy with different lesion volume defining thresholds. **Method**: 15 breast cancer subjects scanned pre and during therapy were studied with in-house 3D box counting and gliding box fractal and lacunarity analysis software following ethical approval and consent. Different threshold Methods were applied to segment PET functional lesions using pixels (a) > contra lateral normal breast uptake or (b) >40% or (c) >50% of maximum FLT lesion uptake. Software generated a regression fit (RF) indicating whether fractal properties existed, then derived lesion irregularity as fractal dimension (FD) and lesion volume utilisation as fractal abundance (FA). Corresponding hysteresis type graphs were generated showing lacunarity curves with these segmentation Methods for pre and post therapy scans. **Results**: Differences in mean FD, FA and RF across patients between pre and post therapy FLT scans were -0.028, -0.006, -0.001; 0.090, 0.073, 0.001 and 0.118, 0.178, 0.001 respectively for segmentation Methods (a) (b) and (c). Individual mean FD and FA were significantly different ($p<0.0001$) between different segmentation Methods pre and post therapy but differences were non-significant between pre and post therapy for the same segmentation technique. The lacunarity curves for segmentation technique (a) were displaced from those acquired using Methods (b) and (c). Indeed in many cases there was also a displacement of curves pre and during therapy suggesting prognostic potential. **Conclusions**: FLT PET-CT breast cancer pre and during therapy exhibits functional fractal and lacunarity characteristics with significant differences in FD and FA between separate (a), (b) and (c) Methods for lesion segmentation. Potential exists to predict outcome using suitable segmentation regimes with 3D fractal analysis and lacunarity.

## P028

### Simultaneous F-18 and Se-75 dual-isotope imaging using TOF-PET scanner: Effect of Down-Scatter

**C. C. Chiang**[1], K. S. Chuang[1], H. H. Lin[1], M. L. Jan[2]; [1]National Tsing Hua University, Hsin-Chu, TAIWAN, [2]Institute of Nuclear Energy Research, Atomic Energy Council, Taoyuan, TAIWAN.

**Aim**: In general, dual-isotope imaging provides both additional diagnostic value to clinical judgment and shorter duration of acquisition. Our previous studies demonstrated the time-of-flight information can be applied in dual-photon emission tomography. This work is the feasibility study of performing simultaneous F-18 and Se-75 imaging with a TOF-PET scanner. The main purpose of present study is to evaluate the down-scatter effect in F-18/Se-75 dual-isotope imaging. **Method**: Monte Carlo simulations were performed by an in-house developed SimGATE, which was an integration of SimSET and GATE simulation codes. A PET with fast temporal resolution was used to collect the coincidence of the two photons

emitted from F-18 and Se-75. Two water phantoms, 5 cm in diameter each and separated by 10 cm, were filled with F-18 and Se-75, separately, both with activity of 0.27 mCi. A triple-energy window centered at 136, 264.7, and 511keV technique was used. The 136 keV and 264.7 keV coincident pair was regarded as from Se-75 and the two 511 keV from F-18. The contribution of down-scattered events in Se-75 energy window from 511 keV photons was characterized. Images of F-18 and Se-75 were reconstructed by TOF MLEM algorithm and simultaneous algebraic reconstruction technique (SART) algorithm, respectively. **Results:** The rod images corresponding to F-18 and Se-75 were well separated without significant artifacts. The fraction of contaminated coincidences from F-18 into Se-75 was 12% (which made of 61.4% of the total scattering events in Se-75) while those from Se-75 into F-18 were less than 0.1%. **Discussion and Conclusion**: Preliminary studies demonstrated the feasibility to acquire F-18 and Se-75 dual-isotope images simultaneously. The effect of F-18 isotopes down-scattered coincidences in Se-75 energy windows is not significant. Therefore, this simultaneous acquisition method might open a way to many potential applications in the future.

P07-1 - Sunday, Oct. 20, 16:00 - 16:30, Poster Exhibition Area

## Molecular & Multimodality Imaging: PET/CT

### P029

### The Role of 18F-FDG-PET/CT in initial staging of patients with locally advanced and/or potentially resectable breast cancer

**N. Testart**, R. Sánchez Sánchez, A. Rebollo Aguirre, M. Navarro-Pelayo Láinez, T. Aroui Luquin, A. Rodríguez- Fernández, J. Llamas-Elvira; Hospital Virgen de las Nieves, Servicio de Medicina Nuclear, Granada, SPAIN.

**Aim**: The presence, extent and localization of distant metastases are key prognostic factors in breast cancer patients and play a central role in therapeutic decision making.This study was conducted evaluate the utility of 18F-FDG-PET/CT in initial staging of patients with locally advanced and/or potentially resectable breast cancer. **Methods**: A total of twenty-four consecutive patients (Mean age: 54 years) with newly diagnosed locally advanced breast cancer (≥T3-N2) and/or potentially resectable breast tumors (>3cm) were evaluated retrospectively from January 2011 to December 2012. Conventional staging was according to routine practice in our institution and included: chest radiography, liver sonography, bone scanning and PET/CT. Positive findings were confirmed by specific image procedures or clinical follow up for at least 1 year. **Results**: Primary tumor was detected by PET/CT and MRI in all cases. At the diagnosis time 22 patients had axillary lymph node involvement showed by PET/CT in all these patients. Nodal involvement was detected by axillary sonography and MRI in 86% and 82% respectively. Extra axillary nodal involvement was diagnosed in 8 patients; Sensitivity of PET/CT and MRI were 62, 5% and 87, 5% respectively and both had Specificity 100%. Distant metastases were diagnosed in 10 patients: bone metastases (n= 9), liver metastases (n=1) and lung metastases (n=1). PET/CT had a higher sensitivity in detection of bone metastases compared to bone scanning (89% vs 56%). The only patient with liver metastases was diagnosed by both PET/CT and liver sonography. In 5 patients (21%) PET/CT was the only imaging procedure that showed distant disease: bone metastases (n=4) undetected by bone scanning and later confirmed by MRI and lung metastases (n=1). **Conclusions** Our preliminary results suggest a potentially utility of PET/CT in initial staging of patients with locally advanced and/or potentially resectable breast cancer, especially for detection of unsuspected distance metastases. With increasing availability of FDG-PET/CT, prospective studies are needed to determine whether it could potentially replace the array of conventional imaging procedures used today.

### P030

### Association between [18F]Fluorodeoxyglucose (FDG)-Positron Emission Tomography (PET) Parameters and Prognostic Factors in Patients with Invasive Ductal Carcinoma of the Breast

**S. Chiacchio**[1], L. Evangelista[2], G. Manca[1], N. Dubbini[3], A. Cervino[2], A. AlSharif[4], E. Filidei[5], M. Tredici[1], G. Puccini[1], A. Cacciato Insilla[6], F. Betti[1], A. Giorgetti[5], D. Volterrani[1], M. Roncella[7], G. Mariani[1]; [1]Regional Center of Nuclear Medicine, University of Pisa, Pisa, ITALY, [2]Istituto Oncologico Veneto- IRCCS, Padova, ITALY, [3]Dipartimento di Matematica, University of Pisa, Pisa, ITALY, [4]Nuclear Medicine Unit, University of Jordan, Jordan, JORDAN, [5]Nuclear Medicine Unit, Fondazione CNR-Regione Toscana "G. Monasterio", Pisa, ITALY, [6]Section of Pathological Anatomy, Department of Surgery, University of Pisa, Pisa, ITALY, [7]Senology Unit, Azienda Ospedaliero-Universitaria Pisana, Pisa, ITALY.

**Aim:** The expression of specific molecular markers in invasive ductal carcinoma (IDC) of the breast, such as estrogen receptor (ER), progesterone-receptor (PR), HER2, as well as tumor size (T), axillary lymph node status (N), and grading (G), has direct prognostic and therapeutic implications in patient's management. The aim of this retrospective study was to evaluate the relationship between tumor glucose use and ER, PR, HER2, T, N, and G in breast cancer patients with IDC. To this purpose, tumor glucose consumption was quantified by PET-derived parameters, such as SUVmax, SUVmean and tumor lesion glycolysis (TLG, determined by multiplying the metabolic tumor volume - at 40% of SUVmax - by SUVmean). **Methods:** Breast tumors from 62 IDC patients who underwent FDG-PET in three different centers for staging prior to neo-adjuvant chemotherapy and surgery were excised and examined for ER, PR, HER2, T, N and G. PET scans were acquired in 26 patients using a Discovery ST/8 scanner (GE Healthcare, Milwaukee, USA) and in 36 patients a Biograph 16 HR (Siemens, USA). The association between SUVmax, SUVmean and TLG with ER, PR, HER2 status, T, N and G was investigated using unpaired Student's t test and linear regression. **Results:** There was a significant association between ER status and lesion SUVmax and SUVmean. ER-negative tumors (n=23; SUVmax=11.73±6.34; SUVmean=5.68±2.49) demonstrated both a significantly higher SUVmax (P=0.002) and SUVmean (P=0.003) than did ER-positive tumors (n=39; SUVmax=7.14±4.75; SUVmean=3.86±2.10). Moreover, there was an inverse correlation between the %ER-positive cells and SUVmax (r=0.387, P=0.002) and SUVmean (r=0.358, P=0.004). The correlation between TLG and ER status was not significant (P=0.158). No significant difference existed between SUVmax or SUVmean and/or TLG and PR status, HER2 status, lymph node involvement or Ki67. A significant association was found between histological grade and lesion SUVmax and SUVmean. Grade 2 breast carcinomas (n=16; SUVmax=4.8±3.01; SUVmean=2.81±1.34) demonstrated both a significantly lower SUVmax (P=0.001) and SUVmean (P=0.001) than did Grade 3 tumors (n=46; SUVmax=10.25±5.88; SUVmean=5.13±2.41). Finally, a significant correlation was found also between tumor size and SUVmean (r=0.316; P=0.013) and TLG (r=0.316; P=0.013), respectively. **Conclusions**: In the present study strong relationships were observed between ER status, tumor grade and tumor glucose consumption (SUVmax and SUVmean) in patients with IDC. These preliminary data support a growing body of evidence that ER-positive and ER-negative breast cancers have distinct disease-specific patterns. Conversely, no correlation was found between TLG and other parameters characterizing patients with IDC.

### P031

### Statistical comparison between SUVmax and SUVpeak of FDG uptake in pancreas cancer: Bland-Altman plot analysis

**K. Yoshikawa**, S. Ohashi, S. Toubaru, M. Hasebe, K. Tamura, T. Shiraishi, K. Tanimoto, S. Yamada, S. Kandatsu, M. Zhang, T. Saga, T. Kamada; National Institute Of Radiological Sciences, INAGE-KU, CHIBA-SHI, JAPAN.

Adoption of metabolic imaging with F-18-FDG in staging and follow up of cancers needs tumor metabolism parameters like standardized uptake value (SUV). SUVmax, the value of the single voxel with the maximum intensity, avoids inter-observer differences, but a major drawback of SUVmax is its susceptibility to noise in the data. SUVpeak defined as the largest possible mean value of a 1 cm3 spherical VOI positioned within a tumor removes inter-observer variation and reduces the susceptibility to noise. In this study we compared SUVpeak against SUVmax of glucose metabolic activity of pancreas cancer, and assessed how much the SUVpeak was likely to differ from SUVmax using Bland-Altman plot. **Method**: A total of 53 patients (35 males, 18 females; mean age, 67 ± 8 y) with pancreas cancer underwent F-18-FDG PET/CT scan in pre- and post-carbon ion radiotherapy. All patients were followed more than 1 year after treatment. The following parameters were measured: maximum standardized uptake value (SUVmax) and peak SUVs (SUVpeak6, SUVpeak10, SUVpeak15). SUVpeak6, SUVpeak10 and SUVpeak15 are measured using spherical VOI with radius 6 mm, 10 mm and 15 mm, respectively, where the volume of spherical VOI of SUVpeak6 is almost 1 cm3. The overall survival was estimated using the Kaplan-Meier method with SUVs as prognostic variables. Bland-Altman plots were used to evaluate difference between SUVmax and SUVpeak in pre- and post-treatment scan. **Results**: Cutoff values for each SUV were defined by ROC analysis, and the probability of survival was significantly lower with increasing FDG uptake measured by all the kinds of SUVs in both pre- and post-treatment. Significant correlations were observed between SUVmax and SUVpeak6, SUVpeak10 or SUVpeak15 in both pre- and post-treatment. However, proportional bias was observed between SUVmax and SUVpeak6, SUVpeak10 or SUVpeak15 in both pre- and post-treatment as revealed by the Bland-Altman plot analysis. The Bland-Altman analysis illustrated that the 95% limits of agreement is smaller between SUVmax and SUVpeak6 (range: pre 0.25, post 0.16) than between SUVmax and SUVpeak10 (range: pre 0.40, post 0.23), and is also smaller between SUVmax and SUVpeak10 than between SUVmax and SUVpeak15 (rang: 0.62, post 0.35). **Conclusions:** SUVmax and SUVpeak were statistically significant prognostic variables for overall survival estimated using the Kaplan-Meire method. SUVmax as FDG-PET uptake parameter was correlated closely to SUVpeak, but there was proportional bias between SUVmax and SUVpeak. The smaller the sphere's radius of SUVpeak the smaller the 95% limits of agreement is.

## P032

### A new approach to estimate the amount of tumor stroma as a prognostic factor using SUVmax and SUVpeak in pancreatic cancer

**K. Tanimoto**[1], K. Yoshikawa[1], T. Shiraishi[1], N. Ishii[1], S. Toubaru[1], S. Ohashi[1], T. Saga[1], M. Tajiri[1], A. Kato[2], M. Miyazaki[2], K. Shibayama[1], H. Tsuji[1], Y. Ando[1], T. Kamada[1]; [1]National Institute Of Radiological Sciences, Chiba, JAPAN, [2]Chiba University, Chiba, JAPAN.

**Objective** Various parameters are used for measuring tumor glucose metabolic activity with $^{18}$F-FDG PET including measuring the single maximum pixel value within the slice with highest radioactivity concentration (SUVmax) or placing a fixed ROI in the area of the tumor with the highest level of $^{18}$F-FDG uptake (SUVpeak), which it defines as the largest possible mean value of a spherical VOI with radius 10 mm positioned within a tumor (SUVpeak10). It is said that the amount of tumor stroma correlates with prognosis of patients with cancer. We estimated the amount of tumor stroma with $^{18}$F-FDG-PET using SUVmax and SUVpeak10, and evaluated the prediction performance of the amount of tumor stroma with $^{18}$F-FDG-PET after surgery of pancreatic cancer. **Methods** Sixteen pre-surgery patients with either proven or suspected primary pancreatic cancer underwent $^{18}$F-FDG-PET/CT. The pathologically confirmation found out 13 malignancy in all cases. According to pathological findings, the stroma of tumors were quantitatively classified in 3 types (Scirrhous type: abundant stroma, Intermediate type: a type intermediate between the scirrhous type and the medullary type, and Medullary type: scanty stroma). We evaluated the correlation between the amount of tumor stroma and each 3 indexes, SUVmax, SUVpeak10 and SUVstroma. SUVstroma was calculated by the following equation: SUVstroma =1- [SUVpeak10] / [$SUV_{max}$] $^{18}$F-FDG accumulates in tumor cells but does not accumulate so much in stromal cells. The tumor with abundant stroma might be low SUVpeak10, so SUVstroma might be high. Because the tumor cell avidly accumulates $^{18}$F-FDG but stroma does not so much. Each 3 indexes of SUV (SUVmax, SUVpeak10 and SUVstroma) were statistically compared with 3 types of stroma classification using the Mann-Whitney's U test. The overall survival (OS) was calculated using Kaplan-Meier method by SUVs found statistically-significant with Mann-Whitney's U test. **Results** There was no patient with Medullary type in our cases. Statistically-significant difference was observed between Scirrhous type and Intermediate type in SUVstroma ($p<0.05$). No statistically-significant difference was observed between Scirrhous type and Intermediate type ($p<1.0$, $p<0.53$) in SUVmax and SUVpeak10. Scirrhous type has a higher SUVstroma than Intermediate type. The patients with SUVstroma>0.3 had markedly lower OS rate than those with SUVstroma<0.3 (0% vs. 50% $p<0.05$). **Conclusion** We think that SUVstroma could estimate the amount of tumor stroma, and it is useful for predicting prognosis of the patients with pancreatic cancer.

## P033

### Impact of respiration on tumor measurements in lung cancer patients using FDG-PET

H. G. Hulshof[1], A. H. J. Oostdijk[2], P. L. Jager[2], C. H. Slump[1], **J. van Dalen**[2]; [1]University of Twente, Enschede, NETHERLANDS, [2]Isala, Zwolle, NETHERLANDS.

**Aim** Respiratory movements cause significant challenges to image quality and quantitative accuracy in PET imaging. Correct usage of CT-based attenuation correction (AC) in PET imaging of lung cancer patients is of particular relevance. It strongly depends on the accuracy of PET/CT co-registration at the transition region between lungs and more dense tissue as the liver. The aim of this study was to quantify possible effects of misregistration due to respiration on tumor size and uptake values in lung cancer patients using FDG-PET. **Methods** Using segmentation techniques misregistration between FDG-PET and CT at the diaphragm was measured for 25 consecutive lung cancer patients who underwent hybrid PET/CT (Discovery STE 16, GE Healthcare). For both modalities, patients followed a free breathing protocol. Furthermore, a 4D PET/CT phantom study was performed using the NEMA IEC Body Phantom, where 6 spheres (diameter 10-37 mm) were filled with FDG. The influence of respiration was simulated by manual phantom movement and by artificially introducing a mismatch between PET and CT up to 50 mm. The cavity of the phantom alternately contained air or water during the PET and CT acquisition to study the effect of a different attenuation medium. Using PET images after CT-based AC, sphere signal was determined by its maximum pixel value. Sphere size was obtained by a contour using a 42% threshold of the signal. Signal measurements were compared to the gold standard where neither movement nor misregistration was simulated. Size measurements were compared to the true sphere size and to the true volume that was covered by the sphere movement. **Results** The patient study showed that for 15 patients (60%) misregistrations were non-negligible and varied from 10 to 28 mm. The phantom study showed that sphere signal decreased more than 50% due to movement, with the largest deviation for the smallest sphere. However, in case of an incorrect AC the PET signal was overestimated by more than 400%. Furthermore, movement led to an overestimation of the sphere size up to 300% for the smallest sphere, but to an underestimation up to 200% of the volume that was covered by the movement. **Conclusion** Respiration during FDG-PET/CT examinations of lung cancer patients may have a huge impact on the measured PET signal and size of a tumor. Especially for small lung tumors near the diaphragm this may severely influence staging, follow-up studies and radiotherapy treatment planning of lung cancer patients using FDG-PET.

## P034

### Subcutaneous and muscular metastasis of the colorectal cancer on F-18 FDG PET/CT

**S. Karyagar**[1], U. Kesici[2], S. S. Karyagar[1], C. Kece[3], A. Guner[3], U. Kucuktulu[3], G. Duman[4]; [1]Trabzon Kanuni Training and Research Hospital, Nuclear Medicine Department, Trabzon, TURKEY, [2]Akcaabat Hackali Baba State Hospital, General Surgery Department, Trabzon, TURKEY, [3]Trabzon Kanuni Training and Research Hospital, General Surgery Department, Trabzon, TURKEY, [4]Kartal Yavuz Selim State Hospital, General Surgery Department, Istanbul, TURKEY.

**Purpose**: The purpose of this study is to reveal the ratio of subcutaneous and muscular metastasis which is determined by F-18 FDG PET/CT imaging on patients diagnosed as colorectal cancer. **Material and Methods**: In this study, F-18 FDG PET/CT imaging findings, those were made at the staging or follow up phase of 292 colorectal cancer patients between July 2009-October 2012 were examined in terms of subcutaneous or muscular metastasis retrospectively. **Results**:In 8 patients (2,73%) subcutaneous or muscular metastasis determined when F-18 FDG PET/CT imaging findings of 292 colorectal cancer patients were examined. The mean age of the patients (5M, 3F) was 67,86 (35-88). Metastasis was determined in one patient at the staging phase, in the others at follow up phase.The average period from the diagnosis of primary tumor in 7 patients at whom metastasis were determined at the follow up stage to F-18 FDG PET/CT imaging was 39 months (5-87). In 2 of 8 patients (0,68%) muscular metastasis, and in 6 of 8 (2,05%) subcutaneous metastasis was determined. While there were subcutaneous or muscular metastasis in each 4 patients; there were 3 lesion in each 3 patients, and in 2 patients there were multiple lesion.The SUVmax. value of lesions was 11,05 (2,58-26,71) on the average. All the patients in whom subcutaneous or muscular metastasis was determined had metastatic illnesses. While one patient has isolated muscular metastasis besides having lung metastasectomy, in the others there were other metastatic lesions accompanying. **Conclusion**:In patients having colorectal cancer F-18 FDG PET/CT imaging is an effective method on determining the subcutaneous and muscular metastasis.

## P035

### The Role of PET/CT in Detecting Peritoneal Metastases

**B. A. Z. Ü. KAMİL KUMANLIOĞLU**; EGE UNIVERCITY MEDICINE FACULTY NUCLEAR MEDICINE DEPARTMENT, İZMİR, TURKEY.

**Aim:** It may be difficult to diagnose peritoneal metastases using only CT. 18F-FDG PET/CT not only shows metastatic sites which cannot be diagnosed with CT, demonstrates additional peritoneal metastasis sites as well. The aim of our study is to evaulate the role of PET/CT in detecting peritoneal metastases and to compare the results within contrast enhanced CT. Our second aim is to identify various metabolic 18F-FDG retainment patterns in patients with proven peritoneal metastases. The third aim is to evaluate the role of PET/CT in determining primary site for cases in whom peritoneal metastasis has been proven cyto/histopathologically but the primary malignancy couldn't be detected. **Materials and Methods:** 29 cases who were investigated with PET/CT and contrast-enhanced abdominopelvic CT in recent time (within 45 days) were included in our study group and they were investigated retrospectively. In patients with no histologic/cytologic diagnosis, the results were correlated by radiologic/clinical follow-up. **Findings:** In 20 of 29 cases, the ultimate diagnosis of peritoneal metastasis was based on histologic(5)/cytologic(5) diagnosis or radiological/clinical observation without any histologic/cytologic investigation (10). Peritoneal aspiration cytology was negative in 3 of 9 patients who had peritoneal metastases according to PET/CT. When the PET/CT and CT images of 29 patients were investigated, in 17 patients peritoneal ascites, and in 5 patients omental cake appearance was observed. In 2 of 17 patients with peritoneal ascites, increased 18F-FDG retention was observed while in remaining 15 patients, SUVmax values were under 2,5. For 20 patients with proven metastases, in 2 patients diffuse metabolic pattern, in 12 patients nodular involvement pattern and in 6 patients both nodular and diffuse involvement patterns were observed. For the 4 patients in whose peritoneal biopsies, malignancy was detected and PET/CT was applied for the exploration of primary site, in 3 of them primary tumour could be detected. **Conclusion:** PET/CT is a useful diagnostic tool for situations in when peritoneal biopsy cannot be used or is non-diagnostic. We identified two patterns of displayable glucose patterns and warned the clinician for the possibility of peritonitis carcinomatosa in relevant clinical cases. In addition, we detected that PET/CT was more successful in locating primary site compared to contrast-enhanced abdominal CT. Due to this high level of success, the most effective treatment can be planned for peritoneal metastases; thus survival time of the patient increases. Our study shows that PET/CT has important contribution to CT in detecting peritoneal metastasis.

P07-1 - Sunday, Oct. 20, 16:00 - 16:30, Poster Exhibition Area

## Molecular & Multimodality Imaging: PET/CT

### P036
### Software registration of CT guided fine-needle aspiration biopsy with PET/CT

**A. Frenkel**[1], A. Bar Shalev[2], R. Rozenberg[1]; [1]Rambam Medical Center, Haifa, ISRAEL, [2]GE Healthcare, Haifa, ISRAEL.

**Aim**: To register PET/CT images with data of CT guided fine-needle aspiration (FNA) in order to improve the accuracy and decrease the false negative rate of histological results in assessment of lung masses**. Materials and Methods**: Patients with diagnosis of lung mass perform FDG-PET/CT for metabolic characterization of findings and CT-guided FNA for histological diagnosis. A software code was developed to register the corresponding images of the CT-guided FNA and PET/CT studies. The data input to the program includes a CT guided FNA image clearly showing the tip of the biopsy needle at the site where the aspiration of the lung mass was done and the transaxial chest slices of the PET/CT study. In cases of biopsy performed in prone or decubitus position PET/CT images are rotated to match the FNA scan. The matching CT slice of the PET/CT ($CT_{PET}$) is registered axially with the selected CT slice demonstrating the FNA needle tip ($CT_{FNA}$). Subsequently the slices are shifted and, when needed, rotated to accurately match the lesion in both CT images. After an accurate and rapid $CT_{PET}/CT_{FNA}$ registration, the same registration is applied to the PET which is inherently registered with the $CT_{PET}$. The use of the code by a radiologist was assessed. Acquisition parameters for both CT and PET were recorded. **Results**: The code was implemented on the Xeleris workstation (GE Healthcare). Training for a "naïve user", a radiologist was performed during a time period of less than 30 minutes. The duration of performing a whole registration process was below 5 minutes. Study parameters of both PET (SUV) and CT (HU) at the location of the tip of the FNA needle and SUV threshold based volumes can be accurately measurd from the respective images and the results are exported to an Excel format file for further processing. **Conclusion:** A software code was designed and implemented aiming to assess whether PET/CT-guided lung FNA can improve the accuracy and false negative rate of histological evaluation of lung masses. A user friendly code was developed employing prior PET/CT images registered with intraprocedural CT scans .

### P037
### Determination of muscular activity in the lower limb during walking using FDG-PET

S. Kolk[1], **E. P. Visser**[1], O. Schenk[2], W. J. G. Oyen[1], M. Gotthardt[1], V. Weerdesteyn[1], N. Verdonschot[1,2]; [1]Radboud University Nijmegen Medical Centre, Nijmegen, NETHERLANDS, [2]University of Twente, Enschede, NETHERLANDS.

***Aim*** The goal of the project "TLEMsafe" is to predict functional outcome of extensive orthopaedic interventions on the lower limb. Functional outcome is predicted using subject-specific musculo-skeletal (M-S) models. The most important model outcome is muscular activity during walking, which thus needs to be extensively validated, initially using healthy subjects. The purpose of this study was to determine the contribution of each muscle of the lower limb to walking. In contrast to other available Methods (e.g. electromyography), FDG-PET allows detailed study of muscular activity in walking, both for deep and superficial muscles [1]. The FDG accumulates in muscles that are active during walking. ***Methods*** Ten healthy subjects walked on a treadmill at their own comfortable walking speed for a total of 90 minutes, 60 minutes before and 30 minutes after intravenous injection of 50 MBq FDG. Subsequently, PET-CT scans of the lower limb were made on a Siemens mCT scanner using 4 min per bed position, time-of-flight detection and HD image reconstruction. Two-dimensional regions-of-interest (ROI) were drawn on cross-sectional slices of 5 mm thickness in 54 muscles by registering the CT images onto detailed anatomical MRI images. The ROIs were then superimposed on the PET images, yielding muscle FDG uptake. Mean standard uptake values ($SUV_{mean}$) were determined for these ROIs in all muscles. The muscle glucose consumption index (MGCI) was defined as $SUV_{mean}$ multiplied by blood glucose concentration and muscle volume of the cross sectional slices. ***Results*** The muscles with the highest MGCI were the soleus, gluteus medius, maximus, minimus, and gastrocnemius medialis with MGCI of $19.9\times10^{-3}$, $9.9\times10^{-3}$, $7.4\times10^{-3}$, $6.4\times10^{-3}$, and $6.2\times10^{-3}$ $g^2$/mL, respectively (averaged over all subjects and over left en right limbs). The corresponding $SUV_{mean}$ in these muscles were 3.03, 1.59, 0.81, 2.65 and 4.4l g/mL, respectively. There were no significant differences within subjects between dominant and non-dominant side (p=0.59), nor between subjects based on age (p=0.44) or gender (p=0.09). ***Conclusions*** Our data indicate that FDG-PET has a high discriminative ability for muscular activity during walking. These data are extremely valuable in the validation of M-S models. A limitation is that we only analyzed single slices, which might not fully represent whole muscle activity. A complete 3D analysis will be subject to future study. REFERENCES [1] N. Oi, et al., "FDG-PET imaging of lower extremity muscular activity during level walking". J Orthop Sci, Vol. 8, pp. 55-61, (2003).

### P038
### Imaging hepatic steatosis with FDG

**G. KERAMIDA**[1], J. Potts[2], J. Bush[1], S. Dizdarevic[2], S. Verma[2], M. A. Peters[2]; [1]Clinical Imaging Science Centre, Brighton, UNITED KINGDOM, [2]Department of Medicine, Brighton Sussex Medical School, Brighton, UNITED KINGDOM.

**Objectives:** Hepatic steatosis (HS) ranges from benign fatty liver to the serious condition of steatohepatitis (SH). No non-invasive Methods are available to diagnose SH before it progresses to cirrhosis. Previous studies on the relation between HS and hepatic FDG accumulation are contradictory. The aim of this study was to re-examine this relation taking into account the effects of blood glucose (BG) on liver FDG kinetics and the 'dilutional' effect of hepatic fat on the liver FDG signal. A positive relation between HS and liver FDG accumulation would provide the impetus to develop FDG-PET for diagnosing SH. **Methods:** FDG-PET/CT scans from 306 patients were retrospectively analysed. SUV was measured over blood pool (left ventricular cavity: $SUV_{LV}$) and liver ($SUV_{average}$ and $SUV_{max}$) at 60 min post-injection, avoiding any focal pathology. Liver fat was estimated from CT density using the equation: %fat = 32.8 - 0.59.Hounsfield units (HU) (Ricci et al; J Hepatol 1997;27:108-13). $SUV_{average}$ was adjusted for fat by division with 1-[%fat/100]. CT density of <40 HU was taken as indicating fatty liver. **Results:** $SUV_{max}$ and $SUV_{average}$ both increased as BG increased up to values of 8-10 mmol/l but tended to decrease at BG >10 mmol/l. $SUV_{max}/SUV_{LV}$ and $SUV_{average}/SUV_{LV}$ were independent of BG, suggesting dynamic equilibrium between blood and hepatocyte FDG. CT density showed no correlation with $SUV_{average}$ (r = -0.08) but correlated inversely with $SUV_{max}$ (r = -0.31; p<0.001). Critically, the difference between $SUV_{max}$ and $SUV_{average}$ correlated more strongly with CT density (r = -0.39), suggesting that $SUV_{average}$ is 'diluted' by hepatic fat. Accordingly, fat-adjusted $SUV_{average}$ continued to increase at BG >10 mmol/l. Moreover, fat-adjusted $SUV_{average}/SUV_{LV}$, unlike non-adjusted $SUV_{average}/SUV_{LV}$, correlated positively with BG. When patients were divided into <40 HU (n=71) and >40 HU (n=235) groups, fat-adjusted $SUV_{average}$ increased with increasing BG in both groups, with the <40 HU group about 0.4 g/ml higher than the >40 HU group. Fat-adjusted $SUV_{average}/SUV_{LV}$ increased with increasing BG in the HU <40 group but not the HU >40 group.**Conclusions:** Because of rapid intrahepatic FDG dephosphorylation, hepatocyte and blood FDG concentrations are linked, suggesting that the majority of the hepatic FDG signal is from blood pool. However, after allowing for BG levels and adjusting for liver fat, an additional significant FDG signal is seen in HS that we speculate arises from infiltrating inflammatory cells. We suggest that with methodological development, FDG-PET may be useful for monitoring patients with HS and identifying those with SH.

### P039
### How we reduce five times brown fat frequency of occurence.

**M. Roudas**, V. Manukova, A. Luosev, E. Panchkovskaya, A. Kopyrin; Central Clinical Hospital at the Management Department of the President of the Russian Federation, Nuclear Medicine Department,, Moscow, RUSSIAN FEDERATION.

**Aim**. Uptake in the so-called brown fat appears to be present of 2-4% of patients. It is thought that this fat is used for nonshivering thermoregulation. Very often brown fat can exhibit strong uptake, extended or local. The location of brown fat is mainly in the neck and shoulders area, but can go also along the spine and around upper abdominal organs in a symmetrical fashion, rare unilateral. It is noted more frequently in patients after chemotherapy, and if not recognized properly, it can be easily mistaken as a pathological lesion. The best way to minimize uptake into brown fat is to control temperature. **Materials and Methods**. Before January 2009 y. 1711 PET studies were performed at our department. All patients were imaged using a standard clinical PET protocol with a time interval between injection and scanning not less than 60 min. 83 patients (4.8%) demonstrated considerable FDG uptake in the brown fat. Getting out of this pitfall the following measures were assumed. **Results**. Firstly, the temperature in the waiting and uptake rooms was raised up to 28-30 C (empirically fitted numbers). Next step was to warm up patients on the inside. We have found the means of doing it by giving them about two glasses of hot water (tea temperature- empirically fitted temperature and volume as well) before injection. New procedure started at the beginning of 2009 y. and we were thrilled by the results. During 2009-2012 yy. 4653 patients were imaged and only 44 (0.9%) had uptake in that bothering brown fat- five times less than before.**Conclusions**. To reduce brown fat frequency five times one should keep quite high temperature in the uptake and waiting rooms and give patients some hot water.

### P040
### Comparison of the intestinal 18F-FDG uptake in diabetic patients treated with metformin versus a control group

**M. Ochoa-Figueroa**[1], D. Cabello-García[2], A. Allende-Riera[2], V. Sánchez-Rodríguez[2], C. Cárdenas-Negro[2], E. Martínez-Gimeno[2], J. Uña-Gorospe[2], J. Muñoz-Iglesias[2], M. De Sequera-Rahola[2]; [1]UMSNH, Morelia, MEXICO, [2]Hospital Universitario de Nuestra Señora de La Candelaria, Santa Cruz de Tenerife, SPAIN.

**Purpose:** To determine the degree of intestinal 18F-FDG uptake in type 2 diabetic patients under treatment with metformin in comparison with a control group, using a low dose 18F-FDG protocol. **Materials and Methods**: A retrospective study which initially included 120 patients referred to our service for a PET-CT scan, excluding 2 diabetic patients because they were not taking metformin, thus studying 118 patients (53 females and 65 males, mean age 60). The PET-CT scans were performed 60-90 minutes after the i.v. injection of a mean 18F-FDG dose of 2.77±0.4MBq/kg. The patients were divided in 2 groups: Group 1 included 58 patients diagnosed of diabetes type 2 under treatment with metformin and in group 2 we included 60 non diabetic patients as controls. 18F-FDG uptake in small intestine and colon was visually graded using a previously published semi-quantitatively scale and semi-quantitatively measured using the maximum standardized uptake value (SUVmax) in both groups, measuring the activity in the duodenum, jejunum, ileum, hepatic flexure, splenic flexure and sigmoid colon, respectively. **Results**: 18F-FDG bowel uptake was significantly increased in group 1 compared with group 2 and was at least twice as much higher in the colon than in the small intestine. Bowel uptake pattern in group 1 was intense, diffuse and continuous along the bowel, predominantly in the colon. The mean SUVmax values for group 1 were as follows: duodenum 3.37, jejunum 3.30, ileum 4.37, hepatic flexure 6.04, splenic flexure 6.10 and sigmoid colon 9.28. For group 2: duodenum 2.46, jejunum 2.37, ileum 2.57, hepatic flexure 2.26, splenic flexure 2.03 and sigmoid colon 3.03. **Conclusion**: Our results suggest that the use of metformin in type 2 diabetic patients significantly increase the uptake of 18F-FDG in the colon and to a lesser extent in the small intestine, strengthening the idea that metformin should be retired previous the performance of a 18F-FDG PET-CT study in patients which require a evaluation of intraabdominal lesions.

## P041

### Evaluation of Normal Adrenal Gland Uptake on 18F-FDG PET/CT

**M. KESKIN**, S. TURKOLMEZ, N. YILDIRIM POYRAZ, Z. KANDEMIR, E. OZDEMIR; Department of Nuclear Medicine, Ataturk Educational and Training Hospital, Ankara, TURKEY.

**PURPOSE:** On visual evaluation of PET / CT images; normal uptake of adrenal glands may vary. While focal uptake is usually an abnormal finding; bilateral involvement may indicate different pathologies, depending on severity of the uptake. Mild adrenal gland uptake is frequently encountered on oncologic PET/CT scans, sometimes leading to difficulties in determining and staging or a requirement for an additional investigation. In a present study, uptake values of normal adrenal glands are intended to provide additional information to interpreters. **METHODS:** 32 patients (16M/16F) referred to the characterization of solitary pulmonary nodules were included and evaluated retrospectively. No pathological uptake of the whole body scan were detected. Liver, spleen and adrenal glands were morphologically normal on the CT images. Same dimensions of regions of interests (ROI) from liver, spleen, adrenal glands were drawn and SUVmax values of these areas, adrenal gland/liver SUVmax ratio and adrenal gland /spleen SUVmax ratios were recorded. **RESULTS:** The normal SUV max values of adrenal glands ranged from 1.51 to 4.58, the mean value was 2.41. Normal SUV max values for the liver ranged from 1.97 to 3.75 (mean: 2.81)and for spleen 1.43 to 3.2 (mean: 2.35). Adrenal gland/liver SUVmax average rate was 0.85, adrenal gland/spleen SUVmax average rate was 1.02. **CONCLUSION:** On PET / CT scans; normal uptake of adrenal glands may vary but usually correlates with liver and spleen uptake values. Therefore, we think that adrenal gland / liver SUVmax ratios and adrenal gland/spleen SUVmax ratios may be useful in the interpretation.

P08-1 - Sunday, Oct. 20, 16:00 - 16:30, Poster Exhibition Area

## Molecular & Multimodality Imaging: SPECT/CT

## P042

### Preoperative $^{99}$mTc-Sestamibi Scintigraphy in Patients with Primary Hyperparathyroidism: Comparison of SPECT/CT and Planar Imaging.

**A. Mhiri**, I. Slim; MF. Ben Slimène.; DEPARTMENT OF NUCLEAR MEDICINE, SALAH AZAIEZ INSTITUT, EL MANAR II UNIVERSITY, TUNIS, TUNISIA., Tunis, TUNISIA.

**INTRODUCTION:** Primary hyperparathyroidism is a common cause of hypercalcemia in the outpatient population. It is usually caused by a single parathyroid adenoma in the majority of cases while less frequent causes include double adenoma, parathyroid hyperplasia, and parathyroid carcinoma. Sestamibi-technetium 99m scintigraphy (sestamibi) has been considered essential component of focused parathyroidectomy often complemented by ultrasound (US). Actually, single-photon emission computed tomography associated to computed tomography (SPECT/CT) imaging is considered as a recent advancement in preoperative parathyroid localization that may have further impact in the planning and success of targeted parathyroidectomy. AIM: The purpose of this study was to compare the diagnostic accuracy of 99mTc-sestamibi planar scintigraphy to SPECT/CT for the localization of abnormal parathyroid glands in patients with primary hyperparathyroidism. **METHODS**: We evaluate 50 patients with biochemical diagnosis of hyperparathyroidism (27 patients with primary hyperparathyroidism (PHP) and 22 patients with secondary hyperparathyroidism (SHP)). All of them underwent an optimized parathyroid scintigraphic protocol based on planar imaging with dual-phase, dual-tracer scintigraphy and an early SPECT-CT study. Scintigraphic imaging protocol included: thyroid exam with 50 MBq of pertechnetate and dual-phase parathyroid planar study (at 10 min and 150 min) post 99mTc-Sestamibi (740 MBq) injection. SPECT /low dose CT of the neck and chest was acquired with a Symbia T camera at early phase (30-40 min after Sestamibi injection). **RESULTS:** Planar imaging identified hyperfunctioning parathyroid glands in 35 patients: 21 with PHP and 14 with SHP, while SPECT/CT detected hyperfunctioning parathyroid glands in 42 patients: 32 with PHP and 10 with SHP. Discordant planar - SPECT/CT information was obtained in 15 patients. DISCUSSION: 99mTc-sestamibi is the most commonly used radiotracer for imaging the parathyroid glands and has been extensively studied in the setting of primary hyperparathyroidism. Sestamibi is taken up by both the thyroid and parathyroid glands, but adenomatous and hyperplastic parathyroid tissue shows more avid uptake of the radiotracer and often retains the radiotracer longer than adjacent thyroid tissue. Asymmetric foci of increased radiotracer uptake on early images can be seen, representing abnormal parathyroid tissue superimposed on the normal thyroid. SPECT/CT of the neck and chest can help to differentiate parathyroid activity from the overlying thyroid and to detect ectopic parathyroid adenomas. Also, it has been shown to increase the sensitivity of scintigraphic parathyroid imaging. **CONCLUSION**: We would suggest the use of SPECT/CT mostly for a workup of all patients with ectopic glands who are scheduled for minimally invasive parathyroid surgery.

## P043

### The Comparison of Operation Results and Tc99m-Sestamibi Parathyroid Scintigraphy SPECT/CT Findings in Patients who were Operated due to Hyperparathyroidism

**M. F. GECER**[1], E. YILMAZ[1], E. G. ISIK[1], S. KUYUMCU[1], Z. G. OZKAN[1], B. OZCINAR[2], Y. ERBIL[2], S. N. UNAL[1]; [1]Istanbul Medicine Faculty, Nuclear Medicine Department, Istanbul, TURKEY, [2]Istanbul Medicine Faculty, General Surgery Department, Istanbul, TURKEY.

**Purpose**: For patients examined due to hyperparathyroidism, it is important to determine and localize the parathyroid lesions for excising them with minimal invasive surgery. With this purpose; we researched the contributions of Tc99m-sestamibi parathyroid scintigraphy findings on anatomically definition of parathyroid lesions in patients who were operated due to hyperparathyroidism,then we compared their cohesiveness with operation results. **Method**: 44 female and 11 male, totally 55 patients who were examined in our department between June 2010 and December 2011, then operated in General Surgery Service were retrospectively evaluated, the mean age was 53.2±10.4 (21-78). 48 patients were in follow-up due to primary hyperparathyroidism, 2 patients had chronic renal failure and were thought to have tertiary hyperparathyroidism, 2 patients were suspected to have parathyroid carcinoma, 3 patients were thought to have parathyroid hyperplasia (2 had Multiple Endocrine Neoplasia (MEN) I syndrome and 1 had MEN II syndrome). The mean parathyroid hormone(PTH) level of patients was 375pg/ml (69-3173) and mean serum calcium level was 11.4mg/dl (9.3-17.8). Among 47 patients examined via ultrasonography; reported findings were parathyroid adenoma in 28 patients, parathyroid hyperplasia in 5 patients, parathyroid carcinoma suspect in 1 patient, and multinodular thyroid gland in 32 patients. After injection of 20mCi Tc99m-sestamibi; double phased MIBI parathyroid scintigraphy was performed through immediate planar imaging at 10$^{th}$ minute, SPECT at 30$^{th}$ minute and delayed planar imaging at 2$^{nd}$ hour. Thyroid scintigraphy was performed with Tc99m-perteknetat at next day. Also in order to determine the anatomical localization, CT was performed in neck and mediastinum regions. Planar imaging and SPECT/CT fusion images were evaluated together,the determined focal MIBI uptakes were reported. Findings: In only 1 of 55 patients, there was no pathologic finding for suspecting the parathyroid lesion as a result of scintigraphy. In 47 of 55 patients (85%), the parathyroid lesion localizations which were anatomically determined in parathyroid scintigraphy were evaluated as true positive with operation results. While there is no pathologic finding in planar imaging in 4 of 47 patients, parathyroid lesion was detected in SPECT/CT images. In rest 8 patients (15%), the scintigraphy misidentified paratyhroid lesions when compared with operation results. **Result**: It is known that SPECT images gives additional information to planar imaging in evaluation of parathyroid lesions,and increases the sensitivity of scintigraphy. When SPECT images are evaluated by fusing with CT slices, it helps the determination and identification of parathyroid

lesion's adjacency with thyroid gland especially in patients with multinodular goiter.

## P044

### SPECT-CT imagings of the thyroid and/or parathyroid glands: reflexions around Mr Hounsfield's contributions

**P. Bourgeois**, B. Vanderlinden; Institute Jules Bordet, Brussels, BELGIUM.

SPECT-CT imaging is now the standard approach for some organs and/or investigations in nuclear medicine. The interest of the SPECT-CT approach has been largely stressed to image and localize the para-thyroid glands. In the case of the thyroid glands, SPECT-CT allows also to define « cold » and/or « hot » nodules better than with planar imagings. However, the informations present in the CT are underused. In fact, (Dr) Hounsfield's units (HU) define the « densities » of the tissues on the classical CT scale and, of interest, normal thyroid tissues contain their « own » specific « contrast agent »··· the iodine-127 which HU are +100 to +110. Consequently, when displaying SPECT-CT results, if you apply on your CT slides a scale between 0 and +110 HU, you put directly in relation the tissular uptake of your radio-tracer (123-I, 99m-TcO4, 99m-Tc-MIBI) with the naturally « iodinated » thyroid tissues. The application of such a scaling to the thyroid and/or parathyroid glands imagings is simply fascinating. The nodules described by the echographist are now on « our » display : around 0 HU, these are cysts : around 40-70 HU, they are solid : but if they are around 100-110 HU, this is normal thyroid tissue. The « structure » of the thyroid tissues may now be said homogenous or heterogenous. A contrario, some tissues with a normal iodine « content » may appear scintigraphically hypo-funtional whereas « hot » nodules may show either a normal, or a decreased iodine content. In one patient with hyper-para-thyroidy, if your MIBI spot does not contain iodine, that is your adenoma? Several examples illustrating these Hounsfield's contributions will be shown on the poster.

## P045

### Iodine-123 MIBG imaging: the incremental value of SPECT-CT fusion images in the detection phéochromocytoma compared to Planar imaging

**A. Mhiri**, I. Slim; I. Yeddes; I. Elbez ; I. Meddeb; A. Bahloul; T. Ben Ghachem; H. Charfi; MF. Ben Slimène.; DEPARTMENT OF NUCLEAR MEDICINE, SALAH AZAIEZ INSTITUT, EL MANAR II UNIVERSITY, TUNIS, TUNISIA., Tunis, TUNISIA.

Pheochromocytoma is the most common tumor of the adrenal medulla and the sympathetic and parasympathetic systems occurring in adults. Iodine-123 metaiodobenzylguanidine (123 I-MIBG) scintigraphy has good sensitivity and specificity of this neoplasm. The aim of our study is to evaluate the impact of SPECT-CT fusion images on the diagnosis of phéochromocytoma. Methods: We evaluate 35 patients (20 M, 15 F) followed for suspected pheochromocytoma based on symptoms of catecholamine excess, CT findings, or elevated catecholamine or metanephrine levels. All patients underwent whole-body planar imaging 18-24 hr following IV administration of 5-8 mCi (185-296 MBq) 123 I-MIBG. SPECT -low dose CT was performed with a Symbia T camera in all patients. Final diagnoses were based on histopathology, correlative imaging, catecholamine or metanephrine measurements, and clinical follow-up. Results: Among the 35 patients with definitive diagnoses (disease present: 17 and disease absent: 18), 123 I-MIBG planar scintigraphy had a sensitivity of 82% and a specificity of 100%. SPECT-CT imaging improve diagnostic confidence in all patient and provide additional diagnostic information in 5 patients with negative planar scans (small extra-adrenal pheochromocytoma in two cases). The addition of SPECT-CT increased the sensitivity to 87% but the specificity decrease to 90%. Discussion-Conclusion: In pheochromocytoma, early detection of relapse is understandably crucial and has a major impact on treatment and prognosis. In the detection of this tumor, using I-123 MIBG, planar imaging alone may not provide conclusive results. SPECT-CT has been shown to demonstrate a higher value of diagnostic information particularly in patients with negative planar scans and should be performed routinely in conjunction with planar imaging.

## P046

### The role of MIBG SPECT/CT in children with neuroblastoma compared to planar images

**A. Mhiri**, I. Slim; I. Elbez; I. Yeddes; I. Meddeb; A. Bahloul; T. Ben Ghachem; H. Charfi; MF. Ben Slimène.; DEPARTMENT OF NUCLEAR MEDICINE, SALAH AZAIEZ INSTITUT, EL MANAR II UNIVERSITY, TUNIS, TUNISIA., Tunis, TUNISIA.

In neuroblastoma, morphologic imaging modalities, such as CT or MRI, offer high sensitivity for the detection of the tumor. 123I-MIBG sintigraphy is also helpful for the detection of extra-adrenal tumor sites. Actually there is an increasing interest with SPECT/CT systems. SPECT in combination with CT enables a direct correlation of anatomic information and functional information, resulting in better localization and definition of scintigraphic findings. Our aim is to evaluate the added value of SPECT/CT over planar images in MIBG scans of children with neuroblastoma. **Methods:** We evaluate 34 children followed for neuroblastoma in different clinical phases (24 for diagnosing and staging and 10 for monitoring response to therapy). All patients underwent planar imaging 18-24 hr following IV administration of 123I-MIBG. SPECT /low dose CT was performed with a Symbia T camera. **Results**: Uptake of 123I-MIBG by the primary tumour occurred in 88%. Planar imaging showed bone and/or bone marrow involvement 10 patients with hepatic metastases in 3 of them. Among the 10 children studied for evaluating the response to therapy 4 patients were in remission (good responders) and 6 were bad responders and they benefit of a change of treatment. Overall, SPECT/CT provided additional information over planar imaging in 60% of studies. Discussion: 11C-HED PET/CT was demonstrated to show a higher spatial resolution and to return a final diagnosis within 30 min. SPECT/CT was compromised by a longer examination time and the need for delayed imaging (24 h after tracer administration). However, no superiority of PET/CT over SPECT/CT was observed. Because of the high cost and low availability of 11C, 123I-MIBG SPECT/CT seems to be appropriate for the imaging of tumors derived from the sympathetic nervous system, such as neuroblastoma. According to literature data, our results confirm the added value of SPECT/CT over planar imaging in the diagnosis, staging and follow-up of neuroblastoma **Conclusion**: SPECT/CT can improve the diagnostic accuracy of MIBG studies in children with neuroblastoma mainly by excluding malignancy in sites of physiologic and benign uptake in the soft tissues.

## P047

### Incrimental Value of SPET/CT Image Fusion in the Assessment of Neuroendocrine Tumours with 111In-Pentetreotide Scintigraphy

**A. Mhiri**, I. Slim; MF. Ben Slimène.; DEPARTMENT OF NUCLEAR MEDICINE, SALAH AZAIEZ INSTITUT, EL MANAR II UNIVERSITY, TUNIS, TUNISIA., Tunis, TUNISIA.

**INTRODUCTION:** Single photon emission computed tomography related to computed tomography (SPECT/CT) imaging is an efficient method which allows the fusion of functional and anatomic information over Somatostatin receptor scintigraphy (SRS) for the investigation of neuroendocrine tumors. This study evaluates the impact of SPECT/CT on routine planar Somatostatin receptor scintigraphy study interpretation. **METHODS**: Thirty five patients were studied with routine planar SRS and SPECT/CT at 4, 24 and optionally 48 h after injection of 185-222MBq 111In-pentetreotide. Eight patients were evaluated for gastric tumours, ten for endocrine pancreatic tumours, nine for midgut tumors, four for other NETs and four others for metastatic NET of unknown primary. SPECT/CT induced improvement in the interpretation of SPECT and conventional CT and resultant clinical management changes were recorded. **RESULTS**: Planar scintigraphy was negative in 12 patients, positive in 15 patients and doubtful in 8 patients. SPECT/CT was positive in 16 patients, confirming doubtful foci in 5 patients and showing unsuspected foci in 6 negative planar images. Fused images affected the diagnostic interpretation of planar imaging in 62 % of cases and induced changes in management in some patients. **DISCUSSION-CONCLUSION**: SRS is a functional imaging modality for neuroendocrine tumors. It has the potential to define the extent of metastatic disease, to localize the primary occult tumor site, and to identify the receptor status of metastases. However, the detection of NET remains challenging, due to their usually reduced dimensions and poorly defined anatomic localization. Its specificity may also be affected by tracer uptake at physiological sites or benign conditions. SPECT/CT offers superior lesion localization, an identification of physiologic activity, and additional anatomic information derived from the non diagnostic CT portion of the study. It improves guidance of invasive diagnostic and therapeutic procedures and may help in monitoring therapeutic outcomes.

## P048

### Quantitative Evaluation of the Somatostatin Receptor SPECT-CT Studies

**E. Schmidt**[1], V. Husz[2], K. Somogyi[2], K. Derczy[3], Z. Szabo[1], S. Szekeres[1], K. Zambo[1]; [1]University of Pecs Department of Nuclear Medicine, PECS, HUNGARY, [2]University of Pecs Medical School, PECS, HUNGARY, [3]University of Pecs Department of Radiology, Pecs, HUNGARY.

Somatostatin analoges play a key role in the diagnosis of neuroendocrine tumors. The aim of our study was to determine such quantitative values, which can help to differentiate the origin of foci, whether they are tumors or not. Between 01-Jan-2008 and 31-Dec-2011 we performed examinations of 55 patients (22 males and 33 females, mean age: 55 years). After the intravenous injection of In111-Octreoscan, in the 24th and 48th hours, planar and SPECT images were performed of the skull, neck, chest, abdomen, pelvic, which was complemented by a low dose CT scan using SPECT/CT fusion technique. During our research 178 foci of 55 patients were evaluated using the images of the 48th hour based on the VOI maximum counts of each focus, which was compared with values of the spleen (higher physiological activity) and with the values of the lungs (lower uptake). Because of the

physiological increased uptake of the liver, we distingished intrahepatic foci and foci with other localisations, and we separated true positive and false positive cases on the results of histological examinations, other imaging Methods (CT, MRI, US) and/or the history of each patients. Out of the examined 178 foci, 60 were detected in the liver and out of them 5 were false-positive. Of the rest foci with other localisations 48 proved to be false positive. While the mean rates of the intrahepatic tumorous foci compared with the spleen is 1.65±2.03, the mean values of false-positive cases amount to 0.67±0.44. A significant difference was found between these two groups (p<0,05). When compared with the lungs, the mean rates of true-positive foci localised in the liver are 21.40±23.23, the values of the false positive cases however are 13.97±12.09. This differece has not proved to be significant. As for the foci located in the other organs or areas, the mean focus/spleen rate was 0.64±1.21, while in the case of false-positive accumulations the rate was 0.21±0.15. The difference was significant (p<0,001) and also a significant difference (p<0,01) was found in true (10.84±10.36) and false (7.99±12.96) positive foci of other localisations in the mean focus/lung activity ratio. **Conclusion:** This quantitative method can help to evaluate patients with foci of unclear origin. Our further aim is to determine such rate values through the refinement and standardisation of this technique (considering localisations and the histology), which could offer a solution to distinguish true and false postive foci thereby increasing the diagnostic accuracy.

## P049

### The role of the hybrid imaging techniques SPECT-CT and PET-CT for diagnostic algorithm in patients with carcinoid tumors

**I. Kostadinova**, S. Ivanova, J. Mihailova; Medical University, Sofia, BULGARIA.

Somatostatin receptor scintigraphy (SRS) is known to be highly sensitive for diagnosis of primary carcinoid tumors, regional lymph nodes' and distant metastasis, in many cases performing superior to CT and MRI. The aim of our study was to show our first experience in the application of the hybrid imaging techniques SPECT-CT and PET-CT in the diagnostic algorithm of patients with a proven carcinoid tumors for staging, localization and evaluation of the therapy. In total 20 patients (with proven or suspected gastroenteropancreatic or lung localization) were investigated, using the new somatostatine analog 99mTc-HYNIC-TOC (Tektrotyd,PL) at activity between 370-550 MBq. The average level of chromogranine was 215ng/ml and that of Ki 67-23%. Whole body and SPECT-CT scintigraphy were performed 2- 4h p.i. In 6/20 of the patients, in whom Ki 67 was above 2% and tumor localization and/ or stage still unclear after the examination, PET-CT (using an average 370 MBq 18F-FDG) was additionally applied within one week. The SRS was true positive in 16/20 of the patients, true negative in 3/20 ( after therapy) and 1/20 false negative, while PET-CT was positive in all investigated 6 patients with more aggressive behavior and helped for localizing of the primary tumor. All patients with positive scintigraphies were referred for surgery or somatostatin therapy and/or chemotherapy depending on the stage and the differentiation of the disease. Our first data showed that 99mTc-HYNIC-TOC was very promising, cheap, convenient and with comparable sensitivity (95%) to the other SR radiopharmaceuticals. In summary, we suggest that SRS using the new 99mTc-HYNIC-TOC and SPECT-CT technique are very reliable in patients with carcinoid tumors. The therapeutic strategy could be optimized additionally applying 18F-FDG PET-CT in some of the patients.

## P050

### The Evaluation of Increased Uptake on Iodine -131 SPECT/CT in Post Thyroidectomy Thyroid Cancer Patient and Its Correlation with Biochemical Markers.

**S. J. Ong**, F. Dambha, E. Nowosinska, J. Buscombe; Addenbrookes Hospital, Cambridge, UNITED KINGDOM.

**Aim**: To assess sites of iodine-131 (I-131) uptake in post ablation SPECT/CT imaging and to correlate these findings with thyroid stimulating hormone (TSH), thyroglobulin (Thb), anti-thyroglobulin antibody (ThbAb) and histological results. **Materials and Methods**: Planar and site specific SPECT/CT were performed 4 days after administration of I-131 for ablation of post surgical thyroid remnant. Sites of uptake were identified and results correlated with plasma TSH, Thb and ThbAb. Histopathology of the primary tumour was reviewed. **Results**: A total of 44 patients were identified over a 12 month period (15male, 39 female) with a mean age of 56.5 (SD 17.1, range 18-84) received ablation doses of I-131 post thyroidectomy. 10 patients had uptake outside the thyroid bed consistent with metastatic disease (5 papillary, 3 follicular, 1 follicular like papillary, 1 other) and 4 patients demonstrated lymph node involvement (2 papillary and 2 follicular). 9 patients demonstrated no abnormal I-131 uptake (8 papillary, 1 follicular) while the remaining patients demonstrated uptake in the residual thyroid bed or thyroglossal tract. Patients with metastatic diseases had an average TSH of 50.4 mU/l, Thb of 122 ug/l and a ThbAb of 39 kU/l. Patients with I-131 avid nodes had average TSH of 71 mU/l, Thb of 22 ug/l and ThbAb of 13.6 kU/l. Patients with thyroid bed/thyroglossal duct activity only had values of 63 mU/l, 48.5 ug/l and 47.8 kU/l while patients with no abnormal I-131 activity had values of 77.6 mU/l, 38.9 ug/l and 16 kU/l respectively. **Conclusion:** Thyroglossal tract and thyroid bed uptake is frequently seen in post thyroidectomy I-131 ablation therapy. However, this does not have a significant effect on the levels of thyroid stimulating hormone, thyroglobulin and anti-thyroglobulin antibody among the patient population undergoing I-131 ablation. However there is a strong trend towards increased markedly levels of thyroglobulin in patients with metastatic lesions identified in SPECT CT. Therefore, we suggest that SPECT CT should be considered over planar imaging in I-131 ablation therapy should the patient present with high thyroglobulin levels.

## P051

### Whole Body Bone Scintigraphy, SPECT and SPECT/CT in Patients with Breast Cancer

**M. Y. Smolyarchuk**, G. Davydov; MRRC of the Russian Ministry of Health, Obninsk, RUSSIAN FEDERATION.

**Aim**: Bone scintigraphy is commonly used as a screening method to search bone metastases of cancer, including breast cancer, which is one of the most common oncologic disease. Due to low specificity in differentiation of specific and degenerative-dystrophic changes, as well as difficulties in visualization of lytic metastases, results of whole body scintigraphy (WBS) with labelled bone imaging pharmaceuticals turn out to be false. The introduction of SPECT/CT into clinical practice raises the question whether this study can improve the sensitivity and specificity of the radionuclide method. **Materials and Methods**: 45 patients (range 44-79 years) with breast cancer were studied. Scintigraphic studies were performed after intravenous injection of 740-925 MBq 99mTc-labelled bone imaging pharmaceuticals. In 3 hours after injection whole-body scintigraphy was performed followed by SPECT/CT with low dose CT mode if there were areas suspicious for metastatic lesions. Images evaluated by WBS, SPECT and SPECT/CT were assessed separately. All the results were verified using MRI, trepanobiopsy and observation over time. **Results:** The results of per lesion analysis were as follows: WBS-sensitivity 78%, specificity 69%; SPECT- sensitivity 85%, specificity 75%; SPECT/CT sensitivity 96% and specificity 90%. Results of per patient analysis were as follows: WBS-sensitivity 80% specificity 65%; SPECT- sensitivity 88%, specificity 76%; SPECT/CT sensitivity 94%, specificity 92%. False negative results by SPECT/CT were associated with metastatic lesions in bone marrow without changes in bone trabecules that were detected on MRI and confirmed histologically. In addition, a single changes in the ribs remained equivocal and were differentiated only in observation over time. A false positive result in one patient was associated with prevalent widespread osteosclerosis of nonspecific genesis. **Conclusion**: SPECT significantly increases the sensitivity and specificity of bone scintigraphy, particularly in the spine and pelvis bones. SPECT/CT dramatically increases information through identification of lytic metastases. However, neither method is not reliable enough in the differentiation of single changes in the ribs.

P09-1 - Sunday, Oct. 20, 16:00 - 16:30, Poster Exhibition Area

## Molecular & Multimodality Imaging: PET/CT

## P052

### Extension of mandibular squamous cell carcinoma with PET/CT dedicated analysis software: 18F-NAF versus 18F-FDG.

**R. Lopez**[1], P. Gantet[2], A. Julian[3], A. Hitzel[3], B. Herbault-Barres[4], C. Fontan[5], P. Celsis[6], P. Payoux[3]; [1]Purpan Hospital Department of Maxillo-Facial Surgery, Toulouse, FRANCE, [2]Paul Sabatier University, Toulouse, FRANCE, [3]Purpan Hospital Department of Nuclear Medicine, Toulouse, FRANCE, [4]Purpan Hospital Department of Anatomopathology, Toulouse, FRANCE, [5]Purpan Hospital Department of Radiopharmacy, Toulouse, FRANCE, [6]Purpan Hospital INSERM Laboratory, Toulouse, FRANCE.

**Aim**: The aim of this work is to propose a new approach in mandibular imaging of squamous cell carcinoma of the oral cavity, with an innovative FDG/NaF image analysis using dedicated software. Patients and Methods: A prospective study was carried out from November 2010 to August 2012. Fifteen patients with oral cavity squamous cell carcinoma extending to the mandible underwent 18F-NaF and 18F-FDG PET/CT. We compared the delineation of bone invasion obtained with 18F-NaF and 18F-FDG PET/CT with the results of pathological analysis of mandibular resection. In order to carry out this comparison, a method for visualisation and quantification of PET images was developed. This new approach was based on the one hand on linear imaging of the mandible, placing hybrid images (CT and PET) in the same spatial reference as that used when cutting histology sections, and, on the other hand, on a process of quantification of radioactive activity within mandibular bone that objectively defined the significant limits of this activity on the PET images. The spatial limits obtained by analysis of the PET/CT images were

compared with those obtained by histopathological examination. **Results:** Take with pathology as reference 18F-NaF PET/CT was significantly more accurate than 18F-FDG PET/CT in assessment of intraosseous extension of oral cavity squamous cell carcinoma. **Conclusion**: 18F-NaF is a more useful bone marker than 18F-FDG for assessment of intraosseous mandibular extension of cancers of the oral cavity. With this radioactive tracer, the dedicated software enables objective delineation of radioactive activity within the bone, with very encouraging results. This new approach to mandibular imaging of cancers of the oral cavity should be tested in routine clinical practice.

## P053

### 18F-FDG-PET/CT in the Evaluation of Solid Pulmonary Nodules (SPN). Role of Dual Phase Imaging

**F. Vlachou**[1], V. Fillippi[1], A. Nikaki[1], D. Savvidou[1], T. Pipikos[1], K. Iliadis[2], S. Merisoglou[1], V. Papoutsis[1], R. Efthymiadou[1], V. Prassopoulos[1]; [1]DTCA Hygeia Department of PET/CT, Athens, GREECE, [2]DTCA Hygeia Thoracic Surgery Clinic, Athens, GREECE.

**AIM:** SPN is a challenging imaging finding for the clinician. In the work-up of an SPN, FDG PET/CT is a very important imaging modality. SUVmax cut-off of 2,5 is the standard method for discrimination between benign and malignant lesions. The value of delayed FDG imaging has been evaluated as well as its contribution to the assessment of SPNs. **Materials and Methods**: After intravenous administration of mean 374 MBq F18-FDG 32 patients underwent PET/CT examination with Siemens Biograph 16, adding a 120 min delayed imaging of the chest to the standard 60 minute acquisition. The size of the SPN and SUVmax at 60 and 120 minutes were measured. Histologic report was available when the SPN was resected; otherwise 1 year follow up was used as end point of the study. **Results**: 23/32 SPNs proved to be malignant. Using the SUVmax cut-off of 2,5 13/23(40%) were identified correctly. Overall the method showed very high specificity (100%), PPV (100%), and low sensitivity (57%) NPV (43%). Dual phase imaging method (increasing SUVmax indicating malignancy) identified 19/23 malignant lesions, having sensitivity, specificity, PPV and NPV respectively: 82%, 67%, 87%, 60%. In the group of SPNs with SUVmax < 2,5 , 10/19 nodules were malignant 8 of which were diagnosed correctly with the delayed imaging method. Two false negative results were to be adenocarcinomas. Three false positive results occurred ;( 1 amartoma, one inflammatory lesion and one granuloma). Careful inspection of the CT characteristics can exclude in some cases at least some of the false positive results. **Conclusion**: The role of late imaging is important for lesions with SUVmax < 2,5 because of the high sensitivity of the method in this group. Malignant lesions that are missed with the standard method can be identified correctly using the rising SUVmax method. However, extra caution is needed because of method's specificity. Careful inspection of the CT images can raise the specificity of the method increasing the diagnostic value.

## P054

### 18F-FDG-PET/CT in Hodgkin Disease (HD) Patients Who Receive Autologous Transplantation

**A. Nikaki**[1], V. Fillippi[1], F. Vlachou[1], D. Savvidou[1], T. Vassilakopoulos[2], M. Aggellopoulou[2], M. Moschogianni[3], R. Efthymiadou[1], V. Prassopoulos[1]; [1]DTCA Hygeia Department of PET/CT, Athens, GREECE, [2]Laiko Hospital Hematologic Department, Athens, GREECE, [3]Apolloneio Hospital Hematologic Department, Athens, GREECE.

**Purpose**: the purpose of this study was to investigate the correlation of pre-transplantation PET/CT with the after- transplantation PET/CT and further outcome of the disease, using Deauville criteria**. Methods**: we retrospectively examined the files of patients with HD who underwent autologous transplantation and were reported for 18F-FDG-PET/CT examination. In total, 27 patients were included in the study. All patients had undergone PET/CT examination before (first) and after (second) transplantation and were surveyed for at least nine months to five years. Additional Chemo- and/or radiotherapy between the two PET examinations were co-evaluated. Visual and SUVmax analysis was used to discriminate positive from negative PET examination. An examination was considered negative or borderline positive or positive according to Deauville criteria. **Results:** 19 patients had a positive first PET/CT; 11/19 (6 received additional therapy between the two examinations) achieved a negative second PET and 7 of them remain in complete response during surveillance. Of the rest 4, two patients relapsed soon after the second negative PET, both had not received additional therapy, and were led for further treatment, one relapsed 18 months after and one was diagnosed with second primary. 2 patients had borderline first PET and negative second; one relapsed 1 year after and the other remains in complete response. 6 patients had a negative first and second PET, none received additional therapy between the two examinations and four of them remain in complete response (CR) during surveillance, while two relapsed 2.5 and 4 years after transplantation respectively. **Conclusions**: In this study, we used Deauville criteria to discriminate positive from negative examinations, although characterization of a PET scan after autologous transplantation needs perhaps further clarification. Whatever the case, a negative before autologous transplantation PET is correlated with a negative after transplantation PET/CT and a prolonged disease free interval. Patients with a positive pre- transplantation PET/CT are more likely to need further therapeutic action in order to achieve complete response. Borderline positive PET examinations require further investigation whether they can be considered positive or negative.

## P055

### 18F-FDG PET/CT in variable presentations of Carcinoma breast

**C. Jora**, P. Pankaj, R. Verma, E. Belho, A. Jain, N. Sharma, P. Gupta, H. Mahajan; Sir Gangaram Hospital, Delhi, INDIA.

**Aim:** To assess the diagnostic impact of 18F-FDG PET/CT in variable presentations of carcinoma breast and to assess its role in T1 disease. **MATERIALS and METHODS:** 12 patients undergoing evaluation for suspicious malignant lesions were imaged 1 h (54-72 min) after 18F-FDG injection on a PET/CT scanner. Tracer uptake was quantified by standardized uptake values (SUVmax) of the lesions. Contrast CT was obtained in 11 of 12 patients. 8 of 12 had no history of breast cancer . Of these 8, 2 patients were being evaluated for breast lump, 1 for pathological fracture, 1 for vertebral lesion, 1 for metastatic supraclavicular node, 1 for recurrent strokes, 1 for space occupying lesions liver and raised tumor markers and 1 for hypercalcemia. 4 of 12 patients were old treated cases of carcinoma breast. **RESULTS:** PET/CT identified a primary tumor in all 8 new cases. After PET study, 6 of 8 with primary tumor were diagnosed with carcinoma breast (3 of 6 had T1 lesion, 1 of 6 had T2 lesion, 1 of 6 had T4 lesion and 1of 6 had multicentric disease), 1 of 8 was diagnosed as breast lymphoma and 1 of 8 as cystosarcoma phylloides. 2 of the 6 primary breast cancer cases had indeterminate mammogram and breast ultrasound. All lesions were well delineated on 18F-FDG PET/CT . Extra axillary nodal metastases were detected in 4 of 6 patients. Distant metastases were picked up in 4 of 6 patients. Of the 4 old treated cases of carcinoma breast, PET/CT identified recurrence in vertebral metastases in 2 cases, lung metastases in 1 case and recurrence at the site of treated primary and liver metastases in 1 case. In this last case, serial PET/CTs helped modulate the treatment. **Conclusion:** PET/CT is a valuable tool to provide information on extra-axillary lymph node involvement, distant metastases and other occult primary cancers. Preoperative $^{18}$F-fluorodeoxyglucose-PET/CT has a substantial impact on initial staging and on clinical management in patients with early-stage breast cancer and even with tumors < 2 cm. Key words: Breast cancer. Staging. PET/CT. Treatment

## P056

### 18F-fluorocholine-PET, 201Thallium-SPECT and MRI in glioma recurrence: diagnostic accuracy and clinical utility.

**N. Testart**[1], R. Sánchez Sánchez[1], E. Yagui Beltrán[2], T. Aroui Luquin[1], G. Guzmán Caro[1], C. Sánchez Toro[3], R. Luque Caro[3], G. Olivares Granados[2], M. Zurita Herrera[4], J. Pastor Rull[5], C. Chamorro Santos[6], A. Rodríguez-Fernández[1], M. Gómez-Río[1], J. Llamas-Elvira[1]; [1]Hospital Virgen de las Nieves, Servicio de Medicina Nuclear, Granada, SPAIN, [2]Hospital Virgen de las Nieves, Servicio de Neurocirugía, Granada, SPAIN, [3]Hospital Virgen de las Nieves, Servicio de Oncología Médica, Granada, SPAIN, [4]Hospital Virgen de las Nieves, Servicio de Oncología Radioterápica, Granada, SPAIN, [5]Hospital Virgen de las Nieves, Servicio de Neurorradiología, Granada, SPAIN, [6]Hospital Virgen de las Nieves, Servicio de Anatomía Patológica, Granada, SPAIN.

**BACKGROUND** Tumor recurrence in brain glioma represents a diagnostic challenge. In some cases when alterations appear in structural imaging, it is difficult to differentiate post-treatment changes and glioma recurrence. In the brain, the utility of 18F-FDG-PET is limited due to the elevated physiological glucose metabolism of the cortex, which makes desirable the use of a more specific oncologic radiotracer. The aim of this work is to evaluate the diagnostic accuracy and clinical utility of 18F-fluorocholine-PET in the follow up of patients treated for Glioma. **METHODS** A longitudinal prospective cohort of 21 glioma patients treated (mean age: 46.9±6.2y; 57% females; 9 high grade [HG]; 12 low grade [LG]) under suspicion of tumor growth, have been studied by MRI, 201Thallium-SPECT and 18F-fluorocholine-PET. The final confirmation of the results has been obtained in 9 patients by histology and in the remaining cases by imaging and clinical follow up (>6 months). **RESULTS** The tumor activity was suspected in 11 patients because of clinical manifestations, in 5 patients for structural changes found on MRi and in 5 patients for both: clinical and imaging alterations. MRI was considered true positive (TP) in 12 explorations (5LG; 7HG), false positive (FP) in 3 (3LG) and inconclusive in 6 (4LG; 2HG). 201Thallium-SPECT shown 15 TP explorations (6LG; 9HG), 3 TN (3LG) and inconclusive in 3 cases (3LG). 18F-fluorocholine-PET shown 16 TP scans (7LG; 9HG), 4 TN (4LG) and only one non-conclusive (1LG). In all positive findings, the 18F-fluorocholine-PET showed a high uptake, to both high grade and low grade lesions. These results were relevant for clinical decisions in 13 patients (9LG; 4HG) and did not modify the clinical attitude in 8 patients (3LG; 5HG). **COMMENTS** Despite the small population and its selection bias (that prevent to reach definitive conclusions) our preliminary results suggest that 18F-fluorocholine-PET could be

useful in the diagnosis of tumor recurrence of gliomas with repercussions in clinical management, especially in low grade gliomas.

## P057

### The forgotten cardiophrenic lymph node: Its role in staging and management as detected by FDG PET/CT

S. Farmakis, K. Vejdani, R. Muzaffar, N. Parkar, **M. M. Osman**; Saint Louis University, Saint Louis, MO, UNITED STATES.

**Objectives:** There is little data on what constitutes a normal sized cardiophrenic lymph node. In addition, its impact on staging is unclear since it is not included in the TNM staging. The purpose of this study was to determine whether PET/CT is more sensitive than CT in detecting metastatic disease in the cardiophrenic space and whether the presence of disease in this location would change the staging and clinical management. **Methods:** We retrospectively reviewed 1200 consecutive FDG PET/CT reports of cancer patients in the span of 20 months for the presence of FDG-avid cardiophrenic lymph nodes. The maximum standardized uptake value (SUVmax) was used to quantify the metabolic activity in each of the lymph nodes. The radiographic data was used for correlation. A retrospective review of diagnostic contrast CT reports performed within a one month period of time of the PET/CT in the same subset of patients determined whether cardiophrenic lymph nodes were mentioned. **Results:** 9 (0.8%) out of the 1200 patients evaluated were found to have FDG-avid cardiophrenic lymph nodes (4 males and 5 females with a mean age of 55 years; range 7-69; median 59). On the CT portion of the PET/CT the nodes demonstrated a mean size of 0.8 cm in the short axis diameter (range 0.4-1.6 cm; median 0.7 cm). The mean SUVmax was 2.5 (range 1.4-7.9; median 1.9). Only 2 of these patients were found to have suspicious lymph nodes on diagnostic contrast CT. The presence of cardiophrenic lymph nodes changed the staging and/or management in 4 out of the 9 patients (44%). **Conclusions:** Our study finds that PET/CT is more accurate in detection of pathologic cardiophrenic lymph nodes, particularly when they are sub centimeter in size. The detection of cardiophrenic lymph nodes is relatively rare. However, when present, detection changes staging and/or management in 44%. Therefore, inclusion of these nodes should be included in TNM staging.

P10-1 - Sunday, Oct. 20, 16:00 - 16:30, Poster Exhibition Area

## Molecular & Multimodality Imaging: SPECT & SPECT/CT

## P058

### Diagnosis of axillary lymph node invasion in patients with breast cancer: comparison of CT with SPECT-CT

**S. N. Novikov**, S. V. Kanaev, P. I. Krgivickiy, V. F. Semiglazov, N. D. Ilin; N.N. Petrov Institute Oncology, St Petersburg, RUSSIAN FEDERATION.

**Purpose:** to compare diagnostic accuracy of conventional computerized tomography (CT) and SPECT-CT in lymph node (LN) staging of patients (pts) with breast cancer (BC). **Material and Methods:** 38 consecutive pts with early BC (T1-2 NxM0) were included in this study. All pts underwent SPECT-CT examination on Symbia-T16 scanner which is consists of dual head gamma-camera combined with 16 slices diagnostic CT. SPECT-CT was performed 15 min after i/v injection of 740-860 MBq of 99mTc-MIBI. Experienced radiologist and specialist in nuclear medicine separately reported on CT and SPECT-CT data. On CT scans all LNs with short diameter more than 10 mm were considered abnormal. On SPECT images all LNs with tracer uptake (TU) on the level of background or slightly (less than 70% above background) increased TU were judged as normal or nonspecific LNs. Metastases were diagnosed if SPECT revealed intensive (70% and more) 99mTc-MIBI accumulation in one or several LNs. Final interpretation of the data was done according to histological verification of removed LNs. **Results:** Postoperative histological evaluation of removed axillary LNs revealed metastatic involvement in 15 cases and normal LN histology - in another 23 pts. CT examination detected axillary LNs with short diameter larger than 10 mm in 14 pts: 8 cases were true positive and 6 - false positive. LNs with diameter less than 10 mm were metastatic on histology in 7 cases, normal - in 17 observations. Sensitivity (Sen), Specificity (Sp) and Accuracy (AC) of CT were as follows: 53%, 74%, 66%. If ovoid LNs with fat center larger than 10 mm were considered as reactive non-metastatic nodes Sp of CT examination raised to 91% on the expense of decreased Sen (40%) and slightly improved AC (71%). SPECT-CT gives unique opportunity for image interpretation when CT is used as a guide for localization of LN and intensity of TU in LN is verified by SPECT part of examination. This technique revealed intensive TU in LN of 12 pts with metastatic axillary involvement and in 3 pts with non-specific LN changes. In all 3 pts with false negative SPECT-CT conclusions histological verification showed microfoci of BC in 1 or 2 sentinel LNs. Remained 19 cases were interpretated as true negative. SPECT-CT combination enables significant improvement in AC (81%), Sp (82%) and Sen (80%). **Conclusion**: In pts wit early breast cancer SPECT-CT with 99mTc-MIBI is very promising method for diagnosis of axillary LN macroinvasion by the tumor.

## P059

### Surgery based on preoperative 99mTc-Sestamibi scintigraphy in patients with primary hyperparathyroidism: concordance between SPECT/CT and histopathological findings

**M. H. Listewnik**[1], A. Borowiecki[2], M. Ostrowski[3], K. Jasiakiewicz[1], M. Wojnarowska[1], M. Chosia[4], H. Piwowarska-Bilska[1], P. Zorga[1], M. Sawrymowicz[1], B. Elbl[1], T. Sulikowski[3], B. Birkenfeld[1]; [1]Dept. of Nuclear Medicine Pomeranian Medical University, SZCZECIN, POLAND, [2]Department of Plastic, Endocrine and General Surgery, Pomeranian Medical University, SZCZECIN, POLAND, [3]Department of Surgery and Transplantation Pomeranian Medical University, SZCZECIN, POLAND, [4]Department of Pathology, Pomeranian Medical University, SZCZECIN, POLAND.

**Introduction**: Preoperative $^{99m}$ Tc-Sestamibi SPECT/CT scintigraphy is an important metabolic method in the diagnosis of parathyroid lesions in primary hyperparathyroidism (PHP). A success of surgical treatment is determined by proper preoperative localization of abnormal parathyroid tissue. This study presents results based on "wash-out" scintigraphy (one tracer, two phases). Aim: To assess concordance between preoperative SPECT/CT "wash-out" $^{99m}$ Tc-Sestamibi scintigraphy, surgery and histopathological findings in proper localization of suspected lesions in patients with PHP**. Methods**: 28 SPECT/CT "wash-out" scans after i.v. administration of $Tc^{99m}$-MIBI were performed on 27F and 1M aged 28-74 years with PHP. SPECT/CT presentation in three dimensional (3D) fusion projections for each localization served as guidelines for the surgeon at the operation theatre. Parathyroidectomy or combined with subtotal/total thyreoidectomy was conducted in 15(53%) and 13(47%) patients respectively. Histopathological (HP) result was obtained in all patients after the surgery. The removed lesions were classified as HP positive, if they proved to be: normal cells (3), hyperplasia (8), adenoma (15) or cancer (3) of parathyroid gland. The removed lesions were classified as HP negative, if proved to be: lymph nodes (2) or thyroid (1). On the basis of SPECT/CT and HP lesions were classified into one of four categories: 1. true positive (TP), visible on SPECT/CT and HP positive; 2. false negative (FN), negative on SPECT/CT but HP positive ("correct" surgeon decision); 3. false positive FP, positive in SPECT/CT but negative in HP; 4. True negative, neither confirmed in SPECT/CT nor HP ("false" decision of the surgeon). **Results:** In 28 patient 32 lesions were found on SPECT/CT and validated in HP. 28 of 32 (87.5%) lesions were TP, TN were in 2(6.3%), FP was 1 (3,1%) and FN was 1(3.1%) lesion. In 3 lesions SPECT/CT findings were not followed by the surgeon during operation. The SPECT/ CT 99mTc-Sestamibi scintigraphy: sensitivity 96.6%, specificity 66.7%, accuracy 93.8%, PPV-96.6% and NPV 66.7%. **Conclusions**: 1. SPECT/CT "washout" protocol parathyroid scintigraphy 3D presentation is useful for localization of suspected lesions during surgery. 2. Parathyroid gland (normal cells, hyperplasia, adenoma and cancer) was successfully detected with the "wash-out" $^{99m}$Tc-Sestamibi scintigraphy protocol.

## P060

### Surgery based on preoperative $^{99}$mTc-Sestamibi scintigraphy in patients with secondary hyperparathyroidism: concordance with SPECT/CT and histopathological findings

**M. H. Listewnik**[1], M. Ostrowski[2], K. Jasiakiewicz[1], M. Wojnarowska[1], H. Piwowarska-Bilska[1], J. Lubiński[3], P. Zorga[1], T. Sulikowski[2], M. Sawrymowicz[1], B. Elbl[1], B. Birkenfeld[1]; [1]Dept. of Nuclear Medicine Pomeranian Medical University, SZCZECIN, POLAND, [2]Department of Surgery and Transplantation Pomeranian Medical University, SZCZECIN, POLAND, [3]Department of Genetics and Pathology, International Hereditary Cancer Centre, Pomeranian Medical University, SZCZECIN, POLAND.

**Introduction**: Due to multiple and usually small volume of parathyroid lesions in secondary hyperparathyroidism (SHP) and presence of serious concurrent diseases in vast majority of patients the parathyroid surgery is more difficult than in case of primary hyperthyroidism. Preoperative $^{99m}$ Tc Sestamibi SPECT/CT scintigraphy is an important metabolic method in the diagnosis of parathyroid lesions in SHP. This study presents results based on wash-out scintigraphy (one tracer, two phases). Aim: To assess the concordance of preoperative "wash-out" $^{99m}$ Tc-Sestamibi SPECT/CT scintigraphy with surgery and histopathological findings in proper detecting (localization) of suspected lesions in patients with SHP. **Methods:** 32 SPECT/CT wash-out scans with i.v. administration of $Tc^{99m}$-MIBI were performed on 16F and 16M aged 22-77 years with SHP. SPECT/CT presentation in three dimensional (3D) fusion projections for each localization served as guidelines for the surgeon at the operation theatre. In 5(16%) patients parathyroidectomy was combined with subtotal/total thyreoidectomy. Histopathological (HP) results were obtained in all patients after the surgery. The removed lesions were classified as HP positive, if they proved to be: normal cells (13), hyperplasia (15), adenoma (32) or suspicious cancer (1) of parathyroid gland. The removed lesions were classified as HP negative, if proved to be: lymph nodes (5), thyroid (9) or fat tissue (1). On the basis of SPECT/CT and HP lesions were classified into one of four categories: 1. true

positive (TP), visible on SPECT/CT and HP positive; 2. false negative (FN), not visible on SPECT/CT but HP positive ("correct" surgeon decision); 3. false positive (FP), positive in SPECT/CT but negative in HP; 4. true negative (TN), neither confirmed in SPECT/CT nor HP ("false" decision of the surgeon**). Results**: In 32 patient 76 lesions were found on SPECT/CT and validated in HP. In 55 (72.4 %) lesions TP results were found, in 8 (10.5%) -TN, 7 (9.2%) -FP, 6(7.9%) -FN. In 6 lesions SPECT/CT findings were not followed by surgeon during operation. The SPECT/ CT 99m Tc- Sestamibi scintigraphy: sensitivity 90.2%, specificity 53.3%, accuracy 82.9%, PPV-88.7%, NPV-57.1%. **Conclusions**: 1. Preoperative $^{99m}$ Tc Sestamibi "wash-out" SPECT/CT is very sensitive tool in imaging in secondary hyperparathyroidis 2. The presence of positive SPECT/CT findings is strong indicator for the surgeon to remove the lesion.

## P061

### SPECT/CT and freehand-SPECT based navigation for sentinel nodes in the groin in patients with penile cancer.

**N. S. Van den Berg**[1,2], G. H. KleinJan[1,2], O. R. Brouwer[1], H. Mathéron[2], T. Wendler[3,1], H. Simon[2], H. Van der Poel[2], R. A. Valdés Olmos[1,2], F. W. B. Van Leeuwen[1]; [1]Leiden University Medical Centre, Leiden, NETHERLANDS, [2]the Netherlands Cancer Institute, Amsterdam, NETHERLANDS, [3]Surgic Eye, Munich, GERMANY.

**Aim** For penile carcinoma, sentinel node (SN) biopsy is a valid method to provide accurate lymph node staging without performing a complete inguinal lymph node dissection. However, in some series false-negative rates up to 18% have been reported. The Declipse® SPECT-system (SurgicEye, Munich, Germany) is a navigation system which allows intraoperative real-time 3D mixed-reality-based navigation to a lesion of interest based on a preoperatively acquired SPECT/CT scan. As such, this technique may increase the accuracy with which a sentinel can be detected as such to help further reduce the false-negative outcome. This study evaluated the accuracy of the 3D SPECT/CT-based navigation in patients with penile cancer**. Materials and Methods** Ten patients with penile cancer scheduled for a sentinel node biopsy were peritumorally injected with indocyanine green (ICG)-99mTc-nanocolloid. After injection lymphoscintigraphy and SPECT/CT imaging were performed to determine the number of sentinel nodes. Before starting the SPECT/CT scan a reference tracker (ReT) was placed on the mons pubis of the patient. The location a ReT was marked with indelible inked, so that prior to the start of the operation a sterile ReT could be placed on the exact same location. This allowed repositioning of the acquired SPECT/CT scan onto the patient. On the gamma probe a second ReT was placed which allowed 3D SPECT/CT-based mixed-reality navigation to the sentinel node and the location was marked on the skin. The error compared to the location pointed to with the conventional gamma probe was then measured. The navigation system also provided the distance from the skin to the actual location of the sentinel node. This was compared to the distance measured on the CT. **Results** The average error in the location of the sentinel node on the skin was 5.0 mm (range 0-10 mm). In three patients, 3D SPECT/CT-based navigation pointed to the exact same location on the skin as the conventional probe. The error in depth estimation indicated by the navigation system compared that measured in Osirix was 5.3 mm. **Conclusion** Navigation towards the sentinel node could be facilitated based on 3D SPECT/CT-mixed-reality. With this approach, imaging data obtained at the nuclear medicine department can be optimally translated into the operating theatre to be mixed with the real environment of the patient and as such help guide the surgeon. Future studies have to shown whether this approach can help to further reduce the false-negative rates associated with sentinel node biopsy.

## P062

### Incidental findings in SPECT/CT

**A. Hunter**[1], T. Wagner[2]; [1]University College London, London, UNITED KINGDOM, [2]Royal Free London NHS Foundation Trust, London, UNITED KINGDOM.

**Background:** Single positron emission tomography (SPECT) with computed tomography (CT) (SPECT/CT) is a recent technology combining functional and anatomical information. Its use is increasing in oncological and non-oncological indications. Hybrid imaging reporting is complex given the amount of data to analyse. Depending on the type of scan, indication, experience and background of the reporter, the focus of the report might be on the SPECT or the CT component of the study. In conventional cross-sectional imaging (CT, MRI) incidental findings are common, reporters are trained in their identification and reporting and published guidelines help manage the most frequent ones. To our knowledge the incidence and impact of incidental findings in SPECT/CT have not been reported. We aimed to study incidental findings on the CT and SPECT components of SPECT/CT. **Methods**: Reports of 292 consecutive SPECT-CT scans performed on 292 patients at the Royal Free Nuclear Medicine Department between August and December 2012 were collected, anonymised and analysed. An incidental finding was defined as an unexpected finding with regard to the primary intent/indication of the scan. Findings reported previously on other scans, congenital variants, anatomical variants and bone degenerative changes were not considered incidental. **Results:** Of the 292 patients 37% of patients had at least one incidental finding reported and 11% of patients had more than one incidental finding reported. Of all incidental findings reported 82% were found on CT review, 18% were found on SPECT and anatomically located on CT and 1% was found on SPECT alone with no corresponding CT abnormality. Of all incidental findings reported those most frequent were lung changes 32% (most commonly lung nodules, pleural nodules, pleural effusions, consolidation, atelectasis), liver changes 10% (cysts, undefined lesions), kidney changes 10% (cysts and calculi), musculoskeletal 8% (trauma, bone lesions, muscle lesions) and gastrointestinal 7% (diverticular change, hernias). **Conclusion**: SPECT/CT incidental findings are frequent. Given the recent advent of hybrid imaging and SPECT/CT there are no guidelines to reporting and managing incidental findings. Reporters of SPECT/CT scans need to be trained in identification, reporting and management of incidental findings.

## P063

### Combined Radionuclide Imaging of Mandibular Fibrous Dysplasia with Tc-99m MDP/MIBI

T. Ones, **M. Aras**, F. Dede, S. Gungor, S. Ozguven, R. Maleki, T. Y. Erdil, S. Inanir, H. T. Turoglu; Marmara University School of Medicine Nuclear Medicine Department, Istanbul, TURKEY.

Fibrous Dysplasia (FD) is a common benign skeletal lesion in which normal bone is replaced by abnormal fibroosseous tissue. Utility of the combined radionuclide imaging with Tc99m MDP/MIBI for evaluation of the potentially operable symptomatic FD lesions have been reported in the literature. Monostotic fibrous dysplasia of the mandible is an unusual manifestation of the disease that is usually benign, occurs in young individuals. In this study we aimed to evaluate the value of Whole Body Tc-99m MDP Bone Scintigraphy (MDPBSc) with Whole Body Dual Phase Tc-99m MIBI Scintigraphy (DuPhMIBISc) in the evaluation of mandiular FD lesions. 6 patients with histopathologically confirmed FD aged between 12-73 years-old (mean age: 36±16 years) were evaluated with MDPBSc and 5 patients with DuPhMIBISc. In all patients, MDPBSc showed increased uptake in all of the FD lesions. Lesions were monostotic in five patients and polyostotic in one patient on MDPBSc. The patients were followed up for a mean duration of 55 months (range:6-143 months) after the initial evaluation. Only one symptomatic lesion showed increased Tc-99m MIBI uptake on the early phase of DuPhMIBISc and showed retention of Tc-99m MIBI on delayed phase of DuPhMIBISc. Although our study did not include any patients with any pathological MIBI uptake in nonsymptomatic lesions, it might have an impact on management of such patients. Therefore, this study may provide a new approach for the clinical work-up of mandibular FD patients with DPMSc imaging on initial evaluation. One of the potential limitations of this study was the relatively small number of patients. However, it is the only combined radionuclide imaging study with a long-term prospective follow-up period with the largest patient group. Tc-99m MIBI uptake within the symptom-positive lesion that need surgical treatment was shown in this study. Although our study did not include patients with any pathological MIBI uptake in nonsymptomatic lesions (i.e. subclinical disease), it might have an impact on management of such patients. In conclusion, whole-body bone scan is useful in determining the site and extent of the skeletal involvement. It seems that DPMSc findings correlate with the symptoms of mandibular FD. This relationship may have a role in improving the preoperative assessment of mandibular FD lesions. DPMSc could be useful in the follow-up of symptomatic lesions of mandibular FD if our results are validated in a larger patient series.

P11-1 - Sunday, Oct. 20, 16:00 - 16:30, Poster Exhibition Area

## Molecular & Multimodality Imaging: New Methods & Tracers

## P064

### Simultaneous SPECT and PET dual-tracer imaging using beam stopper device

**H. H. Lin**[1], K. S. Chuang[1], C. H. Chien[1], K. H. Lue[1], C. C. Chiang[1], M. L. Jan[2]; [1]Department of Biomedical Engineering & Environmental Sciences, National Tsing Hua university, Hsin Chu, TAIWAN, [2]Health Physics Division, Institute of Nuclear Energy Research Atomic Energy Council, Hsin Chu, TAIWAN.

**Aim:** Simultaneous SPECT and PET dual tracer imaging have great potential in clinical and molecular applications, such as two receptor binding studies or differential imaging of physiological and molecular functions. It can help assess these functions under identical physical conditions and reduce the quantitative errors between acquisitions. In this work, we proposed a simultaneous dual tracer technique based on beam stopper device applied in PET scanner. The technique can retain regular PET imaging of $^{18}$F while obtaining SPECT imaging of $^{99m}$Tc using beam stopper device. **Material and Methods:** The beam stopper (BS), a concept of inversing of pinhole collimator, can acquire pinhole-like imaging through mutual

subtraction of the images without and with beam stopper. The size of BS is 0.8 mm diameter, which is large enough to obstruct most of 140 keV gammas but small enough to be ignored by 511 keV gammas. A feasible study with Monte Carlo simulation using GATE was performed to validate the concept. The BS device is designed as a cage insert where eight BS's are distributed uniformly on the periphery. A partially overlapping combination of dual source ($^{99m}$Tc/$^{18}$F) inside a water cylinder of 2 cm diameter and 2 cm height was employed on a preclinical PET scanner. In $^{99m}$Tc energy window (120-160 keV), dual information (w/wo BS) on each projection pertaining to each BS can be obtained for the reconstruction of $^{99m}$Tc images with the rotation of BS cage. Meanwhile, regular acquisitions of $^{18}$F projection were conducted almost without the interference from BS in $^{18}$F energy window (350-650 keV). **Results**: Our preliminary simulation study showed that the proposed method allowed for separation of the two activity distributions and recovered activities with relative errors within 5%. Down scatter effect from 511 keV photons on $^{99m}$Tc images is nicely corrected during the subtraction of projections w/wo BS. Further, similar image resolution for $^{99m}$Tc and $^{18}$F is achieved even though the signal to noise ratio of $^{99m}$Tc images is inferior to that of $^{18}$F images. **Conclusion:** We conclude that the proposed method can acquire PET and SPECT images simultaneously without the cost of PET sensitivity and perform dual functions on individual object, enhancing the ability to detect multiple disease targets.

## P065

### Intraoperative radiolocation of parathyroid adenoma with freehand SPECT probe and comparison with portable gammacamera. Initial experience.

**S. Prado-Wohlwend**[1], I. Casáns-Tormo[1], R. Díaz-Expósito[1], C. Rocafuerte-Avila[1], C. Orozco-Molano[1], H. Bowles-Antelo[1], N. Cassinello-Fernández[2], J. Ortega-Serrano[2]; [1]Nuclear Medicine. Hospital Clínico Universitario, Valencia, SPAIN, [2]Surgery. Hospital Clínico Universitario, Valencia, SPAIN.

**Aim**: Freehand SPECT probe (declipseSPECT®) allows to obtain intraoperative SPECT. It combines gamma probe, infrared detector, optical camera and two tracking targets fixed on patient and on probe, mapping the studied area in the three axis, obtaining 3D reconstruction in the surgical field. There are only 3 patients with 5 adenomas currently published. We present our initial experience with freehand SPECT (FSPECT) comparing with portable gammacamera (PG) Sentinella® in parathyroid adenoma intraoperative radiolocation. **Material and Methods**: Two patients, male(58y/o), female(70y/o) diagnosed of parathyroid adenoma, with previous conventional planar and SPECT parathyroid scintigraphy (99mTc-MIBI), one patient with available fusion SPECT-CT with Syntegra®. After IV administration of 99mTc-MIBI (5 mCi) in the operating room, we obtained from 15 to 90 min, planar static images with PG and scanning-3D reconstruction of cervical area with FSPECT. We determined intraoperative PTH levels pre and post adenoma removal and histopathological study. **Results:** Previous parathyroid scintigraphy provides accurate location of adenomas, one infero-posterior left parathyroid and the other in medium mediastinum, infero-posterior to thyroid gland. During surgery, PG planar images as well as FSPECT 3D reconstruction let us correct identification and location of both adenomas. PG provided images with counts activity information of adenomas and surrounding tissue. With FSPECT we also obtained precise information of lesion depth and distance (mm) to the cutaneous border. After extirpation of adenomas, ex-vivo verification of radioactivity in the excised tissue specimen and in surgical bed was obtained with both devices, confirming successful parathyroidectomy. Intraoperative PTH levels decreased in the two patients from 147-30 and 154-62 pg/ml after surgery and both adenomas were confirmed by histopathological study. **Conclusion**: We obtained accurate intraoperative radiolocation and removal verification of our parathyroid adenomas with PG as well as with FSPECT, that provides real-time depth information added. They are different systems and larger comparative studies are needed. They could have a complementary role in surgical radiolocation to improve minimally invasive surgery of parathyroid adenomas, reducing surgical time with easier patient recovery. Recent developments, as superposition in the surgical field of previous SPECT-TAC (FSPECT) and dynamic images (PG) will contribute to improve surgical radiolocation.

## P066

### Preoperative radioguided tumour-related injection using freehand-SPECT for sentinel lymph node mapping in non-palpable breast cancer

**B. Pouw**, L. J. de Wit- van der Veen, M. P. Stokkel, D. Hellingman, O. R. Brouwer, R. A. Valdés Olmos; Department of Nuclear Medicine, The Netherlands Cancer Institute, Antoni Van Leeuwenhoek Hospital, Amsterdam, NETHERLANDS.

**Aim**. This study was designed to explore the feasibility of replacing conventional ultrasound (US)-guided 99mTc-nanocolloid injections by radioguided tumour-related 99mTc-nanocolloid administration using a novel freehand-SPECT device (DeclipseSPECT; SurgicEye GmbH, Germany) in patients with non-palpable breast cancer scheduled for Sentinel Lymph Node Biopsy (SLNB). The freehand-SPECT procedure is based on the detection of an Iodine-125 (125I) seed, which was implanted a few weeks before SLNB and enables 3D-reconstructions of radioactivity maps. This radioguided injection decreases the workload for the Radiology Department by avoiding the need for a second US-guided procedure. A second advantage is the prevention of potential pitfalls by ultrasonography when other types of markers or calcifications are confounded with the 125I-seed causing an incorrect injection location. **Materials and Methods**. The study included 44 breast cancer patients (mean age= 59, range = 26-89) who were injected in supine position. In the first 10 patients the implanted 125I-seed was primarily localized using freehand-SPECT and subsequently by conventional US. For both techniques the perpendicular 125I-seed depth was determined to guide 99mTc-nanocolloid injection. The following 34 patients were injected using only freehand-SPECT localisation, after which the distance between the 99mTc-nanocolloid-depot and the 125I-seed was evaluated by means of SPECT/CT. Additionally, a control group of 21 patients with US-guided injections was evaluated by means of SPECT/CT to compare the distance between the 99mTc-nanocolloid-depot and the 125I-seed. Distances were measured on SPECT/CTs by a second independent blinded observer to evaluate the limits of agreement. **Results.** The average depth difference measured by US and freehand-SPECT in the first 10 patients was 1.6 mm (SD 1.6 mm, range 0-5 mm). In the following 36 seeds (34 patients) the average difference between the 125I-seed and the centre of the 99mTc-nanocolloid-depot was 10.9 mm (SD 6.8 mm, range 0-29 mm). In the control group of 21 patients with US-guided injections an average difference of 9.7 mm (SD 6.4 mm, range 2-30 mm) was measured. Bland-Altman analyses, used for interobserver agreement analysis, indicated a mean difference for freehand-SPECT guided injections of 0.1 mm (95% CI: 3.1 mm to -3.0 mm). **Conclusion.** Minimal differences for 125I-seed guided injections between conventional US and freehand-SPECT were observed in the present study. Additionally, when comparing the 99mTc-nanocolloid-depot and 125I-localisations on SPECT/CT, the concordance was clinically acceptable. It is concluded that freehand-SPECT guided 99mTc-nanocolloid injections in patients with non-palpable breast cancer, scheduled for SLNB and an implanted 125I-seed, are feasible and appear to be reliable.

## P067

### Mini gamma camera "Sentinela102" in post-neoadjuvant chemotherapy (NAC) for guiding surgical treatment in locally advanced breast cancer (LABC) patients

**L. Evangelista**[1], A. Cervino[1], R. Sanco[1], M. Bignotto[2], T. Saibene[3], S. Michieletto[3], M. Paiusco[2], F. Bozza[3], C. Ghiotto[4]; [1]Radiotherapy and Nuclear Medicine Unit, Istituto Oncologico Veneto I.R.C.C.S., Padova, ITALY, [2]Medical Physic Unit, Istituto Oncologico Veneto I.R.C.C.S., Padova, ITALY, [3]Surgery Oncology Unit, Istituto Oncologico Veneto I.R.C.C.S., Padova, ITALY, [4]Oncology 2 Unit, Istituto Oncologico Veneto I.R.C.C.S., Padova, ITALY.

**Introduction.** The present pilot study was conceived in a multidisciplinary vision with the involvement of radiologists, radiology technicians, clinicians and surgeons. The aim of the present study was to assess the utility of a dedicated gamma cameras for guiding surgical treatment in LABC after NAC. **Materials and Methods**. Ethical committee was requested for the acceptance of the study. From January 2012, at Oncological Institute of Veneto, a mini gamma-camera (Sentinela 102, ONCOVION) has been available. For the evaluation of appropriateness, 99mTc-Sestamibi (740 MBq intravenous-i.v.) was injected before the start of NAC performing a scintimammography (SMM). The analysis of the images were computed according the following formulas: tumor to background ratio (T/B)=[cntsT-cntsB]/ [cntsB] and the most intense uptake of the tumor to background ratio (I/B) [cntsI-cntsB]/ [cntsB]. Furthermore, the percentage washout index (WO%) for T and I were obtained, according to: WO%T,I= [cntsT,I]early image-[cntsT,I]delayed image/[cntsT,I]early image. After at least 6-months at the end of NAC a new injection of 99mTc-Sestamibi (100-150 MBq) was made for the evaluation in operating theater. **Results**. 54 patients were evaluated by SMM and out of them 17 (31.5%) with Sentinela102. All SMM scans were performed using prone and supine planar images in different projections. A focal uptake in the breast with or without lymph nodes was demonstrated in all patients. At quantitative analysis, the mean values of early/late T/B and early/late I/B were 11.21±8.56vs.8.92±5.95 (p=0.004) and 1.10±0.15vs.0.87±0.11 (p=0.001), respectively for the entire tumor and the most intense were obtained. Furthermore, 33 (61.1%) patients had both WO%T and WO%I less than 45%. After the end of NAC, in 17 patients, the 99mTc-sestamibi was administrated before surgery and a single image in anterior projection was made by the standard gamma camera. In the operatory theatre, at least four static planar images were obtained by using Sentinela102. In particular, 10 (58.8%) patients showed a focal uptake of tracer in the breast or lymph nodes before or after the surgical excision (at histological specimen), while 7 did not. The histological specimen concluded for a complete response to NAC in 4 (23.5%) patients and for a partial or no response to treatment in the remnant 13 subjects. The diagnostic accuracy of Sentinela102 was: 70.58% (95% confidence interval: 48.92-92.24%). **Conclusions**. From the present pilot study emerges how a new nuclear imaging device can be useful in the

operatory theater for guiding a radical surgery approach in patients with LABC after NAC.

## P068

### Development of a hybrid probe for specific imaging of bacterial infections

**M. M. Welling**, A. Bunschoten, M. T. M. Rood, T. Buckle, F. W. B. van Leeuwen; Leiden University Medical Center, Interventional Molecular Imaging Laboratory, Leiden, NETHERLANDS.

***Aim:*** Molecular imaging of bacteria can aid the clinical diagnostics of complicated infections after implantation of bioMaterials and prostheses. A probe that facilitates both the specific detection and localization of bacteria may be helpful in the treatment of infections after medical implantation. Recently, a radioactively labeled version of the peptide $UBI_{29-41}$ was tested for imaging of experimental infections. This peptide was also successfully evaluated in various clinical studies. For optimization of the optical evaluation of infections during surgical interventions a fluorescent probe would be of interest. To combine both nuclear and intraoperative optical imaging of infections a radioactive and fluorescent (hybrid) imaging probe would be of great value. ***Materials and Methods*:** In this study we report on the synthesis of a hybrid bacteria targeting probe that contains both a DTPA chelate and a fluorescent dye; $UBI_{29-41}$-MSAP-Cy5. After radiolabeling with indium-111, the binding to various bacterial strains (S. aureus, S. epidermidis, K. pneumoniae, E. coli and B. subtilis) and human leukocytes was evaluated. The binding and uptake in the bacteria was determined using a gamma counter, fluorescence spectroscopy and the binding was visualized with confocal fluorescence microscopy. The binding was evaluated under various conditions including temperature (ranging between 4 and 37°C) and pH (ranging between 3 and 9). ***Results*:** We observed high and highly selective binding of the hybrid probe to all strains of bacteria tested with poor binding to human leukocytes. A follow up study to evaluate the biodistribution of the probe in mice and the detection of experimental thigh muscle infections using a microSPECT imaging system and optical imaging modalities is ongoing. ***Conclusion*:** Hybrid probes for specific imaging of infections can be a worthwhile asset to the array of imaging probes for detection and localization of complicated infections. Here by the integration of diagnostic nuclear imaging and optical guidance during surgical interventions is expected to help optimize the current treatment regimens.

P12-1 - Sunday, Oct. 20, 16:00 - 16:30, Poster Exhibition Area

## Radiopharmaceuticals & Radiochemistry & Dosimetry: Radiopharmaceuticals - PET

## P069

### Radiosynthesis of 5-(2-[18F]fluoroethyl)-sunitinib as inhibitor of VEGFR-2 - first results

**T. Kniess**[1], M. Kuchar[1,2], R. Bergmann[1], J. Steinbach[1,2], J. Pietzsch[1,2]; [1]Helmholtz-Zentrum Dresden-Rossendorf, Institute of Radiopharmaceutical Cancer Research, Dresden, GERMANY, [2]Technical University Dresden, Department of Chemistry and Food Chemistry, Dresden, GERMANY.

**Aim:** Radiolabeled inhibitors of receptor tyrosine kinases (RTK) might be suitable probes for monitoring pathophysiological situations related to enhanced expression of the vascular endothelial growth factor receptor (VEGFR). Imaging of angiogenesis with PET could facilitate for the individual patient the evaluation of e.g. the success of corresponding anti-angiogenic chemotherapy or monitoring the stimulation of the endogenous adaptive vessel growth after implantation of bioMaterials. For this purpose we developed an 18F-radiolabeled probe, 5-(2-[18F]fluoroethyl)-sunitinib basing on the lead structure of sunitinib®, a multi-kinase inhibitor selective to VEGFR-2. **Materials and Methods**: The non-radioactive reference compound 5-(2-fluoroethyl)-sunitinib was synthesized by Knoevenagel condensation of 5-(2-fluoroethyl)-indoline-2-one with N-[2-(diethylamino)ethyl]-2,4-dimethyl-5-formyl-1H-pyrrole-3-carboxamide. Two suitable precursors for radiolabeling, A and B were obtained by reacting a 5-(2-bromoethyl)-substituted sunitinib derivative with silver 4-toluenesulfonate and silver methanesulfonate, respectively. [18F]Fluoride was produced by the 18O(p,n)18F reaction from [18O]H2O in a 18/9 cyclotron (IBA), separated by an anion exchange cartridge (QMA, Waters) and activated by azeotropic drying with acetonitrile in a stream of nitrogen before use. In a set of radiolabeling experiments 4 mg of precursor A or B were reacted with [18F]fluoride in 500µL of solvent at a scheduled temperature regime for 20 min. The yield of 5-(2-[18F]fluoroethyl)-sunitinib was determined by radio-TLC (silicagel, THF/TEA=9/1). **Results:** The non-radioactive 5-(2-fluoroethyl)-sunitinib was investigated in a competition binding assay against VEGFR-2; a Kd value of 9 nM is justifying its classification as specific inhibitor. The radiolabeling reaction of the precursors A and B was performed at temperatures varying from 60, 90, and 120°C in one of the following solvents: acetonitrile, DMF, and DMSO. As result it turned out that for both precursors in DMF and DMSO only poor labeling yields about 2% could be achieved, whereas by using acetonitrile at 90°C the yield of 5-(2-[18F]fluoroethyl)-sunitinib increased to 7-9%. Reaction temperatures higher than 90°C lead to fast and complete decomposition of the precursors as monitored by several non-radioactive by-products on TLC. Notably no difference in yield was observed by using the methanesulfonyl- or the 4-toluenesulfonyl-precursor. **Conclusions:** The new VEGFR-2 targeted radiolabeled probe 5-(2-[18F]fluoroethyl)-sunitinib was successfully synthesized by radiofluorination of the corresponding methanesulfonyl- or 4-toluenesulfonyl-substituted precursor with [18F]fluoride. First attempts to transfer the labeling method to a remote-controlled system were successful. By now a procedure for the purification of the radiotracer by semi-preparative HPLC and SPE is under development to enable the radiopharmacological evaluation.

## P070

### Evaluation and assessment of a 50 mCi $Sn0_2$-based matrix $^{68}Ge/^{68}Ga$ generator

**S. Maus**[1], D. Rossouw[2], D. Prince[2], C. Davids[2], M. Schreckenberger[1], C. Naidoo[2]; [1]University Medical Centre Mainz, Mainz, GERMANY, [2]iThemba LABS,NRF, Somerset West, SOUTH AFRICA.

**Introduction:** iThemba LABS produces $^{68}Ge/^{68}Ga$ generators commercially in a range of activities (generally 10 to 50 mCi). The generator consists of a tin dioxide support which is double loaded with the mother isotope $^{68}Ge$. It is produced under GMP conditions. In this presentation typical characteristics of a 50 mCi generator, measured over a one year period, will be discussed. In addition, labelling data on three important peptide ligands will be presented. **Experimental:** The $^{68}Ga$ was eluted with 0.6 N hydrochloric acid. Elution efficiencies, $^{68}Ge$ breakthrough, total metal contaminants and microbiological purity were monitored over a one year period. Labelling of three peptide ligands, DOTATATE, DOTATOC and DOTANOC was carried out using different amounts of ligand (15 µg, 25 µg and 35 µg) and 2 ml of the eluate. Sodium acetate was used as the buffering agent. Labelling mixtures were heated for 15 minutes in sealed glass vials placed in a heater block at 90°C and labelling efficiencies were determined by means of HPLC. Labelling mixtures were purified on solid phase C18 mini-columns (Sep-Pak) and the labelled peptide was desorbed with a saline/ethanol mixture. **Results:** The following elution data was obtained: Total metal contaminants were less than 10 ppm after 12 months. Endotoxin concentration ranged from 0.72 EU/ml to 1.12 EU/ml. No growth was detected in samples tested for sterility.In the radiolabelling experiments, an amount of 35 µg (9.2-9.4 µM) ligand resulted in labelling efficiencies consistently in excess of 90%, whereas the other two amounts yielded less consistent results for all three peptides. Labelling yields after Sep-Pak purification were in line with the labelling efficiencies and ranged between 60-80%. Radiochemical purities after Sep-Pak, as determined by means of HPLC, were in excess of 95%. Suitable ITLC QC Methods are also being tested and validated. **Discussion and Conclusion:** The data indicates that a good quality eluate is obtained from the iThemba LABS generator. Elution efficiencies are high and minimal $^{68}Ge$ breakthrough has been encountered during the first six months. Labelling efficiencies of peptide ligands are high provided a sufficient amount is used during labelling. The Sep-Pak purification also ensures that any possible traces of $^{68}Ge$ in the eluates are removed after labelling, as this metal is not complexed by the ligands. This eliminates the need for pre-purification of eluates.

## P071

### Differentiation of malignant tumors from granulomas with dynamic [$^{18}$F]-Fluoro-L-α-methyltyrosine PET imaging

**A. Yamaguchi**[1], Y. Iida[1,2], Y. Fujisawa[2], S. Inamoto[2], S. Zhao[3], K. Suzue[1], H. Tominaga[1], K. Kishimoto[1], T. Higuchi[1], H. Hisaeda[1], T. Izumi[1], Y. Kuge[3], Y. Tsushima[1]; [1]Gunma University Graduate School of Medicine, Gunma, JAPAN, [2]Suzuka University of Medical Science, Suzuka, JAPAN, [3]Hokkaido University Graduate School of Medicine, Sapporo, JAPAN.

**Aim**: Increased [$^{18}$F]-Fluoro-2-deoxy-D-glucose ($^{18}$F-FDG) uptake in inflammatory lesions is a frequent cause of false positive results in tumor diagnosis. Previous studies showed that radiolabelled amino acids possess a higher specificity to viable tumor tissue than $^{18}$F-FDG. The aim of this study is to evaluate a usefulness of dynamic [$^{18}$F]-Fluoro-L- α-methyltyrosine ($^{18}$F-FAMT) PET on the differentiation of malignant tumors from granulomas. **Materials and Methods**: The *Mycobacterium bovis bacillus Calmette-Guérin* (BCG) and allogenic C6 giloma cells were inoculated into the left and right calf muscles of rats, respectively. At 20 days after inoculation of BCG and 10 days after inoculation of glioma cells, rats were kept fasting overnight, anesthetized with isoflurane, and administered an intravenous injection of $^{18}$F-FDG (11.7 ± 2.57 MBq). A dynamic PET was performed for 120 min with hind leg region in the field of view. The next day, $^{18}$F-FAMT (19.4 ± 1.91 MBq) was injected intravenously and a dynamic PET was performed similarly. Time-activity curves, static images, mean standardized uptake value (SUV), and ratios of SUVs at a delayed phase ($^{18}$F-FDG : 60 min post injection, $^{18}$F-FAMT : 15 min post injection) to that at an early phase ($^{18}$F-FDG : 30 min post injection, $^{18}$F-FAMT : 2 min post injection) in the lesions were assessed. **Results**: In granuloma lesion, $^{18}$F-FAMT

showed relatively rapid clearance after initial distribution. In contrast, in tumor lesion, a second peak was shown immediately after initial distribution of $^{18}$F-FAMT, followed by gradual clearance compared to granuloma lesion. The ratio of SUVs in tumor lesion (0.92 ± 0.07) was markedly higher than that in the granuloma lesion (0.75 ± 0.06, p<0.001). The mean SUV in the tumor (1.24 ± 0.13) was significantly higher than that in the granuloma (1.08 ± 0.16, p<0.001). The dynamic patterns, the ratio of SUVs, and the mean SUV of $^{18}$F-FDG in the granuloma were comparable to those in the tumor (p = NS). **Conclusion:** Dynamic $^{18}$F-FAMT-PET provides useful information to differentiate malignant tumors from granulomatous lesions.

## P072

### Imaging of α7 nicotinic acetylcholinereceptors (nAChRs): Automated synthesis and biological evaluation of [18F]NS14490 in mice and pig

**S. Rötering**[1], S. Fischer[1], A. Hiller[1], C. Donat[1], M. Scheunemann[1], D. Peters[2,3], R. Bergmann[1], M. Ullrich[1], O. Sabri[4], J. Steinbach[1], W. Deuther-Conrad[1], P. Brust[1]; [1]Helmholtz-Zentrum Dresden-Rossendorf, Institute of Radiopharmaceutical Cancer Research, Leipzig/Dresden, GERMANY, [2]DanPET AB, Malmö, SWEDEN, [3]Aniona ApS, Ballerup, DENMARK, [4]Department of Nuclear Medicine, University of Leipzig, Leipzig, GERMANY.

**Aim** There is evidence that α7nAChRs play an important role in cancer and neurodegenerative diseases. Therefore, quantitative imaging of α7nAChRs using PET represents a new approach for investigation of those diseases. Due to its high target affinity and selectivity [$^{18}$F]NS14490, an oxadiazolyl-diazabicyclononane derivative, is a promising radiotracer for α7nAChRs imaging. Manual radiosynthesis of [$^{18}$F]NS14490 and its in vivo evaluation in mice were already reported [1]. The subsequent assessment of its imaging potential by dynamic PET studies in piglets and PET/CT studies in tumor-bearing mice required the transfer of the manual synthesis to an automated synthesis module. **Materials and Methods** For dynamic PET studies, the manual radiosynthesis of [$^{18}$F]NS14490 [1] was transferred to an automatic synthesis module (Tracerlab FX-N) including azeotropic drying of [$^{18}$F]F$^-$ with Kryptofix K222/$K_2CO_3$ in acetonitrile, direct nucleophilic substitution at the precursor, semipreparative HPLC and solid phase extraction. After evaporation the radiotracer was formulated in phosphate buffered saline containing 5% ethanol. Dynamic PET studies in piglets (female, 15-18 kg) were performed under control and blocking conditions (n=2 each) with a highly selective α7nAChRs ligand (NS6740; bolus: 3 mg kg$^{-1}$ h$^{-1}$; infusion: 1 mg kg$^{-1}$ h$^{-1}$) for 4 hours. The metabolism of [$^{18}$F]NS14490 in piglets was analyzed by chromatography of plasma samples. PET/CT studies were performed in tumor-bearing nude mice under control and blocking conditions with NS6740. **Results and Conclusion** During transfer of radiosynthesis into an automated synthesis module, solid phase extraction was challenging. For desorption of the radiotracer from divinyl/polystyrene cartridge, the elution solvent ethanol/acetic acid used in manual synthesis was replaced by acetonitrile/formic acid resulting in more efficient elution, formerly not accomplished. The radiotracer was achieved within 1.25 hours and radiochemical yields (32%), radiochemical purity (> 90%) and specific activity (> 150 GBq µmol$^{-1}$) were comparable to the manual synthesis [1]. Brain uptake of [$^{18}$F]NS14490 peaked in piglets at 3 min p.i. and is with a value of $SUV_{max}$ = 0.504 about tenfold higher than in mice. Blocking by NS6740 decreased the specific uptake in brain by 28% (SUV 240 min p.i. 0.174 vs. 0.125 under baseline and blocking conditions, respectively).The metabolic stability of [$^{18}$F]NS14490 in piglets is lower than in mice. At 60 min p.i. intact radiotracer represented 30% of plasma activity in piglets compared to 55% in mice. Preliminary animal PET/CT studies in tumor-bearing mice provide evidence that [$^{18}$F]NS14490 may also be suitable for tumor imaging. [1] Rötering, S. et al. *Bioorg. Med. Chem. 2013*

## P073

### Brain and whole body PET evaluation of the novel PDE10A PET radioligand, [$^{11}$C]T-773, in nonhuman primates

**A. Takano**[1], V. Stepanov[1], B. Gulyás[1], R. Nakao[1], N. Amini[1], H. Kimura[2], T. Taniguchi[3], S. Miura[1,3], C. Halldin[1]; [1]Karolinska Institutet, STOCKHOLM, SWEDEN, [2]TAKEDA Pharmaceutical Company, Fujisawa, JAPAN, [3]TAKEDA Pharmaceutical Company, Ltd., Fujisawa, JAPAN.

**Aim** Phosphodiesterase 10A (PDE10A) is considered to be a key target for the treatment of neuropsychiatric diseases such as schizophrenia and Huntington's disease. It is predominantly distributed in the putamen and caudate nucleus in the brain. PDE10A inhibitors have been shown to be effective in several animal models, spanning positive, cognitive and negative symptoms of schizophrenia. [$^{11}$C]T-773 is a novel PET radioligand for PDE10A with high binding affinity and selectivity. The aim of the present PET study was to evaluate whether [$^{11}$C]T-773 has favorable characteristics as a brain PET radioligand and to calculate the effective dose of [$^{11}$C]T-773 using whole body PET. Materials and Methods Brain PET measurements were performed for 120 min at the baseline condition and after administration with 1.8 mg/kg of MP-10, a selective PDE10A inhibitor, at which dose approximately 70-80% PDE10A has been reported to be occupied. Total distribution volume (VT) and binding potential ($BP_{ND}$) were calculated as outcome measures with various kinetic models. The occupancy was calculated by the change of the outcome measures. Whole body PET measurements were performed for approximately 120 min. The effective dose of [$^{11}$C]T-773 was calculated based on the time course of the organ uptake. **Results** In the brain PET study, there was a high accumulation of the radioligand in the striatum, where the peak was reached at around 10 min after radioligand injection. The specific binding (= 'binding in the striatum - binding in the cerebellum') peaked at around 50 min after radioligand injection. The decrease of VT values, which were calculated by a 2-tissue compartment model, after pretreatment with MP-10 was seen in the striatum but not in the cerebellum. $BP_{ND}$ was approximately 1.8 in the putamen when the cerebellum was used as the reference regions. Approximately 70% of PDE10A was occupied by the administration of 1.8 mg/kg of MP-10. In the whole body PET study, the liver, the kidney, the heart and the brain showed high accumulation of the radioligand in the initial phase. The radioligand was partly excreted via bile and the gastrointestinal tract, and partly excreted through the urinary tract. Calculated effective dose was 0.007 mSV/MBq. **Conclusions** [$^{11}$C]T-773 was demonstrated to be a promising PET radioligand for PDE10A with favorable brain kinetics. Dosimetry results support multiple PET measurements per person in human PET study. Further research with [$^{11}$C]T-773 by us would include occupancy studies as well as testing the radioligand's potential clinical applications.

## P074

### Development of [11C]nintedanib as potential TKI-PET tracer for angiogenesis imaging

**A. J. Poot**, P. Slobbe, G. A. M. S. Van Dongen, A. D. Windhorst; VU University Medical Center, Dept. of Radiology & Nuclear Medicine, Amsterdam, NETHERLANDS.

**Aim:** Tumor angiogenesis is one of the hallmarks of cancer.[1] Receptor tyrosine kinases promoting angiogenesis, e.g. vascular endothelial growth factor receptors (VEGFR), are therefore important targets for therapies with tyrosine kinase inhibitors (TKIs). Although several TKIs have reached the market most of them are only effective in a subsets of patients. Also tumor resistance to these therapies is often developed after a period of TKI treatment, which limits the clinical efficacy even further. Therefore, patient selection before treatment and response monitoring early during or after treatment with TKIs is of growing interest.[2] The aim of this study was to develop [*N-methyl*-$^{11}$C]nintedanib as TKI-PET tracer to be used for imaging purposes. Nintedanib is a broad-spectrum angiogenesis inhibitor targeting VEGFR, FGFR and PDGFR. [*N-methyl*-$^{11}$C]nintedanib will be evaluated preclinically for its imaging properties in mice bearing tumor xenografts.[3] **Material and Methods:** The precursor required for radiolabeling is desmethyl-nintedanib. This precursor was synthesized analogues to literature procedures.[3] The total precursor synthesis contained 9 synthetic steps. The optimal radiosynthesis of [*N-methyl*-$^{11}$C]nintedanib was investigated by variation between [$^{11}$C]MeI or [$^{11}$C]MeOTf as methylating agent. Furthermore, other reaction conditions such as base and solvent were varied to obtain optimal reaction conditions to synthesize [*N-methyl*-$^{11}$C]nintedanib. Crude products were purified with semi-preparative HPLC to obtain pure [*N-methyl*-$^{11}$C]nintedanib. Currently, a screening is performed using immunohistochemical staining to select suitable xenografts for preclinical evaluation of [*N-methyl*-$^{11}$C]nintedanib. **Results:** In the synthesis of [*N-methyl*-$^{11}$C]nintedanib, DMF is the superior solvent over MeCN and DMSO. Furthermore, for all bases investigated, $K_2CO_3$ was preferred compared to $Et_3N$ and TBAOH. [$^{11}$C]MeI was the preferred methylating agent in the synthesis of [*N-methyl*-$^{11}$C]nintedanib. Variations in reaction time between 5 and 10 minutes had no beneficial effects for the synthesis. Highest yields of [*N-methyl*-$^{11}$C]nintedanib are 28% d.c. after purification and formulation.[$^{11}$C]MeI in DMF and $K_2CO_3$ at a temperature of 80°C for 5 minutes are optimal conditions to synthesize [*N-methyl*-$^{11}$C]nintedanib. **Conclusions:** A reliable labelling procedure was developed for the synthesis of [*N-methyl*-$^{11}$C]nintedanib. With the synthesis of [*N-methyl*-$^{11}$C]nintedanib, a new angiogenesis PET tracer is obtained to be investigated for its imaging properties in the near future. Research Support: This research was financially supported by the Center for Translational Molecular Medicine (CTMM - Airforce). References: [1] D. Hanahan et al., *Cell*, 2011, *144*, 646; [2] P. Slobbe et al., *Drug Discov Today*, 2012, *17,* 1175; 2012, *33*, 607;[3] F. Hilberg et al., *Cancer Res.,* 2008, *68*, 4774.

## P075

### Validation of a HPLC Method for measuring radiochemical purity [68Ga]DOTANOC

**A. Iudicello**, F. Lodi, C. Malizia, S. Costa, S. Boschi; PET Radiopharmacy, Nuclear Medicine Unit, Azienda Ospedaliero Universitaria di Bologna, Policlinico S. Orsola-Malpighi, Bologna, ITALY.

**Introduction**: Quality, safety and effectiveness of Radiopharmaceutical preparations are essential for their use in clinical practice. This is supported by the implementation of chemical, physical and biological tests in specific monographs of the European Pharmacopoeia. For an Investigational Medicinal Product, specifications for the quality control come from general, raw Materials or other

radiopharmaceutical preparations monographs. Therefore it is necessary to validate the analytical Methods, verifying their suitability for intended use. Aim of this work was to develop and validate a simple and selective RP-HPLC method for the analysis of [68Ga]DOTANOC in radiopharmaceutical preparations Materials e Methods: Isocratic Chromatographic separation was achieved on a C8 column (Eclipse XDB-C8 (5µm, 150mm x 4.6mm) utilizing a mobile phase of water/acetonitrile/ TFA (70:30:0.1 v/v) at 1mL/min flow rate, with UV detection at 220. **Method** validation was performed according to ICH guideline. **Results and conclusion**: Specificity was documented by comparing retention times obtained in the standard solutions of DOTANOC (RT 4.5min) and GaDOTANOC (RT 5.8min) with those obtained from the [68Ga]DOTANOC samples. The minimal difference between retention times (<0.1%) allows confident, highly specific, peak identification. The linearity was studied in the range from 1 to 15 µg/mL of standard solutions of GaDOTANOC and DOTANOC, corresponding approximately to 20-300% of the test concentration. Five concentration points were assayed in triplicate. Good linearity has been demonstrated in the tested range. The R2 was always greater then 0.990. Precision was measured as repeatability and intermediate precision. Repeatability was studied on nine injections of standard solutions of cold GaDOTANOC and DOTANOC (three injection of standard solutions 1µg/mL, three 5µg/mL and three 15µg/mL). The %CV for each concentration of standard solution was less than 2.5%, compared with an acceptance specification of 5%. Intermediate precision was studied by measurements on three different days. The %CV for each concentration of standard solution was generally not greater than 2.5%. Fischer test were not significant for a 95% confidence interval. LOQ and LOD were calculated on the basis of the standard deviation of the response and the slope obtained from the linearity plot. LOQ and LOD, calculated as 3.3α/S and 10α/S, respectively, were 0.26 µg/ml and 0.80 µg/ml for GaDOTANOC, and 0.21 µg/ml and 0.63 µg/ml for GaDOTANOC. The proposed method is proved to be applicable for the quality control and routine analysis of [68Ga]DOTANOC in radiopharmaceutical preparations for human use.

## P076

### Oxygen-18 water: Recycle?

**S. Rötering**[1], K. Franke[2], P. Brust[1], S. Fischer[1], J. Steinbach[1]; [1]Helmholtz-Zentrum Dresden-Rossendorf, Institute of Radiopharmaceutical Cancer Research, Research Site Leipzig, Leipzig, GERMANY, [2]Helmholtz-Zentrum Dresden-Rossendorf, Institute of Radiopharmaceutical Cancer Research and Institute of Resource Ecology, Research Site Leipzig, Leipzig, GERMANY.

**Aim** The standard method for fluorine-18 production relies on proton irradiation of oxygen-18 water. Increased demand and costs of O-18 water forced us to consider its re-use for research purposes. After irradiation and F-18 separation the target water is contaminated with radioactive metal ions and organic solvents disturbing its re-use. Therefore, thorough purification is needed before further irradiation is possible. Here, we present two Methods for the removal of organic contaminants from used target water. **Materials and Methods** Two different Methods were accomplished to oxidize the organic contaminants ethanol and acetone in O-18 water using photo-oxidation (Pen-Ray 254 nm, 5.4 W) [1] and a wet chemical method with $KMnO_4$ and NaOH. Thereafter vacuum distillation was performed and the target water was validated by gas chromatography, ICP-OES, pH value, conductivity and pycnometry. In addition artificially contaminated O-16 water was used to evaluate the potential of both Methods concerning the oxidation of other potential contaminants such as methanol and acetonitrile. Target irradiations were performed at equal parameters of bombarding (beam current on target 35 µA, 11.7 µAh) at a CYCLONE 18/9 (IBA Molecular, Nirtra® Fluor L-target (99.9% niobium): 2 mL, target window: Havar alloy, 50 µm). Radionuclide purity and yields were determined by gamma spectrometry (ORTEC) and an ionization chamber (MED Nuklear-Medizintechnik Dresden GmbH). Produced F-18 was used in nucleophilic substitution reactions in various radiosyntheses of ongoing projects. **Results and Conclusion** Using both purification Methods a comparable decrease of organic contaminants from 400 µg $mL^{-1}$ ethanol and 44 µg $mL^{-1}$ acetone to 10 µg $mL^{-1}$ – 50 µg $mL^{-1}$ ethanol was achieved. Photo-oxidation was approximately 1.5times faster. Important parameters (amount of oxidation agent, temperature, treatment time) for both Methods were defined to ensure reproducibility of the radiosyntheses after comparable proton irradiation as done for the purchased target water. We observed a loss of production yield (19%) compared to purchased water due to a lower O-18 concentration. No influence on radionuclide purity or radiochemical yields was observed. Both Methods enable a multiple re-cycling of target water for successful F-18 production and application for research purposes. The re-cycling process is limited by the amount of F-18 required for radiosyntheses. Starting from 87% enrichment of O-18 in target water we found 83% enrichement after one cycle allowing reasonable production yields and efficient economical usage of the purchased target water including efforts to minimize the contamination of target water. [1] DE 29504388 U1, 1995

## P077

### Synthesis and evaluation of 21-[$^{18}$F]fluoro-17α-hydroxyprogesterone for imaging the activity of CYP17A1 with positron emission tomography

Z. Zhang, M. Pourghiasian, J. Pan, J. Lau, N. Hundal, F. Bénard, **K. Lin**; BC Cancer Agency, Vancouver, BC, CANADA.

**Aim**: Intratumoral androgen production is the key mechanism to sustain growth for castration-resistant prostate cancer (CRPC). CYP17A1 is a cytochrome P450 enzyme that catalyzes the deacetylation of 17α-hydroxypregnenolone and 17α-hydroxyprogesterone. The deacetylated products, dehydroepiandrosterone and androstenedione, are the metabolic intermediates for the biosynthesis of androgen. CYP17A1 has been shown to be up-regulated in CRPC. The ability to image the activity of CYP17A1 will have the potential to improve early diagnosis of CRPC, patient selection/screening for anti-CYP17A1 treatment, and the development of anti-CYP17A1 therapies. For this study, we hypothesized that (1) 21-[$^{18}$F]fluoro-17α-hydroxyprogesterone, a close analog of 17α-hydroxyprogesterone, is a substrate of CYP17A1; (2) the deacetylated by-product 2-[$^{18}$F]fluoroacetate will be trapped inside the cells; and (3) the amount of 2-[$^{18}$F]fluoroacetate generated is proportional to the activity of CYP17A1. Materials and **Methods**: The radiolabelling precursor 17α-hydroxy-21-[(methylsulfonyl)oxy]progesterone was prepared by coupling 17α,21-dihydroxyprogesterone with mesyl chloride in DCM using DIPEA as the base. The standard 21-fluoro-17α-hydroxyprogesterone was prepared by reacting the mesylate precursor with TBAF in THF at reflux for 30 min. 21-[$^{18}$F]fluoro-17α-hydroxyprogesterone was prepared by aliphatic nucleophilic substitution using the mesylate precursor and TBA[$^{18}$F]F in DMF at 70°C for 20 min. The stability of 21-[$^{18}$F]fluoro-17α-hydroxyprogesterone was determined in mouse plasma, and monitored by HPLC. PET imaging and biodistribution studies were performed using male NODSCID/IL2RKO mice. **Results**: The yields of mesylate precursor and standard were 65 and 22%, respectively. After HPLC purification, 21-[$^{18}$F]fluoro-17α-hydroxyprogesterone was obtained in ~8 % decay-corrected yield in 100 minutes with >1 Ci/µmole specific activity at EOS, and >99% radiochemical purity. 21-[$^{18}$F]fluoro-17α-hydroxyprogesterone was stable in mouse plasma as >95% remained intact after 2h incubation at 37°C. Biodistribution and PET imaging studies showed that 21-[$^{18}$F]fluoro-17α-hydroxyprogesterone was excreted mainly through the hepatobiliary pathway (15.8, 12.8 and 8.82 %ID/g for liver, S-intestine and L-intestine, respectively, at 1h post-injection). Significant *in vivo* defluorination was observed as the uptake in bone was 6.04 ± 1.84 %ID/g at 1h post-injection. The uptake (1h post-injection) in the CYP17A1 rich organ, testes, was 1.63 ± 0.26 %ID/g which was not significantly higher than the uptake in muscle (1.39 ± 0.64 %ID/g). **Conclusion**: We successfully synthesized 21-[$^{18}$F]fluoro-17α-hydroxyprogesterone and evaluated its potential for imaging the activity of CYP17A1 with PET. Due to the lack of uptake in testes, 21-[$^{18}$F]fluoro-17α-hydroxyprogesterone is not suitable for use as a CYP17A1 PET imaging agent.

## P079

### Characterization of radiometal chelated benzamide for diagnosis of malignant melanoma.

H. Kim[1], **J. Park**[1], M. Hur[1], S. Yang[1], K. Yu[2]; [1]Korea Atomic Energy Research Institute, Jeongeup, KOREA, REPUBLIC OF, [2]Dongguk University-Seoul, Seoul, KOREA, REPUBLIC OF.

**Aims:** Radiolabeled benzamides are attractive for melanoma imaging as they bind melanin and exhibit high uptake and retention in melanoma. We are developing $^{68}$Ga-labeled benzamide derivative for early diagnosis of melanoma with positron emission tomography (PET). **Methods**: Labeling of $^{68}$Ga was optimized for pH, temperature and time. These compounds were purified by RP-HPLC. Micro-PET imaging and biodistribution studies were performed using B16F10 melanoma bearing C57BL6 mice. **Results**: $^{68}$Ga-SDB was synthesized with ~80% radiochemical yield and high specific activity. The biodistribution studies of $^{68}$Ga-SDB displayed a significant tumor uptake, with 2.51 ± 0.5% ID/g at 1 h (the tumor-to-muscle ratio was 8.1±1.2). Micro-PET imaging revealed clearly visualization of the tumor. The tumor uptake of $^{68}$Ga-SDB accumulated time dependently. The radiotracer was cleared via renal excretion without further metabolism. **Conclusions:** $^{68}$Ga-SDB localized in melanotic melanoma tumor xenografts. $^{68}$Ga-SDB is promising candidates for the PET imaging of melanoma.

## P080

### A facial synthetic route to [18F]FBuEA-peptide via a butyl ethacrynic acid-peptide tosylate

**H. Y. Wu**, H. L. Huang, S. F. Tien, C. S. Yu; Department of Biomedical Engineering and Environmental Sciences, National Tsing Hua University, Hsinchu, TAIWAN.

**Aim**: Based on the application of [18F]FBuEA-peptide conjugate in providing differential cellular accumulation, we wish to report a simplified synthetic route to [18F]FBuEA-peptide, in which only one deprotection step was required post radiofluorination. Through the optimized route, the radiochemical yield was improved thereby ensuring a future in vivo experiment. **Materials and Methods**:

Peptide containing a thiol group was firstly dimerized via a formation of disulfide linkage upon oxidation. The subsequent protection with Boc afforded the well protected dimer. After reduction with PBr3, the released monomer with thiol group was further conjugated with N-Boc protected butyl ethacrynic amide. Followed by introducing a tosyl group, the subsequent radiofluorination and deprotection could be performed as well. **Results**: The four step-synthesis of the well-protected tosylate proceeded uneventfully (30% yield). [18F]FBuEA-peptide complex was obtained in a radiochemical yield of 5% (decay uncorrected). Specific activity and radiochemical purity were obtained in 50 GBq/μmol and 98%, respectively. **Conclusion**: [18F]FBuEA-peptide has been prepared via an optimized synthetic design. An enough radioactivity of [18F]FBuEA-peptide (1.5 mCi) was prepared and the in-vivo imaging experiments is in due course.

## P081

### Synthesis and Biological Evaluation of Novel $^{64}$Cu-Labeled Glucosamine-Dimeric RGD Peptide Conjugates for Improved PET Imaging

**L. Jiwoong**, P. JiAe, L. Yongjin, S. Unchol, P. Hyun, K. Byungil, L. Sangmoo, A. Gwangil, K. Jungyoung, L. Kyochul; Molecular Imaging Center Korea Institute of Radiological & Medical Sciences, Seoul, KOREA, REPUBLIC OF.

**Object:** Recent reports on the use of dimeric RGD peptides for imaging of angiogenesis and targeting of tumors have demonstrated that dimeric RGD is better targeting capability and higher cellular uptake because of the increased $\alpha_v\beta_3$ integrin recognition ability as compared with the monomeric RGD peptide[1, 2]. Based on above studies, we designed a noble dimeric cyclic RGD labeled radioactive Cu-64 for an effective tumor imaging, which was prepared with two cyclic RGDfK, bifunctional chelators (BFCAs) and glucosamine. Glucosamine was used for the purpose of increasing the blood clearance and reducing the liver uptake[3]. Therefore, the aim of this study was Cu-64 labeled glyco-BFCA-di-c(RGDfK) with its synthesis and evaluation *in vivo* for diagnosis and radiotherapy in tumor. **Methods:** The derivatives of glyco-BFCA-di-c(RGDfK) was prepared as three chelator types of NODAGA, NOTA and DOTA. After Cu-64 labeling with analogues of glyco-BFCA-di-c(RGDfK), they were conducted the serum stability test for 24 h, respectively. Imaging studies and biodistribution were performed the nude mice bearing U87MG glioma cancer cell. The organ uptake (10 μCi) in tumor (U87MG) bearing mice was calculated as a percentage of the injected dose per gram of organ tissue (%ID/g). Animal PET imaging of each dimeric RGD peptide was obtained at 1 h, 2.5 h, 4 h, and 16 h as tumor bearing mice injected with 230 μCi into the tail vein.**Result:** Theserum stability of each dimeric RGD peptide derivative was very stable as radiochemical purity of over 95% by ITLC. Biodistribution results of each derivatives were showed higher tumor uptake after 1 h as follows : 3.89 ± 0.56 (glyco-NODAGA-di-c(RGDfK)), 3.99 ± 0.98 (glyco-DOTA-di-c(RGDfK)), 3.81 ± 0.58 (glyco-NOTA-di-c(RGDfK)). In addition, animal PET imaging of the above derivatives were showed the highest uptake of tumor at 1 h in mice bearing tumor belong several time points.**Conclusion:** We introduced three types of Cu-64 labeled glyco-BFCA-di-c(RGDfK) and confirm their ability, possibility, high serum stability and good imaging properties making it an interesting alternative to the monomeric RGD peptide as PET radiopharmaceutical for tumor imaging.Acknowledgements: This research was supported from National Reaserch foundation of Korea(NRF) grant funded by the Korean government(MEST)(2012-0006388).References**:** [1] Yun Wu, et al (2005) J Nucl Med, 46, 1707-1718. [2] Zi-Bo Li, et al (2008) Eur J Nucl Med Mol Imaging, 35, 1100-1108. [3] B.C.Lee, et al (2007) Bioorganic & Medicinal Chemistry, 15, 7755-7764.

P13-1 - Sunday, Oct. 20, 16:00 - 16:30, Poster Exhibition Area

## Radiopharmaceuticals & Radiochemistry & Dosimetry: Radiopharmaceuticals - SPECT

## P082

### Evaluation of radiolabeled 5-iodo-2'-deoxycytidine as a SPECT proliferation imaging probe in a lung tumor xenograft model

**H. Yu**[1], C. Lin[1], W. Kuo[1], J. Kuo[1], M. Weng[1], C. Chien[1], P. Wang[1], M. Wang[1], C. Chen[2], H. Wang[2], W. Lin[1]; [1]Institute of Nuclear Energy Research, Longtan Township,Taoyuan County, TAIWAN, [2]Department of Biomedical Imaging and Radiological Sciences, National Yang-Ming University, Taipei, TAIWAN.

**Objective**: This study aims to evaluate radiolabeled nucleoside analog 5-iodo-2'-deoxycytidine (123I-ICdR) as a SPECT proliferation probe for imaging tumor in A549 lung carcinoma-bearing mouse model. **Methods**: 123I-ICdR was prepared from stannylated precursor 1-(2-deoxy-β-D-ribofuranosyl)-5-tributylstannylcytosine, and its radiochemical purity was determined by using radio thin-layer chromatography and high performance liquid chromatography. Subcutaneous tumor xenografts were produced by inoculation of A549 lung cancer cells in the right flank of 6-week-old nude male mice under anesthesia. Biological characterization studies of 123I-ICdR including in-vitro A549 cellular uptake (0.5, 1, 2, 4, and 24 h), biodistribution and nanoSPECT/CT imaging of A549 tumor-bearing mice were performed (1 h post-intravenous injection). **Results**: 123I-ICdR was prepared in high radiochemical yield (≧85%, decay corrected) and radiochemical purity (≧95%). The accumulations of 123I-ICdR in A549 cells increased with time. The percentage uptake per million cells of 123I-ICdR reached 8.01 ± 0.02 after 24 h incubation. Biodistribution studies showed that the accumulation of 123I-ICdR in A549 xenografts and muscle were 1.18±0.29 %ID/g and 0.25±0.12 %ID/g respectively. Tumor-to-muscle ratio was 4.72±0.32. NanoSPECT/CT imaging of 123I-ICdR in A549 lung carcinoma-bearing mouse clearly delineated the tumor lesion with tumor-to-muscle ratio of 2.79 at 1 h post-injection. **Conclusion:** In this study, the radioiodinated ICdR was successfully prepared with high yield and radiochemical purity. Both results of biodistribution and nanoSPECT/CT imaging showed that 123I-ICdR was accumulated in tumor with desirable tumor-to-normal tissue ratio. 123I-ICdR is demonstrated as a promising radio-probe for tumor proliferation imaging in A549 lung carcinoma-bearing mouse model.

## P083

### Quality Control of $^{99m}$Tc-tektrotyd Kits

**M. Papachristou**[1], I. E. Datseris[2]; [1]General Hospital of Athens "Evaggelismos", Athens, GREECE, [2]General Hospital of Athens, Athens, GREECE.

**Introduction:** Several attempts have been performed in order to label somatostatin analogues with $^{99m}$Tc, which is the most available radionuclide. Tektrotyd ($^{99m}$Tc-EDDA/HYNIC-Tyr$^3$-Octreotide) scintigraphy seems to have significant sensitivity and specificity in GEP's.[1] We report the daily quality controls of this pharmaceutical introduced in our Department. **Materials and Methods:** We perform physicochemical tests, indicate the level of radionuclidic and radiochemical impurities, determine of pH and visual controls. The biological tests (sterility and apyrogenity) performed periodically by an external official laboratory, which checks the QA of our Department. For these controls, the pHmetric papers, the ITLC strips, the solvents or other solutions are described on the product SPC / package insert[2]. The ITLC's strips are counted in a well counter. **Results:** We study the labeling procedure using a radioactivity range from 40 mCi to 75 mCi, different volumes from 0.9 ml to 1.7 ml, different temperatures in heating procedure 80 °C, 90 °C, 100 °C of different times 20 min, 22min, 25min, 30 min. The radiochemical purity was between 91% - 98%. After the quality control, we release the pharmaceutical and the administration takes place. The residual activity was measured after each administration. For the specific protocol the injection dose is 10 mCi to 25 mCi. The residual activity was measured in order to calculate the exact injected dose and was 3- 5 mCi. **Discussion/Conclusion**: We concluded that conditions 75 mCi, in 1.0 ml, heated up to 90 °C for 22 min, give radiochemical purity 98%. These conditions allow us high specific activity, good labeling percentage and high quality imaging under the suggested protocol. We can also administer two patients to achieve abetter cost effective preparation - scintigraphy. Reduction in dosages have significant role to the imaging quality, therefore we inject higher dosages and wash carefully the syringe due to high residual activity. Our release criteria include batch and dose labeling (radioactivity at preparation, time of use and expire time), radiochemical purity, pH, appearance (clear, colorless, free of particulates). References: 1. Plachcinska A. et al, Clinical usefulness of $^{99m}$Tc-EDDA/HYNIC-TOC scintigraphy in oncological diagnostics: a pilot study. Cancer Biother. Radiopharm. 2004; 19:261-270. 2. Package insert of Tektrotyd.

## P084

### 99mTc-exametazime-labelled leucocytes: effect of volume and concentration on labelling yield and image quality.

**I. Bossert**[1], B. Repetto[2], M. Massollo[1], A. Buschiazzo[1], S. Capitanio[1], G. Siclari[2], C. Massara[2], F. Peschiera[2], T. Zino[2], E. Giglio[2], A. Orengo[2], C. Marini[3], G. Sambuceti[1,2]; [1]Nuclear Medicine, University of Genoa, Genoa, ITALY, [2]Nuclear Medicine, Department of Health Science, IRCCS AOU San Martino – IST, Genoa, ITALY, [3]Genoa Section, CNR Institute of Molecular Bioimaging and Physiology, Milan, Genoa, ITALY.

**AIM** Scan of labeled white blood cells (WBC) distribution is commonly used to detect and localize occult sites of infection in various disorders, including osteomyelitis, infected joint and vascular prosthesis. Current clinical practice implies the direct WBC labeling with 99mTc-HMPAO. Crucial determinants for diagnostic quality of this investigation are labeling yield (LY) and total administered radioactivity. The former is directly proportional to tracer concentration in incubating solution up to a certain point when decreases due to appearance of radiolysis. The present study was designed to verify the optimal values of dose and concentration to obtain elevated LY and adequate radioactivity contain to allow best quality images. **MATERIAL AND METHODS** Experimental tests were performed using blood samples collected from seven healthy volunteers. WBC were labeled according to EANM Guidelines and three different concentrations were tested dissolving 555 MBq of 99mTc-HMPAO in 1, 2.5 or 5 ml of saline. Thereafter, we verified the relevance of dose incubating WBC with 1 ml of solution containing five

different doses of 99mTc-HMPAO (111, 370, 444, 555, 1110 MBq). **RESULTS AND CONCLUSION** As expected, LY progressively decreased at decreasing HMPAO concentration. On the contrary, radioactivity dose modified LY with a biphasic pattern characterized by a peak (89%) at a concentration of 444 MBq/ml. This behavior was confirmed in all samples. Thereafter, in a further set of five samples we verified whether the high LY is affected by increasing labeling volume (and dose) at a fixed concentration. This experiment showed that LY does not decrease up to a volume of 2 ml corresponding to a total 99mTc-HMPAO activity of 888 MBq. Any further increase in total dose caused a decrease of LY, that was interpreted as an effect of radiolysis. Our experimental approach indicates that optimal WBC labeling can be best achieved using a fixed concentration of 99mTC-HMPAO approaching 450 MBq/ml and maintaining a labeling volume of 2 ml.

## P085

### Development of Reverse Phase Thin Layer Chromatography (RP-TLC) method for determination of radiochemical purity of 99mTc-Mebrofenin

**V. V. Murhekar**, N. S. Pilkhwal, D. Padmanabhan, P. Saraswathy, G. Samuel; Board of Radiation & Isotope Technology, Navi Mumbai, INDIA.

**Aim**: A simple user friendly method for determination of radiochemical purity of a radiopharmceutical is desired in a radiopharmacy at the hospital. Pharmacopoeias describes HPLC on C18 reverse phase (RP) column as a standard method of analysis for radiochemical purity of $^{99m}$Tc-Mebrofenin in combination with ITLC method. Due to the possibility of presence of reduced hydrolysed $^{99m}$Tc ($^{99m}$Tc-colloid) as an impurity, HPLC alone cannot be used for the purpose. The test is time consuming as well as labor intensive. Our aim was to develop a simple Reverse Phase Thin layer chromatography (RP-TLC) as a rapid and convenient method for radiochemical purity determination of $^{99m}$Tc-Mebrofenin. **Materials and Methods**: Cold kit for $^{99m}$Tc-Mebrofenin was labeled according to manufacturer's instructions. The standardised RP-TLC method for determination of radiochemical purity employs 5mm x 75mm strip of RP modified silica gel on aluminium support (Merck) and a mobile phase consisting of 0.385% ammonium acetate and acetonitrile in a ratio of 55:45. An aliquot of the labeled preparation was spotted and developed in the mobile phase for 10 min. The strip was scanned under a radiochromatogram scanner. The formation of $^{99m}$Tc-Mebrofenin in the preparation was further confirmed by HPLC on HiQ Sil C18W reverse phase column in gradient mode using mobile phase water (0.385% ammonium acetate) and acetonitrile (Acetonitrile, 30% to 60% in 20 min). The flow rate was 1ml/min. UV detection was carried out at 254 nm. **Results and Discussion:** The Rf values observed the developed system were 0-0.1 for $^{99m}$Tc-colloid, 0.4-0.6 for $^{99m}$Tc-Mebrofenin and 0.8-1.0 for $^{99m}TcO_4^-$, giving a clear separation of the different radiochemical species. The reproducibility of the method was checked and the RCP was found to be 98.7% $\pm$ 0.8 (n= 6). $^{99m}$Tc-Mebrofenin complex was additionally confirmed using radio-HPLC ($T_R$=15min). The developed RP-TLC thus is a convenient, reliable and fast (development time ~10 min) method to determine radiochemical purity levels of $^{99m}$Tc-Mebrofenin in a single strip. The method is especially suited in a radiopharmacy environment where speed of analysis is important.

## P086

### Synthesis and biological evaluation of new $[^{99m}Tc^{III}(PS)_2(L)]$ mixed-ligand compounds (PS= phosphino-thiolate; L= dithiocarbamate), useful in design and development of Tc(III)-radiopharmaceuticals

**N. Salvarese**[1], N. Morellato[1], F. Refosco[2], A. Dolmella[1], C. Bolzati[2]; [1]Dipartimento di Scienze del Farmaco, University of Padua, Via Marzolo 5, 35135 Padua, ITALY, [2]ICIS-CNR, Corso Stati Uniti 4, 35127 Padua, ITALY.

**Aim**. The trivalent state is one of the most common and stable oxidation states of technetium and rhenium. In spite of this, none of the radiopharmaceuticals currently in clinical use contains the metal in this oxidation state and only a limited number of studies involving the use of M(III)($^{99m}$Tc/$^{188}$Re) are reported. We present here a general procedure for the preparation of a new series of neutral, six-coordinated mixed ligand $[^{99m}Tc^{III}(PS)_2(L^n)]$ compounds, (PS = bis-aryl-alkyl or tris-alkyl-phosphino-thiolate; $L^n$ = dithiocarbamate) that could be used to design either essential or target specific imaging agents. **Methods.** The synthesis of $[^{99m/99}Tc^{III}(PS)_2(L^n)]$ complexes, and their in-vitro stability as well as their in-vivo biological assay were investigated. Stability studies were performed by considering: *i*) stability toward transchelation with Cysteine, Glutatione, Histidine and EDTA; *ii)* binding to the serum proteins*; iii)* stability in rat serum, human serum and rat liver homogenates. Biodistribution studies of some representative $[^{99m}Tc^{III}(PS)_2(L^n)]$ compounds were performed in healthy Sprague-Dawley rats to investigate their organ uptake, excretion pathways and in-vivo stability. **Results.** $[^{99m}Tc^{III}(PS)_2(L^n)]$ complexes were prepared, in high yield, following a one-pot procedure which required the addition of pertechnetate to a reaction vial containing $SnCl_2$ and the selected PS and $L^n$ ligands. The chemical identity of $^{99m}$Tc-complexes was determined by HPLC comparison with the corresponding $^{99}$Tc-complexes. All complexes are constituted by the presence of the $[^{99m/99}Tc^{III}(PS)_2]^+$ moiety where two phosphino-thiolate ligands are tightly bound to the metal while the remaining two positions are saturated by a dithiocarbamate chelate, also carrying bioactive molecules (e.g. 2-methoxyphenilpiperazine). All complexes were inert toward ligand exchange reactions. No significant in-vitro serum protein binding and no notable biotransformation of the native compounds into different species by the in-vitro action of the serum and liver enzymes were observed. Biodistribution profiles of the complexes were characterized by a rapid blood clearance, a high lung, liver and spleen uptakes followed by slow wash-out. The activity was mainly eliminated through the hepatobiliary system. In all cases, activity in thyroid and increase of the %ID over the time in the stomach were not found, indicating the high in-vivo stability of the complexes. However, structural modifications are required to improve the pharmacokinetic profile of these compounds. **Conclusion.** Stable $[^{99m}Tc^{III}(PS)_2(L^n)]$ compounds were efficiently prepared in high yield and in physiological conditions. These results could be conveniently utilized to devise a novel class of $^{99m}Tc^{III}$-based useful to design either essential or target specific imaging agents.

P14-1 - Sunday, Oct. 20, 16:00 - 16:30, Poster Exhibition Area

## Radiopharmaceuticals & Radiochemistry & Dosimetry: Radiopharmacy

## P087

### Investigation of Radiopharmaceutical Potential of Magnetic Poly(HEMA-APH) Nanoparticles Radiolabeled with Iodine-131 on Experimental Animals

**U. Avcibasi**[1], N. Avcibasi[2], F. Gümüşer[3], D. Uygun[4], S. Akgöl[5], H. Akalın[1], M. Ediz[1], H. Demiroğlu[6], E. Özçalışkan[5], C. Türkcan[5]; [1]Celal Bayar University Faculty of Science and Art, Manisa, TURKEY, [2]Ege University Ege Higher Vocational School, İzmir, TURKEY, [3]Celal Bayar University Faculty of Medicine, Manisa, TURKEY, [4]Faculty of Arts and Science, Aydın, TURKEY, [5]Ege University Faculty of Science Department of Biochemistry, İzmir, TURKEY, [6]Faculty of Science and Art, Manisa, TURKEY.

Nanotechnology is a highly promising application platform to improve therapeutic effectiveness and safety profiles in the treatment of multiple types of cancer, as it is specific to site, limits multi-drug resistance and efficiently delivers anticancer agents [1-4]. The aim of the current study is to synthesize a new generation magnetic poly(HEMA-APH) nanopolymer using surfactant free emulsion polymerization, to radiolabel related compound with 131I and to investigate radiopharmaceutical potential of radiolabeled compound on experimental animals. To achieve this, functional monomer anilinephtalein (APH) molecule was synthesized in the first stage [5], then polymerization reaction was carried out between APH and 2-hydroxyethyl metacrilate (HEMA). In the next stage, mag-poly(HEMA-APH) polymer was radiolabeled with 131I and quality-control studies were done using radiochromatographic method. Radiolabeling yield was found to be about 90%. After that, lipophilicity and stability studies of radiolabeled nanopolymer were done. Consequently, stability in the rat serum was found to be stable for 24 hours and lipophilicity was found to be 0.12±0.02. In the final stage, scintigraphy and biodistribution studies were done. In the result of scintigraphy studies, it was observed that radiolabeled compound showed high uptake in the heart, the lungs, the liver, the kidney and the stomach. After scintigraphy studies, biodistributional experiments were carried out on female and male rats. As a consequence of these, target organs for related experiment animals were determined to be the uterus, the ovarian, the lungs and the prostate, respectively. In conclution, the nanopolymer was successfully radiolabeled with 131I using iodogen method. Showing high uptake of nanopolymer in the uterus, the ovarian, the lung and the prostate reveals the potential of this radioiodinated compound to be used in the diagnostics and therapy in diseases related with these organs. Using mag-poly(HEMA-APH) for this purpose will be able to be possible, if the cell and the xenograft studies planned to be carry out in subsequent stages give positive results. REFERENCES 1. Haley B, Frenkel E, Nanoparticles for drug delivery in cancer treatment, Urol Oncol, 26(1), 2008, 57-64. 2. Sing J, Tremendous potential for cancer treatment: Nanotechnology, The Indian Pharmacist, 8, 2008, 23-26. 3. Torchilin VP, Targeted pharmaceutical nanocarriers for cancer therapy and imaging, AAPS J, 9(2), 2007, Article 15: E128-147. 4. Loo C, Lin A, Hirsch L, Lee M, Marton J, Halas N, West J, Drezek R, Nanoshell-enabled photonics based imaging and therapy of cancer, Technol Cancer Res Treat, 2004, 91-110. 5. Hubacher MH. Anilinephthalein. Notes 1951;73:5885-5886.

## P088

### The Synthesis and Identification of NODA-Lipiodol and NODA-Oleic Acid Derivatives as the Therapeutic Labeling Ligand of Liver Cancer

**Y. Chang**; Institute of Nuclear Energy Research, Taoyuan County, TAIWAN.

Lipiodol is an iodinated and esterified lipid of poppy seed oil which has been found to be retained significantly in liver tumors after infusion via the hepatic artery. Iodine-131 ($^{131}$I) Lipiodol has been investigated as a radioembolizing material and is commercial available. Owing to the above phenomenon, several researcher attempted to label I-131, even Y-90 or Re-188 in Lipiodol. However, the low β energy and high-energy gamma emission of $^{131}$I decrease the competitiveness of $^{131}$I-lipiodol. $^{90}$Y-lipiodol has high possibility of accumulation in the skeletal system which limit its clinical value. $^{188}$Re becomes the most probable isotope for labeling Lipiodol due to its convenient, economical and energy characteristics, then $^{188}$Re-lipiodol is probably effective as a chemotherapeutic agent of liver cancer. This study reported the synthetic route of two novel monoamine-monoamide-dithiol ($N_2S_2$) tetradentate ligand, NODA-Lipiodol and NODA-Oleic acid. The former was directly complexed with $^{188}$Re, and the latter was complexed with $^{188}$Re, then was futher dissolved in Lipiodol. Both are anticipated to have a high and stable tumor accumulation in hepatoma rat model and show the potential to be therapeutic radiopharmaceuticals for hepatoma treatment. All of intermediate and final products are verified by the following instrument. Infrared spectra were run on a Bio-Rad FTS-800 spectrometer. The $^{1}$H and $^{13}$C nuclear magnetic resonance (NMR) spectra were recorded on a Varian Mercury Plus 300 MHz spectrometer. Gas chromatography was scanned on a Shimadzu GCMS-OP 1100EX model

## P089

### Optimization use of the automatic hospital dispenser Trasis® for preparation of 18Fluorodeoxyglucose (18FDG) single patient dose.

**J. Evrard**, D. Matanza, E. Odouard, M. Fraysse; Hospices Civils de Lyon, Centre Hospitalier Lyon Sud, Service de Radiopharmacie, Lyon, FRANCE.

**Introduction:** The unit dose dispenser Trasis® is an automatic system allowing aseptic production of 18FDG single dose packaged in cartridge. Theorical activity concentration (supplier data) and low distributed volume (<0.3mL), decrease the accuracy on the first dose produced from a multi-dose vial, where less activity produced is often observed. In order to make doses with a gap between produced activity and prescribed activity which is more or less 10% (internal limit for approval), the dispenser system produces then an additional cartridge. This leads up to another injection step which constitues a barrier to the acceptance of the system by medical staff. The aim of this study is to improve accuracy on the first unit dose production from a multi-dose vial. **Materials and Methods**: The filling machine accuracy after vial transfer is determined by the activity error on the first cartridge, because the system adjusts concentration activity after production, subsequently limiting errors on dispensation. There is non-conformity when there is an additional cartridge produced and/or more 10% failing dispensed relative prescribed activity. First of all, the error rate on the first cartridge production has been evaluated with 2 operating systems: without rinsing system before the installation of the second multi-dose vial (method 1) or with (method 2). Based on obtained results, a time corrective factor (method 3) has been used to limit the error on dispensed activity which is still high with the 2 previous operation way. This corrective factor consists to anticipate production of first unit dose; to correct the mean error rate of first dispensed dose, as determined previously. **Results** : Method n°1 : On 1214 cartridges made, 9.56% are first unit doses produced after vial transfert and non-conform. This error rate decreases to 0.74% for the second cartridge. Method n°2: 899 cartridge made whose 4.45% are first non-conform doses. The percentage of error is 0.44% for second cartridge. Method n°3: 984 produced cartridges, the non-conformity rate reaches to 1.32% for first cartridge and 0.71% for second. **Conclusion** : Compared with method 1, method 2 increases accuracy of approximately 5% while method 3 improves it of 8%. Corrective capacity system is effective in view of the very low error rate on second cartridge. Optimizing the accuracy on the first unit dose production, the system is better accepted by medical staff who see in this improvement a radiation exposure reduction during injection.

## P090

### Interaction between antiseptic and reduction of 99mTcO4- by SnCl2

**J. Evrard**, D. Matanza, M. Fraysse; Hospices Civils de Lyon, Centre hospitalier Lyon Sud, Service de Radiopharmacie, Lyon, FRANCE.

**Introduction:** Preparations of injectable radiopharmaceutical drugs require particular precautions of preparation and asepsis. Concerning preparations of 99mTc-labelled radiopharmaceuticals, it is necessary to avoid any contact with substances which interfere on 99mTcO4- reduction for good 99mTc-labelling kits. About asepsis, careful disinfection of septum of kits must be made before preparation but much of disinfectants are likely to disturb oxydoreduction reactions. The aim of this study is to evaluate in practice the effect of different antiseptic on oxidation-reduction reaction between 99mTcO4- and SnCl2 for 99mTc-labelling kits. **Materials and Methods**: A mother solution of SnCl2 (5.27x10-3 mol.L-1) and a diluted eluate from 99Mo/99mTc generator (activity concentration: 0.4GBq/mL) are used to reproduce redox environment of radiopharmaceutical kits. 5 antiseptics have been tested: isopropyl alcohol, alcohol 70°, chlorhexidine®, biseptine® and iodine-povidone. For each antiseptic, 4 experiments in vials have been made: negative control (2ml of eluate), positive control (2ml of eluate + 100µl of SncI2), reaction 1 (100µl of SnCl2 then injection of 2ml of eluate through the disinfected septum: usual practice), reaction 2 (100µl of SnCl2, 10µl of antiseptic, 2ml of eluate: extreme case where a significant amount of disinfectant penetrates into the vial). At t=0h, t=2h and t=4h; percentage of 99mTcO4- reduction is determined by thin-layer chromatography (ITLC-SG Varian®/acetone) added to interpretation by radiochromatography instrument (Berthold® Raytest RitaStar). Tests are achieved 5 times by antiseptic. The positive control is the reference test in terms of reduction percentage. **Results**: Without SnCl2 (negative control), no 99mTcO4- reduction have been observed. There is no reduction when iodine-povidone is in contact with 99mTcO4- and SnCl2, so the results for test 2 of iodine-povidone are not included in the following statistical analysis. The average percentage reduction of positive control is 96.3% vs 97.21% for antiseptic. When antiseptic (except for iodine-povidone) are in the reaction environment (worst case), there is no interference on redox reaction (p=0.15, n=60). **Discussion/Conclusion**: Whole of disinfectants used for simple disinfection of septum does not alter quality of redox reaction. In fact more than 95% of 99mTcO4- is reduced in this case. The absence of interaction is shown by the percentages of reduction which are higher or equal to the positive control. Only the presence of iodine in a preparation inhibits the reduction of the 99mTcO4-, and this although SnCl2 is in excess compared to the 99mTcO4-.

## P091

### A practical evaluation of effectiveness of commonly used syringe shields for PET dose dispensing

**J. G. Chan**, K. Young, K. Hickson, S. Gong, G. J. O'Keefe, A. M. Scott; Austin Health, Heidelberg VIC, AUSTRALIA.

**BACKGROUND:** Extremity doses from handling unsealed radioactive sources are a major concern to nuclear medicine staff. Automated and semi-automated syringe dispensers for dispensing FDG doses result in a significant reduction in exposure. However it is not practicable to use the dispenser system for research compounds and it is estimated that this was now contributing around 70% of extremity doses. Thus a review of PET dose dispensing practices was undertaken. **METHOD**: Two experienced operators manually dispensed 20 syringes of PET radiopharmaceutical each, 10 syringes without a syringe shield and 10 with. The syringe shield used was 85 mm tungsten shield designed for PET radiopharmaceuticals. The activity dispensed was 370 MBq, a common dose for research. The operators were timed and the dispensed activities recorded. Exposure measurements were recorded using the instadose™ dosimeter worn around the wrist of the dominant hand. In addition, 10 doses were dispensed using an alternate 30 mm syringe shield available in nuclear medicine departments for SPECT radiopharmaceutical dispensing. The premise for this was to evaluate whether the lighter, easier to handle shield would afford any protection. **RESULTS:** The same extremity exposure and dispensing time is shown by both operators when dispensing with unshielded syringes. Operator A's exposure was 20% less when dispensing using a PET syringe shield, however dispensing time increased threefold. Operator B's exposure rate only decreased slightly when dispensing with PET shielded syringes, probably due to the syringe being removed from the shield when removing the air bubble because of difficulty with visualisation through the syringe shield lead glass. However the easier air removal procedure resulted in only doubling the unshielded syringe dispensing time. Dispensing with the lighter SPECT syringe shield yielded no time advantage over using the PET syringe shield. Additionally the 30 mm syringe shield does not seem to provide enough attenuation for 511 keV photons to provide a benefit to radiation finger dose. **CONCLUSION**: Dispensing PET radiopharmaceuticals using PET syringe shields can lead to a significant reduction in hand exposure. However there is a significant increase in dispensing time due to the awkwardness of handling a heavy shield and difficulties with visualisation through the lead glass. Using a lighter, easier to handle SPECT syringe shield offers no net benefit to radiation finger dose when compared to an unshielded syringe. Decreasing exposure time is not as effective as shielding. Further investigation is warranted.

## P092

### Influence of antiandrogen therapy in $^{18}$F-fluromethylcholine in patients with prostate cancer

W. VALDES, **A. RAMIREZ**, M. NAVARRO-PELAYO LAINEZ, E. TEIJEIRO-VAZQUEZ, G. FERNANDEZ-VASCO, J. LLAMAS-ELVIRA; H.VIRGEN DE LAS NIEVES, GRANADA, SPAIN.

**Aim:** Antiandrogen drugs are essential part of the accepted pharmacological treatment for prostate cancer. They are used to reduce the tumour activity. Diagnosis and clinical following of this cancer is usually realized with $^{18}$F-choline ($^{18}$F-fluoromethylcholine) PET/CT. Choline is a substrate for the synthesis of cellular membranes that accumulates in prostate cancer. Therefore, an influence between these pharmacological treatments and the $^{18}$F-choline PET/CT images is reasonable,

but this influence is not well established. For this reason, our purpose was to analyse whether antiandrogen therapy (AAT) influences in $^{18}$F-choline prostate uptake in patients with prostate cancer. **Patients and Methods:** We retrospectively studied 27 patients diagnosed with prostate carcinoma and didn't undergo to prostatectomy. All of them underwent PET/CT with $^{18}$F-choline. 21 patients were under AAT (androgen antagonist + GnRH agonist) at the time of the PET/CT examination while other 6 didn't undergo any treatment. We calculated the $^{18}$F-choline maximum standardized uptake values (SUVmax) in the prostate gland in all patients and analysed the SUVmax differences between both groups. Moreover we realized a correlation study in the group under treatment, analyzing the relation between the therapy time and the SUVmax in prostate. In the descriptive statistics the SUVmax results were expressed as mean ± variance. In the analytic statistics the SUVmax difference between groups was studied using the statistic *"Student's t"*. **Results:** In the group who had undergone AAT the prostate SUVmax was 3.08±0.41 while in the no AAT group was 6.20±0.41. An univariate analysis detected a significant difference between SUVmax of both groups (p<0.0005). This difference reveals a negative influence of AAT in the prostate SUVmax. Also, in the group who had undergone AAT was found no correlation (r2= 0.036) between the therapy time and the SUVmax in prostate. **Conclusion:** Our preliminary results show that AAT in patients with prostate cancer induces a significantly decreased in $^{18}$F-choline prostate uptake, so it should be considered to evaluate the $^{18}$F-choline PET/CT images in these patients. Our results agree with the therapeutic objective of the AAT. The decreased in the prostate uptake is caused for the reduction of the tumour activity.

## P093

### Influence of several factors on the labelling of leucocytes with 99mTc-HMPAO.

**M. DE GREGORIO VERDEJO**, B. MARTÍNEZ DE MIGUEL, B. SANTOS MONTERO, G. PUERTAS HERNANDO, E. MARTÍNEZ MONTALBÁN, R. PÉREZ PASCUAL, L. MARTÍN CURTO; HOSPITAL UNIVERSITARIO LA PAZ, MADRID, SPAIN.

**AIM** To study several factors that may influence the labelling procedure of autologous $^{99m}$Tc- hexamethylpropyleneamine oxime (HMPAO) white blood cell (WBC). **MATERIAL AND METHODS** Influences of drug treatment, patient's WBC count and inter-operator variability on 131 leucocyte labellings were studied. These were performed under sterile conditions in a laminar flow cabinet (Class A hood in C.) The protocol was evaluated by calculating labelling efficiency (LE) and subsequently, pre and post labelling blood samples were processed in an automated hematology analyzer (CELL-DYN Sapphire). Furthermore, in 120 of them, we observed if there was any relation between $^{99m}$Tc-HMPAO labelling activity (1453-1901 MBq/mL), radiochemical purity (RP) and LE. **RESULTS** Among all the studied drugs, the only ones that may influence our labelling process were: Proton Pump Inhibitors (PPIs), Vitamin B12 and Iron Supplements. Isolating capacity (isolated leucocytes/ initial leucocytes ratio) increases with PPIs from 6.77±1.16 to 7.69±0.80 whereas it decreases if patients take Iron Supplements from 6.77±1.16 to 4.48±2.18. LE is only reduced with Iron Supplements from 74.83±3.36 to 71.58±4.54. The difference between pre and post labelling red cell/ leucocyte ratio decreases with Iron Supplements from |8.67|±2.73 to |4.47|±2.1 and Vitamin B12 from |8.67|±2.73 to |5.74|±2.63. Eosinophil %, eosinophil count/µL and neutrophil count/µL have direct relation to LE (0.325, p<0,001; 0.354, p<0,001 and 0.228, p=0.009 respectively). Neutrophil % and neutrophil count/µL have inverse relation to red cell/ leucocyte ratio in the final sample (-0.195, p=0.026 and -0.346, p<0.001). Neutrophil % has direct relation to the isolating capacity (0.256, p=0,003). Kit radiopharmaceutical preparation (mean Activity (MBq) = 3354±449, mean RP (%) = 90.16±4.39) and LE (mean LE (%) = 74.64 ± 3.14) values were analyzed. There is a significant statistical relation between RP (%) and LE (p=0.016; Pearson's correlation coefficient of 0.219). Inter-operator variability had no statistical significance (p>0.05) with any studied factor. **CONCLUSION** Our protocol for labelling autologous WBC with $^{99m}$Tc-HMPAO is consistent but it may be influenced by drug treatment and patient's WBC count. This study has revealed the potential negative influence of Vitamin B12 and Iron Supplements over the labelling procedure. The presence of high eosinophil and neutrophil patient counts enhance LE. High neutrophil count in the initial blood sample allows improved isolating capacity and decreased red cell/ leucocyte ratio in the final sample. Finally, better LE could be achieved with high RP.

## P094

### Simplified method for in vitro red cells labelling with 99mTc

**I. Gil**[1], M. Roca[1], L. Camacho[1], P. Boya[2], M. Bajén[2], A. Rodriguez[2], P. Notta[2], R. Puchal[2], A. Santapau[2], J. Martin-Comin[1]; [1]Radiopharmacy Unit. Nuclear Medicine Department. Bellvitge-IDIBELL University Hospital, Hospitalet de Llobregat, Barcelona, SPAIN, [2]Nuclear Medicine Department. Bellvitge-IDIBELL University Hospital, Hospitalet de Llobregat, Barcelona, SPAIN.

**Introduction:** We label erythrocytes "in vitro" with 99mTc using Sn2+ as a reducing agent, EDTA for the chelation of Sn2+ in excess and the process involves two centrifugations. With this method we use to obtain labelling efficiencies higher than 96% and it took around 40 minutes. The method that recommends only Sn2+ as a reducing agent and large volumes of saline to reduce Sn2+ in excess sometimes fails to labelling efficiencies below 70% and it takes about 1 hour. Aim: The aim of this study was to evaluate a new method for labelling red cells with 99mTc reducing steps and time spent. **Methods**: We combined different amounts of Sn2+ (0.3 µg to 5 µg / mL blood) and EDTA (0.5 mg to 2.9 mg / mL blood) and performed only one centrifugation. We obtained the best labelling efficiency using 0.8 µg Sn2+ / mL blood and 2.9 mg EDTA / mL blood. Three 4.5 mL blood samples were withdrawed over 0.5 mL of ACD-A from 12 patients scheduled for ventriculography and after their signed informed agreement. One sample was labelled with 99mTc as usual with Sn2+ as a reducing agent, EDTA and 2 centrifugations. The second sample was labelled with 99mTc using only Sn2+ as a reducing agent (Spanish Pharmacopeia recommended method). The third sample was labelled using the new proposed method. Briefly, it is as follows: 0.8 ug Sn2+ / mL blood is added and left at room temperature 5 minutes, followed by 2.9 mg of EDTA / ml blood, 3 mL of saline and 99mTc-pertechnetate. After 5 minutes at room temperature, the blood is centrifuged, the supernatant is removed and replaced by saline. The amount of 99mTc was 1110 MBq ± 10% in all cases in a volume of 0.3 mL - 0.4 mL. Results: Labelling efficiencies and the approximate time of labelling were: 97.3 ± 1.1, 40 min (usual method), 87.6 ± 13.8, 60 min (Spanish Pharmacopeia method), 87.1 ± 3.1, 30 min (simplified method). **Conclusions:** Using the simplified method for in vitro labelling red cells with 99mTc here described, the labelling efficiencies obtained are aproximately 10% lower that that those obtained with our usual method, but performed with less sample manipulations and shortening the process in 10 minutes. The labelling efficiencies are similar to those obtained with the recommended method without EDTA but it is much more fast and reproductible.

## P095

### Radiopharmaceuticals Aseptic Preparation: Feasibility Study of Connectors Use

**E. NEVADO**, J. COSTES, I. QUELVEN; Nuclear Medicine Department, University Hospital Dupuytren, Limoges, FRANCE.

**AIM:** Radiopharmaceuticals are prepared in Nuclear Medicine Department, in a controlled atmosphere area (ISO 8), inside a shielded isolator with laminar flow (ISO 4.8). Preparation of these injectable solutions require to respect severals regulations: good practice preparation (BPP) for the observance of asepsis, and regulation of the Nuclear Safety Authority (ASN) for radiation protection. Most of radiopharmaceuticals are multidose preparations and used for many patients syringes preparations. The aim of this study is to find a secure sampling method which allow to reduce bacterial contamination risk and optimize radioprotection. **MATERIALS AND METHODS**: To avoid perforating several times the septum and manipulate the vial, direct puncture with syringe and needle was excluded. Multisample system was preferred. Among sterile medical devices available, a long needle, as lumbar puncture needle, seem interesting but, between syringes collections, a cap for needle is necessary. An ordinary cap, which need removal for sampling, induce preparations bacterial contamination risk and manipulator contact with radioactive source. Connector systems with two-way valves seem adapted to our needs. This system advantage is to collect the radiopharmaceuticals without having to remove the device. So, we made an inventory of available connectors. Among market references, twenty one was selected and eleven was tested by personnel handling. Several criteria were analyzed to evaluate handling, aseptic and radioprotection. **RESULTS**: After many suppliers contact, twenty-one connector systems with two-way valves and allowing connection to our sampling system was obtained. Among them, those with dead volume estimated by supplier > 0.15 ml were excluded. Furthermore, two connectors were rejected because after needle connection, these systems remained open and induced bacterial contamination risk. Eleven connectors were finally tested on 7 criteria: connection, connector-needle-syringe ability and sealing, handling, sampling facility, asepsis respect, kind of flush. To avoid radioactive contamination, connectors having a bad connection or positive flush were not been selected. Afterwards, dead volume and residual radioactivity in the connector was measured. Connectors with residual radioactivity > 0,5 mCi and/or dead volume > 0,12 ml were excluded. **CONCLUSION**: No system tested performed all choice criteria. Two connector systems standed out from our feasibility study : Bionecteur 2® (Vygon) and Tego® Connector (Hemotech). They presented little dead volume and residual radioactivity, but each have a limit : difficult connection with luer 1 ml syringue for Bionecteur 2® ; drops production after several sampling and price for Tego® Connector. Dedicated system adapted to radiopharmacy specificity may be interesting to develop.

## P096

### UPLC®-RAD the new standard in quality control of PET radiopharmaceuticals

**B. Maas**[1], R. Zijlma[1], A. Bannink[2], M. Lub-de Hooge[1,3], P. H. Elsinga[1], R. A. J. O. Dierckx[1], H. H. Boersma[1,3], G. Luurtsema[1]; [1]Department of Nuclear Medicine and Molecular Imaging, University Medical Centre Groningen,

University of Groningen, Groningen, NETHERLANDS, [2]Waters Corporation, Milford, MA, UNITED STATES, [3]Department of Hospital and Clinical Pharmacy, University Medical Centre Groningen, University of Groningen, Groningen, NETHERLANDS.

**Objectives:** Good Manufacturing Practice (GMP) compliant productions require validated, quality control procedures of the radiopharmaceutical. Quality control of the final product is conventionally performed by High Performance Liquid Chromatography (HPLC) with UV and radioactivity (RAD) detection. To use an ACQUITY Ultra Performance Liquid Chromatography (UPLC®) with an online UV and RAD detector we improved not only the analysis time, but also linearity, resolution, reproducibility, precision, accuracy, signal-to-noise ratio, limit of quantitation (LOQ) and limit of detection (LOD) compared to conventional HPLC quality control analysis. **Materials and Methods:** A Waters H-class UPLC® with a variable UV detector and an online Berthold flowstar LB 513 radioactivity detector was used to measure the (radioactive) concentrations of the radiopharmaceutical and impurities in the samples. The UPLC® columns used were from the Waters ACQUITY UPLC® line, with a 2.1 or 3.0 mm i.d. by 50 mm length and a particle size of 1.7µm. Flow rates can vary from 0.4 till 1.0 ml/min dependent on the procedure. Total run time of a quality control method is 2-3 minutes. Aliquots from 1-10 µL are needed for quality control. To validated new UPLC® analysis Methods we performed a full validation (PQ). As part of the validation of the new UPLC® Methods we performed a comparison with the conventional HPLC Methods. PET radiopharmaceuticals; such as fluorine-18 labeled FLT, FAZA, FDOPA, FES and carbon-11 labeled PK11195, PIB, 5-HTP and methionine were used in this study. **Results:** Due to shorter conditioning- run- and rinse times, the solvents cost reduced up to 80% significantly. The higher resolution and lower LOQ gave a better and more accurate result of the concentration of compounds. Both for the UV and radioactivity signal, the measurability of impurities possible present in the production sample is considerably increased. Indeed, more impurities are detected. However, the total amounts of these impurities are far below the release criteria of 1 $mg.L^{-1}$. Radioactivity concentrations > 0.3 MBq/ml could reliably be measured with the Berthold RAD detector. **Conclusion:** The UPLC®-RAD gave better linearity, reproducibility, sensitivity and higher resolution then conventional HPLC with UV/RAD detection. Especially for the $^{11}C$ radiopharmaceuticals, a reduction in the analysis time of 12 min leads to 34% more released radioactivity, ready for injection. For $^{18}F$-radiopharmaceuticals the profit is still 7%. Thus, UPLC®-RAD might become the new standard in quality control of PET radiopharmaceuticals.

P15-1 - Sunday, Oct. 20, 16:00 - 16:30, Poster Exhibition Area

## Radiopharmaceuticals & Radiochemistry & Dosimetry: Radiometals

### P097
### Cyclotron production of Cu-61

**O. Lebeda**, J. Ralis, D. Seifert; Nuclear Physics Institute AS CR, Husinec-Rez, CZECH REPUBLIC.

**Aim** Copper-61 (3.33 h) is one of the most promising non-conventional positron emitters with excellent imaging properties. However, its half-life and limited availability has been limiting exploration of its potential. We have, therefore, investigated some aspects of its routine cyclotron production via deuteron induced reactions on natural nickel. **Materials and Methods** High purity thick nickel targets (60 µm and 1 mm) were irradiated on external cyclotron deuteron beam of energy varying between 10.6 and 7.5 MeV. After the end of bombardment (EOB), the targets were dismounted, dissolved in 37% hydrochloric acid with 30% hydrogen peroxide and the product was separated from the target matrix via ion-exchange chromatography from HCl adjusted to 8M. In the case of the 1mm thick target, only the thickness corresponding to degrading the beam energy up to the reaction threshold (2–3 MeV) was etched. Intact targets, etched targets and all the solutions from the separation process were measured using calibrated gamma spectrometer equipped with HPGe detector. Evaluated data allowed for estimating achievable activity, radionuclidic purity and separation efficiency of the produced $^{61}Cu$. **Results** The whole target processing took 1.5–2.0 h and separation efficiency was around 80 %. Maximum deuteron energy of 10.6 MeV resulted in physical yield of 85–90 MBq/µAh, but also in rather high content of long-lived cobalt isotopes: $^{56}Co$ (77.233 d, 0.5 % at EOB) and $^{58}Co$ (70.86 d, 1.2 % at EOB) that are not, in contrast to nickel, separated from $^{61}Cu$. Decrease of the incident beam energy up to 7.5 MeV reduced physical target yield to 45 MBq/µAh, while having significantly improved radionuclidic purity: content of $^{56}Co$ and $^{58}Co$ dropped to 0.067 and 0.055 % at EOB, respectively, another, actually inseparable impurity in the product was $^{64}Cu$ (12.70 h) – 0.81 % at EOB, while short-lived $^{65}Ni$ (2.52 h) was efficiently removed. **Conclusion** It is easy to produce $^{61}Cu$ using compact cyclotrons used in PET centres in amounts up to 1 GBq at EOB under moderate conditions (single run, 3 h, 10 µA) with relative content of longer-lived cobalt isotopes around 0.12 % and $^{64}Cu$ around 0.8 %. Further improvement of radionuclidic purity is possible only by employing highly enriched $^{60}Ni$ (26.2 % in natural nickel) that would both increase the yield almost four times and eliminate practically production of $^{64}Cu$ and $^{56}Co$. Acknowledgements This work was supported by Technology Agency of the Czech Republic (project no. TA02010797).

### P098
### Radiosynthesis of [68Ga]Ga-Df-DUPA-Pep as a PSMA Ligand.

**E. Andreolli**[1], E. Al-Momani[2], B. Baur[2], N. Malik[2], H. Machulla[2], C. Solbach[2]; [1]University of Milano-Bicocca, Milano, ITALY, [2]Clinic for Nuclear Medicine, Ulm, GERMANY.

**Aim**: Prostate-specific membrane antigen (PSMA) is a promising target to develop new markers for Molecular Imaging of prostate carcinoma (PCa). Glutamate-urea-based peptides (DUPA) exhibit specific binding to PSMA. In the last years, various ligands having DUPA moiety were synthesized and labelled using different chelating agents or prosthetic groups that have shown excellent binding affinities in PSMA expressing PCa cells. Our goal was the coupling of the chelator Desferrioxamine (Desferal; Df) to DUPA-Pep to enable both the labelling with Ga-68 and Zr-89. In the present study we describe the synthesis of Df-DUPA-Pep labelled with Gallium-68 as a new PSMA ligand. **Materials and Methods**: Custom made DUPA-Aoc-Phe-Phe-NH-(CH2)2-NH2 Trifluoroacetate (DUPA-Pep Trifluoroacetate; DUPA: 2-[3-(1,3-dicarboxypropyl)-ureido]-pentanedioic acid) was coupled with p-isothiocyanatobenzyl-desferrioxamine to give Df-DUPA-Pep by standard procedure. The preparation and purification of [68Ga]GaCl3 were conducted by conventional procedure after acidic elution of a TiO2-based 68Ge/68Ga generator. [68Ga]GaCl3 was neutralized by 2M Na2CO3 and the resulting solution was then added to a solution of Df-DUPA-Pep (1 µg - 0.6 nM, 5 µg - 3 nM and 20 µg - 13 nM; DMSO) and 0.25 M HEPES buffer (pH 7.4, 500 µL). The reaction was carried out at room temperature for 1, 5 and 10 min. Determination of the radiochemical yield and radiochemical purity was performed by radio-TLC (Phosphor Imager) and radio-HPLC. **Results**: Best results were obtained by use of 20 µg precursor for a reaction time of 10 min. The RCY was >90% after 1 min and increased up to 97±1.6% after 10 min. The relation ("specific activity") between [68Ga]Ga-Df-DUPA-Pep (411 MBq) to unlabelled peptide was >30 GBq/µmol. **Conclusion**: An efficient method for the preparation of a new PSMA-ligand ([68Ga]Ga-Df-DUPA-Pep) was developed resulting in an overall RCY of >95% within 10 min providing a radiotracer directly applicable in preclinical studies.

P16-1 - Sunday, Oct. 20, 16:00 - 16:30, Poster Exhibition Area

## Radiopharmaceuticals & Radiochemistry & Dosimetry: Radiopharmakinetics & Drug Development

### P099
### Preclinical Evaluation of Ligand-Target Binding Properties Using Competitive Interaction Analysis in Real-Time Radioimmunoassay on Living Cells

**P. Barta**[1], F. Trejtnar[1], K. Andersson[2]; [1]Faculty of Pharmacy in Hradec Kralove, Charles University in Prague, Hradec Kralove, CZECH REPUBLIC, [2]Department of Radiology, Oncology and Radiation Sciences; Uppsala University, Uppsala, SWEDEN.

**Aim**: The binding characteristics of specific ligands, which are expected to be new promising pharmaceuticals, may be determined with the use of competitive assays. The comparison of a novel ligand with an established ligand upon competing interaction seems to be a basic pharmacodynamic test before a potential further development. The disadvantage of the traditional competition Methods lies in their time and material consumption, especially the consumption of novel ligand, where its preparation may be difficult and costly. These facts led us to the development of a convenient, economic and information rich method to conduct competition assays. Our presented technique is based on the automatic radioimmunoassay carried out on the instrument LigandTracer. **Materials and Methods**: To evaluate the appropriateness of the ligand competiton technique detected with the real-time radioimmunoassay, we used the well-described epidermal growth factor receptor (EGFR) model. EGFR natural ligand epidermal growth factor (EGF) was radioiodinated (131I) using the chloramine-T method. 131I-EGF (3 nM) was left to bind to EGFR for 1-3 hours followed by an addition of an anti-EGFR monoclonal antibody (cetuximab, panitumumab or nimotuzumab) to compete with radioiodinated EGF as already bound to EGFR. The assay was performed in vitro on two different EGFR over-expressing cell lines. **Results**: 131I-EGF bound during the preincubation phase on the targeted receptor was displaced by cetuximab and panitumumab. To induce similar displacement, the required concentration of the cetuximab was 15 times (nM) lower than for panitumumab. Nimotuzumab did not displace EGF even at 10 times higher concentration than the radioiodinated EGFR natural ligand. Thanks to the small working volume (5 ml) per experiment there was used small concentrations (3 to 45 nM) of radiolabelled ligand or unlabelled antibodies, which was sufficient to detect the receptor - ligand interactions. **Conclusion**: The used method enabled to manifest cetuximab and panitumumab as

good binders to EGFR. On the other hand we have demonstrated that nimotuzumab targets different binding site then EGF does, and was confirmed as a poor competitor for EGF. The appropriateness of the novel technique based on the competition assay for convenient, economic and information rich ligand characterization was confirmed. The real time radioimmunoassay detection can reveal the binding characteristics of studied ligands and their binding site preference with the consumption of a less ligand. The study was co-financed by the European Social Fund and the state budget of the Czech Republic, project no. CZ.1.07/2.3.00/30.0061.

## P100

### Comparison of Pharmacokinetics of 188Re-HEDP and 99mTc-HDP in Human Using Scintigraphy

**M. Smolyarchuk**[1], G. Davydov[1], A. Aleksandrova[1], V. Krylov[1], T. Kochetova[1], E. Markova[2]; [1]MRRC Ministry of Health of Russia, Obninsk, RUSSIAN FEDERATION, [2]IAE NRNU MEPHI, Obninsk, RUSSIAN FEDERATION.

Rhenium-188 is a generator isotope, it has very high energy of beta-particles (E(max)=2,12 MeV), gamma component with E=150 keV, short half-time (17 hrs) and radiochemical properties similar to Technecium-99m. One of Re-188 labeled bisphosphonates, 188Re-hydroxyethylidene diphosphonate (HEDP), which has "brother" labeled with Technecium-99m - 99mTc-HDP - is very promising radiopharmaceutical for painful bone metastases therapy. The aim of this work was to evaluate pharmacokinetic of 188Re-HEDP in human and evaluate predictive value of 99mTc-HDP preliminary scan for radionuclide therapy planning. Materials and Methods: 8 patients having painful bone metastases from breast cancer, prostate cancer, thyroid cancer and gastric cancer were studied. Prior to radionuclide therapy patients had scintigraphic studies: static images of pelvis, including kidneys, were made in 1, 3 and 24 hrs, and wholebody scan was performed in 3 hrs after after injection of 800-1000 MBq of 99mTc-HDP. 3-6 days later ~2000 MBq of 188Re-HEDP was injected intravenously followed by static images in 1, 3, 24 and 48 hrs and wholebody scan in 22-24 hrs. Acquired images were assessed visually and semiquantitatively - we used a Differential Uptake Coefficient (DUC), which was calculated as a percentage of lesion/bone uptake. T1/2 from time of maximum uptake was computed for both datasets using exponential estimation and taking half-life of isotopes into concideration. Results: wholebody scans with both radiopharmaceuticals showed same number and localisation of bone pathologic uptake lesions in all patients. DUCs were the same in 5 patients (140% to 390%), higher with 188Re-HEDP in 2 patients (higher up to 80%), higher with 99mTc-HDP in 1 patient (up to 30% difference). T1/2 of 188Re-HEDP in metastases is 36,7±3,4 hrs, in bones 31,5±2,8 hrs. T1/2 of 99mTc-HDP in metastases tends to infinity, in bones is >400 hrs. In addition, WB scans with 188Re-HEDP showed high uptake in kidneys in all patients (220-420% over background), moderate uptake in liver in 7 patients (160%±10%), intensive uptake in thyroid in 2 patients (210-380% over background). Conclusion: 188Re-HEDP shows intensive uptake in bone metastases similar to 99mTc-HDP and it washes off from lesions significantly slower then from healthy bones. Good correllation between uptake of these radiopharmaceuticals indicates that bone scan with 99mTc-HDP can be used to predict 188Re-HEDP uptake in bones and plan radionuclide therapy more effectively. However 188Re-HEDP lower T1/2, its' uptake in liver and thyroid means high binding to blood proteins and decomposition of a radiopharmaceutical in vivo. It definitely needs futher investigation.

## P101

### Biological Behavior of 188Re-Sn Suspension as a Promising Radiopharmaceutical for Radiosynovectomy

**O. E. Klementyeva**, A. O. Malysheva, G. E. Kodina, N. A. Taratonenkova, M. V. Zhukova, K. E. Makarova; Burnasian Federal Medical Biophysical Center FMBA, Moscow, RUSSIAN FEDERATION.

**Objectives**: Radiosynovectomy is a therapy used to relieve pain and inflammation from rheumatoid arthritis and related diseases. Progression of the disease leads to the destruction of the joint or loss of function. Cartilage is relatively radioresistent, so a radioactive agent with effective soft tissue penetration can be administered directly into the joint, causing no harm to the adjacent cartilage. As beta radiation can penetrate only a few hundred cell diameters, microparticles labeled with beta emitting radionuclides are effective in treating the disease by radiation without endangering nearby normal tissues. In this study the 188Re-Sn suspension was synthesized and characterized according to its physico-chemical properties and biological behavior in rats and rabbits. **Methods:** In this study 188Re is the chosen radionuclide as it is readily available on routine basis from the 188W/188Re generator (Russia, Obninsk). The radionuclide 188Re has a β-ray emission of sufficient energy (2.11 MeV) to penetrate 5-10 mm of thickened synovial membrane, and its low-level γ-ray emission (155 keV) makes scintigraphic monitoring possible, without harming patients or practitioners. Its half life (16.9 hr) is adequate in terms of obtaining an appropriate therapeutic effect or for handling of the agent, avoiding hazardous residual effects. The suspension was prepared in two stages. The radiochemical purity was determined by paper chromatography on Whatmann 1 in 0.9 % NaCl. The particle sizes were determined by laser scattering method on NICOMP™ 380 ZLS. All animal experiments were conducted in compliance with the animal protection laws and with the ethical principles and guidelines for scientific animal trials. Biodistribution of 188Re-Sn suspension was studied in normal rats. The scintigraphic images were acquired with a SPECT/CT (Philips) at 24 and 72 hr after intraarticular administration of suspension to rabbits. **Results and conclusion**: We successfully synthesized 188Re-Sn suspension, this suspension is stable more than 3 days after its preparation. Optimal conditions for effective labeling (> 95%) was found. About 90 % of particles in the synthesized suspension was lower than 9.3 μm. The results of biodistribution studies show that the 188Re-Sn suspension solidly fixed in the knee joint of rats. Within 72 hours after injection 188Re-Sn suspension is not redistributed in animals. Similar results were also obtained in rabbits. The scintigraphic images of the rabbits, at 24 hr and 72 hr post administration, indicate relevant activity only in the knee.

P17-1 - Sunday, Oct. 20, 16:00 - 16:30, Poster Exhibition Area

## Radiopharmaceuticals & Radiochemistry & Dosimetry: Antibodies & Peptides

## P102

### 177Lu-DOTA-NOC radiolabelling with the ModularLab PharmTracer® for the treatment of NET patients at the Medical University of Vienna: preliminary results

**H. Eidherr**[1], M. Hoffmann[1], C. Decristoforo[2], F. Girschele[1], M. Mitterhauser[1], L. Nics[1], I. Leitinger[1], H. Sinzinger[1], W. Wadsak[1]; [1]Medical University Of Vienna, Vienna, AUSTRIA, [2]Medical University Of Innsbruck, Innsbruck, AUSTRIA.

**Aim:** The peptide receptor radiotherapy (PRRT) of neuroendocrine tumour (NET) patients using 177Lu-labelled peptide analogues of somatostatin like DOTA-TATE has become very successful over the last years. Yet due to patent legal restrictions of DOTA-TATE the unlabelled peptide is currently not commercially available.Therefore 177Lu-radiolabelling of DOTA-NOC which is free available and which has similar chemical and biological properties compared with DOTA-TATE was evaluated and performed. **Materials and Methods:** The complete 177Lu-radiolabelling was done with a cassette based ModularLab PharmTracer® (Eckert&Ziegler) system, employed activities were around 500MBq of 177LuCl3 (n.c.a.), in 0.5ml 0.04M HCl, (ITG). Radiolabelling of the DOTA-NOC-peptide [fixed amount (80μg) of the DOTA-NOC-peptide, dissolved in deionized water, 1μg/μl, ABX)] took place at 80°C/20min in 0.57M ascorbate buffer, pH 4.5. The complete procedure was performed using the appropriate synthesis sequence. To each formulation 0.2ml DTPA (3mg/ml) solution was added. Quality control according to the pharmacopeia was performed for each lot (RCP by HPLC and TLC, pH, osmolality, sterility and bacterial endotoxins). **Results:** 177Lu-DOTA-NOC could be produced in activities of ~450MBq corresponding to labelling yields of ~90%). RCP always was ~99% with good stability (~98% even after 40h), pH ~5.0, osmolality ~270mosmol/kg. All lots were sterile and the endotoxins below 1EU/ml. **Conclusions**: From the chemical point of view 177Lu-DOTA-NOC can be produced as well as 177Lu-DOTA-TATE. All 177Lu-DOTA-NOC preparations had excellent radiochemical purity and stability. In vitro- and in vivo-studies are planned for the near future to see whether 177Lu-DOTA-NOC can be a good surrogate for 177Lu-DOTA-TATE in NET patients.

## P103

### Aspects on the synthesis of $^{177}$Lu-DOTA-tate and $C_{18}$ purification: re-addition of ascorbic acid is required to maintain radiochemical purity

**S. Maus**[1], E. d. Blois[2], M. Schreckenberger[1], W. A. P. Breeman[2]; [1]University Medical Centre Mainz, Mainz, GERMANY, [2]Erasmus MC, Rotterdam, NETHERLANDS.

**Objectives:** Radio labelled somatostatin analogues, such as $^{177}$Lu-DOTA-tate ([$^{177}$Lu-DOTA$^0$,Tyr$^3$]-Octreotate) play an important role in peptide receptor-targeted radionuclide therapy (PRRT). $^{177}$Lu-DOTA-tate can be produced either manually or by robotics and $C_{18}$ columns are recently introduced as a "safety net" post synthesis in order to remove non-incorporated $^{177}$Lu from the solution for intravenous administration. However, $^{177}$Lu-DOTA-tate is vulnerable to radiolysis, which results in decreased radiochemical purity (RCP). Every % decrease in RCP of $^{177}$Lu-DOTA-tate for PRRT represents 74 MBq of a Lu-labelled compound, which has lost its receptor affinity. Gentisic acid and ascorbic acid are well known ingredients to reduce the effects of radiolysis. With the introduction of this "safety net", however, gentisic acid and ascorbic acid might be removed effectively from the injectate, thus RCP might drop dramatically. Therefore we investigated the effect of $tC_{18}$

purification on RCP of $^{177}$Lu-DOTA-tate in the injectate as a f(t) post labelling *vs.* control (=without $tC_{18}$ purification). **Methods:** The effect of $tC_{18}$ purification on RCP of $^{177}$Lu-DOTA-tate was investigated by HPLC as function of time post radiolabelling *vs.* control (=without $tC_{18}$ purification), and concentration of activity in 5 or 20 mL. In addition, the effects on RCP of with vs. without re-addition of ascorbic or gentisic acid was also quantified time-dependently post radiolabelling. **Results:** After $tC_{18}$ purification gentisic acid and ascorbic acid were indeed effectively removed from the injectate. RCP of the injectate with $tC_{18}$ purification was >95% after 5h in 5 mL, while RCP in 20 mL decreased much more rapidly and resulted in 95% RCP after ~5h and 74% at 24h. RCP of control (=without $tC_{18}$ purification) was ≥95% at ~ 72h in 5 and in 20 mL. RCP of fractions after re-addition of ascorbic acid was ≥95% at ~ 72h. Re-addition of gentisic acid had no beneficial effect on RCP. **Conclusion:** RCP of $^{177}$Lu-DOTA-tate decreases time- and volume-dependently after $tC_{18}$ purification in comparison to control. These results clearly demonstrate the necessity for re-addition of ascorbic acid after $tC_{18}$ purification.

## P104

### Comparative in vitro and in vivo evaluation of three $^{99m}$Tc-labeled CCK2R-targeting gastrin-analogs differing in amino acid chain length

A. Kaloudi[1], E. Lymperis[1], P. J. Marsouvanidis[1,2], E. P. Krenning[2], M. de Jong[2,3], B. A. Nock[1], **T. Maina-Nock**[1]; [1]Molecular Radiopharmacy, INRASTES, NCSR Demokritos, Athens, GREECE, [2]Department of Nuclear Medicine, Erasmus MC, Rotterdam, NETHERLANDS, [3]Department of Radiology, Erasmus MC, Rotterdam, NETHERLANDS.

**Aim:** Radiolabeled gastrin analogs have been proposed for diagnostic imaging and radionuclide therapy of CCK2R-positive human tumors, such as medullary thyroid carcinoma. Modifications in the length of the amino acid (AA) chain and strategic AA-replacements may influence the biological profile of resulting radioligands. With the aim to study such effects, we have coupled the chelator $N_4$ at the N-terminus of gastrin I (GI)-related sequences of varying peptide chain length to allow for $^{99m}$Tc labeling. Accordingly, the following analogs were developed: Sargastrin-6 (SG6= [$(N_4)Gln^1$]GI), Demogastrin-2 (DG2= [$(N_4)Gly^4$,$DGlu^5$]GI(4-17), and Demogastrin-4 (DG4= [$(N_4)DGlu^{10}$]GI(10-17)). **Materials and Methods**: Peptides were labeled with $^{99m}$Tc as previously described and QC was conducted adopting RP-HPLC and ITLC Methods. Time-dependent internalization of $^{99m}$Tc-radiopeptides was conducted at 37°C in confluent monolayers of A431-CCK2R$^+$ cells (±1 μM DG2). Stability was tested by RP-HPLC analysis of blood samples collected 5 min post injection (pi) of $^{99m}$Tc-analogs in healthy Swiss albino mice. Biodistribution was performed at 4 h pi of test $^{99m}$Tc-radiopeptide (100 μL, 5 μCi, 10 pmol total peptide ± 40 nmol DG2: *in vivo* CCK2R-blockade) in SCID mice bearing AR4-2J tumors. **Results:** Internalization in A431-CCK2R$^+$ cells was rapid and CCK2R-specific ranking the three $^{99m}$Tc-radiopeptides as follows: [$^{99m}$Tc]SG6= 7.3% > [$^{99m}$Tc]DG2= 6.7% > [$^{99m}$Tc]DG4= 1.7% (% of total added radioactivity per million cells at 2 h). After injection in mice, the percentage of $^{99m}$Tc-radiopeptides detected intact in the blood at 5 min pi was: [$^{99m}$Tc]DG4 (10%) < [$^{99m}$Tc]SG6 (28%) < [$^{99m}$Tc]DG2 (55%). Biodistribution data were consistent with internalization and stability findings, with [$^{99m}$Tc]DG2 exhibiting the highest AR4-2J tumor uptake (6.5%ID/g) *vs.* [$^{99m}$Tc]SG6 (3.3%ID/g) and [$^{99m}$Tc]DG4 (1.8%ID/g). However, [$^{99m}$Tc]DG2 also presented the most elevated renal uptake (55.6%ID/g) *vs.* [$^{99m}$Tc]SG6 (26.7%ID/g) and [$^{99m}$Tc]DG4 (1.6%ID/g). **Conclusion**: In agreement with previous experience, peptide-chain length greatly affected important biological parameters of the three gastrin-based $^{99m}$Tc-radiopeptides reported herein, such as internalization in CCK2R-expressing cells, metabolic integrity of circulating radioligand and uptake in AR4-2J xenografts. [$^{99m}$Tc]DG2 best combined these properties, but at the expense of unfavourably elevated renal accumulation.

## P105

### $^{99m}$Tc tricarbonyl labelled single chain anti-PSMA antibody fragment: Evaluation in PSMA positive prostate cancer cell lines

S. Nawaz[1], F. Kampmeier[1], G. E. D. Mullen[1], P. J. Blower[1], **J. R. Ballinger**[2]; [1]King's College London, London, UNITED KINGDOM, [2]Guy's & St Thomas' Hospital, London, UNITED KINGDOM.

**Introduction:** The most extensively studied antigen for imaging prostate cancer (PCa) is prostate specific membrane antigen (PSMA). The monoclonal antibody J591 has specificity for an extracellular epitope of PSMA. We prepared a single chain variable fragment (scFv) of J591 incorporating a His-tag for labelling with $^{99m}$Tc tricarbonyl and evaluated its binding using the human PCa cell lines PC3LN3 (PSMA negative) and a variant engineered to express PSMA (PC3LN3-PSMA). **Methods:** J591(scFv) was expressed in HEK293T cells and purified by metal ion affinity chromatography followed by size exclusion chromatography. Stability and monomer/dimer ratios of the purified scFv under different storage conditions were analysed by SDS-PAGE and analytical size exclusion HPLC. J591(scFv) was labelled with $^{99m}Tc(CO)_3^+$ using an Isolink kit, at 37°C for 60 min and labelling was monitored by iTLCsa. Stability of the radiolabelled scFv in human serum was analysed by SDS-PAGE/autoradiography over 24 h. Cell binding studies were performed using PC3LN3 and PC3LN3-PSMA cell lines. **Results:** J591(scFv) was expressed in 293T cells with a yield of 12 mg purified protein/L culture supernatant. J591(scFv) is most stable to dimerisation at -80°C compared to -20°C and 4°C. Site specific labelling via the His-tag results in a radiochemical yield of 85-90% with a final radiochemical purity of >99% after a gel filtration purification step. Liquid chromatography-mass spectrometry using a C18 column shows the formation of radiolabelled J591(scFv) detected in both UV and radioactivity chromatograms. J591(scFv) is radiochemically stable in serum with no dissociation of $^{99m}$Tc over 24 h. Cell binding assay shows specific binding of the radiolabelled protein to PSMA positive cells. **Conclusion:** J591(scFv) can be radiolabelled with $^{99m}Tc(CO)_3^+$ conveniently and efficiently. In these small scale studies the maximum specific activity achieved was 7 MBq/μg. The labelled product is stable in serum. It shows selective binding to PSMA positive cells compared to PSMA negative cells. This potential radiotracer warrants evaluation in PCa xenograft models. Acknowledgement: The J591(scFv) sequence and PC3LN3/PC3LN3-PSMA PCa cell lines were kindly provided by Dr John Maher, King's College London.

P18-1 - Sunday, Oct. 20, 16:00 - 16:30, Poster Exhibition Area

## Radiopharmaceuticals & Radiochemistry & Dosimetry: New Targets

## P106

### In vivo imaging of hEGFR-targeted PEG-based nanocarrier containing magnetic nanoparticles for cancer diagnosis and therapy

**D. Psimadas**[1,2,3], M. Comes-Franchini[4], G. Baldi[5], E. Fragogeorgi[1,3], C. Ravagli[5], T. Tsotakos[1,3], P. Bouziotis[3], P. Georgoulias[2], G. Loudos[1]; [1]Department of Medical Instruments Technology, Technological Educational Institute of Athens, Egaleo, GREECE, [2]University Hospital of Larissa, Larissa, GREECE, [3]Institute of Nuclear and Radiological Sciences and Technology, Energy & Safety, N.C.S.R. "Demokritos", Aghia Paraskevi, GREECE, [4]Department of Industrial Chemistry "Toso Montanari", University of Bologna, Bologna, ITALY, [5]CERICOL, Colorobbia, Firenze, ITALY.

**Aim**: Magnetic nanoparticles (NPs) represent a promising vehicle with application in drug delivery, hyperthermia treatment and imaging. MNPs bearing an iron oxide core can be hybridized with various polymeric chemicals and functionalized with appropriate targeting ligands, resulting in targeted magnetic core-shell nanocarriers. The main advantages of MNPs include their ability to be visualized by magnetic resonance imaging (MRI), guided to target sites by means of an external magnetic field and be heated to provide hyperthermia/ablation of tissues for cancer therapy (magnetic fluid hyperthermia - MFH). Radiolabeling of these nanoformulations with SPECT or PET isotopes can result new and attractive dual-imaging agents and provide the means to obtain of an accurate in vivo biodistribution profile. **Materials & Methods**: In this study we used polyethyleneglycol (PEG)-based polymeric stealth nanoparticles bearing a lipophilic magnetite core, which are useful delivery systems for in vivo applications. In vivo visualization of the fate of these hybrid MNPs targeted with a MoAb (hEGFR) was performed in epidermoid carcinoma (A431) animal mouse models after radiolabelling with 99mTc by the direct SnCl2 method. In vitro stability of the radiolabelled nanocarriers was tested with histidine (His), diethylene triamine pentaacetic acid (DTPA) and serum challenge studies. Ex vivo biodistribution studies in tumor-bearing mice were also performed and were compared against scintigraphic images. **Results**: The final size of the hEGFR-targeted hybrid magnetic nanoformulations was 92.1 + 0.6 nm with a polydispersity index (PDI) of 0.15. They were radiolabeled with 99mTc with high labelling efficiency (>98%), using 40 μg of SnCl2. In vitro stability showed that the radiolabeled complex was relatively stable in His and serum solutions after incubation for 24 h, whereas that was not the case for DTPA where a displacement occurred even at 1 h. Biodistribution studies revealed maximum concentration in the liver, which remains almost constant over time, while a significant concentration is found in spleen as well. Concentration on tumor is higher than 1% and the analysis per gram shows that it is much higher than the concentration in normal tissue. Finally, some concentration in blood and kidneys, suggest that NPs remain in the blood pool for some time. Scintigraphic images agree with the above results and the tumor can be clearly delineated. **Conclusion:** Targeted magnetic-based hybrid nanocarriers can be efficiently applied for tumor imaging using nuclear medicine techniques and can potentially serve as dual-imaging agents as well as become efficacious tools for drug delivery and MFH applications.

## P107

### Radiolabeling of Phytohemagglutinin-L (L-PHA) Conjugated Magnetic Nanoparticles and Investigation In Vitro Biological Affinities

**P. Unak**, O. K. Guldu, F, E. I. Medine, M, A. Y. Kılçar, F. B. Barlas, F. Z. B. Müftüler, S. Timur; Ege University, BORNOVA-IZMIR, TURKEY.

**Introduction**: In recent years, magnetic nanoparticles have attracted much attention because of their unique magnetic properties and widespread application in cell separation, drug delivery, MRI techniques, clinical applications as cancer diagnosis and treatment. The aim of this study is to synthesize L-PHA conjugated magnetic nanoparticles radiolabeled with $^{131/125}$I and to evaluate its in vitro biological behavior. Experimental: Magnetic nanoparticles, $Fe_3O_4$, were prepared by the co-precipitation method from ferrous and ferric ion solutions with a molecular ratio of 1:2 and they coated with TEOS. The obtained silica-coated magnetic particles coated with aminosilane. Finally L-PHA, was conjugated to the NPs by the cross-linker of glutaraldehyde. Magnetic nanoparticles were characterized with Zeta potential, AFM, SEM, FTIR Methods. Finally, phytohemagglutinin-L conjugated magnetic nanoparticles (MNP-L-PHA) were radiolabeled with $^{131}$I by iodogen method. Incorporation studies were carried out on breast cancer cell line (MCF-7) and Human alveolar adenocarcinoma cell line (A-549). Cytotoxicity studies were carried out on MCF-7, A-549 and Vero cell lines for 24, 48 and 72 hours by MTT method. Wound healing studies were carried out on MCF-7 cells. Results: The size of the magnetic nanoparticles were 40-60 nm. L-PHA lectin was conjugated to nanoparticles in 10 minutes with yield over 99 % and 30 minutes with 99.9 % binding was determined as optimum immobilization time. Radiolabeling yields of $^{131}$I labeled L-PHA conjugated silane magnetite nanoparticles and $^{131}$I labeled L-PHA were 97.96 ± 1.98 % and 94.43 ± 4.28 %, respectively. Radiolabeled compounds ($^{131}$I-MNP and $^{131}$I-MNP-L-PHA) could be separated with electrophoresis method and they were positive charged. Experimental lipophilicity value of the $^{131}$I-L-PHA was determined as -0.35 ± 0.11. This value shows that the radiolabeled biomolecule is hydrophilic. Serum stability studies showed that the stability until 24 hours were over 90 %. In vitro bioaffinities of $^{125}$I-MNP-L-PHA and $^{131}$I-L-PHA were performed on A549 (Human lung adenocarcinoma epithelial cell line) and MCF-7 (Breast cancer cell line). Cell uptake studies show that conjugation with magnetic nanoparticles were increased the uptake of radiolabeled compound by the cells. Also applying external magnetic field increase the cell uptake. There were no toxicity both MCF-7 and Vero cells up to 200µg/ml concentration limit till to 48 hours. **Conclusion:** Radioiodinated lectin conjugated radiolabeled magnetic nanoparticles could have a potential as hybrid imaging agent in SPECT-MR imaging systems. Also using this molecule under external magnetic field can increase its affinity for therapeutic purposes.

P19-1 - Sunday, Oct. 20, 16:00 - 16:30, Poster Exhibition Area

## Radiopharmaceuticals & Radiochemistry & Dosimetry: Miscellaneous

## P108

### The study of mechanisms and specificity of 99mTc-ciprofloxacin interaction with St.Aureus cultures.

S. I. Sazonova[1], **Y. N. Ilushenkova**[1], M. R. Karpova[2], N. V. Varlamova[3], Y. B. Lishmanov[1]; [1]Institute of Cardiology of the Siberian Branch of the Russian Academy of Medical Sciences, Tomsk, RUSSIAN FEDERATION, [2]Sibirean medical University, Tomsk, RUSSIAN FEDERATION, [3]Tomsk Politechnical University, Tomsk, RUSSIAN FEDERATION.

The use of radiolabeled antibiotics is technique for infection diagnosis. The clinical usefulness of $^{99m}$Tc-ciprofloxacin ($^{99m}$Tc-CF) has been described previously. However, mechanisms of $^{99m}$Tc-CF action is not studied enough. **The purpose.** To investigate mechanisms of $^{99m}$Tc-CF accumulation in the infection foci. **Methods.** Presumable mechanisms of $^{99m}$Tc-CF accumulation in the pathological foci are associated with antibacterial activity of its substance. However, incorporation of $^{99m}$Tc into the structure of CF may affect mechanism of its antibacterial action consisted in binding with microbial DNA-gyrase. We studied antibacterial activity of CF comparing with $^{99m}$Tc-CF, Na$^{99m}$TsO4 and reagent for $^{99m}$Tc-CF preparation by disk-diffusion method. Control of antimicrobial activity was performed using daily broth culture St.Aureus, seeded on the meat-infusion broth in Petri dishes as a lawn. Over the growth medium with St.Aureus we put sterile disks wetted with solutions of CF, $^{99m}$Tc-CF, $^{99m}$Tc and reagent for $^{99m}$Tc-CF preparation. The diameter of sterile zone was measured after 24 hrs. We also analyzed the extent of $^{99m}$Tc-CF binding with live and heat inactivated St.Aureus culture. 0.7 ml suspension of live or inactivated St.Aureus were incubated with 1 ml (20 MBq) of $^{99m}$Tc-CF or $^{99m}$Tc at 37$^0$C for 15, 30 and 60 min. Each type of suspension was passed through antibacterial filter with a pore diameter 200 nm, followed by filter washing with 10 ml of 0.9% NaCl. The radioactivity of filter and washed solution was measured. As a control we used filters through which 1 ml (20 MBq) of $^{99m}$Tc-CF or Na$^{99m}$TsO4 without S.Aureus was flowed. We made 3 experiment iteration. **Results.** The diameter of sterile zone was 27 mm for CF, $^{99m}$Tc-CF and reagent for $^{99m}$Tc-CF, 0 mm for Na$^{99m}$TsO4. The residual $^{99m}$Tc-CF radioactivity in filter with live St.Aureus was 2,511±0,204, 3,232±0,256, 4,364±0,191 MBq at 15, 30 and 60 min respectively, in filter with inactivated St.Aureus - 5,448±0,201, 4,651±0,154, 5,287±0,067 MBq at the same terms. The Na$^{99m}$TsO4 radioactivity in filter with live St.Aureus was 0,413±0,034, 0,355±0,054, 0,289±0,095 MBq at 15, 30 and 60 min respectively, in filter with St.Aureus - 0,521±0,021, 0,342±0,102, 0,202±0,0094 MBq at the same terms. In control filters radioactivity was 0,244±0,023 in all terms. **Conclusion.** The incorporation of $^{99m}$Tc into the structure of CF does not affect its antibacterial properties and binding with DNA-gyrase. Accumulation of $^{99m}$Tc-CF both in living and dead cultures of S.Aureus indicated presence of additional non-specific mechanisms of its binding with bacteria. Na$^{99m}$TsO4 has no affinity to St.Aureus cultures.

## P109

### Investigation of the Necessary Conditions for Effective Leukocytes' Labeling with the Colloidal Complex

V. Zavadovskaya, O. Kilina, M. Zorkaltsev, **V. Udodov**, M. Zamyshevskaya, A. Kurazhov; Siberian State Medical University, Tomsk, RUSSIAN FEDERATION.

Indication of chronic and subacute inflammation is a diagnostic problem that can be solved by using colloidal complexes. The aim of this study is to find optimal conditions for labeling and to assess the effect of colloidal complex 0,1-1 micron ("Diamed" Ltd., Russia) on the viability and the functional activity of leukocytes. Materials and Methods. Assessment of viability in vitro under different conditions of blood sampling was performed in the following way: by visual inspection (no clots), by microscopy after staining with trypan - blue. There was also estimated the functional activity of leukocytes including the assessment of B-lymphocytes' phagocytosis activity (determination of the immunoglobulins' concentration) and T-lymphocytes' activity (blast-cell transformation response assessment) by immunological Methods. Results. In the first phase there were determined the best and most convenient conditions for the blood's taking: needle's diameter, temperature and duration of incubation. There was performed the functional assessment of the T- and B-lymphocytes' activity by determining the levels of immunoglobulin G in the supernatant, and staging LRBT, NBT test. The greatest number of viable and functionally active cells are stored when using needle with diameter G19, at 37 º C and the incubation time up to 90 minutes. In the next phase of the study under the conditions described above, there was carried on the leukocytes' incubation with the colloidal drug. When comparing the two groups (control (C) - no nanocolloids, and experimental (E) - with nanocolloids) on various findings there were received the following data: viability of M (C) = 97±2, of M (E) = 97.5±1.5 at p = 0.08; NBT test of M (C) = 65±2, of M (E) = 66±2 at p = 0.07; immunoglobulin G of M (C) = 19.8±1.2, of M (E) = 19.4±1.3 at p = 0.09 and reaction blast-cell transformation of M (C) = 74.2±2.1, of M (E) = 76.2±1.8 at p = 0.10. These data show no statistically significant differences in the number of viable white blood cells in contact with the colloid. Conclusion. These results allowed us to formulate the necessary conditions for effective labeling of leukocytes with the colloidal complex: blood's taking with a needle with a diameter not less than 19G, incubation at 37 ºC and the incubation's time is 45-90 minutes. There was also proved that nanocolloid doesn't affect the viability of blood cells.

## P110

### Synthesis of 18F-Labeling Folate Conjugated Silica-Gold Nanocomposite for Tumor Cell Diagnosis

**J. Lee**[1,2], M. Hur[1], S. Yang[1], K. Yu[3], S. Kim[2]; [1]Korea Atomic Energy Research Institute, Jeoneup, REPUBLIC OF KOREA[2], Department of Advanced Material Chemistry, Dongguk University-gyeongju, REPUBLIC OF KOREA, [3]Department of Chemistry, Dongguk University-seoul, Seoul, REPUBLIC OF KOREA.

Silica and gold nanocomposites have been used in the field of medicinal chemistry and heterogeneous catalysis. These Materials are useful in various areas of sciences because of its easy and stable fabrication method and extensive properties. Multifunctional hybrid nanocomposites were synthesized by template method using a range of coupling Materials. The nanocomposites were fully characterized by XRD, DLS, TEM, SEM, Zetasizer, UV-Vis, Fluorescence Spectroscopy and 13C CP-MAS solid state NMR. The accumulation on CT-26 cell was observed by Confocal Lazer Scanning Microscopy. In this research, we have newly synthesized various nanocomposites by incorporating folic acid and fluorescence (FITC) on silica gold composites (FA-FSGNS). Folic acid is essential vitamin for living cells. A cancer cell has are receptor in cell membrane to utilize folic acid as much as possible. In vitro, we successfully carried out biological evaluation on mouse colon cancer cell (CT-26) with folic acid immobilized composite Materials (FA-FSGNs). The results showed that FA-FSGNPs can be accumulated on CT-26 cancer cells. In vivo, we confirm that SGN-18F used effective on the PET imaging. In future, this hybrid nanocomposite is expected to be used as new type of radiopharmaceutical material, which can diagnose various disease By introducing the various functional groups.

## P111

### Influence of medium (plasma vs saline) in labelling autologous leucocyte with 99mTc-hexametazime for inflammation scintigraphy. An "in vitro" and "in vivo" study

**V. Frusciante**, P. Tabacco, M. Totaro, G. Castriotta, G. Valle; Nuclear Medicine, Scientific Institute "Casa Sollievo della Sofferenza", San Giovanni Rotondo (FG), ITALY.

**Background and Aim**: Optimization of white blood cells (WBCs - leucocytes) labelling procedure is critical to get the highest diagnostic sensibility and specificity of the cell labelled scintigraphic studies in inflammation. Critical steps in WBC labelling procedure are the re-suspension procedure of the isolated leukocytes and their incubation with 99mTc- hexametazime (HMPAO - Ceretec). Our research has been aimed to study the influence of the medium (plasma vs saline) in which leucocyte labelling is performed, on the quality of the WBC inflammation scintigraphy. **Patients and Methods**: 23 patients with suspicion of phlogosis after ortopedic protesic implantation and other phlogistic conditions underwent autologous WBC labelling by 99mTc- hexametazime and scintigraphy according with good clinical practice procedures. The patients were divided in two groups: group P (14 pts) in which the re-suspension and labelling of WBC with 99mTc-hexametazime was performed in autologous plasma and group S (9 pts) in which the re-suspension and labelling of WBC with 99mTc- hexametazime was performed in saline. After labelled-WBC re-injection, radioactivity curves in the time were obtained from regions of interest taken on lungs, liver and spleen. In vitro vitality test was performed by dying with May Grunwald-Giemsa staining a drop of the final preparation, taken just before the intravenous injection, and careful microscopical evaluation. **Results:** In the 9 patients of group S the microscopic examination demonstrated aggregates of leucocytes, suggesting the presence of morpho-functional alteration. This is also reflected by the early important accumulation of the radioactivity in the liver and in the lungs and by the continous increase in the spleen activity during the 40 minutes after injection. On the contrary in the 14 subjects of group S at optic microscopy the leucocytes did not present abnormalities and the dynamic scintigraphic study showed a fast lung clearance and only a moderate accumulation of the labelled white cells in the liver and in the spleen. **Discussion and Conclusions**: The medium in which leucocytes are re-suspended and labelled heavily affects the quality of the injected preparation and, therefore, the "in vivo" behaviour of the labelled cells. This, in its turn, affects the quality of the scintigrafic study. The use of autologous plasma as the medium in which to re-suspend and to label the leucocytes with 99m-Tc-hexametazime is a simple, not expensive and easily implementable improvement and can result in an important increase of the quality of 99mTc- hexametazime - WBC scintigraphy.

## P112

### Synthesis of radio hollow silicate as cancer imaging agent

**J. Park**, B. Jang, M. Hur, S. Yang; Korea Atomic Energy Research Institute, Jeongeup, KOREA, REPUBLIC OF.

**Objectives:** A hollow silica nanosphere is a new nanostructured drug carrier for increasing drug loading capability [1,2]. The F-18 loaded hollow silica was synthesized by the sol-gel process with dodecylamine (DDA) and polyvinylpyrrolidone (PVP) for PET imaging agent in comparison to F-18 loaded silica **Methods:** The concentration of DDA was controlled to form self-assembled hexagonal arrays on the surface of the PVP spheres and tetraethylorthosilicate (TEOS) was added and hydrolysised for the formation of silica shell. The hollow silica was obtained by removing the PVP core and template DDA through solvent extraction. The hollow silica were characterized by X-ray diffraction (XRD) measurements, Fourier transform infrared spectroscopy (FT-IR) and high-resolution transmission electron microscopy (HR-TEM). After separation and purification of F-18 using ionic resin, F-18 has been loaded into the hollow silica by soaking method and acid addition. After the mixture was centrifuged, the hollow silica was washed with methanol *In vivo* studies, Images were obtained with Balb/C nude mice with induced CT26 colon cancer cells with a micro PET. **Results:** The diffraction peaks match well with those of the corresponding standard silica, indicating that the hollow silica was successfully synthesized. The FT-IR spectra showed broad and extensive band in the 3,600 ~ 3,400 cm-1 corresponding to the O-H stretching vibration on the silica shell surface. Whereas, the strong absorption bands at 1,080 cm-1 and 1,032 cm-1 are the symmetric and asymmetric stretching vibrations of Si-O-Si. The peaks at 2,980 cm-1 and 2,920 cm-1 are associated with the asymmetric and symmetric $CH_2$ stretching modes. HR-TEM image indicated that the diameter and wall thickness of the synthesized hollow silica was about 100 nm and 20 nm. PET images showed high tumor uptakes of the F-18 loaded hollow silica was higher than that of the silica. **Conclusions:** The F-18 loaded hollow silica was successfully prepared by the sol-gel process with dodecylamine (DDA) and polyvinylpyrrolidone (PVP) as dual template combination. The ability of F-18 storage of hollow silica suggests it has a potential imaging agent as radioisotopes delivery vehicles. **References:** [1] Haam SJ, et al (2008) Langmuir, 24, 3417-3421. [2] Zhou WL, et al (2007) J. Phys. Chem. C, 111, 17473-17477.

P20-1 - Sunday, Oct. 20, 16:00 - 16:30, Poster Exhibition Area

## Cardiovascular: Basic Science

## P113

### The Possible Role of Radionuclide Methods in Assessment of Cardiac Resynchronization Therapy in Patients with Heart Failure

**Y. Lishmanov**[1], I. Efimova[1], S. Minin[2,1], S. Popov[1]; [1]Federal State Budgetary Institution «Research Institute for Cardiology» of Siberian Branch under the Russian Academy of Medical Sciences, Tomsk, RUSSIAN FEDERATION, [2]Federal State Budgetary Institution Research Institute for Complex Issues of Cardiovascular Diseases under the Siberian Branch of the Russian Academy of Medical Sciences, Kemerovo, RUSSIAN FEDERATION.

Cardiac resynchronization therapy (CRT) has been demonstrated as being an extraordinarily effective technique that improves symptoms leading to reverse ventricular remodeling and reducing mortality in patients with a wide QRS complex and congestive heart failure (CHF). However, not all patients respond to CRT, have positive haemodynamic and contractility effects. The aim the study was to elucidate the role of radionuclide Methods in the selection of candidates for cardiac resynchronization therapy (CRT) and in the evaluation of CRT effectiveness. Methods. We studied 28 patients (19 male and 9 female) with dilated cardiomyopathy (DCM) and heart failure (HF). Before implantation of CRT device, all patients underwent SPECT with 99mTc-MIBI at rest to evaluate the myocardial perfusion, 123I-BMIPP to evaluate the myocardial metabolism, and gated cardiac blood pool SPECT (GBPS) to assess the myocardial contractile function. Following CRT, all patients were examined with 99mTc-MIBI SPECT and GBPS 12±3 months after the intervention. Results. All patients after CRT were divided into three groups. The first group included 10 patients with LVEF increased by more than 10% (hyperresponders), the 2nd group included 11 patients with an increase in EF of more than 5% but less than 10% (responders) and third group consisted of 7 males whose LVEF remained unchanged or worsened compared with pre-operative values (nonresponders). Prior to CRT, no statistically significant differences were found between groups in hemodynamic parameters (EF, EDV, ESV, SV), intra- and interventricular dyssynchrony, as well as in the midsize of perfusion defects. Following long-term CRT, we found increase in LVEF and decrease in average size of perfusion defects in groups of hyperresponders and responders ($P<0.05$). Results of SPECT with 123I-BMIPP, performed prior to CRT, showed that nonresponders had more pronounced disturbance of myocardial metabolism compared with the group of hyperresponders (20% vs 14.7%, $p<0.05$). Conclusion. The results of the study demonstrate that the radionuclide Methods can be used as possible indicators in the evaluation effectiveness and selection of candidates on the CRT.

P21-1 - Sunday, Oct. 20, 16:00 - 16:30, Poster Exhibition Area

## Cardiovascular: Perfusion

## P114

### Positron emission tomography versus cardiac magnetic resonance imaging for the assessment of myocardial viability: A meta-analysis

**I. Bandong**, R. Fuentes; St. Luke's Medical Center, Quezon City, PHILIPPINES.

**Background:** Ischemic heart disease is now the leading cause of death worldwide, and it is expected that the rate of coronary artery disease will only accelerate in the next decade with the burden shifting progressively to lower socioeconomic groups. Chronic ischemic heart disease with left ventricular dysfunction is present in a number of clinical syndromes in which myocardial revascularization results in an improvement of patient's survival. Over the past two decades, positron emission tomography (PET) imaging has become more widely accessible for the management of ischemic heart disease. Cardiac magnetic resonance (CMR) is an emerging diagnostic test for the detection of viable myocardium. Several studies comparing cardiac MRI with PET have been done the evaluation of myocardial viability, but each has considered few subjects, thus leaving uncertainty about the diagnostic accuracy of these two modalities. The purpose of this study was to evaluate the diagnostic accuracy of cardiac magnetic resonance (CMR) imaging for the assessment of myocardial viability compared with the gold standard of positron emission tomography (PET) **Methodology**: We searched Medline for literature that evaluated myocardial viability among patients with chronic ischemic heart disease and left ventricular dysfunction using cardiac magnetic resonance imaging (CMI) and positron emission tomography (PET). Data were pooled. Standard approach for meta-analysis for diagnostic tests and a bivariate analysis of sensitivity, specificity, positive predictive value (PPV), and negative predictive value (NPV) were done. **Results:** From the 17 citations identified, 7 relevant original articles were selected. Only 3 fulfilled all of the inclusion criteria, and presented data on segment-based analysis. The overall segment-based analysis demonstrated a sensitivity of 91%

(95% CI: 90-92%), specificity of 88% (95% CI: 85-91%), positive predictive value of 97%, negative predictive value of 69%, positive likelihood ratio of 7.8 and negative predictive value of 0.10 Conclusion: CMR is highly sensitive for detection of viable myocardium but its specificity remains moderate.

## P115

### Prognostic value of thallium ECG-gated myocardial perfusion single-photon emission computed tomography (SPECT) left ventricular parameters in patients with suspected coronary artery disease

**I. Bandong**[1], J. Obaldo[2]; [1]St. Luke's Medical Center, Quezon City, PHILIPPINES, [2]Philippine Heart Center, Quezon City, PHILIPPINES.

**Background:** Thallium ECG-gated myocardial perfusion single-photon emission computed tomography (SPECT) is non-invasive technique for the diagnostic and prognostic assessment of patients with suspected or known coronary artery disease. The aim of this study is to evaluate the prognostic value of thallium ECG-gated myocardial perfusion single-photon emission computed tomography (SPECT) left ventricular parameters in patients with suspected coronary artery disease. **Methodology**: We identified 175 patients who underwent Tl-201 ECG-gated myocardial perfusion SPECT in the Philippine Heart Center between February 2006 and December 2006. The left ventricular parameters, LHR, TID, LVESV, LVEDV and LVEF were obtained and correlated with the development of cardiac events. **Results**: Of the 175 patients, 100 (57%) had normal MPI results and 75 (43%) had abnormal MPI results. The mean values of LVEDV (>85 ml, p =0.024), LVESV (>35 ml, p = 0.019) and LVEF (<60 ml, p = 0.002) in males, as well as the mean values of LHR (>0.30, p= 0.000), TID (>0.90, p = 0.007), SSS (>2, p = 0.000), SRS (>0, p = 0.000), SDS (>1, p = 0.000), number of segments (>2, p =0.000) and severity of the defects (>0, p =0.000) showed significant correlation with the development of cardiac event. The number of segments and severity of the defect showed a sensitivity of 100%, specificity of 82.6%, PPV of 72% and NPV of 100% in predicting cardiac event. The SSS and SDS showed a sensitivity of 90.7% and 88.9%. The SRS showed a specificity of 83.3%. **Conclusion**: Thallium ECG-gated myocardial perfusion SPECT LV parameters provide prognostic information in predicting cardiac event.

## P116

### Long-term prognostic value of coronary artery calcium score and cardiac gated SPECT imaging in asymptomatic individuals

**M. Kaminek**[1], I. Metelkova[1], M. Budikova[1], E. Buriankova[1], R. Formanek[1], L. Henzlova[1], P. Koranda[1], E. Sovova[1], V. Kincl[2]; [1]University Hospital, OLOMOUC, CZECH REPUBLIC, [2]CMI, ICRC-FNUSA, BRNO, CZECH REPUBLIC.

**Purpose:** The aim of this study was to investigate the prognostic value of coronary artery calcium (CAC) score in combination with cardiac SPECT imaging in an asymptomatic population. **Methods:** One hundred twenty-eight consecutive asymptomatic patients (79 men, mean age 54±10 let, 25 with diabetes) with an intermediate 10-year risk of cardiac death or myocardial infarction (MI) underwent stress cardiac gated SPECT imaging and CT assessment of CAC score. Perfusion summed difference score (converted to % of ischemic myocardium), the left ventricular ejection fraction (LVEF) and end-diastolic/end-systolic volumes (EDV/ESV) were automatically calculated using 4D-MSPECT. Cardiac event was defined as cardiac death, nonfatal MI, or symptoms requiring coronary revascularization. **Results:** During an average follow-up of 46±22 months, three patients had severe outcomes (nonfatal MI), and revascularization was required in 8 patients. In the subgroup of 11 patients with cardiac events, the observed parameters was significantly worse than in patients without cardiac event concerning perfusion (9±13% vs. 0±1% ischemic myocardium, P <0.05), the left ventricular function (stress LVEF 56±12% vs. 68±9%, rest LVEF 56±7% vs. 66%±9, stress EDV/ESV 129 ml/59 ml vs. 98 ml/34 ml, *P* <0.05), and CAC score (581±1400 vs. 74±203, *P* <0.05). An annual cardiac event rate depended on the amount of CAC (1.0%, 2.4%, 4.6%, and 8.7% for CAC score 0-10, 11-100, 101-400, and >400, respectively). Moderate and high risk CAC score (≥101) was detected in 27 patients. In twenty of them who simultaneously had normal SPECT, only one patient underwent cardiac event during long-term observation (nonfatal MI treated by angioplasty sixty-one months after SPECT examination). **Conclusion:** CAC scoring combined with cardiac gated SPECT enables evaluation of long-term prognosis in asymptomatic risk individuals. Patients with preclinical atherosclerosis (high CAC and normal stress SPECT) have benign prognosis. However, the examination should be repeated (supposedly after 5 years)

## P117

### Impact of nicorandil on infarct myocardium in comparison with nitrate: Assessed by cardiac magnetic resonance imaging

**K. Yamada**[1], S. Isobe[2], K. Yokouchi[1], H. Iwata[1], K. Sawada[1]; [1]Gifu Social Insurance Hospital, Kani, JAPAN, [2]Nagoya University Graduate School of Medicine, Nagoya, JAPAN.

**Objectives** The complementary intravenous administration of nicorandil, a hybrid compound of ATP-sensitive potassium channel opener and nitric donor, to percutaneous coronary intervention (PCI) reportedly has a protective effect on the infarct myocardium, leading to improve clinical outcome in patients with acute myocardial infarction (AMI). We compared the infarct and edema size in AMI patients intravenously treated by nicorandil with those by nitrate, using cardiac magnetic resonance (CMR) imaging. **Methods** The double-blinded trial was conducted in 54 AMI patients who successfully underwent emergency PCI. The patients were assigned to receive nicorandil or nitrate just before reperfusion at random. For the assessment of infarct and edema areas, short-axis T2w and delayed enhancement (DE) CMR images were acquired 6.1 ± 2.4 days after the onset of AMI. **Results** The edema size on T2w CMR was significantly larger than the infarct size on DE CMR ($p < 0.05$). A significant correlation was observed between the peak creatine kinase (CK) levels and infarct size on DE CMR ($r = 0.62$, $p < 0.05$) as well as the edema size on T2w CMR ($r = 0.7$, $p < 0.05$) in patients treated by nicorandil. A similar correlation was seen between the peak CK and infarct size on DE CMR ($r = 0.84$, $p < 0.05$) as well as the edema size on T2w CMR ($r = 0.84$, $p < 0.05$) in patients treated by nitrate. The maximum serum CK level was significantly lower in patients treated by nicorandil than those by nitrate (2132 ± 1689 IU. vs 2884 ± 2142 IU. ; $p < 0.05$). Both the edema size on T2w CMR and the infarct size on DE CMR were significantly smaller in patients treated by nicorandil than those by nitrate (edema size; 17.7 ± 9.9 % vs 22.4 ± 13.6 % ; infarct size; 10.3 ± 6.0 % vs 12.8 ± 6.7 % ; $p < 0.05$, respectively). **Conclusion** Using CMR imaging, we demonstrate that the complementary intravenous administration of nicorandil to PCI provides more favorable effects in reducing myocardial damage compared with nitrate.

## P118

### Assessment of myocardial damage and prediction of future cardiac function in patients with AMI using $^{99m}$-SESTAMIBI early washout imaging

**R. Tanaka**[1], T. Kasai[2], N. Tomoharu[3], K. Yamamoto[4], C. Takabayashi[5]; [1]Chiba Insttute of Sience, Choshi, Chiba, JAPAN, [2]Jikei University Katsushika Medical Center, Tokyo, JAPAN, [3]Kushiro Sanjikai Hospital, Hokkaido, JAPAN, [4]Toyama College of Welfare Science, Toyama, JAPAN, [5]Niigata College of Nursing, Niigata, JAPAN.

The aim of this study is to elucidate the usefulness of early phase of washout rate of MIBI in predicting future cardiac functional recovery. **Method** Thirty-seven AMI patients were hospitalized within 24 hours of the onset and underwent successful PCI then enrolled in this study. MIBI SPECT was obtained in sub-acute phase and repeated 6 months later. Images were acquired at five minutes (0h), one hour (1h), and six hours (6h) after MIBI injection. Washout rate was calculated as washout index (WI) between 0h and 1h, 1h and 6h, respectively. ECG gated acquisition was performed at 1h and 6 months later (6M). The relationships between washout rate of MIBI and various parameters, such as perfusion defect, peak CPK, BNP, and LVEF were investigated. **Results** There were 17 patients whose WI showed 0 from 0h to 1h (group A) and 20 patients whose WI was accelerated (group B) (0 vs. 13.8±3.2, p<0.01). There was significant difference in WI from 1h to 6h between group A and B (15.3±5.8 vs. 19.1±3.7, p<0.05). No differences were found in the number of perfusion defect segments (NPDS) on SPECT among 0h, 1h and 6M in group A. On the other hand, significant differences were found between 0h and 1h, 1h and 6M, in group B (4.1 ± 3.1 vs. 5.3 ± 3.1, p<0.01; 5.3 ± 3.1 vs. 4.2 ± 3.3, p<0.05, respectively). Both group A and B demonstrated significant difference in NPDS between 0h and 6h (0.06±0.2 vs. 2.9±2.6, p<0.01; 4.1 ± 3.1 vs. 7.3 ± 3.2, p<0.01, respectively). Group B demonstrated much higher peak CPK value than that in group A (4098±1695 IU/l vs. 1452±1006 IU/l, p<0.001). BNP was not different between group A and B in sub-acute phase (384 ± 413pg/ml vs. 319 ± 260pg/ml). Although BNP in group A decreased 6 months later, BNP in group B remained much higher than that in group A in the chronic phase (181±145pg/ml vs. 98±109pg/ml, p<0.05). LVEF improved from 55.4±12.4% to 62.7±8.8% over six months in group A. On the other hand, no improvement was found in group B (from 45.7±12.1% to 48.0±13.1%). LVEF at chronic phase was negatively correlated with early WI (r = -0.565, p<0.001). **Conclusion** It is suggested that in patients with AMI, early myocardial washout rate derived from MIBI SPECT associates with severity of myocardial damage and predicts poorer cardiac functional recovery.

## P119

### Regional LV diastolic dyssynchrony assessing myocardial ischemia by cardioGRAF at post adenosine stress and rest : a comparison with RT3DE

**M. Ota**, M. Nagaya, N. Onishi, S. Tanaka, R. Tanaka, T. Noda, S. Watanabe; Gifu Prefectural General Medical Center, GIFU, JAPAN.

**Background:** Recently, gated myocardial perfusion single photon emission computed tomography (GMPS) was developed, and GMPS with the cardioGRAF

software can provide regional left ventricular (LV) function. The systolic LV dyssynchrony applied by time-volume curves of the each regional LV would elicit a sensitive approach for detecting myocardial ischemia. However, it may remain a pitfall that there is a time-lag for acquiring imaging from loading adenosine administration, which led to be false-negative resulted by recovery from myocardial ischemia. Hence, diastolic dysfunction raised from myocardial ischemia is more prolonged than systolic function raised from that. Purpose: The purpose of this study is to investigate whether the regional LV diastolic dyssynchrony determined by GMPS with adenosine stress is a sensitive and reliable approach for detecting myocardial ischemia by comparing with systolic dyssynchrony, and to assess those with 3-dimensional echocardiography (RT3DE), which might be able to evaluate real-time LV dyssynchrony during adenosine stress. **Method:** The subjects were 22 consecutive patients (16men; mean 68±11 year-old) with suspected stable coronary artery disease (CAD), who received $^{201}$Tl-GMPS and RT3DE at rest and at adenosine-stress (120μg/kg/min.iv). RT3DE were performed during adenosine-stress, $^{201}$Tl-GMPS image were acquired after adenosine stress. Rest (baseline) images of GMPS was acquired 3 hours after stress. The standard deviation (SD) of the Time to end systole calculated by from time-volume curve of the 16 LV segments (echoTES-$SD_{16}$) was considered as the real-time LV dyssynchrony during adenosine stress obtained by RT3D. By using GMPS with cardioGRAF, the 17 segments SD of the Time to end systole (TES-$SD_{17}$) were considered to represent LV systolic dyssynchrony. Those of the Time to Peak Filling (TPF-$SD_{17}$) were considered as diastolic dyssynchrony. We evaluated the relation between echoTES-$SD_{16}$ and TES-$SD_{17}$ or TPF-$SD_{17}$. **Results**: At adenosine stress, a significant correlation was seen between echoTES-$SD_{16}$ and TPF-$SD_{17}$ (r=0.48, p<0.05), however, there had no relation between echoTES-$SD_{16}$ and TES-$SD_{17}$ (r=0.35, p=n.s.). Furthermore, though the change of echoTES-$SD_{16}$ (from adenosine-stress to baseline) had no correlation with those of TES-$SD_{17}$ (r=0.12, p=n.s.), there was a significant correlation between the change of echoTES-$SD_{16}$ and those of TPF-$SD_{17}$ (r=0.44, p<0.05). **Conclusion:** TPF-$SD_{17}$ provided by GMPS was associated with real-time LV dyssynchrony due to myocardial ischemia. This may support that the evaluation of LV diastolic dyssynchrony may be useful for increasing the sensitivity to detect CAD.

## P120

### MPI under the influence of respiratory motion - preliminary qualitative results of an anthopomorphic phantom study

**I. Chrysanthou-Baustert**[1], O. Demetriadou[2], C. Panayidis[3], A. Londos[1,4], A. Antoniou[1,4], S. Christofides[5], L. Livieratos[6,7], I. Polycarpou[6], D. Kaolis[5], C. Yiannakkaras[5], M. Lampaskis[5], A. Kouzalis[1,4], Y. Parpottas[1,8]; [1]Frederick Research Centre, Nicosia, CYPRUS, [2]Nuclear Medicine Department, Limassol General Hospital, Ministry of Health, Limassol, CYPRUS, [3]Nuclear Medicine Department, Nicosia General Hospital, Ministry of Health, Nicosia, CYPRUS, [4]Department of Mechanical Engineering, Frederick University, Nicosia, CYPRUS, [5]Medical Physics Department, Nicosia General Hospital, Ministry of Health, Nicosia, CYPRUS, [6]School of Medicine, Division of Imaging Sciences, King's College, London, UNITED KINGDOM, [7]Guy's and St. Thomas' NHS Foundation Trust, London, UNITED KINGDOM, [8]General Department (Physics - Math), Frederick University, Nicosia, CYPRUS.

**Background:** The sensitivity and specificity of myocardial perfusion (MP) imaging is influenced by cardiac motion, respiratory motion and tissue attenuation. In this work the effects of a respiratory motion and its impact on MPI diagnosis are evaluated qualitatively with the use of a mechanical anthropomorphic phantom exhibiting a beating heart and inflating lungs**. Methods**: A previously developed anthropomorphic phantom with a beating left ventricle [1] was further developed to include computer-controlled respiratory motion. The respiratory system consists of highly-flexible silicon life-sized lungs, a flowing air pumping system for inhalation and exhalation and a computerised heart/lung control system. Small (1x1cm) and large (2x2cm) transmural defects were inserted into the inferior wall of the myocardium. MP Images of the anthropomorphic phantom with cardiac motion as well as cardiac and respiratory motion (RM) have been acquired and processed with/without gating and with/without attenuation correction. The processed datasets were reported by two expert physicians blinded to the prior known phantom conditions. The size and the severity of the lesions were recorded. **Results:** The large defects were correctly diagnosed as lesions with severely reduced perfusion, despite the visually perceived difference in image quality. The small transmural defects were consistently underdiagnosed as lesions with mildly reduced perfusion when acquired with RM. The results improved when acquired without RM and leaving all other acquisition conditions identical. **Conclusions:** The results of our preliminary study support previously published data produced through computer simulations [2]. Assuming that RM causes the decrease in accurate diagnosis, it could be suggested that adding RM correction has the potential to improve the sensitivity and specificity in MPI. Acknowledgments: This project "ΥΓΕΙΑ/ΔΥΓΕΙΑ/0311(BIE)/27" is funded by the Cyprus Research Promotion Foundation and the European Regional Development Fund. References: [1] Parpottas Y, Chrysanthou I et al; Construction of a Dynamic Cardiac Phantom to Optimize the Diagnostic Value in SPECT Myocardial Perfusion Imaging; World J Nucl Med. 2011 Jul-Dec; 10(2): 178-189. [2] Yang YW, Chen JC et al; Evaluation of Respiratory Motion Effect on Defect Detection in Myocardial Perfusion SPECT: A Simulation Study. IEEE Trans Nucl Sci. 2009 Jun 1;56(3):671-676.

## P121

### Should we switch to attenuation corrected myocardial perfusion imaging in clinical practice with SPECT-CT gammacameras

K. Melis[1,2], L. Tack[3], I. Goethals[3], **A. Dobbeleir**[3]; [1]AZ Nikolaas, Sint Niklaas, BELGIUM, [2]AZ Sint-Augustinus, Veurne, BELGIUM, [3]University Hospital Ghent, Gent, BELGIUM.

**Aim**: to determine the number of patients changing the interpretation of myocardial perfusion scintigraphy (MPI) after CT-attenuation correction (AC) compared to non corrected images in patients suggestive of myocardial ischemia. **Material and Methods**: 45 consecutive patients over a 4 month period were referred to a small nuclear medicine department. All patients had one day 180° rest-stress SPECT/CT MPI acquisitions ( Sestamibi or Tetrofosmine-Tc99m, GE Infinia Hawkye ) allowing both non-AC FBP and iterative AC reconstruction. The low-dose CT added 1 mSv to the patient dose per examination. No manual realignment of SPECT-CT data was performed. MPI was interpretated quantitatively using the 20-segment Cedar Sinai myocardial perfusion package. Summed Stress (SSS) and Rest (SRS) score were determined. **Results**: The patient group had an average age of 69,6 +/- 13,2 years and consisted of 20 men and 25 women. The mean SRS was 1,2 without and 1,3 after AC. The mean SSS was 3,2 without and 3,8 after AC. Since low scores were obtained for rest studies we mainly investigated the difference between stress. We considered SSS < 4 normal, 4-8 mildly, 9-13 moderately and > 13 severely abnormal. Concordant results were obtained in 35 out of the 45 patients ( 27 normal and 8 different degrees of abnormality ). In 6 patients, without AC, stress was normal but after AC in 5 patients a mild defect appeared in the apical region, in the sixth patient liver or gastro-intestinal activity created a defect. On the other side in 4 patients reduced lesions were obtained after AC: a mild lateral and moderate septal lesion became normal, a severe inferior lesion became moderately abnormal in the third patient and in the fourth patient liver or gastro-intestinal activity created a severely abnormal score where a mildly score was present after AC. Interpreting the stress study using only the AC study seems to create defects in 6 out of the 45 patients mainly in the apical wall. Eventual liver or gastro-intestinal activity present is amplified after AC. Contrarily only interpreting the non AC stress study in 2 abnormal patients misclassified the patients as abnormal based on quantitative data and exaggerated the lesion extent and severity in 2 other patients.**Conclusion**: departments who dispose of a SPECT-CT might feel more comfortable using both non-AC and AC myocardial perfusion images.

## P122

### Large variability of ischemic extent values in myocardial perfusion scintigraphy decreased when physicians were provided with an automated suggestion of ischemic extent

**E. Tragardh**[1], P. Hoglund[2], L. Edenbrandt[1]; [1]Clinical Physiology and Nuclear Medicine, Skåne University Hospital, Lund University, Malmo, SWEDEN, [2]Competence Center for Clinical Research, Skåne University Hospital, Lund, SWEDEN.

**Aim***:* Visual interpretation of myocardial perfusion scintigraphy (MPS) studies is dependent on the knowledge of the physician, and subject to inter- and intra-observer variability. Recent studies have shown that patients with significant ischemia have a survival benefit from early revascularization. The European Society of Cardiology recommends that patients with >10% area of ischemia should receive revascularization. In this study we wanted to investigate 1) the inter-observer variability for the extent of reversible perfusion defects reported by different physicians in nuclear medicine, 2) the variability for the reversible perfusion defects obtained from different software tools, and 3) if the inter-observer variability is reduced when the physicians are provided with a computerized suggestion of the delineation of the reversible perfusion defects. **Material and method***:* Twenty-five MPS patients who were regarded as ischemic according to the final report were included. Eleven physicians in nuclear medicine from four different countries delineated the extent of the ischemic defects. After at least two weeks, they delineated the defects again, and were provided a suggestion of the defect delineation by EXINI Heart$^{TM}$ (EXINI). Summed difference scores and ischemic extent values were obtained from four software programs (EXINI, Emory Cardiac Toolbox, Quantitative Perfusion SPECT, and 4D-MSPECT). **Results***:* The median extent values obtained from the 11 physicians varied between 8% and 34%, and between 9% and 16% for the software programs. There was a considerable variation in the reported amount of ischemic myocardium between the different programs as well as between the different physicians for the 25 patients. The variability among the physicians was large for both small, medium-sized and large ischemic areas. For all 25 patients, mean ischemic extent obtained from EXINI was 17.0%. Mean extent for physicians was 22.6% for the first delineation and 19.1% for the evaluation where they were provided computerized suggestion (p = 0.002).

Intra-class correlation increased from 0.56 for the first to 0.81 for the second delineation, whereas standard deviation between physicians decreased from 7.8 to 5.9.**Conclusions***:* There was large variability in the estimated ischemic defect size obtained both from different physicians and from different software packages. When the physicians were provided with a suggested delineation, the inter-observer variability decreased significantly. Physicians should be aware of the large differences between both different physicians and different software packages when giving the amount of ischemic myocardium to the referring physician.

## P123

### Interobserver and Intraobserver Agreement in Perfusion and Functional Interpretation of Gated Myocardial Perfusion SPECT

**D. KUSLU**, E. OZTURK; Ufuk University Medical Faculty Nuclear Medicine Department, Ankara, TURKEY.

AIM: To evaluate the intraobserver and interobserver variability in LV perfusion and function interpretation; to define the repeatability of QPS/QGS software quantitative parameters and to compare them with visual parameters. MATERIALS AND METHODS: 139 patients were interpreted by 3 independent observers, with and without knowledge of clinical data, using a 20-segment scoring model in 2 day rest/stress Tc-99m sestamibi gMPS. Standard QPS/QGS algorithm has been applied to derive quantitative parameters. Intraobserver and interobserver agreement for global and vascular (LAD, Cx and RCA) territorries, also agreement between CAG and observers; repeatability of QPS/QGS software perfusion and function parameters were assessed. RESULTS: Intraobserver perfusion agreement in global, LAD, Cx and RCA territorries were %72-100, %83,5-91, %88,5-93 and %85,6-92 respectively (p<0,05). Clinical knowledge had no impact on interpretations. Interobserver perfusion agreement was higher in vascular territorries than global interpretations (%83,5-92,8 vs %64,7-78,4) with the least agreement in the LAD territory (p=0,000). There was significant agreement between observers and CAG results in Cx (%81,6-86) and RCA (%77,2-83,3) (p=0,000) territories but not in LAD territory in any of the observers (p>0,05). When we compared the visual perfusion scores with the QPS software's automatic quantification scores it was seen that there were more differences between the least experienced observer and software than the others'. In general there were significant but not clinically specific interobserver variabilities in the wall motion and thickening scores. When we compared the visual scores with the QGS scores there were significant differences between parameters except rest and stress SMS in Cx territory (p>0,01). There was no impact of the proccesing procedure on QPS/QGS software and the repeatability of this software and EF values were high (p>0,05). CONCLUSIONS: There were significant interobserver and intraobserver agreement in perfusion interpretation either global or each vascular territory. There was significant agreement between the visual interpretation and the CAG results especially in the Cx and RCA arteries. The interobserver and intraobserver agreement was higher in the wall motion scores than thickening scores. There was no significant difference between 3 observers' interpretations, also there was no difference if they're blinded or not. QPS/QGS software quantitative perfusion and motion/thickening scores and LVEF values showed high repeatability.

## P124

### Evaluation of Silent Myocardial Ischemia by Tc-99m MIBI SPECT in welders

**E. Kaya**[1], H. Saglam[2], E. Vardareli[3]; [1]Acibadem Kayseri Hospital, Kayseri, TURKEY, [2]Kayseri Education and Research Hospital Department of Cardiology, Kayseri, TURKEY, [3]Acıbadem University Medical Faculty, Nuclear Medicine, Kayseri, TURKEY.

**Background:** Welding fumes associated with respirable metal particles and toxic gases (carbon dioxide, carbon monoxide, hydrocarbon, nitrogen oxide, nitrogen dioxide and ozone) are primarily lead to respiratory compliants and various systemic symptoms. Histopathological changes (interstitialand pleural fibrosis) in the lungs of welders increases the cardiac afterload. Furthermore, gases and toxic substances can lead to ischemic heart disease, dysrhytmia and death.*Objective*: The aim of this study is to research the prevalence of silent myocardial ischemia by Technetium-99m methoxyisobutylisonitrile (Tc-99m MIBI) single-photon emission computed tomography (SPECT) in welders. ***Materials and Methods:*** The study population consisted of 26 men welders and 20 healthy controls. Welders working period were more than five years. All subjects had no any risk factors for coronary artery disease. Stress/rest electrocardiography (ECG) and echocardiography (ECHO) were performed to all subjects. Tc-99m MIBI SPECT studies were performed at stress and rest in a one-day protocol. Myocardial perfusion scores [summed stress score (SSS), summed rest score (SRS), summed difference score (SDS), and fix defect score (FDS)] and perfusion defect prevalence (stress, rest ischemic, and fix defect) were determined as the percentage of left ventricule (%LV). Coronary angiography (CAG) was performed to the welders who have abnormal myocardial perfusion scintigraphy (MPS). ***Results:*** The mean ages of the welders and control groups were 39.7±6.2 years and 36.3 ±3.4 years, respectively. No statistically significant differences were observed between the two groups regarding clinical features. In welders group, total 4 patients had abnormal findings in their stress and rest ECG. ECHO examination was abnormal in 4 patients. Abnormal MPS was found in 5 (19%) of the welders. Only one (5%) reversible perfusion defects was recorded in the control group. When the two groups were compared regarding the SPECT findings, differences were determined in the following parameters; SSS, SRS, SDS, and stress %LV. In the welders group when the SPECT results were compared between those with and without abnormal MPS, differences were determined in SSS, SRS, SDS, stress and rest %LV (p values <0.05). The mean duration of working was 21.7 ± 8.9 years in welders with abnormal MPS and 16.8±9.3 in welders without it (p<0.05). Four welders accepted CAG study and two of them were normal. ***Conclusions:*** The results of this study is to show that the prevalence of abnormal MPS is high in welders. Myocardial perfusion scintigraphy may be advised for evaluation of silent myocardial ischemia in welders.

## P125

### Prognostic value of myocardial reversibility index in evaluating the effectiveness of surgical treatment in patients with postinfarction left ventricular aneurysm: a gated myocardial perfusion SPECT study

**M. Vakhromeeva**, A. Vakhrameeva, F. Chanakhchyan; Pirogov National Medical Surgical Center, Moscow, RUSSIAN FEDERATION.

**BACKGROUND**: The objective information not only about coronary artery anatomy, left ventricular (LV) structural and functional anomalies, but also myocardial viability is very important in planning the surgical treatment in patients with postinfarction left ventricle aneurysm (LVA). ECG-gated myocardial perfusion imaging with single-photon emission computed tomography (gSPECT) provides valuable information of myocardial viability in order to establish the decision of reconstructive and/or revascularization treatment. **AIM:** To assess the usefulness of the gSPECT myocardial perfusion imaging to assess myocardial viability and to evaluate potentials of preoperative prediction for recovery of hibernating myocardium in patients with postinfarction LVA, directed to the surgical treatment (reconstruction and/or revascularization). **METHODS:** In our study we included 44 patients with postinfarction LVA. All patients were performed "stress/rest" or "rest" gSPECT with $^{99m}$Tc-Technetrill using two-detector rotating gamma-camera ("Forte", Philips) before operation (for assessment viable myocardium) and after surgical treatment (for assessment hibernating myocardium recovery). In all patients before operation we determined myocardial reversibility index (MRI) as a ratio of total hypoperfused zone extent (viable + nonviable myocardium) to the nonperfused zone extent (nonviable myocardium, tracer uptake <25%) on the rest polar maps. This ratio reflects the hibernating myocardium volume. **RESULTS:** After surgical treatment we indentified the perfusion improvement in 35 (79,5%) from 44 patients. The improvement in perfusion didn't depend on extents of only hypoperfused or nonperfused zones, but depend on MRI. Meanwhile, there wasn't significant improvement in myocardial perfusion in patients with MRI = 1,0-2,0. Significant improvement in myocardial perfusion was obtained in patients with postinfarction LVA and with MRI > 2,1 (p<0,05). The perfusion defect in this group of patients decreased over 20% (p<0,05) and more. **CONCLUSIONS:** Improvement of perfusion in patients with postinfarction LVA after the surgical treatment depends on the volume of viable (hibernating) myocardium in postinfarction zone. Using of MRI in these patients obtained by gSPECT could predict the efficiency of surgical treatment, especially in cases, when one of the elements of the operation is the direct myocardial revascularization. Significant improvement in perfusion after revascularization can predicted in patients with MRI ≥ 2,0.

## P126

### Comparison of Gated and Non-gated TI-SPECT Imaging in Detecting Coronary Artery Disease

O. Lammintausta[1], **J. Heikkonen**[2], M.Ventilä, H.Siljander, A.Lampinen; [1]Division of Cardiology, Heart and Lung Center, Helsinki University Central Hospital, Helsinki, FINLAND, [2]Department of Oncology, Helsinki, FINLAND.

The aim of this study was to compare the capability of three different algorithms of thallium scintigraphy to detect left ventricular diseased territories. For this purpose non-gated and gated SPECT algorithms and modified gated SPECT algorithm were constructed. Methods: Twenty seven patients, 22 males and 5 females, were studied with Tl-201 SPECT (110 MBq) during stress and at rest with Siemens c.cam cardiac gamma camera. Seven patients had three-vessel coronary artery disease, 7 patients had two-vessel disease and 13 patients had one-vessel disease. All diseased territories were verified in angiography (>50% diameter). Twenty one stenoses were observed in left descending coronary artery, 10 in the right coronary artery and 17 in left circumflex artery. The time gap between stress and rest study was three hours. The perfusion data was collected using step-and-shoot acquisition method and 180° non-circular orbit with 2x32 angular steps. Matrix size was 64 and frames per cardiac cycle was collected in eight slots. Non-gated data was collected simultaneously with gated study to another data file. Gated SPECT images were reconstructed using all gated data (slots 1-8) and corrected gated SPECT images

were reconstructed from collected gated data (slots 1, 6-8) excluding the systolic phase. All images were displayed as normal tomographic planes with Syngo MI workplace and as washout images with 4-DMSPECT and were compared with coronary angiography. Sensitivity, specificity and accuracy were calculated for three different algorithms. Results: Corrected gated SPECT detected 46/48 diseased vessels, gated SPECT 41 vessels and non-gated SPECT detected 40 vessels. All algorithms gave also false positive findings and were localized in LAD or in RCA region. Non-gated algorithm detected three false positive defects, gated two and corrected gated detected also two false positive findings. For corrected gated study the sensitivity was 92%, specificity 94% and accuracy 93%. For gated study the corresponding values were 81%, 93 %, and 85% and for non-gated study 80%, 90% and 84%, respectively. Conclusions: This study showed that the best sensitivity, specificity and accuracy for coronary artery stenosis were obtained with corrected gated study where the effect of cardiac movement is minimized by excluding the data in systolic phase. Gated study and non-gated studies are also fast and useful scintigraphy Methods.

## P127

### Comparison of Gated SPECT MIBI Early Post Stress Imaging Protocol and Stress Echo in Patients with Intermediate Duke Score

**D. Sobic-Saranovic**, Z. Petrasinovic, S. Pavlovic, L. Bojic, N. Kozarevic, V. Artiko, V. Obradovic; Clinical Center of Serbia, Belgrade, SERBIA.

**Background**: Early post stress gated SPECT MIBI imaging could result in shorter waiting times for patients comparable with stress echo. In addition, it would be possible to better organize nuclear cardiology labs. However, one important factor limiting early imaging protocols with MIBI is a possible increase in artefact defects in the inferior wall due to high sub-diaphragmatic uptake. Aim: To compare Gated SPECT MIBI early post stress findings with stress echo in patients with suspected or known coronary artery disease. To evaluate sensitivity and specificity of Gated SPECT MIBI early post stress protocol in comparison to coronary angiography served as gold standard. **Methodology:** The sample included 63 patients, mean age 58±8 years, 47 men and 16 women with normal or mild impairment of the left ventricular function and intermediate exercise Duke Score. They underwent 2-day stress-rest gated SPECT MIBI protocol with early post stress data acquired 15 minutes after i.v. injection of 740MBq of 99mTc-MIBI. Perfusion and functional parameters were assessed by 4D-MSPECT programme. Stress echo was performed within two days and CA within one month of gated SPECT MIBI investigation. **Results**: There was no significant difference between early gated SPECT and stress echo findings in detection CAD (Mc Nemar, p=1.000) with good agreement between Methods (kappa 0.691, p<0.001). Spearman correlation between early gated SPECT and stress echo was also significant (s=0.448, p<0.01). In addition, early gated SPECT has added value over stress echo findings (NRI index = 0.2466, p<0.001) in detection of ischemia. Overall sensitivity of ES was 96% and specificity 83.33%. **Conclusions**: Our data demonstrate comparative utility of early gated SPECT MIBI imaging and stress echo for non-invasive evaluation of CAD in patients with mild left ventricular dysfunction. The advantage of gated SPECT MIBI over stress echo is ability to concurrently assess perfusion abnormalities in patients with poor acoustic window or wall motion abnormalities in lateral wall.

## P128

### Diagnostic utility of stress dual SPECT using MIBI and Tl-201 for coronary artery disease (CAD).

**T. Tanaka**; HOSPITAL, Tokyo, JAPAN.

Objectives; Generally exercise stress myocardial SPECT is perfomed according to routine protocol i,e, myocardial perfusion tracer is injected at end point. It is believed that for adequate detection of CAD enough stress is necessary . In cace of poor exercise torelance pharmacological stress test is recommended. However there is no reports about ischemic region induced by low degree of exercise stress. For this purpose stress synchronized dual myocardial SPECT using MIBI and Tl -201 is perfomed in pts with CAD. Methods; We studied 120 patients(pts) with CAD in whom coronary angiography is performed. Exercise stress is performed according to Bruce protocol and at 3 minute after beginning of exercise stress 185MBq of MIBI is intravenously infused and at end point 111MBq of Tl-201 is infused. Then another 1 minute exercise is added. Delayed images are collected after 4 hours. Variation of ischemic region is estimated by comparing ischemic region noted at 3 minute after beginning of exercise stress with ischemic region noted at end point. Resulst; In 80 pts among 120 pts ischemic region is noted at 3 minute..In 41 pts of 80 pts no difference is noted between both images.(degree of stenosis 88+10%)..In 14 pts Ischemic region is growed (degree of stenosis;80+10%.In remaining 25 pts ischemic region at end point is smaller than ischemic region at 3 minute.(degree of stenosis 55+15%).In 8 pts of 25 pts it revealed that nearly normal perfusion myocardial images are noted at end point. Conclusion; In 25 pts of 120 pts it revealed that low degree of stress induced transient ischemic region. In 56 pts of 120 pts low degree of stress is enough for detecting ischemic region. Stress synchronized dual myocardial SPECT is useful for diagnosing pts with CAD.

## P129

### Effect of attenuation correction on diagnostic efficacy of myocardial perfusion study

**A. Płachcińska**[1], K. Kovacevic-Kuśmierek[1], M. Włodarczyk[2], M. Bieńkiewicz[1], K. Chiżyński[3], J. D. Kasprzak[4], J. Z. Peruga[4], R. Gawor[5], J. Kuśmierek[2]; [1]Department of Quality Control and Radiological Protection, Medical University, Łódź, POLAND, [2]Department of Nuclear Medicine, Medical University, Łódź, POLAND, [3]Department of Invasive Cardiology, Medical University, Łódź, POLAND, [4]Department of Cardiology, Medical University, Łódź, POLAND, [5]Department of Cardiology, N. Copernicus Regional Hospital, Łódź, POLAND.

The aim of the study was to check whether attenuation correction (AC) of images improves diagnostic efficacy of myocardial perfusion study (MPS), in detection of patients with critical narrowing of coronary arteries. Material and Methods MPS of 90 pts (33F, 57M), mean BMI - 28.8, with no history of myocardial infarction, referred for this study for diagnosis of CAD, were assessed. Study was acquired applying a 2-day protocol, after administration of 99mTc-MIBI in dose of 11 MBq/kg of body mass, with Hawkeye (GE) gamma camera. Study reconstruction was made with FBP (non AC) and with iterative method applying AC (2 iterations, 10 subsets). Images were assessed by 2 nuclear medicine specialists (consensus), with semiquantitative method, dividing myocardium into 17 segments and applying 5-point segmental scoring, with subsequent summing of scores (SSS and SRS). Classification of MPS results as normal/abnormal was based on SSS values. Results of MPS were compared with coronary angiography, which was considered abnormal (positive) when at least 1 of 3 main coronary arteries was narrowed by 70% or more. Results Coronary angiography turned out positive in 39 pts, negative in 51. SSS and SRS values obtained with AC were lower than without AC (median values SSSnonAC and SSSAC amounted to 3.0 and 1.0, respectively, p=0.0004, and of SRSnonAC and SRSAC - 2.0 and 0.5, p=0.007). ROC curves were generated for nonAC and AC Methods in relation to coronary angiography results. Areas under curves (AUC) were equal to 0.86 and 0.80, respectively (p=0.11). Optimal threshold value of SSS=3 for detection of critical coronary artery narrowing was accepted. Sensitivity, specificity and accuracy of nonAC method amounted to 85% (33/39), 73% (37/51) and 78% (70/90), respectively. AC improved, although non-significantly, (p=0.11), specificity of MPS to 84% (43/51), but compromised its sensitivity to 67% (26/39), p=0.05, with almost unchanged accuracy of 77% (69/90). Lowering of detection threshold SSS to 2 did not improve diagnostic efficacy of AC method (sensitivity - 77%, specificity - 76%). In all analyzed subgroups of patients (males, females, obese (BMI>27) patients, obese males) AUCs for ROC curves were smaller, although non-significantly, for AC than nonAC method (0.77 vs 0.84, 0.73 vs 0.85, 0.73 vs 0.85, 0.74 vs 0.86, respectively). Conclusion: Attenuation correction of MPS applied in this group of patients did not improve diagnostic efficacy of the study.

## P130

### The benefit of combined supine-prone myocardial perfusion SPECT in reducing anterior wall artifactual defects.

**M. Stathaki**, S. Koukouraki, E. Papadaki, A. Tsaroucha, O. Bourogianni, K. Galanopoulos, M. Alefantinou, N. Karkavitsas; Department of Nuclear Medicine, University Hospital of Heraklion, Heraklion-Crete, GREECE.

**Aim:** The aim of the study was to determine the use of combined supine-prone approach in overcoming breast attenuation artifacts in females, thus reducing the number of unnecessary rest perfusion studies and patient radiation exposure. **Material-Methods**: We examined 19 female patients with suspected breast attenuation artifacts of the anterior wall. Coronary angiography was used as a "gold standard" for evaluating coronary artery patency. One day stress-rest protocol with Tc-99m tetrofosmin was performed. A dual-headed large field of view gamma camera (Philips, Forte Jetstream AZ) with a low-energy, high resolution collimator was used. Stress images were acquired first in the supine and then in the prone position, using the same acquisition settings. In the presence of a disappearing defect by prone, rest imaging was not done. Quantitative visual interpretation was performed using the 5-point scoring system: 0=normal to 4=no detectable tracer uptake. With the 20-segment model, the summed stress score (SSS) of each supine and prone study was calculated. SSS<4 was considered normal, 4 to 8 mildly abnormal and >8 moderate to severely abnormal. Results were compared with clinical data and coronary angiographic findings. **Results**: Prone imaging revealed normal anterior wall activity in 12 out of 19 patients (63.1%), therefore further scintigraphic study was not done. The normal patency of coronary vessels was angiographically confirmed. The finding was correctly attributed to breast attenuation artifact. Two patients (10.5%) demonstrated a defect that persisted despite positional change and rest study was not avoided. Both had a history of an anterior wall infarction. In spite of normal coronary angiograms and no history of coronary artery disease, 4 patients (21%) revealed remaining defects (false positive). Moreover 1 patient (5.2%) with total occlusion of the first diagonal branch demonstrated prone normal tracer activity (false negative). In patients with normal prone interpretation, the mean SSS of supine

and prone studies were 7.4 and 1.2 respectively. The mean SSS in those with abnormal prone interpretation were 9.5 for supine versus 7.6 for prone studies. These are the preliminary results of an ongoing study. **Conclusion**: The addition of prone to stress supine myocardial scintigraphy seems to accurately overcome breast attenuation artifacts. Moreover it provides a low cost approach in eliminating subsequent rest imaging, so as to limit investigation time, radiation exposure and patient discomfort.

## P131

### Factors affecting the myocardial activity recorded at exercise-SPECT with a high-sensitivity cardiac CZT-camera as compared with conventional Anger-cameras

**A. Verger**[1], L. Imbert[1], Y. Yagdigul[1], R. Fay[1], W. Djaballah[1], F. Rouzet[2], N. Fourquet[3], S. Poussier[4], D. Le Guludec[2], G. Karcher[1], P. Marie[1]; [1]CHU Nancy, Nancy, FRANCE, [2]APHP, Paris, FRANCE, [3]Clinique Pasteur, Toulouse, FRANCE, [4]NancycloTep, Nancy, FRANCE.

Injected doses are difficult to optimize for exercise-SPECT, depending on the myocardial fraction of injected activity (MFI), which is detected by the camera. This study aimed to analyze factors affecting MFI on a cardiac CZT-camera, as compared with conventional Anger-cameras. **Methods.** Factors affecting MFI were comparatively determined in patients who had consecutive recordings of exercise Anger- and CZT-SPECT with $^{201}$Tl (n=84) or $^{99m}$Tc-Sestamibi (n=87). The predictive model was assessed in a validation group of patients routinely referred to $^{201}$Tl (n=78) or $^{99m}$Tc-Sestamibi (n=80) exercise CZT-SPECT. **Results.** The global predictive model involved: 1) camera type, adjusted mean of MFI being 9 fold higher for CZT- than Anger-SPECT, 2) tracer type, adjusted mean of MFI being 2 fold higher for $^{201}$Tl than $^{99m}$Tc-Sestamibi and 3) logarithm of body weight. The use of the CZT-SPECT model led to a +1±26% error in the prediction of the actual MFI from the validation group. The mean values of MFI, which were estimated for the CZT-SPECT, were more than two fold lower for 120 kg of body-weight than for 60 kg whatever tracer-type: respectively, 6.8 and 15.9 parts-per-million for $^{99m}$Tc-Sestamibi and 13.1 and 30.5 parts-per-million for $^{201}$Tl; and for a 14-minutes recording of as much as one million of myocardial counts, corresponding injected activities would be only 186 and 80 MBq for $^{99m}$Tc-Sestamibi (respective radiation doses: 1.4 and 0.6 mSv) and 91 and 39 MBq for $^{201}$Tl (respective radiation doses: 15.4 and 6.6 mSv). **Conclusion.** Myocardial activities, recorded at exercise CZT-SPECT, remain strongly influenced by body weight and tracer type and are dramatically higher than with Anger-cameras, allowing low-dose protocols to be planned.**Key-words:** myocardial SPECT, thallium-201, Sestamibi, exercise, CZT-camera.

## P132

### The significance of MPI with 99mTechnetium-tetrofosmin in patients with stroke

S. Zouroudi, S. Markoula, C. Sioka, M. Spiliotopoulou, K. Naka, L. Michalis, **A. Fotopoulos**, A. Kyritsis, S. Giannopoulos; University Hospital of Ioannina, Ioannina, GREECE.

**Aim**: To estimate the myocardial status in patients with stroke, employing myocardial perfusion imaging (MPI) with 99mTechnetium-tetrofosmin (99mTc-TF) - single photon emission computer tomography (SPECT). **Material and Methods**: Forty one patients with stroke were subjected to 99mTc-TF-SPECT MPI within 1 month after stroke. None of the patients had any history or symptoms of coronary artery (CAD) or other heart disease. Visually was evaluated the MPI using polar map of 17 segments. Summed stress score (SSS) the myocardial ischemia was graded as mild (4-8), moderate (9-13), and severe (> 13**). Results**: Abnormalities in the SSS were found in 23/41 (56.1%) patients. Among them, 15/30 (50%) were male and 8/11 (72.7%) female. MPI grading revealed mostly mild abnormalities (MPI grade: 4-8) in 15/41 (36.6%) patients, 10/30 (33.3%) male and 5/11(45.5%) female. Moderate and severe abnormalities were noted in 8/41 (19.5%) patients. All 99mTc-TF-SPECT abnormalities were clinically silent. **Conclusion:** The study suggested that a significant number of stroke patients without history of cardiac disease may have abnormalities on MPI.

## P133

### Does chest pain during dobutamine stress predict occurrence of perfusion defects on SPECT-MPI?

**M. L. Abrar**, K. Agrawal, R. Kumar, A. Bhattacharya, B. R. Mittal; Postgraduate Institute of Medical Education & Research, PGIMER, CHANDIGARH, INDIA.

**AIM**: Pharmacological stress in conjunction with radionuclide myocardial perfusion imaging (MPI) has become a widely used non-invasive method of assessing patients with known or suspected coronary artery disease who are unable to undergo exercise stress testing. Dobutamine is an inotoropic agent commonly used for pharmacological stress testing, particularly in patients unfit for vasodilator stress testing. This study was carried out to assess whether chest pain during Dobutamine infusion can predict occurrence of perfusion defects on imaging. **METHODS**: This retrospective study included 200 patients who underwent dobutamine stress MPI. Univariate analysis was done for chest pain (limiting and non-limiting) during infusion and also for other factors as age, sex, history of diabetes, h/o hypertension, smoking, dyspnea ,known CAD, regional wall motion abnormalities (RWMA) on echocardiography (ECHO) in predicting perfusion defects on MPI. A p value of <0.05 was considered significant **RESULTS**: On univariate analysis chest pain during Dobutamine infusion did not predict occurrence of perfusion defects (p=0.346). Of all the other factors analysed h/o known CAD (P=0.0001), RWMA on ECHO (p=0.004), age (p=0.05) and h/o alcoholism (P=0.003) predicted the occurrence of perfusion defects on MPI. On the contrary, sex, history of diabetes (p=0.514), h/o hypertension (p=0.613), smoking (p=0.089), h/o dyspnoea on exertion (p=0.331) were not significant predictors of perfusion defects on MPI. **CONCLUSIONS**: Our results suggest that chest pain during dobutamine stress testing is not a predictor of perfusion defects on SPECT MPI.

## P134

### Frequency of myocardial stunning in the population with suspected coronary artery disease referred for stress myocardial perfusion imaging and its relation to the perfusion defect size

**O. Lang**, H. Balon, I. Kunikova, R. Pichova; Charles University, 3rd Medical Faculty, Prague 10, CZECH REPUBLIC.

**Objectives**: Myocardial stunning represent transient left ventricular dysfunction as a result of short lasting myocardial ischemia when early reperfusion precludes myocardial necrosis. The goal of our retrospective study was to identify the frequency of such a phenomenon during stress testing and to test its relation to the perfusion defect size. **Methods:** We analyzed 4411 consecutive patients referred to our department for stress MPI. There were 1775 female and 2636 male with average age of 62 (16-86) years. All were evaluated with one day stress-rest protocol with 99mTc MIBI using gated SPECT. Data were analyzed with QGS™ software. Stress LV EF values were obtained at 45 minutes and rest data at > 3 hours post stress. Myocardial stunning was defined as post stress LV EF at least 5% lower than rest LV EF. Differences were compared with paired t-test. **Results:** Myocardial stunning was present in 725 pts (16.4%). Their average stress perfusion defect size was 15.5%±12.2% of left ventricular myocardium compared to 13.5%±11.4% in pts without stunning (p=0.000). Perfusion defect size in pts with vs without stunning was significantly larger in the LAD territory (12.3% vs 9.5%, p=0.000), defect size did not differ in the LCx and RCA territories (p=0.228 and p=0.064 respectively). We could detect enlargement of left ventricle in patients with stunning. EDV increased from 95.2 to 95.6 (p=0.000) and ESV increased from 43.0 to 50.7 (p=0.000). **Conclusion:** Frequency of myocardial stunning during stress test in unselected patient population is quite high (16.4%). Larger perfusion defect size in pts with stunning was present only in the LAD territory while there was no relation of defect size in the areas supplied by LCx of RCA. Myocardial stunning also caused stress LV dilatation. However, large individual differences exist.

## P135

### Type of myocardial damage after acute myocardial ischemia treated with emergency PCI.

**O. Lang**, H. Balon, I. Kunikova, R. Pichova; Charles University, 3rd Medical Faculty, Prague 10, CZECH REPUBLIC.

**Objectives**: Acute myocardial ischemia is still challenging disease. Emergency PCI is very effective method in clinical trials but it is not clear how it works in daily practice. Therefore, the aim of our study was to assess the effectiveness of PCI in patients referred to community hospital. **Methods**: We evaluated 44 pts without previous MI referred to community hospital for emergency PCI due to acute myocardial ischemia and subsequently for myocardial perfusion imaging. There were 12 f and 32 m, avg age 58 (36-77) y. MPI was performed 58 (32-87) days after PCI. We assessed the type of myocardial damage, its frequency and relation to particular coronary vessel. Chi-square test was used for statistical significance. **Results**: 22 pts had PCI of RCA, 17 of LAD and 5 of LCx. 24/44 (55%) pts had homogenous perfusion, 2/44 (4%) pts had reversible defect and 18/44 (41%) pts had fixed perfusion defect on subsequent MPI. Findings differed significantly among coronary vessels (chi-square test p=0.005). **Conclusions**: PCI was effective in only 55% of pts and no effect (fixed perfusion defect) was observed in 41% of pts. PCI of RCA was most effective and PCI of LCx was less effective. Result of PCI of LAD was balanced between no damage and fixed defect almost equally.

## P136

### Assessment of Left Ventricular Synchrony in Patients with Normal Gated SPECT Myocardial Perfusion Imaging

**L. G. Diaz Gonzalez**[1], R. Ruano Perez[1], M. Diego Dominguez[2], A. S. Rosero Enriquez[1], P. Perdiguero[2], S. Merchan[2], J. R. Garcia-Talavera[1]; [1]Nuclear Medicine.University Hospital of Salamanca, Salamanca, SPAIN, [2]Cardiology.University Hospital of Salamanca, Salamanca, SPAIN.

**Aim**: To correlate the hemodynamic parameters of myocardial ischaemia with left ventricular synchrony by phase analysis in patients with normal gated-SPECT myocardial perfusion images (MPI). **Material and Methods:** retrospective study of 42 consecutive patients from January 2012 to January 2013, with normal stress and resting MPI. We excluded those cases with technical defects or physiological artifacts, and patients with pacemakers. Gated SPECT was performed using stress and rest 99mTc-Tetrofosmin Protocol (1 day). For phase analysis processing Cedars Quantitative Gated SPECT ® software was used. Differences between groups were analyzed using SPSS. **Results:** 51% male, 49% female. Mean age 68 + - 13 years. In 21/42 there was diagnosis of myocardial ischaemia (unstable angina, non-Q). The baseline electrocardiogram (ECG) was normal in 31 patients. There were 4 LBBB, 4 RBBB, 3 AF. 82% with at least 2 coronary risk factors. It was observed that patients with a normal ECG had improved bandwidth (HB) and standard deviation (SD) compared with resting images (p <0.05). No statistical relationship was found between changes in ventricular synchrony and cardiovascular risk factors. However, hypertension in men was associated with lack of synchrony improvement during exercise. No significant differences were found between those patients who performed Bruce protocol versus pharmacologic stress with dipyridamole. Patients with known branch block (LBBB, RBBB) shown values of dyssynchrony in the two studies. **Conclusion:** The phase histogram analysis is a useful tool for the identification, assessment and classification of disorders in ventricular synchrony in patients with adequate myocardial perfusion.

## P137

### Role of attenuation correction in stress MPS interpretation for cardiac risk assessment of obese patients prior to bariatric surgery

**G. Arun Reddy**, M. L. Abrar, K. Agrawal, J. R. Mohan, B. R. Mittal; Postgraduate Institute of Medical Education & Research, PGIMER, CHANDIGARH, INDIA.

**BACKGROUND**: Bariatric surgery has known procedure-related risks and associated serious medical co-morbidities and is thus considered an intermediate to high risk non cardiac surgery. Presence of low functional capacity is common in most of these patients making cardiac risk assessment imperative before surgery. We evaluated the incremental value of attenuation correction as tissue attenuation plays major role while interpreting the scintigraphic images in this group of patients. AIM: To assess the impact of attenuation correction (AC) in image interpretation of stress myocardial perfusion scintigraphy (MPS) in obese patients for cardiac risk assessment prior to bariatric surgery. **MATERIALS & METHODS**: Analysis of pre-surgery stress MPS of 20 obese (BMI ranging from 36.6 to 59.6; Mean: 43.3) patients (3 males & 17 females) was performed using "EC tool box" in 17 segment model. Low dose CT (2.5 mA) was used for attenuation correction. Stress induced perfusion defects (SPD) were characterized into mild, moderate and severe categories using both non-attenuation corrected (NAC) and attenuation corrected (AC) images separately. The segment-based and patient-based change in interpretation of perfusion defect after AC was analyzed. **RESULTS**: 18/20 patients showed SPD in NAC images whereas only 13/20 patients showed SPD in AC images. 31 out of a total of 340 segments showed change in interpretation due to AC. The interpretation was changed from mild to no defect in 24, moderate to mild in 4 and no defect to mild defect in 3 segments. However, AC showed false positive defects in apex (3 segments), which is known as attenuation induced artifact. 4 of the 5 patients that showed complete normalization on AC images had BMI > 40. No incidence of adverse cardiac events was noted in the peri-operative period including the patients that showed new defects on AC. Overall, AC showed incremental value in 14/20 (70 %) patients with more significant role in patients with higher levels of BMI. **Conclusion**: Stress MPS is a non-invasive investigative modality in obese patients undergoing bariatric surgery to evaluate cardiac risk. In this subset of patients, AC has significant incremental value over NAC images in detecting the stress induced perfusion defect. However, caution is advised in view of attenuation induced artefacts.

P22-1 - Sunday, Oct. 20, 16:00 - 16:30, Poster Exhibition Area

## Cardiovascular: Metabolism

## P138

### Nuclear Medicine Assessment of Patients with Atrial Fibrillation Treated with PUFA

**V. Sukhov**, A. Ismailov, V. Nikiforov, P. Kirichenko, A. Marin; Military Medical Academy, St. Petersburg, RUSSIAN FEDERATION.

**Objective**. This study examined the effects of polyunsaturated fatty acids (PUFA) on myocardial perfusion and metabolism in patients with atrial fibrillation (AF) using well known in clinical practice myocardial gated single photon emission computered tomography (G-SPECT) with 99mTc-tetrofosmine (TF) and 123I-beta-metyl-iod-phenyl-pentadecanoic acid (BMIPP) as in vivo Methods for diagnostics of different heart diseases. **Material and Methods**. 56 male patients 45-69 y.o. with persistent AF treated with standard anti-ischemic and anti-arrhythmic agents (control group) were compared with 51 male patients 44-66 y.o. with AF I-II FC NYHA treated with standard anti-arrhythmic + PUFA. All of them underwent standard clinical investigation, Bruce protocol ETT, EchoCG and rest/stress G-SPECT with 99mTc-TF and 123I-BMIPP. Both tracers SPECT data were analyzed with 17-segment model. **Results.** Definite regional abnormality of perfusion tracer uptake at rest/stress were concordant with metabolic defects at the same site. While comparing regions of repolarization disturbancies, shifted metabolism and decreased perfusion tracer uptake in 95 patients, 93% of them were considered match (di=0,615-0,998), 7% - mismatch (di=0,002-0,385). Though sensitivity in detecting of impaired repolarization by ECG and decreased 99mTc-TF/123I-BMIPP uptake regions by SPECT were 19.6% vs 87.1%./89.2%. Moreover, number of sectors with low 99mTc-tetrofosmine and/or 123I-BMIPP uptake (<70%) and with EchoCG signs of cardiac insufficiency, ECG abnormalities and decrease of tracers uptake were equal. Repeated gated SPECT studies after treatment with PUFAs showed increase of perfusion tracer uptake in previously altered sectors compared to patients treated with only standard therapeutic scheme **Conclusion**. Metabolic activity and myocardial perfusion as shown by 123I-BMIPP and 99mTc-TF SPECT allow to perform adequate assessment of changing (decreasing) of myocardial metabolizm (i.e. levels of beta-oxydation in cardiomyocytes) that together with perfusion data can fully represent the state of heart tissue impairments in AF patients. Therefore, this method is feasible and highly informative for assessment of PUFA effects during metabolic treatment and follow-up.

## P139

### Extra-cardiac findings on [18F]- FDG PET-CT scans performed for evaluation of cardiac sarcoidosis.

**D. Ersahin**, A. Sinusas, R. Russell, M. Djekidel; Yale University School of Medicine, New Haven, CT, UNITED STATES.

**Purpose:** To evaluate the prevalence and clinical significance of extra-cardiac findings in patients who underwent an [18F]- FDG PET-CT for the evaluation of cardiac sarcoidosis involvement . **Methods:** Forty-three [18F]- FDG cardiac PET-CT scans performed for the evaluation of cardiac sarcoidosis were retrospectively evaluated by a nuclear medicine physician. Qualitative assessment of extra-cardiac findings using an AW (GE Healthcare) workstation was completed. Studies were accompanied by flow [82Rb]- PET-CT scans. The diagnosis of cardiac sarcoidosis was made using a Wackers-Liu CQ software (MEDX, Inc) by nuclear cardiologists with >11 to > 25 years of experience. This data was extracted from clinical reports **Results:** Ten scans were excluded from the study due to poor extra-cardiac resolution of the PET images. A total of 33 scans were included. The majority of the patients (57.6%) were asymptomatic at the time of the studies. Cardiac involvement by sarcoidosis was present in 51.5 % of the patients (n=17). Extra-cardiac findings were found in 31 of the 33 scans (93.9%). The most common extra-cardiac finding was FDG avid lymphadenopaty in bilateral hila and mediastinum (66.7%). Additional findings included diffuse bone marrow uptake (51.5%), uptake in the distal esophagus ±proximal stomach (30.3%), uptake along the thoracic aortic wall (18.2%), focal skeletal uptake (18.2%), FDG avid lung nodules (9.1%), and diffuse splenic uptake (3%, n=1). **Conclusion**: Extra-cardiac findings are extremely common in patients referred for [18F]-FDG PET-CT scans with suspected cardiac sarcoidosis. The prevalence of widespread sarcoidosis as well as bone marrow involvement is underestimated in the literature. This is likely related to the fact that historically end-organ involvement has been a late diagnosis, once significant involvement is present and clinical or biochemical symptoms are present. It is therefore important to document all the areas of abnormal FDG uptake in order to allow referring physicians to appropriately stage these patients and potentially target more accessible sites for biopsy. Our ongoing study is evaluating relevant clinical information related to the patient's extra-cardiac findings.

## P140

### Clinical utility of I-123BMIPP imaging in patients with Takotsubo cardiomyopathy

**S. Matsuo**, K. Nakajima, S. Kinuya; Kanazawa University, Kanazawa, JAPAN.

**Backgrounds.** Takotsubo cardiomyopathy is a heart syndrome with an acute onset defined by chest symptoms, ST segment elevation on electrocardiograms. Patients with Takotsubo cardiomyopathy are usually misdiagnosed as having acute myocardial infarction (AMI). Transient balloon-like asynergy in the apical regions with hyperkinesis in the basal left ventricle. Several study reported the utility of 123I-BMIPP imaging. However, few data exist regarding the clinical impact of BMIPP on diagnosis of Takotsubo cardiomyopathy. **Methods and Results**. We examined 17 patients of Takotsubo cardiomyopathy and 12 with acute myocardial infarction in the left anterior descending artery (LAD) lesion. Coronary angiography showed the absence of stenotic regions in the subjects of Takotsubo cardiomyopathy and culprit legion in LAD in subjects with AMI. All patients were

studied with resting BMIPP imaging. Planar and SPECT image were obtained at 20 min after the injection of BMIPP and total defect score (TDS) was semi-quantitatively determined with SPECT imaging using 17-segment model. 123I-BMIPP showed reduced uptake in the apical segments of the myocardium (TDS; 5 ± 3), indicating impairment of metabolic abnormalities on 123I-BMIPP in patients with Takotsubo cardiomyopathy. BMIPP defect score was higher than that of perfusion in patients with Takotsubo cardiomyopathy. There was a significantly higher defect score in patient with AMI than in those with Takotsubo cardiomyopathy, especially in apial (3.1±1.1 vs. 1.3±1.1) and mid-anteroseptal segment (2.8±1.1 vs. 0.1±0.1; (p<0.01). BMIPP SPECT images give us information on differential diagnosis on Takotsubo cardiomyopathy. **Conclusion**. These results demonstrate that cardiac metabolic BMIPP imaging can detect myocardial injury and used as an important tool to diagnose the disease.

P23-1 - Sunday, Oct. 20, 16:00 - 16:30, Poster Exhibition Area

## Cardiovascular: Stem Cells

### P142

### Perfusion and metabolism imaging to evaluate the effects of intracoronary bone marrow-derived mesench stem cells on acute myocardial infarction in dogs

L. Hao[1], **X. Wang**[1], W. Fang[2]; [1]Dept. of Nuclear Medicine, Inner Mongolia Medical University, Hohhot, CHINA, [2]Dept. of Nuclear Medicine, Fuwai Hospital of Chinese Academy of Medicine, Beijing, CHINA.

***Aim*:**The method was evaluated using intracoronary delivery of bone marrow-derived mesenchymal stem cells (MSCs) to improve the cardiac function after acute myocardial infarction (AMI) in dog. *Materials and ethods*: Dogs (n=12, 20 to 30Kg weight) were assigned to a graft study (n=6) and control group (n=6). AMI model were prepared by blocking the blood stream of 1/3 of descending branch of coronary artery (LAD) in dogs, and released the branch after ligation 90 minutes. 0.9% NaCl was grafted into each dog of control group and MSCs culture-expanded 2-3 weeks in vitro and labeled in vitro before 24 h were grafted into heart's AMI area in each dog of graft group through intracoronary way respectively. AMI model were succeed by electrocardiogram (ECG) ,blood Biochemical chemical examine and myocardial perfusion imaging (MPI) and(or)metabolism imaging (MMI) in each dogs. MPI and MMI were performed in all dogs in 6 weeks and 10 weeks after graft. Pathology and immunohistochemical analysis were performed in end of trial. MPI and MMI images were scored semi- quantitatively using a 9-segment model of the left ventricle with a 5-point scale (0=normal uptake, 1= mild hypoperfusion, 2=moderate hypoperfusion, 3=severe hypoperfusion and 4=no uptake). *Results*: 1. Three dogs were died in making model (two dogs in control group). 2.Viability myocardial segments of segmental myocardial perfusion defects were found in MPI/ MMI 8/ 20 and 10/26 in control and graft group respectively, which was no significantly in control and graft group (*P*>0.05) .3.Changes in MPI/ MMI were found compared to 5-7 day's and 10 weeks in segmental viable myocardium in graft group(*P*<0.01); however, no changes in segmental no viable myocardium and compared to 5-7 day's and 6 weeks in all segmental myocardial perfusion defects and in graft group(*P*>0.05); And no changes in MPI/ MMI were found among 7-10 day's , 6 weeks and 10 weeks in control group(*P*>0.05). 4. The change value of LVEF between 5-7day's and10 weeks in control and graft group were 5.5±2.69 and 16.2±2.93 respectively,which was significantly higher than that in control group(*P*<0.01). *Conclusions*:MPI and(or)MMI is availability method to evaluate AMI model. MPI and MMI not only can display the part of infarction,area and degree,but also detect viable myocardium after myocardial infarction,and reflect metabolize change after transplantation.

P24-1 - Sunday, Oct. 20, 16:00 - 16:30, Poster Exhibition Area

## Cardiovascular: New & Innovative

### P143

### Initial experience of assessment of left ventricular function with gated blood pool SPECT in Kuwait

**G. Biswas**, S. Panchadar, Y. Mohammad, M. Syed, M. Mohammad; Chest Hospital, Safat, KUWAIT.

**Aims and Objectives**: We performed gated blood pool SPECT [GBPS] in various groups of patients referred for left ventricular[LV] function assessment and compared it to planar radionuclide ventriculography [PRNV] to find out whether GBPS can replace PRNV for LV function assessment in our patients. Materials and **Methods**: We performed GBPS on the same day with PRNV in 60 patients [47 males,13 females, mean age:57yrs] referred for LV function assessment using in vivo labelling of red blood cells with technetium-99m. PRNV imaging was performed first, followed by GBPS using a 24 frame/cycle gated acquisition protocol that included 180° rotation, 64 by 64 matrix and 64 views on a dual headed SPECT gamma camera [GE-infinia].GBPS images were reconstructed with a butterworth filter [cutoff frequency:0.4,power:10] using an automated GBPS processing software installed on a xeleres computer[GE]. **Results**: Mean values of left ventricular ejection fraction[LVEF] for PRNV and GBPS were 46.2% and 49.5% respectively,(r=0.88,p<0.01).Bland-Altman plot demonstrated mean difference of 0.77% to 5.84%[mean±SD] between LVEF from 2 techniques. The 95% limits of agreement are therefore -9.73% to +16.35%.Interoperator reproducibility of GBPS LVEF was excellent [r=0.98,p<0.01]. Mean values of left ventricular end diastolic volume(LVEDV),left ventricular end systolic volume(LVESV),right ventricular end diastolic volume(RVEDV) and right ventricular end systolic volume(RVESV) were found to be 128.7± 47.8ml ,69.3 ± 40.3ml,122 ± 30.2 ml and 60± 25.1ml respectively. Mean right ventricular ejection fraction[RVEF] was found to be 52.1% with GBPS. Regional wall motion abnormalities (RWMA) were better delineated in 60% of patients with color rendered 3D phase, amplitude, wall motion and cine images using GBPS. **Conclusions**: Our study shows that LVEF values of GBBS correlated well with PRNV and showed excellent reproducibilty.In addition GBPS assesses RWMA better than PRNV and estimates RVEF,LV and RV end systolic and end diastolic volumes.

### P144

### PET Imaging of Angiogenesis in Murine Hindlimb Ischemia with a $^{64}$Cu-Labeled Anti-CD105 Monoclonal Antibody

**H. Orbay**, Y. Zhang, H. Hong, T. E. Barnhart, W. Cai; University of Wisconsin-Madison, Madison, WI, UNITED STATES.

**Aim**: Peripheral arterial disease (PAD) affects >10% of adults, which frequently involves the circulation of the lower extremities. Overexpressed on proliferating endothelial cells, CD105 is a promising vascular target for in vivo imaging. The goal of this study was to use $^{64}$Cu-NOTA-TRC105 (TRC105 is a monoclonal antibody that bind to both human and murine CD105) PET for non-invasive and quantitative assessment of angiogenesis in a murine hindlimb ischemia model of PAD, which can be used to guide therapy. **Materials and Methods**: CD105 binding affinity and specificity of NOTA-TRC105 was evaluated by flow cytometry and microscopy. BALB/c mice (n = 15) were anesthetized and the right femoral artery was ligated to induce hindlimb ischemia, which was confirmed with laser Doppler and PET imaging (the left hindlimb served as an internal control). Ischemia-induced angiogenesis was monitored and quantified with $^{64}$Cu-NOTA-TRC105 PET at post-operative days 1, 3, 10, 17, and 24. Biodistribution studies were also performed on days 10 and 24 in separate cohorts of mice. Histology and RT-PCR of the hindlimb muscle tissue were carried out to detect the dynamic CD105 expression after ischemia. **Results:** NOTA-TRC105 specifically bound to CD105 in cultured endothelium. Laser Doppler imaging showed that perfusion in ischemic hindlimbs plummeted to ~10% of the contralateral hindlimb after surgery, similar as observed with PET imaging, and gradually recovered to near normal levels on day 24. The uptake of $^{64}$Cu-NOTA-TRC105 in ischemic hindlimbs was 9.0±2.2, 14.1±1.9, 11.4±1.5, 6.2±1.5, 3.4±1.9 %ID/g at days 1, 3, 10, 17, and 24 after surgery (n = 3) and significantly higher than that of the non-ischemic control hindlimbs (< 3.0 %ID/g; P<0.05). $^{64}$Cu-NOTA-TRC105 uptake in the ischemic limbs on days 3 and 10 were significantly higher than all the other days, which correlated well with biodistribution data. Histological assessment and RT-PCR both revealed increased CD105 expression on days 3 & 10. Administration of a pro-angiogenic drug significantly increased the blood flow of the ischemic hindlimb, as evidenced by laser Doppler imaging and PET. **Conclusion:** This is the first report on PET imaging of CD105 expression during angiogenesis following hindlimb ischemia. Rapid, persistent, and CD105-specific uptake of $^{64}$Cu-NOTA-TRC105 in the ischemic hindlimb was observed, which was validated by various in vitro and in vivo experiments. $^{64}$Cu-NOTA-TRC105 PET can play multiple roles in future PAD-related research, and improve PAD patient management by identifying the optimal time for therapeutic intervention and monitoring the efficacy of therapy.

### P145

### Assessment of global and regional tracer kinetics in isolated perfused rat heart using micro PET system

**T. Yamane**[1], M. J. Park[1,2], D. Richter[1], K. Fukushima[1], T. Higuchi[1,2]; [1]Department of Nuclear Medicine, University of Würzburg, Würzburg, GERMANY, [2]CHFC, University of Würzburg, Würzburg, GERMANY.

**Aim:** Assessment of tissue kinetic parameters of myocardial tracers, such as extraction fraction and washout, requires studies with isolated perfused heart to avoid recirculation of the tracers. A combination of the isolated perfused rat heart and high-resolution micro PET system could offer not only global but also regional parameters of the tracer uptake. **Materials and Methods:** Isolated rat hearts were perfused via the Langendorff method under a constant flow of KH buffer with a rate of 5ml/min and placed in the field of view of micro PET system (SIEMENS Inveon) for dynamic PET imaging (2min/frame). F-18-FDG uptake was studied in a total of 8 hearts in the various conditions such as a model of myocardial infarction induced by coronary artery occlusion and addition of hexokinase II (Hex-II) inhibitor

to the perfusion buffer. Immediately after the PET session, activity of the hearts was measured in the gamma counter to correlate with the PET data of the last frame. **Results:** Dynamic PET imaging of the isolated heart under constant F-18-FDG infusion demonstrated continuous increase of the activity in the heart, which was blocked by the addition of Hex-II inhibitor. Correlations between the value measured by PET and gamma counter were excellent for both whole heart activity (MBq) ($R^2$=0.99) and regional myocardial activity concentration (MBq/cc) ($R^2$=0.81). Images of the heart with myocardial infarction showed clear tracer uptake defect corresponding with localization of scar tissue identified by autoradiography and histology. **Conclusion:** A combination of isolated perfused rat heart and micro PET system allows accurate quantification of global and regional myocardial tissue tracer kinetics. This novel assay could be useful for the characterization of novel myocardial PET tracers.

## P146

### Complex diagnostictics of nonrheumatic myocarditis by means of Nuclear Medicine in conjunction with echodensitometry and CT-MRI

**V. Sukhov**[1], V. Nikiforov[1], K. Zaplatnikov[2], P. Kirichenko[1], A. Marin[1]; [1]Military Medical Academy, ST. PETERSBURG, RUSSIAN FEDERATION, [2]Clinic for Nuclear Medicine MÄZ, Nürnberg, GERMANY.

To date, the diagnosis of myocarditis is an actual and complex issue. Clinical verification of disease is difficult, so different radiologic Methods are increasingly used for diagnostics of myocarditis. **Aim**. To implement complex clinical and instrumental examination including single photon emission computed tomography (SPECT) with the 99Tc-labelled white blood cells (WBC), ultraconographic videodensitometry (USVD) and contrast enhanced magnetic resonance imaging (CE-MRI) in patients with myocarditis. **Material and Methods**. We perform clinical, laboratory and instrumental examination of 152 patients with symptoms of myocarditis at the age between 14 and 50 years. Besides routine investigations study protocol included WBC-SPECT and USVD with cyclic variation indexes calculation (CVI) in all patients. Some of them (n=57) underwent cardiac MRI with gadolinium. **Results**. WBC infiltration was detected in myocardium of patients with clinical signs of myocarditis in 84% of cases (diagnostic value of the method). Features of WBC-infiltration in the cardiac muscle showed diferencies in severity and extent of myocardial damage (deep, widespread and/or limited). Most frequent signs of myocarditis are: increased concentration of LDH, fibrinogen, the migration of the pacemaker, atrial fibrillation, frequent atrial and ventricular arrhythmias, increased diastolic heart size, signs of diastolic dysfunction, cardiac blood detection of antigen and antibodies to the myocytes. USVD revealed wide spectrum of US densities in both acute and chronic myocarditis, despite no one case of normal myocardium. CVI in posterior wall region was 33 ± 9% for the control group; 8,3 ± 19% for the 1-st group; -2,7 ± 19% for the 2-nd group; -11,2 ± 21% for the 3-rd group patients, and the CVI in the septum 38 ± 10%; 10,6 ± 21%; -5,2 ± 22%; -19 ± 23%, respectively. CE-MRI performed after WBC-study in 57 patients with myocarditis. In 52 cases have confirmed the existence of zones of pathological MR signal intensity due to elevated myocardial extracellular water, which completely corresponded to the fixation of labeled WBC. A false-negative MRI result obtained in five cases was associated with technical difficulties. The diagnostic value of the method was 80%. **Resume**. Our results are consistent with the literature data about diagnosis of myocarditis (SPECT, US and MRI) that are almost equivalent to the verification of the inflammatory process in the myocardium and can be used as a noninvasive diagnostic Methods. Sites of leukocyte infiltration in myocardium by WBC-SPECT are fully consistent with pathological areas of intense magnetic resonance signal and CVI changes at USD.

## P147

### Assessment of left ventricular mechanical dyssynchrony using electrocardiographically-gated myocardial perfusion single-photon emission computed tomography

**T. Niimi**[1], H. Maeda[2], M. Nanasato[1], M. Sugimoto[1]; [1]Nagoya Daini Red Cross Hospital, NAGOYA, JAPAN, [2]Nagoya University, Nagoya, JAPAN.

**Purpose**: Regional radial and longitudinal function in patients with coronary artery disease (CAD) is often evaluated by visual inspection of wall motion. This evaluation is subjective and may be difficult in patients with left ventricular (LV) dyssynchrony. We mechanically evaluated synchronization and contraction work in patients with CAD using quantification of segmental function by solving the Poisson equation (QSFP). **Methods and Materials**: We evaluated 32 patients with CAD and 40 healthy individuals (controls), using electrocardiographically-gated technetium-99m-labeled myocardial perfusion agents. Synchronous contraction index (SCI) and contraction work were evaluated mechanically using the QSFP to differentiate abnormal regional contractions in the cardiac wall. SCI was defined as the temporal correlation coefficient between the LV volume and myocardial contraction. Contraction work was estimated as the product of force and displaced distance. The definition of force was based on Laplace's law that considers a thin cardiac wall model. The cardiac wall was divided into 17 segments, and the accumulation of perfusion agents, SCI, and contraction work for each segment were calculated and plotted on polar maps. **Results**: SCI and contraction work values of the 17 segments were 96.6% ± 1.4% and 6.9 ± 1.1 $mJ \cdot cm^{-2} \cdot beat^{-1}$ in healthy individuals, and 85.9% ± 16.7% and 5.8 ± 1.5 $mJ \cdot cm^{-2} \cdot beat^{-1}$, in patients with CAD, respectively. In addition, these values were 60.7% ± 17.9% and 3.9 ± 1.3 $mJ \cdot cm^{-2} \cdot beat^{-1}$ in CAD patients with LV ejection fraction (LVEF) < 40% ($n$ = 11), respectively. SCI and contraction work values were significantly lower in patients with CAD than in controls ($p < 0.005$), and were also significantly lower in CAD patients with LVEF < 40% ($n$ = 11) than in the patients with CAD ($p < 0.05$). SCI and contraction work showed good correlation with LVEF in patients with CAD, with values of 75% and 76%, respectively. Therefore, areas of LV dyssynchrony can be visually delineated on polar maps. **Conclusion**: CAD-associated with LV dyssynchrony could be detected using SCI, and mechanical work during dyssynchrony could be determined as value of contraction work; further, these values indicated the reason for the decrease in the LVEF. SCI and contraction work are thought to aid radiologists and provide them with valuable information in the diagnosis of LV dysfunction.

## P148

### Gated-SPECT evaluation of left ventricular function at rest using a CZT gamma-camera and a fast low-dose clinical protocol: comparison to cardiac Magnetic Resonance Imaging.

**A. Giorgetti**[1], P. Masci[1], D. Genovesi[1], G. Marras[1], Y. K. Rustamova[2], M. Lombardi[1], P. Marzullo[3]; [1]Fondazione CNR/Regione Toscana "G. Monasterio", Pisa, ITALY, [2]Azerbaijan Medical University,department of Internal Medecine Central Customs Hospital, Pisa, ITALY, [3]Istituto di Fisiologia Clinica del CNR, Pisa, ITALY.

**Background** CZT technology allows ultrafast low-dose myocardial scintigraphy but its accuracy in assesing left ventricular function is still to be defined. **Materials and Methods** 55 patients (23 female, mean age 63±9 years) referred for myocardial perfusion scintigraphy were studied at rest using a CZT-camera (Discovery NM530c, GE Healthcare) and a low-dose 99mTc-Tetrofosmin clinical protocol (mean dose 264±38 MBq). Gated-SPECT imaging was performed as a 6 min list mode acquisition, 15 min after radiotracer injection. Images were reframed (8/16-frame) using Lister software on a Xeleris workstation (GE Healthcare) and then reconstructed with a dedicated iterative algorithm. Analysis was performed using Quantitative Gated Spect software (QGS). Within 2 weeks patients underwent cardiac Magnetic Resonance Imaging (cMRI, 1.5-Tesla unit CVi, GE Healthcare) using a 30-frame acquisition protocol and dedicated software for analysis (MASS 6.1, Medis). **Results** QGS 8-frame analysis showed an excellent correlation with cMRI volumes (end-diastolic volume (EDV): r= 0.90; end-systolic volume (ESV): r= 0.94, p<0.001) but a significant underestimation in measures (EDV mean difference:-39,5±29 mL; ESV: -15,4±22 mL, p<0.001). Similarly, QGS 16-frame resulted in an excellent correlation with cMRI volumes (EDV: r= 0.92; ESV: r= 0.95, p<0.001) with a significant underestimation in measures (EDV mean difference:-33.2±26 mL; ESV: -17.9±20 mL, p<0.001). QGS 8-frame mean ejection fraction (EF) resulted closely correlated to cMRI (r= 0.84, p<0.001) despite significantly lower (47.9±16% vs 51.2±15%, p<0.008). QGS 16-frame mean EF showed the best correlation to cMRI (r= 0.91, p<0.001) and similar to mean cMRI values (49.6±16%, p=ns). Regional analysis showed a good correlation between both 8/16-frame and cMRI wall motion score indexes (8-frame WMSI: r= 0.85; 16-frame WMSI: r= 0.89; p<0.01). **Conclusions** Low-dose gated-SPECT with a CZT camera provides ventricular volumes that correlate well with cMRI despite significant underestimation in measures. 16-frame re-formatted images appears more accurate than 8-frame ones in EF estimation.

## P149

### 99mTc-HDP scintigraphy in the diagnostic workup of cardiac amyloidosis: preliminary results.

**D. Genovesi**, A. Giorgetti, M. Emdin, G. Vergaro, A. Bottoni, E. Filidei, A. Gimelli, P. Marzullo; Fondazione Toscana Gabriele Monasterio, Pisa, ITALY.

**AIM**. Amyloidosis constitutes a large group of disorders caused by extracellular deposition of insoluble proteic fibrils which may alter tissues structure and the function of various organs, including the heart. The aim of the present study was to evaluate the usefulness and the accuracy of 99mTc-HDP scintigraphy in the diagnostic pathway of patients with suspected amyloidosis. MATERIALS AND **METHODS.** We evaluated a group of 12 patients (7♀, 5♂; mean age 80 y) admitted to our hospital with hypertrophic cardiomyopathy (septal thickness: 16 ±2.5 mm; posterior wall thickness: 15±2 mm;) and suspected cardiac amyloidosis studied with electrocardiography, echocardiography, magnetic resonance (MR), periumbilical fat analisys (PFA) and/or blood sampling for immunoglobulin light chains (ILC) or transthyretine mutations. Each patient underwent to 99mTc-HDP scintigraphy; planar and tomographic images were collected 3 hours after tracer injection (740 MBq i.v.) using a double headed gamma-camera equipped with LEGP collimators for planars and a CZT multi pin-hole gamma-camera for SPECT. Qualitative (+/-) and semiquantitative analisys (heart to rib-bone [H/B] and heart to

thorax background [H/Bkg] ratios) and regional myocardial distribution of tracer were than performed**. RESULTS**. PFA resulted positive in 5/12 patients (42%) and 6/12 patients showed high levels of ILC or transthyretine mutations (50%). MR showed an "amyloidosis pattern" in 7/12 patients (58%), while 99mTc-HDP scintigraphy showed a cardiac tracer uptake in 4/12 patients (33%). Patients with positive scintigraphy showed a cardiac tracer uptake of 119±18 mean cps/pixel with an H/B ratio of 2.8±1.2 and H/Bkg ratio of 4.2±1.3; PFA was positive in 2/4 patients (50%) while 3/4 patients (75%) had transthyretine mutations and 1/4 (25%) had high levels of ILC. All patients showed an "amyloidosis pattern" at MR. Patients with negative scintigraphy showed a cardiac tracer uptake of 52±41 mean cps/pixel with an H/B ratio of 1.6±1 and H/Bkg ratio of 2.6±0.9; PFA was negative in 5/8 patients (62.5%); 2/8 patients (25%) had high levels of ILC while no patients had transthyretine mutations. 3/8 patients (37.5%) showed an "amyloidosis pattern" at MR (1/3 had high levels of ILC). Overall agreement with histological or molecular analisys was obtained in 8/12 patients (67%) using MR and in 9/12 patients (75%) using 99mTc-HDP scintigraphy. **CONCLUSIONS**. Although the number of patients studied is small, our data suggest an important role of 99mTc-HDP scintigraphy in the diagnostic workup of patients with suspected cardiac amyloidosis. The incidence of false positive appears to be higher for MR than for 99mTc-HDP scintigraphy.

## P150

### Automatic Segmentation Method to Reduce the Influence of Extra-cardiac Radionuclide Activity Using Sinogram Images

**M. Tanaka**[1], R. Kimoto[1], K. Nagahiro[1], Y. Nakamura[1,2], N. Katsuta[2], S. Shiraishi[2], M. Yoshida[2], F. Sakamoto[2], S. Tomiguchi[1]; [1]Kumamoto University, Kumamoto, JAPAN, [2]Kumamoto University Hospital, Kumamoto, JAPAN.

**Aim**: The artifact due to extra-cardiac radionuclide activity affects diagnostic performance for single photon emission computed tomography (SPECT) myocardial perfusion imaging (MPI).The aim of this study was to develop an automatic segmentation method to reduce the effect of extra-cardiac radionuclide activity and evaluate our method in clinical study. **Material and method**: 20 patients within 10 patients who suspected to be extra-cardiac radionuclide activity underwent stress non-gated 201Tl SPECT-MPI with dual detector SPECT system (SKYLight, Philips). Our method was applied for original projection data using siongram image, and made the segmented extra-cardiac radionuclide activity image. These images were reconstructed with filtered back projection (FBP) method (Order 5, cut-off frequency 0.50 cycles/cm) . Regional myocardial uptake on MPI polar map using 17-segment model for the left ventricle was assessed for each segment in high extra-cardiac radionuclide activity group and normal group, and these uptake s were compared between the original data and our method. **Result:** A good agreement was observed between the original data and the segmented data in high activity group (r=0.8229, p<0.0001), and in normal activity group (r=0.8862, p<0.0001) using FBP method. The original myocardial uptake on polar map was lower than the segmented (76.08±14.15% vs 77.97±11.84%, p=0.073) in high activity group, the same trend was observed in normal group (70.07±15.59% vs 76.36±12.04%, p<0.0001). **Conclusion**: Our method can reduce the artifact due to extra-cardiac radionuclide activity, and expect to improve the diagnostic performance for SPECT-MPI.

P25-1 - Sunday, Oct. 20, 16:00 - 16:30, Poster Exhibition Area

## Cardiovascular: Miscellaneous

## P151

### Assessment of regional left ventricular contractile function in patients with known or suspected coronary artery disease : do gated blood pool SPECT and myocardial perfusion scintigraphy data correlate at segmental levels ?

A. HALKOVICH, **D. MARIANO - GOULART**, A. BOURDON, M. SAINMONT, M. BENKIRAN, F. BOUALLEGUE; CHU Lapeyronie, MONTPELLIER, FRANCE.

**Context and objective *:*** In cardiology, regional left ventricular contractile function assessment not only helps diagnosis of coronary artery disease and myocardial viability, but also gives important prognostic information. The aim of our study was to compare local assessments of left ventricular wall kinetics by gated blood pool SPECT (GBPS) and myocardial perfusion scintigraphy (MPS). **Material and Methods *:*** we retrospectively included consecutive patients from January 2004 to December 2012 who had had both GBPS and MPS at close intervals, and thus compared 23 GBPS to 23 $^{99m}$Tc-tetrofosmin MPS, and 50 GBPS to 50 $^{201}$thallium MPS. GBPS segmental ejection fraction (GBPS-sEF) was compared to MPS segmental wall thickening (MPS-T) and wall motion (MPS-M) on a segment by segment basis. Agreement for left ventricular ejection fraction (LVEF), end-diastolic (EDV) and end-systolic (ESV) was also assessed. **Results *:*** GBPS and MPS global left ventricular function parameters strongly correlated (GBPS versus $^{99m}$Tc-tetrofosmin MPS : r = 0.89, 0.81, and 0.86 for LVEF, EDV and ESV respectively ; GBPS versus $^{201}$thallium MPS : r = 0.88, 0.90, and 0.95). Good and highly significant correlations were found between GBPS-sEF and MPS-T (GBPS versus $^{99m}$Tc-tetrofosmin MPS : r = 0.62, and GBPS versus $^{201}$thallium MPS : r = 0.52) or MPS-M (r = 0.59, and 0.49), with similar results for men and women. Those correlations were significantly lower for hypokinetic segments (sEF <50%, wall thickening <20% and wall motion <3) only in the group of patients studied with $^{201}$thallium MPS, who had larger infarction sequelae and more severe cardiomyopathies than in the $^{99m}$Tc-tetrofosmin MPS group, with potential accountability of MPS segmentation difficulties. When the left ventricle wall was divided into anatomical territories, GBPS-sEF and MPS-T correlated quite steadily, whereas correlation between MPS-M and GBPS-sEF varied (lower for the septum than the lateral wall). **Conclusion :** Although using very different approaches, GBPS and MPS gives data about global and segmental left ventricular wall contraction that are well correlated, but which are not strictly interchangeable. Their agreement appeared to be altered in the presence of large infarction sequelae.

## P152

### The role of myocardial perfusion scintigraphy in predicting risk for coronary artery disease in patients with anxiety and depression semptoms; preliminary results of prospective study

**B. Caliskan**, O. Yildirim, T. C. Tuman, N. Kayka, A. Erdem; Abant Izzet Baysal University, Bolu, TURKEY.

**Background and aim:** Relationship between depression and anxiety with cardiovascular disease, has been previously reported on but there are conflicting data about whether chest pain arises from emotional distress or coronary spasms from the onset of coronary artery disease(CAD). Patients with chest pain who do not have known CAD often have been referred to myocardial perfusion scintigraphy (MPS). The aim of the study to predict risk for CAD in patients with anxiety and depression semptoms using MPS. **Methods**: 82 patients (30 males and 52 females, mean age 52 ±11..3 ) with chest pain underwent standart one-day stress-rest Tc99m MIBI myocardial perfusion sintigraphy for diagnosis of coronary artery disease. The emotional status of the patients was evaluated using the Hamilton Depression (HAM-D), Hamilton Anxiety (HAM-A), state and trait anxiety inventory (STAI-I and STAI-II), perceived stress scale (PSS), and the anxiety sensitivity index-3 (ASI). Myocardial perfusion was evaluated using a 17 segment model and a five point scoring system (0:normal, 1:equivocal, 2:moderate, 3: severe and 4:absent). Summed stress scores , summed rest scores and summed difference scores (SDS) were calculated. **Results**: 11/82 patients had reversible perfusion defect and of the 71/82 patients had no perfusion defect on MPS. There were statistically significant correlations between SDS and STAI-I, PSS, HAM-A scores (r: 0.224, p:0.043; r: 0.239, p:0.031; r:0.279, p: 0.01 respectively). Athough there were correlations between SDS and STAI-II, ASI, HAM-D scores, it was not statistically significant (r:0.106, p: 0342; r: 0.157, p: 0.160; r: 0.139, p: 0.212 respectively). **Conclusion:** Our preliminary results showed that there are correlations between myocardial perfusion defect and patients' anxiety and depression semptoms. MPS is a useful method to evaluate of CAD in patients with anxiety and depression semptoms.

## P153

### Radionuclide Ventriculography in the Evaluation of Cardiotoxicity by Chemotherapy

F. Z. T. Huber, W. E. F. Alves, M. J. Santos, **E. T. Rocha**; Fundação Pio XII, Barretos, BRAZIL.

**OBJECTIVES**: The aim was to evaluate the frequency of assessments of left ventricule ejection fraction (LVEF) by radionuclide ventriculography in a sample of patients undergoing chemotherapy for breast cancer and analyze when significant changes ocurred, associating this information with the chemotherapy regimens and doses achieved. **BACKGROUND**: Patients, who are receiving Chemotherapy regimens with anthracycline associated or not with trastuzumab, are at risk of cardiotoxicity and should be monitored for a decrease in LVEF, even when asymptomatic. **METHODOLOGY**: We selected female patients, who were diagnosed with breast cancer and were under monitoring in the Barretos Cancer Hospital, and who had performed at least two tests of radionuclide ventriculography for assessment of cardiotoxicity with anthracyclines or anthracyclines followed by trastuzumab, having performed necessarily an examination in the period from 03/01/2011 to 15/02/2011. These patients were analyzed mainly according to the chemotherapy regimens and the number, frequency, and average results of the examinations. **RESULTS:** Thirty patients were studied, the average age was 48.47 years (SD ± 10.08), 70% were treated with anthracyclines followed by trastuzumab, while 30% were treated with anthracyclines without trastuzumab. The overall mean of performed ventriculographies was 4.70 examinations / patient (SD ± 1.34). These tests were conducted on an average frequency of 129.13 days (SD ± 37.99). The overall mean baseline LVEF was 63.63% (± 5.79 SD), and no patient had ≤ 50%.

However, the basic tests were performed on the average 82.33 days after initiation of chemotherapy treatment with anthracycline, and 40% of the sample began on average 11.83 days before and 60% on average 145 days after initiation of referred treatment. 43.33% of the sample showed overall change in LVEF (decrease> 10%, LVEF ≤ 50% or both) sometime in the study, 7.7% of these belonged to the group that used anthracyclines not followed of trastuzumab and 92.3% belonged to the group which used anthracyclines followed by trastuzumab. Among the groups, 57.14% of patients who used anthracyclines followed by trastuzumab and 11.11% who used anthracyclines not followed by trastuzumab showed changes in LVEF. In the first group, the change in LVEF happened after an average 7.42 cycles of trastuzumab (± 4.72 SD). **CONCLUSION**: It was observed that change in LVEF is higher in the group receiving anthracyclines followed by trastuzumab, and this change when present, appears 7.42 cycles on average after the beginning of therapy with trastuzumab in the sample.

## P154

### Morphophysiological evaluation of the heart of athletes of different sports

D. P. Miranda[1], M. J. Santos[1], E. T. Silva[1], V. M. C. Salemi[2], **E. T. Rocha**[1]; [1]Fundação Pio XII, BARRETOS, BRAZIL, [2]Instituto do Coração da Universidade de São Paulo, Sao Paulo, BRAZIL.

**OBJECTIVES:** Physical training performed consistently and at high intensities causes morphophysiological adaptation in the heart of athletes. This study aimed to investigate the influence of the type of sport practiced on such adaptations and if there is a correlation of structural and functional aspects with the autonomic cardiac innervation. **METHODOLOGY**: The sample consisted of 58 males aged between 19 and 47 divided into three groups: strength group(SG), consisting of 20 bodybuilding athletes; endurance group(EG), consisting of 20 endurance athletes; and control group(CG) consisting of 18 healthy non-athlete subjects. Structural and functional aspects were assessed by two-dimensional Doppler echocardiography, left ventricular function was assessed by radionuclide ventriculography and cardiac sympathetic innervation was assessed by planar images obtained with mIBG-I123, using the early (15min) and late(3,5h), heart-to-mediastinum ratio(H/M) and washout rate(WR). **RESULTS:** Left ventricular mass index(LVMI) was significantly higher both in the SG(88.73±28.71p<0.017) and in the EG (79.25±20.75 p=0.001) when compared to the CG(57.38±14.29). There was no significant difference between the SG and EG(p=0.417). Relative wall thickness (RWT) was significantly higher in the SG(0.39±0.06) compared to the CG(0.32±0.04 p<0.017). Both left ventricular aejection fraction(LVEF) and peak filling rate(PFR) shwed no significant difference between groups p=0.425 and p=0.119, respectively. Resting heart rate(RHR) of the EG (60.40 ±8.58) was significantly lower when compared to the CG (68.67±5.71 p=0.006) and SG (70.45±9.45 p=0.002). The myocardial uptake of mIBG-I123 in the late H/M ratio of the CG was 2.25±0.20 and showed no significant difference with the SG (2.01+_0.25 p=0.57) and EG (2.06+_0.18 p=0.157). On the other hand, the WR was significantly higher in the CG (23.93±5.07) compared to SG(19.39±4.07 p=0.005) and EG (18.84±2.96 p=0.001). There was no correlation of late H/M and RWT for CG(r=0.550 p=0.018). **CONCLUSION**: Therefore, It follows that strength training causes significant cardiac enlargement tending toward concentric hypetrophy and endurance training causes a significant reduction in RHR with a cardiac enlargement less expressive than in strength training. The planar imaging method alone does not seem to be sufficient to evaluate the cardiac sympathetic innervation in mIBG-I123 scintgraphy and the WR was not such a good parameter to explain sinus bradycardia observed in endurance athletes.

## P155

### Tc-99m MIBI myocardial GATE SPECT in the detection of cancer treatment-induced cardiotoxicity

**V. Chernov**[1,2], T. Kravchuk[1], R. Zelchan[1], V. Goldberg[1]; [1]Institute of Oncology, Tomsk, RUSSIAN FEDERATION, [2]Institute of Cardiology, Tomsk, RUSSIAN FEDERATION.

**Purpose:** To compare the possibility of using multiple-gated acquisition scan (MUGA) and Tc-99m MIBI GATE SPECT for evaluation of acute and chronic anthracycline-induced cardiotoxicity. **Materials and Methods**: The study included 80 patients (72 women and 8 men) (mean age 43±4.2 years) with malignant tumor without significant pathology of the cardiovascular system. For the treatment of these patients used doxorubicin in dose of 50 mg/m$^2$ per course in combination with various drugs. All patients were studied by MUGA (40 patients) or GATE SPECT (40 patients) before starting chemotherapy, at 1 hour after the first administration of doxorubicin and after the 4th course. **Results:** After administration of doxorubicin at a dose of 50 mg/m$^2$ was found that 14 patients according MUGA and 16 patients according GATE SPECT had a significant (10% or more) reduction in left ventricular ejection fraction (LVEF). Significant inhibition of systolic function in this patient group remained after the 4th course treatment. In the individual analysis of the MUGA and GATE SPECT results, registered after the administration of doxorubicin at a dose of 200 mg/m$^2$, was revealed that the criterion of LVEF reduction (10% or more) in response to the first dose of doxorubicin can predict the development of chronic cardiotoxicity. **Conclusion**: The MUGA and GATE SPECT can be applied with equal effectiveness for evaluation of acute and chronic anthracycline-induced cardiotoxicity in patients with malignant tumors. The decrease in LVEF (10% or more) in response to the first dose of doxorubicin can predict the development of chronic cardiotoxicity.

## P156

### The role of Tc-99m Myoview gated myocardial perfusion SPECT in evaluation of myocardial viability in ischemic cardiac patients, compared to low-dose Dobutamine echocardiography

**A. Amin**[1], A. Zaher[2], S. Ahmed[3], M. El-Sayed[2]; [1]NEMROCK, Faculty of Medicine; Cairo University, Cairo, EGYPT, [2]NCI, Faculty of Medicine; Cairo University, Cairo, EGYPT, [3]Cardiology, Faculty of Medicine; Cairo University, Cairo, EGYPT.

**Background** Thallium-201 [201Tl] myocardial single-photon emission computed tomography (SPECT) is recognized to be an excellent tool for identifying viability after myocardial infarction, but being expensive and needing a longer time for imaging are among its main limitations. Hence this study was designed to evaluate the effectiveness of low dose dobutamine echocardiography and Tc-99m myoview gated SPECT in assessment of myocardial viability in comparison to 201Tl. **Patients and Methods** 35 patients (30 males and 5 females) were included in this study to identify viable myocardium by defining akinetic or dyskinetic segments and comparing with 201Tl scan that was considered as gold standard. **Results** We compared the segments in patients; we had 560 segments in the myoview, 201Tl SPECT and echocardiography. Low dose dobutamine echocardiography identified 325/560 segments (58%) as viable myocardium compared to 525/560 (83.3%) by Tc-99m Myoview gated SPECT while 201Tl identified 536/560 (85%) viable segments. Sensitivity, specificity PPV and NPV for low dose dobutamine echocardiography and Tc-99m Myoview gated SPECT were [60.6 %, 100%, 100%, 30.8%] and [98%, 100%, 100% and 93.5%] respectively. **Conclusion** Tc-99m Myoview gated SPECT scan is superior to low dose dobutamine echocardiography in assessment of myocardial viability.

## P157

### Influence of Respiratory Gating, Image Filtering and Animal Positioning on High-Resolution ECG-Gated Murine Cardiac SPECT

**C. Wu**[1,2], B. Vastenhouw[1,2,3], P. E. B. Vaissier[1], J. R. de Jong[4], R. H. J. A. Slart[4], F. J. Beekman[1,3]; [1]Delft University of Technology, Delft, NETHERLANDS, [2]University Medical Center Utrecht, Utrecht, NETHERLANDS, [3]MILabs B.V., Utrecht, NETHERLANDS, [4]University Medical Center Groningen, University of Groningen, Groningen, NETHERLANDS.

**Objectives:** Cardiac SPECT images and physiological parameters obtained from these images can be affected by respiratory motion, post-reconstruction image filtering and animal positioning. Here we investigate the influence of these factors on myocardial perfusion SPECT in mice. **Methods**: Five mice were injected with Tc-99m-tetrofosmin and subsequently scanned in supine and prone positions using a U-SPECT-II scanner with simultaneous ECG and respiratory gating. ECG-gated myocardial perfusion images were reconstructed under three different strategies: by using gamma counts of (i) all respiratory gates without applying motion correction, (ii) only six out of eight respiratory gates (that have limited motion) without applying respiratory motion correction, and (iii) all respiratory gates with respiratory motion correction applied. All images were filtered with 3D Gaussian kernels ranging from 0.5–1.0 mm full width at half maximum (FWHM), and were analysed with Corridor4DM in order to compare cardiac parameters. **Results**: No significant visual differences were found in most images reconstructed with or without respiratory motion correction. The average left ventricular volume (LVV) over all mice was 50±11 µl at end diastole (ED) and 22±8 µl at end systole (ES), and the average left ventricular ejection fraction (LVEF) over all mice was 57±7%. Little differences in LVEF were found on average of all mice: <2.0% when changing reconstruction strategies, <4.6% when changing filter kernel sizes, and <2.8% with different animal positioning. However, relatively large LVV differences (>10 µl) were found in three mice as a consequence of their positioning. **Conclusions**: Animal positioning can affect cardiac parameters, while the influence of respiratory gating and different image filtering tested is showed to be limited, even for sub-half-millimetre SPECT. Our results indicate that respiratory gating is probably not necessary, and the selection of a specific image filter is not very critical for obtaining reliable cardiac parameters either.

## P158

### Prognostic value of MIBG scintigraphy for predicting cardiac events

**M. COZAR SANTIAGO**[1], P. GARCIA GONZALEZ[2], M. DEVIS SAIZ[1], F. RIDOCCI SORIANO[3], J. FERRER REBOLLEDA[1]; [1]UNIVERSITY GENERAL HOSPITAL. ERESA-NUCLEAR MEDICINE DEPARTMENT, VALENCIA, SPAIN, [2]UNIVERSITY GENERAL HOSPITAL.CARDIOLOGY DEPARTMENT, VALENCIA, SPAIN, [3]UNIVERSITY GENERAL HOSPITAL. CARDIOLOGY DEPARTMENT, VALENCIA, SPAIN.

**Objectives :** To assess the prognostic value of cardiac innervation scintigraphy with 123I-MIBG in predicting cardiac events in patients with left ventricular dysfunction in class I indication for implantable cardioverter defibrillator (ICD) for primary prevention. **Methods :** We evaluated 44 patients (35 men and 9 women) with a mean age of 64 years who underwent cardiac innervation scintigraphy (CIS) (Philips Brightview SPECT two detectors) with 10 mCi of 123I-MIBG (planar anterior chest images acquired at 20 minutes and 4 hours after injection and thoracic SPECT at 4 h) and we calculated the late heart/mediastinum uptake ratio (HM l). All of them were administered 4ml of 5% lugol one hour before the injection of the tracer and underwent a MRI study to characterize the presence of late gadolinium enhancement and calculate the left ventricular ejection fraction (LVEF) previous CIS. They were followed up for a minimum of 6 months-1 year to assess possible cardiac events. We established possible statistical correlation between the value of the HM l and the presence or absence of cardiac events. We used SPSS software to correlate variables. **Results :** The HM l ratio ranges from 0.92 to 1.96 (mean 1.35 ± 0.22) and LVEF between 10 and 44 (mean 25.77 ± 10.21). The group of patients with cardiac events (1 sudden death, 6 ICD discharges, 6 congestive heart, 1 ventricular tachycardia and 1 acute myocardial infarction) had a more pathological HM l ratio than the event-free group (1.28 vs 1.37, p = 0.212) even with higher LVEF (31% vs 23.8%, p = 0.117), although these differences were not statistically significant.

## P159

### Incidental extra-cardiovascular findings on the computed tomography attenuation correction scan for myocardial perfusion imaging.

**J. AVET**, E. YOUSSOF, P. CROISILLE, A. WAHART, F. DUBOIS; CHU de Saint-Etienne, Saint-Etienne, FRANCE.

*Objective:* The purpose of this study was to evaluate the prevalence and the clinical impact of non cardiac incidental findings (IF) on the computed tomography attenuation correction (CT-AC) scan for myocardial perfusion single photon emission computed tomography (MPI SPECT). *Methods:* Non cardiovascular structures were evaluated with the low-dose, no breath-hold, non ECG gated CT-AC scans performed for SPECT myocardial perfusion imaging. IF were categorized as clinically significant, indeterminate, or clinically not significant. Patient follow-up was performed by telephone, and verified with hospital records and/or communication with physicians (at least 6 months). *Results:* Of 192 patients, there were 85 patients with extracardiac IF (44.3%). The reports made specific follow-up recommendations for 41 patients (21.4%) with significant or indeterminate findings. The most common of which was single or multiple pulmonary nodules (12% of patients). Only 6 patients (3.1%) was found to have malignancy that was subsequently treated. *Conclusion:* Although noncardiac IF are common, clinically significant or indeterminate IF are less prevalent. The failure to follow-up abnormal IF may result in missed opportunities to detect early disease. On the other hand, investigation of IF is not without cost or risk. The difference of cancer death in patients with and without IF still has to be determined.

## P160

### Assessment of Sympathetic Innervation with 23I-MIBG in Patients with Heart Failure in which is Expected Implementation of Resynchronization Therapy.

**J. G. ROJAS CAMACHO**, Y. Ricart, I. Tatjer, N. Manito, A. Rodríguez-Gasén, M. Roca, M. T. Bajen, J. Mora, I. Gil, J. Martín-Comín; Hospital Universitari de Bellvitge-IDIBELL., L'Hospitalet de Llobregat. Barcelona., SPAIN.

**Objective**: To assess sympathetic innervation in patients with heart failure eligible for implantation of cardiac resynchronization therapy (CRT) with or without an automatic implantable cardioverter defibrillator (ICD). **Methods:** We studied 14 patients (p), (12 men) with a mean age of 60 ± 13 years (31-79) with CRT indication. The ejection fraction of the left ventricle was 26 ± 7%. The functional class (NYHA) was II in 3 p, III in 10 p and IV in 1 p. Telediastolic and telesistolic volumes of the left ventricle by echocardiography were of 238± 104 ml and 177 ± 84 ml respectively. Five p had mitral regurgitation grade I, 6 p grade II, 2 p grade III and 1 p grade 0. NT-proBNP pre-CTR was 1825 ± 2222 pg / ml. In all cases, myocardial innervation scan was performed at 15 min and 3 h post-injection with 185 MBq of 123I-MIBG. Heart / lung index (CPI) and washing index were determined. The mean follow-up time was of 17 months (9-24). **Results:** CPI at 15 min was 1.58 ± 0.25, at 4 hours of 1.37 ± 0.14. The washing index was 40.0 ± 17.4%. After implantation of CRT in 7 cases, CRT + ICD in 6 cases and single-chamber ICD in 1 p; we observed improvement in at least one level of the functional grade (NYHA) in all patients. At follow-up: 1 p presented an ICD discharge, 1 p had a non sustained ventricular tachycardia, and 2 p died at 12 and 14 months after implantation. **Conclusion:** Myocardial innervation scintigraphy with 123I-MIBG reflects a severe decrease in sympathetic innervation in heart failure patients who are candidates for CRT implantation. This result is in accordance with the significant left ventricular dysfunction in these patients.

## P161

### Cardiac sympathetic nervous system in arrhythmogenic disorders and in end-stage renal diseases patients

**B. Chrapko**, M. Pachowicz, A. Nocuń, A. Drop, A. Książek; Medical University of Lublin, Lublin, POLAND.

**Background**: The cardiac sympathetic dysfunction is observed in arrhythmogenic disorders as well as in in end-stage renal diseases (ESRD) patients. Aim: We investigated the activity of cardiac sympathetic nervous system (CSNS) by use of iodine-123 meta-iodo-benzylguanidine ($^{123}$I-*m*IBG) in ESRD patients and paroxysmal atrial fibrillation (AF) patients. **Materials and Methods**: 60 patients were divided in two group: ESRD and AF. ESRD group consist of 40 patients (8F/32M; age 53.8±12.5 years); AF group consist of 20 patients (5 F/22M; age 54.2±10.7 years). Patients in poor general condition, with diabetes mellitus, amyloidosis and neoplastic diseases were excluded from the study. In all patients myocardial scintigraphy was performed after injection of 370 MBq $^{123}$I-*m*IBG. Antiarrhythmic drugs were not withdrawn before the study in AF patients. Cardiac sympathetic functions were evaluated semiquantitatively as routine heart to mediastinum ratio (H/M): 15 minute (early eH/M) and 4 hour (delayed dH/M) post administration as well as washout rate (WR). **Results**: In ESRD group eH/M=1.86±0.26; dH/M=1.7±0.28, WR=36.34±15.36; in group AF eH/M=1.85±0.28; dH/M=1.73±0.29, WR=44.7±17.29; No significant differences between studied groups (t-Student test for independent samples) were found among follow indices: eH/M, dH/M. However, there is significant different within WR indices. **Conclusions**: Cardiac sympathetic dysfunction is observed both in patients ESRD and AF patients. The sympathetic drive is higher in AF group, what is suggested by higher WR and thus sympathetic activity in that group.

## P162

### Dietary conditions, hours of fasting and clinical conditions of patients influence the myocardial uptake at 18F-FDG-PET/CT.

**R. BONFIGLIOLI**, C. Nanni, J. J. Morigi, L. Zanoni, V. Ambrosini, S. Fanti; Azienda Ospedaliero-Universitaria S.Orsola-Malpighi, Bologna, ITALY.

**Aim**: High myocardial uptake (MU) of 18F-FDG is often observed in patients (pts) referred for both oncologic and non-oncologic PET/CT. This physiological event could make it difficult to correctly analyze small structures in the heart, such as atherosclerotic plaques in coronary arteries or small infected vegetations produced by endocarditis. The aim of this study is to describe the effect of a last high fat meal (LHFM) prior to a 18F-FDG PET/CT scan and the influence of concomitant conditions (diabetes -DB- and heart failure -HF- with ejection fraction <50%) and hours of fasting on MU. **Materials and Methods**: 81 pts underwent 18F -FDG PET/CT. 23/81 received LHFM, 19/81 had DB, 20/81 had HF. All these pts were organized into sub-groups based on hours of fasting: more than 12 (>12hf) or less than 12 (<12hf). One last group (19/81) consisted of pts with unrestricted dietary preparation (UP), less than 10 hours of fasting and no concomitant conditions. Attenuation-corrected PET imaging was performed with standard procedure. The mean Myocardial SUVmax (mM SUVmax) was calculated on the lateral wall of the left ventricle. **Results**: LHFM group: 23 pts, mM SUVmax: 3.2; 16/23 had >12hf (mM SUV max=3,0±2,7), 7/23 had <12hf (mM SUV max 3,7±2,9). There wasn't any significant difference between the two groups (Wilcoxon test p>0,1). DB group: 19pts, mM SUVmax: 3.4; 3/19 had > 12hf (mM SUV max=1,8±0,5), 16/19 had < 12hf (mM SUV max=3,7±3,4) There wasn't a significant difference between the two groups (Wilcoxon test, p>0,1). HF group: 20 pts, mM SUVmax: 3.7; 13/20 had > 12hf (mM SUV max=2±1) 7/20 had <12hf (mM SUV max=6,8±4,3). There was a significant difference between the two groups (Wilcoxon test, p=0,0008). UP group: 19 pts, mM SUVmax: 4.7 (mean hours of fasting: 7). No statistical difference was found between LHFM and UP (Wilcoxon test, p=0.11), between DB and UP (Wilcoxon test, p=0.2) nor between HF<12hf and UP (Wilcoxon test, p=0.3). A significant difference was found, on the contrary, between HF> 12hf and UP (Wilcoxon test, p=0.02). **Conclusions:** In this study, a long fasting (more than 12 hours) generally reduced the MU in normal and diabetic patients, especially when associated to oral administration of fats, although the difference was not statistically significant. A long fasting was much more important to reduce myocardial physiological uptake in patients with heart failure.

P26-1 - Sunday, Oct. 20, 16:00 - 16:30, Poster Exhibition Area

**Neurosciences: Basic Science**

## P163

### Evaluating the protective effect of dextromethorphan against MDMA-induced neurotoxicity in monkey brain using [$^{123}$I]ADAM/SPECT

**K. Ma**[1], T. Hsu[1], C. Sung[1], C. Cheng[2], W. Huang[3], M. Liao[4]; [1]National Defense Medical Center, Taipei, TAIWAN, [2]Tri-Service General Hospital, Taipei, TAIWAN, [3]Changhua Christian Hospital, Changhua, TAIWAN, [4]Institute of Nuclear Energy Research, Taoyuan, TAIWAN.

**Aim**: 3,4-Methylenedioxymethamphetamine (MDMA) is an illegally recreational drugs that may cause degeneration of serotonergic system in primate brain. In this study, we examined the long-term effect of MDMA in monkey brain and explored whether dextromethorphan (DM) could protect against MDMA-induced neurotoxicity using [$^{123}$I]ADAM/SPECT. **Methods:** Eight monkeys (macaca cyclopis) were tested in this study. Four healthy monkey were employed as normal controls, two monkeys were treated with MDMA (5 mg/kg, s.c.) twice a day for four successive days, and two monkeys were co-treated MDMA (5 mg/kg, s.c.) and DM (5 mg/kg) twice a day for four successive days. All the eight monkeys were performed brain imaging using [$^{123}$I]ADAM coupled with single-photon emission computed tomography (SPECT). In the MDMA-treated group and the MDMA/DM co-treatment group, the brain imaging studies were conducted up to about 2 years after the drugs treatment. The uptake ratios (URs) of [$^{123}$I]ADAM were determined by drawing manually the regions of interest (ROI) in midbrain, thalamus, and striatum of monkey brains that divide to the cerebellum (i.e., ROI/cerebellum). **Results:** The URs of [$^{123}$I]ADAM in the midbrain, thalamus, and striatum of MDMA-treated group were significantly lower than those of normal monkeys. The URs of the MDMA/DM co-treatment group demonstrate no significant difference when compared to the normal values, but obviously higher than those of MDMA-treated group. **Conclusions:** These results indicate that MDMA-induced serotonergic toxicity could persist over two years in nonhuman primate. In addition, DM could alleviate the serotonergic neurotoxicity of MDMA in brain of nonhuman primate.

## P164

### Investigating the brain monoaminergic system in ADHD animal model using [$^{123}$I]-ADAM and [$^{99m}$Tc]-TRODAT-1

**C. Cheng**[1], C. Lin[2], C. Lin[2], M. Liao[3], K. Ma[2], W. Huang[4]; [1]Tri-Service General Hospital, TAIPEI, TAIWAN, [2]National Defense Medical Center, TAIPEI, TAIWAN, [3]Institute of Nuclear Energy Research, Taoyuan, TAIWAN, [4]Changhua Christian Hospital, Changhua, TAIWAN.

**Aim:** Attention-deficit/hyperactivity disorder (ADHD) is a behavioral disorder characterized by impulsivity, difficulty in sustaining attention, and hyperactivity. The symptoms of ADHD in children may persist into adulthood. Presently, the affected monoaminergic systems by ADHD in brain remained to be elucidated. This study was undertaken to investigate brain monoaminergic system in ADHD model using two radiopharmaceuticals and animal single photon emission computed tomography (animal-SPECT**). Methods**: In this study, the spontaneous hypertensve rat (SHR) was employed as ADHD model and the Wistar Kyoto (WKY) rat was used as control. Two radiopharmaceuticals, [$^{123}$I]-ADAM (targeting to serotonin transporters) and [$^{99m}$Tc]-TRODAT-1 (targeting to dopamine transporters) coupled with animal-SPECT were used to image the brain of the ADHD rat models. The mannitol was used to induce a transient disruption of blood-brain barrier for the [$^{99m}$Tc]-TRODAT-1 uptakes in rat brains. Specific uptake ratios (SURs) of [$^{123}$I]-ADAM were determined from the animal-SPECT imaging data in various brain regions and the SURs of [$^{99m}$Tc]-TRODAT-1 was defined in the striatum. The behavior tests of the rats were performed and analyzed with TopScan Lite system. Immunohistochemistry (IHC) was conducted 1 week after the final animal-SPECT scan. **Results**: In the behavior test, the SHR showed hyperactivity compared to the WKY rats. The [$^{99m}$Tc]-TRODAT-1 uptakes in SHR striatum shows significantly higher than those of WKY rat. The [$^{123}$I]-ADAM uptakes in the midbrain, hypothalamus, thalamus, striatum, and frontal cortex of SHR brain also demonstrated obviously higher than those of WKY rat. The results of IHC studies paralleled to those from animal-SPECT studies. **Conclusions**: The results suggest that the brain of ADHD rat model has higher density of serotonin and dopamine transporters than controls. The [$^{123}$I]-ADAM and [$^{99m}$Tc]-TRODAT-1 coupled with animal-SPECT may be feasible imaging Methods for assessing the status of SERT and DAT, respectively, in rat brain.

## P165

### Exploring the effect of amitriptyline against MDMA-induced serotonergic toxicity in rat brain using 4-[$^{18}$F]-ADAM/animal -PET

**W. Huang**[1], Y. Kuo[2], C. Cheng[3], C. Shiue[3], K. Ma[2]; [1]Changhua Christian Hospital, Changhua, TAIWAN, [2]National Defense Medical Center, TAIPEI, TAIWAN, [3]Tri-Service General Hospital, Taipei, TAIWAN.

**Aim:** Numerous studies have demonstrated that the 3, 4-Methylenedioxymethamphetamine (MDMA) induce long-lasting changes in the serotonergic system, including cause decreases in the density of the serotonin transporter (SERT). Recently, we developed a new [$^{18}$F]-labeled SERT radioligand, N,N-dimethyl-2-(2- amino-4-[$^{18}$F]-fluorophenylthio) benzylamine (4-[$^{18}$F]-ADAM). The aim of this study was to examine whether amitriptyline (a tricyclic antidepressant) could protect against MDMA-induced serotonergic toxicity in rat brain using 4-[18F]-ADAM/animal -PET. **Methods:** Male Sprague-Dawley rats were co-administered amitriptyline (5 mg/kg, s.c.) with MDMA (10 mg/kg, s.c.) twice a day for 4 successive days. In another group, the rats were treated only with MDMA (10 mg/kg, s.c.) twice a day for 4 successive days. The imaging studies using 4-[18F]-ADAM and animal-positron emission tomography (animal-PET) were performed on 16 and 30 days after the drugs administration in the rats. The specific uptake ratios (SURs) were determined in the midbrain, thalamus, hypothalamus, striatum, and frontal cortex of the animal-PET images. Immunohistochemistry was executed 1 week after the last animal-PET imaging. **Results:** In MDMA-treated rats, the SURs of 4-[$^{18}$F]-ADAM in all brain regions were significantly lower than those of normal control. The SURs of 4-[$^{18}$F]-ADAM in the amitriptyline and MDMA co-administered rats were markly higher than those of MDMA-treated rats in the midbrain, thalamus, hypothalamus, hippocampus, striatum, and frontal cortex on 16 and 30 days after the drugs treatment . The results of immunohistochemistry were comparable to the results of animal-PET imaging in various brain areas. **Conclusions:** These results suggest that Amitriptyline may provide protection against MDMA-induced loss of serotonin transporters and 4-[18F]-ADAM coupled with animal -PET may provide a feasible method for evaluating the status of serotonin transporters in the rat brain.

## P166

### Decrease of 13N-labeled ammonia uptake in both ipsilateral and contralateral hemispheres after carotid artery endarterectomy in human

T. Wang[1], X. Wang[2], T. Zhang[2], Y. He[2], **C. Han**[3]; [1]Dept. of Neurosurgery, Inner Mongolia Medical University, Hohhot, CHINA, [2]Dept. of Nuclear Medicine, Inner Mongolia Medical University, Hohhot, CHINA, [3]Turku PET Centre, Turku University Central Hospital, Turku, FINLAND.

**Introduction:** Carotid artery plaque is a leading cause for ischemic stroke and carotid artery endarterectomy (CAE) is a major treatment method for it. Cerebral metabolism change is unclear after CAE for human. The current study is designated to evaluate the effect of cerebral metabolism after CAE using PET 13N-labelled ammonia. **Materials and Methods:** Twenty patients were enrolled in this study with a mean age of 59.5 year old, 16 males and 4 females. Eight patients had left side operation and twelve had right. Carotid artery stenosis in all patients were over 80% measured by ultrasound before CAE. 13N-labeled ammonia (740 MBq) PET scanning was performed one day before CAE and between one and four weeks after CAE for every one patient. After injection, static PET data was acquired for 10 minutes. Region of interest (ROI) covering major cerebral hemisphere was drawn and ammonia uptake in ROI was taken into account for ipsilateral and contralateral hemisphere using Carimas2 (PET data analysis tool developed in Turku PET Centre of Finland). **Results:**No significant change of cerebral hemisphere ammonia uptake was found between ipsilateral and contralateral hemispheres before CAE (ratio=0.98, p<0.01) and after CAE (ratio=1.09, p<0.01). Ammonia uptake in both ipsilateral and contralateral hemispheres decreased significantly after CAE, ipsilateral and contralateral uptake decreased 23.2% and 23.5%, respectively. **Conclusion:** 13N-labeled ammonia uptake is significantly decreased after CAE for both ipsilateral and contralateral hemisphere in human. The decrease of ammonia uptake after CAE could be caused by the disturbance of ammonia metabolism in cerebral tissue.

## P167

### Interictal FDG PET Findings in Temporal Lobe Epilepsy Patients Related to Presence of Secondarily Generalized Tonic Clonic Seizures

**Ü. Ö. Akdemir**[1], I. Çapraz[2], T. Sucak[1], G. Kurt[3], N. I. Karabacak[1], E. Bilir[2], L. Ö. Kapucu[1]; [1]Gazi University Medical Faculty, Department of Nuclear Medicine, Ankara, TURKEY, [2]Gazi University Medical Faculty, Department of Neurology, Ankara, TURKEY, [3]Gazi University Medical Faculty, Department of Neurosurgery, Ankara, TURKEY.

**Aim**: We aimed to compare interictal 18F-FDG PET findings of two groups of temporal lobe epilepsy (TLE) patients: one with complex partial and secondarily generalized tonic-clonic seizures (GTCS) and the other with complex partial seizures only (CPS). **Materials and Methods**: Interictal 18F-FDG PET images of patients who were operated for drug-resistant TLE in Gazi University Hospital and post-operatively became seizure free (Engel I) were retrospectively analyzed using the spm2 program. The hypothesis that interictal cerebral hypometabolism was more extensive in patients with GTCS in comparison to patients with CPS was tested. Additionally, PET images of both patient groups were separately compared with the PET data of an aged-matched institutional normal control group. Regarding the lateralization of TLE, PET images of left TLE patients were flip-flopped in y-axis using

the MRIcro program and spm analyses were done as if all patients had right TLE. All spm analyses were run using one-sided two-sample unpaired t-test with a statistical threshold of 0,01 and cluster threshold of 100 voxels. Findings: The GTCS, CPS and control groups included 29, 15 and 16 cases, respectively. When compared to the control group patients in CPS group had ipsilateral temporal and frontal hypometabolism. Similarly, the GTCS group had ipsilateral temporal and frontal hypometabolism when compared to the control group. When the patient groups were compared to each other, the GTCS group had significant hypometabolism in the precentral gyrus of ipsilateral frontal lobe, inferior parietal lobule of ipsilateral parietal lobe and postcentral gyrus of contralateral lobe. **Conclusion**: TLE patients with GTCS had bilateral interictal hypometabolism in sensorimotor cortical regions in addition to the ipsilateral temporal lobe when compared to TLE patients with CPS. Therefore, interictal 18F-FDG PET imaging provided information about functional cortical changes related with seizure semiology in addition to lateralization of epileptogenic region.

## P168

### The preliminary study of measurement of related cerebral metabolism in subacute infarction with a sequential PET/CT-MRI system

**X. LING**, Y. TANG, L. HUANG, Y. ZHANG, C. SHI, Z. TAN, X. LIU, X. Xin, H. XU; Jinan University, Guangzhou, CHINA.

**Background and Purpose**: The abnormal brain uptake distal to the primary lesion after a stroke has been detected by some studies using positron emission teomography (PET) but its potential clinical significance of these dysfunction regions related to the stroke has received little attention. **Methods:** 7 patients with focal cerebral infarction in subactue stage were examined using a sequential PET/computed tomography (CT)-magnetic resonance imaging (MRI) system. The images of PET and MRI were coregistered using the integrated software of an off-line workstation. The primary lesion was determined on MRI. 18F-FDG uptake in the primary lesion and bilateral thalumus, cerebellum was analyzed in visualize and in quantification. The maximize standardized uptake value (SUV), mean SUV and SUV ratio was determined. The behavioral testing of all patients were evaluated before the examination, including MoCA (Montreal cognitive assessment), MMSE (mini-mental state examination). **Results**: 7 focal cerebral infarction from 7 patients detected by MRI, including 5 cases of subcortical infarction (4 in basalganglia and corona radiata area, 1 in pons), 2 cases involved in both cortical and subcortical area (1 in frontal lobe, 1 in parietal-temporal-occipital junction area). Both F18-FDG PET and PET/MRI fusion detected abnormal metabolism in the primary lesion in all patients compared to the mirror area of contralateral side. In four cases of subcortical infarction and one case of cortical and subcortical infarction, hypometabolism regions in the ipsilateral thalumus and the contralateral cerebellum were also identified. While there was no abnormal signal intensity on MRI. A negative correlation was found between SUVmax ratio of primary lesion and MMSE ($P$<0.05), SUVmax ratio of thalumus and MMSE ($P$<0.05), SUVmean ratio in thalumus and MoCA ($P$<0.05).**Conclusion**: The abnormal brain metabolism in subacute infarction has been detected qualitatively and quantitatively using a sequential PET/CT-MRI system. It might contribute to explain the impairment of cognitive function and clinical functional recovery of these patients.

## P169

### Brain FDG-PET in the diagnosis of Alzheimer's disease and frontotemporal dementia in the clinical setting

**S. Rubí**, S. Tarongí, D. Vásquez, A. García, H. Vico, A. Noguera, C. Sampol, M. Giménez, A. Mas, M. J. Picado, C. Peña, G. Amer; Hospital Universitari Son Espases, Palma de Mallorca, SPAIN.

**Aim**: To evaluate the contribution of FDG-PET to the diagnosis of Alzheimer's disease (AD) and frontotemporal dementia (FTD) in the clinical setting**. Materials and Methods**: From April 2012 to March 2013, forty-seven patients with a clinical suspicion of AD or FTD were referred by the Dementia Unit for a brain FDG-PET examination after comprehensive clinical and structural neuroimaging evaluation. Those with psychiatric comorbidity or prominent vascular or extrapyramidal features were excluded. Among the 37 patients included (50-86 years; 16 male), 12 had mild cognitive impairment (MCI) -8 with AD features and 4 with FTD features-, and 25 had established dementia -5 with AD features, 14 with FTD features, 6 undetermined AD/FTD-. Cortical metabolism in FDG-PET was visually rated in 7 regions bilaterally (frontal, anterior and posterior cingulate, anterior and posterior temporal, parietal, and sensorimotor area), thus classifying each FDG-PET scan as "normal", "AD pattern", "FTD pattern" or "uncertain pattern". Cerebrospinal fluid (CSF) AD-biomarkers were obtained in 11 patients. Concordance between FDG-PET pattern, previous clinical diagnosis and CSF biomarkers was assessed. **Results**: Among the 12 MCI patients, 4/8 with AD features showed an AD metabolic pattern in FDG-PET and 1/4 with FTD features had a FTD metabolic pattern. All (5/5) the dementia patients with AD features and 5/14 patients with FTD features had an AD metabolic pattern. In only 3 of the 14 patients with FTD features, a FTD metabolic pattern was seen. Among the 6 patients with undetermined AD/FTD, FDG-PET metabolic pattern was that of AD in 2 cases and of FTD in one. FDG-PET results in the 16 remaining patients were normal or uncertain. When an AD metabolic pattern was seen, it had marked posterior temporal/parietal hypometabolism in 69% of cases and moderate/mild findings in 31%. All cases with FTD metabolic pattern consisted of moderate/mild PET findings. CSF biomarkers were supportive of AD in 4/11 patients, three of them having an AD metabolic pattern. In the 7 patients with uninformative/normal CSF biomarkers, PET was supportive of AD in three. **Conclusion:** The AD metabolic pattern in FDG-PET supports AD clinical suspicion in a significant amount of patients with MCI or dementia. Furthermore , it may also arise when FTD is initially suspected, thus leading to a possible diagnostic shift to AD. Therefore, brain FDG-PET should be regarded as a useful tool, complementary to CSF AD-biomarkers, in the diagnostic work-up of AD and FTD in the clinical setting.

## P170

### SISCOM in Children Epilepsy

**F. Setoain**[1], A. Perissinotti[1], B. Martí[1], S. Rubí[1], J. Aparicio[2], F. Santmartí[2], A. Donaire[1], J. Rumià[1], N. Bargalló[1], M. Carreño[1], F. Pons[1]; [1]Hospital Clínic, Barcelona, SPAIN, [2]Hospital Sant Joan de Deu, Barcelona, SPAIN.

**Aim:** To evaluate the clinical usefulness of SISCOM analysis (subtraction ictal SPECT corregistered to MRI), to localize seizure focus (SF) in pediatric patients with intractable complex partial seizures and to compare the sensitivity of SISCOM image with interictal SPECT, ictal SPECT and MRI . **Methods**: 64 patients (30 male and 34 female, from 1 to 22 years - mean age: 8 years) with intractable complex partial seizures were studied using video-EEG monitoring (V-EEG), MRI, interictal SPECT and ictal SPECT. Both SPECTs were performed after the intravenous injection of 99mTc-ECD in 42 cases and with 99mTc-HMPAO in the remaining 22 cases. Average injection time for ictal SPECT was 17 sec (2-72 sec). SISCOM was obtained using Focus-det software. **Results** of MRI, interictal SPECT, ictal SPECT and SISCOM were compared with V-EEG and clinical data. Ictal SPECT analysis was always compared with interictal SPECT. Results: V-EEG localized SF in 52/64(81%) patients, in two cases indicated the hemisphere of the SF, in 3 cases was multifocal and in 4 cases was diffuse or non-localizing. MRI localized SF in 22 patients (34%) but failed to localize SF in 42 cases. In 16 of these, MRI determined anatomical lesions that did not localize SF and was normal in 26(40%) patients. Interictal SPECT localized SF in 18 (28%) patients. In 13 cases, it identified anatomical lesions that did not localize SF, was normal in 28 (43%) patients and was contra lateral V-EEG in one case. Visual ictal SPECT localized SF in 28 (44%) patients. Ictal SPECT was normal in 20 cases and in 10 cases identified anatomical lesions that did not localize SF. in 4 cases indicated the hemisphere of the SF and showed contralateral uptake in other 2 cases. SISCOM analysis localized SF in 44 (69%) patients, successfully identifying SF in 26 out of the 42 (62%) cases where MRI had failed. SISCOM analysis improve the ability of ictal SPECT to localize the SF in 16 cases where ictal SPECT was normal or identified anatomical lesions that did not localize SF. In percentage, SISCOM improve SF localization of ictal SPECT from 44 to 69%. **Conclusions**: SISCOM analysis (subtraction ictal SPECT corregistered to MRI) improves the sensitivity of visual ictal SPECT in the localization of seizure focus in paediatric patients. So, our data strongly recommend the use of SISCOM analysis in the clinical practice of ictal SPECT in epilepsy.

P27-1 - Sunday, Oct. 20, 16:00 - 16:30, Poster Exhibition Area

## Neurosciences: Clinical Science Psychiatry

## P171

### Association between endothelial dysfunction markers and regional cerebral blood flow (rCBF) changes in cocaine dependent patients under recent abstinence.

T. Massardo[1], **J. Quintana**[2], R. Jaimovich[2], C. Saez[2], J. Pallavicini[1], J. Veliz[1], C. Ibáñez[1], M. Cabreras[2], K. Pereira[2], D. Mezzano[2], J. Pereira[2]; [1]Hospital Clínico Universidad de Chile, Santiago, CHILE, [2]Hospital Clínico Pontificia Universidad Católica de Chile, Santiago, CHILE.

Chronic cocaine use produces multiparenchymal damage and also has been related with accelerated atherosclerosis and even endothelial dysfunction (ED). Our aim was to study whether cocaine induced regional cerebral blood flow (rCBF) abnormalities correlate with ED markers**. Methods** Population: From a group of 27 DSM-IV cocaine dependent patients (mean age 31 year old; 22 of them males); all with recent consumption, we performed a brain single photon emission tomography (SPECT) with 99mTc-ethylen cysteine dimer (ECD) at baseline and after 4 weeks of strict cocaine abstinence. We measured concomitantly: circulating endothelial cells number (CEC), regulated on activation normal T cell expressed and secreted (RANTES), soluble intercellular adhesion molecule-1 (sICAM) and monocyte chemo attracting protein (MCP-1). Analysis: Plasma values were compared with 20 non consumer controls using student non paired t test. We studied 20 out of 27 cocaine consumer patients with statistical parametric mapping

analysis (SPM8) to analyze SPECT rCBF changes using paired t-test as factorial design specification with ED markers levels as single covariates, with a p<0.001 threshold. **Results** A. Baseline CEC number, RANTES, sICAM and MCP-1 values were significantly higher compared with non consumer control subjects (p<0.0001, 0.008, 0.05 and <0.0001, respectively). CEC decreased after abstinence (p<0.006); MCP-1 increased (p=0.04); sICAM and RANTES remained without significant changes but sICAM had a decreasing trend. All parameters after abstinence were still significantly higher than controls. B. SPM analysis demonstrated strong association between increased rCBF after detoxification explained by ED markers change. Perfusion improvement was observed mainly in bilateral posterior brain cortex with all four markers. The strongest predictor of rCBF change was sICAM in a region located at inferior right parietal lobe (Brodmann Area 40). CEC explained rCBF improvement at limbic lobe, occipital lobe, left parietal lobe and right temporal lobe levels; RANTES at occipital and limbic lobes levels; MCP-1 at left parietal and right temporal and in lesser extent in right occipital and left frontal lobes and sICAM mainly at both parietal lobes, left frontal, and right temporal lobe levels**. Conclusion**: We found new evidence of a strong association between rCBF improvement after cocaine detoxification with ED markers and possibly with accelerated atherosclerosis. Grants Fondecyt n°1080253/1110418

## P172

### A succesful treatment of OCD over the orbitofrontal cortex using rTMS is related to a decrease in orbitofrontal cortex and cingulate gyrus metabolisms

**F. LE JEUNE**[1], C. Nauczyciel[2], S. Douabin[2], F. Naudet[2], M. VERIN[3], B. MILLET[2]; [1]Centre Eugène Marquis, Rennes, FRANCE, [2]CHS Guillaume Régnier, Rennes, FRANCE, [3]CHU Pontchaillou, Rennes, FRANCE.

Rationale: This preliminary study assessed the efficacy of low frequency stimulation repetitive trans-cranial magnetic stimulation (rTMS) with the help of a double plan coil of the right Orbito Frontal Cortex (OFC) in patients suffering from Obsessive Compulsive Disorder (OCD). We hypothesized that low frequency stimulation of the OFC cortex would lead to a reduction of the clinical symptoms observed with the Yale Brown Obsessive Compulsive Scale (YBOCS). Method: A randomized, double-blind, crossover design was proposed with two "one week" treatment periods (one period "on stimulation" versus one period "sham stimulation") shared by a 1-month washout period. Concomitantly every patients overcame a [18F]-FDG-PET at the end of each sequence of stimulation. Statistical analysis compared YBOCS scores at the end of the two periods. Results: At day 7, a significant decrease from baseline in the Yale-Brown Obsessive Compulsive Scale (YBOCS) was observed after both active (p < 0.01) and sham stimulation (p = 0.02). This decrease tended to be larger after active stimulation than after sham stimulation with respectively - 6 (-29, 0) points versus - 2 (-20, 4) points (p = 0.07). Using PET, contrast between "on" and "off" stimulation showed that stimulation was related to a decrease in orbitofrontal cortex and cingulate gyrus metabolisms at rest. Conclusion: OFC should be considered as an interesting rTMS neuroanatomical target easier to reach comparing NST target as proposed by deep brain stimulation approaches.

P28-1 - Sunday, Oct. 20, 16:00 - 16:30, Poster Exhibition Area

## Neurosciences: Neurodegeneration

## P173

### Cortical hypoperfusion and beta-amyloid density in Posterior Cortical Atrophy and Progressive Primary Aphasia

**M. J. Santiago-Ribeiro**, E. Beaufils, J. Vercouillie, K. Mondon, V. Camus, D. Guilloteau, C. Hommet; CHRU, INSERM 930, Université François Rabelais, Tours, FRANCE.

**Objectives:** Posterior cortical atrophy (PCA) and progressive primary aphasia (PPA) are characterised by atrophy and hypoperfusion that predominates in the parieto-occipital and temporal cortex for PCA and PPA respectively. In this study we evaluated the relationship between cortical perfusion and cerebral β-amyloid density in PCA and PPA. **Material and Methods**: Eight PCA patients (mean±SD age: 64±8 y, 3 men and 5 women) and 8 PPA patients (mean±SD age: 74±8 y, 5 men and 3 women) were submitted to a cerebral SPECT study using a Symbia T2 gamma-camera (Siemens) 30 min after a mean±SD injected dose of 835±90 MBq of 99mTc-ECD or 99mTc-HMPAO. For all the subjects, we also performed a 10 min PET study, 50 min after the injection of 18F-AV45 (208±15 MBq) using a Gemini Dual PET tomograph (Philips). Regions of interest (ROI) were defined for frontal, posterior cingulate, precuneus, parietal, temporal and occipital cortex as also for cerebellum (used as reference region to obtain SUVr values) for 18F-AV45 images using Syngo.via (Siemens). For SPECT studies we used Scenium (Siemens) to compare perfusion on the left and right parietal, temporal and occipital cortex to a database of normal controls. Results: In the PCA group, a severe hypoperfusion was observed in the parietal-occipital region. In the PPA group, hypoperfusion was found in left temporal cortex for 5 patients and bilaterally for the other three. In the PCA group, SUVrs (mean±SD) were 1.23±0.21, 1.27±0.21, 1.18±0.18, 1.14±0.19, 1.20±0.15 and 1.20±0.15 for frontal, posterior cingulated, precuneus, parietal, temporal and occipital cortex, respectively. For the PPA subjects, SUVr were lower, but not significant different, for all ROIs and were, for the same ROI, 1.07±0.24, 1.20±0.20, 1.06±0.28, 1.05±0.23, 1.05±0.24 and 1.11±0.21. Furthermore, no significant differences between SUVr obtained for left and right parietal, temporal and occipital regions were observed. **Conclusions**: No cortical regional significant differences in 18F-AV45 binding between PCA and PPA whereas cortical focal perfusion patterns were distinct in PCA and PPA were founded. These results suggest that PCA and PPA syndromes are associated with degeneration of functional networks that are not explained by the distribution β-amyloid deposition. This work has been supported in part by grants from French National Agency for Research called Investissements d'Avenir ANR-11-LABX-0018-01; FEDER (Radex programme) and the Fondation Thérèse Planiol.

## P174

### rCBF SPECT in Logopenic Primary Progressive Aphasia: Initial Aspect and Evolution Over 5 Years

**L. BERTHET**[1], E. MAGNIN[2], C. POROT[3], C. UNGUREANU[1], C. CAODURO[1], O. ANGOUE[3], S. FERREIRA[2], L. RUMBACH[2], P. VANDEL[2], H. BOULAHDOUR[1]; [1]Nuclear Medicine Department, University Hospital of Besancon, F-25000, FRANCE, [2]Research and Resources Memory Center, University Hospital of Besancon, F-25000, FRANCE, [3]Radiopharmacy Unit, University Hospital of Besancon, F-25000, FRANCE.

Aim: Logopenic primary progressive aphasia (l-PPA) concerns patients with a lack of words for at least 2 years as the main symptom and caused by a neurodegenerative disease. Regional cerebral blood flow scintigraphy (rCBF SPECT) is a key technique of the diagnosis. The main purpose of our study was to evaluate the scintigraphic appearance of a population of patients with l-PPA at 1 year, 2 years and 5 years of disease progression. The secondary aim was to validate a method of semi-quantitative visual analysis and a method of voxel-based analysis. Material and Methods: Our study focused on a population of 22 patients with l-PPA followed at the Research and Resources Memory Center of the University Hospital of Besançon, France. All patients underwent neuropsychological tests, 19 of them underwent at least one rCBF SPECT. The search for Alzheimer's disease biomarkers in CSF, scintigraphy of dopaminergic neurotransmission, brain MRI and neuropsychological tests were performed for 10, 10 and 18 patients respectively. A visual score has been developed for the study. Voxel-based analysis was performed by the Z-score method using the Neurogam® software. An average scintigraphic aspect of the population was determined by these visual score and voxel-based analyzes at 1 year (8 patients), 2 years (13 patients) and 5 years (5 patients) of disease progression. Results: At 1 year of evolution of symptoms, a left temporo-parietal hypoperfusion was observed, including the inferior parietal lobule. At 2 years, additional anomalies were observed in left inferior frontal and left medial temporal cortex. At 5 years, anomalies were more diffused, affecting the temporoparietal cortex bilaterally, the left frontal cortex and the anterior and posterior cingulate. Visual analysis and voxel-based analysis were generally consistent with literature. Among the 22 patients, 5 evolved in typical Alzheimer's dementia, 1 in fronto-temporal dementia and 3 in others PPA subtypes. Among the 10 CSF biomarkers results, 7 patients had a profile consistent with Alzheimer's disease. Among the 10 scintigraphies of dopaminergic neurotransmission, no anomaly was found. Conclusion: Our study highlights that the clinical and scintigraphic diagnosis of l-PPA is feasible during the first year of symptoms, allowing earlier treatment for patients. Our study showed the feasibility of a semi-quantitative visual assessment of rCBF SPECT, although the qualitative interpretation remains essential. The use of voxel-based analysis software, to better discriminate the territories concerned, seems promising although there are some limits. In this purpose, the creation of reference populations seems crucial.

## P175

### Visualization of Restorative Effect of a Honokiol Derivative on Neurotoxicity in 6-Hydroxydopamine-induced Hemiparkinsonism Mice using [18F]FP-(+)-DTBZ PET

**P. Chen**[1], C. Weng[2], Y. Chang[3], K. Lin[4], I. Hsiao[1,4], M. Kung[5], T. Yen[4], M. Chan[6], S. Wey[1,4]; [1]HARC and Department of Medical Imaging and Radiological Sciences, Chang Gung University, Taoyuan, TAIWAN, [2]Department of Biomedical Engineering and Environmental Sciences, National Tsing Hua University, Hsinchu, TAIWAN, [3]Center for Neuropsychiatric Research, National Health Research Institutes, Zhunan, TAIWAN, [4]Molecular Imaging Center, Department of Nuclear Medicine, Chang Gung Memorial Hospital, Linkou, Taoyuan, TAIWAN, [5]Department of Radiology, University of Pennsylvania, Philadelphia, PA, UNITED STATES, [6]Institute of Neuroscience, National Chengchi University, Taipei, TAIWAN.

**Aim:** The feasibility of cerebral vesicular monoamine transporter subtype 2 (VMAT2) imaging using [18F]FP-(+)-DTBZ ([18F]AV-133) PET has been successfully demonstrated to determine the pathological progress of Aim: The feasibility of cerebral vesicular monoamine transporter subtype 2 (VMAT2) imaging using

[18F]FP-(+)-DTBZ ([18F]AV-133) PET has been successfully demonstrated to determine the pathological progress of Parkinson's disease (PD) in human and neurotoxin-induced animal models. In addition to differential diagnosis of parkinsonism, imaging on brain VMAT2 may serve as a valuable biomarker to measure the effectiveness of therapeutic drugs aiming to restore declined dopaminergic function of PD. We reported herein the in vivo imaging of restorative effect of a synthetic honokiol derivative MH101 on 6-hydroxydopamine (6-OHDA)-induced neurotoxicity in a hemiparkinsonism mouse model using [18F]FP-(+)-DTBZ PET. **Methods**: The 6-OHDA mice (NMRI male weighing 35-45 g) were intraperitoneally and daily administered with MH101 (5 mg/kg) for 7-14 days. A 20-min static brain PET scan was performed 30 min after intravenous injection of [18F]FP-(+)-DTBZ (22.2 MBq) on 6-OHDA-treated mice as well as the 6-OHDA animals receiving 7- and 14-day MH101 treatments, respectively. The specific uptake ratio (SUr) of [18F]FP-(+)-DTBZ was calculated by [(target uptake - cerebellar uptake)/cerebellar uptake] with cerebellum as the reference region. The ipsilateral-to-contralateral (right-to-left) striatal SUr ratio was determined. Ex-vivo autoradiography (ARG) and tyrosine hydroxylase immunohistochemistry (TH-IHC) studies were carried out to confirm the abundance of dopaminergic neurons. **Results**: The striatal [18F]FP-(+)-DTBZ SUr ratios for the normal, the sham, the 6-OHDA-lesioned, and the 7-day and 14-day MH101 treatment groups were 0.98±0.03, 1.02±0.02, 0.35±0.01, 0.44±0.13 and 0.69±0.09 (n=3 for each group), respectively. The percentage of 6-OHDA lesion was -64.3%. The restoration percentages of 6-OHDA lesion after 7-day and 14-day MH101 treatment were +14.0% and +52.9%, respectively. The 6-OHDA-induced decline of [18F]FP-(+)DTBZ uptake and subsequent restoration after MH101 treatment shown on ex-vivo ARG were corroborated with the results of PET studies. TH-IHC results shown on the adjacent brain sections consistently confirmed the 6-OHDA-induced dopaminergic neuron loss and the restoration after MH101 treatment. **Conclusion**: The restoration effect of MH101 on neurotoxicity in 6-OHDA-induced mouse model of PD can be visualized in vivo using [18F]FP-(+)-DTBZ PET. These preliminary results strongly suggest that [18F]FP-(+)-DTBZ PET imaging may serve as a potentially useful approach to evaluate the effectiveness of new drugs for the treatment of PD.

## P176

### Brain 18FDG-PET biodistribution in patients with Semantic Dementia vs Alzheimer's Dementia and Frontotemporal Dementia evaluated with 3D-SSP algorithm.

**F. M. Fringuelli**[1], S. Luzzi[2], V. Cafazzo[2], G. Ascoli[1], L. Provinciali[2]; [1]Nuclear Medicine dpt OSPEDALI RIUNITI, ANCONA, ITALY, [2]Department of Neurology OSPEDALI RIUNITI, Ancona, ITALY.

**Aim**: recent literature has shown an increasing use of 18FDG/PET in neurodegenerative diseases. 18FDG/PET associated with other diagnostic Methods, helps to make early diagnosis and also allows to differentiate different types of dementia, mainly Alzheimer's Dementia (AD) and Frontotemporal Dementia (FTD). Among the various clinical forms of dementia, the Semantic Dementia (SD) is a rare neurodegenerative subtype of frontal dementia, characterized by progressive impairment of language with loss of the meaning of words often associated with paraphasias and prosopoagnosia while the loss of memory occurs only in late stage of the disease. This type of dementia has been little studied with 18FDG-PET. The aim of our study was to evaluate hypometabolic distribution in the patients with SD vs AD patients and FTP patients. **Materials and Methods**: we studied 12 patients with SD (4 female /8 male, mean age 70.8); 13 patients with AD (3 female / 10 male, mean age 67.7) and 12 patients with FTD (7 female / 5 male, mean age 62.6) who fulfilled the clinical criteria for dementia, (MMSE mean score was respectively 23.7 in SD, 22.5 in AD and 17.5 in FTD). Each patient, with resting eyes open, in silent room, received 185 MBq of 18FDG. Imaging 3D-PET/CT scan was performed thirty minutes after injection using "Discovery PET/CT 690 - GE Healthcare", 15' acquisition time. Attenuation correction was performed. Individual PET scan was analyzed with visual inspection and automated Z score method (3D-SSP data); one patient (with FTD)was unable to process the images for the presence of motion artifacts. **Results**: in SD the quantitative analysis showed hypometabolism in correspondence of the temporal lobes, with low prevalence on the right lobe(for 7/12 patients), while mild hypometabolism affects both frontal and parietal lobes, with the exception of two patients with normal metabolism in the frontal right lobes; visual assessment confirms the topographical distribution of hypometabolism. Quantitative analysis confirms in AD hypometabolism mainly in the temporal and parietal lobes, while FTD we showed moderate to severe hypometabolism in the temporal, parietal and frontal lobes with high prevalence in the left hemisphere (for 8/11patients); visual assessment confirms the topographical distribution of hypometabolism. **Conclusion:** The results confirm the different distribution hypometabolism in SD quantitative analysis, compared to AD and FTD, although the data must be further validated on a larger number of patients.

## P177

### Semiquantitative analysis of brain perfusion changes in patients with Alzheimer's disease and control groups using Neurogam program

**R. Pichova**[1], H. Trojanova[1], A. Bartos[1,2], P. Zach[1], O. Lang[1]; [1]University Hospital Kralovske Vinohrady, PRAGUE 10, CZECH REPUBLIC, [2]AD Center, Prague Psychiatric Center, Prague, CZECH REPUBLIC.

Aim: To assess SPECT perfusion in mediotemporal region and posterior cingulate gyrus as potential early indicators of Alzheimer's dementia (AD). Introduction: Since early changes in AD are present in mediotemporal brain region and posterior cingulate gyrus, we selected these parts for analyses of brain SPECT perfusion changes using Neurogam semiquantitative approach. Subjects and Methods: We compared 2 groups in our retrospective study: 1) 18 patients with probable AD (11 females, age range 55-81 years, mean age 73±9) repeatedly examined with 31 brain SPECT scans (subgroup of 7 patients had histopathologically verified AD with 16 brain SPECT scans) and 2) age matched control group of 41 healthy senior volunteers (30 females, age range 56-88 years, mean age 68±7). Both groups were divided into 3 groups (younger, middle, older). Each age category of AD patients was further divided into 2 groups according to median of MMSE scores (lower or higher). We calculated semiquantitative perfusion of predefined regions of interest (ROI) corresponding to the Brodmann areas (mediotemporal 28 (+34), 36 and posterior cingulate gyrus 23, 31) as normalized percentage relative to perfusion of the whole brain. We analyzed both sides of the brain separately. Results: The most significant differences in perfusion between AD and controls were found in Brodmann area 23 - posterior cingulate gyrus. Perfusion in this area was significantly lower for younger patients with low MMSE scores (left AD 50.6±3.9, N 64.1±2.4, p = 0.00036; right AD 55±1.7, N 66.6±3, p = 0.00000015) and also with high MMSE scores (left AD 56.8±4.5, N 64.1±2.4, p = 0.0097; right AD 59.6±4.4, N 66.6±3, p = 0.0103). Significant changes (p = 0.006) in the left mediotemporal area (ROI 28) were found for the middle age groups. In older groups, perfusion impairment was significant for AD patients with lower MMSE scores only (ROI 23 left p = 0.0035, right p = 0.0006, ROI 28 left p = 0.0042; ROI 36 left p = 0.018, ROI 36 right p = 0.0072). Conclusion: Semiquantitative analysis with the Neurogam program from selected Brodmann areas can aid in identification of relevant brain regions depending on age and cognitive impairment. These findings can support early diagnosis of AD, namely with early or middle-age onset. This study was supported by research projects IGA MH CR NT 13183.

P29-1 - Sunday, Oct. 20, 16:00 - 16:30, Poster Exhibition Area

## Neurosciences: Dopamine Imaging

## P178

### Challenge with L-DOPA Reduces Iodine-123-IBZM Binding to the Dopamine D2 Receptor in the Rat Striatum

**S. Nikolaus**[1], M. Beu[1], C. Antke[1], H. Hautzel[1], A. Wirrwar[2], H. W. Müller[1]; [1]University Hospital Düsseldorf, Düsseldorf, GERMANY, [2]Helios Clinics, Krefeld, GERMANY.

Aim: So far, in vivo findings in patients with Parkinson's disease (PD) under chronic L-3,4-dihydroxyphenylalanine (L-DOPA) treatment have not been consistent with reports of either normal or reduced D2 receptor (D2R) binding. In the present study, we assessed the effect of acute L-DOPA in the clinic dose of 10 mg/kg on D2R binding in the rat striatum using iodine-123-IBZM (IBZM) and a dedicated small animal SPECT. Materials & Methods: D2R binding was measured in 10 rats in baseline, after pre-treatment with the peripheral DOPA decarboxylase inhibitor benserazide (10 mg/kg ip), and after pre-treatment with 10 mg/kg L-DOPA methylester plus benserazide (10 mg/kg ip). IBZM (24±4 MBq) was injected into the tail vein 30 min after pharmacological challenge. Measurements were performed 120 min after radioligand administration with the "TierSPECT". Striatal regions of interest and cerebellar reference regions were defined with the MPI-Tool. For baselines and challenges, striatal equilibrium ratios (V3'') were computed as estimation for the binding potential. Striatal V3'' values were compared between baseline and challenges using the paired t-test (two-tailed, $\alpha$ =0.05). In addition, cerebellar radioactivity concentrations were compared between baseline and challenges to account for possible confounding influences of L-DOPA or benserazide. Results: Baseline V3''was 1.68±0.26 (mean±SD). After application of 10 mg/kg L-DOPA/benserazide and benserazide alone striatal V3'' amounted to 1.37±0.36 and 1.49±0.46, respectively. The difference between baseline and L-DOPA/benserazide was significant (p=0.038). There was no difference between baseline and benserazide (p=0.393) and benserazide and L-DOPA/benserazide (p=0.662). Cerebellar radioactivity concentrations amounted to 717±239 (baseline), 880±219 (L-DOPA/benserazide) and 639±132 counts/pixel (benserazide). Differences between treatment were not significant (0.094<p<0.459). Conclusion: Challenge with 10 mg/kg L-DOPA/benserazide induced a 15% reduction of striatal D2R binding. Cerebellar radioactivity concentrations did not differ between baseline and challenges yielding evidence that under the present experimental conditions no confounding effects were exerted on radioligand accumulation, e.g., by affecting cerebral perfusion. Results agree with previous in vivo findings of

reduced neostriatal D2R binding in PD patients under chronic L-DOPA treatment (1). The reduction of D2R binding after acute L-DOPA can be attributed to competition between endogenous dopamine and the exogenous radioligand and/or compensatory D2R down-regulation in response to the increased availability of dopamine in the synaptic cleft. Further investigations are needed to clarify whether the present findings have also implications for the performance of D2R-SPECT or D2R-PET in schizophrenic, depressive or anxiety patients receiving dopaminergic medication. (1) Turjanski et al., Neurology 1997;49:717-23.

## P179

### Synthesis And Preliminary Evaluation Of [18F]AMC-20 As Candidate Dopamine D2/3-Agonist Radioligand For PET

**V. Shalgunov**[1], J. van Wieringen[2], J. W. A. Sijbesma[1], R. A. J. O. Dierckx[1], M. C. Michel[3], H. M. Janssen[4], J. Booij[2], P. H. Elsinga[1]; [1]UMC Groningen, Groningen, NETHERLANDS, [2]AMC Amsterdam, Amsterdam, NETHERLANDS, [3]Johannes Gutenberg University, Mainz, GERMANY, [4]SyMO-Chem BV, TU/e, Eindhoven, NETHERLANDS.

AIM: Dopamine D2/3-receptor agonist PET tracers have greater sensitivity to endogenous dopamine levels than D2/3-antagonists and may offer the opportunity to study in vivo the high-affinity state of D2/3 receptors (D2/3-high), which is possibly implicated in Parkinson's disease, addiction and schizophrenia. All D2/3-agonist tracers currently available for human use are labeled with the short-lived radionuclide 11C, which hampers their widespread application. We have recently evaluated several homologous 18F-labeled D2/3-agonists based on the aminomethyl chromane scaffold and containing [18F]fluoroalkoxy moieties of varying length. The best tracer of that series, [18F]FEt-AMC-13, was not evaluated further due to low signal-to-noise ratio. Here we report the synthesis, in vitro and in vivo evaluation of [18F]AMC-20 - a structurally related compound containing a 18F-fluoroaryl moiety. MATERIALS AND METHODS: In vitro binding experiments with [19F]AMC-20 were carried out in membrane homogenates from HEK-293 cells expressing humane dopamine receptors. [18F]AMC-20 was synthesized via a three-step two-pot approach including the synthesis of 4-[18F]fluorobenzaldehyde, reductive [18F]fluorobenzylation of an amine precursor and removal of protecting group in situ. The tracer was purified by HPLC. In vitro autoradiography was conducted in Sprague-Dawley rat brain slices. In vivo evaluation was carried out in Sprague-Dawley rats using a microPET Focus 220 camera. RESULTS: In vitro affinity of [19F]AMC-20 for D2-high was in the sub-nanomolar range - comparable to that of (+)PHNO and 70-fold higher than that of AMC-13 derivatives evaluated earlier. [18F]AMC-20 was obtained in 24±6% decay-corrected yield and >95% radiochemical purity. End-of-synthesis specific activity was 44±17 GBq/nmol. In rat brain slices the D2/3-specific component of total striatal binding of [18F]AMC-20 was 71% (vs 69% for [18F]FEt-AMC-13). In vivo maximum brain uptake of [18F]AMC-20 reached 1.0%ID. The tracer was preferentially taken up in the striatum, peak striatum-to-cerebellum uptake ratio was 1.98±0.10 in the control group 35 min post-injection. In raclopride-treated group this peak ratio was reduced by 21%. In rats depleted of dopamine by reserpine and alpha-methyltyrosine methyl ester (AMPT) treatment striatum-to-cerebellum uptake ratio peaked at the same level as in the controls but fell down slower, becoming 22% higher than in the control group 68 min post-injection. CONCLUSION: [18F]AMC-20 specifically binds to D2/3-receptors in living rat brain and its signal-to-noise ratio is higher than those of the previously evaluated candidate aminomethyl chromane derivatives. However, it is too low to warrant further use of [18F]AMC-20 in vivo. Still, AMC-20 may yet lead to further optimized D2/3-agonist PET tracers suitable for in vivo application.

## P180

### Does [I-123]FP-CIT SPET correlate with UPDRS in patients with possible or probable Lewy Body Dementia? A single-center, prospective, pilot study

**A. Del Sole**[1], F. Clerici[2], G. Perini[2], L. Dellavedova[1], S. Seghezzi[1], M. Lecchi[1], C. Mariani[2], G. Lucignani[1]; [1]Department of Health Sciences, Centre of Molecular and Cellular Imaging (IMAGO), University of Milan, and Nuclear Medicine Unit, Department of Diagnostic Imaging, San Paolo Hospital, Milan, ITALY, [2]Center for Research and Treatment of Cognitive Dysfunctions, Institute of Clinical Neurology, Department of Biomedical and Clinical Sciences, Luigi Sacco Hospital, University of Milan, Milan, ITALY.

**INTRODUCTION** Dementia with Lewy bodies (DLB) is diagnosed in the presence of dementia associated with at least two "core" clinical features, such as fluctuating cognition, visual hallucinations and parkinsonism. Application of these criteria in clinical settings gives specific results but suboptimal sensitivity. Given the need for objective biomarkers to support the diagnosis, in 2005, neurodegeneration, as detected by $^{123}$I-FP-CIT SPET, was included in the international criteria as a feature suggestive of DLB. AIM To compare the level of $^{123}$I-FP-CIT SPET uptake in basal ganglia with the severity of clinical symptoms measured with the UPDRS III scale in patients with suspected DLB. **MATERIALS AND METHODS** Twenty consecutive patients with probable or possible DLB (13M, 7F), median age 78 years (range 67-90), were enrolled. After a complete neurological examination with UPDRS III assessment, they underwent $^{123}$I-FP-CIT brain scan. Tracer uptake in the basal ganglia was assessed with Basal Ganglia Matching Tools software and results were compared with clinical data. First, results were compared using a dichotomous criterion: scan positive or negative vs presence of parkinsonism (defined as UPDRS >15). Then, we compared two continuous variables: UPDRS score vs striatal uptake of $^{123}$I-FP-CIT, expressed as the percentage deviation (d%) from the expected value for a healthy age-matched subject. **RESULTS** Of the 20 patients studied, 10 had significant motor impairment (UPDRS >15) and 13 a positive $^{123}$I-FP-CIT scan. A high correlation was found with the clinical diagnosis of parkinsonism, 17/20 patients (85%) showing concordant results. In the remaining three patients, no motor impairment was observed, in the presence of a positive scan. A linear correlation between UPDRS and $^{123}$I-FP-CIT uptake was observed in the caudate and putamen (r=0.68 and 0.70 respectively, p<0.001), with uptake close to the expected normal value (d%: 0.2±6.6% and –4.0±7.9% respectively) in patients with UPDRS <7 (group A) and significantly reduced (d%: -46.8±9.8% and 68.5±7.0%, respectively) in those with UPDRS >20 (group C). Interestingly, in patients with mild motor impairment (UPDRS between 7 and 20, group B), uptake of $^{123}$I-FP-CIT was low (d%: -51.6±6.0% and -73.7±11.2%, respectively) and comparable with that observed in patients with major clinical manifestations (p < 0.0005 between A-B and A-C, not significant between B-C). **CONCLUSION** In DLB, neurodegeneration in basal ganglia as measured on $^{123}$I-FP-CIT brain SPET is more sensitive than clinical signs of parkinsonism as measured with UPDRS; $^{123}$I-FP-CIT scans can easily reveal signs of neurodegeneration in patients with mild signs of parkinsonism.

## P181

### Performance of semi quantitative 123I-FP-CIT parameters in Parkinson's Disease.

**J. Haanpää**[1], A. Loimaala[2]; [1]Seinäjoki Central Hospital, SEINÄJOKI, FINLAND, [2]Helsinki University Central Hospital, Helsinki, FINLAND.

**Aim and Purpose** The purpose of this study was to evaluate the performance of semi quantitative 123I-FP-CIT parameters in patients suspected for Parkinson's disease (PD). We also wanted to study the influence of age and gender on dopamine transporter binding using a certain acquisition protocol, imaging technique and reconstruction method. **Materials and Methods** 123I-FP-CIT imaging was performed in 267 consecutive patients suspected for PD (112 PD negative, 155 PD positive pts). 136 males and 131 females were included n the study (age 32 to 88 years, median 64 years). Imaging protocol followed the EANM and supplier´s guidelines and acquisitions were performed with Siemens Ecam dual-head SPET camera and fanbeam collimators. We calculated age and gender corrected specific binding ratios (*SBR*) and left to right ratios (*LRR*) for the whole striatum, caudatus and putamen. Sensitivity and specificity values for each parameter and result was plotted using *ROC* analysis. The diagnostic performance of each parameter was estimated using the surface area under *ROC* curves (AUC). **Results** The SBR of all the parameters was found to be a strong function of age and gender. The influence of age in *SBR* values was stronger in PD negative males than in PD negative females, for example correlation coefficients between age and putamen *SBR* were -0.49 in males and -0.29 in females, P<0.01. Uncorrected *SBR* values in PD negative females were generally higher than in PD negative males. The best diagnostic discrimination between PD positive and negative patients was achieved using *SBR* values of putamen and striatum, *AUC = 0.94*. Diagnostic performance of the commonly used left to right ratio (rectangular ROI) of striatum *SBR* values turned out to be weak tool in diagnosing PD, *AUC = 0.68*. An other commonly used putamen to caudatus ratio, *AUC=0.90,* was found to be more specific than *LRR*s but the sensitivity was not as good as the sensitivity of *SBR*s of striatum and putamen. **Conclusions** The best diagnostic performance in PD was achieved using *SBR* values of putamen and striatum. According to our results age and gender correction should be included into quantification. It must also be pointed out that SBRs depend distinctly on camera detectors, collimators and the reconstruction method used.

## P182

### Dopamine Transporter Binding in the Rat Striatum is Correlated to Parameters of Motor and Exploratory Behavior after Treatment with Therapeutic Doses of L-DOPA

**S. Nikolaus**[1], M. Beu[1], M. A. De Souza Silva[2], H. Hautzel[1], C. Antke[1], A. Wirrwar[3], J. P. Huston[2], H. W. Müller[1]; [1]University Hospital Düsseldorf, Düsseldorf, GERMANY, [2]Heinrich-Heine University, Düsseldorf, GERMANY, [3]Helios Clinics, Krefeld, GERMANY.

Aim: The dopamine precursor L-DOPA is known to affect motor behavior in humans and rats. Previously, we determined the effect of clinical L-DOPA doses on dopamine transporter (DAT) binding in the rat striatum using FP-CIT and a dedicated small animal SPECT. In the present study, we present first in vivo evidence on the association between striatal DAT binding and parameters of motor and exploratory behavior after challenge with 5 or 10 mg/kg L-DOPA. Materials & Methods: Rats received intraperitoneal injections of either 5 (n=10) or 10 mg/kg (n=9) L-DOPA methylester plus the peripheral DOPA-decarboxylase inhibitor

benserazide (10 mg/kg). Subsequently, each rat was placed into an open field. Motor (ambulatory activity, sitting, grooming) and exploratory behavior (rearing, head and shoulder motility) was registered for 30 min using EthoVision XT. FP-CIT (24±4 MBq) was injected into the tail vein 30 min after pharmacological challenge. "TierSPECT" measurements were performed 120 min after radioligand administration. Striatal regions of interest and cerebellar reference regions were defined with the MPI-Tool. For baselines and challenges, striatal equilibrium ratios (V3'') were computed as estimations for the binding potential. For each group, the Pearson product moment correlation (α=0.05) was computed for behavioral data and V3''. Moreover, V3'' was compared between groups using the independent t-test (two-tailed, α=0.05). Results: After 5 mg/kg, striatal V3''correlated negatively with rearing duration in min 1-5 (r=-0.7,p=0.02) and sitting frequency in min 10-15 (r=-0.71,p=0.02). After 10 mg/kg, striatal V3'' correlated positively with the durations of ambulatory activity in min 1-30 (r=0.67,p=0.05) and head and shoulder motility in min 10-15 (r=0.66,p=0.05), whereas negative correlations were observed with sitting duration in min 1-30 (r=-0.68,p=0.045) and 11-15 (r=-0,75,p=0.020). Striatal V3''(5 mg/kg: 0.90±0.24; 10 mg/kg: 1.16±0.30) significantly differed between groups (p=0.047). Conclusion: In the lower dose group, lower DAT binding can be associated with longer duration of rearing behavior in min 1-5 and higher sitting frequency in min 10-15. In the higher dose group, lower DAT binding is related to decreased head and shoulder motility in min 10-15 and to decreased ambulation and increased sitting throughout the trial. Due to the small number of animals findings are but preliminary. However, they indicate an association between striatal DAT and motor and exploratory parameters, which appears to be both behavior-specific and time-dependent.

## P183

### 123-Ioflupane SPECT in Patients with Hemiparkinsonism

**S. Prado-Wohlwend**, C. Rocafuerte-Ávila, R. Díaz-Expósito, I. Casáns-Tormo, C. Orozco-Molano, H. Bowles-Antelo, M. Hassan-Ezz-Eddin, L. Díaz-Platas; Medicina Nuclear. Hospital Clínico Universitario, Valencia, SPAIN.

AIM Parkinson disease (PD) is a progressive chronic disorder with usually unilateral symptoms in the early stages. In this study we analyze our results with 123-ioflupane SPECT in patients referred by hemiparkinsonism symptoms and assess the correlation with the clinical findings. MATERIAL AND METHODS From 435 successive patients, we included 142 (71 men), mean age 64,7 (29-83) year old, with hemiparkinsonism symptoms. We obtained SPECT 3 hours after intravenous injection of 5 mCi of I123-Ioflupane. We assess the presence of bradykinesia, tremor in upper and lower limbs, postural instability and rigidity. We performed an independent visual analysis by 3 observers considering normal, lower or absent uptake in caudate and putamens nucleus. Clinical follow-up was completed whenever possible. RESULTS There were 79/142 patients with right-side and 63/142 with left-side hemiparkinsonism, with predominant homolateral tremor in upper limb in 55/142 (38.73%) and 41/142 (30,98%) respectively. SPECT was normal in 28/142 (19.71%), with clinical confirmation of absence of PD in 21/28 (75%) and showed pathological findings in 114. SPECT revealed bilateral involvement in 86 patients, and only unilateral in 28 (putamen was affected in 19 cases and caudate-putamen in 9). We found bilateral involvement in striatum nucleus in 20/114 (17.54%), bilateral involvement more intense on the left side in 31/114 (27.19%), with clinical match (CM) in 27/31(87.09%), and bilateral involvement more intense on the right side in 35/114 (30.70%) with CM in 33/35 (94.28%). We appreciate unilateral left involvement in 20/114 (17.54%) with CM in 14/20 (70%) and unilateral right involvement in 8/114 (7%) CM in 3/8(37.5%). Globally, patients displaying unilateral or bilateral involvement with one predominant side in SPECT, showed concordance with contralateral clinical symptoms in 77/94 (81.91%) versus the 20 cases displaying bilateral SPECT affectation. CONCLUSIONS Our results with I123-Ioflupane SPECT in patients with hemiparkinsonism symptoms globally shows a high concordance with clinical findings, in particular in those patients displaying only unilateral symptoms or predominantly on one side. A normal SPECT result suggest absence of disease in a high percentage of patients with hemiparkinsonism symptoms.

## P184

### Iodine-123-FP-CIT Binding to the Dopamine Transporter in the Rat Striatum is Reduced by Therapeutic Doses of L-DOPA

**S. Nikolaus**[1], M. Beu[1], H. Hautzel[1], C. Antke[1], A. Wirrwar[2], H. W. Müller[1]; [1]University Hospital Düsseldorf, Düsseldorf, GERMANY, [2]Helios Clinics, Krefeld, GERMANY.

Aim: As dopamine transporter (DAT) function is not altered in essential tremor but impaired to different degrees in idiopathic Parkinson's disease (PD) and "Parkinson Plus" syndromes, DAT imaging is an important tool for differentiating between movement disorders. PD can be treated with the dopamine precursor L-3,4-dihydroxyphenylalanine (L-DOPA), which enhances dopamine synthesis and increases the availability of dopamine in the synaptic cleft. The present study assessed the effect of L-DOPA on DAT binding in the rat striatum using FP-CIT and a dedicated small animal SPECT. Materials & Methods: DAT binding was measured in 32 rats in baseline, after pre-treatment with the peripheral DOPA-decarboxylase inhibitor benserazide (10 mg/kg ip), and after pre-treatment with 5 mg/kg or 10 mg/kg L-DOPA methylester plus benserazide (10 mg/kg ip). FP-CIT (23±3 MBq) was injected into the tail vein 30 min after pharmacological challenge. Measurements were performed 120 min after radioligand administration with the "TierSPECT". Striatal regions of interest and cerebellar reference regions were defined with the MPI-Tool. For baselines and challenges, striatal equilibrium ratios (V3'') were computed as estimations for the binding potential. Within-group and between-group comparisons were performed using the paired and the independent t-test, respectively (two-tailed, α=0.05). Results: After application of 5 mg/kg and 10 mg/kg L-DOPA/benserazide, striatal V3'' was 0.92±0.24 (mean±SD) and 1.35±0.50, respectively. Baseline V3'' was 1.40±0.42 and 1.69±0.44, respectively. V3'' after benserazide amounted to 1.17±0.40 and 1.62±0.47, respectively. After 5 and 10 mg/kg L-DOPA/benserazide differences to baseline were significant (p=0.001 and 0.003). There were no differences between baseline and benserazide or between benserazide and 10 mg/kg L-DOPA/benserazide (0.127<p<0.384). For the comparison between benserazide and 5 mg/kg L-DOPA/benserazide a p of 0.051 was obtained. There were no between-group differences of baseline V3'' (p=0.081). However, V3'' significantly differed between L-DOPA treatment groups (p=0.005). Conclusion: Challenge with 5 mg/kg and 10 mg/kg L-DOPA/benserazide led to mean reductions of DAT binding by 34% and 20%, respectively. Results indicate a biphasic response with a higher effect on DAT after the lower dose of L-DOPA. The reduction of DAT binding may be interpreted in terms of competition between FP-CIT and endogenous dopamine. There is conflicting evidence on DAT binding in PD patients under chronic L-DOPA treatment (1). Thus, further investigations of rats after chronic L-DOPA may be helpful to clarify whether the present findings have implications for the performance of DAT-SPECT in neurologic and psychiatric patients receiving dopaminergic medications. Literature: (1) Nikolaus et al., Rev Neurosci 2011;22:625-645.

P30-1 - Sunday, Oct. 20, 16:00 - 16:30, Poster Exhibition Area

## Neurosciences: Miscellaneous

## P185

### Brain SPECT in evaluation of hypotensive treatment effect on cerebral perfusion in metabolic syndrome patients: relationship with cognitive function

N. Efimova[1], **V. Chernov**[2,1], I. Efimova[1], T. Kalashnikova[1], Y. Lishmanov[1]; [1]Institute of cardiology, Tomsk, RUSSIAN FEDERATION, [2]Institute of Oncology, Tomsk, RUSSIAN FEDERATION.

**Aim:** to evaluate influence of hypotensive treatment on cerebral perfusion and cognitive function in patients (pts) with metabolic syndrome (MetS**). Material and Methods:** The study involved 26 pts (mean age 52±5) with MetS. Fifteen healthy volunteer were investigated as control group. All pts were investigated by brain SPECT with $^{99m}$Tc-HMPAO and comprehensive neuropsychological testing before and after 24 weeks of combination hypotensive therapy verapamil (Ca-channel blocker) and enalapril (angiotensin-converting enzyme inhibitor). Brain SPECT slices were divided into 14 symmetrical (right and left) regions of interest per patients: inferior and superior frontal lobes, temporal, anterior and posterior parietal, occipital lobes and cerebellar hemispheres. Regional cerebral blood flow (rCBF) (ml/100g/min) in these regions was calculated**. Results:** The regional cerebral blood flow in MetS pts was decrease on 7.3% (p=0.003), 6% (p=0.028), 5.9% (p=0.024) in right and left posterior parietal cortex, in right anterior parietal region correspondingly, as well as was decrease on 8.3% (p=0.007) in right superior frontal cortex and 6.6% (p=0.009) in right temporal region, in comparison with control patients. Cognitive dysfunction was detected in 90% MetS patients. Hypotensive 24 weeks' therapy followed by the increase in rCBF relative to baseline in right anterior parietal region (45.9±1.8 vs 43.3±1.1, p=0.006), in right and left posterior parietal regions (48.6±1.2 vs 43.8±1.3, p=0.004; 46.7±1,3 vs 41.3±0,8, p=0.0004, correspondingly), in right temporal cortex (50.7±2.1 vs 44.7±1.2, p=0.0007), in right superior and inferior frontal regions (47.3±1.1 vs 43.3±0.9, p=0.0004 ; 50.0±2.8 vs 47.0+0.8, p=0.02, correspondingly). After treatment these pts demonstrated improvement in immediate and delayed verbal memory, learning, attention, psychomotor speed and mentation. Relationship between the changes of cerebral perfusion and dynamics of cognitive status was found. Improvement of immediate verbal memory correlated well with increase in rCBF in right superior frontal region, left posterior parietal cortex and right temporal region ($R^2$=0.124; p=0.022, $R^2$=0.224; p=0.002, $R^2$=0.214; p=0.002, $R^2$=0.193; p=0.004, correspondingly). Betterment of attention related to growth in cerebral perfusion in right inferior frontal region ($R^2$=0.18; p=0.005), in right anterior parietal region, in right and left posterior parietal regions ($R^2$=0.10; p=0.038, $R^2$=0.14; p=0.013, $R^2$=0.12; p=0.023, correspondingly). **Conclusion:** Our results suggest that brain SPECT is useful technique for evaluation of medical treatment dynamic and understanding of

cognitive disorders mechanisms in MetS pts. Improvement of cognitive functions after treatment in MetS pts was connected with the increase in brain perfusion.

## P186

### Time dependent effects of a single bolus morphine on canine regional brain perfusion.

I. Polis[1], A. Adriaens[1], E. Vandermeulen[1], S. Vermeire[1], T. Waelbers[1], B. De Spiegeleer[2], A. Dobbeleir[1], J. Eersels[3], K. Audenaert[4], **K. Peremans**[1]; [1]Faculty of Veterinary Medicine, Ghent University, Merelbeke, BELGIUM, [2]Faculty of Pharmaceutical Sciences, Ghent University, Ghent, BELGIUM, [3]VU University Medical Centre Amsterdam, Amsterdam, NETHERLANDS, [4]Faculty of Medicine, Ghent University, Ghent, BELGIUM.

Gaining insight on the influence of opioids on brain function is important to understand their effect on pain perception and modulation. **Aim**: To assess the time dependent effects of a single bolus of morphine on rCBF in dogs using $^{99m}$Tc-ECD. **Material and Methods:** In a randomized cross-over experimental study, rCBF was estimated in 8 pain free dogs (female, 5 yo). $^{99m}$Tc-ECD was injected without pretreatment with morphine (baseline), at 30 minutes (T30) and 120 minutes (T120) after a single bolus of morphine (0.5 mg/kg IV), and prior to sedation and induction of general anaesthesia. The dogs were mechanically ventilated (by intermittent positive pressure ventilation) during anesthesia to preserve $PaCO_2$ within the physiologic range, i.e. end tidal $CO_2$ within 35-45 mmHg. SPECT data were acquired with a triple head gamma camera (Trionix, Triad) 20 minutes after tracer injection. The perfusion indices (PI) in the frontal, parietal, temporal and occipital cortex and in the subcortical and cerebellar region were obtained by semiquantification. Total counts were used for normalization. **Results:** A significantly decreased PI was found 30 min after morphine administration compared to baseline in the right frontal cortex (P = 0.047), and PI was increased in the left parietal cortex (P = 0.021). The subcortical region showed a significantly increased PI 30 min after morphine compared to baseline (P = 0.006). No significant differences were noted for the other regions or for all regions at T120 compared to baseline. **Conclusions:** A single bolus of morphine generated a different rCBF pattern at T30 but not at T120 compared to baseline. Alterations were found in structures involved in the cognitive and affective motivational aspects of pain perception (frontoparietal cortex) and pain modulation (subcortical structures). The time dependent effects (T30 versus T120) suggest a time dependent localization of the analgesic effect (supraspinal versus spinal), an interesting focus for future research. This study was supported by the Ghent University Special Research Fund (grant n°01J06109).

## P187

### Use of $^{18}$F-FDG-PET/CT and MRI in patients with refractory epilepsy and possible candidates for surgery: preliminary data

**J. C. Igua Sáenz**; University and Polytechnic La Fe Hospital, Valencia, SPAIN.

**OBJECTIVE** Assess the concordance between FDG PET and MRI in the lateralization and localization of the epileptogenic zone in patients with intractable epilepsy, to select surgical candidates. **MATERIALS AND METHODS** From June 2012 to January 2013, were studied 26 patients, (16 females/ 4 males; mean age 30 years old), with medically refractory epilepsy referred to the epilepsy unit for multidisciplinary evaluation of surgical candidacy. All patients underwent MR imaging (3T-HR), $^{18}$F FDG PET/CT (2mm-iterative reconstruction), PET/MRI fusion and continuous VEEG, and seven of them also underwent SISCOM (MIMvista). Surgical outcomes were clinically evaluated with Engel classification. For the analysis of PET scan were used two standardized colour scales that allowed the evaluation of temporal lobe and other cortical areas separately. **RESULTS** FDG PET and MRI coincided on lateralization of the seizure foci in 11/26 patients (42%). PET scan alone identified metabolic changes in 3/26 patients (11%) without clear structural lesions and in 4/26 (15%) with cortical dysplasia and/or nonspecific findings on MRI, however the epileptogenic zone was not established. SISCOM images detected the seizure foci in 3/7 patients, 2 of them concordant with PET scan. Continuous VEEG lateralize the ictal onset zone in 1 patient without abnormalities on anatomic and functional images. No single imaging modality alone was able to identified the epileptogenic zone in 8/26 patients (30%). Nine patients were candidates for surgical treatment, temporal lobectomy and/or amygdalohippocampectomy were performed in 6/9 patients, cortical dysplasia resection in 2/9 and corpus callosotomy in 1/5. After surgery five patients were seizure free and four reduced seizure frequency. **CONCLUSION** Both imaging modalities are useful for lateralize the epileptogenic zone. Brain PET scan identified metabolism changes in patients without anatomic lesions. In those cases with suspicious lesions on MRI, a normal metabolism with FDG helped to ruled them out as the seizure onset.

## P188

### Interaction between the serotonergic and opioid system: effect of 10 days oral morphine on the canine cerebral 5-HT2A receptor density measured with SPECT

**K. Peremans**[1], A. Adriaens[1], E. Vandermeulen[1], S. Vermeire[1], T. Waelbers[1], J. Eersels[2], L. Duchateau[1], A. Dobbeleir[1], B. De Spiegeleer[3], K. Audenaert[4], I. Polis[1]; [1]Faculty of Veterinary Medicine, Ghent University, Merelbeke, BELGIUM, [2]VU University Medical Centre Amsterdam, Amsterdam, NETHERLANDS, [3]Faculty of Pharmaceutical Sciences, Ghent University, Ghent, BELGIUM, [4]Faculty of Medicine, Ghent University, Ghent, BELGIUM.

Blockade of the serotonergic 2A (5-HT2A) receptor has been suggested as a strategy to augment the effects of conventional psychopharmaca in the treatment of depression. On the other hand, antidepressive effects have also been attributed to μ-opiate receptor agonists and opiates were commonly used to treat depression in the 19$^{th}$ century. A reciprocal physiologic interaction between both receptors exists: downregulation and internalization of μ-opiate receptors can be induced by 5-HT2A receptor activation, and μ-opiate receptor activation can suppress electrophysiological and behavioural effects triggered by 5-HT2A receptor activation. More, activation of the μ-opiate receptor has been reported to increase serotonin levels in the brain. The present study examined the effect of prolonged morphine administration, a μ-opiate receptor agonist, on cerebral 5-HT2A receptors in dogs. Material and Methods Cerebral 5-HT2A receptor availability was estimated in seven healthy and pain free five-year-old female dogs at baseline and after 10 days of prolonged morphine treatment (oral sustained release morphine, 2.86 ± 0.16 mg/kg twice daily) with $^{123}$I-5-I-R-91150, a 5-HT2A selective radioligand. SPECT was performed with a triple head gamma camera (Trionix, Triad) 90 minutes after tracer injection (185 MBq IV). Scans were performed under general anesthesia according to a fixed anesthetic protocol used for this type of studies. 5-HT2A receptor binding indices (BI) for the frontal, parietal, temporal and occipital cortex and the subcortical region were calculated using a semiquantification procedure with the cerebellum as reference region. Results Prolonged morphine treatment significantly lowered 5-HT2A BIs in the right (p=0.038) and left (p=0.004) frontal cortex, the right (p=0.026) and left (0.019) temporal cortex, the right (0.004) and left (0.009) parietal cortex, and the subcortical region (0.012). Conclusion The decreased cerebral 5-HT2A receptor availability following prolonged morphine exposure provides further evidence for an interaction between the opioid and serotonergic system in general and may suggest an interaction between the 5-HT2A receptor and the μ-opioid receptor in particular. The exact mechanism underlying this decreased BI of the 5-HT2A receptor remains to be elucidated. This study was supported by the Ghent University Special Research Fund (grant n°01J06109).

## P189

### Brain artery spasm in hepatic porphyrias demonstration by 99m-Tc-Bicisate (Neurolite) Single Photon Emission Computed Tomography (SPECT)

**V. Frusciante**[1], C. C. Guida[2], M. Totaro[1], F. Aucella[2], L. Di Mauro[3], A. Potenza[4], M. Savino[5], M. Stanislao[6], G. Valle[1]; [1]Nuclear Medicine, Scientific Institute "Casa Sollievo della Sofferenza", San Giovanni Rotondo (FG), ITALY, [2]Nephrology & Dialisis - Interregional Reference Center for the Prevention, Surveillance, Diagnosis and Treatment of Porphyria, Scientific Institute "Casa Sollievo della Sofferenza", San Giovanni Rotondo (FG), ITALY, [3]Transfusional Medicine and Clinical Laboratory, Scientific Institute "Casa Sollievo della Sofferenza", San Giovanni Rotondo (FG), ITALY, [4]Dietology and Clinical Feeding, Scientific Institute "Casa Sollievo della Sofferenza", San Giovanni Rotondo (FG), ITALY, [5]Clinical Laboratory, Scientific Institute "Casa Sollievo della Sofferenza", San Giovanni Rotondo (FG), ITALY, [6]Cardiology, Scientific Institute "Casa Sollievo della Sofferenza", San Giovanni Rotondo (FG), ITALY.

**Background and Aim**: The most common forms of hepatic porphyrias, Acute Intermittent Porphyria (AIP) and Hereditary Copro-Porphyria (HCP), share a common clinical pattern characterized by abdominal pain, neurologic symptoms and psychiatric disorders. Our retrospective study was aimed to investigate the SPECT cerebral perfusional pattern both in AIP and HCP patients (pts). **Patients and Methods**: Perfusional brain SPECT studies collected in a 18 year long time on 15 AIP and 7 HCP pts, were retrospectively re-evaluated by two experienced operators. The studies had been performed according to common nuclear medicine procedures. In 2 AIP and in 3 HCP pts the SPECT was repeated in a time span ranging from 3 up to 43 months. All the pts entered in the study were inpatients admitted for an abdominal pain crisis. All pts underwent electromyography, a brain Magnetic Resonance (MR, without diffusion) and/or Computed Tomography (CT) study close (days) to the SPECT study. **Results:** Perfusional defects at SPECT study were demonstrated in all HCP pts and in all but one AIP subjects. The brain perfusional defects ranged from multiple bilateral mild perfusional cortical defects, moderate side perfusional cortical asymmetry and focal perfusional defects. The most commonly affected areas were temporal (11 pts), frontal (7 pts) and parietal lobes (6 pts). Occipital lobe and basal ganglia involvement were seldom observed and only in AIP patients. Cerebellar involvement was never observed. In the pts that had more than a SPECT study, changes of the perfusional pattern were commonly observed, with recovery or worsening in the hypoperfused areas and

appearance of new defects in other brain regions. In all patients electromyography, MRI and CT resulted normal. **Discussion and Conclusions**: Our study indicates that brain perfusional defects are a constant marker of both AIP and HCP: cerebral perfusion defects were shown in nearly all patients. The severity of the defects, although variable, is usually mild. This could explain the normal pattern observed in CT and MR. The changes in time of the brain hypoperfused areas observed in the cases in which the study was repeated clearly demonstrates that a brain artery vasospasm is a very common finding in AIP and HCP pts. Our study indicates that brain artery vasospasm is probably an important determinant in the psychiatric and neurologic symptomatology observed in AIP and HCP pts. These observations could lead to important advances in porphyrias' clinical pharmacology.

## P190

### Correlates of speech understanding and loudness adaptation in auditory implant users revealed by PET activation studies

**G. Berding**[1], F. Wilke[2], T. Rode[3], C. Haense[1], G. Joseph[3], G. J. Meyer[1], L. Geworski[2], F. Bengel[1], T. Lenarz[3], H. Lim[3]; [1]Department of Nuclear Medicine, Hannover Medical School, Hannover, GERMANY, [2]Department of Medical Physics and Radiation Protection, Hannover Medical School, Hannover, GERMANY, [3]Clinic for Laryngology, Rhinology and Otology, Hannover Medical School, Hannover, GERMANY.

**Aim**: We studied in auditory implant users with PET: activation of the auditory cortex and connected areas during decoding of acoustic information. The purpose was to obtain in these patients further insights regarding auditory function (speech understanding) and dysfunction (loudness adaptation). **Methods**: Five patients with auditory implants (one cochlea, two brainstem, two midbrain) were enrolled. Open speech understanding of number-word pairs was 40% (0-82) and loudness perception during continuous presentation of a multi-tone complex (mtc) decreased to 27% (0-50) in three and stayed 100% (i.e. no loudness adaptation) in two. Always six injections of 740MBq O-15-water each followed by 90s PET acquisition were performed in three conditions: (i) silence, (ii) stimulation with speech and (iii) mtc stimulation. Stimulation was initiated 60s before tracer injection to assure (if existing) loudness adaption during PET scanning. Data was analyzed individually using statistical parametric mapping (SPM2). After spatial normalisation statistical inferences in comparisons between conditions were based on p(uncorrected)<0.001. A volume of interest template according to Brodmann areas (BA's) was used to extract the number of voxels above threshold (e.g. the size of activation) in relevant areas. Deactivations were evaluated as well. **Results:** During speech stimulation four patients with understanding (5-82%) showed activation in "auditory" BA's 41, 42 and 22, while one without understanding (0%) did not. The size of the activated area within BA's 41 and 42 correlated with the degree of understanding (r2=0.97, p=0.002). All three patients with loudness adaptation showed no supra-threshold activation of the auditory cortex during mtc stimulation. However, two with partial loudness adaption (30-50%) showed activation at a lower level (p<0.05), whereas one with complete adaptation (0%) showed deactivation of BA's 41, 42 and 22 at a level of p<0.001. Finally, loudness adaptation after 35-38s of mtc stimulation was associated with activation of the ventral prefrontal cortex (BA's 9, 10) - the extent of activation in this region correlated negatively with the degree of loudness preservation (r2=0.91, p=0.045). **Conclusions:** Speech comprehension in implant users is not dependent on nonexistence of loudness adaptation but sufficiently extended activation of the auditory cortex. Loudness adaptation is reflected in a lack of auditory cortex activation during continuous complex acoustic stimulation and accompanied by activation of the ventral prefrontal cortex. Since the latter area plays a role in processing and discrimination of complex sounds (auditory objects), it might be up-regulated in the situation of (acute) deafferentation from the auditory cortex during loudness adaptation.

P31-1 - Sunday, Oct. 20, 16:00 - 16:30, Poster Exhibition Area

## Neurosciences: Data Analysis & Quantification

## P191

### Validation of a Novel Algorithm for Automated Semi-Quantification of Striatal 123I-FP-CIT Uptake

**P. Tamayo**[1,2], C. Montes[3,2], P. Cacabelos[4], D. Sevillano[4], L. Díaz[1], A. Rosero[1], E. Perez[3], J. R. García-Talavera[1]; [1]Nuclear Medicine Department. University Hospital of Salamanca, Salamanca, SPAIN, [2]Institute of Biomedical Research of Salamanca, Salamanca, SPAIN, [3]Medical Physics Department. University Hospital of Salamanca, Salamanca, SPAIN, [4]Neurology Department. University Hospital of Salamanca, Salamanca, SPAIN.

The aim of the study was to validate a novel fully automated algorithm for semi-quantification of striatal 123I-FP-CIT uptake on an anthropomorphic phantom. **MATERIAL AND METHOD**. The algorithm is based on the design of a specific low resolution template that represent a realistic simulation of the activity distribution from the basal ganglia of a healthy subject. For it, left and right caudate and putamen binary regions were extracted from Automatic Anatomical Labeling (AAL) database in Statistical Parametrical Mapping (SPM) software v.8. Background region was obtained from standard gray and white matter SPM maps. Weighting factors of 4, 2 and 1 were applied to caudate, putamen and background regions, respectively. A Gaussian kernel (FWHW= 8 mm) was applied to the template to obtain a low resolution template resembling striatal activity distribution. Then the subject SPECT images will be co-registered with this template by means of SPM tools. After that, the former binary regions will be projected on the co-registered images to obtain the counts on caudate and putamen regions. Experimental validation of this software was done acquiring four SPECT studies of an anthropomorphic striatal phantom (Alderson DSD phantom) in which left and right striatum were filled with variable concentrations of 123I-iodide solutions. The first acquisition was performed with an activity concentration of approximately 149.5 kBq/ml. After this reference acquisition, another three acquisition were done reducing sequentially the activity concentration in right putamen, left putamen and in left caudate to 109.6 kBq/ml, 54.81 kBq/ml and 87.70 kBq/ml, respectively. The activity concentration in the cortex (background activity) was 18.97 kBq/ml. On the reference SPECT acquisition a binary occipital region was defined for background activity to calculate the binding potential. True experimental BP were obtained counting aliquots of the activity concentrations used to fulfill the chambers of the phantom, in a multichannel analyzer. Correlation analysis was done between true experimental BP and BP obtained with measured counts in caudate and putamen regions. **RESULTS.** True experimental BP values and BP obtained from the phantom SPECT images were 6.57 and 2.69, 5.03 and 2.12, 3.92 and 1.51, and 2.28 and 1.15 for activity concentrations of 149.5 kBq/ml, 109.6 kBq/ml, 87.70 kBq/ml and 54.81 kBq/ml, respectively. A highly correlation was achieved between both experimental BP and measured activities in caudate and putamen regions (mean correlation coefficient r= 0.98). **CONCLUSIONS**. This novel software automatically identified the 123I-FP-CIT uptake in an experimental study performed with an anthropomorphic phantom.

## P192

### Partial Volume Correction for Subregional Analysis of Striatal Uptake in Dopaminergic PET Imaging

**K. H. Lue**[1], H. H. Lin[1], C. H. Kao[2], H. J. Hsieh[2], S. H. Liu[2], K. S. Chuang[1]; [1]National Tsing Hua University, Hsinchu, TAIWAN, [2]Buddhist Tzu Chi General Hospital, Hualien, TAIWAN.

Aim In positron emission tomography (PET) of the dopaminergic system, quantitative measurements of nigrostriatal dopamine function are useful for differential diagnosis. A subregional analysis of striatal uptake enables the diagnostic performance to become more powerful. However, the partial volume effect (PVE) hampers the quantitative accuracy and induces an underestimation of the true radioactivity concentration in small structures. This work proposes a partial volume correction (PVC) method for subregional analysis of striatal uptake in dopaminergic PET imaging. Materials and Methods The proposed PVC method was used to analyze the separate striatal subregions and take into account the PVE based on the recovery coefficient (RC). The RC is defined as the ratio of the PVE-uncorrected to PVE-corrected radioactivity concentration, and is derived from a combination of the traditional volume of interest (VOI) analysis and the large VOI technique. The clinical studies, comprising 11 patients with Parkinson's disease (PD) and 6 healthy controls, were used to assess the impact of PVC on the quantitative measurements of F-18 FDOPA binding. Simulations on a numerical phantom that mimicked realistic healthy and neurodegenerative situations were used to evaluate the performance of the proposed PVC method. In both the clinical and the simulation studies, the striatal-to-occipital ratio (SOR) values for the entire striatum and its subregions were calculated with and without PVC. Results In the clinical studies, the SORs in each structure (caudate, anterior putamen, posterior putamen, putamen, and striatum) were significantly higher by using PVC in contrast to those without. Irrespective of whether PVC was considered, the SORs for different structures in the PD group were significantly smaller than those in the control group. The PD and control group were perfectly distinguished based on the SORs over each structure, with the exception of caudate nuclei. Among the PD patients, the SORs in each structure and quantitative disease severity ratings were shown to be significantly related only when PVC was used. For the simulation studies, the average absolute percentage error of the SOR estimates before and after PVC were 17.30% and 1.75% in the healthy situation, respectively; those in the neurodegenerative situation were 16.75% and 1.49%, respectively. Conclusion We successfully implemented a PVC method for subregional analysis of striatal uptake in dopaminergic PET imaging. The proposed method provides an accurate measure of the SOR in the entire striatum and its subregions, and improves the correlation between the SORs and the clinical disease severity of PD patients.

## P193

### Development of a simple non-invasive microsphere method for cerebral blood flow using 123I-IMP

**A. Ofuji**, K. Yamashita, S. Shiraishi, S. Tomiguchi, S. Ito; Kumamoto University, Kumamoto, JAPAN.

**Objective:** The method of continuous arterial blood sampling on a microsphere using 123I-IMP SPECT (MS method) have mainly been used for measurement of regional cerebral blood flow (rCBF). Non-invasive quantitative measurements are useful for clinical study because these Methods have simple and pain-free procedures. Several non-invasive Methods were developed in the past. However, the accuracy of these Methods is limited, as it has a serious problem in the determination of input function with complex techniques. Therefore, a new non-invasive quantification method based on a simple input function determining protocol is required in order to guarantee the repeatability and reproducibility of its method. The purposes of this study are to develop a simple non-invasive 123I-IMP microsphere method (SMS method) with a simple input function determining protocol based on the MS method and to confirm the clinical usefulness of this method. **Method:** The input function for the SMS method was calculated by multiplying administered counts by an integrated lung washout rate. The administered counts and integrated lung washout rate were obtained by analyzing the count-time activity curve (TAC) of the pulmonary artery (PA) and lung on the chest dynamic images, respectively. The integrated washout rate was defined as the complementary event of a trapping rate of lung. The trapping rate of lung was defined as the ratio of the counts from 0 to 5min to the maximum counts of the lung TAC. To improve the reproducibility and repeatability of the SMS method, we used the 3DSRT algorithm to obtain the anatomically standardized rCBF. The rCBF and input function in 9 patients measured by the SMS method were compared with the values obtained using the MS method. **Result:** A good correlation was observed between the arterial blood sampling counts by the MS method and the estimated counts by the image analysis of the new method (r=0.96, P<0.0001). Similarly, a good correlation was observed between the rCBF values obtained by the MS method and the new method using estimated counts (r=0.89, P<0.0001). The rCBF values by the new method coincided closely with the values by the MS method. **Conclusion:** The SMS method as a simple non-invasive quantification of rCBF method was developed by using the administration dose and integrated lung washout rate obtained by analyzing the dynamic planar images of the chest. This method was good correlation with the MS method. This finding indicates the possibility of clinical routine study.

## P194

### Validation of normal control database from different CT-PET scanners for SPM single-subject analysis of 18FDG PET brain images

**P. Della Rosa**[1], F. Gallivanone[1], I. Castiglioni[1], M. Gilardi[1], D. Perani[2]; [1]IBFM-CNR, Segrate, ITALY, [2]San Raffaele Scientific Institute and Università Vita Salute San Raffaele, Milan, ITALY.

**AIM** Statistical Parametric Mapping (SPM) for 18FDG PET scan analysis in single-subject requires comparison with substantial number of 18FDG PET studies from healthy subjects (HS) measured in similar conditions. This limits SPM use unless large HS database become available. Aim of this work was to assess the consistency of SPM results in single-subject analysis, compared with datasets of HS from different PET-CT scanners, following proper image standardization and normalization procedures. **MATERIALS AND METHODS** 68 HS (mean age=61.76y±5.95), from 4 centres equipped with 4 different PET-CT scanners and divided in 4 groups matched pairwise for age and sex, underwent 18FDG PET brain scan following the same acquisition/reconstruction protocol: 1) voxel scaling to the same average intensity, 2) intensity normalization to the mean of all images; 3) normalization to an 18FDG PET population-specific template created from both neurological patients and age-matched controls, and 4) smoothing. An ANOVA model including linear and nonlinear age as covariates evaluated differences between the 4 HS groups, and assessed influence of age on whole-brain metabolism. 10 probable AD patients underwent 18FDG PET-CT brain study with one PET system. PET images were spatially normalized and smoothed as for HS, and tested for relative 'hypometabolism' by comparison with each of the 4 scanner-specific datasets. 40 t-maps were obtained (age as covariate, grey matter threshold= 0.8, global normalization to 6.5 mg/100 mL/min, use of explicit mask, p = 0.05, FWE-correction at the voxel level). 4 separate group-analysis were performed to verify consistency of hypometabolic patterns by different scanners. Measurements of pattern extent and t-values were obtained for the significant AD scanner-specific patterns. A multiple regression analysis was then performed on the 40 maps coding the different scanners using 4 binary covariates to evaluate significant main effects and differences between CT-PET group maps. 2 F-contrasts were computed to evaluate effects of interest (voxels showing effect for all scanners) and differences between scanners (voxels showing differences between scanners). **RESULTS:** No positive or negative influence of linear and nonlinear age was found by ANOVA; separate group analyses for different CT-PET scans showed overlapped AD-specific patterns (hypometabolism in precuneus, parietal lobules). Multiple regression of 18FDG PET in 10 AD patients revealed significant hypometabolism in typical AD areas with no significant differences between scanners surviving correction for multiple comparisons. **CONCLUSIONS**: Following proper image standardization and normalization, single subject SPM analysis can be performed with datasets of normal controls collected from a different PET-CT scanner.

P32-1 - Sunday, Oct. 20, 16:00 - 16:30, Poster Exhibition Area

## Neurosciences: Movement Disorders

## P195

### [123I]-IBVM SPECT Imaging of cholinergic systems in Dementia with Lewy bodies

**J. Mazère**[1,2,3], F. Lamare[1,2,3], M. Allard[1,2,3], P. Fernandez[1,2,3], W. Mayo[2,3]; [1]Nuclear medicine department of Bordeaux Hospital University, Bordeaux, FRANCE, [2]CNRS, INCIA, UMR 5287, F-33400 Talence, FRANCE, [3]Univ. Bordeaux, INCIA, UMR 5287, F-33400 Talence, FRANCE.

**INTRODUCTION** Cholinergic systems involvement in the pathophysiology of dementia with Lewy bodies (DLB) is supported by the positive effects of anticholinesterase agents on several symptoms including cognitive deficits, hallucinations and sleep disorders (O'Brien, Mc Keith et al. 2006). Cholinergic alterations are widely documented in *post mortem* studies (Pimlott, Piggott et al. 2006) whereas *in vivo* studies are sparse, recently describing a variable degree of cholinergic dysfunction in early phases of DLB (Marcone, Garibotto et al. 2012). In order to evaluate *in vivo* the integrity of cholinergic pathways in DLB, we measured the vesicular acetylcholine transporter (VAChT) expression by using SPECT with [$^{123}$I]-IBVM (Kuhl, Koeppe et al. 1994; Mazere, Prunier et al. 2008; Mazere, Meissner et al. 2012). **MATERIALS AND METHODS** Ten DLB patients (age=72.6±2.16 yrs) and 10 healthy participants (age=71.4±1.4 yrs) underwent a dynamic [$^{123}$I]-IBVM SPECT scan and a magnetic resonance imaging (MRI) scan. MR images were automatically segmented and labeled by using the Freesurfer© software, providing volumes of interest (VOI), including striatum and cholinergic terminals in Ch1 (hippocampus), Ch4 (cortical lobes) and Ch5 (thalamus). Co-registration of SPECT dataset with MR images provided regional time-activity curves (TAC). For each VOI, pharmacokinetic modeling of TAC led to the calculation of [$^{123}$I]-IBVM to VAChT binding potential ($BP_{ND}$) value, proportional to VAChT expression. **RESULTS** Thalamic and striatal $BP_{ND}$ values were significantly lower in DLB patients than in healthy subjects (p<0.006). **DISCUSSION-CONCLUSION** Our results confirm the existence of cholinergic alterations in DLB and demonstrate a specific involvement of the Ch5 pathway and the striatum. Interestingly, the Ch5 is involved in the sleep regulation and its alteration may underlie sleep abnormalities classically reported in DLB.

## P196

### Brain SPECT with DaTSCAN (I-123 Ioflupane). Impact of Uniform Attenuation Correction Using Chang Algorithm in Image Quality and Clinical Decision

**T. Pipikos**, F. Vlachou, A. Nikaki, K. Gogos, K. Dalianis, D. Antoniou, D. Papoutsani, E. Tsiakas, V. Prassopoulos; DTCA Hygeia Department of Nuclear Medicine, Athens, GREECE.

AIM: DaTSCAN functional imaging is important in the clinical management of patients with extrapyramidal diseases. Differentiation between normal and abnormal scans is primarily based on visual assessment. Semi quantitative Methods play complementary role. Deep location of the striatum in the brain leads to lower counts obtained during SPECT study. Chang attenuation correction is a well-established method for brain studies. We inquired the effect of the method on clinical decision and image quality. MATERIALS AND METHODS: We evaluated side by side the corrected and uncorrected DaTSCAN- SPECT images of 64 patients. Imaging was performed with a Philips Brightview γ-camera system and reconstructed with Astonish iterative method on a Philips EBW workstation, with and without Chang attenuation correction. Best 4 slices were fused and the produced image was evaluated visually and semi quantitative. Specific uptake ratios (SUR) [(specific activity - background activity)/background activity] for the whole striatum, caudate and putamen were calculated using occipital lobe as non-specific uptake area. Visual results were graded into 5 levels: 0-normal; 1-asymmetrical reduced uptake in the putamen in one hemisphere; 2-reduced putamen uptake bilateral; 3- no uptake in both putamen and reduced in one caudate; 4- bilateral very reduced uptake in both striatum. Semi-automated ROIs were drawn with Jetpack software. RESULTS: Mean increase of SUR was 31,1% and 32,42% for left and right striatum respectively. The increase was more prominent in putamen (46,17% and 46,32% for left and right respectively). Non attenuation correction results were: 19 grade 0, 11 grade 1, 11 grade 2, 15 grade 3 and 8 grade 4. Images after Chang method were classified as: 25 grade 0, 12 grade 1, 14 grade 2, 9 grade 3 and 4 grade 4. Improvement of image quality led to more confident visual interpretation, resulting decline of scntigraphic grade in 28/64 patients. This fact was very important for 6 patients with borderline decreased uptake in one putamen that were classified as grade 1 with non-attenuated images. After

attenuation correction these patients were graded 0. CONCLUSION: Corrected images were more legible for clinical interpretation because of increased contrast between striatum structures; as well as between striatum and the rest of brain parenchyma. Better image quality led to more accurate patient staging, more confident diagnosis and avoidance of false positive results.

## P197

### 123I-MetalodoBenzylGuanidine (123I-MIBG) cardiac scintigraphy in the differential diagnosis of neurodegenerative movement disorders

**S. Nuvoli**[1], M. R. Piras[2], A. Nieddu[3], G. Dachena[1], A. Spanu[1], G. Madeddu[1]; [1]Unit of Nuclear Medicine, University of Sassari, Sassari, ITALY, [2]Unit of Neurology, University of Sassari, Sassari, ITALY, [3]Geriatrics DPT, Policlinico Sassarese, Sassari, ITALY.

**Aim**: We investigated whether 123I-MIBG cardiac scintigraphy (SC) may be useful in the differential diagnosis of neurodegenerative movement disorders (NMD). **Methods**: We enrolled consecutively 87 NMD patients with inconclusive 123I-Ioflupane SPECT and vascular damage in basal ganglia at MRI. Planar antero-posterior and antero-left oblique views were acquired 15 min (early) and 240 min (delayed) after 123I-MIBG i.v. injection, by a dual head gamma camera integrated with a low-dose X-ray tube (INFINIA; GE Healthcare). The images were evaluated both qualitatively and quantitatively, the latter by early (E) and delayed (D) heart/mediastinum (H/M) ratio calculation in anterior view ROIs manually drawn (cut-off: 1.6). To better define ROIs in patients in whom there was difficulty to determine heart image at planar acquisition, SPECT/CT was also performed with SPECT images reconstructed with iterative method and fused with CT images. **Results:** Normal/homogeneous cardiac uptake at 123I-MIBG was ascertained in 25/87 (28.7%) cases (Group 1) in both E and D acquisitions with H/M mean values of 1.79±0.19 (range:1.70-1.82) and 1.75±0.18 (range1.71-1.80), respectively. A slight to severe reduction of 123I-MIBG uptake was evidenced in the remaining 62/87 (71.3%) cases (Group 2) in both E and D acquisitions with H/M mean values of 1.31±0.22 (range:1.10-1.58) and 1.25±0.18 (range: 1.10-1.49), respectively. In 50/62 patients of Group 2 with slight to moderate reduction of 123I-MIBG uptake, SPECT/CT was determinant to better define the heart ROI. Mean E and D ratios values were significantly ($p<0.00006$ and $p<0.00002$, respectively) lower in Group 2 than Group 1, while no statistical difference was found in both groups when H/M ratios in E and D acquisitions were mutually compared. In the follow up, according to International Clinical Criteria, all Group 1 cases were classified as affected by movement disorders without cardiac sympathetic and striatal dopaminergic impairment such as Progressive Supranuclear Pulsy, Multiple System Atrophy and Alzheimer dementia while, 56/62 Group 2 patients were diagnosed as Parkinson's disease (PD) and 6/62 as Lewy bodies dementia (LBD); **Conclusion**: SC proved useful in ND differential diagnosis in our patients with MRI basal ganglia lesions and inconclusive 123I-Ioflupane SPECT. SC contributed to clarify clinical signs, excluding or confirming sympathetic post ganglionic damage, thus early allowing the most specific treatment. Planar and SPECT/CT combined use permitted a more accurate H/M ratio calculation in those cases with slight to moderate 123I-MIBG uptake reduction.

## P198

### I-123 Ioflupane Brain SPECT and I-131 MIBG Myocardial Scintigraphy as Complementary Diagnostic Tools in Parkinsonism

**T. SAMARDŽIĆ**, R. PETROVIĆ, M. RELJA, S. TELAROVIĆ, V. MILETIĆ, S. TEŽAK; CLINICAL HOSPITAL CENTRE ZAGREB, ZAGREB, CROATIA.

**AIM**: The diagnosis of various parkinsonian syndromes is primary clinical, but sometimes require more time to final diagnosis. Nuclear medicine diagnostic procedures may be helpful in differential diagnosis of parkinsonian syndromes. I-123 ioflupane brain SPECT is established as a diagnostic procedure which allows a differentiation of primary from secondary parkinsonism. Precise diagnosis of different subtypes of diseases with presynaptic deficit is not possible only by performing I-123 ioflupane brain SPECT. **MATERIALS AND METHODS**: Sixteen patients clinically diagnosed to have different parkinsonian syndromes from experienced neurologist (IPD, MSA, EPS) underwent to I-123 ioflupane brain SPECT and I-131 MIBG myocardial scintigraphy, using standard protocols for both procedures. A dose of 185 MBq of 123I-ioflupane was administered and brain SPECT imaging conducted 3-6 hours after radiotracer injection. Images were analyzed visually and results classified in four groups of different stages of dopaminergic deficit: normal, mild, moderate and severe. Planar chest I-131 MIBG imaging was performed 15 min, 2, 3, 4 and 24 hours after the injection of 18,5 MBq of MIBG. Myocardial I-131 MIBG activity was quantified by means of a heart to mediastinum ratio (H/M ratio). Ratio over 1.8 was considered normal, between 1.31 -1.79 decreased, and less than 1.3 severely decreased. None of the patients in this study had clinical findings that suggested heart disease. **RESULTS**: In 13/16 patients (81%) we observed different stages of reduced striatal accumulation of I-123 ioflupane. In 3/16 patients (19%) the striatal uptake was normal. On planar chest MIBG scintigraphy our results showed that H/M ratio was pathologically decreased in 5 patients (31%), 3 with clinical diagnosis of IPD and 2 with clinical diagnosis of EPS. Four patients initially diagnosed as MSA had normal H/M ratios (100%). In total, combining these two procedures we confirmed initially established clinical diagnose of IPD or MSA in 6/9 patients (66,7%), and changed it in 3 patients (33,3%). The results are more interesting in a group of patients clinically diagnosed as EPS in which, after our procedures, we suggest a possible final diagnosis in all patients. **CONCLUSIONS:** In case that clinical diagnosis is not satisfactory, I-123 ioflupane SPECT and myocardial I-131 MIBG scintigraphy can be of great help in establishing final diagnosis in parkinsonian syndromes. Additional studies on greater number of patients are needed to clarify those findings and evaluate effects and results of combined nuclear medicine diagnostic Methods in routine clinical practice.

P33-1 - Sunday, Oct. 20, 16:00 - 16:30, Poster Exhibition Area

# Oncology Basic Science: Preclinical Tumour Biology & Animal Imaging

## P199

### Changes of Glycolytic Pathway in Response to Efficient Inhibition of EGFR Signaling in Non-small Cell Lung Cancer (NSCLC)

**V. De Rosa**[1], F. Iommelli[1], G. Votta[2], M. Monti[3], G. Ortosecco[1], R. Fonti[1], C. Mainolfi[3], M. Stoppelli[2], S. Del Vecchio[3]; [1]Institute of Biostructures and Bioimages, National Research Council, Naples, ITALY, [2]Institute of Genetics and Biophysics, National Research Council, Naples, ITALY, [3]Department of Advanced Biomedical Sciences, University of Naples "Federico II", Naples, ITALY.

To investigate how the glycolytic pathway is affected by the inhibition of EGFR signaling, we selected NSCLC cells that were resistant to erlotinib due to T790M mutation (H1975) or MET amplification (H1993) and treated them with erlotinib (negative control), third generation EGFR TKIs or MET inhibitors (positive controls) so that differential changes of glycolytic pathway could be observed in the same cellular context in response to the efficient inhibition of EGFR signaling. Materials and Methods. To this end H1975 cells were preliminarily tested for GLUT1, GLUT3, Hexokinase (HK) I and II, Pyruvate Kinase (PK) M1 and M2 expression before and after 48-72 h treatment with erlotinib (1μM) and WZ4002 (0.1μM and 1μM) by real time PCR and western blot analysis. In parallel experiments H1993 cells were treated with erlotinib (1μM) and PHA-665,752 (1μM). 18F-FDG uptake and glucose consumption were then determined in untreated and treated cells along with hexokinase activity and PKM2 phosphorylation status. Finally drug-induced changes of glycolytic pathway were compared to the levels of total and phosphorylated forms of EGFR signaling mediators. Results. Effective inhibition of EGFR signaling in H1975 cells treated with WZ4002 was associated with a dramatic reduction of HKII expression and activity, translocation of GLUT3 from membrane to cytosol and reduction of phosphorylated form of PKM2. Accordingly, a parallel decrease of 18F-FDG uptake and glucose consumption was observed in response to effective treatment in those cells. No changes of glycolytic pathway were found in H1975 cells after treatment with erlotinib. Similarly, H1993 cells treated with PHA-665,752 showed a strong reduction of HKII expression, phosphorylated form of PKM2, glucose consumption and 18F-FDG uptake whereas only a slight decrease of phosphorylated form of PKM2 was observed after erlotinib treatment. Furthermore the strong reduction of HKII and phosphorylated form of PKM2 were associated with a decrease of P-EGFR or P-MET in treated H1975 and H1993 cells, respectively, along with a reduction of P-AKT, P-ERK and cyclin D1 in both cell lines. The slight reduction of phosphorylated form of PKM2 in erlotinib treated H1993 cells was associated with a decrease of P-EGFR without inhibition of downstream mediators. Conclusion. Early reduction of 18F-FDG uptake in response to efficient inhibition of EGFR signaling mainly occurs through changes in the expression and activity of HKII and phosphorylation status of PKM2.

## P200

### Propranolol inhibits glucose metabolism and $^{18}$F-FDG PET imaging of breast cancer through post-transcriptional downregulation of hexokinase-2

**F. Kang**, W. Ma, W. Yang, L. Li, J. Wang; Xijing Hospital, Xi'an, CHINA.

**Aim:**he advancement of breast cancer therapy is limited by the biological behaviors of cancer cells, such as metastasis and recurrence. β1 and β2 adrenoceptors (ADRB1/2) are reported to be associated with the biological behaviors of breast cancer and may influence glucose metabolism. Here, we sought to investigate the relationship between the activation of ARDB and the expression of glucose transporter (GLUT)-1 and hexokinase (HK)-2 and to clarify the impact of ARDB on $^{18}$F-FDG PET imaging in breast cancer. **Materials and Methods:** ARDB1/2 expression

in 4T1 breast cancer cells was detected by western blotting and immunofluorescence. ARDB-dependent regulation of GLUT-1 and HK-2 was determined by in vitro pharmacological intervention. 4T1 cells were treated with PBS, 10 μM isoproterenol, or 25 or 50 μM propranolol, and the transcription and expression of GLUT-1 and HK-2 were measured by quantitative RT-PCR and western blotting, respectively. To evaluate the impact of ARDB on $^{18}$F-FDG PET imaging, BALB/c mice bearing tumors derived from 4T1 breast cancer cells were injected with PBS, 10 mg/kg isoproterenol, or 10 mg/kg propranolol, and $^{18}$F-FDG PET imaging was carried out. The T/NT values of tumors and brown adipose tissue (BAT) were calculated by defining the liver as a reference. The in vivo expression of GLUT-1 and HK-2 was observed by immunohistochemical analysis. **Results:** 4T1 breast cancer cells were positive for ARDB1/2 expression. Additionally, the protein expression and post-transcriptional level of HK-2 were significantly decreased by treatment with propranolol in vitro ($p < 0.05$), while GLUT-1 expression was not significantly altered by pharmacological intervention. Mice in the propranolol-treated group exhibited lower T/NT values for the tumors ($p < 0.05$) and BAT ($p < 0.01$), as compared with the control group. Immunohistochemistry analysis revealed reduced HK-2 expression in the tumors of propranolol-treated mice. **Conclusion:** The expression of HK-2 was regulated by the activation of ARDB in 4T1 breast cancer cells primarily at the post-transcriptional level. Additionally, propranolol prevented glucose metabolism and $^{18}$F-FDG PET imaging of 4T1 cell-derived breast cancer tumors.

## P201

### Metformin directly and selectively inhibits hexokinases I and II reducing FDG uptake in cancer.

**C. Marini**[1], B. Salani[2], A. Orengo[3], M. Massollo[3], A. Del Rio[4], S. Ravera[5], A. Amaro[6], M. Passalacqua[7], S. Maffioli[2], U. Pfeffer[6], R. Cordera[2], D. Maggi[2], G. Sambuceti[8]; [1]CNR Institute of bioimages and molecular physiology, Milan, Section of Genoa, ITALY, [2]Dept. of Internal Medicine, University of Genoa, Genoa, ITALY, [3]Nuclear Medicine; IRCCS San Martino - National Institute for Cancer, Genoa, ITALY, [4]Department of Experimental, Diagnostic and Specialty Medicine, Alma Mater Studiorum–University of Bologna, Bologna, ITALY, [5]Department of Pharmacy, University of Genova, Genoa, ITALY, [6]Advanced Molecular Pathology; IRCCS San Martino - National Institute for Cancer, Genoa, ITALY, [7]Department of Experimental Medicine, University of Genova, Genoa, ITALY, [8]Nuclear Medicine; University of Genoa, IRCCS San Martino - National Institute for Cancer, Genoa, ITALY.

Aim: Several studies indicate that metformin has important anticancer properties. This therapeutic potential is usually attributed to its high affinity for mitochondrial respiratory complex-one that hampers cell energy production by metabolite oxidation and switches on the energy sensor pathway AMP-activated protein kinase (AMPK) limiting growth and proliferation in cancer. However, while AMPK phosphorylation should increase glucose consumption, many studies reported a reduced FDG uptake in cancer cells after metformin treatment. Materials and Methods: Labeling was performed by incubating 106 Calu-1 cells in a solution containing 18F-Fluoro-deoxyglucose (FDG) at a concentration of 1microCi/mL for 60 minutes at 37°C. Tracer uptake was measured using a Gamma-Counter (Cobra, Packard/Perkin Elmer, Waltham,USA). The protein expression was evaluated by Western Blot. HK activity was studied on cell lysates as well as on purified HK isoforms. Mitochondrial membrane potential was determined by the cationic dye JC-1 (Life Technologies Ltd, Paisley, UK) and FACS analysis by FACScan (BD Pharmigen, San Jose, CA, USA). Apoptosis was studied by Annexin V-FITC and propidium iodide double staining (eBioscience, San Diego, CA, USA) and FACS analysis. Finally, the conformational states of HK II catalytic domain were modeled with in silico techniques. Results and Conclusion: Drug treatment decreased FDG uptake in a dose and time dependent manner up to its virtual abolition after 24 hours exposure to 10 mM drug concentration (from 32.7±1.0% in controls to 3.1±0.4% in treated cells, p<0.0001). Metformin treatment did not affect hexokinase (HK) I and II availability, while it selectively inhibited glucose phosphorylating activity of both cell lysates and purified enzymes. This effect was paralleled by depolarization of mitochondrial membranes at 24 hours while cell death only occurred after 48 hours exposure without evidence of apoptosis, confirming the direct nature of metabolic drug effect. Finally, in silico model showed that metformin steadily binds glucose-6-phosphate pocket in HK II, thus preventing further glucose phosphorylation. Thus, metformin impairs the enzymatic function of in human non-small-cell lung cancer cell line, Calu-1 reducing entrapment of FDG. This novel effect of metformin on the enzymatic activity of HK I and II contributes to explain the anticancer properties of this drug and opens new strategies in cancer prevention and treatment. From the imaging point of view, this selective effect on tumor metabolism has to be considered in PET studies of cancers characterized by high HKI and II expression.

## P202

### Correlation Between in vitro and in vivo 18F-FDG Uptake and GLUT's expression in Breast Cancer

**M. Casanova Martins**[1,2], C. Matos[2], A. M. Abrantes[2,3], J. Casalta[2,4], R. Silva[1], P. Lapa[1], G. Costa[1], J. Pedroso de Lima[1,5], M. F. Botelho[2,3]; [1]Nuclear Medicine Department, University Hospitals of Coimbra, CHUC, Coimbra, PORTUGAL, [2]Biophysics Unit, IBILI, Faculty of Medicine, University of Coimbra, Coimbra, PORTUGAL, [3]CIMAGO, Faculty of Medicine, University of Coimbra, Coimbra, PORTUGAL, [4]Radiotherapy Department, University Hospitals os Coimbra, Coimbra, PORTUGAL, [5]ICNAS, University of Coimbra, Coimbra, PORTUGAL.

AIM: Breast cancer represents a very heterogeneous group of tumors with high variability regarding 18F-FDG uptake. This variability limits PET's role in the clinical evaluation of patients with breast cancer. The purpose of this study was to determine 18F-FDG uptake pattern in breast cancer cell lines presenting different estrogen, progesterone and HER2/neu receptor's expression and to establish a correlation between GLUT's 1, 3, 5 and 12 profiles and each of the cell lines used. We also compare the previous results with the standardized uptake values (SUVs) determined in 18F-FDG PET/CT scans of breast cancer patients with histologies similar to those of the in-vitro studies. MATERIALS AND METHODS: Three human breast cancer cell lines have been used: MCF-7, HCC1806 and HCC1954. MCF-7 only express estrogen receptors; HCC1806 exhibit neither hormone receptors nor HER2/neu's (triple negative); and HCC1954 only overexpress HER2/neu. In vitro 18F-FDG uptake studies were conducted with these cells and the expression of GLTU-1, GLUT-3, GLTU-5 and GLUT-12 were assessed by flow cytometry. Additionally, SUVs of 51 18F-FDG PET/CT scans from 46 patients, performed between October 2006 and September 2010 were retrospectively analyzed. The inclusion criteria were the presence of 18F-FDG uptake in the primary tumor or in local recurrent disease and the histological similarity to the cell lines studied in vitro. Results: HCC1806 and HCC1954 cells presented higher GLUT-1, GLUT-3 and GLUT-12 expressions than MCF-7. However, concerning 18F-FDG uptake, MCF-7 presented the highest percentage values over time. Moreover, the triple-negative cell line (HCC1806) showed a low and stable (<1.5 %) in vitro uptake. Comparatively, 18F-FDG in-vivo uptake in PET was higher in triple negative tumors (SUVmax mean = 12.6 ± 7.0). Triple negative tumors and tumors expressing estrogen receptors and HER2, but negative for progesterone receptors showed similar 18F-FDG uptake values (respectively mean SUVmax = 5.2 ± 2.5 and mean SUVmax = 6.6 ± 3, 0). We also found an inverse correlation between SUV and Bloom differentiation degree. CONCLUSION: A negative correlation was found between 18F-FDG in vitro uptake and GLUT-1, 3 and 12's expressions in the referred cell lines. The same type of correlation was observed between in vivo 18F-FDG uptake and tumor differentiation degree, in agreement with the known aggressiveness of undifferentiated tumors. Nevertheless, the differences found in uptake profiles, between in vivo and in-vitro studies of breast tumors, warrant further research.

## P203

### Is there a true correlation between cytotoxic effect and uptake of ascorbic acid in colorectal cancer cells?

A. S. Pires[1], C. R. Marques[1], A. R. Almeida[1], A. C. Mamede[2], A. M. Abrantes[3], **J. G. Tralhão**[4], A. B. Sarmento-Ribeiro[5], M. F. Botelho[3]; [1]Biophysics Unit, IBILI, Faculty of Medicine, Faculty of Sciences and Technology, University of Coimbra, Coimbra, PORTUGAL, [2]Biophysics Unit, IBILI, CIMAGO, Faculty of Medicine, University of Coimbra, Coimbra;CICS-UBI, Health Sciences Research Centre, University of Beira Interior, Covilhã, PORTUGAL, [3]Biophysics Unit, IBILI, CIMAGO, Faculty of Medicine, University of Coimbra, Coimbra, PORTUGAL, [4]Biophysics Unit, IBILI, CIMAGO, Faculty of Medicine, University of Coimbra; Surgical Department, Surgery A, HUC, Coimbra, PORTUGAL, [5]Applied Molecular Biology and Hematology Group, CIMAGO, Faculty of Medicine, University of Coimbra, Coimbra, PORTUGAL.

Aim: Colorectal cancer (CRC) is a major health problem, with more than 800,000 new cases diagnosed worldwide every year. Ascorbic acid (AA) may have a pro-oxidant activity, promoting the formation of reactive oxygen species (ROS). These ROS can induce cancer cell death revealing a therapeutic potential of AA in cancer. The increased production of hydrogen peroxide, coupled with the breakdown of the activity of antioxidant enzymes and the presence of transition metals in cancer cells, may result in the selective cytotoxicity of AA. The aim of this study is to ascertain if there is a correlation between the cytotoxic effect of AA and its uptake in two colorectal carcinoma cell lines. Methods: Two human colorectal carcinoma cell lines, the C2BBe1 and LS1034 (a multidrug resistant cell line), were incubated in absence and with different concentrations of AA. The half maximal inhibitory concentration (IC50) was calculated after 24, 48, 72 and 96 hours by the sulphorhodamine B (SRB) assay. In order to evaluate cell survival, clonogenic assays were made and the survival factor determined. The radiolabeling of AA with 99mTc was performed using a previously described method, as well as the respective quality control, that was accessed by HPLC. The complex obtained, 99mTc-AA, was added to a cell suspension at 2x106 cells/ml and uptake studies were performed, allowing the separation of pellet and supernatant. Percentage of 99mTc-AA uptake was calculated after measuring the radioactivity of both fractions. Results: Our results obtained with SRB showed that AA induces a decrease in cell proliferation in

both cell lines, in a dose-dependent way (r2>0.91). The clonogenic assays revealed that, as the concentration of AA increases, the survival factor decreases. These facts were much more evident in C2BBe1 cells (IC50<0.95mM) comparing to LS1034 cells (IC50>4.33mM). AA radiolabeling efficiency was determined by graphic integration and normalization of the peak areas, being 97.5%±2.28%. Preliminary results showed that 99mTc-AA uptake is higher in C2BBe1 (around 6%) and lower in LS1034 cells (not exceeding 1.06%). Conclusion: Our study suggests that AA induces an anti-proliferative effect and a decrease in cell survival in two different CRC cell lines. The higher sensitivity of C2BBe1 cells to AA and its higher uptake lead to a possible correlation between the cytotoxic effect of this compound and its uptake by cells. The data obtained could contribute to the insights of the role of AA in cancer treatment.

## P204

### Sodium butyrate reduces 18F-FDG uptake in two colon cancer cell lines

T. J. Gonçalves[1], A. S. Pires[2], J. C. Encarnação[1], C. R. Marques[2], J. E. Casalta-Lopes[3], **J. G. Tralhão**[4], A. M. Abrantes[5], M. F. Botelho[5]; [1]Biophysics Unit, IBILI, Faculty of Medicine, Faculty of Pharmacy, University of Coimbra, Coimbra, PORTUGAL, [2]Biophysics Unit, IBILI, Faculty of Medicine, Faculty of Sciences and Technology, University of Coimbra, Coimbra, PORTUGAL, [3]Biophysics Unit, IBILI, Faculty of Medicine, University of Coimbra, Coimbra, PORTUGAL, [4]Biophysics Unit, IBILI, CIMAGO, Faculty of Medicine, University of Coimbra; Surgical Department, Surgery A, HUC, Coimbra, PORTUGAL, [5]Biophysics Unit, IBILI, CIMAGO, Faculty of Medicine, University of Coimbra, Coimbra, PORTUGAL.

**Aim:** Butyrate is a short chain fatty acid (SCFA) and it's produced by decomposition of dietary fiber by intestine's bacteria, being the main energy source of colonocytes. It is related with colon cancer mostly because of its capacity to inhibit histone deacetylases (HDAC), and inducing apoptosis and differentiation in contrast to normal cells. Some studies suggest that the Warburg effect may explain why the cancer cells use preferentially glucose rather than other energy sources, inducing butyrate accumulation in the tumor cells. Other studies also suggest that butyrate can be used by tumor cells as energy source when glucose levels are reduced. The aim of this study is to evaluate if butyrate interferes with uptake of the radiolabeled glucose analogue (18F-FDG) and the increased glycolysis in colorectal cancer cells. **Methods**: WiDr and C2BBe1 cell lines were cultured in DMEM with low glucose content (5mM). To perform the uptake studies, cells were incubated with or without butyrate, 3mM for WiDr cells and 15mM for C2BBe1 cells (values chosen taking into account the respective IC50) during 1 and 4 hours, before the incubation with 18F-FDG (25μCi/ml). At 5, 30, 60, 90, and 120 minutes, duplicate samples of 200μl of cell suspension were collected for eppendorfs with iced phosphate buffer solution (PBS). The samples were centrifuged at 10000rpm for 60 seconds, separating the pellet from the supernatant. In order to calculate the 18F-FDG uptake percentage, radioactivity of both fractions was measured in a well-type gamma counter, in counts per minute (CPM). **Results**: 18F-FDG uptake is greater in WiDr cells than in C2BBe1 cells, being the uptake at 120 minutes of 6.91%±0.15% and 5.05%±0.15%, respectively. In both cell lines, we observed that incubation with butyrate decreases the 18F-FDG uptake. This difference was more pronounced in WiDr cell line however, in C2BBe1 cells there seems to be a trend for a decrease in tracer uptake with increasing exposure time to butyrate. **Conclusions**: Our study suggests that butyrate can reduce the 18F-FDG uptake and may interfere with the Warburg effect which influences the agressiveness of the tumor. This also suggests that butyrate can act in cancer cells in an advanced phase of development, and could contribute to the understanding of the importance of our diet in advanced tumor stages.

## P205

### 18F-FDG an alternative to 99mTC-MIBI in the study of multidrug resistance in hepatocellular carcinoma?

A. F. Brito[1], M. Mendes[2], M. Ribeiro[2], A. M. Abrantes[1], A. C. Gonçalves[3], A. B. Sarmento-Ribeiro[3], F. Castro-Sousa[4], **J. G. Tralhão**[4], M. F. Botelho[1]; [1]Biophysics Unit, IBILI, CIMAGO, Faculty of Medicine, University of Coimbra, Coimbra, PORTUGAL, [2]Biophysics Unit, IBILI, Faculty of Medicine, Faculty of Sciences and Technology, University of Coimbra, Coimbra, PORTUGAL, [3]Applied Molecular Biology and Hematology Group, CIMAGO, Faculty of Medicine, University of Coimbra, Coimbra, PORTUGAL, [4]Biophysics Unit, IBILI, CIMAGO, Faculty of Medicine, University of Coimbra; Surgical Department, Surgery A, HUC, Coimbra, PORTUGAL.

**Background and aims**: Hepatocellular carcinoma (HCC) is known to be highly resistant to chemotherapy, which is due in part to overexpression of multidrug resistance proteins (MDR). A method to measure the function of these proteins involves the study of radiolabeled substrate 99mTc-MIBI uptake. Studies have demonstrated that 18F-FDG uptake is associated with MDR proteins expression in HCC. This study aims evaluate the uptake and retention of 18F-FDG and 99mTc-MIBI in three human HCC cell lines and to correlate with the expression of three MDR proteins (Pgp, MRP1 and LRP). **Methods:** Human HCC cell lines used were HepG2(wp53), HuH7(mp53) and Hep3B2.1-7(p53null). Cells were grown in low glucose medium(5mM), and in high glucose medium(25 mM) in order to verify the influence of the glucose level on 18F-FDG and 99mTC-MIBI uptake and retention. Cell suspensions were incubated with 2x106cells/ml with 25μCi/ml of 18F-FDG or 99mTc-MIBI. Samples of 200μl were collected at different periods of time and centrifuged separating the supernatant from the pellet. Activity was measured in a well counter. The retention of 18F-FDG and 99mTc-MIBI was obtained by incubating the cell suspension with radiotracers during 60 minutes. Thereafter, the cells were centrifuged and medium renewed. The following procedure was similar to the uptake studies. Pgp, MRP1 and LRP proteins levels were determined by flow cytometry. To evaluate MDR modulation, retention studies were performed in the presence of verapamil prior to incubation with 18F-FDG or 99mTc-MIBI. **Results:** For all cell lines used, 18F-FDG and 99mTc-MIBI uptake was higher when cells grown on low glucose medium. For both media formulations Hep3B2.1-7 cell line is one that has higher levels of uptake and retention of 18F-FDG and 99mTc-MIBI. HepG2 cell line has a lower uptake and retention and a higher expression of MRP1. Through studies of modulation by incubating the cells with verapamil, a considerable increase in 18F-FDG and 99mTc-MIBI retention in all cell lines was verified. **Conclusions:** It is concluded that the glucose level in the medium influences the uptake and retention of both radiopharmaceuticals. There is an inverse relationship between MRP1 expressions and uptake and retention of 99mTc-MIBI and 18F-FDG. Through modulation studies it was found that Pgp has an active role on MDR phenomenon in HCC. The uptake and retention profiles for the two radiopharmaceuticals are similar, showing that the 18F-FDG can be used to study the action of MDR proteins in HCC cells, presented as an alternative to 99mTc-MIBI.

## P206

### Quercetin: an option in primary liver tumors therapy?

M. Ribeiro[1], A. F. Brito[2], A. M. Abrantes[2], A. C. Gonçalves[3], A. B. Sarmento-Ribeiro[3], F. Castro-Sousa[4], **J. G. Tralhão**[4], M. F. Botelho[2]; [1]Biophysics Unit, IBILI, Faculty of Medicine, Faculty of Sciences and Technology, University of Coimbra, Coimbra, PORTUGAL, [2]Biophysics Unit, IBILI, CIMAGO, Faculty of Medicine, University of Coimbra, Coimbra, PORTUGAL, [3]Applied Molecular Biology and Hematology Group, CIMAGO, Faculty of Medicine, University of Coimbra, Coimbra, PORTUGAL, [4]Biophysics Unit, IBILI, CIMAGO, Faculty of Medicine, University of Coimbra; Surgical Department, Surgery A, HUC, Coimbra, PORTUGAL.

Background and aims: Hepatocellular carcinoma (HCC) is the most common primary liver malignancy followed by cholangiocarcinoma (CC). The mortality is high and the therapeutic options are limited. So it is urgent to find new therapeutic targets as well as complementary therapies. Glucose transporter-1 (GLUT-1) expression is increased in primary liver tumors (PLT's) and promotes tumorigenesis. Flavonoids, including quercetin, have shown potential as GLUT-1 function inhibition and they can be useful as therapeutic weapons against this highly aggressive kind of tumor. The aim of this study is to evaluate the potential anticancer effect of quercetin on two HCC cell lines which differ on p53 expression and one CC cell line, evaluate its effect on 18F-FDG uptake and in GLUT-1 expression. Materials and Methods: Two different HCC cell lines (HepG2 (wp53) and HuH7 (mp53)) and a CC cell line (TFK-1) were used. In order to assess the effect of quercetin in these cell lines, the cells were incubated in the presence of different concentrations of this compound for different periods of time and after cell proliferation was evaluated by the MTT test in order to calculate half maximal inhibitory concentration (IC50). The type of cell death was assessed by flow cytometry using the double staining with annexin-V and propidium iodide. Bax, Bcl-2 and GLUT-1 expression was also assessed by flow cytometry. For uptake studies, 18F-FDG was incubated in a cell suspension in cells pre-incubated with quercetin and control cells. At different times, samples were collected to eppendorf tubes for uptake calculation. Eppendorfs were then centrifuged and radioactivity of pellets and supernatants was measured with a well-type gamma counter. Results: Quercetin inhibits cell proliferation in HepG2, HuH7 and TFK-1 cell lines in a time-dependent manner. This compound does not inhibit GLUT-1 expression, however is able to decrease the 18F-FDG uptake in all cell lines. Flow cytometry results have shown that quercetin has a cytotoxic effect only at high concentrations. When cell death occurs, is mainly by apoptosis and this is accompanied by Bax activation. Conclusions: This study showed that quercetin has a considerable anti-proliferative effect in all cell lines used. This compound probably modifies the function but not the expression of GLUT-1, since it inhibits 18F-FDG (a glucose analogue that is transported into the cell by GLUT-1 and GLUT-3) uptake. In this context quercetin may represent a new therapeutic option in PLT's.

## P207

### Chemoradiation in neuroendocrine-like tumors as a treatment option: preliminary results in pancreas cancer cell lines

**R. Gradiz**[1], A. C. Mamede[2], A. M. Abrantes[3], A. R. Natal[4], A. Mota-Pinto[1], M. F. Botelho[3]; [1]General Pathology Service, CIMAGO, Faculty of Medicine, University of Coimbra, Coimbra, PORTUGAL, [2]Biophysics Unit, IBILI,

CIMAGO, Faculty of Medicine, University of Coimbra, Coimbra;CICS-UBI, Health Sciences Research Centre, University of Beira Interior, Covilhã, PORTUGAL, [3]Biophysics Unit, IBILI, CIMAGO, Faculty of Medicine, University of Coimbra, Coimbra, PORTUGAL, [4]Biophysics Unit, IBILI, Faculty of Medicine, Faculty of Sciences and Technology, University of Coimbra, Coimbra, PORTUGAL.

**Aim:** Pancreatic cancer contributes to high morbidity and mortality worldwide due to the absence of noticeable signs or symptoms in the early stages and due to the symptoms, similar to those experienced in other types of pathologies. Regarding the treatment options, different strategies are available. Metabolic Chemoradiation, a technique that combines chemotherapy and radiation therapy to increase the effects of both, has increasingly been considered as a treatment option in pancreatic cancer. However, and despite the studies already presented to medical community, these treatment strategy remains controversial and more studies are needed to understand the benefits of these type of combined therapy. **Materials and Methods**: Studies were performed in two pancreas cancer cell lines obtained in ATCC with different somatostatin receptors (SR) expression: MIA PaCa-2 (SR++) and Panc-1 (SR+). In order to evaluate cell proliferation after chemotherapy treatment, was used colorimetric test MTT. Cells were incubated with different concentrations of 5-fluorouracil, everolimus and docetaxel for 24h and cell proliferation was evaluated through MTT assay. Through all dose-response curves obtained, a concentration unable to inhibit cellular proliferation was selected. Both cell lines were incubated with selected drug concentration for 24h and uptake studies were then performed with 177Lu-DOTA-TATE. To perform these studies, samples were collected to eppendorfs, centrifuged and radioactivity of cell pellets and supernatants was measured in a well-type gamma counter. The percentage of radiopharmaceutical uptake was calculated by the ratio between the pellet and the pellet plus supernatant. 177Lu-DOTA-TATE uptake studies in cells not submitted to drugs were also performed (controls). **Results:** After 24h of incubation, 5-fluorouracil didn't inhibit 50% of Mia PaCa-2 and Panc-1 cellular proliferation. Everolimus half maximal inhibitory concentration (IC50) calculated for Mia PaCa-2 and Panc-1 are, respectively, 26.795 and 26.794μM. After 24h of docetaxel incubation in Mia PaCa-2 and Panc-1, IC50 calculated is 0.1260 and 0.2350μM, respectively. Preliminary results indicate that previous incubation with all drugs seems to increase the uptake of 177Lu-DOTATATE in Mia PaCa2. Interestingly, this increased uptake does not appear to happen in Panc-1 cell line when is previously exposed to several drugs. **Conclusion:** Previous incubation of 5-fluorouracil, everolimus and docetaxel in Mia PaCa-2 seems to potentiate 177Lu-DOTA-TATE uptake. The same is not true in Panc-1 cell line, indicating that somatostatin receptors expression should be taken into account in the treatment strategy with chemoradiation. Chemoradiation outcome should be further explored for neuroendocrine-like tumors.

P34-1 - Sunday, Oct. 20, 16:00 - 16:30, Poster Exhibition Area

## Oncology Clinical Science: Miscellaneous

### P208

### Serum thyroglobulin (Tg0) at the time of the first ablative radioiodine treatment (RAI) in patients with differentiated cancer thyroid (DTC): prognostic value and follow up with 131I Whole Body Scan (WBS).

**L. Bertolazzi**, V. Barbetti, L. Di Ciolo; C. Cananzi; M. Gaffuri; G. Agnese; C. Motta; E. Piccardo; Nuclear Medicine Unit, Imaging Department of ASL2 Savonese, Santa Corona Hospital, Pietra Ligure (SV), ITALY.

**Aim.** The aim of this research is twofold. To assess retrospectively the initial prognostic factors for treatment efficacy and the relevant cut off of Tg0 in a large cohort of consecutive patients (Pts) submitted to RAI. To evaluate in the follow up which is the best factor to detect functioning recurrence: diagnostic WBS or thyroglobuline (Tgl). **Materials and Methods**. The study included 201 Pts who had had total thyroidectomy and RAI between 2008 and 2012. Tg0 was measured off L-T4 and just before RAI (131I mean dose 2,5 GBq, range 2,2-3,0 GBq). Tg values reported here are the result of duplicate measurements done with RIA in our laboratories (Thyroglobuline IRMA Radim, detection limit <0,5 ng/ml). 12 Pts were excluded for positive anti-Tg antibodies. 189 Pts (134 females and 55 males, age 19-84, mean age 48) were affected by papillary cancer (159 Pts = 84%) and by follicular cancer (30 Pts = 16%). 76 Pts (A) had Tg0 <1,5 ng/ml and 113 Pts >1,5 ng/ml (B): we have considered only A Group (40,21%). After 6-12 months A Group which followed a low iodine diet and off L-T4 (TSH > 40 uU/ml) underwent diagnostic assessment with WBS (131I 185 MBq) and Tg1. **Results**. WBS after RAI in 63/76 Pts 83 % (C) was positive for thyroid remnants (R); in the remaining 13 Pts 17 % (D) WBS was positive for R and for lymph nodes metastases (N). In 43 Pts of C Group Tg0 was undetectable (<0,5 ng/ml), while in D Group 6 Pts Tg0 was >0,6 ng/ml. At diagnostic assessment after 6-12 months from RAI in C Group WBS and TG1 were negative for R and N. In D Group 6 Pts have WBS and Tg1 negative for R and N while 7 Pts have WBS positive for lymph nodes and Tg1 was detectable between 0,6 and 1,5 ng/ml. **Conclusion**. In 69/76 Pts (83 %) with Tg0 undetectable is not necessary to perform a second RAI. In 13/76 Pts (17 %) WBS diagnostic assessment allowed the identification of positive lymph nodes while Tg0 and Tg1 are < 1,5 ng/ml. In 6/13 Pts (46 %) with Tg0 undetectable and with positive lymph nodes only first ablative therapy was sufficient. On the basis of these findings we recommend the complementary diagnostic use of 131I WBS.

P35-1 - Sunday, Oct. 20, 16:00 - 16:30, Poster Exhibition Area

## Oncology Clinical Science: Brain

### P209

### $^{11}$C-choline PET/CT detecting tumour recurrence and predicting survival in post-treatment patients with high-grade Gliomas

**X. Hu**, L. Ma, W. Li, X. Sun, J. Sun, J. Yu; Shandong Cancer Hospital & Institute, Jinan, CHINA.

It is important to distinguish between recurrent glioma and the changes of post-treatment. The objective of the present study is to evaluate the role of $^{11}$C-choline PET/CT for detecting tumour recurrence and predicting survival in post-treatment patients with high-grade gliomas. **Methods**: A total of 16 previously treated histopathologically proven high-grade gliomas patients were included in this study. All patients underwent $^{11}$C-choline PET/CT scan and Gd-DTPA contrast enhanced MRI. Combination of histopathologically by surgery or biopsy, clinical follow-up or repeat imaging was taken as a gold standard. Data was censored, if the patient died of disease or at the end of the study. Survival analysis was done for the results of $^{11}$C-choline PET/CT scan and Gd-MRI. **Results:** Based on visual analysis, the sensitivity and specificity of $^{11}$C-choline PET/CT were 100% and 70% respectively whereas that for Gd-MRI was 83.3% and 60%. Patients with the positive of $^{11}$C-choline PET/CT visual had poorer survival compared the negative ($p$=0.003). Two group patients divided by the result of Gd-MRI scan showed no significant survival difference ($p$=0.194). **Conclusion**: $^{11}$C-Choline PET/CT not only has highly sensitivity for detecting tumour recurrence in post-treatment patients with high-grade gliomas, but has prognostic value.

### P210

### MRI and $^{11}$C-Methionine PET in the Follow-up of Radiation-induced Brain Injury in Patients with Treated Cerebral Gliomas

**T. Skvortsova**, Z. Brodskaya, Z. Savintseva, S. Medvedev; N. P. Bechtereva Institute of the Human Brain of Russian Academy of Sciences, Saint-Petersburg, RUSSIAN FEDERATION.

**The aim** of the study was to monitor the radiological and metabolic evolution of radiation-induced brain lesions (RBL) using MRI and positron emission tomography with [$^{11}$C]methionine (PET-Met). **Material and method**. From our database 96 patients (median age 32 years, range 3-70) with proven RBL after multimodal treatment of primary cerebral tumors ((glioma 88, others 8) were identified. The first PET-Met was performed in view of developing new or progressive MR imaging enhancing brain lesions to differentiate posttreatment radiation effects from brain tumor recurrence. Patients underwent at least one PET follow-up study (range 1-18, median 3) with prior contrast-enhanced MRI to control radiological abnormalities. The median follow-up was 17,5 months (range 6-77). The total 327 PET studies were performed. Histopathological verification of RBL was available in 13 patients. PET examinations were assessed by visual inspection and calculating [$^{11}$C]methionine uptake index (UI) as the ratio of the highest lesion uptake to normal cortex. **Results.** Assessment of RBL and changes over time was based on MRI follow-up studies. We used PET-Met to control RBL and to differentiate theirs from recurrence at each time point. According to our previous results negative or slightly increased $^{11}$C-methionine uptake in site of contrast-enhanced lesion on MRI (UI less than 1,45) was typical for radiation-induced injury. On the other hand high focal tracer uptake (UI more than 1,45) confirmed tumor recurrence (TR). Evolution of RBL could be divided into five forms. Primary progressive course was defined as an increase of lesion volume at least 12 months after appearance (n=14). Secondary progressive course was defined as a decrease followed by an increase of primary lesion (n=3). Second-line radiation therapy aggravated previously existing radiation injury. Remitting course was defined as appearance of new distant contrast-enhanced foci in addition to primary lesion (stable or others) in 19 patients. Reduction or stabilization of the RBI was noted in 60 patients. In 20 patients PET-Met revealed recurrent glioma that had developed in primary tumor bed (n=14) or at a distance (n=6) on average of 19,5 months (range, 4-46) follow-up period. RBL and RT could not match the location and time of development. **Conclusion.** Radiation brain injury has variable evolution. PET with [$^{11}$C]methionine is a valuable additional tool for the follow-up of patients with post radiation reactions in order to distinguish unsteady course of posttreatment brain injury from progressive tumor on timely basis.

P36-1 - Sunday, Oct. 20, 16:00 - 16:30, Poster Exhibition Area

## Oncology Clinical Science: Head & Neck

### P211

### PET volume computer-assisted reading (PET VCAR) software for accurate measurement of tumor volume using 18F-FAMT PET/CT in oral cancer.

**M. Kim**, T. Higuchi, A. Achmad, Y. Arisaka, A. Tokue, S. Sugawara, S. Yokoo, Y. Tsushima; Gunma University, Maebashi Gunma, JAPAN.

Aim: L-3-[$^{18}$F]-fluoro-α-methyl tyrosine ($^{18}$F-FAMT) is an amino acid PET tracer which has been shown useful in complementary with $^{18}$F-FDG PET for diagnosis of malignancies. The evaluation of PET VCAR software accuracy to measure the tumor volume of oral squamous cell carcinoma (OSCC) using $^{18}$F-FAMT PET images has not been performed. Materials and Methods: Forty-one patients with OSCC were enrolled in PET/CT studies using $^{18}$F-FDG and $^{18}$F-FAMT before surgery. The functional tumor volumes ($cm^3$) were measured from volume of interest (VOI) generated by the PET VCAR using the pre-determined cut-off values in both $^{18}$F-FAMT and $^{18}$F-FDG PET images. Semi quantitative measurements of tumor volumes obtained were performed. Post-surgical pathological examination results were used as the reference to determine the final diagnoses and the actual tumor size. Results: $^{18}$F-FAMT uptake correlates with tumor viability. Tumor volumes derived from $^{18}$F-FDG PET were significantly bigger than that derived from $^{18}$F-FAMT images, and the actual tumor size ($P$<0.01). Conclusion: $^{18}$F-FAMT PET/CT tumor volume was closely correlated with the actual size of tumor, compared to that obtained from $^{18}$F-FDG. Accurate determination of tumor border using PET VCAR may optimize the extent of resection in the surgery and maintain the patient's quality of life.

### P212

### Accuracy of 18F-FDG PET/CT in assessing direct osseous invasion by head & neck tumors: A Pathological correlation.

**O. A. Raslan**[1], A. Namin[2], Y. Zhou[3], K. M. Christopher[4], M. Varvares[5], M. M. Osman[1]; [1]Nuclear Medicine division-Saint Louis University, Saint Louis, MO, UNITED STATES, [2]Medical School Saint Louis University, Saint Louis, MO, UNITED STATES, [3]Neuroradiology division Saint Louis University, Saint Louis, MO, UNITED STATES, [4]Biostatistic Division-Saint Louis University, Saint Louis, MO, UNITED STATES, [5]Head&Neck Surgery-Saint Louis University, Saint Louis, MO, UNITED STATES.

Objectives : The aim of this study was to evaluate the accuracy of 18F-FDG PET/CT in prediction of direct bone invasion by head & neck tumors. Data from PET/CT was compared to the pathological findings. Methods : PET/CT images of 28 lesions (4 mandible, 2 tongue, 7 floor of mouth, 3 retromolar trigone, 7 oral cavity, 2 tonsillar & 3 alveolar ridge carcinomas) from 27 patients (16 men, 11women; mean age± SD, 60.5± 11.5 y) referred for PET/CT from April 2005 to March 2012 were independently & retrospectively reviewed for bone invasion by 2 board certified radiologists, unaware of the pathology information. Certainty of lesion characterization was scored on a 5-point scale (0= defiantly no invasion, 1= probably no invasion, 2= equivocal, 3= probably invaded, 4= defiantly invaded). Results : PET/CT images suggested osseous invasion in 13 lesions, no invasion in 10 lesions and equivocal in 5 lesions. Pathology correlation showed 4 false positive & 2 false negative lesions. Sensitivity of PET/CT was 80% (95%CI: 44 to 96), specificity was 69% (95%CI: 39 to 90), PPV was 67% (95%CI: 30 to 88), NPV was 82% (95%CI: 48 to 97), and accuracy was 74%. Variables including the SUV max & volume of tumor, distance between the bone & tumor on CT, cortical or bone marrow FDG uptake, number of metastatic lymph nodes, presence & size of cortical interruption were also analyzed as predictors of bone invasion. These variables were not a significant predictor of invasion (p>.05 for all variables entered). A t-test compared means of SUVmax based on the pathological invasion variable, and showed no significant differences. Conclusions : FDG PET/CT is an important diagnostic tool to detect direct osseous invasion by head and neck tumors with an accuracy of 74%. None of the aforementioned variables were statistically significant as a predictor of osseous

### P213

### Retrospective evaluation of head and neck cancer patients by FDG PET/CT for distant metastases and second primary tumor

**T. Traub-Weidinger**, R. Unterrainer, E. Selzer, M. Mitterhauser, M. Mayerhöfer, G. Karanikas; Medical University of Vienna, Vienna, AUSTRIA.

Recently, FDG-PET/CT has been introduced especially for more accurate evaluation of local lymph node tumor involvement in head and neck cancer (HNC) patients. However, little is known about the value of diagnostic whole-body FDG PET/CT in HNC patients for distant metastases and second primary tumor. The aim of this study was to figure out the frequency of distant metastases and second primary carcinoma (ca) in HNC patients examined by whole-body FDG-PET/CT. Patients and **Methods**: Diagnostic whole-body FDG-PET/CT examinations (n=262) of 163 HNC patients (male, n=105 , female, n=58), who underwent staging and/or restaging at the Medical University of Vienna, were analyzed for distant metastases and for secondary primary tumor. **Results** were compared to histology and/or the clinical management of the patients. Result: Twenty-two (male, n=14, female, n=8) of 163 patients (13.5%) presented distant metastases by FDG PET/CT imaging: 7 patients with a cancer of the oral cavity in, 3 patients with a larynx ca , 3 patients with paranasal sinus ca, 3 patients with oropharynx ca, 3 patients with a hypopharynx ca, 1 patient with a nasopharynx ca, and 1 patient with maxilla ca. The most commonly site of distant metastases was the lung in 18 of 22 patients. In 5 patients bone metastases were seen combined with lung metastases in 3 of them. Liver metastases were found in 3 patients. A second primary tumor was observed in 5 of 163 patients (male, n=2, female, n=3 , 3.1%) localized in the tounge in 2 patients, in the tonsilles in 1 patients, in the maxilla in 1 patients and in the hypopharynx in 1 patient. **Conclusion**: FDG-PET/CT showed to be useful in HNC patients for estimating distant metastases and second primary cancers. However, a diagnostic whole-body imaging PET/CT protocol seems to be reconsidered regarding the high radiation exposure for whole body hybrid imaging.

### P214

### 18F-FDG PET CT in rare choroidal and mucosal melanomas of the head and neck

**A. Agrawal**[1], N. Purandare[1], S. Shah[1], S. Sonawane[2], V. Rangarajan[1]; [1]Tata Memorial Hospital, Mumbai, INDIA, [2]RMC, Tata Memorial Hospital Annexe, Mumbai, INDIA.

Aim – To report our experience in evaluating the role of FDG PET CT in staging, restaging and treatment response evaluation of patients with choroidal and mucosal melanomas of the head and neck. Materials and Methods – All patients with malignant melanoma of the eye and head and neck, who were referred for a PET CT scan to our department between 2006 and 2012, were included in this retrospective evaluation. A total of 30 patients; 19 patients with mucosal malignant melanoma (MMM) of the nasal cavity, paranasal sinusus and oral cavity and 11 patients with choroidal malignant melanoma (CMM) of the eye and were evaluated. Results - There were 12 patients for staging, 5 for restaging and 2 patients for treatment response evaluation in the MMM group. The diagnostic accuracy of FDG PET CT for detection of the primary tumor/recurrence and the metastatic lesions was correlated with either histopathology or subsequent follow up scan. The primary mass/recurrent lesion was detected in all patients (sensitivity and specificity =100%), nodal metastases were detected in 11 out of 19 patients and missed in 1(sensitivity = 92% and specificity =100%), distant metastatic lesions were detected in 10 sites in 5 patients and a frontal lobe lesion was missed on PET (sensitivity = 90% and specificity =100%), but detected on MRI and confirmed histopathologically. The overall sensitivity was 95% and specificity was 100%. The overall PPV was 100% and NPV was 97.36%. In the CMM group there were 3 patients for staging, 4 for restaging and 4 for treatment response evaluation or post-surgery. The primary tumor was detected in all 3 patients, nodal disease was seen in 4 and metastases were detected in 8 sites in 5 patients. The overall sensitivity and specificity was 100%. The high sensitivity for the primary was because of large nodular tumor mass at initial presentation (1-2cm). Conclusion - FDG PET CT is a useful imaging modality for staging, restaging and in post-treatment evaluation of melanomas of the head and neck. It helps in appropriate management of patients by detecting extent of disease and distant metastases in these aggressive tumors.

### P215

### Usefulness of low-dose 18F-FDG PET-CT in the detection of Head and Neck Cancer recurrence in relation to conventional imaging Methods (CT, MRI)

V. Sánchez-Rodríguez[1], A. Allende-Riera[1], D. Cabello-García[1], C. Cárdenas-Negro[1], **M. Ochoa-Figueroa**[2], J. Uña-Gorospe[1], J. Muñoz-Iglesias[1], E. Martínez-Gimeno[1], M. De Sequera-Rahola[1]; [1]Hospital Universitario de Nuestra Señora de La Candelaria, Santa Cruz de Tenerife, SPAIN, [2]UMSNH, Morelia, MEXICO.

AIM: To assess, in terms of diagnostic validity, the usefulness of low-dose 18F-FDG PET-CT in the detection of head and neck cancer recurrence, in treated patients in comparison with conventional imaging Methods (CT, MRI). MATERIAL AND METHODS: A retrospective study of 41 patients with suspected tumour relapse (34 males, 7 females, mean age 54 y.o.), which underwent a low-dose 18F-FDG PET-CT study (a total of 50 18F-FDG PET-CT scans). 18F-FDG PET-CT images were obtained 60-90 min after intravenous injection of a mean dose of 3.19±0.6MBq/Kg. Results of the visual interpretation were compared with conventional imaging Methods in most studies: in 29 studies with CT and 6 with MRI and correlated to the definitive diagnosis by histopathology in 15 studies, clinical follow-up in 35 (mean: 10 months). RESULTS: Of 50 studies, 31 head and neck tumour recurrences were detected. Low-dose 18F-FDG PET-CT had a Sensitivity, Specificity and Accuracy of 100%, 89% and 96% respectively (2FP, 0FN). Three primary tumors were detected

incidentally. Comparing the 29 CT studies, in relation to T-staging we found a Sensitivity, Specificity and Accuracy of 88%, 100% and 93% respectively (0FP, 2FN); whereas for low-dose 18F-FDG PET-CT was of 88%, 92% and 90% respectively (1FP, 2FN). Regarding N-staging the CT we found a Sensitivity, Specificity and Accuracy of 70%, 48% and 61% respectively (11FP, 10FN); whereas for low-dose 18F-FDG PET-CT was of 94%, 68% and 83% respectively (7FP, 2FN). Respect to the distant metastases, the CT showed a Sensitivity, Specificity and Accuracy of 67%, 100% and 74% respectively (0FP, 14FN); whereas for low-dose 18F-FDG PET-CT was of 98%, 90% and 96% respectively (1FP, 1FN). In the comparative study of the 6 MRI scans comparing with 18F-FDG PET-CT, MRI only presented 1FN due to postsurgical changes for T-staging. 18F-FDG PET-CT changed the tumoral stage in 8 patients and therapeutic management in 9 patients. CONCLUSION: Our results suggest that low-dose 18F-FDG PET-CT is superior to the conventional imaging techniques in the evaluation of head and neck cancer recurrence, shows similar results to those achieved with higher 18F-FDG doses in the literature. Nevertheless, it would be necessary to complete this study with a larger number of patients.

P37-1 - Sunday, Oct. 20, 16:00 - 16:30, Poster Exhibition Area

## Oncology Clinical Science: Thyroid

### P216

### Outcome of Radioiodine Therapy in Benign Nodular Non-Toxic Goiter

**K. Del Mundo**, J. De Jesus, J. Torres; University of Santo Tomas Hospital, Manila, PHILIPPINES.

Objectives: This study will investigate the efficacy of I-131 treatment on thyroid function and size reduction in a group of patients with scintigraphic findings of nodular goiter. The primary objective of the study is to compare the thyroid volume and nodule size before and after RAI therapy. Secondary objective is to evaluate changes in the subjective symptoms and thyroid function tests. Methods: This is a prospective study of patients with nodular goiter selected for radioactive iodine therapy in a tertiary hospital from 2011 to 2012. All participating patients underwent both pre- and post- RAI therapy I-131 thyroid scans. Serum concentration of thyroid stimulating hormone was determined before and after radioactive iodine therapy. Results: A total of 40 patients were included in this study. It is composed of 35 females and 5 males with age of 42.48 + 15.33. Mean TSH pre therapy was 1.97 + 6.53 mIU/mL. Mean dose of RAI given was 6.53 +1.64. Mean follow-up interval was approximately 3-6 months. Mean thyroid volume pretreatment was 41.26 + 12.02 cm3 compared to 31.82 + 9.46 cm3 post treatment with a percent reduction of 17.28 + 16.31 cm3. Mean nodule size pre treatment was 6.51 + 4.79 cm2 compared to 2.66 + 3.52 cm2 post-treatment with a percent reduction of 71.39 + 32.59 cm2. In a significant number of patients, there was complete disappearance of nodules. There was clinical improvement of previously noted anterior neck enlargement and obstructive symptoms. There was no increase in thyroid size, or development of new nodules or worsening of obstructive symptoms noted at the end of the study. Conclusions: Radioactive iodine therapy is an effective, non-invasive and safe management that could be used as a primary therapy in patients with benign nodular non-toxic goiter.

### P217

### Impact of patient's specification on clinical outcome for an I-131 ablation therapy with differentiated thyroid carcinoma.

**M. Nakayama**[1], A. Okizaki[1], M. Sakaguchi[2], T. Uno[2], J. Sato[2], S. Ishitoya[1]; [1]Department of Radiology, Asahikawa Medical University, Asahikawa, Hokkiado, JAPAN, [2]Radiological Technology Section, Asahikawa Medical University Hospital, Asahikawa, Hokkiado, JAPAN.

OBJECTIVES: An I-131 whole-body scans (WBS) has been considered the main tool for detecting local recurrence or distant metastases during follow-up of differentiated thyroid carcinoma (DTC). Serum thyroglobulin (Tg) is one of the useful tumor marker as demonstrating a therapeutic effect. Tg is easy to evaluate and it represents DTC activity, but it sometimes affected by other factors including Tg-Ab. Elevated Tg suggests disease and is usually associated with an abnormal uptake of I-131 WBS. However, discordant results between I-131 WBS and Tg have been observed, and discourage the usefulness of them as a diagnostic method. Some Authors reported several patients' specifications such as age, gender, and body mass index (BMI) affected prognosis in other carcinoma. We considered patients' specifications also might have significant correlation with prognosis in DTC. The purpose of this study was to assess the impact of patient's specification on clinical outcome for patients with DTC treated by an I-131 ablation therapy (IAT). Furthermore, we calculated ablation index (AI) and the accuracy using the index. METHODS: A total of 326 patients with DTC (female 211, male 115) underwent total thyroidectomy and IAT (3.7-5.55 GBq). The potential significant variables were composed of age, gender, BMI, the blood urea nitrogen (BUN), serum creatinine (Cr), thyrotrophin (thyroid-stimulating hormone, TSH) and Tg in the analysis. Discriminant analysis was used for the data evaluation. AI was defined as discriminant value. RESULTS: There were 100 successful ablations (female 60, male 40). In a discriminant analysis, however, the only significant variables affecting outcome were age, TSH and Tg. The obtained discriminant formula was as follows: *AI = - 2.9908 + 0.0200(Age) + 0.0108(TSH) + 0.0022(Tg).* The outcome of IAT could be predicted by a negative AI value, with an accuracy of 84.0%. The sensitivity and specificity of AI was 92.9% and 64.0% with a PPV of 85.4% and an NPV of 80.0%. CONCLUSIONS: There was statistically significant relationship between some patients' specifications (age, TSH and Tg) and prognosis of DTC. This simple discriminant function might be useful for predicting the outcome of IAT.

### P218

### Survival of patients with metastases of Hürthle cell thyroid carcinoma

**A. Schwarzbartl - Pevec**, R. Petric, B. Vidergar - Kralj, I. Zagar, N. Besic; Institute Of Oncology, Ljubljana, SLOVENIA.

**Introduction:** It is generally believed that patients with Hürthle cell thyroid carcinoma (HCTC) have poor prognosis. Furthermore, distant metastases represent the most frequent cause of thyroid cancer-related death of patients with HCTC. The aim of this study was to report outcomes of patients with distant metastases. **Methods:** Altogether 109 patients were treated because of HCTC during the period from 1972 to 2011 in our tertiary center and 33 patients (19 females, 14 males; median age 69 years) had either initially metastatic disease (N=12; 9 females, 3 males; median age 66.5 years) or distant progression of HCTC after initial treatment (N=21; 10 females, 11 males; median age 70 years). Patients with metastases were followed for 1-201 (mean 66, median 41) months. The data on gender and age of the patients, disease history, extent of disease, morphologic characteristics, mode of therapy, outcome, and survival were collected. Statistical correlation between possible prognostic factors and cause-specific survival from time of detection of metastases was analyzed by univariate analysis and log-rank test. **Results:** Single organ and multiple organ metastases were diagnosed in 29 and 4 cases, respectively. The most common were lung metastases, followed by bone, mediastinum, kidney and liver in 26, 8, 2, 2 and 1 case, respectively. Total thyroidectomy, lobectomy, subtotal thyroidectomy and neck dissection were performed in 19, 11, 3 and 7 patients, respectively. Radioiodine (RAI) ablation of thyroid remnant was performed in 28 patients, while 27 patients had RAI therapy (median 2 times). Two or more RAI therapies were applied in 18 patients. Chemotherapy and external irradiation was used in 12 and 19 patients, respectively. Locoregional control of disease was achieved in 18/21 (86%) cases who succumbed due to HCTC. Eleven patients are alive and one lost from follow-up. Median disease-specific survival for all patients, pulmonary, bone, single organ, multiple organ metastases, initially metastatic and metastatic after disease-free interval was 41, 41, 93, 36, 141, 131 and 26 months, respectively. 5-year disease-specific survival for all patients, pulmonary, bone, single organ and multiple organ metastases was 42%, 46%, 57%, 32% and 100%, respectively. 10-year disease-specific survival for all patients, pulmonary, bone, single organ and multiple organ metastases was 28%, 29%, 43%, 25% and 66%, respectively. **Conclusion:** Patients with multiple and initially metastatic HCTC may have long survival after multimodal treatment. Patients with bone metastases live longer than patients with lung metastases.

### P219

### Does TSH stimulation for preparation for radioiodine theraphy in thyroid cancer paitents affect thymic findings in F-18 FDG PET/CT?

**E. Choi**[1], S. Kim[1], H. Choi[1], Y. Seo[1], Y. Chung[2], S. Lee[3], E. Han[4], W. Choi[5]; [1]Seoul St. Mary's Hospital, College of Medicine, The Catholic University of Korea, Seoul, KOREA, REPUBLIC OF, [2]Incheon St. Mary's Hospital, College of Medicine, The Catholic University of Korea, Incheon, KOREA, REPUBLIC OF, [3]Uijeongbu St. Mary's Hospital, College of Medicine, The Catholic University of Korea, Uijeongbu, KOREA, REPUBLIC OF, [4]Daejeon St. Mary's Hospital, College of Medicine, The Catholic University of Korea, Daejeon, KOREA, REPUBLIC OF, [5]St. Vincent's Hospital, College of Medicine, The Catholic University of Korea, Suwon, KOREA, REPUBLIC OF.

**Objective**: The purpose of this study was to determine whether the thymic activity and size on F-18 FDG PET/CT of thyroid cancer patients is affected by TSH stimulation, which is performed prior to radioiodine ablation. **Methods**: PET/CT images between January 2009 and March 2010, from 94 (24 men and 70 women; mean age 47±13) patients who underwent total thyroidectomy were retrospectively reviewed. PET/CT images were analyzed for the size (thickness, length) and FDG uptake (SUVmax, SUVmax of thymus/SUVmean of Liver ratio) of thymus. Existing follow up PET/CT images without TSH stimulation were also reviewed for changes in the size and FDG uptake of thymus. Clinical history was reviewed to determine whether the patient was under TSH stimulation when PET/CT was performed, which was analyzed for correlation with thymic findings. **Results**: Of the included 94 PET/CT images, 32 were performed under TSH

stimulation. PET/CT images with TSH stimulation and those without did not show statistically significant difference in size (mean thickness 17.0 ± 7.1 mm and 17.3 ± 5.4 mm, length 40.3 ± 16.5 and 39.1 ± 10.0, each respectively) and FDG uptake (mean SUVmax 1.79 ± 0.73 and 1.56 ± 0.58, thymus/liver ratio 0.81 ± 0.41 and 0.81 ± 0.34, each respectively). From patients with PET/CT images performed under TSH stimulation, 12 had a follow up PET/CT image performed without TSH stimulation. Their initial and follow up PET/CT images did not show statistically significant changes in size (mean thickness 17.6 ± 8.3 mm and 16.1 ± 7.9 mm, length 40.7 ± 24.2 mm and 39.0 ± 24.4 mm, each respectively) and FDG uptake (mean SUVmax 1.65 ± 0.64 and 1.38 ± 0.28, thymus/liver ratio 0.98 ± 0.29 and 0.92 ± 0.23, each respectively). **Conclusion**: TSH stimulation does not affect thymic activity and size in F-18 FDG PET/CT of thyroid cancer patients.

## P220

### Are serum Tg and anti-Tg antibody measurements adequate on follow-up of patients with differentiated thyroid cancer? A brief report on the importance of patient's anamnesis and careful physical examination

**B. E. Akkas**, G. U. Vural, B. B. Demirel, N. Ercakmak; Ankara Oncology Research and Training Hospital Department of Nuclear Medicine, Ankara, TURKEY.

Serum thyroglobulin (Tg) measurements play a key role in the post-surgical follow-up of patients with differentiated thyroid cancer (DTC). These measurements may hampered by the presence of Tg antibodies, which can cause underestimation of Tg concentration. Anti-Tg antibody is the most common one, and can be measured in routine practice. However, some other antibodies which are not routinely measured may exist and interfere with Tg measurements. The aim of this study is to determine the frequency of patients with recurrent/metastatic DTC who also have negative serum Tg and anti-Tg antibody levels. Method: In this study, we retrospectively reviewed data of 3200 patients who previously treated with radioiodine ablation therapy after total thyroidectomy and followed-up in our institution. We searched for patients with recurrent/metastatic DTC who also have negative serum Tg and Anti-Tg antibody. Results: During a 10-yr period, 9 patients were identified. In 8 patients, palpable and non-palpable metastatic cervical lymph nodes were detected on physical examination and neck ultrasound on follow-up. These patients had undetectable serum Tg and anti-Tg levels under TSH stimulation. Patients were referred to surgery for en-bloc or completion compartmental neck dissection if symptomatic metastasis were present. The other patient, who previously treated with total thyroidectomy followed by mediastinal-cervical lymphatic dissection and radioiodine therapy were referred with swelling in sternal region on follow-up. On physical examination, a palpable mass on sternum and an axillary mass 4cm in size was noted. PET/CT scan revealed a destructive bone lesion in sternum and metastatic multiple lymph nodes in the left axilla. Since serum Tg and anti-Tg antibodies were undetectable, our pre-diagnosis was a second primary malignancy. However, a tru-cut biopsy revealed metastasis of papillary thyroid carcinoma. Following axillary lymphadenectomy, 250mCi I-131 was administered and residual lesions showed intense radioiodine uptake. Conclusion: Patient management starts with detailed questioning the patient and careful physical examination. Serum Tg and anti-Tg antibody measurements are crucial on the follow-up of patients with DTC, but it must be kept in mind that serum Tg levels may not be reliable on follow-up in a small percentage of patients. Even though we could not prove in this study due to laboratory facilities, antibodies other than anti-Tg antibody may exist in the patient's serum. Our results proved that paying attention to patients' subjective complaints and careful physical examination followed by radiological imaging and histopathological sampling provides excellent opportunity to detect recurrent or metastatic disease and guide patient management.

## P221

### Stimulated Thyroglobulin (Tg) measured Before or After Radioiodine Therapy has a Clinical Impact on the Management of Patients with Differenciated Thyroid Carcinoma

**M. Bauriaud**[1], S. Brillouet[1], N. Eche[1], L. Dierickx[1], S. Grunewald[2], D. Bastie[2], O. Caselles[1], F. Courbon[1], S. Zerdoud[1]; [1]INSTITUT CLAUDIUS REGAUD, Toulouse, FRANCE, [2]CHU, Toulouse, FRANCE.

AIM Stimulated thyroglobulin (Tg) with administration of recombinant human thyrotropin (rh-TSH) during ablation with iodine-131 is the most important tumor marker in the monitoring of patients with differentiated thyroid carcinoma (DTC). Tg should be measured the third day after the second injection of rh-TSH, but to avoid the postponed due to iodine-131, Tg is often measured the day after the second injection of rh-TSH before the ablation. There is no evidence that Tg measured three days after radioiodine therapy is a more sensitive marker than the Tg measured before the administration of iodine-131. The objective of this prospective study was to evaluate the clinical impact in the choice of one of these two Tg for the follow up of these patients. MATERIALS AND METHODS This study included 140 patients with differentiated thyroid carcinoma (DTC) who underwent thyroidectomy with apparently total tumor resection. All patients had Tg measurement before radioiodine therapy (Tg1), 3 days after the last injection of rh-TSH (Tg2) and one year after ablation (Tg3). All serum Tg were measured using the same sensitive IRMA assay standardized on the European reference standard (CRM 457). ROC curve is a function of both the sensitivity and specificity and take into account the entire range of error rates. Area under the ROC curve is summary measure of the accuracy. Sensitivity and specificity were evaluated with the use of the optimal threshold value calculated to maximize the Youden's index. This index is defined as the sum of sensitivity and specificity minus one. RESULTS The cut-off obtained using the youden index were respectively 2.55 for Tg1 and 3.65 for Tg2. In the two cases, the area under the curve was estimated to 0.66. After backward selection, only Tg1 remain significant (OR=3,8 95%CI=[1,7; 8;47] p<0.001). CONCLUSION Tg stimulated with rh-TSH measured before radioiodine therapy seems to be the most sensitive marker to predict the recurrence of DTC in patients.

## P222

### Role of Tc-99m Pertechnetate for Remnant Scintigraphy Post-Thyroidectomy, and Serum Thyroglobulin and Antithyroglobulin Antibody Levels in the Patients with Differentiated Thyroid Cancer

**F. Aydin**, M. Sipahi, E. Surer Budak, A. Aktas Samur, M. Erkilic, F. Gungor; Akdeniz University, Antalya, TURKEY.

**Aim:**Postoperative scanning may help to identify in patients with differentiated thyroid cancer (DTC), however low dose I-131 can lead to stunning and suboptimal response to ablative therapy. The aim of this retrospective study to compare postablative I-131 scintigraphy with Tc-99m pertechnetate scintigraphy post-thyroidectomy, serum thyroglobulin (Tg), and antithyroglobulin antibody (Atg) levels in the patients with DTC. **Materials Methods:**One hundred seventy four patients (146 women, 28 men) with a mean age of 48.7±13.1 years (range: 12-84) who had undergone surgical thyroidectomy for DTC were evaluated retrospectively. All patients had undergone Tc-99m pertechnetate and postablative I-131 scans. Serum Tg and Atg levels were measured in all subject. Preablative pertechnetate scans of the thyroid bed were viewed blindly then directly compared with postablative I-131 scans, and Tc-99m pertechnetate scintigraphy was compared with serum Tg and Atg levels. **Results:**For the per-patient analysis, pertechnetate scans were considered to be positive if they showed any definite sites of uptake. Of the 174 patients, 6 (3%) had negative I-131 scans, both of which were also negative on pertechnetate. Of the remaining 168 positive I-131 scans, 131 (75%) were positive in at least one site on the pertechnetate scan, 19 (11%) were considered to have equivocal uptake, and 18 (11%) were negative. For the per-site analysis, pertechnetate sites were considered to be accurate if they showed concordant uptake at sites that correlated precisely with those seen on the postablation I-131 scans. There were a total of 356 positive foci on I-131 scans. Of these, 273 foci (77%) were unequivocally positive on pertechnetate scintigraphy, 41 (11%) showed equivocal uptake, and 42 (12%) were not detected. Tg and Atg values were in the range of 0.1- 696.7ng/ml (median: 5 ng/ml) and 10-1109ng/ml (median: 19.2 ng/ml), respectively. There were statistically significant differences (p<0.0001) between the negative and positive foci in terms of Tg level in pertechnetate sites. There were also statistically significant differences (p<0.004) in Tg level in pertechnetate sites between positive and equivocal uptake. Any statistically significant differences in Atg values for pertechnetate sites (p >0.05) could not be found. **Conclusion:**A positive pertechnetate scan is therefore sufficient to guide progression to I-131 ablation in most patients. Pertechnetate scintigraphy may be of particular benefit if it is considered desirable to avoid I-131 in post-thyroidectomy remnant imaging. Tg level is important parameter in detection of remnant thyroid tissue in the patients with DTC.

## P223

### The value of [$^{18}$F]FDG-PET/CT imaging in the detection of recurrence in patients with medullary thyroid cancer as part of multiple endocrine neoplasia-MEN IIA syndrome

**E. Skoura**[1], P. Rondogianni[1], D. Exarhos[2], M. Alevizaki[3], S. Tsagarakis[4], D. Kyprianou[1], I. E. Datseris[1]; [1]Nuclear Medicine Department, Evangelismos General Hospital, Athens, GREECE, [2]Department of Computed Tomography, Evangelismos General Hospital, Athens, GREECE, [3]Department of Endocrinology, Alexandra General Hospital, Athens, GREECE, [4]Department of Endocrinology, Evangelismos General Hospital, Athens, GREECE.

**Aim:** In this report we studied the diagnostic accuracy of [$^{18}$F]FDG-PET/CT in the detection of recurrence in patients with histologically proven medullary thyroid carcinoma (MTC), as part of multiple endocrine neoplasia-MEN IIA syndrome and elevated calcitonin levels. **Materials and Methods**: Between May 2007 and May 2012, 13 [$^{18}$F]FDG-PET/CT scans were performed on 10 patients with MEN IIA syndrome and elevated calcitonin levels for localization of recurrent MTC disease. All patients underwent total thyroidectomy as initial treatment for the MTC and adrenalectomy for pheochromocytoma. Also, in 4 of them subtotal

parathyroidectomy had been performed for glandular parathyroid hyperplasia. All patients had elevated calcitonin levels (26.2-5500pg/ml). **Results:** Among the 13 [$^{18}$F]FDG-PET/CT scans, 3 were positive and 10 negative for MTC recurrence. In positive [$^{18}$F]FDG-PET/CT scans the lesions were located in cervical lymph nodes (2), mediastinal lymph nodes (1), thyroid bed (1), liver (2), and bones (1). The overall per-patient sensitivity of [$^{18}$F]FDG-PET/CT was only 23% and for patients with calcitonin levels <2000pg/ml this fell to zero (0%). Positive were the [$^{18}$F]FDG-PET/CT scans from only 3 patients with very high calcitonin levels: 5500, 2096 and 4800pg/ml, respectively. Also, two of the negative (for MTC) scans had findings due to recurrence of pheochromocytoma **Conclusion:** Although in bibliography, [$^{18}$F]FDG-PET/CT appears a valuable tool for the detection of MTC recurrence in patients with elevated calcitonin levels, our study showed that concerning patients with MTC as part of MEN IIA syndrome, its sensitivity was much lower. The findings are in accordance with them of other studies which support that MEN IIA disease induce more indolent MTCs, and as [$^{18}$F]FDG uptake relies on the biological aggressiveness of the tumor, the detection sensitivity of the method is low.

## P224

### Comparison of Pentagastrin and Calcium Stimulation Test for preoperative Diagnosis of Medullary Thyroid Carcinoma in Patients with nodular Goiter

**P. Ubl**, R. Marculescu, C. Scheuba, B. Niederle, S. Li; Medical University of Vienna, Vienna, AUSTRIA.

AIM: The aim of this study was to compare the accuracy of pentagastrin test (PGT) with calcium stimulation test (CST) for preoperative diagnosis of medullary thyroid carcinoma (MTC) in patients with nodular goiter. MATERIALS AND METHODS: Between 2011 and 2012, a prospective screen for increased basal values of calcitonin (CT) was undertaken in 526 patients with nodular goiter. Patients with elevated basal level of serum CT were subjected to both PGT and CST by injection of 0.5 µg/kg of pentagastrin or 2.5 mg/kg of calcium, respectively. Stimulated levels of CT more than 80 pg/ml by PGT or more than 350 pg/ml by CST or basal values more than 50 pg/ml were indication for surgery. RESULTS: Of 526 patients, 38 with increased basal CT values had both PGT and CST. 23 patients had thyreoidectomy. 14 cases of MTC and seven of C-cell hyperplasia (CCH) were histologically identified. Two patients had negative histological results (neither MTC nor CCH). The basal CT values for MTC, CCH and negative histological results ranged from 8 to 22417 pg/ml (2894 ± 1839 pg/ml), 5 to 28 pg/ml(12 ± 3pg/ml) and 7 to 15 pg/ml (12 ± 4 pg/ml), respectively. Under pentagastrin stimulation, the maximal values of CT for MTC, CCH and negative histological results ranged from 97 to 143556 pg/ml (8780 ± 3851 pg/ml), 19 to 522 pg/ml (127 ± 67 pg/ml)and 30 to 95 pg/ml (63 ± 33 pg/ml), respectively. After stimulation with calcium, the maximal values of CT for MTC, CCH and negative histological results reached from 372 to 209186 pg/ml (32995 ± 17110 pg/ml), 161 to 1163 pg/ml (483 ± 133 pg/ml) and 200 to 489 pg/ml (345 ± 145 pg/ml), respectively. CONCLUSIONS :For preoperative diagnosis, both PGT and CST are specific and sensitive Methods. There is a correlation between PGT and CST.

## P225

### Bone metastasis from differentiated thyroid carcinoma: diagnosis, treatment and outcome Experience of a Tunisian center

N. Essabbah, H. Regaïeg, **K. Chatti**, T. Kamoun, R. Sfar, M. Nouira, M. Ben Fredj, N. Ayachi, M. Guezguez, H. Essabbah; Nuclear Medicine Department, Sousse, TUNISIA.

Bone is the second most frequent target of distant metastasis in patients with differentiated thyroid carcinoma (DTC). Many authors reported that it decreased the 10 years survival by 50%. The aim of our study is to report the diagnosis, treatment and outcome of patients with bone metastasis (BM) from DTC treated in the department of nuclear medicine of Sousse (Tunisia). Patients and Methods: We reviewed retrospectively patient data with bone metastasis from DTC in the university hospital of Sahloul, Sousse, Tunisia. There were 844 patients with DTC from 1992 to 2012. Among them 16 patients had BM. All of them adults with an age of 54±14 years. Most of them were women (14/16). Results: Bone metastasis was present in 2% of CDT. BM were synchronous of the DTC in 12 and metachronous in 4. All the patients had had total thyroidectomy. 12/16 had had lymph node resection. There were four cases with papillary DTC, in one case with tall cell; in one no tumor was detected in the thyroid. In 10 cases there were vesicular DTC, in seven cases of them lymph node resection was performed and was positive in two cases. All but three of the patients with BM were symptomatic. Thyroglobuline was higher than 200ng/ml in 15/16. In one patient it was less than 3ng/ml. The diagnosis of BM was essentially made by radioiodine scintigraphy. Only two cases were non functional and the diagnosis was based on the other imaging techniques and/or anatomo-pathology. In the 14 cases, the treatment was radioiodine associated to surgery in 8 cases with or without external radiotherapy and to external radiotherapy in 6. Only one patient was died in two years. 3 of the eight patients with a follow up more than 10 years died. Among them, only in two cases the survival was less than ten years. Conclusion: BM from DTC was rare. It had decreased the 10 years survival by 30%. In our population, the surgery and external radiotherapy associated to radioiodine had increased the overall survival.

## P226

### IMPACT of 131-I SPECT/CT in STAGING or FOLLOW-UP of DIFFERENTIATED THYROID CARCINOMA

Ö. Ömür, **A. Oral**, B. Tuğral, E. Tekin, K. Kumanlıoğlu; Ege University, Faculty of Medicine; Department of Nuclear Medicine, Izmir, TURKEY.

OBJECTIVE: In cases with differentiated thyroid carcinoma (DTC) although the 131-I whole body scintigraphy (WBS) is a method having very high sensitivity and specificity, absence of anatomical location data on planar imaging protocols may causes difficulties and diagnostic errors in differential diagnosis. In this study, it was aimed to investigate diagnostic efficacy of 131-I SPECT-CT in DTC. METHODS: A total of 60 SPECT-CT images (21 head-neck, 28 thorax, 11 abdomino-pelvic) and WBS findings (39 post-therapeutic, 8 diagnostic) of 47 subjects who has suspected 131-I uptake or could not be distinguished from physiologic accumulations on planar 131-I WBS were retrospectively reviewed. FINDINGS: It was observed that the involvement areas where SPECT-CT is needed most are localized on inferior cervical region, mediastinum and on both hemithorax. On WBS lymph node metastasis which its location not confirmed previously was observed in 8 of the 16 cases where 131-I involvement undistinguishable from residual thyroid tissue was established on inferior cervical region. In addition, a soft tissue mass was found in one case and the presence of metastatic bone lesion in another one. Besides this, metastasis was excluded by determining residual thyroid tissue in 7 of the cases with head-neck SPECT-CT and the physiological reasons in 3. In one patient the cranial bone lesion could be distinguished from the radionuclide contamination on scalp. Through 28 thoracic SPECT-CT, mediastinal metastatic lymh node could be localized in 7 cases, hiler metastatic lymph node in 1 case and soft tissue mass lesion in 1 case. It was determined pulmonary metastasis in 8 patients, benign etiologies and physiological uptake (breast, thymus, consolidation area in lung) in 10 patients. 131-I accumulation was observed over lung area in 1 case belonged to metastatic bone lesion located in costa. In 5 of 10 cases where abdomino-pelvic SPECT-CT was needed, the functional bone metastasis was localized and pulmonary metastasis in 1 case; false-positive (cystic lesion on over and subcutaneous previous injection sites) and physiological 131-I involvement areas in 3 cases were excluded though SPECT-CT. CONCLUSION: After data were obtained it was concluded that 131-I SPECT-CT technique would be as a guide for surgical excision by determining the locations of the metastatic lymph node and the soft tissue mass lesions accumulating 131-I and can play an important role in detection of unknown metastatic bone and lung lesions.

## P227

### Optimisation of $^{99m}$Tc(V)DMSA Scintigraphy in a Postoperative Monitoring of Patients with Medullary Thyroid Cancer

**D. A. Dzhuzha**, G. G. Sukach; National Institute of Cancer, Kyiv, UKRAINE.

**Aim** of the study was to increase the diagnostic efficacy of the scintigraphy with $^{99m}$Tc(V)DMSA in a postoperative monitoring of patients with a medullary thyroid cancer (MTC) by means the analysis of a kinetics of the radiopharmaceutical (RP) in neck and mediastinal metastases. **Materials and Methods:** Results of radionuclide studies of 35 patients aged 21-74 years (10 males, 25 females) after a surgical treatment were analysed. The scintigraphic investigations included subsequent implementation of a radionuclide angioscintigraphy during 1 min after intravenous injection of 500-700 MBq of $^{99m}$Tc(V)DMSA, dynamic scintigraphy during 90 min, and delayed whole body scanning and SPECT in 2 h after beginning study. **Results:** The foci of a RP accumulation estimated visually as lymph node metastases were determined in 16 patients. After complex diagnostics and follow-up the metastases were verified in 10 patients. Angiographic curves “activity-time” received from the large lymph node metastases had dilated asymmetric serrated often peaks. Duration of the angiographic peaks was 8-12 s, ascending segments - 3-6 s, descending segments - 4-6 s. Curves “activity-time” received from lymph node metastases at the dynamic scintigraphy consisted from next segments: a) ascending segment, the mean duration - 16.8±1.7 min; b) “plateau”, the mean duration - 23.8±2.0 min; c) wash out segment beginning after 45-55 min. After subtraction the background curves the most difference between the accumulation in the metastases and background was survived from 20.3±1.8 till 46.8±2.4 min. In 3 cases the clear visualisation of small lymph node metastases was till 50 min after injection of RP only. Curves “activity-time” receiving from the foci of the hyperactivity caused a crossing, superposition of the large vessels of a neck and thorax or a fixation of the part of RP bolus in large veins had the exponential form and were similar to the curves of a blood clearance. Analysis of the dynamic curves permitted to exclude the lymph node metastases in 6 patients. **Conclusions:** The execution the $^{99m}$Tc-DMSA scintigraphy in time interval 20-50 min after intravenous injection of RP can increase the efficacy of diagnosis of the small lymph node metastases in postoperative monitoring of patients with MTC. The complex scintigraphic investigation enables of receiving of the data for differential diagnosis.

## P228

### The Usefulness of Postoperative Diagnostic I123 SPECT-CT in Patients with Differentiated Thyroid Carcinoma.

**O. Bessolova**, V. Vidioukov, O. Perfileva, N. Vyrenkova; Russian Medical Academy of Postgraduate Education, Moscow, RUSSIAN FEDERATION.

Aim: To compare diagnostic values postoperative Diagnostic I123 Whole Body Scan, SPECT and SPECT-CT in Patients with Differentiated Thyroid carcinoma. Materials and Methods: We studied 62 post-thyroidectomy patients (43 women and 19 men) 19-75 years old, mean age 43,5 with differentiated thyroid carcinoma (40 papillar, 22 follicular). Patients were subdivided into two groups: before thyroid remnants ablative treatment (Group1 - 22 patients) and in the follow up after admitted I131therapy (Group2 - 40 patients). Whole body study (WBS) and SPECT of the neck and upper chest area was performed in all patients and in cases of detecting increased uptake foci SPECT-CT was done (GE Infinia Hawkeye 4).The I123studies were performed after 3 week thyroid hormone withdrawal. Pathology report, Tg, Anti-Tg, TSH and ultrasound were evaluated. Results: 10 and 19 increased uptake foci in Group1 and Group2 respectively were detected on WBS. All of them were confirmed on SPECT. Radioiodine uptake in 4 and 11 cases, not seen on planar WB scan, was detected by SPECT in Group1 and Group2. Among them in 5 patients in the both group WBS did not reveal any pathology, in another cases SPECT revealed additional to WBS foci. SPECT-CT localized the uptake in the thyroid bed (12 cases) and cervical and mediastinum lymph nodes (2 cases) in patients Group1 and in the thyroid bed (5 cases), cervical and mediastinum lymph nodes (21 cases) , lung (3 cases ) and bone (1case) in patients of Group2. Conclusion: I123SPECT imaging is more sensitive than WBS in detecting of radioiodine uptake in postoperative patients with differentiated thyroid carcinoma. SPECT-CT technique is a useful modality in accurate localization of the lesion and interpretation of uptake in cervical region.

P38-1 - Sunday, Oct. 20, 16:00 - 16:30, Poster Exhibition Area

## Oncology Clinical Science: Breast

## P229

### Prognostic significance of SPECT-CT in sentinel lymph node mapping in breast cancer

**S. Stanzel**[1], V. Bjelic-Radisic[2], T. Schwarz[1], R. Aigner[1]; [1]Medical University of Graz, Division of Nuclear Medicine, Graz, AUSTRIA, [2]Medical University of Graz, Department of Gynecology and Obstetrics, Graz, AUSTRIA.

The **aim** of this study was to determine the prognostic value of SPECT-CT concerning changes in therapy in comparison to planar imaging within sentinel lymph node scintigraphy in breast cancer. Moreover, we studied the clinical additional value of SPECT-CT in comparison to planar scintigraphy. **Materials and Methods:** 118 patients with invasive breast cancer were included in our retrospective study (group 1). SPECT-CT was performed on a dedicated gamma camera 19 hours after subareolar injection of $^{99m}$Tc-Nanocolloid. Additionally a reference group (group 2) of 50 patients with invasive breast cancer was studied with exclusively planar scintigraphy. The cancer recurrence/metastasis rate was determined for a total of 166 patients with available 2- to 7-year follow-up data. **Results:** The number of patients with changes in therapy due to a with SPECT-CT identified tumor-positive sentinel lymph node (SLN) was significantly greater in group 1 with SPECT-CT than in the reference group without SPECT-CT (31/118, 26,2% vs. 10/50, 20%; p<0.001). In group 1 significantly less patients had recurrence/metastases compared to group 2 after an average of >1 year (6,8% vs. 12,2%, p=0,001). The sensitivity of sentinel lymph node scintigraphy based on the breast recurrence/lymph node metastasis rate over the course of time was 100% in group 1 with SPECT-CT compared to 33% in group 2 without SPECT-CT. SPECT-CT could identify SLNs in significantly more patients than planar scintigraphy in group 1 (99% vs. 97%, p=0,002). **Conclusion:** The application of SPECT-CT led in significantly more patients with breast cancer to changes in therapy in terms of upstaging in comparison with planar sentinel lymph node scintigraphy. The cancer recurrence/metastases rate at long-term follow-up after SPECT-CT was lower than planar. SPECT-CT could identify hot nodes in significantly more patients than planar scintigraphy.

## P230

### Correlation of the value of FDG-uptake - described by SUVmax and SUVavg, metabolic tumor volume (MTV) and total lesion glycolisis (TLG) - to clinicopathological prognostic factors in breast cancer

**K. Kajary**[1], T. Tőkés[2], M. Dank[2], J. Kulka[3], M. Udvardy[1], P. Molnár[1], S. Szakáll Jr.[1], Z. Lengyel[1]; [1]Pozitron PET/CT Center, Budapest, HUNGARY, [2]Semmelweis University, Oncological Division of 1st Dept. of Internal Medicine, Budapest, HUNGARY, [3]Semmelweis University, 2nd Dept. of Pathology, Budapest, HUNGARY.

AIM: Knowledge of the clinicopathological features of the breast cancer is important for optimal choice of treatment. Reported data suggest that the SUVmax of the primary tumour is higher in patients with poor prognostic characteristics resulted from core biopsy than in those who have good prognostic features. This study was carried out to observe the relationship between some clinicopathological factors and the FDG-uptake described by SUVmax, SUVavg, metabolic tumour volume (MTV) and total lesion glycolysis (TLG) - with a threshold of SUV at 2.5. MATERIALS AND METHODS: Forty-seven lesions of 46 women with breast cancer (tumour-size>10 mm) undergone PET/CT imaging after core biopsy. The SUVmax, SUVavg, MTV and TLG in the primary tumour were calculated and compared to the histological type, nuclear grade, oestrogen receptor (ER) status, progesterone receptor status (PR), triple-negativity (ER-, PR-, HER2-), p53 and Ki-67 expression. RESULTS: The SUVmax, SUVavg, MTV and TLG were significantly higher in invasive ductal carcinomas (IDC) than in invasive lobular carcinomas (ILC). There was a significant correlation between the high nuclear grade (GrIII) and the SUVmax or SUVavg or MTV or TLG (p = 0.001, 0.003, 0.002, <0.001, respectively). The SUVmax, SUVavg, MTV and TLG were significantly higher either in the ER- cases (p = 0.003, 0.005, <0.001, <0.001, respectively) or the PR- cases (p = 0.008, 0.014, 0.003, <0.001, respectively). The triple negative tumours had higher SUVmax, SUVavg, MTV and TLG vs. for all other tumours, but the correlation with SUVavg was not statistically significant (p =0.062). Moderately strong positive correlation was found between the Ki-67 expression and the SUVmax or SUVavg (r = 0.591, 0.540, respectively). There was a weak correlation between the Ki-67 expression and the MTV or TLG (r = 0.406, 0.465, respectively). Weak correlation was found between the p53 expression and the SUVavg (r = 0.389) and there was no correlation between the p53 expression and the SUVmax or MTV or TLG. CONCLUSION: Our data confirmed that the FDG-uptake is higher in patients with IDC or high nuclear grade (III) or ER-negativity or PR-negativity or triple-negativity compared with those who have ILC or lower nuclear grade (I-II) or ER-positivity or PR-positivity or non-triple-negativity, respectively. Linear correlation was found between the FDG-uptake and Ki-67 expression, which was statistically stronger in case of SUVmax and SUVavg, then MTV or TLG. TLG or SUVmax seems to be suitable for metabolic characterization of the tumour in the interpretation of PET/CT scans.

## P231

### Axillary lymphadenectomy and metastases in the sentinel lymph node in breast cancer patients

**J. Muñoz Iglesias**, A. Allende Riera, J. Uña Gorospe, L. Almeida, M. De Sequera Rahola, D. Cabello García, E. Martínez Gimeno, C. Cárdenas Negro; Hospital Nuestra Señora de Candelaria, Santa Cruz de Tenerife, SPAIN.

Purpose: to assess the presence of micro and macrometastases in breast cancer patients undergoing to sentinel lymph node biopsy. Subjects and Methods: in the past year, 154 patients with breast cancer have been undergo, to our hospital, to the sentinel lymph node biopsy, age range 27-85 years with no axillary involvement detected by palpation or ultrasound-FNA. We identified the sentinel node (SN) by lymphoscintigraphy through subareolar injections of technetium-99m nanocolloid (4 x 0.2 mL x 37 MBq) the day before surgery and removed in the operating room. The SN was intraoperatively studied by serial sections and immunohistochemical techniques, classified as negative (when the SN was negative and/or with isolated tumor cells) or positive (either micro or macrometastases). When sentinel node was positive, a complete axillary lymphadenectomy was performed. Results: the histological types of breast cancer were: infiltrating ductal carcinoma (88.9 %), ductal carcinoma in situ (6.49 %), lobular carcinoma (3.89 %) and lobular carcinoma in situ (0.65 %). The average number of lymph nodes removed was 1.9. Of all patients, in 84.4% (130) the SN was negative, in 9.7 % (15) resulted in micrometastases and in 9 patients (5.8 %) macrometastases. Of the patients with positive sentinel node underwent lymphadenectomy, the 5.18 % had more nodes involved. Discussion: although the overall prevalence of micro and macrometastases affects a significant number of patients, the percentage of those undergoing lymphadenectomy axillary with more affected lymph nodes, is small. Therefore given the morbidity associated to the axillary dissection, could be adopted more conservative therapies with adjuvant treatments (chemotherapy and radiotherapy).

## P232

### Role of 18F-FDG PET/CT in restaging and management of suspected recurrent breast neoplasm.

**M. Haidar**[1,2], F. CHEHADE[1], M. JRIEGE[3], T. KHOURY[4]; [1]Mount Lebanon Hospital, Nuclear Medicine Department, HAZMIEH - BEIRUT, LEBANON, [2]Lebanese University, Beirut, LEBANON, [3]Saint Joseph University, Radiology Department, Beirut, LEBANON, [4]American University of Beirut Medical Center, Radiology Department, Beirut, LEBANON.

Aim of study: Breast carcinoma is known as the most common cancer in women. This study was carried out to elucidate the role of 18F-FDG PET/CT in restaging of treated breast neoplasm and to determine the impact on the management of suspected recurrence. Material and Methods: Retrospective analysis was performed on the PET/CT examination of 35 women with a suspicion of recurrent breast cancer based on clinical examination, tumor marker values (CA 15-3) and/or negative or equivocal findings on other imaging modalities. Results: PET/CT scan could detect only locoregional recurrence (mainly lymph nodes) in 12 patients, locoregional and distant metastasis in 15 patients, and only distant metastasis in 5 patients. Three patients were without evidence of recurrent disease and did not have any recurrence during a close follow up for 6 months. PET/CT led to management modification from locoregional treatment to systemic chemotherapy in 20/35 patients (57%). Conclusion: This study demonstrates the considerable role of FDG PET/CT in restaging of breast cancer with high tumor marker values and negative or equivocal findings on other conventional imaging modalities. PET/CT led to treatment optimization mainly in cases of single recurrent lesion that could be surgically removed. In addition, PET/CT can change the management by detecting distant metastasis.

## P233

### FDG PET/CT in the preoperative staging of newly diagnosed breast cancer

**K. KAMALESHWARAN**, A. SUGUNAN SHINTO; KOVAI MEDICAL CENTRE AND HOSPITAL LIMITED, Coimbatore, INDIA.

Objectives: To determine the efficacy of 18F-Fluorodeoxyglucose positron emission tomography /computed tomography (FDG -PET/CT) in detecting the primary tumor, lymph node and distant metastasis and assess the impact of this technique in cancer staging in the newly diagnosed breast cancer. Methods: Fifty consecutive patients (45 ±10 yrs) with biopsy proven primary breast cancer who were examined by FDG PET were enrolled in this prospective staging study. Whole body PET images were obtained approximately 60 minute after the intravenous administration of FDG . Visual assessment and the maximum standardized uptake value (SUVmax) of breast lesions for semi-quantitative analysis were obtained. The results were compared with the histopathological results. Results: For the TNM staging ,Fifty were considered eligible based on the criteria which were established for this analysis. Significant differences were noted in SUVmax of lesions according to the primary tumor staging. PET imaging revealed pathologic FDG uptake in 50% of patients with axillary lymph node metastases (25 of 50 patients). Patients with axillary nodal metastasis showed metastasis in liver(10 ),lung (15),bone (18) ,brain (1) and abdominal lymph nodes (2 ). Detection of metastatic lesions revealed by PET/CT scan in 25 of 50 patients resulted in a significant change in the TNM stage. The results revealed that FDG PET upgraded TNM stage in 50% (25/50) of patients and 40% (20/50) of patients were diagnosed as having one or more distant metastases. Conclusions: FDG PET was able to identify extra-axillary nodal and distant metastatic lesions in the newly diagnosed patients with breast cancer and therefore, PET may alter to the staging and therapy managements of newly diagnosed breast cancer patients.

## P234

### High risk breast cancer: prospective data about the role of FDG PET/CT in pre- and post-operative settings

**L. Evangelista**[1], A. Cervino[1], S. Michieletto[2], T. Saibene[2], C. Falci[3], E. Bezzon[4], F. Pomerri[4], F. Bozza[2], C. Ghiotto[3]; [1]Radiotherapy and Nuclear Medicine Unit, Istituto Oncologico Veneto I.R.C.C.S., Padova, ITALY, [2]Surgical Oncology Unit, Istituto Oncologico Veneto I.R.C.C.S., Padova, ITALY, [3]Oncology 2 Unit, Istituto Oncologico Veneto I.R.C.C.S., Padova, ITALY, [4]Radiology Oncology Unit, Istituto Oncologico Veneto I.R.C.C.S., Padova, ITALY.

**Purpose**: who should be evaluated initially with 18F-fluorodeoxyglucose (FDG) hybrid positron emission tomography/computed tomography (PET/CT) among breast cancer patients? For providing an answer to this question, herein we aimed to determine the potential diagnostic and therapeutic impact of pre and post-operative FDG PET/CT in patients with breast cancer at high risk of recurrence. **Materials and Methods**: we prospectively collected data from 165 women (age: 53±12 yrs; range:23-82 yrs) with a locally advanced breast cancer diagnosis at initial staging or after surgical treatment (clinical or pathological stage II-III, respectively)who performed FDG PET/CT examination before (n=85) or after surgery (n=80).The mean period between surgery and PET/CT was 45±22 days. The images were visually and semiquantitatively analyzed and compared with other imaging modalities, biopsy or histology, as appropriate. The treatment was planned by the oncologists, according to the current recommendations. The diagnostic performance was calculated by standard Methods. The differences between categorical data were assessed using Yates-corrected chi-square test. **Results**: FDG PET/CT was negative in 43 out of 80 (53.75%) post-operative subjects, while it resulted positive in all patients at pre-operative setting. In particular, in pre-operative group, PET/CT showed an abnormal FDG-uptake in breast (n=84; 99%), in axillary lymph nodes (n=58; 68.2%), distant lymph nodes (n=20; 23.5%) and in distant organs (n=12; 14.1%). Conversely, four (5%) patients of post-operative subset had a positive PET/CT at breast level, five (6.3%) in axillary lymph nodes, 11 (13.8%) in distant lymph nodes and eight (10.5%) in distant organs. Stage grouping according to AJCC 7th edition was changed in 26/76 (34.2%) and 18/79 (22.8%) patients, respectively for pre and post-operative group (p=0.114). Moreover, the diagnostic accuracy in the post-operative setting for the detection of residual or distant metastases was: sensitivity= 100%; specificity= 71%, positive predictive value= 54%, negative predictive value= 100% and accuracy= 78.5%. Change in treatment was reported in 17 (10.3%) of patients, 4 in pre-operative and 13 in post-operative setting (5 vs. 16%, respectively; p=0.013). **Conclusions**: the decision to carry out an FDG PET/CT scan in initial evaluation of patients with locally advanced breast cancer should be probably taken in account. The change in staging is similar both in pre and post-operative setting, while the change in treatment is higher in post-operative subjects. A cost-effectiveness analysis seems necessary.

## P235

### Evaluation of chemotherapy efficacy in patients with advanced breast cancer: high accuracy of breast scintigraphy

**S. N. Novikov**, S. V. Kanaev, P. V. Krivorotko, T. U. Semiglazova, V. F. Semiglazov, L. A. Jukova, E. A. Turkevich; N.N. Petrov Institute Oncology, St Petersburg, RUSSIAN FEDERATION.

**Purpose:** to determine diagnostic accuracy of breast scintigraphy (BSc) with 99mTc-MIBI when it was used for monitoring efficacy of neoadjuvant chemotherapy (NACHT) in patients (pts) with breast cancer (BC). **Material and Methods:** Efficacy of NACHT was evaluated in 51 primary pts with advanced BC (T3-4, N1-2). BSc was performed before the start of NACHT and after 2-3, 5-6 cycles of taxane-doxorubicin +/- trastuzumab based regimes. Predictive accuracy of BSc was verified by final histological examination (HE) of breast tissues removed after the end of NACHT. Visualization of breast lesions and regional lymph nodes was started 10-15 min after i/v injection of 740 MBq of 99mTc-MIBI. Qualitative and semiquantitative scores were used to qualify changes in tracer uptake (TU) in BC. NACHT efficacy were estimated as follows: progression (grade I) - increase of area and/or intensity of TU; stabilization (II) - unchanged images of BC; partial effect (III) - intermediate (30-80%) decrease in intensity and area of TU in BC; prominent efficacy (IV) -small foci of residual (10-20% above background) TU in BC; complete resolution (V) - TU in BC on the level of background. Histological verification of tumor response was graded according Miller classification: I-II- progression or stabilization, III - 30-90% reduction in tumor cellularity, IV- sparse tumor cells (>90% of cell loss) V -complete disappearance of tumor cells. **Results:** BSc and HE concordantly detected grade IV-V tumor response to NACHT in 14 (27%) of 51 treated pts. In another 31 (60.7%) pts both examinations determined low or moderate (grade I-III) efficacy of NACHT. BSc overestimate tumor response in 3(5.8%) and underestimate - in another 3 (5.8%) cases. Sensitivity, specificity and accuracy of BSc in evaluation of breast cancer response for NACHT were as follows: 82.4%, 91.2%, 88,2%. After 4-6 cycles of NACHT good response (scintigraphic grades IV or V) of primary tumor was detected in 54%, moderate (grade III) - in 21% and poor (grade I-II) - in 25% of evaluated pts. **Conclusion:** BSc can be successfully used as accurate noninvasive tool for monitoring efficacy of taxane+/-doxorubicin+/- trastuzumab based NACHT in pts with breast cancer

## P236

### Scintimammography (SMM) and fluorodeoxyglucose (FDG) hybrid positron emission tomography (PET)/computed tomography (CT) in locally advanced breast cancer (LABC): straightness and weakness for the staging and the prediction of response to neo-adjuvant treatment

**L. Evangelista**[1], A. Cervino[1], R. Sanco[1], S. Michieletto[2], T. Saibene[2], F. Bozza[2], C. Ghiotto[3]; [1]Radiotherapy and Nuclear Medicine Unit, Istituto Oncologico Veneto I.R.C.C.S., Padova, ITALY, [2]Surgery Oncology Unit, Istituto Oncologico Veneto I.R.C.C.S., Padova, ITALY, [3]Oncology 2 Unit, Istituto Oncologico Veneto I.R.C.C.S, Padova, Italy, Padova, ITALY.

**Background:** SMM has shown a great ability in identifying multi-drug resistance to a large number of chemiotherapeutic agents in BC. FDG PET/CT can provide important information in LABC patients detecting unknown lymph nodes metastases outside axilla and occult distant metastases. We aimed to assess the role of SMM and PET/CT in patients with LABC, both in staging and in prediction the response to therapy. **Materials and Methods**:after ethical committee evaluation, we prospectively enrolled 54 women (mean age: 50.24±11.65years; range: 27-76yrs) with LABC who underwent within one week both SMM and FDG PET/CT. Both SMM and PET/CT were qualitatively and semiquantitatively analyzed. For SMM we calculated the tumor to background ratio (T/B) and the most intense uptake of the tumor to background ratio (I/B) according the following formula: T/B=[cntsT-cntsB]/ [cntsB] and I/B [cntsI-cntsB]/ [cntsB]. Furthermore, the percentage washout index (WO%) for T and I were obtained, according to: WO%T,I=[cntsT,I]early image-[cntsT,I]delayed image/[cntsT,I]early image.

Maximum, minimum and average standardized uptake value (SUV) was computed by PET/CT, using a region of interest. The results from SMM and PET/CT were correlated with clinical and histological findings (according to the Luminal classification). Moreover, in 39 patients, we assessed the correlation of SMM and PET/CT results with the response to treatment. **Results:**both at SMM and at PET/CT, a significant uptake of tracer in the primary tumorwas identified. PET/CT showed a slightly higher detection rate for axillary lymph node than SMM (83 vs. 77.8%), moreover it recognized supraclavicular/distant lymph nodes and skeletal metastases in 15 patients (28%). Based on histological findings, only early T/B resulted significantly different between HER-2 and basal-like patients (19.4±15.9 vs. 8.8.67, p=0.040), while both SUVmax and SUVavg resulted significantly different in all categories (ANOVA test, p=0.027 and 0.009, respectively). In accordance with response to therapy, 27 (69.2%) patients showed a partial response, 7 (17.9%) a complete response and 5 (12.9%) no response or progression. Both WO%T and WO%I resulted lower in responders than no/partial-responders, although not statistically significant (33.87±10.41 vs. 41.39±15.71, p=0.237 and 29.94±9.22 vs. 42.57±16.65; p=0.061, respectively). Conversely, SUVmax and SUVavg was significantly higher in responders than no/partial-responders (19.69±10.56 vs. 9.47±5.17, p=0.001 and 7.01±2.13 vs. 4.25±1.37, p=0.000, respectively). **Conclusions**: PET/CT is able to detect distant metastases in ¼ of patients and to predict the metabolic response. SMM can be used for the prediction of chemotherapeutic treatment considering its washout index between early and late images. Table 1. Response to treatment and semiquantitative data

## P237

### Usefulness of the $^{18}$F-FDG PET/CT in the Initial Staging of Locally Advanced Breast Cancer (LABC) Prior to Neoadjuvant Chemotherapy

**C. Sampol**[1], A. Pozo[2], J. Torrecabota[3], T. Avella[4], R. Canet[5], A. Lopez[6], S. Rubi[1], M. Villar[1], M. Gimenez[1], C. Peña[1]; [1]Nuclear Medicine Department. Hospital Universitari Son Espases, Palma de Mallorca, SPAIN, [2]Radiology Department. Hospital Universitari Son Espases, Palma de Mallorca, SPAIN, [3]Gynaecology Department. Hospital Universitari Son Espases, Palma de Mallorca, SPAIN, [4]Oncology Department. Hospital Universitari Son Espases, Palma de Mallorca, SPAIN, [5]Patological Anathomy Department. Hospital Universitari Son Espases, Palma de Mallorca, SPAIN, [6]Plastic Surgery Department. Hospital Universitari Son Espases, Palma de Mallorca, SPAIN.

AIM To determine the usefulness of the $^{18}$F-FDG PET/CT in initial staging of Locally Advanced Breast Cancer (LABC) prior to neoadjuvant chemotherapy. Comparison of the PET/CT results of the axillary lymph nodes with other imaging studies and Sentinell Lymph Node Biopsy (SLNB). MATERIALS AND METHODS Based on 51p with clinical diagnosis of LABC (T>3cms/any T-N1). Staging studies prior to neoadjuvant chemotherapy: breast MRI, axillary ultrasound and fine-needle aspiration (FNA) if required and PET/CT (intravenous contrast dye when possible and SUV max LBM). If clinical and radiological axillary staging is N0, SLNB performed prior to chemotherapy, and, if needed, post-chemotherapy Axillary Lymph Node Dissection (ALND) depending on the histological result. RESULTS Average age 54(25-85).Average size 4.18cms(1.8-10).Histology:44p IDC, 3p ILC, 2p Mucinous, 1p Inflammatory, 1p DCIS. Undetected breast tumor on PET/CT for 2p, detected in 49p, with SUV max average 6.94 g/ml(1.4-18). Sensitivity of FDG-PET for primary tumor 96%.PET/CT detected positive axillary nodes in 32p (average SUV 3.53 g/ml(1.7-14)): 28p confirmed and the rest unconfirmed due to a clearly high SUV and suspected CT. One false positive patient SUV max 2 g/ml (SN negative). PET/CT negative axillary result in 19p: 7 false negative with positive SLNB and 12p true negative. 7/19p SUV were low, less than 1.5 g/ml (considered negatives and SLNB candidates), the SN being positive in 2p (38 total affected axillas).Sensitivity axillary FDG-PET 81.5%, Specificity 90%, PPV 96.8%, NPV 56.25%. In 8p the Internal Mammary Chain (IMC) was affected and 12p showed distant metastasis (all confirmed during follow-up), therefore 15.6% were affected with extra-axillary lymph nodes (IMC, supraclavicular and cervical) and 23.5% with M1, the global staging change being 31.37% (16/ 51p). Metastasis was found as follows: 2p liver, 5p lung, 6p bone, 1p local relapse and brain. No additional lesions were found during follow-up beyond those detected by PET/CT. In 4/51p (7.8%) M1 lesions were undetected by CT (very small bone lesions in 3p and liver metastasis in 1p). CONCLUSIONS Staging LABC with PET/CT has demonstrated a strong sensitivity in detecting the primary tumor and great usefulness in the locoregional staging at both axillar and extra-axillar levels (high specificity and PPV). The percentage of detected metastasis makes PET/CT a required technique for this pathology. Low SUV in axillas should be correlated with axillary ultrasound and FNA to avoid false positives and ensuing ALND after chemotherapy, thanks to the prior performance of the SLNB (37.2% unnecessary ALND were avoided).

## P238

### Predictive value of double -phase scintimammography with 99mTc - MIBI in phyllodes tumors.

**S. Shiryaev**, A. Odzharova; Russian Cancer Research Center RAMS, Moscow, RUSSIAN FEDERATION.

Phyllodes tumors are rare non-epithelial tumors of the breast, accounting for less than 1%, of all breast tumors. Most breast cancers are classified as stages 1 to 4, but that is not case with phyllodes tumors. Depending on how the cells pathological criteria, the tumors is classed as benign (harmless), borderline or malignant. The aim of this study was to evaluate a predictive value of double - phase scintimammography with $^{99m}$Tc - MIBI in benign and malignant phyllodes tumors. We represent 15 cases of phyllodes tumor of the breast (mean - 38 ages) evaluated with $^{99m}$Tc-MIBI double-phase scintimammography (at 15 and 180 min post-injection). Lateral prone and anterior supine early and delayed images were acquired after intravenous administration of 555 MBq $^{99m}$Tc-MIBI. Scintimammography was performed using a dual-head gamma-camera (E.CAM, Siemens). In all patients was evaluated increased concentration with tumor to background ratio (T/B) both in early and delayed images. The findings of imaging studies were compared with pathological results. Firstly, in the case of phyllodes tumor, $^{99m}$Tc-MIBI accumulation was recognized on early images in all cases. The level of B/T in benign phyllodes tumor was lowest on early studies < 2 and practically not changed on delayed study - < 10%. In borderline tumors B/T ratio was > 2 and on delayed images the level of "wash-out" of radiotracer was > 50%. In the case with malignant phyllodes tumor B/T ratio was > 2 and level of "wash-out" > 70 % (up to100%). The biological behavior of phyllodes tumors is unpredictable and local recurrence and even malignant transformation may occur in high-grade malignant phyllodes tumors. All three kinds of phyllodes tumors tend to grow quickly, and they require surgery to reduce the risk of tumor coming back in the breast (local recurrence). Neither a mammogram nor a breast ultrasound can distinguish clearly between fibroadenomas and phyllodes tumors. Regard to this increased accumulation of $^{99m}$Tc-MIBI can offer only in phyllodes tumors $^{99m}$Tc-MIBI delayed imaging may have the potential to distinguish between benign, borderline and malignant phyllodes tumors. Key words: phyllodes tumor -scintimammography - MIBI

## P239

### Accuracy of Sentinel Lymph Node Biopsy After Neoadyuvant Chemotherapy in Locally Advanced Breast Cancer

**J. C. Igua Sáenz**; University and Polytechnic La Fe Hospital, Valencia, SPAIN.

**OBJECTIVE** Determine the accuracy of the sentinel lymph node biopsy (SLNB) in patients with locally advanced breast cancer after neoadjuvant chemotherapy. **MATERIALS AND METHODS** From May 2007 to January 2013 we studied 61 patients mean age 47 years old (range 24-65) that underwent SLNB after neoadjuvant chemotherapy. Fifty-seven (93%) were ductal carcinoma and four (7%) lobular carcinoma, (stage II-III). All patients underwent breast surgery (mastectomy (43%), lumpectomy (54%) and quadrantectomy (3%)), SLNB and axillary lymph node dissection. Immunohistochemistry was performed on all sentinel lymph nodes. **RESULTS** The detection rate of SLN was 77% (47/61). In fourteen patients (23%) SLN localization was unsuccessful and lymph node involvement was seen in ten of them. The average of removed sentinel lymph nodes was 1.26 per patient and 14 in axillary dissection. True positive rate was 38% (18/47). True negative rate was 58% (27/47) and false negative rate was 4% (2/47). In this group of patients the FN rate is slightly higher than the one obtained in our institution for patients with early stage breast cancer. **CONCLUSION** SLNB after neoadjuvant chemotherapy is a reliable and useful technique for assessing axillary lymph node status in patients with locally advanced breast cancer, avoiding unnecessary axillary lymph node dissection and associated morbidity. In our experience we would have been avoided 44.2% of axillary dissection.

## P240

### Medical consequences of LVEF monitoring in patients with breast carcinoma treated with Trastuzumab : a 7 year retrospective study

S. MASSON, **L. MASSON**, B. DAYEZ, D. PAPATHANASSIOU, J. LIEHN, J. REY; Institut Jean GODINOT, Reims, FRANCE.

**Aim** : Cardiotoxicity induced by Trastuzumab may require discontinuation. Regular measurement of the Left Ventricular Ejection Fraction (LVEF) is a validated method to evaluate cardiotoxicity. The measurement by radionuclide ventriculography of LVEF is known to be reliable and reproducibile. Cardiotoxicity of Trastuzumab is reversible, unlike that of other chemotherapeutic agents such as anthracyclines. The recovery usually appears at the end of treatment, but it can also occur spontaneously. The decision to stop and reinstate Trastuzumab should be taken on a case by case basis. In this study we describe the medical consequences of LVEF monitoring during Trastuzumab treatments in patient with breast carcinoma. **Materials and Methods** : A retrospective study was performed in all patients treated with Trastuzumab for breast carcinoma between 2005 and 2012 in our center. Data were extracted from the chemotherapy management software and scintigraphic reports giving the results of the measurement of LVEF. These tests were performed on a ECAM Siemens gamma-camera after injection of $^{99m}$Tc-Albumin. Abnormal results are defined as a at least 10% decrease of LVEF and/or a

value lower then 50%. **Results** : Among the 155 patients in whom at least two measurements were performed, 39 (25%) (group 1) had an abnormal result. 116 had normal result (group 2). The average age in group 1 was 52.9 vs 54.4 in group 2 . Clinical signs of heart failure (dyspnea, orthopnea or edema) were found in 6 patients (15%) of group 1. LVEF decrease occurred mostly during the fourth treatment. In case of LVEF decrease, prescribers adopted different attitudes : - Permanent discontinuation of Trastuzumab for 7 patients (LVEF <50% for 86% of those patients) - A therapeutic break (snooze then repeat) for 11 patients (LVEF <50% for 72% of those patients) - No change in treatment for 21 patients (LVEF <50% for 24% of those patients) Risk factors of the patient (age, BMI, CardioVascular risk factors) and associated treatments (chemotherapy, radiotherapy, hormonotherapy) were compared between the two groups, but no significant difference was found. **Conclusion** : Regular monitoring of LVEF in Trastuzumab is essential because it can detect many cases of heart function alterations which often imply treatment modifications.

## P241

### SUVmax Values in PET/CT at Histolgic Grade Groups According to Bloom Richardson Grading System also Called Nottingham System in Breast Cancer

**A. Ozen**, S. Altınay, E. Bastug, O. Ekmekcioglu; Bagcilar Training and Research Hospital, Istanbul, TURKEY.

The aim of this study was evaluated to SUVmax values in PET/CT according to histopathologically Modified Bloom Richardson grading system also called Nottingham sysem in breast cancer. The majority of tumor grading systems currently employed for breast cancer combine nuclear grade, tubule formation and mitotic rate. In general, each element is given a score of 1 to 3 (1 being the best and 3 the worst) and the score of all three components are added together to give the "grade". This study was included 29 female patients with breast cancer (mean age 53.3±11.3), 27 invasive ductal carcinoma and 2 mixed histologic type. All patients had one lesion bigger than 1 cm. The F-18 FDG between 7.3-14.7 mCi was injected intravenosly after 6 hours fasting while plasma glucose level is <200 mg/dl. Patients were divided 3 groups according to Modified Bloom Richardson grading system, grade 1, 2 and 3. SUVmax levels were 3.833±0.737 (3 patients in grade 1), 5.6±4.035 (8 patients in grade 2) and 9.061±5.647 (18 patients in grade 3), respectively. There was no difference statistically between grade 1-2 and grade 2-3, but p value lower than 0.05 between grade1 and 3. We found that SUVmax value was increasing with histologic grade in this study. As another a result, SUVmax level reflects agressive cancer in breast cancer.

## P242

### The Role of FDG-PET/CT in The Initial Staging of Breast Cancer and The Correlation of Prognostic Factors

M. Ismailoglu, **E. Varoglu**, M. Serdengecti, B. Kaya, O. Sahin, T. Guler; N.Erbakan University, Konya, TURKEY.

**Aim:** To investigate the role of initial staging FDG PET/CT in evaluating distant metastases and in detecting axillary lymph node metastases as well as the other local lymph node metastases in patients diagnosed with breast cancer but not receiving chemotherapy and radiotherapy; and to clarify the relationship between maximum standardized uptake value (SUVmax) of primary lesions and some prognostic factors for the cases in which primary lesions are present. **Methods:** 114 patients diagnosed with breast cancer who underwent FDG PET/CT between March 2008 and September 2012 for the purpose of initial staging were included the study. 113 out of 114 patients with the average age of 57,6 (±13,8) were female, whereas one was male. There were 38 patients with primary lesions who were diagnosed with breast cancer by means of tru-cut/core or fine needle aspiration biopsy (FNAB) which were obtained from the primary lesions or from axillary LAPs, and there were 76 patients without primary lesions who were performed excisional biopsy or mastectomy+axillary dissection. **Results:** Of 114 patients, 48 (42.1%) were found to have distant metastases. In 24 patients (21%) bone/bone marrow metastases, in 11 patients (9.6%) lung metastases, in 10 patients (8.7%) liver metastases, in 27 patients (23.6%) mediastinal and hilar lymph node metastasis, in 6 patients (5.2%) contralateral axillary-supraclavicular-infraclavicular-internal mammarian lymph node metastasis and in 17 patients (14.9%) different metastases were seen. In addition to that, in 17 patients (14.7%) ipsilateral axillary lymph node metastases was detected. In 31 of 43 patients not undergoing invasive intervention to axillary regions, ipsilateral axillary lymph nodes were found positive. A linear correlation between SUVmax of primary lesions of the patients and the size of such primary lesions and Ca 15-3 prognostic factor was revealed; whereas a significant association between SUVmax value and the other prognostic factors including, frequency of distant metastasis, the presence of proto-oncogene c-erbB2 and ER-PR receptor status were not reported. **Conclusion:** It is considered that FDG PET/CT is highly useful method for patients with breast cancer by detecting axillary lymph nodes, and other local lymph nodes that are relatively hard to evaluate and distant metastasis at initial staging. However, there is a need for studies with higher number of patients and longer term follow-up to determine the correlation of different prognostic factors.

## P243

### 18F-FDG-PET/CT in staging, restaging, and treatment response assessment of male breast cancer

**D. Groheux**[1], E. Hindié[2], M. Marty[1], M. Espié[1], L. Vercellino[1], G. Bousquet[1], J. Ohnona[1], M. Toubert[1], P. Merlet[1], J. Misset[1]; [1]Hopital Saint-Louis, PARIS, FRANCE, [2]Haut-Lévêque Hospital, CHU Bordeaux, Bordeaux, FRANCE.

AIM: Male breast cancer (BC) is a rare disease, with patterns different from those found in women. Most tumors are estrogen receptor positive (ER+) and are detected at more advanced stages than in women. The aim of this study was to analyze the performance of [18F]fluorodeoxyglucose positron emission tomography/computed tomography (18F-FDG-PET/CT) in staging, restaging, and therapy response assessment. MATERIALS AND METHODS: We performed a systematic analysis in the database of Saint-Louis Hospital to identify male patients with BC referred for PET/CT. 18F-FDG-PET/CT findings considered suspicious for malignancy were compared to biopsy results, further work-up and/or patient follow-up of at least 6 months. Performances of 18F-FDG-PET/CT were compared to that of conventional imaging (CI) using the McNemar test. The impact of PET/CT on management was evaluated. RESULTS: During 6 consecutive years, among 12692 18F-FDG-PET/CT oncology studies, 30 were performed in 15 men with BC: 7 examinations for initial staging, 11 for restaging, and 12 for response assessment. Tumors profile was ER+ and one had HER2-overexpression. PET/CT sensitivity, specificity, positive predictive value, negative predictive value and accuracy to detect distant metastases, were respectively 100%, 67%, 86%, 100% and 89%. PET/CT was more informative than CI in 40% of studies (p = 0.03 ; 95% confidence interval : 3.26 - 40%). Findings from 18F-FDG-PET/CT led to modification in the planned treatment in 13/30 cases (43%). CONCLUSION: Although all tumors were ER+, primary lesions and metastases were diagnosed with high sensitivity. 18F-FDG-PET/CT seems to be a powerful imaging method to perform staging, restaging and treatment response assessment in male patients with BC.

## P244

### Repeat axillary sentinel lymph node biopsy after neoadjuvant chemotherapy in breast cancer patients with positive sentinel lymph node at presentation

**T. Aroui**[1], A. C. Rebollo[1], R. Sanchez[1], M. Gallego[2], N. Testart[1], J. Garcia[3], S. Menjón[3], J. M. Llamas[1]; [1]Nuclear Medicine. Hospital Universitario Virgen de las Nieves, Granada, SPAIN, [2]Nuclear Medicine. Hospital Universitario Santa Lucía, Cartagena, SPAIN, [3]Gynecology. Hospital Universitario Virgen de las Nieves, Granada, SPAIN.

Aim. To evaluate accuracy of a second sentinel lymph node biopsy (SLNB) in patients with operable breast cancer and clinically negative axilla, with SLN metastasis at diagnosis, treated with primary systemic chemotherapy in order to avoid unnecessary axillary lymphadenectomy in pathologic complete response cases or disease limited to the SLN. Materials and Methods. Prospective study (September 2011-March 2013). 49 women, average age 50.7 years (range 29-73) with invasive ductal carcinoma (2 bilateral), stage II A (cT2N0M0). The axillary status was established clinically including ultrasonography or biopsy. Chemotherapy scheme: epirubicin/ cyclofosfamide x 4, and docetaxel x 4. The day before surgery, 74-111 MBq albumin nanocolloid was injected periareolarly. The SLN was analyzed by OSNA, one-step nucleic acid amplification. Axillary lymph node dissection (ALND) was performed in patients with positive SLN at presentation. Results. The pre-chemotherapy SLN was identified in 96% (49/51) cases. SLN mean: 1.69±0.89 (range 1-4). In 28/49 (57.2%) patients the SLN was positive: 19 macrometastasis, 2 macro/micrometastasis and 7 micrometastasis. At the moment, 39 patients (2 bilateral) have completed the neoadjuvant chemotherapy and surgical treatments (34 lumpectomies, 7 mastectomies), 23 of them with positive pre-chemotherapy SLN (15 macrometastasis, 2 macro/micrometastasis and 6 micrometastasis). Post-chemotherapy SLN was only identified in 11/21 (52.4%) cases. Non migration occurred in 10 patients: 1 patient with ALND involvement (4/12) and 9 patients without ALND involvement (0/10, 0/14, 0/11, 0/10, 0/12, 0/7, 0/11, 0/10 and 0/9, respectively). In 7 cases, the post-chemotherapy SLN was a true positive (2 macrometastasis, 5 micrometastasis), being the only affected in 4 (3/3, 1/1, 1/1 and 1/1 with ALND negative (0/13, 0/10, 0/12 and 0/5, respectively). In 3 patients, the post-chemotherapy SLN was a true negative (0/2, 0/2, and 0/1) with ALND negative (0/6, 0/7 and 0/22 respectively), and it was a false negative only in 1 (12,5%) patient (SLN 0/1 and ALND 1/6). Conclusion. Though the post-chemotherapy SLNB migration percentage is very low, in cases with SLN identification it maintains the predictive value of the axillary status.

## P245

### Sentinel lymph node biopsy after neoadjuvant chemotherapy in operable breast cancer patients with positive axillary nodes at initial diagnosis

**T. Aroui**[1], A. C. Rebollo[1], M. Gallego[2], R. Sanchez[1], E. Pastor[3], J. Garcia[4], C. E. Chamorro[5], S. Menjón[4], J. M. Llamas[1]; [1]Nuclear Medicine. Hospital Universitario Virgen de las Nieves, Granada, SPAIN, [2]Nuclear Medicine. Hospital Universitario Santa Lucía, Cartagena, SPAIN, [3]Radiology. Hospital Universitario Virgen de las Nieves, Granada, SPAIN, [4]Gynecology. Hospital Universitario Virgen de las Nieves, Granada, SPAIN, [5]Pathology. Hospital Universitario Virgen de las Nieves, Granada, SPAIN.

Aim. To evaluate accuracy of sentinel lymph node biopsy (SLNB) in operable breast cancer patients with positive axillary nodes at initial diagnosis treated with neoadjuvant chemotherapy (NAC). Materials and Methods. Prospective study, between January 2008 - December 2012. We studied 52 women with infiltrating breast carcinoma T1-3, N1, M0 (1 bilateral, 7 multifocal) treated with epirubicin/cyclophosphamide, docetaxel and trastuzumab in Her2/neu-positive patients. Axillary evaluation included physical examination, ultrasound, with ultrasound-guided core needle biopsy of any suspicious lymph node. The day before surgery, 74-111 MBq of 99mTc-albumin nanocolloid was injected periareolary. All patients have undergone breast surgery, with SLNB followed by complete axillary lymph node dissection (ALND). SLN were examined hematoxylin-eosin staining (H&E) and immunohistochemical analysis or OSNA (one- step nucleic acid amplification). Results. TNM estadification was: stage IIA (T1N1M0): 9.4% (n = 5), IIB (T2N1M0): 79.3% (n = 42), IIIA (T3N1M0): 11.3% (n = 6). Average age: 50.7 years (range 31-68), 54.7% premenopausal, the tumor mean size was 35.5 mm (range 18-65), 81.1% corresponded to invasive ductal carcinoma and 49% to the luminal-A molecular type. In 84.9% (45/53) of patients, pathologic confirmation of axillary status was obtained. After NAC, 50.9% of patients had a clinical complete response of primary tumor, 43.4% a pathologic complete response and no response in 5.7%. All patients were clinically node-negative after NAC and 42.2% had a pathologic complete response in axillary nodes. Only 15 patients have complete pathologic response in both breast and axilla. The SLN was identified in 84.9% cases, the mean SLN identified was 1.9±0.96 (range 1-5), 6 of 8 patients in whom SLN was not found had positive axilla in histopathological study (3 cases pN1a and 3 cases pN2a). The SLN results were: 23 negative (8 H&E, 15 OSNA), 13 micrometastasis (1 H&E, 12 OSNA) and 9 macrometastasis (9 OSNA). SLN was the only positive node in 68.2% of patients (9 micrometastasis, 6 macrometastasis), and accurately represented the axillary status in 95.5%. In 72.7% of patients with a positive result all SLN identified were affected (1/1: 10 cases, 2/2: 5 cases, 3/3: 1 case). False negative rate was 8.3% (2/24). The mean number of lymph nodes resected in the ALND was 13.2±4.8 (range 3-24). Conclusion. SLN biopsy after NAC is a feasible and accuracy tool in operable breast cancer patients T1-3, N1 and clinically node-negative after therapy.

## P246

### Sentinel Node Detection in Breast Cancer Patients (T1-T4N0) Treated with Neoadjuvant Chemotherapy

**S. Prado-Wohlwend**[1], R. Díaz-Expósito[1], I. Casáns-Tormo[1], C. Orozco-Molano[1], C. Rocafuerte-Ávila[1], H. Bowles-Antelo[1], A. Julve-Parreño[2], Á. Martínez-Agulló[3], A. Caballero-Garate[3]; [1]Medicina Nuclear. Hospital Clínico Universitario, Valencia, SPAIN, [2]Radiología. Hospital Clínico Universitario, Valencia, SPAIN, [3]Cirugía. Hospital Clínico Universitario, Valencia, SPAIN.

AIM Wide controversy persists in sentinel lymph node biopsy (SLNB) in breast cancer patients treated with neoadjuvant chemotherapy (NCH). We asess the differences in the sentinel node detection by two administration pathways: intratumoral (IT) vs periareolar (PA) in patients without clinical-ultrasound axillary affectation before NCH. MATERIAL AND METHODS Retrospective study in 51 women, age 28-83 (53.2) years old, with infiltrative carcinoma T1-T4N0 that received NCH 6 months before. The mean tumor size (measured with sonography) was 32.1 mm preNCH and 8.1 mm postNCH. We found 16 patients with complete tumoral response (CTR), 33 partial (PR) and 2 without response (NR). We administered 2 mCi of 99m-Tc albumin nanocolloid by IT in 28 patients (palpable lesion and ultrasound guided or stereotaxy in the non-palpable lesions) and PA in 23, at the same day of surgery, performing planar lymphoscintigraphy (PL) in different projections, intraoperative detection with hand held gammaprobe, intraoperative pathologic analysis of the SN (OSNA) and differed inmunohistochemistry. RESULTS The global sentinel node detection with PL was 94.1% (48/51), with surgical remove in 43/48. We detected in PA group 22/23 (95.6%) versus 18/28 (64.2%) in IT group (p: 001). We detected SN in 8 patients more through PA reinjection, with a final global detection of 92.8% (26/28) in this group. In 3 patients without migration, there were 2 IT with nodal involvement and 1 PA without (2 CTR and 1 NR). Considering together the patients without sentinel migration, after IT initial injection and after PA injection (n=11), the mean tumor size pre and post NCH tended to be higher (38.1-10.6 mm) than in patients with migration (30.1-7.5 mm), although without significative differences. There was pathological involvement in 4/11 (36.3%). When some sentinel node was removed, there was involvement in 14/44 (31.8%), 4 with CTR and 10 with PR. The lymphadenectomy showed involvement, in addition to sentinel node, in 7 patients, 6 with PR and 1 with CTR (mean tumor size pre and postNCH were 24.2 mm and 7.4 mm). CONCLUSIONS The sentinel node detection in this group of patients with NCH offers good results, similar to the non-treated patients. However, there is higher detection rate in the patients injected PA than IT way. Mean tumor size pre and postNCH tended to be higher in patients without migration. The pathological involvement node predominated in patients with partial response to NCH.

P39-1 - Sunday, Oct. 20, 16:00 - 16:30, Poster Exhibition Area

## Oncology Clinical Science: Lung

## P247

### Is Brain F-18 FDG PET worthwhile in Lung Cancer staging?

**V. Gontu**[1], D. Griffiths[2], R. O'Connor[1], J. Birchall[3]; [1]Nottingham University Hospitals, Nottingham, UNITED KINGDOM, [2]InHealth, Derby, UNITED KINGDOM, [3]Derby Hospitals NHS Foundation Trust, Derby, UNITED KINGDOM.

Introduction: Lung cancer is second commonest cancer in men and women. Surgery remains the mainstay of treatment with curative intent for NSCLC. The majority of patients with SCLC and around 40% of patients with NSCLC have distant metastases at presentation, which precludes radical treatment options. A proportion of these are asymptomatic. The issue of when to investigate patients and with what imaging modality is debated[1]. F-18 FDG PET/CT of the brain is not yet a recommended staging protocol in the UK. Aim: To identify if including brain imaging in staging PET/CT alters management in lung cancer patients with asymptomatic brain metastases Methods: Retrospective analysis of 1146 staging PET/CT imaging reports between 2006 and 2011. Results: Of the 577 Lung cancer patients, 47 had abnormal reported brain findings. 24 were proven to be metastatic disease, with 2 false positives (0.35%). Asymptomatic brain disease was found in 13 (2.3%). Disease was upstaged with alteration in management plan in 10 (1.7%). Survival benefit was seen in the subset that had curative brain radiotherapy. 20 patients subsequently developed proven brain metastasis within a year of PET/CT (96% Negative predictive value). Positive predictive value, sensitivity and specificity of PET/CT in our cohort is 96.4%, 54.5% and 99.6% respectively and equate to experience from other centers[12] Discussion: The prevalence of asymptomatic patients in our cohort was 2.3%. Inclusion of the brain in the whole body PET/CT performed as a part of the local lung cancer staging protocol, helped avoid futile radical management in 10 asymptomatic patients, whilst instituting early management of brain metastases leading to an improvement in survival. We advocate the inclusion of brain in whole body PET/CT, with a small increase in radiation dose (upto 0.2 mSv/ DLP increase of 10-15%) and time (approx 5 mins). Reference: 1. NICE Guideline CG121, 2011 2. Brain metastases detectability of routine whole body (18)F-FDG PET and low dose CT scanning in 2502 asymptomatic patients with solid extracranial tumors. Bochev et al, Hell J Nucl Med. 2012

## P248

### Performance of Beath-Hold PET/CT using Time-of-Flight System

**K. ISHIHARA**[1], K. HAKOZAKI[1], K. AKIYAMA[1], T. TOMIYAMA[2], Y. SUGIHARA[2], Y. KOBAYASHI[2], T. KIRIYAMA[2], H. SATO[2], S. KUMITA[2]; [1]Clinical Imagin Center for Healthcare, Nippon Medical School, Tokyo, JAPAN, [2]Department of Radiology, Main Hospital, Nippon Medical School, Tokyo, JAPAN.

Time-of -Flight PET/CT system reduced acquisition time per bed position, enabling us PET data collection for the target lesion under breath hold condition. The aim of this study was to assess the performance of shallow inspiration breath-hold (BH) FDG PET/CT using Time-of-Flight system for evaluation of middle/lower pulmonary and upper abdominal lesions. Twenty four patients with middle/lower pulmonary or upper abdominal lesions were examined with standard and BH protocols. Following the standard protocol of one min. data acquisition per bed position under shallow breath free (BF) condition, patients were scanned with the BH protocol of 20 sec. BH per bed position. Twenty malignant and eleven benign lesions were compared between the BF and BH protocols using max standardized uptake value (SUV). Image quality of total 31 lesions with the BH protocol were also visually assessed based on 3-point rating scale (excellent, good, and poor) for accuracy of registration. All lesions showed abnormal FDG uptake and higher SUV value with BH that those with BF. In malignant lesions, the mean and the standard deviation values of SUV with BH was significantly higher than those with BF (5.97±3.34 vs. 3.52±2.84, p<0.01). A higher SUV was also observed in benign lesions on BH PET compared on BF PET (3.91±2.53 vs. 2.30±1.32). There was no significant difference of an average increase in SUV between malignant and benign lesions (65±50 vs. 64±49). No lesion was assessed visually as poor on BH PET. Only 20 percent of the lung base lesions were depicted as the excellent image quality. On the other hand, more than 60 percent of the middle pulmonary lesions were classified as excellent. The frequency of excellent point decreased in lesions near the diaphragm. The BH protocol using Time-of-Flight system improved image

quality of PET/CT not only by reducing misregistration but also by increasing image contrast. This protocol requires only 20 sec. additional data acquisition for lesions near the diaphragm detected on the standard PET.

## P249

### The role of fluorodeoxyglucose (FDG) positron emission tomography (PET)/computed tomography (CT) versus diagnostic CT in surgical management of patients (pts) with lung cancer according to the 7th TNM classification

**L. Evangelista**[1], A. Panunzio[2], R. Polverosi[3], P. Muzzio[2], F. Pomerri[2]; [1]Radiotherapy and Nuclear Medicine Unit, Istituto Oncologico Veneto I.R.C.C.S., Padova, ITALY, [2]Radiology Oncology Unit, Istituto Oncologico Veneto I.R.C.C.S., Padova, ITALY, [3]Department of Radiology, San Donà di Piave Hospital, Venice, ITALY.

**Background.** In accordance with the new classification, stages from IA to IIIA are considered surgically resectable with a possible role for neoadjuvant or adjuvant chemotherapy and radiotherapy. In pts at stage IIIB-IV of disease, surgical resection is considered impracticable, and chemotherapy-radiation therapy becomes the primary treatment. The aim of our study was to compare the role of FDG PET/CT vs. diagnostic CT in order to evaluate the impact on surgical management. **Materials and Methods:** We retrospectively reviewed both PET/CT and CT scans of 67 pts (69±9 years) with lung cancer. Based on their findings, the sites of primary lung lesions, lymph nodes and metastases were tabulated and the final staging was computed according to the new classification. A comparison across diagnostic and metabolic imaging was performed. **Results:** Based on CT findings, 19 pts were at stage I; 8 at stage II; 13 at stage IIIA; 7 at stage IIIB and 20 at stage IV. No concordance between imaging modalities was reported in 30 pts, particularly based on PET/CT 15 were downstaged and 15 upstaged. Twenty-nine out of 67 pts underwent surgery. According to PET/CT, 3 pts underwent surgery by a change in staging from IIIB-IV to I and IIIA. On the contrary, no surgical management was adopted in 6 pts due to upstaging (from I-IIIA to IV). Therefore, PET/CT changed the surgical management in 9/67pts. **Conclusion:** According to the new TNM classification, PET/CT contributes to determine the surgical treatment in about 15% of lung cancer pts, thus improving preoperative staging and reducing the number of needless surgery.

## P250

### A correlation study of Rb-82 PET/CT, F-18 FDG PET/CT and histological findings on lung lesions

**E. DESHAYES**[1], V. DUNET[2], P. MITSAKIS[2], J. O. PRIOR[2]; [1]Montpellier Cancer Institute, Montpellier, FRANCE, [2]Lausanne University Hospital, Lausanne, SWITZERLAND.

Aim: Pulmonary incidentalomas can be discovered during cardiac PET/CT. Our purpose was to correlate 82Rb PET/CT, 18FDG PET/CT, and histological findings on lung lesions. Materials: We included patients who performed both a myocardial perfusion imaging (MPI) with 82Rb PET/CT and 18FDG PET/CT with a known pulmonary abnormality included in the limited 82Rb field of view. In all but 1 patient, 18FDG PET/CT was performed for initial staging of a known or suspected malignancy and MPI with 82Rb PET/CT was part of the preoperative assessment; in 1 case, a lung nodule was discovered during cardiac PET/CT. Between July 2011 and January 2013, n=9 patients (5M:4W, 71±6 years) were enrolled. Both PET/CT were performed within 23±17 days and histopathology was obtained in all lesions. Patients did not receive any treatment between the two examinations. Lesion size, SUVmax, SUVmean and respective ratio to liver and contralateral lung background were measured on 18FDG and rest 82Rb images. Comparison and correlation was assessed using Kruskal-Wallis and Spearman's test, respectively. Results: Eight patients had carcinoma (5 lung squamous cell carcinomas, 3 lung adenocarcinomas) and one benign lesion (hamartoma). Lesion size was 47±31mm, five being located in the right lung and four in the left lung. SUVmax and SUVmean were of 13.2±7.1 vs.4.9±2.7g/mL (P=0.43) and 5.2±2.1 vs. 2.3±0.3g/mL (P=0.24) on 18FDG vs. 82Rb PET/CT respectively. There was no significant correlation between 18FDG and 82Rb PET for SUVmax (rho=0.22, P=0.57) or SUVmean (rho=0, P=1). SUVmax and SUV mean were significantly correlated to lesion size with 18FDG (rho=0.86, P=0.01 & rho=0.83, P=0.01, respectively), but not with 82Rb (rho=0.26, P=0.53 & rho=-0.28, P=0.50, respectively). Conclusion: 82Rb uptake of lung lesions is not related to 18FDG uptake and does not appear to have a good positive predictive value of tumor malignancy. Thus, any incidentaloma found on cardiac 82Rb PET/CT should be investigated for a possible malignancy, independently of the lesion size and 82Rb uptake.

## P251

### Impact of Respiration-averaged CT for Attenuation Correction for Texture Parameters in Non-Small-Cell Lung Cancer

**N. Cheng**[1], T. Yen[2,3], Y. D. Fang[2]; [1]Chang Gung Memorial Hospital at Keelung, Keelung, Taiwan, TAIWAN, [2]Chang Gung Memorial Hospital, Linkou, Taiwan, TAIWAN, [3]Chang Gung University College of Medicine, Taoyuan, TAIWAN.

Purpose: Texture parameters of 18F-FDG PET/CT were prognosticators in non-small-cell lung cancer (NSCLC). However, impacts of respiratory motion on those parameters had not been investigated. Respiratory average CT (ACT) for attenuation correction of PET was reported to reduce respiratory artifacts. In this study, we wanted to evaluate the variations of 18F-FDG PET texture parameters with and without average CT. Methods: We retrospectively enrolled patients of NSCLC, with tumour sized more than 1 cm and performed 18F-FDG PET/CT for staging before therapy. Low dose CT and ACT were done in all cases for attenuation correction of PET images. We used 45%, 50% of the maximum standard uptake value (SUVmax) and adaptive threshold for tumour segmentation and texture parameters were derived based on SUV histogram, normalized grey level co-occurrence matrix (NGLCM), neighbourhood gray-tone difference matrix (NGTDM), voxel alignment matrix (VAM), and grey level size zone matrix (GLSZM) in PET with and without ACT for attenuation correction. Results: 36 patients with 42 lesions were enrolled for analysis. For SUV histogram, significantly higher SUVmax, SUV mean, SUV variance and total lesion glycolysis (TLG) were noted for all segmentation Methods in the PET attenuation correction by ACT. Coarseness and busyness derived from NGTDM varied significantly between PET attenuation correction by CT and ACT if using adaptive threshold. However, no prominent variations were found when applying 45%, or 50% SUVmax for segmentation. For parameters driven from NGLCM, VAM, and GLSZM, no significant different were found. Conclusions: Texture parameters were more robust and less variable to respiratory motion when applying 45%, or 50% SUVmax for segmentation and could served as reliable and repeatable markers in patients with NSCLC.

## P252

### Prognostic value of volume-based parameters measured using 18F-fluorodeoxyglucose positron emission tomography/computed tomography in patients with stage I non-small cell lung cancer treated with stereotactic body radiation therapy

**Y. Satoh**; Kofu Neurosurgical Hospital, PET center, Kofu, JAPAN.

Purpose: To evaluate the prognostic significance and predictive performance of volume-based parameters of 18F-fluorodeoxyglucose (18F FDG) positron emission tomography (PET)/computed tomography (CT) in patients with stage I non-small cell lung cancer (NSCLC) after stereotactic body radiation therapy (SBRT). Materials and Methods: We retrospectively evaluated 88 patients with stage I NSCLC (68 T1N0M0 and 20 T2aN0M0) who had undergone pretreatment 18F FDG-PET/CT and then SBRT. We analyzed maximum standardized uptake value ($SUV_{max}$), metabolic tumor volume (MTV), and total lesion glycolysis (TLG). The prognostic significance of PET parameters and other clinicopathological variables was assessed using Cox proportional hazards regression analysis. Results: The median follow-up period was 33 months. At 3 years, overall survival and disease-free survival (DFS) were 70.0% and 49.7%, respectively. In the univariate analyses, $SUV_{max}$ ($p = 0.001$), MTV ($p = 0.002$), TLG50 ($p = 0.001$), and TLG60 ($p = 0.000$) were found to be significantly associated with DFS. In multiple variable analysis, these parameters were also significantly associated with DFS ($p = 0.011$ for $SUV_{max}$, $p = 0.010$ for MTV, $p = 0.004$ for TLG50, and $p = 0.005$ for TLG60). Only volumetric parameters (MTV, TLG50, and TLG60) were significant indicators of DFS in patients with tumors larger than 3 cm. Conclusion: $SUV_{max}$ and volume-based parameters of 18F FDG-PET/CT may have a prognostic role for NSCLC patients treated with SBRT. This study also suggests that MTV and TLG are better prognostic measures than $SUV_{max}$ for tumors larger than 3 cm.

## P253

### Prediction for occult lymph node metastasis using metabolic parameters on pretreatment F-18 FDG PET/CT in clinically node negative squamous cell lung carcinoma

**D. Kim**, S. Son, C. Kim, C. Hong, B. Song, S. Jeong, S. Lee, J. Lee, B. Ahn; Department of Nuclear Medicine, Kyungpook National University School of Medicine and Hospital, Daegu, KOREA, REPUBLIC OF.

**Objectives:** The aim of this study was to investigate predictability of occult lymph node metastasis (OLM) using metabolic parameters on pretreatment F-18 FDG PET/CT in squamous cell lung carcinoma (SqCC) patients who were clinically node-negative before surgery. **Methods**: Sixty-three clinically node-negative SqCC (Based on FDG PET and contrast enhanced CT) patients without any neoadjuvant treatment (M/F=61/2, mean age, 64.1±8.0) who received curative surgery with mediastinal lymph node dissection were enrolled in this study. Metabolic tumor volume (MTV) of primary tumor was obtained with a threshold of SUV 2.5. Total lesion glycolysis (TLG) was calculated by multiplication of the MTV and its SUVmean. Metabolic tumor parameters (SUVmax, MTV and TLG) and pathologic tumor size were analyzed for OLM. **Results:** Twelve (19.0%) of 63 patients were found to have OLM. SUVmax, MTV, TLG and pathologic tumor size were significantly higher in patient with OLM (*P*=0.023, 0.006, 0.011, 0.043 respectively).

The optimal cut-off values determined using a receiver-operating characteristic (ROC) curve were 8.80 for SUVmax, 18.86 $cm^3$ for MTV, 88.40 for TLG and 2.8 cm for pathologic tumor size. Univariate analysis revealed that SUVmax, MTV and TLG correlated with the rate of OLM (*P*=0.013, 0.005, 0.007 respectively). In the multivariate analyses, high SUVmax and MTV were associated with an increased risk of OLM, after adjusting for age, sex and T stage (*P*=0.044, 0.029 respectively, odds ratio=9.65, 19.79 respectively). **Conclusions:** Metabolic parameters on pretreatment F-18 FDG PET/CT demonstrated statistically significant relationship with OLM in clinically node negative squamous cell lung carcinoma patients diagnosed by surgical resection of primary tumor with lymph nodes dissection.

## P254

### Radioguided Surgery of Pulmonary Nodules. Experience and Results.

**J. G. ROJAS CAMACHO**, M. T. Bajen, A. Benitez, A. Sabate, I. Macía, J. Mora, P. Notta, M. Roca, M. Vidal, P. Boya, J. Martín-Comín; Hospital Universitari de Bellvitge-IDIBELL., L'Hospitalet de Llobregat. Barcelona., SPAIN.

Objective: To evaluate the usefulness of the gamma probe radioguided surgery for resection of pulmonary nodules (lung ROLL). Methods: Prospective study of 10 patients (p) with potentially resectable pulmonary nodular lesions, 8 p with previous cancer (solitary pulmonary node and without extrapulmonary metastases). Average age: 61 years (41-81a). All patients had a computed tomography (CT) of the chest between 30 and 75 days prior to surgery. Radioguided surgery was performed at 15-19h of the intratumoral administration of 1110 MBq / ml 0.2 99mTc-MAA, CT guided. Planar images and SPECT/CT of the chest were recorded after 30-90 min post inyection. The following parameters were analyzed: • Scintigraphic and surgical detection rate of pulmonary nodules. • The lesion and surgical specimen's size by CT and histology • The resection margins. • The histology of the lung nodule • The disease-free period after surgery. Results: One patient was excluded due to the presence of multiple bilateral nodules in the chest CT at the time of radiocolloid puncture. Preoperative scintigraphy showed intrapulmonary focal uptake in all remaining patients. There was surgical detection and free of disease resection margins in all patients. The mean lesion size was 6.9 mm (2-11) by CT and 8.3 mm (2-17) by pathology. The pathology report indicated malignancy in 7 p. All patients are disease free after a median follow-up of 8.6 months after surgery (3-10) Conclusions: Despite the small sample studied, the ROLL technique in lung surgery allows an easy location of the small pulmonary nodules with safe margins of resection and free of disease survival at follow-up.

## P255

### Metabolic and anatomic criteria use in evaluation of Erlotinib treatment response

**M. Ippolito**[1], S. Cosentino[1], G. Murè[1], S. Baldari[1], A. Stefano[2], G. Russo[2], M. C. Gilardi[3], C. Messa[2,4], M. G. Sabini[5], D. Sardina[5], L. Valastro[5], R. Bordonaro[6], H. Soto Parra[7]; [1]Nuclear Medicine Department, Cannizzaro Hospital, Catania, ITALY, [2]Istituto di Bioimmagini e Fisiologia Molecolare-Consiglio Nazionale delle Ricerche (IBFM CNR - LATO), Cefalù (PA), ITALY, [3]Istituto di Bioimmagini e Fisiologia Molecolare-Consiglio Nazionale delle Ricerche (IBFM CNR), Segrate (MI) - Cefalù (PA), ITALY, [4]University of Milan-Bicocca, Milan, ITALY, [5]Medical Physics Unit, Cannizzaro Hospital, Catania, ITALY, [6]Medical Oncology Unit, Oncology Department, Garibaldi Nesima Hospital, Catania, ITALY, [7]Medical Oncology Unit, Oncology Department, Policlinico Universitario Hospital, Catania, ITALY.

**Aim**:The aim of this study was to compare the treatment response using EORTC 1999, PERCIST, and RECIST protocols in patients with advanced or metastatic non small cell lung cancer (NSLCL) after failure of at least one prior chemotherapy regimen. Patients were treated with Erlotinib, an epidermal growth factor receptor-tyrosine kinase inhibitor. **Materials and Methods:** Patients with NSCLC stage IV in progression after at least one line of chemotherapy were treated with Erlotinib (150 mg orally once daily). FDG-PET\CT was performed before and 45 days after the treatment. Anatomic response to therapy treatment was evaluated using RECIST: the longest CT lesion anatomic diameter was recorded before and after the treatment. EORTC and PERCIST were used to assess metabolic response. The ratio between maximum SUV calculated in the hottest lesion and mean SUV liver (SUVratio) were used to assess EORTC response. According to the PERCIST protocol, SUV peak normalized to lean body mass (SULpeak) was calculated in the hottest lesion in each patient. Metabolic and anatomic response classifications were compared statistically using Wilcoxon signed-rank test. Overall survival (OS) and Progression-Free Survival time (PFS) of response classifications were calculated by the Kaplan-Meier test. **Results**: 15 patients were enrolled to treatment evaluation. Anatomic responses according to RECIST were as follows: 4 Partial Response (PR) and 11 Progressive Disease (PD). Metabolic responses according to EORTC criteria were as follows: 5 patients showed a Partial Metabolic Response (PMR), 5 patients a Progressive Metabolic Disease (PMD) and 5 patients a Stable Metabolic Disease (SMD). According to PERCIST: 3 PMR, 6 PMD, and 6 SMD. There was a significant difference in response evaluation between metabolic classifications and RECIST ($p<0.05$). The patients achieving PMR according to PERCIST were associated with a longer median PFS (355 days) versus EORTC criteria (229) and versus patients achieving PR according to RECIST protocol (287). Instead the longer median OS was associated with the patients achieving PR according RECIST protocol (480 days) versus the metabolic responders according PERCIST (410) and EORTC criteria (278). **Conclusion:** This study demonstrates that PERCIST, a new standardized evaluation method that uses functional data from PET, is closely related to prognosis and can be considered an appropriate metabolic evaluation method of therapeutic efficacy to discriminate responders from non-responders in patients with advanced NSLCL treated with Erlotinib. Further investigations will be devoted to increment the patient number to better assess the PERCIST classification.

## P256

### FDG PET/CT in the Detection of Lung Cancer Recurrence

**O. Mukhortova**[1], I. Aslanidis[1], I. Ekaeva[1], Z. Shavladze[2]; [1]Bakoulev Scientific Center for Cardiovascular Surgery, Moscow, RUSSIAN FEDERATION, [2]Medical Radiological Research Center, Obninsk, RUSSIAN FEDERATION.

Detection of locoregional recurrence or distant metastases of lung cancer is crucial for appropriate management and prognosis in patients after primary treatment. Purpose: To evaluate the diagnostic impact of FDG PET/CT for detection of lung cancer recurrence. Materials and Methods: FDG PET/CT results of 48 patients suspected for lung cancer recurrence in 7-22 moths after primary treatment were analyzed retrospectively. Whole-body FDG PET/CT was performed for all patients according to standard protocol in 60 - 90 min after 18F-FDG injection (180 - 200 MBq). Visual assessment and SUVmax calculation for pathological focuses in the chest were done. All PET/CT findings were compared to results of conventional diagnostic Methods (CDM). Results: Sensitivity, specificity and accuracy of FDG PET/CT in diagnostic of lung cancer relapse proved to be 91%, 81% and 88% in comparison with CDM which gave 59%, 56% and 58% respectively. FDG PET/CT identified 82% of patients with combined - regional and distant - metastases, while CDM gave 55%. The best ratio of sensitivity and specificity of FDG PET/CT in diagnostic of local lung cancer recurrence was obtained with threshold value of SUVmax > 4,0. Conclusion: FDG PET/CT is an accurate non-invasive method for early detection of lung cancer recurrence. PET/CT helps in the selection of patients for different treatment: to identify the patients who will benefit from surgical re-treatment and patients with unknown distant metastases revealed by FDG PET/CT who will escape unnecessary surgical treatment.

## P257

### Tumour Heterogeneity in Non-small Cell Lung Carcinoma and its Relation with Metabolic Parameters in 18F-FDG PET/CT

**O. V. Gómez López**[1], A. M. García Vicente[1], A. F. Honguero Martínez[2], J. M. Udías[3], G. A. Jiménez Londoño[1], C. H. Vega Caicedo[1], P. León Atance[2], A. M. Soriano Castrejón[1]; [1]Nuclear Medicine Service, Hospital General Universitario de Ciudad Real, Ciudad Real, SPAIN, [2]Thoracic Surgery Service, Complejo Hospitalario Universitario de Albacete, Albacete, SPAIN, [3]Atomic, Molecular and Nuclear Physic Department, Universidad Complutense de Madrid, Madrid, SPAIN.

Objective: The aim of this study was to investigate the relationship between tumour heterogeneity, assessed by texture analysis of 18F-FDG PET images, and the global metabolic parameters of the primary tumor in patients with non-small cell lung carcinoma (NSCLC). Methods: Retrospective analysis of thirty-four patients (31 men and 3 women with a mean age of 63.9 years), with histologically confirmed NSCLC who underwent staging 18F-fluorodeoxyglucose (FDG) PET/CT before surgery. FDG PET/CT acquisitions were performed following a standardized protocol at 60 min after intravenous administration of approx. 370 MBq of FDG, in three-dimensional (3D) mode and 3 min/bed position. Tumors were segmented with 3D-SLICER software, using a standard uptake value (SUV) cut-off of 2.5. Five 3D local textural features, extracted from images of the segmented tumors, with a positive (contrast, correlation and entropy) and negative (energy and homogeneity) relation to heterogeneity of the gray-level distribution, were assessed by using MazDA software. In addition, global semi-quantitative metabolic parameters of the primary tumor, as (SUVmax), mean standard uptake value (SUVmean), metabolic tumor volume (MTV) and total lesion glycolysis (TLG) given as MTV x SUVmean were obtained. Finally, the relation between local textural features and global metabolic parameters was assessed by performing a Pearson's test ($p<0.05$). Results: From 34 tumors, 21 (61.8%) were epidermoid and 13 (38.2%) adenocarcinomas. The mean ± SD values of SUVmax and MTV were 12.45±6.18 and 28.17±24.08 cc respectively. There was a positive relation between SUVmax, SUVmean, MTV, TLG and entropy ($r=0.48$, $p=0.004$; $r=0.48$, $p=0.004$; $r=0.64$, $p<0.001$ and $r=0.63$, $p<0.001$ respectively) and correlation ($r=0.37$, $p=0.03$; $r=0.39$, $p=0.02$; $r=0.70$, $p<0.001$ and $r=0.63$, $p<0.001$ respectively). Also, a positive relation between MTV, TLG and homogeneity ($r=0.80$, $p<0.001$ and $r=0.73$, $p<0.001$ respectively) was seen. On the other hand, all the global metabolic semiquantitative parameters showed a significant negative relation with energy and contrast. Also, statistically significant relationships were observed between

SUVmax, SUVmean and MTV (r=0.33, p=0.06; r=0.35, p=0.04 respectively) and TLG (r=0.57, p<0.001; r=0.58, p<0.001 respectively). Conclusions: Textural features, positive and negative related to tumour heterogeneity, showed significant relations with global metabolic semiquantitative parameters in FDG PET/CT. Thus a wide textural spectrum, assessed by metabolic imaging, could coexist in this group of patients.

## P258

### The feasibility of $^{18}$F-FDG PET/CT in the differential diagnosis of solitary pulmonary nodules with cavity

Y. Zhang, G. Zhang, H. Liu, **X. Lan**; Union Hospital, Tongji Medical College of Huazhong University of Science and Technology, Wuhan, CHINA.

**Aim:** To evaluate the feasibility of $^{18}$F-FDG PET/CT in the differential diagnosis of solid lung nodules with cavity. **Methods:** A total of 50 patients with solid pulmonary nodules with cavity (M: F = 40:10; mean age, 58.8y) were retrospectively analyzed. All patients should fulfill the following criteria: (a) single pulmonary solid nodule with cavity; (b) the size of the lesion should be more than 10mm, but less than 30 mm; (c) the final definitive diagnosis was determined by histopathology or the long-term follow-up of at least 9 months. The data obtained from CT, PET and PET /CT was analyzed separately. The SUVmax was obtained from PET images. The accuracy, sensitivity, specificity, positive predictive value (PPV) and negative predictive value (NPV) were calculated and compared with each different method. **Results:** Of the 50 patients, 23 patients were diagnosed as malignant tumor with histopathology, in which 9 patients were adenocarcinoma and 14 were squamous cell carcinoma. Benign pulmonary nodules were confirmed in the other 27 patients, with lung abscess (n=14) and pulmonary tuberculosis (n =13). The sensitivity, specificity, accuracy, PPV and NPV for CT in the diagnosis of benign and malignant lung nodules with cavity were 82.6%, 74.0%, 78.0%, 67.9% and 83.3%, respectively, and 95.0%, 44.4%, 68.0%, 59.4% and 92.3%, respectively, for PET. PET/CT had better diagnostic performance, and the values could reach 95.6%, 92.5%, 94.0%, 91.7% and 96.2%, respectively. When SUVmax 2.5 was chosen as a cutoff, the diagnostic performance were 100.0%, 7.4%, 50.0%, 47.9% and 100.0%, respectively, which showed the lowest specificity and accuracy among all the Methods. The accuracy of PET/CT was significant higher than that of either CT or PET alone (P<0.01). **Conclusion**: $^{18}$F-FDG PET has high false positive rate in differential diagnosis of benign and malignant solitary pulmonary nodules with cavity. SUmax 2.5, which was commonly used as an indicator for benign and malignant tumor, was not an optimal cutoff in this group of patients with solid lung nodules with cavity. This suggested that SUV should be carefully interpreted in areas with a high incidence of tuberculosis. The combination of PET and CT, the metabolism and morphological analysis, is helpful to improve the diagnostic accuracy of the lesions. Supported by China National 863 program (2008AA02Z426)

P40-1 - Sunday, Oct. 20, 16:00 - 16:30, Poster Exhibition Area

## Oncology Clinical Science: Oesophageal

## P259

### FDG-PET/CT imaging to monitor the response of esophagus cancer to proton-beam therapy

**Y. Nakagami**[1], T. Kobayashi[1], T. Ogawa[1], T. Hara[2], M. Satake[1]; [1]National Cancer Center, Chiba, JAPAN, [2]Fukushima Medical University School of Medicine, Fukushima, JAPAN.

Aim: Proton-beam therapy (PBT) is a promising modality for the management of esophagus cancer. Proton-beam therapy appears to provide distinct therapeutic advantages over conformal x-ray therapy in sparing organs at risk when treating esophageal cancer. These advantages are based on the fundamental physical dose distribution of the proton-beam. However, cases with extended esophageal lesions or with distant regional lymph node metastases are hard to treat with conventional PBT with a single isocentric field. The goal of this study was to evaluate [18F] fluorodeoxyglucose (FDG)-positron emission tomography (PET)/computed tomography (CT) for the detection of persistent disease and recurrence after proton-beam therapy in esophagus cancer. Materials and Methods: Posttreatment FDG-PET/CT was performed in 10 patients on several weeks after proton therapy. FDG-PET/CT was visually analyzed for the entire patient group. The contrast-enhanced CT was separately analyzed blinded to the results of FDG-PET/CT and classified as negative or positive for residual disease. Pathologic findings and clinical follow-up data were served as the reference standard. If there was possibility of invasion of esophagus cancer to other organ before proton-beam therapy, a 3D multi planar reconstruction contrast-enhanced CT was additionally performed. Results and Conclusions: Follow-up data were available for all 10 patients. Regarding the detection of residual disease, the overall sensitivity of FDG-PET/CT was slightly lower than contrast-enhanced CT. The overall specificity of FDG-PET/CT was higher than contrast-enhanced CT. The accuracy of FDG-PET/CT was higher than contrast-enhanced CT. However, a 3D multi planar reconstruction contrast-enhanced CT excelled in evaluating the staging of the tumor than FDG-PET/CT. The metabolic-anatomic information from FDG-PET/CT provided the most accurate assessment for treatment response after the conclusion of proton-beam therapy in esophagus cancer. FDG-PET/CT excelled by a higher specificity, accuracy and overall diagnostic performance than CT imaging alone. A 3D multi planar reconstruction contrast-enhanced CT was useful for evaluating the staging of the tumor in comparison with FDG-PET/CT. These results support a potential clinical role of FDG-PET/CT in the early assessment of therapy response after proton-beam therapy in esophagus cancer.

## P260

### Prognostic Value of Metabolic Tumor Volume Measured by 18F-FDG PET/CT in Esophageal Cancer Patients

**C. Soydal**, C. Yuksel, O. N. Kucuk, I. Okten, E. Ozkan, B. Doganay Erdogan; Tip Fakultesi, Ankara, TURKEY.

**Aim** In this study, we aimed to explore the prognostic importance of preoperative metabolic tumor volumes defined by 18F-FDG PET/CT in esophageal cancer patients. **Material and method** 22 patients who have histologically proven stage IIA-III esophageal cancer and underwent 18F-FDG PET/CT for preoperative staging of disease were included to the study. After 18F-FDG PET/CT, all the patients underwent surgery within 4 weeks period. Patients have been followed up until dead or 15th Sept 2012. Dates of dead were recorded for survival analysis. During evaluation of 18F-FDG PET/CT images, metabolic tumor volumes were calculated by drawing the isocontour region of interests from all visually positive FGD uptake lesions. **Results** 22 patients (14M, 6F; mean age: 65.1±8.4, min-max: 48-80) were underwent 18F-FDG PET/CT for preoperative staging of esophageal cancer. Preoperative diagnosis was squamous cell and adeno cancer in 17(%77) and 5(%23) patients, respectively. Location of primary tumor is distal, proximal and mid-esophagus in 12(%54), 5(%22) and 3(%13) patients, respectively. Primary tumor of all the patients were FDG avid (mean SUVmax: 18.85±7.0; min-max:5.5-35.1). Additionally, 18F-FDG uptake was seen in mediastinal lymph nodes in 13 patients (5.45±8.15; min-max: 2.6-29.9). Mean metabolic tumor volumes of primary esophageal lesions were calculated as 8.77±8.46cm$^3$ (min-max: 2.3-34.2). Mean MTV of lymph nodes was 2.44±1.01cm$^3$ (min-max: 0.4-3.6). Mean total metabolic tumor volume was calculated as 9.99±8.58cm$^3$ (min-max: 2.3-27.3). 10 patients died during 447±121 days follow-up period. Mean survival time was 11.9±1.5 (95%CI: 8.99-14.74) for entire patient group. Total metabolic tumor volume had significant effect on survival (p=0.045) according to Cox proportional hazards regression analysis. One unit increase in TLV caused 1.1 (95%CI: 1.003-1.196) fold increase in hazard, at any time. Conclusion Definition of preoperative metabolic tumor volume is a prognostic value in the prediction of postoperative survival times. Patients who have higher preoperative metabolic tumor volumes could be good candidates for more aggressive chemo-radiation therapy regiments. Review of Discrepancy in Reports: A Three year experience Objective: Discrepant reports can lead to suboptimal patient management. We reviewed discrepant reports with the objective of analyzing the underlying causes and to hence improve the process. Methods: For 3 years, from 2010-2012, 23 discrepant reports were brought to our notice by referring physicians, multidisciplinary review meetings, tumor boards or nuclear medicine physicians. Each discrepant report was then reviewed by a joint committee comprising of 3 nuclear medicine physicians. These reports were categorized as non sustainable if no error was identified, trivial when an error with no impact on the patient management was identified or significant when an error impacted on patient management was dentified Results: No error was identified in nine cases while 14 had errors. Ten cases had errors with no impact on patient management while in four cases the errors could have had an impact on patient management. Multiple causes of errors were identified in 11 of the 14 patients. Most common cause of errors was interpretation error (6/14) followed by failure to correlate with other imaging modalities or biochemical tests (5/14) and technical errors (5/14). Referral errors were identified for 3 patients. Additional checks and guidelines for reporting were implemented. **Conclusion**: Review of discrepant reports helps to identify the underlying causes of errors and hence to improve the process by setting up appropriate checks and reviews.

## P261

### A systematic review of the predictive value of $^{18}$FDG-PET in esophageal and esophagogastric junction cancer after neo-adjuvant chemoradiation on the survival outcome stratification

**P. Schollaert**[1], R. Crott[2], C. Bertrand[1], L. D'Hondt[1], T. Vander Borght[1], B. Krug[1]; [1]Univ. Catholique de Louvain - CHU UCL Mont-Godinne Dinant, YVOIR, BELGIUM, [2]Univ. Catholique de Louvain, Brussels, BELGIUM.

**Aim:** Radical surgery preceded by neoadjuvant chemoradiation or chemotherapy is most common approach to treating patients with advanced esophageal cancer. Only 40% to 50% of the patients respond to neoadjuvant chemoradiation. Quality of life and survival must be balanced against the toxicity of this neoadjuvant treatment as well as surgical mortality and morbidity. A based response

stratification based on non-invasive parameters might help in selecting the appropriate treatment for an individual patient We studied the predictive value of $^{18}$FDG-PET for assessing disease-free (DFS) and overall survival (OS) in advanced esophageal and esophagogastric junction cancer. **Methods:** A literature search (PUBMED/MEDLINE, EMBASE, Cochrane) from 1966 until April 2012 was performed to identify full papers with $^{18}$FDG-PET and survival data, using indexing terms and free text words. Studies with >10 patients, presenting sequential or at least one post-treatment $^{18}$FDG-PET data and Kaplan-Meier survival curves with >6 months median follow-up period were included. We performed a meta-analysis for disease-free survival (DFS) and overall survival (OS) data using the hazard ratio (HR) as outcome measure. Sources of study heterogeneity were also explored. **Results:** We identified 26 eligible studies including a total of 1544 patients (mean age 62 years, 82% males). The TNM distribution was as follows: stage I 7%, II 24%, III 53% and IV 15%. The pooled HRs for complete metabolic response versus no response were 0·51 for OS (95%CI, 0·4 to 0·64; P<0·00001) and 0·47 for DFS (95%CI, 0·38 to 0·57; P<0·00001), respectively. No statistical heterogeneity was present. To explore sources of clinical heterogeneity we also realised subgroup and regression analyses. Taken into account the moderate correlation between OS and DFS (ρ= 0·54), we used joint bivariate random regression model. These analyses did not show a statistically significant impact of study characteristics and PET modalities on the pooled outcomes. **Conclusion** Despite methodological and clinical heterogeneity, complete metabolic response on $^{18}$FDG-PET is a significant predictor of long-term survival outcomes

P41-1 - Sunday, Oct. 20, 16:00 - 16:30, Poster Exhibition Area

## Oncology Clinical Science: Liver

### P262

### Correlation of total lesion glycolysis (TLG) and tumor marker in liver metastases in the follow up of colon rectal cancer.

**C. Gstettner**, S. Kerschbaumer, K. Köfer, D. Heber, R. Aigner; Medical University Graz,Departement of Radiology, Division of Nuclear Medicine, Graz, AUSTRIA.

Aim: TLG is a measure of metabolic tumour activity. We want to investigate the correlation of this $^{18}$F- FDG parameter and the tumor marker. Materials and Methods: We investigate 80 colon rectal cancer patients in the follow up. Every patient underwent a surgical operation and adjuvant chemotherapy. In the follow up the tumour marker CEA increased and a $^{18}$F- FDG PET-CT was performed (GE, Discovery ST). We only enrolled patients with pathological tracer up take in the liver and without further metastases in the PET-CT results. Patients with adjuvant chemotherapy less than 2 month before the PET-CT were excluded. The functional tumor volume (VF) of the liver metastases was determined using a standard uptake value (SUV) thresholding method. The normal liver SUVmax was set as a threshold value. Tumor contours that traced the areas of increased F18 FDG uptake above the liver maximum SUV were drawn in each image slice and summed for the entire data set, thereby defining the functional tumor volume (VF). The total lesion glycolysis (TLG) was determined by multiplying the SUVmax in the tumor by the functional tumor volume (VF). In cases of more than one liver metastases TLGs were added. The Pearson correlation coefficient of TGL and the tumor marker was calculated. Results In this retrospective study in 12/80 patients (7 men and 5 women, mean age 62 years) liver metastases were detected. In 7/12 patients one solitary, in 4/12 patients three and in 1/12 four liver metastases were detected. The FTV ranged from 6.8 to 224cm³, the SUVmax ranged from 4.8 to 11.4 g/cm³ and the TGL of the liver metastases ranged from 59.3 to 1759g. The tumor marker CEA ranged from 6- 95ng/ml. The Pearson correlation coefficient of TLG and CEA was minus 0.37. Conclusion: In this study we detect a weak negative correlation of TLG and the tumor maker CEA. Despite the small number of patients we are able to demonstrate that liver metastases with a higher TGL generally have a smaller increase of CEA. This incidence could be caused by a delayed immune system reaction. These results have to be proven with lager clinical studies.

### P263

### Oncologic diagnosis of liver tumors using [18F]-fluoroacetate PET/CT as compared to [18F]-fluorodeoxyglucose PET/CT. Initial experience.

**T. Higashi**[1], R. Nishii[2], S. Kagawa[1], M. Takahashi[1], Y. Kishibe[1], H. Yamauchi[1], K. Matsumura[3], M. Zaima[4], K. Takemoto[5], E. Hatano[5]; [1]Shiga Medical Center Research Institute, MORIYAMA, SHIGA, JAPAN, [2]Miyazaki University, Miyazaki, JAPAN, [3]Department of Gastroenterology, Shiga Medical Center, MORIYAMA, SHIGA, JAPAN, [4]Department of Surgery, Shiga Medical Center, MORIYAMA, SHIGA, JAPAN, [5]Graduate School of Medicine, Kyoto University, Kyoto, JAPAN.

[Objective] Although [18F]-FDG is a useful oncologic PET tracer, FDG uptake is known to be low in a certain type of hepatocellular carcinoma. [18F]-fluoroacetate (FACE) is an [18F] fluorinated acetate, which is known to be metabolically trapped in TCA cycle and is expected to be a promising oncologic PET tracer. The aim of this study was to evaluate the usefulness of FACE as an oncologic PET tracer in the diagnosis of liver tumors, compared with FDG. [Methods] Eight patients with liver tumor (age: 71+/-8 y.o.; 4 male and 4 female) were included. We performed whole body static PET/CT scan twice using FACE and FDG on each day respectively. Qualitative analysis and quantitative analysis of tumors (4 hepatocellular carcinoma/ HCC, 1 cholangiocellular carcinoma/ CCC, 3 metastatic tumors from colon cancer and P-NET) was performed using SUVmax and TNR (Tumor-to-normal Liver Ratio). [Results] FDG uptake of liver tumors (SUVmax: 6.1+/-3.9, TNR: 2.4+/-1.5) was significantly higher than that of FACE (2.7+/-0.6, 1.5+/-0.4), while normal physiological uptake of FACE (SUVmean: 1.8+/-0.2) was lower than that of FDG (SUVmean: 2.5+/-0.2). In qualitative analysis, FDG was positive in 3 tumors (2 HCC, 1 CCC) and negative in the other 5 tumors, while FACE was also positive in 3 tumors which were the same tumors with positive FDG uptake. Pathological results showed that a case of moderately differentiated HCC showed high FACE uptake (SUVmax=3.0), while FDG also showed high uptake (SUVmax=5.7). [Conclusions] Tumor FACE uptake was positive in three patients with HCC and CCC, but the uptake pattern was similar to FDG. Further evaluation was needed.

### P264

### Evaluation of regional liver function by Tc-99m GSA SPECT or SPECT/CT before and after percutaneous transhepatic portal embolization, Preliminary study

**K. Suzuki**, M. Yoshimura, T. Hashimoto, T. Saguchi, K. Saitou, K. Kasuya, K. Koizumi; Tokyo Medical University Hospital, Tokyo, JAPAN.

Aim: Percutaneous transhepatic portal embolization (PTPE) is the preliminary procedure for the candidates of major hepatic resection to produce regenerative hypertrophy in the non-resected part of the liver. Sometimes verification of the regenerative hypertrophy due to PTPE and prediction of the postoperative hepatic functional reserve are estimated by the liver volume obtained by CT images. But the discrepancy has been described between postoperative liver functional recovery and volumetric liver regeneration. Tc-99m galactosyl human serum albumin (GSA) scintigraphy is beneficial examination for hepatic function, because it can evaluate regional liver function. This time we performed Tc-99m GSA SPECT or SPECT/CT before and after PTPE for right branch of portal vein and accessed the effect of it. Materials and Methods: Three patients who are to undergo right hepatectomy were assessed. They were all non-cirrhotic, with cholangiocarcinoma (1), intraductal papillary neoplasm of bile duct (IPNB)(1), and metastatic liver tumor from colon cancer (1). PTPE for right branch of portal vein was performed a month prior to surgery. Tc-99m GSA scintigraphy was performed just before and a month after PTPE. We drew cutting line on SPECT or SPECT/CT imaging to divide into right and left lobe liver, and calculated the function of each lobe. Results: We used LU15 (liver uptake rate of radioactivity at 15 minutes after injection) as the parameter of liver function. The mean value of LU15 was left lobe / total liver: 7.8 / 24.8 before PTPE, and was 12.0 / 24.9 after PTPE. The percent increase value of left lobe was 54% with LU15. As for the liver volume, left lobe / total liver(cm3): 483 / 1411 before PTPE, and was 625/ 1281 after PTPE. The percent increase value of left lobe was 30% on CT volume images. All cases were confirmed that both the function and the volume of the left lobe increased. Moreover the safe outcome of right hepatectomy was achieved. Conclusion: The outcome of PTPE was assessed by Tc-99m GSA SPECT or SPECT/CT in view of the function and the volume. In these cases, the increase of the function was more obvious than of the volume. The resectability indices using Tc-99m GSA scintigraphy are expected for the verification of PTPE effect and preoperative evaluation of the limitation of hepatic resection.

P42-1 - Sunday, Oct. 20, 16:00 - 16:30, Poster Exhibition Area

## Oncology Clinical Science: Urogenital

### P265

### Characterization of lipid-rich adrenal tumors by FDG PET/CT: hormone-secreting or not?

**K. Takanami**, A. Arai, T. Kaneta, S. Takahashi; Tohoku University, Graduate School of Medicine, Sendai, JAPAN.

Purpose: The purpose of this study was to evaluate the diagnostic ability of FDG PET/CT for the characterization of lipid-rich adrenal tumors. Methods: This study included 44 lipid-rich (CT number < 10HU) adrenal tumors 2 cm or larger in diameter in 43 patients who underwent FDG PET/CT. The diagnoses were based on endocrine examinations including adrenal venous sampling and subsequent surgical resection or biological and morphological imaging follow-up during at least 6 months. FDG uptake of the adrenal tumors were evaluated semi-quantitatively using maximum standardized uptake values ($SUV_{max}$) and a ratio of adrenal SUVmax compared to liver $SUV_{max}$ ($SUV_{ratio}$). Statistical difference was assessed using Mann-Whitney test, and p value < 0.05 was set as statistically significant. Results: The

lipid-rich adrenal tumors were proved to be 20 non-hormone-secreting tumors (19 adenomas and 1 myelolipoma) and 24 hormone-secreting tumors (5 cortisol-producing adenomas, 4 subclinical cortisol-producing adenomas, 12 aldosteron-producing adenomas, and 3 both cortisol and ardosteron producing adenomas). There was no patient with pheochromocytoma nor malignant adrenal tumor. Values are expressed as median and range. $SUV_{max}$ of the hormone-secreting tumors (2.7 , 1.3 - 8.3) was higher than that of the non-hormone-secreting tumors (2.3, 1.5 - 3.3) ($p < 0.05$). Similarly, $SUV_{ratio}$ of the hormone-secreting tumors (0.83, 0.49 - 3.10) was higher than that of the non-hormone-secreting tumors (0.73, 0.54 - 0.95) ($p < 0.05$). Meanwhile, there was no significant difference in tumor diameter between the two groups ($p = 0.8$). The sensitivity, specificity, PPV, NPV, and accuracy of FDG PET/CT for differentiating hormone-secreting tumors from non-hormone-secreting tumors were 66.7, 75.0, 76.2, 65.2, and 70.5 for the cutoff $SUV_{ratio}$ of 0.76, and 33.3, 100, 100, 55.6, and 63.6 for the cutoff $SUV_{ratio}$ of 1, respectively. Conclusions: The result of this study indicates that FDG PET/CT may be useful for the characterization of lipid-rich adrenal tumors. A lipid-rich adrenal tumor presenting increased FDG uptake compared with that of liver is likely to be a hormone-secreting adenoma.

## P266

### How helpful is Imaging of Testicular Carcinoma with 18F-FDG PET/CT?

**K. Nikoletic**[1], J. Mihailovic[1], D. Srbovan[1], R. Avramovic[2], E. Matovina[1]; [1]Institute of Oncology of Vojvodina, SREMSKA KAMENICA, SERBIA, [2]Clinical Center of Vojvodina, Novi Sad, SERBIA.

Aim: is to assess the role of 18F-FDG PET/CT in patients with testicular carcinoma. Materials and Methods: From January 2011 to March 2013, we performed 740 PET/CT studies, among them were 21 patients (aged 23-54, mean 34.9±2) with testicular carcinoma which were further analyzed. Histology type of cancer included: seminoma (7), embryonal carcinoma (3), Yolk sac tumor (2), teratoma (3), choriocarcinoma (1) and mixed forms of more then 1 histological type (5). Before PET/CT study, 20 patients were operated and 1 was treated with chemotherapy. Indications to perform PET/CT study was: suspicious CT or MR finding (14), elevated tumor markers (5), or follow-up (2). PET/CT imaging results were compared to histopathological results, other imaging modalities or follow-up. Results: PET was positive in 6, negative in 14 and equivocal in 1 patient. All positive foci were located in lymph nodes: abdominal lymph nodes (3), inguinal lymph nodes (1), mediastinal and neck nodes (1) and simultaneously abdominal and inguinal (1) with max SUV values from 4.5 to 11.3. In further follow up, only 1 patient (negative PET) was lost for data analysis. Out of remaining 20 patients, 3 with positive PET/CT result were operated: in 2 histopathology showed no cancer cells (granulomatous tissue in mediastinal lymph nodes and benign abdominal lymph nodes) and in 1 patient metastases were confirmed in retroperitoneal lymph nodes. Three patients with positive finding were treated with chemotherapy. Among patients with negative PET/CT, 10 were considered to be disease-free, 2 showed elevation of tumor markers and in 1 follow-up showed increased retroperitoneal lymph nodes on CT that were considered metastatic. Conclusion: Overall sensitivity of 18F-FDG PET/CT as imaging modality in testicular carcinoma was only 57.1% and specificity 83.3%. Among different histological types, seminoma showed highest sensitivity 100%, while embryonal cell carcinoma and Yolk sac tumor had lowest specificity, mostly due to presence of granulomatous tissue or inflammation. The role of PET/CT in imaging of testicular carcinoma should be further analyzed in greater number of patients.

## P267

### A 18-fluoro-Choline PET/CT pitfall: incidental Leydig cell tumor in patient with recurrent prostate cancer disease

**A. Maffione**[1], M. Cimitan[2], M. Hodolic[3], E. Borsatti[2], S. Chondrogiannis[1], M. Marzola[1], L. Rampin[1], D. Rubello[1]; [1]S.M. della Misericordia Hospital, Rovigo, ITALY, [2]National Cancer Institute (IRCCS) - CRO Aviano, Aviano, ITALY, [3]University Medical Centre Ljubljana, Ljubljana, SLOVENIA.

We report a case of 62 year old patient referred to fluorine-18-choline (FCH) PET/CT for biochemical recurrence of prostate cancer showing a second non-prostate malignant tumor. After a radical prostatectomy, confirming a well-differentiated prostate tumor (Gleason score 2+2), serum PSA levels remained below 0.2 ng/ml for 5 years. Then serum PSA level increased to 2.49 ng/ml, suspicious for prostate cancer recurrence. Bone scan and CT were negative for bone and lymph node metastases, therefore the patient was referred to FCH PET/CT. PET/CT scans demonstrated a focal Choline uptake (SUVmax. 9.9) in the right testis thought to be metastasis from prostate cancer. On testis removal, a Leydig cell tumor of 2.5 cm in diameter was found. After orchiectomy, PSA increased further to 4.44 ng/ml, but a following FCH PET did not show pathological findings consistent with prostate cancer relapse. The final conclusion was that PSA increased due to local recurrence of prostate cancer, and the patient was referred for local salvage radiotherapy. This patient had a low-risk to develop distant recurrence, since Gleason score was 2+2 and PSA relapsed 5 years after prostatectomy. However the possibility that prostate cancer may spread in the testis and penis had been reported in the literature. FCH PET/CT has been used in a variety of malignancies other than prostate cancer, as shown by a recent systematic review article on 18F-FCH demonstrating tracer uptake in brain tumors, head and neck tumors, thoracic tumors (lung and mediastinal), hepatocellular carcinoma, gynecologic malignancies (including breast tumors), bladder and upper urinary tract tumors, and bone and soft tissue tumors.

## P268

### Evaluation of FDG-PET/CT in re-staging and therapy response monitoring of penile squamous cell carcinoma

**S. M. Schwarzenböck**[1], A. Sponholz[1], J. Kurth[1], C. Protzel[2], M. Heuschkel[1], A. Erbersdobler[3], O. W. Hakenberg[2], B. J. Krause[1]; [1]Department of Nuclear Medicine, University Medical Centre of Rostock, Rostock, GERMANY, [2]Department of Urology, University Medical Centre of Rostock, Rostock, GERMANY, [3]Institute of Pathology, University Medical Centre of Rostock, Rostock, GERMANY.

Aim Evaluation of F-18 FDG PET/CT for re-staging penile squamous cell carcinoma after primary local surgery with or without inguinal/iliacal lymphadenectomy/chemotherapy and therapy response monitoring after adjuvant chemotherapy. Methods 13 patients (mean age 62 years, range 43-77 years) with penile squamous cell carcinoma were referred for F-18 FDG PET/CT for re-staging before adjuvant chemotherapy. 6/13 patients had a follow up FDG PET/CT after adjuvant chemotherapy, 3/6 patients had more than one follow up PET/CT. SUVmax and mean of each lesion was defined using VOIs comparing 4 different software tools (Hermes® Medical Hybrid Viewer 2.0, Siemens Syngo True D®, Rover® abx GmbH (Threshold only and automatic)). Results: Before adjuvant chemotherapy in 9/13 patients (32 lymph nodes, 2 lung metastases, 6 local penile lesions) no significant difference was shown in SUVmax and SUVmean between the 4 software tools. In 4/13 patients no focal lesions were found. In follow up PET/CT after adjuvant chemotherapy (and additional lymphadenectomy in 2 patients) in 6/13 patients 15 nodal lesions, 2 lung metastases and 2 local penile lesions showed decreases, 6 nodal lesions showed increase of FDG uptake. In nodal metastases Siemens Syngo True D® and Hermes® Medical Hybrid Viewer 2.0 showed a significant difference before and after adjuvant chemotherapy in SUVmean ($p = 0.006$ and $p = 0.038$, respectively), Rover® abx GmbH (Threshold only and automatic) showed a significant difference in SUVmax ($p = 0.028$ and $p = 0.031$, respectively). Conclusion: FDG PET/CT seems to be a valuable tool for re-staging patients with penile squamous cell carcinoma especially to identify lymph node metastases. In re-staging before adjuvant chemotherapy the 4 software tools performed equally. Therapy response monitoring after adjuvant chemotherapy was feasible with FDG as imaging biomarker. Irrespective of the software tool used, there was a decrease of FDG uptake after chemotherapy in nodal, lung and local penile lesions.

P43-1 - Sunday, Oct. 20, 16:00 - 16:30, Poster Exhibition Area

## Oncology Clinical Science: Prostate

## P269

### Staging Patients with High Risk Prostate Cancer: 18F-methylcholine PET/CT Can Not Replace PLND

**K. J. van Os**, E. J. Trip, H. H. E. van Melick, J. F. Verzijlbergen, M. M. C. van Buul; St. Antonius Hospital, Nieuwegein, NETHERLANDS.

Purpose The incidence of (advanced) prostate cancer (PC) is increasing. In patients with high risk prostate cancer, lymph node (LN) metastasis most commonly involve the internal iliac, external iliac, or obturator nodes. For LN staging, pelvic lymph node dissection (PLND) is the gold standard. In this study, it was evaluated if 18F-methylcholine positron emission tomography/ computed tomography (FCH PET/CT) can replace invasive LPLND. Materials and Methods A consecutive series of patients with high risk PC according to D'Amico criteria (or cT3, or PSA>20, or Gleason ≥8), were prospectively included from May 2011 - July 2012. All patients underwent routinely laparoscopic lymph node dissection (LPLND) after FCH PET/CT. Acquisition started 5 min after injection of the radiotracer. The blinded reviewed imaging results were compared with histology. Sensitivity, specificity, positive- and negative predictive value (PPV, NPV) of FCH PET/CT were calculated. Results Sixteen patients were included with a mean age of 69 y (60-77 y), mean PSA 42,9µg/l (2.8-363µg/l), mean Gleason score 8,2, and a chance of ≥ 15% to have disseminated disease according to the MSKCC nomogram. Sensitivity, specificity, PPV and NPV were calculated as 63%, 88%, 83%, and 70% respectively. In none of the patients, distant metastases were found in this early stage of disease. Conclusion In patients with high risk prostate cancer, 18F-Methylcholine PET/CT can not replace laparoscopic pelvic lymph node dissection in the staging procedure. The results are comparable with studies in literature in which FCH PET/CT was

acquired 60 min.p.i. This suggests that bladder activity is not the cause of the low sensitivity of FCH PET/CT in lymph node staging.

## P270

### PET-guided radiotherapy planning in prostate cancer patients

**E. Lopci**, F. Alongi, M. Rodari, E. Villa, M. Scorsetti, A. Chiti; Humanitas Clinical and Research Center, Rozzano (MI), ITALY.

**Aim**: In the era of image-guided radiotherapy (IGRT), PET has grown as a relevant, and sometimes irreplaceable tool, for tumor delineation in several types of cancer. Limited evidence concerns however the use of Choline-PET in prostate cancer patients, therefore in our study we aimed assessing the impact of this imaging modality in treatment planning of patients eligible for radiotherapy (RT). **Materials and Methods**: For the study we prospectively enrolled 23 consecutive patients (mean age 71years, range 58-84) referred to our department for radiation therapy planning with radical intent (n=3), as adjuvant to surgery (n=1), as savage therapy (n=18) or with palliative intent (n=1). Patient were submitted to a single-day protocol, including dedicated CT scan of the pelvis and Choline-PET. Gross-tumor volumes (GTV) , clinical-tumor volumes(CTV), planning-tumor volumes (PTV) and organs at risk (OAR) were outlined on CT with Eclipse Varian Medical System software, whereas GTV-PET was defined as areas with pathologic uptake and contoured with PETVCAR software on Adwantage GE workstation. **Results**: According to the imaging findings, in 17/23 patients the indication for radiation therapy was confirmed: in 4 cases RT was limited to prostatic bed, in 8 cases RT was extended to the entire pelvis, and in 5 patients treatment was performed on extra-pelvic organs. In 26% of cases (6/23), either a negative scan or evidence of extensive disease at PET addressed patients to other treatment options. Overall Choline-PET determined a modification in patient management in 61% of cases (14/23), and of these in 7 patient the impact was exert directly in treated volumes, which were consequently extended. A specific boost in PET-positive lesions was given in total to 41% of irradiated patients (7/17). **Conclusion**: As expected, Choline-PET can have a significant impact on RT planning of prostate cancer patients, by determining a change in therapeutic decision in up to 61% of cases

## P271

### High risk and very high risk prostate cancer and the role of choline PET/CT at initial staging

**L. Evangelista**[1], F. Zattoni[2], A. Guttilla[2], A. Cervino[1], M. Gregianin[1], M. Burei[1], F. Zattoni[2], G. Saladini[1]; [1]Istituto Oncologico Veneto I.R.C.C.S., Padova, ITALY, [2]University of Padova, Padova, ITALY.

**Purpose**: To prospectively evaluate the role of 18F-fluorocholine (FCH) positron emission tomography (PET)/computed tomography (CT) in the preoperative staging of patients with prostate cancer at high and very high risk of recurrence, according to National Comphrensive Cancer Network (NCCN) classification (version 2.2013). **Materials and Methods**: 30 patients with prostate cancer (median age: 67 years; range: 57-85yrs) and very or very high risk of recurrence (cT3-T4 or Gleason score ≥ 8 or PSA value≥ 20 ng/mL) were prospectively enrolled between July 2010 and December 2012. Five patients were subsequently excluded. All patients underwent FCH PET/CT before surgical or other treatments, although seven subjects were already on hormonal therapy (HT) with LH-RH analogues.Imaging was performed with an integrated PET/CT system after injection of 3MBq FCH per kilogram of body weight with acquisition of whole-body images. In 11 patients, radical prostatectomy with extended pelvic lymph node dissection was performed, twowere treated bythe association of external radiation therapy and HT, 10 started HT and two continued on going HT. Statistical analysis was performed on a per-patient basis. **Results**:out of 25 patients, 11 (44%) had a positive PET/CT finding in prostate gland, seven (28%) in prostate and loco-regional lymph nodes, three (12%) in prostate, lymph nodes and bone and in four (16%) cases only in prostate and bone. The median SUVmax in prostate gland was 7.82 (range 3.01-17.91), and the lowest value was found in a patient undergoing HT. The SUVmax of lymph nodes ranged between 1.51-15.89 and the value was correlatedwith the size of lesions($r=0.93$; $p<0.01$). In patients undergoing surgical treatment (n=11), a per-patient analysis revealed that the sensitivity, specificity, positive and negative predictive values and accuracy of FCH PET/CT in the detection of malignant lymph nodes were 100%, 75%, 60%, 100% and 82% respectively. Two false positive lymph nodes showed a SUVmax<2.5 and a diameter <10mm. In sevenpatients were detected bone metastases. Early bone marrow infiltration was detected in onepatient. FCH PET/CT led to a change in therapy in 40% of high and very high-risk patients. **Conclusion**: FCH PET/CT seems useful in the evaluation of patients with prostate cancer who are at high and very-high risk for distant metastases, and it could be used to preoperatively for excludingdistant metastases and for tailoring the best treatment approach.

## P272

### Clinical impact of PET/CT with 18F-FDG and 18F-fluorocholine in the staging of patients with prostate adenocarcinoma

**M. Navarro-Pelayo Lainez**, A. Rodriguez-Fernandez, R. Sanchez-Sanchez, M. Gomez-Rio, W. Valdes, M. Martinez-Carrillo, F. Vazquez-Alonso, J. Llamas-Elvira; Virgen de las Nieves University Hospital, Granada, SPAIN.

**OBJECTIVE:** In prostate cancer, an accurate characterization of the tumour and staging of disease are of great importance in choosing the appropiate therapeutic and surgical management. Morphological imaging techniques (CT and MRI) have no decisive role in the diagnosis of primary prostate cancer. Combined molecular and morphological imaging techniques may improve the diagnostic accuracy in prostate cancer. The role of 18F-FDG has been approved for imaging in several malignancies but its physiologic urinary activity can mask lesions adjacent to bladder. Choline is a substrate for the synthesis of cellular membranes that accumulates in prostate cancer. Therefore, the aim of our study was to evaluate the clinical usefulness of PET/CT with 18F-FDG and 18F-fluorocholine in assesing extra-prostatic disease during the staging of primary prostate cancer. **MATERIAL AND METHODS:** From June 2011 to January 2013 we prospectively evaluated 30 patients, all newly diagnosed with prostate adenocarcinoma and high-risk clinical and pathological features. All patients had CT and bone scan performed as conventional imaging techniques and were subsequently evaluated using 18F-FDG and 18F-fluorocholine, with a maximum interval of one month between them, using an hybrid PET/CT tomograph (Siemens Biograph 16, Knoxville, Milwokee). The scans were analyzed visually and semiquantitatively (SUVmax). All positive results were confirmed by other diagnostic procedures (imaging procedures and histopathology) and the negative results by follow up. **RESULTS:** Our study population showed a mean age 69.47 years old (± 8.60 S.D.), with an average PSA value: 41.17 (± 28.35 ng/ml), Gleason score from 6 to 9 and clinical stage T1c to T3. 24/30 patients (80%) were on androgen deprivation at the time of the PET/CT performance. 18F-fluorocholine-PET/TAC was positive for extra-prostatic fossa disease in 3 patients (10%), with an average SUVmax 13.27 (± 0.89 S.D.) and unsuspected by other diagnostic procedures. One of them showed lymph node metastases with 18F-FDG and 18F-fluorocholine and in 2 (6.67%) 18F-fluorocholine proved tumor activity not evidenced by 18F-FDG: in one case, lymph nodal malignancy and in another lymph nodal and distant metastases (bone lesions). All three aforementioned patients were under androgen blockade at the time of scanning. **CONCLUSION:** Our preliminary results suggest that 18F-fluorocholine can be useful as an "one stop diagnostic procedure" for the staging of primary high-risk prostate cancer, implying a change in the therapeutic approach and offering better results than 18F-FDG.

## P274

### Role of 18F-CHOLINE PET/CT in restaging and management of treated prostate neoplasm with PSA level rising up to7 ng/ml. A single site Lebanese Experience.

**M. Haidar**[1], T. KHOURY[2], M. JRIEGE[2], M. HADDAD[2], F. CHEHADE[3]; [1]Mount Lebanon Hospital, Lebanese University, Nuclear Medicine Department, Beirut, LEBANON, [2]Radiology Department, Beirut, LEBANON, [3]Nuclear Medicin Department, Beirut, LEBANON.

**Objective:** To evaluate the impact of 18F-CHOLINE PET/CT in restaging and management of prostate cancer with PSA level rising up to 7 ng/ml. Material and **Methods:** This retrospective study included 63 patients with a history of treated prostate cancer (status post radical prostatectomy or/and radiotherapy or/and hormonal therapy) and with PSA level rising up to 7 ng/ml. The PET/CT scan was performed immediately after injection of 18F-CHOLINE with dynamic acquisition at the pelvis followed by whole body scan 40-60 minutes later. All the PET/CT scans were evaluated for the presence of active disease within the prostate bed, pelvic, retroperitoneal and/or mediastinal lymph nodes, as well as other metastatic sites such as bone, lungs and liver. **Results**: PET/CT scan was negative in 21 patients (33%). There was positive uptake within the prostate bed in 22/63 pts (35%) which was only localized to the prostate bed in 9/63 pts (14%). There was active nodal disease in 25/63 pts (40%) and extra nodal disease in 19/63 pts (30%). One or more pelvic metastatic lymph nodes were detected in 17/63 pts (27%) which was only localized at the pelvis in 7 pts, retroperitoneal metastatic lymph nodes in 12/63 pts (19%) and mediastinal lymph nodes in 13/63 pts (21%). One or more bone lesions were identified in 18/63 pts (28%) with the most common locations being in the pelvis and lower spine. Lung metastasis was present in 1/63 pts (1.5%). Patients with localized recurrent disease (prostate bed and pelvic nodal metastasis) were treated by radiotherapy 16/63 pts (25%) and patients with multiple metastatic sites were treated by hormonal therapy and/or chemotherapy. Therefore, 18F-CHOLINE PET/CT played a major role in altering the therapeutic management. **Conclusion:** 18F- CHOLINE PET/CT detected local recurrent prostate cancer, loco- regional or distant nodal and extra nodal metastatic disease in patients with treated prostate cancer. This was noteworthy even in cases where PSA level elevation was inferior to7 ng/dl. It also altered the therapeutic management of patients by providing a more suitable treatment modality especially in patients with only pelvic recurrence.

## P275

### 18F-FCH-PET/CT in Prostate Cancer Patients

**A. Nikaki**, D. Kechagias, F. Vlachou, V. Fillippi, T. Pipikos, D. Savvidou, K. Dalianis, K. Gogos, R. Efthymiadou, V. Prassopoulos; DTCA Hygeia Department of PET/CT, Athens, GREECE.

**Purpose:** In this study we retrospectively examined the role of FCH-PET in restaging patients with prostate cancer. **Methods**: 25 patients with prostate cancer, who had previously received the appropriate treatment (surgery, tadiotherapy, hormonal blockade), were reported to our department for FCH-PET/CT due to elevated or increasing serum PSA levels. PET acquisition was performed at Siemens Biograph LSO PET/CT device and was initialized immediately after the administration of the radiopharmaceutical at the field of prostate where 3min images were acquired consecutively for 30 min. Whole body PET/CT was performed 60 min after FCH administration. Findings of PET were correlated with serum PSA values and were compared to those of at least one of the rest imaging procedures (CI: CT, MRI, Bone Scintigraphy) for osseous metastasis, with MRI for local recurrence and lymph node invasion. **Results**: Serum PSA, known for 24 patients, ranged between 0.02-48 ng/ml. All patients (18) who had serum PSA values >0.3 had a positive FCH-PET. Of those 2 had PSA <0.5 and another 5 had PSA <4. All patients with serum PSA < 0.3 but one had negative FCH-PET. Osseous metastasis: CI was positive in 4/25 cases, while PET was positive in 3/4. In 1/4, high density lesions in CT- negative bone scan did not accumulate FCH. CI was equivocal in 5 cases: PET was negative for 3/5 and positive (multiple lesions) for 2/5. CI was negative for 16, while PET was positive for 2/16 and negative for 14/16. Local recurrence (number of available MRI examinations 12): MRI was positive in 3 cases and so was FCH-PET, negative in 7 cases- in one of which PET was positive- and equivocal for 2, of which PET was negative for one and positive for one. Lymph node invasion (number of available MRI examinations 12): MRI was negative for lymph node invasion in 10 cases, of which PET was negative for 7 and positive for 3 (small <1cm lymph nodes). Both MRI and PET were positive in 1 case. In 1 case MRI was equivocal, while PET was negative. In one case PET revealed lymph nodes at the mediastinum, which proved to be second primary of the lung. **Conclusions**: FCH-PET/CT is a whole body imaging procedure promising in prostate cancer patients, especially in cases of biochemical relapse. Its major role relies in the evaluation of small sized lymph nodes, osseous disease and of equivocal findings in conventional imaging.

## P276

### Role of $^{18}$F-Choline PET/CT in detection of prostate cancer recurrence

**E. Skoura**[1], C. Giannopoulou[1], M. Skilakaki[2], G. Bartseas[1], D. Kyprianou[1], I. E. Datseris[1]; [1]Nuclear Medicine Department, Evangelismos General Hospital, Athens, GREECE, [2]Radiology Department, Evangelismos General Hospital, Athens, GREECE.

**Aim**: Aim of our study is the evaluation of the diagnostic value of $^{18}$F-choline PET/CT in detection of prostate cancer recurrence in patients with elevated PSA levels and negative or equivocal findings in conventional imaging (CT, MRI or bone scan). **Materials and Methods**: Between November 2011 and October 2012, 23 $^{18}$F-choline PET/CT scans were performed on 23 patients, with a mean age of 62.7±5.7 years old, with a history of prostate cancer and biochemical suspected recurrent disease. 20 of the patients had received radical prostatectomy, 3 chemotherapy, 6 external radiotherapy/brachytherapy, 6 hormonal therapy and 2 biphosphonate treatment. PSA levels ranged from 0.03 to >1000ng/ml. In all cases conventional imaging Methods (CT, MRI) were performed 10-30 days before PET/CT and had negative or equivocal findings. **Results**: Of the 23 $^{18}$F-choline PET/CT studies, 11 were positive (47.8%) and 12 negative (52.2%). On positive scans, the sites of recurrence located mainly in lymph nodes: iliac (7patients), inguinal (2), mediastinal (2), cervical (1), in bones (5), focal uptake in prostate (2), peritoneal implants (2), a pleural thickness (1), adrenal (1) and brain (1). In patients with a positive PET/CT scan the mean PSA levels were 191ng/ml (0,03 to >1000ng/ml) while in patients with a negative scan the PSA levels were 2.39ng/ml (0.05 to 7.5ng/ml) **Conclusions:** Our findings from this small cohort of patients suggest that $^{18}$F-choline PET/CT provides additional information and it is a useful imaging tool for the detection of prostate cancer recurrence in patients with elevated PSA levels but negative or equivocal conventional imaging findings.

## P277

### The potential value of FDG-PET/CT for staging of patients with biological high-risk prostate cancer: a surgical cohort study

**J. M. Beauregard**[1], A. C. Blouin[2], G. Rimac[2], A. Caron[2], C. Lemay[2], V. Fradet[2], Y. Fradet[2], L. Lacombe[2], T. Dujardin[2], R. Tiguert[2], F. Pouliot[2]; [1]Division of Nuclear Medicine, Department of Radiology, Université Laval, Quebec City, QC, CANADA, [2]Division of Urology, Department of Surgery, Université Laval, Quebec City, QC, CANADA.

**Aim:** Overall, $^{18}$F-fluorodeoxyglucose positron emission tomography/computed tomography (FDG-PET/CT) has a limited utility for staging of prostate cancer (PCa) due to the indolent behaviour and low uptake of most tumours. However, higher-grade PCa tend to exhibit higher FDG uptake and metastatic rate. We aimed to assess the potential value of FDG-PET/CT for staging of biological high-risk PCa in a surgical patient cohort. **Methods:** Of 54 consecutive patients with biopsy-proven biological high-risk PCa (biopsy Gleason sum >7) who were prospectively staged with FDG-PET/CT, 41 underwent surgery and were included in this analysis. FDG-PET/CT was read blinded to any clinical information other than the diagnosis of PCa. Visual score criteria for prostatic uptake was: 0) no definite focal uptake; focal uptake of 1) mild, 2) moderate (similar to liver), 3) intense, or 4) very intense level. Prostatic maximum standardized uptake value (SUVmax) was measured independently, with caution to exclude urinary activity. Suspicious extra-prostatic foci of FDG uptake were considered positive for metastases. Comparison was made with surgical results: pathological Gleason pattern (pGP), pathological Gleason sum (pGS), pathological T stage (pT) and lymph node histopathology. **Results:** Prostatic focal FDG uptake was found in 35 (85%) patients. Thirty-nine patients underwent radical prostatectomy. In only one of these patients the focus of mild uptake was in a prostatic lobe devoid of cancer. Statistically significant positive correlations were found between SUVmax and pGP (Spearman $r$=0.46;$P$=0.004), pGS ($r$=0.44;$P$=0.006) and pT ($r$=0.35;$P$=0.03), as well as between visual uptake score and pGP ($r$=0.58;$P$=0.0001), pGS ($r$=0.50;$P$=0.001) and pT ($r$=0.32;$P$=0.04). Eighteen (90%) of 20 patients with an uptake score of 0 or 1 were downstaged to pGS 6 or 7, or had a primary pGP of 3. Conversely, 5 (71%) of 7 patients with a score of 3 or 4 had a pGS of 8 or 9. All patients underwent pelvic lymph node dissection. Suspicious FDG-avid lymph nodes were detected in 3 of 11 patients with nodal metastases. The sensitivity, specificity, positive and negative predictive values of FDG-PET/CT for nodal metastasis were 27%, 100%, 100% and 78%, respectively. **Conclusions:** Our results suggest that, among patients with biological high-risk PCa at biopsy, FDG-PET/CT may help to prospectively identify patients with poorer pathological features. Although FDG-PET/CT lacks sensitivity for nodal metastasis detection, it remains highly specific. Both increased FDG uptake in primary PCa and the presence of FDG-avid nodal metastasis may have prognostic implications and could be useful to personalize patient management.

## P278

### 18F-choline PET/CT detection of prostate cancer recurrence related to PSA level.

**V. Ptacnik**, J. Kubinyi; Department of Nuclear Medicine, First Faculty of Medicine, Charles University in Prague and General University Hospital Prague, Prague, CZECH REPUBLIC.

Aim: Prostate cancer is the most common neoplasm in men. Although significant part of prostate cancers is diagnosed in early phase and radical treatment is possible, the risk of disease recurrence is quite high. Mainly in patients with less differentiated cancer and advanced local tumor. PSA level is sensitive marker to assess the recurrence. For further treatment the localization of the recurrence is important. PET/CT with $^{18}$F-choline (FCH) seems to be useful imaging technique for recurrence localization. FCH PET/CT is mentioned as a sensitive method for bone metastases detection and also works well in lymph nodes assessment. Some authors present increasing sensitivity of FCH PET/CT according to PSA level. This poster presentation shows the correlation between PSA level and rate of positive FCH PET/CT findings in patients with suspicion for prostate cancer recurrence. Methods: FCH PET/CT was performed in 41 patients with suspicion for prostate cancer recurrence and known PSA level. Before PET contrast enhanced CT was performed, than early PET scan started within 10 minutes after FCH injection (2.5 – 4.5 MBq/kg). If increased accumulation of FCH was observed in soft tissues, late scanning aimed on particular region was performed 60-90 minutes after FCH injection. Than SUVmax in hot lesions was compared on early and late scan. The study was considered to be positive if SUVmax had been stable or increasing in soft tissues. Any focal hyperaccumulation in bones was considered as metastasis. Results: In total 43 PET/CT was performed, 27 were evaluated as positive and 16 as negative. In the group of patients with PSA < 0.2 ng/ml 1 of 7 was positive (14%); 14 patients had PSA 0.2 – 1.99 ng/ml, 6 of them had positive PET/CT (43%); 8 patient had PSA 2 – 4.99 ng/ml, 7 of them had positive PET/CT (88%) and 14 patients had PSA > 5 ng/ml, 13 of them had positive PET/CT (93%). Conclusion: The probability of positive FCH PET/CT finding is increasing with PSA level. According to results of our group of patient FCH PET/CT can be helpful tool for prostate cancer recurrence localization. The chance to detect the site of recurrence is higher in patients with PSA > 2 ng/ml. In our opinion method is not effective in patients with PSA level < 0.2 ng/ml. Further research including histological verification of detected lesions is needed to assess sensitivity and specificity of the method and also to establish recommended indication criteria.

P44-1 - Sunday, Oct. 20, 16:00 - 16:30, Poster Exhibition Area

## Oncology Clinical Science: Gynaecological

## P279

### Ability of 18F-FDG PET/CT scan to detect recurrent ovarian cancer in patients with rising levels of CA-125.

**M. Haidar**[1], F. CHEHADE[1], M. JREIGE[2], T. KHOURY[3]; [1]Mount Lebanon Hospital, Lebanese University, Nuclear Medecine Department, HAZMIEH - Beirut, LEBANON, [2]University Saint Joseph, Radiology Department, Beirut, LEBANON, [3]American University of Beirut Medical Center, Radiology Department, Beirut, LEBANON.

**Aim of this study**: This study was performed to assess the ability of 18F-FDG PET/CT scan to detect recurrent ovarian cancer in patients with rising levels of CA-125 or with clinical signs for recurrence. **Patients and Methods**: We evaluated retrospectively 45 patients with ovarian cancer for suspicion of recurrence based on clinical symptoms and/or rising levels of CA-125 and/or suspicious lesion on other imaging modalities. All patients fasted at least 6 hours before injection of 18F-FDG and the PET/CT scan were performed 45-60 min after radiotracer injection and complete bed rest. All patients received 20 mg of Lasix 20 min before acquisition to increase tracer elimination (urinary voiding). **Results**: The PET/CT scan results were correlated with a follow up after at least 6 months, biopsy and/or surgery, and close radiologic follow up. 18F-PET/CT findings suggested locoregional recurrence in 16 patients and distant metastasis with or without locoregional disease in 24 patients. No evidence of recurrence was noted in 5 patients. PET/CT was helpful in identifying pathologic uptake in sub-centimetric pelvic/abdominal lymph nodes and in detecting small foci of peritoneal carcinomatosis as well as distant metastatic sites. The sensitivity of our study was 98% with 86% specificity. False positive was related to inflammatory processes. **Conclusion:** FDG-PET/CT is a highly accurate non invasive imaging modality, which improves the detection of recurrent ovarian cancer with rising levels of CA-125.

## P280

### PET/CT in Recurrent Carcinoma Ovary: Contrast enhanced CT (CECT) verses Non enhanced low dose CT (NECT)

**A. G. Vyas, Sr**[1], A. Tiwary, Jr[2], S. A. Shamim, Consultant[3]; [1]NMC IMAGING AT VIMHANS HOSPITAL, NEW DELHI, INDIA, [2]Army Hospital R&R, NEW DELHI, INDIA, [3]DCA IMAGING At Shanti Mukund Hospital, NEW DELHI, INDIA.

Aim: To evaluate the role of F-18 FDG PET/CT, Contrast enhanced CT (CECT) verses Non enhanced low dose CT (NECT) in restaging of Recurrent carcinoma ovary (post treatment) Material & Methods: In total 45 F-18FDG PET/CT examinations were performed in patients with carcinoma of ovary, for attenuation correction whole body NECT was performed followed by diagnostic CECT with contrast agent. Post furosemide delayed image were also taken. Criteria for evaluation were signs of vital tumor tissue (extent of lesions, contrast enhancement & maximum standardized uptake value (SUVmax). Findings suspicious for recurrence were considered lesions. Combined analysis of PET/NECT and PET/CECT were evaluated separately by two different PET experts. Findings were verified histologically and/or follow up (12 months). Results: Total 198 lesions were analysed and 129 proved to be metastatic. The sensitivity, specificity, positive predictive value, negative predictive value & accuracy of PET/NECT were 90%, 79.3%, 84.8%, 87.3% and 85% respectively. And for PET/CECT were 98.3%, 90.7%, 94.4%, 97.1% and 95.4% respectively. Compared to PET/NECT the PET/CECT obtained additional 19 lesions-perihepatic/perisplenic deposits (n=5), serosal deposits (n=9), mesenteric deposits (n=3) and small lymph nodes(n=2).PET/NECT had 10 false negative findings- serosal (n=3),perihepatic (n=2), iliac lymph nodes (n=2), mesenteric deposits (n=1) and focal urinary activity in distal ureter (n=2).On PET/CECT two false negative findings occurred (peritoneal deposits). Conclusion: Overall PET/CECT changed staging of 6 out of 45 patients. Our results indicate that PET/CECT instead of PET/NECT may be a better tool for restaging of recurrent carcinoma ovary, prior to selection of the most appropriate therapy. The ability to fully evaluate the patient in one combined imaging modality rather than multiple tests is advantageous if the performance is equal to or better.

## P281

### 18F-FDG PET/CT in patients with locally advanced cervical cancer. Correlation between SUVmax and overall survival, microvessel density and cell proliferation. A preliminary study

**S. Ruiz Solís**, P. Sarandeses Fernández, A. Hernández Martínez, P. Cotrina Monroy, C. Lechuga, J. Pérez-Regadera, A. Tejerizo, R. D'Ambrosi, J. Estenoz Alfaro; Hospital 12 de Octubre, Madrid, SPAIN.

**Aim**: to determine whether the tumor SUVmax (Standardized Uptake Value Maximum) measured by 18F-fluorodeoxyglucose Positron Emission Tomography/Computed Tomography (18F-FDG PET/CT), in patients with locally advanced cervical cancer which will be treated with concurrent chemoradiotherapy, is associated with overall survival, microvessel density and cell proliferation.Materials **and Methods**: 49 patients were included in the current study, from January 2009 to February 2013. All patients underwent 18F-FDG PET/CT before initiation of treatment. The microvessel density and cellular proliferation was measured by immunohistochemical staining Methods with antibodies CD34 and Ki67 respectively. The overall survival was measured by an actuarial method from the completion date of radiotherapy to the date of death from any cause or to the end of the study period. **Results**: three patients were excluded from the study by metastatic spread (one in liver, one in mediastinum, and the last one in left supraclavicular fossa and mediastinum). The mean value of cervical tumor SUVmax was 14.72 (Standard Deviation= 6.68) and the median value was 16,40 ($25^{th}$ percentile= 9.10, $75^{th}$ percentile= 19.43). Patients with SUVmax ≤ $50^{th}$ percentile vs > $50^{th}$ and those that have a SUVmax ≤ $75^{th}$ percentile vs > $75^{th}$, had an overall survival without statistical differences, being three-year overall survival 76% vs 84% and 83% vs 70% respectively. There is some relation between SUVmax and the microvessel density, with a Spearman correlation coefficient of 0.28, although without statiscally significant (p= 0.07). However, there is no association between SUVmax and cell proliferation, with a Spearman correlation coefficient of 0.01 (p = 0.95). Also, there is no association between cell proliferation and microvessel density, with a Spearman correlation coefficient of 0.05 (p= 0.74). **Conclusion**: the metabolic tumor activity measured by SUVmax in patients with locally advanced cervical cancer shows no association with overall survival or cell proliferation. However, in our study, SUVmax shows some relation with microvessel density, although it was not statistically significant presumably due to a small sample size.

## P282

### Preoperative differential diagnosis of minimal deviation adenocarcinoma (MDA) and lobular endocervical glandular hyperplasia (LEGH) of the uterine cervix: Effectiveness of MRI and FDG-PET

**T. Shiozawa**, R. Asaka, T. Miyamoto; Shinshu Univsersity, Matsumoto, JAPAN.

Minimal deviation adenocarcinoma (MDA) of the cervix is an extremely well differentiated mucinous adenocarcinoma. Lobular endocervical glandular hyperplasia (LEGH) is a benign lesion characterized by lobular proliferation of small glands. Although LEGH is similar to MDA in terms of pathological findings and clinical symptoms, precise preoperative diagnosis is important for the proper treatment. To address this issue, we performed a retrospective, multicenter study for the preoperative diagnosis and treatment of MDA and related disorders. In this study, a total of 112 patients who underwent conization or a hysterectomy for suspected MDA were enrolled from 24 hospitals. The pathological diagnosis in each case was determined by a central pathological review (CPR) board. The diagnostic significance of clinicopathological findings including results of magnetic resonance imaging (MRI), Pap smears, and testing for gastric mucin was analyzed. In addition, diagnostic capability of FDG-positron emission tomography (PET) on these lesions was analyzed. The result indicated that the CPR identified 37 cases of Nabothian cyst or tunnel cluster, 54 cases of LEGH, 6 cases of MDA, 11 cases of adenocarcinoma, and 4 cases of benign disease. On MRI, LEGH appeared as a characteristic multicystic lesion with an inner solid component, whereas MDA showed a predominantly solid pattern. FDG-PET revealed that LEGH was characterized by low signal intensity, whereas MDA and adenocarcinoma associated with MDA showed elevated signal intensity. A Pap smear or gastric mucin alone had limited diagnostic power. However, a combination of these findings was useful, i.e., a cystic structure with inner solid components on MRI associated with low FDG-PET signal intensity, mild glandular atypia and gastric mucin strongly suggested LEGH. In contrast, a solid structure on MRI, with elevated FDG-PET signal intensity and atypical glandular cells was indicative of MDA or adenocarcinoma. These data showed that the combination of MRI, FDG-PET, Pap smears, and gastric mucin will improve the accuracy of the preoperative diagnosis of MDA and LEGH.

## P283

### Evaluation of dual-time-point F-18 FDG-PET scans for diagnosis of cancer of the corpus uteri

**S. Ito**[1], K. Kato[2], T. Okuda[3], S. Iwano[1], S. Naganawa[1]; [1]Department of Radiology, Nagoya University Graduate School of Medicine, Nagoya, JAPAN, [2]Department of Radiological and Laboratory Science, Nagoya University Graduate School of Medicine, Nagoya, JAPAN, [3]Department of Radiology, Toyota Memorial Hospital, Toyota, JAPAN.

Purpose: This study was to evaluate the efficacy of dual-time-point F-18 FDG-PET scans for cancer of the corpus uteri. Methods: Twenty-two patients who were histologically suspected cancer of the corpus uteri by biopsy underwent dual-time-point F-18 FDG-PET scans. The first scan was performed at 60 minutes after F-18 FDG administration and the second scan was done at 90 minutes. The maximum standardized uptake value (SUVmax) of the lesions were determined, and the retention index was calculated by dividing the increase in SUVmax from 60 min (SUV-60) to 90 min (SUV-90) by SUV-60. Results: All the patients underwent total hysterectomy within one month after F-18 FDG-PET scans were performed. Eighteen patients were diagnosed as endometrial carcinoma and four patients as carcinosarcoma. Except for one patient with the diameter of tumor below 5 mm, SUV-90 values were higher than SUV-60 values and resulted in a significant increase between SUV-60 and SUV-90. The average retention index was 13.5 %. The SUV-60

and the retention index of endometrial carcinoma were 12.2 ± 7.9 and 14.3 ± 9.2, respectively, and those of carcinosarcoma was 9.1 ± 3.3 and 6.6 ± 5.1, respectively. The retention index of endometrial carcinoma was statistically higher than that of carcinosarcoma (p = 0.03). Low-differentiated endometrial carcinoma tended to show higher uptake of F-18 FDG than high-differentiated endometrial carcinoma, but no significant difference was observed between the retention index of low-differentiated and high-differentiated endometrial carcinoma. Conclusion: Although the number of patients with carcinosarcoma was small, our results suggested that dual-time-point F-18 FDG-PET scans may be useful in distinguishing carcinosarcoma from endometrial carcinoma.

## P284

### PET-CT for Pelvic and Para-Aortic lymph node staging in locally advanced cervical cancer compared with lymphadenectomy.

**M. SIMO**, B. FEIJOO, M. Barios, M. Sabate, E. Franquet, L. Gracia, J. Castell-Conesa, R. Cardenas; Hospital Universitario Vall de Hebron, Barcelona, SPAIN.

BACKGROUND: The most important prognostic recurrence factor in patients with cervical cancer was paraortic nodal status. We proposed FDG PET-CT as diagnostic imaging tool for lymph node staging and its role with laparoscopic verification in the staging management algorithm. PURPOSE: The aim of the study was to evaluate the accuracy of FDG PET-CT for detecting pelvic and para-aortic lymph nodes (LNs) metastases in patients with locally advanced cervical cancer. MATERIAL AND METHODS: This prospective study included 19 consecutive women with recent diagnostic of cervical cancer (mean 43y, range 29-66 ) stage FIGO IIB-IVA. All patients underwent MRI and PET/CT in order to evaluate pelvic and paraortic LN staging. After that a laparoscopic lymphadenectomy (LDN) of the para-ortic and/or pelvic LNs was performed in order to obtain histological verification of imaging results. A median of 13.4LNs/patient were removed in LND. A patient was excluded from surgery because of several metastatic spread diagnosed by PET-CT and histopathologicaly confirmed. RESULTS: PET-CT detected the primary cervical tumor in all patients, with a mean value of SUV max of 16.8 (range 7-40). The tumor local infiltration was assessed with MRI. Pelvic region was studied with PET-CT showing LN involvement in 8/18 patients. Of these 8 patients, 4 were true positive after LND. 1 patient with pelvic LN metastasis in MRI and PET-CT was considered false positive by histological verification . Other 3 patients did not have pelvic LND for histopathological confirmation due to surgeon's decision. All of these three patients had also suspicious nodal infiltration by MRI. Para-ortic region was studied with PET-CT showing LN involvement in 4/18 patients, all of them were true positive after LND. No LN infiltration was obtained in 14 patients with negative PET-CT (true-negatives). Overall, the therapeutic approach was modified in 22.2%. The presence of para-ortic metastases lead to expand the radiation field in 4 patients and 1 more patient with metastases was excluded from surgery and underwent palliative treatment. CONCLUSION: Preliminary results of our study show that PET-CT was able to correctly predict para-ortic lymph node staging in all patients recently diagnosed with a locally advanced cervical cancer. In our study, the therapeutic approach was modified in 22.2% of patients, mostly increasing RT fields. We suggest that PET-CT may be performed as the first diagnostic tool in these patients, reserving laparoscopic LDN for those patients with N1.

## P285

### Role of 18F-FDG PET/CT in detection of recurrence in asymptomatic patients of ovarian carcinoma with normal CA-125 levels after primary treatment.

**R. Kumar**, J. R. Mohan, M. L. Abrar, B. Anish, B. R. Mittal; Postgraduate Institute of Medical Education & Research, PGIMER, CHANDIGARH, INDIA.

AIM To evaluate the role of 18F-FDG PET/CT in asymptomatic patients with epithelial ovarian carcinoma after completion of primary treatment with normal CA-125 levels. MATERIAL AND METHODS In this retrospective study, we evaluated 19 patients (mean age 50.7; range 27 -70 years) of epithelial ovarian carcinoma, who were referred to the nuclear medicine department for disease status assessment from January 2012 to December 2012. All the patients had completed primary treatment (debulking surgery followed by 6 cycles of chemotherapy or 3 cycles of neoadjuvant chemotherapy followed by surgery and 3 cycles of adjuvant chemotherapy). All the 19 patients were asymptomatic on clinical examination and had normal CA125 (<35 U/ml). Whole-body 18 F FDG PET/CT scans was performed on all patients after 4 weeks of chemotherapy. 18 F FDG PET/CT data were interpreted by 2 experienced nuclear medicine physicians and the results were assessed by using clinical follow-up or pathology as gold standard. RESULTS Of the 19 patients, PET revealed no evidence of disease in 8 patients and suggested disease recurrence in 11 patients. Out of these 11 patients, 4 patients had extensive disease, 3 patients had abdominal (loco-regional) disease and 4 patients had pelvic disease (local disease) only. All 11 patients who showed PET evidence of recurrence underwent subsequent chemotherapy. 3 patients in whom tissue diagnosis was done showed positive histopathological evidence of recurrence. 8 patients who had normal findings on PET showed no evidence of disease up to 6 months of clinical follow up. PET/CT revealed an overall sensitivity and specificity of 100% in detection of disease recurrence in patients with normal clinical examination and normal CA125 level. CONCLUSIONS 18 F FDG-PET/CT is a highly sensitive and specific tool for the evaluation of patients of ovarian carcinoma during follow-up period with normal CA125 level and normal clinical examination. PET/CT appropriately modified clinical management in patients, either by excluding the disease or identifying relapse in patients who were apparently disease-free.

P45-1 - Sunday, Oct. 20, 16:00 - 16:30, Poster Exhibition Area

## Oncology Clinical Science: Colorectal Cancer

## P286

### Clinical Usefulness of serum CYFRA 21-1 in Patients with Colorectal Cancer

**J. Lee**, S. Park, D. Park, H. Namgung; Dankook University Hospital, Cheonan, KOREA, REPUBLIC OF.

*Aim* Among diverse tumor markers, pretreatment evaluation and follow up detection of recurrence in colorectal cancer are generally evaluated by serum carcinoembryonic antigen (CEA) levels. However, there have not been many reports about the low accuracy and high false-positive results of CEA in colorectal cancer. We retrospectively evaluated the possibility of clinical application of CYFRA 21-1 in pretreatment and recurrent colorectal cancer. *Methods* Using a solid-phase immunoradiometric assay, serum levels of CYFRA 21-1, CEA and Cancer antigen 19-9 (CA 19-9) were analyzed in 132 patients with primary colorectal cancer, 123 healthy controls, 104 patients with benign colorectal disease and 20 patients with recurrent colorectal cancer. We determined 3 different cutoff values to evaluate the sensitivity of diagnostic performance in pretreatment and recurrent colorectal cancer, using ROC curves. Cutoff levels are determined according to conventional value (CYFRA 21-1 2 ng/ml, CEA 7 ng/ml and CA19-9 38 ng/ml), 95% specificity in healthy controls and benign diseases, comparing colorectal cancer patients. *Results* Significant differences of CYFRA 21-1 levels (1.55±0.17; interquartile range 0.55 - 1.85 ng/ml) were founded between primary colorectal cancer patients and patients with benign colorectal diseases (0.47±0.06; interquartile range 0.23 - 0.78 ng/ml) and healthy controls (0.38±0.03; interquartile range 0.16 - 0.48 ng/ml), ($p < 0.0001$). CYFRA 21-1 (≥ 1.13 ng/mL) had a sensitivity of 47%, compared with 37% for CEA (≥ 3.05 ng/ml) and 32.6% for CA 19-9 (≥ 23.1 ng/ml) in the initial staging of primary colorectal cancer. Using different cutoff values, CYFRA 21-1 showed higher sensitivity for pretreatment colorectal cancer than CEA and CA 19-9 in adenocarcinoma and adenosquamous carcinoma of this study. A mild significant correlative relationship was noted between duke stages and three tumor markers ($p<0.01$). The areas under the receiver operating characteristic curves (ROC-AUCs) of CYFRA 21-1, CEA and CA 19-9 were 0.81±0.03, 0.74±0.03 and 0.62±0.04, respectively, for discriminating colorectal cancer patients from patients with benign colorectal disease. In addition, CYFRA 21-1 was determined as the most sensitive tumor marker for evaluating recurrent colorectal cancer for all cutoff values (Sensitivity: 73.6%, cutoff value: 1.13ng/ml). *Conclusion* This study showed that CYFRA 21-1 could be a useful and dependable tumor marker for pretreatment and recurrent colorectal cancer. Further prospective studies on its usefulness with respect to the prognosis and utility of combined tumor markers are needed.

## P287

### Diffuse and intense FDG uptake in the large intestine

**S. Yasuda**[1], M. Ono[2], Y. Miyatake[2], R. Mikami[2], M. Yoshimura[2], T. Kato[2], M. Akeboshi[2], T. Kojima[2], W. Ko[2], K. Kobayashi[2]; [1]Tokai University School of Medicine, Kanagawa, JAPAN, [2]Yotsuya Medical Cube, Tokyo, JAPAN.

**Aim:** Diffuse and intense uptake (DIU) of 18F-fluorodeoxyglucose (FDG) is occasionally observed in the entire large bowel (LB) during FDG PET studies. The purpose of this study was to determine the frequency and clinical significance of DIU in the LB. **Methods:** Subjects were 697 asymptomatic individuals (men: 430; woman, 267) aged 63.0 ± 11.5 years who underwent FDG PET between January 2011 and December 2011 under our periodical cancer screening program. Grayscale PET images were visually evaluated retrospectively, and subjects were classified into 3 groups according to the intensity and extent of FDG uptake in the LB: typical (T) type (intense uptake nearly equal to that of the urine along the entire LB); intermediate (I) type (uptake apparently higher than that of the liver beyond two colonic segments); and low (others). The following aspects were then examined: 1) frequency of DIU; 2) relationship between DIU and factors such as age, sex, fasting blood sugar (FBS), HbA1C, and constipation; and 3) reproducibility of DIU. Most subjects underwent PET study annually, and 4 consecutive PET images were reviewed for the presence of DIU. **Results:** 1) T type and T+ I type were observed in 5 (0.7%) and 18 (2.6%) of the 697 subjects, respectively. 2) Factors such as age, sex, FBS, HbA1c, and constipation were not significantly associated with DIU. 3) Of the 18 T+ I-type subjects, 17 had undergone annual PET studies, and DIU

was recognized repeatedly in 4 of 5 subjects with T-type (80%) and 5 of 13 subjects with I-type (38%) FDG uptake. None of the 18 subjects with DIU had abdominal symptoms, and 15 were negative for simultaneously performed fecal occult blood test (FOBT). One FOBT-positive subject underwent colonoscopy after one month and no lesions were revealed. Thus, in 16 of the 18 subjects (89%), the presence of diffuse organic lesions in the LB seemed unlikely, and the DIU was considered physiological. **Conclusion:** Typical DIU was observed at a rate of 0.7% and was considered physiological in most cases. Therefore, no further colonic exams are warranted. Typical DIU was observed repeatedly at a rate of 80% and seemed to indicate accelerated glucose metabolism in the LB that is specific to the subject.

## P288

### Clinical Importance of F-18 FDG PET/CT in Colorectal Cancer Restaging

**E. Gencoglu**[1], A. Cinar[2], A. Yapar[3], A. Aktaş[1]; [1]Baskent Universitesi, Ankara, TURKEY, [2]ANKARA EDUCATION AND TRAINING HOSPITAL, Ankara, TURKEY, [3]Baskent Universitesi, Adana, TURKEY.

***Aim:*** The aim of this study was to investigate the clinical impact of the findings of F-18 FDG PET/CT in operated colorectal cancer patients that suspected recurrence/metastasis. For this purpose, F-18 FDG PET/CT findings were compared with CT results and blood levels of CEA. ***Materials and Methods***: A total of 102 patients with operated colorectal cancer (63 female, 39 male, mean age 65.81±4.63 years, mean follow up time 23 months) were included in this retrospective study. All patients were acquired F-18 FDG PET/CT. The results of PET/CT were compared with findings of concurrent CT and serum CEA levels. Data were compared about the localizations of metastatic/reccurrent tumors, the histopathologic verifications of the tumors, the impact to the treatment type, the response to the treatment. ***Results:*** In this study, success rates of detecting pathologic lesions in suspected metastasis/ recurrence for colorectal carcinoma cases were 98% for PET/CT and 64.7% for CT. In 34 cases, pathologic lesions were detected with PET/CT, however, CT findings showed no metastasis/recurrence. In 70 patients with high CEA levels, lesions of 68/70 cases were localized with PET/CT, whereas in only 45/70 cases pathologic findings were observed with CT. Most of the pathologic hypermetabolic lesions were detected in the liver and the lungs with PET/CT. PET/CT was considered 1.8 times successful than CT in detecting recurrent disease. In the liver where was the most detected lesion localization, sensitivity and specificity of PET/CT were 88% and 92%, while sensitivity and specificity of CT were 80% and 76% respectively. ***Conclusion:*** In PET/CT studies focusing on the treatment response after restaging, mediastinum and liver showed the most efficient response to the treatment. In the light of these findings, PET/CT was considered as a beneficial imaging tool in restaging and treatment response of colorectal carcinoma cases with suspected metastasis/ recurrence.

## P289

### SUV parameters in locally advanced rectal cancer before and after neoadjuvant chemoradiotherapy: correlation with tumor regression grade, Ki-67 and GLUT1

M. Koc, **G. Çapa Kaya**, S. Sarioglu, F. Obuz, I. Oztop, I. B Gorken, S. Sokmen; Dokuz Eylul University, School of Medicine, Izmir, TURKEY.

**Aim**: There have been very limited numbers of studies in the literature, comparing SUV parameters and hispathology in patients with locally advanced rectal cancer (LARC). We investigated the correlation between SUV parameters before and after the neoadjuvant chemoradiotherapy and tumor regression grade, Ki-67 and GLUT1 in LARC **Methods**: From 2009 to 2012, 29 patients diagnosed LARC with histopathology was included in our study. SUV before treatment (BT) and after treatment (AT) (early and delay SUVmax- average, LBM SUVmax-average, tumor/liver (T/L) and retention ratios) were calculated. Pathological complete response and tumor regression grade (TRG) were compared in subgroups. Immunohistochemical staining with Ki-67 and GLUT1 were performed for biopsy and surgery specimens. Correlation between staining ratios and SUV parameters were investigated. **Results:** SUV parameters for AT were generally decreased according to SUV parameters for BT (p<0.001). All of the SUV parameters obtained from delayed scans were higher than early scans images (p<0.001). When we separated the patients according to the TRG; there were 12 (%41) patients with TRG1, 10 (%35) patients with TRG2, 7 (%24) patients with TRG3. There was significant difference TSUVaverage/LSUVaverage (p=0.047) and ATdelay TSUVaverageLBM (p=0.036) in ATdelay scans for all three groups. There were 5 (17%) patients with complete response and 24 (83%) patients with non-complete response. There was significant difference in SUVmax-average ATdelay (p=0.012, p=0.025), SUVmax-average LBM (p=0.015, p=0.025) ATdelay and TSUVaverage/LSUVaverage, TSUVmax/LSUVmax both early and delayed scans between complete and non-complete response. TSUVmax (r: 0.51, p: 0.013), TSUVaverage(r: 0.45, p: 0.03), TSUVmax LBM (r: - 0.55, p: 0.007), TSUVaverage LBM (r: - 0.49, p: 0.02), TSUVaverage/LSUVaverage (r: 0.49, p: 0.017), TSUVmaks/LSUVaverage (r: - 0.52, p: 0.012) obtained from early images and Ki-67 values were moderately correlated for the AT. TSUVaverage/LSUVaverage, TSUVmaks/LSUVaverage values and GLUT1 AT were moderately correlated (r = 0.44, p = 0.04 ve r = - 0.48, p = 0.02, respectively). **Conclusion**: PET-CT is an effective method for assessing the response to neoadjuvant CRT in the patients with LARC. T/L ratios and SUV LBM values may more valuable parameters for assessing treatment response between SUV parameters. Since the significant correlation between Ki-67 AT and SUV values, SUV values may be a good metabolic indicator. Because GLUT1 and T/L ratio for AT were correlated, the rate of metabolic activity may be more related T/L ratio than the other SUV parameters in the assessment of treatment response.

## P290

### The role of [18F]FDG-PET/CT in the restaging of patients with colorectal cancer: a comparison with CT and biochemical markers of recurrence

**L. Locantore**, D. Volterrani, P. Erba, G. Mariani; Regional Center of Nuclear Medicine, University of Pisa, Pisa, ITALY.

**BACKGROUND/AIM**: Despite resection with radicals intents and chemoterapy, distant metastases and/or locoregional recurrence of colorectal cancer occur in about one-third of patients within 2 years after surgery. In this retrospective study we evalued the added value and the complementary information of [18F]FDG-PET/CT compared to conventional imaging modalities and laboratory tests in the restaging of patients with suspected relapse of colorectal cancer. **PATIENTS/METHOD:** Seventy-one consecutive patients (40 men, 31 women, mean age 66±10 yr) were included in the study. Nine patients had rectal and 62 colon carcinoma; 24 patients had syncronous liver metastases at initial diagnosis. All patients underwent [18F]FDG-PET/CT for post-surgical restaging, either for routine follow-up (n=40), for suspected recurrence based on rising serum CEA with negative radiologic imaging (n=12), or for inconclusive CT/MRI findings with normal serum CEA (n=19). All results were correlated with the CT and CEA findings. [18F]FDG (3.7 MBq/kg) was injected i.v. in fasting conditions. Images were acquired 60 minutes after tracer administration with a Discovery ST/8 scanner (GE Healthcare, Milwaukee, USA). A low-dose CT was performed for attenuation correction and image co-registration. PET/CT study interpretation was based on abnormal uptake and SUVmax. **RESULTS:** [18F]FDG-PET/CT was positive in 36/71 patients: loco-regional recurrence was detected in 12, nodal involvement in 14, and distant metastases in 31 cases (several patients showing more than one site of disease). In 61 patients PET/CT detected more lesions than CT, with an overall statistically significant difference (P<0.05). For the "T" and "N" parameters, the PET/CT findings were concordant with CT, while there were discordant cases for parameter "M" (P<0.05), most cases being observed in patients with lung nodular lesions at CT with no [18F]FDG uptake, or with [18F]FDG-avid lesions in the liver or at other sites, but undetected at CT. In 62 patients the PET/CT findings were well-related with the CEA results, while there was discordance between the CEA and the CT findings (P<0.05). At long-term follow-up (available for 54 patients), 100% of the patients with a positive PET still showed presence of disease, while only 1 patient with a negative PET later had disease recurrence. **CONCLUSION:** With its high positive and negative predictive value, [18F]FDG-PET/CT has a proven diagnostic value for restaging patients with colorectal cancer. It also provides relevant additional informations on the presence of distant metastases, thus changing clinical and therapeutic management of these patients and optimizing time and resources.

P46-1 - Sunday, Oct. 20, 16:00 - 16:30, Poster Exhibition Area

## Oncology Clinical Science: Gastrointestinal & Pancreas

## P291

### Role of 18F-FDG PET/CT in Diagnosis and Management of Pancreatic Cancer; Comparison with MDCT, MRI and Endoscopic Ultrasonography

**N. Ergül**[1], C. Gundogan[2], M. Tozlu[1], H. Toprak[1], H. Kadıoglu[1], M. Aydın[1], T. F. Çermik[2]; [1]Bezmialem Vakıf University School of Medicine, Istanbul, TURKEY, [2]Istanbul Training and Research Hospital, Istanbul, TURKEY.

**Objectives:** We aimed to analyze the contribution of 18F-fluorodeoxyglucose positron emission tomography/computed tomography (FDG PET/CT) imaging to diagnosis and management of pancreatic cancer comparing with multidetector row computed tomography (MDCT), magnetic resonance imaging (MRI) and endoscopic ultrasonography (EUS). **Patients and Methods**: We retrospectively scanned the data of 52 patients who were referred to FDG PET/CT imaging for evaluating the pancreatic lesions greater than 10 mm. Sensitivity, specificity, positive predictive value (PPV) and negative predictive value (NPV) of all four imaging Methods for differentiation of benign versus malignant lesions were compared statistically. The eligible cut-off value of standardized uptake value (SUV) was determined. The impact of PET/CT to management of pancreatic cancer was defined. **Results:** Pancreatic adenocarcinoma was diagnosed in 33 of 52 patients (63%), 15 patients

had benign diseases of pancreas (29%), and 4 patients were normal (8%). Sensitivities and NPVs of EUS and PET/CT were equal (100%) and higher than MDCT and MRI. Specificity, PPV and NPV of PET/CT were significantly higher than MDCT; however sensitivities of two imaging Methods were not significantly different. There was no significant difference between PET/CT and MRI and EUS for these values. When the cut-off value of SUVmax was 3.2 most effective sensitivity and specificity values were obtained. PET/CT contributed to the management of pancreatic cancer in 30% of patients. **Conclusion:** FDG PET/CT is a valuable imaging method for diagnosis and management of pancreatic cancer, especially when applied along with EUS as first line diagnostic tools.

## P292

### Clinical Application of 18F-FDG PETCT in Gastric Disease

L. Di, **R. Wang**, F. Yan, H. Wang, G. Zhao; Department of Nuclear Medicine,Peking University First Hospital, Beijing, CHINA.

**Objective:** The purpose was to study the pathological results, FDG activity and PET/CT patterns in benign and malignant gastric diseases. Further to assess the value of $^{18}$F-FDG PET/CT imaging in the differential diagnosis of gastric diseases. **Methods:** Forty-nine patients clinically suspicious of gastric diseases underwent $^{18}$F-FDG PET/CT imaging, the data and image of PET/CT studies were reviewed. Imaging Methods: All patients were instructed to fast for at least 4-6 h before imaging. PET/CT scans were obtained at early 60 min and later 120min after $^{18}$F-FDG injection (5.0 MBq/kg). The pathological results and PET/CT image patterns was described. The diagnostic value of SUVmax including early-phase and delay-phase and thickness of lesions was analyzed. SUV= tissue concentration(kBq/ml)/injected FDG dose(kBq)/body weight(g). **Results:** The benign group comprises three examples of stomach ulcer and twelve examples of chronic gastritis. The malignant group comprises eighteen examples of lymphoma and sixteen examples of primary gastric cancer. Thickness of the benign and malignant lesions was 13.800±3.489mm,18.088±8.575mm respectively(t=-2.486,P=0.017). The SUVmax in early-phase of the benign and malignant lesion was respectively 3.607±2.710, 7.277±6.175 (t=-2.891,P=0.006). The SUVmax in early-phase and delay-phase of the benign lesions was3.607±2.710,4.144±1.070 (t=-1.799,P=0.094),that of gastric carcinoma's and lymphoma's was 5.131±2.486 vs 6.156±3.126, 9.183±7.770 vs 11.744±10.222 respectively(t=-3.691, -4.095,P= 0.002, 0.001). **Conclusions:** Our results showed the SUVmax was higher in malignant diseases than benign diseases .And the SUVmax of delay-phase was higher than the early-phase in the malignant group. So $^{18}$F-FDG PET/CT imaging especially dual-phase imaging is a useful differential diagnostic modality for benign and malignant gastric diseases. [Key words]: Gastric; PET/CT; SUVmax; Early-phase; Delay-phase; Thickness

P47-1 - Sunday, Oct. 20, 16:00 - 16:30, Poster Exhibition Area

## Oncology Clinical Science: Lymphoma

## P293

### Our experience in Gallium67 scintigraphy in the era of PET/CT

**B. Al Suqri**, N. Al Belushi, A. Al Saadi, K. Al Busaidi; Royal Hospital, Muscat, OMAN.

**Introduction:** Although $^{18}$F FDG PET/CT has replaced the use of Ga67 in the evaluation and follow up of lymphoma patients, Gallium67 (Ga67) scans are still of value particularly in countries where no PET/CT service is available. The same applies for the evaluation of pyrexia of unknown origin (PUO) and follow up of infections. We present our tertiary care center experience in the evaluation of lymphoma and infection using Ga67 where no PET/CT and no white blood cell labeling facility is available. **Methods:** Retrospective review of all Ga67 scans done from 2007 to 2011 was performed. A total of 74 patients were referred to our department for Ga67 scans during this period. 12 patients were referred from other hospitals and were followed up there, hence excluded from this review. The remaining 62 patients (mean age 43) were referred from departments in our hospital, 28 (44%) patients were males. The main bulk of the referrals came from medical oncology department for the lymphoma patients (24 patients, 40%). Infectious diseases team (9 patients, 15%) and paediatric haematology (7 patients, 12%) came second in terms of the number of referred patients. **Results:** A total of 89 Ga67 scans were performed between 2007 and 2011. 59 scans (66%) were done for Hodgkin and Non-Hodgkin lymphoma patients, 29 scans (33%) for infections and 2 scans for sarcoidosis. The images and the reports of these Ga67 scans were compared to the subsequent clinical and radiological follow-up including CT, PET/CT and biopsies when available. Regarding Ga67 scans done for lymphoma, 20 came as true positive, 30 as true negative, 4 as false positive and 5 as false negative. This gives a sensitivity of 80% and a specificity of 88%. Out of the 13 scans done for PUO, 6 were positive and guided management, 3 were negative and the fever was attributed to the disease process in these patients (SLE, Stills disease, myelodysplastic syndrome) and 4 were negative and were treated empirically for unknown source of infection. **Conclusion:** These results are consistent with reported sensitivity and specificity of Ga67 in the evaluation of lymphoma and infection. Ga67 will remain a very useful tool in this aspect for many coming years in areas where PET/CT cannot be afforded.

## P294

### Quantitative Analysis of FDG PET for Evaluation of Bone Marrow Infiltration in Patients with Non Hodgkin Lymphoma

**L. Ö. Kapucu**[1], Ü. Ö. Akdemir[1], B. Çetin[2], M. Başara[1], U. Aydos[1], N. I. Karabacak[1], M. Benekli[2], S. Büyükberber[2]; [1]Gazi University, Faculty of Medicine, Department of Nuclear Medicine, Ankara, TURKEY, [2]Gazi University, Faculty of Medicine, Department of Internal Medicine, Medical Oncology Unit, Ankara, TURKEY.

**Aim**: To compare quantitative results of 18F-FDG PET imaging for the evaluation of bone marrow involvement of non-Hodgkin lymphoma (NHL) in comparison to findings of bone marrow biopsy. **Materials and Methods**: We retrospectively evaluated 18F-FDG PET data of 50 NHL patients (age= 57.3 ± 1.8; Female/Male = 27/23) who had bone marrow biopsies done within 1 month of PET examination. For the quantitative assessment of PET images cubic volumes of interests were used to measure mean bone marrow 18F-FDG uptake as standardized uptake values from L3-L5 lumbar vertebras (bmSUV). Additionally, normalized bone marrow 18F-FDG uptake values were calculated using mean blood pool, liver and splenic 18F-FDG uptake. All quantitative results were compared between the biopsy proven bone marrow infiltration positive and negative groups using the Mann-Whitney U test. ROC analysis was used to assess the diagnostic value of each quantitative parameter. **Results**: In 8 of 50 (16%) patients bone marrow biopsy revealed infiltration. The bmSUV and normalized bmSUVs were higher in the infiltration positive group in comparison to the infiltration negative group. Area-under-curve values in ROC analyses were 0.722, 0.769, 0.787 and 0.587 for bmSUV, normalized bmSUVs for mediastinum, liver and spleen, respectively. The quantitative parameter with the highest discriminative power was bmSUVs normalized using liver 18F-FDG uptake, with 75% sensitivity and 83% specificity for the detection of bone marrow infiltration when 1.15 was applied as the threshold. **Conclusion:** Bone marrow SUVs were significantly higher in NHL patients with bone marrow infiltration in comparison to NHL patients without bone marrow infiltration. Normalization of bmSUVs using liver 18F-FDG uptake provided the best diagnostic accuracy in detecting bone marrow infiltration with 18F-FDG PET imaging.

## P295

### Are Interleukin-10 (IL-10) and glucose metabolism modifications linked in early prognostication of diffuse large B-cell lymphoma (DLBCL)? A multicentric, prospectic, pilot study.

**S. Seghezzi**[1], L. Ottobrini[1], A. Moro[2], G. Ucci[3], A. Bertolini[4], L. Uziel[1], G. Lucignani[1,5], L. Tagliabue[5]; [1]Department of Health Sciences, University of Milan, Milan, ITALY, [2]San Paolo Hospital, Milan, ITALY, [3]Lodi Hospital, Lodi, ITALY, [4S]ondrio Hospital, Sondrio, ITALY, [5]Nuclear Medicine Unit, San Paolo Hospital, Milan, ITALY.

**Introduction**: DLBCL is the most common aggressive non-Hodgkin lymphoma. ($^{18}$F)-FDG PET/CT, performed at baseline and at the end of the treatment (EOT), has become an integral part of the workup of these patients. Despite the well-known prognostic value of EOT PET/CT, the role of interim-PET/CT in prognostication is debated. The aim of this study was to evaluate the role of interim-PET/CT both in early response assessment and in predicting clinical outcome. **Methods**: 24 previously untreated patients, presenting with a disease burden higher than Ann Arbor stage I and candidates for first-line R-CHOP chemotherapy, were enrolled; all patients performed staging, interim (after 2 cycles of R-CHOP) and EOT PET/CT. A qualitative and semi-quantitative analysis of PET scans, using the maximum standardized uptake value (SUVmax), was performed by three blinded, expert operators. *Interim*-PET/CT were visually interpreted using the *Deauville* 5-point *score*. At every interim and EOT scan a PERCIST-based evaluation was also performed. Serum IL-10 levels were assessed at staging and after 2 cycles of chemotherapy. A mean follow-up of 17 months was available. **Results.** 16/24 (66%) patients had a PERCIST complete response (CR) at interim and at EOT PET/CT. 8/24 (33%) had positive interim-PET/CT, showing either persistent or progressive disease, with a Deauville interim score ≥4; 2/8 (25%) had a PERCIST CR at EOT PET/CT while 6/8 patients showed persistent disease. Serum IL-10 was undetectable in 8/24 Patients at staging time while it was undetectable at interim evaluation in all Patients; IL-10 was higher, but non-significant, in Patients with positive interim-PET/CT. **Discussion:** Interim-PET/CT has a high Predictive Negative Value (PNV) since 16/24 (88%) patients, showing a CR at the EOT, were CR at interim evaluation and 16/16 were disease-free at follow-up. This observation deserves further confirmation, as it could imply interim changes in therapeutic regimens. SUVmax is not superior to a qualitative analysis and Deauville score ≥4 seems to be reliable to evaluate persistent disease at interim assessment. IL-10 tends to be higher in non-responders Patients than in responders, whereas at

interim evaluation, detectable values of IL-10 weren't observed. **Conclusion:** Interim-PET/CT predicts EOT PET/CT results in DLBCL patients with a high PNV and it should be further tested in order to obtain tailored per-patient therapies. IL-10 seems to be an interesting biochemical marker that could identify patients who respond more slowly, or not respond, to therapy, which deserve careful follow-up, although it didn't present a prognostic value in our series.

## P296

### Reader variability in response assessment by revised IWG criteria for malignant lymphoma

**E. Han**[1], E. Choi[1], W. Choi[1], W. Lee[2], J. O[3], Y. Park[1], S. Kim[1]; [1]The Catholic University of Korea, Seoul, KOREA, REPUBLIC OF, [2]Soonchunhyang University Hospital, Bucheon, KOREA, REPUBLIC OF, [3]The Johns Hopkins University, Baltimore, MD, UNITED STATES.

Objective: To evaluate the interobserver variability in response assessment of malignant lymphoma by revised International Working Group (IWG) criteria. Materials & Methods: FDG PET/CT images were performed at baseline, after 3 cycles of rituximab, cyclophosphamide, hydroxydaunomycin, oncovin, and prednisone (R-CHOP) chemotherapy, and after completion of chemotherapy in 61 diffuse large B cell lymphoma (DLBCL) patients. Two blinded nuclear medicine physicians (with 7 and 10 years' experience with FDG PET/CT each) retrospectively assessed response to chemotherapy using the revised IWG response criteria from 2007. The 4 response categories recommended are complete remission (CR), partial remission (PR), stable disease (SD) and progressive disease (PD). Interobserver agreement was analyzed with Kappa statistics. A kappa value of 0.0-0.2 was considered to indicate slight agreement; 0.21-0.4, fair; 0.41-0.6, moderate; 0.61-0.8, substantial; and 0.81-1.0, almost perfect. Results: 114 PET/CT images of 61 DLBCL patients (23 female, 38 male; mean age 53±14 years) were included. At baseline, 11 patients were TNM stage I, 19 were stage II, and 31 had advanced stage. Of 114 cases, observer 1 interpreted 64 cases as CR (56%), 48 as PR (42%), 0 as SD, and 2 as PD (2%). Observer 2 interpreted 64 as CR (56%), 36 as PR (31%), 3 as SD (3%), and 11 as PD (10%). Response agreement occurred in 45 cases for CR, 22 for PR, and 1 for SD. The Kappa statistic for interobserver consistency was 0.25. Conclusion: Low interobserver variability was observed in response assessment to chemotherapy according to revised IWG criteria. Further studies with greater number of cases and readers are required.

## P297

### Assessment of $^{111}$In-Ibritumomab pretreatment imaging in $^{90}$Y-Ibritumomab radioimmunotherapy for relapsed or refractory low-grade B cell lymphoma.

**K. Kaneko**, N. Uike, K. Shinozaki, I. Choi; National Kyushu Cancer Center, Fukuoka, JAPAN.

**Objective:** The objective of this study was to clarify the significance of $^{111}$In-Ibritumomab pretreatment imaging for $^{90}$Y-Ibritumomab radioimmunotherapy (RIT) for relapsed or refractory low-grade B cell lymphoma. **Material and Methods**: This retrospective study includes a total of 55 patients who underwent $^{90}$Y-Ibritumomab RIT for relapsed or refractory low-grade B cell lymphoma. The subjects consisted of 31 men and 24 women (range: 30-84 yrs). We compared $^{111}$In-Ibritumomab pretreatment image findings and $^{18}$F-FDG PET/CT image findings which were also obtained prior to RIT. $^{111}$In-Ibritumomab pretreatment image findings were also compared therapeutic effect and prognosis. **Results:** $^{111}$In-Ibritumomab findings were positive for lymphoma lesions in 31 patients and negative in 24 patients. $^{18}$F-FDG PET/CT image findings were more frequently matched (i.e., $^{111}$In-FDG positive or $^{111}$In-FDG negative) in $^{111}$In positive patients than in $^{111}$In negative patients (97% vs. 63%, $p < 0.001$). Overall response rate (ORR) of 97%, with complete response (CR) in 65% was obtained in $^{111}$In positive patients, and ORR of 79%, with CR in 50% was obtained in $^{111}$In negative patients. The ORR was significantly higher in $^{111}$In positive patients than in $^{111}$In negative patients ($p < 0.04$). In the clinical follow up at least 24 months (24-53months, n=32), disease relapse occured in 46 % (11/24) of $^{111}$In positive patients, in 38% (3/8) of $^{111}$In negetive patients, and no significant difference was found between them. In $^{111}$In negative patients, $^{111}$In-FDG negative patients showed high ORR (100%;9/9) , whereas $^{111}$In negative-FDG positive patients showed relatively low ORR(67%;10/15) and had five non-responders. **Conclusion.** Pretreatment $^{111}$In positive finding for lymphoma lesion was obtained in more than half of the lymphoma patients. $^{111}$In pretreatment image findings were similar to FDG-PET/CT image findings especially in $^{111}$In positive patients. $^{111}$In positive finding would indicate better therapeutic response to RIT than patients with $^{111}$In negative finding, although they had a similar rate of relapse.

## P298

### Usefulness of 18F-FDG PET/CT in the initial staging of ocular adnexal lymphomas

**C. Caoduro**[1], C. Ungureanu[1], P. Helias[2], O. Angoue[1], O. Blagosklonov[1], E. Deconinck[2], H. Boulahdour[1]; [1]Service de Médecine Nucléaire, Centre Hospitalier Régional Universitaire, Hôpital Jean Minjoz, Besançon, FRANCE, [2]Service d'Hématologie clinique, Centre Hospitalier Régional Universitaire, Hôpital Jean Minjoz, Besançon, FRANCE.

**Aim:** The purpose of this study was to evaluate the role of 18F-FDG PET/CT in the initial staging of patients with ocular adnexal lymphoma (OAL). **Materials and Methods:** six consecutive referred patients (male 2, female 4; mean age: 68 years) who were evaluated with 18F-FDG PET/CT for initial staging of OAL were included in this study. Four patients underwent vitrectomy, one patient underwent biopsy of a lesion of the anterior part of the orbit and a biopsy of the conjunctiva was performed on the last patient, two to four weeks before 18F-FDG PET/CT. The histopathological results revealed diffuse large B-cell lymphoma (DLBCL) for five patients and follicular lymphoma for one patient. **Results:** Orbital lesions were demonstrated by 18F-FDG PET/CT in five of six patients (83%), as focal increased FDG uptake in the orbit of these patients, clearly higher than the physiologic uptake of the surrounding soft tissue. Only one patient with DLBCL did not present any pathological focal uptake in the orbit. Furthermore, 18F-FDG PET/CT permitted to confirm systemic lymphomatous involvement suspected on previous CT, with increase FDG uptake of multiple supra-diaphragmatic lymph nodes in one patient and supra and infra-diaphragmatic in another patient. For two other patients 18F-FDG PET/CT also revealed cerebral lesions with increased FDG uptake respectively located in the right frontal lobe and in the left fronto-temporal lobe, secondarily confirmed by MRI. **Conclusion:** To our knowledge, few studies have assessed the value of 18F-FDG PET/CT in the initial staging of patients with OAL. These studies agree that 18F-FDG PET/CT is very useful to find extra-ophthalmologic lymphomatous sites and should be recommended during the initial staging of OAL patients, but they also point out the low sensitivity of 18F-FDG PET/CT in the detection of ophthalmologic lymphomatous sites probably owing to the relatively small tumor volume of adnexal lesions, the large amount of background physiologic activity in the orbits from the extra-ocular muscles and the proximity to the intense physiologic uptake from the brain. Nevertheless, our data show that, beyond its efficiency to evaluate systemic lymphomatous involvement in OAL, 18F-FDG PET/CT can also be a good tool to detect orbital lymphomatous lesions. Of course, further data obtained under a prospective and larger study are warranted to support this finding.

## P299

### Fluorine-18-Fluorodeoxyglucose Positron Emission Tomography/Computed Tomography for Extranodal Staging of Non-Hodgkin Lymphoma and Hodgkin Disease

**Ö. Ömür**[1], B. Yusufoglu[2], A. Oral[1], Y. Ceylan[1]; [1]Ege University Medical Faculty, Department of Nuclear Medicine, Izmir, TURKEY, [2]İzmir Institute of Technology, Department of Molecular Biology and Genetics, Izmir, TURKEY.

**OBJECTIVE:** Lymphomas, predominantly non-Hodgkin lymphoma (NHL), may involve extranodal organs. The presence and diagnosis of organ involvement is important for staging and management of patients. Anatomical imaging techniques have several limitations such as infiltrated organs without structural abnormalities. Aim of this study is to evaluate the role of FDG PET/care dose non contrast-enhanced CT for the detection of extranodal involvement in patients with NHL and Hodgkin Disease (HD). **PATIENTS and METHODS:** One hundred and ten patients with Lymphoma (35 HD, 75 NHL) having diagnostic contrast-enhanced CT (CE-CT) within the last month for FDG PET/CT imaging were included in our study. One hundred and twenty nine PET/CT images and all radiological, clinical and pathological records of these 110 patients were retrospectively reviewed. **RESULTS:** All of 137 hypermetabolic extranodal infiltration sites were detected by FDG PET/CT in 62/110 patients. There were no positive findings by CE-CT that reflect to organ involvement in 40/137. The κ statistics revealed fair agreement between PET/CT and CE-CT for detection of extranodal involvement (κ: 0.60). Organs having disagreement between two modalities were spleen, bone morrow, bone, thyroid and prostate glands. In all of these lesions that were negative at CE-CT, there was diffuse FDG uptake pattern in PET/CT images. Frequency of extranodal involvement was 51% (18/35) and 58% (44/75) in HD and NHL patients, respectively. There was no significant correlation between histological type, grade, and FDG affinity (SUV) of tumor, and detection of extranodal sites with FDG PET/CT or CE-CT ($p<0.05$). Mean SUVmax of the extranodal infiltration sites was 20.6±14.2 in staging/re-staging and 6.3±3.2 in post-therapy PET/CT scans. There was a high positive correlation between SUVmax values of the highest FDG accumulating lymph nodes and extranodal sites (R: 0.67) in patients with nodal and extranodal involvement. **CONCLUSION:** The results of this study demonstrated that FDG PET/CT is more effective technique than CE-CT for evaluation of extranodal involvement in HD and NHL patients. PET/CT has significant advantage for diagnosis of diffusely infiltrating organs without mass lesion or contrast enhancement such as spleen, bone morrow, thyroid gland and prostate as compared to CE-CT. In case, there is the highest SUVmax of the nodal sites, it may provide differential diagnosis of organ infiltrations other than FDG avid benign conditions.

## P300

### F-18 FDG PET/CT quantisation parameters as predictors of outcome in patients with diffuse large B-cell lymphoma

**F. D'Antuono**[1], G. Mansueto[1], S. Giacomobono[1], R. Gallicchio[1], A. Nardelli[2], T. Pellegrino[2], A. Tempone[1], F. Leggiadro[1], D. Gattozzi[3], R. Guariglia[1], G. Storto[1]; [1]IRCCS CROB, Rionero in Vulture, ITALY, [2]IBB CNR, Napoli, ITALY, [3]University of Texas Southwestern, Dallas, TX, UNITED STATES.

**Aim**: diffuse large B-cell lymphomas (DLBCL) exhibit an aggressive behaviour which ultimately contributes to their high cure rate being responsive to chemotherapy. We evaluated the prognostic significance of the quantitative assessment by standardized uptake value (SUVmax) and metabolic tumor volume (MTV) on F-18 FDG PET/CT in patients complying with DLBCL. **Material and Methods:** thirty-two patients (mean age, 67.6±19 years) with DLBCL underwent F-18 FDG PET/CT for staging 2 ±1 months before the initiation of chemotherapy. The maximum standardized uptake mean value and the summed metabolic tumor volume (cm3; 42% threshold) were registered for all the detected lesions. The patients were categorized into two groups according to SUVmax and MTV median values and followed up 22±9 months thereafter. Relapse or disease-related death constituted surrogate end-points. PET/CT results were then compared to the disease outcome (overall survival; OS). **Results**: global mean SUVmax was 15.2±7 and global mean MTV was 50.6± 44 cm3. The median SUVmax value was 14 and median MTV value was 24 (cm3). 6/32 patients (22%) showed relapse and 2/32 (6%) died. The Kaplan-Meier survival analysis for SUVmax showed a significant difference in OS between the two groups (p=0.007; HR, 8.1, log-rank test). Interestingly, the survival analysis for SUVmax showed a significant better OS in patients presenting higher values as compared to those having less than 14; the tumour burden estimated by the summed MTV was not suitable for predicting the outcome (p=0.07; HR, 0.2, log-rank test). **Conclusion**: despite the availability of several new tools for the quantitative appraisal and the estimation of disease activity on F-18 FDG PET/CT, the SUVmax rather than the MTV remains the only feature able to predict the outcome in DLBCL patients. These findings confirm that the magnitude of the glicolitic activity rather than the amount of the metabolically active burden holds a predominant value for determining the response to therapy in DLBCL.

## P301

### 18F-FDG-PET-CT evaluation of response to chemoimmunotherapy in Non-Hodgkin Lymphoma (NHL): a comparison between different reporting criteria in Diffuse Large B-Cell Lymphoma (DLBCL) and Primitive B-Cell Lymphoma of the Mediastinum (PMBCL).

F. Giunta[1], **M. Menga**[1], M. Zotta[1], A. R. Filippi[2], P. Pregno[3], M. Balma[1], M. Bellò[1], G. Bisi[1]; [1]Azienda Ospedaliera Città della Salute e della Scienza, Nuclear Medicine Unit, Internal Medicine Department, University of Turin, Turin, ITALY, [2]Azienda Ospedaliera Città della Salute e della Scienza, Radiotherapy Unit, Department of Oncology, University of Turin, Turin, ITALY, [3]Azienda Ospedaliera Città della Salute e della Scienza, Haematology 2, Department of Oncology and Haematology, Turin, ITALY.

**Aim:** In consideration of the diversity in histology and clinical behaviour between various forms of NHL, we compared, in two histological types of glucose-avid forms, the performance of three different evaluation criterion: International Harmonization Project (IHP), 5-point scale (5-PS) and ΔSUVmax. **Materials and Methods:** 84 patients (31 PLMBCLs, 53 DLBCLs, 22 of which with a bulky lesion at diagnosis) who had undergone baseline (b-PET) and end-of-chemoimmunotherapy (f-PET) 18F-FDG-PET-CT scans at our institution between July 2004 and January 2013 were retrospectively re-evaluated. All received R-CHOP or R-CHOP-like regimens; all PMBCLs and 9/22 bulky DLBCLs also received radiotherapy. Mean clinical follow-up: 26,78+/-19 months. Clinical outcome (complete response -CR, partial response -PR and disease progression -PD) at follow-up was considered gold standard. In non-bulky disease, SUVmax of the hottest lymph node at staging and after therapy were calculated, independently from localisation. In bulky disease, SUVmax of the mass at staging and of its post-therapy CT residue were calculated. Liver and mediastinal blood-pool SUVmax were calculated for all patients. All f-PET-CTs were evaluated dichotomously by IHP, 5-PS (positivity/negativity threshold between scores 3 and 4) and ΔSUVmax (f-PET vs. b-PET ΔSUVs were calculated as a percentage value, considering 66% and 75% decrease as positivity/negativity thresholds). Sensitivity (SE), specificity (SP) and positive predictive value (PPV) were calculated. **Results:** DLBCL:10 PR/PD, 43 CR. IHP: 36 positive, 17 negative. SE:100%; SP:40%; PPV:28%. 5-PS: 21 positive, 32 negative. SE:90%; SP:72%; PPV:43%. ΔSUV75%: 12 positive, 41 negative. SE:50%; SP:84%; PPV:42%. ΔSUV66%: 9 positive, 44 negative. SE:50%; SP:91%; PPV:56%. PMBCL:5 PD, 26 CR. IHP: 30 positive, 1 negative. SE:100%; SP:4%; PPV:17%. 5-PS: 19 positive, 12 negative. SE:100%; SP:46%; PPV:26%. ΔSUV75%: 7 positive, 24 negative. SE:100%; SP:92%; PPV:71%. ΔSUV66%: 6 positive, 25 negative. SE:100%; SP:96%; PPV:83%. **Conclusions:** In PMBCL, ΔSUVmax at threshold 66% appears to strongly predict outcome, possibly because of inflammatory reactions or minimal residual disease sterilized by radiotherapy. In DLBCL, both nodal and bulky, negativity threshold at score 3 5-PS appears to be an acceptably safe tool for prognostic evaluation.

## P302

### The Value of Qualitative and Quantitative Evaluation of Interim-PET/CT in Lymphoma Patients For The Prediction of Metabolic Response

O. Sahin, **M. Serdengecti**, B. Kaya, M. İsmailoglu, T. Guler, E. Varoglu; N.Erbakan University, Konya, TURKEY.

**Aim:** The aim of our study was to evaluate the value of visual interpretation of FDG-PET/CT scanning which is made after the 2nd - 4th chemotherapy cycle while predicting the metabolic response in lymphoma patients and to compare with quantitative assessment. **Methods:** 34 patients are included who have undergone basal PET/CT (PET0) scanning before therapy, interim-PET/CT (PET1) scanning after the 2 - 4. chemotherapy cycle, PET/CT (PET2) scanning for evaluation of response after the therapy. 24 of these patients were Non Hodgkin's Lymphoma (NHL) and 11 of them were Hodking's Lmphoma (HL). Patients are evaluated by visual qualitative interpretation as positive, negative and minimal residual uptake (MRU) as to PET1 results and complete response, partial response, stable disease and progression of disease as to PET2 results. PET1's prediction value for PET2 is evaluated by quantitative assessment by taking the cut-off values of ratios of exchange of PET0 - PET1 SUVmax values as 66% and cut-off value of PET1 SUVmax as 4. The values of qualitative and quantitative Methods were compared to predict metabolic response. **Results:** According to visual qualitative interpretation of PET1 results, 80% of sensitivity, 83% of specifity, 67% of PPV and 91% of NPV were found. According to quantitative assesment by taking cut-off value of ratio of exchange of PET0 - PET1 SUVmax as 66%, 60% of sensitivity, 100% of specifity, 100% of PPV and 86% of NPV and furthermore by taking the cut-off value of PET1 SUVmax as 4, 60% of sensitivity, 96% of specifity, 86% of PPV and 85% of NPV were concluded for prediction of metabolic response. **Conclusion:** Visual interpretation method of interim-PET/CT is considerably successful for prediction of metabolic response to the therapy in lymphoma patients. With additional quantitative Methods to Interim-PET/CT's visual interpretation, ratios of false positivity would be reduced significantly. We concluded that need to transition to a more aggressive treatment, the use of quantitative Methods was found to be more useful. When the reduction of dose or duration of treatment is planned, qualitative visual interpretation of interim-PET/CT will be more useful.

## P303

### Standardized uptake value for F-18 fluorodeoxyglucose associates with high International Prognostic Index and the presence of extranodal involvement in patients with Diffuse Large B-cell Lymphoma

**B. E. Akkas**, G. U. Vural; Ankara Oncology Research and Training Hospital Department of Nuclear Medicine, Ankara, TURKEY.

The aim of this study was to evaluate whether standardized uptake value (SUVmax) for F-18 fluorodeoxyglucose (FDG) associates with international prognostic index (IPI) and the presence of extranodal involvement in patients with Diffuse Large B-cell Lymphoma (DLBCL). Method: Seventy seven patients (40F, 37M, age: 57.2±18.5, age range:14-93) with DLBCL who underwent FDG PET/CT for initial staging were enrolled in this retrospective study. The sites of nodal and extranodal involvement, SUVmax of the predominant lesions were noted. SUVmax were compared to AnnArbor stage, IPI scores, the presence of extranodal involvement and the number of involved extranodal sites. Results: Clinical AnnArbor stage of the patients was as follows; stage I:3 patients, stage II:28 patients, stage III:18 patients and stage IV:28 patients. PET/CT detected nodal and/or extranodal involvement in all patients. PET/CT detected extranodal involvement in 52 patients. In 27 patients, extranodal disease could only be detected by PET/CT. SUVmax of the predominant lesion in patients with extranodal disease was significantly higher than patients who had only nodal disease (25±12 vs. 15.3±10 respectively, p=0.001). We observed that SUVmax significantly correlated with IPI scores; such that, the average SUVmax of the predominant lesion was 13.9±9.5 in patients with low risk (IPI=0-1), 14.2±8.8 in low-intermediate risk group (IPI=2) whereas 26.6±9.5 in high-intermediate risk group (IPI=3) and finally, 25±13.6 in high risk group patients (IPI=4-5) (p=0.002). SUVmax was not correlated with clinical stage, the number of extranodal sites and serum LDH levels. Conclusion: Our study indicates that high FDG uptake of predominant lesion on pretreatment PET/CT correlates with clinical poor prognostic factors such as IPI and extranodal involvement in patients with DLBCL. Thus, the correlation of SUVmax with these prognostic factors may highlight the importance of pretreatment FDG uptake as a poor prognostic metabolic marker for patients with DLBCL. We consider that further prospective studies may provide efficient use of SUVmax in combination with IPI to guide risk- adapted therapies in patients with DLBCL.

## P304

### Can 18F-FDG PET/CT avoid the systematic bone marrow biopsy for initial staging of Hodgkin's Lymphomas?

**D. Cabello García**[1], S. Lakhwani[2], A. Allende Riera[1], J. Raya[2], E. Martínez Gimeno[1], J. Muñoz Iglesias[1], M. Fernández González[2], J. Uña Gorospe[1], C. Stoica[2], M. DeSequera Rahola[1], C. Cárdenas Negro[1]; [1]Nuestra Señora de Candelaria University Hospital, Santa Cruz de Tenerife, SPAIN, [2]De Canarias University Hospital, Santa Cruz de Tenerife, SPAIN.

Aim: To assess whether 18F-FDG PET/CT study alone can replace bone marrow biopsy (BMB) in evaluation of bone marrow involvement (BMI) in initial staging of Hodgkin's Lymphomas (HL). Evaluate the clinical impact of 18F-FDG PET/CT, in relation to BMB, in the clinical management of these patients. Materials and Methods: A total of 36 patients (mean age 36, range 13-76; 16 female, 20 male) with Hodgkin's disease (nodular sclerosis 66.7% and mixed cell 19.4%), underwent 18F-FDG PET/CT and BMB for initial staging of HL. Bone marrow uptake (BMU) level was assessed visually according to liver uptake (1=below liver uptake, 2=corresponding to liver uptake and, 3=above liver uptake) and semi-quantitatively using the maximum standardized uptake value (SUV max) measured in the sacral area. BMB results were correlated with 18F-FDG PET/CT findings. Results: Thirty-four patients had negative BMB and 2 also presented positive BMB. BMI measured by 18F-FDG PET/CT resulted negative for 27 patients and positive for 9 patients. Seven patients presented negative BMB and positive 18F-FDG PET/CT study: 5 showed multifocal FDG uptake and 2 patients presented unifocal FDG uptake. Bone marrow uptake was higher than liver uptake in 77.8% (7/9) of cases with BMI. The 2 patients with positive BMB had a positive 18F-FDG PET/CT. The mean of SUV max of the lesions was 9.0±2.3 (range 5.6-12.5) and the mean of SUV max in sacral area was 3.7±1.1 (range 2.4-6.7). Sensitivity and Specificity for 18F-FDG PET/CT were 100% and 100%, respectively. Sensitivity and Specificity for BMB were 22.2% and 100%, respectively. Diagnostic Accuracy was 100% for 18F-FDG PET/CT and 80.6% for BMB. The 18F-FDG PET/CT study supposed a change in the staging and clinical management of 13.9% (5/36) of the patients in relation to BMB. Conclusion: 18F-FDG PET/CT highly improves the Sensitivity for diagnosis of bone marrow involvement in staging HL compared bone marrow biopsy. In our patients, BMB didn't provide additional information with respect to 18F-FDG PET/CT about bone marrow involvement, underdiagnosing 7 of 36 patients, so 18F-FDG PET/CT study should be the test of choice versus BMB in initial staging of HL. Nevertheless, it would be necessary to complete this study with a larger number of patients.

## P305

### What are the benefits of 18F-Fluorodeoxyglucose positron emission tomography/computed tomography in the initial staging of follicular lymphoma?

**J. Muñoz Iglesias**[1], A. Allende Riera[1], M. Hernández[2], C. Cárdenas Negro[1], J. Uña Gorospe[1], M. De Sequera Rahola[1], D. Cabello García[1], E. Martínez Gimeno[1]; [1]Hospital Universitario Nuestar Señora de Candelaria, Santa Cruz de Tenerife, SPAIN, [2]Hospital Universitario de Canarias, Santa Cruz de Tenerife, SPAIN.

Aim: The purpose of this study was to assess the usefulness of 18F-Fluorodeoxyglucose positron emission tomography/computed tomography (18F-FDG-PET/CT) in staging of patients with follicular lymphoma (FL). Material and method: Data from 31 patients (mean age 58, range 38-71), 17 females and 14 males with newly diagnosed FL WHO grade I-III (21 had FL grade I/II and 10 had FL grade III). All patients had received contrast-enhanced CT, 18F-FDG-PET/CT (mean doses 2,8 MBq/Kg) and bone marrow biopsy (BMB), which was not available at the time of 18F-FDG imaging, in the initial staging. The patients were classified using COTSWOLD Staging System for Lymphoma (CSS) by CT and 18F-FDG-PET/CT. To evaluate disseminated bone marrow involvement the 18F-FDG-uptake in bone marrow (BMU) was visually assessed according to the liver uptake and classified as normal, diffuse and focal positive uptake. Results: 18F-FDG-PET/CT was positive in all patients and detected more nodal (45%) and extranodal (85%) lesions than CT. CSS CT staging was: 2 patients in stage I, 11 in stage II, 13 in stage III and 5 in stage IV. The CT did not detect bone marrow involvement in any patient. CSS PET/CT staging was: 5 patients in stage II, 12 in stage III and 14 in stage IV. 18F-FDG-PET/CT modified CSS staging in 15/31 patients (48%) and the therapeutic management in 27%. The BMB was positive in 14/31 patients, of which 9/14 had pathological BMU. 18F-FDG-PET/CT had a sensitivity, specificity and positive predictive value of 65, 94 and 90 %, respectively, to identify bone marrow involvement. Conclusion: Due to the impact on the initial staging and therapeutic management of follicular lymphomas, we believe that the 18F-FDG-PET/CT should be included in all guidelines. In patients with bone marrow involvement assessed by 18F-FDG-PET/CT, bone marrow biopsy could be avoided or at least could be used as the guide for biopsy.

## P306

### Could the highest standardized uptake value of 18F-Fluorodeoxyglucose be used to distinguish between indolent and aggressive follicular lymphoma in initial staging?

**J. Muñoz Iglesias**[1], A. Allende Riera[1], M. Hernández[2], C. Cárdenas Negro[1], J. Uña Gorospe[1], M. De Sequera Rahola[1], D. Cabello García[1], E. Martínez Gimeno[1]; [1]Hospital Universitario Nuestra Señora de Candelaria, Santa Cruz de Tenerife, SPAIN, [2]Hospital Universitario de Canarias, Santa Cruz de Tenerife, SPAIN.

Aim: The purpose of this study was to assess whether the intensity of [18F]Fluorodeoxyglucose positron emission tomography (18F-FDG-PET) uptake could differentiate between indolent and aggressive follicular lymphoma (FL). Material and method: PET studies of 30 patients (mean age 58, range 38-71), 17 females and 13 males with FL WHO grade I-III (11, 9 and 10 patients), who were untreated disease and had not received treatment within the last 6 months, were analyzed. The images were visually assessed on axial, coronal, sagittal reconstruction and with the multi intensity projection (MIP). A semiquantitative analysis using the highest standardized uptake value (SUV) was applied. SUVs were analyzed considering indolent clinical course (FL grade I and II) and aggressive course (FL grade III) and correlations were made with histopathology. Two-sample comparisons were performed using the Wilcoxon test and a P value less than .05 was considered significant. Results: All patients with follicular lymphoma had a positive 18F-FDG-PET. FDG uptake was lower in indolent than in aggressive lymphoma (SUV, 9.3 ± 5.7 v 15.4 ± 8.5; P < .03). All patients with indolent FL had a SUV ≤ 12, except one patient with a diagnosis of low-grade FL in bone marrow biopsy with SUV 31 (probably because the biopsy was not performed in the lesion with highest uptake). On the other hand, 2 patients with high grade FL showed lesions with a SUV < 12. Conclusion: 18F-FDG-PET is a reliable method in patients with follicular lymphoma irrespective of tumour grading. As FDG uptake is lower in indolent than in aggressive follicular lymphomas, it could be used in cases of discordance between biopsy and clinical behaviour.

P48-1 - Sunday, Oct. 20, 16:00 - 16:30, Poster Exhibition Area

## Oncology Clinical Science: Leukaemia & Myeloma

## P307

### 18F-FDG kinetics in patients with multiple myeloma. Evaluation with dynamic PET-CT

**C. Sachpekidis**[1], L. G. Strauss[1], H. Goldschmidt[2], J. Hillengaß[2], C. Cheng[1], L. Pan[1], A. Dimitrakopoulou-Strauss[1]; [1]Clinical Cooperation Unit Nuclear Medicine, German Cancer Research Center, Heidelberg, GERMANY, [2]Department of Medicine V, Multiple Myeloma Section, University of Heidelberg, Heidelberg, GERMANY.

Aim: During recent years the role of 18F-FDG PET in the diagnostic approach of multiple myeloma (MM) has been upgraded. However, little is known about the kinetics of 18F-FDG in this malignancy. Aim of the study is to acquire quantification data regarding kinetics of 18F-FDG in patients (pts) with MM. Materials and Methods: The ongoing evaluation includes 41 MM pts. Dynamic PET-CT (dPET-CT) studies of the lower lumbar spine and pelvis were performed after the administration of 200-250 MBq of 18F-FDG. Sites of focal increased tracer uptake were considered as highly suspicious of metastatic lesions. The kinetic parameters' values of these lesions were compared with the respective values of lower lumbar spine and pelvic skeleton that served as reference. The evaluation of dPET-CT studies was based on a 2-tissue compartment model and a non-compartmental approach. Results: The number of MM-indicative lesions was 41. The kinetic parameter k1 (1/min) that represents regional blood flow and is related to angiogenesis was 0.27 for MM lesions and 0.21 for reference areas. The kinetic parameter k3 (1/min) indicative of phosphorylation rate was 0.1 for MM lesions, while in references areas 0.04. Conclusion: Both mechanisms of increased perfusion and FDG phosphorylation seem to take place in MM metastases, thus leading to increased FDG-PET expression in this malignancy.

## P308

### Autologous blood stem cell transplantation in multiple myeloma: treatment response evaluation with two different PET tracers

**C. Sachpekidis**[1], L. G. Strauss[1], H. Goldschmidt[2], J. Hillengaß[2], H. Dirk[2], A. Dimitrakopoulou-Strauss[1]; [1]Clinical Cooperation Unit Nuclear Medicine, German Cancer Research Center, Heidelberg, GERMANY, [2]Department of Medicine V, Multiple Myeloma Section, University of Heidelberg, Heidelberg, GERMANY.

Aim: Autologous blood stem cell transplantation (ABSCT) has become the first line standard of care in multiple myeloma (MM). Aim of this ongoing study is to evaluate therapy response in MM patients (pts) who underwent ABSCT, with the use of 18F-FDG and 18F-fluoride PET-CT. Materials and Methods: 7 patients (mean age 64 years) suffering from stage III MM according to the Durie-Salmon staging system underwent 18F-FDG and 18F-fluoride PET-CT scan for baseline evaluation before the onset of high-dose chemotherapy and ABSCT. 5 months after the ABSCT, another combination of 18F-FDG and 18F-fluoride PET-CT studies was performed in each patient, for imaging evaluation of treatment response. Results: On baseline evaluation, the 18F-FDG PET-CT scans showed that 4/7 pts were FDG-positive while

3/7 were FDG-negative for MM. The 18F-fluoride studies demonstrated the MM indicative lesions depicted with FDG, as well as degenerative lesions. The patients subsequently underwent high dose chemotherapy and ABSCT. Their response to treatment was characterized by the hematologists as: complete response (CR) in 3/7, very good partial response (VGPR) in 2/7 and partial response (PR) in 2/7 pts. Approximately 5 months after the ABSCT, the pts went through another combination of 18F-FDG and 18F-fluoride PET-CT scans. These studies showed that 3/7 pts who were FDG-negative on baseline scan remained FDG-negative (2 VGPR, 1 CR). Of those with initial FDG-positive scan, those characterized as CR showed complete remission of the disease and those characterized as PR demonstrated less lesions on FDG-PET scan. These follow-up FDG-PET studies were in agreement with the pts' hematologic status. On the other hand, 18F-fluoride PET demonstrated only minor changes compared with the baseline studies. Conclusions: These cases demonstrate the role of 18F-FDG PET-CT in evaluation of treatment response in FDG-positive MM pts. They also indicate the inability of 18F-fluoride to evaluate early therapy response in this malignancy.

## P309

### Prognostic impact of bone structure in advanced chronic lymphocytic leukemia

**F. Fiz**[1], C. Marini[2], R. Piva[1], M. Miglino[3], M. Massollo[1], F. Bongioanni[1], A. Buschiazzo[1], S. Morbelli[1], G. Bottoni[1], M. Gobbi[4], A. Bacigalupo[5], P. Bruzzi[6], F. Frassoni[7], M. Piana[8], G. Sambuceti[1]; [1]Chair of Nuclear Medicine; Genoa University, IRCCS-AOU San Martino-IST, Genoa, ITALY, [2]CNR Institute of Molecular Bioimaging and Physiology, Milan, Section of Genoa, Genoa, ITALY, [3]3Chair of Hematology, Genoa University, IRCCS-AOU San Martino-IST, Genoa, ITALY, [4]Chair of Hematology, Genoa University, IRCCS-AOU San Martino-IST, Genoa, ITALY, [5]Hematology and Bone Marrow Transplantation Dept., IRCCS-AOU San Martino-IST, Genoa, ITALY, [6]Epidemiology Dept., IRCCS-AOU San Martino-IST, Genoa, ITALY, [7]Stem Cell lab, IRCCS Pediatric Institute G. Gaslini, Genoa, ITALY, [8]Department of Mathematics, University of Genoa, Genoa, ITALY.

**Background**: In experimental models, leukemia can alter osteoblast and osteoclast function causing significant bone thinning, which is quantifiable at microCT scan. This alteration in bone structure contributes to disease progression, simultaneously disrupting normal hematopoiesis and favoring uncontrolled proliferation of clonal elements. The clinical impact of the interaction between leukemia cells and bone microenvironment is to date still uncertain, due to the lack of dedicated Methods for studying bone structure and function throughout the whole skeleton in living humans. **Methods**: The study included 22 patients, hospitalized for suspected disease progression in advanced chronic lymphocytic leukemia (ACLL), and undergoing FDG PET/CT scan for disease status assessment. Data were compared with corresponding values obtained from 22 age and sex matched control subjects, selected according to a case-control criterion from a previously published normalcy database. Images were analyzed using a novel computational approach to PET/CT images to estimate total skeletal volume (SV), intra-bone volume (IBV) and compact bone volume (CBV) from CT data. To this purpose, the algorithm recognized the bone contour on each CT slice and measured the average Hounsfield coefficient value within a two-pixel ring starting from the border. All intraosseous pixels having an attenuation coefficient lower than this cut-off were flagged as IBV, while the others were considered CBV. FDG PET uptake index, extracted from the voxel corresponding to the IBV, were used to tell apart active bone marrow (ABM) from fatty bone marrow (FBM), according to a statistical threshold of glucose analogue uptake. All volumes were then normalized for ideal body weight (IBW). **Results**: ACLL caused compact bone loss and expansion of IBV that was higher in patients than in controls (32±8 vs 27±8 ml/Kg IBW, respectively, p<0.05), despite an only minor increase in ABM. As a consequence, IBV/SV ratio was higher in leukemics (39%±5%) than in controls (31%±7%, respectively, p=<0.001). After stratification according to median value, patients with IBV/SV >37.3% showed an actuarial two-year survival of 18% compared with 76% for those whose IBV/SV was less than 37.3% (p<0.001). Multivariate Cox analysis ruled out any significant contribution of age, gender, biological disease pattern and time elapsed from onset of chronic lymphocytic leukemia to PET/CT. **Conclusion**: Our mathematical approach to PET/CT images documents that ACLL is associated with skeletal alterations whose assessment might represent a new window to predict the clinical course of the disease.

## P310

### 18F-FDG PET/CT features in systemic mastocytosis

S. Djelbani[1], M. Chandesris[2], A. Mekinian[3], O. Monsarrat[1], G. Pop[1], I. Durieu[2], S. Georgin-Lavialle[2], B. Grosbois[2], V. Eder[1], O. Hermine[2], O. Fain[3], **M. Soussan**[1]; [1]Avicenne Hospital, APHP, Department of Nuclear Medicine, Bobigny, FRANCE, [2]Center of reference of mast cells (CEREMAST), University of Paris, Paris, FRANCE, [3]Jean Verdier Hospital, Department of Internal Medicine, Bondy, FRANCE.

Objectives Systemic mastocytosis (SM) is characterized by abnormal accumulation and growth of mast cells in the bone marrow (affected almost invariably) or other extracutaneous organs together with cytological and biochemical signs of systemic disease. SM is divided into the following categories: indolent systemic mastocytosis (ISM), the most common form (> 80%) with good prognosis, aggressive systemic mastocytosis (ASM) associated or not with hematologic non-mast cell lineage disease (SM-AHNMD) and the exceptional mast cell sarcoma. The purpose of this study was to describe the appearance of FDG-PET in different forms of mastocytosis. Materials and Methods Fifteen patients followed at the reference center of mastocytosis (CEREMAST) were retrospectively included. All patients performed an FDG-PET/CT for initial evaluation (n = 14) or follow-up (n = 1). FDG uptake has been graded for bone marrow and lymph node using a 3-point visual scale with the mediastinal blood pool (MBP) as a reference: uptake < or equal to MBP = 0, moderately increased uptake above MBP = 1, markedly increased uptake above MBP = 2. Results ISM was diagnosed in 3 patients, ASM in 5 patients, SM-AHNMD in 6 patients, and a mast cell sarcoma in one patient. PET was positive in 13 patients (87%). Pathological uptake was located in bone marrow (n = 10; SUV max: 12.2), liver and/or spleen (n = 12; SUVmax: 4.8) and in lymph nodes (n = 7; SUVmax: 6.6). The 3 patients with ISM had no significant (score 0, n=2) or slight (score 1, n=1) bone marrow uptake. Three out of 5 patients with ASM had moderately or markedly increased bone marrow uptake. Five out of 6 patients with SM-AHNMD had markedly increased bone marrow uptake. Patients with SM-AHNMD had higher bone marrow uptake than patients with ISM and ASM (p=0.03). Lymph node uptake has been observed in 1/3 ISM patients, 2/5 ASM patients and 2/6 SM-AHNMD patients. The patient with the mast cell sarcoma showed markedly increased bone marrow and lymph node uptakes. Liver and/or spleen uptake was observed in all patients except in the 3 ISM patients. No correlation was found between SUVmax and tryptase levels. Conclusions Systemic mastocytosis appears with different FDG-PET patterns according to their aggressiveness and the presence or absence of AHNMD.

## P311

### Correlation of 18F-fluorodeoxyglucose uptake on PET/CT with MIB-1 labeling index in pheochromocytomas.

**S. Sugawara**, Y. Arisaka, A. Tokue, M. Kim, T. Higuchi, Y. Tsushima; Gunma University Graduate School of Medicine, Maebashi, JAPAN.

**Background and Purpose** 18 F- fulorodeoxyglucose positron emission computed tomography (FDG-PET) is known to have a high sensitivity in detecting pheochromocytomas in which 10 to 15% of the cases are malignant and is associated with poor prognosis after occurrence of multiple metastasis. Reliable pathologic criteria predicting clinical behavior of pheochromocytomas has not been fully established while MIB-1 labeling index (MIB-1 LI) is expected as relatively better marker. The purpose of this study was to investigate the correlation between MIB-1 labeling index and FDG uptake in pheochromocytomas. **Materials and Methods** FDG-PET and MRI were performed in all 22 patients (13 male, 9 female). FDG (5-6 MBq/kg) was administered after fasting for more than 6 hours. Data acquisition was started at 60 minutes by 3D-mode with PET/CT. FDG uptake was evaluated by the maximum standardized uptake value (SUV max.). Diffusion-weighted imaging (DWI) was done in axial images by 1.5 T, spin echo echo-planar imaging (SE-EPI), with TR : 1000 ms. TE 'minimum', 5-mm thickness, with b values of 1000/1500 mm2/s, covering the whole brain. A region of interest (ROI) was set on the lesion of pheochromocytomas. The ADC values were calculated at a workstation. Proliferative activity of the tumor was assessed as the percentage of MIB-1-stained nuclei (MIB-1 labeling index) by immunohistochemical analysis of the resected specimen. Correlation between MIB-1 labeling index and other factors (SUVmax, ADC value and tumor size) was statistically analyzed by using a Spearman's rank correlation coefficient. **Results** All lesions showed positive FDG findings and detected by MRI. Tumor size (mm), MIB-1 index (%), SUVmax and ADC values were 47.4±21.1, 5.20±9.69, 9.16±8.10 and 1.04±0.24, respectively. MIB-1 index significantly correlated with SUV max of FDG (r=0.756, p<0.001), while maximum diameter (r=0.3119, n.s.) and ADC value (r=0.3166, n.s.) showed no significant correlation. **Conclusions** FDG-PET seems to have diagnostic utility in the evaluation of tumor proliferative activity of the patient with pheochromocytomas, thereby, future application to the optimization of patient's management is promising.

## P312

### Chromogranin A, biomarker in GEP-NETs, correlation with Octreoscan; our experience

**S. Rodriguez Martinez de Llano**[1], J. Mendez Mendez[2], I. Candal Casado[1], P. Pais Silva[1]; [1]Nuclear Medicine. Centro Oncologico de Galicia, La Coruña, SPAIN, [2]Medical Oncology. Centro Oncologico de Galicia, La Coruña, SPAIN.

Introduction Chromogranin A (CgA) is the best available biomarker for diagnosis of NET. Elevated CgA may correlate with tumor progression and is elevated 80-100% of the time in these patients. Treatment with proton-pump inhibitors, chronic atrophic gastritis, impaired renal function, irritable bowel syndrome and inflammatory bowel disease, may increase its values. Aim Evaluate its values and

search for a correlation with octreoscan findings, to identify diagnostic and prognostic information and its significance. Material and Methods A three year retrospective study was conducted (09.09-09.12), selecting patients referred to our department to perform an OctreoscanTM (mean injected dose of In-111 Pentectreótide, 111MBq) with a plasma CgA determination (enzyme immunoanalysis) within 15 days of the study (19,4-98,1ng/mL). In addition possible conditions that could cause its elevation, were evaluated. Octreoscan results were assessed qualitatively by three experienced nuclear physicians, with subsequent confirmation of diagnosis by other imaging thecniques or histology. Results 39 out of 146 patients fulfilled our inclusion criteria. 17 women and 22 men (mean age 60.02 years), presented in most cases as low-grade (51.28%) carcinoid tumors (61.53%) from small intestine (33.33%). Whole body and tomographic studies were conducted at 4 and 24 hours for all patients with confirmation of diagnosis mostly with CT in 89,7% and histology in 38.46%. 17 patients (43.58%) did not show an increase in CgA plama levels, 8 of them had a negative Octreoscan study (all true negative, CgA mean value 65,49ng/mL) and 9 of them were positive (all true positive)mostly in liver, with a mean value of 53,55ng/mL. In the 22 (56.41%) that showed it, 14 had a positive Octreoscan (all true positive, CgA mean value 994.65ng/mL) and 8 (43, 33%) did not, all true negative (CgA mean value 263.17 ng/mL) of which, all but one patient presented chronic atrophic gastritis(n=3), irritable bowel syndrome (n=1) and three of them were on treatment with proton-pump inhibitors. Conclusions Plasma CgA is not frequently requested in our area. Elevation of CgA seems to be more related to a positive Octreoscan but some conditions as chronic atrophic gastritis , irritable bowel syndrome and treatment with proton-pump inhibitors may increase it values in true negative scans. This increase does not seem as high as in positive scans. The absence of its elevation could be related with a true positive Octreoscan. Limitations of using CgA should be taken into account. New biomarkers in NET are needed to provide better diagnostic and prognostic information.

## P313

### Lebanese experience with 68Ga-DOTA-TATE PET/CT in the diagnosis and management of Neuroendocrine tumors.

**M. Haidar**[1,2], F. CHEHADE[1], R. ASMAR[1], M. JRIEGE[3], T. KHOURY[4]; [1]Mount Lebanon Hospital, Nuclear Medicine Department, HAZMIEH - BEIRUT, LEBANON, [2]Lebanese University, Beirut, LEBANON, [3]Saint Joseph University, Radiology Department, BEIRUT, LEBANON, [4]American University of Beirut Medical Center, Radiology Department, HAZMIEH - BEIRUT, LEBANON.

OBJECTIVE: Evaluation of the role of 68Ga-DOTA-TATE PET/CT in the diagnosis and management of neuroendocrine tumors (NET). SUBJECTS AND METHODS: 27 patients with NET underwent 68Ga-DOTA-TATE PET/CT which was performed after injection of 111-259 MBq (3-7 mCi) of 68Ga-DOTA-TATE. PET/CT images were compared with conventional imaging by two experienced nuclear medicine physicians. The results of PET/CT were correlated to histopathology results, when available, and with radiological data after close follow up. RESULTS: 68Ga-DOTA-TATE PET/CT showed sensitivity and specificity of 76% and 92%, respectively, for primary tumor and 98% and 100% for metastases. It was superior in the detection of both primary tumor and metastases when compared to conventional imaging modalities. It changed the management strategy in 6 patients (22%). CONCLUSION: Our analysis in this relatively small patient cohort indicates that 68Ga-DOTA-TATE PET/CT is a highly sensitive and specific modality for the detection of NET especially for metastatic lesions, with better results when compared to conventional imaging modalities. This can have a significant impact on patient management.

## P314

### The impact of FDG PET/CT on the management of Merkel cell carcinoma

**C. Sayer**, S. Westwell, V. Raman, G. Burkill, S. Dizdarovic; Brighton and Sussex Universities Trust, Brighton, UNITED KINGDOM.

Aim Merkel cell carcinoma (MCC) is a rare but highly aggressive cutaneous neoplasm which carries a poor prognosis. The overall survival rate is 58-79%. Even after treatment close surveillance is required due to high recurrence; 30%-40% locally within 12 months, 50% regionally within 2 years, and systemic disease in 36%-49%. There is limited data on the optimum imaging strategy. FDG-PET-CT has been suggested as useful in baseline and surveillance imaging due the high metabolic activity of MCC. We aim to document our institutional experience of this modality and its impact on further investigation and management. Materials and Methods A retrospective cohort study of FDG-PET/CT in cases of histologically confirmed MCC in a single institution between 1/1/2008 and 31/12/2012 was performed. A pro-forma was completed for each scan detailing patient demographics, reason for scan, impact on diagnostic management (none, confirmed proposed management or altered management), impact on investigations and impact on therapy (upgraded, downgraded or none). Results 10 scans performed in 6 patients (4 females, 2 males) with a median age of 71.5 years. 80% were performed following treatment (local excision, chemotherapy or radiotherapy) or to increase diagnostic confidence where the CT findings were equivocal. 20% were performed as the baseline investigation. 60% of scans confirmed the proposed diagnostic management plan in all cases by increasing diagnostic confidence from previous imaging findings; 20% altered diagnostic management (i.e. resulted in an ultrasound guided FNA); and 20% had no effect on further investigations. Therapy was upgraded in 40% after PET-CT (chemotherapy commenced due to the presence of distant metastases), but downgraded in 10% (chemotherapy stopped due to a complete response). In 50% of cases there was no effect on the therapeutic management. Conclusion FDG-PET-CT has an impact on therapeutic and diagnostic management of patients with MCC. PET-CT altered therapeutic management in 50% of cases and influenced diagnostic management in 80% of cases by detecting additional lesions not appreciable on CT, or by providing confidence or reassurance where the CT findings were ambiguous. In our experience FDG-PET-CT was performed most commonly to look for residual or metastatic disease following excision of the primary lesion; to problem solve ambiguous CT findings; and to aid decisions to instigate or continue chemo-radiotherapy. Multicentre prospective trials in MCC are needed to investigate the full potential of PET-CT for standard use for staging, assessment of treatment response or plan further therapy for recurrence in MCC.

## P315

### Somatostatin receptor PET/CT in neuroendocrine tumours: update on systematic review and meta-analysis

**H. Geijer**, L. Breimer; Örebro University Hospital, Örebro, SWEDEN.

Aim: neuroendocrine tumours (NET) are uncommon and may be localized in many different places in the body. Traditional imaging has mainly been performed with computer tomography and somatostatin receptor scintigraphy (SRS). Recently, it has become possible to use somatostatin receptor PET/CT (SMSR-PET) instead, which might improve diagnostic quality since PET has higher sensitivity and better spatial resolution than SRS. To evaluate the diagnostic quality of SMSR-PET we have performed a meta-analysis which was performed as an update of a previously published study from 2012. Materials and Methods: a literature search was performed searching MEDLINE, Embase and five other databases with a combination of the expressions ”PET”, ”positron emission tomography”, ”neuroendocrine” and ”NET”. The search was updated until Dec 31, 2012. Studies were selected which evaluated the sensitivity and specificity of SMSR-PET for NET in the thorax or abdomen with a study size of at least eight patients. Reviews, comments and case reports were excluded. Two reviewers read all titles and abstracts independently and chose studies for reading in full-text. Based on this, studies fulfilling the inclusion criteria were selected. Pooled sensitivity and specificity as well as a summary ROC curve were alculated. The quality of the included studies was evaluated with QUADAS-2. Results: Literature search and reading of reference lists found a total of 704 articles. Twenty-two of these were selected for reading in full-text. Nine studies fulfilled the inclusion criteria and were selected for final analysis. Fourteen articles from a previous meta-analysis were added for a total of 23 articles. A total of 2143 patients were included in the studies, an increase from 567 in the previous meta-analysis. The pooled sensitivity was 92% (95% CI 91-94%) and specificity 96% (95% CI 95-98%). The area under the SROC curve was 0.97 (95% CI 0.94-1.0). In the previous meta-analysis the pooled sensitivity was 93% (95% CI 91-95%) with specificity 91% (95% CI 82-97%). Conclusion: SMSR-PET has a good diagnostic performance for evaluation of NET in the thorax and abdomen, better than SRS which has been the previous standard method. This meta-analysis gives further support for switching to SMSR-PET.

## P316

### Ga-68 DOTATATE PET/CT in identification of primary site in patients with carcinoma of unknown primary-neuroendocrine tumors

**B. R. Mittal**, K. Agrawal, J. Shukla, R. Vatsa, A. Bhattacharya, B. Singh; Postgraduate Institute of Medical Education & Research, CHANDIGARH, INDIA.

Aim: To study the role of Ga-68 DOTATATE PET/CT in the detection of unknown primary sites in patients with carcinoma of unknown primary (CUPS) neuroendocrine tumors (NET). Materials and Methods: Retrospective analysis of Ga-68 DOTATATE PET/CT data in patients with histologically proven NET was performed who underwent PET/CT to identify the site of primary tumor. Studies were performed on a dedicated PET/CT scanner (DISCOVERY, STE-16, GE, Milwaukee, USA). Acquisition was started 45-60 min after intravenous injection of approximately 1.5 MBq/kg body weight of Ga-68 DOTATATE. Results: 68Ga-DOTATATE PET/CT was performed in 24 patients (9 male, 15 female; age 18-71 years, mean 48.8 years) with histologically proven NET for detection of unknown primary. Site of primary tumor was identified in 14/24 patients (58.3%) with the help of Ga-68 DOTATATE PET/CT. Ga-68 DOTATATE PET/CT localized the site of the primary as pancreas (n=2), stomach (n=3), caecum/rectum (n=2), meningioma (n=1), nasopharynx (n=1), posterior mediastinum (n=1), adrenal (n=1) and thyroid (n=1). In two patients, multiple sites with primary disease were identified (midgut

carcinoid with bronchial carcinoid in one patient and MEN-I syndrome in other patient). In the remaining 10 patients where site of primary could not be localized, 4 patients did not show Ga-68 DOTATATE uptake even in the site of presentation. Conclusion: Ga-68DOTATATE PET/CT is very useful in detection of primary site in CUPS-NET and should be used for identifying primary site in these tumors for better management.

## P317

### Initial experience in neuroendocrine tumors assessment with 99mTc-HYNIC-Tyr3-Octreotide and comparison with 111In-Octreotide

**S. Prado-Wohlwend**, I. Casáns-Tormo, R. Díaz-Expósito, C. Rocafuerte-Ávila, C. Orozco-Molano, H. Bowles-Antelo, M. Hassan-Ezz-Eddin, L. Díaz-Platas; MEDICINA NUCLEAR. HOSPITAL CLINICO UNIVERSITARIO, VALENCIA, SPAIN.

AIM The 99mTc labeling offers dosimetric advantages to the new available tracer 99m-Tc-HYNIC-Tyr3-octreotide (99mTc-O). We present our initial experience in neuroendocrine tumor diagnosis, analysing the image quality and comparing with 111In-octreotide (111In-O) when it was possible. MATERIAL AND METHODS We studied 11 patients (p) (7 females), age 63±17(28-83) y old, with neuroendocrine tumors (5 gastroentheropancreatic, 2 pulmonary, 1 thymoma, 2 hipofisary and 1 medullary thyroid carcinoma). We performed wholebody scan and SPECT 2 and 4 hours after iv administration of 11-19,3 mCi of 99mTc-O, with SPECT-CT fusion with Syntegra ® in 8 cases and MR comparison in 2. The referral reason was diagnosis (3 p) and follow-up evaluation (8 p). In 6 p was available a previous study with 111In-O, 5 of these without clinical changes between them. Diagnosis was confirmed by other imaging Methods, pathological findings or clinical follow up. RESULTS We found somatostatin receptor positive uptake in 6/11 p and the other 5 were negative, all with diagnostic confirmation. The image quality was excellent in planar scintigraphy, and specially in SPECT. The 2 and 4 h images had similar quality, although sometimes they were necessary to identify correctly intestinal activity. SPECT-CT fusion help to the right location of the lesions in all cases. We found coincidence in the results obtained with the two tracers, although the 99mTc-O planar-SPECT image quality were higher than 111In-O. The acquisition time was shorter with 99mTc-O and the physiological kidney activity was always lower with 99mTc-O, improving the identification of lesions near the kindey CONCLUSIONS In our preliminary study with 99mTc-O we obtained diagnostic confirmation of the results in all cases, with excellent image quality in both planar and SPECT studies. We found concordance between results from 99mTc-O and 111In-O studies. The 99mTc-O provides dosimetic advantages to the patient comparing with 111In-O, with optimal energy for the gammacammera, reduces acquisition times and allows to complete the study in one day, avoiding unnecessary displacement of patients.

## P318

### The Evaluation of Grade 1 and Grade 2 Gastroenteropancreatic Neuro-Endocrine Tumors with Ga-68 Dotatate PET/BT

**D. HAS**[1], S. KUYUMCU[1], F. GECER[1], Z. OZKAN[1], E. YILMAZ[1], Y. SANLI[1], C. TURKMEN[1], F. BUYUKKAYA[2], I. ADALET[1]; [1]ISTANBUL FACULTY OF MEDICINE, ISTANBUL, TURKEY, [2]TAEK CEKMECE NUCLEAR RESEARCH AND TRAINING CENTER, NUCLEAR TECHNICS DEPARTMENT RADIOISOTOPE DIVISION, ISTANBUL, TURKEY.

**AIM**: Gastroenteropancreatic neuroendocrine tumors (GEPNET) are the heterogenic group being slowly progressive, rarely encountered, frequently malign, and including many kinds of tumors. Using the same definition pattern for those tumors occurring in different organs causes problems in diagnosis, treatment and prognosis determination. In order to overcome those problems, in new classification which published by WHO in 2010, it was classified as Grade1, 2 NET and Grade3 neuroendocrine carcinoma (NEC) according to number of mitosis and Ki67 index. Grade3 NEC indicates slowly progressive tumors with weak somatostatin receptor, and people have problems while estimating the route of disease and planning the treatment. But grading system falls short in Grade 1 and 2 NET classes for planning the treatment and distinguishing the patients with low and high risk levels. With this study, it was aimed to investigate the relationship between maximum standard uptake (SUVmax) value and Ki67 index in Grade1 and 2 GEPNETs, and to evaluate the Ga68-DOTATATE PET/BT findings between groups. **METHOD:** With the aim of determining the primary focus and the staging / restaging; the Ga68 - DOTATATE PET / BT images of total 42 patients being in follow up period with GEPNET diagnosis (14 with pancreas, 9 with stomach, 5 with intestine, 3 with colorectal, 3 with appendix and 8 with unknown primer)(21 males and 21 females, mean age is 49.8). By calculating the SUVmax values of detected lesions, its relation with Ki67 proliferation in Grade1 (Ki67 1-2%) and Grade2 (Ki67 3-20%) patients was evaluated. **FINFINGS**: Mean SUVmax a value of all cases was calculated as 35.54, and mean Ki67 index of all cases was calculated as 5%. Also the Grade2 patients were grouped as Grade2a (Ki67: 3-10%) and Grade2b (Ki67: 11-20%). For patient groups; the mean Ki67 index, mean SUVmax values and the numbers of metastatic patients and negative patients according to Ga68-DOTATATE PET/BT findings were given in table. **RESULT**: It was seen that the highest Ga68-DOTATATE PET/BT uptake was in Grade 1 tumors, and that SUVmax values decreased while Ki67 index increased. According to Ga68-DOTATATE PET/BT findings, total 30 metastatic focuses were detected in 33% of Grade 1 patient, although Ki67 indexes were low.

## P319

### Correlation between metabolic tumor burden at [$^{18}$F]FDG-PET/CT and Ki67 index in neuroendocrine tumors

**K. Massri**, V. Duce, S. Margotti, D. Volterrani, R. Boni, M. Grosso, G. Mariani; Dipartiment of Nuclear Medicine, Pisa, ITALY.

**Aim**:Neuroendocrine tumors (NETs) originate from neural crest cells and can be found anywhere in the body including the gastrointestinal tract, pancreas and lung. The WHO's 2010 classification of NETs is based on grading according to the proliferation index (PI), which is determined by immunohistochemical staining of the nuclear antigen Ki67, thus recognizing Ki67 as the most important criterion for tumor grading, influencing patients' prognosis and choice of treatment. The majority of NETs are slow growing and, accordingly, [$^{18}$F]FDG-PET has so far been assumed to have limited value for diagnostic imaging in these patients. However, we have recently shown that [$^{18}$F]FDG-PET does have a certain prognostic value for patients with NETs, though based on a relatively short follow-up. On the other hand, the Ki67 index has a definite prognostic value, highly proliferating tumors being associated with poorer prognosis. In this study we correlated the metabolic tumor burden (TLG) at [$^{18}$F]FDG-PET/CT to the Ki67 index in patients with NETs. **Methods**: We evaluated 30 patients (14 men and 16 women; median age 56 yr) whith confirmed NETs (4 pulmonary NETs, 15 liver metastases from GEP NETs, 8 pancreatic NETs, and 3 ileal NETs). According to the WHO 2010/ENETS classification, patients were stratified into 3 groups: those with grade 1 tumour (Ki67 index ≤2%, 8 patients), with grade 2 tumour (Ki67 index >3% to <20%, 11 patients) and with grade 3 (Ki67 index >20%, 11 patients). Based on [$^{18}$F]FDG-PET/CT, 20 patients were classified as PET-positive (PET$^+$) and 10 as PET-negative (PET$^-$). In this study, the SUV $max_{max}$ was defined as maximum activity concentration the tumor/(injected dose/body weight). TLG was calculated as the product of metabolic tumor volume (at 40% of $SUV_{max}$) by $SUV_{mean}$. **Results:** 6/8 of the patients with grade 1 were PET$^+$ (SUV $max_{max}$ 4.6, $SUV_{mean}$ 2.3, TLG 40.3) and 2 were PET$^-$; 10/11 patients with grade 2 were PET$^+$ (SUV $max_{max}$ 9.7, $SUV_{mean}$ 3.5, TLG 504) and 1 was PET$^-$; all 11/11 patients with grade 3 were PET+ (SUV $max_{max}$ 16,9, $SUV_{mean}$ 5.1, TLG 1898). In multivariate analysis there was a significant association between Ki67 index and SUV $max_{max}$ (P=0.013) and TLG (P=0.034), while the association was borderline with $SUV_{mean}$ (P=0.064). **Conclusion:** The results obtained in this preliminary study demonstrate the high correlation existing in patients with NETS between Ki67 index and metabolic parameters derived from [$^{18}$F]FDG-PET/CT, thus modifying the general attitude against use of such imaging modality in these patients.

P49-1 - Sunday, Oct. 20, 16:00 - 16:30, Poster Exhibition Area

## Oncology Clinical Science: Bone

## P320

### The clinical impact of oncological patients with solitary bone lesions detected on F-18 FDG PET/CT scans

**T. BAHCECİ**[1], A. YAPAR[2], M. REYHAN[2], A. AKTAŞ[1], H. MERTSOYLU[2]; [1]Baskent University, Ankara, TURKEY, [2]Baskent University, Adana, TURKEY.

The clinical impact of oncological patients with solitary bone lesions detected on F-18 FDG PET/CT scans and positive predictive value for detection of these lesions was aimed to be evaluated in our study. 192 patients (117 male and 75 female) with solitary bone lesions (average age was 59,8±13,6) were included in the study. The SUVmax was measured using regions of interest in the each bone lesions. Patients were staged according to TNM classification both before and after PET/CT imaging. The clinical impact of PET/CT on manangement of this patients was estimated. In 175 patients, metastatic lesions were confirmed to be malignant on conventional radiological Methods, follow-up and histopathologic examination (TP), as 17 patients were shown to have non-metastatic lesions (FP). Average SUVmax value of the lesions detected on PET/CT was 8.4±5.2 (1.6-34.5). SUVmax value was found 8.8±5.3 (1.60-34.50) and 4.5±1.3 (2.1-7.3) for TP and FP lesions, respectively. SUVmax value of TP and FP lesions showed statistically significant difference (P=0.001). Positive predictive value (PPV) of F-18 PET/CT for detection of solitary bone lesions was estimated as 91%. Of 192 lesions, 100 (52%) were lytic, 59 (31%) were scleroic and 33 (17%) were mixed on CT. In TP group (n=175), 99 (57%) were lytic, 48 (27%) were sclerotic and 28 (16%) were mixed . Only one lesion (6%) was lytic in FP group, as 11 (65%) were sclerotic and 5 (29%) were mixed. Positive predictive value (PPV) of F-18 PET/CT for detection of solitary bone lesions was

estimated as 99% for lytic lesions, 81% for sclerotic lesions and %85 for mixed lesions. 5 patients with stage I (2%), 9 patients with stage II (6%) and 61 patients with stage III (35%) before PET/CT imaging upstaged to stage IV after PET/CT imaging. The remaining 100 patients remained at stage IV. A total of seventy-five patients (39%) with stage I, II and III disease upstaged to stage IV after PET/CT imaging in our study group. The clinical impact of PET/CT was high in 38 (20%) patients as moderate clinical impact and low clinical impact was observed in 60 (31%) and 65 patients (34%), respectively. We found no impact in 29 (15%) patients who had positive PET/CT findings. Our findings suggest that FDG PET/CT has a high impact on management of patients with solitary bone lesions, as it has a high positive predictive value for detection of solitary bone lesions, similar to multiple bone lesions.

P50-1 - Sunday, Oct. 20, 16:00 - 16:30, Poster Exhibition Area

## Oncology Clinical Science: CUP

### P321

### Detection of the Primary Tumor by F-18 FDG PET/CT in Patients Presenting with Cancer of Unknown Primar

**K. Itoh**[1], K. Kanegae[1], A. Watanabe[2], M. Hosokawa[3]; [1]Radiological Imaging Center, Sapporo, JAPAN, [2]Department of ENT, Sapporo, JAPAN, [3]Department of Digestive Surgery, Sapporo, JAPAN.

**[Background]** Cancer of unknown primary (CUP) is defined as the presence of histologically proven metastatic disease in which the primary tumor is undetectable on presentation. Detection of the primary tumor is important in the appropriate treatment of patients with CUP. F-18 FDG PET/CT (PET/CT) allows whole-body tumor detection. In this study, the utility of FDG PET/CT for the detection of the primary tumor in CUP patients was evaluated. **[Materials and Methods]** PET/CT scans performed in patients presenting with CUP from Jan. 2006 to Dec. 2012 were retrospectively reviewed. Two hundred fifty-six patients (137 men and 119 women, age 30-92 y with median age of 67 y) were included in this study. These patients were classified into four groups, depending on clinical findings on presentation. Group A (49 cases) was comprised of cases of cervical and/or axillary lymphadenopathy. Group B (33 cases) presented with metastatic bone disease. Group C (93 cases) presented with non-osseous metastases in the body. Group D (81 cases) had elevated tumor markers or severe clinical symptoms with no anatomical abnormalities detected by imaging workup. All patients had been instructed to fast for 6 h before intravenous injection of commercially available [F-18] FDG. Sixty minutes after FDG injection, whole body images were obtained in 3-D acquisition mode at one bed position per 20 min using PET/CT (Gemini GXL, Philips Medical Systems Inc., Cleveland, Ohio, USA). **[Results]** Out of 256 patients, the primary tumors were proven histologically in 84 patients (33%). Detectability of primary tumor in CUP by diagnostic work-up was highest in Group C with 49% (46/93) and lowest in group D with 15% (12/81). Out of the eighty-four patients, primary tumor was identified in sixty patients by PET/CT. Sensitivity, specificity, accuracy, and positive and negative predictive value by PET/CT for primary tumor in CUP was 71%, 88%, 83% 75% and 86%, respectively. Positive predictive value with 47% (9/19) in Group D was significantly low. The commonest primary tumor was lung cancer, the second malignant lymphoma. There were twenty false-positive cases, including colorectal uptake in five cases and pulmonary inflammation in three cases. **[Conclusions]** The detectability of the primary tumor in patients with CUP is not always successful with PET/CT. Although clinical indication of PET/CT may be limited in CUP patients presented with no anatomical abnormalities, the study is useful for whole body evaluation of identified metastatic abnormalities and unidentified primary lesion by imaging Methods in CUP patients.

### P322

### Clinical value of FDG-PET in carcinoma of unknown primary: Explorative analysis of retrospective data of 200 patients

**G. Karanikas**, F. Novak, M. Weber, M. Mitterhauser, T. Traub-Weidinger; University of Vienna, Vienna, AUSTRIA.

Aim of the study: Recent literature reports that FDG-PET is a good tool in the diagnostic management of carcinoma of unknown primary (CUP). The aim of this study was to critically assess the diagnostic value of FDG-PET in patients with CUP, based on the collected data of the Department for Nuclear Medicine at Vienna's General Hospital. Material and Methods: 200 patients referred between 1998 and 2009 to our department with the diagnosis CUP. We searched through the retrospective data of those patients for FDG-PET and histology/cytology results (gold standard) in diagnosing CUP. This way true positive, false negative and false positive results were gathered, thus the positive predictive value (PPV), the detection rate and the sensitivity were calculated. Results: Of 200 patients, 27 did not refer to a FDG-PET examination due to CUP, 65 patients of our cohort had insufficient data for statistical analysis, the remaining 108 patients showed adequate data for statistical analysis. In 61 of our 108 patients the primary tumour could be detected correctly by various diagnostic modalities, in 33 of those 61 detected primary tumours the FDG-PET detected the unknown primary. In consistency this means we evaluated a primary tumor detection rate of 31% for the FDG-PET. 52% of the 33 by FDG-PET detected primary tumours were located in the lung. 9% were located in the uterus and head and neck, respectively. Stomach and colon were 6% of the 33 primary locations each; breast, ovary and prostate were 3% each. The FDG-PET was not able to detect cases in which melanoma was the primary tumour or the primary tumour was located in the liver or kidney. The most common cause for a false negative result were primary tumours located in the mamma (n = 4) and melanoma (n = 5), the most common false positive result of the FDG- PET was lung (n = 5) and colon (n = 5). Finally we evaluated a sensitivity of 61% and a PPV of 67% for the primary tumour detection by FDG-PET examination. Conclusion: FDG-PET is, according to our data, a useful and not invasive imaging technique for revealing the unknown primary tumor and a good diagnostic tool in the management of CUP.

### P323

### Value of PET/CT with 18F-Fluorodeoxyglucose in patients with paraneoplastic syndrome

**D. Fuster**, M. Vidal, M. Depetris, M. Mayoral, J. J. Grau, A. Muxi, F. Lomeña, F. Pons; Hospital Clinic, Barcelona, SPAIN.

Aim: The paraneoplastic syndrome is defined as a set of symptoms that affect cancer patients and cannot be explained by the effect of the tumor or the metastases. The aim of this study is to evaluate PET/CT with 18F-FDG as noninvasive imaging modality in patients with suspected paraneoplastic síndrome. Material and Methods: This is a retrospective study of 24 patients (13 men, 11 women) with an age range of 38-87 years with clinically suspected paraneoplastic syndrome: 1) neurological (n=18), 2) hematologic (n =3) and other symptoms (n =3). We performed whole-body and brain PET/CT to all patients. Patients were classified into two groups based on histological confirmation of cancer (cancer group) and negative follow up for at least 6 months (non cancer group). Results: We classified 9 patients in the cancer group (38%) and 15 patients in the non cancer group (62%). The primary tumor was localized in the lung (n =4), central nervous system (n =3), ovary (n =1) and duodenum (n =1). PET/CT was able to identify the primary tumor in 8/9 cases (89%) so it was falsely negative in 1/9 (11%). In the non cancer group PET/CT ruled out cancer in 14/15 patients (93%) and was falsely positive in 1/15 (7%). The sensitivity, specificity, PPV and NPV of PET/CT was 89%, 93%, 89% and 87% respectively. Conclusions: PET/CT can be useful in the diagnosis of primary tumor in patients with paraneoplastic syndrome. PET/CT should be recommended to rule out the presence of cancer in these patients.

P51-1 - Sunday, Oct. 20, 16:00 - 16:30, Poster Exhibition Area

## Oncology Clinical Science: Melanoma

### P324

### Sensitivity and false negative rate of sentinel lymph node biopsy(SLNB) in malignant melanoma of different parts of the body

**H. Ahmadzadehfar**[1], A. Wierzbicki[1], M. Schmid-Wendtner[2], J. Wenzel[3], K. Eichhorn[4], H. Biersack[1], S. Ezziddin[1], A. Sabet[1], T. Hinz[3]; [1]University Hospital Bonn-Department of Nuclear Medicine, BONN, GERMANY, [2]Interdisciplinary Oncology Center, Munich, GERMANY, [3]University Hospital Bonn-Department of Dermatology, BONN, GERMANY, [4]University Hospital Bonn-Department of Otorhinolaryngology, BONN, GERMANY.

Purpose: Aim was to determine the sensitivity and false negative rate(FNR) of SLNB in malignant melanomas (MM) of different body parts. In addition we analyzed the prognostic factors for the progression free survival (PFS). Methods : 621 patients (339 men; mean age:55y/o)with a cN0 MM, who underwent a SLN scintigraphy followed by a SLNB, were included. The primary tumor was in Head & Neck(H&N), extremities and trunk in 10%, 48% and 42%, respectively. The tumor thickness (TT) was 4 mm in 22%, 42%, 25% and 10% respectively, with a median TT of 1.55 mm. The FNR of SLNB calculated as FN/(TP+FN). Results: A total of 766 SLNs were excised. The median follow up time was 31 months. The FNR and sensitivity for MM of H&N, trunk and extremities were 35.7% and 64%, 13.8 % and 86%, and 21% and 79% respectively. The overall FNR and sensitivity were 19% and 81%, respectively. In the univariate analysis the significant prognostic factors affecting PFS were: gender, age, primary tumor site, TT, ulceration, clark level and the results of SLNB, however in the multivariate analysis gender and clark level lost their significance. In both uni- and multivariate analysis the significant prognostic factors for PFS in patients with negative SLN were age, site of the primary tumor and TT (P< 0.001). Conclusions: The FNR and the sensitivity of SLNB have been mentioned in the literatures in different ways, which should be done uniformly as

recommended by some authors with the above formula. The FNR of the Head & Neck MM is the highest compared with other tumor sites. The significant prognostic factors affecting PFS were age, primary tumor site, TT, ulceration and the result of SLNB.

## P325

### The probability of sentinel node positivity in patients with truncal melanoma with more than one drainage basin

**H. Ahmadzadehfar**[1], A. Wierzbicki[1], M. Schmid-Wendtner[2], E. Habibi[1], J. Wenzel[3], M. Muckle[1], H. Biersack[1], S. Ezziddin[1], T. Hinz[3]; [1]University Hospital Bonn-Department of Nuclear Medicine, BONN, GERMANY, [2]Interdisciplinary Oncology Center, Munich, GERMANY, [3]University Hospital Bonn-Department of Dermatology, BONN, GERMANY.

**Purpose:** The aim of this study was to assess whether an association exists between drainage to multiple basins and lymphatic metastasis in patients with truncal melanoma (TM). **Methods:** 260 patients with primary TM (163 men; mean age:59y/o)with a cN0 MM, who underwent a SLN scintigraphy followed by a SLNB, were included. The tumor thickness(TT) was < 1.0mm, 1.01-2.0mm, 2.01-4mm and >4 mm in 21%, 44%, 25% and 10% respectively, with a median TT of 1.51 mm. Majority of patients had a clarck level IV (58.8 %), without ulceration (87,3 %). **Results** : 103 patients (39.6%) showed more than one basin, of these 95 patients had 2, 6 had 3 and 2 had 4 basins of drainage. Nodal histology was positive for metastatic disease in 65 patients (25 %). Of whom, 40 had 1 basin, 24 had 2 basins and 1 had 3 basins of drainage. Of the 193 node-negative patients, 116 had 1 basin, 70 had 2 basins, 5 had 3 basins and 2 had 4 basins of drainage (P= 0.89). In a median follow up time of 30 months 26 patients showed progressive disease (PD), of whom 15 had 1 basin and 11 had 2 basins of drainage (P=0.76). 20 Patients died, of whom 11 had 1 basin and 9 had 2 basins of drainage (P=0.75). **Conclusions:** There is no significant association between the number of drainage basins and sentinel node positivity as well as progress of the disease in patients with TM.

## P326

### Status of Sentinel Lymph Node in Patients with Cutaneous Melanoma- Relations to Clinicopathologic Characteristics of Primary Tumor

**L. Jaukovic**, M. Rajovic, L. Kandolf-Sekulovic, L. Zolotarevski, M. Novakovic, B. Ajdinovic; Military Medical Academy, Belgrade, SERBIA.

Objective: Most important prognostic factor in cutaneous melanoma patients is the status of regional lymph nodes. Sentinel lymph node (SLN) biopsy technique is useful tool to detect regional lymph node involvement Purpose: To investigate the relationship between SNL involvement and patients and primary tumor characteristics. Method: Sentinel lymph node biopsy was performed from 2011-2013 in 88 patients (42 males, 46 females, median age 53.5, 22-81), Dynamic, early and delayed lymphoscintigraphy were performed over the regional basins of drainage after 3-4 intradermal injection of Tc-99m Nanocolloid dose activity 15MBq around the scar. Once the SLN was visualized the mark was set on the skin in the "surgical "position of patient. Methylene blue dye (1%) was injected 15 minutes before the surgery. Histopathology of SLN was done using 2x10 full face serial sections stained with hematoxylin&eosin and S-100 as well as additional Melan-A and HMB- 45 staining. Results: The SLN identification rate was 98.8%. On lymphoscintigraphy, total of 171 SLNs was detected, mean 1.94 (range 1-6) per patient. Drainage to single lymphatic basin was identified in 90% of patients (axila in 49%, groin and laterocervical location in 32% and 19% of them). Trunk was the primary melanoma site in 40.5% of patients, lower extremity, head& neck, upper extremity and acral localization in 20.5; 17.0; 9.1; and 8.0 % respectively. The median Breslow thickness was 2.3 mm (range 0.4 - 16). SLN metastases were found in 20/88 (22.72%) patients. The mean Breslow thickness significantly differed in the groups of patients with positive and negative SLN (4.6 vs. 1.8 mm). In 6/20 (30%) patients metastases were <1 mm in diameter. After complete lymph node dissection (CLND), additional non-SLN involvement was found in 1/6 (16.6%) patient with micrometastases and in 7/14 (50%) patients with extensive SLN involvement. Conclusion: SLN status is in positive correlation with Breslow thickness, as well as the finding of further metastases on CLND. SLN biopsy is effective diagnostic procedure for the precise staging of patients with cutaneous melanoma.

## P327

### Role of serum S100B and PET-CT in follow-up of patients with cutaneous melanoma

B. Peric, **I. Zagar**, S. Novakovic, J. Zgajnar, M. Hocevar; Institute of Oncology, Ljubljana, SLOVENIA.

**Background:** Increased level of serum S100B can serve as a marker of metastatic spread in patients with cutaneous melanoma (CM). In patients with elevated S100 B and/or clinical signs of disease progression PET-CT scan is a valuable tool for discovering metastases and planning treatment. The aims of this study were to determine whether regular measurements of serum S100B are a useful tool for discovering patients with CM metastases and to evaluate the diagnostic value of PET-CT during the follow-up. **Methods:** From September 2007 to February 2010, 115 CM patients included in regular follow up at the Institute of Oncology Ljubljana were appointed to PET-CT. There were 82 (71.3%) patients with clinical signs of disease progression and 33 (28.7%) asymptomatic patients with two subsequent elevated values of S100B. Sensitivity,specificity, positive and negative predictive value (PPV, NPV) of S100B and PET-CT were calculated using standard procedures. **Results:** Disease progression was confirmed in 81.7% of patients (in 86.5% of patients with clinical signs of disease progression and in 69.7% of asymptomatic patients with elevated S100B). Sensitivity, specificity, PPV and NPV of S100B was 33.8%, 90.9%, 96.0% and 17.5% in patients with clinical signs of disease progression. In 20.0% of patients increased serum S100B was the only sign of disease progression. Sensitivity and PPV of S100 in this group of patients were 100.0% and 69.7%. With PET-CT disease progression was diagnosed in 84.2% of symptomatic patients and in 72.7% of asymptomatic patients with elevated S100B. The sensitivity, specificity, PPV and NPV of PET-CT for symptomatic patients was 98.5%, 90.9%, 98.5% and 90.9% and 100%, 90.0%, 95.8% and 100% for asymptomatic patients with elevated S100. **Conclusions:** Measurements of serum S100B during regular follow-up of patients with CM are a useful tool for discovering disease progression in asymptomatic patients. The value of its use increases if measurements are followed by extended whole body PET-CT.

P52-1 - Sunday, Oct. 20, 16:00 - 16:30, Poster Exhibition Area

## Oncology Clinical Science: Soft Tissues & Sarcoma

## P328

### 99mTc-MIBI scintigraphy: different visualizations patterns of the musculoskeletal tumors

V. Zavadovskaya[1], **A. Kurazhov**[1], M. Zorkaltsev[1], E. Choynzonov[2], E. Slonimskaya[2], A. Bogoutdinova[2]; [1]Siberian State Medical University, Tomsk, RUSSIAN FEDERATION, [2]Cancer Research Institute, Tomsk, RUSSIAN FEDERATION.

Introduction. 99mTc-MIBI scintigraphy is used for non-specific visualization of neoplasms. Exploring the diagnostic potential of 99mTc-MIBI scintigraphy we saw some atypical visualization of the tumors of the musculoskeletal system. Purpose: a study of the characteristics of the tumor visualization processes of musculoskeletal system using 99mTc-MIBI scintigraphy. Materials and Methods. 99mTc-MIBI scintigraphy was carried out on 21 patients with malignant (n=19) and benign (n=2) tumors of the musculoskeletal system. SPECT (n=7) or planar (n=14) images (SPECT Philips BrightView) were acquired at 20 min (early) and 3 h (delayed) after intravenous injection of 740 MBq of 99mTc-MIBI. Qualitative assessment of the results of the study consisted of recording the presence or the absence of hyperfixation/hypofixation of 99mTc-MIBI in the region of the interest (ROI), and in cases of an increased accumulation of the marker - its nature (homogeneous or heterogeneous). Results. Tumors were visualized in 20/21 (95.2%) cases (malignancies in 19/19, and benignities in 1/2). In one case (1/21, 4.8%) benign osteochondroma was not identified. Of the remaining 20 we identified three types of tumor visualization - the traditional positive pattern and the rare negative pattern and the rare mixed pattern. In all the cases that pattern observed in the early phase of the study stayed in a deferred one. Positive pattern was expressed by the presence of areas of hyperfixation markers in ROI and occured most frequently (16/20, 80.0%). Negative pattern was significantly less found and it was a resistant photopenic focus of the corresponding tumor tissue against the background of physiological accumulation of the indicator in the surrounding intact tissues (2/20, 10.0%). Mixed pattern was consistent with a combination of high and low parts of the accumulation of the marker (2/20, 10.0%). Positive pattern was found in a variety of histological variants of tumors and didn't have specificity. Negative pattern was observed with patients with primary (n=1) and recurrent (n=1), chondrosarcomas. Mixed pattern was observed with patients with primary chondrosarcoma (n=1) and metastatic tumor of urinary bladder (n=1). Conclusion. Inclusion of the rare pattern of accumulation of 99mTc-MIBI in the region of interest may increase the sensitivity of scintigraphy with the marker indicating the tumors of musculoskeletal system.

## P329

### FDG PET/CT In Staging, Restaging And Response Assessment Of Ewing's Sarcoma Family Of Tumors

**A. Tiwary, Resident**[1], A. G. Vyas, Resident[2], M. Chauhan, Consultant[1], A. Sharma, Consultant[1]; [1]Army Hospital R&R, NEW DELHI, INDIA, [2]NMC IMAGING AT VIMHANS HOSPITAL, NEW DELHI, INDIA.

AIM: To determine the role of FDG PET/CT in staging, restaging and response assessment of Ewing's Sarcoma Family of Tumors (ESFT). MATERIALS & METHODS: 37 patients of histopathologically proven ESFT were subjected to FDG PET/CT.

Patient age ranged between 5-45 years with mean age of 21 years; male to female ratio was 4.2: 1. Response was assessed as per PERCIST criteria by follow up PET/CT in 26 cases after completion of treatment (surgery for resectable tumors & chemotherapy / radiotherapy for advanced tumors). Data was interpreted using qualitative (compared to liver & mediastinal blood pool) & semi-quantitative (Standardized Uptake Value- SUV max) Methods. Resolution of metabolic activity was used as a marker of response to therapy, even if the skeletal changes persisted on anatomic imaging. RESULTS: Out of 37, there were 29 cases of skeletal Ewings sarcoma (ES) - 17spinal & 12 extra-spinal, 4 cases of Extraskeletal Ewings (ESE), 2 cases of Askin`s tumor of chest wall & 2 of PNET (brain in one and orbit in other). There were 16 (43.2%) cases of stage IIa, 1 (2%) of IIb, 1 (2%) of III, 8 (21%) of IVa & 11 (29.7%) of IVb. Spine was the most frequent location of primary involvement followed by extremities. Typically a mixed sclerotic- lytic lesion is seen with associated soft tissue component and variable heterogeneous FDG uptake in most of the cases. SUVmax of primary lesion ranges from 2.5 to 19.3 with the mean SUVmax of 6.1. Regional lymphnodes (57 % cases) were most common site of metastases. Distant metastases were found in 37% of cases, lung (21.6 %) was most common site followed by bone (18.9 %). Out of 26 patients for response assessment there was complete metabolic response in 9 (34.6%), partial metabolic response in 7 (26.9%), stable disease in 1 (3%) & progressive disease in 9 (34.6%) cases respectively. CONCLUSION: FDG PET/CT may be helpful tool for staging & restaging of ESFT as well as for localization of distant metastases. In addition to this it may be a valuable tool in response assessment of all the types of Ewing sarcoma family of tumors by using qualitative & semi-quantitative (SUVmax) Methods.

## P330

### Is an extended field of view 18F FDG PET/CT necessary in patients with sarcoma?

**S. L. Ayesa**, G. P. Schembri; Royal North Shore Hospital, St Leonards, AUSTRALIA.

Aim: Current 18F -FDG PET/CT scanning protocols for assessment of primary sarcoma typically include whole body imaging from vertex to toes. This requirement increases scanning time per patient and radiation dose. The aim of our study was to assess the incidence of relevant PET findings outside of the standard field of view. Materials and Methods: The 18F -FDG PET/CT of 80 patients referred for assessment of primary sarcoma were retrospectively reviewed. Initial diagnosis, pathology and scan findings were obtained from the patients reports and the images reviewed to confirm these findings. Patients were excluded if imaging was vertex to mid-thigh only, if the primary lesion was within the legs or if subsequent histopathology did not confirm sarcoma (23 exclusions). Remaining patients were divided into sarcomas arising from a visceral organ (30 patients) and sarcomas arising from musculoskeletal or soft tissues (27 patients). Records were examined to determine if patients had 18F -FDG avid findings above or below the knee which were relevant to the management of their sarcoma. Further data analysis was conducted based on histopathological subtypes, with sarcoma subclass groupings based on 2002 WHO guidelines. Results: Among patients with visceral primary sarcomas, no patients were found to have lower limb foci of uptake (0%). In patients with a musculoskeletal or soft tissue primary, one patient had a known clacaneal lesion. Three patients had unsuspected findings -one in the distal thigh and two below the knee (11%). These findings were related to presumed folliculitis, subcutaneous injections and likely metastatic disease in one patient. In no patient did these findings alter management. Conclusions: Extended whole body images did not demonstrate additional findings in patients with visceral sarcomas. In patients with a musculoskeletal or soft tissue primary, lower limb findings were evident in 11% but had no impact on patient management.

## P331

### Metabolic Tumor Volume (MTV) and Total Lesion Glycolysis (TLG) Are Predictive of Sarcomatous Transformation in Type-1 Neurofibromatosis

S. Djelbani, E. Sbidian, O. Zehou, A. Chetrit, A. Luciani, M. Sasanelli, J. Chalaye, A. Rahmouni, M. Meignan, P. Wolkenstein, L. Allanore, **E. Itti**; H. Mondor Hospital, Creteil, FRANCE.

**Objective:** Patients with type-1 neurofibromatosis (NF1) have an increased risk of developing neoplasia. An "at-risk" clinical phenotype has been recently defined by the presence of sub-cutaneous neurofibromas (SCNF). Aim of this study was to correlate measures of tumor burden (MTV, TLG) with clinical and pathological features in NF1 patients. **Methods**: Retrospective analysis of 50 patients (31 men, mean age 32 y) who underwent FDG-PET in Henri Mondor NF1 reference center was performed. In all patients, SUVmax, SUVmean, MTV, and TLG were mesured in each hypermetabolic tumor. Total MTV was computed by summing the volumes of all lesions after thresholding at 41% of the SUVmax using a semi-automatic software. TLG was computed by summing the MTV×SUVmean products. MTV, TLG and SUVmax were compared in each group of patients, divided according to standardized phenotypic analysis and pathological data, using a non-parametric Mann-Whitney test. **Results:** The median delay between PET and clinical symptoms (pain, n=44; neurological deficit, n=16; tumor growth, n=19) was 6.3 mo. Concordance between the symptomatic lesion and the most intense lesion on PET was found in 65% of patients. Biopsy was performed in 33 lesions, of which 15 demonstrated a sarcomatous transformation, 5 a dysplastic NF, and 13 an uncomplicated NF. Median MTV and TLG were 77 mL (0-1687) and 142 mL (0-2323), respectively. Median SUVmax was 4.0 (0-18). Univariate analysis showed higher MTV in patients with SCNF (159 vs. 43 mL, P=.01), tumor growth (96 vs. 47 mL, P=.04) and a sarcoma (228 vs. 52 mL, P=.0002). Similarly, higher TLG was found in patients with SCNF (90 vs. 33 mL, P=.04), tumor growth (290 vs. 60 mL, P=.01) and a sarcoma (618 vs. 60 mL, P<.0001). A higher SUVmax was found only in patients with tumor growth (7.9 vs. 2.9, P=.005) and a sarcoma (9.2 vs. 2.8, P<.0001). **Conclusion:** MTV and TLG are reliable measures of tumor burden and are correlated with clinical and pathological prognostic factors in NF1 patients.

P53-1 - Sunday, Oct. 20, 16:00 - 16:30, Poster Exhibition Area

## Oncology Clinical Science: Miscellaneous

## P332

### F-18 FDG PET/CT findings of hemophagocytic lymphohistiocytosis

**E. Han**[1], E. Choi[1], W. Choi[1], W. Lee[2], S. Kim[1], Y. Park[1], S. Lee[1]; [1]The Catholic University of Korea, Seoul, KOREA, REPUBLIC OF, [2]Soonchunhyang University Hospital, Bucheon, KOREA, REPUBLIC OF.

Object: To evaluate F-18 FDG PET/CT findings of hemophagocytic lymphohistiocytosis Method: FDG PET/CT images of 3 patients with hemophagocytic lymphohistiocytosis (HLH) confirmed by bone marrow biopsy were reviewed. Results: All three patients had malignancy-associated hemophagocytic syndrome: T cell lymphoma, anaplastic large cell lymphoma, and NK cell leukemia. The bone marrow showed increased FDG activity in all 3 patients, and contained areas with focal FDG uptake in the 2 patients with lymphoma. Lymphadenopathy was present in all 3 patients, and accompanied prominent FDG uptake in all patients. One patient with leukemia had hepatosplenomegaly, and the FDG activity was diffusely increased in both liver and spleen. The anaplastic lymphoma case also had splenomegaly, and spleen showed diffusely increased FDG activity. Conclusion: HLH is characterized by activation of macrophages or histiocytes with prominent hemophagocytosis in bone marrow and other organs of reticuloendothelial system. Previous studies have demonstrated that macrophages and histiocytes can cause increased FDG uptake. Thus, FDG PET/CT could be a useful tool in assessing the extent of HLH, and evaluating response to treatment.

## P333

### Evaluation of $^{123}$I-MIBG uptake into the adrenal medulla in $^{123}$I-MIBG scintigraphy

**S. Abe**[1], K. Kato[2], T. Odagawa[2], N. Fujita[1], Y. Fujita[2], A. Niwa[2], S. Naganawa[3]; [1]Department of Radiological Technology, Nagoya University Hospital, Nagoya, JAPAN, [2]Department of Radiological and Medical Laboratory Sciences, Nagoya University Graduate School of Medicine, Nagoya, JAPAN, [3]Department of Radiology, Nagoya University Graduate School of Medicine, Nagoya, JAPAN.

Aim $^{123}$I-labeled norepinephrine analog metaiodobenzylguanidine ($^{123}$I-MIBG) has been clinically used for imaging of the adrenal glands. $^{123}$I-MIBG has been proven useful for the scintigraphic imaging of pheochromocytoma. Quantification of the accumulation of $^{123}$I-MIBG is considered useful for diagnosing the abnormalities of the adrenal glands and for analyzing the target changes due to disease processes. To our knowledge, there has been no study on the quantification of the accumulation of $^{123}$I-MIBG into the adrenal glands and on the relationship between the disease groups and the degree of accumulation of $^{123}$I-MIBG into the adrenal glands. The present study was a retrospective analysis of the patients with known or suspected primary or metastatic pheochromocytoma or paraganglioma. Materials and Methods Consecutive 30 patients with a prior history of primary or metastatic pheochromocytoma, suspected pheochromocytoma, or paraganglioma based on symptoms of catecholamine excess, and CT or MRI findings. (male / female 13 / 17, age 25 - 84 average 54.5) underwent $^{123}$I-MIBG scintigraphy. All patients received 111 or 222 MBq of $^{123}$I-MIBG. At 6 h after administration, total-body planar imaging (anterior and posterior whole-body acquisition) was performed. At 24 h after administration, total-body planar imaging was performed, and 20 of 30 study patients were followed by SPECT-CT of the upper abdomen. The region of interests (ROI) was set on the adrenal glands depicted in the total-body planar images and the image fusion of SPECT and CT. In the same way, ROI was set on the liver as the reference, and the mediastinum as the background. The average and maximum counts of the ROI on the adrenal glands and the ratio of counts of the ROI on the adrenal glands to those on the liver were used for estimation of the accumulation of the $^{123}$I-MIBG. This study was performed under the approval of the Ethics Committee for Human Studies of Nagoya University. Results The $^{123}$I-MIBG

accumulation into the adrenal medulla was significantly higher in the patient group that received surgery with the diagnosis of adrenal pheochromocytoma (9 patients) compared with the patient groups with either no pheochromocytoma or adrenal adenoma (8 patients). Capability of the adrenal gland imaging has been improved by SPECT-CT. Conclusion Adrenal medulla scintigraphy using $^{123}$I-MIBG is useful for the diagnosis of pheochromocytoma. This study suggests that not only the visual evaluation but also the quantitative evaluation of adrenal $^{123}$I-MIBG accumulation may be useful indices for the preoperative diagnosis.

## P334

### Incidental finding of increased uptake in the lateral pterygoid muscle in FDG PET/CT: frequency in 1017 patients

**A. ALSHEHRI**, R. Muzaffar, M. Osman; Saint Louis University Hospital, St. Louis, MO, UNITED STATES.

Objective: The standard of care for PET/CT imaging in most institutions is from the base of the skull to upper thighs. Therefore, the head is typically not included in imaged field of view. However, total whole body (TWB) imaging from top of the skull to the feet is performed at our institution. The lateral pterygoid muscle is anatomically and functionally linked with the temporomandibular joint (TMJ). The purpose of this study was to determine the incidence of F18-FDG uptake of lateral pterygoid muscle detected on PET/CT and correlate the FDG PET/CT findings to all available data. Methods: We retrospectively reviewed 1017 consecutive TWB F18-FDG PET/CT reports of cancer patients in the span of a year. Studies reporting focal uptake in the lateral pterygoid muscle were evaluated for further analysis. Quantification of the metabolic activity in the lateral pterygoid muscle was obtained by using the maximum standardized uptake value (SUVmax). Results: Of the 1017 patients evaluated, 4 (0.4%) had incidental focal FDG uptake in the lateral pterygoid muscle (2 males and 2 females) with a mean age of 68 years (range 63-80). The uptake was seen bilaterally in 2 (50%), only right in 1 (25%) and only left in 1 (25%) with mean SUVmax 6.4 (range 5.4-7.1). No differences were seen on the CT portion of the exam. Of the 4 patients, 2 were diagnosed with lung cancer, one with lymphoma and one with head and neck cancer. Conclusions: Intense FDG uptake in the lateral pterygoid muscle on PET/CT is not well documented since it is typically not included in the imaged field. Although incidental uptake in the muscle is a rare finding (0.4%), being aware of the abnormal uptake may aid in differentiating benign from a malignant lesion in patients with a known history of cancer. It is unclear if this represents temporomandibular joint disorder. Further studies are needed to assess this hypothesis.

## P335

### Unilateral physiological FDG uptake in teres minor muscle seems well associated with intravenous tracer injection procedures: prospective observational research

**K. Nakatani**, Y. Nakamoto, M. K. Kanae, K. Kurihara, N. Hayakawa, M. K. Arimoto, S. Koyasu, K. Togashi; Kyoto University Graduate School of Medicine, Kyoto, JAPAN.

AIM: Physiological FDG uptake in teres minor muscle (TM) is often observed regardless of the history of rotor cuff injury or scapulohumeral periarthritis. Since TM acts on lateral rotation, adduction, and extension of the humerus, we hypothesized the TM uptake might be influenced by posture of patients' arm or injection site. The purpose of this prospective observational study was to verify the relationship between TM uptake and their posture or injection site. PATIENTS & METHODS: We evaluated 578 patients who underwent whole-body FDG PET/CT scan in our institute. Those who showed extensive accumulation in skeletal muscles were excluded. We recorded (1) whether IV injection was performed through the pre-existing venous line or after onsite puncture, (2) tracer injection site, (3) failure of venous puncture, (4) posture of upper limb during the scanning, (5) TM uptake score (4: markedly increased uptake > liver, 3: moderately increased uptake > liver, 2: ≤ liver, 1: ≤ mediastinum, 0: none), and (6) the side of TM uptake. The relationship between the presence of significant TM uptake (score ≥ 2) and IV access method, between the presence of TM uptake and upper limb position during the scanning, and between the injection site and TM uptake side, were analyzed. RESULTS: Overall, the TM uptake was seen in 138 (23.9%) of 578 patients. It was observed in 2 (2.9%) of 68 patients who had been administered via pre-existing line and in 136 (26.7%) of 510 patients who had been injected after onsite puncture (Fisher's exact test, $p<0.0001$). In these 510 patients, the incidence of significant TM uptake was 35/160 (21.9%) for those with the arms up during the scanning and 100/348 (28.7%) for those with the arms down ($p = 0.11$). (The remaining two were scanned with one-side up and one-side down.) Of the 126 patients who showed significant TM uptake without pre-existing IV line or puncture failure, 98 (77.8%) of their uptake were seen in ipsilateral side of tracer injection. 10 (7.9%) were seen in contralateral side, and the remaining 18 patients had bilateral TM uptake. The overall Spearman's correlation between the side of injection and that of TM uptake was 0.59 ($p<0.0001$). When confined to those with unilateral TM uptake, it was 0.82 ($p<0.0001$). CONCLUSIONS: TM uptake seems well associated with IV tracer injection procedures, although it would not be a single cause.

## P336

### Clinical value of FDG-PET/CT in suspected occult cancer

**S. Hess**, A. L. Nielsen, A. Thomassen, H. Petersen, P. F. Høilund-Carlsen; Odense University Hospital, Odense, DENMARK.

AIM Patients with clinically suspected occult cancer are a heterogeneous group presenting with a multitude of non-specific symptoms. Confirming or refuting a malignant diagnosis is of paramount importance and a multitude of diagnostic modalities are often employed. Due to an increased use of FDG-PET/CT in these patients at our institution, we performed a retrospective survey of a consecutive series referred to FDG-PET/CT for suspected occult cancer. MATERIAL AND METHODS All patients referred from our hospital during a 2-year period with clinically suspected occult cancer were included. A comprehensive retrospective chart review provided dates and conclusions of all diagnostic procedures and events during a mean follow-up period of 23 months [range 1-36]. Follow-up was at least 12 months in all patients without cancer. A PET/CT scan was considered true positive for cancer, if an increased focal FDG uptake suggestive of malignancy was confirmed by biopsy, and false positive if subsequent investigations could not confirm malignancy during follow-up. A scan was considered true negative, if a normal FDG uptake or an abnormal FDG uptake were reported as reflecting a benign condition, and no malignant disease was found during follow-up, whereas a scan was considered false negative, if no abnormal FDG uptake suggestive of malignancy was reported, and a cancer was diagnosed during follow-up. RESULTS Our series comprised 99 patients, 50 females and 49 males with a mean age of 66 years [range 26-90]. PET/CT was suggestive of cancer in 30 patients (17 true positive, 13 false positive), and showed no cancer in 69 patients (66 true negative, 3 false negative). Thus, the sensitivity, specificity, accuracy, positive and negative predictive values were 85% [61%-95%], 84% [73%-90%], 84% [73%-90%], 57% [38%-74%], and 96% [87%-99%], respectively (95% confidence intervals in brackets). CONCLUSION FDG-PET/CT showed a high diagnostic yield with a very high negative predictive value in this consecutive, unselected and heterogeneous group of patients with clinically suspected occult cancer. Thus, FDG-PET/CT should be at the forefront of the diagnostic workup in this category of patients.

## P337

### FDG PET for assessment of epidermoid carcinoma in patients with inherited epidermolysis bullosa

**L. S. Vercellino**[1], C. Lebbé[1,2], M. Resche-Rigon[1], D. Lussato[1], N. Basset-Seguin[1,2], P. Merlet[1,2], E. Bourrat[1]; [1]Hôpital Saint Louis, APHP, Paris, FRANCE, [2]Université Paris 7, Paris, FRANCE.

Background Cutaneous epidermoid carcinoma (EC) is the most common cause of death in patients with recessive dystrophic epidermolysis bullosa (RDEB). Staging and follow-up can be difficult because of the permanent inflammation (trauma induced blistering of the skin) responsible for lymph node enlargement difficult to characterize with computed tomography, and lymph node (LN) ultrasound assessment can be painful. Aims To describe the results of evaluation with FDG-PET in RDEB patients with aggressive EC. Materials and Methods Patients with RDEB were referred to our department during the follow-up of a previously diagnosed EC. FDG-PET images were analysed qualitatively and semi-quantitatively (SUVmax). The relevance of findings was assessed by confrontation with pathological data and patient follow-up. Results Five patients were included, aged between 23 and 78 year-old. Nine FDG-PET were performed: 4 patients had 2 exams and 1 patient had 1 exam. Seven EC were detected with a mean SUVmax of 8.9 (4-15.6). There was also 1 false negative and 1 non-evaluable skin lesion. Conversely one hypermetabolic lesion (SUVmax=6.6) was considered false positive because there was no suspicious lesion to biopsy. Tumoral LN were correctly identified in 1 patient on her first PET (SUVmax=4.6) and on her second PET with nodal relapse (SUVmax=16.7). This second examination also identified metastatic lung and bone lesions. In another patient PET showed some discordant results with high uptake (SUVmax=7.7) in a LN whose biopsy found infection and hyperplasia, and mild uptake (SUVmax=3) in a necrotic LN with proven disease. In a patient presenting with cellulitis of the left arm, there was high uptake in the axillary LN (SUVmax=5.1). A patient showed suspicious uptake in a LN that could not be evaluated because the patient refused further diagnostic and therapeutic intervention. Finally, in 2 patients PET was relevant for all lesions, and prompted axillary lymphadenectomy in one and carcinologic excision of the skin lesion in the other. In 2 patients PET was concordant with histology for some lesions and not for the others, and in 1 patient it was not relevant for any lesions, with no impact on patient management. Conclusion These preliminary results show that interpretation of metabolic lesions in EB is difficult because of the permanent inflammation, ulceration and infections of skin lesions. The pathological diagnosis is also difficult. The interpretation should thus be conducted in close collaboration with the clinician. However, FDG-PET can help direct biopsies, identify suspicious LN, and detect metatastic lesions.

P54-1 - Sunday, Oct. 20, 16:00 - 16:30, Poster Exhibition Area

## Oncology Clinical Science: Paediatric

### P338

#### 123I-MIBG SPECT/CT for a higher interpretation confidence in neuroblastoma.

**M. WARTSKI**, N. JEHANNO, S. PETRAS, H. BRISSE, C. CELLIER, J. ALBERINI, L. CHAMPION, D. ORBACH, J. MICHON; Curie Hospital, Paris, FRANCE.

123I-MIBG is the reference functional imaging tool in the characterization of primary tumor and the detection of distant metastases in neuroblastoma. However, physiological activities, small focal uptake and inability to distinguish between primary tumor and locoregional lymph nodes affect interpretation of planar imaging and thus staging and follow up of disease. The aim of this prospective study was to assess the additional value of 123I-MIBG SPECT/CT compared to planar imaging in neuroblastoma. Both planar and SPECT/CT imaging were systematically performed in 34 consecutive patients since September 2012 to march 2013 (median age at diagnosis =33 months ; age=2.4years, SD=3.3years, range 1 month-15 years) with neuroblastoma including INSS stage 4 in 20 pts, 4S in 5 pts, 3 in 2 pts, 2 in 3 pts and 1 in 4 pts. MIBG scans were performed in the initial staging in 9 pts, in the follow up in 25 pts ; were performed twice in 17 pts and three times in 2 pts. SPECT/CT field of view included the primary tumor and if removed (20 pts), was performed on the thoraco abdominal area. A total of 53 paired planar and SPECT/CT scans were reviewed by two experienced nuclear medicine physicians and classified as indeterminate (inaccurate uptake localization, equivocal uptake as overlying with physiological activities, difficulty to distinguish between soft tissue and bone, uncertainty of malignacy) or determinate and if indeterminate, the doubtful site was registered. In 36/53 exams, planar 123I-MIBG were classified as indeterminate and one of the SPECT/CT. SPECT/CT changed the interpretation from indeterminate to determinate in 35/36 exams. Doubtful sites on planar imaging were loco regional lymph nodes (n=16), liver (n=3), pleura (n= 4), distant lymph nodes (n= 3), bones (n= 9), primary lesions (n= 4), remaining post surgical tissue (n=2) SPECT/CT is strongly recommended in 123I-MIBG imaging for a high confidence in interpretation in neuroblastoma. Further studies are needed to assess prognostic implication and impact for patient's management.

### P339

#### PET/CT imaging feasibility in pediatric oncology: experience of Curie Institute

**N. JEHANNO**[1], M. WARTSKI[1], S. PETRAS[1], H. BRISSE[2], F. MONTOYA[1], H. PACQUEMENT[3], J. MICHON[3], J. ALBERINI[4]; [1]Institut Curie, Nuclear Medicine Department, PARIS, FRANCE, [2]Institut Curie, Radiology Department, PARIS, FRANCE, [3]Institut Curie, Pediatric Oncology, PARIS, FRANCE, [4]Institut Curie, Nuclear Medicine Department, SAINT CLOUD, FRANCE.

Aim: 18FDG-PET/CT imaging in oncology has shown interesting development in the management of children, particularly in lymphoma and solid tumors. Few PET units perform imaging for children probably due to the supposed constraints of organizational procedures and especially sedation of children. The aim of this study is to share our experience in the management of PET in pediatric oncology. Materials and Methods: Seventy-five consecutive PET/CT scans were performed in 47 children (22F/25M), median age 9.7 years (range 3-18 years). Sixteen PET/CT scans were performed in children aged 3 to 5 years; 38 in children aged 6 to 12 years, and 21 in children aged 13 to 18 years. All PET examinations were performed without any sedation or drug preparation, even for the youngest children. Children would fast for 4 to 6 hours prior to FDG administration and were installed in a warm quiet room with blankets to avoid brown fat activation. Injected FDG activities were calculated according to the EANM-Guidelines 2008. When required, i.v. contrast agent was used to avoid additional diagnostic CT exposure. The parents were allowed to stay with their child during the whole procedure, wearing an external operational dosimeter during both the resting period (behind a lead shield) and PET imaging acquisition, and when necessary during the CT-scan for the youngest child, wearing an additional lead apron. Children audiobooks were played during acquisition, and the dose delivered to the parent was registered at the end of procedure. Results: PET/CT indications were staging and response assessment of lymphoma (71%, n=53), response assessment of gliomas (n=7), neurofibromatosis with suspected Malignant Peripheral Nerve Sheath Tumor (n= 5), rhabdomyosarcomas (n=4), osteosarcomas (n=3), UCNT (n=2) and Gastro-Intestinal Stromal Tumor (n=1) staging. Images reviewed by three experimented nuclear medicine physicians, were all considered as high diagnosis quality. Median effective dose delivered to the parent was 13 µSv ± 11.6 SD (range 4-50) for the whole procedure. The delivered dosimetry to the parent was 21 µSv when the child was below 5 years, 11.5 µSv between 6-12 years and 9 µSv after the age of 12. Conclusion: PET/CT imaging in pediatric oncology is a feasible procedure and may be combined with diagnostic contrast-enhanced CT procedure. Skilled and trained technologists, implication of both parents and children and a reassuring environment allow avoiding sedation. The effective dose to the parent is negligible with regard to the diagnostic and prognostic benefit of PET/CT imaging in patients' care.

P55-1 - Sunday, Oct. 20, 16:00 - 16:30, Poster Exhibition Area

## Conventional & Specialised Nuclear Medicine: Endocrinology

### P340

#### Postsurgical Outcome Prediction by Semiquantification of 1311I-6β-iodomethyl-norcholesterol Adrenal Scintigraphy in Primary Aldosteronism

**C. Lu**, R. Yen, V. Wu, K. Wu, TAIPAI Study Group; National Taiwan University Hospital, Taipei, TAIWAN.

**Background:** Aldosterone-producing adenoma (APA) and idiopathic adrenal hyperplasia (IAH) are two main causes of primary aldosteronism (PA). $^{1311}$I-6β-iodomethyl-norcholesterol (NP-59) adrenal scintigraphy can be used to distinguish the etiology. Postsurgical outcome after adrenalectomy in PA patients has been reported to be associated with numerous factors. Since semiquantification manipulated from SPECT/CT can be easily performed, we designed this study using three semiquantitative parameters to evaluate their relation to pathology result and the ability to predict postsurgical outcome. **Methods:** We retrospectively reviewed 49 patients with clinically confirmed PA by saline infusion and captopril tests who underwent adrenalectomy after NP-59 adrenal scintigraphy within one year. Three semiquantitative parameters generated from NP-59 SPECT/CT, visual scale (VS), adrenal-to-liver ratio (ALR) and lesion-to-contralateral ratio of bilateral adrenal glands (CON), were compared with pathology result and postsurgical outcome to determine the accuracy. **Results:** By pathology result, ALR≧1.84 and CON≧1.15 gave the highest sensitivity and specificity to distinguish adenoma from hyperplasia, with similar ability as VS ($P$ = 0.2143 and 0.1469, respectively). By postsurgical outcome, ALR≧2.28 and CON≧1.11 showed gave the highest sensitivity and specificity to predict outcome after adrenalectomy, and they had superior ability than VS ($P$ = 0.0148 and 0.0718, respectively). Patients with either ALR or CON greater than cutoff gave high probability to have positive postsurgical outcome (n = 36/38), while patients with both ALR or CON less than cutoff gave high probability to have negative postsurgical outcome (n = 2/11). **Conclusion:** Semiquantification of NP-59 SPECT/CT has excellent ability in outcome prediction after adrenalectomy. A ALR or CON greater than cutoff strongly suggested the benefit from adrenalectomy, and combination of ALR and CON both less than the cutoff implied low chance to have postsurgical outcome improvement. By this method, a preoperative assessment can be easily performed to predict the outcome and to avoid unnecessary surgery.

### P341

#### Serum Thyroglobulin (Tg) measurements before I-131 treatment, under rhTSH preparation, as a prognostic indicator in patients with Differentiated Thyroid Carcinoma (DTC).

**J. Koutsikos**[1,2], I. Xirafi[2], A. Velidaki[3], H. Tourkohoriti[2], G. Misichronis[4]; [1]401 General Military Hospital, Nuclear Medicine dept., ATHENS, GREECE, [2]Central Clinic of Athens, Nuclear Medicine Dpt., Athens, GREECE, [3]Laiko General Hospital, Nuclear Medicine dpt., ATHENS, GREECE, [4]Central Clinic of Athens, Endocrinology Dpt., Athens, GREECE.

**Introduction**: Tg measurement can provide useful informations during hypothyroidism, just before radioiodine thyroid ablation. However when rhTSH is used to prepare DTC patients for ablation, its role is questionable. The therapeutic activity and retention of radioiodine in the target volume are decisive parameters. Many authors have proposed that effective half-life (Teff) has a strong dependency on biological half-life, showed no relationship with administered activity (AA). The aim of this study was to investigate the impact of the AA, Teff and Tg concentrations in the ablation success after rhTSH preparation. **Materials and Methods**: Forty-seven patients that were treated with I-131 for DTC after rhTSH preparation were retrospectively reviewed. Patients that underwent initial ablative I-131 treatment were included. Exclusion criteria were Tg>100 ng/ml, I-131 uptake>10% and measurable Tg-specific autoantibodies. Tg measurements (day 1 of the protocol) and exposure rate values [measured immediately (ER1) and 24h post-ablation (ER2)] were collected. The ablation was considered successful if, in a follow-up period over 18 months, both the WBS (185 MBq I-131 dose) was visually negative in the thyroid bed, and there was no iodine-avid tissue seen outside of expected areas and Tg was undetectable. **Results**: Nineteen patients fulfilled the above criteria (5 males, 14 females, mean age 47.2 y.o., follow-up period 18-30 m.). Sixteen patients were ablated successfully (ablation rate 84.2%), while the

remaining 3 had a repeated therapy. The mean AA was 106±25 mCi and 142±10 mCi (P=0.02), RA at 24 hrs was 33.3 and 30.9 mCi (P=NS) respectively, while Teff at 24 hrs was 15 and 11 hrs respectively (P<0.05). The excretion of the AA for the first 24 hrs was calculated to 68.5% and 81.8% respectively (P=NS). ER1 differed significant (18.9 vs. 23.3 mrem/h, P<0.01), while ER2 didn't (5.9 vs. 6.2 mrem/h, P=NS). Tg was increased in the 3 not-cured patients (6.25±0.49 ng/ml vs. 0.68±0.93 ng/ml, P=0.003). **Conclusion**: Serum Tg levels measured before rhTSH preparation for I-131 ablation have a complementary role for predicting persistence or recurrence of disease in the earliest postoperative period, even if the patients aren't hypothyroids. Teff plays also a critical role in the effectiveness of the treatment, instead of AA which didn't result in therapeutic efficacy, although it was significant greater than that of successfully ablated patients.

## P342

### Role of 99mTc - HYNIC Tyr3 Octreotyde scintigraphy in neuroendocrine carcinoid tumours (NEcT) based on localization of primary tumor

**G. A. JIMENEZ LONDOÑO**, A. García Vicente, O. Gomez Lopez, C. Vega Caicedo, A. Leon Martín, A. Soriano Castrejon; Hospital General Universitario de Ciudad Real, Ciudad Real, SPAIN.

*Objetive:* The aim of our work was to determine the accuracy of $^{99m}$Tc - HYNIeC-Tyr$^3$-Octreotyde scintigraphy (TcOS) in detecting active disease in neuroendocrine carcinoid tumors (NEcT) based on embryological origin of primary tumor (foregut, midgut or hindgut). *Methods:* We analyzed retrospectively 45 studies (12 staging, 26 suspicion of recurrence, and 7 follow up) belonging to 33 patients with histological confirmation of NEcT(16 were males and 17 females, mean age 58 years). Whole body scan and static images, followed by SPECT-CT were acquired 4 hours post-injection of 740 MBq of $^{99m}$Tc- HYNIC-Tyr$^3$-Octreotyde. The studies were divided into 3 groups based on the embryological origin of primary tumor [foregut (group 1), midgut (group 2) and hindgut (group3)]. Each study was evaluated by two blinded nuclear medicine physicians. The accuracy of TcOS in each group was assessed, included chi-square analyses. The final diagnosis was established by histopathology or clinical/radiological follow-up greater than 6 months. *RESULTS* The localization of the primary tumor per patient revealed that 58% were from the foregut (19), 30% from the midgut (10) and 12% from the hindgut (4). Per studies basis analysis (45 studies) showed an overall sensitivity, specificity and accuracy of 95%, 92% and 93% respectively. In the group 1, all the studies were correctly classified by TcOS (10 TP and 15 TN). There were 9 TP, 4 TN and 1 FP in the group 2 whereas in the group 3, 4 TN, 1 FP, and 1 FN were found. The only FN was liver metastasis in an atypical carcinoid of rectum and the two FP were a benign ovarian lesion and a physiological uptake in the adrenal gland, respectively. The accuracy per studies for the group 1, 2 and 3 were: 100%, 92% and 66% respectively, demonstrating a better detection of active disease in primary tumors from foregut and midgut compared to hindgut (P< 0.05). *CONCLUSION* It seems that there is a relationship between the embryological origin of carcinoid tumors and the detection of active disease by TcOS, with a better accuracy in NEcT of foregut and midgut origin.

## P343

### Atypical $^{131}$I SPECT/CT Findings of Parotid Gland in two Patients with Differentiated Thyroid Carcinoma

**B. Tuğral**, Ö. Ömür, A. Oral, Z. Özcan; Ege University School of Medicine, Department of Nuclear Medicine, Izmir, TURKEY.

**OBJECTIVE:** Symmetric or asymmetric salivary gland uptake can be observed in post-therapeutic or diagnostic whole body $^{131}$I scintigraphies (WBS) after radioiodine therapy in patients with differentiated thyroid carcinoma. Although the sialadenitis is considered especially in asymmetric $^{131}$I uptake, metastatic lesions in similar locations should be kept in mind. In this case presentation we aimed to present $^{131}$I SPECT-CT and the radiological findings of two cases with atypical findings and $^{131}$I accumulation observed in parotid gland on $^{131}$I WBS. **FINDINGS**: **Case 1:** In 63-year old female patient diagnosed with papillary thyroid carcinoma, residual thyroid tissue and increased $^{131}$I accumulation on the right parotid gland were observed by the post-ablative $^{131}$I WBS after 100mCi radioiodine therapy (TSH: 50mIU/ml, Tg: 2,6ng/ml). On the $^{131}$I WBS taken post-treatment 6th months, it was established that thyroid tissue was ablated and the $^{131}$I accumulation observed at right parotid gland continued (TSH: 50mIU/ml, Tg: 0,7ng/ml). An 18 mm nodular lesion was detected by ultrasonography and MRI consistent with pleomorphic adenoma within the right parotid gland. **Case 2:** In 50-year old female patient diagnosed with follicular thyroid carcinoma and having pulmonary metastases, a diffuse, intense (creating star artifact) $^{131}$I accumulation accompanied by increased density was observed in the right parotid gland on the $^{131}$I WBS and SPECT-CT images after 100mCi radioiodine therapy and this raised the suspicious of metastasis (TSH: 50mIU/ml, Tg: 1600ng/ml)**.** On the parotid gland ultrasonography, heterogeneity in the internal structure of the gland along with the dimension and increased perfusion on the right parotid gland and on the MRI homogenous contrast involvement as well as hyperintense signal changes on T2A images of the right parotid gland was observed. These findings were interpreted as inflammation of right parotid gland (parotitis). **CONCLUSION**: In this case presentation it was concluded that the presence of $^{131}$I accumulation, more than expected or asymmetric, in salivary glands which are from physiological uptake areas on $^{131}$I screening scintigraphies, should suggest the possibility of sialadenitis, benign or malignant primary salivary gland pathologies, intraparotid metastatic lymph nodes and metastatic infiltration. Differential radiological-histological diagnosis should be made for definitive diagnosis.

## P344

### Count rate of 99mTc-pertechnetate thyroid imaging can be used as a surrogate of 24 hour 131I radioactive iodide uptake (RAIU) in a clinically meaningful manner

**M. Pelletier-Galarneau**, O. O. Sogbein, W. Zeng, L. S. Zuckier; University of Ottawa, Ottawa, ON, CANADA.

**Objectives**: To differentiate the etiology of hyperthyroidism, we frequently supplement $^{99m}$Tc-pertechnetate thyroid imaging with a 24hr $^{131}$I-NaI thyroid uptake measurement (RAIU), though this entails additional radiation, cost and a repeat patient visit. We have retrospectively analyzed our patient data to assess when the degree of RAIU can be independently inferred from the prior $^{99m}TcO_4^-$ image count rate. **Methods**: We retrospectively reviewed 104 thyroid studies in patients referred for hyperthyroidism. Thyroid scan was performed following IV injection of 37 MBq of $^{99m}TcO_4^-$. Anterior images were acquired 15 minutes post injection using a pinhole collimator and usual technique. Acquisition was stopped at 300,000 counts. When indicated, 0.37 MBq of $^{131}$I-NaI was then administered orally and 24 hour uptake was measured using the Capintec Thyroid Uptake System (Captus® 3000). For the purpose of this study, the thyroid imaging time to reach 300k counts, an inverse surrogate of count rate, was correlated with probe-performed RAIU **Results**: Thyroid imaging time inversely correlated with 24hr RAIU (R2= 0.54, p<0.0001). When acquisition time was < 1 minute, 23/23 cases demonstrated abnormally high (> 44%) 24hr RAIU. When acquisition time was > 7 mins, 3/3 cases demonstrated low (<1%) 24hr RAIU. **Conclusions**: In patients with hyperthyroidism, high count rate on $^{99m}$Tc-pertechnetate imaging correlated well with 24hr RAIU and could obviate the need for subsequent $^{131}$I-NaI uptake in these patients, especially in a diagnostic setting or where empiric $^{131}$I-NaI therapy is employed. In cases of low count rate (acquisition time > 7 mins), findings correlated with < 1% RAIU, as would be seen in subacute thyroiditis, and administration of $^{131}$I-NaI would not be necessary. In our patient population, these conditions applied in 26 of the 104 patients imaged (25%).

## P345

### Role of 131-I-6β-iodomethyl-19-norcholesterol scintigraphy with SPECT/CT in patient with primary aldosteronism caused by aldosteron secreting cortical adenoma

**A. Baric**[1], V. Marković[1], D. Eterović[1], D. Brdar[1], G. Šošo[1], S. Gračan[1], D. Ljutić[2], D. Kaštelan[3], A. Punda[1]; [1]Department of Nuclear Medicine, University Hospital Centre Split and Split University School of Medicine, Split, CROATIA, [2]Department of Nephrology, University Hospital Centre Split and Split University School of Medicine, Split, CROATIA, [3]University of Zagreb School of Medicine and Department of Internal Medicine, Division of Endocrinology, University Hospital Center Zagreb, Zagreb, CROATIA.

**Aim**: Primary aldosteronism may be caused by bilateral idiopatic adrenal hyperplasia or adrenal cortical adenoma. It is important to distinguish theese two conditions because they require different treatment. Adrenal venous sampling is the gold standard in determining the source of aldosterone excess in patients with primary aldosteronism, but it is invasive and technically demanding with possible severe complications and doubtful success. I-131-6β-iodomethyl-19-norcholesterol (NP-59) scintigraphy is simple, nonivasive, without any complications and may be used as a supplementary diagnostic tool. Patient: 58-year-old man has arterial hypertension during last 10 years, with high levels of blood preasure up to 220/140 mmHg. He has been unsuccesfully treated with various combination of antihipertensive drugs, but only spironolactone had effects. Due to this reaction on aldosterone antagonist the aldosteronism was suspected. He had one cerebrovascular insult with no consequences. He had no hypokalemia. Aldosterone-to-renin ratio indicate primary aldosteronism. MSCT of adrenal glands revealed expansive right adrenal mass, 25 mm in diameter, apsorption coefficient of 9-12 HU. His therapy included beta blockers, ACEI, calcium channel blocking agents and antagonist of aldosterone receptors. During preparation for NP-59 scintigraphy, therapy had been revised. Spironolactone and ACEI were excluded during 6 weeks before applying NP-59, and replaced with monoxydine, amlodipine and doxazosin. **Methods:** Dexamethason suppression has been applyed to decrease ACTH- dependant accumulation of norcholesterol in the zona fasciculata. Patient received 4 mg/day of dexamethasone per os, during seven days before applying radiotracer and throughout the imaging period. NP-59 was intravenously applyed in dose of 37 MBq (1 mCi). Thyroid blocade with Na-perchlorate had been started 30 min before injection of NP-59 and continued during next 10 days.

**Results:** On the third and the fourth day NP-59 planar scintigram showed intensive focal radiotracer accumulation in the right hemiabdomen, under the lower edge of the liver, and abscent accumulation on the left side of lumbar region. Physiological accumulation has been seen in the liver, gallbladder and colon. SPECT/CT confirmed accumulation of NP-59 in the right adrenal mass. Laparoscopic partial right adrenalectomy was done and pathohistology confirmed aldosteronom. After operation patient´s blood preasure is beeing regulated with combination of bisoprolol/hydroclorthiazide, and it is about 140/90 mmHg. **Conclusion:** Considering invasiveness, possible severe complications and doubtful success of adrenal venous sampling, we suggest simple and noninvasive 131-I-6β-iodomethyl-19-norcholesterol scintigraphy using SPECT/ CT as the first localization modality for patients with a clinically confirmed primary aldosteronism.

## P346

### A Case of Misleading Brown Fat Visualization by Parathyroid Scintigraphy/Case Report/

**M. Lázár**[1], J. Furák[2], Z. Besenyi[1], Z. Fejes[1], L. Tiszlavicz[3], G. Lázár[2], A. Palkó[4], B. Iványi[3], L. Pávics[5]; [1]Euromedic Diagnostics Hungary Ltd., Szeged, HUNGARY, [2]Department of Surgery, University of Szeged, Szeged, HUNGARY, [3]Department of Pathology, University of Szeged, Szeged, HUNGARY, [4]Department of Radiology, University of Szeged, Szeged, HUNGARY, [5]Department of Nuclear Medicine, University of Szeged, Szeged, HUNGARY.

Introduction: The diagnosis of primary hyperparathyreoidism is based on laboratory tests and the treatment is primarily surgical, removal of the pathological gland. Skilled surgeon and possibly the knowledge of localization - determined by imaging Methods (parathyroid scintigraphy, US, CT, MR investigation of the neck) - of parathyroid adenoma are necessary. Scintigraphy and intraoperative radioguidance can contribute to the success of the intervention significantly. Case report: Hyperparathyreoidism of a 12 year old girl was suspected in the course of an upper arm fracture due to a minor trauma. Clinical picture and laboratory tests clearly indicated primary hyperparathyreoidism. First ultrasound and MR investigations of the neck were performed, but no parathyroid adenoma was reported. On the parathyroid scintigraphy (99mTc-tetrofosmin, washout method combined with 99mTc-pertechnetate thyroid scintigraphy) pathological isotope accumulation was described on the left side of the neck above the level of the jugular notch. However, during the operation only brown fat tissue was found (confirmed histologically as well). The scintigraphic images were re-evaluated, and a side difference in the activity of the areas between the lobes of the thyroid gland and salivary glands (R>L) was discovered, which appeared to be more marked on the late images. Reviewing the MR images as well a well-circumscribed lesion was found in the area confirmed by the repeated ultrasound investigation. During the second (radioguided) operation the removal of the parathyroid adenoma from the suspected area was successful, confirmed histologically (benign chief cell parathyroid adenoma, 24 x 10 x 6 mm) and by the normalization of laboratory parameters. Conclusions: Asymmetrically situated brown fat tissue can mimic parathyroid adenoma on scintigraphic images, so confirmation with other imaging method is recommended. Parathyroid adenoma can be missed by radiological Methods (UC, CT, MR), therefore in the knowledge of scintigraphic picture (probable location) existing CT or MR images should be reviewed and/or neck ultrasound investigation should be repeated.

## P347

### In-111 Pentetreotide and F18-FDG PET/CT Findings in the Case of Ectopic ACTH-Secreting Bronchial Carsinoid Tumor

**Z. KANDEMIR**, N. YILDIRIM POYRAZ, E. ÖZDEMİR, M. KESKİN, S. TÜRKÖLMEZ; Ankara Atatürk Training and Research Hospital Department of Nuclear Medicine,Ministry of Healt, Ankara, TURKEY.

**INTRODUCTION-AIM** Ectopic ACTH Syndrome (EAS) is one of the most frequent paraneoplastic syndromes and bronchial carcinoid tumors are responsible for about 10 % of these cases. In this study, our aim was to present the images of a patient diagnosed with bronchial carcinoid following the operation and he was examined in connection with the ectopic ACTH syndrome. His computed tomography of thorax (CTT) images displayed a parenchymal nodular lesion in the right lung, whereas in the 18-fluorine-2-deoxyglucose-positron emission tomography / computed tomography (18 F- FDG PET/CT) images no uptake was observed. On the other hand, in the same nodule, during In 111-Pentetreotide whole body scan (WB) and single photon emission computed tomography scan (SPECT), focal activity uptake was observed. **CASE REPORT** A 27-year-old male patient with typical Cushing's syndrome findings was directed to our clinic with the ectopic ACTH syndrome pre-diagnosis since his hipofisis and surrenal magnetic resonance imaging (MRI) were normal and a nodular lesion was detected in the CCT images. During the 18F- FDG PET/CT scanning in our clinic, pathologic FDG uptake was not observed in the nodular lesion region of the right lung which was detected in the thorax CT images.Then, somatostatin receptor-specific agent In-111 Pentetreotide was used in the whole-body scan and focal radiopharmaceutical uptake was detected in the same region. Right lung middle lobe wedge resection was performed in this patient and it was reported as carcinoid tumor according to the pathology result. **CONCLUSION** While searching the patients who may have ectopic ACTH sydrome, it is necessary to consider carcinoid tumor as a differential diagnosis. Because of the low metabolism of the carcinoid tumor, the negative result of FDG uptake was an expected finding. Therefore, in these cases, the diagnostic value of In-111 Pentetreotide scintigraphy is higher.

P56-1 - Sunday, Oct. 20, 16:00 - 16:30, Poster Exhibition Area

## Conventional & Specialised Nuclear Medicine: Thyroid

## P348

### Value of stimulated Tc-99m sestaMIBI Scan in differentiated thyroid cancer; comparative study to unstimulated Tc-99m sestaMIBI, RAI-131 diagnostic whole body scan and Thyroglobulin

**A. Amin**[1], H. El-Sayed[1], H. El-Sayed[2]; [1]NEMROCK, Faculty of Medicine; Cairo University, Cairo, EGYPT, [2]NCI, Faculty of Medicine; Cairo University, Cairo, EGYPT.

Background Differentiated thyroid cancer [DTC] is among the most curable cancers. Diagnostic scan with radioactive iodine [RAI-131X] is among the routines used for follow-up of DTC. RAI-131X necessitates withdrawal of Levothyroxine for 4-6 weeks. The latter has side effects; therefore whole body scanning with Tc-99m sestaMIBI [Unstimulated MIBI] is suggested as there is no need for replacement therapy withdrawal together with Thyroglobulin serum level estimation [TG]. Aim To assess the effect of Levothyroxine hormone withdrawal on Tc-99m sestaMIBI Scan [Stimulated MIBI] outcomes in comparison to Unstimulated MIBI, RAI-131X and Tg. Patients and Methods 50 patients of papillary and follicular DTC were enrolled in this work. All patients underwent RAI-131X, unstimulated and stimulated MIBI scans and serum TG estimation. Results No difference between unstimulated and stimulated MIBI scans were found, however an approximate specificity was found compared to RAI-131X but with a lower sensitivity. TG showed 8% more abnormality in the studied patients compared to the scan modalities. Conclusion Stimulated MIBI scan had added no value over the stimulated MIBI; so confirming the MIBI main advantage in avoiding the patients' replacement therapy withdrawal with its known undesirable side effects.

## P349

### Early Increase in Anti-Thyroglobulin Antibody Predicts Elevated Peak Thyroglobulin in I-131 Therapy with Recombinant Human Thyrotropin

**S. Cho**[1], H. Song[1], A. Chong[1], S. Kang[1], J. Kim[1], H. Park[2], S. Yoo[2], S. Kwon[2], J. Min[2], H. Bom[2]; [1]Chonnam National University Hospital, Gwang-Ju, KOREA, REPUBLIC OF, [2]Chonnam National University Hwasun Hospital, Hwasun-Gun, Jeollanam-Do, KOREA, REPUBLIC OF.

**Purpose**: We aimed to clarify the predictability of thyroglobuiln (Tg) after recombinant human thyrotropin (rhTSH) injection for I-131 therapy, and factors affecting the elevation of peak thyroglobulin on day 3 or 4 post-injection. **Methods:** Totally 53 patients who received rhTSH injection for I-131 therapy from 2008 to 2012 were included. Baseline immunoradiometric assay (IRMA) was done 5 days before rhTSH injection (baseline Tg), then repeated on day 1 (early Tg), and day 3 or 4 post-injection (delayed Tg). We analyzed the correlation of early and delayed Tg, and the possible factors affecting the elevation of delayed Tg in patients with undetectable early Tg (< 1 ng/ml**). Results**: The early Tg showed good correlation with the delayed Tg ($R^2$= 0.927). Thirty-one patients showed undetectable early Tg, but 10 of them showed increases in delayed Tg (NPV 68%, PPV 95%, accuracy 79%). The early/baseline TgAb ratio was significantly higher in patients who showed increase in delayed Tg than who did not (1.58±1.09 vs. 0.96±0.32, p = 0.036). The optimal cutoff value of early/baseline TgAb ratio was 1.28 for prediction of delayed Tg elevation with NPV of 83% and PPV of 71%. **Conclusion**: The early Tg correlates well with delayed Tg, and the early/baseline TgAb ratio was predictive of elevation of delayed Tg after rhTSH injection.

## P350

### Patient with parathyroid adenoma, thyroid toxic adenoma and metastatic papillary thyroid carcinoma

**D. Brdar**[1], A. Punda[1], D. Eterović[1], G. Šošo[1], S. Gračan[1], A. Barić[1], M. Kontić[2], V. Marković[1]; [1]Department of Nuclear Medicine, University Hospital Centre Split and Split University School of Medicine, Split, CROATIA, [2]Department of Otorhinolaryngology, Head and Neck Surgery, University Hospital Split, Split, CROATIA.

**Aim:** The occurrence of primary hyperparathyroidism, toxic adenoma of the thyroid and metastatic papillary thyroid carcinoma simultaneously in the same patient is extremely rare and diagnostically challenging. Only a few cases are reported in the

literature. **Case Report**: A 75-year-old woman with hypercalcemia was referred to our Outpatient Clinic for ultrasound examination of the neck. Sonography revealed large hypoechogenic nodule in the right thyroid lobe that measured 42x32x25 mm. In the upper third of the left lobe there was hypoechogenic nodule with microcalcifications that measured 15x10x11 mm. Behind the midle third of the left thyroid lobe we found hypoechogenic nodule that measured 16x12x5 mm. In the upper third of the left side of the neck there were two small lymph nodes with microcalcifications, larger one measured 16x9x6 mm. Accidental concomitant finding of the toxic adenoma of the thyroid, metastatic thyroid carcinoma and parathyroid adenoma was suspected. Laboratory findings showed T3 thyrotoxicosis and increased serum PTH level. Tc-99m-scintigraphy showed hot nodule in the right thyroid lobe. Parathyroid adenoma was indiscernible on Tc-99m-MIBI scintigraphy because a huge activity was accumulated in the toxic thyroid adenoma, but PTH in the aspirate of the hypoechogenic nodule behind left thyroid lobe was high (> 2 096 pg) and thus confirmed parathyroid adenoma. FNA cytology of the hypoechogenic nodule in the upper third of the left thyroid lobe and the lymph node on the left side of the neck revealed metastatic papillary carcinoma. After short course of thyrostatic preparation, total thyroidectomy, parathyroid adenomectomy and functional dissection of the left side of the neck was performed. **Results:** Pathohistology confirmed papillary thyroid carcinoma of the left thyroid lobe with metastases in cervical lymph nodes, follicular adenoma of the right thyroid lobe and left-upper parathyroid adenoma. Patient received ablative-therapeutic dose of 3,98GBq of I-131 and is now disease-free, 3 years after the operation and radioiodine treatment. PTH and calcium levels remained normal during follow-up. **Conclusions**: This case illustrates the need for clinical awareness of possibility of concomitant multiple thyroid and parathyroid diseases and emphasizes high diagnostic utility of utrasound. It also points out the necessity for PTH determination in aspirate of suspected lesion in patient with concomitant toxic adenoma of the thyroid because scintigraphic visualization of hyperfunctioning parathyroid adenoma is difficult in that case.

## P351

### "Hyperthyroidism": to treat or not to treat ?

C. Caoduro, O. Angoue, **C. M. Ungureanu**, I. Chavot, O. Blagosklonov, H. Boulahdour; University Hospital Besançon, Besançon, FRANCE.

"Hyperthyroidism": to treat or not to treat? Aim: The goal of this case is to sensibilisate the nuclear medicine physicians about a condition where a thyroid toxic adenoma is a benefit for the patient and must not be treated. Materials and Methods: A 66 year-old man was referred to the Nuclear Medicine Department to explore the thyroid gland and eventually to treat by $^{131}$Iodine because the physical examination and the echography showed a thyroid nodule and the level of the thyroid stimulating hormone (TSH) was below the lower normal limit. We performed a thyroid scintigraphy 20 minutes after intravenous injection of 111 MBq of $^{99m}$Tc and we performed also the dosage of triiodothyronine ($T_3$ ) and thyroxine ($T_4$ ) hormones. Results: The thyroid scintigraphy showed an intense uptake of the thyroid nodule without any uptake of the rest of the thyroid gland, typical image of thyroid toxic adenoma. The level of the $T_3$ and $T_4$ hormones was normal but to values near the lower normal limit. Conclusion: An image of thyroid toxic adenoma with TSH level below the lower normal limit, mimicking hyperthyroidism, and $T_3$ and $T_4$ level normal but to values near the lower normal limit is not habitually. The patient had not any treatment for thyroid disease and had not any symptom of thyroid disease. The history of patient revealed surgical ablation of the pituitary gland for non-secretory adenoma. The patient had a hormone replacement therapy for the pituitary gland but no hormone replacement treatment for the thyroid gland. The TSH level below the lower normal limit is explained by the ablation of the pituitary gland. The normal level of $T_3$ and $T_4$ hormones is explained by the thyroid "toxic" adenoma. The thyroid "toxic" adenoma was a benefit for the patient and didn't need any treatment.

## P352

### Comparison between Pinhole and parallel hole collimator for thyroid uptake measurements

**H. Ben Ahmadi**, B. K. Adams, A. Al Rumaithy, S. Al Kindy, M. Agravante; Zayed Military Hospital, AbuDhabi, UNITED ARAB EMIRATES.

**Introduction:** The Society of Nuclear Medicine (SNM) guidelines recommend the pinhole collimator for routine thyroid imaging. However, many NM departments use the parallel hole collimator exclusively and some use both pinhole and parallel hole collimators. Many prefer the parallel hole because of the cost of the pinhole collimator, the time required to change the collimator, and the lack of availability of a pinhole collimator with some camera models. **Aim** To compare thyroid uptake measurements using the pinhole collimator with those obtained using the parallel hole collimator in euthyroid and hyperthyroid patients and to determine the correlation between the respective collimators and TSH values. **Materials and Methods** We performed a prospective study comparing thyroid uptake measurements obtained with pinhole and parallel hole collimators. The study protocol was approved by the ethics committee of the hospital. Patients recruited into the study were referred with clinical hyperthyroidism (24patients 13 females and 11 male) and euthyroid patients with nodular thyroid disease (25patients 19 females and 6 males). Each patient was imaged in the same way. Each was injected intravenously with a single standard dose of 5millicuries (185 MBq) 99mTc sodium pertechnetate. Anterior and anterior oblique views were obtained 20 minutes post injection using the pinhole and then the parallel hole collimator for 5 minutes per view as per SNM guidelines. Uptake measurements were made using Siemens software and compared using the Student T-test. Correlations were made between the uptake measurements by respective collimators and serum TSH levels obtained by electrochemiluminescence immunoassay in each patient. **Results** Forty-nine patients were studied, 32 Females and 17 males with age range of 17 to 77 years; mean age 44 years . Hyperthyroid patients: (n = 24): Pinhole versus parallel hole: p = 0.027 Euthyroid cases: (n = 25): Pinhole versus parallel hole: p =0.009 Total (n = 49): Pinhole versus parallel hole: p= 0.014 Correlation coefficients (r): Hyperthyroid cases: Pinhole and TSH: -0.10; Parallel hole and TSH: 0.27 Euthyroid patients: Pinhole and TSH: 0.16; Parallel hole and TSH: 0.14 Total: Pinhole and TSH: -0.03; Parallel hole and TSH: 0.28 **Conclusion:** The significant differences between Tc-99m pertechnetate uptake values using pinhole and parallel hole collimators indicate that these collimators cannot be used interchangeably. Furthermore, weak correlations between uptake and TSH measurements for each collimator suggest that uptake values do not accurately reflect thyroid function.

## P353

### Thyroglobulin in Fine Needle Aspiration Cytology Washout to Detect Neck Lymph Node Metastasis of Differentiated Thyroid Carcinoma

**R. Sánchez Vañó**, E. Caballero Calabuig, M. Reyes Ojeda, P. Abreu Sánchez, L. Frontado Morales, L. Marbello García, H. Rodríguez Parra, C. Plancha Mansanet, J. Félix Fontestad, R. Sopena Monforte; Hospital Dr Peset, Valencia, SPAIN.

INTRODUCTION Many patients with differentiated thyroid carcinoma (DTC) are selected for fine needle aspiration cytology (FNAC) to detect cervical lymph node metastasis. Insufficient sample or non-determinant result can hinder cytology results. The assessment of thyroglobulin in the FNAC aspirate (FNAC-Tg) can be a useful complement of cytology to diagnose lymph node metastasis. AIM To assess FNAC-Tg value to detect thyroid activity in neck lymph nodes related to cytology in DTC patients. METHOD We conducted a prospective study of 155 DTC patients submitted for neck sonography. We selected 183 neck lymph nodes >0.5 cm for ultrasound-guided-FNAC from 95 patients. Bethesda Criteria were used for cytology. FNAC-Tg measurement was carried out in 1 mL saline for needle washout into a dry tube using IRMA assay. Tg sensitivity in our laboratory is 0.5 ng/mL. We related Tg-FNAC with cytology in all cases and with histology when available. Two control groups were also studied: 76 thyroid nodules from 39 patients (positive controls) and 18 samples from 16 non-thyroidectomized patients with thyroid-unrelated cervical mass (negative controls), in order to calculate sensitivity (S), specificity (E) and predictive values (PPV, NPV) of Tg-FNAC. Association between serum Tg and Tg-FNAC was examined in the positive control group. RESULTS Tg-FNAC in non-malignant cytology was <0.5ng/mL in 125/126 nodes and >600ng/ml in 1/126. Tg-FNAC in malignant cytology ranged between 3 and >600 ng/mL in 20/23 nodes, 11 of them with malignant histology. Tg-FNAC result was <0.5ng/ml in 3/23 nodes (13%, 2 confirmed malignancies). Tg-FNAC result in non-determinant cytology samples was <0.5 ng/ml in 1 case and >50 ng/ml in 2 cases. Tg-FNAC when non sufficient matherial (NSM) was <0.5 ng/ml in 31/31 nodes, 1 of them malignancy proved. Tg-FNAC in positive control group was >500 ng/mL in 68/76 nodules (NSM in 22) and <0.5 ng/mL in 8/76 (2 thyroiditis, 6 NSM). S=89%, PPV= 100%. Mean value serum Tg was 68.4 ng/mL. Association between Tg-FNAC and serum Tg showed $r^2$=0.11. Tg-FNAC in 18/18 negative control cases was <0.5-1 ng/mL. E=100% NPV=100% CONCLUSIONS Tg-FNAC >3ng/mL evidence thyroid cells and could help to decide in case of non-determinant cytology. Tg-FNAC <0.5ng/mL can not exclude thyroid activity in neck lymph nodes of DTC, mainly if NSM is obtained. Tg-FNAC result is independent of serum Tg.

P57-1 - Sunday, Oct. 20, 16:00 - 16:30, Poster Exhibition Area

## Conventional & Specialised Nuclear Medicine: Pulmonology

## P354

### Ventilation/perfusion lung SPECT/ LdCT in children with lung disease show high clinical impact on preoperative evaluation - Preliminary results

**M. Moerk**, J. Mortensen, L. Borgwardt; Department of Clinical Physiology, Nuclear Medicin and PET, Rigshospitalet, University Hospital of Copenhagen, Copenhagen, DENMARK.

**Aim:** To determine the clinical impact of ventilation/perfusion lung SPECT/LdCT in children with lung diseases for preoperative evaluation. **Materials and Methods:** Single photon emission computed tomography (SPECT) with low-dose CT was used to measure the distribution of lung ventilation (V) and perfusion (Q) in 21 scans in 19 children with a median age of 3,7 years between January 2012 and April 2013. The indications were primary abnormalities of the lung and pulmonary vessels/congenital anomalies of the heart and great vessels(n=10), Congenital emphysema(n=6), cystic fibrosis(n=2) and others(n=1). The V and Q were traced with 9000 MBq 81m Krypton and Technetium-labelled albumin macro aggregates, respectively, and the V/Q match-mismatch was visually interpreted by a specialist in nuclearmedicine and the Ld CT was interpreted by a specialist in radiology to determine the extent of lung function impairment. **Results:** 19 children (13 males, 6 females) had V/Q SPECT/CT performed. Clinical impact was found in 20 out of 21 scans, but in 19 out of 19 patients and changed or confirmed the clinical course of the patient. **Conclusion:** V/Q SPECT/LdCT provides unique additional information about regional lung function. The results suggest that the current clinical preoperative evaluation of children with severe lung disease can be improved and/or complemented with V/Q SPECT/LdCT with high clinical impact.

## P355

### Investigating Pulmonary Embolism (PE) In Pregnancy: Single Photon Emission Computed Tomography Ventilation-Perfusion Scintigraphy (SPECT VQ).

**S. Tomas Hernandez**, J. Phillips, N. Bebbington, T. Ogunremi, P. Guest; NHS, Birmingham, UNITED KINGDOM.

PURPOSE SPECT-VQ has replaced planar VQ scanning as imaging investigation of pulmonary embolism in general population. However, in the major studies, pregnant women were not included. In addition to this, protocols for pregnant women differ from the general population ones with the aim of reducing the dose. In our centre, SPECT-VQ is used as primary investigation for suspected PE in pregnant women. Computed tomography pulmonary angiography (CTPA) is performed when SPECT-VQ is not available or patient is unstable. The aim of this study is to verify the value of SPECT-VQ in pregnant women. METHODS 75 consecutive referrals for investigation of PE in pregnant patients during July 2010-September 2012 were retrospectively reviewed. There were 65 SPECT-VQ performed and 10 CTPA. The mean age was 27 years (range 17-45) and mean duration of pregnancy was 29 weeks (11-41). From the hospital information system, the clinical data including diagnostic tests and results (chest X-ray (CXR), leg ultrasound (US), SPECT-VQ, CTPA) were collected. RESULTS There were 65 patients primarily investigated with SPECT-VQ. Of the 65, 25 did not have CXR, 34 had normal CXR, 1 had abnormal CXR and 5 had minor abnormalities. The average interval between CXR and SPECT-VQ was 1.4 days (interval 0-6 days). Eleven patients had bilateral leg US prior to SPECT-VQ, all of them normal. Of the 65 SPECT-VQ, they were diagnostic in 95.4% of cases (no pulmonary embolism in 60, pulmonary embolism in 2) and indeterminate in 4.6% of cases (3 patients). Ten patients were primarily investigated with CTPA. Two did not have CXR prior to CTPA, 5 had normal CXR, 1 had abnormal CXR and 1 had minor abnormalities, 1 was not available for review. The average interval between CXR and CTPA was 1 day (interval 0-2 days). Five patients had bilateral leg US, 3 were normal, 1 reported deep vein thrombosis and 1 was not available for review. CTPA results were: no PE 70% (7 patients), indeterminate 30% (3 patients). Incidental findings included: consolidation and pleural effusions in 2 cases, old PE in 1 case, 6mm pulmonary nodule in 1 case, one suspected aortic root dissection (aortic root was normal on subsequent MRI) and breast implant rupture. CONCLUSION The majority of pregnant patients had SPECT-VQ as primary investigation for suspected PE. SPECT-VQ scan provides very good diagnostic value in excluding PE in pregnant patients being most of the time diagnostic.

## P356

### The diagnostic performance of dual-energy CT and SPECT. Is dual-energy CT truly superior to SPECT in diagnosis of pulmonary embolism?

**S. Kosuda**, A. Kawana, Y. Kyoto, Y. Naoi; National Defense Medical College, Tokorozawa, JAPAN.

Some investigators published that lung perfused blood volume (lung PBV) imaging by dual-energy CT was feasible and comparable to Tc-99m MAA SPECT. **Objectives:** To compare the diagnostic performance of lung PBV and SPECT in the diagnosis of pulmonary diseases including acute and chronic pulmonary thromboembolism (PTE). **Methods:** Seven patients who underwent both lung PBV and SPECT study, enrolled in this study. Those included 3 chronic PTE patients and each one of acute PTE, ASD, COPD, and no abnormality. Ten radiologists of more than ten-year experience read the two series of images: (a) Tc-99m MAA SPECT with 3.56 mm-thick transverse, coronal, and sagittal sections, and (b) contiguous 1-mm thick averaged transverse lung PBV images from both tubes. The image quality was rated using a semi-quantitative 5-point scale. **Results:** The findings of clear defects in patients with acute or chronic PTE showed the excellent scores in both studies, 1.4 for lung PBV and 1.2 for SPECT. The ambiguous or unclear findings showed better scores in SPECT than in lung PBV, 3.8 for lung PBV and 2.2 for SPECT. In a patient with no abnormality, three readers misdiagnosed it as abnormal in lung PBV images though they correctly read it as normal in SPECT. **Conclusions:** SPECT may be replaced with lung PBV in diagnosing diseases with definite findings. On the other hand, SPECT is superior to lung PBV in diagnosing diseases with unclear findings.

## P357

### Clinical application of deep-inspiratory breath-hold pulmonary perfusion SPECT with SPECT-CT combined system in patients with pulmonary thromboembolism

**Y. Fukushima**, S. Kumita, Y. Kobayashi, Y. Sugihara, T. Tomiyama, T. Kiriyama, K. Sohara; Nippon Medical School, Tokyo, JAPAN.

Introduction: Pulmonary perfusion SPECT-CT provides objective and comprehensive assessment of pulmonary function and morphological relationship. However, it hasn't been applied for clinical use since on conventional non-breath-hold SPECT, respiratory lung motion and cyclically varying lung volume changes during image acquisition deteriorate image quality and smear perfusion defects. Recently, SPECT-CT combined system is becoming widespread and it enables CT attenuation correction, obtaining fusion image, and quantitative evaluation by the use of breath-hold acquisition. The purpose of this study was to evaluate the degree of perfusion defect and its distribution in patients suspected of pulmonary artery thromboembolism by deep-inspiratory breath-hold pulmonary perfusion SPECT with SPECT-CT combined system. Methods: A total of 38 patients (20 men and 18 women, 65±16 years) with respiratory failure and suspected of pulmonary thromboembolism (PTE) were included in this study. All patients underwent deep-inspiration breath-hold pulmonary perfusion SPECT-CT. All the SPECT data was reconstructed using FLASH-3D and CT attenuation correction, and SPECT-CT images were created by hardware fusion. Deep-inspiratory breath-hold method was performed with 15 seconds in continuous 360 degrees acquisition in a single breath-hold. It was repeated 16 times (no less than 12 times), and the data was added to create the SPECT images. To diagnose the diseases, pulmonary perfusion defect distribution on SPECT images was compared with pulmonary abnormal shadow distribution on CT images, and percentage of perfusion defect was calculated. The percentage of perfusion defect is perfusion defect volume (derived from SPECT image) divided by lung volume (derived from CT image). In the cases with pulmonary thromboembolism, a CT pulmonary angiography (CTPA) was performed. Mastra score was calculated as an index of pulmonary artery thrombus volume (stenosis) in the CTPA image. The percentage of perfusion defect and Mastra score were compared in the cases with PTE. Results: Final clinical diagnoses were PTE (n=17), pulmonary hypertension (n=10), pulmonary emphysema (n=3), pulmonary inflammatory change (n=5), and interstitial pneumonia (n=3). The percentage of perfusion defect in PTE cases was not significantly higher than that in non-PTE cases. In patients with PTE, it was higher than the Mastra score ($p < 0.0005$). Conclusions: Deep-inspiratory breath-hold pulmonary perfusion SPECT-CT accurately demonstrated pulmonary perfusion abnormality and it enables the calculation of the percentage of perfusion defect. In patients with PTE, the severity of pulmonary perfusion defect doesn't correspond to the severity of pulmonary artery stenosis due to thrombus. Therefore, the detection of perfusion abnormality is important to understand the condition.

P58-1- - Sunday, Oct. 20, 16:00 - 16:30, Poster Exhibition Area

## Conventional & Specialised Nuclear Medicine: Gastroenterology

## P358

### Scintigraphic Evaluation of Liver Transplant Function

**V. Obradovic**, N. Petrovic, D. Sobic-Saranovic, V. Artiko; Clinical Center of Serbia, Faculty of Medicine University of Belgrade, Belgrade, SERBIA.

PURPOSE: The aim is evaluation of the perfusion, morphology and the biliary three patientcy of the liver transplants by two radionuclide Methods. PATIENTS AND METHODS: The study was performed in 10 controls and 10 patients after orthotopic transplantation (up to two years). "First pass" dynamic acquisition was performed with scintillation camera, after bolus injection of 360 MBq 99mTc-diethyl- IDA, (60 frames/60s), continued by 59 minutes (1 frame/min) slower dynamic study. From the liver and kidney activity during "first pass" study, hepatic perfusion index (HPI) was calculated using slope-analysis. Hepatobiliary scintigrams obtained during second phase of the study were analysed for morphology, and parenchymal and hepatobiliary TA curves were generated and analysed according to the time to maximal acitivity (Tmax) and the time to half of maximum acitivity (T/2). RESULTS: In comparison to the controls (HPI=0.64.5±0.05%) portal perfusion was slightly (0.68±0.04%), but not significantly ($p>0.05$) increased. In 3 patients, biliary phase of hepatobiliary scintigraphy showed increased accumulation of

radiopharmaceutical in the left (n=1) or right (n=2) hepatic duct. Uptake of the radiopharmaceutical (Tmax =18.5±2.9min) was slightly, but not significantly (p > 0.05) delayed in comparison to the controls (14.2±3.4min), while excretion was significantly (p 0.05) prolonged (31.3± 3.7 min) in comparison to the controls (25.7±3.5 min) while extrahepatic one is high significantly (p < 0.01) prolonged (89.0±14.3 min) than physiological (45.0±7.2 min). CONCLUSION: Radionuclide Methods are noninvasive, sensitive and valuable for the monitoring liver transplants.

## P359

### Usefulness of FDG-PET/ contrast enhanced CT in the follow-up of patients with high risk of recurrence of colorectal cancer.

**G. A. JIMENEZ LONDOÑO**, V. Sánchez Perez, E. Dominguez Ferreras, A. García Vicente, J. Cano Cano, A. Pinardo Zabala, A. León Martín, C. Vega Caicedo, O. Gomez Lopez, C. Molina Trinidad, J. Espinosa Arranz, A. Soriano Castrejon; Hospital General Universitario de Ciudad Real, Ciudad Real, SPAIN.

**OBJECTIVE:** Assess the accuracy of FDG-PET/contrast enhanced CT (FDG-PET/ ceCT) in the detection of unsuspected recurrence of colorectal cancer (CRC) in patients with high risk of relapse. **METHODS** Prospective study which included 29 patients (12 females and 17 males, mean age: 62, range: 41-78), underwent FDG-PET/ ceCT (55 studies). The inclusion criteria were: 1. Histological diagnosis or recurrence of CRC less than 3 years before the study. 2. CRC stage II (high risk), III and IV. 3. Curative surgery and adjuvant chemotherapy/radiotherapy. 4. Disease-free status. PET was performed 1 hour after the administration of a mean dose of 370 MBq of $^{18}$ F-FDG (standard protocol). After the injection of iodinated contrast agent, a portal venous phase (60 s) delayed CT scan was performed. Each modality (PET and ceCT) was evaluated independently by 2 blinded nuclear medicine physicians and radiologists respectively. An individual and combined assessment of both techniques was performed. Receiver operating characteristic (ROC) analysis was used to compare the area under the curve (AUC) of each modality. The final diagnosis was established by histopathology or clinical/radiological follow-up at least 6 months. **RESULTS** Six out of the 29 patients (7 studies) had a confirmed recurrence and the rest of patients had disease free status (48 studies). Six out of 7 studies with confirmed recurrence were detected by PET and ceCT, whereas both failed to identify malignant peritoneal implant in the same study. There was complete remission in 48 studies: 45 were correctly classified by PET, 46 by ceCT and 47 by PET/ ceCT. The sensitivity, specificity, positive predictive value (PPV), negative predictive value (NPV) and accuracy were: 86%, 94%, 67%, 98% and 92% for PET, 86%, 96%, 75%, 98% and 94% for ceCT, and 86%, 98%, 86%, 98% and 96% for PET/ceCT respectively. ROC analysis resulted in an AUC of 0.907, 0.907 y 0.918 for PET, ceCT and PET/ ceCT respectively. The use of PET/ceCT showed a slightly improved accuracy in the detection of recurrence in CRC compared to each technique separately (p= 0.9). **CONCLUSION:** PET and ceCT seem to have similar value in the detection of unsuspected recurrence of CRC. The added value of the combined assessment (PET/ ceCT) appears to improve the accuracy.

## P360a

### Prevalence of bile acid malabsorption in patients with chronic diarrhea. Causes and resin cholestyramine response.

**J. G. ROJAS CAMACHO**, P. Notta, O. Puig, Y. Ricart, A. Rodríguez-Gasén, M. Vidal, G. Martínez, J. Martín-Comín; Department of Nuclear Medicine. Hospital Universitari de Bellvitge-IDIBELL, L'Hospitalet de Llobregat. Barcelona., SPAIN.

**Objective**: To evaluate the prevalence of bile acid malabsorption (BAM) and the response to treatment with resin cholestyramine (RC) in patients with chronic diarrhea (CD) over one year of evolution. **Materials and Methods:** Two hundred ninety-seven (197 women) patients (p) between 21-90 years with chronic diarrhea were retrospectively evaluated. **Patients** were patients were followed for more than a year without clinical improvement and no established diagnostic. Abdominal bile acid retention was measured in all patients at 7 days after oral administration of 370 kBq of 75 Se-SeHCAT. Patients with a retention index (RI) <10% were considered to have bile acid malabsorption; these were treated with RC and assessed for response time based on changes in depositional rate. **Results**: Of the 297 p evaluated, 132 p (44%) had a low RI. They were classified by etiology of BAM in type I (16 p), type II (52 p) and type III (64 p). Only 113 p were treated with resin cholestyramine and 93 p showed a decrease in the number of stools (82%). In the remaining 165 p other cause. of CD was diagnosed **Conclusion**: The bile acid malabsorption is a common problem in patients with chronic diarrhea (44% prevalence). The absorption measurement of 75 Se-SeHCAT allows its diagnosis. Most of the patients (82%)diagnosed of BAM on the basis of an abnormal 75Se-SeHCAT test respond to therapy.

## P360b

### The effect of a single high caloric meal on [$^{18}$F]FDG uptake in brown adipose tissue in humans

M. Vosselmans[1], W. van Marken Lichtenbelt[1], A. van der Lans[1], R. Wierts[2], P. Schrauwen[1], M. van Baak[1], **B. Brans**[2]; [1]University Maastricht, Maastricht, NETHERLANDS, [2]Maastricht University Medical Center, Maastricht, NETHERLANDS.

**Aim:** The question is addressed whether $^{18}$F-fluoro-deoxyglucose ([$^{18}$F]FDG) can be used to detect diet induced brown adipose tissue (BAT) activity. Previous studies in humans have shown that BAT is negatively correlated with adiposity. Studies in rodents have shown that BAT might play a role in regulating energy balance as it could waste excessive caloric intake. The current study examined the effect of a high-caloric, carbohydrate rich meal on BAT activity in humans. **Material and Methods:** BAT activity was studied in eleven lean human adults (BMI: 22.4 ± 2.1 kg.m$^{-2}$, age: 23.6 ± 2.1 y) after the intake of a liquid meal (1622 ± 222 kcal; 78% C, 12% P, 10% F, Nutrical and Nutriprotein). BAT activity during two hours of mild cold exposure in 6 out of 11 subjects served as a positive control experiment. BAT activity was assessed by static PET/CT-scans, 1 hour after injection of $^{18}$F-fluoro-deoxyglucose ([$^{18}$F]FDG). We analyzed the average SUV ($SUV_{mean}$) in the cold and meal experiment in supraclavicular BAT, subcutaneous WAT and visceral WAT, skeletal muscle, liver, and brain by calculating cubes as volume of interests, placed in selected areas within the relevant tissues (PMOD 3.0; PMOD Technologies) **Results:** Postprandial [$^{18}$F]FDG-uptake in BAT (1.65 ± 0.99 $SUV_{mean}$) was significantly higher than in subcutaneous (0.35 ± 0.15 $SUV_{mean}$, $P < 0.05$) and visceral (0.49 ± 0.24 $SUV_{mean}$, $P < 0.05$) WAT, and liver (0.95 ± 0.28 $SUV_{mean}$, $P < 0.05$), but lower as compared to cold-induced BAT activity (7.19 ± 2.09 $SUV_{mean}$). Most distinctly, there was a pronounced, widespread [$^{18}$F]FDG hyperactivity in skeletal muscle as compared to cold (1.36 ± 0.31 vs. 0.59 ± 0.07 $SUV_{mean}$, $P < 0.05$) in the postprandial scans. **Conclusion:** The intake of the high-caloric meal resulted in enhanced [$^{18}$F]FDG-uptake in supraclavicular BAT in comparison to WAT and the liver. This is a first indication that BAT might be involved in wasting excessive caloric intake in humans. However, the widespread uptake in the large muscle compartment may affect biodisposition and may lead to underestimation of the postprandial BAT activity as judged by [$^{18}$F]FDG uptake. **Funding**: Research related to this abstract was funded by NWO-TOP (Netherlands Science Foundation ZonMw, TOP 91209037) to W.D. van Marken Lichtenbelt.

P59-1 - Sunday, Oct. 20, 16:00 - 16:30, Poster Exhibition Area

# Conventional & Specialised Nuclear Medicine: Haematology

## P361

### Use of Tc-99m sulphur colloid SPECT/CT in the differentiation of ectopic splenic tissue from malignant lesions

J. Chen, T. Wagner, A. Quigley, **S. Navalkissoor**; Royal Free London NHS Foundation Trust, London, UNITED KINGDOM.

**Background** Ectopic splenic tissue is an asymptomatic, benign condition that does not require treatment in the majority of cases. However, it is often discovered incidentally on radiological examination and mistakenly interpreted as neoplastic growth. Furthermore, definitive diagnosis is difficult to reach with computed tomography (CT) or magnetic resonance imaging alone. Tc-99m sulphur colloid scintigraphy has been the historical method of diagnosis in suspected cases of ectopic splenic tissue. However, detection of small nodules may be limited by the resolution of planar images and the location of the lesion (nodules close to the spleen may not be easily visualised due to scatter from the spleen). The addition of SPECT/CT fusion with the improved contrast resolution of SPECT and localisation of CT improves this problem, but has been scarcely reported in the literature. **Aim** To determine the value of Tc-99m sulphur colloid SPECT/CT CT in the identification and differentiation of ectopic splenic tissue from other causes of intra-abdominal soft tissue masses. **Methods** We retrospectively reviewed sulphur colloid SPECT/CT scans performed at our institute over the past 18 months. We looked at the indication for the scan and looked at the follow up and final diagnosis in the patients that did not have uptake on the Tc-99m sulphur colloid SPECT/CT CT. **Results** Six patients were identified. Indications for the study were as follows: nodule adjacent to tail of pancreas (2 patients), para-aortic mass (1 patient), retroperitoneal nodules in patient with previously resected tail of pancreas neuroendocrine tumour (NET) (1 patient), previous traumatic splenectomy, to differentiate splenosis from tumour (2 patients). Ectopic splenic tissue was identified in 4/6 (67%) patients (2 splenosis; 2 accessory spleen). One of the four patients with a history of pancreatic NET treated by distal pancreatectomy and splenectomy (who had 2 retroperitoneal nodules) was shown to have concomitant accessory spleen and tracer negative node (the latter of which increased in size on follow up CT, confirming disease recurrence). Suspected accessory spleen was excluded in 2 patients with peri-pancreatic and para-aortic mass respectively. These were diagnosed on subsequent biopsy as pancreatic NET and prostate cancer

metastasis respectively. **Conclusion** Tc-99m sulphur colloid SPECT/CT is an accurate and sensitive modality to identify and distinguish accessory splenic tissue from malignant lesions. It increases the diagnostic confidence and avoids potential invasive procedures.

## P362

### Functional imaging in diagnosis of bone marrow invasion in patients with Hodgkin's disease: the guide for treatment planning?

**S. V. Kanaev**, M. M. Girshovich, S. N. Novikov, L. A. Gukova; N.N. Petrov Institute Oncology, St Petersburg, RUSSIAN FEDERATION.

**Purpose:** retrospective analysis of 15 year experience of whole body (WB) bone marrow (BM) visualization was performed in order to determine prognostic significance of this diagnostic information. In addition we evaluate the value of this data for final treatment decision. **Material & Methods:** Since 1992 we perform WBBM visualization as a part of routine staging for all primary patients (pts) with HD. At the moment 632 pts with advanced HD and WBBM survey are available for long term (10-15 years) follow-up. All of them were included in this analysis. In pts with scintigraphic sings of BM involvement by HD they were verified and confirmed by biopsy and/or additional instrumental (MRI, bone scan, CT) examinations. All pts received 4-8 cycles of chemotherapy with MOPP-ABVD or ABVD or BEACOPP. In 45 pts visualized BM lesions were irradiated within 20Gy-50Gy (average dose 38.1Gy). BM lesions were outside radiation fields in another 30 cases. **Results:** In 206 pts with extranodal disease BM invasion revealed in 75 (36%) cases: 51 pts had one-two BM lesions and another 21 - multifocal BM involvement. *Overall (OS) and disease free (DFS) 10 year survival in pts with BM invasion (49% and 45%) were significantly (p=0,026) lower than in other pts with extranodal HD (62% and 65%).* In pts with only BM involvement and those with BM and other extranodal invasion OS and DFS were comparable: 50% versus 47.5% and 48.5% versus 41%. On the contrary, OS was significantly different (p=0.014) in pts with 1-2 BM lesions (57%) and multifocal BM disease (26.5%). *Irradiation of BM lesions significantly improve 10 year OS (p=0,00005) and DFS (p=0,006) in pts with HD: from 16% to 68% and from 23% to 58.5% correspondingly*. This differences are evident in subgroup of pts with 1-2 detected BM foci: 10 year OS and DFS in cases of irradiated BM lesions are 72.7% and 57.5% versus 13.5% and 25% - in non irradiated BM lesions (p=0.0006 and p=0.054). **Conclusion:** 1. In pts with advanced HD bone marrow invasion significantly decrease 10 year OS and DFS. 2. Extent of BM involvement determined by whole body visualization has significant prognostic value. 3. Visualization of BM involvement by HD can be used as a guide for radiotherapy planning

P60-1 - Sunday, Oct. 20, 16:00 - 16:30, Poster Exhibition Area

## Conventional & Specialised Nuclear Medicine: Uronephrology

## P363

### Clinical Value of Cystatin C and Beta Trace Protein in Glomerular Filtration Rate in Renal Transplant Cases with Stable Renal Graft Functions; Comparison by Tc 99m DTPA PLlaspma Sample Method

**O. Öner**, F. Aydın, F. Güngör, G. Süleymanlar, H. Akbas; Akdeniz University Faculty of Medicine, Antalya, TURKEY.

Glomerular filtration rate (GFR) is the best indicator of the renal function. Therefore, measurement of the graft's GFR is of paramount importance in renal transplantations. Gold standard for GFR measurement is inulin clearance. However, its measurement is inconvenient and non-economic. Thus, in both scientific studies and routine clinical practice Nuclear medicine Methods (Tc-99m DTPA) are preferred, which are highly correlated with inulin clearance. In addition, recently cystatin C (cys C) and beta trace protein (BTP) are also used for this purpose. In literature, data are limited about the clinical value of cys C and BTP in GFR measurement in transplant cases and the results have been inconclusive. In this study, we aimed to determine the efficiency of cys C and BTP in determination of GFR in transplant patients with stable renal graft functions. A total of 89 (60 males, 29 females) renal transplant patients aged 19 to 67 years were included, who had undergone renal transplantation at least 6 months before study enrollment and had stable graft functions according to clinical and laboratory criteria. GFR was calculated with three different Methods: 1) Using the gold standard Tc-99m DTPA two plasma sample method; 2) Using 8 different formula containing cys C (mg/l) to calculate GFR; 3) Using 3 different formula containing BTP (mg/l). Correlation of GFR values calculated with cys C and BTP with that obtained with Tc-99m DTPA two plasma sample method was assessed. GFRs calculated with both Methods were significantly correlated with that calculated with gold standard method. However, GFR values obtained with cys C had a better correlation compared to those of BTP. Also using regression analysis, performances of cys C and BTP in predicting GFR calculated with Tc-99m DTPA two plasma sample method were compared and a p value < 0,01 was obtained for cys C and 0,706 for BTP. Using Bland Altman analysis, scatter graphics of the differences between GFR values calculated using Tc-99m DTPA method and those calculated with cys C, BTP at a confidence interval of 95% (mean±1.96SD). The GFR value obtained with cys C had the most reliable consistency. As a conclusion, we showed that cys C may be a good marker for GFR of transplanted kidney. We also found that GFR value calculated with BTP failed to show GFR of the transplanted kidney. Based on these results, our study demonstrated that cys C is superior to BTP in reflecting GFR.

## P364

### Demonstration of the kidney functions obtained from a cadaveric donor in a rat model by the dynamic renal scintigraphy

H. Mitil, **Z. Koç**, Y. Guzel, M. Kom, A. Ozer, H. Ozercan, T. Balci; Firat University Hospital, Elazig, TURKEY.

Aim: In this study we aimed to determine the changes in the kidney functions detected through the Tc-99m renal scintigraphy and simultaneous histopathological and biochemical changes in the brain death rats. Materials and Methods: Ten rats were subject of this study. Dynamic renal scintigraphy and image analysis were carried out by Tc-99m DTPA one day before and just after the production of brain death model in ten rats. Tc 99m DTPA renal scintigraphy was performed under entubation and monitorization. Urea and creatinin levels of venous blood samples of the rats were measured before and after the brain death. Wilcoxon test was performed for the comparison of the numeric variables. Results: Significant increase in the GFR, left kidney Tmax, urea and creatinin levels after the brain death were observed in comparision with the levels before the brain death (p<0, 05). Although an increase in the right kidney Tmax levels after the brain death was also observed, it was not statistically significant (p=0, 066). In the visual evaluation of the renogram curves; the loss of the concentration functions and delay in the excretion functions were observed after the brain death. Common principal histopathological changes were the congestion in the veins, hydropic degeneration in the tubule epithelium and focal lymphocytic infiltrations in the kidney graft tissues of the all cases which were consisted with tubular impairment. In addition, all rats brain death were confirmed by histopathology. Conclusion: As a result, the quantitative and visual findings of the Tc-99m DTPA renal scintigraphy were related with the histopathological findings observed in the early periods of the brain death. These results showed that Tc-99m DTPA renal scintigraphy is a reliable and effective method for the graft function evaluation. Comprehensive experimental and even human studies on this topic will increase the number and the success of the renal transplantations. Keywords: Brain death, Tc 99m DTPA, renal functions.

## P365

### Added value of parametric renal clearance images in evaluation of regional renal functional defects following ESWL (extracorporeal shock wave lithotripsy)

**M. Bienkiewicz**[1], T. Konecki[2], I. Frieske[3], W. Woznicki[3], M. Sosnowski[2], A. Plachcinska[1], J. Kusmierek[3]; [1]Department of Quality Control and Radiological Protection, Medical University, Lodz, POLAND, [2]Department of Urology, Medical University, Lodz, POLAND, [3]Department of Nuclear Medicine, Medical University, Lodz, POLAND.

**Aim** Based on previous findings showing an effectiveness of parametric renal clearance images (PRCI) in detection of renal scars and regional kidney dysfunction in diabetic children, we aim to investigate its application to detection of regional renal functional defects following ESWL. Subjects 40 patients (17F,23M, age:54±10) with untreated renal stone disease: single calculus up to 25mm localized in calyces (25) or in kidney pelvic (15); with no urinary tract dilation on ultrasound examination, no urinary tract infection, no renal morphology abnormalities. **Methods** Patients underwent single ESWL session - treatment characteristics randomly assigned, assuming total energy of generated impulses of 50J. Renoscintigraphy (130MBq 99mTc-EC) was performed 3 times - directly before and one week and one month after treatment. Scintigrams were assessed with conventional method based on images of kidney parenchymal phase and with use of PRCI (method of Anderson &Surma). Regional renal function was assessed as with RFD (single-s or multiple-m regions of deteriorated renal function) or without renal function defects (no RFD) - by consensus of two experienced NM specialists. Split renal function (SRF) was calculated from renographic curves by integral method. Mean transit time (MTT) through whole kidney and parenchymal transit time (PTT) were obtained after deconvolution of renographic curves. 99mTc-EC clearance was calculated by multi-sample method. **Results** Week after ESWL parametric images showed RFD in 19(48%) of kidneys, month after - in 16(40%). It was significantly more than for conventional ones: 19 cases (12s,7m) vs. 5 cases (3s,2m) -week after, 16 cases (14s,2m) vs. 5 cases (4s,1m) -month after ESWL. Regional renal defects visible on parametric images week after ESWL, were present in follow-up values of functional parameters of exposed kidney: lower values of SRF

and EC clearance, longer times of MTT and PTT: -week after ESWL (mean values): SRF - 42% vs 49%; MTT - 297 vs 190; PTT - 239 vs 132; Cl - 128 vs 155 -month after ESWL (mean values): SRF - 45% vs 48%; MTT - 199 vs 210; PTT - 152 vs 146; Cl - 142 vs 155 **Conclusions** 1. PRCI detects more cases of regional RFD, week after ESWL, than conventional renoscintigraphic images of radiopharmaceutical uptake in parenchymal phase. 2. Frequency of occurrence and intensity of disturbances in regional renal function drop considerably one month after ESWL. 3. Significant differences in parameters of global renal function (SRF, MTT, PTT, EC clearance) in patients with and without RFD on PRCI show successful application of parametric imaging for assessment of RFD.

P61-1 - Sunday, Oct. 20, 16:00 - 16:30, Poster Exhibition Area

## Conventional & Specialised Nuclear Medicine: Infection & Inflammation

### P366

### The preliminary study of rat model with bisphosphonate-related osteonecrosis of the jaw using F-18 fluoride and F-18 fluorodeoxyglucose positron emission tomography

**Y. Kim**[1], H. Lee[2], B. Kim[3]; [1]Department of Dentistry, Ewha Womans University, School of Medicine, Seoul, KOREA, REPUBLIC OF, [2]Department of Nuclear Medicine, Seoul national University, School of Medicine, Seoul, KOREA, REPUBLIC OF, [3]Department of Nuclear Medicine, Ewha Womans University, School of Medicine, Seoul, KOREA, REPUBLIC OF.

P**urpose:**The aim of this preliminary study was to evaluate the usefulness of F-18 fluoride and F-18 fluorodeoxyglucose (FDG) positron emission tomography (PET) in the diagnosis of bisphosphonate-related osteonecrosis of the jaw (BRONJ) in Sprague-Dawley rat models. **Materials:**Rats were allocated into 4 groups: (1) rats treated with zoledronic acid (ZA) and dexamethosone (DX), (2) rats treated with ZA, (3) rats treated with DX, (4) control rats. Following 4 week period of treatment, upper right molars were extracted under anesthesia. After 4 weeks from the extraction, the animals were clinically examined and underwent PET scans with F-18 fluoride and F-18 (FDG). Then they were sacrificed and histological analysis was performed. Results:F-18 fluoride PET images of all groups, the uptake of extraction side was higher than those of contralateral (unwounded) side. However, ZA/DX groups had 0.66 times lower SUV ratio of ipsi to contralateral side than in control groups. In FDG PET images of all groups, the metabolism of extraction side was higher than those of contralateral (unwounded) side. Furthermore, ZA/DX groups had 1.4 times high SUV ratio of ipsi to contralateral side than in control groups. Animals treated with ZA and DX for 4 week period developed BRONJ-like lesions following extraction of maxillary molars, whereas the extraction sites of control animals underwent predictable healing with rapid epithelialization. Number of exposed necrotic bone sequestra and prevalence of pseudoepitheliomatous hyperplasia were higher in ZA/DX groups than in other groups. The number of terminal deoxynucleotidyl transferase (TdT)-mediated deoxyuridine triphosphate-biotin nick-end label-positive (TUNEL$^+$) osteoclasts increased on the surface of post-tooth extraction alveolar bone of the ZA/DX groups, which is related to the findings of FDG PET. **Conclusion:**In our preliminary study, ZA/DX groups showed similar pathogenesis of human who develop BRONJ and the extraction site of those groups had decreased F-18 fluride uptake ratio and increased FDG metabolism ratio than those of normal control. It is suggested that the PET studies using F-18 fluride and/or FDG could be useful to evaluate the BRONJ.(This research was funded by Basic Science Research Program through the National Research Foundation of Korea (NRF) funded by the Ministry of Education, Science and Technology (2012R1A1A1012913)).

### P367

### Role of Gallium-67 Scintigraphy in the Diagnosis of Tubulointerstitial Nephritis

A. Sabaté-Llobera, E. Noriega Álvarez, P. C. Notta, **O. Puig**, L. Camacho, J. G. Rojas Camacho, J. Mora, A. Benítez Segura, J. Martín-Comín; Servei de Medicina Nuclear, Hospital Universitari de Bellvitge, L'Hospitalet de Llobregat - Barcelona, SPAIN.

AIM To evaluate the role of renal imaging with gallium-67 in the initial diagnosis of tubulointerstitial nephritis. MATERIAL AND METHOD Twenty-seven patients (12 men, 15 women; median age 68 years) referred to our department for a scintigraphy with 67Ga-citrate to rule out tubulointerstitial nephritis. All of them had an acute renal failure with clinical suspicion of tubular or interstitial involvement, mostly due to drug intake, and were not recently treated with steroids. Doses injected were of 148 or 296 MBq (4 or 8 mCi) depending on the wish of performing a half-body scan or static images of the lumbar area (anterior and posterior views in any case). Scanning time was at 48 hours (2 patients), 72 hours (16 patients) or 96 hours (9 patients) after radiotracer injection. Positivity or negativity of the test was based on a visual assessment. Evaluation of scintigraphic results was done retrospectively in correlation with response to treatment and clinical evolution (follow-up 1-35 months). Moreover, 15 patients had a contemporary renal biopsy, also useful in the data analysis to correlate with scintigraphic findings. RESULTS Twenty-two patients were scintigraphically positive for nephritis. Twenty-one of them had good response to steroid treatment and a favourable evolution in time. The remaining patient had a renal biopsy showing an acute tubular necrosis in context of a rectum carcinoma treated with neoadjuvant chemo-radiotherapy and radical surgery the previous 3 months. Renal function improved with haemodialysis and hydration. Five patients had a negative gallium scan. Three of them were classified as “true negative”: two had a negative biopsy for tubulointerstitial nephritis (one was a renal cell carcinoma and one showed changes related to diabetic nephropathy), and the other patient did not have a good response to steroids and was finally diagnosed of diabetic nephropathy, with good evolution after an acute management of symptoms and a better control of diabetes. From the remaining 2 patients, one was a woman with a Sjögren syndrome and a favourable evolution after starting steroid therapy, and the other one had a biopsy-proven tubulointerstitial nephritis with good response to steroids. Sensitivity, specificity, positive and negative predictive values of gallium-67 scintigraphy were calculated with respect to favourable/unfavourable response to treatment and evolution, and were of 91%, 75%, 95% and 60% respectively, with a positive likelihood ratio of 3.6. CONCLUSION Gallium-67 scintigraphy is a useful tool in the diagnosis of tubulointerstitial nephritis. Its positivity is highly indicative of tubulointerstitial involvement.

### P368

### Diagnostic Role of $^{18}$F-FDG PET/CT in Immunocompromised Children with Fever of Unknown Origin

**L. CHANG**[1], M. CHENG[2], K. TZEN[2], R. YEN[2]; [1]Mackay Memorial Hospital and Mackay Medicine, Nursing and Management College, Taipei, TAIWAN, [2]National Taiwan University Hospital and National Taiwan University College of Medicine, Taipei, TAIWAN.

***Purpose:*** Scintigraphy using Gallium-67 (Ga-67) has been used frequently in the evaluation of children with fever of unknown origin (FUO). Owing to superior spatial resolution in less imaging time than Ga-67 scintigraphy, [$^{18}$F]fluorodeoxyglucose (FDG) positron emission and computed tomography (PET/CT) has recently reported to be a promising tool in the evaluation of FUO in adults. However, there are limited studies about the role of FDG PET/CT in evaluation of FUO in immunocompromised children. Here we report our experience using FDG PET/CT in this specific group of patients. ***Material and Methods:*** Nine children of immunocompromised status (median age, 3 year-old; range, 1 month to 11 year-old) underwent FDG PET/CT to evaluate FUO after all other conventional imaging showed negative results. The findings of FDG PET/CT were analyzed and compared with the final diagnosis. ***Results:*** Six children had oncological or hematological diseases (2 leukemia, 1 pheochromocytoma, 1 severe type aplastic anemia, 1 thalassemia, and 1 infantile neutropenia). Three young-aged infants had complex congenital heart disease. Seven of nine FDG PET/CT were true positive, all proved by biopsy or culture results. Prior Ga-67 scintigraphy in 2 of the 7 PET positive patients did not reveal abnormalities compatible with infection. A false-positive FDG PET/CT was noted, leading to additional diagnostic procedures. Additionally, 1 true-negative was found and the fever subsided without treatment shortly thereafter. Thus, FDG PET/CT had an overall accuracy of 88.9% (8/9). ***Conclusions:*** Our preliminary experience suggests FDG PET/CT may be of clinical benefit in the evaluation of FUO in immunocompromised children in whom conventional diagnostic imaging yielded negative results.

P62-1 - Sunday, Oct. 20, 16:00 - 16:30, Poster Exhibition Area

## Conventional & Specialised Nuclear Medicine: Bone & Musculoskeletal - DXA

### P369

### Close analysis of women osteoporosis situation with menopausal age less than 40 years old

**Y. Wang**, M. Liu, Z. Liu, D. Li, Y. Li; Department of Nuclear Medicine, Huashan Hospital of Fudan University, Shanghai, CHINA.

**Objective**: To do retrospective study on osteoporosis state of earlier menopausal age women and to perfect epidemic informations.**Method:** 164 postmenopausal women were divided into 2 groups whose age less than 70 years old and menopausal age less than 40: Group A included 50 cases with age at natural menopause <36 years, Group B 114 cases with age at natural menopause between 36 and 39 years old. To make a detailed inquiry about menopause reasons, analize results of its DXA on lumbar spine and left hip, and blood biochemical parameters such as N-MID, CTX-I, 25-OH-VD, PTH, BGP, CT, bone turnover markers.**Results:** 50.0% (25/50) in Group A diagosed osteoporosis, 42.0% (21/50) for low bone mass; 42.98% (49/114) in group B for osteoporosis, 41.23% (47/114) of patients with low

bone mass. The mean of 25 - hydroxy vitamin D were both lower than normal reference values, and the same as that of osteocalcin N-terminal molecular fragment in group B. There were several factors leading to menopause earlier: 5 cases for congenital diseases or genetic disease, 27 cases for cancer patients who had to take hormone therapy, 45 cases for oophorectomy, 16 cases for endocrine disorders, 36 cases were considered natural menopause, the remaining refuse to discuss. In addtion, there were several epidemic results: 62.20% (102/164) of the patients had a high school education, 7.32% (12/164) had smoking history more than 3 years, 45.73% (75/164) often drunk alcohol, coffee or carbonated drinks, 73.17% (120/164) ate legumes, 51.22% (84/164) drunk milk, 44.81% (69/154) were patients older than 35 years old who had pregnancy, 10.98% (18/164) accounted for poor economic conditions.**Conclusion:** Women in the probability of osteoporosis after menopause will increase significantly and become prone to osteoporosis crowd. At present, the point is to concern the earlier postmenopausal women. It is necessary to conduct regular detection of osteoporosis even if young women to keep abreast of the bone and prevent osteoporosis.

## P370

### Low mineral density in patriens with Hystiocytosis- primary results

**I. Kotsalou**[1], A. Adraktas[2], T. Sidira[1], P. Manoli[1], S. Gerali[1]; [1]Nuclear Medicine Dept, Pammakaristos Hospital, ATHENS, GREECE, [2]General Practice Dept, Pammakaristos Hospital, Athens, GREECE.

**Target**: Hystiocytarosis X (Langerhans Cell Histiocytosis - LCH), is a rare systematic disease, characterized by the infiltration of tissues from Langerhans. This disease infects primary the lungs and secondary the skin, the skull and the femurs, while the corticosteroids are essential part of the symptomatic relief therapy. **Method**: We reviewed the bone mineral densitometry studies (Bone Mineral Density, BMD, DEXA method) of 26 patiens with hystiocytosis, performed in lumbar spine and femoral neck. Our population had mean age±SD 40±22,5years and body mass index BMI)±SD: 28,2 ± 5,3. Studies were reported according the current WHO guidelines. **Results**: Mean bone density appeared to differ statistically significant between patients with hystiocytosis and control heathy volunteers (p 0.03). Furthermore, patient newly diagnosed had higher bone mass comparatively to those who received symptomatic corticoid therapy for the last three years (p 0,08). **Conclusion**: Bone infection in hystiocytosis consists mainly of lytic lesions in skull and ilium. Corticosteroids serve to the symptomatic therapy of the disease, but their negative role to the reduction of bone mass needs to be further researched.

## P371

### The relation of fat-free mass and bone mineral density with exercise performance in patients with chronic obstructive pulmonary disease.

**J. Koutsikos**[1], I. Giannopoulou[2], S. Spetsioti[2,3], S. Episkopopoulou[1], M. Vasilopoulou[2,3], M. Tsakirellis[1], J. Vogiatzis[3,4]; [1]401 General Military Hospital, Nuclear Medicine Dpt., Athens, GREECE, [2]Physical Education & Sports Science Dept, University of Athens, Athens, GREECE, [3]1st Respiratory Medicine Dept, University of Athens, Athens, GREECE, [4]Clinical Exercise & Health Sciences Institute, University of the West of Scotland, Paisley, UNITED KINGDOM.

INTRODUCTION: Exercise limitation is a common manifestation in chronic obstructive pulmonary disease (COPD) patients and has primarily been attributed to airflow limitation. Malnutrition is a common problem in COPD patients and a significant percentage of patients have been reported to be underweight. Although weight loss has been reported to be associated with decreased lung function and respiratory muscle strength, more research is needed on its impact on exercise performance. Furthermore, the relationship between exercise capacity and body composition in COPD patients is not well defined. The aims of this study were to measure the body composition of COPD patients by dual energy x-ray absorptiometry (DXA) and to explore the relationship between these body composition measures and exercise performance. MATERIALS & METHODS: In 21 COPD patients (17 M, 4 F, mean age 67.2±4.7 years), body composition and bone mineral density (BMD) were measured by DXA. Bone mineral content (BMC) and free fat mass (FFM) were assessed. Exercise performance was assessed by an exercise test to volitational fatigue on a cycle ergometer and measurements such as maximal work rate (WRmax) and maximal oxygen uptake (VO2max) were conducted. All patients also underwent a 6-minute walk test (6MWT). Pulmonary function tests (PFTs) were also performed and FEV1, FVC and DLCO were measured. RESULTS: Mean (±SD) of BMC, BMD, FFM, VO2max, WRmax and 6MWT were respectively 2.52±0.42 kg, 1.13±0.09 gr/cm2, 50.61±8.61 kg, 1.48±0.50 l/min, 63.48±26.02 W and 350.29±95.77 m. Strong correlations were found between FEV1 and exercise performance [P<0.01]. BMC and/or BMD correlated significantly with FFM [p<0.0005]. BMC correlated with exercise performance [p<0.05], while BMD and FFM correlated only with WRmax (r= 0.504 [p<0.05] and 0.694 [p<0.001] respectively). No significant correlations was found between FEV1 and either BMC, BMD or FFM. CONCLUSION: We conclude that BMD and FFM, independently of airflow obstruction, are important factors in determining maximum exercise performance in patients with severe COPD. Therefore, should be possibly used in the clinical assessment of COPD patients prior to their participation in exercise rehabilitation programs.

P63-1 - Sunday, Oct. 20, 16:00 - 16:30, Poster Exhibition Area

# Conventional & Specialised Nuclear Medicine: Bone & Musculoskeletal

## P372

### Suspicious single rip lesions in planar bone szintigraphy- Can SPECT-CT clarify the results?

**C. Gstettner**, S. Kerschbaumer, D. Heber, R. Aigner; Medical University Graz,Departement of Radiology, Division of Nuclear Medicine, Graz, AUSTRIA.

**Aim** 30 patients, suffering from a malignant primary disease in clinical history were enrolled retrospectivley in this study. The follow up planar scintigraphy has no clear diagnosis in suspicious single rip lesions. The impact of 3D-SPECT- CT, for differential diagnosis and impact to further patient treatment, was reviewed. **Materials and Methods** A malignant primary disease was histological proven in clinical history in 30 patients (17 male, 13 female with an average age of 57 years). 10 patients suffered from a lung cancer, 9 from a breast cancer, 5 from a prostatic cancer, 2 from a cervix cancer, one from a hepatic cancer, one from a colon cancer, one cancer of unknown primary and one from a osteosarcoma. A Siemens Symbia T16 SPECT- CT (Siemens Medical Solutions USA, Inc., Malvern, PA ) whole body bone scintigraphy was performed three hours after an intravenous application of 700MBq $^{99m}$ Tc DPD. Planar images were done (LEHR, 256 matrix, 2 detectors, 15cm/minute); additionally a SPECT (120 positions a 30seconds, 2 detectors) and a low dose CT (120keV 30mA-effective) of the region of interest was performed. **Results**: Using additional SPECT-CT 13/30 (43%) lesions were diagnosed as posttraumatic chance, 12/30 (40%) lesions as metastatic infested, 1/30 (3.3%) as osteoidosteoma, 1/30 (3.3%) as osteoblastic reaction in chase of local tumour infiltration of lung cancer and 1/30 (3.3) as osteochondrosis at the cartilage bone border. **Conclusion** SPECT CT, as an additional method in planar bone szintigraphy, plays an important role in the clarification of single suspicious rip lesions. This method is capable to distinguish between benign and malignant bone lesions and furthermore influence the individual treatment of the patients.

## P373

### Early monitoring of cartilage degeneration in osteoarthritis using a new radiotracer, 99mTc labeled chondroitin sulfate

**G. Sobal**[1], M. Pagitz[2], K. Velusamy[1], S. Kosik[2], H. Sinzinger[1]; [1]Medical University of Vienna, Vienna, AUSTRIA, [2]University of Veterinary Medicine, Vienna, AUSTRIA.

**Aim** Osteoarthritis is a common disease in aging society. There is a big need for specific radiotracer to image cartilage degeneration, especially at the early stage. We present uptake studies with 99mTc labeled chondroitin sulfate (CS) as a possible new tracer for imaging osteoarthritis. **Methods** We radiolabeled CS (Chondrosulf, IBSA, Lugano, Switzerland) with 99mTc (120-150 MBq) using tin method. For precise evaluation of tracer for further clinical studies we performed in-vitro uptake of 99mTcCS in human chondrocytes cell culture, tissue pieces, autoradiography and in-vivo in dogs. Cartilage tissue from patients undergoing knee arthroplasty (n=4, 63-82a) was divided into areas of mild (control) and heavy degeneration according to histological examination. Chondrocytes were isolated from both tissue areas. Uptake in chondrocytes (cell monolayer 1.5x104cells/well, cell suspension 1x106cells/well), both tissue areas (~5mg) and autoradiography (5µ) was monitored from 0.5h-72 h. In dogs (castrated male dogs, n=10, 4-9a, with 15-51 kg body weight) the tracer was i.v. injected into the external cephalic vein. 6 healthy dogs served as controls and 4 with clinical and radiological signs of osteoarthritis in carpal, elbow, or tarsal joint were examined. Uptake was monitored up to 24h using a gamma camera (Diacam, MiE GmbH, Germany). For whole body scintigraphy animals were under general anaesthesia, for planar under sedation only. **Results** In chondrocytes monolayer the max binding amounted to 0.9 ±0.07 fmol/cell vs. 65.0±4.5 f.mol/cell for mild, vs heavily degenerated cartilage, at 75 nmol/well. In chondrocyte cell suspensions uptake varied from 12.2-22.5% for mild vs. 17.6-27.2% for heavily degenerated at 24-72h, respectively. In tissue pieces uptake amounted to 35.2-42.9% at saturation (72h) vs 54.8-68.2%, respectively. Autoradiography revealed comparable results reaching saturation at the same time. In the diseased dogs suffering from osteoarthritis a significant, specific, persistent uptake between 4-6h in tarsal, carpal and elbow joints was documented. Median target (joint) to background (mid lower arm and lower leg) ratio in the osteoarthritic joints after 4, 6, and 24 hours was 2.6, 2.5, and 2.9, respectively and 1.4, 1.4, and 1.6, respectively, in healthy controls. In contrast, in healthy control dogs we did not detect any specific uptake in cartilage. None of

dogs showed any side effects. **Conclusions** 99mTcCS seems to be a suitable and specific tracer for imaging osteoarthritis. Furthermore, we could show that uptake correlates both in regional chondrocytes and cartilage tissue with the degree of cartilage degeneration. This finding could be crucial for early diagnosis of osteoarthritis.

## P374

### Comparison of the chest X-ray(CXR), bone scintigraphy and thoracic computed tomography(CT) to evaluate primary thoracic cage disorders

**H. Bozkurt**, Y. Akkaş, Ö. Kantarcıoğlu; Sivas Numune hospital, Sivas, TURKEY.

**Introduction**: Chest wall discomfort is a frequently complaint of patient admited to emergency service or primary health care system. Fact that the majority of the causes of pain are musculoskeletal disorders not a life-threatening cause such as cardiac origin. Chest X-ray is usually accepted as the first imaging modality to research thoracic cage disorders. But in many cases, physicians often have dificulty detecting these disorders on CXR because of organs overlap each other. So in our study, we compare CXR, bone scintigraphy and thoracic computed tomography to investigate clinical benefit of bone scintigraphy in primary thoracic cage disorders. **Material and Method**: Between 2008 to 2012 years, including 41 females and 32 males, totally 73 patients with complaint of chest wall discomfort associated with bony part were enrolled into study. Ages ranged from 9 to 80(mean age 37±17). Priorities for detection of metastases were excluded. The results of histopathological, clinical follow-up, chest CXR, bone scintigraphy and toracic CT of patients were compared statistically. **Results**: 7% (5/73) of patient were operated for biopsy. Hisopatologic results were 2 fibrous dysplasia, 2 encondroma and 1 bone cyst respectively. The other patients were evaluated according to clinical follow-up. Clinical distributions of these patients were 1 bifid rib, 14 fracture, 9 osteoarthritis, 15 costochondritis, 1 sternal anomaly and 28 intercostal muscle strain. No malignant lession was detected. CXR, bone scintigraphy and toracic CT were positive of patient respectively 20,5 % (15/73), 39,7% (29/73) and 40% (10/25). There was istatistically difference between CXR and bone scintigrapfy ($p \leq 0,05$, chi square test), but no diference was detected between bone scintigraphy and CT. **Conclusion**: There is so many pathology that affect the chest wall such as congenital/developmental anomalies or inflamatory/enfectious disease or soft tissue/bone tumor etc. Recognizing these pathological processes is the most valuable to make a good clinical impact. So it is thought that bone scintigraphy is still an important imaging modality to evaluate thoracic cage disorders despite many newly advances.

## P375

### The significance of 99m-technetium sestamibi accumulation in bone imaging for gonarthrosis

**R. Tanaka**[1], O. Nishiike[2], J. Nishiike[2]; [1]Chiba Institute of Sience, Choshi, Chiba, JAPAN, [2]Kushiro Sanjikai Hospital, Kushiro, JAPAN.

**Purpose:** Intracellular maintenance of $^{99m}$Tc-sestamibi (MIBI), a myocardial perfusion agent, is considered to be dependent on mitochondrial membrane potential. This study aimed to examine the relationship between images of bone accumulation and those of bone washout following MIBI administration in patients with gonarthrosis. **Methods:** We compared 84 hospitalized patients with gonarthrosis who were scheduled to undergo testing for artificial joint replacement. Ten normal subjects were enrolled as controls. Planar images of the knee joint were collected 30 min (early images) and 4 h (delayed images) after MIBI administration. Single-photon emission computed tomography (SPECT) images of the knee joint were also obtained along with the early images**.** Radioisotope (RI) count was calculated for bone substance in the knee and the quadriceps femoral muscles using the early and delayed planar images. The mean RI counts in the medulla and bone substance were calculated from the SPECT images. Washout of bone substance and femoral muscle was assessed using the washout rate (WR) formula: WR = early image − delayed image/early image × 100. **Results:** The mean RI count calculated from the early and delayed images of the knee joint was significantly higher in the gonarthrosis group (21.12 ± 9.78 and 9.47 ± 3.99, respectively) than in the control group (6.38 ± 1.62 and 4.51 ± 1.05, respectively; $p < 0.001$), as was the WR (53.29 ± 9.19% and 28.7 ± 4.13%; $p < 0.001$). There was no significant difference in the mean RI count of the quadriceps femoral muscles on both early and delayed images between the gonarthrosis group (24.13 ± 7.79 and 17.69 ± 5.76, respectively) and control group (23.76 ± 3.42 and 17.38 ± 3.42, respectively). Furthermore, there was no significant difference in the WR between the gonarthrosis group (26.52 ± 6.76%) and control group (28.7 ± 4.13%).The mean RI count in the medulla and bone substance as calculated from short-axis SPECT images was significantly lower in the control group (41.4%) than in the gonarthrosis group (68.8%; $p < 0.001$). **Conclusion:** MIBI accumulation in the bone requires the presence of cells containing many mitochondria, suggesting that MIBI can visualize the activity of osteoblasts and osteoclasts during the bone remodeling process in patients with gonarthrosis.

## P376

### Nodular fasciitis: A possible differential diagnosis of a hypermetabolic lesion suggestive of a soft tissue metastasis on $^{18}$F-FDG PET/CT during surveillance work up

**J. Kim**, J. Park, S. Lee, Y. Choi; Hanyang University Hospital, Seoul, Korea, REPUBLIC OF.

**Aim:** To report the findings of nodular fasciitis encountered on $^{18}$F-FDG PET/CT which were initially misinterpreted as a soft tissue metastasis during surveillance work up for the patients with malignancy. To recognize nodular fasciitis as FDG-avid benign tumor that may mimic soft tissue metastasis. **Materials and Methods:** Three cases of pathologically proven nodular fasciitis, which showed hypermetabolic activity on $^{18}$F-FDG PET/CT were evaluated. The patients had history of malignancy; Hodgkin's lymphoma (2 year ago), spindle cell sarcoma (8 years ago), and melanoma (9 years ago). Contrast enhanced MRI was also performed within 2 weeks after $^{18}$F-FDG PET/CT. **Results:** All lesions showed round shape. The locations and the longitudinal diameters of each lesion were quadrates femoris muscle, just lateral aspect of rectus femoris tendon, intermuscular space posterior to femoral neck and 2 cm, 1.4 cm, and 1.9 cm, respectively. All presented as FDG-avid lesions and the maximal standardized uptake values (SUVmax) of each lesion were 4.46, 7.96, and 3.40, respectively. On MRI, each lesion had various appearances which showed intermediate signal intensity (SI) on T1-weighted images, high or intermediate SI on T2-weighted images and homogeneous or heterogeneous enhancement on gadolinium-enhanced T1-weighted fat suppressed images. **Conclusion:** Although nodular fasciitis is a benign tumor, it is easily misinterpreted as a soft tissue metastasis because of its clinical and radiologic similarities with more aggressive tumors. Therefore nodular fasciitis may be considered as another possible diagnosis if solitary hypermetabolic soft tissue lesion is located in the muscle, intermuscular space or adjacent tendon on $^{18}$F-FDG PET/CT, especially in the patients with clinically low possibility of tumor recurrence or metastasis during their surveillance work up.

## P377

### Prevalence and correlates of ischial enthesopathy in FDG PET/CT: A retrospective study of 1751 patients

**K. Vejdani**, L. Sarajlic, Y. T. El-Gammal, M. M. Osman; St Louis University, St Louis, MO, UNITED STATES.

**Objectives**: Focal FDG uptake due to inflammatory enthesopathy has not been well addressed in the literature. Such a finding may represent a potential source of false positive interpretation. The purpose of our study was to evaluate the prevalence of peri-ischial FDG uptake and its correlation with gender, age, and weight, and possible persistence in subsequent studies**. Methods**: We reviewed the FDG PET/CT reports of 1751 patients for focal FDG uptake at the ischial tuberosities. All studies had been reported by one experienced nuclear medicine physician. For each patient with ischial enthesopathy, we measured the standard uptake values (SUVmax) for bilateral ischial entheses, and correlated them with patients' gender, age, and body mass index (BMI). When available, the patients' prior or subsequent PET/CTs were also reviewed in the same manner. **Results**: Of 1751 patients, 8 (4 M, 4 F) had increased FDG uptake at the ischial entheses, unilateral in 7 cases and bilateral in one. Male patients with ischial enthesopathy were older than female patients (mean age 79.0 vs. 62.7, p=0.017). SUVmax for the enthesopathic side (or the hotter side) was significantly higher than the contralateral side (mean 3.9 vs. 2.0, p=0.0002). The SUVmax correlated positively with age (r = 0.63) and negatively with BMI (r = -0.46). Three of 8 patients had a normal BMI (<25) and the other 5 were either overweight or obese. Mean BMI was 28.1 (range 19.4 - 40.2). Prior PET/CT studies were available in two patients and a subsequent study was available only in one of them. None of these studies revealed evidence of ischial enthesopathy. **Conclusion:** Metabolically active ischial enthesopathy is a relatively uncommon finding (8/1751 or 0.46%) in FDG PET/CT. When present, it appears to be temporally isolated and mostly unilateral, without gender predominance. On average, men with ischial enthesopathy are older than women with this finding, and the degree of FDG uptake correlates positively with age and negatively with BMI. Clinical significance of ischial enthesopathy remains to be studied.

## P378

### Diagnostic value of SPECT-CT in patients with equivocal lesions on planar bone scans.

**P. I. Krzhivitsky**, S. V. Kanaev, S. N. Novikov, O. I. Ponomoreva, L. A. Jukova; N.N. Petrov Institute Oncology, St Petersburg, RUSSIAN FEDERATION.

***Purpose*** to evaluate importance of SPECT/CT examination in verification of equivocal findings revealed on routine planar whole body bone scans (BS). ***Methods*** We prospectively studied 227 patients (mean age 57 years) with malignant tumors of various localizations. All of them underwent whole-body planar BS 3-4 hours after i/v injection of 740-1000 MBq of $^{99m}$Tc-methylene diphosphonate (MDP) and subsequent SPECT/CT of equivocal regions. BS was

considered equivocal when patient had inconclusive lesion that could not be differentiated as metastatic or benign. The lesions were rated as inconclusive if they have intense focal uptake involving a bone with extension to adjacent joint or solitary focal area of abnormal uptake only. All lesions discovered on BS were visually compared with their appearance on the SPECT/CT. ***Results*** In our study 41 of 227 evaluated patients (18%) had equivocal BS data. SPECT/CT correctly excluded bone metastases in 29 (71%) and confirmed malignant character of bone lesions in another 7 (17%) patients. In 5 patients (12%) scintigraphic changes remained unclear even after SPECT/CT. This patients requires regular follow-up. ***Conclusion*** 1.SPECT/CT was able to verify most (88%) of equivocal changes revealed on routine planar BS permitting dramatical improvement of test specificity. 2. SPECT/CT helps to exclude bone metastases in 71% of patients with equivocal changes on routine planar BS.

## P379

### Tc99m labelled S-HYNIC Certolizumab Pegol for selecting patients for anti-TNFα treatment: a biodistribution and dosimetric study.

**B. LAMBERT**[1], P. Carron[1], Y. D'Asseler[1], K. Bacher[2], F. Van den Bosch[1], L. Jans[1], D. Elewaut[1], G. Verbruggen[1], F. De Vos[2]; [1]UZ Gent, Gent, BELGIUM, [2]Ghent University, Gent, BELGIUM.

**Introduction** Biologicals directed against Tumor Necrosis Factor (TNFα) have proven their therapeutic efficacy in rheumatoid arthritis (RA) and spondyloarthritis (SpA). We initiated a clinical study to verify whether the therapeutic effect of Certolizumab Pegol (UCB Pharma), a PEGylated humanized antibody fragment (Fab') directed against TNFα, could be predicted by a pre-therapeutic scintigraphy with radiolabelled Certolizumab Pegol. **Aim** To perform a biodistribution and dosimetry study of Tc99m labelled S-HYNIC Certolizumab Pegol. **Methods** First, an attenuation map was obtained from a Whole Body (WB) scan using a Co57 floodsource. Subsequently, approximately 740 MBq Tc99m labelled S-HYNIC Certolizumab Pegol (1.25 mg) was injected IV. WBscans and blood sampling were performed immediately pi, at 1h, 4-6h and at 24h with a standard activity 99mTc placed in the FOV. Urinary excretion of the tracer was measured in urine collections up to 24h pi. All visualized organs as well as ROIs for the WB, background and standard activity were delineated on the 4 geometric mean WB images. Residence times in the WB and organs were estimated using mono-exponential fitting and absorbed doses computed by OLINDA/EXM. **Results** We analyzed 8 patients (4 females) with rheumatoid arthritis (1), psoriatic arthritis (2) or spondyloathritis (5). Besides accumulation of the tracer in the affected peripheral joints, high tracer uptake was observed in the bloodpool, liver, spleen and kidneys, with estimated mean absorbed doses for kidneys, spleen, liver, heart wall and urinary bladder wall of 56.1, 34.0, 32.7, 30.6 and 19.9 µGy/MBq. The WB effective dose was 9µSv (1SD)/MBq Tc99m-labelled S-HYNIC-Certolizumab. The urinary excretion was 15.1% (8.1SD) IA at 24h. Blood samples were fitted to a two-compartment model with a distribution half-life of 1.2h (1.5SD) and an elimination half-life of 26.9h (2.7SD). **Conclusion** Following an injection of 690 MBq Tc99m labelled S-HYNIC Certoluzimab Pegol an effective dose of 6.2 (SD0.9) mSv was estimated. The organs receiving the highest absorbed doses are the kidneys, a finding consistent with renal clearance being the major route of elimination for IgGs and Fab fragments. Other organs with relatively high absorbed doses are the spleen, liver, heart and urinary bladder. Urinary excretion was 15.1% of the administered activity at 24h post injection. The elimination half-life in blood was estimated to be 26.9h. There was clear accumulation of the tracer in the affected peripheral joints, encouraging us to apply this tracer in a trial designed to predict the clinical effect of therapeutic doses of Certolizumab Pegol.

## P380

### The role of three phase bone scintigraphy in management of patients with chostochondral pain

**Z. Koç**, M. Ozyurtkan, T. Balci; Firat University Hospital, Elazig, TURKEY.

Aim: The bone scintigrpahy is indicated in patients with chostochondral pain in order to identify organic etiology. We aimed to investigate the local, projecting or incidental findings in three phase bone scintigraphy of the patients who were referred for chostochondral pain. Materials and Methods: We included 50 patients (36K, 24E; mean:41±18 years old) who were referred to our department for three phase bone scintigraphy for chostochondral pain between January 2009-July 2012. Results: Among the 50 patients 22 had normal scintigraphy, and sternoclavicular increased activity accumulation was observed in 12 patients (right in 4, left in 4 and bilateral in 4) only in late phase and in 9 patients (right in 2, left in 1 and bilateral in 6) with increased vascularity. Among projecting pain causes sternal activity in 4 patients, humerus in 2 and in first costae in 2 patients was identified. Additionally increased vascularity associated with malign diseases elsewhere were firstly described in 3 patients (leimyosarcoma, flank mass, humerus metastasis) and benign bone tumor (chondroma) identified in one patient. Conclusion: Bone scintigraphy is an effective diagnostic method in the identification of local, projecting and additionally unexpected incidental pathologies associated with chostochondral pain. Key words: bone scintigrpahy, three phase, chostochondral pain.

## P381

### Osteosarcoma diagnosed by SPECT/CT

**S. Dinning**, B. Sogbein, W. Zeng; The Ottawa Hospital, Ottawa, ON, CANADA.

Bone scan is a sensitive imaging modality for the detection of bony lesions but is known to be non-specific. A diagnosis of bone metastases, especially from a solitary lesion, often requires radiological or pathological correlation. However, with the increased availability of hybrid SPECT/CT, the uncertainty on the bone scan can be greatly improved by the corresponding findings on the low-dose CT and the final diagnosis made by whole body bone scan with SPECT/CT, as illustrated by this case report. A 91 year old male with castration resistant prostate cancer with urinary bladder involvement was referred for a bone scan in January 2013, which showed no evidence of metastases in the axial skeleton. However, there was an unexpected finding of diffuse, heterogeneously increased activity in the left lower leg. Possible radiotracer contamination from radiourine was initially suspected and a SPECT/CT of the lower extremities was performed, which excluded this possibility. The patient stated that his left leg had bothered him on and off for several years but denied any symptoms at the time of the study. A prior bone scan from 2006 was normal. The low-dose CT scan localizes the metabolically active lesion to the left fibula involving two-thirds of the fibular shaft centered at the mid fibula. There is dense osteoid matrix with marked expansion and loss of corticomedullary differentiation. There is also marked circumferential, aggressive periosteal reaction with sunburst and hair on end appearance, typical for osteosarcoma. The subsequent studies consisted of a chest CT, which showed no pulmonary metastases and radiographs of the left tibia/fibula, which confirmed the SPECT/CT findings of classical osteosarcoma. Following consultation with the orthopedic oncology team, it was felt that the imaging findings are diagnostic with a high certainty and treatment without further biopsy confirmation ensued. The standard treatment of the above the knee amputation and chemotherapy were suggested to the patient but he was not keen for either treatment, which may not be unreasonable considering his age and co-morbidities. Consequently, radiation oncology was consulted for consideration of palliative radiation. The educational objectives of this poster are: 1. Review classical findings of osteosarcoma on CT scan and radiographs. 2. Review (with illustrated examples) common indications of SPECT/CT on musculoskeletal imaging. 3. Review prevalence, age and disease distribution of osteosarcoma and associations with secondary osteosarcoma. 4. Provide brief descriptions of CT acquisition parameters and the associated CT radiation exposure.

## P382

### Three-phase Bone Scintigraphy for Imaging Osteoradionecrosis of the Jaw

**C. Bluemel**, C. Linz, C. Lapa, A. Mottok, U. Mueller-Richter, A. Kuebler, P. Schneider, A. Buck, K. Herrmann; University Hospital, Wuerzburg, GERMANY.

**Aim**: This study evaluates the diagnostic utility of 3-phase bone scintigraphy (TPBS) for diagnosing osteoradionecrosis of the jaw (ORNJ). **Methods:** 32 consecutive patients with suspected ORNJ underwent 3-phase bone scans after injection of 520-750 MBq of Tc-99m-DPD. In addition to planar scans, tomographic images (SPECT) were acquired in the second phase and SPECT/CT images during the third phase. Histopathology (n=18) and clinical follow-up (n=14) served as reference standard for osteoradionecrosis. **Results**: The first, second and third phases of planar images were rated positive in 18/32 patients (56.3%), 25/32 (78.1%), and 27/32 patients (84.4%), respectively. The late SPECT was positive in all patients (32/32, 100%), respectively. Histopathology available in 18/32 patients (56.3%) confirmed ORNJ in all subjects. Acute inflammation was histologically proven in 18/18 specimens (100%) and additional chronic inflammation in 12/18 (66.7%). In 13/18 (72.2%) specimens, superinfection was evident histopathologically. A photopenic defect with surrounding hypermetabolism, a reported hallmark of ORJN was found in less than 5%. **Conclusions**: The predominant scintigraphic pattern of osteoradionecrosis includes increased bone mineralization phase in all patients. Central photopenia, reportedly a typical bone scan finding in bisphosphonate-induced osteonecrosis (BIONJ) was not characteristic for ORNJ. A differentiation of acute from chronic inflammatory processes was not possible.

P64-1 - Sunday, Oct. 20, 16:00 - 16:30, Poster Exhibition Area

## Conventional & Specialised Nuclear Medicine: SLN

### P384

### Lymphatic mapping and sentinel node biopsy in endometrial carcinoma: a feasibility study using cervical injection of radiotracer and blue dye

**R. Sadeghi**[1], Z. Shiravani[2], M. Hassanzadeh Mofrad[2], N. Shafiee[3], Z. Yousefi[2], A. Fattahi[4]; [1]Nuclear Medicine Research Center, Mashhad University of Medical Sciences, MASHHAD, IRAN, ISLAMIC REPUBLIC OF, [2]Women's Health Research Center, Mashhad University of Medical Sciences, MASHHAD, IRAN, ISLAMIC REPUBLIC OF, [3]Pathology Department, Ghaem Hospital, Mashhad University of Medical Sciences, MASHHAD, IRAN, ISLAMIC REPUBLIC OF, [4]Minimally Invasive and Endoscopic Surgery Research Center, Mashhad University of Medical Sciences, MASHHAD, IRAN, ISLAMIC REPUBLIC OF.

**Objective:** The aim of this study was to evaluate the feasibility and accuracy of sentinel lymph node detection using preoperative lymphoscintigraphy and intra operative gamma probe/blue dye for endometrial cancer patients. **Methods:** Twenty four consecutive patients with endometrial cancer were recruited. All patients underwent lymphatic mapping and sentinel node biopsy using combined intracervical radiotracer and blue dye injections. Pelvic lymph node dissection was performed for all patients. Para-aortic lymphadenectomy was done in high risk patients. All SLNs were examined by frozen section and H&E permanent sections.**Results:** Pre-operative lymphoscintigraphy showed at least one SLN in 21/24 patients. Intra-operatively, at least one SLN could be harvested by gamma probe and/or blue dye Methods. A total of 95 SLNs were detected. Four SLNs were detected only by blue dye, 42 only by radiotracer, and 49 were hot/blue. Median number of SLN per patient was 3. Three patients had positive pelvic lymph nodes. All of them had positive SLN (no false negative case). Frozen section could identify SLN involvement in two of three patients with positive pathology (33% false negative rate). **Conclusion:** Lymphatic mapping and sentinel node biopsy is feasible and accurate in endometrial cancer patients using combined radiotracer and blue dye Methods. Frozen section accuracy was lower and underscores the importance of expert pathologists for SLN mapping technique.

### P385

### Comparison of SPECT/CT, Gamma Probe and Methylene Blue-Dye For Sentinel Lymph Node Detection in Gynecologic Tumours

**S. Asa**[1], S. Sager[1], G. Demirayak[2], J. Nemetyazar[1], M. Halac[1], C. Onsel[1], K. Sonmezoglu[1], L. Kabasakal[1], H. Sayman[1], B. Kanmaz[1]; [1]Istanbul University Cerrahpasa Medical Faculty Department of Nuclear Medicine, Istanbul, TURKEY, [2]Istanbul University Cerrahpasa Medical Faculty Department of Obstetrics and Gynaecology, Istanbul, TURKEY.

**Aim:** It is known that sentinel lymph node surgery is to determine whether the primary cancer has spread to the very first lymph node or sentinel node. This study was designed to compare the SPECT/CT, gamma probe and methylene blue dye for sentinel lymph node detection in gynecologic tumours. **Materials and Methods:** SPECT/CT, intraoperative gamma probe and metyhylene blue-dye were performed in 30 patient with gynecologic tumours (mean age 60,8 with range 49-87 years). 1-2 mCi of Tc 99m labelled nanocolloid was injected in the uterine cervix in 23 patiens with endometrial cancer and 3 patients with cervical cancer and peritumoral area in 4 patients with vulvar cancer. 60 minutes after injection pelvic planar and SPECT images performed. SPECT/CT fusion images were composed with a PMOD fusion software programme. Methylene blue dye was also injected into the cervix and vulva immediately prior to the surgery. A gamma probe was used during the surgical procedure for sentinel lymph node identification. **Results:** A total of 67 sentinel lymph nodes were detected in 30 patients. The sensitivity of the SPECT/CT and gamma probe for detection of SLN was %86 and %96 respectively. SPECT/CT could not detect SNL in 4 patients. Intraoperative gamma probe was negative in only one patient. Methylene blue-dye was negative in 5 patients. With gamma probe the number of the detected sentinel lymph was more than SPECT/CT and methylene blue-dye. Metastasis of the primary cancer was detected in 8 lymph nodes in 4 patients. All the metastatic lymph nodes were sentinel lymph nodes and these metastatic lymph nodes were detected with SPECT/CT and gamma probe however 3 of metastatic lymph nodes were not positive with methylene blue dye. **Conclusion:** In our study it is shown in that gamma probe and SPECT/CT is more reliable than methylene blue-dye alone in patients with gynecologic cancers. SPECT/CT appears to improve sentinel lymph node detection and gives anatomic localization however gamma probe is the most reliable method for detection of sentinel lymph node in gynecologic cancers.

### P386

### Optimal Detection of Sentinel Node Metastases in Breast Cancer Patients by Intraoperative Radioactivity Threshold

**G. Manca**, S. Mazzarri, M. Tredici, G. Puccini, H. Svirydenka, R. Boni, E. Tardelli, E. Fiasconaro, S. Margotti, V. Duce, G. Boni, D. Volterrani, G. Mariani; Regional Center of Nuclear Medicine University Hospital, Pisa (Italy), Pisa, ITALY.

**Aim:** Many radioactive lymphnodes are often spotted by lymphoscintigraphy for identification of sentinel lymphnode(s) (SLN) in patients with breast cancer. It is still to be understood whether these further lymph nodes are 'true' sentinel nodes, or second-echelon lymphnodes that have collected the radiotracer crossing the SLN. A number of criteria based on the percentage of radioactivity concerning the 'hottest' node have been suggested to establish how many radioactive lymphnodes should be excised to reduce the false negative rate of the procedure. The goals of this study were to determine the frequency by which the hottest node is negative when the less radioactive lymphnodes present metastatic cells; and to determine the lymphoscintigraphic criteria that best define the radioactive lymphnodes to be harvested. **Materials & Methods:** Nine hundred and eighty-seven patients with breast cancer were submitted to lymphoscintigraphy for radioguided SLN biopsy. To establish how often a less radioactive sentinel node is metastatic when the most radioactive lymphnode is not, we classified as SLNs those with the highest counts as well as other radioactive lymphnodes counting 20% or more of the hottest node. We found two sets of pN+ patients, the former in which the most radioactive node was positive and the latter in which the less radioactive lymphnodes presented metastases when the hottest did not. **Results**: Of the 987 patients 201 (20.4%) had sentinel node metastases found by histological examination. We detected 128 positive axillary nodal basins from 128 patients with at least one positive sentinel node, and more than one sentinel node was harvested. In 31 out of these 128 nodal basins, a less radioactive lymphnode was positive when the most radioactive sentinel node was negative. If only the most radioactive sentinel node in each basin had been removed, 24% of these nodal basins with positive sentinel nodes would have been missed. The 'parallel' lymphoscintigraphic pattern (multiple lymphatic channels originating in the region of the primary tumor and running to different lymph nodes) was associated with increased percentage of finding the hottest negative lymphnode, while another less radioactive sentinel node contained metastatic disease (21 of out 31 patients; 68%). **Conclusion:** Our results demonstrate that the intraoperative threshold of ≥20% is necessary for optimal detection of nodal metastases in breast cancer patients, in particular in those presenting a lymphoscintigraphic parallel pattern

P65-1 - Sunday, Oct. 20, 16:00 - 16:30, Poster Exhibition Area

## Conventional & Specialised Nuclear Medicine: Miscellaneous

### P387

### Establishing renal and hepatic kinetics of Tc-99m-hexakis-methoxy-isobutyl isonitrile (MIBI): way towards imaging drug toxicity

**S. Dizdarevic**[1,2], M. Aplin[1], N. Ryan[1], S. Holt[1,3], L. Goldberg[1], K. A. Miles[4,5], A. M. Peters[1,2]; [1]Brighton and Sussex University Hospital NHS Trust, BRIGHTON, UNITED KINGDOM, [2]Brighton and Sussex Medical School, Brighton, UNITED KINGDOM, [3]Royal Melbourne Hospital, Melbourne, AUSTRALIA, [4]University College London, London, UNITED KINGDOM, [5]Molecular Imaging Centre, Princess Alexandra Hospital, Brisbene, AUSTRALIA.

**Objective:** Tc-99m-MIBI is a substrate for the ATP-binding cassette (ABC) transporter proteins, including P-glycoprotein (P-gp), and has been used to image high P-gp expression, mainly in multidrug-resistant cancer. Low P-gp expression also has an important role in development of drug toxicity, but this has not been investigated with Tc-99m-MIBI. Our aim was to study the normal kinetics of Tc-99m-MIBI in the kidney and liver to help understand the physiology of P-gp expression in these organs, and to subsequently develop an imaging assay to monitor toxicity of drugs that are P-gp substrates. **Methods:** Thirty healthy kidney transplant donors received ~400 MBq Tc-99m-MIBI i.v. followed by dynamic

scintigraphy over the abdomen for 20 min (phase-1) and static imaging at 30 and 120 min (phase-2). Time-activity curves were generated from phase-1 data from ROI over parenchymal regions of both organs. An exponential blood Tc-99m-MIBI clearance was assumed, with rate constant 0.3 $min^{-1}$, and used to predict the amount of Tc-99m-MIBI that would have accumulated in the organs over phase-1 had none left. The activities leaving the organs, the elimination curves, were then calculated by subtraction and expressed as percentages of the predicted total accumulated activities. **Results:** Kidney time-activity curves peaked at 2-4 min, then declined to a plateau from ~15 min of 31 (SD 5)% of the total activity accumulated (corresponding to 69 [5]% rapidly eliminated). Bladder activity followed a similar but opposite time course. Between 30 and 120 min, activity left the kidney at 0.36 (0.13)%.$min^{-1}$. Hepatic curves peaked at 6-8 min. Differentiation of the hepatic elimination curve revealed that a variable proportion of tracer (5-58%; mean 30 [14]%) was rapidly excreted over ~11 min. From 30 min, activity left the liver at 1.02 (0.23)% $min^{-1}$. There was no correlation between renal and hepatic elimination rates in either phase or between early and late phase elimination rates in either organ. **Conclusions:** The substantially higher, yet less variable, early renal elimination of tracer compared with hepatic elimination would be consistent with initial renal elimination predominantly through glomerular filtration. P-gp respectively located at the urine/tubule and bile/hepatocyte boundaries likely prevents Tc-99m-MIBI from re-entering cells from tubular lumen and biliary canaliculus, respectively, and thereby influences elimination rates and retention in both phases, although other ABC transporters are probably also involved. P-gp expression is tissue-dependant and understanding physiological renal and hepatic Tc-99m-MIBI handling will be a useful for the development imaging assays for investigating drug toxicity.

## P388

### Measurement of tear clearance with nuclear medicine method

**S. Barna**[1], A. Kiss[1], A. Forgács[1], A. Rentka[2], A. Berta[2], Á. Kemény-Beke[2], I. Garai[1]; [1]ScanoMed Ltd., DEBRECEN, HUNGARY, [2]Ophtalmology, University of Debrecen, HUNGARY.

**Background:** The tear has two phases (water and lipid) and it has 3 layers (lipid, water and mucin). In case of missing lipid phase, which produced by Meibomian glands, the tear layer easily split up. The patients can feel dry eye sensation, which means a constantly stimulus to twinkle. Moreover the evaporation of tear is increase, because of that the tear-clearance is increase accordingly. The aim of our prospective study was to work out a method to measure tear clearance. **Method and Patient:** 10MBq/ml sterile 99mTcO4 was dropped into both of eyes and a dynamic acquisition (90*10sec, 256*256) was started on planar gamma camera, with high spatial resolution (Nucline Th22, MEDISO). ROI was drawn on summed images and time-activity curve was generated. Tear clearance was defined based on the rate or time activity curve (T1/2) (Interview XP, MEDISO).We performed 32 examinations (64 eyes) among them 8 healthy and 24 patients with Meibom-gland dysfunction (MGD). The healthy control group was selected based on previous ophthalmological examinations excluded all types of keratoconjunctivitis sicca, as well as surgical intervention. **Result**: The mean of T1/2 value of tear-clearance of healthy people was 6.26min, median was 6.19 min, in contrast of MGD patients, where the mean value was 29.908 min, the median value was 30.26 min. We found that the tear clearance was significantly slower in patient's (MGD) group (Mann-Whitney Test $p<0.0001$). **Conclusion:** We can summarize that the tear scintigraphy is able to quantify the dry-level of eye based on tear clearance. Practically it is reproducible, a cheap and easy to perform method. Of course it does not replace the routine MGD examinations, but it contains meaningful added information.

P66-1 - Sunday, Oct. 20, 16:00 - 16:30, Poster Exhibition Area

## Therapy & Clinical Trials: Radioisotope Therapy - Miscellaneous

## P389

### Enhancement of Natural Killer Cell Cytotoxicity by Radioiodine Pretreatment in Breast Cancer Cells

**H. Kim**[1], J. Kim[2], Y. Jeon[2], S. Lee[2], J. Lee[2], S. Zeon[3], B. Ahn[2]; [1]Asan Medical Center, College of Medicine, University of Ulsan, Seoul, KOREA, REPUBLIC OF, [2]Kyungpook National University School of Medicine and Hospital, Daegu, KOREA, REPUBLIC OF, [3]Keimyung University School of Medicine, Daegu, KOREA, REPUBLIC OF.

**Purpose:** The purpose of this study was to determine whether death receptors of breast cancer cells are up-regulated by radioiodine (I-131) therapy and whether I-131 therapy can enhance natural killer (NK) cell cytotoxicity in *in vitro* and *in vivo* studies. **Methods:** The MDA-MB 231 breast cancer cell line co-expressing sodium iodide symporter and firefly luciferase genes (MDA-231/NF) and the NK92-MI NK cell line (NK92-MI) were used in the *in vivo* and *in vitro* assays. Flow cytometric analysis was performed in order to investigate the effect of I-131 therapy in surface levels of Fas, DR5, and MIC A/B of MDA-231/NF cells. The cytotoxicity assay was performed for the susceptibility of MDA-231/NF cells to NK cell cytotoxicity in *in vitro* study. BALB/c nude mice were divided into four groups (control, I-131, NK, and combined groups) and PBS, I-131, NK92-MI or NK92-MI with I-131 was given, respectively. The therapeutic results were assessed by bioluminescence imaging. **Results:** The levels of Fas, DR5, and MIC A/B expression in irradiated MDA-231/NF cells were significantly higher than in non-irradiated cells. Results of the cytotoxicity assay showed that the susceptibility of MDA-231/NF cells to NK cells was increased by precedent I-131 therapy *in vitro*. Results of *in vivo* study showed that tumor burdens of the NK and I-131 groups were significantly lower than that of the control group. Tumor burdens of the combined group were significantly lower than those of the I-131 and NK groups. **Conclusions:** Pretreatment with I-131 would result in up-regulation of the level of death receptors in breast cancer cells and improve therapeutic efficiency of NK cell therapy through enhancement of the cytotoxic effect of NK cells to the cancer.

## P390

### Role of FDG-PET/CT in radiotherapy planning (preliminary results)

**Z. Besenyi**[1], K. Hideghéty[2], Z. Lengyel[3], S. Kovács[4], L. Pávics[4]; [1]Euromedic Diagnostics Hungary Ltd., Szeged, HUNGARY, [2]University of Szeged, Department of Oncology, Szeged, HUNGARY, [3]Positron Diagnostics Ltd., Budapest, HUNGARY, [4]University of Szeged, Department of Nuclear Medicine, Szeged, HUNGARY.

**Introduction**: Modern oncologic care utilize FDG-PET/CT imaging not only in cancer detection, diagnosis and staging, but also on radiation therapy planning. Furthermore FDG-PET/CT may also play a role in therapy response monitoring. Aims of the current study were to compare radiotherapy targeted tumor volume based on conventional CT and FDG-PET/CT imaging and to determine weather additional metabolic information leads to a modification of staging and previously devised therapeutic regimens. **Methods**: 85 oncologic patients with primary head-neck, esophagus and lung cancer were enrolled in the current study. /Age 31-75 /. Within 3 weeks difference CT and FDG-PET/CT image acquisition was completed in regards to the planned irradiation position. During radiotherapy planning delineation of target volume and organs at risk were carried out both on conventional CT based topometric slices and FDG-PET/CT images. Radiotherapy target volume was calculated (PTV-cm3) by using both modalities. **Results:** In regards to the total population radiotherapy target volume as assessed by FDG-PET/CT differed in 92 % from target volumes calculated by topoCT. According to metabolic information the planned irradiation field was greater in 14 cases (16 %) (of which in 5 cases involved other regions as well) and smaller in 65 cases (76 %). Previously devised oncologic therapeutic regimen was altered in 18% of the patients based on the FDG PET/CT examination results. **Conclusion:** FDG-PET/CT imaging may allow for better radiation therapy target volume planning and viable tumor mass definition, while lessening organ at risk radiation exposure. Radiotherapy planning based on the combination of structural and metabolic information with implementation of modern radiotherapy techniques (intensity modulated radiotherapy, SIB) may improve the efficacy of cancer therapy.

## P391

### $^{18}$F-FDG PET-CT accuracy to assess lesion response three months after lymph node metastasis stereotatic body radiotherapy

**S. Hassler**, J. Clavier, M. Pop, P. Salze, G. Noel; CLCC Paul Strauss, Strasbourg, FRANCE.

Aim After radiotherapy, PET-CT is useful to determine tumor response but the interpretation is sometimes complicated because of inflammatory process that can remain for months. Inflammation is less after a more targeting radiotherapy, like stereotactic body radiotherapy. That's why an early FDG PET/CT could be efficient to determine lesion response after this kind of radiotherapy. We analysed FDG PET-CT diagnostic accuracy, performed 3 months after stereotactic radiotherapy of lymph nodes metastases. Material and Methods We studied 18 lymph node metastases in 13 patients treated by stereotactic radiotherapy, with a total dose from 33 to 60 Gy, in 3 to 8 fractions. After a mean follow-up period of 12 months (range 3.5- 23), treated lesions were classified as responders or non responders, by means of FDG PET-CT or CT alone if PET-CT was not available. Only lesions with complete response were considered as responders because goal of stereotactic treatment was curative. After treatment, the FDG uptake in lesion was assessed quantitatively, using SUV max, $SUV_{max}$ lesion to $SUV_{max}$ normal tissue ratio (L/N ratio), decrease of $SUV_{max}$ lesion, and qualitatively (no uptake, diffuse uptake, focal uptake). This metabolic analysis was compared to final response in order to define performance of PET-CT to assess response three months after radiotherapy. Results During follow-up, 11 lymph node metastases were described as responders and 7 as non responders. Mean time of first FDG PET CT after the end of stereotactic radiotherapy was 3.4 months (range 1.7- 4.4). On this exam, the mean $SUV_{max}$ and L/N ratio were significantly higher ($p<0.05$) for non-responder lesions compared to

responder ones. For lesion with decreased $SUV_{max}$ after radiotherapy, the decrease was not significantly higher for responder lesions compared to non-responder ones. All non responder lesions showed a focal FDG uptake pattern. The best exam accuracy (sensivity of 100% and specificity of 91%) was obtained with addition of this qualitative pattern to quantitative criteria of L/N > 1,2. Conclusion These initial results demonstrate that PET-CT performed 3 months after lymph node metastasis stereotactic radiotherapy can diagnose lesion response with high accuracy. The addition of qualitative criteria (focal uptake) and quantitative (L/N ratio > 1.2) appears to be the most efficient interpretation criteria.

## P392

### Role of 18F-FDG PET/CT in the clinical work-up of patients with vasculitis.

**D. PENNA**, C. TESTA, V. ARENA, E. PELOSI; IRMET EUROMEDIC PET/CT CENTER, TURIN, ITALY.

**INTRODUCTION** The purpose of our study was to evaluate the potential use of 18F-FDG PET/CT in the management of patients with large vessels vasculitis: at diagnosis and during the treatment. **METHODS** We retrospectively evaluated 13 patients (8 female, 5 male) during 55 months, with a total of 48 PET/CT scans. At the moment of the first scan, 3 pts presented diagnosis of vasculitis (2 Horton, 1 Takayasu), 7 clinical suspicion, 1 fever of unknown origin and 1 patient had a incidental finding of vasculitis during an oncological follow up. The 18F-FDG uptake at the level of ascending thoracic aorta, aortic arch, descending thoracic and abdominal aorta and subclavian, carotid and iliac arteries, was compared with that of the liver background using the SUV max. With a semiquantitative scale (grade 0 = no uptake; grade 1 = uptake lower than liver; grade 2 = similar to the liver; grade 3 = between liver and cerebral) PET findings were considered "negative" in case of grade 0-1 and "positive" in case of grade 2-3. PET results were compared with serological markers of inflammation and clinical evaluation**. RESULTS** First PET was positive in 12 cases and negative in one; these results, compared with clinical data, showed a good correlation both with laboratory data and symptoms. Than all patients were treated with steroids and/or immunosuppressive drugs. At the second exam we had 9 partial response (PR), 2 stable disease (SD), 1 progression of disease (PD) and the confirmation of negativity in 1 patient. At the third exam we had 3 complete response (CR), 9 positivity (PR, SD, PD) while the patient previously negative showed a positivization after withdrawing the treatment. During the treatment we observed a good correlation of PET data with the clinical evaluation in cases of PR and PD. Instead, 3 negative PET cases did not correlate with the still high serologic value of ESR, and 2 stable disease at PET did not correlate with disappearance of symptoms and normalization of inflammatory indices. **DISCUSSION/CONCLUSIONS** In this study the addition of PET helped in confirming the diagnosis of vasculitis in 7 patients and identified vasculitis in 2 patients without specific suspicion. In our study, the use of PET during the treatment is controversial. In particular, the group of "positive" PET highly correlate with clinical and laboratory evaluation (high positive predictive value), while "negative" PET present a low correlation (low negative predictive value).

## P393

### Immediate post operative 18-FDG PET/CT is able to evaluate the success of percutaneous ablative treatment

**E. C. S. C. Etchebehere**, J. Romanato, M. Menezes, R. Bezerra, A. Vicente, A. Santos, G. Cerri, E. Camargo; Sirio Libanes Hospital, Sao Paulo, BRAZIL.

Percutaneous ablative treatments (PA) such as cryoablation or radiofrequency for metastases of solid tumors have increased the possibility of oncological control in non-surgical candidates. After PA it is crucial to evaluate treatment outcome to avoid recurrences. Follow-up studies with CT and MRI are not able to differentiate scar from viable tissue after ablation**. AIM**: Demonstrate if $^{18}$F-FDG PET/CT (FDG PET/CT) performed in the immediate post operative hours after PA (*immediate post operative* FDG-PET/CT) is able to evaluate the success of PA. **MATERIALS AND METHODS:** Twenty patients (13 males, mean age 65.8 years), submitted to PA, were retrospectively reviewed. All patients with solid tumors metastases with indication for PA who exhibited focal uptake of $^{18}$F-FDG prior to PTA were included. The maximum interval between a baseline FDG PET/CT and the PA were 30 days. Exclusion criteria consisted of patients that had a change in chemotherapeutic regimen or that began chemotherapy during the 6 month follow-up period. An *immediate post operative* FDG-PET/CT study to evaluate the presence of residual viable lesion was performed between one and 8 hours after PA. The treatment was considered a success (no viable lesion) if no uptake of $^{18}$F-FDG was noted after PA on the *immediate post operative* FDG-PET/CT. Patient follow-up after 6 months was performed by clinical examination and imaging studies (FDG-PET/CT, MRI or contrast-enhanced CT). **RESULTS:** Twenty-six lesions were submitted to PA with either cryoablation (7/26) or radiofrequency (19/26) with mean lesion size of 2.5 cm. The metastatic lesions locations were liver (13/26), lung (8/26) and other sites in the abdomen (5/26). The *immediate post operative* FDG-PET/CT was performed between 1 and 8 hours after PA and detected viable tumor with a sensitivity, specificity, accuracy, positive and negative predictive values of 66.7%, 95%, 88.5%, 80% and 90.5%, respectively. False-positive cases consisted of two lung metastases (1.5 and 0.7 cm) of colon cancer submitted to cryoablation. The false-negative case consisted of a 3.0 cm lung metastasis of melanoma also submitted to cryoablation. There was a significant agreement between the *immediate post operative* FDG-PET/CT findings and the results on the follow-up study (Kappa = 0.66; $p < 0.01$). **CONCLUSION:** An *immediate post operative* FDG-PET/CT performed between 1 and 8 hours after PA may reliably evaluate the success of these procedures. This strategy may potentially allow early re-intervention of viable lesions and reduce morbidity. A larger number of patients are necessary to confirm these findings.

## P394

### Usefulness of [$^{18}$F]-FDG PET for Early Evaluation Response to Therapy with Sunitinib in Patients with Progressive Gastrointestinal Stromal Tumors

**L. C. Sobral Violante**[1], J. Teixeira[1], M. Soares[2], I. Sampaio[1], L. Pereira[1], L. Costa[1], F. Lopes[1], O. Soares[1], H. Duarte[1]; [1]Department of Nuclear Medicine, Portuguese Institute of Oncology, Porto, PORTUGAL, [2]Department of Medical Oncology, Portuguese Institute of Oncology, Porto, PORTUGAL.

**Aim:** Therapy resistance in advanced gastrointestinal stromal tumor (GIST) represents a major clinical problem. Although [$^{18}$F]-2-fluoro-2-deoxy-D-glucose positron emission tomography (PET) has proved to be useful in staging, imatinib therapy monitorization and patient's follow-up, little is known about its value in therapy with Sunitinib. The establishment of [$^{18}$F] FDG-PET/CT as an accurate and effective diagnostic tool in the early prediction response to sunitinib therapy would allow precocity in dose adaptations or drug substitution in patients (pts) with progressive GIST. **Material and Methods:** Between November 2006 and June 2012, we retrospectively evaluated imaging and medical record of ten pts with histological and immunohistochemical diagnosis of GIST who started Sunitinib therapy due to metastatic disease progression despite maximum tolerated dose of Imatinib. Three of these pts performed baseline [$^{18}$F] FDG-PET/CT (bPET) and early evaluation [$^{18}$F] FDG-PET/CT (ePET) scans less than two months apart from Sunitinib therapy initiation and were included in the study. The remaining pts were excluded due to inappropriate long time intervals between PET scans and treatment initiation. Primary tumour was located in the stomach (1 patient) and in the duodenum or small bowel (2 pts). Tumour response to sunitinib was determined using maximum Standardized Uptake Value (SUVmax) according to EORTC-PET study group recommendations. Clinical and imagiological outcome during the follow-up time was used as gold standard. **Results:** According to EORTC criteria, no pts presented complete metabolic response; early evaluation [$^{18}$F] FDG-PET/ CT showed one case of stable metabolic disease (SMD), other of partial metabolic response (PMR) and one of progressive metabolic disease (PMD). Patient 1: bPET SUVmax = 13,77; ePET SUVmax = 5,77; Δ SUVmax = -58,10% (PMR) - died of disease 8 months after initiating therapy. Patient 2: bPET SUVmax = 9,63; ePET SUVmax = 9,69; Δ SUVmax = +0,62% (SMD) - died of disease 5 months after initiating therapy. Patient 3: bPET SUVmax = 5,33; ePET SUVmax = 8,64; Δ SUVmax = +62,10% - (PMD) - died of disease 13 months after initiating therapy. **Conclusion:** In this small group of patients the absence of complete metabolic response in early evaluation [$^{18}$F] FDG-PET/CT seemed to be predictive of disease progression, independently of the observed degree in SUVmax decrease. A higher number of patients is required to accurately evaluate [$^{18}$F] FDG-PET/CT role in the early prediction of response to sunitinib therapy in GIST and to determine the correlation between SUVmax decrease and patient outcome.

## P395

### Usefulness of brain 99mTc-MIBI SPECT in the early assessment of the response to anti-angiogenic therapy in patients with recurrent high-grade glioma

**N. Yeni**[1,2], G. Petrirena[3], J. Tacchella[2], R. Guillevin[4], J. Delattre[3], A. Kas[1,2]; [1]Service de Médecine Nucléaire, AP-HP CHU Pitié-Salpêtrière, Paris, FRANCE, [2]LIF, INSERM UMR_S 678, Université Pierre et Marie Curie, Paris, FRANCE, [3]Service de Neuro-Oncologie, AP-HP CHU Pitié-Salpêtrière, Paris, FRANCE, [4]Service de Radiologie, CHU Poitiers, Poitiers, FRANCE.

Objectives: The aim of this prospective study was to evaluate the usefulness of brain 99mTc-sestamibi (99mTc-MIBI) SPECT in the early assessment of the response to anti-angiogenic therapy in patients with recurrent high-grade glioma (rHGG). Materials and Methods: 14 patients were included (median age: 62 years, median Karnofsky index: 80%). SPECT acquisition (three heads camera Philips, Irix) was performed 15 minutes after injection of 740 MBq of 99mTc-MIBI. SPECT and 3D T1w MRI with gadolinium injection were performed before and after 1 month of treatment with bevacizumab. Patients were monitored to assess the progression-free survival (PFS). MIBI reconstructed slices were analyzed blinded to MRI findings and patients clinical course. Tumor MIBI uptake was measured using a tumor / background (T/B) ratio calculated by: i) circular regions of interest manually placed on images and ii) an automatic method of extraction of the tumor uptake with

Brainvisa software. Manual segmentation of tumor volumes was performed on the 3D T1w MRI with gadolinium and compared to 99mTc-MIBI SPECT results. Results: Results of T/B ratios of the two Methods were significantly correlated (r = 0.67, p <0.001). Whatever the method used, 99mTc-MIBI SPECT was not predictive of the outcome of patients under treatment (no significant correlation with PFS). However, analyzes showed that tumor volumes defined by gadolinium enhancement on MRI and 99mTc-MIBI uptake on SPECT were strongly and positively correlated (r = 0.86, p <0.001). Conclusion: 99mTc-MIBI SPECT does not allow an early assessment of response to anti-angiogenic therapy in rHGG, even with the semi-automatic method. One hypothesis that could explain this result is the need of a break in the blood-brain barrier for the MIBI to be picked up by tumor cells. However, this barrier tends to be restored under bevacizumab independently of the antitumor efficacy. This phenomenon has been described with gadolinium. The demonstration of a strong correlation between 3D T1w MRI with gadolinium results and 99mTc-MIBI SPECT results reinforces this hypothesis.

## P396

### Assessment of the efficacy of Peptide Receptor Radionuclide Therapy (PRRT) in 6 -year observation.

A. Sowa-Staszczak[1], A. Stefańska[1], **M. Tomaszuk**[1], R. Mikołajczak[2], A. Hubalewska-Dydejczyk[3]; [1]Nuclear Medicine Unit, Department of Endocrinology, University Hospital, Krakow, POLAND, [2]Radioisotope Center POLATOM, National Centre for Nuclear Research, Otwock, POLAND, [3]Department of Endocrinology, Jagiellonian University Medical College, Krakow, POLAND.

**Introduction**: PRRT is a palliative form of treatment in patients with the progression of disease or in case of inoperable primary tumor if the expression of somatostatin receptors was confirmed. The aim of this study was to assess the efficacy of PRRT with the use of 90Y-DOTATATE and the survival rate of patients with disseminated or inoperable neuroendocrine tumors (NETs). **Material and Method**: In the time period from June 2006 to January 2013 72 patients were treated with PRRT in our Department. The 90Y-DOTATATE therapeutic activity was calculated per total body surface area up to a total of 7.4 GBq/m2 administrated in three to five cycles, repeated every four to nine weeks. Before and after the therapy, blood tests for hematology, kidney and liver function were performed. After PRRT, patients have been further treated with cold long acting somatostatin analogues (Sandostatin LAR) to the progression of the disease. **Results**: Out of 72 90Y-DOTATATE treated patients, 22 died after completing the therapy, among them two due to myocardial infarction. After 12 month follow-up, stabilization of disease was observed in 63%, partial remission in 25%, and progression in 12% in this group of patients. The progression free survival (PFS) was found to be 41.27 months and the event-free survival (EFS) - 37.73 months. The median overall survival (OS) was not reached. The mean time to progression and mean time to death were 24.04±18.59 and 20.09±18.59 months, respectively. During follow-up, transient decrease of PLT, WBC and hemoglobin values was observed. A increase of creatinine level and decrease of GFR values over observation period were found, but these were clinically insignificant symptoms of transient nephrotoxicity. **Conclusion**: Long-term patients benefit in the form of long survival rate, symptomatic relief and tumor mass reduction after 90Y-DOTATATE therapy was observed. PRRT is safe method which may extend the survival of disseminated patients with NETs.

## P397

### Reduced efficacy of repeated peptide receptor radionuclide therapy (PRRT) in progressive gastroenteropancreatic neuroendocrine tumours (GEP-NET)?

**J. Schnurr**, M. Reimold, H. Dittmann, J. Kupferschlaeger, R. Bares; Universität Tübingen, Tübingen, GERMANY.

Aim: PRRT has become widely accepted to treat inoperable, Somatostatin receptor positive GEP-NET. In order to avoid renal toxicity usually several low dose treatment courses are given shortly after each other. Aim of this retrospective study was to evaluate the efficacy of single courses of PRRT in patients who had received repeated therapy because of recurrent tumour growth. Materials and Method: Out of 99 patients with histology proven GEP-NET 20 patients (mean age: 60.5 yrs; 16male/4 female; localization of primary: pancreas/10, small intestine/6, large bowel/1, CUP/3) were selected who had received a single dose PRRT because of tumour progression and later on another single dose RPT because of recurrent progression. In 15 patients 90-Y-DOTATOC or 90-Y-DOTATATE was applied in both courses (1. therapy: mean 3770 MBq (3180-7250); 2. therapy: 3730 MBq (2580-5875)), 5 patients had received 177-Lu-DOTATOC as 1. and/or 2. course (mean: 7223 MBq (6700-7805). Response evaluation was primarily based upon CT using RECIST 1.1. In addition data from PET/CT (68-Ga-DOTATOC/TATE; SUVmax), tumour markers, and body weight were analyzed. Treatment response was evaluated after 3 months (tumour shrinkage) and after that until progression took place (time-to-progression (TtP). Results: Three months after initial or repeated PRRT favourable response was documented in 19/20 or 16/20 patients (partial remission in 2/19 or 2/16, n.s.), reduction of lesion diameters was slightly higher after initial PRRT (mean: 8.8% vs. 2.6%; n.s.), similarly weight gain and drop of tumour markers was higher after initial PRRT. TtP was significantly longer after initial PRRT (17 vs. 12 months; p = 0.017). Mean pretherapeutic SUVmax did not differ between initial und repeated PRRT (22.9 vs. 22.0), there was a weak correlation between SUVmax and shrinkage of target lesions (-0,325 or -0,285; p=0.02 or 0.029). Analysis of recurrence localization revealed new lesions as well as local progression after both initial and repeated PRRT. Conclusion: Repeated single dose PRRT is effective, however, response to the second course is moderately reduced possibly due to selection of less radiosensitive tumour cells after first PRRT.

## P398

### Is a rise in chromgranin A post-$^{177}$Lu-DOTATATE therapy significant?

**H. H. Tam**[1], A. Boles[1], P. Drymousis[2], N. Patel[1], A. Frilling[2], A. Al-Nahhas[1]; [1]Department of Nuclear Medicine, Hammersmith Hospital, London, UNITED KINGDOM, [2]Department of Surgery, Hammersmith Hospital, London, UNITED KINGDOM.

**Aim**: We have observed a rise in serum chromogranin A (chrA) levels in neuroendocrine tumour (NET) patients undergoing $^{177}$Lu-DOTATATE therapy. However, its significance is unknown. The aim of this study is to correlate changes in serum chrA levels with imaging based response assessment in patients who received $^{177}$Lu-DOTATATE for NET. **Materials and Methods**: Retrospective review of 9 patients with NET who received 4 cycles of $^{177}$Lu-DOTATATE from 2008 to 2012. Serial serum chrA levels were obtained at clinic visits before and after each cycle. An increase of chrA >25% from the baseline of each treatment cycle was considered significant. Response were assessed on pre-treatment and post-4 cycles CT/MRI according to RECIST 1.1 or $^{68}$Ga-DOTATATE PET/CT (SUVmax reduction of >30% = response; >20% increase or new lesion = progression; stable disease otherwise) where available. **Results**: ChrA was incomplete in 2 patients, resulting in a cohort of 7 patients (6 males, 1 female; 6 carcinoid tumours and 1 small bowel NET), total 28 cycles. A significant rise in chrA was observed in all patients (median 185% (range 25.2% to 798.7% increase). On $^{68}$Ga-DOTATATE, 1 patient showed partial response, 1 showed stable disease and 3 showed progressive disease. The other 2 patients were assessed on CT (1 stable disease and 1 partial response). Neither the percentage increase nor the absolute increase in chrA were significantly different (p = 0.29 and 0.92, respectively; Kruskall-Wallis test) between patients who showed response, stable disease or progressive disease. **Conclusion:** A significant increase in serum chromogranin A level post-$^{177}$Lu-DOTATATE can sometimes be seen in responding patients and should not be interpreted in isolation as a sign of disease progression.

## P399

### Radioisotopic Synoviorthesis. Overall Performance in Our Centre

**D. M. Ruiz Hernández**, C. Castillo Berrio, J. Nogueiras Alonso, O. Rivas Dominguez, A. Serena Puig, S. Martinez Bernardez, F. Loira Bamio, L. Campos Villarino, R. Guitian Iglesias, A. Lopez Lopez; ESG36555100, Pontevedra, SPAIN.

Aim To assess the use of Radioisotopic Synoviorthesis (RS) in our Hospital; its therapeutic efficacy, complication rate and patient satisfaction with this procedure. Materials and Methods Retrospective search of the RS performed in our center from 2005 to 2012. Review of medical records (written and electronic items). Patient satisfaction survey by phone. Method: Rheumatologist prescription. Informed consent. Pregnancy test if appropriate. Intra-articular administration of 185 MBq of 90Yttrium-colloidal and 40 mg of triamcinolone. Compressive bandage and relative rest during 48 hours. Control image at 72 hours p.i.. (Bremstrahlung). Treatment response assessed by: pain and/or joint effusion recurrence or not, its magnitude and frequency; need for fluid drainage; infiltrations and amount of analgesics for clinical control. Initial date of response and duration thereof. Results 42 cases were reviewed in total (Knee RS), excluding 13: 5 contraindication (Baker cyst), 1 by insufficient joint fluid, 1 performed with 186Renio, by meniscus rupture in1 and in 5 by insufficient monotoring. Of the 29 cases finally analyzed, 25 had good response at the initial evaluation (2 months). Follow-up at 18 months was only possible in 26 patients; of them just 18 persisted with positive outcome. In four cases there were never improved. There were slight migration to regional nodes in three patients, but without regional swelling nor other adverse effects. There were no cases of radionecrosis or transient increase of synovitis. Overall assessment of the procedure by the patients was satisfactory in most cases. Conclusion The RS in synovitis associated with chronic inflammatory arthropathy of diverse etiology produces very good short-term therapeutic results in most patients and in a lesser, but significant, percentage of cases a durable response even at two years post treatment. In some patients could be a definitive solution. The RS is a generally very well tolerated technique of high value for patients, usually without complications and, in our opinion, significantly underused.

## P400

### Pharmacokinetics of yttrium-90-labeled epratuzumab in the consolidation radioimmunotherapy of non-Hodgkin's lymphoma

**J. Barbet**[1], A. Rauscher[1], C. Bodet-Milin[2], T. Eugène[2], W. A. Wegener[3], S. Le Gouill[2], P. Soubeyran[4], D. M. Goldenberg[3], F. Kraeber-Bodéré[1], A. Faivre-Chauvet[1]; [1]Inserm, CNRS, Université de Nantes, Nantes, FRANCE, [2]CHU de Nantes, Nantes, FRANCE, [3]Garden State Cancer Center, Center for Molecular Medicine and Immunology, Morris Plains, NJ, UNITED STATES, [4]Institut Bergonié, Bordeaux, FRANCE.

**Aim**: Yttrium-90-labeled epratuzumab has been studied in the consolidation radioimmunotherapy of non-Hodgkin's lymphoma. The pharmacokinetics of the labeled antibody was monitored to assess the variability of its biodistribution and elimination. **Materials and Methods**: Seventy-five elderly patients with diffuse large B-cell lymphoma were accrued in a phase II clinical trial sponsored by the French LYSA group, assessing 6 cycles of R-CHOP14 followed 8 weeks later by 2 infusions of yttrium-90-labeled epratuzumab tetraxetan (555 MBq/m2), 7 days apart. Blood samples were collected at selected time intervals after the first injection and counted. The kinetics of the antibody was assessed by correction for radioactive decay assuming that catabolism products are eliminated faster than the intact molecule. Then a two-compartment pharmacokinetic model was used to simulate the blood kinetics using a population kinetics approach. The kinetics of the circulating yttrium-90 activity was also studied using the same approach to estimate the total number of disintegration in blood and finally the absorbed dose in blood. **Results**: The epratuzumab blood kinetics could be studied in 43 of the 75 accrued patients. They were well-fitted by a two compartment model but were found quite variable from one patient to another. For example the population blood clearance was estimated at 11.5 +/- 5.5 mL/hr, but varied from 0.6 to 25.0 mL/hr with a 33% CV within the population. Part of the variability was due to later time points and the variability of the activity kinetics was more limited (25 % CV). The total number of disintegration in blood thus varied from 3.9 to 11.2 x 1010 disintegrations corresponding to a blood absorbed dose of 4.5 to 12.8 Gy and to a blood-derived bone marrow absorbed dose of 1.3 to 3.8 Gy. These values did not correlate with observed hematological toxicities. **Conclusion**: Blood pharmacokinetics was found quite variable from one patient to another. Part of this variability could be attributed to the methodology, since yttrium-90 is too short lived to accurately trace the very long lived antibody (7 to 225 days terminal half-life). Pharmacokinetic modeling was however useful for the calculation of the total number of disintegrations in blood and ultimately of the blood delivered absorbed dose in bone marrow. The absence of correlation with observed hematological toxicity could be attributed to differences in previous chemo-immunotherapy-related toxicity and bone marrow function.

## P401

### Limoges' Hospital Experience of 90Y-ZEVALIN® in Non-Hodgkin's Lymphoma Treatment

**A. GRULIERE**[1], J. ABRAHAM[2], F. DALMAY[3], J. MONTEIL[1], D. BORDESSOULE[2], I. QUELVEN[1]; [1]Nuclear Medicine Department, University Hospital Dupuytren, Limoges, FRANCE, [2](2) Hematologic Department, University Hospital Dupuytren, Limoges, FRANCE, [3]INSERM UMR1094, Tropical Neuroepidemiology, Limoges, FRANCE.

BACKGROUND Non-Hodgkin's Lymphomas (NHL) B CD20+ are the most common hematological malignancies in France. Many immunochemotherapy protocols are available. However, complete and sustained remission in patients with NHL remains a real issue. Radioimmunotherapy (RIT) with 90Y-ZEVALIN® could be a rational approach, which involves administration of monoclonal anti-CD20 antibody labeled with radionucleide, leading to lymphoma cells significant radiation exposure. MATERIALS AND METHODS Data from 62 patients having received 90Y-ZEVALIN® standard-dose (14.8 MBq/kg for patients with platelet counts ≥ 150,000 cells/µl and 11 MBq/kg for patients with platelet counts between 100,000 and 150,000 cells/µl), between 2005 and 2012, both in monotherapy (n=16) or in addition to autologous stem cell transplant (ASCT) with BEAM conditioning regimen (n=46), have been analyzed in order to evaluate treatment usefulness and to compare results with literature. Disease histologies were diffuse large B-cell (n = 12), follicular (n = 30) and transformed lymphomas (n = 20). Endpoints included overall survival rate (OS), progression-free survival rate (PFS), and safety. RESULTS For patients treated in monotherapy for relapsed NHL B CD20+, our results are lower than those obtained in the literature: after a median follow-up of 47 months, 2-year PFS and OS were 25% and 58% respectively. Hematologic toxicities are frequently observed (70% grade 3-4 cytopenias). These results, both in terms of efficiency and tolerance, could be explained by a delayed RIT in disease progression. For patients treated in addition to ASCT conditioning, with a median follow-up of 6 months (range, 0,5 to 44,6 months) the estimated 2-year PFS and OS were 100% and 73% for patients treated for a relapsed follicular NHL (n=21). These results are very closed to GELA study (Decaudin et al., 2011) without hematologic toxicity increasing versus BEAM alone. For patients treated as first line consolidation for an aggressive NHL (n=16), the estimated 2-year PFS and OS were 76% and 66%. A new GELA study is in progress to evaluate benefit of RIT in this indication but results are not yet published. CONCLUSION Our study suggests 90Y-ZEVALIN® use, in monotherapy, in advanced phases of NHL B CD20+, leads to insufficient results. An earlier use, in addition to ASCT conditioning, seems more promising. The results of this experimental monocenter phase require confirmation in a wide multicenter study.

## P402

### Safety of Strontium-89 therapy in combination with chemotherapy

M. Yoshimura, **K. Suzuki**, T. Hashimoto, K. Koizumi; Tokyo Medical University, Tokyo, JAPAN.

**Aim:** Strontium-89 has long been used for the palliation of skeletal-related metastatic pain. Because of its side effects, particularly myelosuppression, it is difficult to combine with chemotherapy, thus the optimum duration for strontium-89 therapy is thought to be very limited. On the other hand, early administration of strontium-89 is known to be more effective not only for the palliation of bone pain but also in terms of its tumoricidal effect. The aim of this study was to assess the safety of combination therapy of strontium-89 and several types of chemotherapy. **Materials and Methods**: All 71 patients in this study were suffering from metastatic bone pain associated with breast cancer (29 cases), lung cancer (16), prostate cancer (8), and 18 other conditions. Patients underwent chemotherapy within 8 weeks before or 12 weeks after strontium-89 therapy. The degree of myelosuppression after combination therapy was assessed. **Results**: Blood toxicity was evaluated using NCI-CTCAE version 4.0. Hematologic toxicities (anemia, leukopenia, and thrombocytopenia) grade III/IV within 12 weeks after strontium-89 administration were defined as adverse events, and occurred in 28 cases (39%). Adverse events were divided into 3 categories: 1) Grade III/IV leukopenia or thrombocytopenia. However, the degree of WBC or PLT decrease is predictive by adding up the effect of myelosuppression of each therapy (15 cases). 2) Continuous decrease in RBC count leads to grade III/IV with the progress of the disease due to gastrointestinal bleeding, hemoptysis from a primary lesion, or anemia of cancer (9 cases). 3) Rapid deterioration of the general condition triggered by strontium-89 administration (4 cases). Occult DIC or carcinomatosa of bone marrow is thought to be manifested. Categories 1) and 2) were predictive and avoidable, but category 3) was difficult to predict (in case of the patients had no history of chemotherapy), and was sometimes fatal. Two of the 4 cases in category 3) had prostate cancer as shown by super bone scan, and 2 were in a serious end-stage of bladder and lung cancer. **Conclusion:** Hematologic toxicities grade III/IV were observed in 28 cases (39%). Most of these toxicities were predictive and avoidable by proper planning so as not to overlap the each nadir of hematologic toxicities. Patients who are able to undergo chemotherapy safely are also able to undergo combined therapy safely. Patients with super bone scan or serious end-stage conditions should not undergo combined therapy even if the hematologic toxicities are not evident at that time.

P67-1 - Sunday, Oct. 20, 16:00 - 16:30, Poster Exhibition Area

## Therapy & Clinical Trials: Therapy Response Assessment

## P403

### Stunning phenomenon after Radioactive I-131 Diagnostic Whole-Body Scan; is it really a point of clinical consideration?

**A. Amin**, M. Amin, A. Badwey; NEMROCK, Faculty of Medicine; Cairo University, Cairo, EGYPT.

Purpose: Stunning of thyroid remnants after diagnostic scanning [Dx-WBS] using radioactive iodine [RAI-131] may limit efficacy of RAI-131 therapy. We aimed to evaluate this assumption in a prospectively designed study. Methods: forty patients who underwent thyroidectomy for differentiated thyroid carcinoma were studied and divided into two identical groups. In G1 no Dx-WBS was done and ablation dose was given directly based on their risk stratification while in G2; Dx-WBSs were obtained with 185 MBq [5 mCi] of RAI-131 and ablation was given at a mean 11±1.1 days where stunning was found on semiquantitative basis in all of them. At a mean of 6.5±0.3 months ablation success rate [ASR] was evaluated using Dx-WBS, thyroglubline [TG] and neck sonography. Complete ASR was considered when no RAI-131 uptake could be seen in the neck or elsewhere, TG < 2 ng/mL and free neck sonography for any disease related abnormalities. Results: G1 and G2 were completely identical as no significant differences were found between their different characteristics including the mean ablative dose. ASR was 81.7% and 78.3% in G1 and G2 respectively [P 0.6]. Multivariate Cox regression analysis showed the mean ablation dose is the most influential factor in ASR [OR 1.045; 95% CI 0.936-1.1189; P 0.01]. Conclusion: Our data suggest that stunning had no influence on ASR and is not a point of clinical consideration regarding such aspect.

P68-1 - Sunday, Oct. 20, 16:00 - 16:30, Poster Exhibition Area

## Therapy & Clinical Trials: Miscellaneous

### P405

### A Randomized Control Trial to assess the influence of Radioiodine Uptake (RAIU) on 131I Therapy in Graves' Disease : A Paradox Solved

**S. Malapure**, C. Bal, S. Karunanithi, G. K. Parida, S. Ballal; All India Institute of Medical Sciences, New Delhi, INDIA.

**Aim**: It is firmly believed that higher the RAIU lesser is the amount of 131I required for the successful treatment of Graves' disease (GD). Paradoxical observations were made in a recent retrospective cohort study showing that in high RAIU GD patients lesser amount of 131I lead to lesser success rate. Thus we designed a prospective randomized control trial (RCT) with 90% power (alpha= 0.05, n= 170 in each arm) to test the 131I therapy and high uptake paradox. **Materials and Methods**: GD patients with 24h RAIU > 50% were randomized into two groups(gr)- Gr1 patients were administered a fixed dose of 185MBq and Gr2 were administered 259-555 MBq of 131I. Those patients with 24h RAIU less than 50% were excluded from this study. All patients were reassessed clinically and biochemically after 3 months. The cure rate was defined as either euthyroidism or hypothyroidism at 3 months of follow-up. **Results**: From Jan'10 to Oct'12, a total of 415 GD patients fulfilled the inclusion and exclusion criteria and were randomized into Gr1(n=204) or Gr2(211). 100% recruitment was achieved, however, 71 patient lost to follow-up (30 from Gr1 and 41 from Gr2). Final analyses were made on 344 patients-103 males, median age-40yrs and mean 24h RAIU- 64%. The mean administered dose of 131I in Gr1 was 185MBq and in Gr2 was 458 + 65.12MBq. First dose success rate in Gr1 was 61.5% (n=107/174) and in Gr2 was 76.47% (n=130/170). Thus, in Gr1 success rate was significantly lower than those who received high administered dose of 131I in Gr2 (p= 0.005) **Conclusion**: We conclude that GD patients with >50% 24h RAIU need higher 131I dose of to be cured with single therapy. 24h RAIU seems to be an old reliable tool for guiding the dose and predicting the outcome of 131I success rate in Graves' disease patients.

P69-1 - Sunday, Oct. 20, 16:00 - 16:30, Poster Exhibition Area

## Radionuclide Therapy & Dosimetry: MIBG & Peptides

### P406

### Evaluation of two amino acid protocols for kidney protection in patients treated with $^{90}$Y-DOTATOC for neuroendocrine tumors

**A. K. ARVESCHOUG**[1], S. M. J. Kramer[1], P. Iversen[1], J. Frøkiær[1], H. Grønbæk[2]; [1]Aarhus University Hospital, Dept of Nuclear Medicine & PET - Center, Aarhus, DENMARK, [2]Aarhus University Hospital, Dept of Gastroenterology and Hepatology, Aarhus, DENMARK.

**Background:** Peptide receptor radionuclide therapy (PRRT) is an established treatment for progressive neuroendocrine tumours (NET). Nephrotoxicity is the limiting factor using $^{90}$Y-DOTATOC. Although administration of amino acids lowers the radioactive dose to the kidneys, delayed renal damage is a concern following therapy. Studies have indicated that prolonging the infusion of amino acids offers improved kidney protection. The intermittent infusion of amino acids up two days after PRRT has also been shown to further reduce renal uptake of radioactivity in pilot studies. **Aim:** We evaluated whether differences could be detected in GFR in patients treated with two different protocols for kidney protection using commercially available (Vamin-18) amino acid mixture (AAM); a standard protocol with 2 litres of AAM infused over 4 hours or a 24-hour infusion protocol with 3 litres of AAM. **Material and method:** GFR in 18 patients treated with infusion of 2 litres AAM of 4 hours was compared with GFR in 13 patients treated with 3 litres of AAM over 24 hours at 3 months, 6 months and 12 months after therapy with $^{90}$Y DOTATOC. The majority of patients received the standard treatment of 3.7GBq/m$^2$ $^{90}$Y DOTATOC every 8-10 weeks. The glomerular filtration rate (GFR) was estimated using the $^{51}$Cr-EDTA plasma clearance by a single sample technique according to Groth and Aasted. **Results**: Pre-existing risk factors associated with kidney failure were seen in 84 % of the patients. Other identified risk factors associated with kidney failure were former treatment with $^{90}$Y-DOTATOC and/or chemotherapy, hypertension and diabetes. In the whole group of patients a significant fall in renal function was seen up to twelve months after PRRT. The median loss of kidney function was 30 ml/min/1.73m$^2$ (27 %) 12 months after treatment compared to pre-therapeutic values. Although no significant statistical difference was found comparing the two amino acid protocols, the use of a 24-hour amino acid infusion resulted in a continuous reduction in the median loss of renal function compared to the 4 hour infusion, i.e. 13% versus 23 % at 6 months and 19% versus 40 % at 12 months after therapy. **Conclusion**: The use of a kidney protection protocol involving a 24-hour infusion of AAM shows a tendency towards reduction of the loss of kidney function in patients treated with PRRT for NET compared to a less stringent protocol.

### P407

### Acute toxicities of I-131 MIBG therapy in patients with refractory neuroblastoma

**D. Kayano**, H. Wakabayashi, A. Inaki, A. Toratani, M. Fukuoka, S. Kinuya; Kanazawa University Hospital, Kanazawa, JAPAN.

**Objectives:** The aim of this study was to evaluate the acute toxicities of I-131 MIBG therapy in patients with refractory neuroblastoma. **Methods**: This study included 40 patients who underwent I-131 MIBG therapy for refractory neuroblastoma between February 2002 and January 2012. The patients comprised 19 males and 21 females, and the age range at I-131 MIBG therapy was 2 to 27 years (mean = 8.9 years). Therapeutic doses of I-131 MIBG were 1.7 to 18 mCi/kg (mean = 10.5 mCi/kg). We investigated the acute toxicities of I-131 MIBG therapy within a week after I-131 MIBG administration. Toxicities were graded by Common Terminology Criteria for Adverse Events Version 4.0. **Results**: Nausea, vomiting and sialadenitis were seen within a week after I-131 MIBG therapy. Grade 1 and 2 nausea, vomiting and sialadenitis were seen in 33% (13/40), 10% (4/40) and 23% (9/40). Only one patient (2.5%) had grade 3 nausea. In patients who were administrated more than 12mCi/kg I-131 MIBG (n=20), nausea, vomiting and sialadenitis were seen in 50% (10/20), 15% (3/20) and 35% (7/20). In patients who were administrated less than 12mCi/kg I-131 MIBG (n=20), nausea, vomiting and sialadenitis were seen in 20% (4/20), 5% (1/20) and 10% (2/20). **Conclusions**: Although the frequency of acute toxicities of I-131 MIBG therapy increases with the increased doses of I-131 MIBG, severe acute toxicities of I-131 MIBG therapy are rare.

### P408

### Survival Improvement in Patients with Disseminated Medullary Thyroid Carcinoma Treated with $^{131}$I-MIBG Therapy

**I. Mihaljević**[1,2], N. Topuzović[1,2], D. Šnajder[1]; [1]Clinical Institute of Nuclear Medicine and Radiation Protection, University Hospital Centre Osijek, OSIJEK, CROATIA, [2]School of Medicine Osijek, Josip Juraj Strossmayer University of Osijek, Osijek, CROATIA.

**Introduction and aim**: The aim of this paper is to present our experience of $^{131}$I-MIBG therapy in the cases of aggressive form of medullary thyroid carcinoma (MTC) with local and distant metastases. MTC is an uncommon thyroid tumor, accounting from 3-5% of all thyroid malignancies, and arises from parafollicular C cells which produce calcitonin (CT). Prognosis of MTC is related to tumor extension at disease detection, but long-term survival in patients with disseminated MTC is still unsatisfactory**. Methods**: Four female patients with metastatic MTC (63, 69 and 2 patients aged 73 years), which already underwent total thyroidectomy and selective neck dissection, received therapy with 100 mCi $^{131}$I-MIBG in our Institute. Patients had widespread disease with neck recurrences (all 4 cases), liver and bone metastases (2 cases) and lung metastases (1 case). All those patients received the therapy twice, second one 3 months up to 1 year after the first cycle. After therapy, whole body scintigraphy was performed; tumor marker levels (CT, carcinoembryonic antigen - CEA, neuron specific enolase - NSE, chromogranin A - CgA and pro-gastrin releasing peptide - pro-GRP) were measured before and after therapy. **Results**: In one patient we observed a slight decrease in CT level after first MIBG therapy, in another one a slight decrease in CEA serum level, and no lung metastases were visible on whole body scan after second $^{131}$I-MIBG therapy. In one of the two remaining cases there was a significant decrease in CT serum level only after neck dissection. In all cases the patients reported an improvement in subjective symptom reduction. **Conclusion:** $^{131}$I-MIBG therapy could provide additional benefit to patients with MTC and could improve overall survival, but more patient should be treated in order to define the true potential of the therapy. The aim of this paper is to present our experience of $^{131}$I-MIBG therapy in the cases of aggressive form of medullary thyroid carcinoma (MTC) with local and distant metastases. MTC is an uncommon thyroid tumor, accounting from 3-5% of all thyroid malignancies, and arises from parafollicular C cells which produce calcitonin (CT). Prognosis of MTC is related to tumor extension at disease detection, but long-term survival in patients with disseminated MTC is still unsatisfactory.

P70-1 - Sunday, Oct. 20, 16:00 - 16:30, Poster Exhibition Area

## Radionuclide Therapy & Dosimetry: Thyroid

### P409

### Adjuvant radioactive iodine (I131) therapy in patients with papillary thyroid cancer: comparison of ablation outcome post low and high doses of I131

**S. W. Yassin**[1], K. Salman[1], T. Al-Munshy[1], M. Al-Ezzi[1], S. Salem[2], Y. Mohammad[2]; [1]King Abdulla Medical City, Jeddah, SAUDI ARABIA, [2]Cairo University Hospitals, Cairo, EGYPT.

**Introduction:** I131 ablation post total thyroidectomy is a well established adjuvant therapy in patients with papillary thyroid cancer. Many factors can affect ablation outcome including size of remnant thyroid tissue , stage of the disease and given dose of I131. Some authors stated that small doses of I131 can achieve successful complete ablation outcome comparable to high ablative dose **Aim:** The aim of the current study is to compare successful complete ablation rate using low I131 ablation dose (30 mCi) versus high dose (100 mCi) post total thyroidectomy in patients with papillary thyroid cancer confined to the thyroid gland. **Patients and Methods:** 129 patients with papillary thyroid cancer confined to the thyroid gland, with no regional lymph nodal or systemic metastases, candidates for I131 ablation therapy post total thyroidectomy, were included in the current study .61 patients received 30 mCi ablative dose on out patient basis. The remaining 68 patients received high ablation dose (100 mCi) .All patients performed follow up I131 whole body scan, neck ultrasound and unsuppressed serum thyroglobulin level (Tg) 6-9 months post I131 therapy. Successful complete ablation was considered in absence of any I131 avid thyroid tissue in the neck, free neck ultrasound and Tg level < 2 ng/ml. **Results**: Successful complete ablation post 30 mCi of I131 was noted in 36 out of 61 patients (59%).On the other hand, this was observed post 100 mCi in 56 out of 68 patients (82.3%), with a statistically significant difference between both groups ($p<0.05$). **Conclusion**: In patients with papillary thyroid cancer confined to the thyroid gland , candidates for I131 ablation therapy post total thyroidectomy, high ablation dose of I131 (100 mCi) has significantly higher successful complete ablation rate compared to small I131 dose (30 mCi).

## P410

### Comparison of reablation success post low and high radioactive iodine (I131)second ablative dose in patients with papillary thyroid cancer

S. El-Refaei[1], **S. W. Yassin**[2], K. Salman[2], T. Al-Munshy[2], M. abd-El Kareem[1], Y. Mohammad[1], M. Al-Ezzi[2]; [1]Cairo University Hospital, Cairo, EGYPT, [2]King Abdulla Medical City, Jeddah, SAUDI ARABIA.

**Introduction**: I131 ablation is a well established adjuvant therapy post total thyroidectomy in patients with papillary thyroid cancer (PTC) . No single group achieved 100% complete ablation rate post first ablation dose. A second (reablation) dose of I131 is recommended in patients who fail to achieve complete ablation. **Aim**: The aim of the current study is to compare successful complete ablation rate post low reablation dose of I131 (30 mCi) versus high reablation dose (80 or100 mCi) in patients with PTC who fail to achieve complete ablation post first I131 ablative dose of 100 mCi. **Patients and Methods**: The current study includes 81 patients with PTC candidates for post total thyroidectomy ablation. All patients failed to achieve complete ablation post first ablation dose of 100 mCi. Their first follow-up I131 whole body scan (WBS) done 6-8 months post first ablation dose showed partial ablation with remaining small residual functioning thyroid tissue in the thyroid bed and no functioning metastases, this is associated with unsuppressed serum thyroglobulin level (Tg) more than 2 ng/ml. All patients received a second ablation dose. The reablation dose was small (30 mCi) in 37 patients, given on out patient basis. The remaining 44 patients received high reablation dose (80 or 100 mCi). WBS,neck ultrasound and Tg were done 6-9 months post reablation dose. The criteria for successful complete ablation include WBS showing no residual functioning thyroid tissue in the neck ,free neck ultrasound and Tg level less than 2ng/ml. **Results** : Successful complete ablation was achieved post reablation dose in the whole group in 61 out of 81 patients (75.3%). This was achieved in 27 out of 37 patients (72.9%) and in 34 out of 44 patients (77.2%) in patients who received low and high reablation dose respectively, with no statistically significant difference between both groups ($p>0.05$). **Conclusion**: In patients with PTC who failed to achieve complete ablation post 100 mCi first ablation dose of I131, no statistically significant difference between low (30 mCi) and high (80 or 100 mCi) reablation dose in achieving successful complete ablation.

## P411

### Initial radioiodine remnant ablation success rates compared by diagnostic scan Methods: I-123 versus I-131

**W. Choi**[1], E. Choi[2], E. Han[3], I. Yoo[2], S. Lee[4], S. Kim[2], W. Lee[5]; [1]St. Vincent's Hospital, The Cathoic University Of Korea, Suwon, KOREA, REPUBLIC OF, [2]Seoul St. Mary's Hospital, The Cathoic University Of Korea, Seoul, KOREA, REPUBLIC OF, [3]Daejeon St. Mary's Hospital, The Cathoic University Of Korea, Deajeon, KOREA, REPUBLIC OF, [4]Uijeongbu St. Mary's Hospital, The Cathoic University Of Korea, Uijeongbu, KOREA, REPUBLIC OF, [5]Soonchunhyang University Hospital, Bucheon, KOREA, REPUBLIC OF.

**Objective:** To see if diagnostic whole body scan (DxWBS) performed with I-131 prior diminishes the success rate of initial radioiodine remnant ablation (RRA) compared to I-123 DxWBS in differentiated thyroid cancer patients. **Material and Methods:** Consecutive thyroid cancer patients who received total thyroidectomy for differentiated thyroid cancer and then high dose RRA (either 100 mCi or 150 mCi) within 6 months were included. DxWBSs were performed with I-123 or with I-131. Prior to the DxWBSs, all patients followed strict low iodine diet for 2 weeks and withdrew hormone to stimulate TSH above 30 mIU/L. Patients with extra-thyroidal extension of tumor, lymph node metastasis, or distant metastasis were excluded. The initial RRA was defined as successful if the next DxWBS done 6 months to 1 year later was negative and stimulated thyroglobulin level was below 2 ng/ml. **Results**: Of 71 patients who had I-123 DxWBSs, 31 patients went on to receive RRA with 100 mCi and 40 patients received 150 mCi. Of 73 patients who had I-131 DxWBSs, 66 received 100 mCi and 7 patients received 150 mCi. The overall success rate was 79% for patients who had I-123 DxWBS prior to RRA (68% for 100 mCi and 86% for 150 mCi), and 68% for patient who had I-131 DxWBSs (68% for 100 mCi and 71% for 150 mCi). **Conclusion**: For patients who received 100 mCi, the RRA success rate was same for I-123 DxWBS and I-131 DxWBS. For patients treated with 150 mCi, the success rate may be lower in patients who receive RRA following DxWBS with I-131 compared to DxWBS with I-123.

## P412

### Required therapeutic dose of $^{131}$I for thyroid ablation after surgery for differentiated thyroid carcinoma

**M. Yaneva**, A. Botushanova; UMBAL St.George Plovdiv, PLOVDIV, BULGARIA.

After operation for carcinoma of the thyroid gland a lot of patients are treated with radioactive iodine for ablation of the residual thyroid parenchyma. **Aim**: To determine the appropriate dose of radioactive iodine for ablation of the residual thyroid parenchyma in patients operated for differentiated thyroid carcinoma. **Materials and Methods**: The study includes 316 patients who underwent a whole-body scan (WBS) scintigraphy with $^{131}$I,. From 2009 to 2012 year 632 images were taken. Patients range from 21 to 78 years old. The scan was performed on a dual-headed gamma camera SIEMENS after an oral reception of a diagnostic dose $^{131}$I (2mCi). The remnants of thyroid parenchyma were registered in 67 of the patients. 39 patients with registered remnants of thyroid parenchyma and slightly elevated thyroglobulin (TG) values who took therapeutic dose $^{131}$I (80-100mCi) underwent a WBS scintigraphy with $^{131}$I and did not display remnants of thyroid parenchyma or extra thyroid accumulation of the radio nucleotide. 23 patients with several remnants of thyroid parenchyma and elevated values of TG who underwent a WBS scintigraphy with $^{131}$I eight to ten months after reception of the first dose therapeutic iodine (80-100mCi) displayed persisting remnants of thyroid parenchyma. They were treated with a second dose of $^{131}$I (50-100mCi). In 5 patients with high values of TG besides the thyroid remnants 3 of the patients displayed an extra thyroid accumulation in the lungs and 2 of them displayed an extra-thyroid fixation in the thoracic vertebras in addition to the fixation in the lungs. These 5 patients were treated twice with $^{131}$I, but still displayed the remnants of thyroid parenchyma and extra thyroid fixation. That group was treated with a third dose of $^{131}$I (30-50mCi) and no remnants of thyroid parenchyma and extra-thyroid fixation of the radio nucleotide were visualized on the control WBS scintigraphy. **Conclusion**: In the majority of the patients with thyroid remnants after surgery for differentiated thyroid carcinoma one dose of therapeutic $^{131}$I of 80-100 mCi is enough for ablation of the thyroid remnants. The requirement of a second dose of therapeutic $^{131}$I is evaluated by a thorough assessment of the thyroglobulin values.

## P413

### Anxiety and depression related to the hospitalization experience of patients receiving radioiodine ablation

**Z. Koç**, A. Karakoc, T. Balci, F. Kepenek, M. Atmaca; Firat University Hospital, Elazig, TURKEY.

**Objective:** The hospital rooms for radioiodine ablation of differentiated thyroid carcinoma are designed according to radiation safety lows where patients have to remain isolated. The aim of the present study is to investigate depression and anxiety levels of the patients associated with hospitalization experience for radioiodine ablation. **Methods:** Thirty patients (8M, 22F; mean: 45±13 years old) with differentiated thyroid carcinoma were included into study. After withdrawal of thyroid hormone replacement at least for three weeks, the patients were subject of the ablation treatment. After routine psychiatric examination Hamilton Anxiety and Depression scales were administered to the patients before and after complement of hospitalization for 1-3 days. **Results:** According to the statistical analysis there weren't any significant difference between Hamilton depression and anxiety scores and state and trait anxiety scores of the patients before and after treatment ($P>0.05$). However, of the patients 18 patients had depression, with major depression of six, and 21 had high anxiety levels, according to Hamilton Depression and Anxiety Scales. **Conclusion:** Although the patients with differentiated thyroid carcinoma do not experience anxiety or depression related to the hospitalization itself for radioiodine ablation they might frequently have depression or anxiety just before the treatment. Key Words: ablation, depression, anxiety, thyroid carcinoma.

## P414

### The prevalence of thyroid tissue along the thyroglossal tract on SPECT/CT following I-131 ablation therapy after total thyroidectomy for thyroid cancer.

**T. W. Barber**[1], M. H. Cherk[1], K. S. K. Yap[1], D. J. Topliss[2], J. W. Serpell[3], V. Kalff[1]; [1]Department of Nuclear Medicine & PET Centre, The Alfred Hospital, Melbourne, AUSTRALIA, [2]Department of Endocrinology, The Alfred Hospital, Melbourne, AUSTRALIA, [3]Department of Surgery, The Alfred Hospital, Melbourne, AUSTRALIA.

**Aim:** The aims of this study are (1) to determine the prevalence of thyroid tissue along the thyroglossal tract on SPECT/CT and (2) to assess the contribution of this tissue to total neck I-131 activity in patients treated with I-131 ablation therapy after total thyroidectomy for thyroid cancer. **Materials and Methods:** A total of 63 consecutive patients with well differentiated thyroid cancer treated with total thyroidectomy underwent whole body planar imaging and SPECT/CT of the neck 48 hours following ablative I-131 therapy. On SPECT/CT, thyroglossal tract thyroid tissue was defined as radioiodine activity in the anterior neck, superior to the thyroid bed in close proximity to the midline without evidence of localisation to lymph nodes. On planar imaging, thyroglossal tract thyroid tissue was defined as linear radioiodine activity in the midline of the neck superior to the thyroid bed. SPECT/CT and planar images were classified by two independent reviewers as positive, negative or equivocal with interobserver agreement quantified using a Kappa score. Disagreement was resolved using a third reviewer. Quantitation of thyroglossal tract thyroid tissue and total neck I-131 activity was performed using region of interest analysis on planar imaging following localisation on SPECT/CT. **Results:** Thyroglossal tract thyroid tissue was present in 31/63 (49%; 95% CI: 37-61%) patients on SPECT/CT. In these 31 patients, thyroglossal tract thyroid tissue contributed to an average of 49% of total neck activity. Interobserver agreement was substantial on SPECT/CT (Kappa = 0.76; 95% CI: 0.61-0.91) and fair on planar imaging (Kappa = 0.31; 95% CI: 0.15-0.47). **Conclusion:** Thyroid tissue along the thyroglossal tract was present in one half of patients in our study population and can contribute to a significant amount of total neck I-131 activity. Given the high prevalence of thyroglossal tract thyroid tissue, our results suggest that total neck radioiodine activity on planar imaging may not be a suitable parameter to assess the completeness of thyroid bed surgery.

## P415

### Influence of oral rinsing on the exposure of salivary glands during radioiodine therapy

U. Lützen, P. Silvia, Y. Zhao, M. Marx, C. Winkler, **M. Zuhayra**; Christian-Albrechts-Universität zu Kiel, Kiel, GERMANY.

Aim: The salivary glands (SG) constitute a risk organ during a radioiodine therapy of thyroid. A possible side effect is xerostomia. This study investigates whether repeated rinsing of the mouth with water during radioiodine therapy significantly extracts I-131 from the circuit between saliva and the gastrointestinal tract, and thus whether radiation exposure of the patient's SG is reduced. Methods: The control group consisted of 45 patients, ages 32 to 81 years, (mean 62 years, 8 male, 37 female), and received radioiodine therapy without rinsing their mouths. An intervention group of 42 patients, ages 36 to 88 years, (mean 61 years, 8 male, 34 female), with a benign or malignant thyroid disease, were asked 15-17 hours after capsule administration to rinse their mouths hourly with water for the next two days. The intervention group (n = 42) was divided into three groups. A low-risk group (n = 22) received between 0.4 and 1.0 GBq I-131 (mean 0.746), a medium risk group (n = 15) between 1.2 and 2.0 GBq (mean 1.783), and the high-risk group (n = 5) between 3.0 and 6.0 GBq (mean 3.600) respectively. To assess the function of the SG, scintigrams were performed prior to and 3 months after the radioiodine therapy. The estimation of the activity in the gastrointestinal tract was performed using whole-body scintigraphy on the day of release. Both, the SG and the WB scintigraphies were evaluated using the region-of-interest technique. Furthermore, the activity of the collected saliva was quantified using a calibrated well-type detector. Results: The mean values of the activity extracted into the water-saliva mixture were 0.72% ± 0.3% and 0.14% ± 0.05% of the applied dose on the first and second day after capsule administration respectively. The analysis of the SG scintigrams of the low and medium risk groups showed no significant decrease in salivary gland function. Only in the high-risk group a significant loss of salivary gland function was detected ($p < 0.03$). However, in all groups there was no difference in salivary gland function between the intervention and control group. The analysis of WB scintigrams also showed no significant reduction in residual activity in the gastrointestinal tract in the intervention group compared to the control group (p-value = 0.47). Conclusion: This study showed that repeated rinsing of the mouth with water had no significant influence on the radiation exposure of patients receiving radioiodine therapy and did not significantly protect their SG´s.

## P416

### Late follow up results after J - 131 therapy of toxic multinodular goiter

**Z. Petrovski**; Clinical Hospital Bitola Macedonia, Bitola, MACEDONIA, THE FORMER YUGOSLAV REPUBLIC OF.

**Objective**: The aim of this study was to analyze success of radioiodine therapy in patients with toxic multinodular goiter (TMG). **Methods**: The group of 43 patients (36 females / 7 males, aged 47 -+ 11 yrs, range 27 - 75 yrs) with TMG were treated with radioiodine. 28 pts were treated with one dose, 12 pts with two doses and 7 pts with three and more doses according to Marinelli's formula.The administered activity of J -131 was established basing on radioiodine uptake and goiter size ( median 555 MBq, range: 370 - 1100 MBq).Patients were evaluated by clinical and thyroid examination of TSH, FT4, FT3 after 1 - 3 months.Thyroid scintigraphy was performed three months after radioiodine therapy.Prior to treatment with J -131 all patients were treated with antithyroid medications, who were suspended 4 - 7 days and restarted one week after J - 131 therapy. **Results**: In 76,8%(33/43) pts there was control of disease after the first J -131 dose and in 95,2% (40/43) pts after the second and more doses.At 20 years of follow up, there were 84,4% (36/43) pts euthyroid, 13,9% (6/43) pts hypothyroid and 4,6% (2/43) pts hyperthyroid.Reduction of gland weight were in 74,4% (32/43) pts.During 20 yrs of follow up no adverse side effects were observed after J - 131 therapy.**Conclusion**:Radioiodine therapy is the choise of treatment for toxic multinodular goiter and single dose of J -131 is successful in most of the cases. A single higher radioiodine dose diminishes the need for additional J -131 therapy,without increasing of developing hypothyroidism.

## P417

### Predictive factors of failure in radioiodine therapy of Graves' disease

**I. Iakovou**[1], A. Doumas[1], K. Badiavas[1], E. Giannoula[2], E. Kamperidis[1], V. Nikos[1], D. Katsaboukas[1], V. Mpalaris[1], S. Georga[1], D. Lo.Presti[1], G. Arsos[1], N. Karatzas[1]; [1]3rd Nuclear Medicine Dpt Aristotle Univ. Papageorgiou Hsp, THESSALONIKI, GREECE, [2]Theageneio Anticancer Hsp, THESSALONIKI, GREECE.

**Aim**: To retrospectively evaluate any factors that may limit the success rate of radioiodine therapy (RIT) in Graves' disease patients. **Methods**: Eighty Graves' disease patients submitted for RIT in our department in a two years' period (2010-2011) enrolled in the study. A fixed dose of 12mCi (444MBq) of 131I was administered to all patients after antithyroid drug administration, in order to achieve normal FT3 serum values. Thyroid function outcome were assessed 10-12 months after RIT. Patient's sex, age, evidence of ophthalmopathy, ultrasound measurement of the thyroid volume and 99mTc thyroid uptake % prior to RIT were considered as potential interference factors for success. Multiple logistic regression analysis was performed. **Results**: After RIT, 9 patients (11%) became euthyroid, 48 patients (61%) became hypothyroid and 23 (28%) remained hyperthyroid. No statistically significant association between treatment outcome and sex ($p = 0.56$), age ($p=0.61$) and ophthalmopathy ($p = 0.72$) was found. On the contrary, 99mTc thyroid uptake % and thyroid volume were associated with success rate (thyroid uptake<14%, $p< 0.001$, odds ratio 3.9 and thyroid volume <58 ml, $p < 0.001$, odds ratio 7.9). **Conclusions**: A radioiodine fixed dose of 12 mCi (444MBq) for treatment of Graves' disease seems to be a practical and effective approach. However, this administration is not recommended for patients with large goiters and a high pre-RIT thyroid uptake, due to high failure rates observed in patients with thyroid volume more than 58ml and thyroid uptake higher than 14%.

## P418

### Importance of Post-operative Diagnostic 131I SPECT/CT Imaging for Treatment Optimization of Thyroid Carcinoma Patients

**B. Gunalp**, E. Alagoz, S. Ince, A. Ayan, O. Emer, O. Karacakioglu; Gulhane Military Medical Academy and Medical Faculty, Ankara, TURKEY.

Objective: The purpose of this study was to evaluate clinical impact of diagnostic 131I SPECT/CT imaging on staging and determining 131I ablation/treatment dose or need for alternative treatment options such as surgical re-interventions and external beam radiation therapy. Materials and Methods: Twenty seven patients (9 men and 18 women; age range, 14-65 years) with differentiated thyroid carcinoma (DTC) 3-4 weeks after surgery underwent diagnostic 131I planar imaging and SPECT/CT, 24 hours after oral administration of 37MBq (1mCi) 131I . Neck ultrasonography (US) was performed, thyroglobulin (Tg) and TSH levels was measured in all patients just before 131I imaging. Ablation dose adjusted for each patient according to remnant thyroid volume calculated from SPECT/CT images and 24 hours thyroid uptake values. FDG-PET/CT was also performed in four patients due to unfavourable histopathology or non-iodine avid metastases which were detected in 131I-SPECT/CT. Results: SPECT/CT detected unsuspected nodal metastases in two patients and distant metastases in one patient. SPECT/CT was not detected any remnant thyroid tissue in one patient and no ablation dose was given for this patient. SPECT/CT changed prescribed activity in 10 (37%) patients

and post-surgical staging for 3 (11%) patients. Conclusion: Postoperative diagnostic imaging was found very useful for accurate staging and determining 131I ablation/treatment dose or need for radioiodine therapy. Non-iodine-avid metastases can also be detected by CT part of SPECT/CT and alternative treatment options can be considered for these patients. Our preliminary data shows that pre-ablative 131I-SPECT/CT is a very useful tool for optimization of radioiodine treatment of thyroid carcinoma patients.

## P419

### Influence of smoking associated with stress on the outcome of radioiodine therapy in patients with Graves' disease

**V. Sekulic**, M. Rajic, M. Vlajkovic, S. Ilic, M. Stevic; Department of Nuclear Medicine, the University of Nis Medical School and Clinical Centre, Nis, SERBIA.

**Introduction:** Graves' disease (GD) is characterized by activation of the immune system as a result of interactions between genetic predisposition and environmental factors such as iodine intake, stressful events or smoking. Currently, there are no sufficient data on influence of nicotine and other components of tobacco smoking on outcome of radioiodine therapy in GD. **The aim** of this study was to analyze a possible influence of cigarette smoking associated with stress on the outcome of radioiodine therapy (RIT) in the patients with Graves' disease. **Patients and Methods:** The study included 29 patients (23 female) aged from 22 to 73 years, who were subjects of a follow-up within 12 months after RIT. The stressful events were presented in all patients prior to diagnosing the GD. Patients were divided into two groups: 1. smokers - 15 patients who smoked cigarettes before, at the moment and after RIT, and 2. non-smokers - 14 patients who were always non-smokers. Patients were treated using a sliding scale of fixed activity of radioiodine according to the goiter size. Antithyroid drugs were discontinued 7 days before radioiodine therapy. Therapy outcome was assessed by serum TSH and thyroid hormones levels, and clinical evaluation. A successful response (SR) to RIT was defined as euthyroidism and subclinical or clinical hypothyroidism, and unsuccessful response (UR) as persistent hyperthyroidism. **Results:** Comparison of age (48.0±9.39 vs. 49.6±14.3 years, P=0.715), values of TRAb (2.25±0.91 vs. 2.75±1.32 U/l, P=0.560), administered activity of $^{131}$I-NaI (365±75.8 vs. 360±44.4 MBq, P=0.832), and duration of ATDs therapy before RIT (3.34±3.41 vs. 5.06±5.81 years, P=0.397) between smokers and non-smokers showed no significant difference. There was no significant influence of smoking on UR at 3$^{rd}$, 6$^{th}$, 9$^{th}$ and 12$^{th}$ month compared with UR in patients who did not smoke (P=0.597, P=0.837, P=0.876, P=0.812, $\chi^2$ test). The cumulative incidence of SR in smokers and non-smokers was 33.3 vs. 42.9%, 53.3 vs. 57.1%, 60.0 vs. 57.1%, and 60.0 vs. 64.3% after 3, 6, 9 and 12 months, respectively. **Conclusion:** Our results showed that smoking associated with stress before the beginning of Graves' disease was not influential on the outcome of radioiodine therapy within twelve months of follow-up.

## P420

### Does multifocal papillary microcarcinoma require radioiodine ablation?

A. Punda, V. Markovic, **D. Eterovic**; University Hospital Split, Split, CROATIA.

Background: The thyroid carcinomas smaller than 1 cm (microcarcinomas) comprise a significant fraction of papillary carcinomas. Excluding clinical microcarcinomas, which present as metastatic disease, the microcarcinomas diagnosed by ultrasound/FNAC or incidentally have very good prognosis. However, whether or not these papillary microcarcinomas require post-surgical radioiodine ablation remains a matter of debate. Hypothesis: Multifocality is present in majority of clinical papillary microcarcinomas and this characteristic can be used to identify the subset of non-clinical microcarcinomas with greater malignant potential. Methods: The data on types of differentiated thyroid carcinomas diagnosed in the period 2008-2011 in the University Hospital Split were collected. Results: There were 359 patients with thyroid carcinoma, 329 (92%) of which had papillary carcinoma. About 61% (202/329) of papillary carcinomas were microcarcinomas; most of them were diagnosed by ultrasound/FNAC (134/202= 66%), the rest were incidentalomas (48/202=24%) and clinical microcarcinomas (20/202=10%). Sixty percent (12/20) of patients with clinical microcarcinoma and 23 patients with non-clinical microcarcinoma (23/182=13%) had multifocal disease. Conclusion: Multifocal disease is a frequent characteristic of clinical papillary thyroid microcarcinomas, suggesting that multifocality presents an early stage of non-clinical microcarcinomas with more aggressive behaviour. Thus multifocal, but not unifocal papillary microcarcinomas may require radioiodine ablation.

P71-1 - Sunday, Oct. 20, 16:00 - 16:30, Poster Exhibition Area

## Radionuclide Therapy & Dosimetry: Bone Pain Palliation

## P421

### Efficacy of Sm-153 Radionuclide Therapy for Bone Pain Palliation in Metastatic Prostate Cancer

**N. Incili**, B. Gumus, Y. Parlak, G. Gumuser, M. Bigehan Yuksel, E. Sayit; Celal Bayar University, Manisa, TURKEY.

**Aim**: The aim of this study is to evaluate the usefulness and efficacy of radionuclide therapy with Sm-153 in patients with prostate cancer presenting painful osteoblastic osseous metastases. **Materials-Methods**: In our study, 10 patients aged between 59-80 years (mean age=69±6.26 years) with osteoblastic osseous metastases of prostate cancer, treated in our unit between November 2011 and December 2012, were included. All patients had undergone Tc-99m hydroxymethylenediphosphonate (HDP) bone scintigraphy documenting increased multiple osteoblastic activity in the painful sites. Images were obtained from anterior-posterior projection with double headed gamma camera (Infinia, GE, Tirat Hacermel, Israel) equipped with LEHR collimators. Patients were excluded from the study, when their hemoglobin<10g/dl, WBC<4.5x10$^9$/L, platelet count <100x10$^9$/L, treated with systemic chemotherapy or RT in six weeks, spinal cord compression, pathologic fractures, life expectancy less than 3 months. All patients were treated with Sm-153-EDTMP at a standard intravenous dose of 37 MBq/kg and were observed for toxicity and decrease in pain score using visual analog scale (VAS) once in a week up to 6 weeks.A bone scan with Sm-153-EDTMP was performed 4 hours post treatment. **Results**: There was a significant decrease in VAS score from the time of administration up to 6 weeks. Mean pain score was decreased from %79 to %15. Median duration of response to therapy was found to be 8-12 weeks. No serious acute adverse events were observed post-treatment period. When we evaluated hematotoxicity of Sm-153-EDTMP; 2 patients showed a reduced toxicity (grade 1 anemia and grade 0-1 WBC) and other 8 patients did not show hematological toxicity. There was no relationship between the number and/or severity of bone lesions at the beginning of therapy and at the six week. Finally, six of ten patients died from terminal cancer within the mean 31 weeks (8-56 weeks) observation period. **Conclusion**:In our study we conclude that, Sm-153 was found feasible, effective and safe radionuclide therapy for bone pain palliation and reduced the overall-long term cost of pain palliation while improving the quality of life in patients with metastatic prostate cancer. Key Words: Sm-153, prostate cancer, bone pain palliation

## P422

### Myelotoxicity of samarium Sm 153 lexidronam in patients with painful bony metastases

**T. Ben Ghachem**, A. Mhiri; I. Slim; A. Bahloul; I. Yeddes; I. Elbez; I. Meddeb; MF. Ben Slimène.; DEPARTMENT OF NUCLEAR MEDICINE, SALAH AZAIEZ INSTITUT, EL MANAR II UNIVERSITY, TUNIS, TUNISIA., Tunis, TUNISIA.

**Introduction:** The management of bone pain includes analgesia, radiation, hormones, radiofrequency (RF) ablation, chemotherapy, and surgery. Bone pain palliation therapy with radiopharmaceuticals is a cost-effective systemic therapy to relieve pain from skeletal metastases with a consequent decrease in morbidity and an improvement in quality of life. The aim of our study is to evaluate the effect of myelotoxicity of samarium lexidronam (Sm 153) in patients with painful bony metastasis. **Methods:** we reviewed 116 patients aged from 14 to 87 years old, 91 males (78%) and 25 females (22%), having received 1 to 4 treatments of Sm 153 (37 MBq/kg) for painful bony metastases from different primitive tumors: 67 cases of prostate cancer (57.7%), 22 cases of breast cancer (18.9%), 10 cases of pulmonary cancer (8.6%) and others in 14.6% of cases. Clinical follow-up was available for 159 treatments, consisting on blood count each week over at least two months, in order to evaluate myelotoxicity according to WHO classification. **Results:** No patients had grade 4 toxicity after its cures. A grade 2-3 myelotoxicity was observed after 52 treatments (34%) during the second week and after 50 treatments (32.6%) during the fourth week with a satisfactory reversibility. At 10 weeks of treatment, myelotoxicity was reclassified from 0 to 2 for 139 cures (90,8%). Moreover, we found that prior treatment with radiotherapy or chemotherapy did not affect the rates of myelotoxicity. **Conclusion**: Multiple treatments with samarium Sm 153 lexidronam had no significant effect on myelotoxicity. Patients with bone predominant metastatic disease may survive for extended periods of time and may safely be treated with multiple modalities of therapy.

## P423

### Incremental value of metabolic radiotherapy of bone metastases with 153Sm-EDTMP in prostate cancer. About 67 cases

**A. Mhiri**[1], T. Ben Ghachem[1], I. Slim[1], A. Sellem[2], H. Hammami[2], F. Ben Slimène[1]; [1]DEPARTMENT OF NUCLEAR MEDICINE, SALAH AZAIEZ INSTITUT, EL MANAR II UNIVERSITY, TUNIS, TUNISIA., tunis, TUNISIA, [2]DEPARTMENT OF NUCLEAR MEDICINE, MILITARY HOSPITAL, EL MANAR II UNIVERSITY, TUNIS, TUNISIA., Tunis, TUNISIA.

INTRODUCTION: Painful bone metastases are common in advanced prostate cancer. Samarium 153-ethylenediaminetetramethylenephosphonic acid (153Sm-EDTMP; Quadramet) is a beta-particles emitter that concentrates in the areas of enhanced osteoblastic activity and used for palliate pain from bone metastases. Our purpose is to evaluate the incremental value of the 153Sm-EDTMP, in patients affected of cancer of the prostate with painful bony metastasis. METHODS: sixty-seven patients with metastatic prostate cancer received a single bolus infusion of 153Sm (37 MBq/kg). All patients had painful bone metastases to more than one anatomical region. Bone specific pain, analgesic score, and blood count were evaluated before and after treatment with a receding of 38 months. RESULTS: We observed a positive answer in 85% of the cases; this answer was complete in 35% of the cases. The results gotten after multiple administrations show that the cures could be repeated with results comparable to those of the first cure. The therapeutic efficiency is at least equivalent to those of the other therapeutic means, with nearly non-existent secondary effects. The only toxicity is of hematological order; it is the most often moderate and reversible with a complete recuperation at the end of 8 weeks. Besides, the effect on the pain came with an improvement of the quality of life of the patients treaties. CONCLUSION: Due to its half-life of 46 hours and its beta emissions, a high dose rate of 153Sm can be delivered to regions adjacent to enhanced osteoblastic activity over a short period of time with little residual long term activity being left in the bone marrow. Its administration to patients with prostate cancer suffering from painful bone metastases that enhance on bone scans, offered clinical relevant pain relief with tolerable hematological toxicity and then enjoy a better quality of life.

## P424

### The Usefulness of Samarium-135 in Advanced Breast Cancer

**A. Mhiri**, T. Ben Ghachem; A. Bahloul; H. Charfi; I. Yeddes;I. Elbez, I. Meddeb; I. Slim; MF. Ben Slimène; DEPARTMENT OF NUCLEAR MEDICINE, SALAH AZAIEZ INSTITUT, EL MANAR II UNIVERSITY, TUNIS, TUNISIA., Tunis, TUNISIA.

**Introduction**: Breast cancer is a solid cancer which can often be complicated by metastatic bone pain, reducing performance status and decreasing the quality of life. Quadramet® is a radiopharmaceutical consisting of stable complexes of radioactive Samarium (Sm-153) and tetraphosphonate chelators (EDTMP), having a high affinity to the skeleton more intense in osteoblastic lesions. It is indicated as a palliative measure for the relief of pain from metastatic lesions that enhance on bone scans. Our aim was to assess the effect of Sm-153 in breast cancer. **Methods:** The study included 10 patients with breast cancer (mean age 43, 5 years) with multiple bone painful metastases detected by scintigraphy. Each patient received 37 MBq/kg of Sm-153. For assessment of therapy effectiveness; pain relief, a reduction in analgesic requirements and motor activity (Karnofsky scale) were evaluated with a receding of 36 months. **Results**: Palliative therapy using Sm-153 is effective (in 2/3 of cases "good" and "moderate" response rate) and we have observed that the analgesic requirements decreased to 40% of dose on average. The motor activity of the points evaluated according to Karnofsky scale increased from 50 to 70. **Conclusion**: In breast cancer, bone metastasis is a major complication which is most often associated with pain. Bone pain palliation therapy with Sm-153 is a cost-effective systemic therapy to relieve pain from skeletal metastases with a consequent decrease in morbidity and an improvement in quality of life.

P72-1 - Sunday, Oct. 20, 16:00 - 16:30, Poster Exhibition Area

## Radionuclide Therapy & Dosimetry: Dosimetry Models & Treatment Planning

## P425

### The effect of omitting measurement points in the estimation of renal doses from planar and SPECT scans after peptide radionuclide receptor therapy using Lu-177-DOTATATE.

**A. Delker**, C. Zach, H. Ilhan, P. Bartenstein, M. Hacker, A. Haug, G. Böning; Department of Nuclear Medicine, University of Munich, Munich, GERMANY.

**Aim**: Peptide radionuclide receptor therapy is a promising treatment option in metastasized, somatostatine receptor expressing neuroendocrine tumors. A severe side effect of this therapy is radiation induced nephropathy due to renal excretion and reabsorption of the radioactive compound. In this study we investigated the influence of the dynamic scan during the injection and the importance of the following measurement time points to achieve the accumulated activity. **Methods**: SPECT image data and anterior and posterior planar images were acquired in 7 patients (57±14 years) at 1h, 24h, 48h and 72h after administration of Lutetium-177-DOTATATE. Furthermore a dynamic planar scan was acquired with 12 frames during the injection. Scatter correction was performed with the triple-energy window method. A co-registered CT was used for attenuation correction in SPECT OSEM reconstruction and in planar images by estimating the patient size. Total activity in kidneys were fitted to a bi-exponential function in dynamic planar images and to a mono-exponential function in SPECT and whole body planar images with the Levenberg-Marquardt-Algorithm. These functions were integrated over time to estimate the organ dose, by applying the kidney specific S value according the MIRD concept. To investigate the effect of the dynamic measurement (dyn-P) the resulting dose was compared to the same measurement without dynamics (stat-P). Furthermore we studied the influence of reducing the number of time points to the dose estimated from planar and SPECT images by omitting one of the time points 1h, 24h, 48h or 72h after injection. **Results**: A relative mean deviation of 3.0% was discovered by comparing dyn-P and stat-P. The Spearman Rank Correlation Coefficient (SRCC=0.87) indicated strong correlation between SPECT and planar images when all 4 time points were used. With reduced number of time points a deviation of 7.3% (1h, 24h, 48h), 1.8% (1h, 24h, 72h) and 3.3% (1h, 48h, 72h) in SPECT and 12.9%, 12.1% and 16.2% in stat-P were observed. **Conclusions**: We found that dispensing with the initial dynamic measurement resulted in a relatively small error in dose calculation from planar images. The small deviation of estimated dose especially when the 72h measurement was omitted in SPECT processing suggests a further investigation of this approach. This optimization might increase the availability of individualized peptide radionuclide therapy.

P73-1 - Sunday, Oct. 20, 16:00 - 16:30, Poster Exhibition Area

## Radionuclide Therapy & Dosimetry: Clinical Dosimetry

## P426

### Assessment of organ absorbed dose in patients following bone scan with technetium-99m-labeled methylene diphosphonate (MDP) using of MIRD method

**D. Shahbazi-Gahrouei**[1], M. Cheki[2], M. Moslehi[1]; [1]Dept. of Medical Physics, School of Medicine, Isfahan Uni. of Medical Sciences, Isfahan, IRAN, ISLAMIC REPUBLIC OF, [2]Dept. of Medical Physics, School of Medicine, Tehran Uni. of Medical Sciences, Tehran, IRAN, ISLAMIC REPUBLIC OF.

**Objectives:** The aim of study was to describe and compare a method to obtain absorbed dose of organs in patients following bone scan with technetium-99m-labeled methylene diphosphonate (MDP) using of MIRD (Medical Internal Radiation Dosimetry) method with the data of MIRD dose software of report no.13. **Methods:** In this study**,** each patient was injected 25 mCi of $^{99m}$Tc-MDP. Patients were imaged with a gamma camera. Whole-body images from thirty patients were acquired by gamma camera at 10, 60, 90, 180 minutes after $^{99m}$Tc-MDP injection. To evaluate the activity of each organ, total body images were analyzed by the conjugate view method. Based on the MIRD schema, absorbed doses were calculated for the organs of patients. At the end, absorbed dose values obtained in this study was compared with the values of MIRD dose software report no.13. **Results:** The mean uptake activity was measured in different time periods after injection of $^{99m}$Tc-MDP for each organ. The absorbed doses per unit injected activity (mrad/mCi) for liver, bladder, spleen, right kidney and left kidney were 7.78 ± 1.6, 8.17 ± 2.1, 7.96 ± 1.9, 30.0 ± 4.8 and 30.9 ± 5.1 mrad/mCi, respectively. The percentage difference between absorbed dose values obtained in study with the values of MIRD dose software report no.13 for liver, bladder, spleen, right kidney and left kidney were 3 to 56.33%, -10.73 to 51.02%, -9.55 to 47.16%, -21.25 to 8.75% and -19.37 to 12.5%, respectively **Conclusions:** The results of this study were close to with the values of MIRD dose report no.13. The results of this study may be useful to estimate the amount of activity that can be administered to the patient and also showed that Methods used in the study for absorbed dose calculation is in good agreement with the data of MIRDose software and it is possible to use by a clinician. Key Words**:** Absorbed dose, Bone scan, $^{99m}$Tc-MDP, MIRD dose software.

## P427

### Radioactive iodine treatment of a struma ovarii with extensive peritoneal involvement: a dosimetric study.

**D. Métivier**, M. Ricard, L. Lamartina, D. Hartl, C. Lhommé, P. Morice, C. Lepoutre, D. Déandréis, J. Lumbroso, M. Schlumberger, S. Leboulleux; Institut Gustave Roussy, Villejuif, FRANCE.

**Objective:** We report a patient with a very large and unresectable peritoneal involvement from a struma ovarii who was treated with radioactive iodine (3.7 GBq). **Methods:** Whole body retention was measured during hospital stay (10 days), three times a day, using a calibrated automatic gamma counter attached to the ceiling of the room. Radiation protection for the husband was monitored with a radiation dosimeter, during one month after hospital discharge. OLINDA software was used to evaluate the absorbed dose delivered to the red marrow, assuming that radioactive iodine was concentrated mainly in the abdomen. **Results:** A 53-year-old woman, treated 22 years before for bilateral ovarian cysts with thyroid elements (struma ovarii) but no sign of malignancy, was explored for hyperthyroid symptoms with undetectable TSH level (0.07 mUI/ml) and elevated FT3 level (11,6 pmol/l). Thyroglobulin (Tg) level was elevated (15,200 ng/ml). Thyroid uptake was

low. Abdominal ultrasonography revealed liver nodules and multiple intra-abdominal masses, the largest measuring 140, 57 and 53 mm. Coelioscopic exploration and histologic analysis found peritoneal metastasis of a follicular carcinoma. The masses did not disclose any FDG uptake. Lesions were considered non resectable and the patient was referred for total thyroidectomy and radioactive iodine treatment. The post-therapy whole-body scan revealed an intense $^{131}$I uptake in all abdominal masses. Dosimetric study $^{131}$I showed a very long whole body effective half-life (7 days compared to 0.3 days in non-metastatic patients). The mean red marrow dose ranged between 100 and 200 mGy. Effective dose delivered to her husband was 225 µSv. A transient and moderate decrease in lymphocyte (1.15 G/l) and platelet (178 G/l) counts was observed 3 weeks after the $^{131}$I administration. FT3 decreased slowly after treatment. Tumour response according to RECIST will be shown during the congress presentation. **Conclusion:** Malignant struma ovarii with metastases are uncommon. Surgical management is recommended before radioiodine therapy, but in our case the masses were unresectable. The high $^{131}$I uptake observed during radioiodine therapy justifies the need for dosimetry and radiation protection.

P74-1 - Sunday, Oct. 20, 16:00 - 16:30, Poster Exhibition Area

## Radionuclide Therapy & Dosimetry: Miscellaneous

### P428

### Unbounded $^{131}$I Elimination by Means of Hemodialysis After Papillary Thyroid Cancer Radioiodine Therapy in Patients with Terminal Renal Failure: Three Case Reports

**M. Matović**[1], T. Lazarević[1], M. Jeremić[1], S. Janković[1], M. Vlajković[2]; [1]Clinical Center Kragujevac, Kragujevac, SERBIA, [2]Clinical Center Niš, Niš, SERBIA.

**Background and objectives** After its administration for therapeutic purposes, unbounded and circulating $^{131}$I should be eliminated from the body, as it can cause adverse effects to non-thyroid/tumor tissue. If a patient is anuric or severely oliguric, the only way for unbound radioiodine to get eliminated is via hemodialysis. However, the effectiveness of this process is questionable, and furthermore, the patient is not allowed to leave the controlled radiation zone until the radioactivity in their body drops below 400 MBq. **Methods** Three patients (two males and one female, 35, 53 and 66 years of age) with terminal renal failure accompanied by anuria/severe oliguria, who had previously undergone papillary thyroid cancer surgery (pT1NxMx/CSI), received therapeutic doses of 1915, 1880 and 1850 MBq of $^{131}$I, respectively. Prior to this, the patients had received chronic hemodialysis (4 hours every other day) over a 6-month period. Twenty-four hours after the oral administration of radioiodine, each patient was hemodialysed in the controlled zone (veno-venous hemodiafiltration for 4 hours, via MultiFILTRATE device, Fresenius Medical Care). Upon the completion of dialysis, venous blood was sampled from the patients every hour for 4 hours. Moreover, the dialysis effluent was collected hourly, its value was measured and it was sampled. The radioactivity of blood and dialysis effluent samples was measured by means of gamma-counter using peak of $^{131}$ I energy. **Results** The total radioactivity measured in the dialysis effluent after 4 hours amounted to 31.61% of the administered dose. Within the first hour following the dialysis, the radioactivity decreased by 8.31%, whereas after the 2$^{nd}$, 3$^{rd}$ and 4$^{th}$ hour it decreased by 7.23%, 7.77% and 8.30%, respectively. In other words, one hour after the dialysis the radioactivity of blood samples was 91.33% of the pre-dialysis value. After 2, 3 and 4 hours it was 83.34%, 75.23% and 69.88 % respectively. **Conclusions** The four-hour dialysis session removes just over one third of the administered radioiodine, which is insufficient when therapeutic doses are administered. We could conclude on the basis of this case that in anuric patients at least 14-28 hours of hemodialysis is necessary to remove 1850-7400MBq of radioiodine.

### P429

### Adjuvant post-operative radiosynovectomy in patients with knee pigmented villonodular synovitis

**I. Iakovou**[1], A. Doumas[1], K. Badiavas[1], M. Potoupnis[2], E. Giannoula[3], E. Kamperidis[1], V. Nikos[1], V. Mpalaris[1], N. Karatzas[1]; [1]3rd Nuclear Medicine Dpt Aristotle Univ. Papageorgiou Hsp, THESSALONIKI, GREECE, [2]3rd Orhtopedics Dpt Aristotle Univ. Papageorgiou Hsp, THESSALONIKI, GREECE, [3]Theageneio Anticancer Hsp, THESSALONIKI, GREECE.

**Background:** Treatment of extensive diffuse pigmented villonodular synovitis (PVNS) of knee joint by isolated surgical resection is usually suboptimal, with high rates of local recurrence. Adjuvant treatment with intra-articular injection of yttrium-90 is supposed to provide better results. Aim: The aim of this study was to evaluate the efficacy of a combined treatment with radiosynovectomy (RS) and surgical synovectomy (SS). **Methods**: The final effect of 21 RS performed in all 16 patients with PVNS presented in 2 years in our department was assessed. Adjuvant post-operative therapy using intra-articular injection of 5 mCi 90Y was performed within 2-3 months after SS. Five out of 16 patients had to be treated twice, due to a relapse of symptoms 4-6 months after the first treatment. Treatment efficacy was evaluated 8-12 months after the initial RS by a questionnaire reporting the relief of limiting the daily activities knee pain as a percentage of the pretherapeutic joint discomfort using a visual analog scale (VAS). Relative uptake of Tc-99m-diphosphonate in the knee joint involved on the blood pool was also taken into consideration. **Results:** The overall response rate for all knee treatments was 81%. Results in double treated joints were significantly worse than in single treated ones. A significant improvement in blood pool bone scintigraphic signs of inflammation was noticed. On the other hand, there was no influence on late diphosphonate uptake. **Conclusion**: A combination of surgical synovectomy with adjuvant post-operative radiosynovectomy is highly efficacious in treating clinical symptoms of pigmented villonodular synovitis, with excellent results regarding the incidence of local recurrence and functional outcome.

### P430

### Efficacy of radiosynovectomy in the treatment of chronic knee synovitis: systematic review and meta-analysis.

**S. Zakavi**[1], N. Norouzbeigi[1], N. Ayati[1], J. Farahati[2], R. Sadeghi[1], Z. Mirfeizi[3]; [1]Nuclear Medicine Research Center, Mashhad University of Medical Sciences, MASHHAD, IRAN, ISLAMIC REPUBLIC OF, [2]Thyroid Center, Institute of Radiology, Nuclear Medicine and Radiotherapy,, Bottrop, GERMANY, [3]Rheumatic Diseases Research Center, Mashhad University of Medical Sciences,, MASHHAD, IRAN, ISLAMIC REPUBLIC OF.

**Objective***:* Knee joints are commonly involved with various inflammatory and non-inflammatory rheumatoid diseases. Radiosynovectomy is being used as a local therapeutic option to alleviate pain and swelling in involved joints. The present study evaluated the effectiveness of radiosynovectomy for treatment of chronic knee synovitis. **Methods***:* Through a search of Medline and SCOPUS with (Radiosynovectomy OR radio-synovectomy OR "radio synovectomy" OR "radiation synovectomy" OR radiosynoviorthesis OR radio-synoviorthesis OR synoviorthesis OR "radiochemical synovectomy" OR "radioisotope synovectomy") AND (Re-188 OR Y-90 OR SM-153 OR P-32) as key words, 9 RCTs were enrolled in the analysis. The outcomes of interest were odds ratio and risk difference of improvement in the radiosynovectomy group compared to the control group. **Results***:* odds ratio and risk difference for SM-153 plus corticosteroid subgroup was 1.959[0.571-6.725, P=0.285] and 14.9% [-17.1%-47%, P=0.362] respectively. The subgroup of Y-90 plus corticosteroids showed pooled odds ratio and risk difference of 2.366[0.779-7.188, P=0.129] and 23.9% [-1.7%-49.4%, P=0.67] and in the subgroup Y-90 alone were 0.851[0.356-2.036, P=0.717] and -2.3% [-23.3%-18.7%, P=0.829] respectively. **Conclusion:** Combination of Y-90 colloid or Sm-153 with corticosteroids in radiosynovectomy have higher response rate compared to each of radioisotope or corticosteroid therapy alone.

# POSTER SESSIONS – GROUP 2

P01-2 - Tuesday, Oct. 22, 16:00 - 16:30, Poster Exhibition Area

## Physics & Instrumentation & Data Analysis: Instrumentation

### P431

### Effect of time-of-flight (TOF) and point-spread-function (PSF) reconstruction on lesion contrast and detectability in large body-size: a phantom study.

**H. NISHIDA**, A. Ohnishi, T. Nishio, Y. Ikari, M. Senda; Institute of Biomedical Research and Innovation, Kobe, JAPAN.

**Aim**: PET image reconstruction using TOF and/or PSF is known to increase spatial resolution and reduce noise, which is considered effective for large body size. The present study examined the impact of TOF and PSF on lesion contrast and detectability using a large size phantom.**Methods**: A body phantom of 36cm width was created in a design similar to the standard 30cm wide NEMA IEC body phantom. Both 36cm and 30cm phantoms containing a 10mm sphere with F-18 activity concentration being 4:1 to background (5.3kBq/ml) were scanned with Discovery PET/CT 690 (GE, LYSO detector) for 10min to generate images of variable scanning time (1-10min). The images were created using 3D-OSEM, TOF, PSF and TOF+PSF reconstruction, using iterations and subsets optimized for the 30cm phantom, to compute lesion contrast (Q10) and background noise (N10). Detectability of the 10mm sphere was visually evaluated. Apart from it, both phantoms containing six spheres of 10-37mm diameters were scanned for 30min to measure recovery coefficient (RC).**Results:** In the 30cm phantom, all four reconstruction Methods visualized the 10mm sphere in as short as 1-2min scan. In the 36cm phantom, however, TOF and TOF+PSF enabled detection of the 10mm sphere with the 2min scan, while PSF and 3D-OSEM required 4min for visualization. TOF and TOF+PSF provided the highest Q10, while TOF provided the lowest N10. Although RC for the 10mm sphere was highest by TOF+PSF (0.52), followed by TOF (0.48), PSF (0.41) and 3D-OSEM (0.40), TOF+PSF presented Gibbs artifact for the 17mm (RC=1.08) and 22mm spheres. **Conclusion**: TOF with or without PSF is effective in increasing contrast and reducing noise, which allows shorter (or avoids longer) scanning time to visualize lesions in large body size. Although TOF+PSF is qualitatively effective in lesion detection, further optimization of the PSF parameters is necessary for quantitative SUV measurement.

### P432

### Optimal projections subset determination for the reconstruction of 99mTc-DMSA SPECT studies after motion correction

**M. Hesse**[1], G. Demonceau[2], S. Walrand[1], F. Jamar[1]; [1]Cliniques Universitaires Saint-Luc, Brussels, BELGIUM, [2]Sint-Elizabeth Ziekenhuis, Zottegem, BELGIUM.

**Aim**: Most 99mTc-DMSA studies are done on children, and are so often prone to patient motion. Motion correction in pinhole SPECT is quite challenging due to the pinhole magnification that is strongly spatially dependent. Using a previously validated motion correction technique, we investigated whether the reconstruction of a projection subset could be better than using all the projections. **Method**: Six hours after a weight-dependent injection of 99mTc-DMSA, a 25min-pinhole SPECT was performed in 110 patients from 1 month old to 47 years old. First, a motion-free orbit subset was determined, reconstructed and re-projected at all acquisition angles. Then the acquired projections were shifted to match as well as possible those re-projections. This process was repeated on the corrected projections until the orbit subset free of residual motions increased no longer. To define the projection subsets to reconstruct, we used various criteria based on the kidney's position on the motion corrected acquisition, and we selected projections for which these positions were closer to a fitted sinogram or to the re-projected kidney's position. The final reconstruction quality was visually assessed, based on the presence of high background and double contours. **Results**: The selected set of projections differed from the full orbit in more than half the patients. However, no significant improvement with respect to the full orbit reconstruction was observed. This was probably due to the fact that the subsets differed in general only in a few isolated angles, whose effect was reduced by the averaging in the reconstructed image. **Conclusion**: contrary to what could be expected, using some criteria to limit the set of incidences to be reconstructed after our motion correction in PHS did not provide any visual improvement of the final image.

### P433

### Effect of scatter correction on myocardial perfusion imaging: qualitative and quantitative comparison

**P. Bhusari**, M. Parmar, S. Santhosh, B. R. Mittal; Postgraduate Institute of Medical Education & Research, PGIMER, CHANDIGARH, INDIA.

**Introduction**: Soft tissue attenuation on SPECT imaging may cause artifacts resulting in reduced diagnostic accuracy of myocardial perfusion imaging (MPI). This study aimed at comparing scatter corrected to uncorrected gated MPI, qualitatively as well as quantitatively for diagnosis of coronary artery disease (CAD) using Tc99m-Tetrofosmin. **Methods**: One day stress/rest protocol MPI using Tc-99m-Tetrofosmin was performed in 25 patients. Scatter correction was done using Dual-Energy Window Method. Images were reconstructed by filtered back-projection applying Butterworth filter (cutoff 0.66 Nyquist, order 5). Quantification parameters like EF, EDV, ESV and SV were recorded for both stress and rest studies with attenuation correction and with & without scatter correction. Data was analyzed by Nuclear Medicine Physician for perfusion defects. The perfusion images were scored semi-quantitatively (0 to 4 scale). Summed stress score and summed rest scores were determined using 17 segment model. Summed stress, Summed rest and Summed Difference Score were computed for both scatter corrected and scatter uncorrected data. Paired T-test was applied to compare these values. **Results:** Mean Summed Stress Score in uncorrected data significantly differed from that in corrected data (p=0.001). Mean Summed rest Score in uncorrected data varied significantly from that in corrected data (p=0.010). However Mean SDS varied insignificantly (p=0.53). Among Stress parameters, EF significantly increased (p=0.003), EDV significantly decreased (p=0.012), ESV decreased (p=0.0074), SV showed insignificant increase (p=0.618). Among Rest parameters, EF increased significantly (p=0.0014), EDV and ESV decreased significantly with p=0.017 and p=0.0010 respectively. SV showed insignificant increase (p=0.526). Of the 25 studies, 13 were concordant and 12 were discordant. In the discordant cases, a total of 30 perfusion defects were present in various segments of myocardium (20 in Scatter corrected, 10 in non-scatter corrected data), indicating improvement in sensitivity after scatter correction. Among the various segments, septal wall was most affected with increase in defects from 4 in Non-scatter data to 9 in corrected data. Inferior wall had 7 defects in scatter-corrected data and 4 defects in Non-Scatter corrected data. **Conclusion**: This study suggests that scatter corrected images increase sensitivity of detection of mild perfusion defects which aren't resolved on Non-Scatter images. Scatter correction also introduces significant changes in functional quantification parameters. Hence its use must be emphasized both in quantification and visual interpretation.

### P434

### Impact of acquisition time on semi-quantitative index values in whole body FDG PET/CT for evaluating cancer response.

**P. Lovinfosse**, A. Chauvin, T. Ganem, I. Mahdjoub, P. Ménager, L. Vervueren, F. Bouchet, F. Lacœuille, O. Couturier; Nuclear Medicine Department, and Inserm UMR_S 1066 MINT, University of Angers, 49933 Angers, France, Angers, FRANCE.

**Objectives :** Our objective was to evaluate the impact of acquisition time on semi-quantitative uptake values, and lesion volume for FDG-PET/CT. **Methods :** 52 patients among them 40 with at least one tumor lesion underwent a whole body FDG-PET/CT (3D TOF GE 640) in list-mode (2.5min scan per bed position). PET images were reconstructed using different time per bed position, i.e. 1.5min, 2min and 2.5 min. Maximum standardized uptake values (SUVmax) were collected on tumoral lesion (20 lymph node, 5 liver, 5 lung, 4 breast, 4 bone, 2 pancreas), normal brain, normal liver, descending thoracic aorta and muscle (deltoid). Furthermore, a 41% SUVmax thresholding volume was measured on each studied tumor. Repeated measures Anova test were used for statistical analyses. **Results :** For each site, a significant difference of SUVmax was always seen between 1.5min data sets and the two other data sets. Moreover, large maximal individual fluctuations (%max) were observed in different patients. For tumors, SUVmax were 11.3±8.1; 11.1±7.9; 11.1±7.9 ((m±SD for 1.5min, 2min and 2.5min respectively; p<0.01) and %max=13%; for brain: 12.7±4.3; 12.5±4.2; 12.5±4.2; (p<0.0005) and 11%; for liver: 4.1±1.2; 3.8±1.0; 3.8±0.9 (p<0.001) and 23%; for aorta: 2.7±0.7; 2.7±0.7; 2.6±0.6 (p<0.0001) and 20%; and for muscle: 0.7±0.2; 0.6±0.2; 0.6±0.2 (p<0.0009) and 33%. There was no significant difference for tumor volume (mL) (12.2±16; 12.4±16; 12.4±16; p=0.31). **Conclusions :** FDG SUVmax of tumor and normal tissues may vary significantly depending on the time of acquisition with sometimes large maximal individual variations. These results underline the need to perform acquisitions of sufficient duration in the context of clinical research and / or evaluation of response to therapy, especially when a cut-off value is used to define tumor response.

### P435

### The standard uptake value of different image reconstruction Methods for positron emission tomography

**A. Wyszomirska**[1,2,3], A. Gramek[4], S. Cichocka[3], A. Dobek[5], R. Czepczynski[1,2,3], J. Sowinski[1,3], M. Ruchala[1,3]; [1]University of Medical Science, Poznan, POLAND, [2]Department of PET-CT, Euromedic Greaterpoland Medical Center, Poznan, POLAND, [3]H. Swiecicki Clinical Hospital University of Medical Science, Poznan, POLAND, [4]Adam

Mickiewicz University, Poznan, POLAND, [5]Department of Molecular Biophysics, Adam Mickiewicz University, Poznan, POLAND.

The positron emission tomography (PET) is the basic method of imaging the metabolic function of tumors. The standard uptake value (SUV), is the most commonly used by doctors, and is a parameter for evaluating the degree of concentration of fluorodeoxyglucose 18F (18F-FDG) in the tumour. The aim of this study was to investigate the influence of image reconstruction Methods for value SUVmax. In the experiment, PET imaging of the water phantom simulating the patient's body had been performed on 10 patients with bone metastases and one patient without metastases. Images of the phantom for all patients were obtained using the four reconstruction Methods: (OSEM, FBP, FORE OSEM, FORE FBP). For each of the Methods of reconstruction the value of SUVmax was easured in several regions of interest (ROI). Eight of these were selected for the phantom study: the four regions filled with FDG (hot area), two spheres filled with water (cold area), lungs, and background of the phantom. In clinical studies the regions of interest (ROI) were placed in the brain, heart, metastases to the bone and soft tissue of the patients. For each area of the ROI average SUVmax values obtained in different Methods of image reconstruction had been compared. As a result of these comparisons, it was found that significant differences exist between the SUVmax values of the iterative method OSEM and the analytical method FORE FBP in areas characterized by the phantom increased FDG uptake (hot areas). In the other regions of interest, in the phantom, no difference was found. In clinical studies it was found that differences in mean SUVmax was most common in areas of increased uptake of FDG (the biggest variable was for metastases, then for the heart and brain). These differences were mainly observed between the iterative method (OSEM or FORE OSEM), and the analytical method (FBP or FORE FBP). In this work it was found that the value of SUVmax in PET studies is affected by the applied Methods of image reconstruction, and the probability of occurrence of differences in the values of this parameter increases with FDG uptake.

## P436

### Evaluation of Flash3D iterative algorithm for myocardial perfusion SPECT imaging

**F. Palleri**[1], C. Cidda[2], A. Belletti[2], G. Baldari[2], M. Scarlattei[2], F. Zavoli[2], G. Serreli[1], C. Ghetti[1], L. Ruffini[2]; [1]Department of Medical Physics, University Hospital Parma, Parma, ITALY, [2]Nuclear Medicine Department, University Hospital Parma, Parma, ITALY.

**Aim** To evaluate the clinical impact of Flash3D algorithm on myocardial perfusion SPECT imaging. Comparison between Iterative Reconstructions (IR) and standard Filtered Back-Projection (FBP) in terms of image quality and interpretation. Effect of an increasing iteration number has been also evaluated. **Matherials-Methods** 30 myocardial SPECT studies of consecutive patients have been analyzed. They had 2day stress-rest protocol(99mTc-MIBI, 740 MBq each scan). Cardiac SPECT was performed using an integrated system SPECT/CT(SymbiaT6, Siemens). Images were processed with FBP and with an innovative 3D-OSEM (ordered-subsets expectation-maximization) algorithm, Flash3D(Siemens). This software incorporates a 3D parallel hole collimation model. Three IR have been performed using different combinations of iterations and subsets: 8i/4s(default settings), 16i/8s and 24i/16s for a total of 120 reconstructions(4 each patient), each containing stress and rest datasets. Three Nuclear Medicine Physicians, blinded to clinical data, evaluated all the reconstructed images using a subjective-score-system for image quality from 1(acceptable) to 3(excellent). They also evaluated myocardial perfusion abnormalities for ischemia diagnosis, assessing presence of a reversible (positive) or irreversible (negative) perfusion defects. **Results** All physicians gave the highest scores to FBP images. IR performed with 8i/4s demonstrated similar results while increasing the number of iterations images scores decreased; the reason is probably that physicians are used to read FBP cardiac images rather than IR. The diagnosis performed on images processed with FBP were the same for 28/30 patients. In many cases the reading of IR changed diagnosis performed on FBP; in these cases clinical follow-up of patients has been considered to evaluate the correct diagnosis. Physicians gave different images interpretations on IR8i/4s, IR16i/8s, IR24i/16s in comparison with FBP in the following percentage of cases: 10%, 7%, 10% (physician1), 7%, 10%, 20% (physician2), 10, 27%, and 43 % (physician3). The percentage of false positive interpretation was 80%, 72% and 83% for physician 1, 2 and 3, respectively. **Conclusions:** FBP reconstructions demonstrated superior images quality at the subjective evaluation; 3D-OSEM IR with default settings showed performances similar to FBP; IR with an increased number of iterations worsened results, probably because they appear less familiar. The number of IR readings different from FBP grows with the increasing of iterations set and it is correlated with the worst scores given to images reconstructed with IR16i/8s and IR24i/16s. In about 80% of discrepancies the diagnosis made on IR lead to false positive interpretation. Using 3D-OSEM algorithm for myocardial perfusion imaging results misleading and it does not improve clinical diagnosis.

## P437

### The Effects of Time of Flight, Point Spread Function Modelling and Reconstruction Iterations on PET Image Quality

**C. McKeown**, G. Gillen, M. Dempsey, J. Prosser; NHS GG&C, Glasgow, UNITED KINGDOM.

**Aim** This study assesses quantitatively the effects Time of Flight (TOF) and Point Spread Function (PSF) modelling have on PET image quality as a function of the number of iterations used in the reconstruction process. **Materials and Methods** A GE Discovery 690 PET-CT system, which can incorporate TOF and PSF modelling into the standard ordered subset expectation maximization (OSEM) reconstruction algorithm, was used in this study. A NEMA body phantom was filled with F18 resulting in six hot spheres (diameters ranging from 10mm to 37mm) in a background activity (sphere to background activity ratio 4:1; background activity concentration 5kBq/ml). Four reconstruction Methods were used: (1) standard OSEM, (2) OSEM+TOF, (3) OSEM+PSF, and (4) OSEM+TOF+PSF. 18 subsets were used for all reconstructions, with iterations varying from 1 to 30. All other reconstruction parameters were held constant. Images were assessed using Coefficient of Variation (COV) in background regions, and Contrast Recovery Coefficients (CRC) and Signal to Noise Ratios (SNR) for the hot spheres. **Results** COV increased with the number of iterations for all four reconstruction Methods (lowest COV = 0.06 for OSEM+PSF with 1 iteration, highest COV= 0.35 for OSEM+TOF+PSF with 30 iterations). When 10 or less iterations were used, PSF reconstructions achieved lower COV values than non-PSF reconstructions. OSEM+TOF achieved the lowest COV of all reconstructions Methods when >10 iterations were used. Maximum CRC convergence was achieved by OSEM+TOF+PSF for the 5 largest spheres. Smaller spheres required more iterations to reach convergence, and converged to lower values ($CRC_{37mm}$ = 98% after 4 iterations; $CRC_{13mm}$ = 90% after 8 iterations). $CRC_{10mm}$ did not converge for either PSF reconstruction, and exceeded 100% after 10 iterations. Maximum SNR for each sphere was also achieved using OSEM+TOF+PSF. The three largest spheres peaked after one iteration, and then decreased. The 4th and 5th spheres peaked at 2 iterations, and the smallest sphere peaked at 3 iterations. The maximum SNR achieved decreased as sphere size decreased ($SNR_{10mm}$ = 20, $SNR_{37mm}$ = 50). **Conclusions** Results demonstrated a trade-off between SNR and CRC, for all four reconstruction types, as the number of iterations varied. COV increased with the number iterations for all four reconstruction types. The best combination of CRC and SNR for the smallest sphere was achieved by using OSEM+PSF with 10 iterations. However, image noise increased with the number of iterations. Further work is required to identify the optimal reconstruction parameters for different clinical situations.

P02-2 - Tuesday, Oct. 22, 16:00 - 16:30, Poster Exhibition Area

# Physics & Instrumentation & Data Analysis: Data Analysis & Management

## P438

### Analysis of the Scaled Subprole Model on PET-data of schizophrenic patients

J. van Zandwijk[1], J. Doorduin[2], M. Koole[2], A. T. M. Willemsen[2], R. A. J. O. Dierckx[2], R. Renken[3], **J. R. de Jong**[2]; [1]University of Twente, Twente, NETHERLANDS, [2]University Medical Center Groningen, Groningen, NETHERLANDS, [3]University of Groningen, Groningen, NETHERLANDS.

**Aim**: The Scaled Subprofile Model (SSM) has been deployed in neurodegenerative disorders, yielding information about characteristic abnormalities of functional brain organization. This principal components analysis (PCA)-based spatial covariance method focuses on identifying deviating regions between groups. Patients with schizophrenia may display localized regions of neuroinflammation as studied with [11 C]-(R)-PK11195 positron emission tomography (PET). This work investigates the suitability of the SSM approach for analyzing [11 C]-(R) -PK11195 PET data in schizophrenia and whether it can be used to discriminate schizophrenia patients from healthy subjects based on localized regions. **Methods:** An [11 C]-(R)-PK11195 dynamic PET-study of 7 schizophrenic patients and 8 healthy controls was preprocessed to calculate binding potential images. The binding potential data was normalized to a common space using SPM software. The SSM method, consisting of an essential log transformation, double centering with respect to subjects and voxels, and the PCA- based singular value decomposition (SVD), was applied to identify a possible characteristic spatial covariance pattern. An important deviation with the `standard' SSM approach involving this data-set was the use of an external brainmask, on top of an initial threshold. Subject scores of each principal component (PC) were statistically analyzed with a logistic regression model to find the best discriminating component or combination of components. The influence of several parameters in applying SSM was studied, based on their discriminating power of the two groups. **Results**: The variance accounted for in the different principal components was rather more spread out than strongly decreasing from the first component, possibly the result of noise. The Akaike information criterion (AIC) revealed PC11 as the most discriminative component for controls and patients by logistic regression. Linear combinations of multiple components

(PC7,11) yielded more significant discrimination between the two groups with p-value 0.03. No voxels in the resulting pattern were detected in the hippocampus or gray matter. **Conclusion**: The SSM method showed no significant discrimination between healthy subjects and schizophrenic patients. The lowest p-value found was p=0.03 but the resulting patterns were too spread out to substantiate the hypothesis of discriminating regions of tracer uptake in schizophrenic patients. However, the potential of SSM should be researched further, since only a small dataset was used. Finally, pre-processing and processing operations can be optimized further.

## P439

### Prognostic value of standard metabolic indexes and heterogeneity indexes from pre-treatment PET: application to esophageal cancer

P. Gouel[1], P. Michel[2], F. Di Fiore[2], P. Vera[1], **R. Modzelewski**[1]; [1]Department of Nuclear Medicine, Henri Becquerel Cancer Center and Rouen University Hospital, & QuantIF – LITIS [EA 4108], Faculty of Medicine, University of Rouen, Rouen, FRANCE, [2]Digestive Oncology Unit, Hepatogastroenterology Department, Rouen University Hospital and University of Rouen, Rouen, FRANCE.

**Aim.** To investigate the prognostic value of 34 3D PET image based indexes calculated on pre-treatment PET in oesophageal cancer patients undergoing radio/chemotherapy. **Materials and Methods**. We retrospectively selected 12 patients with esophageal cancer with identical TNM stage (T = 3, N = 1, M = 0). Assessment of the 34 indexes to predict response to chemoradiation therapy was performed. The response was evaluated according to RECIST criteria on CT performed 6-8 weeks after the beginning of the treatment.Tumors were delineated using 5 semi-automated Methods (40% of SUVmax, 50% of SUVmax, Black (Black et al., Int J Radiation Oncol Biol Phys, 2004) , Nestle (Nestle et al., EJNMMI, 2008), and Vauclin (Vauclin et al. Phys Med Biol, 2009) on pre-treatment PET examinations .The 34 indexes computed on the segmented tumors were as follows: • 5 standard metabolic indexes (SUV max, SUV peak, Avg SUV, volume (cm3), TLG) • 4 indexes of the first order (entropy, kurtosis, energy, CV) • 12 indexes calculated from cooccurences matrices (CM) (energy, entropy, correlation, contrast, variance, sum average, inertia, cluster shade, cluster tendency, homogeneity, probability max, inverse variance) • 11 indexes calculated from the matrices of uniform length (MLH) (SRE, LRE, GLN, RLN, RP, lightweight, HGRE, SGLGE, SRHGE, LRLGE, LRHGE) • 2 indexes of fractal dimension (box counting differential recovery of white) After 8 weeks of treatment, 7 patients were considered as responders and 5 as non-responders according to RECIST criteria. ROC curves of the 34 indexes were constructed. AUC (± SD) associated were calculated. **Results**. The indexes (coming from tumors delineated with Vauclin semi-automated method) with the best AUC were: TLG (0.94 ± 0.01), volume (0.94 ± 0.06), CV (0.91 ± 0.02) and variance (CM) (0.88 ± 0.03), RLN (0.97 ± 0.008), HGRE (0.97 ± 0.008), SRHGE (0.97 ± 0.008). **Conclusions**. Standard metabolic index like TLG and some indexes to characterize the heterogeneity or texture of intratumoral metabolism (CV, variance, RLN, HGRE, SRHGE) could predict the response to radio/chemotherapy in (T = 3, N = 1, M = 0) esophageal cancer. A larger cohort is under investigation in order to improve the statistical power of this study.

## P440

### Method for SPECT visualisation and characterisation of tumour foci in the liver

**T. Magnander**[1,2], E. Wikberg[2], J. Nilsson[2], J. Svensson[3], P. Gjertsson[4], P. Bernhardt[1,2]; [1]Department of Radiation Physics at Sahlgrenska Academy, Gothenburg University, Gothenburg, SWEDEN, [2]Medical Physics & Medical Bioengineering at Sahlgrenska University Hospital, Gothenburg, SWEDEN, [3]Oncology at Sahlgrenska Academy, Gothenburg University, Gothenburg, SWEDEN, [4]Nuclear Medicine at Sahlgrenska Academy, Gothenburg University, Gothenburg, SWEDEN.

Early and precise detection of tumours in the liver for patients suffering from cancer is critical in determining the mode of treatment. This work aims to in nuclear medicine applications with SPECT accomplish a quantitative method for determination of tumour foci in the liver. The method was developed for SPECT/CT data of In-111-pentetreotide (Octreoscan®). Raw image material (128x128, 120 projections) was reconstructed using OSEM (2 iterations, 10 subsets) and the resulting volume was completely unfiltered. The method analyses a segmented volume of interest by finding the highest voxel value within and localise all disjointed regions (y-axis) for a number of threshold values between zero and the maximum value. On the x-axis is the threshold index, ThI= $(C_{max}-C)/C_{max}$ where C is the voxel value threshold and $C_{max}$ the maximum voxel value. The number of separate uptake foci is calculated at each step and a distribution of the number of uptake foci vs. the threshold index is generated. The method was constructed to be a real time visualisation tool for physicians; the ThI can be adjusted by moving a slider and the corresponding uptake foci will instantly be displayed in a 3D volume of the patient. A large number of simulated tumours were implanted in a healthy liver, this to obtain a robust quality assurance method and to find the diagnostic limitations of the method. They were implanted into image data as randomly shaped spheroids with determined volume and activity. This work explored three parameters for discrimination of liver with and without tumours. When implanting the simulated tumours the most sensitive parameter was the one that used the ThI at the intercept of 0.75 of the maximum number of uptake foci. It was shown that this novel technique can detect a simulated tumour with size less than 1 g if the tumour/background ratio is higher than 6. For higher tumour/background ratios extremely small tumours can be detected. In a patient material the mean ThI for healthy patients (n=48) and patients with malignancy (n=11) was 0.49 and 0.72 respectively. The program was repeatedly tested and found to perform in a robust manner. While the present work focused on SPECT data of $^{111}$In labelled somatostatin analogues in the liver, the method can plausibly be applied to any organ, for other radionuclides and for PET-imaging as well.

## P441

### Optimisation of I-123 Thyroid Cancer SPECT Imaging

**S. J. McQuaid**, S. A. Kilfeather, P. J. Hinton; Royal Surrey County Hospital, Guildford, UNITED KINGDOM.

**Aim.** I-123 NaI SPECT acquisitions for thyroid cancer patients are performed after I-131 therapy to assess metastatic disease. The primary photopeak of I-123 is at 159 keV, but there are also higher-energy gamma emissions, most prominently at 529 keV, which can lead to image degradation due to downscatter and septal penetration. The aim of this study was to assess scatter-correction and collimator choice as strategies for reducing the impact of these high-energy emissions. **Methods.** The NEMA-IEC body phantom (Data Spectrum) was filled with I-123, with a sphere-to-background activity concentration ratio of 4.5:1. Four repeated SPECT-CT acquisitions were obtained for low-energy-general-purpose (LEGP), low-energy-high-resolution (LEHR) and medium-energy-general-purpose (MEGP) collimators, using a GE Infinia Hawkeye system (120 projection views, photopeak energy window: 159±15.9 keV, scatter windows: 195±19.5 keV and 130±13 keV). Projection data were scaled to match typical patient counts, using a random number generator to maintain Poisson statistics, and subsequently corrected for scatter and downscatter. OSEM was used to reconstruct scatter-corrected and non-scatter-corrected data, with the reconstruction parameters optimised separately for each collimator. CT attenuation-correction was applied but resolution-recovery was not employed, as per the current clinical protocol. Reconstructed images were assessed in terms of the root-mean-squared-error (rMSE) of the sphere-to-background ratio of the 17-mm-diameter sphere (to represent a challenging imaging case), calculated over the 4 repeated acquisitions for each scenario. A visual assessment of the appearance of this sphere was also performed by 5 observers, with a score assigned according to how well the sphere was visualised, and t-tests performed to evaluate the statistical significance of results obtained. **Results.** Scatter-correction was found to improve the rMSE of activity ratio estimates of all collimators by up to 20%. The overall best rMSE was achieved with the LEHR collimator with scatter-correction. For visual assessments, LEHR (scatter-corrected and non-scatter-corrected) and LEGP (non-scatter-corrected) images gave the clearest visualisation of the 17-mm sphere and were not statistically significantly different from each other. Inferior results ($P<0.05$) were observed with scatter-corrected LEGP and both MEGP results. **Conclusions.** Despite the higher septal penetration of the low-energy collimators, the LEHR collimator was found to produce the overall best result, both for visualisation and quantification assessments. Although scatter-correction did not improve the appearance of the sphere, quantification results were improved, so should be incorporated if uptake-measurement is performed. Introducing resolution-recovery may improve the relative performance of poorer resolution collimators, and this will be investigated in future studies.

## P442

### PET Uptake Heterogeneity Quantification for Therapy Response in Oncology: Dependency on Image Pre-processing and Tumor Delineation

**M. Hatt**[1], F. Tixier[1], C. Valla[2], C. Cheze Le Rest[2], D. Visvikis[1]; [1]INSERM LaTIM UMR 1101, Brest, FRANCE, [2]CHU Milétrie, Poitiers, FRANCE.

**Aim**: several recent studies have investigated the characterization of tracer uptake heterogeneity within tumors in PET images and its potential clinical value regarding oncology applications of therapy response assessment. Textural features analysis has been proposed in order to quantify this heterogeneity and has shown promising clinical value regarding prediction of response to therapy. However, no study has assessed the potential dependency of this quantification method on pre-processing steps yet. The objective of this study was therefore to determine the variability of heterogeneity quantitative parameters obtained through textural features analysis with respect to partial volume effects (PVE) correction (PVC) as well as the tumor metabolic volume delineation step. **Methods:** pre-treatment FDG PET images of 50 patients with locally advanced esophageal cancer were retrospectively analyzed for the purpose of this work. Each image was corrected for PVE using a previously validated iterative deconvolution incorporating wavelet-

based noise filtering. The tumors metabolic volumes were delineated using three different Methods: a fixed (FT) and an adaptive threshold (AT), and the fuzzy locally adaptive Bayesian (FLAB) method. Uptake heterogeneity was then quantified within the resulting delineations through the following features selected for their reproducibility and robustness, previously established in another study: entropy, homogeneity, dissimilarity, intensity variability (IV), size-zone variability (SZV) and high intensity emphasis (HIE). For the purpose of this comparative study, the heterogeneity parameters values derived from tumor volumes delineated with FLAB (the most accurate method) on the non-corrected image were chosen as reference. Variability of these parameters according to delineation or PVC pre-processing steps, with respect to this reference, was established through Bland-Altman analysis. The impact on the predictive value regarding the identification on non-responders using each parameter was assessed by comparing areas under the receiver operating characteristic curves. **Results**: the delineation method had a higher impact on the parameters' values than the pre-processing PVC. IV and SZV exhibited the highest variability (90-100%). On the contrary, some parameters, such as entropy, homogeneity and HIE (10-50%) were relatively robust and exhibited low variability with respect to the delineation method or PVC. The impact on the associated predictive value was not significant except for HIE and SZV after PVC ($p<0.04$). **Conclusion:** several heterogeneity parameters were shown to be quite sensitive to the PVC pre-processing or metabolic volume delineation steps, whereas others (entropy and homogeneity for instance) could be extracted from PET images with high reliability independently on delineation or PVC.

## P443

### Impact of automated processing technique on I-131 activity quantitation for planar imaging studies.

**M. Kotzassarlidou**, A. Giannopoulou, E. Giannoula, A. Pipintakou, A. Makridou, A. Raptou; "THEAGENIO" Cancer Hospital, Thessaloniki, GREECE.

**Aim:** Activity quantitation of I-131 is the first step towards measurement of thyroid absorbed dose, during treatment of hyperthyroidism. Although conjugate- view method of imaging is a clinically reliable technique to start with, automated processing should be applied for edge definition, in order to achieve reproducible and comparable measurements. We tested three automated processing techniques on conjugate- view images of a thyroid phantom, acquired at 256x256 and 512x512 matrix sizes. Accuracy of I-131 activity quantitation has been assessed and compared to the process including manually drawn region of interest. Materials and **Methods**: A thyroid phantom and a reference source were filled with known activities of I-131. Voxel size for 256x256 and 512x512 matrix during planar acquisition were defined. Serial planar acquisitions of phantom and reference source were performed (256x256 matrix size, 900sec time of projection, zoom 2,66 and 512x512 matrix size, 900sec time of projection, zoom 2,66) on a SOPHA DST-Xli , dual head γ-camera. Processing was performed on Vision software. Dual energy window scatter correction and background subtraction were applied to all planar images before the derivation of geometric mean (GM) images. Contour of thyroid phantom and reference source was performed automatically applying a threshold set at 30%, 50% , 80% and 90% of the maximum value in each ROI respectively. I-131 activity estimation of the thyroid phantom was obtained by the use of a calibration factor derived from the reference source. Measurements were compared with nominal values. **Results**: best correlation between nominal and measured activities by I-131 conjugate view images was obtained at threshold percentage of 30 % and 50% for both 256x256 and 512x512 matrix sizes. Error increased as the threshold value increases ($p<0.001$) and the activity present increases. There was no statistically important difference of I-131 activity quantitation between processes involving manual and automated mode of ROI segmentation. **Conclusions**: Auto threshold technique is effective for in vivo I-131 activity quantitation offering the opportunity to perform comparable, reproducible and acceptable results.

## P444

### Atherosclerosis Imaging in FDG-PET: quantitative accuracy as a function of the lesion features

**P. Huet**[1], S. Burg[1,2], F. Hyafil[2], D. Le Guludec[2], I. Buvat[1]; [1]IMNC-UMR 8165 CNRS, Orsay, FRANCE, [2]Service de Médecine Nucléaire, Bichat Hospital, AP-HP, Paris, FRANCE.

**Aim:** FDG-PET can detect atherosclerotic lesions as demonstrated by several clinical studies, hence may play a role in diagnosing plaque vulnerability, planning treatment or guiding drug development. For these applications, quantification of the pathological metabolic activity is crucial but very challenging given the very small lesion size. We developed a numerical model of atherosclerotic arteries to simulate highly realistic data and assessed Partial Volume Effect (PVE) on plaque relative uptake estimates. **Materials and Methods**: The digital patient was defined based on the XCAT phantom, in which we introduced arterial walls by adaptive dilations. Atherosclerotic lesions were modeled as extruded cylinders further shaped using morphological operations. Activities in the various organs were measured from PET/CT images of 6 subjects who underwent head and neck scans. Simulated plaques differed in length (L=10 to 30mm), angular coverage (A=60 to 300 degrees) and adventitial activity concentration given as Wall to Blood Ratio (WBRtrue=2 to 8). Acquisitions involving the Gemini GXL scanner were simulated with the GATE-6.1 Monte Carlo simulation tool following the clinical protocol: 8min per bed position, 120min after injection of 4MBq/kg FDG. Images were reconstructed using an OP-OSEM algorithm. For each configuration, PVE was calculated by the mean Wall to Blood Ratio (WBRmean) from exact region relative to the blood mean uptake measured in the contra-lateral vein. Max Target to Background Ratio (TBRmax) was computed to mimic expert measurements and was compared to the Total Activity (TA) in the lesion, assumed to describe the lesion severity. **Results**: Measurements in simulated images were consistent with clinical images: for a WBRtrue=4, a 10-30mm long 300 degrees wide lesion, TBRmax varies from 1.9 to 2.3 when clinical images of a 16mm long 300 degrees wide lesion showed a TBRmax at 2.1. WBRmean recovering was 15% to 52%. TBRmax recovery was 20% to 80%. A given TBRmax could often correspond to several (WBRtrue, A, L) combinations, demonstrating the need for improved index to better characterize atherosclerotic lesions. **Conclusions**: Highly realistic simulations of patients with atherosclerotic lesions have been produced and used to assess the quantitative accuracy with which plaque relative uptake can be measured. First results show the large bias introduced by PVE, suggesting that a measured TBRmax corresponds to a 1.2 to 5.4 times greater WBRtrue. PVE correction will be essential to assess pathological metabolic activity of atherosclerotic lesions.

## P445

### Reliability study of the calculated textural parameters for heterogenic activity distribution in PET investigation using special designed phantom

**A. Forgács**[1], Á. K Krizsán[2], I. Garai[1], L. Balkay[2]; [1]ScanoMed Ltd, University of Debrecen, Debrecen, HUNGARY, [2]University of Debrecen, Medical and Health Science Center, Department of Nuclear Medicine, Debrecen, HUNGARY.

**Aim** Positron emission tomography (PET) technique has an increasing importance at in vivo tumor staging, monitoring therapy response and predicting the outcomes. In the recent years, a high number of articles have been published which deal with tumor heterogeneity. Several textural parameters were introduced to characterize inhomogeneity of the radioactive tracer accumulation. However, it is still unclear what the reliability of these parameters is, what can they reflect and what their sensitivity is. These could be tested by using a special heterogenic phantom but such kind of phantom has not been presented in the literature yet. **Materials and Methods** It is a big challenge to construct a phantom having constant inhomogeneous radiotracer distribution; moreover the size scale of the heterogeneity should be comparable or smaller than the spatial resolution of human PET camera. We constructed a plastic phantom which consists of three small distinct but joining compartments with different volumes. We filled the phantom with the mixture of the same diluted F18 and CT contrast solutions, so the real activity concentration in any voxels can be extracted from the CT image too. Thus the high resolution CT image defines the expected PET image voxel by voxel. In the images we calculated the following textural parameters, which already exist in the literature: homogeneity, entropy, correlation, inhomogeneity-contrast, size and intensity-variance. The above mentioned heterogeneity parameters were tested at different activity contrast values in the volumes, typically in the range of 1-10. **Results** In the case of contrast 4, high activity concentration was not detectable, while contrast 10 causes 1.5 times bigger SUV mean value than the background's SUV. The contrast changing from 4 to 10 was followed by 62% increase in entropy, 45% decrease in homogeneity, 41% decrease in correlation, 40% decrease in size variance and 20% decrease in intensity variance and the inhomogeneity-contrast was 10 times bigger. The reproducibility was also tested by measuring the phantom three times with the same contrast ratios and we calculated the % variability of the parameter means as stdev/mean*100. We found that % variability were 1.89%, 1.24%, 4.97%, 6.11%, 13.48%, 16.34% for the homogeneity, entropy, correlation, contrast, size and intensity-variance. **Conclusion** The construction of a heterogenic phantom could provide a precise demonstration of the correlation between the reconstructed clinical image and the real tumor heterogeneity.

## P446

### A tool for automatic classification of heterogeneity of lung cancers based on PET/CT intensity values

**C. M. Pereira**, C. F. Gomes, F. J. Caramelo; Institute of Biomedical Research in Light and Image - Faculty of Medicine of the University of Coimbra, Coimbra, PORTUGAL.

**Aim:** The main goal of the present work was to develop a simple model for computer classification of intratumoral heterogeneity using FDG PET/CT images. This is part of a larger project where we intend to study the possible association between the heterogeneity of lung tumors and other relevant clinical parameters

such as histological grade, invasiveness and response to therapy, using that as a predictor of patient outcome. **Introduction:** Intratumoral heterogeneity, typical of solid tumors, results from the coexistence of multiple neoplasic cell subpopulations with different biological characteristics. PET images show areas with increased metabolic activity, whereas the CT scan shows detailed anatomical locations. The combination of these two images enables both the identification of high metabolic activity regions and its location. **Methods:** We develop a Matlab® routine to extract, from 12 FDG PET/CT lung scans acquired in a GEMINI TF Big Bore PET camera, the parameters for the classification statistical model. After the co-registration of the CT and PET volumes, two independent users have drawn ROI's in each slice where tumors appear. Previously the tumors had been classified by their degree of heterogeneity (4 possible levels). We used the joint histogram of the PET and CT images to calculated 8 parameters for the classification model. Since the number of subjects was small we divided the heterogeneity in only two degrees, which allowed the use of a binary logistic regression implemented in IBM SPSS v20 statistical platform. **Results:** We fitted a logistic regression model to the results obtained from one of the users. The fitting of the model was excellent (Cox Snell R = 0.740, Nagelkerke R = 1.0) in part due to the fact that the number of subjects was small. Thus, to test the model independently we used the data from the other user obtaining an accuracy of 80%. **Conclusion:** The developed model has successfully classified the new tumors according to their heterogeneity degree. However, the number of subjects was small preventing the use of other Methods capable of leading with more levels of classification. On the other hand, it was difficult to test the classifier in a robust fashion. It is very important that more subjects are added to the database to overcome these aspects. Despite the drawbacks the parameters calculated from the joint histogram are a new form for feeding classification algorithms and seem to be robust to different users.

P03-2 - Tuesday, Oct. 22, 16:00 - 16:30, Poster Exhibition Area

## Physics & Instrumentation & Data Analysis: Radiation Exposure & Protection

### P447

### Dosimetric study in a radiopharmacy unit

**F. Rinaldi**[1], D. Bruel[1], N. Machefert[1], C. Cottet[2], C. Boursot[3], C. Naveau-Ploux[4]; [1]Radiopharmacy, Le Mans Hospital, Le Mans, FRANCE, [2]Radiation Protection Unit, Le Mans Hospital, Le Mans, FRANCE, [3]Nuclear Medicine, Le Mans Hospital, Le Mans, FRANCE, [4]Pharmacy, Le Mans Hospital, Le Mans, FRANCE.

Le Mans hospital radiopharmacy unit prepares nearly 1700 radiopharmaceuticals doses and more than 4000 patient injections per year. For risks evaluation, a dosimetric study about ionizing radiations has been lead. Dosimetric measures, without distinction between manipulated radioelements, have been realised from May to June 2012 for 2 radiopharmacists and 3 pharmacist assistants. Doses received at fingers extremities and at fingers basis were measured. Six TLD chips were positioned on the thumb, the index and the major for fifteen days besides finger ring dosimeters usually used within individual monitoring. Six TLD chips were then placed on each hand, on the basis of the thumb, the index and the major for two months. Dosimetric measures of "whole body" were collected during the manipulation of generators and during the measure of iodine 131 capsules. The ratio between received doses on fingers extremities and handled doses was calculated. The 3 pharmacist assistants received 4,2 ; 11,2 and 7,1 µSv per handled GBq. The 2 radiopharmacists received 10,6 and 29,6 µSv per handled GBq. The most penalizing measure for each hand was extrapolated over one year. The dose received at the extremities of fingers differs from the dose received on the basis of fingers by a factor 1 to 5,5. For the pharmacist assistants, the annual equivalent dose in hands is 42 mSv. The annual effective dose is estimated at 0,4 mSv. For a radiopharmacist, the equivalent dose to the hands extrapolated over one year is 24 mSv. The annual effective dose is 0,5 mSv. These values are coherent with those of operational dosimetry. Results of the dosimetry of extremities by TLD chips shows that left index of pharmacist assistants is the most exposed finger (pulp of the finger for 2 people and basis of the finger for 3 people), probably because of the activimeter located on the left during syringe preparations. Difference observed between each person may result from dexterity and manner to handle. In order to integrate the maximum of received radiations, it is advised to the pharmacist assistants and radiopharmacists to carry their dosimeter ring on the left index, detector inward. With radiopharmacy units development, dosimetric studies become essential to improve staff radioprotection. Pharmaceutical staff turnover is sufficient to respect guiding values and to minimize the exposure of each one.

### P448

### The contribution of external irradiation to dose absorbed by patients undergoing radioiodine therapy in stationary conditions

**A. Wyszomirska**[1], K. Suska[1], R. Kopec[2], J. Sowinski[1], M. Budzanowski[2], M. Ruchala[1]; [1]University of Medical Science, Poznan, POLAND, [2]of Individual and Environmental Dosimetry Institute of Nuclear Physics Polish Academy of Sciences (IFJ PAN), Krakow, POLAND.

Medical treatment with the use of radioactive isotopes is at present an integral part of nuclear medicine. In the isotope therapy sodium iodide is used to treat thyroid illnesses(hyperthyroidism, thyroid cancer). Short-ranged and of high energy while going through human tissues, beta rays have therapeutic effects. Beta rays do not cause strong irradation of other organs. The isotope emits one more type of radiation - gamma rays which are used in medical imaging. The goal of the thesis was to find out what influence the presence of other patients on the patient treated is. The study was carried out in the fixe-line isotope therapy hospital ward, in cooperation with Laboratory of Individual and Environmental Dosimetry at The Institute of Nuclear Physics of The Polish Academy of Sciences. The TLD dosimetres have been used to detect and measure the radiation, and the results have been presented in the dissertation below. The research has been conducted at Clinical Endocrinology, Metabolism and Internal Diseases Unit of Święcicki University Hospital in Poznań. The research has been carried out on a group of patients hospitalized in the isotope therapy ward, treated with radioactive iodine doses disconnecting from contact outside the ward for the whole period of treatment. Based on the results given (of the equivalent absorbed radiation dose), and after analysing them, it has been stated that the estimated additional exposure of patients treated to radiation at the Fixed-Line Isotope Therapy Unit, makes slight fraction of the entire dose given to a patient. The average value of the exposure is between 0,6 and 1.9% of the whole risk patient is exposed to and depends on how long the experiment has been carried out. Conclusions drawn and presented in the thesis below, however, might not be completely reliable, because of the limited group of patients, to achieve more exact results, the group investigated should be made larger. This way the statistics of patients exposed to the same level of radiation could be more credible. The essential information could be as well comparing and confronting the research carried out in other units, unfortunately, no such data in literature were found available.

### P449

### Improved Radiation Protection by Introducing a New Application System for Peptide Receptor Radionuclide Therapy (PRRT)

**S. Wiessalla**[1], S. Senftleben[1], A. Rimpler[2], C. Schuchardt[1], C. Zachert[1], M. Wieditz[1], R. P. Baum[1]; [1]Zentralklinik Bad Berka GmbH, Bad Berka, GERMANY, [2]Bundesamt fuer Strahlenschutz, Berlin, GERMANY.

**Aim:** Since the introduction of peptide receptor radionuclide therapy (PRRT), the number of treatments had greatly increased over the past years and we now have a high steady load of treatments at our centre for neuroendocrine tumors (ENETS Centre of Excellence). This increasing use of PRRT led to a higher radiation exposure of the personnel. Originally, the syringe containing the therapeutic activity was loaded with a gripping tool into the syringe pump. This operation particularly led to a radiation exposure of the fingers. The aim of the present study was to examine the realized radiation exposure minimization, especially of the hands, by use of a new semi-automatic filling and application system. **Material and Methods**: While using the new application system, local dose rate was determined at different locations in the workplace and its environment. Additionally, in collaboration with the Bundesamt fuer Strahlenschutz the individual finger doses were determined with TLD tapes. The routinely carried finger rings were included in the analysis. **Results:** Despite the increasing frequency of PRRT and thus higher handled activities, the radiation dose (especially to the fingers) was serially reduced by the new application system. The official ring dosimeters (administration staff) showed the lowest finger dose in the period 2008-2012. Additionally, through improvement in the method of filling of the activity automatic significant dose reduction to the hands was achieved ($^{90}$Y: max 1.9 mSv / GBq, min 0.3 mSv / GBq). For application of the radiopharmaceutical, the shielded syringe is clamped in a special infusion stand, which contains a 20 mm thick tungsten shield. The dose rate in the vicinity of the infusion stand drops to a few µSv/h. **Conclusion:** By the introduction of a new filling and application system, the radiation protection of the staff was improved. Depending on the actual measurements, use of the system is continually optimized to increase the user's safety.

### P450

### Data Mining of Radiological Information Systems (RIS) Records To Generate Automated Nuclear Medicine Dosimetry and Quality Assurance Data

**M. Carroll**; Royal Liverpool University Hospital, Liverpool, UNITED KINGDOM.

**Objectives** : To implement a data mining program in Python Version 3.0 to create and maintain a patient specific radiation exposure database , with the aim of monitoring compliance with national legislation in terms of diagnostic reference levels and to investigate the impact of dose reduction technologies such as

resolution recovery . **Methods** : The National Health System(NHS) within the UK has instigated a National Interim Clinical Imaging Procedures (NICIP) Code set. The NICIP code set is a comprehensive national standard set of codes and descriptions for imaging procedures maintained by the UK Terminology Centre of NHS Connecting for Health. It is for use in all imaging department information systems. Each procedure in nuclear medicine has a unique NCIP code, for example NBONE represents Tc99m labelled MDP bone scan test. Each patient's RIS record includes the NCIP code for each nuclear medicine procedure they have undergone , the associated isotope and the measured injected dose. In nuclear medicine, radiation dose is determined by the radiopharmaceutical and activity administered. This information is automatically available independently of the patient's report with no requirement for complex text recognition within patient test reports or reliance on the test type actually being recorded within the report . Using Python's extensive data structure tools , each NCIP code is used to index the corresponding radiopharmaceutical tabulated organ dose estimates obtainable from the US Department of Health and Human Services and the resulting individual patient radiation dose is calculated and added to that patients dosimetry history. **Results** : 5 years of patient's data representing 50,000 nuclear medicine procedures performed at the Royal Liverpool University Hospital(RLUH) were used to populate a SQlite data base using Python's SQL toolbox. Example dose administration population statistics were generated for Tc99m bone scans and for F18 Fluoride PET bone scans which represent a current change in clinical practice and also display compliance with current limits on injected activities for these tests. **Conclusion:** Large scale personalized dosimetry and legislative compliance monitoring is entirely practicable based on current RIS and national consistent codes for nuclear medicine procedures. Such a database has the potential to efficiently provide evidence based on changes in received patient dose for the efficacy of dose reduction techniques such as resolution recovery . In addition one can monitor impact of changing clinical practice for example in moving from conventional nuclear medicine to PET as in the field of bone scanning.

P04-2 - Tuesday, Oct. 22, 16:00 - 16:30, Poster Exhibition Area

## Physics & Instrumentation & Data Analysis: Quality Control & NEMA

### P451

### Performance Characteristics of the Albira Tri-Modal Pre-clinical Scanner

**T. J. Spinks**, D. Karia, G. Flux, M. Leach; Institute of Cancer Research, Sutton, UNITED KINGDOM.

The Albira Tri-Modal pre-clinical scanner comprises PET, SPECT and CT components in a single gantry. The PET tomograph consists of 24 monolithic (50 x 50 x 10 $mm^3$) LYSO crystals with depth-of-interaction capability, arranged in 3 rings to give a large (148 mm) axial FOV and a transverse FOV of 80 mm. The SPECT component (using a single-pinhole collimator) has two opposing (100 x 100 x 4 $mm^3$) CsI crystals which acquire data in 6° increments over 180° or 360°, for selectable transverse FOVs (25, 50, 80 and 120 mm). The X-ray CT component (co-axial with the SPECT) consists of an X-ray source delivering 35-45 kVp at a current of 200-400 µA onto a flat-panel detector (FOV 70 mm transaxial x 70 mm axial). Spatial resolution, sensitivity and image uniformity have been investigated. **Methods:** Spatial resolution for PET was measured with a NEMA-specified $^{22}$Na point source (< 0.3 mm diam) and for SPECT with a "micro-Derenzo" line source phantom containing $^{99m}$Tc. Sensitivity was measured for PET with the $^{22}$Na point source and for SPECT with a point source (~ 1 mm diam) of $^{99m}$Tc. Image uniformity was investigated with a Perspex cylinder (30 mm diam, 160 mm length) filled with well-mixed solution of $^{18}$F or $^{99m}$Tc. Circular ROIs (20 mm diam) were defined on planes at 5 mm intervals along the axis. The axial variation in ROI counts was determined as well as the C.V. of voxel counts in-plane. Image reconstruction was performed with the standard scanner software: MLEM for PET and OSEM for SPECT. CT resolution was measured with a gold wire of diameter 50 µm and reconstruction performed with FBP. **Results:** At the centre of the FOV, spatial resolution for PET reaches a plateau of 1.5 mm (MLEM, 12 iterations) and for SPECT 0.7 mm (OSEM, 2 iterations). Sensitivity at the centre of the FOV for PET is 6% and for SPECT 0.02%. For both PET and SPECT the C.V. of ROI counts axially was 3-5% for repeated scans. For a 30 min PET scan (uniform cylinder) with 5 MBq (160 M counts), the mean ROI voxel C.V. was about 5% (MLEM, 12 iterations). For SPECT with 37 MBq (0.6 M counts) the C.V. was about 22% (OSEM, 2 iterations). CT resolution is about 90 µm. **Conclusions:** The good resolution and uniformity of response of the Albira provides a sound basis for accurate quantitative studies.

### P452

### Quantative assessment of planar spatial resolution and linearity of gamma cameras using quadrant bar or orthogonal hole patterns

**J. Holzmannhofer**, C. Pirich; Landeskliniken Salzburg, Salzburg, AUSTRIA.

**Objectives**: Basic gamma camera routine quality control of planar spatial resolution and linearity is usually done by assessing extrinsic or intrinsic measurements of quadrant bar or orthogonal hole patterns visually. The results can be quantified if special software is available. **Methods:** A tailored software using MatLab was developed to support quantitative assessment of both spatial resolution and linearity for quadrant bar and orthogonal hole patterns. For the quadrant bar pattern the data calculations are done as close as possible to the Methods described in NEMA No. NU-1:2007 (Performance measurements of gamma cameras): data are summed parallel to the direction of the slits to form line spread functions of width 30 mm or less. Full width half maximum (FWHM) is calculated to assess spatial resolution and the peak center, which is the average of the interpolated half maximum locations, and is used for linearity calculations. For the orthogonal hole pattern the optimum global thresholding using Otsu's method is implemented. For each hole the FWHM and the peak center are calculated for both x- and y-direction. One orthogonal hole phantom (hole diameter 5 mm) and several quadrant bar phantoms are measured on different gamma camera systems from small field of view to large field of view systems. The calculations are done with minimal user input. **Results**: In NEMA No. NU-1:2007 a digital resolution is recommended to be less than or equal to 0.2 FWHM. For large field of view gamma cameras this means that a matrix of 1024×1024 shall be used. Measurements for different count statistics have been undertaken and are presented. **Conclusions:** Quantitative assessment of spatial resolution and linearity based on quadrant bar and orthogonal hole patterns is feasible if the bar spacing / the hole diameter, the pixel size and the count statistics are appropriately chosen. This approach provides the tool for comparing resolution and linearity measures over time.

### P453

### A Method to Assess the Physical Performance of an Imaging Gamma Probe System

**A. J. Britten**, A. G. Irwin, L. Vass, A. Paramithas; St. Georges Hospital, London, UNITED KINGDOM.

Gamma probe system performance has been reported in terms of a range of physical performance parameters, for example following NEMA-NU3 protocols. The recent development of a system (declipseSPECT, Surgiceye GmbH) to track the gamma probe and perform 3D image reconstruction raises the question of how to evaluate the physical performance of such a system. Gamma camera SPECT system performance Methods in terms of spatial resolution and sensitivity do not take into account the specialised nature of the declipse system to localise small hot sources rather than to produce transaxial tomographic images, and so the **aims of this work** are to investigate a method of assessing the performance of intra-operative gamma probe systems which produce images. **Methods**: Since the declipse images are visually assessed, we have used a visual method to assess the spatial resolution by using two equal (+/-10 %) 1 MBq $^{99m}$Tc sources at 30 mm depth ("node sources") and at increasing separation from 10 mm to 50 mm, with a count rate from each source of around 300 cps. The gamma probe used was the Crystal SG04 (Nuclear Fields Inc), with a measured NEMA-NU3 spatial resolution at 30 mm depth in water of 22.3 mm FWHM. This was carried out without background and then with a 100 MBq $^{99m}$Tc source to simulate scatter from an injection site at 15 cm from the node sources. **Results:** The two sources were resolved when 40 mm or further apart, both with and without scatter. The surface localisation error mean was 6.1 mm, excluding some high outlier values seen especially when the background exceeded 15 % of the source count rate. **Conclusions:** We conclude that this visual assessment of spatial resolution by the separation of two sources is relevant to the way that the imaging gamma probe system is used in clinical practice, and that further work is needed to consider the effects of background from the injection site in sentinel node surgery.

P05-2 - Tuesday, Oct. 22, 16:00 - 16:30, Poster Exhibition Area

## Physics & Instrumentation & Data Analysis: Standardisation

### P454

### Determination of the calibration factors of commercially available dose calibrators for beta-emitters

**S. SHARMA**[1], B. SINGH[1], B. R. MITTAL[1], A. KOUL[2]; [1]PGIMER, CHANDIGARH, PUNJAB, INDIA, [2]PANJAB UNIVERSITY, CHANDIGARH, INDIA.

**Introduction**: The therapeutic doses of beta emitters administered to cancer patients must be accurately measured to achieve the best clinical efficacy of radionuclide therapy procedures. The routinely used dose calibrators in the clinical practice do not have proper calibrations for the radioactivity measurements of beta emitters. **Aim**: In the present study, we standardized the calibration factors of two

CAPINTEC (models; CRC-15R & CRC-ultra) dose calibrators for two commonly used therapeutic radionuclides (153-Sm and 177-Lu) available in India. **Materials and Methods:** The calibration settings of the dose calibrators were adjusted for the variations in the volume of the radioactivity measured for the two radionuclides. 137-Cs standard source (7.74 MBq, Benchmark, RadQual, International Isotopes Inc., USA) was used to check the stability of the dose calibrators. The dial setting number for each dose calibrator was determined by using known activities of 153-Sm and 177-Lu separately. The radionuclides were measured in the routinely used syringes (2ml, 5 ml and 10 ml) and the calibration factors were determined by using three Methods i.e. (a) Constant activity method (b) constant specific activity - Volumetric method at a constant specific activity and (c) constant specific activity - Gravimetric method. **Results:** The dial settings for each dose calibrator were determined and found to be 230 and 123 x 10 for 153-Sm and 177-Lu respectively. The volumetric correction factors remained constant for a specific syringe type. However, the factor changed (2.0-4.0%) when the syringes of increasing volume capacity were used. **Conclusion**: The calibration of the dose calibrators and establishing the dial settings for the routinely used therapeutic radionuclides are mandatory for the accurate radioactivity administrations.

P06-2 - Tuesday, Oct. 22, 16:00 - 16:30, Poster Exhibition Area

## Physics & Instrumentation & Data Analysis: New & Innovative

### P455
### SPECT without collimators

**K. S. Chuang**[1], H. H. Lin[1], C. H. Chien[1], C. W. Shen[1], M. L. Su[2], Y. C. Ni[3], M. L. Jan[3]; [1]National Tsing-Hua University, Hsin-Chu, TAIWAN, [2]Oriental Institute of Technology, Taipei, TAIWAN, [3]Institute of Nuclear Energy Research, Long-Tan, TAIWAN.

**[Aim]** The Single Photon Emission Computed Tomography (SPECT) requires collimator to limit the direction of incoming photons. Depending on the shape of the collimator, it can be categorized as a pinhole, converging, parallel, or diverging collimator each with different magnification. The collimator is heavy and difficult to manipulate. In this presentation we replace the collimator with a beam stopper (BS) to perform SPECT and the new system is named BS-SPECT. Image data obtained from the subtraction between scan with and without the BS yields the information similar to the SPECT with collimator. In BS-SPECT, various magnifications can be achieved by adjusting the BS location inside the scanner. The BS is a 0.8 mm diameter sphere made of high Z materials. **[Material and Methods]** A water phantom with Tc-99m injected in an insert and an animal positron emission tomography (PET) were employed to perform the study. A tube consisted of eight BSs distributed uniformly on the periphery was inserted between the PET and subject. The field of view (FOV) passing through each BS casted a projection occupying one-sixteenth of the total detector ring. As a result, the projections of the FOV on the detector ring with and without BS were interchanged each other. For each scan there were eight projections with BS and eight projections without BS. The BS tube rotated 1/160 of the full circle after each scan for a total of twenty scans. Totally 160 differenced projections (=8x20) were generated and can be used for image reconstruction. **[Results and Discussion]** With BS placed in the middle, a 3cm FOV is available for mouse imaging. Preliminary results using Monte Carlo simulation show good image quality demonstrating that the SPECT without collimator is feasible. The advantages of the new system are its light weight, low cost, and flexibility. One possible application of this technique is the simultaneous imaging of dual isotopes (F-18 and Tc-99m) with a PET scanner.

### P456
### Simultaneous dual isotope SPECT-VQ using Kr-81m as ventilation agent; optimisation of technical and practical factors to allow confident clinical implementation

**C. D. Baker**, J. C. Fowler; Royal Brompton & Harefield NHS Foundation Trust, London, UNITED KINGDOM.

**Introduction**: Recent EANM guidelines recommend SPECT-VQ for the scintigraphic investigation of pulmonary emboli. Krypton-81m is an attractive potential SPECT-VQ ventilation agent given ideal physical characteristics, a very low radiation dose and opportunities for simultaneous dual isotope acquisition to allow perfect co-registration and shortened acquisition time. Technical aspects of simultaneous technetium-99m/krypton-81m dual isotope SPECT-VQ (STEKDI-SPECTVQ) acquisition require optimisation given septal penetration by krypton-81m photons, potential for down-scatter of Kr-81m photons into the Tc-99m window and possible difficulties with achieving a steady ventilation state given the short half life of Kr-81m. To our knowledge, no technical guidelines for STEKDI-SPECTVQ have been published. Aim: To optimise technical and practical aspects of STEKDI-SPECTVQ to allow confident clinical implementation. **Materials and Methods**: A specifically developed STEKDI-SPECTVQ phantom was used to establish the optimal SPECT acquisition parameters in terms of collimator choice, matrix size, number of projections, time per projection and reconstruction algorithms to best demonstrate small matched and mismatched defects within the phantom. These parameters were used to establish clinical protocols. The technical success of image acquisition, time for study acquisition and image quality of the first 20 cases were assessed. The rate of CTPA conversion to VQ before and after the implementation of STEKDI-SPECTVQ clinical service was monitored to assess enthusiasm for the new technique amongst referrers and reporters. **Results**: Use of the phantom was successful in establishing acquisition parameters. Practical aspects of clinical application of the dual isotope technique required refinement in early clinical cases particularly in terms of ventilation mask application. In one case the ventilation phase required repetition; all other acquisitions were successful. The STEKDI-SPECTVQ technique took no longer than conventional planar VQ study acquisition. All STEKDI-SPECTVQ image acquisitions resulted in interpretable ventilation and perfusion images. Conversion of CTPA requests to VQ has more than doubled since the introduction of STEKDI-SPECTVQ with substantial savings in terms of radiation exposure to patients. **Conclusions**: Using a specifically developed phantom prior to clinical implementation, STEKDI-SPECTVQ has been successfully introduced clinically and taken up enthusiastically by performing technical staff, reporting imaging specialists and referring clinicians.

### P457
### Phantom Studies of Cyclotron Produced Technetium-99m

X. Hou[1], **A. Celler**[1], M. Vuckovic[2], P. Shaffer[3], F. Benard[2,1]; [1]University of British Columbia, Vancouver, BC, CANADA, [2]BC Cancer Agency, Vancouver, BC, CANADA, [3]TRIUMF, Vancouver, BC, CANADA.

**Objectives:** Cyclotron-based production has been proposed as a new approach for solving the anticipated shortage of 99mTc traditionally obtained from reactors. However, with this method several other technetium isotopes are created (Celler et al., PMB-2011), which may contribute to patient dose (Hou et al., PMB-2012) and degrade image quality by adding background from scatter of high energy photons. The aim of this study was to investigate the characteristics of photon emissions from samples obtained from a cyclotron and to compare them with $^{99m}$Tc from a generator. **Methods**: Identical bottles (33ml and 17ml) containing cyclotron- and reactor-technetium were scanned in a water filled Jaszczak and an acrylic neck phantoms. The cyclotron-technetium was obtained by 1h irradiations of 99.01% enriched $^{100}$Mo targets with 18-10MeV protons. Acquisitions were performed on days 1, 2, 4 and 5 and included SPECT/CT and planar scans of both types of technetium placed in the phantoms, bottles placed directly on the detector and of the background. Three energy windows were used: photopeak (126-154keV), upper (168-312keV) and lower (89-120keV). Photon counts and images from the two types of technetium were evaluated. Additionally, experimental data were compared with theoretical estimates of the primary and scattered photons $^{99m}$Tc contribution in each source. **Results**: All images acquired on days 1-2 (early images) corresponding to the photopeak and lower energy windows from cyclotron- and reactor-technetium were basically identical. In spite of a small increase in total counts (3-6%) in cyclotron-technetium image, there was no difference in the shapes of profiles drawn across the sources and their scatter tails. Although counts in the upper energy window from the cyclotron-technetium were four times higher than those from the reactor, they amounted to only 5-6% of the total counts. In late images (days 4-5), with only trace amounts of $^{99m}$Tc, the counts in the image from the reactor-technetium were at the background level, while those for the cyclotron source were 50% higher than the background. Because the majority of contaminant technetium isotopes emit high energy photons, in the late images of cyclotron-technetium these showed as a uniform scatter background. **Conclusion:** Images from the cyclotron-produced technetium acquired up to 24h post irradiations are of the same quality as those from generator. In agreement with our theoretical predictions, late images show small increase in count rates originating from other technetium isotopes. Quantitative comparison of experimental results with our theoretical predictions is on-going.

P07-2 - Tuesday, Oct. 22, 16:00 - 16:30, Poster Exhibition Area

## Molecular & Multimodality Imaging: PET/CT

### P458
### Utilization of 18F-FDG PET/CT to differentiate PTSD from TBI and the relationship of the hypothalamic-pituitary axis: initial experience

**M. M. Osman**, R. Muzaffar, P. T. Roskos, T. M. Malone, D. Whitson, R. D. Bucholz; Saint Louis University, Saint Louis, MO, UNITED STATES.

**Objectives**: The role of the hypothalamic-pituitary axis has been suspected in post traumatic stress disorder (PTSD) but there has not been a significant imaging research effort to target the relationship. Differentiating PTSD from traumatic brain injury (TBI) has been challenging since there are many pathologic features found in

both, with shared signs and symptoms. In addition, many of these patients present with a normal structural MRI. To date, FDG PET/CT is not playing a role in the diagnosis of PTSD or in the differentiation of PTSD from TBI. The objective of this study is to evaluate the potential use of FDG PET/CT in differentiating PTSD from TBI based on metabolic activity in the pituitary and hypothalamus. **Methods**: We retrospectively reviewed 90 dedicated brain FDG PET/CT studies. All PET images were acquired in the morning and according to standard brain PET/CT protocol. MRI was performed the day before the PET/CT scan with normal findings in all selected cases, as per the read of a fellowship trained neuroradiologist. The 90 cases were divided into 3 groups of 30 which were age and gender matched: normal control, TBI and TBI+PTSD. The PET/CT scans were read by 2 board certified nuclear medicine physicians blinded to the groups, and a log recorded the SUV max of the pituitary gland and the hypothalamus. **Results:** The mean SUV max of the pituitary and the hypothalamus was the greatest in the normal control (pituitary = 3.41; hypothalamus = 6.67). In the TBI group, the SUV max decreased by 2.3% in the pituitary and 6.6% in the hypothalamus when compared to the normal control group (SUV max pituitary 3.33; hypothalamus = 6.23). In the TBI + PTSD group, the SUV max decreased by 10.3% in the pituitary and 13.6% in the hypothalamus when compared to the normal controls (SUV max pituitary 3.06; hypothalamus = 5.76). **Conclusion**: We are continuing to acquire and analyze data. However, our initial results suggest that the metabolic activity in the pituitary and hypothalamus can be used to not only identify PTSD but also differentiate it from TBI.

## P459

### [18F]FDG PET in patients with rheumatologic disease.

**V. A. Manukova**, M. Roudas, E. Panchkovskaya, A. Gordeev, A. Kopyrin, I. Pozharov, A. Luosev; Central Clinical Hospital at the Management Department of the President of the Russian Federation, Nuclear Medicine Department,, Moscow, RUSSIAN FEDERATION.

**Aim.** Because FDG is taken up into activated granulocytes, lymphocytes, and macrophages, PET has the potential to visualize not only infectious but also sterile inflammation that are present in active rheumatologic diseases. Rheumatoid arthritis is a common, chronic, and progressive disease. It has the highest incidence of all autoimmune diseases. Vasculitis includes different diseases presenting with inflammation of the arterial wall. Application PET- FDG is very important as well for definition of a role of this method in complex inspection of patients with large vessel vasculitis, rheumatoid arthritis and other rheumatologic diseases as retroperitoneal fibrosis (Ormond's disease), ankylosing spondylitis etc. FDG-PET can be used for activity inflammatory process assessment and therapy response monitoring . **Materials and Methods**. PET scan it was carried out on patients fasting for at least 6 hours before the scan with blood glucose level less than 9,0 mmol/l. [18F]FDG in a dose of 350-450 MBk was intravenously administered. Acquisition started not until 60 minutes after injection. [18F]FDG-PET studies were performed in 72 patients who were refered for PET with fever of unknow origin (FUO) or rheumatic polymyalgia or Ormond's disease (for therapy response). **Results**. We detected accumulation of FDG in large vessels in 36 patients and after following clinical work up 27 giant cell arteritis and 9 Takayasu`s arteritis was diagnosed. In 30 patients the increased accumulation of FDG was observed around joint surfaces and in some cases in adjoining muscles without signs of vasculitis. In 4 patients with FDG accumulation in spine joints ankylosing spondylitis was diagnosed. 2 patients with Ormond's disease demonstrated increased activity around abdominal aorta (before and during treatment) and in pancreas**. Conclusions**. Whole-body imaging with [18F]FDG-PET is highly effective in assessing the activity and extent of giant cell arteritis and Takayasu`s arteritis. Metabolic imaging using [18F]FDG-PET has been shown to identify more affected vascular regions than MRI in both diseases. In patients with rheumatoid arthritis FDG PET allowed quantification of metabolic changes though this information additional but not defining. All the more FDG uptake is not associated with treatment outcome. The role of PET in patients with Ormond's disease is still under investigation. We believe this method can be used for detection inflammatory lesions all over the body as well therapy response monitoring.

## P460

### Strong correlation between 18F-FDG PET positive bone involvement and increased serum IL-2R levels in patients with untreated sarcoidosis under surveillance.

**D. Kalkanis**[1], A. Kalkanis[2], D. Drougas[3], N. Karagiannidis[2], M. Mpountali[3], P. Chroni[3], A. Mpournazos[3], D. Exarhos[4], I. Datseris[3]; [1]Department of Nuclear Medicine, 251 General Airforce Hospital, Athens, GREECE, [2]Third Pulmonary Medicine Department, Sismanoglion General Hospital, Maroussi, GREECE, [3]Department of Nuclear Medicine and PET/CT, Evangelismos Hospital, Athens, GREECE, [4]Department of Radiology, Evangelismos Hospital, Athens, GREECE.

Introduction: F-18 fluorodeoxyglucose positron emission tomography and computed tomography (FDG PET/CT) has been shown to be able to detect osseous involvement in patients with sarcoidosis. Aims and objectives: Our aim was to use FDG PET/CT to assess bone involvement in patients with an established diagnosis of sarcoidosis who are therapy-naive and to examine if there is any correlation between FDG-avid bone involvement and biochemical markers. Methods: All patients with an established diagnosis of sarcoidosis were identified from a local database in our hospital. Patients who had not received any therapy and were under routine surveillance were enrolled in this study. All enrolled patients prospectively underwent a whole-body combined FDG PET/CT scan, as well as biochemical lab tests, which included serum interleukin-2 receptor (IL-2R), C-reactive protein (CRP), serum angiotensin-I converting enzyme (SACE), serum calcium and urine calcium levels. Bone involvement was identified in PET scans as any abnormal focus of increased FDG uptake, and in CT scans as any lytic or sclerotic abnormality in the skeleton. Results: Thirty patients (10 male, 48.2 ±11.6 years) were included. PET(+) bone lesions were identified in 20% of the patients (6/30), while no lesions were noted on the CT. Bone lesions were present in both axial and appendicular skeleton in 4/6 patients and in axial skeleton only in 2. SUVmax of the most FDG-avid bone lesion was 9.3 ±3.4. In patients with PET(+) bone involvement IL-2R was significantly higher (3000 ±1588), than in the rest (1022 ±587)($p<0.001$). There was significant positive correlation between PET(+) bone involvement and abnormal IL-2R levels (Spearman's rho=0.5, p=0.005). No significant correlation was found between PET(+) bone involvement and abnormal CRP, SACE, serum or urine calcium levels. Conclusions: The prevalence of FDG PET(+) bone involvement in untreated sarcoidosis is 20% in our series. All PET(+) bone lesions were negative on corresponding CT. There is strong correlation between PET(+) bone involvement and increased IL-2R levels, while no correlation is identified between PET(+) bone involvement and abnormal CRP, SACE, serum or urine calcium levels in patients with untreated sarcoidosis.

## P461

### Review : Can FLT PET-CT predict treatment response?

**B. Sanghera**[1], L. Sonoda[1], D. Woolf[2], A. Makris[2], W. Wong[1]; [1]Paul Strickland Scanner Centre, Mount Vernon Hospital, Northwood, UNITED KINGDOM, [2]Mount Vernon Hospital, Northwood, UNITED KINGDOM.

**Objectives:** Review evidence of FLT PET-CT in predicting response to cancer treatment regimes and suggest future improvements to increase the evidence base. **Methods**: FLT PET studies looking at lesion proliferation with therapy are assessed. We review 32 studies and include information about FLT scan regimes including treatment regimes, scan timings, injected activity regimes, fasting, uptake times /acquisition parameters, reconstruction, numbers scanned and Ki-67 correlations. **Results**: FLT PET has a role in monitoring tumour response during treatment particularly in brain, lung and breast cancers where strong correlation with Ki-67 is observed, despite a multiplicity of different parameters implemented between separate studies. We advocate a more unified approach towards FLT PET use as essential to establish true efficacy in evaluating treatment response. This may be achieved with a strict regime of scanner QA/QC, PET protocol and analysis technique compliance for all centres. **Conclusions:** FLT PET in therapy is currently 'a work in progress' with need for harmonisation in future. Evidence suggests promise for this proliferation tracer especially for brain, lung and breast cancers where strong correlation with Ki-67 is observed. Larger scale multi-centre trials are recommended to investigate the true potential of FLT in the treatment response pathway.

## P462

### Comparison of image quality and quantification between Philips Ingenuity TF PET/MRI and Gemini TF PET/CT data in prostate cancer patients

**D. E. Oprea-Lager**, M. Yaqub, F. Jongsma, I. Pieters-van den Bos, R. Reinhard, O. S. Hoekstra, A. A. Lammertsma, R. Boellaard; VU University Medical Center, Amsterdam, NETHERLANDS.

**Aim:** To compare image quality and quantification of PET/MRI with PET/CT in metastatic prostate cancer (PCa). **Methods:** Six patients (64±7 years) with relapsing metastatic PCa were examined. Whole body (WB) PET/CT scans were acquired on a Philips Gemini TF PET/CT system, 30 minutes post injection (p.i.) of 344±44 MBq [$^{18}$F]Fluoromethylcholine (FCH). Next, WB PET/MRI studies were performed on a Philips Ingenuity TF PET/MRI scanner, 90 min p.i.. This tracer was selected because of the relative stable uptake from 30 to 90 min after administration. During the latter scan acquisition time was increased with 50% compared with the PET/CT scan to (partially) compensate for radioactive decay. Visual evaluation of number and localization of soft tissue and bone lesions on both PET/MRI and PET/CT images was performed to compare the diagnostic performance of these techniques. Images were independently interpreted by two radiologists and two nuclear medicine specialists who were aware of the clinical history of the patients. Lesions were defined as choline avid structures, incompatible with physiological uptake, showing anatomical substrate on MRI or CT. They were deemed benign/ malignant, based on the metastatic pattern of PCa. Furthermore, [$^{18}$F]FCH uptake in all lesions and various normal tissues was assessed semi-quantitatively. Maximum and 3D peak SUV normalised to body weight (SUVmax & SUVpeak) were obtained for all lesions. In addition, mean SUV using a 2-3 cm diameter volume of interest

was derived for healthy tissues. **Results:** A total of 9 benign and 18 suspected malignant lesions were identified on both PET/MRI and PET/CT. Visual inspection showed comparable PET image quality for both modalities. A difference of 6±28% in SUV values of lesions between PET/MRI and PET/CT data was observed ($R^2$=0.80, slope=1.04). In normal tissues, PET/MRI SUV values were 17±9% lower than corresponding values derived from PET/CT ($R^2$=0.99, slope=0.85). The largest quantitative deviations (up to -40%) were found in the lungs. Moreover, 2 out of 6 patients showed severe artefacts in the thorax region in the PET/MRI images. These errors were due to incorrect lung segmentation in the MRI attenuation map. **Conclusion:** In absence of PET/MRI artefacts, good correspondence in [$^{18}$F]FCH uptake in both healthy tissues and suspected lesions was found, although PET/MRI data suffered from negative bias. For clinical use of PET/MRI it is essential that readers are able to interpret both attenuation and non-attenuation corrected images to avoid incorrect conclusions from severe attenuation correction artefacts.

## P463

### Biodistribution of Ga-68 labelled Prostate Specific Membrane Antigen Ligand Glu-NH-CO-NH-Lys-(Ahx)-[68Ga (HBED-CC)] in Patients with Prostate Cancer: Characterization of Uptake in Normal Organs and Tumour Lesions

**H. R. Kulkarni**[1], R. P. Baum[1], H. Wester[2]; [1]THERANOSTICS Center for Molecular Radiotherapy and Molecular Imaging, Bad Berka, GERMANY, [2]Pharmaceutical Radiochemistry, Faculties of Chemistry and Medicine, Technische Universität München, Munich, GERMANY.

Aim: Prostate-specific membrane antigen (PSMA) is a transmembrane cell surface antigen which is significantly higher expressed in prostate cancer cells when compared to normal tissue. The Ga-68 labelled PSMA ligand Glu-NH-CO-NH-Lys-(Ahx)-[68Ga (HBED-CC)] (Ga-68 PSMA) is a novel PET tracer with high potential for the better detection of residual / recurrent disease and of metastases in prostate cancer. The aim of this study was to determine the biodistribution of Ga-68 PSMA in normal tissue as well as in tumour lesions. Materials and Methods: The maximum standardized uptake values (SUVmax) of Ga-68 PSMA were evaluated in normal organs and 168 tumour lesions in 9 prostate cancer patients (mean age 68±3 years) presenting with rising serum prostate specific antigen (PSA). The mean injected activity of Ga-68 PSMA was 190±71 MBq, the mean acquisition time after injection was 87±14 minutes. All but one patient had undergone prostatectomy. SUVmax of 123 skeletal, 39 lymph node and 6 lung metastases were documented. Results: Intense tracer uptake was noted in both kidneys. The salivary glands showed a moderately intense uptake. Notable in all patients was a moderate to intense accumulation in the small intestine, particularly the 3rd part of the duodenum. Moderate uptake was seen in the lacrimal glands followed by spleen and liver. Results of SUVmax (mean±SD) were as follows: lacrimal gland 7.8±3.7, parotid gland 17.4±7.4, submandibular gland 20.3±6.8, lung 1.0±0.4, liver 6.0±1.5, spleen 8.4±3.3, small intestine 13.8±4.8, kidney 51.0±9.6, gluteal muscle 0.9±0.4 and blood pool 2.6± 1.4. The normal prostate had a SUVmax of 7.7 in one patient. Quantitative assessment of the tumour lesions revealed a maximum SUV of 29.0±7.5 for skeletal metastases (n=123), 36.3±13.3 for lymph node (n=39), and 2.9 for pulmonary metastases (n=6). The mean tumour-to-background ratio was 30.6±10.9 for skeletal metastases, 40.0±17.4 for lymph nodes and 3.3 for pulmonary metastases. Corresponding CT detected only 45/123 skeletal metastases, 27/39 lymph nodes and all 6 lung lesions. The highest SUV was found for lymph node metastases (74.7) followed by bone metastases (53.4) Conclusion: Normal biodistribution of Ga-68 PSMA tracer revealed maximum uptake in the kidneys. Significant uptake was found in salivary and lacrimal glands and in the duodenum. Tumour lesions exhibit a high target-to-background ratio, which allows detection of very small lesions - the smallest detectable lymph node metastases measured only 3 mm in diameter - and also detection of early bone marrow metastases (negative on conventional imaging).

## P464

### Respiratory gating 4D-PET/CT and 4D-CT simulation acquisitions for radiotherapy target volumes definition

**L. Santoro**, L. Bedos, M. Capdepon, D. Azria, P. Kotzki; Montpellier Cancerology Institute, Montpellier, FRANCE.

18F-FDG hybrid positron emission tomography/computed tomography (PET/CT) is now recognized as an important diagnostic tool for oncologic applications. This ability to perform functional images and to identify active disease from normal tissue makes it an interesting tool for radiotherapy planning. Huge recent evolutions in radiotherapy technology allowed more targeted dose delivery but with a still imprecise initial tumor volume delineation. Since a PET/CT was acquired in 2012 by the nuclear medicine department, nuclear physicians, radiation oncologists and medical physicists work in close collaboration to optimize planning radiotherapy by using registration of PET/CT and CT simulation images. To obtain a more accurate target volumes definition and to minimize the respiratory organ motion, a respiratory gating (RG) 4D-PET/CT acquisition technique was installed in addition to the RG 4D-CT simulation. After RG 4D-CT simulation, a RG 4D-PET/CT is performed in the same conditions: rigid flat table, positioning and immobilization devices and external lasers. As soon as the patient is properly positioned and immobilized, the Real Time Position Management (RPM by Varian Medical Systems) system is used to synchronize the patient respiratory cycle with the CT-PET acquisition system. Once acquired RG 4D-PET/CT data are processed and sorted into the same number of phases than the RG 4D-CT. Each phase corresponds to a specific phase of the respiratory cycle. First, a registration between the two CT Maximun Intensity Projection (MIP) (CT simulation and CT of PET) is performed. Then, this registration matrix is applied to all the RG 4D-PET phases. Finally, these registrated images are used by physicians to validate target volumes definition. We will present at the congress the technique used to perform RG 4D-PET/CT acquisition with data processing and registration. We will also show the contribution in radiotherapy contouring and review the potential uncertainties in using this technique.

## P465

### Incidental findings on the CT component of hybrid imaging: a literature review

**S. Parthiban**, T. Wagner; Royal Free Hospital, London, UNITED KINGDOM.

Background: Single positron emission tomography (SPECT) with computed tomography (CT) (SPECT/CT) and positron emission tomography (PET) with computed tomography (CT) (PET/CT) are recent technologies combining functional and anatomical information. Their use is increasing in a wide range of clinical indications, including oncology, neurology, cardiology, inflammatory and musculoskeletal diseases. Hybrid imaging reporting is complex because of the large amount of data to analyse. Incidental findings are frequent in conventional cross-sectional imaging (CT, MRI) and there is extensive literature on the frequency and management of incidentalomas. To our knowledge there has been no review of the literature for incidental findings from the CT component of hybrid SPECT/CT and PET/CT scans. We decided to perform a literature search for incidental findings from the CT component of hybrid scans. Materials and Methods: We performed a literature search using PUBMED for articles mentioning incidental findings on the CT component of SPECT/CT and PET/CT. We searched the words: SPECT/CT AND Incidental findings; Incidental findings; PET/CT AND Incidental findings; CT AND Incidental findings. Findings were classified depending on their severity as 'major' or 'minor'. Major incidental findings were considered to be ones that require immediate medical attention and could be life threatening. Results: Major incidental findings were relatively infrequent (3%-4%). More than 50% of scans mentioned at least one minor incidental finding. Pulmonary nodules (>7mm) seemed to be the most frequent with one study finding 184 cases in 321 patients. Abdominal aortic aneurysms were the most common major finding with 2 being found across 2 major studies (321 and 250 patients). Discussion: There is a high frequency of incidental findings on the CT component of SPECT/CT and PET/CT. Reporters of hybrid imaging scans need to be trained in the identification, reporting and management of incidental findings. There is also a need for appropriate guidelines for the management of the most common incidental findings in hybrid imaging.

## P466

### Assessment of statistical comparison between TNR and SUVs of MET-PET/CT using Kaplan-Meier method and Bland-Altman plot.

**S. Ohashi**, K. Yoshikawa, s. toubaru, M. Hasebe, K. Tamura, T. Shiraishi, K. Tanimoto, N. Yamamoto, S. Kandatsu, M. Zhang, T. Saga, T. Kamada; National Institute Of Radiological Sciences, Chiba, JAPAN.

Purpose Standardized quantitative assessment of metabolic tumor response with PET necessitates a consistent and reliable measure of tumor activity. TNR, tumor to normal tissue ratio, is a simple but relatively stable uptake index which compares the tumor uptake to reference uptake in the body, usually uptake of muscle around the spine. But a major drawback of TNR is its inter-observer difference. By SUVpeak, which it defines as the largest possible mean value of a 1cm3 spherical VOI positioned within a tumor, inter-observer variation is removed, and the susceptibility to noise is reduced. We compared the usefulness of TNR with SUV-based indexes driven from Methionine PET/CT, for assessment of patient's prognosis with lung cancer treated by Carbon-ion beam therapy using Kaplan-Meier method and Bland-Altman plot. Material and Method A total of 67 patients (32 males, 35 females; mean age, 73 ± 9 y) with lung cancer underwent C-11-MET PET/CT scan in pre- and post-carbon ion radiotherapy. All patients were followed more than 2 year after treatment. We measured TNR calculated with mean activity of circular ROI drawn in the tumor divided by mean normal muscle ROI in para-spinal column. Maximum standardized uptake value (SUVmax), SUVpeak6 and SUVpeak15. SUVpeak6 and SUVpeak15 are measured using spherical VOI with radius 6 mm and 15 mm, respectively. The overall survival was estimated using the Kaplan-Meier method with each index as prognostic variables. We calculated the other TNRs from SUVs. TNRmax is TNR calculated using tumor SUVmax and normal muscle SUVmax. In the same manner TNRpeak6 and TNRpeak15 is calculated from

SUVpeak6 and SUVpeak15, respectively. Bland-Altman plots were used to evaluate difference between TNR and the other TNRs in pre- and post-treatment scan. Result Cutoff values for each MET uptake indexes were defined by ROC analysis, and the probability of survival was significantly lower with increasing MET uptake measured by all the kinds of TNR, TNRpeak6, TNRpeak15 and SUVs but SUVmax in pretreatment. In post-treatment, only TNRpeak6 among all indexes was statistically significant index on the treatment outcome by Kaplan-Meier analysis. TNRpeak6 avoids inter-observer difference and reduces the susceptibility to noise. However, proportional bias was observed between TNR and TNRpeak6 and TNRpeak15 in both pre- and post-treatment as revealed by the Bland-Altman plot analysis. Conclusions: TNRpeak6 in both pre- and post-treatment was statistically significant prognostic variable for overall survival estimated using the Kaplan-Meier method, and it avoids inter-observer difference and reduces the susceptibility to noise.

## P467

### Exploratory human PET study of the effectiveness of 11C-ketoprofen methyl ester, a potential biomarker of neuroinflammatory processes for Alzheimer's disease

**A. Ohnishi**[1], M. Senda[1], T. Yamane[1], M. Sasaki[1], Y. Ikari[1], H. Nishida[1], T. Nishio[1], T. Mikami[1], Y. Yamamoto[2], M. Syukuri[3], Y. Watanabe[3], H. Onoe[3]; [1]Institute of Biomedical Research and Innovation, Kobe, JAPAN, [2]Department of Psychiatry Kobe University Graduate School of Medicine, Kobe, JAPAN, [3]RIKEN, Center for Molecular Sciences, Kobe, JAPAN.

Aim: Microglial activation plays an important role in the pathogenesis of Alzheimer's disease (AD). As a biomarker of neuroinflammatory processes we have designed 11C-ketoprofen methyl ester (11C-KTP-Me) (JNM 52:1094, 2011) to increase blood-brain barrier permeability of ketoprofen (KTP), which is a selective inhibitor of cyclooxygenase-1. Animal studies indicated that 11C-KTP-Me entered the brain and was retained in inflammatory model lesions as it accumulated in activated microglia, while it was washed out from normal tissues. In a preliminary study, We indicated that 11C-KTP-Me was a safe PET tracer and entered the human brain and that the activity was washed out from normal cerebral tissue . This human study explored the effectiveness of 11C-KTP-Me as a biomarker of AD process. Methods: 9subjects(ages 54 to 90), consisting of 4 healthy subjects, 2 PiB-positive MCI and 3 PiB-positive AD patients, underwent a dynamic brain PET scan for 70min starting injection of 11C-KTP-Me (474 to 554 MBq). We evaluated differences in the cortical retention and washout rate from brain among three groups. Results: The cortical activity was washed out biphasically to 63 % of the peak at 10 min and to 40 % at 50 min, and the late phase images showed blood pool much higher than cortex, suggesting very low permeability of the metabolite. No significant difference was observed in the cortical retention or in the wash out rate between healthy subjects, MCI and AD patients. Conclusion: 11C-KTP-Me enters the human brain, and the activity is washed out from cerebral tissue. However, No significant difference was observed in the cortical retention or in the wash out rate between healthy subjects and patients, Suggesting limited the effectiveness of 11C-KTP-Me as a potential biomarker for Alzheimer's disease.

## P468

### Functional state of anterior cingulate cortex at early stage of the disease is altered in both patients with multiple sclerosis and HIV positive subjects as revealed by H1-MRS data.

**G. V. Kataeva**[1], A. Korotkov[1], A. Trofimova[1], A. Bogdan[1], T. Trofimova[1], N. Belyakov[2], S. Medvedev[1]; [1]N.P.Bechtereva Institute of the Human Brain of the Russian Academy of Sciences, St.Petersburg, RUSSIAN FEDERATION, [2]St.Petersburg Center for Control of AIDS and Infectious Diseases, St.Petersburg, RUSSIAN FEDERATION.

OBJECTIVE Functional neuroimaging studies have shown that functional state of the anterior cingulate cortex (ACC) is altered in many neurological diseases including multiple sclerosis (MS). Recently the reduced functional activity of ACC in asymptomatic HIV subjects was shown (Towgood et al. 2012). Our aim was to study the functional state of ACC with H1-magnetic resonance spectroscopy (MRS). SUBJECTS AND METHODS We studied two groups of patients: 1) 10 patients (6 males and 4 females) with relapsing remitting multiple sclerosis in remission (EDSS<2) and 2) 16 (8 males and 8 females) HIV positive patients. Subjects of both groups had no prominent neurological deficit and cognitive decline. HIV positive subjects were without any history of neurological and somatic pathology and drug abuse. 17 healthy subjects (9 males and 8 females) constitute the control group. NAA/Cr, Cho/Cr, NAA/Cho ratios in supraventricular plane were measured using multivoxel 1H-MRS (2D PRESS (TE/TR = 144/1500, voxel size 10*10*15 mm). The twelve voxels were chosen for analysis in groups of four for anterior, central and posterior cingulate. RESULTS Significant changes of metabolite ratios were revealed only for ACC region. Significant decrease ($p<0.001$) of NAA/cr was found in both patient groups in comparison with control that indicate the neuronal deterioration. On the contrary the significant alteration of other metabolite ratios (decrease of NAA/Cho ($p<0.001$) and increase of Cho/Cr ($p<0.001$)) was found only for HIV group indication the presence of inflammatory and ischemic/hypoxic processes. CONCLUSION Our findings suggest that neuronal deterioration in ACC is common feature at early stages of both MS and asymptomatic HIV infection while underlying metabolic alterations may be different.



Abstract P469 withdrawn at author's request due to inadvertent miscalculation

## P470

### Imaging serotonin and dopamine transporters with dynamic 123I-β-CIT SPECT in mouse brain

**M. Pitkonen**[1,2], E. Hippeläinen[1,2], M. Raki[3], S. Savolainen[1,2], J. Andressoo[4], M. Saarma[4], K. Bergström[1,3]; [1]HUS Medical Imaging Center, Helsinki University Central Hospital, Helsinki, FINLAND, [2]Department of Physics, University of Helsinki, Helsinki, FINLAND, [3]Center for Drug Research, Faculty of Pharmacy, University of Helsinki, Helsinki, FINLAND, [4]Program of Molecular Neurobiology, Institute of Biotechnology, University of Helsinki, Helsinki, FINLAND.

Aims: A high-resolution pinhole single-photon emission computed tomography (SPECT) is capable of accurate, repeatable and semiquantitative measurement of 123I-β-CIT dopamine transporter (DAT) binding in mouse brain (EJNMMI Res. 2012 Sept 29; 2(1):55). However, 123I-β-CIT has affinity also to serotonin transporter (SERT), which could be useful for research of SERT associated neurodegenerative diseases. Currently, there are only postmortem autoradiography data of mice SERT kinetics available. The aim of the work is to verify 123I-β-CIT binding kinetics to SERT and DAT with SERT blocking agent paroxetin. Materials and Methods: Two healthy wild type mice were scanned twice; with and without pretreatment of paroxetin. There was eight days between first (baseline) and second (pretreatment) scan. Mice received similar doses (46 ± 0.4 MBq, mean ± SD) of 123I-β-CIT (MAP Medical Technologies Oy, Finland) intravenously. Before pretreatment scan, mice received 5 mg/kg paroxetin to block SERT binding of 123I-β-CIT. Dynamic SPECT acquisitions were performed with NanoSPECT/CT system (Bioscan inc.,USA) from 5 minutes post injection until 4 hours, covering 13 time points. Images were reconstructed and co-registered with the DAT-SPECT-template, created in our previous study. The template was modified to include also a volume of interest of midbrain region to extract time activity curves from both striata, cerebellum and midbrain regions. We used the binding potential (BP), which represents the ratio of the distribution volumes of the specifically and the non-specifically bound compartment, to analyze the 123I-β-CIT kinetics. Results and Conclusion: The SPECT images showed striatal and midbrain uptake over the baseline scanning. Post-injection uptake was more rapid in the midbrain volume, peaking within 1 hour while striatum peaked around 2 hours. In the midbrain volume, there was a marked signal loss in the pretreatment scan compared to the baseline scan. This result refers to the successful SERT blocking. This study confirmed that we can

image dynamically 123I-β-CIT kinetics of SERT and DAT in a mouse brain using SPECT.

P08-2 - Tuesday, Oct. 22, 16:00 - 16:30, Poster Exhibition Area

## Molecular & Multimodality Imaging: SPECT/CT

### P471

### Application of SPECT-CT in patients with suspicion of a vascular graft infection

**I. Kostadinova**, S. Ivanova, D. Zlatareva, S. Dineva; Medical University, Sofia, BULGARIA.

Vascular graft infection is a rare, but serious complication with a high rate of morbidity and mortality. Labeled leucocytes imaging could ensure its prompt and specific visualization for an efficient treatment. The aim of the study was to apply SPECT-CT in patients with suspicion of a vascular graft infection. We have examined 21 patients (Pts), aged 60-80 years, for a period of 4 years of whom 14 were with aortobifemoral, 2-with femorofemaral, 2-with axillofemoral and 3-with ileofemoral bypass. Fourteen of the patients were still under the antibiotic therapy, not enough clinically influenced by it. We have used "in vitro" labeled leukocytes with 99mTc-HMPAO (370MBq) and the following protocol of investigation: static/whole body SPECT-CT/low dose CT/, 2h p.i. The results of all patients were verified microbiologically, by surgery or by follow-up. An index of accumulation (IA) was used for an objective quantification of the results and for evaluation of the activity of the infection process. IA was calculated as the activity of the suspected area divided by the activity of the contralateral area, after both were normalized to the background activity. The infection was ruled out when IA was below 1.1 (in 2 Pts), low grade of activity was considered at IA of 1.1-1.3 (in 11 Pts) and active infection at IA above 1.3 (in 8 Pts). Using CT, exact localization of the infection was possible, differentiating infection along the vascular graft and/or infection in the soft tissues adjacent to the graft (in 4/21 Pts) or superimposed on bone marrow (in 2/21 Pts). In two of the patients additional fistula was visualized and in one - a perigraft abscess. As a whole, there were 2 false negative results (one of the Pts was still and another had recent antibiotic therapy), 1 false positive (due to non-infectious reaction to the graft), 16 true positive and 2 true negative results, yielding a sensitivity of 88.9%, specificity of 66.7% and accuracy of 85.7%. For 30% of the patients SPECT-CT contributed important additional information, which changed the therapy. In summary, we suggest that combining hybrid imaging with quantitative criteria for evaluation of the activity of the vascular graft infection ensures exact localization and measurement of the activity of the infectious process. In addition, collected information for the state of the surrounding tissues can influence the therapeutic strategy.

### P472

### Diagnosis of hip prosthesis infection by means of Nuclear Medicine: aiming to get maximal fidelity

**E. Servuli**[1], D. Strabykina[1], I. Znamensky[1], K. Zaplatnikov[2], V. Sukhov[3]; [1]Central Clinical Hospital of RAS, Moscow, RUSSIAN FEDERATION, [2]Clinic for Nuclear Medicine MÄZ, Nürnberg, GERMANY, [3]Military Medical Academy, St. Petersburg, RUSSIAN FEDERATION.

Introduction Endoprosthesis replacement after cervical hip fracture is the best option with the high rehabilitation potential. It has, however, complications, such as inflammatory changes and abarticulations. Routine clinical investigations: blood chemistry, X-ray, CT and MRI studies and synovial fluid aspiration may non-diagnostic or equivocal for this purpose. Differentiating infection from aseptic prosthetic failure (mechanical loosening) is especially important because of different types of therapeutic strategies. Aim To estimate efficiency of bone/WBC scans in diagnostics of non-/inflammatory changes as complications after total endoprosthesis replacement. Materials and Methods A total of 147 patients (mean age 57 ± 12 years) with total endoprosthesis replacement and postoperative hip pain were prospectively enrolled in our study. All patients underwent routine clinical and radiological examination and EDTMP/ZDA and/or HMPAO-WBC WB and SPECT/CT scans. Bone imaging was performed at arterial, soft tissue and metabolic phases. Tomographic data were reconstructed in orthogonal planes and compared with surgical and pathological findings. Results Bone scanning (especially with ZDA) showed increased tracer uptake in all patients with hip pains. Ten patients had osteoarthrosis of hip joint, and inflammation in soft tissues was revealed in 23 cases. Also high level uptake was associated with malrotation of femoral component (n=48). Revision surgery confirmed aseptic inflammation in 32 patients with high racer uptake. However, 34 cases of both bone-scan and WBC-evident inflammation had confirmed infections. Bone imaging had sensitivity of 100% in detecting prosthesis infections, but low specificity up to 62%. Routine WBC-scans (1-3 hrs p.i.) were less sensitive (50% vs 85%) and less specific (80% vs 100%) than delayed (24 hrs). All tests had a high negative predictive value for excluding infection (95%-100%). However, both bone (10%-24%) and routine WBC-imaging (38%) showed poor positive predictive value (PPV), whereas delayed WBC-imaging had PPV and diagnostic accuracy of 100% . Conclusions Bone scan with different tracers is an efficient (100%-sens) method for diagnostics of complications after total endoprosthesis replacement. WBC scan may show the inflammatory nature (septic or aseptic) more precisely, and may provide information for adequate patient management. Delayed WBC-imaging improves the specificity of diagnosis and should be combined with three-phase bone scintigraphy in studies of patients with painful joint replacement.

### P473

### Cardiac neurotransmission imaging with 123i-meta-iodobenzylguanidine in patients with atrial fibrillation

**Y. Lishmanov**, Y. Saushkina, I. Efimova, S. Minin, I. Kisteneva; Institute of Cardiology of the Siberian Branch of the Russian Academy of Medical Sciences, Tomsk, RUSSIAN FEDERATION.

**Introduction.** The mechanisms underlying the majority of cardiac arrhythmias are unclear. The disturbance sympathetic innervation of the heart may be the cause of atrial fibrillation (AF), but also reason of myocardial dysfunction of the left ventricle (LV). The aim of this study was assessment of cardiac sympathetic activity in patients with atrial fibrillation by planar scintigraphy with 123I-metaiodbenzilguanidine (123I-MIBG). **Materials and Methods.** The study included 39 (30 men and 9 women, average age 57,4 ± 11,6 years) patients with suspected coronary artery disease, hypertension 2-3 class. All patients to divide 3 groups: 15 patients (group 1) with paroxysmal AF (PAF), 12 patients (group 2) with long-standing persistent AF (LSPAF) and 12 patients with no signs of AF (group 3). Planar imaging was performed to study initial (imaging started 20 minutes after MIBG injection 148 MBq 123I-MIBG) and delayed (imaging started 4 hours after 123I-MIBG injection). For the anterior planar 123I-MIBG images, regions of interest were constructed for the heart and upper mediastinum, and the heart-mediastinal ratio (HMR) and corrected 123I -MIBG washout were calculated. **Results.** The delayed HMR in patients with PAF and LSPAF was significantly lower compared that in patients third group (1,59±0,16, 1,54±0,17 and 1,82±0,11, respectively, p <0,05). The washout rate of 123I-MIBG in patients with PAF and LSPAF was significantly highest compared that in patients with no signs of AF (33,4±17,5, 29±11,7 and 17,2±9,6, respectively, p <0,05). **Conclusion.** Results of this study indicated, that the patients with atrial fibrillation has of regional LV myocardial, according with 123I-MIBG imaging. More sympathetic innervation abnormality was observed in patients with atrial fibrillation.

### P474

### Clinical application of fusion image of myocardial perfusion / fatty acid metabolism SPECT and coronary CTA in patients with Takotsubo cardiomyopathy

**Y. Sugihara**, Y. Fukushima, S. Kumita, H. Hayashi, Y. Kobayashi, S. Imai; Nippon Medical School, Tokyo, JAPAN.

Clinical application of fusion image of myocardial perfusion / fatty acid metabolism SPECT and coronary CTA in patients with Takotsubo cardiomyopathy Takotsubo cardiomyopathy (TTC) is similar to acute coronary syndromes (ACS) in the pattern of onset. However, TTC is known for good prognosis compared with ACS. Although TTC causes apical hypokinesis and myocardial damage, the pathogenic mechanism hasn't been definitely understood. Fusion image of myocardial SPECT and coronary CTA (CCTA) is reported to improve the interpretation of coronary artery disease. In this study, we examined the diagnostic performance of SPECT/CTA fusion image in patients with TTC. Methods: Twenty consecutive patients (from January 1, 2007 to January 31, 2013) who were suspected TTC with apical hypokinesis were included in this study. All patients underwent perfusion (99mTc-MIBI 555MBq) / fatty acid metabolism (123I-BMIPP 148MBq) SPECT and coronary CTA within 2 weeks from the onset. All patients were classified to 2 groups according to the final clinical diagnosis: TTC (n=11) and ACS (n=9). LVEF, total defect score (TDS), and total mismatch score (TMS) were compared between 2 groups. Mismatch score (MS) in distal, middle, and proximal region was compared between 2 groups. Diagnostic accuracy was compared between SPECT only and SPECT/CTA fusion study. Image findings were determined under the agreement of 2 experienced nuclear cardiology specialists. Results: Although there were no significant differences between 2 groups in ages, sexes, LVEF, TDS, and TMS, significant differences were seen in distal MS ($P < 0.005$) and middle MS ($P < 0.05$). In the diagnostic accuracy of TTC, myocardial SPECT/ CTA fusion image was excellent (sensitivity: 82%, specificity: 100%, accuracy: 85%) contrast to myocardial SPECT (sensitivity: 64%, specificity: 78%, accuracy: 67%). Conclusions: Only with myocardial SPECT image, in a portion of the cases, it was hard to determine the diagnosis between TTC and ACS due to absence of coronary territory information. SPECT/CCTA fusion image enables to improve diagnostic performance of TTC.

### P475

### Artifacts in Attenuation-Corrected Myocardial Perfusion SPECT Introduced by Misalignment Between SPECT and CT About one case

**A. Benabderrahmane**, E. Haffaf; CENTRAL HOSPITAL OF ARMY, Kouba, ALGERIA.

Nonuniform soft-tissue attenuation affects the diagnostic accuracy of SPECT in myocardial perfusion imaging. The attenuation map required for attenuation correction can be acquired using x-ray tomography (CT). Frequent findings in attenuation-corrected images are defects in the apical and anterior myocardial wall. We assume that these artifacts are produced by misalignment of SPECT images and the attenuation map. PATIENTS AND METHODS: • A patient underwent myocardial perfusion imaging. • Review Protocol: physical stress test negative clinically and electrically issue followed by an injection of 15 mCi of 99mTc-MIBI. SPECT -CT acquisition 15 minutes after. • Gamma camera Bright View new XCT with dedicated software heart: Auto SPECT pro for image processing and Auto Quant to see the results. • Image processing using the following steps: Quality Control, Generation attenuation map (Map Generation AC) Reconstruction Astonish, Reorientation (short axis, horizontal long axis and vertical long axis) then Display. RESULTS: 1. The SPECT has demonstrated a decreased uptake at the lower wall. 2. Facing the negativity of the stress test was suspected attenuation level of the inferior wall attenuation correction. 3. The SPECT with attenuation correction has objectified a marked improvement in lower level with another hypofixation appearance at the antero-apical??? 4. After proper alignment of the two acquisitions (SPECT & CT) images and reprocessing ,we eliminated two artifacts (one of a diaphragmatic attenuation and the other to a misalignment of the two images (SPECT & CT) CONCLUSION: Misalignment between SPECT and the attenuation map can lead to artifacts in the apical and anterior wall, which will appear as defects. The coregistration of SPECT and the attenuation map needs to be verified for every patient.

## P476

### Prostate cancer imaging using a PSMA-targeted small-molecule, $^{99m}$Tc-MIP-1404: A phase I clinical study in patients undergoing radical prostatectomy

**S. Vallabhajosula**[1], D. Green[1], J. R. Osborne[1], A. Nikolopoulou[1], B. Robinson[1], S. J. Goldsmith[1], T. Armor[2], D. S. Scherr[1], J. W. Babich[2]; [1]Weill Cornell Medical College, New York, NY, UNITED STATES, [2]Progenics Pharmaceuticals, Inc., Tarrytown, NY, UNITED STATES.

**Introduction:** Critical challenges in imaging prostate cancer (PCa) are differentiating clinically significant from indolent disease within the gland and to identify metastatic and recurrent disease. Imaging PCa lesions within the gland is challenging with CT or MRI. Since prostate specific membrane antigen (PSMA) is up-regulated in aggressive PCa, a PSMA targeted radiotracer has potential as an imaging biomarker. We have previously reported the development of a number of small molecules which bind with high affinity to the enzymatic domain of PSMA (EJNMMI 2011;38:S202). We report here results from a pilot study of $^{99m}$Tc-MIP-1404 in patients scheduled for radical prostatectomy (RP) and pelvic lymph node dissection. **Methods:** Subjects (n=8) diagnosed with localized PCa (Gleason Scores (GS) ≥7 with ≥3 biopsy cores positive; at least one core ≥30%) and scheduled for RP participated in this study. Within two weeks prior to surgery, subjects received a single dose of $^{99m}$Tc-MIP-1404 (20 mCi) and had planar whole body and pelvic SPECT/CT images between 2-4 hours post-injection. Tracer uptake in prostate lesions was quantified and imaging results compared to CT/MR, histopathology and PSMA staining by immunohistochemistry (IHC). **Results:** All subjects completed the study yielding 60 evaluable prostate sectors. Greater than 80% of the sectors contained a PSMA-positive PCa nodule. The dominant tumor nodule was detectable by SPECT imaging in all patients and correlated with pathological location within the prostate. The lesion detection depended upon both PSMA expression and tumor volume. The tumor/background ratio was 10.8±2.2 with GS of 7, and 30±10 with GS of 9. In all subjects with GS $\geq$7, $^{99m}$Tc-MIP-1404 SPECT clearly identified the PCa foci confirmed by histopathology and PSMA by IHC. **Conclusion:** The small molecule PSMA inhibitor, $^{99m}$Tc-MIP-1404 rapidly detected primary and metastatic PCa with high specificity. $^{99m}$Tc uptake in the lesions correlated well with both GS and PSMA expression. The trend towards improved detection with increasing Gleason grade suggests the novel PSMA based small molecule SPECT imaging probe may be able to distinguish aggressive from indolent disease. Further development of this modality should include exploring its role in guiding focal therapy and active surveillance. Limitations of the study include small sample size and limits of SPECT resolution. A multi-center, international phase II study with $^{99m}$Tc-MIP-1404 in patients scheduled for prostatectomy is ongoing.

## P477

### Can 99mTc-etarfolatide (EC20) SPECT imaging identify ovarian cancer patients who are most likely to benefit from folate-receptor-targeted agent vintafolide (EC145)?

**R. W. Naumann**[1], W. Harb[2], J. Symanowski[1], C. Lovejoy[3], R. T. Morris[4]; [1]Levine Cancer Institute, Carolinas Medical Center, Charlotte, NC, UNITED STATES, [2]HORIZON ONCOLOGY CENTER, Lafayette, IN, UNITED STATES, [3]Endocyte, Inc., West Lafayette, IN, UNITED STATES, [4]Barbara Ann Karmanos Cancer Institute, Wayne State University, Detroit, MI, UNITED STATES.

Background: The folate receptor (FR) is overexpressed in ovarian cancer (OC) tumors and may be useful as both a biomarker for patient selection and as a therapeutic target. Vintafolide is a potent conjugate of folic acid and the vinca alkaloid desacetylvinblastine hydrazide. 99mTc-etarfolatide, a technetium-labeled folate, allows for full-body, real-time single-photon emission computed tomography (SPECT) imaging of FR expression of individual tumors. These 2 companion agents are co-developed in several clinical programs and the aim of this analysis was to evaluate the correlation of FR expression identified by 99mTc-etarfolatide imaging with benefit from vintafolide therapy in OC patients. Methods: In this phase 2 study, heavily pre-treated OC patients were first evaluated using 99mTc-etarfolatide to assess uptake in target lesions (identified per RECIST 1.0 criteria). Patients were categorized as FR(100%) (all target lesions FR positive), FR(10−90%) (≥1 but not all target lesions FR positive), or FR(0%) (no FR-positive target lesions). Patients then received vintafolide in an induction phase (1.0 mg intravenous [IV] bolus daily x 5 days for 3 weeks of a 4-week cycle x 2 cycles) followed by a maintenance phase (2.5 mg IV bolus daily x 3 days, weeks 1 and 3 of a 4-week cycle). Patients continued therapy until disease progression or unacceptable toxicity. Results: Patients with FR(100%) status demonstrated the greatest efficacy in both tumor response and survival endpoints. These patients experienced a doubling in median progression-free survival (PFS) (15.2 vs 7.4 weeks) and improvement in median overall survival (OS) (63.6 vs 41.7 weeks) compared with FR(10−90%) patients. PFS and OS hazard ratios (95% CI) were 0.797 (95% CI 0.362, 1.756) and 0.574 (0.213, 1.542), respectively, between the 2 FR-positive subgroups. FR(100%) patients also had >50% improvement in disease control rate (57.1% vs 36.4%) compared to FR(10-90%) patients. Furthermore, achievement of partial response (5.6% vs 0%) or stable disease (38.9% vs 33.3%) was numerically greater in FR-positive lesions than in FR-negative lesions, supporting the target-specific mechanism of action of vintafolide. Both 99mTc-etarfolatide and vintafolide were generally safe and well tolerated. Drug-related adverse events were reported in 4.7% of patients for 99mTc-etarfolatide (1.6% grade 3, no grade 4) and 89.8% of patients for vintafolide (30.6% grade 3, no grade 4), most commonly constipation, fatigue, nausea, anorexia, and neuropathy. Conclusions: These data in heavily pre-treated OC patients support this combined approach to personalized, predictive medicine using 99mTc-etarfolatide to identify patients most likely to benefit from FR-targeted treatment with vintafolide.

## P478

### The Contributions of SPECT-CT to Planar Whole Body Bone Scan

**A. Oral**, Ö. Ömür, B. Tuğral, E. Tekin, M. Argon; Ege University, Faculty of Medicine; Department of Nuclear Medicine, Izmir, TURKEY.

**Objective**: Bone scintigraphy is an imaging method which has low specificity despite its high sensitivity. In this study to investigate the contributions of SPECT-CT technique to whole body bone scintigraphy (WBBS) results was aimed in cases where anatomical localization data or differential diagnosis were required to be supported on the planar images of WBBS. **Methods**: Between August 2012 and January 2013 a total of 50 SPECT/CT of 47 cases were examined retrospectively. The patients were referred for Tc-99m MDP WBBS through different indications. The SPECT/CT images were performed if there was Tc-99m MDP uptake other than typical radiopharmaceutical accumulation sites in soft tissue or CT data were needed or certain locations could not be determined on planar images. Findings: Of the cases, 41 referred for malignancies (prostate carcinoma in 12, breast in 9, lung in 5 and other malignancies in 15) and 6 for WBBS for reasons other than malignancy. In 47 cases, 53 hyperactive foci were visualized by SPECT/CT images on a total of 50 visualization areas (3 patients had 2 different lesions on a SPECT/CT visualization area). 6 of the SPECT/CT images were obtained from cranium, 24 from thorax and 20 from abdomino-pelvic region. A differential diagnose was made by determining that the activity uptakes observed on planar WBBS and SPECT/CT images were associated with degenerative/traumatic changes in 16 patients (8 thorax, 8 abdomino-pelvic), metastatic lesions in 17 patients (11 thorax, 6 abdomino-pelvic). Besides this, to determine the anatomic location in 16 patients (6 cranium, 6 thorax and 4 abdomino-pelvic areas), to confirm that Tc-99m MDP accumulation is located in soft tissue out of bone in 3 cases (2 thorax, 1 abdomino-pelvic) and to establish that contamination of radiopharmaceutical in 1 patient could be possible through SPECT/CT images. **Conclusion**: When the results obtained were evaluated it was concluded that SPECT/CT technique is a method which increases specificity of the test significantly by providing differential diagnosis in areas where especially degenerative changes are observed on planar WBBS.

## P479

### In Vivo High Quality SPECT Imaging of Mouse Brains using I-125 Labeled Compounds

**K. Inoue**[1], I. O. Umeda[2], K. Tani[2], T. Saitou[2], N. Moriyama[3], M. Satake[2], M. Fukushi[1], H. Fujii[2]; [1]Tokyo Metropolitan University, Tokyo, JAPAN, [2]National Cancer Center Hospital East, Kashiwa, JAPAN, [3]National Cancer Center, Tokyo, JAPAN.

**Aim**: While iodine-125 (I-125) labeled compounds are commonly used in the research fields of life sciences, the energy of gamma rays emitted from I-125 is too low to clearly visualize the biodistribution of its radioactive compounds in vivo by routine SPECT tests. This study aimed at clear visualization of intracerebral distribution of I-125 labeled compounds by optimizing the conditions of image acquisition and reconstruction. **Materials and Methods**: A SPECT/CT scanner dedicated for small animal imaging (NanoSPECT/CT scanner, Bioscan, Washington, D.C., USA) was used to clearly acquire brain images of I-125 labeled iomazenil (IMZ)-treated mice. To establish the optimal conditions for image acquisition, spatial resolution, sensitivity and linearity of this device were measured, and the best projection numbers and acquisition counts for small animal imaging were studied. The proper injection dose of I-125 labeled compounds was determined through these investigations. Furthermore, to optimize the reconstruction of the SPECT images obtained, iteration numbers and size of pre-processing filter were examined. The SPECT images of mouse brains treated with I-125 labeled IMZ were acquired under the optimized conditions. These images were compared with those treated with I-123 labeled IMZ because the energy of gamma rays emitted from I-123 was similar to that of Tc-99m and the image quality of I-123 labeled compounds was usually acceptable. **Results**: The best spatial resolution and sensitivity of this scanner for I-125 were 1.1 mm and 2054 cps/MBq, respectively. Good linearity was shown between 0.05 and 3.18 MBq/ml. The optimal projection number and acquisition counts were determined as 24 projections and 40 Mcounts, respectively, in experiments using phantoms imitating small animals. This optimal acquisition counts were twice as high as that of Tc-99m. The optimal injection dose of I-125 labeled compounds was 13.2 MBq. The best iteration number and size of pre-processing filter were 72 and 35%, respectively. The quality of SPECT images of I-125 IMZ-treated brains acquired under the best conditions was comparable to that of I-123 IMZ. **Conclusion:** The optimized conditions of image acquisition and reconstruction for I-125 could successfully improve the quality of SPECT images of I-125 labeled compounds in vivo and enabled clear visualization of their intracerebral distribution.

## P480

### Method for Dialysate Volume Measurement throughout Peritoneal Dialysis in Small Animals using Micro-SPECT

I. CALM[1], A. ZALOSZYC[1], A. SAYEH[2], J. DILLENSEGER[2], C. GOETZ[2,3], M. FISCHBACH[1], **P. CHOQUET**[2,3]; [1]Hôpitaux Universitaires de Strasbourg - Nephrology Dialysis Transplantation Children's Unit, STRASBOURG, FRANCE, [2]Hôpitaux Universitaires de Strasbourg - Preclinical Imaging Lab UF6237, STRASBOURG, FRANCE, [3]ICube, CNRS, Strasbourg, FRANCE.

AIM: Peritoneal dialysis (PD) efficiency depends on physical parameters such as dialysate volume and peritoneal surface. Studying the progress of PD in small animals suffers from their small size: limiting dialysate sampling for measuring volume, is mandatory. We propose to monitor the volume of dialysate during a PD process in mice using micro-SPECT, combined with peritoneal surface measurement with micro-CT. We first evaluated the uncertainty of these measurements, to ensure that they could be useful. To this end, phantoms, with known geometrical characteristics, were used to compare the results obtained from images to the ones calculated from their geometry. This methodology will be then applied in live animals. MATERIALS AND METHODS: Syringes of 60 ml and 5 ml were filled with a solution that contained water, 10% of an iodinated contrast agent, (Visipaque 320 mg I/ml, GE Healthcare) and 150 to 200 MBq of $^{99m}$Tc labeled macro-aggregates of albumin (Technescan LyoMAA, Mallinckrodt). Images were obtained using a microSPECT-CT (eXplore speCZT 120 Vision, GE). The CT scan was done at 70kV/32mA leading to reconstructed voxels of 100x100x100 µm$^3$. 5 slits and 8 slits collimators were employed for SPECT acquisitions, for the 60 ml and 5 ml syringes respectively. Total scan time was approximately 5 minutes. Volumes were calculated from the distribution of the labeled nanocolloids after thresholding (Otsu's method) and peritoneal surface was extracted from CT data [Breton & al. Peritoneal Dialysis International, 2008]. RESULTS: We found out a strong linear relationship between the values obtained by SPECT and the volume calculated from phantom's geometry ($R^2$ = 0,99) for a range of volumes from 5 ml to 40 ml, as well as for volumes from 2 ml to 5 ml ($R^2$ = 1). In addition, the linear relationship between the internal surface of our phantom obtained by µCT and the surface calculated from geometry was $R^2$ = 0.99 for both ranges of volumes. The relative error was smaller than 5% for all the cases. CONCLUSION: Taking into account that the fill volume in mice is 1 to 2 ml, 25 to 45 ml in rats, we can confirm that our method is precise and accurate enough in order to evaluate the volume and the peritoneal surface area during DP in small animals.

P09-2 - Tuesday, Oct. 22, 16:00 - 16:30, Poster Exhibition Area

## Molecular & Multimodality Imaging: PET/CT

## P481

### Dynamic FDG PET in liver metastases of colorectal cancer: repeatability of dynamic and static FDG PET parameters.

**L. Heijmen**[1], H. W. M. van Laarhoven[2], J. W. de Wilt[1], J. Bussink[1], W. J. G. Oyen[1], E. P. Visser[1], L. de Geus-Oei[1]; [1]Radboud University Medical Centre, Nijmegen, NETHERLANDS, [2]Academic Medical Centre, University of Amsterdam, Amsterdam, NETHERLANDS.

**Aim:** The aim of this study was to assess repeatability of dynamic FDG PET in colorectal liver metastases. We compared the repeatability of quantitative analysis to the repeatability of static FDG PET parameters. **Methods:** Eleven patients scheduled for metastasectomy of colorectal liver metastases were approached for study participation. Two 60-minute dynamic FDG PET scans were performed within one week. In the last time frame (50-60 minutes) the tumors were delineated with a background corrected threshold method (41% above background) and a 70% isocontour, to determine the $SUV_{MAX}$, $SUV_{SBR}$ and $SUV_{70}$. The metabolic rate map was calculated and the tumors were delineated using a 50% and 70% isocontour to determine maximum metabolic rate ($MR_{glu}$), $MR_{glu50}$ and $MR_{glu70}$. The coefficient of repeatability (CR) was calculated. **Results:** Nine patients had 15 FDG PET positive lesions; two patients had no FDG uptake in the liver metastases. The CR of $MR_{glu}$ was superior compared to semi-quantitative PET parameters. The CR was 32.5%, 33.4% and 30.1% for the maximum $MR_{glu}$, $MR_{glu70}$ and $MR_{glu50}$. The CR was 40.9% for the $SUV_{MAX}$, 41.6% for the $SUV_{70}$ and 37.7% for the $SUV_{SBR.}$ Repeatability of volume measurements slightly improved by delineation on the parametric maps (best CR: $MR_{glu50}$ volume 68%). Volumes on the 70% isocontour did not significantly differ between the $MR_{glu}$ and SUV measurements (2470 mm$^3$ vs. 2926 mm$^3$ respectively, p=0.07). **Conclusion:** Repeatability of $MR_{glu}$ was superior to the repeatability of semi-quantitative PET parameters, but only mildly improved repeatability

## P482

### Comparison of different metabolic indices for therapeutic response evaluation by PET in metastatic breast cancer.

**D. GOULON**[1], B. HENAFF[1], H. NECIB[1], T. CARLIER[1], C. ROUSSEAU[2], F. KRAEBER-BODERE[1]; [1]CHU, NANTES, FRANCE, [2]ICO, NANTES, FRANCE.

**Aims**: FDG PET/CT is useful in therapeutic response evaluation in breast cancer. This retrospective study aimed at comparing the performance of metabolic assessment, according to PERCIST criteria, using 6 different indices and defining their best threshold, for metastatic breast cancer patients treated by chemo or hormone-therapy. **Methods**: Seventeen patients, who underwent from 2 to 6 PET, during the follow-up were included. For each lesion, 6 indices were measured: maximum standardized uptake value (SUVmax), SUVpeak, standardized added metabolic activity (SAM), metabolic volume (MV) and SUVmean using an adaptative threshold, and total lesion glycolysis (TLG). The % change for each lesion between each PET was calculated for the 6 indices. The gold standard was defined by clinical, biological and RECIST 1.1 evaluation using CT-scan or MRI. A per-lesion and a per-patient analysis were performed to determine the best cut-off of each indices and compare **Results**: For the per-lesion analysis, a total of 48 lesions and 108 evaluations, 69 responding (R) and 39 non-R, were analyzed. Using ROC curves, no significant difference was found between each indices, except VM. SUVmax, SUVpeak, and SUVmean showed the best area under the curve (AUC) 0.88, 0.88, 0.84, respectively, and a Youden correlation coefficient of 0.72, 0.66, and 0.67, respectively. SAM, TLG and VM appeared less accurate (AUC: 0.75, 0.73 and 0.53, respectively). Using the best threshold defined at -36%, -24% and -34% for SUVmax, SUVpeak, SUVmean respectively, SUVmax appeared as the most accurate parameter (accuracy: 83%). Sensitivity of SUVmax, SUVpeak, SUVmean were 74%, 76%, 70%, and specificity 98%, 90%, 98%, respectively. For the per-patient analysis, a total of 36 pairs of PET scans (R=21 and NR=15) were analyzed. Only SUVmax and SUVpeak were significantly correlated with the gold standard, with a Youden correlation coefficient of 0.74 and 0.81. SUVpeak appeared the most accurate parameter with an accuracy of 89% (86% for SUVmax). Sensitivity of SUVmax and SUVpeak was 81% for both, specificity 93% and 100%, positive predictive value 94% and 100%, and negative predictive value 78% and 79%, respectively. **Conclusion**: This study showed that SUVmax and SUVpeak are the best indices to assess therapy response in metastatic breast cancer.

## P483

### The Influence of Misalignment Artifact Due to Global and Respiratory Motion on Interpretation of Cardiac PET/CT Examination: Clinical and Phantom Studies

**P. Ghafarian**[1,2], M. R. Ay[3,4,5]; [1]Chronic Respiratory Disease Research Center, NRITLD, Masih Daneshvari Hospital, Shahid Beheshti University of Medical Sciences, Tehran, IRAN, ISLAMIC REPUBLIC OF, [2]Telemedicine Research Center, NRITLD, Masih Daneshvari Hospital, Shahid Beheshti

University of Medical Sciences, Tehran, IRAN, ISLAMIC REPUBLIC OF, [3]Department of Medical Physics and Biomedical Engineering, Tehran, IRAN, ISLAMIC REPUBLIC OF, [4]Medical Imaging Group, Research Center for Molecular and Cellular Imaging,, Theran, IRAN, ISLAMIC REPUBLIC OF, [5]Research Center for Nuclear Medicine, Tehran University of Medical Sciences, Tehran, IRAN, ISLAMIC REPUBLIC OF.

**Introduction**:In cardiac PET/CT imaging, as CT images are used for attenuation correction (CTAC), erroneous myocardial uptake values in PET images can produce due to global physical motion of patients and also with respect with different temporal resolution between two modules. In this study the influence patient motion and various respiratory and cardiac cycles on apparent uptake value of myocardium PET images were evaluated. **Methods:** for consideration of physical motion, the attenuation and emission data were obtained using both RSD phantom and 3 patients including one perfusion and two viability examinations acquired on the Biograph TP 64 PET/CT scanners. The manually shifted CT from 0 to 20 mm in steps of 5mm in six different directions was applied. The reconstructed PET images using misaligned CT were compared with the original PET images. The impact various respiratory and cardiac phases in CTAC on the reconstructed myocardium PET image were investigated using the XCAT phantom applied to generate activity and attenuation maps. Emission data reconstructed using forward projection by STIR software. The analyses of the PET images were performed by VOI-based analysis in corporation to the Box and Whisker plots and semi-quantitative analysis were also considered by the bull's eye view model. Furthermore for better qualitative consideration, PET images were also reoriented along the short axis, horizontal and vertical long axis views. **Results:** In patient images, especially in 20-mm shift between the CT and PET data, the significant errors were observed in the anteroseptal (23.6±9.9) and lateroinferior (33.0±9.7) segments of the myocardium in backward and forward directions, respectively. The XCAT study revealed that the PET images reconstructed with attenuation map at end-exhalation can induced overestimated activity in all segments of the myocardium that in contrast to end-inhalation of respiratory phase. Moreover the amplitude of the erroneous uptake value in myocardium were more sever in end-exhalation versus to end-inhalation respiratory cycle. **Conclusion:** Errors in uptake values of PET images even with a 5-mm shifted CT especially in right, backward and forward directions caused to misinterpretation of PET images. Although the mismatch can lead to the variation in all segments of myocardium but the anterior and lateral walls were more vulnerable regions. Using of attenuation map at mid-inhalation and mid-exhalation of the respiratory phase can introduce to significantly decrease of errors in myocardium but also a little overestimation of activity in all segments of myocardial wall were also observed.

## P484

### A Nomogram to Improve Outcome Prediction of Patients with Hodgkin Lymphoma Treated with Chemotherapy

**L. Strigari**[1], A. Chiaravalloti[2], A. Duggento[3], A. Attili[4], M. Guerrisi[3], O. Schillaci[5]; [1]Regina Elena National Cancer Institute IFO, Roma, ITALY, [2]Dept. of Biomedicine and Prevention, University of Rome Tor Vergata, Roma, ITALY, [3]Medical Physics Section, Dept. Biomedicine and Prevention, University of Rome Tor Vergata, Roma, ITALY, [4]Istituto Nazionale Fisica Nucleare, sez. Torino, Torino, ITALY, [5]Dept. of Biomedicine and Prevention, University of Rome Tor Vergata, Roma, ITALY.

**Aim:** During last years the interim-PET has been reported as a powerful tool to predict the outcome of Hodgkin Lymphoma(HL) treated with chemotherapy. However, as a major drawback, the predictive power is limited by the lack of an uniform and reliable criteria for imaging interpretation. In addition, the information from CT images are not currently used in the algorithm for predicting relapse. Aim of the present study is to improve the prognostic value of basal and interim-PET/CT in patients with HL through the use of quantitative analysis. **Materials and Methods**:A cohort of 70 patients, undergo to basal(PET/CT0) for HL staging and an interim(PET/CT2) with 18F-FDG after 2 cycles of chemotherapy, were examined. From the cohort two subsets of 7 patients were selected, one set with a positive PET/CT2 scan and the other set with a negative PET/CT2 scan. Matches have been based on tumour stage and patient age. After PET/CT0, all the patients were treated with ABVDx2 cycles consisting in Doxoroubicin(Adriamycin), Bleomycin, Vinblastine,Decarbazine for 2 months. PET/CT2 examination has been carried out 15±5 days after ABVD treatment. According to standard guidelines in HL treatment, after PET/CT2 chemotherapy was ABVD or BEACOPP in 10 and 4 Patients, respectively. A Discovery ST16(GE,Medical Systems,Tennessee,USA) using a 3D-mode standard technique in 128x128 matrix, was used to acquire PET/TC. A total of 10 lymph-node lesions showing a good response to chemotherapy were contoured on the co-registered PET/CT images of the patients with a positive PET/CT2 scan; 6 responder and 12 relapsing lymph-node lesions were selected on the co-registered PET/CT images of patients with a negative PET2 scan. SUV and Hounsfield Unit(HU) values included in the volumes contoured on PET/CT0 and PET/CT2 were extracted and used to generate a database including stage, weight, sex and age of patients. A linear regression model was used to identify the predictor of relapse at the voxel levels and was presented as a nomogram. **Results and conclusion:** SUV at the basal/interim study and HU values resulted as predictor of poor prognosis. In particular, the higher points were associated to lower values of SUV at PET/CT0, at the higher values of SUV at PET/CT2 study, and at the lower basal HU numbers. A nomogram was generated to identify the subvoxels at the highest risk of relapse, using the full information from basal/interim PET/CT study.

## P485

### Seasonal difference in presence of inflammatory cervical lymph nodes in patients undergoing whole body FDG-PET/CT scans

**T. Vask**, L. Karusoo, R. Brand, M. Paris, S. Nazarenko, A. Samarin; North Estonia Medical Centre, Tallinn, ESTONIA.

**Aim** There is a substantial increase in upper respiratory tract infections in Estonia during a cold season from September till April. The aim of the study was to investigate whether it will result in higher prevalence of inflammatory cervical lymph nodes on FDG-PET/CT scans. **Methods** The imaging data of 168 patients who underwent whole body PET/CT scan during years 2009-2011 was retrospectively analyzed for the presence of the cervical lymph nodes with an increased FDG uptake compared to surrounding soft tissues. Only the patients with primary tumor below the diaphragm and melanoma were selected for the study. A two-year minimum clinical follow-up and absence of chemo- or radiotherapy during this period ensured the inflammatory and not metastatic nature of increased FDG uptake. **Results** 18 patients showed increased FDG uptake in cervical lymph nodes consistent with inflammatory changes with the mean SUVmax 3.1+/-0.94 (range 2.1-5.5). There was substantially higher number of patients with inflammatory lymph nodes during the cold season from September till April compared to the period from May till August, 12 patients (SUVmax 3.0+/-1.1) and 6 patients (SUVmax 3.2+/-0.6), respectively. **Conclusion** According to our study about 10% of patients undergoing whole body FDG PET/CT scan can present with inflammatory cervical lymph nodes. The prevalence of inflammatory lymph nodes is markedly higher during the cold season from September till April - an important consideration in interpretation of oncological whole-body PET/CT scans.

## P486

### The Influence of Respiratory Motion Induced Artifacts on SUV Calculation in Lung PET/CT Imaging

**H. Soufi**[1], P. Ghafarian[2,3], S. M. R. Aghamiri[1]; [1]1 Department of Radiation Medicine, Shahid Beheshti University, Tehran, IRAN, ISLAMIC REPUBLIC OF, [2]Chronic Respiratory Disease Research Center, NRITLD, Masih Daneshvari Hospital, Shahid Beheshti University of Medical Sciences, Tehran, IRAN, ISLAMIC REPUBLIC OF, [3]Telemedicine Research Center, NRITLD, Masih Daneshvari Hospital, Shahid Beheshti University of Medical Sciences, Tehran, IRAN, ISLAMIC REPUBLIC OF.

Introduction:Although CT image is acquired in afew seconds and PET image is achieved in a several minutes, respiratory motion artifact is the natural result in PET/CT imaging, so some errors can be produced in the estimation of activity in PET/CT images. In this study, we evaluated variations in Standardized Uptake Values (SUVs) in different location of the lung region. Methods: The XCAT software phantom used for simulation of the body and lung lesions with 8,15 and 30 mm in diameter in different location of lung region. The XCAT phantom has a high potential in the field of breathing and heart motion modeling. The Phantom also is able to show the distribution of activity and attenuation coefficients for the various organs in any desired energy. PET/CT datasets reconstructed with STIR software. This software is an image reconstruction software which allows providing a three-dimensional reconstruction of the raw data set obtained from the PET scanner or simulation. Atenuation maps were abtained at end-inhalation and end-exhalation respiratory phases and emision data were acquired in averaging respiratory phase. The corrected PET image at averaging phase used as a reference because of smaller mismatch. SUV and the lesion volume in PET image at end-inhalation and end-exhalation respiratory phases were evaluated and compared with reference PET image. Results: We analyzed 11 tumor's datasets in various parts of left and right lung region. This investigation showed that the overestimate of 87.98% and 44.47% for tumor's SUV in end-exhalation breathing protocol for lesion with 8 and 15 mm diameter that were located in the lower right lung and above the liver. Most changes were observed in the size of lesions at end-inhalation respiratory phase, for lower left lung tumor with values 86.98% and 66.67% for the primary tumor diameter of 8 and 15 mm. Morover the underestimation SUV lesions of 43.99%, 39.85% and 3.23% were clear in end-inhalation for tumor with 8, 15 and 30mm in diameter respectively. Conclusion: Misalignment due to respiratory motion, in end-exhalation cycle produced greater SUV than the average respiratory cycle in the lung tumors. It should be noted that the amplitude of the errors were increased when the tumors were in the lower versus upper lung region. Furthermore smaller lesions were more sensitive to respiratory motion than larger lesions and the artifact due to respiratory motion were more obvious for lesions in the lower lung region close to the liver dome.

## P487

### Reduction of activity in time-of-flight PET FCH in initial stadging or biochemical recurrence in prostate cancer

**L. Michaud**, J. Ohnona, K. Kerrou, V. Huchet, M. Wartki, F. Montravers, S. Balogova, J. Talbot; Tenon hospital, Paris, FRANCE.

**Introduction** : The superiority of fluorocholine (18F) (FCH) PET/CT compared with fluorodeoxyglucose PET/CT has been showed in prostate cancer and hepatocellular carcinoma. It is underused because of its high cost. Currently, time-of-flight cameras can increase the sensitivity of PET exams. We decided to study the reduction of activity in time-of-flight PET FCH in initial staging or biochemical reccurence in prostate cancer. **Methods** : To simulate half activity, we used a « low dose » reconstruction protocol. 41 exams were performed prospectively and reconstructed in 2 minutes increments and 1 minute increment (the latter simulating half activity). First of all we compared SUV max between the images of 2 minutes and 1 minute on two regions considered as background noise : L5 vertebra and liver. Then, all 82 exams obtained were read blinded by 2 nuclear physicians experts. For readings blinded images were analyzed by regions (prostate, seminal vesicles, lymph nodes under the diaphragm, bones and other). **Results** : Semi-quantitative analysis showed that the reconstructed images in 1 minute were noiser than those reconstructed in 2 minutes. The inter-observer analysis showed a difference between readers only for the interpretation of seminal vesicles. The intra-observer analysis showed only one significant difference for the analysis of seminal vesicles for one of the reader. **Conclusion :** A reduction of FCH activity is possible for targeted indications namely therapeutic monitoring of prostate cancer or possibly its biochemical reccurence. Our study requires further investigations to confirm the feasibility.

P10-2 - Tuesday, Oct. 22, 16:00 - 16:30, Poster Exhibition Area

## Molecular & Multimodality Imaging: SPECT & SPECT/CT

## P488

### The Added Value of 99mTc-sestamibi SPECT/CT Over Combined Radionuclide Imaging with Tc-99m MDP/MIBI: A Pilot Study for Patients with Fibrous Dysplasia

T. Ones, **M. Aras**, F. Dede, S. Gungor, S. Ozguven, R. Maleki, T. Y. Erdil, S. Inanir, H. T. Turoğlu; Marmara University School of Medicine Nuclear Medicine Department, Istanbul, TURKEY.

Fibrous Dysplasia (FD) is a non-neoplastic developmental disorder of bone, in which normal bone is replaced by abnormal fibro-osseous tissue. Utility of the combined radionuclide imaging with Tc99m MDP/MIBI for evaluation of the potentially operable symptomatic FD lesions have been reported in the literature. However, because of the physiological biodistribution of Tc-99m MIBI some lesions could not be evaluated in these procedures. In this study we aimed at assessing the impact of 99mTc-sestamibi SPECT/CT over combined radionuclide imaging for these equivocal lesions. We also aimed to establish whether 99mTc-sestamibi SPECT/CT add further information about the potentially operable symptomatic lesions. Six patients with histopathologically confirmed FD aged between 15-55 years-old (mean age: 36±13 years) were evaluated with Whole Body Tc-99m MDP Bone Scintigraphy (MDPBSc) and Whole Body Dual Phase Tc-99m MIBI Scintigraphy (DuPhMIBISc). All of the equivocal and symptomatic lesions evaluated with 99mTc-sestamibi SPECT/CT. In all patients, MDPBSc showed increased uptake in all of the FD lesions. A total of 23 bone lesions in six patients and five symptomatic lesions in two patients were evaluated. Lesions were monostotic in four patients and polyostotic in two patients on MDPBSc. The patients were followed up for a mean duration of 78 months after the initial evaluation. Among all of the lesions, 99mTc-sestamibi SPECT/CT images have been provided additional information in two patients with four lesions. In one patient with SPECT/CT images, the symptomatic FD lesions (3 lesions) have been evaluated more accurately and these findings improved the preoperative assessment for guiding surgical treatment. In another patient, an equivocal nonsymptomatic lesion showed no pathological uptake in the SPECT/CT images. Compared to the literature, our 99mTc-sestamibi SPECT/CT findings have provided additional information about "dual-phase planar MIBI imaging" in patients FD who were positive for all lesions on bone scans. This study is the only one to date that to assess the impact of 99mTc-sestamibi SPECT/CT over combined radionuclide imaging in FD patients. MDPBSc is useful in determining the extent of the skeletal involvement. It seems that 99mTc-sestamibi SPECT/CT imaging of the FD lesions may have a role in improving the preoperative assessment. Also, it seems 99mTc-sestamibi SPECT/CT imaging have been provided additional information about "Dual Phase Planar MIBI Imaging" in FD patients.

## P489

### SPECT / CT with 99mTc-labeled leukocytes HMPAO in patients with suspected prosthetic infection.

**R. García Jiménez**[1], J. Lojo Ramirez[1], F. Luis Simon[2], R. M. Alvarez Pérez[1], R. Vazquez Albertino[1]; [1]UGC Diagnostico por Imagen Hospital Universitario Virgen del Rocío, Sevilla, SPAIN, [2]UGC Radiofísica Hospital Universitario Virgen del Rocío, Sevilla, SPAIN.

**Objective**: To determine the diagnostic utility of SPECT / CT bone scan studies with 99mTc-labeled leukocytes HMPAO in suspected septic prosthetic mobilization. **Methods**: We analyzed retrospectively the results of examinations of 49 patients (30 women and 19 men) from January 2010 to December 2012, with a mean age of 63.73 (21-83) years, with clinically suspected prosthetic infection. All planar images were performed at 1 hour and 4 hours post-injection, after administration of a dose of 240-370 MBq of 99mTc-labeled leukocytes HMPAO. In addition, they performed at 4 hours, a SPECT / CT in the region studied. Diagnostic confirmation was made by biopsy or clinical follow-culture (6-30 months). **Results:** 49 prostheses were studied: 36 total knee and total hip replacement 13. The results obtained when planar scintigraphy is evaluated were 7 true positive (TP), 36 true negative (TN), 0 false positives (FP) and 6 false negative (FN), with values of sensitivity (S ), specificity (Sp), positive predictive value (PPV), negative predictive value (NPV) and accuracy of 53.8%, 100%, 100%, 85.7% and 87.75% respectively. With the SPECT / CT images , the final diagnosis was modified in three patients initially regarded as negative, thus obtaining results of 10VP, 36 VN, 0FP and 3 FN, with values of S , E, PPV, NPV, and accuracy of 76.9%, 100%, 100%, 92.3% and 93.8% respectively. **Conclusion**: The completion of the SPECT / CT as complementary planar scintigraphy added to, increased sensitivity, diagnostic accuracy and negative predictive value of the study in patients with suspected septic prosthetic mobilization, being especially effective in initially considered negative.

## P490

### Added Value of Technetium-99m HMPAO-Labelled Leukocyte SPECT/CT in Diagnosing and Management of Patients with Suspected Infection; the Singapore Experience.

**S. Mok**, B. M. Magsombol, W. W. Lam; Singapore General Hospital, Singapore, SINGAPORE.

Value of Technetium-99m HMPAO-Labelled Leukocyte SPECT/CT in Diagnosis and Management of Patients with Suspected Infection; the Singapore Experience. The diagnostic accuracy and management of patients with suspected infection can be augmented with the use of functional imaging Methods such as radio-labelled leukocyte (Technetium-99m [Tc-99m] hexamethylpropyleneamine oxime [HMPAO]-labelled white blood cell [WBC]) scan. **Methods:** Retrospective evaluation of Tc-99m HMPAO-WBC scintigraphy combined with SPECT/CT imaging dated from August 2008 to December 2012 was performed. Scintigraphy results were correlated with outcome stated in the electronic hospital inpatient discharge summary (HIDS) records, electronic surgical reports or follow-up imaging. **Results:** From August 2008 to December 2012, 300 Tc-99m HMPAO-WBC studies were performed. Additional SPECT/CT imaging with hybrid scanner was done in 88 studies (29.3%). Forty-seven of the 88 scans were reported as positive on SPECT/CT imaging (53.4%) with 34 male patients (age range 14 to 86 years) and 13 female patients (age range 43 to 82 years). The sites of infection were categorised into: vascular graft (12.8%), prosthesis/external device (6.4%), head and neck region (21.3%), intra-thoracic (17.0%), intra-abdominal (25.5%), extremities (6.4%), skeletal system (6.4%) and other sites (4.2%). Fifteen of these scans (17.2%, 15/88) resulted in either surgical or medical intervention. Intervention included removal/revision/ligation of a vascular graft, localisation of biopsy site and change of antibiotic regime. **Conclusion:** Tc-99m HMPAO-WBC scintigraphy combined with SPECT/CT imaging provides additional information in localisation of infective sites in cases where the source of sepsis is not obvious on clinical findings or via other imaging modalities. Our results show that addition of SPECT/CT to planar functional imaging such as Tc-99m HMPAO-WBC scintigraphy augments the diagnostic accuracy in difficult cases. Therefore, SPECT/CT can be also incorporated into other nuclear medicine imaging procedures such as tagged red blood cell scan (for localisation of bleeding points) or ventilation/perfusion lung scan (for localisation of segmental defects) to aid clinicians in improving patient management.

## P491

### Usefulness of fusion imaging of $^{201}$Tl-SPECT and brain MRI in diagnosis of malignancy of gliomas

**A. Abe**, S. Oya, T. Matsui; Saitama Medical Center, Kawagoe, JAPAN.

*Aim* The aim of this study is to investigate the usefulness of the fusion imaging of the $^{201}$Thallium ($^{201}$Tl)-single photon emission computed tomography (SPECT) and brain magnetic resonance imaging (MRI) in the diagnosis of the malignancy of the gliomas. *Materials and Methods* Twenty patients who underwent both the $^{201}$Tl SPECT and the brain MRI before the operation and proved histopathologically between 2006 and 2012 were included in this study. The early imaging and the delayed imaging were acquired 15 minutes and 3 hours 15minutes after the intravenous injection of $^{201}$TlCl respectively. The circular region of interest (ROI) was placed over the brain tumor (T) of the fusion image of the $^{201}$Tl-SPECT and T2-weighted image of the brain MRI. The ROI placements over the brain tumors were

possible using the fusion images even when the uptake of the brain tumor were so slight that the perfect placements of the ROI were difficult. And the fusion images confirmed that the increased uptake were over the intraaxial tumors. The same-size ROI was placed in the background (N) on the contralateral side and the uptake ratio was defined as T/N. The uptake ratios of the early imaging (ER) and the delayed imaging (DR) were calculated and the retention index (RI) was defined as follows: RI= (DR-ER)/ER. *Results* The precise ROI placements over the intraaxial tumors were possible with the fusion images which were impossible with the $^{201}$Tl-SPECT alone. Both the ERs and DRs of all the benign gliomas were 3.6 or less (100%). The ERs or DRs over 3.6 of the intraaxial tumors, therefore, indicate malignancy. RIs were not directly contributed to the diagnosis of the malignancy of the gliomas. *Conclusion* The fusion images of the $^{201}$Tl-SPECT and brain MRI were useful to diagnose the malignancy of the intraaxial brain tumors. Although the delayed imaging of $^{201}$Tl-SPECT is believed to represent the malignancy of the tumors, the results suggest that the fusion imaging of the early images is sufficient to diagnose the malignancy of the gliomas and the delayed imaging is not necessary.

## P492

### Comparison of SPECT/CT, Planar Imaging and Conventional Ultrasonography in Localization of Parathyroid Adenomas

**S. Ince**, A. O. Karacalioglu, O. Emer, E. Alagoz, N. Arslan, B. Gunalp, M. A. Ozguven; Gulhane Military Medical Academy, Ankara, TURKEY.

OBJECTIVE: Parathyroid scintigraphy is helpful to localize the lesions in patients with biochemically proven hyperparathyroidism before initial surgery and is mandatory before reoperative surgery for persistent or recurrent disease. The aim of this study is to evaluate the efficacy of different imaging techniques and modalities to localize the parathyroid lesions. MATERIAL AND METHOD: Fifty-two patients (35 women, 17 men, mean age±SD:52±35) with elevated serum parathyroid hormone and calcium levels were included into the study. MIBI, a lipophylic compound, was radiolabeled with 99mTc and it was injected to the patients in a dose of 20±5 mCi. Planar imaging at 20 min and 2 h and tomoscintigraphy (SPECT/CT) acquisition at 120 min were performed. Ultrasonography (US) was also performed to each patient for anatomic correlation. RESULTS: Lesions were detected in 32, 34 and 36 patients by planar imaging, US and tomoscintigraphy, respectively. 13 patients had no lesions at all imaging modalities. Two lesions localized at retrotracheal region were only detected by tomoscintigraphy because it's outside the field of view of US. Besides, two small lesions detected by ultrasonography were not imaged by planar imaging. CONCLUSION: Tomoscintigraphy seems to be superior imaging modality to detect parathyroid lesions. Tomoscintigraphy may also detect adenomas prolapsed behind the lower pole of the thyroid gland. These adenomas can be located paraesophageal or retroesophageal locations and may be missed by neck ultrasound or planar scintigraphy as in our study. SPECT may provide improvement in sensitivity in comparison to planar imaging. Small parathyroid adenomas detected by US are usually missed by planar scintigraphy. Therefore anatomic correlation is a complementary workup in parathyroid lesion detection.

P11-2 - Tuesday, Oct. 22, 16:00 - 16:30, Poster Exhibition Area

## Molecular & Multimodality Imaging: New Methods & Tracers

## P494

### PET/MRI/SPECT/CT in vivo longitudinal imaging of Earthworm (Lumbricus terrestris L.), as a novel aspect for toxicological testing

F. Budán[1], N. Kovács[1], I. Horváth[2], D. Veres[2], P. Engelmann[3], P. Németh[3], **K. Szigeti**[2], D. Máthé[1]; [1]CROmed Ltd, Budapest, HUNGARY, [2]Semmelweis University, Budapest, HUNGARY, [3]University of Pécs, Pecs, HUNGARY.

**Introduction**. Anellid species are used widely in toxicological (carcinogens and noxious metals) tests. Most toxic heavy metals in vivo mimic physiological ions and some of them form covalent bonds with sulfhydryl groups of proteins. Animal tests end-points are mostly the alteration in body mass and in reproductive capacity. Aims. The purpose of this study was to offer to the aforementioned tests a valuable longitudinal quantitative in vivo molecular imaging supplement based on PET/MRI and SPECT/CT. Reducing animal number, experiment duration and increasing data robustness and repeatability are all in favor of in vivo imaging tests. **Materials and Methods.** To visualize organs with higher resolution, larger sized earthworm Lumbricus terrestris species were used. To detect glucose metabolism after intra-coelomic (ic.) injection of cca. 3 MBq of 18F-Fluoro-D-deoxyglucose (FDG) we recorded whole body PET data with a nanoScan PET/MRI (Mediso, Hungary). Data were acquired in list mode PET during 60 minutes in 4 animals. For MRI imaging T1 weighted spoiled gradient echo sequence was used with 3 dimensional acquisition scheme. [201Tl]Thallous chloride solution (cca. 12 MBq per animal) was injected ic. in other 4 animals, while in 3 animals [123I]Iodide solution was ic. applied. SPECT/CT (NanoSPECT/CTPLUS, Mediso, Hungary) imaging was performed to detect 201Tl in vivo accumulation, iodine metabolism, and to obtain information on the adequacy of SPECT resolution and CT contrast. **Results**. Employing propan-2-ol caused immobilization on earthworms during examination. Using MRI the morphology of the reproductive organs of the animals was visualised. FDG-PET allowed to determine metabolic uptake in discernable organs as nehpridia, gut and genital organs. The sulfhydryl group bindig propeties of 201Tl were visualized as uptake througout the body as well as in the urinary system. With the same modality, complete body imaging with water soluble 123I ions enabeled to elucidate the distribution of small hydrophylic molecules. **Discussion**. The reported tests could supplement carcinogene and toxicity tests. According to 201Tl results we can suppose that this model is capable to demonstrate toxicokinetic features of certain toxic metal ions (e.g. silver), which mimic in vivo potassium ions. Reactive (soft electrophylic) heavy metals (such as quicksilver (Hg) and cadmium (Cd) inter alia) with analogous toxicodynamic feature as 201Tl could be elucidated, in a reliable and quantificated manner. According to MRI results, reproductive capacity alterations could be demonstrated. Using FDG, the metabolic aspects of toxicodynamic effect of carcinogens, radioactivity or toxic heavy metal exposures could be tested, as well.

## P495

### [18F] Flutemetamol amyloid-beta PET imaging compared with [11C] PIB across the spectrum of Alzheimer's disease

**S. Hatashita**, H. Yamasaki, Y. Suzuki, K. Tanaka, K. Taniguchi, T. Wakebe, H. Hayakawa; Shonan-Atsugi Hospital, Atsugi, JAPAN.

Background: We have demonstrated that a diagnostic framework with an Aβ deposition by [11C]-PIB PET allows for an earlier and more specific AD diagnosis. The aim is to identify the beta amyloid (Aβ) deposition by PET imaging with [18F]-labeled PIB derivate [18F]-Flutemetamol (FMM) across the spectrum of Alzheimer's disease (AD). Furthermore, we clarify the association in Aβ between [18F]-FMM and [11C]-PIB PET imaging. Method: Twenty-eight patients with AD, 44 with mild cognitive impairment (MCI) and 32 subjects with healthy control (HC) were studied. All 104 subjects (age: 56-89 years) underwent 30-min static [18F]-FMM PET acquired 85 min after injection (193.5 ± 6.6 MBq), 60-min dynamic [11C]-PIB PET, and cognitive test. [18F]-FMM scans were assessed visually by 3 blind readers as abnormal or normal cortical uptake, and the standardized uptake value ratios (SUVR) were defined quantitatively in regions of interest defined on co-registered MRI (cerebellar gray as a reference region). The PIB distribution volume ratios (DVR) were determined in same cortical regions. Result: The visual assessments of [18F]-FMM scans had a increased uptake in 27 of 28 scans with AD patients and 4 of 32 scans with HC subjects, corresponding to an overall sensitivity of 96.4% and a specificity of 87.7%. Inter-reader agreement between 3 visual readers was excellent (Kappa score=0.84), and intra-reader agreement was 93.3%. Fourteen (31.8%) of 44 MCI patients showed a increased uptake of [18F]-FMM. The [18F]-FMM SUVR of whole cortical regions in AD was significantly greater than in [18F]-FMM negative HC (1.85 ± 0.25 vs 1.24 ± 0.09, P<0.01). MCI patients had a bimodal distribution of SUVRs. The SUVRs in 14 patients with [18F]-FMM positive MCI and 30 patients with negative MCI were 1.89 ± 0.27 and 1.21 ± 0.10, respectively. The [18F]-FMM SUVR of all cortical regions except for medial temporal cortex, were greater in AD than HC or MCI. The [18F]-FMM SUVR values in all individual subjects were strongly correlated with [11C] PIB DVR values (r=0.94, n=63, p<0.001). Cortical FMM SUVR was significantly correlated negatively with MMSE scores (r=-0.23, P<0.05), and positively to CDR SB scores (r=-0.23, P<0.05), when all groups were analyzed together. Conclusion: [18F] amyloid tracer Flutemetamol has imaging properties very similar to [11C] PIB and is the best alternative. The PET imaging with [18F] Flutemetamol is a reliable biomarker of Aβ deposition along the continuum from normal cognitive status to dementia of AD, and facilitates integration of Aβ imaging into clinical practice.

## P496

### Preparation and Evaluation of fluorine-18 labeled galactosyl-neoglycoalbumin

**X. Gu**, G. Cai, M. Jiang, Y. Zhou, R. Zhang; Key Laboratory of Nuclear Medicine, Ministry of Health, Jiangsu Key Laboratory of Molecular Nuclear Medicine, Jiangsu Institute of Nuclear Medicine, Wuxi, CHINA.

**Objective**: To evaluate the feasibility of fluorine-18 labeled galactosyl-neoglycoalbumin ([18F]FNGA) as a liver Asialoglycoprotein receptor (ASGPR) functional imaging agent. **Methods:** [18F]FNGA was prepared with 18F by conjugation with N-succinimidyl-4-18F-fluorobenzoate ([18F]SFB) under a slightly basic condition, and purified with PD-10 desalting column. The radiolabeling yield and radiochemical purity of [18F]FNGA were determined by radio-HPLC. Biodistribution of [18F]FNGA was investigated in normal mice after injection through the tail vein. MicroPET images in mice were acquired with and without block after injection of the radiotracer (3.7 MBq/mouse), respectively. For the

chronic liver disease model, the mice were injected with 3.7MBq of [18F]FNGA through tail vein under isoflurane anesthesia and then subjected to a 30-min dynamic scan. **Results**: Starting with [18F]F-, the total reaction time for [18F]FNGA was about 100 min. The radiochemical purity of [18F]FNGA was more than 99%. The specific radioactivity of [18F]FNGA was 58.4TBq/mmol. Biodistribution in mice showed that the peak of liver uptake of [18F]FNGA was within 10min after injection. MicroPET imaging of [18F]FNGA in normal mice showed that [18F]FNGA can be uptaken rapidly by liver specifically, the liver imaging was very clear, and the optimal imaging of liver can be obtained during the 10-30 minutes after injected. And the imaging of heart was faint at 5min after injection. On the contrary, the liver accumulation was significant lower after block, indicating the specific binding to ASGP receptor. Comparing the normal mice with the chronic liver disease model, there was low liver activity accumulation in the model mice with slow clearance and vague images. **Conclusions**: [18F]FNGA could be used as a receptor-specific radiopharmaceutical with potential applications in liver imaging for the evaluation of liver function.

## P497

### Synthesis and evaluation of chalcone derivatives as probes targeting amyloid-beta plaques in alzheimer's disease

**Y. Park**, S. Seung, M. Hur, S. Yang; Korea atomic energy research institute, Jeongeup-si, KOREA, REPUBLIC OF.

**Objectives:** Alzheimer's disease (AD), the most common form of dementia, involves the progressive accumulation of amyloid-beta (A$\beta$) plaques in the brain parenchyma and neurofibrillary tangles (NFTs) in neurons. We hypothesized that the structure of 1,3-diarylprop-2-en-1-ones could be used to exploited to create a probe that exhibited certain changes in fluorescence properties upon binding to A$\beta$ plaques. Furthermore, the hydrophobic planarized system of chalcones is an advantage, promoting the binding of A$\beta$ aggregates through hydrophobic interactions. **Methods:** Two 1,3-diarylprop-2-en-1-ones derivatives were prepared using the synthesis sequence. Compound **1** was reacted with benzaldehyde after treatment with potassium iodide and triphenylphosphine to produce trans-isomer. We evaluated the fluorescent properties of 2 compounds at 10 μM in PBS before and after mixing with aggregated A$\beta$40 peptides (10 μM, aggregated in PBS buffer for 3 days at 35 $^{\circ}$C). Two compounds showed a greater than 10-fold fluorescence intensity increase in their emission spectra, indicating that these compounds bind to the A$\beta$ aggregates. To determine whether compounds could be used as the basis of a fluorescence probe for detecting A$\beta$ aggregates, we tested compound **4** in brain sections from 15-month-old transgenic AD model mice (APP/PS1). **Results:** we show that dimethylamino group-containing the chalcones derivative (**4**) has fluorescence characteristics appropriate for imaging Aβ aggregates. Compound **4** exhibited a strong fluorescence response ($F_{Ab}/F_0$ = 58.9) and binding affinity ($K_d$ = 2.31 uM) to A$\beta$ aggregates, and it clearly stained both intracellular A$\beta$ aggregates and A$\beta$ plaques in the transgenic AD model mice (APP/PS1). **Conclusions:** chalcones derivatives may be good candidates as alternative fluorescence imaging agents for the study of AD. Based on the above results, our next study will focus on radiolabeled chalcones derivatives as potentially useful PET imaging agents for cerebral A$\beta$ plaques.

P12-2 - Tuesday, Oct. 22, 16:00 - 16:30, Poster Exhibition Area

## Radiopharmaceuticals & Radiochemistry & Dosimetry: Radiopharmaceuticals - PET

## P498

### Synthesis of Gallium based Phosphonate Macrocyclic Chelate (68Ga-DOTP): Its Preclinical Evaluation as PET Agent for Diagnosis of Skeletal Metastases

**A. Datta**[1], K. Ganesh Kadiyala[1], K. Chauhan[1], A. Adhikari[1], K. Chuttani[1], A. Kaul[1], M. Thirumal[2], A. K. Mishra[1]; [1]INMAS, DELHI, INDIA, [2]University of Delhi, DELHI, INDIA.

**Aim** Positron emission tomography is one of most common invasive technique in the field of molecular imaging. Several $^{68}$Ge/$^{68}$Gagenerator systems have been developed to provide reliable source of the positron-emitter $^{68}$Ga (half-life 68min) that can readily be converted into radiopharmaceuticals for positron emission tomography (PET) studies. Phosphate and phosphonic acid derivatives are known to have a very high affinity for various inorganic hydroxidic and oxidic materials which make them ideal targeting groups for HAP and bone.[1,2] This has justified the use of many phosphonate-based molecules as bone-seeking agents over the years. The potential of $^{68}$Ga-DOTP as a bone-seeking pharmaceutical was evaluated by understanding its deposition pattern in osseous tissues after its synthesis and radiolabeling with $^{68}$Ga. **Method** This work describes the potential of $^{68}$Ga- DOTP as diagnostic pharmaceutical by evaluating its deposition in bone after the synthesis and radiolabeling of (1,4,7,10-tetraazacyclododecane-1,4,7,10-tetrayl)tetrakis(methylene)tetraphosphonic acid, DOTP.Synthesis was performed by using 1,4,7,10-tetraazacyclododecane as a precursor. 1,4,7,10-Tetraazacyclododecane was converted in to tert-butyl 2,2',2'',2'''-(1,4,7,10-tetraazacyclododecane-1,4,7,10-tetrayl)tetraacetate. The acetate arms are cleaved by using Tri-flouroacetic acid to convert in to 2,2',2'',2'''-(1,4,7,10-tetraazacyclododecane-1,4,7,10-tetrayl)tetraacetic acid and the carboxylic acid groups are modified in to phosphonate groups to get (1,4,7,10-tetraazacyclododecane-1,4,7,10-tetrayl)tetrakis(methylene)tetraphosphonic acid (DOTP).Finally compound was labeled with $^{68}$Ga for scintigraphic studies. Biodistribution studies were performed in BALB/c mice to check the uptake of compound in bone. **Results** Synthesis of DOTP was confirmed by $^{1}$H NMR, $^{13}$C NMR and ESI-MS spectroscopy. Radiolabeling efficiency of DOTP with $^{68}$Ga was found to be >93%. Blood clearance showed quick washout from the circulation via renal route and biological half life were determined. Biodistribution characteristics of $^{68}$Ga- DOTP were examined in BALB/c mice and it shows prominent accumulation in bone. Accumulation of $^{68}$Ga- DOTP in bone was determined at various intervals of time. **Conclusion** $^{68}$Ga- DOTP was prepared in high radiochemical yield. $^{68}$Ga-DOTP has high accumulation in bone and it is showing high affinity towards HAP. Further investigation of $^{68}$Ga- DOTP on the bone metastasis induced by different cell lines is in progress. References 1. J. Tanwar, A. Datta, A. K. Tiwari, M. Thirumal, K. Chuttani, A. K. Mishra , Bio conjugate Chem., 2011, 22, 244-255. 2. A. Datta, P. Panwar., K. Chuttani, A. K. Mishra, Cancer Biother. Radiopharm., 2009, 24, 123-128.

## P499

### A Novel PET ligand 8-[O-methyl-11C]2-((4-(2-methoxyphenyl)piperazin-1-yl)methyl)quinoline for 5HT1Areceptor Imaging: Synthesis, Characterization and Evaluation

**R. Sandhya**[1,2], R. Varshney[1], S. K. Sethi[1,2], S. K. Ghumman[2], A. K. Mishra[1]; [1]INMAS, Delhi, INDIA, [2]University of Delhi, Delhi, INDIA.

Abstract: Aim: serotonin(5HT) receptors are group of G-protein coupled receptors has its importance in central nervous system and variousneuropsychiatric disorders. 5HT1A has been implicated in major depression, Schizophrenia, dementia of the Alzheimer type, insomnia, anxiety etc. 1-(2-Methoxyphenyl)pipearazine (MPP)act as a potent antagonist of presynaptic and postsynaptic 5HT1Areceptor. An attempt to develop brain imaging radiopharmaceuticals, selective for 5HT1A, we have synthesized and evaluated8-[O-methyl-11C]-2-((4-(2-methoxyphenyl)piperazin-1-yl)methyl)quinoline.
Methods:The 8-hydroxyquinoline-2-carbaldehyde was synthesized by selenium dioxide oxidation of 2-methylquinolin-8-ol. The oxidized 8-hydroxyquinoline-2-carbaldehyde was conjugated MPP and reduced to give desired ligand with a good yield (75%). We have developed novel short-lived 11C (t1/2=20min) labelled methoxyphenylpiperazine based derivative with high specific activity for PET. [11C]Carbon dioxide is converted to [11C]methyl iodide which is produced by iodinations of recirculated [11C]methane, then reacted with the precursor (0.5mg) in ethanol and 1M NaOH solution. Results:The synthesized ligand has been fully characterized by NMR and MASS spectroscopic techniques.Radiolabeling was achieved above 50%. The overall synthesis time, from EOB to HPLC analysis of 8-[O-methyl-11C]2-((4-(2-methoxyphenyl)piperazin-1-yl)methyl)quinolonewas 40 min. Specific activity was 122-174 GBq/mmol. Radiochemical purity determined by analytical Radio-HPLC was higher than 98%.Cytotoxity were determined by MTT assay. Conclusion:We were successful in synthesizing 8-[O-methyl-11C]2-((4-(2-methoxyphenyl)piperazin-1-yl)methyl)quinoline.In vitro studies with the novel compound are under progress. References: European journal of pharmacology 394 (2000), 47-50 Journal of medicinal chemistry 44 (2001), 3175-3186 Journal of medicinal chemistry 48 (2005), 839-848

## P500

### Synthesis and evaluation of F-18 labeled stabilized bombesin analogues for GRPR imaging

**Z. Yu**[1,2], A. Kuipers[3], H. J. K. Ananias[2], G. Carlucci[2], H. D. Hoving[2], R. Rink[3], R. A. J. O. Dierckx[1], W. Helfrich[4], F. Wang[5], G. N. Moll[3], I. de Jong[2], P. H. Elsinga[1]; [1]Department of Nuclear Medicine and Molecular Imaging, University Medical Center Groningen, University of Groningen, Groningen, NETHERLANDS, [2]Department of Urology, University Medical Center Groningen, University of Groningen, Groningen, NETHERLANDS, [3]Lanthio Pharma, Groningen, NETHERLANDS, [4]Department of Surgery, Surgical Research Laboratory, University Medical Center Groningen, University of Groningen, Groningen, NETHERLANDS, [5]Medical Isotopes Research Center, Peking University, Beijing, CHINA.

**Introduction:** To enhance the resistance against proteolytic enzymes and to improve the gastrin releasing peptide receptor (GRPR) targeting ability of radiolabeled bombesin, we developed a series of lanthionine-stabilized full-length bombesin analogues by introducing internal thioether cross-links to connect two amino acids of the peptide. **Methods:** The binding affinity of lanthionine-stablized bombesin analogues was determined with *in vitro* competitive binding assay in PC-

3 prostate cancer cell line, the affinity of reference compounds was determined as well. The best two candidates (C5 and C6) with the highest *in vitro* affinity were labeled with $^{18}$F by using N-succinimidyl 4-[$^{18}$F]fluorobenzoate ($^{18}$F-SFB) for positron emission tomography (PET) imaging of GRPR-expressing prostate cancer. The *in vitro* and *in vivo* behaviour of the $^{18}$F-labeled bombesins were compared to reveal the effects of the variation of internal cross-links. The GRPR targeting ability and imaging potential of $^{18}$F-labeled stabilized bombesin analogues were investigated in PC-3 prostate cancer bearing mouse. **Results:** When coupled with $^{19}$F-SFB, the $IC_{50}$ value of C5 and C6 increased from 248±6 and 26±1 nM to 1299±249 and 35±14 nM, respectively. The radiochemical yield of $^{18}$F-C5 and $^{18}$F-C6 was ~10 % and ~30%. The specific activity of $^{18}$F-C5 and $^{18}$F-C6 was 1437±329 and 218±135 MBq/µmol, respectively. The PC-3 tumor uptake of $^{18}$F-C5 and $^{18}$F-C6 at 1 h post-injection was 0.7 ± 0.1 %ID/g and 3.5±0.9 %ID/g, respectively. For both tracers, PC-3 tumors were clearly visible from PET images at 2 h and 3 h post injection. For $^{18}$F-C6, high liver and abdomen background were observed from all images. The absolute uptake of $^{18}$F-C6 in liver, kidney and small intestine was 4.0 ± 0.1, 9.0 ± 3.0 and 14.9 ± 5.5 %ID/g at 1 h post injection. For $^{18}$F-C6, the major organs with high radioactivity accumulation were kidneys (2.9 ± 0.1 %ID/g at 1 h p.i.) and intestines (2.6 ± 0.4 %ID/g at 1 h p.i.). The tumor-to-background contrast of both tracers was better at 2 h than 1h and 3 h post-injection. **Conclusion:** Two promising lanthionine-stabilized full-length bombesin peptides were successfully labeled with $^{18}$F. Both radio-tracers showed GRPR targeting potential *in vitro* and in animal model. * This work was made possible by a financial contribution from CTMM, project PCMM, project number 03O-203 and IAG2, Province of Groningen.

## P501

### $^{64}$Cu-labelled compounds with dithiocarbamate ligands for theragnostic applications: preliminary in vitro studies

**N. Morellato**[1], G. Cicoria[2], V. Gandin[1], N. Salvarese[1], C. Marzano[1], S. Costa[3], C. Malizia[3], F. Lodi[3], C. Bolzati[4]; [1]Dip. di Scienze del Farmaco, University of Padua, Via Marzolo, 5, 35135 Padua, ITALY, [2]Medical Physics, Azienda Ospedaliero Universitaria di Bologna, Policlinico S. Orsola-Malpighi, Bologna, ITALY, [3]PET Radiopharmacy, Nuclear Medicine Unit, Azienda Ospedaliero Universitaria di Bologna, Bologna, ITALY, [4]ICIS-CNR, Corso Stati Uniti 4, 35127 Padua, ITALY.

**Aim.** Recently DEDC (diethyl-dithiocarbamate) and PDTC (pyrrolidine-dithiocarbamate) have been recognized to act as copper chelators able to spontaneously form stable Cu(II)-complexes. It was found that Cu-DEDC and Cu-PDTC complexes display potent proteasome-inhibitory and apoptosis-inducing activities in cultured human cancer but not in normal cells [1, 2]. Despite the *in-vitro* investigation of the mechanism responsible of the cytotoxicity of these compounds is well documented, little is known of the mechanism involved in the cell uptake, accumulation patterns and efflux of this family of compounds as well as their *in- vivo* pharmacokinetic profile.Using the corresponding $^{64}$Cu-complexes, as chemical probes, we investigate here the accumulation of $^{64}$Cu-DEDC and $^{64}$Cu-PDTC in human normal and cancer cells under a range of conditions. **Method.** The cellular accumulation of both Cu-complexes was assessed, working both in carried added ($^{64}$Cu/Cu) and carrier free condition ($^{64}$Cu), in Human Embryonic Kidney (HEK293) and human breast cancer cell lines (MCF-7), at 4 and 37 °C, in presence or not of copper-transporter 1 (Ctr1) inhibitor. The chemical integrity of the $^{64}$Cu-complexes after cellular incubation and in cytosolic fraction was determined. **Results.** A selective accumulation of the $^{64}$Cu-complexes was found in human cancer cell (% cell uptake in MCF7 = 40 ± 5; % cell uptake HEK= 7 ± 2.02). For both $^{64}$Cu-complexes a linear increase of the cellular accumulation was observed over the time and did not reach a plateau even in carried added conditions where a relatively high concentration of compounds (50 µM) was used. After 15 min of incubation the % of cell uptake was quantified to be 20%, at 60 min this amount was ranging 30-40%. No variation of the cellular accumulation was observed in temperature-dependent experiments suggesting for these compounds a passive mechanism of uptake. The complexes were effluxed from the cells in the form of ionic Cu. **Conclusion**. These results support a model in which the ligand acts as an ionophore for the metal ion. Intracellular metal accumulation is maximized when the cells were treated with the Cu-complexes; copper and ligand follow different uptake kinetics and reach different intracellular concentrations. The high lipid solubility of these complexes allows them to rapidly cross the membrane reaching a high intracellular concentration. Copper overload, originated by the complex dissociation could be responsible for the cytotoxic effects. 1. Giovagnini L et. al. Inorg Chem, 2008, 47, 6336-6343. 2. Yu Z., et al. Int. J Mol Med, 2007, 20: 919-925.

## P502

### Synthesis and biological evaluation of F-18 labeled 8-(3-(4-(3-fluoropropyl)-1H-1,2,3-triazol-1-yl)propyl)-1-phenyl-1,3,8-triazaspiro[4.5]decan-4-one for PET imaging of D2 receptor.

**S. K. Sethi**[1,2], R. Varshney[1], R. Sandhya[1,2], M. D. Milton[2], A. K. Mishra[1]; [1]INMAS, Delhi, INDIA, [2]University of Delhi, Delhi, INDIA.

**Aim**: The signalling process through dopamine D2 receptor governs physiological functions related to locomotion, hormone production. D2 receptor is also the known target of antipsychotic drugs that are used to treat neuropsychiatric disorders. Thus, the use of radiolabeled neurotransmitter antagonist ligands for visualization and quantifying their binding sites in the normal and diseased brain offers a noninvasive way to monitor the functional interaction at the synaptic level between different regions in the human brain. A peripheral and central D2 receptor antagonist like spiperone stimulates the sympathetic nervous system and may alter autonomic modulation. Spiperone is one of the most well-known ligands for PET as it possesses inherent high sensitivity and capability of imaging quantitation which is highly useful for the imaging of the dopamine receptor. The triazaspirodecnone moiety is the key to its antagonism and its activity is preserved even after a large chemical modification has been carried on it. **Materials and Methods**: The triazspirodecanone moiety was subjected to nucleophilic substitution using 1-bromo-3-chloropropane to give 8-(3-chloropropyl)-1-phenyl-1,3,8-triazaspiro[4.5]decan-4-one (yield 82%) which was further converted into its corresponding azide. The 4-pentyn-1-ol was tosylated to give pent-4-ynyl-4-methylbenzenesulfonate (yield 56%). "Click" chemistry was performed with the tosylated alkyne and triazaspirodecanone based azide to yield a triazole based conjugated, viz., 3-(1-(3-(4-oxo-1-phenyl-1,3,8-triazaspiro[4.5]decan-8-yl)propyl)-1H-1,2,3-triazol-4-yl)propyl 4-methylbenzenesulfonate. The radio-fluorinated conjugate, 8-(3-(4-(3-fluoropropyl)-1H-1,2,3-triazol-1-yl)propyl)-1-phenyl-1,3,8-triazaspiro[4.5]decan-4-one was obtained after labeling with short-lived 18F (t1/2=110min). Radiolabelling: The tosylated click conjugate was radio fluorinated with K18F/Kryptofix at high temperature of 100°C-110°C in FX-N module to yield fluorinated ligand. The radiolabelling efficiency was found to be >95%. The Radiochemical purity was higher than 98% which was determined by analytical Radio-HPLC. The cytotoxity were determined by MTT assay. Results: All the intermediates and final compound were fully characterized by 1H, 13C NMR and Mass Spectroscopy. Radiolabeling was achieved above >95%. Further biological evaluation is in progress. **Conclusions**: We have optimized, successfully synthesized and characterized the ligand 8-(3-(4-(3-fluoropropyl)-1H-1,2,3-triazol-1-yl)propyl)-1-phenyl-1,3,8-triazaspiro[4.5]decan-4-one utilizing the efficient, reliable and robust click chemistry based methodology. This class of imaging agents holds a promising future in imaging D2 receptor for the effective treatment of neuropathological disorders. References: 1.) Clinical Autonomic Research 2003, 13, 275-280. 2.) Journal of Inclusion Phenomena and Macrocyclic Chemistry 2007, 59, 323-329

## P503

### Optimised radiosynthesis of [$^{18}$F]Fluorobenzaldehyde on the GE FASTlab: Effect of chemical impurities on the tumour uptake of [$^{18}$F]AH113804

**G. McRobbie**[1], M. Battle[1], H. Betts[1], G. Tang Dalsgaard[1], K. Drystad[2], T. Engell[2], P. Evans[1], G. Getvoldsen[1], J. Grigg[1], I. Khan[1]; [1]GE Healthcare, Amersham, UNITED KINGDOM, [2]GE Healthcare, Oslo, NORWAY.

The tyrosine kinase c-Met receptor has been shown to be involved in tumour growth, invasion and metastasis in many human cancers of epithelial origin. c-Met is expressed by most carcinomas and its elevated expression relative to normal tissue has been detected in lung, breast, colorectal, prostate, pancreatic, head and neck, gastric, hepatocellular, ovarian, renal, glioma, melanoma cancers and a number of sarcomas. [$^{18}$F]AH113804 is a peptide-based Positron Emission Tomography (PET) imaging agent being developed as a marker for c-Met expression in tumours. [$^{18}$F]AH113804 is manufactured in a two-step radiosynthesis on the GE Healthcare FASTlab™ automated synthesiser followed by high performance liquid chromatography (HPLC) purification. In the first step $^{18}$F-fluorobenzaldehyde (FBA) is formed and in the second step FBA is reacted with the peptide precursor. The aim of this study was to produce FBA in good radiochemical yield whilst reducing the amount of the major chemical impurity, dimethylaminobenzaldehyde (DMAB). DMAB reacts like FBA with the peptide precursor and forms a DMAB-peptide conjugate which is the major chemical impurity in the drug product (DP). Reducing the amount of DMAB formed in the first step will thus decrease the chemical impurity of the drug product. A "Plackett-Burman" experimental design was chosen due to the number of variables under investigation. Interpretation of the results generated confirms a positive correlation between FBA yield and DMAB (i.e. the more FBA you have, the more DMAB). In conclusion, the amount of DMAB was reduced 40-fold with a radiochemical yield of > 60%. The tumour uptake and efficacy of [$^{18}$F]AH113804 is dependent on the level of DMAB-peptide present in the DP. In xenograft mice, retention of radioactivity in the tumour at 30 minutes pi decreases with DMAB-peptide levels (ca. 4% id/g with 5 µg/mL vs. ca. 2% id/g with 145 µg/mL).

## P504

### Microfluidic preparation of [18F]altanserin for clinical trials

**C. Philippe**, J. Ungersboeck, L. Nics, G. Karanikas, M. Mitterhauser, W. Wadsak; Medical University Of Vienna, Vienna, AUSTRIA.

**AIM** The selective 5-$HT_{2A}$ receptor antagonist [$^{18}$F]altanserin has become an important positron emission tomography (PET) tracer used in clinical trials regarding depression and behavioural studies, Alzheimer's disease and pain research. We developed an automated microfluidic preparation method with subsequent purification using a conventional synthesis module in series. A clinical study is going to start within the next couple of weeks, what would be - to the best of our knowledge - the first application of a tracer prepared with a microfluidic device in a human PET study. **MATERIALS & METHODS** Radiosynthesis in the microfluidic device (Advion NanoTek®): n.c.a [$^{18}$F]fluoride was trapped on an anion exchange cartridge and released with a solution containing tetrabutylammonium hydroxide (20 mg/ml) or Kryptofix 2.2.2 (20 mg/ml)/potassium carbonate (4.5 mg/ml) in acetonitrile/ water (70/30 v/v). After azeotropic drying, [$^{18}$F]fluoride was dissolved in DMSO. The [$^{18}$F]fluoride-solution and the precursor solution (nitro-altanserin: 4 mg/ml in DMSO) were loaded into the respective loops. 450 µl of both solutions were pushed simultaneously through the microreactor at 220°C with a flow rate of 10 µl/min. Subsequently, the crude product solution was swept out of the microreactor with a defined volume of 300 µL DMSO. Purification via a conventional synthesis module (Nuclear Interface®): The crude product solution was dissolved with 10 ml 1N HCl and passed over a C18-SepPak cartridge. The here trapped [$^{18}$F]altanserin was eluted with 2ml methanol. After evaporation of the methanol, [$^{18}$F]altanserin (and lipophilic by-products and precursor) were dissolved in 1.5 ml 0.025 N $NH_4OAc$ and subsequently injected onto the semi-preparative HPLC column. The [$^{18}$F]altanserin fraction was cut, pushed over another C18-SepPak cartridge and eluted with 1.5 ml ethanol. Formulation was done with physiological saline solution, 3% saline solution and phosphate buffer. Radiochemical and chemical purity, residual solvents, ph and osmolality were checked. **RESULTS** The use of Kryptofix 2.2.2/potassium carbonate for the [$^{18}$F]fluoride elution resulted repeatedly in clogging of the microcapillary. The radiosynthesis could only be conducted reliably using tetrabutylammonium hydroxide. Starting from 33 ± 3 GBq [$^{18}$F]fluoride, 433 ± 117 MBq (3.3 ± 0.2% EOB) of formulated [$^{18}$F]altanserin were obtained within ≤ 140 min. Specific activity was 74 ± 21 GBq/µmol and all other quality control parameters were in accordance with the standards for human application. **CONCLUSION** [$^{18}$F]altanserin was successfully synthesized in a commercial microfluidic flow-through reactor, purified on a serial conventional synthesizer and is now ready to be applied in a human PET study.

## P505

### Labeling NOTA coupled peptides with F18: steps toward the development of an automated synthesis procedure.

**M. Aurilio**[1], M. Malinconico[1], A. Morisco[1], R. Farese[1], L. Aloj[2], S. Lastoria[2]; [1]INT Fondazione Pascale-CROM, Mercogliano (AV), ITALY, [2]INT Fondazione Pascale, Napoli, ITALY.

Radiolabeled receptor binding peptides are being extensively utilized as radiopharmaceuticals. For PET imaging, Ga-68 labeled compounds have been used in recent years. Fluorine-18, however, has physical characteristics that would make it more appealing than Ga-68 for labeling of small peptides. It has a slightly longer half-life than Ga-68 and lower positron energy that improves imaging resolution, particularly for preclinical imaging. There have been different attempts at labeling peptides with F-18. We are currently working on a simple method based on the chelation of Aluminum 18F-Fluoride (ALF) by 1,3,7-triazacyclononane-1,4,7-triacetic acid (NOTA). The method is being applied for the synthesis of 18F-NOTA-Octreotate. We are developing a fully automated method which makes use of the commercially available synthesis module GE TracerLabFX-FDG utilized to produce 18F-FDG. The aim is to allow automated high yield production of the labeled peptide while minimizing exposure of involved staff. The method can also be extended to the synthesis of similar NOTA coupled compounds. Methods: optimal labeling conditions were first determined by manual reactions performed in glass conical vials by adding 200µL of saline solution containing 18F- to 3-8 microliters of 2 mM AlCl3 in 0.1M sodium acetate buffer (pH4). This solution was heated to 90-110 °C then purified with a Sep-PaK C18, HLB or Allumina-n cartridges. Other buffer systems were also investigated such as sodium citrate and Hepes Buffer (0,1M, pH 4.1). Varying peptide concentrations were also investigated. Radio-TLC was used to determine radiochemical yield. Results: Among the different labeling conditions tested with the manual procedure, the one that yielded the highest yield was obtained by utilizing 8µL of 2 mM Al-Cl3, F-18, 20 µg of peptide in sodium acetate buffer, and incubation at 100 °C for 15 minutes. Under these conditions radiochemical yield was 81.5 ± 17.6%. Cartridge purification with the three Methods mentioned was ineffective in removing free fluoride (less than 50% removed). We are currently scaling up the optimized procedure for use in the synthesis module. Conclusions: Although technically challenging, standardization of automated synthesis of NOTA coupled compounds with ALF will allow to greatly increase their use in radiopharmaceutical research.

## P506

### NOPO-based 68Ga and 64Cu PET radiopharmaceuticals

**J. Simecek**, J. Notni, K. Pohle, T. Kapp, M. Weineisen, M. Schottelius, H. Kessler, H. Wester; TU Muenchen, Garching, GERMANY.

Aim: The phosphinic chelator NOPO exhibits superior 68Ga-labelling properties compared to the carboxylic derivatives NODAGA and DOTA. Motivated by high labelling yields, high specific activities and convenient handling, we employed NOPO for further development of peptidic bioconjugates. Here we report on the preparation and initial preclinical assessment of 68Ga/64Cu-NOPO-c(RGDfK), 68Ga-NOPO-NOC, 68Ga-NOPO-PSMA, 68Ga-NOPO-BASS and 68Ga-NOPO-AmB-CPCR4. Materials and Methods: The conjugates were prepared by reaction of NOPO with primary amines of peptides in DMSO containing HATU and DIPEA. 68Ga labelling using fractionated eluate from 68Ge/68Ga generator (iThemba Labs, South Africa) was performed in a fully automated cGMP-compliant module (SCINTOMICS, Germany). Labelling with 64Cu (Acom, Italy) was done manually. IC50´s of conjugates were determined using immobilised αvβ3 integrins, AR42J cells (sst2), LNCaP cells (PSMA) and Jurkat cells (CXCR4). Biodistribution, PET imaging studies and metabolic stability of 68Ga/64Cu-NOPO-c(RGDfK) and 68Ga-NOPO-sst analogues were performed using mice bearing αvβ3+/αvβ3- M21/M21L human melanomas and AR42J rat pancreatic carcinomas, respectively. Results: IC50´s showed improved affinity of NOPO-c(RGDfK) (0.94±0.06 nM), Cu-NOPO-c(RGDfK) (0.51±0.06 nM) and Ga-NOPO-c(RGDfK) (1.02±0.09 nM) for αvβ3 integrin compared to c(RGDfK) (1.33±0.09 nM), whereas coupling of NOPO to AmB-CPCR4 resulted in a conjugate with only moderate affinity. The reported NOPO-peptides were labelled with 68Ga to high yields and specific activities up to 7 TBq/µmol with radiochemical purity >99 %. The tracers were stable towards decomplexation and metabolic degradation. 68Ga-NOPO-c(RGDfK) showed M21 tumour uptake 2.02±0.34 % ID/g at 1 h p.i., fast urinary excretion and low liver uptake. Results from biodistribution studies were confirmed by µPET imaging. Both 68Ga- and 64Cu-labelled NOPO-c(RGDfK) allowed for comparable tumour localisation. Moreover, using the 64Cu tracer, integrin expression was detectable even 18 hours p.i. Specificity of uptake was demonstrated by co-injection of the cold competitor. 68Ga-NOPO-NOC showed fast excretion kinetics and high AR42J tumour uptake (13.87±4.93 % ID/g at 2 h p.i.). Administration of 68Ga-NOPO-BASS resulted in tumour uptake of 4.73±0.89 % ID/g at 1 h p.i. 68Ga-NOPO-PSMA showed high affinity to PSMA (IC50=56.5±3.5 nM) and internalisation rate 4.1±0.7, 6.2±0.3, 7.3±0.4 % at 5, 30 and 60 minutes, respectively. Conclusion: Together with excellent labelling properties and highly reproducible GMP-compliant automated labelling procedure, in vivo performance of 68Ga-NOPO-conjugates proved NOPO an excellent framework for development of new generation of 68Ga-PET radiopharmaceuticals. Moreover, when excellent image resolution is required for preclinical studies with rodents, 64Cu-labelled NOPO-conjugates could be considered as an alternative. Acknowledgement: Financial support by DFG (SFB 824, projects Z1/B5) is gratefully acknowledged.

## P507

### Fully Automated Production of 68Ga-DOTANOC with a Trasis miniAIO® Synthesizer.

**M. Léonard**[1], J. Aerts[1], S. Voccia[2], C. Lemaire[1], J. Morelle[2], G. Philippart[1], A. Luxen[1]; [1]Université de Liège, Liège, BELGIUM, [2]Trasis SA, Liège, BELGIUM.

**Aim:** Our objective was to develop a fast and reproducible fully automated method for the preparation of 68Ga-labelled DOTA-peptide with the miniAIO® synthesis module made by Trasis. The labelling of an easy available peptide, DOTANOC, was designated as a proof of concept for this purpose. **Materials and Methods**: The synthesis of 68Ga-DOTANOC was performed on a miniAIO® synthesizer which has the advantages of using single-use cassette, monitoring the radiosynthesis by means of radioactivity detectors and being small and easily implantable in GMP hot cells. The leachable of metallic impurities was taken in account for the choice of the cassette materials. The synthesis includes the following steps: elution of 68Ga from a 68Ge/68Ga generator with 6 to 10 ml of a HCl solution. Two different generators were used: iThemba's 370 MBq eluted with HCl 0.6N and Eckert-Ziegler's 1850 MBq eluted with HCl 0.1N. The eluate was loaded with NaCl and then passed through a strong anion exchange resin (Waters OASIS MAX) to concentrate 68Ga. 68Ga was then eluted from the resin with 200 µl of HCl 0,02N directly into a reaction vial containing the peptide solubilized in acetate buffer. The mixture was heated at 95°C for 5 min. The reaction media was passed through a hydrophilic/lipophilic resin (Waters OASIS HLB) and the resin was rinsed with NaCl 0,9% solution and HCl 0,02N to remove free 68Ga3+. 68Ga-DOTANOC was eluted with 0.5 ml of ethanol and diluted with NaCl 0.9% solution and filtered with a 0.22 µm filter. The quality of the product was assessed by UPLC with UV and radiochemical detection, GC, pH determination, radionuclidic purity by gamma spectroscopy. **Results and conclusions:** 68Ga-DOTANOC was obtained with reproducible yields of 60% (decay corrected, calculated on the total activity eluted from the generator) within 25 minutes including generator elution, clean-up and concentration of the eluate, radiolabeling, final SPE purification and formulation. Radiochemical purity was > 99.5% ; ethanol concentration was less than 10% v/v ; acetic acid content was below 5000 ppm ; pH was around 6.5. No 68Ge was detected in the vial after decay of 68Ga. Using miniAIO® from Trasis, the method

described allows a safe, fast and reliable synthesis of 68Ga-DOTANOC from a 68Ge/68Ga generator and should be easily transposable for the production of any other 68Ga-labelled DOTA-peptides.

## P508

### New Purification Road of Three Fluorous Radiotracer FBA, EFB and SFB using SPE based on Molecularly Imprinted Polymers

C. Perollier, **S. Bayoudh**, K. Naraghi; POLYINTELL, Val de Reuil, FRANCE.

**Aims:** Aromatic nucleophilic substitution is widely used to synthesize fluorous radiotracers. Due to the short lifetime of 18F radiotracers, the purification is a key step of the synthesis. It must be fast and effective to ensure a high radiochemical purity. This poster shows the effectiveness of the purification method for Fluorobenzaldehyde (FBA), Ethyl 4-Fluorobenzoate (EFB) and N-succinimidyl fluorobenzoate (SFB), using an new Molecularly Imprinted Polymers SPE cartridge for Aromatic Nucleophilic Substitution. **Methods and Results**: Aromatic nucleophilic fluoration using p-substituted phenyltrialkylammonium compounds as precursors, has been purified using a new MIP SPE cartridge. At 95°C were mixed 5 mg of ammonium salt, 6.7 mg of Kryptofix 2.2.2 and 1 mg of potassium fluoride in 400 µL of ACN. After 15 minutes and the cooling of the reaction mixture, 2 mL of water were added to obtain the loading solution (L). The details of each step are as follows: • Condition the SPE Cartridge with 5mL of Acetonitrile (ACN) • Load the loading solution (L) • Wash the cartridge with 5mL of 80-20 Water-ACN • Dry the cartridge. Force the water down into the cartridge and out the bottom or apply vacuum 30 seconds • Elute the fluorous radiotracer with 1-2mL of ACN until dryness (E1). Ethanol can be used as the elution solvent in some cases depending on the nature of the radiotracer/impurity. Recovery of more than 95 % of the fluorous radiotracer was obtained without any contamination of other identified compounds (phenolic and dimethylaminobenzylic compounds, precursor and fluoride). **Conclusions**: The use of a new MIP sorbent cartridge is a simple, fast, and selective tool for the purification of a reaction mixture issued from an aromatic nucleophilic substitution. The fluorous radiotracer is obtained without any identified impurities such as Kryptofix, dimethylammonium/phenolic derivatives or precursor.

## P509

### Test of SOLA AX columns for Separation and Concentration of 18F Isotopes

**P. Mikecz**, N. Pótári, T. Miklovicz, E. Németh, Z. Rácz, D. Szikra, I. Jószai; Dept. of Nuclear Medicine, Medical and Health Science Center, University of Debrecen, Debrecen, HUNGARY.

**Objectives:** The separation of 18F from enriched water on SPE cartridge and its elution into the reaction vessel are crucial in the application of this isotope in PET radiochemistry. In the most application Water's Sep-Pak Accell Plus QMA Light cartridge is used that has a capacity of 30 µeq. This capacity is far more than required to adsorb the produced maximum 2 µmol 18F. Since the carrier fluorine originates from the reagents, mostly from the potassium carbonate used for the elution from the SPE cartridge, decreasing the size of the separation cartridge seems desirable. Our aim was to test a new anion exchange cartridge that has less adsorbent than the recently available ones, in order to obtain the fluoride in less eluent volume and with less water content, and test the eluate in well-established syntheses. **Methods and materials**: For the adsorption experiments the target rinsing water containing 1-2 GBq F-18 produced on a GE PETtrace cyclotron using niobium targets was used. . Two types of solid phase extraction cartridges were compared, Water's Sep-Pak Accell Plus QMA Plus with 130 mg adsorbent, and Thermo Scientific's SOLA AX cartridge with 10 mg adsorbent. The F-18 isotopes were adsorbed on the cartridges during the direct transport from the cyclotron. The elution solutions contained either K2CO3 /Kryptofix 2.2.2., or tetrabutylammonium hydrogen carbonate in 80 % acetonitrile . **Results**: Under direct flow from the cyclotron about 2/3 (range 52%-65%) of the activity was trapped on the Sola AX columns. When flow restriction was applied, the retention increased up to 92%. In case of SOLA AX the elution could take place with 100 µl of elution mixture and 100 µl acetonitrile with 96±2% efficiency. The eluate was used to synthesize of FDG and fallypride with decreased precursor quantity.. **Conclusions:** Using the small size SOLA AX column limited - up to 92 % - 18F adsorption was achieved. The adsorption depended very much on the speed of the passing liquid. This way one could obtain a significantly higher 18F concentration and lower amount of water in the eluate compared to the traditional method, allowing to apply only a single short drying step, which would be advantageous for all applications including microfluidic techniques. Furthermore, higher specific activity could be achieved because of the lower amount of potassium carbonate, a well-known source of carrier fluorine. Decreasing the amount of Kryptofix is also desirable because of its carcinogenic properties.

## P510

### 68Ga-labeled tracers for targeted imaging of glycolysis in cancer cells

**I. Tworowska**[1], D. Ranganathan[2], S. Thamake[2], E. Delpassand[1]; [1]RadioMedix Inc.; RITA Foundation, Houston, TX, UNITED STATES, [2]RITA Foundation, Houston, TX, UNITED STATES.

**Objectives**: The Warburg effect defines the enhanced conversion of glucose to lactate observed in proliferating tumor cells. Increased dependence on glycolysis for generation of ATP molecules by cancer cells is compensated by higher uptake of glucose. This process is supported by over-expression of glucose transporters, especially GLUT1 and over-activation of hexokinase enzyme. Here, we present our results on the synthesis, structure optimization and in vivo validation of two generations of radiotracers targeting metabolic pathways in cancer cell, glucosamine conjugates (RMX-GC) **Methods**: RMX-GC conjugates were synthesized by standard peptide coupling reaction and Cu-catalyzed and Cu-free click chemistry. Compounds were analyzed by ESI-MS and HPLC and radiolabeled with 68GaCl3 in 0.5M NaOAc pH=4.1 at 95oC for 10min (68Ge/68Ga generator -ITG GmbH Germany) and purified using C18 Sep-pak cartridges. 68Ga-labeled agents were evaluated in vitro in multiple cancer cell lines such as SKBr3-breast, PC-3 prostate, A549-small lung cancer. Radiotracers were also validated in vivo as PET metabolic agents in biodistribution and microPET static imaging studies. **Results**: All 68Ga-labeled RMX-GC conjugates have shown tumor-specific accumulation with no uptake by brain and heart and relatively fast elimination through kidneys. Differences in pharmacokinetic properties of agents (e.g. tmax of tumor accumulation) reflect dissimilarities in their physic-chemical properties. Click conjugates have shown the highest accumulation in tumor compared to other glucosamine conjugates as quantified by analysis of PET images and biodistribution studies. **Conclusions:** 68Ga-labeled RMX-GC conjugates allow for detection of GLUT-1 over-expressing tumors and provide competitive advantages over 18F-FDG in imaging of metabolic pathways.

P13-2 - Tuesday, Oct. 22, 16:00 - 16:30, Poster Exhibition Area

## Radiopharmaceuticals & Radiochemistry & Dosimetry: Radiopharmaceuticals - SPECT

## P511

### Novel radiolabeled liposomes with excellent background clearance for tumor diagnostic imaging and radionuclide therapy

**I. O. Umeda**[1], Y. Koike[1,2], S. Kimura[1], S. Hamamichi[1], K. Moribe[2], K. Yamamoto[2], M. Satake[1], N. Moriyama[3], H. Fujii[1]; [1]National Cancer Center, Kashiwa, JAPAN, [2]Chiba University, Chiba, JAPAN, [3]National Cancer Center, Tokyo, JAPAN.

**Objective:** Radionuclide-carrying liposomes are promising radiopharmaceuticals for tumor imaging and radionuclide therapy because of their capacity to accumulate in the tumors. However, liposomes have also been shown to accumulate non-specifically in the reticuloendothelial systems (RES), such as the liver and spleen, even though they are PEGylated to avoid trapping. Consequently, radionuclides encapsulated in liposomes were accumulated in the RES, and it has hindered their clinical application. In this study, we devised a new strategy, i. e., to quickly expel radionuclides from the RES after the accumulation, and promptly remove them through rapid urinary excretion. For this aim, we generated novel liposomes encapsulating $^{111}$In-ethylenedicysteine (EC) that demonstrated rapid RES clearance. **Methods:** Liposomes encapsulating $^{111}$In-EC or $^{111}$In-nitrilotriacetic acid (NTA) were prepared using the active loading method and they were intravenously injected to sarcoma-180-bearing mice. Their biodistribution patterns were evaluated and the mechanism of rapid clearance of $^{111}$In-EC from RES was investigated. Their biodistribution patterns were also visualized by SPECT/CT imaging. **Results:** Striking time-dependent contrasts were observed in the biodistribution of novel $^{111}$In-EC-liposomes and conventional $^{111}$In-NTA-liposomes. While $^{111}$In-EC-liposomes were taken up by the RES (similar to the conventional radiolabeled liposomes), $^{111}$In radioactivity was subsequently cleared from the RES while maintaining good retention in the tumor. Urinary excretion of $^{111}$In was very rapid, and the original complex structure of $^{111}$In-EC was kept intact in the urine. In contrast, regarding$^{111}$In-NTA-liposomes, large amount of $^{111}$In remained in the RES for a long time and subcellular fractionation studies revealed that most of them were found in the mitochondria-lysosome fraction. HPLC analyses of tumor and liver cytosolic fractions demonstrated that both liposomes remained intact in the tumor whereas most were degraded in the liver. These findings suggested that liposomes were broken in the liver, releasing encapsulated radionuclide-ligand complexes, and $^{111}$In-EC released from the liposomes were able to escape from lysosomal trap in the liver and consequently be excreted in urine. This may explain the rapid clearance of $^{111}$In-EC-carrying liposomes from the RES. *In vivo* SPECT imaging at 24 hr after the injection successfully visualized these different biodistribution patterns. **Conclusions:** $^{111}$In-EC-liposomes could be excellent tumor imaging agents

because they accumulated sufficiently in the tumor and remained significantly less in the RES. Radionuclide therapy using $^{90}$Y instead of $^{111}$In would be also promising.

## P512

### In vitro and in vivo evaluation of an anthraquinone molecule labelled with 99mTc designed as anticancer agent

**S. AGGARWAL**[1,2], A. K. TIWARI[1], G. SINGH[2], A. K. MISHRA[1]; [1]INMAS, Delhi, INDIA, [2]DEPARTMENT OF CHEMISTRY ,UNIVERSITY OF DELHI, Delhi, INDIA.

Aim: In the recent years the research work related to cancer has led to the recognition of abundant molecular targets critical for cancer growth and evolution. In common, the known anthracycline drugs, stimulates the production of double-strand DNA breaks, therefore appears likely that intercalation into DNA is necessary for antitumor activity. The present study examines the DNA intercalative abilities of an anthraquinone analogue using molecular docking, a computational approach used universally and spectroscopic results, used to determine the structural features, the binding mode and the association constants. Consequently, the photo-kinetics of molecule with 99mTc, a radioactive metal for SPECT imaging purposes, helps to elucidate the nature of this biologically important complexation process in vitro. Preliminary biological studies include in vivo imaging of radiolabelled molecule. Materials and Methods: X-ray crystal structure of DNA was taken from the protein databank and the Glide version as a part of Maestro 9.3 suite of programs was used for molecular docking. Alkylation reaction was carried out and the synthesis was confirmed from the various characterisation techniques. Absorbance, fluorescence and quenching measurements were performed spectrophotometrically. Biodistribution, blood kinetics and SPECT imaging was done of the 99mTc radiolabeled molecule. Results: Molecular docking results show intercalative nature of the molecule and good binding affinity with DNA considered from the Glide Gscore comparable with a known anticancer drug, Doxorubicin. Synthesized molecule was radiolabelled with 99mTc and the complex was found to be stable over a period of 24 hrs with high radiolabeling efficiency (98%). Blood clearance kinetics were described for the therapeutic efficiency of the drug showing quick wash out while renal excretion route was followed for the molecule in the bio-distribution studies, also showing accumulation at the tumor site. Similar distribution pattern was observed in the scintigraphic imaging. Conclusion: The analysis of molecule binding for its target site is of considerable importance as knowledge of this basic experimental parameter allows predicting drug efficiency and photo-kinetics analysis reveals the molecule as an efficient radiopharmaceutical used for nuclear medicine applications.

## P513

### [$^{99m}$Tc(N)PNP]-moiety: a suitable scaffold for the developmant of radiolabeled probes for SPECT of multidrug resistance. In vitro study

**C. Bolzati**[1], V. Gandin[2], N. Morellato[2], N. Salvarese[2], C. Marzano[2], F. Refosco[1]; [1]ICIS-CNR, Corso Stati Uniti, 4, 35127 Padua,, ITALY, [2]Dip. di Scienze del Farmaco, University of Padua, Via Marzolo 5, 35135 Padua, ITALY.

**Aim**. $^{99m}$Tc(N)-DBODC(**5**) [DBODC = bis(N -ethoxyethyl)dithiocarbamato; and **5** = bis(dimethoxypropylphosphinoethyl)ethoxyethylamine], is a lipophilic cationic mixed-compound originally investigated as myocardial imaging agent. This compound has been recently identified as a suitable scaffold for the design of new $^{99m}$Tc-based agents for the noninvasive imaging of P-gp and closely related transporter activities [1]. The possibility to control the hydrophobicity and pharmacological activity of this heterocomplex through the independent variation of the substituents on the two ligand backbones, without affecting the $P_2S_2$ coordinating sphere, makes $^{99m}$Tc(N)-DBODC(5) an appropriate platform for the preparation of different molecular probes for SPECT of MDR. To evaluate the impact of the [$^{99m}$Tc(N)PNP]-moiety on the tumor cell accumulation and on the MDR recognition different $^{99m}$Tc(N)-DBODC(5) like complexes were synthesized varying the substituents on the PNP ligand and their in-vitro biological behaviors on selected human cancer cell lines and in the corresponding sub-lines were investigated. **Method.** $^{99m}$Tc(N)-DBODC(**n**) complexes were efficiently prepared as previously described [2], [**n** is PNP3 bis(dimethoxypropylphosphinoethyl)-methoxyethylamine, PNP7 (bis(dimethoxyethylphosphinoethyl)-ethoxyethylamine) and PNP10 (bis(dimethoxyethylphosphinoethyl)-methoxyethylamine). Basic parameters such as the kinetic of uptake, at 4 and 37 °C, of the $^{99m}$Tc(N)-DBODC(**n**) complexes were evaluated in-vitro in selected cell lines such us MCF7 (human breast cancer) and 2008 (human ovarian cancer), and in the corresponding sub-lines by using $^{99m}$Tc-sestamibi and $^{99m}$Tc(N)-DBODC(5) as references. **Results.** In drug-sensitive cell lines a significant increase of the % of cell accumulation of $^{99m}$Tc(N)-DBODC(7) and $^{99m}$Tc(N)-DBODC(10) complexes was observed with respect to $^{99m}$Tc-sestamibi and $^{99m}$Tc(N)DBODC(5). At steady-state level, this amount was quantified to be two or three times the % of uptake value of the reference compounds. At 4 °C a significant reduction of cellular accumulation was observed for all $^{99m}$Tc agents. After 60 min, the nonspecific uptake was assessed as around 2 % (p<0.001). A reduction of the net cell uptake between drug-sensitive cells and drug-resistant tumor cells was detected (p< 0.001 for the $^{99m}$Tc-complexes in all cell lines). **Conclusion**. Variation of the chemical-physical properties (lipophilicity, dimension, shape, etc.) of [$^{99m}$Tc(N)PNP]-moiety significantly affect the capability of the complexes to cross the plasma membrane increasing their cellular accumulations and their affinity for the MDR transporters. Hence, $^{99m}$Tc(N)-DBODC(7) and $^{99m}$Tc(N)-DBODC(10) represent good candidates for the in-vivo exploration of P-gp/MRP functions. This research was supported by the Italian Ministero dell'Istruzione, dell'Università e della Ricerca (PRIN20097FJHPZ-004). [1] Bolzati, C. et al (2013) J Biol Inorg Chem DOI 10.1007/s00775-013-0997-1 [2] Bolzati C, et al (2010) Bioconjug Chem 21:928-939.

## P514

### DaTSCAN™ (Ioflupane I 123 Injection), a radiopharmaceutical indicated for visualization of the striatal dopamine transporter using SPECT: Safety Results

**I. D. Grachev**[1], P. Sherwin[1], D. Lane[1], E. Moreno[2], J. Freid[1], D. Grosset[3], N. Bajaj[4], R. A. Hauser[5], J. Seibyl[6], K. Marek[6]; [1]GE Healthcare, Princeton, NJ, UNITED STATES, [2]GE Healthcare, Madrid, SPAIN, [3]The Institute of Neurological Sciences, Glasgow, UNITED KINGDOM, [4]Nottingham University, Nottingham, UNITED KINGDOM, [5]USF Byrd Parkinson's Disease and Movement Disorders Center, Tempa, FL, UNITED STATES, [6]The Institute for Neurodegenerative Disorders, New Haven, CT, UNITED STATES.

***Objective:*** To assess DaTSCAN™([$^{123}$I]Ioflupane Injection) safety data from 11 clinical trials (Phases I-IV) in GE Healthcare's clinical development and post-marketing experience. ***Background:*** DaTSCAN™ is a radiopharmaceutical, approved in Europe (2000) and the USA (under the trade name DaTscan™ in 2011) for SPECT imaging to visualize the striatal dopamine transporter in the brain. **Design/Methods:** In GE Healthcare's clinical trials, DaTSCAN™ was administered intravenously to 1236 subjects (1171 patients and 65 healthy volunteers). Clinical trials collected information on adverse events (AEs), and collected data on laboratory parameters (e.g., serum biochemistry, hematology and urinalysis), vital signs and electrocardiograms (ECG). Administered activity of [$^{123}$I]ioflupane ranged from 3 to 5 mCi (111 to 185 MBq; a maximum mass dose of 0.325 microgram), comparable to administered activities for other commercially available $^{123}$I-labeled imaging products. The calculated whole body effective dose was 4 to 6 mSv, comparable to 1 year of natural background radiation in the USA (3 to 4 mSv). ***Results:*** Review of clinical trial data on non-serious AEs, vital signs, laboratory parameters, and ECG identified no safety issues. There were mild and infrequently reported AEs and no SAEs or deaths that were considered related to DaTSCAN™ administration. The most common AE ascribed to DaTSCAN™ by the investigator was headache (1%), followed by nausea, and vertigo, dry mouth, hunger, dizziness, and formication (<1 % each). Most of these AEs were mild. The safety profile established in clinical trials is supported by limited AE reports (including hypersensitivity reported as rash and pruritis shortly after dosing) from post-marketing exposure in over 300,000 patients who have been imaged with DaTSCAN™. ***Conclusions:*** Comprehensive review of the safety data from clinical trials and 11 years of post-marketing use shows that adverse events associated with diagnostic radiopharmaceutical DaTSCAN™ are mild and infrequently reported, and DaTSCAN™ is a safe product to use. DaTSCAN™ is also considered to be low risk from a radiation dosimetry perspective. Study Supported by: This study was sponsored and conducted by GE Healthcare, Princeton, NJ, USA

## P515

### Cyclotron produced Tc-99m: testing compatibility with established kits

**O. Lebeda**[1], J. Ralis[1], P. Hradilek[1], P. Hanc[1], E. J. van Lier[2], A. Zyuzin[2], M. Mosa[3]; [1]Nuclear Physics Institute AS CR, Husinec-Rez, CZECH REPUBLIC, [2]Advanced Cyclotron Systems Inc., Richmond, BC, CANADA, [3]General University Hospital, Prague, CZECH REPUBLIC.

Aim Global shortage of $^{99}$Mo and anticipated shut-down of multiple aging reactors has triggered the development for alternative production routes of $^{99}$Mo and $^{99m}$Tc. One of the most promising technologies is direct cyclotron production of $^{99m}$Tc. It has already been proven that it is feasible to produce TBq amount of $^{99m}$Tc by (p,2n) reaction on highly enriched $^{100}$Mo (24 MeV, 500 μA and 6h irradiation) while keeping levels of radionuclidic impurities sufficiently low for clinical applications. Significant progress was achieved also in R&D of separation process and recycling of the highly enriched targets. An outstanding challenge to be resolved is compatibility of commercially available kits for $^{99m}$Tc radiopharmaceuticals with cyclotron-produced $^{99m}$Tc. We have, therefore, tested several kits for routine production of widely used $^{99m}$Tc radiopharmaceuticals with $^{99m}$Tc produced on cyclotron U-120M at 24 MeV. Materials and Methods Thick targets from 99.03 % enriched $^{100}$Mo were irradiated on external 24MeV proton beam of the cyclotron U-120M at Nuclear Physics Institute, Rez. After the end of bombardment (EOB), the targets were processed on ACSI designed Cyclotec™ Tc-99m automated separation module. The final product in 0.9% NaCl was analyzed and combined with majority

of kits for production of $^{99m}$Tc radiopharmaceuticals. Each product was characterized by Methods recommended by the respective producer. Results and Conclusion In all the cases, prepared $^{99m}$Tc radiopharmaceuticals complied with the tests for radiochemical purity as described by their respective producers. Moreover, in majority of cases, no radiochemical impurities were detected in the products at all, even if very low $^{99m}$Tc concentrations were used for labellings (5 MBq/ml). From that point of view, we have not observed any difference between generator $^{99}$Mo/$^{99m}$Tc eluate and $^{99m}$Tc solution prepared from proton-irradiated $^{100}$Mo targets on the Cyclotec™ Tc-99m automated separation module. Acknowledgements The work was supported by the Nuclear Physics Institute of the Academy of Sciences of the Czech Republic (RVO 61389005) and by Natural Resources Canada's Non-reactor-based Isotope Supply Contribution Program (NISP).

P14-2 - Tuesday, Oct. 22, 16:00 - 16:30, Poster Exhibition Area

## Radiopharmaceuticals & Radiochemistry & Dosimetry: Radiopharmacy

### P516

### Usability of radionuclide activity meters in assaying 68Ge breakthrough in 68Ga generators

**F. Zagni**[1], G. Cicoria[1], D. Pancaldi[1], G. Lucconi[2], S. Vichi[3], F. Lodi[4], M. Marengo[1]; [1]Medical Physics Department, University Hospital "S.Orsola - Malpighi", Bologna, ITALY, [2]Postgraduate School in Medical Physics, Physics Department, University of Bologna, Bologna, ITALY, [3]Nuclear Engeneering Laboratory of Montecuccolino, University of Bologna, Bologna, ITALY, [4]PET Radiopharmacy Unit, University Hospital "S.Orsola - Malpighi", Bologna, ITALY.

**Aim**. Radionuclide activity meters have been proposed for use in quality control procedures, such as the evaluation of radionuclidic purity of $^{68}$Ga generators. This requires the capacity of measuring very low ionization currents. The aim of this work was to measure the minimum detectable activity (MDA) of widely diffuse models of activity meters, in order to evaluate the feasibility of measuring the amount of $^{68}$Ge breakthrough in fresh elutions of $^{68}$Ga. **Materials and Methods**. The amount of impurity due to $^{68}$Ge, typically evaluated from the day after the elution after the complete decay of initially eluted $^{68}$Ga, must not exceed 0.01% of the total activity assayed right after the elution. This means that, for the typical elution range (400 – 1500 MBq of $^{68}$Ga), the activity meter should be capable to reliably measure less than 10 kBq of $^{68}$Ge . A Capintec CRC-15 PET and a Comecer Talete activity meters, placed within a shielded hot cell were used; no interfering radioactive sources were present. Vials containing an initial activity of 1 MBq of purified $^{68}$Ga ($^{68}$Ga-DOTANOC) were prepared and assayed, recording measurements at fixed time intervals of 5 minutes. The ratio between the activity measured and expected values, based on decay, were plotted as a function of the activity; the first derivative of the curve was evaluated, in order to compare the half-life estimation with the expected value. Moreover, the % Coefficient of Variation (%CV) was calculated for the decay-corrected time-activity curves. **Results**. As the measured activity decreases, the discrepancy between measured and expected activity, and the %CV gradually increase; a criteria of 10% difference may be selected as a threshold of significance to asses the MDA. For example, for the CRC15 PET the %CV was 1.5%, 6.7% and 13% respectively at 100, 35 and 20 kBq. According to the criteria adopted, the MDA was found at activities in the range of 20 – 30 kBq for both type of meters. **Conclusions.** These results show that activity meters, known to be accurate when measuring relatively large amounts of activity, can be used in the assessment of $^{68}$Ge breakthrough only in limited cases (i.e. measure of a whole eluate of a new generator), Conversely, these devices cannot be validated as sufficiently sensitive for routine testing of radionuclidic purity of $^{68}$Ga labelled radiopharmaceuticals, nor for assessment of eluates obtained from a several months aged generator.

### P517

### 99mTc-HMPAO labelled white blood cell scintigraphy in pediatric patients. Our experience.

**M. DE GREGORIO VERDEJO**, A. MARTÍNEZ LORCA, M. MARTÍN FERRER, B. MARTÍNEZ DE MIGUEL, R. PÉREZ PASCUAL, I. SANTOS GÓMEZ, E. MARTÍNEZ MONTALBÁN, L. MARTÍN CURTO; HOSPITAL UNIVERSITARIO LA PAZ, MADRID, SPAIN.

**AIM** Our aim is to evaluate the usefulness of the labelling $^{99m}$Tc HMPAO white blood cell (WBC) procedure and the leucocytes scintigraphy in pediatric patients. **MATERIAL AND METHODS** We evaluated retrospectively 49 patients (19 girls and 30 boys: mean age 12.61±3.99 ranging from 2 to 17 years) with suspicion of inflammatory bowel disease. The study was conducted between February 2008 and January 2013. Leucocytes were labelled with $^{99m}$Tc-HMPAO using our Radiopharmacy Unit routine protocol. We adjusted blood mL, acid-citrate-dextrose anticoagulant solution mL, 2-hydroxiethyl starch mL and activity MBq according to children weights. $^{99m}$Tc-HMPAO kit preparation was done with freshly eluted $^{99m}$Tc-pertechnetate. Radiochemical purity (RP) control was performed by solvent extraction ($CHCl_3$: NaCl 0.9%1:1). Anterior abdomen, anterior pelvis and pelvis caudal images were acquired at 30minutes and 3 hours after injection, by using a single-headed gamma camera. Images were interpreted by a nuclear physician using a qualitative score (positive/negative/undefined). Final inflammatory bowel disease diagnosis was done according to histopathology diagnosis (85.71%; n=42) and clinical follow up (14.28%; n=7). **RESULTS** Radiochemical purity (mean RP (%) = 90.43 ±3.7), injected activity (12.95MBq/kg) and labelling efficiency (mean LE (%) = 70.42±7.04) values were analyzed. Injected activity has direct relation to LE ($p<0.05$, Spearman's correlation coefficient of 0.695). $^{99m}$Tc-HMPAO labelled WBC scintigraphy has been found to be true positive in 15 cases, true negative in 26 cases, false positive in 4 cases, false negative in 3 cases and 1 undefined case. The sensitivity, specificity, positive predictive value and negative predictive value were 83.33%, 86.67%, 78.95% and 89.66%, respectively. **CONCLUSION** These results suggest that our labelling procedure of autologous 99mTc-HMPAO WBC is appropriate in pediatric population. We conclude that, due to high sensitivity and specificity, WBC scintigraphy is a valuable tool in the diagnosis of suspicion of inflammatory bowel disease.

### P518

### Clinical peptide receptor radionuclide therapy: Kit preparation of $^{90}$Y, $^{177}$Lu, and $^{111}$In DOTATATE

**J. R. Ballinger**[1], Y. Tan[1], S. J. Allen[1], V. J. Lewington[2]; [1]Guy's & St Thomas' Hospital, London, UNITED KINGDOM, [2]King's College London, London, UNITED KINGDOM.

Peptide receptor radionuclide therapy (PRRT) is an expanding area of nuclear medicine which is showing promising results. $^{90}$Y and $^{177}$Lu DOTATATE have been brought into routine use in our department for PRRT of neuroendocrine tumours and $^{111}$In DOTATATE for the corresponding pre-therapy scan. For $^{177}$Lu DOTATATE the standard administered activity is 7400 MBq while $^{90}$Y DOTATATE is given at 3700 MBq/sq-m. Our experience in preparation of these doses over four years has been reviewed. Methods: Records of radiolabelling DOTATATE kits (Polatom) with $^{90}$Y chloride (Eckert & Ziegler), $^{177}$Lu chloride (ITG Munich) or $^{111}$In chloride (Covidien) since 2009 were reviewed. The contents of a DOTATATE kit are dissolved in 1-1.5 mL saline and transferred into the vial of trivalent radiometal in dilute HCl. The kit is heated at 100°C for 30 min ($^{90}$Y, $^{111}$In) or 20 min ($^{177}$Lu). $^{90}$Y or $^{177}$Lu doses are drawn into a 20 mL syringe for infusion whereas $^{111}$In is transferred to a fresh vial. All transfers from the reaction vial are performed using a spinal needle with the vial upright and a filtered vent needle in the septum; these precautions are to avoid contamination with unreacted radiometal which may remain near the top of the vial. Radiochemical purity (RCP) testing by thin layer chromatography is performed on every preparation before release. Results: The numbers of preparations were: $^{90}$Y, 65; $^{177}$Lu, 94; $^{111}$In, 90. There were no production failures and reprocessing was required on only one occasion. Average (±SD) % yields (activity in syringe/initial activity) were: $^{90}$Y, 91 ± 9; $^{177}$Lu, 94 ± 2; $^{111}$In, 94 ± 4. Average % RCP values were: $^{90}$Y, 99.4 ± 0.7; $^{177}$Lu, 99.5 ± 0.3; $^{111}$In, 99.4 ± 0.5 (limit 95%). Labelling with $^{90}$Y or $^{177}$Lu is always performed by a radiopharmaceutical scientist but labelling with $^{111}$In has now been handed over to radiopharmacy technicians. The yields and RCP were slightly lower when labelling was performed by technicians (91 ± 4 and 98.9 ± 0.7, respectively, n = 8). Based on the above analysis, a 10% excess of $^{90}$Y and 5% excess of $^{177}$Lu should be ordered so that the prescribed dose can be obtained. Conclusions: Preparation of radiolabelled peptides was reproducible and labelling efficiency generally exceeded 99%. A robust kit procedure with commercially available ingredients made this possible.

### P519

### Radiopharmaceutical formulation of $^{90}$Y-labelled minigastrin analogues for application in targeted radiotherapy

**E. von Guggenberg**, C. Decristoforo, I. J. Virgolini; Department of Nuclear Medicine, Innsbruck Medical University, Innsbruck, AUSTRIA.

**Aim:** Targeting of cholecystokinin receptor subtype 2 (CCK2R) expressing malignancies, mainly medullary thyroid carcinoma, neuroendocrine gut tumours, as well as stromal tumours, up to now has been limited by high kidney retention or low in vivo stability of the developed radioligands. Within the trans-European collaborative project COST BM0607 on targeted radionuclide therapy three new DOTA-peptides with optimal properties for CCK2R targeting in terms of tumour uptake and tumour to kidney ratio have been identified. One of these peptide derivatives was DOTA-cyclo-MG1, a cyclic minigastrin analogue which was developed and preclinically evaluated in our center. Using this peptide derivative we have developed a radiopharmaceutical formulation which could be used for first clincal studies. **Materials and Methods:** Radiolabelling of DOTA-cyclo-MG1 with $^{90}$Y was performed at a specific activity of 30 MBq/µg and using a commercially available kit based on ascorbic acid (Polatom, Otwock, Poland) for pH adjustment. The radiolabelling procedure was performed in an automated cassette

based synthesis module (Eckert&Ziegler, Berlin, Germany) including a final purification step by solid phase extraction. The reaction conditions were optimized to reduce methionine oxidation to a minimum. Besides determination of radiochemical yield and radiochemical purity using radio-HPLC and ITLC, other quality control testing included endotoxin and sterility testing. **Results:** $^{90}$Y-DOTA-cyclo-MG1 was obtained in <15 ml saline containing <5% ethanol, and a 20-fold molar excess of calcium-trisodium-pentetate (Ditripentat-Heyl, Berlin, Germany). Based on losses of radioactivity in the $^{90}$Y-chloride vial and in the waste the end product was obtained with radiochemical yield of 85%. The radiochemical purity of $^{90}$Y-DOTA-cyclo-MG1 always exceeded 95%. All bachtes passed the quality control and were compliant with the product specifications. Methionine oxidation was kept below 5% when a reaction temperature of 80°C was combined with an incubation time of 15 min. By using a stabilizing buffer containing ascorbic acid the product was stablized aganist oxidation and radiolysis for 24 h when stored at -20°C. **Conclusions:** The presented radiolabelling process based on an automated synthesis module has been optimized for the preparation of $^{90}$Y-DOTA-cyclo-MG1 meeting high quality standards for therapeutic application. The radiopharmaceutical formulation could be easily adapted also for the preparation of other CCK2R targeting peptide analogues.

## P520

### Is there a variability between trained operators in labelling leucocytes with 99mTc-HMPAO?

**J. Gleize**[1], D. Matanza[1], A. Foucher[1], F. Hallouard[1,2], M. Fraysse[1]; [1]Hospices Civiles de Lyon, Lyon, FRANCE, [2]LAEGP, Universtité Lyon 1, Lyon, FRANCE.

Introduction Autologous leucocytes isolation and labelling with 99mTc-HMPAO is a long and delicate procedure performed twice daily (approx. 300 per year) by trained pharmacy technicians in our structure. However, an organization based on a pooling of human resources between the different pharmacy sectors imply an increased versatility of staff members. Thus, the question of a loss of specialization and an alteration of the qualities of the preparation may arise. Aim The aim of this study is to evaluate the variability between already trained technicians in performing this operation. Method We chose the labelling efficiency, defined as the ratio between the amount of radioactivity in the pellet (labelled leucocytes) and the sum of this activity and the radioactivity of the supernatant (soluble 99mTc-compounds), as our primary variable. We compared the ratios obtained by 4 trained technicians (more than a year's practice) since 2005 using Student's t-test. As the delays between the blood count (taken from the patient's record) and the labelling varied greatly (a few hours to 98 days), we normalized the data by restricting to a maximum delay of one week. Preliminary studies showed a correlation between the labelling efficiency and the leucocytes count ($r(155) = 0.36$, $p < 0.001$). This correlation disappeared when looking at the patients with a high leucocytes count (> 10 G/L) ($r(48) = 0.13$, $p > 0.3$). We consequently refined our results focusing on the normal leucocytes count (4 to 10 G/L). Results In these conditions, when combining the normal leucocytes count and the one week delay there were no significant difference of the labelling efficiency between the four technicians ($t(97) = 1.61$, $p > 0.10$). Discussion/Conclusion The study shows that the differences between the output of the process are more influenced by the patient's biological factors than by the variability between the technicians' skills. This implies that flexibility between technicians would not degrade the quality of the process, provided that the technicians follow the standard operating procedure and go through an initial validation of their ability to carry out the procedure. Our study is based on an in vitro measurement, the labelling efficiency, which is influenced by a lot of patient's related factors. It would therefore be interesting to take into account in vivo parameters as well, such as lung uptake and liver to spleen ratio to complete the evaluation.

## P521

### Clinical application for single-vial ready-for-use formulation of $^{111}$In- or $^{177}$Lu-labelled somatosatin, bombesin and minigastrin analogs

**E. de Blois**, H. S. Chan, R. de Zanger, W. A. P. Breeman; Erasmus MC, Rotterdam, NETHERLANDS.

**Aim:** For the sake of safety it would be desirable to store and transport ready-for-use liquid formulation (diagnostics and therapeutics) of radiolabelled peptides. Therefore, the effectiveness of quenchers on the stability of radiolabelled somatostatin (SS), Bombesin (BN) and minigastrin (MG) analogs was investigated and radiochemical purity (RCP) monitored up to 7 days after radiolabelling. These radiolabelled regulatory peptides are applied in Nuclear Medicine for Peptide Receptor Scintigraphy (PRS) and Peptide Receptor Radionuclide Therapy (PRRT). Regulatory peptides, such as SS-, MG- and BN-analogues contain i.e, tryptophan and methionine in their pharmacophore. Whereas methionine is rapidly oxidized in to methionine-sulfoxide, as described for DOTA-MG11 (MG-analog) and DOTA-AMBA (BN-analog) and results in loss of receptor affinity. Here we present our Methods of quantification and how to protect radiolabelled SS-, MG- and BN-analogues against radiolysis by the addition of different mixes of quencher(s). **Methods and Materials:** RCP of radiolabelled DTPA- and DOTA-peptides was quantified by RP $C_{18}$ HPLC in samples, as function of time post radiolabelling at room temperature. After optimization of single quenchers, quenchers (single or mixtures) were applied and RCP's were monitored by HPLC up to 7 days after radiolabelling. **Results:** Addition of either ascorbic and gentisic acid and Se-methionine or melatonin, histidine and methionine to $^{111}$In- or $^{177}$Lu-labelled MG- and BN-analogs containing solutions clearly show stabilizing effect. For SS analogs, ethanol, in combination with a mixture of gentisic- and ascorbic acid, has superior effect in stabilizing radiolabelled SS analogs up to 7 days. **Conclusions:** As a consequence, $^{111}$In- or $^{177}$Lu-labelled SS-, BN- and MG-analogues can be stored and transported in a single-vial ready-for-use liquid formulation up to 7 days after radiolabelling.

## P522

### Bacteriological controls in radiopharmacy: towards our quality requirements

**S. Dupont**, M. Rannou, C. Fessier, J. Legrand, T. Prangère, D. Huglo; Nuclear medicine, University Hospital, Lille, FRANCE.

**Aim** Bacteriological controls were established in April 2011 to test our techniques of bio cleaning and check our working condition. They apply to four equipments available: two laminar flow hood for blood cell labelling, an automated hot cell for positron preparations and a manual hot cell for other radiopharmaceuticals. The two laminar flow hoods are in clean room with an air classification C (ISO 7) and the two hot cells are in clean room with an air classification D (ISO 8). The aim of this study is to make an assessment of bacteriological controls to identify risk area and implement corrective actions. **Materials and Methods** Three types of samples are carried out on different equipments: contact agar for flat surface, swab and count agar for surface difficult to access and Brain Heart Infusion for needles. There is 12 sampling points for each equipment that are controlled every 3 weeks alternatively. Samples are incubated 72h at 37°C then are interpreted after 72h at room temperature. We have a target threshold below 1 CFU and an action threshold above 5 CFU. **Results** There were 103 samples on laminar flow hood used to white blood cells labelling, 4.8% (5) of these samples were positive (> 1 CFU). For laminar flow hood used to other blood cells labelling, there were 97 samples with 4.1% (4) positive. These results are good because no samples have reached the action threshold. The positive results can be explained by the fact that it's an opened system and they were related to areas where the garbage and shielded syringe carrier are placed. In automated hot cell for positron preparation, there were 100 samples with 34% (34) positive whose 8 > to the action threshold. The bench is the largest critical point with 17 positive samples; it's the place where we store the shielded materials. In manual hot cell, there were 114 samples with 45.6% (52) positive. 12 samples exceeded the action threshold; all are located in the work area, which contains most of exchanges with outside materials. Despite its find 10% of critical results, bacteriological controls on radiopharmaceuticals prepared in two hot cells were always negative. **Conclusion** These results have shown few contaminations for laminar flow hoods, which are the most critical point of bacteriological risk. Nevertheless, the two hot cells have revealed too much positive samples that leads to improve techniques of bio cleaning and staff training.

## P523

### Self shielded radiosynthesis box as a tool for fully automated preparation of radiolabeled peptides

M. Kroselj[1], A. Socan[1], T. Dreger[2], R. Knopp[2], **P. Kolenc Peitl**[1]; [1]University Medical Centre Ljubljana, Ljubljana, SLOVENIA, [2]Eckert and Ziegler Eurotope GmbH, Berlin, GERMANY.

**Aim.** Appropriate shielding is in the field of PET radiopharmaceuticals crucial both for preparation (synthesis) and application of prepared radiopharmaceuticals due to high energy of emitted gamma rays. Automated systems for appliciation of PET radiopharmaceuticals were developed and are already used in everyday clinical practice. However, production is still limited to fully automated modules which stand in big and heavy shielded boxes. By using smaller and self shielded radiosynthesis boxes the lack of space can be overcome, thus can be fitted almost everywhere in hospital inviroment. With the introduction of new Modular-Lab MicroCell, shielding becomes an integral part of the synthesis system. The modules to actuate valves, syringes or other moving parts are located outside the shielding and only the sterile, single-use cassettes are placed inside the shielding area as fluid path. Here we describe a fully automated synthesis of $^{68}$Ga, $^{177}$Lu and $^{90}$Y radiolabeled peptides in the self-shielded box. **Materials and Methods.** Fractionated and cation exchange prepurification method were used for $^{68}$Ga peptide radiosynthesis. $^{68}$Ga generator (IGG100, Eckert&Ziegler) was eluted with 0.1M HCl. $^{177}$Lu n.c.a. and $^{90}$Y were purchased from ITG and Perkin Elmer. Reaction conditions such as buffers, pH range, reaction temperature and time and volume of reaction solution were optimized for labelling DOTA-Tyr$^3$-octreotate (DOTATATE). Sterile and single-use cassetes were specially designed for MicroCell. Dose rates

were measured at surface and at 1m distance from shielded unit. **Results** 40 µg of peptide (27,8 nmol) were successfully labeled with $^{68}$Ga (300 MBq) with radiochemical purity >99%. Overall reaction yields were around 60%. With final purification step using SepPak (Waters) $^{68}$Ge breakthrough was 2,4 Bq 68Ge/ MBq $^{68}$Ga. Dose rates at surface were 1,3 uSv/h and at 1m distance were normal background rates. $^{177}$Lu-DOTATATE (3GBq) was synthesised reproducibly with radiochemical purity of > 99%. Dose rates at surface and 1m distance were normal background rates. **Conclusions** A self-shielded radiosynthesis box is a unique solution for Nuclear Medicine departments which lack space for standard automated synthesis systems set in large and heavy dedicated PET boxes. It's main advantage is small size and low weight (app. 450kg). Newly designed single-use cassettes enable same range of synthesis as previously developed cassette systems. Results show reproducible $^{68}$Ga, $^{177}$Lu and $^{90}$Y peptide radiolabeling. With adequate $^{68}$Ge/$^{68}$Ga generator shielding, MicroCell provides sufficient shielding for both PET and β- radioisotopes.

## P524

### Design and development of Arylpiperazine based Homobivalent radioligand (DO3A-(MPP)$_2$): Synthesis based on 'Click Chemistry' and Preclinical Evaluation for Imaging Oligomeric GPCR using SPECT and PET.

**S. Chaturvedi**[1], A. Kaul[1], S. Mishra[1], N. Yadav[2], B. Singh[2], A. K. Mishra[1]; [1]Institute of Nuclear Medicine and Allied Sciences, Delhi, INDIA, [2]Banaras Hindu University, Varanasi, INDIA.

Molecular tracers designed on the paradigm of highly promising 'bivalent ligand' approach are effective contenders for investigating dimerization and clustering of GPCRs. The formation of dimerised and higher- order oligomers, both hetero and homo is an important event in the functioning of GPCR proteins. Dopamine ($D_2$ / $D_3$) and serotonin (5-$HT_{1B}$) receptors exist as homomeric or heteromeric complexes. Based on this, the study focuses on the development aspects of homo-bivalent ligand (DO3A-(MPP)$_2$), as a tracer. As no single imaging modality can be regarded as a perfect solution, the compound is evaluated as both SPECT and PET tracer after radiolabeling with $^{99m}$Tc and $^{68}$Ga, respectively. Aryl piperazines exhibit attractive pharmacophore features with strong affinity for monoaminergic receptors- a class of GPCR receptors. The bivalent ligand with two units of 1-(2-methoxyphenyl) piperazine (MPP) was synthesized as follows. 1,4,10-tris-tert-butoxycarbonylmethyl-7-[2-(di-prop-2-ynyl-amino)-ethyl]-1,4,7,10tetraaza-cyclododecane derived from trisubstituted cyclen was click conjugated with MPP azide. Cyclen scaffold was further used for labeling with radiometals. Intermediates and the compound were characterized by $^{1}$H, $^{13}$C and mass spectrometry. Radiolabeling with $^{99m}$Tc and $^{68}$Ga has been carried to evaluate efficacy as a SPECT and PET tracer. The salient properties for include high radiolabeling yield (>95%) and radiochemical purity (>98% for $^{99m}$Tc, □ 90% for $^{68}$Ga) using very low ligand concentration. Biodistribution indicated predominantly renal excretion. Activity-time relationship was studied using Dynamic imaging wherein the tracer uptake for peak value was studied as a function of time using SPECT camera. Static PET images were obtained which indicate localization in the brain region. Regional localization in brain after isolating hippocampus, cortex and rest of the brain was also evaluated. Other pharmacokinetics parameters including blood kinetics and stability studies have also been evaluated. Cellular uptake and MTT assays using HEK cell-lines have been performed. No significant toxicity has been observed at nanomolar concentrations. Hill coefficients found approximately 2 reflect the homodimeric binding of pharmacophores and cooperative binding. Molecular modeling studies were carried out for a deeper understanding in terms of interactions involved in binding. Monomeric models of $D_2$, $D_3$ and 5-$HT_{1B}$ receptors, built using Homology modeling were subsequently used to build oligomeric models using *Prime* module of *Schrödinger Software*. The receptor models at each step have been refined and evaluated based on Ramachandran plots. Docking studies are underway. The results indicate that (DO3A-(MPP)$_2$), holds a promising future in imaging oligomeric receptors for the effective evaluation of GPCR receptors ($D_2$/$D_3$/5-$HT_{1B}$) responsible for various neuropsychiatric diseases.

## P525

### Evaluation of a strip test for rapid visual determination of tin in 99mTc-radiopharmaceticals

**H. Kvaternik**, C. Barowitsch, S. Kerschbaumer, R. M. Aigner; Division of Nuclear Medicine, Medical University of Graz, AUSTRIA.

**AIM:** Tin (Sn) is present as reducing agent in most of the kits for the preparation of 99mTc- radiopharmaceuticals (99mTc-RPH). These kits may contain up to 1.1 mg stannous chloride dihydrate (SnCl2.2H2O), equivalent up to 610 µg Sn. Our intention was to verify a commercial available tin strip test for the semi quantitative determination of tin in several 99mTc-RPH samples. **METHODS**: For experiments, a universal tin strip test (110028, Merck, Darmstadt) was used. The measuring principle based on the reduction of all tin ions to tin(II) and forming a red dye by the reaction with toluene-3,4-dithiol. 1,0 mL 99mTc-RPH sample placed in a round bottom vial was mixed with 40 µl reagent containing thioglycolic acid. Then the reaction zone of the test strip was placed in the vial for 5 min. The tin concentration was measured by visual comparison of the reaction zone on the test strip with the fields of a colour scale indicator in a range from 10 - 200 µg/mL Sn. Samples with an expected concentration more than 200 µg/mL Sn were diluted with saline before testing. **RESULTS**: Test strips, test reagent, and handling were evaluated by tin standard solutions. Samples of 99mTc-MDP, 99mTc-DPD, 99mTc-Phytate, 99mTc-DTPA and 99mTc-DMSA have been successfully tested. The results of these samples meet the specifications of the tin content which were given in the corresponding SPC. If the 99mTc-kit contained in total <100 µg SnCl2.2H2O we get results below quantification limit. No results were obtained with 99mTc-IDA and 99mTc-MIBI due to interferences with the reagent. **CONCLUSION:** It could be shown that the tin concentration in selected 99mTc-kits, containing more then 100 µg SnCl2.2H2O, can be measured with a commercial available tin strip test. The semi quantitative test leads to a sufficient visual result within 5 min and is suitable for routine quality control.

## P526

### Radiopharmacy - a scarce skill in South Africa

**S. M. Rubow**, J. le Roux; Tygerberg Hospital and Stellenbosch University, Tygerberg, SOUTH AFRICA.

The Nuclear Technologies in Medicine and the Biosciences Initiative (NTeMBI) in South Africa is investigating scarce skills in their fields of interest. Skills in Radiopharmacy are required in two fields, manufacture of radiopharmaceuticals at reactor or cyclotron centres, and compounding and dispensing of radiopharmaceuticals in nuclear medicine units or central radiopharmacies. South African regulations require that a pharmacist be responsible for the production of all medicines, including radiopharmaceuticals, and that production facilities be GMP compliant. In South Africa, the preparation of radiopharmaceuticals in nuclear medicine units is traditionally seen as a laboratory function under supervision of the nuclear physician, and these laboratories are not regarded as pharmacies. Questionnaires to investigate staff numbers, staff training and the perceived need for specialists in Radiopharmacy, were sent to supervisors in radiopharmaceutical companies and Nuclear Medicine units in hospitals. Information from the responses confirmed that pharmacists are mostly employed in radiopharmaceutical industry, with extremely limited involvement in Hospital Radiopharmacy. Currently, radiopharmacy tasks are carried out by the following categories of people in South Africa: • Pharmacists who have a specific post-graduate degree in radiopharmacy, and are registered as specialists with the SA Pharmacy Council • Pharmacists who have either in-house training or non-degree post-graduate training, employed at manufacturing sites or in a hospital • Scientists with a degree in chemistry and further training and/or experience in radiochemistry and radiopharmacy • Nuclear Medicine radiographers (technologists) The situational analysis indicates that 11 specialist radiopharmacists and 14 pharmacists with some specialised training should ideally be employed in the different radiopharmacy sites including industry, retail and hospitals. Until such persons are available, ways should be sought to recognize the experience and knowledge of non-pharmacists involved in radiopharmacy, and to improve their knowledge and understanding of pharmaceutical aspects of and quality management in radiopharmacy. Two South African universities currently offer MSc degrees with Radiopharmacy as an option. Shorter courses such as post-graduate diplomas or certificates of competence should be considered to provide accredited training in selected aspects of Radiopharmacy. NTeMBI has suggested a national plan to address the shortage of human resources in Radiopharmacy, which includes amongst others, engaging authorities to establish specialist posts for radiopharmacists.

P15-2 - Tuesday, Oct. 22, 16:00 - 16:30, Poster Exhibition Area

## Radiopharmaceuticals & Radiochemistry & Dosimetry: Radiometals

## P527

### First Decade of a State Teaching-Hospital-Based PET Radiopharmaceutical Production & Development Facility Including Solid Targetry Production of Radiometal Isotopes $^{61}$Cu, $^{64}$Cu $^{89}$Zr & $^{45}$Ti

**R. I. Price**, RAPID PET Labs Team; RAPID PET Labs, Sir Charles Gairdner Hospital, Nedlands (Perth), AUSTRALIA.

OUTLINE**:** Perth, Australia is one of the world's most isolated cities, being 3000km from the nearest external medical cyclotron. Conventional PET isotopes must be synthesized and utilized locally; however this is not so for several PET radiometals. Following establishment of a routine sole-supplier State PET-radiopharmaceuticals service our group has seen growth from around 1760 patient-doses in 2003 to 8800 in 2012, serving 4 PET cameras (6 by mid 2013). As experienced elsewhere this is represented by 95% FDG; however 8 other radiolabels are available for the clinic,

the most popular being $^{68}$Ga-octeotrate and $^{11}$C-PiB. CONTEXT: An 18/9MeV cyclotron and asociated laboratory was originally installed without significant research capabilities (funding constraints). It has run daily; undergoing a major upgrade in mid-2012, converting to 18/18 and dual-beam, plus doubling of beam-currents. This revised single unit will serve Western Australia's (population 2.5M) clinical PET needs for at least 4yr. Following establishment of the routine service, work by the group of the late Michael J. Welch, Washington University (plus a notable discussion with him in 2008) inspired our team that PET radiometal isotopes were strategically important - particularly since (at the time) no radiometal PET sources were readily available in Australia. Subsequent work exemplified what is achievable with a cyclotron embedded in a sophisticated medical physics/engineering environment. Local development of solid-targetry engineering & chemistry has enabled quasi-routine production of $^{61}$Cu, $^{64}$Cu, $^{45}$Ti and $^{89}$Zr as validated products for fostering preclinical research nationally - particularly in experimental oncology. Collaborative research utilizing novel radiopharmaceuticals is underway, including a first-in-human investigation of a therapeutic antibody. Opportunities including imminent commissioning of Western Australia's first preclinical microPET/SPECT/CT/MRI systems have motivated development of adjunctive facilities in our laboratory for antibody radiolabeling, plus cell culturing & small-animal imaging. CONCLUSION: In establishing a regional PET radiopharmaceuticals service with strategic objectives, many-fold increases in the palette and magnitude of services, plus R&D opportunities must be considered, given that the facility's lifetime exceeds 25yr. In strategic developments of a PET radiopharmaceutical production centre, a strong connection with physics/engineering expertise is as important as the obligatory 'joined-at-the-hip' relationship with clinical services.

## P528

### Study of 68Ga sorption-desorption mechanism in mixed media

**A. Larenkov**[1], A. Bruskin[1], E. Lesik[1], G. Kodina[1], Y. Zubavichus[2]; [1]Burnasyan Federal Medical Biophysical Center, Moscow, RUSSIAN FEDERATION, [2]National Research Centre "Kurchatov Institute", Moscow, RUSSIAN FEDERATION.

Chemical form of 68Ga in the eluate of the 68Ge/68Ga generator, theoretically means, that it can be directly used as universal source of 68Ga for RPs synthesis, provided the availability of a suitable chelating agent. After long experience of 68Ge/68Ga generator application in various research groups, the presence of non-isotopic carrier and parent radionuclide in the eluate still is one of the main problems. In FMBC, Russia, two Methods for purification and concentration of 68Ga are developed. Both of these Methods are based on combined cation-anion exchange in mixed media (HCl-acetone or HCl-ethanol). Note, that conditions found allow to obtain effective transport of 68Ga from cation exchanger to anion exchanger at the concentration of HCl not higher than 2.5M. After that 68Ga is eluted from the anion-exchange resin with 0.02 - 0.1 M hydrochloric acid. [1]. It was found that it is exactly an addition of organic solvent, that allows to use low HCl concentrations. Trying to understand speciation of Ga, determining its ion-exchange behavior, we studied EXAFS spectra of Ga in different mixed media. The study was carried out in Kurchatov Center for Synchrotron Radiation and Nanotechnology. Few series of samples (GaCl3 5 mmol in 0.1-3 M HCl) were studied. In each series concentration of ethanol was varied from 0 % to 90 %. In each series of samples an abrupt change in the spectrum was observed above a certain threshold concentration of ethanol. This change is appeared to be connected with transformation of Ga coordination from octahedral cation [Ga(H2O)6]3+ to tetrahedral anion [GaCl4]-. It was found, that higher concentration of hydrochloric acid corresponds to the lower concentration of alcohol, which is needed for transition from an octahedral aqua complex to the tetrahedral chloride complexes. These data obtained from XANES spectra have been confirmed by quantitative analysis of the EAXFS spectra and correlate with our data on variability in ion-exchange behavior of Ga. 1. Kodina G., Larenkov A., Lesik E. Ion exchange processes in HCL-ethanol media for high-purified 68Ga solutions. Eur. J. Nucl. Med. Mol. Imaging V39-Supp2-October 2012, p. S527

P16-2 - Tuesday, Oct. 22, 16:00 - 16:30, Poster Exhibition Area

## Radiopharmaceuticals & Radiochemistry & Dosimetry: Radiopharmakinetics & Drug Development

## P529

### Quantification of DOTA-peptide content and purity by titration with metal ions

**W. A. P. Breeman**[1], E. de Blois[1], H. S. Chan[1], J. L. Erion[2]; [1]Erasmus MC, Rotterdam, NETHERLANDS, [2]BioSynthema, St Louis, MO, UNITED STATES.

Aim: Radiolabelled DOTA-peptides are in use for Peptide Receptor Radionuclide Scintigraphy and Therapy. Quality control of DOTA-peptide, such as quantification of content and purity can be performed with various Methods, including and most commonly by UV. There are numerous conditions in which this is hampered, e.g. impurities may also have UV-absorption. Our aim was quantification of DOTA-peptide content and purity. Methods an Materials: An alternative method was developed, which include titration of the DOTA-moiety with metal ions, such as Lu, In and Y. Initially at concentrations of metal ion ≤ peptide, and increasing, always with known amounts of metal ions. One molecule DOTA-peptide can incorporate 1 metal ion. Titration is performed with ≥4 ratios of metal ions *vs.* DOTA-peptide. After incorporation (=labelling) the reaction mixture was subsequently analysed by reversed phase $C_{18}$ HPLC or UPLC, which include base-to-base separation of metal-DOTA-peptide (A) from DOTA-peptide (B) (Asti *et al.*, Nucl Med Biol, 2012). Subsequently peak area of A and B are determined, and ratio of peak area of A *vs.* B calculated. If peak B does not fully shift to peak A, this is an indication of the presence of impurities with similar chemical characteristics as the DOTA-peptide, but cannot incorporate metal ions. By plotting the fraction of metal-DOTA-peptide over total DOTA-peptide will result in a point in which all DOTA-peptide has incorporated metal ions, thus 100% incorporation, and, at a known amount of metal ion. Eventually the concordant DOTA-peptide content can be calculated. For radiochemistry the "available" DOTA-moiety is of interest, while for pharmacists the total DOTA-peptide is of relevant. Results: Increasing metal ions in the reaction mixture clearly shows the decrease of DOTA-peptide (peak B), concordant increase of metal-DOTA-peptide (peak A), and increase of ratio peaks A *vs.* B. Reproducibility was 100±0.3%, n=10 at 1 nmol, 100±2%, n=10 at 10 pmoles. Lower level of detection of DOTA-peptide was 10 pmoles. Variation in ratio of peak area of A *vs.* B was <2% at ≥10 pmoles DOTA-peptide. In addition, metals, such as Fe, Zn and Cu were always present, already incorporated in the DOTA, even up to 10% of the DOTA-moiety (and also confirmed by MS). DOTA-peptide content was always lower (range -10% to -55%) *vs.* quantification by UV-absorption. Conclusion: DOTA-peptide content and purity can be quantified accurately.

## P530

### Correlations and FTIR characterization studies on 99mTc labelled complexes

**I. C. GRIEROSU**[1], M. Drobota[2], C. Stefanescu[1]; [1]Department of Biophysics and Medical Physics - Nuclear Medicine, U.M.F."Gr.T.Popa", Iasi, ROMANIA, [2]Petru Poni Institute of Macromolecular Chemistry, Iasi, ROMANIA.

Aim. In order to gain some insight about new understanding of the radiotracers mechanism and biodistribution we focused on labelled complexes Fourier Transform Infrared (FTIR) studies. FTIR data can be used as molecular signatures for physiological status once the spectral patterns are correlated with biological properties. We look after posibil conformational modification of the radiotracer in standard solution and in plasma. Material and method. Nanocolloidal labelled complexes FTIR spectra were recorded on a Bruker Vertex 70 FTIR spectrometer, equipped with a diamond ATR device (Golden Gate, Bruker). Specac's High Temperature Golden Gate™ ATR Accessory is a high performance single reflection (45° angle) monolithic diamond ATR product offer for spectroscopic sample analysis of samples up to 200°C. The absorption was measured in a wave number range from 4000 to 600 cm-1. For a spectrum 64 scans were taken, with a baseline correction. Results. The prominent absorption peak 3300 cm-1 is due to the N-H stretching mode (amide A) of proteins. The strong absorption band at 1630 cm-1 correspond to C=O stretching vibrations (amide I) whereas the vibration band at 1580 cm-1 is attributed as amide II arising of N-H bending vibrations strongly coupled with C-N stretching of proteins, as related with literature data. This spectral region is sensitive to changes in the molecular geometry and hydrogen bindings of peptide groups. In the protein amide I (with vmax in the range 1660-1650 cm-1) and II (with vmax in the range 1594-1548 cm-1) regions, significant shifts of the maxima can be observed. Though amide I upshifts toward 1640 cm−1, amide II downshift to 1580 cm−1. Conclusions: Our results suggest the idea that secondary structure modifications appear, most likely due to the elimination of the β-sheets and formation or replacement with the alpha or random coil structure. These data will be further correlated with analytical studies in order to better understand radiotracer localization mechanisms.

## P531

### Preparation of 131I- Pentamidine and Evaluation for scintigraphy of experimentally Leishmania tropica infected Hamsters

T. İnceboz[1], F. Y. Lambrecht[2], M. S. Eren[3], N. Girginkardeşler[4], **R. Bekis**[3], O. Yılmaz[5], Ö. Er[2], A. Özbilgin[4]; [1]Department of Parasitology, Dokuz Eylul University, School of Medicine, Izmir, TURKEY, [2]Department of Nuclear Applications, Institute of Nuclear Sciences, Ege University, Izmir, TURKEY, [3]Department of Nuclear Medicine, Faculty of Medicine, Dokuz Eylul University, Izmir, TURKEY, [4]Department of Parasitology, Celal Bayar

University, School of Medicine, Izmir, TURKEY, [5]Department of Laboratory Animal Science, Dokuz Eylul University, Izmir, TURKEY.

Aim: To assess the ability of 131I- Pentamidine scintigraphy to detect the lesions of Leishmania tropica (L. tropica) infection. Materials and Methods: Three groups of male hamsters were formed, each composed of 10 eight-week old hamsters and in control hamsters without induced lesions. A concentration of L. tropica (1x108 promastigotes/ml) 0.3 ml promastigote suspension was injected subcutaneously into the right posterior soles of the feet of all the hamsters, and infection established. An animal model of L. tropica infection was developed. The success of implantation was controlled 40 days after implantation. Five infected and two healthy animals were studied. Pentamidine was radioiodinated with I-131 using the iodogen method. In visual evaluation, first normal 131I- Pentamidine uptake pattern was demonstrated in healthy Syrian hamsters (Mesocricetus auratus). After that 131I- Pentamidine uptake in infected animals was evaluated visually, after the injection of 3.7 MBq (0.13 mg/rat) 131I- Pentamidine intravenously. Static images from the whole body were obtained at 5. and 30 minutes, 2, 6 and 24 hours. Visual and semiquantitative analyses were performed. In semiquantitative analysis, an irregular region of interest was drawn over infected animal's right feet and liver and a second region of interest was drawn over normal animal's right feet and liver as control. Infected/control ratios for right feet and liver were calculated using the mean counts. Results: 131I- Pentamidine was accumulated in the stomach, liver, bladder and right feet of the infected animals. In the visual evaluation, it was noticed that there was increased 131I- Pentamidine uptake in the right feet and liver of the infected animals according to the control. Although there is no statistically difference in mean counts between the infected and healty animals, the ratio for mean counts of infected animals to the control in the liver and right feet were over 2 at the 6 hours images and later. Conclusion: In concluding, 131I-Pentamidine might be useful as an agent for diagnosis of Leishmania tropica (L. tropica) infection especially involvement of soft tissue and liver Imaging at 2 hours and 6 hours seems to be more suitable imaging time for the diagnosis of Leishmaniasis.

P17-2 - Tuesday, Oct. 22, 16:00 - 16:30, Poster Exhibition Area

## Radiopharmaceuticals & Radiochemistry & Dosimetry: Antibodies & Peptides

### P532

### Influence of chelator type on in vitro receptor binding and stability in 177Lu-labeled anti-EGFR monoclonal antibodies

**Z. Novy**[1], A. Laznickova[2], J. Mandikova[2], M. Laznicek[2], F. Trejtnar[2]; [1]Institute of Molecular and Translational Medicine, Palacky University Olomouc, Olomouc, CZECH REPUBLIC, [2]Faculty of Pharmacy, Charles University in Prague, Hradec Kralove, CZECH REPUBLIC.

Aim: Monoclonal antibodies are used in therapy of various diseases. Thanks to highly specific uptake in the target tissue the antibodies could be utilized as carriers of radioisotopes to the tumors in case of targeted radioimmunotherapy and/or diagnosis. However, important characteristics of antibodies such as binding to the target or stability in the organism may be affected by various structural parameters. In this study we have focused on potential influence of selected chelators on radiochemical quality and in vitro receptor binding capacity of two modified monoclonal antibodies. Materials and Methods: We have chosen cetuximab and panitumumab, both ligands of epidermal growth factor receptor (EGFR). These two antibodies were coupled with three macrocyclic bifunctional chelators (DOTA, NOTA and PTCA) and labeled with lutetium-177. The stability of the preparations was checked in HPLC and the rate of binding to EGFR expressing cell lines (A431, HaCaT and HepG2) was examined. Results: The used method led to very stable radiolabeled preparations for all three chelators. Binding rate of labeled antibodies varied from 15% to 45% of applied dose according to used cell line. The results showed that the binding to the target cells was not affected by the type of chelator. Conclusion: We conclude that recent chelators (NOTA and PCTA) could be convenient for radiolabeling of anti-EGFR antibodies with lutetium-177 as well as established chelator DOTA. Therefore NOTA and PCTA could be useful tools in future preclinical studies with these radiopharmaceuticals.

### P533

### Preliminary results of microwave radiolabelling of DOTA-gastrin analogue with 90Y

**D. Pawlak**, M. Maurin, P. Garnuszek, R. Mikolajczak; Radioisotope Centre POLATOM, National Centre for Nuclear Research, Otwock, POLAND.

Introduction. A macrocyclic chelator DOTA (1,4,7,10-tetraazocyclododecane-1,4,7,10-tetraacetic acid) is one of the most often used chelators for coupling to peptides for PRRT (peptide receptor radionuclide therapy), however the reaction kinetics differ for each radiometal. Hence, depending whether the 90Y, 111In or 177Lu are planned to be used, the optimization of radiolabelling conditions is required. In addition, the elevated temperature and incubation time may influence the rate of undesired radiochemical species formation. Contrary to traditional heating devices used for radiolabelling, the microwave heating assures that desired temperatures are reached rapidly in a fully controlled radiolabelling process. Thus, microwave heating shortens incubation time, which might be critical in case of oxidation-sensitive peptides. Aim. The aim of this work was to use microwave heating for optimization of 90Y radiolabelling conditions of a gastrin analogue known as CP04 (DOTA-DGlu-DGlu-DGlu-DGlu-DGlu-DGlu-Ala-Tyr-Gly-Trp-Met-Asp-Phe-NH2). Methods. For radiolabelling 600 MBq of 90Y (ItraPol, NCBJ OR POLATOM) was added to 20 ug of CP04 (Pichem, Austria) dissolved in 0.2 mL of ascorbic acid solution (50 mg/mL, pH 4.5) and incubated in microwave oven (Bioteg Initiator). The influence of temperature and reaction time on the labeling yield and radiochemical purity were investigated using HPLC: column Ace 3 C18 150x4.6; isocratic F = 0.5 mL/min; mobile phase: 25% Acetonitrile/0.1% TFA/Water, using UV 215 nm and on-line radiometric detection. Results. Radiolabeling yield greater than 99% (calculated in reference to unbound 90Y radioactivity) was obtained already after 5 min incubation in a microwave oven at 95oC. Isocratic HPLC allowed good resolution and quantitation of observed peaks. HPLC radiochromatograms revealed several peaks that can be attributed to radiolabelled CP04 and to impurities (including oxidized form of CP04 due to the methionine oxidation). Radiochemical purity of 90Y-CP04 (Rt ca. 10.9 min) depended on the time of incubation and was decreasing with increase of incubation time. At 5, 15 and 25 min incubation time the radiochemical purity was 94.4%, 91.1% and 88.5%, respectively. Contribution of radioactive oxidized forms of CP04 (Rt ca. 3.5-3.8 min) increased with incubation time (from 0.8% to 4.6% after 5 and 25 min, respectively). Therefore, we conclude that incubation time should be as low as possible to obtain 90Y-DOTA-gastrin of high RCP. Acknowledgement. This project was financed from the funds of the National Science Centre (Poland) allocated on the basis of the decision number DEC-2011/03/B/ST5/02734.

### P534

### Development of new radionuclide nanocarriers to overcome the radioresistance of stem-like glioblastoma cells

**D. Séhédic**[1,2], M. Mougin-Degraeff[2], F. Hindré[1], F. Davodeau[2], E. Garcion[1]; [1]U1066 MINT, Angers, FRANCE, [2]U892 CRCNA, Nantes, FRANCE.

Although only palliative, external beam radiation remains to date the standard treatment of dramatic brain glioblastoma (GBM). Radiotherapy effectiveness is indeed largely limited by resistance mechanisms combining intrinsic properties of tumour cells to the influence of the microenvironment in which they develop (e.g. hypoxia). The recent discovery of stem-like cancer cells (SLCC) in GBM supports the presumption that the failure of conventional antitumor strategies could be attributed to a problem of target cells. Thus, the present work deals with the development of a new-targeted internal radiotherapy to radio-resistant SLCC through the use of nanocarriers loaded with α- or β- radiation emitters. As CXCR4 receptor has been associated with radio-resistance and with SLCC occurrence, we focused on the targeting of these proteins in a human GBM models known to express it: A172. We primarily developed 50 nm lipid nanocapsules (LNCs) functionalized with monoclonal antibodies (mAbs) directed against CXCR4 (or isotype control). LNCs will then be combined to 188Re (beta emitter) and 211At (alpha-emitter) for further evaluation. By using blocking antibodies, our investigations merged the interest of targeting SLCC associated epitopes to the one of inhibiting CXCR4 signaling pathways to overcome radioresistance. In line with this, by using immunofluorescence flow cytometry, we found that CXCR4 expression is correlated with radiation doses: we found 41% expression when are radiated at 32Gy versus 10% expression when they are radiated at 0Gy. Finally, new encapsulation of 125I (β-emitter and halogen), which will help for the development of 211At (halogen), has been developed. Preliminary results show a relatively stable SIB encapsulation over time in different medium. Efficacies of β- versus α-nanocarrier based radiotherapies will then be compared in vivo after othotopic implantation of human GBM cells in immunodeprived SCID mice and loco-regional infusion of the treatment.

### P535

### Is Necessary the Detection of Human Anti-Mouse Antibody (HAMA) Previous to the Administration of Radiopharmaceutical Tc99m-Besilesomab (Scintimun®)?

**A. LIMA**, M. QUERA, M. MARTINEZ, A. HERNANDEZ, M. MOGA; UNIVERSITARY VALL D´HEBRON HOSPITAL, BARCELONA, SPAIN.

AIM: The radiopharmaceutical Tc99m-Besilesomab (Scintimun®) is a monoclonal antibody (IgG1) of murine origin which allows the granulocytes tagging "in vivo". The objective was to determine the significance of the detection of Human Anti-Mouse Antibody (HAMA), pre-administration of the radiopharmaceutical. MATERIAL AND METHODS: 33 patients were examined, age 58.6±19.9 (18 women) with suspicion of infection/inflammation of peripheral skeleton bone, and bone scan compatible with septic process. It was made a blood extraction (5ml) on the

day of the bone scan and then, we proceeded to the quantitative blood serum detection of HAMA, by ELISA technique (commercial test: MEDAC®). The test is calibrated against anti-mouse IgG antibodies. The measuring range of the HAMA-ELISA Medac® is 40 to 2000ng/ml. The reference values are: <40ng/ml, HAMA negative and ≥40-2000ng/ml HAMA positive. The patients' medical records were reviewed up to 3 years prior to the completion of the detection, in an attempt to relate HAMA values obtained with the immune pathology and/or treatment with antibodies of murine origin before the administration of Scintimun® which could influence the results. RESULTS: From 33 patients, there were 31 cases (94%) of HAMA negative (<40ng/ml) 0.4±1.6ng/ml, and 2 cases (6%) of HAMA positive (≥40-2000ng/ml) 53.8±13.4ng/ml. From the two patients with positive HAMA, one of the patients had rheumatoid arthritis and the other one had nonspecific osteoarthritis and had presented an episode of nonspecific allergy. Among the patients with negative HAMA, three presented rheumatoid arthritis (9.6%), and one had nonspecific osteoarthritis (3.2%). No patients were treated with murine origin antibodies in the mentioned time period. Tc99m-Besilesomab was administered only to patients with negative HAMA. HAMA positive results forced a change in the labeling of leukocytes with Scintimun® from "in vivo" to "in vitro" labeling (Tc99m-HMPAO-leukocytes). CONCLUSION: The finding of positive HAMA in 2 patients, suggests that HAMA determination is advisable, prior to the administration of 99mTc-Besilesomab, to avoid the risk of hypersensitivity reactions. Although such low figures, together with the lack of relation with immune pathology (3HAMA negative patients showed rheumatoid arthritis) and/or biological treatment, it cannot be ruled out that these positive figures could be false positives. This is the reason that we will perform two additional tests to verify if it actually is a false positive or not. Complementary tests: Rheumatoid Factor and Heterophile Antibody. Future-directions: Monitoring these patients to see if after the administration of Antibody, the HAMA values become positive.

P18-2 - Tuesday, Oct. 22, 16:00 - 16:30, Poster Exhibition Area

## Radiopharmaceuticals & Radiochemistry & Dosimetry: New Targets

### P536

### Radiolabeling and biodistribution properties comparison of hybrid nanoparticles bearing CoFe2O4 and Fe3O4 magnetic cores

**D. Psimadas**[1,2,3], G. Baldi[4], C. Ravagli[4], T. Tsotakos[1,3], E. Fragogeorgi[1,3], M. Comes-Franchini[5], V. Valotassiou[2], P. Georgoulias[2], G. Loudos[1]; [1]Department of Medical Instruments Technology, Technological Educational Institute of Athens, Egaleo, GREECE, [2]University Hospital of Larissa, Larissa, GREECE, [3]Institute of Nuclear and Radiological Sciences and Technology, Energy & Safety, N.C.S.R. "Demokritos", Aghia Paraskevi, GREECE, [4]CERICOL, Colorobbia, Firenze, ITALY, [5]Department of Industrial Chemistry "Toso Montanari", University of Bologna, Bologna, ITALY.

Aim: Magnetic NPs (MNPs) are well-established nanomaterials that offer controlled size and have the ability to be manipulated by an external magnetic field and enhance contrast in magnetic resonance imaging (MRI). Radiolabeling of MNPs provides an additional imaging modality allowing hybrid dynamic imaging and visualization of their in vivo route. MNPs bear iron oxide cores with favorable superparamagnetic properties and can be hybridized with various biocompatible polymers, resulting in small and versatile nanoformulations. In this study we compare the radiolabeling and biodistribution behavior of hybrid micelle-like MNPs bearing Fe3O4 and CoFe2O4 metal cores. Materials & Methods: The two nanoformulations studied here are PLGA-PEG-Fe3O4 [PLGA: poly(D,L-Lactic-co-glycolic acid); PEG: polyethylene glycol] and BSA stabilized PLGA-CoFe2O4 (BSA: bovine serum albumin). Radiolabeling with 99mTc was performed by the direct method using SnCl2. The assessment of their in vitro stability was performed by histidine (His), diethylene triamine pentaacetic acid (DTPA) and serum challenge assays. Biodistribution analysis was performed using anatomic as well as scintigraphic techniques in normal mice by intravenous administration of the radiolabeled nano-preparations (4-6 μg of Fe3O4/CoFe2O4 per animal) via the tail vein (100 μL, 3-5 MBq per animal). Results: Direct radiolabeling was performed in high yields (<98%) using 40μg SnCl2 with neither radiocolloid nor free pertechnetate present in the final preparations. Radiolabeled nanoformulations proved to be stable after incubation for 2 h in the conditions tested. At 24 h 99mTc dissociated from 99mTc-PLGA-BSA-CoFe2O4 in a larger percentage than from 99mTc-PLGA-PEG-Fe3O4, indicating greater robustness of the magnetite nanoformulations. Both 99mTc-labeled MNPs showed primarily liver and spleen uptake. One major difference between them is that the uptake of magnetite MNPs remains relatively constant until after 24 h, while the uptake of the cobalt ferrite MNPs, which was greater at 1 h, presented significant reduction at 24 h. Additionally 99mTc-PLGA-PEG-Fe3O4 present significant bone marrow uptake which is clearly visible at the γ-camera images. Conclusion: After studying some of the major properties of one magnetite and one cobalt ferrite hybrid nanoformulation, it can be concluded that even though the metal core can have significant influence in a number of properties such as hyperthermic, magnetic, etc, the radiolabeling and most importantly the in vivo biodistribution properties of the nanoformulations cannot be considered to be significantly affected. It is mainly the shell structure as well as the size that determines the in vivo fate of hybrid MNPs.

### P537

### Synthesis and quality control of $^{111}$In labeled PSMA-minibody (IAb2-M-DOTA)

**D. Mueller**[1], I. Klette[1], H. Kulkarni[1], C. Schuchardt[1], S. Wiessalla[1], D. Bartlett[2], D. Ho[2], C. P. Behrenbruch[2], A. Wu[2], R. P. Baum[1]; [1]THERANOSTICS Center for Molecular Radiotherapy and Molecular Imaging, Zentralklinik Bad Berka GmbH, Bad Berka, GERMANY, [2]ImaginAb, Inc., Inglewood, CA, UNITED STATES.

**Aim** Prostate Specific Membrane Antigen(PSMA) is expressed by normal prostate and elevated considerably in prostate cancer. Therefore a radiolabeled antibody with high affinity to PSMA is of particular interest. The DOTA conjugated protein IAb2-M-DOTA (huJ591 antibody fragment) combines both, a ligand for radio-metal labeling and a molecule to bind to PSMA with a high affinity. Usually labeling of DOTA- conjugated peptides requires higher reaction temperature. On the other hand a lower labeling temperature is needed in order to preserve the affinity of the protein moiety. The aim of our study was to devise a procedure for optimal labeling and quality control Methods. **Materials & Methods** All reagents were purchased from commercial sources and used as received. $^{111}$In was purchased from Mallinckrodt Medical B.V. / Covidien. To examine free $^{111}$In by TLC, ITLC-SG[Varian] and 0.4M citric acid as solvent was used. The radiochemical purity is expressed as the % of the main peak activity, vs. total activity. The radiochemical yield is expressed as percentage and is not decay corrected. The radiochemical purity was also determined using size exclusion HPLC (pump: Jasco PU-1580; quaternary gradient unit: Jasco LG-1580-04; radio detector: biostep IsoScan LC; Multiwavelength Detector: Jasco MD 1510, column: GPC BIO-SIL SEC 250; solvent: 0.1 M phosphate buffer, 1.2 mL/min). The affinity was checked with the help of Recombinant Human PSMA/FOHL1. Synthesis of $^{111}$In labeled IAb2-M-DOTA: 410 MBq $^{111}$In was added into a solution of 2 mg IAb2-M-DOTA in 1 mL of 1M sodium acetate buffer (pH= 6.2). After heating the reaction mixture for 30 minutes at 40 °C, the solution was sterile filtered and samples were taken for quality control, sterility and endotoxin test. **Results** After 30 minutes, $^{111}$In was completely bound to the DOTA moiety of IAb2-M-DOTA. The radiochemical yield was 85%. Using radio ITLC no unbound $^{111}$In could be detected in the final product. The radiochemical purity was greater than 95 % as determined by SE-HPLC. The product is stable for 24 h. The affinity of the $^{111}$In labeled IAb2-M-DOTA was similar to that of the unlabeled protein**. Conclusion** We developed a simple procedure for the labeling of IAb2-M-DOTA with $^{111}$In. The quality control Methods allowed rapid check of the final product. The labeling of IAb2-M-DOTA with $^{177}$Lu would be investigated in further studies.

P19-2 - Tuesday, Oct. 22, 16:00 - 16:30, Poster Exhibition Area

## Radiopharmaceuticals & Radiochemistry & Dosimetry: Miscellaneous

### P538

### Laws versus Quality scheme: an opportunity to improve

**G. Chittò**, E. Di Domenico, P. Gandolfo, S. Papa, G. Pedrinelli, F. Ria, C. Tafuri; CDI Centro Diagnostico Italiano Spa, Milan, ITALY.

**Aim** European and national legislation for radiation protection, standards and certification schemes of quality and the new Compounding of Radiopharmaceutical (PHARMEUROPA Vol.23, No.4, Oct. 2011) are elements that affect and influence an Healthcare Organization and, as a result, a Department of Nuclear Medicine. In a complex system such as healthcare, can be easy to be disoriented and even dangerous for its economic consequences. The work aims to propose the "state of the art" of our analysis, able to provide a reference tool and consideration in order to rationalize typical processes of Nuclear Medicine Department. The re-engineering of processes and some available tools can be driven by means that make it easier the path to follow. **Materials and Methods** Comparing the requirements of the European Rules as the requirements of the new Compounding of Radiopharmaceutical, Italian Laws (as Italian D.M. Health Office 30/03/2005 Good Radiopharmaceutical Preparation Practice in Nuclear Medicine), Quality Certification/Accreditation Schemes, both ISO 9001 Quality Rules and Joint Commission International (JCI) Standards, offer interesting ideas for simplification and rationalization. The regulations have been clustered in different topics. Then, for each topic is been chosen the most strict among the examined requirement. **Results and conclusion** The rationalization process has become essential for various causes, from the economic to those related to the dispute raised by the patients, the provisions of the Statutes and, not insignificant, the competition

among health care organizations. In conclusion of the work, CDI advances that the implementation of quality standard recognized by the organization to support processes, diagnosis and treatment, can reduce some index of risk associated with the daily activity of a department. Moreover, it could improve a better management of the available resources and the satisfaction of patients. Comparing law and quality scheme is so a useful tool to promote the improvement. The compliance to the requirements of law is at least what an organization needs but if it would be in evidence it has to go beyond it.

## P539

### Assessment of Mass Spectrometric Detection for Quality Control of PET Radiopharmaceuticals

**R. Canales Candela**[1], M. Allen[2], M. Baumert[2], F. I. Aigbirhio[1]; [1]University of Cambridge, Wolfson Brain Imaging Centre, Cambridge, UNITED KINGDOM, [2]Advion, Harlow, UNITED KINGDOM.

**Introduction:** The use of mass spectrometers for the quality control (QC) of PET radiopharmaceuticals is not a common practice due to concerns related to sensitivity and reproducibility during routine analysis, as well as instrument size and the costs associated to implementation and maintenance. However, advances in instrumentation have drastically reduced the investment and footprint of mass spectrometers which can now be installed into standard QC laboratories. In this work we assess mass detection of radiopharmaceutical preparations routinely produced for PET clinical imaging, using a new single-quadrupole instrument. Consideration was given to the ease of use and times for analysis, both important parameters for analysis radiopharmaceuticals labelled with short half-life radioisotopes. **Methods:** Mass data was acquired using an Advion expression CMS instrument equipped with a ESI source connected to a gradient HPLC. The samples were analyzed after decay without further treatment (0.1 mL/min, methanol / 0.05 % formic acid or acetonitrile / 50 mM ammonium formate); and had been formulated in 0.9 % saline, 0-10 % EtOH and various buffers. Fast flow injection analysis (FIA) in either positive or negative ionization IM mode was used for compound profiling and identity confirmation. **Results:** Mass determination was within 0.1-1.6 m/z of the expected, depending on the analyte. Increased hydrophobicity gave higher signal intensities probably due to the stable generation of charged droplets by the electrospray, producing ions that enter the gas phase more readily. The minimum detection level was found to be between 25 pg and 2.5 ng for $^{11}$C ( PIB, PK11195, Metomidate) and $^{18}$F (FLT, Fallypride, FMISO). **Conclusion:** Our preliminary assessment shows that the observed sensitivity range is within the level required for PET product identification. ESI is suitable for ionizing various radiopharmaceuticals including polar compounds; with a typical turn around time of less than one minute per analysis. Spectra vary with types and intensity of ions depending on the source conditions applied, mobile-phase, buffers and additives. The use of a compact mass detector has clear advantages to be applied to underpin GMP quality control of radiopharmaceutical, especially when coupled with HPLC, adding more accurate and robust chemical identification. Our preliminary result has established this potential for further development to be integrated into QC systems, complementing other standardised detection Methods more widely available in the radio-analytical laboratory.

## P540

### Risk assessment and economic impact evaluation of the application of the Compounding of Radiopharmaceutical (PHARMEUROPA, Vol.23, No.4, October2011)

G. Chittò, E. Di Domenico, P. Gandolfo, S. Papa, G. Pedrinelli, **F. Ria**, C. Tafuri; CDI Centro Diagnostico Italiano Spa, Milan, ITALY.

***Aim*** The new *Compounding of Radiopharmaceutical*, published on PHARMEUROPA, Vol. 23, No. 4, Oct. 2011, shows many patterns similar to the Italian D.M. Health Office 30/03/2005 "*Good Radiopharmaceutical Preparation Practice in Nuclear Medicine*". Aim of this study is to provide a representation of all the necessary costs, after one year from the application of Italian law into a department of Nuclear Medicine, in order to guarantee a great quality of the radiopharmaceuticals, and a positive impact to the patient and to the sanitary organization on the risk evaluation. The presented results can become a useful guideline for hospitals facing similar pathways in the future. ***Materials and Methods*** In order to assess the economic impact of the new Compounding, fixed costs of a nuclear medicine department were calculated, (i.e. costs non depending on the new regulations). Subsequently were estimated only the emerging costs of the new activities consequent to the switch on of the new European Rules. These amounts were averaged over the total number of provided services. The simultaneous process of Risk Management is divided into four key operational phases: 1. identification of risks; 2. assessment and risk analysis, which aims to determine the probability and severity (magnitude); 3. treatment of risks, which identifies the most appropriate actions to be taken to reduce risk; 4. monitoring process carried out. The relative risk of the threat, realized as expected damage from an uncertain event, is the product of gravity of injuries, or damage, and the associated probability of occurrence: Risk = Probability (P) × gravity (G) The probability (P) is given by the estimation of the possibility that the critical event occurs, while gravity is given by: Severity = amplitude of the potential damage (D) - Relative attenuation (A) ***Results and conclusion*** The risk assessment and cost assessment made at the CDI shows that in the future, the application of the new Compounding of Radiopharmaceutical can allow a positive impact on risk indexes ( about 25%), with an increasing operational costs of about 30%.

## P541

### Protection Efficiency Against Skin Radioactive Contamination in Nuclear Medicine by Medical and Isolator Gloves

C. GUINOT[1], L. HACHON[2], D. LEGULUDEC[3], R. LEBTAHI[1,4], N. PONS-KERJEAN[2], **M. BEN REGUIGA**[1,2,4]; [1]APHP - Hôpital Beaujon - Service de Médecine Nucléaire, Clichy, FRANCE, [2]APHP - Hôpital Beaujon - Radiopharmacie/Service Pharmacie, Clichy, FRANCE, [3]APHP - Hôpital Bichat- Service de Médecine Nucléaire, Paris, FRANCE, [4]INSERM U773, Paris, FRANCE.

Introduction: Preparation of radiopharmaceuticals, their handling and administration to patients may expose nuclear medicine workers to external radioactive contaminations. The use of isolator and medical gloves is commonly supposed to be efficient tool against skin contamination. In fact, gloves materials are expected to be effective barriers to retain radioactive substances and prevent them to reach the skin. The aim of this study was to assess whether gloves usually used in Nuclear Medicine and Radiopharmacy are efficient against radioactive contamination and how long this protection is assured. Material & Methods: 5 types of gloves made in different materials and thicknesses were tested: thin medical (vinyl, latex and neoprene) and thick isolator (neoprene and rubber) gloves. Testing method was adapted from EN374 European-Standard "Protective gloves against chemicals". Briefly, each glove was suspended to an adapted support and filled with 250mL of saline (equivalent to one hand volume). Gloves were then immersed in a contamination bath made of 4L water heated at 32°C (skin temperature) and added 250MBq of pertechnetate (99mTcO4-, Na+). 1mL samples were then withdrawn from gloves and their contaminating bath at 0, 3, 5, 8, 10, 15, 20, 30, 45 and 60 minutes post-contamination. Radioactivity (A) was measured in each sample using Perkin-Elmer-Wallac-1470 Gamma-Counter previously calibrated for Tc-99m. Results were expressed as mean±SD (Bq/mL, n=3-4/glove). Gloves permeability was described in terms of Tp (time of first radioactivity passage trough gloves) and Rp (relative fraction of radioactivity that crosses the glove=ratio Aglove/Abath). Results:99mTcO4- crossed rapidly gloves barrier and radioactivity was detected significantly few minutes post-contamination: 4.3±1.2min for latex to 6.0±1.7 for neoprene gloves. Fractions of radioactivity that crosses gloves (Rp) varied from 8.3.10-5±2.5.10-5 in vinyl to 1.3.10-4±5.3.10-5 in thin neoprene gloves corresponding respectively to 1.3±0.4kBq and 2.1±0.8kBq of Tc-99m. Rp increased then with time following the first detection moment. Discussion and Conclusion: Our results show that common examination gloves or isolator gloves used in nuclear medicine and radiopharmacy are not protective against radioactive contamination more that few minutes. Contamination levels were initially low (about 10-4 of contaminating activity crosses the glove) and increased with time. Thick neoprene and vinyl gave the lowest contamination rates and should be preferred to other materials. Regarding these results, we recommend to change regularly working gloves during unsealed sources handling and in case of suspicion of radioactive contamination, not to use the glove more than 4 minutes.

## P542

### Impact evaluation of the application of Italian law "Good Radiopharmaceutical Preparation Practice in Nuclear Medicine": cheery or heavy becoming of quality?

**P. Gandolfo**, P. Puglia, Andrea Bonfanti, Ruggero Baroni, Riccardo Buffa, Mila Montevecchi, Alessio Pisano, Luciano Abate, Martina Bianchi, Serena Padelli, Roberto Moltrasi, Antonio Triulzi; Casa di Cura Igea S.p.A., Milano, ITALY.

**Aim:** The goal of Italian D.M. Health Office 30/03/2005 "Good Radiopharmaceutical Preparation Practice in Nuclear Medicine" is to establish necessary standards of best practice to guarantee a great quality in preparation of radiopharmaceuticals. Aim of this study is to provide a reference tool for upgrading and managing internal organization of a Department of Nuclear Medicine according to new legal requirements. **Materials and method**:Quality system was built throughout structural and environmental modifications. Relevant promises and equipment were designed, built and maintained to defend product, personnel, patients, taking into account radiation safety and prevent of contamination by personnel and environmental microbial conditions. Personnel involved was qualified, receiving necessary background, and appropriately continuing trained in quality system, to perform new procedures and operations in classified areas. The responsabilities and duties were clearly identified. All resources to enable personnel to perform their functions were assured. A quality control unit oversee preparation operations to ensure that a radiopharmaceutical of sufficiency quality was prepared. The system of documentation includes operative procedures and records related to any

relevant step of the process, in order to allowing the traceability of the entire process itself. Regular quality reviews are carried out and documented with the objective of verifying the consistency of the existing process. Continual improvement is facilitated through the implementation of quality strategies appropriate to current level of process and product knowledge. **Results and conclusion:** After about one year from the application of Italian law into a department of Nuclear Medicine, our team has really got a positive return in terms of great quality of radiopharmaceutical, positive impact to the patient, to the personnel and to the sanitary organization. The new Compounding of Radiopharmaceutical, published on PHARMEUROPE, vol. 23, No.4, Oct. 2011, shows many patterns similar to the Italian law; our team believes that the above mentioned process and the awareness of a higher competence can become an useful guideline for all European department facing similar pathways in the future.

P20-2 - Tuesday, Oct. 22, 16:00 - 16:30, Poster Exhibition Area

## Cardiovascular: Basic Science

### P543

### The important of incidental thyroid gland uptake during Tc-99m MIBI myocardial perfusion SPECT

**S. Karacavus**[1], H. Ede[2], N. Delibas[3], E. Kaya[4], A. Erbay[2]; [1]Bozok University School of Medicine Nuclear Medicine Department, Yozgat, TURKEY, [2]Bozok University School of Medicine, Cardiology Department, Yozgat, TURKEY, [3]Hacettepe University School of Medicine, Department of Biochemistry, Ankara, TURKEY, [4]Acıbadem Kayseri Hospital, Department of Nuclear Medicine, Kayseri, TURKEY.

**Aim:** One of the most important steps in myocardial perfusion single photon emission computed tomography study (SPECT) interpretation is to review the raw data consisting of the projection images. Tc-99m sestamibi (MIBI) has been previously reported to have an useful role in detection thyroid diseases. The purpose of study was to investigate whether incidental thyroid gland uptake had an important during Tc-99m MIBI myocardial perfusion SPECT. **Methods:** Between January 2012 and March 2013, 968 consecutive patients were evaluated for the presence or absence of thyroid gland uptake in the raw data of the Tc-99m MIBI myocardial perfusion SPECT studies. All of the patients had thyroid gland uptake of the Tc-99m MIBI underwent laboratory evaluation of thyroid function, ultrasonographic imaging, and hystopathological examination. **Results:** The thyroid gland uptake was detected in 14 of 968 (1.4 %) consecutive patients during the evaluation of raw images of Tc-99m MIBI myocardial perfusion SPECT studies. Among these 14 patients, 4 had subacute thyroiditis, 7 multinodular goiter, 3 Graves disease by ultrasonographic imaging and hystopathological examination. TSH levels of all of these patients were <0.01 µU/ml. **Conclusion:** Tc-99m MIBI uptake by thyroid gland has been explained with associated clinical thyrotoxicosis. Although the primary goal of myocardial perfusion imaging is the evaluation of myocardial perfusion, the interpretation of myocardial perfusion imaging should not be limited to the heart. During this detailed examination, it is possible to observe extracardiac radioactivity accumulation, which may then lead to the diagnosis of a noncardiac disease.

P21-2 - Tuesday, Oct. 22, 16:00 - 16:30, Poster Exhibition Area

## Cardiovascular: Perfusion

### P544

### Is there any correlation between Troponin-T levels and infarct size in patients early after primary PTCA?

**T. Christoforidis**[1], A. Doumas[1], I. Iakovou[1], V. Mpalaris[1], D. Mpountas[2], V. Nikos[1], D. Katsaboukas[1], S. Georga[1], D. Lo.Presti[1], N. Karatzas[1]; [1]3rd Nuclear Medicine dpt Aristotle Univ. Papageorgiou hsp, THESSALONIKI, GREECE, [2]Hippokratis Nuclear Medicine center, THESSALONIKI, GREECE.

AIM: During the acute phase of a myocardial infarction, the extent of the infarcted area plays a major role to the patient's future quality of life, directly related to the left ventricular ejection fraction (LVEF). We investigated if there is any relationship between Troponin-T (TnT) levels and the extent of the infarcted area, using gated SPECT myocardial perfusion imaging (SPECT-MPI) in patients early after primary Percutaneus Transluminal Coronary Angioplasty (PTCA). METHODS: A total number of 86 patients, mean age 59+/-14 years (58 male), underwent primary PTCA due to an acute myocardial infarction (MI). All of them had angiographically proven one vessel coronary artery disease, which was angioplastized. Serial TnT samples were assessed during the first 4 hours from the onset of chest pain and the higher titer was recorded. Five to seven days after the procedure, SPECT-MPI was performed to all of them. The infarcted area was quantitatively assessed as a percentage of the total left ventricular mass, using dedicated software. RESULTS: Twenty four patients presented with TnT values <1ng/ml (group I), 30 patients with TnT between 1 and 2ng/mL (group II), 28 patients between 2 and 3ng/mL (group III) and 14 with TnT values >3ng/mL (group IV). The mean infarct size in Group I was 12%, in Group II 14%, in Group III 10% and in Group IV 16% of the total left ventricular mass. The regression analysis revealed a poor correlation (r=0.35) between the TnT levels and the infarcted area. CONCLUSION: During the acute phase of a myocardial infarction, and early post primary PTCA, the levels of Troponin-T do not correlate well to the extent of the infarcted zone, as it is estimated using SPECT-MPI.

### P545

### Quantitative measurement of myocardial perfusion with PET using 11C-acetate

**B. Botond**[1], L. Zsolt[2], M. Mónika[1], T. Gyula[2], K. Gábor[1], S. István[1]; [1]Medical Centre, Hungarian Defence Forces, Budapest, HUNGARY, [2]Pozitron-Diagnostics Health Centre, Budapest, HUNGARY.

Our goal was to measure myocardial perfusion of patients with ischaemic heart disease quantitatively using 11C-acetate PET method. Patients and Methods. 11 patients with diagnosed ischaemic hearth disease were examined. Stress and rest myocardial perfusion was measured with 185-550 MBq 11C-acetate iv. injection after pharmacological stress (4 minutes infusion of dipyridamole 0,56 mg/kg). List-mode data acquisition was performed with a Biograph HD 6 PET-CT camera (Siemens) during 330 seconds. CT-based attenuation-corrected frames (2x3, 12x5, 7x10 and 7x20 seconds) were constructed. Data quantification was performed with PMOD software, based on a one-compartment model. Regional perfusion was represented on a standard 17-segments myocardial map in mL/min/g. Our results were compared with results of invasive coronary angiography (n=8) or the CT coronary angiography (n=3) and with stress-rest 99mTc myocardial SPECT (n=5) using standard semiquantitative evaluation. Results: 90 % of the segments with normal perfusion on SPECT and normal coronary angiogram had stress flow higher than 2,5 mL/min/g calculated by the PET study. Ischaemic segments had less than 2 mL/min/g. Statistical analysis could not be performed because of the low number of patients. Our results with 11C-acetate were similar to data in the literature. Our preliminary results demonstrated that quantitative measurement of myocardial perfusion with 11C-acetate seems to be clinically useful.

### P546

### Quantitative evaluation of myocardial perfusion of stress-induced SPECT / CT in the assessment of hemodynamic significant intermediate coronary artery stenose s: a comparative study with fractional flow reserve measurements

**V. Solomyanyy**, I. Sergienko; Russian Cardiology Research and Production Complex, Moscow, RUSSIAN FEDERATION.

**Background**: FFR is currently used to determine the management of intermediate coronary artery stenosis. FFR more 0.80 used in clinical practice to guide revascularization. Advances in noninvasive imaging test (SPECT / CT) require revaluation FFR in intermediate stenosis severity against noninvasive imaging **Methods and Results:** In this study, 60 patients (mean age 56 + / - 9.1 years, 10 women) with ischemic heart disease and 50% to 70% coronary stenosis (target vessel). All perfusion scans were performed using a camera (BrightView XCT Philips) equipped with a low-energy, high-resolution collimator and with cardiac gating. Antianginal medication was discontinued 48 h before the study, and patients abstained from caffeine for 24 hours prior to the study protocol one day stress (bicycle test) /rest use with 900 MBq (25 mCi) of technetium 99m-MIBI. During the 4 (+ / -9) days, coronary angiography, which was defined as angiographic moderate (50-70%) was assessed by QCA and pressure wires received FFR (RADI Medical Systems). Normal FFR,> or = 0.8). Mean FFR all patients was 0.76 + / - 0.15. Summed stress scores (SSS) and summed difference scores (SDS) in the LDA, RCA and RCX artery territory according to the 20 segment model were calculated. A summed stress score of ≥ 3 and an SDS of ≥ 2 were assumed as pathologic, indicating significance of the lesion; a cutoff value of 0.80 was used to define abnormal FFR. Both visual and quantitative assessment results were compared with FFR using Chi-square ($\chi^2$). FFR was normal in 45 and abnormal in 15 patients. Given the results of FFR as the gold standard method for assessing the significance of lesions, the sensitivity and specificity of the quantitative analysis of abnormal flow reserve were 85% and 90% respectively. **Conclusion**: The quantitative analysis of myocardial perfusion SPECT / CT increases the specificity in assessing the value of the average degree of coronary artery disease.

### P547

### Is Attenuation Correction Useful to Avoid False Positive Findings in MPS of Women? Our Preliminary Results

**S. Czibor**[1], I. Szilvási[1], A. Radácsi[2]; [1]Semmelweis University, Budapest, HUNGARY, [2]Euromedic Kft. Péterfy Hospital, Budapest, HUNGARY.

**Aim.** Purpose of the study was to evaluate the clinical relevance of CT-based attenuation correction (AC) in Myocardial Perfusion Scintigraphy (MPS) of women to avoid false-positive findings in detecting ischaemia on the anterior wall caused by attenuation of the breast. **Materials and Methods**. We studied a group of 55 consecutive female patients (mean age: 65,71±12,1) referred for MPS with suspected myocardial ischaemia, 8 of them with known CAD. All patients underwent a 2-day Tc-99m-tetrofosmin stress/rest imaging with dipyridamole stress. Images were acquired by a Siemens Symbia T2 SPECT/CT using low-dose 2-slice CT for AC. Both corrected and uncorrected studies were evaluated with Corridor 4DM software, using 17-segments model, 5-point segmental scoring scale from 0 (normal) to 4 (absent). We compared corrected and uncorrected summed stress score (SSS), summed rest score (SRS) , summed difference score (SDS) of the anterior left ventricle wall (anterior, anterolateral, anteroseptal and anteroapical segments). Results. SSS, SRS, and SDS for AC versus non-AC were 3,04±4,51 vs 2±4,03; 3±3,93 vs 1,58±2,93; and 1,53±2,74 vs 1±2,18, respectively. There were statistically significant differences for SSS and SRS (p<0,005) while difference for SDS was nonsignificant (p=0,07). SDS values were similar, thus the quantitative assessment of ischaemia was unaffected by AC. SSS and SRS values were consistently higher with AC than without AC, probably due to overcorrection, as the normals database was the same for uncorrected and corrected studies. However, quality of the images acquired with AC was better than without AC, making qualitative analysis easier. **Conclusion**. In our patient population of 55 women, AC did not prove to provide incremental advantage for quantitative analysis in detecting myocardial ischaemia, but by improving the qualitiy of the images, it allowed a more confident qualitative analysis.

## P548

### High negative predictive value of workload ≥7 METS on exercise testing in patients with normal gated myocardial perfusion imaging in Pakistani population: Was imaging really required?

**M. u. Zaman**[1,2], N. Fatima[3,4], U. Zaman[5], M. Ishaq[2], D. Baloch[2]; [1]AKUH, Karachi, PAKISTAN, [2]Karachi Institute of Heart Diseases (KIHD), Karachi, Pakistan, Karachi, PAKISTAN, [3]Dr Ziauddin Medical University, Karachi, PAKISTAN, [4]Karachi Institute of Heart Diseases (KIHD), Karachi, PAKISTAN, [5]Year II MBBS, Dow University of Health Sciences (DUHS), Karachi, PAKISTAN.

**Objective:** to evaluate negative predictive value (NPV) of functional capacity during treadmill exercise in patients with normal gated myocardial perfusion imaging (GMPI) in Pakistani population. **Design:** Prospective **Place & duration of study:** KIHD, Karachi. December 2008 till December 2011. **Patients & Methods:** Study included 1318 individuals with normal exercise GMPI studies. On the basis of maximal age predicted heart rate (MAPHR) and metabolic equivalents (METS) achieved, these patient were divided into Group A: ≥ 85% MAPHR and ≥7 METS (714 patients), Group B: ≥85% MAPHR and <7METS (145 patients), Group C: <85% MAPHR and ≥7 METS (289 patients) and Group D: <85% MAPHR and <7 METS (170 patients). These patients were followed up on telephone (15 ±3 months) for fatal or non-fatal myocardial infarction (MI). **Results:** Follow-up data revealed no evidence of MI in any group and non-fatal MI in Group A and C. Non-fatal MI was reported in 2.07% in Group B and 2.35% in Group D. NPV of a normal GMPI in relation with functional capacity was found to be 100% for Group A and C (≥7METS), 97.9% and 97.6% for Group B and D (<7METS) respectively **Conclusion:** We conclude that (1) patients with ≥7 METS with a normal GMPI had 100% NPV for fatal and non-fatal MIs; (2) patients with <7 METS with a normal GMPI had a NPV of about 98% for non-fatal and 100% for fatal MIs; (3) Omitting GMPI in patients with ≥7 METS would save cost and avoid radiation exposure.

## P549

### Adenosine triphosphate stress 99mTc-MIBI single-photon emission computed tomography in the diagnosis of cardiac syndrome X

**L. E. Samoylenko**, G. N. Soboleva, I. E. Karpova, A. N. Rogoza, J. A. Karpov, V. B. Sergiyenko; Russian Cardiology Reserch Complex, Moscow, RUSSIAN FEDERATION.

Background: Generalize abnormality in vascular endothelial function and reduced coronary flow reserve has been reported in Cardiac Syndrome X (CSX) patients. Purpose: To evaluate the feasibility of 99mTc-MIBI-SPECT with intravenous adenosine triphosphate (ATP) infusion and digital reactive hyperemia as measured by computer photoplethysmography in patients with CSX. Methods: 18 patients with angina, positive exercise stress testing and normal coronary angiogram were included in the study. Patients with diabetes, hypertension, autoimmune diseases, prior myocardial infarction and coronary spasm during the coronary angiography were excluded. Antianginal medication was discontinued for>5 drug half-lives before investigation. Patients underwent a three-phase 99m Tc-MIBI-SPECT scan: rest, exercise stress test (Ex) and pharmacological stress with ATP infusion (0.16 mg/kg body weight per min for 5 min). Results: We evaluated non-smokers 18 patients (89% female, mean ages of 53,8±11 yrs, BMI 27±4 kg/m2, cholesterol and LDL cholesterol levels 5,6±0,9 mmol/l, 3,5±0,9 mmol/l accordingly. Generalized abnormality in microvascular function was determined by computer photoplethysmography in 61% patients of CSX. SPECT image was divided into 20 segments. Perfusion was graded on scale of 0-4, with 0 representing normal perfusion and 4 representing a very severe perfusion defect. 18 patients completed ATP-SPECT and 17 of them had also Ex-SPECT. In 14 cases out of 18 (78%) developed chest pain during ATP stress, and 7 cases out of 17 (41%) - during exercise. Stress ECG showed ischemic changes in 12 cases from 17 (71%), whereas ATP stress ECG demonstrated ischemic changes in 13 cases from 18 (72%). Comparison Exercise stress/ATP stress SPECT images showed mild reversible perfusion defects in 10 cases out of 17 (59%) vs. 6 cases out 18 (33%); moderate - in 6 cases out of 17 (35%) vs. 8 cases out 18 (45%) and severe - in 1 cases out of 17 (6%) vs. 4 cases out 18 (22%) accordingly. Conclusions: Our results demonstrate that adenosine triphosphate stress 99mTc-MIBI SPECT is comparable with exercise 99mTc-MIBI SPECT in detection of ischemia and may be useful tool for the diagnosis of cardiac syndrome X.

## P550

### Higher Events Rate in Patients with A Normal Gated MPI With Dipyridamole than Exercise: "Run For Reliability".

**N. Fatima**[1,2], M. Zaman[3,2], M. Ishaq[2], R. Omar[2]; [1]Department of Nuclear medicine, Dr Ziauddin Medical University, Karachi, PAKISTAN, [2]Karachi Institute of Heart Diseases (KIHD), Karachi, PAKISTAN, [3]Department of Radiology, The Aga Khan University Hospital (AKUH), Karachi, PAKISTAN.

**Objective:** Evaluate the negative predictive value (NPV) of a normal gated myocardial perfusion imaging (NGMPI) with exercise and dipyridamole in a propensity matched population. **Methods:** This is a prospective study conducted at Nuclear Cardiology Department of Karachi Institute of Heart Diseases (KIHD), Karachi from December 2008 till June 2010. Total 809 patients with a NGMPI with adequate exercise (558/809) or dipyridamole (251/809) stress were included and followed-up for 12-30 months (mean 24 ±3 months) for fatal or non-fatal infarctions (MI). **Results:** Mean ejection fraction (EF %), end diastolic volume (EDV, ml) and end systolic volume (ESV, ml) in exercise and dipyridamole cohorts were (72 ±08, 66 ±11), (68 ±13, 81 ±17), and (19 ±11, 26 ±12) respectively. On follow up, in dipyridamole cohort 2 fatal and 6 non-fatal MIs were reported. While in exercise cohort only 2 non-fatal MIs were reported. The NPV of a NGMPI with exercise was 99.7% (95% confidence interval [CI] 98.93%-99.96%) with an event rate of 0.3% (95% CI; 0.03% to 0.6%) and annualized event rate of 0.15%. The NPV of NGMPI with dipyridamole was 96.80% (95% CI; 2.2% to 4.3%) with an event rate of 3.2% (95% CI; 1.39% to 3.83%) and annualized event rate of approximately 1.6%. Event free survival for dipyridamole group was significantly lower than exercise analyzed by Logrank test (14.509, p<0.001). **Conclusion:** A NGMPI with dipyridamole stress has higher event rate (low NPV) as compared with exercise and this raises concern over its credibility to label these patients into low risk group.

## P551

### Increased FDG uptake in the right ventricle indicates a poor prognosis in patients with CTEPH: A comperative study between hemodynamic parameters and FDG PET/CT

**S. Ozguven**[1], F. Dede[1], B. Yıldızeli[2], S. Tas[3], M. Yanartas[3], S. Gungor[1], M. Aras[1], T. Ones[1], S. Inanir[1], T. Y. Erdil[1], H. T. Turoglu[1]; [1]Marmara University Department of Nuclear Medicine, Istanbul, TURKEY, [2]Marmara University Department of Thoracic Surgery, Istanbul, TURKEY, [3]Kartal Kosuyolu EAH Department of Cardiovascular Surgery, Istanbul, TURKEY.

**Introduction**: Chronic thromboembolic pulmonary hypertension (CTEPH), is a rare disease that occurs after acute pulmonary embolism and causes significant morbidity and mortality. Hemodynamical parameters plays a great role in the assessment of prognosis and severity of the disease. Right ventricular overload is an expected finding. In this study we investigated the relationship between right ventricular FDG uptake and the measured hemodynamical parameters. **Methods**: We performed FDG PET/CT before endarterectomy operation in order to distinguish thrombus / endovascular malignancy (angiosarcoma, etc.) which is seen as filling defects in main pulmonary artery and its branches. In FDG PET/CT study we measured the SUVmaximum (SUVmax) values of right (RV) and left ventricles(LV) and detected the RV-SUVmax and RV/LV SUVmax ratio. After this we compared the RV-SUVmax and RV/LV SUVmax ratio with the systolic (SPAP) and mean (MPAP) pulmonary artery pressures and pulmonary vascular resistance (PVR) values which are measured by echocardiography and/or right heart cateterization. **Results**: 20 patients (11 women, 9 men) with a mean age of 52.2 ± 12.1 years were included in this study. We found statistically significant positive relationship between the mean (± standard deviation) values of RV-SUVmax and SPAB (Spearman r = 0.48, P = 0.037), and between PVR and RV / LV ratio (Spearman r = 0.50, P = 0.024). There was no significant correlation found between other parameters. **Conclusion**: Hemodynamic measurements are important objective parameters in determining the severity and prognosis in patients with CTEPH.

Increase in these values indicates poor prognosis. On the other hand, in those patients who had RV hypertrophy and decreased systolic function due to pulmonary hypertension, can be detected by routine echocardiography, right heart catheterization and CT-pulmonary angiography in the evaluation stage. In the literature, only few studies reported the relationship between the level of the RV FDG uptake in FDG PET/CT and the severity of pulmonary hypertension in pulmonary hypertensive patients. In this study, we observed a positive correlation between the level of the right ventricular FDG uptake, PVR and SPAP in patients with CTEPH. Also increased RV-FDG uptake was shown to be a poor prognostic marker for these group of patients.

## P552

### Can stress induced changes in left ventricular mechanical dyssynchrony predict the presence of multivessel coronary artery disease on Thallium-201 gated myocardial perfusion SPECT?

**C. D. Patel**, H. Singh, P. Sharma, A. Malhotra; All India Institute of Medical Sciences, New Delhi, INDIA.

Aim: Evaluation of diagnostic value of stress induced changes in left ventricular mechanical dyssynchrony (LVMD) assessed by stress-rest Thallium-201 gated myocardial perfusion SPECT (Tl-201 MPS) for the diagnosis of multivessel coronary artery disease (CAD). Material and Methods: Data of one hundred and fifty patients who underwent Exercise stress-rest Tl-201 MPS and coronary angiography within 3 months, was retrospectively evaluated. Patients were divided into 2 groups: single vessel CAD (n=45) and multivessel CAD (n=105). LV perfusion parameters [Summed stress score (SSS), summed rest score (SRS), Summed difference score (SDS)], LV function parameters [LVEF, ΔLVEF (Post stress LVEF - Rest LVEF)] and LVMD parameters [phase standard deviation (PSD), phase histogram bandwidth (PHB), ΔPSD (Post stress PSD - Rest PSD), ΔPHB (Post stress PHB - Rest PHB)] were assessed. Receiver Operated Characteristic Curve, univariate and multivariate analysis were performed. Results: No statistically significant difference was observed between the 2 groups with regard to age, sex, prevalence of hypertension, diabetes mellitus, obesity, hyperlipidemia, SRS score, Rest LVEF, Rest PSD and PHB. However, prevalence of smoking habit was more in group with multivessel CAD (p 0.04). On ROC analysis, the following cut-offs were obtained for detection of multivessel CAD: SSS score >11 (sensitivity-80%, specificity-44.5%), SDS score >6 (sensitivity-60%, specificity-75.6%), ΔPSD value >-4.8 (sensitivity-53.3%, specificity-64.4%), and ΔPHB value >-17 (sensitivity-53.3%, specificity-64.4%). On Univariate analysis, SSS (p 0.002, Odds ratio 0.312, 95% CI 0.146-0.667), SDS (p 0.0001, Odds ratio 4.636, 95% CI 2.116-10.154), ΔPSD (p 0.047, Odds ratio 2.071, 95% CI 1.007-4.259) and ΔPHB (p 0.047, Odds ratio 2.071, 95% CI 1.007-4.259) were significant predictors for presence of multivessel CAD. While on multivariate analysis, SSS (p 0.015, Odds ratio 0.365, 95% CI 0.162-0.822), SDS (p 0.001, Odds ratio 4.209, 95% CI 1.868-9.483) and ΔPHB (0.049, Odds ratio 2.195, 95% CI 1.003-4.805) were found to be significant predictors for presence of multivessel CAD. Conclusion: Stress induced changes in left ventricular mechanical dyssynchrony (ΔPHB) can aid perfusion analysis (SSS, SDS) in predicting the presence of multivessel coronary artery disease on Thallium-201 gated myocardial perfusion SPECT.

## P553

### Contributions of myocardial perfusion imaging for myocardial ischemia in patients with diabetes

**M. AIT IDIR**, S. TALEB, A. GUENSI, M. KEBBOU; Nuclear Medicine Department, Ibn Rochd UH, Casablanca, MOROCCO.

Diabetes is an important risk factor of myocardial ischemia. Myocardial perfusion imaging (MPI) is used for diagnostic, prognostic assessment and for post-therapeutic follow-up of coronary artery disease (CAD). Its usefulness has been documented extensively in the general population. CAD is more severe and more frequent among diabetic patients. The goal of our work was to study, the usefulness of MPI among diabetic patients. This work includes 44 diabetic patients (22 women, 22 men), investigated by stress MPI, referred to the nuclear medicine department of Ibn Rochd UH of Casablanca. The studied parameters concerned: age, antecedents of CAD, risk factors of CAD associated to diabetes, duration of the diabetes, diabetes complications, diabetes treatment, indication of MPI, presence or not of anomaly on the ECG performed at rest, existence or not of typical or atypical clinical signs of CAD, investigations and therapy prescribed as well as the occurrence or not of cardiac event during monitoring after MPI. Results of MPI have been compared to clinical, therapeutic and monitoring data of patients. Mean age of patients was 55 years (39 to 75 years), mean diabetes duration was 8.6 years (1 to 30 years), at least one complication has been noted in 18 patients. The most frequent complication was diabetic retinopathy. MPI has been achieved for diagnosis of ischemia in 37 patients and assessment of anti-ischemic treatment in 7 cases. Treadmill exercise has been achieved in 34 cases and a pharmacological stress in 10 others. During follow-up which was between 1 and 36 months (mean: 14.9 months), 6 cardiac events occurred among the 44 patients. Patients with abnormal findings at stress MPI had two cardiovascular risk factors or more associated to diabetes (91.3% Vs 9.5% among patients having normal findings, p <0.001) and had diabetic retinopathy more often (56.5% Vs 9.5% among patients with normal findings, p <0.001). Cardiac events were more frequent among men (85.7% Vs 43.2% of patients who didn't have a coronary event, p <0.01). Patients with stress MPI showing ischemia in 3/17 segments or more have presented a cardiac event more often during the follow-up (4/12 Vs 2/32 among patients with normal MPI or defect in less than 3/17 segments, p <0.01). In this series, coronary artery disease was found more frequently among patients having more than 2 cardiovascular risk factors. In addition, risk of cardiac event seems related to extent of uptake decrease.

## P554

### 99mTc Tetrofosmin gated SPECT with Nitrate in assessment of myocardial viability - study at patients who underwent Myocardial Revascularization

**C. BUZUMURGA**[1], C. SUCIU[2], A. TUDOSE[3]; [1]Oncology Diagnostic and Treatment Center, Brasov, ROMANIA, [2]"N.Stancioiu" Heart Institute, Cluj-Napoca, ROMANIA, [3]ICCO Cardiology, Brasov, ROMANIA.

The aim of this study was to demonstrate the accuracy of 99mTc Tetrofosmin gated SPECT MPI in detection of myocardial viability.Methods:we study 42 patients (50+/-11y;38 male,4 female) with previous infarction and severe left ventricular disfunction (EF=29+/-6%).All patients underwent rest 99m Tc Tetrofosmin gated SPECT MPI and postnitate 99m Tc Tetrofosmin gated SPECT MPI.Scintigraphic analysis was performed using quantitative perfusion SPECT (QPS) providing the percentage radiotracer uptake and defect severity in a 17 segments model, with the same day protocol.6 patients had single vessel coronary disease,14 patients had double vessels and 22 patients had triple vessels coronary disease.At patients with myocardial viability 99mTc Tetrofosmin gated SPECT was repet at 9 months after myocardial revascularization. Results: In analysis of SPECt perfusion at rest and after nitrate 714 segments was analysed .In 343 segments (48%) were dysfunction on QGS analysis and 371 segments (52%) were with normal regional motion.In 582 segments the mean regional percentage of 99m Tc Tetrofosmin uptake at rest was 57+/-15% and increased significantly after nitrate administration (79,1+/-11%)Similary,the mean perfusion defect severity at rest was 2,80+/-1,5SD and decreased significantly after nitrate .In 297/343 segments (86,5%) after nitrate the uptake increased and the wall motion was impoved (viability ).After myocardial revascularisation at 9 months the uptake of 99mTc Tetrofosmin was impoves in 240/297 segments (81%)-semnificative statistical.Conclusion:In patients with severe LV dysfunction after myocardial infarction ,postnitrate imaging is a accurate tool to assess myocardial viability.

## P555

### Preliminary results: Influence of the software and the type of reconstruction, in the processing time and the volumes calculation

**C. M. Hernández Heredia**, L. Villares Garcia, P. Gálvez Diez, R. De La Fuente, J. Rodriguez Zarauz; Hospital Central de la Defensa, Madrid, SPAIN.

**OBJECTIVE:** Compare the results obtained with different processing programs in the calculation of cardiac volumes, left ventricular dilatation transient (TID) and the processing time. **MATERIAL AND METHODS:** A retrospective study, randomized, including 20 patients from December 2012 to march 2013. All patients had undergone myocardial perfusion SPECT after stress and basal as standard protocol in our service. Each study process with three different programs: QGS / QPS ®, MYOMETRIX ®, EC-TOOLBOX ® and different reconstruction: filtered back projection (FBP) and iterative (OSEM). In each method were obtained systolic and diastolic volumes, TID and load time of each software. The data are analyzed with a normality test of Shapiro Wilk, Pearson linear correlation and Student t test. **RESULTS:** Positive linear correlation was obtained statistically significant in calculating volumes even comparing different programs and processed. The time spent was lower for processed with OSEM over FBP, with a positive linear correlation, statistically significant. The TID has a statistically significant linear relationship, comparing the same sofware with different reconstruction type. We found a significant linear relationship between the TID to compare different software. **CONCLUSION:** FBP processing is faster than OSEM and the results for volumes and TID have good statistically significant correlation. The volumes have a statistically significant linear correlation between the different programs, with a tendence to have higher values with EC-TOOLBOX®, respect to others. The sample size can not allowed us to test the relationship of TID, between different software.

## P556

### Severity of coronary atherosclerosis in patients with coronary artery disease with moderate myocardial perfusion abnormalities

K. Zavadovsky, M. Gulja, **Y. Lishmanov**; Institute of Cardiology, Tomsk, RUSSIAN FEDERATION.

**Aim.** To estimate the severity of coronary atherosclerosis in patients with coronary artery disease with moderate myocardial perfusion abnormalities. **Materials and Methods.** The study group consisted 34 patients (21 men and 13 women; average age 59,2±7,7 y) who were referred for both myocardial perfusion SPECT (adenosine test and rest) and multislice CT coronary angiography because of clinically suspected CAD and who underwent these investigations within 1 day of each other. Including criteria: clinical signs of CAD in combination with adenosine induced perfusion defect ≤10% (according myocardial perfusion SPECT data). Excluding criteria: acute coronary syndrome, previous myocardial infarction, coronary revascularization, cardiomyopathy, inflammatory cardiac diseases, renal insufficiency. All studies were performed on the hybrid SPECT/CT unit GE Discovery NM/CT 570c. Data analysis was performed on workstations GE Advanced Workstation and Xeleris 3 Workstation.The following parameters were analyzed: coronary calcification, the presence of atherosclerotic plaques, their impact on the lumen of the vessel, the location and depth of myocardial perfusion defects at the peak of the pharmacological test (adenosine) and rest. **Results**. Myocardial perfusion defects were found in 26 patients out of 34 (82%). The average summed stress score (SSS) was 3,1 ± 2,3; the average summed rest score (SRS) 0,7±0,9 and the summed difference score (SDS) was 2,35±1,72. The average coronary calcium score per coronary was 163,76±258,72; in LMA 2,96±11,78; in LAD 75,03±79,36; in LCX 23,33±53.21, in RCA 62,42±170,41. Depending on the degree of stenosis of the coronary arteries has been allocated four cohorts of patients: 1 - without evidence of coronary atherosclerosis, 2 - insignificant stenosis (<40% luminal narrowing), 3 - intermediate stenosis of 40 to 70%, 4 - significant stenosis (≥70% luminal narrowing). For further analysis, it has been allocated two groups of patients: with normal and abnormal myocardial perfusion. In the group with abnormal myocardial perfusion the average SSS was 3.7±1.95, in a vascular territory of the LAD - 1.35 ±1.39, LCX - 1.14±1.17, RCA - 1.21±1.1. The average SRS was 0.85±0.89, and the average SDS was 2.85±1.45 . A comparative analysis showed that the level of coronary calcium (both in general, and in the vascular regions), the number of atherosclerotic lesions segments and the degree of stenosis were not significantly different. **Conclusion**. In patients with stable angina pectoris with moderate myocardial perfusion disturbances, we have expressed in different degrees of atherosclerotic coronary arteries. In this group patient we should use hybrid SPECT/CT approach for CAD diagnostic.

## P557

### Effects of age, gender, body weight and mild airway diseases on the safety and tolerability of adenosine as a pharmacological stressor in myocard perfusion imaging

**N. Yildirim Poyraz**[1], E. Ozdemir[1], B. Poyraz[2], Z. Kandemir[1], M. Keskin[1], S. Turkolmez[1]; [1]Ankara Ataturk Training and Research Hospital, Ankara, TURKEY, [2]Private TOBB ETU Hospital, Department of Pulmonary Diseases, Ankara, TURKEY.

**Aim**: Stress gated single photon emission computed tomography myocardial perfusion imaging (SPECT MPI) is a validated, noninvasive method for evaluating patients with known or suspected coronary artery disease (CAD) . Pharmacologic stress (PS) agents are indicated for the patients who are not suitable for exercise testing. Adenosine is a potent PS agent, however some side-effects observed with adenosine can be assigned to the nonselective activation of other adenosine receptor subtypes. The aim of this study was to investigate the effects of gender, age, body weight and mild airway disease (AD) of the patients on the safety and tolerability of adenosine during stress MPI. Materials and **Methods:** Total of 281 patients ( 109 M, 192 F; mean age: 62,6±10) were included in the study with 48 patients with mild AD (mild-intermittent asthma and mild/moderate chronic obstructive pulmonary disease-COPD). Patients with mild AD were pretreated with 2 puffs of inhaled beta2-adrenergic agonist before adenosine infusion. After PS, MPI on an integrated SPECT/CT system was applied to all patients. The frequency of side-effects of adenosine were determined and patients with mild AD and others were compared in terms of the safety and tolerability of the adenosine stress test. **Results:** Infusion protocole was completed in 227 patients (80%), dose reduction was required in 31 pts (11%), and infusion was terminated early in 23 pts (8%). Flushing (31.3%), dyspnea (27.9%), and chest pain (23.1%) were the most common side effects, however most of those were transient and did not require any intervention, aminophylline was given to only 3 patients. Totally side effects (68.8%) were observed more common in patients with mild AD than the others (60.5%)but the difference was not statistically significant, except for dyspnea (p=0.027). Only 6 (12.5 %) of the patients with mild AD developed bronchospasm, manifested as wheezing and aminophylline was not required in any case. The sensitivity, specificity and diagnostic accuracy of adenosine MPI with SPECT/CT were 85%, 94% and 92% respectively. **Conclusion:** Adenosine is a safe, well tolerated and currently available PS agent for MPI in patients who are not suitable for exercise stress test as well as patients with mild AD. Most of the side-effects due to nonselective receptor stimulation are transient and do not require any intervention. However, it is probably safe to exclude patients with severe airway disease from adenosine stress MPI until the results of the larger number of series are reported.

## P558

### The Value of Summed Scores Obtained From MPS SPECT Study to Predict Cardiac Events

**S. Kirac**[1], L. Akca[2], O. Yaylali[1], D. Yuksel[1], D. Dursunoglu[3]; [1]Pamukkale University Medical Faculty, Dept of Nuclear Medicine, DENIZLI, TURKEY, [2]Corlu State Hospital, Dept of Nuclear Medicine, Tekirdag, TURKEY, [3]Pamukkale University Medical Faculty, Dept of Cardiology, DENIZLI, TURKEY.

**Aim**: To investigate the value of the summed stress (SSS), summed rest (SRS) and summed difference scores (SDS) to predict the early and long-term cardiac prognosis in the patients with known myocardial ischemia.**Materials and Methods**: Total 153 cases (91 M, 62 F; 57 ± 10 years) who underwent stress-rest MPS gated SPECT with Tc-99m labeled radiopharmaceuticals were investigated. From the LV polar map, SSS, SRS and SDS values were semiquantitatively calculated using the 20 segments/5 points scoring model. SSS and SRS were classified as 13 severe ischemia; SDS groups were 5 severe ischemia. LVEF was quantitatively calculated from the gated images. Following MPS SPECT, the cardiac deaths and non-fatal MI were accepted as hard and PTCA, coronary stenting, by-pass were accepted as soft cardiac event. **Results**: The rate of soft and hard cardiac events highly raised by SSS and SRS increased. SSS and SRS were higher in the low LVEF group than normal one. Meaningful relationship among SSS, SRS values and the breast, and between SSS and the diaphragm were found. Gender, DM, SSS and SRS were independent prognostic indicators in the Cox regression analysis. However, the power of SSS and SRS was higher than DM and gender in the prediction of cardiac events. The survival period was shorter for ≥ 9 than <9 of SSS and SRS in the Kaplan-Meier analysis (Log Rank, Mantel-Cox p= 0.01 for SSS and p= 0.03 for SRS).**Conclusion**: SSS value obtained from MPS SPECT study is the most significant and reliable prognostic factor to predict early and late cardiac prognosis. Adding the SRS to SSS parameter association with visual interpretation and quantitative analysis will strengthen the power of the foresight to cardiac event, but the importance of the SDS value is still controversial.

## P559

### Validation of PSF-based 3D reconstruction for myocardial blood flow measurements with Rb-82 PET

**L. P. Tolbod**, N. L. Christensen, L. W. Møller, J. F. A. Aanerup, K. Bouchelouche; Department of Nuclear Medicine & PET-Center, Aarhus University Hospital, Aarhus N, DENMARK.

**Aim**:The use of PSF-based 3D reconstruction algorithms (PSF) is desirable in most clinical PET-exams due to their superior image quality. Rb-82 cardiac PET is inherently noisy due to short half-life and prompt gammas and would presumably benefit from PSF. However, the quantitative behavior of PSF is not well validated and problems with both edge-effects and unphysical contrast-recovery have been reported.[1] In this study, we compare myocardial blood flow (MBF) and coronary flow reserve (CFR) obtained using GEs implementation of PSF, SharpIR, with the conventional method for reconstruction of dynamic images, filtered backprojection (FBP). Furthermore, since myocardial segmentation might be affected by image quality, two different approaches to segmentation implemented in standard software (Carimas (Turku PET Centre) and QPET (Cedar Sinai)) are utilized. **Method**:14 dynamic rest-stress Rb-82 patient-scans performed on a GE Discovery 690 PET/CT were included. Images were reconstructed in an isotropic matrix (3.27x3.27x3.27 mm) using PSF (SharpIR: 3 iterations and 21 subsets) and FBP (FORE FBP) with the same edge-preserving filter (3D Butterworth: cut-off 10 mm, power 10). Analysis: The dynamic PET-data was analyzed using a 1-tissue model corrected for incomplete extraction.[2] Two different approaches to orientation and segmentation were performed: 1) individual segmentation (IN) of PSF and FBP data (in QPET), 2) identical segmentation (ID) of PSF and FBP data using the same ROIs on both datasets (in Carimas). **Results**: Good correlation between values of MBF was found regardless of segmentation approach for both global (R2=0.98 in both cases) and segmental data (ID: R2=0.95, IN: R2=0.94). This was also the case for global CFR (ID: R2=0.96, IN: R2=0.89) and segmental CFR (ID: R2=0.89, IN: R2=0.85). However, PSF results were slightly higher than FBP when using identical segmentation (Global: 10±6%, p>0.05, Segment: 8±2%, p>0.05). This was not observed when using individual segmentation. **Conclusion:** Good correlation between PSF and FBP MBF and CFR values on both global and segmental level was found. The slightly higher MBF for PSF than FBP when using identical segments can be understood in terms of better resolution using PSF (less spill-over between myocardium and input ROIs). The difference of less than 10% must, however, is most likely clinically irrelevant. Thus, the data suggest that SharpIR reconstruction can be used for myocardial blood flow measurements with Rb-82. References:1) Rapisarda et al, Phys Med Biol 2010;55:4131-4151 2) Lortie et al, Eur J Nucl Med Mol Imaging 2007;34:1765-1774

## P560

### Possible adverse effect of external radiation on myocardial perfusion in patients with breast cancer

**M. Eftekhari**[1,2], H. Zamani[1], B. Fallahi[3], R. Anbiaee[4], A. Ameri[4], A. Emami Ardekani[1], A. Fard-Esfahani[1], D. Beki[1]; [1]Shariati Hospital, Tehran, IRAN, ISLAMIC REPUBLIC OF, [2]Research Center for Nuclear Medicine, Tehran University of Medical Sciences, Tehran, IRAN, ISLAMIC REPUBLIC OF, [3]Shariati Hospital, Tehran University of Medical Sciences, Tehran, IRAN, ISLAMIC REPUBLIC OF, [4]Imam Hossein Hospital, Shahid Beheshti University of Medical Sciences, Tehran, IRAN, ISLAMIC REPUBLIC OF.

Objectives: This study was designed to evaluate possible myocardial perfusion abnormality following external radiation for treatment of patients with left sided breast cancer. Method: Seventy one patients who were candidates for local radiation therapy entered in this study, 35 with left-sided breast cancer as the exposed group with their heart being at least partially in the field of radiation therapy and 36 patients with right-sided breast cancer as controls. All patients did not have any sign or symptoms related to cardiovascular disease with "Farmington Risk" of less than 5%. The same treatment protocols were applied for both groups. Six months after radiation therapy, myocardial perfusion imaging (MPI) with SPECT was performed for each case. Stress and rest MPI findings were compared between study groups. For statistical analysis, SPSS-16 software was applies using Mann-Whitney and Chi-square tests. Results: There were no significant differences between the study and control groups (P >0.05) as far as age, CAD risk factors or left ventricular ejection fraction were concerned, so the groups were comparable. Visual perfusion abnormalities were detected in 15 (42.9 %) of left-sided and 6 (16.7 %) of right-sided patients (P=0.020) showing a risk ratio of exposed to control group of 1.46 (CI95%=1.06-2.01) even after adjusting for age and percent of heart received more than 50% of radiation (DVH50%). The most affected parts of myocardium were apex and anterolateral walls. Conclusion:Exposure of the heart to radiation as in the cases of left sided breast cancer may increase the risk of perfusion abnormalities. MPI-SPECT is a valuable method for early detection and proper management of these patients.

## P561

### Inferior wall attenuation artifact on CZT gamma camera. Is prone imaging better than stand-alone CT attenuation correction (CTAC)?

**S. Piszczek**, M. Dziuk, A. Gizewska-Krasowska, A. Mazurek; Military Institute of Medicine, Warsaw, POLAND.

AIM: Attenuation can mimic the coronary artery disease (CAD) in myocardial SPECT imaging. Cardiac dedicated CZT gamma camera improves myocardial perfusion imaging with higher energy and spatial resolution but yet attenuation phenomenon has to be taken into consideration while analyzing the study. The goal of this study is to assess the feasibility and efficacy of CTAC and prone imaging in detecting the diaphragmatic attenuation. METHODS: The 20 male patients without history of myocardial infarction and with sinus rhythm were estimated (mean age 61 years, mean BMI 28 kg/m2). Every patient had 99mTc-sestamibi stress MPI with assessed EF >50%, no significant left ventricle contractility abnormalities were observed. We analyzed studies of patients with inferior wall stress myocardial perfusion defects, if elicited by attenuation. We performed CTAC (CT attenuation correction with stand-alone low dose CT) by overlapping perfusion images on CT scans and prone position imaging. For the analysis we used commercially available QGS/QPS software. The 5-point scale was used to establish perfusion abnormalities and image improvements on 20-segment polar map with percentage uptake of radionuclide (0-normal to 4-absent). We evaluated adjacent segments of inferior and lateral wall on the supine, CTAC and prone images (basal, mid and apical - 6 segments per patient). RESULTS: The means of perfusion scores, according to 5-point scale (±SD) in all patients for inferior basal segments were 1.30±0.47, 0.45±0.60 and 0.95±0.39 (supine, CTAC and prone images, respectively, P<0.001, 99%IC). In comparison to supine polar maps, scores increased at least for 1 point in 80% and 35% of segments in CTAC and prone images, respectively. The statistically significant differences were obtained also among inferior mid segments, means (±SD) were 0.85±0.48, 0.10±0.30 and 0.25±0.44 (supine, CTAC and prone images, respectively, P<0.001, 99%IC) with score improvements in 75% (CTAC) and 50% (prone) segments comparing to supine imaging. No statistical significance was observed in apical segments of inferior wall. Mean ESV, EDV and EF were 35ml, 100ml and 65%, respectively. CONCLUSIONS: Both CTAC and prone imaging are feasible in detecting diaphragmatic attenuation. The analysis of inferior segments revealed predominance of CTAC over prone imaging in improving the basal segments scores (80% vs 35% of segments, respectively).

## P562

### Assessment of right ventricular myocardial perfusion of patients with pulmonary arterial hypertension - utility consideration of CT-guided LAO planar imaging

**H. Miyauchi**[1], T. Iimori[2], Y. Kuwabara[1], K. Sawada[2], Y. Masuda[2], S. Sakao[3], Y. Kobayashi[1]; [1]Department of Cardiovascular Medicine, Chiba University Graduate School of Medicine, Chiba, JAPAN, [2]Department of Radiological Technology, Chiba University Hospital, Chiba, JAPAN, [3]Department of Respirology, Chiba University Graduate School of Medicine, Chiba, JAPAN.

[Background and Aim] Qualitative and quantitative evaluation of right ventricular function could be useful as diagnostic and prognostic indicator because some cardiovascular diseases develop with advancing RV dysfunction. In patients with pulmonary arterial hypertension (PAH), enlargement and hypertrophy of right ventricle (RV) occurs in according with increase of RV pressure. As a result, myocardial perfusion in RV consequently shows absolute increase. Therefore, quantitative assessment by myocardial perfusion imaging (MPI) can be applied to evaluate the severity of PAH. The aim of this study is to quantitatively evaluate right ventricular myocardial perfusion by planar thallium-201 (201Tl) imaging, and to compare them between pulmonary arterial hypertension (PAH) patients and normal controls. [Method] The study group comprised 10 patients with PAH and 10 healthy controls. PAH was diagnosed by echocardiography and cardiac catheterization. All subjects underwent cardiac CT by SPECT-CT (Infinia Hawkeye 4 GE Healthcare Japan Co. Ltd) in order to the get the optimal angle to differentiate RV from LV. Planar acquisition was performed 5 minutes after intravenously administration of 111 MBq of 201Tl from the optimal LAO degree with extended LEGP parallel hole collimators. In the planar image, we set ROI at left ventricle (LV), RV, and mediastrinum(M), and measured total and mean counts of these regions. Then, mean and total count ratio of (1) RV/LV and (2) RV/M were calculated as the indices for RV myocardium perfusion. [Results] 1) RV/LV ratio: The scores obtained from total counts were 0.394±0.884 for normal control, and 0.619±0.159 for PAH patient. The score of PAH patients was higher than that for normal. 2) RV/M ratio: The scores obtained from total counts were 23.6±5.01 for normal control, and 41.1±14.8 for PAH patient. The score of PAH patients was higher than that for normal controls. These data were statistically significant. [Conclusion] We examined rightventricular myocardial perfusion (RVMP) using CT-guided LAO planar imaging. Patients with PAH had significantly high RVMP. It is suggested that CT-guided LAO planar imaging are useful for quantification of RVMP.

## P563

### The efficacy of attenuation correction with stand-alone CT scans in diaphragmatic attenuation investigation in cardiac dedicated CZT gamma camera imaging - feasibility study.

**S. Piszczek**, M. Dziuk, A. Gizewska-Krasowska, A. Mazurek; Military Institute of Medicine, Warsaw, POLAND.

AIM: Attenuation decreases amount of radioactivity detected by gamma camera, resulting in partial loss in counts and can appear as regional perfusion defects. Even in patients with previous myocardial infarction (MI), treated with primary percutaneous coronary intervention of right coronary artery, it could cause considerable clinical evaluation disruption, when no relevant contractility disorders can be observed. The goal of this study is to assess the efficacy of CT attenuation correction with stand-alone CT in inferior wall perfusion abnormalities. METHODS: We estimated 20 male patients (mean age 61 years) without history of MI, 99mTc-sestamibi stress MPI was performed. Every patient had sinus rhythm and EF >50%, no significant left ventricle contractility abnormalities were observed. The images of patients with inferior wall myocardial perfusion defects were analyzed, whether induced by attenuation. We performed CT attenuation correction with stand-alone low dose CT by overlapping perfusion images on CT scans. Commercially available QGS/QPS software was used to estimate the studies. The data were received from 20-segment polar map with percentage uptake of radiotracer, we used 5-point scale (0-normal to 4-absent) to establish perfusion abnormalities and image improvements. The adjacent segments of inferior and lateral walls were evaluated on the supine and CTAC images (basal, mid and apical - 6 segments per patient). RESULTS: All the images were of diagnostic quality. Means of perfusion scores obtained from polar maps (±SD) for inferior basal segments were 1.30±0.47 and 0.45±0.60 (supine and CTAC images, respectively, P<0.001, 99%IC). There was significant improvement in CTAC images in comparison to supine polar maps, scores increased at least for 1 point in 80% of basal segments. The statistically significant differences were obtained also among inferior mid segments, means (±SD) were 0.85±0.48 and 0.10±0.30 (supine and CTAC images, respectively, P<0.001, 99%IC) with score improvement in 75% CTAC segments, comparing to supine imaging. No statistical significance was observed in apical segments of inferior wall. Mean ESV, EDV and EF were 35ml, 100ml and 65%, respectively. CONCLUSIONS: CTAC with stand-alone CT is useful in detecting diaphragmatic attenuation. In male patients with no evidence of MI and contractility abnormalities there was improvement in 80% and 75% of basal and mid inferior segments, respectively.

## P564

### Epidemiology of coronary artery disease in diabetics type 2 without anginal symptoms - retrospective study

**I. Kotsalou**[1], A. Kotsalos[2], N. Dimakopoulos[1], C. Koutis[3], N. Zakopoulos[4]; [1]Nuclear Medicine Dept, NIMTS Hospital, Athens, GREECE, [2]Cardiovascular Surgery Dept, NIMTS Hospital, Athens, GREECE, [3]Technological Educational Institute, Athens, GREECE, [4]University of Athens, Alexandra Hospital, Athens, GREECE.

**Introduction**: Worldwide, the prevalence of coronary artery disease (CAD) in diabetics is extremely high. Therefore, we studied the role of myocardial perfusion scintigraphy (MPS) and the incidence of CAD in asymptomatic diabetics comparing them to symptomatic ones, thus aiming to their best stratification into high and low risk category of CAD. **Material and method:** 78 diabetics type 2, mean age 62 years, which proceeded Cardiothoracic Department of NIMTS. Inclusion criteria were appropriate control of diabetes, of hypertention, no damage in organ-targets and absence of coronary intervention. We reported the risk factors for CAD, hereditary history, possible acute coronary syndrome referrals, or angina symptoms and medication and all diabetics were subjected in myocardial perfusion study. **Results**: Our study revealed the high prevalence (73%) of CAD in asymptomatic diabetics included and statistically higher prevalence of CAD in male than in women (*p<0,01*). Statistical correlationwas reported between severity of ischemia findings and typical angina symptoms (*p <0,05*), duration of diabetes mellitus (DM) (*p=0,003*), while type of therapy (*p=0,37*) and number of risk factors of CAD (*p =0,23)* were independent. **Conclusions:** MPS aids the detection of silent ischemia and diabetic autonomic neuropathy in DM patients, especially the asymptomatic ones, though DM is currently thought as a CAD equivalent independently of the presence of hypertension. Thus, MPS can help to early application of appropriate medication according to the recommendations of American Society of Diabetes.

## P565

### Comparison of stress-test, single-photon emission computed tomography, and coronarography results in IHD patients.

**A. Ansheles**, V. Sergienko; Russian Cardiology Research Center, Moscow, RUSSIAN FEDERATION.

**Aim**: Comparison of stress-test, SPECT and CAG results in patients with various IHD forms. **Material and Methods**: 204 patients with verified IHD and performed CAG. 140 (68.6%) underwent bicycle ergometer stress-test and rest-stress gated SPECT. During methodical comparison patients were divided into groups based on IHD clinical manifestations and CA stenosis severity. **Results**: 38% showed positive stress-test results, 35% - negative, 14% - equivocal, 13% - nondiagnostic. Whith positive stress-test, SPECT revealed transient myocardial ischemia (TMI) in 100% of cases, while with other stress-test results TMI was not diagnosed only in 35%. In groups with angina pectoris (1), painless ischemia (2) and atypical angina (3) stress-test referral rates were 79.3%, 49.2%, 67.6%, while SPECT ischemia detection rates in group 1 and 2 were similar. In groups without CA stenoses, 1-, 2-, 3-vessel involvement, stress-test referral rates were 50.0%, 70.0%, 93.8% and 52.5%, rates of equivocal and nondiagnostic stress-test results - 21%, 14%, 25% and 47%, SPECT ischemia detection rates - 13.8%, 90.9%, 76.2% and 54.5%, respectively. Summary and discussion: Refusing stress-test execution in IHD patients without evident manifestations, and also equivocal and nondiagnostic stress-test results may cause myocardial ischemia underestimation. Negative stress-test results with no TMI revealed by SPECT predict normal CAG results, while SPECT enables non-stenotic IHD cases detection. Low stress-test referral rate, highest equivocal and nondiagnostic stress-test results rate in patients with 3-vessel involvement, leading to SPECT myocardial ischemia underestimation in this group, is noted.

## P566a

### Myocardial perfusion scintigraphy, osteoprotegerin, and bone mineral density to determine cardiovascular risk in rheumatoid arthritis: Preliminary results

**S. Karacavus**[1], I. Gunaydın[2], S. Sarıkaya[3], A. Y. Gocmen[4], M. Korkmaz[5], A. R. Erbay[3], N. Delibas[4]; [1]Bozok University, Medical Faculty, Department of Nuclear Medicine, Yozgat, TURKEY, [2]Bozok University, Medical Faculty, Department of Internal Medicine/Rheumatology, Yozgat, TURKEY, [3]Bozok University, Medical Faculty, Department of Cardiology, Yozgat, TURKEY, [4]Bozok University, Medical Faculty, Department of Biochemistry, Yozgat, TURKEY, [5]Bozok University, Medical Faculty, Department of Orthopedics and Traumatology, Yozgat, TURKEY.

**Aim:** Rheumatoid arthritis (RA) is a chronic multi-organ inflammatory disease that leads to progressive joint deformity, osteoporosis and to premature death. The high mortality and morbidity rates in RA patients, are primarily due to an increase of cardiovascular events. The aim of study is to determine risk of cardiovascular disease using osteoprotegerin level, myocardial perfusion scintigraphy and bone mineral density in patients with rheumatoid arthritis. **Methods:** A total of 76 patients (M/F: 42/34; mean age 49±9.4 years) with Rheumatoid arthritis were prospectively enrolled. All the patients were performed gated myocardial perfusion scintigraphy (GSPECT) and dual-energy X-ray absorptiometry and measured osteoprotegerin level (OPG). The results obtained by these techniques were compared each other. All patients are following for cardiovascular events. **Results:** Sixteen patients were diagnosed with myocardial ischemia by GSPECT documented angiographically . OPG levels were significantly higher in the myocardial ischemia group than in the non-myocardial ischemia group (p<0.001). Also, there were statistically difference serum concentrations of OPG among normal, osteopenic and osteoporotic patients with RA (p<0.001). Furthermore, compared with non-ischemia group, ischemia group showed significantly lower bone mineral density (BMD) (p<0.05). **Conclusion:** GSPECT, OPG levels and BMD values together with other conventional factors, can help to better define the RA population with an increased likelihood for myocardial ischemia.

## P566b

### Evaluation of post-stress ejection fraction decrease detected by early gated myocardial perfusion SPECT in patients after coronary stenting

**E. Takács**[1], K. Bús[1], Z. Varga[1], M. Janecskó[2], G. Dabasi[1], I. Szilvási[1]; [1]Semmelweis University Dept. of Nuclear Medicine, Budapest, HUNGARY, [2]Semmelweis University Dept. of Anaesthesiology and Intensive Care Unit, Budapest, HUNGARY.

**Objectives**: Assessment of post-stress left ventricular function impairment (myocardial stunning) is useful in risk-stratification of patients with CAD. Aim of study was to investigate the prevalence of post-stress ejection fraction (EF) decrease ≥ 5% without reliable ischemia detected by early gated myocardial perfusion SPECT (eGSPECT) in patients after coronary stenting. **Patient and Methods**: 20 patients (average age 63,8 years) who underwent coronary stenting within two years and 21 patients (average age 55,5 years) with suspected CAD were studied. We performed eGSPECT (15 min after exercise) and resting GSPECT using one-day Tc99m-tetrofosmin protocol. Difference between post-stress and rest EF (ΔEF), summed difference score (SDS), total perfusion deficit (TPD) were evaluated using a quantitative software (QPS/QGS, 17 segments model, scoring system). **Results**: Although no reliable ischemia was detected in the two groups of patients (SDS≤5), post-stress EF decrease ≥ 5 % was more frequent and more severe in patients with stenting (7 patients vs 2 patients, mean ΔEF - 9,3 % vs - 5,5 %). Stress TPD values were higher in patients with myocardial stunning, but the difference was not significant (12,7 ± 6,2 vs. 9,7 ± 2,4, p=0,126). **Conclusions**: Our results show that stunning occurs more frequently in patients underwent coronary stenting than in the control group. According to literature data the cardiac event rate of patients with stunning even without detectable inducible ischemia is relatively high, so the evaluation of post-stress left ventricular EF decrease using early GSPECT can help in risk-stratification of patients after coronary stenting.

P22-2 - Tuesday, Oct. 22, 16:00 - 16:30, Poster Exhibition Area

## Cardiovascular: Metabolism

## P567

### Myocardial viability testing PET - $^{18}$F-FDG and SPECT - $^{99m}$Tc on prognosis in patients with coronary artery disease and left ventricular function

**I. V. Shurupova**, I. P. Aslanidis, T. A. Trifonova, E. P. Derevyanko, T. A. Katunina, L. A. Bokeria; Bakoulev Scientific Center for Cardiovascular Surgery, Moscow, Moscow, RUSSIAN FEDERATION.

**Purpose:** to evaluate the predicting capabilities of the combination of gated single-photon emission computed tomography with $^{99m}$Tc-technetril ($^{99m}$Tc-tn SPECT) and positron emission tomography (PET) with $^{18}$F-FDG Methods in evaluation of LV function improvement after revascularization. **Material and Methods:** 21 patients with CAD (mean age 56,7±12,8 yrs) were studied. Nineteen of them (90%) had history of myocardial infarction, 16 patients had heart failure, 9/16 of them had functional class III as per NYHA. Average left ventricular ejection fraction (LVEF) was 44,9±9,6% (from 25 to 50%). The results of rest $^{99m}$Tc-tn SPECT and $^{18}$F-FDG-PET were analyzed. Using 20 segments model, myocardial perfusion was estimated for all segments (comparing to normal data pool). Based on the results of comparison of the non-attenuation corrected gated-SPECT and $^{18}$F-FDG PET images (tomographic slice and polar diagrams) the perfusion/metabolic (P/M) match (scar) and mismatch (hibernation) regions of LV were identified. LVEF was calculated out of gated-SPECT using «QGS» software. For evaluation of LVEF changes in dynamics, myocardial perfusion gated-SPECT was repeated in all patients within 127±56 days after revascularization. **Results:** resting hypoperfusion was detected in 193 LV segments, P/M mismatch was found in 88/193 (45%), P/M match - in 105/193 (55%). Hibernation myocardium in 3 and more segments was diagnosed in 11/21 pts (group 1), <3 segments- in 10/21 pts (group 2). After revascularization LVEF increased by ≥5% in 8/11 pts of group 1 (positive predicted value 73%) and only in 1/10 pt of group 2 (negative predicted value 90%). Sensitivity and specificity of the combination of $^{18}$F-FDG PET and $^{99m}$Tc-tn SPECT in LVEF improvement prediction was 89% and 70% respectively, diagnostic accuracy - 77%. Left ventricular EF

increase was noted in group 1 (55±5,8% compared to 45,4±7,6%, p<0,05), in group 2 LVEF increased from 43,7±7,8% to 49,7±4,0% (p=NS). **Conclusion:** 1.Combination of $^{18}$F-FDG PET and $^{99m}$Tc-tn SPECT Methods demonstrates high accuracy of hibernation myocardium diagnostics in patients with LV ischemic dysfunction. 2. Availability of hibernation myocardium of more then 15% of LV (≥3 segments) allows to predict considerable LVEF increase after revascularization.

## P568

### Long-term follow-up of patients with cardiac sarcoidosis using $^{18}$F-FDG PET

**K. Koyama**[1], S. Kodaira[1], A. Tokue[2], T. Higuchi[2], Y. Arisaka[2], T. Toyama[1], H. Hoshizaki[1], S. Ooshima[1], Y. Tsushima[2]; [1]Gunma Prefectural Cardiovascular Center, Maebashi, JAPAN, [2]Gunma Faculty of Medicine, Maebashi, JAPAN.

**Introduction**: Cardiac $^{18}$F-FDG PET (PET) is useful Methods for identification of cardiac sarcoidosis (CS). How ever, normal myocardial cells use not only free fatty acids but also glucose as their energy sources, thus $^{18}$F-FDG can accumulate in normal myocardium. The purpose of this study was to assess significant $^{18}$F-FDG accumulation in patients with CS. **Methods**: PET was performed in 18 patients (Male: 1, Female: 17) diagnosed CS. Mean age of the patients was 65.3 (range 49-81). Total study times were 81. Theses studies were divided into three groups, Group A was pre- steroid treatment (n: 11), Group B was monitoring response to steroid treatment (interval of two studies was with in few months (n: 21)) and Group C was follow up the activity of CS (interval of two studies was over 10 months, without cardiac event (n: 49)). Myocardial images were divided into 17 myocardial segments. The standardized uptake value (SUV) of PET was calculated. **Results**: Mean SUV of Group A, B and C were 3.32, 2.03 and 2.21, respectively. Maximum SUV of Group A, B and C were 6.92, 2.74 and 4.05, respectively. Ratio of maximum to minimum SUV in patients of Group A, B, and C were 3.66, 2.08 and 3.14, respectively. **Conclusions**: PET using SUV was useful Methods for monitoring response to steroid treatment in patients of CS. In case of follow up the activity of CS, maximum SUV and ratio of maximum to minimum SUV in patients seemed to be more useful than mean SUV.

## P569

### Impact of different factors on myocardial 18F-FDG uptake

A. Sałyga[1,2], **R. Czepczynski**[1,2], A. Wyszomirska[1,2], R. Oleksa[1], S. Cichocka[1], M. Ruchała[1], J. Sowiński[1]; [1]Department of Endocrinology and Metabolism, Poznan University of Medical Sciences, Poznan, POLAND, [2]Euromedic Diagnostics, Poznan, POLAND.

**Introduction** Physiological 18F-fluorine-deoxyglucose (FDG) activity in myocardium is observed in some patients in routine PET/CT studies. It is known that FDG uptake depends on the substrates currently utilized by myocardium. In case of oncological indications the myocardial activity is undesirable, as it may relatively decrease uptake in the malignant tissue and impair the interpretation of the images, particularly in mediastinum. Aim of this investigation was to evaluate the role of several patient-related factors that may potentially influence the non-specific cardiac FDG uptake. **Materials and Methods**. We retrospectively evaluated 405 consequent PET/CT studies performed in patients with suspected or known malignancy. After exclusion of 43 patients with history of myocardial infarction, the study population comprised 362 patients aged 13-87 years (median age 60 yrs.). Cardiac FDG uptake was assessed by the measurement of SUVmax. Correlation of the resulting values of SUVmax with 17 factors was studied using Spearman correlation test. Following factors were analysed: age, gender, body mass index (BMI), glucose level, time between FDG injection and image acquisition, previous oncological treatment (radiotherapy of mediastinum, chemotherapy), concomitant diabetes as well as the most frequent medication (beta-blockers, calcium channel blockers, angiotensin-converting enzyme inhibitors, diuretics, statins, oral hypoglycemic drugs (metformin, sulfonamides), insulin and levothyroxine. **Results.** Average value of myocardial SUVmax was 3.5 (range 0.9 - 15.4, median 2.4). Statistical analysis showed correlation of SUVmax with patient's sex, age and BMI. Cardiac FDG uptake was higher in men than women and was higher in younger subjects (under 35 years). Negative correlation was found in case of BMI values. Some correlations were found also in respect to the current medication. Myocardial FDG uptake was lower in patients receiving calcium channel blockers, and higher in patients treated with insulin. There was no correlation between SUVmax and the other factors studied. **Conclusion**. In the studied population patient's sex, age and BMI, as well as medication with calcium channel blockers or insulin had impact on the cardiac FDG uptake. Potential use of calcium channel blockers to decrease unnecessary myocardial FDG activity should be studied.

## P570

### Comparison between 18F-FDG Blood Pool Activity in Ascending Aorta and in Superior Vena Cava. Are They non Dependent on the Presence of Atheroma Indistinct as a Reference of FDG Vascular Activity?

**C. Lavado-Pérez**, Z. Bravo -Ferrer, R. Quirce, I. Martínez-Rodríguez, I. Banzo, J. F. Jiménez-Bonilla, A. Rubio-Vassallo, R. Del Castillo-Matos, F. Ortega-Nava, S. Ibañez-Bravo, N. Martínez-Amador, J. M. Carril; University Hospital Marqués de Valdecilla. Cantabria University ,, Santander, SPAIN.

**AIM:** To assess vascular activity of 18F-FDG (FDG) in the ascending aorta and superior cava in order to evaluate which region could provide an optimal reference for target/background ratio in the assessment of vasculitis and atheroma FDG uptake. **MATERIAL AND METHODS:** We performed a retrospective study which inclued 10 patients in whom an FDG-PET/CT (images acquired 90´ after the administration of 7 MBq/kg) was performed. A semiquantitative assessment of images (SUV max), was carried out in the blood pool of ascending aorta and superior vena cava at the same level. Atheromatous plaques were evident in the CT in 4 of the 10 patients studied with FDG. **RESULTS:** In the 10 FDG patients, the mean SUVmax in ascending aorta was 1.48 ± 0.24 and in the superior vena cava was 1.40 ± 0.27. Aorta/cava ratio was 1.07 ± 0.15. In patients with atheromatous plaques the mean SUVmax observed in aorta and cava was 1.51 ± 0.3 and 1.33 ± 0.24 respectively, aorta/cava ratio was 1.14 ± 0.14. In patients without atherosclerotic plaques the mean SUVmax in aorta and cava was 1.43 ± 0.12 and 1.51 ± 0.12, with an aorta/cava ratio of 0.95 ± 0.08. These results yielded no statistically significant differences. **CONCLUSIONS**: This preliminary work shows that FDG activity in the blood pool is not uniform, althought there was not statistically significant differences. These findings should be taken into account when comparing vessel wall/ blood pool ratios (TBR) obtained with different vascular ROIs as reference.

P23-2 - Tuesday, Oct. 22, 16:00 - 16:30, Poster Exhibition Area

# Cardiovascular: Stem Cells

## P571

### Effect of marrow cells auto transplantation on the status of damaged myocardium at various periods after infarction

**A. Yalfimov**[1], A. Ivanova[2]; [1]Pediatric Medical University, St. Petersburg, RUSSIAN FEDERATION, [2]Scientific Center of Radiology and Surgical Technology, St. Petersburg, RUSSIAN FEDERATION.

Despite the high level of pharmacological and surgical expertise the cardiovascular diseases are the predominant cause of death. The new advanced and long term method in cardiology proposed is an application of marrow auto logical cells. Many problems that arise due to cell types, infiltration method and transplantation time still remain unsolved. Purposes Compare an effect of auto transplantation of nucleated cells (NC) and multi potent mesenchymal stromal marrow cells (MMSC) upon the clinical course of acute myocardial infarction. Compare the Methods of marrow cells infiltration (intra myocardial and intravenous) by simulating an acute myocardial infarction Assess an effect of intra myocardial auto transplantation of nucleated marrow cells on the status of damaged myocardium by simulating post infarction cardiosclerosis. The Methods and materials. Cardiac infarction has been simulated on Chinchilla rabbit males by applying deligation of the anterior descending branch of the left coronary artery. In the model of acute myocardial infarction the damaged area or auricle acentric veins was injected intra myocardially with the MMSC culture or marrow NC right after coronary occlusion occurred. In the postinfarction aterosclerotic cardiosclerosis model the marrow NC were injected into the peri-infarction area in an intra myocardial manner. The results of transplantation were assessed functionally (electrocardiography, SPECT, echocardiography), macroscopically and histomorphologically. In each group the investigation was carried out prior to transplantation and in 10, 45, 90, 180 and 360 days after cells transplantation. Results. In the acute infarction model. The groups of animals exposed to the marrow NC and MMSC culture auto transplantation demonstrated in a 6 months time after the operation was performed complete normalization of the myocardium perfusion in the abnormal zone; a perfusion defect was detected in control at all the periods. Intravenous marrow cell infiltration did not result in any changes of the functional and morphological indices, and marked cells were detected in myocardium. In the post infarction cardio sclerosis model was performed a considerable improvement of the myocardium perfusion in the abnormal zone (35±4%). Conclusion. Marrow MMSC auto transplantation resulted in a marked positive influence on the reparation of the myocardium damaged; marrow NC transplantation resulted at various periods after infarction resulted in a considerably higher perfusion of the ischemic myocardium; however, NC transplantation at the most acute myocardial infarction phase did not result in a better systolic functioning of the sinister ventricle and was accompanied with a worsening of the reparation processes.

## P572

### Evaluation of CD34+ HPCs labelled with 99mTc-HMPAO

**A. Socan**, M. Sever, B. Vrtovec, P. Kolenc Peitl, L. Lezaic; University Medical Centre Ljubljana, Ljubljana, SLOVENIA.

AIM Several clinical studies showed the potential of the treatment with progenitor cells (PCs) when delivered to myocardium. Monitoring and evaluation of the therapy "in-vivo" is difficult and optimal method remains to be developed, although different Methods for cell labelling can be used (111In-oxine, 111In-tropolone, 18FDG, 64Cu-oxine, 99Tc-exametazime). The aim of our study was to label and evaluate influence of 99mTc-HMPAO labeling on CD34+ hematopoietic PCs (HPCs) during time period suitable for SPECT "in-vivo" monitoring of labeled cells myocardial homing. MATERIALS Human HPCs were mobilized with G-CSF and collected by aphaeresis. CD34+ cells were enriched with an immunomagnetic separation device (MACS®). A fraction of the collected cells (25%), number was patient dependent (78 to 285 mio), was labeled with 99mTc-HMPAO, incubated for 20 min at room temperature, unbound radioactivity was removed by washing the cells with cell free media. Cell viability was assessed by Trypan Blue exclusion assay at different time points before and after labelling. CFC Assay (MethoCult®) of labelled and unlabelled HPCs was performed. Labelling stability of HPCs was assessed 150 min after cell labelling. Labelled cells (48-343 MBq) were injected through a micro catheter during coronarographic procedure together with unlabelled HPCs. SPECT images were obtained 2 and 18 hours after HPC injection. RESULTS Labelling efficiency of HPCs was up to 65.7% depending on the amount of cells available for radiolabelling.Viability of HPCs before and immediately after the labelling was 91,3 ± 4,7% and 90,6 ± 5,1% , whereas viabilities 150 min and 18 hours after labeling were 95,8 ± 3,4% and 84 ± 16,7% for unlabelled HPCs and 92,7 ± 6,8% and 83,4 ± 12,5% for labelled ones. CFC Assay results of labelled compared to unlabelled HPCs showed unchanged proliferation. Labelling stability of HPCs 150 min after cell labelling was 75±11,2%. SPECT images obtained 2 and 18 hours after HPCs injection enabled evaluation of the arrangement and percentage of transplanted HPCs accumulated in the heart muscle. CONCLUSIONS Labelling procedure of HPCs with 99mTc-HMPAO is feasible resulting in high cell viability, unchanged proliferative ability and high labelling stability. It enables imaging with SPECT, which proves to be a suitable non-invasive method for "in-vivo" monitoring of cell trafficking with good spatial resolution.

P24-2 - Tuesday, Oct. 22, 16:00 - 16:30, Poster Exhibition Area

## Cardiovascular: New & Innovative

## P573

### Blood pool left ventricular ejection fraction from reprojected planar images obtained with a CZT dedicated cardiac SPECT camera

**D. Emond**, S. Prévost; Sherbrooke University Hospital Centre,Department of Nuclear Medicine and Radiobiology, Sherbrooke, QC, CANADA.

**Aim:** In our institution, left ventricular ejection fraction (LVEF) is calculated from the analysis of planar acquisition images obtained on a dual head GE Infinia camera. Although new dedicated semi-conductor cardiac cameras using CZT (cadmium-zinc-telluride) technology have the potential for shorter acquisition time and have shown promise in myocardial perfusion imaging, they have yet to be applied to LVEF calculation. In order to expand the new technology's indications, we evaluated the accuracy of LVEF values based on reprojected gated planar images obtained on CZT cardiac cameras by comparing them to LVEF values obtained using images from the conventional dual head GE Infinia cameras. **Materials and Methods**: Planar blood pool gated images were obtained on a standard camera from 31 consecutive patients in best septal view as determined from a SPECT acquisition. A second set of tomographic images was acquired for 8 minutes on the CZT camera. Recently released software from GE was used to process the data. Both the standard planar and the reprojected pseudo-planar datasets were analyzed semi-automatically and manually using "EF Analysis" software from GE to determine left ventricular ejection fraction. Data were analyzed independently by two observers. **Results**: The difference in LVEF values obtained on the planar (Infinia) and pseudo-planar (NM530) datasets averaged -1,4 ± 4,0 in automatic mode and -0,8 ± 3,0 in manual mode .The correlation coefficients between the LVEF values obtained on the two cameras were r = 0,94 (p 0,01) and r = 0,97 (p 0,001) respectively in automatic and manual mode . The correlation coefficients between the two observers using either mode or cameras were all greater than 0,94 (p<0.001) **Conclusion**: LVEF measured on planar reprojections derived from gated blood-pool SPECT images acquired on a dedicated cardiac SPECT camera are equivalent to those obtained on standard planar images. We expect that ongoing trial should confirm the accuracy of CZT technology for measuring other parameters such as peak filling rate, end diastolic volume and end systolic volume are equivalent as well.

## P574

### Tetrofosmin-Tc-99m Right Ventricular Uptake as a New Surrogate Marker of Subclinical Pulmonary Hypertension in Rheumatoid Arthritis

**T. Vieira**[1], M. Bernardes[2], A. Oliveira[1], P. Oliveira[1], T. Faria[1], V. Alves[1], E. Martins[3], J. G. Pereira[1]; [1]Nuclear Medicine Department of Hospital de São João, Porto, PORTUGAL, [2]Rheumatology Department of Hospital de São João, Porto, PORTUGAL, [3]Cardiology Department of Hospital de São João, Porto, PORTUGAL.

**Aim**: Cardiovascular diseases are a leading cause of death in patients with rheumatoid arthritis (RA). Pulmonary arterial hypertension (PAH) associated with rheumatic diseases carries a particularly grim prognosis with faster progression of disease and poor response to therapy, which may be explained by an underlying inflammatory component. New noninvasive parameters would be helpful to assess early subclinical PAH and direct therapeutic efforts. It was recently published that right ventricular to left ventricular uptake ratio (RV/LV) from SPECT myocardial perfusion images of an unselected population can identify patients with high pulmonary artery pressure or right ventricular hypertrophy; however that study included patients with abnormal ejection fraction. We aimed to study the usefulness of RV/LV as a new marker of subclinical PAH in a RA population with normal LV perfusion and function. **Materials and Methods**: Thirty RA patients performed a clinical evaluation of the disease activity (DAS28-CRP(3), DAS28-CRP(4), DAS28-SR(3) and DAS28-SR(4)) and duration, and of the corticotherapy duration, a brain natriuretic peptide (BNP) evaluation and a tetrofosmin-Tc-99m gated myocardial perfusion SPECT with adenosine. All patients had normal SPECT LV perfusion and ejection fraction. For RV/LV calculation an investigator with no knowledge of the clinical and analytical data placed 6×6 pixel ROIs in the RV and LV free walls of a mid-ventricular short-axis SPECT slice. RV/LV was calculated as the ratio of myocardial counts in each ROI. A Spearman's analysis was conducted to study the correlations of RV/LV with clinical and analytical parameters and of BNP with clinical parameters, adjusted for age and sex. Results: Twenty-one patients were female (70%). Mean age was 54.7 years-old. There were significant correlations of RV/LV with DAS28-CRP(3) (r=0.434; p=0,017), DAS28-CRP(4) (r=0.405; p=0,026), DAS28-SR(3) (r=0.428; p=0,018) and DAS28-SR(4) (r=0.427; p=0,019). BNP correlated significantly with the disease duration time and with the corticotherapy duration time. **Conclusion:** These results suggest that the RV/LV from tetrofosmin-Tc-99m myocardial perfusion SPECT can be an useful new early marker of subclinical PAH in RA, which is dependent of inflammatory disease activity. This new marker could possibly help in the decision of early biological therapy introduction for symptomatic PAH prevention. Long-term follow-up of a larger sample of patients will be obviously necessary to ascertain the impact of RV/LV on the prognosis of RA patients.

## P575

### Planar $^{123}$I-MIBG heart-to-mediastinum ratio: the impact of a predefined ROI and collimator type on reproducibility

**D. O. Verschure**[1,2], V. Bongers[3], P. J. Hagen[3], C. E. E. van Ofwegen-Hanekamp[3], G. A. Somsen[2,4], B. L. F. van Eck – Smit[1], H. J. Verberne[1]; [1]Academic Medical Center, Amsterdam, NETHERLANDS, [2]Onze Lieve Vrouwe Gasthuis, Amsterdam, NETHERLANDS, [3]Diakonessenhuis, Utrecht, NETHERLANDS, [4]Cardiology Centers of the Netherlands, Amsterdam, NETHERLANDS.

**Aim:** The $^{123}$I-metaiodobenzylguanidine ($^{123}$I-MIBG) myocardial scintigraphically derived late heart-to-mediastinum (H/M) ratio is a prognostic marker in heart failure (HF). The purpose of this study was to assess the impact of mediastinal region of interest (ROI) definition on intra- and inter-observer variability in relation to collimator type used for image acquisition. **Methods:** 35 subjects with HF (mean age 65±7.8 years, 80% male, LVEF 29±8.4) referred for $^{123}$I-MIBG were enrolled. At 4 hours (late H/M) after the administration of 185 MBq $^{123}$I-MIBG, anterior planar thoracic images were acquired with a low energy high-resolution (LEHR) collimator and a medium energy (ME) collimator. The late H/M ratio was calculated based on the mean count densities from the manually drawn ROI over the left ventricle and a ROI placed in the upper mediastinum. First analysis: 2 observers used an observer-defined mediastinal ROI. Second analysis: the same 2 observers used a fixed mediastinal ROI. A third observer analysed the images twice with a fixed mediastinal ROI. The intra- and inter-observer variability of the late H/M were assessed using Lin's concordance coefficient (LCC) and Bland-Altman analysis. **Results:** Agreement was substantial between the three observers in the assessment of the late H/M ratios when using a predefined fixed mediastinum ROI. The LCCs for the LEHR collimator were 0.98, 0.96 and 0.95, respectively and for the ME collimator 0.98, 0.97 and 0.97 respectively. However, compared to the predefined mediastinal ROI, the observer-defined mediastinal ROI resulted in a poor to moderate agreement. The LCCs for the late H/M ratios between the three observers with LEHR collimator were 0.82, 0.94 and 0.70, respectively and for the ME collimator 0.77, 0.91 and 0.80, respectively. Intra-observer analysis for the observer using a predefined fixed mediastinal ROI showed a substantial agreement. The LCCs for the LEHR collimator was 0.97 and for the ME collimator 0.96, respectively. The intra-observer Bland-Altman 95% limits of agreement were -0.01 (-0.12 - 0.10) using LEHR collimator and -0.04 (-0.27 - 0.19) using ME collimator. **Conclusion:** A predefined fixed mediastinal ROI results in a low intra- and inter-observer variability of the late H/M and is therefore to be preferred over an

observer defined mediastinal ROI. In addition the intra- and inter-observer variability of the late H/M is not influenced by collimator type used.

## P576

### Correlations of Left Ventricular Mechanical Dyssynchrony with Myocardial Perfusion and Functional Parameters Assessed by Tetrofosmin-Tc-99m Gated SPECT in Patients with Left Bundle Branch Block

**T. Vieira**[1], V. Ribeiro[2], E. Martins[2], V. Alves[1], P. Oliveira[1], A. Oliveira[1], T. Faria[1], M. B. Pérez[1], J. G. Pereira[1]; [1]Nuclear Medicine Department of Hospital de São João, Porto, PORTUGAL, [2]Cardiology Department of Hospital de São João, Porto, PORTUGAL.

Aim: Left bundle branch block (LBBB) may induce abnormalities in left ventricular performance due to abnormal asynchronous contraction patterns and has received much renewed attention since biventricular pacing to restore synchrony (CRT) has become a frequently used modality to treat patients with heart failure. In patients with left ventricular dysfunction, the presence of LBBB remains the main criterion for CRT selection although not allowing the prediction of success in clinical response. Phase analysis by gated myocardial perfusion SPECT has been supported to evaluate left ventricular mechanical dyssynchrony (LVMD). Using the same technique, we aimed to identify predictors of LVMD in patients with LBBB. Materials and Methods: The study included 65 patients (32 males; 70.26 ± 9.41 years-old) with LBBB consecutively referenced for stress (adenosine) tetrofosmin-Tc-99m ECG-gated myocardial perfusion SPECT between January 2007 and October 2010 due to suspected coronary artery disease. LV perfusion and functional parameters were measured, and phase analysis was performed to quantify LV dyssynchrony. The following two parameters obtained from the phase analysis were evaluated, as they have been shown to best identify LV dyssynchrony: phase histogram bandwidth and phase histogram standard deviation. LV dyssynchrony was considered to be present if at least one of the parameters was above the cut-off value. Pearson's chi-square and Student's t tests were used for the statistical analysis of the correlations between LVMD and perfusion and functional parameters. Results: Myocardial perfusion defects (MPD) were present in 40/65 (61.5%) patients, and the mean post-stress left ventricular ejection fraction (LVEF) was 39.48 ± 16.43%. LVMD was present in 53/65 (81.5%) patients. Student's t test revealed post-stress LVEF (p = 0.011), summed thickening scores (p = 0.013) and summed motility scores (p = 0.003) as predictors of LVMD. In chi-square test there were verified significant associations of LVMD with the presence of global motility (p = 0.001) and thickening (p = 0.011) abnormalities, the presence of motility abnormalities in the lateral (p = 0.003), apical (p = 0.005), anterior (p = 0.007) and inferior (p = 0.015) regions, the presence of lateral thickening abnormalities (p = 0.023) and the presence of apical MPD (p = 0.033). Conclusion: In patients with LBBB, the response to CRT may be dependent on intraventricular dyssynchrony due to the presence of certain motility and perfusion LV regional parameters. Phase analysis by gated myocardial perfusion SPECT could be a complementary imaging tool for CRT planning.

## P577

### Evaluation of Ventricular Function by Gated Blood Pool SPECT: A Simulation Study

**S. Mohseni**[1], A. Bitarafan-Rajabi[2], A. Kamaliasl[1], S. M. Entezarmahdi[1], Z. Shahpouri[1], P. Segars[3], M. Bordbar[4]; [1]Department of Nuclear Engineering, Shahid Beheshti University, Tehran, IRAN, ISLAMIC REPUBLIC OF, [2]Cardiovascular Interventional Research Centre, Department of Nuclear Medicine, Rajaei Cardiovascular, Medical & Research Centre, Tehran University of Medical Science, Tehran, IRAN, ISLAMIC REPUBLIC OF, [3]Departments of Radiology and Radiological Science, Johns Hopkins University School of Medicine, Baltimore, MD, UNITED STATES, [4]Electrical Engineering Faculty, Sahand University of Technology, IRAN, ISLAMIC REPUBLIC OF.

Background. We evaluated the accuracy of three difference Surface-Based, Count-Based Calculation and Count-Based Volumes electrocardiogram (ECG)- gated blood pool single-photon emission computed tomography (GBPS) algorithms for assessment of right ventricle end- diastolic (RVEDV), end-systolic volume (RVESV), and ejection fraction (RVEF) compared with the determine NCAT phantoms parameters as gold standard. Methods and materials. Eleven digital NCAT phantoms including the normal and abnormal phantoms with known RV end-diastole volumes, RV end-systole volumes and ejection fractions (EF)were generated. The SIMIND Monte Carlo program was used to create raw data. The studies were reconstructed by FBP and then filtered with Butterworth without the attenuation and scatter correction. Three different algorithms Surface-based, Count-based calculation and Count-based volumes available in Cedars-Sinai quantitative blood-pool SPECT (QBS) package were used to quantify the datasets. Results. The QBS calculated RVEDV: [166:220] in SB method, [224:291] in CB method and [224:291] in VB method and RVESV: [112:141] in SB, [134:162] in CB and [146:183] in VB Methods. The QBS outputs were more correlated with simulated heart in SB method for RVEDV r= 0.98 and in CB method for EF value with r= 0.99. Conclusion. As the results show the QBS with Surface-Based (SB) method is an appreciate tool for ventricular volumes quantitative analysis and with Count-Based algorithm in determination of ventricular ejection fraction. This software has high potential in researches for Gated blood pool SPECT. Otherwise, all of these RV and LV function measurements by this software may require further validation using a gold standard clinical data.

## P578

### Scintigraphic myocardial profile of diabetics type 2, independently of anginal symptoms

**I. Kotsalou**[1], A. Kotsalos[2], N. Zakopoulos[3], N. Dimakopoulos[1], M. Dimopoulos[3]; [1]Nuclear Medicine Dept, NIMTS Hospital, ATHENS, GREECE, [2]Cardiovascular Surgery Dept, NIMTS Hospital, ATHENS, GREECE, [3]University of Athens, Alexandra Hospital, ATHENS, GREECE.

AIM: Autonomic Dysfunction is common in patients with diabetes (DM)causing silent coronary artery disease (CAD). Our study searched the prognostic role of anginal or atypical symptoms of diabetics undergoing myocardial perfusion (SPECT) studies. METHODS: We retrospectively included 78 patients, of both sexes, with known Diabetes and duration 1-15 years (64% Group 1) and 16-25years (36 Group 2). 22 (28%- Group A) of included diabetics claimed angina symptoms, 23 subjects (29%- Group B) mentioned atypical angina symptoms, whereas 33 (43%- Group C) were asymptomatic. Patients with known CAD were excluded. Gated- single photon emission tomography was performed using a one-day stress/rest protocol with Tc-99m tetrofosmin (n=65:physical exercise, n=13:adenosine). We also analyzed for statistical significance multiple risk and clinical prediction factors like the duration of DM, the presence of peripheral vascular disease, dyslipidemia, hypertension, smoking, family history of CAD and obesity. RESULTS: Using the 20- segments scoring model for SPECT analysis, we found that 77% of perfusion studies in Group A were positive for CAD (scar and/or ischemia) and 48%, 73% for Group B and Group C respectively. Incidence of Ischemia showed no significant difference in groups 1 and 2 (Duration of Diabetes Mellitus). CONCLUSIONS: Myocardial perfusion scintigraphy study is a sensitive mean for screening of subclinical CAD in patients with DM type 2 and may help the referring cardiologist to handle properly and consider right controversial and confusing "angina" symptoms of diabetics. Finally, the absence or not of anginal symptoms doesn't increase more the definite high cardiovascular risk profile of diabetics type 2, because of high incidence of silent ischemia in those patients.

## P579

### Effect of stress modality on left ventricular synchrony parameters (LVSP) in patients with normal myocardial perfusion scintigraphy (MPS) and normal contractile function

**G. Arun Reddy**, K. Parveen, A. Sood, A. Bhattacharya, P. Madan, B. R. Mittal; Postgraduate Institute of Medical Education & Research, PGIMER, CHANDIGARH, INDIA.

Aim: To analyze the effect of stress modality on left ventricular synchrony parameters using phase analysis on gated SPECT MPS in patients with normal perfusion studies and normal left ventricular ejection fraction. Materials and Methods: In this retrospective study, 45 patients who underwent 99mTc Tetrofosmin stress/rest myocardial perfusion imaging with no known CAD, LVEF > 50 %, no history of conduction abnormalities, QRS < 120 ms, and normal MPS study were included. Of the 45, 27 patients had undergone treadmill exercise stress study (ESS) and 18 had undergone dobutamine stress study (DSS). Phase analysis was performed using QGS software. The first harmonic phase angles obtained from Fourier transformed time dependent signals were used by the software to obtain LVSP automatically. Global and regional (wall based) LVSP including histogram mean (μ), Standard deviation SD (σ), mode (m), bandwidth (b) and entropy (e) were analyzed separately for ESS and DSS groups. Values were expressed as mean + SD except for entropy which was expressed as percentage. Student's t-test was utilized to compare the means of LVSP of both groups. Results: ESS and DSS groups included 27(11-males, 16-females; Mean age-52.7 yrs) and 18 patients (6-males, 12-females; Mean age-62.1 yrs) respectively. Global LVSP of the ESS and DSS groups were: μE- 135.26 + 14.75, σE- 8.26+5.73, mE- 136.33+ 14.54, bE- 32.89+20.68, eE- 48.56+9.25 and μD- 137.05+ 13.99, σD- 5.89 + 2.02, mD- 139 + 14.4, bD- 24.67 + 7.09, eD- 45.33 +8.48 respectively. No significant difference between LVSP of both groups was noted (Pμ =0.686, Pσ=0.151, Pm =0.548, Pb =0.113, Pe=0.242). Regional wall based LVSP were also analyzed for each group and compared in a similar manner which proved no significant difference between both the groups Conclusion: Type of stress modality (exercise vs. dobutamine) has no effect on left ventricular synchrony parameters in patients with normal myocardial perfusion study. However, further evaluation is needed to validate these findings.

P25-2 - Tuesday, Oct. 22, 16:00 - 16:30, Poster Exhibition Area

**Cardiovascular: Miscellaneous**

## P580

### Increased right ventricular function in patients with liver cirrhosis awaiting TIPS procedure

**L. Dercle**, T. Cognet, C. Christol, O. Lairez, M. Galinier, D. Carrié, I. Berry, M. Robic, C. Bureau; CHU Toulouse, Toulouse, FRANCE.

Introduction In patients with liver cirrhosis, there is clinical evidence of cardiac dysfunction involving left ventricle after a compensatory phase but the influence of the hyperdynamic circulation on right heart remains unclear. The aim of this study was therefore to evaluate non-invasively the effects of end stage liver disease on right ventricular function. Subjects and Methods From June 2012 to March 2013, cirrhotic patients waiting for a TIPS (Transjugular Intrahepatic Porto systemic Shunt) procedure were prospectively included and compared to 11 age and gender matched healthy controls subjects. Patients with a history, ECG, echocardiography or CMR suggesting a concomitant heart disease were excluded. Global cardiac function was assessed by two physicians blinded for the clinical information using a fully automatic software BPGS (Blood Pool Gated SPECT) on ERNV (Equilibrium Radionuclide Ventriculography). Regional and diastolic cardiac function was evaluated using semi-automatic software with manual correction (TomPool). Data were compared to results of right heart catheterization. Results Eleven patients (9 men, mean age 59±11) with Child-Pugh grade B and C (10/1) cirrhosis mainly due to alcohol (9/11) were prospectively included. Mean Child-Pugh score was 8.3 ± 1.2, mean MELD score was 8.4 ± 2.8 and was <16 for all patients. Right ventricular ejection fraction (RVEF) and normalized RVEF were significantly increased in the pre-TIPS population in comparison with controls subjects (70.2 ± 9.9 vs. 57.7 ± 6.8, p=0.01 and 74.2 ± 10.8 vs. 62.3 ± 8.3; p=0.028, respectively) and did not depend on Child-Pugh score, ascites, levels of transaminase or BNP. Mean Filling Rate (edv/systole) was increased in pre-TIPS population for both left (4.9 ± 1.5 vs. 2.8 ± 1.5, p=0.004) and right ventricle (3.90 ± 1.30 vs. 2.68 ± 0.82, p=0.026). Wall motion and synchrony did not differ. Right cardiac index (r=0.61; p≤0.05) and right ventricular stroke volume (r=0.61; p≤0.05) were significantly correlated with MELD score. The estimated right ventricle cardiac index with BPGS was well correlated with catheter measurement (r = 0.91; p = 0.0001). The inter-observer reproducibility was excellent for right ventricular parameters (>0.95 for EF, cardiac index and end diastolic volume). Conclusion/Discussion Right ventricular function and filling rate are increased in patients with end-stage liver disease and waiting for a TIPS procedure.

## P581

### Diagnosis of portal hypertension and prediction of pulmonary consequences of liver cirrhosis on Equilibrium Radionuclide Ventriculography

**L. Dercle**, M. Sinigaglia, T. Cognet, O. Lairez, D. Bastié, C. Bureau, I. Berry; CHU Toulouse, Toulouse, FRANCE.

Introduction In patients with liver cirrhosis, the hyperdynamic circulation and portal hypertension are responsible for hepato-pulmonary syndrome and portopulmonary hypertension. Equilibrium Radionuclide Ventriculography [ERNV] is efficient to diagnose the hyperdynamic circulation. With the same data as ERNV, the aim of this study was to identify a quick and easy score and to assess if it was able to diagnose portal hypertension and to estimate the probability of pulmonary complications. Subjects and Methods Patients referred for ERNV were retrospectively and consecutively included in two groups: control group and group with portal hypertension and without hepato-pulmonary syndrom (gold standard: echography and right catheterization). Patients with liver cancer, acute symptoms or abnormal blood count were excluded. Two physicians performed a blind analysis of the tomographic view of ERNV and recorded: the longest splenic diameter [LSD], the longest hepatic diameter [LHD], the mean activity per pixel at the center of the right liver in a 25 pixel ROI [H25], at the center of the spleen [S25]. Except the LSD, all the data were recorded with the front view of the sum image of tomography. The spleno-hepatic index [SHI] was calculated according to the formula: SHI=(S25*LSD)/(H25*LHD). Results 71 patients were included. 11 patients suffered from portal hypertension and their mean SHI was 1.14 ± 0.79. 60 patients were in the control group and their mean SHI was 0.38 ± 0.15. Inter-observer reproducibility was 0.93. The area under the ROC curve was 0.99 (95%CI 0.98-1.00). The best cut off point was 0.71 (sensitivity of 100%, specificity of 95%). In the liver cirrhosis group, correlation with mean pulmonary arterial pressure was r=0.79, p=0.002. Conclusion/Discussion SHI allows the diagnosis of the typical vascular redistribution of portal hypertension. It is a simple, accurate and reproducible score. SHI was strongly and positively correlated with the mean pulmonary arterial pressure and therefore must warn of the risk of pulmonary complications.

## P582

### 18F-FDG PET-CT imaging for the evaluation of small- and medium-size vessel vasculitis, including Wegener's granulomatosis

**S. Vöö**, M. Kemna, P. van Paassen, J. Cohen-Tervaert, M. van Kroonenburgh; Maastricht University Medical Center, Maastricht, NETHERLANDS.

**Background.** Small- and medium-size blood vessel vasculitis, including Wegener's granulomatosis, is a rather rare clinical entity which leads in most of the cases to life-threatening complications. Early diagnosis of active disease is therefore crucial in preventing a rapid fatal disease progression. Routine diagnostic tools, such as serum inflammatory markers and plasma antineutrophil cytoplasmic antibodies (ANCA), may often produce inconclusive results. 18F-FDG PET-CT is commonly used to identify active inflammatory lesions. This study evaluated the diagnostic value of 18F-FDG PET-CT in patients with suspected relapse of small- and medium-size vessel vasculitis. **Material&Methods**. Twenty three patients with a history of small- and medium-size vessel vasculitis underwent 18F-FDG PET-CT imaging between December 2006 and June 2012 due to suspected relapse of their disease. CRP, as an inflammatory marker, and ANCA levels were determined at the time of scanning. **Results.** Despite no significant increase in CRP levels and inconclusive ANCA levels, PET-CT identified foci of active inflammation in 19/23 cases with suspicion of active vasculitis. Common PET-positive sites were nasopharynx (12/19), lungs (11/19), and larynx (10/19). Corresponding tissue biopsies confirmed the diagnosis of active small- and medium-size vessel vasculitis in all these sites. Additional PET-positive sites were found in bone marrow (10/19), aorta (7/19), and thyroid gland (5/19), suggesting a multiorgan involvement in majority of patients (17/19). **Conclusions**. PET-CT is able to accurately depict active sites of small- and medium-size vessel vasculitis, including in those in whom other diagnostic markers have been inconclusive. Majority of patients with relapsing disease show a multiorgan involvement on PET-CT.

## P583

### F18 FDG- PET/CT in evaluation of malignant and benign cardiovascular lesions

**S. Puri**, H. Son, S. Hobbs, S. Voci; University of Rochester, Rochester, NY, UNITED STATES.

Purpose: While vascular FDG uptake within the inflammatory process associated with atherosclerosis and endovascular grafts has been well documented, there is a paucity of data on PET/CT findings in other malignant and benign conditions affecting the cardiovascular system. We present FDG avid uncommon benign and malignant cardiovascular lesions identified by PET/CT and subsequently confirmed by other imaging modalities, histology, and/or clinical follow up. Material and Methods: This is a retrospective analysis of the significance of focal FDG avid Cardiovascular lesions identified in a series of 25 patients during oncologic whole body FDG-PET/CT imaging at University of Rochester medical center from January 1, 2007- April 1, 2013. Our series include benign and malignant lesions with the diagnosis confirmed by another imaging modality (MRI, CECT, US, and Echocardiography), histology, and/or clinical follow-up including response to targeted therapies. Cases with well established causes of cardiovascular FDG-uptake related to aortic atherosclerosis, endovascular grafts, physiologic papillary muscle and interatrial septal fat uptake were excluded. Results: Of the 25 patients with FDG avid cardiovascular lesions, 12 were malignant (48%) and 13 benign (52%). Of the 12 patients with malignant lesions 8 had hyper-metabolic vascular tumor thrombi and/or direct invasion of the vessels by adjacent tumor, sometimes representing the only sign of disease recurrence. Example include GI malignancies involving the portal vein, SMA/SMV, and IVC, lymphoma involving the pulmonary veins extending into the left atrium, and a sacral chordoma with associated common iliac vein thrombus necessitating stenting). Three patients had cardiac metastases (1 esophagus, 2 malignant melanoma), and 1 patient had pulmonary artery angiosarcoma. Of the 13 benign lesions, 6 had nonspecific radiation related uptake within the right atrium/atrial appendage, 1 carotid artery dissection, 1 benign thrombus of the jugular vein, 1 focal left ventricular hypertrophy, and 3 had a well defined inflammatory cause of FDG uptake (1retroperitoneal fibrosis, 1 erdheim-chester disease involving the right atrium, and 1 disseminated sarcoidosis). Some of these lesions were not initially detected on preceding contrast enhanced CT, but present on retrospective review of CT CONCLUSION: FDG-avid lesions involving the cardiovascular system are uncommon and not well defined in the literature. Familiarity with their wide range of etiologies, their PET/CT appearance, as well as correlation with other imaging modalities and clinical presentation is essential to facilitate accurate diagnosis. Their early detection may influence patient management and clinical outcome.

## P584

### Performance of QBS Software in the Processing of Gated Blood Pool SPECT Increases With OSEM as Compared to Filtered Backprojection

**D. Daou**[1,2], O. Kotbi[1], C. Coaguila[3]; [1]Cochin Hospital APHP, PARIS, FRANCE, [2]Université Paris 7, Paris, FRANCE, [3]Centre Hospitalier Sud Francilien, Corbeil-Essonnes, FRANCE.

**Aim**: Gated blood pool SPECT radionuclide angiography (GSPECT RNA) is interesting for the evaluation of cardiac function. We previously validated the use of QBS software (Cedars Sinai) for the quantification of left ventricular (LV) ejection fraction (EF) using filtered backprojection reconstruction (FBP). We then reported its better performances when using iterative reconstruction combined to resolution recovery (3D-Flash, Siemens) as compared to FBP. In this study, we aim to compare its performances when using iterative reconstruction (OSEM) without resolution recovery versus FBP. **Materials and Methods**: Our study included 140 patient addressed for LV function evaluation with planar (left anterior oblique view, $planar_{LAO}$) and GSPECT RNA. Studies were acquired on a two-headed gamma-camera (Symbia, Siemens). $Planar_{LAO}$ studies were processed with the NXT program (Vision, GEMS) and provided $planar_{LAO}$ LVEF. GSPECT RNA studies were reconstructed using 2 different Methods (FBP and OSEM) and then processed with the QBS software. For each of the 2 reconstruction Methods, the 3 different LVEF values provided by QBS were noted: LVEF_actratio (ratio of activities of maximal activity threshold method - MAT method), LVEF_volratio (ratio of LV volumes of MAT method), and LVEF_Gd (gradient method). For comparison of the performance of FBP versus OSEM, $planar_{LAO}$ LVEF was considered gold standard. LVEF mean±SD were reported and linear correlations of GSPECT RNA LVEF values vs $planar_{LAO}$ LVEF were studied as well as corresponding Bland Altman analysis. **Results**: LVEF provided by $planar_{LAO}$ (58±10%) was significantly lower ($p$<0.01) than GSPECT RNA LVEF_actratio_OSEM (70±15%), LVEF_actratio_FBP (70±15%), LVEF_Gd_OSEM (63±14%), and LVEF_Gd_FBP (62±14%). But it was NS different from both LVEF_volratio_OSEM (60±14) and LVEF_volratio_FBP (59±14%). $Planar_{LAO}$ LVEF is highly correlated to both OSEM and FBP GSPECT RNA LVEF ($P$ <0.0001): LVEF_actratio_OSEM (r=0.78), LVEF_volratio_OSEM (r=0.77), LVEF_Gd_OSEM (r=0.78), LVEF_actratio_FBP (r=0.74), LVEF_volratio_FBP (r=0.72), LVEF_Gd_FBP (r=0.73). Note these correlations are slightly higher with OSEM than those with FBP for the 3 LVEF values. On Bland Altman analysis, the limits of agreement of LVEF (mean±1.96*SD) were slightly tighter with OSEM than with FBP versus $planar_{LAO}$ are: -11.3±18.3% and -11.3±19.8% for LVEF_actratio, -1.5±17.1% and -0.4±19.1% for LVEF_volratio, and -4.5±17.5% and -3.1±19.4% for LVEF_Gd, respectively. **Conclusion**: QBS performances seem better when using OSEM than FBP reconstruction for LVEF measurement.

## P585

### Could interobserver variability modify the greatest prognostic value of the 123I-MIBG scintigraphy in patients with severe left ventricular dysfunction?

**M. COZAR SANTIAGO**[1], P. GARCIA GONZALEZ[2], R. SANCHEZ JURADO[1], F. RIDOCCI SORIANO[2]; [1]GENERAL UNIVERSITARY HOSPITAL. ERESA-NUCLEAR MEDICINE DEPARTMENT, VALENCIA, SPAIN, [2]GENERAL UNIVERSITARY HOSPITAL. CARDIOLOGY DEPARTMENT, VALENCIA, SPAIN.

Objective: It is known that the late cardiomediastinum ratio (H/Mt) has prognostic value in the detection of cardiac events in patients with severe ventricular failure. The aim of our study is to evaluate the interobserver variability of this index and assess whether there is a possible change in the values that conditions its usefulness. Material and Methods: Patients 37 (31 male / 6 female) with a mean age 64 properly treated and severe heart failure. All of them were underwent a scintigraphy study with I123-MIBG. Planar images were obtained 20 minutes and 4 hours after injection of 10mCi. We use the region of interest (ROIS) analysisin the early (e) and late (l) image to calculate the index H/M and the washout rate. Each patient is evaluated by two independent observers, none of whom know the demographic or baseline disease of individual patients. We used the Pearson correlation coefficient (PCC) and the Bland and Altman method to evaluate de results. Results: We evaluated the H/M early and late ratio, and the washout of the ROIs obtained by each of the observers and a possible correlation between them is established. We get a good interobserver correlation measurements of H/Me (PCC = 0.697, p=0.00) in the valuation of H/Ml (PCC = 0.936, p=0.00), but a little worse in the washout (PCC = 0.475, p=0.003). Bland and Altman method confirm the findings. Conclusion: Standardized method for measuring the H/Me, H/Ml ratios and the washout is reproducible and not submitted to variation by the observers, which it describes as reliable and useful in the prognostic evaluation of patients with severe left ventricular dysfunction.

## P586

### Myocardial abnormal uptake of 99m Tc DPD whole body scan in systemic senile amyloidosis

P. Ghassibi[1], C**. Benhabib Mekkakia**[2], H. Garrigue[2], P. Goube[3]; [1]Cardiologie, Viry Chatillon, FRANCE, [2]Medecine Nucleaire - Centre Hospitalier Sud Francilien, Corbeil, FRANCE, [3]Cardiologie - Centre Hospitalier Sud Francilien, Corbeil, FRANCE.

*Aim* : systemic amyloidisis is a multisystem disease caused by the deposition of fibrillar no soluble proteins in the interstitium of various tissues and organs. More than 25 proteins are able to form amyloid fibrils but cardiac involvement is mainly caused by three types of amyloidisis. -AL amyloidosis associated with the deposition of light chains monoclonal immunoglobulins produced by the plasma cells in the bone marrow. -ATTR or hereditary transtyretin amyloidosis associated with mutated transtyretin deposition (transtyretin is the protein that transport the thyroid hormones and the vitamin A and it is produced in the liver). -SSA or senile systemic amyloidosis associated with a non mutated transtyretin or wild type. Technetium 99 diphosphono-propano-dicarboxylic acid (99 Tc DPD) scintigraphy may help in the differential diagnosis of hypertrophic cardiomyopathies at a low cost as it has a higt affinity for transtyretin. *Method* : we describe 4 cases illustrating the benefit of whole body scan with 99Tc DPD to differentiate transtyretin amyloidosis from other causes of myocardial hypertrophy. Whole body scan was obtained at 5 minutes (early) and 3 hours (late). Figures show the strong cardiac uptake in the late phase in cases 1 and 2 (SSA amyloidosis) and absent uptake for cases 3 ans 4 (hypertensive cardiomyopathy and hypertrophic cardiomyopathy). Case 1 : 86 yr ol male presenting with congestive heart failure. After a course of diuretics, the echocardiography shows a hypertrophic cardiomyopathy with a restrictive pattern. Case 2 : 82 yr old male admitted for congestive heart failure, followed previously for a hypertensive hypertrophic cardiomyopathy. After a course of diuretics, the echocardiogram shows a hypertrophic cardiomyopathy with a restrictive pattern. Case 3 : 18 yr old mal with a history of very severe hypertension, asymptomatic. The echocardiography shows a hypertrophic cardiomyopathy without a restrictive pattern but with a speckle tracking images in favor of amyloidosis (ATTR). Case 4 : 50 yr old female, followed for an obstructive hypertrophic cardiomyopathy and a thickened mitral valve favoring an infiltrative disease. *Conclusion* : whole body scan helps limit expensive investigations in the geriatric age goup with senil amyloidosis since there is no specific treatment for the disease.

## P587

### Estimation of Pericardial Fat, Novel cardiovascular disease risk factor, with Low dose CT (of PET/CT)

**S. Raja**[1,2], K. Das[2], S. George[1], A. ALRASHED[2], H. Ghunaim[2], S. Rumyantsev[2], s. raja[1]; [1]Baylor College of Medicine, Houston, TX, UNITED STATES, [2]KFMC, Riyadh, SAUDI ARABIA.

A strong association between pericardia;l;l;kll fat (PAT) estimated by diagnostic CT (diagCT), and CAD, especially vulnerable plaques, has been documented. Recently PAT has been touted as an independent risk factor for CAD. However, significant variability in PAT estimates have been reported, including ethnicity, technical factors (CT acquisition parameters) etc. Currently low dose CT (lowCT) is routinely obtained as part of SPECT/PET-CT. We sought to explore the feasibility of estimating PAT on lowCT in comparison to PAT estimated on diagCT. **Materials and Methods**: A subset of 16 pts (male =11, female =5; mean age = 27 yrs (range=6-70)) referred to PET-CT, and with history of prior diagnostic CT, were randomly selected for further analysis. All lowCT were acquired on GE STE 960 PET-CT scanner (General Electric, Wakusha, Milwaukee, USA). at 50-80 milliamp, based on vender specifications. To estimate PAT, axial CT slices were post processed utilizing the volume analysis toolbox on a AW-4 .6 GE workstation. To exclude extra-visceral thoracic fat, the heart and pericardium were manually contoured and extracted. The extracted datasets ware threshoulded semiautomatically (-190 to -30 Hounsfield units), to obtain the voxels containing PAT. **Results:** The estimated PAT were statistically analyzed using Excel and Medcal (statistical analysis suite). The mean and standard deviation for lowCT=36.47 +/- 26.6, while for diagCT =21.84 +/- 19.5 ml. The correlation coefficient 'r' value was 0.9174, p-value =0.0005, 95% CI for r = 0.7645 to 0.9726. While Bland Altman plots (mean difference Vs. PAT estimated on diagCT) revealed good agreement between the two techniques. **Discussion:** We have demonstrated the feasibility of estimating PAT on lowCT. To the best of our knowledge this is the first report of estimating PAT on lowCT. Our pilot study demonstrates a tight correlation between the two techniques, and Bland Altman plot analysis suggests PAT estimated via low dose CT may be clinically acceptable . However, significant differences observed in the estimated means and reasons for the wider standard deviation of PAT estimates by lowCT, needs further explortion. **Conclusion**: Our small series suggests that PAT can be estimated on lowCT, however, the technique needs to be refined and automated. Additionally, a larger series is needed to obtain normal ranges in different ethnic populations prior to routine clinical usage. Finally, with recent trends towards ever low radiation exposure rates and lower CT doses, PAT by lowCT can be obtained from all chest CT.

## P588

### Incremental Prognostic Value of Delayed Post-stress Tetrofosmin-Tc-99m Pulmonary Uptake

**T. Vieira**[1], A. Oliveira[1], A. Azevedo[2], P. Oliveira[1], T. Faria[1], V. Alves[1], E. Martins[3], J. G. Pereira[1]; [1]Nuclear Medicine Department of Hospital de São João, Porto, PORTUGAL, [2]Department of Clinical Epidemiology, Predictive Medicine and Public Health - University of Porto Medical School, Porto, PORTUGAL, [3]Cardiology Department of Hospital de São João, Porto, PORTUGAL.

Aim: The incremental value of Tl-201 lung/heart ratio (LHR) for the prediction of cardiac events has long been reported. Subsequent experience suggests that sestamibi-Tc-99m LHR has a comparable role. Given the similar biodistributions of tetrofosmin and sestamibi, it is plausible that the same would also apply to tetrofosmin-Tc-99m LHR. Recently published literature proposes that early (4-6 min after radiotracer injection) post-stress tetrofosmin-Tc-99m LHR appears to add value to other variables for the prediction of cardiac events. The disadvantage of early imaging is that it negates much of the convenience and scheduling efficiency of technetium labeled radiopharmaceuticals over Tl-201. We aimed to evaluate the incremental prognostic value of delayed post-stress tetrofosmin-Tc-99m lung uptake for cardiovascular events. Materials and Methods: Our study included 89 consecutive patients referred for myocardial perfusion scintigraphy (MPS) with cardiac stress induced by the Bruce protocol. Patients were followed for cardiovascular events (cardiac death, non-fatal acute myocardial infarction, unstable angina, coronary revascularization and stroke). Stress imaging was performed by gated SPECT, 30-60min after tetrofosmin-Tc-99m administration. QGS/QPS® software was used for perfusion and function assessment of the left ventricle (LV). We summed all LV coronal slices from SPECT acquisition to improve count statistics for the purpose of LHR determination. Manually generated ROIs in the LV and in the left lung of the resulting summed images were used for LHR calculation as the simple ratio of the average pixel counts in the lung and LV ROIs. Cox regression analysis was conducted for prognostic evaluation. Results: Seventy-three patients (82%) were male. Mean age was 56.6 years-old (range 17 to 82). Thirty-four patients (38.2%) had an abnormal MPS and 9 patients (10.1%) had a LV ejection fraction < 45%. Mean LHR was 0.33. There was a positive correlation of tetrofosmin-Tc-99m LHR with myocardial perfusion defects (MPD) severity (Spearman's correlation = 0.28; p = 0.01) and a negative correlation with LV ejection fraction (-0.31; p = 0.004). There were 9 events over a median follow-up of 4 years (range 3 months to 4 years). Cox regression analysis yielded a hazard ratio of 1.18 [95% confidence interval (CI): 1.06-1.32], for each 0.01 increase in LHR, adjusting for age, MPD severity and LV ejection fraction. Conclusion: Delayed post-stress tetrofosmin-Tc-99m pulmonary uptake evaluation is easy to obtain from exercise gated SPECT and adds value for the prediction of cardiovascular events.

## P589

### Cardiac mIBG Scintigraphy in a Selected Hypertensive Population

**T. Vieira**[1], E. Martins[2], A. Oliveira[1], T. Faria[1], P. Oliveira[1], V. Alves[1], M. B. Pérez[1], J. G. Pereira[1]; [1]Nuclear Medicine Department of Hospital de São João, Porto, PORTUGAL, [2]Cardiology Department of Hospital de São João, Porto, PORTUGAL.

Aim: Radiodine labeled metaiodobenzylguanidine (mIBG), a sympathetic neurotransmitter analog, was developed to visualise tumours of the adrenal medulla, such as pheochromocytoma. More recently mIBG has been used for the study of abnormalities of sympathetic cardiac activity. Cardiac autonomic function plays a key role in maintaining hemodynamic and electrophysiologic harmony and it is adversely altered in many disease states, such as congestive heart failure, myocardial ischemia, and diabetes. Arterial hypertension is a risk factor for all of these diseases. Our purpose was to evaluate the prevalence of abnormal cardiac mIBG uptake in a hypertensive population with suspected, but subsequently not confirmed, pheochromocytoma. Materials and Methods: Our study included 15 hypertensive patients, not under any pharmacologic therapy known to decrease mIBG uptake, consecutively referenced during the year of 2008 for pheocromocytoma evaluation with mIBG scintigraphy. Follow-up did not confirm pheocromocytoma. Cardiac mIBG uptake was evaluated by the delayed heart-to-mediastinum ratio (H/M) in a planar whole-body image, 3 to 4 hours after radiopharmaceutical administration. We calculated H/M from the average counts per pixel in left ventricular and mediastinal regions of interest. An H/M value <1.7 was considered abnormal. Finally the prevalence of abnormal cardiac mIBG uptake was calculated. Results: Eight patients (53.3%) were female. Mean age was 57 years-old (males: 54 years-old; females: 60 years-old). Abnormal cardiac mIBG uptake was present in 40% of the patients (4 males and 2 females). Mean H/M in patients with abnormal cardiac mIBG uptake was 1.592 (males: 1.598; females: 1.580). Mean H/M in patients with normal cardiac mIBG uptake was 2.081. Conclusion: Our selected hypertensive population revealed a high prevalence of abnormal cardiac mIBG uptake. These results seem to indicate that cardiac mIBG scintigraphy performed in suspected, but not confirmed, pheochromocytoma patients may represent an opportunity for cardiac autonomic function evaluation and risk stratification.

## P590

### Similar Diagnostic Value of HMPD and DPD for the Detection of Cardiac Involvement in TTR-familial Amyloid Neuropathy

**F. Rouzet**[1], V. Algalarrondo[2], R. Chequer[1], F. Hyafil[1], R. Ben Azzouna[1], D. Adams[3], M. Slama[2], D. Le Guludec[1]; [1]Bichat Hospital, Paris, FRANCE, [2]Antoine Béclère Hospital, Clamart, FRANCE, [3]Bicetre Hospital, Bicetre, FRANCE.

Background. Familial amyloid neuropathy (FAN) is a severe hereditary disease, due to production by the liver of a genetic variant of transthyretin (TTR) resulting in tissue amyloid deposits. Cardiac involvement is of major prognostic value. Diphosphonate scintigraphy has been proposed as a diagnostic tool for TTR-related cardiac amyloidosis. We compared the relative value of 99mTc-hydroxymethylene diphosphonate (HMDP) and 99mTc-diphosphono-1,2-propanedicarboxylic acid (DPD) scintigraphy for the diagnosis of cardiac involvement in patients with TTR-FAN. Methods and results. We prospectively included 50 consecutive patients with proven TTR-FAN. Cardiac involvement was based on the combination of criteria derived from EKG, echocardiography, heart rate variability, right catheterization, 123I-MIBG scintigraphy and cardiac MRI, and classified as absent, moderate, or severe. Patients' characteristics are presented in Table. Acquisitions were performed 3 h (planar and SPECT) after i.v. injection of 740 MBq of tracer (HMDP in the first 24 patients). Myocardial uptake was visually scored on planar images (absent, moderate, or intense compared to bone uptake), and quantified (myocardium to lung ratio [MLR]) on tomographic slices to avoid bone uptake. In patients with cardiac involvement of amyloidosis, 9/21 (43%) were positive with HMDP and 14/24 with DPD (58%; p=0.4), all but one with severe forms. The main determinant of a positive scan was left ventricular wall thickness assessed by echo, and MLR was correlated to relative wall thickness both with HMDP (r=0.6;p=0.05) and DPD (r=0.6;p=0.04). In patients without cardiac involvement of amyloidosis, none was positive whatever the tracer. Conclusion. Since it failed to detect moderate forms, diphosphonate scintigraphy seems unfit to be used as a screening tool in this population, but mostly as marker of severity. There was no significant difference in diagnostic accuracy between HMDP and DPD.

## P591

### Extra-cardiac findings on [18F]- FDG PET-CT scans performed for evaluation of cardiac sarcoidosis

**D. Ersahin**[1], A. Sinusas[2], V. Tsatkin[3], R. Russell[2], M. Djekidel[1]; [1]Yale University School of Medicine, Department of Radiology- Section of Nuclear Medicine., New Haven, CT, UNITED STATES, [2]Yale University School of Medicine, Department of Internal Medicine- Section of Cardiovascular Medicine., New Haven, CT, UNITED STATES, [3]Yale New Haven Hospital, New Haven, CT, UNITED STATES.

Purpose: To evaluate the prevalence and clinical significance of extra-cardiac findings in patients who underwent an [18F]- FDG PET-CT for the evaluation of cardiac sarcoidosis involvement . Methods: Forty-three [18F]- FDG cardiac PET-CT scans performed between September 2010 and August 2012 for the evaluation of cardiac sarcoidosis were retrospectively evaluated by a nuclear medicine physician. Qualitative assessment of extra-cardiac findings using an AW (GE Healthcare) workstation was completed. Studies were accompanied by flow [82Rb]- PET-CT scans. The diagnosis of cardiac sarcoidosis was made using a Wackers-Liu CQ software (MEDX, Inc) by nuclear cardiologists with >11 to > 25 years of experience. This data was extracted from clinical reports. Results: Ten scans were excluded from the study due to poor extra-cardiac resolution of the PET images. A total of 33 scans were included. The majority of the patients (57.6%) were asymptomatic at the time of the studies. Cardiac involvement by sarcoidosis was present in 51.5 % of the patients (n=17). Extra-cardiac findings were found in 31 of the 33 scans (93.9%). The most common extra-cardiac finding was FDG avid lymphadenopaty in bilateral hila and mediastinum (66.7%). Additional findings included diffuse bone marrow uptake (51.5%), uptake in the distal esophagus ±proximal stomach (30.3%), uptake along the thoracic aortic wall (18.2%), focal skeletal uptake (18.2%), FDG avid lung nodules (9.1%), and diffuse splenic uptake (3%, n=1). The most common extra-cardiac finding in patients with cardiac sarcoidosis was FDG avid lymphadenopaty in bilateral hila and mediastinum (64%). Conclusion: Extra-cardiac findings are extremely common in patients referred for [18F]-FDG PET-CT scans with suspected cardiac sarcoidosis. The prevalence of widespread sarcoidosis as well as bone marrow involvement is underestimated in the literature. This is likely related to the fact that historically end-organ involvement has been a late diagnosis, once significant involvement is present and clinical or biochemical symptoms are present. It is therefore important to document all the areas of abnormal FDG uptake in order to allow referring physicians to appropriately stage these patients and potentially target more accessible sites for biopsy. Our ongoing study is evaluating relevant clinical information related to the patient's extra-cardiac findings.

## P592

### Clinical Impact of a Solid-State CZT SPECT Camera for Myocardial Perfusion Imaging

**M. Urhan**, H. San; GATA Haydarpasa Training Hospital, Istanbul, TURKEY.

Aim: Cardiac cameras with cadmium-zinc-telluride (CZT)-based detectors have been recently introduced into myocardial perfusion imaging. In this study we assessed the clinical performance of a novel ultra fast cardiac CZT camera GE DNM 530 and compared the results with those of conventional cardiac SPECT cameras. Methods: A total of 126 patients (86 men, 50 women; mean age 62.2) were enrolled the

study in this prospective study. After IV injection of approximately 185 MBq of Tc-99m MIBI, all patients imaged with CZT cardiac camera GE DNM 530c for 4 and 6 minutes scan times and then with dual-head conventional SPECT camera in supine position. Clinical agreement (normal, ischemia, and scar) was assessed for each coronary territory using coronary angiography as the reference point (gold-standard). Left ventricular ejection fraction (LVEF) estimated with CZT camera system and conventional imaging modalities were compared with each other. Results: The time needed for both stress and rest imaging with CZT camera were significantly lower as compared with the conventional Anger cameras. This resulted in shorter imaging time (4 min vs. 15 min). Clinical correlations between CZT camera and conventional cameras on per-patient and per-vessel territory basis were 93.4 and 95.1, respectively. Myocardial count rate was higher with 6-minute imaging compared with imaging for 4 minutes and conventional imaging (9.8 +/- 0.57 KCts/s vs 7.8+/-0.63 KCts/s and 6.9+/-0.45 KCts/s, respectively). Quality of images obtaine with CZT cameras was better in 48%, the same in 32% and worse in 20% of cases. Conclusion: This new ultrafast cardiac CZT cameras enables better cardiac imaging in shorter imaging time and significantly lower radiation dose compared to conventional Anger SPECT cameras

P26-2 - Tuesday, Oct. 22, 16:00 - 16:30, Poster Exhibition Area

## Neurosciences: Basic Science

### P593

### Comparing Cerebrospinal Fluid Biomarker, Brain Perfusion, Glucose Metabolism, and Hippocampal Atrophy in Mild Cognitive Impairment.

**J. M. Nogueiras Alonso**, C. Castillo Berrio, D. Ruiz Hernández, O. Rivas Domínguez, A. López López, F. Loira Bamio, A. Serena Puig, L. Campos Villarino, J. Outomuro Perez, L. Campos Villarino, R. Guitian Iglesias; Hospital do Meixoeiro, Vigo, SPAIN.

AIM:This study compares the degree of alteration of cerebrospinal fluid (CSF) fluid biomarker, glucose metabolism, brain perfusion and hippocampal volume reductions (T1-MRI) in mild cognitive impairment (MCI). METHODS:From fourteen MCI patients, we obtained Amyloid-beta 1-42(A-beta), total tau (t-tau) in CSF samples evaluation, visual and semiquantitative assessment of Neuroimaging (18F-FDG PET/TC, 99mTc-HMPAO brain SPECT and T1-MRI in a double-blind study by specialists in nuclear medicine and radiology,performed in our center in 2012) and were used to compare biomarkers across MCI patients, and relative to fourteen 18F-FDG PET/TC normal controls (with other indications for PET/CT without neurological impairment). RESULTS:All MCI patients had significantly elevated t-tau protein in CSF and glucose hypometabolism compared to controls. We found pathological SPECT in half of the cases and only one case with hippocampal volume loss on MRI. PET/TC abnormalities (7 hippocampal, 4 posterior cingulated, 4 parietotemporal and 2 temporal cortex hypometabolism regions) were more pronounced in good correlation with the CSF t-tau values. CONCLUSIONS:In line with the current pathophysiological model of AD, the earliest changes correspond to the deposition of Amyloid-beta and regional hypometabolism. Thus 18F-FDG PET/TC and cerebrospinal fluid (CSF) markers of pathology improve the early detection of AD.

### P594

### To evaluate the value of 18F-FDG and 11C-CHO PET-CT in differentiation of brain annular enhanced lesion on MRI imaging

**X. Wang**, Z. Zhao, X. Bai; Dept. of Nuclear Medicine, The First Affiliated Hospital of Inner Mongolia Medical University, Hohhot, CHINA.

**Aim**: To evaluate the value of (18)F-FDG and (11)C-CHO PET-CT in differentiation of brain annular enhanced lesion on MRI imaging. Materials and **Methods**: Forty patients with the brain annular enhanced lesion on MRI imaging and atypical clinical in our hospital from September 2007 to May 2012 underwent (18)F-FDG and (11)C-CHO PET-CT brain scan in adjacent two days. Among them, 10 patients who were suspected to have brain metastasis received body scan by (18)F-FDG PET-CT. Both images were analyzed visually and semi-quantitatively and all of lesion were confirmed by pathology . Results: Fourty-eight of 56 brain of annular enhanced lesions on MRI of 40 patients were found in (18)F-FDG PET-CT brain imaging , including 17 low metabolism lesions ,20 moderate metabolism lesions and 10 high metabolism lesions. Twenty-seven lesions were correctly diagnosted tumor by (18)F-FDG PET-CT , 17 lesions of false negative and 3 lesions false positive. Sensitivity, specificity and accuracy of the diagnostic malignant neoplasm were respectively 61.4%(27/44),34.6%(9/26)and64.3%(36/56). Fifty-six of 56 brain annular enhanced lesions on MRI of 40 patients were found in the (11)C-CHO PET-CT brain imaging , including 8 low metabolism lesions ,10 moderate metabolism lesions and 38 high metabolism lesions, Fourty lesions of $^{18}$F-FDG PET-CT correct diagnostic tumor , 7 cases of false negative and 2 cases of false positive. Sensitivity, specificity and accuracy of the diagnostic malignant neoplasm are respectively 85.0%(40/47),77.8%(7/9)and 83.9%(47/56). Conclusions: Both (18)F-FDG and (11)C-CHO PET-CT are useful in differentiation of brain ringlike-enhanced lesions on MRI imaging. (11)C-CHO PET-CT is far superior to (18)F-FDG especially for low malignant neoplasm and metastatic tumor. (18)F-FDG PET-CT body scanning is helpful for founding primary tumor.Combination of (18)F-FDG and (11)C-CHO PET-CT scans can improve the accuracy of differential diagnosis for annular enhanced brain lesions on MRI imaging.

### P595

### Role of 99Tc-HMPAO SPECT in the assessment of cerebral hemodynamic parameters after superficial temporal artery-middle cerebral artery bypass in patients with severe steno-occlusive disease of intracranial carotid and middle cerebral artery

**A. SINHA**, V. K Sharma, N. Chow, Y. Tseng Tsai, T. Hock Luen, B. PL Chan,, R. C Seet, C. Vincent F; National University Hospital, Singapore, SINGAPORE, SINGAPORE.

**Background and Objective-** Although superficial temporal artery-middle cerebral artery (STA-MCA) bypass surgery in patients with symptomatic carotid occlusion failed to demonstrate any benefit, its role in symptomatic intracranial steno-occlusive disease has been evaluated scarcely. We evaluated changes in hemodynamic parameters in patients with severe steno-occlusive disease of intracranial internal carotid (ICA) or middle cerebral artery (MCA) who underwent STA-MCA bypass for impaired cerebral vasodilatory reserve (CVR). **Methods-** Patients with severe steno-occlusive disease of intracranial ICA or MCA underwent transcranial Doppler (TCD) evaluation and CVR assessment using breath-holding index (BHI). Patients with impaired BHI (<0.69) were further evaluated with acetazolamide-challenged 99Tc-HMPAO-SPECT. STA-MCA bypass surgery was offered to patients with impaired CVR on SPECT. TCD and SPECT were repeated in all patients at 4±1 months and they were followed-up for cerebral ischemic events. **Results**- Of the 126 patients (80 male, mean age 56yrs; range 23-78yrs) that fulfilled our inclusion criteria, 84 (67%) showed impaired CVR HMPAO-SPECT. Fifty (60%) of them underwent STA-MCA bypass while 34(40%) received best medical treatment. TCD and acetazolamide-challenged HMPAO-SPECT repeated 4±1 months after surgery showed significant improvement in STA-MCA bypass group. TCD BHI improved from a median (IQR) of -0.05 to 1.1 (p<0.001). Compared to 98% patients with impaired CVR on pre-operative SPECT, only 20% showed abnormal results on post-operative imaging (p<0.001). During follow-up (mean 35 months; range 8 to 49months), only 6/50 (12%) patients in bypass group developed cerebral ischemic events as compared to15/34 (44%) cases on medical therapy (absolute risk reduction 32%, p=0.006). **Conclusion**- 99Tc-HMPAO SPECT with acetazolamide challenge is a reliable tool for the assessment of cerebral vasodilatory reserve in patients with severe steno-occlusive disease of intracranial ICA or MCA. STA-MCA bypass surgery in carefully selected patients results in significant improvement in hemodynamic parameters and reduction in stroke recurrence.

### P596

### Endovascular embolization of intracranial arteriovenous malformations- perfusion changes visualized by $^{99m}$Tc-ECD SPECT

**A. Nocuñ**[1], M. Szajner[2], K. Obszańska[3], K. Gil[3], B. Chrapko[1]; [1]Department of Nuclear Medicine, Lublin, POLAND, [2]Department of Interventional Radiology and Neuroradiology, Lublin, POLAND, [3]Clinic of Neurosurgery and Paediatric Neurosurgery, Lublin, POLAND.

**Introduction:** Cerebral arteriovenous malformations (AVMs) comprise abnormal direct communications between feeding arteries and draining veins (the nidus). Although AVMs are relatively uncommon (the incidence of 0.01%-0.001%), they are a major cause of intracranial haemorrhage in the young population. Published data describing perfusion changes in patients with AVMs after embolization are very scarce. The aim of our study was to evaluate these changes by using $^{99m}$Tc-ECD SPECT. **Material and Methods:** The study group consisted of 20 patients with cerebral AVM (13 women, 7 men, mean age 34.3 ± 13.4 years). The nidus size, evaluated on the basis of the digital subtraction angiography (DSA), was 0.5 ml-97.8 ml (mean 15.7±22.3 ml). $^{99m}$Tc-ECD SPECT was performed before and after endovascular embolization with n-butyl cyanoacrylate and lipiodol. For semi-quantitative assessment of SPECT voxel-based analysis was employed. Hypoperfusion in basal SPECT was diagnosed when asymmetry index (AI) was higher than 10% in a cluster volume (CV) greater than 10.0 ml. The change of perfusion between basal and control studies was considered significant when relative difference (RD) was higher than 10% in a CV greater than 10 ml. **Results:** Obliteration of AVMs was total in 12 patients and partial in 8 patients. No serious complications were observed after the procedure. Two patients developed transient hemiparesis and four patients severe headache. The symptoms regressed in a few days. Before embolization hypoperfusion in the region of an AVM was seen in 17 cases, perfusion defects in areas distant from an AVM were found in 12

patients. After embolization, perfusion around an AVM deteriorated in 11 patients (CV=10.7-68.7ml, mean 28.6±18.4, RD=14-26%, mean 17.8±4.5). Improvement was seen in 3 cases (CV=13.7-17.7ml, mean 16±2, RD=16.5-20.1%, mean 18.2±1.8). The nidus of AVMs with perfusion improvement (mean 53.0± 38.1) was significantly (p=0,001) larger than in the rest of the group (mean 9.0±9.7ml). In areas distant from AVMs, perfusion deterioration was found in 9 cases, improvement in 3 cases. **Conclusions**: The changes of perfusion caused by endovascular embolization of AVM can rely on both deterioration and improvement. They occur in the parenchyma surrounding the AVM and in the distant regions of the brain. Perfusion improvement around an AVM is more likely in larger lesions. Perfusion deterioration was not related with serious complications, however it suggested more frequent follow-up. $^{99m}$Tc-ECD-SPECT with voxel based analysis is a useful tool for the management of AVM, which can supplement the data obtained from CT, MRI and DSA.

## P597

### The Role of 18F-FDG PET/CT in the Pre-Surgical Evaluation of Patients with Refractory Temporal Lobe Epilepsy

M. Schütze, P. T. Aguiar, H. M. Mendes, D. V. Rosa, B. C. Silva, **M. Mamede**, M. A. Romano-Silva; Universidade Federal Minas Gerais, BELO HORIZONTE - MG, BRAZIL.

**Aim:** This study aimed to assess the use of automatic $^{18}$F-FDG PET image analysis through 3-dimentional stereotactic surface projection (3D-SSP) in the pre-surgical evaluation of patients with refractory epilepsy. **Material and Methods:** A group of 27 patients with refractory temporal lobe epilepsy (TLE) and surgical indication and 23 healthy subjects were subjected to a $^{18}$F-FDG PET/CT exam, followed by manual and automatic analysis of the images. Patients had a fasting period of at least six hours and the injected $^{18}$F-FDG dose was 5,18 MBq/Kg (mean 304,14 ± 88,8 MBq). Images were obtained after an uptake period of 50 minutes. The images were reconstructed in a 192 x 192 matrix, using an OSEM (Ordered Subsets Expectation Maximization) algorithm, with 2 iterations and 20 subsets. Automatic analysis was performed on a GE Workstation using the software CortexID (GE Healthcare, Millwalke, EUA). **Results:** The results of the comparison between patients and controls showed significant metabolism differences in the temporal, frontal, occipital and hemisphere mean regions. The asymmetry index for the temporal lobe, which is the difference of metabolism between the left and the right side, showed a sensibility of 53,8% with a specificity of 100% in the identification of patients. The metabolism of the right temporal lobe showed a sensibility of 50% and a specificity of 100% in the identification of the epileptic focus on the right side. These values are bigger than for the manual analysis, which yielded a sensibility of 33,3% and a specificity of 100% for patient identification. The comparison between metabolism values and the age of disease onset, disease duration, presence of initial precipitating factors and surgical response did not show any significant relationship. In fact, a large variation of metabolism between patients in the studied regions was observed, which explains the low sensibility of the method in this group. **Conclusions:** It is likely that differences in metabolism between patients is due to the heterogeneity of their diseases. It is known that TLE is a complex syndrome that can have different causes. Further studies with a larger number of patients are important to reduce the effect of these differences and possibly find relations between metabolism and certain groups of patients.

## P598

### 99mTc-HMPAO brain SPECT imaging in patients with olfactory dysfunction after craniofacial traumas

**I. Iakovou**[1], I. Konstantinidis[2], V. Nikos[1], E. Tsakiropoulou[2], V. Mpalaris[1], D. Katsaboukas[1], A. Doumas[1], N. Karatzas[1]; [1]3rd Nuclear Medicine Dpt Aristotle Univ. Papageorgiou hsp, THESSALONIKI, GREECE, [2]2nd ORL Dpt, Aristotle Univ. Papageorgiou hsp, THESSALONIKI, GREECE.

Background: Hyposmia or even anosmia following head trauma are relatively common and in many cases are persistent and irreversible. The ability to objectively measure such a decline in smelling, for both clinical and medicolegal goals, is very important. Aim: To assess the role of 99mTc-HMPAO brain SPECT imaging in patients with olfactory dysfunction after craniofacial traumas. Methods: Nineteen male and thirteen female patients with olfactory dysfunction after craniofacial traumas (14 traffic accidents, 5 assaults, 3 sport injuries, 4 occupational accidents, 6 other) enrolled in our study. They were all were assessed in the smell and taste clinic. Olfactory function was measured with the Sniffin'sticks battery test revealing 21 anosmic and 11 hyposmic patients. The brain perfusion state was evaluated by means of the SPECT with 99mTc-HMPAO infusion- before and after olfactory stimulation. The orbitofrontal lobe of the brain was assumed as the region of interest and changes in perfusion of this area before and after the stimulations were assessed. Conventional imaging correlated with the brain SPECT and Sniffin'sticks findings. Results: 99mTc-HMPAO SPECT had a 100% recognition of anosmics, however this was not the case with hyposmics (65%). Brain perfusion imaging not only showed areas of brain hypofunction unobserved in MRI (4 cases) but it also revealed function in areas of MRI brain damage (2 pts). Finally 99mTc-HMPAO SPECT could detect two cases of malingering. Conclusions: The 99mTc-HMPAO brain SPECT is an objective technique suitable for evaluating anosmia following the head trauma. It may also be used with other diagnostic modalities resulting in significant additional patient information.

## P599

### 99mTc-HM PAO Brain SPECT qualitative (QL) and quantitative (QN) analyses in mild cognitive impairment (MCI)

**S. Nuvoli**[1], M. R. Piras[2], A. Nieddu[3], G. Dachena[1], A. Spanu[1], G. Madeddu[1]; [1]Unit of Nuclear Medicine, University of Sassari, Sassari, ITALY, [2]Unit of Neurology, University of Sassari, Sassari, ITALY, [3]Geriatrics DPT, Policlinico Sassarese, Sassari, ITALY.

**Aim**: To further investigate the usefulness of brain perfusion SPECT QL and QN analyses in MCI diagnosis and follow-up. **Methods**: We studied 40 patients, clinically classified as MCI (EHDC criteria). Perfusion brain SPECT was performed after 740 MBq 99mTc-HM PAO i.v. injection and the images were analyzed by both QL and QN, the latter by a software based on a voxel comparative analysis (Talairach technique) with normal healthy age matched controls (C). QN for each lobe and Brodman areas was expressed as standard deviation (SD) than C (cut-off: -1.5 SD). **Results:** QL showed normal perfusion in 19/40 MCI patients (Group A) and focal perfusion defects in the remaining 21/40 patients (Group B), 11 cases in temporal lobes (8 in both hemispheres and 3 only in left fronto-temporal lobe), 8 in temporo-occipital cortex (6 in both hemispheres and 2 only in left side) and 2 in left fronto-temporal cortex. In Group A, QN showed low SD values in both limbic lobes of 17/19 cases (SD values ranging from -1.8 to 4.6) and normal values in the remaining 2 cases. In Group B, QN showed low SD values in all hypoperfused areas identified by QL and in 2 further areas in temporal right lobes incorrectly defined normal at QL. All MCI patients were monitored overtime (range:2-5 years) and 34/40 had no variations at both clinical and scintigraphic evaluations; the remaining 6/40 cases developed clinical signs of dementia. In these cases both basal and follow up brain SPECT images correlated with clinical data, but only QN correctly identified perfusion defects earlier than QL showing the greatest SD in hippocampal areas (BA28) in 2 amnesic cases, in hippocampal areas (BA 36 and BA 28), parahippocampal gyri (BA 20) and part of inferior parietal left lobe (BA 39) in 3 multiple-domain cases and in posterior inferior temporal gyrus, middle temporal gyrus, fusiform gyrus and angular gyrus (BA 37 and BA 39) in the remaining non memory case. **Conclusion**: Brain perfusion SPECT proved useful in early MCI clinical assessment. However, in our cases only the combined use of QL and QN analyses achieved the best performance to correctly detect MCI in the early stage of cognitive disorders. Moreover, larger series of cases followed with longer follow-up are necessary to evaluate if the data from the combined QL and QN analyses may give in MCI patients early information to identify those cases who may convert to dementia.

## P600

### Use of $^{99m}$Tc-HMPAO SPECT with Brodmann areas mapping for the assessment of language impairment in Corticobasal Degeneration/Progressive Supranuclear Palsy and language variants of Frontotemporal dementia.

**V. Valotassiou**[1], J. Papatriantafyllou[2], N. Sifakis[3], C. Tzavara[1], J. Tsougos[1], D. Psimadas[1], E. Kapsalaki[4], G. Chadjigeorgiou[5], J. Fezoulidis[4], P. Georgoulias[1]; [1]Department of Nuclear Medicine, University Hospital of Larissa, Larissa, GREECE, [2]Memory & Cognitive Disorders Clinic, Department of Neurology, "G.Gennimatas" Hospital, Athens, GREECE, [3]Department of Nuclear Medicine, "Alexandra" University Hospital, Athens, GREECE, [4]Department of Radiology, University Hospital of Larissa, Larissa, GREECE, [5]Department of Neurology, University Hospital of Larissa, Larissa, GREECE.

**AIM:** Corticobasal degeneration (CBD) and progressive supranuclear palsy (PSP) may develop speech and language disorders, as a result of motor impairment, causing significant clinical overlap with the language variants of frontotemporal dementia (FTD), semantic dementia (SD) and progressive non-fluent aphasia (PNFA). The aim of our study was the evaluation of perfusion in specific Brodmann areas (BA) in CBD/PSP and SD/PNFA patients, using automated 3D-voxel-based processing software, in order to reveal more localised perfusion differences between these disorders. **MATERIALS AND METHODS:** We studied 70 consecutive patients from an outpatient Memory Clinic. We used the established criteria for the diagnosis of dementia and the specific established criteria for the diagnosis of CBD/PSP and SD/PNFA, and a neuropsychological evaluation with a battery of tests including the mini-mental state examination (MMSE). All the patients had a CT and/or MRI of the brain in order to exclude the presence of anatomical lesions. Thirty-one patients received the clinical diagnosis of CBD/PSP: age(±SD) 64±9 years, MMSE(±SD) 18±7, education(±SD) 10±4.3 years, duration of disease(±SD) 2.8±1.4 years. Thirty-nine patients received the clinical diagnosis of SD/PNFA: age(±SD) 68±7 years, MMSE(±SD) 15±9, education(±SD) 10±5.3 years, duration of disease(±SD) 3.6±2.6 years. All the patients underwent a brain SPECT 20 min after the intravenous administration of 740MBq $^{99m}$Tc-HMPAO. We applied the

NeuroGam™ software on the reconstructed data, for the semi-quantitative evaluation of brain perfusion in BA areas in the right(R) and left(L) hemispheres. We also evaluated the proportion of patients with BA perfusion values more than 2SDs below the mean of a data base of normal subjects of the same gender and age. **RESULTS:** CBD/PSP patients had lower mean perfusion values in BA 4R, 5R, 6R, 8R, 9R, 10R, 19R, 22R, 23R, 31R, 40R, 45R and 46R and higher mean values in BA 20L, 21L, 25L, 28L, 36L and 38L, compared to SD/PNFA patients. In multiple analysis, BA 6R [OR(95% CI)=1.19(1.06-1.34), P=0.002] and 20L[OR(95% CI)= 0.80(0.69-0.92), P=0.002] were found to independently differentiate CBD/PSP from SD/PNFA. Compared with normal data base, statistically significant differences in proportions between CBD/PSP and SD/PNFA patients were found in 9R, 18L, 18R, 20L, 38L, 45R. The proportions were: 9R=87.1%, 18L=58.1%, 18R=54.8%, 20L=74.2%, 38L=87.1%, 45R=83.9% in CBD/PSP and 9R=66.7%, 18L=48.7%, 18R=20.5%, 20L=94.9%, 38L=100%, 45R=59% in SD/PNFA. **CONCLUSION:** The clinical, genetic and pathological relationship between CBD/PSP and SD/PNFA may lead to misdiagnosis. The use of $^{99m}$Tc-HMPAO SPECT with BA mapping may provide additional information in the differential diagnosis between these disorders.

P27-2 - Tuesday, Oct. 22, 16:00 - 16:30, Poster Exhibition Area

## Neurosciences: Clinical Science Psychiatry

### P601

### Initial observation of PET cerebral metabolism imaging in the Mental Retardation

**R. Wang**[1], L. Tang[2]; [1]Department of Nuclear Medicine,Peking University First Hospital, Beijing, CHINA, [2]Department of Nuclear Medicine,Fuxing Hospital, Beijing, CHINA.

**Objective** As is well-known, psychiatric disorders are one of functional diseases rather than structural diseases, so it is crucial to choose an effective imaging study to understand the pathophysiology and treatment of them. A large body of positron emission tomography(PET)studies has documented that psychiatric disorders are associated with significant alterations in regional cerebral metabolism of specific biomolecules. The purpose of this study is to observe the cerebral metabolic changes in the patients with Mental Retardation (MR). **Methods** 32 patients with MR by clinical diagnosis were examined with $^{18}$F-FDG PET imaging undergone a brain PET scanning and to observe the distribution change of glucose metabolic in patient's $^{18}$F-FDG PET cerebral images through visual of cerebral hypometabolism lesions observed by at least 3 PET or PET/CT physicians. The detailed relationships of patient's low-intelligence quotient with PET,MRI and electroencephalogram (EEG) were analyzed by statistical package SPSS 10.0. **Results** There were 19 cases with abnormal PET images in the 32 patients, The positive rate was 59.4%. Their performance was all hypometabolism without any hypermetabolism localized respectively on: 6 cases in the frontal lobe(the positive rate is 33.3%), 15 cases in the temporal lobe(the positive rate is 83.3%) , 12 cases in the parietal lobe (the positive rate is 66.7%), and 4 cases in the occipital lobe and cerebellum(the positive rate is 21.1%). There were 13 cases with 2 and more than 2 of affected areas and the positive rate is 72.2%. **Conclusion** $^{18}$F-FDG PET is very useful in the diagnosis of MR implying the abnormal cerebral glucose metabolism with the character is that the increase of radioactive distribution in the area to be involved .**Key world:** Mental Retardation, PET, $^{18}$F-FDG, Cerebral metabolism, Hypometabolism

### P602

### Changes in regional cerebral blood flow in patients with eating disorders

**R. Petrovic**, T. Samardzic, R. Gregurek, D. Marcinko; Clinical Hospital Centre Zagreb, Zagreb, CROATIA.

Aim: This study is part of a continuing effort to understand the pathophysiology of the brain in eating disorders and to correlate any abnormalities in blood flow with eating disorder psychopathology. Method: Ten newly referred patients with a diagnosis of bulimia nervosa and four with anorexia nervosa underwent regional cerebral blood flow (rCBF) examination using single-photon computerized tomography (SPECT). Brain rCBF SPECT data from age- and sex-matched healthy volunteers were used as controls. Patients were diagnosed following DSM-IV criteria and were off psychoactive medication. SPECT scans were started 30 minutes after administration of 740 MBq of 99mTc-HMPAO in resting state, eyes closed and with low ambient noise. Tomograms were normalized to the mean brain activity and analysed visually and semi quantitatively using region-of-interest based method. Results: Detailed neurologic and laboratory examinations, including EEG and CT, were within normal limits in all patients. Nevertheless, SPECT studies revealed that all anorexic and bulimic patients had asymmetry (hypoperfusion) of blood flow in at least one area. For all 14 patients rCBF changes were caused by decreased perfusion in the prefrontal and temporal areas which was more prominent in the left hemisphere. Regions of the brain showing hypoperfusion included the prefrontal cortex (n = 12), temporal lobe (n = 10) and in one case global hypoperfusion was observed. In five patients hypoperfusion was found exclusively in left hemisphere. Nine patients had two or more hypoperfused areas. Bulimic patients with two or more hypoperfused areas had higher EDE scale scores than those with single hypoperfused area, but the differences were not statistically significant. Conclusions: Compared with the normals, all patients with eating disorders were characterized by abnormal rCBF, predominantly affecting prefrontal cortex and the temporal lobes. Disturbances of these brain regions have been found in people with eating disorders, but it was not certain whether they were a cause or consequence of symptoms. Different factors might explain areas of decreased rCBF in eating disorders. It might be the consequence of neurophysiological changes following nutritional deficiencies and/or the result of some associated symptoms such as anxiety or depression. We also hypothesize that either a pathological prefrontal and temporal cortex hypoperfusion in eating disorders reflects dysfunction in neuronal activity which is responsible for the disturbances in psychological processes it mediates.

### P603

### Brain metabolic and neurocognitive function disorders in patients with somatoform disorders and dissociative disorders: a preliminar PET study

**G. Capriotti**[1], L. Sonni[1], S. Di Traglia[1], M. Basili[2], A. Del Casale[1], A. Comparelli[1], S. Ferracuti[1], P. Girardi[1], M. Tuccimei[1], D. Prosperi[1], P. Pizzichini[1], F. Scopinaro[1]; [1]Sapienza University, Rome, ITALY, [2]Tor Vergata University, Rome, ITALY.

Somatoform (DS) and dissociative disorders (DD) considered in this preliminary PET study represent the two major diagnostic categories of DSM-IV-TR; in the classical psychopathology they were considered part of "hysteria". The **aim of this study** was to evaluate whether 18F-FDG PET-CT brain scans show specific abnormality patterns in patients affected by DD and DS to better define these disorders; other end point was to identify correlations of brain metabolic pattern with neurocognitive functions of patients. **Methods.** We enrolled 10 patients, 5 affected by DD (3 male, 2 female; mean age 35.4) and 5 affected by DS (5 female; mean age 44.6), diagnosed according to the DSM-IV-TR criteria. All patients underwent physical examination, electrocardiogram, laboratory evaluation, and clinical MRI to exclude those with anatomical brain lesions or diagnoses other than DD and DS and FDG PET/CT scan. All patients were assessed through a neuropsychological battery: Selective Reminding Buschke Fuld, Rey's Picture copy, Trail Making subtest B-A, Stroop Colour Word test, Wisconsin Card Sorting Test and Visual Verbal test and a psychopathological evaluation (BPRS, HAM -A, HAM-D). FDG PET scans were obtained with a head-dedicated scanner. We injected 5 mCi-FDG and processed the images as described. Patients fasted overnight, and their blood glucose was checked immediately before scanning. We enrolled 10 healthy volunteers (8 female and 2 male, mean age 52) who were underwent PET/CT. 18F-FDG-PET and neurocognitive tests was performed prior and after 1 months to 3 months after the diagnosis. **Results and Conclusion**. DS and DD patients groups did not show statistically significant differences in the levels of anxiety (HAM-A), depression (HAM-D) and psychopathological aspect assessed by BPRS (total scores). Patients with DS have performed significantly worse when compared with DD to test Wisconsin, with a greater number of total errors (p = 0.032), perseverative errors (p = 0.032) and perseverative responses (p = 0.032). In the same patients PET scan showed reduction of metabolism in was demonstrated a reduction in the metabolism in the left temporal lobe (Test of Fisher = 0.004), striatum of the left (Test of Fisher = 0.024), parietal lobe (Pearson's chi-squared test= 0.058; Fisher's test=0,103) when compared with DD patient group. Our data suggest that DS patients are associated with impairment of neurocognitive functions and brain metabolism greater than DD patients. PET scan can identify DS and DD patients group.

P28-2 - Tuesday, Oct. 22, 16:00 - 16:30, Poster Exhibition Area

## Neurosciences: Neurodegeneration

### P604

### Is there any role for 18F-FDG PET/CT in the differentiation of patients with Mild Cognitive Impairment from those with Alzheimer's Dementia?

F. M. C. Carvalho, A. R. Peixoto, P. T. Aguiar, M. A. C. Bicalho, **M. Mamede**, M. A. Romano-Silva; Universidade Federal Minas Gerais, BELO HORIZONTE - MG, BRAZIL.

***Aim:*** The goal of this case-control study is to differentiate individuals with mild cognitive impairment (MCI) from elderly patients with early Alzheimer`s dementia through a possible pattern of cerebral atrophy and/or glucose hypometabolism assessed by $^{18}$F-FDG PET/CT. ***Materials and Methods:*** $^{18}$F-FDG PET/CT was performed in 35 elderly patients with clinical and neuropsychological diagnosis of

MCI and 34 patients with early Alzheimer`s dementia (CDR 1) between May 2011 and May 2012. Visual scale was used for analysis of medial temporal atrophy on computed tomography coronal images. Glucose brain metabolism with $^{18}$F-FDG PET was assessed by visual analysis and by automated software based in 3D-SSP Method. ***Results:*** Visual scale for medial temporal atrophy was not completely effective in differentiating MCI cases from early Alzheimer`s dementia cases (sensibility=7,1%; specificity=77,1%; PPV = 66,7%; NPV = 60%; accuracy=62,3%). The role of $^{18}$F-FDG PET in differentiating the two groups of patients was important. There was significant difference between MCI and DA, especially when considering the average metabolic Z-scores of the following cortical areas: parietal association (p=0,002), temporal association (p=0,001), medial parietal (p=0,003) and posterior cingulate (p=0,013). We determined Z-scores cutoff values (based on ROC analyses) for each region in order to separate the two sample groups, but none proved great performance to make differential diagnosis between MCI and early Alzheimer`s dementia. Finally, we noticed patterns of $^{18}$F-FDG PET as a predictor of conversion and regression of cognitive deficit when applying these cutoff points in four MCI patients who developed Alzheimer`s dementia and in one MCI elderly who reverted to normal status at one-year follow-up period. ***Conclusion:*** Despite the advances of $^{18}$F-FDG PET for diagnostic and prognostic purposes, further longitudinal researches with large samples and specific radiotracers are still needed in order to standardize the use of PET/CT in Alzheimer's disease evaluation.

## P605

### 11C-PIB Retention Patterns Compared to 18F-FDG Uptake Distribution in Amnesic and non Amnesic Mild Cognitive Impairment Patients and in a Control Population.

**F. Ortega-Nava**, J. Jiménez-Bonilla, I. Banzo, I. Martínez-Rodríguez, R. Quirce, M. De Arcocha-Torres, S. Ibañez-Bravo, N. Martínez-Amador, C. Lavado-Pérez, Z. Bravo-Ferrer, J. Vázquez-Higuera, E. Rodríguez, J. Carril; HUMV, Santander, SPAIN.

**Aim:** To evaluate the regional distribution of 11C-PIB cortical retention and to compare the patterns found with FDG uptake in a control group and in patients with Mild Cognitive Impairment (MCI). **Methods:** A control group with 10 subjects and 35 patients with MCI were included in the study: 11 patients with non amnesic MCI (NA-MCI) and 24 with predominantly amnesic MCI (A-MCI). All patients had a 30-minutes PET/CT acquisition 60 minutes after intravenous injection of 481 MBq of 11C-PIB and 24 hours later, a 15-minutes PET/CT, 20-minutes after intravenous injection of 185 MBq of 18F-FDG was acquired. A blind interpretation of the randomly distributed images was done by two experienced readers. Regional PIB retention was classified according to the intensity in each region into the following patterns: A(frontal, basal ganglia and anterior cingulate); B(posterior cingulate, parietal, temporal and occipital) and C (global). **Results**: In the 10 controls, PIB was negative in 9 and positive in 1(A-pattern) and FDG showed hypometabolism in another 1. In the 11 NA-MCI patients, PIB was positive in 1(A-pattern) and FDG negative in all of them. Of the 24 A-MCI patients PIB was positive in 17 and negative in 7. In 7 of the 17 PIB positive the retention pattern corresponded to the A-pattern, all of them with a negative FDG; in 3 there was a B-pattern, 2 of them with a positive FDG, and in 7 there was a C-pattern, 4 of them with a positive FDG scan. **Conclusions:** While PIB was positive in only 1 of the 11 NA-MCI patients, in 17 of the 24(71%) of the A-MCI PIB was positive. The results show an association between PIB retention pattern and glucose metabolism: A-pattern was strongly linked to normal glucose metabolism, suggesting an early stage of the disease. However in B and C patterns, glucose metabolism was abnormal in 6 of 10 A-MCI patients. Therefore in addition to the presence of PIB retention, the retention pattern could provide additional information regarding the stage of the disease. These results are encouraging for a deeper evaluation including a larger number of patients.

## P606

### Cortical metabolic changes in normal aging brain: a 18F FDG PET/CT study.

**A. Chiaravalloti**[1], M. Pagani[2], B. Di Pietro[1], C. Di Russo[1], S. Pizzi[1], A. Lacanfora[1], P. Abbatiello[1], E. Paolombo[1], L. Travascio[1], O. Schillaci[1]; [1]Department of Biomedicine and Prevention, University Tor Vergata, Rome, ITALY, [2]Institute of Cognitive Sciences and Technologies, CNR, Rome, ITALY.

**Aim:** The aim of our study was to investigate the effects of aging on brain glucose metabolism by means of 18F FDG PET/CT. **Materials and Methods**: 73 healthy subjects were enrolled in the study (34 women and 39 men, mean age 56±16.8 years old; age range 20-89 years). All of them were chemotherapy-naïve subjects undergoing a whole body 18F FDG PET/CT for a suspect of malignancies and found to be completely negative at whole body images evaluation. Prior PET/CT, all the patients were examined by an experienced neurologist and found negative for neurological or psychiatric diseases. MMSE did not show any cognitive impairment. A contrast enhanced brain CT, performed contextually to 18F FDG PET/CT examination, was negative in all of them. PET/TC was acquired with a Discovery ST16 (GE Medical Systems, Tennessee, USA) using a 3D mode standard technique in a 128x128 matrix. Regression analysis for brain 18F-FDG uptake and age was performed by statistical parametric mapping (SPM8). **Results**: The main result of our study is a negative relationship between age and 18F-FDG uptake in a wide portion of the right anterior cingulated cortex (BA 32). As expected, no significant areas of age-related increase of glucose consumption have been found in our series. **Conclusions**: the results of our study suggest a mild and limited decrease of 18F-FDG brain uptake with age in normal brain. An age-related physiological reduction of glucose consumption in the anterior cingulated cortex could be considered during the evaluation of brain 18F FDG PET/CT scan in the elderly.

## P607

### Differential diagnosis of Progressive Supranuclear Palsy and Corticobasal Degeneration from behavioural variant of Frontotemporal Dementia using $^{99m}$Tc-HMPAO and Brodmann areas mapping. Comparison with normal data base.

**V. Valotassiou**[1], J. Papatriantafyllou[2], N. Sifakis[3], C. Tzavara[1], J. Tsougos[1], D. Psimadas[1], E. Kapsalaki[4], G. Chadjigeorgiou[5], P. Georgoulias[1]; [1]Department of Nuclear Medicine, University Hospital of Larissa, Larissa, GREECE, [2]Memory & Cognitive Disorders Clinic, Department of Neurology, "G.Gennimatas" Hospital, Athens, GREECE, [3]Department of Nuclear Medicine, "Alexandra" University Hospital, Athens, GREECE, [4]Department of Radiology, University Hospital of Larissa, Larissa, GREECE, [5]Department of Neurology, University Hospital of Larissa, Larissa, GREECE.

**AIM:** Progressive supranuclear palsy (PSP) and corticobasal degeneration (CBD) are clinically characterized by parkinsonism and dementia, although behavioural changes and impaired executive functions frequently occur, showing considerable clinical overlap with behavioural variant of frontotemporal dementia (bvFTD). The aim of this study was the evaluation of perfusion in specific Brodmann areas (BA) in bvFTD and CBD/PSP patients and the comparison with a normal data base, using an automated 3D-voxel-based processing software, in order to highlight perfusion differences between these disorders. **MATERIALS-METHODS:** We studied 52 consecutive patients from an outpatient Memory Clinic. We used the established criteria for the diagnosis of dementia and the specific established criteria for the diagnosis of CBD/PSP and bvFTD, as well as a neuropsychological evaluation with a battery of tests including the mini-mental state examination (MMSE). All the patients had a CT and/or MRI of the brain in order to exclude the presence of anatomical lesions. Thirty-one patients received the clinical diagnosis of CBD/PSP: age(±SD) 64±9 years, MMSE(±SD) 18±7, education(±SD) 10±4.3 years, duration of disease(±SD) 2.8±1.4 years. Twenty-one patients received the clinical diagnosis of bvFTD: age(±SD) 62±11 years, MMSE(±SD) 18±7, education(±SD) 10.5±4.5 years, duration of disease(±SD) 2.4±1.7 years. All the patients underwent a brain SPECT 20 min after the intravenous administration of 740MBq $^{99m}$Tc-HMPAO. We applied the NeuroGam$^{TM}$ software on the reconstructed data, for the semi-quantitative evaluation of brain perfusion in BA areas in the right(R) and left(L) hemispheres. We also evaluated the proportion of patients with BA perfusion values more than 2SDs below the mean of a data base of normal subjects of the same gender and age. **RESULTS:** CBD/PSP patients had lower mean perfusion values in BA 5R and 7R (somatosensory association cortex), and higher mean perfusion values in BA 10L, 24L-24R, 32L-32R (anterior prefrontal, ventral and dorsal anterior cingulate cortex) compared to bvFTD patients. Multiple logistic regression analysis demonstrated that BA 7R [OR(95% CI)*=1.11(1.02-1.2), p=0.012] and 32R [OR(95% CI)*=0.90(0.82-0.98), p=0.015] could discriminate CBD/PSP from bvFTD. The proportions of CBD/PSP patients with mean BA perfusion more than 2SDs below the mean of healthy subjects were: 5R=90.3%, 7R=87.1%, 10L=83.9%, 24L=35.5%, 24R=90.3%, 32L=45.2%, 32R=54.8%. Similarly, in bvFTD the proportions were: 5R=90.5%, 7R=81%, 10L=95.2%, 24L=52.4%, 24R=95.2%, 32L=71.4%, 32R=66.7%. **CONCLUSION:** Our findings are consistent with impairment of specific BA in CBD/PSP and bvFTD patients. Brain perfusion SPECT with BA mapping would contribute in a more accurate differential diagnosis of bvFTD from CBD/PSP, especially when overlapping of clinical features occurs.

P29-2 - Tuesday, Oct. 22, 16:00 - 16:30, Poster Exhibition Area

## Neurosciences: Dopamine Imaging

## P608

### Uptake of $^{18}$F-FDOPA in the heart muscle of normal humans in $^{18}$F-FDOPA PET

**K. Kato**[1], S. Abe[2], T. Odagawa[1], A. Niwa[1], Y. Fujita[1], S. Naganawa[1]; [1]Nagoya University Graduate School of Medicine, Nagoya, JAPAN, [2]Nagoya University Hospital, Nagoya, JAPAN.

Purpose: $^{18}$F-FDOPA uptake has been reported to decrease in the corpus striatum in Parkinson's disease. As the first step of our studies to seek the other organs or tissues which show changes in $^{18}$F-FDOPA uptake, we try to test a possibility that

$^{18}$F-FDOPA uptake is changed in the heart muscle of patients with Parkinson's disease. Confirmation of the normal level of $^{18}$F-FDOPA uptake in the heart muscle is necessary for the judgment of modified $^{18}$F-FDOPA uptake in the heart muscle. This study was conducted to determine the normal level of $^{18}$F-FDOPA uptake in the heart muscle. Methods: We examined 10 patients with choroidal malignant melanoma who underwent $^{18}$F-FDOPA PET for the measurement of heart muscle $^{18}$F-FDOPA uptake. All the 10 study patients had no pathological changes in their hearts. $^{18}$F-FDOPA PET was performed 60 minutes after intravenous administration of $^{18}$F-FDOPA using a PET camera (Siemens Biograph 16). The maximal standardized uptake value (SUVmax) of $^{18}$F-FDOPA in the heart muscle and mediastinam was measured and the ratio of SUVmax in the heart muscle to SUVmax in the mediastinum (the heart-to-mediastinum ratio, HMR) was calculated. Besides the 10 study patients, 1 patient with suspected parkinsonism was examined for comparison. Results: The range and mean of HMRs in the 10 study patients were 1.105 to 1.805 (mean±SD, 1.396± 0.223). HMRs in 1 patient with suspected parkinsonism as 0.804. Conclusion: The range of HMRs (mean±SD) in 10 study patients with normal heart examined in this study was 1.105 to 1.805 (1.396± 0.223). Further studies will be conducted with increased numbers of study patients.

## P609

### Diagnostic accuracy of MIBG scintigraphy in patients with Parkinson's disease who was diagnosed with dopamine PET.

**S. Fujita**[1], Y. Tashiro[1], S. Nagamachi[2], S. Tamura[2], T. Fujimoto[1]; [1]Fujimoto General Hospital, Miyazaki, JAPAN, [2]Miyazaki University, Miyazaki, JAPAN.

PURPOSE: A diagnosis of Parkinson's disease (PD) can be difficult in early period of onset, and precision improvement is planned by using a function image with nuclear medicine. Cardiac (123)I-labelled metaiodobenzylguanidine (MIBG) scintigraphy is one of the diagnosis biomarker which availability establishes of PD, but the example which does not recognize abnormality is in particular present early. The aim of this study is to evaluate the diagnostic potential of MIBG scintigraphy in idiopathic PD with diagnosis was confirmed by positron emission tomography (PET) imaging with (11)C-N-(3-iodoprop-2E-enyl)-2beta-carbomethoxy-3beta-(4-methylphenyl)nortropane (PE2I) and (11)C-raclopride (together designated as dopamine PET). METHODS: For from July, 2011 to June, 2012, cardiac MIBG scintigraphy, MRI, FDG PET and dopamine PET were performed for 66 patients with parkinsonism. To estimate the cardiac MIBG uptake, heart to mediastinum (H/M) ratios and wash out rate in early and delayed images were calculated. We compared MIBG uptake with age at onset, Yahr severity and occipital lobe FDG metabolism. RESULTS: On the basis of established clinical criteria and our dopamine PET findings, 14 patients were classified into PD group (male 5, woman 9, 75.4 +/-7.9 years old, Yahr 1.78+/- 0.70), and 3 patients were DLB group (male 2, woman 1). In PD group, Yahr1 was 5 cases, Yahr2 was 7 cases, and Yahr3 was 2 cases. When it evaluates MIBG every Yahr stage, early H/M was Yahr1: 1.42+/-0.31, Yahr2: 1.30+/-0.20, Yahr3: 1.13+/-0.02, delayed H/M was Yahr1: 1.23+/-0.23, Yahr2: 1.13+/-0.15, Yahr3: 1.12+/-0.06, and wash out rate was Yahr1:70.4+/-10.9, Yahr2: 77.2+/-12.9, Yahr3: 43.8+/-33.9. CONCLUSION: We were able to confirm that a Yahr stage of PD moved as for the Cardiac MIBG uptake, and it was important that early PD diagnosis was careful to wash out rates for early diagnosis. In the Parkinson's disease who was diagnosed with dopamine PET, cardiac MIBG was effective as a diagnosis marker in early period of onset.

## P610

### Social Exclusion, Dopamine Function and Psychosis Risk: A [123I]IBZM-SPECT Study in Young Adults with Serious Hearing Impairment

**M. Gevonden**[1,2,3], J. Booij[1], W. van den Brink[1], J. van Os[2,4], J. Selten[3,2]; [1]Academic Medical Center, Amsterdam, NETHERLANDS, [2]MUMC+, Maastricht, NETHERLANDS, [3]Rivierduinen, Leiden, NETHERLANDS, [4]King's College London, London, UNITED KINGDOM.

**Aim:** According to the social defeat hypothesis the long-term experience of social exclusion or social defeat leads to enhanced baseline activity and/or sensitization of the mesolimbic dopamine (DA) system and puts the individual at increased risk for psychotic disorder and/or schizophrenia. Such increased risk has been found in migrants and in people with hearing impairment. This study tests the social defeat hypothesis by comparing dopaminergic function in two groups who differ greatly in the experience of social exclusion and are also expected to differ in DA release: (1) young adults (age 18-30) with a serious hearing impairment (HI); (2) normal hearing peers. **Subjects and Methods:** Nineteen subjects with HI (3 males; 4 smokers, mean age 25y10m, *SD* = 8m) and 19 control subjects individually matched on age, sex and smoking behaviour (mean age 26y2m, *SD* = 9m), were examined using SPECT imaging with the well-validated DA $D_{2/3}$ receptor tracer [$^{123}$I]iodobenzamide (IBZM) on a brain-dedicated system (Neurofocus; 12 detectors). In one session, baseline striatal $D_{2/3}$ receptor binding and endogenous DA release after stimulation with D-amphetamine sulphate (0.3 mg/kg i.v.) were assessed (bolus/constant infusion technique). Questionnaires were administered to measure social defeat, depression and sub-clinical psychotic experiences (lifetime, before and after D-amph). Group differences in baseline $D_{2/3}$ receptor binding and DA release were tested using ANOVAs. Associations between subjective measures and DA release were tested using linear regression and adjusted for sex, age and smoking. **Results:** HI and control subjects did not differ in baseline $D_{2/3}$ receptor binding, $F$ (1, 36) = .09, $p$ = .77. [$^{123}$I]IBZM binding potential decreased 13.6% after D-amphetamine administration in the HI group and 10.6% in the control group, reflecting DA release, but showing no significant between-group difference, $F$ (1, 35) = .48, $p$ = .49. HI subjects had stronger subjective responses to D-amphetamine, $F$ (1, 36) = 4.73, $p$ = .04. While HI participants had higher social exclusion and depression scores, neither HI, nor social exclusion, nor depression scores predicted DA release. Higher lifetime psychotic symptom scores, however, were associated with greater DA release, $b$ = -2.25, $t$(32) = 2.45, $p$ = .02. **Discussion:** While this study provides no evidence for hyperdopaminergia in socially excluded individuals, and therefore does not support the social defeat hypothesis, it demonstrates a relationship between a measure of psychotic experiences and DA release in a non-clinical population. This finding contributes to the understanding of the biological mechanisms underlying psychosis risk.

## P611

### Can the Putamen-to-Caudate ratio (P/C) serve as an additional quantitative index worth mentioning in the quantification process of 123I-FPCIT SPECT studies? Does it enhance or deteriorate the method's sensitivity and specificity?

**K. Badiavas**[1], I. Iakovou[2], A. Doumas[2], G. Arsos[2], S. Georga[2], D. Lo Presti[2], V. Balaris[2], V. Nikos[2], D. Katsampoukas[2], M. Tsolaki[3], A. Kotzamani-Psarrakou[4], A. Sioundas[4], N. Karatzas[2]; [1]Medical Physics Dept, "Papageorgiou" General Hospital, THESSALONIKI, GREECE, [2]3rd Nuclear Medicine Dept, Aristotle University Medical School, "Papageorgiou" General Hospital, THESSALONIKI, GREECE, [3]Neurology Dept, Aristotle University Medical School, "Papanikolaou" General Hospital, THESSALONIKI, GREECE, [4]Medical Physics Dept, Aristotle University Medical School, THESSALONIKI, GREECE.

Aim. To explore whether the Putamen-to-Caudate ratio (P/C), a quantitative index that can be derived from a number of quantification Methods applied in 123-I FPCIT SPECT studies, affects sensitivity and specificity. Materials and Methods. We randomly selected 15 patients (9 men and 6 women, aged 68.7±9.8 years) from those referred for confirming or excluding Parkinsonism. Imaging was done in a dual-head ADAC Vertex Plus γ-camera with the standard 123-I FPCIT SPECT protocol. We applied two semiquantification Methods suitable for deriving the Putamen-to-Caudate ratio (P/C). For the manually positioning ROIs method, reconstruction and semiquantification was done on the ADAC PEGASYS workstation. For the "crescent" semiautomated method of the QuantiSPECTTM software package, reconstruction, Chang attenuation correction and semiquantification were done with the package itself. Except for the "all-time classic" specific uptake index, Putamen-to-Caudate ratio (P/C) was calculated in order to explore whether it affects sensitivity and specificity of the Methods. The final diagnoses were taken from the referring neurologists and were based on the overall patient's clinical status, various tests e.g. UPDRS, nuclear medicine imaging results and response to medical treatment, if such. Results. From the studies of 15 patients (5 free, while 10 suffering from Parkinson's disease or other parkinsonian syndrome), sensitivity for the "manual" and the "crescent" method, based on the specific uptake index, was found to be 100% and 50% respectively, while, specificity was found to be 100% and 80% respectively. Using our department's normal database Putamen-to-Caudate ratio (P/C) values, 0.58±0.09 and 0.80±0.10 for the "manual" and "crescent" Methods respectively, sensitivity was 60% and 10% and specificity was 80% and 100%, respectively for each method. Conclusion. This study, for a really small number of 15 patients, confirms that the "manual" semiquantification method based on the specific uptake index, shows great sensitivity and specificity and worth its place next to visual assessment, which is the method of choice for diagnosing 123I-FPCIT SPECT studies. The "crescent" method, when based on the specific uptake index, gives much poorer results. The use of the Putamen-to-Caudate ratio (P/C) as an index, while worsens the sensitivity and specificity of the "manual" method and sinks the sensitivity of the semiautomated "crescent" method, greatly favors the specificity of this last method. Therefore, the semiautomated "crescent" method, with the use of the Putamen-to-Caudate ratio (P/C) as an index, can serve as a good method to exclude Parkinson's disease or other Parkinsonian syndrome.

## P612

### Effects of Thyroid Blockade on Brain Imaging of Dopamine Transporter in Normal Mice

**A. Greco**[1,2], A. Zannetti[3], A. R. D. Coda[3], S. Albanese[2], A. Nardelli[3], A. Roca[1], S. Pappatà[3], A. Brunetti[1], A. Cuocolo[1]; [1]University of Naples - Federico II, Napoli, ITALY, [2]CEINGE scarl, Napoli, ITALY, [3]National Council of Research, Napoli, ITALY.

**Aim**: Single-photon emission computed tomography (SPECT) using [123I] 2b-carbomethoxy-3b-(4-iodophenyl)-N-(3-fluoropropyl)nortropane (FP-CIT), as

radioligand for the dopamine transporter (DAT), is a widely used tool to evaluate and monitor the integrity of the nigrostriatal dopaminergic projection in patients with Parkinson's disease. [123I] FP-CIT has been also applied in experimental studies in monkeys and rats, but it has not yet been extensively validated in mice. We assessed whether thyroid blockade improves the quality of microSPECT-DAT images and in turn the semi-quantitative assessment of the striatum specific binding (SB) in mice. We also compared the results of microSPECT-DAT imaging to those of phosphorimaging autoradiogradiography on ex vivo mice brain tissue slices. **Material and Methods**: Male c57/balck healthy mice (8 weeks old, weighing 25-30 g) were studied. MicroSPECT images were obtained using the YAP-(S)PET scanner (ISE) in 4 mice pre-treated with oral Lugol solution (1 µl, one hour before tracer administration) and 4 untreated mice. A dose of 700-800 µCi of [123I] FP-CIT was injected in the tail vein in anesthetized mice (isoflurane 4% and oxygen 1 L/min). MicroSPECT images were acquired in list mode (128 views over an angle of 360 degrees). The acquisition started 2-3 hours after radiotracer administration and lasted 2 hours. At the end of the microSPECT study, animals were sacrificed and the brain was removed for autoradiographic analysis using 600 dpi resolution Cyclone Storage Phosphor System (Perkin-Elmer). In each animal, regions of interests were drawn on microSPECT and autoradiographic images on the striatum and on the cerebral cortex. Striatum-cortex/cortex ratios were calculated to evaluate SB. **Results**: Both visual inspection and semiquantitative analysis of microSPECT images revealed higher striatal [123I] FP-CIT uptake in mice pre-treated with Lugol. In particular, SB was 1.61±0.2 in pre-treated mice and 0.59±0.05 in untreated mice (P<0.01). Autoradiographic data confirmed in vivo microSPECT analysis showing a higher [123I] FP-CIT binding in pre-treated mice in comparison to untreated mice (SB: 1.36±0.14 vs. 0.63±0.04, P<0.01). Finally, a significant correlation between radioligand SB calculated in vivo with microSPECT and ex-vivo with phosphoroimaging autoradiogradiography was found (r=0.92, P<0.01). **Conclusions**: Our results show that thyroid blockade improves by two-three times the striatal SB and suggest that Lugol pre-treatment should be always used in microSPECT-[123I] FP-CIT experimental protocols in mice. Our data also demonstrate a good correlation between in vivo and ex-vivo striatal [123I] FP-CIT binding in mice.

## P613

### Brain SPECT with 123I-IBZM in the Diagnosis of Patients with Suspected Atypical Parkinsonism

**C. Gamazo**, P. Garcia-Talavera, J. G. Villanueva, A. Sainz-Esteban, M. A. Ruiz, M. L. Gonzalez, R. Olmos; Hospital Clínico Universitario, Valladolid, SPAIN.

Aim: to assess the clinical impact of brain SPECT imaging of postsynaptic dopaminergic receptors in the diagnosis of patients with suspected atypical parkinsonism. Material and Methods: We included 48 patients (28 women; mean age=74 ± 11) with clinical parkinsonism (progression time 5,2 ± 3,3 years). A brain SPECT with 123I-Iodobenzamide (IBZM) was performed to all patients (from february 2010 to august 2012). The acquisition was carried out 2-3 hours after the injection of 185 MBq of the radiotracer (matrix 128x128, fan-beam, 128 images, 35 seconds/image). The indication to perform the SPECT was the presence of atypical clinic (32 cases), the lack of response to treatment (8), and both reasons (8). Patients were divided into two groups according to the clinical pre-test probability of atypical parkinsonism: group A, low probability (21 patients) and group B, high probability (27 patients). The results of the SPECT were correlated with clinical follow-up (10.7 ± 9,3 months). Results: In group A, 19 out of 21 123I-IBZM SPECT were normal. In 16 out of these (16/19), Parkinson's disease was confirmed whereas in three cases the neurologist didn't achieve a definitive diagnosis (PNV 100%). One of the pathological 123I-IBZM SPECT was diagnosed with Parkinson's disease and in the other one a clinical diagnosis was not reached. In Group B, 17 out of 27 123I-IBZM SPECT were normal. Eleven were consistent with clinical judgment and 4 were not congruent. In two cases a definitive diagnosis was not reached (PNV of 73%). Nine out of 10 pathological 123I-IBZM were confirmed as postsynaptic parkinsonisms (PPV = 90%). Conclusions: Brain SPECT with 123I-IBZM is a useful tool in the diagnosis of patients with suspected of postsynaptic parkinsonism, especially to confirm the diagnosis in patients with high clinical suspicion (PPV of 90%), as well as to exclude it in patients with lower probability of this disease (PNV 100%).

## P614

### Increased dopamine release induced by acute exercise in the brain of healthy human volunteers

**M. TASHIRO**[1], T. FUJIMOTO[2], T. ARAI[1], M. MASUD[1], M. MIYAKE[1], S. WATANUKI[1], K. SHIBUYA[3], A. INAMI[1], K. HIRAOKA[1], R. IWATA[1], K. YANAI[1], M. ITOH[1,3]; [1]Tohoku University Cyclotron and Radioisotope Center, Sendai, JAPAN, [2]Tohoku University Center for the Advancement of Higher Education, Sendai, JAPAN, [3]Sendai Medical Imaging Clinic, Sendai, JAPAN.

Exercise may have various psychophysiological effects characterized by increased positive emotion and reduced stress and anxiety. However, its underlying mechanism has not been studied well yet. Though it is very probable that certain biochemical changes may be taking place in the brain of athletes, clinical neuroimaging study with positron emission tomography (PET) has been quite rare. In addition to the measurement of regional cerebral perfusion and metabolism, the measurement of neurotransmission would be a very powerful tool for exercise psychophysiology. Eight healthy young male volunteers (mean age: 22.1 +/- 2.3 years old) were recruited for the present study, based on the approval from the ethics committee of Tohoku University Graduate School of Medicine. The volunteers were scanned twice by PET immediately following intravenous injection of [11C]raclopride (approximately 230 MBq) once in resting condition and the other in exercise condition. The scan lasted for 90 min creating 23 frames. In the exercise condition, exercise loading with an ergometer bicycle was initiated 20 min prior to injection and lasted for 50 min. The exercise loading ended at 30 min post-injection, and the study subjects were scanned quietly another 60 min during the period of 30 to 90 min post-injection. Regions of interest (ROIs) were applied to the dynamic PET data on the bilateral putamen and caudate nuclei, and binding potential (BP) values were calculated using Logan noninvasive model using the cerebellum as a reference tissue (PMOD 3.0). Time activity curves of the putamen and caudate nuclei demonstrated higher counts in the resting than in the exercise condition during the first 60 min post-injection. Furthter analysis demonstrated significantly lower BP in the right putamen and in the left caudate nucleus in the resting than in the exercise condition, suggesting the increased dopamine release in exercise condition. But there was no difference between the 2 conditions during the period of 60 to 90 min post-injection, suggesting that the dopamine release increase lasted only 30 min or so following cessation of exercise load. Our hypothesis that dopamine release may increase in the basal ganglia of healthy volunteers due to acute whole body exercise has been partially proved using PET and [11C]raclopride in spite of small number of study subjects. Neuroreceptor PET studies seem to be very useful in research in health promotion sciences.

P30-2 - Tuesday, Oct. 22, 16:00 - 16:30, Poster Exhibition Area

## Neurosciences: Miscellaneous

## P615

### Transient Changes in the Endocannabinoid System after Acute and Chronic Ethanol Exposure and Abstinence in the Rat: a Combined PET and Microdialysis Study

**J. Ceccarini**[1,2], C. Casteels[1,2], M. Koole[1,2], G. Bormans[3,2], K. Van Laere[1,2,4]; [1]Division of Nuclear Medicine, University Hospitals and KU Leuven, Leuven, BELGIUM, [2]MoSAIC, Molecular Small Animal Imaging Center, KU Leuven, Leuven, BELGIUM, [3]Laboratory of Radiopharmaceutical Chemistry, KU Leuven, Leuven, BELGIUM, [4]LIND, Leuven Institute for Neurobiology and Disease, KU Leuven, Leuven, BELGIUM.

AIM: Recent biochemical and post-mortem evidence suggest involvement of the endocannabinoid system (ECS) in alcohol drinking behavior and dependence. Using [18F]MK-9470 small-animal PET imaging, our primary objective was to evaluate in vivo type 1 cannabinoid receptor (CB1R) binding changes in rats subjected to several ethanol conditions: (i) at baseline, (ii) after acute administration of ethanol (4g/kg intraperitoneal) or saline, and (iii) after 7-days of forced chronic ethanol consumption, followed by a 7 and 14-days abstinence period. Secondly, levels of brain anandamide (AEA) in the nucleus accumbens (NAcc) were investigated in the same animals using in vivo microdialysis and correlated to the changes in CB1R binding. MATERIALS AND METHODS: In total, thirty-one male Wistar rats were investigated. Small-animal PET was done on a FOCUS-220 with ~12 MBq of [18F]MK-9470. Images were normalized to Paxinos space and analyzed voxel-wise using SPM8 (pheight = 0.005; kext = 200). AEA content was quantified using HPLC with tandem mass spectrometry detection. RESULTS: Acute ethanol administration increased relative CB1R binding in the bilateral NAcc (+7.7%) that positively correlated to the change in AEA level of that region (r = 0.99). Chronic ethanol exposure decreased relative CB1R binding in the hippocampus (-5.2%) and caudate-putamen (-5.7%), whereas same regions were increased by +8.9% and +14.2% after 7 and 14-days of abstinence as compared to baseline. Also, after 7-14 days of abstinence, relative CB1R binding additionally decreased in the orbitofrontal cortex (> -20.1%). The magnitude of these hippocampal and frontal changes was highly correlated to daily ethanol intake (r = 0.99 and r = -0.99, respectively). CONCLUSION: This study provides in vivo evidence that acute ethanol consumption is associated with an enhanced endocannabinoid signaling in the NAcc, indicated by an increased CB1R binding and AEA content. In addition, chronic ethanol exposure points to regional dysfunctions in CB1R levels, incorporating hippocampus and caudate-putamen that are reversible within two weeks in this animal model.

## P616

### Early brain perfusion improvement after ventriculoperitoneal shunt surgery in patients with idiopathic normal pressure hydrocephalus in $^{99m}$Tc-HMPAO SPECT- preliminary report

**A. Nocuñ**[1], A. Mosiewicz[2], R. Kaczmarczyk[2], B. Chrapko[1]; [1]Department of Nuclear Medicine, Lublin, POLAND, [2]Clinic of Neurosurgery and Paediatric Neurosurgery, Lublin, POLAND.

**Introduction:** Perfusion improvement resulting from successful shunt surgery in patient with idiopathic normal pressure hydrocephalus (INPH) is described in the literature months after the procedure. However, early reperfusion is not well documented. The aim of the present study was to determine brain perfusion changes earlier than one week after the ventriculoperitoneal shunting in patients with INPH by using $^{99m}$Tc-HMPAO SPECT. **Material and Methods:** Fourteen patients with INPH (8 women, 6 men, mean age 64.7±13.4 years), who underwent ventriculoperitoneal shunt surgery, were included into the study group. $^{99m}$Tc-HMPAO SPECT was performed 1-2 days before and 3-6 days after the surgical treatment. Radiopharmaceutical dose was 740 MBq. Brain SPECT was carried out using a rotating, double-head, large field of view gamma camera (Varicam, GE Medical Systems) equipped with low-energy, high-resolution collimators. The data were collected in a 128 × 128 matrix through 360° rotation at 3° intervals for 25 s per view. Data reconstruction was performed by filtered back projection with Metz filter. Regional cerebral blood flow was evaluated visually and semiquantitatively using voxel- based analysis with Brain SPECT Quantification software (Compart, Poland). The change of perfusion between basal and control studies was considered significant when relative difference (RD) was higher than 10% in a cluster volume (CV) greater than 10 ml **Results:** No serious side effects were observed after the surgery. Perfusion improvement after the shunting was observed in 10 patients (71.4%). Perfusion increased in the whole brain (3 patients) or in the separate cerebral regions (7 patients): right frontal, bilateral frontal, bilateral frontal and left cerebellum, left frontal and left parietal, right cerebral hemisphere, right temporal, right cingulate gyrus. Perfusion improved predominantly in the frontal lobes (4 cases). **Conclusion:** In patients with INPH perfusion improves promptly after ventriculoperitoneal shunt surgery. It may be global or regional in different cerebral areas with prevalence of the frontal lobes.

## P617

### The cognitive interference-related brain activity during Stroop task performance - H2O15 PET study - initial results.

M. Wrobel[1], A. Markowska[2], L. Balszewski[1], M. Piec[1], **B. Malkowski**[1]; [1]Department of Nuclear Medicine Oncology Centre, Bydgoszcz, POLAND, [2]Department of Psychiatry Nursing, CM, Nicolaus Copernicus University, Bydgoszcz, POLAND.

The existing data on brain activation during performance on commonly used Stroop Test showed the role of different cortical regions. The aim of the study was to examine the differences in brain activation during the color-word congruent and incongruent part of the Stroop Test compared with the baseline activation. [15O]H2O PET studies was performed using a high-resolution, time-of-flight, 3-rings Biograph128 mCT scanner, equipped with LSO crystals and a 2x64-slice spiral CT scanner. Color-word congruent (A), incongruent (B) and baseline (C) conditions were presented to 5 healthy, righthanded subjects (aged 20-30 years old) during 8 [15O]H2O PET scans. The sequence of scans is as following: C, A, C, B, C, A, C, B. A bolus of 550 MBq of [15O]H2O in 2.5 ml of normal saline was injected for each emission scan. It is done via the intravenous cannula over 15s and then the solution was flushed in with the automatic pump at a rate 60 ml/min for 10s. The emission data was acquired after 15s of the end phase of the injection. The acquisition was performed in a list mode in 60s epochs, began 5s before the raising phase of the radioactivity head curve. The subject initiates the task 15s before the onset of the injection phase in order to ensure that the performance of the task was coincided with the maximum activity level of isotope in the brain. SPM analysis of the PET scans showed interference-related activations of superior frontal gyrus, medial frontal gyrus, left Inferior frontal gyrus, left middle frontal gyrus, precentral gyrus, left cingulate gyrus, left insula and cerebellum. Interference - related deactivations were observed bilaterally in the postcentral gyrus, angular gyrus, middle frontal gyrus, left superior temporal gyrus, left superior frontal gyrus, left paracentral lobule, right medial temporal gyrus, right precuneus, right Superior occipital gyrus, right anterior cingulated, right uncus and cerebellum. These findings may provide some additional knowledge about the role of anterior cingulate and prefrontal cortical contributions to performing the Stroop interference task. These are preliminary data that are planned to be conducted on larger group.

## P618

### Inter-Ictal FDG PET in Temporal Lobe Epilepsy. Correlation with ictal EEG, ictal SPECT, MRI, Neuropsychology and Outcome

**L. Pushpalatha Sudhakar**, S. SITA JAYALAKSHMI, S. PRAVEEN, P. MANAS; KRISHNA INSTITUTE OF MEDICAL SCIENCES, HYDERABAD, INDIA.

**Aim**: To identify inter-ictal FDG PET patterns and to correlate with ictal EEG, ictal SPECT, MRI, neuropsychology and surgical outcome in patients with refractory temporal lobe epilepsy(TLE). **Materials & Methods:** Retrospective analysis of inter-ictal FDGPET, Ictal EEG, ictal SPECT neuropsychology and MRI data was performed in 88 patients with refractory TLE with at least one year post-surgery follow up. Ictal SPECT was performed in 65. **Results**: Mean follow up was 42(12-92) months; 55% were males; Mean age at surgery was 26.5(5-52) years. Pathology was hippocampal sclerosis(HS) in 68; Favorable outcome (Engel's Class I&IIA) was noted in 81.81%. PET showed unilateral hypometabolism in 82, bilateral- 4 and contralateral- 2, extended hypometabolism -7 patients. PET correlated with MRI in 98.6% , ictal EEG -86.8% and neuropsychology - 80.7%. Sensitivity of ictal SPECT & inter-ictal PET was 93% and 93% and specificity 97% and 88% respectively. Ictal EEG onset was discordant/uncertain in 10(11.3%) but ictal SPECT and interictal PET were concordant. MRI was normal in 16 and surgery was performed after concordant ictal EEG, ictal SPECT & interictal PET; 9(56%) had favorable outcome. After multiple regression analysis using the McHenry's algorithm, abnormal imaging, unilateral interictal spikes, ipsilateral PET Hypometabolosm and typical ictal SPECT pattern were predictors of favorable outcome. **Conclusion**: Inter-ictal FDGPET is specific and sensitive non-invasive modality during pre-surgical evaluation of patients with refractory TLE. Ictal SPECT and Inter- ictal FDG PET are complimentary , together obviate the need for invasive EEG in resource poor countries.

## P619

### Imaging of brain TSPO expression in a mouse model of stroke with [18F]DPA-714 and micro-PET

**C. Vicidomini**[1,2], A. Vinciguerra[3], A. Greco[4,2], M. R. Panico[1], S. Gargiulo[1,2], M. Gramanzini[1,2], A. R. D. Coda[1], G. Pignataro[3], M. Quarantelli[1], B. Tavitian[5], F. Dollé[6], A. Brunetti[2,4], M. Salvatore[4], L. Annunziato[3], S. Pappatà[1,2]; [1]Institute of Biostructure and Bioimaging of CNR, Naples, ITALY, [2]Ceinge, Biotecnologie Avanzate, scarl, Naples, ITALY, [3]Department of Neurosciences and Reproductive and Odontostomatologic Sciences, University Federico II, Naples, ITALY, [4]Department of Advanced Biomedical Sciences, University Federico II, Naples, ITALY, [5]Inserm U970, Paris, FRANCE, [6]CEA, Institute for Biomedical Imaging, Orsay, FRANCE.

**Aim:**The translocator protein (18 kDa) is a promising biochemical markers of reactive gliosis and inflammation associated with neurological disorder. Marked increase in TSPO expression characterizes ischemic brain tissue and experimental stroke models are considered a useful tool to validate new TSPO radioligands (1). [18F]DPA-714 is a new TSPO radioligand recently validated in models of neuroinflammation (NI) in rat (1). Here we have evaluated the feasibility and the sensitivity of [18F]DPA-714 in a mouse model of transient MCAO (tMCAO). This might be of relevance for future applications of [18F]DPA-714 in mouse model of stroke or other NI disorders. **Methods:** C57BL/6 male mice were subjected to twenty minute of right tMCAO (age: 10-21 weeks; weight: 20-30g). We performed in vivo microPET-CT imaging in three group of animals at 2 (n=3), 4 (n=2) and 6-7 (n=3) days after reperfusion (GE Explore Vista,PET spatial resolution=1.6 mm). PET scans were acquired in dynamic, 3D mode (12 x 5 min frames) starting 10 minutes after i.v. tail injection of 18F-DPA-714 (5.36 ± 1.74 MBq; SRA: 185 ± 98 GBq/ µmol) in anesthetized mice (Isoflurane 2% Oxygen, 2 L/min). TTC staining or MRI were used to assess the infarct size/location. ROI were drawn on the core infarct (CI), peri-infarcted region (PI) and the contralateral hemisphere (CH), based on CT images. **Results:** At 2 days post tMCAO, [18F]DPA-714 uptake was reduced in the CI and almost unchanged or mildly increased in PI (CI/CH=0.498±0.192; PI/CH=0.989±0.203). At 4 days, [18F]DPA-714 uptake was reduced in the CI (CI/CH= 0.444) and mildly increased in the PI (PI/CH=1.136) in one mouse whereas it was increased in the CI-PI (PI/CH=1.529) in the other mouse. At 6-7 days, [18F]DPA-714 uptake was increased in the CI-PI regions in two mice and only in PI in one mouse (PI/CH=1.632±0.29). **Conclusions**: The preliminary results suggest that increased [18F]DPA-714 uptake can be measured with microPET on the occluded side of mice brain between 4 and 7 days after tMCAO, in agreement with the well known increase in TSPO expression reported in this model. The relationships between the location and the magnitude of [18F]DPA-714 uptake in the occluded hemisphere and the extent/severity of infarct and time window after tMCAO deserve further investigations. (1)Jacobs AH, Tavitian B and the INMiND consortium. J Cereb Blood Flow Metab 2012; 32:1393-1415 Supported in part by INMiND-LSIP 278850

## P620

### SPECT CT Radionuclide Cisternography proves cerebrospinal fluid fistula causing pleural effusion after partial corporectomy

**G. Pina**[1,2], T. Montvuagnard[3], C. Scheiber[1]; [1]Médecine Nucléaire, Groupement Hospitalier Est, Hospices Civils de Lyon, Université de Lyon, Lyon, FRANCE, [2]Centre de recherche en Neuroscience, Equipe BioRan, Université Lyon 1, Université de Lyon, Lyon, FRANCE, [3]Radiologie, Groupement Hospitalier Est, Hospices Civils de Lyon, Université de Lyon, Lyon, FRANCE.

Aim Contribution of SPECT-CT Radionuclide cisternography (RC) to prove and localise CerebroSpinal Fluid (CSF) dural leakage and fistula in patient with suspected dural CSF leak and pleural effusion. Materials & Methods A 59 year old

patient with a history of liver transplant for hepatocarcinoma was hospitalized for partial L1 corporectomy for solitary bone metastasis. Secondary to partial corporectomy, the patient developed infection. As CSF leakage was observed on the surgical site and iterative thorax radiography showed increasing right pleural effusion, history was suggestive of CSF pleural fistula. However Computerized Tomography (CT) with myelography was conducted and showed no sign of CSF leakage and CSF pleural fistula. SPECT CT RC was then performed by intrathecal injection into the lumbar subarachnoidal space (LP) of 67 MBq of [111In] DTPA. Planar imaging of thorax and abdomen were acquired 6 and 24 hours after LP with a dual head hybrid gamma camera equipped with CT (SYMBIA T2 ® Siemens, Germany). A thoraco-lumbal SPECT/CT study with a slice thickness of 2.5mm for CT and 3.9 mm for SPECT was acquired 24 hours after LP. Results Planar images were positive for CSF lumbar leakage and fistula into the pleural space with increasing activity in pleural effusion between 6 and 24 hours after LP. Fused SPECT/CT images located the leakage on the right side of the surgical site and showed the fistula route to the right pleural space. Conclusion CSF leakage is a potentially life threatening situation. Its treatment is surgical. Therefore, CSF leak imaging should confirm and locate the main site of leakage, indicate its source and help planning the surgical approach. This case highlights the complementarity of RC imaging for diagnosis confirmation of CSF leakage and localization of CSF leakage and fistula route. In this case, CT myelography showed no evidence of CSF leak or CSF fistula, probably due to the low cinetic of CSF fistula. Radionucleide cisternography SPECT/CT was conclusive for CSF leakage and CSF pleural fistula, and the fusion images could give anatomical localisation. The dural fistula was shortly afterwards operated successfully.

P31-2 - Tuesday, Oct. 22, 16:00 - 16:30, Poster Exhibition Area

## Neurosciences: Data Analysis & Quantification

### P621

### Dedicated colour-scale for visual analysis of 18F-DOPA PET images in brain tumours

**J. Darcourt**[1,2], R. Guignard[1], J. Olivain[3], J. Barriere[1], O. Clatz[3], D. Fontaine[4], V. Bourg[4], L. Mondot[4], S. Chanalet[4], P. Bondiau[1], F. Vandenbos[4]; [1]Centre Antoine Lacassagne, Nice, FRANCE, [2]University of Nice, Nice, FRANCE, [3]INRIA, Sophia-Antipolis, FRANCE, [4]CHU, Nice, FRANCE.

DOPA is an amino-acid substrate of the amino-acid transporter which is over-expressed in brain tumours. Therefore 18F-DOPA PET has proven its usefulness for imaging such lesions. Unlike other labelled amino-acids, 18F-DOPA also binds to normal striatum which can be used as an internal reference. Indeed, Chen et al. (JNM 2006) demonstrated that quantitative analysis could take advantage of this property and that the best quantitative parameter was tumour/striatum ratio with an optimal diagnostic threshold of 0.75. We propose an adapted colour-scale which allows using this criterion by simple visual analysis. Materials and Methods We developed a dedicated rainbow colour scale which maximum can be set on the normal striatum and in which the red colour changes to yellow when reaching 75% of the mean striatal value. Visualisation of the images using this scale allows a simple direct reading, considering a positive uptake when the tumour area appears in red colour. This approach was tested on 15 patients referred for suspicion of brain tumour recurrence in whom the diagnosis could be confirmed either by surgery (5 patients) or by 6 months follow-up including repeated F-DOPA PET. 8 patients had recurrence and 7 did not. Ten minutes static PET acquisitions were performed 20 minutes post injection of 2 MBq/kg of 18F-DOPA on a PET/CT camera (mCT Siemens). Images were reconstructed by OSEM 5 iteration 24 subsets and visualized with the dedicated colour-scale. All patients underwent an MRI within 3 weeks of the PET study. Contrast-enhanced 3D T1 images were systematically coregistered to the PET data. Visual analysis was compared to quantitative measures of tumour (T) uptake using 3D VOIs. Nine quantitative parameters were measured: TSUVmax, TSUVmean, TSUVpeak, TSUVmax/bkg, TSUVmean/bkg, TSUVpeak/bkg, MTV, TSUVmean/striatum and TSUVpeak/striatum and tested by ROC analysis. Results However visual analysis using the adapted colour scale showed a sensitivity of 100% and a specificity of 57%. The best quantitative parameters were SUVpeak, TSUVpeak/bkg and TSUVpeak/striatum. Their sensitivity were equal or inferior to visual analysis. Conclusion The proposed dedicated colour scale which takes advantage of the physiological striatal uptake of F-DOPA allows direct visual quantification at the voxel base which is equivalent to the best VOI quantitative analysis.

### P622

### Use of SOR index as quantification tool in FDOPA PET/CT to evaluate Parkinson's Disease

**C. Villano**[1], G. Pigotti[2], L. Curatola[3], V. De Francesco[4], D. Martini[2], E. Baldassarrini[2], P. Panichelli[2], G. Valentini[2]; [1]U.O.C. Medicina Nucleare Ospedale Civile "Spirito Santo", Pescara, ITALY, [2]ACOM SPA, MONTECOSARO, ITALY, [3]Neurologia, Marche, ITALY, [4]U.O.C. Medicina Nucleare Ospedale Civile, Pescara, ITALY.

Parkinson's Disease (PD) is a common neurodegenerative disorder of unknown etiology, characterised by a progressive loss of dopaminergic neurons in the nigrostriatal pathway and it is clinically featured by its motor symptoms consisting of an insidious (asymmetric) onset of bradykinesia, rigidity and (rest) tremor. The aim of our study is to assess the striatal FDOPA (L-3,4-dihydroxy-6-18F-fluoro-phenylalanine) uptake in FDOPA PET/CT to quantify the loss of striatal dopaminergic terminal function in vivo in PD and to obtain an analytic parameter to help in discriminating PD patients from healthy subjects. We decided to evaluate the performance of SOR (striatal-to-occipital ratio) index due to its practical advantage because it can be determined by static data acquisition and not dynamic scans over a longer time. After pretreatment with 125 mg carbidopa to block peripheral dopa-decarboxylase activity, 250-300 MBq of FDOPA was intravenously injected in 19 patients and after 50-60 min they underwent a cerebral PET/CT scanning (Biograph 6 Truepoint PET/CT, Siemens) 15 min length with 128x128 matrix. A set of standard elliptic ROIs (Region of Interest) were placed over the right and left caudates, putamen and occipital cortex in the mean image and the values for the left and right sides were averaged to reduce noise. Specific FDOPA uptake was expressed as SOR index for caudate (SORc) and putamen (SORp) following the equation: SOR index = (CROI-CREF)/CREF (CROI=average (left and right) ROI activity concentration; CREF=average occipital activity in the occipital reference region). As reported in other studies by several groups, both FDOPA uptake indices of PD patients showed significant decrease compared with the healthy subjects and SORp values were lower than SORc ones. Moreover, in PD the reduction of SORp values is greatly more evident than SORc values. In this clinical assessment of nigrostriatal dopaminergic function in PD, it is very important the assumption of carbidopa 1 hr before injection to enhance FDOPA cerebral bioavailability and to avoid underestimated values of SOR indices. Female subjects showed higher FDOPA uptake compared to males. These results demonstrate that both SORc and SORp parameters significantly discriminate PD patients from healthy subjects and show that SOR is a reliable imaging indicator of PD disease.

### P623

### How to increase normal database in SPM analysis of $^{18}$F-FDG brain PET.

**R. Stoico**, P. Baruzzi, G. Gianduia, L. Maffioli; A.O. Ospedale Civile di Legnano, Legnano (MI), ITALY.

**AIM**: Database of normal $^{18}$F-FDG brain studies often represents critical point for general medium hospital. In this study we tried to use HR brain PET scans of non-neurological patients to increase the normal sample size. **MATERIALS AND METHODS:** 38 $^{18}$F-FDG PET studies were performed. 28 patients underwent $^{18}$F-FDG PET brain examinations: 8 without (Group A) and 20 with brain disorders (Group B). 10 oncologic but non-neurological patients underwent $^{18}$F-FDG PET head and neck examination (Group C). In all patients, images were acquired by Philips TF Gemini system (2 mm slice thickness, 2 mm pixel size). The acquired images of all patients were processed according to SPM procedure: DICOM images converted to header and image files, spatial alignment, normalization with a PET template and smooth. The normal patients database was created by using Group A. An intra-database SPM analysis was made in order to find statistical significant differences ($p<0.05$) voxel-by-voxel between the images. Then SPM analysis ($p<0.05$) was performed for Group B so as to find hypo- or hyper-metabolic areas. The original dataset of Group C was cropped to the healthy brain volume. The images were processed according SPM procedure. An intra-group SPM analysis was performed in order to find statistical significant differences voxel-by-voxels ($p<0.05$). Then SPM analysis ($p<0.05$) was performed between Group B and Groups A+C. SPM analysis was matched with NM visual reports previously written by two blinded experienced NM physicians. **RESULTS**: The first intra-database (Group A) SPM analysis showed no statistically significant differences between images. SPM analysis of Group B vs Group A was in 6 cases concordant and 14 discordant with NM visual reports. The second intra-group SPM analysis (Group C) showed statistically significant differences (hypo-metabolic area) only for one case that was excluded. SPM analysis of Group B vs Groups A+C was in 14 cases concordant and 6 discordant with NM visual reports. **CONCLUSION**: The study shows: 1) a normal database can be increased by adding HR head and neck PET scans with a decrease of classification errors; 2) therefore, SPM software represents robust tool also with an "extended" normal database to support NM physicians visual analysis, in particular for borderline cases.

### P624

### The effect of number of iterations on quantitative DaTscan results and the repeatability of studies processed using an automated analysis program

**G. Roberts**, H. Richardson, A. Small; NHS Lothian, Edinburgh, UNITED KINGDOM.

Aims In a 2010 phantom study, Dickson et al. concluded that 10 iterations and 10 subsets (100 MLEM equivalent iterations) provided adequate convergence of the OSEM algorithm. We use OSEM with 2 iterations and 10 subsets. We aimed to determine the number of iterations needed for convergence in clinical images. The GE software DaTQUANT, which automatically registers images to a normal template, was used to obtain uptake values. A secondary aim was to investigate the variation in DaTQUANT results introduced from reorienting the transverse slices during processing. Method. Ten clinical DaTscans (I123-FP-CIT studies) reported as clearly normal and ten reported as clearly abnormal were selected based on the radiologist report. All studies were acquired at the same centre on a GE Discovery 670 camera using consistent acquisition and reconstruction parameters (OSEM with Chang AC). Studies were processed by a single operator with 2, 4, 6, 8, 10, 15, 20 and 30 iterations and 10 subsets. Studies were reconstructed to give transverse slices orientated parallel to the AC-PC line (as per EANM guidance). Transaxial slices were also reconstructed along the original acquisition frame of reference. Both orientations were analysed with DaTQUANT. Uptake ratios relative to background for the striata, putamen and caudate were extracted. Results were plotted against number of iterations and assessed for convergence (values stable within 5%). Due to variable results, the processing was repeated trying to be more consistent in transverse slice placement. One of the normal subjects was processed 10 times (using 10 iterations), repeating the transverse reorientation each time, to assess the variation this introduces. Results Based on the transaxial (non-reformatted) images, 8/10 of the normal and 6/10 abnormal patient images achieved convergence by 10 iterations. All normal and 9/10 abnormal images converged by 15 iterations. Some of the transverse (reformatted) did not converge at all (3/10 normal, 5/10 abnormal). Uptake results on transverse images varied by up to 25% between 10 and 30 iterations, reducing to 7% when processed the second time. The repeatability study on the single subject showed approximately 5% variation in uptake when processed as consistently as possible. Conclusion We have shown that clinical images acquired with our protocol require up to 15 iterations for convergence. DaTQUANT image registration appears highly sensitive to changes in the input image given by reformatting. Adjusting the transverse plane to obtain consistent orientation between patients is necessary but this step makes DaTQUANT uptake values unreliable.

P32-2 - Tuesday, Oct. 22, 16:00 - 16:30, Poster Exhibition Area

## Neurosciences: Movement Disorders

### P625

### Cardiac Scintigraphy with 123I-MIBG. Clinical Utility in Patients with Atypical Parkinsonism

**A. Rubió Rodríguez**[1], M. Negre Busó[1], N. Ferran Sureda[1], D. Genís Batlle[2], I. Martínez Sánchez[1], I. Trias Davesa[1], M. Sánchez García[1], A. Ruíz Rodríguez[1]; [1]Unitat Medicina Nuclear. Centre IDI, Hospital Universitar Dr Josep Trueta. Girona, SPAIN, [2]Neurology Department, Hospital Universitar Dr Josep Trueta. Girona, SPAIN.

AIM The aim of the study was to evaluate the clinical utility of 123I-MIBG cardiac scintigraphy, in order to establish a differential diagnosis between Parkinson's disease (PD)/Lewy Body Dementia (LBD) and Multisystemic Atrophy (MSA). MATERIAL AND METHODS We performed a prospective analysis of patients with atypical parkinsonism or clinical symptoms suggesting MSA, referred from Neurology Department between July 2007 and December 2010. Patients with diabetes or myocardiopathy were excluded from the study. The farmacological MIBG interactions were assessed in order to avoid misinterpretation in the results. A cardiac scintigraphy with 123I-MIBG was performed in all patients, acquiring planar images at 15 minutes and at 4 hours after radiopharmaceutical administration (4 mCi). A fifteen minutes heart/mediastinum ratio was obtained, considering a ≥ 1.8 value as normal and a ≤ 1.6 value as pathological (suggesting myocardial denervation). Patients with ratios between 1.6 and 1.8, were evaluated with delayed images, considering it as a pathological those with a clear decrease in the ratio value. The final diagnose was clinically established by the neurologist, assessing a clinical follow-up until December 2011. RESULTS We evaluated the scintigraphics results of 35 patients (mean age 66 ± 9.6 y). 24 of them showed denervation criteria and 10 were considered normal. One patient showed an heterogeneous myocardial uptake and therefore the study was considered not assessable. During the clinical follow-up, 20 patients were diagnosed of PD or LBD showing all of them signs of myocardial denervation (true positives). In 10 patients a MSA diagnosis was established, with normal cardiac scintigraphy in 7 patients (true negatives) and signs of denervation in 3 (false positives). One patient with normal cardiac scintigraphy, was diagnosed of idiopathic cranial dystonia. In 3 patients, it was not possible to establish a clear clinical diagnosis by follow-up. Comparing scintigraphics results with the clinical follow up, we saw that the 82.36% (28/34) of patients showed concordance results, and the rest 8.82% (3/34) of the studies showed discordance results. Only in this three cases, the image technique was not helpful for the neurologist. CONCLUSION 123I-MIBG cardiac scintigraphy is a useful tool to assess myocardial denervation, and this result helps neurologists to make a correct differential diagnosis between PD/LBD and MSA.

### P626

### 18F-DOPA qualitative brain PET/CT in patients with movement disorders: first two years experience

**L. Antunovic**, M. Rodari, G. Pepe, A. Chiti; Humanitas Clinical and Research Center, Milan, ITALY.

**Purpose**: 18F-deoxiphenilalanine (DOPA) is a radiolabelled amino acid precursor of dopamin, applied for the evaluation of striatal activity in patients with movement disorders; here we present our first two years experience on the clinical impact of 18F-DOPA qualitative brain PET/CT in differential diagnosis between parkinsonism and essential tremor. Subjects and Methods: 56 patients (26 females, 30 males, middle age 72,5±8,1 range 50-88 years) underwent 18F-DOPA PET/CT over two years period (02/2011-02/2013). Before the imaging, all patients were clinically evaluated and the diagnosis was suggested to be essential tremor in 7 patients and parkinsonism in 49 cases (41 idiopathic Parkinson disease, 3 Lewy body dementia, 1 vascular origin parkinsonism, 3 progressive supranuclear palsy, 1 multiple system atrophy). A visual analysis of PET/CT scans was made by an experienced nuclear medicine physician. One or more clinical controls were conduced after PET/CT imaging and diagnosis modification was evaluated in all cases. **Results:** in 24 patients the striatal activity resulted normal; the uptake of 18F-DOPA was reduced in 32 cases. In 38/56 patients (68%) the initial clinical diagnosis was confirmed by PET/CT results. In 16/56 patients (29%) the diagnosis was modified after PET/CT results; all patients resulted normal on PET/CT imaging, thus the diagnosis of parkinsonism was excluded. In two case (3%) there was a disagreement between PET/CT results and further clinical evaluation. **Conclusions:** Our experience confirm brain qualitative PET/CT with 18F-DOPA as a useful diagnostic tool in management of patients with movement disorders, since in around one third of patients there is a change of diagnosis based on imaging results. Future studies should be focused on developing quantification Methods in order to improve diagnostic accuracy of this imaging methodology.

### P627

### Support Vector Machine classifier (SVM) in investigating the ability of two Methods of semiquantitative analysis of $^{123}$I-FP-CIT brain SPECT to correctly diagnose Parkinson's disease

**B. Palumbo**[1], S. Nuvoli[2], F. Pompili[3], M. L. Fravolini[3], I. Sabalich[1], N. Tambasco[4], A. Spanu[2], G. Madeddu[2]; [1]University of Perugia- Section of Nuclear Medicine, Perugia, ITALY, [2]University of Sassari- Unit of Nuclear Medicine, Sassari, ITALY, [3]University of Perugia- Dept. of Electronic Engineering, Perugia, ITALY, [4]University of Perugia- Dept. of Neurosciences, Perugia, ITALY.

**Aim:** The different performance of two Methods of semiquantitative analysis of $^{123}$I-FP-CIT brain SPECT data, Basal Ganglia V2 software (BasGan) and Neurotrans3D (Segami Corp.), was compared to obtain differential diagnosis between Parkinson's disease (PD) and normal subjects. The features extracted from the two Methods were fed into a Support Vector Machine classifier (SVM), a powerful supervised classification algorithm based on ground-truth training data. **Materials and Methods:** $^{123}$I-FP-CIT brain SPECT with semiquantitative analysis (according to EANM guidelines) with the 2 mentioned Methods was performed in 62 patients with mild symptoms (bradykinesia-rigidity) to confirm or exclude PD, resulted 35 PD and 27 normal subjects. A clinical follow up of at least six months confirmed final diagnosis. Each patient was described by 4 descriptors (caudate-nucleus left/right - CL, CR- putamen left/right - PL, PR -) and a class label: '1' for PD and '2' for normal subjects. For each semiquantitative method a nonlinear SVM with Radial Basis Function kernel was trained to predict the diagnostic categories. A "leave-one-out" classification protocol was performed to assess the method accuracy and for each round a 10-fold cross-validation was performed on the training set for SVM parameters tuning. The same protocol was used in two further subsequent classification experiments on specific subsets of the initial features to assess their prediction capabilities: the first one using only caudate-nucleus left/right, the second one using only putamen left/right. **Results:** Both Methods were able to correctly classify labels in the experiment using all the 4 descriptors; BasGan and Neurotrans3D showed respectively an accuracy of 96.8% and 93.6%. When using a subset of descriptors, a high accuracy value (respectively 95.2% for BasGan and 93.6% Neurotrans3D) was reached by using only putamen left/right, while a significant loss in accuracy (74.5% and 76% respectively for BasGan and Neurotrans3D) resulted by using only caudate-nucleus left/right. Therefore putamen descriptors alone were able to correctly discriminate patients and controls. **Conclusion:** Both BasGan and Neurotrans3D were similarly accurate to identify PD patients. Among the different features used to classify patients, putamen (either left or right) resulted as the most discriminative descriptor for mild disease in both semiquantitative Methods.

## P628

### 123I-Ioflupane in Late Onset Postanoxic Dystonias. Preliminary Results.

**C. CALVO MORON**, M. BORBON ARCE, J. GARCIA MORENO, P. DE LA RIVA PEREZ, T. CAMBIL MOLINA, J. CASTRO MONTAÑO; HOSPITAL VIRGEN MACARENA, SEVILLA, SPAIN.

Dystonia is defined as an abnormal movement, produced by an involuntary muscle contraction that can lead to abnormal sustained postures and / or abnormal torsional movements. The late onset dystonias are a rare consequence of diffuse brain injury after perinatal anoxia. The time period between the hypoxic insult and onset of the symptoms is variable. The anatomical location of the lesion is variable, ranging from diffuse brain injury to the involvement of the caudate and lentiform nucleus, thalamus and internal capsule, however usually morphological tests (CT and MRI) are normal. AIM:123I-Ioflupane utility in assessing the involvement of the basal ganglia in patients with late-onset dystonias secondary to perinatal anoxia. MATERIALS AND METHODS: We present five cases of male patients with a mean age of 42 years, diagnosed with late-onset dystonia, all had history of perinatal anoxia and a pathological electrotmyography study. The average period from brain damage to the appearance of symptoms was10 years. All patients underwent through a brain SPECT, 4 hours after injection of 185 MBq of 123I-Ioflupane, 128 matrix, 128 images, 30 seconds per image. RESULTS: In the visual analysis of the images we found severe bilateral involvement (2 patients), moderate unilateral (one patient), mild (1 patient), normal (1 patient). MRI showed no pathological findings in all cases. CONCLUSION: The late-onset postanoxic dystonia is uncommon but well known. The anatomic location that justify the symptoms can be a diffuse cerebral lesion. But a theory of involvement of the circuit connecting the basal ganglia and the thalamus has been postulated. In our cases the 123I-Ioflupane SPECT (DATSCAN) was the only diagnostic technique able to show the location and extension of the basal ganglia lesions. Despite the small number of patients and how infrequent this cases are We think this technique can be useful because most of the morphological studies in these patients appear to be normal and don't give information about the exact injury location. However, we need to increase the number of patients to confirm our data.

P33-2 - Tuesday, Oct. 22, 16:00 - 16:30, Poster Exhibition Area

## Oncology Basic Science: Preclinical Tumour Biology & Animal Imaging

## P629

### Bevacizumab enhances efficiency of radiotherapy in a lung adenocarcinoma rodent model: an angiogenesis αvβ3 imaging study

**S. Becker**, A. C. Bouyeure-Petit, P. Bohn, R. Modzelewski, D. Gensanne, M. Chastan, J. Picquenot, P. Vera; Centre Henri Becquerel, Rouen, FRANCE.

**Background** : Numerous studies show the central role of the tumour microenvironment and more particularly the angiogenesis in the response to anticancer treatment such as radiotherapy. The current study was conducted to evaluate whether αvβ3 imaging could provide information to determine the optimal combination schedule of bevacizumab and radiotherapy on a lung adenocarcinoma model. **Materials and Methods**: Subcutaneously implanted human lung adenocarcinoma cells in nude mice served as tumour model. The tumours volume and angiogenesis changes induced after bevacizumab and radiation treatment were evaluated using [99mTc]HYNIC-RGD on a microSPECT/CT device. Firstly, we determined the optimal dose regimen for bevacizumab and radiotherapy alone compared to controls. Secondly the combined effects of bevacizumab and radiation were evaluated according to the combination timing (radiation 1, 24, 48h after bevacizumab) and compared to controls. Tumour volume and RGD uptake were determined in vivo by SPECT/CT at days 0, 2, 5 and 9 after treatment and expressed as % of variation compared to day 0. Ex vivo tumour activity was measured and expressed as % of the injected activity by gram of tissue (% IA/g). Results were correlated to histology percentage tumour necrosis. **Results** : The optimal dose regimens is 20 mg/kg for bevacizumab and 12.5 Grays for radiotherapy with a significant decrease of tumoral uptake and volume at day 9 compared to controls (+8%, +6%, +31% volume respectively and +10%, -40%, +134% uptake respectively). Those results were confirmed ex vivo (0.40, 0.22 and 2.83 %IA/g respectively). When bevacizumab treatment was combined with 12.5 Grays of radiation, the best combination appears to be the administration of bevacizumab 1 hour prior radiation with better result than single treatments (-21% volume and -43% uptake). Bevacizumab administration 24 h or 48 h prior radiation leads to a weaker tumour response but slightly better than single agent (+4%, -6% volume and +5%, -4% uptake respectively). Moreover there is a strong correlation between percentage necrosis and RGD uptake (r=-0.96), slightly higher than CT correlation and necrosis (r=-0.95). **Conclusion :** These data suggest an optimal combination of bevacizumab and radiation consisting in chemotherapy administration 1 hour prior 12.5 Gray radiation therapy. αvβ3 imaging is strongly correlated to tumour necrosis and would be accurate to assess tumour response after combined therapy.

## P630

### Pioglitazone, a peroxisome proliferator-activated receptor γ (PPARγ) agonist, impairs the growth and induces differentiation and/or apoptosis in human leiomyosarcoma cells

**Y. Zhao**[1], J. Culman[2], I. Cascorbi[2], M. Marx[1], M. Zuhayra[1], U. Lützen[1]; [1]Department of Nuclear Medicine, Molecular Image, Diagnostics and Therapy, University Hospital of Schleswig-Holstein, Campus Kiel, Kiel, GERMANY, [2]Institute of Experimental and Clinical Pharmacology,University Hospital of Schleswig-Holstein, Campus Kiel, Kiel, GERMANY.

Aim: The human uterine leiomyosarcoma is one of the most malignant tumours and has poorly prognosis. The role of the peroxisome proliferator-activated receptor γ (PPARγ) in the tumour biology has been intensively studied. Pioglitazone, a PPARγ agonist, is currently used in the treatment of diabetes type 2. The present study, conducted in a human leiomyosarcoma cell line, SK-UT-1 cells, and employing pioglitazone and the natural PPARγ agonist, 15-deoxy-Δ12,14-prostaglandin J2 (15-PGJ2), clarifies the role of the PPARγ in proliferation, differentiation and apoptosis of SK-UT-1 cells. Methods: SK-UT-1 cells were treated with pioglitazon (10 and 25 μM) or 15-PGJ2 (0.5, 1 and 2 μM) in the presence or absence of the selective PPARγ antagonist, GW9662, (1 μM). The cellular toxicity of the PPARγ agonists was assessed by lactate dehydrogenase (LDH) release in normal primary human smooth muscle cells (HutSMC). The following parameters were investigated in SK-UT-1 cells after the treatments: differentiation (expression of the smooth muscle differentiation markers, SM22α and calponin); apoptosis (expression of the members of the Bcl-2 protein family and the cleaved caspase-3); cellular death (release of LDH); cellular glucose metabolism (uptake of 18F-FDG). Time- and dose - dependent uptake of 99mTc-MIBI was determined to evaluate the mitochondrial activity and P-glycoprotein (P-gp) function. The induction of the multiple-drug-resistance protein after treatment of tumour cells with pioglitazon was also investigated. Results: 1) Pioglitazone and 15-PGJ2 at the lower dose did not display any toxic effects in HutSMC. 2) Pioglitazone and 15-PGJ2 significantly reduced the numbers of proliferating as well as quiescent SK-UT-1 cells. 3) Pioglitazone increased the PPARγ and calponin expression but did not change the expression of SM22α. 4) In SK-UT-1 cells, pioglitazon, but not 15-PGJ2, dose- and time dependently induced cleaved caspase-3 and cell death, partially via mitochondrial pathway. Pioglitazone increased the 18F-FDG uptake at 24 h but decreased it 48 h after stimulation. 5) Exposure of SK-UT-1 cells to pioglitazon time- and dose-dependently increased 99mTc-MIBI uptake. Conclusion: Our results demonstrate that pioglitazone promotes differentiation, inhibits growth and induces apoptosis in leiomyosarcoma cells but not in HutSMC. Pioglitazone can thus prevent the leiomyosarcoma cells re-entering the cell cycle. Patients suffering from leiomyosarcoma and receiving chemotherapy may benefit from the additional treatment with pioglitazone in terms of a better response and longer progression-free survival.

## P631

### In vivo PET imaging using polo-box domain targeted Peptide for diagnosis of tumor

S.-M. Kim,1 Min, K. Chae, 1 M.S. Yim, E.-K. Ryu,* C. Lee*; Division of Magnetic Resonance Research, Korea Basic Science Institute, 804-1 Ochang, Chungbuk 363-883, Republic of Korea

Polo-like kinase 1 (Plk1) is a regulator of cell cycle progression during mitosis; it is overexpressed in many different tumors and has been implicated as a potential antimitotic target. Plks are characterized by the presence of a highly conserved C-terminal polo-box domain (PBD) that is involved in regulating kinase activity. The phosphopeptide Pro-Leu-His-Ser-p-Thr (PLHSpT) is reportedly a potent and selective inhibitor of the PBD of human plk1 that acts by inducing mitotic arrest and apoptotic cell death in cancer cells with high binding affinity ($K_d$ ~ 0.45 μM). In this study, we synthesized cRGDyK-S-S-PLHSpT to exploit the drug delivery and molecular imaging using PET. To determine of inhibition of plk-1 kinase and apoptotic effect of cRGDyK-S-S-PLHSpT, we performed polo-like kinase 1 assay, FACs, western blotting, RT-PCR, and anticancer therapy using the mice bearing tumor xenografts. $^{68}$Ga-NOTA-cRGDyK-S-S-CPLHSpT (3.7 MBq) was injected into the tail veins of the mice and PET scanning was performed for 20 min at 30, 60, and 120 min post-injection. For studies of the biodistribution, the mice bearing the tumor xenografts were injected with the radioligand (3.7 MBq) in 0.2 mL of saline via a tail vein. The mice were then sacrificed at 30, 60, and 120 min post-injection. Samples of the organs (blood, bone, heart, lung, liver, kidney, spleen, tumor, and brain) were then collected, weighed, and their radioactivity was determined with a γ counter. The cRGDyK-S-S-PLHSpT was blocked dramatically proliferation and survive of tumor in vitro and in vivo. Cell proliferation was inhibited by cRGDyK-S-S-PLHSpT due to the induction of apoptosis. The anticancer effects in vivo, tumor

growth was significantly reduced compared with untreated and PLHSpT-treated mice. Tumor uptake of radioligand was high in both the PET images and in the biodistribution study at 60 min postinjection with 1.45±0.1%ID/g and 3.40±1.10%ID/g, respectively. The biodistribution of the radioligand was correlated with the PET analysis results. Our results demonstrated that the new peptide, cRGDyK-S-S-PLHSpT, is promising not only as an anticancer agent, but also as a radioligand for tumor diagnosis. We expect that our contribution will provide new insights into the design of novel plk1 peptide inhibitors and have significant implications for anticancer therapy and tumor diagnosis.

## P632

### Radiolabeled polyethyleneiminomethyl phosphonic acid as a molecule with potential for diagnosis and therapy. Comparative study on models of bladder cancer and osteossarcoma

**S. Ferreira**[1], A. M. Abrantes[2], A. F. Brito[2], M. Laranjo[2], A. C. Gonçalves[3], A. B. Sarmento-Ribeiro[3], L. Metello[4], J. Zeevart[5], W. Louw[5], I. Dormehl[6], M. F. Botelho[2]; [1]Biophysics Unit, IBILI, Faculty of Medicine, University of Coimbra, Coimbra; School of Sciences, University of Minho, Braga; Nuclear Medicine Course, High Institute of Allied Health Technologies of Porto's Polytechnic Institute, Porto, PORTUGAL, [2]Biophysics Unit, IBILI, CIMAGO, Faculty of Medicine, University of Coimbra, Coimbra, PORTUGAL, [3]Applied Molecular Biology and Hematology Group, CIMAGO, Faculty of Medicine, University of Coimbra, Coimbra, PORTUGAL, [4]Nuclear Medicine Course, High Institute of Allied Health Technologies of Porto's Polytechnic Institute, Porto, PORTUGAL, [5]Radiochemistry Department, NECSA, Pretoria, SOUTH AFRICA, [6]Department of Internal Medicine, University of Pretoria, Pretoria, SOUTH AFRICA.

Introduction: The polymer PEI-MP (polyethyleneiminomethyl phosphonic acid) that might be labeled with 99mTc and 188Re, have a strong potential for diagnosis and metabolic radiotherapy, respectively. The aim of this study was to evaluate the efficacy of 99mTc-PEI-MP for diagnosis and 188Re-PEI-MP as therapeutic agent, in a comparative study using in vitro and in vivo models of bladder cancer and osteossarcoma. Material and Methods: In vitro studies were performed using the cell lines of bladder cancer (CRL-1472) and of osteossarcoma (MNNG-HOS). Cytotoxicity of PEI-MP was investigated using the MTT test and flow cytometry. Radiochemical purity of 188Re-PEI-MP and 99mTc-PEI-MP was achieved using ascending microchromatography. Celular uptake studies were performed using the complexes 188Re-PEI-MP, 99mTc-PEI-MP, Na188ReO4 and Na99mTcO4. Cell samples were collected during four hours, centrifuged to separate supernatant and pellet. Subsequently, the radioactivity of each portion was counted to determine percentage of uptake. The in vivo studies were performed using twelve groups of Balb/c nu/nu mice: four normal groups injected with Na188ReO4, 188Re-PEI-MP, Na99mTcO4 and 99mTc-PEI-MP, four with bladder carcinoma xenotransplants and four with osteosarcoma xenotransplants injected with the same complexes. After injection of the radiopharmaceuticals, were acquired dynamic and static images for 2 and 4 hours. For biodistribution proposes, mice were euthanized 2 and 4 hours after injection and organ samples where weighted and counted in a well-counter to obtain percentage injected activity per gram of organ (%ID/g). Results: The MTT assay and flow cytometry tests showed that PEI-MP is not cytotoxic. The radiochemical purity of 188Re-PEI-MP and 99mTc-PEI-MP was higher than 85%. The uptake studies demonstrated that the uptake was higher for 188Re-PEI-MP and 99mTc-PEI-MP in relation to their controls, and higher for 188Re-PEI-MP e relation to 99mTc-PEI-MP. Biodistribution results, with Na188ReO4 and Na99mTcO4, showed a higher uptake by the thyroid, bladder and stomach, following a normal biodistribution. The biodistribution with 188Re-PEI-MP and 99mTc-PEI-MP showed that the excretion of these complexes occurs primarily through the renal system, with a small fraction being eliminated by the hepatobiliary system. Tumor/muscle ratio for 188Re-PEI-MP was >1 for the xenotransplants of osteosarcoma and >1.5 to xenotransplants of bladder cancer. Conclusions: Considering the results, 188Re-PEI-MP seems to be promising in the treatment of both types of cancer, but with a greater potential for bladder cancer. 99mTc-PEI-MP seems to be optimal for diagnosis of both types of cancer.

## P633

### Boron concentration in experimental tumor measured by means of F-18 FBPA and PET/CT

**K. Hanaoka**[1], T. Watabe[1], S. Naka[1], Y. Kanai[2], H. Ikeda[1], H. Watabe[2], H. Kato[1], E. Shimosegawa[1], J. Hatazawa[1]; [1]Department of Nuclear Medicine and Tracer Kinetics, Osaka University, Suita, JAPAN, [2]Department of Molecular Imaging in Medicine, Osaka University, Suita, JAPAN.

Objectives : In the boron neutron capture therapy (BNCT) for cancer treatment, boron-10 (10B) concentration in tumor and normal tissue is critical. Borono-phenylalanine (BPA) is utilized to deliver 10B to tumors. In order to predict relative 10B concentration in tumor, 4-borono-2-18F-fluoro-phenylalanine (FBPA) PET has been employed (Imahori, et al., J Nucl Med, 1998). We aimed to quantify absolute 10B concentration in normal organs and tumor of rats by PET/CT. Methods : The glioma cells (1.9×10^7) were injected in the back of 4 male F344 rats. FBPA solution (30.5±0.7MBq) was injected via the tail vein. On the 20 days after tumor implantation, whole body scan using PET/CT (Inveon, SIEMENS) was performed at 1 hour after injection of FBPA. Accumulation of FBPA as percentage of injected doze per gram (%ID/g) was estimated in the brain, lung, heart, liver, pancreas, kidney, small intestine, and tumor on PET images by referring CT images. After PET/CT scanning, 10B BPA-fr (40mg) were injected intravenously. Rats were dissected at 1 hour after 10B BPA-fr injection. Absolute 10B concentration in autopsied tissue and blood were measured by inductively coupled plasma optical emission spectrometry (ICP-OES). Results : The estimated 10B concentration using FBPA PET/CT in the brain, lung, heart, liver, pancreas, kidney, small intestines, and tumor was 0.37±0.06, 0.40±0.06, 0.59±0.14, 0.76±0.13, 2.63±0.34, 2.62±0.54, 0.48±0.07, and 1.52±0.33 %ID/g, respectively. In almost all parts, the measured value by PET/CT and ICP-OES show the similar values. On the other hand, in the lung and small intestine, the concentration using PET/CT were underestimated more than 50% ($p<0.01$). In the kidney, the concentration was overestimated more than 40% ($p<0.01$). 10B concentration in the blood was 0.44±0.07 %ID/g. Conclusions: We demonstrated quantification of boron concentration in tumor and normal organs of rats by FBPA PET/CT. This non-invasive in vivo tool in monitoring the drug distribution before BNCT method can be extended to FBPA PET in candidate patients of BNCT.

## P634

### Evaluation of the Effect of MicroRNA-148a on Hepatocellular Carcinoma Proliferation and Metastasis by FDG Small-Animal PET

L. Kang[1], X. Xu[2], **R. Wang**[1], Z. Fan[2], P. Yan[1], C. Zhang[1], Q. Ye[2]; [1]Department of Nuclear Medicine,Peking University First Hospital, Beijing, CHINA, [2]Department of Medical Molecular Biology, Beijing Institute of Biotechnology, Beijing, CHINA.

**Objective:** MicroRNA-148a (miR-148a) has been found down-regulated in cancerous specimens, despite lack of convenient and noninvasive Methods to evaluate *in vivo*. Small-animal positron emission tomography (PET) can provide interior molecular information of tumor cells noninvasively. The objective of this study is to investigate the value of 2-deoxy-2-[$^{18}$F] fluoro-D-glucose ($^{18}$FDG) PET in assessing the role of miR-148a in hepatocellular carcinoma (HCC) xenograft and metastasis models. **Methods:** After the stably overexpressed miR-148a HCC cell lines (HepG2 and MHCC97H) were constructed by lentiviral vector transfection, *in vitro* studies were performed evaluating the ability of miR-148a in FDG uptake, tumor proliferation and metastasis by colony formation and Matrigel invasion assay. Moreover, *in vivo* small-animal PET and biodistribution studies were performed in HepG2 xenografts or MHCC97H metastasis models. Besides, the expression of markers in insulin-like growth factor-1 receptor (IGF-1R)/ phosphatidyl- inositol-3-kinase (PI3K)/AKT pathways and glucose metabolism in HCC cell lines and tumor xenografts were evaluated by Western blot assay. **Results:** The proliferated and invaded abilities were inhibited in miR-148 overexpressed HCC cells *in vitro*, as well as the FDG cellular uptake. The inhibited FDG uptake by miR-148a in HCC cells was correlated with the suppression of IGF-1R/PI3K/AKT pathway and glucose transporter-1 (GLUT1) protein. For HepG2 tumor xenografts, small-animal PET clearly showed relatively low FDG accumulation in the miR-148a group, which was verified by the suppressed FDG uptake and IGF-1R/PI3K/AKT pathway of ablated tumors. Quantitative analysis showed that the tumor-to-muscle ratios of maximum counts decreased significantly in the miR-148a overexpressed tumors, especially in the PET delayed images. For MHCC97H metastasis model, the FDG PET images of living mice and the ablated organs discovered less metastatic nodules in livers and lungs in the miR-148a group, which were consistent with anatomy. **Conclusion:** $^{18}$FDG small-animal PET is useful for evaluating the negative role of miR-148a in HCC living models. MiR-148a may suppress the FDG uptake in HCC via the inhibition of IGF-1R/PI3K/AKT pathway in glucose metabolism. **[Key Words]** miR-148a; $^{18}$FDG PET; HCC; IGF-1R; Glucose metabolism

## P635

### Effect of starvation alone or in combination with chemotherapy on glucose consumption in cancer tissue. An " in vivo" microPET study.

**M. MASSOLLO**[1,2], G. Bottoni[1,2], C. Marini[3], L. Raffaghello[4], C. Massara[1], G. Bianchi[4], L. Emionite[5], R. Martella[4], S. Capitanio[1,2], S. Morbelli[1], R. Gamba[1], M. Cilli[5], M. Sanguineti[5], B. Dib[1,2], G. Sambuceti[1,2]; [1]IRCCS San Martino IST, Nuclear Medicine Unit, Genoa, ITALY, [2]University of Genoa, Genoa, ITALY, [3]CNR Institute of Bioimages and Molecular Physiology, Milan, Section of Genoa, ITALY, [4]Laboratory of Oncology, G. Gaslini Institute, Genoa, Genoa, ITALY, [5]Animal facility, IRCCS AOU San Martino – IST, Genoa, Genoa, ITALY.

**AIM**. Chemotherapy (CT) can extend survival in patients diagnosed with a wide range of tumors. However, the CT dose intensity and its efficacy can be compromised by several side effects. Thus, reduction of undesired toxicity by

selective protection of normal cells represents a promising strategy to enhance cancer treatment. Previous studies demonstrated that short term starvation (STS) not only protects normal cells but also sensitized tumor cells to chemotherapeutic drugs. The aim of our translational research study was to verify whether STS, in combination with CT, can modify cancer metabolism and whether this functional effect can be detected by dynamic micro-PET imaging in vivo. **MATERIALS AND METHODS.** A total of 500.000 colonic cancer cells (CT-26) were inoculated subcutaneously in the dorsal hip of syngeneic 6 weeks-old female BALB/c mice one week before imaging. We analyzed 25 mice divided into four groups: untreated (n=7) with tumor and no treatment, STS mice (n=6) that were submitted to 48-hour STS (absence of food and free access to water) before imaging, CT (n=6) treated with oxaliplatin (OXP 10 mg/Kg intraperitoneally, one somministration two days before imaging), CT-STS mice (n=6) submitted to both CT and STS. In vivo imaging was performed according to a protocol validated in our lab. To this purpose, a bolus of 3-6 MBq of 18F-fluorodeoxyglucose was injected through a tail vein during a list mode acquisition lasting one hour using a dedicated microPET system (Albira, Carestream Inc.). After framing rate optimization, tumor glucose consumption was measured using Patlak graphical approach and normalizing the slope of regression line for serum glucose level. **RESULTS AND CONCLUSION**. STS significantly reduced tumor glucose consumption (6±3 vs 12±6 microMol X g-1 X min-1, in STS and untreated mice, respectively, p<0.05). CT alone did not produce any significant change (16.05±11.1 microMol X g-1 X min-1, ns vs untreated). By contrast, the combination of CT and STS caused a marked reduction in cancer glucose metabolism down to 1.9±1.4 microMol X g-1 X min-1 (p<0.05 vs all other conditions). In conclusion, for the development of novel treatments in oncology there is the need to improve the efficacy of traditional therapeutic approaches such as chemotherapy. In this respect, STS has been proposed as strategy to optimize the traditional protocols in cancer patients. Measurement of glucose consumption by dynamic micro-PET imaging can provide a comprehension of the effects exerted by these interventions in order to optimize their utilization in cancer therapy.

## P636

### Assessing cancer metabolic remodeling in animal models using PET imaging

**I. Raccagni**[1,2,3], D. Gaglio[2,3], S. Valtorta[1,2,3], S. Belloli[1,2,3], G. Di Grigoli[1,2,3], M. Vanoni[3,4], F. Mastroianni[2,3,4], S. Todde[1,2], L. Alberghina[3,4], R. M. Moresco[1,2,3]; [1]Tecnomed Foundation and Department of Health Sciences University of Milan-Bicocca; Nuclear Medicine Department, San Raffaele Scientific Institute, Milan, ITALY, [2]Institute of Molecular Bioimaging and Physiology, National Research Council, Segrate, ITALY, [3]SysBio, Centre of Systems Biology, Milan, ITALY, [4]Department of Biotechnology and Biosciences University of Milan-Bicocca, Milan, ITALY.

**Aim**: K-ras proteins have been found mutated in about 35% of human tumors and appear to be an important factor for tumorigenesis. Its expression correlates with metabolic alterations such as increased glycolysis and glutamine consumption. This ability of cancer cells to decouple glucose and glutamine uptake reprogramming their metabolism leads to a more efficient use of nutrients in order to support cell proliferation and represents an interesting target for cancer therapy. Aim of this study is to investigate the metabolic alterations occurring in k-ras transformed fibroblasts combining in vivo and in vitro studies. **Materials and Methods**: nu/nu mice were subcutaneously implanted with 2.5 x $10^5$ k-ras transformed murine NIH3T3 fibroblasts (oncogenic k-ras) or with 2.5 x $10^5$ murine fibroblasts with the dominant negative mutation on GEF protein that attenuates k-ras activation reverting to the wild type phenotype (reverted). Lesions size was constantly monitored with calliper and volumes calculated as (L x $l^2$)/2 $mm^3$. Animals performed [$^{18}$F]FDG- and [$^{18}$F]FLT-PET studies at several time points starting with a tumor dimension consistent with animal PET spatial resolution (approximately 2mm). Images were calibrated, corrected for isotope half-life and elaborated with PMOD software to calculate Standardized Uptake Value (SUVmax). Finally, animals were sacrificed and tumor collected for metabolomic analysis. **Results**: All animals injected with oncogenic k-ras fibroblasts develop in few days fast growing, aggressive and highly glycolytic tumors that appear homogeneous for both [$^{18}$F]FDG and [$^{18}$F]FLT SUV values. On the contrary, 40% of k-ras reverted animals develop heterogeneous tumors at later time. Among k-ras reverted animals, two distinct tumor phenotypes can be observed: small, slow growing and poor glycolitic tumors with low uptake of both tracers, and small, slow growing but highly glycolytic and proliferating tumors that present SUVmax values comparable to those of k-ras oncogenic tumors. A good correlation, even if not significant, between tumor volume and [$^{18}$F]FLT SUVmax has been observed for oncogenic k-ras animals. **Conclusions**: PET imaging is an accurate in vivo technique able to visualize and monitor tumor development in the k-Ras fibroblasts mouse model. K-Ras transformed fibroblasts give rise to aggressive and fast-growing tumors that represent a good model to study the efficacy of cell metabolism based therapy. Finally, K-Ras reverted tumors need further investigations to understand the interaction among tumor microenvironment, metabolic alterations and genetic component that may trigger tumor development.

## P637

### Micro-PET pilot study of 18F-FDG labeled T-lymphocytes distribution : a model to study T cell trafficking in intestinal graft versus host disease.

**M. MASSOLLO**[1,2], A. M. Orengo[1], L. Emionite[3], M. Cilli[3], R. Benelli[4], C. Vitale[5], S. Minghelli[6], M. Sanguineti[3], E. Monteverde[1,2], A. Bacigalupo[7], G. Sambuceti[1,2], C. Marini[8]; [1]IRCCS San Martino IST, Nuclear Medicine Unit, Genoa, ITALY, [2]University of Genoa, Genoa, ITALY, [3]Animal facility, IRCCS AOU San Martino – IST, Genoa, Genoa, ITALY, [4]IRCCS San Martino IST, Genoa, Genoa, ITALY, [5]DIMES, University of Genoa, Genoa, ITALY, [6]G. Gaslini Institute, Genoa, Genoa, ITALY, [7]IRCCS San Martino IST, Haematology Unit, Genoa, ITALY, [8]CNR Institute of Bioimages and Molecular Physiology, Milan, Section of Genoa, ITALY.

**Aim**. After allogeneic bone marrow (BM) transplantation, grafted T lymphocytes can recognize the recipient as foreign and attack host's tissues generating graft-versus-host-disease (GVHD). This syndrome is associated with lesions caused by T lymphocytes infiltration of the intestinal tract and is one of the major causes of morbidity and mortality following BM transplantation. This life threatening complication can be prevented using ex-vivo T-cell-depleted BM transplants. However, this procedure has several drawbacks : (a) it increases the risk of rejection , (b) it reduces the graft-versus-tumor effect increasing the risk of relapse and (c) it causes delayed immune recovery and infectious complications. To better understand the pathogenesis of gut GvHD one needs to study trafficking of T cells across endothelial barriers. The present study was designed to verify whether micro-PET visualization of 18F-FDG labeled T-lymphocytes could help to evaluate the distribution of xenogenic T cells. **Materials and Methods**. Human purified CD3+ T lymphocytes, after short-term in vitro activation with Phytohemoagglutinin and Interleukin-2, were labeled with 18F-FDG according to a modified procedure developed and validated in our laboratory. One million labeled T cells were injected in a tail vein of five severely immunodeficient NOG mice (Charles River, Italy). After four hours, lymphocyte distribution was evaluated by micro-PET imaging (Albira, Carestream Inc., US). The intestinal fraction of the injected dose was calculated on the basis of ten minutes static imaging. At the end of image acquisition animals were sacrificed, the whole intestine was removed and ileum and colon were separated at the ileo-caecal level. The gut segments of three mice were counted using a gamma-counter (Hewlett Packard, US), while immunohistochemical analysis with an anti-human CD3 antibody (Bio-optica, Italy) was performed on corresponding intestinal segments of two others. **Results and Conclusion**. Activated T-cells showed a high affinity for the gut as radioactivity content was similar in the abdomen and in the lungs , 4 hours after injection (20±5% vs 23±5% of the dose, respectively, p=ns). Ex-vivo counting revealed a marginal contamination from radioactivity accumulated within the intestinal content ranging 6-12% of the whole gut counts. Immunohistochemistry analysis confirmed a good relationship between intestine radioactivity and presence of T-lymphocytes infiltrating the aggregated lymphoid nodules. These data support the feasibility of using micro-PET to evaluate the trafficking and homing of activated T lymphocytes. This approach can quantify T-cell recruitment in the gut offering early correlates for innovative approaches aiming to reduce GVHD severity.

## P638

### Synthesis of 99mTc-anti-CD56 Monoclonal Antibody for Molecular Imaging of NK Cells: in Vitro and in Vivo Studies

**F. Galli**[1], A. Rapisarda[1], H. Stabile[2], G. Malviya[3], E. Bonanno[4], A. Gismondi[2], A. Santoni[2], R. Dierckx[3], A. Signore[1,3]; [1]Nuclear Medicine Unit, Faculty of Medicine and Psychology, Department of Medical-Surgical Sciences and Translational Medicine, "Sapienza" University of Rome, Rome, ITALY, [2]Department of Molecular Medicine, "Sapienza" University of Rome, Rome, ITALY, [3]Department of Nuclear Medicine and Molecular Imaging, University Medical Center Groningen, University of Groningen, Groningen, NETHERLANDS, [4]Department of Biopathology and Image Diagnostics, Tor Vergata University of Rome, Rome, ITALY.

**Introduction**: Natural killer (NK) cells are important effectors of the innate immune system directed against cancer cells. In vivo imaging of their trafficking may be relevant to follow-up the efficacy of new therapeutic approaches aiming at increasing NK cell infiltration in tumors. Several attempts to image NK cells have been done in the past years using a direct in vitro cell-labeling approach which has several limitations such as laborious cell manipulation and high radiation dose to the cells. **Aim**: to develop a radiopharmaceutical suitable for the imaging of NK cell trafficking in vivo. For this purpose, an anti-CD56 mAb was radiolabelled with 99mTechnetium and tested in vitro and in animal models. **Material and Methods**: The anti-human CD56 mAb was radiolabelled with 99mTc through a two-step method using the hetero-bi-functional linker succinimidyl-6-hydrazinonicotinate hydrochloride (SHNH/S-HYNIC). Titrations of the reagents were performed to optimize the labelling protocol and in vitro quality controls were performed to evaluate its labelling efficiency and retained biological activity (including SDS, stability, IRF, binding assay). In vivo biodistribution was studied in 12 nude mice sacrificed at different time points (1, 3, 6, 24h). Major organs were collected,

weighted and counted for radioactivity. In-vivo studies included a cell targeting experiment in athymic nude mice subcutaneously injected in the right thigh with increasing number of human NK cells (CD56+) or CD56- cells as control. In vivo trafficking of NK cells was evaluated injecting i.v. increasing amounts of human NK cells in nude mice bearing a ARO tumor xenograft in the right thigh. 24h after injection of cells, the 99mTc-anti-CD56 was injected i.v. and images acquired at 1, 3, 6 and 24 h. At each time point, 3 mice were also sacrificed for organ counting and histology. **Results**: The antibody was labelled with high efficiency (90%) and retained in vitro binding activity. Biodistribution studies showed high circulating activity and high uptake in the liver and kidneys. Cell targeting experiment demonstrated a high uptake of radiolabelled mAb to NK cells with highest target-to-background ratio at 6h. The radiopharmaceutical was also able to follow in vivo NK cells infiltrating tumor xenografts. **Conclusions**: Radiolabelled anti-CD56 mAb is able to bind to CD56 positive NK cells and could be a promising tool for the imaging human NK cell trafficking.

P35-2 - Tuesday, Oct. 22, 16:00 - 16:30, Poster Exhibition Area

## Oncology Clinical Science: Brain

### P639

### The role of $^{11}$C-methionine positron emission tomography in prediction of meningioma recurrence and progression

**Y. Terakawa**, N. Tsuyuguchi, J. Abe, H. Ikeda, T. Goto, K. Ohata; Department of Neurosurgery, Osaka City University Graduate School of Medicine, Osaka, JAPAN.

*Aim* Meningioma is one of the most common primary brain tumours in adults, accounting for 34.4% of all brain tumours. It is mostly a benign tumour, but the recurrence rate of meningioma after surgical treatment and the progression rate during observation are not negligible. Currently, a definitive method to predict recurrence or progression of this disease has not yet been established. In this study, we used $^{11}$C-methionine (MET) positron emission tomography (PET) in patients with meningioma to determine whether MET PET can be used to predict tumour recurrence or progression. *Materials and Methods* A total of 37 patients newly diagnosed as intracranial meningioma were examined using MET PET before treatment. They were 14 men and 23 women, and the mean age of the patients was 54.5 ± 12.9 years. The lesion-to-normal tissue (L/N) ratios were generated by dividing the mean MET uptake of the lesion by that of the contralateral frontal-lobe gray matter. Patient characteristics, location and histopathology of tumor, extent of resection, Ki-67 labeling indices, and L/N ratios were analyzed to determine the role of MET PET in examining meningiomas, especially with respect to tumor recurrence and progression. *Results* Among 37patients enrolled in this study, 33 patients were surgically treated and four patients were followed without surgery. Recurrence occurred in six of 33 surgically treated patients and progression was seen in two of four observed patients during a mean follow-up period of 80 months. Multivariate analysis found high L/N ratios, small extent of resection, and high WHO grade to be significant risk factors for recurrence and progression. Receiver operating characteristic curve analysis indicated that an L/N ratio of greater than 3.18 provided the best sensitivity and specificity for recurrence and progression, 63% and 79%, respectively. *Conclusion* Although the number of patients in this study is still limited, our preliminary data suggest that MET PET may provide quantitative values in prediction of meningioma recurrence and progression, even though they are not absolute indicators.

### P640

### Comparison of FET- and F-DOPA-PET/CT in Primary and Recurrent Glioblastoma Patients

**C. Bluemel**[1], T. Linsenmann[1], C. Lapa[1], J. Czernin[2], A. Buck[1], R. Ernestus[1], M. Löhr[1], K. Herrmann[1]; [1]University Hospital, Wuerzburg, GERMANY, [2]University of California, Los Angeles, CA, UNITED STATES.

Aim: Amino acid tracers such as F-DOPA, FET and C-MET have been reported to be highly sensitive for detection of primary and recurrent glioblastoma (GBM). FET is mainly used in Europe, whereas due to regulatory issues F-DOPA is the tracer of choice in the US. Aim of this study is to compare FET- and F-DOPA-PET/CT in GBM patients (pts) to find out potential superiority of one tracer. Material/Methods: A prospective ongoing trial was designed for a total of 60 pts with primary or recurrent GBM. Up to date, 10 pts (2 primary GBM, 8 recurrent GBM) have been included and underwent FET- and F-DOPA-PET/CT. PET/CT scans were performed according to standard protocols. Image analysis comprised visual comparability, semi-quantitative evaluation of the tumor (SUVmax, SUVpeak, 50% isocontour), the background (SUVmax and SUVpeak), as well as calculation of tumor-to-background ratios (TBR). Background was defined as a 2.5 diameter ROI on the contralateral side. Results: No difference in tumor uptake pattern was revealed in visual analysis, but physiological F-DOPA uptake in the striatum makes tumor delineation in this area more challenging. Mean SUVmax and SUVpeak for FET were 4.3 and 3.3, and for F-DOPA 3.7 (p=0.058) and 2.9 (p=0.050), respectively. Corresponding mean background SUVmax and SUVpeak were 1.5 and 0.9 for FET, and for F-DOPA 1.3 (p=0.02) and 0.9 (p=0.30). TBR for mean SUVmax and SUVpeak were similar for FET and F-DOPA (SUVmax: 2.8. vs. 2.9, p=0.68; SUVpeak 3.6 and 3.4, p=0.57). Conclusions: Visual analysis revealed no difference in uptake pattern for FET and F-DOPA in pts with primary or recurrent GBM. After inclusion of 10/60 pts in this ongoing prospective trial semi-quantitative analysis revealed for FET higher tumor and background uptake values (SUVpeak and SUVmax) than for F-DOPA, not reaching statistical significance yet. However, TBR values were similar for both tracers supporting the impression that both tracers are equally feasible for imaging of primary and recurrent GBM pts.

P36-2 - Tuesday, Oct. 22, 16:00 - 16:30, Poster Exhibition Area

## Oncology Clinical Science: Head & Neck

### P641

### The Role of SPECT/CT in Detecting Parathyroid Pathology

O. Bessolova, **V. Vidioukov**, O. Perfileva, N. Vyrenkova; Russian Medical Academy of Postgraduate Education, Moscow, RUSSIAN FEDERATION.

Aim: To evaluate the role of SPECT/CT in detection and preoperative localization of parathyroid adenomas with 99mTc MIBI (dual-phase study) in patients with primary hyperparathyroidism. Materials and Methods: Our study included 57 patients (57 women with average age 44±6.1 years old) with laboratory features of hyperparathyroidism. After intravenous injection of 555 MBq 99mTc MIBI each patient received dual-phase planar images at 15 and 120 minutes and SPECT after second phase investigation. If we determined lesions of increased uptake on planar or SPECT images also fusion SPECT/CT investigation additional performed using GE Infinia Hawkeye 4. Results: 22 patients had lesions of increased uptake in typical parathyroid area on planar images. 9 cases of solitary foci were discovered additionally using SPECT. We had no case of ectopic parathyroid adenoma. SPECT/CT method used for 31 patients which had lesions on preceding study for installation localization of lesions. Out of these patients parathyroid adenoma was localised in 29 patients, 2 tumour were localized in thyroid gland. Conclusion: Our results demonstrated that SPECT/CT improves the sensitivity and localization ability parathyroid scintigraphy. SPECT/CT can locate parathyroid adenomas and differentiate between thyroid tissue and pathological parathyroid tissue.

### P642

### Incidental Focal 18F-FDG Uptake in the Pituitary Gland of Head and Neck Cancer Patients: Clinical Significance and MRI Findings

**P. Kao**[1,2], C. Huang[3], J. Weng[1,2]; [1]Department of Nuclear Medicine, Chung Shan Medical University Hospital, Taichung, TAIWAN, [2]School of Medicine, Chung Shan Medical University, Taichung, TAIWAN, [3]Molecular Imaging Laboratory, Chung Shan Medical University Hospital, Taichung, TAIWAN.

[Aim] The purpose of this study was to determine the incidence and clinical significance of incidental pituitary uptake on whole body FDG PET/CT scans for head and neck cancer patients. The pituitary FDG PET/CT findings were correlated with the MRI findings. [Materials and Methods] The FDG PET/CT images for head and neck cancer staging and treatment monitoring were retrospectively reviewed over a three-year period. The types of head and neck cancers include nasopharyngeal, oral, tongue, and hypopharyngeal cancers. The FDG PET/CT scan was acquired one hour after intravenous injection of 185 to 370 MBq of FDG. If the PET/CT scan revealed abnormal FDG uptake in the pituitary gland, the MRI, serum pituitary hormone levels, and follow-up PET scan were reviewed. The maximum standardized uptake value (SUVmax) of the pituitary gland was measured. [Results] 1,630 FDG PET/CT scans were retrospectively reviewed. Normal pituitary glands do not accumulate FDG and are not visualized by FDG-PET/CT scans. Thirty-three scans from 26 patients revealed visualization of pituitary gland FDG activity. The PET/CT images revealed repeated pituitary FDG uptake in five patients. The SUVmax of the pituitary activity was >5 in 4 scans, 5-3 in 22 scans and <3 in 7 scans. Only five FDG PET/CT scans reported abnormal pituitary FDG uptake in the original reports and three MRIs reported abnormal pituitary findings, including one pathologically proved pituitary adenoma. In two of eight patients (25%) who had serum hormone tests, one had an abnormal increased prolactin level and the other had an abnormal increased growth hormone level. [Discussion and Conclusion] In this study, 2.0% (33/1,630) of FDG PET/CT scans for head and neck cancer patients showed incidental pituitary uptake. The pituitary gland was usually included in both FDG PET/CT and MRI image fields of these head and neck cancer patients. However, pituitary gland abnormality was often overlooked during FDG PET/CT imaging interpretation because of the high normal cerebral cortex FDG activity. In addition, the TNM staging of head and neck cancer includes skull base invasion but does not specifically include the pituitary gland. The correlation between FDG PET/CTs and MRIs may facilitate accurate diagnosis of incidental pituitary

adenoma. In conclusion, the incidence of pituitary FDG uptake in head and neck cancer patients was low. When reading the FDG PET/CT for head and neck cancer staging, pituitary gland lesions should be identified with MRI for correlation.

## P643

### Role of F18 FDG PET CT in follow up of Head and Neck Cancers

**L. Pushpalatha Sudhakar**, S. Praveen, P. Amber, S. Sheethal Kumar, T. Prathap Reddy; KRISHNA INSTITUTE OF MEDICAL SCIENCES, HYDERABAD, INDIA.

Aim : The highest recurrence rate in Head and Neck cancers demands frequent follow up . The aim of our study is to evaluate the role of PET CT in the follow up of Head and Neck cancer patients Materials and Methods: A total PET CT scans of 35 patients who were on follow up after the definitive treatment for Head and Neck cancer from 2010 to 2012 were retrospectively evaluated. The local recurrence, regional and distant metastatic disease were assessed in each scan. Impact of PET CT scans on clinical management was assessed by means of Disease free status and therapeutic interventions following the scan. Results : A total of 35 patients were evaluated , male 29 and female 6. The mean duration of follow up after the initial treatment was six months. Of 35 patients , fifteen ( 43%) were negative on PET CT for loco regional or distant disease., out of which 86.6 % were disease free up to a minimum follow up of six months. Recurrent disease was seen in 20 patients, of which six ( 30%) were asymptomatic. Local recurrence alone was seen in 5 patients, loco regional disease in 2 and local recurrence with distant metastases in 11 patients. In asymptomatic group two patients had distant metastases and rest had local / loco regional recurrence. In symptomatic or clinically positive patients ( 14) distant metastases were seen in eight patients ( 57%). Conclusion : PET CT plays a vital role in the follow up of Head and Neck cancer patients to detect the recurrence . Our study showed high disease free rate in negative scan group (86.6%). PET CT helped in detecting recurrence in asymptomatic patients ( 30%) and diagnosed the distant metastases in 57% of symptomatic or clinically evident disease group resulted in initiation of appropriate clinical management at the earliest.

## P644

### Intraoperative freehand SPECT for localization and minimal invasive resection of hard to find sentinel lymph nodes in the neck area of early stage malignancies

**C. M. Hernández Heredia**, P. Paredes, A. Vilalta, C. Marti, F. Pons, S. Vidal-Sicart; Hospital Clinic, Barcelona, SPAIN.

Objectives Prove feasibility of freehand SPECT in hard to find sentinel lymph nodes (SLNs) in the neck area for early stage melanomas and squamous cell carcinomas Methods 3 patients with head/neck malignancies (2x melanoma, 1x tongue) scheduled for SLN biopsy underwent (dynamic and static) planar scintigraphy followed by low-dose SPECT/CT (Hawkeye, GE; 111 MBq peritumoral injection day before surgery). Due to possible difficult localization, also freehand SPECT images (declipseSPECT, SurgicEye) were acquired after SPECT/CT in order to confirm localization of SLNs and skin marking. On the day of surgery freehand SPECT was used to image SLNs before incision and to confirm complete removal before suture. Freehand SPECT images were used to define depth of SLNs, guide incision and navigate surgeon during access. Gamma probe of freehand SPECT system was used for additional acoustic guidance. Results Preoperatively, 3 SLNs were located in areas of difficult surgical access in planar scintigraphy, SPECT/CT and freehand SPECT (1x possible intramuscular node, 1x subclavicular node at apex of lung, 1x submental node very close to injection site). Intraoperatively freehand SPECT confirmed the localization of 1 intramuscular node inside the sternocleidomastoid muscle, 1 subclavicular node 2cm deep from skin at clavicular fossa close to lung apex and 1 little submental node directly next to injection site. Depth information and navigation gave confidence to surgeon to broach SLNs, which otherwise would not be resected. All nodes resulted to be radioactive as measured by gamma probe of freehand SPECT. Post-excision images showed complete resection of radioactivity in the wound. Conclusion Preliminary experience indicates that intraoperative imaging with freehand SPECT for lymphatic mapping enables more intuitive and faster detection and localization of SLNs than conventional gamma probe alone in hard to find SLNs in the neck area of early stage malignancies. Without major changes in surgical workflow, surgeons could find the target SLNs faster and gained confidence when broaching SLNs in difficult access areas. Moreover the possibility of controlling complete resection of radioactivity played as quality insurance mean. As preliminary experience more cases are required to make broader conclusions, but freehand SPECT seems to be a potential useful tool towards reducing the number of SLNs that are not retrieved with conventional means due to difficult access. Thus we see a potential to lower the false negative rate in complex anatomies.

## P645

### PET /CT for Detecting Second Primary Tumors in Head and Neck Area

**C. PANIAGUA CORREA**, M. BALSA BRETON, M. CASTILLEJOS RODRIGUEZ, M. GARCIA ALONSO, E. RODRIGUEZ PELAYO, A. MENDOZA PAULINI, M. FERNANDEZ RODRIGUEZ, F. PENIN GONZALEZ; HOSPITAL UNIVERSITARIO DE GETAFE, GETAFE, MADRID., SPAIN.

The frequency of multiple malignancies of the head and neck area is high and varies from 7-20%. The larynx is the most common location of the primary tumors. Lung and head-neck comprises the vast majority of second primary tumors (SPT). OBJECTIVE: To evaluate the role of PET/CT in detecting second primary tumors following head and neck cancer patients. MATERIAL AND METHODS: Retrospective review of 99 patients with a first primary head and neck cancer (HNC), between Mayo/09 and October/12, performing a total of 122 PET / CT studies. They were 77 men and 23 women, with a mean age of 59.5 years. RESULTS: Thirteen (13%) second primary tumors occurred in the original 99 patients. Synchronous tumors were detected in 3 patients (larynx and lung; lip, colon and lung; larynx and esophagus). In 10 patients studied for suspected recurrence, other tumor lesions were found (Metachronous T.): 8 patients with laryngeal cancer associated primary lung lesion in 5 cases, and colon, esophagus and lymphoma for the rest patients, respectively. A patient associated tongue cancer and primary lung lesion, and other had oral cavity cancer and pancreatic neuroendocrine tumor. Sixteen of the primary head and neck cancer had previous history of tumor disease, with lung and head- neck disease (laryngeal mainly). CONCLUSION: This study confirms the high rate of SPT in patients with initial HNC and the usefulness of our technique for detection of synchronous or metachronous tumors in HNC follow-up. The most common primary tumor was the larynx and, lung and head-neck had the highest incidence of second primary, as shown in most studies. Accurate diagnosis is critical for selection of the appropriate treatment strategy. Multiple tumor lesions also involves changing patient management (early diagnosis and prioritize the worst prognosis).

P37-2 - Tuesday, Oct. 22, 16:00 - 16:30, Poster Exhibition Area

# Oncology Clinical Science: Thyroid

## P646

### Parathyroid dual tracer, dual phase scintigaphy in thyroid nodular disease and solitary parathyroid adenoma: pearls, miscellaneous and pitfalls

**A. Koljevic Markovic**, Gordana Pupic, Radan Dzodic; National Cancer Research Center Serbia, Belgrade, SERBIA.

**Aim**: Evaluation of double tracer dual phase parathyroid scintigraphy in histopathology verified solitary parathyroid adenoma in concomitant thyroid nodular disease in relation to parathormone (PTH) levels. MM: The study group of 50 patients with histopathology verified parathyroid adenomas and elevated serum PTH (> 65 pg/ml) were included. Double tracer parathyroid scintigraphy was performed: 99m Tc-pertecnetate and 99mTc-MIBI dual- phase technique: 150 MBq 99m Tc; 500 MBq MIBI dynamic acquisition 35 min and delay images after 60 (120 min). All patients were surgically treated and histopathology revealed concomitant thyroid pathology: thyroid follicular adenoma 38 (76%) pts, thyroditis in 6 (12%) pts, and thyroid carcinoma in 6 (12%) pts. We correlated scintigraphy findings, to histology results and PTH levels. **Results**: In 43 (87%) patients solitary adenoma was localized predominantly behind thyroid (only 1 outside the thyroid border), hyperplasia in 6 (12%) patients and in 1 (2%) parathyroid carcinoma. Concomitant thyroid disease was in high percent presented as malignancy 7/50 pts (14%): as thyroid carcinoma in 6 (two MEN I) and 1 pts adenocarcinoma. A misscelanious case of parathyroid adenoma, follicular carcinoma and B cell lymphoma in neck was present. One patient had intrathyroid parathyroid adenoma and another patient rare case of metastatic adenocarcinoma in thyroid. PTH levels were: median 140 pg/ml and range 75, 8- 658 pm/ml. Cutoff value of positive scintigraphic finding was 102, 6 pg/ml and correlated to sensitivity 80%. The standard scan processing that includes analysis of subtraction image, delayed scans and additional positioning scans in 11 cases failed in localizing parathyroid adenoma adjunct to enlarged thyroid nodule: parathyroid volumes were median 796 range 120- 1630 $mm^3$ and PTH levels median 170,9 range 85- 244 pg/ml. Subtraction image was either negative or presented thyroid and/ or nodule as well as delayed scans. An additional retrospective ROI processing revealed in projection of solitary parathyroid adenoma late peak on time activity curves, comparing to thyroid tissue while thyroid nodules showed different patterns of prolonged accumulation of MIBI. **Conclusion**: In our study we had high diagnostic accuracy localize parathyroid adenoma in concomitant thyroid nodular disease. Increased PTH level is in excellent correlation with cut of value 102.6 pg/ml for positive scan findings of parathyroid adenoma. In our group high percent of thyroid malignancy and parathyroid adenoma was present.

## P647

### Pyramidal thyroid lobe carcinomas- a rare and atypical localization

**L. M. Vija**[1], T. Meas[2], I. Faugeron[2], M. Toubert[2]; [1]Paris Sud University, Le Kremlin-Bicetre, FRANCE, [2]St Louis Hospital Nuclear Medicine Department, Paris, FRANCE.

Aim: The pyramidal lobe is an anatomical variant of thyroid tissue, representing the inferior part of the thyroglossal duct and an accessory lobe of the thyroid gland identified in approximately 41-44% of people, more commonly in women. The purpose of the present monocentric study was to evaluate the clinico-pathological characteristics and short-term outcomes of thyroid carcinomas located in the pyramidal lobe. Material and Methods: From more than 1400 patients with total thyroidectomy and regular follow-up for differentiated thyroid cancer in St Louis' Nuclear Medicine Department since 1998, we identified 9 women, aged between 21 and 71 years (mean 50.44), all presenting with papillary thyroid carcinoma located in the pyramidal lobe. Results: Pyramidal tumor was identified as a unifocal tumor site in 6 patients, two of them discovered during ultrasonography follow-up of apparently benign thyroglossal cysts. Interestingly, while tumor size varied between 1 and 4.5 cm (mean 2.19 cm), extra thyroidal extension and bilateral node involvement were frequent (respectively 8/9 and 4/9). Tumor removal was associated with total thyroidectomy, and completed by radioiodine (RI) ablation. At that time, only 2 patients had undetectable serum thyroglobulin (Tg) concentration without Tg antibodies, while the 7 others had higher Tg level (mean: 14.07 ng/ml, ranging between 0.1 and 38 ng/ml). With a median seven-year follow-up, RI therapy was repeated in 4 cases (mean cumulative dose 5487 MBq), after surgery of lateral lymph node recurrences (n=3) and/or local tumor recurrence (n=2) invading thyroid, cricoid cartilages and/or prelaryngeal muscles. Progressive lung and mediastinal lymph node recurrence was noticed once, requiring tyrosine kinase inhibitor treatment. All patients, except this later, are at present in complete remission. Conclusion: Thyroid carcinomas located in the pyramidal lobe are exceptional (we registered a local prevalence of 0.6%), occult primary localizations, with very few cases reported. We describe 9 pyramidal lobe papillary carcinomas, with frequent extra thyroidal extension, lateral cervical lymph node extension and potential aggressiveness (invasion of the medial cervical structures or distant metastases). These findings indicate that total thyroidectomy with appropriate pyramidal lobe excision and LN dissection completed by RI treatment is important to prevent the presence of residual tissue and diminish the risks of disease recurrence.

## P648

### Differentiated thyroid cancer localized in the thyroid isthmus

**L. M. Vija**[1], T. Meas[2], I. Faugeron[2], M. Toubert[2]; [1]Paris Sud University, Le Kremlin-Bicetre, FRANCE, [2]St Louis Hospital Nuclear Medicine Department, Paris, FRANCE.

Aim: Few data have been reported on the particularities of thyroid carcinomas localized in the isthmus. The purpose of the present monocentric study was to evaluate the clinico-pathological characteristics and short-term outcomes of isthmic differentiated thyroid cancer (DTC) and to compare to local and referenced data from the literature related to tumors of the isthmus or other thyroid regions. Material and Methods: Total thyroidectomy and follow-up for DTC in St Louis' Nuclear Medicine Department were performed in more than 1000 patients between March 2004 and March 2013. After exclusion of lobar localizations extending towards the isthmus, we have identified 35 patients with DTC in the isthmus. Results: The frequency of DTC with isthmus localization in our cohort was 3.5% (35 of 1000 patients) with similar age and gender ratio (4:1 female/male ration, aged between 19-76 years) compared to data reported in the literature. The principal histological form was papillary (29/35 patients); other forms were: oncoytic (n=2), diffuse sclerosing variant (n=1) and follicular (n=4) thyroid carcinomas. The mean primary tumor size was 1.44 cm (tumor size ranging between 0.1-3.8 cm, median 1.2cm); extra thyroidal extension was found in 43% (15/35 patients) and multifocality in 48 % (17/35 patients). Central and/or lateral lymph node (LN) involvement was found respectively in 8 (23 %), and 9 patients (26 %). At the time of postoperative radioiodine (RI) ablation, 61% had a detectable serum thyroglobulin (Tg) concentration (mean level: 104.13 ng/ml) while anti Tg antibodies were present in 13/35 (37 %). During the 6 yrs of follow-up, 17% recurrences occurred: 4 in lateral cervical LN, one in bones and one local tumor recurrence. The mean cumulated RI activity was 5200 MBq. Long-term outcome was comparable to usual DTC; 29 patients (83%) are at present in complete remission. Conclusion: Although our study is limited by the small number of patients, characteristics of tumors located in the isthmus do not seem to differ from the usual presentation of DTC, except that bilateral LN extension was noticed in 9/35 (26%). In our series, multifocality (isthmus and other) was found in 17/35 (48%). A multicentric study would allow a better knowledge of this localization of DTC.

## P649

### 18F Ffluorodeoxyglucose-Positron Emission Tomography/Computed Tomography (PET) in patients with Differentiated Thyroid Cancer (DTC) and increased Thyroglobulin serum levels (Tg) with negative 131I Whole Body scan (WBS): comparison with CT findings

**S. Panareo**[1], I. Santi[1], R. Rossi[2], C. Cittanti[1], V. De Cristofaro[1], C. Peterle[1], E. degli Uberti[2], L. Feggi[1]; [1]University Hospital - Nuclear Medicine Unit, Ferrara, ITALY, [2]Section of Endocrinology, University of Ferrara, ITALY.

**AIM**: to evaluate the role of PET in patients with DTC already treated with therapeutic 131I after thyroidectomy presenting with increased Tg and negative WBS during follow up, comparing PET results with Tg and radiological findings (US, CT, MRI). **METHODS**: Twenty-five patients with DTC underwent PET because of a negative WBS and Tg >1.5 ng/mL. PET was performed after the administration of RhTSH as stimulation. PET data were compared with Tg and US, CT or MRI. **RESULTS:** PET was positive in 20 patients and negative in 5 patients. Out of the 20 PET positive patients, 12 showed focal FDG uptake in lymph nodes (overall 16 lymph nodes: 2 right II compartment, 3 left III compartment, 3 right III compartment, 4 left IV compartment, 1 supraclavicular, 3 supraclavicular), 4 in thyroid bed, 2 in bone and 2 in lung parenchyma. Negative PET patients showed lower Tg levels (1,4+/-0,21 ng/mL) than positive PET patients (5,2+/-1,94 ng/mL). Tg was significantly higher in patients with bone (4,02+/-1,31 ng/mL) and lung (5,12+/-1,27 ng/mL) PET positive lesions than in patients with PET positive lymph nodes (2,7+/-0,94 ng/mL). PET pathological findings in thyroid bed were confirmed by US in 3 cases (75%). PET positive lesions in lung and bone were all confirmed by CT (100%). Out of 16 lymph node detected by PET, 11 (68,75%) - 9 laterocervical and 2 supraclavicular - were confirmed by CT while 5 (31.25%) - 2 supraclavicular and 3 laterocervical - were not identified by either CT and MRI. **CONCLUSION**: PET is a powerful and useful tool for assessing patients with DTC. Particularly, it can provide additional information in patients with high Tg and negative WBS at follow-up detecting distant metastatic sites. Our data are consistent with literature and show a correlation between Tg trend and site of focal PET uptake: distant metastatic lesions (bone and lung) seem to be more likely to occur in patients with higher Tg. A positive PET scan could also represent a prognostic tool combined with Tg. Attenuation correction and morphological findings provided by CT in PET hybrid imaging increase the specificity of both PET standing alone and morphological imaging (US, CT, MRI). Moreover PET seems to be better than conventional imaging particularly in the detection of lymph node disease relapse. Our data need to be confirmed by studies with larger series.

## P650

### Thyroid Cancer: Ultrasonographic Appearance of Neck Metastases

**S. Kusacic Kuna**, G. Horvatic Herceg, I. Bracic, H. Tomic Brzac, Z. Bence Zigman; University Hospital Centre Zagreb, Zagreb, CROATIA.

AIM: Enlarged neck lymph nodes appear in many diseases and they are echographicaly presented with high accuracy. Benign lymph nodes seems to have typical sonomorphology as well as malignant. The aim of study was to evaluate echographic appearance of metastases in the neck of patients with thyroid cancer, and to determine the frequency of thyroid cancer neck metastases at the moment of the presentation of disease. METHODS: The study included 578 enlarged nodes in which ultrasound (US) guided fine needle aspiration biopsy (FNAB) was performed and their echographic appearance like size, shape, echogenicity (the presence of hilum, calcification, cystic portions) and position in the neck were noted. All citologically verified malignant nodes were confirmed histologically after surgical removal. RESULTS: 19.67 % patients had metastases at the time when disease presented. In majority of cases metastases were roundly shaped and of different echostructure with predomination of hypoechogenic nodes, without hilum. Nodal size alone has been shown to be unreliable criterion for diferentiation of benign from malignant diseases. Although there were statistical differences in size among metastatic and benign nodes in terms of maximum, minimum diameter and volume, among them, minimum diameter and shape of the nodes (longitudinal/transversal ratio) seems to be far more reliable in sugesting of malignancy. Great majority of metastases were roundly shaped with longitudinal/transversal ratio (L/T ratio) of less than 2, and of various echostructure. Cystic portions and calcifications are also suspitious on malignancy. In addition to morphological criteria it is necessary to consider the position of nodes when diagnosing them ultrasonically. Most metastatic nodes were situated in lower third of neck. Reactively enlarged nodes occure more frequently in upper part of neck. CONCLUSION: The morphologic criteria of size, shape, internal architecture and localization of nodes in the neck are helpful in selection of the correct node to aspirate with US-guided FNAB that is crucial for final diagnosis.

## P651

### Benign Tumours of the Parotid Gland may Mimic Metastatic Thyroid Carcinoma on 131I-NaI Whole Body Scintigraphy

**M. Pelletier-Galarneau**, L. S. Zuckier; University of Ottawa, Ottawa, ON, CANADA.

**Objective:** Post treatment whole body $^{131}$I-NaI scintigraphy following total thyroidectomy in patients with well-differentiated thyroid carcinoma (WDTC) allows evaluation of thyroid remnant and possibly detection of metastatic lesions that will impact both treatment and follow-up. Cellular iodide uptake is mediated by the sodium-iodide symporters (NIS). Different benign and malignant tumors express NIS and therefore accumulate radio-iodide, potentially resulting in false positive studies. **Case presentation:** A 72 year-old male underwent total thyroidectomy with left neck dissection for thyroid carcinoma. Pathological examination of the thyroid revealed a papillary thyroid carcinoma measuring 2.0 x 1.8 x 1.0 cm and containing 10% tall cell variant with 8/40 involved lymph nodes (levels II, III and IV). Patient received 150 mCi of $^{131}$I-NaI 3 months after surgery. Five days post treatment whole body scan with SPECT-CT revealed faint uptake in cervical lymph nodes at level III-R and a focus of moderate uptake in the left parotid corresponding to a well-defined cystic lesion with a solid component on CT. Subsequent ultrasound (US) revealed a mixed cystic and solid lesion in the left parotid. A computed tomography (CT) scan with contrast showed a ring enhancing lesion in the parotid. Patient underwent a second surgery consisting of a left parotidectomy and right neck dissection. Pathological examination of the left parotid revealed a Warthin's tumor. Follow-up whole body $^{131}$I-NaI scintigraphy under rTSH stimulation was negative for lymph nodes and distant metastasis while serum thyroglobulin was 1.9 pmol/L. **Discussion:** The sodium-iodide symporter (NIS) is a membrane glycoprotein mediating active cellular iodide uptake. It is found in thyroid tissue as well as non-thyroid tissues including salivary glands, stomach, thymus and breast. Grave's disease and toxic multinodular goiter are associated with increased thyroidal NIS expression. In breast, lactating mammary gland and malignancy are associated with increased NIS expression. In salivary glands, benign tumors including Warthin's tumor and oncocytoma, originating from NIS-expressing ductal epithelial cells, express NIS whereas malignant tumors usually do not. Because radio-iodide uptake depends on NIS expression in different tissues, asymmetrically increased radio-iodide uptake in salivary glands can be due to metastatic lymph nodes of WDTC versus benign salivary gland tumors including Warthin's tumor and oncocytoma. Increased radio-iodide uptake has also been described in parotitis and partial obstruction of major salivary duct.

## P652

### Implementation of a dual tracer study protocol (18F-FDG and I-131) in the evaluation of patients diagnosed of differentiated thyroid carcinoma with oncocytic variant.

**H. Portilla Quattrociocchi**, I. Tobalina, A. Montero, C. Moreno, I. Alonso, P. Alcorta, D. Garcia Hernandez; Hospital Universitario de Araba - Sede Santiago, Vitoria - Gasteiz, SPAIN.

AIM Establish a dual tracer study protocol (18F-FDG and I-131) after rh-TSH stimulation for the correct assessment on the first control post ablative therapy in patients diagnosed of differentiated thyroid carcinoma (DCT) with oncocytic variant. MATERIAL AND METHODS The Hurthle cell carcinoma is 2.5% - 1.4% of all DCT, being considered by WHO as an oncocytic variant of follicular thyroid carcinoma. Is well know that the Radioactive iodine therapy is effective in follicular carcinoma, however, Hurthle cell carcinoma usually do not presents uptake of iodine so that the use of I-131 in the monitoring and therapy is controversial. RESULT A study by the department of endocrinology of our hospital (2005-2012) In a study by the Department of Endocrinology of our hospital on 110 patients diagnosed of CDT, revealed that tumors with oncocytic variant represented 2.7% of all differentiated thyroid carcinomas, but 14% within the follicular . Due to the different cell lines with different metabolic behavior, proposed in oncology committee of our hospital this protocol. Protocol dual tracer after rh-TSH stimulation: 1. Analytical before rh-TSH (Monday): thyroglobulin and thyroglobulin antibodies 2. Intramuscular injection of rh-TSH for two days every 24 hours (Monday and Tuesday) 3. Standar study PET/CT with 18F-FDG and images localized of the cervical region. (Wednesday) 4. After completing study PET/CT, oral administration of 185 MBq of I-131. 5. Whole body I-131 supplemented with SPET/CT cervicothoracic and analytical post rh-TSH. (Friday): thyroglobulin and thyroglobulin antibodies. CONCLUSIONS The development of appropriate protocols within a multidisciplinary medical team support the smooth initial follow post ablative treatment in patients diagnosed of DCT with variant oncocytic and allow us to choose the most appropriate tool for further evolutionary controls.

## P653

### Comparison of Salivary Gland Function Side Effect of 30-100 mCi versus <30 mCi of Radioiodine Therapy

**A. Fard-Esfahani**, M. Karimi, B. Fallahi, D. Beiki, M. Saghari, A. Emami-Ardekani, M. Eftekhari; Tehran University of Medical Sciences, Reseach Center for Nuclear Medicine, Tehran, IRAN, ISLAMIC REPUBLIC OF.

Aim: It is known that high doses of radioactive iodine can adversely affect salivary gland function. This study is aimed to evaluate effect of radioactive iodine (RAI) with doses 30-100 mCi compared to lower doses of <30 mCi. Method: 54 patients (13 men and 41 women; age: 21-71, mean age 42.3±14.35) were enrolled in the study. 27 patients were hyperthyroid cases who received < 30 mCi of I-131 for treatment, and 27 patients had thyroid carcinoma who were treated with 30-100 mCi of I-131. All patients underwent Tc-99m pertechnetate scintigraphy before and three months after receiving radioiodine, and salivary gland excretion fraction (EF) were compared. EF decrease of 5% was considered significant. Clinical symptoms including voice hoarseness and mouth dryness were also recorded. To analyze the data, Statistical Package for the Social Sciences was used. Results: There is a significant decrease in salivary gland function after radioiodine administration ($p<0.05$). The total frequency of salivary dysfunction is 41.7%. In patients received a dosage of 30-100 mCi of I-131this frequency is 49.1% while in those treated with <30 mCi it is 34.3% ($p<0.01$). The right parotid gland was affected more than other salivary glands after 30-100 mCi treatment. Risk ratio of salivary gland involvement using 30-100 mCi versus <30 mCi was significant ($p=0.019$). The study found no particular relation between the side effects and age or sex ($p=0.2$); also there was no significant difference in xerophthalmia or xerostomia symptoms between two groups. Conclusion: The current study shows that RAI can reduce salivary gland function and this effect is more prominent in higher doses of 30-100 mCi used for thyroid carcinoma compared to lower dose of <30 mCi used for treatment of hyperthyroidism. However the significant presence of this complication even in using low dose of radioiodine notifies that all necessary precautions should be taken seriously into consideration to reduce this effect.

## P654

### Is Adding Hounsfield Unit Measurement on Standardized Uptake Value Helpful in Differentiating Thyroid Nodules?

**H. B. Sayman**, L. Uslu, O. Vural Topuz, S. Sager, M. Halac, K. Sonmezoglu; Istanbul University Cerrahpasa Medical Faculty Department of Nuclear Medicine, Istanbul, TURKEY.

Objectives : Focally increased F-18 FDG uptake in thyroid nodules is not a reliable indicator of thyroid gland malignancy, since several benign diseases such as infection and inflammation also can cause falsely inflated F-18 FDG uptakes on PET/CT scans. Therefore, in order to differentiate malignant thyroid nodules from benign ones, other parameters apart from standardized uptake value (SUV) is needed. We investigated if addition of Hounsfield unit (HU) measurement, a radiodensity parameter obtained by CT component of PET/CT imaging, may help in seperation of malignant nodules from benign ones. Methods : Thirty patients, with incidental finding of focally increased FDG uptake in thyroid gland were included in this study. Patients underwent routine thyroid ultrasonography, thyroid function tests, thyroid scintigraphy and thyroid fine needle aspiration biopsy. The patients with malignant nodules on aspiration biopsy were referred to the department of surgery for thyroidectomy. SUVmax and SUVmean values obtained by PET, also HUmax and HUmean values obtained by CT were measured and compared with cytopathology or postoperative pathology results. Results : Pathology examinations revealed malignant nodules in 11 patients (36,7%). Mean values for HUmax and HUmean were found to be 136,7±9,9 and 60,5±9,5, respectively and mean values for SUVmax and SUVmean were found to be 7,43±3,68 and 3,87±3,0, respectively. There was no statistically significant correlation between any of SUV values or HU values with either benign or malignant pathology results. Similarly SUV values and HU values were also found not to be correlated with each other. Conclusions : The measurement of HU values does not have an additional effect on SUV values in evaluating incidental thyroid nodules with increased F-18 FDG uptake on PET/CT scans, in terms of differentiating malignant from benign conditions.

## P655

### The value of thyroglobulin measurement in fine needle aspirates from cervical lymph nodes of thyroid cancer patients

**H. Sayman**, S. YILMAZ, S. Nisli, M. Ozhan, L. Uslu, R. Akyel, F. Eren, E. Erginöz, S. Sager, B. Kanmaz; CERRAHPASA MEDICAL FACULTY, Istanbul, TURKEY.

Objectives : There are various Methods for follow-up of well differentiated thyroid cancer (DTC). Among these, serum Tg level is not optimal in detecting small lymph node metastases and it does not localize metastatic foci. Additionally, high circulating serum thyroglobulin antibodies (TgAb) may obscure the disease. In order to improve the sensitivity of FNA cytolgy, several studies have reported the recurrences or metastases of differentiated thyroid cancer could be shown by the Tg detection in FNA washout. We aimed to evaluate utility of Tg detection in FNA for accurate diagnosis of lymph node involvement in patients with DTC. Methods : 47 consecutive thyroid cancer patients (9 male, 38 female) underwent ultrasound-guided (USg) FNA biopsy and FNA-Tg measurement for suspicious metastatic cervical lymph nodes of thyroid carcinoma in our department. USg-FNA biopsy was performed with a 23-gauge needle attached to a 10 mL disposable plastic syringe in 55 lymph nodes from the study population. The materials obtained from FNA biopsy were smeared on glass slides. The remaining aspirates in the syringe and

needle were rinsed with normal saline and 2 mL of rinsed washout was submitted for Tg measurements (FNA-Tg). An adequate volume of patients' blood was drawn and sent to laboratory for serum Tg measurement as well. Cytological examinations were performed by experienced cytopathologists. FNA-Tg and serum Tg levels were compared by chi-square test. Results : The FNA-Tg cut-off value of 2,1 ng/p offers the best diagnostic performances showing 93% sensitivity, 61% specificity, 72% accuracy in detecting lymph node metastases of DTC. The positive and negative predictive value was 55% and 95%, respectively. Conclusions : FNA-Tg determination is a valuable technique for diagnosis of metastatic lymph nodes of patients with differentiated thyroid cancer. It has additional value in pinpointing the metastatic focus in the body.

## P656

### The Clinical Role of F-18 FDG PET/CT in the Follow-Up of Differentiated Thyroid Carcinoma Patients

**S. DEMİRELLİ**, E. S. BUDAK, M. SİPAHİ, A. BOZ, M. ERKILIÇ, B. KARAYALÇIN; AKDENİZ UNIVERSITY HOSPITAL DEPARTMENT OF NUCLEAR MEDICINE, Antalya, TURKEY.

OBJECTIVE: In this study, it was aimed to investigate the diagnostic role of F-18 FDG PET/CT and its effects on the clinical outcome in the follow-up of differantiated thyroid carcinoma (DTC) patients with suspicious scanning and laboratory findings for metastasis/recurrence. MATERİALS and METHODS: 71 PET/CT images of 52 DTC patients (44 papillary carcinoma, 8 follicular carcinoma, age ranges 21-84, median: 51.7) performed between december 2008-november 2012 and their clinical data were evaluated retrospectively. RESULTS: In 34 of 52 patients (46 images), iodine 131 diagnostic whole body scan (I-131 dxWBS) was negative, while in 7 of 52 patients (8 images) were suspicious for malignancy. Also in 11 of 52 patients (17 images) without performing I-131 dxWBS, suspicious findings were detected with other imaging techniques like ultrasound(US), computed tomography (CT). In all of the patients, serum thyroglobulin (sTg) levels were higher than normal. Hence F-18 FDG PET/CT was performed in order to find out any metastatic focus correlating with other imaging techniques or to explain the reason of high sTg levels. In the 51 of 72 PET/CT images findings correlating with metastasis were detected and 9 patients were referred to surgery (8 malignant/1 benign pathology) while 25 patients were treated with high dose I-131 therapy (9 patients had therapy after surgery) and remaining 27 patients were followed up clinically (1-33 months). As a result, approach imaging has changed the treatment and clinical approach in the 50% of 51 patients (18% of these group was referred to surgery and pathology was malignant in 90% of them). CONCLUSION: F-18 FDG PET/CT is thought to be a useful tool in the follow-up/diagnosis of DTC patients with high sTg levels and suspicious imaging findings on US/CT while no metastatic focus was detected by I-131 dxWBS. F-18 FDG PET/CT can also change the clinical treatment/follow-up options of these patients.

## P657

### Recombinant Thyrotropin (Rh-TSH) stimulated Positron Emission Tomography/Computed Tomography with [18F]fluoro-2-deoxy-D-glucose (PET) to improve detection of recurrence of well-Differentiated Thyroid Carcinoma (DTC) in patients with increased serum Thyroglobulin (Tg) and negative [131]I Whole Body Scan (WBS)

**S. Panareo**[1], I. Santi[1], R. Rossi[2], C. Cittanti[1], V. De Cristofaro[1], C. Peterle[1], E. degli Uberti[2], L. Feggi[1]; [1]University Hospital - Nuclear Medicine Unit, Ferrara, ITALY, [2]Section of Endocrinology, University of Ferrara, Ferrara, ITALY.

**Aim**: to assess how the stimulation with Rh-TSH in patients with DTC, increased serum Tg and negative WBS should improve the sensitivity of PET for the detection of DTC recurrence**. Method**: we studied 31 patients (15 women, 16 men - mean age 63.7+/-2 yo) with previously operated DTC, increased Tg serum levels, negative WBS and negative PET performed six months earlier than enrolment. All patients were revaluated with PET scan: Two consecutive days before PET, all patients were pre-treated with i.m. injection of Rh-TSH. Tg and TSH levels were assessed before and 24-48 hours after Rh-TSH administration. **Results:** Tg levels after Rh-TSH ranged from 2,1 to 28,7 ng/ml and they were substantially unchanged in all patients compared to serum Tg evaluated 6 months earlier. PET during stimulation with Rh-TSH resulted positive in 20 patients (64.5% - mean SUVmax 7,5) showing Tg levels ranging from 8,1 to 28,7 ng/ml (mean 20.55 ng/ml). Eleven negative PET patients (35,5%) showed Tg serum within 1,4 and 11,7 ng/dl (mean 7.61 ng/ml). Tg levels resulted greater in PET positive patients compared to Tg levels in PET negative patients and the difference resulted statistically significant ($p<0.05$). Out of 11 patients with negative PET, 5 (45,5%), with serum Tg levels within 3 and 3,4 ng/ml were closely followed-up. Six (54,5%) patients with negative both PET and WBS and Tg levels within 8 and 11,7 ng/ml were however re-treated with [131]Iodine because of loco-regional disease recurrence identified by Ultra Sonography. All PET were confirmed by histological analysis after surgery. **Conclusions**: Our results suggest that Rh-TSH stimulation could improve the diagnostic sensitivity of PET in patients with DTC relapse. There seems to be a direct correlation between serum Tg and SUVmax. According to literature PET should be perform when Tg is greater than 10 ng/ml: our experience shows that PET is positive when serum Tg is greater than about 8 ng/ml. This could possibly represent a criterion redefine threshold to select patient eligible for PET examination to detect DTC recurrence. Moreover PET after Rh-TSH administration could change the therapeutic strategy and patient's follow-up. Our data must be confirmed in larger series.

## P658

### Quality of life and associated factors in radio-iodine treated patients with differentiated thyroid carcinoma

**B. Fallahi**[1], S. Razavi Ratki[1], D. Beiki[1], M. Eftekhari[1], A. Fard-Esfahani[1], A. Emami Ardekani[1], N. Namiranian[2], M. Saghari[1]; [1]Research Center for Nuclear Medicine, Tehran University of Medical Sciences, TEHRAN, IRAN, ISLAMIC REPUBLIC OF, [2]Tehran University of Medical Sciences, Tehran, Iran, TEHRAN, IRAN, ISLAMIC REPUBLIC OF.

Background: Radio-active iodine (RAI) therapy and other modern treatment protocols have led to excellent prognosis and an overall 10-year survival rate reaching to 95% in patients with differentiated thyroid carcinoma (DTC). However, individual insight of patient to the life in relation to life-long goals, concerns and standards of living are of considerable importance in the success of management and are reflected on the quality of life (QL). Methods: A study was designed to evaluate the QL and the related factors in DTC patients. Four hundred and thirty five patients entered in the study and a standard questionnaire (EORTC QLQ-C30 version 3.0) was applied to assess the global QL scores as well as its sub-domains including physical, social, role, cognitive and emotional functions, symptom scales and financial difficulties. The socio-demographic and management data were also recorded. All data were analyzed to explore the associations between different sub-domains of QL and the background factors such as income, education, job, marital status, the number of surgeries and cumulative dose of RAI therapies. Results: The mean age of participants was 42.11 years (± 14.25) ranged between 18 and 83. Three hundred and thirty seven patients were female (77.5%) and most of them (343) were married (78.8%). Global QL score was higher in women, single and higher educated patients. QL and its sub-domains were adversely affected by increasing the number of RAI therapies, radio-iodine cumulative dose and the number of surgeries. In functioning domains the most unaffected part was social function and the worst was emotional function. Conclusion: Fear, hesitation and uncertainty related to cancer diagnosis, radical or partial surgical treatments and RAI therapies are associated with lower quality of life. A majority of socio-economic and management variables may influence the QL. Availability of professional support may be an important part of the management in patients with DTC.

## P659

### Incidental Thyroid Lesions Detected with FDG PET Scanning

E. Kalender[1], **U. Elboga**[1], Y. Celen[1], H. Demir[1], E. Sahin[2], M. Yilmaz[1], M. Ozkaya[1]; [1]Gaziantep University, Gaziantep, TURKEY, [2]Namik Kemal University, Tekirdag, TURKEY.

**Aim:** As FDG PET scanning has become more popular in recent years, it has also become more frequent means of detecting incidental thyroid lesions. The aim of this study is to investigate to prevalance of incidentally found thyroid lesions in patients undergoing FDG PET and determine the risk for thyroid cancer. **Material and Methods:** FDG PET was performed on 5758 patients for eveluation of suspected or known cancer without any history of thyroid disease between January 2006 and May 2012 in our clinic. Patients with incidental thyroid abnormalities were identified. Medical records related to the FDG PET findings including SUVmax and pattern of FDG uptake, FNA diagnosis and histopathology after thyroid surgery were reviewed retrospectively. **Results:** One hundred twenty three patients (2.1%) were identified to have focal incidental thyroid lesions and 52 patients (0.9%) were identified diffuse incidental thyroid lesions on FDG PET. Twenty four patients with focal and 5 patients with diffuse incidental thyroid lesion underwent FNA. The malignant diagnosis was detected 41.6% of focal lesions. In diffuse lesions, malignant diagnosis was not observed. There was a significiant difference in the SUVmax between the benign and malignant lesions (5.7±2.2 and 10.1±5.3). Malignant diagnosis was noted in 57.1% of male patients and 20% of female patients who underwent FNA. **Conclusion:** The results of this study suggest that focal FDG uptake, high SUV and male gender have high risks for thyroid malignancy in incidentally found thyroid lesions by FDG PET. Further diagnostic work-up is needed in patients with these findings.

P38-2 - Tuesday, Oct. 22, 16:00 - 16:30, Poster Exhibition Area

## Oncology Clinical Science: Breast

## P660

### Prognostic impact of intratumoral metabolic heterogeneity in invasive ductal breast cancer patients

**S. Son**; Kyungpook National University Hospital, Daegu, KOREA, REPUBLIC OF.

Purpose: The purpose of this study was to evaluate prognostic implication of intratumoral metabolic heterogeneity on pretreatment F-18 FDG PET/CT in patients with invasive ductal breast cancer (IDC). Methods: Eighty two female IDC patients who underwent pretreatment PET/CT were enrolled. The heterogeneity factor, defined as the derivative (dV/dT) of a volume threshold function from 40% to 80%, was computed for primary breast tumor. Other metabolic PET parameters [SUVmax, metabolic tumor volume (MTV) and total lesion glycolysis (TLG)] were also measured. Heterogeneity factor was compared with clinicopathological and other PET parameters by two-tailed Spearman correlation. Univariate and multivariate analyses for overall survival (OS) were performed by Kaplan-Meier method and Cox proportional hazards models. Results: The heterogeneity factor ranged from -6.72 to -0.02 (mean, -0.41 [SD, 0.96]) and was significantly higher in patients with higher T (r=-0.451; p<0.0001) stage, ER-negative tumors (r=0.363; p=0.0008) and PR-negative tumors (r=0.361; p=0.0009). And the heterogeneity factor was significantly correlated with MTV (r=-0.662; p<0.0001) and TLG (r=-0.606; p<0.0006). The optimal cut-off values determined using a receiver-operating characteristic (ROC) curve were -0.3588 for heterogeneity factor, 10.86 $cm^3$ for MTV and 14428.8 for TLG. The OS rate among the 82 patients was 20.7%. According to the results of Kaplan-Meier analysis, T stage (p<0.0001), N stage (p<0.0001), ER status (p=0.0034), PR status (p=0.0101), SUVmax (p<0.0001), MTV (p<0.0001), TLG (p<0.0001), and heterogeneity factor (p<0.0001) significantly affected OS. However, none of them was statistically significant on multivariate analysis. Conclusion: The intratumoral metabolic heterogeneity significantly correlated with clinicopathological and PET parameters, and significantly affected outcome. Therefore, as the other metabolic PET parameters, the heterogeneity factor could be used as a good surrogate marker for the prediction of OS in IDC patients.

## P661

### Ultrasound-guided radionuclide injection for sentinel lymph node detection in breast cancer: a preliminary results

**G. Horvatic Herceg**, S. Kusacic-Kuna, I. Bracic, A. Mutvar; Department of Nuclear Medicine and Radiation Protection, University Hospital Centre Zagreb, Zagreb, CROATIA.

Axillary lymph node status is the most important prognostic factor in early-stage breast cancer. General availability of ultrasound (US) could at least partially resolve the current controversy about the method of radiocolloid application in the sentinel lymph node (SLN) detection in breast cancer. US-guided technique opens new possibilities for more accurate peritumoral injection even in case of small nonpalpable primary cancer. Purpose: This study aims to evaluate the success rate of different radiocolloid injection techniques (US-guided vs. non-guided) in the detection of SLNs in early breast cancer. In a prospective study, the visualization and identification rates of the US-guided tracer injection technique for nonpalpable breast tumors were evaluated. Methods: In 34 consecutive patients (range: 35-75 years) with $T_{1-2}N0$ breast cancer, sentinel lymph node biopsy was performed following peritumoral tracer injection in two-day protocol. In the case of nonpalpable breast lesions (the smallest one 5 mm in diameter), Tc-99m nanocolloid injections were given using a 7.5 or 10 MHz US probe. Results: In 18 patients with nonpalpable breast lesions radiotracer was applied peritumorally under the guidance of US. The lymphoscintigraphic visualization and surgical retrieval rates of axillary SLNs were 100%. In 3 patients SLNs were detected in axillary region as well as in internal mammary chain. Majority of sentinel nodes appeared during initial dynamic study. In 16 patients with palpable lesions radiotracer was injected peritumorally without the US-guidance. In 5/16 cases from this group sentinel nodes were not visualized within the scope of two-day protocol. Detection rate was 68.75%. In all 34 patients axillary ultrasound was negative. Axillary metastases were detected in 4/33 patients, although pathohystology revealed only micrometastasis or individual atypical cells. Conclusion: Our preliminary results indicate better identification rate of sentinel lymph nodes in patients with breast cancer in case of US-guided radionuclide injection. In nonpalpable breast lesions, the US-guided injection technique is an accurate technique for SLN identification and retrieval. Early appearance of SLNs makes this method more convenient for one-day protocol.

## P662

### Simultaneous detection of non-palpable breast lesion with $^{99m}$Tc-MAA and SLN with $^{99m}$Tc-nanocolloid

**A. Valković-Mika**, S. Grbac Ivanković, P. Valković Zujić, A. Valković; Clinical Hospital Centre Rijeka, Croatia Faculty of Medicine, University of Rijeka, Rijeka, CROATIA.

Detection of breast cancer in its earliest stage is of utmost importance because it increases the probability of complete cure, the surgical procedure is minimally invasive and the disability and suffering of the patient is lesser. **Aim:** Our aim was to determine the reliability of the diagnostic procedure of radioguided occult lesions localization (ROLL) with $^{99m}$Tc-MAA under ultrasound guidance and detecting sentinel lymph node (SLN) with $^{99m}$Tc-nanocolloids in breast cancer, identifying them simultaneously and removing them surgically. **Materials and Methods:** We evaluated a total of 40 patients aged between 41 and 71 years in whom screening mammography detected a high risk occult lesion. The average size of the lesions was 0.6 mm (from 0.3 mm to 0.9 mm). All underwent breast ultrasound, while on more than one half of the patients' fine-needle aspiration cytology was performed.The day before surgery (12 hours earlier), under ultrasonic guidance we injected into the localized breast lesion 74.0 MBq $^{99m}$Tc-MAA (from 55.5 MBq to 92.5 MBq) in a volume of 0.2 ml. After ten minutes we outlined the breast contour with a flexible marker ($Co^{57}$) and acquired anterior and lateral images. On the day of surgery 15 MBq of $^{99m}$Tc-nancolloids in a volume of 0.2 ml was subdermally injected above the marked localized breast lesion. Images made twenty minutes later in anterior and anterior/lateral positions revealed a sentinel lymph node. **Results:** In all patients scintigraphy demonstrated activity in the lesion and a SLN. When a preoperative diagnosis was not available using a hand-held gamma-detecting probe we removed the defined occult localized breast lesion and an intraoperative frozen section examination of the breast lesion was performed. In the presence of invasive cancer the sentinel node biopsy (SNB) was then carried out. If the cytological diagnosis of the lesion confirmed the cancer SNB was done first and the primary tumor was removed as a second step. **Conclusion:** The obtained results show that a method of choice for a safe and quick localization of the occult breast lesion and a sentinel lymph node is the combination of simultaneous detection of the occult localized breast lesion with $^{99m}$Tc-MAA under ultrasound guidance and the detection of a sentinel lymph node with a subdermal injection of $^{99m}$Tc-nanocolloids.

## P663

### The Usefulness of SPECT/CT Imaging for SN Mapping in Breast Cancer.

**E. Ozalp**, M. T. Do, L. Baeyens, T. Masson, P. Bergmann; CHU Brugmann Hospital, Brussels, BELGIUM.

AIM: To show our experience and the additional value of SPECT/CT sentinel node (SN) scintigraphy in breast cancer. MATHERIAL AND METHODS: A total of 94 women (mean age: 61± 12 yr) diagnosed with breast cancer addressed to our department for SN mapping between December 2010 and September 2012 were retrospectively analyzed. Three pts had bilateral breast cancer. SPECT/low-dose CT (Siemens Symbia T6) was performed 3 hours after periareolar injection of (99m) Tc-nanocoloid. The number and localization of SN obtained by SPECT/CT lymphoscintigraphy were compared with gamma-detecting intraoperative probe and with histopathologic results. RESULTS: In all 94 pts (97 breasts) at least one SN was localized using gamma probe. SPECT/CT enabled the mapping of at least one SN in 92/97 (95%) of the breasts. Of 5 pts for whom SPECT/CT lymphoscintigraphy failed, 1 had metastatic involvement in SN. SNs were found in the axilla in 93% pts. In 4 pts internal mammary SN, in 2 pts intramammary SN, in 1pt supraclavicular SN were detected. Lymph node metastases were found in 16 of 97 breasts (17%). According to histopathology, 3 pts had FN results with both SPECT/CT and gamma probe (metastases in another lymph node without any metastatic involvement of SN). CONCLUSION: SPECT/CT allows highly accurate and precise anatomical localization of SN prior to surgery. Therefore it facilitates the exploration of SN in breast cancer with gamma probe in operating room.

## P664

### Excised mammary volume and margin involvement in palpable and non-palpable breast cancer tumors

**M. A. Depetris**[1], F. Caparros[2], M. Velasco[3], X. Bargalló[3], J. Munrós[2], F. J. Barranco[2], P. L. Fernández[4], M. Mayoral[1], P. Paredes[1], I. Alonso[2], S. Vidal-Sicart[1], F. Pons[1]; [1]Nuclear medicine Department. Hospital Clinic, Barcelona, SPAIN, [2]Gynecology Department. Hospital Clinic, Barcelona, SPAIN, [3]Radiology Department. Hospital Clinic, Barcelona, SPAIN, [4]Pathology Department. Hospital Clinic, Barcelona, SPAIN.

Aim To assess the surgical accuracy in palpable and non-palpable breast cancer harvesting by measuring the total excised volume and involvement of surgical sample margins. Methods This is a retrospective study including 81 patients with conservative breast cancer surgery from January to December 2011. Patients with ductal in situ carcinoma, multifocal or multicentric tumors, previous neoadjuvant chemotherapy or surgery were excluded from the analysis. In non-palpable lesions the tissue excision was guided by means a needle or radioguided occult lesion localization (ROLL). Data included histological tumor type, tumor size, surgical re-excision and involvement of sample's surgical margins. The excised tissue volume (ETV) was calculated, as well as the optimal volume (OV) to be excised (by considering tumor as a sphere with 1 cm free margin surrounding it). A ratio

between ETV and OV was obtained to quantify the amount of excised surgical sample volume that exceeded the optimum. Results Thirty (37%) out of 81 patients presented palpable tumors. In the remaining 51 patients a needle into the tumor was previously inserted before surgical localization in 23 (28.4%) and with an intratumoral depot of radiotracer (99mTc-nanocoll; ROLL technique) in 28 (34.6%) patients. After surgical tumor excision, involved margins were observed in 10.7%, 10.3% and 13%, respectively (p = 0.948). The ratio between ETV and OV was 2.7 for palpable lesions, 1.6 in the needle group and 2.8 in the ROLL patients (needle vs ROLL, p = 0.01). The mean excess harvested tissue volume was 2.5 times higher than the OV (range 0.04-11.3). Conclusions In breast cancer conservative surgery there is, in our hands, an excess of harvested healthy tissue for this type of surgery with a suboptimal involvement ratio of surgical margins. It seems that needle-guided excision for non-palpable lesions offers the best approach in our experience. It is mandatory improving the surgical accuracy both in palpable and non-palpable lesions.

## P665

### Sentinel Node Mapping with SPECT/CT in Breast Cancer

**A. Mutvar**, D. Huić, G. Horvatić-Herceg, M. Dobrenić, M. Trogrlić, D. Grošev, A. Dujmović, M. Duduković; University Hospital Centre Zagreb, Zagreb, CROATIA.

**AIM**: The aim of this study is to investigate whether single photon emission computed tomography with computed tomography (SPECT/CT) is of additional value compared to conventional sentinel node (SN) lymphoscintigraphy in patiens with breast cancer. **METHOD**: 65 consecutive patients with breast cancer scheduled for sentinel node biopsy, underwent conventional lymphoscintigraphy with dynamic and static planar imaging and subsequently SPECT/CT. Tc99m-colloid was injected in the breast tissue around the tumor. Hand-held gamma probe was used for identification of the SLNs. We studied whether SPECT/CT; showed additional sentinel nodes, provided better information on the location of the sentinel nodes, and whether this additional anatomic information had an impact on surgical approach or patient menagement.The results were collected prospectively. **RESULTS:** SPECT-CT detected 97 SNs in 61out of 65 patient (94% of patients) and conventional lymphoscintigraphy 84 SNs in 56 patients (86% of patients). SPECT-CT found 13 additional radioactive nodes (13,4%) in eleven patients (17 %) of whom 5 patients had non-visualization of SN on planar images (7.7%). We didn't find SN either on conventional scintigraphy or SPECT-CT in 4 patients (6%). SPECT/CT had positive impact on menagement of 20 patients by providing additional information that led to an adjustment of the surgical approach or further patient menagement (30,7%). **CONCLUSION:** SPECT/CT detected additional sentinel nodes and revealed the exact anatomical location of sentinel nodes. SPECT/CT provided relevant additional information in 20 (30,7%) of the 65 patients. Our preliminary results suggest that routine use of SPECT/CT in addition to conventional lymphoscintigraphy may improve sentinel lymph node detection, surgical procedure and patient menagement.

## P668

### Comparison of the Efficiency for Tc-99m Tin-colloid and Tc-99m Phytate in Sentinel Node Detection in Breast Cancer Patients.

**J. Seok**; Chung-Ang University, Colleage of Medicine, Seoul, KOREA, REPUBLIC OF.

Objectives: Lymphoscintigraphy and sentinel node biopsy has become a standard method for detection of axillary lymph node metastasis in breast cancer patients, but the standard radiopharmaceutical was not prepared. About detection of axillary lymph node metastasis by lymphoscintigraphy and sentinel node biopsy in breast cancer patient, we compared the results of Tc-99m Tin-colloid and Tc-99m Phytate by subareolar injection. Methods: This study included 679 breast cancer patients who were performed operation during 2001-2013. Four hundred twelve patients was injected 0.8 ml of Tc-99m Tin-colloid (37-185 MBq) by subareolar injection. Two hundred sixty seven patients was injected 0.8 ml of Tc-99m Phytate (37-185 MBq). Lymphoscintigraphy was performed in supine position and sentinel node localization was performed by hand-held gamma probe in operation. Results: Among 412 patients by Tc-99m Tin-colloid, 374 cases (90.8%) localized the sentinel node by lymphoscintigraphy and 367 cases (89.1%) localized by gamma probe. Among 267 patients by Tc-99m Phytate, 258 cases (96.6%) localized by lymphoscintigraphy and 256 cases (95.9%) localized by gamma probe. Detection rate by lymphoscintigraphy and gamma probe was superior for Tc-99m Phytate compared to that with Tc-99m Tin-colloid, with a statistically significant difference. ($p<0.05$, $p<0.05$) Conclusions: Tc-99m Phytate is a better choice for localization of sentinel node than Tc-99m Tin-colloid in breast cancer patients.

## P669

### Comparison of Subareolar Injection Lymphoscintigraphy with the 1 Day and the 2 Day Protocol for the detection of Sentinel Lymph Nodes in Patients with Breast Cancer.

**J. Seok**; Chung-Ang University, Colleage of Medicine, Seoul, KOREA, REPUBLIC OF.

Objectives: Lymphoscintigraphy and sentinel node biopsy were used for the detection of axillary lymph node metastasis in breast cancer patients. We compared the results of subareolar injections on the day of surgery (1 day protocol) with injections the day before surgery (2 day protocol). Methods: This study included 679 breast cancer patients who underwent surgery between 2001 and 2013. For the 1 day protocol 0.8 ml of Tc-99m Tin-Colloid (37MBq) was injected in 393 in the subareolar region on the morning of the surgery. For the 2 day protocol 0.8 ml of Tc-99m Tin-Colloid (185MBq) was injected in 286 patients on the afternoon before surgery. Lymphoscintigraphy was performed in the supine position and sentinel node identification was performed by hand-held gamma probe during surgery. Results: Among 393 patients with the 1 day protocol, 368 cases (93.6%) were identified by sentinel node lymphoscintigraphy, and 369 cases (93.9%) were identified by gamma probe. Among the 286 patients, in the 2 day protocol, 264 cases (92.3%) had the sentinel node identified by lymphoscintigraphy, and 254 cases (88.8%) had the sentinel node identified by the gamma probe. There was no significant difference in the identification rate of the sentinel node between the 1 day and 2 day protocol by lymphoscintigraphy and the gamma probe. Conclusions: The results of the identification of the sentinel node according to 1 day or 2 day protocols showed no significant differences. Because the 2 day protocol allows for an adequate amount of time to perform the lymphoscintigraphy, it is a more useful protocol for the identification of sentinel nodes in patients with breast cancer.

## P670

### The feasibility, acceptability and safety of Molecular Breast Imaging (MBI) using a breast specific gamma camera* and 99mTc-sestamibi in patients with a high risk of breast cancer

**K. Y. Gulenchyn**[1], A. Singnurkar[1], L. Bordeleau[2], M. N. Levine[3], K. Dhamanaskar[1], J. Valliant[4], A. Goodbody[4], K. Cline[3], G. R. Pond[3]; [1]Hamilton Health Sciences, HAMILTON, ON, CANADA, [2]Juravinski Cancer Centre, HAMILTON, ON, CANADA, [3]McMaster University, HAMILTON, ON, CANADA, [4]Centre for Probe Development and Commercialization, HAMILTON, ON, CANADA.

Aim: We investigated the use of MBI in subjects at high risk of breast cancer, hypothesizing the study would be feasible (recruitment rate of ≥2 patients per month), acceptable (refusal rate of ≤ 30% and more women would prefer MBI than MRI) and safe (a reportable incident rate for MBI of 0%). Materials and Methods: A prospective cohort undergoing annual breast MRI was approached to undergo MBI. Subjects with a positive MBI but a negative MRI were to have further investigations as clinically indicated. Subjects with no evidence of disease were followed for one year and underwent an additional set of MBI/MRI exams. Preferences were obtained following completion of their first MBI/MRI using a brief, self-administered questionnaire. MBI was obtained 10 minutes post IV injection of 740 MBq 99mTc-sestamibiwith craniocaudal and mediolateral oblique 10-minute views of each breast (8 images, 40 minutes, total). MRI, at either 1.5T or 3T magnet field strength, was obtained with and without gadolinium contrast using a dedicated breast coil and standard institutional protocol (45 minutes total). Results: 42 of 62 subjects approached agreed to participate at an average of 2.8 per month; the refusal rate of 32% just exceeded the preplanned criteria for success. 1 patient had a positive pregnancy test and 1 withdrew prior to baseline imaging. 2 of 40 patients who underwent baseline MBI could not tolerate MRI. 31 subjects (4 others withdrew, 1 had bilateral prophylactic mastectomy, 1 developed disease and 1 had a positive pregnancy test) completed the 1 year scans. There were no reportable incidents with MBI. Just under half indicated they felt no discomfort during MBI and 75% were quite a bit or very much satisfied with MBI. 66% experienced no pain during MBI, while 29% experienced a little bit. 18 of 34 subjects who responded (52.9%, 95% confidence interval: 35.1% to 70.2%) preferred or strongly preferred MBI over MRI. Conclusion: This study demonstrates that MBI is safe, feasible and at least potentially acceptable to women who are at high risk of developing breast cancer. A majority of women who underwent MBI preferred or strongly preferred the new technology, rating it superior to MRI for patient comfort and satisfaction. *GE Discovery NM750b

## P671

### Relationship between the expression of Estrogenic/Progestinic receptors, grading and sentinel lymph nodes status, identified by linfoscintigraphy in patients with breast cancer

**A. Niccoli Asabella**, M. Renna, V. Loseto, D. Rubini, F. Iuele, C. Ferrari, G. Rubini; Nuclear Medicine Unit, D.I.M., University of Bari "Aldo moro", Bari, Italy, Bari, ITALY.

**Aim** To evaluate the association between the expression of E/P receptors, grading and lymph nodal status in breast cancer patients. The status of the axillary sentinel nodes (SNs) is the most important prognostic factor for patients with breast cancer.

Preoperative lymphoscintigraphy with 99mTc-labeled human albumin colloid is an essential tool in identifying SNs. One Step Nucleic Acid Amplification (OSNA) method is actually recognized as a sensitive and specific technique for intraoperative research of SNs metastasis. The expression of estrogenic or progestinic (E/P) receptors plays an important role for an appropriate therapeutic choice. **Matherials and Methods** From May 2012 to January 2013, we enrolled 62 pts (mean age 57 years) affected by breast cancer. Grading of lesions was: G1 in 20/62 (25%), G2 in 24/62 (38%) and G3 in 18/62 (29%). All patients underwent preoperative lymphoscintigraphy. Planar images were acquired using a dual-head gamma camera, after 15 minutes from the radiopharmaceutical injection. On the same day patients were submitted to surgery and sentinel node biopsy (SNB). Sensibility of lymphoscintygraphy was assessed. Chi squared-test (X2) was used to evaluate the association between E/P receptors expression, grading and lymph nodal status. **Result** Lymphoscintigraphy showed a sensitivity of 100%, because SNs were identified and removed in all patients. High expression of estrogenic receptors was found in 46/62 patients (74%), low in 11/62 (18%) and absent in 5/62 (8%); progestinic receptors expression was high in 34/62 patients (44%), low in 14/62 (22%) and absent in 14/62 (22.5%). There was not a statistically significant association between the expressivity of E/P receptors and lymph nodes positivity (X2 = 3.719; p= 0,617). A statistically significant association was found between the expression of hormone receptors and the grading, for estrogenic receptors (X2 = 14,581; p= 0,024), and for progestinic one (X2 = 15,81; p= 0,015), with low expression of receptors for high grading. **Conclusions** Lymphoscintigraphy and SNs histological examination remain the most reliable techniques for the detection of SNs, early staging of breast cancer and clinical and surgical management of these patients. Performing both lymphoscintigraphy and sentinel node analysis with OSNA method allowed to reduce the invasiveness of breast surgery. High grading of the tumor is related to sentinel lymph nodes positivity and to a low expression of E/P receptors, but the absence of E/P receptors is not always correlated with lymph node status in the early stage of disease.

## P672

### Upstaging of Locally Advanced Breast Cancer with PET/CT

**J. Duch**, V. Camacho, A. Montes, C. Achury, L. Geraldo, J. Deportós, M. Estorch, I. Carrió; Hospital de la Santa Creu i Sant Pau, Barcelona, SPAIN.

Aim: PET/CT has shown to be useful in the staging of locally advanced breast cancer. We aimed to evaluate the additional information provided by FDG PET/CT compared with conventional imaging procedures. Materials and Methods: We prospectively evaluated 94 patients (mean age 63+/-15 years) with locally advanced breast cancer, who underwent FDG PET/CT and convencional imaging procedures (bone scan, chest x-ray and liver ultrasonography) for initial staging. Findings were histologically confirmed; otherwise a follow-up for at least 6 months was required. Results: PET/CT showed significant FDG uptake (SUVmax 7,7) in 92 out of 94 patients. N3 stage was found in 14 patients, which forces to change the radiotherapy field. Overall, PET/CT showed a sensitivity and specificity for axillary lymph node metastases of 90% and 73% respectively. Bone metastasis were diagnosed in 14 patients (5 of them with negative bone scan). Liver metastasis were diagnosed in 3 patients (all of them with positive liver ultrasonography). Lung metastases were diagnosed in 5 pacients (all of them with negative chest x-ray). Moreover, PET/CT showed distant lymph node metastases in 4 patients. With these results, PET/CT led to a change in initial staging in 20% of patients. Conclusions: FDG PET/CT yields useful information for the initial staging of locally advanced breast cancer.

## P673

### The role of breast scintigraphy with breast-specific γ-camera (BSGC) and SPECT/CT in the preoperative identification of residual breast tumor and axillary lymph node metastases following neoadjuvant therapy.

**A. Spanu**[1], F. Chessa[1], I. Gelo[1], L. Mele[1], S. Sanna[1], G. Sarobba[2], G. Sanna[2], S. Nuvoli[1], G. Madeddu[1]; [1]Unit of Nuclear Medicine. University of Sassari, Sassari, ITALY, [2]Unit of Oncology. University of Sassari, Sassari, ITALY.

**Aim.** The aim of the present study was to assess the role of BSGC scintigraphy and SPECT/CT in the preoperative identification of residual breast tumor and axillary lymph node metastases in patients with locally advanced primary breast cancer (LAPBC) following neoadjuvant therapy. **Methods.** Forty consecutive LAPBC patients, aged 26 to 82 yrs, scheduled to surgery following neoadjuvant chemo (32 cases) or hormone (8 cases) therapy were studied. Starting 10 min. after the i. v. injection of 740 MBq of 99mTc-tetrofosmin, all patients underwent breast scintigraphy in both cranio-caudal and medio-lateral oblique views (600 sec./view) using a high resolution BSGC. A SPECT/CT study was then acquired, including both breasts and also both axillae in the field of view, using a dual head gamma camera integrated with a x-ray tube for low-dose CT. SPECT images were corrected for attenuation and scattering, reconstructed by iterative method (OSEM) and fused with CT images using a dedicated package. All patients had breast surgery, with associated axillary lymph node sampling in 35/40 cases. Scintigraphic data were correlated with surgical histopathological findings in all cases. **Results.** Thirty-three/40 patients (82.5%) had residual breast cancer following neoadjuvant therapy, while the remaining 7/40 patients (17.5%) had no residual breast disease. Axillary lymph node metastases were ascertained in 24/35 cases (68.6%), while the remaining 11/35 cases (31.4%) were free of metastases. BSGC scintigraphy detected residual tumors in 32/33 cases and SPECT/CT in 28/33 (sensitivity: 97 and 84.8%, respectively; p>0.05), while both procedures were true negative in the 7 patients without residual disease (specificity: 100%). The accuracy values of BSGC scintigraphy and SPECT/CT in detecting residual breast tumor were 97.5 and 87.5%, respectively (p>0.05). SPECT/CT detected axillary lymph node metastases in 17/24 patients (sensitivity: 70.8%) and resulted true negative in 9/11 patients free of metastases (specificity: 81.8%), showing a diagnostic accuracy value of 74.3%. **Conclusion.** In the present study, both BSGC scintigraphy and SPECT/CT proved highly accurate diagnostic tools in the preoperative identification of residual breast carcinomas following neoadjuvant therapy, although BSGC scintigraphy showed a higher sensitivity than SPECT/TC; however, this latter procedure gave useful information on the preoperative axillary lymph node status. According to our data, the combined use of both procedures may guide the surgeon to the most appropriate breast surgical treatment (radical mastectomy or conservative surgery) and to eventually select the most suitable axillary lymph node sampling (axillary lymph node dissection or sentinel node biopsy).

## P674

### Initial Staging with $^{18}$F-FDG PET/CT in Breast Cancer, Accuracy Detecting Distance Metastases

**A. MARTINEZ LORCA**, I. SANTOS GOMEZ, R. COUTO CARO, S. RODADO MARINA, I. HERNANDEZ PEREZ, D. MENDEZ MAREQUE, L. MARTIN CURTO; Hospital Universitario La Paz, Madrid, SPAIN.

**AIM** Evaluate diagnostic accuracy $^{18}$F-FDG PET/CT to detect bone and other location metastases in initial staging breast cancer in our clinical setting. **MATERIAL AND METHODS** A total of 266 women (p), mean age 58,6 years (range 25-93), were evaluated retrospectively between 2009-2012. Previously, they had been diagnosed of locally advanced breast cancer or early breast cancer with risk factors (triple negative, hormonal receptors, HER2/neu, high Ki67) without distant metastases suspicious. Detailed breast cancer data: invasive ductal carcinoma (222p/83,4%), invasive lobular carcinoma (30p/11,2%), 14p other histological patterns but not inflammatory. Tumour markers: estrogenic receptor (positive 185p/69,5%) progesterone receptor (positive 162p-60,9%), HER2/Neu (negative 202p-75,9%), triple-negative 41p. Ki67≥ 15% (196p-73,6%). All patients underwent $^{18}$F-FDG PET/CT initial staging scan as part of their diagnostic work-up. Evaluated distance hipermatabolic uptake lesions not corresponding to physiological uptake or inflammation /infection pattern was recorded as positive for metastases. PET/CT findings were divided into: suspicious of bone metastases and other localizations. Final diagnosis for metastases was determined: for bone metastases by imaging procedures (259p bone scintigraphy, 40p CT, 18p MRI and 13p revaluated PET/CT) 4p clinical follow-(up more than 12 months) and 3p pathologic analysis. For other metastases: 44p imaging procedures (29p CT, 6p MRI, 8p revaluated PET/CT, 1p ecography) 11p clinical follow-(up more than 12 months) and 9p pathologic analysis **RESULTS** PET/CT bone findings: 229p without osseous uptake (228/232p true negative and 1/232p false negative), 33p suspicious bone metastases (33/33p true positive), 4p undefined for bone metastases. PET/CT has shown sensitivity of 97% and specificity of 100%, a positive predictive value of 100% and negative predictive value of 99% for bone metastases. For other locations metastases PET/CT has found: 231p without uptake (231/231p true negative), 32p suspicious of metastases: 29/32p true positive (12p pulmonary metastases, 10p liver metastases and 7p lymph nodes) and 3/33p false positive (3p inflammation, 1p benign suprarenal) and 3p undefined for other locations metastases. In our study PET/CT sensitivity was 100%, specificity 98%, positive predictive value 90% and negative predictive value of 100% Total metastases detected were 45p(16,9%): bone metastases: 33p, other organ metastases 29p and both 17p. **CONCLUSION** $^{18}$F-FDG PET/CT in our experience offers important diagnostic information to detect distant metastases; bone metastases and other location metastases, in breast cancer patients due to sensitivity and specificity values.

## P675

### Comparison of different metabolic parameters used in dual phase FDG PET imaging

**M. Tuncel**, O. Kupik, E. Akdemir, B. Erbas; Hacettepe University, Ankara, TURKEY.

AIM: As an estimate of metabolic acitivity of tumor, several parameters have been described, regarding measurement method and volume definition. Although most widely used estimate has been SUVmax, peak SUV (SUVpeak) has been recommended as a more robust alternative to SUVmax, which is adversely affected by noise. It is defined as the average SUV within a small, fixed-size region of interest (ROIpeak) placed on the region of high uptake. We aimed to compare

several metabolic activity estimates MATERIAL and METHOD: Standard and 2.hr 18-FDG PET/BT images of 26 patients (50±10 yrs) with various primary tumors were included. Tumor size ranged from 17 mm to 80 mm (mean: 35±13 mm). SUVmax, SUVpeak and SUVmean values were measured corrected for body weight (bw) and lean body mass (ln). Total lesion glycolysis values (TLG) were calculated for the VOIs drawn with adapted (visually best threshold) and fix threshold values (50%). In addition, heterogenity and noise levels were calculated for standard and late studies, respectively. RESULTS: SUV values increased significantly in the late study (SUVmax bw :10,4±6,7 to 11,2±6,7, SUVmean bw: 4,7±2,7 to 4,9±2,6, SUVmax ln :7,2±5 to7,7±4,7, SUVmean ln:3,3±2 to 3,4±1,8, SUVpeak bw: 8,3±5,3 to 8,5±4,8, SUVpeak ln: 5,8±4 to 5,8±3,3). Although TLG values measured with adapted VOIs increased significantly (TLGa-bw: from 290±423 to 318±500,p=0.037; TLGa-lean: from 218±342 to 238±396, p=0,047), TLG values measured using VOIs with fixed threshold level did not change significantly (TLG50-bw: from 151±243 to 154±247, TLG50-lean: from 117±190 to 114±192). Tumor volume measured with adapted threshold level was significantly higher compared to fixed threshold level in both studies (p=0.001). Adapted volume did not differ significantly, but fixed threshold level volume decreased in the late study (p=0,001). Tumor heterogenity and noise increased in the late study (33±12 to 35.8±11.3, p=0.037 ; 10,4±2,1 to 12,1±3,3, p=0,04). Adapted threshold value was negatively correlated with tumor heterogenity in both studies (r=0-0,93 and r=-0,86, p<0,0001). CONCLUSION: The metabolic parameters except SUV peak lean and TLG 50 increased in the late phase. The heterogenity of the tumor significantly affect the appropriate threshold needed for optimum tumor coverage with TLGa VOI

## P676

### Role of SPECT-CT Scintimammography in Recurrent Breast Cancer

**S. Sergieva**[1], E. Alexandrova[2], G. Baichev[3], M. Dimcheva[1]; [1]Sofia Cancer Center, Sofia, BULGARIA, [2]National Oncological Hospital, Sofia, BULGARIA, [3]Military Medical Academy, Sofia, BULGARIA.

Introduction: The value of scintimammography with 99mTc-Sestamibi/ 99mTc-Tetrofosmin is well known. Both of these radiopharmaceuticals have proved to manifest tumorotropic uptake mainly dependent on neoangiogenesis and increased proliferation activity of tumor cells. Additional diagnostic information of performed SPECT-CT studies has recently been analyzed. Aim: To determine role of SPECT-CT scintimammography for detecting ipsilateral breast tumour relapse and/or regional recurrence in women previously treated for primary breast cancer. Patients and Methods: This study included 57 women (age 32-80) with breast cancer after complex treatment - surgical, radiotherapy, chemo-/hormonotherapy. SPECT-CT scintimammography were performed 15-20 min after i.v. application of 99mTc-Sestamibi/ 99mTc-Tetrofosmin (740-925 MBq per dose) in all of them due to some clinical and laboratory indices suspicious for relapse. SPECT-CT camera Symbia T2, Siemens with low-dose CT was used. Fusion images were analyzed retrospectively. Focal tracer uptake was described as likely benign, malignant and equivocal. All SPECT-CT data were compared to the clinical status, radiological data and histological findings. Results: SPECT-CT images were positive for local relapse in 41 out of 57 women (in 26 pts radical mastectomy was performed; 15 were with partial resection), proved histologically after excision or biopsy. Infiltration of surrounding tissues were diagnosed in 6 of them. Regional lymph node metastases were visualized in the following areas: ipsilateral axilla I-III levels - in 11 pts; contralateral axilla - in 6 pts; parasternal nodes - in 4 pts; mediastinal nodes - in 3 pts; cervical nodes - in 2 pts. Metastatic lesions in the contralateral breast were imaged in 6 pts. Distant metastases (osteolytic bone lesions; pulmonary and pleural) were obtained in 10 pts. SPECT-CT changed the treatment management of these women - to indicate surgery and/or radio-/chemotherapy. In the rest 16 pts benign changes were visualized. SPECT was positive in 13 pts with fibrocystic alteration, mastopathy and postoperative parenchymal changes. SPECT was negative in 3 pts with fibroadenoma. In 6 of these pts SPECT was positive due to radiation pulmonitis after radiotherapy of the ipsilateral breast; in 3 - due to mediastinal granulomatosis and axillary inflammation. SPECT-CT was very useful in these cases to differentiate morphological changes of benign lesions and physiological uptake. Conclusion: By using functional SPECT modalities to complete anatomical CT imaging clinicians can obtain more information after scintimammography to plan their surgical and/or therapeutic management of women with recurrent breast cancer. SPECT-CT data are applicable for planning in radiotherapy to target precise tumor volume delineation.

P39-2 - Tuesday, Oct. 22, 16:00 - 16:30, Poster Exhibition Area

## Oncology Clinical Science: Lung

## P677

### Assessing the Feasibility of Using the Maximum Standardized Uptake Value as a Guiding Parameter for Lung Cancer Diagnosis and Prognosis

Y. Cui[1], X. Liao[1], **R. Wang**[1], Y. Fan[1], L. Di[1], H. Liu[1], Y. Zhao[2]; [1]Department of Nuclear Medicine,Peking University First Hospital, Beijing, CHINA, [2]Beijing Chinese Medicine University,Dongfang Hospital, Beijing, CHINA.

**Objective:** The aim of this study is to validate correlations of the maximum standardized uptake value ($SUV_{max}$) with the short diameters of pulmonary lesions and the pathology of lung cancer, and assess the feasibility of using $SUV_{max}$ as an important evaluation parameter for lung cancer diagnosis and prognosis **Methods**:$^{18}$F-deoxyglucose PET/CT imaging results of in our center between July, 2010 and February, 2012 from 127 patients with clinically suspected lung cancer were analyzed. In each case, the $SUV_{max}$ and the short diameter of the lesions were measured and calculated from the PET images. Statistical comparisons of these values were made between malignant and benign groups, and among patient groups of different pathological origins. **Results**:Our studies clearly show a positive correlation between the $SUV_{max}$ and the short diameter of the lesions in both malignant and benign groups. There is a statistical difference in $SUV_{max}$ between the malignant group and the benign group ($P$=0.0002), but not in the short diameters of the lesions ($P$=0.0938). The $SUV_{max}$ and the short diameters of squamous cell carcinoma are statistically different from those of a denocarcinoma, with $P$=0.0059 and $P$=0.0041, respectively. However, such statistical differences were not observed between non-small cell lung cancer and small cell lung cancer groups ($P$=0.8932 for the $SUV_{max}$, and $P$=0.6355 for the short diameters). **Conclusion**:These results reveal that $^{18}$FDG $SUV_{max}$ can be used as an important parameter to differentiate malignant tumors from benign ones, also to help evaluate the lung cancer pathology. [Key words] Lung cancer, PET/CT, Standardized uptake value, $^{18}$F-FDG,Metabolic imaging

## P678

### Evaluation of clinical value of 18F-PETCT and tumor markers in diagnosis of solitary pulmonary lesion

**R. Wang**, Q. Wang; Department of Nuclear Medicine,Peking University First Hospital, Beijing, CHINA.

**Objective:** $^{18}$F-FDG PET/CT plays an important role in diagnosing and differential diagnosis of pulmonary lesion. The aim of this study was to investigate the clinical value of $^{18}$F-FDG PET/CT functional imaging combined with tumor markers in the diagnosis of solitary pulmonary lesion. **Methods:** A retrospective analysis of PET/CT and TMs diagnosis results of forty-nine patients with solitary pulmonary lesions, and all lesions were confirmed by pathological or clinical follow-up results. All of the solitary pulmonary lesions from PET/CT images were blindingly diagnosed by three experienced nuclear medicine physicians and two experienced radiologists The diagnostic results of PET/CT, TMs and the combined examination were compared. The relationship between SUV $_{max}$ and TMs value were investigated. **Results:** The size of benign and malignant solitary pulmonary lesions didn't have statistics different(t=0.487,P<0.5). The sensitivity of $^{18}$F-FDG PET/CT,TMs and combined the two examinations were 87.9%,63.6%,97.0%($\chi^2$=13.778,P <0.01),respectively. The specificity of $^{18F\text{-}FDG\ PET/CT}$,TMs and combined the two examinations were 85.7%,71.4%,89.8%($\chi^2$=6.261,P <0.05),respectively. There were no significant correlation between $SUV_{max}$ and three TMs in diagnosis solitary pulmonary lesion(P >0.05). **Conclusion:** The combination of $^{18}$F-FDG PET/CT and TMs could improve the diagnosis and differential diagnosis in solitary pulmonary lesions. There were no correlation between $SUV_{max}$ and TMs numerical value. **[Keywords]** $^{18}$F-FDG;PET/CT;Tumor markers;Solitary pulmonary lesion

## P679

### Feasibility of parametric imaging in 18F-FDG PETCT dynamic multi-bed scanning for pulmonary lesions

**R. Wang**, Q. Wang, J. Zhang, Y. Zhou; Department of Nuclear Medicine,Peking University First Hospital, Beijing, CHINA.

**Objective:** The aim was to investigate the feasibility of ki parametric imaging in diagnosis of pulmonary lesions. **Methods:** There were fifty patients who have pulmonary lesions perform dynamic multi-bed scanning and followed by routine examination. The fifty patients can be divided into malignant and benign groups. The number of cases and lesions between the malignant and benign groups were 6(9) and 9(12), respectively. The left ventricular was used for image derived input function. The ki of pulmonary lesions and ki parametric images were generated with patlake plot method. In our study, the difference of ki between the malignant and benign lesions were analyzed, at the same time, we investigate the correlation of ki and $SUV_{max}$. **Results**: The results showed that the maximum diameter of pulmonary lesions were not significant different between malignant and benign lesions ($P$>0.05).The ki and SUV in malignant lesions were significantly higher than benign lesions ($P$<0.05). The ki were highly correlated with SUV in pulmonary lesions($P$<0.01). The malignant lesions showed a gradually increasing time activity curves, whereas, benign lesions were gradually decreasing curves. The parametric images of ki were useful to distinguish malignant lesions from normal tissue. **Conclusion**: The ki parametric imaging in $^{18}$F-FDG PET/CT dynamic multi-bed scanning can play a very important role in diagnosis for pulmonary lesion. [Keywords] $^{18}$F-FDG PET/CT, pulmonary lesions, parametric imaging, caner

## P680

### Real-time systemic leakage monitoring with 99mTc-labeled red blood cells during hyperthermic isolated lung perfusion with Melphalan and Tumor Necrosis Factor-α

**G. Villa**, F. Fiz, E. Ferrari, M. T. Piras, G. B. Ratto, G. Sambuceti; IRCCS Az Ospedaliera Universitaria San Martino - IST, Genoa, ITALY.

**Aim:** Isolated limb perfusion (ILP) with Melphalan and Tumor Necrosis Factor-α (TNFα) is currently used in the treatment of advanced tumor arising in the extremities or within a single organ such as liver or lung. Severe systemic toxicity and haemodynamic changes have been reported and are reduced when leakage is adequately controlled. Critical steps for ILP are the technique of isolation perfusion and an accurate and real-time monitoring of the leakage. The most diffuse procedure for the evaluation of the systemic leakage is based on utilization of human soluble serum albumin (HSA) labelled with 131I and an external scintillation detector. Due to the non commercial availability of HSA-131I, we have adopted a method based on the in vivo red blood cells (RBC) labelled with 99mTc-stannous pyrophosphate (Angiocis®). In vivo stability of the 99mTc-labelled RBC was previously assessed by monitoring precordial activity in normal subjects. **Material and Methods**: Twelve subjects with pulmonary metastatic adenocarcinoma underwent to this procedure. A small calibration dose of RBC labelled with 99mTcb (4 MBq) was administered into the systemic circulation after surgical isolation of the lung; it allows the evaluation of the blood volume and efficiency of a NaI(Tl) scintillation probe (Neoprobe 2000®) positioned above the controlateral temporal artery. This position was selected in order to minimize the confounding effects of radioactive spill-over from the isolated lung as well as from the unbound 99mTc fraction. A 10-times higher dose of tracer was injected into the perfusion circuit. Any increase in the counting rate, corrected for the 99mTc half-life, was interpreted as a leakage from the isolated circuit to the systemic circulation. The leakage factor (LF) was calculated by following equation: LF= (CPMsyst - CPMbas)/CPMbas x DSyst/Dperf x Vtotal/Vsyst x 100%, where CPMsyst is the systemic count rate, CPMbas the systemic count rate at the beginning of the perfusion, Dsyst the dose injected into systemic circulation, Dperf the dose injected into the perfusion circuit, Vtotal the total blood volume and Vsyst the blood volume of the systemic circulation. **Results and conclusion**: The mean isotopically measured leakage was 7.5% per hour. From our preliminary data, patients with a low leakage rate showed reduced adverse effect. Real time monitoring of the leakage during ILP obtained with radioisotopic procedure seems to be in our experience easy, safe and accurate, and serves as a good guide for the effectiveness of isolation during perfusion.

## P681

### The role of 18F-FDG PET/TC in the diagnostic of the mediastinal lymph nodes. Pathological correlation with EBUS.

**P. Sarandeses Fernández**, A. Hernández Martínez, S. Ruiz Solís, P. Cotrina Monroy, R. García Luján, J. Estenoz Alfaro; Hospital 12 de Octubre, Madrid, SPAIN.

**AIM** Histological confirmation of mediastinal lymph node is usually required in lung cancer proven or suspected staging, other tumors staging (not lung), and less frecuently CT findings. The aim of this study was to evaluate the diagnostic accuracy of 18F-fluoro-2-deoxy-D-glucose (18F-FDG) positron emission tomography/computed tomography (PET/TC) compared to endobronchial ultrasound-guided transbronchial needle aspiration (EBUS-TBNA). **MATERIAL AND METHODS** Retrospective study of 93 patients (p) (116 lymph nodes), 20 women and 73 men, with mean age 65.66 ± 10.05 years. PET/CT and EBUS-TBNA was performed in all of them: in 61 p for lung cancer staging, 22 p for other tumors staging and 10 p for diagnosis of lymphadenopathy observed in TC. Surgical staging/diagnostic procedures (mediastinoscopy or thoracotomy) were recommended in lymph nodes with no conclusive results with EBUS-TBNA. Using logistic regression, we evaluated the discriminatory power of SUVmax, giving the p value and area under ROC curve (AURC). Sensitivity (S), specificity (Sp), positive predictive value (PPV) and negative predictive value (NPV) were studied for differents SUVmax cutoff. **RESULTS** Abnormal uptake in PET/CT (interpreted as tumor) was observed in 88/116 lymphadenopathy. EBUS-TBNA proved malignancy in 65/116, no evidence of malignancy in 18/116 and lymphoid hyperplasia in 33/116. PET/CT values of S, Sp, PPV and NPV compared with EBUS-TBNA were: 100%, 54,9%, 73.8%, 100% respectively (Kappa coefficient of 0.57). 8 p subsequently underwent mediastinoscopy, with histology positive for malignancy in 4 p (4 TP), and negative for the other 4p (2 FP and 2 TN). 6 p underwent thoracotomy with histology positive for malignancy in 3 (2 TP, 1 FN) and negative for the other 3 (2 FP, 1 VN). We established a cutoff value of SUVmax 4,5 to discriminate between malignancy and benignity, and obtained S: 93.85%, Sp: 62.75%, PPV: 76.25% and NPV: 88 , 89% (p value <0.0001 and AURC of 0.78). If we consider the group of lung tumors (in which mediastinal staging is important in determining its resectability) using a cutoff value of 4,5, the S was 94.44%, Sp: 68, 42%, PPV: 89.47% and NPV: 81.85% (p value of 0,001 and AURC of 0.86). **CONCLUSION** PET/CT demostrated high agreement with EBUS-TBNA. Negative findings in PET/CT would avoid histological confirmation, however positive findings indicate it.

## P682

### 18F-FDG PET/CT SUV and CT Net Contrast Enhacement Correlations with size and histology of Lung Cancer

M. L. De Rimini, **F. Porcaro**, C. Landolfi, M. Bifulco, G. Borrelli, G. Mazzarella, S. Piccolo, P. Muto; Nuclear Medicine Dept- AO Ospedali dei Colli-Monaldi, Naples, ITALY.

**Aim:** to identify correlations between the results of dynamic multiphase multi detector CT (MDCT) and [F18] fluorodeoxyglucose standardised uptake value (SUV) with tumor size and cytology in patient affected with lung cancer. **Materials and Methods:** we retrospectively reviewed a total of 50 patients who underwent total body 16 slice MDCT and 18F-FDG PET/CT for staging of lung cancer including: adenocarcinoma, small cell lung cancer, non small cell lung cancer, squamous cell carcinoma. Based on lesion size, 68 patients (pts) were enrolled: 25 pts with solitary pulmonary nodules (SPN) and 25 with a pulmonary lesion measuring between 3 and 7 cm (Mass). Contrast CT Net-enhancement (C-NE) was calculated by subtracting peak pre-contrast density from peak post-contrast one of each lesion. The following lesion parameters were evaluated: maximum diameter, NE, SUV max and cytology. Correlation coefficient and p-value were computed for each pair of variables. **Results**: In malignant SPNs the correlation between SPN size, C-NE and SUV showed increasing in C-NE (r=0.982; p=0.284) and SUV (r=0.789; p=0.421) with an increase of SPNs diameter; - in Mass, a weak correlation (r=0.32; p=0.048) was found between SUV max and tumour size. This correlation was stronger for masses larger than 31 mm (r=0.4515; p=0.0268). No other correlations were found among the variables examined. Regarding the cytological classification, the correlation between tumour size and SUV max was slightly stronger in the case of adenocarcinomas. **Conclusions**: Our data indicate that a lot of prognostic data will be obtained with the multidisciplinary approach, particularly in SPN lesion, prospectively resulting in a better therapeutic outcome. However, owing to the small number of patients in our study, it is difficult to identify clinically important results, requiring a larger numbers of patients and more histological subtypes to determine the full potential and clinical impact of MDCT and PET/CT combined use.

## P683

### Accuracy of F-18 FDG-PET/CT in characterization of lung lesions in correlation with size

**T. Kakhadze**[1,2], A. Fijolek-Warszewska[1], M. Bryszewska[1], G. Łapińska[1], I. Kozłowicz-Gudzińska[1]; [1]Maria Sklodowska-Curie Memory Cancer Center-Institution of Oncology, Warsaw, POLAND, [2]High Technology Medical Center University Clinic, Tbilisi, GEORGIA.

Purpose- The aim of this retrospective study is to evaluate the accuracy of PET/CT in detecting cancer lesions. We assess the accuracy of SUV uptake in lung lesion and its correlation with tumor size and histo types. Additionally correlation between N stagings based on FDG PET/CT and cytology or HP results was assessed. Material and Methods - Our study includes 67 patients referred to FDG PET/CT. 32 patients with unverified lung lesion due to evaluation of FDG metabolism and character of a lesion, 35 patients were diagnosed with cancer and referred for staging. Overall in 51 cases lung lesions were confirmed cytologically or histologically We collected these lesions regarding the sizes: Among 14 small lesions 2cm or smaller in CT scan 8 were neoplasmatic with average suv max 3.9 (range 1.4-9.6). From 16 lession with diameter 2-3 cm 12 were confirmed as Malignant suv max -6.5 (2.8-11.8). From 16 lesion diameters of 2-5cm 13 revealed malignant origin suv max9.2 (4.1-25.0). From 14 lesion diameter 5-7 cm 12 were malignant suv max 10.3(5.7-14.3). From 5 lesion with diameter > 7 cm suv max 11.2(8.2-14.3) all 5 were malignant. The average suv max for adeno-ca was 7,9 (1.4-15.9); squamouscell- 8.3(2.0-14.3); other types of cancer cancer-8.1(3.6-14.4); without malignant cell- 3.1(1,1-6.4); 6 lesions smaller than 2cm with FDG uptake 1,1-2,8 revealed to be granuloma but 3 lesions smaller than 2 cm with FDG uptake less than 2,5 SUV revealed to be malignant 2 lesions with diameter 4 and 5 cm with FDG uptake 4, 6 and 4,4 revealed to be inflammation and granulomatosis. In 30 cases lymph nodes were assessed by cytology or histopathology. In 13 cases FDG PET/CT was truly negative .In 1 case FDG PET/CT gave false negative result,. In 8 cases FDG PET/CT gave true positive result, but same number (8) false positive results although in 2 of those cases imaging findings suggested reactive origin. Conclusion: PET CT is an efficient method of imaging for characterization of lung lesion.. We should take under consideration that small tumor size with faint FDG uptake doesn't not exclude malignant process. Cutoff value of SUV predicting of malignancy should be considered regarding to the tumors sizes. FDG PET CT in lung cancer N staging have high negative predicative value, When positive mediastinal lymph nodes are detected, invasive mediastinal staging must be performed before qualified to surgery.

## P684

### Stage III-IV non small cell lung cancer: the impact of SUVmax and %ΔSUVmax in predicting survival after chemotherapy

A. Cistaro[1,2], **N. Quartuccio**[3], A. Mojtahedi[4], P. Fania[1], M. Cucinotta[3], A. Campennì[3], U. Ficola[5], S. Baldari[3]; [1]Positron Emission Tomography Centre IRMET S.p.A., Euromedic Inc., Turin, ITALY, [2]Co-ordinator of National PET Pediatric Group, Turin, ITALY, [3]Nuclear Medicine Unit, Department of Biomedical Sciences and of the Morphological and Functional Images, University of Messina, Messina, ITALY, [4]Nuclear Medicine Service, Memorial Sloan-Kettering Cancer Center, New York, NY, UNITED STATES, [5]Department of Nuclear Medicine, La Maddalena Hospital, Palermo, ITALY.

**Aim**: To investigate the impact of SUVmax, size of primary lung lesion and %ΔSUVmax on outcome (overall survival:OS, and 2years disease-free survival:2years-DFS) of patients with advanced (stage III-IV) non-small-cell lung cancer (NSCLC). undergoing chemotherapy. We evaluated also the correlation between the pre-treatment SUVmax and the initial response to therapy (best response) and between size and best response. **Materials & Methods**: 86 patients (M=67, F=19; mean age=63.5 years; range=37-80) with advanced NSCLC were included in the study. Thirteen patients (15%) were at stage IIIA, 18 (21%) at stage IIIB and 55 (64 %) at stage IV. Patients underwent 2 FDG-PET/CT scans, before and after chemotherapy and were further classified in subgroups according to the tumor response (EORTC criteria). OS was calculated for patients in disease progression (PD) and PET responders [stable disease (SD), partial response (PR), complete response (CR)]. Correlations between pre-treatment SUVmax and outcome, size and outcome, SUVmax and best response, size and best response were assessed by Student-t test. Correlation between %ΔSUVmax and outcome was assessed using the chi-square test. **Results:** The patients showed an average baseline SUVmax of 12.5 ± 7.43 and a diameter of the primary lesion of 42 ± 20 mm. At the end of the first-line chemotherapy 20/86 patients were in PD, 24/86 were in SD, 35/86 had a PR, and 7/86 showed a CR. In patients in PD (20/86) the recorded average pre-treatment SUVmax was 11.8 ± 5.23 and the mean size of the primary lesion was 43.35 mm ± 16.63. 13/20 patients had already died at the end of the follow-up (OS:35%). In patients in SD, PR or CR (66/86) the average value of pre-treatment SUVmax was 12.7 ± 8.05 and the mean size of the primary lesion was 41.6 mm ± 21.15. 24/66 patients passed away at the end of the follow-up (OS:64%). No significant correlation was discovered between the following couples of parameters: pre-treatment SUVmax and outcome, size and outcome, SUV max and best response, size and best response (p = n.s.). From the analysis of the relationship between %ΔSUVmax and OS we found that patients with Δ<+25%(CR, PR and SD) showed a better OS (p = 0.0235). **Conclusions:** In stage III-IV NSCLC, no useful correlation between SUVmax, tumor size and clinical outcome could be proved. In patients with advanced disease, only %ΔSUVmax can be considered as a useful prognostic factor.

## P685

### Role of 18F-FDG-PET/CT (PET) in addition to fiberoptic bronchoscopy (FOB) in solitary pulmonary nodules differentiation.

**I. Santi**[1], V. de Cristofaro[1], F. Ravenna[2], V. Conti[2], M. Marchi[2], C. Peterle[1], C. Cittanti[1], S. Panareo[1], R. Rinaldi[3], P. Maniscalco[4], S. Fabbri[5], L. M. Feggi[1]; [1]Sant'Anna University Hospital, Nuclear Medicine Unit, Department of Diagnostic Imaging and Laboratory Medicine, Ferrara, ITALY, [2]Sant'Anna University Hospital, Pneumology Unit, Department of Emergency, Ferrara, ITALY, [3]Sant'Anna University Hospital, Pathology Unit, Department of Diagnostic Imaging and Laboratory Medicine, Ferrara, ITALY, [4]Sant'Anna University Hospital, Thoracic and General Surgery Unit, Surgical Department, Ferrara, ITALY, [5]Sant'Anna University Hospital, Medical Physics Unit, Ferrara, ITALY.

**Aim**: to evaluate the diagnostic performance of 18F-FDG-PET/CT combined with fiberoptic bronchoscopy (PET+FOB) compared to the single techniques (PET and FOB) in solitary pulmonary nodule (SPN) characterization. **Materials and Methods**: we studied 39 patients presenting with SPN (1-3 cm) identified by CT scan who underwent both PET and FOB for lesion differentiation. FOB included Trans-Bronchial Biopsy (TBB), Trans-Bronchial Needle Aspiration (TBNA) and bronchial washing (BW). Findings were considered positive as follows: PET, when SUVmax of lesion FDG uptake was ≥ 2.5; FOB, in case either TBB, TBNA or BW was positive for malignancy; PET+FOB, when at least one was positive. Results were validated through histology after surgery or follow-up, as reference standard. Sensitivity, specificity, accuracy, positive predictive value (PPV) and negative predictive value (NPV) of PET, FOB and PET+FOB were respectively calculated. Statistical comparison of frequencies was carried out through Fisher Exact Test. **Results**: out of the 39 patients PET, FOB and PET+FOB respectively resulted true positive (TP) in 31, 18 and 32 cases, true negative (TN) in 5, 6 and 5, false positive (FP) in 1, 0 and 1, false negative (FN) in 2, 15 and 1. PET was FP in 1 TN FOB case (inflammatory lesion), and FN in 2 cases: 1 TP FOB case (bronchioloalveolar carcinoma), and 1 FN FOB case (lung neuroendocrine neoplasm). FOB was FN in 14 TP PET cases. The diagnostic performance of PET, FOB and PET+FOB respectively resulted in: sensitivity 93.9, 54.5 and 97.0 %; specificity 83.3, 100.0 and 83.3 %; accuracy 92.3, 61.5 and 94.9 %; PPV 96.9, 100.0 and 97,0 %; NPV 71.4, 28.6 and 83.3 %. No statistically significant difference was found between PET and PET+FOB results, as well as in specificity and PPV of the three Methods. Statistically significant difference was found both between FOB and PET, and between FOB and PET+FOB in sensitivity (p<0.001) and accuracy (<0.01), and between FOB and PET+FOB in NPV (p<0.05). **Conclusions**: despite the small series presented, PET showed high sensitivity and accuracy playing an important diagnostic role especially in cases of FN FOB. The addition of PET to FOB resulted in a statistically significant improvement in sensitivity, accuracy and NPV that strengthens the value of multimodal patient management. Further studies based on larger series may lead to the setting of a consistent diagnostic flow-chart involving PET and FOB, and to a better selection of patients with small pulmonary lesions addressed to surgery.

## P686

### Significance of lesions: single lesion, five lesions and whole body lesions, in prediction of Progression Free Survival (PFS) & Overall Survival (OS) and response evaluation in NSCLC patients treated with EGFR tyrosine kinase inhibitor therapy by PERCIST criteria - A comparative prospective study.

**A. Bhoil**[1], B. R. Mittal[2], R. Kashyap[3], B. Singh[3], N. Singh[3]; [1]Nuclear Medicine Centre, Regional Cancer Centre, I.G.M.C., Shimla, INDIA, [2]Post Graduate Institute Of Medical Education and Research, Chandigarh, INDIA, [3]Post Graduate Institute of Medical Education and Research, Chandigarh, INDIA.

AIM: To compare the significance of hottest single lesion, five lesions and whole body lesions in prediction of OS & PFS in NSCLC patient treated with EGFR inhibitor therapy. MATERIAL and METHODS: 23 patients(14M, Mean age 55yrs) with stage ≥IIIb NSCLC treated with EGFR inhibitor therapy were prospectively analysed with 18F-FDG PET/CT at 3weeks (early) and 6weeks (late) for response evaluation with PERCIST criteria. Patient analyses were done with SUVmax and TLG in 3 categories 1) Hottest lesion, 2) Five hottest lesions 3) SUVmax of hottest lesion and TLG of whole body lesions. The patients were classified as responder vs non-responders and as having progressive and non progressive disease. PFS and OS was estimated with Kaplan-Meier analysis RESULTS: Hottest lesion: The PFS in early and late FDG studies of the SUVmax and TLG in responders was (p<0.04 &0.09) and (p<0.72 &0.84) and in non progressive disease was (p<0.11 &0.37) and (p<0.34 &0.34). The OS in early and late FDG studies of SUVmax and TLG in responders was (p<0.04 &0.34) and (p<0.74 &0.37) and in non progressive disease was (p<0.05 &0.12) and (p< 0.46 &0.46). Five lesions: The PFS in early and late FDG studies of the SUVmax and TLG in responders was (p<0.04 & 0.09) and (p<0.18 &0.44) and in non progressive disease was (p<0 .11 &0.37) & (p<0.11 &0.11). The OS in early and late FDG studies of the SUVmax and TLG in responders was (p< 0.32 &0.17) and (p<0.25 &0.43) and in non progressive disease was (p< 0.049 &0.115) and (p<0.05 &0.05). Whole body lesions: The PFS in early and late FDG studies of the SUVmax and TLG in responders was (p< 0.04 &0.09) and (p< 0.72 &0.46) and in non progressive disease was (p <0 .11 &0.37) & (p< 0.34 &0.34) in non progressive disease. The OS in early and late FDG studies of the SUVmax and TLG in responders was (p<.04 &0 .34) and (p<0.74 &0.37) and in non progressive disease was & (p< 0.05 &0.12) & (p< 0.46 &0.84). CONCLUSION: The prediction of PFS and OS with SUVmax were similar in all 3groups. TLG of five lesions was better predictor of PFS and OS. Hence SUVmax of hottest lesion and TLG of 5 lesions would be a better to define the tumor response as per PERCIST criteria. Also FDG study at 3weeks was better predictor of response and PFS and OS compared to 6weeks study.

## P687

### Pulmonary Lesions Associated with Hypermetabolic Lymph Nodes: Are They All Malignant?

**M. Sipahi**[1], A. Cengiz[2], E. Budak[1], A. Öner[1], S. Demirelli[1], F. Aydın[1]; [1]Akdeniz University Medical School, Departmen of Nuclear Medicine, Antalya, TURKEY, [2]Adnan Menderes University Medical School, Departmen of Nuclear Medicine, Aydin, TURKEY.

Aim: The aim of this retrospective study to evaluate the accuracy of F-18 FDG PET/CT in differentiating benign from malignant pulmonary lesions in patients with associated mediastinal lymph nodes. Methods: A total of 81 patients (23 women, 58 men, mean age: 63.5) referred to our department between January 2011 - December 2012 for the metabolic characterization of pulmonary lesions with F-18 FDG PET/ CT were included in the study. Lesions were classified according to their size, metabolic activity (maximum standardized uptake value: SUVmax) and associated lymph nodes. The diagnosis was confirmed by histopathology. Results: The size of pulmonary lesions varied between 1-12 cm, and SUVmax was calculated between 2.1-30. On histopathologic examination, while 56 (69%) of the hypermetabolic pulmonary lesions were determined to be malign, 25 (31%) were found as benign lesion. Eighteen (72%) of the benign hypermetabolic lesions were associated with lymph nodes demonstrating metabolic activity (1.2-2 cm in size and with SUVmax: 3.6-21). Conclusion: We found that not all hypermetabolic pulmonary lesions associated with hypermetabolic lymph nodes were malignant.

We believe that pulmonary lesions associated with lymph nodes should be confirmed with histopathologic examination regardless of their metabolic activity.

## P688

### Implications of metabolic maximum in the primary lung tumour versus the metastatic lesions

**P. C. Holdgaard**, A. D. Nygaard, K. G. Spindler, N. Pallisgaard, A. Jakobsen; Sygehus Lillebælt, Vejle, DENMARK.

Background: Patients with advanced non small-cell lung cancer (NSCLC) are treated with chemotherapy and sometimes radiotherapy. Metabolic positron emission tomography imaging (PET) with $^{18}$F-fluorodeoxyglucose (FDG) provides information of prognostic significance and can aid the delineation of metabolically active target volumes for radiation therapy. We wished to study the implications of a metabolic maximum located outside of the primary tumour, as it may affect the areas intended for dose escalation. Methods: Patients with newly diagnosed NSCLC being candidates for first-line chemotherapy were enrolled into a prospective biomarker trial (2007-2010) at the Department of Oncology, Vejle Hospital, Denmark. Patients who had a FDG PET scan within a month prior to enrolment were included in this study. The FDG uptake was assessed using the maximum standardized uptake value (SUVmax). Metabolic tumour volumes (MTV) were calculated semi-automatically using a threshold of 2.5 SUV. Patients were dichotomized by the location of SUVmax: Primary tumour versus metastases, including mediastinal lymph nodes. Data were analyzed by non-parametric statistics and reported as median values. Results: Fifty-three of the 246 patients were included. Two patients had no metastases and one patient had no measurable primary tumour. 35 patients (66%) had SUVmax (12.8) located in the primary tumour (PRIM-group) and 15 patients (28%) had SUVmax (8.8) located in one of the metastatic lesions (METS-group). There was no significant difference in overall survival (OS) between the PRIM-group (17.2 months) and the METS-group (12.4 months) (p=0.8). Overall SUVmax (p=0.04) and primary tumour MTV (PRIM: 55.1 ml vs. METS: 16.0 ml), (p=0.02) were lower in the METS-group. SUVmax in the primary tumour was neither correlated to primary tumour size (r=0.60, p=0.09) nor total tumour burden (r=0.48, p=0.10). Patients with a total tumour burden above the median, had a significantly shorter OS than patients below the median (p=0.02). The same did not apply to patients with a primary tumour size above versus below (p=0.8). Conclusion: In personalized radiotherapy of NSCLC-patients it is important to notice that a substantial proportion has SUVmax located outside of the primary tumour, but the OS is not influenced by the location of the baseline SUVmax. Patients with SUVmax located in the metastases have a significantly smaller primary tumour and an overall lower metabolic maximum, indicating a different tumour growth and metastatic potential. Furthermore, a large total tumour burden had a prognostic value in OS.

P40-2 - Tuesday, Oct. 22, 16:00 - 16:30, Poster Exhibition Area

## Oncology Clinical Science: Oesophageal

## P689

### Additional value of MDCT over F-18 FDG-PET/CT in assessment of lymph nodes metastases in patients with esophageal carcinoma

**M. Ishihara**[1], M. Shiiba[1], H. Udagawa[2], H. Maruno[3], K. Ishihara[4], S. Kumita[4]; [1]Department of Diagnostic Imaging, Toranomon Hospital, Tokyo, JAPAN, [2]Department of Surgery, Toranomon Hospital, Tokyo, JAPAN, [3]Department of Radiology, Toranomon Hospital, Tokyo, JAPAN, [4]Department of Radiology, Nippon Medical School, Tokyo, JAPAN.

In patients with esophageal carcinoma (EC), lymph nodes metastases occur even in the early stage. Furthermore, most of the metastatic nodes are less than 1cm in diameter, which can be misdiagnosed by conventional PET as well as CT images. Integrated PET/CT equipping multidetector CT (MDCT) provides high specificity in nodal metastases owing to easy anatomical registration, however, better sensitivity has been required to alternate with endoscopic ultrasound (EUS) which has a limited specificity especially in deep lymph node area. The purpose of this retrospective study is to assess whether MDCT over PET/CT provides additional value on nodal metastases in EC using “EUS-like" diagnostic criterion. Ninety-one patients with EC (80 males and 11 females, 10 T1a, 28 T1b, 17 T2, 33 T3 and 3 T4 patients as T stage, 2 cervical, 19 upper thoracic, 39 middle thoracic, 47 lower thoracic, 6 abdominal totally lesions as primary location) who underwent PET/CT and received three-field lymph node dissection surgery within 6 months were participated. Thirty-seven cases received preoperative chemotherapy. We obtained F-18 FDG-PET/CT images using an integrated PET/CT scanner with 16-slice CT system. PET/CT images were visually assessed by the consensus of two diagnostic and nuclear medicine specialists as follows. The lymph node was considered positive for metastasis if the FDG uptake was higher than that of background (PET/CT criterion). For “EUS-like” (PET/CT+MDCT) criterion, the lymph node was defined positive when short axis of the node was more than 5mm and the shape was oval or round regardless of the FDG uptake. Regional (region1; cervical ~ upper mediastinal, region2; subcarinal ~ supradiaphragmatic, region3; abdominal) nodal metastases were evaluated by each criterion and correlated with pathologic results, respectively. Of the 273 regions of 91 patients, 42 were positive and 231 were negative in PET/CT criterion whereas 64 were positive and 209 were negative in PET/CT+MDCT criterion, obtaining 44% vs. 55% sensitivity, 98% vs. 91% specificity and 81% vs.80% accuracy, respectively. Regionally, PET/CT+MDCT had higher sensitivity in region 1 (53% vs. 65%) and region 3 (47% vs. 68%) compared with those of PET/CT. Accuracy, however, did not improve in any regions. In assessment of lymph node metastases in patients with EC, MDCT over PET/CT is useful to improve sensitivity especially in abdomen where lymph nodes are likely to be distant from the intestinal wall, but challenging problem still exists to achieve high diagnostic performance.

## P690

### 18F-FDG PET in gastro-oesophageal cancer: clinical impact of Partial Volume Correction in treatment monitoring

**C. Canevari**[1], F. Gallivanone[2], L. Gianolli[1], M. Gilardi[2], I. Castiglioni[2]; [1]San Raffaele Scientific Institute, Milan, ITALY, [2]IBFM-CNR, Segrate, ITALY.

**AIM:** To assess the clinical impact of Partial Volume Correction (PVC) on 18F-FDG PET/CT studies for the monitoring of treatment response in gastric malignancies. **MATERIALS AND METHODS**: 30 biopsy-proven gastro-oesophageal cancer patients were enrolled in a clinical protocol, requiring a basal 18F-FDG PET/CT study and a follow up 18F-FDG PET/CT study after neoadjuvant chemotherapy. For each GC lesion detected on both basal and follow up 18F-FDG PET/CT studies, averaged Body-Weight Standardized Uptake Value (SUVBW) was calculated. A PVC method based on Recovery Coefficients as a function of PET measured sphere-to-background ratios and PET measured sphere volumes [1] allowed to obtain Partial Volume Corrected SUVBW (PVC-SUVBW) for the GC lesions. SUVBW and PVC-SUVBW changes during follow up (ΔSUVBW and ΔPVC-SUVBW) were calculated for each detected lesion. The effect of PVC was evaluated in terms of tumour response classification (EORTC 1999 [2]). **RESULTS**: PVC affected basal and follow up SUV values up to 85%. In 5/30 patients (17%), PVC modified the tumour response classification. For 2 lesions the classification changed from “Partial metabolic response” to “Stable metabolic disease”, and for 3 lesions the classification changed from “Progressive metabolic disease” to “Stable metabolic disease”. In the remaining 83% of cases, PVC did not affect the tumour response classification, but significantly modified the SUV changes during follow up: 1) in 19 lesions classified as “Partial metabolic response”, ΔSUV modified up to 25% with PVC, averaged ΔSUVBW=-66%±16% and averaged ΔPVC-SUVBW =-64%±16%; 2) in 6 lesions classified as “Progressive metabolic disease”, ΔSUV modified up to 55% with PVC, averaged ΔSUVBW=78%±52% vs averaged ΔPVC-SUVBW=60%±36%, 3) in 2 lesions classified as “Stable metabolic disease”, ΔSUV modified up to 15% with PVC, averaged ΔSUVBW=-3.9%±0.3% vs averaged ΔPVC-SUVBW=-8%±8%. **CONCLUSIONS** PVC has a clinical impact on PET/CT studies and has to be considered for the monitoring of treatment response in gastric malignancies. REFERENCES [1] F. Gallivanone, et al. (2011) “PVE correction in PET-CT whole-body oncological studies from PVE-affected images”, IEEE Trans Nucl Sci, vol. 58(3), pp. 736-747. [2] H. Young, et al. (1999) “Measurement of clinical and subclinical tumour response using [18F]-fluorodeoxyglucose and positron emission tomography: Review and 1999 EORTC recommendations,” Eur. J.Canc, vol. 35, pp. 1773-1782.

## P691

### Can the maximum standardised uptake value (SUVmax) predict regional lymph node (LN) metastasis in oesophageal cancer? : preliminary study

**G. Koh**, H. Lee, J. Kim, S. Kim, K. Hwang; Gil Hospital, Incheon, KOREA, REPUBLIC OF.

BACKGROUND According to a report from National Cancer Information Centre in South Korea, oesophageal cancer was the 17th leading cancer in both genders in 2009. It occurred more commonly in men by about twelvefold than women. In oesophageal cancer, surgery is the most preferable treatment method if indicated (patients with stage I, II and some III) and there are various surgical procedures associated with the disease. Authors evaluated whether SUVmax of the primary one can give information about regional LN metastasis. METHOD We retrospectively investigated 30 histopathologically confirmed oesophageal cancer patients (29 men, 1 woman, aged from 51 to 84 with a median of 67) who underwent pre-operative PET-CT examination from April 2007 to December 2012. SUVmax of the oesophageal cancer was measured and we compared the SUVmax values in patients with regional LN metastasis to those in patients with only primary cancer. Regional LN metastasis was confirmed by histopathologically or follow-up imaging study. RESULTS 19 patients had proven regional LN metastasis and the remaining 11 did not. The SUVmax of the former ranged from 5.21 to 24.97 with a median of 10.65, mean of 11.96, standard deviation (SD) of 5.35 and from 2.71 to 18.25 with a median of 6.1, mean of 7.4, SD of 5.29 for the latter. There was statistically significant difference between the two groups ($p$=0.03). CONCLUSION

This study showed a significant difference in SUVmax of primary oesophageal cancer between the patients with regional LN metastasis and without. Further study is warranted with more cases.

P41-2 - Tuesday, Oct. 22, 16:00 - 16:30, Poster Exhibition Area

## Oncology Clinical Science: Liver

### P692

### Prognostic Factors of Bile Duct Cancers in Patients Receiving Pretreatment FDG PET/CT

**M. CHENG**[1], Y. WU[2], R. YEN[1], K. TZEN[1], H. WANG[1]; [1]National Taiwan University Hospital and National Taiwan University College of Medicine, TAIPEI, TAIWAN, [2]Far Eastern Memorial Hospital, New Taipei, TAIWAN.

**Purpose:** This study aims to assess the prognostic factors for survival in bile duct cancer patients receiving [$^{18}$F]fluorodeoxyglucose (FDG) positron emission and computed tomography (PET/CT) before treatment. **Material and Methods:** Information on 107 consecutive patients with bile duct cancers before treatment and FDG PET/CT was entered into a prospective database at a single institution. Forty-eight patients (44.9%) underwent curative surgical resection and the remaining 59 subjects (55.1%) were unresectable. All patients were followed up until 5 years or death. The effects of clinicopathological factors including primary tumor standardized uptake value (SUV) were assessed by univariate (Kaplan-Meier curves and log-rank test) and multivariate analyses (Cox-proportional hazard model). **Results:** The median overall survivals were 19.7 months for the entire cohort and 29.0 months for curative resection. In all 107 patients, multivariate analysis showed that surgical resection (risk ratio 3.9, 95% confidence interval [CI] 2.14-7.26, *P*=0.005) and advanced AJCC stage (3.7, 1.99-6.94, *P*=0.005) were independent predictors of survival regardless of the primary tumor SUV. In the 48 patients who received surgical resection, multivariate analysis identified pathological lymph node metastasis (4.3, 1.79-10.56, *P*=0.0004), involved surgical margin (2.6, 1.30-5.28, *P*=0.005), and lymphovascular invasion (2.4, 0.96-5.86, *P*=0.05) as independent prognostic factors for overall and disease-free survival. Also, primary tumor SUV>5 showed a significant relationship with pathological lymph node metastasis (*P*=0.027). **Conclusions:** Our data suggest that surgery offers the most beneficial outcome in bile duct cancer, emphasizing the importance of resectability as a major prognostic factor. The present study also identified SUV>5 of primary tumor is associated with pathological lymph node metastasis.

### P693

### Head to head comparison of abdominal binding 18F-FDG PET/CT versus magnetic resonance imaging in metastatic liver lesions

**V. Soubeyran**, V. Bettschart, S. Anchisi, C. Constantin, J. Feilchenfeldt, J. Coppey, E. M. Kamel; CHCVs, Sion, SWITZERLAND.

**Aim:** To prospectively investigate the performance of abdominal binding $^{18}$F-FDG PET/CT in identifying metastatic liver lesions versus that of MRI as the current radiological standard of reference. **Material and Methods:** Twenty one cancer patients were enrolled. All patients were subjected to abdominal binding $^{18}$F-FDG PET/CT and MRI no more than 2 weeks apart. Abdominal binding free breathing PET/CT was achieved after applying a conventional abdominal binder over the right hypochondreal region. Each binder was fastened at the front with Velcro over a cylindrical sponge appropriate to patient's size. This approach was previously shown to improve the overall PET/CT performance through reducing the craniocaudal liver movements during the acquisition. Double blinded abdominal binding $^{18}$F-FDG PET/CT and MRI interpretations were done by different readers. The final diagnosis was established by histological examination or radiological follow-up (>6months). **Results:** Abdominal binding $^{18}$F-FDG PET/CT was tolerated by all patients since no technical failure was reported. There were 55 liver lesions (45 liver metastases and 10 benign lesions). Thirteen (62%) of the 21 patients had liver metastases, whereas 8 (38%) patients with- and without-structural liver alterations were free from hepatic involvement by their cancers. On lesion based analysis, PET failed to detect 4/45 (9%) metastases of 3 and 4mm in 1 patient who had already other FDG avid liver metastasis. These 4 lesions were detected by MRI. On the other hand, MRI mistook 3 microabscesses in sub-acute phase and 1 atypical hemangioma for liver metastases in 2 patients. These 4 lesions did not show FDG accumulation and accordingly they were successfully characterized by PET as of benign nature. The overall sensitivity, specificity, and accuracy of abdominal binding $^{18}$F-FDG PET/CT were 91%, 100%, and 98%. Corresponding values of MRI were 100%, 64%, and 98%. **Conclusion:** Abdominal binding has the potential to improve the overall performance of $^{18}$F-FDG PET/CT in the work-up of liver metastases versus that of MRI showing comparable sensitivity and better specificity.

### P694

### Evaluation of Hepatocellular Carcinoma (HCC) before and after Vascular Endothelial Growth Factor Antibody Therapy (Bevacizumab) and Transarterial Chemoembolisation by using C-11-Acetate PET and F-18-FDG PET

**P. Ubl**, M. Peck-Radosavljevic, H. Eidherr, M. Mitterhauser, W. Wadsak, S. Li; Medical University of Vienna, Vienna, AUSTRIA.

Aims: The hepatocellular carcinoma (HCC) is one of the most malignant tumours and its incidence continues growing. The aim of this study was to compare the results of C-11-acetate PET with F-18-FDG PET in patients with HCC before and after treatment with transarterial chemoembolisation (TACE) and VEGF-antibody (Bevacizumab). Patients and Methods: 15 patients with histopathological verified HCC were prospectively investigated. CT/MR, C-11-acetate PET and F-18-FDG PET were undertaken for each patient. The results were analyzed before and after treatment with Bevacizumab and TACE. Results: Positive results were found in 11 of 15 patients (73 %) and 24 of 58 HCC lesions (41%) were shown by using C-11-acetate PET. Only 7 of 15 patients (47 %) and 14 of 58 lesions (24 %) were demonstrated by F-18-FDG-PET. After treatment with TACE and Bevacizumab, positive results were shown only in 3 of 11 patients (27 %) and in 4 of 44 HCC lesions (9 %) by C-11-acetate as well as by F-18-FDG. Conclusion: Higher sensitivity of C-11-acetate PET was shown as compared with F-18-FDG PET in the detection of HCC lesions. The results suggests that C-11-acetate PET and F-18-FDG PET may be useful in the diagnosis and follow-up of patients with HCC.

### P695

### Can we predict microvascular invasion in HCC on FDG PET-CT imaging parameters?

**V. Agarwal**, S. PANDE, S. KRISHAN, B. SUNEETHA, D. JANGID; MEDANTA THE MEDICITY HOSPITAL, GURGAON, INDIA.

**Objectives :** The purpose of this study is to correlate clinicopathologic and PET-CT parameters with the presence of microvascular invasion at histopathologic examination in patients with hepatocellular carcinoma (HCC) who have undergone liver transplantation **Methods :** In this retrospective single-center study, we assessed 224 patients (187 men and 37 women; mean age, 52 years) with HCC who underwent liver transplantation and pretransplant PET-CT (performed within 20 days before liver transplantation). Three physicians (two nuclear medicine specialist and one radiologist) analyzed the following tumor parameters in consensus: size, multi-focality, pattern of uptake, quantitative FDG uptake (SUV), pattern of enhancement and distance to closest vessel. The size and number of lesions, tumor differentiation and the presence or absence of microvascular invasion were determined at histopathologic examination. Histopathological findings were analysed vis-a-vis to the imaging parameters on PET-CT to determine any useful indicator for predicting microvascular invasion. **Results :** . None of the clinical parameters was predictive of microvascular invasion; however on univariate analysis, MVI was statistically significantly associated with morphologic features of multi-focality, uptake pattern and distance to the closest vessel; on FDG PET-CT. By applying multiple logistic regression analysis, uptake pattern (heterogeneous and peripheral FDG uptake) was found to be the only independent risk factor for MVI. **Conclusions :** Heterogeneous and peripheral FDG uptake on FDG PET-CT was the only parameter that correlated significantly with microvascular invasion.

P42-2 - Tuesday, Oct. 22, 16:00 - 16:30, Poster Exhibition Area

## Oncology Clinical Science: Urogenital

### P696

### Comparison between $^{18}$F-fluoride PET/CT and $^{99m}$Tc-MDP bone scintigraphy in the detection of bone metastases from clear cell renal carcinoma (RCC): a prospective pilot study.

**C. FUCCIO**[1], R. PALUMBO[1], M. FRASCAROLI[1], E. SPINAPOLICE[1], P. CASTELLUCCI[2], F. CECI[2], E. LATELLA[1], D. D'AMBROSIO[1], A. BERNARDO[1], G. TRIFIRO'[1]; [1]FONDAZIONE MAUGERI, PAVIA, ITALY, [2]POLICLINICO SANT'ORSOLA-MALPIGHI, BOLOGNA, ITALY.

**Aim**: the study aim was to prospectively compare the diagnostic value of $^{18}$F-fluoride PET/CT and $^{99m}$Tc-MDP bone scintigraphy in the detection of bone metastases in the restaging of patients affected by metastatic RCC. **Materials and Methods**: consecutive patients affected by bone metastases from RCC and treated with Sunitinib as first-line therapy for the metastatic disease were enrolled. There were 10 males and 1 female, median age 65 years (range 53-86); Fuhrman grade at nephrectomy was G2 in 7, G3 in 3 and G4 in 1. All underwent $^{18}$F-fluoride PET/CT and $^{99m}$Tc-MDP bone scintigraphy. The time elapsed from two investigations ranged from 7 days to 67 days. Images were interpreted visually by two experienced readers and results were compared. Validation of results was established by follow-

up and, when possible, by biopsy. **Results**: eleven patients were currently evaluable for the study endpoints. On a patient-based analysis, results of the two Methods were in accordance: $^{99m}$Tc-MDP bone scintigraphy and $^{18}$F-fluoride PET/CT were positive in 8 patients and negative in 3 patients. On a lesion-based analysis, $^{99m}$Tc-MDP bone scintigraphy showed a total of 21 lesions, while $^{18}$F-fluoride PET/CT identified a total of 32 lesions. Three out of 32 lesions detected by $^{18}$F-fluoride PET/CT were osteoblastic, 14/32 were mixed and 12/32 lesions were lytic. The remaining 3 lesions did not show any structural changes at CT. The eleven lesions identified by PET/CT and not by bone scintigraphy were located in: scapula (3 lesions), rib (1),sternum (1), vertebra (3) and pelvis (3). The bone structure of these lesions were lytic in 7 cases, mixed in 1, osteoblastic in 1(lesion size= 9.3 mm) and without significant alterations in 2. **Conclusion**: $^{18}$F-fluoride PET/CT demonstrated a higher sensitivity when compared to bone scintigraphy in the detection of lytic bone lesions. $^{18}$F-fluoride PET/CT could also add information in case of small osteoblastic lesions or without any structural alteration. The main limitations of the study were the limited number of patients and the validation of positive findings only based on a longitudinal follow up of each lesion. The accrual is ongoing to confirm such preliminary results on a larger population, aiming to a better definition of the potential advantages of $^{18}$F-fluoride PET/CT in metastatic RCC. Specifically, these findings could be of value in the debated field of the evaluation of response in RCC patients with bone metastases treated with biological multitargeted therapies as Sunitinib.

## P697

### FDG PET/CT in patients with nonseminoma testicular cancer with elevated surveillance tumor markers and negative conventional imaging

Y. Bocheva, **P. Bochev**, A. Klisarova; Mbal St. Marina Varna, Varna, BULGARIA.

Nonseminoma testicular cancer is a heterogeneous group of malignancies. This specific type of cancer is a rare condition whose initial management include surgery and subsequent chemotherapy with further follow up. The follow up itself includes serial testing of alpha-fetoprotein (AFP), h-BCG (human chorion gonadotropin) and lactate dehydrogenase (LDH) as serum tumor markers as well as conventional imaging with CT. FDG PET/CT is not routinely indicated at any step of the patients' management. A specific clinical situation appears when tumor markers are elevated during surveillance but conventional imaging techniques fail to localize disease. Aim of the study was to assess the value of FDG PET/CT in patients with nonseminoma testicular cancer, treated with curative intent, with elevated tumor markers during follow up, in whom conventional CT imaging fail to localize disease. Materials and Methods: the files of all patients with testicular cancer, referred to our nuclear medicine department for FDG PET/CT in the period 2009-11 were retrospectively reviewed. Inclusion criteria consisted of nonseminoma hystologies, no objective persistence of disease after initial treatment, elevated AFP and/or hBCG and negative abdominal/pelvic CT scan and chest X-ray or CT. Only 5 patients met the inclusion criteria with AFP elevated in 4, hBCG in 2 (both markers in one patient). Final diagnosis was based on histology or follow up data. Results: FDG PET/CT was read as positive in 4/5 patients - two with paraaortic lymph node involvement, one with lung metastases , one with mediastinal lymph node involvement and one with more extensive disease. All patients were verified as true positive by histology (2) or follow up (2). The single patient with negative PET had follow up data for 36 months , but no evidence of recurrence was detected by either CT of subsequent PET/CT and the case was accepted true negative. FDG detected recurrence in 4 cases and correctly classified all 5 cases. The elevated tumor marker classified correctly 4/5 patients. Conclusion: Although based on very limited number of cases the study results supports the use of FDG PET/CT in patients with nonseminoma testicular cancer with elevated tumor markers, but no disease localization by conventional imaging Methods.

## P698

### 18F-FDG PET/CT in the Evaluation of Lymphnode metastasis in penile cancer patients

A. L. Salazar[1], C. E. C. Fonseca[1], M. Viana[1], G. Bretas[1], T. P. Pena[1], P. F. Perdigão[2], **M. Mamede**[1]; [1]Universidade Federal Minas Gerais, BELO HORIZONTE - MG, BRAZIL, [2]Instituto Mario Penna, BELO HORIZONTE - MG, BRAZIL.

**Aim:** We prospectively evaluated $^{18}$F-fluorodeoxyglucose ($^{18}$F-FDG) positron emission tomography-computerized tomography (PET/CT) to assess inguinal lymph node status, the main prognostic factor in invasive squamous cell carcinoma of the penis. **Material and Methods**: 21 patients with invasive squamous cell carcinoma of the penis from our institution were prospectively included in this study. Lymph node status was assessed preoperatively by $^{18}$F-FDG PET/CT to detect subclinical metastasis in 9 patients with initially cN0 disease and quantify inguinal lymph node invasion in 12 with cN+. **Results**: In the 9 cN0 cases, $^{18}$F-FDG PET/CT were positive in 6 patients (total of 9 inguinal lymph node basis analyzed) with maxSUVlbm 4.3 ± 2.1. In the remaining 12 cN+ patients, $^{18}$F-FDG PET/CT were positive in all cases (total of 33 inguinal lymph node basis analyzed) with maxSUVlbm 7.6 ± 4.9. Interesting to mention that the primary lesions showed significantly higher $^{18}$F-FDG uptake (maxSUVlbm 16.7 ± 5.3) compared to those from cN0 cases (maxSUVlbm 9.7 ± 4.8). In 2 cases staged clinically as cN1 $^{18}$F-FDG PET/CT revealed several metabolically active lesions on the same side (pN2) and/or active lesions in the pélvis (pN3), up-staging these cases. **Conclusions**: $^{18}$F-FDG PET/CT is a useful staging examination for invasive penile cancer. It confirms inguinal lymph node invasion and can detect subclinical inguinal lymph node invasion.

## P699

### The Spinal Nerve Invasion Detected with 18 F FDG-PET/CT in a Operated with Penile Cancer

**Z. KANDEMIR**[1], N. YILDIRIM POYRAZ[1], E. ÖZDEMİR[1], H. F. ERDİL ERYILMAZ[2], M. KESKİN[1], S. TÜRKÖLMEZ[1]; [1]Ministry of Health Atatürk Training and Research Hospital Department of Nuclear Medicine, Ankara, TURKEY, [2]Ministry of Health Atatürk Training and Research Hospital Department of Radiology, Ankara, TURKEY.

**Introduction** Penile cancers compose less than 1% of all urogenital cancers. Genital infections and HPV 16-18 increase the incidence rates. Bad hygiene and phimosis are among the most important risk factors. Through local invasion, the tumor leads to corpus cavernosum and urethra involvement and also it may cause metastasis by means of lymphatic system. Metastasis to body parts and organs such as lungs, liver, brain and bones accompanied with vascular involvement is rare. PET/CT is an imaging technique which is used to detect regional and distant metastasis. In this paper, our aim was to present the PET/CT images of a patient who had radical penectomy surgery due to penile cancer. FDG PET/CT scan was performed to this patient in terms of restaging and treatment procedures. At the right S-2 (sacral 2) foramen level, pathologic FDG uptake was detected. The PET/CT images were correlated with contrast-enhanced MRI. **Case Presentation** Following the detection of a soft tissue lesion in the right obturator region during abdominopelvic CT imaging, a 57-year-old male patient was directed to our clinic for PET/CT scanning to determine restaging and treatment procedures. In the PET/CT images, in the right obturator region, high pathologic F-18 FDG uptake was observed in a soft tissue lesion attached to the right piriformis muscle containing hipometabolic parts(SUV max: 16.8). In addition, at the right S-2 foramen level, a gradually increased focal F-18 FDG uptake was observed in the late images (SUV max: 5.9). This finding was not significant in the bone images of the CT scan and a radiological correlation was recommended considering spinal nerve invasion. Following the iv Gad-DTPA injection, a sacral MRI scan was performed. According to this, the bone structures were normal. At the S2 level, in the right S2 nerve root, asymmetric contrast uptake was seen. In addition, inside the spinal canal at this level, nodular contrast uptake was observed in the filum terminale. In both PET/CT and MRI images, the findings concerning the right S2 nerve root were associated with the spinal nerve invasion. **Conclusion** Spinal nerve invasion is seen rarely and it is difficult to detect it. As PET/CT whole body scan has the advantage to perform anatomical and functional imaging at the same time, it detected the spinal nerve invasion. This finding was also verified with MRI imaging.

P43-2 - Tuesday, Oct. 22, 16:00 - 16:30, Poster Exhibition Area

# Oncology Clinical Science: Prostate

## P700

### 18F-Fluorocholine PET/CT versus PSA in Patients with Recurrent Prostatic Cancer

**R. Silva**[1], M. Martins[1], P. Lapa[1], G. Costa[1], J. Pedroso de Lima[1,2]; [1]Centro Hospitalar Universitário de Coimbra, COIMBRA, PORTUGAL, [2]Instituto de Ciências Nucleares Aplicadas à Saúde, Coimbra, PORTUGAL.

AIM: Relapse after treatment of localized prostate cancer is not uncommon. 18F-Fluorocholine PET/CT allows evaluation of local recurrence and distant metastases in a single step. This information is essential for treatment planning. However, PET/CT has limited sensitivity at low PSA levels. The purpose of this work was to evaluate the impact of PSA levels in the sensitivity of 18F-Fluorocholine PET/CT for the detection of recurrent disease in prostatic cancer patients with biochemical failure. MATERIAL AND METHODS: The clinical charts of 50 patients, median age of 65.5 (1ºQ:60;2ºQ:65.5;3ºQ:70;48-81) years and median PSA of 1.34 (1ºQ:0.6;2ºQ:1,34;3ºQ:2.8;0.2-50) ng/ml, submitted to radical prostatectomy with biochemical failure, who performed 18F-Fluorocholine PET/CT, were reviewed. PET studies were obtained after injection of 4MBq/Kg of 18F-Fluorocholine (dynamic pelvic acquisition followed by whole body acquisition and a late image of the pelvis). Three different, nonexclusive, recurrence patterns were considered: 1) Local recurrence in the prostatectomy bed; 2) Loco-regional metastases in pelvic lymph nodes; 3) distant metastases (nodal or osseous). An independent samples Mann-Whitney U test was used to compare the PSA values of patients with and without evidence of disease. RESULTS: PET evidence of disease was found in 25 of 50 patients (50%), 9(18%) with local recurrence, 14(28%) with loco-regional pelvic lymph nodes metastases and 12(24%) with distant metastases. Considering only

patients with PSA < 2ng/dl, PET evidence of disease was found in 11 of 34 patients (32%), 5(15%) with local recurrence, 2(6%) with loco-regional pelvic lymph nodes metastases and 4(12%) with distant metastases. Considering only patients with PSA ≥ 2ng/dl, PET evidence of disease was found in 14 of 16 patients (87.50%), 4(25%) with local recurrence, 12(75%) with loco-regional pelvic lymph nodes metastases and 8(50%) with distant metastases. A statistical significant difference ($p<0.05$) in PSA values was found between patients with (n=25) and without (n=25) PET evidence of disease. CONCLUSION: A statistical significant difference in PSA values was found between patients with and without PET evidence of recurrent prostatic cancer. The detection rate of 18F-Fluorocholine PET was closely related to PSA values, with an overall detection rate of 32% in patients with PSA < 2ng/ml versus a global detection rate of 87.50% in patients with PSA ≥ 2ng/ml. Considering only the detection rate of distant metastases an increase from 12% in patients with PSA < 2 to 50% in patients with PSA ≥ 2ng/ml was found, with consequences in the treatment planning.

## P701

### Do we need bone scintigraphy when 18F-choline PET is performed for suspicion of prostate cancer recurrence?

H. Lahousse, **H. Kolesnikov-Gauthier**, A. Oudoux, P. Nickers, R. Renaud, E. Lartigau, P. Carpentier; Centre Oscar Lambret, Lille Cedex, FRANCE.

**Aim :** Retrospective analysis to study the discordance between 18F-fluorocholine (FCH) PET and planar bone scintigraphy (BS) for the diagnosis of bone metastasis in recurrent prostate cancer patients. **Methods** Between 2011 and April 2012, 52 patients were addressed for an increase in PSA after local treatment. FCH PET results on bone status were compared to BS findings, only if the two tests were performed in delays of 4 months. We analysed the discordance between the FCH and BS. Results were classified as true/false positive/negative in comparison with radiological findings and biological follow-up (mean of 19 months). Therapeutic impact was also studied. **Results** 38 patients were eligible (20 radical prostatectomy, 18 external beam radiotherapy/or curietherapy, mean PSA : 9.2 ng/ml). FCH PET and BS were concurrently positive or negative in 32 patients (28 negative and 4 positive results). No false positive or false negative result was reported. The management plan was changed in these 4 positive cases (3 introduction of hormonotherapy, 1 modification of hormonotherapy). In only 1 out of 4 positive cases, FCH showed more lesions than BS, but this result didn't change treatment plan. FCH PET and BS were discordant in 6 patients. In 5 cases, FCH was positive and BS negative. Anatomical imaging and follow-up confirmed FCH results. No false positive FCH PET was observed. Hormonotherapy was proposed for 4 patients and a nadir in PSA levels was observed few months later. Radiotherapy of a solitary bone lesion (L4) was proposed to the last patient. In one case FCH TEP was negative and BS positive. Focal uptake of 99mTC-HDP was observed on 7$^{e}$ rib, with osteocondensation on CT. However, etiology of this lesion was not determined 1 year later. **Conclusion** Discordance between FCH PET and BS was observed in 6/38 cases (16%). FCH was more sensitive than BS with positive predictive value of 100% for bone metastasis. We think that BS should not be performed if there is an indication to FCH PET (especially in case of unexplained rising PSA after local therapy).

## P702

### The Value of Bone Scans to Predict Survival Time in Patients with Diagnosed Prostate Cancer

**E. Marangoz**[1], D. Yüksel[1], O. Yaylalı[1], F. S. Kıraç[1], S. Eskiçorapçı[2]; [1]Pamukkale University, Medical Faculty, Dept. of Nuclear Medicine, Denizli, TURKEY, [2]Pamukkale University, Medical Faculty, Dept. of Urology, Denizli, TURKEY.

**AIM:** We aimed to investigate the significance of the bone scan results as a prognostic factor to predict the survival by comparing age, serum PSA level, and Gleason score in patients with prostate cancer. **MATERIALS AND METHODS:** Medical records of 313 patients with prostate cancer performed Tc 99m-MDP whole body bone scan in our institution between 2002 and 2010 were retrospectively examined. Patiens' age, Gleason score, total PSA values before the bone scan were recorded. It was asked for whether the patients are alive or dead. Of those who died, the cause of death and time of death were recorded. The death patients were excluded if there was an additional malignancy among of them or the cause of death was non-malign. Two hundred sixty five patients of 313 were included in the study. Patients were divided into several groups according to bone scan results, age, PSA and Gleason scores. Kaplan-Meier method was used for survival analysis. Multivariate Cox regression analysis was used to evaluate potential prognostic variables affecting survival. **RESULTS**: Patients' mean estimated survival times who had bone metastases, had no and suspicious bone metastases were 47.4±5.4 months, 159.1±8.6 months and 71.1±14.4 months respectively. Significant difference was determined among these three groups ($p=0.0001$). The mean estimated survival of patients who are younger than 70 years old was 137.1±9.4 months, while the older ones was 78.2±5.0 months. In the survival analysis, significant difference was determined between these two groups ($p=0.031$). Two hundred fourty three patients with known PSA values, of those whose PSA levels <10 ng/ml, 10-20 ng/ml, >20-50 ng/ml and >50 ng/ml, estimated mean survival was 106.9±4.2 months, 118.1±14.8 months, 87.6±7.4 months and 51.7±6.2 months respectively and significant difference was determined among them ($p=0.0001$). Patients whose Gleason score <7, 7 and >7, mean estimated survival was 167.5±10.8 months, 86.8±5.5 months and 61.0±5.4 months respectively and significant difference was determined between these three groups ($p=0.0001$). Results of Cox regression analysis showed that the most important independent prognostic factor for the survival is the findings of the bone scan. We identified in this study that the estimated mean survival of the patients who had bone metastases, had high level of PSA, had high level of Gleason score and were older than 70 years old was shorter than other groups. **CONCLUSION:** The bone metastases detected in the bone scan is an important independent prognostic factor in the estimation of the survival time.

## P703

### Bone Scan Index: a strong predictor of outcome in metastatic hormone naive prostate cancer patients

**J. Rasmussen**[1], M. Poulsen[2], A. Johansen[1], L. Lund[2], P. Høilund-Carlsen[1], O. Gerke[1,3], L. Edenbrandt[4]; [1]Department of Nuclear Medicine, Odense University Hospital, Odense, DENMARK, [2]Department of Urology, Odense University Hospital, Odense, DENMARK, [3]Department of Business and Economics, University of Southern Denmark, Odense, DENMARK, [4]Nuclear Medicine Unit, Skåne University Hospital, Lund University, Malmö, SWEDEN.

*Aim* Prostate cancer patients are M-staged using whole-body bone scintigraphy (WBS) and categorized as M0 or M1. However, within the M1 group, there is a wide range of clinical outcome. The standard clinical and pathological tests provide some prognostic tools, but more is needed. A decade ago, the Bone Scan Index (BSI) was introduced, which provides a quantification of bone metastases by estimating the percentage of bone involvement. However, it was time consuming and, as a consequence, it has had limited clinical use. Recently, computer-assisted diagnosis software was developed for automated detection and quantification of bone metastases. The few studies published so far have reported promising results. The aim of this retrospective study was to evaluate the prognostic capabilities of BSI when using an automated platform to predict castration resistance as well as prostate cancer specific survival. *Materials and Methods* A total of 88 patients with prostate cancer awaiting initiation of androgen deprivation due to metastases (bone, lymph nodes, or both) were included. WBS was performed prior to androgen deprivation. Whole-body images were obtained with a two-headed gamma camera after intravenous injection of $^{99m}$Tc-MDP/DPD. BSI was obtained using the automated platform EXINI bone (EXINI Diagnostics AB, Lund, Sweden) and assessed by multivariate analyses of PSA, Gleason score and BSI towards time to castration resistance and prostate cancer specific survival, respectively. For Kaplan-Meier estimates, BSI groups were dichotomously split into: BSI <1 and BSI ≥ 1. *Results* The mean age of the patients was 72 years (range 52-92). The median PSA level was 73 µg/L (range 4-5740, SD 726). The average Gleason score was 7.7 (range 5-10, SD 1.3). BSI mean was 1.0 (range 0-9.2, SD 1.8). Mean follow up was 26 months (range 8-49, SD 11), 48 patients became castration resistant, and 15 died, the majority (13) of prostate cancer. In time-to-event analyses, PSA, Gleason score and BSI were used as explanatory factors. Regarding time to castration resistance, only BSI proved statistically significant at the 5% level as respective p-values were 0.47, 0.07, and 0.0005. Regarding prostate cancer specific survival, again only BSI was a statistically significant factor ($p=0.11$, $p=0.95$, $p=0.01$, respectively). *Conclusion* BSI obtained by an automated computer-assisted algorithm seems to be a useful predictor of outcome with regard to castration resistance and prostate cancer specific survival in patients with metastatic hormone sensitive prostate cancer.

## P704

### Myocardial Up-take of 99mTc-HDP in Patients with Prostate Cancer

**P. Santoro**, L. Fattizzi, M. Monti, G. Calo' - Gabrieli; Di Venere Hospital, Bari, ITALY.

**Aim**. To verify if 99mTc-HDP heart up-take in bone scintigraphy may give clinical, diagnostic and prognostic informations and to verify if it can be correlated with hormonal therapy. **Materials and Methods**. In a period of 4 years (01.01.2009 - 31.12.2012) we enrolled and submitted to bone scintigraphy 1869 patients (PTs) with prostate cancer. Bone scan images revealed in 18 PTs 99mTc-HDP intense homogeneous myocardial up-take . Their Gleason score was between 2 and 8. Total prostate specific antigen was between 0 and 27 ng/ml, while freePSA was between 0 and 5 ng/ml. 6 of them were previously submitted to radical prostatectomy; the other 12 PTs used only ormonal therapy without surgery (bicalutamide [Casodex] or bicalutamide + Leuprorelina acetate [Enantone]). All PTs who were performed to bone scan in the same day of men with myocardial up-take didn't showed myocardial activity. Bone scans of all these PTs were negative for bone metastases,

except for 1 PT examined in 2012 who had vertebral metastases. Clinical situation of these 18 men was studied at the moment of bone scan and they were submitted to a follow-up until January 2013. During follow-up we observed presence of heart diseases, therapy changing of and other clinical setting modifications. **Results**. During follow-up we discovered that a man who was submitted to bone scan in Genruary 2010, died suddenly 2 months later for a diffuse myocardial infarction. He used bicalutamide [Casodex] after prostatectomy, previously he wasn't an heart patient and, after bone scan, he did electrocardiogram and echocardiography with evidence of pericardial pouring, so he was treated with diuretic therapy (furosemide and ramipril). Another PT caring only with bicalutamide showed pericardial pouring in echocardiography, so he was submitted to furosemide therapy. After 6 months, he died. 2 years before discovering prostate cancer, he was submitted to dissection of a basal-cell carcinoma of the skin of his head and then a metastasis localized in the neck. The other PTs hadn't hearth diseases or other important clinical events during follow-up. PT with bone metastases was performed to radiotherapy. All other Pts hadn't history of chemotherapy, radiotherapy, cardioversion, heart diseases, chest pain or hyperparathyroidism which are the main literature described causes of myocardial 99mTc-HDP uptake. **Conclusions**. We think that heart activity in bone scintigraphy must be underlined in refertation because it seems to be a negative prognostic factor, considering 2 deaths in 18 pts (11%) during follow-up.

## P705

### Initial assessment of prostate cancer by Fluoromethylcholine (FCH) positron emission tomography (PET)/computed tomography (CT): who and why?

**C. Villano**[1], G. Pigotti[2], V. De Francesco[1], E. Baldassarrini[2], F. Zattoni[3], L. Evangelista[4]; [1]U.O.C. Medicina Nucleare e Terapia Radiometabolica Ospedale Civile "Spirito Santo", Pescara, ITALY, [2]ACOM S.p.A., Montecosaro (MC), Località Cavallino, ITALY, [3]Department of Urology, University of Padova, Padova, ITALY, [4]Radiotherapy and Nuclear Medicine Unit, Istituto Oncologico Veneto I.R.C.C.S., Padova, ITALY.

**Purpose**. The aim of this bicentric study was to evaluate the role of FCH PET/CT in patients who received the diagnosis of prostate cancer. **Materials and Methods**. For the end-point, we retrospectively recovered the data of 70 patients (mean age: 69.80±8.23yrs; range: 56-86yrs) who had a cytologic diagnosis of prostatic carcinoma by fine-needle aspiration biopsy. Demographic and clinical information were retrieved by medical archives or by an interview with each patient. All subjects underwent whole-body FCH PET/CT scan after 60-90min from the tracer injection. Biograph 6 HR and 16 HR PET/CT scans by Siemens were used by two Institutions. The images were visually and semiquantitatively evaluated. The maximum standardized uptake value (SUVmax) was automatically calculated. A patient-based analysis was performed**. Results**. The Gleason score (GS) was ranged between 4 and 10; in particular 19 (27%) patients had a GS between 4 and 6; 21 (30%) had a GS=7 and finally 27 (38%) had a GS>7 (8-10). The data was missed in 3 cases. The PSA value, before PET/CT scan, was 34.37±68.67ng/mL (range: 0.98-500ng/mL). PSA measurement resulted significantly different among three GS categories (13.36±15.83 vs. 19.61±18.05 vs. 62.29±103.61, respectively; ANOVA test p=0.029). 67/70 patients showed a significant FCH-uptake in prostate gland; although SUVmax resulted similar among three GS subsets (5.52±2.54 vs. 6.28±2.15 vs. 6.72±2.83; respectively ANOVA test p=0.311). Skeletal disease and loco-regional or distant lymph node lesions were mainly demonstrated in subjects with GS≥7 (15/48=31.2% and 16/48=33.3%, respectively) than their counterpart (2/19=10% and 4/19=21%, respectively). A concomitant systemic treatment based on hormonal therapy was started in 53.9 and 71.1% of patients with GS<7 and GS≥7 (p=0.256). **Conclusions**. FCH PET/CT could be helpful in men with intermediate-high risk of prostate cancer for stratifying the risk of distant metastases at initial staging, and therefore for planning an appropriate treatment. A prospective and well-structured trial is mandatory.

## P706

### Evaluation of 18F-Choline PET/CT and MRI diagnostic performances in prostate cancer local recurrence detection after non surgical treatment: correlation with biopsies.

**L. CHAMPION**[1], M. Wartski[2], N. Jehanno[2], V. Servois[2], O. Abdelli[2], A. Hottelart[2], V. Edeline[1], D. Pontvert[2], P. Meria[2], J. Alberini[1], S. Petras[2]; [1]Institut Curie Hopital Rene Huguenin, Saint Cloud, FRANCE, [2]Institut Curie, Paris, FRANCE.

**Objectives:** The aims of the study were to (1) evaluate the clinical value of 18F-Choline PET/CT in prostate cancer local recurrence detection in patients treated by nonsurgical treatment, (2) compare the diagnostic performances of 18F-Choline PET/CT and MRI in correlation with biopsies. **Material and Methods**: Thirty-eight consecutive patients with rising PSA, mean age 70 years (range: 57-88), previously treated by external radiotherapy (23 pts, 61%) and interstitial brachytherapy (15 pts, 39%) were included. Dual phase 18F-Choline PET/CT scan followed by MRI and prostate biopsies were performed in all patients. Findings were compared with MRI and correlated with biopsies. **Results:** Mean initial pre-therapeutic PSA was 18,8 ng/ml (range: 4,4-88) in patients having Gleason scores 5-8. During follow-up (mean 94 months, range 24-192), increased PSA showed values from 1,4 to 25 ng/mL (mean: 5,7) before imaging. F-Choline PET/CT showed positive prostate uptake in 25 (66%) and MRI was positive in 28 pts (74%). Concordant F-Choline PET/CT and MRI results were found in 30 pts (79%) and discordant in 8 pts (21%). Biopsies revealed local recurrences in 29 pts (76%). In pts having histological confirmation of local recurrence, F-Choline PET/CT was positive in 23/29 pts (79%) and MRI in 26/29 (90%). In 9 cases of negative biopsies (24%), 5 matched negative (56%) F-Choline PET/CT and MRI results were observed.**Conclusion:** 18F-Choline PET/CT is an important diagnostic tool in prostate cancer local recurrence detection after nonsurgical treatment in patients with rising PSA. Diagnostic performances are comparable to those of MRI when correlated to biopsies.

## P707

### Prostate cancer isolated local recurrence diagnosed by 18F-Choline PET/CT and/or MRI, confirmed by biopsies and leading to salvage therapy in 22 consecutive patients.

**L. CHAMPION**[1], M. Wartski[2], N. Jehanno[2], V. Servois[2], O. Abdelli[2], A. Hottelart[2], V. Edeline[1], D. Pontvert[2], P. Meria[2], J. Alberini[1], S. Petras[2]; [1]Institut Curie Hopital René Huguenin, Saint Cloud, FRANCE, [2]Institut Curie, Paris, FRANCE.

**Objectives:** The aim of the study was to demonstrate the clinical impact of 18F-Choline PET/CT imaging in detection of isolated prostate cancer local recurrence, leading to different options of individualized salvage therapy. **Material and Methods:** Twenty-two consecutive prostate cancer patients with rising post-therapeutic PSA, mean age 70 years (range: 57-88), previously treated by external radiotherapy, interstitial brachytherapy or prostate surgery were included. Twelve of them showed initial Gleason 7 (55%), 8 patients Gleason 6 (36%), and 2 Gleason 5 and 8 (9%) scores. Dual phase 18F-Choline PET/CT imaging and prostate biopsies were performed in all patients. Twenty subjects (91%) were examined by pelvic MRI. **Results:** Mean initial pre-therapeutic PSA was 15,2 ng/mL (range: 4,4-88). At diagnosis of biochemical recurrence and before imaging, post-therapeutic PSA showed values from 1,5 to 25 ng/mL (mean: 6,8). F-Choline PET/CT exam demonstrated positive prostate focal and/or diffuse uptake pattern in 18/22 pts (82%) and pelvic MRI was positive in 19/20 cases (95%). Concordant positive F-Choline PET/CT and MRI results were found in 16/20 pts (80%) and discordant in 4/20 subjects (20%). F-Choline PET/CT did not find any positive lymph node or distant metastasis in all examined patients. Histological findings revealed local recurrences in all 22 patients. After biopsies, they benefited from local salvage therapy, i.e. with external radiotherapy in 10 patients (45%), interstitial brachytherapy in 6 patients (27%), surgery in 3 patients (14%), and high-intensity focused ultrasound (HIFU (14%) in 3 patients. **Conclusion:** 18F-Choline PET/CT is an efficient imaging technique to detect prostate cancer local recurrence and in the same time distant metastases in a "one-stop" shop procedure, in patients with rising PSA, showing an important clinical impact on post-therapeutic patient's management. Positive 18F-Choline PET/CT results are concordant to those obtained by pelvic MRI in majority of patients, and when confirmed by biopsies, they might lead to different options of individualized salvage therapy.

## P708

### Role of $^{18}$F-choline PET/CT in disease detection in patients with biochemical relapse after radical prostatectomy

**S. RODADO MARINA**, M. Coronado Poggio, D. Mendez Mareque, M. Marin Ferrer, A. Martinez Lorca, Y. Ramirez Escalante, I. Hernandez Perez, L. Martin Curto; La Paz Universitary Hospital, Madrid, SPAIN.

**Objective:** To evaluate the utility of $^{18}$F-Choline positron-emission tomography/ computed tomography ($^{18}$F-PET/CT) for detecting clinical recurrence in patients with increasing prostate-specific antigen (PSA) levels after radical prostatectomy (RP). **Materials and Methods**: We retrospectively studied 33 patients with prostate cancer (age mean: 66 years, 50-81) (Gleason range 6-10, median 7) (initial T staging : 14 T2, 15 T3 and 4 unknown) treated with RP and referred for a $^{18}$FCH PET/CT because of biochemical relapse (BR) from January 2010 and January 2013; 18 of them had a previous relapse treated with radiotherapy. 18FCH PET/CT was performed following standard procedures. Mean PSA level at diagnosis was 9 ngr/ml (3,2-20) and at PET/CT 2,8ngr/ml (0,12-16,90 ), mean PSA doubling time (PSADT) was 7,5 months (1-40). We evaluated the overall detection rate of $^{18}$FCH PET/CT and its correlation with age, Gleason score, initial T staging, previous BR, PSA levels at diagnosis and at PET/CT, PSA nadir and PSA doubling time (PSADT). The results were correlated with clinical follow up and imaging data. Negative PET/CT scans were considered false negative, since all patients had serum PSA levels suggestive of relapse**. Results:** $^{18}$FCH PET/CT showed positive findings in 15 of 33 patients (45,5%), all true positive (PPV 100%), and negative in 18 (54,5 %), all false negative . In detail, 18F-FCH PET/CT detected: local relapse in 1, regional lymph node metastases in 8 and disseminated disease in 6 patients. Mean PSA level at diagnosis was 7,5 ngr/ml (SD 2,8) in PET-positive patients and 10,2 ngr/ml

(SD:4,8) in PET negative (p: 0,098). Mean PSA level at PET/CT was 4 ngr/ml (SD 4,4) in PET-positive and 1, 83 (SD 0,41) in PET-negative (p: 0,073). In 2 patients with disseminated disease the PSA level was < 1 ngr/ml. Mean age was 68,4 years in PET-positive patients and 64 in PET-negative (p: 0,099). PSA NADIR, PSADT, Gleason score, initial T staging and previous BR had a p> 0,1. No parameter was statistically significant to predict positive PET/CT (p=NS). **Conclusions:** 18FCH PET/CT detected recurrent disease in 45,5% of the patients, PPV 100%. We found disseminated disease with PSA at PET/CT < 1 ngr/ml. There were no statistical significant differences in the parameters analyzed between PET-positive and negative results; however, our results shown that PSA value at diagnosis, PSA value at PET/CT and age might be related with positive PET/TC and should be studied in a larger sample.

## P709

### Clinical impact of an early dynamic acquisition of 18F-Choline PET/CT for staging and restaging of prostate cancer

**E. Orunesu**[1], K. Siczek[2], L. Florimonte[1], V. Longari[1], M. Castellani[1], F. Zito[1], L. S. Maffioli[2], R. Benti[1]; [1]Fondazione IRCCS Ca' Granda - Ospedale Maggiore Policlinico, Milano, ITALY, [2]Ospedale Civile di Legnano, Legnano, ITALY.

**Introduction**: Numerous studies evaluating the diagnostic accuracy of 18F-Choline PET/CT for prostate cancer staging or restaging can be found in literature. For this kind of evaluation, the analysis is based on definite positive or negative PET-results for calculation of sensitivity, specificity, positive- and negative-predictive value of the test, not taking into account the indeterminate test results. Nevertheless, we have to acknowledge the presence of indeterminate test results in everyday clinical practice. In literature this fact often disappears due to review of PET-data by several nuclear medicine physicians, which find a consensus and "force" the findings in either positive or negative reports. Aim of our study was to evaluate how the availability of an early dynamic acquisition mode, could help to reduce the amount of indeterminate "grey zone" PET results, which can substantially reduce the cost-effectiveness and the clinical impact of these technique. **Methods**: We evaluated 127 consecutive patients, 21 for staging and 106 for restaging of prostate cancer after treatment with radical prostatectomy and/or radiotherapy, who presented a biochemical recurrence. Positive findings were validated by a) surgical lymphadenectomy or b) other imaging techniques including bone scintigraphy, abdominal ultrasound, MRI or contrast-enhanced CT. PET/CT imaging was performed at two time points: a 10 minutes dynamic acquisition on the pelvic region was performed at injection time and a whole-body acquisition 60 minutes after injection. All whole body static images were first evaluated and a preliminary report was drafted. For all the indeterminate reports, a thorough evaluation of the early dynamic PET/CT was made, which if possible, yielded either a positive or negative final report. For prostate cancer staging or restaging in surgically untreated patients, prostate gland uptake was not considered a positive finding. Results: Of all 127 fluorocholine PET/CTs, the preliminary reports (without considering the dynamic acquisition images), yielded 59% negative (N=75), 17% positive (N= 22) and 24% (N= 30) indeterminate results. After evaluation of the early dynamic acquisition of all 30 indeterminate results, 57% (N= 17) turned to negatives, 20% (N=6) to positives and 23% (N= 7) remained indeterminate, so that the conclusive results of all studies were 72% negatives, 22% positives and 6% indeterminates. **Conclusion:** Our preliminary results show an overall significant reduction of indeterminate results from 24% to 6% and an increase of negative ( from 59% to72%) and positive results (from 17% to 22%) with a substantial clinical impact and overall cost-reduction in sparing further diagnostic tests.

P44-2 - Tuesday, Oct. 22, 16:00 - 16:30, Poster Exhibition Area

## Oncology Clinical Science: Gynaecological

## P710

### Initial Staging of Locally Advanced Cervical Cancer with FDG-PET/CT

**A. Caresia Aróztegui**[1], M. Barahona Orpinell[2], C. Gámez Cenzano[1], L. Rodriguez Bel[1], M. Cortés Romera[1], J. Ponce Sebastià[2]; [1]Institut De Diagnòstic Per La Imatge, L'HOSPITALET DE LLOBREGAT, SPAIN, [2]Hospital Universitari de Bellvitge, L'HOSPITALET DE LLOBREGAT, SPAIN.

Aim: To evaluate the value of FDG-PET/CT for primary staging of locally advanced cervical cancer (LACC). Material and Methods: This prospective study included 25 women (25-78 years old; mean age = 53.3) diagnosed with LACC. All cases were squamous cell carcinoma (100%) and distribution according to International Federation of Gynecology and Obstetrics (FIGO) stage was as follows: IB2 (n=3), IIA2 (n=2), IIB(n=14), III (n=1) and IVA (n=5). All patients underwent a whole-body FDG-PET/CT for primary staging. PET positive findings were described (site, maximum diameter and SUVmax) and correlated with para-aortic lymphadenectomy (PAL) and histopathologic confirmation in case of distant metastasis. Results: All the primary tumors showed FDG uptake (SUVmax range 8-36; mean 15,5). FDG-PET/CT showed positive para-aortic nodes in 6 patients: 5 TP (1 with a positive PAL and 4 with confirmed metastasis) and 1 FP with a negative PAL ( inflammatory node related to infected tumor). FDG-PET/CT was negative in para-aortic región in 19 patients ;16 TP + 3FN (lymph node metastasis <7 mm). PET/CT showed distant metástasis in 4 patients, sited in lung, liver and mediastinal nodes. PAL was technically feasible in 22/25 women: positive in 5 (2 TP and 3FN by PET) and negative in 17 (16 TN and 1 FP by PET). NPV was 84,2%. The treatment was modified in 4/25 (16%) women that received chemotherapy because of detection of unsuspected distant metastasis. Conclusions: This study suggests that PET/CT is an effective imaging technique in the initial staging of LACC. It may help to evaluate para-aortic nodal metastasis and to plan the management, especially when unsuspected distant metastasis are detected.

## P711

### Impact of FDG-PET/CT in Initial Staging of Primary Advanced Ovarian Cancer: Preliminary Results

**A. Caresia Aróztegui**[1], C. Gámez Cenzano[1], C. Capó Pons[2], M. Martí Cardona[2], M. Cortés Romera[1], J. Robles Barba[1], S. Rossi Seoane[1], J. Ponce Sebastià[2]; [1]Institut De Diagnòstic Per La Imatge, L'HOSPITALET DE LLOBREGAT, SPAIN, [2]Hospital Universitari de Bellvitge, L'HOSPITALET DE LLOBREGAT, SPAIN.

Aim To evaluate clinical impact value of PET/CT in initial staging of primary advanced ovarian cancer. Materials and Methods This study included 22 patients (Mean age 61.3 years; Range 45-81) with solid-cystic adnexal masses in CT, all of them suspicious of primary advanced ovarian cancer. All patients underwent PET/CT before diagnostic laparoscopy. PET/CT findings were described (maximum diameter, SUVmax and site) and correlated with histopathological confirmation. The impact on patient management was tested by comparing the intention before and after FDG-PET/CT. Results Adnexal masses in PET-CT were FDG-positive (solid component) in 20/22 patients and FDG-negative in 2/22. All FDG-positive masses were malignant consistent with serous adenocarcinoma (SUVmax mean = 11.56g/ml; Maximum diameters mean=89mm). A clear cell carcinoma and a benign cystoadenofibroma were found in the 2 cases with FDG-negative masses. PET/CT revealed hypermetabolic peritoneal metastasis in 18 patients, while prior CT scan showed them in 16 patients. PET/CT detected distant metastasis in 9/22 patients (40%), mainly in supradiaphragmatic nodes (7/9 patients), associated with additional metastasis in pleura, bone and liver metastasis. The FIGO staging was modified in 11/22 (50%) women: 6/11 patients were upstaged because of unsuspected peritoneal or distant metastasis, and 5/11 patients were downstaged (false positive CT findings). In 11 patients CT and PET/CT results were similar. Overall, the implementation of FDG-PET-CT led to modify therapeutic intention in 8/22 (36%): 5/8 patients were finally operated of intra-abdominal disease (extra-abdominal CT finding were negative at PET scan) and 3/8 patients received chemotherapy (distant metastasis solely detected by PET scan) Conclusion Initial staging of advanced ovarian cancer can be improved using FDG-PET/CT instead of diagnostic CT, mainly due to the detection of suspected distant metastasis. Supradiaphragmatic lymph nodes were the most frequent site of metastasis. FDG-PET/CT could make a decisive contribution to final management al least in a third of patients.

## P712

### Impact of 18F- FDG PET/CT in detection and management of recurrent cervical cancer.

**A. Bhoil**[1], B. Mittal[2], A. Bhattacharya[2], K. Manohar[2], F. Patel[2]; [1]Nuclear Medicine Centre, Regional Cancer Centre, I.G.M.C, Shimla, INDIA, [2]Post Graduate Institute of Medical Education and Research, Chandigarh, INDIA.

AIM: Role of 18F-FDG PET/CT in detection of recurrent cervical cancer with impact of PET/CT on its management. MATERIAL and METHODS: Fifty patients (Age range 32-70 yrs, median 51yrs,) FIGO stage ≥ stage IB suspicious of cervical cancer on clinical symptoms or equivocal radiological findings for recurrence were retrospectively analysed with 18F-FDG PET/CT. All the patients had histologically diagnosed cervical cancer at the time of initial diagnosis and were treated with curative intent. 18F-FDG PET/CT was done as per institutional protocol. Delayed and post lasix studies were acquired wherever found necessary. All results were confirmed by histopathological or clinical/imaging minimal follow up of 6month RESULTS: The distant metastasis/recurrence and local recurrence were noted in 26 & 13 patients. Eight patients had normal scan and secondary carcinoma was seen in 3 patients (lung primary =2, colonic malignancy =1) of these 50 patients. 26patients with distant recurrence/metastasis were also followed up clinically and repeat CT imaging was done after 3 months and FNAC was done where deemed necessary. Four patients were diagnosed as falsely positive, lung nodule (n=2), mediastinal lymphadenopathy (n=1) and supraclavicular with multiple abdominal lymphadenopathy (n=1). Sensitivity and specificity for distant metastasis was 100% and 92% and positive and negative predictive values were 85% and 100 % respectively for the distant metastasis. Change in management in treatment was noted in of the patient with recurrence was noted in 50% of the patients (n=25/50),

(Distant metastasis=22 & secondary malignancy=3) 13 patients with local recurrence were progressively followed up clinically and PET/CT repeated after 6 month. 1 patient with local recurrence on 6 month of follow up had a normal scan after 6 months suggestive of falsely positive PET/CT finding. In these patients with clinically equivocal recurrences disease, 18F-FDG PET/CT had a sensitivity of 87%, a specificity of 67%, a positive predictive value of 87%, and a negative predictive value of 91%. CONCLUSION: 18F-FDG PET/CT was highly sensitive and had high negative predictive value in detection of the distant metastasis in recurrence of cervical cancer. The change in management was seen in 50% (n=25/50) of our patients who were then subsequently treated as per institute treatment protocol making whole body PET/CT highly beneficial and having a major impact on treatment in these patients. The high negative predictive value in this study suggests that the 18F-FDG PET should be given considered in patient suspected of recurrence depending on its availability and cost -effectiveness.

## P713

### Relationship between Ca-125 serum levels and FDG PET-CT in recurrent ovarian cancer

**A. Palomar Muñoz**, J. Cordero García, O. Gómez López, A. García Vicente, G. Giménez Londoño, Á. Soriano Castrejón; Hospital General Ciudad Real, Ciudad Real, SPAIN.

**AIM** To establish the relation between the behavior of serum levels of Ca 125 and the result of FDG PET-CT study in the evaluation of recurrence of ovarian cancer. **MATERIAL AND METHODS** Retrospective study carried out in 26 patients with suspected recurrence of ovarian cancer. The two last determinations of Ca 125 were taken into account (the second one less than 30 days before the date of the FDG PET-CT study). The difference, the difference percentage, as well as the rising speed between these values were calculated and compared with the FDG PET-CT study (U Mann-Whitney-Wilcoxom test). The final diagnosis was obtained by histological analysis or clinical follow up greater than 6 months. **RESULTS** The final FDG PET-CT study was positive in 18 patients (TP) and negative in 8 (TN). No false negative or positive results were found. The difference in Ca 125 values ranged between -9.70 and 350.8 UI/ml, with a percentage of rising between -0.46 and 36.5, whilst the rising speed ranged between -0.88 and 101.1 UI/ml/month. Statistically significant differences were obtained between PET positive and PET negative patients in the total difference between Ca 125 values of both groups, as well as in the rising speed (mean difference 67.82 UI/ml, SD 98.72 in the PET positive group, mean =5.96 UI/ml with SD 18.3, p=0.011 in PET negative group; rising speed 16.82 UI/ml/month, SD 26.09 vs. 2.18 UI/ml/month, SD 5.88, p 0.019). Altogether, a greater rising percentage seem to be present in the PET positive group (mean= 6.11%, SD 9.73 vs. 0.42%, SD=0.88), near the limit of statiscal significance (p=0.062). **CONCLUSION** The FDG PET-CT shows a high diagnostic performance in the suspicion of recurrent ovarian cancer, highly related with the behavior of the Ca 125 values (difference, rising speed and percentage of difference between the last two determinations).

## P714

### Usefulnees of 18F-FDG in monitoring cervical cancer: Our Experience

**D. Mendez Mareque**, C. Escabias del Pozo, I. Rodriguez, A. Martinez Lorca, I. Hernandez Perez, S. Rodado Marina, M. Coronado Poggio, I. Santos Gomez, M. Marin Ferrer; Hospital Universitario La Paz, Madrid, SPAIN.

**Purpose / objective** The aim of this study was to evaluate the qualitative response using post-therapy molecular imaging with [$^{18}$F] Fluorodeoxyglucose (FDG) PET/CT and to compare it with clinical response in patients with locally advanced cervical carcinoma treated with radio-chemotherapy followed by brachytherapy. **Material and Methods** This was a retrospective cohort study of 30 patients new diagnosis of cervical carcinoma with stage IB2-stage IIIB who underwent pre- and post-treatment whole-body FDG-PET-CT. All patients were treated with external beam radiotherapy and concurrent chemotherapy followed by high-dose rate (HDR) brachytherapy between August 2009 and February 2013. Median age was 53 years (31-79). Post-therapy FDG-PET-CT was performed with a median of 13 weeks (11-20) after completing brachytherapy. The qualitative analyse persistent or negative of PET-CT pre and post-therapy were recorded by 2 independent observers and correlated with clinical response at the same time. All patients were followed (clinical/imaging procedures) was 19 months (7-33). **Results** Clinical assessment after treatment showed complete response (not tumor) in 20/30, local persistence (tumor) in 1/30 and partial response (doubt) in 9/30. The post-therapy PET-CT showed persistent FDG uptake in 8/30 and was negative in 22/30 cases. In 8/30: 1/8 persistent uptake correlated well with clinical findings, while 4/8 still showed partial response and the remaining 3/8, complete response. In 2 patients PET-CT showed new sites of increased FDG uptake that were distant metastases. One of them presented negative uptake in cervix where as the other one had persistent uptake in cervix. The FDG-PET proved to be a useful tool to clarify 40% of the cases (12/30). In patients who were partial response clinical examination, 4 were positive PET-CT and 5 were negative PET-CT .The patients were classified as complete response, the PET-CT discovered 3 persistent disease. However, all patients who were negative in PET-CT remained disease free **Conclusion** The FDG-PET proved to be a useful tool for monitoring cervical cancer and post-therapy persistent FDG uptake might be predictive of clinical persistent loco regional disease and can detect unsuspected distant metastases. Increasing evidence has documented the value of FDG-PET-CT in Oncology, but only limited data comparing PET findings pre and post-treatment with clinical response in patients with cervical carcinoma is available.

## P715

### Impact of 18F-Fluordesoxyglucose PET/CT on the Clinical Management of Women with Ovarian Cancer

**J. Deportos**, A. Domènech, R. E. Jaller, A. Montes, J. Duch, V. Camacho, M. Estorch, I. Carrió; Hospital de la Santa Creu i Sant Pau, Barcelona, SPAIN.

AIM To evaluate the impact of PET/CT with 18F-FDG on the clinical management of women with ovarian cancer. MATERIAL AND METHODS One hundred twenty-seven studies performed with 18F-FDG PET/CT in our center between September 2010 and December 2012 in women with ovarian cancer were retrospectively reviewed. From these 127 studies we selected 60 that corresponded to 30 patients (28-86 years, mean 60.5 years) who had two consecutive PET/CT studies in order to evaluate possible disease progression or remission (partial or complete) after treatment. We evaluated the changes in clinical management after the follow-up PET/CT (surgery; start, maintenance or change of chemotherapeutic regimen; beginning of radiotherapy; control of tumor markers). RESULTS Comparison of the follow-up PET/CT with the first study showed tumor progression in 21 out of 30 patients (70%). Subsequently, 13 of these patients started chemotherapy, two patients changed their treatment regimen and one extended chemotherapy. Four patients underwent surgery and one patient received cranial radiotherapy for brain metastases. PET/CT changed the clinical management in all 21 patients with disease progression. Comparison of the follow-up PET/CT showed partial response after chemotherapy in 3 out of 30 patients (10%). One of them extended chemotherapy treatment, another patient changed chemotherapy and the last one followed analytical controls and died seven months later. PET/CT changed the therapeutic management in 2 of the 3 patients with partial response. Comparison of the follow-up PET/CT showed that 6 out of 30 patients (20%) were in complete remission after chemotherapy. All of them followed analytical controls only. Overall, PET/CT changed the therapeutic management in 23 out of 24 patients (95.8%) with disease progression or persistence of tumor. CONCLUSION Our results show that PET/CT with 18F-FDG has significant impact on the clinical management of women with ovarian cancer. In 95.8% of our patients, the findings of the follow-up PET/CT resulted in a change in clinical management.

P45-2 - Tuesday, Oct. 22, 16:00 - 16:30, Poster Exhibition Area

## Oncology Clinical Science: Colorectal Cancer

## P716

### Role of FDG PET/CT in the initial staging of primary colorectal cancer

**K. Agrawal**, A. Sharma, A. Bhattacharya, R. Gupta, B. R. Mittal; Postgraduate Institute of Medical Education & Research, PGIMER, CHANDIGARH, INDIA.

Aim: 18F-Fluorodeoxyglucose (FDG)-positron emission tomography (PET) and computed tomography (CT) is widely accepted in the staging of different cancers. Only a few studies had evaluated the role of FDG PET/CT in the initial staging of primary colorectal cancers. The aim of the present study was to assess the role of FDG PET/CT in the initial staging of primary colorectal cancers. Materials and Methods: Data of 23 patients (13 M, 10 F; mean age 59 years; range 24-78 years) with newly diagnosed colorectal cancer who underwent contrast enhanced FDG PET/CT were retrospectively reviewed. Discordant findings between ceCT and FDG PET/CT were noted and were confirmed by imaging follow-up. Results: FDG PET/CT identified discordant findings in 10/23 patients (43%). FDG PET/CT upstaged the disease in 3/10 patients by identifying subcentimetric lymph node metastases in two and distant metastases in one patient. FDG PET/CT downstaged the disease in 3/10 patients by showing no FDG avidity in presumed distant metastases in ceCT scan in lung lesion, liver lesion and mediastinal lesion. Follow up imaging in these 3 patients showed no increase in size or FDG avidity of the lesion. In rest 4/10 patients, PET/CT identified additional lymph nodal metastases, but the stage was not changed as three patients had distant metastases in liver and one had lymph nodal metastases. Thus, FDG PET/CT changed the staging in 6/23 (26%) patients. Conclusion: FDG PET/CT has additional value over ceCT in the initial staging of patients with colorectal cancer and may have an impact on subsequent patient management.

## P717

### Predictive Value of Volumetric Parameters Measured by F-18 FDG PET/CT for Lymph Node Status in Patients with Surgically Resected Rectal Cancer

**S. Kim**, H. Jo, I. Kim, S. Ko, S. Kim; Pusan National University Hospital, Busan, KOREA, REPUBLIC OF.

**Aim:** The aim of the current study was to investigate the predictive value of volumetric parameters (MTV and TLG) measured by F-18 FDG PET/CT for lymph node (LN) metastasis in patients with rectal cancer. **Methods**: A retrospective review identified 74 patients with surgically resected rectal cancer patients who received F-18 FDG PET/CT at diagnosis of cancer. The F-18 FDG PET/CT findings for all primary cancer and LN involvement were compared with the pathologic diagnosis within 5weeks after surgical resection. The pathologic diagnoses of LN state were confirmed by surgical resection. Univariate and multivariate analyses were used to analyze the associations among the pathologic LN status and age, sex, T stage, AJCC stage, $SUV_{max}$, lymphatic invasion, venous invasion, neural invasion, MTVs, and TLGs. **Results:** The LN(+) group showed statistically significant higher values of MTV2.5 ($p<0.0001$), MTV3 ($p<0.0001$), MTV3.5 ($p=0.0001$), TLG2.5 ($p=0.0007$), TLG3 ($p=0.0011$), and TLG3.5 ($p=0.0024$) than those of LN(-) group. In univariate analysis, T stage, AJCC, neural invasion, MTVs and TLGs were factors significantly associated with pathologic LN involvement. However, in multivariate analysis, the advanced T stage, high AJCC stage, MTV2.5, and TLG2.5 were factors significantly associated with pathologic LN involvement in rectal cancer. **Conclusion:** Based on the presented results, not only T stage and AJCC stage, the volumetric parameters such as MTV2.5 and TLG2.5 measured by F-18 FDG PET/CT are useful factors for the prediction of pathologic LN status in rectal cancer patients.

## P718

### PET / CT 18F-FDG for diagnosis of recurrent colorectal cancer. HUG

**A. Mendoza Paulini**, M. Fernández Rodríguez, E. Rodríguez Pelayo, P. García Alonso, L. Castillejos Rodríguez, M. Balsa Bretón, A. Ortega Valle, J. Penín González; HOSPITAL UNIVERSITARIO DE GETAFE, Getafe, SPAIN.

INTRODUCTION: PET / CT is not recommended for routine oncological follow up, but could be of great help when there is suspicion on recurrence because early and exact detection of local recurrence, distant lymph node metastases or haematological spread out is very important to optimise therapy regimes. AIM: The objective was to assess the effect of PET / CT in suspected recurrent colorectal cancer. MATERIAL AND METHODS: We retrospectively evaluated 56 patients, mean age 67 ± 9 years, 37 males (66%). Indications for PET / CT were rising tumour markers, inconsistent conventional diagnosis or suspicious clinical or radiological findings. The results were confirmed by pathology or clinical outcome. RESULTS: A. - In 31 patients (55.4%) findings on PET/TAC were true positive (TP): . 27 (48.2%) had liver metastases, of which 6 (10.5%) had a greater number of metastases compared with CT. . 2 lymph node metastasis (3.6%). PET/TAC showed greater extension than CT in all of them. . 2 metastatic lung nodules (3.6%). B. - In 21 patients (37.5%) PET/TAC did not show any pathological findings and PET/TAC was true negative (TN). C. - In 4 patients (7.1%) PET/TAC show false positive (FP) resuts: . 2 (3.5%) inflammatory pathologies (abscess and peritonitis) . 2 (3.5%) histological nonspecific pulmonary nodules D. - There were no false negative cases. The PET / CT showed high sensitivity (100%), Especificity: 84.0%, PPV: 88.5%, NPV: 100% and certainty: 92.9%. CONCLUSION: PET/TAC distinguishes absence of tumour manifestation, local recurrence and systemic spread out with high accuracy, sensitivity and negative predective value.

## P719

### Assessment of the response in patients with colorectal carcinoma treated with neoadjuvant chemotherapy by PET and CT.

**M. Ribelles**, J. Arredondo, E. Prieto, L. Sancho, M. García-Velloso, J. Hernández, J. Richter; Clinica Universidad de Navarra, Pamplona, SPAIN.

AIM Neoadjuvant chemotherapy followed by radical surgery is a novel therapeutic approach for locally advanced colon cancer (LACC). This study let us correlate radiological and metabolical changes with pathologic response after neoadjuvant treatment. MATERIALS AND METHODS 15 patients with LACC (cT3-4 N-/+) were staged at baseline and after chemoterapy (XELOX) by Computed Tomography (CT) and fluorodeoxyglucose-positron Emission Tomography (18F-FDG-PET). The percentage of SUVmax reduction in the primary lesion and the change in the measured volume after neoadjuvant treatment were correlated to the pathologic response according Memorial score (MSKCC ). RESULTS The mean SUVmax of primary lesions at diagnosis was 19.1± 2.9 with a reduction after treatment of 34.8 ± 9.6% (p = .03). Mean volume of the primary lesion at diagnosis was 58.1 ± 11.6 and the percentage of reduction was 50.6 ± 7.1% (p = .001). In the three patients with the highest level of response (> 66% MSKCC), the percentage of SUVmax reduction after treatment was 74.8 ± 21.8%, being that response significantly higher than in the 12 patients with reduced response (<66% MSKCC). In those 12 patients, SUVmax reduction was 33 ± 32.4 (p = .048). The change in volume of the primary lesion in patients with greater pathologic response was not significantly higher 87.5 ± 21.6 %(p = .573) compared to patients with lower levels of response 49.3 ± 24.3 %. The correlation between FDG-PET and CT tests was not significant (RS=.324 p = .304). CONCLUSION Although these results may be preliminary it could be considered that 18F-FDG-PET is an useful technique in the assessment of response to neoadjuvant therapy in patients with LACC.

## P720

### Role of FDG PET/CT in evaluation of suspected recurrence of disease in patients of colon carcinoma in relation to carcino-embryonic antigen (CEA) levels

**G. Arun Reddy**, M. L. Abrar, K. Rajender, B. Anish, B. R. Mittal; Postgraduate Institute of Medical Education & Research, PGIMER, CHANDIGARH, INDIA.

AIM: To evaluate the role of FDG PET/CT in evaluating patients with suspected recurrence of colon carcinoma, in correlation with CEA levels. MATERIALS AND METHODS: In this retrospective study, 32 patients (males- 7, females - 25; mean age 57.7 yrs) of postoperative colorectal cancer with suspected recurrence were included. Patients were grouped into low and high CEA level groups with a cutoff value of 5 ng/ml. All the patients were followed up either by imaging or clinically for mean follow up duration of 18.2 months (range: 4 - 32 months). A diagnosis of recurrent colon carcinoma was made in patients who underwent subsequent chemotherapy or revision surgery. The sensitivity, specificity, positive predictive value (PPV) & negative predictive value (NPV) of the FDG PET / CT were compared with the final diagnosis in both the groups of patients. RESULTS: Of the 32 patients, 19 patients had a CEA level of less than 5 ng/ml & 13 patients had a CEA level of of > 5 ng/ml at the time of initial FDG PET/CT study. FDG PET/CT was positive for disease recurrence in a total of 20/32 patients. On follow up the total number of 15/32 patients underwent revision surgery/chemotherapy and were considered diagnostic for recurrent disease. The overall sensitivity, specificity, PPV and NPV of the FDG PET/CT in colon carcinoma was 93.33 %; 64.70 %; 70 % and 91.66 % respectively. In patients with CEA 5ng/ml it was 100 %; 80 %; 88.88 % and 100 % respectively. It was found that in patients with higher levels of CEA the specificity and PPV was significantly improved. CONCLUSION: FDG PET/CT has a high sensitivity and NPV in evaluation of suspected recurrence in patients with colon carcinoma. The specificity and PPV of FDG PET/CT is increased in patients with higher levels of CEA. In patients with CEA < 5ng/ml, findings on FDG PET/CT must be confirmed by pathological correlation due to poor specificity.

P46-2 - Tuesday, Oct. 22, 16:00 - 16:30, Poster Exhibition Area

## Oncology Clinical Science: Gastrointestinal & Pancreas

## P721

### Detection of suspected recurrent pancreatic adeno-carcinoma: comparison of fluorine-18-fluoro-2-deoxy-D-glucose Positron Emission Tomography/Computed Tomography (PET) with contrast-enhanced Computed Tomography (CT) and serum CA 19.9

**S. Panareo**, I. Santi, C. Cittanti, V. De Cristofaro, C. Peterle, L. Feggi; University Hospital - Nuclear Medicine Unit, Ferrara, ITALY.

**AIM**: To establish the value of PET in the detection of suspected recurrent pancreatic adeno-carcinoma previously operated in comparison to contrast-enhanced multidetector CT and serum CA19.9. **METHODS:** Twenty-two patients (6 men, 16 women - mean age 77.6+/-2), previously operated for pancreatic adeno-carcinoma with suspected disease recurrence (increased CA19.9 > 40U/ml) were enrolled. Both PET and CT were performed in all cases. After visual analysis, maximum Standardized Uptake Values (SUVmax) of PET focal uptakes were calculated. PET data were compared to CT findings. The value of serum CA19.9 was also compared with the SUVmax obtained from each patient (in case of a patient with multiple lesions we considered the one with greater SUV max). **RESULTS**: Out of 22 patients enrolled, 5 (22.7%) negative results at both PET and CT. In the 17 positive cases (77.3%) PET overall showed 26 areas of focal uptake divided as follow: 3 in pancreatic bed, 9 hepatic, 2 pulmonary, 9 nodal (7 sub diaphragmatic, 2 supra diaphragmatic) and 3 peritoneal. On the other hand CT overall showed 50 areas of contrast enhancement divided as follow: 1 in pancreatic bed, 6 in bone, 19 hepatic, 5 pulmonary, 17 nodal (12 sub diaphragmatic, 5 supra diaphragmatic), 1 peritoneal and 1 in adrenal gland. From the comparison between CA19.9 and SUVmax obtained for each patients, in 12 out of 17 positive PET cases we observed a statistically significant correlation ($p<0,05$) between CA 19.9 trend and SUVmax. Five patients (22,7%) with positive PET showed a not significant correlation

between CA19.9 and SUVmax trend. The five cases with negative both PET and CT showed lower CA 19.9 levels than patients with positive PET. **CONCLUSION**: In patients with suspected pancreatic adeno-carcinoma relapse after surgery, PET reliably detected local and peritoneal recurrences, whereas CT seemed to be more sensitive for the detection of hepatic, bone, nodal and lung metastases. Although less reliable in the identification of lymph nodes, PET is able to clearly highlight mediastinal lymph nodes. Furthermore, PET does not appear to be advantageous for the detection of non locoregional and extra-abdominal recurrences. Our experience showed a significant direct correlation between CA 19.9 increase and SUVmax. Negative PET and CT cases with positive CA19.9 are probably due to the small size of recurrent disease. To confirm our data an improvement in casuistry is required.

## P722

### The Effect of ERCP as a Predictor of Diffuse Splenic FDG Uptake in Patients with Cholangiocarcinoma

**S. Kim**, K. Kim; Pusan National University Hospital, Busan, KOREA, REPUBLIC OF.

**ABSTRACT** Although diffuse splenic F-18 FDG uptake exceeding hepatic activity is considered abnormal, its clinical significance is discussed sparsely in the literature. The aim of this study was to determine the contributing factors of diffusely increased splenic FDG uptake in patients with cholangiocarcinoma. **Methods:** From January 2010 to March 2013, 153 patients (94 men, 59 women) were enrolled in this study. All patients were diagnosed with cholangiocarcioma and underwent F-18 FDG PET/CT for the pretreatment staging work up. Clinical records were reviewed retrospectively. Various hematological parameters, C-reactive protein (CRP) level, CEA, CA19-9 and liver function test were conducted within 3 days before and after the F-18 FDG PET/CT study. **Results:** Endoscopic retrograde cholangiopancreastography (ERCP) was performed in 8 days before F-18 FDG PET/CT in 91 patients (59.5 %). Sixty two (40.5 %) patients received ERCP after F-18 FDG PET/CT. Diffuse splenic uptake was visualized in twenty four patients (15.7%). Others (84.3%) did not show abnormal glucose metabolism in the spleen. The CRP level (p=0.002) and white blood cell level (p=0.0407) were significantly higher in the group of patients with diffuse splenic FDG uptake. The hemoglobin level (p=0.0001) and the hematocrit level (p=0.001) were significantly lower in patients who showed diffuse splenic FDG uptake. Liver function test and tumor markers were not significantly different between the groups divided according to splenic FDG uptake. Under multiple regression analysis, the CRP level (Odds ratio [OR], 14.05; 95% CI, 3.23-60.14) and conducting ERCP (OR, 13.37; 95 CI, 1.36-131.23) before F-18 FDG PET/CT were the significant predictors for diffuse splenic FDG uptake. **Conclusion:** In conclusion, our study demonstrated that concurrent inflammation could be associated with diffusely increased splenic FDG uptake. We suggest that performing ERCP before F-18 FDG PET/CT could induce increased splenic FDG activity. As ERCP is an invasive procedure, it cause acute inflammatory condition.

P47-2 - Tuesday, Oct. 22, 16:00 - 16:30, Poster Exhibition Area

## Oncology Clinical Science: Lymphoma

## P723

### Effects of first-line lymphoma chemotherapy on metabolism and extension of hematopoietic bone marrow as quantified by a computational analysis of PET/CT scans

**F. Fiz**[1], C. Marini[2], M. Gobbi[3], M. Miglino[3], A. Bacigalupo[4], F. Frassoni[5], F. Bongioanni[1], A. Buschiazzo[1], G. Bottoni[1], R. Piva[1], S. Morbelli[1], S. Fiordoro[1], M. Piana[5], C. Campi[6], G. Sambuceti[1]; [1]Chair of Nuclear Medicine; Genoa University, IRCCS-AOU San Martino-IST, Genoa, ITALY, [2]CNR Institute of Molecular Bioimaging and Physiology, Milan, Section of Genoa, Genoa, ITALY, [3]Chair of Hematology, Genoa University, IRCCS-AOU San Martino-IST, Genoa, ITALY, [4]Hematology and Bone Marrow Transplantation Dept., IRCCS-AOU San Martino-IST, Genoa, ITALY, [5]Stem Cell lab, IRCCS Pediatric Institute G. Gaslini, Genoa, ITALY, [6]Department of Mathematics, University of Genoa, Genoa, ITALY.

**AIMS**: Bone marrow (BM) toxicity by chemotherapy (CHT) largely varies in different patients. Measuring this damage and the subsequent reaction might help in fitting treatment regimen, yet it would imply an estimation of both extension and activity of hematopoietic tissue. While the latter variable can be derived by FDG uptake in specific bone districts, the former has never been assessed. The present study utilizes a new computational analysis to quantify BM extension and metabolism during and after CHT in the clinical model of lymphoma. **METHODS**: The study comprised 23 patients, affected either by Hodgkin (n=5) or non-Hodgkin Lymphoma (n=18), evaluated with whole body PET/CT scan (from skull vertex to toes), at three different time points: staging (PET1), in the course of CHT (PET2) and one month after treatment completion (PET3). Criteria of exclusion were: suspected BM disease localization at PET1, change of CHT protocol within the study period, use of BM stimulating drugs as well as presence of overt anemia, leukopenia or thrombocytopenia at any time point during the study. A computational approach to PET/CT image was used to estimate total intra-bone volume (IBV) and compact bone volume (CBV) normalized for ideal body weight (IBW). The algorithm recognizes bone contours on each CT slice and measured the average Hounsfield value within a two-pixel ring starting from the border. All intraosseous pixels having an attenuation coefficient lower than this threshold were flagged as IBV, the others as CBV. FDG uptake index, extracted from IBV, was used to distinguish active from fatty BM, according to a statistical threshold determined in a published series of control subjects. Metabolic volumetric product is obtained multiplying active BM volume for its average SUV. **RESULTS**: IBV and CBV remained constant throughout the study. By contrast, active BM volume increased from PET1 to PET2 by 15% (10.4±3.9 vs 11.9±5.1 ml/Kg IBW, p<0.02) and returned to baseline levels at PET3 (10.2±3.1 ml/Kg IBW, p=ns vs PET1, p<0.05 vs PET 2). Average SUV showed a more noticeable response, increasing by 29% from PET1 to PET2 (1.7±0.2 vs 2.2±0.8, p<0.01) and returning to baseline levels at PET3 (1.67±0.2, p=ns vs PET1). As a consequence, the same biphasic response was observed when the metabolic volumetric product of active BM was analyzed. **CONCLUSIONS**: Computational analysis of PET/CT scans shows that hematopoietic reaction to CHT is immediate and transient, especially implying an increased metabolism of active BM, which is more pronounced than its expansion.

## P724

### The Role of Indices Obtained from Positron Emission Tomography for Predicting Prognosis in Patients with Non-Hodgkin's Lymphomas

**B. DIRLIK SERIM**[1], E. ÜMİT[2], F. ÜSTÜN[1], S. AKSOY[3], M. DEMİR[2], G. DURMUŞ ALTUN[1]; [1]Nuclear Medicine, Trakya University Faculty of Medicine, Edirne, TURKEY, [2]Hematology, Trakya University Faculty of Medicine, Edirne, TURKEY, [3]Nuclear Medicine, Trakya University Faculty of Medicine, Edirne, TURKEY.

Aim: Non-hodgkin's lymphoma (NHL) is a heterogeneous group of klonal proliferative disease that originate in lymph nodes or extranodal lymphatic tissues. Identifying prognostic factors and clinical staging is important for choosing the adequate initial therapy. F18 FDG PET/CT scan is a functional imaging tool for NHL patients in staging, re-staging, defining the adequate biopsy side, theraphy response, chemosensitivity and residual disease after therapy. Since there are several studies for predicting prognosis with PET/CT scan, it direct us to investigate about the contribution of quantitative parameters obtained from PET/CT scan to predict prognosis, IPI score system and therapy response criteria. In this study the role of liver, mediastinum and brain indices obtained from initial PET/CT scan for predicting prognosis in NHL patients were evaluated. Materials and mehods: PET/CT images of 31 patients with NHL who were referred to our center in between December 2009 and August 2011 for staging and posttheraphy response were evaluated retrospectively. The ratio of SUVmax value of primary lesion to SUVmean values of mediastinum, liver and brain obtained from initial PET/CT scan were defined as pre-treatment mediastinum, liver and brain indices. Spleen/liver ratio were also investigated as a quantitive parameter for contribution to predict prognosis. Indices and spleen/liver ratio were compared with each other and with post theraphy response. Results: Mean age of patients was 58±13 years. There was statistically significant relationship between mediastinum (p=0.008), liver (p=0.02), brain (p=0.022) indicis and pre-treatment staging. There was statistically significant relationship between spleen/liver ratio and mediastinum (p=0.007), liver (p=0.002), brain (p=0.001) indices. We found no significant relationship between indices and posttheraphy response. Conclusion: In our study, mediastinum, liver and brain indices obtained from initial PET/CT scan were significantly related with pre-treatment staging. In the patients those are not truly staged because of the inadequate or ineffective bone marrow biopsy and inflamatuar reactivity, predicting the initial staging is crucial for therapeutic approach; so this may avoid side effects of unnecessary intense chemotherapy in a low grade patient, or give chance to apply an intensive regime for high grade patients at the initial stage. In our study with limited number of patients, there is no correlation between indices and prognosis. The significant relation between initial staging and indices may lead to a brand new parameter for staging beside clinical parameters in NHL patients. Multicentric studies with larger patients groups are needed to identify parameters contributing prognosis prediction in NHL.

## P725

### Liver and Mediastinal Blood Pool 18F FDG Standard Uptake Value changes during ABVD chemotherapy in Hodgkin s disease.

**A. Chiaravalloti**, R. Danieli, M. Cantonetti, M. Guazzaroni, M. Tavolozza, D. Di Biagio, P. Abbatiello, A. Orlacchio, G. Simonetti, O. Schillaci; Depatment of Biomedicine and Prevention, University Tor Vergata, Rome, ITALY.

**Aim:** The aim of our study was to assess the intrasubject variability of 18F FDG uptake in the liver and in themediastinum among patients with Hodgkin's disease

(HD) treated with ABVD chemotherapy (CHT). **Patients and Methods**: 68 patients (30 men, 38 women; mean age 32±11 years old) with biopsy proven HD. 6 were Stage I, 34 were Stage II, 12 were Stage 3 and 16 were Stage 4 according to Ann Arbor Criteria. All of them underwent a baseline (PET0) and an interim (PET2) 18F-FDG whole body PET/CT. All patients were treated after PET0 with ABVDx2 cycles consisting in Doxoroubicin (Adriamycin), Bleomycin, Vinblastine, Decarbazine for 2 months that ended 15±5 days prior PET2 examination. All patients were further evaluated 15±6 days after four additional ABVD cycles (PET6). No one of the patients presented serum glucose level higher than 107 mg/dl. SUVmean and SUVmax of the liver and of MBP were calculated using the same standard protocol for PET0, PET2 and PET6 respectively. Data have been examined by means of Wilkoxon matched pairs test and Linear regression analysis. **Results**: The main results of our study is an increased liver SUV mean in PET2 (1.76±0.35) as compared to that of PET0 (1.57±0.31; P<0.0001) and PET6 (1.69±0.28;P=0.0407). Same results were obtained when considering liver SUV max in PET2(3.13±0.67) as compared to that of PET0 (2.82±0.64; P<0.0001) and PET6 (2.96±0.52; P=0.0105). No significant differences were obtained when comparing mediastinum SUV mean and SUV max in PET0, PET2 and PET6 (P>0.05). Another finding is a relationship in PET0 between liver SUVmean and SUVmax with the stage, being lower in those patients with an advanced disease (R square=0.1456 and P=0.0013 for SUVmean and R square=0.1277 and P=0.0028 for SUVmax). **Conclusions**: the results of our study suggest that liver 18F-FDG uptake is variable in patients with HD during the CHT treatment and the disease course and should be considered carefully when used to define therapy response in the interim PET in HD.

## P726

### Bone marrow uptake of 18F-FDG PET/CT and bone marrow biopsy in initial staging of diffuse large B-cell lymphoma patients

**A. Nicoletti**, A. Niccoli-Asabella, F. Antonica, A. Notaristefano, M. Polito, C. Ferrari, G. Rubini; Nuclear Medicine Unit, D.I.M., University of Bari "Aldo Moro", Bari, Italy, ITALY.

**Aim**: to evaluate the relationship between bone marrow uptake of 18Fluorine-fluorodeoxyglucose positron-emission-tomography/computed-tomography (18F-FDG PET/CT), bone marrow biopsy (BMB), in initial staging of patients with diffuse large B-cell lymphoma (DLBCL). **Materials and Methods**: the study population comprised 98 patients (mean age 54, range 3-82) who had performed 18F-FDG PET/CT (dose of 3,7 MBq/Kg) for initial staging of DLBCL. All patients underwent a BMB at least 30 days before the 18F-FDG PET/CT scan and hadn't started chemotherapy. The bone marrow uptake was evaluated qualitatively (Visual PET) and quantitatively calculating standard uptake value (SUV) by building a region of interest (ROI) on the L3 vertebral body. The SUV measurement site was different from biopsy site in all patients to avoid false increase of SUV. Concordance was evaluated by Cohen's K. ROC Curve Analysis was used to evaluate diagnostic accuracy of SUV on the L3 vertebral body. Analysis of covariance was performed to evaluate differences in SUV mean between BMB+ and BMB- patients with weight and age as covariates. **Results**: 56/98 patients (57.1%) were negative to BMB while 42/98 (42.9%) were BMB positive. Visual PET results negative in 83/98 patients (84.7%) and positive in 15/98 patients. Concordance between Visual PET and BMB is low [K=0.343 p=0.000], 28 patients with BMB positive were not detected by Visual PET analysis. In 83/98 patients negative at the Visual PET the SUV mean is 2.86 (s.d. 0.58), while in the remaining 15 patients positive at the Visual PET, the SUV mean is 4.15 (s.d. 2.9) [t=1.91; p=0.076]. From a quantitative point of view, SUV diagnostic capacity results quite high at the ROC curve analysis with (Area Under the Curve) AUC=0.793 (95% IC: 0.699-0.868); the best cut-off value resulted 2.9 with a sensitivity of 66.7% and a specificity of 83.9%. The analysis of covariance reports that differences between SUV mean of the two groups of patients (BMB+ and BMB-) is significant (F=13.55 p=0.000) and SUV do not depend on age [F=0.0009 p=0.925] and weight [F=0 p=0.983]. **Conclusions**: weight and age do not influence bone marrow uptake. Concordance between Visual PET analysis and BMB is low, while the predictive accuracy of SUV is high. It's important to evaluate bone marrow uptake because the qualitative analysis by itself isn't sufficient to assess disease activity. Even if BMB is the gold standard for initial staging of DLBCL, SUV >2.9 of the bone marrow has a good predictivity of positive bone marrow biopsy.

## P727

### Interim FDG PET/CT in Hodgkin's Lymphoma - does binary response assessment criteria have any prognostic value?

**P. Arce-Calisaya**[1], A. Scarsbrook[1], H. Thygesen[2], F. Chowdhury[1], C. Patel[1]; [1]Saint James's University Hospital, Nuclear Medicine department, Leeds, UNITED KINGDOM, [2]Leeds Institute of Molecular Medicine, Statistics group, Leeds, UNITED KINGDOM.

Aim: 18F-FDG PET/CT is now routinely used in the assessment of patients with Hodgkin's Lymphoma (HL) for initial staging of disease and assessment of response to therapy. More recently, early response assessment with interim PET/CT has been shown to provide important prognostic information but there remains debate as to what criteria should be used to evaluate interim studies. These include qualitative evaluation (binary or 5-point scale) or semi-quantitative assessment (e.g. ΔSUVmax). The aim of this study was to evaluate whether binary response assessment criteria (positive or negative) has any prognostic significance after 2 cycles of ABVD therapy. Methods and Materials: Newly diagnosed adult patients with advanced-stage HL undergoing baseline and interim (post-2 cycles ABVD) 18F-FDG PET/CT were included in this retrospective study. Interim PET/CT studies were retrospectively reviewed to assign a binary result of positive (i.e. partial metabolic response) or negative (i.e. complete metabolic response). Positive was defined as residual FDG uptake above mediastinal blood-pool. Negative was defined as any FDG uptake similar to/below mediastinal blood-pool. Patients were followed up to determine final remission status following primary therapy and any subsequent disease relapse. Data analyzed using Kaplan-Meier survival analysis. Results: A total of 99 patients (median age: 38 years, range: 18-77, 44 female, 55 male) underwent baseline and interim PET/CT. 70 patients were categorized as negative (CMR) after 2 cycles ABVD and 29 as positive (PMR) of which 23 achieved CMR at subsequent assessment with PET/CT. 6 patients did not achieve CMR following chemotherapy. For those achieving a complete remission (93 patients), the 1-year recurrence-free survival was 89% in the negative (CMR) interim PET/CT group and 86% in the positive (PMR) interim PET/CT group. There was no statistically significant difference between groups. Conclusions: Our study shows that binary response assessment criteria (positive or negative) for interim PET/CT in Hodgkin's lymphoma does not provide any prognostic significance for early recurrence.

## P728

### Early treatment intensification with escalated BEACOPP after interim PET in advanced Hodgkin Lymphoma patients not responding to ABVD therapy .

**B. Malkowski**[1], I. Danielewicz[2], K. Leśniewski-Kmak[2], M. Zalewska[3], R. Zaucha[4], J. Szefer[1], J. Zaucha[2]; [1]Oncology Centre, Bydgoszcz, POLAND, [2]Gdynia Oncology Center, Gdynia, POLAND, [3]Department of the Prevention of Environmental Hazards and Allergology, Warsaw, POLAND, [4]Department of Oncology and Radiotherapy Medical University of Gdańsk, Gdansk, POLAND.

The prognosis of Hodgkin Lymphoma (HL) patients treated with ABVD and having interim positron emission tomography (PET) positive scans is dismal; therefore, treatment intensification in such patients is justified. Escalated BEACOPP seems to be the treatment of choice due to its high efficacy. However, the data confirming the utility of BEACOPP intensification is scarce and the optimal number of BEACOPP cycles is not known. Here, we present the results of early BEACOPP intensification (6 cycles) in 8 out of 64 patients treated for advanced HL. All patients, median age 35 (21-61) years, had positive interim PET after 1 and 2 ABVD cycles. FDG PET/CT studies were made by using the Siemens Biograph mCT and Biograph 16 scanners, 60±10 min after 7 MBq /kg FDG injection. Studies were performed at staging, after 1 and 2 ABVD, 2±1 days cycles before the next cycle of chemotherapy. Seven patients responded and became PET negative. With a median follow up of 23.7 (7.1-42.5) months, only 1 patient relapsed. One patient died during a third BEACOPP cycle due to bacterial sepsis. We conclude that early intensification with 6 escBEACOPP cycles in HL patients not responding to ABVD is feasible and effective.

## P729

### Does FDG-PET uptake correlate with grade and Ki67 in follicular lymphoma?

L. Colleter, **J. Ohnona**, D. Lussato, C. Thieblemont, P. Brice, C. De Bazelaire, J. Briere, P. Merlet, E. De Kerviler; CHU Saint-Louis, Paris, FRANCE.

Aim: To determine whether Standardized Uptake Value (SUV) correlates with the histologic grade and Ki-67 antigen expression in follicular lymphoma (FL) assessed by image-guided biopsies. Materials and Methods: From 2007 to 2012, we reviewed the data from 92 patients with FL who underwent both image-guided biopsies and FDG-PET. Biopsies were performed on the largest or more easily accessible lesion blindly from PET results. We compared the SUV at biopsy site and the maximal SUV on whole-body examination with pathologic feature (Ki67 antigen expression and follicular lymphoma histologic grade). Wilcoxon tests were used to compare SUV between measurement sites, SUV between tumor grade and Ki-67 between tumor grades. Spearman tests were used to compare Ki-67 and SUV. Results: The SUV at biopsy site was lower (mean=8.1, SD=3.49) than the maximal SUV on whole-body (mean=10.4, SD=3.49, p<0.0001). Eighty-five patients had a histologic grade 1-2, 7 were grade 3. The mean Ki-67 index was higher in grade 3 (47.6, SD=35.7) than in lower grades (17.6 SD=17.3, p=0.0337). Both maximal SUV at biopsy site and on whole-body were slightly correlated with Ki-67 expression (rs=0.239, p=0.0220 and rs=0.280, p=0.0069 respectively). Conclusion: Both SUV measured at biopsy site and maximal SUV correlate with the Ki-67 proliferation rate, but not with the grade. However, there is no need to perform FDG-PET prior to the biopsy in the aim of targeting tissue sampling in follicular lymphoma.

## P730

### Early 18F-FDG PET/CT Response Assessment in Agressive Lymphoma: Comparison Between Visual and Semiquantitative Analysis. Preliminary Results

**M. CORTES ROMERA**[1], S. MERCADAL VILCHEZ[2], A. CARESIA ARÓZTEGUI[1], S. ROSSI SEOANE[1], J. ROBLES BARBA[1], L. RODRIGUEZ BEL[1], E. DOMINGO DOMÉNECH[2], E. GONZÁLEZ BARCA[2], C. GÁMEZ CENZANO[1]; [1]INSTITUT DE DIAGNOSITC PER LA IMATGE, L'HOSPITALET DE LLOBREGAT, SPAIN, [2]DEPARTMENT OF HEMATOLOGY, L'HOSPITALET DE LLOBREGAT, SPAIN.

Aim: The aim of this study was to compare visual and semiquantitative analysis in the early response evaluation with PET/CT (interim PET) in the aggressive lymphomas and its correlation with the final response. Material and Methods: Thirty patients with newly diagnosed aggressive lymphoma,19 diffuse large B cell lymphoma and 11 Hodgkin lymphoma were included in this prospective study. Median age patient was 43 years (range 19-79) and 19 of them were men. Stages were: II in 5, III in 3 and IV in 22. All patients underwent PET/CT at 3 times: at initial staging (baseline), at midtherapy or interim (after 3-4 cycles) and at the end of therapy. Interim PET studies were interpreted according to visual and maximal standardized uptake value reduction compared to baseline PET. Interim PET images were considered negative (good responders) when FDG uptake in the residual mass was less than liver uptake (score ≤ 3 in London criteria for visual analysis) and SUVmax reduction ≥ 65.7% (after 3 cycles) or ≥ 72.4% (after 4 cycles) for the semiquantitative analysis. Correlation study was performed between two Methods. The results of interim PET were compared with the end of therapy (complete metabolic response) and the follow-up (>6 months). Results: All baseline PET studies had positives lesions. Twenty-two out of 30 patients were classified as negative interim PET according to visual analysis and 23 out of 30 according to SUVmax reduction (22 out of 23 concordant results and 1 out of 23 discordant). All of them achieved complete response at the end of treatment and remain free of disease in the follow-up. All patients classified as positive interim PET (8 according to visual analysis and 7 to semiquantitative analysis) finally progressed. The correlation between two Methods was good (Kappa=0.8; Standard Error=0.13). Conclusion: Interim PET is a good predictor of the response at the end of treatment. In our study a good correlation between visual and SUVmax reduction analysis was found.

## P731

### Bone marrow biopsy has no routine role in the staging of Hodgkin's lymphoma in the modern era of 18F-FDG PET/CT

**P. Arce-Calisaya**[1], R. Johnson[2], F. Chowdhury[1], A. Scarsbrook[1], C. Patel[1]; [1]Saint James's University Hospital, Nuclear Medicine department, Leeds, UNITED KINGDOM, [2]Saint James's University Hospital, Clinical Haematology, Leeds, UNITED KINGDOM.

Purpose Current international guidelines recommend 18F-FDG PET-CT for the initial staging of patients with Hodgkin's lymphoma but many centres continue to perform invasive bone marrow biopsies (BMB) to evaluate bone marrow involvement at baseline. The aim of this study was to evaluate whether BMB provides any additional information in patients having staging PET-CT scans. Methods Retrospective analysis of 64 patients with newly diagnosed Hodgkin's lymphoma (median age: 28 years, range: 11-79, 27 female, 37 male) undergoing baseline 18F-FDG PET-CT and diagnostic BMB. Bone marrow activity was assessed visually to determine the degree of uptake compared to background liver and the pattern of uptake as either homogeneous (considered negative for bone marrow disease) or multifocal/heterogeneous (considered positive for bone marrow disease). This was correlated with the BMB findings and any subsequent change in management. Results: In the study population of 64 patients, 45 (70%) were found to have a normal pattern of bone marrow uptake on FDG PET-CT and all had a negative BMB. 19 (30%) patients had increased bone marrow uptake of which 8 (13%) was diffuse/homogeneous and 11 (17%) was multifocal/heterogeneous. In the homogeneous group, 1 of 8 patients had a positive BMB but this did not change stage of disease or management due to concurrent pulmonary involvement (stage IV). If normal or homogeneous bone marrow uptake is considered negative for disease, the overall negative predictive value (NPV) of FDG PET-CT is 98%. In the multifocal/heterogeneous group, only 2 of 11 patients had a positive BMB but the remaining 9 had advanced stage disease and therefore not associated with any change in management. Conclusion: FDG-PET-CT has high NPV for bone marrow involvement in patients with newly-diagnosed Hodgkin's lymphoma. It probably also has greater sensitivity than BMB for detecting multifocal bone marrow disease, although this is difficult to prove without multiple biopsies for correlation. Our study suggests that bone marrow biopsy is not routinely required in patients being staged with FDG PET-CT.

## P732

### Standardized Uptake Value (SUV) Based Differentiation of Thymic Rebound from Anterior Mediastinal Lymphoma and Lymphoma Recurrence at Positron Emission Tomography/Computerized Tomography (PET/CT) of Young Adults

**P. Rondogianni**[1], M. Skylakaki[2], E. Vlontzou[1], G. Mpartseas[1], D. Kyprianou[1], A. Samartzis[1], C. Giannopoulou[1], M. Bountali[1], I. Datseris[1]; [1]Nuclear Medicine Department -"Evangelismos"General Hospital, Athens, GREECE, [2]Radiology Department-"Evangelismos" General Hospital, Athens, GREECE.

AIM In young adults it is often difficult to distinguish 18-Fluoro-deoxyglucose (18FDG) uptake due to post chemotherapy thymic rebound from residual or recurrent mediastinal disease .In this study we examined if SUVmax value of the mediastinal lesions can help in the differentiation of these entities. MATERIALS-METHODS Eighty PET CT studies of 71 young adults( mean age 27,7y) were reviewed retrospectively. Patients were divided into five groups: Anterior mediastinal lymphoma at initial staging(group A) , post treatment residual mediastinal mass (group B ), lymphoma recurrence in mediastinum (group C) , lymphoma outside the mediastinum ( group D) and other malignant tumors outside the mediastinum post treatment ( Group D ) .Mediastinal uptake in groups D and E was attributed to thymic rebound. Analysis concerned measurements of maximum Standardized uptake values of anterior mediastinal mass and thymus on PET images. RESULTS: Mean prechemotherapy mediastinal mass SUV was 15,86 for group A , 7,5 for group B and 10,6 for group C .Mean thymus SUV was 2,7 for group D and 3,37 for group E .The difference between pretreatment and post treatment mediastinal uptake and mediastinal uptake in recurrence was statistically significant (p<0,001) CONCLUSION: Uptake is usually high in mediastinal lymphoma before treatment or in lymphoma mediastinal recurrence. Residual masses post treatment have lower uptake but still higher than thymic rebound postchemotherapy. SUV value higher than 4 seems to be in favor of active mediastinal disease.

## P733

### The Role of Positron Emission Tomography/ Computed Tomography (PET/CT) in the Estimation of Bone Marrow Involvement (BMI) in Hodgkin Lymphoma (HL) During Initial Staging

**P. Rondogianni**[1], T. Vassilakopoulos[2], E. Vlontzou[1], D. Exarhos[3], D. Kyprianou[1], G. Mpartseas[1], A. Samartzis[1], I. Houssianakou[1], J. Meletis[2], I. Datseris[1]; [1]Nuclear Medicine Department -"Evangelismos"General Hospital, ATHENS, GREECE, [2]Department of Haematology- National and Kapodistrian University, Athens, Greece., ATHENS, GREECE, [3]CT and MRI Department-"Evangelismos" General Hospital, ATHENS, GREECE.

Introduction: PET/CT is a sensitive tool for HL staging. BMI is observed in ~6% of HL patients (pts) at initial diagnosis and recent data suggest that very few pts may have a positive bone marrow biopsy ( BMB) in the absence of PET/CT evidence, thus questioning the need of BMB. The aim of this study was correlate BMB and BM-PET/CT findings in a series of 148 HL pts and to assess the ability to omit BMB in selected or even all pts. Patients and Methods: PET/CT data were reviewed by two experienced Nuclear Medicine physicians and bone marrow uptake was visually graded as follows: (1) no increased BM FDG uptake; (2) diffusely increased BM FDG uptake ≤liver; (3)diffusely increased BM FDG uptake >liver; (4) solitary osseous/BM focus without CT correlate; (5) multiple osseous/BM foci. Pts were also classified according to clinical data (based on age, B-symptoms, pre-BMB stage, inguinal/iliac involvement, hemoglobin, leukocyte count) as low-, standard- and high-risk for BMI Results: PET/CT was negative for BMI in 122 pts (82%;)and positive in 26 pts (18%): 3 (2%) had a single focus and 23 (16%) had multiple foci. Only 10 pts had BMI by BMB (6.8%). None of the pts of PET/CT categories 1,2,3 or even 4 had a positive BMB; 10/23 pts graded as "5" had positive BMB (44%). .PET/CT-based BMI was effectively predicted: it was 0% in low-risk, 6.5% in standard-risk and 40% in the high-risk group. The outcome of the 10 pts with BMI by BMB was marginally inferior with 3-yr FFS 43% vs. 85% (p=0.055). The difference was even more pronounced for the 23 pts with BMI by PET/CT (3-yr FFS 43% vs. 85%; p=0.0002). Pts with BMI by PET/CT and negative or positive BMB had similar outcomes (3-yr FFS 28% vs 52%, p=0.33). Conclusions: PET/CT appears more efficient than BMB in detecting BMI, revealing ~2.5 times more cases. There was no case of positive BMB in the absence of BMI by PET/CT. These data confirm that BMB can be safely omitted in HL pts staged by PET/CT. Furthermore, this study suggests that omission of BMB is feasible in all pts, since there was no high-risk group who might obtain a benefit from the combination of PET/CT and BMB.

## P734

### Value of PET / CT 18F-FDG in the evaluation of recurrence in patients with diffuse large B-cell lymphoma responders to first-line therapy. HUG.

**A. Mendoza Paulini**, M. Fernández Rodríguez, E. Rodríguez Pelayo, L. Castillejos Rodríguez, M. Balsa Bretón, P. García Alonso, A. Ortega Valle, J. Penín González; HOSPITAL UNIVERSITARIO DE GETAFE, Getafe, SPAIN.

INTRODUCTION: The value of PET / CT in monitoring patients with diffuse large B-cell lymphoma (DLBCL) at the end of first-line therapy is not completely

understood, which is why there is still no consensus best time to ask for a PET / CT and often depends on the clinical and / or radiological. AIM : The objective was to evaluate the clinical significance of PET / CT in the detection of recurrence in patients with (DLBCL) responders to first-line therapy. MATERIAL AND METHODS: We retrospectively studied 60 patients, mean age 60 ± 12 years, 31 (51.6%) women, during a three year follow up. They all had a PET / CT negative after the treatment of 6 cycles of chemotherapy. We conducted a PET / CT in suspected clinical or radiological recurrence. We determined the number of relapses, the disease-free time (TLE). Relapse was confirmed by biopsy or clinical course. RESULTS: Of the 60 patients studied, the PET / CT confirmed 12 (20.0%) cases of recurrence (VP), 46 (76.7%) cases were VN, 2 (3.3%) cases FP (2 nonspecific adenitis, a and one of them axillary jugular chain) and no cases of FN. 80.7% of patients were free of disease at 3 years. We found a S: 100%, E: 93.8%, PPV 96.7% and NPV 100%. CONCLUSION: PET / CT was useful in the evaluation of recurrence in patients with (DLBCL), showing a high NPV, and detecting 20% of recurrences.

## P735

### 18F-FDG PET / CT in post treatment and follow-up Hodgkin´s disease

**A. Mendoza Paulini**, E. Rodríguez Pelayo, M. Fernández Rodríguez, P. García Alonso, L. Castillejos Rodríguez, A. Ortega Valle, M. Balsa Bretón, J. Penín González; HOSPITAL UNIVERSITARIO DE GETAFE, Getafe, SPAIN.

INTRODUCCION: 18F-FDG PET / CT is an accurate imaging technique in staging and assessing response to therapy in Hodgkin lymphoma (HL). However, usefulness in monitoring patients already treated, in order to detect subclinical relapse, is controversial. Some authors get high number of false positives results, increasing costs and limiting its value when compared to other imaging techniques. AIM: To determine PET / CT utility in monitoring patients with HL already treated. MATERIAL AND METHODS: We retrospectively evaluated 47 patients already treated, followed for a minimum three-year period , mean age 47 ± 19 years, 27 (57.4%) women. We determined the free-disease interval and the number of relapses. All the patients had completed first-line therapy achieving complete response to treatment. Relapses were confirmed by pathology or clinical outcome. RESULTS: Of the 47 patients studied: 7 (14.9%) were PET/TAC TP (relapses), 1 (2.1%) was FP (axillary lymph reagent), 39 (83.0%) were TN, and there were no FN cases. PET/TAC detected unespected relapses in 15% of the patients. We found a Sensitivity of 100%, E: 97.5%, PPV 87.5%, NPV 100% and an accuracy of 97.8%. CONCLUSION: 18F-FDG PET / CT is a useful tool in monitoring Hodgkin Lymphoma already treated, detecting unsuspected relapses in about 15% of the patients.

## P736

### FDG PET-CT diffuse bone marrow uptake and bone marrow reactive changes in staging of Hodgkin's Lymphoma patients

**M. Gregianin**[1], A. Colpo[2], E. De March[2], F. Lessi[2], M. Ermani[3], L. Alessandrini[4], L. Iaria[4], F. Marino[4], L. Evangelista[1], A. R. Cervino[1], M. Burei[1], G. Saladini[1], G. Semenzato[2], L. Trentin[2]; [1]Radiotherapy and Nuclear Medicine Unit, Istituto Oncologico Veneto IOV-IRCCS, Padova, ITALY, [2]Department of Medicine, Hematology and Clinical Immunology Unit, University of Padova, Padova, ITALY, [3]Department of Neurological Sciences, University of Padova, Padova, ITALY, [4]Department of Diagnostic Medical Sciences, Pathology Section, University of Padova, Padova, ITALY.

**Aim.** To evaluate the correlation between FDG-diffuse bone marrow uptake (BMU) and bone marrow reactive changes in initial staging of Hodgkin's Lymphoma (HL). Bone marrow aspirate (BMA) and bone marrow biopsy (BMB) are routinely performed in the staging of HL. A relatively high percentage of patients is characterized by non-specific lesions that indicate a reactive condition that is likely to account for the FDG-diffuse BMU observed and that does not seem to be related to malignant involvement. **Material and Methods.** 92 HL patients (median age 33 yy) undergoing staging BMA, BMB and FDG PET-CT were included in this retrospective study. BMU was assessed visually according to liver uptake (0<liver uptake, 1=liver uptake, 2>liver uptake). Clinical and laboratory characteristics were collected. The scans were acquired employing a dedicated PET/CT tomograph (Biograph 16, Siemens), 71±11 min after the 18F-FDG injection (2.8-3 MBq/kg/bw). **Results.** BMB was positive for bone marrow infiltration (BMI) in 6.5% of patients, whereas focal skeletal FDG-uptake was seen in 9.8%. BMB and PET/CT were concordant in 90.2% of cases. In BMA smears we found hypercellular marrow in 44.6%, disgranulopoiesis in 61.9%, myeloid hyperplasia in 5.4%, eosinophil hyperplasia in 29.3%, dyserythropoiesis in 8.7%, erythroid hypoplasia in 15.2%, reactive lymphocytosis in 4.3% and higher values of plasma cells in 10.9%. FDG-PET scans of 62 patients were analyzed: diffuse BMU was detected in 51.6% (grade 0:8.3%, grade 1:29.2%, grade 2:62.5%). Univariate analysis found a correlation between BMU and bone marrow biopsy cellularity (p=0.05), hypercellular marrow at BMA (p=0.02), myeloid hyperplasia (p=0.003), erytroid hypoplasia (p<0.001), WBC values (p=0.02) and CRP level (p=0.05). In multivariate analysis only hypercellular marrow at BMA (p=0.01), erytroid hypoplasia (p<0.001) and CRP level (p=0.005) were correlated with BMU. No statistical link was found between BMU and other factors analysed, in particular BMI, detected by BMB. After a median follow-up to 36 months (range 7-88), the 2-year OS and PFS were 93% and 82%, respectively. By univariate analysis diserythropoiesis (p=0.03), erythroid hypoplasia (p=0.001), elevated CRP level (p=0.03) and advanced stage (p=0.04) were predictors of lower PFS. The presence and the degree of BMU were not related to PFS (p=0.42 and p=0.1 respectively). **Conclusions.** Diffusely increased BMU is frequently seen in FDG PET-CT at initial staging in HL and it is due to reactive changes seen at BMA and BMB. BMA findings, such as diserythropoiesis, could be predictors of outcome.

P48-2 - Tuesday, Oct. 22, 16:00 - 16:30, Poster Exhibition Area

# Oncology Clinical Science: Leukaemia & Myeloma

## P737

### Comparison of FDGPET/CT and 111In-Pentetreotide SPECT/CT for Neuroendocrine Tumours: a Lesion Based Analysis

**K. Kubota**, M. Okasaki, R. Minamimoto, M. Morooka, Y. Miyata, K. Nakajima, T. Sato; National Center for Global Health and Medicine, Tokyo, JAPAN.

Somatostatin receptor scintigraphy using $^{111}$In-pentetreotide(SRS) has been a standard for diagnosis of neuroendocrine tumours(NET) in most of the country except Japan. Recently, possibility of $^{18}$F-FDGPET for the evaluation of aggressiveness of NET has been reported. However, lesions based analysis of each patient has not been well studied. In order to characterize the heterogeneity of metastatic lesions of NET, we have compared FDG uptake and SRS uptake of individual lesions. *Methods:* Thirteen patients of various NETs, for staging or re-staging have been studied by FDGPET/CT, and by SRS SPECT/CT with attenuation correction within 3 days interval. 30 lesions having both FDG uptake and SRS uptake confirmed as mass lesion by CT were evaluated by SUV for FDG uptake, and by tumour/muscle ratio for SRS uptake. Also the correlation of WHO classification and the tracers uptake were evaluated. The study was approved by IRB and informed consent was obtained from all patients. *Results*. Lesions having higher SRS uptake showed variable FDG uptake, but generally lower level. While the lesions having high FDG uptake showed uniformly lower SRS uptake. SRS T/M ratio ranged from 192.7 to 1.9 and its distribution is logarithmic, FDG SUV ranged from 13.8 to 0.77 and its distribution is linear. Two tracers uptake of each lesion showed significant inverse logarithmic correlation (p<0.05). 9 patients have multiple metastatic lesions and the tracers uptake in each lesion in a same patient showed wide variation, especially SRS uptake variation in the same patient was larger than that of FDG. The Grade 3 NET lesions showed significantly higher FDG uptake than the Grade 2 lesions (10.39±4.88(5) vs 3.09±1.75(25)). SRS uptake of Grade 3 was lower than Grade 2 as expected but not significant due to large variation (9.32±14.56(5) vs 48.58±57.57(25)). *Conclusion*. An inverse correlation of SRS uptake and FDG uptake in metastatic lesions of NET observed in this study may be consistent with the opposed idea of differentiation and proliferation. Large variation of SRS uptake in Grade 2 tumours lesions might suggest the limitation of SRS based therapy for patient having multiple heterogeneous metastases.

## P738

### Pulmonary carcinoid tumor diagnosis and follow up: a 111In-pentetreotide SPECT/CT study.

**A. Spanu**[1], O. Schillaci[2], B. Piras[1], A. Falchi[1], R. Danieli[2], P. Ferro[3], A. Chiaravallotti[2], S. Nuvoli[1], F. Dore[3], G. Madeddu[1]; [1]Unit of Nuclear Medicine. University of Sassari, Sassari, ITALY, [2]Unit of Nuclear Medicine. University of Rome Tor Vergata, Rome, ITALY, [3]Unit of Nuclear Medicine. Hospital of Trieste, Trieste, ITALY.

**Aim**. Pulmonary carcinoid tumours (PCT) are low grade malignancies which usually arise in lobar, segmental or proximal subsegmental bronchi. However, atypical forms can be discovered which can be aggressive and metastasize. Conventional imaging procedures (CIP) may be inconclusive in diagnosing PCT in some cases. We evaluated $^{111}$In-Pentetreotide SPECT/CT incremental value than CIP, such as US, CT and MRI, in PCT diagnosis and follow-up. **Methods**. We enrolled 107 ascertained PCT patients, 47 at initial staging and 60 in follow-up; primary tumors had been excised in 81 cases. All patients underwent at least 2 CIP before scintigraphy. Whole body scan was followed by SPECT/CT of chest and other suspect regions at 4h and 24h after $^{111}$In-Pentetreotide injection using a dual head gamma camera including a low-dose x-ray tube (Infinia, GE Medical System). SPECT images were reconstructed with iterative method and fused with CT images. **Results**. Primary PCT and/or metastatic lesions were ascertained in 72/107 patients and SPECT/CT was positive in 66/72 cases, while CIP in 58/72. Comparing SPECT/CT with CIP, per-patient sensitivity (91.7 vs 80.6%), specificity (100 vs 100%) and accuracy (94.4 vs 86.9%) showed no statistical difference. SPECT/CT and CIP were concordantly true

positive in 52 patients and true negative in 35; only SPECT/CT was true positive in 14 pts and only CIP in 6. In the 72 positive patients, 273 lesions were ascertained, with SPECT/CT detecting 234/273 foci and with CIP 198/273 (per-lesion sensitivity 85.7 vs 72.5%, p<0.0001). In the 72 positive patients, 61 primitive lesions were ascertained, with SPECT/TC detecting 51/61 foci and with CIP 46/61 (per-lesion sensitivity 83.6 vs 75.4%); 212 secondary lesions were identified and SPECT/CT detected 183/212 and CIP 152/212 (per-lesion sensitivity 86.3 vs 71.7% p<0.0001). SPECT/CT provided further information than CIP in 25/72 (34.7%) cases correctly localizing lesion anatomical sites and well determining involved organs and lesion relationship with adjacent structures in 15 unclear cases, excluding malignancy in sites reported as positive in 3 patients, while revealing unsuspected mediastinal or bone metastases in 7 cases. **Conclusion.** In the present study, $^{111}$In-Pentetreotide SPECT/CT proved more sensitive and accurate than CIP, thus enhancing its role in PCT diagnosis and follow-up. SPECT/CT could define lesion anatomical sites and surrounding tissue invasion and differentiate tumor lesions from benign tracer uptakes. Thus, SPECT/CT more correctly classified the affected patients giving useful information for the most appropriate therapeutic strategy. However, SPECT/CT and CIP combined use achieved the highest accuracy values.

## P739

### The value of 99mTc EDDA/HYNIC-TOC SPECT/CT in assessment of patients with metastatic neuroendocrine tumours of unknown primary or suspicion of NET, Initial Experience

**M. Trogrlic**, S. Tezak, M. Zuvic; University Hospital Centre Zagreb, Zagreb, CROATIA.

AIM: Radiolabeled somatostatin analogs have proved very useful in localization of somatostatin receptor expressing tumours. The aim was to evaluate the potential usefulness of 99mTc EDDA/HYNIC-Tyr3-octreotide (TOC) SPECT/CT in patients with metastatic NETs of unknown primary and in patients with suspected NET. MATERIALS AND METHODS: In this retrospective study 32 patients (20 males and 12 females; age group 19-90 years, mean age 61 year) were examined with 99mTc EDDA/HYNIC-TOC between November 2010 and April 2012 and divided in two groups: Group 1: 21 patients with biochemical (increased tumour markers: chromogranin A (n=14), 5-HIAA (n=5), NSE (n=2)) and/or clinical suspicion of NET, Group 2: 11 patients with histologically proven metastatic NET of unknown primary. SPECT/CT results were compared with conventional imaging (CT, MRI, EUS) and clinical follow up of at least one year. Whole body and tomographic acquisition were taken 2 and 4 hours after administration of 666 MBq of 99mTc EDDA/HYNIC-TOC. All the patients underwent SPECT/CT 4 hours after injection of the tracer. RESULTS: In group 1 somatostatin receptor positive lesions were found in 9 of 21 (43%) patients and negative in 12 of 21 (57%) patients. SPECT/CT results were true-positive (confirmed by conventional imaging and clinical follow up of at least one year) in 6 cases, true-negative in 12 and false-positive in 3 cases. 99mTc EDDA/HYNIC-TOC had an overall sensitivity of 100%, specificity of 80%, a positive predictive value (PPV) of 67%, and a negative predictive value (NPV) of 100%. The diagnostic accuracy of 99mTc EDDA/HYNIC-TOC was 86%. The prevalence of NETs in the studied population was 29% (6 of 21). In group 2 the primary tumor was not identified in any of the patients. In terms of initial staging, somatostatin receptor positive lesions were found in 9 of 11 (82%) patients and negative in 2 of 11 (18%) patients. SPECT/CT results were true-positive in 8 cases, true-negative in 1, false-negative in 1 and false-positive in 1 case. 99mTc EDDA/HYNIC-TOC had an overall sensitivity of 89%, specificity of 50%, PPV of 89%, and NPV of 50%. The diagnostic accuracy was 82%. CONCLUSIONS: 99mTc EDDA/HYNIC-TOC SPECT/CT is useful functional imaging modality in evaluation of patients with suspicion of NETs. Excellent sensitivity in group 1 was probably due to relatively short (one year) follow-up period. Even if 99mTc EDDA/HYNIC-TOC SPECT/CT doesn´t give exact localization of primary tumor it may provide an accurate staging of metastatic NETs.

## P740

### Functional imaging in paragangliomas with $^{68}$Ga-DOTA-TOC PET/CT, $^{18}$F-DOPA PET and $^{123}$I-MIBG SPECT/CT imaging

**A. Kroiss**[1], D. Putzer[2], A. Frech[3], C. Decristoforo[1], C. Uprimny[1], L. Posch[3], R. Gasser[4], C. Goetsch[4], G. Fraedrich[3], B. Shulkin[5], C. Url[6], G. Widmann[2], I. Virgolini[1]; [1]Department of Nuclear Medicine, Innsbruck Medical University, AUSTRIA, [2]Department of Radiology, Innsbruck Medical University, AUSTRIA, [3]Department of Vascular Surgery, Innsbruck Medical University, AUSTRIA, [4]Department of Endocrinology, Innsbruck Medical University, AUSTRIA, [5]Department of Nuclear Medicine, St. Jude Children´s Research Hospital, Memphis, TN, UNITED STATES, [6]Department of Otorhinolaryngology, Innsbruck Medical University, AUSTRIA.

Introduction/Purpose: CT and MRI are the morphological imaging modalities of choice in localizing paragangliomas (PGLs), as they provide excellent anatomical detail and high sensitivity. Functional imaging, for example metaiodobenzylguanidine (MIBG), labeled with $^{123}$I, achieves moderate sensitivity in localizing PGLs. However, functional imaging is limited in detecting localizing multifocal/malignant PGLs due to limited resolution of planar scintigraphy and of single photon emission computed tomography (SPECT), respectively. $^{18}$F-DOPA has high sensitivity in the detection of nonmetastatic PGLS, but sensitivity decreases in malignant disease. We compared functional imaging modalities in the diagnosis and staging of paragangliomas (PGLs), using $^{68}$Ga-DOTA-TOC PET, $^{18}$F-DOPA PET, and $^{123}$I-MIBG imaging including SPECT/CT ("low-dose" CT). Diagnostic CT imaging referred as reference standard. Methods: Three male and eight female patients (age range 26 to 73 years) with anatomical and/or histologically proven disease were included in this study. Three patients were either suffering from metastatic head and neck paragangliomas (HNPGLs) or multifocal PGLs and eight patients from nonmetastastic disease. Comparative evaluation included morphological imaging with CT, functional imaging with $^{68}$Ga-DOTA-TOC PET, $^{18}$F-DOPA PET and $^{123}$I-MIBG imaging including SPECT/CT. Imaging results were analyzed on a per-lesion basis. Results: On a per-lesion basis, $^{68}$Ga-DOTA-TOC PET/CT showed a sensitivity of 100% (McNemar p<0.5), $^{18}$F-DOPA PET 67.9% (McNemar p<0.01), when compared with anatomical imaging. Sensitivity of $^{123}$I-MIBG was 7.1% (McNemar p<0.0001), and that of SPECT/CT 10.7% (McNemar p<0.0001), respectively. Overall, $^{68}$Ga-DOTA-TOC PET and CT identified 28 lesions, $^{18}$F-DOPA PET 19 lesions. $^{123}$I-MIBG imaging identified 2 lesions and SPECT/CT 3 lesions. Conclusion: $^{68}$Ga-DOTA-TOC PET is more sensitive than $^{18}$F-DOPA PET and $^{123}$IMIBG SPECT/CT imaging, providing valuable clinical information for staging of paragangliomas.

## P741

### Analysis of additional 68Ga-DOTATATE thyroid uptake in patients with neuroendocrine tumors.

**J. Kunikowska**[1], R. Matyskiel[1], P. Pawliszak[1], A. Zemczak[2], D. Pawlak[3], M. Plazinska[1], B. Kos-Kudła[2], L. Królicki[1]; [1]Medical University of Warsaw, Warszawa, POLAND, [2]Division of Endocrinology, Department of Pathophysiology and Endocrinology, Silesian Medical University, Katowice, POLAND, [3]National Centre for Nuclear Research, Radioisotope Centre POLATOM, Otwock-Swierk, POLAND.

Incidental 68Ga-DOTATATE uptake seen in the thyroid gland is not a rare finding on diagnostic PET-CT scans performed in patients with neuroendocrine tumors (NET). AIM: was to evaluate the prevalence of unexpected thyroid uptake of 68Ga-DOTATATE PET/CT in patients referred to Nuclear Medicine Department for evaluation of NETs. MATERIAL AND METHODS: We retrospectively evaluated 1150 patients with NET, who underwent 68Ga-DOTATATE PET /CT imaging between January 2010 and March 2013. Clinical history, serum TSH levels, thyroid antibodies (TAb), ultrasonography and cytological assessment of the material from fine-needle aspiration biopsy of the thyroid lesion were investigated. Visual analysis of uptake and the distribution pattern with measurement of maximum standardized uptake value (SUVmax) were performed in order to asses 68Ga-DOTATATE uptake. RESULTS: Our study revealed unexpected abnormalities in 47/1150 (4.1%)patients in the thyroid gland defined as focal or diffuse 68Ga-DOTATATE uptake. 35/47 patients showed diffuse 68Ga-DOTATATE thyroid uptake. Laboratory test and ultrasound revealed : 24 pts (68.6%) had an active autoimmune thyroiditis, 9 pts had a benign goiter and the remaining 2 pts had thyroid glands without any pathology. The SUV max mean was 4.55 ±1.59 (range 2.0-10.9) 12/47 pts showed focal uptake in the thyroid. 1 pt had papillary thyroid carcinoma (SUVmax 11.6) associated with Hashimoto's thyroiditis (HT). 4 pts had category III lesion among them 2 pts with nodular goiter (SUVmax 9.8 , 11.8) and 2 pts with nodular goiter associated with HT (SUVmax 3.9; 12.6). 2 pts with nodular goiter had category II lesions (SUV max 4.2 and 4.3) and the remaining 5 pts had an active HT with L-thyroxine substitution(SUV max range from 5.9 to 8.8). CONCLUSIONS: Patients with focal 68Ga-DOTATATE uptake should undergo further examination due to considerable risk of malignancy. Diffuse 68Ga-DOTATATE uptake was predominantly associated with active autoimmune thyroiditis. In pts with diffuse uptake of 68Ga DOTA-TATE visual assessment had better correlation with presence of active autoimmune thyroiditis than SUVmax value.

## P742

### [111In-DTPA]-octreotide whole body and SPECT scintigraphy in the evaluation of patients with NET: comparison with CgA assay and CT imaging.

A. Niccoli Asabella, **C. Ferrari**, C. Altini, A. Nicoletti, A. Notaristefano, M. Polito, G. Rubini; Nuclear Medicine Unit, D.I.M., University of Bari "Aldo Moro", Bari, Italy, ITALY.

**Aim**: Neuroendocrine diseases (NETs) diagnostic management is still discussed due to the lack of a standardized workflow. We evaluate the role of ["In-DTPA]-octreotide (OCT) in patients (pts) who previously performed Chromogranin-A (CgA) assay and morphological imaging as computed tomography (CT) for the diagnosis or restaging of NETs. **Materials and Methods**: We retrospectively analyzed 99 OCT performed in 90 pts. All the 99 OCT was performed with whole-body technique and SPECT acquisition from the neck to the thigh roots. Pts underwent 36/99 OCT for diagnosis of NETs and 63 scans for restaging of NETs. Thirtyfive/90 pts had clinical

suspect of NETs (for SCLC in 4/35 cases and for GEP tumors in 31/35) and 55/90 pts restaged NETs after therapy. Restaging was for well-differentiated neuroendocrine tumors in 33/55 (16 lung and 17 GEP); well-differentiated neuroendocrine carcinomas in 10/55 (7 GEP and 3 neuroendocrine carcinomas of unknown origin); poorly differentiated neuroendocrine carcinomas in 12/55 (8 GEP and 4 SCLC). All pts performed previously (30-60 days before) the CgA assay (normal values: 0-18 U/l) and 58/90 also a performed whole-body CT. The comparison between OCT and CgA, and OCT and CT were performed by K of Cohen. **Results** The comparison between OCT and CgA showed that the two Methods were concordant in 41/99 cases (positive concordant in 18/41 and negative concordant in 23/41); instead they were discordant in 58/99 cases (OCT positive and CgA normal levels in 4/58 pts; OCT negative and CgA high levels in 54/58 pts). The correlation between this two Methods was very low (K=0.065, 95%CI:-0.075 to 0.15). The comparison between OCT and CT showed that the two Methods were concordant in 36/58 cases (positive concordant in 15/36 and negative concordant in 21/36), while they were discordant in 22/58 cases (OCT positive and CT negative in 3/22 patients; OCT negative and CT positive in 19/22 patients). The correlation between this two Methods was low (K=0.288, 95%CI:0.037 to 0.429). In the 58 pts who performed all the techniques, they were all concordant in 20/58 patients (positive concordant in 13/20 and negative concordant in 7/20), while they were discordant in 38/58 patients. **Conclusion** The rarity and the heterogeneous clinical behavior of NETs make difficult their clinical management, requiring a multidisciplinary approach. Whole body and SPECT OCT have to be performed even if CgA or CT doesn't indicate the presence of NET, because the combined use of the techniques improves the diagnostic performance.

## P743

### Sensitivity of 111In-DTPA-exendin-4 SPECT/CT in patients with endogenous hyperinsulinaemic hypoglycaemia

**K. Antwi**[1], E. Christ[2], M. Béhé[3], T. Zumbrunn[4], M. E. Chaplin[5], M. Brändle[6], S. Fischli[7], H. R. Maecke[3], A. Perren[8], J. C. Reubi[8], F. Forrer[1], D. Wild[1,3,9]; [1]Department of Radiology, Division of Nuclear Medicine, University of Basel Hospital, Basel, SWITZERLAND, [2]Division of Endocrinology, Diabetology and Clinical Nutrition, University Hospital of Berne, Berne, SWITZERLAND, [3]Department of Nuclear Medicine, University Hospital Freiburg, Freiburg, GERMANY, [4]Clinical Trial Unit, University of Basel Hospital, Basel, SWITZERLAND, [5]Neuroendocrine Tumour Unit, Royal Free Hospital, London, UNITED KINGDOM, [6]Division of Endocrinology, Diabetes and Osteology, Kantonsspital St.Gallen, St. Gallen, SWITZERLAND, [7]Division of Endocrinology, Diabetes and Clinical Nutrition, Kantonsspital Luzern, Luzern, SWITZERLAND, [8]Institute of Pathology, University of Berne, Berne, SWITZERLAND, [9]Institute of Nuclear Medicine, University College Hospital, London, UNITED KINGDOM.

**Aim:** Preoperative localization of benign insulinomas is critical in order to plan and minimize the surgical intervention. Due to the small size of these tumours difficulties remain to localize them. The goal of this study was to prospectively evaluate the insulinoma detection rate (sensitivity) of the novel imaging modality 111In-DTPA-exendin-4 (111In-[Lys40(Ahx-DTPA)NH2]-exendin-4) SPECT/CT and the comparison with CT or MRI. **Materials and Methods**: A prospective open-label phase 2 trial was undertaken at 3 centres in 3 countries. Twenty-five consecutive patients (age≥25 years) with proven clinical and biochemical endogenous hyperinsulinaemic hypoglycaemia, no or maximal one suspect lesion on conventional imaging and verified histopathology were evaluated. Whole body planar images and SPECT/CT of the abdomen were performed up to 168 h after injection of 111In-DTPA-exendin-4. CT or MRI was performed using a standard protocol. **Results:** 111In-DTPA-exendin-4 SPECT/CT showed a significantly higher sensitivity than CT or MRI (95% [95% CI 75-100) vs 47% [95% CI 27-68), p=0.011, per patient based analysis). 111In-DTPA-exendin-4 SPECT/CT detected at least one insulinoma in all 19 patients with benign insulinomas and four additional positive lesions (2 islets hyperplasia, 2 uncharacterized lesions) resulting in a positive predictive value of 83% (95% CI 62-94). Further, one patient with islet hyperplasia and one with malignant insulinoma were negative. In two patients with MEN-1 gene mutation multiple insulinomas (3 benign insulinomas each) were detected: three Insulinomas less than 7 mm could not be localized with 111In-DTPA-exendin-4 SPECT/CT. In 7 of 25 patients surgery planning was only based on 111In-DTPA-exendin-4 SPECT/CT findings. Five of these patients had a confirmed insulinoma with normalization of hyperinsulinism after surgery, confirming the clinical benefit of 111In-DTPA-exendin-4 SPECT/CT. **Conclusion:** 111In-DTPA-exendin-4 SPECT/CT shows a high sensitivity in detecting insulinomas and is superior to CT or MRI.

## P744

### Clinical utility of SPECT/CT compared to SPECT alone in patients with neuroendocrine tumours

**Z. Varga**, K. Bus, R. Jóba, E. Takács, G. Dabasi, I. Szilvási; Semmelweis University, Budapest, HUNGARY.

**Objectives:** to assess the clinical performance of SPECT/CT compared to SPECT alone and usefulness of the late (24-hours) images of somatostatin receptor scintigraphy (SRS) with Tc-99m-Tektrotyd in patients with neuroendocrine tumours (NET). **Patients and Methods:** 40 patients (28 women, 12 men, average age: 56,6 years) with diagnosis or strong clinical suspicion of NET were studied between October 2011 and December 2012. SRS with Tc-99m-Tektrotyd was performed using SPECT/CT. After iv. administration of Tc-99m-Tektrotyd we made planar and SPECT examination after 1 and 4 hours, and we completed the 4 hours SPECT with native, low-dose CT as well. In 24 patients we performed late planar and - if required - SPECT images after 24 hours. Planar, SPECT and SPECT/CT images were analysed. First we evaluated the planar and SPECT images, than the additional SPECT/CT images. All cases were analysed independently by two nuclear medicine specialists, in conflicting opinions by consensus. **Results:** 26 patients had abnormal SRS. 127 lesions were found. SPECT images helped the localisation of 124 lesions compared to the planar images. The SPECT/CT gave more accurate localisation in 24 of the 26 patients (in 87 of the 127 lesions), compared to SPECT, especially in the upper abdomen. In 2 patients, where the SPECT/CT did not give any additional information, the patients had intrahepatic lesions only. In those 24 studies of the 26 abnormal SRS, where 24 hours images were taken, late images were helpful in 7 patients, in differentiating physiological uptake in the bowels and extrahepatic intraabdominal lesions. In 17 patients late images did not give any plus information. **Conclusions:** SPECT/CT of SRS using Tc-99m-Tektrotyd provides extra information in the great majority of the examinations of patients with NETs compared to SPECT, therefore routine application of SPECT/CT is suggested in SRS. Late images could be useful in the differentiation between extrahepatic abdominal lesions and physiological bowel-uptake, so they are indicated in doubtful cases, but not routinely.

## P745

### First Announcement of GLP-1 Receptor Imaging Results in Patients with Other Diseases than Insulinoma.

A. Sowa-Staszczak[1], A. Stefańska[1], **M. Tomaszuk**[1], R. Mikołajczak[2], B. Janota[2], A. Jabrocka-Hybel[1], E. Przybylik-Mazurek[3], A. Gilis-Januszewska[3], A. Hubalewska-Dydejczyk[3]; [1]Nuclear Medicine Unit, Department of Endocrinology, University Hospital, Krakow, POLAND, [2]Radioisotope Center POLATOM, National Centre for Nuclear Research, Otwock, Otwock, POLAND, [3]Department of Endocrinology, Jagiellonian University Medical College, Krakow, POLAND.

Introduction: Glucagon-like peptide 1 (GLP-1) labelled analogues have been considered as a very useful tool for visualization of benign insulinoma [1]. The expression of GLP-1 receptors is also observed in different neoplasmas including medullary thyroid carcinoma (MTC), pheochromocytoma and gastrinoma. The objective of this study is to present a new applications of [Lys40(Ahx-HYNIC-99mTc/EDDA)NH2]-exendin-4 in patients with other diseases than benign insulinoma. Material and method: 99mTc-GLP-1 receptor scintigraphy was performed in 8 patients (54±18 years): 4 patients with recurrence or dissemination of MTC suspected, 3 patients with pheochromocytoma and 1 patient with dissemination of gastrinoma suspected. The lyophilized kit prepared Radioisotope Center POLATOM was used for preparing the tracer. WB scans were performed at 5 time points and SPECT/CT at 2 points. Results: In 1 patient with malignant MTC 99mTc-GLP-1 receptor scintigraphy revealed inhomogenous liver uptake and focally increased tracer uptake at the location of previously confirmed liver metastases. Moreover, an additional liver lesion not seen on SRS, was detected. In 2 patient with sporadic MTC small focal uptake in the neck was found. The images were comparable with SRS findings. In 3 patient with MEN2a and suspicion of recurrence, the GLP-1 receptor scintigraphy showed the tracer uptake in the same place as 99mTc and 131I scans. In 4 patient tracer uptake at the location of the neck and chest lesions seen on CT was detected. In 1 of 2 patients with benign pheochromocytoma the uptake in the lesion in left adrenal gland was observed. In 3 patient with malignant pheochromocytoma tracer accumulation was observed in numerous metastases in bones and soft tissues. In patient with gastrinoma focal uptake in pancreas tail was observe additionally with one focus in segment 5/6 of the liver. Conclusion: [Lys40(Ahx-HYNIC-99mTc/EDDA)NH2]-exendin-4 seems to be an promising new tracer for clinical practice also in case of patients with other diseases than benign insulinoma. Reference: [1] Sowa-Staszczak A, Pach D, Mikołajczak R, Mäcke H, et al. Glucagon-like peptide-1 receptor imaging with [Lys40(Ahx-HYNIC-99mTc/EDDA)NH2]-exendin-4 for the detection of insulinoma. Eur J Nucl Med Mol Imaging 2013:40-524-531

## P746

### Correlation Between the 111In-Pentetreotide Uptake and Histological Grade of Differentiation of Neuroendocrine Tumours

**A. Sainz-Esteban**, P. García-Talavera, C. Gamazo, J. G. Villanueva, M. L. González, M. Á. Ruiz, R. Olmos; Nuclear Medicine. Hospital Clínico Universitario de Valladolid, Valladolid, SPAIN.

**Aim**: The aim of the study was to evaluate the correlation between the 111In-pentetreotide uptake and histological grade of differentiation of neuroendocrine

tumours (NET). **Material and Methods**: We have included 43 histological samples generated from 38 patients (13 women; mean age: 60±15 years old) with histologically documented NET and we have compared the histological grade of differentiation of each lesion with the 111In-pentetreotide uptake observed in the whole-body scintigraphy (WBS) performed at 4h and 24h after the intravenous administration of 185 MBq of 111In-pentetreotide. Lesions were given a score from 0 to 4 depending on the uptake of the radiopharmaceutical (0 being lowest and 4 highest) in the 4h (early) and 24h (delayed) WBS. Histological samples included 20 low-grade NET with Ki67 index <3%, 3 intermediate-grade NET with Ki67 index ranging from 3 to 20%, and 20 high-grade NET with Ki67 index >20%. **Results:** In the early images the uptake score was 0 in 11 lesions, 1 in 12, 2 in 4, 3 in 8 and 4 in 8, and in the delayed images the uptake score was 0 in 8 lesions, 1 in 13, 2 in 3, 3 in 10 and 4 in 9. There was a good correlation between the early and delayed scores (kappa index 0.73; p-value: 0.000). There was a significant correlation between the histological grade of differentiation and the uptake score in the early and in the delayed images. There was higher 111In-pentetreotide uptake in low-grade NET compared with 111In-pentetreotide uptake in high-grade NET (Spearman coefficient for early images: -0.407; p-value: 0.007; Spearman coefficient for delayed images: -0.474; p-value: 0.001). **Conclusion:** There was a significant inverse correlation between the histological grade of differentiation and the radiotracer uptake in the early and in the delayed images. There was a good correlation between the early and the delayed uptake score although more lesions were detected in the delayed images.

## P747

### 99mTc-EDDA/HYNIC-TOC in imaging of patients with confirmed or suspected gastroenteropancreatic neuroendocrine tumors; pilot study

**H. A. Nasr**[1,2], H. R. Farghaly[1,3]; [1]Radiology Department, PSMMC, Riyadh, SAUDI ARABIA, [2]Nuclear Medicine, Kasr Al-Aini Cairo University Hospital, Cairo, EGYPT, [3]Nuclear Medicine, Assute University Hospital, Assute, EGYPT.

**Introduction:** The clinical use of somatostatin receptor scintigraphy (SRS) using 99mTc labeled agents had been addressed in few limited previous studies and probably remains an interesting focus for more research. In this pilot study we are shedding light on such imaging modality as an available and feasible option for imaging gastroenteropancreatic (GEP) neuroendocrine tumors. Objectives: To assess accuracy of 99mTc-EDDA/HYNIC-TOC scintigraphy in detection of GEP tumors. **Methods:** We included 17 patients (9 males, mean age 53 ± 18.4 years) with confirmed histopathological diagnosis of carcinoid in 13 patients and gastrinoma in 1 patient from which 10 patients had already surgical resection at the time of imaging. The rest of the patients had suspected carcinoid with one suspected insulinoma. Eight patients at time of study had elevated markers (24 hr urinary 5HIAA, serum CgA, serum gastrin). All patients underwent 99mTc-EDDA/HYNIC-TOC (Tektrotyd) scan at 2 and 4 hrs ± imaging at 24 hrs post IV injection of 740 MBq of the tracer. SPECT was done for selected body parts at 4 hrs. All patients had CT scan within 1 month from the SRS. The detected lesions were correlated with one or more of the following as a gold standard: biopsy, tumor markers, clinical or imaging follow-up using SRS, CT or MRI. Sensitivity, specificity, PPV and NPP and accuracy to detect lesions for SRS and for CT were calculated. We also compared number of lesions detected by SRS or CT as an organ based lesion score or a total lesion score. **Results:** The mean age in patients with positive disease on SRS was higher than for negative SRS group; 60.46±10.24 vs. 28.75±19.12 (P<0.001). SRS revealed metastases in 13 (76.5%) patients; in 4 (23.5%) of these patients, the metastatic lesions had not been diagnosed previously. Metastases were mainly localised in liver and abdominal lymph nodes followed by lungs and bone in 11 (65%), 10 (59%), 3 (18%) and 2 (12%) patients respectively. In 1 patient liver metastases near to gall bladder activity was only detected in SPECT images. Sensetivity, specificity, PPV, NPV, and accuracy for overall and organ based lesion detection were 100% for SRS with lower values for CT. **Conclusions**: 99mTc-EDDA/HYNIC-TOC imaging is more accurate than CT scan in our small study series of mainly carcinoid tumors. Imaging using this gamma emitting agent represents an accessible and promising alternative for better staging and follow up of GEP neuroendocrine tumors.

## P748

### Long-acting somatostatine analogues affect the physiological distribution of $^{68}$Ga-DOTANOC

**A. Papa**[1,2], F. Cicone[1,2], D. Prosperi[2], C. Del Mastro[2], G. Franchi[2], I. Sonni[1,2], P. Pizzichini[2], F. Scopinaro[1,2]; [1]Faculty of Medicine and Psychology, "Sapienza" University of Rome, Rome, ITALY, [2]Department of Nuclear Medicine, Sant'Andrea Hospital, Rome, ITALY.

**Aim**. Patients with neuroendocrine tumors (NETs) are often under medication with long acting somatostatine analogues (SA). Because of the long half-lives, significant receptor blockade by the "cold" analogue can not be excluded even after 3-4 weeks withdrawal. Our aim was to investigate the influence of SA treatment on physiological $^{68}$Ga-DOTANOC uptake. **Matherials and Methods.** All patients referred for $^{68}$Ga-DOTANOC PET/CT at our institution between March 2012 and March 2013 were analysed. Images were acquired on a Philips Gemini camera, 30 ± 10 minutes after the administration of 135 ± 30 MBq $^{68}$Ga-DOTANOC. Standardized Uptake Values (SUVmax) were recorded in sites of physiological uptake: pituitary gland, adrenals, liver and spleen. We also identified cases of significant uptake by the uncinate process of the pancreas (UPP). At study entry, patients were classified in two groups (i.e. non-SA vs SA) according to the presence of concomitant treatment with SA. Adequate statistical analysis was applied to evaluate differences of physiological uptake between the two groups. **Results.** Seventy-four patients were analysed. Tumour types included pancreatic NETs (19 pts), extrapancreatic gastro-intestinal NETs (34 pts), carcinoid lung tumors (9 pts) and other histologies (12 pts), including 4 suspected neuroendocrine shifts of prostate cancer, 4 paragangliomas, 2 small-cell lung cancers, 2 medullary thyroid carcinomas. Seventeen patients (23%) were on active SA medication (SA group), while the remaining 57 pts (77%) were receiving other treatments or no treatment at all (non-SA group). Median SUVs of the pituitary gland (2.5 vs 1.8, $p$=0.02), liver (3.7 vs 3.2, $p$<0.05) and spleen (15.1 vs 8.5, $p$=0.01) were significantly higher in the non-SA group than in the SA group (two-sided Student's $T$ test). No significant difference of adrenal uptake between groups was found. Uptake of the UPP was evaluable in 69 patients only, because 5 patients (4 from the non-SA group, 1 from the SA group) had previously undergone a cephalopancreasectomy. Remarkable UPP uptake (SUVmax: 2.9 ± 0.9) was found in 19/53 (36%) patients of the non-SA group and in 2/16 (12.5%) patients of the SA group. The trend was highly suggestive of a significant increased UPP uptake in the non-SA group as compared to the SA group ($\chi^2$ test). **Conclusion**. Treatment with SA significantly reduces uptake of pituitary glands, liver and spleen and is likely to reduce the incidence of remarkable UPP uptake. This should be taken into account when interpreting PET images and in-vivo quality controls.

P49-2 - Tuesday, Oct. 22, 16:00 - 16:30, Poster Exhibition Area

## Oncology Clinical Science: Bone

## P749

### 99mTc-MIBI scintigraphy in the diagnostics of tumors and inflammations of musculoskeletal system, including patients after surgeries

V. Zavadovskaya[1], **A. Kurazhov**[1], M. Zorkaltsev[1], E. Choynzonov[2], E. Slonimskaya[2], A. Bogoutdinova[2]; [1]Siberian State Medical University, Tomsk, RUSSIAN FEDERATION, [2]Cancer Research Institute, Tomsk, RUSSIAN FEDERATION.

Introduction. 99mTc-MIBI scintigraphy is available method for visualization of tumors and, probably, inflammatory processes of musculoskeletal system. But capabilities of 99mTc-MIBI scintigraphy in detection tumors and inflammatory processes in patients after surgeries are not quite clear. Purpose: assess the diagnostic efficiency of tumors and inflammations visualization using 99mTc-MIBI scintigraphy, including patients after surgeries. Materials and Methods. 61 patients with malignant (n=19) and benign (n=2) tumors, and inflammatory processes (n=40) of musculoskeletal system underwent 99mTc-MIBI scintigraphy. 23 patients of 61 were studied after surgeries (11 patients after sternotomy due cardiosurgeries, 7 patients after removal malignant tumors, and 5 patients after osteotomy due osteomyelitis). SPECT (n=47) or planar (n=14) images (SPECT Philips BrightView) were acquired at 20 min (early) and 3 h (delayed) after intravenous injection of 740 MBq of 99mTc-MIBI, and the early ratio (ER), delayed ratio (DR) and retention index (RI) were measured (RI=DR/ER). Results. Tumors were visualized in 20/21 (95.2%) cases (malignancies in 19/19, and benignities in 1/2). Recurrent malignant tumors after surgeries were detected in 7/7 (100.0%) cases. Summary, sensitivity, specificity, positive, negative predictive value and accuracy 99mTc-MIBI scintigraphy in diagnostics of tumors were 95.2%, 5.0%, 34.5%, 66.7%, and 36.1%, respectively. Inflammations were revealed in 38/40 (95.0%) cases. Inflammatory processes in patients after surgeries were visualized in 15/16 (93.8%) cases. Summary, sensitivity, specificity, positive, negative predictive value and accuracy 99mTc-MIBI scintigraphy in diagnostics of inflammations were 95.0%, 4.8%, 65.5%, 33.8%, and 63.9%, respectively. There are statistically significant correlation between DR and WBC (r=0.47, p=0.03) in inflammations. There are no statistically significant differences between ER, DR, and RI in tumors and inflammations (p=0.87, p=0.70, and p=0.89, respectively). Conclusion. 99mTc-MIBI scintigraphy is sensitive tool for diagnostics of tumors and inflammations, including patients after surgery, but absolutely not suitable for differentiating tumor and inflammatory processes.

P50-2 - Tuesday, Oct. 22, 16:00 - 16:30, Poster Exhibition Area

## Oncology Clinical Science: CUP

### P751

### Role of $^{18}$F-FDG PET/CT in patients with metastatic cervical lesions of carcinoma of an unknown primary site: a retrospective study

**X. Lan**, A. Gungadin, H. Liu, Y. Zhang; Union Hospital, Tongji Medical College, Huazhong University of Science and Technology, Wuhan, CHINA.

**Aim** Carcinoma of unknown primary (CUP) represents a heterogeneous group of metastatic malignancies for which no primary tumor site can be identified after extensive routine diagnostic workup. The aim of this study was to assess the potential of $^{18}$F-FDG PET/CT imaging in patients referred for metastatic cervical lymph nodes of CUP in detecting the primary tumor and to detect the presence of any common prognostic factors to this heterogeneous group of tumors. **Methods** Patients with cervical metastasis of CUP (CCUP) who had previously undergone PET/CT between January 2010 and September 2012 were retrospectively analyzed. All patients had histologically proven cervical metastatic carcinomas and relevant diagnostic workup prior to $^{18}$F-FDG PET/CT. The average time of follow-up was 18 months. The primary tumors suggested by PET/CT were compared with the golden standard histopathological diagnosis. Multivariate analyses were also performed to obtain the prognostic factors in this group of patients. **Results** Eighty patients were included in this study, and 20 patients died at the end of the follow-up.$^{18}$F-FDG PET/CT scan detected the primary tumor in 55% (44 of 80). The sensitivity, specificity, accuracy, positive predictive value and negative predictive value were 91.6%, 90.6%, 91.25%, 93.6% and 87.8%, respectively. The lung and head/neck were the two most commonly detected primary tumor sites (36% each). Furthermore, in 25% (20 out of 80) of patients, $^{18}$F-FDG PET/CT detected extra-nodal metastases leading to a re-staging influencing subsequent treatment plans. Multivariate analyses revealed a significant difference in overall survival between patients presenting with extra-nodal metastases (M stage), excluding those subsequently re-diagnosed with lymphoma, with a relative risk value of 4.561 (95% CI 1.820-11.433, P=0.001). SUVmax was found to be a poor prognostic factor with a relative risk value of 1.074 (95% CI 1.002-1.152, P=0.044). **Conclusions** The present study indicates that whole body $^{18}$F-FDG PET/CT scan is a significant and valuable tool in the identification of the primary tumor site in patients with CCUP. Furthermore, PET/CT scans are of value in the assessment of the extent of nodal involvement and in detecting the presence of extra-nodal metastases, further optimizing the management of these patients. Supported by China National 863 program (2008AA02Z426)

### P752

### Whole body F-18FDG PET/CT imaging in detection of primary tumour site in patients with suspected brain metastasis of unknown origin

**S. J. Rayamajhi**, K. Agrawal, R. Kumar, A. Sood, A. Bhattacharya, B. R. Mittal; Postgraduate Institute of Medical Education & Research, PGIMER, CHANDIGARH, INDIA.

Objective: The aim of the study is to evaluate the role of F-18 FDG PET/CT in detection of the primary tumor site in patients with suspected brain metastasis of unknown origin. Secondary aim was to evaluate the value of F-18 FDG PET/CT in detecting secondaries to other sites apart from brain. Method: Data of 26 patients (18 males and 8 females; age range 40-75years) suspected to have brain metastasis on brain MRI or CT performed for various indications like seizure, headache, raised intracranial pressure etc, was retrospectively analyzed. All these patients had undergone F-18 FDG PET/CT scan for detection of the primary site. Site of primary tumor was confirmed by histopathological examination, when available. Results: The F-18 FDG PET/CT scan detected primary site of cancer in 20 of the 26 patients (77%). The site of primary was lung in 16 patients and kidney, bowel, prostate and adnexae in one patient each. The F-18 FDG PET/CT scan was unable to find primary site in 6 patients (23 %). Metastases to organs other than brain were detected in 8 patients (30.7 %) with 7 lung primaries and 1 renal primary. The patients with only isolated brain metastases had lower SUV values in the primary site (average 6.7, range 2.8-14.4), compared to patients with multiple sites of metastases (average 8.5, range 4.6-16.6). Conclusion: Our results suggest that whole body F-18 FDG PET/CT imaging has a high rate of detection of a primary tumor in patients with brain secondary compared to approximately 30% as reported in the literature. Furthermore, F-18 FDG PET/CT helped in detecting other metastatic sites apart from brain.

### P753

### Clinical impact of (18)F-FDG PET-CT in the management of patients with carcinoma of unknown primary:our experience

**G. Paone**, G. Treglia, T. Ruberto, L. Ceriani, L. Giovanella; Department of Nuclear Medicine and PET/CT Center, Oncology institute of Southern Switzerland, Bellinzona, SWITZERLAND.

Aim: The purpose of this study was to evaluate the role of (18) F-FDG PET-CT (FDG PET-CT) in highlighting the sites of primary tumors in patients with carcinoma of unknown primary (CUP) and its impact on the management of these patients. Materials and Methods: We reviewed retrospectively 35 patients with CUP who underwent a FDG PET-CT at our center between 2006 and 2012. Before 18F-FDG injection, the patient had fasted for at least 6 hours and images were acquired one hour after intravenous injection of 18F-FDG according to the body mass index (4 MBq/Kg). The histological and follow-up findings were used to confirm the FDG PET-CT results. Results: FDG PET-CT was able to identify sites of primary tumors in 24/35 (69%) patients. Overall, primary tumors were localized to the lung (n = 5), oropharynx (n = 4), laryngopharynx (n = 1), stomach (n = 3), small intestine (n = 1), ovary (n = 1), bladder (n = 1), rectum (n = 1), adrenal gland (1), other (n = 6) and were confirmed by pathology in all cases. False-positive and false-negative FDG PET-CT results occurred in 1 patient (mediastinal and pulmonary granulomatosis) and 5 patients (1 bladder ca, 1 lung ca, 1 digestive ca, 1 uterine ca and 1 malignant melanoma), respectively. The sensitivity, specificity, PPV, NPV and accuracy of FDG PET-CT were 83%, 83%, 96%, 50% and 83%. A better prognosis emerged in patients with head and neck primary malignancies as compared to other localizations. Conclusion: FDG PET-CT is a useful non-invasive imaging tool to identify unknown primary malignancies and plan therapeutic strategies. Prolonged follow-up is required to evaluate the relationship between primary tumor localization and prognosis.

P51-2 - Tuesday, Oct. 22, 16:00 - 16:30, Poster Exhibition Area

## Oncology Clinical Science: Melanoma

### P754

### Early response evaluation to combination therapy with ipilimumab and vemurafenib in stage IV melanoma patients: Initial results of an ongoing dynamic FDG PET-CT study.

**C. Sachpekidis**[1], A. Dimitrakopoulou-Strauss[1], L. G. Strauss[1], C. Schulz[2], J. Hassel[2]; [1]Clinical Cooperation Unit Nuclear Medicine, German Cancer Research Center, Heidelberg, GERMANY, [2]Department of Dermatology, University Hospital Heidelberg, Skin Cancer Center, Heidelberg, GERMANY.

Objectives: Ipilimumab is a CTLA-4 inhibitor and vemurafenib a BRAF inhibitor. The combination of ipilimumab and vemurafenib provides a strong promise on the current treatment approach of metastatic melanoma. Dynamic PET-CT (dPET-CT) studies with 18F-FDG were performed in patients (pts) with stage IV melanoma who received combination of these targeted therapies. Aim of the study was to evaluate the FDG metabolism with regard to the preliminary therapy outcome. Methods: The ongoing evaluation includes 5 pts. All pts were examined prior, after two cycles and after four cycles of ipilimumab and vemurafenib treatment. The evaluation of dPET-CT studies was based in addition to the conventional SUV evaluation, on a 2-tissue compartment model and a non-compartmental approach. These results were compared with treatment response evaluation, performed by clinicians in accordance with the RECIST criteria. Results: The number of metastatic lesions before the onset of therapy was 17, after 2 cycles of treatment 19 and after 4 cycles of therapy the number of lesions was 15. Mean SUV prior therapy was 5.8, in comparison to 4.3 SUV after 2 cycles and 4.0 SUV after 4 cycles (31% reduction). Maximal SUV prior therapy was 10.2 in comparison to 6.5 SUV after 2 therapy cycles and 6.9 SUV after 4 cycles (32% reduction). The perfusion-dependent parameter k1 remained stable after 4 cycles. However, the phosphorylation-dependent kinetic parameters k3 was more than 50% decreased after completion of therapy. These results are in consistence with the clinical data, which revealed stable disease in 3 pts and partial response in 2 patients. No patient was characterized as having progressive disease. Conclusions: On the basis of these results, dPET-CT studies after 2 and 4 cycles of ipilimumab-vemurafenib combination treatment were predictive for early therapeutic outcome after completion of therapy.

### P755

### Dynamic FDG PET-CT in stage IV melanoma: early therapy response evaluation to ipilimumab.

**C. Sachpekidis**[1], A. Dimitrakopoulou-Strauss[1], L. G. Strauss[1], C. Schulz[2], J. Hassel[2]; [1]Clinical Cooperation Unit Nuclear Medicine, German Cancer Research Center, Heidelberg, GERMANY, [2]Department of Dermatology, University Hospital Heidelberg, Skin Cancer Center, Heidelberg, GERMANY.

Objectives: Ipilimumab is a monoclonal antibody that blocks cytotoxic T-lymphocyte-associated antigen 4 (CTLA-4), thus potentiating an antitumor T-cell response. Dynamic PET-CT (dPET-CT) studies with 18F-FDG were performed in patients (pts) with stage IV melanoma who received palliative therapy with ipilimumab. Aim of the study was to evaluate the FDG metabolism with regard to the preliminary therapy outcome. Methods: The ongoing evaluation includes 9 pts. All pts were examined prior, after two cycles and after four cycles of ipilimumab. The evaluation of dPET-CT studies was based in addition to the conventional SUV evaluation, on a 2-tissue compartment model and a non-compartmental approach.

These results were compared with treatment response evaluation, performed by clinicians and according to the RECIST criteria. Clinical data served as reference. Results: The number of metastatic lesions before the onset of therapy was 27, after 2 cycles of Ipilimumab 29 and after 4 cycles of therapy the number of lesions was 36. Mean SUV prior therapy was 6.1, in comparison to 7.3 SUV after 2 cycles of Ipilimumab and 6.0 SUV after 4 cycles. Maximal SUV prior therapy was 10.1 in comparison to 12.3 SUV after 2 therapy cycles and 9.9 SUV after 4 cycles. The perfusion-dependent parameter k1 showed reduction after 4 cycles. The phosphorylation-dependent kinetic parameters k3 was moderately increased after completion of therapy. These results are in consistence with the clinical data, which revealed progressive disease in 4 pts, stable disease in 4 pts and partial response in only 1 patient. Notably, the patient with partial response demonstrated a reduction of the number of his lesions, of SUV, as well as of all the kinetic parameters. Conclusions: On the basis of these results, dPET-CT studies after 2 and 4 cycles of ipilimumab were predictive for early therapeutic outcome after completion of therapy.

## P756

### Introduction of US- guided FNAC in preoperative staging prior to sentinel lymph node biopsy: benefit for patients with cutaneous melanoma

**G. Horvatic Herceg**, I. Bracic, S. Kusacic-Kuna, A. Mutvar, J. Antulov, D. Herceg; University Hospital Centre Zagreb, Zagreb, CROATIA.

Regional lymph nodes involvement is critical to the overall survival of patients with stage I/II melanoma. Sentinel lymph node biopsy (SLNB) is widely accepted as a screening method for assessing the extent of metastases to regional lymph nodes for the purpose of planning a complete lymph node dissection (CLND). This study was designed to evaluate the value and possible benefits of preoperative ultrasound (US) examination and US-guided fine needle aspiration cytology (FNAC) for the detection of non-palpable lymph node metastases in patients with cutaneous melanoma. Methods: The prospective study included 78 consecutive patients with cutaneous melanoma (38 females and 40 males; mean age 56 years, range: 21-81 years) planned for SLNB. All patients were examined by US before preoperative lymphoscintigraphy. FNAC was performed in suspicious lymph nodes (round or broad oval shaped lymph node, eccentric cortical hypertrophy, and a loss of normal hilar vascularization, with multiple peripheral, capsular vessels penetrating the nodal cortex). In cases of malignant findings, patients were submitted to CLND. The findings were correlated with pathohistological outcomes after CLND. Results: US and US-guided FNAC were true positive in 13 cases, with no false positive results. All FNAC findings were confirmed by pathohistology. There were 6 false negative results out of 64 patients with negative echographic findings. In those patients pathohistology revealed metastases, mostly in form of small foci of tumor cells or individual atypical cells. The sensitivity, specificity, positive predictive value, and negative predictive value of US combined with FNAC were 68.42%, 100%, 100% and 90.77%. Conclusion: Detection of possible regional melanoma metastases by US, combined with power Doppler and FNAC to be performed before sentinel lymphoscintigraphy can spare patients unnecessary surgical sentinel node staging. In our study, 17% (13/78) of our patients with FNAC-proven regional metastasis were sent directly to CLND without previous surgical staging. For patients with a negative US finding, SLNB remains the best diagnostic option. The introduction of US-guided FNAC as a preoperative algorithm for all patients with cutaneous melanoma, as a less invasive and complementary method to SLNB, significantly improves the course and decreases the cost of treatment.

## P757

### Lymphatic mapping and sentinel lymph node biopsy in the management of atypical melanocytic neoplasms

**C. De Gaudio**[1], R. Cecchi[2], V. Ciliberti[1], M. Cerone[3], E. Banti[1], M. Pellegri[1]; [1]Nuclear Medicine Unit, Lucca, ITALY, [2]Dermatology Unit, Pistoia, ITALY, [3]Surgical Unit, Pistoia, ITALY.

**Aim:** atypical spitzoid melanocytic neoplasms (ASMN) are cutaneous lesions of uncertain malignant potential, which can be difficult to distinguish from cutaneous melanoma. Sentinel lymph node biopsy (SLNB) is a safe and useful prognostic tool for staging melanoma, but its role in staging ASMN is still controversial. The aim of this study was to evaluate the incidence of lymph node metastases in patients with (ASMN) after (SLNB) and during follow-up, and to assess the diagnostic value of this procedure. **Patients and Methods***:* Patients with ASMNs referred to our Service from 2004 to 2011 were identified and scheduled for a prospective database. The clinical and histopathologic features of all patients referred to us in those period, with ASMN were studied. All patiens underwent SLNB and were reviewed and correlated in base of the presence or absence of metastatic findings in their corresponding sentinel lymph node. A total of 18 patients with ASMNs were treated during the time analyzed. Four males and 14 females; age range 14-52 years (median age 32 years); 15 were classified as Athypical Spitz Nevi (83%) , 3 cases (17%) were classified as Spitzoid Melanomas. Mean Breslow thickness was 1.72 (range 0.64-3.0) mm. The majority of lesions were found on the extremities (14 of 18 lesions), whereas 3 lesions were located on the trunk, and 1 lesion was located in the scalp; 2 of the 18 tumors were ulcerated. All underwent wide local excision and after a few days were submitted to SLNB by a combination of preoperative lymphatic scan with unfiltered $^{99m}$TC-nanocolloid and intraoperative lymphatic mapping using both a handling γ probe. **Results***:* Two of 18 patients (11%) had a positive SLN biopsy. Out of the two patients with positive SLNB, none had further recurrence after completion lymphadenectomy. All patients with a negative SLNB remain disease free at mean follow-up of 60 months (range: 22-104 months). Also the two patients with positive SLNB, submitted to regional lymphadenectomy were desease-free after a follow up of 22 and 41 months respectively. **Conclusion:** as published, the most powerful predictor of overall survival for melanocytic tumors is the status of the regional lymph nodes and SLNB is a useful adjunct in the management of histologically difficult melanocytic lesions. Our results confirm that some of the ASMN metastasize to regional lymph nodes so that SLNB is a valuable adjunct tool in staging these tumors.

P52-2 - Tuesday, Oct. 22, 16:00 - 16:30, Poster Exhibition Area

## Oncology Clinical Science: Soft Tissues & Sarcoma

## P758

### Merkel Cell Carcinoma. Sentinel Lymph Node Biopsy. Review of Our Experience

**M. P. Boya Román**, M. T. Bajen, J. Mora, Y. Ricart Brulles, A. Benítez-Segura, I. Gil, O. Puig, L. Camacho; U. Hospital of Bellvitge-IDIBELL, . L'Hospitalet de Llobregat. Barcelona, SPAIN.

Objetives The aim of this study is to analyze the results of the application of the sentinel node biopsy (SNB) in patients with Merkel cell carcinoma (MCC) in our hospital. Materials and Methods A retrospective study of 12 patients (p) (48-86 years old, median 70) diagnosed with MCC (cT1-T2N0) operated from 2001-2012. Preoperative lymphoscintigraphy (55.5 MBq 99mTc-nanocolloid-albumin) and SNB took place the same day (betwenn 30 minutes and 2h p.i.). Lymphadenectomy was only performed if the sentinel lymph node (SLN) showed metastasis. The following parameters were analyzed: the most common site of the primary tumor, surgical and scintigraphic detection rate of the (SLN), pathological status of the SLN and of the lymphadenectomy (in cases in which it was performed), the clinical course of patients and their survival rate to date. Results The most common location of MCC were the limbs 8/12 p (66%), followed by head and neck 4/12 p (33%). Scintigraphic and surgical detection of the SLN was 100%. The SLN was free of metastases in 7/12 p (58%) with a median survival of 24 months. Two patients died of other neoplasms, and one of them also presented nodal progression in the context of a local MCC recurrence. The SLN was positive in 5/12 p (42%), of which 2 p (40%) had metastasis in the regional lymphadenectomy. Median survival was of 18 months in 3 of these 5 patients. Two patients were lost to follow-up. Conclusions Despite the short number of patients studied, these results show the utility of the SNB in the staging and prognosis of Merkel cell carcinoma. Survival is somewhat higher in patients with negative SLN.

## P759

### Detection of skeletal muscle metastasis - a reality with 18F-FDG PET/CT

**V. Sousa**, C. Loewenthal, M. Vieira; Hospital da Luz, 1500-650, PORTUGAL.

**Aim** - Although skeletal muscles comprise nearly 40% of the total human body mass, skeletal muscle is rarely a site of reported malignant metastasis. The incidence is generally described as less than 1.5%. The aim of this study was to evaluate the contribution of $^{18}$F-fluoro-desoxyglucose ($^{18}$F-FDG) positron emission tomography (PET)/ computed tomography (CT) in identifying skeletal muscle metastasis, to report our experience and to compare with the literature. **Materials and Methods** - Of 2483 oncologic patients examined by $^{18}$F-FDG PET/CT during the period from January 2008 to February 2013, 10 patients with skeletal muscle metastases were identified. Hematologic, dermatologic and soft tissue primitive tumors were excluded. Clinicopathological findings for these patients were retrospectively reviewed. The source of literature search (English language) was international Medline database and was performed using the terms "muscle metastases" and "muscle metastasis". **Results -** The average age of the selected patients (*N=10*) was 68(SD: 11.99). Eighty percent (n=8) were males. All of the patients (*n=10*) had metastatic disease elsewhere at the time of skeletal muscle metastasis detection (stage IV). None of the patients (*n=10*) presented any signs or symptoms suggesting skeletal muscle involvement and $^{18}$F-FDG PET/CT was the first method to identify these lesions. The standardized uptake value (SUV) determined for the muscle lesions ranged from 5 to 18.44 (average 8.872, median 8.33, SD 3.619). The most common primaries were lung (*n=4*), esophagus (*n=2*), bowel (*n=2*), prostate (*n=1*) and urothelium (*n=1*). Fifty percent (*n=5*) presented with a single skeletal muscle lesion. Muscles most commonly involved were the psoas (*n =*

5), deltoid (*n* = 3), adductor of the thigh (*n* = 2), and intercostal (*n* = 2) muscles. **Conclusions** - Metastatic carcinoma involving skeletal muscle is extremely rare and our very low detection of such lesions (0.403%) is concordant with the literature. These lesions, which tend to be found in people with advanced-stage neoplasms, occur more frequently in males and there seems to be a slight preponderance of lung and esophageal primaries, as also referred in the literature. With the increase use of PET/CT with $^{18}$F-FDG, it is likely that muscle metastic lesions will be referred more often, as future studies might confirm.

## P760

### FDG PET/CT in staging of Ewings group of tumors - comparison with conventional imaging modalities.

**A. Puranik**, S. Shah, A. R. Agrawal, N. Purandare, B. Arora, T. Vora, V. Rangarajan; Tata Memorial Centre, Mumbai, INDIA.

Introduction: Routine staging for Ewing's group of tumor includes a 99mTc MDP bone scan, CT thorax and a MRI of the local region. FDG PET/CT scans are being increasingly used for staging various malignancies. The role of FDG PET/CT in the staging is not yet established. AIM: To evaluate the incremental value of 18 F FDG PET/CT over conventional imaging modality (CIM) in staging Ewing's group of tumors. Materials and Methods: This is a retrospective analysis of 66 histological proven untreated cases of Ewing's group of tumors. A 99mTc MDP planar bone scan and FDG PET/CT scan were done within a span of five days. A breath- hold CT chest was done after completion of the PET/CT study. Abnormalities on an MDP bone scan at primary and metastatic sites and the areas of abnormal FDG uptake in the skeletal system on a PET/CT study in all the patients were noted. A comparison of the skeletal lesions identified by both modalities was done. Additional sites of metastases on a FDG PET/CT were also evaluated. Results: MDP bone scan identified in 4/66 (6%) patients while FDG PET/CT identified skeletal disease in 12/66 (18%). 50% (6/12) of the lesions identified on PET/CT were purely marrow lesions. FDG PET/CT delineated 22 (33/3%) patients with non skeletal metastases (15 - lung and 7- nodes), this group consisted of 19 (28.8%) patients who showed only non skeletal metastases while 3 patients had both skeletal and non skeletal metastases. Conclusion: FDG PET/CT in view of its better sensitivity (incremental value of 12%) in delineating skeletal metastases over MDP bone scan and its ability to detect non skeletal metastases (which accounted for 33% in our study) can be considered as a useful modality for staging Ewings group of tumors. All sites of metastases which are located by conventional imaging modalities can be identified in a single modality - one stop modality

## P761

### Role of 18F-FDG PET/CT in detecting of recurrence in patients with soft tissue sarcomas

**S. A. Shamim**[1], S. Jeph[1], M. Gairola[2], S. Khatri[2], N. Jain[1], B. Aggarwal[1], A. Aggarwal[1]; [1]DCA imaging and research centre, New Delhi, INDIA, [2]HCG Oncology, New Delhi, INDIA.

Purpose To evaluate the role of 18F-FDG PET/CT in detection of recurrence in patients with soft tissue sarcomas. Methods Fourty-four patients (22 males; 22 females each) with histopathological diagnosis of soft tissue sarcoma underwent 18F - FDG PET/CT for detection of recurrence. The median age for males was 38.5 years and for females 27 years. PET/CT studies were analyzed by two experienced nuclear medicine physicians independently. PET/CT results were validated with histopathologic correlation/conventional radiologic imaging and clinical follow up. Results Out of 44 patients, 28 patients were reported as positive for recurrence, 24 of these as having active local recurrence and 4 patients with metastatic recurrence only. 15 out of 24 patients with local recurrence also had concomitant distant metastasis. Remaining 16 patients were reported as negative for recurrence. The lung was the most common distant metastatic site. Based on histopathological correlation, conventional radiologic imaging and follow up one patient was identified as falsely positive and two other as falsely negative. The sensitivity, specificity, positive and negative predictive value were derived to be 92.5%, 82.3%, 89.2% and 87.5 %, respectively. Conclusions 18F FDG PET/CT is a good modality for the detection of recurrence and metastatic workup in patients with soft tissue sarcoma. It is useful in targeting biopsy sites in suspected cases of recurrence. It may also be clinically helpful in tumor grading.

P53-2 - Tuesday, Oct. 22, 16:00 - 16:30, Poster Exhibition Area

## Oncology Clinical Science: Miscellaneous

## P762

### Our Initial Experience For The Role of 18F-FDG PET-CT in the Detection of Unknown Primary Malignancy

**O. Yaylali**, F. S. Kıraç, D. Yüksel; Pamukkale University Medical Faculty, Denizli, TURKEY.

AIM: To retrospectively evaluate the role of Fluor-18 fluorodeoxyglucose positron emission tomography/computed tomography (18F-FDG PET/CT) imaging in the detection of unknown primary tumor site in patients with a suspicious malignancy. MATERIALS AND METHODS: We retrospectively examined 18F-FDG PET/CT images of 82 consecutive patients with unknown primary malignancy and negative conventional diagnostic procedures (including CT/MRI/endoscopic procedures). However only 50 patients had histopathologically proven data of primary malignancy or metastatic disease. We analysed only these 50 patients, because the histopathology were used as the gold standard to evaluate PET/CT results. The PET/CT images (Philips GEMINI TF TOF PET-CT scanner) of 50 patients were analyzed with visual and semi-quantitative Methods for locating the primary. The PET/CT images were read by two experienced nuclear medicine physicians. Hypermetabolic 18F-FDG findings at the pathological lymph nodes or lesion sites were the criteria for malignancy. The probable site of primary tumor was decided according to combined findings of PET and CT. The PET/CT findings were later confirmed by histopathological examination. RESULTS: Of total 50 patients, 29 were male and 21 were female with age group between 18-85 years (mean ± SD: 61.64 ± 16.26 yrs). The lesion localisations of 50 patients on 18F-FDG PET/CT were evaluated. The 18F-FDG PET/CT depicted the lesions accurately as malign in 28 patients (meanSUVmax ± SD: 8.27 ± 7.22) and as benign in 12 patients (meanSUVmax ± SD: 3.62 ± 3.07) with histopathological confirmation. There were 32 malign and 18 benign results by histopathological evaluation. So, in 4 patients, our PET/CT results were false negative (liver in one, lung in one, lymph nodes in one, soft tissue in one) and in 6 patients the PET/CT results were false positive (benign cytomorphology in three and inflammatory changes in three) (meanSUVmax ± SD: 0.95 ± 1.10 and 4.57 ± 1.50, respectively) on the basis of histopathology data. The PET/CT correctly detected the primary tumor site in 14 (44%) of 32 patients: liver in four, lung in three, lymph nodes in two, ovary in one, cerebellum in one, stomach in one, soft tissue in two. PET/CT failed in identifying the primary tumor site in 18 (56%) patients. Histopathological findings confirmed the diagnosis in all patients. CONCLUSION: 18F-FDG-PET/CT identified the primary tumour site quite well in 44% of our cases. Therefore the present study supports that the 18F-FDG PET/CT may be a helpful method for exact determination of lesion site in patients with unknown primary tumor.

## P763

### Yield of 18F-FDG PET/CT in patients with paraneoplastic neurological syndrome for detection of primary malignancy

**P. S. Chakraborty**, P. Sharma, R. Soundararajan, S. Karunanithi, H. Singh, R. Kumar, A. Malhotra, C. Bal; All India Institute of Medical Sciences, New Delhi, INDIA.

**Aim:** To evaluate the yield and utility of $^{18}$F-FDG PET/CT in patients with paraneoplastic neurological syndrome (PNS) for detection of primary malignancy. **Material and Methods:** Data of 65 patients (mean age: 65±13 years; Male/Female: 44/21) with PNS who underwent $^{18}$F-FDG PET/CT for detection of primary malignancy was retrospectively analyzed. The diagnosis of PNS was established based on European Federation of Neurological Societies task force criteria. $^{18}$F-FDG PET/CT images were analyzed by two nuclear medicine physicians in consensus. PET/CT studies were classified into normal, malignant and benign. Histopathology and/or clinical/imaging follow up (minimum-6 months) were used as reference standard. **Results:** PNS was classified as either "possible PNS" (n=37) or "definite PNS" (n=28). The neurological indication for PET/CT were polyneuropathy in 34, cerebellar syndrome in 10, myasthenia/myopathy in 7, cranial nerve palsy in 5, encephalitis ( including limbic) in 5, stiff man syndrome in 2 and motor neuron disease in 2. Positive Anti Hu antibody was available in 12 patients. PET/CT demonstrated 14 malignant lesions in 14 patients. The site of suspected malignant lesions was thyroid in 4, lung 2, lymphoma 2, colon 2, breast 1, prostate 1, brain metastasis in 1 and bone metastasis in 1 patient. Based on the reference standard 11/65 patients were found to have a malignancy. Patient based sensitivity was 100%, specificity was 94.4%, PPV was 78.5%, NPV was 100% and accuracy was 95.3%, for PET/CT. PET/CT also demonstrated infective/inflammatory findings in 8 patients and was normal in 43 patients. **Conclusion:** $^{18}$F-FDG PET/CT demonstrates high sensitivity and accuracy for detection of malignancy in patients with PNS. Because of very high sensitivity and NPV it can be used the first imaging investigation for whole body screening of malignancy in patients with PNS.

## P766

### A semi-quantitative lympho-scintigraphic approach to determine the timing of breast-cancer related lymphedema

**A. Lorenzoni**[1], M. Maccauro[1], M. Gennaro[2], C. Sigari[3], G. Aliberti[1], C. Vellani[1], L. Bedodi[3], M. Castellani[1], E. Seregni[1], A. Caraceni[3], R. Agresti[2], E. Bombardieri[1]; [1]Foundation IRCCS Istituto Nazionale dei Tumori, Nuclear Medicine, Milan, ITALY, [2]Foundation IRCCS Istituto Nazionale dei Tumori, Breast Unit Surgery, Milan, ITALY, [3]Foundation IRCCS Istituto Nazionale dei Tumori, Rehabilitation and Palliative Care, Milan, ITALY.

**Aim:** lymphedema is a chronic, progressive and disabling medical condition. Secondary lymphedema of the upper limbs results in substantial functional impairment and severe morbidity in 10-20% of patients after axillary dissection. Breast-cancer related lymphedema can be successfully treated only when diagnosed at an early, ideally latent, stage. Misdiagnosis and/or delayed diagnosis are common and the treatment-critical recognition of the latent disease stages is poorly evaluated. A few published quantitative evaluation techniques lack sufficient reliability, sensitivity and accuracy and no reliable, clinically accepted, quantitative evaluation of the upper-limb lymphoscintigraphy is at disposal. Lymphoscintigraphy may be used to assess disease extent, for early detection of disease progression, and can be used to direct therapy. The aim of this study is to evaluate the efficacy of semi-quantitative lymphoscintigraphy to early diagnose lymphedema after axillary dissection in patients with breast cancer. **Materials and Methods:** Fifty-five consecutive patients underwent to semi-quantitative lymphoscintigraphy at 1, 6 and 12 months after axillary dissection and every 6 months during follow up. After subcutaneous injection of $^{99m}$Tc-nanocolloid (37 MBq, 0.2ml) into the dorsum of both hands dynamic and static images of the arms and axillary was acquired using the gamma-camera after 20, 90, and 180 minutes. A comparative and semi-quantitative analysis was made based on velocity of axillary lymph node visualization, intensity of uptake and % of radiotracer uptake in drainage nodal basin. Scintigraphic data was correlated with the clinical evaluation. **Results:** Scintigraphic data obtained 1 months after axillary dissection showed the presence of lymphatic stasis in 90% of the cases associated with normal clinical examination. After 6 months 70% of patients showed lymphatic stasis and/or lymphatic slowdown, but in the majority of cases clinical examination remained negative. After 12 months scintigraphic findings showed in 90% of patients which underwent to early therapy based on nuclear medicine data, an improvement of lymphedema or stable edema. In the remaining cases the following scintigraphic evaluations showed clinical worsening associated with appearance of lymphedema. **Conclusions:** The lymphoscintigraphy had high diagnostic yield, allowing early treatment of lymphedema. Semi-quantitative scintigraphic evaluation is important for recognition of the early (latent) stages of the disease. The persistence of pathological scintigraphic findings after 12 months from axillary dissection, may be considered as a prognostic marker to develop severe/irreversible lymphedema. **Acknowledgment:** the study is partially supported by Fondazione Umberto Veronesi

## P767

### The Role of 18F-FDG PET/CT in Pretreatment Evaluation of Anterior Mediastinal Lesions

**A. Tabain**[1], A. Balenović[1], M. Jakopović[2], M. Janković[2], M. Milošević[3]; [1]Polyclinic Medikol, PET/CT Center, Zagreb, CROATIA, [2]University Hospital Center Zagreb, Department for Respiratory Diseases, Zagreb, CROATIA, [3]School of Public Health Andrija Štampar, Department of Environmental and Occupational Health, Zagreb, CROATIA.

AIM:To assess the role of 18F-FDG PET/CT in pretreatment evaluation of patients (pts) with newly diagnosed anterior mediastinal mass.METHODS:During the period of five years, we performed 44 PET/CT sudies in 22 pts, age range 14 to 70 years, reffered for further evaluation of newly diagnosed (by CT or MRI) lesion localized in anterior mediastinum. PET/CT was indicated to determine the further therapeutic procedure. We compared SUVmax, size of lesion (maximal transverse diameter by CT/MRI) and patohistology in operated and non-operated pts . Pts without surgical treatment were followed up clinicaly and with different diagnostic procedures. PET/"low-dose"CT and PET/"contrast enhanced"CT studies with 18F-FDG were performed on Philips Gemini TF 64 hybrid scanner (dose range 211-259 MBq), according to the standard oncologic protocol. RESULTS: Out of all patients, 45.5% (10/22) were PET/CT positive, with SUVmax values (range, mean, median) of 2.7-11.2, 5.86, 5.05, and lesion size (in mm) of 23-116, 63.5, 62.5. All of them underwent surgery. Open byopsy, lymph node extraction or complete resection was conducted in region of anterior mediastinum, except in 2/10 pts in which procedure was transfered to more accessible region due to intensive pathological metabolism in multiple lymph nodes. Pathohistologycal findings confirmed 8 thymomas, 1 lymphoma and 1 granulomatous inflammatory disease (TBC). Out of those PET/CT negative pts (12/22), with SUVmax (range, mean, median) 0-3.2, 0.9, 0 and size 6-100, 34.3, 26; 9 had metabolically inactive lesions while 3 were caracterized as thymic hyperplasia considering both intensity/pattern of FDG accumulation and age of the patient. Due to high dimensional lesion, surgery was performed in 2/12 pts and confirmed benign tumour (1 angiolipoma and 1 mediastinal cyst). Remaining PET/CT negative pts were followed-up free of malignancy.In surgically treated pts lowest SUVmax (2.4) was detected in angiolipoma, while highest SUVmax (11.2) was detected in patient with TBC, which was also the only one false positive PET/CT finding. SUVmax was significantly higher in PET/CT positive (p=0.001) and surgicaly treated pts (p=0.021); also size positively correlated to patohistology (p=0.015) and conducted surgery (p<0.001). Sensitivity, specificity, PPV, NPV were 100%, 92%, 90%, 100%. CONCLUSION: PET/CT is valuable diagnostic method that can direct type and region of further surgical procedure in pts with anterior mediastinal mass. Relation between SUVmax and patohistology should be further investigated in purpose of better pretreatment patient menagement. There should be awereness of possible positive results caused by other malignant systemic or inflammatory diseases.

## P768

### Pattern of 18F-FDG PET/CT in Patients with neurofibromatosis type I

**H. M. M. Vasconcelos**, S. Almeida, N. A. Resende, L. O. C. Rodrigues, M. Mamede, D. M. Miranda; Universidade Federal Minas Gerais, BELO HORIZONTE - MG, BRAZIL.

**Aim:** The aim of this study was to use to characterize malignant transformation of plexiform neurofibroma (PN) in neurofibromatosis type I (NF-1) patients using $^{18}$F-FDG PET/CT. **Material and Methods:** A group of 20 patients with NF-1 (55% female and 45% male), from 4-50 years old with symptomatic PN or suspected of malignization underwent an $^{18}$F-FDG PET/CT exam followed by the lesion biopsy or 12-month clinical and/or radiological follow-up. **Results:** A total of 30 peripheral nerve sheath tumors (PNSTs) were identified and 1 malignant transformation. Among the patients, 20% submitted a core-biopsy. Semi-quantitative analysis showed a range of SUVmax 3.9-6.9 on benign lesions and a 10.3 on the malignant PNST (MPNST). **Conclusions:** Neurofibromatosis is understood as a group of pathologies predisposing to malignant transformation, thus having good applicability of $^{18}$F-FDG PET/CT, especially in the evaluation of the PN in NF-1 patients. The PNST presented a potential for transformation into MPNST of up to 13% throughout life and is the leading cause of early mortality in individuals with NF-1. Due to frequency and severity of MPNST, routine evaluation of tumors with malignant potential is essential. The present study revealed important insights of malignant transformation of PNSTs, however further information is needed to better correlation of the PET findings.

P54-2 - Tuesday, Oct. 22, 16:00 - 16:30, Poster Exhibition Area

## Oncology Clinical Science: Paediatric

## P769

### A multicentre retrospective study on the additional value of 18F-FDG -PET/CT findings over conventional imaging in the follow-up of hepatoblastoma patients

A. Cistaro[1,2], **N. Quartuccio**[3], G. Treglia[4], M. Pagano[5], M. E. Basso[6], P. Fania[1], V. Bova[7], A. Piccardo[8], E. Lopci[9], F. Fagioli[10], U. Ficola[11]; [1]Positron Emission Tomography Centre IRMET S.p.A., Euromedic Inc., Turin, ITALY, [2]Co-ordinator of National PET Pediatric Group, Turin, ITALY, [3]Nuclear Medicine Unit, Department of Biomedical Sciences and of the Morphological and Functional Images, University of Messina, Messina, ITALY, [4]Department of Nuclear Medicine and PET/CT Centre, Oncology Institute of Southern Switzerland, Bellinzona, SWITZERLAND, [5]Pediatric Unit, Hospital Cirie' ALS To4, Turin, ITALY, [6]Paediatric Oncohematologic Unit, Department of Paediatric Oncology, Regina Margherita Children's Hospital, Turin, ITALY, [7]Department of Radiological Sciences, Unit of Nuclear Medicine, hSR Giglio, Cefalù, ITALY, [8]Nuclear Medicine Unit, Galliera Hospital, Genoa, ITALY, [9]Nuclear Medicine Department, IRCCS Humanitas, Rozzano, Milan, ITALY, [10]Regina Margherita Children's Hospital, Department of Haematology, Oncology, Immunology and Infectious Diseases, Turin, ITALY, [11]Department of Nuclear Medicine, La Maddalena Hospital, Palermo, ITALY.

**Aim**: A rising of level of serum alpha-fetal protein (α-FP) during the follow-up of patients affected by hepatoblastoma (HB) is generally associated with tumour relapse. Conventional imaging (CI), such as Computed Tomography (CT), Magnetic Resonance Imaging (MRI) and Ultrasonography (US), may detect neoplastic lesions. However, negative findings at the morphological study cannot completely rule out cancer. **Materials and Methods**: We retrieved nine patients (mean age:5.9 years; range:3.1-12 years) from the hospital databases of multiple centres in Italy. Patients were surgically treated for hepatoblastoma and were followed up by serum α-FP monitoring and ultrasonography. CI and 18F-FDG -PET/CT were performed to better assess the disease extent in case of suspicion of relapse. Fine-needle aspiration biopsy (FNAB) was executed for recurrence confirmation and was

considered as reference of standard. Imaging findings were compared on a peer scan basis (18F-FDG-PET/CT vs. CI). **Results**: α-FP level was suggestive for disease recurrence in 8/9 patients. All the patients underwent CI and PET/CT. Biopsy was performed in 8/9 cases. CI and 18F-FDG-PET/CT resulted to be concordant in 5/9 patients (CI identified recurrence of disease but 18F-FDG-PET/CT provided a better definition of disease extent); in 4/9 cases CI diagnostic information resulted in negative findings, whereas PET/CT correctly detected recurrence of disease. 18F-FDG-PET/CT showed an agreement of 100% (8/8) with FNAB results, while CI findings were confirmed by FNAB in 4/8 patients. **Conclusion**: 18F-FDG-PET/CT scan seems to better asses tumor recurrence in HB respect to CI and may provide incremental diagnostic value in the follow-up of this group of patients.

## P770

### Information derived from "non-specific" uptake on FDG PET/CT before and during therapy of paediatric lymphoma

**L. Jorgov**[1], F. Montravers[2], J. Landmann-Parker[3], J. Talbot[2]; [1]Semmelweis University, Department of Nuclear Medicine, Budapest, HUNGARY, [2]Department of Nuclear Medicine and PET Centre, Hôpital Tenon, Paris, FRANCE, [3]Department of Paediatric Oncology, Hôpital Trousseau, Paris, FRANCE.

"Non-specific" uptake of FDG is frequently observed in the paediatric patients with lymphoma, either on the initial FDG PET/CT or on the interim one. Prediction of response to chemotherapy is based on the decrease of FDG uptake in the lymphomatous lesions, but the actual incidence and the signification of the "non-specific" uptake has been overlooked. It could bring some information which somehow reflects metabolic status of the patient, possibly in relation with some aspects of the disease. The research was performed at Hôpital-Tenon PET/CT centre, part of the EuroNet-PHL-C1 study which has different objectives. We could use multimodality data that had been gathered over 3 years. 19 Hodgkin lymphoma patients (age range 6-17) referred between October 2009 and December 2011 had FDG PET/CT at baseline and as an interim examination (iPET) after 2 cycles of chemotherapy. We searched visually for "non-specific" uptake i.e. more intense than the liver uptake: diffuse uptake by the thymus, the bone marrow, the spleen, or the spinal cord (Th12), or for visualisation of the brown fat. We also made semiquantitative analysis (with SUVmax). Based on the visual interpretation, at least one site of "non-specific" uptake was observed at baseline in 14/19 patients (74%) and on iPET in 7/19 (37%). Diffuse thymus hyperactivity was detected in 3/19 (16%) at baseline and in just 1/19 (5%) on iPET; diffuse bone marrow hyperactivity in 7/19 (37%) at baseline and in 3/19 (16%) on iPET; diffuse spleen hyperactivity in 9/19 (48%) at baseline and in 1/19 (5%) on iPET; diffuse spinal cord hyperactivity in 6/19 (31%) at baseline and in 3/19 (16%) on iPET; brown adipose tissue uptake both at baseline and iPET in 1/19 (5%) patient. The semiquantitative analysis showed a significant decrease in uptake under treatment in spleen and bone marrow, and a significantly increased uptake by the liver. Comparing with literature data, diffuse spleen hyperactivation at baseline was more frequent in paediatric Hodgkin lymphoma than in adults. At interim PET/CT, the "non-specific" uptake was reduced, both in number and intensity of sites. This is probably in relation to the effect of the treatment, but this part of the study is not yet available. The liver uptake rose after 2 cycles of treatment, which may have some influence when liver uptake is taken as a reference for visual analysis, but is not sufficient to account for the drop of SUVmax in "non-specific" sites at interim PET.

P55-2 - Tuesday, Oct. 22, 16:00 - 16:30, Poster Exhibition Area

# Conventional & Specialised Nuclear Medicine: Endocrinology

## P772

### Localising Ectopic Parathyroid Adenomas: A Pictorial Review of $^{99m}$Tc Sestamibi SPECT/CT

**R. M. Chakravartty**, D. Ruiz, B. Corcoran, C. Hooker, E. Kalogianni, G. Galata, D. Gialvalis, N. Mulholland, S. Diaz-Cano, K. M. Schulte, G. Vivian; Kings College Hospital, London, UNITED KINGDOM.

**AIM:** Localization of ectopic parathyroid adenomas is important in guiding surgical decisions with the aim of minimising post-operative morbidity. This pictorial review explores the role of 99mTc Sestamibi SPECT/CT imaging for localising these unusual sites and the subsequent surgical approach to these adenomas. **MATERIALS AND METHODS:** We retrospectively reviewed 164 imaging studies of patients clinically suspected to have primary hyperparathyroidism and referred for localisation of adenomas between January 2010 and March 2013. All patients had $^{99m}$Tc Sestamibi imaging with early and delayed SPECT/CT performed 20 minutes and 3 hours after the tracer injection respectively. SPECT/CT images were reconstructed to provide fused axial images as well as with volume rendering of the CT using recovery software. All patients also underwent an ultrasound of the neck to confirm absence of adenomas in the usual location. The pre-operative imaging results were correlated with operative decisions and findings as well as histopathology. **RESULTS:** In our series, 11 patients demonstrated an ectopic parathyroid adenoma which suggested an incidence of 6.7% of all patients referred for parathyroid imaging, lower than the 20-25% incidence rate reported in world literature. Ectopic locations demonstrated on SPECT/CT included the superior and anterior mediastinum (3 and 4 adenomas respectively), tracheoesophageal groove (3 adenomas) and retropharyngeal space (1 adenoma). Surgical plans required the addition of sternotomy in 2 patients. Surgical and histopathological findings confirmed the diagnosis of ectopic parathyroid adenoma in 8/ 9 patients. (2 patients are awaiting surgery) **CONCLUSION:** SPECT/CT imaging provided accurate localisation of ectopic parathyroid adenomas and helped guide surgical approach in these patients.

## P773

### Primary hyperparathyroidism presented as multipl brown tumours on bone scintigraphy due to an ectopic parathyroid lesion: A case report

**E. G. Işık**, E. Yılmaz, S. Kuyumcu, D. Has, M. F. Geçer, S. Ünal, I. Adalet; Istanbul Medical Faculty, Department of Nuclear Medicine, Istanbul, TURKEY.

***Introduction*** Primary hyperparathyroidism is a disease characterized by hypercalcemia due to overproduction of parathyroid hormone (PTH) by one or more parathyroid glands. With widespread use of laboratory tests, the incidence of bone lesions has decreased form 80% to as low as %15. Herein we aimed to highlight the utility of bone scintigraphy in depicting metabolic bone disease and importance of dual phase Tc99m-MIBI parathyroid scintigraphy in ectopic localization of parathyroid lesions. ***Case*** A 59 years old female was performed CT due to left arm pain and CT images revealed an expansive lytic lesion at distal ulnar localization. Differential diagnosis included ossifying fibroma, aneurysmal bone cyst and malignancy. Further evaluation with 3 phase bone scan revealed increased blood pool activity as well as increased osteoblastic activity at bilateral carpal-metacarpal junctions, ribs, metatarsal bones and expansive osteoblastic lesions at tibia and fibula. Diffuse uptake in the cranium was also evident. The findings were reported as a possible metabolic bone disease and the impression suggested clinical and biochemical evaluation in order to differentiate brown tumour secondary to hyperparathyroidism. Serum calcium (12.2mg/dl) and PTH (891pg/ml) levels were elevated however ultrasonographic evaluation of the parathyroid glands were normal. The patient was performed dual-phase Tc99m-MIBI scintigraphy. Planar and SPECT/CT images revealed a soft tissue lesion anterior to arcus aortae. The lesion was surgically removed and histopathologic examination confirmed parathyroid adenoma. ***Conclusion*** Although bone scintigraphy is not first-line modality of choice in detecting metabolic bone disease, it may be beneficial in detecting its complications such as brown tumours. Additionally dual phase tc99m-MIBI scintigraphy can assist the ectopic localization of parathyroid adenomas even if not detected by ultrasonography. *Keywords* Brown tumor; bone scintigraphy; MIBI Parathyroid scintigraphy, Primary hyperparathyroidism

## P774

### The success rates of conventionel imaging technics on preoperative localisation of enlarged parathyroid glands in the primary hyperparathyroidism

**U. Elboga**[1], E. Sahin[2], E. Kalender[1], H. Demir[1], S. Zincirkeser[1], M. Yilmaz[1], G. Maralcan[1], A. Gokalp[1], S. Erkilic[1], M. Ozkaya[1], E. Akarsu[1], Z. Celen[1]; [1]Gaziantep University, Gaziantep, TURKEY, [2]Namik Kemal University, Tekirdag, TURKEY.

***Objective:*** We aimed to evaluate the diagnostic and preoperative localisation capacity of MIBI scintigraphy and USG in enlarged parathyroid glands in the primary hyperparathyroidism and the relationship between the success rate of these techniques and biochemical values (PTH, Ca) ). ***Material and Methods:*** In this study, we retrospectively evaluated 39 patients ( 27 women and 12 men mean age 41 ± 8,3; age range 19-58 years ) who had clinical and biological evidence of primary hyperpar[[Unsupported Character - Codename ]]athyroidism presented to the university hospial over a 4-years period ( June 2007 to June 2011 ) for 99mTc-sestamibi parathyroid scintigraphy test. Patients were examined with ultrasonography (USG) and double-phase 99mTc-MIBI parathyroid scintigraphy, for detection of enlarged parathyroid gland/glands. Preoperative serum intact parathyroid hormone(PTH) levels, calcium(Ca), phosphate(P) and alkaline phosphatase measurements were obtained. Concomitant thyroid pathology was also recorded. ***Results:*** A total of 45 parathyroid lesions in 39 patients were reviewed. 34 patients had a single adenoma and 5 patients with multigland disease had 11 abnormal parathyroid glands including three adenomas, whereas the remaining eight glands showed hyperplasia. The combination of MIBI and USG had both a high sensitivity and positive predictive value for localization of abnormal

parathyroid glands. The overall sensitivities of MIBI, USG and combined these technics was 85.3 % , 72.5% and 90.4 %; positive predictive value (PPV) was 89.7 %, 85.2 % and 92.6%, respectively. There was significant difference in the detection of parathyroid lesions between patients with and without thyroid pathology for both scintigraphy (p=0.01), and USG(p=0.01). Both PTH and serum calcium levels showed significant differences between scintigraphy positive and negative patients(p=0.01; p =0.013). PTH levels showed significant differences between ultrasonographic examinations positive-negative patients (p=0.011), but no significant differences in the serum calcium could be found between patients with positive and negative ultrasonographic examinations(p=0.29). The weight of gland was significantly associated with the detection rate of either scintigraphy or USG in localizing the enlarged parathyroid gland (p=0.001; p =0.024). ***Conclusions:*** The most successful technique is both USG and scintigraphy modalities were applied together to detect the enlarged parathyroid glands. The concomitancy of thyroid disease, as it decreases the sensitivity of parathyroid scintigraphy and USG in enlarged parathyroid glands. The increased preoperative serum PTH and glands weight were correlated with positive 99mTc-MIBI and USG study for pathologic glands.

## P775

### Do Serum Calcium Levels Affect The Success Rate of Parathyroid Scintigraphy in Primary Hyperparathyroidism Patients?

**S. GUNGOR**, F. Dede, S. Ozguven, M. Aras, F. Novruzov, R. Maleki, T. Ones, S. Inanir, T. Y. Erdil, H. T. Turoglu; Marmara University School of Medicine Department of Nuclear Medicine, Istanbul, TURKEY.

**Aim:** Most of the primary hyperparathyroidism patients are asymptomatic and only 20% of them become symptomatic with increasing levels of calcium. The effect of serum calcium levels on lesion detection rate with parathyroid sintigraphy in patients with high levels of serum PTH was evaluated in this retrospective study. **Methods:** Thyroid scintigraphy, dual phase Tc-99m-MIBI parathyroid scitntigraphy and early phase SPECT/BT images were acquired in primary hyperparathyroidism patients without chronic renal failure. Serum calcium levels above 10.5 mg/dl were regarded as hypercalcemia. **Results:** The mean serum PTH levels (±SD) in normacalcemic **(**nCa, n:35, 9.56±0.6mg/dL) and hypercalcemic (hCa, n:45, 11.57±0.6mg/dL) patients were found as 157±102pg/ml and 198±131pg/ml respectively in total 80 patients (F/M, 67/13) (p>0.05). Lesion detection rates with parathyroid scintigraphy in nCa and hCa groups were %37 (13/35) and %89 (40/45) respectively and the difference between these two groups were statistically significant (p<0.0001). All the parathyroid lesions in nCa group were solitary ( 1 ectopic) and no statistical difference were found between scintigraphy (+) and scintigraphy (-) patients in terms of mean serum calcium levels (p>0.05). In hCa group, 3 patients had multiple and 42 patients had solitary parathyroid lesions. **Conclusion:** High serum PTH and Ca levels prior to parathyroid scintigraphy is important in terms of preventing possible false (-) results in primary hyperparathyroidism patients.

## P776

### MIBG scintigraphy with 131 Iodine in pheochromocytoma : experience of nuclear medicine department in Ibn Rochd Hospital in Casablanca

**S. TALEB**, M. AIT IDIR, A. GUENSI, G. CHERKAOUI, M. KEBBOU; Nuclear medicine department in Ibn Rochd Hospital, Casablanca, MOROCCO.

Pheochromocytoma diagnosis can be difficult due to variable clinical presentation: the triad headache, sweating, palpitations, aren't always present and because of presence of wrong positives in urine catecholamines measurement. MIBG scintigraphy with 131 Iodine allowed affirmation of neuroendocrine tumor, and to confirm diagnosis of pheochromocytoma. Aim of this study was to evaluate reliability of this exam in pheochromocytoma diagnosis and to determine scintigraphic aspects found in our experience. Twenty patients (9 M and 11 F), aged 10 years to 60 years (mean: 30 yrs), were studied in nuclear medicine department of Ibn Rochd UH, in Casablanca, between January 2006 and December 2012 who underwent MIBG scintigraphy for pheochromocytoma suspicion. Indications were: clinical signs (10 cases) including HTA or adrenergic symptoms, high urinary catecholamines (5 cases), suspected recurrence or metastasis in patients previously operated (4 cases), in Multiple Endocrine Neoplasia syndrome type II (1 case) MIBG scintigraphy was negative in 12 cases; in 7 cases diagnosis of unilateral adrenal neuroendocrine tumor was confirmed, and bilateral pheochromocytoma in one case. No secondary location was found. MIBG scintigraphy is essential in exploration of pheochromocytoma, providing important information for tumor localization, but also staging.

## P777

### Intense uptake of Technetium 99m Pertechnetate by Parathyroid Carcinoma-A rare case report

**G. Rijju**, J. Vibin, G. Nissy, D. Davies; Malabar Institute of Medical Sciences(MIMS), Calicut, Kerala, INDIA.

Parathyroid carcinoma is an uncommon cause of PTH dependent hypercalcemia. In most of the study series the entity accounts for less than 1% of patients with primary hyperparathyroidism. We herewith report an unusual case of parathyroid tumor which shows avid uptake of Technetium 99m-Pertechnetate. An eighty two year old lady referred with history of nephrocalcinosis,severe generalized bone pain, fracture neck of femur and right neck swelling with a tentative diagnosis of primary hyperparathyroidism .The biochemical profile revealed significantly elevated serum calcium and PTH levels. As the part of pre operative evaluation Technetium-MIBI subtraction scan done as per dual -isotope protocol and SPECT CT. Technetium 99m pertechnetate was administered was administered first which show moderate uptake of tracer in the thyroid gland and a focalized area of intense uptake inferior to right lobe of thyroid. The subsequent sestamibi image does not show any significant additional uptake in the same area or elsewhere in neck or chest region. The delayed image continues to show persistent residual retention of tracer in the initial focal area of intense Tc 99m Pertechnetate uptake. The SPECT CT image demonstrated a cystic mass lesion in the inferolateral aspect of the right lobe of thyroid with focalized intense uptake .The lesion was surgically removed and the HPR reported as parathyroid carcinoma. The exact mechanism of Technetium 99m pertechnetate uptake by the parathyroid carcinoma is unclear possibly due to hypervascularity. The search of literature does not show many cases of parathyroid carcinomas which significantly accumulated Tc-99m pertechnetate.

P56-2 - Tuesday, Oct. 22, 16:00 - 16:30, Poster Exhibition Area

## Conventional & Specialised Nuclear Medicine: Thyroid

## P778

### Prognostic value of post-ablation scan and pre-ablation stimulate thyroglobulin in differentiated thyroid cancer.

**A. Garcia Vicente**[1], C. Vega Caicedo[1], A. León Martín[2], J. Sastre Marcos[3], O. Gomez Lopez[1], G. Jimenez Londoño[1], A. Soriano Castrejón[1]; [1]Nuclear Medicine Department. University General Hospital, Ciudad Real, SPAIN, [2]Investigation Unit. University General Hospital, Ciudad Real, SPAIN, [3]Endocrinology Department. Complejo Hospitalario, Toledo, SPAIN.

Aim: To evaluate the ability of the post-ablative I-131 whole body scan (PA-WBS) and pre-ablation stimulate thyroglobulin (PA-t) blood level as a predictor of the outcome in patients with differentiated thyroid cancer (DTC). Methods: We retrospectively included 91 patients (83 females and 8 males, mean age of 46 y) with DTC treated at our Metabolic Therapy Unit between May 2006 and December 2008. Pre-ablative thyroglobulin (PA-t), after levothyroxine withdrawal or TSH-rh stimulation, was obtained. In all cases thyroglobulin antibodies were negative. Risk classification was established following the recommendations of ATA guidelines. A PA-WBS was obtained 7-8 days after I-131 ablative treatment, using empirical doses depending on risk and clinical classification of patients. The patterns of PA-WBS were: (1) isolated remnant thyroid, (2) lymph node in neck area or/and upper mediastinum or (3) distant metastases. Furthermore PA-WBS patterns were grouping in advanced disease (pattern 3) and loco-regional disease (1 and/or 2 patterns). Patients underwent conventional follow-up at least 4 years and their status was classified into ablation success (disease-free status) or ablation failure (persistent disease requiring new ablative dose). Relations between risk, PA-t and PA-WBS patterns with final evolution was assessed (X2Pearson). Results: PA-WBS demonstrated isolated remnant thyroid, lymph node in neck area or/and upper mediastinum or distant metastases in 82.2%, 14.5% and 3.3% of patients respectively. PA-t value (mean±SD) was 51±192 ng/ml. In 87.6% and 10.1 % of patients was demonstrated ablation success and ablation failure respectively. Recurrent disease was diagnosed in one patient and another dead for other reason during the follow-up. Ablation success was found in 73.3% and 91.8% of patients classified as high and low risk respectively (p=0.04). Statistical significant differences (p=0.02) were found between the percentage of advanced vs loco-regional disease in PA-WBS and risk status (13.3% and 86.7% in high risk and 1.4% and 98.6% in low risk respectively). Mean PA-t values were significantly higher in patients with advanced vs loco-regional disease in PA-WBS (620.7 vs 2.7 ng/ml; p<0.001) and in cases with ablation success vs ablation failure (22.4 vs 128.8 ng/ml; p<0.001). Ablation failure was detected in 8.1% and 66.7% of patients with loco-regional vs advanced disease in PA-WBS (p<0.001). Conclusions: PA-WBS and PA-t values demonstrated predictive value of disease status after radioiodine ablation with a higher and significant response rate in patients with loco-regional disease in PA-WBS and lower values of PA-t with respect to patients with advanced disease pattern and higher PA-t.

## P779

### Is it useful a delayed post-therapeutic 131I whole-body scanning in patients with thyroid cancer?

**A. S. Rosero Enriquez**, R. Ruano Perez, L. G. Diaz Gonzalez, P. Tamayo, E. Martin Gomez, M. E. Martin Gomez, J. R. Garcia-Talavera; Nuclear Medicine.University Hospital of Salamanca, Salamanca, SPAIN.

**Aim:** To assess the added value of a delayed post-therapeutic 131I whole body scanning (WBS) compared with an early WBS in patients with differentiated thyroid carcinoma (DTC)**. Methods:** This study included 43 patients (16 men and 27 women) with DTC who underwent early (2 or 3 days after administration) and delayed (7 days after administration) WBS after postsurgical 131 I treatment for thyroid remnant ablation or metastases treatment. The early and delayed scan images were visually analyzed and compared the thyroid remnants and the number of regional and distant lesions found. In positive scanning cases a complementary SPECT-CT was performed for a better location. **Results**: delayed WBS was positive in 33 patients, 20 of them only showed thyroid remnants in accordance with the early WBS, 9 patients also showed regional or distant lesions (6 cervical and 3 thoracic) not observed in the early WBS. The delayed WBS detected a new metastatic lesion in one of the 3 patients with known metastases in the early WBS, and we also found a pathologic cervical lymph node in a patient with early negative WBS. 10 patients presented a negative delayed WBS, 7 had already a negative early WBS and 3 had a positive early WBS. One corresponded to small thyroid remnants (false negative of delayed scan). Other was a deposit in the chest because of a gastroesophageal reflux (early false positive, SPECT-CT was determined in this patient). And the third case was an abnormal chest uptake in the mammary tissue of a young woman located by SPECT-CT and negative in the delayed WBS (rapid wash out of a benign breast). **Conclusions**: Delayed post-therapeutic 131I WBS in patients with differentiated thyroid cancer after 131 I treatment for thyroid remnant ablation or treatment, showed a higher detection rate of cervical and distant metastases than early WBS probably because of the washout of the physiological distributions. Additional delayed scanning and a SPECT-TC is recommended, especially for high-risk patients or those with intensive physiological distribution on early scanning.

## P780

### Factors Influencing the Success of Radioiodine Therapy in Patients with Graves' Disease

**S. Gaberscek**, D. Sfiligoj, P. Jaki Mekjavic, K. Zaletel, E. Pirnat, S. Hojker; University Medical Centre Ljubljana, Ljubljana, SLOVENIA.

AIM. For decades, radioiodine (I-131) therapy has been effectively used for the treatment of Graves' disease. However, not all patients are successfully cured with the first dose of I-131. Our aim was to evaluate factors influencing the success of I-131 therapy when used in a fixed-dose manner considering thyroid volume. METHODS. We reviewed records of 725 patients, 570 females and 155 males, who were for the first time diagnosed with Graves' disease between 2005 and 2009 and later treated with I-131. In all subjects, thyrotropin (TSH), free thyroxine (fT4), free triiodothyronine (fT3), and TSH receptor antibodies (TSHRAb) were measured at the first examination and before treatment with I-131. We calculated the fT4/fT3 ratio. Graves' disease was diagnosed by biochemical hyperthyroidism and positive TSHRAb. Thyroid volume was measured by ultrasound. After initial treatment with antithyroid drugs, all patients were eventually treated with I-131. With respect to thyroid volume they received 555, 740, 925 or 1110 MBq of I-131. Treatment was considered successful if hypothyroidism or euthyroidism was achieved. RESULTS. Out of 725 patients, 656 (90.5%) were successfully treated with the first dose of I-131 (Group 1). In 69 patients (9.5%) a second or a third dose (in 4 patients) of I-131 was needed (Group 2). In Group 1, the mean applied dose of I-131 was significantly lower than in Group 2 (626±107 and 708±139 MBq, respectively, p<0.001). At the first examination, patients from Group 1 were significantly younger than those from Group 2 (mean 45.5±14.8 and 50.1±15.8 years, respectively, p=0.017), they had a lower fT4 (54.8±26.1 and 72.1±34.1 pmol/L, respectively, p<0.001), a lower fT3 (21.1±8.4 and 24.7±8.8 pmol/L, respectively, p<0.001), a lower fT4/fT3 ratio (2.6±0.7 and 2.9±0.8, respectively, p=0.002), a similar TSHRAb (15.2±11.4 and 17.6±13.4 U/L, respectively, p=0.103), and a smaller thyroid volume (21.1±12.5 and 38±23.7 mL, respectively, p<0.001). Before treatment with I-131, patients from Group 1 had a lower fT4 (24.2±14.5 and 29.3±27 pmol/L, respectively, p=0.014), a lower fT3 (9.6±5.9 and 11.3±7.6 pmol/L, respectively, p=0.028), a higher fT4/fT3 ratio (2.7±0.6 and 2.4±0.7, respectively, p=0.002), and a lower TSHRAb (8.7±9.4 and 13.6±14.5 U/L, respectively, p<0.001) when compared with the patients from Group 2. CONCLUSIONS. Patients who were successfully treated with the first dose of I-131 were younger, less severely hyperthyroid and had a smaller thyroid volume at the first examination. Also, they were less severely hyperthyroid and had a lower TSHRAb before treatment with I-131.

## P781

### Comparison of Different Scintigraphic Methods in Determination of Recurrence in Medullary Thyroid Carcinoma Patients

**M. F. GECER**[1], Z. G. OZKAN[1], S. KUYUMCU[1], G. ALCIN[1], E. YILMAZ[1], A. K. UZUM[2], Y. SANLI[1], C. TURKMEN[1], F. ARAL[2], I. ADALET[1]; [1]Istanbul Medicine Faculty, Nuclear Medicine Department, Istanbul, TURKEY, [2]Istanbul Medicine Faculty, Internal Medicine Endocrinology Department, Istanbul, TURKEY.

**Aim:** Detection of recurrence is important during follow-up of medullary thyroid carcinoma patients in the case of increasedtumor markers or clinically suspicious metastases. Different scintigraphic Methods are used in order to evaluate recurrence. In this study, we aimed to evaluate and compare the findings of Ga-68 DOTATATE PET/CT, F-18 FDG PET/CT, Penta-DMSA scintigraphy and Tc99m-MDP bone scintigraphy in determination of recurrence in medullary thyroid carcinoma patients who had been directed to our department with purpose of restaging. **Method:** 6 female and 8 male, totally 14 patients who had different scintigraphic examinations in our department due to suspected recurrence between July 2011 and December 2012 were evaluated retrospectively. The mean age was 47±10 (21-70). The mean calcitonin value of patients was 1600pg/ml (134-5495) and mean CEA value was 37.5ng/ml (2-188.8). The scintigraphy results obtained in 6 months were compared with each other. **Results:** Within 14 patients involved in the study; 11 Ga-68 DOTATATE PET-CT, 9 F-18 FDG PET/CT, 11 Penta-DMSA scintigraphy and 12 Tc99m-MDP bone scintigraphy were performed. In 8 of those patients, pathological uptakes were reported as metastases. There were suspicious radiopharmaceutical uptakes in 6 patients, but no exact interpretation could be done in terms of recurrence. When the different scintigraphic Methods which have been performed within 6 months in 8 metastatic patients were compared, it was seen that Ga-68 DOTATATE(51 foci) and F-18 FDG PET/CT(30 foci) were more successful in detecting lesions than Penta-DMSA(8 foci) and bone scintigraphy(7 foci). Ga-68 DOTATATE PET/CT detected more lesions than F-18 FDG PET/CT. **Conclusion:** It was found that Ga-68 DOTATATE PET/CT and F-18 FDG PET/CT were more effective than Penta-DMSA and bone scintigraphy in determination of recurrence in medullary thyroid carcinoma patients. Also, Ga-68 DOTATATE PET/CT could detected more lesions than F-18 FDG PET/CT.

## P782

### Oral administration of diluted lemon juice to differentiate between agenesis and ectopia of thyroid gland by 99mTc-pertechnetate scintigraphy in young infant.

**T. Kamoun**, H. Regaieg, M. Ben Fredj, H. Zanzouri, A. Toumi, M. Nouira, R. Sfar, N. Ayachi, K. Chatti, M. Guezguez, H. Essabbah; Nuclear Medicine department, Sahloul University Hospital, Sousse, TUNISIA.

AIM: We present the 99mTc-pertechnetate scintigraphy findings before and after oral administration of diluted lemon juice for an 11-month-old girl, diagnosed with thyroid dysgenesis. Patient and Methods: An 11-month-old girl with hypothyroidism symptoms: psychomotor retardation, constipation, drowsiness and infiltrated skin. The diagnosis of primary hypothyroidism is confirmed by the assays of the thyroid stimulating hormone (TSH) and free thyroxine (FT4). The patient underwent a thyroid 99mTc scintigraphy to look for the etiology of this primary hypothyroidism. The patient did not had thyroid hormone treatment. Results: 99mTc-pertechnetate scintigraphy revealed no activity in the thyroid bed or elsewhere particularly along the path of the descent of the thyroid during its embryological development. It shows a gastric activity eliminating the diagnosis of Iodide Transport Defect. Because in young ages, the overlapping images of salivary gland and ectopic thyroid in thyroid scintigraphy are a source of pitfalls, we decided to administer orally diluted lemon juice and to repeat acquisition. The second acquisition shows tracer accumulation in the lingual region confirming the presence of lingual thyroid. In this case, it allowed differentiating between agenesis and ectopia of thyroid gland. Conclusion: 99mTc-pertechnetate scintigraphy after oral administration of diluted lemon juice improves the sensitivity of the test in young ages for the diagnosis of thyroid ectopic. It may replace I-123 thyroid scintigraphy in countries where the I-123 is not available.

## P783

### Influence of a Recent Contrast-Enhanced CT on Image Quality of Thyroid Scintigraphy: A retrospective Study of 197 Patients.

**T. B. Andersen**[1], R. Aleksyniene[1], L. C. Gormsen[2], L. J. Petersen[1]; [1]Aalborg University Hospital, AALBORG, DENMARK, [2]Aarhus University Hospital, AARHUS C, DENMARK.

**Background:** It is well-known that uptake of technetium-99m-pertechnetat in the thyroid is impaired by excess free iodide in the blood, e.g. due to recently administered iodinated contrast media. Most references recommend 6-8 weeks

between an iodide contrast-enhanced CT scan (IC-CT) and thyroid scintigraphy. However, limited evidence supports this recommendation. The aim of this study was to investigate the quality of thyroid scintigraphy in patients who had had an IC-CT scan within 3 months before scintigraphy. **Methods:** Thyroid scintigraphies of 197 patients (age 28-92 years, mean 64) were analyzed retrospectively. All had had IC-CT performed 1-90 days (median 66) before the scintigraphy. Exclusion criteria were elevated TSH (>4.5 miu/L) and suspected thyroiditis. Thyroid scintigraphy was performed in accordance with EANM guidance using pin hole collimators. Two nuclear medicine specialists reviewed and reported the images simultaneously, but independently as diagnostic or not ("Is the quality of the scintigraphy sufficient to evaluate the up-take pattern (presence/ absence of a cold nodule; diffuse/ multinodular/ adenoma?")). Clinical information was available during image reading. Logistic regression was performed to calculate the probability for a diagnostic scintigraphy including 95% confidence intervals (CI). Number of days since IC-CT was the independent variable. Decreased TSH was included in a secondary analysis as a potential confounder. Furthermore, the prevalence of diagnostic scintigraphy was reported. **Results:** The specialists agreed on the diagnostic outcome in 86% of the patients and reached consensus in the remaining 14% of the scintigraphies. The prevalence of diagnostic thyroid scintigraphies was 44% from 0 to 30 days: 71% from day 31 to 60 days, and 71% from day 61 to 90. Preliminary results from the logistic regression analysis revealed that the probability of a diagnostic scintigraphy after IC-CT was 54% (95% CI: 45-62%) at day 30, 72% (95% CI: 64-80%) at day 60, and 85% (95% CI: 76-94%) at day 90. 100% probability was not reached within the studied period. There was no statistically significant effect of including TSH as a variable. **Conclusion:** A notable proportion of thyroid scans was of non-diagnostic quality 3 months after contrast-enhanced CT, though the probability of obtaining scans of diagnostic quality increased almost linearly with time after the IC-CT. Whether 100 % diagnostic scans is an achievable goal is unclear at present. Further analysis are planned to report the prevalence of diagnostic scintigraphies in a population of patients with no recent IC-CT.

P57-2 - Tuesday, Oct. 22, 16:00 - 16:30, Poster Exhibition Area

## Conventional & Specialised Nuclear Medicine: Pulmonology

### P784

### A pilot study of Simultaneous Dual Isotope SPECT-VQ with krypton-81m in the District General Hospital setting - SPECT-VQ breathes fresh life into pulmonary embolism scintigraphy in the UK.

**J. C. Fowler**[1,2], C. Baker[2], S. Rostampour[1], N. Bassett[1]; [1]Luton and Dunstable NHS Foundation Trust, Luton, UNITED KINGDOM, [2]Royal Brompton and Harefield NHS Foundation Trust, Harefield, UNITED KINGDOM.

Introduction: VQ appeared to be in terminal decline in our centre prior to EANM guidelines recommending Single Photon Emission Computed Tomography - Ventilation/Perfusion scintigraphy (SPECT-VQ); the lowered sensitivity and increased frequency of indeterminate results of planar-VQ relative to multi-slice Computed Tomographic Pulmonary Angiography (CTPA) made CTPA a more attractive option for authorising emergency radiologists despite the lower patient radiation exposure of planar-VQ. On the basis of EANM guidelines recommending SPECT-VQ with reports of equivalent sensitivity to CTPA and low frequency of indeterminate results, the possibility of replacing planar-VQ with SPECT-VQ as an emergency radiologist led service was explored by a pilot study. Krypton-81m was the ventilation agent of choice due to ideal physical characteristics and excellent dosimetry. Krypton-81m SPECT-V should allow simultaneous technetium-99m/krypton-81m dual isotope SPECT-VQ (STEKDI-SPECTVQ) image acquisition. It would also result in perfect V-Q image registration and halved acquisition time compared to alternative technetium based ventilation agents (an important consideration in our busy centre). Aim: To perform a pilot study to assess the feasibility of introducing an emergency STEKDI-SPECTVQ radiologist led service in a district general hospital. Materials and Methods: Four aspects were addressed in preparation for the introduction of the pilot study. 1. In view of the paucity of dual isotope SPECT-VQ guidelines and concerns about the feasibility of krypton-81m SPECT use, a specifically developed phantom was used to confirm STEKDI-SPECTVQ success and to develop optimal acquisition parameters. 2. Provision was made for high quality cross sectional SPECT-VQ image display and manipulation to be available for reporting radiologists. 3. Training was carried out for technical staff and reporting radiologists. 4. Referring clinicians were informed of the benefits of the SPECT-VQ technique. 20 STEKDI-SPECTVQ studies were performed. These cases were reviewed and assessed in terms of reported acquisition problems, image acquisition time, raw and processed image quality, report accuracy and reporter confidence compared to planar-VQ. Demand for VQ was compared over equivalent referral periods before and after introduction of the pilot study. Results: The first patient required repetition of ventilation images due to suboptimal mask fit, requiring modification of the mask. Otherwise there was successful acquisition of images. Raw and processed image were very good quality. There was improved reporting accuracy and radiologist confidence comparing SPECT-VQ with previous planar-VQ studies. Demand for the service has nearly trebled since planar-VQ was replaced by SPECT-VQ. Conclusion: Introduction of a novel STEKDI-SPECTVQ radiologist led emergency service was successful.

### P785

### Myocardial Tc-99m-MAA uptake on V/Q SPECT/CT in Eisenmenger Syndrome

**S. GUNGOR**, F. DEDE, M. ARAS, F. NOVRUZOV, S. OZGUVEN, T. ONES, T. Y. ERDIL, S. INANIR, H. T. TUROGLU; Marmara University School of Medicine, Istanbul, TURKEY.

**Aim:** Eisenmenger syndrome (ES) is a cardiac disease caused by ventricular or atrial septal defect and accompanied by pulmonary hypertension. Initially the direction of the shunt is from left to right. However, by the progressive increase in the pulmonary pressure, right to left shunt predominates. Extrapulmonary uptake of Tc-99m-MAA on routine lung perfusion scan is a rare finding and the reason is entry of the radiopharmaceutical into the systemic circulation instead of pulmonary circulation due to right to left shunt. Herein, we reported myocardial and other extrapulmonary uptakes of Tc-99m-MAA on V/Q SPECT/CT in a patient with ES. **Case Presentation:** A 50-year-old female patient with atrial septal defect and ES was referred to V/Q scintigraphy due to sudden deterioration of her complaints suspicious for pulmonary embolism. According to our departmental protocol, first ventilation (Technegas) and 5 hours later perfusion (Tc-99m-MAA) SPECT/CT images were obtained on the same day. It showed nonventilating and severly hypoperfused left lung and a subsegmental match V/Q defect in the inferior lob of rigt lung. Additionally, unusual Tc-99m-MAA uptake within the heart resembling myocardial perfusion imaging studies was also seen on perfusion SPECT/CT images. Moreover, Tc-99m-MAA images revealed abnormal uptake in the kidneys and brain suggestive for right to left cardiac shunt. **Conclusion:** Extrapulmonary Tc-99m-MAA uptake due to the right to left cardiac shunt is a very rare entity that is seen in nearly 4% of patients investigated for pulmonary embolism. Myocardial Tc-99m-MAA uptake is even more rare and needs > 40% right to left shunt and increased myocardial blood flow due to the ventricular hypertrophy. In our case, the severe hypoperfusion of the neighbouring left lung and fusion SPECT/CT images made it easier for us to depict myocardial Tc-99m-MAA uptake.

### P786

### Diagnostic utility of perfusion scintigraphy in pregnant women with suspected pulmonary embolic disease.

**A. SELLEM**, Y. MAHJOUB, W. EL AJMI, H. HAMMAMI; MILITARY HOSPITAL, TUNIS, TUNISIA.

The aim of this study was to retrospectively determine the efficacy of perfusion scintigraphy as the first line investigation in pregnant women with suspected PE. One hundred and sixteen consecutive pregnant patients had perfusion scintigraphy (Q scan). Q scans were the first line investigation in all patients. Seventy-eight (67,2%) scans were normal, twenty-two (19%) were non-diagnostic and sixteen (13,8%) was high probability. Pulmonary embolic disease is uncommon in pregnancy. Perfusion scintigraphyin pregnant patients has an excellent diagnostic yield. The percentage of non-diagnostic scans is much lower than in other patient groups.Scintigraphy imparts a significantly lower breast dose than CTPA and should be used as the first-line investigation in most pregnant patients with suspected PE.

### P787

### Effect of combined Bleomycin and irradiation therapy on the alveolar clearance

**I. Garai**[1], G. Szilágyi[2], S. Barna[1], A. Forgács[1], L. Galuska[3], Á. Illés[4], Z. Miltényi[4]; [1]ScanoMed Ltd., DEBRECEN, HUNGARY, [2]Medical School, University of Debrecen, HUNGARY, [3]Nuclear Medicine, University of Debrecen, HUNGARY, [4]Internal Medicine, University of Debrecen, HUNGARY.

Background: Bleomycin is a cytostatic drug frequently used in the treatment of different cancer. The major limitation of Bleomycin therapy is that, it can induce pulmonary inflammation that may progress to fibrosis approximately in 10 percent of cases. In our prospective study we examined the synergism side effect of Belomycin and irradiation in connection with the alveolar clearance. Patients and Method: 107 non-smoking patients with Hodgkin lymphoma without any history of lung disease were included in the study. We also exluded 12 patients, who did not get Bleomycin in their therapy. Dynamic inhalation lung study was performed after chemo- or combined therapy. After the inhalation of Tc99m DTPA aerosol dynamic acquisition was performed with planar gamma-camera (NuclineAP, Mediso). Based on DTPA clearance calculation we identified the alveolar capillary membran dysfunction. We analysed the relative frequency of presence of pathological

alveolar clearance. Results: We grouped the patients into two groups: 40 pts got only chemotherapy (inc. Bleomycin) and combined therapy was applied in case of 55. In only chemotherapy group we found 9 pts, and in combined therapy group we found 8 pts with pathological clearance. Chi-square test was applied which did not indicate significant difference between the frequency of pathological alveolar clearance in the two groups. Conclusion: Knowing that the dynamic inhalation scintigraphy is a sensitive method to measure alveolar clearance we can suppose that the additional irradiation does not worse whole lung alveolar function. However further examination is needed to confirm it. Furthermore dynamic inhalation lung study seems to be sensitive to recognise early pulmonary side effect of Bleomycin.

P58-2 - Tuesday, Oct. 22, 16:00 - 16:30, Poster Exhibition Area

## Conventional & Specialised Nuclear Medicine: Gastroenterology

### P788

#### The importance of the SeHCAT study in evaluating chronic diarrhoea

J. E. Sarkodieh, R. S. Malliwal, **Y. Bouchareb**, A. Nunes, A. Haroon, H. Jan, T. Szyszko; Barts Health NHS trust, London, UNITED KINGDOM.

**Purpose** Bile salt malabsorption is a reversible cause of chronic diarrhoea. Tauroselcholic Selenium-75 acid (SeHCAT) is an established test for investigation bile acid malabsorption and is recommended in symptomatic patient groups without ileal resection. The aim of this study was to assess the prevalence, severity and treatment of bile acid malabsorption in the local population. **Materials and Methods** 82 patients underwent SeHCAT scans (day 1 after injection of 370 kBq and day 7) in 2012. The scans were performed on the Millennium VG Hawkeye gamma camera; GE Healthcare. Mild malabsorption was defined as 10-14.9% SeHCAT retention at 7 days; moderate malabsorption 5-9.9% retention and severe malabsorption as <4.9%. The patients with abnormal results were followed up on the electronic patient record. **Results** 53/82 (62%) of patients had abnormal results with 27% demonstrating mild bile acid malabsorption; 12% demonstrating moderate malabsorption and 23% demonstrating severe malabsorption. 26/53 (49%) were commenced on a bile acid sequestrant; of whom 11/26 (42%) had documented evidence of symptom improvement and only 2/26 (8%) experienced side effects from treatment. Interestingly, 4/53 (11%) of patients with abnormal bile acid malabsorption suffered from graft versus host disease. **Conclusions** SeHCAT is a sensitive test for diagnosing bile salt malabsorption with 62% having an abnormal result and 23% demonstrating severe malabsorption. A good proportion of patients diagnosed with malabsorption, who were prescribed bile acid sequestrants, demonstrated symptomatic improvement. Hence, the SeHCAT study is an essential investigation for patients with chronic diarrhoea.

### P789

#### Radioguided small intestine lesion localization: Meckel's diverticulum and neuroendocrine multifocal tumor.

**S. Neubauer**, J. Godoy, U. Kronberg, A. Ibarra; Clinica Las Condes, Santiago, CHILE.

We report on laparoscopic radioguided surgery for Meckel's diverticulum and open surgery of a multifocal small intestine neuroendocrine tumor. Case 1 : CS, 7 month old male. Due to two bloody stools Tc99m-pertechnetate scintigraphy was done. The presence of ectopic gastric mucosa was confirmed. On a first diagnostic laparoscopy no abnormality could be found. One month later a second laparoscopic attempt was done at our hospital. Immediately before surgery we injected 92 MBq (2.5 mCi) Tc99m- pertechnetate i.v. and imaged the abdomen on a Siemens ECAM with a LEHR collimator for 5 minutes. The position of the abnormal focal uptake, visible in the lower right quadrant of the abdomen, was marked on the skin using a radioactive pointer. Surgery was began immediately. As soon as the laparoscopic instruments and the gammaprobe (Europrobe) were in place, a very radioactive spot confirmed a small Meckel's diverticulum in the ileum. Histopathology confirmed the diagnosis. Case 2 : IA, 63 year old women. After many years of repeated episodes of abdominal pain and lipotimia, recently also with diarrhea, nausea and cutaneous flushing, a carcinoid syndrome was diagnosed. A Ga68-DOTATATE PET/CT confirmed a multifocal midgut neuroendocrine tumor, probably a carcinoid. Five hours before surgery, Somatostatin receptor imaging was done with 814 MBq (22 mCi) of Tc99m-Hyanic/TATE (CGM Nuclear) on a Siemens ECAM with a LEHR collimator. Planar and SPECT images showed several spots of progressive abnormal uptake in the central abdomen, in coincidence with the findings of Ga68-DOTATATE. Intense gallbladder uptake of Tc99m-Hyanic/TATE was also seen. During surgery, several abnormal palpable nodes in the ileum and at the root of the ileal mesentery showed between two and eight times the background radioactivity in the normal intestine with the handheld probe. Partial ileal resection and cholecystectomy were performed. Conclusion: this preliminary experience confirms the feasibility of radioguided surgery for small intestine lesions. Laparoscopic radioguided localization of ectopic gastric mucosa has not been reported before.

### P790

#### Evaluation and comparison of the salivary gland scintigraphy and diffusion weighted MRI findings in patients with rheumatic disease complaining xerostomia

**A. Comak**, G. Koca, M. Korkmaz; Ankara Training and Research Hospital, Nuclear Medicine Department, Ankara, TURKEY.

**Aim:** The aim of this study was to determine decreased functions of salivary glands using salivary gland scintigraphy in rheumatoid arthritis and ankylosing spondilitis patients complaining xerostomia and compare the findings with ADC (Aperant diffusion coefficient) values obtained from diffusion-weighted magnetic resonance imaging (DW-MRI). **Material and Methods:** 55 patients, mean age 46,6 year (40 F, 15 M), followed-up in romatology policlinic with diagnosis of rheumatoid arthritis and ankylosing spondilitis, 35 controls without rheumatic disease, mean age 42,8 year (26 F, 9 M) were included the study. All subjects underwent dynamic salivary gland scintigraphy and diffusion-weighted magnetic resonance imaging. With quantitative evaluation, maximum accumulation (MA), maximum secretion (MS), secretion velocity (SV), time at maximum count ($T_{max}$), time interval from stimulation to minimum count ($T_{min}$) and uptake ratio (UR) values of parotid and submandibular salivary glands were obtained. After that T2 weighted MR images and diffusion-weighted MR images with b-800 and b-1000 factor of parotid and submandibular glands were obtained. ADC values were calculated from the diffusion-weighted images. **Results:** In the groups rheumatoid arthritis and ankylosing spondilitis, MA, MS, SV ve UR values were lower than the control group statistically. In rheumatoid arthritis, ankylosing spondilitis and control groups parotid glands' mean values were MA: 59.04, 54,10, 67,27; MS: 51.73, 53.09, 61.83; SV: 43.10, 44.40, 52.36; UR: 3.84, 3.85, 5.18 respectively. In submandibular glands MA: 31.07, 28,09, 47,92; MS: 41.15, 43.19, 50.93; SV: 23.74, 26.93, 38.77; UR: 1.95, 1.89, 2.39 were respectively. In control, rheumatoid arthritis and ankylosing spondilitis groups, parotid glands mean ADC values were 1.23, 1.12, 1.11 at b=800; 1.12, 1.03, 1.06 at b=1000 factors respectively. There was difference in the comparision of ADC values of parotid glands between rheumatic patients and control subjects. In the statistically analysis, significant correlation were acquired between quantitative scintigraphic parameters and ADC values of parotid glands at ankylosing spondilitis patients. **Conclusion:** We established decrease at salivary gland parameters and ADC values in DW-MRI. Non-invasive Methods like salivary gland scintigraphy contrarily biopsy, can be used for early diagnosis of secondary Sjögren Syndrome at rheumatology patients complaining xerostomia.

### P791

#### The Value of Cr-51 Labeled Erythrocytes in Demonstrating Gastrointestinal Tract Blood Loss as a Silent Cause of Iron Deficiency

E. Modebe[1,2], **A. Ellmann**[1], L. Wood[3], P. Jacobs[3]; [1]Stellenbosch University, Tygerberg, SOUTH AFRICA, [2]Department of Radiation Medicine, University of Nigeria Teaching Hospital, Enugu, NIGERIA, [3]The Heamatology Research Group, Pathcare, Claremont, SOUTH AFRICA.

Background Assessing patients with iron deficiency anaemia, possibly due to occult blood loss from the gastrointestinal (GI) tract, can be diagnostically and therapeutically challenging. This is because stool testing may be negative, endoscopy poorly informative in view of intermittent bleeding while barium studies can potentially overlook superficial lesions. These limitations can be approached using two different radioactive isotopes to first reliably demonstrate the appearance of a significant volume of Cr-51 labelled red blood cell (RBC) in the stool and then localise the site anatomically using Tc-99m labelled RBC. Aim To demonstrate the usefulness of Cr-51 labelled RBC in detecting and quantifying blood loss from the GI tract and aid in the timing of a Tc-99m labelled RBC study, improving the sensitivity of the study to localize the site of GI bleeding. Finally to correlate these findings with clinical outcome. Method In this retrospective review, records of patients referred for evaluation of iron deficiency due to possible GI blood loss were reviewed. All patients had Cr-51 RBC studies performed after blood was labelled with Cr-51, injected intravenously and daily counts from faeces measured in the whole body counter over a period up to 30 days. Where this exceeded 50 ml in any 24-hour period a localising study with Tc-99m labelled erythrocytes followed immediately (within 24hrs) to identify a site of bleeding. The results of these studies were reviewed. Finally, these studies were correlated with clinical findings. Results The patient group comprised 36 female and 21 males (n = 57), with a total of 59 studies (one patient had 3 studies). In 32 (54%) of the 59 chromium studies the results were positive. Tc-99m RBC studies were performed in

17 of these. In 14 (82%) of these the technetium imaging was positive. Clinicians then successfully defined a specific anatomical bleeding site in 10. Half of these were diagnosed with small-bowel angiodysplasia. Conclusion This combination of Cr-51 labelled erythrocytes for confirming GI blood loss and timing of bleeding and Tc-99m RBC for localisation of bleeding site (twin isotope method) is practical in revealing otherwise silent intestinal haemorrhage. It has good patient acceptability and clinical as well as diagnostic utility in managing these patients.

P59-2 - Tuesday, Oct. 22, 16:00 - 16:30, Poster Exhibition Area

## Conventional & Specialised Nuclear Medicine: Haematology

### P792

### Patophysiological mechanism of thrombocytopenia in pediatric population investigated by autologous platelets labeled with In-111 oxinate

**M. Todorovic-Tirnanic**, S. Pavlovic, D. Sobic-Saranovic, V. Artiko, V. Obradovic; Center for Nuclear Medicine, Clinical Center of Serbia, and Faculty of Medicine, University of Belgrade, Belgrade, SERBIA.

**Aim**: To investigate patophysiological mechanism of thrombocytopenia with In-111 oxinate labeled autologous platelets in children with chronic thrombocytopenia. **Methods**: Autologous platelet separation and (In-111 oxinate) labeling; quality control: general and differential yields of Pt labeling (GYL&DYL) and initial platelet accumulation in the liver (IPAL); Pt lifespan; production index (PI); sequestration index and site estimation. Out of 473 investigated patients with clinical diagnosis of chronic immune thrombocytopenic purpura (ITP), there were 69 children (44 girls and 25 boys) aged from 3.1-18 yrs (median=11 yrs). Body height was 100-187 cm (mean=147 cm), weight 15-98 kg (median 34 kg). **Results:** Platelet blood count (BC) in 69 children ranged from 1-122 G/l (median=21 G/l). Blood sample volume for platelet separation and labeling was 30-75 ml (mean=55 ml). Radioactivity used for Pt labeling was 300 µCi. GYL ranged from 33,9-90,2 % (mean=65.9 %). Platelet DYL was 55.7-99.6 % (mean=92.6 %). RBC+WBC DYL was 0.0-41.5 % (median=1.6 %). Plasma DYL was 0.2-7.3 % (median=0,7 %). Injected radioactivity: 70.2-272.2 µCi (mean=181 µCi). IPAL ranged from 3.0-36.8 % (median=11.9 %). Platelet lifespan was 0.7-21.6 h (median=12 h). In two children normal quantity of platelets was separated despite low platelet blood count (35 and 122 G/l; platelet lifespan=8.4 and 9.0 days). In four patients normal platelet lifespan was obtained, while platelet PI was low (0.1; 0.2; 0.2; 0.2; PtBC: 5, 21, 30, 55 G/l). Platelet lifespan in children with confirmed ITP ranged from 0.7-93.6 h (median=9.6h). Platelet PI in ITP was 0.2-23.4 (median=1.8). Sequestration index values were 0.3-9.4 (median=1.8). Sequestration site was the spleen in 26 (41,94 %), predominantly spleen in 9 (14,52 %), liver in 3 (4.84 %) and mixed sequestration (in liver and spleen) in 24 (38.7 %) ITP patients. **Conclusion**: In 6/69 children initial diagnosis of ITP was changed (in 2 to pseudothrombocytopenia, in 4 to inadequate platelet production). In 63/69 children diagnosis of ITP was confirmed. Help in decision whether to perform splenectomy or not was enabled in 61.3 %.

### P793

### Comparaison between gamma camera and external counting in $^{111}$Indium labeled platelet exam : a prospective study

S. Levesque, S. Couderc, M. Terroir, C. Fontan, J. Simon, **P. Payoux**; CHU Purpan, Toulouse, FRANCE.

**Introduction and objectives** $^{111}$Indium labeled platelets exam is the gold standard for sequestration measurement. Unfortunatly there's no consensus for technical procedure. The present study was conducted to validate if the 2 main Methods for $^{111}$Indium platelets sequestration sites determination in Idiopathic Thrombocytopenic Purpura (ITP), gamma camera and external counting, provided similar results or not. **Methods:** From November 2012 until April 2013, a prospective study was done in 15 patients suffering from chronic ITP. For all of them a kinetic and sequestration study of $^{111}$Indium platelet was requested with the following procedure :thirty minutes after injection of labeled platelets and daily after over a week, both gamma camera and external scintillation probe were used for the measurement of $^{111}$Indium radioactivity in the liver, spleen and heart. Quantification data with the 2 Methods were analyzed independently by 2 raters and classified in 4 types: spleen sequestration, liver sequestration, mixed sequestration and no sequestration. We selected 3 index values for spleen/heart ratio and liver/heart ratio among those currently used to evaluate $^{111}$Indium platelets sequestration sites. The degree of agreement between gamma camera and external counting results was calculated for each index. The degree of interobserver agreement for gamma camera quantification was also collected. **Results:** A contingency table was used to calculate percentage of observed agreement (proportion of common and similar observations) as well as percentage of random agreement. Using the Cohen's kappa coefficient, agreement between the 2 Methods was poor for the 3 given indices (0.10, 0.13 and 0.33 ) However, the value of Cohen's kappa itself conveys no information about the reliability of this assessment. Despite of this statistical result, gamma camera and external counting provided the same clinical diagnosis in 80 % cases when a sensible index is preferred to a specific one to predict a splenic sequestration. In cases of hepatic sequestration, observed agreement of 67% is observed with the 3 indices. The investigation in term of interobserver agreement conducted only for the gamma camera data concluded at 0.79 Cohen's kappa coefficient. **Conclusion:** Our results demonstrate that gamma camera and external counting are not comparable Methods from a statistical point of view. Therefore, switching from one to another method is not trivial. In most of cases, the platelet isotopic study performed with those 2 techniques appears to be well comparable for the observed agreement but discordances exist and may lead to inappropriately categorize splenic and hepatic sequestration.

P60-2 - Tuesday, Oct. 22, 16:00 - 16:30, Poster Exhibition Area

## Conventional & Specialised Nuclear Medicine: Uronephrology

### P794

### Cr-51-EDTA-glomerular filtration rate (Cr-51-GFR): differences between the slope-intercept 2-sample method and the 10-sample kinetic plasma clearance analysis in relation to GFR categories

G. Arsos[1], **C. Sachpekidis**[2], D. Katsampoukas[1], E. Manou[3], G. Miserlis[4], I. Tsechelidis[5], A. Sioulis[6], D. Tsakiris[3], N. Karatzas[1]; [1]3rd Department of Nuclear Medicine, Aristotle University of Thessaloniki Medical School, Papageorgiou Hospital, Thessaloniki, GREECE, [2]Clinical Cooperation Unit Nuclear Medicine, Heidelberg, GERMANY, [3]Department of Nephrology, Papageorgiou Hospital, Thessaloniki, GREECE, [4]Transplantation Clinic, Aristotle University of Thessaloniki Medical School, Hippokration Hospital, Thessaloniki, GREECE, [5]1st Department of Nuclear Medicine, Aristotle University of Thessaloniki Medical School, Hippokration Hospital, Thessaloniki, GREECE, [6]1st Clinic of Internal Medicine, Aristotle University of Thessaloniki Medical School, AHEPA Hospital, Thessaloniki, GREECE.

Introduction: GFR categories are essential for chronic kidney disease (CKD) staging. Plasma clearance of exogenous tracer is the gold standard for clinical GFR assessment. The "slope-intercept" technique (2-3 plasma samples during the 2-5 hours p.i. plus empirical correction for the fast neglected component) is routinely applied. Detailed elimination analysis requires more plasma samples starting soon after tracer injection, but does not rely upon any correction. We aim to study the differences between the two Methods in relation to GFR categories according to KDIGO-2012 and their importance for CKD staging. Subjects and Methods : In 300 subjects with CKD (58.0±16.1 years, 33.0% females), after bolus i.v. injection of 3.7 MBq Cr-51-EDTA and 10 plasma samples between 5 min-4 hours p.i., GFR was calculated by biexponential kinetic (GFR10) and by "slope-intercept" analysis and Brochner-Mortrensen correction of 2 samples at 120 and 240 min p.i. (GFR2). GFR was indexed by body surface area (ml/min/1.73 m2) and allocated according to KDIGO-2012 as G1, G2, G3a, G3b and G4-5 (≥90, 60-89, 45-59, 30-44 and ≤29 ml/min/1.73 m2 respectively). For each patient the absolute (D=GFR10-GFR2) and relative (DR=100xD/GFR10) differences calculated and grouped according to KDIGO-2012. The correlations GFR10-GFR2 and GFR10-D were assessed by linear and non-linear regression analysis respectively. D and DR differences between the KDIGO-2012 groups were studied by ANOVA and Bonferroni post hoc analysis (significance for p<0.05). Results: GFR10, GFR2, D (ml/min/1.73 m2) and DR (%) were (mean±SD): 109.0±17.0, 97.4±13.2, 11.5±7.0, 8.4±5.3; 72.3±9.3, 65.3±9.5, 7.0±4.3, 9.7±5.7; 51.2±4.3, 46.9±5.2, 4.3±3.7, 8.3±7.2; 36.6±4.4, 32.6±4.8, 3.9±3.0, 10.7±8.4; 21.3±5.7, 20.4±4.9, 0.9±3.9, -0.8±35.2 for G1, G2, G3a, G3b and G4-5 groups respectively. GFR10-GFR2 correlation was strong (r=0.985, p<0.0001) but slope was less than unity (0.876±0.008). GFR10-D correlation was positive, best approximated be 3rd order polynomial (r = 0.686, p<0.001). Significant, between KDIGO-2012 groups, differences were detected for both D and DR (ANOVA, p<0.0001). All but the G3a-G3b pair-wise comparisons were significant for D but only G4-5 group differed significantly from all other groups for DR. Conclusions: The "slope-intercept" GFR measurement with Brochner-Mortensen correction systematically underestimates GFR. The absolute underestimation is maximum at G1 and becomes progressively negligible at the G4-5 levels. The relative underestimation is stable around 10% in all but the G3-4 groups. Our data suggest that with the exception of G3-4 category, GFR categorization using the slope-intercept" GFR measurement with Brochner-Mortensen correction is biased in comparison to the plasma tracer kinetic analysis.

## P795

### Comparison of Glomerular Filtration Rate Measurements with the Two Plasma Sample and Single Plasma Sample, Creatinine Clearance, and Prediction Equation Methods in Renal Transplant Patients with Stable Greft Functions

**E. S. BUDAK**[1], F. AYDIN[1], S. DEMİRELLİ[1], A. ÖNER[1], G. SÜLEYMANLAR[2], H. AKBAŞ[3], M. ERKILIÇ[1], F. GÜNGÖR[1]; [1]AKDENİZ UNIVERSITY HOSPITAL DEPARTMENT OF NUCLEAR MEDICINE, ANTALYA, TURKEY, [2]AKDENİZ UNIVERSITY HOSPITAL DEPARTMENT OF NEPHROLOGY, ANTALYA, TURKEY, [3]AKDENİZ UNIVERSITY HOSPITAL DEPARTMENT OF BIOCHEMISTRY, ANTALYA, TURKEY.

OBJECTİVE: Glomerular filtration rate (GFR) is one of the most effective Methods in the assesment of renal functions. Because of that, quick and accurate measurement of GFR takes great care. In renal transplant patients, decrease in the GFR is closely associated with rejection and cardiac complications. In the assessment of greft functions, GFR measurement has great importance. In this study, Tc-99m DTPA two-plasma sampling method (TPSM) was accepted as reference method and it was aimed to compare it with single-plasma sampling method (SPSM) and creatinine clearance (Ccr) formulations [Cockgroft-Gault (CGf) ve Modification of renal disease (MDRDf)]. MATERİALS and METHODS: Ninety-six renal transplant patients (63 males, 33 females; age ranges 19-67 years, median: 38.15) with stable greft functions (defined as clinical and laboratory) at least 6 months after transplantation were prospectively included in the study. Blood samples were taken at 120 min, 180 min, and 240 min after the injection of 111-148 MBq Tc 99m DTPA. SPSMs used were those of Constable (CM), Dakubu (DM), Groth and Aasted (GAM), Morgan (MM), Russel (RM), and Christensen and Groth modified by Watson (CGmW) 180 min and 240 min. Slope- intercept method was used for TPSM (120 min and 240 min samples). The appropriate formulas were used for MDRDf and CGf. Pearson's correlation and Bland-Altman analyses were used to compare the results. RESULTS: There were strong statistically significant correlation between the TPSM and all SPSMs. Among them, GAM showed the best correlation and the lowest "Standard error of estimation" (see) (r=99%; p<0.0001, see=5.39 ml/min/1.73m2). The correlation coefficient values were calculated as r=0.52, r=0.60 (p<0.0001), for CGf and MDRDf, respectively. According to Bland-Altman analysis, all SPSMs showed good agreement (95% limits of agreement) with TPSM. Mean absolute difference ±1.96SD value between TPSM and GAM was found as 3.7 ± 7.6 ml/min/1.73m2 . CGf and MDRDf did not show good agreement with TPSM. CONCLUSION: Since all SPSMs showed high correlation and good agreement with TPSM, they can be routinely used for determination of GFR. As GAM had the highest correlation value and showed the highest concordance with TSPM, it could be regarded as an alternative method. This study indicated that CGf and MDRDf are not accurate in the measurement of GFR.

## P796

### Follow up of renovascular hypertensive disease post angioplasty

**I. Kotsalou**[1], A. Kotsalos[2], M. Bazigos[2], N. Dimakopoulos[3], A. Zoumboulidis[3], A. Hatzioannou[4]; [1]Nuclear Medicine Dept, Pammakaristos Hospital, Athens, GREECE, [2]Cardiovascular Surgery Dept, NIMTS Hospital, Athens, GREECE, [3]Nuclear Medicine Dept, NIMTS Hospital, Athens, GREECE, [4]Radiology Dept, University of Athens, Aretaieion Hospital, Athens, GREECE.

**Target:** Renovascular hypertensive disease counts about 1-3% of hypertension causes worldwide, mainly due to critical stenosis of renal arteries. Late therapy may lead to serious loss of renal function and deficiency. **Method:** We studied 60 patients who were subjected to renal angioplasty after a pathological diagnostic renogram with 99m-Tc DTPA. All patients performed a renal scintigraphic study as a follow up method (6 months post angiography), in order to evaluate non-invasively the functional results of the invasive method. **Results:** Comparison of renal flow pre and post angioplasty show a statistically significant increase in previously stenosed arteries (mean 257 counts/pixel vs 546 counts/pixel). Relative contribution in renal function appeared indicatively improved, approximately 14% (*p:0.10*) in 63% of the cases, perhaps due to progressively in each case recovery of renal dysfunction. Patients with poor short-term improvement in hypertension and renal function were consequently subjected to myocardial perfusion scintigram and were referred for coronary angioplasty when needed. **Conclusions**: The present study stressed the need of accurate improvement of renal artery stenosis in patients with pathologic radionuclide renogram and hypertention resistant to medication. Renal scintigraphic study is useful in diagnosis of renal artery stenosis, the quantification of renal deficiency and prognosis of reversibility of renal loss, but also can help to evaluate recovery or renal function post angioplasty.

P61-2 - Tuesday, Oct. 22, 16:00 - 16:30, Poster Exhibition Area

## Conventional & Specialised Nuclear Medicine: Infection & Inflammation

## P797

### Clinical assessment of patients with suspected infection or inflammatory condition with F-18 FDG PET-CT

**N. Shuke**, C. Miyazaki, T. Aburano, T. Onishi, A. Ando, H. Harada, H. Nomura, N. Saito, H. Yamamoto, K. Saito; Kushiro Kojinkai Memorial Hospital, Kusiro, JAPAN.

Objective: The objective of this study was to address clinical significance and role of FDG PET-CT in assessment of patients (pts) with suspected infection or inflammatory condition. Methods: A total of 44 pts (69.6 ± 12.2 years old, M/F=27/17) with suspected infection and inflammatory condition from clinical manifestations and blood tests were retrospectively studied. FDG PET-CT was performed on these pts using a PET-CT system with BGO PET detectors and 16-row detector helical CT (Discovery STE, GE) to localize infection or inflammatory sites. PET-CT findings were evaluated in relation to results of blood tests (C-reactive protein (CRP), white blood cell count (WBC)), implemented treatment, and prognosis. Results: Ten pts (22.7%) showed negative findings on FDG PET-CT. All these pts recovered with conservative antibiotic treatment and favorable prognosis except two pts (one with viral encephalitis who had severe neurological sequelae and the other with acute renal failure who had died). Thirty-three pts (75%) showed positive findings suggesting infection or inflammation in various regions: bone and soft tissue, 9; colon, 5; mediastinum, 4; lung, 4; heart and pericardium, 3; retroperitoneum,3; peritoneum, 2; gall bladder, 1; kidney,1; vascular graft,1; pace maker lead, 2; great vessels, 1. Esophageal cancer was found in one patient in these 33 pts unexpectedly. One patient (2.3%) showed positive finding suggesting not infection but malignant lymphoma and was diagnosed with diffuse large B cell lymphoma subsequently. In PET-positive pts, surgical treatments, abscess drainage, or removal of pace maker lead were done in 9 pts. In PET positive pts, 4 pts had died due to multiple organ failure, MRSA endocarditis, lymphoma, myelodysplastic syndrome, and unknown cause. Remaining 30 pts recovered by appropriate surgical and medical treatment. In PET-negative and PET-positive pts, CRP (mg/dl) was 9.0±9.0 and 8.6±7.6, WBC (/μl) was 8600±3300 and 10000±6600, showing no significant difference. Conclusion: FDG PET-CT was useful in initial assessment of pts with suspected infection or inflammatory condition, providing important information regarding location and severity of the disease. PET-negative pts tended to have mild disease however, presence of PET-negative severe disease such as viral encephalitis should be kept in mind.

## P798

### Usefulnes of FDG-PET/CT Imaging in Patients with Suspected Septic Choc but Without Evidence of Infectious Focus

**E. MATHIAS**[1], A. TATOPOULOS[2], C. BESSEAU[1], O. MOREL[1], A. VERGER[1], P. BOLLAERT[3], G. KARCHER[1], S. GIBOT[3], P. OLIVIER[1], P. MARIE[1]; [1]Service de Médecine Nucléaire CHU NANCY, Vandoeuvre-les-nancy, FRANCE, [2]Réanimation, Polyclinique Louis Pasteur, Essey-Les-Nancy, FRANCE, [3]Service de Réanimation Médicale CHU NANCY, Nancy, FRANCE.

A definite identification of infectious foci is frequently difficult to obtain in patients with suspected septic choc, in spite of the use of numerous biologic tests and imaging techniques (X-ray computed tomography (CT), planar radiography, echography). Positron Emission Tomography with 18F-fluorodesoxyglucose (FDG - PET) is currently recorded with CT on hybrid systems and the dual FDG-PET / CT exams are highly sensitive for detecting septic foci. This study was aimed at assessing the additional diagnostic value of FDG-PET / CT exams in patients with suspected septic choc but without evidence of septic focus with conventional medical imaging (CT, planar radiography, echography) Materials and Methods. FDG-PET / CT exams were performed in 17 patients (10 men / 7 women, from 19 to 82 years old), who had a known or suspected septic choc and for whom no infectious focus had been evidenced with conventional imaging techniques (echography and planar radiographies had been previously performed in all patients and CT in 10 of them). The FDG-PET / CT images were analyzed on the day of the test by a consensus of two senior physicians. Results. Ten among the 17 patients (59%) had positive hemocultures. The day of FDG-PET / CT, 16 patients (94%) had antibiotics, 14 had a continuous intravenous administration of sympathomimetic drugs (84%) and mean SOFA score was 10 (from 2 to 16). Two serious but reversible adverse events were documented during the exams: one arterial hypotension and one marked decrease in blood oxygen saturation. At least one infectious focus was documented on the FDG-PET / CT of 13 patients and 2 of them could subsequently considered as false positives and 11, as true positives. No infectious focus was documented in the 4 remaining patients. On overall, the use of FDG-PET / CT was associated with a sensitivity of 100% and with a specificity of 67% for identifying patients with septic focus; and the FDG-PET / CT results led to therapeutic changes (changes in antibiotherapy and/or surgical intervention) in 12

among the 17 patients (71%). Conclusion. When performed in patients with suspected septic choc, but without evidence of infectious focus, FDG-PECT / CT exhibits a high sensitivity for detecting actual infectious foci, and has a marked impact on therapy.

## P799

### 99mTc-HDP/67Ga scintigraphy in the assessment of patients with suspected postoperative spinal infection. Our experience.

**E. Rodríguez Pelayo**, A. Mendoza Paulini, M. Fernández Rodríguez, M. Balsa Bretón, M. García Alonso; Hospital Universitario de Getafe, Getafe, SPAIN.

INTRODUCTION: Emergence of new techniques for diagnose postoperative spinal infection (18F-FDG-PET/CT), has questioned the role of dual tracer 99mTc-HDP and 67Ga scintigraphy to be questioned. AIM: To assess the usefulness of dual tracer 99mTc-HDP/67Ga scintigraphy in patients with suspicion of postoperative spinal infection. MATERIAL AND METHOD: We retrospectively reviewed 35 studies of 29 patients , 21 women (60%), aged 59 ± 17, with clinical suspicion of infection after spinal fusion surgery and nonspecific or doubtful radiological tests (Rx, NMR). Elevated CRP and ESR were used as clinical suspicion markers. No patient received prior antibiotic therapy. 99mTc-HDP/67Ga scintigraphy was used as diagnostic test and results were confirmed by microbiological culture and / or clinical follow up. RESULTS: Of the 35 studies evaluated, we found: In 4 patients (11.4%) dual tracer scintigraphy showed infection (TP). In 24 patients (68.6%) it was negative (TN). In1 patient (2.8%) we obtained a FP result; patient with recent surgery (<6 months). And in 6 (17.1) test result was falsely negative (FN). Sensitivity obtained was 40%, Specificity 96%, PPV 80%, NPV 80% and diagnostic accuracy 80%. CONCLUSION: Dual tracer 99mTc-HDP/67Ga scintigraphy is useful to confirm postsurgical spinal infection, considering the high specificity obtained. It can be considered as a useful tool in diagnosis of this pathology despite of newer diagnostic techniques.

P62-2 - Tuesday, Oct. 22, 16:00 - 16:30, Poster Exhibition Area

# Conventional & Specialised Nuclear Medicine: Bone & Musculoskeletal - DXA

## P800

### Whole body dual-energy X-ray absorptiometry as a "one stop" study in the clinical evaluation of patients with chronic obstructive pulmonary disease.

**J. Koutsikos**[1], I. Giannopoulou[2], S. Bakalis[1], K. Athanasiou[1], G. Koniaris[1], I. Vogiatzis[3,4]; [1]401 General Military Hospital, Nuclear Medicine Dpt., ATHENS, GREECE, [2]Physical Education & Sports Science Dept, University of Athens, ATHENS, GREECE, [3]1st Respiratory Medicine Dept, University of Athens, ATHENS, GREECE, [4]Clinical Exercise & Health Sciences Institute, University of the West of Scotland, Paisley, UNITED KINGDOM.

INTRODUCTION: Dual-energy X-ray absorptiometry (DXA) is an accurate and reproducible method with very low radiation exposure and it is applicable in clinical practice to analyze bone mineral content (BMC) and bone mineral density (BMD) of subregional compartments (particularly of the hip). Whole body DXA (WBDXA) can differentiate BMC and the soft tissue surrounding the bone by measuring the amount of fat and lean tissue. Also, BMD of the WBDXA can be assessed. Depletion of fat-free mass (FFM) commonly occurs in patients with chronic obstructive pulmonary disease (COPD). Loss of BMD may also occur, with lumbar spine fractures reported in nearly 50% of steroid-naive male patients. There is little evidence linking FFM and BMD loss in COPD. The aim of our study was to determine whether WBDXA is an applicable method in the clinical evaluation of FFM and BMD in COPD. MATERIALS & METHODS: Twenty-five pts with mild to moderate COPD (19 M, 6 F, mean [±SD] age 66.2±5 y.o., mean [±SD] FEV 1 47.4±16.2) underwent both WBDXA and regional DXA. BMC, BMD and FFM were assessed by WBDXA. BMD was also measured by the regional (hip) DXA. RESULTS: WBDXA revealed mean values [±SD] of BMC, BMD and FFM, 2.5±0.42 kg, 1.13±0.1 gr/cm2 and 50.43±8.51 kg, respectively. Significant correlation was found between BMC and FFM (r= 0.721, p<0.001). The BMD at the hip (mean value±SD = 0.92±0.15 gr/cm2) was also significant correlated to BMD at the WBDXA (r=0.777, p<0.001). CONCLUSION: WBDXA, an easily applicable method, appears to be suitable in identifying bone mineral loss in COPD patients. It is also informative for clinically evaluating the body composition of these patients. We propose that WBDXA should be performed instead of regional DXA, considering however the higher values for BMD it gives.

## P801

### Antiepileptic treatment including new drug regimens is associated with bone loss

**M. Assadi**[1], H. Salimipour[2], S. Kazerooni[3], M. Seyedabadi[1], I. Nabipour[4], R. Nemati[2], D. Iranpour[1]; [1]The Persian Gulf Nuclear Medicine Research Center, Bushehr University of Medical Sciences (BUMS), BUSHEHR, IRAN, ISLAMIC REPUBLIC OF, [2]Department of Nurology, Faculty of Medicine, Bushehr University of Medical Sciences, BUSHEHR, IRAN, ISLAMIC REPUBLIC OF, [3]Department of Pediatrics, Faculty of Medicine, Bushehr University of Medical Sciences, BUSHEHR, IRAN, ISLAMIC REPUBLIC OF, [4]The Persian Gulf Tropical Medicine Research Center, Bushehr University of Medical Sciences, BUSHEHR, IRAN, ISLAMIC REPUBLIC OF.

Introduction: The effects of antiepileptic drugs (AEDs) on bone mineral density (BMD) are well-addressed; but, data in children especially with new antiepileptic medications is scarce. This study aimed to provide the impact of these drugs on BMD of ambulatory patients with epilepsy. Method: BMD and detailed clinical information were obtained in 113 patients as well as 38 controls using Dual X-ray absorptiometry (DXA). The patients were also categorized to two enzyme-inducing AEDs (EIAEDs) and non-enzyme-inducing AEDs ( non-EIAEDs) groups. Also, they classified to monotherapy and multiple therapy groups. All patients filled a questionnaire of 63 questions. In this study, the raw value of BMD, T-score and Z-score of the spine, neck of femur, total hip and forearm were analyzed. Results: Patients receiving antiepileptic drugs showed lower lumbar BMD compared to the control (p<0.05), regardless of the type of antiepileptic drug (enzyme inducer (EIAEDs) or non-inducer (non-EIAEDs). In addition, there was a significant decrease in femoral neck BMD of patients receiving EIAEDs (0.922± 0.161, p<0.05) but not those treated with non-EIAEDs. Patients undergoing carbamazepine monotherapy (33 patients) showed lower lumbar and femoral neck BMD, while those receiving valproate (22 patients) or undergoing polytherapy showed similar BMD to that of control in all studied regions of interestThere was not a notable change of BMD in ward, trochanter or total hip in either EIAEDs or non-EIAEDs groups Conclusion: antiepileptic drugs therapy especially new generations diet are associated with low bone density. The presented these data stressing the clinical and diagnostic points, in hope of stimulating a high index of suspicion to facilitate early diagnosis and preventive care.

## P802

### Impact of adding distal forearm DXA to hip and spine measurements on DXA report

**M. u. Zaman**[1], N. Fatima[2], Z. Sajjad[1], U. Zaman[3]; [1]AKUH, Karachi, PAKISTAN, [2]Dr Ziauddin Medical University, Karachi, PAKISTAN, [3]Year II, MBBS, Dow University Health Sciences (DUHS), Karachi, PAKISTAN.

Dual energy X-ray absorptiometry (DXA) is the gold standard modality for non-invasive diagnosis of osteoporosis but controversy exists about the optimal site (s) for bone mineral density (BMD) measurement. The objective was to find out impact of adding distal forearm BMD to hip and spine measurements on final diagnosis of a DXA study. This prospective study recruited 279 consecutive patients [female 256 (92%); male 23 (8%)] with a mean age of 63.25 ± 10.62 years from April 2011 to April 2012. The BMD was measured over hip (total hip and femoral neck), spine and distal forearm in all patients. Based on T-Score values of hip and spine (2 sites), diagnosis was normal in 34%, low bone mass in 40% and osteoporosis in 26% patients. However, adding distal forearm BMD and T-score (3 sites), diagnosis was normal in 28%, low bone mass in 37% and osteoporosis in 35%. Therefore, distal forearm BMD has upstaged the diagnosis from normal to low bone mass in 14%, from normal to osteoporosis in 2% and from low bone mass to osteoporosis in 18% patients. We conclude that combining distal forearm BMD with spine and hip can identify more patients with low bone mass or osteoporosis.

P63-2 - Tuesday, Oct. 22, 16:00 - 16:30, Poster Exhibition Area

# Conventional & Specialised Nuclear Medicine: Bone & Musculoskeletal

## P803

### Trench foot differs from freezing environmental cold-induced injuries on HDP-Tc99m-SPECT-CT

**L. Dercle**, M. Sinigaglia, G. Victor, W. Ajmi, P. Pascal, I. Berry; CHU Toulouse, Toulouse, FRANCE.

Introduction Environmental cold-induced injuries [CI] are frequent. Trench foot is an unknown and underestimated non-freezing CI. We describe, for the first time, its characteristics on bone scan and highlight how SPECT-CT may revolutionize the management of CI. Subjects and Methods A literature review was performed up to March 2013, including the words: "trench foot", "CI", "bone scan", "HDP-Tc99m" and "SPECT-CT". From January 2010 to March 2013, a physician retrospectively reviewed all the bone scans performed more than 72 hours after the CI and with known follow-up (results of surgery or patient outcome). 3 patients with clinically the most extended and severe lesions were included: 1 trench foot and 2 freezing CI. A physician, blinded for the clinical information, analysed the bone phase and

performed a lesion mapping of every bone and muscle in each foot. The intensity of the uptake was recorded compared with healthy tissue. Results 78 articles were reviewed, none of which described trench foot on bone scan. In accordance with the results of the literature, trench feet were caused by cold and wet exposure, compression, dietary inadequacy, fatigue (absence of removal of boots and prolonged stay outside for 10 days) and the symptoms were oedema, numbness, and pain. Biology revealed a mild rhabdomyolysis. The SPECT-CT showed an increased uptake in 13 muscles and 22 bones, a decreased uptake in 2 bones. The pattern of uptake differed from freezing CI, abnormalities were not peripherals but were at the pressure points of the boots and at the plantar arch. For the 3 patients, the lesion mapping revealed: an increased uptake in 26 muscles and 24 bones, a decreased uptake in 2 bones, no uptake in 28 muscles and 20 bones. Absence of uptake after 72h was a strong predictor of infarction (48/48 become necrotic), decreased and increased uptake may recover (52/52 healed). Conclusion/Discussion The pattern of uptake of trench foot differs from freezing CI. SPECT-CT may improve surgeon decision and patient prognosis because it may accurately describe the degree and extent of tissue necrosis.

## P804

### Gastric Uptake of TC-99M-HDP in Bone Scintigraphy: a Decision-Making Algorithm

**L. Dercle**, G. Victor, F. Breibach, M. Alonso, I. Berry; CHU Toulouse, Toulouse, FRANCE.

Introduction Gastric uptake used to occur in 2.2% of bone scans. We hypothesized that a review of the literature and of 1000 bone scans would lead to a decision-making algorithm. Subjects and Methods The literature review was performed up to April 2013 including the words: “bone scan/scintigraphy” and “gastric/stomach uptake or artifact or visualization or calcification or accumulation or concentration” or “extraosseous uptake”. Two physicians blinded for the clinical information retrospectively reviewed 1000 consecutive bone scans in our department up to April 2012. A physician recorded all the relevant information from past medical history, biology, radiology and biopsy. All the patients with a gastric uptake or with known gastric biopsy were included. Results 82 cases of non-artifactual gastric uptake were recorded: 80 cases in the literature (27 articles including 2 cases of gastric cancers) and 2 cases (0.2%) in our department whose histological diagnosis were gastritis and metastatic calcifications from parathyroid adenoma. In our department, 5 cases (0.5%) of biopsy-proven gastric cancer showed neither gastric uptake nor micro or macro-calcifications on the preoperative CT-scan. It leads to the following decision making algorithm. A defect of the imaging kit may be confirmed if: all the patients injected with the same kit present the same abnormalities (stomach, thyroid, salivary glands, choroid plexus uptake); quality control parameters are altered or the incubation is long. Metastatic calcifications must lead to etiological investigations and may be confirmed if: stomach, lungs and kidney uptake; medical history of renal failure or hypercalcemia; Total-Ca x Pi is above 5.6 $mmol^2/L^2$ (70 $mg^2/dL^2$); CT-scan or biopsy show soft tissue microcalcification; reversibility on the control bone scintigraphy. Gastric cancer is not a frequent diagnosis (less than 5% are calcified) but physicians must always look for: risk factors or symptoms of gastric cancer; typical feature of adenocarcinoma on CT-scan (focal thickening of the gastric wall, diffuse infiltration, mass, stenosis, lymphadenopathy) and early gastric cancer may never be excluded. Conclusion/Discussion This decision making algorithm based on 82 cases of non-artifactual gastric uptake may prevent unnecessary tomography, CT-scan or biopsy because the most relevant information comes from past medical history, quality control and biology. Frequency of gastric uptake is decreasing due to improved imaging kits and quality control.

## P805

### Evaluation of retention and pharmacokenetics of Iodine-131 labeled recombinant human Bone Morphogenetic Protein-2 (I-131-rhBMP-2) following implantation of rhBMP-2/absordable collagen sponge at orthotropic site in rats by using nanoSPECT/CT

**H. Yu**[1], C. Chien[1], P. Wang[1], J. Kuo[1], C. Chen[1], C. Ho[1], W. Yu[2], S. Shen[2], M. Wang[1], W. Lin[1]; [1]Institute of Nuclear Energy Research, Longtan Township,Taoyuan County, TAIWAN, [2]Biomedical Technology and Device Research Laboratories, Industrial Technology Research Institute, Hsinchu, TAIWAN.

Objective: Recombinant human Bone Morphogenetic Protein-2 (rhBMP-2) is disulfide-linked dimeric protein molecule and plays an important role in the development of bone and cartilage. The absordable collagen sponge (ACS) is a soft, white, pliable, absorbent implantable matrix for rhBMP-2. ACS is made from bovine Type I collagen obtained from deep flexor tendon. The ACS acts as a carrier for the rhBMP-2 and acts as a scaffold for new bone formation at the site of implantation. The new bone formation depends on the concentration of rhBMP-2 in ACS. So the release/retention profile of rhBMP-2 in ACS is an important information for its efficacy. This study aims to evaluate the retention and pharmacokenetics of radiolabeled rhBMP-2 (I-131-rhBMP-2) following implantation of rhBMP-2/ACS at orthotropic sites in rats by using nanoSPECT/CT. Methods: rhBMP-2 was radioabeled with iodine-131 by standard Iodogen method. Its radiochemical purity was determined by radio thin-layer chromatography. I-131-rhBMP-2 was injected into ACS directly. For the orthotopic animal model, a section of right radius (2mm) of 8-week-old male SD rat was removed under anesthesia and replaced with I-131-rhBMP-2/ACS (3 mCi/rat). NanoSPECT/CT imaging of I-131-rhBMP-2/ACS implanted rats were performed everyday for first week and three days (Mon, Wed, Fri) per week for next three weeks (total 16 scans/rat in 1 month). ROIs at imlpanted site and other major organs were selected from the SPECT/CT images and the radioactivities of the ROIs were calibrated and decay corrected. Results: I-131-rhBMP-2 was prepared in radiochemical purity (≧95%). The results of nanoSPECT/CT studies showed that almost entire radioactivity was accumulated at implanted site and no obvious radioactivity was observed in any organ and tissue. I-131-rhBMP-2 was slowly released from the implant site with an averaged half-life of approximately 16 days. On 29 days after implatation, about 43% of original radioactivity was still retained at the implanted site. Conclusion: The radioiodinated rhBMP-2 was successfully prepared with high yield and high radiochemical purity. After implantation of I-131-rhBMP-2/ACS into the orthotopic site in rat, the release/retention profile of I-131-rhBMP-2 could be monitored by using nanoSPECT/CT for more than one month. Most I-131-rhBMP-2 was accumulated at implanted site and I-131-rhBMP-2 could be slowly released from the ACS at the implant site with desirable half-life.

## P806

### Value of SPECT/CT Bone Scintigraphy in the Diagnosis and Management of Patients with Mandibular Unilateral Condylar Hyperplasia

**S. Tiskevicius**[1], M. Stalnionis[1], S. Grybauskas[2,3], M. Stacevicius[2,3]; [1]Institute of Oncology of Vilnius University, Vilnius, LITHUANIA, [2]Vilnius University Zalgirio Hospital, Vilnius, LITHUANIA, [3]Vilnius Implantology Center, Vilnius, LITHUANIA.

***Aim***: Mandibular condylar hyperplasia is an idiopathic unilateral disorder of jaw growth resulting functional problems and psychological aspects due to facial asymmetry. Unilateral condylar hyperplasia (UCH) patient management, optimal surgical timing and approach are largely dependent on the growth activity of the mandibular condyles. Therefore, an adequate assessment of disease activity is of utmost importance. We present this case series in order to demonstrate the potential clinical utility of SPECT/CT imaging in a patient with suspected UCH. *Materials and Methods*: From July 2012 to December 2012, 6 patients (all females; age range 15-36 with a mean 27) underwent 99mTc-MDP bone scintigraphy due to mandibular asymmetry and clinical signs of UCH. Planar anteroposterior and lateral images of the head followed by maxillofacial SPECT/CT were aquired in all subjects. The scans were analyzed both qualitatively (visually) and quantitatively (using 3D Volumetric analysis). The relative activity of each condylar region and right-to-left condylar ratio were calculated. The additional value of SPECT/CT in the diagnosis and managment of UCH (surgical vs. conservative) was discussed with the maxillofacial surgeon. *Results*: The qualitative visual interpretation of the bone scintigrams revealed 2 subjects with a symmetric activity in the left and right condylar region. The right-to-left condylar ratio calculated from the SPECT/CT VOIs was 1.13 and 0.96, respectively. One of the patients with symmetric condylar uptake showed increased osteoblastic activity in left ramus of mandible suggesting that the cause of progressive mandibular asymmetry was not in the condylar process. Asymmetry was observed visually in 4 patients. The right-to-left condylar ratio showed a large difference in condylar activity (0.68, 0.51, 0.82 and 2.81). The mean percentage of the affected condyle calculated from the planar images was lower comparing with the calculated from the SPECT/CT (59% ±1.6 and 68%±4.0, respectively). *Conclusion*: The SPECT/CT imaging adds extra qualitative and quantitative information to the study compared with planar or SPECT imaging alone. The fused SPECT/CT multiplanar reconstructions can be very useful for maxillofacial surgeon in clinical decision making. The quantification of the bone activity is more precise employing 3D Volumetric analysis compared with quantification from the planar images due to anatomical contours from the CT component. Our series of cases suggest that the SPECT/CT imaging modality appears to be useful in the managment of patients with UCH.

## P807

### Role of SPECT/CT in the therapeutic management of patients with unspecific pain of the wrist

**A. MURE**[1], T. Kapandji[2], T. Waitzenegger[2], F. Cavailloles[1], H. Nasser[1]; [1]HOPITAL PRIVE D' ANTONY, antony, FRANCE, [2]clinique de l'Yvette, Longjumeau, FRANCE.

**Purpose** Wrist pain remains a diagnostic challenge for the surgeon because it is often difficult to localize clinically the origin of the pain and radiologic imaging fails to detect the patient’s main pathology. Bone scan is reported to be sensitive in detecting wrist injuries because it allows the detection of metabolic pathologies

within the bone. The adjunction of SPECT/CT offers the advantage of distinguishing individual carpal bones and the small joints. **Methods** We present a study of 27 patients with persisting wrist pain. The diagnostic was made by the referring hand surgeon based on patient history , clinical examination, plain radiography and if necessary MRI and arthro-CT. In 9 the main pathology was rhizarthrosis, 7 had ligament lesions and 11, bone pathologies. Therapeutic management took into account the results of all modalities. **Results** In the rhizarthrosis group, 5 patients had tracer uptake in the TM joint confirming the surgical indication, 2 were normal, one had uptake in the radio-carpal joint changing the surgeon strategy and one patient had uptake in the trapezoide bone. In the ligament lesions, three patients had no joint uptake and the surgical indication was ruled out, one had a reflex sympathtic dystrophy instead of a local disease . In two patients, SPECT/CT confirmed the surgical indication demonstrating secondary degenerative ulnocarpal changes due to advancing instability. In the last patient SPECT/CT confirmed metacarpophalangeal inflammation. In the bone pathologies, 5 were suspected of Kienböck's disease, confirmed in 2 cases, 3 were normal. Within 4 patients with a scaphoid geode on plain radiography, two showed an uptake on SPECT/CT and were operated. The other 2 were normal. In one patient, SPECT/CT excluded an osteoid osteoma of P2's head of the middle finger, and in the last case, SPECT/CT confirmed necrosis of the head of third metacarpal. In all cases, SPECT/CT had a positive concordance with the final clinical diagnosis, and had a significant impact on therapeutic strategy, especially when the conventional imaging shows several abnormalities. **Conclusion** Thus the major additional value of SPECT/CT was in confirming the diagnosis towards the clinically more relevant lesion and in helping the surgical decision. On the contrary, in case of a negative bone scan the surgeon can rule out patients without causative lesions with confidence.

## P808

### Longitudinal Follow Up of Bone Remodeling with Quantitative Planar Scintigraphy in a Mouse Model with Osteoblast Specific PKC Knock Out and Chronic Kidney Disease

A. ZALOSZYC[1], A. SAYEH[2], I. CALM[1], U. HUEGEL[3], M. FISCHBACH[1], C. P. SCHMITT[3], **P. CHOQUET**[2,4]; [1]Hôpitaux Universitaires de Strasbourg - Nephrology Dialysis Transplantation Children's Unit, STRASBOURG, FRANCE, [2]Hôpitaux Universitaires de Strasbourg - Preclinical Imaging Lab UF6237, STRASBOURG, FRANCE, [3]University of Heidelberg - Center for Pediatric and Adolescent Medicine, HEIDELBERG, GERMANY, [4]iCube, CNRS, Strasbourg, FRANCE.

AIM: Parathyroid hormone is an important regulator of bone remodeling, which binds to osteoblasts. Among the pathways activated, the role of the $G\alpha_{q/11}$-PKC pathway remains poorly understood. Chronic Kidney Disease (CKD) induces hyperparathyroidism, which leads to bone disease. We create a model based on induced CKD in transgenic (Tg) mice, with osteoblast specific ablation of $G\alpha_q$ and global ablation of $G\alpha_{11}$. Bone planar scintigraphy was used for longitudinal follow up of bone remodeling in this model. MATERIAL AND METHODS: Tg mice were generated using a Cre Lox recombination technic. CKD was created in 13 female Tg (vs 16 sham Tg) and 6 WT (vs 7 sham WT) mice by right cortical electrocautery and left nephrectomy at the age of 10 (10W) and 12 weeks, respectively. Planar scintigraphy was performed before first operation and 12 weeks later (22W). A dedicated Anger type gamma camera was used with 2mm hole diameter's pinhole collimator (Gaede Medizinsysteme GmbH, Freiburg, Germany). 5 to 10mCi of $^{[99m}$Tc]-HMDP (CIS bio international, Gif-sur-Yvette, France), was administered to the mice under gaseous anesthesia (isoflurane 3%), through a tail vein. After tracer administration, animals were allowed to wake up before acquisition. Activity of the tracer in the syringe before and after administration were measured and time of measurement recorded. Pinhole whole-body acquisitions (15min) were performed 1.5 hours after, keeping the individual under gaseous anesthesia (isoflurane 2%) in an imaging cell. Rectangular ROIs were drawn on each knee. Counts (expressed by pixels and seconds) were corrected for activity administered, decay between administration and imaging, and individual weights. RESULTS: Mean corrected counts in the knees ROIs were as follows: At 10W, $1.57x\ 10^{-6}\pm0.55x\ 10^{-6}$ in WT and $1.84x\ 10^{-6}\pm0.42x10^{-6}$ counts.s$^{-1}$.pixel$^{-1}$.MBq$^{-1}$.g$^{-1}$ in Tg mice. At 22W, $0.35x10^{-6}\pm0.65x10^{-6}$ in WT and $1.00x10^{-6}\pm0.44x10^{-6}$ counts.s$^{-1}$.pixel$^{-1}$.MBq$^{-1}$.g$^{-1}$ in Tg sham operated mice; $1.18x10^{-6}\pm0.70x10^{-6}$ in WT CKD and $1.40x10^{-6}\pm0.65x10^{-6}$ counts.s$^{-1}$.pixel$^{-1}$.MBq$^{-1}$.g$^{-1}$ in Tg CKD mice. CONCLUSION: Tg mice show a higher bone uptake than WT at 10W and 22W. We found the same tendency in hyperparathyroid CKD mice, PKC pathway inactivation in Tg mice increases tracer uptake sign of osteoblastic increased activity.

## P809

### Muscle Perfusion Assessment with Planar Scintigraphy in a Mouse Model of Chronic Critical Limb Ischemia

A. LEJAY[1,2], J. ZOLL[3,2], F. THAVEAU[1,2], A. CONSTANTINESCO[4], B. GENY[3,2], **P. CHOQUET**[4,5]; [1]Hôpitaux Universitaires de Strasbourg - Service de Chirurgie Vasculaire et Transplantation Rénale, Strasbourg, FRANCE, [2]Equipe d'Accueil 3072, Université de Strasbourg, Fédération de Médecine Translationelle, Strasbourg, FRANCE, [3]Hôpitaux Universitaires de Strasbourg - Service de Physiologie et d'Explorations Fonctionnelles, Strasbourg, FRANCE, [4]Hôpitaux Universitaires de Strasbourg - Preclinical Imaging Lab UF6237, Strasbourg, FRANCE, [5]ICube, CNRS, Strasbourg, FRANCE.

AIM: Chronic critical limb ischemia mouse models are difficult to obtain. A new model is proposed, based on a double arterial ligature (femoral then iliac) to reproduce the onset of critical limb ischemia in human beings and avoid effect of collateral arteries. To be able to evaluate the model, we propose to use muscle perfusion scintigraphy with $^{99m}$Tc-sestamibi. The object of this work is the longitudinal follow-up of the progress of ischemia to validate the model and to compare with clinical scoring. MATERIAL AND METHODS: At D0, femoral ligature was performed on the right hind limb of 18 Swiss mice (8 to 13 weeks old). At D4, iliac ligature was performed on the same side. Left hind limb was considered as control. Planar scintigraphies were done at D0, D4, D6, D10 and D20, D30 for some individuals. A dedicated Anger type gamma camera (field of view 170mm x 170mm, 25 photomultiplicators) was used with 2mm hole diameter's pinhole collimator (Gaede Medizinsysteme Gmbh, Germany). 5 to 10mCi of $^{99m}$Tc-sestamibi (CIS bio international, France), was administered under general gaseous anesthesia (isoflurane 3%), through a tail vein. About 0.5 hours after, they are put in a large warmed (38°C) bed under general gaseous anesthesia (isoflurane 2%), in a position with their hind limbs spreaded as much as possible and secure to the bed. 256x256 pinhole whole-body images were acquired (15min, with a 10% window centered at 140keV). Rectangular ROIs were drawn on each lower limb and ratio between left and right calculated. Comparisons were done with tissue and functional clinical scores. RESULTS: A marked increase of the ratio was observed at D6 showing the larger difference between normal and ischemic limbs. Then the ratio decreased but never go back to one. The parallel behaviour was noted for clinical scores, without the decrease after peak at D6. CONCLUSION: We demonstrated that a scintigraphic semi-quantitative approach of muscle perfusion is able to monitor the evolution of a surgically induced ischemia in mice. We believe that scintigraphy should be able to measure in vivo the efficiency of proposed novel therapies in this new model of critical limb ischemia. Scintigraphy could be a non invasive way to follow clinically patients suffering from critical limb ischemia.

## P810

### Bone scan features in a case of Ollier disease.

**A. K. AYAN**, B. SEVEN, E. ORSAL, A. MAMAN; Ataturk University School of Medicine Department of Nuclear Medicine, Erzurum, TURKEY.

The authors report the case of a 17-year-old man with Ollier disease, a rare form of a nonhereditary disorder characterized by multiple enchondromas with a predilection for unilateral distribution who was presented with short stature. The whole body scan is performed for determining extent and distribution of disease. Bone scan demonstrated Tc-99m MDP uptake in shoulders and proximal humerus bilaterally. Tc-99m MDP uptake was also shown in the left knee and left ankle.

## P811

### PET/CT Finding of a Rare Skeletal System Variation; Eagle Syndrome

**Ü. Yararbas**[1], M. Argon[1], R. Savas[2]; [1]Ege University Medical Faculty Department of Nuclear Medicine, IZMIR, TURKEY, [2]Ege University Medical Faculty Department of Radiology, IZMIR, TURKEY.

Styloid process is a thin outgrowth at the base of the temporal bone and its length is normally 2.5-3.0 cm. Eagle Syndrome is described as the elongation of the styloid process and calcification of stylohyoid ligament. Main clinical symptom caused by this phenomenon is the pain along the glossopharyngeal nerve while swallowing, extending tongue or rotating head. We present a case of Eagle syndrome detected on F18-FDG PET/CT study. Twenty three years old female was referred to nuclear medicine department with the purpose of metabolic characterization of a mediastinal soft tissue mass. Patient suffered also from choreiform movements that are under evaluation. In the evaluation of head and neck structures, increased FDG accumulation was observed on bilaterally elongated styloid processes. Additionally the tongue muscles were hypermetabolic due to choreic movements. Mediastinal mass was found to have low metabolic activity on FDG PET/CT study. According to our knowledge, this is the first case with Eagle Syndrome described to have hypermetabolic appearance on FDG PET/CT study.

## P812

### Planar bone scintigraphy in bone metastases of nasopharyngeal carcinoma (257 cases)

**A. MALIKA**[1], G. CHERKAOUI[1], S. TALEB[1], A. GUENSI[1], M. MOKHLISSI[2], M. KEBBOU[1]; [1]Nuclear Medicine Department, Ibn Rochd UH, Casablanca, MOROCCO, [2]Radiotherapy and Oncology Department, Ibn Rochd UH, Casablanca, MOROCCO.

Bone scintigraphy (BS) is a sensitive exploration of bone metastases. Emphasis on BS in nasopharyngeal carcinoma (NC) depends on disease stage, but also on

availability of investigations. The aim of this work is to evaluate results of BS in patients with NC. These 257 patients, with diagnosis of NC, aged between 13 and 77 yrs (Mean of 43.6 yrs), referred for BS, between January 2011 and December 2012, to nuclear medicine department of university hospital in Casablanca (6.5% of all BS performed during the same period), 70% were male. Planar BS has been made two to three hours after injection of 13 to 19 mCi of hydroxymethylene diphosphate (HMDP) Tc99m labeled.Whole body scan was completed by static images if necessary. Indication of BS was : extension assessment, 226 cases, bone pain, 18 cases, post therapy assessment, 13 cases. Histological type was specified in 66 cases, 89% had undifferentiated carcinoma (UCNT). BS revealed bone secondary locations signs in 88 cases (34.2%) : single localization, 25 cases, multiples, 54 cases or diffuse uptake skeleton, 9 cases. Bone sites affected were mainly in axial skeleton (64.5%). One hundred twenty two patients had just uptake localized to nasopharyngeal area, without uptake abnormality elsewhere (47.5%). Remaining cases had no detected abnormality uptake (18.3%). For post treatment assessment, performed in 13 cases, BS showed decrease of uptake bone foci in 3/13 cases, one case among them had inconclusive results due to recent chemotherapy. BS is an integral part of NC assessment, both during initial assessment and follow-up. However, false negative findings are not unusual. There are other means of functional investigations, such as SPECT-CT or PET-CT, which remain less accessible in our context.

## P813

### The Role of Bone SPECT- CT and SPECT-RMN Fusion in the Diagnosis of Unusual Localisations of Osteoid Osteoma

**F. Kallel**, W. Amouri, F. Hamza, I. Jardak, S. Charfeddine, F. Guermazi; Habib Bourguiba Hospital Nuclear Medicine Department, Sfax, TUNISIA.

Bone scintigraphy has demonstrated its effectiveness for many years, thanks to its good sensitivity, its low irradiation and its non invasive character. However, it may cause be faulted because of the lack of specificity of tracer uptake. The use of additional morphological imaging is often necessary to establish the final diagnosis. The aim of our work is to present the contribution of this combination in the diagnosis of unusual localisations of osteoid osteoma. .Materials and Methods: we present 3 cases of uncommon localisations of osteoid osteoma where SPECT-CT and SPECT-RMN fusion had an important role in exploration and diagnosis. Results: In all cases SPECT-CT and SPECT-MRI fusion allowed correct initial diagnosis and discover osteoid osteoma images of the acetabulum, of the fourth lumbar vertebra and of a rib that where unsuspected by conventional imaging alone. Conclusion: the multimodality imaging has shown interest in the interpretation of bone scans allowing a significant increase in specificity comparatively to either planar mode or SPECT alone.

P64-2 - Tuesday, Oct. 22, 16:00 - 16:30, Poster Exhibition Area

## Conventional & Specialised Nuclear Medicine: SLN

## P814

### The value of isotopic detection of the sentinel lymph node in breast cancer patients.

**A. Bahloul**, A. Mhiri; I. Slim; I. Elbez ; T. Ben Ghachem; I. Yeddes; I. Meddeb; MF. Ben Slimène.; DEPARTMENT OF NUCLEAR MEDICINE, SALAH AZAIEZ INSTITUT, EL MANAR II UNIVERSITY, Tunis, TUNISIA., Tunis, TUNISIA.

Introduction: The concept of sentinel lymph node biopsy in breast cancer surgery relates to the fact that the tumor drains from the first lymph node “sentinel node” to upper levels via the lymphatic system. Sentinel lymph node (SNL) biopsy is indicated for women with small invasive breast cancers and clinically negative nodes and would represent a significant advantage as a mini-invasive procedure, considering that, after operation, about 70% of patients are found to be free from metastatic disease, making possible to avoid axillary node dissection which can lead to significant morbidity. We present our experience in this field. Methods: Our study involved 150 consecutive patients with breast cancer who underwent isotopic detection of SLN. Of these, 100 were classified T1N0M0 and 50 T2N0M0. All patients had subcutaneous injection of Tc-99m sulfur colloid (Nanocoll). Endpoints included successful SLN localization by lymphoscintigraphy, successful SLN localization at surgery, and blue dye-isotope concordance in more than half of the cases (uptake of dye and isotope by the same SLN). Results: Isotopic SLN localization was successful in 90% of cases by lymphoscintigraphy and in 88 of cases by intraoperative isotopic detection. When isotope was combined with blue dye, SLN were found in 95% of cases. Out of a total of 150 patients, having isotopic detection of SLN, we report the following results: sensitivity 83%, specificity 100%, positive predictive value 100% and negative predictive value 95%. Conclusion: In small breast cancer, the isotopic detection of the sentinel node decreases the morbidity of axillary staging and the duration of hospital stay for the patients. Furthermore, the optimal use of a peroperative hand-held gamma probe requires some training for the surgeon. A good selection of the indications is essential for a successful detection.

## P815

### Reliability on sentinel node biopsy for staging breast cancer treated with neoadjuvant chemotherapy

**R. Ruano Perez**[1], A. S. Rosero Enriquez[1], L. G. Diaz Gonzalez[1], M. Ramos Boyero[2], T. Ramos Grande[2], P. Tamayo[1], J. R. Garcia-Talavera[1]; [1]Nuclear Medicine.University Hospital of Salamanca, Salamanca, SPAIN, [2]Surgery.University Hospital of Salamanca, Salamanca, SPAIN.

**Aim:** assess the reliability on axillary staging with sentinel node (SN) in patients with breast cancer (BC) treated with neoadjuvant chemotherapy. **Method**: studied 70 consecutive patients with BC and neoadjuvant chemotherapy in 2007-2012. Neoadjuvant chemotherapy was intended to conservative treatment of breast, existing axillary involvement prior chemotherapy in 11 patients (with complete response after chemotherapy). The combined technique ($^{99m}$Tc-collodial rhenium and blue dye) was the approach for sentinel lymph node detection. Axillary lymphadenectomy (AL) was completed in all cases after identification of the SN. **Results:** The histological type was 60 invasive ductal, 5 invasive lobular and 5 multifocal lobular cancer. Of the 70 cases complete tumor response was achieved in 20 and partial in 50. Only the GC was not located in 1 patient. In 74% the SN was negative for metastases and also negative were the nodes of AL in all patients. In 13% with micrometastases only 1 patient presented a positive node in AL. In 50% of the cases with metastatic SN (which included 3 with axillary involvement at diagnosis) the SN was the only metastatic node. Mean SN analyzed by patient was 1.72 (range 1-4), and mean total lymph analyzed was 14.05 (range 5-27). **Conclusion**: The sentinel node biopsy in breast cancer treated with neoadjuvant chemotherapy is safe and accurately achieves adequate staging. The subsequent lymphadenectomy can be safely avoided after a negative sentinel node.

## P816

### Sentinel lymph node detection in patients with Squamous Cell Vulvar Cancer (SCVC)

**S. Nieves Maldonado**, S. Argibay Vazquez, M. Garrido Pumar, V. Pubul Nuñez, J. Lopez Urdaneta, M. Pombo Pasín, M. Seone Villaverde, M. Veiga Lopez, A. Ruibal Morel, A. Novo Dominguez; Hospital Clínico Universitario de Santiago de Compostela, Santiago de Compostela, SPAIN.

Aims: Sentinel lymph node (SLN) lymphoscintigraphy is a feasible technique in patients with primary vulvar cancer, and the SLN biopsy (SLNB) was established for less invasive lymph node (LN) staging than inguinal lymphadenectomy (ILND). We assessed the feasibility and accuracy of preoperative SLN mapping in patients with primary vulvar cancer, and evaluated the outcome in routine clinical setting. Materials: We analyzed the data of 22 patients diagnosed of vulvar SCVC who underwent preoperative SLN mapping in our department since 2009, including 5 patients on the validation phase and 17 patients on the therapeutic phase. After intradermal injection of 111 MBq of tc99m nanocolloid around the tumor, dynamic and static images were acquired for SLN identification. A SLNB using a hand-held gamma probe was performed, with ILND when indicated. For pathological staging, samples were evaluated using haematoxylin/eosin and immunohistochemistry. We evaluated during the follow-up (median 18 months): the drainage, the performance of SLNB, histological results, surgical complications, recurrence, and causes of death. Results: Preoperative SLN visualization by scintigraphy was successful in 21 (95.5%) patients, showed unilateral drainage in 16 (72.7 %) and bilateral drainage in 5 (22.7%) of the cases. All SLN were detected intraoperatively, before performing the vulvectomy. On the histological results of SLNB 6 (28,5%) of the 21 cases analyzed were metastatic, 3 patients resulted with macrometastases (14.2 %) and 3 patients with micrometastases (14.2%). All of the patients with positive results underwent lymphadenectomy. There was no false negative SLN result in patients who underwent ILND. Eight patients presented with post-surgical complications, 7 were related to mild wound dehiscence or infection. During the follow-up period there was no groin recurrences in initially negative SLNB patients (n:15/21). Three patients developed local recurrence on the vulvar scar area (14,2%); the first one was a positive SLNB with no LN affected on the ILND. The other two patients had negative SLNB and relapsed on the remaining vulvar skin, one of them had contralateral lymphatic metastases. On the follow-up four patients died (19.1%): 3 of oncological causes (one of cholangiocarcinoma and 2 of progression disease), and 1 of heart failure. Conclusions: According to our experience the SLN identification permits the pathological study of regional nodes, and accurately predicts LN status of vulvar SCC. SLNB is a reliable method in a clinical routine setting to identify nodal negative patients in vulvar cancer who do not profit by a complete ILND.

## P817

### Accuracy of sentinel node mapping of breast cancer using traditional intra-operative γ-probe

**M. Rodari**[1], L. Branchini[2], L. Antunovic[1], G. Pepe[1], E. Lopci[1], A. Chiti[1]; [1]Humanitas Clinical and Research Center, Milano, ITALY, [2]Humanitas Mater Domini, Castellanza, ITALY.

**Aim**: Sentinel lymph node (SLN) biopsy is standard of care for lymph node staging in breast cancer patients in order to limit axillary lymph node dissection. Axillary

node status is a major prognostic factor in early breast cancer and staging with sentinel node biopsy leads to a substantial reduction in surgical morbidity. In this study we evaluated the opportunity to localize the sentinel lymph node in patients with breast cancer, only with a traditional intra-operative γ-probe. **Material and method**: from November 2009 to February 2013 we studied 584 patients (mean age 58 years) affected by invasive carcinoma of the breast. Sub-dermal injection of 25-40 MBq of 99mTc-nanocolloid was injected over the tumor site according to the EANM procedure guidelines. Patients were not subjected to scintigraphic γ-camera control before surgery. A traditional γ-probe was used during surgery for intraoperative sentinel lymph node localization at least 3 hours after injection. **Results**: 431(78%) of 548 total patients with operable breast carcinoma and clinically negative axilla, underwent sentinel lymph node evaluation. Axillary sentinel node was detected in 432 patients (98%). Metastatic sentinel node invasion was found in 128 patients (29%), 50 of which showed neoplastic disease only in the sentinel node; in the other 78 patients two or more pathological lymph nodes were found after axillary dissection. **Conclusion**: sentinel node localization by means of γ-probe during surgery yields axillary sentinel node detection in 98% of cases. These finding are consistent with recent literature, that shows identification rate of sentinel node to be over 95%. Our results suggest that for sentinel lymph node localization a scintigraphic γ-camera control is not strictly necessary.

P65-2 - Tuesday, Oct. 22, 16:00 - 16:30, Poster Exhibition Area

## Conventional & Specialised Nuclear Medicine: Miscellaneous

### P818

### Intrahepatic Echinococcus multilocularis lesions leading to false-positive findings in a patient with adeno carcinoma of the jejunum

**T. M. Haslerud**, F. Huertos-Lopez, A. Sabet, B. Simon, H. Ahmadzadehfar, S. Ezziddin; Uniklinikum Bonn, Bonn, GERMANY.

Objectives: Human manifestations of E. multilocularis are rare, but the incidence is increasing in urban areas. Vital echinococcus multilocularis lesions are known to be FDG-avid and most commonly affect the liver. We present a case, in which FDG-avid E. multilocularis lesions in the liver could have caused a therapeutic relevant false-positive finding in a FDG-PET/CT. The patient is a 72 year old, asymptomatic woman with a malignant suspicious tumour in the jejunum. Methods: A whole body FDG-PET/CT including delayed imaging of the abdomen (2 beds) was performed prior to surgery. Additionally biopsies were taken from some of the liver lesions during surgery. Results: The whole body scan showed a large FDG-positive tumour in the jejunum (SUV max: 22,0) and numerous small discrete FDG-positive intrahepatic lesions (SUV max: 3,4; SUV max (delayed images): 3,5). Other lesions suspicious of malignancy were not present. The primary was resected and multiple biopsies of the liver lesions were performed. The pathology report described an adeno carcinoma of the upper jejunum (TNM: pT3) as well as multiple Echinococcus multilocularis manifestations in the liver. As a consequence the planned chemotherapy was cancelled and an Albendazole therapy was initiated instead. Conclusions: Due to the increase of E. multilocularis in urban areas, FDG-avidity of the lesions and frequent hepatic manifestation, E. multilocularis can be a potential pitfall of FDG-avid liver lesions, even if the patient is asymptomatic and has no previous records of E. multilocularis. This parasite infection has to be considered a potential differential diagnosis of FDG-avid liver lesions, especially in endemic areas.

P66-2 - Tuesday, Oct. 22, 16:00 - 16:30, Poster Exhibition Area

## Therapy & Clinical Trials: Radioisotope Therapy - Miscellaneous

### P819

### The SAMDOCET study: 153Sm-EDTMP and Docetaxel versus Docetaxel in Taxane-naïve patients with metastatic castration-refractory prostate cancer.

**E. Borsò**[1], S. Mazzarri[1], G. Boni[1], C. Cianci[2], D. Tosi[7], M. Sansovini[4], S. Baldari[3], J. Vuillez[8], O. Morel[9], M. Veltri[5], R. Schiavo[6], C. Orlandini[2], S. Ricci[2], G. Mariani[1]; [1]Regional Center of Nuclear Medicine, Hospital of Pisa, Pisa, ITALY, [2]Unit of Medical Oncology, Hospital of Pisa, Pisa, ITALY, [3]Nuclear Medicine Service, University Hospital, Messina, ITALY, [4]Scientific Institute of Romagna for the Study and Treatment of Cancer, Meldola, ITALY, [5]Nuclear Medicine Service, Town Hospital, Cosenza, ITALY, [6]Nuclear Medicine Service, Town Hospital, Viterbo, ITALY, [7]Unit of Medical Oncology, University Hospital, Montpellier, FRANCE, [8]Nuclear Medicine Service, University Hospital, Grenoble, FRANCE, [9]Centre Paul Papin, Angers, FRANCE.

**Aim**: The primary objective was to compare the time-to-progression (TTP) after combined therapy with 153Sm-EDTMP and Docetaxel + Prednisone (Arm 1) versus Docetaxel + Prednisone (Arm 2) in patients with histologically documented castration-refractory prostate cancer and bone metastases, scheduled for treatment with Docetaxel. The secondary objectives were to compare tumor response, overall survival (OS) and safety**. Materials and Methods**: Thirty-seven patients were randomized in a 1:1 ratio. Patients in Arm 1 (age 69±8 yr, mean PSA 131.5 ng/mL) received Docetaxel 75 mg/sqm i.v. on day 1 every 21 days for a maximum of 9 cycles, and 153Sm-EDTMP 37 MBq/kg i.v. 6 to 15 hours before Docetaxel at cycles 1, 5 and 9. Patients in Arm 2 (age 66±19 yr, mean PSA 53.3 ng/mL) received Docetaxel 75 mg/sqm i.v. on day 1 every 21 days for a maximum of 9 cycles. Prednisone 10 mg/day orally was given continuously as a concomitant medication for both arms. Patients have been evaluated at every cycle with complete blood chemistry including serum PSA, and at screening and during follow-up with serum PSA, bone scan and CT until disease progression. The last-patient last-visit of the study took place in March 2013, while extended follow-up for OS is still ongoing. **Results:** Three patients had ≤2 chemotherapy cycles and were therefore not evaluable for response. Out of the 29 patients with evaluable data at the current follow-up time-point, 12 had 3 to 8 cycles, while 17 completed the planned administration schedule for a total of 102 cycles in Arm 1 and 115 cycles in Arm 2. Although patients in Arm 1 (combination regimen) had starting serum PSA almost 2.5-fold patients in Arm 2, median TTP was identical in the two arms (5.6 months). Mean PSA response was -29% in Arm 1 and -38% in Arm 2. Although OS data are still being collected, preliminary data show OS of 30.1 months in Arm 1 (versus 21-22 months reported for Docetaxel alone). Haematological toxicities in Arm 1 were less frequent than in Arm 2: neutropenia G4 in 14/102 cycles (13.7%) versus 26/115 cycles (22.6%, p = n.s.), respectively; no thrombocytopenia G3/G4 were recorded in either arm. **Conclusions:** Although these preliminary data do not allow to draw definite conclusions regarding advantages of the combined treatment versus standard Docetaxel in terms of TTP and tumor response, they do show that the experimental combined therapy is as safe as standard Docetaxel chemotherapy.

### P820

### Tc-99m mebrophenin hepatobiliary scintigraphy for assessment of lobar functional liver status by liver mebrophenin clearance rate in patients who will undergo Y-90-microsphere treatment

**L. Kabasakal**[1], S. Yılmaz[1], H. Tanyildizi[2], M. Ocak[3], R. Ozcan[4], A. Aygun[1], G. Atun[4], A. Araman[3], B. Kanmaz[1]; [1]University of Istanbul, Cerrahpasa Medical Faculty, Istanbul, TURKEY, [2]University of Istanbul, Faculty of Sciences, Department of Nuclear Physics, Istanbul, TURKEY, [3]University of Istanbul, Faculty of Pharmacy, Department of Pharmaceutical Technology, Istanbul, TURKEY, [4]University of Istanbul, Faculty of Engineering, Department of physical chemistry, Istanbul, TURKEY.

Objectives : Ytrium-90 microsphere (Y90) therapy data depicted that local efficacy correlated to tumor absorbed dose and the mean absorbed dose is associated with toxicity. Accurate measurement of liver function before Y-90 therapy is crucial especially in patients with underlying paranchymal disease. Nuclear imaging techniques have the advantage of measuring both lobar and total liver function. In this study, we aimed to examine the measurement of hepatic function by Tc-99m mebrophenin hepatobiliary scintighraphy and compare these results with blood biochemical parameters.Methods : 32 patients who were planned to give Y90 therapy were included to the study. After i.v injection of Tc-99m mebrofenin, dynamic hepatobiliary scintigraphy was performed and mebrophenin clerance rate is calculated (HER). Radioactivity counts acquired between 150 and 350 seconds postinjection were used for calculation. SPSS 15 was used for statistical anaysis.Results : We found a negative correlation between the right lobe HER and AST (p=0,008), DBil (p=0,002), TBil (p=0,01) and INR (p=0,04) and positive correlation between the right lobe HER and albumin (p=0,03). A high negative correlation was seen between the global HER and AST (p=0,03), DB (p=0,002), TB (p=0,001), INR(p=0,003) and also positive correlation between the global HER and albumin (p=0,01). There is no correlation between the left lobe HER and any biochemical parameters (p>0,05).Conclusions : The HER allows us assessment of both global and lobar liver function which can not be done by one single test. It seems to be a valuable liver function test especially in Y-90 microsphere therapy planning.

### P821

### Evaluation of the impact of $^{90}$Y selective internal radiation therapy in patients with non-resectable liver tumors

**Á. O. Rabines Juárez**, P. Serra Arbeloa, A. Martínez de la Cuesta, E. Goñi Gironés, F. Mañeru Cámara, I. Elizalde Apestegui, A. Viudez Berral, F. Lozada Delgado, M. Martínez Lozano; Complejo Hospitalario de Navarra, Pamplona, SPAIN.

Aim: To analize the influence of $^{90}$Y selective internal radiation therapy (SIRT) in overall survival of patients with non-resectable liver tumors. Methods: Observational, prospective and non-randomized study in a cohort of 18 patients with non-resectable liver tumors treated with $^{90}$Y SIRT between August 2011 and

October 2012 and followed-up until March 2013. Basal characteristics of cohort were evaluated by descriptive statistics. All the patients have undergone $^{99m}$Tc-MAA scintigraphy within 2 weeks before the treatment.Uptake patterns were considered as total congruent, partial congruent and non-congruent according to CT findings. Initial therapeutic response was evaluated by RECIST criteria. Overall survival was evaluated by Kaplan-Meier curves and stratified by initial radiological response and $^{99m}$Tc-MAA uptake patterns. The association between initial radiological response and $^{99m}$Tc-MAA uptake patterns was studied. Results: All the patients that received SIRT treatment were included (18), 94.4% men, mean age 68.50±10.73 years, (range: 46-79), mean body surface area 1.76±0.17 m² (range 1.45-2.14). 61.1% of patients were diagnosed with a hepatocellular cancer and 38.9% with liver metastases. The tumoral involvement was 12.63±19.4% (range 0.2-70). The mean treatment dose was estimated as 1.41 ±0.43 GBq (range: 0.9-2). Median overall survival was 8 months (95% CI: 4.49-11.51) and accumulated survival 50% at the end of the observational period. Hazard ratio (HR) calculated was 3.095 (95%IC: 0.767-2.478) stratified by initial radiological response. No differences between $^{99m}$Tc-MAA uptake patterns and overall survival (p=0.548) or initial radiological response (p=0.144) were found. Conclusions: Patients with initial radiological response have an overall survival rate three times higher than non-responders. It could be considered as a prognostic factor. $^{99m}$Tc-MAA uptake pattern is not an associated factor of initial radiological response and overall survival in patients treated with $^{90}$Y-SIRT, so its utility could be restricted to evaluate the presence of extrahepatic shunt.

## P822

### Therapeuric Choices of Rheumatoid Arthritis in 2013. Role of Radiosynoviorthesis in the Treatment Protocol Film /Dvd / 12 min.

**M. Szentesi**, P. Géher, Á. Balog; Semmelweis Univ., Chair of Rheumatology and Physiotherapy, Polyclinic of the Hospitaller Brothers of St. John of God.,, Budapest, HUNGARY.

This film is about the treatment possibilities of rheumatoid arthritis /RA/. It describes the role of DMARD medications, physiotherapy and biological therapy in the therapeutic protocol. It shows the way how radiosynoviorthesis/RSO/ is carried out and tells its indications in the era of biological therapies. In the film, patients tell their experiences in connection with the different ways of treatement. When we manage to diminish the activity of the disease significantly with DMARD or biological therapy, we recommend the use of RSO to treat one or two joints with active synovitis since the other alternatives such as open surgical and arthroscopic synovectomies can only be carried out when biological therapy is suspended .

## P823

### A prospective observational study on long-term results of 90Yttrium radiosynoviorthesis of chronic knee synovitis in rheumatoid arthritis and osteoarthritis patients.

**M. Szentesi**[1], Z. Nagy[2], P. Géher[1], I. Papp[1]; [1]Semmelweis Univ. Chair of Rheumatology and Physiotherapy, Dept. of Rheumatology, Polyclinic of the Hospitaller Brothers of St. John of God,, Budapest, HUNGARY, [2]Semmelweis Univ. Chai Polyclinic of the Hospitaller Brothers of St. John of God,, Budapest, HUNGARY.

Patients:Long-term follow-up after radiosynovectomy was offered for a prospective observational study to 486 patients, 40 to 86 years of age, suffering either from rheumatoid arthritis or osteoarthritis of the knee joint, starting 5 years after intra-articular administration of 90yttrium citrate. 312 of 345 patients with rheumatoid arthritis were seropositive, 33 seronegative. Mean age of 108 male and 237 female patients was 61.6 years (range 40-84) years. In 180 patients the right knee, in 165 the left knee was treated by radiosynovectomy. Steinbrocker functional stadium II was observed in 165, stadium III in 165 and stadium IV in 15 of them. By radiography grades I (n= 9 ), II (n=201), III (n= 135), and IV (n=15) were observed. Grading was done according to Steinbrocker anatomic score. Mean duration of disease was 7.3 years (range 0.5-25), of synovitis (6.4 years (range 0.5-24) Mean number of punctions of the treated joint prior to radiosynovectomy was 12.3 per patient and of steroid administrations prior to radiosynovectomy 10.2. In 195 patients a systemic steroid therapy has been performed. 141 patients suffered from osteoarthritis (m: 46; female:96). Mean age was 61.5 years (range 40-86). The right knee was treated by radiosynovectomy in 71, the left in 70 patients. Mean duration of disease was 12.3 years (range 5-20), of synovitis 8.2 years (range 5-20). The mean number of punctions prior to radiosynovectomy was 8.7/patient and of intra-articular steroid administration 9.3. Following the Kellgren-Lawrence score in 9 patients grade I, 60 garde II, and 72 grade III was diagnosed. During the follow up period up to 10 years the individual response after radiosynovectomy was evaluated by an objective and subjective point system. Results: In the first ten years excellent and good results were recorded in 71%. They achieved excellent as well as good results at 83% of patients with rheumatoid arthritis, and at 55% of patients with osteoarthritis. Ten years after radiosynoviorthesis 72% of patients did not need another punction. Conclusions: Radiosynoviorthesis is as effectiv method of treating chronic synovitis as surgical synovectomy. Even after a ten-years period 71% the findings were rated as excellent or good. 72% of the patients do not need another punction even after a ten years period. The effectiveness is worsened significantly by the stadium of the disorder and the local x ray phase and diagnosis. P 0.00001.

## P824

### Knees Synovectomy in Rheumatoid Arthritis with 153-Samarium Hydroxypatite

**J. U. M. Calegaro**[1], F. A. C. Lima[2], D. P. Hage[1], D. C. Landa[1], J. Mengatti[3], A. P. Paula[1]; [1]Hospital de Base do Distrito Federal, Brasília, BRAZIL, [2]Hospital Universitário de Brasília, Brasília, BRAZIL, [3]Radiopharmacy Center - IPEN/CNEN, São Paulo, BRAZIL.

Background- 90Y is the most appropriated material in knee synovectomy in rheumatoid arthritis due to the higher penetration of its beta energy. However, the use of higher activities of 153Sm-hydroxyapatite (153Sm-HA) may show therapeutic equivalence (1). Aim- To show the initial experience in knee synovetomy in patients with rheumatoid arthritis using only 153Sm-HA. Material and Methods- The treatment was made with an intraarticular injection of a fixed dose of 20mCi (740Mbq) of 153Sm-HA in 14 knees of 9 patients (3 males, 6 females), average age=54,5years (range from 30 to 80 years old) and affected by arthropathy with an evolution of 15,8 years (range from 2 to 35 years). This protocol used particle size between 2-10µm, described elsewhere (1). No corticosteroid was co-injected and immobilization was not specifically recommended. Early (1-2h) and late (7 days) scintigraphic studies were performed after the procedure. The patients were evaluated 16,1 months after the synovectomy using the following criteria: reduction in the number of effusions and reduction in pain, evaluated by a visual analogic scale. The occurrence of adverse effects was considered as mild, moderate or accentuated. The statistical analysis used p<0, 05. Results- There was a significant reduction in the frequency of effusions (in 72,7% of the knees) and in occurrence of pain (in 46,2% of the knees). Five cases of reactive synovitis were observed, being four being of moderate and one of mild intensity. The scintigraphic controls showed adequate intra-articular distribution of the radioactive material, without detection of scape from the joint until up to 7 days. Conclusion- Knees synovetomy in patients with rheumatoid arthritis using 153Sm-HA showed good results in this initial study. This therapeutic agent may probably also be employed in others inflammatory synovitis of this joint.

## P825

### Patch radiation therapy : Breakthrough in keloid management

**P. Gupta**[1], A. Malhotra[1], K. K. Verma[1], S. P. Lochab[2], S. Gupta[1], P. Kumar[1], S. Singla[1], G. P. Bandopadhyaya[1]; [1]All India Institute Of Medical Sciences, New Delhi, INDIA, [2]IUAC, New Delhi, INDIA.

Aim: The present study was aimed to analyze the efficacy and toxicity profile of patch radiation therapy (PRT) using Phosphorus-32 (P-32) and Rhenium-188 (Re-188) in keloids. Materials and Methods: 16 patients (M/F=6/10) with 42 keloid lesions were recruited for prospective study using PRT. The study was approved by the ethical committee of the institute and written informed consent was obtained from all patients. Baseline hemogram, liver function tests (LFT) and kidney function tests (KFT) were obtained. Shape of the lesions were traced and surface area calculated. Patches conforming to the shape and size of the individual lesions were applied superficially so as to deliver 50 Gy/sq. cm of surface radiation dose. Results: The mean age of the patients was 33 ± 12 (range: 19-59) years. The patients were randomly chosen for treatment with P-32 and Re-188. The patients were matched for age, sex, number and extent of lesions in both the groups (p>0.05). Ten, nine and eight lesions demonstrated a reduction in lesion size of 50-80%, 80-99% and complete disappearance, respectively. There was a greater than 50% decrease in lesion size in 27 (64%) lesions. Ten (77%) lesions in P-32 group demonstrated decrease in lesion size of more than 50% as compared to 17 (59%) lesions in Re-188 group, the difference not being statistically significant (p = 0.664). The median follow up of the patients after patch application was 6 months (range: 4 - 12 months). Maximum reduction of lesion size was noted after a median duration of 8 weeks (range 4-10 weeks) after patch application. Spectrum of radiation dermatitis ranging from pain, itching, erythema, crusting, desquamation and re-epithelialization was observed in patients. Serious radiation dermatitis requiring antibiotic treatment was noted in 6 (38%) patients while mild to moderate skin changes in 10 (62%) patients. None required hospitalization. Median duration of onset of radiation dermatitis was 2 weeks for both P-32 and Re-188 (p=0.723) and disappearance in 8 weeks in both the groups (p=0.509). Serious toxicity was noted in 43% patients with P-32 patches compared to 50% patients with Re-188 patches, the difference not being significant. There were no changes observed in the hemogram, KFT, LFT during the entire duration of treatment and follow up. Conclusion: Patch radiation therapy is an effective and safe therapeutic option for treatment of keloids. P-32 patch demonstrated similar efficacy and toxicity profile as Re-188 patch for PRT.

## P826

### Copper PET/CT vs Fluoromethylcholine in prostate cancer: staging and diapeutic action

**C. Villano**[1], G. Pigotti[2], V. De Francesco[3], A. D. Di Nicola[3], G. Camplone[3], D. Martini[2], E. Baldassarrini[2], P. Panichelli[2], G. Valentini[2]; [1]U.O.C. Medicina Nucleare Ospedale Civile "Spirito Santo", Pescara, ITALY, [2]ACOM SPA, MONTECOSARO, ITALY, [3]U.O.C. Medicina Nucleare Ospedale Civile, Pescara, ITALY.

Prostate cancer is the most common noncutaneous cancer in men with several new cases diagnosed every year in all the world. Our aim is to demostrate and to evaluate the potential of 64Cu PET/CT in the detection of recurrent disease or distant metastases in prostate cancer patients in a better way than the other common tracer 18F-FCH. 64Cu can link cell DNA and it is characterized by long half-life (12.7 h) and decays by electron capture (43.6%), β+ (17.4%) and β- (39%) decay accompanied by Auger electron emission with its therapeutic effect thanks to high linear energy transfer (LET) that is able to destroy tumor cells, as reported in literature references. Prior patient's consent, 18F-FCH and 64Cu PET/CT has been evaluated in men with metastatic prostate cancer 60-90 minutes after e.v. injection, according to whole-body acquisition protocol (2.5 min/bed), including cranial region, with 168x168 matrix (Biograph 6 Truepoint PET/CT, Siemens). Axial, coronal and sagittal 64Cu images showed increased uptake in the same lesions of 18F-FCH ones, but they can highlight more pathological areas that aren't detected by FCH scans. In fact, FCH metabolite excretion into the urinary system, unlike the hepatobiliary copper excretion, enable us to correctly detect occult disease in prostate region due to bladder filling. Furthermore, 64Cu has a better spatial resolution to reveal primary lesions and/or local recurrent disease in prostate cancer. In all cases, no uptake was detected in hepatic parenchymal lesions. Following up patients over months after PET/CT exam, we reported improved sense of well-being with recorded significant reduction of PSA levels (87%) and hepatic values as gamma GT levels (53%), blood bilirubin (74%) and alkaline phosphatase (62%). The obtained results are very promising to introduce 64Cu tracer in staging and restaging prostate cancer as a diapeutic agent with both diagnostic and therapeutic action. It would replace 18F-FCH PET/CT with 64Cu PET/CT to have a more powerful tool due to its better PET imaging properties. However, we need to examine in depth copper human biodistribution to assess the optimal activity which can be administered in accordance with regulatory limitations and radiotoxicity.

## P827

### Radioembolization using Y-90 resin microspheres for patients with advanced hepatocellular carcinoma

**W. Choi**[1], E. Choi[2], E. Han[3], S. Lee[4], Y. Park[1], I. Yoo[2], W. Lee[5]; [1]St. Vincent's Hospital, The Cathoic University Of Korea, Suwon, KOREA, REPUBLIC OF, [2]Seoul St. Mary's Hospital, The Cathoic University Of Korea, Seoul, KOREA, REPUBLIC OF, [3]Daejeon St. Mary's Hospital, The Cathoic University Of Korea, Daejeon, KOREA, REPUBLIC OF, [4]Uijeongbu St. Mary's Hospital, The Cathoic University Of Korea, Uijeongbu, KOREA, REPUBLIC OF, [5]SoonChunHyang University Hospital, Bucheon, KOREA, REPUBLIC OF.

PURPOSE: To investigate the antitumor effect of resin microspheres loaded with Y-90 against hepatocellular carcinoma (HCC) and their safety. PATIENTS AND METHODS: Data from 22 consecutive patients with HCC treated by radioembolization in the period from July 2009 to May 2012 were reviewed. Response was assessed with modified Response Evaluation Criteria in Solid Tumors (mRECIST) at 3 months after radioemblization. RESULTS: Complete response in 4 (18%), partial response in 7 (32%), stable disease in 6 (27%), and progressive disease was observed in 5 (23%) of the 22 patients. Gastrointestinal toxicity (nausea, vomiting, abdominal pain etc) was seen in 11 patients. Acute Renal failure was observed in 1 patient. 1 patient showed a transient increase in total bilirubin level. Liver parenchymal injury on the FU MR images was noted in 2 patients. CONCLUSION: In this single-center study, radioembolization using resin microspheres has a significant antitumor effect against HCC.

## P828

### Long-Term Effects of Correction of Anemia with Recombinant Human Erythropoietin (rEPO) on Blood Volume in Chronic Hemodialysis Patients

**N. Topuzović**, I. Mihaljević, V. Rupčić; University Hospital Centre Osijek, Osijek, CROATIA.

AIM: To investigate blood volume changes in chronic hemodialysis patients before and after long-term treatment for their anemia with rEPO. PATIENTS AND METHODS: This study included forty patients undergoing regular hemodialysis (mean age 38 ± 11 years, mean duration of dialysis 5.3 ± 3 years) with severe renal anemia (hematocrit < 0.25). There was no iron deficiency; serum folic acid and vitamin B12 were in normal range. All patients were treated with rEPO intravenously three times in week in adjustable doses. Blood volume were evaluated at three occasions: a) basal - before EPO therapy, b) intermediate - after reaching target hemoglobin (Hb) of 100g/L, and c) late - after 12 ± 2 months of therapy with rEPO. Blood volume was measured with Tc-99m-labeled human serum albumin using dilution technique adjusted and validated in our department. RESULTS: At the beginning mean Hb was 72 ± 8 g/L, increased to 111 ± 12 g/L at intermediate studies during 3.8 ± 1.6 months, and was maintained thereafter. The mean hematocrit value was 24.4 ± 0.9% at the basal studies, rose to 29.7 ± 1.1% intermediate ($p < 0.01$), and was further increase to 36.7 ± 1.5%, $p < 0.01$, at late studies. After correction of anemia, red-cell volume was significantly increased from 12 ± 3 to 16 ± 3 mL/kg in intermediate studies, $p < 0.0001$. However, no further significant change between intermediate and late studies (14 ± 4 mL/kg) was found. Consequently, plasma volume was significantly decreased from basal 48 ± 9 to 42 ± 9 mL/kg at intermediate examinations, $p < 0.2$, and was further decreased to 38 ± 7 mL/kg in late studies, $p < 0.001$. In contrast, total blood volume remained unchanged at intermediate studies (58 ± 11 vs. 57 ± 10 mL/kg, p = NS), whereas blood volume was significantly reduced to 52 ± 8 mL/kg, $p < 0.001$, in late investigation. CONCLUSIONS: Significant increase in red-cell volume occurred shortly after correction of anemia with EPO in patients on chronic hemodialysis, followed by decrease in plasma volume. However, total blood volume only decrease after a long-term treatment of anemia in chronic hemodialysis patients.

## P829

### Muscular and cerebral glucose metabolic changes by chiropractic spinal manipulation in neck pain patients

**A. INAMI**[1], T. OGURA[1,2], S. WATANUKI[1], M. MASUD[1], K. SHIBUYA[3], M. MIYAKE[1], K. HIRAOKA[1], M. ITOH[3,1], K. YAMAGUCHI[1,4], K. YANAI[1,5], M. TASHIRO[1]; [1]Tohoku University Cyclotron and Radioisotope Center, Sendai, JAPAN, [2]Japan Chiropractic Doctor College, Sendai, JAPAN, [3]Sendai Medical imaging Clinic, Sendai, JAPAN, [4]Sendai Kousei Hospital, Sendai, JAPAN, [5]Tohoku University Graduate School of Medicine, Dept. of Pharmacology, Sendai, JAPAN.

Neck pain is often accompanied by muscle stiffness ranging from the neck to shoulder region, and its pathophysiological mechanism has not been elucidated yet. It is also still unknown how a certain manual therapy such as chiropractic spinal manipulation (CSM) is sometimes very effective in neck pain patients. To date, few studies have been conducted to examine the effects of CSM on the skeletal and cerebral metabolism using positron emission tomography (PET). Therefore, the aim of the present study was to investigate the muscular and cerebral metabolic responses to the CSM intervention using PET with [$^{18}$F]fluorodeoxyglucose (FDG PET). Twelve male volunteers were recruited for the present study, based on the approval from the ethics committee of Tohoku University Graduate School of Medicine. FDG PET scanning was performed twice on each subject; at rest (control condition) and after CSM intervention (treatment condition). Measuring the glucose metabolism of the skeletal muscles and brain, we compared standardized uptake values (SUVs) between the 2 conditions. The regional brain metabolic changes between the 2 conditions were examined using statistical parametric mapping (SPM) software package. In addition, we measured the muscle tone of the trapezius before and after CSM. As a subjective measure, intensity of pain was rated by each subject before and after CSM using a visual analogue scale. Finally, specific brain regions associated with the skeletal muscle tones or muscular glucose metabolism were explored using correlation analysis. In results, the left splenius muscle showed reduction of SUV in the treatment than in the control condition. In addition, the brain regions correlated to skeletal muscle tones were the prefrontal cortex, anterior cingulate gyrus, and caudate nucleus. The brain regions associated with skeletal muscle glucose metabolism were the prefrontal cortex, cingulate gyrus, motor associated area and insular cortex. There was no significant correlation among subjective pain score, muscle tone and skeletal muscle glucose metabolism, respectively. There was no significant correlation between the muscle tone changes and skeletal muscle glucose metabolic changes, neither. The results indicated that the muscle activity was functionally connected with the regional brain activity though the subjective pain sensation did not show significant correlation to muscle activities. It was speculated that the brain regions, especially the limbic and paralimbic structures, seemed to be playing a certain role in symptom relief by the CSM intervention even when the physical intervention is given to the local musculoskeletal tissue.

## P830

### A nuclear medicine approach to treat metastatic or locally advanced evolutive radio-iodine "resistant" differentiated thyroid carcinomas (DTC) using 13-cis-retinoic acid; report of 7 cases.

**P. Bourgeois**, B. Ahmed, B. Vanderlinden; Institute Jules Bordet, Brussels, BELGIUM.

Introduction : Few therapeutic options can be now practically proposed to patients with metastatic or locally advanced evolutive DTC who are said resistant after 131-I treatments. Redifferenciation approaches using retinoic acids (RA) have however been proposed since 1990 to treat them. We report here our results in such 7

patients treated "simply" using 13-cis-RA. Methods: The protocol (approved by our institutional ethical committee) is as follows: 1° the "metabolic" status and the iodine metabolism of their lesions were evaluated using 18F-DG and 124-I PET-CT under rh-TSH stimulation, 2° they were thereafter treated (RAT) using 13-cis-RA (Ro-Accutane ®: 1 mg/kg) during 2 months and Tg controlled every 2 weeks, 3° after and under RAT, their metabolic responses were evaluated as in 1°, 4° if metabolic changes were observed, patients were treated by 131-I (740 GBq) and thereafter maintained under RAT, 5° they were followed biologically (Tg: every two weeks) and metabolically (18F-DG PET-CT: one and three months). Results: - 4 patients showed increased iodine uptake thus improving the radio-biological effects of administered 131-I activities with transient biological and/or metabolic responses, - 1 patient showed before any 131-I administration a biological and RECIST response allowing a surgical approach of her lesion, - at least 1 patient showed a complete response at the level of some of his lesions. Conclusions: Despite the limited number of cases here reported but also on the basis of the past and recent literature supporting our results, the therapeutic approach here proposed (the administration of one unexpensive and commercially available drug) represents a valuable and rationale option for patients with metastatic or locally advanced evolutive DTC who are said resistant after radio-iodine treatments.

## P831

### Prognostic predictors of treatment outcome of hyperthyroid patients receiving Radioactive Iodine (RAI) therapy.

**A. Ab. Aziz**, S. Zainudin; Universiti Kebangsaan Malaysia Medical Centre (UKMMC), KUALA LUMPUR, MALAYSIA.

**Aims:** To determine prognostic predictors of radioactive iodine (RAI) treatment outcome of hyperthyroid patients with respect to the underlying cause, patients' age-group, timing to treatment and dosage of radio-iodine received. **Materials and Methods:** Retrospective analysis of 720 patients' records who received RAI treatment (dose 10-15 mCi) for hyperthyroidism in Nuclear Medicine Department, Universiti Kebangsaan Malaysia Medical Centre (UKMMC), between 1999-2009. Patients between 8 to 65 years old and those with available follow up free thyroxine 4 (fT4), and thyroid stimulating hormone (TSH) levels at 6, 9 and 12 months post RAI treatment were included. 275 patients (248 females and 27 males) had adequate data for analysis. Underlying Graves' disease (GD) were in the overwhelming majority (90.2%) and 9.8% were toxic nodular goitre (TNG). Eighty,128 and 67 patients were between 18-35, 36-50 and 51-65 year-old age-groups respectively. Only 57 (20.7%) received RAI treatment within 18-month of initial diagnosis. Two hundred patients received 10mCi of RAI whilst 68 and 7 patients received 15mCi and 12mCi of RAI respectively. Free T4 and TSH levels at diagnosis, 6, 9 months and one year post RAI treatment were recorded to determine outcome status. **Results:** The relationship between underlying cause and resolution of hyperthyroidism was not significant (p=0.516). However, there was significant relationship (p<0.01) between the underlying cause and the thyroid status in those 157 patients with resolved hyperthyroidism after the RAI therapy. After RAI therapy, patients with GD were more likely to develop hypothyroidism as compared to TNG patients (55% vs 11.8%); and patients with TNG were more likely to obtain euthyroid status as compared to patients with GD (88.2% vs 45%). Resolution of hyperthyroidism vary significantly among the age groups (p=0.035) and highest (47.8%) in patients between 36-50. The treatment outcome was not statistically significant (p=0.256) between the 3 different doses of RAI received. Resolution of hyperthyroidism after 6 months of RAI was achieved in 70.8% of patients who received early-treatment, and only 54.2% of patients who received late-treatment (p = 0.034). **Conclusion:** Those in 36-50 year age-group and received early-RAI therapy tend to have favourable outcome.The underlying cause of hyperthyroidism and RAI dosage received, do not lend significant prognostic difference. Nevertheless, patients with GD are more likely to develop hypothyroidism than TNG post RAI therapy, hence long term follow up is recommended in GD patients.

## P832

### Evaluation of high-dose radioiodine therapy in differentiated and poorly differentiated metastatic thyroid cancer

**M. Enzian**, A. H. Hering, A. Odparlik, M. Bähre, B. Meller; Martin-Luther-University Halle-Wittenberg, Halle, GERMANY.

*Aim:* It is well known, that patients with metastatic differentiated (papillary PTC, follicular FTC) or with metastatic poorly differentiated thyroid cancer (PDTC) have a poor prognosis. Since radioiodine therapy (RIT) remains the most effective treatment modality in these patients, we determined the effects of single high $^{131}$I activities applied in curative intention. For this purpose, thyroglobulin (TG) levels were monitored and side effects were recorded. *Materials and Methods:* Treatment of 23 patients (9 with FTC, 8 with PTC, 6 with PDTC) was monitored 20 to 180 weeks (m=82 weeks). Bone metastases were detected in 8 cases, pulmonary metastases in 11, lymphogenic metastases in 10 cases. 6 patients suffered from a combination of metastatic disease. Each patient received an initial RIT (4.0 - 25.4 GBq, m=15.4 GBq), 9 of them a second RIT (4.2 - 28.2 GBq, m=18.1 GBq) after 16 - 77 weeks. TG, TG antibody and TSH levels were measured and only data collected under TSH suppression were considered. Prior to the first RIT initial TG level amounted from 1.6 to 14,251 ng/ml (m=1,048 ng/ml). *Results:* After the first RIT, TG was ≤0.5 ng/ml in 10 out of 23 the patients, 6/10 patients suffered from lymphogenic, 4/10 from bone and/or pulmonary metastases. 9 showed a partial remission with significant decrease of the TG level ranging from 25 to 98 %. After the second RIT only in 4 out of 10 patients decreasing TG levels could be detected (30 - 90 %). One of these 4 patients suffered from lymphogenic, 3 from bone and/or pulmonary metastases. Patient prognosis depended on the initial TG level and the $^{131}$I avidity of the metastases. In 9 patients, side effects like a temporary dysfunction of taste or xerostomia were recorded. Only 1 case with severe bone marrow depression as a grade 3/4 side effect could be observed, but was successfully treated with granulocyte colony stimulating factor. *Conclusions:* Even in metastatic disease first RIT's with high activities are very effective, providing a response rate of 19/23, compared to usual results in oncology. In contrast, second RIT's are less effective. 4/8 patients with bone metastases achieved a TG level ≤0.5 ng/ml after the first RIT (20.1 - 25.4 GBq, m=22.4 GBq). The number of harmful secondary effects of high-dose RITs was very low. Therefore, primary therapy in patients with known metastatic disease should be performed with high activities, because subsequent RIT's are less effective.

P67-2 - Tuesday, Oct. 22, 16:00 - 16:30, Poster Exhibition Area

## Therapy & Clinical Trials: Therapy Response Assessment

## P833

### Evaluation of efficacy of $^{90}$Y Microspheres therapy (TARE) for metastatic liver cancers using $^{18}$F FDG PET-CT.

**A. C. Gandhi**, R. Kabnurkar, A. Zade, S. Shah, A. Agarwal, N. Purandare, S. Kulkarni, N. Shetty, V.Rangarajan.; Tata Memorial Centre, Mumbai, INDIA.

Introduction: $^{90}$Y Microspheres is considered as one of the treatment for primary and secondary liver malignancies along with chemoembolization and radio-frequency ablation. $^{18}$F FDG PET-CT scan is an established investigation for treatment response assessment in cancers. In view of this, $^{18}$F FDG PET-CT scan similarly be used to assess therapeutic response to radioembolization. Aim: To assess therapeutic treatment response to radioembolization for liver metastases, using pre transarterial radioembolization (TARE) and post TARE $^{18}$F FDG PET-CT studies. Material & Methods: 11 patients with metastatic liver cancer were studied: 9 patients of colorectal carcinoma and two patients of neuroendocrine tumors. Total numbers of sessions for $^{90}$Y Microspheres transarterial radioembolization were 16; fourteen for colorectal liver metastases and two for metastatic neuroendocrine tumors. $^{90}$Y Microspheres were delivered with all the aseptic precautions and considering all the radiation safety procedure from intra-arterial route. All the patients underwent contrast enhanced $^{18}$F FDG PET-CT scan 1 week prior to the therapy. $^{18}$F FDG PET-CT scan was also performed after 2 months of the TARE to evaluate the response to therapy. Lesion to lesion assessment for maximum SUV values was done on pre and post TARE FDG PET images. Reduction in SUV max values by 50 % or more was considered as response to treatment. Also, clinical and biochemical parameters (liver function tests) were assessed. Results & discussion: Based on the above criteria, all the treated liver lesions showed response to TARE, except for one lesion on FDG PET-CT images. All the lesions from colorectal carcinoma showed response (100%). Only one of two patients with metastatic neuroendocrine tumor showed response. All these patients are under regular clinical & imaging follow up. Conclusion: Based on this preliminary data, it can be concluded that $^{90}$Y Microspheres transarterial radioembolization (TARE) is an effective method for treatment of metastatic liver cancer.

## P834

### Early complications in patients treated with selective intra-arterial radioembolization with 90Y-glass microspheres. Our experience

**M. Falgás Lacueva**, P. Bello Arques, A. Repetto, J. Martí Vidal, C. Igua Saenz, P. Borrelli, J. Loaiza Góngora, C. Ruiz Llorca, J. Vercher Conejero, D. Pérez Enguix; HUP La Fe, Valencia, SPAIN.

AIM: To evaluate the development of early complications in patients with hepatocellular carcinoma or liver metastases, treated with selective intra-arterial

radioembolization with 90Y-glass microspheres. MATERIAL AND METHODS: We performed 23 treatments to 21 patients (9 women/12 men), between April 2009 and January 2013, with an average age of 56 (28-82). The indication was hepatocellular carcinoma in 16 patients and liver metastases in 7 patients (5 Neuroendocrine tumors, 1 colorectal carcinoma and 1 Medullary thyroid carcinoma). Mean follow-up was 14 months (1-38). Each lobe was treated separately, except one segmental treatment. Pre-therapy planar imaging and SPECT (or SPECT/CT) with intra-arterial 99mTc-labelled albumin macroaggregate were obtained. After 90Y-glass microspheres infusion, Bremsstrahlung images were obtained to predict side effects to extrahepatic flight of the radiopharmaceutical. RESULTS: 7 (30%) patients died during follow-up, with a mean of 14 (1-35) months after radioembolization. The pre-treatment average of liverlung shunting was 5.15% (0.7-34.5%) and 2.43% of gastrointestinal reflux (0 - 45%). No case suggestive of extrahepatic leak was found with Bremsstrahlung images. 7 (30%) patients presented complications secondary to treatment: 3 liver complications (2 severe hepatic insufficiency and 1 extensive venous thrombosis). The only extrahepatic complication was gastrointestinal bleeding 1 month after treatment (without image of gastrointestinal leak). Other three patients developed biliar complications (in all of them, the right hepatic lobe was treated). There was no postirradiation pneumonitis. Between 3 days and 2 weeks after treatment, 5 (22%) patients developed self-limiting syndrome postembolization (abdominal pain, nausea and fever). CONCLUSION: Radioembolization of liver tumors with 90Y-glass microspheres has proven, in our experience, to be a safe therapy with a low rate of early complications.

P68-2 - Tuesday, Oct. 22, 16:00 - 16:30, Poster Exhibition Area

## Therapy & Clinical Trials: Miscellaneous

### P835

### Characteristics and trends of research on positron emission tomography: Comparison between 2007 and 2012

**S. Baek**[1], D. Yoon[2], E. Yoon[2], Y. Seo[2], K. Lim[2], K. Min[2]; [1]Department of Nuclear Medicine, Kangdong Seong-Sim Hospital, Hallym University College of Medicine, Seoul, KOREA, REPUBLIC OF, [2]Department of Radiology, Kangdong Seong-Sim Hospital, Hallym University College of Medicine, Seoul, KOREA, REPUBLIC OF.

Purpose: We performed a comparative bibliometric analysis of the scientific publications on positron emission tomography (PET) in 2007 and 2012. Materials and Methods: The MEDLINE (PubMed) and ISI Web of Knowledge databases were searched for English-language original articles on PET published from SCI/SCIE-indexed journals in 2007 and 2012. We selected those documents whose title included "PET" or "positron emission." The following information has been obtained from each article: topic of study, tracer used, type of research (basic, clinical, combined, or others) affiliation of the first author, and country of origin (for the purpose of our research, the country of the first author was considered as the country of origin of the paper). In addition, all the variables examined were compared between 2007 and 2012. Results: The yearly publication on PET increased from 1056 (2007) to 1846 (2012). The most common topic of study was oncology (1410 of 2092, 48.6%), followed by neurology (423, 14.6%). A total of 1518 (52.3%) articles used FDG as radiotracer, 2075 (71.5%) were clinical research articles, 1310 (45.1%) were written by the first author who was from a department of nuclear medicine/radiology or related specialties. The United State published 811 (27.9%) articles, followed by Japan (277, 9.5%), Germany (277, 9.5%), and South Korea (166, 5.7%). The following variables demonstrated a statistically significant increase from 2007 to 2012: China (2.4% vs. 4.5%) and India (0.2% vs. 1.6%) as country of origin. On the other hand, nuclear medicine/radiology department of the first author (49.7% vs. 42.6%), and the United States (33.5% vs. 24.8%) and Israel (1.7% vs. 0.3%) as country of origin demonstrated a statistically significant decrease. Conclusion: The publications on PET have grown at a rapid rate over the last decade. This bibliometric analysis revealed characteristics and trends of the current PET research, which may provide useful information to researchers.

P69-2 - Tuesday, Oct. 22, 16:00 - 16:30, Poster Exhibition Area

## Radionuclide Therapy & Dosimetry: MIBG & Peptides

### P836

### Paget disease revealed by Lu-177-DOTATATE post-therapy whole-body scan.

**F. Minutoli**, A. Sindoni, G. Restifo Pecorella, C. Vigneri, M. Licari, D. Cardile, S. Baldari; University of Messina, Messina, ITALY.

**Aim.** Visualization of Paget disease after In-111-Pentetreotide for diagnostic purposes has been previously reported. We report a case of Paget disease revealed by a whole-body scan performed after Lu-177-DOTATATE administration for therapeutic purposes. **Patient.** A 45-year-old female patient underwent duodenocefalopancreasectomy because of a neuroendocrine carcinoma of Vater ampulla (Chromogranin A+, Sinaptofisin+, Ki-67=5%). Post-surgery biochemical and imaging controls showed no abnormalities. At two-year follow-up, Chromogranin A levels were higher than the previous control (63 *vs* 18 ng/ml, normal values <100 ng/ml), even if in the normal range. Contrast enhanced CT scan revealed the presence of multiple hyperdense hepatic lesions, up to 25-mm in maximum diameter, some of which with central necrotic areas. Somatostatin receptor scintigraphy (SRS) performed with 185 MBq of In-111-pentetreotide showed high radiopharmaceutical accumulation in these liver lesions and increased uptake in the right hemi-pelvis. The patient underwent peptide receptor radionuclide therapy with Lu-177-DOTATATE (7400 MBq). Biochemical findings at hospitalization, including serum calcium (8.96 mg/dl, n.v. 8.2 - 10.4) and phosphate (2.5 mg/dl, n.v. 2.5 - 4.6) were normal, with the exception of alanine aminotransferase (56 U/L, n.v. 0 - 50) and alkaline phosphatase (397 UI/L, n.v. 45 - 132). **Results.** Post-therapy whole body scan (PTWBS) confirmed high radiopharmaceutical accumulation in hepatic metastases and revealed with better advantage than SRS increased radiopharmaceutical accumulation extensively involving the right hemi-pelvis. Whole body images acquired after Tc-99m-hydroxymethane diphosphonate administration (700 MBq) showed high radiotracer uptake in the right hemi-pelvis with a pattern suggestive of Paget disease. Corresponding bone window CT images demonstrated typical sclerotic features of Paget disease in the right hemi-pelvis. **Conclusion.** To the best of our knowledge, this is the first report about visualization of Paget disease after Lu-177-DOTATATE administration. Correlation with CT may improve the diagnostic accuracy when a bone uptake of radiolabeled somatostatin analogues uptake is seen, allowing discrimination between benign Paget disease and neoplastic lesions.

### P837

### Repeated administrations of peptide receptor radionuclide therapy: long term follow-up of renal function.

**F. Minutoli**, D. Cardile, A. Sindoni, V. Gangemi, M. Bertia, G. Restifo Pecorella, S. Baldari; University of Messina, Messina, ITALY.

**Aim.** The aim of this study is to evaluate renal function modifications at renal dynamic scintigraphy (RDS) with GFR estimation in neuroendocrine tumor (NET) patients treated with peptide receptor radionuclide therapy (PRRT). **Materials and Methods.** We reviewed clinical records of 31 patients with NET (15 F and 16 M, mean age 59.8 years, range 37-79) referred to the Unit of Nuclear Medicine of our University Hospital for PRRT. Histological diagnoses were: pancreatic neuroendocrine carcinoma (NEC) in 10, ileal NEC in 4, NEC of unknown origin in 4, duodenal NEC in 1, mediastinal NEC in 1, thymic NEC in 1, mesenterial NEC in 1, lung carcinoid in 2, carcinoid of unknown origin in 2, pancreatic carcinoid in 1, ileal carcinoid in 1, medullary thyroid carcinoma in 1 and intracranial meningiomatosis in 2 patients. All patients were treated with $^{111}$In-Pentetreotide (1-7 cycles, median 4 cycles, activity range per cycle 1.1-7.5 GBq, median activity per cycle 5.5 GBq, mean cumulative activity 16.2 GBq) and/or $^{90}$Y-DOTATOC/DOTATATE (1-7 cycles, median 3 cycles, activity range per cycle 0.74-2.6 GBq, median activity per cycle 1.9 GBq, mean cumulative activity 10.3 GBq) and/or $^{177}$Lu-DOTATATE (1-4 cycles, median 2 cycles, activity range per cycle 3.7-7.0 GBq, median activity per cycle 5.5 GBq, cumulative activity 11.9 GBq). Each patient underwent 1 to 13 PRRT cycles. Intravenous aminoacids were always administered prior to PRRT for reducing tubular peptide uptake and minimize renal damage. Nineteen patients had comorbility factors (diabetes, hypertension, dyslipidemia). Renal function evaluation by RDS was performed before each PRRT cycle; creatinine and azothemia serum levels were also recorded. **Results**. Baseline GFR ranged 58 to 129 ml/min/1.73 m$^2$. GFR decrease ranged 4 to 52.4% (mean: 22.7%). A statistical significant correlation between GFR percentage reduction with cumulative administered activity was found only for $^{90}$Y-DOTATOC/DOTATATE (Spearman test:R=0.4818, P=0.0232), but not for $^{111}$In-Pentetreotide or $^{177}$Lu-DOTATATE. Oppositely, creatinine and azothemia values did not show such a statistical correlation. In 11 patients (35.5%) the decreased GFR led to adjustment of the therapeutic activity and/or of the radiopharmaceutical used for PRRT; azothemia and/or creatinine serum levels were normal in 7/11 patients with decreased GFR. **Conclusion**. Neither creatinine serum concentration nor azothemia serum concentration can be recommended for evaluation of renal function in patients undergoing PRRT. GFR evaluation with RDS is a reliable and simple method to evaluate renal function, which allows to manage PRRT for reaching the therapeutic purpose with the minimum renal function impairment.

### P838

### $^{111}$In-Pentetreotide therapy in patients with inoperable benign intracranial tumors.

**F. Minutoli**, A. Sindoni, D. Cardile, E. Amato, L. Cassalia, A. Herberg, S. Baldari; University of Messina, Messina, ITALY.

**Aim.** In the last years Peptide Receptor Radionuclide Therapy (PRRT) acquired greater importance as an alternative or complementary treatment of neuroendocrine tumors (NETs) and other somatostatin receptor positive (sstr+) tumors. Many studies about PRRT using different radiopharmaceuticals, mainly $^{90}$Y and $^{177}$Lu (β-emitters) labelled peptides, are reported in the literature. $^{177}$Lu-labeled

somatostatin analogues seem to be more effective because of their favourable physical properties and the better objective response. On the other hand, only few reports exist on PRRT using $^{111}$In-Pentetreotide, an Auger-emitter. The aim of this study is to evaluate the usefulness of $^{111}$In-Pentetreotide therapy in patients with sstr+ inoperable benign intracranial tumors in which the use of β-emitters radiopharmaceuticals (characterized by higher penetration range) could be unsafe and questionable since lesions were close to critical anatomical structures, such as optic chiasm or medulla oblongata. **Materials and Methods.** We retrospectively reviewed clinical records of 9 patients (7F and 2M) affected by sstr+ benign intracranial tumors (mean age 58.4 years, range 50-81): 8 patients had meningiomas/meningiomatosis and 1 patient had a pituitary macroadenoma. A previous diagnostic scintigraphy with $^{111}$In-Pentetreotide demonstrated high intralesional radiotracer uptake. All patients underwent PRRT with high therapeutic activities of $^{111}$In-Pentetreotide (1-7 cycles, median 4 cycles, activity per cycle 3.7-7.5 GBq, median activity per cycle 7 GBq, cumulative activity range 13.7-66 GBq). Efficacy of PRRT was evaluated according to RECIST criteria. Toxicity was also assessed considering hematological parameters and GFR value estimated by renal dynamic scintigraphy. **Results.** No patient had acute damage. Complete response was observed in 1 patient (11.1%). Partial response was observed in 2 patients (22.2%); stable disease was observed in 5 patients (55.6%) and progressive disease in only 1 case (11.1%). PRRT is still ongoing in 2 patients. Mild hematological toxicity (characterized by transient leucopenia and/or thrombocytopenia grade I WHO) was observed in 4 patients (44.4%). No impairment of renal function was noted. **Conclusion.** Our data demonstrate that PRRT with $^{111}$In-Pentetreotide is safe, well tolerated and effective on disease control in patients with intracranial sstr+ benign lesions. Because of the short range of penetration of Auger electrons that results in a modest oedemigenous effect, $^{111}$In-Pentetreotide should be a valid alternative therapy in sstr+ benign intracranial tumors not responsive to other medical approaches or without any other therapeutic option available.

P70-2 - Tuesday, Oct. 22, 16:00 - 16:30, Poster Exhibition Area

## Radionuclide Therapy & Dosimetry: Thyroid

### P839

### Estimation of effective dose at thyroid cancer patients treated with 131I

**M. Zdraveska Kochovska**[1], V. Majstorov[1], V. Spasic Jokic[2], A. Bogdanovska[1], N. Ristevska[1]; [1]Medical Faculty, Skopje, MACEDONIA, THE FORMER YUGOSLAV REPUBLIC OF, [2]Technicall Faculty, Novi Sad, SERBIA.

Radioiodine therapy for thyroid cancer patients and hyperthyroid patients at the Institute of Pathophysiology and nuclear medicine is performed in a form of capsules. During the oral application it is reasonable to presume that 15 minutes in stomach is long enough to make additional exposure to stomach as well to other organs nearby. It is almost impossible to perform direct measurements to estimate internal doses of organs, so it is rather recommended to estimate the dose by calculation. Absorbed energy per unit transformation in stomach and surrounding organs has been calculated. The dose equivalents in several internal organs have been calculated in aim to determine the effective doses using appropriate tissue weighting factor values. The MCNP 4b model was used for this calculation. The phantom model was created using three major sections: - an elliptical cylinder representing the trunk and arms - two truncated circular cones representing the legs and feet - a circular cylinder on which sits an elliptical cylinder capped by half an ellipsoid representing the neck and head. The stomach wall is represented by the volume between two concentric ellipsoids and the contents by the volume within the inner ellipsoid. Also TLD measurements were performed over gastric region for limited time of fifteen minutes. Estimated effective dose was highest in stomach 7,43 E-02 Sv. The estimated values for other organs like colon, liver, lungs, ovary and bone surface was less than the estimated effective dose of stomach

### P840

### Cardiac, choroidal and subcutaneous metastases of a follicular thyroid carcinoma

**W. AMOURI**, F. HAMZA, I. JARDAK, F. KALLEL, S. CHARFEDDINE, F. GUERMAZI; Department of Nuclear Medicine; Habib Bourguiba Hospital, Sfax, TUNISIA.

AIM: To describe an unusual case of follicular carcinoma of the thyroid with uncommon metastases at the left atrium, the pulmonary vessels, the right eye and a subcutaneous mass. MATERIALS AND METHODS: The patient record was reviewed retrospectively. We analysed clinical outcomes and thyroglobulin rate as well as imaging findings after radio-iodine therapy. RESULTS: We report the case of 43-year-old woman operated in 1995 for multi-nodular goitre by total thyroidectomy. Histopathologic findings were typical of follicular thyroid carcinoma with vascular invasion. The patient was then lost of sight and consulted in 2000 for a neck swelling. She was reoperated for lymphadenectomy with resection of two peri-jugular tumoral masses that deviate vascular axes. Histopathologic findings concluded for residual follicular thyroid carcinoma with insular component without lymph node metastasis. The initial chest CT revealed a macronodular lungs miliairy and the whole body scan post 100 mci Iodine-131 showed intense cervical uptake and multiple bilateral thoracic fixations. The evolution after 10 cures of Iodine-131 has been marked by a persistently high thyroglobulin levels superior to 800 ng/ml with disappearance of cervical uptake and the persistence of pulmonary fixations. Bone scintigraphy scan was negative. Later, the patient complained of a decreased visual acuity. The last whole body spect/ct scan revealed multiple fixations of I-131 located at the right eyeball, lungs, left atrium, liver, sacrum as well as an abdominal subcutaneous solid mass. MRI confirmed a right choroid metastasis. CONCLUSION: Follicular thyroid carcinoma comprises 15% of all thyroid cancers and usually metastasises to the lymph nodes, lungs and bone. Other rare sites of metastases are the brain, pituitary, maxilla, larynx, and thymus. Distant metastases of these sites, particularly choroidal are exceptional. Metastatic cardiac involvement occurs most often during the terminal stage. They are frequently asymptomatic, but when symptoms develop these tend to be severe and often fatal. To our knowledge, only a few cases have been reported in the entire literature. Our case is unique in the presence of metastases in cardiac, choroidal and subcutaneous sites. We highlight the contribution of the spect/ct in the assessment of these distant metastases.

### P841

### False-Positive Iodine-131 Whole-Body Scan Due to a Benign Dermal Lesion; Intradermal Nevus

**N. Yildirim Poyraz**, E. Ozdemir, C. Amutkan, N. Adiyaman, S. Kilinc, Z. Kandemir, F. Saglam, S. Turkolmez, B. Cakir; Ankara Ataturk Training and Research Hospital, Ankara, TURKEY.

Whole body Iodine-131 (131I) scanning (WBS) and serum thyroglobuline (Tg) mesurement are the reference method for detecting residual tissue or metastases in patients with differentiated thyroid cancer (DTC) after thyroidectomy, however a considerable number of false-positive WBS findings have been reported. The recognition of a scan as false positive is important in avoiding additional costly investigations and unnecessary therapies. We present a case of 47-year-old female patient with Hashimoto's autoimmune tiroiditis and DTC with false-positive 131I uptake in an intradermal nevus, mimicking cutaneous metastases in post therapeutic WBS with low Tg level. The scan showed an unexpected focus in the right hemithorax-on the anterior chest wall with lateral images- as well as residual thyroid tissue in the thyroid bed. There was a rised, dome shaped tan coloured dermal lesion on the right breast skin in physical examination. Histopathological evaluation and immunohistochemistry revealed a benign intradermal melanocytic nevus. A considerable number of false-positive WBS findings mimicking cutaneous metastases of DTC and unexpected radioiodine uptakes in various benign tumors have been reported but to our knowledge this is the first report of such cases intradermal nevus in the literature. External contamination by physiological or pathological body secretions or excretions, inflammatory and cystic structures are the common causes of false-positive cutaneous radioiodine accumulation. On the other hand skin exhibits typical abnormalities in thyroid dysfunction especially in patients with autoimmune thyroiditis due to a number of interesting similarities between cells of melanocytic and thyrocytic origin. This case report provides a description of possible mechanisms of false-positive radioiodine uptake in cutaneous lesions.

### P842

### Hyperthyroïdism relapse after Iratherapy in Graves'disease : influence of iodine uptake heterogeity

M. Dumuis, G. Pop, O. Monsarrat, A. Neuman, **V. Eder**; APHP, Bobigny, FRANCE.

We evaluated outcome of patients after 131I therapy for Graves' disease. 18 out 120 patients(15%) relapsed Graves' disease 9±4months [5;25] after treatment with fixed dose of 555mCi. Thyroid scintigraphy was characterised as homogenous or heterogeneous. Planar image was segmented using a threshold at 50% of maximal activity measured in thyroid gland. Heterogeneous fixation was defined as more than half of thyroid gland do not achieved the maximal activity although total uptake was increased allowing radioiodine treatment. Heterogeneity of the fixation was observed in 88% of patients with relapse contrarily to 33% without relapse. Heterogeneity of radioiodine repartition on thyroid gland before treatment was the only predictive factor for relapse; Iodide uptake, hormone dosage (TSH, T3L, T4L), age, sex, TSH receptors or other antibodies positivity rate were not significantly different between the two groups of patients with or without relapse. In patients with relapse, iodine uptake was not different than before treatment but scintigraphy was homogenous for 8 of them and the 10 others shown an increase uptake in the area without high fixation on the first scintigraphy. TSH receptors were positive for 12 patients before the first treatment and was more increase when relapse occurred (31±14 vs 13±12; $p<0.05$). In conclusion : Heterogenity of iodine uptake is predictive of hyperthyroidism relapsed in Graves'disease. Recommendations for radioiodine treatment in this particular population should be reconsidered.

## P843
### High-dose Radioiodine Therapy of Graves disease.

V. Solodky, D. Fomin, **E. Pestritskaya**; Russian Scientific Center of Roentgenoradiology., Moscow, RUSSIAN FEDERATION.

Objectives: To estimate the effectiveness and safety of the disease treatment under different modes of applying RIT. Materials and Methods: 67 patients with the thyrotoxicosis condition associated with Graves disease were researched. The patients were divided into two groups: control one with 25 people (18 women and 7 men), who underwent a low-dose therapy of 150-500 MBq; and a main group of 42 people (32 women and 10 men), who underwent a high-dose therapy of 550 and 800 MBq. The volume of thyroid prior to the treatment made up 23.8 ± 20 ml in the main group and 30.2 ± 23 ml in the control one. The average age in the high-dose group was 44.6 ±23 years old and in the low-dose - 47.2±24 years old. In terms of the hormone level before the RIT, 52% of the main group patients experienced euthyroidism, while 48% - thyrotoxicosis. The corresponding indices in the control group were 42% and 58% respectively. The cessation of the thyrostatic therapy came on 5th to 21st day prior to the treatment, with the average of 14±7 days in both groups. The diagnosis of the disease was based on ultrasonography, planar scintigraphy, the hormone level and antibody titer. The performance was assessed through the attainment of hypothyrosis and the transition to a substitutive hormonal therapy with L-thyroxine in 6 months or more. The attainment of euthyroidism was seen as a partial effect due to a possibility of relapse. Results: In 6 months a positive result in the form of hypothyrosis achieved 39 patients in the main group, which accounted for 93%, and 3 patients (7%) experienced euthyroidism. No symptomatic thyrotoxicosis relapses were revealed. In the control group, hypothyrosis was achieved by 18 patients, which accounted for 72%; euthyroidism came up to 12%; 4 patients needed a refresher course of RIT, which made up 16% of the group. 93% of the main group patients tolerated the treatment favourably. Three patients complained of the edema of the neck area condition, which was blocked in a course of 3 to 5 days, without any additional prescriptions. In the control group, 1 patient complained of the same condition. Conclusion: Implementing of a high-dose RIT provides a 21% higher likability of Graves disease recovery as well as a four-time as much decline in relapse occurrences, with an equally favourable tolerance.

## P844
### Radio-iodine treatment under rh-TSH stimulation for differentiated thyroid cancer

**P. Bourgeois**; Institute Jules Bordet, Brussels, BELGIUM.

Radio-iodine treatment (RAIT) under rh-TSH stimulation is now currently proposed to patients operated for differentiated thyroid carcinoma (DTC). Hereafter is reported our limited experience of these treatments. Population : Twelve patients ((11 women, 1 man : age = 30-62 years) with pNx or pN0 and cM1 DTC (1 pTx, 2 pT1, 5 pT1m, 3 pT2 : 1 follicular, 11 papillary : 5 with anti Tg antibodies above normal) have received RAIT (ten had 3700 MBq and two 5290 MBq) after rh-TSH stimulation. Results : Ablation was observed in 8/12. Seven had Tg < 5 ng/ml when RAIT was given (TgD0) and one had Tg 5.6 ng/ml. Absorbed dosis in thyroid tissues (calculated on the basis of post-therapeutic imagings) was in 6/8 patients higher than 80 J per ng TgD0. On the opposite, the 4 patients without ablation (3 papillary , 1 follicular : 1pT1, 1 pT1m and 2 pT2) had TgD0 higher than 5 and the absorbed dosis was lower than 80 J per ng TgD. Conclusions : Although the present series is limited, two factors appear predictive of the RAIT results : the TgD0 (< 5 ng/mL) and the absorbed dosis (> 80 J per ng TgD0).

## P845
### Empiric $^{131}$I Treatment of High Thyroglobulin Levels in Differentiated Thyroid Carcinoma After Remmant Ablation

E. Kalender[1], **U. Elboga**[1], Y. Celen[1], H. Demir[1], E. Sahin[2], M. Yilmaz[1]; [1]Gaziantep University, Gaziantep, TURKEY, [2]Namik Kemal University, Tekirdag, TURKEY.

Objective: Serum thyroglobulin (Tg) measurements are usually the best marker of residual or metastatic disease after the treatment of differentiated thyroid carcinoma (DTC). It is not rare to find patients with detectable serum Tg levels after ablative $^{131}$I treatment (AIT). The objective of this study is to establish the efficacy of empiric $^{131}$I treatment (EIT) given for patients whose Tg levels remained high after AIT. Materials and Methods: Twenty-eight patients (23 women, 5 men; mean age 47.4±16.8) without distant metastasis, who were treated empirically for high Tg levels after AIT in our clinic were studied retrospectively. In all patients stimulated Tg levels before AIT (Tg I) and 6 months after AIT (Tg II) were measured. The Tg cutoff level for EIT was accepted 10 ng/ml. After EIT, posttherapeutic whole-body scintigraphy (PWBS) was performed to all patients. $^{18}$F-FDG PET CT was performed to patients who had negative PWBS but continued high Tg II levels. Results: PWBS was positive in 14 patients (50%) and negative in 14 patients (50%). Fourteen patients did not respond to EIT (50%), and 14 patients (50%) responded to EIT at different rates. Eight patients (28.6%) responded to EIT completely, and 6 patients (21.4%) responded to EIT partially. Tg I was 60.7±40 ng/ml and Tg II was 31±20.4 ng/ml in responded patients. Tg I was 87.6±96 ng/ml and Tg II was 114.3±106 ng/ml in unresponded patients. $^{18}$F-FDG PET CT was performed to 14 patients who had negative PWBS. $^{18}$F-FDG PET CT was positive in 11 patients and negative in 3 patients. $^{18}$F-FDG PET CT positive patients were referred to surgery. Conclusion: Our findings, suggested that the EIT is not beneficial in patients who have higher Tg II than Tg I and the cure rate is low in increasing Tg levels. The patients who have high Tg II but lower than Tg I can be treated empirically with $^{131}$I. In these patients EIT may be beneficial.

## P846
### Thymic Uptake After High Dose I-131 Treatment in Patients with Differentiated Thyroid Carcinoma: Interpretation and therapeutical management.

**M. Borbón Arce**, Teresa Cambil Molina, Tomás Martín Hernández, María de La Cinta Calvo Morón, Pablo De La Riva Pérez, Cristina Hernández Herrero, Juan Castro Montaño; Hospital Universitario Virgen Macarena, Seville, SPAIN.

AIM: I-131 is a very important for initial staging, treatment and monitoring of differentiated thyroid carcinoma after a total thyroidectomy. Doubtful uptake foci may appear due to physiological tracer distribution or true concomitant pathology. Increased functional activity of the thymus may be physiological in children and adolescents. In adults is associated with thymic hyperplasia, primary neoplasms, metastases, inflammatory processes or even in normal parenchyma. Thymic uptake after high dose radioiodine treatment is frequent in young adults and deciding the need of additional therapy is difficult in some cases. Materials and Methods: We present five cases of female patients with a mean age of 36.6 years(24-43), which were treated with a mean dose of 106 mCi of I-131(100-150 mCi) that showed tracer uptake in the thymic area. A blind therapeutic dose of I-131 was administered to 3 patients due to high Tg levels. In the remaining two, one corresponds to a 131I-WBS after remnants ablation treatment and the remaining one to a 131I-WBS after a treatment dose given for lymph node metastases. The 131I-WBS was performed 7 days after treatment. Conventional anterior and posterior planar images and SPECT / CT of head, neck and upper mediastinum were performed in all patients. Tg levels were measured with and without hormone replacement therapy in all cases. In every case thymic samples were sent to pathology for analysis. Results: In one patient an elective total thymectomy was performed due to the macroscopic appearence and the prominent tracer uptake. In a second one also a total thymectomy was decided due to the intense tracer uptake and because the patient was catalogued as high risk and had history of several bilateral lung metastases on a previous 131I-WBS which disappeared. In the remaining three, non additional invasive procedure was considered due to the normal previous pathology reports of the thymus parechyma from the initial thyroidectomy that involved compartment VII dissection. In the first two cases a thymic hyperplasia was reported. Conclusion: With the characteristics of the cases mentioned above and what its described in literature we can include thymus as a region of normal physiological uptake in most young adults. We also propose to include I-131 therapy as a possible cause of true thymic or transitory hyperplasia in these type of patients. Reminding the importance to always take the precaution of studying each case separately to exclude all risk factors of potential thymic metastasis or primary tumors

## P847
### Low-activity Radioiodine for Remnant Ablation after Surgery for Differentiated Thyroid Cancer- Initial Experience

**L. C. Sobral Violante**[1], J. Teixeira[1], I. Sampaio[1], R. Martins[2], J. Couto[2], A. Fonseca[1], L. Costa[1], F. Lopes[1], O. Soares[1], H. Duarte[1]; [1]Department of Nuclear Medicine, Portuguese Institute of Oncology, Porto, PORTUGAL, [2]Department of Endocrinology, Portuguese Institute of Oncology, Porto, PORTUGAL.

**Aim:** Residual thyroid tissue ablation with radioiodine after total thyroidectomy is one of the key elements in differentiated thyroid carcinoma (DTC) therapy. Clinicians worldwide have been trying to address what is the lowest effective radioiodine activity to successful ablation. This study intents to show our initial results using a low $^{131}$I activity -1850 MBq (50mCi) - for that purpose in patients (pts) with low-risk DTC. **Material and Methods:** Thirteen patients (12 female, 1 male; mean age 43.7 years; range 23-66 years), with histologically confirmed DTC (12 cases of papillary thyroid carcinoma- 3 pT1a N0, 1 pT1a N1, 4 pT1b N0, 2 pT2 N0 and 2 pT3 N0 and 1 case of follicular thyroid carcinoma - pT3 N0), underwent total thyroidectomy followed by an ablative $^{131}$I activity of 1850 MBq. An $^{131}$I whole

body scan (WBS) was performed six months after the ablative activity as well as thyroglobulin (Tg) level determination. Ablative therapy, WBS and Tg measurements were performed at least four weeks after thyroid hormone withdrawal. Six months after ablative therapy, patients with negative WBS and stimulated Tg levels <2ng/mL were considered to have successful ablation. **Results:** Complete thyroid tissue ablation was obtained in 9/13 pts with a success rate of 69.2%. Of the four remaining pts: one (pT1bN0) presented positive WBS; one (pT1aN0) showed both positive WBS and elevated Tg levels and the other two (pT2N0; pT3N0) presented Tg levels above the considered limit despite negative WBS. Three of those patients who didn't achieve a successful complete ablation presented high Tg levels (> 30 ng/ mL) at the time of radioiodine treatment. **Conclusion:** Although several studies have demonstrated good rates of ablation using low $^{131}$I activities, each center must assess whether the same results are found in its particular context. Our preliminary data reveals a successful ablation rate for post-thyroidectomy remnant thyroid tissue, in patients with low-risk DTC using 1850 MBq $^{131}$I, not far from the results obtained with 3700 MBq. These early results seem to support its feasibility, but a higher number of patients is required to accurately evaluate the effectiveness of thyroid remnant ablation with low-activity $^{131}$I.

## P848

### Miliary lung metastases of differentiated thyroid carcinoma

**A. MALIKA**, S. TALEB, G. CHERKAOUI, A. GUENSI, M. KEBBOU; Nuclear Medicine Department, Ibn Rochd UH, Casablanca, MOROCCO.

Lungs and bones are the most common distant metastases sites for differentiated thyroid cancer (DTC). Comparing with bone metastases, radioiodine therapy (RAI) has been an effective measure of treating lung metastases especially in micronodular (miliary) lung metastases. Management of disease differs considerably and outcome of RAI varies in series reported. The goal of study was to evaluate characteristics and outcome of RAI in patients with miliary lung metastases of DTC, in our experience. Forty four patients (34F and 10 H), with miliary lung metastases in the first therapeutic131I whole body scintigraphy (WBS), were retrospectively analysed, between January 2007 and December 2011. Patients with macronodular lung metastases and those with bone metastases were excluded. Age, gender, histological findings, diagnostic and therapeutic WBS, CT scan, thyroglobulin levels, RAI activity, evolution after de last RAI course, were studied. Patients were aged 20 to 81 yr (mean of 45 yr); they all underwent total thyroid surgery before being sent to nuclear medicine department for RAI. Papillary thyroid cancer was the most frequent histological variety (35%), with local lymph node metastases (50%). Miliary was diagnosed on diagnostic WBS in 13/22 cases (59%), CT scan was positive in 15/38 cases (39%). Initial stimulated thyroglobulin (Tg) level was very high in 14/22 cases (63%). All patients benefited hormone suppressive therapy and RAI. A total of 3.7-27.75 GBq (100-750 mCi) 131I was given. Effect of RAI and prognostic values of patient data were examined. Therapeutic efficacy was evaluated based on change in WBS findings and stimulated Tg level after the last RAI course. During follow-up which was between 2 and 5 yr (mean: 3 yr): 25% had negative WBS with stimulated Tg level under 1ng/ml. Among all variables studied, a better prognosis would be accomplished in patients without lymph node metastases, in those who had low level of initial stimulated Tg and by early diagnosis during post surgery 131I scanning of radiologicaly inapparent metastases.

## P849

### Repeatitive use of recombinant human TSH in radioiodine therapy of follicular thyroid cancer with multiple skeletal metastasis

**P. Pradhan**, Jain S,Gambhir S,Arya A,Verma S,Murthy S.Yadav N,Shukla AK; Sanjay Gandhi Post Graduate Inst. of Medical Sciences, Lucknow, INDIA.

Follicular thyroid cancer constitutes 30% of our thyroid cancer population among which 10% patients present with lung and skeletal metastasis.The goal of the study for assessment of effectiveness and side effects of repeated use of rh TSH in radioiodine therapy in patients of follicular thyroid cancer with multiple skeletal metastasis. Nine patients of follicular cancer thyroid with multiple skeletal metastasis ,6 females and 3 males,age more than 45 years had undergone repeated radioiodine therapy at 6-9 months interval with intramuscular injection of two doses of 0.9mg rhTSH on compassionate ground.Each patient have received at least twice rhTSH and maximum 4 times for radioiodine therapy and whole body radioiodine scan in same sitting.These patients did not reveal any obvious neurological deficit on clinical examination.Patients with compressive myelopathy were excluded from the study. Serum TSH were found to be mean of 46.75 (29.2-77.85 IU/L) following 24 hrs of 1st intramuscular injection and 107.42 (77.87-150 IU/L) following 24 hrs of 2nd intramuscular injection. Serum thyroglobulin was found to be more than 300 ng/dl except one patient with 0.2ng/dl in spite of demonstrable multiple skeletal metastasis on whole body radioiodine scan and antithyroglobulin antibodies were negative .Most of the patients did not develop any side effects besides mild nausea or fever except one patient who developed severe pain on both occasion following rhTSH administration at 6 month interval. First time the pain could be relieved with higher doses of analgesics and steroid.However,the second time,it required spinal decompression for relief of pain. Repeated administration of rh TSH in radioiodine therapy in follicular cancer thyroid with multiple skeletal metastasis could be possible because of rise of serum TSH >30 IU/L and no serious side effects or complications which lead to easy acceptability of this alternative procedure.Metastatic lesions were seen in diagnostic whole body radioiodine scan as well as in post therapy scan at the time of discharge. rhTSH can be used repeatedly in safe and effective manner in follicular thyroid cancer with multiple skeletal metastasis without obvious features of compressive myelopathy.

## P850

### Exogenous or endogenous TSH stimulation before radioiodine therapy of metastatic thyroid cancer patients? The answer from post-therapy whole-body scan

**L. M. P. Pires**, G. Costa, A. Albuquerque, J. Pedroso de Lima; Centro Hospitalar da Universidade de Coimbra, Coimbra, PORTUGAL.

Aim: Human thyroid-stimulating hormone (rhTSH) is a well establish preparation method for ablation therapy with 131I in patients with differentiated thyroid cancer (DTC). However, for residual or metastatic disease, the advantage of rhTSH-aided 131I compared with the conventional preparation with thyroid hormone withdrawal (THW) still is a subject of discussion. The aim of our study was to compare the efficacy of rhTSH versus THW preparation for 131I therapy of metastatic DTC, based on the post-therapeutic whole body scan (ptWBS) information. Material and Methods: Ten DTC patients (4 female and 6 males; age: 53±19yr) with iodine-avid metastasis (5 patients with lung, 2 with bone, 1 with lymph node, 1 with lung+bone+lymph node and 1 with lung+bone+hepatic), were submitted to several (mean per patient: 3.6) radioiodine therapeutic courses, between January 2004 and February 2013. Endogenous TSH stimulation was used in most treatments (n=28) but rhTSH was the choice in 12 therapies (once in 8 patients and twice in 2 patients). For every patient, the interval between two consecutive treatments with different stimulation Methods was less than 11 months. Post-therapy WBS was performed one week after radioiodine administration. The radioiodine avidity for the metastatic lesions seen on the rhTSH-aided ptWBS was compared, on a within-patient comparison basis, to the radioiodine avidity for the metastatic lesions seen on the THW-aided ptWBS. Results: In patients with positive metastasis on ptWBS after THW, no visible radioiodine uptake was seen on rhTSH-aided ptWBS in 4 patients (2 cases of lung metastasis, 1 case of lymph node and 1 case of bone metastases). A significant reduction of 131I uptake was recorded in 4 cases (2 with pulmonary, 1 with lung+bone+lymph node and 1 with lung+bone+hepatic). No significant differences were detected between both TSH stimulation Methods in the other 2 patients, 1 with pulmonary and the other with bone metastases. Conclusions: In our study, metastates showed much less intense radioiodine uptake on patients treated after rhTSH stimulation when compared with those treated after THW stimulation, supporting the option for an endogenous stimulation when metastatic disease is known or suspected.

P71-2 - Tuesday, Oct. 22, 16:00 - 16:30, Poster Exhibition Area

## Radionuclide Therapy & Dosimetry: Bone Pain Palliation

## P851

### Samarium 153 in metastatic bone pain: palliative to curative benefits?

**T. Ben Ghachem**, A. Mhiri; I. Slim; A. Bahloul; H. Charfi; I. Yeddes; I. Elbez ; I. Meddeb; MF. Ben Slimène.; DEPARTMENT OF NUCLEAR MEDICINE, SALAH AZAIEZ INSTITUT, EL MANAR II UNIVERSITY, TUNIS, TUNISIA., Tunis, TUNISIA.

Samarium 153 has many benefits for the treatment of metastatic bone disease, including early onset and length of pain relief, predictable and reversible myelosuppression and ease of administration; furthermore curative effect on malignant cells was discussed in some studies. The aim of our cases is to assess the effectiveness of Samarium 153 (QUADRAMET) as a tumoricidal agent. The first case concerns a 58 years old woman with breast cancer who has received 5 cures of Samarium 153 with complete response. In fact analgesics were stopped completely after complete remission of bone pain and the patient Karnofsky Performance Score (KPS) improved by about 40 points (from 50 to 90). Also a decreasing uptake

of costal lesions was observed. The second case was about a 73 years old man with prostate adenocarcinoma. After 6 cures life quality was improved and pain-free period was adequate associated with disappearance of multiple metastases on bone scan. In the follow-up we have notated a significant reduction of PSA to normal level. Moreover, mild and transient myelosuppression was seen in both two patients. After radionuclide treatment a decrease in metabolic activity in a large portion of metastases was seen. Also in some studies, a major regression of bone metastases has been shown, with almost total regression of those up to 20 mm and with features of calcification in the bigger ones. Other studies suggest weak tumoricidal effects of radionuclide therapy including samarium153, both in clinical studies and animal models. It may be hypothesized that both local tumoricidal effect and prevention of pathological fractures may have a positive impact on improving the clinical outcome and survival shown by some studies. Then, if the cost / effectiveness of this treatment remains unknown, preliminary studies are extremely encouraging, and the impact on quality of life is formally established.

## P852

### Samarium-153 oksabifor in the treatment of metastatic bone disease

**O. Solodyannikova**, N. Voit, G. Sukach, D. Sagan; National Cancer Institute, Kiev, UKRAINE.

Aim. Bone metastases (BM) are one of the most common complications of solid cancers. Frequency of metastatic bone breast cancer (BC) at different stages of the disease ranges from 47 to 85%, for prostate cancer (PC) - from 33 to 85%, for lung cancer - from 30 to 60%, kidneys - from 33 to 40%, thyroid cancer - from 28 to 60%. Initial stages of BM are often clinically asymptomatic, but later manifested with fractures and pain which greatly reduces patients' quality of life. In world practice for palliative treatment of BM are widely used isotopes 32P, 89Sr, 186Re, 188Re, 153Sm, and 177Lu. Materials and Methods. The results of examination and treatment with 153Sm of 25 BM patients were analyzed. Among them 5 men and 20 women, mean age 61.2± 7.9 (min - 51.1, max 73.0). In 4 patients PC was diagnosed, 2 - lung cancer, 17 - BC, 1 - kidney cancer, 1 - cervical cancer. All patients after preliminary survey (bone scan, blood count, blood biochemical analysis) have got administration of 153Sm-oksabifor in doses of 1 mCi (37 MBq) per 1 kg of weight. To determine the dynamics of BM re-scan with 99mTc Tehnefor carried out in 1.5 and 3 months after starting treatment. Results. Reduction of pain intensity appeared at 6 + 4.6 days (min 2, max-18). There was a decline consumption of analgetics. According to the assessment of bone pain scales and efficiency, we can say that the therapy was effective and 90% of patients have got pain relief for three months and only in two patients pain-free period lasted 70 days. Quality of life was assessed by Karnofsky scale and improved statistically significantly. Most patients return to normal life. Only one patient's quality of life did not change (remained at 50%) and one - has changed slightly (from 50% to 60% on the Karnofsky scale). However, this is due to progression of primary disease and not related to pain symptoms. According to our data, 10 patients had stabilization process, in 15 patients - reducing the number of foci and the level of radiopharmaceutical uptake in them. Conclusions. Radionuclide therapy in patients with BM can effectively suppress pain and significantly reduce the number of analgesics. Post-treatment patients, life quality statistically significantly improved. Samarium-153 has the ability to reduce BM number and intensity of radiopharmaceutical accumulation in spots in the control study.

## P853

### Results of treatment of osteoblastic lesions from prostate cancer with strontium-89.

**G. Gerasimou**[1], E. Moralidis[1], E. Papanastasiou[1], I. Tzitzikas[2], G. Liaros[1], I. Hilidis[1], A. Sofos[3], K. Mellisourgidis[3], K. Pistevou-Gombaki[2], A. Gotzamani-Psarrakou[1]; [1]Clinical Lab of Nuclear Medicine-AHEPA University Hospital, THESSALONIKI, GREECE, [2]Oncology Department-AHEPA University Hospital, THESSALONIKI, GREECE, [3]1st Pathologic Clinic-AHEPA University Hospital, THESSALONIKI, GREECE.

Prostate cancer is a neoplasm frequently spreading to the bones, producing pain, discomfort and analgesics intake, with side effects. External beam radiation is one of chosen treatments. However, this kind of treatment is uncomfortable in terms of patients' transition to the hospital and can be applied in a limited field. Application of radiopharmaceuticals emitting β radiation has been proven an effective alternative treatment which is distributed to the whole skeleton, reducing pain and improving quality of life. We are herewith trying to evaluate the usefulness of radionuclide treatment (RT) with strontium-89 (89Sr ) in patients with prostate cancer presenting osteoblastic osseous metastases. Twenty patients aged 61-78 years with osteoblastic osseous metastases from prostate cancer, reported in bone scan with Tc-99m-HDP, no responders to analgesics, were recruited for the study. All patients were treated with 89Sr at a dose 150MBq, at least 5 days apart of prior treatment with zoledronic acid and one month after possible external beam radiation. Twelve patients received two courses and eight of them three courses of RT. The extent of bone disease was evaluated using the extent of disease grade (EOD) nomenclature (scale from 1 that equals to less than 6 bony metastases, to 4 that represents a "super scan" or equivalent). The beneficial effect was estimated by the Scoring System for Evaluating Pain (SSEP) using a severity score from 0 (normal mobility), to 4 (unendurable). Blood samples were taken 20 days post RT in order to estimate possible myelosuppression. Fifteen of the above mentioned patients (75%) responded well to RT with a remarkable improvement from a median level of 3.1+0.6 pre-treatment to a respective one of 1.4+0.3 post RT ($p<0.01$). Ten of those patients referred a partial relief of pain, whilst five an almost complete relief. A better therapeutic outcome was achieved after the second application of RT in 6 patients, whilst 9 of them responded well after the first application. A grade I myelosuppression in terms of white cells' level reduction between 3,000 and 3,400/mm3 was mentioned in 4 patients plus mild reduction of platelets (grade I) in 2 out of the above mentioned 4 patients. However this effect was transient and reset to normal levels was mentioned after 10-15 days. RT with 89Sr is of benefit for patients with prostate cancer and painful osteoblastic involvement, in terms of improvement of life quality. Mild myelosuppression is a transient side-effect.

P72-2 - Tuesday, Oct. 22, 16:00 - 16:30, Poster Exhibition Area

## Radionuclide Therapy & Dosimetry: Dosimetry Models & Treatment Planning

## P854

### Assessing absorbed dose heterogeneities for organ S-value calculation in mice

**T. Mauxion**[1], D. Villoing[1], S. Marcatili[1], M. P. Garcia[1], J. Suhard[2], J. Barbet[2], M. Poirot[1], M. Bardiès[1]; [1]UMR 1037 INSERM/UPS, Toulouse, FRANCE, [2]UMR 892 INSERM/Université de Nantes-Angers, Nantes, FRANCE.

Introduction and aim: S-values calculated according to the MIRD scheme strongly depend on the size of source/target regions and particle ranges(1). Several mean organ S-values were recently calculated for mice in the context of targeted radionuclide therapy and molecular imaging(2). However, the heterogeneity of energy deposition at the sub-organ level is seldom taken into account and the relevance of mean organ S-values is not systematically evaluated. This study aims at assessing spatial variations associated to mean S-values for small animals to estimate energy deposition heterogeneity at the sub-organ or voxel level. Materials and Methods: A 29g-mouse-model generated at high spatial sampling (200x200x200 µm3) from the Moby software was used to calculate S-values for several radionuclides of interest(3). Monte Carlo simulations were performed with GATE (v6.2), in which specific corrections were implemented and validated to improve the accuracy of voxel energy-scoring. Mean S-values and standard deviations were calculated from 3D-voxel-based energy deposition maps for several source/target organ pairs. As the standard deviation associated to the mean S-value in a given target organ includes both spatial and statistical fluctuations, we simulated an increasing number of primary particles (typically from 10E+06 to 10E+10) to estimate the impact of relative statistical/spatial fluctuations for several source/target pairs. A spatial dispersion factor (HS-value for Heterogeneity of S-value) was obtained when the standard deviation converged to a stable value. Results: Several HS-values calculated for source organs were significant in case of self-irradiation for all considered radionuclides, but remained very low as compared to values obtained for short and large source/target distances. For example, for 131I sources located in the thyroid, S(thyroid←thyroid)=1.80E-09 Gy.Bq-1.s-1 and HS(thyroid←thyroid)=3.09E-10 Gy.Bq-1.s-1, leading to a fractional HS-value of 17%. Fractional HS-values for (bone marrow←thyroid) and (total body←thyroid) were 996% and 3579%, respectively. Besides, fractional HS-values converged above a threshold that varied from one source/target combination to the other (131I source: from 246% to 68% for (brain← thyroid) with a number of simulated particles varying from 5E+06 to 6E+09). Discussion and conclusion: Heterogeneity of energy depositions in mice at the sub-organ level increases with source/target distances and for diffuse target organs. We demonstrated that mean S-values are not always relevant in these situations. The method described in this work allows a reliable and systematic assessment of mean organ S-values relevance for small animal dosimetry. (1) Hindorf et al., JNM, 2004 (2) Xie et al., PMB, 2013 (3) Mauxion et al., Med Phys, in press

P73-2 - Tuesday, Oct. 22, 16:00 - 16:30, Poster Exhibition Area

## Radionuclide Therapy & Dosimetry: Clinical Dosimetry

### P855

#### A Patient-Specific Dose Estimation in 18F-FDG Examination from External TLD Measurement

**K. S. Chuang**[1], J. C. Lu[2], H. H. Lin[1], S. L. Dong[2], Y. C. Ni[3], M. L. Jan[3]; [1]National Tsing-Hua University, Hsin-Chu, TAIWAN, [2]Chung-Shan Medical University, Tai-Chung, TAIWAN, [3]Institute of Nuclear Energy Research, Long-Tan, TAIWAN.

[Aim] There are a growing number of patients undergoing nuclear medicine examination each year and dose estimation becomes a very important issue. The time-activity curves (TAC) of all source organs are required before one can estimate patient-specific body dose during the whole treatment period. However, TAC is known to be difficult to obtain for each individual. The purpose of this paper is to develop a patient-specific dose estimation system from the dose measured outside the body without any TAC information. [Materials and Methods] The method involves two steps. First, to compute the S values on the body surface for each source organ based on nuclear image using Monte Carlo simulation. Second, to measure the dose externally from the TLD placed on the body surface during nuclear examination. Since the doses in TLD are contributed from all source organs, they can be expressed by simultaneous equations with the S values as known variables and the cumulative activities of source organs unknown. Solving the simultaneous equations, the cumulative activities of all source organs can be obtained and subsequently the total body dose calculated. A NEMA phantom and an ORNL mathematical phantom were used to validate this method. A static activity was used for NEMA phantom and the dynamic activity distribution of each source organ obtained from MIRD dose estimate Report 19 was used in ORNL phantom. Eight simulations were performed at 15min, 30min, 45min, 60min, 120min, 180min, 240min, and 300min after intravenous administration of 18F-FDG. Numerous TLDs were placed on the surface nearest to each source organ. After each simulation, the TLD reading and S values were used to compute the cumulated activity of each organ. [Results and Discussion] The percent error in estimations of cumulative activity of the source organs and the error caused by inaccurate positioning the TLD will be investigated. Preliminary results on the NEMA phantom indicate it is an accurate, robust, and efficient method. Effectiveness of this method was validated by the ORNL phantom study.

### P856

#### Slice-based Thresholding Method for Dosimetric Evaluation of Ga-68 DONATOC

**S. Ballal**, S. Singla, G. Arora, C. Bal; All India Institute of Medical Sciences, Delhi, INDIA.

**Aim:** The role of Gallium-68 (Ga-68) labeled somatostatin analogues in the management of neuroendocrine tumors (NETs) is well established. Though its clinical application has been studied extensively, studies reporting the radiation dosimetry aspects are few. Internal dosimetry is based on many assumption, the most common being homogeneous radioactive uptake in organs. This assumption, however, does not hold true for most organs and doses are rather over-estimated. Herein, we have evaluated the dosimetry of Ga-68 DOTANOC in NETs patients based on slice-by-slice thersholding method. **Methods:** 5 patients (3 males; 2 females) with known NET were recruited in the study. Mean age of patients was 43 y (35-56 y). Patients were injected mean activity 60.01 MBq followed by whole body PET acquisition at 5 time points: 10, 20, 30, 70 and 120 minutes post-injection. Quantification (Bq/ml) for each organ (spleen, liver, kidneys, heart, urinary bladder and pituitary) was done using ROI based method in each slice with automatic thresholding. Whole body counts were taken at respective time points for all the patients. Dosimetric calculations were performed using OLINDA/EXM 1.1 software. **Results:** The highest mean effective dose equivalent was observed in liver (8.18E-03 mSv/MBq) followed by Spleen (4.30E-03 mSv/MBq). The mean dose to kidneys, urinary bladder, heart and pituitary were 2.97E-03, 4.10E-03, 1.68E-03 and 5.23E-07 mSv/MBq, respectively. The mean whole body effective dose and effective dose equivalent were calculated to be 1.29E-02 and 2.28E-02 mSv/MBq. **Conclusion:** Renal and bladder doses are attributed to the renal route of excretion of Ga-68-DOTANOC. The dose to other organs is owing to the physiological presence of somatostatin receptors on these organs. The evaluated doses in the present study are significantly lower than the ones reported in literature which is mainly because of the processing methodology. The dosimetric calculations in the already reported studies are based on the assumption of homogenous radioactive uptake in each organ. However, the present study employed more accurate thresholding of each organ derived from per slice and hence these values are considered to be more accurate.

P74-2 - Tuesday, Oct. 22, 16:00 - 16:30, Poster Exhibition Area

## Radionuclide Therapy & Dosimetry: Miscellaneous

### P857

#### Calculation OF Absorbed Dose in Target Tissue and Equivalent Dose in Sensitive Tissues of Patients Treated by BNCT Using MCNP4C

**M. Zamani**; Atomic Energy Organization of Iran, Tehran, Iran, ISLAMIC REPUBLIC OF.

Today BNCT (Boron Neutron Capture Therapy) is used for treatment of many diseases, including brain tumors, in many medical centers. In this method, a target area (e.g. head of patient) is irradiated by using some optimized and suitable neutron fields such as research reactors. Due to the importance of healthy tissues which are located in the vicinity of irradiated tissue, and based on the ALARA principle, it is required to prevent unnecessary exposure of these vital organs. In this study, by using stimulation method (MCNP4C Code), the absorbed dose in target tissue and the equivalent dose in different tissues of a patient treated by BNCT are calculated. For this purpose, we have used the MIRD Standard Phantom. Equivalent dose in 11 sensitive organs, located in the vicinity of the target, and the total equivalent dose in whole body was calculated. The results show that the absorbed dose in tumor tissue is equal to 1.52Gy and the total equivalent dose in 11 sensitive organs is equal to 14mGy. The maximum equivalent dose in organs, other than brain and tumor, belongs to the tissues of lungs and thyroid and are equal to 7.36 mSv and 3.00 mSv, respectively. Key words: BNCT, tumor, vital organs, absorbed dose, equivalent dose, total dose

### P858

#### Comparison of Hepatopulmonary shunt calculated by planer and SPECT $^{99m}$Tc MAA studies.

**A. K. Jha**, Zade AA, Shah SA, Agrawal A, Purandare N , Kulkarni SS, Shetty N, Rangarajan V.; Tata Memorial Hospital, Mumbai, INDIA.

**INTRODUCTION:** Transarterial-radioembolisation (TARE) is the treatment of choice in inoperable primary and metastatic liver malignancies. Estimation of hepatopulmonary shunt (HPS) plays a significant role in the planning of TARE to avoid radiation-induced pneumonitis. HPS estimation is done by gamma camera imaging method in most centers because of unavailability of software to estimate HPS by Single Photon Emission Computed Tomography/ Computed Tomography (SPECT/CT). This study aims at using a self-developed software for quantification in SPECT imaging and comparing its results with that of planar imaging. **MATERIALS AND METHODS:** 10 - 12 mCi of 99mTc-MAA was administered transarterially, selectively to the tumor feeding artery. Scans were performed on Infinia Hawkeye, GE Medicals, and were acquired in anterior and posterior views with lungs and liver in the field of view and SPECT/CT was also performed similarly. Static images were acquired in 256 × 256 matrix (1000KCnts) and SPECT in 128 X 128 matrix with 64 frames (20s/frame); CT parameters were 140 kV, 2.5 mAs, and 1-cm slices. Self-developed software on dedicated workstation, Xeleris 1.1, GE Medicals, was used for analysis. HPS estimation: Planar: Left and right lung and liver ROIs (region of interest) with three background ROIs were drawn on anterior and posterior image. Pixel normalized background subtraction (PNBS) was done. Geometric mean was calculated for both the lung and liver ROI, HPS was calculated by formula-1. Formula 1: HPS = (Total Lung count X 100)/(Total Lung count + Total Liver count) SPECT/CT: Attenuation and Scatter corrected Transaxial slice were generated by iterative reconstruction. CT and SPECT trans axial slices were loaded on self developed software and available Left and right lung and liver and two background ROI were drawn on each CT slice which were copied on SPECT slices. PNBS lung and liver counts were summated over the slices and HPS was calculated by formula 1. **RESULTS:** 17 patients who underwent TARE of hepatic neoplasm were evaluated. HPS fraction calculated from pre therapeutic Planar and SPECT/CT images for 99m Tc MAA study was 4.97% and 3.72% respectively. There is good correlation in the HPS fraction values by both Methods (coefficient of correlation=0.97) **CONCLUSION**: HPS calculated by both Methods correlates with each other in range of 0-10% , but HPS calculated by SPECT/CT can be considered as more accurate because it gives the true representation of three dimensional organs.

## P859

### Radiation Exposure Of Owners And Veterinary Staff Members After Treatment Of Hyperthyroid Cats With 131I

E. Vandermeulen[1], K. Bacher[2], A. Dobbeleir[1], M. Monsieurs[2], **K. Peremans**[1]; [1]Faculty of Veterinary Medicine, Ghent University, Merelbeke, BELGIUM, [2]Faculty of Medicine and Health Sciences, Ghent University, Ghent, BELGIUM.

Aim: The present study aims to evaluate radiation exposure of owners and veterinary staff members after 131I treatment of hyperthyroid cats. Additionally, radiation dose rates from the treated cats were measured at different time points to analyze the effective half-life of 131I within the cat. Materials and Methods: 28 cats received a mean activity of 173±84MBq of 131I. During the 5 day hospitalization period, the veterinary staff (3 persons) involved in the care for these cats wore waterproof bracelets and rings (at left and right hand) containing calibrated (LiF:Mg,Cu,P)thermoluminescent dosimeters (TLDs). TLDs were read out after 5 days and readings were converted in a dose value using an in-house measured calibration factor. Further, equivalent dose rates (µSv/h) were registered at 1m distance from the cat at 4h, 24h, 48h and 72h after injection. The dose rates were plotted against time and fitted to an exponential function. From the fitting results, the effective half-life (T1/2eff) could be calculated. Owners were also given waterproof bracelets containing TLDs at the moment their cat was released from the Veterinary Nuclear Medicine Division. They were given strict instructions concerning the management of the cat at home (emphasizing limited time, keeping distance and waste management). The bracelets were returned by mail after 1 week together with the owners' estimation of the time spent with the cat. TLDs doses were analyzed using the aforementioned procedure. Results: 4 hours after injection, mean equivalent dose rate at 1m was 9±4 µSv/h. This value further decreased to 4±3 µSv/h. Based on the dose rate measurements a mean T1/2eff of 3.0±1.6 days was found. Over 7 days, the average accumulated wrist dose of the owners was 504 µSv (range 26-2682 µSv). Concerning staff members, mean accumulated wrist doses over 5 days were 101µGy and 120µGy for left and right wrists respectively, and mean finger doses of 257µGy and 198µGy were found for left and right hand respectively. No correlation was found for any of the latter values and the amount of injected activity or time spent with the cats. Discussion: radiation exposure of both owners and veterinary staff members after 131I treatment of hyperthyroid cats is acceptable. The hand/wrist doses can be regarded as the maximum dose an individual will receive as manipulation of the cat is done by hand. Nevertheless, measured values indicate the need of appropriately instructing owners on radiation protection to keep the dose as low as possible.

# TECHNOLOGIST POSTER SESSIONS

TP01 - Tuesday, Oct. 22, 8:00 - 9:30, Poster Exhibition Area

## Technologist Poster Session 1

### TP001

#### Patient's Respiratory Motion Management in PET/CT Procedures

**L. Pavanello**[1], F. Sciume'[1], M. Ferdeghini[1], M. Zuffante[1], C. Cavedon[2], M. Giri[2]; [1]Nuclear Medicine Unit AOUI Verona, Verona, ITALY, [2]Medical Physics Unit AOUI Verona, Verona, ITALY.

**AIM** This study wants to show the importance of the respiratory training session in the use of the procedures 4D-PET/CT. They have been valued the regularity of the respiration during the training and the phase of acquisition and finally the necessary time for the positioning of the patient before the acquisition of the images. **MATERIALS AND METHODS** At the Nuclear Medicine Unit of Verona University Hospital, 4D imaging is obtained using a PET/CT Gemini Big Bore system (with TOF reconstruction) and a respiratory synchronization system Varian RPM. Through Varian RPM , the respiratory cycles to monitor can be evaluated. 4D-PET/CT with 18F-FDG is performed once the planned amplitude and regularity respiration are achieved. Pitch is adapted to number of breaths per minute before the CT acquisition and PET parameters in nominal phase is 25% and 2 minutes for phase. Retrospective reconstruction is used for each respiratory cycle phase. The breath curve is analyzed considering the respiratory cycle amplitude. 53 patients were studied with 4D-PET/CT and only 28 patients performed respiratory training session. For the 4D PET/CT studies and RT treatment, a complete collaboration of the patients is essential. Therefore it was decided to perform a Training Session to obtain a regular and reproducible respiratory condition. Simulation was performed in a dedicated room before the diagnostic study. The responsible trainer is a technician that calculates free breaths for 5 minutes, assessing the number per minute. The average score obtained will be kept by the patient during PET/CT and RT treatment. **RESULTS** In 28 patients who performed training session we have obtained a good collaboration during the images acquisition and 22/28 held a constant breath for minute (bpm) during the CT and PET acquisition. Only 9/25 patients, who did not perform training session, held a constant bpm during the examination. The time consuming of the training session allows to obtained a good patient's collaboration, reducing positioning and immobilization management of 4-7 minutes in the examination procedure. Consequently radiation dose to technicians staff was reduced. **CONCLUSIONS** Respiratory motion management, optimized with Training Session, becomes an important chapter in both diagnostic and RT applications. 4D-PET/CT allows compensation of degradation and artifacts induced by respiratory movements. In addition 4D-PET/CT provides information on target motion, which can be used to personalize RT treatment planning.

### TP002

#### Incidence of exposure in PET/CT compared to the total dose taken by the nuclear medicine technical staff

**R. Raschillà**, S. Caputo, B. Dell'Anno, R. Cantini, L. Antonacci, F. Betti, G. De Laurentiis, D. Panariello, L. Paglialunga, F. Picchi, D. Fontanelli, G. Mariani; Regional Center of Nuclear Medicine, Pisa, ITALY.

**Aim**: The 511-keV photons originated by the annihilation event have a penetration capacity 10-fold greater than the 140 keV gamma rays emitted by 99mTc. The resulting increased radiation risk for technical staff is sometimes underestimated. The results of a prior pilot investigation had shown that, in our center, radiaton exposure for technologists working with PET/CT before installation of the automatic injector was higher than for those working with conventional Nuclear Medicine, and was directly related to the number of scans performed. In this work we measured the actual radiation exposure for the technical staff employed for PET/CT and for conventional Nuclear Medicine, respectively, considering that for PET/CT we minimized radiation exposure by using an automatic injector. **Methods**: To measure the actual percentage of whole-body and extremities exposures (normally measured every 4 months with chest and wrist film dosimeters, respectively), throughout 2012 each technologist was equipped with two dosimeters, one of which was used only during the PET/CT sessions. Over that period each technologist performed about 500 conventional Nuclear Medicine scans (using mostly 99mTc, but also 131I, 123I and 111In) and about 250 PET/CT scans (almost exclusively with [18F]FDG). Results: The range of exposures in 2012 turned out to be 0.5±0.3 mSv (range 0.23-1.04) for the chest dosimeter used in PET/CT, while it was 0.6±0.3 (range 0.21-1.24) for conventional Nuclear Medicine. Regarding the extremities, the dosimeter used only for PET/CT recorded 1.4±0.8 mSv (range 0.69-3.02), while they recorded 5.7±4.17 mSv (range 1.0-13.84) for conventional Nuclear Medicine. **Conclusion**: These results demonstrate that similar whole-body exposures are reached with about half the PET/CT scans versus the conventional Nuclear Medicine scans (0.5 mSv versus 0.6 mSv deriving from 250 versus 500 scans, respectively). The additional exposure from PET/CT activity to the extremieties is instead less important 1.4 mSv for 250 PET scans versus 5.7 mSv for 500 conventional scans), most likely because of the reduced risk due to use of an automatic injector for PET. Instead, for conventional Nuclear Medicine the technologist has to handle more closely the radiopharmaceuticals prepared in the radiopharmacy. In order to further reduce the average dose accumulated by the technical staff, the development of optimal environmental pathways is required to ensure an adequate distance between the injected patient and the technologists.

### TP003

#### The Effects of Cradle and Mobile Table on CT Attenuation Correction in PET/CT/MRI Trimodality Device

H. Chae, **H. Park**, H. Lee, K. Kim, Y. Go, W. Cha, Y. Kim, S. Kim, K. Lyu; Shingu College, Seongnam, Korea, REPUBLIC OF.

We introduce TriModality system that MRI merged to PET/CT. The artifact was founded on cradle's certain part(screw part) that used in examination. We evaluate the CT metal artifact caused from cradle and Mobile table that used in PET/CT/MRI-examination effect the SUV in PET/CT image evaluate. In this Study, we use the 1994NEMA PhantomTM(NU2-1994). in the hot spot, we injected the water 289 ml with 0.29 MBq of 18F-FDG, and in the background radioactive, we injected the water 4180 ml and 22.5 MBq of 18F-FDG. We acquired the CT image in 120 Kvp of tube voltage and 50 mA, 80 mA, 200 mA, 240 mA, 400 mA of Tube curren. we reconstructed the PET image with the each of CT image, compare the SUV values in same parts. We verified the significance, Use the Kruskall-wallis test which is Nonparametric analysing Methods. Each of table's condition and SUV value in ROI according to CT dose was unsignificant each other($P<0.05$). We evaluated about the CT metal artifact that caused from cradle and Mobile table, effects to SUV in PET/CT image evaluate. in The current Trimodality system, it is considered that Cradle will be suitable to using in clinical condition.

### TP004

#### Evaluation of spatial resolution of Siemens Biograph mCT PET scanner for TOF and non-TOF reconstruction algorithms

A. Suljic[1], L. Jensterle[2], **B. Vidovic**[2], M. Suhadolnik[2], P. Tomse[2], D. Škrk[3]; [1]Faculty of Health Sciences, Ljubljana, SLOVENIA, [2]University Medical Centre, Ljubljana, SLOVENIA, [3]Ministry of Health, Ljubljana, SLOVENIA.

**Aim** The aim of this study was to measure the spatial resolution of Biograph mCT Positron Emission Tomography (PET) scanner in air and in scattering medium for various time of flight (TOF) and non-TOF reconstruction algorithms available at the accompanying workstation. **Materials and Methods** Measurements were performed with a triple line source phantom consisting of capillaries with internal diameter of ~ 1 mm. Phantom was filled with 130 MBq of 18F solution, assuring that the percentage of dead time losses and randoms were not higher than 5% of the total event rate. PET image was acquired in list mode in air and in water as the scattering medium, using Biograph mCT that combines 3 ring PET and 128-slice CT scanner. Total single count rate was varied by collecting 11 data sets of 5 minute frames over 14 hours and was in the range of routine nuclear medicine scans. Each of the data sets was reconstructed using analytical Filtered Back Projection (FBP) algorithm, Iterative Ordered Subsets Expectation Maximization (OSEM) algorithm (4 iterations, 24 subsets) and Iterative TrueX algorithm incorporating a specific correction for the point spread function (4 iterations, 21 subsets), each with and without TOF information. Spatial resolution was evaluated as the full-width at half-maximum (FWHM) of the reconstructed intensity profile of the line source**. Results** For our measurements in the air as well as in the water, FWHM values were constant within 1% in the interval of observed total single count rate, for each of the studied reconstruction Methods. FWHM in air was 5.2 mm, 4.1 mm and 2.4 mm for FBP, OSEM and TrueX; and 5.3 mm, 4.0 mm, and 2.4 mm for FBP+TOF, OSEM+TOF and TrueX+TOF respectively. FWHM in water was 5.4 mm, 4.6 mm and 2.6 mm for FBP, OSEM and TrueX; and 5.5 mm, 4.8 mm, and 2.8 mm for FBP+TOF, OSEM+TOF and TrueX+TOF respectively. **Conclusion** Our study confirms spatial resolution values for Biograph mCT PET scanner cited by Siemens. Both in air and in water, TrueX reconstruction algorithm resulted in best value of FWHM, followed by OSEM and FBP. Water degraded spatial resolution in comparison to the measurements in air for all reconstruction algorithms. Incorporation of TOF information resulted in marginally improved FWHM only in the case of OSEM reconstruction of measurement in air; therefore we may conclude that for PET spatial resolution evaluated with minute-dimensional phantom capillaries improvement due to TOF is negligible.

## TP005

### Work flow with manual re-registration of cardiac 18F-FDG PET and attenuation correction CT to compensate for respiratory motion: Effects and inter-operator variability.

**C. S. D. Juhl**[1], N. L. Christensen[1], L. W. Møller[1], R. Nielsen[2], K. Bouchelouche[1], L. P. Tolbod[1]; [1]Department of Nuclear Medicine & PET-Center, Aarhus University Hospital, Aarhus N, DENMARK, [2]Department of Cardiology, Aarhus University Hospital, Aarhus N, DENMARK.

**Aim**: Cardiac PET exams with CT for attenuation correction are increasing in number. However, due to different natures of the PET (average over many respiratory cycles) and the CT exam (snap-shot during one respiratory cycle) and the large difference in density of the cardiac and lung tissue, attenuation artefacts are often observed on the lateral wall of the left ventricle. Many strategies has been proposed to reduce these artefacts, including averaging multiple CTs, respiratory gating and manual re-registration[1-3]. However, for scanner platform-independent implementation, manual re-registration is currently the most feasible. In this study, we examine both the effect on misalignment artefacts and the inter-operator variability of manual re-registration performed by the technologist in a step before the final image reconstruction and verified by a second technologist before image analysis. **Method**: 40 18F-FDG viability scans were examined. After the patient scan, a fast image reconstruction of low quality was made and used for manual re-registration of PET and AC CT, before starting the high quality reconstruction used for analysis. The left ventricle was reoriented and segmented in QPS (Cedar-Sinai) and quantified using AHA-17-scores. Comparisons were made between 1) no re-registration, 2) re-registration by two independent technologists. Differences of 10% on the segment level were considered significant [2-3]. Results and conclusion: When no manual re-registration was performed, significant artefacts were observed in 15 % (6/40) of the scans, and, as expected, mainly in lateral segments. It was estimated that 80% (5/6) of these artefacts could be reduced using manual re-registration procedure. This is in agreement with previous reports[1-3]. The inter-operator variability was generally low, except in a few cases where the manual re-registration resulted in new artefacts. These were, however, easily identified and eliminated by second technologist in the verification-step resulting in an overall insignificant inter-operator variability. In conclusion, manual re-registration reduces artefacts due to misalignment in 18F-FDG viability studies and can be performed with insignificant inter-operator variability. We suggest that manual re-registration is performed routinely in daily clinical practise combined with control by a second person. References:1)Kennedy J.A. et al., *J Nucl Med 2009;* 50:1471-1478, 2)Lautamäki R. et al., *Eur J Nucl Mol Imaging 2008;35:*305-310, 3)Martinez-Möller A. et al., *J Nucl Med 2007;48:*188-193

## TP006

### Advanced 18F-FDG PET reconstruction method for detection low accumulation tumors adjacent to the bladder

**M. Yamamoto**, Y. Okura; Hiroshima International University, Higashihiroshima,Hiroshima, JAPAN.

Background and purpose: In 18F-FDG PET study, it is difficult to detect small tumors adjacent to the bladder with low accumulation of 18F-FDG, because of the high activity in the bladder. By the suppression of the effect of high activities in the bladder, detection of tumors in the area of pelvis will be more easily. The purpose of this study is to develop improved reconstruction method to suppress the effect of high activity in the bladder. Methods: We propose improved reconstruction algorithm consisted of three steps. First, "initial" reconstruction process are performed by OSEM and the bladder area is determined by bladder detection algorithm which we developed. Second, pixel value in the sinogram corresponding to the bladder area was suppressed using cutting value technique and interpolation processing. In our algorithm, the interpolation method was applied along the curve in the sinogram according to the pixel position of reconstructed image. Finally, we got the final reconstructed images from the processed sinogram using OSEM reconstruction method. For evaluate our method, we used five numerical phantoms and projection data which were calculated by Geant4 application for tomographic emission (GATE v6.2). In the numerical phantom, pelvis bone, bladder and small tumor were modeled. Reconstructed images by our method were evaluated subjectively by three physicians and three technologists. Evaluation was carried out with comparison to normal OSEM reconstruction method by categorizing the grade of detection difficulty from 1 to 5(difficult). Results and Discussion: As results, our method showed better performance than normal reconstruction method for 18F-FDG PET images of pelvic lesion. 75% of subjective results demonstrated that small activities (tumor) adjacent a high activity area (bladder) of reconstructed images by our method were detected apparently. Since our method was well focused on bladder area, the effect to reconstructed images of other area (e.g. brain, abdomen) should be investigated carefully.

## TP007

### The usability evaluation according to the application of bismuth shields in PET/CT examination

**J. Kim**[1], S. Nam-Kung[2], J. Lee[3], H. Park[4]; [1]Seoul Medical Center, Seoul, KOREA, REPUBLIC OF, [2]Konkuk Univeristy Medical Center, Seoul, KOREA, REPUBLIC OF, [3]Philips Heathcare Korea, Seoul, KOREA, REPUBLIC OF, [4]Shingu College, Seongnam, KOREA, REPUBLIC OF.

**Purpose**: Recently PET/CT with the development of CT, reduction of exposure dose for various studies is underway. Study of bismuth shields in these studies is actively underway, and has already been applied in the clinical. However, the application of the PET/CT examination was not activated. Therefore, through this study, depending on the application of bismuth shields in the PET/CT examination the quality of the image, and to identify the impact on the SUV. Materials and Methods: In this study, to apply to the shielding of the breast, by using the bismuth shields that contains 0.06 mm Pb ingredients, was applied to the PET/CT GEMINI TF 64 (Philips Healthcare, Cleveland, USA). Phantom experiments using the NEMA IEC Body Phantom, images were acquired according to the presence or absence of bismuth shields apply. Also, When applying, images were obtained by varying the spacing 0, 1, 2 cm each image set to the interest range in the depth of the phantom by using EBW-NM ver.1.0. Results: When image of the PET Emission acquires, the SUV was in increased depending on the use of bismuth shields, difference in the depth to the surface from deep in the phantom increasingly SUV increased ($P<0.005$). Also, when using shields, as the more gab decreased, SUV is more increased ($P<0.005$). Conclusion: Through this study, PET/CT examination by using of bismuth shields which is used as purpose of reduction dose be considered. When using shields, the difference of SUV resulting from the application of bismuth shields exist and that difference is more decreased as gab of shields and surface is wider. Therefore, setting spacing of shield should be considered, if considering the reduction of the variation of SUV and image quality, disease of deep or other organs should be a priority rather than superficial disease. Through this study, when applying identified to clinical examination, the reduction of unnecessary exposure is considered.

## TP008

### Dose rate from patients after PET/CT scan with $^{18}$F (FDG and Choline)

**A. Canudo**[1], D. Dantas[1], B. Martins[1], B. Freitas[1], S. Chaves[1], V. Santos[1], C. Oliveira[2], D. Costa[2], R. Parafita[1]; [1]Medical Consult SA/ Fundação Champalimaud, Lisboa, PORTUGAL, [2]Fundação Champalimaud, Lisboa, PORTUGAL.

**Introduction**: Recommended activities from international organizations (ICRP, EANM ARSAC) for all kind of Nuclear Medicine investigations are set to provide good image quality with the lowest possible dose rate. These recommendations are based in the ALARA principle (As Low As Reasonable Achievable). Since the beginning of our clinical activity, at the Nuclear Medicine-Radiopharmacology Unit of the Champalimaud Foundation, all staff engages in that principle and developed a practice to verify its performance. The main objective of this study is to prove that after the administration of $^{18}$F-DG or $^{18}$F-Choline (37MBq/10kg), the dose rate from patients leaving the department is well below 50μSv/h (Florida Administrative Code, NUREG 1492), ensuring safety of general public and environment. Material and Methods: The dose rate (μSv/h) was measured from 257 patients (132 women and 125 men) after undergoing PET/CT investigations, with $^{18}$F labeled FDG or Choline just before leaving the unit. Measurements were made at 1 meter in front of the bladder, after micturition. A Geiger-Muller (Thermo Scientific - Radeye B20-ER) equipment was used. The obtained data - dose rate adjusted to the background - was related to the patient's Body Mass Index, the administered activity and the time between injection and measurement. All patients received an activity according to their weight and remained in the Unit for periods between a minimum of 1 to a maximum of 5 hours after intravenous injection. Results: Dose rate became smaller with longer stays at the Unit. The longer stays were related with the need for delayed studies during staging and restaging of oncological diseases. For administered activities of 37MBq/10Kg of $^{18}$F-DG or $^{18}$F-Choline, all patients left the Unit with dose rates lower than 50μSv/h (the average was 6,5μSv/h). On average, patients remain in the department about 3-4hours, and the mean dose rate in this time range did not exceed 6μSv/h in 39% of the sample. Considering the worst case scenario, in which patients remained 1 to 2hours in the department (7%), the mean dose rates never exceeded 11μSv /h. Conclusion: Our data demonstrates that for recommended administered activities of $^{18}$F-DG or $^{18}$F-Choline the dose rate is 8 times lower than the proposed limit, when patients remain 3-4hours in the Unit. Even in the worst case scenario (1-2hours), the dose rate is 4.5 times lower than the limit. Therefore, this type of diagnostic procedures do not add significant radiological risk to patients relatives, general public and environment.

## TP009

### Study to Protocol of PET Acquisition time for Patient Body Type in PET/CT Scan

**S. Cho**[1], J. Ham[1], K. Kang[1], Y. Ban[1], S. Lee[1], H. Park[2], H. Lim[1], C. Lee[1]; [1]Yonsei University Health System, Seoul, KOREA, REPUBLIC OF, [2]Shingu College, Seoul, Korea, REPUBLIC OF.

**Purpose** Whole-body PET using radiopharmaceutical is one of the imaging study Methods for physiological changes of body. High specificity of the PET-CT examination is used to detect an early stages of cancer and metastatic cancer by imaging a physiological changes. During the imaging process, PET image has been characterized by a relatively low image quality due to its low sensitivity and the acquisition of random and scatter coincidences as well as patients figure. Therefore, the image quality as the changes of the acquisition times of patient weight was evaluated in this study. **Materials and Methods** Thirty patients who presented to our hospital were enrolled. They were divided to normal, overweight, and obese group using BMI index, respectively. The patients with a liver disease and diabetes were excluded. $^{18}$F-FDG was administered to the patients as 5.2MBq per Kg. After an hour from an injection, image acquisition was obtained as List mode in a part of liver in 1 bed. SNR (signal-to-noise ratio) of each groups acquisition times were confirmed from the caculated radiation counts and random fractions. The statistical significance of three groups was confirmed through one-way ANOVA test. On the basis of the counts of 2 minutes on normal group, the SNR of overweight group and obese group were compared. **Results** The SNR were increased with loger aquisition time in 3 groups. In the condition of same acquistion time, the SNR had a statistical significance($p$<0.05). The SNR were decreased to the normal, overweight, and obese, respectively. Liver activity had no significance difference on each group and RF had the significance differences ($p$<0.05). On the basis of the counts of 2 minutes on normal group, there were no statistical significance in a three minute aquisitions of overweight group and two minute aquisitions of obese group($p$=0.150). **Conclusion** In this study, the administrated amount of radiation dose did not adjust as the change of the patients weight. Increasing the acquisition time when the administration of the same amount of dose was able to get a good result of SNR. When the Based 2 minute on normal group, if overweight and obese case the increased acquisition time of 3 minute was able to obtain a similar SNR. On the basis of the normal group, the acquisition times of overweight and obese group were increased to 3 minutes per bed and the SNR were similer to the normal group.

## TP010

### CT findings from a PET/CT scanner assessment

**T. F. Vaz**[1], D. C. Costa[2], R. Parafita[3]; [1]Nuclear Medicine - Escola Superior de Tecnologia da Saúde de Lisboa, Instituto Politécnico de Lisboa, Lisbon, PORTUGAL, [2]Nuclear Medicine - Radiopharmacology, Champalimaud Centre for the Unknown, Champalimaud Foundation, Lisbon, PORTUGAL, [3]Nuclear Medicine - Radiopharmacology, Champalimaud Centre for the Unknown, Champalimaud Foundation / Medical Consult, Lisbon, PORTUGAL.

**Aim** To assess and identify acquisition parameters for the Computed Tomography (CT) component of a Positron Emission Tomography (PET)/CT scanner, using the lowest dose possible, without compromising image quality (linearity, uniformity and noise). **Materials and Methods** CT acquisitions (Philips Gemini TF PET/CT 16) of Catphan®503 phantom were undertaken with different protocols, varying voltage (90, 120, 140 kVp) and exposure (20, 25, 30, 35, 40, 45, 50, 55, 60, 100, 230, 265, 305 mAs), but keeping all remaining acquisition parameters of the standard protocol of low dose CT constant (viz. thickness=5mm; increment=-5mm; collimation=16x1.5mm, pitch=0.813; rotation=0.5s, FOV=600mm; matrix=512x512 pixels). Hounsfield Units (HU) in the CT images were measured in regions of interest (ROI): a) CTP404 Module with slice width, sensitometry and pixel size (seven ROI placed in sensitometry targets made from different density materials: Air, PolyMethylPentene (PMP), Low Density PolyEthylene (LDPE), Polystyrene, Acrylic, Delrin® and Teflon®); b) CTP486 Image uniformity module (one ROI placed in center and four in periphery). Each measurement was repeated 5 times to obtain mean HU and their standard deviation (SD). Linearity was studied for different acquisitions via Pearson coefficient correlation. Uniformity was evaluated using control charts for variables. Analysis of variance (two-way ANOVA) and multiple mean comparisons (Games-Howell test) were used to evaluate noise ($p < 0.05$ was considered statistically significant). Results There was a strong linear correlation ($r > 0.99$) between the attenuation coefficients and HU measured, indicating the contrast scale for several CT numbers to be constant. As expected, the attenuation coefficients decreased and HU increased, when increasing tube voltage. Materials with average HU were outside the specified limits, for the majority of mAs applied, included low density materials, such as PMP, LDPE and Polystyrene. The noise decreased with increasing beam CT energy, being the noisiest measurements from materials close to the HU scale limits (Air and Teflon®), showing statistically significant differences in acquisitions with 90 kVp. The variations of exposure affected more the noise measurements than the average materials HU. Conclusion Specific features of the CT component of the Philips Gemini TF PET/CT 16 scanner were obtained and characterized, including strong linear correlation between AC and HU, as well as its dependency on tube voltage.

## TP011

### Quality assurance in daily PET/CT practice: Do we meet the challenge?

**C. Baun**, K. Falch, O. Gerke; Odense University Hospital, Odense, DENMARK.

**Introduction:** The number of FDG PET/CT scans has increased dramatically in the last decade. The modality has an important role in staging of and therapy assessment in oncological patients. This has led to an increased focus on standardized protocols and compliance to guideline procedures. The EANM procedure guidelines for FDG PET/CT imaging prescribe a time interval from injection to image acquisition of 60 min ± 5 min. As our department participates in several multicenter studies the EANM guidelines provides the basis for the daily work routine. In our department the technologist records the injection- and acquisition time manually amongst others. The aim of this study was to assess a) to which degree this guidelines are followed and b) the agreement between the written and electronically obtained time via DICOM. **Methods and materials:** Manual data were obtained by extracting scan data from one random weekday per month in 2012 in the departmental database. These data were compared to the electronically registered DICOM data for each scan which served as the gold standard. 263 FDG PET/CT scans were included in the study. Scans performed with other tracers, dual- or triple time point protocols and incomplete dataset were not included. Descriptive statistics were performed. **Results:** Of a total of 263 scans 116 patients (44%) were scanned at 60 min ± 5 min, 70 patients (27%) were scanned 66-70 min and 42 patients (16%) were scanned 71-75 min after injection according to the DICOM data. In the manual data 151 patients (57%), 61 patients (23%) and 23 patients (9%) were scanned within the same intervals, respectively. All patients were scanned 50 to 120 min after injection. DICOM data showed a mean time between injection and acquisition of 69 min [range 55; 118]. The corresponding value for the manual data was 67 min [range 50; 120]. The mean time from injection to scanning start was 2 min [range -10 ; 31] shorter with manual registration than with electronical registration ($p = 0.002$, paired t test). **Conclusion:** The study shows that only 44% of the scans meet the European PET/CT guidelines. There is discordance between the electronic and the manual registration of the time. The results indicates that the technologists should pay more attention to the time slot emphasizing that 60 min describes time between the injection and the start of the PET acquisition – not the start of the CT scan.

## TP012

### 18F-Fluorid-PET-CT: Patient expectations and experiences

**C. Andersson**[1], C. Wassberg[1], S. Johansson[1], H. Ahlström[1], B. Wikehult[2]; [1]Dept. of Radiology, Oncology and Radiation Sciences, Uppsala University, Uppsala, SWEDEN, [2]Dept. of Surgical Sciences, Uppsala University, Uppsala, SWEDEN.

**Aim** To investigate if there is a need for improvement of the information to the patients before, and patients´ satisfaction during an $^{18}$F-Fluorid-PET-CT examination. **Materials & Methods** A total of 50 consecutive patients who were scheduled for $^{18}$F-Fluorid-PET-CT were asked to participate in this prospective study. Using a descriptive survey design, the data collection started November 2011 and is still ongoing. Inclusion criteria for the patients were; prostate cancer, 18 years or older and speaking and understanding the Swedish language. All patients were asked to participate in the study after the examination was completed. If the patient agreed to participate he received a questionnaire which consisted of four sections, such as; patients´ characteristics, EORTC-QLQ-C30 and EORTC-QLQ-PR25 which both are valid quality of life instruments and a section of questions constructed for this study regarding the patients´ expectations and experiences of the $^{18}$F-Fluorid-PET-CT examination. The questionnaire also offered possibilities to write comments. Each patient could choose to either complete the questionnaire directly after the examination or take it home and send it back later (within 1 month). **Results** The study is still ongoing. There are 47 patients included, and the response rate is 42 returned questionnaires. Preliminary findings showed that 62 % did not know at all or little about how an $^{18}$F-Fluorid-PET-CT examination was performed. 95 % of the participants were satisfied or very satisfied with the treatment from the clinical staff that performed the examination. Only 17 % thought the examination was quite, or very much exhausting. The comments the participants wrote (n=11) indicate that it is the time spent in the camera and the fixed positions of the body during the PET acquisition and registration that is the most strenuous for the patients (n=9). None of the participants felt claustrophobic. **Conclusion** The information to the patient before the examination needs to be improved. Different interventions are suggested to be tested in the future to improve patient satisfaction during $^{18}$F-Fluorid-PET-CT examinations.

## TP013

### The assessment of tracer extravasation in patients undergoing PET/CT examination

**G. Zonzin**, M. Bortolami, G. Masiero, M. Zappalà, S. Zampieri, R. Sanco, M. Laura, E. Zaramella, G. Saladini, L. Evangelista; Istituto Oncologico Veneto I.R.C.C.S., Padova, ITALY.

**Purpose:** The pitfall of the tracer extravasation is a common problem in nuclear medicine. Its presence can determine a misinterpretation of the images both in scintigraphic and PET exams. The aim of this study was to determine a handle method for the evaluation of tracer extravasation, using a tool normally presents in a PET/CT department. The early evidence of extravasation would avoid: 1) an examination with an uncorrected dose; 2) an examination with low quality images;and 3) an useless patient exposure to CT examination. **Materials and Methods**: For the detection of the extravasation an "Hand-Foot-Clothing" probe (HFC Monitor MOD.CMS 60D, years 2011) was used. Different values of counts were computed for verifying a possible linear response to different activities of the tracer. The parameters and measurement modality, after the shielding of the patient's body, were fixed exposing the arm employed for the tracer injection. A database of consecutive patients sent for examination PET was created. In none of our patients, a cutaneous sign of obvious tracer extravasation was reported. Finally, PET images of all enrolled patients were analyzed. **Results:** from August to October 2012, 15 out of a total of 720 patients, were included, in whom a possible extravasation was suspected due to the presence of cutaneous manifestations. In these 15 patients, only two were positive for extravasation after the evaluation by HFC probe. In both cases the calculated activity was lower than 10MBq. In these patients, a PET/CT scan was performed without determining a loss on the image quality. **Conclusions:** the above-described method for calculating the extravasation is easy to apply and feasible in all PET centers where a HFC probe is disposable for the control of staff contamination. This modality allows to verify and to quantify the extravasation, eventually thanks to the correction for decay, permitting the calculation of the real administered dose.

## TP014

### [18F] Fluorocholine PET/CT Scanning Protocol Optimisation

**B. Vidovic**, S. Rep, B. Trebec, M. Hodolic; University Medical Centre Ljubljana, Department of Nuclear Medicine, Ljubljana, SLOVENIA.

Aim: To reduce the radiation load in patients with prostate cancer using the "old" Acquisition protocol for Positron Emission Tomography combined whit Computed Tomography (PET/CT) using [18F] Fluorocholine (FCH). Materials and Methods: 815 FCH PET/CT scans of patients with prostate cancer were examined; patients were referred to this investigation for staging of primary disease or for localization of recurrence. 236 patients had early dynamic scan of the pelvis (less than 10 seconds after the intravenous injection of FCH) and delayed whole body scan (45 min after the intravenous injection of FCH). 565 patients had only delayed whole body scan with head. 14 patients had delayed whole body scan combined with early whole body scan. Meanwhile, we also reduced administered dose of FCH from standard 250 MBq/patient (in 186 patients) to 2.5 MBq/kg of body weight (in 629 patients). Results: In only 8,1% of the patients (21/236), early dynamic scan of the pelvis was necessary to get final information. In 215 patients, it was enough to start the PET/CT acquisition approx. 3 min after urination. The total effective dose, due to CT scan and FCH kinetics, in delayed whole body imaging with head decreased in average from 0,9 mSv to 2,5 mSv. Conclusion: Only one delayed whole body scan with head, performed 45 min after FCH injection, is enough to obtain good quality results and at the same time to avoid false-positive uptake related to urinary excretion. According to that, the dose reduction is more than in favor for this scanning protocol. Our new Scanning Protocol showed a relevant impact on patient management in terms of easier programming and planning of FCH PET/CT investigations.

## TP015

### (FDG) PET/CT scan with contrast enhanced CT: Which benefits for the patient?

**F. TAMBURINI**, M. VALERIA, N. CRISTINA; S. ORSOLA-MALPIGHI HOSPITAL, Bologna, ITALY.

**BACKGROUND:** Generally FDG PET/CT is performed with a low dose non diagnostic CT, after a diagnostic CT acquired in a separate session. **PURPOSE:** To evaluate the advantages of adding combined 18F- fluorodeoxyglucose (FDG) PET /CT scan with contrast enhanced CT, both acquired by a last generation PET/CT system versus two separate exams in oncologic patient. **MATERIAL AND METHODS:** In our centre we performe 1/ week hybrid session for oncologic patients. All the patients are referred by our hospital's oncology specialists. They undergo both a standard FDG PET /CT and a diagnostic contrast enhanced CT in the same imaging session. We use a PET/CT tomograph with 16 slices (GE, discovery, STE). So far FDG PET is performed with standard protocol while CT acquisition technique depends on the disease under a valuation. **RESULTS:** So far no patients complained about the procedure. We had no significant adverse reactions. We noticed an increase in time for image acquisition of approximately 15 minutes/ patient on average, providing, on the other side, fully diagnostic image series and conclusive reports. The execution of PET/ce CT in the same session on the same hybrid tomograph is convenient for the patient in term of time sparing and costs. The patient is admitted to the hospital once and must bear the costs for one trip only. If the two Methods are carried out separately, the patient waists more time and travel expenses doubles. Furthermore, since most of oncologycal patients come to the hospital with a companion, the social costs for work permits are reduced too. In addition since both the Methods require fasting, one session exam leads to a reduced discomfort for the patient. **DISCUSSION:** Despite a mild increase in time for image acquisition, a fully hybrid exam is very convenient for the patient in terms of time saving and costs.

## TP016

### $^{18}$F-FDG Colonic Uptake by Oral Anti-Diabetic Drugs Including Metfomin in PET/CT Scan

**S. Kim**[1], H. Park[2], J. Kim[1], Y. Bahn[1], H. Lim[1], J. Kim[1], C. Lee[1]; [1]Yonsei University Health System, Seoul, KOREA, REPUBLIC OF, [2]Department of Radiological Technology in Shingu College, Seongnam, KOREA, REPUBLIC OF.

**Purpose:** The uptake of $^{18}$F-FDG is often observed in normal cell of colon to patients who have non-insulin-dependent diabetes mellitus and had taken anti-diabetic drugs including Metformin in PET/CT scan. In this study, the region of colon was compared between the patients who took anti-diabetic drugs including Metfomin and other patients who took the other anti-diabetic drugs through SUV measurements. **Materials and Methods**: A hundred-eighty patients were studied. 120 patients who have non-insulin-dependent diabetes mellitus (Including Metformin : 60, Excluding Metformin : 60) and 60 patients as a control group were composed. The patient fasted at least 6 hours before receiving an intravenous injection of 370-592 MBq (10~16mCi) of $^{18}$F-FDG. Scanning from the base of the skull though the mid thigh was performed using the Discovery STe PET/CT Equipment (GE Healthcare, Milwaukee, WI, USA). The highest uptake region was measured SUV among ascending, transverse and descending colon. **Results**: The values of patients who took the anti-diabetic drugs including Metformin were 6.16±3.64 g/ml, 4.41±2.94 g/ml, and 5.46±2.44 g/ml. The patients who took the anti-diabetic drugs which does not have Metformin were 3.05±1.39 g/ml, 2.08±0.97 g/ml, and 3.15±1.85 g/ml. The control group were 2.02±0.88 g/ml, 1.68±0.87 g/ml, and 2.19±1.88 g/ml. **Conclusion:** The effect of the intake of Metformin was observed from the SUV on region of large bowel in this study. Thus, it could be helpful for the results by identifying the ingredient of anti-diabetic drug before the examination and the possibility of interpretation of false-positive will be reduced.

## TP018

### Usefulness of CTAC Shift Correction Method of Artifact by Diaphragm in PET/CT

**J. HAM**, C. Kang, S. Cho, Y. Bahn, S. Lee, H. Lim, J. Kim, C. Lee; Yonsei University Health System, Seoul, KOREA, REPUBLIC OF.

**Purpose:** Cold artifacts are often found in decrement correction image by mismatch between LDCT image and Emission image near diaphragm due to patient's respiration. This research studied reduction of cold artifact by patient's respiration using CTAC Shift among correction Methods. **Object and Method:** From March to September in 2012, 30 patients who had cold artifacts by respiration were targeted using PET/CT Discovery 600 (GE Healthcare, MI, USA) equipment. Patients with cold artifacts were additionally scan in diaphragm area, and the image shown cold artifacts at whole body scan were corrected using CTAC Shift. Cold artifacts including image, additional scan image and CTAC Shift correction image were evaluated as 1~5 points with naked eye by one nuclear medicine expert, 4 radiological technologists with over 5 year experience. Also, standard uptake value of 3 images was compared using ANOVA. **Results:** Additional scan image and CTAC Shift correction image received relatively higher score in naked eye evaluation than cold artifacts including image. The additional scan image and CTAC Shift correction image had high correlation as the results of ANOVA of standard uptake value and did not show significant difference. **Conclusion:** When cold artifacts are appeared by patient's respiration at PET/CT, it causes not only patient inconvenience but troubles in scan schedule due to extra radiation exposure and time consumption by additional scan. But if CTAC Shift correction image can be acquired without additional scan, it is considered to be helped in exact diagnosis without unnecessary extra radiation exposure and additional scan.

## TP019

### A novel C-11-2DG PET application for cognitive mapping of the brain's functional response

**M. Li**; Institute of Nuclear Energy Research, Taoyuan, TAIWAN.

**Objectives:** It has been argued that brain research has contributed to understanding of economics, marketing, law, and neuro-strategy fields. Cognitive neuroscientists are also interested in these issues. This paper examines the potential contributions of imaging brain functions with [1-C-11]2-Deoxy-D-Glucose to visual-auditory-cognitive research and practice. Our project is an interdisciplinary collaboration at the intersection of neuroscience and management studies, which we study by examining brain activity in visual-auditory-cognitive stimulations. This study integrates the two approaches, using cognitive neuroscience and PET imaging to enhance our understanding of functional maps in vivo related to both body region and modality of sensory information in the human brain. **Methods:** This research by using the [1-C-11]2-Deoxy-D-Glucose technique was used to measure human cerebral glucose utilization during functional activation by ex-ante controlled. The normal volunteer subjected to sensory stimulation (visual, auditory, or cognitive) after [1-C-11]2-Deoxy-D-Glucose injection showed focal increases in glucose metabolism in reply to these stimulus. The definitions of the visual-auditory-cognitive: Visual:1. To close the eyes and image nothing. 2. To open the eyes and imaging music for piano. Auditory:1. To close the eyes and image nothing. 2. To open the eyes and listening music for piano. Cognitive:1. To close the eyes and image nothing. 2. To open the eyes and stroking the fingers with the rhythm of the music for piano. **Results:** Fig.1 left presents the image of the brain of subject stimulated visually, whereas the visual stimulation causes a higher glucose metabolism in striate cortex (white arrow). Emission tomography of the brain of subject listening to the music for piano showed in Fig.1-middle, whereas the region of auditory cortex was more extensive activation (white arrow). The image Fig.1-right of subject obtained during somatosensory stimulation. An extensive area of the cortex, of which the postcentral gyrus is the only part, was activated by the cognitive stimulation. **Conclusions:** The local glucose metabolic activities of the human brain during visual-auditory-cognitive stimulation that can be provide PET images by the [1-C-11]2-Deoxy-D-Glucose method. We aim to advance this research to examine neural activity that capture the essential features for social science application.

## TP020

### Routine preparation of 68Ga-DOTA-Substance P doses for locoregional administration follow up of 213Bi-DOTA-Substance P in the course of glioma therapy

**D. Pawlak**[1], J. Kunikowska[2], L. Krolicki[2], A. Kopatys[2], W. Tkacz Garnuszek[1], M. Maurin[1], R. Mikolajczak[1]; [1]Radioisotope Centre POLATOM, National Centre for Nuclear Research, Otwock, POLAND, [2]Nuclear Medicine Department, Medical University of Warsaw, Warsaw, POLAND.

**Introduction**: Targeted alpha-radionuclide therapy of functionally critically located gliomas with 213Bi-DOTA-[Thi8,Met(O2)11]-Substance P can be performed after locoregional administration of radiopharmaceutical to the tumor cavity after tumor resection via catheter. We proposed to use 68Ga-DOTA-[Thi8,Met(O2)11]-Substance P prior to therapeutic dose administration to exclude any leakage of the radiopharmaceutical. In addition, PET imaging using 68Ga-DOTA-[Thi8,Met(O2)11]-Substance P co-injected with 213Bi-DOTA-[Thi8,Met(O2)11]-Substance P therapeutic dose administered to the glioma patient allowed assessing the uniformity of dose distribution. Aim: The aim of this work was to establish the procedure for preparation of 68Ga-labeling of Substance P and QC in hospital radiopharmacy conditions. **Methods**: First 3 mL of eluate of the 68Ge/68Ga generator (iThembaLABS) with radioactivity of 350 - 780 MBq of 68Ga were used for labeling of 100 µg DOTA-[Thi8,Met(O2)11]-Substance P (piChem, Austria) dissolved in 2.4 mL of 1.25 M AcONa, pH of about 3.7. Incubation was carried out at 95oC for 15 min using heating oven. Radiochemical purity was assessed by ITLC-SG with 0.05M sodium citrate as a developing solution. The suitability of this TLC system for routine QC was prior validated by HPLC using Jupiter 4µ Proteo 90A (150x4.8 mm, Phenomenex) column with isocratic elution (25% of 0.1%TFA/ACN, 75% of 0.1%TFA/H2O, 0.6 mL/min). After radiolabelling the solution of 68Ga-DOTA-[Thi8, Met(O2)11]-Substance P was purified by SPE method using Waters OASIS HLB columns, then diluted to about 10 mL and sterilized by membrane filtration 0.22 µm directly to syringes. **Results and conclusions**: Radiochemical purity of 68Ga-DOTA-[Thi8,Met(O2)11]-Substance P before purification was in the range 73.9 to 92.3% (mean 85.7 ± 5.8) and after purification was in the range 96.0 to 99.7% (mean 98.3 ± 1.1) in 18 consecutive labeling runs in the procedure lasting 20-25 min. High radiochemical purity of 68Ga-labelled Substance P allowed its use in patients. PET images acquired directly after administration of mixed 68Ga/213Bi-DOTA-[Thi8,Met(O2)11]-Substance P dose showed orthotopic radioactivity distribution. Acknowledgement: IAEA co-ordinated research project No. 16476: Development of 68Ga based PET-Radiopharmaceuticals for Management of Cancer and other Chronic Diseases.

## TP021

### Effects of Time of Flight image reconstruction on myocardial perfusion $^{13}$N-ammonia PET/CT

**B. Olsson**[1], S. Saran[1], K. Ekholm[1], E. Evetovics[2], F. Hedeer[1], J. Jögi[1], J. Oddstig[2], C. Hindorf[2]; [1]Department of Clinical Physiology, LUND, SWEDEN, [2]Radiation Physics, Lund, SWEDEN.

**Aim** Modern PET/CT cameras enable reconstruction with time of flight (TOF) technique to improve the image quality by reducing the noise. The ASNC (American Society of Nuclear Cardiology) guidelines for myocardial perfusion with PET/CT have omitted recommendations on whether TOF should be applied since this is considered as a new technique. $^{13}$N-ammonia is used for assessing myocardial perfusion in rest and stress. The aim of this study was to evaluate the effect of TOF reconstruction on cardiac volumes and image quality. **Material and Methods** Six male patients (mean BMI 27.4) underwent a one-day rest-stress examination. All images were acquired using a whole-body 64-slice PET/CT scanner (GE Discovery 690). The imaging sessions (19 minutes) began at the time of injection of 500-700 MBq $^{13}$N-ammonia (rest and stress). The stress examination was performed with adenosine at least 50 minutes after the beginning of the rest examination. The images (static and gated) were reconstructed with and without TOF. The time for reconstruction with TOF was increasedfrom 12 minutes to 16 minutes in relation to the reconstruction without TOF. The images were evaluated for EDV (End Diastolic Volume), ESV (End Systolic Volume) and EF (Ejection Fraction) using GE CardIQ Physio. The images were also visually analyzed for subjective image quality by one reader. **Results** EDV was 10% higher and ESV was 14% higher when TOF reconstruction was used. EF was not affected by the type of reconstruction. The visual evaluation of the images showed an improvement of the image quality using TOF. The nosie was reduced and an increased contrast was experienced. **Conclusion** Image quality is subjectively improved and cardiac volumes are increased when TOF reconstruction is used in 13N-ammonia PET/CT. This may have impact on image interpretation.

## TP022

### Biological validation of the novel dopamine transporter (DAT) PET radioligand [$^{18}$F]FEPE2I in the rodent brain: A pilot study in rats using a Concorde R4 pre-clinical scanner

**B. Gulyas**[1], P. Padmanabhan[2], J. Lu[3], M. Kan Enci[3], L. Zheng[4], R. Keddal Thulasiraman[4], C. Halldin[1]; [1]Karolinska Institute, Stockholm, SWEDEN, [2]Lee Kong Chian School of Medicine, Singapore, SINGAPORE, [3]Defence Medical and Environmental Research Institute, Singapore, SINGAPORE, [4]Singhealth Experimental Medicine Centre, Singapore, SINGAPORE.

**Aims** [$^{18}$F]FEPE2I is a novel PET radioligand for the in vivo quantification of the dopamine transporter (DAT) in both non-human primates and humans (Schou et al., 2009; Varrone et al., 2009, Sasaki et al., 2012). With the aim of evaluating the suitability of [$^{18}$F]FEPE2I as a radioligand of choice in "humanised" small animal disease models of dopamine system related pathologies, we measured whole brain and striatal uptake (%SUV) and striatal binding ($BP_{ND}$) of the radioligand in rats. **Materials and Methods** Three male Sprague Dawley rats (weight: 326.25±8.66 g; anesthesised with 1.3-1.5 % isoflurane) were given an injection of 19.03±2.17 MBq [$^{18}$F]FEPE2I via the tail vein. Using a Concorde R4 pre-clinical PET scanner (Knoess et al., 2003), dynamic data acquisition lasted for 60 min. Image reconstruction was done with the ASI Pro VM™ Micro PET Analysis software, using 10 min reconstruction time frames. The ROI's were manually delineated on the following regions: whole brain, left and right striatum, cerebellum. %SUV values in whole brain and striatum (between 10 and 60 min) as well as $BP_{ND}$ values in the striatum were calculated; for the $BP_{ND}$ calculation the cerebellum was used as the reference region. **Results** The average %SUV value in the left striatum was 160±15, in the right striatum 159±9, in total striatum it was 160±11. The average %SUV value in the whole brain (without the striatum) was 59±3 and in the cerebellum it was 42±4. The $BP_{ND}$ in the striatum was 2.13±0.32. **Conclusions** The present investigation, using a Concorde R4 pre-clinical PET imaging system and Sprague Dawley rats, demonstrate that [$^{18}$F]FEPE2I appears to be a suitable radioligand for the in vivo quantification of DAT in the rodent brain, with special regard to the striatum. However, the assessment of $BP_{ND}$ in other brain structures than the striatum was not possible due to the resolution characteristics of the scanner (FWHM = 1.65 mm). Consequently, further experiments using a high resolution (FWHM « 1 mm) pre-clinical PET scanner with high sensitivity (Nagy et al., 2013) are required to explore the fine modalities of the binding in extra-striatal brain structures as well as the usefulness of the radioligand in various small animal disease models. References Knoess et al. Eur J Nucl Med Mol Imaging 2003(5):737-747. Nagy et al., J Nucl Med. 2013 (submitted) Sasaki et al. J Nucl Med. 53(2012):1065-73. Schou et al. 19(2009):4843-4845. Varrone et al. Synapse 63(2009):871-880.

## TP023

### Correlation Between in vitro and in vivo 18F-FDG Uptake and GLUT's expression in Breast Cancer

**M. Casanova Martins**[1], C. Matos[2], A. M. Abrantes[2], J. Casalta[2], R. Silva[1], P. Lapa[1], G. Costa[1], J. Pedroso de Lima[3], M. F. Botelho[4]; [1]Nuclear Medicine Department, University Hospitals of Coimbra, CHUC, Coimbra, PORTUGAL, [2]Biophysics Unit, IBILI, Faculty of Medicine, University of Coimbra, Coimbra, PORTUGAL, [3]ICNAS, University of Coimbra, Coimbra, PORTUGAL, [4]CIMAGO, Faculty of Medicine, University of Coimbra, Coimbra, PORTUGAL.

**AIM**: Breast cancer represents a very heterogeneous group of tumors with high variability regarding 18F-FDG uptake. This variability limits PET's role in the clinical evaluation of patients with breast cancer. The purpose of this study was to determine 18F-FDG uptake pattern in breast cancer cell lines presenting different estrogen, progesterone and HER2/neu receptor's expression and to establish a correlation between GLUT's 1, 3, 5 and 12 profiles and each of the cell lines used. We also compare the previous results with the standardized uptake values (SUVs) determined in 18F-FDG PET/CT scans of breast cancer patients with histologies similar to those of the in-vitro studies. **MATERIALS AND METHODS**: Three human breast cancer cell lines have been used: MCF-7, HCC1806 and HCC1954. MCF-7 only express estrogen receptors; HCC1806 exhibit neither hormone receptors nor HER2/neu's (triple negative); and HCC1954 only overexpress HER2/neu. In vitro 18F-FDG uptake studies were conducted with these cells and the expression of GLTU-1, GLUT-3, GLTU-5 and GLUT-12 were assessed by flow cytometry. Additionally, SUVs of 51 18F-FDG PET/CT scans from 46 patients, performed between October 2006 and September 2010 were retrospectively analyzed. The inclusion criteria were the presence of 18F-FDG uptake in the primary tumor or in local recurrent disease and the histological similarity to the cell lines studied in vitro. **Results:** HCC1806 and HCC1954 cells presented higher GLUT-1, GLUT-3 and GLUT-12 expressions than MCF-7. However, concerning 18F-FDG uptake, MCF-7 presented the highest percentage values over time. Moreover, the triple-negative cell line (HCC1806) showed a low and stable (<1.5 %) in vitro uptake. Comparatively, 18F-FDG in-vivo uptake in PET was higher in triple negative tumors (SUVmax mean = 12.6 ± 7.0). Triple negative tumors and tumors expressing estrogen receptors and HER2, but negative for progesterone receptors showed similar 18F-FDG uptake values (respectively mean SUVmax = 5.2 ± 2.5 and mean SUVmax = 6.6 ± 3, 0). We also found an inverse correlation between SUV and Bloom differentiation degree. **CONCLUSION**: A negative correlation was found between 18F-FDG in vitro uptake and GLUT-1, 3 and 12's expressions in the referred cell lines. The same type of correlation was observed between in vivo 18F-FDG uptake and tumor differentiation degree, in agreement with the known aggressiveness of undifferentiated tumors. Nevertheless, the differences found in uptake profiles, between in vivo and in-vitro studies of breast tumors, warrant further research.

## TP024

### Difference between early and delayed acquisition of 18F-Methylcholine PET/CT in prostate cancer

**V. Mautone**[1], E. Sintuzzi[1], A. Biagioli[2], A. Moretti[2], P. Caroli[1], A. Musto[2], R. Galassi[2], F. Matteucci[1]; [1]Nuclear Medicine Unit, IRCCS Istituto Scientifico Romagnolo per lo Studio e la Cura dei Tumori (IRST), Meldola, ITALY, [2]Nuclear Medicine Unit, Department of Radiology, Morgagni Pierantoni Hospital, Forlì, ITALY.

**AIM** 18F-Methylcholine is a radiopharmaceutical used for the diagnosis of prostate cancer and it also plays a definitive role in restaging when PSA levels are increasing. Our study was based on the assumption that Choline has a rapid clearance rate from the blood-pool and on the fact that the gold standard for acquisition has been established at 50 minutes post injection (P.I.). We evaluated whether early acquisition (5 minutes P.I.) is equivalent to delayed acquisition (standard acquisition) and also compared standardized uptake values (SUVbw, g/ml). **MATERIAL and Methods** Twelve patients between 70 and 90 years of age with a median weight of 88 kg and a median BMI of 29 were studied at IRCCS IRST in Meldola. Following administration of a dose of 3MBq/ kg of 18F-methylcholine, patients underwent two PET/CT scans on a GE Discovery LS, the first after 5 minutes and the second after 50 minutes. The protocol was performed with a CT value of 120 kW and 80-140 mAs at 5 minutes P.I. and 120 KW and 80-140 mAs at 50 minutes P.I, whit a pitch of 1.5 and a scan time of 30-40 second. The scan started from the root of the thigh and ended at the base of the skull. The time of acquisition for the PET, normally established at 3 minutes per bed, was increased by about 30 seconds per bed during the second scan, for a total time of 3 minutes and 30 seconds per bed. After acquisition we measured and compared the SUVs of physiological uptake in healthy organs ( liver, salivary glands, spleen, kidneys, bones and muscles) and metastatic lesions via the Xeleris 1.1, with a ROI of 2 cm in diameter. **RESULTS** The Wilcoxon test was used to process data as the SUVs of healthy organs and metastatic lesions were not normally distributed. Two different SUVs were registered for the physiological uptake; early acquisition SUV=8.97 and delayed acquisition SUV=7.28 ($p< 0.0001$). With respect to lesions, early acquisition SUV was 5.73, while delayed acquisition SUV was 7.12 ($p=0.0005$) **CONCLUSIONS** On the basis of our results, it can be concluded that acquisition at 50 minutes P.I. was more effective than the early acquisition as a much higher resolution was obtained between lesions and background, which is essential for restaging and treatment monitoring.

## TP025

### The best way for glycaemia measurement in patients undergoing 18F Fluorodeoxyglucose (FDG) positron emission tomography (PET)/computed tomography (CT)

**M. Trevisan**, E. Carpin, A. Biscotto, G. Zonzin, G. Saladini, L. Evangelista; Radiotherapy and Nuclear Medicine Unit, Istituto Oncologico Veneto I.R.C.C.S., Padova, ITALY.

**Background**: as suggested by European and American guidelines, the blood level glucose should be checked before 18F-FDG administration, because tumour FDG-uptake is reduced by hyperglycaemic states. European guidelines reports that a glucometer or a similar bedside device should be used for this purpose. The aim of our study was to assess the difference in blood glucose levels between two Methods of glycaemia measurement, it means capillary vs. venous in a subset of oncological patients performing PET/CT examination. **Materials and Methods**. We prospectively evaluated 103 patients who underwent FDG PET/CT for the evaluation of oncological status. We performed a double check of capillary and venous blood glucose levels by using a dedicated stick that was calibrated and validated with a control solution (three times per week). The continuous data were compared by parametric tests (paired and un-paired t-Student test). The p value <0.05 was considered statistically significant. **Results**. Out of 103 patients, 10 were diabetic and 93 were non-diabetic. The capillary blood glucose levels were significantly lower than venous values (102.61±22.59 vs. 110.92±24.57; p=0.0001). In particular, the difference resulted statically different between diabetic and non-diabetic patients, being 144.50±31.89 vs. 159.20±39.1 and 98.11±15.97 vs. 105.73±15.45, respectively (both p<0.05). The percentage of variability between venous and capillary blood glucose levels was similar between diabetic and non-diabetic subjects (p=0.662). **Conclusion**. The venous and capillary blood glucose levels are different from each others, although similar for diabetic and non-diabetic patients. Therefore, in patients who perform FDG PET/CT examination, a preferential way of blood glucose level measurement should be established, because they are not interchangeable.

## TP026

### High impact of a simple warming regime on the FDG uptake in brown adipose tissue.

**E. Abrahamsson**, M. Federspiel, S. Holm, C. B. Christensen, L. Borgwardt; Copenhagen University Hospital, Riqshospitalet, Copenhagen, DENMARK.

**Aim**: Uptake of 18F-FDG in brown adipose tissue (BAT) is a well-known phenomenon, especially seen in children and young adolescents. The activation of BAT helps maintaining normal body temperatures in newborns and the tissue is reduced with age. 18F-FDG uptake in BAT can complicate interpretation and quantification of PET images, especially in regions of possible lymph node metastases such as the axilla and the mediastinum and is a potential source of false-positive interpretation. The aim of this study was to prospectively evaluate the effect of patient preparation using a simple warming regime to prevent 18F-FDG uptake in BAT in paediatric patients referred for 18F-FDG PET/CT. **Materials and Methods:** 244 scans of paediatric patients (aged 0-18 years) referred for 18F-FDG PET/CT were included. A cohort of 115 scans were imaged without an intervention, and a second cohort of 129 scans (67 patients, 42 males and 25 females. Some patients were scanned >1 time during the study period.) the patients were prepared according to a new protocol that included a warming regime; After establishing the IV access, the patient was packed carefully under a warm duvet for 30 minutes. If the child was already hospitalized, the staffs at the referring department were instructed of the procedure. After the initial warming period, the 18F-FDG was injected as usual and the child was placed under the duvets for 60 minutes more during tracer uptake until the scan was started 60 minutes after injection. The generated images were visually assessed for the presence of 18F-FDG at the location of fat-density tissue on CT images. **Results**: In the cohort without intervention, relevant 18F-FDG uptake in BAT was identified in 29 scans (25%); in the cohort prepared according to the proposed protocol, in only 8 scans (6%). We also compared the distribution of the months, and confirmed the tendency for increased uptake during winter and fall. **Conclusion**: In the group of paediatric patients, 18F-FDG uptake in BAT can be reduced by a forth using a simple warming procedure in the resting room.

TP02 - Tuesday, Oct. 22, 8:00 - 9:30, Poster Exhibition Area

## Technologist Poster Session 2

### TP027

#### Interest of a multidisciplinary and two-step consultation in radioiodine therapy to improve patient's support

**C. Guillaumon**, M. Eberlé, E. Deshayes, B. Savry, B. Vinson, P. Kotzki; Montpellier Cancer Institute, Montpellier, FRANCE.

**Aim** Surgery of differentiated thyroid cancer may be followed by radioiodine therapy (I-131). This therapy requires a three-day hospital stay in an isolation room without family visits, but also many precautions before, during and after the hospital stay. This clinical environment can give rise to increased anxiety for a number of patients. This is why we have set up a dedicated consultation, aimed at improving preparation of the hospital stay. The aim of our work was to assess the efficiency of such consultation for patient's understanding of their disease, related apprehensions, and coordination between the nuclear medicine (NM) unit and inpatient ward. **Material and Methods** We followed the recommendations of the first French Cancer Plan regarding the diagnosis or treatment announcement and the project was reviewed in the frame of Professional Practices Evaluation. Consultations were carried out according to a two-step procedure in the NM unit. First, patients were informed by the NM physician about disease and treatment. Then, a technologist evaluated social and psychological conditions, and checked proper understanding of disease and treatment. He/she paid a special attention to radiation protection measures, especially for the discharge period. Patients received a guidance manual document, and when necessary were oriented towards the supportive care staff. A dedicated computerized form was used to share patient information between the NM unit and inpatient ward. These consultations ran every day (2 per day). To evaluate procedure efficiency, patients were asked to fulfill a satisfaction questionnaire. Inpatient ward nurses were also surveyed for patient's understanding of their disease, level of anxiety, and quality of care. **Results** At Montpellier Cancer Institute, a total of 30 thyroid cancer patients and 15 nurses were surveyed about their perceptions about the consultation before radioiodine therapy from April to May 2011. Patient satisfaction rates were high with 88% of patients answering that this consultation met their expectations. Ninety-three (93%) of inpatient ward nurses reported an improved coordination between both Departments, 78% observed reduction in patient anxiety, and 70% noted positive impact on the quality of patient care. **Conclusion** This pilot study showed that a dedicated pre-consultation involving both NM physicians and technologists before radioiodine therapy improved not only coordination between NM department and inpatient ward, but also reduced patient anxiety related to treatment. Since this study, pre-consultation has been routinely performed for thyroid cancer patients in our NM Department.

### TP028

#### Evaluation of the basic characteristics of the cardiac focusing-collimators

**A. Niwa**[1], S. Abe[2], T. Odagawa[1], N. Fujita[2], H. Kono[2], T. Kumazawa[2], Y. Fujita[1], K. Kato[1]; [1]Department of Radiological and Medical Laboratory Sciences, Nagoya University Graduate School of Medicine, Nagoya, JAPAN, [2]Department of Radiological Technology, Nagoya University Hospital, Nagoya, JAPAN.

Aim Recently IQ-SPECT, which consists of the SMARTZOOM collimator, the cardio-centric acquisition, and the IQ-SPECT reconstruction, has been developed in the field of nuclear cardiology. This study was performed to evaluate the basic characteristics of the SMARTZOOM collimator such as the influences on the SPECT uniformity and resolution. Materials and Methods For the evaluation of the SPECT uniformity, Siemens Symbia T was used by setting NEMA body phantom. For the evaluation of the SPECT resolution, Siemens Symbia T6 was used by setting the line source phantom made of expanded polystyrene and fluororesin tube. In both cases of experiments, the Tc-99m solution was enclosed into the phantoms, and the data acquisitions were made by regarding the center of the phantoms as the center of the heart in IQ-SPECT. Both the SMARTZOOM and the LEHR collimators were set on the SPECT equipment, image reconstructions were performed, and the images obtained using these collimators were compared. Results When the images were collected with the SMARTZOOM collimator, the SPECT images were uniform at the areas near the rotation center and the center of body axis of the phantom compared to that when collected with the LEHR collimator. However, when the SMARTZOOM collimator was used the SPECT resolution was inferior to that when the LEHR collimator was used. The full width at half maximum was higher in the former than that in the latter. The uniformity and resolution of the SPECT images collected with the SMARTZOOM collimator were maintained within a certain range around the rotation center or the center of the body axis of the phantom, but they worsened outside the ranges. Discussion The findings that the uniformity and resolution of the SPECT images change dependently on the distance from the centers are due to the experimental conditions under which the beam collection is carried out by adjusting the focus to the centers and the sweet spot of the SMARTZOOM collimator corresponds to the center of the phantoms. Conclusion When the SMARTZOOM collimator is used, the uniformity of images were better but their resolution were worse than those when the LEHR collimator is used.

### TP029

#### Comparison of lesion detection efficiency of different detector techologies in breast phantom

**T. Haciosmanoglu**, A. O. Karacalioglu, S. Ince, O. Emer, E. Alagoz, N. Arslan, B. Gunalp, M. Ozguven; Gulhane Military Medical Academy, Ankara, TURKEY.

**Background** Cadmium zinc telluride, (CdZnTe) or CZT, is a compound of cadmium, zinc and tellurium or, in other words, an alloy of cadmium telluride and zinc telluride. Radiation detectors using CZT can operate in direct-conversion (or photoconductive) mode at room temperature, unlike some other materials (particularly germanium) which require liquid nitrogen cooling. Their relative advantages include high sensitivity for x-rays and gamma-rays, due to the high atomic numbers of Cd and Te, and better energy resolution than scintillator detectors. CZT can be formed into different shapes for different radiation-detecting applications, and a variety of electrode geometries, thereby improving energy resolution. The aim of this study was to evaluate the lesion detection efficiency in breast phantom of the gamma camera equipped with CZT detectors by comparing the results between CZT detectors and conventional scintillation detectors. **Material and Method** Left part of the breast phantom (model, ECT/FIL-BR/P) was filled with 890 ml and 2 mCi Tc-99m pertechnetate was added in it for simulating background activity. Four different radiactive sources, containing activities of 20, 40, 60, 800.1 ml respectively were placed in the left part of the fillable breast phantom. SPECT acquisition of the breast phantom was performed in a two headed gamma camera (Optima, GE, USA) equipped with low energy high resolution collimator and conventional scintillation detectors in 20 minutes. Later, similar SPECT acquisition was performed in a gamma camera (Discovery 530c, GE, Israel) equipped with CZT detectors in 10 minutes. Same acquisitions with similar activities in the breast phantom were repeated in several times in different time points. **Results**: Although both gamma cameras are dedicated cardiac cameras, the breast imaging can also be acquired in both gamma cameras. The radiactive source containing the least activity was not clearly identified on scans derived from the conventional scintillation detectors in every time. On the other hand all, four radiactive sources were clearly identified on scans derived from the CZT detectors every time. **Conclusion**: According to our results, CZT detectors seem to be superior than the conventional scintillation detectors in lesion detection efficiency.

### TP030

#### Examination of the Patient's Movements During Myocardial Perfusion SPECT Imaging by Cardiac Phantom

**E. ERIM**[1], T. ERTAY[2], I. EVREN[2], M. EREN[2], H. DURAK[2]; [1]DOKUZ EYLUL UNIVERSITY, INSTITUE OF HEALTH SCIENCES,DEPARTMENT OF MEDICAL PHYSICS, IZMIR, TURKEY, [2]DOKUZ EYLUL UNIVERSITY, DEPARTMENT OF NUCLEAR MEDICINE, IZMIR, TURKEY.

Movement of the patient during myocardial perfusion SPECT scintigraphy leads to some artifacts that make interpretation of the image difficult. In this study myocardial perfusion imaging protocol was performed by using cardiac phantom and SPECT studies were done by simulating patient movements. A lesion model with dimensions of 1,2x2x2 cm was created on inferoseptal wall of cardiac phantom. Imaging was done circular in 64x64 matrix, zoom step 1 mode. First image taken under no effect of movement was referred as reference image. During imaging, patient movement was simulated by moving the phantom in ±X and ±Y directions between the frames starting from $8^{th}$ frame to $16^{th}$ frame. At the end of imaging, moving images were compared with Bull's eye maps of reference images. Bull's eye maps obtained by an experienced nuclear medicine physician were evaluated. In shifting patient's movement in all directions by ±1 and ±2 cm, it was noted that lesion was displaced mildly and this did not prevent evaluation. However, it was observed that movements of ±3 or ±4 cm resulted in artifacts which in turn caused partial or no visualization of the lesion. In image processing steps done by correction of movement, lesion could be evaluated in ±1 and ±2 cm movements while lesion could not be evaluated in ±3 and ±4 cm movements. As a result, movement greater than ±3 cm causes significant image artifacts and this should be considered as a potential source of error in myocardial perfusion studies.

### TP031

#### The effect of DRAMA on estimating human nuro-receptor binding potential with PET

**T. Shiraishi**, Y. Kimura, H. Ito, N. Ishii, H. Iwakami, T. Maeda, K. Tanimoto, S. Ohashi, S. Toubaru, K. Yoshikawa, H. Takano, H. Tsuji, Y. Ando, T. Kamada, K. Shibayama; National Institute Of Radiological Sciences, Chiba, JAPAN.

**Objectives**: FBP is a standard method for quantitative analysis in human neuroreceptor binding assay, while OS-EM is used widely in tumor PET imaging. Owing to noise propagation from projection data, especially at high subset number, OS-EM leads to loss of signal to noise (SNR) and quantitative accuracy. A novel

reconstruction algorithm DRAMA can suppress the noise propagation by using dynamic relaxation parameter with faster convergence compared to OSEM algorithm. In this study, we compared regional radioactivity concentrations and binding potential (BP) values between FBP, OS-EM and DRAMA to assess the effect of DRAMA algorithm on estimating human nuroreceptor binding. **Methods:** The PET scanning was carried out with Eminence Sophia (shimadzu corp.) . After 4min pre-injection transmission scan, [11C] FLB457, 90min dynamic PET scans were performed with 3D acquisition mode. To compare reconstruction parameter, a phantom scan was done with same scan protocol. Images were reconstructed with FBP, OSEM and DRAMA to assess quantitative accuracy and noise characteristics. **Results***:* To evaluate the SNR, we performed the image quality tests along with NEMA NU-2 2007. Noise of DRAMA was 7% lower than that of FBP. On the other hands, Q10/N10 number of DRAMA was 5.3% higher than that of FBP, similarly, it is 3.5% higher than that of OS-EM. In patient study, the difference of BP by OSEM with iteration 4, subset 16 compared to FBP was +3.17% at maximum in the caudate, while that of DRAMA was +1.59%. **Conclusions***:* There were no significant differences of BP values in thalamus, frontal cortex, temporal cortex and occipital cortex between DRAMA and FBP. Furthermore, noise propagation was not shown in DRAMA in phantom studies. These results indicated that DRAMA could provide similar performance of FBP with the improved SNR, therefore, DRAMA can be a novel standard reconstruction method of neuroreceptor PET studies.

## TP032

### Evaluation of new reconstruction algorithm for attenuation correction.

**A. Ando**, N. Shuke, H. Nakamura, T. Onishi, K. Saito, K. Yamamoto; Kushiro Kojinkai Memorial Hospital, Kushiro, JAPAN.

**Objectives**: Attenuation correction for PET-CT is performed using a μMAP created from the CT image. Low dose CT is enough for attenuation correction and even better for exposure reduction. HU value is not dependent on the dose in principle, however underestimation of HU value in FOV center by low dose has been reported. Reconstruction algorithm for solving this problem has been mounted to a newly introduced PET-CT system (Discovery PET-CT 710,GE). The objective of this study was to compare this low dose attenuation correction (Q.AC: Quantitation Achieved Consistently) to those of an old PET-CT system (Discovery ST Elite, GE) using the same scanning parameters. **Methods**: Two cylinder phantoms, which were 20cm in diameter, were filled with FDG solution in different radioactivity concentration. Two phantoms were set within the same FOV and were acquired in the old and new PET-CT systems. CT scanning parameters used were the same for both PET-CT systems: tube voltage was fixed to 120kVp and tube current was changed in the range of 5 to 200 mAs. The PET images were reconstituted using μMAPs from these CT images, and radioactivity measured as quantitative voxel values on the PET images were compared.**Results:** When low dose CT was applied on the old PET-CT, the quantitative values were underestimated in the center of FOV, but were constant in the new PET-CT. **Conclusions:** The reconstruction algorithm for attenuation correction of the new PET-CT could improve quantitative values of PET images even in low dose CT and could provide superior images to those of the old PET-CT.

## TP033

### Absorbed Dose Values After Radionuclide Therapy with LU-177 DOTA TATE in Patients with Neuroendocrine Tumor

**M. Demir**[1], N. Yeyin[1], T. Toklu[2], L. Uslu[1], I. Çavdar[3], L. Kabasakal[1]; [1]Istanbul University, Cerrahpasa Medical Faculty, Department of Nuclear Medicine, Istanbul, TURKEY, [2]Yeditepe University, Medical Faculty, Department of Nuclear Medicine, ISTANBUL, TURKEY, [3]Istanbul University, Science Faculty, Department of Physics, Istanbul, TURKEY.

**Aim:** Lu-177 DOTA TATE has been introduced to be a successful treatment modality in neuroendocrine tumors. Kidneys and bone marrow may be affected adversely due to high radiation dose in peptide receptor radionuclide therapy (PRRT). Our aim is to calculate total organ absorbed dose in patients treated with single or multiple cycles of PRRT. **Material and Methods:** Total 67 patients (35 male, 32 female, mean age: 54.4±12.2) treated with single or multipl cycles of Lu-177 DOTA TATE (total 149 treatment) were included in the study. Right and left kidney, liver, spleen, bone marrow, tumor and whole body dosimetry were performed. Bone marrow dosimetry was done with the blood samples taken in 3rd, 15th, 30th, 60th, 180th minutes and 24th, 48th and 72nd hours after the infusion. Organ, tumor and whole body dosimetry were calculated with anterior and posterior planar scintigraphic images taken in 4th, 24th, 48th and 72nd hours after the infusion. The necessary organ thickness, body thickness and organ Hounsfield unit values to calculate photon decrease were obtained from CT images. Time-activity curve of all data was drawn and fit in biexponential curves. Regression curves were integrated for all organs, thus cumulative activity for each organ was calculated and organ dose was calculated via MIRD method. **Results:** Total 3.8-24.2 GBq (mean:12.2±5.5 GBq) Lu-177 DOTA TATE was given to patients. Twenty-two patients received only one cycle, 19 patients received 2 cycles, 17 patients received 3 cycles, 7 patients received 4 cycles and 2 patients received 5 cycles of treatment. Dosimetry was performed for left kidney, right kidney, bone marrow, tumor and whole body. Doses were calculated separately for each patient in units of Gray (Gy). When all patients were taken into consideration, calculated mean dose value was counted as 10.6±5.7, 11.2±6.0, 0.4±0.2, 176.7±126.7 and 0.7±0.5 Gy for left kidney, right kidney, bone marrow, tumor and whole body, respectively **Conclusion:** This study demonstrated that absorbed radiation dose in high dose Lu-177 DOTA TATE treatment is in safe range. At the end of all cycles of treatments, dose limits did not exceed safe limits in the all patients.

## TP034

### An investigation of neck uptake with I-131 through a quantitative analysis: relationship to therapeutic effect in patient with thyroid carcinoma

**T. Uno**, J. Sato, M. Sakaguchi, N. Nakagami, K. Nakayama, M. Nakayama, A. Okizaki; Asahikawa Medical University Hospital, Asahikawa, Hokkaido, JAPAN.

An I-131 whole body scintigraphy (I-131 WBS) is useful to evaluate the patient with differentiated thyroid carcinoma (DTC) after total thyroidectomy and I-131 ablation therapy. An uptake of I-131 in the neck may relate to therapeutic effect because the ablated dose around the neighbor tissue of accumulation should be large. On the other hand, much accumulation may represent plenty residual tissue derived from thyroid, it suggests many times of treatments are necessary. Whichever idea is true, there might be significant correlation between the uptake in the neck and required ablation times. Therefore, quantitative neck uptake analysis might be able to indicate quantity of I-131 ablation. We hypothesized that quantitative neck uptake is a predictor of required total ablation times to complete. The purpose of this study was to clarify the relationship between the neck uptake at the first I-131 ablation and required total ablation times. The subject was twenty eight patients (male: 8, female: 20 ) who were completed treatment among 547 patients with DTC underwent total thyroidectomy and then I-131 ablation therapy. The each ablation dose was from 3.7 to 5.55GBq. Twice of ablations were needed in 16 patients and 3 times of ablations were required in 12 patients. Using the anterior view of the I-131 WBS, a region of interest (ROI) for accumulation in the neck was set as 10% and more of the maximum count at the uptake. Another ROI in the head was also set as same size and shape of ROI in the neck to obtain background counts in each I-131 WBS. The average of uptake was calculated as count in the ROI divided by size of the ROI. Neck uptake index (NUI) was defined as follows; ( Neck average uptake ) - ( Head average uptake ) Gamma statistic was used to evaluate the relationship between NUI and total ablation times to complete. There was statistically significant negative correlation between NUI and total ablation times to complete (Gamma statistic = -0.3863, $p < 0.05$). In other words, patient with small NUI required many times of I-131 ablation. In conclusion, NUI might be useful to estimate the required I-131 ablation times.

## TP035

### Causes and Actions in Relation to Defaulting Patients

**T. Godskesen**; Odense University Hospital, Odense, DENMARK.

**Aim**: With the in creased focus on use of resources in Healthcare; defaulting patients are an area of interest due to the wasted capacity of hospital's equipments and staff. The aim of this study was to find causes of the high number of defaulting patients at our department and to find possible actions to decrease this number in order to improve capacity utilization and ensure patients the necessary studies. **Materials and Methods**: Twenty five patients were invited to participate in telephone interviews. Inclusioncriteria were outpatients who were defaulting from scheduled appointments within the last two months and patients with available telephone numbers. It was attempted to ensure a representative group based on sex, age, diagnosis and type of examination. In the interview the patient was asked about the course of the defaulting, information received prior to the appointment, issues important to the patient and ideas for actions for decreasing the number of defaulting patients. Two referring physicians were interviewed regarding their point of view on defaulting patients, the level of patient information and ideas for improvements. **Results**: Seventeen defaulting patients participated in the study. Reasons for defaulting: Forgetfulness (9 patients), missing appointment letter (5 patients), negligence (1 patient), mistook date of appointment (1 patient), and unknown reasons (1 patient). The information received prior to the appointment varied: no information (10 patients), some information (6 patients), wrong information (1 patient). Important issues to the patients were waiting time, information from the referring doctor, information in the appointment letter, parking facilities, transportation and availability to the department. Ideas for improvements: Better parking facilities, reminders, online-booking, better coordination with other departments and better availability to booking staff. Results of the interviews with the two referring physicians: Patients default because of forgetfulness, uncertainties regarding the examination and lack of information. The seventeen patients and two physicians were asked their opinion about fines for defaulting patients: 11 patients were for and 6 against. Both the referring physicians were against fines. **Conclusion**: Causes for defaulting patients were forgetfulness, lack of appointment letters, lack of information and uncertainties regarding the examination. Actions to reduce the number of defaulting patients may include reminders, better information, better coordination with other departments and better availability to The Department of Nuclear Medicine. There was not a clear conclusion regarding the use of fines.

## TP036

### The impact of wearing lead aprons on the effective dose of staff working in Nuclear Medicine departments during diagnostic procedures using Technetium-99m

**M. I. Larg**, I. C. Pestean, A. Sabo, M. M. Crisan, A. Bara, D. Piciu; Ion Chiricuta Institute of Oncology, Cluj-Napoca, ROMANIA.

**Aim.** The aim of this study is to investigate the usefulness of lead aprons of thicknesses of 0,5 mm, in shielding staff from photons of energies of 140 keV during eluation process of a $^{99m}$Tc generator, preparation of radiopharmaceutical and administration of radiopharmaceutical to patients. We also estimated the impact of these protective measures on the effective dose of the staff. From a radiation point of view we want to discuss the necesity of wearing those aprons taking into account the reduction of the exposure in relation with dose limit established by European regulations and recommandations for exposed workers [1,2] **Material and Methods**. This study was conducted over a period of 2 couple weeks where one physicist and one technologist were involved and they worn lead aprons and thyroid shields. Each of them had an electronic dosimeter DMC2000S under the lead apron and one above the lead apron. The energy of photons to which staff was exposed is 140 keV and a total activity of 44 GBq has been manipulated. The physicist spent 1 hour and 50 minutes for doses preparation for the entire period of the study. The technologist spent 4 hours and 9 minutes for radiopharmaceutical administration to the patients. To minimize the time spent with patients after injection patients received all necessary explanations before the procedure. All the procedures were performed with shields of tungsten for syringes and vials. **Results.** Technologist's dosimeter situated under the lead apron measured an effective dose of 0,018 µSv and the other one situated above the lead apron measured 0,022 µSv. The exposure dose has been reduced with 0,004 µSv, which means a reduction of 18,18 %. Physicist's dosimeter worn above the lead apron measured 0,023 and the one situated under the lead apron measured 0,020 µSv which means a reduction of 0,003 µSv (13,04 %). **Conclusions.** Considering the work conditions described above as usual working conditions over a year we estimated that the dose reduction wearing lead aprons would have a value of 0,096 µSv which represents 0,48% from the dose limit for exposed workers. Having the fact that the reduction of effective dose is minimal and the difficulty with which certain procedures are performed when wearing the lead apron, we believe it is reasonable to not wear it. Bibliography 1. Draft Euratom Basic Safety Standard Directive. [Online]. 2010 [cited 2013 April]; [67 screens]. Available from: URL: http://ec.europa.eu/energy/nuclear/radiation_protection/doc/art31/2010_02_24_draft_euratom_basic_safety_standards_directive.pdf

## TP037

### The Effect of Filtrating and Reconstruction Method on Ventricular Function by the Gated Blood Pool SPECT

**S. Mohseni**[1], A. Kamaliasl[1], A. Bitarafan-Rajabi[2], S. M. Entezarmahdi[1], N. Yaghoobi[2], Z. Shahpouri[1]; [1]Department of Nuclear Engineering, Shahid Beheshti University, Tehran, IRAN, ISLAMIC REPUBLIC OF, [2]Cardiovascular Interventional Research Centre, Department of Nuclear Medicine, Rajaei Cardiovascular, Medical& Research Centre, Tehran University of Medical Science, Tehran, IRAN, ISLAMIC REPUBLIC OF.

**Background**. Gated Blood Pool Single Photon Emission Computed Tomography (GBPS) offers the possibility of obtaining additional functional information from blood pool studies, including evaluation of left and right ventricular function simultaneously. The calculation of ventricular volumes based on the identification of the endocardial surface, which will be influenced by the spatial resolution in the reconstructed images. This study was performed to evaluate the effect of different filtering Methods on the ventricular function. **Methods & Materials**. The normal NACT phantom with known RV and LV end-diastole volume and ejection fraction was generated. The SIMIND Monte Carlo program was used to create projections. The studies were reconstructed by FBP, MLEM, OSEM and Flash 3D, then filtered separately with Butterworth, Gaussian, Hanning, Shep-logan, Metz and Wiener in 167 different statuses. Using with Cedars-Sinai QBS package, the ventricular function parameters were computed. The calculated values were analyzed and compared with the normal NCAT results. **Results.** The results imply that the closer RVEDV calculated by QBS to the NCAT output (1.2% relative difference) gathered with FBP and Butterworth filtration (cut of freq. =0.3 c/p, n= 5), while the closer RVESV (1% relative difference) gathered with MLEM and Weiner filter (FWHM=20, SNR= 15). The closer RVEF (3% relative difference) obtained with FBP and Metz filter (FWHM=20, n= 15). The Gaussian filter has significant difference with indicator values. Also, the order parameters in Butterworth and Metz filter does not considerable effect on calculated quantity. **Conclusion**. The resolution recovery and Butterworth filters tend to give more comparable ventricular volumes and ejection fraction with the determined normal NCAT values. To achieve more accurate results need extra simulation and clinical studies.

## TP038

### The road to Telemedicine: mobile solutions for Nuclear Medicine

**D. Vieira**, P. Costa, L. Cunha, L. F. Metello; Nuclear Medicine Department, High Institute for Allied Health Technologies of Porto - Polytechnic Institute of Porto, Porto, PORTUGAL.

**Aim:** The present dimension of the concept "Telemedicine" includes the application of mobile communication technologies and information systems to provide Health Care at distance. In the medical imaging field, and particularly in Nuclear Medicine, this concept is broader, involving the application of a variety of software and mobile applications at several steps of the process: digital imaging display and processing, data transfer and storage, but also decay calculations and inherent corrections, often in real-time and automatically performed, as well as the exchange of theoretical information. This paper aims to review the current status concerning available software and applications, with a clear accent on those with a close relation to cloud computing and interfacing with smart phones and/or tablets. **Materials and Methods:** This paper presents a literature review in this field, complemented by a general description of the solutions available in the market. A small introduction based on the relevance and justification of Telemedicine will be presented, followed by the proof-of-concept using several independent solutions. Finally, our vision about this each-day increasingly important issue will be pointed and justified, including the enumeration of the correspondent limitations and predictable difficulties for its wide implementation. **Results and Conclusion:** Main applications found were related with support guidelines, learning games, DICOM viewers, scientific and education articles access, portal news, technical remote support/equipment assessment and augmented reality. It is widely recognized that this is a complex process, since it ideally requires a change of the mind setting, at different levels, of the distinct players, with some of them more able - and willing to do so - than others. Nevertheless, the added value of these sorts of applications seems to win more and more acceptation, clearly tending to become quite consensual ···and so the need and overall interest to adapt the daily practice of medicine to the commonly available technological tools, assumedly with an extra-urgency created by the present socio-economic reality.

## TP039

### Easy - to - implement

**M. Porto**; UniversitätsSpital Zürich, Zürich, SWITZERLAND.

**Aim**: This project was conceived to assure that the maximum number of patients will voluntarily and wittingly participate in the research projects of our PET/ CT - MR tri-modality centre. We were convinced that, with the correct approach, the patients will easily participate, and that we will be able to effectively increase our research numbers in a sustainable way. Despite the natural limitations for an MR procedure (pacemakers, claustrophobia, etc···) the average of 7 in 10 patients doing MR could be achieved. **Materials and Methods** We've introduced a much more personal and humanized approach to the patient, supported by mother language documentation and, if available, a mother language speaker to clarify any patient's doubt. We are now using six different languages in a regular basis in our centre: German, English, French, Italian, Spanish and Portuguese. The study was conducted from May till November 2012, for a population of 604 patients, doing PET/CT exams in our centre. May was used has a control reference month, before the implementation of this new approach, June till November, as field data for the effects of the implementation and sustainability of the procedure. **Results** The results were slightly over our expectations. We've had an average of 7,6 in 10 patients accepting to participate during the six months of the study, witch represents an average of 88% real increase regarding May control values. At the same time, we were also able to have a clear view of the amount of non-German speakers in our centre: slightly over 37% is the average population for the six month study, with a net peak in August, where they represent 50% of the population for that month. **Conclusion** In a world were numbers are the new motor force, especially in health related matters, humanizing can be the tool to give you the numbers. By taken into account the different language needs of patients, numbers concerning participation in clinical research project can be substantially and sustainable improved.

## TP040

### Variation of radiaoactive iodine thyroid uptake rate on attenuation effects with change of thyroid depth

**J. Oh**, J. Kim, S. Oh, H. Park, J. Kim, K. Oh, C. Lee; Yonsei University Health System, Seoul, KOREA, REPUBLIC OF.

**Purpose** It is certain that radioactive iodine thyroid uptake (RAIU) rate should be measured with the standard counts considering the thyroid gland depth in enlarged thyroid patients for the variation from geometric factors. The purpose of this paper is to consider the effects of geometric factors according to detector to source

distance and effective thyroid depth on RAIU rate with experimental tests. **Materials and Methods** $^{131}$I 370 kBq point source was measured by Captus-3000 thyroid uptake system with a change detector-source distance from 20 cm to 30 cm at an interval of 1 cm. And we changed the neck surface-source depth with 1 cm, 2 cm, 5 cm using the neck phantom in order to reproduce the effective thyroid depth. **Results** Every experimental group follows power curve as inverse square curve ($R^2$≧0.915). The average count rates between the case of not using a phantom and every case of applied the effective thyroid depth 1 cm using a phantom in every energy ROI were significantly different ($p$=0.00). There were significant fluctuations of count rates applied the effective thyroid depth above 1 cm in 364.4 keV±10% energy ROI ($p$=0.000). But there were not significant differences between 1 cm and 2 cm in 364.4 keV±20% and 637.1 keV±6.2% ($p$=0.354, $p$=0.397). In assumed RAIU rate, 364.4 keV±20% was lower difference than 364.4 keV±10% as 6.42% and 5.09% per 1 cm. Every change of count rate upon depth appears decreased line on Linear Regression, but the case of 284.3 keV±10% increased only. And also, the graphs of coefficient of variation increased as for the straight line on every experimental group when distance increase. **Conclusion** In this study, we demonstrated that measurement errors can increase when radioactive iodine thyroid uptake rate increase, effective thyroid depth deepen, detector-thyroid distance shorten, and set up inappropriate energy ROIs. It seems that checking the patient's thyroid depth with sonographic images or CT images before administration radioactive iodine and applying appropriate distance or neck phantom depth when measure standard count before administration in accordance with thyroid depth reduce errors of RAIU rate effectively. And also, it is thought that the error from thyroid depth can reduce through applying correction factor as thyroid depth, set up 364.4 keV±20% energy ROIs.

## TP041

### Practices in radiopharmacy: Is the use of a breathing needle a concern on the radiochemical purity of $^{99m}$Tc-radiopharmaceuticals?

**M. Oliveira**[1], T. Oliveira[2], A. Rebelo[2], C. Sousa[1], A. Silva[1], J. Nery[1], I. Amorim[1], R. Castro[1]; [1]Santo António General Hospital, Oporto Hospital Center, Porto, PORTUGAL, [2]High Institute for Allied Health Technologies, Polytechnic Institute of Porto, ESTSP.IPP, Gaia, PORTUGAL.

**Aim:** The action of collecting the patient's individual doses isn't subjected to any followed protocol, unlike most practices in the Nuclear Medicine department. In certain departments, the individual doses are withdrawn by perforating the rubber septum at every dose while others choose to keep a needle in the *kit* to avoid multiple perforations. Radiochemical purity is typically the primary concern for $^{99m}$Tc-radiopharmaceuticals so the potential presence of impurities will affect the radiochemical stability of the radiopharmaceutical and, after being injected to a patient, result in an altered biodistribution and poor image quality. Therefore, it's important to verify every practice used on the product, which results in a need to learn if the needle kept in the *kit* at some departments is affecting the radiopharmaceutical's stability. It is aimed to disseminate the results obtained on a large study performed to evaluate whether there is any correlation between keeping the needle in the *kit,* during the clinical practice and during the stability period of two different radiopharmaceuticals. **Material and Methods:** Two commonly used $^{99m}$Tc-radiopharmaceuticals, $^{99m}$Tc-Tetrofosmin (n=20) and $^{99m}$Tc-HDP (n=20), were included. The radiopharmaceuticals were prepared strictly according to manufacturer's instructions. All preparations were stored at room temperature. To assess the radiochemical stability, the reference sample was withdrawn directly from the vial, immediately after radiolabelling, and subsequent aliquots were tested for each time-point predefined (1h, 3h and 6h after radiolabelling). Radiochemical purity was assessed by thin-layer chromatography, according to manufacturer's or EU Pharmacopeia instructions. Student's t-Test was used to evaluate differences between means for each hour. **Results:** At 0h, the results were identical since the labeling was performed similarly in both situations. However, at 6h, a variation of 1,32% and 0,61% is seen on the radiochemical purity, for $^{99m}$Tc-HDP and $^{99m}$Tc-Tetrofosmin, respectively, with the smaller values obtained when a needle is kept in the *kit*. Still at 6h, the free pertecnetate values differ 0,20% and 0,20% and the $^{99m}$Tc-colloid impurities values present variations of 1,12% and 0,42%, for $^{99m}$Tc-HDP and $^{99m}$Tc-Tetrofosmin, respectively, being higher when the needle is kept in the *kit*. **Conclusion:** Results demonstrate that a higher percentage of $^{99m}$Tc-radiopharmaceuticals is obtained when the needle isn't kept in the *kit*. This can have a positive impact on subsequent clinical images, due to a highest concentration of radioactivity in the target organs.

## TP042

### A New Approach of Tc-99m Sestamibi Resting Early and Delayed Myocardial Perfusion images in Patients with Vasospastic Angina Pectoris

**M. Hara**, N. Itou, N. Fujimoto, I. Hamada, Y. Sasaki, T. Sakaue, H. Habara, S. Sueda; Prefectual Niihama Hospital, Niihama, JAPAN.

**Aim:** Previous study have suggested that Tc-99m sestamibi(MIBI) shows very slow washout from the heart after its initial uptake, which is related to mitochondrial function.On he other hand, some investigators have reported that reverse redistribution(washout) of MIBI was observed in patients with acute myocardial infarction after PCI, dilated cardiomyopathy, and hypertrophic cardiomyopathy. However, the clinical usefulness of myocardial MIBI washout was not established yet. The purpose of this study was to investigate whether the myocardial washout of MIBI is thought to be a tool for the evaluation of vasospastic angina pectoris(VSA). **Meterials and Methods**: This study was performed on 14 patients with VSA(9 men and 5 women, mean age, 69.9±10 years) and 5 normal subjects(2 men and 3 women, mean age, 34.6±9 years). We also performed coronary vasospasm induced test with acetylcholine or ergonovine in all patients. The resting MIBI SPECT myocardial perfusion imaging was obtained 1 hour(early image) and 6 hours(delayed image) after 600 MBq of MIBI injection. We divided the patients in two groups: Group A(9 patients; coronary spasm induced test(+)) and group B(5 patients; coronary spasm induced test(-)). We calculated global myocardial MIBI washout rate from the early and delayed images in all subjects. **Results:** The global myocardial MIBI washout rate was significantly lower in group A(25.0±7.8) than in group B(33.9±9.0, p=0.04) and in normal subjects(34.1±6.2, p=0.02) respectively. These results indicate that the myocardial MIBI washout in gruop A patients aws almost done on the early imaging phase(1 hour after MIBI injection). **Conclusion**: This approach may provide a useful information on the evaluation for the patient management of VSA. Further studies are needed to obtain the early image within 1 hour after MIBI injection.

## TP043

### Evaluation of different strategies for reduction of extra cardiac activity in myocardial perfusion imaging

**M. G. Schalken**[1], I. A. C. Rutten-Vermeltfoort[1], P. G. H. M. Raijmakers[2], J. A. F. de Jong[1], R. J. Pijpers[1], A. B. van Dijk[1]; [1]Institute Verbeeten, Tilburg, NETHERLANDS, [2]VUMC, Amsterdam, NETHERLANDS.

**Aim** In technetium (Tc)-99m myocardial perfusion imaging (MPI), abdominal activity often interferes with the evaluation of the perfusion of the inferior wall. Increased abdominal activity necessitates repeated imaging of some patients and may reduce the diagnostic accuracy of MPI. The aim of the study was to compare the efficacy of consuming a sausage roll versus our conventional preparation in reducing infra-cardiac activity. In this study we examined the effect of sausage roll, chocolate bar versus (chocolate)milk upon the image quality of MPI studies. **Methods** Data of 1804 consecutive MPI studies in Institute Verbeeten were prospectively collected. This includes all studies with exercise, adenosine and rest. Patients consumed a sausage roll, (chocolate)milk or a chocolate bar prior to SPECT imaging. The frequency of intestinal activity adjacent to the inferior myocardial wall resulting in the need for a repeated scan, was evaluated by observers on SPECT images. **Results** The frequency of a poor quality scan due tot abdominal activity in the sausage roll group was 7.2% (43/597); in the chocolate bar group 7.7% (54/700); vs. 5.3% in the (chocolate)milk group (27/507). There was no significant difference between the three groups. In the subgroup of patients undergoing exercise there was no need to rescan due to adequate image quality. **Conclusion** This study shows no significant improvement of infra-cardiac activity in MPI using sausage roll, in comparison to our conventional schedule (chocolate bar or (chocolate)milk). During exercise abdominal activity is a far less frequent problem, and in this respect is the preferred modality.

## TP044

### How to increase the distance between myocardia and subdiaphragmatic $^{82}$Rubidium uptake in PET

**E. Lindell**, M. Pejtersen, M. L. Lassen; Rigshospitalet, PET-center, Copenhagen University Hospital, Copenhagen, DENMARK.

**Aim** High gastric activites are often seen in $^{82}$Rb myocardial Positron Emission Tomography (PET) scans. These subdiaphragmal activites may interfere with the myocardium and could mask out true defects. Studies have shown oral uptake of sparklingwater ten minutes prior to scanstart may increase the cardio-subdiphragmal distance when performing $^{99}$mTc SPECT (Single-photon emission tomography) scans(1). The aim of this study was to investigate if the distance between myocardia and subdiaphragmatic organs would increase after an oral uptake of 300 ml sparkelingwater in $^{82}$Rb PET scans. **Methods** In this study 72 patients were analyzed for evaluation of myocardial blood-flow using $^{82}$Rb. The patients were scanned for 9 minutes in a rest-setup. Static images were reconstructed for clinical evaluation. The static images were reconstructed from the 2$^{nd}$ to the 9$^{th}$ minute of the scan, using an iterative OSEM-reconstrution (3 iterations and 8 subsets) method using 5mm Full-Width at Half-Maximum (FWHM) Gaussian filtration, image size 128 X 128, zoom 2. The patients were divided into three groups. Group one, the controlgroup, were not given any sparkelingwater, group two were given sparkelingwater one minute before the scan and group three were given sparkelingwater ten minutes before the scan. The shortest distance between the inferior wall and the gastric activity closest to the heart was measured in the coronal plane. **Results** In the controlgroup (n=30), the average distance between myocardia and gastric activity was 2,9 cm and with a standard deviation of 1,5. In group two (n=19), the average distance was 3 cm (p=0,94 compared to

the controlgroup) with a standard deviation of 1,8. In group three (n=23), the average distance was 3,7 cm (p=0,12 compared to the controlgroup) with a standard deviation of 2,3. **Conclutions** In this study we could not show that the distance between myocardia and subdiaphragmatic organs were significantly increased after oral uptake of sparkelingwater. Since we could see a visual increasement of the distance between patients drinking sparkelingwater and those who did not, a larger study with a larger patientgroupe could be made in the future 1. Alice J. van Dongen and Peter P.van Rijk. Minimizing Liver, Bowel, and Gastric Activity in Myocardial Perfusion SPECT. *J Nucl Med* 2000; 41:1315-1317

## TP045

### Reduction of extra-myocardial abdominal uptake in myocardial perfusion-gated studies by means of ingestion of meals with different fat content

J. F. Tomè Pereira[1], S. M. Azevedo Oliveira[1], **G. Testanera**[2], B. Nardi[2], G. Pepe[2], T. F. Vaz[1], L. Vieira[1], L. Leonardi[2], A. Chiti[2]; [1]Escola Superior de Tecnologia da Saude de Lisboa, Lisboa, PORTUGAL, [2]Istituto Clinico Humanitas, Rozzano (MI), ITALY.

The extra-cardiac activity can be a problem in the quantitative and qualitative assessment of the infero-septal region in myocardial perfusion gated-SPECT studies. The aim of this study was to evaluate the effect of meals with different fat content in the reduction of extra-myocardial uptake in the daily routine practice. **Materials and Methods**: 30 male patients referred for myocardial perfusion gated-SPECT were enrolled in this prospective study. All patients underwent 1-day-protocol studies with 99mTc-Sestamibi, performing the stress study (pharmacological plus 3 minutes light cycling) (administered activity 370±7 MBq) in the morning and the rest study (640±7 MBq) in the afternoon. Patients, selected on the basis of common clinical characteristics, were randomly divided into three groups as follows: Group I (GI): patients ingesting 125 ml of apple juice; Group II (GII): patients ingesting 125 ml of apple juice and croissant with chocolate; Group III (GIII): patients ingesting 125 ml of apple juice, croissant with chocolate and chocolate pudding. The patients had food soon after the radiopharmaceutical injection both at stress and rest studies. Images were acquired 45-60 minutes after the injection. Static images of the left anterior oblique (45º) and anterior projections were acquired prior to the normal SPECT acquisition. We performed qualitative assessment of SPECT and quantitative assessment of myocardium/liver (M/L), myocardium/stomach (M/S) and myocardium/bowel (M/B)ratios, by drawing square (4x4 pixels) regions of interest over those areas. **Results:** Uptake values (UV) of M/L and M/B were lower than UV of M/S in all groups. Patients from GII and GIII showed better UV of M/L than the patients from GI at both stress and rest studies. The qualitative results showed that there are significant differences only between the patients belonging to GI and GIII, in stress and rest studies. There were no significant differences between the GII and GIII, in any study. Analyses of quantitative results is ongoing. **Conclusion**: Eating food with fat content after 99mTc-Sestamibi injection increases the biliary excretion of the radiopharmaceutical in myocardial perfusion gated-SPECT studies. Slight changes in the fat content of meals subministrated to patients did not showed relevant differences in myocardial images assessment while more significant changes were found relevant and evaluable.

## TP046

### About the usefulness of the 123 I-MIBG scintigraphy of Parkinson's disease and a Levy snug type dementia judgment

**N. OGAWA**, T. HIGUCHI, Y. ARISAKA, A. TOKUE, M. KINN, H. SHIMADA, H. OTAKE, T. SUTOU, Y. TSUSHIMA; GUNMA UNIVERSITY HOSPITAL, GUNMA, JAPAN.

**(Introduction)** I-123 metaiodobenzylguanidine (I-123 MIBG) has been used as a myocardial perfusion scintigraphy for the evaluation of sympathetic nerve activity since 1992. It was reported that the grade of accumulation of I-123 MIBG in the cardiac muscle could be used as predictor of prognosis in patients with chronic heart failure. Quantification of its accumulation in cardiac muscle is also useful in the evaluation of Parkinson's disease and differential diagnosis with other diseases related with the symptom of Parkinsonism becomes possible. (Purpose) In myocardial scintigraphy, heart to mediastinum ratio (H/M ratio) is a simple index showing the relative MIBG uptake in the cardiac muscle. H/M ratio can be used to make the differential diagnosis of Alzheimer disease (AD) and Levy body type dementia (DLB), and it is also applicable to making therapeutic plan. In our current study, the usefulness of MIBG myocardial scintigraphy for diagnosis of AD or DLB was evaluated. **(Method)** During the period from January 2011 to March 2013, 175cases with Parkinsonism were enrolled and H/M ratio and wash out rates were calculated and these were correlated with final clinical diagnosis. (Result) In 122 out of 175 cases, diagnosis form H/M ratio and washout rate were compatible with clinical final diagnosis. In these patients, 55 cases with PD and 24 cases with DLB were 24 cases were contained and final diagnostic accuracy was 69.7%**. (Discussion and Conclusion)** In the differential diagnosis of PD and DLB with other disease showing Parkinsonism, I-123 MIBG cardiac scintigraphy seems useful.

## TP047

### Predictive indicator for prognosis of residual thyroid carcinoma with liver uptake on I-131 whole-body scintigraphy

**M. Sakaguchi**[1], M. Nakayama[2], A. Okizaki[2], J. Sato[1], T. Uno[1]; [1]Radiological Technology Section, Asahikawa Medical University Hospital, Asahikawa Hokkaido, JAPAN, [2]Department of Radiology, Asahikawa Medical University, Asahikawa Hokkaido, JAPAN.

OBJECTIVES: Thyroglobulin (Tg) concentration is a useful tumor marker in follow-up differentiate thyroid carcinoma (DTC) patient after total thyroidectomy. Tg and radioactive iodine whole-body scintiglaphy (I-131 WBS) is also a useful diagnostic method for evaluation therapeutic effect of I-131 ablation. Tg might be affected by some factors such as anti-thyroglobulin antibody (Tg-Ab) or measurement system error. Discordant results of Tg and I-131 WBS have been sometimes observed in the follow-up study and it is difficult to interpretation of WBS in these cases. Diffuse liver uptake of I-131 represents organo-iodine, which interfered with residual thyroid tissue. Its uptake is often evaluated by visual approach. We considered that quantitative liver uptake might be a useful indicator to evaluate the activity of DTC. The purpose of this study was to evaluate the usefulness of quantitative liver uptake as an indicator of need for retreatment with I-131 ablation. METHODS: One hundred twenty two consecutively patients were analyzed, who were diagnosed with DTC and underwent I-131 ablation at doses of 3.7-5.55GBq after total thyroidectomy. Patients were categorized into two groups as: group 1, necessary for retreatment (n = 78), and group 2, unnecessary for retreatment (n = 44). Liver uptake ratio was calculated using liver and head uptake on I-131 WBS. A head uptake was obtained as background. Region of interests were drawn manually over the whole liver and part of head. Liver uptake ratio was defined as follows; ( Liver uptake ) / ( Head uptake ) Receiver operating characteristic (ROC) curve analysis was performed to evaluate the usefulness of liver uptake ratio and Tg. First of all, ANOVA was used to examine whether there was statistically significant difference or not. Second, DBM MRMC was performed to compare area under the curve (AUC) on ROC of liver uptake ratio and Tg. According to ANOVA, there was statistically significant difference between the AUC on each ROC. RESULTS: The results were summarized in the table. The AUC on ROC of Liver uptake ratio was significantly larger than that of Tg ($p < 0.0001$). CONCLUSIONS: In conclusion, liver uptake ratio might be a useful indicator of need for retreatment with I-131 ablation.

## TP048

### Validation of a Scintigraphy Technique for the Evaluation of Patients with Gastric Pull-Up Esophagectomy

**F. Sciume'**, L. Pavanello, F. Longo, E. Cuozzo, M. Zuffante, M. Ferdeghini; Nuclear Medicine Unit AOUI Verona, Verona, ITALY.

**AIM** The aim of this study was to verify and validate our scintigraphic technique in the evaluation of the dynamics of swallowing and the time of gastric emptying in patients with gastric pull-up esophagectomy. **MATERIALS AND METHODS** The study included 10 esophagectomized patients with gastric pull-up reconstruction. All subjects studied, fasted (no food and drink) for 6 hours before the exam. We used a Gamma-camera Picker Prism 1500 with parallel holes LEHR collimator and a computer Odyssey Fx. A semisolid balanced meal (80g, protein 5.2%, carbohydrates 7.1%, fat 2.5%) was labeled with 40 MBq of 99mTc-nanocolloid. Patients were positioned seated in vertical position close to gamma camera (FOV from the jugular notch to the upper abdomen, images matrix 128 x 128, zoom 1). To study the transit of esofageal remnant and gastric conduit we used a first phase with a dynamic acquisition of 400 frames per 0.5 sec/frame. These dynamic images was acquired during oral administration of 6 radioactive bolus of about 10 ml every 30 sec. To study gastric emptying first we acquired dynamic images of 60 sec/frame for 30 minutes with the patient sitted, then we acquired a series of static images of 60 sec/frame every 10 min until 120 min post oral administration. During the intervals we invited the patients to stand-up and walk to mimic physiological situation of post-prandial phase. The compacted images were aligned and analyzed using ROIs placed on the gastric conduit and stomach. Parametric images and time/activity curves are created. **RESULTS** Two patients had swallowing difficulties. The study of the gastric emptying recognized two distinct groups of patients. The first group showed an early and fast emptying when the patient was sitted. The second group showed a slow emptying in the first phase which was then accentuated by the deambulation. The time to half of gastric empting was from 2 min to 145 min. **CONCLUSION** This method was well tolerated by the patients. Our scintigraphic procedure allowed us to evaluate swallowing and gastric emptying in patients with gastric pull-up esofagectomy, mimicking their physiological situation.

## TP049

### Quantitative sacroiliac evaluation in paediatric population - our standard values

**N. S. Silva**, D. Calado, A. Alvernaz; Hospital da Luz, Lisboa, PORTUGAL.

**AIM:** The aim of this study is to define the standard values for sacroiliac (SI) quantification in paediatric population, based in our experience. The goal is to use this standard values to distinguish normal from abnormal sacroiliac uptake.

**METHOD:** Bone scan were performed in a Siemens E-Cam gamma camera. We used $^{99m}$Tc- HMDP and the injected dose was prepared accordingly to EANM recommendation for paediatric patients. Images were acquired 2 hours after the administration of the radiopharmaceutical. Whole body acquisition in both anterior and posterior view was performed with a speed of 10cm/min, a 256 x1024 matrix. **RESULTS:** We analyzed 30 patients aged from 7 to 17 years old. All the patients were clinically reported with normal uptake in both sacroiliac bones. In order to proceed to the quantitative evaluation, 3 ROI's were obtained, 1 in the right sacroiliac, 1 in the left sacroiliac and 1 in the sacrum. All the ROI's were performed by the same operator, in order to reduce the potential error. A ratio between each sacroiliac/sacrum was determined. **CONCLUSION:** These results prove that the paediatric population may have different standard values in comparison with adult population. More studies should be assessed in an effort to establish a reliable standard value, to help with the diagnosis of sacroiliitis in paediatric population.

## TP050

### Usefulness of the Salivagram for the Diagnosis of Brain Lesions in Patients with Aspiration Pneumonia

**S. Oh**[1], Y. Choi[1], D. Ro[1], H. Nam-Koong[1], H. Park[2], J. Kim[1], C. Lee[1]; [1]Yonsei University Health System, Seoul, KOREA, REPUBLIC OF, [2]Department of Radiological Technology in Shingu College, Seongnam, KOREA, REPUBLIC OF.

**Purpose:** Aspiration pneumonia is an acute inflammatory respiratory disease infected from foreign substances or pathogens in lung and bronchus. Staying in bed for a long time is required in adult patients with brain lesions. It can be caused to patients who stay in bed for a long time from stroke, traumatic brain injury, and Parkinson's disease, causing pneumonia and respiratory diseases may be due to aspiration of food or saliva. In patients with recurrent pneumonia or pulmonary symptoms, there is a need to determine the possibility of pulmonary aspiration due to aspiration of saliva. In this study, a usefulness of the salivagram for diagnosing aspiration pneumonia with patients who had brain lesions was evaluated. **Materials and Methods**: To diagnose aspiration pneumonia due to saliva, 10 patients (male : 6, female : 4) with brain lesions were objected. Patients were fasted before the test, $^{99m}TcO_4$ 185 MBq (5 mCi) of less than 1 mL of solution was administered in the oral cavity. 20 minutes of dynamic imaging acquired after the administration, immediately and the static images were acquired, respectively. Additional static images were obtained after 2 and 4 hours if $^{99m}TcO_4$ was still on the mouth. In addition, a positive study result was defined as radionuclide tracer being present in the tracheobronchial tree. **Results**: Positivity rate of all 10 patients was 60%, 4 patients showed the aspiration after the administration of oral cavity in a 20-minute of dynamic imaging. In the remaining 2 patients of the positive, the aspiration was shown in four hours of additional delay tests. One patient confirmed with aspiration of saliva had a re-examination after treatment. In the dynamic imaging and 4-hour delayed imaging shows a negative reaction, and the aspiration of saliva could not be confirmed. **Conclusion:** In this study, we believe Salivagram takes comparatively short time with simple examination procedure, provide the image information for the diagnosis and treatment-planning in aspiration pneumonia without changing patients posture.

## TP051

### Manifestation of a urinoma in a cervix cancer patient in a bone scan image

**I. Paula**, L. Pereira, B. Ferreira, L. S. Violante, H. Duarte; Instituto Portugés Oncologia Francisco Gentil S.A., Porto, PORTUGAL.

**Aim** Urinomas generally are a contained collection of urine outside of the normal pathways where urine travels and may have a variety of aetiologies. Urinomas may cause sensations of pressure or pain due to their mass effect, but they may also be asymptomatic and discovered as an incidental finding, for example, in a bone scan. **Materials and Methods** A 31-year-old woman, with history of cervix carcinoma diagnosed in 2012, treated with radiotherapy and chemotherapy. In February 2013, during a routine visit, the patient refers bone pain in lumbar and sacral vertebral region. A bone scan was performed, which didn't show any abnormal uptake in the skeleton that could justify the patient symptoms. Instead, an accumulation of the radiopharmaceutical in the posterior right perirenal region was seen. For better anatomic localization of the incidental finding, a SPET/CT was performed using the PET/CT device in our department and after the fusion of both images (SPET and abdominal CT scan), a marked right-sided perirenal fluid collection was confirmed, suggesting urinoma, probably secondary to an obstructive uropathy. The urology department was contacted and drainage of the fluid collection was performed, which alleviated the patient symptoms, confirmed the urinoma as their etiology and defined the therapeutic attitude- nephrostomy and antibiotic treatment. **Conclusion** The renal excretion in $^{99m}$Tc-HMDP bone scan allows the kidneys visualization, accessing some functional and/or morphologic changes. The bone scan in the present case led to the detection of an unsuspected urinoma in a patient with cervix cancer.

## TP052

### Adapted recommendations for radioprotection in daily practice, after a radioactive aerosol emission study in a nuclear medicine department during ventilation scintigraphy using 99mTc-aerosols

**S. AMIOT**[1], P. BOMBARDIER[2], C. Houzard[1]; [1]CHLS, PIERRE-BENITE, FRANCE, [2]Laboratoire InterUniversitaire des Systèmes Atmosphériques, Créteil, FRANCE.

AIM We expose practical procedures for radioprotection optimization after a scientific work realized in our medicine department, with measure the leakage of radioactive particles during pulmonary scintigraphy examinations using 99mTc-aerosols MATERIAL AND METHOD This initial study used a specially designed enclosure for our Technegas™ generator (2006) connected to a specific hood including patient's head and mouthpiece, permitting accurate measure of radioactivity diffusion, with recording of short time events; best location for air contaminations sensors were defined with a numerical model of our department. Combining staff position information, simulation of the dissemination for the aerosol released were used to confirm the exposure levels for professional groups and enhance the workplace studies (radioactivity released in the air by the generator leakage was equal to that deposited in the patients' lungs by inhalation - 6%- of that introduced into the generator). These results were used to establish a list of procedures to minimize professional and patients exposure. RESULTS Main recommendations for professional and for department radioprotection procedures are listed 1-Positionning optimization of technician -during aerosol preparation in the generator: it is the main recommendation, especially for eye lens radioprotection : rapid work, with the head more far as possible of the recipient, because of the importance of the radioactivity released at this precise moment - during patient inhalation : a great variability of radioactivity diffusion around the mouthpiece is presumed, depending of the age, medical status of the patient, morphologic adaptation between mask and patient's face, even if the measure realized in live with one patient with the specific hood showed a very low diffused activity (around 0.4MBq). It's more difficult for specific recommendations, others than the usual ones (time, distance). 2-Correct use of aspiration hood (hood position and prior functioning verification) 3-Surgical mask use after inhalation, including time of acquisition with gamma-camera 4-Use of the shortest way between inhalation room and gamma camera room 5-A paradoxical result of this study is now taken in account: more important air flow, with more distant contamination in the corridor were observed when the door of the inhalation room was closed vs opened (abnormal high pressure inside the room generating higher air flow under door bottom); the differential pressure between the inhalation room and the corridor has been adjusted and the door is closed CONCLUSION From the quantitative results of a dedicated scientific study, we could preconize effective procedures for radioprotection purpose, for technicians and patients.

## TP053

### What are the main attributes of cohesive team work and qualities of team member in delivering health care to patients?

**E. Bagi**[1], A. Vara[2], L. Jenkins[2], H. Campbell[2], S. Dizdarevic[2], L. Vieira[3], F. Lucena[3]; [1]Nuclear Medicine Student, ESTeSL-IPL, PORTUGAL and ERASMUS student at Brighton and Sussex University Hospitals, NHS Trust, UNITED KINGDOM, [2]Brighton and Sussex University Hospitals, NHS Trust, UNITED KINGDOM, [3] Nuclear Medicine, ESTeSL-IPL, PORTUGAL.

**Aim** Professional Multidisciplinary team work is essential in delivering high quality healthcare to patients. In some departments, the approach of collective work is more frequent then the real concept of cohesive teamwork. The following describes the two scenarios in approaching collective working: 1. Group working: Formulation of professional groups i.e. Clinical, Physics, technical, which has limited links between these professional groups, or a specific functional articulation between the group's elements, though each group performs their tasks individually. 2. Team working: Team of professionals who together hold a common purpose, who meet together to communicate, collaborate and consolidate knowledge. The aim of this study was to investigate the main attributes of the team work evaluating the satisfaction and motivation of the professionals and to identify the most important qualities of a team member. **Methods:** We designed a questionnaire that allowed the evaluation of: communication, job satisfaction, motivation and teamwork within our Department. The results were statistically analyzed, by non- parametric test, classified in ordinal scale. **Results:** The questionnaire was answered by 24 professionals. 81% of professionals were satisfied with their job. 67% felt the team worked well together all the time, whilst 33% felt that only on occasions the team works well together. 67% of professionals felt motivated to teach and learn with others team members. The most important qualities of a team member are as follows: • Good Communication between team members - 92% • Knowledge and Collaboration skills - 67% • Performance and Technical Skills - 63% • Respect and following rules - 58% 36% and 28% of the professionals would like to improve the working environment and the

communication respectively. **Conclusions:** Collaboration and communication were the most useful skills and personal attributes for the integration of the team members. The main attributes of cohesive team work are collaboration and negotiation through discussion, since the tasks are usually collective. Team approach is required to deliver efficient service; however regular departmental staff's survey may be helpful to identify priorities for each team member in conjunction with their appraisal and performance review.

TP03 - Tuesday, Oct. 22, 8:00 - 9:30, Poster Exhibition Area

## Technologist Poster Session 3

### TP054

### Study on repeatability detection and influence factors of $^{13}$C-urea breath test with mass spectrometer

**Y. Wang**, M. Liu; Department of Nuclear Medicine, Huashan Hospital, Fudan University, Shanghai, CHINA.

Objective: The "gold standard" of H. pylori detection is $^{13}$C-urea breath test with mass-spectrometer. Reproducibility of mass spectrometry will be investigated. Methods: It was Dual-channel sample gas-isotope ratio mass spectrometry to obtain and analyze the results -- the $^{13}CO_2$ excess values of δ. The gas sample in vitro is the first blowing breath of people who is not infected with H. pylori before taking the $^{13}$C labeled urea. Then the Friedman two-way analysis of variance according to rank of the data was carried out analysis of repeatability. The second blowing breath were gas sample detected of people who had been infected with H. pylori with the mass spectrometry assay confirmed after taking the $^{13}$C labeled urea. Then 18 tubes which had been placed 2-10h were detected by "replicates 3" and analyzed by paired t-test.Results: Negative in vitro test: δ values the twice retest obtained (± SD) was -24.54 ± 0.86, -24.37 ± 0.81, paired t-test t = -7.657, P <0.001. Friedman rank two-way ANOVA analysis showed that the average rank of the two groups were respectively 1.16, 1.84, P <0.001. This two statistical Methods showed that the retest results were elevated and statistically significant. According to Friedman rank two-way ANOVA analysis, the mean rank of δ values were respectively 1.77, 1.77, 2.98, 3.63, 4.86, P <0.001, there was statistically significant. Positive test-tube test: according to the rank of two-way analysis of variance results, the average rank of 18 pairs of the δ values were, respectively, 1.28, 1.89, 2.89, 4.06, 4.89, P <0.001. This two statistical Methods proved that the measurement results rose with the increasing frequency (time variation), and there was a significant difference. Conclusion: $^{13}$C mass spectrometric analysis of H. pylori urea breath test. Results will be affected by the test tubes long-time placed, changes in the temperature of the machine, but the influence is not obvious. In the mass spectrometric analysis of the urea breath test and relevant experiments, each test tube should be detected as soon as possible, and not suitable for doing multiple measurements.

### TP055

### Optimal number of iterations and attenuation correction method for the quantification of liver radioactivity on $^{99m}$Tc-GSA SPECT/CT imaging

**Y. Nakamura**[1], S. Tomiguchi[2], N. Katsuda[1], M. Hashida[1]; [1]Division of Medical Technology, Kumamoto University Hospital, Kumamoto, JAPAN, [2]Faculty of Life Sciences, Kumsmoto University, Kumamoto, JAPAN.

**Background and Purpose** $^{99m}$Tc-GSA SPECT/CT imaging is performed for quantitative evaluation of a liver functional reserve. Recently, ordered subsets-expectation maximization (OS-EM) method with attenuation correction by using CT image has been used for the image reconstruction. However, optimal numbers of iterations and attenuation correction method for the quantification of liver radioactivity have not been precisely evaluated. The aim of this study was to assess the optimal number of iterations for OS-EM method with attenuation correction in the quantification of liver radioactivity. Usefulness of Chang's attenuation correction method using CT values in the liver(Chang's method) was also evaluated. **Material and Method** Liver phantom with total 160 MBq of $^{99m}$Tc radioactivity in the liver was used and 16 donors who performed $^{99m}$Tc-GSA SPECT/CT imaging before the liver transplantation were enrolled in this study. In phantom and clinical studies, SPECT images were obtained by OS-EM method with change in the number of iteration from 1 to 30 times. Then, the optimal numbers of iteration were defined by accuracy of estimated radioactivity in the liver and image uniformity (C.V.) of the liver. The usefulness of Chang's method using CT values of the liver was also assessed by compared it with that performed using CT image (CT method). **Results** Optimal number of iteration was considered to be 6 that were feasible to obtain the accurate liver radioactivity. C.V. in the liver increased by increase in the numbers of iteration. Chang's method was superior to CT method for radioactivity quantification in the liver. The Chang's method showed more uniform SPECT image than CT method. **Conclusion** Reconstructed SPECT image obtained at 6 iterations using Chang's method is feasible for the quantification of $^{99m}$Tc-GSA radioactivity in the liver.

### TP056

### Brain blood flow quantity method with fixed quantity-vein blood one point blood collection by time series medicine movement analysis in brain

**A. TSUNEKAWA**, Y. OKUMURA, T. KAWACHI, M. NAKAMURA, M. FURUKAWA, F. NIWA, H. NISHIWAKI, Y. SONE, H. OYAMA, K. AKIRA; Ogaki Municipal Hospital, OGAKI, JAPAN.

Microsphere model (MS) which did sustained artery blood sampling by the SPECT in cerebral blood flow calculation conventionally if essential was appreciated in precision. In late years one point of artery drawing blood Autoradiography ( ARG )simple and easy is used. We developed an examination of minimally invasive vein revision ARG method this time and inspected precision. We got the amount of change in the brain count (radioactivity) by dynamic image collection just after the 123I-labeled N-isopropyl-p-iodamphetamine (IMP) dosage more for 18 minutes. We estimated an artery blood count at 10 minutes after the IMP intravenous injection, and estimated a vein blood count 43 minutes later after the IMP intravenous injection. We supposed an artery count from quantity of radioactivity and the venous blood count in the brain which I got. We supposed actual measurement arterial blood counts from cerebral counts and venous blood counts using multiple linear regression analysis. Independent's factors are total 19 factors;18 factors of time series cerebral counts and venous blood counts. 34 patients presented with major cerebral artery occlusion disease.The study protocol was approved by the local ethical committer. All patients and subjects gave written informed consent prior to the study. The actual survey artery drawing blood count and estimated artery count that I got from and a multiple regression analysis got coefficient of correlation r=0.8836 and high correlation. In addition, I extracted 22 cases from 34 cases at random number selection and made an estimated function and inspected precision in other 12 cases for validation. There was a high association between r=0.7 and Ca10(Ca10 is the arterial blood radioactivity at 10 min ) and calculated arterial radioactivity at ten minutes 12 cases. And they are a high correlation(r=0.78)within rCBF by ARG method. We think so this method can apply for clinical laboratory diagnosis.

### TP057

### Chronic myocardial ischemia assessment: an experimental comparative study between histology and microPET imaging quantification

**E. Fleury**[1], M. Ndengera[1], W. Mrowczynski[2], J. Tille[2], L. Wuarin[2], B. Walpoth[2], O. Ratib[2]; [1]Haute école de santé Genève - University of Applied Sciences: Western Switzerland, Geneva, SWITZERLAND, [2]University Hospital of Geneva, Geneva, SWITZERLAND.

**Aim** The myocardial infarction model in small animals is widely used in cardiovascular research, to study aspects such as revascularization, preventing cardiac remodelling, pharmacology support and cellular therapy. Experimental chronic myocardial ischemia-remodelling and regeneration studies require sequential non-invasive follow-up Methods. The gold standard to assess an infarction zone or scar remains histology, requiring the euthanasia of the animal. The aim of the study is to correlate the extent of myocardial infarction obtained by microPET with histology. **Materials and Methods** Twelve male Dawley Sprague rats (400g) underwent permanent left coronary artery (LCA) ligation. The microPET scans were performed 2 and 30 days after ischemia according to the following protocol. Intravenous injection of 20MBq of 18-FDG was followed by 30min of gated acquisition. 3D images were reconstructed from sinograms and analyzed with clinically used software (Corridor 4DM). At 30 days animals were sacrificed, hearts harvested, divided into 4 equal short axis slices (Apical, Lower medial, Upper medial and Basal) and colored with Massons' trichrome stain. The percentages of viable myocardium assessed by microPET were compared to histology slices. **Results** There was a significant underestimation of the myocardial infarction zone in the microPET imaging quantification against histologic planimetry. Histology quantification assessed a mean ischemia percentage of the LV at 14.08%, ± 8.67; median 13.68, interquartile range 4.44-25.0, whereas microPET quantification assessed a mean non-viable muscle percentage of the LV at 10.98% ± 7.56; median 8.67, interquartile range 3.40-18.53, this difference was significant (p = 0.028). The non-parametric Spearman correlation coefficient is high, r = 0.85, which suggests a strong correlation between histology and microPET imaging quantification. **Conclusion** This study shows that, despite minimal discrepancies with the microPET imaging quantification underestimating the ischemia when compared to histology. The underestimation of microPET can be attributed to the fact that both Methods do not evaluate the same entities. PET with 18-F FDG only assesses viable vs. non-viable myocytes; whereas histology assesses scar tissue with all accompanying cellular reactions (collagen, fibroblasts, and capillaries). However, the correlation is sufficiently promising that future studies could be based on this non-invasive imaging technique. Permanent LCA occlusion yields variable infarction areas and therefore the non-invasive microPET method, especially when performed early and late, can provide myocardial infarction quantification but also its remodelling if reperfusion or regenerative protocols are used.

## TP058

### A simplified noninvasive method for estimation of $^{123}$I-IMP arterial blood activity using $^{123}$I-IMP acquisition data from the lungs and brain

**Y. Fujita**[1], S. Abe[2], T. Odagawa[1], N. Fujita[2], H. Kono[2], T. Kumazawa[2], A. Niwa[1], K. Kato[1]; [1]Department of Radiological and Medical Laboratory Sciences, Nagoya University Graduate School of Medicine, Nagoya, JAPAN, [2]Department of Radiological Technology, Nagoya University Hospital, Nagoya, JAPAN.

**Aim**: The $^{123}$I-IMP autoradiography (ARG) method has been used well for quantification of the cerebral blood flow (CBF). This method requires the $^{123}$I-IMP activity in an arterial blood sample obtained at 10 min after intravenous injection of $^{123}$I-IMP by arterial puncture (Ca10). Arterial puncture is invasive for patients, and they benefit from the avoidance of arterial puncture. Previously we devised a method for estimating of Ca10 using multiple regression analysis without any blood sampling and proposed the noninvasive $^{123}$I-IMP ARG method for estimating CBF. In our previous study, the correlation (r=0.907, n=23) was detected between the estimated Ca10 values and the Ca10 values measured directly with an actual blood sample. The purpose of this study is to develop a more simplified method for estimation of Ca10. **Methods:** In our previous study, we acquired planar dynamic lung images, static brain images before and after brain SPECT, and brain SPECT images. In this study, we acquired planar dynamic lung images and brain SPECT images only from 36 patients. Multiple regression analysis was employed to estimate Ca10 using 4 parameters such as an integral corresponding to the area under the curve of dynamic lung counts, the counts of brain projection data, the sum of an integral of dynamic lung counts and the counts of brain projection data, and the body weight were used as explanatory variables and the Ca10 directly measured with the actual arterial blood sample as objective variable, and the regression equation was calculated. **Results**: The regression equation was calculated by multiple regression analysis as follows: Estimated Ca10=($1.79\times10^{-3}$•UCL)+($1.99\times10^{-3}$•CB)-($1.75\times10^{-3}$•S(L&B))-(5.71•BW)+762, where UCL: the area under the curve of dynamic lung counts, CB: the counts of brain projection data, S(L&B): the sum of UCL and CB, and BW: body weight. The estimated Ca10 values closely correlated with the directly measured Ca10 values (r=0.855). **Conclusion**: The noninvasive method for estimating Ca10 proposed in this study is more simplified compared with the previous method. The correlation coefficient between the estimated Ca10 values and the directly measured Ca10 values (r=0.855) is equivalent to that obtained by the previous method (r=0.907).

## TP059

### Glomerular Filtration Rate - Comparison of Manchester Rutland and Gates Methods

P. Chilra[1], **S. Batanete**[1], F. Lucena[1], L. Vieira[1], P. Delgado[2], S. Pintão[2]; [1]Escola Superior de Tecnologia da Saúde de Lisboa, Lisboa, PORTUGAL, [2]Hospital de Santa Cruz - CHLO, EPE, Lisboa, PORTUGAL.

Glomerular Filtration Rate (GFR) is considered a standard measure of renal function and it can be determinate by the renogram with $^{99m}$Tc-Diethylenetriaminepentaacetic acid ($^{99m}$Tc-DTPA). This quantification is important in several clinical situations, for example in the evaluation of potential kidney donors. However renogram processing is associated with some problems, such as difficulty in correcting the background activity, so there are several tools available to solve these problems. Manchester-Rutland Background Subtraction method optimizes background subtraction and considers soft tissues and vascular background in the quantification of GFR. Gates method determines GFR taking into account pre-, pos-syringe counts and optimizing the quantification of the real administered radioactivity of the radiopharmaceutical. The aim of this study is to evaluate the accuracy of GFR determination through the renogram with $^{99m}$Tc-DTPA using Manchester Rutland Backgroud Subtraction and Gates Methods, comparatively to the plasma sample method. Data from 30 patients who underwent renograms with plasma sample method for pre-nephrectomy evaluation between 2009 and 2012 were collected retrospectively. The sample included female patients, age >18 years, with normal renal morphology and anatomical position and without hypertension, diabetes mellitus and renal diseases. Patient preparation and image acquisition was performed according to the department protocol: oral hydration prior to imaging; image acquisition: static pré- and pos-syringe; dynamic renogram: 1sec/frame (phase 1), 15sec/frame (phase 2); 128*128matrix; zoom 1.33. Renograms were processed by the commercial Manchester-Rutland Background Subtraction and Gates Methods in the nuclear medicine workstation - Xeleris 3$^{TM}$. For each method semiautomatic processing was performed by one Nuclear Medicine Technologist and repeated five times/patient for reproducibility evaluation. Quantification of renal functional parameters were obtained. Plasma sample method GFR results were also collected from the patient's file and used as reference method for the determination of accuracy. It is expected that the accuracy differences between the two Methods studied might contribute to the optimization of the standard protocol for renogram in Nuclear Medicine departments, especially in the quantification of GFR for potential kidney donors.

## TP060

### Comparison of Image Quality According to Collimator, Distance, Acquisition Time in SPECT

C. Kim, **H. Park**, B. Kim, Y. Kim, J. Kim, K. Kong, M. Seo, B. Seo, K. Lyu; Shingu College, Seongnam, KOREA, REPUBLIC OF.

Images obtained in the SPECT, contrast, resolution, noise, etc. can be evaluated. This report is comparing contrast and resolution by the performance of the collimators, the change of distance, and the change of acquisition time. The kinds of collimator are LEAP(Low Energy All Purpose) and LEHR(Low Energy High Resolution) collimators and the factor of changeable distance is 10~25 cm. The acquisition time was between 5 and 20 seconds. Line source in phantom for SPECT imaging was diluted with water 99mTcO4. Resolution measurements phantom was NEMA SPECT resolution phantom and Hoffman phantom. Using measure contrast, Contrast phantom was used to measure the contrast of shape of myocardium. Line profile is obtained and each of the five subjects, we calculated the average value of the radial/tangential FWHM(full width half maximum) and FWTM(full width tenth maximum) of the five point. The highest and lowest values were excluded and the remaining three values. In between that, them were calculated and the average obtained the FWHM resolution. We also used organ part contrast and background contrast in evaluating the cardiac phantom's contrast. The resolution result of LEHR is higher than the LEAP. Also, the LEHR collimator's contrast is 78.2 % and the value of LEHR collimator's contrast is 79.1 %. Therefore, LEHR collimator's contrast value is higher than LEAP collimator's contrast. After eye sight test, we found out that LEHR collimator's brain image using Hoffman phantom is better than LEAP collimator's brain image. Of the distance, if the distance is increased, resolution is decreased. In testing, the contrast by using 15 cm, 20 cm and 25 cm distances, 78.2 %, 71.6 %, 64.1 % were obtained, respectively. Thus, we found out that if the distance is increased, the contrast is decreased as well as the resolution. The acquisition time in the internal line profile has greater resolution than out of external line profile. The contrast values obtained were 82.7 % by 5 s, 83.8 5% by 10 s 84.2 % by 30 s acquisition time. Therefore, higher acquisition time, the higher the contrast value.

## TP061

### To optimize the CT scanner in SPECT/CT equipment of Nuclear medicine

**Y. Wang**, Z. Liu; Department of Nuclear Medicine, Huashan Hospital, Fudan University, Shanghai, CHINA.

**Objective**: Since the invention of SPECT/CT, more and more nuclear medicine physicians are adding the CT scanner to improve the efficiency of diagnosis. However, in order to improve the diagnostic accuracy, in the meantime,also increase the patients' radiative dose. Summarized empirical Methods from the previous practice work, we hope to draw an optimized scheme of CT scanner, to reduce patients' radiation doses and dicrease the exposure time of the CT Tube. **Methods**: To optimize voltage, current , exposure time, front and back of collimator, pitch factor, matrix and a series of acquisition parameters, we analysis the continuous clinical examples in four months, change the different levels of parameter sloely, and retrospect the CT radiative dose. We also compare to the quality of the image and constantly try to optimize the improvement. In the meantime, we statistics the monthly CT Bulb exposure time, exposure time per capita tube data and so on. **Results:** Compared with former optimization, the average CT radiational dose per person is decreased by 84.72%, Which conventional bone group radiation reduced by 83.82% (t = 24.362, P <0.001), the small joints of the bone group radiation reduced by 88.80% (t = 24.914, P <0.001), cerebral group radiation reduced by 86.78% (t = 61.008, P <0.001 ), the heart group radiation reduced by 84.49% (t = 52.994, P <0.001), the differences are statistically significant. Optimized CT Tube exposure time is 2031 seconds monthly. Bulb exposure time per capita is significantly decreased, The fourth month per capita ball of tube exposure time is 16.73% of the first month, and the difference is statistically significant (t = 17.458, P <0.001). **Conclusion**: In this study, it shows that using the CT scan optimization scheming has great efforts in practice of clinical nuclear medicine, while reducing the exposure time of the CT Tube and improving the lifetime of the bulb.It can be widely used.

## TP062

### The role of SPECT/CT (Single Photon Emission Computed Tomography/Computed Tomography) in bone diseases. The additional benefits of the multi-modality imaging.

**A. PALMIERI**, S. COLA, G. BIGI, L. BELLONI, V. CATTINI, M. MANFREDINI; SANTA MARIA NUOVA HOSPITAL, REGGIO EMILIA, ITALY.

**Background:** Radionuclide bone scanning is used to diagnose or to evaluate various malignant and nonmalignant bone diseases. However, increased radionuclide uptake by a lesion is not specific, and differentiating malignant from nonmalignant disorders may therefore be difficult. Single-photon emission computed tomography (SPECT) combined with computed tomography (CT) provides both structural and

functional information. **Aim**: The purpose of this study was to determine the additional benefits of SPECT/CT over traditional bone scan, planar or whole-body imaging, in the evaluation of bone diseases. **Material and Method**: To acquire data we used a Symbia T2 SPECT-CT scanner (Siemens Medical Solutions) that incorporates 2 slice CT scanners with their dual-detector system. Patients were studied 2-4 hours after receiving 740-925 MBq of 99mTc-Ossidronato. All patients were scanned with planar imaging and/or WB (whole-body) imaging. Planar images were acquired with 256x256 matrix, 500-1000 Kcts, zoom 1. WB was performed in both anterior and posterior projections, with a table speed of 12 cm/min for a total time of 20 min (1024x256 matrix). SPECT/CT was added for patients whose planar findings were inconclusive; in particular when the localization of lesions accumulating 99mTc-Ossidronato was unclear or a malignant origin could not be ruled out. From 1st October 2011 until 1st October 2012 we scanned 79 patient with SPECT/CT (36 men and 43 women; the ages ranged from 19 to 91 year, mean 59 y). SPECT/CT scans was performed using the clinical protocol, with LEHR parallel hole collimators, over 360 degrees at 64 angles, 25 seconds/angle, 128x128 matrix. CT images were performed using the follow parameters: 130 kV, 80-100 mAs, pitch 2, thickness 5 mm. SPECT projections were reconstructed with OSEM-Flash 3D algorithm (8 iterations, 4 subsets, cubic voxel of 4.8mm) and corrected for scatter and attenuation. Results: SPECT/CT fusion images provided better identification and interpretation of the uptake foci, more correct anatomic localization and characterization, and precise differentiation between pathologic and physiologic uptake when not obtained from the planar images. SPECT/CT was considered contributory if it accurately localized the anatomic site of a hot spot. The hybrid SPECT/CT imaging provided a significant contribution in 61 patients on 79, up to 75% of patients whose planar imaging findings were inconclusive, thus having a substantial impact on the clinical management of DTC patients. **Conclusion:** Fusion of SPECT and CT images gives an incremental value over planar imaging in increasing diagnostic accuracy, reducing pitfalls, and increasing the confidence in interpreting the scans.

## TP063

### Clinical usefulness of Whole-Body SPECT/CT

**S. van Lierop**, M. Cramer, G. Engizek; Érasmus MC, Rotterdam, NETHERLANDS.

Objective: The objective of this project is to test the added value of the Whole-Body SPECT/CT and to introduce a new scan method for the department. The project also aims to determine the advantages and disadvantages of this method. Material and Methods: The patients in scope for this project are post-Lutetium-177-octreotaat therapy patients. All patients had an annual follow-up somatostatine scan. For all patients, the clinical question was to determine progression or regression of the Neuro Endocrine Tumor (NET). In this project a scan was made of the entire abdomen and/or thorax with the use of Whole-Body SPECT/CT. The Whole-Body SPECT/CT research was conducted on a Siemens Symbia T16 system. The scan includes 60 views of 20 sec per view in a continuous mode with a matrix by 128 x 128. This equals approximately 20 minutes per SPECT for two bed positions with 1cm overlap. The overall research takes about 40 minutes. The processing was performed with Siemens software. For reconstruction, Flash 3D processing with 15 subsets, 5 iterations and a 8mm Gaussian filter was used. Results: 6 patients have participated in the Whole-Body SPECT/CT research. Three different nuclear medicine physicians have independently reviewed the scans and have indicated that the scans meet their review requirements. A great advantage is that one scan can be used to measure the entire target area. Artefacts are visible in the overlap areas of the two scans but this doesn't affect the research results. Further research proved that adding the Auto Recon activity to the processing workflow could eliminate artefacts. The Whole-Body SPECT/CT scan allows us to reduce the error rate. Contrary to current scans, this new method only needs one topogram and one low-dose CT, so that radiation can be reduced. The risk of motion artefacts is large due to the duration of the scan. Therefore a precise fixation is evident. Conclusion: Based on the research results, it can be concluded that the Whole-Body SPECT/CT has an added value for the department. However, the research can be optimalised if the scan time can be reduced.

## TP064

### Quarter millimeter resolution pre-clinical SPECT with quarter-mm pinholes

**O. Ivashchenko**[1], F. van der Have[2], J. Villena[1], F. J. Beekman[2]; [1]MILabs B.V., Utrecht, NETHERLANDS, [2]Section Radiation Detection and Medical Imaging, Delft University of Technology, Delft, NETHERLANDS.

**Aim:** Pre-clinical applications of molecular imaging are often hampered by limited spatial resolution. Collimators with the appropriate resolution-sensitivity trade-off for the task at hand need to be selected. In the present work we evaluate a new focused mouse collimator with 75 micro-pinholes of 250 micrometers diameter, dedicated for focused imaging in small anatomical structures like joints, thyroid and tumors. **Materials and Methods:** The collimator was tested in the U-SPECT+/CT (MILabs, Utrecht, The Netherlands). Images were obtained from the list-mode data using pixel-based ordered subset expectation maximization (POSEM) reconstruction with resolution recovery through use of an accurate PSF model during reconstruction. The spatial resolution of reconstructed images was characterized for 1 hour scans of $^{99m}$Tc and $^{125}$I filled Jaszczak hot rod phantoms (rod diameter equals rod distance). **Results:** Resolution of in terms of visible rod size was 0.25 mm for $^{99m}$Tc and 0.3 mm for $^{125}$I. The peak sensitivity of the collimator for $^{99m}$Tc was 380 cps/MBq. Scanning of a 20 mm diameter uniform filled cylinder yielded highly uniform images. **Conclusions** The U-SPECT+ scanner equipped with ultra-high-resolution collimators reaches as high as ¼ mm resolution over the entire system field of view. Excellent uniformity allows highly quantitative molecular imaging. In-vivo mouse SPECT imaging will begin shortly and results will be presented at the conference.

## TP065

### Tri-Modality Image Fusion Accuracy with a "Home made" designed Shuttle system

**M. Hofbauer**; PET/ CT-MR Wagi, Schlieren, SWITZERLAND.

**Aim**: Several challenges are on the table when we think of integrating the tree modalities (PET, CT and MR) in a single exam. Times to respect, patient displacement between the systems, accurate positioning for the perfect match between the images taken in different systems··· One of the biggest challenges when working in a Tri-Modality centre is the handling of the patient between the different systems, MR and PET-CT, in order to get the same image registration in all of them. Our Nuclear Medicine department developed a unique mechanism that allows patient transfer between the different systems, with almost no patient movement, improving the image registration accuracy. **Materials and Methods**: This study was conducted in our PET/CT-MR center, where a PET/CT Discovery 690 and a 3.0T MR 750w GEM, both from General Electric, are placed in two contiguous rooms. This study comprises 60 MR/PET-CT patients witch exams were performed from top of the head till mid-thighs, in axial slices, in all the tree systems, during last year. Patients were placed in the shuttle and the same zero position was applied in the different systems. The displacement of the patient between the systems is done in the shuttle, so, from the moment that the MR starts, till the end of the PET/CT exam, the patient remains in the same position. Images were automatically fused with Volume Share 5.0 (General Electric). **Results**: The shuttle reveals to be very "user friendly" from different perspectives: • The limitation of patient movement, from starting the MR exam, till the end of the PET/CT, totally improves the image registration accuracy between the tree modalities; • Patient transfer from MR to PET/CT, is done in a very easy way and with reduced time spent in the procedure: we have an average of less then 3 minutes, from the end of the MR exam till the beginning of the PET/CT exam. • The fact that the zero point is the same for the 3 modalities, improves the accuracy of the fused images. **Conclusion**: When commercial answers do not provide good enough results, department's creativity can be the motor for innovative solutions, solve problems, and a factor of improved diagnostic accuracy.

## TP066

### Implementation Through Conventional Tools of a Processing Protocol for Registration and Fusion of SPECT-PET-MRI Studies in Neurology

C. Castillo Berrio, **S. Martínez Bernárdez**, D. Ruiz Hernández, A. Serena Puig, J. Nogueiras Alonso, M. Serrano Pérez, O. Rivas Dominguez, F. Loira Bamio, L. Campos Villarino, E. Vale Goncalves, A. Gil Rodriguez, A. Lopez Lopez, R. Guitian Iglesias, J. Outomuro Perez; SERGAS, Vigo, SPAIN.

INTRODUCTION: Brain pathology requires the use of morphological and functional techniques that assess different aspects of the disease. The joint and simultaneous assessment of both technologies facilitates the interpretation of the findings. Objective: To perform a protocol for registration and fusion of images coming from different modalities (SPECT, PET, MRI, CT) and manufacturers using tools and trading platforms. MATERIAL AND METHODS: Equipment (modalities and manufacturers): SPECT: eCAM® (Siemens); SPECT-CT: Infinia HawkEye® (GE); PET/CT (GE Discovery STE ®); RM (Philips, ACHIEVA); TC (Biograph® Siemens; GE). Processing platforms: eSOFT Siemens MI; Xeleris and Advance GE. PACS Sectra®. DICOM editors: DicomWorks, eFILM, etc. RESULTS: Several protocols have been developed in the eSOFT-MI Station for registration and fusion of studies coming from different modalities: 1) 123I-FP-CIT SPECT vs. FLAIR RM; 2) 18F- FDG PET vs FLAIR or T2 MRI; 3) 99mTc-Perfusion SPECT vs. FLAIR or T2 MRI; 4) PET/SPECT/ MRI. Registration is done manually by rigid transformations (vertical and horizontal translations; rotations in all three planes) by using emission PET, SPECT as object and MRI or CT as target, with good results. The assessment and congruence of the registered and fused images is performed interactively. The registered series can be stored at the station as well as summary screens. We found some incompatibilities between manufacturers (for differences in location and orientation information in DICOM header) that have not been possible to solve with DICOM editors. CONCLUSIONS Many hospitals now have devices enabling multimodality fusion PET/ SPECT/ MRI easily using commercial tools. This option is often underutilized. Multimodality imaging in Neurology helps verify the presence of normal variants or concurrent and confusing pathology (vascular pathology at striatum: DaTSCAN; ventricular dilatation, ischemic lesions, atrophy, etc.. for Perfusion SPECT or PET-FDG) and improves the diagnostic yield.

## TP067

### 99mTc-ECD brain SPECT are significantly correlated in patients with Craniosynostosis: a case-control study.

**M. Barik**, M. Bajpai, A. Malhotra, J. Samantaray, S. Dwivedi; AIIMS, New Delhi, INDIA.

**OBJECTIVES:** To assess subclinical central nervous system (CNS) involvement in Craniosynostosis(CS), by comparing standard brain MRI and (99m)Tc-ECD brain single-photon emission computed tomography (SPECT) of patients with CS with matched controls. **METHODS:** We performed a retrospective analysis of 85 subjects attending pediatric surgery clinic for CS in a tertiary care hospital from January 2007 to 2013. **RESULTS:** Out of 85 patients, 55 were cases and 30 were controls (age, 16- 38 months). Observed detection rates were 96%, 68%, 82%, and 72%, using SPECT/CT, X-ray, NCCT, and MRI respectively. Combination of NCCT and SPECT revealed sensitivity, specificity, positive predictive value (PPV) and negative predictive value (NPV) of 80.5%, 19.5%, 18.2%, 8.3% respectively. Combination of X-ray and SPECT showed sensitivity, specificity, PPV and NPV of 75%, 8.1%, 90.9%, and 100% respectively. However, combination of MRI and SPECT revealed a high sensitivity, PPV and NPV of 85.7%, 100%, 75%, respectively but with low specificity of 14.3%. $^{99m}$Tc-ECD SPECT/CT revealed regional hypoperfusion in the cerebral hemisphere in preoperative patients of craniosynostosis, corresponding to the fused sutures while postoperative studies revealed disappearance of these perfusion abnormalities. **CONCLUSIONS:** Although uncommon, intracranial complications of CS may present with clinical signs or symptoms. Computed tomography of the temporal bone with contrast is essential for identifying asymptomatic complications. Craniectomy remains the mainstay of surgical treatment. We should focus Onlay periosteoplasty and Partial craniectomy. $^{99m}$Tc-ECD SPECT/CT gives the better picture in our observation for Closed sutures. Postoperative vigilance is crucial, as complications may evolve despite aggressive therapy.At the same time follow-up of the patient is more important. We thanks to ICMR, India for funding.

## TP068

### Labeling and Evaluation of Receptor Affinity in Rats for Three Different Types Amino Acid Sequenced Peptide Molecules

**T. Ertay**[1], P. UNAK[2], O. OZDOGAN[1], Z. BIBER[2], O. ULKER[1], R. YESILAGAC[2], H. DURAK[1]; [1]DOKUZ EYLUL UNIVERSITY, MEDICAL SCHOOL, NUCLEAR MEDICINE, IZMIR, TURKEY, [2]EGE UNIVERSITY, INSTITUE OF NUCLEAR SCIENCES, IZMIR, TURKEY.

INTRODUCTION: Recent years, the use of receptor-specific peptide molecules has continuously increasing importance for nuclear medicine applications in imaging and therapy. A modification in the primary peptide structure alters its biological activity. AIM: The aim of this study is to increase receptor specificity with alteration in amino acid sequences in peptide chain and evaluate their radiopharmaceutical potential. METHODS: In this study, amino acid sequences were designed for three different types of peptide molecules. Designed peptide molecules; Tyr-Pro-Phe-Cis-Glu-Cis(ADL), Tyr-Pro-Phe-Pro-Gly-Pro(ADM), Arg-Tyr-Leu-Gly-Tyr-Leu-Glu(ADN) were synthesized by PepMetric Technologies. Amino acid sequenced peptide molecules were labeled with Tc-99m using glucoheptonate (GH) as bifunctional chelating agent. Quality-control studies of the labeled compounds were done using ITLC and HPLC Methods. To determine the lypophilicity of the labeled compounds, Tc-99m GH-ADL, Tc-99m GH-ADM and Tc-99m GH-ADN, log octanol/water partition coefficient was calculated. For imaging studies, 200 µCi Tc-99m labeled molecule was injected via the tail vein to the female rats. Rats were imaged at 5., 10., 15., 20., 30., 60., 120., 180., and 1440. minutes using gamma camera. Region of interests were drawn on organs and time-activity curves were generated for quantitative evaluation. Biodistribution studies were also performed using resection of the organs. The rats were sacrificed at 5., 10. and 30. minutes by ether narcotization and organs were removed. The activity per gram tissue was calculated. Receptor saturation studies were performed on another group of rats in similar conditions. For receptor saturating, 5 µg peptide molecule was administered to the rats 5 min. before injecting the Tc-99m labeled peptide molecule. RESULTS: The labeling efficiencies of each of three radiopharmaceuticals were found to be ≥ 95% in quality control studies. Labeled molecules were stable for 3 hours at room temperature. The prominent activity was observed in ovary and uterus. Main excretion route for three radiopharmaceuticals was kidneys. The more lipophilic Tc-99m-GH-ADL molecule showed hepatobiliary excretion besides renal excretion. The results were evaluated statistically by applying analysis of variance. CONCLUSION: It is seen that the affinity of molecule to the receptors can be modified and enhanced by changing the configuration in the peptide molecule. The results show that designed radiopharmaceuticals may have a potential for the diagnosis of uterus and ovarian pathologies.

## TP069

### A New Processing Method of Generator-Produced Ga-68 Nuclide for Ga-68-DOTA Peptide Radiopharmaceuticals

**M. Li**; Institute of Nuclear Energy Research, Taoyuan, TAIWAN.

Obectives: The Ge-68/Ga-68 generator system is one of the most important sources for preparing radiopharmaceuticals for clinical positron emission tomography (PET), because it produces the short-lived Ga-68 from its long lived parent Ge-68, separation of Ga-68 from Ge-68 is essential for the utilization of Ga-68. However, the available impurities such as stable Zn(II) generated by the decay of Ga-68, Ti(IV) as a constituent of the column material, and Fe(III) as a general impurity are not necessary for the synthesis of Ga-68-labeled radiopharmaceuticals. The positron emitting radionuclide Ga-68 (T½ = 68 min) shows great potential for clinical Positron Emission Tomography (PET). The present procedure purifies initial Ge-68/Ga-68 generator eluates chemically and radiochemically and involves the syntheses of Ga-68-labelled radiopharmaceuticals. Methods: We have developed an efficient route for the processing of generator-derived Ga-68 eluates, including the labeling and purification of radiopharmaceuticals. Purification of the initial generator eluate are performed using a miniaturized column with organic cation-exchanger resin(50WX4 @ BioRad) and 9N hydrochloric acid eluent for Ga-68-ion adsorbed, and to use the 2N hydrochloric acid eluent for Ga-68-ion de-adsorbed. The purified fraction was used for the labeling of nanomolar amounts of DOTA-petide derivatives. Results: Using the generator post-eluate processing system, 95% of the initially eluated Ga-68 activity was obtained within 5min as a 0.5 mL volume of a 2N hydrochloric acid. The initial amount of Ge-68, Zn, Ti, and Fe ions all were reduced by factors of $10^5$. Conclusion: Processing on a organic cation-exchanger resin(50WX4 @ BioRad) system in 9N/2N hydrochloric acid represents an efficient strategy for the purification of generator-derived Ga-68 eluates. This developed method guarantees high yields and safe preparation of injectable Ga-68-labeled radiopharmaceuticals for routine application and is easy for the use of automatic synthesizer. Thus, it is being successfully used in clinical validations and might contribute to the new direction for clinical PET from Ge-68/Ga-68 generator. The purified ionic Ga-68 obtained in this way has been used to label several radiopharmaceuticals. Reference Meyer G-J, Macke HR, Schuhmacher J, Knapp WH, Hofmann M. 68Ga-Labelled DOTA-derivatised peptide ligands. Eur J Nucl Med. 2004;31:10971104. Strelow FWE, Victor AH, van Zyl CR, Eloff C. Distribution coefficient and cation exchange behavior of elements in hydrochloric acid-acetone. Anal Chem. 1971;43:870876.

## TP070

### Scintigraphic evaluation of renal functional activity in early period after coronary artery by-pass grafting

**Z. Vesnina**, Y. Podoksrenov, Y. Lishmanov; Institute of Cardiology, Tomsk, RUSSIAN FEDERATION.

**Purpose.** To evaluate the possibility of radionuclide renoscintigraphy in assessing of kidney function in patients with coronary heart disease (CHD) in the early postoperative period after coronary artery bypass graft (CABG) under extracorporeal circulation (EC). **Methods.** The study included 32 CHD patients (all mans, mean age 53,1 ± 1,8 years) with heart failure (HF) of NYHA class II or III who underwent CABG under EC condition. Dynamic radionuclide renoscintigraphy with 99m Tc-DTPA was performed before and 6-7 days after surgery. The parameters of filtration and excretory renal functions, including glomerular filtration rate (GFR), blood clearance, parenchymal and collecting system half-time of indicator clearance were calculated. **Results.** Patients were divided into two groups. The first Group included patients (17 men) with moderate or significant disturbances of filtration and/or excretory renal function after CABG. Fifteen patients that had not postoperative renal dysfunction or it was insignificant formed Group II. Statistically significant changes of parameters of functional activity of the kidneys we observed only in patients of the Group I. Thus, there has been a significant decreasing of the mean values of total GFR and GFR for each kidney, cortical index delay indicator for both kidneys, as well as significantly increasing of blood clearance and the period of excretion of the radiopharmaceutical from the renal parenchyma and pyelocaliceal system. Comparative groups of patients were differed significantly from each other in the average duration of aortic clamping during the operation (respectively, 84,9 ± 7,5 and 52,9 ± 3,7 min; p = 0,001) and the time of EC (respectively, 131, 4 ± 8,5 and 89,7 ± 5,5 min; p = 0,001). Regression statistical analysis allowed us to identify the high correlation between the duration of the EC and values of majority of scintigraphic parameters of kidney function in the early postoperative period in Group I patients. **Conclusions.** Radionuclide renoscintigraphy allows objectively and with high informativeness to determine the extent and nature of the impact of CABG on the kidney function.

## TP071

### Impaired vasodilatory reserve on acetazolamide-challenged 99Tc-HMPAO-SPECT is a strong predictor of stroke recurrence in patients with severe steno-occlusive disease of intracranial carotid or middle cerebral artery

**A. SINHA**, V. K Sharma, C. Ning, Y. Tseng Tsai, H. Teoh, B. PL Chan,, R. C Seet, V. F Chong; National University Hospital, SINGAPORE, SINGAPORE.

**Background:** Intracranial stenosis carries an increased risk for cerebrovascular ischemia. In severe stenosis, cerebral autoregulation may be impaired due to inadequate cerebral vasodilatory reserve (CVR) & intracranial steal phenomenon (reversed-Robin Hood syndrome-RRHS). Identification of patients with inadequate CVR and RRHS may help in identifying high-risk patients. **Methods:** In this prospective study, we included patients with symptomatic and severe stenosis of intracranial carotid (ICA) & middle cerebral artery (MCA). CVR was evaluated with transcranial Doppler (TCD) and breath-holding index (BHI) <0.69 determined inadequate CVR. RRHS was detected as transient velocity reduction in affected artery when flow increased in the reference artery. Patients with RRHS were further evaluated with acetazolamide-challenged 99Tc-HMPAO-SPECT. **Results:** 126 patients (80 male, mean age 56yrs; range 23-78yrs) fulfilled our TCD criteria for inadequate CVR. HMPAO-SPECT showed impaired CVR in 84 (67%) patients. RRHS noted on TCD in 38 (45%) patients (median steal magnitude 14%; inter-quartile range, IQR 10) was confirmed by acetazolamide-challenged HMPAO-SPECT (median perfusion deficit 8%; IQR 13%) in 35 (92%) cases (sensitivity 82%, specificity 96% with positive predictive value 96%). A strong relationship between RRHS on TCD and SPECT was noted on ROC curve analysis (area under curve 0.93; 95% confidence interval 0.87-0.98;p<0.00001). Linear relationship was observed between impaired vasodilatory reserve and stroke recurrence during follow up (mean 35months; range 8 to 49months)- 56% in patients with RRHS versus 20% in patients with moderately impaired CVR versus 4% in patients with mildly impaired CVR (chi-square 18.42; df=2; p<0.001 for trend). RRHS on HMPAO-SPECT was an independent predictor of recurrent cerebral ischemic events (RR 1.9, 95%CI 1.2-4.2; p=0.03). **Conclusions:** Among patients with severe intracranial stenosis, intracranial steal phenomenon is associated with high risk of cerebral ischemic events. Acetazolamide-challenged HMPAO-SPECT is reliable in the quantification of vasodilatory reserve for selecting a target group of patients for possible revascularization.

## TP072

### A multi-disciplinary approach to the education and operative responsibilities ensures an efficient adoption of PET/MR in clinical routine.

**K. Stahr**, J. Poulsen, M. Federspiel, A. Hansen, S. H. Keller, H. H. Johannesen, T. Bayer, J. Löfgren; Rigshospitalet, University Hospital of Copenhagen, Copenhagen, DENMARK.

**Objective**: Combined PET/MR is a new imaging modality that challenges the radiographer and the nuclear medicine technologist alike. Ideally, the radiographer should use his/her expertise in MR imaging but expand on his/her PET experience, including know-how on handling radioactive PET tracers. The nuclear medicine technologist should use his/her experience in PET imaging but accumulate knowhow on MR imaging techniques and MR safety issues. **Materials and Methods**: A PET/MR (mMR, Siemens) was installed in our PET department. A multi-disciplinary team of one physicist, one radiologist, one nuclear medicine physician, one computer scientist, two nuclear medicine technologists and one radiographer was formed for PET/MR operations. The radiographer and the two technologists had min. 5 years experience in MR and PET/CT respectively. Both technologists and the radiographer attended external professional training classes in their complementary specialties in order to acquire essential knowledge. Together they designed and ordered all necessary MR compatible equipment for the system. They attended all training programmes provided and deemed necessary and wrote a pre-scan PET/MR patient instruction and a questionnaire concerning MR security for the patients. **Results**: After an inital year of set-up of the PET/MR the radiographer and nuclear medicine technologists are working side-by-side to run daily operations of this new and complex combined technique continuously optimizing patient flow and imaging protocols with no more need for support than on a PET/CT system. In addition both professions do now understand how to handle both MR safety issues and radiation protection for PET tracers on their own in daily clinical routine. **Conclusion**: The radiographer and the nuclear medicine technologist are responsible for running the daily quality control, ensuring that all patients are questioned about MRI safety such as metal implants and metal fragments, and to obtain consent forms. The multi modality approach gives a lot of advantages in upgrading competencies for both radiographers and nuclear medicine technologists fast and while still operating the PET/MR system. It gives a high level of flexibility and a valuable understanding for each other's competencies in a highly specialized environment with a need of very different professional backgrounds in the team.

## TP073

### Artifacts and sources of error in V/Q SPECT

**M. Casanova Martins**[1], R. Silva[1], T. Saraiva[1], J. Isidoro[1], A. P. Moreira[1], G. Costa[1], J. Pedroso de Lima[2]; [1]Nuclear Medicine Department, University Hospitals of Coimbra, CHUC, Coimbra, PORTUGAL, [2]ICNAS, University of Coimbra, Coimbra, PORTUGAL.

Aim: SPECT ventilation/perfusion (V/Q) imaging presents several advantages over traditional planar imaging: greater sensitivity in detecting pulmonary embolism (PE), greater specificity, superior reproducibility, reduced number of inconclusive results while not consuming significantly greater time. SPECT also eases the display of V/Q data in ways that may further enhance diagnostic accuracy, namely ventilation/perfusion quotient images. Objective quantification also improves the diagnostic accuracy of V/Q SPECT in patients with inconclusive or indeterminate scans. The purpose of this study is to identify possible sources of error and artifacts that may impair the value of lung SPECT technique's diagnostic accuracy, either by producing false positive or false negative results. We also aim to point out possible ways of preventing the occurrence of these artifacts. Materials and Methods: V/Q SPECT studies of 202 patients with clinical suspicion of PE were reviewed (126 women, 76 men; 18-95 years, mean age 73.2 years). Sequential Technegas ventilation and MAA perfusion SPECT images were acquired in each patient. A clinically validated software developed in our department was used for processing: subtraction of ventilation background to perfusion images, normalization and calculation of V/Q quotient images. V/Q mismatch quantification was performed in all studies and PE extension quantified. Results: Lung SPECT showed ventilation images with low statistics in 7.4% of the studies (15/202). Of these, 20% (3/15) could not be clinically analyzed. In 8.9% (18/202) V/Q SPECT showed mismatched defects, consistent with patient movement. In 1% (2/202) Technegas retention in the lingula was detected. No artifacts related to incorrect handling of the 99mTc-MAA preparation have been detected. However, lung SPECT showed low statistics in perfusion images in 1.49% (3/202) studies. V/Q SPECT also showed detector contamination in 1.98% studies (4/202). Conclusion: Despite the many error sources that can be considered in V/Q SPECT, a correct patient preparation can reduce the occurrence of artifacts to a minimum level. However, respiratory conditions may hinder proper cooperation during Technegas' inhalation. The use of ambu masks has shown to be very helpful preventing inadequate Technegas administration and improving statistics in ventilation images. Considering detector contamination, Technegas can be administered in a different room, although every effort should be made for the patient to ventilate in supine position, in the same position that 99mTc-MAA should be administered. Although motion artifacts are easily identifiable, patient immobilization is critical, especially when it comes to the precise calculation of V/Q ratios.

## TP074

### 111In labelled platelets for patients with Idiopathic Thrombocytopaenia Purpura - an accurate indication for splenectomy? A Technical Perspective for Nuclear Medicine Department

**N. Swadling**, A. Nunes, M. Luqman, L. Biassoni, H. Jan, A. Haroon, T. Szyszko, N. Hartman, M. Newell, E. O'Mahoney; Barts Health NHS Trust, London, UNITED KINGDOM.

Idiopathic thrombocytopenic purpura (ITP) is an illness of primary acquired thrombocytopenia with normal bone marrow and absence of other causes. Splenectomy was first used as a treatment for Idiopathic thrombocytopenic purpura in 1913. The significance of the determination of the site of platelet sequestration as indication for splenectomy in idiopathic thrombocytopenic purpura is of the utmost importance considering that this surgical technique is currently one of the most effective therapies for ITP. The demand for a reliable procedure that provides such indication has been steadily increasing over the last decade and we are currently experiencing a high demand in our institution with referrals from all over the world. We routinely perform 111In labelled platelets scans as pre-surgical predictor of efficacy outcome. This presentation outlines our technical procedures and experience regarding patient preparation, blood labelling, imaging and venous blood sampling to ensure highest quality of diagnostic test is performed. The results of the procedure are usually indicated as purely or predominantly splenic versus mixed or hepatic sequestration. Examples of these different outcomes are included in order to increase the knowledge of a procedure that is infrequently performed across Europe and the rest of the World.

## TP075

### Labeling activated autologous cytotoxic T lymphocytes with $^{111}$In tropolone and $^{99m}$Tc-HMPAO

**T. S. Lundby**[1], W. Fischer[2], J. Mortensen[1]; [1]Dept. of Clinical Physiology & Nuclear Medicine, Rigshospitalet, Copenhagen, DENMARK, [2]Dept. of neurosurgery, Rigshospitalet, Copenhagen, DENMARK.

**Background***:* Shared cancer testis (CT) antigens are expressed in various tumors and are attractive tumour-specific targets for polyclonal immunotherapy. ALECSAT is a new medical product for cancer immunotherapy and consists predominantly of autologous cytotoxic T lymphocytes activated against CT antigens, and NK cells. Isolated CD8+ cells from this product kills a broad spectrum of tumour cells in vitro including the U87 lioblastoma (GBM) cell line and show cytolytic activity on tumour biopsy material from patients with GBM. To determine the effect of the immunotherapy in vivo, two types of labelling with $^{111}$In tropolone or $^{99m}$Tc-HMPAO were performed. After labelling the activated T lymphocytes, these were injected into the GBM patients and both planar scans and SPECT/CT images were acquired. One experienced nuclear medicine physician reviewed both scans with regard to the presence and location of any focus of abnormal radioactivity accumulation. **Aim:** To compare the efficiency of the two labelling Methods*. Materials and* **Methods***: Labeling with $^{111}$In tropolone*: ALECSAT cells suspended in 1-2 ml buffer called "plasma-light" were mixed with 20-30 MBq of $^{111}InCl_3$ and 0.1 ml of 0.0044 M tropolone. Following centrifugation, resuspension and quality control, a dose of 9-12 MBq of labeled ALECSAT cells was injected intravenously within 1 h after labeling. *Labeling with $^{99m}$Tc-HMPAO*: using almost similar steps as described above except that the mixture added to the cells then were 900-1100 MBq of $^{99m}$Tc-HMPAO (Ceretec). After centrifugation, resuspension and quality control, a dose of 150 - 200 MBq of labeled ALECSAT cells were injected into the patient, although the expected dose would be 300 - 500 MBq. **Results:** Radiolabeling efficiency was always between 64% and 97%, for the ALECSAT cell labeling with $^{111}$In tropolone and between 5% and 34% for the ALECSAT cells labeled with $^{99m}$Tc-HMPAO (Ceretec). The viability of the radiolabeled ALECSAT cells was tested by the trypan blue exclusion test before reinfusion in the first 2 patient examinations. Both types of labeling showed normal physiological distribution of ALECSAT cells, similar to the white blood cell scintigraphy distribution in red bone marrow, liver and spleen. In addition, there was an uptake of the labeled ALECSAT cells in GBM brain tumours. **Conclusion***:* Labelling of activated autologous cytotoxic T lymphocytes was possible with both $^{111}$In tropolone and $^{99m}$Tc-HMPAO, however, the labelling method with $^{111}$In tropolone gave the best efficiency.

## TP076

### How to successfully optimise the sequence of renography in children

**B. Ingvardsen**, P. Lemvig, L. Søndergaard, S. Møller, D. Cortes; Hvidovre Hospital, Copenhagen, DENMARK.

Background Use of chloral hydrate for sedation of paediatric patients can be associated with adverse side-effects, for example arterial desaturation wherefore the children should be observed during the sedation-procedure. The sedation period is up to 8 hours, the children need to fast and should be hydrated intravenously. Therefore, from June 2010 we changed the regimen to use melatonin in renography in children. Melatonin is a native neurohormone that induces sleep without reported side-effects. Melatonin is well-tolerated in children below 3 years. Nevertheless, some children may have a light sleep and may wake-up during motional disturbances. A pilot study showed that the changed procedure with the use of melatonin resulted in an increased time consumption (110 minutes versus 60 minutes). The ratio of disturbed children and cancelled renography studies were similarly increased. Aim The aim of this study was to optimise the course during renographies in paediatric patients younger than 3 years. Material and Methods A special form was elaborated for the registration of data in all paediatric patients admitted for renography. The following variables were implemented and monitored: 1. Number of children treated with melatonin. 2. Time consumption for each study. 3. Type of transport from the Department of Paediatrics to the Department of Clinical Physiology (baby-carriage, bed etc.) 4. Type of removal (sheet, placement in paediatric-box specially suited for nuclear-medicine-studies.) 5. Number of successful studies. 6. The condition of the child during the study (sleeping, restless, in pain etc.). A total of 383 patients were included. The filled-in forms were analysed every third month. Hereafter, the results were discussed with the staff of the Department of Paediatrics and necessary adjustments were secured. Results In the study period, the number of successful renography studies increased from 78% to 87% ($p < 0.05$). The average time consumption decreased from 108 to 52 minutes ($p < 0.05$). Out-clinic patients were discharged faster after end of the study since sustained observation is not required after use of melatonin. The staff from the Department of Clinical Physiology and the Department of Paediatrics experienced excess time for other purposes due to this more efficient procedure. Conclusions and perspectives The changed sedation regime improved the number and quality of successful renographies. Since the results of the project were very promising, the new procedure has been implemented in the department and cooperation with the Department of Paediatrics will be expanded to other fields and studies.

## TP077

### Study on the Evaluation of Renal Function according to set a partial Region of Interest in $^{99m}$Tc-DMSA scan of the Pediatric Patient with a Duplicated Ureter.

**H. Nam-Koong**, S. Oh; Severance Hospital, Yonsei University Health System, Seoul, KOREA, REPUBLIC OF.

**Purpose:** Patients with duplicated ureter are in force to $^{99m}$Tc-DMSA scan at surgery before and after. In existing examination, at produce result after $^{99m}$Tc-DMSA scan, didn't compare to upper pole and lower pole with malformed kidney and compared to only relative uptake ratio. Therefore, this study will examine about utility of set a partial region of interest and to functional recovery of renal cell through change of upper pole uptake ratio of malformed kidney by setting each partial region of interest in upper pole and lower pole of malformed kidney in $^{99m}$Tc-DMSA examination in surgery before and after. **Materials and Methods:** Pediatric patients with malformed kidney of incomplete duplicated ureter, 15 patients were enrolled in this study. Scanning were scan 3 to 4 hours after injection of $^{99m}$Tc-DMSA 1.5 ~ 1.9 MBq / Kg. Region of interest were each set in normal kidney, upper pole and lower pole with malformed kidney. Region of interest were set with same condition and method to images of surgery before and after that radio technologist 1 person, resident of nuclear medicine 1 person and doctor of urology together. Therefore, this study were compared to uptake ratio (A: B: C) that normal kidney (A), lower pole of malformed kidney (B) and upper pole of malformed kidney (C) about uptake ratio changes of malformed kidney in follow-up examination of surgery before and after. **Results:** When compared to 15 patients, uptake ratios were increased 7 persons and decreased 8 persons. Among increased 7 persons, it were periods of follow-up examination that 2 persons were 14 months, 4 persons were 12 months and 1 person was 8 months after surgery. Among decreased 8 persons, it were periods of follow-up examination that 4 persons were 12 months 3 persons were 6 months and 1 persons were 4 months after surgery. **Conclusion:** Existing study could not see the exact uptake ratio changes of malformed kidney because using only the overall Left-Right kidney uptake ratios. But a setting partial region of interest was able to see exactly what changes in the uptake of each upper pole and lower pole of malformed kidney. Because recovery of renal parenchymal cells is difficult in an evaluation of short period of time, follow-up examination should be made in long period of time. How to set up partial region of interest be thought that it would be useful.

## TP078

### A survey of the clinical use of exogenous isotopes to measure GFR, and details of measurement in Denmark

**N. S. Nielsen**; Aalborg University Hospital, Aalborg, DENMARK.

**Aim** To perform a survey of the different GFR-protocols using radioactive isotopes (Cr-51 EDTA or Tc-99m DTPA) in Denmark, in order to put our own protocol in perspective. **Materials and Methods** By questioning all nuclear medicine departments in Denmark about their GFR-protocol, it is sought to develop an overview of the differences in our protocols. In addition to the questionnaire some information were derived from the departments' published protocol. **Results** Of the 19 nuclear medicine department in Denmark the survey enrolled all 19 departments. Overall the procedure is mainly the same all over Denmark with minor differences. The differences include: Type of radioactive isotope (Cr-51 EDTA: 14 dep. Tc-99m DTPA: 5 dep.), Patient preparation, Patient conditions during examination, Activity administered to the patient (Cr-51 EDTA: 2.5 - 8 MBq; Tc-99m DTPA: 20 - 40 MBq or 1.25 MBq/kg), Number of blood samples (1-5 samples), Definition of child (age limit ranging from 12 to 16 years). **Conclusion** All department use radioactive isotopes (Cr-51 EDTA or Tc-99m DTPA) to calculate GFR and use separate protocols for adult and children. The use of other non-radioactive tracers such as iohexol is not implemented in Denmark. Most department use adjusted/specific protocols depending on the estimated kidney function (mostly eGFR on behalf of the individual P-creatinine), to increase the accuracy of the protocol. There are a number of small variations in GFR-protocols in Denmark, but the reasons for these variations were not investigated in this survey. The main reason is probably due to local conditions, such as the number of patients, equipment and medical experience with the used protocol. Based on this survey our own department is currently discussing whether some patient (patients with high kidney function i.e. eGFR > 100 mL/min/1.73m2) could undergo a protocol using only 1 sample instead of 4 samples. This could save time when analyzing the samples.

## TP079

### Quality Strategies in Nuclear Medicine Technologies Education - Lisbon experience

**T. F. Vaz**, M. Carapinha, F. Lucena, E. Sousa, L. Vieira; Escola Superior de Tecnologia da Saúde de Lisboa, Lisboa, PORTUGAL.

Introduction: Nuclear Medicine Education (NME) in Portugal is provided by two public Higher Education Institutions, in Lisbon and Porto. In Lisbon, the school is installed in a new building since 2001, projected to accomplish the mission of excellence in teaching, research and community service within the Health Sciences, helping to promote health and improve its quality. The higher standards in NME at the Lisbon School have been sustained by the consolidation of theoretical knowledge with practical lessons in the laboratories of Nuclear Medicine. The aim of this study was to evaluate the impact of the adoption of Quality Strategies in Nuclear Medicine Laboratories (QSNML) in the improvement of practical teaching. Methods: SWOT analysis of QSNML was developed from the perspective of the NME provider: strengths, weaknesses, opportunities and threats of the NML were identified for the years of 2004 and 2012 by NM teachers based on brainstorm methodology. Results/Discussion: The comparison of SWOT analysis of 2004 and 2012 allows the evidence of adequacy of NML to excellence in teaching and research and in the improvement of its quality. The weaknesses identified in 2004 and 2012 point the necessity of structural changes (e.g. lack of working equipment, insufficient laboratory area), although the absence of funds support their persistence. The main strengths identified in 2004 were related to the potentiality of NML infrastructures, intellectual resources and teachers' knowhow and creativity, and allowed the development of new opportunities, such as creative and innovative pedagogic strategies for practical lessons in NML. The Authorization from the Health Ministry (lacking in 2004) for use of radioactivity in the laboratories for teaching and research purposes was one of the main pillars for improvement in practical teaching quality. Also the acquisition of new working equipment and the development of the Security Manual (SM) of the NML permitted the offer of an improved teaching/learning environment, according to the radiation protection regulation and the written procedures of the SM. This allows the students to acquire practical competencies and experience in an academic and controlled environment before the clinical experience at partners Health Institutions. Conclusion: The adoption of Quality Strategies in Nuclear Medicine Laboratories contributes positively for the improvement of practical teaching, providing the implementation of norms in the academic environment.

# Author Index

# EANM'14

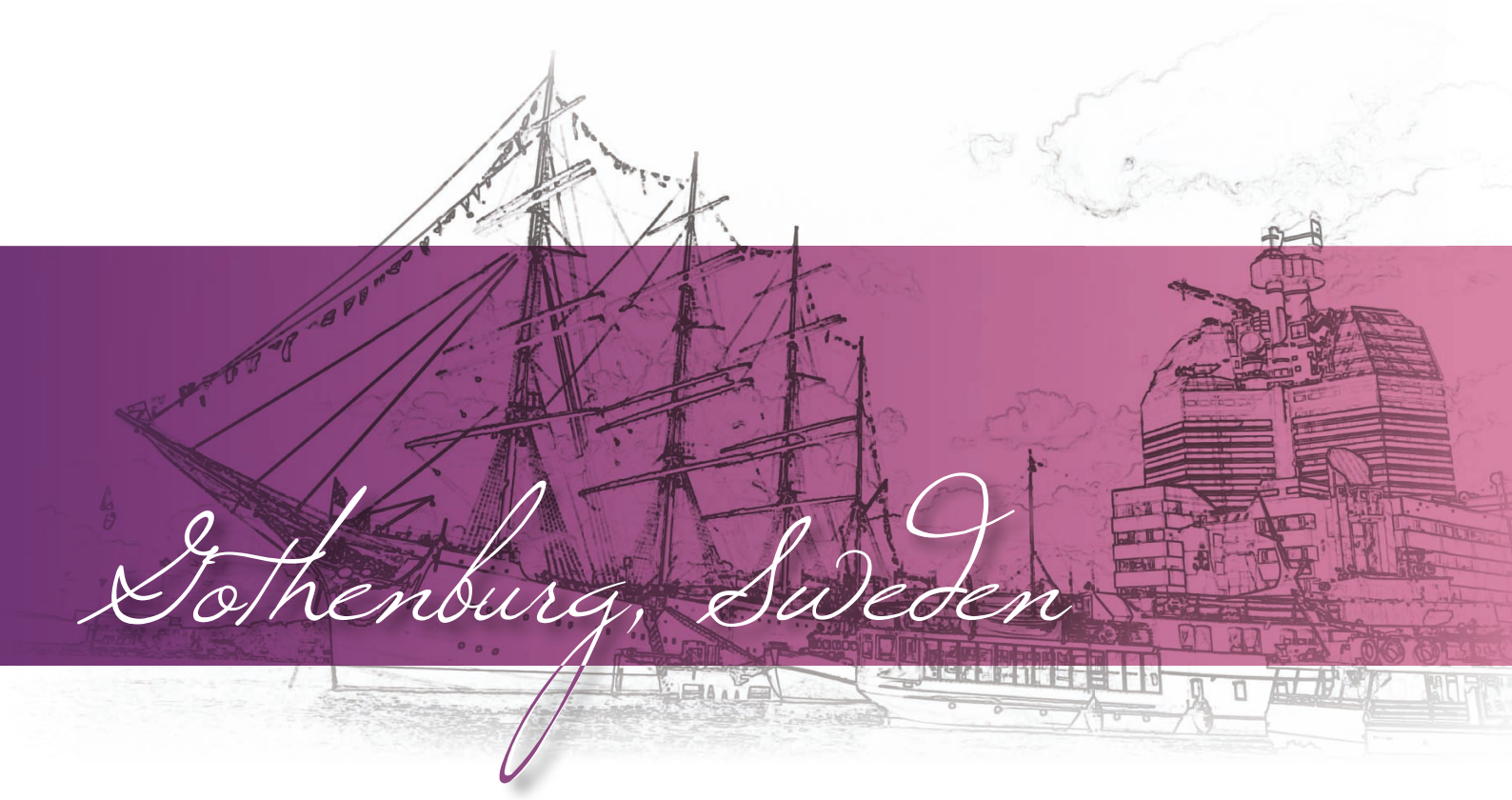


## Annual Congress of the European Association of Nuclear Medicine

October 18–22, 2014
Gothenburg, Sweden

www.eanm.org